

ICMEs, Geostorms, Forbush decreases

NOAA SPACE WEATHER SCALES

<https://www.swpc.noaa.gov/noaa-scales-explanation>

Space Weather Live

<https://www.spaceweatherlive.com/en.html>

Solar cycle 25 Shocks Catalog

<https://data.serpentine-h2020.eu/catalogs/shock-sc25/>

See:

An Overview of Solar Orbiter Observations of Interplanetary Shocks in Solar Cycle 25

Review

D. Trotta, [A. Dimmock](#), [H. Hietala](#), [X. Blanco-Cano](#), [T. S. Horbury](#), +++

ApJ 2024

<https://arxiv.org/pdf/2410.24007>

SCOSTEP/PRESTO

Predictability of the Solar-Terrestrial Coupling

<https://scostep.org/presto/>

Collection, Collation, and Comparison of 3D Coronal CME Reconstructions

Catalogs

[C. Kay](#), [E. Palmerio](#)

Space Weather. [Volume22, Issue1](#) e2023SW003796 2024

<https://arxiv.org/pdf/2311.10712.pdf>

<https://agupubs.onlinelibrary.wiley.com/doi/epdf/10.1029/2023SW003796>

A **catalogue** of observed geo-effective CME/ICME characteristics

R. [Mugatwala](#), [S. Chierichini](#), [G. Francisco](#), [G. Napoletano](#), [R. Foldes](#), [L. Giovannelli](#), [G. De Gasperis](#), [E. Camporeale](#), [R. Erdélyi](#), [D. Del Moro](#)

Journal of Space Weather and Space Climate 2023

<https://arxiv.org/pdf/2311.13429.pdf>

See <https://zenodo.org/records/8063404>

Five significant geomagnetic storms in 2023: Jan. 15 (0.59 TW), Feb. 16 (0.62 TW), Feb. 27 (0.78 TW), Mar. 24 (1.04 TW), and April 24 (1.02 TW)

We perform hindcasts Мы делаем ретроспективные прогнозы

Minor, Moderate, Strong, Severe, Extreme

Data Availability

The solar-wind plasma and IMF data are available at NASA's OMNIWeb (omniweb.gsfc.nasa.gov/). The CME information is available at the Coordinated Data Analysis Workshops (CDAW; cdaw.gsfc.nasa.gov/). The coronal hole images are available at the Solar Dynamics Observatory (SDO; sdo.gsfc.nasa.gov/). The geomagnetic indices are available at the World Data Center for Geomagnetism, Kyoto, Japan (WDC: wdc.kugi.kyoto-u.ac.jp/). The F10.7F10.7 solar fluxes are available at the Laboratory for Atmospheric and Space Physics Interactive Solar Irradiance Data Center (lasp.colorado.edu/lisird/). The CIR event list is obtained from the Electronic Supplementary Material available at [DOI](#).

Top 50 geomagnetic storms by years and Cycles

<https://www.spaceweatherlive.com/en/auroral-activity/top-50-geomagnetic-storms.html>

Table 1 The largest storm intensity for each SC from 1932 to 2016

Table 4 The GGSs during SCs 17 – 24 ($Dst \leq -200$ nT).

Source Locations and Solar-Cycle Distribution of the Major Geomagnetic Storms ($Dst \leq -100$ nT) from 1932 to 2018

Gui-Ming Le, [Ming-Xian Zhao](#), [Wen-Tao Zhang](#) & [Gui-Ang Liu](#)

[Solar Physics](#) volume 296, Article number: 187 (2021)

<https://link.springer.com/content/pdf/10.1007/s11207-021-01927-w.pdf>

<https://doi.org/10.1007/s11207-021-01927-w>

The Solar Orbiter mission

[Astronomy & Astrophysics](#) Volume 642 2020 SPECIAL ISSUES

<https://www.aanda.org/component/toc/?task=topic&id=1082>

<https://www.aanda.org/articles/aa/abs/2020/10/contents/contents.html>

[Solar Orbiter First Results \(Cruise Phase\)](#): many papers on ³He-rich SEPs, near-relativistic electrons, [stealth](#) CME, ICMEs, GCR flux, Forbush

[Astronomy & Astrophysics](#) Volume 656 (December 2021)

<https://www.aanda.org/articles/aa/abs/2021/12/contents/contents.html>

A **Catalog of Interplanetary Coronal Mass Ejections** Observed by Juno between 1 and 5.4 AU

Emma E. [Davies](#) (1,2), [Robert J. Forsyth](#) (2), [Réka M. Winslow](#) (1), [Christian Möstl](#) (3), [Noé Lugaz](#) (1)

2021 *ApJ* **923** 136

<https://arxiv.org/pdf/2111.11336.pdf>

<https://doi.org/10.3847/1538-4357/ac2ccb>

Astronomy & Astrophysics

Volume 650 (June 2021)

Parker Solar Probe: Ushering a new frontier in space exploration

<https://www.aanda.org/articles/aa/abs/2021/06/contents/contents.html>

Earth-affecting Solar Transients: A **Review** of Progresses in Solar **Cycle 24**

Jie **Zhang**, [Manuela Temmer](#), [Nat Gopalswamy](#), +++

Progress in Earth and Planetary Science, Volume 8, Issue 1, article id.56, **2021**

<https://progearthplanetsci.springeropen.com/counter/pdf/10.1186/s40645-021-00426-7.pdf>

<https://arxiv.org/ftp/arxiv/papers/2012/2012.06116.pdf> **File 2021**

2020 <https://arxiv.org/abs/2012.06116>

ICMEs-IH	HEL-CAT S	STEREO HI event catalogs including HICAT, HIJoinCAT, HIGeoCAT http://www.helcats-fp7.eu/	(Harrison et al. 2018)
ICMEs-IS	--	ACE ICMEs since 1996 compiled by Richardson & Cane http://www.srl.caltech.edu/ACE/ASC/DATA/level3/icmetable2.htm	(I. G. Richardson and Cane 2010)
ICMEs-IS	--	WIND ICME catalog (1995-2015) https://wind.nasa.gov/ICME_catalog/ICME_catalog_viewer.php	(T. Nieves-Chinchilla, Vourlidas, et al. 2018)
ICMEs-IS	--	WIND Magnetic Cloud list (1995-2006) https://wind.nasa.gov/mfi/mag_cloud_pub1.html	(Lepping and Wu 2007)
ICMEs-IS	--	WIND ICME catalog (1995-2015) http://space.ustc.edu.cn/dreams/wind_icmes/	(Chi et al. 2016)
ICMEs-IS	--	ICMEs and other large scale structures in solar wind ftp://www.iki.rssi.ru/pub/omni/	(Yu. I. Yermolaev et al. 2009)
Shocks	--	CfA Interplanetary Shock Database https://www.cfa.harvard.edu/shocks/	--
Shocks	--	Heliospheric shock database at the University of Helsinki http://ipshocks.fi/	(E. K. J. Kilpua et al. 2015)
ICMEs-CMEs	--	ICMEs and their solar sources in solar cycle 24 from GMU http://solar.gmu.edu/heliophysics/index.php/GMU_CME/ICME_List	(Hess and Zhang 2017)

Solar and Geomagnetic Indices (SGI) Plots and Data Files

http://www.timed.jhuapl.edu/WWW/scripts/mdc_browse.pl#Instruments

The revisited ICMEs catalog is at https://idoc.ias.u-psud.fr/sites/idoc/files/CME_catalog/html/ACE-ICMEs-list-dates-quality-nosheath-forweb.html

20 Years of ACE Data: How Superposed Epoch Analyses Reveal Generic Features in Interplanetary CME Profiles

F. **Regnault**, [M. Janvier](#), [P. Démoulin](#), [F. Auchère](#), [A. Strugarek](#), [S. Dasso](#), [C. Noùs](#)

JGR **2020**

Review

<https://arxiv.org/pdf/2011.05050.pdf>

1 minute SYM-H indices; HILDCAAs, The auroral SME and SML indices

See **The Complex Space Weather Events of 2017 September**

Rajkumar **Hajra**¹, Bruce T. Tsurutani², and Gurbax S. Lakhina³

2020 ApJ 899 3 **File**

<https://doi.org/10.3847/1538-4357/aba2c5>

WHPI, the Whole Heliosphere and Planetary Interactions

The Astrophysical Journal Supplement Series

[Volume 246](#), Number 2, 2020 February

Early Results from **Parker Solar Probe**: Ushering a New Frontier in Space Exploration

<https://iopscience.iop.org/issue/0067-0049/246/2>

The theme issue '**Solar eruptions and their space weather impact**'. **Reviews**

Philosophical Transactions of the Royal Society A: Mathematical, Physical and Engineering Sciences

v. 377 [Issue 2148](#) 2019

<https://royalsocietypublishing.org/toc/rsta/377/2148>

Extreme Events in Geospace

Origins, Predictability, and Consequences

Book

Editor: Natalia **Buzulukova**, Elsevier, 2018, 798 p. **File**

Site <https://www.sciencedirect.com/science/article/pii/B9780128127001099921>

Download PDF --> Download full book

<https://www.sciencedirect.com/book/9780128127001/extreme-events-in-geospace>

Publications of the Athens Neutron Monitor Group

<http://cosray.phys.uoa.gr/index.php/publications-menu/publications>

The websites http://www.olen.info/solar/coronal_holes.html and

http://cdaw.gsfc.nasa.gov/CME_list/, providing data for the **coronal holes** and for the **coronal mass ejections**, respectively,

Table : An updated catalogue of High-Speed Solar Wind Streams (HSSWSs) from 2009 to 2016.

Supplementary material [11207_2018_1348_MOESM1_ESM.docx](#)

High-Speed Solar Wind Streams and Geomagnetic Storms During Solar Cycle 24

M. **Gerontidou**, H. Mavromichalaki, T. Daglis

[Solar Physics](#) September 2018, 293:131

<https://link.springer.com/article/10.1007/s11207-018-1348-8>

An updated catalog is created of 303 well-defined high-speed solar wind streams that occurred in the time period 2009–2016. These streams are identified from solar and interplanetary measurements obtained from the OMNIWeb database as well as from the Solar and Heliospheric Observatory (SOHO) database. This time interval covers the deep minimum observed between the last two Solar Cycles 23 and 24, as well as the ascending, the maximum, and part of the descending phases of the current Solar Cycle 24. The main properties of solar-wind high-speed streams, such as their maximum velocity, their duration, and their possible sources are analyzed in detail. We discuss the relative importance of all those parameters of high-speed solar wind streams and especially of their sources in terms of the different phases of the current cycle. We carry out a comparison between the characteristic parameters of high-speed solar wind streams in the present solar cycle with those of previous solar cycles to understand the dependence of their long-term variation on the cycle phase. Moreover, the present study investigates the varied phenomenology related to the magnetic interactions between these streams and the Earth's magnetosphere. These interactions can initiate geomagnetic disturbances resulting in geomagnetic storms at Earth that may have impact on technology and endanger human activity and health.

we use the timings of different structures/features of **ICMEs and CIRs** detected during solar cycle 23 (1995–2009) from the **catalogue prepared and made available by L. Jian** (http://www-ssc.igpp.ucla.edu/~jlan/ACE/Level3/ICME_List_from_Lan_Jian.pdf) and (http://www-ssc.igpp.ucla.edu/~jlan/ACE/Level3/SIR_List_from_Lan_Jian.pdf).

Topical collections: [Earth-affecting Solar Transients](#) **CMEs/ICMEs**
Solar Phys. 2017

https://link.springer.com/journal/11207/topicalCollection/AC_74be62d9d035e23ca163bf5434bd2877

См. <http://www.youtube.com/watch?v=QAs73yvZ7eY> и представленные там фильмы-лекции

Near-Earth Interplanetary Coronal Mass Ejections Since January 1996 (to December 2016)

Compiled by Ian **Richardson**(1) and Hilary **Cane**(2),

<http://www.srl.caltech.edu/ACE/ASC/DATA/level3/icmetable2.htm>

2013 LWS TR&T Steering Committee recommendations 11/30/2013

Physics--based Predictive Capability Development

http://lwstrt.gsfc.nasa.gov/LWS_2013_SCReport.pdf

<http://solarnews.nso.edu/2015/20150415.html>

A catalog of Earth-directed coronal mass ejections (CMEs) observed by STEREO

http://sprg.ssl.berkeley.edu/~liuxying/CME_catalog.htm

Solar Phys. Volume 284, Issue 1, May 2013

Topical Issue

Flux-Rope Structure of Coronal Mass Ejections / Guest Editors: N. Gopalswamy, T. Nieves-Chinchilla, M. Hidalgo, J. Zhang, and P. Riley

Recurrent Magnetic Storms: Corotating Solar Wind Streams

Editor(s): Bruce Tsurutani, Robert McPherron, Gang Lu, José H. A. Sobral, Natchimuthukonar Gopalswamy
AGU Monograph, Vol. 167, 2006 (?), 2013
<http://onlinelibrary.wiley.com/book/10.1029/GM167>

Магнитные бури и магнитосферные суббури

Калегаев В.В., Алексеев И.И., Кропоткин А.П.
<http://nuclphys.sinp.msu.ru/cosm/index-15.htm>

Physics of Space Storms

From the Solar Surface to the Earth

Hannu E. J. **Koskinen**

2011, ISBN 978-3-642-00310-3 e-ISBN 978-3-642-00319-6

DOI 10.1007/978-3-642-00319-6

Springer Heidelberg Dordrecht London New York

<http://www.springerlink.com/content/978-3-642-00310-3/#section=845487&page=1&locus=49>

<http://www.springer.com/earth+sciences+and+geography/atmospheric+sciences/book/978-3-642-00310-3>

File of Contents

In addition to light and other wavelengths of electromagnetic radiation the Sun affects our environment through complicated plasma physical processes. The study of these interactions is known as solar–terrestrial physics. Already long before the space era there were indications that solar activity and geomagnetic perturbations must somehow be connected. **A remarkable event was the large flare on the Sun observed, independently, by Carrington [1859] and Hodgson [1859] on September 1, 1859, after which a major magnetic storm commenced only 17 hours later.**

Today we understand that the storm was caused by a magnetic cloud associated with a coronal mass ejection (CME) that reached the Earth exceptionally quickly. The storm was very strong, evidently much stronger than any event recorded during the present era of space weather sensitive equipment in space and on the ground.

Journal of Atmospheric and Solar-Terrestrial Physics

Volume 73, Issue 10, Pages 1077-1292 (20 June 2011)

Three dimensional aspects of CMEs, their source regions and interplanetary manifestations

Edited by Marilena Mierla, Nandita Srivastava and Luciano Rodriguez

ICMEs, Topical issue

REMOTE SENSING OF THE INNER HELIOSPHERE

Solar Phys (2010) 265: 1–3

Preface

M. M. Bisi, A. R. Breen, L. van Driel-Gesztelyi and C. H. Mandrini

Общие сведения о методах

Space Science Reviews (2006), v. 123

This volume is the result of a series of workshops during the years 2000–2004 to

study in detail origin, development, and effects of coronal mass ejections (CMEs).

Special Issue: Coronal Mass Ejections

Guest Editors: N. U. Crooker, J. A. Linker and R. Schwenn

1-2

Foreword

H. Kunow, N. U. Crooker, J. A. Linker, R. Schwenn and R. von Steiger

[Show Summary](#)

[Download PDF \(69.4 KB\)](#)

3-11

A Brief History of CME Science

David Alexander, Ian G. Richardson and Thomas H. Zurbuchen

[Show Summary](#)

[Download PDF \(148.8 KB\)](#)

13-30

Coronal Mass Ejections: Overview of Observations

H. S. Hudson, J.-L. Bougeret and J. Burkepile

[Show Summary](#)

[Download PDF \(518.9 KB\)](#)

31-43

In-Situ Solar Wind and Magnetic Field Signatures of Interplanetary Coronal Mass Ejections

Thomas H. Zurbuchen and Ian G. Richardson

[Show Summary](#)

[Download PDF \(348.7 KB\)](#)

45-56

An Introduction to CMEs and Energetic Particles

H. V. Cane and D. Lario

[Show Summary](#)

[Download PDF \(745.2 KB\)](#)

57-80

An Introduction to Theory and Models of CMEs, Shocks, and Solar Energetic Particles

Z. Mikić and M. A. Lee

[Show Summary](#)

[Download PDF \(289.3 KB\)](#)

81-92

An Introduction to the Pre-CME Corona

David Alexander

[Show Summary](#)

[Download PDF \(155.0 KB\)](#)

93-109

Solar Imprint on ICMEs, Their Magnetic Connectivity, and Heliospheric Evolution

N. U. Crooker and T. S. Horbury

[Show Summary](#)

[Download PDF \(291.2 KB\)](#)

111-126

ICMEs in the Outer Heliosphere and at High Latitudes: An Introduction

R. von Steiger and J. D. Richardson

[Show Summary](#)

[Download PDF \(572.5 KB\)](#)

127-176

Coronal Observations of CMEs

Report of Working Group A

R. Schwenn, J. C. Raymond, D. Alexander, A. Ciaravella and N. Gopalswamy, et al.

[Show Summary](#)

[Download PDF \(1.3 MB\)](#)

177-216

Understanding Interplanetary Coronal Mass Ejection Signatures

Report of Working Group B

R. F. Wimmer-Schweingruber, N. U. Crooker, A. Balogh, V. Bothmer and R. J. Forsyth, et al.

[Show Summary](#)

[Download PDF \(1.0 MB\)](#)

217-250

Energetic Particle Observations

Report of Working Group C

B. Klecker, H. Kunow, H. V. Cane, S. Dalla and B. Heber, et al.

[Show Summary](#)

[Download PDF \(529.3 KB\)](#)

251-302

CME Theory and Models

Report of Working Group D

T. G. Forbes, J. A. Linker, J. Chen, C. Cid and J. Kóta, et al.

[Show Summary](#)

[Download PDF \(1.5 MB\)](#)

303-339

The Pre-CME Sun

Report of Working Group E

N. Gopalswamy, Z. Mikić, D. Maia, D. Alexander and H. Cremades, et al.

[Show Summary](#)

[Download PDF \(1.1 MB\)](#)

341-382

Multi-Wavelength Observations of CMEs and Associated Phenomena

Report of Working Group F

M. Pick, T. G. Forbes, G. Mann, H. V. Cane and J. Chen, et al.

[Show Summary](#)

[Download PDF \(934.5 KB\)](#)

383-416

ICMEs in the Inner Heliosphere: Origin, Evolution and Propagation Effects

Report of Working Group G

R. J. Forsyth, V. Bothmer, C. Cid, N. U. Crooker and T. S. Horbury, et al.

[Show Summary](#)

[Download PDF \(1.1 MB\)](#)

417-451

ICMEs at High Latitudes and in the Outer Heliosphere

Report of Working Group H

P. R. Gazis, A. Balogh, S. Dalla, R. Decker and B. Heber, et al.

[Show Summary](#)

[Download PDF \(1.4 MB\)](#)

453-470
CME Disturbance Forecasting
G. Siscoe and R. Schwenn
Show Summary
Download PDF (345.2 KB)

471-480
Coronal Mass Ejections
A Personal Workshop Summary
R. F. Wimmer-Schweingruber
Show Summary
Download PDF (382.5 KB)

481-484
Glossary
Show Summary
Download PDF (72.4 KB)

ILWS WORKSHOP

**Solar Influence on the Heliosphere and Earth's Environment:
Recent Progress and Prospects**

N. Gopalswamy and A. Battacharyya (Editors),

Quest Publications, Mumbai, 453 pages, hardbound, 2006, ISBN 81-87099-40-2

http://cdaw.gsfc.nasa.gov/publications/ilws_goa2006/

Measurements of the Time-Dependent Cosmic-Ray Sun Shadow with Seven Years of IceCube Data -- Comparison with the Solar Cycle and Magnetic Field Models

[M. G. Aartsen](#), [R. Abbasi](#), [M. Ackermann](#), [J. Adams](#), [J. A. Aguilar](#), and many others

2020

<https://arxiv.org/pdf/2006.16298.pdf>

Observations of the time-dependent cosmic-ray Sun shadow have been proven as a valuable diagnostic for the assessment of solar magnetic field models. In this paper, seven years of IceCube data are compared to solar activity and solar magnetic field models. A quantitative comparison of solar magnetic field models with IceCube data on the event rate level is performed for the first time. Additionally, a first energy-dependent analysis is presented and compared to recent predictions. We use seven years of IceCube data for the Moon and the Sun and compare them to simulations on data rate level. The simulations are performed for the geometrical shadow hypothesis for the Moon and the Sun and for a cosmic-ray propagation model governed by the solar magnetic field for the case of the Sun. We find that a linearly decreasing relationship between Sun shadow strength and solar activity is preferred over a constant relationship at the 6.4sigma level. We test two commonly used models of the coronal magnetic field, both combined with a Parker spiral, by modeling cosmic-ray propagation in the solar magnetic field. Both models predict a weakening of the shadow in

times of high solar activity as it is also visible in the data. We find tensions with the data on the order of 3σ for both models, assuming only statistical uncertainties. The magnetic field model CSSS fits the data slightly better than the PFSS model. This is generally consistent with what is found previously by the Tibet AS-gamma Experiment, a deviation of the data from the two models is, however, not significant at this point. Regarding the energy dependence of the Sun shadow, we find indications that the shadowing effect increases with energy during times of high solar activity, in agreement with theoretical predictions.

Slow Solar Wind: Observations and Modeling

Review

L. **Abbo**, L. Ofman, S. K. Antiochos, V. H. Hansteen, L. Harra, Y.-K. Ko, G. Lapenta, B. Li, P. Riley and 3 more

Space Sci. Rev. Volume 201, [Issue 1](#), pp 55–108 2016

While it is certain that the fast solar wind originates from coronal holes, where and how the slow solar wind (SSW) is formed remains an outstanding question in solar physics even in the post-SOHO era. The quest for the SSW origin forms a major objective for the planned future missions such as the Solar Orbiter and Solar Probe Plus. Nonetheless, results from spacecraft data, combined with theoretical modeling, have helped to investigate many aspects of the SSW. Fundamental physical properties of the coronal plasma have been derived from spectroscopic and imaging remote-sensing data and in situ data, and these results have provided crucial insights for a deeper understanding of the origin and acceleration of the SSW. Advanced models of the SSW in coronal streamers and other structures have been developed using 3D MHD and multi-fluid equations.

However, the following questions remain open: What are the source regions and their contributions to the SSW? What is the role of the magnetic topology in the corona for the origin, acceleration and energy deposition of the SSW? What are the possible acceleration and heating mechanisms for the SSW? The aim of this review is to present insights on the SSW origin and formation gathered from the discussions at the International Space Science Institute (ISSI) by the Team entitled “Slow solar wind sources and acceleration mechanisms in the corona” held in Bern (Switzerland) in March 2014 and 2015.

Prediction of the SYM-H Index Using a Bayesian Deep Learning Method With Uncertainty Quantification

Yasser **Abduallah**, [Khalid A. Alobaid](#), [Jason T. L. Wang](#), [Haimin Wang](#), [Vania K. Jordanova](#), [Vasyl Yurchyshyn](#), [Huseyin Cavus](#), [Ju Jing](#)

Space Weather [Volume22, Issue2](#) February 2024 e2023SW003824

<https://agupubs.onlinelibrary.wiley.com/doi/epdf/10.1029/2023SW003824>

We propose a novel deep learning framework, named SYMHnet, which employs a graph neural network and a bidirectional long short-term memory network to cooperatively learn patterns from solar wind and interplanetary magnetic field parameters for short-term forecasts of the SYM-H index based on 1- and 5-min resolution data. SYMHnet takes, as input, the time series of the parameters' values provided by NASA's Space Science Data Coordinated Archive and predicts, as output, the SYM-H index value at time point $t + w$ hours for a given time point t where w is 1 or 2. By incorporating Bayesian inference into the learning framework, SYMHnet can quantify both aleatoric (data) uncertainty and epistemic (model) uncertainty when predicting future SYM-H indices. Experimental results show that SYMHnet works well at quiet time and storm time, for both 1- and 5-min resolution data. The results also show that SYMHnet generally performs better than related machine learning methods. For example, SYMHnet achieves a forecast skill score (FSS) of 0.343 compared to the FSS of 0.074 of a recent gradient boosting machine (GBM) method when predicting SYM-H indices (1 hr in advance) in a large storm (SYM-H = -393 nT) using 5-min resolution data. When predicting the SYM-H indices (2 hr in advance) in the large storm, SYMHnet achieves an FSS of 0.553 compared to the FSS of 0.087 of the GBM method. In addition, SYMHnet can provide results for both data and model uncertainty quantification, whereas the related methods cannot.

Comment, by Armando [Collado-Villaverde](#), [Pablo Muñoz](#), [Consuelo Cid](#). Space weather [Volume22, Issue8](#) August 2024 e2024SW003909

Main Time Characteristics of Cosmic Ray Variations and Related Parameters in Magnetic Clouds.

Abunina, M.A., Belov, A.V., Shlyk, N.S. et al.

Geomagn. Aeron. 64, 24–31 (2024).

<https://doi.org/10.1134/S0016793223600856>

The behavior of the main parameters of the interplanetary medium, cosmic ray variations, and geomagnetic activity as magnetic clouds pass the Earth (466 events from 1967 to 2021) was studied. Time distributions of these parameters during magnetic clouds passage are considered. It is shown that the maximum values of the solar wind velocity, interplanetary magnetic field strength, and geomagnetic activity indices are more often recorded in the front part of the magnetic cloud, while the minimum values of the temperature index, density, and equatorial component of cosmic ray anisotropy can be observed in any part of the studied structure.

Peculiar solar sources and geospace disturbances on 20-26 August 2018

A.A. [Abunin](#), [M.A. Abunina](#), [A.V. Belov](#), [I.M. Chertok](#)

Solar Phys. **295**, 7 (2020)

<https://arxiv.org/ftp/arxiv/papers/1912/1912.08153.pdf>

<https://doi.org/10.1007/s11207-019-1574-8>

<https://link.springer.com/content/pdf/10.1007/s11207-019-1574-8.pdf>

On the approach to minimum of Solar Cycle 24, on 26 August 2018, an unexpectedly strong geomagnetic storm (GMS) suddenly occurred. Its Dst index reached -174 nT, that is the third of the most intense storms during the cycle. The analysis showed that it was initiated by a two-step long filament eruption, which occurred on 20 August in the central sector of the solar disk. The eruptions were accompanied by two large-scale divergent ribbons and dimmings of a considerable size and were followed by relatively weak but evident Earth-directed coronal mass ejections. In the inner corona, their estimated speed was very low of about 200-360 km/s. The respective interplanetary transients apparently propagated between two high-speed solar wind streams originated from a two-component coronal hole and therefore their expansion was limited. The resulting ejecta arrived at the Earth only on 25 August and brought an unexpectedly strong field of $B_t \sim 18.2$ nT with a predominantly negative B_z component of almost the same strength. The geospace storm also manifested itself in the form of a peculiar Forbush decrease (FD). Its magnitude was about 1.5%, which is rather small for the observed G3-class GMS. The main unusual feature of the event is that large positive bursts with an enhancement up to 3% above the pre-event level were recorded on the FD background. We argue that these bursts were mainly caused by an unusually large and changeable cosmic ray anisotropy combined with lowering of the geomagnetic cutoff rigidity in the perturbed Earth's magnetosphere under conditions of the cycle minimum.

Ring of Stations Method in Cosmic Rays Variations Research

M. A. [Abunina](#), [A. V. Belov](#), [E. A. Eroshenko](#), [A. A. Abunin](#), [V. G. Yanke](#), [A. A. Melkumyan](#), [N. S. Shlyk](#) & [I. I. Pryamushkina](#)

Solar Physics volume 295, Article number: 69 (2020)

<https://link.springer.com/content/pdf/10.1007/s11207-020-01639-7.pdf>

For over 60 years, neutron monitors have been the main standard and high precision detectors for measuring cosmic rays with energy from 400 MeV to hundreds GeV. In order to obtain sufficiently complete information about the distribution of cosmic rays outside the magnetosphere, it is necessary to have a network of detectors spaced evenly around the globe. The ring of stations method is one of the most useful methods for studying the properties of the angular distribution of cosmic rays without expressing the cosmic ray intensity in terms of spherical harmonics. The method allows one to get the hourly longitude distribution of the cosmic ray intensity without modeling. The main objective of this work is to expand the use of the ring of stations method, as it is a convenient and useful method of studying cosmic ray variation. Using the ring of stations method, it is possible to study specific angular distributions of cosmic ray variation that are described poorly by the sum of the first spherical harmonics. The ring of stations method is primarily used to study Forbush decreases. Detailed descriptions of Forbush decrease investigation by the ring of stations method are presented in this study. The application of the method to the study of the precursors of Forbush decreases and cosmic rays behavior inside the solar wind disturbances is shown. **25 September 2001, 1 February 2003, 13 September 2004, 23 June 2013, 15 February 2014, 17 March 2015, 6 November 2015, 25 August 2018**

Forbush-decreases in 19th solar cycle

A [Abunin](#)¹, M [Abunina](#)¹, A [Belov](#)¹, E [Eroshenko](#)¹, V [Oleneva](#)¹ and V [Yanke](#)

2013 J. Phys.: Conf. Ser. 409 012165

The abnormally high solar activity was observed in the late 50's – the early 60's of the 20th century, but not many possibilities was available that time of its observation to which we have got in use during the last years. Ground level cosmic ray observations, along with geomagnetic activity, are one of a few kinds of the continuous measurements, allowing to judge on the events of 19th cycle. The IZMIRAN Database in which all Forbush-decreases are collected since July, 1957 has been used for the analysis. To make the statistics of 19th cycle fuller, the catalogue by Lockwood containing rather big Forbush-decreases (>3 %), picked out from the data of one neutron monitor (Mount Washington),

was involved. Comparison of the events in cosmic rays with solar and geomagnetic activity has shown that the quantity and intensity of geomagnetic storms in 19th cycle correspond to abnormally high number of the sunspots. However in this cycle there is a certain deficiency of Forbush-effects of the large size. Apparently, deficiency of the big Forbush-decreases during this period means that coronal mass ejections (CMEs/ICMEs) in the 19th cycle distinguished from later CMEs and differently affected of the cosmic ray modulation and geomagnetic activity. Probably, the most powerful CMEs of the 19th cycle had, as a whole, the smaller size, than the greatest emissions of solar plasma in later period.

PROPERTIES OF MAGNETIC FIELDS IN CORONAL HOLES AND GEOEFFECTIVE DISTURBANCES IN SOLAR CYCLE 24

Maria **Abunina**, Artem Abunin, Anatoly Belov, Sergey Gaidash, Yordan Tassev*, Peter I.Y. Velinov*, Lachezar Mateev*, Peter Tonev*

Comptes rendus de l'Academie bulgare des Sciences Tome 67, No 5, 2014

<http://spaceweather.izmiran.ru/papers/abunina2014.pdf>

The coronal holes (CH) are sources of high-speed flows of solar wind, and, in its turn, are one of the main sources of geomagnetic disturbances. The coronal holes differ very much one from another and their geoeffectivity varies in a wide range. In this paper we implement a study to answer the question how the coronal holes characterized by different location on the Sun and by their polarity influence the geomagnetic activity. We considered 53 coronal holes observed in the period 2011-2012 of solar cycle 24, and separated them into groups by the heliolatitude and their polarity. A conclusion is made that the trans-equatorial group is the most effective one. Less, but yet sufficiently effective, are the holes of negative polarity at north latitudes and those of positive polarity at south latitudes. The much smaller number of coronal holes of opposite polarity (CH of negative polarity in south hemisphere and CH of positive one in north hemisphere) are less effective

Forecasting Geomagnetic Conditions in near-Earth space

M **Abunina**¹, A Papaioannou², M Gerontidou², P Paschalis², A Abunin¹, S Gaidash¹, I Tsepakina³, A Malimbayev³, A Belov¹, H Mavromichalaki², O Kryakunova³ and P Velinov

2013 J. Phys.: Conf. Ser. 409 012197

<http://iopscience.iop.org/article/10.1088/1742-6596/409/1/012197/pdf>

Geomagnetic conditions in near-Earth space have been a constantly evolving scientific field, especially during the latest years when the dependence of our everyday life on space environment has significantly increased. The scientific community managed to implement centers for the continuous monitoring of the geomagnetic conditions which resulted into short and long term forecasting of the planetary geomagnetic index Ap. In this work, the centers that have been established and are in operational mode in Russia (IZMIRAN), Greece (Athens), Kazakhstan (Almaty) and Bulgaria (Sofia) are presented. The methods that have been used for the forecasting of Ap index are demonstrated and the forecasted results in comparison to the actual Ap measurements are also discussed.

Geoeffectivity of Solar Coronal Holes with Different Magnetic Field Polarity

Abunina, Maria; Abunin, Anatoly; Belov, Anatoly; Gaidash, Sergey; Tassev, Yordan; Velinov, Peter; Mateev, Lachezar; Tonev, Peter

Bulgarian Academy of Sciences. Space Research and Technology Institute. Aerospace Research in Bulgaria. Vol. 25, p. 70-77, 2013

The coronal holes (CH) are sources of high-speed flows of solar wind, and, in its turn, are one of the main sources of geomagnetic disturbances. The coronal holes differ very much one from another and their geoeffectivity varies in a wide range. In this paper we implement a study to answer the question how the coronal holes characterized by different location on the Sun and by their polarity influence the geomagnetic activity. We consider several tens of coronal holes observed in a few recent years, and separate them into groups by the solar latitude and their polarity. A conclusion is made that the transequatorial group is the most effective one, and that almost all coronal holes in this group have a negative polarity. Less, but yet sufficiently effective, are the holes of negative polarity at north latitudes and those of positive polarity at south latitudes. The much smaller number of coronal holes of opposite polarity (CH of negative polarity in south hemisphere and CH of positive one in north hemisphere) are less effective.

A limit for the values of the Dst geomagnetic index

F.J. **Acero**, J.M. **Vaquero**, M.C. **Gallego**, J.A. **García**

2024

<https://arxiv.org/pdf/2402.00437.pdf>

The study of the extreme weather space events is important for a technological dependent society. Extreme Value Theory could be decisive to characterize those extreme events in order to have the knowledge to make decisions in technological, economic and social matters, in all fields with possible impacts. In this work, the hourly values of the Dst geomagnetic index has been studied for the period 1957-2014 using the peaks-over-threshold technique. The shape parameter obtained from the fit of the generalized Pareto distribution to the extreme values of the $|Dst|$ index leads to a negative value implying an upper bound for this time series. This result is relevant, because the estimation of this limit for the extreme values lead to 850 nT as the highest expected value for this geomagnetic index. Thus, from the previous characterization of the Carrington geomagnetic storm and our results, it could be considered the worst case scenario. **13-15 March 1989**

Modeling of Joint Parker Solar Probe–Metis/Solar Orbiter Observations

L. Adhikari¹, G. P. Zank¹, D. Telloni², and L.-L. Zhao¹

2022 ApJL 937 L29

<https://iopscience.iop.org/article/10.3847/2041-8213/ac91c6/pdf>

We present the first theoretical modeling of joint Parker Solar Probe (PSP)–Metis/Solar Orbiter (SolO) quadrature observations. The combined observations describe the evolution of a slow solar wind plasma parcel from the extended solar corona (3.5–6.3 R_{\odot}) to the very inner heliosphere (23.2 R_{\odot}). The Metis/SolO instrument remotely measures the solar wind speed finding a range from 96 to 201 km s⁻¹, and PSP measures the solar wind plasma in situ, observing a radial speed of 219.34 km s⁻¹. We find theoretically and observationally that the solar wind speed accelerates rapidly within 3.3–4 R_{\odot} and then increases more gradually with distance. Similarly, we find that the theoretical solar wind density is consistent with the remotely and in-situ observed solar wind density. The normalized cross helicity and normalized residual energy observed by PSP are 0.96 and -0.07, respectively, indicating that the slow solar wind is very Alfvénic. The theoretical NI/slab results are very similar to PSP measurements, which is a consequence of the highly magnetic field-aligned radial flow ensuring that PSP can measure slab fluctuations and not 2D ones. Finally, we calculate the theoretical 2D and slab turbulence pressure, finding that the theoretical slab pressure is very similar to that observed by PSP.

A Solar Coronal Hole and Fast Solar Wind Turbulence Model and First-orbit Parker Solar Probe (PSP) Observations

L. Adhikari¹, G. P. Zank^{1,2}, and L.-L. Zhao¹

2020 ApJ 901 102

<https://doi.org/10.3847/1538-4357/abb132>

We propose a turbulence-driven solar wind model for a fast solar wind flow in an open coronal hole where the solar wind flow and the magnetic field are highly aligned. We compare the numerical results of our model with Parker Solar Probe measurements of the fast solar wind flow and find good agreement between them. We find that (1) the majority quasi-2D turbulence is mainly responsible for coronal heating, raising the temperature to about $\sim 10^6$ K within a few solar radii, which leads in turn to the acceleration of the solar wind; (2) the heating rate due to quasi-2D turbulence near the coronal base is larger than that due to nearly incompressible/slab turbulence; (3) the quasi-2D energy in forward-propagating modes decreases with increasing distance, while the nearly incompressible/slab energy in forward-propagating modes increases, reaching a peak value at $\sim 11.7 R_{\odot}$ before decreasing with increasing heliocentric distance; (4) the correlation length increases with increasing distance from the coronal base; and (5) the variance of the density fluctuations decreases as a function of heliocentric distance.

Impacts On Proton Fluxes Observed During Different Interplanetary Conditions

Binod Adhikari, Niraj Adhikari, Binil Aryal, Narayan P. Chapagain, and Ildiko Horvath

Solar Phys. 294:61 **2019**

sci-hub.se/10.1007/s11207-019-1450-6

Interplanetary coronal mass ejections (ICMEs) and Corotating Interaction Regions (CIRs) are the major characteristic events of the solar wind. We utilized the proton flux data of different energy level measured by the Low Energy Magnetic Spectrometers (LEMS) 120 system of the Electron, Proton and Alpha Monitor (EPAM) for studying different ICME-driven and CIR-driven storms. Our main aim was to find out from the observational results the nature of proton flux during solar storms driven by different forces, in our cases, ICMEs and CIRs, in the interplanetary regions. We analysed the different parameters provided by the LEMS 120 system and compared them during the different storm types and during the quietest day as well. We studied four events: a geomagnetically quiet day, two ICME-driven storms

and one CIR-driven storm. We also analysed the IMF magnitude (B_{mag}) and the different parameters of the solar wind during all these events. We observed that the prolonged particle precipitations during CIRs and the intense particle precipitations during ICMEs result in the different nature of the proton flux of different energy level in comparison to other parameters such as B_{mag} , and solar wind velocity (V_{sw}). Our results show that there is strong correlation between the higher energy proton fluxes and $B_{\text{mag}}-V_{\text{sw}}$ during the quiet period and weak correlation in the case of lower energy protons during the quiet event. But, when the storm is either driven by ICMEs or CIRs, the lower energy also starts to show positive correlations with B_{mag} and V_{sw} with a 0 min time lag during ICMEs and a ~ 100 min time lag during CIRs. During the quiet day, the proton flux observed was due to the perturbations created by ionization and the higher energy of the protons sufficiently weakened. Whereas, CMEs speed, preceding CMEs, and the presence of pre-existing Solar Energetic Particles (SEPs) in the ambient medium, the makeup of CIRs wind, and the nature of precipitation during both ICMEs and CIRs caused the fluxes of protons of different energy level during storm times. **19 April 2003, 20 November 2003 and 25 July 2004, 8 May 2005**

The Role of Magnetic Reconnection–associated Processes in Local Particle Acceleration in the Solar Wind

L. [Adhikari](#)¹, O. Khabarova², G. P. Zank^{1,3}, and L.-L. Zhao
2019 ApJ 873 72

[sci-hub.se/10.3847/1538-4357/ab05c6](https://doi.org/10.3847/1538-4357/ab05c6)

Recent studies of unusual or atypical energetic particle flux events (AEPEs) observed at 1 au show that another mechanism, different from diffusive shock acceleration, can energize particles locally in the solar wind. The mechanism proposed by Zank et al. is based on the stochastic energization of charged particles in regions filled with numerous small-scale magnetic islands (SMIs) dynamically contracting or merging and experiencing multiple magnetic reconnection in the super-Alfvénic solar wind flow. A first- and second-order Fermi mechanism results from compression-induced changes in the shape of SMIs and their developing dynamics. Charged particles can also be accelerated by the formation of antireconnection electric fields. Observations show that both processes often coexist in the solar wind. The occurrence of SMIs depends on the presence of strong current sheets like the heliospheric current sheet (HCS), and related AEPEs are found to occur within magnetic cavities formed by stream–stream, stream–HCS, or HCS–shock interactions that are filled with SMIs. Previous case studies comparing observations with theoretical predictions were qualitative. Here we present quantitative theoretical predictions of AEPEs based on several events, including a detailed analysis of the corresponding observations. The study illustrates the necessity of accounting for local processes of particle acceleration in the solar wind.

Impacts on Cosmic-Ray Intensity Observed During Geomagnetic Disturbances

Binod [Adhikari](#), Nirakar Sapkota, Prashrit Baruwal, Narayan P. Chapagain, Carlos Roberto Braga
[Solar Physics](#) October **2017**, 292:149

Geomagnetic disturbances are the results of interplanetary causes such as high-speed streamers (HSSs), interplanetary coronal mass ejections (ICMEs), corotating interaction regions (CIRs), and magnetic clouds. During different forms of geomagnetic disturbances, we observed changes in the count rate at neutron monitors that are kept at various locations. We studied the count rates measured by neutron monitors at four stations at various latitudes during different categories of geomagnetic events and compared them. We analysed five events: a geomagnetically quiet event, a non-storm high-intensity long-duration continuous AE activity (HILDCAA) event, a storm-preceded HILDCAA event, a geomagnetic substorm event, and a geomagnetic moderate storm event. We based our analysis on geomagnetic indices, solar wind parameters, and interplanetary magnetic field (IMF) parameters. We found that the strength of the modulation was least during the quiet event and highest during the storm-preceded HILDCAA. By analysing the cause of these geomagnetic disturbances, we related each decrease in the neutron monitor data with the corresponding solar cause. For the ICME-driven storm, we observed a decrease in neutron monitor data ranging from 6% to 12% in all stations. On the other hand, we observed a decrease ranging from 2% to 5% for the HSS-driven storm. For the non-storm HILDCAA, we observed a decrease in neutron monitor data of about 1% to 1.5%. For the quiet event, the neutron monitor data fluctuated such that there was no overall decrease in all stations. **19 – 24 April 2003, 16 November 2003, 21 January 2005, 14 – 19 May 2005, 18 – 21 July 2006,**

Constraints on the Alfvénicity of Switchbacks

O.V. [Agapitov](#) (1), [J. F. Drake](#) (2,3), [M. Swisdak](#) (3), [K.-E. Choi](#) (1), [N. Raouafi](#) (4)
2023

<https://arxiv.org/ftp/arxiv/papers/2312/2312.01011.pdf>

Switchbacks (SBs) are localized structures in the solar wind containing deflections of the magnetic field direction relative to the background solar wind magnetic field. The amplitudes of the magnetic field deflection angles for different SBs vary from ~40 to ~160-170 degrees. Alignment of the perturbations of the magnetic field and the bulk solar wind velocity is observed inside SBs and causes spiky enhancements of the radial bulk velocity inside SBs. We have investigated the deviations of SB perturbations from Alfvénicity by evaluating the distribution of the parameter defined as the ratio of the parallel to ΔB^{\rightarrow} component of ΔV^{\rightarrow} to $\Delta V^{\rightarrow} A = \Delta B^{\rightarrow} / 4\pi n m_i$ inside SBs, i.e. $\alpha = V_{\parallel} / |\Delta V^{\rightarrow}|$ ($\alpha = \Delta V^{\rightarrow} / |\Delta V^{\rightarrow}|$ when $\Delta V^{\rightarrow} \parallel \Delta B^{\rightarrow}$), which quantifies the deviation of the perturbation from an Alfvénic one. Based on Parker Solar Probe (PSP) observations, we show that α inside SBs has systematically lower values than it has in the pristine solar wind: α inside SBs observed during PSP Encounter 1 were distributed in a range of 0.2-0.9. The upper limit on α is constrained by the requirement that the jump in velocity across the switchback boundary be less than the local Alfvén speed. This prevents the onset of shear flow instabilities. The consequence is that the perturbation of the proton bulk velocity in SBs with deflection greater than 60 degrees cannot reach $\alpha=1$ (the Alfvénicity condition) and the highest possible α for a SB with the full reversal of B is 0.5. These results have consequences for the interpretation of switchbacks as large amplitude Alfvén waves. **November 6, 2018**

Flux rope merging and the structure of switchbacks in the solar wind

O. Agapitov, J. F. Drake, M. Swisdak, S. D. Bale, T. S. Horbury, J. C. Kasper, R. J. MacDowall, F. S. Mozer, T. D. Phan, M. Pulupa, N.E. Raouafi, M. Velli

2022 *ApJ* 925 213

<https://arxiv.org/ftp/arxiv/papers/2109/2109.04016.pdf>

<https://iopscience.iop.org/article/10.3847/1538-4357/ac4016/pdf>

A major discovery of Parker Solar Probe (PSP) was the presence of large numbers of localized increases in the radial solar wind speed and associated sharp deflections of the magnetic field - switchbacks (SB). A possible generation mechanism of SBs is through magnetic reconnection between open and closed magnetic flux near the solar surface, termed interchange reconnection that leads to the ejection of flux ropes (FR) into the solar wind. Observations also suggest that SBs undergo merging, consistent with a FR picture of these structures. The role of FRs merging in controlling the structure of SB in the solar wind is explored through direct observations, through analytic analysis, and numerical simulations. Analytic analysis reveals key features of the structure of FR and their scaling with the heliocentric distance R that are consistent with observations and that reveal the critical role of merging in controlling the SB structure. FR merging is shown to be energetically favorable to reduce the strength of the wrapping magnetic field and drive the observed elongation of SBs. A further consequence is the resulting dominance of the axial magnetic field within SBs that leads to the characteristic sharp rotation of the magnetic field into the axial direction at the SB boundary that is revealed in observations. Finally, the radial scaling of the SB area in the FR model of SBs suggests that the observational probability of SB identification should be insensitive to R, which is consistent with the most recent statistical analysis of SB observations from PSP. **November 4, 2018**

Sunward propagating whistler waves collocated with localized magnetic field holes in the solar wind: Parker Solar Probe observations at 35.7 Sun radii

O.V. Agapitov, T. Dudok de Wit, F.S. Mozer, J. W. Bonnell, ...

2020 *ApJL* 891 L20

<https://arxiv.org/ftp/arxiv/papers/2002/2002.09837.pdf>

<https://doi.org/10.3847/2041-8213/ab799c>

Observations by the Parker Solar Probe mission of the solar wind at about 35.7 solar radii reveal the existence of whistler wave packets with frequencies below 0.1 f/fce (20-80 Hz in the spacecraft frame). These waves often coincide with local minima of the magnetic field magnitude or with sudden deflections of the magnetic field that are called switchbacks. Their sunward propagation leads to a significant Doppler frequency downshift from 200-300 Hz to 20-80 Hz (from 0.2 f/fce to 0.5 f/fce). The polarization of these waves varies from quasi-parallel to significantly oblique with wave normal angles that are close to the resonance cone. Their peak amplitude can be as large as 2 to 4 nT. Such values represent approximately 10% of the background magnetic field, which is considerably more than what is observed at 1 a.u. Recent numerical studies show that such waves may potentially play a key role in breaking the heat flux and scattering the Strahl population of suprathermal electrons into a halo population. **4-7 Nov 2018**

Non-conventional Approach for Deriving the Radial Sizes of Coronal Mass Ejections at Different Instances: Discrepancies in the Estimates Between Remote and In Situ Observations

Anjali Agarwal, Wageesh Mishra

MNRAS Volume 534, Issue 3, November 2024, Pages 2458–2474,

<https://doi.org/10.1093/mnras/stae2260>

<https://arxiv.org/pdf/2409.18851?>

<https://academic.oup.com/mnras/article-pdf/534/3/2458/59713264/stae2260.pdf>

Understanding the evolution of radial sizes and instantaneous expansion speeds of coronal mass ejections (CMEs) is crucial for assessing their impact duration on Earth's environment. We introduce a non-conventional approach to derive the CME's radial sizes and expansion speeds at different instances during its passage over a single-point in situ spacecraft. We also estimate the CME's radial sizes and expansion speeds during its journey from the Sun to 1 AU using the 3D kinematics of different CME features, including the leading edge (LE), center, and trailing edge (TE). The continuous 3D kinematics of the CME is estimated by employing the GCS and SSSE reconstruction methods on multi-point observations from coronagraphs and heliospheric imagers combined with the drag-based model. We choose the **2010 April 3** CME as a suitable case for our study, promising a more accurate comparison of its remote and in situ observations. We show that the introduced non-conventional approach can provide better accuracy in estimating radial sizes and instantaneous expansion speeds of CMEs at different instances. We examine the aspect ratio of the CME, which influences its expansion behavior and shows the discrepancy between its value in the corona and interplanetary medium. Our study highlights significant inconsistencies in the arrival time, radial size, and expansion speed estimates obtained from remote and in situ observations. We advocate for future studies leveraging multi-spacecraft in situ observations and our non-conventional approach to analyze them to improve the comprehension of CME dynamics in the solar wind.

Forbush decrease on September 6-13, 2017 observed by the Tanca water-Cherenkov detector de **Aguiar**, R ; Fauth, AC

37TH INTERNATIONAL COSMIC RAY CONFERENCE, ICRC2021 Article Number 1267, 2022

<https://pos.sissa.it/395/1267/pdf>

Solar activity was intense in September 2017 and its effects were observed in different detectors placed at the Earth's surface. Three halo Coronal Mass Ejections (CME) hit the planet and caused magnetic storms. The effects of the CMEs on the flux of galactic cosmic rays at ground level were observed by the Tanca detector, which is one of the water-Cherenkov detectors (WCD) that make up the Latin American Giant Observatory (LAGO). In this paper we present the detection of Forbush events observed by Tanca during the month of September 2017. This WCD is installed on the campus of the University of Campinas, in Brazil, having three photomultiplier tubes that detect Cherenkov photons produced by cosmic radiation in 11400 liters of ultra pure water. We present the description and performance of the experimental apparatus and the observation on days 6(th), 8(th) and 13(th) of the Forbush events originated by the CMEs. A decrease in the cosmic rays flux due to a stream interaction region was also observed on 14(th) September. These results were compared with observations made by neutron monitors and indices of the Earth's magnetic activity.

Numerical MHD models of stream interaction regions (SIRs) and corotating interaction regions (CIRs) using sunRunner3D: comparison with observations

E **Aguiar-Rodríguez**, J J González-Avilés, P Riley, M Ben-Nun, M Rodríguez-Martínez, R F González, M A Pérez-Rivera, A C Raga-Rasmussen

MNRAS Volume 529, Issue 2, April 2024, Pages 1250–1257,

<https://doi.org/10.1093/mnras/stae640>

<https://academic.oup.com/mnras/article-pdf/doi/10.1093/mnras/stae640/56916491/stae640.pdf>

In this work, we present numerical simulations of Stream Interaction Regions (SIRs) and Corotating Interaction Regions (CIRs) using the SUNRUNNER3D tool that employs as a coronal model the boundary conditions obtained by CORHEL/MAS with the PLUTO code that describes the global 3D structure of the solar wind using the magnetohydrodynamics (MHD) approach in the inner heliosphere. Specifically, we selected a set of SIRs and CIRs observed by the Parker Solar Probe (PSP) and STEREO-A (STA) missions during the Carrington rotations (CRs) 2207 to 2210 and CRs from 2020 to 2022. In order to describe the dynamics of the plasma that constitutes the solar wind background conditions for the selected CRs, we solve the ideal MHD equations in an inertial frame of reference, managing the solar rotation by rotating the boundary values in ϕ (longitude) at a rate corresponding to the sidereal rotation rate of the solar equator. We show that our results using SUNRUNNER3D can globally reproduce the plasma parameters, such as radial velocity, number proton density, and radial magnetic field strength of these large-scale structures, observed by PSP and STA at distances near the Sun and around 1 au, respectively. These results allow exploring the global evolution of SIRs/CIRs in the inner heliosphere using SUNRUNNER3D.

Comparison of Solar Wind Speeds Using Wavelet Transform and Fourier Analysis in IPS Data

E. [Aguilar-Rodriguez](#), J. C. Mejia-Ambriz, B. V. Jackson, A. Buffington, E. Romero-Hernandez, J. A. Gonzalez-Esparza, M. Rodriguez-Martinez, P. Hick, M. Tokumaru and 1 more
Solar Phys. **2015**

The power spectra of intensity fluctuations in interplanetary scintillation (IPS) observations can be used to estimate solar-wind speeds in the inner heliosphere. We obtain and then compare IPS spectra from both wavelet and Fourier analyses for 12 time series of the radio source 3C48; these observations were carried out at Japan's Solar-Terrestrial Environment Laboratory (STEL) facility, at 327 MHz. We show that wavelet and Fourier analyses yield very similar power spectra. Thus, when fitting a model to spectra to determine solar-wind speeds, both yield comparable results. Although spectra from wavelet and Fourier closely match each other for solar-wind speed purposes, those from the wavelet analysis are slightly cleaner, which is reflected in an apparent level of intensity fluctuations that is enhanced, being $\approx 13\%$ higher. This is potentially useful for records that show a low signal-to-noise ratio.

Interplanetary Scintillation (IPS) of the Radio Source 3C48 During Periods of Low and High Solar Activity

E. [Aguilar-Rodriguez](#), S. A. Tyul'bashev, I. V. Chashei, E. Romero-Hernandez
[Solar Physics](#) September **2015**, Volume 290, Issue 9, pp 2567-2575

We present a comparative study of three techniques used to estimate the scintillation index using interplanetary scintillation (IPS) observations carried out by the Big Scanning Array (BSA), which operates at a frequency of 111 MHz. These techniques are based on: rms analysis on-source and off-source (classic), Fourier, and wavelet transforms. IPS data are analyzed separately for the period of low solar activity (2007 – 2009), and for the year 2013, near the solar-activity maximum. Our results show that, in general, these methods are equivalent. We analyze the radial dependence of the scintillation index at meter wavelengths during these two periods. It is found that the observed radial dependence of the scintillation index during both periods of U.C. cycle 24 is flatter than the theoretical dependence expected for the case of solar-wind spherical symmetry. This flattening can be explained in terms of the influence of the heliospheric current sheet during the low solar-activity period, and the influence of solar disturbances, such as coronal mass ejections (CMEs), for the high solar-activity period.

May 2005 Halo CMEs and Galactic Cosmic Ray Flux Changes at Earth's Orbit

H. S. [Ahluwalia](#), M. V. Alania, A. Wawrzynczak, R. C. Ygbuhay, M. M. Fikani
Solar Physics, May **2014**, Volume 289, Issue 5, pp 1763-1782

The pressure corrected hourly data from the global network of cosmic ray detectors, measurements of the interplanetary magnetic field (IMF) intensity (B) at Earth's orbit and its components B_x , B_y , B_z (in the geocentric solar ecliptic coordinates) are used to conduct a comprehensive study of the galactic cosmic ray (GCR) intensity fluctuations caused by the halo coronal mass ejection of **13 May 2005**. Distinct differences exist in GCR timelines recorded by neutron monitors (NMs) and multidirectional muon telescopes (MTs), the latter respond to the high rigidity portion of the GCR differential rigidity spectrum. The Forbush decrease (FD) onset in MTs is delayed (~ 5 h) with respect to the onset of a geomagnetic storm sudden commencement (SSC) and a large pre-increase is present in MT data before, during, and after the SSC onset, of unknown origin. The rigidity spectrum, for a range of GCR rigidities (≤ 200 GV), is a power law in rigidity (R) with a negative exponent ($\gamma = -1.05$) at GCR minimum intensity, leading us to infer that the quasi-linear theory of modulation is inconsistent with observations at high rigidities (> 1 GV); the results support the force field theory of modulation. At present, we do not have a comprehensive model for the FD explaining quantitatively all the observational features but we present a preliminary model listing physical processes that may contribute to a FD timeline. We explored the connections between different phases of the FD and the power spectra of IMF components but did not find a sustained relationship.

Characteristics and development of the main phase disturbance in geomagnetic storms ($Dst \leq -50$ nT)

Osman M. [Ahmed](#), [Badruudin Zaheer Ahmad](#), [Moncef Derouich](#)

Advances in Space Research **2024**

<https://arxiv.org/pdf/2402.03261.pdf>

We present geomagnetic storms (GSs) selected from three solar cycles, spanning the years 1995 to 2022. We studied the development of the main phase of storms within disturbance storm time (Dst) amplitudes ranging from $Dst = -64$ nT to $Dst = -422$ nT. In order to determine the solar wind (SW) parameters that mainly influence the main phase development of a GS, which can best describe the SW-magnetosphere coupling, we divided our selected GSs into four groups based on main phase duration. Superposed epoch analysis was performed on the selected geomagnetic indices, SW plasma and field parameters, and their derivatives separately for each group. To that end, the dynamics of GS main phase development is mainly guided by interplanetary driver magnetic field southward component, (-Bz). It has been determined that there is a temporal difference between the peak values of Bz and Dst. As a result, Dst is delayed from Bz by 1-4 hours, which is crucial for space weather forecasting. The peak of Dst has a direct relationship with the amplitude of storm sudden commencement (SSC) and an inverse relationship with the duration of SSC. The inter-relationship between the peaks of the three indices (Dst, AE, and ap) during GS, is also obtained. Dst is found to be more closely related to ap than AE. To determine the best fit SW parameter to the geomagnetic activity indices, we used a linear correlation between the peak values of individual geomagnetic indices and SW plasma and field parameters and their derivatives. An electric field related function involving speed and IMF ($v_4/3Bz$) when coupled with a viscous term ($\rho^{1/2}$) correlates very well with the intensity of the GS (Dst_{min} or ΔDst) and the magnitude of (ap_{max}) and (AE_{max}) during storms. However, a related function ($v_4/3B\rho^{1/2}$) represents slightly better the peak of AE_{max} during the storms.

Table 1. List of the selected 57 GS events profile 1995-2018

Magnetic Interaction of a Super-CME with the Earth's Magnetosphere: Scenario for Young Earth

Vladimir S. [Airapetian](#), Alex Gloer, William Danchi

Proceedings of 18th Cambridge Workshop on Cool Stars, Stellar Systems, and the Sun

Proceedings of Lowell Observatory (9-13 June **2014**) Edited by G. van Belle & H. Harris

<http://arxiv.org/pdf/1410.7355v2.pdf>

Solar eruptions, known as Coronal Mass Ejections (CMEs), are frequently observed on our Sun. Recent Kepler observations of superflares on G-type stars have implied that so called super-CMEs, possessing kinetic energies 10 times of the most powerful CME event ever observed on the Sun, could be produced with a frequency of 1 event per 800-2000 yr on solar-like slowly rotating stars. We have performed a 3D time-dependent global magnetohydrodynamic simulation of the magnetic interaction of such a CME cloud with the Earth's magnetosphere. We calculated the global structure of the perturbed magnetosphere and derive the latitude of the open-closed magnetic field boundary. We also estimated energy fluxes penetrating the Earth's ionosphere and discuss the consequences of energetic particle fluxes on biological systems on early Earth.

Solar Origins of 26th August 2018 Geomagnetic Storm: Responses of the Interplanetary Medium and Equatorial/low-latitude Ionosphere to the Storm

A. O. [Akala](#), [O. J. Oyedokun](#), [P. O. Amaechi](#), [K. G. Simi](#), [A. Ogwala](#), [O.A. Arowolo](#),

Space Weather **Volume 19, Issue 10** e2021SW002734 **2021**

<https://agupubs.onlinelibrary.wiley.com/doi/epdf/10.1029/2021SW002734>

<https://doi.org/10.1029/2021SW002734>

This geomagnetic storm was initiated by a solar filament eruption of **20th August, 2018**, and driven by an aggregation of weak CME transients and CIR/HSSs. The weak PPEF during the storm, which is associated with the extreme quietness of year 2018 caused plasma densities to localize at locations that are not up to the EIA crests. A clear hemispherical asymmetry, with higher TEC in the northern hemisphere was observed. The determining factors for ionospheric responses to this storm are; local time of the storm's onset, local time of storm's minimum SYM-H, and changes in thermospheric O/N₂. Furthermore, one major factor that is hindering our progress in developing robust prediction capabilities for geomagnetic storm is the characteristic peculiarity of each storm. **26th August 2018** geomagnetic storm is peculiar due to the intertwined physical processes that led to its occurrence. To develop future forecasting capabilities for this type of a complex storm, a comprehensive understanding of the intertwined physical processes is required, which this study provided.

A Review of Studies of Geomagnetic Storms and Auroral/Magnetospheric Substorms Based on the Electric Current Approach **Review**

Syun-Ichi **Akasofu**

Front. Astron. Space Sci. 7:604750. 2021 |

<https://www.frontiersin.org/articles/10.3389/fspas.2020.604750/full>

<https://doi.org/10.3389/fspas.2020.604750>

The progress of space physics is reviewed from my personal point of view, particularly how I have reached my present understanding of auroral substorms and geomagnetic storms from the time of the earliest days of space physics. This review is somewhat unique in two ways. First of all, instead of taking the magnetic field line approach (including magnetic reconnection), I have taken the electric current approach; it consists of power supply (dynamo), transmission (currents/circuits), and dissipation (auroral/magnetospheric substorms). This is the basic way to study electromagnetic phenomena and it is much more instructive in understanding the physics involved in the chain processes. Secondly, this is not a textbook-like review, but it is hoped that my humble experience may be useful to see how a new science of space physics has evolved with a number of controversies. On the other hand, it can be seen that the electric current approach is still in a very rudiment stage. Thus, new generations of researchers are most welcome in taking this new way of studying auroral/magnetospheric substorms and geomagnetic storms.

Electric Current Approach Studying Both Auroral Substorms and Solar Flares Together **Review***

Syun-Ichi **Akasofu***

Front. Astron. Space Sci., 7:4 2020 | <https://doi.org/10.3389/fspas.2020.00004>

<https://www.frontiersin.org/articles/10.3389/fspas.2020.00004/pdf>

Auroral substorms and solar flares are basically various manifestations of electromagnetic energy dissipation processes, so it is useful to consider both phenomena in terms of a chain of processes, consisting of power supply (dynamo), transmission (currents/circuits), and dissipation (auroral substorms, solar flares), the electric current approach. In this short review, we briefly describe both phenomena together on the basis of the chain process. It is shown that the introduction of a dynamo process in this consideration provides a step-by-step way of studying both phenomena. It is shown that (a) both the solar wind–magnetosphere dynamo and a photospheric dynamo proposed by [Lee et al. \(1995\)](#) have enough power to accumulate enough energy for the explosive features of both phenomena, respectively. (b) For substorms, the power is accumulated in the inner magnetosphere and inflates it, and for flares, the power is likely to be accumulated in a loop current along and above two-ribbon flares. (c) For substorms, the energy release (unloading) process deflates the inner magnetosphere, resulting in an earthward electric field, and for flares, the disruption of the loop current suggested by [Alfvén \(1950\)](#) may be responsible for the energy release.

A Historical Review of the Geomagnetic Storm-Producing Plasma Flows from the Sun

Syun-Ichi **Akasofu**

Space Science Reviews, Volume 164, Numbers 1-4, 85-132, 2012; **File**

The concept of geomagnetic storm-producing solar plasma flows has evolved and advanced considerably over the last 100 years or so. This particular field of study began in an effort to understand geomagnetic disturbances and the aurora. The purpose of this paper is try to follow the ways in which early concepts evolved to later ones, not to review each concept in detail. It is fascinating to see a step-by-step buildup of these concepts, from the earliest idea of flow of solar electrons to coronal mass ejections (CMEs). The time line, though tentative, of the studies of geomagnetic storm-producing plasma flows is presented. The author hopes that this paper will serve young researchers in particular to consider how they plan to advance further this scientific field. There is still much uncertainty about geomagnetic storm-producing solar plasma flows. Some of the major questions are listed from the point of view of a geophysicist in the summary sections by grouping them in terms of the quiet-time solar wind, solar streams from corona holes and CMEs associated with solar flares.

Space Weather Investigation Frontier (SWIFT)

Mojtaba **Akhavan-Tafti**, Les Johnson, Rohan Sood, +++

Front. Astron. Space Sci. 10: 1185603. 2023

doi: 10.3389/fspas.2023.1185603

<https://www.frontiersin.org/articles/10.3389/fspas.2023.1185603/pdf>

The Space Weather Investigation Frontier (SWIFT) mission will aim at making major discoveries on the three-dimensional structure and dynamics of heliospheric structures that drive space weather. The focus will be on

Interplanetary Coronal Mass Ejections (ICMEs) that originate from massive expulsions of plasma and magnetic flux from the solar corona. They cause the largest geomagnetic storms and solar energetic particle events, threatening to endanger life and disrupt technology on Earth and in space. A big current problem, both regarding fundamental solar-terrestrial physics and space weather, is that we do not yet understand spatial characteristics and temporal evolution of ICMEs and that the existing remote-sensing and in-situ observatories are not suited for resolving multi-layered and evolutionary structures in these massive storm drivers. Here, we propose a groundbreaking mission concept study using solar sail technology that, for the first time, will make continuous, in-situ multi-point observations along the Sun-Earth line beyond the Lagrange point L1 (sub-L1). This unique position, in combination with L1 assets, will allow distinguishing between local and global processes, spatial characteristics, temporal evolution, and particle energization mechanisms related to ICMEs. In addition, measurements of the magnetic field in earthbound ICMEs and their sub-structures from the SWIFT location will double the current forecasting lead-times from L1. This concept also paves the way for missions with increasingly longer forecasting lead-times, addressing NASA and NOAA's space weather goals, as set forth by the Decadal Survey. The objective of this communication is to inform the community of the ongoing effort, including plans to further develop the mission concept, supported by the Heliophysics Flight Opportunities Studies (HFOS) program under NASA's Research Opportunities in Space and Earth Sciences (ROSES). **20-21 Apr 2020**

Interplanetary Magnetic Flux Rope Observed at Ground Level by HAWC

S. **Akiyama**, R. Alfaro, C. Alvarez, J. R. Angeles Camacho, +++

2020 ApJ 905 73

<https://doi.org/10.3847/1538-4357/abc344>

<https://arxiv.org/pdf/2101.03243.pdf>

We report the ground-level detection of a Galactic cosmic-ray (GCR) flux enhancement lasting ~17 hr and associated with the passage of a magnetic flux rope (MFR) over the Earth. The MFR was associated with a slow coronal mass ejection (CME) caused by the eruption of a filament on **2016 October 9**. Due to the quiet conditions during the eruption and the lack of interactions during the interplanetary CME transport to the Earth, the associated MFR preserved its configuration and reached the Earth with a strong magnetic field, low density, and a very low turbulence level compared to local background, thus generating the ideal conditions to redirect and guide GCRs (in the ~8–60 GV rigidity range) along the magnetic field of the MFR. An important negative B Z component inside the MFR caused large disturbances in the geomagnetic field and a relatively strong geomagnetic storm. However, these disturbances are not the main factors behind the GCR enhancement. Instead, we found that the major factor was the alignment between the MFR axis and the asymptotic direction of the observer.

A Study of Coronal Holes Observed by SoHO/EIT and the Nobeyama Radioheliograph

S. **Akiyama**, N. Gopalswamy, S. Yashiro, and P. Mäkelä

Publ. Astron. Soc. Japan 65, No SP1, S15 [10 pages] (**2013**)

<http://pasj.asj.or.jp/v65/sp1/65S015/65S015.pdf>

Coronal holes (CHs) are areas of reduced emission in EUV and X-ray images that show bright patches of microwave enhancements (MEs) related to magnetic network junctions inside the CHs. A clear correlation between the CH size and the solar wind (SW) speed is well known, but we have less information about the relationship between MEs and other CH and SW properties. We studied the characteristics of 21 equatorial CHs associated with corotating interaction regions (CIRs) during 1996 to 2005. Our CHs were divided into two groups according to the intensity of the associated geomagnetic storms: $Dst \leq -100$ nT (10 events) and $Dst > -100$ nT (11 events). Using EUV 284 Å images obtained by SOHO/EIT and 17 GHz microwave images obtained by the Nobeyama Radioheliograph (NoRH), we found a linear correlation not only between the maximum SW speed and the area of EUV CH ($r = 0.62$), but also between the maximum SW speed and the area of the ME ($r = 0.79$). We also compared the EUVCH areas with and without an overlapping ME. The area of the CHs with an ME is better correlated with the SW speed ($r = 0.71$) than the area of those without an ME ($r = 0.36$). Therefore, the radio ME may play an important role in understanding the origin of SW. **Tables of geomagnetic storms from CHs.**

Deriving the Topological Properties of the Magnetic Field of Coronal Mass Ejections from In Situ Measurements: Techniques

Nada **Al-Haddad**, [Mitchell Berger](#)

ApJ **2024**

<https://arxiv.org/pdf/2408.04608>

Coronal mass ejections (CMEs) are magnetized plasma systems with highly complex magnetic topology and evolution. Methods developed to assess their magnetic configuration have primarily focused on reconstructing three-dimensional representations from one-dimensional time series measurements taken in situ using techniques based on the "highly twisted magnetic flux rope" approximations. However, the magnetic fields of CMEs is known to have more complicated geometries. Their structure can be quantified using measures of field line topology, which have been primarily used for solar physics research. In this work, we introduce a novel technique of directly quantifying the various forms of magnetic helicity within a CME in the interplanetary space using synthetic in situ measurements. We use a relatively simple three-dimensional simulation of a CME initiated with a highly-twisted flux rope. We find that a significant portion of the magnetic helicity near 1 AU is contained in writhe and mutual helicity rather than just in twist. We discuss the implications of this finding for fitting and reconstruction techniques.

Multipoint Observations of the Dynamics at an ICME Sheath–Ejecta Boundary

Matti [Ala-Lahti](#)^{1,2}, Tuija I. [Pulkkinen](#)¹, Julia [Ruohotie](#)², Mojtaba [Akhavan-Tafti](#)¹, Simon W. [Good](#)², and Emilia K. J. [Kilpua](#)²

2023 ApJ 956 131

<https://iopscience.iop.org/article/10.3847/1538-4357/acf99e/pdf>

The radial evolution of interplanetary coronal mass ejections (ICMEs) is dependent on their interaction with the ambient medium, which causes ICME erosion and affects their geoefficiency. Here, an ICME front boundary, which separates the confined ejecta from the mixed, interacted sheath–ejecta plasma upstream, is analyzed in a multipoint study examining the ICME at 1 au on **2020 April 20**. A bifurcated current sheet, highly filamented currents, and a two-sided jet were observed at the boundary. The two-sided jet, which was recorded for the first time for a magnetic shear angle $<40^\circ$, implies multiple (patchy) reconnection sites associated with the ICME erosion. The reconnection exhaust exhibited fine structure, including multistep magnetic field rotation and localized structures that were measured only by separate Cluster spacecraft with the mission inter-spacecraft separation of 0.4–1.6 RE. The mixed plasma upstream of the boundary with a precursor at 0.8 au lacked coherency at 1 au and exhibited substantial variations of southward magnetic fields over radial (transverse) distances of 41–237 RE (114 RE). This incoherence demonstrates the need for continuous (sub)second-resolution plasma and field measurements at multiple locations in the solar wind to adequately address the spatiotemporal structure of ICMEs and to produce accurate space weather predictions.

Spatial Coherence of Interplanetary Coronal Mass Ejection Sheaths at 1 AU

Matti [Ala-Lahti](#), Julia [Ruohotie](#), [Simon Good](#), Emilia K. J. [Kilpua](#), [Noé Lugaz](#)

JGR [Volume 125, Issue 9](#) September 2020 e2020JA028002

<https://agupubs.onlinelibrary.wiley.com/doi/epdf/10.1029/2020JA028002>

<https://doi.org/10.1029/2020JA028002>

The longitudinal spatial coherence near 1 AU of the magnetic field in sheath regions driven by interplanetary coronal mass ejection (ICME) is studied by investigating ACE and Wind spacecraft measurements of 29 sheaths. During 2000–2002 Wind performed prograde orbits, and the non-radial spacecraft separation varied from 0.001 to 0.012 AU between the studied events. We compare the measurements by computing the Pearson correlation coefficients for the magnetic field magnitude and components and estimate the magnetic field coherence by evaluating the scale lengths that give the extrapolated distance of zero correlation between the measurements. The correlation is also separately examined for low- and high-pass filtered data. We discover magnetic fields in ICME sheaths have scale lengths that are larger than those reported in the solar wind but that, in general, are smaller than the ones of the ICME ejecta. Our results imply that magnetic fields in the sheath are more coherently structured and well correlated compared to the solar wind. The largest sheath coherence is reported in the GSE y-direction that has the scale length of 0.149 AU while the lengths for B_x , B_z , and $|B|$ vary between 0.024 and 0.035 AU. The same sheath magnitude ordering of scale lengths also apply for the low-pass filtered magnetic field data. We discuss field line draping and the alignment of preexisting discontinuities by the shock passage giving reasoning for the observed results. **15 May 2005**

Alfvén Ion Cyclotron Waves in Sheath Regions Driven by Interplanetary Coronal Mass Ejections

Matti [Ala-Lahti](#), Emilia K. J. [Kilpua](#), [Jan Souček](#), Tuija I. [Pulkkinen](#), [Andrew P. Dimmock](#)

JGR [Volume 124, Issue 6](#) June 2019 Pages 3893–3909

[sci-hub.se/10.1029/2019JA026579](https://doi.org/10.1029/2019JA026579)

We report on a statistical analysis of the occurrence and properties of Alfvén ion cyclotron (AIC) waves in sheath regions driven by interplanetary coronal mass ejections (ICMEs). We have developed an automated algorithm to identify AIC wave events from magnetic field data and apply it to investigate 91 ICME sheath regions recorded by the Wind

spacecraft. Our analysis focuses on waves generated by the ion cyclotron instability. AIC waves are observed to be frequent structures in ICME-driven sheaths, and their occurrence is the highest in the vicinity of the shock. Together with previous studies, our results imply that the shock compression has a crucial role in generating wave activity in ICME sheaths. AIC waves tend to have their frequency below the ion cyclotron frequency, and, in general, occur in plasma that is stable with respect to the ion cyclotron instability and has lower ion β_{\parallel} than mirror modes. The results suggest that the ion beta anisotropy $\beta_{\perp}/\beta_{\parallel} > 1$ appearing in ICME sheaths is regulated by both ion cyclotron and mirror instabilities.

Temporal Changes in the Rigidity Spectrum of Forbush Decreases Based on Neutron Monitor Data

M. V. [Alania](#), A. Wawrzynczak, V. E. Sdobnov, M. V. Kravtsova
Solar Physics, September 2013, Volume 286, Issue 2, pp 561-576,

The Forbush decrease (Fd) of the Galactic cosmic ray (GCR) intensity and disturbances in the Earth's magnetic field generally take place simultaneously and are caused by the same phenomenon, namely a coronal mass ejection (CME) or a shock wave created after violent processes in the solar atmosphere. The magnetic cut-off rigidity of the Earth's magnetic field changes because of the disturbances, leading to additional changes in the GCR intensity observed by neutron monitors and muon telescopes. Therefore, one may expect distortion in the temporal changes in the power-law exponent of the rigidity spectrum calculated from neutron monitor data without correcting for the changes in the cut-off rigidity of the Earth's magnetic field. We compare temporal changes in the rigidity spectrum of Fds calculated from neutron monitor data corrected and uncorrected for the geomagnetic disturbances. We show some differences in the power-law exponent of the rigidity spectrum of Fds, particularly during large disturbances of the cut-off rigidity of the Earth's magnetic field. However, the general features of the temporal changes in the rigidity spectrum of Fds remain valid as they were found in our previous study. Namely, at the initial phase of the Fd, the rigidity spectrum is relatively soft and it gradually becomes hard up to the time of the minimum level of the GCR intensity. Then during the recovery phase of the Fd, the rigidity spectrum gradually becomes soft. This confirms that the structural changes of the interplanetary magnetic field turbulence in the range of frequencies of $10^{-6} - 10^{-5}$ Hz are generally responsible for the time variations in the rigidity spectrum we found during the Fds.

Rigidity spectrum of Forbush decrease calculated by neutron monitors data corrected and uncorrected for geomagnetic disturbances

M V [Alania](#)^{1,2}, A Wawrzynczak³, V E Sdobnov⁴ and M V Kravtsova
2013 J. Phys.: Conf. Ser. 409 012184

Forbush decreases (Fd) of the galactic cosmic ray (GCR) intensity and geomagnetic storms are observed almost at the same time. Geomagnetic storm is a reason of significant disturbances of the magnetic cut off rigidity causing the distortion of the time profile of the Fd of the GCR intensity. We show some differences in the temporal changes of the rigidity spectra of Fd calculated by neutron monitors experimental data corrected and uncorrected for the changes of the geomagnetic cut off rigidity. Nevertheless, the general features of the temporal changes of the rigidity spectrum of Fd maintain as it was found in our previous investigations. Namely, at the beginning phase of Fd rigidity spectrum is relatively soft and gradually becomes hard up to reaching the minimum level of the GCR intensity; then the rigidity spectrum gradually becomes soft during the recovery phase of Fd. We also confirm that for the established temporal profiles of the rigidity spectrum of Fd a structural changes of the interplanetary magnetic field turbulence in the range of frequencies, $10^{-6} - 10^{-5}$ Hz are responsible.

Editorial: Interplanetary Medium Variability as Observed in the New Era of Spacecraft Missions

Tommaso [Alberti](#), Lina Hadid, Valeria Mangano, and Beatriz Sánchez-Cano
Front. Astron. Space Sci. 9:1002727 2022

<https://doi.org/10.3389/fspas.2022.1002727>

<https://www.frontiersin.org/articles/10.3389/fspas.2022.1002727/full>

Since 1970s an increasing number of heliospheric and planetary space missions have been launched as Helios ([Porsche, 1981](#)), Ulysses ([Carvell, 1986](#)), Wind ([Acuña et al., 1995](#)), ACE ([Garrard et al., 1997](#)), MAVEN ([Jakosky and MAVEN Science Team, 2008](#)), Rosetta ([Wood, 1987](#)), Cassini ([Prange, 1985](#)) collected a huge amount of data to characterize the interplanetary medium variability through the Heliosphere. Nowadays, the recently launched space missions BepiColombo ([Benkhoff et al., 2021](#)), Parker Solar Probe ([Bale et al., 2016](#)), and Solar Orbiter ([Müller et al., 2020](#)) provide more accurate in situ measurements through high-resolution instruments for monitoring the evolution of solar

wind parameters at different heliocentric distances ranging from ~ 0.05 A.U. to ~ 10 A.U., and for providing new insights into the physics of various plasma processes related to the Sun and the interplanetary medium.

Tracking of magnetic helicity evolution in the inner heliosphere

A radial alignment study

T. **Alberti**¹, Y. Narita², L. Z. Hadid³, D. Heyner⁴, A. Milillo¹, C. Plainaki⁵, H.-U. Auster⁴ and I. Richter⁴
A&A 664, L8 (2022)

<https://www.aanda.org/articles/aa/pdf/2022/08/aa44314-22.pdf>

Context. Magnetic helicity is one of the invariants in ideal magnetohydrodynamics, and its spectral evolution has a substantial amount of information to reveal the mechanism that are behind turbulence in space and astrophysical plasmas.

Aims. The goal of our study is to observationally characterize the magnetic helicity evolution in the inner heliosphere by resolving the helicity transport in a scale-wise fashion in the spectral domain.

Methods. The evolution of the magnetic helicity spectrum in the inner heliosphere was tracked using a radial alignment event achieved by Parker Solar Probe at a distance of 0.17 astronomical units (AU) from the Sun and BepiColombo at 0.58 AU with a delay of about 3.5 days.

Results. The reduced magnetic helicity resolved in the frequency domain shows three main features: (1) a coherent major peak of a highly helical component at the lowest frequency at about 5×10^{-4} Hz, (2) a damping of helicity oscillation at the intermediate frequencies from 10^{-3} to 10^{-2} Hz when observed at 0.58 AU, and (3) a coherent nonhelical component in the ion-kinetic range at frequencies of about 0.1 – 1 Hz.

Conclusions. Though limited in the frequency range, the main message from this work is that the solar wind develops into turbulence by convecting large-scale helicity components on the one hand and creating and annihilating helical wave components on the other hand. Excitation of waves can overwrite the helicity profile in the inner heliosphere. By comparing this with the typical helicity spectra at a distance of 1 AU (that is, a randomly oscillating helicity sign in the intermediate frequency range up to about 1 Hz), the helicity evolution reaches a nearly asymptotic state at the Venus orbit (about 0.7 AU) and beyond. **25 Sep 2020**

Observations of Forbush Decreases of Cosmic-Ray Electrons and Positrons with the Dark Matter Particle Explorer

Francesca **Alemanno**^{1,2}, Qi An^{3,4}, Philipp Azzarello⁵, Felicia Carla Tiziana Barbato^{1,2}, Paolo Bernardini^{6,7}, XiaoJun Bi^{8,9}, MingSheng Cai^{10,11}, Elisabetta Casilli^{6,7}, Enrico Catanzani¹², Jin Chang^{10,11}Show full author list

2021 *ApJL* 920 L43

<https://iopscience.iop.org/article/10.3847/2041-8213/ac2de6/pdf>

<https://doi.org/10.3847/2041-8213/ac2de6>

The Forbush decrease (FD) represents the rapid decrease of the intensities of charged particles accompanied with the coronal mass ejections or high-speed streams from coronal holes. It has been mainly explored with the ground-based neutron monitor network, which indirectly measures the integrated intensities of all species of cosmic rays by counting secondary neutrons produced from interaction between atmospheric atoms and cosmic rays. The space-based experiments can resolve the species of particles but the energy ranges are limited by the relatively small acceptances except for the most abundant particles like protons and helium. Therefore, the FD of cosmic-ray electrons and positrons have just been investigated by the PAMELA experiment in the low-energy range (<5 GeV) with limited statistics. In this paper, we study the FD event that occurred in **2017 September** with the electron and positron data recorded by the Dark Matter Particle Explorer. The evolution of the FDs from 2 GeV to 20 GeV with a time resolution of 6 hr are given. We observe two solar energetic particle events in the time profile of the intensity of cosmic rays, the earlier, and weaker, one has not been shown in the neutron monitor data. Furthermore, both the amplitude and recovery time of fluxes of electrons and positrons show clear energy dependence, which is important in probing the disturbances of the interplanetary environment by the coronal mass ejections.

Geomagnetic signatures during the intense geomagnetic storms of 29 October and 20 November 2003

S. **Alex**, S. Mukherjee, G.S. Lakhina

Journal of Atmospheric and Solar-Terrestrial Physics, Volume 68, Issue 7, April 2006, Pages 769-780

Solar cycle 23 in its declining phase witnessed the most pronounced space weather events during October–November 2003. A series of powerful solar flares and associated geoeffective Coronal Mass Ejections (CMEs) travelling at 2000 km/s drove shock fronts that impacted the Earth's magnetic field consecutively on 29 and 30 October, resulting in intense geomagnetic disturbances during 29–31 October. Another intense geomagnetic storm activity occurred during 20–21 November, resulting from a solar flare that had an associated geoeffective CME travelling at a speed of 1100 km/s. Digital ground magnetic field measurements from the equatorial and low-latitude locations in the Indian longitude zone, in conjunction with the interplanetary solar wind and magnetic field parameters, are used to study the characteristics of these storms. Maximum magnitude of the total magnetospheric energy injected into the magnetosphere during the mainphase of the three major storm amounts to approximately 4.5×10^{13} , 3.6×10^{13} , 2.8×10^{13} W. Another salient feature brought out is the close correspondence between the magnitude of the peak of the southward component of the interplanetary magnetic field B_z and the strength of the storm intensity as inferred from the Dst and low-latitude digital magnetic records.

Exploring the Coronal Magnetic Field with Galactic Cosmic Rays: The Sun Shadow Observed by HAWC

R. Alfaro¹, C. Alvarez², J. C. Arteaga-Velázquez³, K. P. Arunbabu⁴, D. Avila Rojas¹, R. Babu⁵, E. Belmont-Moreno¹, K. S. Caballero-Mora², T. Capistrán⁶, A. Carramiñana⁷ Show full author list
2024 ApJ 966 67

<https://iopscience.iop.org/article/10.3847/1538-4357/ad3208/pdf>

Galactic cosmic rays (GCRs) are charged particles that reach the heliosphere almost isotropically in a wide energy range. In the inner heliosphere, the GCR flux is modulated by solar activity so that only energetic GCRs reach the lower layers of the solar atmosphere. In this work, we propose that high-energy GCRs can be used to explore the solar magnetic fields at low coronal altitudes. We used GCR data collected by the High-Altitude Water Cherenkov observatory to construct maps of GCR flux coming from the Sun's sky direction and studied the observed GCR deficit, known as Sun shadow (SS), over a 6 yr period (2016–2021) with a time cadence of 27.3 days. We confirm that the SS is correlated with sunspot number, but we focus on the relationship between the photospheric solar magnetic field measured at different heliolatitudes and the relative GCR deficit at different energies. We found a linear relationship between the relative deficit of GCRs represented by the depth of the SS and the solar magnetic field. This relationship is evident in the observed energy range of 2.5–226 TeV, but is strongest in the range of 12.4–33.4 TeV, which implies that this is the best energy range to study the evolution of magnetic fields in the low solar atmosphere.

Investigating The Cross-section of Coronal Mass Ejections Through the Study of Non-Radial Flows with STEREO/PLASTIC

N. Al-Haddad, A. B. Galvin, N. Lugaz, C. J. Farrugia, W. Yu
ApJ 927 68 2022

<https://arxiv.org/pdf/2110.10682.pdf>

<https://iopscience.iop.org/article/10.3847/1538-4357/ac32e1/pdf>

The solar wind, when measured close to 1 au, is found to flow mostly radially outward. There are, however, periods when the flow makes angles up to 15° away from the radial direction, both in the east-west and north-south directions. Stream interaction regions (SIRs) are a common cause of east-west flow deflections. Coronal mass ejections (CMEs) may be associated with non-radial flows in at least two different ways: 1) the deflection of the solar wind in the sheath region, especially close to the magnetic ejecta front boundary, may result in large non-radial flows, 2) the expansion of the magnetic ejecta may include a non-radial component which should be easily measured when the ejecta is crossed away from its central axis.

In this work, we first present general statistics of non-radial solar wind flows as measured by STEREO/PLASTIC throughout the first 13 years of the mission, focusing on solar cycle variation. We then focus on the larger deflection flow angles and determine that most of these are associated with SIRs near solar minimum and with CMEs near solar maximum. However, we find no clear evidence of strongly deflected flows, as would be expected if large deflections around the magnetic ejecta or ejecta with elliptical cross-sections with large eccentricities are common. We use these results to develop a better understanding of CME expansion and the nature of magnetic ejecta, and point to shortcomings in our understanding of CMEs. **2010 September 11, 2012 July 11, 24-25 Jul 2017**

The Magnetic Morphology of Magnetic Clouds: Multi-spacecraft Investigation of Twisted and Writhed Coronal Mass Ejections

N. Al-Haddad¹, S. Poedts², I. Roussev², C. J. Farrugia³, W. Yu³, and N. Lugaz

2019 ApJ 870 100

sci-hub.tw/10.3847/1538-4357/aaf38d

We present a study about the structure of the magnetic field inside coronal mass ejections (CMEs) with consideration of the helicity property of the magnetic field lines. We perform reconstructions and fittings of the magnetic field of two simulated CMEs: (1) a CME with writhed magnetic field lines and minimum twist, and (2) a CME with a twisted flux rope structure. Our aim is to gain insight into the structure of the CMEs' magnetic field through comparing the outcome of the fitting techniques with the actual structure of the simulated CMEs. Reconstructions are performed at 12 different locations using the Grad–Shafranov reconstruction technique and a force-free fitting technique. These locations correspond to different impact parameters, as well as different longitudinal planes in the CME "legs." We find that a flux rope CME and a writhed CME cannot be distinguished by comparing the best-fit orientation at different locations. We also find that the reconstructed shapes and impact parameters may provide some clues about the presence of substantial writhe. Because of the difficulty for present codes to detect writhe, we conclude that reconstruction codes and fitting techniques have to be significantly improved, by taking into consideration the writhe of the magnetic field lines.

Fitting and Reconstruction of Thirteen Simple Coronal Mass Ejections

[Nada Al-Haddad](#), [Teresa Nieves-Chinchilla](#), [Neel P. Savani](#), [Noe Lugaz](#), [Ilia I. Roussev](#)

Solar Phys. **2018**

<https://arxiv.org/pdf/1804.02359.pdf>

Coronal mass ejections (CMEs) are the main drivers of geomagnetic disturbances, but the effects of their interaction with Earth's magnetic field depend on their magnetic configuration and orientation. Fitting and reconstruction techniques have been developed to determine the important geometrical and physical CME properties. In many instances, there is disagreement between such different methods but also between fitting from in situ measurements and reconstruction based on remote imaging. Here, we compare three methods based on different assumptions for measurements of thirteen CMEs by the Wind spacecraft from 1997 to 2015. These CMEs are selected from the interplanetary coronal mass ejections catalog on [this https URL](#) due to their simplicity in terms of 1) small expansion speed throughout the CME and 2) little asymmetry in the magnetic field profile. This makes these thirteen events ideal candidates to compare codes that do not include expansion nor distortion. We find that, for these simple events, the codes are in relatively good agreement in terms of the CME axis orientation for six out of the 13 events. Using the Grad-Shafranov technique, we can determine the shape of the cross-section, which is assumed to be circular for the other two models, a force-free fitting and a circular-cylindrical non-force-free fitting. Five of the events are found to have a clear circular cross-section, even when this is not a pre-condition of the reconstruction. We make an initial attempt at evaluating the adequacy of the different assumptions for these simple CMEs. The conclusion of this work strongly suggests that attempts at reconciling in situ and remote-sensing views of CMEs must take in consideration the compatibility of the different models with specific CME structures to better reproduce flux ropes. **1997-01-10, 1998-08-19, 2000-07-01, 2001-04-21, 2002-09-29, 2008-05-23, 2009-09-30, 2012-05-16, 2012-11-12, 2013-06-27, 2013-12-24, 2014-04-11, 2015-05-06**

Table 1. List of 13 CMEs used in this study

Magnetic Field Configuration Models and Reconstruction Methods for Interplanetary Coronal Mass Ejections

N. [Al-Haddad](#), T. Nieves-Chinchilla, N. P. Savani, C. Möstl, K. Marubashi, M. A. Hidalgo, I. I. Roussev, S. Poedts, C. J. Farrugia

Solar Phys. Volume 284, Issue 1, pp 129-149, **2013**; **File**

This study aims to provide a reference for different magnetic field models and reconstruction methods for interplanetary coronal mass ejections (ICMEs). To understand the differences in the outputs of these models and codes, we analyzed 59 events from the Coordinated Data Analysis Workshop (CDAW) list, using four different magnetic field models and reconstruction techniques; force-free fitting, magnetostatic reconstruction using a numerical solution to the Grad–Shafranov equation, fitting to a self-similarly expanding cylindrical configuration and elliptical, non-force-free fitting. The resulting parameters of the reconstructions for the 59 events are compared statistically and in selected case studies. The ability of a method to fit or reconstruct an event is found to vary greatly; this depends on whether the event is a magnetic cloud or not. We find that the magnitude of the axial field is relatively consistent across models, but that the axis orientation of the ejecta is not. We also find that there are a few cases with different signs of the magnetic helicity for the same event when we leave the boundaries free to vary, which illustrates that this simplest of parameters is not necessarily always clearly constrained by fitting and reconstruction models. Finally, we examine three unique cases in depth to provide a comprehensive idea of the different aspects of how the fitting and reconstruction codes work.

26 – 28 June 1999, 27 July 2000, 6 – 7 November 2000

ON THE INTERNAL STRUCTURE OF THE MAGNETIC FIELD IN MAGNETIC CLOUDS AND INTERPLANETARY CORONAL MASS EJECTIONS: WRITHE VERSUS TWIST

N. **Al-Haddad**^{1,2}, I. I. Roussev¹, C. Möstl^{3,4}, C. Jacobs², N. Lugaz¹, S. Poedts² and C. J. Farrugia
2011 ApJ 738 L18

In this study, we test the flux rope paradigm by performing a "blind" reconstruction of the magnetic field structure of a simulated interplanetary coronal mass ejection (ICME). The ICME is the result of a magnetohydrodynamic numerical simulation and does not exhibit much magnetic twist, but appears to have some characteristics of a magnetic cloud, due to a writhe in the magnetic field lines. We use the Grad-Shafranov technique with simulated spacecraft measurements at two different distances and compare the reconstructed magnetic field with that of the ICME in the simulation. While the reconstructed magnetic field is similar to the simulated one as seen in two dimensions, it yields a helically twisted magnetic field in three dimensions. To further verify the results, we perform the reconstruction at three different position angles at every distance point, and all results are found to be in agreement. This work demonstrates that the current paradigm of associating magnetic clouds with flux ropes may have to be revised.

Testing the empirical relationship between Forbush decreases and cosmic ray diurnal anisotropy

Jibrin Adejoh **Alhassan**, [Ogbonnaya Okike](#), [Augustine Ejikeme Chukwude](#)

Research in Astronomy and Astrophysics (RAA) 2022

<https://arxiv.org/pdf/2203.08883.pdf>

The abrupt aperiodic modulation of cosmic ray (CR) flux intensity, often referred to as Forbush decrease (FD), plays a significant role in our understanding of the Sun-Earth electrodynamics. Accurate and precise determination of FD magnitude and timing are among the intractable problems in FD-based analysis. FD identification is complicated by CR diurnal anisotropy. CR anisotropy can increase or reduce the number and amplitude of FDs. It is therefore important to remove its contributions from CR raw data before FD identification. Recently, an attempt was made, using a combination of Fourier transformed technique and FD-location machine to address this. Thus, two FD catalogs and amplitude diurnal variation (ADV) were calculated from filtered (FD1 and ADV) and raw (FD2) CR data. In the current work, we test the empirical relationship between FD1, FD2, ADV, and solar-geophysical characteristics. Our analysis shows that two types of magnetic fields-interplanetary (IMF) and geomagnetic (Dst) govern the evolution of CR flux intensity reductions. 30 Oct 2003

Tables

Testing the Simultaneity of Forbush Decreases with Algorithm-Selected Forbush Event Catalogue

J. A. **Alhassan**, [O. Okike](#), [A. E. Chukwude](#)

J. Astrophys. Astr. 2021

<https://arxiv.org/pdf/2111.05332.pdf>

Accurate detection and precise timing of transient events such as X-ray photons, $\{\gamma\}$ -ray burst, coronal mass ejections (CMEs), ground level enhancements (GLEs) and Forbush decreases (FDs) frequently raise issues that remain on the cutting edge of research in astrophysics. In an attempt to automate FD event selection, a combination of Fast Fourier transform as well as FD detection algorithms implemented in the statistical computing software R was developed and recently used to calculate the magnitude and FD event timing. The R-FD code implemented in the present study includes several different calculations. Some subroutines detect both small and large transient intensity reductions (minima/pits) as well as increases (maxima/peaks) in cosmic ray (CR) data. Others calculate event amplitude, timing and cataloging of the events identified. As the current work focuses on reductions in CR flux (FDs), the subroutine that identifies increases was disabled. Totals of 229 FDs at Magadan neutron monitor (NM), 230 (Oulu NM) and 224 (Inuvick NM) were identified with daily averaged data, while 4032 (Magadan), 4144 (Oulu) and 4055 (Inuvick) were detected with hourly averages. FDs identified as simultaneous at the three stations totaled 99 for the daily and 261 for the hourly CR averages respectively. 12-13 Feb 2000, 23 May 2002

Table 2. Forbush Decreases from INVK (FD1%), MGDN (FD2%) and OULU (FD3%) (1998-2002)

Investigation of the Relation between Space-Weather Parameters and Forbush Decreases Automatically Selected from Moscow and Apatity Cosmic Ray Stations during Solar Cycle 23

Jibrin A. **Alhassan**, [Ogbonnaya Okike](#), [Augustine E. Chukwude](#)

Research in Astronomy and Astrophysics (RAA) 2021

<https://arxiv.org/pdf/2108.09371.pdf>

We present the results of an investigation of the relation between space-weather parameters and cosmic ray (CR) intensity modulation using algorithm-selected Forbush decreases (FDs) from Moscow (MOSC) and Apatity (APTY) neutron monitor (NM) stations during solar cycle 23. Our FD location program detected 408 and 383 FDs from MOSC and APTY NM stations respectively. A coincident computer code employed in this work, detected 229 FDs that were observed at the same universal Time (UT) at the two stations. Out of the 229 simultaneous FDs, we formed a subset of 139 large FDs ($\Delta I \leq -4$) at Moscow station. We performed a two dimensional regression analysis between the FD magnitudes and the space-weather data on the two samples. We find that there were significant space-weather disturbances at the time of the CR flux depressions. The correlation between the space-weather parameters and galactic cosmic ray (GCR) intensity decreases at the two NM stations are statistically significant. The implications of the present space-weather data on cosmic ray (CR) intensity depressions are highlighted.

Table 1: Selected FDs at MOSC and APTY Stations from 1996-2005

Testing the Effect of Solar Wind Parameters and Geomagnetic Storm Indices on Galactic Cosmic Ray Flux Variation with Automated-Selected Forbush Decreases

Jibrin A. Alhassan, Ogbonnaya Okike, Augustine E. Chukwude

Research in Astronomy and Astrophysics Volume: 21. Issue: 9. 2021

<https://arxiv.org/pdf/2108.09066.pdf>

<https://iopscience.iop.org/article/10.1088/1674-4527/21/9/234/pdf>

Forbush decrease (FD), discovered by Scott E. Forbush about 80 years ago, is referred to as the non-repetitive short-term depression in galactic cosmic ray (GCR) flux, presumed to be associated with large-scale perturbations in solar wind and interplanetary magnetic field (IMF). It is the most spectacular variability in the GCR intensity which appear to be the compass for investigators seeking solar-terrestrial relationships. The method of selection and validation of FD events are very important to cosmic ray scientists. We have deployed a new computer software to determine the amplitude and timing of FDs from daily-averaged cosmic ray (CR) data at OULU neutron monitor station. The code selected 230 FDs between 1998 and 2002. In an attempt to validate the new FD automated catalog, the relationship between the amplitude of FDs, and IMF, solar wind speed (SWS) and geomagnetic storm indices (Dst, kp, ap) is tested here. A two-dimensional regression analysis indicates significant linear relationship between large FDs ($\Delta I \leq -3$) and solar wind data and geomagnetic storm indices in the present sample. The implications of the relationship among these parameters are discussed.

Table 2: 129 Oulu NM station FDs (All FDs) and Associated Solar Wind Data and Geomagnetic Activity Indices from 1998-2002

Properties of the HPS-ICME-CIR Interaction Event of 9–10 September 2011

Duraid A. Al-Shakarchi, Huw Morgan

JGR **Volume 123, Issue 4** Pages 2535-2556 **2018**

<https://agupubs.onlinelibrary.wiley.com/doi/full/10.1002/2017JA024849>

During 9–10 September 2011 the ACE, Wind, and SOHO spacecraft measured the complex interaction between an interplanetary coronal mass ejection (ICME) and a corotating interaction region (CIR) associated with the heliospheric sector boundary. Except for a few short periods, the suprathermal electrons are unidirectional, suggesting that the ICME magnetic field has opened through interchange reconnection. Signatures of interaction are distributed throughout the event suggesting that the structures have become entangled or embedded. Since the ICME speed is relatively low, the strong forward shock must be caused by the ICME-CIR interaction. Other interesting features are the upstream heating flux discontinuity, the very high proton density in the frontal boundary of the heliospheric plasma sheet and the forward shock, the significant speed elevation within the sheath, the distortion of Bz in the magnetic cloud, the indistinct location of the stream interface, the unidirectional domination of the suprathermal electrons, and the reverse shock at the CIR rear boundary. There is an unusual delay between the proton density and temperature profiles. Furthermore, large differences in proton speed and forward shock density measured between L1 spacecraft indicate high variation at small spatial scales. A few days earlier, STEREO B recorded the undisturbed CIR, which shows that (i) some general features of the CIR are preserved, (ii) the CIR is compressed by a factor of ~ 4 by the ICME, and (iii) a magnetic exhausted region at the front of the CIR is a continuous feature and is not formed due to the ICME interaction

Study of the Coronal Mass Ejections for the Down Phase of the Solar Cycle 24, the Events, Verifications and Simulation of the Plasma speed in the Sheath and ICME

Hamza A Ali, Alaa F Ahmed, Wafaa Zaki

Indian Journal of Natural Sciences Vol.8 / Issue 49 / August /2018

Coronal mass ejections CMEs are large amount ejections of plasma and magnetic field from solar corona which propagate through interplanetary space, and usually it affects Earth and other planets of solar system , In our study, we've identified all the events and sun activities through the global Labs, SOHO LASCO, (2014-2015), then we've filtered all the events that could reach the earth, the events that have more the 500 km/s as a speed of the coronal mass ejections, after identifying the events in SOHO LASCO and filtering the events, we did compare the results of the proposed events with other Lab (ERNE) in order to figure out if these events are clear showed with ERNE or not, for the clear event, will be considered as real events, other events will be neglected, once comparing done, we worked on mathematical methods for tripled check and verifications, between the times evaluated and the times assumed, and this was the last method to identify where the events are earth reaching or not, using lognormal model to study the probability of the speed distributions in the sheath and ICME.

Studying the Characteristics of Shock waves associated with CMEs using solar radio bursts.

Khaled [Alielden](#)₁ and Ayman Mahrousy₂

CESRA 2016, p.89

http://cesra2016.sciencesconf.org/conference/cesra2016/pages/CESRA2016_prog_abs_book_v3.pdf

Fast CME/shocks propagating in the Corona and the interplanetary medium can generate metric and kilometric Type II radio emissions at the local plasma frequency and/or its harmonic, respectively. So these radio emissions provide a means of remotely tracking CME/shocks. We apply analysis technique, using the frequency drift of metric spectrum obtained by ground station e-Callisto (Compound Astronomical Low cost Low frequency Instrument for Spectroscopy and Transportable Observatory) in Space Weather Monitoring Center (SWMC) { Helwan University, and estimated by using electron density model the propagation speed of CME/shocks in the corona, and the km-TII spectrum obtained by the WIND/WAVES experiment, to infer, at some adequate intervals, the propagation speed of CME/shocks in the interplanetary medium. We applied this technique on _ve CME/shocks. We combine these results with previously reported speeds from coronagraph white light and interplanetary scintillation observations, and in-situ measurements, to study the temporal speed evolution of the _ve events. The speed values obtained by the metric and km-TII analysis are in a reasonable agreement with the speed measurements obtained by other techniques at di_ erent heliocentric distance ranges. The combination of all the speed measurements show a gradual deceleration of the CME/shocks as they propagate to 1 AU. This technique can be useful in studying the evolution and characteristics of fast CME/shocks when adequate intervals of km-TII emissions are available.

Predictive capabilities and limitations of stream interaction region observations at different solar longitudes

R.C. [Allen](#), [G.C. Ho](#), [L.K. Jian](#), [G.M. Mason](#), [S.K. Vines](#), [D. Lario](#)

Space Weather [Volume18, Issue4](#) 2020 e2019SW002437

sci-hub.si/10.1029/2019SW002437

<https://doi.org/10.1029/2019SW002437>

<https://agupubs.onlinelibrary.wiley.com/doi/epdf/10.1029/2019SW002437>

Advanced warning of a Stream Interaction Region (SIR) or Co-rotating Interaction Region (CIR) impinging upon the magnetosphere of Earth is important for space weather forecasting, due to the ability of SIRs/CIRs to trigger geomagnetic storms and affect ionospheric composition and winds. However, a focused investigation of the likelihood that either an L5 monitor or Earth-trailing “string-of-pearl” constellation of satellites would be able to serve as an effective warning buoy for SIRs/CIRs that will affect the near-Earth space environment has yet to be extensively performed. Through comparing 10 years of SIRs/CIRs observed at L1 and at STEREO, we have investigated the probability of sequentially detecting SIRs/CIRs at two locations as a function of the difference in heliospheric longitude and latitudinal separation between the two spacecraft. By examining the probability of repeat detection of SIRs/CIRs using variable separation distances between two observing points, we explore the utility of an Earth trailing monitor for SIR/CIR predictability (i.e., 74.6% of SIRs observed at L5 reach L1 within ± 3 days of rigid co-rotation). While the

probability of predicting the occurrence of SIRs/CIRs at another spacecraft decreases with longitudinal separation, there is not a significant dependence on latitude. The primary source of error in reliably predicting the arrival time of an SIR/CIR is uncertainty in the rotational speed of the structure. While an L5 monitor would be an advancement in our operational warning ability, an Earth-trailing “string-of-pearls” constellation utilizing multiple point of measurements would engender much more certainty in predicting the arrival time of SIRs/CIRs.

Prediction of Geoeffective CMEs Using SOHO Images and Deep Learning.

Alobaid, K.A., Wang, J.T.L., Wang, H. et al.

Sol Phys 299, 159 (2024).

<https://doi.org/10.1007/s11207-024-02385-w>

<https://link.springer.com/content/pdf/10.1007/s11207-024-02385-w.pdf> **File**

The application of machine learning to the study of coronal mass ejections (CMEs) and their impacts on Earth has seen significant growth recently. Understanding and forecasting CME geoeffectiveness are crucial for protecting infrastructure in space and ensuring the resilience of technological systems on Earth. Here we present GeoCME, a deep-learning framework designed to predict, deterministically or probabilistically, whether a CME event that arrives at Earth will cause a geomagnetic storm. A geomagnetic storm is defined as a disturbance of the Earth’s magnetosphere during which the minimum Dst index value is less than -50 nT. GeoCME is trained on observations from the instruments including LASCO C2, EIT, and MDI on board the Solar and Heliospheric Observatory (SOHO), focusing on a dataset that includes 136 halo/partial halo CMEs in Solar Cycle 23. Using ensemble and transfer learning techniques, GeoCME is capable of extracting features hidden in the SOHO observations and making predictions based on the learned features. Our experimental results demonstrate the good performance of GeoCME, achieving a Matthew’s correlation coefficient of 0.807 and a true skill statistics score of 0.714 when the tool is used as a deterministic prediction model. When the tool is used as a probabilistic forecasting model, it achieves a Brier score of 0.094 and a Brier skill score of 0.493. These results are promising, showing that the proposed GeoCME can help enhance our understanding of CME-triggered solar-terrestrial interactions. **17 September 2022**

Ensemble Learning for CME Arrival Time Prediction

Khalid A. **Alobaid**, [Jason T. L. Wang](#)

2023

<https://arxiv.org/pdf/2305.00258.pdf>

The Sun constantly releases radiation and plasma into the heliosphere. Sporadically, the Sun launches solar eruptions such as flares and coronal mass ejections (CMEs). CMEs carry away a huge amount of mass and magnetic flux with them. An Earth-directed CME can cause serious consequences to the human system. It can destroy power grids/pipelines, satellites, and communications. Therefore, accurately monitoring and predicting CMEs is important to minimize damages to the human system. In this study we propose an ensemble learning approach, named CMETNet, for predicting the arrival time of CMEs from the Sun to the Earth. We collect and integrate eruptive events from two solar cycles, #23 and #24, from 1996 to 2021 with a total of 363 geoeffective CMEs. The data used for making predictions include CME features, solar wind parameters and CME images obtained from the SOHO/LASCO C2 coronagraph. Our ensemble learning framework comprises regression algorithms for numerical data analysis and a convolutional neural network for image processing. Experimental results show that CMETNet performs better than existing machine learning methods reported in the literature, with a Pearson product-moment correlation coefficient of 0.83 and a mean absolute error of 9.75 hours.

Alobaid, K.A., Abdullah, Y., Wang, J.T.L., Wang, H., Fan, S., Li, J., Cavus, H., Yurchyshyn, V.: 2023, Estimating coronal mass ejection mass and kinetic energy by fusion of multiple deep-learning models. *Astrophys. J. Lett.* 958, L34. DOI.

Alobaid, K.A., Abdullah, Y., Wang, J.T.L., Wang, H., Jiang, H., Xu, Y., Yurchyshyn, V., Zhang, H., Cavus, H., Jing, J.: 2022, Predicting CME arrival time through data integration and ensemble learning. *Front. Astron. Space Sci.* 9, 1013345. DOI.

Plasma Data Sources in the OMNI Database

B. L. Alterman

2022 Res. Notes AAS 6 135

<https://iopscience.iop.org/article/10.3847/2515-5172/ac7a2f>

The OMNI data set is a tool well situated for analysis with advanced machine learning (ML) and artificial intelligence (AI) techniques. Because OMNI incorporates data from multiple instruments and spacecraft, care must be taken when interpreting these results. We discuss the OMNI/Lo plasma data sources and one potential challenge with interpreting the results of ML and AI techniques when applied to it.

Geoeffectiveness of solar wind interplanetary magnetic structures

M.V. **Alves**, a, , , E. Echer and W.D. Gonzalez

Journal of Atmospheric and Solar-Terrestrial Physics, Volume 73, Issues 11-12, 2011, Pages 1380-1384

We address the geoeffectiveness of three interplanetary structures in the interplanetary space: magnetic clouds (MCs), interplanetary shocks (IPs), and corotating interaction regions (CIRs). The geoeffectiveness is evaluated using the geomagnetic indices K_p , AE, and Dst. We find that MCs are more geoeffective than IPs, or CIRs. The average values of magnetic indices are significantly enhanced during disturbed periods associated with MCs, IPs and CIRs, compared to the whole interval. The highest effect is noted for MC disturbed periods.

Results obtained for the three data sets are used to derive a theoretical (continuous) probability distribution function (PDF) by fitting the histograms representing the percentage of events against the intervals of magnetic index. PDFs allow estimation of the probability of a given level of geomagnetic activity to be reached after the detection, by in situ solar wind observations, of a given interplanetary structure approaching the Earth.

Empirical forecasting models for peak intensities of energetic storm particles at 1 AU

Dheyaa **Ameri** a b, Rami Vainio b, Eino Valtonen b

Advances in Space Research Volume 73, Issue 1, 1 January 2024, Pages 1050-1063

<https://doi.org/10.1016/j.asr.2023.11.021>

<https://www.sciencedirect.com/science/article/pii/S0273117723009067>

We have investigated the dependence of the peak intensities of energetic storm particles (ESPs) on various parameters characterising the coronal mass ejections (CMEs) and associated phenomena. The aim of this study is to suggest empirical models for forecasting the peak intensities of ESP events at 1 AU based on solar and interplanetary (IP) space observations.

For this study we searched for the associations of front-side full and partial halo CMEs with linear speeds >400 km s^{-1} during the years 1996–2015 with IP shocks at 1 AU and ESP events observed near the time when the shock passes the observer. We found 88 CME-driven IP shocks associated with ESP events at proton energy range 5.0–7.2 MeV (nominal energy 6.0 MeV) and 59 shocks at the energy range 15.1–21.9 MeV (nominal energy 18.2 MeV). At these two energies 71 % and 68 % of the ESP events were associated with solar energetic particle (SEP) events, 85 % and 84 % were associated with decametric–hectometric (DH) type II radio bursts while 67 % and 66 % were associated with both. For each CME - shock pair we calculated the predicted shock transit speed (VTR) by using the method of [Belov et al. \(2022\)](#) and used this as the primary parameter in the investigation. We performed correlation analyses between the logarithm of the peak intensities of the ESP events (\log_{10} [IESP_{peak}]) and the solar parameters related to the CMEs, solar flares, IP shocks, SEP events, and type II radio bursts. When using a single explanatory variable, we found best correlation coefficients for VTR (0.68 ± 0.05 and 0.71 ± 0.06), the CME space speed (VCME_{space}) (0.59 ± 0.05 and 0.68 ± 0.07), and the logarithm of SEP peak intensity (\log_{10} [ISEP_{peak}]) (0.55 ± 0.08 and 0.70 ± 0.08) at 6.0 and 18.2 MeV, respectively. Weak to moderate correlations were found for the logarithm of the soft X-ray flux (\log_{10} [SXRF]) and the logarithm of the duration of DH type II radio burst (\log_{10} [DTII]).

Using linear combinations of two or more variables improved the correlations. The best two-variable combination explaining \log_{10} [IESP_{peak}] was VTR combined with \log_{10} [ISEP_{peak}] and the best three- and four-variable combinations also included these two parameters. We found two methods for forecasting ESP peak intensities, one of which can be used for long lead time and the other for medium lead time forecasting. For long lead time forecasting VTR, VCME_{space} and \log_{10} [SXRF] are used. The correlation coefficients between the calculated and observed \log_{10} [IESP_{peak}] were 0.71 ± 0.05 at 6.0 MeV and 0.74 ± 0.06 at 18.2 MeV. This method only depends on the coronagraph and X-ray observations at the Sun. For medium lead time forecasting the four parameters used are VTR, \log_{10} [ISEP_{peak}], VCME_{space} (or \log_{10} [SXRF]), and \log_{10} [DTII]. The correlation coefficients were 0.80 ± 0.04 at 6.0 MeV and 0.84 ± 0.05 at 18.2 MeV. Coronagraph observations at the Sun and solar energetic particle and DH type II burst measurements in IP space are required for this method. The medium lead time forecasting provides an average warning time of 30 ± 16 h.

Relationships between energetic storm particle events and interplanetary shocks driven by full and partial halo coronal mass ejections

D. Ameri, E. Valtonen, A. Al-Sawad, R. Vainio

Adv. Space Res., **Volume 71, Issue 5**, (2023), pp. 2521-2533,

<https://doi.org/10.1016/j.asr.2022.12.014>

<https://www.sciencedirect.com/science/article/pii/S0273117722011061>

We have analysed energetic storm particle (ESP) events in 116 interplanetary (IP) shocks driven by front-side full and partial halo coronal mass ejections (CMEs) with speeds $>400 \text{ km s}^{-1}$ during the years 1996–2015. We investigated the occurrence and relationships of ESP events with several parameters describing the IP shocks, and the associated CMEs, type II radio bursts, and solar energetic particle (SEP) events. Most of the shocks (57 %) were associated with an ESP event at proton energies $>1 \text{ MeV}$.

The shock transit speeds from the Sun to 1 AU of the shocks associated with an ESP event were significantly greater than those of the shocks without an ESP event, and best distinguished these two groups of shocks from each other. The occurrence and maximum intensity of the ESP events also had the strongest dependence on the shock transit speed compared to the other parameters investigated. The correlation coefficient between ESP peak intensities and shock transit speeds was highest (0.73 ± 0.04) at 6.2 MeV. Weaker dependences were found on the shock speed at 1 AU, Alfvénic and magnetosonic Mach numbers, shock compression ratio, and CME speed. On average all these parameters were significantly different for shocks capable to accelerate ESPs compared to shocks not associated with ESPs, while the differences in the shock normal angle and in the width and longitude of the CMEs were insignificant.

The CME-driven shocks producing energetic decametric–hectometric (DH) type II radio bursts and high-intensity SEP events proved to produce also more frequently ESP events with larger particle flux enhancements than other shocks.

Together with the shock transit speed, the characteristics of solar DH type II radio bursts and SEP events play an important role in the occurrence and maximum intensity of ESP events at 1 AU.

Potential role of energetic particle observations in geomagnetic storm forecasting

Dheyaa Ameri, Eino Valtonen

Advances in Space Research **Volume 64, Issue 3**, 1 August 2019, Pages 801-813

<https://sci-hub.se/10.1016/j.asr.2019.05.012>

We have searched for solar proton events consisting of both solar energetic particles (SEPs) accelerated near the Sun and energetic storm particles (ESPs) accelerated by interplanetary shocks driven by coronal mass ejections (CMEs) and observed near the time when the shock passes the observer. The purpose of this study is to investigate the possibilities and advantages of using energetic particle observations for mid-term (warning time several hours) forecasting of geomagnetic storms or as a support for longer-term forecasting methods based on solar observations. The study period extends from May 1996 to December 2017 covering the entire solar cycle 23 and the major part of solar cycle 24. Using two particle energies, 2 and 20 MeV, we found 95 SEP–ESP events of which 65 were associated with geomagnetic storms with $Dst \leq -50 \text{ nT}$ caused by CMEs. We performed correlation analysis between $\log_{10}|Dst \text{ (nT)}|$ and various parameters characterising the particle events or the associated CMEs. We found the best correlations for the single independent variables $\Delta t_{ESP-SEP}$ ($r = -0.47 \pm 0.08$), which is the difference between the ESP peak time and SEP onset time, the CME direction parameter DP ($r = 0.47 \pm 0.10$), and the logarithm of the maximum ESP energy $\log_{10}[E_{ESPmax} \text{ (MeV)}]$ ($r = 0.44 \pm 0.11$). Using a linear combination of these three variables improves the correlation ($r = 0.68 \pm 0.07$). We suggest that an empirical equation based on these three parameters and requiring only coronagraph observations of CMEs and energetic particle measurements in interplanetary space can be used for mid-term forecasting of geomagnetic storm strengths. We found that 74% of the strongest storms ($Dst \leq -200 \text{ nT}$) during the study period were associated with energetic particle events. The average warning time and its standard deviation for all geomagnetic storms associated with SEP–ESP events was (15 ± 10) hours. **5-6 Aug 2011**

Table A.3 SEP–ESP events and associated CME direction parameters and values of the minimum Dst in 1996–2017.

Investigation of the Geoeffectiveness of Disk-Centre Full-Halo Coronal Mass Ejections

Dheyaa Ameri, Eino Valtonen

Solar Physics June 2017, 292:79 **File**

<https://link.springer.com/content/pdf/10.1007%2Fs11207-017-1102-7.pdf>

We studied the occurrence and characteristics of geomagnetic storms associated with disk-centre full-halo coronal mass ejections (DC-FH-CMEs). Such coronal mass ejections (CMEs) can be considered as the most plausible cause of geomagnetic storms. We selected front-side full-halo coronal mass ejections detected by the Large Angle and

Spectrometric Coronagraph onboard the Solar and Heliospheric Observatory (SOHO/LASCO) from the beginning of 1996 till the end of 2015 with source locations between solar longitudes E10 and W10 and latitudes N20 and S20. The number of selected CMEs was 66 of which 33 (50%) were deduced to be the cause of 30 geomagnetic storms with $Dst \leq -50$ nT. Of the 30 geomagnetic storms, 26 were associated with single disk-centre full-halo CMEs, while four storms were associated, in addition to at least one disk-centre full-halo CME, also with other halo or wide CMEs from the same active region. Thirteen of the 66 CMEs (20%) were associated with 13 storms with $-100 \text{ nT} < Dst \leq -50$ nT, and 20 (30%) were associated with 17 storms with $Dst \leq -100$ nT. We investigated the distributions and average values of parameters describing the DC-FH-CMEs and their interplanetary counterparts encountering Earth. These parameters included the CME sky-plane speed and direction parameter, associated solar soft X-ray flux, interplanetary magnetic field strength, B_t , southward component of the interplanetary magnetic field, B_s , solar wind speed, V_{sw} , and the y -component of the solar wind electric field, E_y . We found only a weak correlation between the Dst of the geomagnetic storms associated with DC-FH-CMEs and the CME sky-plane speed and the CME direction parameter, while the correlation was strong between the Dst and all the solar wind parameters (B_t , B_s , V_{sw} , E_y) measured at 1 AU. We investigated the dependences of the properties of DC-FH-CMEs and the associated geomagnetic storms on different phases of solar cycles and the differences between Solar Cycles 23 and 24. In the rise phase of Solar Cycle 23 (SC23), five out of eight DC-FH-CMEs were geoeffective ($Dst \leq -50$ nT). In the corresponding phase of SC24, only four DC-FH-CMEs were observed, three of which were non-geoeffective ($Dst > -50$ nT). The largest number of DC-FH-CMEs occurred at the maximum phases of the cycles (21 and 17, respectively). Most of the storms with $Dst \leq -100$ nT occurred at or close to the maximum phases of the cycles. When comparing the storms during epochs of corresponding lengths in Solar Cycles 23 and 24, we found that during the first 85 months of Cycle 23 the geoeffectiveness rate of the disk-centre full-halo CMEs was 58% with an average minimum value of the Dst index of -146 nT. During the corresponding epoch of Cycle 24, only 35% of the disk-centre full-halo CMEs were geoeffective with an average value of Dst of -97 nT. **Table 2** Storms and ICMEs associated with single DC-FH-CMEs.

Table 6 Dates and properties of disk-centre full-halo CMEs from May 1996 to December 2015

See **Near-Earth Interplanetary Coronal Mass Ejections Since January 1996** (to December 2016)

Compiled by Ian [Richardson](#)(1) and Hilary [Cane](#)(2),

<http://www.srl.caltech.edu/ACE/ASC/DATA/level3/icmetable2.htm>

Evaluation of CME arrival prediction using ensemble modeling based on heliospheric imaging observations

Tanja [Amerstorfer](#), [Jürgen Hinterreiter](#), [Martin A. Reiss](#), [Christian Möstl](#), [Jackie A. Davies](#), [Rachel L. Bailey](#), [Andreas J. Weiss](#), [Mateja Dumbović](#), [Maike Bauer](#), [Ute V. Amerstorfer](#), [Richard A. Harrison](#)

Space Weather **Volume19, Issue1** e2020SW002553 **2021**

<https://arxiv.org/pdf/2008.02576.pdf>

<https://agupubs.onlinelibrary.wiley.com/doi/epdf/10.1029/2020SW002553>

In this study, we evaluate a coronal mass ejection (CME) arrival prediction tool that utilizes the wide-angle observations made by STEREO's heliospheric imagers (HI). The unsurpassable advantage of these imagers is the possibility to observe the evolution and propagation of a CME from close to the Sun out to 1 AU and beyond. We believe that by exploiting this capability, instead of relying on coronagraph observations only, it is possible to improve today's CME arrival time predictions. The ELLipse Evolution model based on HI observations (ELEvoHI) assumes that the CME frontal shape within the ecliptic plane is an ellipse, and allows the CME to adjust to the ambient solar wind speed, i.e. it is drag-based. ELEvoHI is used to perform ensemble simulations by varying the CME frontal shape within given boundary conditions that are consistent with the observations made by HI. In this work, we evaluate different set-ups of the model by performing hindcasts for 15 well-defined isolated CMEs that occurred when STEREO was near L4/5, between the end of 2008 and the beginning of 2011. In this way, we find a mean absolute error of between 6.2 ± 7.9 h and 9.9 ± 13 h depending on the model set-up used. ELEvoHI is specified for using data from future space weather missions carrying HIs located at L5 or L1. It can also be used with near real-time STEREO-A HI beacon data to provide CME arrival predictions during the next ~ 7 years when STEREO-A is observing the Sun-Earth space. **12 Dec 2008, 26 Oct 2010**

Table 1. Overview of events used in this study (2008-2011)

Ensemble Prediction of a Halo Coronal Mass Ejection Using Heliospheric Imagers

T. [Amerstorfer](#), [C. Möstl](#), [P. Hess](#), [M. Temmer](#), [M. L. Mays](#), [M. Reiss](#), [P. Lowrance](#), [Ph.-A. Bourdin](#)

Space Weather **Volume16, Issue7** Pages 784-801 **2018**

<https://arxiv.org/pdf/1712.00218.pdf>

<https://agupubs.onlinelibrary.wiley.com/doi/epdf/10.1029/2017SW001786>

The Solar TERrestrial RELations Observatory (STEREO) and its heliospheric imagers (HI) have provided us the possibility to enhance our understanding of the interplanetary propagation of coronal mass ejections (CMEs). HI-based methods are able to forecast arrival times and speeds at any target and use the advantage of tracing a CME's path of propagation up to 1 AU. In our study we use the ELEvoHI model for CME arrival prediction together with an ensemble approach to derive uncertainties in the modeled arrival time and impact speed. The CME from **3 November 2010** is analyzed by performing 339 model runs that are compared to in situ measurements from lined-up spacecraft MESSENGER and STEREO-B. Remote data from STEREO-B showed the CME as halo event, which is comparable to an HI observer situated at L1 and observing an Earth-directed CME. A promising and easy approach is found by using the frequency distributions of four ELEvoHI output parameters, drag parameter, background solar wind speed, initial distance and speed. In this case study, the most frequent values of these outputs lead to the predictions with the smallest errors. Restricting the ensemble to those runs, we are able to reduce the mean absolute arrival time error from 3.5 ± 2.6 h to 1.6 ± 1.1 h at 1 AU. Our study suggests that L1 may provide a sufficient vantage point for an Earth-directed CME, when observed by HI, and that ensemble modeling could be a feasible approach to use ELEvoHI operationally.

Parametric Study of ICME Properties Related to Space Weather Disturbances via a Series of Three-Dimensional MHD Simulations

Junmo An, Tetsuya Magara, Keiji Hayashi, Yong-Jae Moon

Solar Physics October 2019, 294:143

<https://link.springer.com/content/pdf/10.1007%2Fs11207-019-1531-6.pdf>

Interplanetary coronal mass ejections (ICMEs) are important drivers of space-weather disturbances observed at the Earth. We use a parameterized ICME model to investigate the relation between the physical properties of an ICME and these disturbances. Compared to those studies focused on deriving a best set of ICME parameter values matched with observed disturbances, this study is aimed at investigating the role of each parameter in producing space-weather disturbances. Toward this end, we performed a series of three-dimensional magnetohydrodynamic (MHD) simulations with different sets of ICME parameter values. These parameters are the location, speed, mass, magnetic field strength, and magnetic field orientation of a spheromak-shaped ICME, which is injected into the solar wind reconstructed from near-Sun data and interplanetary scintillation (IPS) data via an MHD-IPS tomography method. By comparing simulation results to in situ observations near the Earth we discuss how the physical properties of an ICME affect space-weather disturbances at the Earth.

Internal structure of a coronal mass ejection revealed by Akatsuki radio occultation observations†

H. Ando, D. Shiota, T. Imamura, M. Tokumaru, A. Asai, H. Isobe, M. Pätzold, B. Häusler, M. Nakamura
JGR 2015

A coronal mass ejection (CME) was observed at the heliocentric distance of 12.7 Rs by radio occultation measurements using the Akatsuki spacecraft. The temporal developments of the bulk velocity and the electron column density along the ray path traversing the CME were obtained, and under the assumption that the irregularities are transported across the ray path, the internal structure of the CME covering the region from the core to the tail was retrieved. The suggested internal structure was compared with LASCO coronagraph images, a numerical study and previous radio occultation observations of CMEs to propose a CME model: the bulk velocity and the electron density have relatively large values in the core, decrease behind the core, and increase again in the tail region where the fast plasma flow associated with the magnetic reconnection converges. This implies that the magnetic reconnection behind the CMEs might continue up to at least the heliocentric distance of ~ 13 Rs.

Analysis of the substructure within a complex magnetic cloud on 3–4 September 2008

K.A. Andréová, E.K. Kilpua, H.H. Hietala, H.E.K. Koskinen, A.I. Isavnin, and R.V. Vainio
Ann. Geophys., 31, 555-562, 2013

<http://www.ann-geophys.net/31/555/2013/>

In this paper we have analyzed a substructure found within a leading part of a north–south-oriented magnetic cloud (MC) observed on **3–4 September 2008** in the near-Earth solar wind by multiple spacecraft (ACE, Wind, THEMIS B and C). The MC was preceded by a stream interface (SI) and followed by a high-speed stream (HSS). The identified substructure featured a strong depletion of suprathermal halo electrons and showed distinct magnetic field and plasma signatures. It occurred where suprathermal electron flow within a cloud changed from bidirectional to unidirectional, indicating change in the field line connectivity to the Sun. We found that the substructure maintained roughly its

integrity from the first Lagrangian point to the vicinity of the Earth's bow shock in the front edge of the MC, but revealed small changes in the structure which could be explained either by temporal evolution or spatial configuration of the spacecraft.

Relevance vector machines as a tool for forecasting geomagnetic storms during years 1996–2007

T. **Andriyas**, S. Andriyas

JASTP, Volumes 125–126, April 2015, Pages 10–20

In this paper, we investigate the use of relevance vector machine (RVM) as a learning tool in order to generate 1-h (one hour) ahead forecasts for geomagnetic storms driven by the interaction of the solar wind with the Earth's magnetosphere during the years 1996–2007. This epoch included solar cycle 23 with storms that were both ICME (interplanetary coronal mass ejection) and CIR (corotating interaction region) driven. Merged plasma and magnetic field measurements of the solar wind from the Advanced Composition Explorer (ACE) and WIND satellites located upstream of the Earth's magnetosphere at 1-h cadence were used as inputs to the model. The magnetospheric response to the solar wind driving measured by the disturbance storm time or the Dst index (measured in nT) was used as the output to be forecasted. The model was first tested on previously reported storms in [Wu and Lundstedt \(1997\)](#) and it gave a linear correlation coefficient, ρ , of above 90% and prediction efficiency (PE) above 80%. During 1996–2007, several storms (within each year) were chosen as test cases to analyze the forecasting robustness of the model. The top three forecasts per year were analyzed to assess the generalization ability of the model. These included storms with varying intensities ranging from weak (–53.01 nT) to strong (–422.02 nT) and durations (119–445 h). The top RVM forecast in a given year had ρ above 85% (87.00–96.85%), PE >73% (73.59–93.59%), and a root mean square error (RMSE) ranging from 9.31 to 33.45 nT. A qualitative comparison is made with model forecasts previously reported by [Ji et al. \(2012\)](#). We found that the robustness of the model with regards to fast learning and generating forecasts within acceptable error bounds makes it a very good proposition as a prediction tool (given the solar wind parameters) for space weather monitoring.

Forecasting the Dst index during corotating interaction region events using synthesized solar wind parameters

Andriyas, T.; Spencer, E.; Raj, A.; Sojka, J.; Mays, M. L.

J. Geophys. Res., Vol. 117, No. A3, A03204, 2012; **File**

sci-hub.se/10.1029/2011JA017018

Observations from SOHO, STEREO, and ACE during the declining phase of the solar cycle towards the deep minimum in 2008 are analyzed to establish the timing of CIR activity. This analysis is then employed to synthesize signals of the z component of the interplanetary magnetic field (IMF B_z), solar wind radial velocity v_x , and solar wind proton density N_p at 1 AU. The synthesized signals are used as a substitute for ACE measurements to represent solar wind forcing due to coronal hole driven CIR events occurring during multiple Bartel rotations (BR 2381 - BR 2393). The signals drive a low order physics based model of the magnetosphere called WINDMI, one of whose outputs is the ground based measurement of the Dst index. Estimating the arrival of CIR events for future rotations using ACE and SOHO data during BR 2381 produced what we refer to as an uncalibrated yearly forecast. We next generated a video calibrated estimate of the arrival times of CIR events in addition to information from BR 2381 using SOHO and STEREO images of the Sun in order to produce a simulated 3.5 day ahead forecast of possible geomagnetic activity. The time of arrival of CIR events is taken to be the travel time of density compressions as seen in a non-inertial frame according to a radial solar wind speed of 500 km/s and a distance of 1 AU. We were able to forecast the timing of CIR induced geomagnetic activity to within 12 hours for 17 out of 28 events by using the expected recurrence of the events through multiple Bartel rotations together with SOHO and STEREO coronal hole sightings made 3.5 days before every event. The uncertainty in the IMF B_z led to a forecast of levels of geomagnetic activity on an ensemble basis, yielding a distribution of different possible Dst signatures. We used a 10 sample ensemble and a 50 sample ensemble to obtain typical representations of geomagnetic activity. Depending on the periodicity and intensity of fluctuations in B_z , we obtained higher or lower levels of activity, and shorter or longer times for the recovery of the Dst to quiet levels.

Periodicities in solar wind-magnetosphere coupling functions and geomagnetic activity during the past solar cycles

T. **Andriyas**, S. Andriyas

[Astrophysics and Space Science](#) September 2017, 362:160

In this paper, we study the solar-terrestrial relation through the wavelet analysis. We report periodicities common between multiple solar wind coupling functions and geomagnetic indices during five solar cycles and also the strength of this correspondence. The DstDst (found to be most predictable in Newell et al., *J. Geophys. Res. Space Phys.* 112(A1):A01206, 2007) and ALAL (least predictable in Newell et al., *J. Geophys. Res. Space Phys.* 112(A1):A01206, 2007) indices are used for this purpose. During the years 1966–2016 (which includes five solar cycles 20, 21, 22, 23, and 24), prominent periodicities $\leq 720 \leq 720$ days with power above 95% confidence level were found to occur around 27, 182, 385, and 648 days in the DstDst index while those in the ALAL index were found in bands around 27, 187, and 472 days. Ten solar wind coupling functions were then used to find periodicities common with the indices. All the coupling functions had significant power in bands centered around 27, 280, and 648 days while powers in fluctuations around 182, 385, and 472 days were only found in some coupling functions. All the drivers and their variants had power above the significant level in the 280–288 days band, which was absent in the DstDst and ALAL indices. The normalized scale averaged spectral power around the common periods in the coupling functions and the indices indicated that the coupling functions most correlated with the DstDst index were the Newell (27 and 385 days), Wygant (182 days), and Scurry-Russell and Boynton (648 days) functions. An absence of common power between the coupling functions and the DstDst index around the annual periodicity was noted during the even solar cycles. A similar analysis for the ALAL index indicated that Newell (27 days), Rectified (187 days), and Boynton (472 days) were the most correlated functions. It was also found that the correlation numbers were relatively weaker for the ALAL index, specially for the 187 day periodicity. It is concluded that as the two indices respond to solar wind forcing with varying levels of strength at various prominent scales and the coupling function used, the response might be dependent on the scale (days or months or years) of interest at which the solar wind driving is to be predicted.

Solar Filaments and Interplanetary Magnetic Field Bz

V. **Aparna** and Petrus C. Martens

2020 ApJ 897 68

<https://doi.org/10.3847/1538-4357/ab908b>

<https://sci-hub.tw/10.3847/1538-4357/ab908b> File

The direction of the axis of an interplanetary coronal mass ejection (ICME) plays an important role in determining if it will cause a geomagnetic disturbance in the Earth's magnetosphere upon impact. Long period southward-pointing ICME fields are known to cause significant space weather impacts and thus geomagnetic storms. We present an extensive analysis of CME–ICME directionality using 86 halo-CMEs observed between 2007 and 2017 to compare the direction of the source filament axial magnetic field on the Sun and the direction of the interplanetary magnetic field near the Earth at the L1 Lagrangian point. Excluding 12 cases that were too ambiguous to determine, for the remaining 74 ICMEs, we find an agreement in terms of the northward/southward orientation of Bz between ICMEs and their CME source regions in 85% of cases. Some of the previous studies discussed here have obtained an agreement of 77% and 55%. We therefore suggest that our method can be meaningful as a first step in efficiently predicting geoeffective ICMEs by observing and analyzing the source regions of CMEs on the Sun. **2012-03-26, 2013.04.11-16, 2013.12.07-13, 2014-12-21, 2016-01-01,**

Search for Large-scale Anisotropy in the Arrival Direction of Cosmic Rays with KASCADE-Grande

W. D. **Apel**, J. C. Arteaga-Velázquez, K. Bekk, M. Bertaina, J. Blümer, R. Bonino, H. Bozdog, I. M. Brancus, E. Cantoni, A. Chiavassa, F. Cossavella, K. Daumiller,...

2019 ApJ 870 91

<http://iopscience.iop.org/article/10.3847/1538-4357/aaf1ca/pdf>

We present the results of the search for large-scale anisotropies in the arrival directions of cosmic rays performed with the KASCADE-Grande experiment at energies higher than 10^{15} eV. To eliminate spurious anisotropies due to atmospheric or instrumental effects we apply the east–west method. We show, using the solar time distribution of the number of counts, that this technique allow us to remove correctly the count variations not associated to real anisotropies. By applying the east–west method we obtain the distribution of number of counts in intervals of 20 minutes of sidereal time. This distribution is then analyzed by searching for a dipole component; the significance of the amplitude of the first harmonic is 3.5σ , therefore, we derive its upper limit. The phase of the first harmonic is determined with an error of a few hours and is in agreement with the measurements obtained in the $10^{14} < E < 2 \times 10^{15}$ eV energy range by the EAS-TOP, IceCube, and IceTop experiments. This supports the hypothesis of a change of the phase of the first harmonic at energies greater than $\sim 2 \times 10^{14}$ eV.

Comparing the Performance of a Solar Wind model from the Sun to 1 AU using Real and Synthetic Magnetograms

Kalpa Henadhira [Arachhige](#), 1, 2 Ofer Cohen, 1, 2 Andres Muñoz Jaramillo[~], 3 and Anthony R. Yeates⁴
ApJ **938** 39 **2022**

<https://arxiv.org/pdf/2208.13668.pdf>

<https://iopscience.iop.org/article/10.3847/1538-4357/ac8d59/pdf>

The input of the Solar wind models plays a significant role in accurate solar wind predictions at 1 AU. This work introduces a synthetic magnetogram produced from a dynamo model as an input for Magnetohydrodynamics (MHD) simulations. We perform a quantitative study that compares the Space Weather Modeling Framework (SWMF) results for the observed and the synthetic solar magnetogram input. For each case, we compare the results for Extreme Ultra-Violet (EUV) images and extract the simulation data along the earth trajectory to compare with in-situ observations. We initialize SWMF using the real and synthetic magnetogram for a set of Carrington Rotations (CR)s within the solar cycle 23 and 24. Our results help quantify the ability of dynamo models to be used as input to solar wind models and thus, provide predictions for the solar wind at 1 AU.

Proposed Resolution to the Solar Open Magnetic Flux Problem

C.Nick Arge (1), [Andrew Leisner](#) (2), [Samantha Wallace](#) (1), [Carl J. Henney](#) (3)

2024 ApJ **964** 115

<https://arxiv.org/pdf/2304.07649.pdf>

<https://iopscience.iop.org/article/10.3847/1538-4357/ad20e2/pdf>

The solar magnetic fields emerging from the photosphere into the chromosphere and corona are comprised of a combination of "closed" and "open" fields. The closed magnetic field lines are defined as those having both ends rooted in the solar surface, while the open field lines are those having one end extending out into interplanetary space and the other rooted at the Sun's surface. Since the early 2000's, the amount of total unsigned open magnetic flux estimated by coronal models have been in significant disagreement with in situ spacecraft observations, especially during solar maximum. Estimates of total open unsigned magnetic flux using coronal hole observations (e.g., using extreme ultraviolet (EUV) or Helium (He) I) are in general agreement with the coronal model results and thus show similar disagreements with in situ observations. While several possible sources producing these discrepancies have been postulated over the years, there is still no clear resolution to the problem. This paper provides a brief overview of the problem and summarizes some proposed explanations for the discrepancies. In addition, two different ways of estimating the total unsigned open magnetic flux are presented, utilizing the Wang-Sheeley-Arge (WSA) model, and one of the methods produce surprisingly good agreement with in situ observations. The findings presented here suggest that active regions residing near the boundaries of mid-latitude coronal holes are the probable source of the missing open flux. This explanation also brings in line many of the seemingly contradictory facts that have made resolving this problem so difficult.

How are Forbush decreases related to interplanetary magnetic field enhancements?

[Arunbabu](#), K. P. ; [Antia](#), H. M. ; [Dugad](#), S. R. ; [Gupta](#), S. K. ; [Hayashi](#), Y. ; [Kawakami](#), S. ; [Mohanty](#), P. K. ; [Oshima](#), A. ; [Subramanian](#), P.

Astronomy & Astrophysics, Volume 580, id.A41, **2015**

<https://www.aanda.org/articles/aa/pdf/2015/08/aa25115-14.pdf>

<https://doi.org/10.1051/0004-6361/201425115>

Aims: A Forbush decrease (FD) is a transient decrease followed by a gradual recovery in the observed galactic cosmic ray intensity. We seek to understand the relationship between the FDs and near-Earth interplanetary magnetic field (IMF) enhancements associated with solar coronal mass ejections (CMEs).

Methods: We used muon data at cutoff rigidities ranging from 14 to 24 GV from the GRAPES-3 tracking muon telescope to identify FD events. We selected those FD events that have a reasonably clean profile, and magnitude >0.25%. We used IMF data from ACE/WIND spacecrafts. We looked for correlations between the FD profile and that of the one-hour averaged IMF. We wanted to find out whether if the diffusion of high-energy protons into the large scale magnetic field is the cause of the lag observed between the FD and the IMF.

Results: The enhancement of the IMF associated with FDs occurs mainly in the shock-sheath region, and the turbulence level in the magnetic field is also enhanced in this region. The observed FD profiles look remarkably similar to the IMF enhancement profiles. The FDs typically lag behind the IMF enhancement by a few hours. The lag corresponds to the time taken by high-energy protons to diffuse into the magnetic field enhancement via cross-field diffusion.

Conclusions: Our findings show that high-rigidity FDs associated with CMEs are caused primarily by the cumulative diffusion of protons across the magnetic field enhancement in the turbulent sheath region between the shock and the CME.

Appendices are available in electronic form at <http://www.aanda.org>

Forbush decrease precursors observed using GRAPES-3

Arunbabu, K. P. ; [Antia, H. M. ;](#) [Dugad, S. ;](#) [Gupta, S. K. ;](#) [Hayashi, Y. ;](#) [Kawakami, S. ;](#) [Mohanty, P. K. ;](#) [Oshima, A. ;](#) [Subramanian, P.](#)

Proceedings of the 34th International Cosmic Ray Conference (ICRC2015). 30 July - 6 August, 2015. The Hague, The Netherlands. Online at <http://pos.sissa.it/cgi-bin/reader/conf.cgi?confid=236>, id.44 **2015**
<https://pos.sissa.it/236/044/pdf>

Earth-directed Coronal mass ejections (CMEs) emanating from the Sun and the shock associated with it are the primary drivers of space weather disturbances. Forbush decrease precursors are advance warning of these upcoming magnetic field disturbances. GRAPES-3 tracking muon telescope which is a part of GRAPES-3 experiment located in Ooty, India, provides high statistics measurement of the muon flux with good temporal resolution. In this study we are using data from GRAPES-3 muon telescope and making use of its multidirectional observations to study the Forbush decrease precursors in greater detail. We have identified few Forbush decrease precursor signatures in muon flux well before the arrival of the actual shock. We can use these Forbush decrease precursors to study the characteristics of magnetic field compression associated with the upcoming CME shock-sheath system. **29 October 2003, 14 December 2006**

Relation of Forbush decrease with interplanetary magnetic fields.

Arunbabu, K. P. ; [Antia, H. M. ;](#) [Dugad, S.](#) Proceedings of the 34th International Cosmic Ray Conference (ICRC2015). 30 July - 6 August, 2015. The Hague, The Netherlands. Online at <http://pos.sissa.it/cgi-bin/reader/conf.cgi?confid=236>, id.43 **2015**
<https://pos.sissa.it/236/043/pdf>

The relation between the Forbush decreases (FDs) and near-Earth interplanetary magnetic field (IMF) enhancements associated with the solar coronal mass ejections (CMEs) is studied. We have used data from GRAPES-3 tracking muon telescope to identify the Forbush decrease events. We have chosen events that are having a reasonably clean profile, and magnitude >0.25%. We have used IMF data from ACE/WIND spacecrafts to investigate how closely the FD profile follow the IMF enhancements. We found that the enhancement of magnetic field responsible for the FD takes place mainly in the sheath region and also the MHD turbulence level get enhanced in this region. We found that the FD profile looks remarkably similar to that of IMF enhancement, yielding good correlation with a time lag. The FD profile lags behind the IMF by few hours. This observed lag corresponds to the time taken by high energy protons to diffuse into the magnetic field enhancement through cross-field diffusion. **24 November 2001**

Table 2: Events for which the FD profile correlates well only with the perpendicular component of the IMF enhancement. 2001-2004

How are Forbush decreases related with IP magnetic field enhancements ?

Arunbabu, K. P. ; [Subramanian, P. ;](#) [Gupta, Sunil ;](#) [Antia, H. M.](#)

ASI Conference Series, **2013**, Vol. 10, pp 95 - 100 Edited by N. Gopalswamy, S. S. Hasan, P. B. Rao and Prasad Subramanian

<https://articles.adsabs.harvard.edu/pdf/2013ASInC..10...95A>

Cosmic ray Forbush decreases (FDs) are usually thought to be due to Earth-directed coronal mass ejections (CMEs) from the Sun and their associated shocks. When CMEs and their shocks reach the Earth, they cause magnetic field compressions. We investigate the relation between these magnetic field compressions and FDs at rigidities between 12 and 42 GV using data from the GRAPES-3 instrument at Ooty. We find that the shapes of the Forbush decrease profiles show a startling similarity to that of the magnetic field compression in the near-Earth IP medium. We seek to understand the implications of this interesting result. **24 November 2001**

Forbush Decreases and <2 Day GCR Flux Non-recurrent Variations Studied with LISA Pathfinder

M. **Armano**¹, H. Audley², J. Baird³, S. Benella^{4,5}, P. Binetruy^{6,24}, M. Born², D. Bortoluzzi⁷, E. Castelli⁸, A. Cavalleri⁹, A. Cesarini^{4,5}[Show full author list](#)
2019 ApJ 874 167

sci-hub.se/10.3847/1538-4357/ab0c99

<https://arxiv.org/pdf/1904.04694.pdf>

Non-recurrent short-term variations of the galactic cosmic-ray (GCR) flux above 70 MeV n^{-1} were observed between **2016 February 18 and 2017 July 3** on board the European Space Agency LISA Pathfinder (LPF) mission orbiting around the Lagrange point L1 at 1.5×10^6 km from Earth. The energy dependence of three Forbush decreases is studied and reported here. A comparison of these observations with others carried out in space down to the energy of a few tens of MeV n^{-1} shows that the same GCR flux parameterization applies to events of different intensity during the main phase. FD observations in L1 with LPF and geomagnetic storm occurrence are also presented. Finally, the characteristics of GCR flux non-recurrent variations (peaks and depressions) of duration < 2 days and their association with interplanetary structures are investigated. It is found that, most likely, plasma compression regions between subsequent corotating high-speed streams cause peaks, while heliospheric current sheet crossing causes the majority of the depressions.

Characteristics and Energy Dependence of Recurrent Galactic Cosmic-Ray Flux Depressions and of a Forbush Decrease with LISA Pathfinder

M. **Armano**¹, H. Audley², J. Baird³, M. Bassan⁴, S. Benella^{5,6}, P. Binetruy^{7,24}, M. Born², D. Bortoluzzi⁸, A. Cavalleri⁹, A. Cesarini⁵

2018 ApJ 854 113

<http://sci-hub.tw/http://iopscience.iop.org/0004-637X/854/2/113/>

<https://arxiv.org/pdf/1802.09374.pdf>

Galactic cosmic-ray (GCR) energy spectra observed in the inner heliosphere are modulated by the solar activity, the solar polarity and structures of solar and interplanetary origin. A high counting rate particle detector (PD) aboard LISA Pathfinder, meant for subsystems diagnostics, was devoted to the measurement of GCR and solar energetic particle integral fluxes above 70 MeV n^{-1} up to 6500 counts s^{-1} . PD data were gathered with a sampling time of 15 s. Characteristics and energy dependence of GCR flux recurrent depressions and of a Forbush decrease dated **2016 August 2** are reported here. The capability of interplanetary missions, carrying PDs for instrument performance purposes, in monitoring the passage of interplanetary coronal mass ejections is also discussed.

Correlations between Sunspot numbers, Interplanetary Parameters and geomagnetic trends over solar cycles 21, 22 and 23

Kusumita **Arora**, N. Phani Chandrasekhar, Nandini Nagarajan, Ankit Singh

JASTP, Volume 114, Pages 19–29, **2014**

We have analyzed correlations between sunspot numbers, solar wind, ion density, interplanetary magnetic field vis-à-vis magnetic activity. Planetary geomagnetic index (A_p) and local residual measure of magnetic activity ($I\Delta H$) from low-latitude Magnetic Observatory, CSIR-NGRI, Hyderabad (IMO-HYB) spanning solar cycles 21 – 23 are used for this study.

Using correlation coefficients between and wavelet decomposition of sunspot numbers, interplanetary parameters and measures of magnetic activity, the complex and time varying nature of these inter-relationships are brought out. The overall influence of sunspot number could be separated and combined episodic effects of other solar parameters could be distinguished. The demonstrated correlation or lack of it, between measures of magnetic activity (A_p and $I\Delta H$), and all the parameters of solar activity, presented here corroborate established mechanisms as well as delineated clearly the relative impact of different solar mechanisms over phases of three solar cycles. The possible role of non-sunspot related activity from high latitude regions of the sun is indicated.

Comparative study of electric currents and energetic particle fluxes in a solar flare and Earth magnetospheric substorm

[Anton Artemyev](#), [Ivan Zimovets](#), [Ivan Sharykin](#), [Yukitoshi Nishimura](#), [Cooper Downs](#), [James Weygand](#), [Robyn Fiori](#), [Xiao-Jia Zhang](#), [Andrei Runov](#), [Marco Velli](#), [Vassilis Angelopoulos](#), [Olga Panasenco](#), [Christopher Russell](#), [Yoshizumi Miyoshi](#), [Satoshi Kasahara](#), [Ayako Matsuoka](#), [Shoichiro Yokota](#), [Kunihiro Keika](#), [Tomoaki Hori](#), [Yoichi Kazama](#), [Shiang-Yu Wang](#), [Iku Shinohara](#), [Yasunobu Ogawa](#)
<https://arxiv.org/pdf/2105.03772.pdf>

ApJ 923 151 2021

<https://arxiv.org/pdf/2105.03772.pdf>

<https://doi.org/10.3847/1538-4357/ac2dfc>

Magnetic field-line reconnection is a universal plasma process responsible for the conversion of magnetic field energy to the plasma heating and charged particle acceleration. Solar flares and Earth's magnetospheric substorms are two most investigated dynamical systems where magnetic reconnection is believed to be responsible for global magnetic field reconfiguration and energization of plasma populations. Such a reconfiguration includes formation of a long-living current systems connecting the primary energy release region and cold dense conductive plasma of photosphere/ionosphere. In both flares and substorms the evolution of this current system correlates with formation and dynamics of energetic particle fluxes. Our study is focused on this similarity between flares and substorms. Using a wide range of datasets available for flare and substorm investigations, we compare qualitatively dynamics of currents and energetic particle fluxes for one flare and one substorm. We showed that there is a clear correlation between energetic particle bursts (associated with energy release due to magnetic reconnection) and magnetic field reconfiguration/formation of current system. We then discuss how datasets of in-situ measurements in the magnetospheric substorm can help in interpretation of datasets gathered for the solar flare. **2015 June 22**

How are Forbush decreases related with interplanetary magnetic field enhancements ?

K. P. **Arunbabu**, H. M. Antia, S. R. Dugad, S. K. Gupta, Y. Hayashi, S. Kawakami, P. K. Mohanty, A. Oshima, P. Subramanian

A&A 580, A41 2015

<http://arxiv.org/pdf/1504.06473v1.pdf>

<http://www.aanda.org/articles/aa/pdf/2015/08/aa25115-14.pdf>

Aims. Forbush decrease (FD) is a transient decrease followed by a gradual recovery in the observed galactic cosmic ray intensity. We seek to understand the relationship between the FDs and near-Earth interplanetary magnetic field (IMF) enhancements associated with solar coronal mass ejections (CMEs).

Methods. We use muon data at cutoff rigidities ranging from 14 to 24 GV from the GRAPES-3 tracking muon telescope to identify FD events. We select those FD events that have a reasonably clean profile, and magnitude $> 0.25\%$. We use IMF data from ACE/WIND spacecrafts. We look for correlations between the FD profile and that of the one hour averaged IMF. We ask if the diffusion of high energy protons into the large scale magnetic field is the cause of the lag observed between the FD and the IMF.

Results. The enhancement of the IMF associated with FDs occurs mainly in the shock-sheath region, and the turbulence level in the magnetic field is also enhanced in this region. The observed FD profiles look remarkably similar to the IMF enhancement profiles. The FDs typically lag the IMF enhancement by a few hours. The lag corresponds to the time taken by high energy protons to diffuse into the magnetic field enhancement via cross-field diffusion. **Conclusions.** Our findings show that high rigidity FDs associated with CMEs are caused primarily by the cumulative diffusion of protons across the magnetic field enhancement in the turbulent sheath region between the shock and the CME.

Table 2. Shock arrival time, time of maximum magnetic field enhancement, magnetic cloud start and end timings and FD onset timings for different directions for FD events which have a well defined shock and magnetic clouds associated with them.

Table B.1. List of FD events for which the correlation coefficient between the profiles of the FD and the IMF enhancement $\geq 70\%$.

How are Forbush decreases related with IP magnetic field enhancements ?

Arunbabu K. P., P. Subramanian, Sunil Gupta, H. M. Antia

E-print, **2014**; International Symposium on Solar Terrestrial Physics 2012, IISER Pune

Bull. Astr. Soc. India (**2012**)

<http://arxiv.org/pdf/1406.4967v1.pdf>

Cosmic ray Forbush decreases (FDs) are usually thought to be due to Earth-directed coronal mass ejections (CMEs) from the Sun and their associated shocks. When CMEs and their shocks reach the Earth, they cause magnetic field compressions. We seek to understand the relation between these magnetic field compressions and FDs at rigidities between 12 and 42 GV using data from the GRAPES-3 instrument at Ooty. We find that the shapes of the Forbush decrease profiles show a startling similarity to that of the magnetic field compression in the near-Earth IP medium. We seek to understand the implications of this interesting result. **24 November 2001**

High-rigidity Forbush decreases: due to CMEs or shocks?*

K. P. [Arunbabu](#)¹, H. M. Antia^{2,3}, S. R. Dugad^{2,3}, S. K. Gupta^{2,3}, Y. Hayashi⁴, S. Kawakami⁴, P. K. Mohanty^{2,3}, T. Nonaka⁴, A. Oshima⁵ and P. Subramanian
A&A 555, A139 (2013)

Aims. We seek to identify the primary agents causing Forbush decreases (FDs) in high-rigidity cosmic rays observed from the Earth. In particular, we ask if these FDs are caused mainly by coronal mass ejections (CMEs) from the Sun that are directed towards the Earth, or by their associated shocks.

Methods. We used the muon data at cutoff rigidities ranging from 14 to 24 GV from the GRAPES-3 tracking muon telescope to identify FD events. We selected those FD events that have a reasonably clean profile, and can be reasonably well associated with an Earth-directed CME and its associated shock. We employed two models: one that considers the CME as the sole cause of the FD (the CME-only model) and one that considers the shock as the only agent causing the FD (the shock-only model). We used an extensive set of observationally determined parameters for both models. The only free parameter in these models is the level of MHD turbulence in the sheath region, which mediates cosmic ray diffusion (into the CME for the CME-only model, and across the shock sheath for the shock-only model).

Results. We find that good fits to the GRAPES-3 multi-rigidity data using the CME-only model require turbulence levels in the CME sheath region that are only slightly higher than those estimated for the quiescent solar wind. On the other hand, reasonable model fits with the shock-only model require turbulence levels in the sheath region that are an order of magnitude higher than those in the quiet solar wind.

Conclusions. This observation naturally leads to the conclusion that the Earth-directed CMEs are the primary contributors to FDs observed in high-rigidity cosmic rays.

Evolution of the anemone AR NOAA 10798 and the related geo-effective flares and CMEs

Ayumi [Asai](#), Kazunari Shibata,⁴ Takako T. Ishii,⁴ Mitsuo Oka,^{4,5} Ryuho Kataoka,⁶
Ken'ichi Fujiki,⁷ and Nat Gopalswamy

JOURNAL OF GEOPHYSICAL RESEARCH, VOL. 114, A00A21, doi:10.1029/2008JA013291, 2009

We present a detailed examination of the features of the active region (AR) NOAA 10798. This AR generated coronal mass ejections (CMEs) that caused a large geomagnetic storm on 24 August 2005 with the minimum **Dst index of -216 nT**. We examined the evolution of the AR and the features on/near the solar surface and in the interplanetary space. The AR emerged in the middle of a small coronal hole, and formed a sea anemone like configuration. Ha filaments were formed in the AR, which have southward axial field. Three M class flares were generated, and the first two that occurred on 22 August 2005 were followed by Halo-type CMEs. The speeds of the CMEs were fast, and recorded about 1200 and 2400 km s⁻¹, respectively. The second CME was especially fast, and caught up and interacted with the first (slower) CME during their travelings toward Earth. These acted synergically to generate an interplanetary disturbance with strong southward magnetic field of about -50 nT, which was followed by the large geomagnetic storm.

22 Aug 2005

Anemone structure of Active Region NOAA 10798 and related geo-effective flares/ CMEs

A. [ASAI](#) et al.

Suzaku Detection of Solar Wind Charge Exchange Emission from a Variety of Highly-ionized Ions in an Interplanetary Coronal Mass Ejection

Kazunori [Asakura](#), [Hironori Matsumoto](#), [Koki Okazaki](#), [Tomokage Yoneyama](#), [Hirofumi Noda](#), [Kiyoshi Hayashida](#), [Hiroshi Tsunemi](#), [Hiroshi Nakajima](#), [Satoru Katsuda](#), [Daiki Ishi](#), [Yuichiro Ezo](#)

PASJ 2021

<https://arxiv.org/pdf/2102.11298.pdf>

X-ray emission generated through solar-wind charge exchange (SWCX) is known to contaminate X-ray observation data, the amount of which is often significant or even dominant, particularly in the soft X-ray band, when the main target is comparatively weak diffuse sources, depending on the space weather during the observation. In particular, SWCX events caused by interplanetary coronal mass ejections (ICMEs) tend to be spectrally rich and to provide critical information about the metal abundance in the ICME plasma. We analyzed the SN1006 background data observed with Suzaku on **2005 September 11** shortly after an X6-class solar flare, signatures of which were separately detected together with an associated ICME. We found that the data include emission lines from a variety of highly ionized ions

generated through SWCX. The relative abundances of the detected ions were found to be consistent with those in past ICME-driven SWCX events. Thus, we conclude that this event was ICME-driven. In addition, we detected a sulfur XVI line for the first time as one from the SWCX emission, the fact of which suggests that it is the most spectrally-rich SWCX event ever observed. We suggest that observations of ICME-driven SWCX events can provide a unique probe to study the population of highly-ionized ions in the plasma, which is difficult to measure in currently-available in-situ observations.

Correlation of the sunspot number and the waiting time distribution of solar flares, coronal mass ejections, and solar wind switchback events observed with the Parker Solar Probe

[Markus J. Aschwanden](#), [Thierry Dudok de Wit](#)

ApJ 912 94 2021

<https://arxiv.org/pdf/2102.02305.pdf>

<https://doi.org/10.3847/1538-4357/abef69>

Waiting time distributions of solar flares and coronal mass ejections (CMEs) exhibit power law-like distribution functions with slopes in the range of $\alpha\tau\approx 1.4-3.2$, as observed in annual data sets during 4 solar cycles (1974-2012). We find a close correlation between the waiting time power law slope $\alpha\tau$ and the sunspot number (SN), i.e., $\alpha\tau = 1.38 + 0.01 \times \text{SN}$. The waiting time distribution can be fitted with a Pareto-type function of the form $N(\tau)=N_0(\tau_0+\tau)^{-\alpha\tau}$, where the offset τ_0 depends on the instrumental sensitivity, the detection threshold of events, and pulse pile-up effects. The time-dependent power law slope $\alpha\tau(t)$ of waiting time distributions depends only on the global solar magnetic flux (quantified by the sunspot number) or flaring rate, independent of other physical parameters of self-organized criticality (SOC) or magneto-hydrodynamic (MHD) turbulence models. Power law slopes of $\alpha\tau\approx 1.2-1.6$ were also found in solar wind switchback events, as observed with the Parker Solar Probe (PSP). We conclude that the annual variability of switchback events in the heliospheric solar wind is modulated by flare and CME rates originating in the photosphere and lower corona.

Solar wind drivers of energetic electron precipitation†

T. [Asikainen](#), M. Ruopsa

JGR 2016

Disturbances of near-Earth space are predominantly driven by coronal mass ejections (CME) mostly originating from sunspots and high-speed solar wind streams (HSS) emanating from coronal holes. Here we study the relative importance of CMEs and HSSs as well as slow solar wind in producing energetic electron precipitation. We use the recently corrected energetic electron measurements from the MEPED instrument onboard low altitude NOAA/POES satellites from 1979 to 2013. Using solar wind observations categorized into three different flow types we study the contributions of these flows to annual electron precipitation and their efficiencies in producing precipitation. We find that HSS contribution nearly always dominates over the other flows and peaks strongly in the declining solar cycle phase. CME contribution mostly follows the sunspot cycle but is enhanced also in the declining phase. The efficiency of both HSSs and CMEs peaks in the declining phase. We also study the dependence of electron precipitation on solar wind southward magnetic field component, speed and density and find that the solar wind speed is the dominant factor affecting the precipitation. Since HSSs enhance the average solar wind speed in the declining phase they also enhance the efficiency of CMEs during these times and thus have a double effect in enhancing energetic electron precipitation.

Long-term evolution of corrected NOAA/MEPED energetic proton fluxes and their relation to geomagnetic indices

Timo [Asikainen](#), Kalevi Mursula

JASTP, 2014

We study the relationship between energetic 120–250 keV proton fluxes and geomagnetic Ap, AE, Dxt indices using the recently corrected measurements of the MEPED instrument onboard the low-altitude NOAA/POES satellites. Corrected database spans from 1979 to present, and allows us to reliably study the long-term variation of energetic proton fluxes over several solar cycles. Contrary to uncorrected fluxes, which can be more than an order of magnitude too low, the corrected fluxes display a systematic solar cycle variation closely resembling the variation of Ap and AE indices with a maximum in the declining solar cycle phase and a minimum in solar minimum. We also find that trapped fluxes are enhanced relative to precipitating fluxes in the declining phases and solar minima. This supports the fact that high-speed solar wind streams are the most significant driver of energetic proton fluxes. We compute the correlations between fluxes and indices in a range of time scales, and show that they are significantly improved by the flux correction. We find that precipitating fluxes correlate better than trapped fluxes with Ap/AE indices at all time scales, and the highest correlation is found with Ap. For precipitating fluxes these correlations depend weakly on time scale, but for trapped

fluxes the correlation significantly increases from daily scale to solar rotation and longer time scales. Comparing the fluxes to Dxt index shows a complex relationship, where the fluxes depend not only on Dxt value but also on its time derivative.

The source of the 2017 cosmic ray half-year modulation event

O.P.M. [Aslam](#), D. MacTaggart, R. Battiston, M.S. Potgieter, M.D. Ngobeni

ApJ **2024**

<https://arxiv.org/pdf/2412.14907>

In 2017, as the solar cycle approached solar minimum, an unusually long and large depression was observed in galactic cosmic ray (GCR) protons, detected with the Alpha Magnetic Spectrometer (AMS-02), lasting for the second half of that year. The depression, as seen in the Bartel rotation-averaged proton flux, has the form of a Forbush decrease (FD). Despite this resemblance, however, the cause of the observed depression does not have such a simple explanation as FDs, due to coronal mass ejections (CMEs), typically last for a few days at 1 AU rather than half a year. In this work, we seek the cause of the observed depression and investigate two main possibilities. First, we consider a mini-cycle - a temporary change in the solar dynamo that changes the behavior of the global solar magnetic field and, by this, the modulation of GCRs. Secondly, we investigate the behavior of solar activity, both CMEs and co-rotating/stream interactions regions (C/SIRs), during this period. Our findings show that, although there is some evidence for mini-cycle behavior prior to the depression, the depression is ultimately due to a combination of recurrent CMEs, SIRs and CIRs. A particular characteristic of the depression is that the largest impacts that help to create and maintain it are due to four CMEs from the same, highly active, magnetic source that persists for several solar rotations. This active magnetic source is unusual given the closeness of the solar cycle to solar minimum, which also helps to make the depression more evident.

Modulation of Cosmic-Ray Antiprotons in the Heliosphere: Simulations for a Solar Cycle

O. P. M. [Aslam](#)¹, M. S. Potgieter^{1,2}, Xi Luo (罗熙)¹, and M. D. Ngobeni³

2023 ApJ 953 101

<https://iopscience.iop.org/article/10.3847/1538-4357/ace31e/pdf>

The precision measurements of galactic cosmic-ray protons from the Payload for Antimatter Matter Exploration and Light-nuclei Astrophysics and the Alpha Magnetic Spectrometer are reproduced using a well-established three-dimensional numerical model for the period 2006 July–2019 November. The resulting modulation parameters are applied to simulate the modulation for cosmic antiprotons over the same period, which includes the times of minimum modulation before and after 2009, the maximum modulation from 2012 to 2015, including the reversal of the Sun's magnetic field polarity, and the approach to new minimum modulation in 2020. Apart from their local interstellar spectra, the modulation of protons and antiprotons differ in their charge sign and consequent drift pattern. The lowest proton flux was in 2014 February–March, but the lowest simulated antiproton flux is found to have been in 2015 March–April. These simulated fluxes are used to predict the proton-to-antiproton ratios as a function of rigidity. The trends in these ratios contribute to clarifying, to a large extent, the phenomenon of charge-sign dependence of heliospheric modulation during vastly different phases of the solar activity cycle. This is reiterated and emphasized by displaying so-called hysteresis loops. It is also illustrated how the values of the parallel and perpendicular mean free paths, as well as the drift scale, vary with rigidity over this extensive period. The drift scale is found to be at its lowest level during the polarity reversal period, while the lowest level of the mean free paths is found to be in 2015 March–April.

Unfolding Drift Effects for Cosmic Rays over the Period of the Sun's Magnetic Field Reversal

O.P.M. [Aslam](#), [Xi Luo](#), [M.S. Potgieter](#), [M.D. Ngobeni](#), [Xiaojian Song](#)

ApJ **947** 72 **2023**

<https://arxiv.org/pdf/2212.13397.pdf>

<https://iopscience.iop.org/article/10.3847/1538-4357/acc24a/pdf>

A well-established, comprehensive 3-D numerical modulation model is applied to simulate galactic protons, electrons and positrons from May 2011 to May 2015, including the solar magnetic polarity reversal of Solar Cycle 24. The objective is to evaluate how these simulations compare with corresponding AMS observations for 1.0-3.0 GV, and what underlying physics follows from this comparison in order to improve our understanding on how the major physical modulation processes change, especially particle drift, from a negative to a positive magnetic polarity cycle. Apart from their local interstellar spectra, electrons and positrons differ only in their drift patterns, but they differ with protons in other ways such as their adiabatic energy changes at lower rigidity. In order to complete the simulations for oppositely charged particles, antiproton modeling results are obtained as well. Together, the observations and the corresponding modeling indicate the difference in the drift pattern before and after the recent polarity reversal and clarify to a large

extent the phenomenon of charge-sign dependence during this period. The effect of global particle drift became negligible during this period of no well-defined magnetic polarity. The resulting low values of all particles' MFPs during the polarity reversal contrast their large values during solar minimum activity, and as such expose the relative contributions and effects of the different modulation processes from solar minimum to maximum activity. We find that the drift scale starts recovering just after the polarity reversal, but the MFPs keep decreasing or remain unchanged for some period after the polarity reversal.

Study of the Geoeffectiveness and Galactic Cosmic-Ray Response of VarSITI-ISEST Campaign Events in Solar Cycle 24

O. P. M. [Aslam](#), Badruddin

[Solar Physics](#) September 2017, 292:135

We analyze and compare the geomagnetic and galactic cosmic-ray (GCR) response of selected solar events, particularly the campaign events of the group International Study of Earth-affecting Solar Transients (ISEST) of the program Variability of the Sun and Its Terrestrial Impact (VarSITI). These selected events correspond to Solar Cycle 24, and we identified various of their features during their near-Earth passage. We evaluated the hourly data of geomagnetic indices and ground-based neutron monitors and the concurrent data of interplanetary plasma and field parameters. We recognized distinct features of these events and solar wind parameters when the geomagnetic disturbance was at its peak and when the cosmic-ray intensity was most affected. We also discuss the similarities and differences in the geoeffectiveness and GCR response of the solar and interplanetary structures in the light of plasma and field variations and physical mechanism(s), which play a crucial role in influencing the geomagnetic activity and GCR intensity. **14 July 2012, 8 Oct 2012, 17 March 2013, 31 May 2013, 17 March 2015, 21 June 2015,**

Study of Cosmic-Ray Modulation during the Recent Unusual Minimum and Mini Maximum of Solar Cycle 24

O.P.M. [Aslam](#), Badruddin

Solar Phys. Volume 290, Issue 8, pp 2333-2353 **2015**

<http://arxiv.org/ftp/arxiv/papers/1507/1507.07917.pdf>

After a prolonged and deep solar minimum at the end of Cycle 23, the current Solar Cycle 24 is one of the lowest cycles. These two periods of deep minimum and mini maximum are separated by a period of increasing solar activity. We study the cosmic-ray intensity variation in relation with the solar activity, heliospheric plasma and field parameters, including the heliospheric current sheet, during these three periods (phases) of different activity level and nature: (a) a deep minimum, (b) an increasing activity period and (c) a mini maximum. We use neutron monitor data from stations located around the globe to study the rigidity dependence on modulation during the two extremes, i.e., minimum and maximum. We also study the time lag between the cosmic-ray intensity and various solar and interplanetary parameters separately during the three activity phases. We also analyze the role of various parameters, including the current sheet tilt, in modulating the cosmic-ray intensity during the three different phases. Their relative importance and the implications of our results are also discussed.

The Dynamic Coupling of Streamers and Pseudostreamers to the Heliosphere

V. [Aslanyan](#), [D. I. Pontin](#), [A. K. Higginson](#), [P. F. Wyper](#), [R. B. Scott](#), [S. K. Antiochos](#)

ApJ **929** 185 **2022**

<https://arxiv.org/pdf/2201.02388.pdf>

<https://iopscience.iop.org/article/10.3847/1538-4357/ac5d5b/pdf>

The slow solar wind is generally believed to result from the interaction of open and closed coronal magnetic flux at streamers and pseudostreamers. We use 3-dimensional magnetohydrodynamic simulations to determine the detailed structure and dynamics of open-closed interactions that are driven by photospheric convective flows. The photospheric magnetic field model includes a global dipole giving rise to a streamer together with a large parasitic polarity region giving rise to a pseudostreamer that separates a satellite coronal hole from the main polar hole. Our numerical domain extends out to 30 solar radii and includes an isothermal solar wind, so that the coupling between the corona and heliosphere can be calculated rigorously. This system is driven by imposing a large set of quasi-random surface flows that capture the driving of coronal flux in the vicinity of streamer and pseudostreamer boundaries by the supergranular motions. We describe the resulting structures and dynamics. Interchange reconnection dominates the evolution at both streamer and pseudostreamer boundaries, but the details of the resulting structures are clearly different from one another. Additionally, we calculate in situ signatures of the reconnection and determine the dynamic mapping from the inner heliosphere back to the Sun for a test spacecraft orbit. We discuss the implications of our results for interpreting

observations from inner heliospheric missions, such as Parker Solar Probe and Solar Orbiter, and for space weather modeling of the slow solar wind.

Effects of Pseudostreamer Boundary Dynamics on Heliospheric Field and Wind

V. **Aslanyan**¹, D. I. Pontin², P. F. Wyper³, R. B. Scott⁴, S. K. Antiochos⁵, and C. R. DeVore⁵
2021 ApJ 909 10

<https://doi.org/10.3847/1538-4357/abd6e6>

<https://iopscience.iop.org/article/10.3847/1538-4357/abd6e6/pdf>

Interchange reconnection has been proposed as a mechanism for the generation of the slow solar wind, and a key contributor to determining its characteristic qualities. In this paper we study the implications of interchange reconnection for the structure of the plasma and field in the heliosphere. We use the Adaptively Refined Magnetohydrodynamic Solver to simulate the coronal magnetic evolution in a coronal topology containing both a pseudostreamer and helmet streamer. We begin with a geometry containing a low-latitude coronal hole that is separated from the main polar coronal hole by a pseudostreamer. We drive the system by imposing rotating flows at the solar surface within and around the low-latitude coronal hole, which leads to a corrugation (at low altitudes) of the separatrix surfaces that separate open from closed magnetic flux. Interchange reconnection is induced both at the null points and separators of the pseudostreamer, and at the global helmet streamer. We demonstrate that a preferential occurrence of interchange reconnection in the "lanes" between our driving cells leads to a filamentary pattern of newly opened flux in the heliosphere. These flux bundles connect to but extend far from the separatrix-web (S-Web) arcs at the source surface. We propose that the pattern of granular and supergranular flows on the photosphere should leave an observable imprint in the heliosphere.

Powerful non-geoeffective interplanetary disturbance of July 2012 observed by muon hodoscope URAGAN

I.I. **Astapova**, , N.S. Barbashina^a, A.A. Petrukchina, V.V. Shutenkoa, I.S. Veselovsky

Advances in Space Research Volume 56, Issue 12, 15 December 2015, Pages 2833–2838

<http://www.sciencedirect.com/science/article/pii/S0273117715001854>

The most powerful coronal mass ejection of the 24th solar cycle took place on the opposite side of the Sun on **July 23, 2012** and had no geomagnetic consequences. Nevertheless, as a result of passing of the ejection through the heliosphere, variations of galactic cosmic rays flux were observed on the Earth. These variations were registered by the muon hodoscope URAGAN (MEPhI, Moscow). Muon flux angular distributions on the Earth's surface are reported and analyzed.

Modelling a multi-spacecraft coronal mass ejection encounter with EUHFORIA

[E. Asvestari](#), [J. Pomoell](#), [E. Kilpua](#), [S. Good](#), [T. Chatzistergos](#), [M. Temmer](#), [E. Palmerio](#), [S. Poedts](#), [J. Magdalenic](#)

A&A 2021

<https://arxiv.org/pdf/2105.11831.pdf>

Coronal mass ejections (CMEs) are a manifestation of the Sun's eruptive nature. They can have a great impact on Earth, but also on human activity in space and on the ground. Therefore, modelling their evolution as they propagate through interplanetary space is essential. EUropean Heliospheric FOrecasting Information Asset (EUHFORIA) is a data-driven, physics-based model, tracing the evolution of CMEs through background solar wind conditions. It employs a spheromak flux rope, which provides it with the advantage of reconstructing the internal magnetic field configuration of CMEs. This is something that is not included in the simpler cone CME model used so far for space weather forecasting. This work aims at assessing the spheromak CME model included in EUHFORIA. We employed the spheromak CME model to reconstruct a well observed CME and compare model output to in situ observations. We focus on an eruption from **6 January 2013** encountered by two radially aligned spacecraft, Venus Express and STEREO-A. We first analysed the observed properties of the source of this CME eruption and we extracted the CME properties as it lifted off from the Sun. Using this information, we set up EUHFORIA runs to model the event. The model predicts arrival times from half to a full day ahead of the in situ observed ones, but within errors established from similar studies. In the modelling domain, the CME appears to be propagating primarily southward, which is in accordance with white-light images of the CME eruption close to the Sun. In order to get the observed magnetic field topology, we aimed at selecting a spheromak rotation angle for which the axis of symmetry of the spheromak is perpendicular to the direction of the polarity inversion line (PIL). The modelled magnetic field profiles, their amplitude, arrival times, and sheath region length are all affected by the choice of radius of the modelled spheromak.

Using the Evolution of Coronal Dimming Regions to Probe the Global Magnetic Field Topology

[Attrill, G.](#); [Nakwacki, M. S.](#); [Harra, L. K.](#); [van Driel-Gesztelyi, L.](#); [Mandrini, C. H.](#); [Dasso, S.](#); [Wang, J.](#)
Solar Physics, Volume 238, Issue 1, pp.117-139, **2006**; **File**

We demonstrate that study of the evolving magnetic nature of coronal dimming regions can be used to probe the large-scale magnetic structure involved in the eruption of a coronal mass ejection (CME). We analyse the intensity evolution of coronal dimming regions using 195 Å data from the Extreme ultraviolet Imaging Telescope (EIT) on board the Solar and Heliospheric Observatory (SOHO). We measure the magnetic flux, using data from the SOHO/Michelson Doppler Imager (MDI), in the regions that seem most likely to be related to plasma removal. Then, we compare these magnetic flux measurements to the flux in the associated magnetic cloud (MC). Here, we present our analysis of the well-studied event on 12 May 1997 that took place just after solar minimum in a simple magnetic configuration. We present a synthesis of results already published and propose that driven “interchange reconnection” between the expanding CME structure with “open” field lines of the northern coronal hole region led to the asymmetric temporal and spatial evolution of the two main dimming regions, associated with this event. As a result of this reconnection process, we find the southern-most dimming region to be the principal foot-point of the MC. The magnetic flux from this dimming region and that of the MC are found to be in close agreement within the same order of magnitude, 10^{21} Mx.

The 2015 Summer Solstice Storm: one of the major geomagnetic storms of solar cycle 24 observed at ground level

C. R. A. [Augusto](#), [C. E. Navia](#), [M. N. de Oliveira](#), [A. A. Nepomuceno](#), [J. P. Raulin](#), [E. Tueros](#), [R. R. de Mendonça](#), [A. C. Fauth](#), [H. Vieira de Souza](#), [V. Kopenkin](#), [T. Sinzi](#)

Solar Phys. May 2018, 293:84

<https://arxiv.org/pdf/1805.05277.pdf>

<https://link.springer.com/content/pdf/10.1007%2Fs11207-018-1303-8.pdf>

We report on the **22-23 June 2015** geomagnetic storm. There has been a shortage of intense geomagnetic storms during the current solar cycle 24 in relation to the previous cycle. This situation changed after mid-June 2015 when one of the biggest solar active regions (AR 2371) of current solar cycle 24, close to the central meridian produced several coronal mass ejections (CMEs) associated with M-class flares. The CMEs impact on the Earth's magnetosphere resulted in a moderately-severe G4-class geomagnetic storm on 22-23 June 2015 and a G2 (moderate) geomagnetic storms on **24 June**. The G4 solstice storm was the second biggest (so far) geomagnetic storms of cycle 24. We highlight the ground level observations made by New-Tupi, Muonca and the CARPET El Leoncito cosmic ray detectors that are located within the South Atlantic Anomaly (SAA) region. These observations are studied in correlation with data obtained by space-borne detectors and other ground-based experiments. The CME designations are from the Computer Aided CME Tracking (CACTus) automated catalog. As expected, Forbush Decreases (FD) associated with the passing CMEs were recorded by these detectors. We noticed a peculiar feature linked to a severe geomagnetic storm event. The 21 June 2015 CME 0091 was likely associated with the 22 June summer solstice FD event. The angular width of CME 0091 was very narrow and measured 56 degrees seen from Earth. In most cases, only CME halos and partial halos, lead to severe geomagnetic storms. We performed a cross-check analysis of the FD events detected during the rise phase of the current solar cycle 24, the geomagnetic parameters, and the CACTus CME catalog. Our study suggests that narrow angular-width CMEs that erupt in the western region of the ecliptic plane can lead to moderate and severe geomagnetic storms.
18-22 June 2015

Muon Excess at Sea Level during the Progress of a Geomagnetic Storm and High Speed Stream Impact Near the Time of Earth's Heliospheric Sheet Crossing

C. R. A. [Augusto](#), [C. E. Navia](#), [M. N. de Oliveira](#), [A. A. Nepomuceno](#), [V. Kopenkin](#), [T. Sinzi](#)

Solar Phys. 292:107 **2017**

<https://arxiv.org/pdf/1706.00775.pdf>

In this article we present results of the study on the association between the muon flux variation at ground level, registered by the `\textit{New-Tupi}` muon telescopes (22053'00"S, 43006'13"W; 3 m above sea level) and a geomagnetic storm of **25--29 August 2015** that has raged for several days as a result of a coronal mass ejection (CME) impact on Earth's magnetosphere. A sequence of events started with an M3.5 X-ray class flare on **22 August 2015** at 21:19 UTC. The `\textit{New-Tupi}` muon telescopes observed a Forbush decrease (FD) triggered by this geomagnetic storm, with onset on 26 August 2015. After the Earth crossed a heliospheric current sheet (HCS), an increase in the particle flux was observed on 28 August 2015 by spacecrafts and ground level detectors. The observed peak was in temporal coincidence with the impact of a high speed stream (HSS). We study this increase, that has been

observed with a significance above 1.5% by ground level detectors in different rigidity regimes. We also estimate the lower limit of the energy fluence injected on Earth. In addition, we consider the origin of this increase, such as acceleration of particles by shock waves on the front of the HSS and the focusing effect of the HCS crossing. Our results show possible evidence of a prolonged energetic (up to GeV energies) particle injection within the Earth atmosphere system, driven by the HSS. In most cases these injected particles are directed to polar regions. However, the particles from the high energy tail of the spectrum can reach middle latitudes, and that could have consequences for the atmospheric chemistry, for instance, the creation of NO_x species may be enhanced and can lead to increased ozone depletion. This topic requires further study.

VARIATIONS OF THE MUON FLUX AT SEA LEVEL ASSOCIATED WITH INTERPLANETARY ICMEs AND COROTATING INTERACTION REGIONS

C. R. A. [Augusto](#)¹, V. Kopenkin¹, C. E. Navia¹, K. H. Tsui¹, H. Shigueoka¹, A. C. Fauth², E. Kemp², E. J. T. Manganote², M. A. Leigui de Oliveira³, P. Miranda⁴, R. Ticona⁴, and A. Velarde

2012 ApJ 759 143

We present the results of an ongoing survey on the association between the muon flux variation at ground level (3 m above sea level) registered by the Tupi telescopes (Niteri-Brazil, 229S, 432W, 3 m) and the Earth-directed transient disturbances in the interplanetary medium propagating from the Sun (such as coronal mass ejections (CME), and corotating interaction regions (CIRs)). Their location inside the South Atlantic Anomaly region enables the muon telescopes to achieve a low rigidity of response to primary and secondary charged particles. The present study is primarily based on experimental events obtained by the Tupi telescopes in the period from 2010 August to 2011 December. This time period corresponds to the rising phase of solar cycle 24. The Tupi events are studied in correlation with data obtained by space-borne detectors (SOHO, ACE, GOES). Identification of interplanetary structures and associated solar activity was based on the nomenclature and definitions given by the satellite observations, including an incomplete list of possible interplanetary shocks observed by the CELIAS/MTOF Proton Monitor on the Solar and Heliospheric Observatory (SOHO) spacecraft. Among 29 experimental events reported in the present analysis, there are 15 possibly associated with the CMEs and sheaths, and 3 events with the CIRs (forward or reverse shocks); the origin of the remaining 11 events has not been determined by the satellite detectors. We compare the observed time (delayed or anticipated) of the muon excess (positive or negative) signal on Earth (the Tupi telescopes) with the trigger time of the interplanetary disturbances registered by the satellites located at Lagrange point L1 (SOHO and ACE). The temporal correlation of the observed ground-based events with solar transient events detected by spacecraft suggests a real physical connection between them. We found that the majority of observed events detected by the Tupi experiment were delayed in relation to the satellite triggers. This result agrees with theoretical expectations. Our experimental data indicate that the Tupi experiment is able to add new information and can be complementary to other techniques designed to interpret the origin of some interplanetary disturbances observed by satellites.

Confined plasma transition from the solar atmosphere to the interplanetary medium



[Nicolas, Aurélien, Corentin Poirier](#)

2022

<https://arxiv.org/abs/2208.11637>

The last 60 years of space exploration have shown that the interplanetary medium is continually perturbed by a myriad of different solar winds and storms that transport solar material across the whole heliosphere. If there is a consensus on the source of the fast solar wind that is known to originate in coronal holes, the question is still largely debated on the origin of the slow solar wind (SSW). The abundance of heavy ions measured in situ provides a precious diagnostic of potential source regions, because the composition is established very low in the solar atmosphere at the interface between the dense chromosphere and the tenuous corona, and remains invariant during transport in the collisionless solar wind. The similar composition measured in situ in the SSW and spectroscopically in coronal loops suggests that a significant fraction of the SSW originates as plasma material that was initially trapped along corona loops and subsequently released in the solar wind. The recent observations from the Parker Solar Probe (PSP) mission also provide new insights on the nascent solar wind. A great challenge remains to explain both the composition and bulk properties of the SSW in a self-consistent manner. For this purpose we exploit and develop models with various degrees of complexity. This context constitutes the backbone of this thesis which is structured in four major steps: we begin by presenting a new technique that exploits white-light (WL) observations of the SSW taken from multiple vantage points to constrain global models of the solar atmosphere. We then exploit the first images taken by the Wide-Field Imager for Solar PRobe (WISPR) from inside the solar corona to test our global models at smaller scales because WISPR offers an

unprecedented close-up view of the fine structure of streamers and of the nascent SSW. This work provides further evidence for the transient release of plasma trapped in coronal loops into the solar wind, that we interpret by exploiting high-resolution magneto-hydro-dynamics (MHD) simulations. Finally we develop and exploit a new multi-specie model of coronal loops called the Irap Solar Atmosphere Model (ISAM) to provide an in-depth analysis of the plasma transport mechanisms at play between the chromosphere and the corona. ISAM solves for the coupled transport of the main constituents of the solar wind with minor ions through a comprehensive treatment of collisions as well as partial ionization and radiative cooling/heating mechanisms near the top of the chromosphere. We use this model to study the different mechanisms that can preferentially extract ions according to their first-ionization-potential (FIP), from the chromosphere to the corona. In this process we compare the relative roles of frictional and thermal diffusive effects in enriching coronal loops with low-FIP elements that could be subsequently expelled in the SSW through the mechanisms discussed in the first part of this thesis.

A different interpretation of the annual and semiannual anomalies on the magnetic activity over the Earth

[Azpilicueta](#), F., and C. Brunini

J. Geophys. Res., 117, A08202, 2012

The H component of the magnetic field measured at the terrestrial surface presents several periodic signals caused by changes in the ring current that flows within the terrestrial magnetosphere. One of the most important of them is associated to the phenomenon known as the Semiannual Anomaly which produces two significant minima during the equinoxes. This phenomenon is global, i.e., every observatory registers a similar effect independently of the hemisphere where it is located. A second important signal is due to the phenomenon known as the Annual Anomaly that produces significant different values for solstices, with a particular feature: the effect depends on the hemisphere where the observatory is located, with maximum during local summer. In spite of the time since their discoveries (more than a hundred years ago) the physical processes behind them are still open to discussion. In this work we present a new physical interpretation for the combined effects of both anomalies. The main concept developed is that along the year the shape of the magnetospheric cavities within which the ring current flows is deformed according to the geometric configuration between the solar wind and the magnetosphere.

The geomagnetic semiannual anomaly on the four Dst-fundamental observatories: Dependences with Sun-Earth physical parameters

[Azpilicueta](#), Francisco; Brunini, Claudio; CamiliCn, Emilio

J. Geophys. Res., Vol. 117, No. A7, A07204, 2012

<http://dx.doi.org/10.1029/2012JA017730>

The semiannual anomaly (also known as semiannual variation) on the magnetic activity is a phenomenon that produces clear minima during March and September and maxima in June and December on the horizontal components of the geomagnetic field. This phenomenon has been known since the middle of the nineteenth century, but in spite of the accumulation of measurements and the development of three theoretical models, a conclusive physical explanation for it has not been developed. The usual approach to study the semiannual anomaly is by means of geomagnetic indices like the disturbance storm time, Dst, which is based on combining measurements registered on four magnetic observatories. This work follows a different approach based on the raw horizontal components registered at the four observatories. The analyses performed aimed to study and assess the impact of several external parameters, characteristics of the Sun-Earth environment, on the semiannual anomaly. The influence of the global geomagnetic activity level, the solar activity level, the solar magnetic polarity, and the rising/declining phase of the solar radiation cycle is analyzed in detail. The most important finding is that the semiannual anomaly is always present and that none of the previously mentioned parameters significantly favor the development of it. A second result is the presence of a 27 day signal superposed to the semiannual anomaly which is significantly affected by the solar activity level.

Coronal Mass Ejections from the Sun - Propagation and Near Earth Effects

Arun [Babu](#)

THESIS, 2014

<http://arxiv.org/pdf/1407.4258v1.pdf>

Owing to our dependance on spaceborne technology, an awareness of disturbances in the near-Earth space environment is proving to be increasingly crucial. Earth-directed Coronal mass ejections (CMEs) emanating from the Sun are the primary drivers of space weather disturbances. Studies of CMEs, their kinematics, and their near-Earth effects are therefore gaining in importance.

The effect of CMEs near the Earth is often manifested as transient decreases in galactic cosmic ray intensity, which are called **Forbush decreases (FDs)**. In this thesis we probe the structure of CMEs and their associated shocks using FD observations by the GRAPES-3 muon telescope at Ooty. We have established that the cumulative diffusion of galactic cosmic rays into the CME is the dominant mechanism for causing FDs (Chapter 3).

This diffusion takes place through a turbulent sheath region between the CME and the shock. One of our main results concerns the turbulence level in this region. We have quantitatively established that cross-field diffusion aided by magnetic field turbulence accounts for the observed lag between the FD and the magnetic field enhancement of the sheath region (Chapter 4).

We have also investigated the nature of the driving forces acting on CMEs in this thesis. Using CME data from the SECCHI coronagraphs aboard STEREO spacecraft, we have found evidence for the non-force-free nature of the magnetic field configuration inside these CMEs, which is the basis for the (often-invoked) Lorentz self-force driving (Chapter 5).

Taken together the work presented in this thesis is a comprehensive attempt to characterise CME propagation from typical coronagraph fields of view to the Earth.

2000-02-27, 2001-11-24, 10-12 Apr 2001, 17 August 2001, 7 September 2002, 20 November 2003, 26 July 2004, 21 June 2010,

Table 3.1: Forbush decrease event short listed by FD profile and magnitude

High rigidity Forbush decreases: due to CMEs or shocks?

Arun **Babu**, H. M. Antia, S. R. Dugad, S. K. Gupta, Y. Hayashi, S. Kawakami, P. K. Mohanty, T. Nonaka, A. Oshima, P. Subramanian

E-print, April 2013; A&A

<http://arxiv.org/abs/1304.5343>

Aims. We seek to identify the primary agents causing Forbush decreases (FDs) observed at the Earth in high rigidity cosmic rays. In particular, we ask if such FDs are caused mainly by coronal mass ejections (CMEs) from the Sun that are directed towards the Earth, or by their associated shocks.

Methods. We use the muon data at cutoff rigidities ranging from 14 to 24 GV from the GRAPES-3 tracking muon telescope to identify FD events. We select those FD events that have a reasonably clean profile, and can be reasonably well associated with an Earth-directed CME and its associated shock. We employ two models: one that considers the CME as the sole cause of the FD (the CME-only model) and one that considers the shock as the only agent causing the FD (the shock-only model). We use an extensive set of observationally determined parameters for both these models.

The only free parameter in these models is the level of MHD turbulence in the sheath region, which mediates cosmic ray diffusion (into the CME, for the CME-only model and across the shock sheath, for the shock-only model).

Results. We find that good fits to the GRAPES-3 multi-rigidity data using the CME-only model require turbulence levels in the CME sheath region that are only slightly higher than those estimated for the quiet solar wind. On the other hand, reasonable model fits with the shock-only model require turbulence levels in the sheath region that are an order of magnitude higher than those in the quiet solar wind.

Conclusions. This observation naturally leads to the conclusion that the Earth-directed CMEs are the primary contributors to FDs observed in high rigidity cosmic rays.

11/04/01, 17/08/01, 29/09/01, 24/11/01, 23/05/02, 7/09/02, 30/09/02, 20/11/03, 26/07/04

Prediction and Verification of Parker Solar Probe Solar Wind Sources at 13.3 R_☉

Samuel T. **Badman**, [Pete Riley](#), [Shaela I. Jones](#), [Tae K. Kim](#), [Robert C. Allen](#), [C. Nick Arge](#), [Stuart D. Bale](#), [Carl J. Henney](#), [Justin C. Kasper](#), [Parisa Mostafavi](#), [Nikolai V. Pogorelov](#), [Nour E. Raouafi](#), [Michael L. Stevens](#), [J. L. Verniero](#)

JGR [Volume 128, Issue 4](#) April 2023 e2023JA031359

<https://arxiv.org/pdf/2303.04852.pdf>

<https://doi.org/10.1029/2023JA031359>

Drawing connections between heliospheric spacecraft and solar wind sources is a vital step in understanding the evolution of the solar corona into the solar wind and contextualizing *in situ* timeseries. Furthermore, making advanced predictions of this linkage for ongoing heliospheric missions, such as Parker Solar Probe (PSP), is necessary for achieving useful coordinated remote observations and maximizing scientific return. The general procedure for estimating such connectivity is straightforward (i.e. magnetic field line tracing in a coronal model) but validating the resulting estimates difficult due to the lack of an independent ground truth and limited model constraints. In its most recent orbits, PSP has reached perihelia of 13.3R_☉ and moreover travels extremely fast prograde relative to the solar

surface, covering over 120 degrees longitude in three days. Here we present footpoint predictions and subsequent validation efforts for PSP Encounter 10, the first of the 13.3R \odot orbits, which occurred in November 2021. We show that the longitudinal dependence of $\textit{in situ}$ plasma data from these novel orbits provides a powerful method of footpoint validation. With reference to other encounters, we also illustrate that the conditions under which source mapping is most accurate for near-ecliptic spacecraft (such as PSP) occur when solar activity is low, but also requires that the heliospheric current sheet is strongly warped by mid-latitude or equatorial coronal holes. Lastly, we comment on the large-scale coronal structure implied by the Encounter 10 mapping, highlighting an empirical equatorial cut of the Alfvén surface consisting of localized protrusions above unipolar magnetic separatrices. **15-26 Nov 2021**

Coronal Electron Temperature Inferred from the Strahl Electrons in the Inner Heliosphere: Parker Solar Probe and Helios Observations

Magnetic connectivity of the ecliptic plane within 0.5 AU : PFSS modeling of the first PSP encounter

Samuel T. [Badman](#), [Stuart D. Bale](#), [Juan C. Martinez Oliveros](#), [Olga Panasenco](#), [Marco Velli](#), [David Stansby](#), [Juan C. Buitrago-Casas](#), [Victor Reville](#), [John W. Bonnell](#), [Anthony W. Case](#), [Thierry Dudok de Wit](#), [Keith Goetz](#), [Peter R. Harvey](#), [Justin C. Kasper](#), [Kelly E. Korreck](#), [Davin E. Larson](#), [Roberto Livi](#), [Robert J. MacDowall](#), [David M. Malaspina](#), [Marc Pulupa](#), [Michael L. Stevens](#), [Phyllis L. Whittlesey](#)
ApJ **2019**

<https://arxiv.org/pdf/1912.02244.pdf>

We compare magnetic field measurements taken by the FIELDS instrument on Parker Solar Probe (PSP) during its first solar encounter to predictions obtained by Potential Field Source Surface (PFSS) modeling. Ballistic propagation is used to connect the spacecraft to the source surface. Despite the simplicity of the model, our results show striking agreement with PSPs first observations of the heliospheric magnetic field from 0.5 AU (107.5 Rs) down to 0.16 AU (35.7 Rs). Further, we show the robustness of the agreement is improved both by allowing the photospheric input to the model to vary in time, and by advecting the field from PSP down to the PFSS model domain using *in situ* PSP/SWEAP measurements of the solar wind speed instead of assuming it to be constant with longitude and latitude. We also explore the source surface height parameter (RSS) to the PFSS model finding that an extraordinarily low source surface height (1.3-1.5Rs) predicts observed small scale polarity inversions which are otherwise washed out with regular modeling parameters. Finally, we extract field line traces from these models. By overlaying these on EUV images we observe magnetic connectivity to various equatorial and mid-latitude coronal holes indicating plausible magnetic footpoints and offering context for future discussions of sources of the solar wind measured by PSP. **2018-10-15 to 2018-11-30**

Forbush decreases and Geomagnetic Storms during a Highly Disturbed Solar and Interplanetary Period, 4-10 September 2017

B. [Badruddin](#), [O. P. M. Aslam](#), [M. Derouich](#), [H. Asiri](#), [K. Kudela](#)
Space Weather [Volume17, Issue3](#) Pages 487-496 **2019**

sci-hub.se/10.1029/2018SW001941

Features and peculiarities of the cosmic ray intensity (CRI) and the geomagnetic activity, along with several solar plasma and interplanetary magnetic field during the period 4-10 September 2017 are studied. The period was characterized by strong solar activity: several solar flares occurred, several halo Coronal Mass Ejections (CMEs) were ejected in space. In the near-Earth interplanetary space, the CMEs driving shock(s) and sheath(s) were identified. At the Earth, strong Forbush decreases (FD) in CRI and geomagnetic storms (GS) were observed. Several large solar flares, one of them of very high X-ray importance (X 9.3) and three halo CMEs were detected in the solar atmosphere. Two shock-associated Interplanetary Coronal Mass Ejections were observed during that interval in near-Earth space; the latter and faster one arrived even as the ejecta of earlier one was still crossing. Variations in interplanetary plasma and field parameters during, before and after the FD and GS that occurred during the considered period were examined. A detailed time-lagged correlation analysis using data at three different temporal resolutions (hourly, 5-min and 1-min) was also performed. Cross-correlations of time series of CRI with geomagnetic activity during the period 4 – 10 September 2017 are computed. This cross-correlation analysis between CRI variability (defined as the difference of the CRI count rate between the current and the previous time step) and the Dst indicates a delay of Dst by 3-4 hours.

Geomagnetic response of interplanetary coronal mass ejections in the Earth's magnetosphere

[Badruddin](#), [F.Mustajab](#) [M.Derouich](#)

[Planetary and Space Science](#) [Volume 154](#), May **2018**, Pages 1-4

<https://www.sciencedirect.com/science/article/pii/S0032063317304695>

A [coronal mass ejections](#) (CME) is the huge mass of plasma with embedded [magnetic field](#) ejected abruptly from the Sun. These CMEs propagate into [interplanetary space](#) with different speed. Some of them hit the [Earth's magnetosphere](#) and create many types of disturbances; one of them is the disturbance in the [geomagnetic field](#). Individual geomagnetic disturbances differ not only in their magnitudes, but the nature of disturbance is also different. It is, therefore, desirable to understand these differences not only to understand the physics of geomagnetic disturbances but also to understand the properties of solar/interplanetary structures producing these disturbances of different magnitude and nature. In this work, we use the spacecraft measurements of CMEs with distinct [magnetic properties](#) propagating in the interplanetary space and generating disturbances of different levels and nature. We utilize their distinct plasma and field properties to search for the interplanetary parameter(s) playing important role in influencing the geomagnetic response of different coronal mass ejections.

Study of the geoeffectiveness of coronal mass ejections, corotating interaction regions and their associated structures observed during Solar Cycle 23

A. [Badruddin](#), Z. Falak

Astrophysics and Space Science August 2016, 361:253

<https://link.springer.com/content/pdf/10.1007%2Fs10509-016-2839-4.pdf>

The interplanetary coronal mass ejections (ICMEs) and the corotating interaction regions (CIRs) are the two most important structures of the interplanetary medium affecting the Earth and the near-Earth space environment. We study the solar wind-magnetosphere coupling during the passage of ICMEs and CIRs, in the Solar Cycle 23 (Jan. 1995–Dec. 2009), and their relative geoeffectiveness. We utilize the timings of different features of these structures, their arrival and duration. As geomagnetic parameter, we utilize high time resolution data of Dst and AEAE indices. In addition to these geomagnetic indices, we utilize the simultaneous and similar time resolution data of interplanetary plasma and field, namely, solar wind velocity, interplanetary magnetic field, its north-south component and dawn-dusk electric field. We apply the method of superposed epoch analysis. Utilizing the properties of various structures during the passage of ICMEs and CIRs, and variations observed in plasma and field parameters during their passage along with the simultaneous changes observed in geomagnetic parameters, we identify the interplanetary conditions, plasma/field parameters and their relative importance in solar wind-magnetosphere coupling. Geospace consequences of ICMEs and CIRs, and the implications of these results for solar wind-magnetosphere coupling are discussed.

Study of the Cosmic-Ray Modulation During the Passage of ICMEs and CIRs

[Badruddin](#) , Anand Kumar

Solar Phys Vol. 291, Issue 2, pp.559-580 2016

<https://link.springer.com/content/pdf/10.1007%2Fs11207-015-0843-4.pdf>

We compare the cosmic-ray response to interplanetary coronal mass ejections (ICMEs) and corotating interaction regions (CIRs) during their passage in near-Earth space. We study the relative importance of various structures/features identified during the passage of the ICMEs and CIRs observed during Cycle 23 (1995–2009). The identified ICME structures are the shock front, the sheath, and the CME ejecta. We isolate the shock arrival time, the passage of the sheath region, the arrival of ejecta, and the end time of their passage. Similarly, we isolate the CIR arrival, the associated forward shock, the stream interface, and the reverse shock during the passage of a CIR. For the cosmic-ray intensity, we utilize the data from high counting rate neutron monitors. In addition to neutron monitor data, we utilize near-simultaneous and same time-resolution data of interplanetary plasma and field, namely the solar-wind velocity, the interplanetary magnetic field (IMF) vector, and its variance. Further, we also utilize some derived interplanetary parameters. We apply the method of the superposed-epoch analysis. As the plasma and field properties are different during the passage of different structures, both in ICMEs and CIRs, we systematically vary the epoch time in our superposed-epoch analysis one by one. In this way, we study the role and effects of each of the identified individual structures/features during the passage of the ICMEs and CIRs. Relating the properties of various structures and the corresponding variations in plasma and field parameters with changes of the cosmic-ray intensity, we identify the relative importance of the plasma/field parameters in influencing the amplitude and time profiles of the cosmic-ray intensity variations during the passage of the ICMEs and CIRs.

Study of the Forbush Decreases, Geomagnetic Storms, and Ground-Level Enhancements in Selected Intervals and Their Space Weather Implications

Badruddin & Anand Kumar

Solar Phys. Volume 290, [Issue 4](#), pp 1271-1283 **2015, File**

We analysed geomagnetic storms, ground-level enhancements (GLEs), and Forbush decreases in cosmic-ray intensity that occurred in selected intervals. We used data of ground-based neutron monitors for the cosmic-ray intensity. We used the geomagnetic index Dst as a measure of the geomagnetic storm intensity. Solar observations and interplanetary plasma/field parameters were used to identify the solar cause(s), interplanetary structure(s), and physical mechanism(s) responsible for the geomagnetic storms, the Forbush decreases, and the GLEs of different amplitudes and time profiles; all of them occurring within four selected periods of one month each. The observed differences in cosmic-ray and geomagnetic-activity responses to the same solar sources were used to distinguish the structures and mechanisms responsible for transient cosmic-ray modulation and geomagnetic storms. **July 2000 , April 2001, Jan 2005, 5-18 Dec 2006**

Fluctuations in the interplanetary electric potential and energy coupling between the solar-wind and the magnetosphere

Badruddin and Aslam, O.P.M.

E-print, Dec **2013**; Proc. International Symposium on Solar-Terrestrial Physics 2012 (ISSTP 2012)

We utilize solar rotation average geomagnetic index ap and various solar wind plasma and field parameters for four solar cycles 20-23. We perform analysis to search for a best possible coupling function at 27-day time resolution. Regression analysis using these data at different phases of solar activity (increasing including maximum/decreasing including minimum) led us to suggest that the time variation of interplanetary electric potential is a better coupling function for solar wind-magnetosphere coupling. We suspect that a faster rate of change in interplanetary electric potential at the magnetopause might enhance the reconnection rate and energy transfer from the solar wind into the magnetosphere. The possible mechanism that involves the interplanetary potential fluctuations in influencing the solar wind-magnetosphere coupling is being investigated.

Study of the solar wind-magnetosphere coupling on different time scales

Badruddin and Aslam, O.P.M.

E-print, Nov **2013**; Planetary and Space Science

Solar wind-magnetosphere coupling, its causes and consequences have been studied for the last several decades. However, the assessment of continuously changing behaviour of the sun, plasma and field flows in the interplanetary space and their influence on geomagnetic activity is still a subject of intense research. Search for the best possible coupling function is also important for space weather prediction. We utilise four geomagnetic indices (ap, aa, AE and Dst) as parameters of geomagnetic activity level in the earth's magnetosphere. In addition to these indices, we utilise various solar wind plasma and field parameters for the corresponding periods. We analyse the geomagnetic activity and plasma/field parameters at yearly, half-yearly, 27-day, daily, 3-hourly, and hourly time resolutions. Regression analysis using geomagnetic and solar wind data of different time resolutions, over a continuous long period, and at different phases of solar activity (increasing including maximum/decreasing including minimum) led us to suggest that two parameters BV/1000(mV/m) and BV2(mV/s) are highly correlated with the all four geomagnetic activity indices not only at any particular time scale but at different time scales. It probably suggests for some role of the fluctuations/variations in interplanetary electric potential, its spacial variation [i.e., interplanetary electric field BV (mV/m)] and/or time variation [BV2 (mV/s)], in influencing the reconnection rate.

Using Gradient Boosting Regression to Improve Ambient Solar Wind Model Predictions

R. L. **Bailey**, [M. A. Reiss](#), [C. N. Arge](#), [C. Möstl](#), [C. J. Henney](#), [M. J. Owens](#), [U. V. Amerstorfer](#), [T. Amerstorfer](#), [A. J. Weiss](#), [J. Hinterreiter](#)

Space Weather [Volume19, Issue5](#) May **2021** e2020SW002673

<https://agupubs.onlinelibrary.wiley.com/doi/epdf/10.1029/2020SW002673>

<https://doi.org/10.1029/2020SW002673>

Studying the ambient solar wind, a continuous pressure-driven plasma flow emanating from our Sun, is an important component of space weather research. The ambient solar wind flows in interplanetary space determine how solar storms evolve through the heliosphere before reaching Earth, and especially during solar minimum are themselves a driver of activity in the Earth's magnetic field. Accurately forecasting the ambient solar wind flow is therefore imperative to space weather awareness. Here, we present a machine learning approach in which solutions from magnetic models of the solar corona are used to output the solar wind conditions near the Earth. The results are compared to observations and existing models in a comprehensive validation analysis, and the new model outperforms existing models in almost all measures.

In addition, this approach offers a new perspective to discuss the role of different input data to ambient solar wind modeling, and what this tells us about the underlying physical processes. The final model discussed here represents an extremely fast, well-validated and open-source approach to the forecasting of ambient solar wind at Earth.

Improving ambient solar wind model predictions with machine learning

R.L. [Bailey](#), [M.A. Reiss](#), [C.N. Arge](#), [C. Möstl](#), [M.J. Owens](#), [U.V. Amerstorfer](#), [C.J. Henney](#), [T. Amerstorfer](#), [A.J. Weiss](#), [J. Hinterreiter](#)

2020

<https://arxiv.org/pdf/2006.12835.pdf>

The study of ambient solar wind, a continuous pressure-driven plasma flow emanating from our Sun, is an important component of space weather research. The ambient solar wind flows in interplanetary space determine how solar storms evolve through the heliosphere before reaching Earth, and especially during solar minimum are themselves a driver of activity in the Earth's magnetic field. Accurately forecasting the ambient solar wind flow is therefore imperative to space weather awareness. Here we present a novel machine learning approach in which solutions from magnetic models of the solar corona are used to output the solar wind conditions near the Earth. The results are compared to observations and existing models in a comprehensive validation analysis, and the new model outperforms existing models in almost all measures. The final model discussed here represents an extremely fast, well-validated and open-source approach to the forecasting of ambient solar wind at Earth.

Prediction of Dst during solar minimum using in situ measurements at L5

R. L. [Bailey](#), [C. Möstl](#), [M.A. Reiss](#), [A. J. Weiss](#), [U. V. Amerstorfer](#), [T. Amerstorfer](#), [J. Hinterreiter](#), [W. Magnes](#), [R. Leonhardt](#)

Space Weather **Volume18, Issue5** e2019SW002424 2020

<https://agupubs.onlinelibrary.wiley.com/doi/pdf/10.1029/2019SW002424>

<https://arxiv.org/pdf/2005.00249.pdf>

Geomagnetic storms resulting from high-speed streams can have significant negative impacts on modern infrastructure due to complex interactions between the solar wind and geomagnetic field. One measure of the extent of this effect is the Kyoto Dst index. We present a method to predict Dst from data measured at the Lagrange 5 (L5) point, which allows for forecasts of solar wind development 4.5 days in advance of the stream reaching the Earth. Using the STEREO-B satellite as a proxy, we map data measured near L5 to the near-Earth environment and make a prediction of the Dst from this point using the Temerin-Li Dst model enhanced from the original using a machine learning approach. We evaluate the method accuracy with both traditional point-to-point error measures and an event-based validation approach. The results show that predictions using L5 data outperform a 27-day solar wind persistence model in all validation measures but do not achieve a level similar to an L1 monitor. Offsets in timing and the rapidly-changing development of Bz in comparison to Bx and By reduce the accuracy. Predictions of Dst from L5 have an RMSE of 9 nT, which is double the error of 4 nT using measurements conducted near the Earth. The most useful application of L5 measurements is shown to be in predicting the minimum Dst for the next four days. This method is being implemented in a real-time forecast setting using STEREO-A as an L5 proxy, and has implications for the usefulness of future L5 missions.

Shock Connectivity in the August 2010 and July 2012 Solar Energetic Particle Events Inferred from Observations and ENLIL Modeling

H. M. [Bain](#), M. L. Mays, J. G. Luhmann, Y. Li, L. K. Jian, and D. Odstrcil

2016 ApJ 825 1 **File**

During periods of increased solar activity, coronal mass ejections (CMEs) can occur in close succession and proximity to one another. This can lead to the interaction and merger of CME ejecta as they propagate in the heliosphere. The particles accelerated in these shocks can result in complex solar energetic particle (SEP) events, as observing spacecraft form both remote and local shock connections. It can be challenging to understand these complex SEP events from in situ profiles alone. Multipoint observations of CMEs in the near-Sun environment, from the Solar Terrestrial Relations Observatory "Sun Earth Connection Coronal and Heliospheric Investigation and the Solar and Heliospheric Observatory Large Angle and Spectrometric Coronagraph, greatly improve our chances of identifying the origin of these accelerated particles. However, contextual information on conditions in the heliosphere, including the background solar wind conditions and shock structures, is essential for understanding SEP properties well enough to forecast their characteristics. Wang "Sheeley? Arge WSA-ENLIL + Cone modeling provides a tool to interpret major SEP event periods in the context of a realistic heliospheric model and to determine how much of what is observed in large SEP events depends on nonlocal magnetic connections to shock sources. We discuss observations of the SEP-rich periods of **2010 August and 2012 July** in conjunction with ENLIL modeling. We find that much SEP activity can only be

understood in the light of such models, and in particular from knowing about both remote and local shock source connections. These results must be folded into the investigations of the physics underlying the longitudinal extent of SEP events, and the source connection versus diffusion pictures of interpretations of SEP events.

Observational Evidence of S-Web Source of the Slow Solar Wind

D. Baker, P. Demoulin, S.L. Yardley, T. Mihalescu, L. van Driel-Gesztelyi, et al.

ApJ 950:65 2023

<https://arxiv.org/pdf/2303.12192.pdf>

From 2022 March 18-21, active region (AR) 12967 was tracked simultaneously by Solar Orbiter (SO) at 0.35 au and Hinode/EIS at Earth. During this period, strong blue-shifted plasma upflows were observed along a thin, dark corridor of open field originating at the AR's leading polarity and continuing towards the southern extension of the northern polar coronal hole. A potential field source surface (PFSS) model shows large lateral expansion of the open magnetic field along the corridor. Squashing factor Q-maps of the large scale topology further confirm super-radial expansion in support of the S-Web theory for the slow wind. The thin corridor of upflows is identified as the source region of a slow solar wind stream characterised by approx. 300 km s⁻¹ velocities, low proton temperatures of approx. 5 eV, extremely high density over 100 cm⁻³, and a short interval of moderate Alfvénicity accompanied by switchback events. When connectivity changes from the corridor to the eastern side of the AR, the in situ plasma parameters of the slow wind indicate a distinctly different source region. These observations provide strong evidence that the narrow open field corridors, forming part of the S-Web, produce extreme properties in their associated solar wind streams.

Solar Orbiter science nuggets #11 2023 <https://www.cosmos.esa.int/web/solar-orbiter/-/observational-evidence-of-s-web-source-of-slow-solar-wind>

The Major Solar Eruptive Event in July 2012: Defining Extreme Space Weather Scenarios

Daniel Baker

Presentation at Space Weather Workshop in Boulder, April 8-11, 2014; File

http://www.swpc.noaa.gov/sww/SWW_Agenda_w_attached_presentations.pdf

A major solar eruptive event in July 2012: Defining extreme space weather scenarios

D. N. Baker, X. Li, A. Pulkkinen, C. M. Ngwira, M. L. Mays, A. B. Galvin and K. D. C. Simunac
Space Weather, Volume 11, Issue 10, pages 585–591, October 2013

<http://onlinelibrary.wiley.com/doi/10.1002/swe.20097/pdf>

A key goal for space weather studies is to define severe and extreme conditions that might plausibly afflict human technology. On 23 July 2012, solar active region 1520 (~141°W heliographic longitude) gave rise to a powerful coronal mass ejection (CME) with an initial speed that was determined to be 2500 ± 500 km/s. The eruption was directed away from Earth toward 125°W longitude. STEREO-A sensors detected the CME arrival only about 19 h later and made in situ measurements of the solar wind and interplanetary magnetic field. In this paper, we address the question of what would have happened if this powerful interplanetary event had been Earthward directed. Using a well-proven geomagnetic storm forecast model, we find that the 23–24 July event would certainly have produced a geomagnetic storm that was comparable to the largest events of the twentieth century (Dst ~ -500 nT). Using plausible assumptions about seasonal and time-of-day orientation of the Earth's magnetic dipole, the most extreme modeled value of storm-time disturbance would have been Dst = -1182 nT. This is considerably larger than estimates for the famous Carrington storm of 1859. This finding has far reaching implications because it demonstrates that extreme space weather conditions such as those during March of 1989 or September of 1859 can happen even during a modest solar activity cycle such as the one presently underway. We argue that this extreme event should immediately be employed by the space weather community to model severe space weather effects on technological systems such as the electric power grid.

Signatures of Interchange Reconnection: STEREO, ACE and Hinode Observations Combined

D. Baker¹, A. P. Rouillard^{2,3}, L. van Driel-Gesztelyi^{1,4,5}, P. D'émoulin⁴, L. K. Harra¹, B. Lavraud^{6,7}, J.A. Davies³, A. Opitz^{6,7}, J. G. Luhmann⁸, J.-A. Sauvaud^{6,7}, and A. B. Galvin⁹

E-print, Sept 2009; Ann. Geophys., 27, 3883–3897, 2009, File

Combining STEREO, ACE and Hinode observations has presented an opportunity to follow a filament eruption and coronal mass ejection (CME) on the 17th of October 2007 from an active region (AR) inside a coronal hole (CH) into the heliosphere. This particular combination of 'open' and closed magnetic topologies provides an ideal scenario for interchange reconnection to take place. With Hinode and STEREO data we were able to identify the emergence time and type of structure seen in the in-situ data four days later. On the 21st, ACE observed in-situ the passage of an ICME with 'open' magnetic topology. The magnetic field configuration of the source, a mature AR located inside an equatorial CH,

has important implications for the solar and interplanetary signatures of the eruption. We interpret the formation of an 'anemone' structure of the erupting AR and the passage in-situ of the ICME being disconnected at one leg, as manifested by uni-directional suprathermal electron flux in the ICME, to be a direct result of interchange reconnection between closed loops of the CME originating from the AR and 'open' field lines of the surrounding CH.

[Solar Dynamics and its Effects on the Heliosphere](#)

Baker, D.N., Klecker, B., Schwartz, S.J. (et al.) (Eds.)

Space Sciences Series of ISSI, Vol. 22, 2007, VIII, 372 p., 168 illus., 72 in colour,

Reprinted from **Space Science Reviews journal**, Vol. 124/1-4, 2006

Statistics of solar wind electron breakpoint energies using machine learning techniques

M. R. **Bakrania**¹, I. J. Rae¹, A. P. Walsh², D. Verscharen^{1,3}, A. W. Smith¹, T. Bloch⁴ and C. E. J. Watt⁴
A&A 639, A46 (2020)

<https://www.aanda.org/articles/aa/pdf/2020/07/aa37840-20.pdf>

Solar wind electron velocity distributions at 1 au consist of a thermal "core" population and two suprathermal populations: "halo" and "strahl". The core and halo are quasi-isotropic, whereas the strahl typically travels radially outwards along the parallel or anti-parallel direction with respect to the interplanetary magnetic field. Using Cluster-PEACE data, we analyse energy and pitch angle distributions and use machine learning techniques to provide robust classifications of these solar wind populations. Initially, we used unsupervised algorithms to classify halo and strahl differential energy flux distributions to allow us to calculate relative number densities, which are of the same order as previous results. Subsequently, we applied unsupervised algorithms to phase space density distributions over ten years to study the variation of halo and strahl breakpoint energies with solar wind parameters. In our statistical study, we find both halo and strahl suprathermal breakpoint energies display a significant increase with core temperature, with the halo exhibiting a more positive correlation than the strahl. We conclude low energy strahl electrons are scattering into the core at perpendicular pitch angles. This increases the number of Coulomb collisions and extends the perpendicular core population to higher energies, resulting in a larger difference between halo and strahl breakpoint energies at higher core temperatures. Statistically, the locations of both suprathermal breakpoint energies decrease with increasing solar wind speed. In the case of halo breakpoint energy, we observe two distinct profiles above and below 500 km s⁻¹. We relate this to the difference in origin of fast and slow solar wind.

Testing the estimated hypothetical response of a major CME impact on Earth and its implications to space weather

Ramkumar **Bala**, Patricia Reiff, C. T. Russell

JGR Volume 120, Issue 5 May 2015 Pages 3432–3443

The high-speed coronal mass ejection (CME), ejected on **23 July 2012**, observed by STEREO-A on the same day as the leading edge of the CME arrived at 1AU was unique both in respect to the observed plasma and magnetic structure and the large solar energetic particle flux that dynamically regulated the shock front. Because of its great intensity, it has been hailed as "Carrington 2" by some, warning that, had that CME been heading toward the Earth, it might have caused a major space weather event. We used the Rice Artificial Neural Network algorithms with the solar wind and interplanetary magnetic field parameters measured in situ by STEREO-A as inputs to infer what the "geoeffectiveness" of that storm might have been. We have also used an MHD model in Open Geospace General Circulation Model to understand the global magnetospheric process in time sequence. We presently show our neural network models of Kp and Dst on our real-time prediction site: <http://mms.rice.edu/realtime/forecast.html>. Running this event through our models showed that, in fact, this would have been an exceptional event. Our results show a prediction resulting in a Kp value of 8+, a Dst of nearly -250 nT, but when assumptions about maximum dipole angle tilt and density are made, predictions resulting in Kp of 11- and Dst dipping close to -700 nT are found. Finally, when solar energetic proton flux is included, the Kp and Dst predictions drop to 8- and ≈-625 nT, respectively.

Improvements in short-term forecasting of geomagnetic activity

Bala, Ramkumar; Reiff, Patricia

Space Weather, Vol. 10, No. 0, S06001, 2012

<http://dx.doi.org/10.1029/2012SW000779>

We have improved our space weather forecasting algorithms to now predict Dst and AE in addition to Kp for up to 6 h of forecast times. These predictions can be accessed in real time at <http://mms.rice.edu/realtime/forecast.html>. In

addition, in the event of an ongoing or imminent activity, e-mail “alerts” based on key discriminator levels have been going out to our subscribers since October 2003. The neural network–based algorithms utilize ACE data to generate full 1, 3, and 6 h ahead predictions of these indices from the Boyle index, an empirical approximation that estimates the Earth's polar cap potential using solar wind parameters. Our models yield correlation coefficients of over 0.88, 0.86, and 0.83 for 1 h predictions of Kp, Dst, and AE, respectively, and 0.86, 0.84, and 0.80 when predicting the same but 3 h ahead. Our 6 h ahead predictions, however, have slightly higher uncertainties. Furthermore, the paper also tests other solar wind functions—the Newell driver, the Borovsky control function, and adding solar wind pressure term to the Boyle index—for their ability to predict geomagnetic activity.

A scheme for forecasting severe space weather

N. **Balan**, Y. Ebihara, R. Skoug, K. Shiokawa, I. S. Batista, S. Tulasi Ram, Y. Omura, T. Nakamura, M.-C. Fok

JGR **2017** DOI: 10.1002/2016JA023853

<http://sci-hub.cc/doi/10.1002/2016JA023853>

A scheme is suggested and tested for forecasting severe space weather (SvSW) using solar wind velocity (V) and the north-south component (Bz) of the interplanetary magnetic field (IMF) measured using the ACE (Advanced Composition Explorer) satellite from 1998 to 2016. SvSW has caused all known electric power outages and telegraph system failures. Earlier SvSW events such as the Carrington event of 1859, Quebec event of 1989 and an event in 1958 are included with information from the literature. Dst storms are used as references to identify 89 major space weather events ($Dst_{Min} \leq -100$ nT) in 1998–2016. The coincidence of high CME front (or CME shock) velocity ΔV (sudden increase in V over the background by over 275 km/s) and sufficiently large Bz southward at the time of the ΔV increase is associated with SvSW; and their product ($\Delta V \times Bz$) is found to exhibit a large negative spike at the speed increase. Such a product ($\Delta V \times Bz$) exceeding a threshold seems suitable for forecasting SvSW. However, the coincidence of high V (not containing ΔV) and large Bz southward does not correspond to SvSW, indicating the importance of the impulsive action of large Bz southward and high ΔV coming through when they coincide. The need for the coincidence is verified using the CRCM (Comprehensive Ring Current Model) model, that produces extreme Dst storms ($\langle Dst_{MP} \rangle < -250$ nT) characterizing SvSW when there is coincidence. **15–16 July 2000, 30–31 March 2001, 03–26 November 2001, 26 Oct–25 Nov 2003, 30–31 October 2003,**

CME front and severe space weather

N. **Balan**^{1,2,6,*}, R. Skoug³, S. Tulasi Ram⁴, P. K. Rajesh², K. Shiokawa¹, Y. Otsuka¹, I. S. Batista⁵, Y. Ebihara⁶ and T. Nakamura⁷

JGR, Volume 119, Issue 12, pages 10041–10058, December **2014**

<http://onlinelibrary.wiley.com/doi/10.1002/2014JA020151/pdf>

Thanks to the work of a number of scientists it is known that severe space weather can cause extensive social and economic disruptions in the modern high-tech society. It is therefore important to understand what determines the severity of space weather, and whether it can be predicted. We present results obtained from the analysis of coronal mass ejections (CME), solar energetic particle (SEP) events, interplanetary magnetic field (IMF), CME-magnetosphere coupling and geomagnetic storms associated with the major space weather events since 1998 by combining data from the ACE and GOES satellites with geomagnetic parameters, and the Carrington event of 1859, the Quebec event of 1989, and an event in 1958. The results seem to indicate that (1) it is the impulsive energy mainly due to the impulsive velocity and orientation of IMF Bz at the leading edge of the CMEs (or CME front) that determine the severity of space weather. (2) CMEs having high impulsive velocity (sudden non-fluctuating increase by over 275 km s⁻¹ over the background) caused severe space weather (SvSW) in the heliosphere (failure of the SWI mode of SWEPAM in ACE) probably by suddenly accelerating the high energy particles in the SEPs ahead directly or through the shocks. (3) The impact of such CMEs which also show the IMF Bz southward from the leading edge caused SvSW at the Earth including extreme geomagnetic storms of mean $Dst_{MP} < -250$ nT during main phases; and the known electric power outages happened during some of these SvSW events. (4) The higher the impulsive velocity, the more severe the space weather, like faster weather fronts and tsunami fronts causing more severe damage through impulsive action. (5) The CMEs having IMF Bz northward at the leading edge do not seem to cause SvSW on Earth though, later when the IMF Bz turns southward, they can lead to super geomagnetic storms of intensity (Dst_{Min}) less than even -400 nT.

Table 1. Characteristics of the Geomagnetic Storms Associated With 13 Major Space Weather Events Since 1998 and the Carrington Event of September 1959, the Quebec Event of March 1989, and an Event in February

Complex Systems Methods Characterizing Nonlinear Processes in the Near-Earth Electromagnetic Environment: Recent Advances and Open Challenges

Review

Georgios **Balasis**, [Michael A. Balikhin](#), [Sandra C. Chapman](#), [Giuseppe Consolini](#), +++
[Space Science Reviews](#) volume 219, Article number: 38 (2023)
<https://link.springer.com/content/pdf/10.1007/s11214-023-00979-7.pdf>

Learning from successful applications of methods originating in statistical mechanics, complex systems science, or information theory in one scientific field (e.g., atmospheric physics or climatology) can provide important insights or conceptual ideas for other areas (e.g., space sciences) or even stimulate new research questions and approaches. For instance, quantification and attribution of dynamical complexity in output time series of nonlinear dynamical systems is a key challenge across scientific disciplines. Especially in the field of space physics, an early and accurate detection of characteristic dissimilarity between normal and abnormal states (e.g., pre-storm activity vs. magnetic storms) has the potential to vastly improve space weather diagnosis and, consequently, the mitigation of space weather hazards. This review provides a systematic overview on existing nonlinear dynamical systems-based methodologies along with key results of their previous applications in a space physics context, which particularly illustrates how complementary modern complex systems approaches have recently shaped our understanding of nonlinear magnetospheric variability. The rising number of corresponding studies demonstrates that the multiplicity of nonlinear time series analysis methods developed during the last decades offers great potentials for uncovering relevant yet complex processes interlinking different geospace subsystems, variables and spatiotemporal scales. **16 March 1997**

Universality in solar flare, magnetic storm and earthquake dynamics using Tsallis statistical mechanics

G. **Balasis**, I. A. Daglis, A. Anastasiadis, C. Papadimitriou, M. Mandea, K. Eftaxias
E-print, Sept 2010; Accepted for publication in : *Physica A* (2010)

The universal character of the dynamics of various extreme phenomena is an outstanding scientific challenge. We show that X-ray flux and Dst time series during powerful solar flares and intense magnetic storms, respectively, obey a nonextensive energy distribution function for earthquake dynamics with similar values for the Tsallis entropic index q . Thus, evidence for universality in solar flares, magnetic storms and earthquakes arise naturally in the framework of Tsallis statistical mechanics. The observed similarity suggests a common approach to the interpretation of these diverse phenomena in terms of driving physical mechanisms that have the same character.

A solar source of Alfvénic magnetic field switchbacks: *in situ* remnants of magnetic funnels on supergranulation scales

S. D. **Bale**, [T. S. Horbury](#), [M. Velli](#), [M. I. Desai](#), [J. S. Halekas](#), [M. D. McManus](#), [O. Panasenco](#), [S. T. Badman](#), [T. A. Bowen](#), [B. D. G. Chandran](#), [J. F. Drake](#), [J. C. Kasper](#), [R. Laker](#), [A. Mallet](#), [L. Matteini](#), [T. D. Phan](#), [N. E. Raouafi](#), [J. Squire](#), [L. D. Woodham](#), [T. Wooley](#)

ApJ **923** 174 **2021**

<https://arxiv.org/pdf/2109.01069.pdf>

<https://doi.org/10.3847/1538-4357/ac2d8c>

One of the striking observations from the Parker Solar Probe (PSP) spacecraft is the prevalence in the inner heliosphere of large amplitude, Alfvénic magnetic field reversals termed 'switchbacks'. These $\delta B/B \sim O(1)$ fluctuations occur on a range of timescales and in *in situ* patches separated by intervals of quiet, radial magnetic field. We use measurements from PSP to demonstrate that patches of switchbacks are localized within the extensions of plasma structures originating at the base of the corona. These structures are characterized by an increase in alpha particle abundance, Mach number, plasma β and pressure, and by depletions in the magnetic field magnitude and electron temperature. These intervals are in pressure-balance, implying stationary spatial structure, and the field depressions are consistent with overexpanded flux tubes. The structures are asymmetric in Carrington longitude with a steeper leading edge and a small ($\sim 1^\circ$) edge of hotter plasma and enhanced magnetic field fluctuations. Some structures contain suprathermal ions to ~ 85 keV that we argue are the energetic tail of the solar wind alpha population. The structures are separated in longitude by angular scales associated with supergranulation. This suggests that these switchbacks originate near the leading edge of the diverging magnetic field funnels associated with the network magnetic field - the primary wind sources. We propose an origin of the magnetic field switchbacks, hot plasma and suprathermals, alpha particles in interchange reconnection events just above the solar transition region and our measurements represent the extended regions of a turbulent outflow exhaust. **27 Sep 2020**

Highly structured slow solar wind emerging from an equatorial coronal hole

S. D. **Bale**, [S. T. Badman](#), [J. R. Wygant](#)

[Nature](#) volume 576, pages237–242 (2019)

<https://www.nature.com/articles/s41586-019-1818-7.pdf>

During the solar minimum, when the Sun is at its least active, the solar wind^{1,2} is observed at high latitudes as a predominantly fast (more than 500 kilometres per second), highly Alfvénic rarefied stream of plasma originating from deep within coronal holes. Closer to the ecliptic plane, the solar wind is interspersed with a more variable slow wind³ of less than 500 kilometres per second. The precise origins of the slow wind streams are less certain⁴; theories and observations suggest that they may originate at the tips of helmet streamers^{5,6}, from interchange reconnection near coronal hole boundaries^{7,8}, or within coronal holes with highly diverging magnetic fields^{9,10}. The heating mechanism required to drive the solar wind is also unresolved, although candidate mechanisms include Alfvén-wave turbulence^{11,12}, heating by reconnection in nanoflares¹³, ion cyclotron wave heating¹⁴ and acceleration by thermal gradients¹. At a distance of one astronomical unit, the wind is mixed and evolved, and therefore much of the diagnostic structure of these sources and processes has been lost. Here we present observations from the **Parker Solar Probe**¹⁵ at 36 to 54 solar radii that show evidence of slow Alfvénic solar wind emerging from a small equatorial coronal hole. The measured magnetic field exhibits patches of large, intermittent reversals that are associated with jets of plasma and enhanced Poynting flux and that are interspersed in a smoother and less turbulent flow with a near-radial magnetic field. Furthermore, plasma-wave measurements suggest the existence of electron and ion velocity-space micro-instabilities^{10,16} that are associated with plasma heating and thermalization processes. Our measurements suggest that there is an impulsive mechanism associated with solar-wind energization and that micro-instabilities play a part in heating, and we provide evidence that low-latitude coronal holes are a key source of the slow solar wind.

The FIELDS instrument suite for solar Probe plus. Measuring the coronal plasma and magnetic field, plasma waves and turbulence, and Radio signatures of solar transients.

Bale, S. D., Goetz, K., Harvey, P. R., Turin, P., Bonnell, J. W., Dudok de Wit, T., et al.

(2016). *Space Sci. Rev.* 204, 49–82.

doi:10.1007/s11214-016-0244-5

NASA's Solar Probe Plus (SPP) mission will make the first in situ measurements of the solar corona and the birthplace of the solar wind. The FIELDS instrument suite on SPP will make direct measurements of electric and magnetic fields, the properties of in situ plasma waves, electron density and temperature profiles, and interplanetary radio emissions, amongst other things. Here, we describe the scientific objectives targeted by the SPP/FIELDS instrument, the instrument design itself, and the instrument concept of operations and planned data products.

Sub-Alfvénic Solar Wind Observed by the Parker Solar Probe: Characterization of Turbulence, Anisotropy, Intermittency, and Switchback

R. **Bandyopadhyay**¹, W. H. Matthaeus^{2,3}, D. J. McComas¹, R. Chhiber^{2,4}, A. V. Usmanov^{2,4}, J.

Huang⁵, R. Livi⁶, D. E. Larson⁶, J. C. Kasper^{5,7}, A. W. Case⁸Show full author list

2022 *ApJL* 926 L1

<https://iopscience.iop.org/article/10.3847/2041-8213/ac4a5c/pdf>

In the lower solar coronal regions where the magnetic field is dominant, the Alfvén speed is much higher than the wind speed. In contrast, the near-Earth solar wind is strongly super-Alfvénic, i.e., the wind speed greatly exceeds the Alfvén speed. The transition between these regimes is classically described as the "Alfvén point" but may in fact occur in a distributed Alfvén critical region. NASA's Parker Solar Probe (PSP) mission has entered this region, as it follows a series of orbits that gradually approach more closely to the Sun. During its 8th and 9th solar encounters, at a distance of $\approx 16 R_{\odot}$ from the Sun, PSP sampled four extended periods in which the solar wind speed was measured to be smaller than the local Alfvén speed. These are the first in situ detections of sub-Alfvénic solar wind in the inner heliosphere by PSP. Here we explore properties of these samples of sub-Alfvénic solar wind, which may provide important previews of the physical processes operating at lower altitude. Specifically, we characterize the turbulence, anisotropy, intermittency, and directional switchback properties of these sub-Alfvénic winds and contrast these with the neighboring super-Alfvénic periods.

Geometry of Magnetic Fluctuations near the Sun from PSP

Riddhi **Bandyopadhyay**, [David J. McComas](#)

ApJ 2021

<https://arxiv.org/ftp/arxiv/papers/2110/2110.14756.pdf>

Solar wind magnetic fluctuations exhibit anisotropy due to the presence of a mean magnetic field in the form of the Parker spiral. Close to the Sun, direct measurements were not available until the recently launched Parker Solar Probe (PSP) mission. The nature of anisotropy and geometry of the magnetic fluctuations play a fundamental role in

dissipation processes and in the transport of energetic particles in space. Using PSP data, we present measurements of geometry and anisotropy of the inner heliosphere magnetic fluctuations, from fluid to kinetic scales. The results are surprising and different from 1 au observations. We find that fluctuations evolve characteristically with size scale. However, unlike 1 au solar wind, at the outer scale, the fluctuations are dominated by wavevectors quasi-parallel to the local magnetic field. In the inertial range, average wave vectors become less field-aligned, but still remain more field aligned than near-Earth solar wind. In the dissipation range, the wavevectors become almost perpendicular to the local magnetic field in the dissipation range, to a much higher degree than those indicated by 1 au observations. We propose that this reduced degree of anisotropy in the outer scale and inertial range is due to the nature of large-scale forcing outside the solar corona.

Observations of Energetic-particle Population Enhancements along Intermittent Structures near the Sun from the Parker Solar Probe

Riddhi [Bandyopadhyay](#)¹, W. H. Matthaeus^{1,2}, T. N. Parashar^{1,2}, R. Chhiber^{1,3}, D. Ruffolo⁴, M. L. Goldstein^{3,5}, B. A. Maruca^{1,2}, A. Chasapis⁶, R. Qudsi¹, D. J. McComas⁷Show full author list
2020 ApJS 246 61

<https://doi.org/10.3847/1538-4365/ab6220>

Observations at 1 au have confirmed that enhancements in measured energetic-particle (EP) fluxes are statistically associated with "rough" magnetic fields, i.e., fields with atypically large spatial derivatives or increments, as measured by the Partial Variance of Increments (PVI) method. One way to interpret this observation is as an association of the EPs with trapping or channeling within magnetic flux tubes, possibly near their boundaries. However, it remains unclear whether this association is a transport or local effect; i.e., the particles might have been energized at a distant location, perhaps by shocks or reconnection, or they might experience local energization or re-acceleration. The Parker Solar Probe (PSP), even in its first two orbits, offers a unique opportunity to study this statistical correlation closer to the corona. As a first step, we analyze the separate correlation properties of the EPs measured by the Integrated Science Investigation of the Sun (IS \odot IS) instruments during the first solar encounter. The distribution of time intervals between a specific type of event, i.e., the waiting time, can indicate the nature of the underlying process. We find that the IS \odot IS observations show a power-law distribution of waiting times, indicating a correlated (non-Poisson) distribution. Analysis of low-energy ($\sim 15 - 200$ keV/nuc) IS \odot IS data suggests that the results are consistent with the 1 au studies, although we find hints of some unexpected behavior. A more complete understanding of these statistical distributions will provide valuable insights into the origin and propagation of solar EPs, a picture that should become clear with future PSP orbits.

Enhanced Energy Transfer Rate in Solar Wind Turbulence Observed near the Sun from Parker Solar Probe

Riddhi [Bandyopadhyay](#), [M. L. Goldstein](#), [B. A. Maruca](#), [W. H. Matthaeus](#), [T. N. Parashar](#), [D. Ruffolo](#), [R. Chhiber](#), [A. Usmanov](#), [A. Chasapis](#), [R. Qudsi](#), [Stuart D. Bale](#), [J. W. Bonnell](#), [Thierry Dudok de Wit](#), [Keith Goetz](#), [Peter R. Harvey](#), [Robert J. MacDowall](#), [David M. Malaspina](#), [Marc Pulupa](#), [J.C. Kasper](#), [K.E. Korreck](#), [A. W. Case](#), [M. Stevens](#), [P. Whittlesey](#), [D. Larson](#), [R. Livu](#), [K.G. Klein](#), [M. Velli](#), [N. Raouafi](#)
Astrophysical Journal Supplement, PSP special issue **2020**

<https://arxiv.org/pdf/1912.02959.pdf>

Direct evidence of an inertial-range turbulent energy cascade has been provided by spacecraft observations in heliospheric plasmas. In the solar wind, the average value of the derived heating rate near 1 au is $\sim 103 \text{ J kg}^{-1} \text{ s}^{-1}$, an amount sufficient to account for observed departures from adiabatic expansion. Parker Solar Probe (PSP), even during its first solar encounter, offers the first opportunity to compute, in a similar fashion, a fluid-scale energy decay rate, much closer to the solar corona than any prior in-situ observations. Using the Politano-Pouquet third-order law and the von Kármán decay law, we estimate the fluid-range energy transfer rate in the inner heliosphere, at heliocentric distance R ranging from $54R_{\odot}$ (0.25 au) to $36R_{\odot}$ (0.17 au). The energy transfer rate obtained near the first perihelion is about 100 times higher than the average value at 1 au. This dramatic increase in the heating rate is unprecedented in previous solar wind observations, including those from Helios, and the values are close to those obtained in the shocked plasma inside the terrestrial magnetosheath.

Tracking Cosmic-Ray Spectral Variation during 2007–2018 Using Neutron Monitor Time-delay Measurements

C. [Banglieng](#)^{1,2}, H. Jantaloet¹, D. Ruffolo^{1,2}, A. Sáiz¹, W. Mitthumsiri¹, P. Muangha^{1,2}, P. Evenson³, T. Nataro⁴, R. Pyle⁵, S. Seunarine⁶Show full author list

2020 ApJ 890 21

<https://doi.org/10.3847/1538-4357/ab6661>

The energy spectrum of Galactic cosmic-ray (GCR) ions at Earth varies with solar activity as these ions cross the heliosphere. Thus, this "solar modulation" of GCRs provides remote sensing of heliospheric conditions throughout the ~11 yr sunspot cycle and ~22 yr solar magnetic cycle. A neutron monitor (NM) is a stable ground-based detector that measures cosmic-ray rate variations above a geomagnetic or atmospheric cutoff rigidity with high precision (~0.1%) over such timescales. Furthermore, we developed electronics and analysis techniques to indicate variations in the cosmic-ray spectral index using neutron time-delay data from a single station. Here we study solar modulation using neutron time-delay histograms from two high-altitude NM stations: (1) the Princess Sirindhorn Neutron Monitor at Doi Inthanon, Thailand, with the world's highest vertical geomagnetic cutoff rigidity, 16.7 GV, from 2007 December to 2018 April; and (2) the South Pole NM, with an atmosphere-limited cutoff of ~1 GV, from 2013 December to 2018 April. From these histograms, we extract the leader fraction L , i.e., inverse neutron multiplicity, as a proxy of a GCR spectral index above the cutoff. After correction for pressure and precipitable water vapor variations, we find that L roughly correlates with the count rate but also exhibits hysteresis, implying a change in spectral shape after a solar magnetic polarity reversal. Spectral variations due to Forbush decreases, 27 day variations, and a ground-level enhancement are also indicated. These methods enhance the high-precision GCR spectral information from the worldwide NM network and extend it to higher rigidity.

Multi spacecraft study with the Icarus model: Modelling the propagation of CMEs to Mercury and Earth

Tinatín [Baratashvili](#), [Benjamin Grison](#), [Brigitte Schmieder](#), [Pascal Demoulin](#), [Stefaan Poedts](#)

A&A 689, 98 2024

<https://arxiv.org/pdf/2405.17988>

<https://doi.org/10.1051/0004-6361/202450430>

<https://www.aanda.org/articles/aa/pdf/2024/09/aa50430-24.pdf>

Coronal Mass Ejections (CMEs) are the main drivers of the disturbances in interplanetary space. Understanding the CME interior magnetic structure is crucial for advancing space weather studies. Assessing the capabilities of a numerical heliospheric model is crucial, as understanding the nature and extent of its limitations can be used for improving the model and the space weather predictions based on it. The present paper aims to test the capabilities of the recently developed heliospheric model Icarus and the linear force-free spheromak model that has been implemented in it.

To validate the Icarus space weather modeling tool, two CME events were selected that were observed by two spacecraft located near Mercury and Earth, respectively. This enables testing the heliospheric model computed with Icarus at two distant locations. The source regions for the CMEs were identified, and the CME parameters were determined and later optimized. Different adaptive mesh refinement levels were applied in the simulations to assess its performance by comparing the simulation results to in-situ measurements.

The first CME event erupted on SOL2013-07-09T15:24. The modeled time series were in good agreement with the observations both at MESSENGER and ACE. The second CME event started on SOL2014-02-16T10:24 and was more complicated, as three CME interactions occurred in this event. It was impossible to recover the observed profiles without modeling the other two CMEs that were observed, one before the main CME and one afterward. For both CME studies, AMR level 3 was sufficient to reconstruct small-scale features near Mercury, while at Earth, AMR level 4 was necessary due to the radially stretched grid that was used.

The effect of AMR and grid stretching on the magnetized CME model in Icarus

[Baratashvili](#) Tinatín, [Poedts Stefaan](#)

A&A 2024

<https://arxiv.org/pdf/2401.02504.pdf>

Context. Coronal mass ejections (CMEs) are the main driver of solar wind disturbances near Earth. When directed towards us, the internal magnetic field of the CME can interact with the Earth's magnetic field and cause geomagnetic storms. In order to better predict and avoid damage coming from such events, the optimized heliospheric model Icarus has been implemented. Aims. The impact of a CME at Earth is greatly affected by its internal magnetic field structure. The aim of this work is to enable modelling the evolution of the magnetic field configuration of the CME throughout its

propagation in Icarus. The focus of the study is on the global magnetic structure of the CME and its evolution and interaction with the solar wind. **Methods.** The magnetized CME model that is implemented in Icarus is the Linear Force-Free Spheromak and is imported from EUHFORIA. Advanced techniques, such as grid stretching and AMR are applied. Different AMR levels are applied in order to obtain high resolution locally, where needed. The results of all the simulations are compared in detail and the wall-clock times of the simulations are provided. **Results.** The results from the performed simulations are analyzed. The arrival time is better approximated by the EUHFORIA simulation, with the CME shock arriving 1.6 and 1.09 hours later than in the AMR level 4 and 5 simulations, respectively. The profile features and variable strengths are best modelled by Icarus simulations with AMR level 4 and 5. **Conclusions.** The arrival time is closer to the observed time in the EUHFORIA simulation, but the profiles of the different variables show more features and details in the Icarus simulations. Considering the small difference in the modelled results, and the large difference in computational resources, the AMR level 4 simulation is considered to have performed the best. **July 12, 2012**

Exploring the effects of numerical methods and slope limiters in heliospheric modeling

Tinatini [Baratashvili](#), [Christine Verbeke](#), [Rony Keppens](#), [Stefaan Poedts](#)

Sun and Geosphere **2023**

<https://arxiv.org/ftp/arxiv/papers/2305/2305.14905.pdf>

Coronal mass ejections (CMEs) are large eruptions close to the solar surface, where plasma is ejected outwards into space at large speeds. When directed towards Earth, they interfere with Earth's magnetic fields and cause strong geoeffective storms. In order to mitigate the potential damage, forecasting tools are implemented. Recently, a novel heliospheric modelling tool, Icarus, has been implemented, which exploits the open-source framework MPI-AMRVAC as its core MHD solver. This new model efficiently performs 3D MHD simulations of the solar wind and the evolution of interplanetary CMEs with the help of advanced techniques, such as adaptive mesh refinement and gradual radial grid stretching. The numerical methods applied in the simulations can have significant effects on the simulation results and on the efficiency of the model. In this study, the effect of different combinations of numerical schemes and slope limiters, for reconstructing edge-based variables used in fluxes, is considered. We explore frequently exploited combinations from the available numerical schemes in MPI-AMRVAC: TVDLF, HLL and HLLC along with the slope limiters 'woodward', 'minmod', 'vanleer', and 'koren'. For analysis purposes, we selected one particular solar wind configuration and studied the influence on variables at 1 AU in the equatorial plane. The goal is to find the optimal combination to produce accurate results fast and in a robust way so that the model can be reliable for day-to-day use by space weather scientists. As a conclusion, the best result assessed with these two criteria is the combination of the TVDLF scheme with the 'woodward' limiter.

Improving CME evolution and arrival predictions with AMR and grid stretching in Icarus

T. [Baratashvili](#)1, C. Verbeke1,2, N. Wijzen1 and S. Poedts1,3

A&A 667, A133 (2022)

<https://www.aanda.org/articles/aa/pdf/2022/11/aa44111-22.pdf>

Context. Coronal mass ejections (CMEs) are one of the main drivers of disturbances in interplanetary space. Strong CMEs, when directed towards the Earth, cause geomagnetic storms upon interacting with the Earth's magnetic field, and can cause significant damage to our planet and affect everyday life. As such, efficient space weather prediction tools are necessary to forecast the arrival and impact of CME eruptions. Recently, a new heliospheric model called Icarus was developed based on MPI-AMRVAC, which is a 3D ideal magnetohydrodynamics model for the solar wind and CME propagation, and it introduces advanced numerical techniques to make the simulations more efficient. In this model the reference frame is chosen to be co-rotating with the Sun, and radial grid stretching together with adaptive mesh refinement (AMR) can be applied to the numerical domain.

Aims. Grid stretching and AMR speed up simulation results and performance. Our aim is to combine the advanced techniques available in the Icarus model in order to obtain better results with fewer computational resources than with the equidistant grid. Different AMR strategies are suggested, depending on the purpose of the simulation.

Methods. In this study, we model the CME event that occurred on **July 12, 2012**. A cone model was used to study the CME's evolution through the background solar wind, and its arrival at and impact with the Earth. Grid stretching and AMR were combined in the simulations by using multiple refinement criteria, to assess its influence on the simulations' accuracy and the required computational resources. We compare simulation results to the EUHFORIA model.

Results. We applied different refinement criteria to investigate the potential of solution AMR for different applications. As a result, the simulations were sped up by a factor of ~ 17 for the most optimal configuration in Icarus. For the cone CME model, we found that limiting the AMR to the region around the CME-driven shock yields the best results. The results modelled by the simulations with radial grid stretching and AMR level 4 are similar to the results provided by the

original EUHFORIA and Icarus simulations with the ‘standard’ resolution and equidistant grids. The simulations with 5 AMR levels yielded better results than the simulations with an equidistant grid and standard resolution. Conclusions. Solution AMR is flexible and provides the user the freedom to modify and locally increase the grid resolution according to the purpose of the simulation. We find that simulations with a combination of grid stretching and AMR can reproduce the simulations performed on equidistant grids significantly faster. The advanced techniques implemented in Icarus can be further used to improve the forecasting procedures, since the reduced simulation time is essential to make physics-based forecasts less computationally expensive. **July 12-15, 2012**

Slow solar wind sources

High-resolution observations with a quadrature view★

Krzysztof [Barczynski](#)^{1,2}, Louise Harra^{2,1}, Conrad Schwanitz^{1,2}, Nils Janitzek^{1,2}, David Berghmans³, Frédéric Auchère⁴, +++
A&A 673, A74 (2023)

Context. The origin of the slow solar wind is still an open issue. One possibility that has been suggested is that upflows at the edge of an active region can contribute to the slow solar wind.

Aims. We aim to explain how the plasma upflows are generated, which mechanisms are responsible for them, and what the upflow region topology looks like.

Methods. We investigated an upflow region using imaging data with the unprecedented temporal (3 s) and spatial (2 pixels = 236 km) resolution that were obtained on 30 March 2022 with the 174 Å channel of the Extreme-Ultraviolet Imager (EUI)/High Resolution Imager (HRI) on board Solar Orbiter. During this time, the EUI and Earth-orbiting satellites (Solar Dynamics Observatory, Hinode, and the Interface Region Imaging Spectrograph, IRIS) were located in quadrature (~92°), which provides a stereoscopic view with high resolution. We used the Hinode/EIS (Fe XII) spectroscopic data to find coronal upflow regions in the active region. The IRIS slit-jaw imager provides a high-resolution view of the transition region and chromosphere.

Results. For the first time, we have data that provide a quadrature view of a coronal upflow region with high spatial resolution. We found extended loops rooted in a coronal upflow region. Plasma upflows at the footpoints of extended loops determined spectroscopically through the Doppler shift are similar to the apparent upward motions seen through imaging in quadrature. The dynamics of small-scale structures in the upflow region can be used to identify two mechanisms of the plasma upflow: Mechanism I is reconnection of the hot coronal loops with open magnetic field lines in the solar corona, and mechanism II is reconnection of the small chromospheric loops with open magnetic field lines in the chromosphere or transition region. We identified the locations in which mechanisms I and II work.

A comparison of the active region upflow and core properties using simultaneous spectroscopic observations from IRIS and Hinode

[Krzysztof Barczynski](#), [Louise Harra](#), [Lucia Kleint](#), [Brandon Panos](#), [David H. Brooks](#)

A&A 2021

<https://arxiv.org/pdf/2104.10234.pdf>

The origin of the slow solar wind is still an open issue. It has been suggested that upflows at the edge of active regions (AR) can contribute to the slow solar wind. Here, we compared the upflow region and the AR core and studied how the plasma properties change from the chromosphere via the transition region to the corona. We studied limb-to-limb observations NOAA 12687 (14th - 25th Nov 2017). We analysed spectroscopic data simultaneously obtained from IRIS and Hinode/EIS in six spectral lines. We studied the mutual relationships between the plasma properties for each emission line, as well as comparing the plasma properties between the neighbouring formation temperature lines. To find the most characteristic spectra, we classified the spectra in each wavelength using the machine learning technique k-means. We found that in the upflow region the Doppler velocities of the coronal lines are strongly correlated, but the transition region and coronal lines show no correlation. However, their fluxes are strongly correlated. The upflow region has lower density and lower temperature than the AR core. In the upflow region, the Doppler and non-thermal velocity show a strong correlation in the coronal lines, but the correlation is not seen in the AR core. At the boundary between the upflow region and the AR core, the upflow region shows an increase in the coronal non-thermal velocity, the emission obtained from the DEM, and the domination of the redshifted regions in the chromosphere. The obtained results suggest that at least three parallel mechanisms generate the plasma upflow: (1) the reconnection between closed loops and open magnetic field lines in the lower corona or upper chromosphere; (2) the reconnection between the chromospheric small-scale loops and open magnetic field; (3) the expansion of the magnetic field lines that allows the chromospheric plasma to escape to the solar corona.

Periodic behaviour of coronal mass ejections, eruptive events, and solar activity proxies during solar cycles 23 and 24

Tatiana [Barlyaeva](#) [JulienWojak](#) [PhilippeLamy](#) [BriceBoclet](#) [ImreToth](#)

[Journal of Atmospheric and Solar-Terrestrial Physics](#)

Volume 177, October 2018, Pages 12-28

<http://sci-hub.tw/10.1016/j.jastp.2018.05.012>

We report on the parallel analysis of the periodic behaviour of [coronal mass ejections](#) (CMEs) based on 21 years [1996–2016] of observations with the SOHO/LASCO–C2 coronagraph, [solar flares](#), prominences, and several proxies of [solar activity](#). We consider values of the rates globally and whenever possible, distinguish solar hemispheres and [solar cycles](#) 23 and 24. Periodicities are investigated using both frequency (periodogram) and time-frequency (wavelet) analysis. We find that these different processes, in addition to following the ≈ 11 -year Solar Cycle, exhibit diverse statistically significant oscillations with [properties common](#) to all solar, coronal, and heliospheric processes: variable periodicity, intermittence, asymmetric development in the northern and southern solar hemispheres, and largest amplitudes during the maximum phase of solar cycles, being more pronounced during solar cycle 23 than the weaker cycle 24. However, our analysis reveals an extremely complex and diverse situation. For instance, there exists very limited commonality for periods of less than one year. The few exceptions are the periods of 3.1–3.2 months found in the global occurrence rates of CMEs and in the [sunspot](#) area (SSA) and those of 5.9–6.1 months found in the northern hemisphere. Mid-range periods of ≈ 1 and ≈ 2 years are more wide spread among the studied processes, but exhibit a very distinct behaviour with the first one being present only in the northern hemisphere and the second one only in the [southern hemisphere](#). These periodic behaviours likely results from the complexity of the underlying physical processes, prominently the emergence of [magnetic flux](#).

SIR-HUXt -- a particle filter data assimilation scheme for assimilating CME time-elongation profiles

Luke [Barnard](#), [Mathew Owens](#), [Chris Scott](#), [Matthew Lang](#), [Mike Lockwood](#)

Space Weather Volume 21, Issue 6, June 2023 e2023SW003487

<https://arxiv.org/pdf/2210.02122.pdf>

<https://doi.org/10.1029/2023SW003487>

<https://agupubs.onlinelibrary.wiley.com/doi/epdf/10.1029/2023SW003487>

We present the development of SIR-HUXt, the integration of a sequential importance resampling (SIR) data assimilation scheme with the HUXt solar wind model. SIR-HUXt is designed to assimilate the time-elongation profiles of CME fronts in the low heliosphere, such as those typically extracted from heliospheric imager data returned by the STEREO, Parker Solar Probe, and Solar Orbiter missions. We use Observing System Simulation Experiments to explore the performance of SIR-HUXt for a simple synthetic CME scenario of a fully Earth directed CME flowing through a uniform ambient solar wind, where the CME is initialised with the average observed CME speed and width. These experiments are performed for a range of observer locations, from 20 deg to 90 deg behind Earth, spanning the L5 point where ESA's future Vigil space weather monitor will return heliospheric imager data for operational space weather forecasting.

We show that SIR-HUXt performs well at constraining the CME speed, and has some success at constraining the CME longitude. The CME width is largely unconstrained by the SIR-HUXt assimilations, and more experiments are required to determine if this is due to this specific CME scenario, or is a general feature of assimilating time-elongation profiles. Rank-histograms suggest that the SIR-HUXt ensembles are well calibrated, with no clear indications of bias or under/over dispersion. Improved constraints on the initial CME speed lead directly to improvements in the CME transit time to Earth and arrival speed. For an observer in the L5 region, SIR-HUXt returned a 69% reduction in the CME transit time uncertainty, and a 63% reduction in the arrival speed uncertainty. This suggests SIR-HUXt has potential to improve the real-world representivity of HUXt simulations, and therefore has potential to reduce the uncertainty of CME arrival time hindcasts and forecasts.

Quantifying the uncertainty in CME kinematics derived from geometric modelling of Heliospheric Imager data

L. [Barnard](#), [M. J. Owens](#), [C. J. Scott](#), [M. Lockwood](#), [C. A. de Koning](#), [T. Amerstorfer](#), [J. Hinterreiter](#), [C. Möstl](#), [J. A. Davies](#), [P. Riley](#)

Space Weather [Volume 20, Issue 1](#) e 2021SW002841 2022

<https://arxiv.org/pdf/2111.13337>

<https://agupubs.onlinelibrary.wiley.com/doi/epdf/10.1029/2021SW002841>

<https://doi.org/10.1029/2021SW002841>

Geometric modelling of Coronal Mass Ejections (CMEs) is a widely used tool for assessing their kinematic evolution. Furthermore, techniques based on geometric modelling, such as ELEvoHI, are being developed into forecast tools for space weather prediction. These models assume that solar wind structure does not affect the evolution of the CME, which is an unquantified source of uncertainty. We use a large number of Cone CME simulations with the HUXt solar wind model to quantify the scale of uncertainty introduced into geometric modelling and the ELEvoHI CME arrival times by solar wind structure. We produce a database of simulations, representing an average, a fast, and an extreme CME scenario, each independently propagating through 100 different ambient solar wind environments. Synthetic heliospheric imager observations of these simulations are then used with a range of geometric models to estimate the CME kinematics. The errors of geometric modelling depend on the location of the observer, but do not seem to depend on the CME scenario. In general, geometric models are biased towards predicting CME apex distances that are larger than the true value. For these CME scenarios, geometric modelling errors are minimised for an observer in the L5 region. Furthermore, geometric modelling errors increase with the level of solar wind structure in the path of the CME. The ELEvoHI arrival time errors are minimised for an observer in the L5 region, with mean absolute arrival time errors of 8.2 ± 1.2 h, 8.3 ± 1.0 h, and 5.8 ± 0.9 h for the average, fast, and extreme CME scenarios.

Extracting Inner-Heliosphere Solar Wind Speed Information From Heliospheric Imager Observations

L. A. [Barnard](#), [M. J. Owens](#), [C. J. Scott](#), [S. R. Jones](#)

Space Weather 2019

sci-hub.se/10.1029/2019SW002226

We present evidence that variability in the STEREO-A Heliospheric Imager (HI) data is correlated with in situ solar wind speed estimates from WIND, STEREO-A, and STEREO-B. For 2008–2012, we compute the variability in HI differenced images in a plane-of-sky shell between 20 to 22.5 solar radii and, for a range of position angles, compare daily means of HI variability and in situ solar wind speed estimates. We show that the HI variability data and in situ solar wind speeds have similar temporal autocorrelation functions. Carrington rotation periodicities are well documented for in situ solar wind speeds, but, to our knowledge, this is the first time they have been presented in statistics computed from HI images. In situ solar wind speeds from STEREO-A, STEREO-B, and WIND are all correlated with the HI variability, with a lag that varies in a manner consistent with the longitudinal separation of the in situ monitor and the HI instrument. Unlike many approaches to processing HI observations, our method requires no manual feature tracking; it is automated, is quick to compute, and does not suffer the subjective biases associated with manual classifications. These results suggest we could possibly estimate solar wind speeds in the low heliosphere directly from HI observations. This motivates further investigation, as this could be a significant asset to the space weather forecasting community; it might provide an independent observational constraint on heliospheric solar wind forecasts, through, for example, data assimilation. Finally, these results are another argument for the potential utility of including a HI on an operational space weather mission. **2009-05-01**

Testing the current paradigm for space weather prediction with heliospheric imagers

Luke A. [Barnard](#), Curt A. de Koning, Christopher J. Scott, Mathew J. Owens, Julia Wilkinson, Jackie A. Davies

Space Weather Volume 15, Issue 6 June 2017 Pages 782–803

<http://onlinelibrary.wiley.com/doi/10.1002/2017SW001609/full>

<http://sci-hub.cc/10.1002/2017SW001609>

Predictions of the arrival of four coronal mass ejections (CMEs) in geospace are produced through use of three CME geometric models combined with CME drag modeling, constraining these models with the available Coronagraph and Heliospheric Imager data. The efficacy of these predications is assessed by comparison with the Space Weather Prediction Center (SWPC) numerical MHD forecasts of these same events. It is found that such a prediction technique cannot outperform the standard SWPC forecast at a statistically meaningful level. We test the Harmonic Mean, Self-Similar Expansion, and Ellipse Evolution geometric models, and find that, for these events at least, the differences between the models are smaller than the observational errors. We present a new method of characterizing CME fronts in the Heliospheric Imager field of view, utilizing the analysis of citizen scientists working with the Solar Stormwatch project, and we demonstrate that this provides a more accurate representation of the CME front than is obtained by experts analyzing elongation time maps for the studied events. Comparison of the CME kinematics estimated independently from the STEREO-A and STEREO-B Heliospheric Imager data reveals inconsistencies that cannot be explained within the observational errors and model assumptions. We argue that these observations imply that the

assumptions of the CME geometric models are routinely invalidated and question their utility in a space weather forecasting context. These results argue for the continuing development of more advanced techniques to better exploit the Heliospheric Imager observations for space weather forecasting. **2012-08-31, 2012-09-28, 2012-10-05, 2012-11-20**

Differences between the CME fronts tracked by an expert, an automated algorithm, and the Solar Stormwatch project

L. **Barnard**, C. J. Scott, M. Owens, M. Lockwood, S. R. Crothers, J. A. Davies and R. A. Harrison
Space Weather 13(10) (pages 709–725) **2015**

<http://onlinelibrary.wiley.com/doi/10.1002/2015SW001280/epdf>

Observations from the Heliospheric Imager (HI) instruments aboard the twin STEREO spacecraft have enabled the compilation of several catalogues of coronal mass ejections (CMEs), each characterizing the propagation of CMEs through the inner heliosphere. Three such catalogues are the Rutherford Appleton Laboratory (RAL)-HI event list, the Solar Stormwatch CME catalogue, and, presented here, the J-tracker catalogue. Each catalogue uses a different method to characterize the location of CME fronts in the HI images: manual identification by an expert, the statistical reduction of the manual identifications of many citizen scientists, and an automated algorithm. We provide a quantitative comparison of the differences between these catalogues and techniques, using 51 CMEs common to each catalogue. The time-elongation profiles of these CME fronts are compared, as are the estimates of the CME kinematics derived from application of three widely used single-spacecraft-fitting techniques. The J-tracker and RAL-HI profiles are most similar, while the Solar Stormwatch profiles display a small systematic offset. Evidence is presented that these differences arise because the RAL-HI and J-tracker profiles follow the sunward edge of CME density enhancements, while Solar Stormwatch profiles track closer to the antisunward (leading) edge. We demonstrate that the method used to produce the time-elongation profile typically introduces more variability into the kinematic estimates than differences between the various single-spacecraft-fitting techniques. This has implications for the repeatability and robustness of these types of analyses, arguably especially so in the context of space weather forecasting, where it could make the results strongly dependent on the methods used by the forecaster. **14-20/12/2009, 9-17/02/2010**

The Solar Stormwatch CME catalogue: Results from the first space weather citizen science project

L. **Barnard**, C. Scott, M. Owens, M. Lockwood, K. Tucker-Hood, S. Thomas, S. Crothers, J. A. Davies, R. Harrison, C. Lintott, R. Simpson, J. O'Donnell, A. M. Smith, N. Waterson, S. Bamford, F. Romeo, M. Kukula, B. Owens, N. Savani, J. Wilkinson, E. Baeten, L. Poefel and B. Harder
Space Weather, **2015, File**

Solar Stormwatch was the first space weather citizen science project, the aim of which is to identify and track coronal mass ejections (CMEs) observed by the Heliospheric Imagers aboard the STEREO satellites. The project has now been running for approximately 4 years, with input from >16,000 citizen scientists, resulting in a data set of >38,000 time-elongation profiles of CME trajectories, observed over 18 preselected position angles. We present our method for reducing this data set into a CME catalogue. The resulting catalogue consists of **144 CMEs over the period January 2007 to February 2010, of which 110 were observed by STEREO-A and 77 were observed by STEREO-B**. For each CME, the time-elongation profiles generated by the citizen scientists are averaged into a consensus profile along each position angle that the event was tracked. We consider this catalogue to be unique, being at present the only citizen science-generated CME catalogue, tracking CMEs over an elongation range of 4° out to a maximum of approximately 70°. Using single spacecraft fitting techniques, we estimate the speed, direction, solar source region, and latitudinal width of each CME. This shows that at present, the Solar Stormwatch catalogue (which covers only solar minimum years) contains almost exclusively **slow CMEs, with a mean speed of approximately 350 km s⁻¹**. The full catalogue is available for public access at www.met.reading.ac.uk/~spate/solarstormwatch. This includes, for each event, the unprocessed time-elongation profiles generated by Solar Stormwatch, the consensus time-elongation profiles, and a set of summary plots, as well as the estimated CME properties. **2008-06-02**

CMEs in the Heliosphere: III. A Statistical Analysis of the Kinematic Properties Derived from Stereoscopic Geometrical Modelling Techniques Applied to CMEs Detected in the Heliosphere from 2008 to 2014 by STEREO/HI-1

D. **Barnes**, J. A. Davies, R. A. Harrison, J. P. Byrne, C. H. Perry, V. Bothmer, J. P. Eastwood, P. T. Gallagher, E. K. J. Kilpua, C. Möstl, L. Rodriguez, A. P. Rouillard, D. Odstrcil

Solar Phys. **295**, Article number: 150 **2020**

<https://arxiv.org/pdf/2006.14879.pdf>

<https://link.springer.com/content/pdf/10.1007/s11207-020-01717-w.pdf>

We present an analysis of coronal mass ejections (CMEs) observed by the Heliospheric Imagers (HIs) on board NASA's Solar Terrestrial Relations Observatory (STEREO) spacecraft. Between August 2008 and April 2014 we identify 273 CMEs that are observed simultaneously, by the HIs on both spacecraft. For each CME, we track the observed leading edge, as a function of time, from both vantage points, and apply the Stereoscopic Self-Similar Expansion (SSSE) technique to infer their propagation throughout the inner heliosphere. The technique is unable to accurately locate CMEs when their observed leading edge passes between the spacecraft, however, we are able to successfully apply the technique to 151, most of which occur once the spacecraft separation angle exceeds 180 degrees, during solar maximum. We find that using a small half-width to fit the CME can result in observed acceleration to unphysically high velocities and that using a larger half-width can fail to accurately locate the CMEs close to the Sun because the method does not account for CME over-expansion in this region. Observed velocities from SSSE are found to agree well with single-spacecraft (SSEF) analysis techniques applied to the same events. CME propagation directions derived from SSSE and SSEF analysis agree poorly because of known limitations present in the latter. This work was carried out as part of the EU FP7 HELCATS (Heliospheric Cataloguing, Analysis and Techniques Service) project ([this http URL](#)). **20110602, 20131026**

Remote Sensing Estimates of CME Density in the Ecliptic Using the STEREO Heliospheric Imagers

David **Barnes**

JGR [Volume125, Issue2](#) February 2020 e2019JA027175

<https://agupubs.onlinelibrary.wiley.com/doi/epdf/10.1029/2019JA027175>

We present a method to estimate electron densities in the ecliptic plane using the STEREO Heliospheric Imagers (HIs). The nature of Thomson scattering of photospheric light by solar wind electrons is such that visible-light observations by HI provide a means to infer information about plasma density from afar. This is achieved using discrete tomography, whereby line-of-sight integrals from HI are used to estimate electron density in the heliosphere over a predefined grid. The technique is applied to the Earth-impacting coronal mass ejection (CME) launched on 12 **December 2008**. The two vantage points afforded by STEREO are insufficient to reproduce the density structure of the CME in detail; however, the technique is successful in locating the presence of a density enhancement associated with the CME. When applied to consecutive images, we are able to use the technique as a means to track the CME through interplanetary space. From these observations we make estimates of the CME radial velocity and density profiles, the results of which are consistent with measurements made in situ by Wind at L1. This method is presented as a new approach to determine CME propagation from HI observations, one that avoids many of the assumptions of CME morphology and dynamics that are often applied when tracking CMEs in such data. We also expect that this technique will prove useful, and a test of the long-standing heliospheric reconstruction technique employed by using single images over time (Jackson et al., 2006, <https://doi.org/10.1029/2004JA010942>) when views from many wide-angle imagers become available.

CMEs in the Heliosphere: II. A Statistical Analysis of the Kinematic Properties Derived from Single-Spacecraft Geometrical Modelling Techniques Applied to CMEs Detected in the Heliosphere from 2007 to 2017 by STEREO/HI-1

D. **Barnes**, [J. A. Davies](#), [R. A. Harrison](#), [J. P. Byrne](#), [C. H. Perry](#)...

[Solar Physics](#) May 2019, 294:57

<https://link.springer.com/content/pdf/10.1007%2Fs11207-019-1444-4.pdf>

Recent observations with the Heliospheric Imagers (HIs) onboard the twin NASA Solar Terrestrial Relations Observatory (STEREO) spacecraft have provided unprecedented observations of a large number of coronal mass ejections (CMEs) in the inner heliosphere. In this article we discuss the generation of the **HIGeoCAT CME catalogue** and perform a statistical analysis of its events. The catalogue was generated as part of the EU FP7 HELCATS (Heliospheric Cataloguing, Analysis and Techniques Service) project (www.helcats-fp7.eu/). It is created by generating time/elongation maps for CMEs using observations from the inner (HI-1) and outer (HI-2) cameras along a position angle close to the CME apex. Next, we apply single-spacecraft geometric-fitting techniques to determine the kinematic properties of these CMEs, including their speeds, propagation directions, and launch times. The catalogue contains a total of 1455 events (801 from STEREO-A and 654 from STEREO-B) from April 2007 to the end of August 2017. We perform a statistical analysis of the properties of CMEs in HIGeoCAT and compare the results with those from the Large Angle Spectrometric Coronagraph (LASCO) CDAW catalogues (Yashiro et al. *J. Geophys. Res. Space Phys.* 109, A07105, [2004](#)) and the COR-2 catalogue of Vourlidas et al. (*Astrophys. J.* 838, 141, [2004](#)) during the same

period. We find that the distributions of both speeds and latitudes for the HIGeoCAT CMEs correlate with the sunspot number over the solar cycle. We also find that the HI-derived CME speed distributions are generally consistent with coronagraph catalogues over the solar cycle, albeit with greater absolute speeds due to the differing methods with which each is derived. **2011/01/30-31**,

HUXt -- An open source, computationally efficient reduced-physics solar wind model, written in Python

Luke [Barnard](#), [Mathew Owens](#)

Snakes on a Spaceship - An Overview of Python in Space Physics special issue of Frontiers in Astronomy and Space Science - Space Physics **2022**

<https://arxiv.org/pdf/2210.00455>

HUXt is an open source numerical model of the solar wind written in Python. It is based on the solution of the 1D inviscid Burger's equation. This reduced-physics approach produces solar wind flow simulations that closely emulate the flow produced by 3-D magnetohydrodynamic solar wind models at a small fraction of the computational expense. While not intended as a replacement for 3-D MHD, the simplicity and computational efficiency of HUXt offers several key advantages that enable experiments and the use of techniques that would otherwise be cost prohibitive. For example, large ensembles can easily be run with modest computing resources, which are useful for exploring and quantifying the uncertainty in space weather predictions, as well as for the application of some data assimilation methods. We present the developments in the latest version of HUXt, v4.0, and discuss our plans for future developments and applications of the model. The three key developments in v4.0 are: a restructuring of the models solver to enable fully time-dependent boundary conditions, such that HUXt can in principle be initialised with in-situ observations from any of the fleet of heliospheric monitors; new functionality to trace streaklines through the HUXt flow solutions, which can be used to track features such as the Heliospheric Current Sheet; introduction of a small test-suite so that we can better ensure the reliability and reproducibility of HUXt simulations for all users across future versions. Other more minor developments are discussed in the article.

Future applications of HUXt are discussed, including the development data assimilation schemes for assimilation of both remote sensing and in-situ plasma measures. We discuss the progress of transitioning HUXt into an operational model at the UK's Met Office Space Weather Operations Center as part of the UK governments SWIMMR programme.

Ensemble CME Modeling Constrained by Heliospheric Imager Observations

L. [Barnard](#) , [M. J. Owens](#) , [C. J. Scott](#) , [C. A. de Koning](#)

AGU Advances [Volume1, Issue3](#) September **2020** e2020AV000214

<https://doi.org/10.1029/2020AV000214>

<https://agupubs.onlinelibrary.wiley.com/doi/epdf/10.1029/2020AV000214>

Predicting the arrival of coronal mass ejections (CMEs) is one key objective of space weather forecasting. In operational space weather forecasting, solar wind numerical models are used for this task and ensemble techniques are being increasingly explored as a means to improve these forecasts. Currently, these forecasts are not constrained by the available in situ and remote sensing observations, such as those from the heliospheric imagers (HIs) on the National Aeronautics and Space Administration's (NASA's) STEREO spacecraft, which record white-light images of solar wind and CMEs. We report case studies of four CMEs and show how HI observations can be used to improve the skill and reduce the uncertainty of ensemble hindcasts of these events. Using a computationally efficient solar wind model, we produce 200-member ensemble hindcasts, perturbing the modeled CME parameters within uniform distributions about the best estimates. By comparing the trajectory of the modeled CME flanks with HI observations, we compute a weight for each ensemble member. Weighting the ensemble distribution of CME arrival times improves the skill and reduces the hindcast uncertainty of each event. For these four events, the weighted ensembles show a mean reduction in arrival time error of $20.1 \pm 4.1\%$, and a mean reduction in arrival time uncertainty of $15.0 \pm 7.2\%$, relative to the unweighted ensembles. This technique could be applied in operational space weather forecasting, if real-time HI observations were available. Therefore, as NASA and the European Space Agency are currently planning the next space weather monitoring missions, our proof-of-concept study provides some evidence of the potential value of including HIs on these missions. **2012-09-01, 2012-09-04, 2012-09-30, 2012-10-08, 2012-11-24**

Extracting inner-heliosphere solar wind speed information from Heliospheric Imager observations

L.A. [Barnard](#), [M.J. Owens](#), [C.J. Scott](#) , [S.R. Jones](#)

Space Weather [Volume17, Issue6](#) Pages 925-938 **2019**

[sci-hub.se/10.1029/2019SW002226](https://doi.org/10.1029/2019SW002226)

We present evidence that variability in the STEREO-A Heliospheric Imager (HI) data is correlated with in-situ solar wind speed estimates from WIND, STEREO-A, and STEREO-B. For 2008-2012, we compute the variability in HI differenced images in a plane-of-sky shell between 20-22.5 solar radii, and, for a range of position angles, compare daily means of HI variability and in-situ solar wind speed estimates.

We show that the HI variability data and in-situ solar wind speeds have similar temporal autocorrelation functions. Carrington rotation periodicities are well documented for in-situ solar wind speeds, but, to our knowledge, this is the first time they have been presented in statistics computed from HI images. In-situ solar wind speeds from STEREO-A, STEREO-B, and WIND are all correlated with the HI variability, with a lag that varies in a manner consistent with the longitudinal separation of the in-situ monitor and the HI instrument.

Unlike many approaches to processing HI observations, our method requires no manual feature tracking; it is automated, quick to compute, and does not suffer the subjective biases associated with manual classifications. These results suggest we could possibly estimate solar wind speeds in the low heliosphere directly from HI observations. This motivates further investigation as this could be a significant asset to the space weather forecasting community; it might provide an independent observational constraint on heliospheric solar wind forecasts, through, for example, data assimilation.

Finally, these results are another argument for the potential utility of including a HI on an operational space weather mission. **2009-05-01**

The Solar Stormwatch CME catalogue: Results from the first space weather citizen science project

L. Barnard¹, C. Scott¹, M. Owens¹, et al.

Space Weather, [Volume 12, Issue 12](#), pages 657–674, December **2014**

<http://onlinelibrary.wiley.com/doi/10.1002/2014SW001119/pdf>

Solar Stormwatch was the first space weather citizen science project, the aim of which is to identify and track coronal mass ejections (CMEs) observed by the Heliospheric Imagers aboard the STEREO satellites. The project has now been running for approximately 4 years, with input from >16,000 citizen scientists, resulting in a data set of >38,000 time-elongation profiles of CME trajectories, observed over 18 preselected position angles. We present our method for reducing this data set into a CME catalogue. The resulting catalogue consists of 144 CMEs over the period January 2007 to February 2010, of which 110 were observed by STEREO-A and 77 were observed by STEREO-B. For each CME, the time-elongation profiles generated by the citizen scientists are averaged into a consensus profile along each position angle that the event was tracked. We consider this catalogue to be unique, being at present the only citizen science-generated CME catalogue, tracking CMEs over an elongation range of 4° out to a maximum of approximately 70°. Using single spacecraft fitting techniques, we estimate the speed, direction, solar source region, and latitudinal width of each CME. This shows that at present, the Solar Stormwatch catalogue (which covers only solar minimum years) contains almost exclusively slow CMEs, with a mean speed of approximately 350 km s⁻¹. The full catalogue is available for public access at www.met.reading.ac.uk/~spate/solarstormwatch. This includes, for each event, the unprocessed time-elongation profiles generated by Solar Stormwatch, the consensus time-elongation profiles, and a set of summary plots, as well as the estimated CME properties. **2008-06-02**

Radio Observational Constraints on Turbulent Astrophysical Plasmas **Review**

Tim Bastian, James Cordes, Justin Kasper, Adam Kobelski, Kelly Korreck, Gregory Howe, Steven Spangler, Chadi Salem, Angelos Vourlidas

White paper submitted to the Astronomy and Astrophysics decadal survey **2019**

<https://arxiv.org/pdf/1904.05807.pdf>

Remarkable progress has been made in understanding turbulent astrophysical plasmas in past decades including, notably, the solar wind and the interstellar medium. In the case of the solar wind, much of this progress has relied on in situ measurements from space-borne instruments. However, ground-based radio observations also have played a significant role and have the potential to play an even bigger role. In particular, using distant background sources (quasars, pulsars, satellite beacons) to transilluminate the foreground corona and solar wind, a variety of radio propagation phenomena can be used to map plasma properties of the solar corona and heliosphere, as well as the warm interstellar medium. These include angular broadening, interplanetary and interstellar scintillations, and differential Faraday rotation. These observations are highly complementary to in situ observations of the solar wind, and could be a mainstay of investigations into turbulence of the ISM. We point out that the Next Generation Very Large Array (ngVLA) fulfills all the requirements necessary to exploit radio observations of astrophysical turbulence fully.

Predicting CMEs using ELEvoHI with STEREO-HI beacon data

Maïke [Bauer](#), [Tanja Amerstorfer](#), [Jürgen Hinterreiter](#), [Andreas J. Weiss](#), [Jackie A. Davies](#), [Christian Möstl](#), [Ute V. Amerstorfer](#), [Martin A. Reiss](#), [Richard A. Harrison](#)

Space Weather **Volume19**, **Issue12** e2021SW002873 **2021**

<https://arxiv.org/pdf/2108.08072.pdf>

<https://agupubs.onlinelibrary.wiley.com/doi/epdf/10.1029/2021SW002873>

<https://doi.org/10.1029/2021SW002873>

Being able to accurately predict the arrival of coronal mass ejections (CMEs) at Earth has been a long-standing problem in space weather research and operations. In this study, we use the ELlipse Evolution model based on Heliospheric Images (ELEvoHI) to predict the arrival time and speed of 10 CME events that were observed by HI on the STEREO-A spacecraft between 2010 and 2020. Additionally, we introduce a Python tool for downloading and preparing STEREO-HI data, as well as tracking CMEs. In contrast to most previous studies, we use not only science data, which has a relatively high spatial and temporal resolution, but also low-quality beacon data, which is - in contrast to science data - provided in real-time by the STEREO-A spacecraft. We do not use data from the STEREO-B spacecraft. We get a mean absolute error of 8.81 ± 3.18 h / 59 ± 31 kms⁻¹ for arrival time/speed predictions using science data and 11.36 ± 8.69 h / 106 ± 61 kms⁻¹ for beacon data. We find that using science data generally leads to more accurate predictions, but using beacon data with the ELEvoHI model is certainly a viable choice in the absence of higher resolution real-time data. We propose that these differences could be minimized if not eliminated altogether if higher quality real-time data was available, either by enhancing the quality of the already available data or coming from a new mission carrying a HI instrument on-board. **8 April 2010, 24 May 2010, 16 June 2010, 1 August 2010, 15 February 2011, 2 August 2011, 7 Sep 2011, 22 October 2011, 12 July 2012, 9 July 2020**

Table

,

Solar energetic particle events in 2006-2012 in the PAMELA experiment data

G A [Bazilevskaya](#) et al

2013 J. Phys.: Conf. Ser. 409 012188

The PAMELA magnetic spectrometer launched in June 2006 has observed the last strong energetic solar particle event of the 23rd solar cycle in December 2006. Subsequent long minimum of solar activity and weak development of the 24th solar cycle led to a deficit in the solar energetic particle events on the Earth orbit. As a result, only few events with protons accelerated above 100 MeV occurred in 2010-2012. The paper gives the preliminary results on energetic solar particles in the beginning of the 24th solar circle as measured with the PAMELA instrument.

Magnetic axis safety factor of finite beta spheromaks and transition from spheromaks to toroidal magnetic bubbles

Paul M. [Bellan](#) and Roberto Paccagnella

Physics of Plasmas, **2015**

<http://arxiv.org/pdf/1502.01656v1.pdf>

The value of the safety factor on the magnetic axis of a finite-beta spheromak is shown to be a function of beta in contrast to what was used in P. M. Bellan, Phys. Plasmas 9, 3050 (2002); this dependence on beta substantially reduces the gradient of the safety factor compared to the previous calculation. The method for generating finite-beta spheromak equilibria is extended to generate equilibria describing toroidal magnetic ?bubbles? where the hydrodynamic pressure on the magnetic axis is less than on the toroid surface. This ?anti-confinement? configuration can be considered an equilibrium with an inverted beta profile and is relevant to interplanetary magnetic clouds as these clouds have lower hydrodynamic pressure in their interior than on their surface.

On the Most Interesting Solar-Wind and Cosmic-Ray Events in February–April 2023.

Belov, S.M., Shlyk, N.S., Abunina, M.A. et al.

Sol Phys 299, 164 (2024).

<https://doi.org/10.1007/s11207-024-02406-8>

The article focuses on identifying and studying several large-scale solar-wind disturbances and associated Forbush effects in the first months of 2023. Variations of the cosmic-ray flux (with 10 GV rigidity) are obtained using the Global Survey Method with data from the global network of neutron monitors. The beginning of 2023 is characterized by a relatively large number of Forbush effects; the largest ones were recorded on **26 – 28 February, 15 – 16 March, 23 – 25 March, and 23 – 24 April**. These events and their relationship with solar-wind parameters, geomagnetic activity, and associated solar sources are discussed in detail. In terms of the number and magnitude of interplanetary disturbances and corresponding cosmic-ray variations, February–April 2023 proves to be the first active period since the beginning of Solar Cycle 25.

Forbush Effects and Geomagnetic Storms.

Belov, A.V., Belova, E.A., Shlyk, N.S. *et al.*

Geomagn. Aeron. **64**, 289–301 (2024).

<https://doi.org/10.1134/S0016793224600097>

Forbush effects in galactic cosmic rays (according to the neutron monitor network data) and accompanying geomagnetic disturbances over a long period from 1957 to 2022 have been identified and studied. Statistical relationships between various parameters of cosmic ray flux variations and geomagnetic activity indices are analyzed. It has been established that the magnitude of Forbush effects depends nonlinearly on the class of geomagnetic storm. A moderate correlation (up to 0.67) was found between the extreme values of various geomagnetic activity indices (*Ap*, *Kp*, *Dst*) and cosmic ray characteristics. It is shown that the extreme values of cosmic ray and geomagnetic activity parameters are not always detected simultaneously: it depends on the sign of the *Bz*-component of the interplanetary magnetic field in a specific event.

Study of the radial dependence of Forbush decreases at 0.28–1 au using data from the *Helios 1* and *2* spacecraft

Anatoly **Belov**, [Nataly Shlyk](#), [Maria Abunina](#), [Artem Abunin](#), [Athanasios Papaioannou](#), [Ian G Richardson](#), [David Lario](#)

Monthly Notices of the Royal Astronomical Society, Volume 521, Issue 3, May 2023, Pages 4652–4668,

<https://doi.org/10.1093/mnras/stad732>

We identify and investigate cosmic ray Forbush decreases (FDs) observed in the $E > 50$ MeV data from the *Helios 1* and *2* spacecraft, spanning from 1974–1985 and covering heliocentric distances in the range 0.28–1 au. A *Helios* FD catalogue is compiled, including the characteristics of the cosmic ray variations, as well as those of the solar wind (SW) and the interplanetary magnetic field (IMF) of the associated interplanetary disturbances. An extended statistical study considers the radial dependence of the FD magnitude, the SW velocity, and the IMF intensity in these disturbances. It is found that the *Helios* FD sizes at different distances from the Sun are determined by the parameters of the interplanetary disturbances. In particular, the FD magnitudes observed at *Helios*, as well as near Earth, correlate well with VB, which is the product of the maximum SW velocity and the IMF intensity when normalized by the average values of these parameters at the radial distance of the observations. However, we found that, on average, the *Helios* FD sizes are statistically independent of the radial distance in the range of 0.28–1 au.

Estimating the Transit Speed and Time of Arrival of Interplanetary Coronal Mass Ejections Using CME and Solar Flare Data

Belov, Anatoly ; [Shlyk, Nataly](#) ; [Abunina, Maria](#) ; [Abunin, Artem](#) ; [Papaioannou, Athanasios](#)

Universe **2022**, 8(6), 327;

<https://doi.org/10.3390/universe8060327>

The dependence of Interplanetary Coronal Mass Ejections' (ICMEs) transit speed on the corresponding Coronal Mass Ejections' (CMEs) initial speed is investigated. It is shown that the transit speed and transit time depend not only on the CME's initial speed, but also on the longitude of the solar source. The longitudinal dependence of the expected transit speeds and times are obtained from the analysis of 288 CMEs, associated with solar flares, observed from 1995 to 2020. A model, estimating the transit and maximum speeds, as well as the time of arrival of an ICME to Earth, based on the initial CME speed and the longitude of the associated solar flare has been created. It is shown that taking into account the longitude of the solar source in addition to the initial CME speed significantly improves the quality of the model, especially for events in the central part of the solar disk ($E10^{\circ}$ – $W10^{\circ}$). The simplicity of the described model makes it accessible to a wide range of users and provides opportunities for further improvement as the statistics and the number of input parameters increase.

Solar Energetic Particle Events and Forbush Decreases Driven by the Same Solar Sources

Belov, Anatoly ; [Shlyk, Nataly](#) ; [Abunina, Maria](#) ; [Belova, Elena](#) ; [Abunin, Artem](#) ; [Papaioannou, Athanasios](#)

Universe **2022**, 8(8), 403;

<https://doi.org/10.3390/universe8080403>

<https://www.mdpi.com/2218-1997/8/8/403/pdf>

The characteristics of Forbush decreases (FDs) and solar energetic particle (SEP) events driven by the same solar source (i.e., coronal mass ejection and associated solar flare) are investigated. The part of the solar disk (04° E– 35° W) in

which most of the solar events lead both to an FD and SEP event on Earth was chosen. SEPs for different energies ($E > 10$ MeV, $E > 100$ MeV, and Ground Level Enhancements) and with different flux thresholds were considered independently. The obtained results were compared with the control group of FDs that had solar sources within the same longitudinal zone but were not accompanied by any SEPs. It is shown that coronal mass ejections (CMEs) followed by SEPs have a very high probability of creating a large FD in the Earth's orbit and to further cause a geomagnetic storm. It is also found that the accelerative and modulating efficiencies of powerful solar events are well correlated; this can be explained mostly by high speeds of the corresponding CMEs. **15–16 May 1997, 14–15 December 2006., 5–7 October 2011, 14–17 July 2012, 12–14 September 2014**

On the Rigidity Spectrum of Cosmic-Ray Variations within Propagating Interplanetary Disturbances: Neutron Monitor and SOHO/EPHIN Observations at ~1–10 GV

Anatoly **Belov**¹, Athanasios Papaioannou², Maria Abunina¹, Mateja Dumbovic³, Ian G. Richardson^{4,5}, Bernd Heber⁶, Patrick Kuhl⁶, Konstantin Herbst⁶, Anastasios Anastasiadis², Angelos Vourlidas^{2,7}Show full author list

2021 ApJ 908 5

<https://doi.org/10.3847/1538-4357/abd724>

The rigidity dependence of all Forbush decreases (FDs) recorded from 1995 to 2015 has been determined using neutron monitor (NM) and Solar and Heliospheric Observatory (SOHO) (EPHIN) spacecraft data, covering the energy (rigidity) range from ~433 MeV (1 GV) to 9.10 GeV (10 GV). We analyzed a total of 421 events and determined the spectrum in rigidity with an inverse power-law fit. As a result, the mean spectral index was identified to be $\langle \gamma F \rangle = 0.46 \pm 0.02$. The majority (~66%) of the FDs have γF within the range 0.3–0.7. The remaining one-third of the events (~33%) have either (very) soft or hard FD spectra, with the latter being more common than the former. Significant variations of γF occur within almost every FD event. During the initial FD decay phase the spectrum becomes gradually harder, in contrast to the recovery phase, when it becomes softer. Additionally, low energies (rigidities) seem to be better suited for studying the fine structure of interplanetary disturbances (primarily interplanetary coronal mass ejections) that lead to FDs. In particular, FDs recorded by the EPHIN instrument on SOHO better capture a two-step structure than FDs observed by NMs. Finally, the ejecta of an ICME, especially when identified as a magnetic cloud, often leads to abrupt changes in the slope of γF .

Virtual Laboratory for the comprehensive analysis of Forbush-Effects and Interplanetary Disturbances

A. **Belov**, A. Abunin, E. Eroshenko, M. Abunina, V. Yanke, V. Oleneva
VarSITI Newsletter Vol. 21 p.1-3 **2019**

http://newserver.stil.bas.bg/varsiti/newsL/VarSITI_Newsletter_Vol21.pdf

7-9 September 2017

Galactic Cosmic Ray Density Variations in Magnetic Clouds

A. **Belov**, A. Abunin, M. Abunina, [E. Eroshenko](#), [V. Oleneva](#), [V. Yanke](#), [A. Papaioannou](#), [H. Mavromichalaki](#)

[Solar Physics](#) May **2015**, Volume 290, [Issue 5](#), pp 1429-1444

We investigate the characteristics of Galactic cosmic rays in events associated with magnetic clouds that reach Earth. A mathematical model, capable of describing the distribution of the cosmic-ray density in a magnetic cloud is considered. We show that in most cases the behavior of the cosmic-ray density within magnetic clouds at 1 AU can be described accurately by a parabolic function of the distance to the center of the magnetic cloud measured in gyroradii. As expected, the majority of magnetic clouds modulate cosmic rays, resulting in a reduction of their density. However, there is a group of events (about one fifth of the total sample) in which the density of cosmic rays in a magnetic cloud increases. Furthermore, the extremum (a minimum or a maximum) of the cosmic-ray density is found closer to the cloud center and not at its edges. We consider a number of the factors contributing to the model and estimate the effect of each factor.

Coronal Mass Ejections and Non-recurrent Forbush Decreases

Belov, A.; Abunin, A.; Abunina, M.; Eroshenko, E.; Oleneva, V.; Yanke, V.; Papaioannou, A.; Mavromichalaki, H.; Gopalswamy, N.; Yashiro, S.

Solar Physics, Volume 289, Issue 10, pp.3949-3960, 2014 **File**

<http://cosray.phys.uoa.gr/publications/D105.pdf>

Coronal mass ejections (CMEs) and their interplanetary counterparts (interplanetary coronal mass ejections, ICMEs) are responsible for large solar energetic particle events and severe geomagnetic storms. They can modulate the intensity of Galactic cosmic rays, resulting in non-recurrent Forbush decreases (FDs). We investigate the connection between CME manifestations and FDs. We used specially processed data from the worldwide neutron monitor network to pinpoint the characteristics of the recorded FDs together with CME-related data from the detailed online catalog based upon the Solar and Heliospheric Observatory (SOHO)/ Large Angle and Spectrometric Coronagraph (LASCO) data. We report on the correlations of the *FD magnitude to the CME initial speed, the ICME transit speed*, and the maximum solar wind speed. Comparisons between the features of CMEs (mass, width, velocity) and the characteristics of FDs are also discussed. FD features for halo, partial halo, and non-halo CMEs are presented and discussed.

Ground level enhancements of the solar cosmic rays and Forbush decreases in 23rd solar cycle

A. V. **Belov**, E. A. Eroshenko, V. A. Oleneva, V. G. Yanke

PROCEEDINGS OF THE 31st ICRC, ŁÓDŹ 2009 **File**

The outstanding effects of solar activity in 23rd solar cycle, such as ground level enhancements of solar cosmic rays and the largest Forbush decreases (FD), are investigated. The analysis shows that both GLEs and great Forbush effects are connected with anomalously fast ejections of solar matter with similar properties. The main difference between those is in the longitude: the sources of the greatest Forbush effects (FE) are usually located in a central part of visible solar disk whereas flares associated with GLEs are mostly in the western part of disk. It is shown that accelerative and modulative efficiencies of the solar events are tightly correlated. Coronal mass ejection followed by GLE creates with a big probability a very large FE in the Earth orbit. **April, 15-22 2001, 28 Oct - 4 Nov 2003**

TABLE I: GLEs of 23rd cycle

TABLE II: The largest Forbush effects of 23-rd solar cycle

Forbush effects and their connection with solar, interplanetary and geomagnetic phenomena

A.V. **Belov**

'Universal Heliophysical Processes' Proceedings IAU Symposium No. 257, P. 439-450, 2009. **File**

sci-hub.tw/10.1017/S1743921309029676

Forbush decrease (or, in a broader sense, Forbush effect) - is a storm in cosmic rays, which is a part of heliospheric storm and very often observed simultaneously with a geomagnetic storm. Disturbances in the solar wind, magnetosphere and cosmic rays are closely interrelated and caused by the same active processes on the Sun. Thus, it is natural and useful to investigate them together. Such an investigation in the present work is based on the characteristics of cosmic rays with rigidity of 10 GV. The results are derived using data from the world wide neutron monitor network and are combined with relevant information into a data base on Forbush effects and large interplanetary disturbances.

Effects of strong geomagnetic storms on Northern railways in Russia.

Belov, A.V., Gaidash, S.P., Eroshenko, E.A., Lobkov, S.L., Pirjola, R., Trichtchenko, L., 2007. In: Proceedings of the 7th International Symposium on Electromagnetic Compatibility and Electromagnetic Ecology, Saint-Petersburg, Russia, 26–29 June 2007, pp. 280–282.

Magnetospheric effects in cosmic rays during the unique magnetic storm on November 2003

Belov A., Baisultanova L., Eroshenko E. et al.

J. Geophys. Res. 2005. V. 110, A09S20, doi:10.1029/2005JA011067, **File**.

Cosmic ray variations due to changes in the magnetosphere are evaluated for severe magnetic storm on November 20, 2003 using data from the worldwide neutron monitor network and the global survey method. From these results the changes in the planetary distribution of magnetic cutoff rigidities during this disturbed period are obtained in dependence of latitude. A correlation between Dst index and cutoff rigidity variations was defined for each cosmic ray station. The maximum changes in cutoff rigidities occurred while Dst index was around -472 nT. Geomagnetic effect in cosmic ray intensity reached at some stations 6-8%, and it seems to be the greatest one over the history of neutron monitor observations. The latitudinal distribution shows a maximum changes at geomagnetic cutoff rigidities around 7-8 GV. This corresponds to unusually low latitudes for maximal effect. Cutoff rigidity variations were also calculated utilizing the last model of Tsyganenko for a disturbed magnetosphere (T01S). A comparison between experimental and modeling results revealed a big discrepancy at cutoff rigidities less than 6 GV. The results on the geomagnetic effect in cosmic rays can be used for validating magnetospheric field models during very severe storms.

What determines the magnitude of forrush decreases?

A. V. **Belov**, E. A. Eroshenko, V. A. Oleneva, A. B. Struminsky and V. G. Yanke

[Advances in Space Research](#), **Volume 27, Issue 3**, 2001, Pages 625-630; **File**

Cosmic ray Forbush effects (FEs) have been studied for more than 60 years, but even today this phenomenon has no universally accepted definition, which leads to misunderstanding among researchers. There are no complete and convincing answers to the following questions: What are the distinctive features of FEs? What determines the magnitude of FEs and their variety? How are FEs associated with disturbances of the interplanetary medium, coronal mass ejections and high speed flows of the solar wind? What relation exists between FEs and geomagnetic storms? In order to answer these and other questions a data base of transient effects in cosmic rays and in the interplanetary medium is constructed and is being upgraded continuously. It combines variations in cosmic ray densities and anisotropies obtained from data of the world-wide neutron monitor (NM) network, characteristics of solar wind disturbances, solar and geomagnetic data. This data base presently contains more than 1400 events, observed during 1978–1996. The preliminary analysis allowed us to get the main characteristics of FEs, to determine what distinguishes this phenomenon among other cosmic ray variations, and propose a definition of the Forbush effect. In addition, an interplanetary disturbance parameter was derived, which is most closely associated with the magnitude of a FE. Using this large observational database, a relation between FEs and geomagnetic activity was analyzed statistically as a dependence of the FE magnitude on the maximum Kp-index measured during the associated magnetic storm.

Relation the forbush effects to the interplanetary and geomagnetic activity

Belov, A. V., Eroshenko, E. A., Oleneva, V. A., & Yanke, V. G.

Proceedings of the 27th International Cosmic Ray Conference. 07-15 August, 2001. Hamburg, Germany. Under the auspices of the International Union of Pure and Applied Physics (IUPAP), p.3552, **File**

<http://articles.adsabs.harvard.edu/full/2001ICRC....9.3552B/0003552.000.html?high=4afba3082a18300>

Properties of the Forbush effects (FE) and their relation to the sources and different parameters of the interplanetary medium and geospace, are the complex topic till now due to the great variety of FEs origin and manifestation. More definite relations appear to be derived employing the cosmic ray (CR) observations and different related parameters in the space and Earth's environment. To provide the statistical estimations a special database is created, which includes variations of the cosmic ray density and anisotropy, solar wind characteristics, interplanetary magnetic field, solar and geomagnetic data for about 2000 events observed in 1977-1980 and 1986-1997. The preliminary analysis allowed the main characteristics of the FEs and their relation with the solar wind and geomagnetic parameters to be derived and studied. A parameter of the interplanetary disturbance was found which is most closely correlated with the magnitude of the FE. A relation of the FE magnitude to the geomagnetic activity was derived as a dependence of the FE amplitude on the maximal Ap-index throughout the associated magnetic storm.

Combining White Light and UV Lyman-alpha Coronagraphic Images to determine the Solar Wind Speed: the Quick Inversion Method

Alessandro **Bemporad**, [Silvio Giordano](#), [Luca Zangrilli](#), [Federica Frassati](#)

A&A 654, A58 2021

<https://arxiv.org/pdf/2107.06811.pdf>

<https://doi.org/10.1051/0004-6361/202141276>

<https://www.aanda.org/articles/aa/pdf/2021/10/aa41276-21.pdf>

This work focuses on the combination of White Light (WL) and UV (Ly-alpha) coronagraphic images to demonstrate the capability to measure the solar wind speed in the inner corona directly with the ratio between these two images (a technique called "quick inversion method"), thus avoiding to account for the line-of-sight (LOS) integration effects in the inversion of data. After a derivation of the theoretical basis and illustration of the main hypotheses in the "quick inversion method", the data inversion technique is tested first with 1D radial analytic profiles, and then with 3D numerical MHD simulations, in order to show the effects of variabilities related with different phases of solar activity cycle and complex LOS distribution of plasma parameters. The same technique is also applied to average WL and UV images obtained from real data acquired by SOHO UVCS and LASCO instruments around the minimum and maximum of the solar activity cycle. Comparisons between input and output velocities show overall a good agreement, demonstrating that this method that allows to infer the solar wind speed with WL-UV image ratio can be complementary to more complex techniques requiring the full LOS integration. The analysis described here also allowed us to quantify the possible errors in the outflow speed, and to identify the coronal regions where the "quick inversion method"

performs at the best. The "quick inversion" applied to real UVCS and LASCO data allowed also to reconstruct the typical bimodal distribution of fast and slow wind at solar minimum, and to derive a more complex picture around solar maximum. The application of the technique shown here will be very important for the future analyses of data acquired with multichannel WL and UV (Ly-alpha) coronagraphs, such as Metis on-board Solar Orbiter, LST on-board ASO-S, and any other future WL and UV Ly-alpha multi-channel coronagraph.

Exploring the Inner Acceleration Region of Solar Wind: A Study Based on Coronagraphic UV and Visible Light Data

A. **Bemporad**

2017 ApJ 846 86

<http://iopscience.iop.org/sci-hub.cc/0004-637X/846/1/86/>

This work combined coronagraphic visible light (VL) and UV data to provide with an unprecedented view of the inner corona where the nascent solar wind is accelerated. The UV ($H\ i$ Ly α) and VL (polarized brightness) images (reconstructed with SOHO/UVCS, LASCO, and Mauna Loa data) have been analyzed with the Doppler dimming technique to provide for the first time daily 2D images of the radial wind speed between 1 and 6 R_{\odot} over 1 month of observations. Results show that both polar and equatorial regions are characterized at the base of the corona by plasma outflows at speeds > 100 km s $^{-1}$. The plasma is then decelerated within $\sim 1.5 R_{\odot}$ at the poles and $\sim 2.0 R_{\odot}$ at the equator, where local minima of the expansion speeds are reached, and gently reaccelerated higher up, reaching speeds typical of fast and slow wind components. The mass flux is highly variable with latitude and time at the equator and more uniform and stable over the poles. The polar flow is asymmetric, with speeds above the south pole lower than those above the north pole. A correlation (anticorrelation) between the wind speed and its density is found below (above) $\sim 1.8 R_{\odot}$. The 2D distribution of forces responsible for deceleration and reacceleration of solar wind is provided and interpreted in terms of Alfvén waves. These results provide a possible connection between small-scale outflows reported with other instruments at the base of the corona and bulk wind flows measured higher up.

Variations of the electron fluxes in the terrestrial radiation belts due to the impact of Corotating Interaction Regions and Interplanetary Coronal Mass Ejections

R. **Benacquista**, D. Boscher, S. Rochel and V. Maget

JGR **Volume 123, Issue 2** Pages 1191-1199 2018

<http://onlinelibrary.wiley.com/doi/10.1002/2017JA024796/epdf>

<http://sci-hub.tw/10.1002/2017JA024796>

In this paper, we study the variations of the radiation belts electron fluxes induced by the interaction of two types of solar wind structures with the Earth magnetosphere: the corotating interaction regions and the interplanetary coronal mass ejections. We use a statistical method based on the comparison of the pre- and post-events fluxes. Applied to the NOAA-POES data, this gives us the opportunity to extend previous studies focused on relativistic electrons at geosynchronous orbit. We enlighten how CIRs and ICMEs can impact differently the electron belts depending on the energy and the Lshell. In addition, we provide a new insight concerning these variations by considering their amplitude. Finally, we show strong relations between the intensity of the magnetic storms related to the events and the variation of the flux. These relations concern both the capacity of the events to increase the flux and the deepness of these increases.

A New Method to Model Magnetic Cloud-driven Forbush Decreases: The 2016 August 2 Event

Simone **Benella**^{1,2,6}, Monica Laurenza³, Rami Vainio⁴, Catia Grimani^{1,2}, Giuseppe Consolini³, Qiang Hu⁵, and Alexandr Afanasiev⁴

2020 ApJ 901 21

<https://doi.org/10.3847/1538-4357/abac59>

Interplanetary coronal mass ejections (ICMEs), generally containing magnetic clouds (MCs), are associated with galactic-cosmic ray (GCR) intensity depressions known as Forbush decreases (FDs). An ICME was observed at L1 between **2016 August 2** at 14:00 UT and **August 3** at 03:00 UT. The MC region was identified and its magnetic configuration was retrieved by using the Grad-Shafranov (GS) reconstruction. A weak FD in the GCR count-rate was observed on 2016 August 2 by a particle detector on board the European Space Agency LISA Pathfinder mission. The spacecraft orbited around L1 and the particle detector allowed us to monitor the GCR intensity at energies above 70 MeV n $^{-1}$. A 9% decrease in the cosmic-ray intensity was observed during the ICME passage. The first structure of the

ICME caused a 6.4% sharp decrease, while the MC produced a 2.6% decrease. A suited full-orbit test-particle simulation was performed on the MC configuration obtained through the GS reconstruction. The FD amplitude and time profile obtained through the simulation show an excellent agreement with observations. The test-particle simulation allows us to derive the energy dependence of the MC-driven FD providing an estimate of the amplitude at different rigidities, here compared with several neutron monitor observations. This work points out the importance of the large-scale MC configuration in the interaction between GCRs and ICMEs and suggests that particle drifts have a primary role in modulating the GCR intensity within the MC under study and possibly in at least all slowly expanding ICMEs lacking a shock/sheath region.

Coronal Electron Temperature inferred from the Strahl Electrons in the Inner Heliosphere: Parker Solar Probe and Helios observations

Laura [Bercic](#), [Davin Larson](#), [Phyllis Whittlesey](#), [Milan Maksimovic](#), [Samuel T. Badman](#), [Simone Landi](#), [Lorenzo Matteini](#), [Stuart D. Bale](#), [John W. Bonnell](#), [Anthony W. Case](#), [Thierry Dudok de Wit](#), [Keith Goetz](#), [Peter R. Harvey](#), [Justin C. Kasper](#), [Kelly E. Korreck](#), [Roberto Livi](#), [Robert J. MacDowall](#), [David M. Malaspina](#), [Marc Pulupa](#), [Michael L. Stevens](#)

ApJ **892** 88 2020

<https://arxiv.org/pdf/2003.04016.pdf>

<https://doi.org/10.3847/1538-4357/ab7b7a>

The shape of the electron velocity distribution function plays an important role in the dynamics of the solar wind acceleration. Electrons are normally modelled with three components, the core, the halo, and the strahl. We investigate how well the fast strahl electrons in the inner heliosphere preserve the information about the coronal electron temperature at their origin. We analysed the data obtained by two missions, Helios spanning the distances between 65 and 215 RS, and Parker Solar Probe (PSP) reaching down to 35 RS during its first two orbits around the Sun. The electron strahl was characterised with two parameters, pitch-angle width (PAW), and the strahl parallel temperature ($T_{s\parallel}$). PSP observations confirm the already reported dependence of strahl PAW on core parallel plasma beta ($\beta_{c\parallel}$) (Bercic2019). Most of the strahl measured by PSP appear narrow with PAW reaching down to 30°. The portion of the strahl velocity distribution function aligned with the magnetic field is for the measured energy range well described by a Maxwellian distribution function. $T_{s\parallel}$ was found to be anti-correlated with the solar wind velocity, and independent of radial distance. These observations imply that $T_{s\parallel}$ carries the information about the coronal electron temperature. The obtained values are in agreement with coronal temperatures measured using spectroscopy (David et al. 2998), and the inferred solar wind source regions during the first orbit of PSP agree with the predictions using a PFSS model (Bale et al. 2019, Badman et al. 2019).

On Fields and Mass Constraints for the Uniform Propagation of Magnetic-Flux Ropes Undergoing Isotropic Expansion

Daniel Benjamín [Berdichevsky](#)

[Solar Physics](#) May 2013, Volume 284, [Issue 1](#), pp 245–259

<https://link.springer.com/content/pdf/10.1007%2Fs11207-012-0176-5.pdf>

An analytical 3-D magnetohydrodynamic (MHD) solution of a magnetic-flux rope (FR) is presented. This FR solution may explain the uniform propagation, beyond ~ 0.05 AU, of coronal mass ejections (CMEs) commonly observed by today's missions like The Solar Mass Ejection Imager (SMEI), Solar and Heliospheric Observatory (SOHO) and Solar Terrestrial Relations Observatory (STEREO), tracked to tens of times the radius of the Sun, and in some cases up to 1 AU, and/or beyond. Once a CME occurs, we present arguments regarding its evolution based on its mass and linear momentum conservation. Here, we require that the gravitational and magnetic forces balance each other in the framework of the MHD theory for a simple model of the evolution of a CME, assuming it interacts weakly with the steady solar wind. When satisfying these ansätze we identify a relation between the transported mechanical mass of the interplanetary CME with its geometrical parameters and the intensity of the magnetic field carried by the structure. In this way we are able to estimate the mass of the interplanetary CME (ICME) for a list of cases, from the Wind mission records of ICME encountered near Earth, at 1 AU. We obtain a range for masses of ~ 109 to 1013 kg, or assuming a uniform distribution, of ~ 0.5 to 500 cm^{-3} for the hadron density of these structures, a result that appears to be consistent with observations.

Correction: [Solar Physics](#) November 2019, 294:167 <https://link.springer.com/content/pdf/10.1007%2Fs11207-019-1557-9.pdf>

DERIVING THE PHYSICAL PARAMETERS OF A SOLAR EJECTION WITH AN ISOTROPIC MAGNETOHYDRODYNAMIC EVOLUTIONARY MODEL

Daniel B. [Berdichevsky](#)¹, Guillermo Stenborg² and Angelos Vourlidas

2011 ApJ 741 47

The time-space evolution of a $\sim 50^\circ$ wide coronal mass ejection (CME) on 2007 May 21 is followed remotely with the Solar Terrestrial Relations Observatory heliospheric imager HI-1, and measured in situ near Venus by the MESSENGER and Venus-Express spacecraft. The paper compares the observations of the CME structure with a simple, analytical magnetohydrodynamic force-free solution. It corresponds to a self-similar evolution, which gives a consistent picture of the main spatial-temporal features for both remote and in situ observations. Our main findings are (1) the self-similar evolution allows us to map the CME bright front into about 1/3 of the whole interplanetary counterpart of the coronal mass ejection (ICME, i.e., corresponding to the in situ observed passage of the plasma and magnetic field structure), in good quantitative agreement with the imaging measurements, (2) the cavity following the CME front maps into the rest of the ICME structure, 80% or more of which is consistent with a force free, cylindrically shaped flux rope, and (3) time and space conditions constrain the translational speed of the FR center to 301 km s^{-1} , and the expansion speed of the FR core to 26 km s^{-1} . A careful determination of the ICME cross-section and volume allows us to calculate the mass of the CME bright region ($4.3 \pm 1.1 \cdot 10^{14} \text{ g}$) from the in situ measurements of the proton number density, which we assume to be uniform inside the bright region, of excellent agreement with the value estimated from the SECCHI HI-1 observations for the same structure. We provide model estimates for several global parameters including FR helicity ($\sim 2 \times 10^{26}$ Weber²).

Extreme Event Statistics in Dst, SYM-H, and SMR Geomagnetic Indices

A. [Bergin](#), [S. C. Chapman](#), [N. W. Watkins](#), [N. R. Moloney](#), [J. W. Gjerloev](#)

Space Weather [Volume 21, Issue 3](#) e2022SW003304 2023

<https://doi.org/10.1029/2022SW003304>

<https://agupubs.onlinelibrary.wiley.com/doi/10.1029/2022SW003304>

<https://agupubs.onlinelibrary.wiley.com/doi/epdf/10.1029/2022SW003304>

Extreme space weather events are rare, and quantifying their likelihood is challenging, often relying on geomagnetic indices obtained from ground-based magnetometer observations that span multiple solar cycles. The Dst index ring-current monitor, derived from an hourly average over four low-latitude stations, is a benchmark for extreme space weather events, and has been extensively studied statistically. We apply extreme value theory (EVT) to two geomagnetic ring current indices: SYM-H (derived from 6 stations) and SMR (derived from up to 120 stations). EVT analysis reveals a divergence between the return level found for Dst, and those for SYM-H and SMR, that increases non-linearly with return period. For return periods below 10 years, hourly averaged SYM-H and SMR have return levels similar to Dst, but at return periods of 50 and 100 years, they respectively exceed that of Dst by about 10% and 15% (SYM-H) and about 7% and 12% (SMR). One minute resolution SYM-H and SMR return levels progressively exceed that of Dst; their 5, 10, 50, and 100 year return levels exceed that of Dst by about 10%, 12%, 20% and 25% respectively. Our results indicate that consideration should be given to the differences between the indices if selecting one to use as a benchmark in model validation or resilience planning for the wide range of space weather sensitive systems that underpin our society.

Forecasting the Geomagnetic Activity Several Days in Advance Using Neural Networks Driven by Solar EUV Imaging

Guillaume [Bernoux](#), [Antoine Brunet](#), [Éric Buchlin](#), [Miho Janvier](#), [Angélica Sicard](#)

JGR e2022JA030868 [Volume 127, Issue 10](#) 2022

<https://doi.org/10.1029/2022JA030868>

<https://agupubs.onlinelibrary.wiley.com/doi/epdf/10.1029/2022JA030868>

Many models of the near-Earth's space environment (radiation belts, ionosphere, upper atmosphere, etc.) are driven by geomagnetic indices, representing the state of disturbance of the Earth's magnetosphere. Over the past decade, machine learning-based methods for forecasting geomagnetic indices from near-Earth solar wind parameters have become popular in the space weather community. These methods often prove to be very accurate and skilled. However, these approaches have the notable drawback of being effective in an operational context only for limited forecasting horizons (often up to a couple of hours ahead at best). In order to increase this prediction horizon, we introduce SERENADE, a novel deep learning-based proof-of-concept model using images delivered by the Atmospheric Imaging Assembly instrument onboard the Solar Dynamics Observatory spacecraft to directly provide probabilistic forecasts of the daily maximum of the geomagnetic index Kp up to a few days ahead. We show in particular that SERENADE is able to capture information on the geomagnetic dynamics from solar imaging alone. In addition, despite it being a prototypical

model, our model is more accurate in most situations than three empirical baseline models. However, the model still shows some strong limitations inherent to its structure and the used data set, which could be the focus of future works. This opens the way to a better mid-to-long term data-driven magnetospheric modeling within space weather and geophysical pipelines. **8 September 2017**

Characterizing extreme geomagnetic storms using Extreme Value Analysis: a discussion on the representativeness of short datasets

G. [Bernoux](#), [V. Maget](#)

Space Weather **Volume 18, Issue 6** e2020SW002450 **2020**

<https://sci-hub.tw/10.1029/2020SW002450>

<https://agupubs.onlinelibrary.wiley.com/doi/epdf/10.1029/2020SW002450>

One of the main goals when studying Space Weather is to characterize extreme events occurrences and related characteristics. To do so, dedicated statistical methods from the so-called Extreme Value Analysis (EVA) field have been developed. In this study we used Ca index, derived from aa, in order to characterize geoeffectiveness from the radiation belts point of view with a 150-year long dataset. The analysis performed in this study thus focuses on this newsworthy index to provide clues on the reliability of EVA methods. The first main result we present here is that the 1-in-10, 1-in-50 and 1-in-100 year events respectively match Ca values of 100.39, 131.39 and 142.84 nT. Consequently the only 1-in-100 event observed during the Space Era would be the “Halloween Storm” in 2003 that reached a Ca value of 147.6 nT. The second main result highlighted in this work is that performing the same analysis with shorter subsets (20-year long) can give significantly different results for two reasons. The first reason is that some short time periods do not display the same distribution of events as the full period. The second reason is that the choice of the correct threshold (when using a Peaks Over Threshold approach) is made difficult with a short dataset and leads to inaccurate results. This is a strong result as for accurate estimation of the induced effects of extreme events in radiation belts, we may only rely on short flux datasets from one or another mission (mostly shorter than 20 years). **28 September and 28 October 2013, 15 April-15 May 2017**

Table 1: List of the 15 most extreme events since 1868 with their dates, intensities and empirical return period (1848-2004)

The Great Aurora of 4 February 1872 observed by Angelo Secchi in Rome

Francesco [Berrilli](#), [Luca Giovannelli](#)

Journal of Space Weather and Space Climate **12, 3** **2022**

<https://arxiv.org/pdf/2201.01171.pdf>

<https://www.swsc-journal.org/articles/swsc/pdf/2022/01/swsc210083.pdf>

Observation of auroras at low latitudes is an extremely rare event typically associated with major magnetic storms due to intense Earth-directed Coronal Mass Ejections. Since these energetic events represent one of the most important components of space weather, their study is of paramount importance to understand the Sun-Earth connection. Due to the rarity of these events, being able to access all available information for the few cases studied is equally important. Especially if we refer to historical periods in which current accurate observations from ground-based instruments or space were not available. Certainly, among these events, we must include the great aurora of February 4, 1872. An event whose effects have been observed in different regions of the Earth. What we could consider today a global event, especially for its effects on the communication systems of the time, such as the transatlantic cable that allowed a connection between the United States and Europe since 1866. In this paper, we describe the main results of the observations and studies carried out by Angelo Secchi at the Observatory of the Roman College and described in his Memoria sull’Aurora Elettrica del 4 Febbraio 1872 for the Notes of the Pontifical Academy of new Lincei. This note is extremely modern both in its multi-instrumental approach to the study of these phenomena and in its association between solar-terrestrial connection and technological infrastructures on the Earth. The Secchi’s note definitely represents the first example of analysis and study of an event on a global scale, such as the Atlantic cable, affecting the Earth. What we nowadays call an extreme space weather event.

Complex **Catalogue of High Speed Streams Associated with Geomagnetic Storms During Solar Cycle 24**

Diana [Besliu-Ionescu](#), [Georgeta Maris Muntean](#) & [Venera Dobrica](#)

[Solar Physics](#) volume 297, Article number: 65 (2022)

<https://doi.org/10.1007/s11207-022-01998-3>

A complex catalogue of high speed streams produced by coronal holes and their effects in the terrestrial magnetosphere – the so-called geomagnetic storms – for Solar Cycle 24 (2009 to 2019) is presented here. This catalogue is structured in

three parts describing the high-speed stream characteristics, the interplanetary magnetic field state, and the properties of the associated geomagnetic storms. The catalogue is available online at <http://www.geodin.ro/varsiti/>.

Geoeffectiveness Prediction of CMEs

[Diana Besliu-Ionescu](#) and [Marilena Mierla](#)

Front. Astron. Space Sci., 8:672203 2021 |

<https://www.frontiersin.org/articles/10.3389/fspas.2021.672203/full>

<https://doi.org/10.3389/fspas.2021.672203>

Coronal mass ejections (CMEs), the most important pieces of the puzzle that drive space weather, are continuously studied for their geomagnetic impact. We present here an update of a logistic regression method model, that attempts to forecast if a CME will arrive at the Earth and it will be associated with a geomagnetic storm defined by a minimum Dst value smaller than -30 nT. The model is run for a selection of CMEs listed in the LASCO catalogue during the solar cycle 24. It is trained on three fourths of these events and validated for the remaining one fourth. Based on five CME properties (the speed at 20 solar radii, the angular width, the acceleration, the measured position angle and the source position – binary variable) the model successfully predicted 98% of the events from the training set, and 98% of the events from the validation one.

Solar flare associated coronal mass ejections causing geo-effectiveness and Forbush decreases

[Bhatt, B.](#) & [Chandra, H.](#)

Astrophys Space Sci (2017) 362: 41.

doi:10.1007/s10509-017-3024-0

https://www.researchgate.net/publication/313238149_Solar_flare_associated_coronal_mass_ejections_causing_geo-effectiveness_and_Forbush_decreases

In the present study, we have selected 35 halo Coronal Mass Ejections (CMEs) associated with solar flares, Geomagnetic Storms (GSs) and Forbush decrease (Fd) chosen from 1st January 2000 to 31st December 2007 (i.e., the descending phase of solar cycle 23) observed by the Large Angle Spectrometric Coronagraph (LASCO) on board the SOHO spacecraft. Statistical analyses are performed to look at the distribution of solar flares associated with halo CMEs causing GSs and Fd and investigated the relationship between solar flare and halo CME parameters with GSs and Fd. Forbush decrease is the phenomenon of rapid decrease in cosmic ray intensity following the CME. Our analysis indicates that during 2000 to 2007 the northern region produced 44 % of solar flares associated with halo CMEs, GSs, and Fd, whereas 56 % solar flares associated with halo CMEs, GSs, and Fd were produced in the southern region. The northern and the southern hemispheres between 10° to 20° latitudinal belts are found to be more effective in producing events leading to Fd. From our selected events, we found that about 60 % of super-intense storms ($Dst \leq -200$ nT) caused by halo CMEs are associated with X-class flares. Fast halo CMEs associated with X-class flares originating from 0° to 25° latitudes are better potential candidates in producing super-intense GSs than the slow halo CMEs associated with other classes of flares.

Forecasting of SYMH and ASYH indices for geomagnetic storms of solar cycle 24 including St. Patrick's day, 2015 storm using NARX neural network

Ankush [Bhaskar](#) and Geeta Vichare

J. Space Weather Space Clim. 2019, 9 A12

<https://www.swsc-journal.org/articles/swsc/pdf/2019/01/swsc180011.pdf>

– Artificial Neural Network (ANN) has proven to be very successful in forecasting a variety of irregular magnetospheric/ionospheric processes like geomagnetic storms and substorms. SYMH and ASYH indices represent longitudinal symmetric and the asymmetric component of the ring current. Here, an attempt is made to develop a prediction model for these indices using ANN. The ring current state depends on its past conditions therefore, it is necessary to consider its history for prediction. To account for this effect Nonlinear Autoregressive Network with exogenous inputs (NARX) is implemented. This network considers input history of 30 min and output feedback of 120 min. Solar wind parameters mainly velocity, density, and interplanetary magnetic field are used as inputs. SYMH and ASYH indices during geomagnetic storms of 1998–2013, having minimum SYMH < 85 nT are used as the target for training two independent networks. We present the prediction of SYMH and ASYH indices during nine geomagnetic storms of solar cycle 24 including the recent largest storm occurred on St. Patrick's day, 2015. The present prediction model reproduces the entire time profile of SYMH and ASYH indices along with small variations of ~ 10 – 30 min to the good extent within noise level, indicating a significant contribution of interplanetary sources and past state of the magnetosphere. Therefore, the developed networks can predict SYMH and ASYH indices about an hour before, provided, real-time upstream solar wind data are available. However, during the main phase of major storms, residuals (observed-modeled) are found to be large, suggesting the influence of internal factors such as magnetospheric processes.

RELATIVE CONTRIBUTION OF THE MAGNETIC FIELD BARRIER AND SOLAR WIND SPEED IN ICME-ASSOCIATED FORBUSH DECREASES

Ankush [Bhaskar](#)¹, Prasad Subramanian^{2,3}, and Geeta Vichare

2016 ApJ 828 104

We study 50 cosmic-ray Forbush decreases (FDs) from the Oulu neutron monitor data during 1997–2005 that were associated with Earth-directed interplanetary coronal mass ejections (ICMEs). Such events are generally thought to arise due to the shielding of cosmic rays by a propagating diffusive barrier. The main processes at work are the diffusion of cosmic rays across the large-scale magnetic fields carried by the ICME and their advection by the solar wind. In an attempt to better understand the relative importance of these effects, we analyze the relationship between the FD profiles and those of the interplanetary magnetic field (B) and the solar wind speed (V_{sw}). Over the entire duration of a given FD, we find that the FD profile is generally (anti)correlated with the B and V_{sw} profiles. This trend holds separately for the FD main and recovery phases too. For the recovery phases, however, the FD profile is highly anti-correlated with the V_{sw} profile, but not with the B profile. While the total duration of the FD profile is similar to that of the V_{sw} profile, it is significantly longer than that of the B profile. Using the convection–diffusion model, a significant contribution of advection by solar wind is found during the recovery phases of the FD.

The roles of the magnetic field barrier and solar wind speed in ICME-associated Forbush decreases

Ankush [Bhaskar](#), Prasad Subramanian, Geeta Vichare

2016

<http://arxiv.org/pdf/1605.09537v1.pdf>

We study 50 cosmic ray Forbush decreases (FDs) from the Oulu neutron monitor data during **1997-2005** that were associated with Earth-directed interplanetary coronal mass ejections (ICMEs). Such events are generally thought to arise due to the shielding of cosmic rays by a propagating diffusive barrier. The main processes at work are the diffusion of cosmic rays across the large-scale magnetic fields carried by the ICME and their advection by the solar wind. In an attempt to better understand the relative importance of these effects, we analyse the relationship between the FD profiles and those of the interplanetary magnetic field (B) and the solar wind speed (V_{sw}). Over the entire duration of a given FD, we find that the FD profile is generally well (anti)correlated with the B and V_{sw} profiles. This trend holds separately for the FD main and recovery phases too. For the recovery phases, however, the FD profile is highly anti-correlated with the V_{sw} profile, but not with the B profile. While the total duration of the FD profile is similar to that of the V_{sw} profile, it is significantly longer than that of the B profile.

Table 1: Observed parameters of the ICMEs and associated FD Events

Role of solar wind speed and interplanetary magnetic field during two-step Forbush decreases caused by Interplanetary Coronal Mass Ejections

Ankush [Bhaskar](#), Geeta Vichare, K. P. Arunbabu, Anil Raghav

Astrophysics and Space Science July **2016**, 361:242

The relationship of Forbush decreases (FDs) observed in Moscow neutron monitor with the interplanetary magnetic field (B) and solar wind speed (V_{sw}) is investigated in detail for the FDs associated with Interplanetary Coronal Mass Ejections (ICMEs) during 2001–2004. The classical two-step FD events are selected, and characteristics of the first step (mainly associated with shock), as well as of complete decrease (main phase) and recovery phase, are studied here. It is observed that the onset of FD occurs generally after zero to a few hours of shock arrival, indicating in the post-shock region that mainly sheath and ICME act as important drivers of FD. A good correlation is observed between the amplitude of B and associated FD magnitude observed in the neutron count rate of the main phase. The duration of the main phase observed in the neutron count rate also shows good correlation with B. This might indicate that stronger interplanetary disturbances have a large dimension of magnetic field structure which causes longer fall time of FD main phase when they transit across the Earth. It is observed that V_{sw} and neutron count rate time profiles show considerable similarity with each other during complete FD, especially during the recovery phase of FD. Linear relationship is observed between time duration/e-folding time of FD recovery phase and V_{sw} . These observations indicate that the FDs are influenced by the inhibited diffusion of cosmic rays due to the enhanced convection associated with the interplanetary disturbances. We infer that the inhibited cross-field diffusion of the cosmic rays due to enhanced B is mainly responsible for the main phase of FD whereas the expansion of ICME contributes in the early recovery phase and

the gradual variation of V_{sw} beyond ICME boundaries contributes to the long duration of FD recovery through reduced convection–diffusion.

Comparison of Solar Activity Parameters and Associated Forbush Decreases in Solar Cycles 23 and 24

Beena **Bhatt** & [Harish Chandra](#)

Solar Phys. 298, Article number: 132 (2023)

<https://doi.org/10.1007/s11207-023-02227-1>

We examine the Forbush decreases (FDs) associated with solar flares and coronal mass ejections (CMEs) from January 2008 to December 2019, covering the whole of Solar Cycle 24, and we compare them to our earlier study of Solar Cycle 23 (Bhatt and Chandra, Adv. Space Res. 71, 1098, 2023). On a sample of 56 events, we conducted a statistical analysis using solar and geomagnetic parameters to examine their effect on interplanetary space and the decrease in the galactic cosmic rays (GCR). Our research concentrated on an in-depth analysis of the two most significant events. The first event with an FD magnitude of 11.2% on **8 March 2012** and the second with an FD magnitude of 7.7% on **7 September 2017**, respectively. We discovered that compared to other latitude bands, the northern 11 – 20° latitude band had the highest number of FD-associated flare events. We conducted a statistical analysis of FD magnitude, geomagnetic Dst-index, solar and interplanetary parameters.

23rd solar cycle: Solar activity parameters and associated Forbush decreases

Bhatt, Beena; Chandra, Harish

Advances in Space Research, Volume 71, Issue 1, p. 1098-1107. 2023

<https://www.sciencedirect.com/science/article/pii/S027311772200984X/pdf>

We report Forbush decreases (FD) in cosmic ray intensity from January 1996 to December 2008, the whole Solar Cycle 23rd. Statistical analysis is done for only 152 events for which associated solar flare position, flare classes, and Coronal Mass Ejections (CME) speed are given. We applied FD parameters taken from the Forbush Effects and Interplanetary Disturbances databases maintained by the Pushkov Institute of Terrestrial Magnetism, Ionosphere, and Radiowave Propagation (IZMIRAN), obtained by processing the data of the worldwide neutron monitor network using the global survey method (GSM) (A. Belov et al., 2018). For the said number of events, we examine their effect on interplanetary space and the decrease of the galactic cosmic rays (GCR) near Earth. We found that the 11-20° latitudinal belt shows more FD- associated flare events than the other latitudinal belts, and on this belt, the Southern hemisphere is more active. The results reveal that FDs and solar flares are well correlated. Statistical analysis is carried out for the magnitude of the CR decrease with solar and geomagnetic parameters. **May 21–27, 1997**

Table 1 The selected FDs of the cosmic ray Intensity with their associated solar parameters during 1996–2008

On the specific energy and pressure in near-Earth magnetic clouds

Debesh **Bhattacharjee**, [Prasad Subramanian](#), [Angelos Vourlidis](#), [Teresa Nieves-Chinchilla](#), [Niranjana Thejaswi](#), [Nishtha Sachdeva](#)

A&A 669, A153 2022

<https://arxiv.org/pdf/2210.16571.pdf>

<https://www.aanda.org/articles/aa/pdf/2023/01/aa43603-22.pdf>

The pressure and energy density of the gas and magnetic field inside solar coronal mass ejections (in relation to that in the ambient solar wind) is thought to play an important role in determining their dynamics as they propagate through the heliosphere. We compare the specific energy (erg g^{-1}) [comprising kinetic (H_k), thermal (H_{th}) and magnetic field (H_{mag}) contributions] inside MCs and the solar wind background. We examine if the excess thermal + magnetic pressure and specific energy inside MCs (relative to the background) is correlated with their propagation and internal expansion speeds. We ask if the excess thermal + magnetic specific energy inside MCs might make them resemble rigid bodies in the context of aerodynamic drag. We use near-Earth in-situ data from the WIND spacecraft to identify a sample of 152 well observed interplanetary coronal mass ejections and their MC counterparts. We compute various metrics using these data to address our questions. We find that the total specific energy (H) inside MCs is approximately equal to that in the background solar wind. We find that the the excess (thermal + magnetic) pressure and specific energy are not well correlated with the near-Earth propagation and expansion speeds. We find that the excess thermal+magnetic specific energy \geq the specific kinetic energy of the solar wind incident on 81--89 % of the MCs we study. This might explain how MCs retain their structural integrity and resist deformation by the solar wind bulk flow.

Turbulence and Anomalous Resistivity inside Near-Earth Magnetic Clouds

Debesh **Bhattacharjee**, [Prasad Subramanian](#), [Teresa Nieves-Chinchilla](#), [Angelos Vourlidis](#)

MNRAS 2022

<https://arxiv.org/pdf/2210.17359.pdf>

We use in-situ data from the Wind spacecraft to survey the amplitude of turbulent fluctuations in the proton density and total magnetic field inside a large sample of near-Earth magnetic clouds (MCs) associated with coronal mass ejections (CMEs) from the Sun. We find that the most probable value of the modulation index for proton density fluctuations ($\delta n_p/n_p$) inside MCs ranges from 0.13 to 0.16, while the most probable values for the modulation index of the total magnetic field fluctuations ($\delta B/B$) range from 0.04 to 0.05. We also find that the most probable value of the Mach number fluctuations (δM) inside MCs is ≈ 0.1 . The anomalous resistivity inside near-Earth MCs arising from electron scattering due to turbulent magnetic field fluctuations exceeds the (commonly used) Spitzer resistivity by a factor of ≈ 500 – 1000 . The enhanced Joule heating arising from this anomalous resistivity could impact our understanding of the energetics of CME propagation.

On modeling ICME cross-sections as static MHD columns

Debesh [Bhattacharjee](#), [Prasad Subramanian](#), [Volker Bothmer](#), [Teresa Nieves-Chinchilla](#), [Angelos Vourlidas](#)

Solar Phys. 297, Article number: 45 2022

<https://arxiv.org/pdf/2203.06996.pdf>

<https://link.springer.com/content/pdf/10.1007/s11207-022-01982-x.pdf>

Solar coronal mass ejections are well known to expand as they propagate through the heliosphere. Despite this, their cross-sections are usually modeled as static plasma columns within the magnetohydrodynamics (MHD) framework. We test the validity of this approach using in-situ plasma data from 151 magnetic clouds (MCs) observed by the WIND spacecraft and 45 observed by the Helios spacecrafts. We find that the most probable cross-section expansion speeds for the WIND events are only ≈ 0.06 times the Alfvén speed inside the MCs while the most probable cross-section expansion speeds for the Helios events is ≈ 0.03 . MC cross-sections can thus be considered to be nearly static over an Alfvén crossing timescale. Using estimates of electrical conductivity arising from Coulomb collisions, we find that the Lundquist number inside MCs is high (≈ 1013), suggesting that the MHD description is well justified. The Joule heating rates using our conductivity estimates are several orders of magnitude lower than the requirement for plasma heating inside MCs near the Earth. While the (low) heating rates we compute are consistent with the MHD description, the discrepancy with the heating requirement points to possible departures from MHD and the need for a better understanding of plasma heating in MCs.

Table 1. The list of the 151 WIND ICME events we use in this study. 1995-2015

Table 2. The list of 45 magnetic clouds (MCs) shortlisted by Bothmer & Schwenn (1998) using in-situ data from the Helios 1 and 2 spacecrafts 1974–1981

[Two-dimensional MHD modelling of switchbacks from jetlets in the slow solar wind](#) L14

Ruggero Biondo, Alessandro Bemporad, Paolo Pagano and Fabio Reale

Published online: 28 November 2023

A&A Volume 679, L14, November 2023

DOI: <https://doi.org/10.1051/0004-6361/202347696>

<https://www.aanda.org/articles/aa/pdf/2023/11/aa47696-23.pdf>

Solar wind switchbacks are polarity reversals of the magnetic field, recently frequently measured by Parker Solar Probe inside 0.2 AU. In this Letter we show that magnetic switchbacks, similar to those observed by PSP, are reproduced by injecting a time-limited collimated high-speed stream in the Parker spiral. We performed a 2D magnetohydrodynamics simulation with the PLUTO code of a slightly inclined jet at 1000 km s^{-1} between 5 and $60 R_{\odot}$. The jet rapidly develops a field inversion at its wings and, at the same time, it is bent by the Parker spiral. The match with the radial outward wind field creates two asymmetric switchbacks, one that bends to the anti-clockwise and one that bends to the clockwise direction in the ecliptic plane, with the last one being the most extended. The simulation shows that such S-shaped magnetic features travel with the jet and persist for several hours and to large distances from the Sun (beyond $20 R_{\odot}$). We show the evolution of physical quantities as they would be measured by a hypothetical detector at a fixed position when crossed by the switchback, for comparison with in situ measurements.

Tracing the ICME plasma with a MHD simulation★

Ruggero **Biondo**^{1,2}, Paolo Pagano^{1,3}, Fabio Reale^{1,3} and Alessandro Bemporad²
A&A 654, L3 (2021)

<https://www.aanda.org/articles/aa/pdf/2021/10/aa41892-21.pdf>

<https://arxiv.org/pdf/2211.12993>

The determination of the chemical composition of interplanetary coronal mass ejection (ICME) plasma is an open issue. More specifically, it is not yet fully understood how remote sensing observations of the solar corona plasma during solar disturbances evolve into plasma properties measured in situ away from the Sun. The ambient conditions of the background interplanetary plasma are important for space weather because they influence the evolutions, arrival times, and geo-effectiveness of the disturbances. The Reverse In situ and MHD Approach (RIMAP) is a technique to reconstruct the heliosphere on the ecliptic plane (including the magnetic Parker spiral) directly from in situ measurements acquired at 1 AU. It combines analytical and numerical approaches, preserving the small-scale longitudinal variability of the wind flow lines. In this work, we use RIMAP to test the interaction of an ICME with the interplanetary medium. We model the propagation of a homogeneous non-magnetised (i.e. with no internal flux rope) cloud starting at 800 km s⁻¹ at 0.1 AU out to 1.1 AU. Our 3D magnetohydrodynamics (MHD) simulation made with the PLUTO MHD code shows the formation of a compression front ahead of the ICME, continuously driven by the cloud expansion. Using a passive tracer, we find that the initial ICME material does not fragment behind the front during its propagation, and we quantify the mixing of the propagating plasma cloud with the ambient solar wind plasma, which can be detected at 1 AU.

Preface: Radio Heliophysics: Science and Forecasting

[Bisi, Mario M.](#); [Americo Gonzalez-](#)

[Esparza, J.](#); [Jackson, Bernard V.](#); [Tokumaru, Munetoshi](#); [Leibacher, John](#)

Solar Physics, Volume 290, Issue 9, pp.2393-2396, 2015

<https://link.springer.com/content/pdf/10.1007%2Fs11207-015-0784-y.pdf>

From the Sun to the Earth: The 13 May 2005 Coronal Mass Ejection

M.M. **Bisi** · A.R. Breen · B.V. Jackson · R.A. Fallows · A.P. Walsh · Z. Mikić · P. Riley · C.J. Owen · A. Gonzalez-Esparza · E. Aguilar-Rodriguez · H. Morgan · E.A. Jensen · A.G. Wood · M.J. Owens · M. Tokumaru · P.K. Manoharan · I.V. Chashei · A.S. Giunta · J.A. Linker · V.I. Shishov · S.A. Tyul'bashev · G. Agalya · S.K. Glubokova · M.S. Hamilton · K. Fujiki · P.P. Hick · J.M. Clover · B. Pintér
Solar Phys (2010) 265: 49–127

We report the results of a multi-instrument, multi-technique, coordinated study of the solar eruptive event of 13 May 2005. We discuss the resultant Earth-directed (halo) coronal mass ejection (CME), and the effects on the terrestrial space environment and upper Earth atmosphere. The interplanetary CME (ICME) impacted the Earth's magnetosphere and caused the most-intense geomagnetic storm of 2005 with a Disturbed Storm Time (*Dst*) index reaching -263 nT at its peak. The terrestrial environment responded to the storm on a global scale. We have combined observations and measurements from coronal and interplanetary remote-sensing instruments, interplanetary and near-Earth *in-situ* measurements, remote-sensing observations and *in-situ* measurements of the terrestrial magnetosphere and ionosphere, along with coronal and heliospheric modelling. These analyses are used to trace the origin, development, propagation, terrestrial impact, and subsequent consequences of this event to obtain the most comprehensive view of a geo-effective solar eruption to date. This particular event is also part of a NASA-sponsored Living With a Star (LWS) study and an on-going US NSF-sponsored Solar, Heliospheric, and INTERplanetary Environment (SHINE) community investigation.

THREE-DIMENSIONAL RECONSTRUCTIONS AND MASS DETERMINATION OF THE 2008 JUNE 2 LASCO CORONAL MASS EJECTION USING STELab INTERPLANETARY SCINTILLATION OBSERVATIONS

M. M. **Bisi**¹, B. V. Jackson¹, P. P. Hick^{1,3}, A. Buffington¹, J. M. Clover¹, M. Tokumaru², and K. Fujiki²
Astrophysical Journal Letters, 715:L104–L108, 2010 June

We examine and reconstruct the interplanetary coronal mass ejection (ICME) first seen in space-based coronagraph

white-light difference images on 2008 June 1 and 2. We use observations of interplanetary scintillation (IPS) taken with the Solar-Terrestrial Environment Laboratory (STELab), Japan, in our three-dimensional (3D) tomographic reconstruction of density and velocity. The coronal mass ejection (CME) was first observed by the LASCO C3 instrument at around 04:17 UT on 2008 June 2. Its motion subsequently moved across the C3 field of view with a plane-of-the-sky velocity of 192 km s⁻¹. The 3D reconstructed ICME is consistent with the trajectory and extent of the CME measurements taken from the CDAW CME catalog. However, excess mass estimates vary by an order of magnitude from *Solar and Heliospheric Observatory* and *Solar Terrestrial Relations Observatory* coronagraphs to our 3D IPS reconstructions of the inner heliosphere. We discuss the discrepancies and give possible explanations for these differences as well as give an outline for future studies.

Scintillation Observations of Stream Interaction Regions in the Solar Wind

M. M. Bisi, R. A. Fallows, A. R. Breen & I. J. O'Neill

Solar Phys., 261(1), Page: 149 – 172, 2010

We present a summary of results from ten years of interplanetary scintillation (IPS) observations of stream interaction regions (SIRs) in the solar wind. Previous studies had shown that SIRs were characterized by intermediate-velocity solar wind and – in the case of compressive interactions – higher levels of scintillation. In this study we considered all cases of intermediate velocities in IPS observations from the *European Incoherent SCATter* (EISCAT) radar facility made at low- and mid-heliographic latitudes between 1994 and 2003. After dismissing intermediate-velocity observations which were associated with solar-wind transients (such as coronal mass ejections) we found that the remaining cases of intermediate velocities lay above coronal structures where stream interaction would be expected. An improved ballistic mapping method (compared to that used in earlier EISCAT studies of interaction regions) was used to identify the regions of raypath in IPS observations which might be expected to include interaction regions and to project these regions out to the distances of *in-situ* observations. The early stages of developing compression regions, consistent with their development on the leading edges of compressive stream interaction regions, were clearly detected as close to the Sun as 30 R_{\odot} , and further ballistic projection out to the distances of *in-situ* observations clearly associated these developing structures with density and velocity features characteristic of developed interaction regions in *in-situ* data in the cases when such data were available. The same approach was applied to study non-compressive interaction regions (shear layers) between solar-wind streams of different velocities where the stream interface lay at near-constant latitude and the results compared with those from compressive interaction regions. The results confirm that intermediate velocities seen in IPS observations above stream boundaries may arise from either detection of intermediate-velocity flow in compression regions, or from non-compressive shear layers. The variation in velocity about the mean determined from IPS measurements (representing the spread in velocity across that part of the raypath associated with the interaction region in the analysis) was comparable in compressive and non-compressive regions – a potentially interesting result which may contain important information on the geometry of developing SIRs. It is clear from these results that compressive and non-compressive interaction regions belong to the same class of stream – stream interaction, with the dominant mode determined by the latitudinal gradient of the stream interface. Finally, we discuss the results from this survey in the light of new data from the *Heliospheric Imagers* (HI) on the *Solar TERrestrial RELations Observatory* (STEREO) spacecraft and other instruments, and suggest possible directions for further work.

3-D reconstructions of the early-November 2004 CDAW geomagnetic storms: analysis of Ooty IPS speed and density data

M. M. Bisi¹, B. V. Jackson¹, J. M. Clover¹, P. K. Manoharan², M. Tokumaru³, P. P. Hick^{1,4}, and A. Buffington¹

Ann. Geophys., 27, 4479-4489, 2009; **File**

www.ann-geophys.net/27/4479/2009/

Interplanetary scintillation (IPS) remote-sensing observations provide a view of the solar wind covering a wide range of heliographic latitudes and heliocentric distances from the Sun between ~0.1 AU and 3.0 AU. Such observations are used to study the development of solar coronal transients and the solar wind while propagating out through interplanetary space. They can also be used to measure the inner-heliospheric response to the passage of coronal mass ejections (CMEs) and co-rotating heliospheric structures. IPS observations can, in general, provide a speed estimate of the heliospheric material crossing the observing line of site; some radio antennas/arrays can also provide a radio scintillation level. We use a three-dimensional (3-D) reconstruction technique which obtains perspective views from outward-flowing solar wind and co-rotating structure as observed from Earth by iteratively fitting a kinematic solar wind model to these data. Using this 3-D modelling technique, we are able to reconstruct the velocity and density of CMEs as they travel through interplanetary space. For the time-dependent model used here with IPS data taken from the Ootacamund

(Ooty) Radio Telescope (ORT) in India, the digital resolution of the tomography is 10° by 10° in both latitude and longitude with a half-day time cadence. Typically however, the resolutions range from 10° to 20° in latitude and longitude, with a half- to one-day time cadence for IPS data dependant upon how much data are used as input to the tomography. We compare reconstructed structures during early-November 2004 with in-situ measurements from the Wind spacecraft orbiting the Sun-Earth L_1 -Point to validate the 3-D tomographic reconstruction results and comment on how these improve upon prior reconstructions.

Low-Resolution STELab IPS 3D Reconstructions of the Whole Heliosphere Interval and Comparison with in-Ecliptic Solar Wind Measurements from STEREO and *Wind* Instrumentation

M.M. Bisi · B.V. Jackson · A. Buffington · J.M. Clover · P.P. Hick · M. Tokumaru

Solar Phys (2009) 256: 201–217, DOI 10.1007/s11207-009-9350-9, **2009**

STEREO SCIENCE RESULTS AT SOLAR MINIMUM

We present initial 3D tomographic reconstructions of the inner heliosphere during the Whole Heliosphere Interval (WHI) – Carrington Rotation 2068 (CR2068) – using Solar-Terrestrial Environment Laboratory (STELab) Interplanetary Scintillation (IPS) observations. Such observations have been used for over a decade to visualise and investigate the structure of the solar wind and to study in detail its various features. These features include co-rotating structures as well as transient structures moving out from the Sun. We present global reconstructions of the structure of the inner heliosphere during this time, and compare density and radial velocity with multi-point *in situ* spacecraft measurements in the ecliptic; namely STEREO and *Wind* data, as the interplanetary medium passes over the spacecraft locations.

Three-dimensional reconstructions of the early November 2004 Coordinated Data Analysis Workshop geomagnetic storms: Analyses of STELab IPS speed and SMEI density data,

Bisi, M. M., Jackson, B. V., Hick, P. P., Buffington, A., Odstrcil, D., and Clover, J. M.:

J. Geophys. Res., 113, A00A11, doi:10.1029/2008JA013222, **2008a.**

Combined interplanetary scintillation (IPS) and Solar Mass Ejection Imager (SMEI) remote-sensing observations provide a view of the solar wind at almost all heliographic latitudes and covering distances from the Sun between 0.1 AU and 3.0 AU. They are used to study the development of the solar wind and coronal transients as they move out into interplanetary space, and also the inner heliospheric response to the passage of corotating solar structures and coronal mass ejections (CMEs). The observations take place in both radio scintillation level and speed for IPS, and in Thomson-scattered white light brightness for SMEI. With colleagues at the Solar Terrestrial Environment Laboratory (STELab), Nagoya University, Japan, we have developed a data analysis system for the STELab IPS data which can also be applied to SMEI white light data. This employs a three-dimensional (3-D) reconstruction technique that obtains perspective views from solar corotating plasma and outward flowing solar wind as observed from the Earth by iterative fitting of a kinematic solar wind model to the data. This 3-D modeling technique permits reconstructions of the density and speed of CMEs and other interplanetary transients at relatively coarse spatial and temporal resolutions. For the time-dependent model (used here), these typically range from 5° to 20° in latitude and longitude, with a 1/2 to 1 day time cadence. For events during early November 2004 we compare these reconstructed structures with in situ measurements from the ACE and Wind (near-Earth) spacecraft to validate the 3-D tomographic reconstruction results and provide input to the ENLIL 3-D magnetohydrodynamic (MHD) numerical model.

A Prolonged Southward IMF-Bz Event of May 02--04, 1998: Solar, Interplanetary Causes and Geomagnetic Consequences

Susanta Kumar Biso, D. Chakrabarty, P. Janardhan, R.G. Rastogi, A. Yoshikawa, K. Fujiki, M. Tokumaru, Y. Yan

JGR Vol: 121, Pages: 3882–3904 **2016**

<http://arxiv.org/pdf/1604.04959v1.pdf>

A detailed investigation was carried out to understand a prolonged (~44 hours) weakly southward interplanetary magnetic field (IMF-Bz) condition during **May 02--04, 1998**. In-situ observations, during the period, showed the passage of an expanding magnetic cloud embedded in an interplanetary coronal mass ejection (ICME), followed up by a shock and an interplanetary discontinuity driven by another ICME. It is the arrival of the ICMEs and the upfront shocks that cause the prolonged southward IMF-Bz condition. The magnetic configuration of the source regions of the IMF associated with the ICME interval were also examined, which showed open magnetic field structures, emanating from a small active region on the north of the heliospheric current sheet (HCS). The structures remained constantly to the north of the HCS, both on April 29 and May 01, suggesting no change in their polarity. The draping of these outward directed

radial field lines around the propagating CMEs in the shocked plasma explained the observed polarity changes of the IMF-Bz at 1 AU. In addition, multiple enhancements were also detected in the geomagnetic field variations, which showed a distinct one-to-one correspondence with the density pulses observed at 1 AU, during 0700--1700 UT on May 03. The spectral analysis of both the variations showed the same discrete frequencies of 0.48, 0.65 and 0.75 mHz, demonstrating that the solar wind density enhancements can cause detectable global geomagnetic disturbances. The observations, thus, provide a deeper insight into the possible causes and geomagnetic consequences of a prolonged weakly southward IMF-Bz condition.

Are Switchback boundaries observed by Parker Solar Probe closed?

[Nina Bizien](#), [Thierry Dudok de Wit](#), [Clara Froment](#), [Marco Velli](#), [Anthony W. Case](#), [Stuart D. Bale](#), [Justin Kasper](#), [Phyllis Whittlesey](#), [Robert MacDowall](#), [Davin Larson](#)

ApJ **958** 23 **2023**

<https://arxiv.org/pdf/2310.12134.pdf>

<https://iopscience.iop.org/article/10.3847/1538-4357/acf99a/pdf>

Switchbacks are sudden and large deflections in the magnetic field that Parker Solar Probe frequently observes in the inner heliosphere. Their ubiquitous occurrence has prompted numerous studies to determine their nature and origin. Our goal is to describe the boundary of these switchbacks using a series of events detected during the spacecraft's first encounter with the Sun. Using FIELDS and SWEAP data, we investigate different methods for determining the boundary normal. The observed boundaries are arc-polarized structures with a rotation that is always contained in a plane. Classical minimum variance analysis (MVA) gives misleading results and overestimates the number of rotational discontinuities. We propose a robust geometric method to identify the nature of these discontinuities, which involves determining whether or not the plane that contains them also includes the origin ($B=0$). Most boundaries appear to have the same characteristics as tangential discontinuities in the context of switchbacks, with little evidence for having rotational discontinuities. We find no effect of the size of the Parker spiral deviation. Furthermore, the thickness of the boundary is within MHD scales. We conclude that most of the switchback boundaries observed by Parker Solar Probe are likely to be closed, in contrast to previous studies. Our results suggest that their erosion may be much slower than expected. **2018-11-02, 2018 November 7**

Animations available at [this https URL](#)

Space weather effects on Earth's environment associated to the 24–25 October 2011 geomagnetic storm

E. [Blanch](#), S. Marsal, A. Segarra, J. M. Torta, D. Altadill and J. J. Curto

Space Weather, Volume 11, Issue 4, pages 153–168, April 2013

<http://onlinelibrary.wiley.com/doi/10.1002/swe.20035/abstract>

Space weather studies have increased due to human society dependence on spaceborne and terrestrial infrastructure vulnerable to its effects. In this paper, we present an interdisciplinary study of the effects of solar activity on the Earth's environment; specifically, we focus on the effects on the ionosphere and the geomagnetic field. A timeline of effects occurring on the Earth produced by one of the first relevant events of the present solar cycle (24–25 October 2011) is given. We have analyzed the solar wind shockwave from satellite data, the storm-time development, the ionospheric effects at global and local scales using the National Center for Atmospheric Research Thermosphere-Ionosphere-Electrodynamics General Circulation Model fed with geomagnetic field-aligned current data from the Active Magnetosphere and Planetary Electrodynamics Response Experiment, and ground ionosonde data from both hemispheres, at Ebre Observatory and Port Stanley locations. We have compared observed geomagnetic variations at high latitudes with those modeled by the National Center for Atmospheric Research Thermosphere-Ionosphere-Electrodynamics General Circulation Model. We have analyzed rapid geomagnetic variations (e.g., solar flare effect, storm commencement, Pi2) also on both hemispheres, at Ebre Observatory and Livingston Island locations. Finally, we have estimated geoelectric field and geomagnetically induced currents in the northeast of Spain (Catalonia) produced by this geomagnetic disturbance.

Energetic-particle-flux decreases related to magnetic cloud passages as observed by the Helios 1 and 2 spacecraft

J. J. [Blanco](#)¹, M. A. [Hidalgo](#)¹, R. [Gómez-Herrero](#)¹, J. [Rodríguez-Pacheco](#)¹, B. [Heber](#)², R. F. [Wimmer-Schweingruber](#)² and C. [Martín](#)

A&A 556, A146 (2013)

It has been observed that a magnetic cloud (MC) can affect the propagation conditions of solar energetic particles and low-energy cosmic rays. This effect is commonly observed as a decrease in the energetic-particle fluxes, which are partially excluded from the interior of the cloud. The twin spacecraft Helios 1 and Helios 2 explored the inner heliosphere between 0.29 AU and 1 AU from the mid 1970s to early 1980s. The E6 Experiment onboard Helios is the energetic-particle detector able to measure electrons, protons and alphas in the range of 300 keV/n to >50 MeV/n. It has been shown previously that, in absence of strong solar-particle events, the single detector rates of the E6 anti-coincidence and sapphire Cherenkov detectors are sensitive to cosmic rays with rigidities above GV. Because their statistical precision is in the order of hundreds of counts per second, both detectors are very well suited for studying the short-term decreases observed in their count rates during magnetic cloud passages. A total of 35 magnetic clouds have been identified at the Helios locations. Nineteen of them were free of solar energetic-particle contamination. This subset led us to investigate the effect of magnetic clouds on the galactic cosmic ray (GCR) flux. The depth of the decreases are studied in terms of the solar wind and magnetic field properties of the magnetic cloud. We found dependences with the MC magnetic field strength, magnetic rigidity and with the MC time of flight, with the latter supporting the idea of magnetically closed MCs, i.e. with the two legs rooted in the Sun. We also studied MC properties and found evidence of MC expansion during its journey through the inner heliosphere. **Table**

Observable Effects of Interplanetary Coronal Mass Ejections on Ground Level Neutron Monitor Count Rates

J. J. **Blanco**, E. Catalán, M. A. Hidalgo, J. Medina, O. García, J. Rodríguez-Pacheco
Solar Phys., Volume 284, Issue 1, pp 167-178, 2013

In this work, **non-recurrent Forbush decreases (FDs)** triggered by the passage of shock-driving interplanetary coronal mass ejections (ICMEs) have been analyzed. Fifty-nine ICMEs have been studied, but only 25 % of them were associated to a FD. We find that shock-driving magnetic clouds (MCs) produce deeper FDs than shock-driving ejecta. This fact can be explained regarding the observed growing trends between decreases in neutron monitor (NM) count rate and MC/ejecta speed and its associated rigidity. MCs are faster and have higher associated rigidities than ejecta. Also the deceleration of ICMEs seems to be a cause for producing FDs, as can be inferred from the decreasing trend between NM count rate and deceleration. This probably implies that the interaction between the ICME traveling from the corona to the Earth and the solar wind can play an important role in producing deeper FDs. Finally, we conclude that ejecta without flux rope topology are the ones less effective in unchaining FDs.

Interaction between magnetic clouds and the heliospheric current sheet at 1 AU as it is observed by one single observation point

J.J. **Blanco**, a, , M.A. Hidalgo, J. Rodríguez-Pacheco and J. Medina

Journal of Atmospheric and Solar-Terrestrial Physics, Volume 73, Issues 11-12, 2011, Pages 1339-1347

The effect of Magnetic Clouds (MCs) on the Heliospheric Current Sheet (HCS) local structure is yet an open question. Although it is widely accepted that a magnetic cloud has an important effect on the HCS shape, their structural relation, either the MC is part of the HCS or not, is not completely solved. Moreover, the problem grows up when trying to investigate three dimensional structures using one single observation point. We propose an approach to the MC-HCS study using magnetic models for the MC and local HCS structures, which are able of determining their relative orientation from one single spacecraft data. Three events have been selected in which an MC passage was observed close to HCS crossings. The results confirm the strong effect of MC passage on the HCS local orientation and they seem to be consistent with MCs propagating out of the HCS at 1 AU.

Interplanetary shocks and foreshocks observed by STEREO during 2007–2010†

X. **Blanco-Cano**, P. Kajdič, E. Aguilar-Rodríguez, C. T. Russell, L. K. Jian, J. G. Luhmann
JGR 2015

Interplanetary shocks in the heliosphere modify the solar wind through which they pass. In particular, shocks play an important role in particle acceleration. During the extended solar minimum (2007–2010) STEREO observed 65 forward shocks driven by stream interactions (SI), with magnetosonic Mach numbers $M_{ms} \approx 1.1-4.0$ and shock normal angles $\theta_{Bn} \sim 20-87^\circ$. We analyze the waves associated with these shocks and find that the region upstream can be permeated by whistler waves ($f \sim 1$ Hz) and/or ultra low frequency (ULF) waves ($f \sim 10^{-2}-10^{-1}$ Hz). While whistlers appear to be

generated at the shock, the origin of ULF waves is most probably associated with local kinetic ion instabilities. We find that when the Mach number (M_{ms}) is low and the shock is quasi-perpendicular ($\theta_{Bn} > 45^\circ$) whistler waves remain close to the shock. As M_{ms} increases, the shock profile changes and can develop a foot and overshoot associated with ion reflection and gyration. Whistler precursors can be superposed on the foot region, so that some quasi-perpendicular shocks have characteristics of both subcritical and supercritical shocks. When the shock is quasi-parallel ($\theta_{Bn} < 45^\circ$) a large foreshock with suprathermal ions and waves can form. Upstream there are whistler trains at higher frequencies whose characteristics can be slightly modified probably by reflected and/or leaked ions, and by almost circularly polarized waves at lower frequencies that may be locally generated by ion instabilities. In contrast with planetary bow shocks, most of the upstream waves studied here are mainly transverse and no steepening occurs. Some quasi-perpendicular shocks ($45^\circ < \theta_{Bn} < 60^\circ$) are preceded by ULF waves and ion foreshocks. Fluctuations downstream of quasi-parallel shocks tend to have larger amplitudes than waves in the sheath of quasi-perpendicular shocks. We compare SI driven shock properties with those of shocks generated by interplanetary coronal mass ejections (ICMEs). During the same years, STEREO observed 20 ICME driven shocks with $M_{ms} \approx 1.2-4.0$ and $\theta_{Bn} \sim 38-85^\circ$. We find that shocks driven by ICMEs tend to have larger proton foreshocks ($dr \sim 0.1$ AU) than shocks driven by stream interactions ($dr \leq 0.05$ AU). This difference of ion foreshock size should be linked to shock age: ICME driven shocks form at shorter distances to the Sun and therefore can energize particles for longer times as they propagate to 1 AU, while stream interaction shocks form closer to Earth's orbit, and have been accelerating ions for a shorter interval of time.

Kuramoto Model of Nonlinear Coupled Oscillators as a Way for Understanding Phase Synchronization: Application to Solar and Geomagnetic Indices

Elena M. [Blanter](#), Jean-Louis Le Mouél, Mikhail G. Shnirman, Vincent Courtillot
Solar Physics, Volume 289, Issue 11, pp 4309-4333 2014

We apply a Kuramoto model of nonlinear coupled oscillators to the simulation of slow variations of the phase difference between sunspot number [R I] and geomagnetic indices [aa and ζ]. The Kuramoto model is described for the particular case of two oscillators connected by symmetric coupling with quasi-stationary behavior, and its properties are investigated. By solving an inverse problem, we reconstruct the evolution of the couplings between pairs of indices [R I and aa , R I and ζ , aa and ζ], and interpret these in terms of the physics of the solar dynamo. The de-correlation between R I and geomagnetic indices found in Solar Cycle 20 by Le Mouél et al. (J. Geophys. Res. 117, A09103, 2012) is successfully reproduced by the Kuramoto model and corresponds to the alternation of the leading oscillator. Application of the Kuramoto model to the cross-correlations [$C(R I, \zeta)$ and $C(aa, \zeta)$] for ζ -indices computed in eight geomagnetic stations shows the latitudinal dependence of the mean phase difference. We discuss these results in terms of the solar-wind contribution to local geomagnetic indices [ζ].

Loss of synchronization in the 27-day spectral component of geomagnetic indices and its relationship with solar activity

Elena [Blanter](#), Jean-Louis Le Mouél, Mikhail Shnirman, Vincent Courtillot,
JASTP, v. 117, pp. 71-80, 2014

<http://www.sciencedirect.com/science/article/pii/S1364682614000868>

We investigate the “27-day” spectral component of different global (aa and Dst) and local (ζ) geomagnetic indices in two period ranges relevant to the Sun's synodic rotation, as manifested by magnetic activity: 24–28 days (short) and 28–32 days (long). Cross-correlation analysis of the respective energies of the short and long periods of the 27-day rotation signal in the same geomagnetic index reveals well-defined de-synchronization events during certain solar cycles. The largest de-synchronization in the past century occurred during Solar Cycle 21. De-synchronization events first occur in indices of the Dst (and ζ) family, and then in indices of the aa family. We found no evidence that the strength of the de-synchronization of the solar rotation signal in the ζ -index would depend on geomagnetic latitude. Applying the same analysis to proper solar indices (sunspot number, $F10.7$ radio flux, interplanetary magnetic field (IMF) series, solar wind speed), we find that only the B_z component of the IMF demonstrates a de-synchronization, during Solar Cycle 21, between the energies of the 27-day solar rotation signal in the short and long period ranges. We discuss possible implications of these results with respect to the evolution of the toroidal and poloidal components of the Sun's magnetic field and to its large-scale structures.

Data-Driven Classification of Coronal Hole and Streamer Belt Solar Wind

Téo [Bloch](#), [Clare Watt](#), [Mathew Owens](#), [Leland McInnes](#) & [Allan R. Macneil](#)

[Solar Physics](#) volume 295, Article number: 41 (2020)

<https://link.springer.com/content/pdf/10.1007/s11207-020-01609-z.pdf>

<https://doi.org/10.1007/s11207-020-01609-z>

We present two new solar wind origin classification schemes developed independently using unsupervised machine learning. The first scheme aims to classify solar wind into three types: coronal-hole wind, streamer-belt wind, and 'unclassified' which does not fit into either of the previous two categories. The second scheme independently derives three clusters from the data; the coronal-hole and streamer-belt winds, and a differing unclassified cluster. The classification schemes are created using non-evolving solar wind parameters, such as ion charge states and composition, measured during the three Ulysses fast latitude scans. The schemes are subsequently applied to the Ulysses and the Advanced Compositional Explorer (ACE) datasets. The first scheme is based on oxygen charge state ratio and proton specific entropy. The second uses these data, as well as the carbon charge state ratio, the alpha-to-proton ratio, the iron-to-oxygen ratio, and the mean iron charge state. Thus, the classification schemes are grounded in the properties of the solar source regions. Furthermore, the techniques used are selected specifically to reduce the introduction of subjective biases into the schemes. We demonstrate significant best case disparities (minimum $\approx 8\%$, maximum $\approx 22\%$) with the traditional fast and slow solar wind determined using speed thresholds. By comparing the results between the in- (ACE) and out-of-ecliptic (Ulysses) data, we find morphological differences in the structure of coronal-hole wind. Our results show how a data-driven approach to the classification of solar wind origins can yield results which differ from those obtained using other methods. As such, the results form an important part of the information required to validate how well current understanding of solar origins and the solar wind match with the data we have.

A Nonlinear System Science Approach to Find the Robust Solar Wind Drivers of the Multivariate Magnetosphere

S. [Blunier](#) , [B. Toledo](#) , [J. Rogan](#) , [J. A. Valdivia](#)

Space Weather e2020SW002634 2021

<https://agupubs.onlinelibrary.wiley.com/doi/epdf/10.1029/2020SW002634>

We propose a method, based on Neural Networks, that detects the non-linear robust interplanetary solar wind variables, with varying delays, driving the coupled behavior of three geomagnetic indices (Dst, AL, and AU). As opposed to minimizing a prediction error, the method is based on degrading the prediction by distorting the inputs of the trained Neural Networks in order to highlight the most sensible drivers. We show that the z component of the magnetic field, the duskward oriented electric field, and the speed of the particles of the interplanetary medium, at particular time delays, seem to be the most efficient drivers of the three coupled geomagnetic indices. Using only the sensible or robust drivers in the model, we demonstrate that iterated predictions during geomagnetic storm are significantly improved from models that only use one of the outstanding drivers with multiple time delays. The derived robust non-linear Neural Network model is also a significant improvement over linear approximations, specially when used as iterated predictors.

HELCASTS Prediction of Planetary CME arrival times

[Boakes](#), Peter; [Moestl](#), Christian; [Davies](#), Jackie; [Harrison](#), Richard; [Byrne](#), Jason; [Barnes](#), David; [Isavnin](#), Al exey; [Kilpua](#), Emilia; [Rollett](#), Tanja

EGU General Assembly 2015, held 12-17 April, 2015 in Vienna, Austria. id.3601, 2015

We present the first results of CME arrival time prediction at different planetary locations and their comparison to the in situ data within the HELCASTS project. The EU FP7 HELCASTS (Heliospheric Cataloguing, Analysis & Techniques Service) is a European effort to consolidate the exploitation of the maturing field of heliospheric imaging. HELCASTS aims to catalogue solar wind transients, observed by the NASA STEREO Heliospheric Imager (HI) instruments, and validate different methods for the determination of their kinematic properties. This validation includes comparison with arrivals at Earth, and elsewhere in the heliosphere, as well as onsets at the Sun (<http://www.helcats-fp7.eu/>). A preliminary catalogue of manually identified CMEs, with over 1000 separate events, has been created from observations made by the STEREO/HI instruments covering the years 2007-2013. Initial speeds and directions of each CME have been derived through fitting the time elongation profile to the state of the art Self-Similar Expansion Fitting (SSEF) geometric technique (Davies et al., 2012). The technique assumes that, in the plane corresponding to the position angle of interest, CMEs can be modelled as circles subtending a fixed angular width to Sun-center and propagating anti-sunward in a fixed direction at a constant speed (we use an angular width of 30 degrees in our initial results). The model has advantages over previous geometric models (e.g. harmonic mean or fixed phi) as it allows one to predict whether a CME will 'hit' a specific heliospheric location, as well as to what degree (e.g. direct assault or glancing blow). We use correction formulae (Möstl and Davies, 2013) to convert CME speeds, direction and launch time to speed and arrival time at any in situ location. From the preliminary CME dataset, we derive arrival times for over 400 Earth-directed CMEs, and for over 100 Mercury-, Venus-, Mars- and Saturn-directed CMEs predicted to impact each planet. We

present statistics of predicted CME arrival properties. In addition, we independently identify CME arrival at in situ locations using magnetic field data from the Venus Express, Messenger, and Ulysses spacecraft and show first comparisons to predicted arrival times. The results hold important implications for space weather prediction at Earth and other locations, allowing model and predicted CME parameters to be compared to their in situ counterparts.

Estimation of the modulation level of cosmic rays at high energies

Pavol [Bobik](#), [M Putis](#), [Y L Kolesnyk](#), [B A Shakhov](#)

Monthly Notices of the Royal Astronomical Society, Volume 503, Issue 3, May 2021, Pages 3386–3393,

<https://doi.org/10.1093/mnras/stab597>

<https://watermark.silverchair.com/stab597.pdf>

In this article, we focus on the modulation of cosmic rays at high energies. The aim is to determine the limits of the ability of the heliosphere to modulate the intensities of cosmic rays in the inner heliosphere. We address the following questions: how large is the variation in cosmic rays intensities at high energies, i.e. close to 50, 100, and 200 GeV and above? What is the maximum energy at which modulation effects can be measured near the Earth? Specifically, we look at the magnitudes of the variation in cosmic rays intensity at 1 au over the period 1990–2012, at high energies. Attention is paid to energies of around 50, 100, and 150 GeV, where we can expect experimental results within the next decade.

Statistical Analysis of Solar Events Associated with Storm Sudden Commencements over One Year of Solar Maximum during Cycle 23: Propagation from the Sun to the Earth and Effects

K. [Bocchialini](#), [B. Grison](#), [M. Menvielle](#), [A. Chambodut](#), [N. Cornilleau-Wehrin](#), [D. Fontaine](#), [A.](#)

[Marchaudon](#), [M. Pick](#), [F. Pitout](#), [B. Schmieder](#), [S. Regnier](#), [I. Zouganelis](#)

Solar Phys. 293:75 2018

<https://arxiv.org/pdf/1803.07593.pdf>

<https://link.springer.com/content/pdf/10.1007%2Fs11207-018-1278-5.pdf>

Taking the 32 storm sudden commencements (SSCs) listed by the International Service of Geomagnetic Indices (ISGI) of the Observatory de l'Ebre during 2002 (solar activity maximum in Cycle 23) as a starting point, we performed a multi-criterion analysis based on observations (propagation time, velocity comparisons, sense of the magnetic field rotation, radio waves) to associate them with solar sources, identified their effects in the interplanetary medium, and looked at the response of the terrestrial ionized and neutral environment. We find that 28 SSCs can be related to 44 coronal mass ejections (CMEs), 15 with a unique CME and 13 with a series of multiple CMEs, among which 19 (68%) involved halo CMEs. Twelve of the 19 fastest CMEs with speeds greater than 1000 km s⁻¹ are halo CMEs. For the 44 CMEs, including 21 halo CMEs, the corresponding X-ray flare classes are: 3 X-class, 19 M-class, and 22 C-class flares. The probability for an SSC to occur is 75% if the CME is a halo CME. Among the 500, or even more, front-side, non-halo CMEs recorded in 2002, only 23 could be the source of an SSC, i.e.5%. The complex interactions between two (or more) CMEs and the modification of their trajectories have been examined using joint white-light and multiple-wavelength radio observations. The detection of long-lasting type IV bursts observed at metric–hectometric wavelengths is a very useful criterion for the CME–SSC events association. The events associated with the most depressed Dst values are also associated with type IV radio bursts. The four SSCs associated with a single shock at L1 correspond to four radio events exhibiting characteristics different from type IV radio bursts. The solar-wind structures at L1 after the 32 SSCs are 12 magnetic clouds (MCs), 6 interplanetary coronal mass ejections (ICMEs) without an MC structure, 4 miscellaneous structures, which cannot unambiguously be classified as ICMEs, 5 corotating or stream interaction regions (CIRs/SIRs), one CIR caused two SSCs, and 4 shock events; note that one CIR caused two SSCs. The 11 MCs listed in 3 or more MC catalogs covering the year 2002 are associated with SSCs. For the three most intense geomagnetic storms (based on Dst minima) related to MCs, we note two sudden increases of the Dst, at the arrival of the sheath and the arrival of the MC itself. In terms of geoeffectiveness, the relation between the CME speed and the magnetic-storm intensity, as characterized using the Dst magnetic index, is very complex, but generally CMEs with velocities at the Sun larger than 1000 km s⁻¹ have larger probabilities to trigger moderate or intense storms. The most geoeffective events are MCs, since 92% of them trigger moderate or intense storms, followed by ICMEs (33%). At best, CIRs/SIRs only cause weak storms. We show that these geoeffective events (ICMEs or MCs) trigger an increased and combined auroral kilometric radiation (AKR) and non-thermal continuum (NTC) wave activity in the magnetosphere, an enhanced convection in the ionosphere, and a stronger response in the thermosphere. However, this trend does not appear clearly in the coupling functions, which exhibit relatively weak correlations between the solar-wind energy input and the amplitude of various geomagnetic indices, whereas the role of the southward component of the solar-wind magnetic field is confirmed. Some saturation appears for Dst values <-100<-100 nT on the integrated values of the polar and auroral indices. **15 March 2002 , 22 March 2002, 17 April 2002**

Table 1. The 32 SSCs observed during 2002

Table 3. The 44 CMEs associated with the 32 SSCs

CESRA nugget #1895 July 2018 <http://www.astro.gla.ac.uk/users/eduard/cesra/?p=1895>

Correction Solar Phys (2019) 294:38 <https://link.springer.com/content/pdf/10.1007%2Fs11207-019-1426-6.pdf>

Diagnostics of Corotating Interaction Regions with the kinetic properties of iron ions as determined with STEREO/PLASTIC

P **Bochsler**, M A Lee, R Karrer, L Ellis, C J Farrugia, A B Galvin, L M Kistler, H Kucharek, E Moebius, M A Popecki, K D C Simunac, L M Blush, H Daoudi, P Wurz, B Klecker, R F Wimmer-Schweingruber, B Thompson, J G Luhmann, C T Russell, L Jian, and A Optiz

Ann. Geophys., 28, 491-497, **2010**

STEREO/PLASTIC determines three-dimensional distributions of solar wind iron ions with unprecedented time resolution. Typically 300 to 1000 counts are registered within each 5 min time interval. For the present study we use the information contained in these distributions to characterize CIRs (Corotating Interaction Regions) in two test cases. We perform a consistency test for both the derived physical parameters and for the analytical model of CIRs of Lee (2000). At 1 AU we find that apart from compositional changes the most indicative parameter for marking the time when a CIR passes a spacecraft is the angular deflection of the flow vector of particles. Changes in particle densities and the changes in magnitudes of speeds are apparently less reliable indicators of stream interfaces.

Langmuir waves associated with magnetic holes in the solar wind

J. J. **Boldú**^{1,2}, D. B. Graham¹, M. Morooka¹, M. André¹, Yu. V. Khotyaintsev¹, T. Karlsson³, J.

Souček⁴, D. Piša⁴ and M. Maksimovic⁵

A&A 674, A220 (**2023**)

<https://www.aanda.org/articles/aa/pdf/2023/06/aa46100-23.pdf>

Context. Langmuir waves (electrostatic waves near the electron plasma frequency) are often observed in the solar wind and may play a role in the energy dissipation of electrons. The largest amplitude Langmuir waves are typically associated with type II and III solar radio bursts and planetary foreshocks. In addition, Langmuir waves not related to radio bursts occur in the solar wind, but their source is not well understood. Langmuir waves have been observed inside isolated magnetic holes, suggesting that magnetic holes play an important role in the generation of Langmuir waves. *Aims.* We provide the statistical distribution of Langmuir waves in the solar wind at different heliocentric distances. In particular, we investigate the relationship between magnetic holes and Langmuir waves. We identify possible source regions of Langmuir waves in the solar wind, other than radio bursts, by analyzing the local plasma conditions. *Methods.* We analyzed data from Solar Orbiter's Radio and Plasma Waves (RPW) and Magnetometer (MAG) instruments. We used the triggered electric field snapshots and onboard statistical data (STAT) of the Time Domain Sampler (TDS) of RPW to identify Langmuir waves and investigate their properties. The plasma densities were derived from the spacecraft potential estimated by RPW. The MAG data were used to monitor the background magnetic field and detect magnetic holes, which are defined as regions with an isolated decrease in $|B|$ of 50% or more compared to the background level. The statistical analysis was performed on data from 2020 to 2021, comprising heliocentric distances between 0.5 AU and 1 AU.

Results. We show that 78% of the Langmuir waves in the solar wind not connected to radio bursts occur in regions of local magnetic field depletions, including the regions classified as isolated magnetic holes. We also show that the Langmuir waves occur more frequently inside magnetic holes than in any other region in the solar wind, which indicates that magnetic holes are important source regions of solar wind Langmuir waves. We find that Langmuir waves associated with magnetic holes in the solar wind typically have lower amplitudes than those associated with radio bursts.

Dynamics of coronal mass ejections in the interplanetary medium:

A. **Borgazzi**, A. Lara, E. Echer and M. V. Alves

A&A 498 (**2009**) 885-889; **File**

Context. Coronal mass ejections (CMEs) are large plasma structures expelled from the low corona to the interplanetary space with a wide range of speeds. In the interplanetary medium CMEs suffer changes in their speeds because of interaction with the ambient solar wind.

Aims. To understand the interplanetary CME (ICME) dynamics, we analyze the interaction between these structures and the ambient solar wind (SW), approaching the problem from the hydrodynamic point of view.

Methods. We assume that the dynamics of the system is dominated by two kinds of drag-force dependence on speed (U), as $\sim U$ and $\sim U^2$. Furthermore, we propose a model that takes variations of the ICME radius (R) and SW density (ρ_{sw})

) into account as a function of the distance (x) as $R(x) = x^{0.78}$ and $\rho_{sw}(x) = 1/x^2$, respectively. Then, we solve the equation of motion and present exact solutions

Results. Considering CME speeds measured at a few solar radii and at one AU, we were able to constrain the values of the constants (viscosity and drag coefficient) for the linear (U) and quadratic (U^2) speed dependences, which seems to reproduce the ICME – SW system well. We found different solutions in which the concavity of the curves of the ICME speed profile changes, depending on the dominant factor, either the ICME radius or the SW density.

Conclusions. This work shows that the macroscopic ICME propagation may be described by the hydrodynamic theory and that it is possible to find analytical solutions for the ICME-SW interaction.

A Statistical Analysis of the Fluctuations in the Upstream and Downstream Plasmas of 109 Strong-Compression Interplanetary Shocks at 1 AU

Joseph E. **Borovsky**

JGR [Volume 125, Issue 6](#) June 2020 e2019JA027518

<https://agupubs.onlinelibrary.wiley.com/doi/10.1029/2019JA027518>

https://agupubs.onlinelibrary.wiley.com/doi/pdf/10.1029/2019JA027518?casa_token=fK3j0CL6N9oAAAAA:nVyVvLmO5v_RdDb-K8ywPdrvLiRa92BiFlibPrE3tjveR-AP2SiSPW4s6Jfq_h1rIq5xNSo1IwrZF2B4

The upstream and downstream plasmas of 109 strong-compression forward interplanetary shocks are statistically analyzed using 3-s measurements from the WIND spacecraft. The goal is a comparison of the fluctuation properties of downstream plasmas in comparison with the fluctuation properties of upstream plasmas in the inertial range of frequencies and the magnetic-structure range of spatial scales. The shocks all have density compression ratios of ~ 2 or more. When possible, each shock is categorized according to the type of solar wind plasma it propagates through: 15 shocks are in coronal-hole-origin plasma, 42 shocks are in streamer-belt-origin plasma, 36 shocks are in sector-reversal-region plasmas, and 11 shocks are in ejecta plasma. The statistical study examines magnetic field and velocity spectral indices, the Alfvénicity, the fluctuation amplitudes, Alfvén ratios, the degree of plasma inhomogeneity, and Taylor microscales, looking in particular at (1) fluctuation values downstream that are related to fluctuation values upstream and (2) systematic differences in fluctuation values associated with the type of plasma. It is argued that inhomogeneity of the downstream plasma can be caused by spatial variations in the shock normal angle θ_{Bn} caused by field direction variations in the upstream magnetic structure. The importance of determining the type of plasma that the shock propagates through is established. **23 January 2001**

Table 1 The Collection of 109 Strong-Compression Forward Interplanetary Shocks as Seen by the WIND Spacecraft and the Type of Solar Wind Plasma They Are Propagating Through (1995-1999)

Plasma and Magnetic-Field Structure of the Solar Wind at Inertial-Range Scale Sizes Discerned From Statistical Examinations of the Time-Series Measurements **Review**

Joseph E. **Borovsky**

Front. Astron. Space Sci., **2020** |

<https://doi.org/10.3389/fspas.2020.00020>

This paper reviews the properties of the magnetic and plasma structure of the solar wind in the inertial range of spatial scales ($500\text{--}5 \times 10^6$ km), corresponding to spacecraft timescales from 1 s to a few hr. Spacecraft data sets at 1 AU have been statistically analyzed to determine the structure properties. The magnetic structure of the solar wind often has a flux-tube texture, with the magnetic flux tube walls being strong current sheets and the field orientation varying strongly from tube to tube. The magnetic tubes also exhibit distinct plasma properties (e.g., number density, specific entropy), with variations in those properties from tube to tube. The ion composition also varies from tube to tube, as does the value of the electron heat flux. When the solar wind is Alfvénic, the magnetic structure of the solar wind moves outward from the Sun faster than the proton plasma does. In the reference frame moving outward with the structure, there are distinct field-aligned plasma flows within each flux tube. In the frame moving with the magnetic structure the velocity component perpendicular to the field is approximately zero; this indicates that there is little or no evolution of the magnetic structure as it moves outward from the Sun. Large sudden velocity shears are seen across the boundaries between the magnetic flux tubes as the magnetic field rotates and the field-aligned flow rotates. The effect of the solar-wind current sheets on the magnetic power spectral density of the solar wind is examined: the current sheets are found to dominate the spectral properties of the solar wind.

On the Motion of the Heliospheric Magnetic Structure Through the Solar Wind Plasma

Joseph E. **Borovsky**

JGR [Volume125, Issue2](#) February 2020 e2019JA027377

<https://agupubs.onlinelibrary.wiley.com/doi/pdf/10.1029/2019JA027377>

A reference frame in the solar wind can often be found wherein the flow vector v is everywhere approximately parallel to the magnetic field vector B . This is the frame of the heliospheric magnetic structure moving relative to the plasma. Since $v \perp B$ is very small in this reference frame, the magnetic structure appears to have little temporal evolution. The structure moves outward away from the Sun faster than the plasma flow. Even for highly Alfvénic plasma, the structure does not move at the Alfvén speed relative to the proton plasma, rather it moves at $\sim 0.7 v_A$. This may be caused by the spread in the vector directions of the local magnetic field. The degree of inhomogeneity of the plasma is hypothesized to control the motion of the magnetic structure through the plasma. If so, non-Alfvénicity may be owed to an inability of Alfvénic perturbations to coherently propagate from Alfvénic injections at the Sun. Schemes that mathematically advect magnetic and plasma structure from upstream solar wind monitors to the Earth may be improved by calculating and including the motion of the structure relative to the solar wind velocity vector.

Some Properties of the Solar Wind Turbulence at 1 AU Statistically Examined in the Different Types of Solar Wind Plasma

Joseph E. **Borovsky**, Michael H. Denton, Charles W. Smith

JGR [Volume124, Issue4](#) April 2019 Pages 2406-2424

sci-hub.se/10.1029/2019JA026580

A four-plasma classification scheme is used to categorize the ACE solar wind data set into four types of plasma: (1) coronal-hole-origin plasma, (2) streamer-belt-origin plasma, (3) sector-reversal-region plasma, and (4) ejecta. The statistical properties of the solar wind fluctuations at 1 AU are analyzed for each of the four types of plasma in the years 1998–2008 using ACE magnetic field and plasma measurements. Between the four types of solar wind plasma there are subtle statistical differences in the spectral indices of (a) trace- B , (b) trace- v , (c) total energy, (d) magnetic intensity, and (e) plasma number density. Between the four types of plasma there are significant statistical differences (a) in the Elsässer inward and outward spectral indices, (b) in the outward imbalance, (c) in the Alfvénicity, (d) in the normalized vector- B , vector- v , magnetic intensity, and number density fluctuation amplitudes, (e) in the population of strong current sheets, (f) in the population of sudden velocity shears, (g) in the anisotropies of magnetic field and velocity fluctuations, and (h) in the parallel-to- B magnetic field fluctuation spectral index. It is argued that the four-plasma categorization scheme is superior to a slow-versus-fast categorization for the study of turbulence and fluctuations in the solar wind.

On the Origins of the Intercorrelations between Solar-Wind Variables

Joseph E. **Borovsky**

JGR Volume 123, Issue 1 January 2018 Pages 20–29

<http://sci-hub.tw/10.1002/2017JA024650>

sci-hub.se/10.1002/2017JA024650

It is well known that the time variations of the diverse solar-wind variables at 1 AU (e.g. solar-wind speed, density, proton temperature, electron temperature, magnetic-field strength, specific entropy, heavy-ion charge-state densities, electron strahl intensity) are highly intercorrelated with each other. In correlation studies of the driving of the Earth's magnetosphere-ionosphere-thermosphere system by the solar wind, these solar-wind intercorrelations make determining cause and effect very difficult. In this report analysis of solar-wind spacecraft measurements and compressible-fluid computer simulations are used to study the origins of the solar-wind intercorrelations. Two causes are found: (1) synchronized changes in the values of the solar-wind variables as the plasma types of the solar wind are switched by solar rotation and (2) dynamic interactions (compressions and rarefactions) in the solar wind between the Sun and the Earth. These findings provide an incremental increase in the understanding of how the Sun-Earth system operates.

Is the Dst Index Sufficient to Define All Geospace Storms?

Joseph E. **Borovsky**, Yuri Shprits

JGR 2017

<http://onlinelibrary.wiley.com/doi/10.1002/2017JA024679/pdf>

The purpose of this commentary is (1) to raise awareness about some shortcomings of the use of the Dst index to identify storms, to gauge storm intensity, and to represent stormtime space-weather phenomena and (2) to initiate discussions about different types of storms and about improved identifiers for different types of storms.

The trailing edges of high-speed streams at 1 AU

Joseph E. Borovsky, Michael H. Denton

JGR Volume 121, Issue 7 July 2016 Pages 6107–6140

The trailing-edge rarefactions of 54 high-speed streams at 1 AU are analyzed. The temporal durations of the trailing-edge rarefactions agree with ballistic calculations based on the observed speeds of the fast and slow wind bounding the rarefactions. A methodology is developed to measure solar-wind compression and rarefaction using the orientations of solar-wind current sheets. One focus is to determine the signature that best describes the location of the trailing-edge stream interface between coronal-hole-origin plasma and streamer-belt-origin plasma; based on the current-sheet orientations, on the magnetic-field strength, on the intensity of the electron strahl, and on the intensity of the negative vorticity, an inflection point in the temporal profile of the solar-wind velocity is taken as the best indicator of the trailing-edge stream interface. Computer simulations support this choice. Using superposed-epoch analysis, the plasma properties and turbulence properties of trailing-edge rarefactions are surveyed. Whereas the signatures of the coronal-hole/streamer-belt (slow-wind/fast-wind) boundary in the leading edge (corotating interaction region) stream interface are simultaneous, they are not simultaneous in the trailing edge, with ion-charge-state signatures occurring on average 13.7 h prior to the proton entropy signature. It is suggested that differences in the leading and trailing edges of coronal holes on the Sun might account for the differences in the leading and trailing edges of high-speed streams at 1 AU: the formation timescales, heating timescales, and charge-state-equilibration timescales of closed flux loops in the corona might be involved.

The differences between storms driven by helmet streamer CIRs and storms driven by pseudostreamer CIRs.

Borovsky JE, Denton MH

(2013) JGRA 118: 5506-5521

Differences between CME-driven storms and CIR-driven storms.

Borovsky, J. E., and Denton, M. H.

2006. J. Geophys. Res., 111, A07S08, doi:10.1029/2005JA011447.

sci-hub.se/10.1029/2005JA011447

Twenty one differences between CME-driven geomagnetic storms and CIR-driven geomagnetic storms are tabulated. (CME-driven includes driving by CME sheaths, by magnetic clouds, and by ejecta; CIR-driven includes driving by the associated recurring high-speed streams.) These differences involve the bow shock, the magnetosheath, the radiation belts, the ring current, the aurora, the Earth's plasma sheet, magnetospheric convection, ULF pulsations, spacecraft charging in the magnetosphere, and the saturation of the polar cap potential. CME-driven storms are brief, have denser plasma sheets, have strong ring currents and Dst, have solar energetic particle events, and can produce great auroras and dangerous geomagnetically induced currents; CIR-driven storms are of longer duration, have hotter plasmas and stronger spacecraft charging, and produce high fluxes of relativistic electrons. Further, the magnetosphere is more likely to be preconditioned with dense plasmas prior to CIR-driven storms than it is prior to CME-driven storms. CME-driven storms pose more of a problem for Earth-based electrical systems; CIR-driven storms pose more of a problem for space-based assets.

Propagation of Cosmic Rays in Heliosphere: the HelMod Model

M.J. Boschini, S. Della Torre, M. Gervasi, G. La Vacca, P. G. Rancoita

Advances in Space Research 62 (2018) 2859-2879

<https://arxiv.org/pdf/1704.03733.pdf>

The heliospheric modulation model \helmod{} is a two dimensional treatment dealing with the helio-colatitude and radial distance from Sun and is employed to solve the transport-equation for the GCR propagation through the heliosphere down to Earth. This work presents the current version 3 of the \helmod{} model and reviews how main processes involved in GCR propagation were implemented.~The treatment includes the so-called particle drift effects -- ~e.g., those resulting, for instance, from the extension of the neutral current sheet inside the heliosphere and from the curvature and gradient of the IMF --, which affect the transport of particles entering the solar cavity as a function of their charge sign.~The \helmod{} model is capable to provide modulated spectra which well agree within the experimental errors with those measured by AMS-01, BESS, PAMELA and AMS-02 during the solar cycles 23 and 24.~Furthermore, the counting rate measured by Ulysses at +/- 80degree of solar latitude and 1 to 5\,AU was also found in agreement with that expected by \helmod{} code version 3.

A Twenty-First Century View of the March 1989 Magnetic Storm

D.H. Boteler

Space Weather [Volume17, Issue10](#) Pages 1427-1441 2019

<https://doi.org/10.1029/2019SW002278>

<https://agupubs.onlinelibrary.wiley.com/doi/10.1029/2019SW002278>

sci-hub.se/10.1029/2019sw002278

On March 13, 1989, the largest magnetic storm of the last century caused widespread effects on power systems including a blackout of the Hydro-Québec system. Since then this event has become the archetypal disturbance for examining the geomagnetic hazard to power systems. However, even 30 years on from 1989, the story of exactly what happened in March 1989 is far from complete. This paper re-examines the information available about the March 1989 event and uses this to construct a timeline and description of the space weather phenomena and how they caused the power system effects. The evidence shows that the disturbance was caused by two coronal mass ejections (CMEs): the first associated with a X4.5 flare on March 10 and the second linked to a M7.3 flare on March 12. The arrival of the interplanetary coronal mass ejection (ICME) shock fronts caused storm sudden commencements (SSC) at 01.27 UT and 07.43 UT on March 13. The transit time and speed of the first (second) ICME shock are 54.5 hrs (31.5 hrs) and 760 km/sec (1320 km/sec). Empirical relations are used to estimate solar wind speed and southward IMF, B_s , and give values of $v=980$ km/sec, $B_s=40$ nT to 60nT at the peak of the storm. Key findings are that the second SSC occurred at the same time as the substorm that impacted the Hydro-Québec system and indicates that external triggering of the substorm may have contributed to a faster substorm onset than might otherwise have occurred. This caused the production of larger geomagnetically induced currents (GIC) that caused the Hydro-Québec blackout. The March 1989 storm had the largest recorded value of the Dst index representing the size of the magnetic storm main phase, but the Hydro-Québec blackout occurred early in the storm when the Dst value was less disturbed. Only later in the storm did Dst reach its peak value. At this time an expansion of the auroral oval brought disturbances to lower latitudes where they caused power system problems in the US, UK and Sweden.

Comparison of CME and ICME Structures Derived from Remote-Sensing and In Situ Observations

V. Bothmer, N. Mrotzek

[Solar Physics](#) November 2017, 292:157

<https://link.springer.com/article/10.1007/s11207-017-1171-7>

We present results from the comparison of the near-Sun and in situ analysis of two Earth-directed coronal mass ejections (CMEs) with different 3D orientations and solar source region characteristics. The CME on **14 July 2000**, the so-called Bastille Day storm, a well-studied event, was observed from a single-point perspective by the Large Angle and Spectrometric Coronagraph (LASCO) onboard the Solar and Heliospheric Observatory (SOHO). It caused a major geomagnetic storm with a peak K_p of 9. The CME originated from a magnetic bipolar photospheric source region with the polarity inversion line being oriented rather parallel to the heliographic equator. In contrast, the CME on **29 September 2013**, which caused a geomagnetic storm with a peak K_p intensity of 8-, originated from a magnetic quadrupolar photospheric source region with the polarity inversion line between the two bipoles almost vertically oriented with respect to the heliographic equator. The results of a graduated cylindrical shell (GCS) analysis of the CMEs near the Sun are compared with the minimum variance analysis (MVA) of the magnetic field structure of the interplanetary CME (ICME) measured in situ near Earth's orbit. The results are in good agreement for the September 2013 CME and ICME, whereas the July 2000 ICME appears substantially inclined near Earth's orbit. The discrepancy can likely be explained taking into account kinks in the CME's near-Sun structure of the CME that expands into the interplanetary medium.

Sources of magnetic helicity over solar cycle

Bothmer, V.

Proc. ISCS Symp. ESA-SP-535, 2003, File

The magnetic field characteristics of a sample set of helical magnetic flux rope ICMEs (magnetic clouds) observed by the Wind and ACE satellites in solar cycle 23 and their related space weather effects are investigated. The solar source regions of the magnetic clouds were identified using remote sensing observations of the SOHO, Yohkoh and TRACE spacecraft together with ground-based $H\alpha$ images. Each cloud observed at 1 AU could be uniquely associated with a well defined frontside halo CME some days before the cloud's arrival at 1 AU. The hemispheric origin is consistent with

the expected hemispheric helicity pattern. The space weather effects of the clouds were quite variable, depending on their internal magnetic field configuration and speed of propagation

The structure and origin of magnetic clouds in the solar wind

V. [Bothmer](#)^{1*} and R. Schwenn

Ann. Geophysicae 16, 1±24 (1998), [File](#)

Plasma and magnetic field data from the Helios 1/2 spacecraft have been used to investigate the structure of magnetic clouds (MCs) in the inner heliosphere. 46 MCs were identified in the Helios data for the period 1974-1981 between 0.3 and 1 AU. 85% of the MCs were associated with fast-forward interplanetary shock waves, supporting the close association between MCs and SMEs (solar mass ejections). Seven MCs were identified as direct consequences of Helios-directed SMEs, and the passage of MCs agreed with that of interplanetary plasma clouds (IPCs) identified as white-light brightness enhancements in the Helios photometer data. The total (plasma and magnetic field) pressure in MCs was higher and the plasma- β lower than in the surrounding solar wind. Minimum variance analysis (MVA) showed that MCs can best be described as large-scale quasi-cylindrical magnetic flux tubes. The axes of the flux tubes usually had a small inclination to the ecliptic plane, with their azimuthal direction close to the east-west direction. The large-scale flux tube model for MCs was validated by the analysis of multi-spacecraft observations. MCs were observed over a range of up to $\sim 60^\circ$ in solar longitude in the ecliptic having the same magnetic configuration. The Helios observations further showed that over-expansion is a common feature of MCs. From a combined study of Helios, Voyager and IMP data we found that the radial diameter of MCs increases between 0.3 and 4.2 AU proportional to the distance, R , from the Sun as $R^{0.8}$ (R in AU). The density decrease inside MCs was found to be proportional to $R^{-2.4}$, thus being stronger compared to the average solar wind. Four different magnetic configurations, as expected from the flux-tube concept, for MCs have been observed in situ by the Helios probes. MCs with left- and right-handed magnetic helicity occurred with about equal frequencies during 1974-1981, but surprisingly, the majority (74%) of the MCs had a south to north (SN) rotation of the magnetic field vector relative to the ecliptic. In contrast, an investigation of solar wind data obtained near Earth's orbit during 1984-1991 showed a preference for NS-clouds. A direct correlation was found between MCs and large quiescent filament disappearances (disappearance brusques, DBs). The magnetic configurations of the filaments, as inferred from the orientation of the prominence axis, the polarity of the overlying field lines and the hemispheric helicity pattern observed for filaments, agreed well with the in situ observed magnetic structure of the associated MCs. The results support the model of MCs as large-scale expanding quasi-cylindrical magnetic flux tubes in the solar wind, most likely caused by SMEs associated with eruptions of large quiescent filaments. We suggest that the hemispheric dependence of the magnetic helicity structure observed for solar filaments can explain the preferred orientation of MCs in interplanetary space as well as their solar cycle behavior. However, the white-light features of SMEs and the measured volumes of their interplanetary counterparts suggest that MCs may not simply be just $H<\alpha>$ -prominences, but that SMEs likely convect large-scale coronal loops overlying the prominence axis out of the solar atmosphere.

Eruptive prominences as sources of magnetic clouds in the solar wind,

[Bothmer](#), V. and Schwenn, R. ,

Space Sci. Rev. 70, 215, 1994

Towards an AI-based understanding of the solar wind: A critical data analysis of ACE data.

[Bouriat](#) S, Vandame P, Barthélémy M and Chanutot J

(2022) Front. Astron. Space Sci. 9: 980759.

doi: 10.3389/fspas.2022.980759

<https://www.frontiersin.org/articles/10.3389/fspas.2022.980759/pdf>

All artificial intelligence models today require preprocessed and cleaned data to work properly. This crucial step depends on the quality of the data analysis being done. The Space Weather community increased its use of AI in the past few years, but a thorough data analysis addressing all the potential issues is not always performed beforehand. Here is an analysis of a largely used dataset: Level-2 Advanced Composition Explorer's SWEPAM and MAG measurements from 1998 to 2021 by the ACE Science Center. This work contains guidelines and highlights issues in the ACE data that are likely to be found in other space weather datasets: missing values, inconsistency in distributions, hidden information in statistics, etc. Amongst all specificities of this data, the following can seriously impact the use of algorithms: Histograms are not uniform distributions at all, but sometime Gaussian or Laplacian. Algorithms will be inconsistent in the learning samples as some rare cases will be underrepresented. Gaussian distributions could be overly brought by Gaussian noise from measurements and the signal-to-noise ratio is difficult to estimate.

Models will not be reproducible from year to year due to high changes in histograms over time. This high dependence on the solar cycle suggests that one should have at least 11 consecutive years of data to train the algorithm.

Rounding of ion temperatures values to different orders of magnitude throughout the data, (probably due to a fixed number of bits on which measurements are coded) will bias the model by wrongly over-representing or under-representing some values.

There is an extensive number of missing values (e.g., 41.59% for ion density) that cannot be implemented without pre-processing. Each possible pre-processing is different and subjective depending on one's underlying objectives

A linear model will not be able to accurately model the data. Our linear analysis (e.g., PCA), struggles to explain the data and their relationships. However, non-linear relationships between data seem to exist.

Data seem cyclic: we witness the apparition of the solar cycle and the synodic rotation period of the Sun when looking at autocorrelations.

Some suggestions are given to address the issues described to enable usage of the dataset despite these challenges.

Turbulence Characteristics of Switchback and Nonswitchback Intervals Observed by Parker Solar Probe

Sofiane [Bourouaine](#)^{1,2}, Jean C. Perez¹, Kristopher G. Klein³, Christopher H. K. Chen⁴, Mihailo Martinović³, Stuart D. Bale^{4,5,6,7}, Justin C. Kasper⁸, and Nour E. Raouafi²

2020 ApJL 904 L30

<https://doi.org/10.3847/2041-8213/abbd4a>

<https://iopscience.iop.org/article/10.3847/2041-8213/abbd4a/pdf>

We use Parker Solar Probe (PSP) in situ measurements to analyze the characteristics of solar wind turbulence during the first solar encounter covering radial distances between 35.7R_☉ and 41.7R_☉. In our analysis we isolate so-called switchback (SB) intervals (folded magnetic field lines) from nonswitchback (NSB) intervals, which mainly follow the Parker spiral field. Using a technique based on conditioned correlation functions, we estimate the power spectra of Elsasser, magnetic, and bulk velocity fields separately in the SB and NSB intervals. In comparing the turbulent energy spectra of the two types of intervals, we find the following characteristics: (1) The decorrelation length of the backward-propagating Elsasser field z^- is larger in the NSB intervals than the one in the SB intervals; (2) the magnetic power spectrum in SB intervals is steeper, with spectral index close to $-5/3$, than in NSB intervals, which have a spectral index close to $-3/2$; (3) both SB and NSB turbulence are imbalanced with NSB having the largest cross-helicity, (4) the residual energy is larger in the SB intervals than in NSB, and (5) the analyzed fluctuations are dominated by Alfvénic fluctuations that are propagating in the sunward (antisunward) direction for the SB (NSB) turbulence. These observed features provide further evidence that the switchbacks observed by PSP are associated with folded magnetic field lines giving insight into their turbulence nature.

Inner-Heliosphere Signatures of Ion-Scale Dissipation and Nonlinear Interaction

Trevor A. [Bowen](#), [Alfred Mallet](#), [Stuart D. Bale](#), [J. W. Bonnell](#), [Anthony W. Case](#), [Benjamin D. G. Chandran](#), [Alexandros Chasapis](#), [Christopher H. K. Chen](#), [Die Duan](#), [Thierry Dudok de Wit](#), [Keith Goetz](#), [Jasper Halekas](#), [Peter R. Harvey](#), [J. C. Kasper](#), [Kelly E. Korreck](#), [Davin Larson](#), [Roberto Livi](#), [Robert J. MacDowall](#), [David M. Malaspina](#), [Marc Pulupa](#), [Michael Stevens](#), [Phyllis Whittlesey](#)

2020

<https://arxiv.org/pdf/2001.05081.pdf>

We perform a statistical study of the turbulent power spectrum at inertial and kinetic scales observed during the first perihelion encounter of Parker Solar Probe. We find that often there is an extremely steep scaling range of the power spectrum just above the ion-kinetic scales, similar to prior observations at 1 AU, with a power-law index of around -4 . Based on our measurements, we demonstrate that either a significant ($>50\%$) fraction of the total turbulent energy flux is dissipated in this range of scales, or the characteristic nonlinear interaction time of the turbulence decreases dramatically from the expectation based solely on the dispersive nature of nonlinearly interacting kinetic Alfvén waves.

Ion Scale Electromagnetic Waves in the Inner Heliosphere

Trevor [Bowen](#), [Alfred Mallet](#), [Jia Huang](#), [Kristopher G. Klein](#), [David M. Malaspina](#), [Michael L. Stevens](#), [Stuart D. Bale](#), [John W. Bonnell](#), [Anthony W. Case](#), [Benjamin D. Chandran](#), [Christopher Chaston](#), [Christopher H. Chen](#), [Thierry Dudok de Wit](#), [Keith Goetz](#), [Peter R. Harvey](#), [Gregory G. Howes](#), [Justin C. Kasper](#), [Kelly Korreck](#), [Davin E. Larson](#), [Roberto Livi](#), [Robert J. MacDowall](#), [Michael McManus](#), [Marc Pulupa](#), [J Verniero](#), [Phyllis Whittlesey](#)

ApJ **2019**

<https://arxiv.org/pdf/1912.02361.pdf>

Understanding the physical processes in the solar wind and corona which actively contribute to heating, acceleration, and dissipation is a primary objective of NASA's **Parker Solar Probe (PSP)** mission. Observations of coherent electromagnetic waves at ion scales suggests that linear cyclotron resonance and non-linear processes are dynamically relevant in the inner heliosphere. A wavelet-based statistical study of coherent waves in the first perihelion encounter of PSP demonstrates the presence of transverse electromagnetic waves at ion resonant scales which are observed in 30-50% of radial field intervals. Average wave amplitudes of approximately 4 nT are measured, while the mean duration of wave events is of order 20 seconds; however long duration wave events can exist without interruption on hour-long timescales. Though ion scale waves are preferentially observed during intervals with a radial mean magnetic field, we show that measurement constraints, associated with single spacecraft sampling of quasi-parallel waves superposed with anisotropic turbulence, render the measured quasi-parallel ion-wave spectrum unobservable when the mean magnetic field is oblique to the solar wind flow; these results imply that the occurrence of coherent ion-scale waves is not limited to a radial field configuration. The lack of strong radial scaling of characteristic wave amplitudes and duration suggests that the waves are generated $\{\em{in-situ}\}$ through plasma instabilities. Additionally, observations of proton distribution functions indicate that temperature anisotropy may drive the observed ion-scale waves. **Oct 31- Nov 11, 2018**

THE SOLAR ERUPTION OF 2005 MAY 13 AND ITS EFFECTS: LONG-BASELINE INTERPLANETARY SCINTILLATION OBSERVATIONS OF THE EARTH-DIRECTED CORONAL MASS EJECTION

Data derived NARMAX Dst model

Boynton, R. J.; Balikhin, M. A.; Billings, S. A.; Sharma, A. S.; Amariutei, O. A.

Annales Geophysicae, Volume 29, Issue 6, **2011**, pp.965-971

<http://www.ann-geophys.net/29/965/2011/angeo-29-965-2011.pdf>

The NARMAX OLS-ERR methodology is applied to identify a mathematical model for the dynamics of the Dst index. The NARMAX OLS-ERR algorithm, which is widely used in the field of system identification, is able to identify a mathematical model for a wide class of nonlinear systems using input and output data. Solar wind-magnetosphere coupling functions, derived from analytical or data based methods, are employed as the inputs to such models and the outputs are geomagnetic indices. The newly deduced coupling function, $p1/2V4/3BT\sin6(\theta/2)$, has been implemented as an input to model the Dst dynamics. It was shown that the identified model has a very good forecasting ability, especially with the geomagnetic storms.

Inner Structure of CME Shock Fronts Revealed by the Electromotive Force and Turbulent Transport Coefficients in Helios-2 Observations

Philippe-A. **Bourdin** (1), **Bernhard Hofer** (1,2), **Yasuhito Narita** (1,2,3)

ApJ **855** 111 **2018**

<https://arxiv.org/pdf/1802.10111.pdf>

<http://sci-hub.tw/10.3847/1538-4357/aaae04>

Electromotive force is an essential quantity in dynamo theory. During a coronal mass ejection (CME), magnetic helicity gets decoupled from the Sun and advected into the heliosphere with the solar wind. Eventually, a heliospheric magnetic transient event might pass by a spacecraft, such as the Helios space observatories. Our aim is to investigate the electromotive force, the kinetic helicity effect (α term), the turbulent diffusion (β term) and the cross-helicity effect (γ term) in the inner heliosphere below 1 au. We set up a one-dimensional model of the solar wind velocity and magnetic field for a hypothetical interplanetary CME. Because turbulent structures within the solar wind evolve much slower than this structure needs to pass by the spacecraft, we use a reduced curl operator to compute the current density and vorticity. We test our CME shock-front model against an observed magnetic transient that passes by the Helios-2 spacecraft. At the peak of the fluctuations in this event we find strongly enhanced α , β and γ terms, as well as a strong peak in the total electromotive force. Our method allows us to automatically identify magnetic transient events from any in-situ spacecraft observations that contain magnetic field and plasma velocity data of the solar wind.

Scaling Laws for Dynamic Solar Loops

Stephen J. **Bradshaw**¹ and A. Gordon Emslie²

2020 ApJ 904 141

<https://doi.org/10.3847/1538-4357/abbf50>

The scaling laws that relate the peak temperature T_M and volumetric heating rate E_H to the pressure P and length L for static coronal loops were established over 40 yr ago; they have proved to be of immense value in a wide range of studies. Here we extend these scaling laws to dynamic loops, where enthalpy flux becomes important to the energy balance, and study impulsive heating/filling characterized by upward enthalpy flows. We show that for collision-dominated thermal conduction, the functional dependencies of the scaling laws are the same as for the static case, when the radiative losses scale as $T^{-1/2}$, but with a different constant of proportionality that depends on the Mach number M of the flow. The dependence on the Mach number is such that the scaling laws for low to moderate Mach number flows are almost indistinguishable from the static case. When thermal conduction is limited by turbulent processes, however, the much weaker dependence of the scattering mean free path (and hence thermal conduction coefficient) on temperature leads to a limiting Mach number for return enthalpy fluxes driven by thermal conduction between the corona and chromosphere.

Coronal mass ejection deformation at 0.1 au observed by WISPR

Carlos R. **Braga**, [Angelos Vourlidis](#), [Paulett C. Liewer](#), [Phillip Hess](#), [Guillermo Stenborg](#), [Pete Riley](#)

ApJ 938 13 2022

<https://arxiv.org/pdf/2209.13057.pdf>

<https://iopscience.iop.org/article/10.3847/1538-4357/ac90bf/pdf>

Although coronal mass ejections (CMEs) resembling flux ropes generally expand self-similarly, deformations along their fronts have been reported in observations and simulations. We present evidence of one CME becoming deformed after a period of self-similarly expansion in the corona. The event was observed by multiple white-light imagers on **January 20-22, 2021**. The change in shape is evident in observations from the heliospheric imagers from the Wide-Field Imager for Solar Probe Plus (WISPR), which observe this CME for ~ 44 hours. We reconstruct the CME using forward-fitting models. In the first hours, observations are consistent with a self-similar expansion but later on the front flattens forming a dimple. Our interpretation is that the CME becomes deformed at ~ 0.1 au due to differences in the background solar wind speeds. The CME expands more at higher latitudes, where the background solar wind is faster. We consider other possible causes for deformations, such as loss of coherence and slow-mode shocks. The CME deformation seems to cause a time-of-arrival error of 16 hours at ~ 0.5 au. The deformation is clear only in the WISPR observations and, it thus, would have been missed by 1-AU coronagraphs. Such deformations may help explain the time-of-arrival errors in events where only coronagraph observations are available.

Coronal mass ejections observed by heliospheric imagers at 0.2 and 1 au

The events on April 1 and 2, 2019

Carlos R. **Braga**^{1,2} and Angelos Vourlidis

A&A 650, A31 (2021)

<https://arxiv.org/pdf/2011.05229.pdf>

<https://www.aanda.org/articles/aa/pdf/2021/06/aa39490-20.pdf>

<https://doi.org/10.1051/0004-6361/202039490>

Context. We study two coronal mass ejections (CMEs) observed between **April 1 to 2, 2019** by both the inner Wide-Field Imager for Parker Solar Probe (WISPR-I) onboard the Parker Solar Probe (PSP) spacecraft (located between about 46 and 38 solar radii during this period) and the inner heliospheric imager (HI-1) onboard the Solar Terrestrial Relations Observatory Ahead (STEREO-A) spacecraft, orbiting the Sun at about 0.96 au. This is the first study of CME observations from two viewpoints in similar directions but at considerably different solar distances.

Aims. Our objective is to derive CME kinematics from WISPR-I observations and to compare them with results from HI-1. This allows us to understand how the PSP observations affect the CME kinematics, especially due to its proximity to the Sun.

Methods. We estimated the CME positions, speeds, accelerations, propagation directions, and longitudinal deflections using imaging observations from two spacecrafts and a set of analytical expressions that consider the CME as a point structure and take the rapid change in spacecraft position into account. We derived the kinematics using each viewpoint independently and both viewpoints as a constraint.

Results. We found that both CMEs are slow (< 400 km s^{-1}), propagating eastward of the Sun-Earth line (westward of PSP and STEREO-A). The second CME seems to accelerate between ~ 0.1 and ~ 0.2 au and deflect westward with an angular speed consistent with the solar rotation speed. We found some discrepancies in the CME solar distance (up to

0.05 au, particularly for CME #1), latitude (up to $\sim 10^\circ$), and longitude (up to 24°) when comparing results from different fit cases (different observations or set of free parameters).

Conclusions. Discrepancies in longitude are likely due to the feature that is tracked visually, rather than instrumental biases or fit assumptions. For similar reasons, the CME #1 solar distance, as derived from WISPR-I observations, is larger than the HI-1 result, regardless of the fit parameters considered. Error estimates for CME kinematics do not show any clear trend associated with the observing instrument. The source region location and the lack of any clear in situ counterparts (both at near-Earth and at PSP) support our estimate of the propagation direction for both events.

Predicting the Time-of-Arrival of Coronal Mass Ejections at Earth From Heliospheric Imaging Observations

Carlos Roberto [Braga](#), [Angelos Vourlidis](#), [Guillermo Stenborg](#), [Alisson Dal Lago](#), [Rafael Rodrigues Souza de Mendonça](#), [Ezequiel Echer](#)

JGR [Volume125, Issue9](#) e2020JA027885 2020

<https://arxiv.org/pdf/2008.09005.pdf>

<https://doi.org/10.1029/2020JA027885>

The Time-of-Arrival (ToA) of coronal mass ejections (CME) at Earth is a key parameter due to the space weather phenomena associated with the CME arrival, such as intense geomagnetic storms. Despite the incremental use of new instrumentation and the development of novel methodologies, ToA estimated errors remain above 10 hours on average. Here, we investigate the prediction of the ToA of CMEs using observations from heliospheric imagers, i.e., from heliocentric distances higher than those covered by the existent coronagraphs. In order to perform this work we analyse 14 CMEs observed by the heliospheric imagers HI-1 onboard the twin STEREO spacecraft to determine their front location and speed. The kinematic parameters are derived with a new technique based on the Elliptical Conversion (ElCon) method, which uses simultaneous observations from the two viewpoints from STEREO. Outside the field of view of the instruments, we assume that the dynamics of the CME evolution is controlled by aerodynamic drag, i.e., a force resulting from the interaction with particles from the background solar wind. To model the drag force we use a physical model that allows us to derive its parameters without the need to rely on drag coefficients derived empirically. We found a CME ToA mean error of 1.6 ± 8.0 hours ToA and a mean absolute error of 6.9 ± 3.9 hours for a set of 14 events. The results suggest that observations from HI-1 lead to estimates with similar errors to observations from coronagraphs. **2010-03-19, 03-Apr-2010, 09-Apr-2010, 15-Feb-2011, 26-Mar-2011, 2011-06-14, 14-Sep-2011, 20-Apr-2012, 15-Jun-2012, 13-Jul-2012, 28-Sep-2012, 06-Oct-2012, 28-Oct-2012, 15-Mar-2013, 11-Apr-2013**
Table 1. List of CMEs and corresponding ICMEs 92010-2013)

The Solar Eruption of 2005 May 13 and Its Effects: Long-Baseline Interplanetary Scintillation Observations of the Earth-Directed Coronal Mass Ejection

A. R. [Breen](#),¹ R. A. Fallows,¹ M. M. Bisi,² R. A. Jones,³ B. V. Jackson,² M. Kojima,⁴ G. D. Dorrian,¹ H. R. Middleton,¹ P. Thomasson,⁵ and G. Wannberg⁶

Astrophysical Journal, 683: L79–L82, 2008

<http://www.journals.uchicago.edu/toc/apjl/2008/683/1>

Long-baseline observations of interplanetary scintillation (IPS) provide a unique source of information on solar wind speed and meridional direction across the inner regions of the solar system. We report the results of a series of coordinated IPS observations of an Earth-directed CME. A significant development in the interpretation of these data is the use of 3D tomographic reconstructions of solar wind structure derived from STELab IPS data to better constrain the analysis of extremely long baseline observations from EISCAT and MERLIN. The combination of these two approaches leads to a significantly better understanding of the interaction of the CME with the background solar wind than would be possible with either technique alone, revealing a significant rotation in the meridional flow direction of the background wind associated with the passage of the CME. The CME itself is decelerated significantly between its emergence through the corona and its arrival in the IPS ray path, with comparatively little change in speed from then until arrival at ACE.

Gleissberg Cycle Dependence of Inner Zone Proton Flux

Emily J. [Bregou](#), [Mary K. Hudson](#), [Brian T. Kress](#), [Murong Qin](#), [Richard S. Selesnick](#)

Space Weather e2022SW003072 2022

<https://doi.org/10.1029/2022SW003072>

<https://agupubs.onlinelibrary.wiley.com/doi/epdf/10.1029/2022SW003072>

Inner zone proton flux from 1980 to mid-2021 is examined using NOAA POES satellite data, indicating a long-term increase corresponding to a one hundred year minimum in solar activity consistent with the Centennial Gleissberg Cycle. Variation of inner belt protons is correlated with decreasing F10.7 maxima over the 40-year period, serving as proxy for solar EUV input to Earth's atmosphere. Extending an earlier study (Qin et al., 2014) of > 70 MeV protons from 1980 – 2021 using the South Atlantic Anomaly (SAA) peak flux, and at fixed L = 1.3, a comparison is made between the > 35, > 70 and > 140 MeV energy channels on POES. All three energies show an increase in proton flux over the period 1998 – 2021 using a single spacecraft. The observed flux increase is correlated with decreasing F10.7 over the longer 40-year time interval, as with the ~11-year solar cycle. A phase lag during Solar Cycle 24 (January 2010 – June 2021) between the F10.7 minimum and proton flux maximum was determined to be ~500 days, the same at all energies studied. A model calculation of the inner zone proton flux is found to generally confirm the long-term trend examined both in absolute magnitude and phase lag. It is concluded that this long-term trend is a manifestation of the concurrent Gleissberg cycle minimum and accompanying decrease in solar EUV. Reduced EUV at solar maximum (F10.7 proxy) reduces proton loss to the atmosphere following solar maximum, thus explaining the long-term flux increase observed.

Formation, shape, and evolution of magnetic structures in CIRs at 1 AU

Broiles, T. W.; Desai, M. I.; McComas, D. J.

J. Geophys. Res., Vol. 117, No. A3, A03102, 2012, File

<http://dx.doi.org/10.1029/2011JA017288>

We have surveyed the properties of **153 co-rotating interaction regions (CIRs) observed at 1 AU from January, 1995 through December, 2008**. We identified that 74 of the 153 CIRs contain planar magnetic structures (PMSs). For planar and non-planar CIRs, we compared distributions of the bulk plasma and magnetic field parameters. Our identification of CIRs and their features yields the following results: (1) The different pressures within CIRs are strongly correlated. (2) There is no statistical difference between planar and non-planar CIRs in the distributions and correlations between bulk plasma and magnetic field parameters. (3) The mean observed CIR azimuthal tilt is within 1 σ of the predicted Parker spiral at 1 AU, while the mean meridional tilt is about 20°. (4) The meridional tilt of CIRs changes from one solar rotation to the next, with no relationship between successive reoccurrences. (5) The meridional tilt of CIRs in the ecliptic is not ordered by the magnetic field polarity of the parent coronal hole. (6) Although solar wind deflection is a function of CIR shape and speed, the relationship is not in agreement with that predicted by Lee (2000). We conclude the following: (1) PMSs in CIRs are not caused by a unique characteristic in the local plasma or magnetic field. (2) The lack of relationship between CIR tilt and its **parent coronal hole** suggests that coronal hole boundaries may be more complex than currently observed. (3) In general, further theoretical work is necessary to explain the observations of CIR tilt.

The Formation and Lifetime of Outflows in a Solar Active Region

David H. **Brooks**^{1,2}, Louise Harra^{3,4}, Stuart D. Bale⁵, Krzysztof Barczynski^{3,4}, Cristina Mandrini⁶, Vanessa Polito^{7,8}, and Harry P. Warren⁹

2021 ApJ 917 25

<https://doi.org/10.3847/1538-4357/ac0917>

Active regions are thought to be one contributor to the slow solar wind. Upflows in EUV coronal spectral lines are routinely observed at their boundaries, and provide the most direct way for upflowing material to escape into the heliosphere. The mechanisms that form and drive these upflows, however, remain to be fully characterized. It is unclear how quickly they form, or how long they exist during their lifetimes. They could be initiated low in the atmosphere during magnetic flux emergence, or as a response to processes occurring high in the corona when the active region is fully developed. On **2019 March 31** a simple bipolar active region (AR 12737) emerged and upflows developed on each side. We used observations from Hinode, SDO, IRIS, and Parker Solar Probe (PSP) to investigate the formation and development of the upflows from the eastern side. We used the spectroscopic data to detect the upflow, and then used the imaging data to try to trace its signature back to earlier in the active region emergence phase. We find that the upflow forms quickly, low down in the atmosphere, and that its initiation appears associated with a small field-opening eruption and the onset of a radio noise storm detected by PSP. We also confirmed that the upflows existed for the vast majority of the time the active region was observed. These results suggest that the contribution to the solar wind occurs even when the region is small, and continues for most of its lifetime.

The Drivers of Active Region Outflows into the Slow Solar Wind

David H. **Brooks**^{1,13}, Amy R. Winebarger², Sabrina Savage², Harry P. Warren³, Bart De Pontieu^{4,5}, Hardi Peter⁶, Jonathan W. Cirtain⁷, Leon Golub⁸, Ken Kobayashi², Scott W. McIntosh⁹Show full author list

2020 ApJ 894 144

<https://doi.org/10.3847/1538-4357/ab8a4c>

Plasma outflows from the edges of active regions have been suggested as a possible source of the slow solar wind. Spectroscopic measurements show that these outflows have an enhanced elemental composition, which is a distinct signature of the slow wind. Current spectroscopic observations, however, do not have sufficient spatial resolution to distinguish what structures are being measured or determine the driver of the outflows. The High-resolution Coronal Imager (Hi-C) flew on a sounding rocket in 2018 May and observed areas of active region outflow at the highest spatial resolution ever achieved (250 km). Here we use the Hi-C data to disentangle the outflow composition signatures observed with the Hinode satellite during the flight. We show that there are two components to the outflow emission: a substantial contribution from expanded plasma that appears to have been expelled from closed loops in the active region core and a second contribution from dynamic activity in active region plage, with a composition signature that reflects solar photospheric abundances. The two competing drivers of the outflows may explain the variable composition of the slow solar wind.

Full-Sun observations for identifying the source of the slow solar wind

David H. [Brooks](#), Ignacio Ugarte-Urra, Harry P. Warren

Nature Communications **2015**

<http://arxiv.org/pdf/1605.09514v1.pdf>

Fast (>700 km/s) and slow (~400 km/s) winds stream from the Sun, permeate the heliosphere and influence the near-Earth environment. While the fast wind is known to emanate primarily from polar coronal holes, the source of the slow wind remains unknown. Here we identify possible sites of origin using a slow solar wind source map of the entire Sun, which we construct from specially designed, full-disk observations from the Hinode satellite, and a magnetic field model. Our map provides a full-Sun observation that combines three key ingredients for identifying the sources: velocity, plasma composition and magnetic topology and shows them as solar wind composition plasma outflowing on open magnetic field lines. The area coverage of the identified sources is large enough that the sum of their mass contributions can explain a significant fraction of the mass loss rate of the solar wind.

Attention-based machine vision models and techniques for solar wind speed forecasting using solar EUV images

Edward J. E. [Brown](#), [Filip Svoboda](#), [Nigel P. Meredith](#), [Nicholas Lane](#), [Richard B. Horne](#)

Space Weather **Volume 20, Issue 3** e2021SW002976 **2022**

<https://agupubs.onlinelibrary.wiley.com/doi/epdf/10.1029/2021SW002976>

<https://doi.org/10.1029/2021SW002976>

Extreme ultraviolet images taken by the Atmospheric Imaging Assembly on board the Solar Dynamics Observatory make it possible to use deep vision techniques to forecast solar wind speed - a difficult, high-impact, and unsolved problem. At a four day time horizon, this study uses attention-based models and a set of methodological improvements to deliver an 11.1% lower RMSE and a 17.4% higher prediction correlation compared to the previous work testing on the period from 2010 to 2018. Our analysis shows that attention-based models combined with our pipeline consistently outperform convolutional alternatives. Our study shows a large performance improvement by using a 30 minute as opposed to a daily sampling frequency. Our model has learned relationships between coronal holes' characteristics and the speed of their associated high speed streams, agreeing with empirical results. Our study finds a strong dependence of our best model on the phase of the solar cycle, with the best performance occurring in the declining phase. **2011-06-07**

The low-frequency break observed in the slow solar wind magnetic spectra★

R. [Bruno](#)¹, D. Telloni², L. Sorriso-Valvo^{3,4}, R. Marino⁵, R. De Marco¹ and R. D'Amicis¹

A&A 627, A96 (2019)

[sci-hub.se/10.1051/0004-6361/201935841](https://doi.org/10.1051/0004-6361/201935841)

Fluctuations of solar wind magnetic field and plasma parameters exhibit a typical turbulence power spectrum with a spectral index ranging between $\sim 5/3$ and $\sim 3/2$. In particular, at 1 AU, the magnetic field spectrum, observed within fast corotating streams, also shows a clear steepening for frequencies higher than the typical proton scales, of the order of $\sim 3 \times 10^{-1}$ Hz, and a flattening towards $1/f$ at frequencies lower than $\sim 10^{-3}$ Hz. However, the current literature reports observations of the low-frequency break only for fast streams. Slow streams, as observed to date, have not shown a clear break, and this has commonly been attributed to slow wind intervals not being long enough. Actually, because of the longer transit time from the Sun, slow wind turbulence would be older and the frequency break would be shifted to lower frequencies with respect to fast wind. Based on this hypothesis, we performed a careful search for long-lasting

slow wind intervals throughout 12 years of Wind satellite measurements. Our search, based on stringent requirements not only on wind speed but also on the level of magnetic compressibility and Alfvénicity of the turbulent fluctuations, yielded 48 slow wind streams lasting longer than 7 days. This result allowed us to extend our study to frequencies sufficiently low and, for the first time in the literature, we are able to show that the $1/f$ magnetic spectral scaling is also present in the slow solar wind, provided the interval is long enough. However, this is not the case for the slow wind velocity spectrum, which keeps the typical Kolmogorov scaling throughout the analysed frequency range. After ruling out the possible role of compressibility and Alfvénicity for the $1/f$ scaling, a possible explanation in terms of magnetic amplitude saturation, as recently proposed in the literature, is suggested.

Forecasting high-speed solar wind streams based on solar extreme-ultraviolet images

X. Bu , B. Luo, C. Shen , S. Liu, J. Gong, Y. Cao , H. Wang

Space Weather **Volume17, Issue7** Pages 1040-1058 **2019**

[sci-hub.se/10.1029/2019SW002186](https://doi.org/10.1029/2019SW002186)

High-speed solar wind streams that originate from coronal holes play an important role in space weather disturbances, especially during the declining phase of the solar cycle. Space weather forecasters attempt to find good coronal hole indices that can be used to predict high speed streams days in advance. Several indices related to the coronal hole area, brightness, or magnetic field expansion factor have been reported in the literature. Empirical solar wind forecast models have been developed and used in operational service by several organizations by constructing prediction functions that relate the coronal hole index to the solar wind speed. In this paper, we present a new empirical modeling method, and test its validity by comparing it with a previously reported method when applied to different coronal hole indices. In total, six empirical models are tested for a long period of time (2011--2018), with a 27-day persistence model as a comparison benchmark. The results show that while all these empirical models can capture the temporal patterns of the solar wind observations well, the new modeling method and utilization of a composite coronal hole index PCH as an input parameter indeed improves the forecast accuracy. The high speed streams can be predicted approximately 3 days in advance, with a probability of detection (POD) of 0.78, a positive predictive value (PPV) of 0.73, and a threat score (TS) of 0.61. The uncertainty of the high-speed stream arrival time is approximately 1 day and the uncertainty of the peak speed is approximately 80 km/s. **February 28, 2011**

Extended Cosmic Ray Decreases with Strong Anisotropy after Passage of Interplanetary Shocks

Nutthawara **Buatthaisong**¹, David Ruffolo¹, Alejandro Sáiz¹, Chanoknan Banglieng², Warit

Mitthumsiri¹, Tanin Nutaro³, and Waraporn Nuntiyakul⁴

2022 ApJ 939 99

<https://iopscience.iop.org/article/10.3847/1538-4357/ac96ea/pdf>

The passage of an interplanetary shock and/or interplanetary coronal mass ejection often causes a rapid decrease in the Galactic cosmic-ray (GCR) flux, known as a Forbush decrease, followed by a recovery of the flux over some days. These local effects are of short duration and strongly rigidity dependent, with higher-rigidity particles exhibiting much weaker effects. In contrast, we present data for two events in which the cosmic-ray flux gradually decreased for about 1 week after shock passage, then recovering over the following week, with the highest anisotropy levels observed throughout Solar Cycle 24. These extended decreases have a weak rigidity dependence and are much more prominent in observations at higher cutoff rigidity, where the initial Forbush decrease is not clearly detected and other variations are generally weak, as we demonstrate using data from the Princess Sirindhorn Neutron Monitor at Doi Inthanon, Thailand with a cutoff rigidity of about 17 GV. We propose that these extended decrease events were initiated upon the passage of an interplanetary shock that inhibited the inflow of GCRs along the interplanetary magnetic field, possibly due to magnetic mirroring at the shock. We also discuss the general behavior of GCR anisotropy as observed at this high cutoff rigidity.

Abundances of Suprathermal Heavy Ions in CIRs During the Minimum of Solar Cycle 23

R. **Bučík**, U. Mall, A. Korth, G. M. Mason

Solar Physics, November **2012**, Volume 281, Issue 1, pp 411-422

In this paper we examine the elemental composition of the 0.1 – 1 MeV nucleon⁻¹ interplanetary heavy ions from H to Fe in corotating interaction regions (CIRs) measured by the SIT (Suprathermal Ion Telescope) instrument. We use observations taken on board the STEREO spacecraft from January 2007 through December 2010, which included the unusually long solar minimum following Solar Cycle 23. During this period instruments on STEREO observed more than 50 CIR events making it possible to investigate CIR ion abundances during solar minimum conditions with unprecedented high statistics. The observations reveal annual variations of relative ion abundances in the CIRs during

the 2007–2008 period as indicated by the He/H, He/O and Fe/O elemental ratios. We discuss possible causes of the variability in terms of the helium focusing cone passage and heliolatitude dependence. The year 2009 was very quiet in CIR-event activity. In 2010 the elemental composition in CIRs were influenced by sporadic solar energetic particle (SEP) events. The 2010 He/H and He/O abundance ratios in CIRs show large event-to-event variations with values resembling the SEP-like composition. This finding suggests that the suprathermal SEPs could be the source population for CIR acceleration.

An Empirical Relationship Between Coronal Density and Solar Wind Velocity in the Middle Corona With Applications to Space Weather

Kaine A. [Bunting](#), [Huw Morgan](#)

Space Weather [Volume21, Issue3](#) e2023SW003448 2023

<https://doi.org/10.1029/2023SW003448>

<https://agupubs.onlinelibrary.wiley.com/doi/epdf/10.1029/2023SW003448>

Accurate predictions of ambient solar wind conditions are a central component of space weather forecasting. A recent advancement is to use the distribution of electron density at a heliocentric distance of $8 R_{\odot}$, gained by applying coronal rotational tomography to coronagraph data, as an inner boundary condition for the time-dependent Heliospheric Upwind eXtrapolation solar wind model. This approach requires conversion of densities into solar wind velocity at the inner boundary. Based on comparison of the distribution of in situ measurements of density and velocities, this work finds a scaled exponential equation relating the density and outflow velocity at $8 R_{\odot}$, with three key parameters found as a function of time between years 2007–2021. Based on this relationship, comparison of modeled and in situ measurements of velocities at Earth, STEREO A and STEREO B over the past solar cycle give a mean absolute error of 61.2, 69.0, and 66.1 km s⁻¹ respectively. An analysis of thousands of events (defined as solar wind streams above 450 km s⁻¹) gives an accuracy score of 76%. This agreement validates the density-velocity relationship, and shows that an inner boundary based on coronagraph observations is a robust complement, or alternative, to commonly-used magnetic model constraints for solar wind modeling and forecasting.

Heliocentric Distance and Solar Activity Dependence of Sustained Quasi-radial Interplanetary Magnetic Field Occurrence

Brandon L. [Burkholder](#)^{1,2}, Li-Jen Chen², Norberto Romanelli^{2,3}, +

2023 ApJ 953 85

<https://iopscience.iop.org/article/10.3847/1538-4357/ace328/pdf>

Planets close to their stars experience an interplanetary magnetic field (IMF) that is dominantly quasi-radial. Our solar system serves as a laboratory to study how the occurrence of quasi-radial IMF varies away from the star and under different stellar activities. Furthermore, on time and spatial scales relevant to magnetospheric physics, solar wind variability prevails in the form of structures generated both at the Sun and locally in the interplanetary space. The stationary Parker spiral model only approximates the large-scale structure of the IMF. Deviations from the Parker spiral often result in strongly radial magnetic fields that give rise to kinetic foreshock turbulence, which in turn can impact planetary magnetospheres. The relative significance of this type of interaction can be estimated statistically based on the occurrence rate of cases where the IMF is directed along the radial direction, leading to the entire day-side magnetosphere being downstream of the ion foreshock. We use observations covering radial distances from 0.1 to 10 au and more than 2 solar cycles to quantify the prevalence of radial IMFs throughout the heliosphere. Near Earth's orbit, it is found that the occurrence rates of quasi-radial and southward IMF orientations are similar, and that the Pearson correlation coefficient is $R_{xy} \sim -0.7$ calculated between quasi-radial IMF occurrence rate and solar activity. A negative correlation is demonstrated for radial distances extending to at least Mars but not to Saturn.

Magnetic Reconnection of Solar Flux Tubes and Coronal Reconnection Signatures in the Solar Wind at 1 AU

B. L. [Burkholder](#), [A. Otto](#)

JGR [Volume124, Issue11](#) November 2019 Pages 8227-8254

<https://doi.org/10.1029/2019JA027114>

The origin of interplanetary magnetic field that is frozen-in to the solar wind plasma flow is clearly magnetic flux from the Sun's corona. However, the filamented structure of magnetic fields observed in the solar wind cannot be accounted for quite so simply. Given the 2 days or more for solar wind to travel from the Sun to 1 AU, some argue that many current sheets are present due to turbulence and other in-transit effects in the dynamic plasma outflow. Alternatively, it is postulated that a “flux tube texture” of the solar wind exists as fossil structure of the corona. In this paper we examine the possible influence of magnetic reconnection occurring close to the Sun or in the solar wind on the character of

current sheets observed by Magnetospheric Multiscale at 1 AU. Photospheric convection is used to perturb a magnetic carpet-like configuration, which has well-segmented open flux tubes defined by topological elements of the magnetic field. Flux tube boundaries in the model are defined by magnetic separatrix surfaces which are a preferential location for strong currents and magnetic reconnection. Reconnection is associated with signatures in the magnetic field and plasma that may advect with the solar wind all the way to 1 AU. Aided by three-dimensional coronal modeling and two-dimensional simulation examples of reconnection layers, we examine properties of current sheets observed by Magnetospheric Multiscale and how these solar wind boundaries may relate to reconnection operating earlier in the solar wind or corona.

Successive CMEs and complex ejecta.

Burlaga, L.F., Plunkett, S.P., Cyr St., O.C.,

2002. J. Geophys. Res. 107 (A10), 1266. doi:10.1029/2001JA000255.

A magnetic cloud and a coronal mass ejection.

Burlaga LF, Klein L, Sheeley NR Jr, Michels DJ, Howard RA, Koomen MJ, Schwenn R, Rosenbauer H (1982) GRL 9:1317-1320

Extreme Events in Geospace

Origins, Predictability, and Consequences

Book

Editor: Natalia **Buzulukova**, Elsevier, **2018**, 798 p. **File**

Site <https://www.sciencedirect.com/science/article/pii/B9780128127001099921>

Download PDF --> Download full book

Impact of Solar Wind on the Earth Magnetosphere: Recent Progress in the Modeling of Ring Current and Radiation Belts

A Review

Natalia **Buzulukova**, Mei-Ching Fok and Alex Gloer

In: Exploring the Solar Wind, Ed. Marian Lazar, **2012**,

<http://www.intechopen.com/books/exploring-the-solar-wind>

Propagation of an Earth-directed coronal mass ejection in three dimensions

Jason P. **Byrne** 1 , Shane A. Maloney 1 , R.T. James McAteer 1 , 3 , Jose M. Refojo 2 & Peter T. Gallagher 1
Nature Communications 1 , Article number: 74 doi:10.1038/ncomms1077, **2010**, **File**

Solar coronal mass ejections (CMEs) are the most significant drivers of adverse space weather on Earth, but the physics governing their propagation through the heliosphere is not well understood. Although stereoscopic imaging of CMEs with NASA's Solar Terrestrial Relations Observatory (STEREO) has provided some insight into their three-dimensional (3D) propagation, the mechanisms governing their evolution remain unclear because of difficulties in reconstructing their true 3D structure. In this paper, we use a new elliptical tie-pointing technique to reconstruct a full CME front in 3D, enabling us to quantify its deflected trajectory from high latitudes along the ecliptic, and measure its increasing angular width and propagation from 2 to 46 R_{\odot} (~ 0.2 AU). Beyond 7 R_{\odot} , we show that its motion is determined by an aerodynamic drag in the solar wind and, using our reconstruction as input for a 3D magnetohydrodynamic simulation, we determine an accurate arrival time at the Lagrangian L1 point near Earth.

Probabilistic Drag-Based Ensemble Model (DBEM) Evaluation for Heliospheric Propagation of CMEs

Jaša Čalogović, [Mateja Dumbović](#), [Davor Sudar](#), [Bojan Vršnak](#), [Karmen Martinić](#), [Manuela Temmer](#), [Astrid Veronig](#)

Solar Phys. **296**, Article number: 114 **2021**

<https://arxiv.org/pdf/2107.06684.pdf>

<https://link.springer.com/content/pdf/10.1007/s11207-021-01859-5.pdf>

<https://doi.org/10.1007/s11207-021-01859-5>

The Drag-based Model (DBM) is a 2D analytical model for heliospheric propagation of Coronal Mass Ejections (CMEs) in ecliptic plane predicting the CME arrival time and speed at Earth or any other given target in the solar system. It is based on the equation of motion and depends on initial CME parameters, background solar wind speed, w and the drag parameter γ . A very short computational time of DBM ($< 0.01s$) allowed us to develop the Drag-Based Ensemble Model (DBEM) that takes into account the variability of model input parameters by making an ensemble of n different input parameters to calculate the distribution and significance of the DBM results. Thus the DBEM is able to calculate the most likely CME arrival times and speeds, quantify the prediction uncertainties and determine the confidence intervals. A new DBEMv3 version is described in detail and evaluated for the first time determining the DBEMv3 performance and errors by using various CME-ICME lists as well as it is compared with previous DBEM versions. The analysis to find the optimal drag parameter γ and ambient solar wind speed w showed that somewhat higher values ($\gamma \approx 0.3 \times 10^{-7} \text{ km}^{-1}$, $w \approx 425 \text{ km s}^{-1}$) for both of these DBEM input parameters should be used for the evaluation compared to the previously employed ones. Based on the evaluation performed for 146 CME-ICME pairs, the DBEMv3 performance with mean error (ME) of -11.3 h, mean absolute error (MAE) of 17.3 h was obtained. There is a clear bias towards the negative prediction errors where the fast CMEs are predicted to arrive too early, probably due to the model physical limitations and input errors (e.g. CME launch speed).

Analysis of an Interplanetary Coronal Mass Ejection by a Spacecraft Radio Signal: A Case Study

G. Molera **Calvés**, E. Kallio, G. Cimo, J. Quick, D. A. Duev, T. Bocanegra Bahamón, M. Nickola, M. A. Kharinov, A. G. Mikhailov

Space Weather 16 November 2017 Vol: 15, Pages: 1523–1534

<http://sci-hub.tw/10.1002/2017SW001701>

Tracking radio communication signals from planetary spacecraft with ground-based telescopes offers the possibility to study the electron density and the interplanetary scintillation of the solar wind. Observations of the telemetry link of planetary spacecraft have been conducted regularly with ground antennae from the European Very Long Baseline Interferometry Network, aiming to study the propagation of radio signals in the solar wind at different solar elongations and distances from the Sun. We have analyzed the Mars Express spacecraft radio signal phase fluctuations while, based on a 3-D heliosphere plasma simulation, an interplanetary coronal mass ejection (ICME) crossed the radio path during one of our observations on **6 April 2015**. Our measurements showed that the phase scintillation indices increased by a factor of 4 during the passage of the ICME. The method presented here confirms that the phase scintillation technique based on spacecraft signals provides information of the properties and propagation of the ICMEs in the heliosphere.

Using Mutual Information to Determine Geoeffectiveness of Solar Wind Phase Fronts With Different Front Orientations

T. G. **Cameron**, B. Jackel, D. M. Oliveira

JGR [Volume 124, Issue 3](#) March 2019 Pages 1582-1592

sci-hub.se/10.1029/2018JA026080

The geoeffectiveness of solar wind shocks depends on angle with respect to the Sun-Earth line, with highly angled solar wind shocks being less geoeffective than nearly frontal solar wind shocks. However, it is unclear whether this holds for the orientation of structures in nonshocked solar wind. In this paper, we perform a mutual information analysis of 18 years of in situ solar wind and ground magnetometer data in order to investigate the effects of solar wind phase front orientation on solar wind geoeffectiveness (indicated by SuperMAG SME, the SuperMAG enhanced version of the AE index). Since geomagnetic response is strongly influenced by interplanetary magnetic field (IMF) B_z , and IMF B_z affects phase front orientation, we use conditional mutual information to account for the effect of B_z on geomagnetic activity. In contrast to what has been found for solar wind shocks, we find that during times of IMF $B_z > 0$, phase fronts aligned with the average Parker spiral direction (45° azimuth, 0° inclination) tend to be associated with higher geomagnetic activity (SME > 500 nT) than would be expected if IMF B_z and phase front orientation quantities were unrelated. During times of IMF $B_z < 0$, there is no connection between solar wind phase front orientation and geomagnetic activity (SME). We believe that Parker spiral-aligned phase fronts being associated with higher geomagnetic activity during times of IMF $B_z > 0$ is due to constant phase front orientation allowing for more efficient energy transfer either through viscous interaction or high-latitude reconnection.

Classification of Solar Wind With Machine Learning

Enrico **Camporeale**, Algo Carè, Joseph E. Borovsky

JGR November 2017 Vol: 122, Pages: 10,910–10,920

<http://sci-hub.tw/10.1002/2017JA024383>

We present a four-category classification algorithm for the solar wind, based on Gaussian Process. The four categories are the ones previously adopted in Xu and Borovsky (2015): ejecta, coronal hole origin plasma, streamer belt origin plasma, and sector reversal origin plasma. The algorithm is trained and tested on a labeled portion of the OMNI data set. It uses seven inputs: the solar wind speed V_{sw} , the temperature standard deviation σ_T , the sunspot number R , the F10.7 index, the Alfvén speed v_A , the proton specific entropy S_p , and the proton temperature T_p compared to a velocity-dependent expected temperature. The output of the Gaussian Process classifier is a four-element vector containing the probabilities that an event (one reading from the hourly averaged OMNI database) belongs to each category. The probabilistic nature of the prediction allows for a more informative and flexible interpretation of the results, for instance, being able to classify events as “undecided.” The new method has a median accuracy larger than 90% for all categories, even using a small set of data for training. The Receiver Operating Characteristic curve and the reliability diagram also demonstrate the excellent quality of this new method. Finally, we use the algorithm to classify a large portion of the OMNI data set, and we present for the first time transition probabilities between different solar wind categories. Such probabilities represent the “climatological” statistics that determine the solar wind baseline.

Interplanetary coronal mass ejections in the near-Earth solar wind during 1996–2002

H. V. [Cane](#)¹ and I. G. Richardson

JOURNAL OF GEOPHYSICAL RESEARCH, VOL. 108, NO. A4, 1156, 2003, [File](#)

We summarize the occurrence of interplanetary coronal mass ejections (ICMEs) in the near-Earth solar wind during 1996–2002, corresponding to the increasing and maximum phases of solar cycle 23. In particular, we give a detailed list of such events. This list, based on in situ observations, is not confined to subsets of ICMEs, such as “magnetic clouds” or those preceded by “halo” coronal mass injections (CMEs) observed by the Solar and Heliospheric Observatory/Large Angle and Spectrometric Coronagraph, and provides an overview of 214 ICMEs in the near-Earth solar wind during this period. The ICME rate increases by about an order of magnitude from solar minimum to solar maximum (when the rate is ~ 3 ICMEs per solar rotation period). The rate also shows a temporary reduction during 1999 and another brief, deeper reduction in late 2000 to early 2001, which only approximately track variations in the solar 10-cm flux. In addition, there are occasional periods of several rotations duration when the ICME rate is enhanced in association with high solar activity levels. We find an indication of a periodic variation in the ICME rate, with a prominent period of ~ 165 days similar to that previously reported in various solar phenomena. It is found that the fraction of ICMEs that are magnetic clouds has a solar cycle variation, the fraction being larger near solar minimum. For the subset of events that we could associate with a CME at the Sun the transit speeds from the Sun to the Earth were highest after solar maximum.

(See [Richardson & Cane, 2010](#))

CORONAL MASS EJECTIONS AND FORBUSH DECREASES

Review

HILARY V. [CANE](#)

Space Science Reviews 93: 41–62, 2000, [File](#)

Coronal Mass Ejections (CMEs) are plasma eruptions from the solar atmosphere which involve previously closed field regions which are expelled into the interplanetary medium. Such regions and the shocks which they may generate, have pronounced effects on cosmic ray densities both locally and at some distance away. These energetic particle effects can often be used to identify CMEs in the interplanetary medium, where they are usually called “ejecta”. When both the ejecta and shock effects are present the resulting cosmic ray event is called a “classical, two-step” Forbush decrease. This paper will summarize the characteristics of CMEs, their effects on particles and the present understanding of the mechanisms involved which cause the particle effects. The role of CMEs in long term modulation will also be discussed.

Cosmic ray decreases: 1964-1994

[Cane](#), H. V.; Richardson, I. G.; von Roseninge, T. T.

Journal of Geophysical Research, Volume 101, Issue A10, p. 21561-21572, 1996

We have studied 30 years (1964-1994) of neutron monitor data in order to understand the principle mechanisms causing short-term (<20-day duration) cosmic ray decreases seen at Earth. By examining the characteristics of associated low energy (<200 MeV) particle enhancements in combination with the neutron monitor data, we have determined the responsible solar wind disturbances for 153 of the 180 $\geq 4\%$ decreases. The vast majority (86% of the 153 events) are caused by coronal mass ejections and the shocks that they generate. The ejecta is intercepted only when the solar event

originates within 50° of the Sun's central meridian. For more distant events, only the shock is intercepted at Earth. We present a list of all 180 events seen in the years 1964-1994 together with the associated solar event, when this can be determined, and some details about the solar wind structures based on in situ solar wind data, if available. This list represents a compendium of major solar wind disturbances affecting a large section of the inner heliosphere over this time period. We also discuss enhanced daily variations in some events which are related to radial gradients caused by strong disturbances inside the Earth's orbit.

Unveiling the Journey of a Highly Inclined CME: Insights from the March 13, 2012 Event with 110° Longitudinal Separation

F. Carcaboso, M. Dumbovic, C. Kay, D. Lario, L. K. Jian, L. B. Wilson III, R. Gómez-Herrero, M. Temmer, S. G. Heinemann, T. Nieves-Chinchilla, A. M. Veronig

A&A 2024

<https://arxiv.org/pdf/2401.17501.pdf>

A fast and wide Coronal Mass Ejection (CME) erupted from the Sun on **2012-03-13**. Its interplanetary counterpart was detected in situ two days later by STEREO-A and near-Earth spacecraft. We suggest that at 1 au the CME extended at least 110° in longitude, with Earth crossing its east flank and STEREO-A crossing its west flank. Despite their separation, measurements from both positions showed very similar in situ CME signatures. The solar source region where the CME erupted was surrounded by three coronal holes (CHs). Their locations with respect to the CME launch site were east (negative polarity), southwest (positive polarity) and west (positive polarity). The solar magnetic field polarity of the area covered by each CH matches that observed at 1 au in situ. Suprathermal electrons at each location showed mixed signatures with only some intervals presenting clear counterstreaming flows as the CME transits both locations. The strahl population coming from the shortest magnetic connection of the structure to the Sun showed more intensity. The study presents important findings regarding the in situ measured CME on **2012-03-15**, detected at a longitudinal separation of 110° in the ecliptic plane despite its initial inclination being around 45° when erupted. This suggests that the CME may have deformed and/or rotated, allowing it to be observed near its legs with spacecraft at a separation angle greater than 100° . The CME structure interacted with high-speed streams generated by the surrounding CHs. The piled-up plasma in the sheath region exhibited an unexpected correlation in magnetic field strength despite the large separation in longitude. In situ observations reveal that at both locations there was a flank encounter, where the spacecraft crossed the first part of the CME, then encountered ambient solar wind, and finally passed near the legs of the structure.

Characterisation of suprathermal electron pitch-angle distributions

*Bidirectional and isotropic periods in solar wind**

Fernando Carcaboso, Raúl Gómez-Herrero, Francisco Espinosa Lara, Miguel A. Hidalgo, Ignacio Cernuda and Javier Rodríguez-Pacheco

A&A 635, A79 (2020)

<https://doi.org/10.1051/0004-6361/20193660>

Context. Suprathermal electron pitch-angle distributions (PADs) contain substantial information about the magnetic topology of the solar wind. Their characterisation and quantification allow us to automatically identify periods showing certain characteristics.

Aims. This work presents a robust automatic method for the identification and statistical study of two different types of PADs: bidirectional suprathermal electrons (BDE, often associated with closed magnetic structures) and isotropic (likely corresponding to solar-detached magnetic field lines or highly scattered electrons).

Methods. Spherical harmonics were fitted to the observed suprathermal PADs of the 119–193 eV energy channel of STEREO/SWEA from March 2007 to July 2014, and they were characterised using signal processing analysis in order to identify periods of isotropic and bidirectional PADs. The characterisation has been validated by comparing the results obtained here with those of previous studies.

Results. Interplanetary coronal mass ejections (ICMEs) present longer BDE periods inside the magnetic obstacles. A significant amount of BDE remain after the end of the ICME. Isotropic PADs are found in the sheath of the ICMEs, and at the post-ICME region likely due to the erosion of the magnetic field lines. Both isotropy and BDE are solar-cycle dependent. The isotropy observed by STEREO shows a nearly annual periodicity, which requires further investigation. There is also a correspondence between the number of ICMEs observed and the percentage of time showing BDE.

Conclusions. A method to characterise PADs has been presented and applied to the automatic identification of two relevant distributions that are commonly observed in the solar wind, such as BDE and isotropy. Four catalogues (STEREO-A and STEREO-B for isotropic and BDE periods of at least 10 min) based on this identification are provided for future applications.

ACE SWICS observations of solar cycle variations of the solar wind

A. Cardenas-O'Toole, [E. Landi](#)

ApJ 2022

<https://arxiv.org/pdf/2201.05535.pdf>

In the present work we utilize ACE/SWICS in-situ measurements of the properties of the solar wind outside ICMEs in order to determine whether, and to what extent are the solar wind properties affected by the solar cycle. We focus on proton temperatures and densities, ion temperatures and differential speeds, charge state distributions and both relative and absolute elemental abundances. We carry out this work dividing the wind in velocity bins to investigate how winds at different speeds react to the solar cycle. We also repeat this study, when possible, to the subset of SWICS measurements less affected by Coulomb collisions. We find that with the only exception of differential speeds (for which we do not have enough measurements) all wind properties change as a function of the solar cycle. Our results point towards a scenario where both the slow and fast solar wind are accelerated by waves, but originate from different sources (open/closed magnetic structures for the fast/slow wind, respectively) whose relative contribution changes along the solar cycle. We also find that the signatures of heating and acceleration on one side, and of the FIP effect on the other, indicate that wave-based plasma heating, acceleration and fractionation remain active throughout the solar cycle, but decrease their effectiveness in all winds, although the slow wind is much affected than the fast one.

Space storm measurements of the July 2005 solar extreme events from the low corona to the Earth

[Caroubalos](#), C.; Preka-Papadema, P.; Mavromichalaki, H.; Moussas, X.; Papaioannou, A.; Mitsakou, E.; Hillaris, A.

Advances in Space Research, Volume 43 , Issue 4, p. 600-604, 2009.

<http://arxiv.org/pdf/1009.3579v1.pdf>

The Athens Neutron Monitor Data Processing (ANMODAP) Center recorded an unusual Forbush decrease with a sharp enhancement of cosmic ray intensity right after the main phase of the Forbush decrease on 16 July 2005, followed by a second decrease within less than 12 h. This exceptional event is neither a ground level enhancement nor a geomagnetic effect in cosmic rays. It rather appears as the effect of a special structure of interplanetary disturbances originating from a group of coronal mass ejections (CMEs) in the **13-14 July 2005** period. The initiation of the CMEs was accompanied by type IV radio bursts and intense solar flares (SFs) on the west solar limb (AR 786); this group of energetic phenomena appears under the label of Solar Extreme Events of July 2005. We study the characteristics of these events using combined data from Earth (the ARTEMIS IV radioheliograph, the Athens Neutron Monitor (ANMODAP)), space (WIND/WAVES) and data archives. We propose an interpretation of the unusual Forbush profile in terms of a magnetic structure and a succession of interplanetary shocks interacting with the magnetosphere.

Space Storm Measurements of 17 and 21 April 2002 Forbush Effects from Artemis-IV Solar Radio-Spectrograph, Athens Neutron Monitor Station and Coronas-F Satellite

C. [Caroubalos](#), X. Moussas, P. Preka-Papadema, A. Hillaris, I. Polygiannakis, H. Mavromichalaki, C.

Sarlanis, G. Souvatzoglou, M. Gerontidou, C. Plainaki, S. Tatsis, S. N. Kuznetsov, I.N. Myagkova, K. Kudela

<http://arxiv.org/abs/1009.3650>

In this report we present two complex eruptive solar events and the associated Cosmic Ray effects (Forbush decrease). We use combined recordings from a number of Earthbound Receivers, Space Experiments and data archives (such as the ARTEMIS-IV Radio spectrograph, the Athens NEUTRON MONITOR, the LASCO CME Lists, the SONG of the {CORONAS-F} satellite, etc.). The influence of solar transients on the interplanetary medium conditions and the cosmic ray flux is analysed and discussed. The observed time sequence of events of this time period indicates that the initiation of CMEs is closely related to the appearance of type II and IV radio bursts and strong solar flares. Their effects extend from the lower corona to the near Earth vicinity affecting Cosmic Ray measurements and space weather. As regards the Forbush decrease our data indicate significant amplification at the presence of a MHD shock.

Portuguese eyewitness accounts of the great space weather event of 1582

Víctor Manuel Sánchez [Carrasco](#)^{1,2*} and José Manuel Vaquero^{2,3}

J. Space Weather Space Clim. 2020, 10, 4

<https://www.swsc-journal.org/articles/swsc/pdf/2020/01/swsc190083.pdf>

Newly discovered descriptions about the great aurora observed in March 1582 are presented in this work. These records were made by Portuguese observers from Lisbon. Both records described the aurora like a great fire in the northern part of the sky. It was observed during three consecutive nights, according to one of the sources. Thus, we present a discussion of these auroral records in order to complement other works that studied the aurora sighted in March 1582.

Reply to comment by H. Q. Feng, D. J. Wu, and J. K. Chao on "Comparison of small-scale flux rope magnetic properties to large-scale magnetic clouds: Evidence for reconnection across the HCS"?

Cartwright, M. L.; Moldwin, M. B.

J. Geophys. Res., Vol. 115, No. A10, A10110, 2010

Validation of an operational product to determine L1 to Earth propagation time delays

Authors

M. D. **Cash**, S. Witters Hicks, D. A. Biesecker, A. A. Reinard, C. A. de Koning, D. R. Weimer

Space Weather 2016

We describe the development and validation of an operational space weather tool to forecast propagation delay times between L1 and Earth using the Weimer and King (2008) tilted phase front technique. A simple flat plane convection delay method is currently used by the NOAA Space Weather Prediction Center (SWPC) to propagate the solar wind from a monitoring satellite located at L1 to a point upstream of the magnetosphere. This technique assumes that all observed solar wind discontinuities, such as interplanetary shocks and interplanetary coronal mass ejection boundaries, are in a flat plane perpendicular to the Sun-Earth line traveling in the GSE X direction at the observed solar wind velocity. In reality, these phase plane fronts can have significantly tilted orientations, and by relying on a ballistic propagation method, delay time errors of ± 15 min are common. In principle, the propagation time delay product presented here should more accurately predict L1 to Earth transit times by taking these tilted phase plane fronts into account. This algorithm, which is based on the work of Weimer and King (2008), is currently running in real time in test mode at SWPC as part of the SWPC test bed. We discuss the current algorithm performance, and via our detailed validation study, show that there is no significant difference between the two propagation methods when run in a real-time operational environment.

See <https://eos.org/research-spotlights/new-space-weather-forecast-technique-fails-to-improve-forecasts>

Ensemble Modeling of the 23 July 2012 Coronal Mass Ejection

M. D. **Cash**, D. A. Biesecker, V. Pizzo, C. A. de Koning, G. Millward, C. N. Arge, C. J. Henney and D.

Odstrcil

Space Weather Volume 13, Issue 10 (pages 611–625) 2015

On 23 July 2012 a significant and rapid coronal mass ejection (CME) was detected in situ by the Solar Terrestrial Relations Observatory (STEREO) A. This CME was unusual due to its extremely brief Sun-to-1 AU transit time of less than 21 h and its exceptionally high impact speed of 2246 km/s. If this CME had been Earth directed, it would have produced a significant geomagnetic storm with potentially serious consequences. To protect our ground- and space-based assets, there is a clear need to accurately forecast the arrival times of such events using realistic input parameters and models run in near real time. Using Wang-Sheely-Arge (WSA)-Enlil, the operational model currently employed at the NOAA Space Weather Prediction Center, we investigate the sensitivity of the 23 July CME event to model input parameters. Variations in the initial CME speed, angular width, and direction, as well as the ambient solar wind background, are investigated using an ensemble approach to study the effect on the predicted arrival time of the CME at STEREO A. Factors involved in the fast transit time of this large CME are discussed, and potential improvements to modeling such events with the WSA-Enlil model are presented.

Characterizing interplanetary shocks for development and optimization of an automated solar wind shock detection algorithm

M. D. **Cash**^{1,2,*}, J. S. Wrobel³, K. C. Cosentino⁴ and A. A. Reinard

JGR, Volume 119, Issue 6, pages 4210–4222, June 2014

Human evaluation of solar wind data for interplanetary (IP) shock identification relies on both heuristics and pattern recognition, with the former lending itself to algorithmic representation and automation. Such detection algorithms can potentially alert forecasters of approaching shocks, providing increased warning of subsequent geomagnetic storms.

However, capturing shocks with an algorithmic treatment alone is challenging, as past and present work demonstrates. We present a statistical analysis of 209 IP shocks observed at L1, and we use this information to optimize a set of shock identification criteria for use with an automated solar wind shock detection algorithm. In order to specify ranges for the threshold values used in our algorithm, we quantify discontinuities in the solar wind density, velocity, temperature, and magnetic field magnitude by analyzing 8 years of IP shocks detected by the SWEPAM and MAG instruments aboard the ACE spacecraft. Although automatic shock detection algorithms have previously been developed, in this paper we conduct a methodical optimization to refine shock identification criteria and present the optimal performance of this and similar approaches. We compute forecast skill scores for over 10,000 permutations of our shock detection criteria in order to identify the set of threshold values that yield optimal forecast skill scores. We then compare our results to previous automatic shock detection algorithms using a standard data set, and our optimized algorithm shows improvements in the reliability of automated shock detection.

A New Method Linking the Solar Wind Speed to the Coronal Magnetic Field

Marta **Casti**^{1,2}, Charles N. Arge¹, Alessandro Bemporad³, Rui F. Pinto^{4,5}, and Carl J. Henney⁶
2023 ApJ 949 42

<https://iopscience.iop.org/article/10.3847/1538-4357/acc85d/pdf>

The release and acceleration of the solar wind is still an outstanding question. There are several aspects related to this phenomenon that still need to be investigated, and one of these is the identification of the region within the inner corona where the larger fraction of acceleration occurs. To address this matter, it is necessary to have reliable measurements of the solar wind speed between 1 and 10 solar radii (R_{\odot}). Moreover, in order to describe the coronal plasma behavior, it is important to consider its interaction with the magnetic field. Within this context, our intent is to investigate a method to combine measurements of the solar wind with the extrapolated magnetic field in the corona to derive how the solar wind velocity evolves along the magnetic field lines, aiming at better understanding the sources, origins, and acceleration of the solar wind. To this purpose, we used outflow speed measurements of the coronal plasma derived by applying the Doppler dimming technique, as well as the global magnetic field configuration derived from the measured photospheric magnetic field by using the Wang–Sheeley–Arge model. These two sets of data are then combined for heliocentric distances between 2.6 and 5 R_{\odot} . This paper presents the proposed method and the results obtained over two different Carrington rotations (CR 1923 and CR 1924), demonstrating the applicability of the method and the capability to link measured solar wind velocity to the extrapolated coronal magnetic field in order to derive the velocity profile.

Relating 27-Day Averages of Solar, Interplanetary Medium Parameters, and Geomagnetic Activity Proxies in Solar Cycle 24

Yvelice **Castillo**, [Maria Alexandra Pais](#), [João Fernandes](#), [Paulo Ribeiro](#), [Anna L. Morozova](#) & [Fernando J. G. Pinheiro](#)

[Solar Physics](#) volume 296, Article number: 115 (2021)

<https://link.springer.com/content/pdf/10.1007/s11207-021-01856-8.pdf>

<https://doi.org/10.1007/s11207-021-01856-8>

Correlations between solar, interplanetary-medium parameters, and geomagnetic-activity proxies in 27-day averages (a Bartels rotation) were analyzed for the 2009 – 2016 time interval. In this analysis, two new proxies were considered: i) BzsBzs GSM (Geocentric Solar Magnetic), calculated as the daily percentage of the IMF southward component along the GSM zz-axis and then averaged every 27 days; ii) four magnetospheric indices (T-indices), calculated from the local north–south (xx) contributions of the magnetosphere’s cross-tail (TAIL), the symmetric ring current (SRC), the partial ring current (PRC), and the Birkeland current (FAC), derived from the Tsyanenko and Sitnov (J. Geophys. Res. 110, A03208, [2005](#); TS05) semi-empirical magnetospheric model. Our results suggest that, among the parameters tested in this study, solar facular areas, interplanetary magnetic-field intensity and new proxies derived from the TS05 model could be taken into account in an empirical model, with a 27-day resolution, to explain geomagnetic activity felt on the Earth’s surface in terms of solar-surface features and the IMF condition. We further retrieve a clear annual oscillation in series of 27-day-mean values of toward/away asymmetries of geomagnetic-activity indices, which can be interpreted in the light of the Russell–McPherron hypothesis for the semiannual variation of geomagnetic activity.

Solar and interplanetary triggers of the largest Dst variations of the solar cycle 23

Y. **Cerrato**, E. Saiz, C. Cid, , , W.D. Gonzalez, J. Palacios

Journal of Atmospheric and Solar-Terrestrial Physics, Voume 80, May 2012, Pages 111–123, **File**

We present the results of an investigation from the Sun to the Earth of the sequence of events that caused major Dst decreases ($\Delta Dst \leq -100$ nT during 1 h) that occurred during 1996–2005. These events are expected to be better related to

geomagnetic induced current (GIC) events than those events where any geomagnetic index is far from its quiet time value. At least one full halo CME with a speed on the plane of sky above 900 km/s participates in every studied event. The seven events were triggered by interplanetary signatures, which arise as a consequence of interaction among different solar ejections. The interaction arises at different stages from the solar surface, between segments of a filament, to the interplanetary medium, appearing as ejecta or multiple-magnetic clouds (MultiMCs). In other cases, shock waves overtake or compress previous ICMEs and at other times the interaction also appears between magnetic clouds (MCs) and streams.

Ionospheric response to Strong Geomagnetic Storms during 2000-2005: An IMF clock angle perspective

[Sumanjit Chakraborty](#), [Sarbani Ray](#), [Abhirup Datta](#), [Ashik Paul](#)

Radio Science **2020**

<https://arxiv.org/pdf/2008.06765.pdf>

This paper presents the equatorial ionospheric response to eleven strong-to-severe geomagnetic storms that occurred during the period 2000-2005, the declining phase of the solar cycle 23. The analysis has been performed using the global ion density plots of Defense Meteorological Satellite Program (DMSP). Observations show that for about 91% of the cases, post-sunset equatorial irregularities occurred within 3h from the time of northward to southward transition of the Interplanetary Magnetic Field (IMF) clock angle, thus bringing out the importance of the role played by IMF By in the process of Prompt Penetration of Electric Field (PPEF) in addition to the IMF Bz. This is an improvement from the previously reported (Ray et al., 2015) 4h window of ESF generation from the southward IMF Bz crossing -10 nT. **April 05-07, 2000, May 29-31, 2005**

Table 1. Minimum Dst values with the corresponding Day of Year and Date (DOY(DD)) of minimum for the severe storms analyzed during 2000-2005

Probabilistic prediction of geomagnetic storms and the Kp index

Shibaji [Chakraborty](#) and Steven Karl Morley

J. Space Weather Space Clim. **2020**, 10, 36

<https://www.swsc-journal.org/articles/swsc/pdf/2020/01/swsc190086.pdf>

Geomagnetic activity is often described using summary indices to summarize the likelihood of space weather impacts, as well as when parameterizing space weather models. The geomagnetic index K_p in particular, is widely used for these purposes. Current state-of-the-art forecast models provide deterministic K_p predictions using a variety of methods – including empirically-derived functions, physics-based models, and neural networks – but do not provide uncertainty estimates associated with the forecast. This paper provides a sample methodology to generate a 3-hour-ahead K_p prediction with uncertainty bounds and from this provide a probabilistic geomagnetic storm forecast. Specifically, we have used a two-layered architecture to separately predict storm (K_p ≥ 5-) and non-storm cases. As solar wind-driven models are limited in their ability to predict the onset of transient-driven activity we also introduce a model variant using solar X-ray flux to assess whether simple models including proxies for solar activity can improve the predictions of geomagnetic storm activity with lead times longer than the L1-to-Earth propagation time. By comparing the performance of these models we show that including operationally-available information about solar irradiance enhances the ability of predictive models to capture the onset of geomagnetic storms and that this can be achieved while also enabling probabilistic forecasts. **22-28 July 2004**

Table 3. List of storm events (2001-2006)

Probabilistic forecasting of the disturbance storm time index: An autoregressive Gaussian process approach

M. [Chandorkar](#), E. Camporeale, S. Wing

Space Weather Volume 15, Issue 8 August **2017** Pages 1004–1019

<http://sci-hub.cc/10.1002/2017SW001627>

We present a methodology for generating probabilistic predictions for the Disturbance Storm Time(Dst) geomagnetic activity index. We focus on the One Step Ahead prediction task and use the OMNI hourly resolution data to build our models. Our proposed methodology is based on the technique of Gaussian Process Regression. Within this framework we develop two models; Gaussian Process Autoregressive (GP-AR) and Gaussian Process Autoregressive with exogenous inputs (GP-ARX). We also propose a criterion to aid model selection with respect to the order of autoregressive inputs. Finally, we test the performance of the GP-AR and GP-ARX models on a set of 63 geomagnetic storms between 1998 and 2006 and illustrate sample predictions with error bars for some of these events. **2003/11/20-22**

Table 4. Storm events used for model selection of GP-AR and GP-ARX

Table 5. Storm events used to evaluate GP-AR and GP-ARX models

How can a Negative Magnetic Helicity Active Region Generate a Positive Helicity Magnetic Cloud ?

R. **Chandra** · E. Pariat · B. Schmieder · C.H. Mandrini · W. Uddin ·

Solar Phys., 261(1), 127-148, **2010**, **File**

The geoeffective magnetic cloud (MC) of **20 November 2003**, has been associated to the **18 November 2003**, solar active events in previous studies. In some of these, it was estimated that the magnetic helicity carried by the MC had a positive sign, as well as its solar source, active region (AR) NOAA 10501. In this paper we show that the large-scale magnetic field of AR 10501 had a negative helicity sign. Since coronal mass ejections (CMEs) are one of the means by which the Sun ejects magnetic helicity excess into the interplanetary space, the signs of magnetic helicity in the AR and MC should agree. Therefore, this finding contradicts what is expected from magnetic helicity conservation. However, using for the first time correct helicity density maps to determine the spatial distribution of magnetic helicity injection, we show the existence of a localized flux of positive helicity in the southern part of AR 10501. We conclude that positive helicity was ejected from this portion of the AR leading to the observed positive helicity MC.

Over-expansion of a coronal mass ejection generates sub-Alfvénic plasma conditions in the solar wind at Earth

E. **Chané**¹, B. Schmieder^{1,2}, S. Dasso^{3,4}, C. Verbeke¹, B. Grison⁵, P. Démoulin^{2,6} and S. Poedts^{1,7}

A&A 647, A149 (**2021**)

<https://doi.org/10.1051/0004-6361/202039867>

<https://www.aanda.org/articles/aa/pdf/2021/03/aa39867-20.pdf>

Context. From **May 24–25, 2002**, four spacecraft located in the solar wind at about 1 astronomical unit (au) measured plasma densities one to two orders of magnitude lower than usual. The density was so low that the flow became sub-Alfvénic for four hours, and the Alfvén Mach number was as low as 0.4. Consequently, the Earth lost its bow shock, and two long Alfvén wings were generated.

Aims. This is one of the lowest density events ever recorded in the solar wind at 1 au, and the least documented one. Our goal is to understand what caused the very low density.

Methods. Large Angle and Spectrometric Coronagraph (LASCO) and in situ data were used to identify whether something unusual occurred that could have generated such low densities

Results. The very low density was recorded inside a large interplanetary coronal mass ejection (ICME), which displayed a long, linearly declining velocity profile, typical of expanding ICMEs. We deduce a normalised radial expansion rate of 1.6. Such a strong expansion, occurring over a long period of time, implies a radial size expansion growing with the distance from the Sun to the power 1.6. This can explain a two-orders-of-magnitude drop in plasma density. Data from LASCO and the Advanced Composition Explorer show that this over-expanding ICME was travelling in the wake of a previous ICME.

Conclusions. The very low densities measured in the solar wind in May 2002 were caused by the over-expansion of a large ICME. This over-expansion was made possible because the ICME was travelling in a low-density and high-velocity environment present in the wake of another ICME coming from a nearby region on the Sun and ejected only three hours previously. Such conditions are very unusual, which explains why such very low densities are almost never observed.

Observations of interplanetary scintillation of the 2005 May 13 coronal mass ejection: numerical models

O **Chang**, R F **González**, M M **Bisi**, R A **Fallows**

MNRAS, Volume 508, Issue 1, **2021**, Pages 1314–1320,

<https://doi.org/10.1093/mnras/stab2664>

The 2005 May 13 eruption was an Earth-directed coronal mass ejection (CME) observed using the Multi-Element Radio-Linked Interferometer Network telescope system in the UK as it traversed the Interplanetary Medium on 2005 May 14. Observations of interplanetary scintillation (IPS) provide information on the solar wind conditions, which include velocities and density. In addition, it is also possible to calculate other parameters related to the turbulence and geometry of density irregularities in the solar wind from observations of IPS. Previous analyses have shown that IPS information can be difficult to interpret when a complex structure is crossing the line of sight since the physical properties of the plasma may change quite drastically with distance from the Sun. In order to compare and relate the internal structure of a CME and its physical changes, with the results from observations of IPS obtained previously, we

carried out a numerical simulation of the 2005 May 13 eruptive event as it propagates into the IPM, adapting the geometrical properties derived by IPS analysis. In this work, we give a possible explanation of some signatures of CME sub-structure from the point of view of the IPS technique combined with what the modelling reveals. **13-14 May 2005**

Multiple-point Modeling the Parker Spiral Configuration of the Solar Wind Magnetic Field at the Solar Maximum of Solar Cycle 24

Qing [Chang](#)¹, Xiaojun Xu¹, Qi Xu¹, Jun Zhong², Jiaying Xu¹, Jing Wang¹, and Tielong Zhang^{3,4}
2019 ApJ 884 102

<https://doi.org/10.3847/1538-4357/ab412a>

By assuming that the solar wind flow is spherically symmetric and that the flow speed becomes constant beyond some critical distance $r = R_0$ (neglecting solar gravitation and acceleration by high coronal temperature), the large-scale solar wind magnetic field lines are distorted into a Parker spiral configuration, which is usually simplified to an Archimedes spiral. Using magnetic field observations near Mercury, Venus, and Earth during solar maximum of Solar Cycle 24, we statistically surveyed the Parker spiral angles and obtained the empirical equations of the Archimedes and Parker spirals by fitting the multiple-point results. We found that the solar wind magnetic field configurations are slightly different during different years. Archimedes and Parker spiral configurations are quite different from each other within 1 au. Our results provide empirical Archimedes and Parker spiral equations that depend on the solar wind velocity and the critical distance (R_0). It is inferred that R_0 is much larger than that previously assumed. In the near future, the statistical survey of the near-Sun solar wind velocity by Parker Solar Probe can help verify this result.

Single-Site IPS Power Spectra Analysis for Space-Weather Products Using Cross Correlation Function Results from EISCAT and MERLIN IPS Data

O. [Chang](#) [M.M. Bisi](#) [E. Aguilar-Rodriguez](#) [R.A. Fallows](#) [J.A. Gonzalez-Esparza](#) [I. Chashei](#) [S. Tyulbashev](#)

Space Weather **Volume17, Issue7** Pages 1114-1130 **2019**

sci-hub.se/10.1029/2018SW002142

Interplanetary scintillation (IPS) manifests itself as a variation in the radio signal received from a distant, compact radio source on the sky. The intensity fluctuations of the radio waves are caused by density inhomogeneities in the outflowing solar plasma across the heliosphere. IPS allows us to infer solar wind speed and density variations along the line of sight (LOS). There are two types of techniques in the literature to infer solar wind speed using IPS data sets: single-site analysis (SSA), where the power spectra from single time series' are analysed to obtain solar wind parameters; and multi-site analysis, where the cross-correlation function (CCF) of data from two or more widely-separated sites is used. The selection of the analysis technique depends on the number of sites available to each IPS system. In order to combine and complement solar wind speed determinations from different instruments, it is important to validate results and methodologies of the two techniques. In this paper, we analysed previously well-studied European Incoherent SCATter (EISCAT) and Multi-Element Radio-Linked Interferometer Network (MERLIN) observations of IPS with well-known results from the CCF methodology. We applied the SSA technique to each of the individual EISCAT and MERLIN IPS power spectra. This work shows the capabilities of the SSA to describe complex events and seeks to obtain improved parameter fits using the SSA methodology.

Comparison of solar wind speed estimates from nearly simultaneous IPS observations at 327 and 111 MHz

I.V. [Chashei](#), [V.R. Lukmanov](#), [S.A. Tyulbashev](#), [M. Tokumaru](#)

Solar Phys. **296**, Article number: 63 **2021**

<https://arxiv.org/ftp/arxiv/papers/2102/2102.08767.pdf>

<https://link.springer.com/content/pdf/10.1007/s11207-021-01804-6.pdf>

<https://doi.org/10.1007/s11207-021-01804-6>

Results are presented of a comparison between solar wind speed estimates made using the time delays between 3 pairs of 327 MHz antennas at ISEE and estimates made by modeling the temporal power spectra observed with the 111 MHz BSA antenna at LPI. The observations were made for 6 years in the descending phase of solar cycle 24. More than 100 individual records were obtained for the compact source 3C48 and the extended and anisotropic source 3C298. The correlation between the daily speed estimates from 3C48 is 50%. Their annual averages agree within the error estimates and show the expected solar cycle variation. However the correlation between speeds from 3C298 is only 25% and their annual averages do not agree well. We investigate possible causes of this bias in the 3C298 estimated speeds.

Coronal Mass Ejections in September 2017 from Monitoring of Interplanetary Scintillations with the Large Phased Array of the Lebedev Institute of Physics

I. V. **Chashei**, S. A. Tyul'bashev, V. I. Shishov & I. A. Subaev
[Astronomy Reports](#) May 2018, Volume 62, [Issue 5](#), pp 346–351
Astronomicheskii Zhurnal, 2018, Vol. 95, No. 5, pp. 366–371.

<https://link.springer.com/content/pdf/10.1134%2FS1063772918050025.pdf>

Results of monitoring of interplanetary scintillations with the Large Phased Array of the Pushchino Radio Astronomy Observatory at 111 MHz during a period of flare activity of the Sun in the first ten days of September 2017 are presented. Enhancements of scintillations associated with interplanetary coronal mass ejections propagating after limb flares have been recorded. The propagation velocities are estimated to be about 2000 km/s for an ejection on September 7 and about 1000 km/s for an ejection on September 6. It is shown that, during the propagation from the Sun, the lateral part of the ejections decelerates faster than its leading part. Night-time enhancements of second-timescale scintillations during periods of high geomagnetic activity have an ionospheric origin.

Interplanetary and ionosphere scintillation produced by ICME 20 December 2015

I. V. **Chashei**, S. A. Tyul'bashev, V. I. Shishov, I. A. Subaev
Space Weather Volume 14, Issue 9 September 2016 Pages 682–688

Observational data of scintillation monitoring with typical time about 1 s at the frequency 111 MHz are presented for the period between 18 and 23 December when interplanetary coronal mass ejection (ICME) of flare origin resulted in the geomagnetic storm on **20–21 December 2015** with $Dst \approx -200$ nT. Our estimates show that the mean ICME speed between the solar corona and the start of interplanetary scintillation enhancement is close to the mean speed between the corona and the Earth. The strong increase of the nighttime scintillation level is observed after ICME coming to the Earth. Scintillation analysis of the individual radio sources shows that the 1 s night scintillation is of ionospheric origin and can be explained by an order increase of irregularity drift speed in the disturbed ionosphere.

Global Structure of the Turbulent Solar Wind during 24 Solar Activity Maxima from IPS Observations with the Multibeam Radio Telescope BSA LPI at 111 MHz

I. V. **Chashei**, V. I. Shishov, S. A. Tyul'bashev, [I. A. Subaev](#), [V. V. Oreshko](#), [S. V. Logvinenko](#)
Solar Phys. Volume 290, Issue 9, pp 2577-2587 **2015**

Study of a Large Forbush Decrease of July 2017

D.M.L. **Chauhan**, V. Chaudhary and M.K. Richharia
[PoS\(ICRC2019\) id.047](#) **2019**

<https://pos.sissa.it/358/047/pdf>

A large Forbush decrease (Fd) has been recorded by Moscow neutron monitoring station on 17th July 2017. An attempt has been made to understand the probable causes which have contributed for the occurrence of the large Fd. During the period of investigation extreme solar and interplanetary events i.e. sun spot numbers, disturbance storm time (Dst) index and Ap index has been investigated. The Dst index is suddenly increased during the event period indicating high geomagnetic activity during event time. The rise in sun spot numbers earlier the onset of forbush decrease reveals that it should have some connection with the occurrence of solar flares which further effects the cosmic ray variation. Probably this decrease is a result of high activity on the sun. The forbush decrease under investigation is probably due to the solar flare generated shock wave magnetic perturbation.

Interplanetary Magnetic Field Parameters Affecting Cosmic Ray Forbush Decrease

D.M.L. **Chauhan**, M.K. Richharia and B. Soni
PoS(ICRC2019) , id.045 , **2019**

<https://pos.sissa.it/358/045/pdf>

Coronal mass ejections (CMEs) hurl huge volumes of magnetized plasma into interplanetary space often referred to as ICMEs or ejecta. They are an important component of solar wind and can cause enhanced geomagnetic activity when they interact with the Earth's magnetosphere. When the ejecta have an average speed greater than the upstream solar wind speed they create a shock. The large IMF variations due to interplanetary shocks cause depression in the cosmic ray intensity (CRI) called Forbush Decrease (FD). Large Fds caused by fast CMEs are specifically associated with energetic X-ray flares. In the present paper, the author has studied seven largest Forbush decrease events selected from Moscow Neutron Monitor Station during a period of twelve years (1996- 2008), i.e., 23rd solar cycle. The analysis of CRI data with interplanetary magnetic field $|B|$, its southward component B_z , solar wind velocity, Kp and Dst indices

shows that all the three phenomena- solar, interplanetary and geomagnetic are connected to FD. The relationship between interplanetary parameters and FDs is discussed in detail. Moreover the solar cycle effect is found to be slightly shifted for large FDs as the frequency of occurrence of major FD events is more in the descending phase of the solar cycle. **9-15 April 2001, 4-10 November 2001, 22-28 November 2001, 28 October-3 November 2003, 24-30 July 2004, 13- 19 May 2005 & 9-15 September 2005**

How Nanoflares Produce Kinetic Waves, Nano-Type III Radio Bursts, and Non-Thermal Electrons in the Solar Wind

H. **Che**

Proceedings of 17th Annual International Astrophysics Conference, Santa Fe, 2018 **2018**

<https://arxiv.org/pdf/1807.10942.pdf>

Observations of the solar corona and the solar wind discover that the solar wind is unsteady and originates from the impulsive events near the surface of the Sun's atmosphere. How solar coronal activities affect the properties of the solar wind is a fundamental issue in heliophysics. We report a simulation and theoretical investigation of how nanoflare accelerated electron beams affect the kinetic-scale properties of the solar wind and generate coherent radio emission. We show that nanoflare-accelerated electron beams can trigger a nonlinear electron two stream instability, which generates kinetic Alfvén and whistler waves, as well as a non-Maxwellian electron velocity distribution function, consistent with observations of the solar wind. The plasma coherent emission produced in our model agrees well with the observations of Type III, J and V solar radio bursts. Open questions in the kinetic solar wind model are also discussed.

Formation of a Magnetic Cloud from the Merging of Two Successive Coronal Mass Ejections

Chong **Chen**, [Ying D. Liu](#), [Bei Zhu](#), [Huidong Hu](#), [Rui Wang](#)

ApJ **969** L4 **2024**

<https://arxiv.org/pdf/2406.13603>

<https://iopscience.iop.org/article/10.3847/2041-8213/ad53ca/pdf>

On **2022 March 28** two successive coronal mass ejections (CMEs) were observed by multiple spacecraft and resulted in a magnetic cloud (MC) at 1 AU. We investigate the propagation and interaction properties of the two CMEs correlated with the MC using coordinated multi-point remote sensing and in situ observations from Solar Orbiter, STEREO A, SOHO, and Wind. The first CME was triggered by a filament eruption with a high inclination angle. Roughly 9 hr later, the second CME originating from the same active region erupted with a smaller tilt angle and faster speed compared to the first one. The second CME overtook the preceding CME and formed a merged front at approximately $75 r_{\text{sun}}$, which developed into a complex ejecta at 1 AU. The descending speed and low proton temperature inside the complex ejecta suggest that the two CMEs have fully merged before reaching 1 AU, leading them to begin expanding rather than compressing against each other. The complex ejecta appears to have the magnetic field and plasma signatures of an MC, although there is a discontinuity in the magnetic field implying previous interactions. The cross section of the complex ejecta, reconstructed from in situ data using a Grad-Shafranov technique, exhibits a right-handed flux rope structure. These results highlight that an MC-like complex ejecta lacking interaction features could arise from the complete merging of two CMEs.

The effect of continuous geomagnetic storms on enhancements of ultrarelativistic electrons in the Earth's outer radiation belt

Jingrun **Chen**, Jingrun Chen, Chaoling Tang, and Xinxin Chu

Front. Astron. Space Sci. **11**: 1381764. **2024**

<https://doi.org/10.3389/fspas.2024.1381764>

<https://www.frontiersin.org/articles/10.3389/fspas.2024.1381764/full>

Ultrarelativistic electrons ($E_k > 3$ MeV) are the most energetic electrons in the Earth's outer radiation belt, which can cause serious damage to equipments on satellites. The evolutions of ultrarelativistic electrons during geomagnetic storm have been well understood, but the effects of continuous geomagnetic storm on ultrarelativistic electrons are still unclear. Using the data of the Van Allen Probes, we study the evolutions of ultrarelativistic electrons in the Earth's outer radiation belt during the three continuous geomagnetic storm events. These continuous geomagnetic storm events include the two geomagnetic storms. During the recovery phase of the first geomagnetic storm, enhanced relativistic and ultrarelativistic electrons with lower energies (≥ 3.4 MeV) are observed. These enhanced relativistic electrons could be the source of ultrarelativistic electrons and contribute to ultrarelativistic electron acceleration during the second geomagnetic storm. While 3.4 MeV electrons could be further enhanced during the second geomagnetic storm. During the recovery phase of the second small or moderate geomagnetic storm, ultrarelativistic electrons with higher cutoff energies (≥ 5.2 MeV) and higher fluxes are observed. Compared to an isolated geomagnetic storm with similar solar

wind and geomagnetic conditions, ultrarelativistic electrons with higher cutoff energies and higher fluxes are observed during the recovery phase of the second geomagnetic storm. We also find that continuous geomagnetic storm events may contribute even more to enhancements of ultrarelativistic electrons in the outer radiation belt if the second geomagnetic storm is a small or moderate storm with a low solar wind dynamic pressure and short-duration main phase. These can help us to further understand the evolutions of ultrarelativistic electrons in the Earth's outer radiation belt during geomagnetic storms. **18-25 May 2013, 1-7 June 2013, 20-25 April 2017**

Parallel Diffusion Coefficient of Energetic Charged Particles in the Inner Heliosphere from the Turbulent Magnetic Fields Measured by Parker Solar Probe

Xiaohang **Chen**¹, Joe Giacalone¹, Fan Guo², and Kristopher G. Klein¹

2024 ApJ 965 61

<https://iopscience.iop.org/article/10.3847/1538-4357/ad33c3/pdf>

Diffusion coefficients of energetic charged particles in turbulent magnetic fields are a fundamental aspect of diffusive transport theory but remain incompletely understood. In this work, we use quasi-linear theory to evaluate the spatial variation of the parallel diffusion coefficient κ_{\parallel} from the measured magnetic turbulence power spectra in the inner heliosphere. We consider the magnetic field and plasma velocity measurements from Parker Solar Probe made during Orbits 5–13. The parallel diffusion coefficient is calculated as a function of radial distance from 0.062 to 0.8 au, and the particle energy from 100 keV to 1 GeV. We find that κ_{\parallel} increases exponentially with both heliocentric distance and energy of particles. The fluctuations in κ_{\parallel} are related to the episodes of large-scale magnetic structures in the solar wind. By fitting the results, we also provide an empirical formula of $\kappa_{\parallel} = (5.16 \pm 1.22) \times 10^{18} r^{1.17 \pm 0.08} E^{0.71 \pm 0.02} \text{ (cm}^2 \text{ s}^{-1}\text{)}$ in the inner heliosphere, which can be used as a reference in studying the transport and acceleration of solar energetic particles as well as the modulation of cosmic rays.

Earth's Alfvén wings driven by the April 2023 Coronal Mass Ejection

Li-Jen **Chen**, [Daniel Gershman](#), [Brandon Burkholder](#), [Yuxi Chen](#), + + +

2024

<https://arxiv.org/ftp/arxiv/papers/2402/2402.08091.pdf>

In this paper, we report Magnetospheric Multiscale (MMS) observations of the dayside magnetosphere when the upstream Alfvén speed rises above the solar wind speed (sub-Alfvénic), causing the windsock-like magnetosphere to transform into Alfvén wings. The event occurred in the magnetic cloud of a Coronal Mass Ejection (CME) on April 24, 2023. We highlight the following outstanding features: (1) a layer of accelerated cold CME flow directly adjacent to the wing and to the magnetopause, which represents a rare regime of the terrestrial magnetosphere interaction with unshocked CME plasma; (2) moving filaments of the Alfvén wing created by magnetic reconnection, which represent new channels of connection between Earth's magnetosphere and the foot points of the Sun's erupted flux rope; (3) cold CME ion deceleration with little heating across the magnetopause. The reported MMS measurements advance our knowledge of CME interaction with planetary magnetospheres, and open new opportunities to further understand how sub-Alfvénic plasma flows impact astrophysical bodies such as Mercury, moons of Jupiter, and exoplanets that are close to their host stars. **24 Apr 2023**

Small-scale Magnetic Flux Ropes in Stream Interaction Regions from Parker Solar Probe and Wind Spacecraft Observations

Yu **Chen**¹, Qiang Hu^{1,2}, Robert C. Allen³, and Lan K. Jian⁴

2023 ApJ 943 33

<https://iopscience.iop.org/article/10.3847/1538-4357/aca894/pdf>

Using in situ measurements from the Parker Solar Probe and Wind spacecraft, we investigate the small-scale magnetic flux ropes (SFRs) and their properties inside stream interaction regions (SIRs). Within SIRs from ~ 0.15 to 1 au, SFRs are found to exist in a wide range of solar wind speeds with more frequent occurrences after the stream interface, and the Alfvénicity of these structures decreases significantly with increasing heliocentric distances. Furthermore, we examine the variation of five corresponding SIRs from the same solar sources. The enhancements of suprathermal electrons within these SIRs persist at 1 au and are observed multiple times. An SFR appears to occur repeatedly with the recurring SIRs and is traversed by the Wind spacecraft at least twice. This set of SFRs has similarities in variations of the magnetic field components, plasma bulk properties, density ratio of solar wind alpha and proton particles, and unidirectional suprathermal electrons. We also show, through the detailed time-series plots and Grad–Shafranov reconstruction results, that they possess the same chirality and carry comparable amounts of magnetic flux. Lastly, we discuss the possibility for these recurring SFRs to be formed via interchange reconnection, maintain the connection with the Sun, and survive up to 1 au. **2018 Aug 14-16, 2018 Sep 10-11, 2018 Oct 7, 2018 Nov 4-5, 2019 August 24**

Multispacecraft Remote Sensing and In Situ Observations of the 2020 November 29 Coronal Mass Ejection and Associated Shock: From Solar Source to Heliospheric Impacts

[Chong Chen](#), [Ying D. Liu](#), [Bei Zhu](#)

ApJ **937** 44 **2022**

<https://arxiv.org/pdf/2207.07534.pdf>

<https://iopscience.iop.org/article/10.3847/1538-4357/ac7ff6/pdf>

We investigate the source eruption, propagation and expansion characteristics, and heliospheric impacts of the **2020 November 29** coronal mass ejection (CME) and associated shock, using remote sensing and in situ observations from multiple spacecraft. A potential--field source--surface model is employed to examine the coronal magnetic fields surrounding the source region. The CME and associated shock are tracked from the early stage to the outer corona using extreme ultraviolet and white light observations. Forward models are applied to determine the structures and kinematics of the CME and the shock near the Sun. The shock shows an ellipsoidal structure, expands in all directions, and encloses the whole Sun as viewed from both SOHO and STEREO A, which results from the large expansion of the CME flux rope and its fast acceleration. The structure and potential impacts of the shock are mainly determined by its radial and lateral expansions. The CME and shock arrive at Parker Solar Probe and STEREO A. Only based on the remote sensing observations, it is difficult to predict whether and when the CME/shock would arrive at the Earth. Combining Wind in situ measurements and WSA-ENLIL simulation results, we confirm that the far flank of the CME (or the CME leg) arrives at the Earth with no shock signature. These results highlight the importance of multipoint remote sensing and in situ observations for determining the heliospheric impacts of CMEs.

RU-net: A Residual U-net for Automatic Interplanetary Coronal Mass Ejection Detection

Jun [Chen](#)^{1,2}, Hao Deng^{6,1}, Shuxin Li^{3,4,5}, Weifu Li¹, Hong Chen^{6,1}, Yanhong Chen^{3,5}, and Bingxian Luo^{3,4,5}

2022 ApJS 259 8

<https://iopscience.iop.org/article/10.3847/1538-4365/ac4587/pdf>

Detection methods for interplanetary coronal mass ejections (ICMEs) from in situ spacecraft measurements are mostly manual, which are labor-intensive and time-consuming, being prone to the inconsistencies of identification criteria and the incompleteness of the existing catalogs. Therefore, the automatic detection of ICMEs has aroused the interest of the astrophysical community. Of these automatic methods, the convolutional neural network--based methods show the advantages of fast speed and high precision. To further improve the computing feasibility and detection performance, this paper proposes a method called residual U-net (RU-net), from the perspective of time-series segmentation. With the help of U-net architecture, we design an encoder--decoder network with skip connection to capture multiscale information, where the end-to-end architecture with an embedded residual element is formulated to accelerate the algorithmic convergence. For the in situ data from 1997 October 1 to 2016 January 1 collected by the Wind spacecraft, the results of our experiments demonstrate the competitive performance of the proposed RU-net in terms of accuracy and efficiency (178 of 230 ICMEs are detected in the test set, and the F1 score is 80.18%). **1997 October 10-13**

Small-scale magnetic flux ropes and their properties based on in-situ measurements from Parker Solar Probe

Yu [Chen](#), [Qiang Hu](#)

ApJ **924** 43 **2022**

<https://arxiv.org/pdf/2111.09261.pdf>

<https://iopscience.iop.org/article/10.3847/1538-4357/ac3487/pdf>

We report small-scale magnetic flux ropes via the Parker Solar Probe in situ measurements during the first six encounters and present additional analyses to supplement our prior work in [Chen et al. 2021](#). These flux ropes are detected by the Grad-Shafranov-based algorithm with the duration and scale size ranging from 10 seconds to $\lesssim 1$ hour and from a few hundred kilometers to 10^{-3} au, respectively. They include both static structures and those with significant field-aligned plasma flows. Most structures tend to possess large cross helicity, while the residual energy distributes in wide ranges. We find that these dynamic flux ropes mostly propagate anti-sunward, with no preferential sign of magnetic helicity. The magnetic flux function follows a power law and is proportional to scale size. We also present case studies showing reconstructed two-dimensional (2D) configurations, which confirm that the static and dynamic flux ropes have the common configuration of spiral magnetic field lines (also streamlines). Moreover, the existence of such events hints at the interchange reconnection as a possible mechanism to generate flux rope-like structures near the Sun. Lastly, we summarize the major findings and discuss the possible correlation between these flux

rope-like structures and turbulence due to the process of local Alfvénic alignment. **2019 Mar 30-Apr 11, 2020 Jan 23-Feb 8**

Macro Magnetic Holes Caused by Ripples in Heliospheric Current Sheet from Coordinated Imaging and Parker Solar Probe Observations

Chong **Chen**^{1,2}, Ying D. Liu^{1,2}, and Huidong Hu¹

2021 ApJ 921 15

<https://doi.org/10.3847/1538-4357/ac1b2b>

Macro magnetic holes (MMHs), which are significant magnetic field decreases in the solar wind lasting tens of minutes, were found during the first four orbits of the Parker Solar Probe (PSP). We performed a detailed analysis of the **2020 January 30** event and found the possible cause of the MMH using coordinated remote sensing observations from STEREO A and PSP in situ measurements. The results indicate that an MMH represents a brief encounter with the rippled heliospheric current sheet (HCS). Out of the data from the first four orbits of PSP, we identified 17 MMHs and carried out a statistical analysis. Basic characteristics of MMHs include (1) MMHs usually last tens of minutes; (2) the magnetic field strength inside the events is much lower than that in the ambient solar wind; (3) enhanced plasma density, radial velocity, and plasma β are usually found inside the MMHs; and (4) the radial magnetic field has the same polarity before and after an MMH. Based on potential field-source surface and magnetohydrodynamics models, for each of the events we roughly estimate the radial size and the lower limit of the vertical size (i.e., the separation distance between PSP and the HCS), which are $2 R_{\odot}$ and $10 R_{\odot}$ on average, respectively. These results suggest that MMHs are a frequent phenomenon that may shed light on the dynamics of the HCS and the origins and evolutions of the solar wind structures in the heliosphere.

Small-scale Magnetic Flux Ropes with Field-aligned Flows via the PSP In Situ Observations

Yu **Chen**¹, Qiang Hu^{1,2}, Lingling Zhao^{1,2}, Justin C. Kasper^{3,4}, and Jia Huang⁴

2021 ApJ 914 108

<https://doi.org/10.3847/1538-4357/abfd30>

Magnetic flux rope, formed by the helical magnetic field lines, can sometimes maintain its shape while carrying significant plasma flow that is aligned with the local magnetic field. We report the existence of such structures and static flux ropes by applying the Grad-Shafranov-based algorithm to the Parker Solar Probe in situ measurements in the first five encounters. These structures are detected at heliocentric distances, ranging from 0.13 to 0.66 au, in a 4-month time period. We find that flux ropes with field-aligned flows, although they occur more frequently, have certain properties similar to those of static flux ropes, such as the decaying relations of the magnetic fields within structures with respect to heliocentric distances. Moreover, these events are more likely with magnetic pressure dominating over the thermal pressure. About one-third of events are detected in the relatively fast solar wind. Taking into account the high Alfvénicity, we also compare with switchback spikes identified during three encounters and interpret their interrelations. We find that some switchbacks can be detected when the spacecraft traverses flux-rope-like structures. The cross-section maps for selected events are presented via the new Grad-Shafranov-type reconstruction. Finally, the possible evolution of the magnetic flux rope structures in the inner heliosphere is discussed.

Small-scale Magnetic Flux Ropes in the First two Parker Solar Probe Encounters

Yu **Chen**, [Qiang Hu](#), [Lingling Zhao](#), [Justin C. Kasper](#), [Stuart D. Bale](#), [Kelly E. Korreck](#), [Anthony W. Case](#), [Michael L. Stevens](#), [John W. Bonnell](#), [Keith Goetz](#), [Peter R. Harvey](#), [Kristopher G. Klein](#), [Davin E. Larson](#), [Roberto Livi](#), [Robert J. MacDowall](#), [David M. Malaspina](#), [Marc Pulupa](#), [Phyllis L. Whittlesey](#)

ApJ **903** 76 **2020**

<https://arxiv.org/pdf/2007.04551.pdf>

<https://doi.org/10.3847/1538-4357/abb820>

Small-scale magnetic flux ropes (SFRs) are a type of structures in the solar wind that possess helical magnetic field lines. In a recent report (Chen & Hu 2020), we presented the radial variations of the properties of SFR from 0.29 to 8 au using in situ measurements from the Helios, ACE/Wind, Ulysses, and Voyager spacecraft. With the launch of the Parker Solar Probe (PSP), we extend our previous investigation further into the inner heliosphere. We apply a Grad-Shafranov-based algorithm to identify SFRs during the first two PSP encounters. We find that the number of SFRs detected near the Sun is much less than that at larger radial distances, where magnetohydrodynamic (MHD) turbulence may act as the local source to produce these structures. The prevalence of Alfvénic structures significantly suppresses the detection of SFRs at closer distances. We compare the SFR event list with other event identification methods, yielding a dozen well-matched events. The cross-section maps of two selected events confirm the cylindrical magnetic flux rope configuration.

The power-law relation between the SFR magnetic field and heliocentric distances seems to hold down to 0.16 au. **2018 November 13**

Table 3. List of Small-scale Flux Ropes identified during PSP Encounter 1 & 2.

Effects of Radial Distances on Small-scale Magnetic Flux Ropes in the Solar Wind

Yu **Chen**¹ and Qiang Hu²

2020 ApJ 894 25

<https://doi.org/10.3847/1538-4357/ab8294>

Small-scale magnetic flux ropes (SFRs) in the solar wind have been studied for decades. Statistical analysis utilizing various in situ spacecraft measurements is the main observational approach to investigating the generation and evolution of these small-scale structures. Based on the Grad–Shafranov reconstruction technique, we use the automated detection algorithm to build the databases of these small-scale structures via various spacecraft measurements at different heliocentric distances. We present the SFR properties, including the magnetic field and plasma parameters at different radial distances from the Sun near the ecliptic plane. It is found that the event occurrence rate is still of the order of a few hundreds per month, the duration and scale-size distributions follow power laws, and the flux-rope axis orientations are approximately centered around the local Parker spiral directions. In general, most SFR properties exhibit radial decays. In addition, with various databases established, we derive scaling laws for the changes in average field magnitude, event counts, and SFR scale sizes, with respect to the radial distances, ranging from ~ 0.3 au for Helios to ~ 7 au for the Voyager spacecraft. The implications of our results for comparisons with the relevant theoretical works and for applications to the Parker Solar Probe mission are discussed.

The Evolution and Role of Solar Wind Turbulence in the Inner Heliosphere

C. H. K. **Chen**, [S. D. Bale](#), [J. W. Bonnell](#), [D. Borovikov](#), [T. A. Bowen](#), [D. Burgess](#), [A. W. Case](#), [B. D. G. Chandran](#), [T. Dudok de Wit](#), [K. Goetz](#), [P. R. Harvey](#), [J. C. Kasper](#), [K. G. Klein](#), [K. E. Korreck](#), [D. Larson](#), [R. Livi](#), [R. J. MacDowall](#), [D. M. Malaspina](#), [A. Mallet](#), [M. D. McManus](#), [M. Moncuquet](#), [M. Pulupa](#), [M. Stevens](#), [P. Whittlesey](#)

ApJ **2019**

<https://arxiv.org/pdf/1912.02348.pdf>

The first two orbits of the Parker Solar Probe (PSP) spacecraft have enabled the first in situ measurements of the solar wind down to a heliocentric distance of 0.17 au (or 36 Rs). Here, we present an analysis of this data to study solar wind turbulence at 0.17 au and its evolution out to 1 au. While many features remain similar, key differences at 0.17 au include: increased turbulence energy levels by more than an order of magnitude, a magnetic field spectral index of $-3/2$ matching that of the velocity and both Elsasser fields, a lower magnetic compressibility consistent with a smaller slow-mode kinetic energy fraction, and a much smaller outer scale that has had time for substantial nonlinear processing. There is also an overall increase in the dominance of outward-propagating Alfvénic fluctuations compared to inward-propagating ones, and the radial variation of the inward component is consistent with its generation by reflection from the large-scale gradient in Alfvén speed. The energy flux in this turbulence at 0.17 au was found to be $\sim 10\%$ of that in the bulk solar wind kinetic energy, becoming $\sim 40\%$ when extrapolated to the Alfvén point, and both the fraction and rate of increase of this flux towards the Sun is consistent with turbulence-driven models in which the solar wind is powered by this flux. **6th October 2018 to 18th April 2019**

Characteristics of a Gradual Filament Eruption and Subsequent CME Propagation in Relation to a Strong Geomagnetic Storm

Chong **Chen**, [Ying D. Liu](#), [Rui Wang](#), [Xiaowei Zhao](#), [Huidong Hu](#), [Bei Zhu](#)

ApJ **884** 90 **2019**

<https://arxiv.org/pdf/1908.11100.pdf>

<https://doi.org/10.3847/1538-4357/ab3f36>

An unexpected strong geomagnetic storm occurred on **2018 August 26**, which was caused by a slow coronal mass ejection (CME) from a gradual eruption of a large quiet-region filament. We investigate the eruption and propagation characteristics of this CME in relation to the strong geomagnetic storm with remote sensing and in situ observations. Coronal magnetic fields around the filament are extrapolated and compared with EUV observations. We determine the propagation direction and tilt angle of the CME flux rope near the Sun using a graduated cylindrical shell (GCS) model and the Sun-to-Earth kinematics of the CME with wide-angle imaging observations from STEREO A. We reconstruct the flux-rope structure using a Grad-Shafranov technique based on the in situ measurements at the Earth and compare it with those from solar observations and the GCS results. Our conclusions are as follows: (1) the eruption of the filament was unusually slow and occurred in the regions with relatively low critical heights of the coronal field decay index; (2)

the axis of the CME flux rope rotated in the corona as well as in interplanetary space, which tended to be aligned with the local heliospheric current sheet; (3) the CME was bracketed between slow and fast solar winds, which enhanced the magnetic field inside the CME at 1 AU; (4) the geomagnetic storm was caused by the enhanced magnetic field and a southward orientation of the flux rope at 1 AU from the rotation of the flux rope.

Analysis of Small-scale Magnetic Flux Ropes Covering the Whole Ulysses Mission

Yu **Chen**, **Qiang Hu**, **Jakobus le Roux**

ApJ **881** 58 **2019**

<https://arxiv.org/pdf/1905.00986.pdf>

sci-hub.se/10.3847/1538-4357/ab2ccf

Small-scale magnetic flux ropes, in the solar wind, have been studied for decades via the approach of both simulation and observation. Statistical analysis utilizing various in-situ spacecraft measurements is the main observational approach. In this study, we extend the automated detection of small-scale flux ropes based on the Grad-Shafranov reconstruction to the complete dataset of *Ulysses* spacecraft in-situ measurements. We first discuss the temporal variation of the bulk properties of 22,719 flux ropes found through our approach, namely, the average magnetic field and plasma parameters, etc., as functions of the heliographical latitudes and heliocentric radial distances. We then categorize all identified events into three groups based on event distributions in different latitudes separated at 30°, at different radial distances, and under different solar activities, respectively. By the detailed statistical analysis, we conclude as follows. (1) The properties of flux ropes, such as the duration, scale size, etc., follow the power-law distributions, but with different slope indices, especially for distributions at different radial distances. (2) Also, they are affected by the solar wind speed which has different distributions under the different solar activities, which is manifested as the latitudinal effect. (3) The main difference in flux rope properties between the low and high latitudes is attributed to possible Alfvénic structures or waves. (4) Flux ropes with longer duration and larger scale sizes occur more often at larger radial distances. (5) With more strict Walén slope threshold, more events are excluded at higher latitudes. The entire database is published online at [this http URL](#).

Table 2. Category of small-scale magnetic flux ropes (1991-2009).

Ionospheric response to CIR-induced recurrent geomagnetic activity during the declining phase of Solar Cycle 23†

Yanhong **Chen**, Wenbin Wang, Alan G. Burns et al.

JGR **2015**

This paper presents an epoch analysis of global ionosphere responses to recurrent geomagnetic activity during **79 corotating interaction region (CIR) events from 2004-2009**.

A comparison of the effects of CIR- and CME-induced geomagnetic activity on thermospheric densities and spacecraft orbits: Statistical studies

Guang-ming **Chen**^{1,*}, Jiyao Xu¹, Wenbin Wang² and Alan. G. Burns

JGR, Volume 119, Issue 9, pages 7928–7939, **2014**

Enhanced energy input from the magnetosphere to the upper atmosphere during geomagnetic storms has a profound effect on thermospheric density and consequently near-Earth satellite orbit decay. These geomagnetic storms are caused by two different processes. The first is coronal mass ejections (CMEs) and the second is corotating interaction regions (CIRs). CME-driven storms are characterized by large maximum energy input but relatively short duration, whereas CIR-driven storms have relatively small maximum energy input but are of a considerably longer duration. In this paper we carried out a statistical study to assess the relative importance of each kind of storm to satellite orbital decay. The results demonstrate that CIR storms have a slightly larger effect on total orbital decay than CME storms do in a statistical sense. During the declining phase and the minimum years of a solar cycle, CIR storms occur frequently and quasiperiodically. These storms have a large effect on thermospheric densities and satellite orbits because of their relatively long duration. Thus, it is important to fully understand their behavior and impact.

Bayesian prediction of geomagnetic storms: Wind data, 1996–2010,

Chen, J., S. P. Slinker, and I. Triandaf

(2012), Space Weather, 10, S04005,

The feature-based Bayesian method previously developed by Chen et al. (1996, 1997) to predict the occurrence, severity, and duration of large geomagnetic storms has been run on a daily basis on the Wind/Magnetic Fields Investigation (MFI) data from January 1996 until March 2010. The algorithm uses as input real-time solar wind magnetic field data obtained **at the L1 Lagrange point**, and the output is the probability prediction of the magnetic field structure of the upstream solar wind that has yet to arrive, and its geoeffectiveness, where geoeffectiveness is measured by the traditional Dst index. The performance characteristics of the method are evaluated using a four-level contingency table: nonstorm disturbances ($-80 \text{ nT} < \text{Dst} \leq -50 \text{ nT}$), weak storms ($-120 \text{ nT} < \text{Dst} \leq -80 \text{ nT}$), moderate storms ($-160 \text{ nT} < \text{Dst} \leq -120 \text{ nT}$), and strong storms ($\text{Dst} \leq -160 \text{ nT}$). It is found that the greater the level of disturbances, the more accurate the prediction is. With moderate and strong storms combined, the algorithm correctly predicted 30 out of 37 storms (81%). The false negatives are caused by solar wind structures with short durations ($\leq 1\text{--}2$ hrs) of strong southward magnetic field (say, $B_z \leq -30 \text{ nT}$), which are sparsely represented in the probability distribution functions constructed using prior solar wind data (OMNI data set from 1973–1981). The algorithm does not predict the storm onset time, but the results of the present and previous tests show that the average warning time ranges from a few hours to a maximum of 10–15 hours.

Key Signatures of Prominence Materials and Category of Cold Materials Identified by Random Forest Classifier

Zexin **Cheng**¹, Shuo Yao¹, and Shuyi Meng¹

2023 ApJS 268 25

<https://iopscience.iop.org/article/10.3847/1538-4365/ace447/pdf>

The origin of cold materials identified by different criteria is unclear. They are highly suspected to be erupted prominences. However, some cold materials defined by charge depletion exist in both quiet solar wind and interplanetary coronal mass ejections (ICMEs). Recently, solar observations show failed prominence eruption in coronal mass ejections (CMEs) that the prominence sometimes did not propagate into interplanetary space. This work uses Random Forest Classifier (RFC), which is an interpretable supervised machine-learning algorithm to study the distinct signatures of prominence cold materials (PCs) compared to quiet solar wind (QSW) and ICMEs excluding cold materials (ICMEEs). Twelve physical features measured by ACE at 1 au and the monthly averaged sunspot number are used in this study. The measurements from ACE are proton moments, magnetic field component B_z , He/H, He/O, Fe/O, mean charge of oxygen and carbon, $C6+/C5$, $C6+/C4+$, and $O7+/O6+$. According to the returned weights from RFC that are checked by support vector machine classifier, the most important in situ signatures of PCs are obtained. Next, the trained RFC is used to check the category of the cold materials not related to CME observations. The results show that most segments of the cold materials are from prominences, but four of them are possibly from ICMEEs; another one segment is possibly from QSW. The most distinct signatures of PCs are lower ($C6+/C5+$)/($O7+/O6+$), proton temperature, and He/O. Considering the obvious overlaps on key physical features between QSW, ICMEEs, and PCs, the multifeature classifier shows an advantage in identifying them than solid criteria.

Using Stereoscopic Observations of Cometary Plasma Tails to Infer Solar Wind Speed

Long **Cheng**^{1,2,3}, Quanhao Zhang^{1,2,3}, Yuming Wang^{1,2,3}, Xiaolei Li^{1,2,3}, and Rui Liu

2020 ApJ 897 87

<https://sci-hub.tw/https://iopscience.iop.org/article/10.3847/1538-4357/ab93b6>

Detection of the solar wind speed near the Sun is significant in understanding the heating and acceleration of the solar wind. Cometary plasma tails have long been used as natural probes for solar wind speed; previous solar wind speed estimates via plasma tails, however, were based on comet images from a single viewpoint, and the projection effect may influence the result. Using stereoscopic observations from the Solar Terrestrial Relations Observatory and the Solar and Heliospheric Observatory, we three-dimensionally reconstruct the plasma tails of three comets C/2012 S1 (ISON), C/2010 E6, and C/2011 W3 (Lovejoy) and infer the ambient solar wind speed. The first comet is located between 3.5 and 6 solar radii (R_s) away from the Sun at high latitudes; the estimated solar wind speed is about 300–500 km s^{-1} . The second comet is located within 10 R_s and about 20° away from the ecliptic; the estimated solar wind speed is about 200–320 km s^{-1} . The third comet is also located at low latitudes but farther ($>20 R_s$) away from the Sun; the estimated solar wind speed is about 100–600 km s^{-1} . For comets near the ecliptic, our results are close to those predicted by MHD models, whereas for the comet at high latitudes, the deviation between our estimate and the model results is notable. This consistency and difference could be used to constrain and improve solar wind models. We will seek opportunities to apply the method to comet 322P, whose tail may sweep the Parker Solar Probe. **2010 March 12, 2011 December 18, 2013 November 28**

Sun-Earth connection Event of Super Geomagnetic Storm on **March 31, 2001**: the Importance of Solar Wind Density

Li-Bin [Cheng](#), [Gui-Ming Le](#), [Ming-Xian Zhao](#)

Research in Astronomy and Astrophysics

2019

<https://arxiv.org/pdf/1910.07932.pdf>

An X1.7 flare at 10:15 UT and a halo CME with a projected speed of 942 km/s erupted from NOAA solar active region 9393 located at N20W19, were observed on **2001 March 29**. When the CME reached the Earth, it triggered a super geomagnetic storm (hereafter super storm). We find that the CME always moved towards the Earth according to the intensity-time profiles of protons with different energies. The solar wind parameters responsible for the main phase of the super storm occurred on March 31, 2001 is analyzed taking into account the delayed geomagnetic effect of solar wind at the L1 point and using the SYM-H index. According to the variation properties of SYM-H index during the main phase of the super storm, the main phase of the super storm is divided into two parts. A comparative study of solar wind parameters responsible for the two parts shows the evidence that the solar wind density plays a significant role in transferring solar wind energy into the magnetosphere, besides the southward magnetic field and solar wind speed.

Tracking the Evolution of A Coherent Magnetic Flux Rope Continuously from the Inner to the Outer Corona

X. [Cheng](#), M. D. Ding, Y. Guo, J. Zhang, A. Vourlidis, Y. D. Liu, O. Olmedo, J. Q. Sun, and C. Li

E-print, Oct 2013, File; 2014 ApJ 780 28

http://sprg.ssl.berkeley.edu/~liuxying/pubs/2014_apj_cheng.pdf

The magnetic flux rope (MFR) is believed to be the underlying magnetic structure of coronal mass ejections (CMEs). However, it remains unclear how an MFR evolves into and forms the multi-component structure of a CME. In this paper, we perform a comprehensive study of an extreme-ultraviolet (EUV) MFR eruption on **2013 May 22** by tracking its morphological evolution, studying its kinematics, and quantifying its thermal property. As EUV brightenings begin, the MFR starts to rise slowly and shows helical threads winding around an axis. Meanwhile, cool filamentary materials descend spirally down to the chromosphere. These features provide direct observational evidence of intrinsically helical structure of the MFR. Through detailed kinematical analysis, we find that the MFR evolution experiences two distinct phases: a slow rise phase and an impulsive acceleration phase. We attribute the first phase to the magnetic reconnection within the quasi-separatrix-layers surrounding the MFR, and the much more energetic second phase to the fast magnetic reconnection underneath the MFR. We suggest that the transition between these two phases be caused by the torus instability. Moreover, we identify that the MFR evolves smoothly into the outer corona and appears as a coherent structure within the white light CME volume. The MFR in the outer corona was enveloped by bright fronts that originated from plasma pile-up in front of the expanding MFR. The fronts are also associated with the preceding sheath region followed the outmost MFR-driven shock.

On the Relationship Between Transit Time of ICMEs and Strength of the Initiated Geomagnetic Storms

I.M. [Chertok](#)

Solar Phys. 295, Article number: 74 2020

<https://arxiv.org/abs/2004.14894>

<https://arxiv.org/ftp/arxiv/papers/2004/2004.14894.pdf>

More than 140 isolated non-recurrent geomagnetic storms (GMSs) of various intensities from extreme to weak are considered, which are reliably identified with solar eruptive sources (coronal mass ejections, CMEs). The analysis aims to obtain a possibly complete picture of the relationship between the transit time of propagation of CMEs and interplanetary coronal mass ejections (ICMEs) from the Sun to the Earth (more precisely, the time interval dtp from the moment of an eruption until the peak of the corresponding GMS) and the maximum intensity of this GMS, as measured by the disturbance storm time geomagnetic index Dst. Two groups of events are singled out: one includes GMSs, the source of which was an eruption from an active region (AR events), the other GMSs caused by filament eruptions from quiescent areas of the Sun located outside ARs (QS events). The distribution of the large number of the analyzed events on a dtp - Dst plane confirms and substantially clarifies the known regularities. The AR events are characterized by a shorter transit time ($\text{dtp} \sim 1\text{-}4$ days) and much stronger GMSs (Dst up to -600 nT mainly) in comparison with the QS events ($\text{dtp} \sim 3\text{-}5$ days, Dst > -200 nT). For events of both groups, the shorter transit time of CMEs/ICMEs, the more intense GMSs; in particular, for AR events when dtp declines from 4 to 1 day, Dst decreases on average from -100 to -470 nT and can reach -900 nT. From the point of view of the nature of GMSs and their sources on the Sun, the obtained results mean that both the speed of CMEs/ICMEs and the strength of the magnetic field transferred by them are largely

determined by the parameters of the corresponding eruptions, in particular, by the eruptive magnetic flux and the released energy.

Solar Eruptions, Forbush Decreases and Geomagnetic Disturbances from Outstanding Active Region 12673

I.M. **Chertok**, [A.V. Belov](#), [A.A. Abunin](#)

Space Weather, [Volume 16, Issue 10](#) Pages 1549-1560, 2018

<https://doi.org/10.1029/2018SW001899>

<https://arxiv.org/ftp/arxiv/papers/1809/1809.07961.pdf>

Based on our tool for the early diagnostics of solar eruption geoeffectiveness (EDSEG tool; Chertok et al., 2013, 2015, 2017), we have analyzed space weather disturbances that occurred in early September 2017. Two flares, SOL2017-09-04T20:33 (M5.5) and SOL2017-09-06T12:02 (X9.3), accompanied by Earth-directed halo coronal mass ejections (CMEs) were found to be geoeffective. We extracted the associated EUV dimmings and arcades and calculated their total unsigned magnetic flux. This calculation allowed us to estimate the possible scales of the Forbush decreases (FDs) and geomagnetic storms (GMSs) in the range from moderate to strong, and they are close to the observed scales. More precisely, after the first eruption, an FD approximately equal to 2% and almost no GMS occurred because the Bz magnetic field component in front of the corresponding interplanetary CME (ICME) was northern. The stronger second eruption produced somewhat larger composite disturbances (FD ~ 9.3% and GMS with indexes Dst ~ -144 nT, Ap ~ 235) than expected (FD ~ 4.4%, Dst ~ -135 nT, Ap ~ 125) because the second ICME overtook the trailing part of the first ICME near Earth, and the resulting Bz component was more intense and southern. Both ICMEs arrived at Earth earlier than expected because they propagated in the high-speed solar wind emanated from an extended coronal hole adjacent to AR12673 along their entire path. Overall, the presented results provide further evidence that the EDSEG tool can be used for the earliest diagnostics of actual solar eruptions to forecast the scale of the corresponding geospace disturbances.

An Early Diagnostics of the Geoeffectiveness of Solar Eruptions from Photospheric Magnetic Flux Observations: The Transition from SOHO to SDO

I.M. **Chertok** (1), V.V. Grechnev (2), A.A. Abunin

Solar Physics **292**: 62.

2017 doi:10.1007/s11207-017-1081-8

<https://arxiv.org/pdf/1702.05905.pdf>

<http://link.springer.com/content/pdf/10.1007%2Fs11207-017-1081-8.pdf>

In our previous articles (Chertok et al.: 2013, Solar Phys. 282, 175, and 2015, Solar Phys. 290, 627), we presented a preliminary tool for the early diagnostics of the geoeffectiveness of solar eruptions based on the estimate of the total unsigned line-of-sight photospheric magnetic flux in accompanying extreme-ultraviolet arcades and dimmings. This tool was based on the analysis of eruptions observed in 1996-2005 with SOHO/EIT and MDI. Empirical relationships were obtained to estimate the probable importance of upcoming space weather disturbances caused by an eruption, which just occurred, without data on the associated coronal mass ejections. It was possible to estimate the intensity of a non-recurrent geomagnetic storm (GMS) and Forbush decrease (FD), as well as their onset and peak times. After 2010-2011, data on solar eruptions are obtained with SDO/AIA and HMI. We use relatively short intervals of overlapping EIT-AIA and MDI-HMI detailed observations and a number of large eruptions over the next five years with the 12-hour cadence EIT images to adapt the SOHO diagnostic tool to SDO data. The adopted brightness thresholds select from the EIT 195 \AA and AIA 193 \AA image practically the same areas of arcades and dimmings with a cross-calibration factor of 3.6-5.8 (5.0-8.2) for the AIA exposure time of 2.0 s (2.9 s). For the same photospheric areas, the MDI magnetic flux systematically exceeds the HMI flux by a factor of 1.4. Based on these results, the empirical diagnostic relationships obtained from SOHO data are adjusted to SDO instruments. Examples of a post-diagnostics based on SDO data are presented. As before, the tool is applicable to non-recurrent GMSs and FDs caused by nearly central eruptions from active regions, provided that the southern component of the interplanetary magnetic field near the Earth is predominantly negative, which is not predicted by this tool.

Relationship between the Magnetic Flux of Solar Eruptions and the Ap Index of Geomagnetic Storms

I. M. **Chertok**, M. A. Abunina, A. A. Abunin, A. V. Belov, V. V. Grechnev

Solar Phys. February 2015, Volume 290, [Issue 2](#), pp 627-633

<http://arxiv.org/pdf/1410.1646v1.pdf>

Solar coronal mass ejections (CMEs) are main drivers of the most powerful non-recurrent geomagnetic storms. In the extreme-ultraviolet range, CMEs are accompanied by bright post-eruption arcades and dark dimmings. The analysis of events of the Solar Cycle 23 (Chertok et al., 2013, Solar Phys. 282, 175) revealed that the summarized unsigned magnetic flux in the arcades and dimming regions at the photospheric level, Φ , is significantly related to the intensity (Dst index) of geomagnetic storms. This provides the basis for the earliest diagnosis of geoeffectiveness of solar eruptions. In the present article, using the same data set, we find that a noticeable correlation exists also between the eruptive magnetic flux, Φ , and another geomagnetic index, Ap. As the magnetic flux increases from tens to approx. 500 (in units of 10^{20} Mx), the geomagnetic storm intensity measured by the 3-hour Ap index, enhances in average from Ap approx. 50 to a formally maximum value of 400 (in units of 2 nT). The established relationship shows that in fact the real value of the Ap index is not limited and during the most severe magnetic storms may significantly exceed 400.

Magnetic Flux of EUV Arcade and Dimming Regions as a Relevant Parameter for Early Diagnostics of Solar Eruptions – Sources of Non-recurrent Geomagnetic Storms and Forbush Decreases

I. M. [Chertok](#), V. V. Grechnev, A. V. Belov, A. A. Abunin
Solar Physics, January 2013, Volume 282, Issue 1, pp 175-199

<http://arxiv.org/pdf/1209.2208v1.pdf>

This study aims at the early diagnostics of the geoeffectiveness of coronal mass ejections (CMEs) from quantitative parameters of the accompanying EUV dimming and arcade events. We study events of the 23th solar cycle, in which major non-recurrent geomagnetic storms (GMS) with $Dst < -100$ nT are sufficiently reliably identified with their solar sources in the central part of the disk. Using the SOHO/EIT 195 Å images and MDI magnetograms, we select significant dimming and arcade areas and calculate summarized unsigned magnetic fluxes in these regions at the photospheric level. The high relevance of this eruption parameter is displayed by its pronounced correlation with the Forbush decrease (FD) magnitude, which, unlike GMSs, does not depend on the sign of the Bz component but is determined by global characteristics of ICMEs. Correlations with the same magnetic flux in the solar source region are found for the GMS intensity (at the first step, without taking into account factors determining the Bz component near the Earth), as well as for the temporal intervals between the solar eruptions and the GMS onset and peak times. The larger the magnetic flux, the stronger the FD and GMS intensities are and the shorter the ICME transit time is. The revealed correlations indicate that the main quantitative characteristics of major non-recurrent space weather disturbances are largely determined by measurable parameters of solar eruptions, in particular, by the magnetic flux in dimming areas and arcades, and can be tentatively estimated in advance with a lead time from 1 to 4 days. For GMS intensity, the revealed dependencies allow one to estimate a possible value, which can be expected if the Bz component is negative.

Dependence of Forbush-decrease characteristics on parameters of solar eruptions

I M [Chertok](#)¹, A A Abunin¹, A V Belov¹ and V V Grechnev
2013 J. Phys.: Conf. Ser. 409 012150

We analyze relations between characteristics of an extended ensemble of Forbush decreases (FDs) caused by CMEs from the central zone of the solar disk during the 23rd solar cycle, on the one hand, and such solar eruption parameter as a summarized unsigned magnetic flux of CME-associated EUV dimmings and arcades, on the other hand. This eruption parameter is shown to have a pronounced direct correlation with the FD magnitude and a conspicuous reverse correlation with the ICME transit time from the Sun to the Earth. The revealed correlations indicate that main quantitative characteristics of major non-recurrent FDs (and geomagnetic storms as well) are largely determined by parameters of solar eruptions, in particular such as the summarized magnetic flux of dimmings and arcades.

First measurement of interplanetary scintillation with the ASKAP radio telescope: implications for space weather

Rajan [Chhetri](#), [John Morgan](#), [Vanessa Moss](#), [Ron Ekers](#), [Danica Scott](#), [Keith Bannister](#), [Cherie K. Day](#), [Adam T. Deller](#), [Ryan M. Shannon](#)

Advances in Space Research (ASR) entitled "COSPAR Space Weather Roadmap 2022: Scientific Research and Applications" 2022

<https://arxiv.org/pdf/2208.04981.pdf>

We report on a measurement of interplanetary scintillation (IPS) using the Australian Square Kilometre Array Pathfinder (ASKAP) radio telescope. Although this proof-of-concept observation utilised just 3 seconds of data on a single source, this is nonetheless a significant result, since the exceptional wide field of view of ASKAP, and this validation of its ability to observe within 10 degrees of the Sun, mean that ASKAP has the potential to observe an interplanetary coronal mass ejection (CME) after it has expanded beyond the field of view of white light coronagraphs, but long before it has reached the Earth. We describe our proof of concept observation and extrapolate from the measured noise parameters to determine what information could be gleaned from a longer observation using the full field of view. We demonstrate that, by adopting a 'Target Of Opportunity' (TOO) approach, where the telescope is triggered by the detection of a CME in white-light coronagraphs, the majority of interplanetary CMEs could be observed by ASKAP while in an elongation range <30 degrees. It is therefore highly complementary to the colocated Murchison Widefield Array, a lower-frequency instrument which is better suited to observing at elongations >20 degrees.

Large-scale Structure and Turbulence Transport in the Inner Solar Wind: Comparison of Parker Solar Probe's First Five Orbits with a Global 3D Reynolds-averaged MHD Model

Rohit [Chhiber](#)^{1,2}, Arcadi V. Usmanov^{1,2}, William H. Matthaeus¹, and Melvyn L. Goldstein^{2,3}

2021 ApJ 923 89

<https://doi.org/10.3847/1538-4357/ac1ac7>

Simulation results from a global magnetohydrodynamic model of the solar corona and solar wind are compared with Parker Solar Probe (PSP) observations during its first five orbits. The fully three-dimensional model is based on Reynolds-averaged mean-flow equations coupled with turbulence-transport equations. The model includes the effects of electron heat conduction, Coulomb collisions, turbulent Reynolds stresses, and heating of protons and electrons via a turbulent cascade. Turbulence-transport equations for average turbulence energy, cross helicity, and correlation length are solved concurrently with the mean-flow equations. Boundary conditions at the coronal base are specified using solar synoptic magnetograms. Plasma, magnetic field, and turbulence parameters are calculated along the PSP trajectory. Data from the first five orbits are aggregated to obtain trends as a function of heliocentric distance. Comparison of simulation results with PSP data shows good agreement, especially for mean-flow parameters. Synthetic distributions of magnetic fluctuations are generated, constrained by the local rms turbulence amplitude given by the model. Properties of this computed turbulence are compared with PSP observations.

Random Walk and Trapping of Interplanetary Magnetic Field Lines: Global Simulation, Magnetic Connectivity, and Implications for Solar Energetic Particles

Rohit [Chhiber](#), [David Ruffolo](#), [William H. Matthaeus](#), [Arcadi V. Usmanov](#), [Paisan Tooprakai](#), [Piyanate Chuychai](#), [Melvyn L. Goldstein](#)

ApJ 2020

<https://arxiv.org/pdf/2011.06620.pdf>

The random walk of magnetic field lines is an important ingredient in understanding how the connectivity of the magnetic field affects the spatial transport and diffusion of charged particles. As solar energetic particles (SEPs) propagate away from near-solar sources, they interact with the fluctuating magnetic field, which modifies their distributions. We develop a formalism in which the differential equation describing the field line random walk contains both effects due to localized magnetic displacements and a non-stochastic contribution from the large-scale expansion. We use this formalism together with a global magnetohydrodynamic simulation of the inner-heliospheric solar wind, which includes a turbulence transport model, to estimate the diffusive spreading of magnetic field lines that originate in different regions of the solar atmosphere. We first use this model to quantify field line spreading at 1 au, starting from a localized solar source region, and find rms angular spreads of about 20° - 60° . In the second instance, we use the model to estimate the size of the source regions from which field lines observed at 1 au may have originated, thus quantifying the uncertainty in calculations of magnetic connectivity; the angular uncertainty is estimated to be about 20° . Finally, we estimate the filamentation distance, i.e., the heliocentric distance up to which field lines originating in magnetic islands can remain strongly trapped in filamentary structures. We emphasize the key role of slab-like fluctuations in the transition from filamentary to more diffusive transport at greater heliocentric distances. 2012 May 12

Clustering of Intermittent Magnetic and Flow Structures near Parker Solar Probe's First Perihelion -- A Partial-Variance-of-Increments Analysis

Rohit [Chhiber](#), [M. Goldstein](#), [B. Maruca](#), [A. Chasapis](#), [W. Matthaeus](#), [D. Ruffolo](#), [R. Bandyopadhyay](#), [T. Parashar](#), [R. Qudsi](#), [T. Dudok de Wit](#), [S. Bale](#), [J. Bonnell](#), [K. Goetz](#), [P. Harvey](#), [R. MacDowall](#), [D. Malaspina](#), [M. Pulupa](#), [J. Kasper](#), [K. Korreck](#), [A. Case](#), [M. Stevens](#), [P. Whittlesey](#), [D. Larson](#), [R. Livi](#), [M. Velli](#), [N. Raouafi](#)

ApJ 2019

<https://arxiv.org/pdf/1912.03608.pdf>

During the Parker Solar Probe's (PSP) first perihelion pass, the spacecraft reached within a heliocentric distance of $\sim 37 R_{\odot}$ and observed numerous magnetic and flow structures characterized by sharp gradients. To better understand these intermittent structures in the young solar wind, an important property to examine is their degree of correlation in time and space. To this end, we use the well-tested Partial Variance of Increments (PVI) technique to identify intermittent events in FIELDS and SWEAP observations of magnetic and proton-velocity fields (respectively) during PSP's first solar encounter, when the spacecraft was within 0.25 au from the Sun. We then examine distributions of waiting times between events with varying separation and PVI thresholds. We find power-law distributions for waiting times shorter than a characteristic scale comparable to the correlation time, suggesting a high degree of correlation that may originate in a clustering process. Waiting times longer than this characteristic time are better described by an exponential, suggesting a random memory-less Poisson process at play. These findings are consistent with near-Earth observations of solar wind turbulence. The present study complements the one by Dudok de Wit et al. (2020, present volume), which focuses on waiting times between observed "switchbacks" in the radial magnetic field.

2018.11.01-09

Contextual Predictions for Parker Solar Probe II: Turbulence Properties and Taylor

Hypothesis

Rohit [Chhiber](#), [Arcadi V. Usmanov](#), [William H. Matthaeus](#), [Tulasi N. Parashar](#), [Melvyn L. Goldstein](#)

2019

<https://arxiv.org/pdf/1902.03340.pdf>

The Parker Solar Probe (PSP) primary mission extends seven years and consists of 24 orbits of the Sun with descending perihelia culminating in a closest approach of ($\sim 9.8 R_{\odot}$). In the course of these orbits PSP will pass through widely varying conditions, including anticipated large variations of turbulence properties such as energy density, correlation scales and cross helicities. Here we employ global magnetohydrodynamics simulations with self-consistent turbulence transport and heating [\citep{usmanov2018}](#) to preview likely conditions that will be encountered by PSP, by assuming suitable boundary conditions at the coronal base. The code evolves large-scale parameters -- such as velocity, magnetic field, and temperature -- as well as turbulent energy density, cross helicity, and correlation scale. These computed quantities provide the basis for evaluating additional useful parameters that are derivable from the primary model outputs. Here we illustrate one such possibility in which computed turbulence and large-scale parameters are used to evaluate the accuracy of the Taylor "frozen-in" hypothesis along the PSP trajectory. Apart from the immediate purpose of anticipating turbulence conditions that PSP will encounter, as experience is gained in comparisons of observations with simulated data, this approach will be increasingly useful for planning and interpretation of subsequent observations.

Contextual Predictions for Parker Solar Probe I: Critical Surfaces and Regions

Rohit [Chhiber](#), [Arcadi V. Usmanov](#), [William H. Matthaeus](#), [Melvyn L. Goldstein](#)

2018 *ApJS* 241 11

<https://arxiv.org/pdf/1806.00570.pdf>

<https://doi.org/10.3847/1538-4365/ab0652>

The solar corona and young solar wind may be characterized by critical surfaces -- the sonic, Alfvén, and first plasma- β unity surfaces -- that demarcate regions where the solar wind flow undergoes certain crucial transformations. Global numerical simulations and remote sensing observations offer a natural mode for the study of these surfaces at large scales, thus providing valuable context for the high-resolution in-situ measurements expected from the soon-to-be-launched Parker Solar Probe (PSP). The present study utilizes global three-dimensional magnetohydrodynamic simulations of the solar wind to characterize the critical surfaces and investigate the flow in propinquitous regions. Effects of solar activity are incorporated by varying source magnetic dipole tilts and employing magnetogram-based boundary conditions. A magnetohydrodynamic turbulence model is self-consistently coupled to the bulk flow equations, enabling investigation of turbulence properties of the flow in the vicinity of critical regions. The simulation results are compared with a variety of remote sensing observations. A simulated PSP trajectory is used to provide contextual predictions for the spacecraft in terms of the computed critical surfaces. Broad agreement is seen in the interpretation of the present results in comparison with existing remote sensing results, both from heliospheric imaging and from radio scintillation studies. The trajectory analyses show that the period of time that PSP is likely to spend inside the $\beta=1$, sonic and Alfvén surfaces depends sensitively on the degree of solar activity and the tilt of the solar dipole and location of the heliospheric current sheet.

Direct Observations of a Shock Traversing Preceding Two Coronal Mass Ejections: Insights from Solar Orbiter, Wind, and STEREO Observations

Yutian **Chi**¹, Chenglong Shen^{2,3}, Zhiyong Zhang⁴, Mengjiao Xu¹, Dongwei Mao⁴, Junyan Liu⁴, Can Wang⁴, Bingkun Yu¹, Jingyu Luo⁴, Zhihui Zhong⁴Show full author list

2024 ApJL 975 L25

<https://iopscience.iop.org/article/10.3847/2041-8213/ad87e8/pdf>

The three successive coronal mass ejections (CMEs) that erupted from **2023 November 27–28**, provide the first opportunity to shed light on the entire process of a shock propagating through, sequentially compressing, and modifying two preceding CMEs using in situ data from Solar Orbiter, Wind, and STEREO-A. We describe the interaction of the three CMEs as follows: CME-1 and CME-2 interacted with each other at distances close to the Sun. Subsequently, the shock (S3) driven by CME-3 caught up with and compressed ICME-2 before 0.83 au, forming a typical shock–ICME interaction event observed by the Solar Orbiter. The S3 continued to propagate, crossing ICME-2 and propagating into ICME-1 as observed by Wind, and completely overtaking both ICME-1 and ICME-2 at STEREO-A. The interaction between S3 and the preceding two ICMEs leads to a clear compression of preceding ICMEs including an increase in magnetic field (~150%) and a reduction in the interval of ICMEs. It presents direct and compelling evidence that a shock can completely traverse two preceding CMEs, accompanied by a significant decrease in shock strength (magnetic compression ratio decrease from 1.74 to 1.49). Even though the three ICMEs interact significantly in the heliosphere, their magnetic field configurations exhibit coherence at different observation points, especially for ICME-3. Those results highlight the significant implications of shock–CME interactions for CME propagation and space weather forecasting.

The Dynamic Evolution of Multipoint Interplanetary Coronal Mass Ejections Observed with BepiColombo, Tianwen-1, and MAVEN

Yutian **Chi**¹, Chenglong Shen^{2,3}, Junyan Liu⁴, Zhihui Zhong⁴, Mathew Owens⁵, Christopher Scott⁵, Luke Barnard⁵, Bingkun Yu¹, Daniel Heyner⁶, Hans-Ulrich Auster⁶

2023 ApJL 951 L14

<https://iopscience.iop.org/article/10.3847/2041-8213/acd7e7/pdf>

We present two multipoint interplanetary coronal mass ejections (ICMEs) detected by the Tianwen-1 and Mars Atmosphere and Volatile Evolution spacecraft at Mars and the BepiColombo (0.56 au ~0.67 au) upstream of Mars from 2021 December 5 to 31. This is the first time that BepiColombo is used as an upstream solar wind monitor ahead of Mars and that Tianwen-1 is used to investigate the magnetic field characteristics of ICMEs at Mars. The Heliospheric Upwind Extrapolation time model was used to connect the multiple in situ observations and the coronagraph observations from STEREO/SECCHI and SOHO/LASCO. The first fast coronal mass ejection event (~761.2 km s⁻¹), which erupted on December 4, impacted Mars centrally and grazed BepiColombo by its western flank. The ambient slow solar wind decelerated the west flank of the ICME, implying that the ICME event was significantly distorted by the solar wind structure. The second slow ICME event (~390.7 km s⁻¹) underwent an acceleration from its eruption to a distance within 0.69 au and then traveled with the constant velocity of the ambient solar wind. These findings highlight the importance of background solar wind in determining the interplanetary evolution and global morphology of ICMEs up to Mars distance. Observations from multiple locations are invaluable for space weather studies at Mars and merit more exploration in the future. **2021 December 4–8, 2021 December 28–31**

Interplanetary Coronal Mass Ejections and Stream Interaction Regions Observed by Tianwen-1 and MAVEN at Mars

Yutian **Chi**¹, Chenglong Shen^{2,3}, Long Cheng⁴, Bingkun Yu¹, Bin Miao^{2,3}, Yuming Wang^{2,3,5}, Tielong Zhang^{6,7}, Zhuxuan Zou⁴, Mengjiao Xu¹, Zonghao Pan

2023 ApJS 267 3

<https://iopscience.iop.org/article/10.3847/1538-4365/acd191/pdf>

The Tianwen-1 spacecraft is China's first Mars exploration mission. The Mars Orbiter Magnetometer (MOMAG) is a scientific instrument on board the Tianwen-1 mission that is designed to study magnetic fields at Mars, including the solar wind to the magnetosheath and the ionosphere. Using the first Tianwen-1/MOMAG data that is publicly available, we present an interplanetary coronal mass ejection (ICME) and stream interaction region (SIR) list based on in situ observations at Mars between 2021 November 16 and 2021 December 31. We compared the magnetic field intensity and vector magnetic field measurements from Tianwen-1/MOMAG and Mars Atmospheric Volatile Evolution (MAVEN)/Magnetometer (MAG) during the ICME and SIR interval and found a generally good consistency between them. Due to MAVEN's orbital adjustment since 2019, the Tianwen-1/MOMAG instrument is almost unique in its status as an interplanetary magnetic field monitor currently at Mars. The observations indicate that the MOMAG instrument on

Tianwen-1 is performing well and can provide accurate measurements of the vector magnetic field in the near-Mars solar wind space. The multipoint observations combining MOMAG, MINPA, and MEPA on board Tianwen-1 with MAG, SWIA, and STATIC on board MAVEN will help develop systematic studies of the characteristics of ICMEs and SIRs at Mars, and their influences on the Martian atmosphere and ionosphere.

Predictive Capabilities of Corotating Interaction Regions using STEREO and Wind in-situ observations

Yutian [Chi](#), [Chenglong Shen](#), [Christopher Scott](#), [Mengjiao Xu](#), [Mathew Owens](#), [Yuming Wang](#), [Mike Lockwood](#)

Space Weather **Volume20, Issue7** e2022SW003112 **2022**

<https://agupubs.onlinelibrary.wiley.com/doi/epdf/10.1029/2022SW003112>

<https://doi.org/10.1029/2022SW003112>

Solar wind stream interaction regions (SIRs) and corotating interaction regions (CIRs) can cause geomagnetic storms and change energetic particle environment, ionospheric composition on Earth. Therefore advanced warning of SIRs/CIRs is vital for mitigating the effect of space weather on critical infrastructures in modern society. Recently, several solar missions, e.g., Vigil mission (Luntama et al., 2020) and Solar Ring mission (Wang et al., 2020), that can be served as a space weather monitor, have been proposed. To evaluate the capabilities of these future missions of predicting SIRs/CIRs, the STEREO-B spacecraft is used to investigate the correlation between SIRs/CIRs detected by STEREO-B and Wind spacecraft. The correlation coefficients of solar wind velocity in SIRs/CIRs are significantly higher than that of magnetic field intensity or plasma density. It indicates that the velocity structure of solar wind is more persistent than magnetic field and ion density. By assuming the SIR/CIR structures are stable and ideal corotation, 58.9% of SIRs/CIRs in the STEREO-B CIR catalogue can be used to predict CIR arrival time in near-Earth space. With increasing longitudinal and latitudinal separations between STEREO-B and Wind, the percentage of accurately predicted CIRs decreases gradually from 100% to 20%. If the separation angle between STEREO-B and Wind is within 30° in longitude and approximately ± 5° in latitude, more than 93.2% of SIRs/CIRs can be accurately predicted several days in advance. This demonstrates that a spacecraft situated 30° trailing Earth in its orbit, can optimize our space weather-predicting capabilities for the Earth and lessen the risk of missing or “false alarms” CIRs. **May 1–3, 2010**

Using the "Ghost Front" to Predict the Arrival Time and Speed of CMEs at Venus and Earth

Yutian [Chi](#)^{1,2,3}, [Christopher Scott](#)², [Chenglong Shen](#)^{1,3}, [Mathew Owens](#)², [Matthew Lang](#)², [Mengjiao](#)

[Xu](#)¹, [Zhihui Zhong](#)¹, [Jie Zhang](#)⁴, [Yuming Wang](#)¹, and [Mike Lockwood](#)²

2020 ApJ 899 143

<https://doi.org/10.3847/1538-4357/aba95a>

<https://iopscience.iop.org/article/10.3847/1538-4357/aba95a/pdf>

Using in situ measurements and remote-sensing observations, we study two coronal mass ejections (CMEs) that left the Sun on **2012 June 13–14** and impacted both Venus and Earth while the planets were in close radial alignment. The two CMEs generate multiple fronts in Solar Terrestrial Relations Observatory (STEREO)/Heliospheric Imager (HI) images, which can also be observed in the "J-map" as bifurcated features. We present the "ghost front" model to combine remote observations from STEREO/SECCHI and in situ observations from the Wind and Venus Express (VEX) spacecraft, and to derive the kinematics and propagation directions of the CMEs. By fitting the observations of multiple fronts to a kinematically evolving flux rope model and assuming the CMEs undergo deceleration through frictional drag with a steady-state solar wind, we confirm that the outer and inner fronts of the CMEs as detected in HI images are consistent with peaks in Thomson scattered light returned from the flank and nose of a single front for each CME. An interaction takes place between CME-1 and CME-2 that can be observed in the HI-1 field of view (FOV) before CME-1 encounters Venus. The multipoint in situ observations of the shock–CME interaction event serve as further evidence of the interaction between CMEs. The arrival times calculated from the ghost front model are within 2.5 hr of those observed at VEX and Wind. Our analysis indicates that ghost fronts could provide information about the longitudinally extended shape of the CME in the FOV of HI-1, which can be used to improve the forecast of interplanetary CME arrival time at Earth.

Geoeffectiveness of Stream Interaction Regions From 1995 to 2016

Yutian [Chi](#) [Chenglong Shen](#) [Bingxian Luo](#) [Yuming Wang](#) [Mengjiao Xu](#)

Space Weather 16?, 12, 1960-1971 **2018**

<http://sci-hub.tw/10.1029/2018SW001894>

Stream interaction regions (SIRs) are important sources of geomagnetic storms. In this work, we first extend the end time of the widely used SIR catalog developed by Jian et al. (2006, <https://doi.org/10.1007/s11207-006-0132-3>), which covered the period from 1995 to 2009, to the end of 2016. Based on this extended SIR catalog, the geoeffectiveness of

SIRs is discussed in detail. It was found that 52% of the SIRs caused geomagnetic storms with $Dst_{min} \leq -30$ nT, but only 3% of them caused intense geomagnetic storms with $Dst_{min} \leq -100$ nT. Furthermore, we found that 10 of the intense geomagnetic storms caused by SIRs were associated with complex structures due to interactions between SIRs and interplanetary coronal mass ejections (ICMEs). In such a structure, an ICME is embedded in the SIR and located between the slow and fast solar wind streams. In addition, we found that the geoeffectiveness of SIRs interacting with ICMEs is enhanced. The possibility of SIR-ICME interaction structures causing geomagnetic storms is markedly higher than that of isolated SIRs or isolated ICMEs. In particular, the geoeffectiveness of SIR-ICME interaction structures is similar to that of the Shock-ICME interaction structures, which have been demonstrated to be the main causes of geomagnetic storms.

Statistical Study of the Interplanetary Coronal Mass Ejections from 1995 to 2014

Yutian **Chi**, Chenglong Shen, Yuming Wang, Pinzhong Ye, S. Wang

Solar Phys. **2015**

<http://arxiv.org/pdf/1504.07849v1.pdf>

In this work, we establish an ICME list from 1996 to 2014 based on the in-situ observations from the WIND and ACE satellites. Based on this ICME list, we extend the statistical analysis of the ICMEs to the solar maximum phase of solar cycle 24th. The analysis of the annual variations of the properties of ICMEs show that the number of ICMEs, the number of shocks, the percentage of ICMEs drove shocks, the magnetic field and plasma properties of ICMEs are well correlated with the solar cycle variation. The number of MCs do not show any correlation with sunspot number. But, the percentage of the MCs in ICMEs show good anti-correlation with the sunspot number. By comparison the parameters of MCs with None-MC ICMEs, we found that the MCs are stronger than the None-MC ICMEs. In addition, we compare the parameters of ICMEs with and without shocks. It is found that the ICMEs with shocks are much stronger than the ICME without shocks. Meanwhile, we discuss the distribution of the magnetic field and solar wind plasmas parameters of the sheath regions of ICMEs at first time. We find that the magnetic field and solar wind velocity in the sheath region are higher than them in the ejecta of ICMEs from statistical point of view.

ICME Catalogue http://space.ustc.edu.cn/dreams/wind_icmes/

22 - 24 September 1999, 17 - 18 September 2008

GENESIS OF INTERPLANETARY INTERMITTENT TURBULENCE: A CASE STUDY OF ROPE-ROPE MAGNETIC RECONNECTION

Abraham C.-L. **Chian**^{1,2,9,10}, Heng Q. Feng³, Qiang Hu⁴, Murray H. Loew¹, Rodrigo A. Miranda⁵, Pablo R. Muñoz⁶, David G. Sibeck⁷, and De J. Wu

2016 ApJ 832 179

In a recent paper, the relation between current sheet, magnetic reconnection, and turbulence at the leading edge of an interplanetary coronal mass ejection was studied. We report here the observation of magnetic reconnection at the interface region of two interplanetary magnetic flux ropes. The front and rear boundary layers of three interplanetary magnetic flux ropes are identified, and the structures of magnetic flux ropes are reconstructed by the Grad-Shafranov method. A quantitative analysis of the reconnection condition and the degree of intermittency reveals that rope-rope magnetic reconnection is the most likely site for genesis of interplanetary intermittency turbulence in this event. The dynamic pressure pulse resulting from this reconnection triggers the onset of a geomagnetic storm.

Observation of the Solar Corona Using Radio Scintillation with the Akatsuki Spacecraft: Difference Between Fast and Slow Wind

[Shota Chiba](#), [Takeshi Imamura](#), [Munetoshi Tokumaru](#), [Daikou Shiota](#), [Takuma Matsumoto](#), [Hiroki Ando](#), [Hiroshi Takeuchi](#), [Yasuhiro Murata](#), [Atsushi Yamazaki](#), [Bernd Häusler](#) & [Martin Pätzold](#)
[Solar Physics](#) volume 297, Article number: 34 (2022)

<https://link.springer.com/content/pdf/10.1007/s11207-022-01968-9.pdf>

The properties of the coronal plasma at heliocentric distances of 1.5 – 8.9 R_{\odot} (solar radii) were studied with radio-occultation observations using JAXA's Akatsuki spacecraft in 2016. Physical parameters that characterize the solar wind were retrieved from the intensity-scintillation time series by fitting a theoretical spectrum to the observed power spectra. The derived solar-wind velocity clearly shows a difference between the fast wind and the slow wind, which was identified based on IPS observations. The inner scale, at which fluid motions dissipate and kinetic energy is converted to heat, increases with the heliocentric distance, and the fast wind has larger inner scales than the slow wind. By applying wavelet analysis to the frequency time series, we detected quasi-periodic fluctuations in the electron density. The density oscillations are considered to be manifestations of acoustic waves, which were generated from Alfvén waves originating from the photosphere, and the energy fluxes of those acoustic waves were estimated. The relative density-amplitude

peaks around $4 - 6 R_{\odot}$ and the wave-energy flux decreases beyond $\approx 6 R_{\odot}$, implying that the acoustic waves dissipate to heat the corona. The phase-scintillation spectrum that we obtained cannot be expressed by a single power law. A break is seen around the frequency of $0.5 - 2$ Hz beyond $\approx 6 R_{\odot}$, suggesting an excess power other than turbulence at lower frequencies. The enhancement of the relative density amplitude around $6 R_{\odot}$ found by the wavelet analysis might explain this excess power. The acoustic wave-energy flux in the fast solar wind tends to exceed that in the slow wind, suggesting that the fast wind is powered by a larger injection of Alfvén-wave energy than the slow wind.

DETECTION OF CURRENT SHEETS AND MAGNETIC RECONNECTIONS AT THE TURBULENT LEADING EDGE OF AN INTERPLANETARY CORONAL MASS EJECTION

Abraham C.-L. [Chian](#)^{1,2} and Pablo R. Muñoz

2011 ApJ 733 L34

The relation between current sheets, turbulence, and magnetic reconnections at the leading edge of an interplanetary coronal mass ejection detected by four Cluster spacecraft on **2005 January 21** is studied. We report the observational evidence of two magnetically reconnected current sheets in the vicinity of a front magnetic cloud boundary layer with the following characteristics: (1) a Kolmogorov power spectrum in the inertial subrange of the magnetic turbulence, (2) the scaling exponent of structure functions of magnetic fluctuations exhibiting multi-fractal scaling predicted by the She-Leveque magnetohydrodynamic model, and (3) bifurcated current sheets with the current density computed by both single-spacecraft and multi-spacecraft techniques.

A Bayesian approach to the drag-based modelling of ICMEs

Simone [Chierichini](#)^{1,2*}, Gregoire Francisco^{2,3}, Ronish Mugatwala^{1,2}, Raffaello Foldes^{4,5}, +++
J. Space Weather Space Clim. **2024**, 14, 1

<https://www.swsc-journal.org/articles/swsc/pdf/2024/01/swsc230044.pdf>

Coronal Mass Ejections (CMEs) are huge clouds of magnetised plasma expelled from the solar corona that can travel towards the Earth and cause significant space weather effects. The Drag-Based Model (DBM) describes the propagation of CMEs in an ambient solar wind as analogous to an aerodynamic drag. The drag-based approximation is popular because it is a simple analytical model that depends only on two parameters, the drag parameter γ and the solar wind speed w . DBM thus allows us to obtain reliable estimates of CME transit time at low computational cost. Previous works proposed a probabilistic version of DBM, the Probabilistic Drag Based Model (P-DBM), which enables the evaluation of the uncertainties associated with the predictions. In this work, we infer the “a-posteriori” probability distribution functions (PDFs) of the γ and w parameters of the DBM by exploiting a well-established Bayesian inference technique: the Monte Carlo Markov Chains (MCMC) method. By utilizing this Bayesian method through two different approaches, an ensemble and an individual approach, we obtain specific DBM parameter PDFs for two ensembles of CMEs: those travelling with fast and slow solar wind, respectively. Subsequently, we assess the operational applicability of the model by forecasting the arrival time of CMEs. While the ensemble approach displays notable limitations, the individual approach yields promising results, demonstrating competitive performances compared to the current state-of-the-art, with a Mean Absolute Error (MAE) of 9.86 ± 4.07 h achieved in the best-case scenario.

Direct observations of a complex coronal web driving highly structured slow solar wind

L. P. [Chitta](#), [D. B. Seaton](#), [C. Downs](#), [C. E. DeForest](#), [A. K. Higginson](#)

Nature Astronomy **2022**

<https://arxiv.org/ftp/arxiv/papers/2211/2211.13283.pdf>

<https://www.nature.com/articles/s41550-022-01834-5.pdf>

The solar wind consists of continuous streams of charged particles that escape into the heliosphere from the Sun, and is split into fast and slow components, with the fast wind emerging from the interiors of coronal holes. Near the ecliptic plane, the fast wind from low-latitude coronal holes is interspersed with a highly structured slow solar wind, the source regions and drivers of which are poorly understood. Here we report extreme-ultraviolet observations that reveal a spatially complex web of magnetized plasma structures that persistently interact and reconnect in the middle corona. Coronagraphic white-light images show concurrent emergence of slow wind streams over these coronal web structures. With advanced global MHD coronal models, we demonstrate that the observed coronal web is a direct imprint of the magnetic separatrix web (S-web). By revealing a highly dynamic portion of the S-web, our observations open a window into important middle-coronal processes that appear to play a key role in driving the structured slow solar wind.

2D solar wind speeds from 6 to 26 solar radii in solar cycle 24 by using Fourier filtering

Il-Hyun [Cho](#), [Yong-Jae Moon](#), [Valery M. Nakariakov](#), [Su-Chan Bong](#), [Jin-Yi Lee](#), [Donguk Song](#), [Harim Lee](#), [Kyung-Suk Cho](#)

<https://arxiv.org/pdf/1806.08540.pdf>

Measurement of the solar wind speed near the Sun is important for understanding the acceleration mechanism of the solar wind. In this study, we determine 2D solar wind speeds from 6 to 26 solar radii by applying Fourier motion filters to \textit{SOHO}/LASCO C3 movies observed from 1999 to 2010. Our method successfully reproduces the original flow speeds in the artificially generated data as well as streamer blobs. We measure 2D solar wind speeds from 1-day to 1-year timescales and their variation in solar cycle 24. We find that the solar wind speeds at timescales longer than a month in the solar maximum period are relatively uniform in the azimuthal direction, while they are clearly bimodal in the minimum period, as expected from the \textit{Ulysses} observations and IPS reconstruction. The bimodal structure appears at around 2006, becomes most distinctive in 2009, and abruptly disappears in 2010. The radial evolution of the solar wind speeds resembles the Parker's solar wind solution.

Comparison of Helicity Signs in Interplanetary CMEs and Their Solar Source Regions

K.-S. **Cho**, S.-H. Park, K. Marubashi, N. Gopalswamy, S. Akiyama, S. Yashiro, R.-S. Kim, E.-K. Lim
Solar Physics, May 2013, Volume 284, Issue 1, pp 105-127; **File**

If all coronal mass ejections (CMEs) have flux ropes, then the CMEs should keep their helicity signs from the Sun to the Earth according to the helicity conservation principle. This study presents an attempt to answer the question from the Coordinated Data Analysis Workshop (CDAW), "Do all CMEs have flux ropes?", by using a qualitative helicity sign comparison between interplanetary CMEs (ICMEs) and their CME source regions. For this, we select 34 CME-ICME pairs whose source active regions (ARs) have continuous SOHO/MDI magnetogram data covering more than 24 hr without data gap during the passage of the ARs near the solar disk center. The helicity signs in the ARs are determined by estimation of cumulative magnetic helicity injected through the photosphere in the entire source ARs. The helicity signs in the ICMEs are estimated by applying the cylinder model developed by Marubashi (Adv. Space. Res., 26, 55, 2000) to 16 second resolution magnetic field data from the MAG instrument onboard the ACE spacecraft. It is found that 30 out of 34 events (88 %) are helicity sign-consistent events, while four events (12 %) are sign-inconsistent. Through a detailed investigation of the source ARs of the four sign-inconsistent events, we find that those events can be explained by the local helicity sign opposite to that of the entire AR helicity (**28 July 2000 ICME**), incorrectly reported solar source region in the CDAW list (**20 May 2005 ICME**), or the helicity sign of the pre-existing coronal magnetic field (**13 October 2000** and **20 November 2003 ICMEs**). We conclude that the helicity signs of the ICMEs are quite consistent with those of the injected helicities in the AR regions from where the CMEs erupted.

An empirical relationship between coronal mass ejection initial speed and solar wind dynamic pressure

Cho, K.-S.; Bong, S.-C.; Moon, Y.-J.; Dryer, M.; Lee, S.-E.; Kim, K.-H.

J. Geophys. Res., Vol. 115, No. A10, A10111, 2010

Interplanetary shocks that precede coronal mass ejections (CMEs) are mainly responsible for sudden impulses, which are characterized by a simple step-like increase in the horizontal H component. Such a magnetic field change has been explained as a compression of the magnetosphere by the passage of a sudden increase in the solar wind dynamic pressure. Strong compression of the dayside magnetopause could cause geosynchronous satellites to be exposed to solar wind environments where large fluctuations of the interplanetary magnetic field and highly energetic particles are present. In this study, we chose 26 event pairs consisting of a type II burst/CME occurring in conjunction with a sudden commencement/sudden impulse (SC/SI) whose solar wind, and Earth magnetic field data are available. We then investigated relationships among three physical properties (kinetic energy, directional parameter, and speed) of near-Sun CMEs, solar wind dynamic pressure, and SC/SI amplitude. As a result, we found that (1) the CME speed is more highly correlated with SC/SI amplitude than its kinetic energy and direction parameter; (2) by adopting the empirical relationship between solar wind dynamic pressure and amplitude of symmetric H (a step-like increase in the horizontal H component at low latitude), we could derive an empirical formula for the relationship between solar wind dynamic pressure near the Earth and the CME speed; (3) the CME speed has a linear relationship with the difference of magnetopause locations derived by using the model of Shue et al. (1998) at the subsolar point before and after the shock arrivals; (4) a fast CME greater than 1600 km s⁻¹ could be a driver of the magnetopause crossing of a spacecraft at geosynchronous orbit. Our results show that the CME speed is an important parameter for early prediction of geosynchronous magnetopause crossing.

Series of Small-scale Low Plasma β Magnetic Flux Ropes Originating from the Same Longitudinal Region: Parker Solar Probe Observations

Kyung-Eun **Choi**¹, Dae-Young Lee², Sung-Jun Noh³, and Oleksiy Agapitov

2024 ApJ 961 3

<https://iopscience.iop.org/article/10.3847/1538-4357/ad02f6/pdf>

In this study, we report on small-scale magnetic flux ropes (SMFRs) observed as a compact series in a narrow Carrington longitudinal range during three Parker Solar Probe (PSP) encounters. First, during ~ 1.5 days of PSP's inbound part of Encounter 4, we identified a series of 11 SMFRs within $1^\circ 4'$ in longitude over the radial distance of $\sim 8.4 R_\odot$ (from ~ 44 to $35 R_\odot$). The identified SMFRs lasted from ~ 0.5 to 1.8 hr, and adjacent events were separated mostly by a few hours and up to ~ 6.5 hr at the longest, but some events were very closely spaced with intervals of a few \sim tens of minutes or less apart. Most of the identified SMFRs are successfully fitted to the force-free model. The SMFRs are clearly distinguished from the surroundings by a notable reduction in plasma β , which itself was comparably low (less than unity) in the background plasma. Furthermore, the magnetic field and plasma flow within the SMFRs fluctuated significantly less than the more turbulent surroundings. The fluctuations in the surrounding medium exhibited occasional Br polarity reversal (possibly switchbacks) and were Alfvénic to a large extent with far weaker compressional components. The majority of these key features with some differences have also been found in the series of SMFRs and their surroundings identified within $1^\circ 3'$ or less in longitude during Encounters 1 and 5. We speculate that these SMFRs were repetitively generated by successive reconnection within a very narrow angular zone located close to the Sun but not necessarily at the same radial position. **2-3 Nov 2018, 3-4 Jun 2020, 2020-01-25-26**

Near-orthogonal Orientation of Small-scale Magnetic Flux Ropes Relative to the Background Interplanetary Magnetic Field

Kyung-Eun [Choi](#)¹, Dae-Young Lee¹, Katsuhide Marubashi², and Seunguk Lee¹

2022 ApJ 931 98

<https://iopscience.iop.org/article/10.3847/1538-4357/ac69d3/pdf>

Small-scale magnetic flux ropes (SMFRs) have been identified at a large range of heliospheric distances from the Sun. Their features are somewhat similar to those of larger-scale flux rope structures such as magnetic clouds (MCs), while their occurrence rate is far higher. In this work, we examined the orientations of a large number of SMFRs that were identified at 1 au by fitting to the force-free model. We find that, while most of the SMFRs lie mostly close to the ecliptic plane, as previously known, their azimuthal orientations relative to the Sun–Earth line are found largely at two specific angles (slightly less than 45° and 225°). This latter feature in turn leads to a strong statistical trend in which the axis of SMFRs lies at a large tilt angle relative to (most often nearly orthogonal to) the corresponding background interplanetary magnetic field directions in the ecliptic plane. This feature is different from previous reports on SMFRs—and in stark contrast to the cases of MCs. This is an important observational constraint that should be considered for understanding SMFR generation and propagation. **6-7 Aug 1999, 21 Feb 2006**

Characteristics of Suprathermal Electrons in Small-Scale Magnetic Flux Ropes and Their Implications on the Magnetic Connection to the Sun

Kyung-Eun [Choi](#), [Dae-Young Lee](#), [Hee-Eun Wang](#), [Seunguk Lee](#), [Kyung-Chan Kim](#) & [Kyung Sun Park](#)

Solar Physics volume 296, Article number: 148 (2021)

<https://link.springer.com/content/pdf/10.1007/s11207-021-01888-0.pdf>

<https://doi.org/10.1007/s11207-021-01888-0>

Small-scale magnetic flux ropes (SMFRs) are observed more frequently than larger-scale magnetic flux ropes (e.g., magnetic clouds) in interplanetary space. We selected 235 SMFRs by applying cylindrical linear force-free fitting to 20-year observations of the Wind satellite, which meets the criteria of low beta, low temperature, an enhanced magnetic field, and a rotation feature. By examining the pitch angle distribution of suprathermal electrons for these events, we found that approximately 45.1% of the SMFRs were accompanied by unidirectional beams (strahl). A much smaller percentage of SMFRs ($\sim 10.7\%$) were associated with bidirectional beams. We also found a small percentage ($\sim 7.2\%$) of (sunward) conic distributions during SMFR events. Last, the remaining $\sim 37.0\%$ of SMFRs were associated with complex electron distributions. The unidirectional beams and most of the conics (together corresponding to $\sim 50\%$ of the total 235 SMFRs) imply open-field SMFRs with only one end connected to the Sun. For $\sim 37.7\%$ of the unidirectional beam SMFRs, the local IMF field polarity was orthogonal or inverted (possibly due to interchange reconnection). Based on the solar wind conditions around the bidirectional beams, we suggest that more than half of the bidirectional beams were not necessarily closed-field-line SMFRs. **2 Dec 1995, 16 Jun 1996, 12 Aug 1998, 10 Oct 1999, 14 September 2004, 8 Jul 2011,**

Table 2 List of characteristics of unidirectional beam-type SMFRs

Table 3 List of characteristics of bidirectional beam-type SMFRs. (1995-2014)

Origin of Solar Rotational Periodicity and Harmonics Identified in the Interplanetary Magnetic Bz Component Near the Earth During Solar Cycles 23 and 24

Kyung-Eun **Choi**, Dae-Young Lee

Solar Physics April 2019, 294:44

<https://link.springer.com/content/pdf/10.1007%2Fs11207-019-1433-7.pdf>

Periodic variations in solar-wind and geomagnetic parameters have long been recognized. In this work, we examine the periodic properties in the interplanetary magnetic field (IMF) near the Earth using satellite observations from 1996 to 2017. We pay particular attention to short-term periodicities (solar rotational period and its harmonics) of IMF Bz by distinguishing between the geocentric solar ecliptic (GSE) and the geocentric solar magnetospheric (GSM) coordinates. We find that, for nearly all of the years in Solar Cycles 23 and 24, IMF Bz exhibits periodic changes with a period of the solar rotation or its harmonics or both. We emphasize that these changes are far more pronounced in the GSM coordinates than in the GSE coordinates and during the northern hemisphere spring and fall seasons than the other two seasons. We attribute this result to an exquisite harmony between the Russell–McPherron effect and a well-defined IMF polarity that shows either a two- or four-sector structure for a long period of time.

Statistical properties and geoeffectiveness of southward interplanetary magnetic field with emphasis on weakly southward Bz events

Kyung-Eun **Choi**, Dae-Young Lee, Kyu-Cheol Choi, Jaehun Kim

JGR 2017

<http://onlineibrary.wiley.com/doi/10.1002/2016JA023836/pdf>

In this work we analyze the statistical properties and geoeffectiveness of southward IMF Bz (Bs) events measured near the Earth from 1996 to 2015. We classify the Bs events into six contrasting classes according to the duration and intensity of Bs: two subclasses of long-lasting major-intensity, two subclasses of long-lasting weak-intensity and two subclasses of short-lasting weak-intensity. We find the following results. (1) The occurrence rate of Bs events is lowest for the long-lasting major-intensity Bs classes, and increases toward shorter-lasting and weaker-intensity Bs classes. (2) Many of the Bs events in nearly all classes are associated with regions other than interplanetary coronal mass ejections and coronal-hole high-speed streams. (3) Alfvén waves account for a significant fraction of the Bs events (e.g., ~60% for the short-lasting and weak-intensity Bs classes). (4) There are clear differences in solar cycle dependence of Bs events among the different Bs classes. (5) Even either the long-lasting or short-lasting weak-intensity class Bs events can often be geoeffective by triggering substorms of weak-to-medium intensity and by enhancing geosynchronous relativistic electron fluxes. In conclusion, we emphasize that even the weakly (in terms of either intensity or duration) southward IMF Bz should be considered significant from the viewpoint of their high occurrence rate and their geoeffectiveness compared to those of long-lasting major-intensity.

Statistical Analysis of the Relationships among Coronal Holes, Corotating Interaction Regions, and Geomagnetic Storms

Yunhee **Choi** · Y.-J. Moon · Seonghwan Choi · Ji-Hye Baek · Sungsoo S. Kim · K.-S. Cho · G.S. Choe

Solar Phys (2009) 254: 311–323; **File**

We have examined the relationships among coronal holes (CHs), corotating interaction regions (CIRs), and geomagnetic storms in the period 1996 – 2003. We have identified 123 CIRs with forward and reverse shock or wave features in ACE and *Wind* data and have linked them to coronal holes shown in National Solar Observatory/Kitt Peak (NSO/KP) daily He I 10 830 Å maps considering the Sun – Earth transit time of the solar wind with the observed wind speed.

A sample of 107 CH – CIR pairs is thus identified. We have examined the magnetic polarity, location, and area of the CHs as well as their association with geomagnetic storms ($Dst \leq -50$ nT). For all pairs, the magnetic polarity of the CHs is found to be consistent with the sunward (or earthward) direction of the interplanetary magnetic fields (IMFs), which confirms the linkage between the CHs and the CIRs in the sample. Our statistical analysis shows that (1) the mean longitude of the center of CHs is about 8°E, (2) 74% of the CHs are located between 30°S and 30°N (*i.e.*, mostly in the equatorial regions), (3) 46% of the CIRs are associated with geomagnetic storms, (4) the area of geoeffective coronal holes is found to be larger than 0.12% of the solar hemisphere area, and (5) the maximum convective electric field E_y in the solar wind is much more highly correlated with the Dst index than any other solar or interplanetary parameter. In addition, we found that there is also a semiannual variation of CIR-associated geomagnetic storms and discovered new tendencies as follows: For negative-polarity coronal holes, the percentage (59%; 16 out of 27 events) of CIRs associated with geomagnetic storms in the first half of the year is much larger than that (25%; 6 out of 24 events) in the second half of the year and the occurrence percentage (63%; 15 out of 24 events) of CIR-associated storms in the southern

hemisphere is significantly larger than that (26%; 7 out of 27 events) in the northern hemisphere. Positive-polarity coronal holes exhibit an opposite tendency.

Constraining the Charge-, Time- and Rigidity-Dependence of Cosmic-Ray Solar Modulation with AMS-02 Observations during Solar Cycle 24

Ilias **Cholis**, [Ian McKinnon](#)

2022

<https://arxiv.org/pdf/2207.12447.pdf>

Our basic theoretical understanding of the sources of cosmic rays and their propagation through the interstellar medium is hindered by the Sun, that through the solar wind affects the observed cosmic-ray spectra. This effect is known as solar modulation. Recently released cosmic-ray observations from the Alpha Magnetic Spectrometer (AMS-02) and publicly available measurements of the solar wind properties from the Advanced Composition Explorer and the Wilcox observatory allow us to test the analytical modeling of the time-, charge- and rigidity-dependence of solar modulation. We rely on associating measurements on the local heliospheric magnetic field and the heliospheric current sheet's tilt angle, to model the time-dependence and amplitude of cosmic-ray solar modulation. We find evidence for the solar modulation's charge- and rigidity-dependence during the era of solar cycle 24. Our analytic prescription to model solar modulation can explain well the large-scale time-evolution of positively charged cosmic-ray fluxes in the range of rigidities from 1 to 10 GV. We also find that cosmic-ray electron fluxes measured during the first years of cycle 24 are less trivial to explain, due to the complex and rapidly evolving structure of the Heliosphere's magnetic field that they experienced as they propagated inwards.

Constraining the Charge-Sign and Rigidity-Dependence of Solar Modulation

Ilias **Cholis**, [Dan Hooper](#), [Tim Linden](#)

2020

<https://arxiv.org/pdf/2007.00669.pdf>

Our ability to identify the sources of cosmic rays and understand how these particles propagate through the interstellar medium is hindered by the combined effects of the solar wind and its embedded magnetic field, collectively known as solar modulation. In this paper, we build upon our previous work to model and constrain the effects of solar modulation on the cosmic-ray spectrum, using data from AMS-02 and BESS Polar II collected between 2007 and 2012, during which the heliospheric magnetic field was in a state of negative polarity. Our model uses measurements of the heliospheric magnetic field and the tilt angle of the heliospheric current sheet to accurately predict the effects of solar modulation as a function of time, charge, and rigidity. By incorporating data from a period of negative polarity, we have been able to robustly observe and constrain the charge-dependent effects of solar modulation.

Prediction of Amplitude and Timing of Solar Cycle 25

[Partha Chowdhury](#), [Rajmal Jain](#), [P. C. Ray](#), [Dipali Burud](#) & [Amlan Chakrabarti](#)

[Solar Physics](#) volume 296, Article number: 69 (2021)

<https://link.springer.com/content/pdf/10.1007/s11207-021-01791-8.pdf>

<https://doi.org/10.1007/s11207-021-01791-8>

We study the geomagnetic activity Ap-index in relation to sunspot number and area for the interval covering Solar Cycles 17 to 24 (1932 – 2019), in view of the availability of data for the Ap-index from 1932 on, in order to predict the amplitude of Sunspot Cycle 25. We examine the statistical relationship between sunspot-maximum amplitude and Ap-index, and similarly that between sunspot area and Ap-index. We apply the χ^2 -test for the best fit between two parameters and obtain the correlation coefficient. We also derive the standard deviation for the error limits in the predicted results. Our study reveals that the amplitude of the Sunspot Cycle 25 is likely to be $\approx 100.21 \pm 15.06$ and it may peak in April 2025 ± 6.5 months. On the other hand, the sunspot area will have maximum amplitude $\approx 1110.62 \pm 186.87 \mu$ Hem and may peak in February 2025 ± 5.8 months, which implies that Solar Cycle 25 will be weaker than or comparable to Solar Cycle 24. In view of our results as well as those of other investigators, we propose that the Sun is perhaps approaching a global minimum.

Short-term periodicities in interplanetary, geomagnetic and solar phenomena during solar cycle 24

Partha **Chowdhury**, D. P. Choudhary, S. Gosain, Y.-J. Moon

[Astrophysics and Space Science](#) March 2015, Volume 356, [Issue 1](#), pp 7-18

In this paper we study the quasi-periodic variations of sunspot area/number, 10.7 cm solar radio flux, Average Photospheric Magnetic Flux, interplanetary magnetic field (B_z) and the geomagnetic activity index A_p during the ascending phase of the current solar cycle 24. We use both Lomb-Scargle periodogram and wavelet analysis technique and find evidence for a multitude of quasi-periodic oscillations in all the data sets. In high frequency range (10 days to 100 days), both methods yield similar significance periodicities around 20–35 days and 45–60 days in all data sets. In the case of intermediate range, the significant periods were around 100–130 days, 140–170 days and 180–240 days. The Morlet wavelet power spectrum shows that all of the above-mentioned periods are intermittent in nature. We find that the well-known “Rieger period” of (150–160 days) and near Rieger periods (130–190 days) were significant in both solar, interplanetary magnetic field and geomagnetic activity data sets during cycle 24. The geomagnetic activity is the result of the solar wind-magnetosphere interaction. Thus the variations in the detected periodicity in variety of solar, interplanetary and geomagnetic indices could be helpful to improve our knowledge of the inter-relationship between various processes in the Sun-Earth-Heliosphere system.

Relativistic electron model in the outer radiation belt using a neural network approach

Xiangning Chu, [Donglai Ma](#), [Jacob Bortnik](#), [W. Kent Tobiska](#), [Alfredo Cruz](#), [S. Dave Bouwer](#), [Hong Zhao](#), [Qianli Ma](#), [Kun Zhang](#), [Daniel N. Baker](#), [Xinlin Li](#), [Harlan Spence](#), [Geoff Reeves](#)

Space Weather e2021SW002808 2021

<https://agupubs.onlinelibrary.wiley.com/doi/epdf/10.1029/2021SW002808>

<https://doi.org/10.1029/2021SW002808>

We present a machine-learning-based model of relativistic electron fluxes >1.8 MeV using a neural network approach in the Earth’s outer radiation belt. The Outer Radiation belt Electron Neural net model for Relativistic electrons (ORIENT-R) uses only solar wind conditions and geomagnetic indices as input. For the first time, we show that the state of the outer radiation belt can be determined using only solar wind conditions and geomagnetic indices, without any initial and boundary conditions. The most important features for determining outer radiation belt dynamics are found to be AL, solar wind flow speed and density, and SYM-H indices. ORIENT-R reproduces out-of-sample relativistic electron fluxes with a correlation coefficient of 0.95 and an uncertainty factor of ~ 2 . ORIENT-R reproduces radiation belt dynamics during an out-of-sample geomagnetic storm with good agreement to the observations. In addition, ORIENT-R was run for a completely out-of-sample period between March 2018 and October 2019 when the AL index ended and was replaced with the predicted AL index (lasp.colorado.edu/home/personnel/xinlin.li). It reproduces electron fluxes with a correlation coefficient of 0.92 and an out-of-sample uncertainty factor of ~ 3 . Furthermore, ORIENT-R captured the trend in the electron fluxes from low-earth-orbit (LEO) SAMPEX, which is a completely out-of-sample dataset both temporally and spatially. In sum, the ORIENT-R model can reproduce transport, acceleration, decay, and dropouts of the outer radiation belt anywhere from short timescales (i.e., geomagnetic storms) and very long timescales (i.e., solar cycle) variations. **Feb 20-Mar 20, 2017**

REDEFINING THE BOUNDARIES OF INTERPLANETARY CORONAL MASS EJECTIONS FROM OBSERVATIONS AT THE ECLIPTIC PLANE

C. Cid, J. Palacios, E. Saiz, and A. Guerrero

2016 ApJ 828 11

<http://arxiv.org/pdf/1609.01199v1.pdf>

On **2015 January 6–7**, an interplanetary coronal mass ejection (ICME) was observed at L1. This event, which can be associated with a weak and slow coronal mass ejection, allows us to discuss the differences between the boundaries of the magnetic cloud and the compositional boundaries. A fast stream from a solar coronal hole surrounding this ICME offers a unique opportunity to check the boundaries’ process definition and to explain differences between them. Using Wind and ACE data, we perform a complementary analysis involving compositional, magnetic, and kinematic observations providing relevant information regarding the evolution of the ICME as travelling away from the Sun. We propose erosion, at least at the front boundary of the ICME, as the main reason for the difference between the boundaries, and compositional signatures as the most precise diagnostic tool for the boundaries of ICMEs.

A Carrington-like geomagnetic storm observed in the 21st century

Consuelo Cid*, Elena Saiz, Antonio Guerrero, Judith Palacios and Yolanda Cerrato

J. Space Weather Space Clim., 5, A16 (2015)

<http://www.swsc-journal.org/articles/swsc/pdf/2015/01/swsc140015.pdf>

In **September 1859** the Colaba observatory measured the most extreme geomagnetic disturbance ever recorded at low latitudes related to solar activity: the Carrington storm. This paper describes a geomagnetic disturbance case with a

profile extraordinarily similar to the disturbance of the Carrington event at Colaba: the event on **29 October 2003** at Tihany magnetic observatory in Hungary. The analysis of the H-field at different locations during the “Carrington-like” event leads to a re-interpretation of the 1859 event. The major conclusions of the paper are the following: (a) the global Dst or SYM-H, as indices based on averaging, missed the largest geomagnetic disturbance in the 29 October 2003 event and might have missed the 1859 disturbance, since the large spike in the horizontal component (H) of terrestrial magnetic field depends strongly on magnetic local time (MLT); (b) the main cause of the large drop in H recorded at Colaba during the Carrington storm was not the ring current but field-aligned currents (FACs); and (c) the very local signatures of the H-spike imply that a Carrington-like event can occur more often than expected.

On extreme geomagnetic storms

Consuelo **Cid**, Judith Palacios, Elena Saiz, Antonio Guerrero and Yolanda Cerrato

J. Space Weather Space Clim. 4 (2014) A28; **File**

<http://www.swsc-journal.org/articles/swsc/pdf/2014/01/swsc140014.pdf>

Extreme geomagnetic storms are considered as one of the major natural hazards for technology-dependent society. Geomagnetic field disturbances can disrupt the operation of critical infrastructures relying on space-based assets, and can also result in terrestrial effects, such as the **Quebec electrical disruption in 1989**. Forecasting potential hazards is a matter of high priority, but considering large flares as the only criterion for early-warning systems has demonstrated to release a large amount of false alarms and misses. Moreover, the quantification of the severity of the geomagnetic disturbance at the terrestrial surface using indices as Dst cannot be considered as the best approach to give account of the damage in utilities. High temporal resolution local indices come out as a possible solution to this issue, as disturbances recorded at the terrestrial surface differ largely both in latitude and longitude. The recovery phase of extreme storms presents also some peculiar features which make it different from other less intense storms. This paper goes through all these issues related to extreme storms by analysing a few events, highlighting the **March 1989 storm**, related to the Quebec blackout, and the **October 2003 event**, when several transformers burnt out in South Africa.

Clarifying some issues on the geoeffectiveness of limb halo CMEs

Cid, Consuelo; Cremades, Hebe; Aran, Angels; Mandrini, Cristina; Sanahuja, Blai; Schmieder, Brigitte; Menvielle, Michel; Rodriguez, Luciano; Saiz, Elena; Cerrato, Yolanda; Dasso, Sergio; Jacobs, Carla; Lathuillere, Chantal; Zhukov, Andrei

Nature of Prominences and their role in Space Weather, Proceedings of the International Astronomical Union, IAU Symposium, Volume 300, pp. 285-288, **2014**

A recent study by Cid et al. (2012) showed that full halo coronal mass ejections (CMEs) coming from the limb can disturb the terrestrial environment. Although this result seems to rise some controversies with the well established theories, the fact is that the study encourages the scientific community to perform careful multidisciplinary analysis along the Sun-to-Earth chain to fully understand which are the solar triggers of terrestrial disturbances. This paper aims to clarify some of the polemical issues arisen by that paper.

Modeling the recovery phase of extreme geomagnetic storms

C. **Cid**, J. Palacios, E. Saiz, Y. Cerrato, J. Aguado, A. Guerrero

J. Geophys. Res. Space Physics, **2013**, 118, 1-8

<http://arxiv.org/pdf/1405.4804v1.pdf>

The recovery phase of the largest storms ever recorded has been studied. These events provide an extraordinary opportunity for two goals: (1) to validate the hyperbolic model by Aguado et al. [2010] for the recovery phase after disturbances as severe as the Carrington event, or that related to the Hydro-Quebec blackout in March 1989, and (2) to check whether the linear relationship between the recovery time and the intensity of the storm still complies. Our results reveal the high accuracy of the hyperbolic decay function to reproduce the recovery phase of the magnetosphere after an extreme storm. Moreover, the characteristic time that takes the magnetosphere to recover depends in an exponential way on the intensity of the storm, as indicated by the relationship between the two parameters involved in the hyperbolic decay. This exponential function can be approached by a linear function when the severity of the storm diminishes.

Table 1. Chronological list of large geomagnetic storms analyzed in this paper

Event #	Year	Month	Day	Observatory	H range (nT)	Geomagnetic latitude ^a
1	1859	September	1-2	Bombay	1720	9.74
2	1921	May	13-16	Alibag	>700	9.46
3	1928	July	7	Alibag	780	9.45
4	1938	April	16	Alibag	530	9.37
5	1957	September	13	Alibag	580	9.29
6	1958	February	11	Alibag	660	9.29
7	1989	March	13	Kakioka	640	26.6

Can a halo CME from the limb be geoeffective?

Cid, C., H. Cremades, A. Aran, C. Mandrini, B. Sanahuja, B. Schmieder, M. Menvielle, L. Rodriguez, E. Saiz, Y. Cerrato, S. Dasso, C. Jacobs, C. Lathuillere, and A. Zhukov
J. Geophys. Res., 117, A11102, doi:10.1029/2012JA017536, **2012**

The probability for a halo coronal mass ejection (CME) to be geoeffective is assumed to be higher the closer the CME launch site is located to the solar central meridian. However, events far from the central meridian may produce severe geomagnetic storms, like the case in April 2000. In this work, we study the possible geoeffectiveness of full halo CMEs with the source region situated at solar limb. For this task, we select all limb full halo (LFH) CMEs that occurred during solar cycle 23, and we search for signatures of geoeffectiveness between 1 and 5 days after the first appearance of each CME in the LASCO C2 field of view. When signatures of geomagnetic activity are observed in the selected time window, interplanetary data are carefully analyzed in order to look for the cause of the geomagnetic disturbance. Finally, a possible association between geoeffective interplanetary signatures and every LFH CME in solar cycle 23 is checked in order to decide on the CME's geoeffectiveness. After a detailed analysis of solar, interplanetary, and geomagnetic data, we conclude that of the 25 investigated events, there are only four geoeffective LFH CMEs, all coming from the west limb. The geoeffectiveness of these events seems to be moderate, turning to intense in two of them as a result of cumulative effects from previous mass ejections. We conclude that ejections from solar locations close to the west limb should be considered in space weather, at least as sources of moderate disturbances.

Comment on “Interplanetary conditions leading to superintense geomagnetic storms (Dst _ 250 nT) during solar cycle 23”,

Cid, C., E. Saiz, and Y. Cerrato,
Geophys. Res. Lett., 35, L21107, DOI: [10.1029/2008GL034731](https://doi.org/10.1029/2008GL034731), **2008**.
sci-hub.se/10.1029/2008gl034731

Sources of intense geomagnetic storms over the rise of solar cycle 23.

Cid, C., Hidalgo, M.A., Saiz, E., Cerrato, Y., Sequeiros, J.,
2004. Sol. Phys. 223, 231–243.

In this work we present a study of the triggers of intense geomagnetic storms since the launch of the WIND spacecraft, November 1995 until December 2001. Reviewing the signatures of solar wind flow, we looked for two different kinds of interplanetary events associated with intense geomagnetic storms: ejecta and corotating solar wind streams. We also looked for the solar origin related to both events. We provide a list of the solar terrestrial events during the rising phase of this solar cycle. The paper includes statistical conclusions that shed light onto the paradigm of geomagnetic storms.

Large Sunspot Groups and Great Magnetic Storms: Magnetic Suppression of CMEs

Edward W. **Cliver**¹, Werner Pötzi², and Astrid M. Veronig^{2,3}
2022 ApJ 938 136

<https://iopscience.iop.org/article/10.3847/1538-4357/ac847d/pdf>

A solar spot group with a large area is not a requirement for a great magnetic storm. Nearly half (14/30) of all storms with a minimum Dst value ≤ -300 nT from 1932–2014 originated in spot groups with corrected areas ≤ 1000 millionths of a solar hemisphere (μ sh) on the day of the associated eruption. Over the same interval, spot groups with area 3000–4000 μ sh were ~ 250 times more likely to give rise to a great storm than those with areas from 100–1000 μ sh, with the high percentage of great storms originating in small spot groups attributed primarily to the much higher occurrence

frequency of such groups. Above $\sim 3500 \mu\text{sh}$, the ability of a spot group to produce a great storm appears to drop abruptly. For the 1932–2014 interval, we find that for the 71 days when a spot group had a measured daily area of 3000–3500 μsh , five great storms were observed versus none for the 67 times when a group spot with an area from 3500 to $\sim 6000 \mu\text{sh}$ was observed on the Sun. This is consistent with recent studies indicating that large spot groups on the Sun and stars can suppress coronal mass ejections. **May 1951, Sep 1957, Oct 2014**

Table 1 Great Geomagnetic Storms (Dst \square –300 nT) and Their Solar Sources (1932–2014)

Extreme solar events

Review

[Edward W. Cliver](#), [Carolus J. Schrijver](#), [Kazunari Shibata](#) & [Ilya G. Usoskin](#)

[Living Reviews in Solar Physics](#) volume 19, Article number: 2 (2022)

<https://link.springer.com/content/pdf/10.1007/s41116-022-00033-8.pdf>

We trace the evolution of research on extreme solar and solar-terrestrial events from the 1859 Carrington event to the rapid development of the last twenty years. Our focus is on the largest observed/inferred/theoretical cases of sunspot groups, flares on the Sun and Sun-like stars, coronal mass ejections, solar proton events, and geomagnetic storms. The reviewed studies are based on modern observations, historical or long-term data including the auroral and cosmogenic radionuclide record, and Kepler observations of Sun-like stars. We compile a table of 100- and 1000-year events based on occurrence frequency distributions for the space weather phenomena listed above. Questions considered include the Sun-like nature of superflare stars and the existence of impactful but unpredictable solar "black swans" and extreme "dragon king" solar phenomena that can involve different physics from that operating in events which are merely large. **774 AD, 17 Sep 1770, 1 September 1859, 4 Feb 1872, 14-15 May 1921, 28 Feb 1942, 5 April 1947, 23 May 1967, 2–11 August 1972, 29 Apr 1973, 21 Apr 2002, 28 October 2003; 6, 13, 14 Dec 2006, 9 Nov 2011, 28 Oct 2013, 4 Nov 2015**

Table 5 Historical fast transit ICME events

Minimal Magnetic States of the Sun and the Solar Wind: Implications for the Origin of the Slow Solar Wind

Review

E. W. [Cliver](#), R. von Steiger

[Space Science Reviews](#) September 2017, Volume 210, [Issue 1–4](#), pp 227–247

sci-hub.tw/10.1007/s11214-015-0224-1

During the last decade it has been proposed that both the Sun and the solar wind have minimum magnetic states, lowest order levels of magnetism that underlie the 11-yr cycle as well as longer-term variability. Here we review the literature on basal magnetic states at the Sun and in the heliosphere and draw a connection between the two based on the recent deep 2008–2009 minimum between cycles 23 and 24. In particular, we consider the implications of the low solar activity during the recent minimum for the origin of the slow solar wind.

The 1859 Space Weather Event Revisited

Ed [Cliver](#)

RHESSI Science Nugget, No. 213, Nov. 2013

http://sprg.ssl.berkeley.edu/~tohban/wiki/index.php/The_1859_Space_Weather_Event_Revisited

The 1859 space weather event revisited: limits of extreme activity

Edward W. [Cliver](#)^{1*} and William F. Dietrich²

J. Space Weather Space Clim., Volume 3, 2013, A31; **File**

sci-hub.se/10.1051/swsc/2013053

The solar flare on **1 September 1859** and its associated geomagnetic storm remain the standard for an extreme solar-terrestrial event. The most recent estimates of the flare soft X-ray (SXR) peak intensity and Dst magnetic storm index for this event are: SXR class = X45 (± 5) (vs. X35 (± 5) for the 4 November 2003 flare) and minimum Dst = -900 ($+50$, -150) nT (vs. -825 to -900 nT for the great storm of May 1921). We have no direct evidence of an associated solar energetic proton (SEP) event but a correlation between >30 MeV SEP fluence (F30) and flare size based on modern data yields a best guess F30 value of $\sim 1.1 \times 10^{10}$ pr cm^{-2} (with the $\pm 1\sigma$ uncertainty spanning a range from $\sim 10^9$ – 10^{11} pr cm^{-2}) for a composite (multi-flare plus shock) 1859 event. This value is approximately twice that of estimates/measurements – ranging from ~ 5 – 7×10^9 pr cm^{-2} – for the largest SEP episodes (July 1959, November 1960, August 1972) in the modern era.

Great geomagnetic storm of 9 November 1991: Association with a disappearing solar filament

E. W. Cliver, K. S. Balasubramaniam, N. V. Nitta, X. Li

J. Geophys. Res., 114, A00A20, 2009, doi:10.1029/2008JA013232. **File**

<http://dx.doi.org/10.1029/2008JA013232>

sci-hub.se/10.1029/2008JA013232

We attribute the great geomagnetic storm on 8–10 November 1991 to a large-scale eruption that encompassed the disappearance of a $\sim 25^\circ$ solar filament in the southern solar hemisphere. The resultant soft X-ray arcade spanned $\sim 90^\circ$ of solar longitude. The rapid growth of an active region lying at one end of the X-ray arcade appears to have triggered the eruption. This is the largest geomagnetic storm yet associated with the eruption of a quiescent filament. The minimum hourly *Dst* value of **−354 nT on 9 November 1991** compares with a minimum *Dst* value of -161 nT for the largest 27-day recurrent (coronal hole) storm observed from 1972 to 2005 and the minimum -559 nT value observed during the flare-associated storm of 14 March 1989, the greatest magnetic storm recorded during the space age. Overall, the November 1991 storm ranks 15th on a list of *Dst* storms from 1905 to 2004, surpassing in intensity such well-known storms as 14 July 1982 (-310 nT) and 15 July 2000 (-317 nT). We used the Cliver et al. and Gopalswamy et al. empirical models of coronal mass ejection propagation in the solar wind to provide consistency checks on the eruption/storm association.

The 1859 Solar-Terrestrial Disturbance And the Current Limits of Extreme Space Weather Activity

Cliver, E. W., and Svalgaard, L.:

2004, *Solar Phys.* 224, 407, **File**.

<https://link.springer.com/content/pdf/10.1007%2Fs11207-005-4980-z.pdf>

sci-hub.se/10.1007/s11207-005-4980-z

It is generally appreciated that the **September 1859** solar-terrestrial disturbance, the first recognized space weather event, was exceptionally large. How large and how exceptional? To answer these questions, we compiled rank order lists of the various measures of solar-induced disturbance for events from 1859 to the present. The parameters considered included: magnetic crochet amplitude, solar energetic proton fluence (McCracken et al., 2001a), **Sun-Earth disturbance transit time, geomagnetic storm intensity**, and low-latitude auroral extent. While the 1859 event has close rivals or superiors in each of the above categories of space weather activity, it is the only documented event of the last ~ 150 years that appears at or near the top of all of the lists. Taken together, the top-ranking events in each of the disturbance categories comprise a set of benchmarks for extreme space weather activity.

How big was the Carrington 1859 Flare?

Cliver, E. W., Svalgaard, L., and Neidig D.F.

American Geophysical Union, Spring Meeting 2004, abstract #SH43A-03

The 1859 space weather event was distinguished by its great geomagnetic storm, widespread low-latitude aurora, and intense solar energetic particle event (inferred from the NO₃ concentration in polar ice cores). Arguably each of these three effects was the largest ever observed. What can we say about the size of the associated solar flare? We have two observations with which to make such an assessment: (1) Carrington's and Hodgson's report of the white-light flare and (2) the solar flare effect or magnetic crochet observed in the Kew and Greenwich magnetograms. Estimates of the area, duration, spectrum, and intensity of the white-light emission indicate a large ($\sim 2 \times 10^{30}$ erg) but not unequalled event (the white-light emission of the 24 April 1984 >X13 flare contained $\sim 6 \times 10^{30}$ erg). The magnetic crochet of 130 nT in the horizontal force, however, exceeds that for all >X10 soft X-ray flares observed from 1984–2002 (we are presently compiling magnetic data for the recent October–November 2003 activity for comparison with the 1859 event). Thus at this point, we can conservatively say that Carrington's flare likely had a soft X-ray classification >X10 and was at least comparable to the largest flares recorded during the spacecraft era.

Mountains versus valleys: Semiannual variation of geomagnetic activity,

Cliver, E. W., Y. Kamide, and A. G. Ling (2000),

J. Geophys. Res., 105, 2413–2424.

The semiannual variation in geomagnetic activity is generally attributed to the Russell-McPherron effect. In that picture, enhancements of southward field *B_s* near the equinoxes account for the observed higher geomagnetic activity in March and September. In a contrary point of view, we argue that the bulk of the semiannual variation results from an equinoctial effect (based on the ψ angle between the solar wind flow direction and Earth's dipole axis) that makes *B_s*

coupling less effective (by ~25% on average) at the solstices. Thus the semiannual variation is not simply due to "mountain building" (creation of Bs) at the equinoxes but results primarily from "valley digging" (loss of coupling efficiency) at the solstices. We estimate that this latter effect, which clearly reveals itself in the diurnal variation of the am index, is responsible for ~65% of the semiannual modulation. The characteristic imprint of the equinoctial hypothesis is also apparent in hourly/monthly averages of the time-differential Dst index and the AE index.

Energetic Particle Increases Associated with Stream Interaction Regions

C. M. S. [Cohen](#), [E. R. Christian](#), [A. C. Cummings](#), [A. J. Davis](#), [M. I. Desai](#),

ApJS Volume 246, Issue 2, id.20 2020

<https://arxiv.org/ftp/arxiv/papers/1912/1912.08244.pdf>

<https://sci-hub.tw/10.3847/1538-4365/ab4c38>

The **Parker Solar Probe** was launched on 2018 August 12 and completed its second orbit on 2019 June 19 with perihelion of 35.7 solar radii. During this time, the Energetic particle Instrument-Hi (EPI-Hi, one of the two energetic particle instruments comprising the Integrated Science Investigation of the Sun, ISOIS) measured seven proton intensity increases associated with stream interaction regions (SIRs), two of which appear to be occurring in the same region corotating with the Sun. The events are relatively weak, with observed proton spectra extending to only a few MeV and lasting for a few days. The proton spectra are best characterized by power laws with indices ranging from -4.3 to -6.5, generally softer than events associated with SIRs observed at 1 au and beyond. Helium spectra were also obtained with similar indices, allowing He/H abundance ratios to be calculated for each event. We find values of 0.016-0.031, which are consistent with ratios obtained previously for corotating interaction region events with fast solar wind < 600 km s⁻¹. Using the observed solar wind data combined with solar wind simulations, we study the solar wind structures associated with these events and identify additional spacecraft near 1 au appropriately positioned to observe the same structures after some corotation. Examination of the energetic particle observations from these spacecraft yields two events that may correspond to the energetic particle increases seen by EPI-Hi earlier.

Quantitative Comparison of Methods for Predicting the Arrival of Coronal Mass Ejections at Earth based on multi-view imaging†

R. C. [Colaninno](#)*, [A. Vourlidas](#), [C. C. Wu](#)

Journal of Geophysical Research: Space Physics, Nov 2013; File

<http://arxiv.org/pdf/1310.6680v2.pdf>

[1] We investigate the performance of six methods for predicting the coronal mass ejection (CME) time of arrival (ToA) and velocity at Earth using a sample of nine Earth-impacting CMEs between March 2010 and June 2011. The CMEs were tracked continuously from the Sun to near Earth in multi-viewpoint imaging data from STEREO SECCHI and SOHO LASCO. We use the Graduate Cylindrical Shell (GCS) model to estimate the three-dimensional direction and height of the CMEs in every image out to ~200 R_⊙. We fit the derived three-dimensional (deprojected) height and time (HT) data with six different methods to extrapolate the CME ToA and velocity at Earth. We compare the fitting results with the in situ data from the Wind spacecraft. We find that a simple linear fit above a height of 50R_⊙ gives the ToA with an error ±6 hours for seven (78%) of the CMEs. For the full sample, we are able to predict the ToA to within ±13 hours. These results are a half day improvement over past CME arrival time methods that only used SOHO LASCO data. We conclude that heliographic height-time measurements of the CME front made away from the Sun-Earth line and beyond the coronagraphic field of view are sufficient for reasonably accurate predictions of their ToA.

A Framework for Evaluating Geomagnetic Indices Forecasting Models

Armando [Collado-Villaverde](#), [Pablo Muñoz](#), [Consuelo Cid](#)

Space Weather e2024SW003868 [Volume22, Issue3](#) 2024

<https://agupubs.onlinelibrary.wiley.com/doi/epdf/10.1029/2024SW003868>

The use of Deep Learning models to forecast geomagnetic storms is achieving great results. However, the evaluation of these models is mainly supported on generic regression metrics (such as the Root Mean Squared Error or the Coefficient of Determination), which are not able to properly capture the specific particularities of geomagnetic storms forecasting. Particularly, they do not provide insights during the high activity periods. To overcome this issue, we introduce the Binned Forecasting Error to provide a more accurate assessment of models' performance across the different intensity levels of a geomagnetic storm. This metric facilitates a robust comparison of different forecasting models, presenting a true representation of a model's predictive capabilities while being resilient to different storms duration. In this direction, for enabling fair comparison among models, it is important to standardize the sets of geomagnetic storms for model training, validation and testing. To do this, we have started from the current sets used in the literature for forecasting the

SYM-H, enriching them with newer storms not considered previously, focusing not only on disturbances caused by Coronal Mass Ejections but also addressing High-Speed Streams. To operationalize the evaluation framework, a comparative study is conducted between a baseline neural network model and a persistence model, showcasing the effectiveness of the new metric in evaluating forecasting performance during intense geomagnetic storms. Finally, we propose the use of preliminary measurements from ACE to evaluate the model performance in settings closer to an operational real-time scenario, where the forecasting models are expected to operate.

Table 5 Details of the SYM-H Index Storms Used to Train, Validate and Test the Model 1998-2022

Deep Neural Networks With Convolutional and LSTM Layers for SYM-H and ASY-H Forecasting

Armando [Collado-Villaverde](#), [Pablo Muñoz](#), [Consuelo Cid](#)

Space Weather 2021

<https://agupubs.onlinelibrary.wiley.com/doi/epdf/10.1029/2021SW002748>

<https://doi.org/10.1029/2021SW002748>

Geomagnetic indices quantify the disturbance caused by the solar activity on a planetary scale or in particular regions of the Earth. Among them, the SYM-H and ASY-H indices represent the (longitudinally) symmetric and asymmetric geomagnetic disturbance of the horizontal component of the magnetic field at midlatitude with a 1-min resolution. Their resolution, along with their relation to the solar wind parameters, makes the forecasting of the geomagnetic indices a problem that can be addressed through the use of Deep Learning, particularly using Deep Neural Networks (DNNs). In this work, we present two DNNs developed to forecast respectively the SYM-H and ASY-H indices. Both networks have been trained using the Interplanetary Magnetic Field (IMF) and the related index for the solar storms occurred in the last two solar cycles. As a result, the networks are able to accurately forecast the indices 2 h in advance, considering the IMF and indices values for the previous 200 min. The evaluation of both networks reveals a great forecasting precision, including good predictions for large storms that occurred during the solar cycle 23 and comparing with the persistence model for the period 2013–2020.

Corotating Interaction Regions as Seen by the STEREO Heliospheric Imagers 2007–2010

T. M. [Conlon](#), S. E. Milan, J. A. Davies

Solar Phys., Volume 290, Issue 8, pp 2291-2309 2015

NASA's Solar Terrestrial Relations Observatory (STEREO) mission has coincided with a pronounced solar minimum. This allowed for easier detection of corotating interaction regions (CIRs). CIRs are formed by the interaction between fast and slow solar-wind streams ejected from source regions on the solar surface that rotate with the Sun. High-density plasma blobs that have become entrained at the stream interface can be tracked out to large elongations in data from the Heliospheric Imager (HI) instruments onboard STEREO. These blobs act as tracers of the CIR itself such that their HI signatures can be used to estimate CIR source location and radial speed. We estimate the kinematic properties of solar-wind transients associated with 40 CIRs detected by the HI instrument onboard the STEREO-A spacecraft between 2007 and 2010. We identify in-situ signatures of these transients at L1 using the Advanced Composition Explorer (ACE) and compare the in-situ parameters with the HI results. We note that solar-wind transients associated with CIRs appear to travel at or close to the slow solar-wind speed preceding the event as measured in situ. We also highlight limitations in the commonly used analysis techniques of solar-wind transients by considering variability in the solar wind.

Table 2 Timing and propagation speed of the 40 events used in this study. The start time is the start time of the time–elongation profile that starts at $\varphi = 180^\circ$ to the nearest hour in the format dd mmm yyyy hh.

Assessing the Effect of Spacecraft Motion on Single-Spacecraft Solar Wind Tracking Techniques

T. M. [Conlon](#), S. E. Milan, J. A. Davies

Solar Phys., 289, Issue 10, pp.3935-3947 2014

Recent advances in wide-angle imaging by the Solar Mass Ejection Imager (SMEI) on board the Coriolis spacecraft and more recently by the Heliospheric Imagers (HI) aboard NASA's Solar Terrestrial Relations Observatory (STEREO), have enabled solar wind transients to be imaged and tracked from the Sun to 1 AU and beyond. In this paper we consider two of the techniques that have been used to determine the propagation characteristics of solar wind transients based on single-spacecraft observations, in particular propagation direction and radial speed. These techniques usually assume that the observing spacecraft remains stationary for the duration of observation of the solar wind transient. We determine the inaccuracy introduced by this assumption for the two STEREO spacecraft and find that it can be

significant, and it can lead to an overestimation of the transient velocity as seen from STEREO-A and an underestimation as seen by STEREO-B. This has implications for the prediction of solar wind transients at 1 AU and hence is important for the study of space weather.

Хорошее Введение.

Forecasting Geomagnetic Storm Disturbances and Their Uncertainties Using Deep Learning

D. Conde, [F. L. Castillo](#), [C. Escobar](#), [C. García](#), [J. E. García](#), [V. Sanz](#), [B. Zaldívar](#), [J. J. Curto](#), [S. Marsal](#), [J. M. Torta](#)

Space Weather [Volume 21, Issue 11](#) e2023SW003474 **2023**

<https://agupubs.onlinelibrary.wiley.com/doi/epdf/10.1029/2023SW003474>

Severe space weather produced by disturbed conditions on the Sun results in harmful effects both for humans in space and in high-latitude flights, and for technological systems such as spacecraft or communications. Also, geomagnetically induced currents (GICs) flowing on long ground-based conductors, such as power networks, potentially threaten critical infrastructures on Earth. The first step in developing an alarm system against GICs is to forecast them. This is a challenging task given the highly non-linear dependencies of the response of the magnetosphere to these perturbations. In the last few years, modern machine-learning models have shown to be very good at predicting magnetic activity indices. However, such complex models are on the one hand difficult to tune, and on the other hand they are known to bring along potentially large prediction uncertainties which are generally difficult to estimate. In this work we aim at predicting the SYM-H index characterizing geomagnetic storms multiple-hour ahead, using public interplanetary magnetic field (IMF) data from the Sun-Earth L1 Lagrange point and SYM-H data. We implement a type of machine-learning model called long short-term memory (LSTM) network. Our scope is to estimate the prediction uncertainties coming from a deep-learning model in the context of forecasting the SYM-H index. These uncertainties will be essential to set reliable alarm thresholds. The resulting uncertainties turn out to be sizable at the critical stages of the geomagnetic storms. Our methodology includes as well an efficient optimization of important hyper-parameters of the LSTM network and robustness tests.

Calculating travel times and arrival speeds of CMEs to Earth: An analytic tool for space weather forecasting

P. [Corona-Romero](#), J. A. Gonzalez-Esparza, C. A. Perez-Alanis, E. Aguilar-Rodriguez, V. de-la-Luz, J. C. Mejia-Ambriz

Space Weather Vol: 15, Pages: 464–483 **2017**

<http://sci-hub.cc/10.1002/2016SW001489>

Coronal mass ejections (CME) are one of the most important phenomena derived from solar activity that potentially perturb space weather of Earth. In this work we present a semiempirical arrival forecasting tool for Earth-directed halo CMEs. This tool combines the piston shock model and an empirical relationship to estimate in situ arrivals of halo CMEs. The empirical relationship uses the initial conditions of CMEs to calculate the value of free parameter of the piston shock model, a parameter which is closely related to the initial inertia of CMEs. Such a value will let the model to simultaneously approximate the travel time and arrival speed of CMEs (i.e., CME arrivals). We test the forecasting capabilities of our model and its empirical relationship by calculating the arrivals of 40 halo CMEs detected during the period of 1995–2015. Our results indicate that, together, the piston shock model and its empirical relationship approximate CME arrivals with average errors of 7 h for travel times, and 100 km s⁻¹ for arrival speeds. Our results show that our model is suitable for arrival forecasting of isolated events propagating through quiet interplanetary medium.

Table 1. Data and results from the analysis of 21 events (Section 2.2).

Kinematics of ICMEs/shocks: blast wave reconstruction using type II emissions

P. [Corona-Romero](#), J.A. Gonzalez-Esparza, E. Aguilar-Rodriguez, V. de-la-Luz, J.C. Mejia-Ambriz

Solar Phys. Volume 290, Issue 9, pp 2439-2454 **2015**

<http://arxiv.org/pdf/1501.05551v1.pdf>

We present a physical methodology to reconstruct the trajectory of interplanetary shocks using type II radio emission data. This technique calculates the shock trajectory assuming that the disturbance propagates as a blast wave in the interplanetary medium. We applied this Blast Wave Reconstruction (BWR) technique to analyze eight fast Earth-directed ICMEs/shocks associated with type II emissions. The technique deduces a shock trajectory that reproduces the type II frequency drifts, and calculates shock onset speed, shock transit time and shock speed at 1~AU. There were good agreements comparing the BWR results with the type II spectra, with data from coronagraph images, { \it in situ }

measurements, and interplanetary scintillation (IPS) observations. Perturbations on the type II data affect the accuracy of the BWR technique. This methodology could be applied to track interplanetary shocks causing TII emissions in real-time, to predict the shock arrival time and shock speed at 1~AU. **6 Jun 2000, 14 July 2000, 26 Apr 2001, 24 Sept 2001, 20011104, 20011122, 20040725, 20050513**

Propagation of Fast Coronal Mass Ejections and Shock Waves Associated with Type II Radio-Burst Emission: An Analytic Study

P. **Corona-Romero**, J. A. Gonzalez-Esparza and E. Aguilar-Rodriguez

Solar Physics, July **2013**, Volume 285, Issue 1-2, pp 391-410

Coronal mass ejections (CMEs) are large-scale eruptive events in the solar corona. Once they are expelled into the interplanetary (IP) medium, they propagate outwards and “evolve” interacting with the solar wind. Fast CMEs associated with IP shocks are a critical subject for space weather investigations. We present an analytic model to study the heliocentric evolution of fast CME/shock events and their association with type II radio-burst emissions. The propagation model assumes an early stage where the CME acts as a piston driving a shock wave; beyond this point the CME decelerates, tending to match the ambient solar wind speed and its shock decays. We use the shock speed evolution to reproduce type II radio-burst emissions. We analyse four fast CME halo events that were associated with kilometric type II radio bursts, and in-situ measurements of IP shock and CME signatures. The results show good agreement with the dynamic spectra of the type II frequency drifts and the in-situ measurements. This suggests that, in general, IP shocks associated with fast CMEs evolve as blast waves approaching 1 AU, implying that the CMEs do not drive their shocks any further at this heliocentric range.

Numeric and analytic study of interplanetary coronal mass ejection and shock evolution: Driving, decoupling, and decaying

Corona-Romero, P.; Gonzalez-Esparza, J. A.

J. Geophys. Res., Vol. 116, No. A5, A05104, **2011**

<http://dx.doi.org/10.1029/2010JA016008>

We analyze the heliocentric evolution of fast interplanetary counterparts of coronal mass ejections (ICMEs) and their transient shocks to investigate how and where they decelerate in the interplanetary medium. We employ two one-dimensional hydrodynamic models, analytic and numeric, to study three fast CME events. We focus on the transferring of momentum from the ICME to the shock. The two models show that initially the fast ICME propagates at about a constant speed and drives the shock (driving stage) until it reaches a certain distance from which it decelerates and decouples from the shock (decoupling process). Then the ICME and its shock decelerate (decaying stage). This deceleration depends on the speed difference with respect to the ambient wind and tends to a negligible value when the ICME-shock approaches to the ambient wind speed. The location and duration of these propagation stages depend on the initial CME conditions and the ambient wind characteristics. We present a parametric study to compare the results by the analytic and numeric models, showing the variations of their results as a function of the initial conditions. We perform three study cases to compare the model's predictions with a set of speed measurements of ICME-shock events.

Constraining the global heliospheric transport of galactic cosmic rays in solar cycles 23 and 24

Claudio **Corti** (1 and 2), [Peter Sadowski](#) (1), [Nikolay Nikonov](#) (1), [Marius Potgieter](#) (3), [Veronica Bindi](#) (1)

Proceedings of the 38th International Cosmic Ray Conference (ICRC23) **2023**

<https://arxiv.org/pdf/2307.15848.pdf>

Galactic cosmic rays (GCRs) are affected by solar modulation while they propagate through the heliosphere. The study of the time variation of GCR spectra observed at Earth can shed light on the underlying physical processes, specifically diffusion and particle drifts. We combine a state-of-the-art 3D numerical model of GCR transport in the heliosphere with a neural-network-accelerated Markov chain Monte Carlo to constrain the rigidity and time dependence of the global transport coefficients, using precise GCR data from the PAMELA and AMS-02 experiments between 2006 and 2019.

Test of validity of the force-field approximation with AMS-02 and PAMELA monthly fluxes

Claudio **Corti** (1), [Veronica Bindi](#) (1), [Cristina Consolandi](#) (1), [Christopher Freeman](#) (1), [Andrew Kuhlman](#) (1), [Christopher Light](#) (1), [Matteo Palermo](#) (1), [Siqi Wang](#) (1) ((1) University of Hawaii at Manoa)

Proceeding of the 36th International Cosmic Ray Conference (ICRC19) **2019**

<https://arxiv.org/pdf/1910.00027.pdf>

Galactic cosmic rays (GCRs) entering the heliosphere are disturbed by the magnetic field of the Sun, which varies the shape and intensity of their local interstellar spectrum. The force-field approximation is a popular way of dealing with

solar modulation, especially for studies focused on galactic transport of cosmic rays. The validity of this approach to reproduce the modulated GCR fluxes at Earth is tested using monthly proton fluxes measured by PAMELA between July 2006 and January 2014 and monthly proton and helium fluxes measured by AMS-02 between May 2011 and May 2017. We show that the precision of the new AMS-02 data requires a rigidity-dependent modification of the force-field approximation.

Effects of different geomagnetic storm drivers on the ring current: CRCM results

W.D. **Cramer**^{1,*}, N.E. Turner, I. M.-C. Fok², N.Y. Buzulukova

JGR, Volume 118, Issue 3, pages 1062–1073, March 2013

The storm-time magnetic disturbance at the Earth's equator, as commonly measured by the Dst index, is induced by currents in the near-Earth magnetosphere. The ring current is generally considered the most important contributor, but other magnetospheric currents have also been found to have significant effects. Of the two main types of solar geomagnetic storm drivers, Coronal Mass Ejections (CMEs) tend to have a much greater impact on Dst than Corotating Interaction Regions (CIRs). Ring current models have been found to underestimate Dst, particularly during storms driven by CIRs. One possible explanation is that the models neglect to handle some aspect of ring current physics that is particularly important for CIRs. This study uses the Comprehensive Ring Current Model (CRCM) to estimate the ring current contribution to Dst for a selection of storms of various strengths and different drivers (CMEs and CIRs) that have solar wind parameters that fit a typical profile. The model boundary is set to 10 RE at the equator, encompassing the entire ring current region. The magnetic field is held fixed, based on average storm parameters, which limits our model results to the effects of convection and plasma sheet density at the model boundary. Our model results generally show good agreement with the size and timing of fluctuations in Dst, which indicates that convection and boundary conditions play an important role in shaping Dst. We also find excellent agreement with the magnitude of Dst for CME-driven storms. For CIR-driven storms, however, the magnitude at the peak of the storm frequently deviates from actual Dst. In general, we agree with the results of previous research that CIR-driven storms are more underpredicted. However, this study includes some weaker CIR-driven storms for which Dst is actually overpredicted. Overall, when examining the dependence of modeled Dst* on actual Dst* at storm peak, we find that there is a statistically significant difference between CME- and CIR-driven storms. We also find that approximately half of the total ring current energy lies beyond an L-value of 6.6. However, this figure could be overestimated due to the use of a static magnetic field, which limits radial transport.

The Sun's Alfvén Surface: Recent Insights and Prospects for the Polarimeter to Unify the Corona and Heliosphere (PUNCH) Review

Steven R. **Cranmer** (CU Boulder), [Rohit Chhiber](#) (U. Del., GSFC), [Chris R. Gilly](#) (SwRI, CU Boulder), [Iver H. Cairns](#) (U. Sydney), [Robin C. Colaninno](#) (NRL), [David J. McComas](#) (Princeton), [Nour E. Raouafi](#) (JH/APL), [Arcadi V. Usmanov](#) (U. Del., GSFC), [Sarah E. Gibson](#) (HAO/NCAR), [Craig E. DeForest](#) (SwRI)

Solar Physics 298, Article number: 127 2023

<https://arxiv.org/pdf/2310.05887.pdf>

<https://doi.org/10.1007/s11207-023-02220-8>

The solar wind is the extension of the Sun's hot and ionized corona, and it exists in a state of continuous expansion into interplanetary space. The radial distance at which the wind's outflow speed exceeds the phase speed of Alfvénic and fast-mode magnetohydrodynamic (MHD) waves is called the Alfvén radius. In one-dimensional models, this is a singular point beyond which most fluctuations in the plasma and magnetic field cannot propagate back down to the Sun. In the multi-dimensional solar wind, this point can occur at different distances along an irregularly shaped "Alfvén surface." In this article, we review the properties of this surface and discuss its importance in models of solar-wind acceleration, angular-momentum transport, MHD waves and turbulence, and the geometry of magnetically closed coronal loops. We also review the results of simulations and data analysis techniques that aim to determine the location of the Alfvén surface. Combined with recent perihelia of Parker Solar Probe, these studies seem to indicate that the Alfvén surface spends most of its time at heliocentric distances between about 10 and 20 solar radii. It is becoming apparent that this region of the heliosphere is sufficiently turbulent that there often exist multiple (stochastic and time-dependent) crossings of the Alfvén surface along any radial ray. Thus, in many contexts, it is more useful to make use of the concept of a topologically complex "Alfvén zone" rather than one closed surface. This article also reviews how the Polarimeter to Unify the Corona and Heliosphere (PUNCH) mission will measure the properties of the Alfvén surface and provide key constraints on theories of solar-wind acceleration.

Inward-propagating Plasma Parcels in the Solar Corona: Models with Aerodynamic Drag, Ablation, and Snowplow Accretion

Steven R. **Cranmer**¹, Craig E. DeForest², and Sarah E. Gibson³

2021 ApJ 913 4

<https://doi.org/10.3847/1538-4357/abf146>

Although the solar wind flows primarily outward from the Sun to interplanetary space, there are times when small-scale plasma inflows are observed. Inward-propagating density fluctuations in polar coronal holes were detected by the COR2 coronagraph on board the STEREO-A spacecraft at heliocentric distances of 7–12 solar radii, and these fluctuations appear to undergo substantial deceleration as they move closer to the Sun. Models of linear magnetohydrodynamic waves have not been able to explain these deceleration patterns, so they have been interpreted more recently as jets from coronal sites of magnetic reconnection. In this paper, we develop a range of dynamical models of discrete plasma parcels with the goal of better understanding the observed deceleration trend. We found that parcels with a constant mass do not behave like the observed flows, and neither do parcels undergoing ablative mass loss. However, parcels that accrete mass in a snowplow-like fashion can become decelerated as observed. We also extrapolated OMNI in situ data down to the so-called Alfvén surface and found that the initial launch point for the observed parcels may often be above this critical radius. In other words, in order for the parcels to flow back down to the Sun, their initial speeds are probably somewhat nonlinear (i.e., supra-Alfvénic), and thus the parcels may be associated with structures such as shocks, jets, or shear instabilities.

Origins of the Ambient Solar Wind: Implications for Space Weather **Review**

Steven R. **Cranmer** (CU Boulder), [Sarah E. Gibson](#) (HAO), [Pete Riley](#) (PSI)

Space Science Reviews. Special issue connected with a 2016 ISSI workshop on "The Scientific Foundations of Space Weather." 2017

<https://arxiv.org/pdf/1708.07169.pdf>

The Sun's outer atmosphere is heated to temperatures of millions of degrees, and solar plasma flows out into interplanetary space at supersonic speeds. This paper reviews our current understanding of these interrelated problems: coronal heating and the acceleration of the ambient solar wind. We also discuss where the community stands in its ability to forecast how variations in the solar wind (i.e., fast and slow wind streams) impact the Earth. Although the last few decades have seen significant progress in observations and modeling, we still do not have a complete understanding of the relevant physical processes, nor do we have a quantitatively precise census of which coronal structures contribute to specific types of solar wind. Fast streams are known to be connected to the central regions of large coronal holes. Slow streams, however, appear to come from a wide range of sources, including streamers, pseudostreamers, coronal loops, active regions, and coronal hole boundaries. Complicating our understanding even more is the fact that processes such as turbulence, stream-stream interactions, and Coulomb collisions can make it difficult to unambiguously map a parcel measured at 1 AU back down to its coronal source. We also review recent progress -- in theoretical modeling, observational data analysis, and forecasting techniques that sit at the interface between data and theory -- that gives us hope that the above problems are indeed solvable.

Pursuing forecasts of the behavior and arrival of coronal mass ejections through modeling and observations. **Review**

Cremades, H.:

2018, In: Foullon, C., Malandraki, O. (eds.) Space Weather of the Heliosphere: Processes and Forecasts, Proc. Inter. Astron. Union #335 July 2017, V.13, 58-64.

<https://doi.org/10.1017/S1743921317010882>

https://www.cambridge.org/core/services/aop-cambridge-core/content/view/39F647356FF46DEE4BD0DC3DCE038353/S1743921317010882a.pdf/pursuing_forecasts_of_the_behavior_and_arrival_of_coronal_mass_ejections_through_modeling_and_observations.pdf

Sophisticated instrumentation dedicated to studying and monitoring our Sun's activity has proliferated in the past few decades, together with the increasing demand of specialized space weather forecasts that address the needs of commercial and government systems. As a result, theoretical and empirical models and techniques of increasing complexity have been developed, aimed at forecasting the occurrence of solar disturbances, their evolution, and time of arrival to Earth. Here we will review groundbreaking and recent methods to predict the propagation and evolution of coronal mass ejections and their driven shocks. The methods rely on a wealth of data sets provided by ground- and space-based observatories, involving remote-sensing observations of the corona and the heliosphere, as well as detections of radio waves.

Describe and Forecast the Propagation of 71 CMEs/Shocks

H. Cremades, F. A. Iglesias, O. C. St. Cyr, H. Xie, M. L. Kaiser, N. Gopalswamy
Solar Phys. Volume 290, Issue 9, pp 2455-2478 2015

Motivated by improving predictions of arrival times at Earth of shocks driven by coronal mass ejections (CMEs), we have analyzed 71 Earth-directed events in different stages of their propagation. The study is primarily based on approximated locations of interplanetary (IP) shocks derived from Type-II radio emissions detected by the Wind/WAVES experiment during 1997–2007. Distance–time diagrams resulting from the combination of white-light corona, IP Type-II radio, and in-situ data lead to the formulation of descriptive profiles of each CME’s journey toward Earth. Furthermore, two different methods for tracking and predicting the location of CME-driven IP shocks are presented. The linear method, solely based on Wind/WAVES data, arises after key modifications to a pre-existing technique that linearly projects the drifting low-frequency Type-II emissions to 1 AU. This upgraded method improves forecasts of shock-arrival times by almost 50 %. The second predictive method is proposed on the basis of information derived from the descriptive profiles and relies on a single CME height–time point and on low-frequency Type-II radio emissions to obtain an approximate value of the shock arrival time at Earth. In addition, we discuss results on CME–radio emission associations, characteristics of IP propagation, and the relative success of the forecasting methods.

Low-frequency type II radio detections and coronagraph data to describe and forecast the propagation of 71 CMEs/shocks

H. Cremades, F. A. Iglesias, O. C. St. Cyr, H. Xie, M. L. Kaiser, N. Gopalswamy
Solar Phys. 2015

<http://arxiv.org/pdf/1505.01730v1.pdf>

The vulnerability of technology on which present society relies demands that a solar event, its time of arrival at Earth, and its degree of geoeffectiveness be promptly forecasted. Motivated by improving predictions of arrival times at Earth of shocks driven by coronal mass ejections (CMEs), we have analyzed 71 Earth-directed events in different stages of their propagation. The study is primarily based on approximated locations of interplanetary (IP) shocks derived from type II radio emissions detected by the Wind/WAVES experiment during 1997-2007. Distance-time diagrams resulting from the combination of white-light corona, IP type II radio, and in situ data lead to the formulation of descriptive profiles of each CME's journey toward Earth. Furthermore, two different methods to track and predict the location of CME-driven IP shocks are presented. The linear method, solely based on Wind/WAVES data, arises after key modifications to a pre-existing technique that linearly projects the drifting low-frequency type II emissions to 1 AU. This upgraded method improves forecasts of shock arrival time by almost 50%. The second predictive method is proposed on the basis of information derived from the descriptive profiles, and relies on a single CME height-time point and on low-frequency type II radio emissions to obtain an approximate value of the shock arrival time at Earth. In addition, we discuss results on CME-radio emission associations, characteristics of IP propagation, and the relative success of the forecasting methods.

Table 1.: CME-kmTII-shock associations and main characteristics of the 71 analyzed events.

Coronal Transient Events During Two Solar Minima: Their Solar Source Regions and Interplanetary Counterparts

H. Cremades, C. H. Mandrini und S. Dasso

Solar Physics, Volume 274, Numbers 1-2, 233-249, 2011, File

In the frame of two coordinated observational and research efforts, two full solar rotations were investigated in the times of two distinct solar minima. These two campaigns were dubbed Whole Sun Month (WSM; **10 August – 8 September 1996**) and Whole Heliosphere Interval (WHI; **20 March – 16 April 2008**). The nearly uninterrupted gathering of solar coronal data since the beginning of the Solar and Heliospheric Observatory (SOHO) era offers the exceptional possibility of comparing two solar minima for the first time, with regard to the coronal transient aspect. This study characterizes the variety of outward-traveling transients observed in the solar corona during both time intervals, from very narrow jet-like events to coronal mass ejections (CMEs). Their solar source regions and ensuing interplanetary structures were identified and characterized as well, toward a global-scale description of their role in determining the heliosphere’s conditions. Multi-wavelength images provided by the space missions SOHO, Yohkoh (only WSM), and Solar-Terrestrial Relations Observatory (STEREO; only WHI) and ground-based observatories were analyzed for coronal ejecta and their solar sources, while data registered by the Advanced Composition Explorer (ACE) spacecraft were inspected for interplanetary CMEs and magnetic clouds. Notable differences arise from the analysis of the detailed survey of events: more (fewer) ejecta during WHI (WSM), 12% (40%) were produced by active regions during WHI (WSM), and nearly no (high) deflection from the radial direction was observed during WHI (WSM). Instrumental

aspects such as dissimilar resolution, cadence, and fields of view are considered in order to discern instrumentally driven disparities from inherent differences between solar minima.

A tool to improve space weather forecasts: Kilometric radio emissions from Wind/WAVES

To improve predictions of the arrival time of magnetohydrodynamic shock, which can occur as coronal mass ejections propagate through interplanetary space, scientists study low frequency radio emissions detected by the WIND/WAVES satellite.

Cremades, H.; St. Cyr, O. C.; Kaiser, M. L.
Space Weather, Vol. 5, No. 8, S08001, 2007, File
<http://dx.doi.org/10.1029/2007SW000314>

For decades, space environment forecasters have used the appearance of metric Type II radio emission as a proxy for eruptions in the solar corona. The drift rate of these near-Sun emissions is often turned into a speed, commonly assumed to be that of an MHD shock. However, their utility to forecast shock arrival times has not proved to be conclusive. Metric emissions can be detected by ground-based antennae, while lower-frequency components of these slowly drifting emissions can also be tracked by spacecraft in interplanetary space, as far down in frequency as that of the local plasma frequency. For a spacecraft at L1, this corresponds to about 25 kHz, or an electron density of about 7 cm^{-3} in the ambient solar wind. Here we report a recent study that aims to improve the predictions of shock arrival time at L1 by means of the low-frequency emissions detected by WIND/WAVES. This technique, implemented on an extensive sample of hectometric and kilometric type II radio bursts, has yielded promising results.

Table

Comparison of interplanetary signatures of streamers and pseudostreamers

N. U. **Crooker**^{1,*}, R. L. McPherron² and M. J. Owens
JGR, Volume 119, Issue 6, pages 4157–4163, June 2014

If the source of the slow solar wind is a web comprising pseudostreamer belts connected to the streamer belt, then one expects the properties of interplanetary pseudostreamer flows to be similar to those of streamer flows. That expectation is tested with data from the slow wind preceding stream interfaces in stream interaction regions at 1 AU, where the interfaces separate what was originally slow and fast wind. Pseudostreamer cases were separated from streamer cases with the aid of the streamer identification tool developed by Owens et al. (2013), and superposed epoch analysis was performed to compare the patterns of a number of plasma and composition parameters. The results reveal that pseudostreamer flows have all of the slow-wind characteristics of streamer flows except that they are slightly less pronounced than streamer characteristics when compared to fast wind. The results are consistent with the concept that the solar wind displays a continuum of dynamic states rather than only slow and fast states.

Suprathermal electron flux peaks at stream interfaces: Signature of solar wind dynamics or tracer for open magnetic flux transport on the Sun?

Crooker, N. U.; Appleton, E. M.; Schwadron, N. A.; Owens, M. J.
J. Geophys. Res., Vol. 115, No. A11, A11101, 2010

The high variability of the intensity of suprathermal electron flux in the solar wind is usually ascribed to the high variability of sources on the Sun. Here we demonstrate that a substantial amount of the variability arises from peaks in stream interaction regions, where fast wind runs into slow wind and creates a pressure ridge at the interface. Superposed epoch analysis centered on stream interfaces in 26 interaction regions previously identified in Wind data reveal a twofold increase in 250 eV flux (integrated over pitch angle). Whether the peaks result from the compression there or are solar signatures of the coronal hole boundary, to which interfaces may map, is an open question. Suggestive of the latter, some cases show a displacement between the electron and magnetic field peaks at the interface. Since solar information is transmitted to 1 AU much more quickly by suprathermal electrons compared to convected plasma signatures, the displacement may imply a shift in the coronal hole boundary through transport of open magnetic flux via interchange reconnection. If so, however, the fact that displacements occur in both directions and that the electron and field peaks in the superposed epoch analysis are nearly coincident indicate that any systematic transport expected from differential solar rotation is overwhelmed by a random pattern, possibly owing to transport across a ragged coronal hole boundary.

SOLAR IMPRINT ON ICMES, THEIR MAGNETIC CONNECTIVITY, AND HELIOSPHERIC EVOLUTION

N. U. **CROOKER**^{1,*} and T. S. HORBURY

Space Science Reviews (2006) 123: 93–109; **File**

Interplanetary outflows from coronal mass ejections (ICMEs) are structures shaped by their magnetic fields. Sometimes these fields are highly ordered and reflect properties of the solar magnetic field. Field lines emerging in CMEs are presumably connected to the Sun at both ends, but about half lose their connection at one end by the time they are observed in ICMEs. All must eventually lose one connection in order to prevent a build-up of flux in the heliosphere; but since little change is observed between 1 AU and 5 AU, this process may take months to years to complete. As ICMEs propagate out into the heliosphere, they kinematically elongate in angular extent, expand from higher pressure within, distort owing to inhomogeneous solar wind structure, and can compress the ambient solar wind, depending upon their relative speed. Their magnetic fields may reconnect with solar wind fields or those of other ICMEs with which they interact, creating complicated signatures in spacecraft data.

Evidence in magnetic clouds for systematic open flux transport on the Sun,

Crooker, N. U., S. W. Kahler, J. T. Gosling, and R. P. Lepping (2008)

J. Geophys. Res., 113, A12107, (2008)

<http://dx.doi.org/10.1029/2008JA013628>

Most magnetic clouds encountered by spacecraft at 1 AU display a mix of unidirectional suprathermal electrons signaling open field lines and counterstreaming electrons signaling loops connected to the Sun at both ends. Assuming the open fields were originally loops that underwent interchange reconnection with open fields at the Sun, we determine the sense of connectedness of the open fields found in 72 of 97 magnetic clouds identified by the Wind spacecraft in order to obtain information on the location and sense of the reconnection and resulting flux transport at the Sun. The true polarity of the open fields in each magnetic cloud was determined from the direction of the suprathermal electron flow relative to the magnetic field direction. Results indicate that the polarity of all open fields within a given magnetic cloud is the same 89% of the time, implying that interchange reconnection at the Sun most often occurs in only one leg of a flux rope loop, thus transporting open flux in a single direction, from a coronal hole near that leg to the foot point of the opposite leg. This pattern is consistent with the view that interchange reconnection in coronal mass ejections systematically transports an amount of open flux sufficient to reverse the polarity of the heliospheric field through the course of the solar cycle. Using the same electron data, we also find that the fields encountered in magnetic clouds are only a third as likely to be locally inverted as not. While one might expect inversions to be equally as common as not in flux rope coils, consideration of the geometry of spacecraft trajectories relative to the modeled magnetic cloud axes leads us to conclude that the result is reasonable.

Space weather: science and effects

Norma B. **Crosby**

Universal Heliophysical Processes Proceedings IAU Symposium No. 257, 2008 N. Gopalswamy & D.F. Webb, eds. Volume 4 / Symposium S257, pp 47 – 56, 2009, File

From the point-of-view of somebody standing outside on a cold winter night looking up at a clear cloudless sky, the space environment seems to be of a peaceful and stable nature. Instead, the opposite is found to be true. In fact the space environment is very dynamic on all spatial and temporal scales, and in some circumstances may have unexpected and hazardous effects on technology and humans both in space and on Earth. In fact the space environment seems to have a weather all of its own – its own “space weather”. Our Sun is definitely the driver of our local space weather. Space weather is an interdisciplinary subject covering a vast number of technological, scientific, economic and environmental issues. It is an application-oriented discipline which addresses the needs of “space weather product” users. It can be truly said that space weather affects everybody, either directly or indirectly. The aim of this paper is to give an overview of what space weather encompasses, emphasizing how solar-terrestrial physics is applied to space weather. Examples of “space weather product” users will be given highlighting those products that we as a civilization are most dependent on.

Compressible Turbulence in the Near-Sun Solar Wind: Parker Solar Probe's First Eight Perihelia

Manuel Enrique **Cuesta**¹, Rohit Chhiber^{1,2}, Xiangrong Fu^{3,4}, Senbei Du⁴, Yan Yang¹, Francesco Pecora¹, William H. Matthaeus¹, Hui Li⁴, John Steinberg⁴, Fan Guo⁴Show full author list
2023 ApJL 949 L19

<https://iopscience.iop.org/article/10.3847/2041-8213/acd4c2/pdf>

Many questions remain about the compressibility of solar wind turbulence with respect to its origins and properties. Low plasma beta (ratio of thermal to magnetic pressure) environments allow for the easier generation of compressible turbulence, enabling study of the relationship between density fluctuations and turbulent Mach number. Utilizing Parker Solar Probe plasma data, we examine the normalized proton density fluctuations $\langle \delta n_p^2 \rangle^{1/2} / \langle n_p \rangle = \delta n_{p,rms} / \langle n_p \rangle$ as a function of turbulent Mach number M_t conditioned on plasma beta and cross helicity. With consideration of statistical error in the parameters computed from in situ data, we find a general result that $\delta n_{p,rms} / \langle n_p \rangle \sim M_t^{1.18 \pm 0.04}$, consistent with both linear-wave theory and nearly incompressible turbulence in an inhomogeneous background field. We compare observational results conditioned on plasma beta and cross helicity with 3D magnetohydrodynamic simulations and observe rather significant similarities with respect to how those parameters affect the proportionality between density fluctuations and turbulent Mach number. This study further investigates the complexity of compressible turbulence as viewed by the density scaling relationship and may help better understand the compressible environment of the near-Sun solar wind.

Tracking Solar Active Region Outflow Plasma from its Source to the near-Earth Environment

J.L. **Culhane**, D.H. Brooks, L. van Driel-Gesztelyi, P. Demoulin, D. Baker, M.L. DeRosa, C.H. Mandrini, L. Zhao, T.H. Zurbuchen

Solar Phys., Volume 289, Issue 10, pp 3799-3816, **2014**

<http://arxiv.org/pdf/1405.2949v1.pdf>

Seeking to establish whether active region upflow material contributes to the slow solar wind, we examine in detail the plasma upflows from Active Region (AR)10978, which crossed the Sun's disc in the interval **8 to 16 December, 2007** during Carrington rotation (CR)2064. In previous work, using data from the Hinode/EUV Imaging Spectrometer, upflow velocity evolution was extensively studied as the region crossed the disc while a linear force-free magnetic extrapolation was used to confirm aspects of the velocity evolution and to establish the presence of quasi-separatrix layers at the upflow source areas. The plasma properties, temperature, density and first ionisation potential bias (FIP-bias) were measured with the spectrometer during the disc passage of the active region. Global potential field source surface (PFSS) models showed that AR 10978 was completely covered by the closed field of a helmet streamer that is part of the streamer belt. Thus it is not clear how any of the upflowing AR-associated plasma could reach the source surface at 2.5 R(Sun) and contribute to the slow solar wind. However a detailed examination of solar-wind in-situ data obtained by the Advanced Composition Explorer (ACE) spacecraft at the L1 point shows that the increase in O⁷⁺/O⁶⁺, C⁶⁺/C⁵⁺ and Fe/O - a FIP-bias proxy - are present before the heliospheric current sheet crossing. These increases, along with an accompanying reduction in proton velocity and an increase in density are characteristic of both AR and slow-wind plasma. Finally we describe a two-step reconnection process by which some of the upflowing plasma from the AR could reach the heliosphere.

Study of CME transit speeds for the event of 07-NOV-2004

J.L. **Culhane**, S. Pohjolainen, L. van Driel-Gesztelyi, P.K. Manoharan and H.A. Elliott

[Advances in Space Research](#)

[Volume 40, Issue 12, 2007](#), Pages 1807-1814

Several methods for CME speed estimation are discussed. These include velocity derivation based on the frequency drifts observed in metric and decametric radio wave data using a range of coronal density models. Coronagraph height–time plots allow measurement of plane-of-sky and expansion speeds. These in turn can enable propagation speeds to be derived from a range of empirical relations. Simple geometric e.g., cone, models can provide propagation velocity estimates for suitable halo or partial halo events. Interplanetary scintillation observations allow speed estimates at large distances from the Sun detecting in particular the deceleration of the faster CMEs. Related interplanetary shocks and the arrival times and speeds of the associated magnetic clouds at Earth can also be considered. We discuss the application of some of these methods to the transit to Earth of a complex CME that originated earlier than 16:54 U.T. on 07-NOV-2004. The difficulties in making velocity estimates from radio observations, particularly under disturbed coronal conditions, are highlighted.

On the Acceleration Site of Anomalous Cosmic Rays: Voyager 2 Observations of Their Anisotropy in the Heliosheath

A. C. **Cummings**¹, J. Kóta², J. D. Richardson³, J. S. Rankin⁴, and B. C. Heikkilä⁵

2024 ApJ 977 76

<https://iopscience.iop.org/article/10.3847/1538-4357/ad8e66/pdf>

We present the diffusive flow anisotropy vector components for ~0.5–35 MeV anomalous cosmic-ray (ACR) protons observed during Voyager 2 roll maneuvers for the magnetometer instrument in the inner heliosheath. The diffusive flow results are derived from the differences between the observed anisotropy components presented in A. C. Cummings et al. (2021) and the Compton–Getting anisotropies based on measurements of the solar wind speeds from the Plasma Science instrument. We find that the tangential component of the derived diffusive anisotropy vector is in reasonable agreement, both in direction and magnitude, with a numerical model of the acceleration and transport of ACRs by diffusive shock acceleration along a nonspherical solar wind termination shock (TS). The results suggest that there exists a diffusive flow of these particles from the flank or tail of the heliosphere toward the nose, and support models in which higher-energy ACRs are accelerated in the flank or tail of the TS.

Geomagnetic solar flare effects: a review

Juan José **Curto***

J. Space Weather Space Clim. 2020, 10, 27

<https://www.swsc-journal.org/articles/swsc/pdf/2020/01/swsc190079.pdf>

<https://doi.org/10.1051/swsc/2020027>

Solar flare effects (Sfe) are rapid variations in the Earth's magnetic field and are related to the enhancement of the amount of radiation produced during Solar flare events. They mainly appear in the Earth's sunlit hemisphere at the same time as the flare observation and have a crochet-like shape. Much progress has been made since Carrington's first observations in 1859 which are considered to represent the first direct evidence of the connection between the Sun and the Earth's environment but there is still much to discover. In this paper, we review state-of-the-art developments and the advances made in the knowledge concerning Sfe phenomena while also looking at the challenges that lie ahead. First, we offer a historical approach with a comprehensive description that allows for a better understanding of the main characteristics of Sfe. This frames specific topics like the puzzling reversed-Sfe or the nighttime Sfe. The role played by the Service of Rapid Magnetic variations (SRMV) is also assessed, followed by a discussion of the main current limiting factors in the process of detection and proposed ways to overcome challenges such as by creating an automatic detection method. The paper clarifies some aspects related to the geo-effectiveness of the solar flares producing magnetic disturbances. The importance of the global modelling studies covering critical aspects needed to understand this Sun–Earth system is assessed. Also, we provide an overview of the temporal evolution of the electric currents producing Sfe. The importance of key subjects such as the dynamic aspects of Sfe is developed in another section. Finally, estimations of the size of large flares using ionospheric and magnetic data are reviewed as well as the prospects of these large flare events putting technological systems in danger.

Effect of the Heliospheric State on CME Evolution

Fithanegest Kassa **Dagnew**^{1,2,3}, Nat Gopalswamy², Solomon Belay Tessema¹, Sachiko Akiyama^{2,3}, and Seiji Yashiro^{2,3}

2022 ApJ 936 122

<https://arxiv.org/ftp/arxiv/papers/2208/2208.03536.pdf>

<https://iopscience.iop.org/article/10.3847/1538-4357/ac8744/pdf>

The culmination of solar cycle 24 by the end of 2019 has created the opportunity to compare the differing properties of coronal mass ejections (CMEs) between two whole solar cycles: solar cycle 23 (SC 23) and solar cycle 24 (SC 24). We report on the width evolution of limb CMEs in SCs 23 and 24 in order to test the suggestion by Gopalswamy et al. that CME flux ropes attain pressure balance at larger heliocentric distances in SC 24. We measure CME width as a function of heliocentric distance for a significantly large number of limb CMEs (~1000) and determine the distances where the CMEs reach constant width in each cycle. We introduced a new parameter, the transition height (h_c) of a CME, defined as the critical heliocentric distance beyond which the CME width stabilizes to a quasi-constant value. Cycle and phase-to-phase comparisons are based on this new parameter. We find that the average value of h_c in SC 24 is 62% higher than that in SC 23. SC 24 CMEs attain their peak width at larger distances from the Sun than SC 23 CMEs do. The enhanced transition height in SC 24 is new observational ratification of the anomalous expansion. The anomalous expansion of SC 24 CMEs, which is caused by the weak state of the heliosphere, accounts for the larger heliocentric distance where the pressure balance between CME flux rope and the ambient medium is attained. **2014 May 6**

Magnetic clouds in the solar wind: a numerical assessment of analytical models

G. Dalakishvili^{1,2,3}, J. Kleimann¹, H. Fichtner¹ and S. Poedts

A&A 536, A100 (2011)

Context. Magnetic clouds (MCs) are “magnetized plasma clouds” moving in the solar wind. MCs transport magnetic flux and helicity away from the Sun. These structures are not stationary but feature temporal evolution as they propagate in the solar wind. Simplified analytical models are frequently used to describe MCs, and they fit certain observational data well.

Aims. The goal of the present study is to numerically investigate the validity of an analytical model that is widely used to describe MCs, and to determine under which conditions this model’s implied assumptions cease to be valid.

Methods. A numerical approach is applied. Analytical solutions derived in previous studies are implemented in a 3D magnetohydrodynamic simulation code as initial conditions. Besides the standard case in which MCs only expand and propagate in the solar wind, the case of an MC rotating around its axis of symmetry is also considered, and the resulting influence on the MC’s dynamics is studied.

Results. Initially, the analytical model represents the main observational features of the MCs. However, these characteristics prevail only if the structure moves with a velocity close to the velocity of the background flow. In this case an MC’s evolution can quite accurately be described using an analytic, self-similar approach. The dynamics of the magnetic structures that move with a velocity significantly above or below that of the velocity of the solar wind is investigated in detail.

Conclusions. Comparison of the numerical results with observational data indicates reasonable agreement especially for the intermediate case, in which the MC’s bulk velocity and the velocity of the background flow are equal. In this particular case, analytical solutions obtained on the basis of a self-similar approach indeed describe the MC’s evolution quite accurately. In general, however, numerical simulations are necessary to investigate the evolution as a function of a wide range of the parameters, which define the initial conditions.

Investigation of dynamics of self-similarly evolving magnetic clouds

G. Dalakishvili^{1,4}, A. Rogava^{2,3}, G. Lapenta⁴, and S. Poedts⁴

A&A 526, A22 (2011)

Context. Magnetic clouds (MCs) are “magnetized plasma clouds” moving in the solar wind. MCs transport magnetic flux and helicity away from the Sun. These structures are not stationary but experience temporal evolution. Simplified MC models are usually considered.

Aims. We investigate the dynamics of more general, *radially expanding* MCs. They are considered as cylindrically symmetric magnetic structures with low plasma β .

Methods. We adopt both a self-similar approach method and a numerical approach.

Results. We demonstrate that the forces are balanced in the considered self-similarly evolving, cylindrically symmetric magnetic structures. Explicit analytical expressions for magnetic field, plasma velocity, density, and pressure within MCs are derived. These solutions are characterized by conserved values of magnetic flux and helicity. We also investigate the dynamics of self-similarly evolving MCs by means of the numerical code “Graale”. In addition, their expansion in a medium of higher density and higher plasma β is studied. It is shown that the physical parameters of the MCs maintain their self-similar character throughout their evolution.

Conclusions. After comparing different self-similar and numerical solutions, we are able to conclude that the evolving MCs are quite adequately described by our self-similar solutions – they retain their self-similar, coherent nature for quite a long time and over large distances from the Sun.

Dal Lago, A., L.E.A. Vieira, E. Echer, W.D. Gonzalez, A.L.C. de Gonzalez, F.L. Guarnieri, N.J. Schuch and R. Schwenn, Comparison between halo cme expansion speeds observed on the Sun, the related shock transit speeds to Earth and corresponding ejecta speeds at 1 AU, *Solar Physics*, **222**(2), 323, 2004.

Suprathermal Population Associated with Stream Interaction Regions Observed by STEREO-A: New Insights

Bijoy Dalal^{1,2}, Dibyendu Chakrabarty¹, Nandita Srivastava³, and Aveek Sarkar¹

2024 ApJ 960 16

<https://iopscience.iop.org/article/10.3847/1538-4357/ad08c6/pdf>

Stream interaction regions (SIRs) are often thought to be responsible for the generation of suprathermal population in the interplanetary medium. Even though the source is the same, wide variations in the spectral indices of suprathermal populations are observed at 1 au during SIRs. This poses a significant uncertainty in understanding the generation of suprathermal ion populations by SIRs and indicates an interplay of multiple source mechanisms. By analyzing variations in suprathermal 4He, O, and Fe for 20 SIR events recorded by STEREO-A during 2007–2014, we find that the spectral indices of these elements vary in the range of 2.06–4.08, 1.85–4.56, and 2.11–4.04 for 19 events. However, in one special case, all three suprathermal elements show nearly identical (~1.5) spectral indices. We describe possible mechanisms that might cause significant variations in the spectral indices of suprathermal particles. More importantly, we show the possible role of merging and/or contraction of small-scale magnetic islands near 1 au in producing nearly identical spectral indices for three different elements with different first ionization potentials and mass-to-charge ratios. The occurrence of these magnetic islands near 1 au also supports the minimal modulation in the spectral indices of these particles. We also suggest that a possible solar flare may have played a role in generating these magnetic islands near the heliospheric current sheet. **2012 June 12**

Table 1 List of SIR Events 2007-2014

EVOLUTION OF PILED-UP COMPRESSIONS IN MODELED CORONAL MASS EJECTION SHEATHS AND THE RESULTING SHEATH STRUCTURES

Indrajit Das¹, Merav Opher^{1,2}, Rebekah Evans¹, Cristiane Loesch³, and Tamas I. Gombosi⁴

Astrophysical Journal, 729:112 (7pp), **2011** March, **File**

We study coronal mass ejection (CME)-driven shocks and the resulting post-shock structures in the lower corona (2–7R_⊙). Two CMEs are erupted by modified Titov–D’emoulin (TD) and Gibson–Low (GL) type flux ropes (FRs) with the Space Weather Modeling Framework. We observe a substantial pile-up of density compression and a narrow region of plasma depletion layer (PDL) in the simulations. As the CME/FR moves and expands in the solar wind medium, it pushes the magnetized material lying ahead of it. Hence, the magnetic field lines draping around the CME front are compressed in the sheath just ahead of the CME. These compressed field lines squeeze out the plasma sideways, forming PDL in the region. Solar plasma being pushed and displaced from behind forms a strong piled-up compression (PUC) of density downstream of the PDL. Both CMEs have comparable propagation speeds, while GL has larger expansion speed than TD due to its higher initial magnetic pressure. We argue that high CME expansion speed along with high solar wind density in the region is responsible for the large PUC found in the lower corona. In case of GL, the PUC is much wider, although the density compression ratio for both the cases is comparable. Although these simulations artificially initiate out-of-equilibrium CMEs and drive them in an artificial solar wind solution, we predict that PUCs, in general, will be large in the lower corona. This should affect the ion profiles of the accelerated solar energetic particles.

Magnetic clouds along the solar cycle: expansion and magnetic helicity.

Dasso S, Démoulin P, and Gulisano AM

(2012) *IAU Symposium No. 286, edited by C. H. Mandrini and D. F. Webb*, No 286:139-148

Magnetic helicity content in solar wind flux ropes

Sergio **Dasso**

Proceedings of the International Astronomical Union / Volume 4 / Symposium S257, pp 379 – 389,

Published online: 16 Mar 2009

<http://journals.cambridge.org/action/displayIssue?iid=4866212>

Magnetic helicity (H) is an ideal magnetohydrodynamical (MHD) invariant that quantifies the twist and linkage of magnetic field lines. In magnetofluids with low resistivity, H decays much less than the energy, and it is almost conserved during times shorter than the global diffusion timescale. The extended solar corona (i.e., the heliosphere) is one of the physical scenarios where H is expected to be conserved. The amount of H injected through the photospheric level can be reorganized in the corona, and finally ejected in flux ropes to the interplanetary medium. Thus, coronal mass ejections can appear as magnetic clouds (MCs), which are huge twisted flux tubes that transport large amounts of H through the solar wind. The content of H depends on the global configuration of the structure, then, one of the main difficulties to estimate it from single spacecraft in situ observations (one point - multiple times) is that a single spacecraft can only observe a linear (one dimensional) cut of the MC global structure. Another serious difficulty is the intrinsic mixing between its spatial shape and its time evolution that occurs during the observation period. However, using some simple assumptions supported by observations, the global shape of some MCs can be unveiled, and the associated H and magnetic fluxes (F) can be estimated. Different methods to quantify H and F from the analysis of in situ observations in MCs are presented in this review. Some of these methods consider a MC in expansion and going through possible magnetic reconnections with its environment. We conclude that H seems to be a 'robust' MHD quantity in MCs, in the sense that variations of H for a given MC deduced using different methods, are typically lower than changes of H when a different cloud is considered. Quantification of H and F lets us constrain models of coronal formation and ejection of flux ropes to the interplanetary medium, as well as of the dynamical evolution of MCs in the solar wind.

Linking two consecutive nonmerging magnetic clouds with their solar sources,

Dasso, S., C. H. Mandrini, B. Schmieder, H. Cremades, C. Cid, Y. Cerrato, E. Saiz, P. Demoulin, A. N. Zhukov, L. Rodriguez, A. Aran, M. Menvielle, and S. Poedts (2009),

J. Geophys. Res., 114, A02109, <http://dx.doi.org/10.1029/2008JA013102> , February 2009, File

On 15 May 2005, a huge interplanetary coronal mass ejection (ICME) was observed near Earth. It triggered one of the most intense geomagnetic storms of solar cycle 23 ($Dst_{peak} = -263$ nT). This structure has been associated with the two-ribbon flare, filament eruption, and coronal mass ejection originating in active region 10759 (NOAA number). We analyze here the sequence of events, from solar wind measurements (at 1 AU) and back to the Sun, to understand the origin and evolution of this geoeffective ICME. From a detailed observational study of in situ magnetic field observations and plasma parameters in the interplanetary (IP) medium and the use of appropriate models we propose an alternative interpretation of the IP observations, different to those discussed in previous studies. In our view, the IP structure is formed by two extremely close consecutive magnetic clouds (MCs) that preserve their identity during their propagation through the interplanetary medium. Consequently, we identify two solar events in H α and EUV which occurred in the source region of the MCs. The timing between solar and IP events, as well as the orientation of the MC axes and their associated solar arcades are in good agreement. Additionally, interplanetary radio type II observations allow the tracking of the multiple structures through inner heliosphere and pin down the interaction region to be located midway between the Sun and the Earth. The chain of observations from the photosphere to interplanetary space is in agreement with this scenario. Our analysis allows the detection of the solar sources of the transients and explains the extremely fast changes of the solar wind due to the transport of two attached (though nonmerging) MCs which affect the magnetosphere.

Progressive Transformation of a Flux Rope to an ICME Comparative Analysis Using the Direct and Fitted Expansion Methods

S. **Dasso** · M.S. Nakwacki · P. Démoulin · C.H. Mandrini

Solar Phys (2007) 244: 115–137

The solar wind conditions at one astronomical unit (AU) can be strongly disturbed by interplanetary coronal mass ejections (ICMEs). A subset, called magnetic clouds (MCs), is formed by twisted flux ropes that transport an important amount of magnetic flux and helicity, which is released in CMEs. At 1 AU from the Sun, the magnetic structure of MCs is generally modeled by neglecting their expansion during the spacecraft crossing. However, in some cases, MCs present a significant expansion. We present here an analysis of the huge and significantly expanding MC observed by the Wind spacecraft during 9 - 10 November 2004. This MC was embedded in an ICME. After determining an approximate orientation for the flux rope using the minimum variance method, we obtain a precise orientation of the cloud axis by

relating its front and rear magnetic discontinuities using a direct method. This method takes into account the conservation of the azimuthal magnetic flux between the inbound and outbound branches and is valid for a finite impact parameter (i.e., not necessarily a small distance between the spacecraft trajectory and the cloud axis). The MC is also studied using dynamic models with isotropic expansion. We have found $(6.2 \pm 1.5) \times 10^{20}$ Mx for the axial flux and $(78 \pm 18) \times 10^{20}$ Mx for the azimuthal flux. Moreover, using the direct method, we find that the ICME is formed by a flux rope (MC) followed by an extended coherent magnetic region. These observations are interpreted by considering the existence of a previously larger flux rope, which partially reconnected with its environment in the front. We estimate that the reconnection process started close to the Sun. These findings imply that the ejected flux rope is progressively peeled by reconnection and transformed to the observed ICME (with a remnant flux rope in the front part).

Large scale MHD properties of interplanetary magnetic clouds

Dasso, S., Mandrini, C.H., D'emoulin, P., Luoni, M.L., et al.

Advances in Space Research, Volume 35, Issue 5, p. 711-724, **2005**.

Magnetic Clouds (MCs) are the interplanetary manifestation of Coronal Mass Ejections. These huge astrophysical objects travel from the Sun toward the external heliosphere and can reach the Earth environment. Depending on their magnetic field orientation, they can trigger intense geomagnetic storms. The details of the magnetic configuration of clouds and the typical values of their magnetohydrodynamic magnitudes are not yet well known. One of the most important magnetohydrodynamic quantities in MCs is the magnetic helicity. The helicity quantifies several aspects of a given magnetic structure, such as the twist, kink, number of knots between magnetic field lines, linking between magnetic flux tubes, etc. The helicity is approximately conserved in the solar atmosphere and the heliosphere, and it is very useful to link solar phenomena with their interplanetary counterpart. Since a magnetic cloud carries an important amount of helicity when it is ejected from the solar corona, estimations of the helicity content in clouds can help us to understand its evolution and its coronal origin. In situ observations of magnetic clouds at one astronomical unit are in agreement with a local helical magnetic structure. However, since spacecrafts only register data along a unique direction, several aspects of the global configuration of clouds cannot be observed. In this paper, we review the general properties of magnetic clouds and different models for their magnetic structure at one astronomical unit. We describe the corresponding techniques to analyze in situ measurements. We also quantify their magnetic helicity and compare it with the release of helicity in their solar source for some of the analyzed cases.

Forecast of solar ejecta arrival at 1 AU from radial speed

S. **Dasso**, N. Gopalswamy, and A. Lara

Geofisica Internacional, Vol. 43, Num. 1, pp. 47-52, **2004**, **File**

Solar ejecta produce changes in the interplanetary magnetic field of the terrestrial environment. When the magnetic polarity of the ejecta is suitable, it may trigger intense geomagnetic storms. Therefore, prediction of the arrival of solar ejecta in the geospace is of crucial importance for space weather applications. We implement a simple model, developed by Gopalswamy et al., (2000) to estimate the time of arrival for solar ejecta at 1AU. This model requires just one input parameter: the radial speed of the associated coronal mass ejection (CME) at the moment of its expulsion from the Sun. When the speed of the CME is measured from a location on the Sun-Earth line, only the plane of the sky speed can be obtained. Since the prediction model depends on the initial speed of the CMEs observed remotely, it is important to obtain this speed as accurately as possible. One of the major uncertainties in the measured initial speed is the extent of projection effects. We attempt to correct for projection effects using the solar surface location of the eruption and assuming a width to the CME. We found that the correction is in agreement with a model obtained from stereoscopic observations from the past.

Study of Interplanetary and Geomagnetic Response of Filament Associated CMEs

Kunjal **Dave**, [Wageesh Mishra](#), [Nandita Srivastava](#), [R. M. Jadhav](#)

Proceedings IAU Symposium No. 340, **2018**

<https://arxiv.org/pdf/1807.00809.pdf>

It has been established that Coronal Mass Ejections (CMEs) may have significant impact on terrestrial magnetic field and lead to space weather events. In the present study, we selected several CMEs which are associated with filament eruptions on the Sun. We attempt to identify the presence of filament material within ICME at 1AU. We discuss how different ICMEs associated with filaments lead to moderate or major geomagnetic activity on their arrival at the Earth. Our study also highlights the difficulties in identifying the filament material at 1AU within isolated and in interacting CMEs. **23 May 2010, 6 Oct 2010, 23 Sep 2012**

Flux rope modeling of the 2022 Sep 5 CME observed by Parker Solar Probe and Solar Orbiter from 0.07 to 0.69 au

Emma E. [Davies](#) (1), [Hannah T. Rüdiger](#) (1), [Ute V. Amerstorfer](#) (1), [Christian Möstl](#) (1), [Maike Bauer](#), + + +
ApJ **973** 51 **2024**

<https://arxiv.org/pdf/2405.10810>

<https://iopscience.iop.org/article/10.3847/1538-4357/ad64cb/pdf>

As both Parker Solar Probe (PSP) and Solar Orbiter (SolO) reach heliocentric distances closer to the Sun, they present an exciting opportunity to study the structure of CMEs in the inner heliosphere. We present an analysis of the global flux rope structure of the **2022 September 5** CME event that impacted PSP at a heliocentric distance of only 0.07 au and SolO at 0.69 au. We compare in situ measurements at PSP and SolO to determine global and local expansion measures, finding a good agreement between magnetic field relationships with heliocentric distance, but significant differences with respect to flux rope size. We use PSP/WISPR images as input to the ELEvoHI model, providing a direct link between remote and in situ observations; we find a large discrepancy between the resulting modeled arrival times, suggesting that the underlying model assumptions may not be suitable when using data obtained close to the Sun, where the drag regime is markedly different in comparison to larger heliocentric distances. Finally, we fit the SolO/MAG and PSP/FIELDS data independently with the 3DCORE model and find that many parameters are consistent between spacecraft, however, challenges are apparent when reconstructing a global 3D structure that aligns with arrival times at PSP and Solar Orbiter, likely due to the large radial and longitudinal separations between spacecraft. From our model results, it is clear the solar wind background speed and drag regime strongly affects the modeled expansion and propagation of CMEs and needs to be taken into consideration.

Solar Orbiter Science Nuggets #37 Sep 2024 <https://www.cosmos.esa.int/web/solar-orbiter/-/science-nugget-modelling-the-global-structure-of-a-coronal-mass-ejection>

The effect of magnetic field line topology on ICME-related GCR modulation

Emma E. [Davies](#) (1 and 2), [Camilla Scolini](#) (1), [Réka M. Winslow](#) (1), [Andrew P. Jordan](#) (1), [Christian Möstl](#) (2)

ApJ **959** 133 **2023**

<https://arxiv.org/pdf/2310.11310.pdf>

<https://iopscience.iop.org/article/10.3847/1538-4357/ad046a/pdf>

The large-scale magnetic structure of interplanetary coronal mass ejections (ICMEs) has been shown to affect the galactic cosmic ray (GCR) flux measured in situ by spacecraft, causing temporary decreases known as Forbush decreases (Fds). In some ICMEs, the magnetic ejecta exhibits a magnetic flux rope (FR) structure; the strong magnetic field strength and closed field line geometry of such ICME FRs has been proposed to act as a shield to GCR transport. In this study, we identify four ICMEs near Earth that drove Fds with similar mean magnetic field strengths (20 - 25 nT); two ICMEs with more typical mean speeds (~400 km/s), and two fast (~750 km/s) ICMEs. Within each speed pairing, we identify an ICME that exhibited an open magnetic field line topology and compare its effect on the GCR flux to that which exhibited a mostly closed topology. We investigate the different mechanisms that contribute to the resulting ICME-related Fds and their recovery, and determine which properties, if any, play a more important role than others in driving Fds. We find that much of the GCR response to the ICME events in this study is independent of the open or closed magnetic field line topology of the flux rope, and that features such as the fluctuations in speed, magnetic field structure, and expansion within the FR may play more of a role in determining the smaller-scale structure of the Fd profile. **2002-09-30_Oct 1, 2004-11-09-10, 2005-05-15-16, 2022 March 31_Apr 1**

Characterizing ICME-related Forbush Decreases at Mercury using MESSENGER

Observations: Identification of a One or Two-Step Structure

Emma E. [Davies](#) (1), [Réka M. Winslow](#) (1), [David J. Lawrence](#) (2)

ApJ **2022**

<https://arxiv.org/pdf/2212.02707.pdf>

The large-scale magnetic structure of interplanetary coronal mass ejections (ICMEs) has been shown to cause decreases in the galactic cosmic ray (GCR) flux measured in situ by spacecraft, known as Forbush decreases (Fds). We use measurements of the GCR count rate obtained by MESSENGER during its orbital phase around Mercury to identify such Fds related to the passage of ICMEs and characterize their structure. Of the 42 ICMEs with corresponding high-quality GCR data, 79% are associated with a Fd. Thus a total of 33 ICME-related Fds were identified, 24 of which

(73%) have a two-step structure. We use a superposed epoch analysis to build an average Fd profile at MESSENGER and find that despite the variability of individual events, a two-step structure is produced and is directly linked with the magnetic boundaries of the ICME. By using results from previous studies at Earth and Mars, we also address whether two-step Fds are more commonly observed closer to the Sun; we found that although likely, this is not conclusive when comparing to the wide range of results of previous studies conducted at Earth. Finally, we find that the percentage decrease in GCR flux of the Fd is greater at MESSENGER on average than at Earth and Mars, decreasing with increasing heliocentric distance. The relationship between the percentage decrease and maximum hourly decrease is also in agreement with previous studies, and follows trends relating to the expansion of ICMEs as they propagate through the heliosphere. **19-22 May 2011, 21 Jun 2011, 23 Nov 2011**

Table 1. Sample of the Forbush Decreases identified 2011

Multi-spacecraft Observations of the Evolution of Interplanetary Coronal Mass Ejections between 0.3 and 2.2 au: Conjunctions with the Juno Spacecraft

Emma E. **Davies**^{1,2}, Réka M. Winslow¹, Camilla Scolini^{1,3}, Robert J. Forsyth², Christian Möstl⁴, Noé Lugaz¹, and Antoinette B. Galvin¹

2022 *ApJ* 933 127

<https://iopscience.iop.org/article/10.3847/1538-4357/ac731a/pdf>

We present a catalog of 35 interplanetary coronal mass ejections (ICMEs) observed by the Juno spacecraft and at least one other spacecraft during its cruise phase to Jupiter. We identify events observed by MESSENGER, Venus Express, Wind, and STEREO with magnetic features that can be matched unambiguously with those observed by Juno. A multi-spacecraft study of ICME properties between 0.3 and 2.2 au is conducted: we first investigate the global expansion by tracking the variation in magnetic field strength with increasing heliocentric distance of individual ICME events, finding significant variability in magnetic field relationships for individual events in comparison with statistical trends. With the availability of plasma data at 1 au, the local expansion at 1 au can be compared with global expansion rates between 1 au and Juno. Despite following expected trends, the local and global expansion rates are only weakly correlated. Finally, for those events with clearly identifiable magnetic flux ropes, we investigate the orientation of the flux rope axis as they propagate; we find that 64% of events displayed a decrease in inclination with increasing heliocentric distance, and 40% of events undergo a significant change in orientation as they propagate toward Juno. The multi-spacecraft catalog produced in this study provides a valuable link between ICME observations in the inner heliosphere and beyond 1 au, thereby improving our understanding of ICME evolution. **14-23 Nov 2012**

Table 1 Sample of Multi-spacecraft Events Identified 2011-2013

A Catalog of Interplanetary Coronal Mass Ejections Observed by Juno between 1 and 5.4 AU

Emma E. **Davies** (1,2), [Robert J. Forsyth](#) (2), [Réka M. Winslow](#) (1), [Christian Möstl](#) (3), [Noé Lugaz](#) (1)

2021 *ApJ* **923** 136

<https://arxiv.org/pdf/2111.11336.pdf>

<https://doi.org/10.3847/1538-4357/ac2ccb>

We use magnetic field measurements by the Juno spacecraft to catalog and investigate interplanetary coronal mass ejections (ICMEs) beyond 1 AU. During its cruise phase, Juno spent about 5 years in the solar wind between 2011 September and 2016 June, providing measurements of the interplanetary magnetic field (IMF) between 1 and 5.4 AU. Juno therefore presents the most recent opportunity for a statistical analysis of ICME properties beyond 1 AU since the Ulysses mission (1990-2009). Our catalog includes 80 such ICME events, 32 of which contain associated flux-rope-like structures. We find that the dependency of the mean magnetic field strength of the magnetic flux ropes decreases with heliocentric distance as $r^{-1.24 \pm 0.43}$ between 1 and 5.4 AU, in good agreement with previous relationships calculated using ICME catalogs at Ulysses. *We combine the Juno catalog with the HELCATS catalog to create a dataset of ICMEs covering 0.3-5.4 AU.* Using a linear regression model to fit the combined dataset on a double-logarithmic plot, we find that there is a clear difference between global expansion rates for ICMEs observed at lesser heliocentric distances and those observed farther out beyond 1 AU. The cataloged ICMEs at Juno present a good basis for future multispacecraft studies of ICME evolution between the inner heliosphere, 1 AU, and beyond. **29 Jan-3 Feb 2013, 20 Feb 2013**

On the Radial and Longitudinal Variation of a Magnetic Cloud: ACE, Wind, ARTEMIS and Juno Observations

Emma E. **Davies**, [Robert J. Forsyth](#), [Simon W. Good](#) & [Emilia K. J. Kilpua](#)
Solar Physics volume 295, Article number: 157 (2020)

<https://link.springer.com/content/pdf/10.1007/s11207-020-01714-z.pdf>

We present observations of the same magnetic cloud made near Earth by the Advance Composition Explorer (ACE), Wind, and the Acceleration, Reconnection, Turbulence and Electrodynamics of the Moon's Interaction with the Sun (ARTEMIS) mission comprising the Time History of Events and Macroscale Interactions during Substorms (THEMIS) B and THEMIS C spacecraft, and later by Juno at a distance of 1.2 AU. The spacecraft were close to radial alignment throughout the event, with a longitudinal separation of 3.6° between Juno and the spacecraft near Earth. The magnetic cloud likely originated from a filament eruption on **22 October 2011** at 00:05 UT, and caused a strong geomagnetic storm at Earth commencing on **24 October**. Observations of the magnetic cloud at each spacecraft have been analysed using minimum variance analysis and two flux rope fitting models, Lundquist and Gold–Hoyle, to give the orientation of the flux rope axis. We explore the effect different trailing edge boundaries have on the results of each analysis method, and find a clear difference between the orientations of the flux rope axis at the near-Earth spacecraft and Juno, independent of the analysis method. The axial magnetic field strength and the radial width of the flux rope are calculated using both observations and fitting parameters and their relationship with heliocentric distance is investigated. Differences in results between the near-Earth spacecraft and Juno are attributed not only to the radial separation, but to the small longitudinal separation which resulted in a surprisingly large difference in the in situ observations between the spacecraft. This case study demonstrates the utility of Juno cruise data as a new opportunity to study magnetic clouds beyond 1 AU, and the need for caution in future radial alignment studies. **22-24 Oct 2011**

Establishing a Stereoscopic Technique for Determining the Kinematic Properties of Solar Wind Transients based on a Generalized Self-similarly Expanding Circular Geometry

J. A. **Davies**¹, C. H. Perry¹, R. M. G. M. Trines^{2,3}, R. A. Harrison¹, N. Lugaz⁴, C. Möstl^{5,6,7}, Y. D. Liu⁸, and K. Steed

2013 ApJ 777 167

http://sprg.ssl.berkeley.edu/~liuxying/pubs/2013_apj_davies.pdf

The twin-spacecraft STEREO mission has enabled simultaneous white-light imaging of the solar corona and inner heliosphere from multiple vantage points. This has led to the development of numerous stereoscopic techniques to investigate the three-dimensional structure and kinematics of solar wind transients such as coronal mass ejections (CMEs). Two such methods—triangulation and the tangent to a sphere—can be used to determine time profiles of the propagation direction and radial distance (and thereby radial speed) of a solar wind transient as it travels through the inner heliosphere, based on its time-elongation profile viewed by two observers. These techniques are founded on the assumption that the transient can be characterized as a point source (fixed, FP, approximation) or a circle attached to Sun-center (harmonic mean, HM, approximation), respectively. These geometries constitute extreme descriptions of solar wind transients, in terms of their cross-sectional extent. Here, we present the stereoscopic expressions necessary to derive propagation direction and radial distance/speed profiles of such transients based on the more generalized self-similar expansion (SSE) geometry, for which the FP and HM geometries form the limiting cases; our implementation of these equations is termed the stereoscopic SSE method. We apply the technique to two Earth-directed CMEs from different phases of the STEREO mission, the well-studied event of **2008 December** and a more recent event from **2012 March**. The latter CME was fast, with an initial speed exceeding 2000 km s⁻¹, and highly geoeffective, in stark contrast to the slow and ineffectual 2008 December CME.

Predicting the arrival of high-speed solar wind streams at Earth using the STEREO Heliospheric Imagers

Davis, C. J.; Davies, J. A.; Owens, M. J.; Lockwood, M.

Space Weather, Vol. 10, No. 2, S02003, **2012**

<http://dx.doi.org/10.1029/2011SW000737>

High-speed solar wind streams modify the Earth's geomagnetic environment, perturbing the ionosphere, modulating the flux of cosmic rays into the Earth atmosphere, and triggering substorms. Such activity can affect modern technological systems. To investigate the potential for predicting the arrival of such streams at Earth, images taken by the Heliospheric Imager (HI) on the STEREO-A spacecraft have been used to identify the onsets of high-speed solar wind streams from observations of regions of increased plasma concentrations associated with corotating interaction regions, or CIRs. In order to confirm that these transients were indeed associated with CIRs and to study their average properties, arrival times predicted from the HI images were used in a superposed epoch analysis to confirm their identity in near-Earth solar wind data obtained by the Advanced Composition Explorer (ACE) spacecraft and to observe their influence on a number of salient geophysical parameters. The results are almost identical to those of a parallel superposed epoch

analysis that used the onset times of the high-speed streams derived from east/west deflections in the ACE measurements of solar wind speed to predict the arrival of such streams at Earth, assuming they corotated with the Sun with a period of 27 days. Repeating the superposed epoch analysis using restricted data sets demonstrates that this technique can provide a timely prediction of the arrival of CIRs at least 1 day ahead of their arrival at Earth and that such advanced warning can be provided from a spacecraft placed 40° ahead of Earth in its orbit.

A comparison of space weather analysis techniques used to predict the arrival of the Earth-directed CME and its shockwave launched on 8 April 2010

Davis, C. J.; de Koning, C. A.; Davies, J. A.; Biesecker, D.; Millward, G.; Dryer, M.; Deehr, C.; Webb, D. F.; Schenk, K.; Freeland, S. L.; MJKstl, C.; Farrugia, C. J.; Odstrcil, D.

Space Weather, Vol. 9, No. 1, S01005, 2011, **File**

The Earth-directed coronal mass ejection (CME) of **8 April 2010** provided an opportunity for space weather predictions from both established and developmental techniques to be made from near-real time data received from the SOHO and STEREO spacecraft; the STEREO spacecraft provide a unique view of Earth-directed events from outside the Sun-Earth line. Although the near-real time data transmitted by the STEREO Space Weather Beacon are significantly poorer in quality than the subsequently downlinked science data, the use of these data has the advantage that near-real time analysis is possible, allowing actual forecasts to be made. The fact that such forecasts cannot be biased by any prior knowledge of the actual arrival time at Earth provides an opportunity for an unbiased comparison between several established and developmental forecasting techniques. We conclude that for forecasts based on the STEREO coronagraph data, it is important to take account of the subsequent acceleration/deceleration of each CME through interaction with the solar wind, while predictions based on measurements of CMEs made by the STEREO Heliospheric Imagers would benefit from higher temporal and spatial resolution. Space weather forecasting tools must work with near-real time data; such data, when provided by science missions, is usually highly compressed and/or reduced in temporal/spatial resolution and may also have significant gaps in coverage, making such forecasts more challenging.

Assessing the Accuracy of CME Speed and Trajectory Estimates from STEREO Observations Through a Comparison of Independent Methods

C.J. **Davis** · J. Kennedy · J.A. Davies

Solar Phys (2010) 263: 209–222, DOI 10.1007/s11207-010-9535-2; **File**

We have estimated the speed and direction of propagation of a number of Coronal Mass Ejections (CMEs) using single-spacecraft data from the STEREO Heliospheric Imager (HI) wide-field cameras. In general, these values are in good agreement with those predicted by Thernisien, Vourlidis, and Howard in *Solar Phys.* **256**, 111 – 130 (2009) using a forward modelling method to fit CMEs imaged by the STEREO COR2 coronagraphs. The directions of the CMEs predicted by both techniques are in good agreement despite the fact that many of the CMEs under study travel in directions that cause them to fade rapidly in the HI images. The velocities estimated from both techniques are in general agreement although there are some interesting differences that may provide evidence for the influence of the ambient solar wind on the speed of CMEs. The majority of CMEs with a velocity estimated to be below 400 km s⁻¹ in the COR2 field of view have higher estimated velocities in the HI field of view, while, conversely, those with COR2 velocities estimated to be above 400 km s⁻¹ have lower estimated HI velocities. We interpret this as evidence for the deceleration of fast CMEs and the acceleration of slower CMEs by interaction with the ambient solar wind beyond the COR2 field of view. We also show that the uncertainties in our derived parameters are influenced by the range of elongations over which each CME can be tracked. In order to reduce the uncertainty in the predicted arrival time of a CME at 1 Astronomical Unit (AU) to within six hours, the CME needs to be tracked out to at least 30 degrees elongation. This is in good agreement with predictions of the accuracy of our technique based on Monte Carlo simulations.

Within the set of studied CMEs, there are two clear events that were predicted from the HI data to travel over another spacecraft; *in-situ* measurements at these other spacecraft confirm the accuracy of these predictions. The ability of the HI cameras to image Corotating Interaction Region (CIR)-entrained transients as well as CMEs can result in some ambiguity when trying to distinguishing individual signatures.

In-Situ Multi-Spacecraft and Remote Imaging Observations of the First CME Detected by Solar Orbiter and BepiColombo

E. E. [Davies](#) (1), [C. Möstl](#) (2 and 3), [M. J. Owens](#) (4), [A. J. Weiss](#) (2 and 3), [T. Amerstorfer](#) (2), [J. Hinterreiter](#) (2 and 5), [M. Bauer](#) (2), [R. L. Bailey](#) (6), [M. A. Reiss](#) (2 and 3), [R. J. Forsyth](#) (1), [T. S. Horbury](#) (1), [H. O'Brien](#) (1), [V. Evans](#) (1), [V. Angelini](#) (1), [D. Heyner](#) (7), [I. Richter](#) (7), [H-U. Auster](#) (7), [W. Magnes](#) (2), [W. Baumjohann](#) (2), [D. Fischer](#) (2), [D. Barnes](#) (8), [J. A. Davies](#) (8), [R. A. Harrison](#) (8)
A&A 2020

<https://arxiv.org/pdf/2012.07456.pdf>

On April 19th 2020 a CME was detected in-situ by Solar Orbiter at a heliocentric distance of about 0.8 AU. The CME was later observed in-situ on April 20th by the Wind and BepiColombo spacecraft whilst BepiColombo was located very close to Earth. This CME presents a good opportunity for a triple radial alignment study, as the spacecraft were separated by less than 5° in longitude. The source of the CME, which was launched on April 15th, was an almost entirely isolated streamer blowout. STEREO-A observed the event remotely from -75.1° longitude: an exceptionally well suited viewpoint for heliospheric imaging of an Earth directed CME. The configuration of the four spacecraft has provided an exceptionally clean link between remote imaging and in-situ observations of the CME. We have used the in-situ observations of the CME at Solar Orbiter, Wind and BepiColombo, and the remote observations of the CME at STEREO-A in combination with flux rope models to determine the global shape of the CME and its evolution as it propagated through the inner heliosphere. A clear flattening of the CME cross-section has been observed by STEREO-A, and further confirmed by comparing profiles of the flux rope models to the in-situ data, where the distorted flux rope cross-section qualitatively agrees most with in-situ observations of the magnetic field at Solar Orbiter. Comparing in-situ observations of the magnetic field between spacecraft, we find that the dependence of the maximum (mean) magnetic field strength decreases with heliocentric distance as $r^{-1.22 \pm 0.42}$ ($r^{-1.10 \pm 0.20}$), in disagreement with previous studies. Further assessment of the axial and poloidal magnetic field strength dependencies suggests that the expansion of the CME is likely neither self-similar nor cylindrically symmetric. **15-21 Apr 2020**

A synoptic view of solar transient evolution in the inner heliosphere using the Heliospheric Imagers on STEREO

[Davies](#), J. A.; [Harrison](#), R. A.; [Rouillard](#), A. P.; [Sheeley](#), N. R.; [Perry](#), C. H.; [Bewsher](#), D.; [Davis](#), C. J.; [Eyles](#), C. J.; [Crothers](#), S. R.; [Brown](#), D. S.

Geophysical Research Letters, Volume 36, Issue 2, CiteID L02102, **2009**

By exploiting data from the STEREO/heliospheric imagers (HI) we extend a well-established technique developed for coronal analysis by producing time-elongation plots that reveal the nature of solar transient activity over a far more extensive region of the heliosphere than previously possible from coronagraph images. Despite the simplicity of these plots, their power in demonstrating how the plethora of ascending coronal features observed near the Sun evolve as they move antisunward is obvious. The time-elongation profile of a transient tracked by HI can, moreover, be used to establish its angle out of the plane-of-the-sky an illustration of such analysis reveals coronal mass ejection material that can be clearly observed propagating out to distances beyond 1AU. This work confirms the value of the time-elongation format in identifying/characterising transient activity in the inner heliosphere, whilst also validating the ability of HI to continuously monitor solar ejecta out to and beyond 1AU.

Polytropic behavior in the structures of Interplanetary Coronal Mass Ejections

Maher A [Dayeh](#), [George Livadiotis](#)

2022 *ApJL* **941** L26

<https://arxiv.org/ftp/arxiv/papers/2209/2209.12988.pdf>

<https://iopscience.iop.org/article/10.3847/2041-8213/aca673/pdf>

The polytropic process characterizes the thermodynamics of space plasma particle populations. The polytropic index, γ , is particularly important as it describes the thermodynamic behavior of the system by quantifying the changes in temperature as the system is compressed or expanded. Using Wind spacecraft plasma and magnetic field data during 01/1995–12/2018, we investigate the thermodynamic evolution in 336 Interplanetary Coronal Mass Ejection (ICME) events. For each event, we derive the index γ in the sheath and magnetic ejecta structures, along with the pre- and post- event regions. We then examine the distributions of all γ indices in these four regions and derive the entropic gradient of each, which is indicative of the ambient heating. We find that in the ICME sheath region, where wave turbulence is expected to be highest, the thermodynamics takes longest to recover into the original quasi-adiabatic process, while it recovers faster in the quieter ejecta region. This pattern creates a thermodynamic cycle, featuring a near adiabatic value $\gamma \sim \gamma_a$ ($=5/3$) upstream of the ICMEs, $\gamma_a - \gamma \sim 0.26$ in the sheaths, $\gamma_a - \gamma \sim 0.13$ in the ICME ejecta, and recovers again to $\gamma \sim \gamma_a$ after the passage of the ICME. These results expose the turbulent heating rates in the ICME

plasma: the lower the polytropic index from its adiabatic value and closer to its isothermal value, the larger the entropic gradient, and thus, the rate of turbulent heating that heats the ICME plasma.

The Highly Structured Outer Solar Corona

C. E. [DeForest](#)¹, R. A. Howard², M. Velli³, N. Viall⁴, and A. Vourlidas

2018 ApJ 862 18

<http://iopscience.iop.org/article/10.3847/1538-4357/aac8e3/pdf>

We report on the observation of fine-scale structure in the outer corona at solar maximum, using deep-exposure campaign data from the Solar Terrestrial Relations Observatory-A (STEREO-A)/COR2 coronagraph coupled with postprocessing to further reduce noise and thereby improve effective spatial resolution. The processed images reveal radial structure with high density contrast at all observable scales down to the optical limit of the instrument, giving the corona a "woodgrain" appearance. Inferred density varies by an order of magnitude on spatial scales of 50 Mm and follows an f^{-1} spatial spectrum. The variations belie the notion of a smooth outer corona. They are inconsistent with a well-defined "Alfvén surface," indicating instead a more nuanced "Alfvén zone"—a broad trans-Alfvénic region rather than a simple boundary. Intermittent compact structures are also present at all observable scales, forming a size spectrum with the familiar "Sheeley blobs" at the large-scale end. We use these structures to track overall flow and acceleration, finding that it is highly inhomogeneous and accelerates gradually out to the limit of the COR2 field of view. Lagged autocorrelation of the corona has an enigmatic dip around $10 R_{\odot}$, perhaps pointing to new phenomena near this altitude. These results point toward a highly complex outer corona with far more structure and local dynamics than has been apparent. We discuss the impact of these results on solar and solar-wind physics and what future studies and measurements are necessary to build upon them.

FADING CORONAL STRUCTURE AND THE ONSET OF TURBULENCE IN THE YOUNG SOLAR WIND

C. E. [DeForest](#)¹, W. H. Matthaeus², N. M. Viall³, and S. R. Cranmer⁴

2016 ApJ 828 66

Above the top of the solar corona, the young, slow solar wind transitions from low- β , magnetically structured flow dominated by radial structures to high- β , less structured flow dominated by hydrodynamics. This transition, long inferred via theory, is readily apparent in the sky region close to 10° from the Sun in processed, background-subtracted solar wind images. We present image sequences collected by the inner Heliospheric Imager instrument on board the Solar-Terrestrial Relations Observatory (STEREO/HI1) in 2008 December, covering apparent distances from approximately 4° to 24° from the center of the Sun and spanning this transition in the large-scale morphology of the wind. We describe the observation and novel techniques to extract evolving image structure from the images, and we use those data and techniques to present and quantify the clear textural shift in the apparent structure of the corona and solar wind in this altitude range. We demonstrate that the change in apparent texture is due both to anomalous fading of the radial striae that characterize the corona and to anomalous relative brightening of locally dense puffs of solar wind that we term "flocculae." We show that these phenomena are inconsistent with smooth radial flow, but consistent with the onset of hydrodynamic or magnetohydrodynamic instabilities leading to a turbulent cascade in the young solar wind. See Wendel, J. (2016), Scientists get first glimpse of solar wind as it forms, *Eos*, 97, doi:10.1029/2016EO059053. Published on 09 September 2016.

TRACKING CORONAL FEATURES FROM THE LOW CORONA TO EARTH: A QUANTITATIVE ANALYSIS OF THE 2008 DECEMBER 12 CORONAL MASS EJECTION

C. E. [DeForest](#)¹, T. A. Howard¹, and D. J. McComas

2013 ApJ 769 43, [File](#)

We have tracked a slow magnetic cloud associated coronal mass ejection (CME) continuously from its origin as a flux rope structure in the low solar corona over a four-day passage to impact with spacecraft located near Earth. Combining measurements from the STEREO, ACE, and Wind space missions, we are able to follow major elements with enough specificity to relate pre-CME coronal structure in the low corona to the corresponding elements seen in the near-Earth in situ data. Combining extreme ultraviolet imaging, quantitative Thomson scattering data throughout the flight of the CME, and "ground-truth" in situ measurements, we: (1) identify the plasma observed by ACE and Wind with specific features in the solar corona (a segment of a long flux rope); (2) determine the onset mechanism of the CME (destabilization of a filament channel following flare reconnection, coupled with the mass draining instability) and demonstrate that it is consistent with the in situ measurements; (3) identify the origin of different layers of the sheath material around the central magnetic cloud (closed field lifted from the base of the corona, closed field entrained during passage through the corona, and solar wind entrained by the front of the CME); (4) measure mass accretion of the system via snowplow effects in the solar wind as the CME crossed the solar system; and (5) quantify the kinetic energy

budget of the system in interplanetary space, and determine that it is consistent with no long-term driving force on the CME. **2008 December 12**

DISCONNECTING OPEN SOLAR MAGNETIC FLUX

C. E. DeForest¹, T. A. Howard¹, and D. J. McComas^{1,2}

Astrophysical Journal, 745:36 (9pp), **2012**

http://www.boulder.swri.edu/~howard/Papers/2012_Disconnection.pdf - **File**

Disconnection of open magnetic flux by reconnection is required to balance the injection of open flux by coronal mass ejections and other eruptive events. Making use of recent advances in heliospheric background subtraction, we have imaged many abrupt disconnection events. These events produce dense plasma clouds whose distinctive shape can now be traced from the corona across the inner solar system via heliospheric imaging. The morphology of each initial event is characteristic of magnetic reconnection across a current sheet, and the newly disconnected flux takes the form of a "U"-shaped loop that moves outward, accreting coronal and solar wind material. We analyzed one such event on 2008 December 18 as it formed and accelerated at 20 m s^{-2} to 320 km s^{-1} , thereafter expanding self-similarly until it exited our field of view 1.2 AU from the Sun. From acceleration and photometric mass estimates we derive the coronal magnetic field strength to be $8 \mu\text{T}$, $6R_{\odot}$ above the photosphere, and the entrained flux to be $1.6 \times 10^{11} \text{ Wb}$ ($1.6 \times 10^{19} \text{ Mx}$). We model the feature's propagation by balancing inferred magnetic tension force against accretion drag. This model is consistent with the feature's behavior and accepted solar wind parameters. By counting events over a 36 day window, we estimate a global event rate of 1 day^{-1} and a global solar minimum unsigned flux disconnection rate of $6 \times 10^{13} \text{ Wb yr}^{-1}$ ($6 \times 10^{21} \text{ Mx yr}^{-1}$) by this mechanism. That rate corresponds to $\sim -0.2 \text{ nT yr}^{-1}$ change in the radial heliospheric field at 1 AU, indicating that the mechanism is important to the heliospheric flux balance.

OBSERVATIONS OF DETAILED STRUCTURE IN THE SOLAR WIND AT 1 AU WITH STEREO/HI-2

C. E. DeForest¹, T. A. Howard¹ and S. J. Tappin

2011 ApJ 738 103

We present images of solar wind electron density structures at distances of 1 AU, extracted from the STEREO/HI-2 data. Collecting the images requires separating the Thomson-scattered signal from the other background/foreground sources that are 103 times brighter. Using a combination of techniques, we are able to generate calibrated imaging data of the solar wind with sensitivity of a few $\times 10^{-17} \text{ B}$, compared to the background signal of a few $\times 10^{-13} \text{ B}$, using only the STEREO/HI-2 Level 1 data as input. These images reveal detailed spatial structure in coronal mass ejections (CMEs) and the solar wind at projected solar distances in excess of 1 AU, at the instrumental motion-blur resolution limit of 1° - 3° . CME features visible in the newly reprocessed data from 2008 December include leading-edge pileup, interior voids, filamentary structure, and rear cusps. "Quiet" solar wind features include V-shaped structures centered on the heliospheric current sheet, plasmoids, and "puffs" that correspond to the density fluctuations observed in situ. We compare many of these structures with in situ features detected near 1 AU. The reprocessed data demonstrate that it is possible to perform detailed structural analyses of heliospheric features with visible light imagery, at distances from the Sun of at least 1 AU.

Interplanetary shock wave extent in the inner heliosphere as observed by multiple spacecraft

A. de Lucasa, , R. Schwennb, , A. dal Lagoa, , E. Marschb and A.L. Clúa de Gonzalez

Journal of Atmospheric and Solar-Terrestrial Physics, Volume 73, Issue 10, **2011**, Pages 1281-1292

For over an entire solar cycle, from the end of 1974 until the beginning of 1986, the twin Helios spacecraft explored the inner heliosphere. These in situ, high-resolution plasma and magnetic field measurements covered heliocentric distances between 0.3 and 1 AU from the Sun and are of particular interest to studies of space weather phenomena. During this period the two spacecraft detected 395 ICME-driven shocks and these waves were found to be driven by interplanetary coronal mass ejections (ICMEs). Based on these multi-spacecraft measurements, which include a third vantage point with the observations from ISEE-3/IMP-8, the longitudinal extent of the shock waves were measured in the inner heliosphere. It was found that shock waves have about a 50% chance to be observed by two different locations separated by 90° . In practice, one can expect with about a 50% chance that the shock driven by a limb coronal mass ejections (CMEs) will hit the Earth, considering the expansion in longitude of shock waves driven by their associated ICMEs. For

a larger separation the uncertainty increases, as only a few cases could be observed. With the absence of simultaneous solar disk observations one can then no longer unequivocally identify the shock waves observed at each spacecraft.

Research highlights

► Shock waves can extend to large longitudinal angles. ► A limb CME driven shock has about 50% chance to hit the Earth. ► A significant number of single-spacecraft observations were found for small angular distances between the observations locations.

See **Proceedings of the International Astronomical Union (2008), 4: 481-487, 2009**

<http://journals.cambridge.org/action/displayIssue?iid=4866212>

On the Differences in the Ambient Solar Wind Speed Forecasting Caused by Using Synoptic Maps from Different Observatories

M. L. [Demidov](#), [Y. Hanaoka](#), [X. F. Wang](#) & [P. N. Kirichkov](#)

[Solar Physics](#) volume 298, Article number: 120 (2023)

We consider the problem of forecasting the solar wind speed using not only well-known magnetic field data sets, such as the Wilcox Solar Observatory (WSO) and the Global Oscillations Network Group (GONG) but others, such as the Infrared Magnetograph (IRmag) at the National Astronomical Observatory of Japan and the Solar Telescope for Operative Prediction (STOP) in Russia. We use these observations to study Carrington rotation (CR) 2164 (21 May – 17 June 2015). Our initial calculations are based on the Wang-Sheeley-Argé (WSA) model and include determining the coronal magnetic field using the potential field source surface (PFSS) approximation. The speed of the ambient solar wind near the Sun is calculated using an empirical equation that considers the flux tube expansion factor (FTEF) and the distance of the flux tube footpoint from the coronal hole boundary (DCHB) at the photospheric level. The solar wind bulk speed at the Earth's orbit is calculated using the Heliospheric Upwind eXtrapolation (HUX) model. It is shown that the discrepancies in the speed values from four different data sets could reach $\approx 200 \text{ km s}^{-1}$, which is significant. We compare our predictions with in situ data from the Advance Composition Explorer (ACE) and demonstrate that a better coincidence between calculated and empirical results, accounting for the magnetic field strength in coronal holes, can be achieved.

Contribution of the aging effect to the observed asymmetry of interplanetary magnetic clouds

P. [Démoulin](#) (1 and 2), [S. Dasso](#) (3 and 4), [V. Lanabere](#) (4), [M. Janvier](#) (5), [C. Noël](#)

A&A 639, A6 2020

<https://arxiv.org/pdf/2005.05049.pdf>

<https://www.aanda.org/articles/aa/pdf/2020/07/aa38077-20.pdf>

Large magnetic structures are launched away from the Sun during solar eruptions. They are observed as (interplanetary) coronal mass ejections (ICMEs or CMEs) with coronal and heliospheric imagers. A fraction of them are observed in situ as magnetic clouds (MCs). Fitting these structures properly with a model requires a better understanding of their evolution. In situ measurements are done locally when the spacecraft trajectory crosses the magnetic configuration. These observations are taken for different elements of plasma and at different times, and are therefore biased by the expansion of the magnetic configuration. This aging effect leads to stronger magnetic fields measured at the front than at the rear of MCs, an asymmetry often present in MC data. However, can the observed asymmetry be explained quantitatively only from the expansion? Based on self-similar expansion, we derive a method to estimate the expansion rate from observed plasma velocity. We next correct for the aging effect both the observed magnetic field and the spatial coordinate along the spacecraft trajectory. This provides corrected data as if the MC internal structure was observed at the same time. We apply the method to 90 best observed MCs near Earth (1995-2012). The aging effect is the main source of the observed magnetic asymmetry only for 28% of MCs. After correcting the aging effect, the asymmetry is almost symmetrically distributed between MCs with a stronger magnetic field at the front and those at the rear of MCs. The proposed method can efficiently remove the aging bias within in situ data of MCs, and more generally of ICMEs. This allows one to analyse the data with a spatial coordinate, such as in models or remote sensing observations.

Re-analysis of Lepping's Fitting Method for Magnetic Clouds: Lundquist Fit Reloaded

Pascal [Démoulin](#), [Sergio Dasso](#), [Miho Janvier](#) & [Vanina Lanabere](#)

[Solar Physics](#) volume 294, Article number: 172 (2019)

<https://link.springer.com/content/pdf/10.1007/s11207-019-1564-x.pdf>

<https://arxiv.org/pdf/1912.09829.pdf>

http://www.lesia.obspm.fr/perso/pascal-demoulin/19/Demoulin19_Lundquist_reload.pdf

Magnetic clouds (MCs) are a subset of ejecta, launched from the Sun as coronal mass ejections. The coherent rotation of the magnetic field vector observed in MCs leads to envision MCs as formed by flux ropes (FRs). Among all the methods

used to analyze MCs, Lepping's method (Lepping, Burlaga, and Jones in *J. Geophys. Res.* 95, 11957, [1990](#)) is the broadest used. While this fitting method does not require the axial field component to vanish at the MC boundaries, this idea is largely spread in publications. We revisit Lepping's method to emphasize its hypothesis and the meaning of its output parameters. As originally defined, these parameters imply a fitted FR which could be smaller or larger than the studied MC. We rather provide a re-interpretation of Lepping's results with a fitted model limited to the observed MC interval. We find that typically the crossed FRs are asymmetric with a larger side both in size and magnetic flux before or after the FR axis. At the boundary of the largest side we find an axial magnetic field component distributed around zero which we justify by the physics of solar eruptions. In contrast, at the boundary of the smaller side the axial field distribution is shifted to positive values, as expected with erosion acting during the interplanetary travel. This new analysis of Lepping's results has several implications. First, global quantities, such as magnetic fluxes and helicity, need to be revised depending on the aim (estimating global properties of FRs just after the solar launch or at 1 au). Second, the deduced twist profiles in MCs range quasi-continuously from nearly uniform, to increasing away from the FR axis, up to a reversal near the MC boundaries. There is no trace of outsider cases, but a continuum of cases. Finally, the impact parameter of the remaining FR crossed at 1 au is revised. Its distribution is compatible with weakly flattened FR cross-sections.

Magnetic Flux and Helicity of Magnetic Clouds

Demoulin P., Janvier M., Dasso S.

A&A

2018

<http://arxiv.org/pdf/1509.01068v1.pdf>

Context. Magnetic clouds (MCs) are formed by flux ropes (FRs) launched from the Sun as part of coronal mass ejections (CMEs). They carry away an important amount of magnetic flux and helicity. Aims. The main aim of this study is to quantify these quantities from in situ measurements of MCs at 1 AU.

Methods. The fit of these data by a local FR model provides the axial magnetic field strength, the radius, the magnetic flux and the helicity per unit length along the FR axis. Results. We show that these quantities are statistically independent of the position along the FR axis. We then derive the generic shape and length of the FR axis from two sets of MCs. These results improve the estimation of magnetic helicity. Next, we evaluate the total magnetic flux and helicity crossing the sphere of radius of 1 AU, centered at the Sun, per year and during a solar cycle. We also include in the study two sets of small FRs which do not have all the typical characteristics of MCs. Conclusions. While small FRs are at least ten times more numerous than MCs, the magnetic flux and helicity are dominated by the contribution from the larger MCs. They carry in one year the magnetic flux of about 25 large active regions and the magnetic helicity of 200 of them. MCs carry away an amount of unsigned magnetic helicity comparable to the one estimated for the solar dynamo and the one measured in emerging active regions. **Note:** This article will be published in *Solar Physics* but is set in the A&A format because of LaTeX compilation problem with SP style.

Exploring the biases of a new method based on minimum variance for interplanetary magnetic clouds

Pascal Démoulin, Sergio Dasso, Miho Janvier

A&A

2018

<https://arxiv.org/pdf/1809.00522.pdf>

http://www.lesia.obspm.fr/perso/pascal-demoulin/18/Demoulin18_mv_flux_balance.pdf

Context. Magnetic clouds (MCs) are twisted magnetic structures ejected from the Sun and probed by in situ instruments. They are typically modeled as flux ropes (FRs).

Aims. Magnetic field measurements are only available along the 1D spacecraft trajectory. The determination of the FR global characteristics requires the estimation of the FR axis orientation. Among the developed methods, the minimum variance (MV) is the most flexible, and features only a few assumptions. However, as other methods, MV has biases. We aim to investigate the limits of the method and extend it to a less biased method.

Methods. We first identified the origin of the biases by testing the MV method on cylindrical and elliptical models with a temporal expansion comparable to the one observed in MCs. Then, we developed an improved MV method to reduce these biases.

Results. In contrast with many previous publications we find that the ratio of the MV eigenvalues is not a reliable indicator of the precision of the derived FR axis direction. Next, we emphasize the importance of the FR boundaries selected since they strongly affect the deduced axis orientation. We have improved the MV method by imposing that the same amount of azimuthal flux should be present before and after the time of closest approach to the FR axis. We emphasize the importance of finding simultaneously the FR axis direction and the location of the boundaries corresponding to a balanced magnetic flux, so as to minimize the bias on the deduced FR axis orientation. This method

can also define an inner flux-balanced sub-FR. We show that the MV results are much less biased when a compromise in size of this sub-FR is achieved.

Conclusions. For weakly asymmetric field temporal profiles, the improved MV provides a very good determination of the FR axis orientation. The main remaining bias is moderate (lower than 6°) and is present mostly on the angle between the flux rope axis and the plane perpendicular to the Sun-Earth direction.

Quantitative model for the generic 3D shape of ICMEs at 1 AU

P. **Demoulin**, M. Janvier, J.J. Masias-Meza and S. Dasso

A&A 595, A19 2016

<http://arxiv.org/abs/1608.08550>

Interplanetary imagers provide 2D projected views of the densest plasma parts of interplanetary coronal mass ejections (ICMEs), while in situ measurements provide magnetic field and plasma parameter measurements along the spacecraft trajectory, that is, along a 1D cut. The data therefore only give a partial view of the 3D structures of ICMEs. By studying a large number of ICMEs, crossed at different distances from their apex, we develop statistical methods to obtain a quantitative generic 3D shape of ICMEs. In a first approach we theoretically obtained the expected statistical distribution of the shock-normal orientation from assuming simple models of 3D shock shapes, including distorted profiles, and compared their compatibility with observed distributions. In a second approach we used the shock normal and the flux rope axis orientations together with the impact parameter to provide statistical information across the spacecraft trajectory. The study of different 3D shock models shows that the observations are compatible with a shock that is symmetric around the Sun-apex line as well as with an asymmetry up to an aspect ratio of around 3. Moreover, flat or dipped shock surfaces near their apex can only be rare cases. Next, the sheath thickness and the ICME velocity have no global trend along the ICME front. Finally, regrouping all these new results and those of our previous articles, we provide a quantitative ICME generic 3D shape, including the global shape of the shock, the sheath, and the flux rope. The obtained quantitative generic ICME shape will have implications for several aims. For example, it constrains the output of typical ICME numerical simulations. It is also a base for studying the transport of high-energy solar and cosmic particles during an ICME propagation as well as for modeling and forecasting space weather conditions near Earth.

Magnetic Flux and Helicity of Magnetic Clouds

Demoulin P., Janvier M., Dasso S.

Solar Phys. Vol. 291, Issue 2 2015

http://www.lesia.obspm.fr/perso/pascal-demoulin/15/demoulin15_helicity_MCs.pdf

<http://arxiv.org/pdf/1509.01068v1.pdf>

Note: This article will be published in Solar Physics but is set in the A&A format because of LaTeX compilation problem with SP style.

Magnetic clouds (MCs) are formed by flux ropes (FRs) launched from the Sun as part of coronal mass ejections (CMEs). They carry away an important amount of magnetic flux and helicity. The main aim of this study is to quantify these quantities from in situ measurements of MCs at 1 AU. The fit of these data by a local FR model provides the axial magnetic field strength, the radius, the magnetic flux and the helicity per unit length along the FR axis. We show that these quantities are statistically independent of the position along the FR axis. We then derive the generic shape and length of the FR axis from two sets of MCs. These results improve the estimation of magnetic helicity. Next, we evaluate the total magnetic flux and helicity crossing the sphere of radius of 1 AU, centered at the Sun, per year and during a solar cycle. We also include in the study two sets of small FRs which do not have all the typical characteristics of MCs. While small FRs are at least ten times more numerous than MCs, the magnetic flux and helicity are dominated by the contribution from the larger MCs. They carry in one year the magnetic flux of about 25 large active regions and the magnetic helicity of 200 of them. MCs carry away an amount of unsigned magnetic helicity comparable to the one estimated for the solar dynamo and the one measured in emerging active regions.

Evolution of interplanetary coronal mass ejections and magnetic clouds in the heliosphere

Review

Demoulin, P.

E-print, Sept 2013, **File**; IAU S300 proceedings; IAUS, 300, 245-254 (2014)

Interplanetary Coronal Mass Ejections (ICMEs), and more specifically Magnetic clouds (MCs), are detected with in situ plasma and magnetic measurements. They are the continuation of the CMEs observed with imagers closer to the Sun. A

review of their properties is presented with a focus on their magnetic configuration and its evolution. Many recent observations, both in situ and with imagers, point to a key role of flux ropes, a conclusion which is also supported by present coronal eruptive models. Then, is a flux rope generically present in an ICME? How to quantify its 3D physical properties when it is detected locally as a MC? Is it a simple flux rope? How does it evolve in the solar wind? This paper reviews our present answers and limited understanding to these questions.

Does the spacecraft trajectory strongly affect the detection of magnetic clouds?

Demoulin, P., Dasso, S., Janvier, M.

E-print, Dec **2012**, A&A, 550, A3 (**2013**)

Magnetic clouds (MCs) are a subset of interplanetary coronal mass ejections (ICMEs) where a magnetic flux rope is detected. Is the difference between MCs and ICMEs without detected flux rope intrinsic or rather due to an observational bias? As the spacecraft has no relationship with the MC trajectory, the frequency distribution of MCs versus the spacecraft distance to the MCs axis is expected to be approximately flat. However, Lepping and Wu (2010) confirmed that it is a strongly decreasing function of the estimated impact parameter. Is a flux rope more frequently undetected for larger impact parameter? In order to answer the questions above, we explore the parameter space of flux rope models, especially the aspect ratio, boundary shape, and current distribution. The proposed models are analyzed as MCs by fitting a circular linear force-free field to the magnetic field computed along simulated crossings. We find that the distribution of the twist within the flux rope, the non-detection due to too low field rotation angle or magnitude are only weakly affecting the expected frequency distribution of MCs versus impact parameter. However, the estimated impact parameter is increasingly biased to lower values as the flux-rope cross section is more elongated orthogonally to the crossing trajectory. The observed distribution of MCs is a natural consequence of a flux-rope cross section flattened in average by a factor 2 to 3 depending on the magnetic twist profile. However, the faster MCs at 1 AU, with $V > 550$ km/s, present an almost uniform distribution of MCs vs. impact parameter, which is consistent with round shaped flux ropes, in contrast with the slower ones. We conclude that either most of the non-MC ICMEs are encountered outside their flux rope or near the leg region, or they do not contain any.

Interaction of ICMEs with the Solar Wind (Review)

Demoulin P.

E-print, Sept **2009**, SW12 proceedings; **File**

Interplanetary Coronal Mass Ejections (ICMEs) are formed of plasma and magnetic field launched from the Sun into the Solar Wind (SW). These coherent magnetic structures, frequently formed by a flux rope, interact strongly with the SW. Such interaction is reviewed by comparing the results obtained from in situ observations and with numerical simulations. Like fast ships in the ocean, fast ICMEs drive an extended shock in front. However, their interaction with the SW is much more complex than that of the ship analogy. For example, as they expand in all directions while traveling away from the Sun, a sheath of SW plasma and magnetic field accumulates in front, which partially reconnects with the ICME magnetic field. Furthermore, not only ICMEs have a profound impact on the heliosphere, but the type of SW encountered by an ICME has an important impact on its evolution (e.g. increase of mass, global deceleration, lost of magnetic flux and helicity, distortion of the configuration).

Magnetic cloud models with bent and oblate cross-section boundary

Demoulin P., Dasso S.

E-print, Sept **2009**; A&A 507, 969-980 (**2009**); **File**

Magnetic clouds (MCs) are formed by magnetic flux ropes that are ejected from the Sun as coronal mass ejections. These structures generally have low plasma beta and travel through the interplanetary medium interacting with the surrounding solar wind (SW). Thus, the dynamical evolution of the internal magnetic structure of a MC is a consequence of both the conditions of its environment and of its own dynamical laws, which are mainly dominated by magnetic forces. With in-situ observations the magnetic field is only measured along the trajectory of the spacecraft across the MC. Therefore, a magnetic model is needed to reconstruct the magnetic configuration of the encountered MC. The main aim of the present work is to extend the widely used cylindrical model to arbitrary cross-section shapes. The flux rope boundary is parametrized to account for a broad range of shapes. Then, the internal structure of the flux rope is computed by expressing the magnetic field as a series of modes of a linear force-free field. We analyze the magnetic field profile along straight cuts through the flux rope, in order to simulate the spacecraft crossing through a MC. We find that the magnetic field orientation is only weakly affected by the shape of the MC boundary. Therefore, the MC axis can

approximately be found by the typical methods previously used (e.g., minimum variance). The boundary shape affects mostly the magnetic field strength. The measure of how much the field strength peaks along the crossing provides an estimation for the aspect ratio of the flux-rope cross-section. The asymmetry of the field strength between the front and the back of the MC, after correcting the time evolution (i.e., its aging during the observation of the MC), provides an estimation of the cross-section global bending. A flat or/and bent cross-section requires a large anisotropy of the total pressure imposed at the MC boundary by the surrounding medium. The new theoretical model developed here relaxes the cylindrical symmetry hypothesis. It is designed to estimate the cross-section shape of the flux rope using the in-situ data of one spacecraft. This allows a more accurate determination of the global quantities, such as magnetic fluxes and helicity. These quantities are especially important for both linking an observed MC to its solar source and for understanding the corresponding evolution.

Why Temperature and Velocity have Different Relationships in the Solar Wind and in Interplanetary Coronal Mass Ejections?

P. **Démoulin**¹

E-print, April **2009**; Solar Phys., 257(1), 169 – 184, DOI: 10.1007/s11207-009-9338-5

In-situ observations of the solar wind (SW) show temperature increasing with the wind speed, while such dependence is not observed in interplanetary coronal mass ejections (ICMEs). The aim of this paper is to understand the main origin of this correlation in the SW and its absence in ICMEs. For that purpose both the internal-energy and momentum equations are solved analytically with various approximations. The internal-energy equation does not provide a strong link between temperature and velocity, but the momentum equation does. Indeed, the observed correlation in the open magnetic-field configuration of the SW is the result of its acceleration and heating close to the Sun. In contrast, the magnetic configuration of ICMEs is closed, and moreover the momentum equation is dominated by magnetic forces. It implies no significant correlation between temperature and velocity, as observed.

Causes and consequences of magnetic cloud expansion

P. **Démoulin**¹ and S. Dasso

E-print, March **2009**; A&A, 498, 551–566 (**2009**), DOI: [10.1051/0004-6361/200810971](https://doi.org/10.1051/0004-6361/200810971)

Context. A magnetic cloud (MC) is a magnetic flux rope in the solar wind (SW), which, at 1 AU, is observed \sim 2-5 days after its expulsion from the Sun. The associated solar eruption is observed as a coronal mass ejection (CME).

Aims. Both the in situ observations of plasma velocity distribution and the increase in their size with solar distance demonstrate that MCs are strongly expanding structures. The aim of this work is to find the main causes of this expansion and to derive a model to explain the plasma velocity profiles typically observed inside MCs.

Methods. We model the flux rope evolution as a series of force-free field states with two extreme limits: (a) ideal magnetohydrodynamics (MHD) and (b) minimization of the magnetic energy with conserved magnetic helicity. We consider cylindrical flux ropes to reduce the problem to the integration of ordinary differential equations. This allows us to explore a wide variety of magnetic fields at a broad range of distances to the Sun.

Results. We demonstrate that the rapid decrease in the total SW pressure with solar distance is the main driver of the flux-rope radial expansion. Other effects, such as the internal over-pressure, the radial distribution, and the amount of twist within the flux rope have a much weaker influence on the expansion. We demonstrate that any force-free flux rope will have a self-similar expansion if its total boundary pressure evolves as the inverse of its length to the fourth power. With the total pressure gradient observed in the SW, the radial expansion of flux ropes is close to self-similar with a nearly linear radial velocity profile across the flux rope, as observed. Moreover, we show that the expansion rate is proportional to the radius and to the global velocity away from the Sun.

Conclusions. The simple and universal law found for the radial expansion of flux ropes in the SW predicts the typical size, magnetic structure, and radial velocity of MCs at various solar distances.

Expected *in Situ* Velocities from a Hierarchical Model for Expanding Interplanetary Coronal Mass Ejections

P. **Démoulin** · M.S. Nakwacki · S. Dasso · C.H. Mandrini

Solar Phys (**2008**) 250: 347–374

<http://springerlink.metapress.com/content/e334866jk04n4047/fulltext.pdf>

In situ data provide only a one-dimensional sample of the plasma velocity along the spacecraft trajectory crossing an interplanetary coronal mass ejection (ICME). Then, to understand the dynamics of ICMEs it is necessary to consider some

models to describe it. We derive a series of equations in a hierarchical order, from more general to more specific cases, to provide a general theoretical basis for the interpretation of in situ observations, extending and generalizing previous studies. The main hypothesis is a self-similar expansion, but with the freedom of possible different expansion rates in three orthogonal directions.

Quantitative links between CMEs and magnetic clouds

P. Démoulin

E-print, Sept. 2007, *Ann. Geophys.*, **2008**, 26, 3113, **File**

Magnetic clouds (MCs), and more generally interplanetary coronal mass ejections (ICMEs), are believed to be the interplanetary counterparts of CMEs. The link has usually been shown by taking into account the CME launch position on the Sun, the expected time delay and by comparing the orientation of the coronal and interplanetary magnetic field. Making such a link more quantitative is challenging since it requires the relation of very different kinds of magnetic field measurements: (i) photospheric magnetic maps, which are observed from a distant vantage point (remote sensing) and (ii) in situ measurements of MCs, which provide precise, directly measured, magnetic field data merely from one-dimensional linear samples. The association between events in these different domains can be made using adequate coronal and MC models. Then, global quantities like magnetic fluxes and helicity can be derived and compared. All the associations criteria are reviewed, with a description of the general trends found. A special focus is given on the cases which do not follow the earlier derived mean laws since interesting physics is usually associated to them.

Recent theoretical and observational developments in magnetic helicity studies

Adv. Space Res. 39(11), *Pages 1674-1693*, **2007**

Review

P. Démoulin

Magnetic helicity quantifies how the magnetic field is sheared and twisted compared to its lowest energy state (potential field). Such stressed magnetic fields are usually observed in association with flares, eruptive filaments, and coronal mass ejections (CMEs). Magnetic helicity plays a key role in magnetohydrodynamics because it is almost preserved on a timescale less than the global diffusion time scale. Its conservation defines a constraint to the magnetic field evolution.

Only relatively recently, scientists have realized that magnetic helicity can be computed from observations, and methods have been derived to bridge the gap between theory and observations. At the photospheric level, the rate (or flux) of magnetic helicity can be computed from the evolution of longitudinal magnetograms. The coronal helicity is estimated from magnetic extrapolation, while the helicity ejected in magnetic clouds (interplanetary counter-part of CMEs) is derived through modelling of in situ magnetic field measurements. Using its conserved property, a quantitative link between phenomena observed in the corona and then in the interplanetary medium has been achieved.

Magnetosphere response to high-speed solar wind streams: A comparison of weak and strong driving and the importance of extended periods of fast solar wind.

Denton MH, Borovsky JE
(2012) *JGRA* 117:A00L05

Geomagnetic storms driven by ICME- and CIR-dominated solar wind.

Denton MH, Borovsky JE, Skoug RM, Thomsen MF, Lavraud B, Henderson M, McPherron, RL, Zhang JC, Liemohn MW
(2006) *JGRA* 111:7

Suprathermal Ion Energy spectra and Anisotropies near the Heliospheric Current Sheet crossing observed by the Parker Solar Probe during Encounter 7

M. I. **Desai**, **D. G. Mitchell**, **D. J. McComas**, **J. F. Drake**, **T. Phan**, **J. R. Szalay**, ...
2021

<https://arxiv.org/ftp/arxiv/papers/2111/2111.00954.pdf>

We present observations of >10-100 keV/nucleon suprathermal (ST) H, He, O, and Fe ions associated with crossings of the heliospheric current sheet (HCS) at radial distances <0.1 au from the Sun. Our key findings are: 1) very few heavy ions are detected during the 1st full crossing, the heavy ion intensities are reduced during the 2nd partial crossing and peak just after the 2nd crossing; 2) ion arrival times exhibit no velocity dispersion; 3) He pitch-angle distributions track the magnetic field polarity reversal and show up to ~10:1 anti-sunward, field-aligned flows and beams closer to the HCS

that become nearly isotropic further from the HCS; 4) the He spectrum steepens either side of the HCS and the He, O, and Fe spectra exhibit power-laws of the form $\sim E^{-4-6}$; and 5) maximum energies EX increase with the ion's charge-to-mass (Q/M) ratio as EX/EH proportional to $[(QX/MX)]^\alpha$ where $\alpha \sim 0.65-0.76$, assuming that the average Q-states are similar to those measured in gradual and impulsive solar energetic particle events at 1 au. The absence of velocity dispersion in combination with strong field-aligned anisotropies closer to the HCS appears to rule out solar flares and near-sun coronal mass ejection-driven shocks. These new observations present challenges not only for mechanisms that employ direct parallel electric fields and organize maximum energies according to E/Q, but also for local diffusive and magnetic reconnection-driven acceleration models. Re-evaluation of our current understanding of the production and transport of energetic ions is necessary to understand this near-solar, current-sheet-associated population of ST ions. **2021 Jan 17**

Three Dimensional Simulations of Solar Wind Preconditioning and the 23 July 2012 Interplanetary Coronal Mass Ejection

Ravindra T. [Desai](#), [Han Zhang](#), [Emma E. Davies](#), [Julia E. Stawarz](#), [Joan Mico-Gomez](#), [Pilar Iváñez-Ballesteros](#)

Solar Phys. **295**, Article number: 130 **2020**

<https://arxiv.org/pdf/2009.02392.pdf>

<https://link.springer.com/content/pdf/10.1007/s11207-020-01700-5.pdf>

Predicting the large-scale eruptions from the solar corona and their propagation through interplanetary space remains an outstanding challenge in solar- and helio-physics research. In this article, we describe three dimensional magnetohydrodynamic simulations of the inner heliosphere leading up to and including the extreme interplanetary coronal mass ejection (ICME) of 23 July 2012, developed using the code PLUTO. The simulations are driven using the output of coronal models for Carrington rotations 2125 and 2126 and, given the uncertainties in the initial conditions, are able to reproduce an event of comparable magnitude to the **23 July** ICME, with similar velocity and density profiles at 1 au. The launch-time of this event is then varied with regards to an initial **19 July** ICME and the effects of solar wind preconditioning are found to be significant for an event of this magnitude and to decrease over a time-window consistent with the ballistic refilling of the depleted heliospheric sector. These results indicate that the 23 July ICME was mostly unaffected by events prior, but would have travelled even faster had it erupted closer in time to the 19 July event where it would have experienced even lower drag forces. We discuss this systematic study of solar wind preconditioning in the context of space weather forecasting.

MULTI-SCALE STRUCTURE AND COMPOSITION OF ICME PROMINENCE MATERIAL FROM THE SOLAR WIND ANALYSER SUITE

Ryan M. [Dewey](#)¹, Susan T. Lepri¹, Stefano Livi^{1,2}, Christopher J. Owen³, Philippe Louarn⁴, Raffaella D'Amicis⁵, and the Solar Orbiter/SWA team

Solar Orbiter nugget #4 **2023** <https://www.cosmos.esa.int/web/solar-orbiter/science-nuggets/multi-scale-structure-and-composition-of-icme-prominence-material-from-the-solar-wind-analyser-suite>

31 Oct-6 Nov 2021

Switchbacks in the near-Sun magnetic field: long memory and impact on the turbulence cascade

Thierry Dudok [de Wit](#), [Vladimir V. Krasnoselskikh](#), [Stuart D. Bale](#), [John W. Bonnell](#), [Trevor A. Bowen](#), [Christopher H. K. Chen](#), [Clara Froment](#), [Keith Goetz](#), [Peter R. Harvey](#), [Vamsee Krishna Jagarlamudi](#), [Andrea Larosa](#), [Robert J. MacDowall](#), [David M. Malaspina](#), [William H. Matthaeus](#), [Marc Pulupa](#), [Marco Velli](#), [Phyllis L. Whittlesey](#)

ApJS **2020**

<https://arxiv.org/pdf/1912.02856.pdf>

One of the most striking observations made by Parker Solar Probe during its first solar encounter is the omnipresence of rapid polarity reversals in a magnetic field that is otherwise mostly radial. These so-called switchbacks strongly affect the dynamics of the magnetic field. We concentrate here on their macroscopic properties. First, we find that these structures are self-similar, and have neither a characteristic magnitude, nor a characteristic duration. Their waiting time statistics shows evidence for aggregation. The associated long memory resides in their occurrence rate, and is not inherent to the background fluctuations. Interestingly, the spectral properties of inertial range turbulence differ inside and outside of switchback structures; in the latter the $1/f$ range extends to higher frequencies. These results suggest that

outside of these structures we are in the presence of lower amplitude fluctuations with a shorter turbulent inertial range. We conjecture that these correspond to a pristine solar wind.

In Situ Observation of Alfvén Waves in an ICME Shock-Sheath Indicating the Existence of Alfvénic Turbulence.

Dhamane, O., Raghav, A., Shaikh, Z. et al.

Sol Phys 299, 29 (2024).

<https://doi.org/10.1007/s11207-024-02271-5>

<https://link.springer.com/content/pdf/10.1007/s11207-024-02271-5.pdf>

The dynamic evolution of a coronal mass ejection (CME) in the interplanetary space generates a highly turbulent, compressed, and heated shock-sheath. This region provides an exceptional setting for investigating the intricate fluctuations occurring at small scales and offers a valuable opportunity to unravel the underlying physical processes responsible for turbulence dissipation and plasma heating. Understanding the role of turbulence in controlling the energy transport process in a magnetized plasma, within space and astrophysics, remains an enticing challenge of the twenty-first century. In this article, we study sheath regions observed by the Wind spacecraft from 1995 to 2021. We find 80 sheath events out of the studied 384 events that show a significant Alfvénic nature ($\approx 21\%$). These fluctuations are interpreted as Alfvénic wave packets propagating either parallel or antiparallel to the background magnetic field, quantified by the normalized crosshelicity (σ_{\diamond}). We find 47 sheath events with outward-propagating Alfvénic fluctuations and 33 events with inward Alfvénic characteristics. The Alfvénic sheaths had a mean value of $\sigma_{\diamond} = 0.46 \pm 0.03$ and -0.43 ± 0.02 for outward- and inward-directed Alfvénic sheaths, respectively. Furthermore, we compare the average interplanetary parameter values of both the Alfvénic sheaths and the ambient solar wind. The study has strong implications in the domain of interplanetary space plasmas, its interaction with planetary plasmas, and astrophysical plasmas.

Observation of Alfvén Ion Cyclotron Waves in ICME Magnetic Clouds at 1 au

Omkar **Dhamane**¹, Vinit Pawaskar¹, Anil Raghav¹, Zubair Shaikh ⁺⁺⁺

2023 ApJ 957 38

<https://iopscience.iop.org/article/10.3847/1538-4357/acf19f/pdf>

Waves in plasma play an essential role in the energy transfer and plasma-heating processes. This article discusses the in situ observation of Alfvén ion cyclotron (AIC) waves and their characteristics within interplanetary coronal mass ejection (ICME) flux ropes. We analyzed 401 ICME flux ropes, observed by WIND spacecraft from 1995 to 2021 at 1 au. We found only five ICME flux ropes that show an explicit presence of AIC waves; two have normalized magnetic helicity $\sigma_m \leq -0.5$, and the remaining three show $\sigma_m \geq 0.5$ polarization. The angle between velocity and magnetic field (θ_{VB}) for $\sigma_m \leq -0.5$ is $< 40^\circ$, whereas for $\sigma_m \geq 0.5$, $\theta_{VB} > 140^\circ$. This result supports the existence of quasi-parallel and quasi-antiparallel left-handed polarized AIC waves within ICME flux ropes. We suggest that AIC waves are possibly triggered by (i) proton temperature anisotropy $T_{p\perp}/T_{p\parallel} > 1$ driven by cyclotron instability and (ii) low-frequency Alfvén waves through the magnetohydrodynamic turbulent cascade. This study shows evidence of fluid and kinetic scales coupling in the ICME flux rope.

Observation of Alfvén wave in ICME-HSS interaction region

Omkar **Dhamane**, [Anil Raghav](#), [Zubair Shaikh](#), [Utsav Panchal](#), [Kalpesh Ghag](#), [Prathmesh Tari](#), [Komal Chorgha](#), [Ankush Bhaskar](#), [Wageesh Mishra](#)

Solar Physics volume 298, Article number: 34 (2023)

<https://arxiv.org/pdf/2209.04682.pdf>

<https://doi.org/10.1007/s11207-023-02127-4>

The Alfvén wave (AW) is the most common fluctuation present within the emitted solar wind from the Sun. Moreover, the interaction between interplanetary coronal mass ejection (ICME) and high-speed stream (HSS) has been observed on several occasions. However, can such interaction generate an AW? What will be the nature of AW in such a scenario remains an open question. To answer it, we have investigated an ICME-HSS interaction event observed on **21st October 1999** at 1 AU by Wind spacecraft. We have used the Walén test to identify AW and estimated Elsasser variables to find the characteristics of the AWs. We explicitly find that ICME were dominant with Sunward AWs, whereas the trailing HSS has strong anti-Sunward AW. We suggest that the ICME-HSS interaction deforms the MC of the ICME, resulting in the AWs inside the MC. In addition, the existence of reconnection within the ICME early stage can also be the leading cause of the origin of AW within it.

Deep learning reconstruction of sunspot vector magnetic fields for forecasting solar storms

Dattaraj B. [Dhuri](#), [Shamik Bhattacharjee](#), [Shravan M. Hanasoge](#), [Sashi Kiran Mahapatra](#)
ApJ **2022**

<https://arxiv.org/pdf/2209.09944.pdf>

Solar magnetic activity produces extreme solar flares and coronal mass ejections, which pose grave threats to electronic infrastructure and can significantly disrupt economic activity. It is therefore important to appreciate the triggers of explosive solar activity and develop reliable space-weather forecasting. Photospheric vector-magnetic-field data capture sunspot magnetic-field complexity and can therefore improve the quality of space-weather prediction. However, state-of-the-art vector-field observations are consistently only available from Solar Dynamics Observatory/Heliioseismic and Magnetic Imager (SDO/HMI) since 2010, with most other current and past missions and observational facilities such as Global Oscillations Network Group (GONG) only recording line-of-sight (LOS) fields. Here, using an inception-based convolutional neural network, we reconstruct HMI sunspot vector-field features from LOS magnetograms of HMI as well as GONG with high fidelity (~ 90% correlation) and sustained flare-forecasting accuracy. We rebuild vector-field features during the 2003 Halloween storms, for which only LOS-field observations are available, and the CNN-estimated electric-current-helicity accurately captures the observed rotation of the associated sunspot prior to the extreme flares, showing a striking increase. Our study thus paves the way for reconstructing three solar cycles worth of vector-field data from past LOS measurements, which are of great utility in improving space-weather forecasting models and gaining new insights about solar activity. **2003-10-26-31**

Backstreaming ions at a high Mach number interplanetary shock Solar Orbiter measurements during the nominal mission phase

A. P. [Dimmock](#)¹, M. Gedalin², A. Lalti^{1,3}, D. Trotta⁴, Yu. V. Khotyaintsev¹, D. B. Graham¹, A. Johlander^{5,1}, R. Vainio⁶, X. Blanco-Cano⁷, P. Kajdič⁷, C. J. Owen⁸ and R. F. Wimmer-Schweingruber⁹
A&A 679, A106 (**2023**)

<https://www.aanda.org/articles/aa/pdf/2023/11/aa47006-23.pdf>

Context. Solar Orbiter, a mission developed by the European Space Agency, explores in situ plasma across the inner heliosphere while providing remote-sensing observations of the Sun. The mission aims to study the solar wind, but also transient structures such as interplanetary coronal mass ejections and stream interaction regions. These structures often contain a leading shock wave that can differ from other plasma shock waves, such as those around planets. Importantly, the Mach number of these interplanetary shocks is typically low (1–3) compared to planetary bow shocks and most astrophysical shocks. However, our shock survey revealed that on **30 October 2021**, Solar Orbiter measured a shock with an Alfvén Mach number above 6, which can be considered high in this context.

Aims. Our study examines particle observations for the **30 October 2021** shock. The particles provide clear evidence of ion reflection up to several minutes upstream of the shock. Additionally, the magnetic and electric field observations contain complex electromagnetic structures near the shock, and we aim to investigate how they are connected to ion dynamics. The main goal of this study is to advance our understanding of the complex coupling between particles and the shock structure in high Mach number regimes of interplanetary shocks.

Methods. We used observations of magnetic and electric fields, probe-spacecraft potential, and thermal and energetic particles to characterize the structure of the shock front and particle dynamics. Furthermore, ion velocity distribution functions were used to study reflected ions and their coupling to the shock. To determine shock parameters and study waves, we used several methods, including cold plasma theory, singular-value decomposition, minimum variance analysis, and shock Rankine-Hugoniot relations. To support the analysis and interpretation of the experimental data, test-particle analysis, and hybrid particle in-cell simulations were used.

Results. The ion velocity distribution functions show clear evidence of particle reflection in the form of backstreaming ions several minutes upstream. The shock structure has complex features at the ramp and whistler precursors. The backstreaming ions may be modulated by the complex shock structure, and the whistler waves are likely driven by gyrating ions in the foot. Supra-thermal ions up to 20 keV were observed, but shock-accelerated particles with energies above this were not.

Modeling the Geomagnetic Response to the September 2017 Space Weather Event Over Fennoscandia Using the Space Weather Modeling Framework: Studying the Impacts of Spatial Resolution

A. P. [Dimmock](#), [D. T. Welling](#), [L. Rosenqvist](#), [C. Forsyth](#), [M. P. Freeman](#), [I. J. Rae](#), [A. Viljanen](#), [E. Vandegriff](#), [R. J. Boynton](#), [M. A. Balikhin](#), [E. Yordanova](#)

Space Weather [Volume19, Issue5](#) May **2021** e2020SW002683

<https://agupubs.onlinelibrary.wiley.com/doi/epdf/10.1029/2020SW002683>

<https://doi.org/10.1029/2020SW002683>

We must be able to predict and mitigate against geomagnetically induced current (GIC) effects to minimize socio-economic impacts. This study employs the space weather modeling framework (SWMF) to model the geomagnetic response over Fennoscandia to the September 7–8, 2017 event. Of key importance to this study is the effects of spatial resolution in terms of regional forecasts and improved GIC modeling results. Therefore, we ran the model at comparatively low, medium, and high spatial resolutions. The virtual magnetometers from each model run are compared with observations from the IMAGE magnetometer network across various latitudes and over regional-scales. The virtual magnetometer data from the SWMF are coupled with a local ground conductivity model which is used to calculate the geoelectric field and estimate GICs in a Finnish natural gas pipeline. This investigation has led to several important results in which higher resolution yielded: (1) more realistic amplitudes and timings of GICs, (2) higher amplitude geomagnetic disturbances across latitudes, and (3) increased regional variations in terms of differences between stations. Despite this, substorms remain a significant challenge to surface magnetic field prediction from global magnetohydrodynamic modeling. For example, in the presence of multiple large substorms, the associated large-amplitude depressions were not captured, which caused the largest model-data deviations. The results from this work are of key importance to both modelers and space weather operators. Particularly when the goal is to obtain improved regional forecasts of geomagnetic disturbances and/or more realistic estimates of the geoelectric field. **7-8 Sep 2017**

Anomalous dynamics of the extremely compressed magnetosphere during 21 January 2005 magnetic storm

A. V. **Dmitriev**, A. V. Suvorova, J.-K. Chao, C. B. Wang, L. Rastaetter, M. I. Panasyuk, L. L. Lazutin, A. S. Kovtyukh, I. S. Veselovsky and I. N. Myagkova

JGR, Volume 119, Issue 2, pages 877–896, February **2014**

The dayside magnetosphere and proton radiation belt were analyzed during unusual magnetic storm on **21 January 2005**. We have found that from 1712 to 2400 UT, the subsolar magnetopause was continuously located inside geosynchronous orbit due to strong compression. The compression was extremely strong from 1846 to 2035 UT when the dense plasma of fast erupting filament produced the solar wind dynamic pressure that peaked up to > 100 nPa, and during the first time, the upstream solar wind was observed at geosynchronous orbit for almost 2 h. Under the extreme compression, the outer magnetosphere at $L > 5$ was pushed inward, and the outer radiation belt particles moved earthward, became adiabatically accelerated, and accumulated in the inner magnetosphere at $L < 4$ that produced the intensified ring current with an exceptionally long lifetime. The observations were compared with predictions of various empirical and first-principles models. All the models failed to predict the magnetospheric dynamics under the extreme compression when the minimal magnetopause distance was estimated to be ~ 3 RE. The inconsistencies might result from distortions of plasma measurements by extreme heliospheric conditions consisting in very fast solar wind streams and intense fluxes of solar energetic particles. We speculated that anomalous dynamics of the magnetosphere could be well described by the models if the He abundance in the solar wind was assumed to be $> 20\%$, which is well appropriate for erupting filaments and which is in agreement with the upper 27% threshold for the He/H ratio obtained from Cluster measurements.

Interplanetary sources of space weather disturbances in 1997 to 2000,

Dmitriev, A. V., N. B. Crosby, and J.-K. Chao; **File**

(**2005**), *Space Weather*, 3, S03001, doi:10.1029/2004SW000104.

Seventy-five disturbed intervals from 1997 through 2000 were analyzed and selected on the basis of space weather effect occurrences such as significant compression of the dayside magnetosphere, strong magnetic storms, ionospheric perturbations, relativistic electron enhancements, and increases in the rate of data failures and radiation doses on board the Mir station. Solar wind disturbances were considered as the main factor influencing the Earth's magnetosphere. We distinguished four geoeffective interplanetary (IP) phenomena: interplanetary coronal mass ejections (ICME), interplanetary forward shocks with compressed region (IS), fast solar wind streams from coronal holes (CH), and corotating interaction regions (CIR) between the CH and relatively slow ambient solar wind. Each selected interval was studied and classified under the IP phenomena that it was a direct consequence of. It was found that IP phenomena “containing” ISs, ICMEs, and CIRs were mostly responsible for geosynchronous magnetopause crossings, strong geomagnetic storms, and intensification of geomagnetically induced currents. The fast solar wind streams from coronal holes controlled mainly geosynchronous relativistic electron enhancements. The rate of data failures and variations of the radiation dose on board the Mir station were related to both IS-ICME and CIR-CH phenomena. Such a relationship was interpreted in terms of (1) decrease of cutoff

threshold for solar energetic particles due to the magnetospheric compression and/or ring current intensification on the main phase of geomagnetic storms and (2) intensive relativistic electron precipitation from the outer radiation belt and its contribution to the radiation conditions at low altitudes during recovery phase of recurrent magnetic storms.

Mapping the solar wind HI outflow velocity in the inner heliosphere by coronagraphic ultraviolet and visible-light observations★

S. [Dolei](#)¹, R. Susino², C. Sasso³, A. Bemporad², V. Andretta³, D. Spadaro¹, R. Ventura², E. Antonucci², L. Abbo², V. Da Deppo⁴, S. Fineschi², M. Focardi⁵, F. Frassetto⁴, S. Giordano², F. Landini⁵, G. Naletto^{6,4}, G. Nicolini², P. Nicolosi⁷, M. Pancrazzi⁵, M. Romoli⁸ and D. Telloni²
A&A 612, A84 (2018)

<http://sci-hub.tw/https://www.aanda.org/articles/aa/abs/2018/04/aa32118-17/aa32118-17.html>

We investigated the capability of mapping the solar wind outflow velocity of neutral hydrogen atoms by using synergistic visible-light and ultraviolet observations. We used polarised brightness images acquired by the LASCO/SOHO and Mk3/MLSO coronagraphs, and synoptic Ly α line observations of the UVCS/SOHO spectrometer to obtain daily maps of solar wind H I outflow velocity between 1.5 and 4.0 R \odot on the SOHO plane of the sky during a complete solar rotation (from 1997 June 1 to 1997 June 28). The 28-days data sequence allows us to construct coronal off-limb Carrington maps of the resulting velocities at different heliocentric distances to investigate the space and time evolution of the outflowing solar plasma. In addition, we performed a parameter space exploration in order to study the dependence of the derived outflow velocities on the physical quantities characterising the Ly α emitting process in the corona. Our results are important in anticipation of the future science with the Metis instrument, selected to be part of the Solar Orbiter scientific payload. It was conceived to carry out near-sun coronagraphy, performing for the first time simultaneous imaging in polarised visible-light and ultraviolet H I Ly α line, so providing an unprecedented view of the solar wind acceleration region in the inner corona.

A Machine Learning and Computer Vision Approach to Geomagnetic Storm Forecasting

Kyle [Domico](#), [Ryan Sheatsley](#), [Yohan Beugin](#), [Quinn Burke](#), [Patrick McDaniel](#)

Presented at ML-Helio 2022

<https://arxiv.org/pdf/2204.05780.pdf>

Geomagnetic storms, disturbances of Earth's magnetosphere caused by masses of charged particles being emitted from the Sun, are an uncontrollable threat to modern technology. Notably, they have the potential to damage satellites and cause instability in power grids on Earth, among other disasters. They result from high sun activity, which are induced from cool areas on the Sun known as sunspots. Forecasting the storms to prevent disasters requires an understanding of how and when they will occur. However, current prediction methods at the National Oceanic and Atmospheric Administration (NOAA) are limited in that they depend on expensive solar wind spacecraft and a global-scale magnetometer sensor network. In this paper, we introduce a novel machine learning and computer vision approach to accurately forecast geomagnetic storms without the need of such costly physical measurements. Our approach extracts features from images of the Sun to establish correlations between sunspots and geomagnetic storm classification and is competitive with NOAA's predictions. Indeed, our prediction achieves a 76% storm classification accuracy. This paper serves as an existence proof that machine learning and computer vision techniques provide an effective means for augmenting and improving existing geomagnetic storm forecasting methods.

Space weather and dangerous phenomena on the Earth: principles of great geomagnetic storms forecasting by online cosmic ray data

L. I. [Dorman](#)

ANGEOS - Volume 23, Number 9, 2005, Page(s) 2997-3002

[Abstract](#) [Full Article](#) (PDF, 700 KB) [Special Issue](#)

Cosmic-ray forecasting features for big forrush decreases

[L.I.Dorman](#)[a](#)[G.Villoresic](#)[A.V.Belova](#)[E.A.Eroshenko](#)[N.Iuccid](#)[V.G.Yanke](#)[K.F.Yudakhina](#)[B.Bavassano](#)[N.G.Ptitsyna](#)[M.I.Tyastoe](#)

[Nuclear Physics B - Proceedings Supplements](#) Volume 39, Issue 1, February 1995, Pages 136-143

It is well known that big geomagnetic storms have an adverse influence on technological devices and radio wave propagation. Major geomagnetic storms, associated with Forbush decreases (FDs) in cosmic ray (CR) intensity, have also been found to increase the incidence of some diseases (in particular, the frequency of myocardial infarction increases by $13 \pm 1.4\%$). We discuss here three phenomena that can be used for forecasting FDs: 1) CR intensity

increase, of non solar-flare origin, occurring before sudden commencement of a major geomagnetic storm connected with FD (preincrease effect), 2) CR intensity decrease before FD (predecrease effect), 3) change in CR fluctuations before FD. First we investigate several such events by the global survey method for the years 1989–1991. We analyse the behaviour of the isotropic CR intensity and of the 3-dimensional vector of CR anisotropy before FDs, as well as results on CR scintillation of 1-hour and 5-minute data. We discuss a possible procedure of data treatment for future FD-forecasting analyses.

On 17 and 22 January 2005 Events in Space Weather

Dorotovič, I., Kudela, K., Lorenc, M., & Rybanský, M.

2008a, *Solar Phys.*, 250, 339-346

<https://doi.org/10.1007/s11207-008-9222-8>

<https://link.springer.com/content/pdf/10.1007/s11207-008-9222-8.pdf>

This contribution is a follow-up to the recent paper of Kuznetsov et al. (Contrib. Astron. Obs. Skalnaté Pleso36, 85, 2006) on the ground level enhancement (GLE) on 20 January 2005. We focused on a study of Forbush decrease (FD) of 17 - 18 and 21 - 22 January 2005, respectively. The data from the neutron monitor at Lomnický Štít (1 min counts) and from the Geomagnetic Observatory in Hurbanovo, both in Slovakia, were used as the basis for our investigation. The data on magnetic field and solar wind from GOES 10 and 12, SOHO-CELIAS, ACE and WIND satellites were used for better understanding of the global evolution of the event. The magnetic field is transformed to the RTN (Radial - Tangential - Normal) system where only the disturbed part of the field is compared, i.e., daily variations and a constant part are subtracted. The field reduction method is described. Our results are temporal vector diagrams of variation of all parameters at all positions from where we used the data. The amplitudes of $|B|$ exceed 100 nT and variations during the arrival of the wavefront of CME take place simultaneously at the ground-based station and at GOES satellites. The character of the variations is as if there would be regions with the dominant electric charge of opposite signs, or electric currents with different orientations in the CME. On the basis of the values v_p and n_p and using certain assumptions we determined the mass of CME on 17 January and 21 January, respectively, of 1012 kg. A decrease of the cosmic ray level runs suddenly (during 10 minutes), starting, however, about two hours after a sudden change of the magnetic field.

Magnetic Lasso: A New Kinematic Solar Wind Propagation Method

M. **Dósa**, A. Opitz, Z. Dály, K. Szegő

Solar Physics September 2018, 293:127

<https://link.springer.com/content/pdf/10.1007%2Fs11207-018-1340-3.pdf>

Solar wind propagation from the point of measurement to an arbitrary target in the heliosphere is an important input for heliospheric, planetary and cometary studies. In this paper a new kinematic propagation method, the magnetic lasso method is presented. Compared to the simple ballistic approach our method is based on reconstructing the ideal Parker spiral connecting the target with the Sun by testing a previously defined range of heliographic longitudes. The model takes into account the eventual evolution of stream-stream interactions and handles these with a simple model based on the dynamic pressure difference between the two streams. Special emphasis is given to input data cleaning by handling interplanetary coronal mass ejection events as data gaps due to their different propagation characteristics. The solar wind bulk velocity is considered radial and constant. Density and radial magnetic field are propagated by correcting with the inverse square of the radial distance. The model has the advantage that it can be coded easily and fitted to the problem; it is flexible in selecting and handling input data and requires little running time.

Long-term Longitudinal Recurrences of the Open Magnetic Flux Density in the Heliosphere

M. **Dósa** and G. Erdős

2017 ApJ 838 104

<http://iopscience.iop.org/article/10.3847/1538-4357/aa657b/pdf>

<http://iopscience.iop.org/sci-hub.cc/0004-637X/838/2/104/>

Open magnetic flux in the heliosphere is determined from the radial component of the magnetic field vector measured onboard interplanetary space probes. Previous Ulysses research has shown remarkable independence of the flux density from heliographic latitude, explained by super-radial expansion of plasma. Here we are investigating whether any longitudinal variation exists in the 50 year long OMNI magnetic data set. The heliographic longitude of origin of the plasma package was determined by applying a correction according to the solar wind travel time. Significant recurrent enhancements of the magnetic flux density were observed throughout solar cycle 23, lasting for several years. Similar, long-lasting recurring features were observed in the solar wind velocity, temperature and the deviation angle of the solar

wind velocity vector from the radial direction. Each of the recurrent features has a recurrence period slightly differing from the Carrington rotation rate, although they show a common trend in time. Examining the coronal temperature data of ACE leads to the possible explanation that these long-term structures are caused by slow-fast solar wind interaction regions. A comparison with MESSENGER data measured at 0.5 au shows that these longitudinal magnetic modulations do not exist closer to the Sun, but are the result of propagation.

Are switchbacks signatures of magnetic flux ropes generated by interchange reconnection in the corona?

J. F. [Drake](#), [O. Agapitov](#), [M. Swisdak](#), [S. T. Badman](#), [S. D. Bale](#), [T. S. Horbury](#), [Justin C. Kasper](#), [R. J. MacDowall](#), [F. S. Mozer](#), [T. D. Phan](#), [M. Pulupa](#), [A. Szabo](#), [M. Velli](#)

A&A **2020**

<https://arxiv.org/pdf/2009.05645.pdf>

The structure of magnetic flux ropes injected into the solar wind during reconnection in the coronal atmosphere is explored with particle-in-cell simulations and compared with *in situ* measurements of magnetic "switchbacks" from the Parker Solar Probe. We suggest that multi-x-line reconnection between open and closed flux in the corona will inject flux ropes into the solar wind and that these flux ropes can convect outward over long distances before disintegrating. Simulations that explore the magnetic structure of flux ropes in the solar wind reproduce key features of the "switchback" observations: a rapid rotation of the radial magnetic field into the transverse direction (a consequence of reconnection with a strong guide field); and the potential to reverse the radial field component. The potential implication of the injection of large numbers of flux ropes in the coronal atmosphere for understanding the generation of the solar wind is discussed. **Nov. 5, 2018**

Efficiency of particle acceleration at interplanetary shocks: Statistical study of STEREO observations

N. [Dresing](#), S. Theesen, A. Klassen and B. Heber

A&A 588, A17 (2016)

<https://www.aanda.org/articles/aa/pdf/2016/04/aa27853-15.pdf>

doi:10.1051/0004-6361/201527853

Context. Among others, shocks are known to be accelerators of energetic charged particles. However, many questions regarding the acceleration efficiency and the required conditions are not fully understood. In particular, the acceleration of electrons by shocks is often questioned.

Aims. In this study we determine the efficiency of interplanetary shocks for <100 keV electrons, and for ions at ~0.1 and ~2 MeV energies, as measured by the Solar Electron and Proton Telescope (SEPT) instruments aboard the twin Solar Terrestrial Relations Observatory (STEREO) spacecraft.

Methods. We employ an online STEREO *in situ* shock catalog that lists all shocks observed between 2007 and mid 2014 (observed by STEREO A) and until end of 2013 (observed by STEREO B). In total 475 shocks are listed. To determine the particle acceleration efficiency of these shocks, we analyze the associated intensity increases (shock spikes) during the shock crossings. For the near-relativistic electrons, we take into account the issue of possible ion contamination in the SEPT instrument.

Results. The highest acceleration efficiency is found for low energy ions (0.1 MeV), which show a shock-associated increase at 27% of all shocks. The 2 MeV ions show an associated increase only during 5% of the shock crossings. In the case of the electrons, the shocks are nearly ineffective. Only five shock-associated electron increases were found, which correspond to only 1% of all shock crossings.

Injection of solar energetic particles into both loop legs of a magnetic cloud

Nina [Dresing](#), Raquel Gómez-Herrero, Bernd Heber, Miguel Angel Hidalgo, Andreas Klassen, Manuela Temmer, Astrid Veronig

A&A **2016**

<http://arxiv.org/pdf/1601.00491v1.pdf>

Context. Each of the two Solar Terrestrial Relations Observatory (STEREO) spacecraft carries a Solar Electron and Proton Telescope (SEPT) which measures electrons and protons. Anisotropy observations are provided in four viewing directions: along the nominal magnetic field Parker spiral in the ecliptic towards the Sun (SUN) and away from the Sun (Anti-Sun / ASUN), and towards the north (NORTH) and south (SOUTH). The solar energetic particle (SEP) event on 7 November 2013 was observed by both STEREO spacecraft, which were longitudinally separated by 68° at that time. While STEREO A observed the expected characteristics of an SEP event at a well-connected position, STEREO B

detected a very anisotropic bi-directional distribution of near-relativistic electrons and was situated inside a magnetic-cloud-like structure during the early phase of the event.

Aims. We examine the source of the bi-directional SEP distribution at STEREO B. On the one hand this distribution could be caused by a double injection into both loop legs of the magnetic cloud (MC). On the other hand, a mirroring scenario where the incident beam is reflected in the opposite loop leg could be the reason. Furthermore, the energetic electron observations are used to probe the magnetic structure inside the magnetic cloud.

Methods. We investigate in situ plasma and magnetic field observations and show that STEREO B was embedded in an MC-like structure ejected three days earlier on **4 November** from the same active region. We apply a Graduated Cylindrical Shell (GCS) model to the coronagraph observations from three viewpoints as well as the Global Magnetic Cloud (GMC) model to the in situ measurements at STEREO B to determine the orientation and topology of the MC close to the Sun and at 1 AU. We also estimate the path lengths of the electrons propagating through the MC to estimate the amount of magnetic field line winding inside the structure.

Results. The relative intensity and timing of the energetic electron increases in the different SEPT telescopes at STEREO B strongly suggest that the bi-directional electron distribution is formed by SEP injections in both loop legs of the MC separately instead of by mirroring farther away beyond the STEREO orbit. Observations by the Nancay Hadioheliograph (NRH) of two distinct radio sources during the SEP injection further support the above scenario. The determined electron path lengths are around 50% longer than the estimated lengths of the loop legs of the MC itself (based on the GCS model) suggesting that the amount of field line winding is moderate.

The correlation between solar and geomagnetic activity – Part 3: An integral response model

Z. L. Du

Ann. Geophys., 29, 1005-1018, 2011

An integral response model is proposed to describe the relationship between geomagnetic activity (aa index) and solar activity (represented by sunspot number R_z): The aa at a given time t is the integral of R_z at past times ($t' \leq t$) multiplied by an exponential decay factor of the time differences ($e^{-(t-t')/\tau}$), where τ is the decay time scale (~40 months). The correlation coefficient of aa with the reconstructed series based on this model ($r_f=0.85$) is much higher than that of aa with R_z ($r_0=0.61$). If this model is applied to each solar cycle, the correlation coefficient will be higher ($r_f=0.95$). This model can naturally explain some phenomena related to aa and R_z , such as (i) the significant increase in the aa index (and its baseline) over the twentieth century; (ii) the longer lag times of aa to R_z at solar cycle maxima than at minima; and (iii) the variations in the correlations related to solar and Hale cycles. These results demonstrate that aa depends not only on the present R_z but also on past values. The profile of aa can be better predicted from R_z by this model than by point-point correspondence.

Interplanetary Coronal Mass Ejections Observed by *Ulysses* Through Its Three Solar Orbits

D. Du · P.B. Zuo · X.X. Zhang

Solar Phys (2010) 262: 171–190

<https://sci-hub.ru/10.1007/s11207-009-9505-8>

An extended *Ulysses* interplanetary coronal mass ejections (ICMEs) list is used to statistically study the occurrence rate of ICMEs, the interaction of ICMEs with solar wind, and the magnetic field properties in ICMEs. About 43% of the ICMEs are identified as magnetic clouds (MCs). It is found that the occurrence rate of ICMEs approximately follows the solar activity level, except for the second solar orbit; the rate is higher in the southern heliolatitude than in the northern heliolatitude; and it roughly decreases with the increase of ICME speeds. Our results show that the speed difference between the ICME and the solar wind in front of it shows a slight decrease with increasing heliocentric distance for ICMEs preceded by a shock, whereas no such dependence is found for the ICMEs without shock association. It is also found that approximately 23% of the ICMEs are associated with radial field events, in which the interplanetary magnetic field with near-radial direction lasts for many hours, in the *Ulysses* detected range, and these associated events are not necessarily confined to fast ICMEs or the trailing portions of ICMEs. Nearly all these associated events occur during the period of declining solar wind speed and most of them occur at low heliolatitudes.

Anomalous geomagnetic storm of 21–22 January 2005: a storm main phase during northward IMFs.

Du, A.M., Tsurutani, B.T., Sun, W.,

2008. J. Geophys. Res. 113, A10214. doi:10.1029/2008JA013284.

<https://agupubs.onlinelibrary.wiley.com/doi/epdf/10.1029/2008JA013284>

The major (minimum Dst = -105 nT) magnetic storm which occurred on **21–22 January 2005** is highly anomalous because the storm main phase (identified by the SYM-H indices) developed during northward interplanetary magnetic fields (IMFs). We believe this to be the first event of its type to be reported in the literature. Interplanetary ACE and Cluster C1 data are used for solar wind diagnostics, and LANL 90 and 97, GOES 10 and 12 and GEOTAIL data are used for magnetospheric diagnostics. An unusually strong (magnetosonic Mach number equal to 5.4) shock detected at ~1647 UT, 21 January 2005 by ACE causes a SI+ (of 57 nT) at ~1712 UT at Earth. Southward magnetic fields in the sheath following the shock caused a decrease of SYM-H with a peak value ~-41 nT. A dynamic pressure jump across a double discontinuity in the solar wind at 1823 UT observed by ACE induced a second SI+ (of 25 nT) at 1847 UT at Earth. Southward magnetic fields following this event led to a second SYM-H decrease with peak intensity -2 nT. However, when the storm main phase developed starting at 1946 UT, the IMF Bz turned northward. The IMF was northward from the portion of the main phase from ~1946 UT to 0124 UT (almost 6 h). By comparing solar wind energy input (represented by integrated interplanetary E_y) with accumulated energy in the ring current (represented by integrated SYM-H), we arrive at a possible explanation that there is first energy storage in the magnetotail and then a delayed energy injection (after storage in the magnetotail) into the magnetosphere. Other interpretations/mechanisms are possible.

CME Deflection and East-West Asymmetry of Energetic Storm Particle Intensity during Solar Cycles 23 and 24

A. Santa Fe **Dueñas**^{1,2}, R. W. Ebert^{1,2}, Gang Li³, Zheyi Ding⁴, M. A. Dayeh^{1,2}, M. I. Desai^{1,2}, and L. K. Jian⁵

ApJ **2024**

<https://arxiv.org/pdf/2404.01993.pdf>

We investigate the East-West asymmetry in energetic storm particle (ESP) heavy ion intensities at interplanetary shocks driven by coronal mass ejections (CMEs) during solar cycles (SCs) 23 and 24. We use observations from NASA's ACE and STEREO missions of helium (He), oxygen (O), and iron (Fe) intensities from ~0.13 to 3 MeV/nucleon. We examine the longitudinal distribution of ESP intensities and the correlation of ESP intensities with the near-Sun CME speed and the average transit CME speed for eastern and western events. We observed an East-West asymmetry reversal of ESP heavy ion intensities from SC 23 to 24. We have determined that this change in asymmetry is caused by a shift in the heliolongitude distribution of the CME speed ratio (the ratio of CME near-Sun speed to CME average transit speed) from west to east. **November 10 and 11, 2012**

Comparing Energetic Storm Particle Heavy-ion Properties in Solar Cycles 23 and 24

A. Santa Fe **Dueñas**^{1,2}, R. W. Ebert^{1,2}, M. A. Dayeh^{1,2}, M. I. Desai^{1,2}, L. K. Jian³, and G. Li⁴
2023 ApJ 953 176

<https://iopscience.iop.org/article/10.3847/1538-4357/acdede/pdf>

We examine variations in energetic storm particle (ESP) heavy-ion average intensities and energy spectra between ~0.1 and 75 MeV nucleon⁻¹ at coronal mass ejection (CME)-driven interplanetary shocks for events observed at the ACE spacecraft. We compare ESP events observed during the weaker solar cycle (SC) 24 and the relatively stronger SC 23 to investigate any effects on the strength of an SC, including the associated transient events, on ESP properties at 1 au. We find that the number of clearly defined heavy-ion ESP events at ACE during SC 23 is about twice that observed during SC 24 (76 versus 41). The average transit speed of the driving interplanetary CMEs (ICMEs) at 1 au is 20% higher during SC 23 than during SC 24 (859.4 km s⁻¹ versus 729.1 km s⁻¹). The correlation of ESP average intensities with ICME speeds shows that lower-speed ICMEs in SC 24 can be as efficient as the higher-speed events in SC 23 at producing ESPs below 2 MeV nucleon⁻¹. The distribution and magnitude of the average intensities for energies below ~1 MeV nucleon⁻¹ are consistent between both SCs. However, events with intensity enhancements at higher energies (>~10 MeV nucleon⁻¹) are more frequent and their intensity distributions are harder for SC 23, resulting in an increase in the rollover energy (E₀) for their spectra profiles. This suggests more efficient ESP acceleration at >10 MeV nucleon⁻¹ during SC 23. **2005 September 15**

Table 1. List of ESP Events Used in This Study, Including the Shock Arrival Time, the Average Intensity at 0.1365 MeV nucleon⁻¹, the Spectral Index (γ), and the e-folding Energy (E₀) for He, O, and Fe 1998-2017

Dependence of Energetic Storm Particle Heavy Ion Peak Intensities and Spectra on Source CME Longitude and Speed

A. Santa Fe **Dueñas**^{1,2}, R. W. Ebert^{1,2}, M. A. Dayeh^{1,2}, M. I. Desai^{1,2}, L. K. Jian³, G. Li⁴, and C. W. Smith⁵

2022 ApJ 935 32

<https://iopscience.iop.org/article/10.3847/1538-4357/ac73f5/pdf>

We examine variations in energetic storm particle (ESP) heavy ion peak intensities and energy spectra at CME-driven interplanetary shocks. We focus on their dependence with heliolongitude relative to the source region of their associated CMEs, and with CME speed, for events observed in Solar Cycle 24 at the STEREO-A, STEREO-B, and/or ACE spacecraft. We find that observations of ESP events at 1 au are organized by longitude relative to their CME solar source. The ESP event longitude distribution also showed organization with CME speed. The near-Sun CME speeds (V_i) for these events ranged from ~ 560 to 2650 km s^{-1} while the average CME transit speeds to 1 au were significantly slower. The angular width of the events had a clear threshold at V_i of $\sim 1300 \text{ km s}^{-1}$, above which events showed significantly larger angular extension compared to events with speeds below. High-speed events also showed larger heavy ion peak intensities near the nose of the shock compared to the flanks while their spectral index was smaller near the nose and larger near the flanks. This organization for events with $V_i < 1300 \text{ km s}^{-1}$ was not as clear. These ESP events were observed over a narrower range of longitudes though the heavy ion peak intensities still appeared largest near the nose of the shock. Their heavy ion spectra showed no clear organization with longitude. These observations highlight the impact of spacecraft position relative to the CME source longitude and V_i on the properties of ESP events at 1 au. **28 Nov 2011**

Table 1 List of ESP Events Used in This Study, Including the Shock Arrival Time, Observing Spacecraft (SC), Source Flare Location and the Near-Sun and Average Transit CME Speeds 2011-2018

A new method of measuring Forbush decreases

M. [Dumbovic](#), [L. Kramaric](#), [I. Benko](#), [B. Heber](#), [B. Vrsnak](#)

A&A 683, A168 (2024)

<https://arxiv.org/pdf/2401.09000.pdf>

Forbush decreases (FDs) are short-term depressions in the galactic cosmic ray flux and one of the common signatures of coronal mass ejections (CMEs) in the heliosphere. They often show a two-step profile, the second one associated with the CMEs magnetic structure (flux rope, FR), which can be described by the recently developed model ForbMod. The aim of this study is to utilise ForbMod to develop a best-fit procedure to be applied on FR-related FDs as a convenient measurement tool. We develop a best-fit procedure that can be applied to a data series from an arbitrary detector. Thus, the basic procedure facilitates measurement estimation of the magnitude of the FR-related FD, with the possibility of being adapted for the energy response of a specific detector for a more advanced analysis. The non-linear fitting was performed by calculating all possible ForbMod curves constrained within the FR borders to the designated dataset and minimising the mean square error (MSE). In order to evaluate the performance of the ForbMod best-fit procedure, we used synthetic measurements produced by calculating the theoretical ForbMod curve for a specific example CME and then applying various effects to the data to mimic the imperfection of the real measurements. We also tested the ForbMod best-fit function on the real data, measured by detector F of the SOHO-EPHIN instrument on a sample containing 30 events, all of which have a distinct FD corresponding to the CMEs magnetic structure. Overall, we find that the ForbMod best-fit procedure performs similar to the traditional algorithm-based observational method, but with slightly smaller values for the FD amplitude, as it is taking into account the noise in the data. Furthermore, we find that the best-fit procedure has an advantage compared to the traditional method as it can estimate the FD amplitude even when there is a data gap at the onset of the FD.

Table A.1. Full sample of analysed ICMEs and FDs 2008-2019

Generic profile of a long-lived corotating interaction region and associated recurrent Forbush decrease

M. [Dumbović](#)¹, [B. Vršnak](#)¹, [M. Temmer](#)², [B. Heber](#)³ and [P. Kùhl](#)³

A&A 658, A187 (2022)

<https://www.aanda.org/articles/aa/pdf/2022/02/aa40861-21.pdf>

<https://doi.org/10.1051/0004-6361/202140861>

Context. Corotating interaction regions (CIRs), formed by the interaction of slow solar wind and fast streams that originate from coronal holes (CHs), produce recurrent Forbush decreases, which are short-term depressions in the galactic cosmic ray (GCR) flux.

Aims. Our aim is to prepare a reliable set of CIR measurements to be used as a textbook for modeling efforts. For that purpose, we observe and analyse a long-lived CIR, originating from a single CH, recurring in 27 consecutive Carrington rotations 2057–2083 in the time period from June 2007–May 2009.

Methods. We studied the in situ measurements of this long-lived CIR as well as the corresponding depression in the cosmic ray (CR) count observed by SOHO/EPHIN throughout different rotations. We performed a statistical analysis, as

well as the superposed epoch analysis, using relative values of the key parameters: the total magnetic field strength, B, the magnetic field fluctuations, dBrms, plasma flow speed, v, plasma density, n, plasma temperature, T, and the SOHO/EPHIN F-detector particle count, and CR count.

Results. We find that the mirrored CR count-time profile is correlated with that of the flow speed, ranging from moderate to strong correlation, depending on the rotation. In addition, we find that the CR count dip amplitude is correlated to the peak in the magnetic field and flow speed of the CIR. These results are in agreement with previous statistical studies. Finally, using the superposed epoch analysis, we obtain a generic CIR example, which reflects the in situ properties of a typical CIR well.

Conclusions. Our results are better explained based on the combined convection-diffusion approach of the CIR-related GCR modulation. Furthermore, qualitatively, our results do not differ from those based on different CHs samples. This indicates that the change of the physical properties of the recurring CIR from one rotation to another is not qualitatively different from the change of the physical properties of CIRs originating from different CHs. Finally, the obtained generic CIR example, analyzed on the basis of superposed epoch analysis, can be used as a reference for testing future models.

Table 1. Polarity and characteristic timings of CH-CIR throughout different rotations.2007-2009

Drag-based model (DBM) tools for forecast of coronal mass ejection arrival time and speed

Review

Mateja **Dumbovic**, [Jasa Calogovic](#), [Karmen Martinic](#), [Bojan Vrsnak](#), [Davor Sudar](#), [Manuela Temmer](#), [Astrid Veronig](#)

Frontiers March 24th 2021

<https://arxiv.org/pdf/2103.14292.pdf>

Forecasting the arrival time of CMEs and their associated shocks is one of the key aspects of space weather research. One of the commonly used models is, due to its simplicity and calculation speed, the analytical drag-based model (DBM) for heliospheric propagation of CMEs. DBM relies on the observational fact that slow CMEs accelerate whereas fast CMEs decelerate, and is based on the concept of MHD drag, which acts to adjust the CME speed to the ambient solar wind. Although physically DBM is applicable only to the CME magnetic structure, it is often used as a proxy for the shock arrival. In recent years, the DBM equation has been used in many studies to describe the propagation of CMEs and shocks with different geometries and assumptions. Here we give an overview of the five DBM versions currently available and their respective tools, developed at Hvar Observatory and frequently used by researchers and forecasters. These include: 1) basic 1D DBM, a 1D model describing the propagation of a single point (i.e. the apex of the CME) or concentric arc (where all points propagate identically); 2) advanced 2D self-similar cone DBM, a 2D model which combines basic DBM and cone geometry describing the propagation of the CME leading edge which evolves self-similarly; 3) 2D flattening cone DBM, a 2D model which combines basic DBM and cone geometry describing the propagation of the CME leading edge which does not evolve self-similarly; 4) DBEM, an ensemble version of the 2D flattening cone DBM which uses CME ensembles as an input and 5) DBEMv3, an ensemble version of the 2D flattening cone DBM which creates CME ensembles based on the input uncertainties. All five versions have been tested and published in recent years and are available online or upon request. We provide an overview of these five tools, of their similarities and differences, as well as discuss and demonstrate their application. **April 3rd 2010**

Drag-based model (DBM) tools for forecast of coronal mass ejection arrival time and speed

Review

Mateja **Dumbovic**, [Jasa Calogovic](#), [Karmen Martinic](#), [Bojan Vrsnak](#), [Davor Sudar](#), [Manuela Temmer](#), and [Astrid Veronig](#)

Front. Astron. Space Sci., 8:639986 2021 |

<https://doi.org/10.3389/fspas.2021.639986>

<https://www.frontiersin.org/articles/10.3389/fspas.2021.639986/full>

Forecasting the arrival time of coronal mass ejections (CMEs) and their associated shocks is one of the key aspects of space weather research. One of the commonly used models is the analytical drag-based model (DBM) for heliospheric propagation of CMEs due to its simplicity and calculation speed. The DBM relies on the observational fact that slow CMEs accelerate whereas fast CMEs decelerate and is based on the concept of magnetohydrodynamic (MHD) drag, which acts to adjust the CME speed to the ambient solar wind. Although physically DBM is applicable only to the CME magnetic structure, it is often used as a proxy for shock arrival. In recent years, the DBM equation has been used in many studies to describe the propagation of CMEs and shocks with different geometries and assumptions. In this study, we provide an overview of the five DBM versions currently available and their respective tools, developed at Hvar Observatory and frequently used by researchers and forecasters (1) basic 1D DBM, a 1D model describing the

propagation of a single point (i.e., the apex of the CME) or a concentric arc (where all points propagate identically); (2) advanced 2D self-similar cone DBM, a 2D model which combines basic DBM and cone geometry describing the propagation of the CME leading edge which evolves in a self-similar manner; (3) 2D flattening cone DBM, a 2D model which combines basic DBM and cone geometry describing the propagation of the CME leading edge which does not evolve in a self-similar manner; (4) DBEM, an ensemble version of the 2D flattening cone DBM which uses CME ensembles as an input; and (5) DBEMv3, an ensemble version of the 2D flattening cone DBM which creates CME ensembles based on the input uncertainties. All five versions have been tested and published in recent years and are available online or upon request. We provide an overview of these five tools, as well as of their similarities and differences, and discuss and demonstrate their application. **April 3, 2010**

Evolution of coronal mass ejections and the corresponding Forbush decreases: modelling vs multi-spacecraft observations

Mateja [Dumbović](#), [Bojan Vršnak](#), [Jingnan Guo](#), [Bernd Heber](#), [Karin Dissauer](#), [Fernando Carcaboso](#), [Manuela Temmer](#), [Astrid Veronig](#), [Tatiana Podladchikova](#), [Christian Möstl](#), [Tanja Amerstorfer](#), [Anamarija Kirin](#)
Solar Phys. **295**, Article number: 104 **2020**

<https://arxiv.org/pdf/2006.02253.pdf>

<https://link.springer.com/content/pdf/10.1007/s11207-020-01671-7.pdf>

One of the very common in situ signatures of interplanetary coronal mass ejections (ICMEs), as well as other interplanetary transients, are Forbush decreases (FDs), i.e. short-term reductions in the galactic cosmic ray (GCR) flux. A two-step FD is often regarded as a textbook example, which presumably owes its specific morphology to the fact that the measuring instrument passed through the ICME head-on, encountering first the shock front (if developed), then the sheath and finally the CME magnetic structure. The interaction of GCRs and the shock/sheath region, as well as the CME magnetic structure, occurs all the way from Sun to Earth, therefore, FDs are expected to reflect the evolutionary properties of CMEs and their sheaths. We apply modelling to different ICME regions in order to obtain a generic two-step FD profile, which qualitatively agrees with our current observation-based understanding of FDs. We next adapt the models for energy dependence to enable comparison with different GCR measurement instruments (as they measure in different particle energy ranges). We test these modelling efforts against a set of multi-spacecraft observations of the same event, using the Forbush decrease model for the expanding flux rope (ForbMod). We find a reasonable agreement of the ForbMod model for the GCR depression in the CME magnetic structure with multi-spacecraft measurements, indicating that modelled FDs reflect well the CME evolution. **2014 February 12-15**

Unusual plasma and particle signatures at Mars and STEREO-A related to CME-CME interaction

Mateja [Dumbovic](#), [Jingnan Guo](#), [Manuela Temmer](#), [M. Leila Mays](#), [Astrid Veronig](#), [Stephan Heinemann](#), [Karin Dissauer](#), [Stefan Hofmeister](#), [Jasper Halekas](#), [Christian Möstl](#), [Tanja Amerstorfer](#), [Jürgen Hinterreiter](#), [Sasa Banjac](#), [Konstantin Herbst](#), [Yuming Wang](#), [Lukas Holzknicht](#), [Martin Leitner](#), [Robert F. Wimmer-Schweingruber](#)

2019

<https://arxiv.org/pdf/1906.02532.pdf>

On **July 25 2017** a multi-step Forbush decrease (FD) with the remarkable total amplitude of more than 15% was observed by MSL/RAD at Mars. We find that these particle signatures are related to very pronounced plasma and magnetic field signatures detected in situ by STEREO-A on July 24 2017, with a higher than average total magnetic field strength reaching more than 60 nT. In the observed time period STEREO-A was at a relatively small longitudinal separation (46 degrees) to Mars and both were located at the back side of the Sun as viewed from Earth. We analyse a number of multi-spacecraft and multi-instrument (both in situ and remote-sensing) observations, and employ modelling to understand these signatures. We find that the solar sources are two CMEs which erupted on July 23 2017 from the same source region on the back side of the Sun as viewed from Earth. Moreover, we find that the two CMEs interact non-uniformly, inhibiting the expansion of one of the CMEs in STEREO-A direction, whereas allowing it to expand more freely in the Mars direction. The interaction of the two CMEs with the ambient solar wind adds up to the complexity of the event, resulting in a long, sub-structured interplanetary disturbance at Mars, where different sub-structures correspond to different steps of the FD, adding-up to a globally large-amplitude FD. **23-25 July 2017**

Forbush decrease model for expanding CMEs (ForbMod)

Mateja [Dumbović](#)

An Analytical Diffusion-Expansion Model for Forbush Decreases Caused by Flux Ropes

Mateja **Dumbović**, [Bernd Heber](#), [Bojan Vršnak](#), [Manuela Temmer](#), [Anamarija Kirin](#)

2018 *ApJ* 860 71

<https://arxiv.org/pdf/1805.00916.pdf>

We present an analytical diffusion-expansion Forbush decrease (FD) model ForbMod which is based on the widely used approach of the initially empty, closed magnetic structure (i.e. flux rope) which fills up slowly with particles by perpendicular diffusion. The model is restricted to explain only the depression caused by the magnetic structure of the interplanetary coronal mass ejection (ICME). We use remote CME observations and a 3D reconstruction method (the Graduated Cylindrical Shell method) to constrain initial boundary conditions of the FD model and take into account CME evolutionary properties by incorporating flux rope expansion. Several flux rope expansion modes are considered, which can lead to different FD characteristics. In general, the model is qualitatively in agreement with observations, whereas quantitative agreement depends on the diffusion coefficient and the expansion properties (interplay of the diffusion and the expansion). A case study was performed to explain the FD observed **2014 May 30**. The observed FD was fitted quite well by ForbMod for all expansion modes using only the diffusion coefficient as a free parameter, where the diffusion parameter was found to correspond to expected range of values. Our study shows that in general the model is able to explain the global properties of FD caused by FR and can thus be used to help understand the underlying physics in case studies.

The Drag-based Ensemble Model (DBEM) for Coronal Mass Ejection Propagation

Mateja **Dumbović**, Jaša Čalogović, Bojan Vršnak, Manuela Temmer, M. Leila Mays, Astrid Veronig, and Isabell Piantschitsch

2018 *ApJ* 854 180

<http://sci-hub.tw/http://iopscience.iop.org/0004-637X/854/2/180/>

The drag-based model for heliospheric propagation of coronal mass ejections (CMEs) is a widely used analytical model that can predict CME arrival time and speed at a given heliospheric location. It is based on the assumption that the propagation of CMEs in interplanetary space is solely under the influence of magnetohydrodynamical drag, where CME propagation is determined based on CME initial properties as well as the properties of the ambient solar wind. We present an upgraded version, the drag-based ensemble model (DBEM), that covers ensemble modeling to produce a distribution of possible ICME arrival times and speeds. Multiple runs using uncertainty ranges for the input values can be performed in almost real-time, within a few minutes. This allows us to define the most likely ICME arrival times and speeds, quantify prediction uncertainties, and determine forecast confidence. The performance of the DBEM is evaluated and compared to that of ensemble WSA-ENLIL+Cone model (ENLIL) using the same sample of events. It is found that the mean error is $ME = -9.7$ hr, mean absolute error $MAE = 14.3$ hr, and root mean square error $RMSE = 16.7$ hr, which is somewhat higher than, but comparable to ENLIL errors ($ME = -6.1$ hr, $MAE = 12.8$ hr and $RMSE = 14.4$ hr). Overall, DBEM and ENLIL show a similar performance. Furthermore, we find that in both models fast CMEs are predicted to arrive earlier than observed, most likely owing to the physical limitations of models, but possibly also related to an overestimation of the CME initial speed for fast CMEs.

Validation of the CME Geomagnetic Forecast Alerts Under the COMESEP Alert System

Mateja **Dumbović**, Nandita Srivastava, Yamini K. Rao, Bojan Vršnak, Andy Devos, Luciano Rodriguez
[Solar Physics](#) August 2017, 292:96 **File**

<https://link.springer.com/content/pdf/10.1007%2Fs11207-017-1120-5.pdf>

Under the European Union 7th Framework Programme (EU FP7) project Coronal Mass Ejections and Solar Energetic Particles (COMESEP, <http://comesep.aeronomy.be>), an automated space weather alert system has been developed to forecast solar energetic particles (SEP) and coronal mass ejection (CME) risk levels at Earth. The COMESEP alert system uses the automated detection tool called Computer Aided CME Tracking (CACTus) to detect potentially threatening CMEs, a drag-based model (DBM) to predict their arrival, and a CME geoeffectiveness tool (CGFT) to predict their geomagnetic impact. Whenever CACTus detects a halo or partial halo CME and issues an alert, the DBM calculates its arrival time at Earth and the CGFT calculates its geomagnetic risk level. The geomagnetic risk level is calculated based on an estimation of the CME arrival probability and its likely geoeffectiveness, as well as an estimate of the geomagnetic storm duration. We present the evaluation of the CME risk level forecast with the COMESEP alert system based on a study of geoeffective CMEs observed during 2014. The validation of the forecast tool is made by comparing the forecasts with observations. In addition, we test the success rate of the automatic forecasts (without

human intervention) against the forecasts with human intervention using advanced versions of the DBM and CGFT (independent tools available at the Hvar Observatory website, <http://oh.geof.unizg.hr>). The results indicate that the success rate of the forecast in its current form is unacceptably low for a realistic operation system. Human intervention improves the forecast, but the false-alarm rate remains unacceptably high. We discuss these results and their implications for possible improvement of the COMESEP alert system.

Forbush Decrease Prediction Based on the Remote Solar Observations

Mateja **Dumbovic**, Bojan Vrsnak, Jasa Calogovic

Solar Phys. January 2016, Volume 291, Issue 1, pp 285-302

<http://arxiv.org/pdf/1510.03282v1.pdf>

We employ remote observations of coronal mass ejections (CMEs) and the associated solar flares to forecast the CME-related Forbush decreases, i.e., short-term depressions in the galactic cosmic-ray flux. The relationship between the Forbush effect at the Earth and remote observations of CMEs and associated solar flares is studied via a statistical analysis. Relationships between Forbush decrease magnitude and several CME/flare parameters was found, namely the initial CME speed, apparent width, source position, associated solar-flare class and the effect of successive-CME occurrence. Based on the statistical analysis, remote solar observations are employed for a Forbush-decrease forecast. For that purpose, an empirical probabilistic model is constructed that uses selected remote solar observations of CME and associated solar flare as an input, and gives expected Forbush-decrease magnitude range as an output. The forecast method is evaluated using several verification measures, indicating that as the forecast tends to be more specific it is less reliable, which is its main drawback. However, the advantages of the method are that it provides early prediction, and that the input is not necessarily spacecraft-dependent.

Geoeffectiveness of Coronal Mass Ejections in the SOHO era

Mateja **Dumbovic**, Andy Devos, Bojan Vrsnak, Davor Sudar, Luciano Rodriguez, Domagoj Ruzdjak, Kristoffer Leer, Susanne Vennerstrom, Astrid Veronig

Solar Phys., February 2015, Volume 290, Issue 2, pp 579-612

<http://arxiv.org/pdf/1410.3303v1.pdf> **File**

sci-hub.se/10.1007/s11207-014-0613-8

<https://link.springer.com/content/pdf/10.1007%2Fs11207-014-0613-8.pdf>

The main objective of the study is to determine the probability distributions of the geomagnetic Dst index as a function of the coronal mass ejection (CME) and solar flare parameters for the purpose of establishing a probabilistic forecast tool for the geomagnetic storm intensity. Several CME and flare parameters as well as the effect of successive-CME occurrence in changing the probability for a certain range of Dst index values, were examined. The results confirm some of already known relationships between remotely-observed properties of solar eruptive events and geomagnetic storms, namely the importance of initial CME speed, apparent width, source position, and the associated solar flare class. In this paper we quantify these relationships in a form to be used for space weather forecasting in future. The results of the statistical study are employed to construct an empirical statistical model for predicting the probability of the geomagnetic storm intensity based on remote solar observations of CMEs and flares. **15 June 2000, 24 June 2000, 13 December 2006**

Cosmic ray modulation by different types of solar wind disturbances

M. **Dumbović**, B. Vršnak, J. Čalogović and R. Župan

A&A 538, A28 (2012), **File**

Context. Solar wind disturbances such as interplanetary coronal mass ejections (ICMEs) and corotating interaction regions (CIRs) cause short-term cosmic ray depressions, generally denoted as Forbush decreases.

Aims. We conduct a systematic statistical study of various aspects of Forbush decreases. The analysis provides empirical background for physical interpretations of short-term cosmic ray modulations.

Methods. Firstly, we analyzed the effects of different types of solar wind disturbances, and secondly, we focused on the phenomenon of over-recovery (the return of the cosmic ray count to a value higher than the pre-decrease level). The analysis is based on ground-based neutron monitor data and the solar wind data recorded by the Advanced Composition Explorer. The correlations between various cosmic ray depressions and solar wind parameters as well as their statistical

significance are analyzed in detail. In addition, we performed a normalized superposed epoch analysis for depressions and magnetic field enhancements.

Results. The analysis revealed differences in the relationship between different solar wind disturbances and cosmic ray depression parameters. The amplitude of the depression for ICMEs was found to correlate well with the amplitudes of magnetic field strength and fluctuations, whereas for CIRs we found only the correlation between the amplitude of the depression and the solar wind disturbance dimension proxy v_tB . Similar behavior was found for shock and no-shock events, respectively. The CIR/ICME composites show a specific behavior that is a mixture of both ICMEs and CIRs. For all analyzed categories we found that the duration of the depression correlates with the duration of the solar wind disturbance. The analysis of the over-recovery showed that there is no straightforward relationship to either "branching-effect" or geomagnetic effects, therefore we propose a scenario where the "branching-effect" is caused by several factors and is only indirectly related to the over-recovery.

Cosmic ray modulation by solar wind disturbances

M. **Dumbović**, B. Vršnak, J. Čalogović and M. Karlica

Astronomy & Astrophysics, Volume 531, id.A91, 17 pp., **2011, File**

Aims: We perform a systematic statistical study of the relationship between characteristics of solar wind disturbances, caused by interplanetary coronal mass ejections and corotating interaction regions, and properties of Forbush decreases (FDs). Since the mechanism of FDs is still being researched, this analysis should provide a firm empirical basis for physical interpretations of the FD phenomenon.

Methods: The analysis is based on the ground-based neutron monitor data and the solar wind data recorded by the Advanced Composition Explorer, where the disturbances were identified as increases in proton speed, magnetic field, and magnetic field fluctuations. We focus on the relative timing of FDs, as well as on the correlations between various FD and solar wind parameters, paying special attention to the statistical significance of the results.

Results: It was found that the onset, the minimum, and the end of FDs are delayed after the onset, the maximum, and the end of the magnetic field enhancement. The t-test shows that at the 95% significance level the average lags have to be longer than 3, 7, and 26 h, respectively. FD magnitude ($|FD|$) is correlated with the magnetic field strength (B), magnetic field fluctuations (δB), and speed (v), as well as with combined parameters, BtB , Bv , v_tB , and $BvtB$, where tB is the duration of the magnetic field disturbance. In the $|FD|(B)$ dependence, a "branching" effect was observed, i.e., two different trends exist. The analysis of the FD duration and recovery period reveals a correlation with the duration of the magnetic field enhancement. The strongest correlations are obtained for the dependence on combined solar wind parameters of the product of the FD duration and magnitude, implying that combined parameters are in fact true variables themselves, rather than just a product of variables.

Conclusions: From the time lags we estimate that "the penetration depth" in the disturbance, at which FD onset becomes recognizable, is on the order of 100 Larmor radii and is comparable to a typical shock-sheath dimension. The results for the FD time profile indicate "shadow effect" of the solar wind disturbance before and after it passes the observer. The importance of reduced parallel diffusion during the passage of the disturbance is discussed, along with the influence of terrestrial effects on the observed "branching effect".

A new method to detect the ICMEs boundaries

Cristiana **Dumitrache**, Nedelia A. Popescu

2014

<http://arxiv.org/pdf/1405.6002v1.pdf>

A new method to infer the boundaries of the interplanetary coronal mass ejections is proposed. The local minima of a proton temperature anisotropy are used as potential boundaries of the interplanetary event. The low-beta plasma values are then invoked to detect at least four boundaries, two for the beginning and two for the end of an interplanetary coronal mass ejection (ICME). Intermediate boundaries can be identified, as indicated by other plasma and magnetic field signatures, and mark substructures of an event. Using the algorithm we propose here, we have compiled a list with ICME events boundaries registered by *Ulysses* spacecraft during 2000-2002. Three magnetic clouds (observed on **23 January 2001**, **10 June 2001** and **24 August 2001**) are analysed with details. This method provides premises for an alternative way of automatic detection of the ICMEs boundaries.

ICMEs list for a period of three important years of the solar cycle 23: 2000, 2001 and 2002.

The interplanetary mass ejections behaviour in the heliosphere

Cristiana **Dumitrache**, Nedelia A. Popescu

Review

Romanian Journal of Physics, 58, 3-4, p.383-394, **2013**

<http://arxiv.org/pdf/1406.3245v1.pdf>

We present here an overview of an important solar phenomenon with major implication for space weather and planetary life. The coronal mass ejections (CMEs) come from the Sun and expand in the heliosphere, becoming interplanetary coronal mass ejections (ICMEs). They represent huge clouds of plasma and magnetic fields that travel with velocities reaching even 2000 km/s and perturbing the planetary and interplanetary field. The magnetic clouds (MC) are a special class of ICMEs. We summarize some aspects as the ICMEs identification, propagation and track back to the Sun, where the solar source could be found. We notice here few known catalogs of the ICMEs and magnetic clouds.

Tracking a *Ulysses* High-latitude ICME Event Back to Its Solar Origins

C. **Dumitrache** · N.A. Popescu · A. Oncica

Solar Phys (2011) 272:137–157, **File**

High-latitude interplanetary mass ejections (ICMEs) observed beyond 1 AU are not studied very often. They are useful for improving our understanding of the 3D heliosphere. As there are only few such events registered by the *Ulysses* spacecraft, the task of detecting their solar counterparts is a challenge, especially during high solar activity periods, because there are dozens coronal mass ejections (CMEs) registered by SOHO that might be chosen as candidates. We analyzed a high-latitude ICME registered by the *Ulysses* spacecraft on 18 January 2002. Our investigation focused on the correlation between various plasma parameters that allow the identification to be made of the ICME and its components such as the forward shock, the magnetic cloud and the reverse shock.

Using a linear approach and a graphical method we have been able to track the ICME event back to the Sun and to compute the day of the occurrence of the solar CME. In order to decide among several CME candidates which one is the right solar counterpart of our event, we have performed a follow-up computation of these CMEs from the Sun to *Ulysses*, by using two different speed formulas. First, the computation was simply based on the initial CME velocity, while the other was based on the ICME velocity estimated from the CME initial speed (Lindsay et al. 1999). Differences of hours have been obtained between the arrival time predicted in these two ways, but the second one gave the best results. Both methods indicated the same two CMEs as the solar counterparts. We have found the solar source of these CMEs as being a huge polar filament that erupted in several steps.

This ICME event displayed a double magnetic cloud configuration. A minimum variance analysis helped us to detect the smooth rotation of the clouds and their helicity. Both magnetic clouds show the same helicity as the filament that erupted and released them. A cylinder-shape model of both clouds gives the same helicity sign.

Filament eruption of 8 January 2002.

A PSP Perihelion

Jessie **Duncan**, Hugh Hudson

RHESSI Science Nugget, No. **369** Jan **2020** http://sprg.ssl.berkeley.edu/~tohban/wiki/index.php/A_PSP_Perihelion

An expert team (WHPI, the Whole Heliosphere and Planetary Interactions) group has tackled this problem, with a helpful Web site at https://whpi.hao.ucar.edu/whpi_campaign-cr2226.php

CMEs' speed, travel time and temperature: A Thermodynamic approach

Héctor J. **Durand-Manterola**, Alberto Flandes, Ana Leonor Rivera, Alejandro Lara and Tatiana Niembro

JGR Volume 122, Issue 12 Pages 11,810–11,834 **2017**

<http://onlinelibrary.wiley.com/doi/10.1002/2017JA024369/epdf>

<http://sci-hub.cc/10.1002/2017JA024369>

Due to their important role in Space weather, Coronal Mass Ejections or CMEs have been thoroughly studied in order to forecast their speed and transit time from the Sun to the Earth. We present a Thermodynamic analytical model that describes the dynamics of CMEs. The thermodynamic approach has some advantages with respect to the hydrodynamic approach. First, it deals with the energy involved, which is a scalar quantity. Second, one may calculate the work done by the different forces separately and sum all contributions to determine the changes in speed, which simplifies the problem and allows us to obtain fully rigorous results. Our model considers the drag force, which dominates the dynamics of CMEs and the solar gravitational force, which has a much smaller effect, but it is, still, relevant enough to be considered.

We derive an explicit analytical expression for the speed of CMEs in terms of its most relevant parameters and obtain an analytical expression for the CME temperature. The model is tested with a CME observed at three different heliocentric distances with three different spacecraft (SOHO, ACE and *Ulysses*); also, with a set of 11 CMEs observed with the SOHO, Wind and ACE spacecraft and, finally, with two events observed with the STEREO spacecraft. In all cases, we

have a consistent agreement between the theoretical and the observed speeds and transit times. Additionally, for the set of 11 events, we estimate their temperatures at their departure position from their temperatures measured near the orbit of the Earth.

Table 2. CMEs data parameters for the 11 selected CMEs. 2001-2007

Evolution of the α -proton Differential Motion across Stream Interaction Regions

Tereza [Đurovcová](#), Zdeněk Němeček, and Jana Šafránková

2019 ApJ 873 24

<https://doi.org/10.3847/1538-4357/ab01c8>

A corotating interaction region (CIR) develops between the solar wind streams with different bulk speeds emanating from distinct coronal sources. The arising pressure perturbations redistribute momentum between adjacent streams forming the regions of the compressed solar wind around the stream interface. We focus on properties of α -particles with respect to protons in CIRs using measurements of the Wind and Helios spacecraft. In the slow solar wind in front of CIRs, the relative helium abundance A_{He} is usually low (about 1%) and the α -proton differential drift, $V_{\alpha p}$ is close to zero. In the high-speed stream behind CIRs, both of these characteristics are significantly higher. Inside CIRs, a large enhancement of A_{He} accompanied by a decrease in $V_{\alpha p}$ is often observed in the compressed and slowed down fast solar wind close to the CIR leading edge. On the other hand, a depletion of A_{He} is sometimes present in the compressed and accelerated slow solar winds. We explain these observations in terms of magnetic mirroring of the multicomponent solar wind in a converging magnetic field that develops within CIRs.

The Vigil Magnetometer for Operational Space Weather Services From the Sun-Earth L5 Point

J. P. [Eastwood](#), [P. Brown](#), [W. Magnes](#), [C. M. Carr](#), [M. Agu](#), [R. Baughen](#), [G. Berghofer](#), [J. Hodgkins](#), [I. Jernej](#), [C. Möstl](#), [T. Oddy](#), [A. Strickland](#), [A. Vitkova](#)

Space Weather [Volume22, Issue6](#) June 2024 e2024SW003867

<https://doi.org/10.1029/2024SW003867>

<https://agupubs.onlinelibrary.wiley.com/doi/epdf/10.1029/2024SW003867>

Severe space weather has the potential to cause significant socio-economic impact and it is widely accepted that mitigating this risk requires more comprehensive observations of the Sun and heliosphere, enabling more accurate forecasting of significant events with longer lead-times. In this context, it is now recognized that observations from the L5 Sun-Earth Lagrange point (both remote and in situ) would offer considerable improvements in our ability to monitor and forecast space weather. Remote sensing from L5 allows for the observation of solar features earlier than at L1, providing early monitoring of active region development, as well as tracking of interplanetary coronal mass ejections through the inner heliosphere. In situ measurements at L5 characterize the solar wind's geoeffectiveness (particularly stream interaction regions), and can also be ingested into heliospheric models, improving their performance. The Vigil space weather mission is part of the ESA Space Safety Program and will provide a real-time data stream for space weather services from L5 following its anticipated launch in the early 2030s. The interplanetary magnetic field is a key observational parameter, and here we describe the development of the Vigil magnetometer instrument for operational space weather monitoring at the L5 point. We summarize the baseline instrument capabilities, demonstrating how heritage from science missions has been leveraged to develop a low-risk, high-heritage instrument concept.

The Scientific Foundations of Forecasting Magnetospheric Space Weather

Review

J. P. [Eastwood](#), R. Nakamura, L. Turc, L. Mejnertsen, M. Hesse

[Space Science Reviews](#) 2017

<https://link.springer.com/content/pdf/10.1007%2Fs11214-017-0399-8.pdf>

The magnetosphere is the lens through which solar space weather phenomena are focused and directed towards the Earth. In particular, the non-linear interaction of the solar wind with the Earth's magnetic field leads to the formation of highly inhomogeneous electrical currents in the ionosphere which can ultimately result in damage to and problems with the operation of power distribution networks. Since electric power is the fundamental cornerstone of modern life, the interruption of power is the primary pathway by which space weather has impact on human activity and technology. Consequently, in the context of space weather, it is the ability to predict geomagnetic activity that is of key importance. This is usually stated in terms of geomagnetic storms, but we argue that in fact it is the substorm phenomenon which contains the crucial physics, and therefore prediction of substorm occurrence, severity and duration, either within the context of a longer-lasting geomagnetic storm, but potentially also as an isolated event, is of critical importance. Here

we review the physics of the magnetosphere in the frame of space weather forecasting, focusing on recent results, current understanding, and an assessment of probable future developments. **20-30 Oct 2001**

Possible Cause of Extremely Bright Aurora Witnessed in East Asia on 17 September 1770

Yusuke [Ebihara](#) [Hisashi Hayakawa](#) [Kiyomi Iwahashi](#) [Harufumi Tamazawa](#) [Akito Davis Kawamura](#) [Hiroaki Isobe](#)

[Space Weather](#) [Volume 15, Issue 10](#) **2017**

sci-hub.tw/10.1002/2017SW001693

Extremely bright aurora was witnessed in East Asia on **17 September 1770**, according to historical documents. The aurora was described as “as bright as a night with full moon” at magnetic latitude of 25° . The aurora was dominated by red color extending from near the horizon up beyond the polar star (corresponding to elevation angle of $\sim 35^\circ$). We performed a two-stream electron transport code to calculate the volume emission rates at 557.7 nm (OI) and 630.0 nm (OI). Two types of distribution of precipitating electrons were assumed. The first one is based on the unusually intense electron flux measured by the DMSP satellite in the March 1989 storm. The distribution consists of hot (peaking at 3 keV) and cold (peaking at 71 eV) components. The second one is the same as the first one, but the hot component is removed. We call this high-intensity low-energy electrons (HILEEs). The first spectrum results in an auroral display with a bright, lower green border. The second one results in red-dominated aurora extending up to the elevation angle of 35° when the equatorward boundary of the electron precipitation is located at 32° invariant latitude. The poleward boundary of the precipitation would be 42° invariant latitude or greater to explain the auroral display extending from near the horizon. The origin of the HILEEs is probably the plasma sheet or the plasmasphere that is transported earthward to $L \sim 1.39$ due to enhanced magnetospheric convection. Local heating or acceleration is also plausible.

Solar-Wind High-Speed Stream (HSS) Alfvén Wave Fluctuations at High Heliospheric Latitudes: Ulysses Observations During Two Solar-Cycle Minima

Ezequiel [Echer](#), [Adriane Marques de Souza Franco](#), [Edio da Costa Junior](#), [Rajkumar Hajra](#) & [Mauricio José Alves Bolzan](#)

[Solar Physics](#) volume 297, Article number: 143 (**2022**)

<https://doi.org/10.1007/s11207-022-02070-w>

We study Alfvén wave fluctuations in solar-wind high-speed streams (HSSs) at high heliolatitudes during the last two solar-cycle minima (SCM). Solar-wind plasma and interplanetary magnetic field (IMF) measured by Ulysses during four 50-day intervals in 1994, 1995, 2007, and 2008 were analyzed using wavelet and Fourier analyses, cross-correlation and kurtosis techniques. Intervals during 1994 and 1995 (2007 and 2008) correspond to the Ulysses polar passes through the southern and northern solar hemispheres, respectively, during the minimum between Cycles 22 and 23 or SCM22–23 (the minimum between Cycles 23 and 24 or SCM23–24). The solar-wind plasma density [NpNp], IMF magnitude [B0B0], and IMF-component variances are found to be lower during SCM23–24 than during SCM22–23 by $\approx 20 - 30\%$. The cross-correlation between the plasma velocity and IMF vector components, an indicative of Alfvénicity, is smaller during SCM23–24 than during SCM22–23. The Alfvén wave periodicity exhibits a large range, from $\approx 8 \sim 8$ hours to 10 days, with peak occurrences near 1 – 5 days during both minima. The statistical kurtosis analysis shows that the IMF distributions are mostly sub-Gaussian. Further, the Fourier power law analysis reveals a higher spectral power of transverse IMF components BtBt and BnBn than the radial field-aligned component BrBr. The power spectrum shows a spectral break near 10–4 Hz, with its high-frequency portion following a -1.7 power law dependence (Kolmogorov spectrum), while the low-frequency portion shows an $\approx -1.0 \sim -1.0$ power law index dependence. This low-frequency index is slightly higher during SCM22–23 (-0.65 to -0.87) than during SCM23–24 (-0.49 to -0.78). We conclude that while the Alfvénicity of the high-latitude HSSs does not vary substantially between the two minima, the amplitude of the Alfvén wave fluctuations is reduced during SCM23–24 compared to SCM22–23.

Interplanetary origins of moderate ($-100 \text{ nT} < \text{Dst} \leq -50 \text{ nT}$) geomagnetic storms during solar cycle 23 (1996–2008)

E. [Echer](#)¹, B. T. Tsurutani², W. D. Gonzalez

JGR, Volume 118, Issue 1, pp. 385-392, **2013**

<http://onlinelibrary.wiley.com/doi/10.1029/2012JA018086/pdf>

sci-hub.se/10.1029/2012JA018086

The interplanetary causes of 213 moderate-intensity ($-100 \text{ nT} < \text{peak Dst} \leq -50 \text{ nT}$) geomagnetic storms that occurred in solar cycle 23 (1996–2008) are identified. Interplanetary drivers such as corotating interaction regions (CIRs), pure high-speed streams (HSSs), interplanetary coronal mass ejections (ICMEs) of two types [those with magnetic clouds (MCs) and those without (nonmagnetic cloud or ICME_nc)], sheaths (compressed and/or draped sheath fields), as well

as their combined occurrence were identified as causes of the storms. The annual rate of occurrence of moderate storms had two peaks, one near solar maximum and the other in the descending phase, around 3 years later. The highest rate of moderate storm occurrence was found in the declining phase (25 storms year⁻¹). The lowest occurrence rate was 5.7 storms year⁻¹ and occurred at solar minimum. All moderate-intensity storms were associated with southward interplanetary magnetic fields, indicating that magnetic reconnection was the main mechanism for solar wind energy transfer to the magnetosphere. Most of these storms were associated with CIRs and pure HSSs (47.9%), followed by MCs and noncloud ICMEs (20.6%), pure sheath fields (10.8%), and sheath and ICME combined occurrence (9.9%). In terms of solar cycle dependence, CIRs and HSSs are the dominant drivers in the declining phase and at solar minimum. CIRs and HSSs combined have about the same level of importance as ICMEs plus their sheaths in the rising and maximum solar cycle phases. Thus, CIRs and HSSs are the main driver of moderate storms throughout a solar cycle but with variable contributions from ICMEs, their shocks (sheaths), and combined occurrence within the solar cycle. This result is significantly different than that for intense ($Dst \leq -100$ nT) and superintense ($Dst \leq -250$ nT) magnetic storms shown in previous studies. For superintense geomagnetic storms, 100% of the events were due to ICME events, while for intense storms, ICMEs, sheaths, and their combination caused almost 80% of the storms. CIRs caused only 13% of the intense storms. The typical interplanetary electric field (E_y) criteria for moderate magnetic storms were identified. It was found that ~80.1% of the storms follow the criterion of $E_y \geq 2$ mV m⁻¹ for intervals longer than 2 h. It is concluded that southward directed interplanetary magnetic fields within CIRs/HSSs may be the main energy source for long-term averaged geomagnetic activity on Earth.

Extremely low geomagnetic activity during the recent deep solar cycle minimum.

Echer E, Tsurutani BT, Gonzalez WD
(2012) IAUS 286:200-209

Statistical studies of geomagnetic storms with peak $Dst \leq -50$ nT from 1957 to 2008

E. **Echer**, W.D. Gonzalez and B.T. Tsurutani

Journal of Atmospheric and Solar-Terrestrial Physics, Volume 73, Issues 11-12, 2011, Pages 1454-1459, **File**
A catalog of 1377 geomagnetic storms with peak Dst (Dst_p) ≤ -50 nT for the period 1957–2008 has been compiled. The dependence of Dst_p on the solar cycle and annual variation are studied in this paper. It is found that geomagnetic storm peak intensity distribution can be described by an exponential form, where P is the probability of geomagnetic storm occurrence with a given value Dst_p . The updated solar cycle and annual distribution of geomagnetic storms have confirmed the expected behavior. For the solar cycle variation, geomagnetic storms display a two-peak distribution, with one peak close to solar maximum and the other a few years later in the beginning of the declining phase. Geomagnetic storms follow the well-known seasonal variation of geomagnetic activity. More intense storms show a peak in probability occurrence in July, confirming previous observations. These results are of practical importance for space weather applications.

See [Echer_geostorm_100nT_list.doc](#)

Interplanetary fast forward shocks and their geomagnetic effects: CAWSES events

E. **Echer**, , B.T. Tsurutanib, c, F.L. Guarnierid and J.U. Kozyra

Journal of Atmospheric and Solar-Terrestrial Physics, Volume 73, Issues 11-12, 2011, Pages 1330-1338

The seven CAWSES interplanetary fast forward shocks and their geomagnetic effects during 2004–2005 have been analyzed. It is found that the arrival time of the shocks at Earth can be estimated within an accuracy of 5 min. Furthermore, AL decreases are found to occur within 10 min of shock impingement on the magnetopause. It was also determined that there is a direct correlation between the interplanetary magnetic field southward directed (IMF B_s) prior to shock arrival and substorms triggered by the shocks. If the IMF is northward prior to shock arrival, the geomagnetic activity is present but is low. One interpretation of this result is that the preconditioning energy stored in the magnetotail leaks away rapidly. A correlation between substorm peak AL and shock strength (Mach number) has also been noted, which could imply that shock strength is important for the amount of energy released into the magnetosphere/ionosphere.

High Speed Stream Properties and Related Geomagnetic Activity During the Whole Heliosphere Interval (WHI): 20 March to 16 April 2008.

Echer, E, Tsurutani BT, Gonzalez WD, Kozyra JU
(2011a) Sol Phys 274:303-320

Solar and interplanetary origins of the November 2004 superstorms

Ezequiel **Echer**, Bruce T. Tsurutani^b and Fernando L. Guarnieric

[Advances in Space Research](#), [Volume 44, Issue 5](#), 1 September 2009, Pages 615-620, 2009

During the first half of November 2004, many solar flares and coronal mass ejections (CMEs) were associated with solar active region (AR) 10696. This paper attempts to identify the solar and interplanetary origins of two superstorms which occurred on 8 and 10 November with peak intensities of $Dst = -373$ nT and -289 nT, respectively. Southward interplanetary magnetic fields within a magnetic cloud (MC), and a sheath + MC were the causes of these two superstorms, respectively. Two different CME propagation models [Gopalswamy, N., Yashiro, S., Kaiser, M.L. et al. Predicting the 1-AU arrival times of coronal mass ejections. *J. Geophys. Res.* 106, 29207–29219, 2001; Gopalswamy, N.S., Lara, A., Manoharan, P.K. et al. An empirical model to predict the 1-AU arrival of interplanetary shocks. *Adv. Space Res.* 36, 2289–2294, 2005] were employed to attempt to identify the solar sources. It is found that the models identify several potential CMEs as possible sources for each of the superstorms. The two Gopalswamy et al. models give the possible sources for the first superstorm as CMEs on 2330 UT 4 November 2004 or on 1454 UT 5 November 2004. For the second superstorm, the possible solar source was a CME that on 0754 UT 5 November 2004 or one that occurred on 1206 UT 5 November 2004. We note that other propagation models sometimes agree and other times disagree with the above results. It is concluded that during high solar/interplanetary activity intervals such as this one, the exact solar source is difficult to identify. More refined propagation models are needed.

Interplanetary conditions causing intense geomagnetic storms ($Dst = -100$ nT) during solar cycle 23 (1996-2006),

Echer, E., W. D. Gonzalez, B. T. Tsurutani, and A. L. C. Gonzalez

J. Geophys. Res., 113, A05221, 2008, **File**

<http://dx.doi.org/10.1029/2007JA012744>

The interplanetary causes of intense geomagnetic storms and their solar dependence occurring during solar cycle 23 (1996–2006) are identified. During this solar cycle, all intense ($Dst \leq -100$ nT) geomagnetic storms are found to occur when the interplanetary magnetic field was southwardly directed (in GSM coordinates) for long durations of time. This implies that the most likely cause of the geomagnetic storms was magnetic reconnection between the southward IMF and magnetopause fields. Out of 90 storm events, none of them occurred during purely northward IMF, purely intense IMF B_y fields or during purely high speed streams. We have found that the most important interplanetary structures leading to intense southward B_z (and intense magnetic storms) are magnetic clouds which drove fast shocks (sMC) causing 24% of the storms, sheath fields (Sh) also causing 24% of the storms, combined sheath and MC fields (Sh+MC) causing 16% of the storms, and corotating interaction regions (CIRs), causing 13% of the storms. These four interplanetary structures are responsible for three quarters of the intense magnetic storms studied. The other interplanetary structures causing geomagnetic storms were: magnetic clouds that did not drive a shock (nsMC), non magnetic clouds ICMEs, complex structures resulting from the interaction of ICMEs, and structures resulting from the interaction of shocks, heliospheric current sheets and high speed stream Alfvén waves. During the rising phase of the solar cycle, sMC and sheaths are the dominant structure driving intense storms. At solar maximum, sheath fields, followed by Sh+MCs and then by sMC were responsible for most of the storms. During the declining phase, sMC, Sh and CIR fields are the main interplanetary structures leading to intense storms. We have also observed that around 70% of the storms follow the interplanetary criteria of $E_y \geq 5$ mV/m for at least 3 h. Around 90% of the storms used in the study followed a less stringent set of criteria: $E_y \geq 3$ mV/m for at least 3 h. Finally, we obtain the approximate rate of intense magnetic storms per solar cycle phases: minimum/rising phase 3 storms.year⁻¹, maximum phase 8.5 storms.year⁻¹, and declining/minimum phases 6.5 storms.year⁻¹.

Table

Interplanetary conditions leading to superintense geomagnetic storms ($Dst \leq -250$ nT) during solar cycle 23

Echer, E., W. D. Gonzalez, B. T. Tsurutani

Geophysical Research Letters, Volume 35, Issue 6, CiteID L06S03, 2008, File

<http://adsabs.harvard.edu/abs/2008GeoRL..3506S03E>

<https://agupubs.onlinelibrary.wiley.com/doi/epdf/10.1029/2007GL031755>

The interplanetary causes of superintense geomagnetic storms (superstorms, $Dst \leq -250$ nT) that occurred during solar cycle 23 are studied. Eleven superstorms occurred during the cycle, five close to solar maximum (2000-2001) and six in the post-maximum/declining phase (2003-2004). About 1/3 of the superstorms were caused by magnetic clouds (MCs), 1/3 by a combination of sheath and MC fields, and 1/3 by sheath fields alone. The interplanetary parameter best correlated with peak Dst was the time-integrated E_y during the storm main phase (in contrast with peak B_z and/or peak E_y for less intense geomagnetic storms). The range of peak Dst for these storms was -263 to -422 nT. The storm main phase durations had a range of 3-33 h. We conclude from this study that: (1) only MCs and/or interplanetary sheaths had fields intense enough and with long enough durations to cause superstorms; (2) superstorms occurred only in the maximum and declining phases; (3) the total energy transferred from the solar wind to the magnetosphere is best correlated with the time-integrated solar wind E_y parameter.

Table

See Cid, C., Saiz, E., Cerrato, Y., 2008. Comment on "Interplanetary conditions leading to superintense geomagnetic storms ($Dst \leq -250$ nT) during solar cycle 23" by E. Echer et al.

Geophys. Res. Lett. 35, L21107. doi:10.1029/2008GL034731.

<http://onlinelibrary.wiley.com/doi/10.1029/2008GL034731/pdf>

See Reply to comment by C. Cid, E. Saiz, and Y. Cerrato on "Interplanetary conditions leading to superintense geomagnetic storms ($Dst \leq -250$ nT) during solar cycle 23"

W. D. Gonzalez, E. Echer and B. T. Tsurutani

<http://onlinelibrary.wiley.com/doi/10.1029/2008GL035164/pdf>

Influence of Non-Potential Coronal Magnetic Topology on Solar-Wind Models

S. J. Edwards, A. R. Yeates, F.-X. Bocquet,

Solar Phys. 2015

By comparing a magneto-frictional model of the low-coronal magnetic-field to a potential-field source-surface model, we investigate the possible impact of non-potential magnetic structure on empirical solar-wind models. These empirical models (such as Wang–Sheeley–Arge) estimate the distribution of solar-wind speed solely from the magnetic-field structure in the low corona. Our models are computed in a domain between the solar surface and 2.5 solar radii, and they are extended to 0.1 AU using a Schatten current-sheet model. The non-potential field has a more complex magnetic skeleton and quasi-separatrix structures than the potential field, leading to different sub-structure in the solar-wind speed proxies. It contains twisted magnetic structures that can perturb the separatrix surfaces traced down from the base of the heliospheric current sheet. A significant difference between the models is the greater amount of open magnetic flux in the non-potential model. Using existing empirical formulae this leads to higher predicted wind speeds for two reasons: partly because magnetic-flux tubes expand less rapidly with height, but more importantly because more open-field lines are further from coronal-hole boundaries.

Coronal Radio Occultation Experiments with the Helios Solar Probes: Correlation/Spectral Analysis of Faraday Rotation Fluctuations

A. I. Efimov, L. A. Lukanina, A. I. Rogashkova, L. N. Samoznaev, I. V. Chashei, M. K. Bird, M. Pätzold
Solar Phys. 2015

The coronal Faraday rotation (FR) experiments using the linearly polarized signals of the *Helios-1* and *Helios-2* interplanetary probes remain a unique investigation of the magnetic field of the solar corona and its aperiodic and quasi-periodic variations. The unexpectedly long lifetime of these spacecraft (1974 – 1986) enabled studies from very deep solar-activity minimum (1975 – 1976) into the strong activity maximum (1979). Important experimental data were also obtained for the rising (1977 – 1978) and declining (1980 – 1984) branches of the solar-activity cycle. Previous publications have presented results of the initial experimental data only for coronal-sounding experiments performed during individual solar-conjunction opportunities. This report is a more detailed analysis of the *Helios* FR measurements for the entire period 1975 – 1984. Radial profiles of the FR fluctuation (FRF) intensity recorded during the deepest solar-

activity minimum in 1975 – 1976 are shown to differ distinctly from those during the strong solar-activity maximum in 1979. In particular, the decrease of the FRF intensity with solar-offset distance is substantially steeper in 1979 than in 1975/1976. In all cases, however, the FR data reveal quasi-periodic wave-like fluctuations in addition to the random background with a power-law spectrum. The dominant period of these fluctuations, recorded during 35 % of the total measurement time, is found to be close to five minutes. Large-scale FR variations at considerably longer periods (1.1 – 2.7 hours) were observed during 20 % of the measurement time. Knowing the intrinsic motion of the radio ray path from spacecraft to Earth and making a reasonable assumption about the solar-wind velocity, FRF observations at widely spaced ground stations have been used to estimate the velocity of coronal Alfvén waves. The velocity values range between 290 and 550 km s⁻¹ at heliocentric distances between 3.5 and 4.5 R_⊙ and are marginally lower (150 – 450 km s⁻¹) at distances between 5.5 and 6.5 R_⊙. Occasional FR variations with a period near 160 minutes and harmonics with periods 60, 30, and 20 minutes were also observed.

The Interconnection between the Periodicities of Solar Wind Parameters Based on the Interplanetary Magnetic Field Polarity (1967–2018): A Cross Wavelet Analysis

M. A. [El-Borie](#), [A. M. El-Taher](#), [A. A. Thabet](#) & [A. A. Bishara](#)

[Solar Physics](#) volume 295, Article number: 122 (2020)

<https://link.springer.com/content/pdf/10.1007/s11207-020-01692-2.pdf>

In this article, we have examined the possible interconnection and phase asynchrony between the periodicities of solar wind parameters (solar wind velocity VV, plasma density NN, and dynamic pressure PP), and the interplanetary magnetic field (IMF) magnitude BB, taking into account the polarity state, toward (TT) and away (AA) from the Sun, of the IMF. For this purpose, the daily measurements of VV, NN, PP, and BB during the period 1967–2018, thus covering almost five solar cycles, were sorted into two groups according to the IMF sense. Days of mixed IMF polarity or having no data were eliminated from our analysis during the entire period. The monthly averages of TT and AA polarity groups have been calculated for each parameter. BTBT (BABA), VTVT (VAVA), NTNT (NANA), and PTPT (PAPA), refer to the monthly averages of TT (AA) polarity group for BB, VV, NN, and PP, respectively. In this study, three techniques were applied, including the running correlation analysis, cross-wavelet transform (XWT) and wavelet coherence (WTC) to the monthly means of each polarity group. Our results reveal that the running correlation coefficient for toward and away groups of each parameter reflect a positive correlation value during most of the entire period. The long-term periodicities within the 8–16 yr band are also detected for all toward and away components of the considered parameters with a significant common power during most of the entire period. Moreover, the WTC reflects an almost in-phase relationship behavior between the toward and away groups of each parameter during this range. On the other hand, within the 4–8 yr, 2–4 yr, and 1–2 yr bands, the toward and away groups of each solar wind parameter show mid-term periodicities at different periods, displaying sometimes significant powers.

The impact of asymmetrical distribution of solar activity on geomagnetic indices throughout five solar activity cycles

M.A. [El-Borie](#), [A.M. El-Taher](#), [A.A. Thabet](#), [A.A. Bishara](#)

[Advances in Space Research](#) Volume 64, Issue 1, 1 July 2019, Pages 278-286

[sci-hub.se/10.1016/j.asr.2019.03.040](https://doi.org/10.1016/j.asr.2019.03.040)

The [irregularity](#) of the [solar activities](#) based on [sunspot numbers](#) (SSNs) and areas (SSAs) over the solar disk has been considered. More activities phenomena occurred in one of the solar hemispheres than the other at the same time, which they are referred to as the North-South (N-S) [asymmetry](#) of solar activity. Daily averages of geomagnetic indices aa, Ap, Kp, and Dst over the period 1967–2016 have been examined according to the asymmetrical distribution of both solar hemispheric activities. The possible connection between the geomagnetic activity disturbances and the sign of [non-uniformity](#) of solar activity, i.e. the N-S asymmetry for each geomagnetic index has been confirmed. The dependence of the sign of geomagnetic disturbances on the solar activity cycle, has been examined. We have classified the considered data into two groups according to the activity of northern (N) or southern (S) solar hemisphere. The [solar cycles](#) 20 and 24 have [northern hemisphere](#) dominance. These activities shifted from northern to [southern hemisphere](#) in solar cycles 21, 22, and 23. The geomagnetic disturbances exhibited significant asymmetrical states at different periods. The most significant northern and southern peaks occurred at/near the minimum of the solar cycle or in periods of descending phase of the solar cycle. The geomagnetic activity has southern dominance during solar cycle 22 and it favoured the northern activity during solar cycle 23. The dependence of the geomagnetic activity disturbance of aa, Ap, Kp, and Dst indices over the solar activity cycle is confirmed and the sign of the asymmetry changes from one solar cycle to another.

The Dependence of Solar, Plasma, and Geomagnetic Parameters' Oscillations on the Heliospheric Magnetic Field Polarities: Wavelet Analysis

M. A. [El-Borie](#)¹, A. M. El-Taher^{2,4}, A. A. Thabet³, and A. A. Bishara

2019 ApJ 880 86

[sci-hub.se/10.3847/1538-4357/ab12d8](https://doi.org/10.3847/1538-4357/ab12d8)

We investigate the dependence of solar, plasma, and geomagnetic parameters' periodicities on the heliospheric magnetic field polarities for the past five solar activity cycles (1967–2016). For this purpose, the Morlet wavelet technique has been performed to extract information about significant periods. The monthly averages of toward (T) and away (A) polarity groups have been calculated for each parameter. The solar and plasma parameters used in this work are the interplanetary magnetic field (B), sunspot numbers (R), and solar plasma speed (V), and the geomagnetic indices aa, Kp, and Ap. We found that the wavelet power spectra (WPS) for the monthly averages of BT and BA nearly showed a symmetrical power spectra distribution. The global wavelet spectra (GWS) for BT and BA displayed a coupling at some level between 3.2–3.5, 10.7, and 18.3 yr of variations. The GWS for VA provided two significant peaks, within the 95% confidence level, at 9.8 and 15.2 yr, as well as at 1 and 9.8 yr, for VT. In addition, the existence of a periodicity of 1 yr is obvious for VT spectra and it shifted to a 1.5 yr variation in VA spectra. Both the WPS and GWS for RT and RA reflect symmetric power spectra for both groups in the northern and southern hemispheres. The aa spectra exhibited prominent periodicities at 10.7 yr for aaA and 9.8 yr for aaT. Also, the well-known 9.8 yr periodicity variation is a dominant variation in both the spectra of ApT and ApA. On the other hand, within the cone of influence, the periodicities of 10.7 and 13.9 yr are observed for the KpA spectra and 9.8 yr for KpT spectra. The GWS showed double-peak structure for the spectrum of KpA.

Long-term variation of the semiannual amplitude in the aa index

Ana G. [Elias](#), Virginia M. Silbergleitner, c, , and Alicia L. Clua de Gonzalez

Journal of Atmospheric and Solar-Terrestrial Physics, Volume 73, Issues 11-12, 2011, Pages 1492-1499

The long-term variation of the semiannual amplitude in the geomagnetic activity index aa is analyzed with the purpose of contributing to the understanding of solar variability, directly linked to geomagnetic variability. The time series of the semiannual oscillation amplitude, obtained through a wavelet analysis of the daily aa series, presents a long-term variation similar to that shown by solar and geomagnetic indices, like aa itself or Dst. However, the maximum in the semiannual amplitude series occurs around 1947, almost 10 years before it occurs in solar and geomagnetic indices time series. The phase of the semiannual oscillation fluctuates around the values predicted by the equinoctial and Russell–McPherron models, with a predominance of the equinoctial mechanism during the period of maximum semiannual amplitude. A possible source of changes in the equinoctial mechanism would be the secular variation of the Earth's dipole tilt. But, since it does not follow the semiannual amplitude trend, at first sight, it seems not to be responsible for the equinoctial predominance around 1947. The analysis of quiet and disturbed days separately indicates that only disturbed days present the semiannual annual amplitude maximum around 1947, so the 10 year time shift could be due to the mechanism responsible for the semiannual variation in geomagnetically active periods.

Improving Multiday Solar Wind Speed Forecasts

H. A. [Elliott](#), [C. N. Arge](#), [C. J. Henney](#), [M. A. Dayeh](#), [G. Livadiotis](#), [J.-M. Jahn](#), [C. E DeForest](#)

Space Weather e2021SW002868 **Volume 20, Issue 9** 2022

<https://doi.org/10.1029/2021SW002868>

<https://agupubs.onlinelibrary.wiley.com/doi/epdf/10.1029/2021SW002868>

We analyze the residual errors for the Wang-Sheeley-Arge (WSA) solar wind speed forecasts as a function of the photospheric magnetic field expansion factor (f_p) and the minimum separation angle (d) in the photosphere between the footpoints of open field lines and the nearest coronal hole boundary. We find the map of residual speed errors are systematic when examined as a function of f_p and d . We use these residual error maps to apply corrections to the model speeds. We test this correction approach using 3-day lead time speed forecasts for an entire year of observations and model results. Our methods can readily be applied to develop corrections for the remaining WSA forecast lead times which range from 1 to 7 days in 1-day increments. Since the solar wind density, temperature, and the interplanetary magnetic field strength all correlate well with the solar wind speed, the improved accuracy of solar wind speed forecasts enables the production of multiday forecasts of the solar wind density, temperature, pressure, and interplanetary field strength, and geophysical indices. These additional parameters would expand the usefulness of ADAPT-WSA forecasts for space weather clients.

The Multifaceted M1.7 GOES-class Flare Event of 21 April 2023 in AR13283.

[Elmhamdi](#), A., Marassi, A., Romano, P. et al.

Sol Phys 299, 109 (2024).

<https://doi.org/10.1007/s11207-024-02355-2>

On **21 April 2023**, a significant M1.7 solar flare erupted from Active Region 13283, accompanied by a filament eruption and a full-halo Coronal Mass Ejection, which reached Earth on **23 April**, triggering a severe geomagnetic storm, with Kp reaching 8 (G4) and Dst plummeting to -212 nT together with a sharply distinguished long-lasting negative double-dip behavior of the z-component of the interplanetary magnetic field. This event led to remarkable auroral displays, even at mid-latitudes in Europe. The flare-induced filament eruption caused distinct intensity dimming in the solar corona, observed in specific EUV wavelengths. We observed the dimming region growing at its fastest rate before the flare reached its peak of intensity. Notably, the proximity of the flare to a large southern coronal hole influenced the expansion and propagation of the coronal mass ejection toward Earth, probably impacting the solar wind speed and density. Additionally, we observed a sudden expansion of the coronal hole during the flare, leading us to speculating that the adjacent flare may have further stimulated the flow of solar-wind particles along the open magnetic-field lines. In accordance with the severe Dst-index disturbance, we also report changes in the potential of the pipeline of an Italian energy infrastructure company with respect to the surrounding soil as well as double-dip variation in the H-component of the terrestrial magnetic field observed locally (reminiscent to what reported in Dst-index and IMF Bz) temporal profiles, confirming the effects of the geomagnetic storm at Italy mid-latitudes. Several solar radio events have been observed too. Therefore this study provides insights into the dynamic solar phenomena and their potential geomagnetic implications.

Estimating the occurrence of geomagnetic activity using the Hilbert-Huang

S. Elvidge

Space Weather 2020 e2020SW002513

<https://doi.org/10.1029/2020SW002513>

In this paper extreme value theory (EVT) has been used to estimate the return levels for geomagnetic activity based on the aa index. The aa index is the longest, continuously recorded, geomagnetic dataset (from 1868 – Present). This long, 150 year, dataset is an ideal candidate for extreme value analysis. However the data are not independent and identically distributed as required for EVT since they are impacted by the approximately 11 year solar cycle. The Hilbert-Huang Transform has been used to identify the solar cycle component in the data and the data has been split into solar maximum and minimum times. In these two regimes the generalised extreme value distribution has been fit to the datasets. These have also been combined for an estimate of the overall return times. The results suggest that the largest event in the database (March 1989) is a one in 25 year event. However, considering separate solar maximum and minimum times has a large impact on the return times. During solar minimum conditions the return time of the March 1989 event is 130 years. This suggests that the occurrence of extreme space weather events is conditionally dependent on where in the Solar Cycle we are.

Theory of Cosmic Ray Transport in the Heliosphere

Review

N. Eugene [Engelbrecht](#), [F. Effenberger](#), [V. Florinski](#), [M. S. Potgieter](#), [D. Ruffolo](#), [R. Chhiber](#), [A. V. Usmanov](#), [J. S. Rankin](#) & [P. L. Els](#)

[Space Science Reviews](#) volume 218, Article number: 33 (2022)

<https://link.springer.com/content/pdf/10.1007/s11214-022-00896-1.pdf>

Modelling the transport of cosmic rays (CRs) in the heliosphere represents a global challenge in the field of heliophysics, in that such a study, if it were to be performed from first principles, requires the careful modelling of both large scale heliospheric plasma quantities (such as the global structure of the heliosphere, or the heliospheric magnetic field) and small scale plasma quantities (such as various turbulence-related quantities). Here, recent advances in our understanding of the transport of galactic cosmic rays are reviewed, with an emphasis on new developments pertaining to their transport coefficients, with a special emphasis on novel theoretical and numerical simulation results, as well as the CR transport studies that employ them. Furthermore, brief reviews are given of recent progress in CR focused transport modelling, as well as the modelling of non-diffusive CR transport.

Solar Event Simulations using the HAWC Scaler System

O. [Enriquez-Rivera](#), A. Lara, R. Caballero-Lopez, for the HAWC Collaboration
the 34th International Cosmic Ray Conference (ICRC2015), The Hague, The Netherlands.

<http://arxiv.org/pdf/1508.07285v1.pdf>

The High Altitude Water Cherenkov (HAWC) Observatory is an air shower array located near the volcano Sierra Negra in Mexico. The observatory has a scaler system sensitive to low energy cosmic rays (the geomagnetic cutoff for the site is 8 GV) suitable for conducting studies of solar or heliospheric transients such as Ground Level Enhancements (GLEs)

and Forbush decreases. In this work we present the simulation of the HAWC response to these phenomena. We computed HAWC effective areas for different array configurations (different selection of photomultiplier tubes per detector) relevant for Forbush decreases and GLEs. 2014 September 14

Effects of strong geomagnetic storms on Northern railways in Russia.

[Eroshenko](#), E.A., Belov, A.V., Boteler, D., Gaidash, S.P., Lobkov, S.L., Pirjola, R., Trichtchenko, L., 2010. *Advances in Space Research* 46 (9), 1102–1110. doi:10.1016/j.asr.2010.05.017.

Anomalous Forbush effects from remote by longitude solar sources

E. [Eroshenko](#)¹, Belov A.1, Mavromichalaki, H.2, Oleneva, V.1, Papaioannou, A.2, Yanke V. Proceedings IAU Symposium No. 257, 2008, **File**

The Forbush effects associated with far western and eastern powerful sources on the Sun and occurred on the background of unsettled and moderate interplanetary and geomagnetic disturbance have been studied by the data from neutron monitor network and relevant measurements of the solar wind parameters. These Forbush effects may be referred to a special sub-class of events, with the characteristics closed to the event in July 2005, and incorporated by the common conditions: absence of a significant disturbance in the Earth vicinity; absence of the strong geomagnetic storm; slow decrease of cosmic ray intensity during the main phase of the Forbush effect. General features and separate properties in behavior of density and anisotropy of 10 GV cosmic rays for this subclass are investigated.

Compositional Metrics of Fast and Slow Alfvénic Solar Wind Emerging from Coronal Holes and Their Boundaries

Tamar [Ervin](#)^{1,2}, Stuart D. Bale^{1,2}, Samuel T. Badman³, Yeimy J. Rivera³, Orlando Romeo^{2,4}, Jia Huang², Pete Riley⁵, Trevor A. Bowen², Susan T. Lepri⁶, and Ryan M. Dewey⁶ 2024 ApJ 969 83

<https://iopscience.iop.org/article/10.3847/1538-4357/ad4604/pdf>

We seek to understand the composition and variability of fast solar wind (FSW) and slow Alfvénic solar wind emerging from coronal holes (CHs). We leverage an opportune conjunction between Solar Orbiter and Parker Solar Probe (PSP) during PSP Encounter 11 to include compositional diagnostics from the Solar Orbiter Heavy Ion Sensor as these variations provide crucial insights into the origin and nature of the solar wind. We use potential field source surface and magnetohydrodynamic models to connect the observed plasma at PSP and Solar Orbiter to its origin footprint in the photosphere and compare these results with the in situ measurements. A very clear signature of a heliospheric current sheet crossing as evidenced by enhancements in low first ionization potential (FIP) elements, ion charge state ratios, proton density, low Alfvénicity, and polarity estimates validates the combination of modeling, data, and mapping. We identify two FSW streams emerging from small equatorial CHs with low ion charge state ratios, low FIP bias, high Alfvénicity, and low footprint brightness, yet anomalously low alpha particle abundance for both streams. We identify high-Alfvénicity slow solar wind emerging from the overexpanded boundary of a CH having intermediate alpha abundance, high Alfvénicity, and dips in ion charge state ratios corresponding to CH boundaries. Through this comprehensive analysis, we highlight the power of multi-instrument conjunction studies in assessing the sources of the solar wind. 2022-02-24-28, 2022/02/21-03/04

In situ measurement of slow solar wind emerging from a pseudostreamer: a conjunction study with Parker Solar Probe and Solar Orbiter

Tamar [Ervin](#), [Stuart D. Bale](#), [Samuel T. Badman](#), [Yeimy J. Rivera](#), [Orlando Romeo](#), [Jia Huang](#), [Pete Riley](#), [Trevor A. Bowen](#), [Susan T. Lepri](#), [Ryan M. Dewey](#)

ApJ 2023

<https://arxiv.org/pdf/2309.07949.pdf>

We seek to identify the source regions of the slow solar wind (SSW) through combining models with in situ observations. We leverage an opportune conjunction between Solar Orbiter and Parker Solar Probe (PSP) during PSP Encounter 11 to include compositional diagnostics from the Solar Orbiter heavy ion sensor (HIS) as these variations provide crucial insights into the origin and nature of the solar wind. We use Potential Field Source Surface (PFSS) and Magnetohydrodynamic (MHD) models to connect the observed plasma at PSP and Solar Orbiter to its origin footprint in the photosphere, and compare these results with the in situ measurements. A very clear signature of a heliospheric

current sheet (HCS) crossing as evidenced by enhancements in low FIP elements, ion charge state ratios, proton density, low-Alfvénicity, and polarity estimates validates the combination of modeling, data, and mapping. Fast wind from a small equatorial coronal hole (CH) with low ion charge state ratios, low FIP bias, high-Alfvénicity, and low footpoint brightness mostly fits together, yet includes anomalously low alpha particle abundance. We identify slow wind from many different sources, with broad variation in composition and Alfvénicity. We distinguish between classical non-Alfvénic and high-Alfvénicity SSW and make the association of low-Alfvénicity, decreased alpha-to-proton abundance, high charge state ratios, and FIP bias with streamer wind while intermediate alpha abundance, high-Alfvénicity, and dips in ion charge state ratios correspond to CH boundaries. Through this comprehensive analysis, we highlight the power of multi-instrument conjunction studies in assessing the sources of the solar wind. **2022-02-24-27**

Solar Wind Laws Valid for any Phase of a Solar Cycle **A Review**

V.G. **Eselevich**

In: Exploring the Solar Wind, Ed. Marian Lazar, **2012**, File

<http://www.intechopen.com/books/exploring-the-solar-wind>

Comment on the Paper “CAWSES November 7–8, 2004, Superstorm: Complex Solar and Interplanetary Features in the Post_Solar Maximum Phase,” B. T. Tsurutani, E. Echer, F. L. Guarnieri, and J. U. Kozyra, Geophys. Res. Lett. 35 (2008)

V. G. **Eselevich**, V. M. Bogod**b**, I. V. Chasheyc, M. V. Eselevicha, and Yu. I. Yermolaev**d**

Geomagnetism and Aeronomy, **2009**, Vol. 49, No. 1, pp. 133–135, File.

Original Russian Text published in Geomagnetizm i Aeronomiya, **2009**, Vol. 49, No. 1, pp. 142–144.

The solar sources of the magnetic storms of November 8 and 10, 2004, are analyzed. The preliminary results of such an analysis [Yermolaev et al., 2005] are critically compared with the results of the paper [Tsurutani et al., 2008], where solar flares were put in correspondence with these magnetic storms. The method for determining solar sources that cause powerful magnetospheric storms is analyzed. It has been indicated that an optimal approach consists in considering coronal mass ejections (CMEs) as storm sources and accompanying flares as additional information about the location of CME origination.

LEARNING FROM THE OUTER HELIOSPHERE: INTERPLANETARY CORONAL MASS EJECTION SHEATH FLOWS AND THE EJECTA ORIENTATION IN THE LOWER CORONA

R. M. **Evans**¹, M. Opher^{1,2}, and T. I. Gombosi³

Astrophysical Journal, 728:41 (7pp), **2011** February

The magnetic field structure of the ejecta of a coronal mass ejection (CME) is not known well near the Sun. Here we demonstrate, with a numerical simulation, a relationship between the subsonic plasma flows in the CME-sheath and the ejecta magnetic field direction. We draw an analogy to the outer heliosphere, where Opher et al. used *Voyager 2* measurements of the solar wind in the heliosheath to constrain the strength and direction of the local interstellarmagnetic field. We simulate three ejections with the same initial free energy, but different ejectamagnetic field orientations in relation to the global coronal field. Each ejection is launched into the same background solar wind using the Space Weather Modeling Framework. The different ejecta magnetic field orientations cause the CME-pause (the location of pressure balance between solar wind and ejecta material) to evolve differently in the lower corona. As a result, the CME-sheath flow deflections around the CME-pauses are different. To characterize this non-radial deflection, we use $\theta_F = \tan^{-1} v_{N/V_T}$, where V_N and V_T are the normal and tangential plasma flow as measured in a spacecraft-centered coordinate system. Near the CME-pause, we found that θ_F is very sensitive to the ejecta magnetic field, varying from 45° to 98° between the cases when the CME-driven shock is located at $4.5R_\odot$. The deflection angle for each case is found to evolve due to rotation of the ejecta magnetic field. We find that this rotation should slow or stop by $10R_\odot$ (also suggested by observational studies). These results indicate that an observational study of CME-sheath flow deflection angles from several events (to account for the interaction with the solar wind), combined with numerical simulations (to estimate the ejecta magnetic field rotation between eruption and $10R_\odot$) can be used to constrain the ejecta magnetic field in the lower corona.

Impulsive Increase of Galactic Cosmic Ray Flux Observed by IceTop

P. **Evenson**, IceCube Collaboration, P.S. Mangedard, P. Muangha, R. Pyle, D. Ruffolo and A. Sáiz
Proc. 35th Int. Cosmic Ray. Conf. Busan, PoS(ICRC2017)133 (**2017**).

<https://pos.sissa.it/301/133/pdf>

On 2017 January 18 scaler rates in the IceTop detectors at the South Pole revealed an impulsive increase in the galactic cosmic ray flux lasting a few hours. In addition to the neutron monitor at Pole the event was detected clearly by the Mawson neutron monitor and faintly at Jang Bogo. No other neutron monitors appear to have seen the increase. The event was in many ways reminiscent of the 2015 June 22 event observed by the GRAPES muon detectors. Both events occurred during the declining phase of a Forbush decrease, at a time of increasing geomagnetic activity, and were observed by a limited number of neutron monitors with similar asymptotic directions. The magnitude of the impulse was in both cases such that the flux returned briefly to approximately the pre-decrease level. Distinctly unlike the 2015 June 22 event, a changing geomagnetic cutoff cannot explain the 2017 January 18 event because the cutoff at South Pole is nearly zero and the detector response is atmosphere limited. We therefore interpret the 2017 January 18 event in terms of the structure of the Forbush decrease and (possibly changing) asymptotic directions. With our interpretation of the January event in mind we also comment on possible alternative interpretations of the GRAPES event. **2015 June 22, 2017 January 18**

The heliospheric imagers onboard the STEREO mission.

Eyles, C. J., Harrison, R. A., Davis, C. J., Waltham, N. R., Shaughnessy, B. M., Mapson-Menard, H. C. A., ... & Howard, R. A.

(2009). *Solar Physics*, 254(2), 387-445

<http://sci-hub.tw/10.1007/s11207-008-9299-0>

Mounted on the sides of two widely separated spacecraft, the two Heliospheric Imager (HI) instruments onboard NASA's STEREO mission view, for the first time, the space between the Sun and Earth. These instruments are wide-angle visible-light imagers that incorporate sufficient baffling to eliminate scattered light to the extent that the passage of solar coronal mass ejections (CMEs) through the heliosphere can be detected. Each HI instrument comprises two cameras, HI-1 and HI-2, which have 20° and 70° fields of view and are off-pointed from the Sun direction by 14.0° and 53.7°, respectively, with their optical axes aligned in the ecliptic plane. This arrangement provides coverage over solar elongation angles from 4.0° to 88.7° at the viewpoints of the two spacecraft, thereby allowing the observation of Earth-directed CMEs along the Sun – Earth line to the vicinity of the Earth and beyond. Given the two separated platforms, this also presents the first opportunity to view the structure and evolution of CMEs in three dimensions. The STEREO spacecraft were launched from Cape Canaveral Air Force Base in late October 2006, and the HI instruments have been performing scientific observations since early 2007. The design, development, manufacture, and calibration of these unique instruments are reviewed in this paper. Mission operations, including the initial commissioning phase and the science operations phase, are described. Data processing and analysis procedures are briefly discussed, and groundtest results and in-orbit observations are used to demonstrate that the performance of the instruments meets the original scientific requirements.

Evaluating predictions of ICME arrival at Earth and Mars

T. V. **Falkenberg**,¹ A. Taktakishvili,² A. Pulkkinen,^{2,3} S. Vennerstrom,¹ D. Odstrcil,² D. Brain,⁴ G. Delory,⁴ and D. Mitchell⁴

SPACE WEATHER, VOL. 9, S00E12, doi:10.1029/2011SW000682, 2011, File

We present a study of interplanetary coronal mass ejection (ICME) propagation to Earth and Mars. Because of the significant space weather hazard posed by ICMEs, understanding and predicting their arrival and impact at Mars is important for current and future robotic and manned missions to the planet. We compare running ENLILv2.6 with coronal mass ejection (CME) input parameters from both a manual and an automated method. We analyze shock events identified at Mars in Mars Global Surveyor data in 2001 and 2003, when Earth and Mars were separated by <80° in heliocentric longitude. The shocks identified at Mars were also identified at Earth, and the majority of the shock sources were identified through the Solar and Heliospheric Observatory–Large Angle and Spectrometric Coronagraph catalogue. We find that arrival times predicted by the two methods at both planets are statistically similar, dynamic pressures predicted when using the automated method are better, and the automated method tends to underestimate both CME width and speed. Using the location of the related flare as the CME direction did not improve results. In addition, changing the CME speed toward the plane- of- sky speed at 20 RS improves the match to observations, mainly because the speed found by the automated method is underestimated. The time lapse between the shock arrival at Earth and Mars, for the events studied here, is shorter than expected from simulations, and the presence of high speed streams can enable an ICME to arrive almost simultaneously at Earth and Mars. This work will be applied to improve the input parameter methods for ENLIL.

Multipoint observations of coronal mass ejection and solar energetic particle events on Mars and Earth during November 2001

Falkenberg, T. V.; Vennerstrom, S.; Brain, D. A.; Delory, G.; Taktakishvili, A.

J. Geophys. Res., Vol. 116, No. A6, A06104, **2011**

Multipoint spacecraft observations provide unique opportunities to constrain the propagation and evolution of interplanetary coronal mass ejections (ICMEs) throughout the heliosphere. Using Mars Global Surveyor (MGS) data to study both ICME and solar energetic particle (SEP) events at Mars and OMNI and Geostationary Operational Environmental Satellite (GOES) data to study ICMEs and SEPs at Earth, we present a detailed study of three CMEs and flares in late November 2001. In this period, Mars trailed Earth by 56° solar longitude so that the two planets occupied interplanetary magnetic field lines separated by only $\sim 25^\circ$. We model the interplanetary propagation of CME events using the ENLIL version 2.6 3-D MHD code coupled with the Wang-Sheeley-Arge version 1.6 potential source surface model, using Solar and Heliospheric Observatory (SOHO) Large Angle and Spectrometric Coronagraph (LASCO) images to determine CME input parameters. We find that multipoint observations are essential to constrain the simulations of ICME propagation, as two very different ICMEs may look very similar in only one observational location. The direction and width of the CME as parameters essential to a correct estimation of arrival time and amplitude of the ICME signal. We find that these are problematic to extract from the analysis of SOHO/LASCO images commonly used for input to ICME propagation models. We further confirm that MGS magnetometer and electron reflectometer data can be used to study not only ICME events but also SEP events at Mars, with good results providing a consistent picture of the events when combined with near-Earth data.

Investigations of the sensitivity of a coronal mass ejection model (ENLIL) to solar input parameters

Falkenberg, T. V.; Vršnak, B.; Taktakishvili, A.; Odstrcil, D.; MacNeice, P.; Hesse, M.

Space Weather, Volume 8, Issue 6, CiteID S06004, **2010**

Understanding space weather is not only important for satellite operations and human exploration of the solar system but also to phenomena here on Earth that may potentially disturb and disrupt electrical signals. Some of the most violent space weather effects are caused by coronal mass ejections (CMEs), but in order to predict the caused effects, we need to be able to model their propagation from their origin in the solar corona to the point of interest, e.g., Earth. Many such models exist, but to understand the models in detail we must understand the primary input parameters. Here we investigate the parameter space of the ENLILv2.5b model using the CME event of 25 July 2004. ENLIL is a time-dependent 3-D MHD model that can simulate the propagation of cone-shaped interplanetary coronal mass ejections (ICMEs) through the solar system. Excepting the cone parameters (radius, position, and initial velocity), all remaining parameters are varied, resulting in more than 20 runs investigated here. The output parameters considered are velocity, density, magnetic field strength, and temperature. We find that the largest effects on the model output are the input parameters of upper limit for ambient solar wind velocity, CME density, and elongation factor, regardless of whether one's main interest is arrival time, signal shape, or signal amplitude of the ICME. We find that though ENLILv2.5b currently does not include the magnetic cloud of the ICME, it replicates the signal at L1 well in the studied event. The arrival time difference between satellite data and the ENLILv2.5b baseline run of this study is less than 30 min.

Application of Novel Interplanetary Scintillation Visualisations using LOFAR: A Case Study of Merged CMEs from September 2017

R.A. **Fallows**, **K. Iwai**, **B.V. Jackson**, **P. Zhang**, **M.M. Bisi**, **P. Zucca**

Advances in Space Research **2022**

<https://arxiv.org/pdf/2210.02135.pdf>

Observations of interplanetary scintillation (IPS - the scintillation of compact radio sources due to density variations in the solar wind) enable the velocity of the solar wind to be determined, and its bulk density to be estimated, throughout the inner heliosphere. A series of observations using the Low Frequency Array (LOFAR - a radio telescope centred on the Netherlands with stations across Europe) were undertaken using this technique to observe the passage of an ultra-fast CME which launched from the Sun following the X-class flare of **10 September 2017**. LOFAR observed the strong radio source 3C147 at an elongation of 82 degrees from the Sun over a period of more than 30 hours and observed a

strong increase in speed to 900km/s followed two hours later by a strong increase in the level of scintillation, interpreted as a strong increase in density. Both speed and density remained enhanced for a period of more than seven hours, to beyond the period of observation. Further analysis of these data demonstrates a view of magnetic-field rotation due to the passage of the CME, using advanced IPS techniques only available to a unique instrument such as LOFAR.

Clustering of magnetic reconnection exhausts in the solar wind: An automated detection study

Naïs **Fargette**^{1,2}, Benoît Lavraud^{3,2}, Alexis P. Rouillard², Pierre S. Houdayer⁴, Tai D. Phan⁵, Marit Øieroset⁵, Jonathan P. Eastwood¹, Georgios Nicolaou⁶, Andrei Fedorov², Philippe Louarn², Christopher J. Owen⁶ and Tim S. Horbury¹

A&A 674, A98 (2023)

<https://www.aanda.org/articles/aa/pdf/2023/06/aa46043-23.pdf>

Context. Magnetic reconnection is a fundamental process in astrophysical plasmas that enables the dissipation of magnetic energy at kinetic scales. Detecting this process in situ is therefore key to furthering our understanding of energy conversion in space plasmas. However, reconnection jets typically scale from seconds to minutes in situ, and as such, finding them in the decades of data provided by solar wind missions since the beginning of the space era is an onerous task.

Aims. In this work, we present a new approach for automatically identifying reconnection exhausts in situ in the solar wind. We apply the algorithm to Solar Orbiter data obtained while the spacecraft was positioned at between 0.6 and 0.8 AU and perform a statistical study on the jets we detect.

Methods. The method for automatic detection is inspired by the visual identification process and strongly relies on the Walén relation. It is enhanced through the use of Bayesian inference and physical considerations to detect reconnection jets with a consistent approach.

Results. Applying the detection algorithm to one month of Solar Orbiter data near 0.7 AU, we find an occurrence rate of seven jets per day, which is significantly higher than in previous studies performed at 1 AU. We show that they tend to cluster in the solar wind and are less likely to occur in the tenuous solar wind ($< 10 \text{ cm}^{-3}$ near 0.7 AU). We discuss why the source and the degree of Alfvénicity of the solar wind might have an impact on magnetic reconnection occurrence.

Conclusions. By providing a tool to quickly identify potential magnetic reconnection exhausts in situ, we pave the way for broader statistical studies on magnetic reconnection in diverse plasma environments.

The preferential orientation of magnetic switchbacks and its implications for solar magnetic flux transport

Naïs **Fargette**¹, Benoit Lavraud^{1,2}, Alexis P. Rouillard¹, Victor Réville¹, Stuart D. Bale^{3,4} and Justin Kasper⁵

A&A 663, A109 (2022)

<https://www.aanda.org/articles/aa/pdf/2022/07/aa43537-22.pdf>

Context. Magnetic switchbacks in the solar wind are large deflections of the magnetic field vector, which often reverse their radial component, and are associated with a velocity spike consistent with their Alfvénic nature. The Parker Solar Probe (PSP) mission revealed them to be a dominant feature of the near-Sun solar wind. Where and how they are formed remains unclear and subject to discussion.

Aims. We investigate the orientation of the magnetic field deflections in switchbacks to determine if they are characterized by a possible preferential orientation.

Methods. We compute the deflection angles, $\psi = [\phi, \theta]T$, of the magnetic field relative to the theoretical Parker spiral direction for encounters 1 to 9 of the PSP mission. We first characterize the distribution of these deflection angles for quiet solar wind intervals and assess the precision of the Parker model as a function of distance from the Sun. We then assume that the solar wind is composed of two populations, the background quiet solar wind and the population of switchbacks, the latter of which is characterized by larger fluctuations. We model the total distribution of deflection angles we observe in the solar wind as a weighed sum of two distinct normal distributions, each corresponding to one of the populations. We fit the observed data with our model using a Monte Carlo Markov chain algorithm and retrieve the most probable mean vector and covariance matrix coefficients of the two Gaussian functions, as well as the population proportion. This method allows us to quantify the properties of both the quiet solar wind and the switchback populations without setting an arbitrary threshold on the magnetic field deflection angles.

Results. We first confirm that the Parker spiral is a valid model for quiet solar wind intervals at PSP distances. We observe that the accuracy of the spiral direction in the ecliptic is a function of radial distance, in a manner that is consistent with PSP being near the solar wind acceleration region. We then find that the fitted switchback population presents a systematic bias in its deflections, with a mean vector consistently shifted toward lower values of ϕ (-5.52° on average) and θ (-2.15° on average) compared to the quiet solar wind population. This results holds for all encounters but

encounter 6, and regardless of the magnetic field main polarity. This implies a marked preferential orientation of switchbacks in the clockwise direction in the ecliptic plane, and we discuss this result and its implications in the context of the existing switchback formation theories. Finally, we report the observation of a 12-hour patch of switchbacks that systematically deflect in the same direction, such that the magnetic field vector tip within the patch deflects and returns to the Parker spiral within a given plane. **1-10 Apr 2019**

Characteristic Scales of Magnetic Switchback Patches Near the Sun and Their Possible Association With Solar Supergranulation and Granulation

Naïs **Fargette**¹, Benoit Lavraud^{1,2}, Alexis P. Rouillard¹, Victor Réville¹, Thierry Dudok De Wit³, Clara Froment³, Jasper S. Halekas⁴, Tai D. Phan⁵, David M. Malaspina^{6,7}, Stuart D. Bale⁵ [Show full author list](#)
2021 ApJ 919 96

<https://doi.org/10.3847/1538-4357/ac1112>

Parker Solar Probe (PSP) data recorded within a heliocentric radial distance of 0.3 au have revealed a magnetic field dominated by Alfvénic structures that undergo large local variations or even reversals of the radial magnetic field. They are called magnetic switchbacks, they are consistent with folds in magnetic field lines within a same magnetic sector and are associated with velocity spikes during an otherwise calmer background. They are thought to originate either in the low solar atmosphere through magnetic reconnection processes or result from the evolution of turbulence or velocity shears in the expanding solar wind. In this work, we investigate the temporal and spatial characteristic scales of magnetic switchback patches. We define switchbacks as a deviation from the nominal Parker spiral direction and detect them automatically for PSP encounters 1, 2, 4, and 5. We focus in particular on a 5.1 day interval dominated by switchbacks during E5. We perform a wavelet transform of the solid angle between the magnetic field and the Parker spiral and find periodic spatial modulations with two distinct wavelengths, respectively consistent with solar granulation and supergranulation scales. In addition we find that switchback occurrence and spectral properties seem to depend on the source region of the solar wind rather than on the radial distance of PSP. These results suggest that switchbacks are formed in the low corona and modulated by the solar surface convection pattern.

A Machine Learning Approach to Understanding the Physical Properties of Magnetic Flux Ropes in the Solar Wind at 1 AU

Hameedullah **Farooki**, [Yasser Abdulllah](#), [Sung Jun Noh](#), [Hyomin Kim](#), [George Bizos](#), [Youra Shin](#), [Jason T. L. Wang](#), [Haimin Wang](#)

ApJ **961** 81 **2024**

<https://arxiv.org/pdf/2311.09345.pdf>

<https://iopscience.iop.org/article/10.3847/1538-4357/ad0c52/pdf>

Interplanetary magnetic flux ropes (MFRs) are commonly observed structures in the solar wind, categorized as magnetic clouds (MCs) and small-scale MFRs (SMFRs) depending on whether they are associated with coronal mass ejections. We apply machine learning to systematically compare SMFRs, MCs, and ambient solar wind plasma properties. We construct a dataset of 3-minute averaged sequential data points of the solar wind's instantaneous bulk fluid plasma properties using about twenty years of measurements from `{Wind}`. We label samples by the presence and type of MFRs containing them using a catalog based on Grad-Shafranov (GS) automated detection for SMFRs and NASA's catalog for MCs (with samples in neither labeled non-MFRs). We apply the random forest machine learning algorithm to find which categories can be more easily distinguished and by what features. MCs were distinguished from non-MFRs with an AUC of 94% and SMFRs with an AUC of 89% and had distinctive plasma properties. In contrast, while SMFRs were distinguished from non-MFRs with an AUC of 86%, this appears to rely solely on the $\langle B \rangle > 5$ nT threshold applied by the GS catalog. The results indicate that SMFRs have virtually the same plasma properties as the ambient solar wind, unlike the distinct plasma regimes of MCs. We interpret our findings as additional evidence that most SMFRs at 1 au are generated within the solar wind, and furthermore, suggesting that they should be considered a salient feature of the solar wind's magnetic structure rather than transient events.

Magnetic Field Dropouts at Near-Sun Switchback Boundaries: A Superposed Epoch Analysis

W. M. **Farrell**, R. J. MacDowall, J. R. Gruesbeck, S. D. Bale, and J. C. Kasper

2020 ApJS 249 28

<https://doi.org/10.3847/1538-4365/ab9eba>

During Parker Solar Probe's first close encounter with the Sun in early 2018 November, a large number of impulsive rotations in the magnetic field were detected within 50 R_s; these also occurred in association with short-lived impulsive solar wind bursts in speed. These impulsive features are now called "switchback" events. We examined a set of these

switchbacks where the boundary transition into and out of the switchback was abrupt, with fast B rotations and simultaneous solar wind speed changes occurring on timescales of less than ~ 10 s; these thus appear as step function-like changes in the radial component of B and V . Our objective was to search for any diamagnetic effects that might occur especially if the boundaries are associated with quick changes in density (i.e., a steep spatial density gradient at the switchback boundary). We identified 25 switchback entries where the radial component of B , B_r , quickly transitioned from large negative to positive values and V_r simultaneously abruptly increased (i.e., step-up transitions) and 28 switchback exits where B_r quickly transitioned from large positive to negative values and V_r simultaneously abruptly decreased (i.e., step-down transitions). We then performed a superposed epoch analysis on each of these sets of events. We found these fast-transitioning events typically had a clear and distinct decrease in the magnetic field magnitude by 7%–8% detected exactly at the boundary. The presence of the $|B|$ dropout suggests there is a diamagnetic current present at the boundary.

How Magnetic Reconnection May Affect the Coherence of Interplanetary Coronal Mass Ejections

C. J. **Farrugia**¹, B. J. Vasquez¹, N. Lugaz¹, N. A. Al-Haddad¹, I. G. Richardson^{2,3} +++
2023 ApJ 953 15

<https://iopscience.iop.org/article/10.3847/1538-4357/acdcf7/pdf>

On **2020 April 19–20**, a solar ejection was seen by spacecraft in a radial alignment that included Solar Orbiter and Wind. The ejection contained a magnetic flux rope where magnetic field and plasma parameters were well correlated between spacecraft. This structure is called an "unperturbed magnetic flux rope" (UMFR). Ahead of the UMFR is a portion of the ejection (not sheath) that is referred to as "upstream" (US). We focus on the US and inquire why the correlation is so much weaker there. Specifically, we analyze data collected by Solar Orbiter at 0.81 au and Wind at L1. We show that a plausible cause for the lack of coherence in the US is a combination of front erosion and internal reconnection occurring there. Front erosion is inferred from an analysis of azimuthal magnetic flux balance in the UMFR. In the present case, we contend that the US, rather than the UMFR, is the source of the eroded field lines. The presence of erosion is supported further by a direct comparison of the magnetic field data at both spacecraft that shows, in particular, a massive shrinkage of the front portion of the US. Internal reconnection is also happening at thin current sheets inside the US. Strong nonradial flows are reconfiguring the structure. As a result of these reconnection processes, a whole section of the US is disrupted and field lines move down the flanks of the ejection and out of view of Wind.

A Study of a Magnetic Cloud Propagating Through Large-Amplitude Alfvén Waves

C. J. **Farrugia**, **N. Lugaz**, **B. J. Vasquez**, **L. B. Wilson III**, **W. Yu**, **K. Paulson**, **R. B. Torbert**, **F. T. Gratton**
 JGR **Volume 125, Issue 6** June **2020** 019JA027638

<https://agupubs.onlinelibrary.wiley.com/doi/10.1029/2019JA027638>

https://scholar.google.com/scholar_url?url=https://agupubs.onlinelibrary.wiley.com/doi/pdf/10.1029/2019JA027638%3Fcasa_token%3DRjUP4ktG9egAAAAA:j6PT7FZ_T-IUyvveBw1_yRSPldFz2rCPdQiAD8MEXFPhZTJpcFMOZuvkOgXzORc3KGINvJt_iIhuslv&hl=ru&sa=T&oi=ucasa&ct=ucasa&ei=YtT1XriwAq-Sy9YP09mnqAU&scisig=AAGBfm39CeYHizJbOCux_ndbzK8hL-nYpA

We discuss Wind observations of a long and slow magnetic cloud (MC) propagating through large-amplitude Alfvén waves (LAAWs). The MC axis has a strong component along GSE X , as also confirmed by a Grad-Shafranov reconstruction. It is overtaking the solar wind at a speed roughly equal to the upstream Alfvén speed, leading to a weak shock wave 17 hr ahead. We give evidence to show that the nominal sheath region is populated by LAAWs: (i) a well-defined de Hoffmann-Teller frame in which there is excellent correlation between the field and flow vectors, (ii) constant field and total pressure, and (iii) an Alfvén ratio (i.e., ratio of kinetic-to-magnetic energy of the fluctuations) near unity at frequencies much lower than the ion cyclotron frequency in the spacecraft frame. In the region where the LAAWs approach the MC's front boundary there are field and flow discontinuities. At the first, magnetic reconnection is taking place, as deduced from a stress balance test (Walén test). This severs connection of some field lines to the Sun and the solar wind strahl disappears. There follows a 2-hr interval where the magnetic field strength is diminished while pressure balance is maintained. Here the bidirectionality of the suprathermal electron flows is intermittently disrupted. This interval ends with a slow expansion fan downstream of which there is a dropout of halo electrons just inside the front boundary of the MC. This study illustrates an untypical case of a slow MC interacting with LAAWs in the slow solar wind. **3-5 Feb 1998**

Features of the interaction of interplanetary coronal mass ejections/magnetic clouds with the Earth's magnetosphere

C.J. **Farrugia**, N.V. Erkaev, V.K. Jordanova, N. Lugaz, P.E. Sandholt, S. Mühlbacher, R.B. Torbert

JASTP, 99, July 2013, Pages 14–26

The interaction of interplanetary coronal mass ejections (ICMEs) and magnetic clouds (MCs) with the Earth's magnetosphere exhibits various interesting features principally due to interplanetary parameters which change slowly and reach extreme values of long duration. These, in turn, allow us to explore the geomagnetic response to continued and extreme driving of the magnetosphere. In this paper we shall discuss elements of the following: (i) anomalous features of the flow in the terrestrial magnetosheath during ICME/MC passage and (ii) large geomagnetic disturbances when total or partial mergers of ICMEs/MCs pass Earth. In (i) we emphasize two roles played by the upstream Alfvén Mach number in solar wind–magnetosphere interactions: (i) It gives rise to wide plasma depletion layers. (ii) It enhances the magnetosheath flow speed on draped magnetic field lines. (By plasma depletion layer we mean a magnetosheath region adjacent to the magnetopause where magnetic forces dominate over hydrodynamic forces.) In (ii) we stress that the ICME mergers elicit geoeffects over and above those of the individual members. In addition, features of the non-linear behavior of the magnetosphere manifest themselves.

Deep Solar Activity Minimum 2007 – 2009: Solar Wind Properties and Major Effects on the Terrestrial Magnetosphere

C. J. [Farrugia](#), B. Harris, M. Leitner, C. Möstl, A. B. Galvin, K. D. C. Simunac, R. B. Torbert, M. B. Temmer, A. M. Veronig, N. V. Erkaev, ...

Solar Physics, November 2012, Volume 281, Issue 1, pp 461–489

We discuss the temporal variations and frequency distributions of solar wind and interplanetary magnetic field parameters during the solar minimum of 2007 – 2009 from measurements returned by the IMPACT and PLASTIC instruments on STEREO-A. We find that the density and total field strength were significantly weaker than in the previous minimum. The Alfvén Mach number was higher than typical. This reflects the weakness of magnetohydrodynamic (MHD) forces, and has a direct effect on the solar wind–magnetosphere interactions. We then discuss two major aspects that this weak solar activity had on the magnetosphere, using data from Wind and ground-based observations: i) the dayside contribution to the cross-polar cap potential (CPCP), and ii) the shapes of the magnetopause and bow shock. For i) we find a low interplanetary electric field of 1.3 ± 0.9 mV m⁻¹ and a CPCP of 37.3 ± 20.2 kV. The auroral activity is closely correlated to the prevalent stream–stream interactions. We suggest that the Alfvén wave trains in the fast streams and Kelvin–Helmholtz instability were the predominant agents mediating the transfer of solar wind momentum and energy to the magnetosphere during this three-year period. For ii) we determine 328 magnetopause and 271 bow shock crossings made by Geotail, Cluster 1, and the THEMIS B and C spacecraft during a three-month interval when the daily averages of the magnetic and kinetic energy densities attained their lowest value during the three years under survey. We use the same numerical approach as in Fairfield's (J. Geophys. Res. 76, 7600, 1971) empirical model and compare our findings with three magnetopause models. The stand-off distance of the subsolar magnetopause and bow shock were 11.8 R_E and 14.35 R_E, respectively. When comparing with Fairfield's (1971) classic result, we find that the subsolar magnetosheath is thinner by ~ 1 R_E. This is mainly due to the low dynamic pressure which results in a sunward shift of the magnetopause. The magnetopause is more flared than in Fairfield's model. By contrast the bow shock is less flared, and the latter is the result of weaker MHD forces.

Multiple, distant (40°) in situ observations of a magnetic cloud and a corotating interaction region complex

C.J. [Farrugia](#), , , D.B. Berdichevskyb, C. Möstlc, A.B. Galvina, M. Leitnerd, M.A. Popeckia, K.D.C. Simunaca, A. Opitze, B. Lavraude, K.W. Ogilvief, A.M. Veronigg, M. Temmerc, J.G. Luhmannh and J.A. Sauvaud

Journal of Atmospheric and Solar-Terrestrial Physics, Volume 73, Issue 10, 2011, Pages 1254–1269

We report a comprehensive analysis of in situ observations made by Wind and the STEREO probes (STA, STB) of a complex interaction between a magnetic cloud (MC) and a corotating interaction region (CIR) occurring near the heliospheric current sheet (HCS) on **November 19–21, 2007**. The probes were separated by 0.7 AU (40°) with a spread in heliographic latitudes (4.8°, 2.2°, and –0.4°, for STB, Wind and STA, respectively). We employ data from the MFI, SWE and 3DP instruments on Wind, and the PLASTIC and IMPACT suites on STEREO. STB, located east of Earth, observed a forward shock followed by signatures of a MC. The MC took the role of the HCS in that the polarity of the interplanetary magnetic field (IMF) on exit was the reverse of that on entry. A passage through a plasma sheet was observed. Along the Sun–Earth line Wind observed a stream interface (SI) between a forward and a reverse shock. A MC, compressed by the CIR, was entrained in this. STA, located 20° to the west of Earth, saw a MC which was not preceded by a shock. A SI trailed the transient. The shocks are examined using various methods and from this it is concluded that the forward shock at Wind—but not at STB—was driven by the MC. Examining the MC by Grad–Shafranov reconstruction, we find evidence of a double-flux rope structure at Wind and STA and possibly also at STB.

The orientations are at variance with the notion of a large-scale flux tube being observed at the three spacecraft. We find consistency of this with the directional properties of the solar wind “strahl” electrons. We examine aspects of the geomagnetic response and find a double-dip storm corresponding to the two interplanetary triggers. The minimum Dst phase was prolonged and the geoeffects were intensified due to the interaction. We conclude that while the formation of compound streams is a common feature of interplanetary space, understanding their components when CIRs are involved is a complicated matter needing numerical simulations and/or more in situ observations for its complete elucidation.

Research highlights

► Three-spacecraft observations and analysis of a complex interaction between a magnetic cloud (MC) and a corotating interaction region (CIR). ► A MC cloud consisting of two flux ropes and distorted by the interaction with the CIR. ► Force-free and Grad Shafranov modeling challenge the classic picture of a MC as a large-scale, bent coherent flux tube. ► An element of the geomagnetic response consists of a double-dip magnetic storm.

A two-ejecta event associated with a two-step geomagnetic storm

C. J. [Farrugia](#), C.J., Jordanova, V.K., Thomsen, M.F., Lu, G., Cowley, S.W.H., Ogilvie, K.W., JGR, VOL. 111, A11104, 2006

A new view on how large disturbances in the magnetosphere may be prolonged and intensified further emerges from a recently discovered interplanetary process: the collision/merger of interplanetary (IP) coronal mass ejections (ICMEs; ejecta) within 1 AU. As shown in a recent pilot study, the merging process changes IP parameters dramatically with respect to values in isolated ejecta. The resulting geoeffects of the coalesced (“complex”) ejecta reflect a superposition of IP triggers which may result in, for example, two-step, major geomagnetic storms. In a case study, we isolate the effects on ring current enhancement when two coalescing ejecta reached Earth on **31 March 2001**. The magnetosphere “senses” the presence of the two ejecta and responds with a reactivation of the ring current soon after it started to recover from the passage of the first ejection, giving rise to a double-dip (DD) great storm (each min $Dst < -250$ nT). A drift-loss global kinetic model of ring current buildup shows that in this case the major factor determining the intensity of the storm activity is the very high (up to ~ 10 cm⁻³) plasma sheet density. The plasma sheet density, in turn, is found to correlate well with the very high solar wind density, suggesting the compression of the leading ejecta as the source of the hot, superdense plasma sheet in this case. This correlation is similar to that obtained in a previous investigation extending over several years, but the present case study extends the range of plasma sheet densities from ~ 2 to ~ 10 cm⁻³. Since the features of the ejecta interaction in this example are fairly general, we propose that interacting ejecta are a new, important IP source of DD major storms. Peculiarities in the behavior of the magnetopause current during these extreme events are briefly discussed in the light of recent work. In a brief discussion of a second example (**21–23 October 2001**), we suggest that by strengthening the leading shock, the ejecta merger may have added to the “shock-driver gas” origin of DD geomagnetic storms by increasing the ability of the shock to compress preexisting $B_z < 0$ magnetic fields.

Relating near-Earth observations of an interplanetary coronal mass ejection to the conditions at its site of origin in the solar corona

[Fazakerley](#), A. N.; [Harra, L. K.](#); [Culhane, J. L.](#); [van Driel-Gesztelyi, L.](#); [Lucek, E.](#); [Matthews, S. A.](#); [Owen, C. J.](#); [Mazelle, C.](#); [Balogh, A.](#); [Rème, H.](#)

Geophysical Research Letters, Volume 32, Issue 13, CiteID L13105, 2005

File from *Proceedings of the 11th European Solar Physics Meeting - The Dynamic Sun: Challenges for Theory and Observations, 11-16 September 2005 (ESA SP-596, December 2005)*

January 20, 2004

We demonstrate that signatures of both the arcade material and the flux rope material are clearly identifiable in the Cluster and ACE data, indicating that the **magnetic field orientations changed little as the material traveled to the Earth**, and that *the methods we used to infer coronal magnetic field configurations are effective*.

Observations of magnetic flux ropes opened or disconnected from the Sun by magnetic reconnection in interplanetary space

HengQiang [Feng](#), Yan Zhao, Jiemin Wang, Qiang Liu, and Guoqing Zhao
Front. Phys., 12 May 2021 |

<https://doi.org/10.3389/fphy.2021.679780>

<https://www.frontiersin.org/articles/10.3389/fphy.2021.679780/full>

During solar eruptions, many closed magnetic flux ropes are ejected into interplanetary space, which contribute to the heliospheric magnetic field and have important space weather effect because of their coherent magnetic field. Therefore, understanding the evolution of these closed flux ropes in the interplanetary space is important. In this paper, we examined all the magnetic and plasma data measured in 1997 by the Wind spacecraft and identified 621 reconnection exhausts. Of the 621 reconnection events, 31 were observed at the boundaries of magnetic flux ropes and were thought to cause the opening or disconnection magnetic field lines of the adjacent ropes. Of the 31 magnetic reconnection events, 29 were interchange reconnections and the closed field lines of these related flux ropes were opened by them. Only 2 of the 31 magnetic reconnection events disconnected the opened field lines of the original flux ropes. These observations indicate that interchange reconnection and disconnection may be two important mechanisms changing the magnetic topology of the magnetic flux ropes during their propagation during the interplanetary space. **Nov 9, 1997, Nov 16, 1997**

Table 1. The magnetic reconnection exhausts and their related flux ropes. (1997)

Statistical Study of ICMEs with Low Mean Carbon Charge State Plasmas Detected from 1998 to 2011

Xuedong Feng^{1,2}, Shuo Yao¹, Dongni Li¹, Gang Li^{1,3}, and Xiaoli Yan⁴

2018 ApJ 868 124

<http://iopscience.iop.org/article/10.3847/1538-4357/aae92c/pdf>

We present a statistical study of 219 ICMEs measured by both ACE and WIND from 1998 to 2011. ICME plasmas are defined as possessing cold materials if the carbon average charge states are lower than those of the preceding solar wind by three standard deviations and the carbon ionic temperature is lower than 106.05 K. A total of 69 ICMEs were identified as containing cold materials. These ICMEs tend to have speeds in the range of 300–600 km s⁻¹, with durations between 2 and 6 hr. Cold materials tend to be present once or twice per ICME. We further identify two special types of cold materials: the ionic-cold type (IC) shows simultaneous lower average charge states of O, Mg, Si, and Fe ions than those of the preceding solar wind, while the carbon-only cold type (COC) shows a totally opposite trend in that these ions show higher average charge than in the preceding solar wind. We found that the IC has a higher proton temperature than the ICME mean value, whereas the COC has a lower proton temperature than the ICME mean value, and the COC is most often measured in magnetic cloud. A detailed examination of the IC and the COC material suggests that they are related to solar filaments. Their special mean charge indicates that the filaments are a mixture of coronal and chromospheric materials. Heating and collision processes beyond the carbon freeze-in height are crucial in generating the two distinct types.

Observations on the Magnetic Disconnections of a Magnetic Cloud from the Sun through Magnetic Reconnection

H. Q. Feng, J. M. Wang, G. Q. Zhao, and Y. Zhao

2018 ApJ 864 101

Most coronal mass ejections (CMEs) originally exhibit closed magnetic flux rope (MFR) structures near the Sun. Moreover, the amount of magnetic field magnitude in the heliosphere can continually increase when CMEs propagate from the Sun to interplanetary space. To solve the problem of increased magnetic field magnitude, the closed field lines of MFRs should be opened and disconnected through magnetic reconnections. Here, we report a magnetic cloud (MC) associated with a magnetic reconnection exhaust measured by Wind over the period of 2001 **October 31 to November 1**. Observations of unidirectional suprathermal electron strahls revealed that part of the field lines before the rear boundary of the MC was opened. The magnetic reconnection event was disconnecting the opened field lines of the MC by merging with open field lines after the MC. These observations indicated that MFRs could be opened or disconnected in no particular order.

Data-driven modeling of the solar wind from 1 Rs to 1 AU

Xueshang Feng, Xiaopeng Ma, Changqing Xiang

JGR 2016

We present here a time-dependent three-dimensional magnetohydrodynamic (MHD) solar wind simulation from the solar surface to the Earth's orbit driven by time-varying line-of-sight solar magnetic field data. The simulation is based on the three-dimensional (3-D) solar-interplanetary (SIP) adaptive mesh refinement (AMR) space-time conservation

element and solution element (CESE) MHD (SIP-AMR-CESE MHD) model. In this simulation, we first achieve the initial solar wind background with the time-relaxation method by inputting a potential field obtained from the synoptic photospheric magnetic field and then generate the time-evolving solar wind by advancing the initial 3-D solar wind background with continuously varying photospheric magnetic field. The model updates the inner boundary conditions by using the projected normal characteristic method, inputting the high-cadence photospheric magnetic field data corrected by solar differential rotation, and limiting the mass flux escaping from the solar photosphere. We investigate the solar wind evolution from **1 July to 11 August 2008** with the model driven by the consecutive synoptic maps from the Global Oscillation Network Group. We compare the numerical results with the previous studies on the solar wind, the solar coronal observations from the Extreme ultraviolet Imaging Telescope board on Solar and Heliospheric Observatory, and the measurements from OMNI at 1 astronomical unit (AU). Comparisons show that the present data-driven MHD model's results have overall good agreement with the large-scale dynamical coronal and interplanetary structures, including the sizes and distributions of the coronal holes, the positions and shapes of the streamer belts, the heliocentric distances of the Alfvénic surface, and the transitions of the solar wind speeds. However, the model fails to capture the small-sized equatorial holes, and the modeled solar wind near 1 AU has a somewhat higher density and weaker magnetic field strength than observed. Perhaps better preprocessing of high-cadence observed photospheric magnetic field (particularly 3-D global measurements), combined with plasma measurements and higher resolution grids, will enable the data-driven model to more accurately capture the time-dependent changes of the ambient solar wind for further improvements. In addition, other measures may also be needed when the model is employed in the period of high solar activity.

Counterstreaming electrons in small interplanetary magnetic flux ropes†

H. Q. Feng, G. Q. Zhao, J. M. Wang

JGR Volume 120, Issue 12 Pages 10,175–10,184 2015

<http://onlinelibrary.wiley.com/doi/10.1002/2015JA021643/full>

Small interplanetary magnetic flux ropes (SIMFRs) are commonly observed by spacecraft at 1 AU, and their origin still remains disputed. We investigated the counterstreaming suprathermal electron (CSE) signatures of 106 SIMFRs measured by Wind during 1995–2005. We found that 79 (75%) of the 106 flux ropes contain CSEs, and the percentages of counterstreaming vary from 8% to 98%, with a mean value of 51%. CSEs are often observed in magnetic clouds (MCs), and this indicates these MCs are still attached to the Sun at both ends. CSEs are also related to heliospheric current sheets (HCSs) and the Earth's bow shock. We divided the SIMFRs into two categories, as follows: The first category is far from HCSs, and the second category is in the vicinity of HCSs. The first category has 57 SIMFRs, and only 7 of 57 ropes have no CSEs. This ratio is similar to that of MCs. The second category has 49 SIMFRs, however, 20 of the 49 events have no CSEs. This ratio is larger than that of MCs. These two categories have different origins. One category originates from the solar corona, and most ropes are still connected to the Sun at both ends. The other category is formed near HCSs in the interplanetary space. **12 October 2004, 11 November 2005**

Table 1. Percent Counterstreaming in SIMFRs

Observations of Several Unusual Plasma Compositional Signatures within Small Interplanetary Magnetic Flux Ropes

H. Q. Feng¹ and J. M. Wang

2015 ApJ 809 112

Interplanetary coronal mass ejections (ICMEs) often show unusual plasma compositional signatures (high He/P ratio, high O^{7+}/O^{6+} ratio, and high Fe charge states), and their enhanced charge states of oxygen and iron are caused by flare-related heating in the corona. We investigated the abnormal plasma composition of small interplanetary magnetic flux ropes (IMFRs) in terms of He/P ratio, O^{7+}/O^{6+} ratio, and mean Fe charge state. We discover that 18 of the 24 small IMFRs showed high He/P ratios. In addition, 12 and 8 of the 24 events showed high Fe charge states and O^{7+}/O^{6+} ratios, respectively. This observation implies that these small IMFRs and ICMEs may be caused by the same coronal eruptions.

MORPHOLOGICAL EVOLUTION OF A THREE-DIMENSIONAL CORONAL MASS EJECTION CLOUD RECONSTRUCTED FROM THREE VIEWPOINTS

L. Feng^{1,2}, B. Inhester², Y. Wei², W. Q. Gan¹, T. L. Zhang³, and M. Y. Wang

2012 ApJ 751 18

The propagation properties of coronal mass ejections (CMEs) are crucial to predict its geomagnetic effect. A newly developed three-dimensional (3D) mask fitting reconstruction method using coronagraph images from three viewpoints

has been described and applied to the CME ejected on **2010 August 7**. The CME's 3D localization, real shape, and morphological evolution are presented. Due to its interaction with the ambient solar wind, the morphology of this CME changed significantly in the early phase of evolution. Two hours after its initiation, it was expanding almost self-similarly. The CME's 3D localization is quite helpful to link remote sensing observations to in situ measurements. The investigated CME was propagating to Venus with its flank just touching STEREO B. Its corresponding interplanetary CME in the interplanetary space shows a possible signature of a magnetic cloud with a preceding shock in Venus Express (VEX) observations, while from STEREO B only a shock is observed. We have calculated three principal axes for the reconstructed 3D CME cloud. The orientation of the major axis is, in general, consistent with the orientation of a filament (polarity inversion line) observed by SDO/AIA and SDO/HMI. The flux rope axis derived by the Minimal Variance Analysis from VEX indicates a radial-directed axis orientation. It might be that locally only the leg of the flux rope passed through VEX. The height and speed profiles from the Sun to Venus are obtained. We find that the CME speed possibly had been adjusted to the speed of the ambient solar wind flow after leaving the COR2 field of view and before arriving at Venus. A southward deflection of the CME from the source region is found from the trajectory of the CME geometric center. We attribute it to the influence of the coronal hole where the fast solar wind emanated from.

Magnetic reconnection exhausts at the boundaries of small interplanetary magnetic flux ropes

H. Q. **Feng**^{1,2}, D. J. Wu³, J. M. Wang¹ and J. W. Chao
A&A 527, A67 (2011)

Context. Small interplanetary magnetic flux ropes (SIMFRs) are commonly observed by spacecraft at 1 AU.

Aims. We provide a mechanism to decrease the dimensions of some SIMFRs as they propagate away from the Sun.

Methods. We carefully examined the high-resolution magnetic field and plasma data from the Wind spacecraft during the period 1995–2005 to identify X-line magnetic reconnection exhausts at the boundaries of SIMFRs.

Results. We identified nine X-line magnetic reconnection exhausts at the boundaries of SIMFRs, which were destroying the flux within the related SIMFRs.

Conclusions. These observational facts indicate that the boundaries of some SIMFRs were still evolving through interaction with the background solar wind, and their spatial scales would diminish gradually.

Are all leading shocks driven by magnetic clouds?,

Feng, H. Q., D. J. Wu, J. K. Chao, L. C. Lee, and L. H. Lyu (2010),
J. Geophys. Res., 115, A04107, doi:10.1029/2009JA014875

Magnetic clouds (MCs) are commonly observed in association with shocks at 1 AU, and many authors have claimed that the leading shocks are driven by MCs, without any direct evidence. In this work we surveyed the relations between MCs and their associated shocks. Using the interplanetary plasma and magnetic field data measured by Wind, we have identified 97 MCs near Earth during 1995 to 2007. Sixty-two (64%) of the MCs were associated with leading shocks. As Lepping et al. have pointed out, if a leading shock is driven by an MC, the axis of the driver should be approximately perpendicular to the shock normal. We calculated the angle between the axis of the MC and its leading shock normal and found that the angle for 21 of the 62 MCs deviates from 90° by more than 25°. Seventeen of the 21 MCs also have the following signatures: (1) The MC leading edge moves more slowly than the preceding shock; and (2) the time interval between the preceding shock and the front boundary of the MC is always long, with an average period of 15.4 h. The speed profiles of the other four events revealed that the leading shock was driven not directly by the MC but by the immediately subsequent flow, and their sheath durations are shorter than the time interval between the preceding shocks and the MC front boundaries. Therefore, at least 21 (34%) of 62 leading shocks were not directly driven by MCs.

An operational method for shock arrival time prediction by one-dimensional CESE-HD solar wind model

Feng, X. S., Y. Zhang, L. P. Yang, S.T. Wu, M. Dryer
J. Geophys. Res., Vol. 114, No. A10, A10103, 2009
<http://dx.doi.org/10.1029/2009JA014385>

With the purpose of operational real-time forecasting for arrival times of flare/coronal mass ejection associated shocks in the vicinity of the Earth, a one-dimensional hydrodynamic (HD) shock propagation model is established by a novel numerical scheme, the space-time conservation element and solution element (CESE) method. The required observational data inputs to this new one-dimensional CESE-HD model are the low coronal radio Type II drift speed, the duration estimation, and the background solar wind speed for a solar eruptive event. Applying this model to 137 solar events during the period of February 1997 to August 2002, it is found that our model could be practically

equivalent to the STOA, ISPM, HAFv.2, and SPM models in forecasting the shock arrival time. The absolute error in the transit time from our model is not larger than those of the other four models for the same set of events. These results may demonstrate the potential capability of our model in terms of improving real-time forecasting because the CESE method can be extended to three-dimensional magnetohydrodynamics (3D-MHD) from the solar photosphere to any heliospheric position.

A practical database method for predicting arrivals of average interplanetary shocks at Earth,

Feng, X. S., Y. Zhang, W. Sun, M. Dryer, C. D. Fry, and C. S. Deehr

J. Geophys. Res., 114, A01101, (2009), <http://dx.doi.org/10.1029/2008JA013499>

A practical database method for predicting the interplanetary shock arrival time at L1 point is presented here. First, a shock transit time database (hereinafter called Database-I) based on HAFv.1 (version 1 of the Hakamada-Akasofu-Fry model) is preliminarily established with hypothetical solar events. Then, on the basis of the prediction test results of 130 observed solar events during the period from February 1997 to August 2002, Database-I is modified to create a practical database method, named Database-II, organized on a multidimensional grid of source location, initial coronal shock speed, and the year of occurrence of the hypothetical solar event. The arrival time at L1 for any given solar event occurring in the 23rd solar cycle can be predicted by looking up in the grid of Database-II according to source location, the initial coronal shock speed, and the year of occurrence in cycle 23. Within the hit window of ± 12 h, the success rate of the Database-II method for 130 solar events is 44%. This could be practically equivalent to the shock time of arrival (STOA) model, the interplanetary shock propagation model (ISPM), and the HAFv.2 model. To explore the capability of this method, it is tested on new data sets. These tests give reasonable results. In particular, this method's performance for a set of events in other cycles is as good as that of the STOA and ISPM models. This gives us confidence in its application to other cycles. From the viewpoint of long-term periodicity for solar activity, it is expected that the Database-II method can be applicable to the next solar cycle 24.

Geoeffective Analysis of CMEs Under Current Sheet Magnetic Coordinates,

Xueshang **Feng** and Xinhua Zhao,

[Astrophysics and Space Science, Volume 305, Number 1](#), 37-47, 2006

Using 100 CME-ICME events during 1997.01-2002.11, based on the eruptive source locations of CMEs and solar magnetic field observations at the photosphere, a current sheet magnetic coordinate (CMC) system is established in order to statistically study the characteristics of the CME-ICME events and the corresponding geomagnetic storm intensity.

A New Prediction Method for the Arrival Time of Interplanetary Shocks,

Xueshang **Feng** and Xinhua Zhao,

Solar Physics, Volume 238 Number 1, p. 167-186, 2006. **File**

Solar transient activities such as solar flares, disappearing filaments, and coronal mass ejections (CMEs) are solar manifestations of interplanetary (IP) disturbances. Forecasting the arrival time at the near Earth space of the associated interplanetary shocks following these solar disturbances is an important aspect in space weather forecasting because the shock arrival usually marks the geomagnetic storm sudden commencement (SSC) when the IMF B_z component is appropriately southward and/or the solar wind dynamic pressure behind the shock is sufficiently large. Combining the analytical study for the propagation of the blastwave from a point source in a moving, steady-state, medium with variable density (Wei, 1982; Wei and Dryer, 1991) with the energy estimation method in the ISPM model (Smith and Dryer, 1990, 1995), we present a new shock propagation model (called SPM below) for predicting the arrival time of interplanetary shocks at Earth. The duration of the X-ray flare, the initial shock speed and the total energy of the transient event are used for predicting the arrival of the associated shocks in our model. Especially, the background speed, i.e., the convection effect of the solar wind is considered in this model. Applying this model to 165 solar events during the periods of January 1979 to October 1989 and February 1997 to August 2002, we found that our model could be practically equivalent to the prevalent models of STOA, ISPM and HAFv.2 in forecasting the shock arrival time. The absolute error in the transit time in our model is not larger than those of the other three models for the same sample events. Also, the prediction test shows that the relative error of our model is $\leq 10\%$ for 27.88% of all events, $\leq 30\%$ for 71.52%, and $\leq 50\%$ for 85.46%, which is comparable to the relative errors of the other models. These results might demonstrate a potential capability of our model in terms of real-time forecasting.

Numerical modeling of cosmic rays in the heliosphere: Analysis of proton data from AMS-02 and PAMELA

Emanuele [Fiandrini](#), [Nicola Tomassetti](#), [Bruna Bertucci](#), [Federico Donnini](#), [Maura Graziani](#), [Behrouz Khiali](#)
2020

<https://arxiv.org/pdf/2010.08649.pdf>

Galactic cosmic rays (GCRs) inside the heliosphere are affected by solar modulation. To investigate this phenomenon and its underlying physical mechanisms, we have performed a data-driven analysis of the temporal dependence of the GCR proton flux over the solar cycle. We have modeled the solar modulation effect by means of stochastic simulations of cosmic particles in the heliospheric plasma. We have constrained our model using the recent time-resolved measurements of GCR proton fluxes reported by AMS-02 and PAMELA experiments, on monthly basis, from mid-2006 to mid-2017. With a global statistical analysis, we have determined the key model parameters that rules the GCR transport, its dependence on the particle rigidity, and its evolution over the solar cycle. Our data sample comprises epochs of solar minimum, solar maximum, as well as epochs with magnetic reversal and opposite polarities. Along with the evolution of the GCR transport parameters, we study their relationship with solar activity proxies and interplanetary parameters. We find that the rigidity dependence of the parallel mean free path of GCR diffusion shows a remarkable time dependence, indicating a long-term variability in the interplanetary turbulence that interchanges across different regimes over the solar cycle. The evolution of GCR diffusion parameters show a delayed correlation with the sunspot number, reflecting the dynamics of the heliospheric plasma, and different dependencies for opposite states of magnetic polarity, reflecting the influence of charge-sign dependent drift in the GCR modulation.

Characterizing Auroral-Zone Absorption Based on Global Kp and Regional Geomagnetic Hourly Range Indices

R. A. D. [Fiori](#), [L. Trichtchenko](#), [C. Balch](#), [E. Spanswick](#), [S. Groleau](#)

Space Weather e2020SW002572 **2020**

<https://agupubs.onlinelibrary.wiley.com/doi/10.1029/2020SW002572>

Increased ionization in the auroral oval leads to the absorption of high-frequency radio waves in the auroral zone, or auroral absorption. Auroral absorption is typically characterized by global geomagnetic activity indices, such as the Kp index. In this paper the hourly range of the magnetic field (HR) is examined as an alternative to the 3-hr Kp index for describing the dynamic and localized features of auroral absorption represented by the hourly range of absorption (HRA). Kp, magnetometer, and riometer data were examined for a 3-year period for stations spread across typical auroral latitudes. A general linear relationship was shown to exist between Kp and LOG10(HRA) for Kp < 4; for Kp ≥ 4 the correlation was weaker. A stronger linear correlation was demonstrated between LOG10(HRA) and LOG10(HR) for HR > 50 nT, characterized by a correlation coefficient of R = 0.63. Increased variability in the relationship between HRA and Kp was attributed to the following factors: the variability of the magnetic field within the 3-hr window characterized by the Kp index, which was better represented by a 1-hr HR; the dependence of the Kp index on subauroral magnetic data, which is not subject to the geomagnetic variations typically experienced within the auroral region; and reduced statistics for Kp > 6.

Global Circulation of the Open Magnetic Flux of the Sun

L. A. [Fisk](#) and J. C. Kasper

2020 ApJL 894 L4

<https://doi.org/10.3847/2041-8213/ab8acd>

The global circulation of the open magnetic flux of the Sun, the component of the solar magnetic field that opens into the heliosphere, and the consequences of the global circulation were proposed by Fisk and coworkers in the early 2000s. The Parker Solar Probe, on its initial encounters with the Sun, has provided direct confirmation of both the global circulation and the physical mechanism by which the circulation occurs, transport by interchange reconnection between open magnetic flux and large coronal loops. The implications of this confirmation of the global circulation of open magnetic flux and the importance of interchange reconnection is discussed.

Data-driven solar wind model and prediction of type II bursts

M. S. L. [Florens](#), Iver H. Cairns, S. A. Knock, P. A. Robinson

GEOPHYSICAL RESEARCH LETTERS, VOL. 34, L04104, doi:10.1029/2006GL028522, **2007**

Type II solar radio bursts are produced by shock waves moving through the corona and solar wind. An existing theory predicts Type II dynamic spectra by considering electron acceleration at the shock, growth of Langmuir waves, and their conversion into radiation. Two contributions are presented, both relevant to space weather research and missions like STEREO. First, a more realistic 2-dimensional model for the solar wind is developed, based on spacecraft data at 1 AU, and illustrated for a specific period. It relates time to longitude and extrapolates to different heliocentric distances using MHD style equations and power-law temperature models. Second, the type II theory is combined with the data-driven solar wind model to predict the dynamic spectrum of a specific Type II burst. The results show reasonable semiquantitative agreement with observations. Issues and possible improvements are outlined.

Comparing the Properties of ICME-Induced Forbush Decreases at Earth and Mars

Johan L. Freiherr von [Forstner](#), [Jingnan Guo](#), [Robert F. Wimmer-Schweingruber](#), [Mateja Dumbović](#), [Miho Janvier](#), [Pascal Démoulin](#), [Astrid Veronig](#), [Manuela Temmer](#), [Athanasios Papaioannou](#), [Sergio Dasso](#), [Donald M. Hassler](#), [Cary J. Zeitlin](#)

JGR [Volume125, Issue3](#) March 2020 e2019JA027662

sci-hub.ru/10.1029/2019JA027662

Forbush decreases (FDs), which are short-term drops in the flux of galactic cosmic rays, are caused by the shielding from strong and/or turbulent magnetic structures in the solar wind, especially interplanetary coronal mass ejections (ICMEs) and their associated shocks, as well as corotating interaction regions. Such events can be observed at Earth, for example, using neutron monitors, and also at many other locations in the solar system, such as on the surface of Mars with the Radiation Assessment Detector instrument onboard Mars Science Laboratory. They are often used as a proxy for detecting the arrival of ICMEs or corotating interaction regions, especially when sufficient in situ solar wind measurements are not available. We compare the properties of FDs observed at Earth and Mars, focusing on events produced by ICMEs. We find that FDs at both locations show a correlation between their total amplitude and the maximum hourly decrease, but with different proportionality factors. We explain this difference using theoretical modeling approaches and suggest that it is related to the size increase of ICMEs, and in particular their sheath regions, en route from Earth to Mars. From the FD data, we can derive the sheath broadening factor to be between about 1.5 and 1.9, agreeing with our theoretical considerations. This factor is also in line with previous measurements of the sheath evolution closer to the Sun.

2.2. [Catalogs](#) of FDs at Earth and Mars

Tracking and validating ICMEs propagating towards Mars using STEREO Heliospheric Imagers combined with Forbush decreases detected by MSL/RAD

Johan L. Freiherr von [Forstner](#), [Jingnan Guo](#), [Robert F. Wimmer-Schweingruber](#), [Manuela Temmer](#), [Mateja Dumbović](#), [Astrid Veronig](#), [Christian Möstl](#), [Donald M. Hassler](#), [Cary J. Zeitlin](#), [Bent Ehresmann](#)

Space Weather [Volume17, Issue4](#) Pages 586-598 2019

<http://sci-hub.se/10.1029/2018SW002138>

The Radiation Assessment Detector (RAD) instrument onboard the Mars Science Laboratory (MSL) mission's Curiosity rover has been measuring galactic cosmic rays (GCR) as well as solar energetic particles (SEP) on the surface of Mars for more than 6 years since its landing in August 2012. The observations include a large number of Forbush decreases (FD) caused by interplanetary coronal mass ejections (ICMEs) and/or their associated shocks shielding away part of the GCR particles with their turbulent and enhanced magnetic fields while passing Mars.

This study combines MSL/RAD FD measurements and remote tracking of ICMEs using the STEREO Heliospheric Imager (HI) telescopes in a statistical study for the first time. The large dataset collected by HI makes it possible to analyze 149 ICMEs propagating towards MSL both during its 8-month cruise phase and after its landing on Mars. We link 45 of the events observed at STEREO-HI to their corresponding FDs at MSL/RAD and study the accuracy of the ICME arrival time at Mars predicted from HI data using different methods.

The mean differences between the predicted arrival times and those observed using FDs range from -11 h to 5 h for the different methods, with standard deviations between 17 and 20 hours. These values for predictions at Mars are very similar compared to other locations closer to the Sun, and also comparable to the precision of some other modeling approaches.

Forecasting GOES 15 >2 MeV electron fluxes from solar wind data and geomagnetic indices

C. [Forsyth](#), [C. E. J. Watt](#), [M. K. Mooney](#), [I. J. Rae](#), [S. D. Walton](#), [R. B. Horne](#)

Space Weather e2019SW002416 2020

<https://agupubs.onlinelibrary.wiley.com/doi/epdf/10.1029/2019SW002416>

The flux of > 2 MeV electrons at geosynchronous orbit is used by space weather forecasters as a key indicator of enhanced risk of damage to spacecraft in low, medium or geosynchronous Earth orbits. We present a methodology that uses the amount of time a single input dataset (solar wind data or geomagnetic indices) exceeds a given threshold to produce deterministic and probabilistic forecasts of the > 2 MeV flux at GEO exceeding 1000 or 10000 cm⁻² s⁻¹ sr⁻¹ within up to 10 days. By comparing our forecasts with measured fluxes from GOES 15 between 2014 and 2016, we determine the optimum forecast thresholds for deterministic and probabilistic forecasts by maximising the ROC and Brier Skill Scores respectively. The training dataset gives peak ROC scores of 0.71 to 0.87 and peak Brier Skill Scores of -0.03 to 0.32. Forecasts from AL give the highest skill scores for forecasts of up to 6-days. AL, solar wind pressure or SYM-H give the highest skill scores over 7-10 days. Hit rates range over 56-89% with false alarm rates of 11-53%. Applied to 2012, 2013 and 2017, our best forecasts have hit rates of 56-83% and false alarm rates of 10-20%. Further tuning of the forecasts may improve these. Our hit rates are comparable to those from operational fluence forecasts, that incorporate fluence measurements, but our false alarm rates are higher. This proof-of-concept shows that the geosynchronous electron flux can be forecast with a degree of success without incorporating a persistence element into the forecasts.

ICMES IN THE INNER HELIOSPHERE: ORIGIN, EVOLUTION AND PROPAGATION EFFECTS

Report of Working Group G

R. J. **FORSYTH**^{1,*}, V. BOTHMER², C. CID³, N. U. CROOKER⁴, T. S. HORBURY¹,
K. KECSKEMETY⁵, B. KLECKER⁶, J. A. LINKER⁷, D. ODSTRCIL⁸, M. J. REINER⁹,
I. G. RICHARDSON¹⁰, J. RODRIGUEZ-PACHECO³, J. M. SCHMIDT¹¹
and R. F. WIMMER-SCHWEINGRUBER

Space Science Reviews (2006) 123: 383–416; **File**

This report assesses the current status of research relating the origin at the Sun, the evolution through the inner heliosphere and the effects on the inner heliosphere of the interplanetary counterparts of coronal mass ejections (ICMEs). The signatures of ICMEs measured by in-situ spacecraft are determined both by the physical processes associated with their origin in the low corona, as observed by space-borne coronagraphs, and by the physical processes occurring as the ICMEs propagate out through the inner heliosphere, interacting with the ambient solar wind. The solar and in-situ observations are discussed as are efforts to model the evolution of ICMEs from the Sun out to 1 AU.

Multi-Spacecraft Study of the **January 21, 2005 ICME: Evidence of Current Sheet Substructure at the Periphery of a Strongly Expanding, Fast, Magnetic Cloud**

Foullon, C., Owen, C.J., Dasso, S., Green, L.M., Dandouras, I., Elliott, H.A.,
Fazakerley, A.N., Bogdanova, Y.V. and Crooker, N.U.

E-print, March 2007, Solar Phys (2007) 244: 139–165

Travel time classification of extreme solar events: Two families and an outlier

Freed, A. J.; Russell, C. T.

Geophysical Research Letters, Volume 41, Issue 19, pp. 6590-6594, 2014; **File**

Extreme solar events are of great interest because of the extensive damage that could be experienced by technological systems such as electrical transformers during such periods. In studying geophysical phenomena, it is helpful to have a quantitative measure of event strength so that similar events can be intercompared. Such a measure also allows the calculation of the occurrence rates of events with varying strength. We use historical fast travel time solar events to develop a measure of strength based on the Sun-Earth trip time. We find that these fast events can be grouped into two distinct families with one even faster outlier. That outlier is not the Carrington event of 1859 but the extremely intense solar particle event of August 1972. **1 September 1859, 20 October 1989, 23 July 2012**

Neural network applications in geomagnetic storm prognosis based on the pre-storm occurrence of magnetic islands in the solar wind

Mikhail **Fridman**

EGU2020-1848 May 2020

<https://meetingorganizer.copernicus.org/EGU2020/displays/36057>

So far, the problem of a short-term forecast of geomagnetic storms can be considered as solved. Meanwhile, mid-term prognoses of geomagnetic storms with an advance time from 3 hours to 3 days are still unsuccessful (see <https://www.swpc.noaa.gov/sites/default/files/images/u30/Max%20Kp%20and%20GPRPRA.pdf>) This fact suggests a necessity of looking for specific processes in the solar wind preceding geomagnetic storms. Knowing that magnetic cavities filled with magnetic islands and current sheets are formed in front of high-speed streams of any type (Khabarova et al., 2015, 2016, 2018; Adhikari et al., 2019), we have performed an analysis of the corresponding ULF variations in the solar wind density observed at the Earth's orbit from hours to days before the arrival of a geoeffective stream or flow. The fact of the occurrence of ULF-precursors of geomagnetic storms was noticed a long time ago (Khabarova 2007; Khabarova & Yermolaev, 2007) and related prognostic methods were recently developed (Kogai et al. 2019), while the problem of automatization of the prognosis remained unsolved.

A new geomagnetic storm forecast method, which employs a Recurrent Neural Network (RNN) for an automatic pattern search, is proposed. An ability of self-teaching and extracting deeply hidden non-linear patterns is the main advantage of Deep Neural Networks (DNNs) with multiple layers over traditional Machine Learning methods. We show a success of the RNN method, using either the unprocessed solar wind density data or Wavelet analysis coefficients as the input parameter for a DNN to perform an automatic mid-term prognosis of geomagnetic storms.

Direct evidence for magnetic reconnection at the boundaries of magnetic switchbacks with Parker Solar Probe

C. [Froment](#), [V. Krasnoselskikh](#), [T. Dudok de Wit](#), [O. Agapitov](#), [N. Fargette](#), [B. Lavraud](#), [A. Larosa](#), [M. Kretzschmar](#), [V. K. Jagarlamudi](#), [M. Velli](#), [D. Malaspina](#), [P. L. Whittlesey](#), [S. D. Bale](#), [A. W. Case](#), [K. Goetz](#), [J. C. Kasper](#), [K. E. Korreck](#), [D. E. Larson](#), [R. J. MacDowall](#), [F. S. Mozer](#), [M. Pulupa](#), [C. Revillet](#), [M. L. Stevens](#)

A&A, PSP special issue **2021**

<https://arxiv.org/pdf/2101.06279.pdf>

Parker Solar Probe's first encounters with the Sun revealed the presence of ubiquitous localised magnetic deflections in the inner heliosphere; these structures, often called switchbacks, are particularly striking in solar wind streams originating from coronal holes. We report the direct evidence for magnetic reconnection occurring at the boundaries of three switchbacks crossed by Parker Solar Probe (PSP) at a distance of 45 to 48 solar radii of the Sun during its first encounter. We analyse the magnetic field and plasma parameters from the FIELDS and SWEAP instruments. The three structures analysed all show typical signatures of magnetic reconnection. The ion velocity and magnetic field are first correlated and then anti-correlated at the inbound and outbound edges of the bifurcated current sheets with a central ion flow jet. Most of the reconnection events have a strong guide field and moderate magnetic shear but one current sheet shows indications of quasi anti-parallel reconnection in conjunction with a magnetic field magnitude decrease by 90%. Given the wealth of intense current sheets observed by PSP, reconnection at switchbacks boundaries appears to be rare. However, as the switchback boundaries accommodate currents one can conjecture that the geometry of these boundaries offers favourable conditions for magnetic reconnection to occur. Such a mechanism would thus contribute in reconfiguring the magnetic field of the switchbacks, affecting the dynamics of the solar wind and eventually contributing to the blending of the structures with the regular wind as they propagate away from the Sun. **1-2 Nov 2018**

Estimating the Open Solar Flux from In-Situ Measurements

[Anna Marie Frost](#), [Mathew Owens](#), [Allan Macneil](#) & [Mike Lockwood](#)
[Solar Physics](#) volume 297, Article number: 82 (2022)

<https://link.springer.com/content/pdf/10.1007/s11207-022-02004-6.pdf>

A fraction of the magnetic flux threading the solar photosphere extends to sufficient heliocentric distances that it is dragged out by the solar wind. Understanding this open solar flux (OSF) is central to space weather, as the OSF forms the heliosphere, magnetically connects the Sun to the planets, and dominates the motion of energetic particles. Quantification of OSF is also a key means of verifying global coronal models. However, OSF estimates derived from extrapolating the magnetic field from photospheric observations are consistently smaller than those based on heliospheric magnetic field (HMF) measurements, by around a factor two. It is therefore important to understand the uncertainties in estimating OSF from in-situ HMF measurements. This requires both an assumption of latitudinal invariance in the radial component of the HMF in the heliosphere, and that structures without an immediate connection to the Sun, such as local magnetic field inversions (or 'switchbacks'), can be correctly accounted for. In this study, we investigate the second assumption. Following an established methodology, we use in-situ electron and magnetic data to determine the global topology of the HMF and correct for inversions that would otherwise lead to an overestimation of the OSF. The OSF estimation is applied to the interval 1994 – 2021 and combines measurements from the Wind and ACE spacecraft. This extends the time range over which this methodology has previously been applied from 13 years

(1998 – 2011) to 27 years. We find that inversions cannot fully explain the discrepancy between heliospheric and photospheric OSF estimations, with the best heliospheric estimate of OSF still, on average, a factor 1.6 higher than the values extrapolated from photospheric observations.

The contribution and FIP bias of three types of materials inside ICMEs associated with different flare intensities

Hui Fu, [Xinzheng Shi](#), [Zhenghua Huang](#), [Youqian Qi](#), [Lidong Xia](#)

ApJ **956** 129 **2023**

<https://arxiv.org/pdf/2309.09434.pdf>

<https://iopscience.iop.org/article/10.3847/1538-4357/acfa76/pdf>

The studies on the origination and generation mechanisms of ICME materials are crucial for understanding the connection between CMEs and flares. The materials inside ICMEs can be classified into three types, coming from corona directly (corona-materials), heated by magnetic reconnection in corona (heated-corona-materials), and generated by chromospheric evaporation (chromospheric-evaporation-materials). Here, the contribution and First Ionization Potential (FIP) bias of three types of materials inside ICMEs associated with different flare intensities are analyzed and compared. We find that the speeds and scales of near-Earth ICMEs both increase with flare intensities. The proportions of heated-corona-materials are nearly constant with flare intensities. The contributions of corona-materials (chromospheric-evaporation-materials) are significantly decreased (increased) with flare intensities. More than two-thirds of materials are chromospheric-evaporation-materials for ICMEs associated with strong flares. The FIP bias of corona-materials and heated-corona-materials is almost the same. The FIP bias of chromospheric-evaporation-materials is significantly higher than that of corona-materials and heated-corona-materials, and it is increased with flare intensities. The above characteristics of FIP bias can be explained reasonably by the origination and generation mechanisms of three types of ICME materials. The present study demonstrates that the origination and generation mechanisms of ICME materials are significantly influenced by flare intensities. The reasons for the elevation of FIP bias, if ICMEs are regarded as a whole, are that the FIP bias of chromospheric-evaporation-materials is much higher, and the chromospheric-evaporation-materials contributed significantly to the ICMEs which associated with strong flares.

Variations of the Galactic Cosmic Rays in the Recent Solar Cycles

Shuai Fu, [Xiaoping Zhang](#), [Lingling Zhao](#), [Yong Li](#)

Astrophysical Journal Supplement **254** 37 **2021**

<https://arxiv.org/pdf/2104.07862.pdf>

<https://iopscience.iop.org/article/10.3847/1538-4365/abf936/pdf>

<https://doi.org/10.3847/1538-4365/abf936>

In this paper, we study the galactic cosmic ray (GCR) variations over the solar cycles 23 and 24, with measurements from the NASA's ACE/CRIS instrument and the ground-based neutron monitors (NMs). The results show that the maximum GCR intensities of heavy nuclei (nuclear charge 5-28, 50-500 MeV/nuc) at 1 AU during the solar minimum in 2019-2020 break their previous records, exceeding those recorded in 1997 and 2009 by ~25% and ~6%, respectively, and are at the highest levels since the space age. However, the peak NM count rates are lower than those in late 2009. The difference between GCR intensities and NM count rates still remains to be explained. Furthermore, we find that the GCR modulation environment during the solar minimum P24/25 are significantly different from previous solar minima in several aspects, including remarkably low sunspot numbers, extremely low inclination of the heliospheric current sheet, rare coronal mass ejections, weak interplanetary magnetic field and turbulence. These changes are conducive to reduce the level of solar modulation, providing a plausible explanation for the record-breaking GCR intensities in interplanetary space.

The high helium abundance and charge states of the interplanetary CME and its material source on the Sun

Hui Fu, [R.A. Harrison](#), [J.A. Davies](#), [LiDong Xia](#), [XiaoShuai Zhu](#), [Bo Li](#), [ZhengHua Huang](#), [D. Barnes](#)

ApJL **900** L18 **2020**

<https://arxiv.org/pdf/2008.08816.pdf>

<https://doi.org/10.3847/2041-8213/abb083>

Identifying the source of the material within coronal mass ejections (CMEs) and understanding CME onset mechanisms are fundamental issues in solar and space physics. Parameters relating to plasma composition, such as charge states and He abundance (λ_{He}), may be different for plasmas originating from differing processes or regions on the Sun. Thus, it is crucial to examine the relationship between in-situ measurements of CME composition and activity on the Sun. We

study the CME that erupted on **2014 September 10**, in association with an X1.6 flare, by analyzing AIA imaging and IRIS spectroscopic observations and its in-situ signatures detected by Wind and ACE. We find that during the slow expansion and intensity increase of the sigmoid, plasma temperatures of 9 MK, and higher, first appear at the footpoints of the sigmoid, associated with chromospheric brightening. Then the high-temperature region extends along the sigmoid. IRIS observations confirm that this extension is caused by transportation of hot plasma upflow. Our results show that chromospheric material can be heated to 9 MK, and above, by chromospheric evaporation at the sigmoid footpoints before flare onset. The heated chromospheric material can transport into the sigmoidal structure and supply mass to the CME. The aforementioned CME mass supply scenario provides a reasonable explanation for the detection of high charge states and elevated $\langle n_e \rangle$ in the associated ICME. The observations also demonstrate that the quasi-steady evolution in the precursor phase is dominated by magnetic reconnection between the rising flux rope and the overlying magnetic field structure.

Helium abundance and speed difference between helium ions and protons in the solar wind from coronal holes, active regions, and quiet Sun

Hui Fu, [Maria S. Madjarska](#), [Bo Li](#), [LiDong Xia](#), [ZhengHua Huang](#)

MNRAS **2018**

<https://arxiv.org/pdf/1805.02880.pdf>

Two main models have been developed to explain the mechanisms of release, heating and acceleration of the nascent solar wind, the wave-turbulence-driven (WTD) models and reconnection-loop-opening (RLO) models, in which the plasma release processes are fundamentally different. Given that the statistical observational properties of helium ions produced in magnetically diverse solar regions could provide valuable information for the solar wind modelling, we examine the statistical properties of the helium abundance (A_{He}) and the speed difference between helium ions and protons ($v_{\alpha,p}$) for coronal holes (CHs), active regions (ARs) and the quiet Sun (QS). We find bimodal distributions in the space of A_{He} and $v_{\alpha,p}/v_A$ (where v_A is the local Alfvén speed) for the solar wind as a whole. The CH wind measurements are concentrated at higher A_{He} and $v_{\alpha,p}/v_A$ values with a smaller A_{He} distribution range, while the AR and QS wind is associated with lower A_{He} and $v_{\alpha,p}/v_A$, and a larger A_{He} distribution range. The magnetic diversity of the source regions and the physical processes related to it are possibly responsible for the different properties of A_{He} and $v_{\alpha,p}/v_A$. The statistical results suggest that the two solar wind generation mechanisms, WTD and RLO, work in parallel in all solar wind source regions. In CH regions WTD plays a major role, whereas the RLO mechanism is more important in AR and QS.

Charge States and FIP Bias of the Solar Wind from Coronal Holes, Active Regions, and Quiet Sun

Hui Fu¹, Maria S. Madjarska^{2,1}, LiDong Xia¹, Bo Li¹, ZhengHua Huang¹, and Zhipeng Wangguan

2017 ApJ 836 169

10.3847/1538-4357/aa5cba

Connecting in situ measured solar-wind plasma properties with typical regions on the Sun can provide an effective constraint and test to various solar wind models. We examine the statistical characteristics of the solar wind with an origin in different types of source regions. We find that the speed distribution of coronal-hole (CH) wind is bimodal with the slow wind peaking at ~ 400 km s⁻¹ and the fast at ~ 600 km s⁻¹. An anti-correlation between the solar wind speeds and the O7+/O6+ ion ratio remains valid in all three types of solar wind as well during the three studied solar cycle activity phases, i.e., solar maximum, decline, and minimum. The range and its average values all decrease with the increasing solar wind speed in different types of solar wind. The range (0.06–0.40, first ionization potential (FIP) bias range 1–7) for active region wind is wider than for CH wind (0.06–0.20, FIP bias range 1–3), while the minimum value of (~ 0.06) does not change with the variation of speed, and it is similar for all source regions. The two-peak distribution of CH wind and the anti-correlation between the speed and O7+/O6+ in all three types of solar wind can be explained qualitatively by both the wave-turbulence-driven and reconnection-loop-opening (RLO) models, whereas the distribution features of in different source regions of solar wind can be explained more reasonably by the RLO models.

Coronal Sources and In Situ Properties of the Solar Winds Sampled by ACE During 1999 – 2008

Hui Fu, [Bo Li](#), [Xing Li](#), [Zhenghua Huang](#), [Chaozhou Mou](#), [Fangran Jiao](#), [Lidong Xia](#)

Solar Phys. May 2015, Volume 290, [Issue 5](#), pp 1399-1415 **2015**

We identify the coronal sources of the solar winds sampled by the ACE spacecraft during 1999 – 2008 and examine the in situ solar wind properties as a function of wind sources. The standard two-step mapping technique is adopted to establish the photospheric footpoints of the magnetic flux tubes along which the ACE winds flow. The footpoints are then placed in the context of EIT 284 Å images and photospheric magnetograms, allowing us to categorize the sources

into four groups: coronal holes (CHs), active regions (ARs), the quiet Sun (QS), and “undefined”. This practice also enables us to establish the response to solar activity of the fractions occupied by each type of solar wind, and of their speeds and O7+/O6+ ratios measured in situ. We find that during the maximum phase, the majority of ACE winds originate from ARs. During the declining phase, CHs and ARs are equally important contributors to the ACE solar winds. The QS contribution increases with decreasing solar activity and maximizes in the minimum phase when the QS appears to be the primary supplier of the ACE winds. With decreasing activity, the winds from all sources tend to become cooler, as represented by the increasingly low O7+/O6+ ratios. On the other hand, during each activity phase, the AR winds tend to be the slowest and are associated with the highest O7+/O6+ ratios, while the CH winds correspond to the other extreme, with the QS winds lying in between. Applying the same analysis method to the slow winds alone, here defined as the winds with speeds lower than 500 km s⁻¹, we find basically the same overall behavior, as far as the contributions of individual groups of sources are concerned. This statistical study indicates that QS regions are an important source of the solar wind during the minimum phase.

Relationship Between Solar Wind Speed and Coronal Magnetic Field Properties

Ken'ichi **Fujiki**, Munetoshi Tokumaru, Tomoya Iju, Kazuyuki Hakamada, Masayoshi Kojima
Solar Phys. Volume 290, Issue 9, pp 2491-2505 **2015**

<http://arxiv.org/pdf/1507.03301v2.pdf>

We have studied the relationship between the solar-wind speed [V] and the coronal magnetic-field properties (a flux expansion factor [f] and photospheric magnetic-field strength [Bs]) at all latitudes using data of interplanetary scintillation and solar magnetic field obtained for 24 years from 1986 to 2009. Using a cross-correlation analyses, we verified that V is inversely proportional to f and found that V tends to increase with Bs if f is the same. As a consequence, we find that V has extremely good linear correlation with Bs/f. However, this linear relation of V and Bs/f cannot be used for predicting the solar-wind velocity without information on the solar-wind mass flux. We discuss why the inverse relation between V and f has been successfully used for solar-wind velocity prediction, even though it does not explicitly include the mass flux and magnetic-field strength, which are important physical parameters for solar-wind acceleration.

PRECURSORS OF THE FORBUSH DECREASE ON 2006 DECEMBER 14 OBSERVED WITH THE GLOBAL MUON DETECTOR NETWORK (GMDN)

A. **Fushishita**, T. Kuwabara, C. Kato et al.

Astrophysical Journal, 715:1239–1247, **2010** June

We analyze the precursor of a Forbush decrease (FD) observed with the Global Muon Detector Network on **2006 December 14**. An intense geomagnetic storm is also recorded during this FD with the peak Kp index of 8+. By using the “two-dimensional map” of the cosmic ray intensity produced after removing the contribution from the diurnal anisotropy, we succeed in extracting clear signatures of the precursor. A striking feature of this event is that a weak loss-cone (LC) signature is first recorded more than a day prior to the storm sudden commencement (SSC) onset. This suggests that the LC precursor appeared only 7 hr after the coronal mass ejection eruption from the Sun, when the interplanetary (IP) shock driven by the interplanetary coronal mass ejection was located at 0.4 AU from the Sun. We find the precursor being successively observed with multiple detectors in the network according to the Earth’s spin and confirmed that the precursor continuously exists in space. The long lead time (15.6 hr) of this precursor which is almost twice the typical value indicates that the interplanetary magnetic field (IMF) was more quiet in this event than a typical power spectrum assumed for the IMF turbulence. The amplitude (−6.45%) of the LC anisotropy at the SSC onset is more than twice the FD size, indicating that the maximum intensity depression behind the IP shock is much larger than the FD size recorded at the Earth in this event. We also find the excess intensity from the sunward IMF direction clearly observed during ~10 hr preceding the SSC onset. It is shown that this excess intensity is consistent with the measurement of the particles accelerated by the head-on collisions with the approaching shock. This is the first detailed observation of the precursor due to the shock reflected particles with muon detectors.

To the question about perturbations of solar-terrestrial characteristics

E. A. **Gavryuseva** (Institute for Nuclear Research RAS)

2018

<https://arxiv.org/pdf/1802.04348.pdf>

Data obtained over the last three solar cycles have been analysed to reveal the relationships between the intensity of the photospheric field measured along the line of sight by the WSO group at heliolatitudes from -75 to 75 degrees and the

intensity of the interplanetary magnetic field and absolute values of the perturbations of the different characteristics of the solar wind at the Earth orbit, and geomagnetic parameters. provided by the OMNI team.
The heliospheric and geomagnetic data are found to be divided into two groups characterized by their response to variability of the solar magnetic field latitudinal structures on short and on long time scales.

Relations between variability of the photospheric and interplanetary magnetic fields, solar wind and geomagnetic characteristics

E. A. [Gavryuseva](#) (Institute for Nuclear Research RAS)

2018

<https://arxiv.org/pdf/1802.03135.pdf>

Large scale solar magnetic field topology has a great influence on the structure of the corona, heliosphere and geomagnetic perturbations.

Data obtained over the last three solar cycles have been analysed to reveal the relationships between the photospheric field measured along the line of sight by the WSO group at 30 levels of heliolatitudes from -75 to 75 degrees and the interplanetary magnetic field. The main aim of this first paper is to make a direct comparison between the basic structure and dynamics of the photospheric magnetic field and components and intensity of the interplanetary magnetic field, solar wind and geomagnetic parameters without using theoretical assumptions, models, physical expectations, etc.

The second paper by Gavryuseva, 2018d presents the reports between different characteristics of the solar wind at the Earth orbit, and geomagnetic parameters provided by the OMNI team. % Data obtained over the last three solar cycles have been analysed % to reveal the relationships % between the photospheric field measured along the line of sight % by the WSO group % at heliolatitudes from -75 to 75 degrees averaged over one year % and the interplanetary magnetic field, different characteristics % of the solar wind at the Earth orbit, and geomagnetic parameters. % provided by the OMNI team.

The heliospheric and geomagnetic data are found to be divided into two groups characterized by their response to variability of the solar magnetic field latitudinal structures on short and on long time scales.

ICMES AT HIGH LATITUDES AND IN THE OUTER HELIOSPHERE

Report of Working Group H

P. R. [GAZIS](#)^{1,*}, A. BALOGH², S. DALLA³, R. DECKER⁴, B. HEBER⁵, T. HORBURY²,
A. KILCHENMANN⁶, J. KOTA⁷, H. KUCHARAK⁸, H. KUNOW⁵, D. LARIO⁹,
M. S. POTGIETER⁹, J. D. RICHARDSON¹⁰, P. RILEY¹¹, L. RODRIGUEZ¹²,
G. SISCOE¹³ and R. VON STEIGER

Space Science Reviews (2006) 123: 417–451

Magnetic Clouds and Major Geomagnetic storms

[Georgieva](#) K., Kirov B.

2nd Intern. Symp. SEE-2005, Armenia, p. 214-217, File.

See IAU Symp. 226. p. 470, 2005, Book

High-Speed Solar Wind Streams and Geomagnetic Storms During Solar Cycle 24

M. [Gerontidou](#), H. Mavromichalaki, T. Daglis

[Solar Physics](#) September 2018, 293:131

<https://link.springer.com/article/10.1007/s11207-018-1348-8>

An updated catalog is created of 303 well-defined high-speed solar wind streams that occurred in the time period 2009 – 2016. These streams are identified from solar and interplanetary measurements obtained from the OMNIWeb database as well as from the Solar and Heliospheric Observatory (SOHO) database. This time interval covers the deep minimum observed between the last two Solar Cycles 23 and 24, as well as the ascending, the maximum, and part of the descending phases of the current Solar Cycle 24. The main properties of solar-wind high-speed streams, such as their maximum velocity, their duration, and their possible sources are analyzed in detail. We discuss the relative importance of all those parameters of high-speed solar wind streams and especially of their sources in terms of the different phases of the current cycle. We carry out a comparison between the characteristic parameters of high-speed solar wind streams in the present solar cycle with those of previous solar cycles to understand the dependence of their long-term variation on the cycle phase. Moreover, the present study investigates the varied phenomenology related to the magnetic interactions between these streams and the Earth's magnetosphere. These interactions can initiate geomagnetic disturbances resulting in geomagnetic storms at Earth that may have impact on technology and endanger human activity and health.

Table : An updated catalogue of High-Speed Solar Wind Streams (HSSWSs) from 2009 to 2016.
Supplementary material [11207_2018_1348_MOESM1_ESM.docx](#)

Structure of the Photospheric Magnetic Field During Sector Crossings of the Heliospheric Magnetic Field

Tibebu [Getachew](#), Ilpo Virtanen, Kalevi Mursula

[Solar Physics](#) November **2017**, 292:174

The photospheric magnetic field is the source of the coronal and heliospheric magnetic fields (HMF), but their mutual correspondence is non-trivial and depends on the phase of the solar cycle. The photospheric field during the HMF sector crossings observed at 1 AU has been found to contain enhanced field intensities and definite polarity ordering, forming regions called Hale boundaries. Here we separately study the structure of the photospheric field during the HMF sector crossings during Solar Cycles 21 – 24 for the four phases of each solar cycle. We use a refined version of Svalgaard's list of major HMF sector crossings, mapped to the Sun using the solar wind speed observed at Earth, and the daily level-3 magnetograms of the photospheric field measured at the Wilcox Solar Observatory in 1976 – 2016. We find that the structure of the photospheric field corresponding to the HMF sector crossings and the existence and properties of the corresponding Hale bipolar regions varies significantly with solar cycle, solar cycle phase, and hemisphere. The Hale boundaries in more than half of the ascending, maximum, and declining phases are clear and statistically significant. The clearest Hale boundaries are found during the (+,-) HMF crossings in the northern hemisphere of odd Cycles 21 and 23, but less systematic during the (+,-) crossings in the southern hemisphere of even Cycles 22 and 24. No similar difference between odd and even cycles is found for the (-,+) crossings. This shows that the northern hemisphere has a more organized Hale pattern overall. The photospheric field distribution also depicts a larger area for the field of the northern hemisphere during the declining and minimum phases, in a good agreement with the bashful ballerina phenomenon.

Interaction of a coronal mass ejection and a stream interaction region: A case study

Paul [Geyer](#)¹, Mateja [Dumbović](#)¹, Manuela [Temmer](#)², Astrid [Veronig](#)², Karin [Dissauer](#)³ and Bojan [Vršnak](#)¹
A&A 672, A168 (2023)

<https://doi.org/10.1051/0004-6361/202245433>

<https://www.aanda.org/articles/aa/pdf/2023/04/aa45433-22.pdf>

We investigated the interaction of a coronal mass ejection (CME) and a coronal hole (CH) in its vicinity using remote-sensing and 1 AU in situ data. We used extreme-ultraviolet images and magnetograms to identify coronal structures and coronagraph images to analyze the early CME propagation. The Wind spacecraft and the Advanced Composition Explorer (ACE) provide plasma and magnetic field data of near-Earth interplanetary space. We applied various diagnostic tools to the images and to the time-series data. We find that the CME erupts under a streamer and causes the evacuation of material at its far end, which is observable as dimming and subsequent CH formation. The CME is likely deflected in its early propagation and travels southwest of the Sun-Earth line. In situ data lack signatures of a large magnetic cloud, but show a small flux rope at the trailing edge of the interplanetary CME (ICME), followed by an Alfvénic wave. This wave is identified as exhaust from a Petschek-type reconnection region following the successful application of a Walén test. We infer that the two spacecraft at 1 AU most likely traverse the ICME leg that is in the process of reconnection along the heliospheric current sheet that separates the ICME and the high-speed stream outflowing from the CH. **2014: January 25, February 4-10, February 17**

Properties of stream interaction regions at Earth and Mars during the declining phase of SC 24

Paul [Geyer](#), [Manuela Temmer](#), [Jingnan Guo](#), [Stephan G. Heinemann](#)

A&A 649, A80 2021

<https://arxiv.org/pdf/2102.05948.pdf>

<https://www.aanda.org/articles/aa/pdf/2021/05/aa40162-20.pdf>

<https://doi.org/10.1051/0004-6361/202040162>

We inspect the evolution of SIRs from Earth to Mars (distance range 1-1.5 AU) over the declining phase of solar cycle 24 (2014-2018). So far, studies only analyzed SIRs measured at Earth and Mars at different times. We compare existing catalogs for both heliospheric distances and arrive at a clean dataset for the identical time range. This allows a well-sampled statistical analysis and for the opposition phases of the planets an in-depth analysis of SIRs as they evolve with distance. We use in-situ solar wind data from OMNI and the MAVEN spacecraft as well as remote sensing data from

SDO. A superposed epoch analysis is performed for bulk speed, proton density, temperature, magnetic field magnitude and total perpendicular pressure. Additionally, a study of events during the two opposition phases of Earth and Mars in the years 2016 and 2018 is conducted. SIR related coronal holes with their area as well as their latitudinal and longitudinal extent are extracted and correlated to the maximum bulk speed and duration of the corresponding high speed solar wind streams following the stream interaction regions. We find that while the entire solar wind HSS shows no expansion as it evolves from Earth to Mars, the crest of the HSS profile broadens by about 17%, and the magnetic field and total pressure by about 45% around the stream interface. The difference between the maximum and minimum values in the normalized superposed profiles increases slightly or stagnates from 1-1.5 AU for all parameters, except for the temperature. A sharp drop at zero epoch time is observed in the superposed profiles for the magnetic field strength at both heliospheric distances. Maximum solar wind speed has a stronger dependence on the latitudinal extent of the respective coronal hole than on its longitudinal extent. We arrive at an occurrence rate of fast forward shocks three times as high at Mars than at Earth. **2016-06-03, 06-29, 07-26, 08-21, 09-17**

The role of extreme geomagnetic storms in the Forbush decrease profile observed by neutron monitors

Ghag, K ; Tari, P ; Raghav, A ; +++

JOURNAL OF ATMOSPHERIC AND SOLAR-TERRESTRIAL PHYSICS V. 252, Article 106146, **2023**

DOI 10.1016/j.jastp.2023.106146

<https://arxiv.org/pdf/2112.09918.pdf>

The Forbush decrease (FD) and Geomagnetic storm (GS) are the two distinct space weather events having common causing agents like interplanetary coronal mass ejection (ICME) or corotating interacting region (CIR). Generally, large-amplitude FDs and extreme GSs are caused by ICME. Here, we studied eight ICME induced extreme storms and their effects on respective FD profiles as observed by neutron monitors. We observed the sudden storm commencement of the GS coincides with the FD onset. Interestingly, we also noted a gradual increase in neutron counts during the main and recovery phases of GS. The maximum enhancement in neutron counts coincides with the minimum value of the Sym-H index. The enhancement is visible primarily in all the neutron monitors but significantly pronounced in high-energy neutrons compared to low-energy neutrons. We observed that the enhancement in cosmic ray flux during Forbush decrease as observed by neutron monitors is contributed by magnetospheric disturbance of geomagnetic storm. Thus we conclude that the weakening of Earth's magnetic shield due to ICME-Magnetosphere interaction allows more cosmic rays to reach the ground. Thus, we conclude that the geomagnetic storm conditions highly influence the FD profile along with the external causing agent. Therefore, it is essential to include the effect of geomagnetic field variation in the models that are used to reproduce the FD profile. **13 July 1992 and 10 May 1991 , 24th November 2001 , 20 November 2003, 26 August 2018**

Distinct polytropic behavior of plasma during ICME-HSS Interaction

Kalpesh **Ghag**, [Anil Raghav](#), [Zubair Shaikh](#), [Georgios Nicolaou](#), [Omkar Dhamane](#), [Utsav Panchal](#) **2022**

<https://arxiv.org/pdf/2210.04065.pdf>

Interplanetary Coronal Mass Ejections (ICMEs) and High Speed Streams (HSSs) are noteworthy drivers of disturbance of interplanetary space. Interaction between them can cause several phenomena, such as; generation of waves, enhanced geo-effectiveness, particle acceleration, etc. However, how does thermodynamic properties vary during the ICME-HSS interaction remain an open problem. In this study, we investigated the polytropic behavior of plasma during an ICME-HSS interaction observed by STEREO and Wind spacecraft. We find that the ICME observed by the STEREO-A has polytropic index $\alpha=1.0$, i.e., exhibiting isothermal process. Moreover, Wind spacecraft observed the HSS region, non-interacting ICME, and ICME-HSS interaction region. During each regions we found $\alpha=1.8$, $\alpha=0.7$, and $\alpha=2.5$, respectively. It implies that the HSS region exhibits a nearly adiabatic behaviour, ICME region is closely isothermal, and the ICME-HSS interaction region exhibits super-adiabatic behaviour. The insufficient expansion of the ICME due to the interaction with HSS triggers the system for heating and cooling mechanisms which dependent on the degrees of freedom of plasma components.

ICME pancaking: a cause of two-step severe storm (Dst \sim -187 nT) of 25th solar cycle observed on 23 April 2023

Kalpesh **Ghag**, [Anil Raghav](#), [Ankush Bhaskar](#), [Shirish Soni](#), [Bhagyashri Sathe](#), [Zubair Shaikh](#), [Omkar Dhamane](#), [Prathmesh Tari](#)

JGR: Space Weather **2023**

<https://arxiv.org/pdf/2305.05381.pdf>

Interplanetary Coronal Mass Ejections (ICMEs) are prominent drivers of space weather disturbances and mainly lead to intense or extreme geomagnetic storms. The reported studies suggested that the planar ICME sheath and planar magnetic clouds (MCs) cause extreme storms. Here, we investigated the severe two-step geomagnetic storm ($Dst \sim -187$ nT) of 25th solar cycle. Our analysis demonstrates flattened (pancaked) ICME structures, i.e., quasi-planar magnetic structures (PMS). The study corroborates our earlier reported finding that the less adiabatic expansion in quasi-PMS transformed ICME enhanced the strength of the southward magnetic field component. It contributes to the efficient transfer of plasma and energy in the Earth's magnetosphere to cause the observed severe storm.

Galactic Cosmic Rays Modulation in the Vicinity of Corotating Interaction Regions: Observations During the Last Two Solar Minima

Keyvan **Ghanbari**^{1,2}, Vladimir Florinski^{1,2}, Xiaocheng Guo³, Qiang Hu^{1,2}, and Richard Leske⁴

2019 ApJ 882 54

<https://doi.org/10.3847/1538-4357/ab31a5>

[sci-hub.se/10.3847/1538-4357/ab31a5](https://arxiv.org/abs/1905.05381)

Corotating interaction regions (CIRs) are responsible for short-term recurrent cosmic-ray modulation, prominent near solar minima. Using the OMNI data sets for two periods of low solar activity near the beginning and end of solar cycle 24, superposed epoch analysis was performed on the solar wind plasma features for 53 and 43 events during periods 2007–2008 and 2017–2018, respectively. Turbulent properties of the solar wind were studied using the variance method for each CIR. Power spectra have been constructed for overlapped subintervals in the vicinity of stream interfaces (SIs). Using measured correlation lengths and turbulent energies, parallel and perpendicular diffusion mean free paths for cosmic-ray ions have been inferred based on two distinct theoretical formulations. For the two periods with opposite solar polarities, our results show that unlike solar wind speed, magnetic field strength, flow pressure, and proton density are relatively higher during the latest period. Increased turbulent energy and reduced parallel transport coefficients of energetic particles at the SIs are observed. The diffusion coefficients follow the same trends during both periods. The perpendicular diffusion starts increasing nearly a day before SIs and is higher in the fast wind. Superposed epoch analysis is performed on the >120 MeV proton count rate obtained from the CRIS instrument on board the ACE spacecraft for the same events. The recorded proton rates have peaks half a day before a SI and reach their minimum more than a day after a SI and have a high anticorrelation with the perpendicular diffusion coefficient.

Anomalous Cosmic Rays and Heliospheric Energetic Particles

Review

J. **Giacalone**, **H. Fahr**, **H. Fichtner**, **V. Florinski**, **B. Heber**, **M. E. Hill**, **J. Kóta**, **R. A. Leske**, **M. S. Potgieter** & **J. S. Rankin**

[Space Science Reviews](https://arxiv.org/abs/2201.00001) volume 218, Article number: 22 (2022)

<https://link.springer.com/content/pdf/10.1007/s11214-022-00890-7.pdf>

We present a review of Anomalous Cosmic Rays (ACRs), including the history of their discovery and recent insights into their acceleration and transport in the heliosphere. We focus on a few selected topics including a discussion of mechanisms of their acceleration, escape from the heliosphere, their effects on the dynamics of the heliosheath, transport in the inner heliosphere, and their solar cycle dependence. A discussion concerning their name is also presented towards the end of the review. We note that much is known about ACRs and perhaps the term Anomalous Cosmic Ray is not particularly descriptive to a non specialist. We suggest that the more-general term: “Heliospheric Energetic Particles”, which is more descriptive, for which ACRs and other energetic particle species of heliospheric origin are subsets, might be more appropriate.

Energetic Particles Associated with a Coronal Mass Ejection Shock Interacting with a Convected Magnetic Structure

J. **Giacalone**¹, D. Burgess², S. D. Bale^{2,3,4,5}, M. I. Desai⁶, J. G. Mitchell^{7,8}, D. Lario⁸, C. H. K. Chen², E. R. Christian⁸, G. A. de Nolfo⁸, M. E. Hill⁹Show full author list

2021 ApJ 921 102

<https://doi.org/10.3847/1538-4357/ac1ce1>

On **2020 November 30**, Parker Solar Probe (PSP) was crossed by a coronal mass ejection (CME)-driven shock, which we suggest was also crossing a convected, isolated magnetic structure (MS) at about the same time. By analyzing PSP/FIELDS magnetic field measurements, we find that the leading edge of the MS coincided with the crossing of the shock, while its trailing edge, identified as a crossing of a current sheet, overtook PSP about 7 minutes later. Prior to the

arrival of the shock, the flux of 30 keV–3 MeV ions and electrons, as measured by PSP/Integrated Science Investigation of the Sun (ISOIS)/Energetic Particle Instrument (EPI-Lo), increased gradually, peaking at the time of the shock passage. However, during the crossing of the MS downstream of the shock, the energetic-ion flux dropped dramatically, before recovering at about the time of the crossing of the trailing edge of the MS. Afterwards, the ion fluxes remained approximately constant within the sheath region of the CME shock. We interpret this depletion of energetic ions within the MS as the result of insufficient time to accelerate particles at the shock within the MS, given that the structure moves along the shock surface owing to its advection with the solar wind. We present results from a quantitative numerical model of the interaction of an idealized MS with a shock, which supports this interpretation.

Partially ejected flux ropes: Implications for interplanetary coronal mass ejections,

Gibson, S. E., and Y. Fan,

E-print, March 2007; *J. Geophys. Res.*, 113, A09103 (2008), **File**

<http://dx.doi.org/10.1029/2008JA013151>

Connecting interplanetary coronal mass ejections (ICMEs) to their solar pre-eruption source requires a clear understanding of how that source may have evolved during eruption. Gibson and Fan (2006a) have presented a three-dimensional numerical magnetohydrodynamic simulation of a CME, which showed how, in the course of eruption, a coronal flux rope may writhe and reconnect both internally and with surrounding fields in a manner that leads to a partial ejection of only part of the rope as a CME. In this paper, we will explicitly describe how the evolution during eruption found in that simulation leads to alterations of the magnetic connectivity, helicity, orientation, and topology of the ejected portion of the rope so that it differs significantly from that of the pre-eruption rope. Moreover, because a significant part of the magnetic helicity remains behind in the lower portion of the rope that survives the eruption, the region is likely to experience further eruptions. These changes would complicate how ICMEs embedded in the solar wind relate to their solar source. In particular, the location and evolution of transient coronal holes, topology of magnetic clouds ("tethered spheromak"), and likelihood of interacting ICMEs would differ significantly from what would be predicted for a CME which did not undergo writhing and partial ejection during eruption.

Forming tori: Implications and possible origins of a "tethered spheromak" topology for magnetic clouds

Gibson, S. E.; Fan, Y.

American Geophysical Union, Spring Meeting 2008, abstract #SH31C-06, **2008**

We present a "tethered spheromak" model for magnetic clouds. The proposed topology differs from previous magnetic cloud models invoking spheromaks in that large portions of the field remain connected to the sun. This magnetic configuration may explain observed departures from the standard magnetic cloud model of a cylindrically-symmetric magnetic flux rope, such as magnetic fields which rotate more than 180 degrees. It is also topologically complex enough to include intermingled detached, doubly attached, and apparently open fields in a manner consistent with observations of sporadic heat flux dropouts within otherwise bidirectional or unidirectional streaming electrons. We use a numerical simulation to demonstrate how, for solar eruptions where the kink instability drives significant rotation of an erupting flux rope, such a tethered spheromak may form during that rope's partial ejection. It does so because writhing motions and reconnections create twist about two distinct axes of rotation: the first associated with the rotated portion of the original rope axis, and the second formed in situ via reconnections between the erupting rope and surrounding coronal arcade fields.

Partially-ejected flux ropes: implications for space weather

Sarah E. **Gibson**¹ and Yuhong Fan

Solar Activity and its Magnetic Origin, Proc.IAU Symposium No. 233, **2006**, Volker Bothmer, ed., **File**

The structure and evolution of the sources of solar activity directly affects the nature of space weather disturbances that reach the Earth. We have previously demonstrated that the loss of equilibrium and partial ejection of a coronal magnetic flux rope matches observations of coronal mass ejections (CMEs) and their precursors. In this paper we discuss the significance of such a partially-ejected rope for space weather. We will consider how the evolution and bifurcation of the rope modifies it from its initial, source configuration. In particular, we will consider how reconnections and writhing motions lead to an escaping rope which has an axis rotated counterclockwise from the original rope axis orientation, and which is rooted in transient coronal holes external to the original source region.

Solar-MACH: An open-source tool to analyze solar magnetic connection configurations

Jan [Gieseler](#), [Nina Dresing](#), [Christian Palmroos](#), [Johan L. Freiherr von Forstner](#), [Daniel J. Price](#), [Rami Vainio](#), [Athanasios Kouloumvakos](#), [Laura Rodríguez-García](#), [Domenico Trotta](#), [Vincent Génot](#), [Arnaud Masson](#), [Markus Roth](#), [Astrid Veronig](#)

2022

<https://arxiv.org/pdf/2210.00819.pdf>

The Solar MAGnetic Connection HAUS tool (Solar-MACH) is an open-source tool completely written in Python that derives and visualizes the spatial configuration and solar magnetic connection of different observers (i.e., spacecraft or planets) in the heliosphere at different times. For doing this, the magnetic connection in the interplanetary space is obtained by the classic Parker Heliospheric Magnetic Field (HMF). In close vicinity of the Sun, a Potential Field Source Surface (PFSS) model can be applied to connect the HMF to the solar photosphere. Solar-MACH is especially aimed at providing publication-ready figures for the analyses of Solar Energetic Particle events (SEPs) or solar transients such as Coronal Mass Ejections (CMEs). It is provided as an installable Python package (listed on PyPI and conda-forge), but also as a web tool at [this http URL](#) that completely runs in any web browser and requires neither Python knowledge nor installation. The development of Solar-MACH is open to everyone and takes place on GitHub, where the source code is publicly available under the BSD 3-Clause License. Established Python libraries like sunpy and pfsspy are utilized to obtain functionalities when possible. In this article, the Python code of Solar-MACH is explained, and its functionality is demonstrated using real science examples. In addition, we introduce the overarching SERPENTINE project, the umbrella under which the recent development took place. **9 October 2021, 28 October 2021**

Analysis of Geoeffective Impulsive Events on the Sun During the First Half of Solar Cycle 24

Agnieszka [Gil](#), [Monika Berendt-Marchel](#), [Renata Modzelewska](#), [Agnieszka Siluszyk](#), [Marek Siluszyk](#), [Anna Wawrzaszek](#) & [Anna Wawrzynczak](#)

[Solar Physics](#) volume 298, Article number: 26 (2023)

<https://link.springer.com/content/pdf/10.1007/s11207-023-02119-4.pdf>

A coronal mass ejection (CME) is an impulsive event that emerges rapidly from the Sun. We observed a quiet Sun without many spectacular episodes during the last decade. Although some fast halo and partial halo CMEs had taken place, among them was the backside CME on 23 July 2012. In this work, we verify the link between the variability of solar-wind, heliospheric and geomagnetic parameters and the transmission grid failures registered in southern Poland during 2010 – 2014 when many geomagnetic storms appeared, caused by halo and partial halo CMEs. We aim to apply three machine learning methods: Principal Components Analysis, Self-Organizing Maps, and Hierarchical Agglomerative Clustering to analyze sources on the Sun and the impacts of the intense geomagnetic storms in the first half of Solar Cycle 24. The conducted analyzes underline the importance of solar-wind proton temperature and point out other solar-wind and geomagnetic parameters independently indicated by all the methods used in this study. **26 – 27.09.2011, 19.02.2014**

The Solar Event of 14 – 15 July 2012 and Its Geoeffectiveness

Agnieszka [Gil](#), [Renata Modzelewska](#), [Szczepan Moskwa](#), [Agnieszka Siluszyk](#), [Marek Siluszyk](#), [Anna Wawrzynczak](#), [Mariusz Pozoga](#) & [Lukasz Tomasiak](#)

[Solar Physics](#) volume 295, Article number: 135 (2020)

<https://link.springer.com/content/pdf/10.1007/s11207-020-01703-2.pdf>

During Solar Cycle 24, which started at the end of 2008, the Sun was calm, and there were not many spectacular geoeffective events. In this article, we analyze the geomagnetic storm that happened on **15 July 2012** during the 602nd anniversary of the Polish Battle of Grunwald, thus we propose this event to be called the “Battle of Grunwald Day Storm”. According to NOAA scale, it was a G3 geomagnetic storm with a southward component of the heliospheric magnetic field, BzBz, falling to -20 nT, minimum Dst index of -139 nT, AE index of 1368 nT, and Ap index of 132 nT. It was preceded by a solar flare class X1.4 on **12 July**. This geomagnetic storm was associated with the fast halo coronal mass ejection at 16:48:05 UT on 12 July, first appearance in the Large Angle and Spectroscopic Coronagraph C2, with a plane-of-sky speed of 885 km s $^{-1}$ and maximum of 1415 km s $^{-1}$. This geomagnetic storm was classified as the fourth strongest geomagnetic storm of Solar Cycle 24. At that time, a significant growth in the failures of the Polish electric transmission lines was observed, which could have a solar origin.

An Anisotropic Cosmic-Ray Enhancement Event on 07-June-2015: A Possible Origin

Agnieszka [Gil](#), Gennady A. Kovaltsov, Vladimir V. Mikhailov, Alexander Mishev, Stepan Poluianov, Ilya G. Usoskin

[Solar Physics](#) November 2018, 293:154

<https://link.springer.com/content/pdf/10.1007%2Fs11207-018-1375-5.pdf>
sci-hub.tw/10.1007/s11207-018-1375-5

A usual event, called anisotropic cosmic-ray enhancement (ACRE), was observed as a small increase ($\leq 5\%$) in the count rates of polar neutron monitors during 12 – 19 UT on **07 June 2015**. The enhancement was highly anisotropic, as detected only by neutron monitors with asymptotic directions in the southwest quadrant in geocentric solar ecliptic (GSE) coordinates. The estimated rigidity of the corresponding particles is ≤ 1 GV. No associated detectable increase was found in the space-borne data from the Geostationary Operational Environmental Satellite (GOES), the Energetic and Relativistic Nuclei and Electron (ERNE) on board the Solar and Heliospheric Observatory (SOHO), or the Payload for Antimatter Matter Exploration and Light-nuclei Astrophysics (PAMELA) instruments, whose sensitivity was not sufficient to detect the event. No solar energetic particles were present during that time interval. The heliospheric conditions were slightly disturbed, so that the interplanetary magnetic field strength gradually increased during the event, followed by an increase of the solar wind speed after the event. It is proposed that the event was related to a crossing of the boundary layer between two regions with different heliospheric parameters, with a strong gradient of low-rigidity (< 1 GV) particles. It was apparently similar to another cosmic-ray enhancement (e.g., on **22 June 2015**) that is thought to have been caused by the local anisotropy of Forbush decreases, with the difference that in our case, the interplanetary disturbance was not observed at Earth, but passed by southward for this event.

Comparing two intervals of exceptionally strong solar rotation recurrence of galactic cosmic rays

A. **Gil** and K. Mursula

JGR **2018** DOI 10.1029/2018JA025523

<http://sci-hub.tw/https://onlinelibrary.wiley.com/doi/abs/10.1029/2018JA025523>

Two intervals of exceptionally strong recurrence of galactic cosmic ray (GCR) intensity at solar rotation period stand out in recent history, one in 2007-2008, the other in 2014-2015. We use neutron monitor data from Oulu and Hermanus, solar wind (SW) data and coronal images to study these intervals. We find that in both cases the source of solar rotation period recurrence was a coronal hole (CH), but CH structures were different. While a large, longitudinally asymmetric CH existed at high southern latitudes in 2014-2015, a low-latitude CH caused the recurrence in 2007-2008. Spectral properties of GCR and SW parameters reflect these differences. In 2014-2015 the GCR power spectrum density was broad and peaked at a period of 28.9 days, longer than the simultaneous recurrence period of SW speed. In 2007-2008 the GCR power spectrum was narrow and peaked at 27.5 days, exactly the same as for SW speed. The effect of CHs to GCRs was somewhat different in the two cases because of opposite solar polarities in the two intervals. In 2014-2015, during positive polarity when GCRs drift inward from high latitudes, the convection of fast SW from CH reduces the inward GCR drift over a wide range of high heliolatitudes at certain heliolongitudes. In 2007-2008, during negative polarity when GCRs drift inward via the heliospheric current sheet (HCS), a low-latitude CH depletes the GCR flux not only by convection but also by deflecting HCS away from the ecliptic, whence GCR drift to higher latitudes in a limited longitude range. **25 September 2007, 30 January 2015**

FIRST MEASUREMENTS OF THE COMPLETE HEAVY-ION CHARGE STATE DISTRIBUTIONS OF C, O, AND Fe ASSOCIATED WITH INTERPLANETARY CORONAL MASS EJECTIONS

J. A. **Gilbert**, S. T. Lepri, E. Landi, and T. H. Zurbuchen

2012 ApJ 751 20

We present the first analysis of the complete charge state distributions of heavy ions in interplanetary coronal mass ejections (CMEs), from singly charged to fully ionized. We develop a novel analysis technique that requires the combination and cross-calibration of two different data sets from the Solar Wind Ion Composition Spectrometer on the Advanced Composition Explorer. The first contains ions of higher charge states, and includes an identification of their mass, mass-per-charge, and energy-per-charge. The second data set contains singly and low-charge ions, and identifies only their mass-per-charge and energy-per-charge. Focusing on C, O, and Fe, we find ionic charge states representative of temperatures from $\leq 60,000$ K to over 5,000,000 K contained within interplanetary CMEs observed near 1 AU. We interpret these data in the context of near-Sun observations of filament material associated with CMEs. We find that singly charged ions are embedded within selected interplanetary CMEs, and we examine their densities and durations. These data thus provide the most unambiguous in situ diagnostic of solar prominence plasma in the heliosphere.

Multi-fractal Analysis of Cosmic Rays over Mid- and High-Latitude Stations During Severe Geomagnetic Storms.

Giri, A., Adhikari, B., Dahal, S. et al.

Sol Phys 299, 148 (2024).

<https://doi.org/10.1007/s11207-024-02393-w>

This study explores the multi-fractal properties of cosmic-ray (CR) counts collected from two mid-latitude neutron-monitor stations, Newark (NEWK) and Irkutsk 3 (IRK3), and two high-latitude stations, Thule (THUL) and Inuvik (INVK), during periods of severe geomagnetic storms. By employing multi-fractal along with time-series analysis, we did an in-depth examination of CR count variations to demonstrate the effectiveness of these methods in analyzing complex signals associated with astrophysical and solar phenomena. The findings reveal that CR count rates across stations at different latitudes exhibit multi-fractal characteristics, reflecting a range of scaling exponents that capture varying degrees of correlation and variability within the system. The results underscore that solar activity, geomagnetic events, and interactions with Earth's magnetic field play a more crucial role in determining multi-fractality than the geographic location of the measurement station. Moreover, the study shows that geomagnetic events exert a stronger influence on the multi-fractal properties of CR count rate than the geographic location of station, underscoring the impact of solar storms and Earth's magnetic field on the distribution and intensity of CRs. This work emphasizes the value of multi-fractal analysis as a powerful tool for investigating the complex nature of CR counts and its sensitivity to both extraterrestrial and terrestrial factors.

A 30-Year Simulation of the Outer Electron Radiation Belt

S. A. [Glauert](#) [R. B. Horne](#) [N. P. Meredith](#)

Space Weather Volume16, Issue10 October 2018 Pages 1498-1522

<https://doi.org/10.1029/2018SW001981>

As society becomes more reliant on satellite technology, it is becoming increasingly important to understand the radiation environment throughout the Van Allen radiation belts. Historically most satellites have operated in low Earth orbit or geostationary orbit (GEO), but there are now over 100 satellites in medium Earth orbit (MEO). Additionally, satellites using electric orbit raising to reach GEO may spend hundreds of days on orbits that pass through the heart of the radiation belts. There is little long-term data on the high-energy electron flux, responsible for internal charging in satellites, available for MEO. Here we simulate the electron flux between the outer edge of the inner belt and GEO for 30 years. We present a method that converts the >2-MeV flux measured at GEO by the Geostationary Operational Environmental Satellites spacecraft into a differential flux spectrum to provide an outer boundary condition. The resulting simulation is validated using independent measurements made by the Galileo In-Orbit Validation Element-B spacecraft; correlation coefficients are in the range 0.72 to 0.88, and skill scores are between 0.6 and 0.8 for a range of L* and energies. The results show a clear solar cycle variation and filling of the slot region during active conditions and that the worst case spectrum overlaps that derived independently for the limiting extreme event. The simulation provides a resource that can be used by satellite designers to understand the MEO environment, by space insurers to help resolve the cause of anomalies and by satellite operators to plan for the environmental extremes.

Variations in Energetic Particle Fluxes around Significant Geomagnetic Storms Observed by the Low-Altitude DEMETER Spacecraft.

Gohl, S.; N'emece, F.; Parrot, M.

Universe 2021, 7, 260.

<https://www.mdpi.com/2218-1997/7/8/260/htm>

<https://doi.org/10.3390/universe7080260>

A superposed epoch analysis is conducted for five geomagnetic storms in the years 2005 and 2006 with the aim to understand energetic particle flux variations as a function of L-shell, energy and time from the Dst minimum. Data measured by the low-altitude DEMETER spacecraft were used for this purpose. The storms were identified by a Dst index below -100 nT, as well as their being isolated events in a seven-day time window. It is shown that they can be categorized into two types. The first type shows significant variations in the energetic particle fluxes around the Dst minimum and increased fluxes at high energies (>1.5 MeV), while the second type only shows increased fluxes around the Dst minimum without the increased fluxes at high energies. The first type of storm is related to more drastic but shorter-lasting changes in the solar wind parameters than the second type. One storm does not fit either category, exhibiting features from both storm types. Additionally, we investigate whether the impenetrable barrier for ultra-relativistic electrons also holds in extreme geomagnetic conditions. For the highest analyzed energies, the obtained barrier L-shells do not go below 2.6, consistent with previous findings. **15 May 2005, 13 June 2005, 24 August 2005, 31 August 2005, 15 December 2006**

Dependence of Radiation Belt Flux Depletions at Geostationary Orbit on Different Solar Drivers During Intense Geomagnetic Storms

Sneha **Gokani**, De-Sheng Han, R Selvakumaran, R Selvakumaran, and Tarun Pant

Front. Astron. Space Sci. 9:952486. 2022

doi: 10.3389/fspas.2022.952486

<https://www.frontiersin.org/articles/10.3389/fspas.2022.952486/pdf>

The loss of electron flux of the outer radiation belt has been widely studied in terms of the mechanism that brings in these losses. There are a few studies which have attempted to explain the interplanetary conditions that favor the depletions. As the Sun is the prime cause of any change happening in the magnetosphere, it is important to look at the solar drivers that bring in such changes. In this study, we attempt to understand the effect of solar structures and substructures on the loss of radiation belt high-energy electrons during intense geomagnetic storms. The superposed epoch analysis is used to observe any peculiar changes in GOES electron flux data during the storms that are associated with solar structures such as CME and CIR, ICME substructures such as the magnetic cloud, magnetic cloud with sheath, ejecta, ejecta with sheath, and only sheath. The long-term data also give an opportunity to compare the flux decrease during solar cycles 23 and 24. It has been observed that 1) CIR-associated storms cause a comparatively higher flux decrease than CME-associated storms, 2) sheath-related storms bring out a higher flux decrease, and 3) there is no significant change in flux for the storms of both the solar cycles. The flux decrease in intense storms at the geostationary orbit is essentially triggered by the “Dst effect.” Apart from this, the minimum IMF Bz and northward IMF Bz before turning southward add to the flux decrease. These results hold true for the electron depletions occurring only during intense geomagnetic storms and may alter otherwise.

Extended MHD modeling of the steady solar corona and the solar wind

Review

Tamas I. **Gombosi**, Bart van der Holst, Ward B. Manchester, Igor V. Sokolov

[Living Reviews in Solar Physics](#) December 2018, 15:4

<https://link.springer.com/content/pdf/10.1007%2Fs41116-018-0014-4.pdf>

<https://arxiv.org/pdf/1807.00417.pdf>

The history and present state of large-scale magnetohydrodynamic modeling of the solar corona and the solar wind with steady or quasi-steady coronal physics is reviewed. We put the evolution of ideas leading to the recognition of the existence of an expanding solar atmosphere into historical context. The development and main features of the first generation of global corona and solar wind models are described in detail. This historical perspective is also applied to the present suite of global corona and solar wind models. We discuss the evolution of new ideas and their implementation into numerical simulation codes. We point out the scientific and computational challenges facing these models and discuss the ways various groups tried to overcome these challenges. Next, we discuss the latest, state-of-the-art models and point to the expected next steps in modeling the corona and the interplanetary medium. 29 March 2006, 2011 March 7

Clustering of fast Coronal Mass Ejections during the solar cycles 23 and 24 and implications for CME-CME interactions

[Jenny M. Rodríguez Gómez](#), [Tatiana Podladchikova](#), [Astrid Veronig](#), [Alexander Ruzmaikin](#), [Joan Feynman](#), [Anatoly Petrukovich](#)

ApJ 2020

<https://arxiv.org/pdf/2006.10404.pdf>

We study the clustering properties of fast Coronal Mass Ejections (CMEs) that occurred during solar cycles 23 and 24. We apply two methods: the Max spectrum method can detect the predominant clusters and the de-clustering threshold time method provides details on the typical clustering properties and time scales. Our analysis shows that during the different phases of solar cycles 23 and 24, CMEs with speed ≥ 1000 km/s preferentially occur as isolated events and in clusters with on average two members. However, clusters with more members appear particularly during the maximum phases of the solar cycles. Over the total period and in the maximum phases of solar cycles 23 and 24, about 50% are isolated events, 18% (12%) occur in clusters with 2 (3) members, and another 20% in larger clusters ≥ 4 , whereas in solar minimum fast CMEs tend to occur more frequently as isolated events (62%). During different solar cycle phases, the typical de-clustering time scales of fast CMEs are $\tau_c = 28-32$ hrs, irrespective of the very different occurrence frequencies of CMEs during solar minimum and maximum. These findings suggest that τ_c for extreme events may reflect the characteristic energy build-up time for large flare and CME-prolific active ARs. Associating statistically the clustering properties of fast CMEs with the Disturbance storm index $\{Dst\}$ at Earth suggests that fast CMEs occurring in clusters tend to produce larger geomagnetic storms than isolated fast CMEs. This may be related to CME-

CME interaction producing a more complex and stronger interaction with the Earth magnetosphere. **2000-11-23-25, 2005-08-22-23, 2017-09-09-10**

5. GEO-EFFECTIVENESS OF CME CLUSTERS

Sunward-propagating Solar Energetic Electrons inside Multiple Interplanetary Flux Ropes

Raúl **Gómez-Herrero**¹, Nina Dresing², Andreas Klassen², Bernd Heber², Manuela Temmer³, Astrid Veronig³, Radoslav Bučík^{4,5}, Miguel A. Hidalgo¹, Fernando Carcaboso¹, Juan J. Blanco

2017 ApJ 840 85

<http://sci-hub.cc/10.3847/1538-4357/aa6c5c>

On **2013 December 2 and 3**, the SEPT and STE instruments on board STEREO-A observed two solar energetic electron events with unusual sunward-directed fluxes. Both events occurred during a time interval showing typical signatures of interplanetary coronal mass ejections (ICMEs). The electron timing and anisotropies, combined with extreme-ultraviolet solar imaging and radio wave spectral observations, are used to confirm the solar origin and the injection times of the energetic electrons. The solar source of the ICME is investigated using remote-sensing observations and a three-dimensional reconstruction technique. In situ plasma and magnetic field data combined with energetic electron observations and a flux-rope model are used to determine the ICME magnetic topology and the interplanetary electron propagation path from the Sun to 1 au. Two consecutive flux ropes crossed the STEREO-A location and each electron event occurred inside a different flux rope. In both cases, the electrons traveled from the solar source to 1 au along the longest legs of the flux ropes still connected to the Sun. During the December 2 event, energetic electrons propagated along the magnetic field, while during the December 3 event they were propagating against the field. As found by previous studies, the energetic electron propagation times are consistent with a low number of field line rotations $N < 5$ of the flux rope between the Sun and 1 au. The flux rope model used in this work suggests an even lower number of rotations. **2013 November 29**

On Short-Duration Intense and Strongly Geoeffective (ICME) Sheath Magnetic Fields

Walter D. **Gonzalez**

JGR [Volume 129, Issue 4](#) April **2024** e2023JA032222

<https://agupubs.onlinelibrary.wiley.com/doi/epdf/10.1029/2023JA032222>

This Commentary article deals with the important role of large-amplitude, short-duration (<1 hr) and southwardly directed magnetic field incursions within the Sheath region of an interplanetary coronal mass ejection, which were recently shown to have led to extreme auroral activity during the early part of the Halloween storm (Ohtani, 2022, <https://doi.org/10.1029/2022ja030596>). For such largely geoeffective magnetic field structures some suggestions are given toward their possible interplanetary causes, which could also be associated with the origin of similar Sheath-structures observed during other events with very intense geomagnetic activity. A particular attention is given to a Sheath-incorporated and largely geoeffective flux rope-hypothesis. At the end we add some comments on further related magnetospheric and space weather issues. **29–30 Oct 2003**

Using sunRunner3D to interpret the global structure of the heliosphere from in situ measurements

José Juan **González-Avilés**^{1*}, Pete Riley², Michal Ben-Nun², Prateek Mayank³ and Bhargav Vaidya³

J. Space Weather Space Clim. **2024**, 14, 12

<https://www.swsc-journal.org/articles/swsc/pdf/2024/01/swsc230061.pdf>

Understanding the large-scale three-dimensional structure of the inner heliosphere, while important in its own right, is crucial for space weather applications, such as forecasting the time of arrival and propagation of coronal mass ejections (CMEs). This study uses sunRunner3D (3D), a 3-D magnetohydrodynamic (MHD) model, to simulate solar wind (SW) streams and generate background states. SR3D employs the boundary conditions generated by corona-heliosphere (CORHEL) and the PLUTO code to compute the plasma properties of the SW with the MHD approximation up to 1.1 AU in the inner heliosphere. We demonstrate that SR3D reproduces global features of corotating interaction regions (CIRs) observed by Earth-based spacecraft (OMNI) and the Solar Terrestrial Relations Observatory (STEREO)-A for a set of Carrington rotations (CRs) that cover a period that lays in the late declining phase of solar cycle 24. Additionally, we demonstrate that the model solutions are valid in the corotating and inertial frames of references. Moreover, a comparison between SR3D simulations and in situ measurements shows reasonable agreement with the observations, and our results are comparable to those achieved by Predictive Science Inc.'s Magnetohydrodynamic Algorithm outside a Sphere (MAS) code. We have also undertaken a comparative analysis with the Space Weather Adaptive Simulation Framework for Solar Wind (SWASTi-SW), a PLUTO physics-based model, to evaluate the precision of various initial boundary conditions. Finally, we discuss the disparities in the solutions derived from inertial and rotating frames.

Observations of Low-Latitude Red Aurora in Mexico During the 1859 Carrington Geomagnetic Storm

González-Esparza, J. A.; Cuevas-Cardona, M. C.

Space Weather, Volume 16, Issue 6, pp. 593-600, 2018

<http://sci-hub.tw/10.1029/2017SW001789>

One of the most intense geomagnetic storm that has been documented in recent history occurred on 1 September 1859. This storm is known as the Carrington Event. In the morning of 1 September at around 11:15 UT, Richard Carrington and Richard Hodgson observed in England, independently and for the first time, an intense white light solar flare. About 17 hr after this solar event, there occurred the strongest geomagnetic perturbation ever recorded as well as a greatly extended red aurora, which covered unusually at low latitudes. The red auroral display on 2 September was reported in regions where this kind of phenomena is very rare, like in Cuba and Hawaii. Until now however, it was not known to scientists that the low-latitude red aurora is also registered in Mexico. At that time, Mexico was in a civil war, and there were very difficult conditions in where to establish astronomical and magnetic observatories. Nevertheless, the geomagnetic storm was observed with a maximum intensity between 7:00 and 8:00 UTC and was reported to a Mexican newspaper from five different locations (Mexico City, Querétaro, Guadalajara, Hidalgo, and Guanajuato) and registered also from at least in two additional sites (Michoacán and San Luis Potosí) in other historical documents. These records confirm that the Carrington geomagnetic storm was a global event with planetary repercussions, and that the Mexican low-latitude region is susceptible to significant effects associated with intense space weather events.

See Space Weather Quarterly Vol. 15, Issue 2, 2018 <https://agupubs.onlinelibrary.wiley.com/doi/epdf/10.1002/swq.18>

Study of Corotating Interaction Regions in the Ascending Phase of the Solar Cycle: Multi-spacecraft Observations

J. A. Gonzalez-Esparza, E. Romero-Hernandez, P. Riley

Solar Physics, July 2013, Volume 285, Issue 1-2, pp 201-216

We combined simultaneous solar wind observations from five different spacecraft: Helios 1, Helios 2, IMP-8, Voyager 1 and Voyager 2, from November 1977 to February 1978 (Carrington rotations 1661 – 1664, ascending phase of Solar Cycle 21). The concurrence of the five trajectories makes this interval unique for the purpose of studying solar wind dynamics during this phase of the cycle. We analyzed the observations identifying five corotating interaction regions (CIRs) and produced maps of interplanetary large-scale features, unifying and summarizing the data. The maps show the compressive events and the magnetic sectors associated with the solar wind streams causing the CIRs. We analyzed the relative position of the stream interfaces immersed within the CIRs. About 70 % of the stream interfaces in this study were located closer to the forward edge of the CIR. From the analysis of the geometry of the stream interfaces, we found that all the CIRs presented latitudinal tilts, having their fronts pointing towards the ecliptic plane and their tails northwards or southwards. These results are in agreement with the origin of the fast streams coming from mid-latitude coronal holes and the predominance of forward shocks over reverse shocks bounding the CIRs, which characterize this phase of the cycle. From the analysis of the ratio of dynamic pressures between fast and slow solar wind streams associated with the CIRs, we found that in about 60 % of the cases the fast stream was transferring momentum to the slow one ahead, but in the rest of the cases the momentum was flowing sunward. This result indicates significant inhomogeneities in the solar wind streams during the ascending phase of the cycle that affect the local form and evolution of CIR events. We did a limited comparison between a global magneto-hydrodynamic (MHD) model of SW flows and the orientation of the SI from in-situ observations, we found, in general, a qualitative agreement between the pressure profiles at 1 AU predicted by the model and the inclinations of the stream interfaces deduced from the data analysis.

Extreme geomagnetic storms, recent Gleissberg cycles and space era-superintense storms

W.D. Gonzalez, , E. Echera, , A.L. Clúa de Gonzalez, , B.T. Tsurutanib, , and G.S. Lakhinac, Journal of Atmospheric and Solar-Terrestrial Physics, Volume 73, Issues 11-12, 2011, Pages 1447-1453 sci-hub.se/10.1016/j.jastp.2010.07.023

http://ac.els-cdn.com/S1364682610002191/1-s2.0-S1364682610002191-main.pdf?_tid=1bbe6824-a9ab-11e3-ac70-0000aab0f27&acdnat=1394603992_13c70fe75e41148720b352c2e9055341

Extreme historical and space era geomagnetic storms (ΔH or ΔI) are studied in terms of their sunspot and Gleissberg solar cycle distributions. Interplanetary and magnetospheric processes associated with the Carrington storm are summarized and the intense storm of August 4, 1972 is discussed in the context of the possibility of having occurred as an extreme storm instead, if the polarity of the related magnetic cloud would have been opposite. We also discuss about

superintense geomagnetic storms () that occurred in the space era, showing their solar cycle and seasonal distributions and also providing averages for the peak values of their main associated interplanetary parameters. A discussion about the possible occurrence of more Carrington type storms is also addressed.

Table 1
List of superstorms ($Dst \leq -250$ nT) during the space era.

Date	Dst	Date	Dst
1957/01/21	-250	1989/03/14	-589
1957/03/02	-255	1989/09/19	-255
1957/09/05	-324	1989/10/21	-267
1957/09/13	-427	1989/11/17	-266
1957/09/23	-303	1990/04/10	-281
1958/02/11	-426	1991/03/25	-298
1958/07/08	-330	1991/10/29*	-254
1958/09/04	-302	1991/11/09	-354
1958/07/15	-429	1992/05/10	-288
1960/04/01	-327	2000/04/07*	-288
1960/04/30	-325	2000/07/16*	-301
1960/10/07	-287	2001/03/31*	-387
1960/11/13	-339	2001/04/11*	-271
1961/10/28	-272	2001/11/06*	-292
1967/05/26	-387	2003/10/30*	-353
1970/03/08*	-284	2003/10/30*	-383
1981/04/13*	-311	2003/11/20*	-422
1982/07/14*	-325	2004/11/08*	-373
1982/09/06*	-289	2004/11/10*	-289
1986/02/09	-307	2005/05/15*	-263

The events with asterisk are those for which solar wind measurements were available.

Interplanetary Origin of Intense, Superintense and Extreme Geomagnetic Storms Review

Walter D. [Gonzalez](#) · Ezequiel Echer · Bruce T. Tsurutani · Alicia L. Clúa de Gonzalez · Alisson Dal Lago
Space Sci Rev (2011) 158: 69–89, [File](#)

We present a review on the interplanetary causes of intense geomagnetic storms

($Dst \leq -100$ nT), that occurred during solar cycle 23 (1997–2005). It was reported that the most common interplanetary structures leading to the development of intense storms were: magnetic clouds, sheath fields, sheath fields followed by a magnetic cloud and corotating interaction regions at the leading fronts of high speed streams. However, the relative importance of each of those driving structures has been shown to vary with the solar cycle phase.

Superintense storms ($Dst \leq -250$ nT) have been also studied in more detail for solar cycle 23, confirming initial studies done about their main interplanetary causes. The storms are associated with magnetic clouds and sheath fields following interplanetary shocks, although they frequently involve consecutive and complex ICME structures. Concerning extreme storms ($Dst \leq -400$ nT), due to the poor statistics of their occurrence during the space era, only some indications about their main interplanetary causes are known. For the most extreme events, we review the Carrington event and also discuss the distribution of historical and space era extreme events in the context of the sunspot and Gleissberg solar activity cycles, highlighting a discussion about the eventual occurrence of more Carrington type storms.

Interplanetary origin of intense geomagnetic storms ($Dst < -100$ nT) during solar cycle 23,

[Gonzalez](#), W. D., E. Echer, A. L. Clua-Gonzalez, and B. T. Tsurutani
Geophys. Res. Lett., 34, L06101, doi:10.1029/2006GL028879, (2007), [File](#).

We study the interplanetary causes of intense geomagnetic storms ($Dst < -100$ nT) that occurred during solar cycle 23 (1997–2005). It was found that the most common interplanetary structures leading to the development of an intense storm were: magnetic clouds, sheath fields, sheath fields followed by a magnetic cloud and corotating interaction regions leading high speed streams. However, the relative importance of each of those driving structures was found to vary with the solar cycle phase. We divide the cycle in three phases (rising, maximum and declining) and explain the differences. We also discuss about the geoeffectiveness of each of the four main interplanetary driving structures.

(See Yermolaev, 2008)

Magnetic cloud field intensities and solar wind velocities,

Gonzalez WD, Gonzalez ALC, Dal Lago A, Tsurutani BT, Arballo JK, Lakhina GS, Buti B., Ho GM, Wu ST
(1998), GRL 25:963

What is a geomagnetic storm?, **Review**

Gonzalez WD, Joselyn JA, Kamide Y, Kroehl HW, Rostoker G, Tsurutani BT, Vasyliunas V
(1994), JGRA 99(4):5771
[sci-hub.se/10.1029/93ja02867](https://doi.org/10.1029/93ja02867)

After a brief review of magnetospheric and interplanetary phenomena for intervals with enhanced solar wind-magnetosphere interaction, an attempt is made to define a geomagnetic storm as an interval of time when a sufficiently intense and long-lasting interplanetary convection electric field leads, through a substantial energization in the magnetosphere-ionosphere system, to an intensified ring current sufficiently strong to exceed some key threshold of the quantifying storm time Dst index. The associated storm/substorm relationship problem is also reviewed. Although the physics of this relationship does not seem to be fully understood at this time, basic and fairly well established mechanisms of this relationship are presented and discussed. Finally, toward the advancement of geomagnetic storm research, some recommendations are given concerning future improvements in monitoring existing geomagnetic indices as well as the solar wind near Earth.

Impact of Inner Heliospheric Boundary Conditions on Solar Wind Predictions at Earth

Siegfried **Gonzi** , [M. Weinzierl](#) , [F.-X. Bocquet](#) , [M. M. Bisi](#) , [D. Odstrcil](#) , [B. V. Jackson](#) , [A. R. Yeates](#) , [D. R. Jackson](#) , [C. J. Henney](#) , [C. Nikolos Arge](#)

Space Weather **Volume19, Issue1** e2020SW002499 **2021**

<https://doi.org/10.1029/2020SW002499>

<https://agupubs.onlinelibrary.wiley.com/doi/epdf/10.1029/2020SW002499>

Predictions of the physical parameters of the solar wind at Earth are at the core of operational space weather forecasts. Such predictions typically use line-of-sight observations of the photospheric magnetic field to drive a heliospheric model. The models Wang-Sheeley-Arge (WSA) and ENLIL for the transport in the heliosphere are commonly used for these respective tasks. Here we analyse the impact of replacing the potential field coronal boundary conditions from WSA with two alternative approaches. The first approach uses a more realistic non-potential rather than potential approach, based on the Durham Magneto Frictional Code (DUMFRIC) model. In the second approach the ENLIL inner boundary conditions are based on Inter Planetary Scintillation observations (IPS). We compare predicted solar wind speed, plasma density and magnetic field magnitude with observations from the WIND spacecraft for two six-months intervals in 2014 and 2016. Results show that all models tested produce fairly similar output when compared to the observed time series. This is not only reflected in fairly low correlation coefficients (<0.3) but also large biases. For example for solar wind speed some models have average biases of more than 150 (km/s). On a positive note, the choice of coronal magnetic field model has a clear influence on the model results when compared to the other models in this study. Simulations driven by IPS data have a high success rate with regard to detection of the high speed solar wind. Our results also indicate that model forecasts do not degrade for longer forecast times.

Turbulence Properties of Interplanetary Coronal Mass Ejections in the Inner Heliosphere: Dependence on Proton Beta and Flux Rope Structure

S. W. **Good**, [O. K. Rantala](#), [A.-S. M. Jylhä](#), [C. H. K. Chen](#), [C. Möstl](#), [E. K. J. Kilpua](#)

ApJ **2023**

<https://arxiv.org/pdf/2307.09800.pdf>

Interplanetary coronal mass ejections (ICMEs) have low proton beta across a broad range of heliocentric distances and a magnetic flux rope structure at large scales, making them a unique environment for studying solar wind fluctuations. Power spectra of magnetic field fluctuations in 28 ICMEs observed between 0.25 and 0.95 au by Solar Orbiter and Parker Solar Probe have been examined. At large scales, the spectra were dominated by power contained in the flux ropes. Subtraction of the background flux rope fields reduced the mean spectral index from $-5/3$ to $-3/2$ at $k\Delta l \leq 10-3$. Rope subtraction also revealed shorter correlation lengths in the magnetic field. The spectral index was typically near $-5/3$ and radially invariant in the inertial range regardless of rope subtraction, and steepened to values consistently below -3 with transition to kinetic scales. The high-frequency break point terminating the inertial range evolved almost

linearly with radial distance and was closer in scale to the proton inertial length than the proton gyroscale, as expected for plasma at low proton beta. Magnetic compressibility at inertial scales did not grow with radial distance, in contrast to the solar wind generally. In ICMEs, the distinctive spectral properties at injection scales appear mostly determined by the global flux rope structure while transition-kinetic properties are more influenced by the low proton beta; the intervening inertial range appears independent of both ICME features, indicative of a system-independent scaling of the turbulence. **2019-03-24**

Table 1. List of ICMEs Analyzed 2018-2022

Cross helicity of interplanetary coronal mass ejections at 1 au

S. W. [Good](#), [L. M. Hatakka](#), [M. Ala-Lahti](#), [J. E. Soljento](#), [A. Osmane](#), [E. K. J. Kilpua](#)

MNRAS Volume 514, Issue 2, Pages 2425–2433 **2022**

<https://arxiv.org/pdf/2205.07751.pdf>

<https://doi.org/10.1093/mnras/stac1388>

<https://watermark.silverchair.com/stac1388.pdf>

Interplanetary coronal mass ejections (ICMEs) contain magnetic field and velocity fluctuations across a wide range of scales. These fluctuations may be interpreted as Alfvénic wave packets propagating parallel or anti-parallel to the background magnetic field, with the difference in power between counter-propagating fluxes quantified by the cross helicity. We have determined the cross helicity of inertial range fluctuations at 10^{-3} – 10^{-2} Hz in 226 ICME flux ropes and 176 ICME sheaths observed by the Wind spacecraft at 1 au during 1995-2015. The flux ropes and sheaths had mean, normalised cross helicities of 0.18 and 0.24, respectively, with positive values here indicating net anti-sunward fluxes. While still tipped towards the anti-sunward direction on average, fluxes in ICMEs tend to be more balanced than in the solar wind at 1 au, where the mean cross helicity is larger. Superposed epoch profiles show cross helicity falling sharply in the sheath and reaching a minimum inside the flux rope near the leading edge. More imbalanced, solar wind-like cross helicity was found towards the trailing edge and laterally further from the rope axis. The dependence of cross helicity on flux rope orientation and the presence of an upstream shock are considered. Potential origins of the low cross helicity in ICMEs at 1 au include balanced driving of the closed-loop flux rope at the Sun and ICME-solar wind interactions in interplanetary space. We propose that low cross helicity of fluctuations is added to the standard list of ICME signatures. **3-5 Apr 2004**

Cross Helicity of the November 2018 Magnetic Cloud Observed by the Parker Solar Probe

S. W. [Good](#), [E. K. J. Kilpua](#), [M. Ala-Lahti](#), [A. Osmane](#), [S. D. Bale](#), [L.-L. Zhao](#)

ApJL **900** L32 **2020**

<https://arxiv.org/pdf/2008.07868.pdf>

<https://doi.org/10.3847/2041-8213/abb021>

Magnetic clouds are large-scale transient structures in the solar wind with low plasma β , low-amplitude magnetic field fluctuations, and twisted field lines with both ends often connected to the Sun. Their inertial-range turbulent properties have not been examined in detail. In this Letter, we analyze the normalized cross helicity, σ_c , and residual energy, σ_r , of plasma fluctuations in the November 2018 magnetic cloud observed at 0.25 au by the Parker Solar Probe. A low value of $|\sigma_c|$ was present in the cloud core, indicating that wave power parallel and anti-parallel to the mean field was approximately balanced, while the cloud's outer layers displayed larger amplitude Alfvénic fluctuations with high $|\sigma_c|$ values and $\sigma_r \sim 0$. These properties are discussed in terms of the cloud's solar connectivity and local interaction with the solar wind. We suggest that low $|\sigma_c|$ is likely a common feature of magnetic clouds given their typically closed field structure. Anti-sunward fluctuations propagating immediately upstream of the cloud had strongly negative σ_r values. **November 11-12, 2018**

Radial Evolution of Magnetic Field Fluctuations in an Interplanetary Coronal Mass Ejection Sheath

S. W. [Good](#)¹, [M. Ala-Lahti](#)¹, [E. Palmerio](#)^{1,2}, [E. K. J. Kilpua](#)¹, and [A. Osmane](#)¹

2020 ApJ **893** 110

<https://arxiv.org/pdf/2003.05760.pdf>

<https://doi.org/10.3847/1538-4357/ab7fa2>

The sheaths of compressed solar wind that precede interplanetary coronal mass ejections (ICMEs) commonly display large-amplitude magnetic field fluctuations. As ICMEs propagate radially from the Sun, the properties of these fluctuations may evolve significantly. We have analyzed magnetic field fluctuations in an ICME sheath observed by MESSENGER at 0.47 au and subsequently by STEREO-B at 1.08 au while the spacecraft were close to radial alignment. Radial changes in fluctuation amplitude, compressibility, inertial-range spectral slope, permutation entropy,

Jensen–Shannon complexity, and planar structuring are characterized. These changes are discussed in relation to the evolving turbulent properties of the upstream solar wind, the shock bounding the front of the sheath changing from a quasi-parallel to quasi-perpendicular geometry, and the development of complex structures in the sheath plasma. **5-7 Nov 2010**

Self-Similarity of ICME Flux Ropes: Observations by Radially Aligned Spacecraft in the Inner Heliosphere

S. W. [Good](#), [E. K. J. Kilpua](#), [A. T. LaMoury](#), [R. J. Forsyth](#), [J. P. Eastwood](#), [C. Möstl](#)

JGR [Volume 124, Issue 7](#) July 2019 Pages 4960-4982

[sci-hub.se/10.1029/2019JA026475](https://doi.org/10.1029/2019JA026475)

Interplanetary coronal mass ejections (ICMEs) are a significant feature of the heliospheric environment and the primary cause of adverse space weather at the Earth. ICME propagation and the evolution of ICME magnetic field structure during propagation are still not fully understood. We analyze the magnetic field structures of **18 ICME** magnetic flux ropes observed by radially aligned spacecraft in the inner heliosphere. Similarity in the underlying flux rope structures is determined through the application of a simple technique that maps the magnetic field profile from one spacecraft to the other. In many cases, the flux ropes show very strong underlying similarities at the different spacecraft. The mapping technique reveals similarities that are not readily apparent in the unmapped data and is a useful tool when determining whether magnetic field time series observed at different spacecraft are associated with the same ICME. Lundquist fitting has been applied to the flux ropes, and the rope orientations have been determined; macroscale differences in the profiles at the aligned spacecraft may be ascribed to differences in flux rope orientation. Assuming that the same region of the ICME was observed by the aligned spacecraft in each case, the fitting indicates some weak tendency for the rope axes to reduce in inclination relative to the solar equatorial plane and to align with the solar east-west direction with heliocentric distance.

Table (2007-2013)

Correlation of ICME Magnetic Fields at Radially Aligned Spacecraft

S. W. [Good](#), [R. J. Forsyth](#), [J. P. Eastwood](#), [C. Möstl](#)

[Solar Physics](#) March 2018, 293:52

<https://link.springer.com/content/pdf/10.1007%2Fs11207-018-1264-y.pdf>

The magnetic field structures of two interplanetary coronal mass ejections (ICMEs), each observed by a pair of spacecraft close to radial alignment, have been analysed. The ICMEs were observed in situ by MESSENGER and STEREO-B in November 2010 and November 2011, while the spacecraft were separated by more than 0.6 AU in heliocentric distance, less than 4° in heliographic longitude, and less than 7° in heliographic latitude. Both ICMEs took approximately two days to travel between the spacecraft. The ICME magnetic field profiles observed at MESSENGER have been mapped to the heliocentric distance of STEREO-B and compared directly to the profiles observed by STEREO-B. Figures that result from this mapping allow for easy qualitative assessment of similarity in the profiles. Macroscale features in the profiles that varied on timescales of one hour, and which corresponded to the underlying flux rope structure of the ICMEs, were well correlated in the solar east–west and north–south directed components, with Pearson’s correlation coefficients of approximately 0.85 and 0.95, respectively; microscale features with timescales of one minute were uncorrelated. Overall correlation values in the profiles of one ICME were increased when an apparent change in the flux rope axis direction between the observing spacecraft was taken into account. The high degree of similarity seen in the magnetic field profiles may be interpreted in two ways. If the spacecraft sampled the same region of each ICME (i.e. if the spacecraft angular separations are neglected), the similarity indicates that there was little evolution in the underlying structure of the sampled region during propagation. Alternatively, if the spacecraft observed different, nearby regions within the ICMEs, it indicates that there was spatial homogeneity across those different regions. The field structure similarity observed in these ICMEs points to the value of placing in situ space weather monitors well upstream of the Earth. **5-6 November 2010, 5-6 November 2011**

Interplanetary Coronal Mass Ejections Observed by MESSENGER and Venus Express

S. W. [Good](#), [R. J. Forsyth](#)

[Solar Phys.](#) January 2016, Volume 291, [Issue 1](#), pp 239-263 **Open Access**

Interplanetary coronal mass ejections (ICMEs) observed by the MESSENGER and Venus Express spacecraft have been catalogued and analysed. The ICMEs were identified by a relatively smooth rotation of the magnetic field direction consistent with a flux rope structure, coinciding with a relatively enhanced magnetic field strength. A total of 35 ICMEs were found in the surveyed MESSENGER data (primarily from March 2007 to April 2012), and 84 ICMEs in the

surveyed Venus Express data (from May 2006 to December 2013). The ICME flux rope configurations have been determined. Ropes with northward leading edges were about four times more common than ropes with southward leading edges, in agreement with a previously established solar cycle dependence. Ropes with low inclinations to the solar equatorial plane were about four times more common than ropes with high inclinations, possibly an observational effect. Left- and right-handed ropes were observed in almost equal numbers. In addition, data from MESSENGER, Venus Express, STEREO-A, STEREO-B and ACE were examined for multipoint signatures of the catalogued ICMEs. For spacecraft separations below 15° in heliocentric longitude, the second spacecraft observed the ICME flux rope in 82 % of cases; this percentage dropped to 49 % for separations between 15 and 30°, to 18 % for separations between 30 and 45°, and to 12 % for separations between 45 and 60°. As the spacecraft separation increased, it became increasingly likely that only the sheath and not the flux rope of the ICME was observed, in agreement with the notion that ICME flux ropes are smaller in longitudinal extent than the shocks or discontinuities that they often drive. Furthermore, this study has identified 23 ICMEs observed by pairs of spacecraft close to radial alignment. A detailed analysis of these events could lead to a better understanding of how ICMEs evolve during propagation.

Table 1 The MESSENGER (200501- 201203) and *Venus Express* (200601-201312) ICME catalogue. Parenthesised table entries indicate uncertainty in the stated values.

Radial Evolution of a Magnetic Cloud: MESSENGER, STEREO, and Venus Express Observations

S. W. [Good](#)¹, R. J. Forsyth¹, J. M. Raines², D. J. Gershman³, J. A. Slavin², and T. H. Zurbuchen
2015 *ApJ* 807 177

The Solar Orbiter and Solar Probe Plus missions will provide observations of magnetic clouds closer to the Sun than ever before, and it will be good preparation for these missions to make full use of the most recent in situ data sets from the inner heliosphere—namely, those provided by MERcury Surface, Space ENvironment, GEochemistry, and RANGing (MESSENGER) and Venus Express—for magnetic cloud studies. We present observations of the same magnetic cloud made by MESSENGER at Mercury and later by Solar TERrestrial RElations Observatory-B (STEREO-B), while the spacecraft were radially aligned in **2011 November**. Few such radial observations of magnetic clouds have been previously reported. Estimates of the solar wind speed at MESSENGER are also presented, calculated through the application of a previously established technique. The cloud's flux rope has been analyzed using force-free fitting; the rope diameter increased from 0.18 to 0.41 AU (corresponding to an $r_H^{0.94}$ dependence on heliocentric distance, r_H), and the axial magnetic field strength dropped from 46.0 to 8.7 nT (an $r_H^{-1.84}$ dependence) between the spacecraft, clear indications of an expanding structure. The axial magnetic flux was ~ 0.50 nT AU² at both spacecraft, suggesting that the rope underwent no significant erosion through magnetic reconnection between MESSENGER and STEREO-B. Further, we estimate the change in the cloud's angular width by assuming helicity conservation. It has also been found that the rope axis rotated by 30° between the spacecraft to lie close to the solar equatorial plane at STEREO-B. Such a rotation, if it is a common feature of coronal mass ejection propagation, would have important implications for space weather forecasting.

Intense Geomagnetic Storms during Solar Cycles 23-25

N. [Gopalswamy](#), [S. Akiyama](#), [S. Yashiro](#), [P. Makela](#), [H. Xie](#)

Proceedings of the Fifteenth Workshop Solar Influences on the Magnetosphere, Ionosphere and Atmosphere, June, 2023 **2024**

<https://arxiv.org/ftp/arxiv/papers/2401/2401.03524.pdf> **File**

Intense geomagnetic storms are characterized by a minimum value of the Dst index at or below -100 nT. It is well known that these storms are caused by the southward magnetic fields in coronal mass ejections (CMEs) and corotating interaction regions (CIRs). While CIR storms are confined to Dst values at or above -150 nT, CME storms can reach Dst -500 nT or lower. In this report, we illustrate the need to understand the storm evolution based on solar source and solar wind parameters using a recent storm (**2023 April 24**) by way of providing the motivation to catalog such events for a better understanding of the main phase time structure of geomagnetic storms

The Solar Cause of the 2022 February 3 Geomagnetic Storm that Led to the Demise of the Starlink Satellites

Nat [Gopalswamy](#), [Hong Xie](#), [Seiji Yashiro](#), [Sachiko Akiyama](#)

Sun and Geosphere **2023**

<https://arxiv.org/ftp/arxiv/papers/2303/2303.02330.pdf>

We report on the solar source of the **2022 February 3** geomagnetic storm of moderate strength that contributed to the loss of 39 Starlink satellites. The geomagnetic storm was caused by the **2022 January 29** halo coronal mass ejection (CME) that was of moderate speed (about 690 km/s) originating from NOAA active region 12936 located in the northeast quadrant (N18E06) of the Sun. The eruption was marked by an M1.1 flare, which started at 22:45 UT, peaked at 23:32 UT on January 29 and ended at 00:24 UT the next day. The CME ended up as a shock-driving magnetic cloud (MC) observed at Sun-Earth L1 and at STEREO-Ahead (STA) located about 34 deg behind Earth. The geomagnetic storm was caused by a strong southward component of the MC that was boosted by a high speed solar wind stream behind the MC. Even though Earth and STA were separated by only about 34 deg, the MC appeared quite different at Earth and L1. One possibility is that the MC was writhed reflecting the curved neutral line at the Sun. In-situ observations suggest that the MC was heading closer to STA than to Earth because of the earlier arrival at STA. However, the shock arrived at STA and Earth around the same time, suggesting a weaker shock at Earth due to flank passage.

What is Unusual about the Third Largest Geomagnetic Storm of Solar Cycle 24?

[N. Gopalswamy](#), [S. Yashiro](#), [S. Akiyama](#), [H. Xie](#), [P. Mäkelä](#), [M.-C. Fok](#), [C. P. Ferradas](#)

JGR **Volume127, Issue8** e2022JA030404 2022

<https://arxiv.org/ftp/arxiv/papers/2207/2207.11630.pdf>

<https://agupubs.onlinelibrary.wiley.com/doi/epdf/10.1029/2022JA030404>

We report on the solar and interplanetary (IP) causes of the third largest geomagnetic storm (**2018 August 26**) in solar cycle 24. The underlying coronal mass ejection (CME) originating from a quiescent filament region becomes a 440 km/s magnetic cloud (MC) at 1 au after ~5 days. The prolonged CME acceleration (for about 24 hrs) coincides with the time profiles of the post-eruption arcade intensity and reconnected flux. Chen et al. (2019) obtain lower speed since they assumed that the CME does not accelerate after about 12 hrs. The presence of multiple coronal holes near the filament channel and the high-speed wind from them seem to have the combined effect of producing complex rotation in the corona and IP medium resulting in a high-inclination MC. The Dst time profile in the main phase steepens significantly (rapid increase in storm intensity) coincident with the density increase (prominence material) in the second half of the MC. Simulations using the Comprehensive Inner Magnetosphere-Ionosphere (CIMI) model shows that a higher ring current energy results from larger dynamic pressure in MCs. Furthermore, the Dst index is highly correlated with the main-phase time integral of the ring current injection that includes density, consistent with the simulations. A complex temporal structure develops in the storm main phase if the underlying MC has a complex density structure during intervals of southward interplanetary magnetic field. We conclude that the high intensity of the storm results from the prolonged CME acceleration, complex rotation, and the high density in the 1-au MC.

Table 1 Solar Wind Parameters Associated With the Geomagnetic Storms on **26 August 2018, 29 May 2010, and 11 April 2014** From the OMNI Data

Table 2 List of 32 Storms Considered for Correlation Analysis, the First 17 Being Very Intense 1998-2018

The Multiview observatory for solar terrestrial science (MOST),

Gopalswamy, N., Christe, S., Fung, S. F., Gong, Q., Jian, L., Kanekal, S. G., et al.

in The decadal survey for solar and space physics (Heliophysics), 2024–2033. Submitted White Paper. (2022).

https://ntrs.nasa.gov/api/citations/20220013621/downloads/GopalswamyNat_MOST_WP.pdf

Understanding the emergence of magnetic flux from the solar interior through the photosphere and its global impact on the inner heliosphere is a key scientific goal of the heliophysics community. This white paper outlines the concept of the Multiview Observatory for Solar Terrestrial Science (MOST) mission, which will make measurements of solar variability from the solar interior, atmosphere, and the interplanetary (IP) medium. MOST will be a 4- spacecraft mission with one each at L4 (MOST1) and L5 (MOST2) and the other two (MOST3 and MOST4) at variable locations along Earth orbit. MOST1 and MOST2 will each carry seven remote-sensing and 3 in-situ instruments. All four spacecraft will carry elements of a novel radio package known as the Faraday Effect Tracker of Coronal and Heliospheric structures (FETCH). FETCH will systematically probe the magnetic content of transient IP structures including coronal mass ejections (CMEs) and stream interaction regions (SIRs). The Faraday rotation measurements will provide magnetic information of these structures at various heliocentric distances from the outer corona to Earth's vicinity. Photospheric and chromospheric magnetograms will cover >70% of the solar surface providing synchrotron maps needed for accurately modeling the corona and solar wind. EUV, coronagraph, radio spectrograph, and heliospheric imager (HI) observations from multiple viewpoints provide 3-d information on CMEs/CME-driven shocks, SIRs, and other solar wind structures. The Hard X-ray imagers will provide the flare aspects of solar eruptions to complement the CME aspects. MOST, a 10-year mission, is well aligned with NASA's Heliophysics objectives and will

provide an unprecedented opportunity to achieve these objectives with broad participation from the heliophysics community.

Effect of the Weakened Heliosphere in Solar Cycle 24 on the Properties of Coronal Mass Ejections

N. [Gopalswamy](#), [S. Akiyama](#), [S. Yashiro](#), [G. Michalek](#), [H. Xie](#), [P. Mäkelä](#)

Proc. 19th International Astrophysics Conference held in Santa Fe, New Mexico, March 9 - 13, 2020

<https://arxiv.org/ftp/arxiv/papers/2007/2007.08291.pdf>

Solar cycle (SC) 24 has come to an end by the end of 2019, providing information on two full cycles to understand the manifestations of SC 24, the smallest cycle in the Space Age that has resulted in a weak heliospheric state indicated by the reduced pressure. The backreaction of the heliospheric state is to make the coronal mass ejections (CMEs) appear physically bigger than in SC 23, but their magnetic content has been diluted resulting in a lower geoeffectiveness. The heliospheric magnetic field is also lower in SC 24, leading to the dearth of high-energy solar energetic particle (SEP) events. These space weather events closely follow fast and wide (FW) CMEs. All but FW CMEs are higher in number in SC 24. The CME rate vs. sunspot number (SSN) correlation is high in both cycles but the rate increases faster in SC 24. We revisit the study of limb CMEs (those with source regions within 30 degrees from the limb) previously studied over partial cycles. We find that limb CMEs are slower in SC 24 as in the general population but wider. Limb halo CMEs follow the same trend of slower SC-24 CMEs. However, the SC-24 CMEs become halos at a shorter distance from the Sun. Thus, slower CMEs becoming halos sooner is a clear indication of the backreaction of the weaker heliospheric state on CMEs. We can further pin down the heliospheric state as the reason for the altered CME properties because the associated flares have similar distributions in the two cycles, unaffected by the heliospheric state. **2002-09-06**

Table 3. Halo CMEs originating within 30° from the limb in solar cycles 23 and 24

The State of the Heliosphere Revealed by Limb Halo Coronal Mass Ejections in Solar Cycles 23 and 24

Nat [Gopalswamy](#), [Sachiko Akiyama](#), [Seiji Yashiro](#)

ApJL 897:L1 2020

<https://arxiv.org/ftp/arxiv/papers/2006/2006.05844.pdf>

<https://iopscience.iop.org/article/10.3847/2041-8213/ab9b7b/pdf>

We compare the properties of halo coronal mass ejections (CMEs) that originate close to the limb (within a central meridian distance range of 60 to 90 deg) during solar cycles 23 and 24 to quantify the effect of the heliospheric state on CME properties. There are 44 and 38 limb halos in the cycles 23 and 24, respectively. Normalized to the cycle-averaged total sunspot number, there are 42 percent more limb halos in cycle 24. Although the limb halos as a population is very fast (average speed 1464 km s⁻¹), cycle-24 halos are slower by 26 percent than the cycle-23 halos. We introduce a new parameter, the heliocentric distance of the CME leading edge at the time a CME becomes a full halo; this height is significantly shorter in cycle 24 (by 20 percent) and has a lower cutoff at 6 Rs. These results show that cycle-24 CMEs become halos sooner and at a lower speed than the cycle-23 ones. On the other hand, the flare sizes are very similar in the two cycles, ruling out the possibility of eruption characteristics contributing to the differing CME properties. In summary, this study reveals the effect of the reduced total pressure in the heliosphere that allows cycle-24 CMEs expand more and become halos sooner than in cycle 23. Our findings have important implications for the space-weather consequences of CMEs in cycle 25 (predicted to be similar to cycle 24) and for understanding the disparity in halo counts reported by automatic and manual catalogs. **2011 September 22**

Table 1. List of Limb Halo CMEs from Solar Cycles 23 and 24

Sun-to-Earth Propagation of the 2015 June 21 Coronal Mass Ejection Revealed by Optical, EUV, and Radio Observations

N. [Gopalswamy](#), [P. Makela](#), [S. Akiyama](#), [S. Yashiro](#), [H. Xie](#), [N. Thakur](#)

JASTP [Volume 179](#), Pages 225-238 **2018**

<https://arxiv.org/ftp/arxiv/papers/1807/1807.10979.pdf>

We investigate the propagation of the **2015 June 21** CME-driven shock as revealed by the type II bursts at metric and longer wavelengths and coronagraph observations. The CME was associated with the second largest geomagnetic storm of solar cycle 24 and a large solar energetic particle (SEP) event. The eruption consisted of two M-class flares, with the first one being confined, with no metric or interplanetary radio bursts. However, there was intense microwave burst, indicating accelerated particles injected toward the Sun. The second flare was eruptive that resulted in a halo CME. The CME was deflected primarily by an equatorial coronal hole that resulted in the modification of the intensity profile of the associated SEP event and the duration of the CME at Earth. The interplanetary type II burst was particularly intense

and was visible from the corona all the way to the vicinity of the Wind spacecraft with fundamental-harmonic structure. We computed the shock speed using the type II drift rates at various heliocentric distances and obtained information on the evolution of the shock that matched coronagraph observations near the Sun and in-situ observations near Earth. The depth of the geomagnetic storm is consistent with the 1-AU speed of the CME and the magnitude of the southward component.

A New Technique to Provide Realistic Input to CME Forecasting Models

Nat **Gopalswamy** (a1), [Sachiko Akiyama](#) (a2), [Seiji Yashiro](#) (a2) and [Hong Xie](#)

Proc. IAU [Volume 13, Symposium S335](#) July 2017 , pp. 258-262

[sci-hub.se/10.1017/S1743921317011048](https://doi.org/10.1017/S1743921317011048)

We report on a technique to construct a flux rope (FR) from eruption data at the Sun. The technique involves line-of-sight magnetic fields, post-eruption arcades in the corona, and white-light coronal mass ejections (CMEs) so that the FR geometric and magnetic properties can be fully defined in addition to the kinematic properties. We refer to this FR as FRED (Flux Rope from Eruption Data). We illustrate the FRED construction using the **2012 July 12** eruption and compare the coronal and interplanetary properties of the FR. The results indicate that the FRED input should help make realistic predictions of the components of the FR magnetic field in the heliosphere.

Extreme Solar Eruptions and their Space Weather Consequences

Review

Nat **Gopalswamy**

In: Extreme Events in Geospace

Origins, Predictability, and Consequences

Book

Editor: Natalia **Buzulukova**, Elsevier, 2018, 798 p. **File**

p. 37-63 [sci-hub.se/10.1016/B978-0-12-812700-1.00002-9](https://doi.org/10.1016/B978-0-12-812700-1.00002-9)

<https://arxiv.org/ftp/arxiv/papers/1709/1709.03165.pdf> **File**

Solar eruptions generally refer to coronal mass ejections (CMEs) and flares. Both are important sources of space weather. Solar flares cause sudden change in the ionization level in the ionosphere. CMEs cause solar energetic particle (SEP) events and geomagnetic storms. A flare with unusually high intensity and/or a CME with extremely high energy can be thought of examples of extreme events on the Sun. These events can also lead to extreme SEP events and/or geomagnetic storms. Ultimately, the energy that powers CMEs and flares are stored in magnetic regions on the Sun, known as active regions. Active regions with extraordinary size and magnetic field have the potential to produce extreme events. Based on current data sets, we estimate the sizes of one-in-hundred and one-in-thousand year events as an indicator of the extremeness of the events. We consider both the extremeness in the source of eruptions and in the consequences. We then compare the estimated 100-year and 1000-year sizes with the sizes of historical extreme events measured or inferred.

Carrington flare , 2003 October 28, 2004 November 10, October 2014

Table 1. Integral fluence values for different models in units of 10^{10} p cm⁻²

Table 2. Expected 100-year and 1000-year event sizes estimated from the tail of observed distributions fitted to various functions.

Coronal Flux Ropes and their Interplanetary Counterparts

N. **Gopalswamy**, S. Akiyama, S. Yashiro, H. Xie

J. Atmos. Solar-Terr. Phys. 2017 **File**

<https://arxiv.org/pdf/1705.08912.pdf>

We report on a study comparing coronal flux ropes inferred from eruption data with their interplanetary counterparts constructed from in situ data. The eruption data include the source-region magnetic field, post-eruption arcades, and coronal mass ejections (CMEs). Flux ropes were fit to the interplanetary CMEs (ICMEs) considered for the 2011 and 2012 Coordinated Data Analysis Workshops (CDAWs). We computed the total reconnected flux involved in each of the associated solar eruptions and found it to be closely related to flare properties, CME kinematics, and ICME properties. By fitting flux ropes to the white-light coronagraph data, we obtained the geometric properties of the flux ropes and added magnetic properties derived from the reconnected flux. We found that the CME magnetic field in the corona is significantly higher than the ambient magnetic field at a given heliocentric distance. The radial dependence of the flux-rope magnetic field strength is faster than that of the ambient magnetic field. The magnetic field strength of the coronal flux rope is also correlated with that in interplanetary flux ropes constructed from in situ data, and with the observed peak magnetic field strength in ICMEs. The physical reason for the observed correlation between the peak field strength in MCs is the higher magnetic field content in faster coronal flux ropes and ultimately the higher reconnected flux in the

eruption region. The magnetic flux ropes constructed from the eruption data and coronagraph observations provide a realistic input that can be used by various models to predict the magnetic properties of ICMEs at Earth and other destination in the heliosphere. **1999 June 24**

Estimation of Reconnection Flux using Post-eruption Arcades and Its Relevance to 1-au Magnetic Clouds

N. [Gopalswamy](#), S. Yashiro, S. Akiyama, H. Xie

Solar Phys. 292: 65. **2017**

<https://arxiv.org/pdf/1701.01943v1.pdf> **File**

We report on a new method to compute the flare reconnection (RC) flux from post-eruption arcades (PEAs) and the underlying photospheric magnetic fields. In previous work, the RC flux has been computed using cumulative flare ribbon area. Here we obtain the RC flux as half of that underlying the PEA associated with the eruption using an image in EUV taken after the flare maximum. We apply this method to a set of 21 eruptions that originated near the solar disk center in solar cycle 23. We find that the RC flux from the arcade method (Φ_{rA}) has excellent agreement with that from the ribbon method (Φ_{rR}) according to: $\Phi_{rA} = 1.24(\Phi_{rR})^{0.99}$. We also find Φ_{rA} to be correlated with the poloidal flux (Φ_P) of the associated magnetic cloud at 1 au: $\Phi_P = 1.20(\Phi_{rA})^{0.85}$. This relation is nearly identical to that obtained by Qiu et al. (2007) using a set of only 9 eruptions. Our result supports the idea that flare reconnection results in the formation of flux rope and PEA as a common process.

1997 May 12, 2000 July 14, 2001 April 26, 2003 October 29, 2004 April 11

Table 1. List of solar eruptions that were associated with magnetic clouds at Earth

Table 2. List of Events with RC flux Computed from H-alpha or TRACE 1600 A Ribbons

History and development of coronal mass ejections as a key player in solar terrestrial relationship

Review

N. [Gopalswamy](#)

[Geoscience Letters](#) volume 3, Article number: 8 (2016) **File**

<https://geoscienceletters.springeropen.com/track/pdf/10.1186/s40562-016-0039-2>

<http://arxiv.org/pdf/1602.03665v1.pdf>

DOI 10.1186/s40562-016-0039-2

Coronal mass ejections (CMEs) are relatively a recently discovered phenomenon—in 1971, some 15 years into the Space Era. It took another two decades to realize that CMEs are the most important players in solar terrestrial relationship as the root cause of severe weather in Earth's space environment. CMEs are now counted among the major natural hazards because they cause large solar energetic particle (SEP) events and major geomagnetic storms, both of which pose danger to humans and their technology in space and ground. Geomagnetic storms discovered in the 1700s, solar flares discovered in the 1800s, and SEP events discovered in the 1900s are all now found to be closely related to CMEs via various physical processes occurring at various locations in and around CMEs, when they interact with the ambient medium. This article identifies a number of key developments that preceded the discovery of white-light CMEs suggesting that CMEs were waiting to be discovered. The last two decades witnessed an explosion of CME research following the launch of the Solar and Heliospheric Observatory mission in 1995, resulting in the establishment of a full picture of CMEs.

Short-term variability of the Sun-Earth system: an overview of progress made during the CAWSES-II period

Review

[Gopalswamy](#), Nat; Tsurutani, Bruce; Yan, Yihua

Progress in Earth and Planetary Science, Volume 2, article id. #13, 41 pp., **2015**

<http://arxiv.org/pdf/1504.06332v1.pdf> **File**

sci-hub.se/10.1186/s40645-015-0043-8

This paper presents an overview of results obtained during the CAWSES-II period on the short-term variability of the Sun and how it affects the near-Earth space environment. CAWSES-II was planned to examine the behavior of the solar-terrestrial system as the solar activity climbed to its maximum phase in solar cycle 24. After a deep minimum following cycle 23, the Sun climbed to a very weak maximum in terms of the sunspot number in cycle 24 (MiniMax24), so many of the results presented here refer to this weak activity in comparison with cycle 23. The short-term variability that has immediate consequence to Earth and geospace manifests as solar eruptions from closed-field regions and high-speed streams from coronal holes. Both electromagnetic (flares) and mass emissions (coronal mass ejections - CMEs) are

involved in solar eruptions, while coronal holes result in high-speed streams that collide with slow wind forming the so-called corotating interaction regions (CIRs). Fast CMEs affect Earth via leading shocks accelerating energetic particles and creating large geomagnetic storms. CIRs and their trailing high-speed streams (HSSs), on the other hand, are responsible for recurrent small geomagnetic storms and extended days of auroral zone activity, respectively. The latter leads to the acceleration of relativistic magnetospheric 'killer' electrons. One of the major consequences of the weak solar activity is the altered physical state of the heliosphere that has serious implications for the shock-driving and storm-causing properties of CMEs. Finally, a discussion is presented on extreme space weather events prompted by the **23 July 2012** super storm event that occurred on the backside of the Sun. Many of these studies were enabled by the simultaneous availability of remote sensing and in situ observations from multiple vantage points with respect to the Sun-Earth line.

TABLE 2 Major geomagnetic storms of cycle 24 (Dst < -100 nT)

Properties and Geoeffectiveness of Magnetic Clouds during Solar Cycles 23 and 24†

N. **Gopalswamy**, S. Yashiro^{1,2}, H. Xie^{1,2}, S. Akiyama^{1,2} and P. Mäkelä

JGR Volume 120, Issue 11 November 2015 Pages 9221–9245 **2015**

<http://arxiv.org/pdf/1510.00906v1.pdf>

sci-hub.tw/10.1002/2015JA021446

We report on a study that compares the properties of magnetic clouds (MCs) during the first 73 months of solar cycles 23 and 24 in order to understand the weak geomagnetic activity in cycle 24. We find that the number of MCs did not decline in cycle 24, although the average sunspot number is known to have declined by ~40%. Despite the large number of MCs, their geoeffectiveness in cycle 24 was very low. The average Dst index in the sheath and cloud portions in cycle 24 was -33 nT and -23 nT, compared to -66 nT and -55 nT, respectively in cycle 23. One of the key outcomes of this investigation is that the reduction in the strength of geomagnetic storms as measured by the Dst index is a direct consequence of the reduction in the factor VBz (the product of the MC speed and the out-of-the-ecliptic component of the MC magnetic field). The reduction in MC-to-ambient total pressure in cycle 24 is compensated for by the reduction in the mean MC speed, resulting in the constancy of the dimensionless expansion rate at 1 AU. However, the MC size in cycle 24 was significantly smaller, which can be traced to the anomalous expansion of coronal mass ejections near the Sun reported by Gopalswamy et al. (2014a). One of the consequences of the anomalous expansion seems to be the larger heliocentric distance where the pressure balance between the CME flux ropes and the ambient medium occurs in cycle 24.

CMEs during the Two Activity Peaks in Cycle 24 and their Space Weather Consequences

N. **Gopalswamy**, P. Mäkelä, S. Akiyama, S. Yashiro, N. Thakur

Sun and Geosphere, **2015**

<http://arxiv.org/pdf/1509.04216v1.pdf> **File**

We report on a comparison between space weather events that occurred around the two peaks in the sunspot number (SSN) during solar cycle 24. The two SSN peaks occurred in the years 2012 and 2014. Even though SSN was larger during the second peak, we find that there were more space weather events during the first peak. The space weather events we considered are large solar energetic particle (SEP) events and major geomagnetic storms associated with coronal mass ejections (CMEs). We also considered interplanetary type II radio bursts, which are indicative of energetic CMEs driving shocks. When we compared the CME properties between the two SSN peaks, we find that more energetic CMEs occurred during the 2012 peak. In particular, we find that CMEs accompanying IP type II bursts had an average speed of 1543 km/s during the 2012 peak compared to 1201 km/s during the 2014 peak. This result is consistent with the reduction in the average speed of the general population of CMEs during the second peak. All SEP events were associated with the interplanetary type II bursts, which are better than halo CMEs as indicators of space weather. The comparison between the two peaks also revealed the discordant behavior CME rate and SSN is more pronounced during the second peak. None of the 14 disk-center halo CMEs was associated with a major storm in 2014. The lone major storm in 2014 was due to the intensification of the (southward) magnetic field in the associated magnetic cloud by a shock that caught up and propagated into the magnetic cloud. **23-24 Apr 2012; 18-19 Feb 2014**

Table 2. List of DH-km type II bursts in 2012, the associated CMEs and SEP events

Table 3. List of DH-km type II bursts in 2014, the associated CMEs and SEP events

The Mild Space Weather in Solar Cycle 24

Nat **Gopalswamy**, [Sachiko Akiyama](#), [Seiji Yashiro](#), [Hong Xie](#), [Pertti Makela](#), [Grzegorz Michalek](#)

Proc. 14th International Ionospheric Effects Symposium on 'Bridging the gap between applications and research involving ionospheric and space weather disciplines' May 12-14, **2015**, Alexandria, VA

<http://arxiv.org/ftp/arxiv/papers/1508/1508.01603.pdf>

The space weather is extremely mild during solar cycle 24: the number of major geomagnetic storms and high-energy solar energetic particle events are at the lowest since the dawn of the space age. Solar wind measurements at 1 AU using Wind and ACE instruments have shown that there is a significant drop in the density, magnetic field, total pressure, and Alfvén speed in the inner heliosphere as a result of the low solar activity. The drop in large space weather events is disproportionately high because the number of energetic coronal mass ejections that cause these events has not decreased significantly. For example, the rate of halo CMEs, which is a good indicator of energetic CMEs, is similar to that in cycle 23, even though the sunspot number has declined by about 40%. The mild space weather seems to be a consequence of the anomalous expansion of CMEs due to the low ambient pressure in the heliosphere. The anomalous expansion results in the dilution of the magnetic contents of CMEs, so the geomagnetic storms are generally weak. CME driven shocks propagating through the weak heliospheric field are less efficient in accelerating energetic particles, so the particles do not attain high energies. Finally, we would like to point out that extreme events such as the 2012 July 23 CMEs that occurred on the backside of the Sun and did not affect Earth except for a small proton event. **March 17, 2015**

The Peculiar Behavior of Halo Coronal Mass Ejections in Solar Cycle 24

N. **Gopalswamy**, H. Xie, S. Akiyama, P. Mäkelä, S. Yashiro, G. Michalek

ApJL **2015**

<http://arxiv.org/ftp/arxiv/papers/1504/1504.01797.pdf>

We report on a remarkable finding that the halo coronal mass ejections (CMEs) in cycle 24 are more abundant than in cycle 23, although the sunspot number in cycle 24 has dropped by about 40%. We also find that the distribution of halo-CME source locations is different in cycle 24: the longitude distribution of halos is much flatter with the number of halos originating at central meridian distance ≥ 60 degrees twice as large as that in cycle 23. On the other hand, the average speed and the associated soft X-ray flare size are the same in the two cycles, suggesting that the ambient medium into which the CMEs are ejected is significantly different. We suggest that both the higher abundance and larger central meridian longitudes of halo CMEs can be explained as a consequence of the diminished total pressure in the heliosphere in cycle 24 (Gopalswamy et al. 2014). The reduced total pressure allows CMEs expand more than usual making them appear as halos.

Anomalous Expansion of Coronal Mass Ejections during Solar Cycle 24 and its Space Weather Implications

Nat **Gopalswamy**, Sachiko Akiyama, Seiji Yashiro, Hong Xie, and Pertti Mäkelä, Grzegorz Michalek
E-print, April **2014**; GRL 41:2673-2680

<http://arxiv.org/pdf/1404.0252v1.pdf>

<http://sci-hub.tw/10.1002/2014GL059858>

The familiar correlation between the speed and angular width of coronal mass ejections (CMEs) is also found in solar cycle 24, but the regression line has a larger slope: for a given CME speed, cycle 24 CMEs are significantly wider than those in cycle 23. The slope change indicates a significant change in the physical state of the heliosphere, due to the weak solar activity. The total pressure in the heliosphere (magnetic + plasma) is reduced by $\sim 40\%$, which leads to the anomalous expansion of CMEs explaining the increased slope. The excess CME expansion contributes to the diminished effectiveness of CMEs in producing magnetic storms during cycle 24, both because the magnetic content of the CMEs is diluted and also because of the weaker ambient fields. The reduced magnetic field in the heliosphere may contribute to the lack of solar energetic particles accelerated to very high energies during this cycle.

Testing the empirical shock arrival model using quadrature observations

N. **Gopalswamy**^{1,*}, P. Mäkelä^{1,2}, H. Xie^{1,2}, S. Yashiro

Space Weather, Volume 11, Issue 11, pages 661–669, November **2013**

http://cdaw.gsfc.nasa.gov/publications/gopal/gopal2013SW_testESA.pdf

The empirical shock arrival (ESA) model was developed based on quadrature data from Helios (in situ) and P-78 (remote sensing) to predict the Sun-Earth travel time of coronal mass ejections (CMEs). The ESA model requires

earthward CME speed as input, which is not directly measurable from coronagraphs along the Sun-Earth line. The Solar Terrestrial Relations Observatory (STEREO) and the Solar and Heliospheric Observatory (SOHO) were in quadrature during 2010–2012, so the speeds of Earth-directed CMEs were observed with minimal projection effects. We identified a set of 20 full halo CMEs in the field of view of SOHO that were also observed in quadrature by STEREO. We used the earthward speed from STEREO measurements as input to the ESA model and compared the resulting travel times with the observed ones from L1 monitors. We find that the model predicts the CME travel time within about 7.3 h, which is similar to the predictions by the ENLIL model. We also find that CME-CME and CME-coronal hole interaction can lead to large deviations from model predictions. **2011 February 15, 2012 July 12**

Table 1. List of shocks detected at L1 and the corresponding halo CMEs observed by SOHO

Table 2. List of events with coronal holes visible on the disk.

Table 3. The number of preceding CMEs within a 24 h interval preceding the CMEs in Table 1

The Solar Connection of Enhanced Heavy Ion Charge States in the Interplanetary Medium: Implications for the Flux-rope Structure of CMEs

N. **Gopalswamy**, P. Mäkelä, S. Akiyama, H. Xie, S. Yashiro, and A. A. Reinard
Solar Physics, Volume 284, Issue 1, pp 17-46, **2013**, **File**

We investigated a set of 54 interplanetary coronal mass ejection (ICME) events whose solar sources are very close to the disk center (within ± 15 degrees from the central meridian). The ICMEs consisted of 23 magnetic cloud (MC) events and 31 non-MC events. Our analyses suggest that the MC and non-MC ICMEs have more or less the same eruption characteristics at the Sun in terms of soft X-ray flares and CMEs. Both types have significant enhancements in charge states, although the non-MC structures have slightly lower levels of enhancement. The overall duration of charge state enhancement is also considerably smaller than that in MCs as derived from solar wind plasma and magnetic signatures. We find very good correlation between the Fe and O charge state measurements and the flare properties such as soft X-ray flare intensity and flare temperature for both MCs and non-MCs. These observations suggest that both MC and non-MC ICMEs are likely to have a flux-rope structure and the unfavorable observational geometry may be responsible for the appearance of non-MC structures at 1 AU. We do not find any evidence for active region expansion resulting in ICMEs lacking a flux rope structure because the mechanism of producing high charge states and the flux rope structure at the Sun is the same for MC and non-MC events.

Table: http://iopscience.iop.org/0004-637X/710/2/1111/fulltext/apj_710_2_1111.tables.html

1999 September 19, 2001-03-19, 2002 May 27

Energetic Particle and Other Space Weather Events of Solar Cycle 24

N. **Gopalswamy**

E-print, Jan 2013,; In Space Weather: The space Radiation Environment, Ed. Q. Hu, G. Li, G. P. Zank, X. Ao, O. Verkhoglyadova, J. H. Adama, AIP Conf Proc. 1500, pp. 14-19, **2012**; **File**

We report on the space weather events of solar cycle 24 in comparison with those during a similar epoch in cycle 23. We find major differences in all space weather events: solar energetic particles, geomagnetic storms, and interplanetary shocks. Dearth of ground level enhancement (GLE) events and major geomagnetic storms during cycle 24 clearly stand out. The space weather events seem to reflect the less frequent solar eruptions and the overall weakness of solar cycle 24.

TABLE 1. List of large SEP events from solar cycle 24.

2010/08/14; 2011/03/08; 2011/03/21; 2011/06/07; 2011/08/04; 2011/08/09; 2011/09/23; 2011/11/26; 2012/01/23; 2012/01/27; 2012/03/07; 2012/03/13; 2012/05/17; 2012/05/27; 2012/06/16; 2012/07/07; 2012/07/09; 2012/07/12; 2012/07/17; 2012/07/19; 2012/07/23

TABLE 2. Major geomagnetic storms of cycle 24 (Dst < -100 nT)

2011/09/27; 2011/10/25; 2012/03/09; 2012/04/24; 2012/07/15

Radio-loud CMEs from the disk center lacking shocks at 1 AU

N. **Gopalswamy**, P. Makela, S. Akiyama, S. Yashiro, H. Xie, R. J. MacDowall, M. L. Kaiser
E-print, June **2012**, JGR, 117, A08106, **2012**

A coronal mass ejection (CME) associated with a type II burst and originating close to the center of the solar disk typically results in a shock at Earth in 2-3 days and hence can be used to predict shock arrival at Earth. However, a significant fraction (about 28%) of such CMEs producing type II bursts were not associated with shocks at Earth. We examined a set of 21 type II bursts observed by the Wind/WAVES experiment at decameter-hectometric (DH) wavelengths that had CME sources very close to the disk center (within a central meridian distance of 30 degrees), but did not have a shock at Earth. We find that the near-Sun speeds of these CMEs average to ~644 km/s, only slightly higher than the average speed of CMEs associated with radio-quiet shocks. However, the fraction of halo CMEs is only ~30%, compared to 54% for the radio-quiet shocks and 91% for all radio-loud shocks. We conclude that the disk-center radio-loud CMEs with no shocks at 1 AU are generally of lower energy and they drive shocks only close to the Sun and dissipate before arriving at Earth. There is also evidence for other possible processes that lead to the lack of shock at 1 AU: (i) overtaking CME shocks merge and one observes a single shock at Earth, and (ii) deflection by nearby coronal holes can push the shocks away from the Sun-Earth line, such that Earth misses these shocks. The probability of observing a shock at 1 AU increases rapidly above 60% when the CME speed exceeds 1000 km/s and when the type II bursts propagate to frequencies below 1 MHz.

Universal Heliophysical Processes

Gopalswamy, N.

In: *The Sun, the Solar Wind, and the Heliosphere*, ed. M. P. Miralles and J. Sanchez Almeida, IAGA Special Sopron Book Series, Vol 4, Chapter 2, Springer, pp 9-20, **2011, File**, DOI: 10.1007/978/90-481-9787-3_2

The physical processes in the heliospace are a direct consequence of the influenced by Sun's mass and electromagnetic emissions. There has been enormous progress in studying these processes since the dawn of the space age half a century ago. The heliospace serves as a great laboratory to study numerous physical processes, using the vast array of ground and space-based measurements of various physical quantities. The observational capabilities collectively form the Great Observatory to make scientific investigations not envisioned by individual instrument teams. The International Heliophysical Year (IHY) program has been promoting scientific investigations on the universality of physical processes such as shocks, particle acceleration, dynamo, magnetic reconnection, magnetic flux ropes, plasma-neutral matter interactions, turbulence, and so on. This paper highlights scientific deliberations on these and related topics that took place during the IAGA sessionon "Universal Heliophysical Processes" in Sopron, Hungary. The session featured several invited and contributed papers that focused on observations, theory and modeling of the universal heliophysical processes.

Earth-Affecting Solar Causes Observatory (EASCO): A Potential International Living with a Star Mission from Sun-Earth L5*

N. Gopalswamy¹, J. Davila¹, O. C. St. Cyr¹, E. Sittler¹, F. Auchère², T. Duvall¹, T. Hoeksema³, M. Maksimovic⁴, R. MacDowall¹, A. Szabo¹, and M. Collier¹
JASTP, **2011, File** in press.

This paper describes the scientific rationale for an L5 mission and a partial list of key scientific instruments the mission should carry. The L5 vantage point provides an unprecedented view of the solar disturbances and their solar sources that can greatly advance the science behind space weather. A coronagraph and a heliospheric imager at L5 will be able to view CMEs broadsided, so space speed of the Earth-directed CMEs can be measured accurately and their radial structure discerned. In addition, an inner coronal imager and a magnetograph from L5 can give advance information on active regions and coronal holes that will soon rotate on to the solar disk. Radio remote sensing at low frequencies can provide information on shock-driving CMEs, the most dangerous of all CMEs. Coordinated helioseismic measurements from the Sun-Earth line and L5 provide information on the physical conditions at the base of the convection zone, where solar magnetism originates. Finally, in situ measurements at L5 can provide information on the large-scale solar wind structures (corotating interaction regions (CIRs)) heading towards Earth that potentially result in adverse space weather.

Solar Sources of "Driverless" Interplanetary Shocks,

Gopalswamy N, Mäkelä P, Xie H, Akiyama S, Yashiro S

(**2010d**) Twelfth International Solar Wind Conference, AIP Conference Proceedings, Volume 1216, p. 452

INTERPLANETARY SHOCKS LACKING TYPE II RADIO BURSTS

N. [Gopalswamy](#)¹, H. Xie², P. Mäkelä², S. Akiyama², S. Yashiro³, M. L. Kaiser¹, R. A. Howard⁴, and J.-L. Bougeret⁵

Astrophysical Journal, 710:1111–1126, 2010 February, [File](#)

We report on the radio-emission characteristics of 222 interplanetary (IP) shocks detected by spacecraft at Sun–Earth L1 during solar cycle 23 (1996 to 2006, inclusive). A surprisingly large fraction of the IP shocks (~34%) was radio quiet (RQ; i.e., the shocks lacked type II radio bursts). We examined the properties of coronal mass ejections (CMEs) and soft X-ray flares associated with such RQ shocks and compared them with those of the radio-loud (RL) shocks. The CMEs associated with the RQ shocks were generally slow (average speed ~535 km s⁻¹) and only ~40% of the CMEs were halos. The corresponding numbers for CMEs associated with RL shocks were 1237 km s⁻¹ and 72%, respectively. Thus, the CME kinetic energy seems to be the deciding factor in the radio-emission properties of shocks. The lower kinetic energy of CMEs associated with RQ shocks is also suggested by the lower peak soft X-ray flux of the associated flares (C3.4 versus M4.7 for RL shocks). CMEs associated with RQ CMEs were generally accelerating within the coronagraph field of view (average acceleration ~+6.8 m s⁻²), while those associated with RL shocks were decelerating (average acceleration ~-3.5 m s⁻²). This suggests that many of the RQ shocks formed at large distances from the Sun, typically beyond 10 Rs, consistent with the absence of metric and decameter–hectometric (DH) type II radio bursts. A small fraction of RL shocks had type II radio emission solely in the kilometric (km) wavelength domain. Interestingly, the kinematics of the CMEs associated with the km type II bursts is similar to those of RQ shocks, except that the former are slightly more energetic. Comparison of the shock Mach numbers at 1 AU shows that the RQ shocks are mostly subcritical, suggesting that they were not efficient in accelerating electrons. The Mach number values also indicate that most of these are quasi-perpendicular shocks. The radio-quietness is predominant in the rise phase and decreases through the maximum and declining phases of solar cycle 23. About 18% of the IP shocks do not have discernible ejecta behind them. These shocks are due to CMEs moving at large angles from the Sun–Earth line and hence are not blast waves. The solar sources of the shock-driving CMEs follow the sunspot butterfly diagram, consistent with the higher-energy requirement for driving shocks.

ICME Data Table

[Gopalswamy](#), 2010

List of shock-driving ICMEs during the solar cycle 23 ($E15^\circ \leq$ source longitude $\leq W15^\circ$)

http://cdaw.gsfc.nasa.gov/meetings/2010_fluxrope/LWS_CDAW2010_ICMEtbl.html

LARGE GEOMAGNETIC STORMS ASSOCIATED WITH LIMB HALO CORONAL MASS EJECTIONS

NAT [GOPALSWAMY](#), SEIJI YASHIRO†, HONG XIE, SACHIKO AKIYAMA, and PERTTI MÄKELÄ

Advances in Geosciences, Volume 21: Solar Terrestrial (ST). Edited by Marc Duldig. Singapore: World Scientific, 2010, p.71, 2010, [File](#)

http://arxiv.org/pdf/0903.2776.pdf?origin=publication_detail

Solar cycle 23 witnessed the observation of hundreds of halo coronal mass ejections (CMEs), thanks to the high dynamic range and extended field of view of the Large Angle and Spectrometric Coronagraph (LASCO) on board the Solar and Heliospheric Observatory (SOHO) mission. More than two thirds of halo CMEs originating on the front side of the Sun have been found to be geoeffective ($Dst \leq -50$ nT). The delay time between the onset of halo CMEs and the peak of ensuing geomagnetic storms has been found to depend on the solar source location (Gopalswamy et al., 2007). In particular, limb halo CMEs (source longitude $> 45^\circ$) have a 20% shorter delay time on the average. It was suggested that the geomagnetic storms due to limb halos must be due to the sheath portion of the interplanetary CMEs (ICMEs) so that the shorter delay time can be accounted for. We confirm this suggestion by examining the sheath and ejecta portions of ICMEs from Wind and ACE data that correspond to the limb halos. Detailed examination showed that three pairs of limb halos were interacting events. Geomagnetic storms following five limb halos were actually produced by other disk halos. The storms followed by four isolated limb halos and the ones associated with interacting limb halos, were all due to the sheath portions of ICMEs.

CME link to the geomagnetic storms

Nat **Gopalswamy**

Solar and Stellar Variability: Impact on Earth and Planets, Proceedings IAU Symposium No. 264, 2009, p. 326-335, A.G. Kosovichev, A.H. Andrei & J.-P. Rozelot, eds.; **File**

sci-hub.tw/10.1017/S1743921309992870

The coronal mass ejection (CME) link to geomagnetic storms stems from the southward component of the interplanetary magnetic field contained in the CME flux ropes and in the sheath between the flux rope and the CME-driven shock. A typical storm-causing CME is characterized by (i) high speed, (ii) large angular width (mostly halos and partial halos), and (iii) solar source location close to the central meridian. For CMEs originating at larger central meridian distances, the storms are mainly caused by the sheath field. Both the magnetic and energy contents of the storm-producing CMEs can be traced to the magnetic structure of active regions and the free energy stored in them.

Coronal mass ejections and space weather

Nat **Gopalswamy**

Climate and Weather of the Sun-Earth System(CAWSES):Selected Papers from the2007 KyotoSymposium, Edited by T. Tsuda, R. Fujii, K. Shibata, and M. A. Geller, pp. 77–120.

c_TERRAPUB, Tokyo, 2009, **File**.

Solar energetic particles (SEPs) and geomagnetic storms are the two primary space weather consequences of coronal mass ejections (CMEs) and their interplanetary counterparts (ICMEs). I summarize the observed properties of CMEs and ICMEs, paying particular attention to those properties that determine the ability of CMEs in causing space weather. Then I provide observational details of two the central issues: (i) for producing geomagnetic storms, the solar source location and kinematics along with the magnetic field structure and intensity are important, and (ii) for SEPs, the shock-driving ability of CMEs, the Alfvén speed in the ambient medium, and the connectivity to Earth are crucial parameters.

CME Interaction with Coronal Holes and their Interplanetary Consequences

N. **Gopalswamy**¹, P. Mäkelä^{1,2}, H. Xie^{1,2}, S. Akiyama^{1,2}, and S. Yashiro^{1,2}

JGR, 2009; **File**; J. Geophys. Res., Vol. 114, No. A3, A00A22

A significant number of interplanetary (IP) shocks (~17%) during cycle 23 were not followed by drivers. The number of such “driverless” shocks steadily increased with the solar cycle with 15%, 33%, and 52% occurring in the rise, maximum, and declining phase of the solar cycle. The solar sources of 15% of the driverless shocks were very close to the central meridian of the Sun (within ~15°), which is quite unexpected. More interestingly, all the driverless shocks with their solar sources near the solar disk center occurred during the declining phase of solar cycle 23. When we investigated the coronal environment of the source regions of driverless shocks, we found that in each case there was at least one coronal hole nearby suggesting that the coronal holes might have deflected the associated coronal mass ejections (CMEs) away from the Sun-Earth line. The presence of abundant low-latitude coronal holes during the declining phase further explains why CMEs originating close to the disk center mimic the limb CMEs, which normally lead to driverless shocks due to purely geometrical reasons. We also examined the solar source regions of shocks with drivers. For these, the coronal holes were located such that they either had no influence on the CME trajectories, or they deflected the CMEs towards the Sun-Earth line. We also obtained the open magnetic field distribution on the Sun by performing a potential field source surface extrapolation to the corona. It was found that the CMEs generally move away from the open magnetic field regions. The CME-coronal hole interaction must be widespread in the declining phase, and may have a significant impact on the geoeffectiveness of CMEs.

Halo coronal mass ejections and geomagnetic storms

Nat **Gopalswamy**

Earth Planets Space, 61, 1–3, 2009, **File**

In this letter, I show that the discrepancies in the geoeffectiveness of halo coronal mass ejections (CMEs) reported in the literature arise due to the varied definitions of halo CMEs used by different authors. In particular, I show that the low geoeffectiveness rate is a direct consequence of including partial halo CMEs. The geoeffectiveness of partial halo CMEs is lower because they are of low speed and likely to make a glancing impact on Earth

Large Geomagnetic Storms: Introduction to Special Section

Nat [Gopalswamy](#)

J. Geophys. Res., 114, A00A00, 2009 File

Solar cycle 23 witnessed the accumulation of rich data sets that reveal various aspects of geomagnetic storms in unprecedented detail both at the Sun where the storm causing disturbances originate and in geospace where the effects of the storms are directly felt. During two recent coordinated data analysis workshops (CDAWs) the large geomagnetic storms ($Dst \leq -100$ nT) of solar cycle 23 were studied in order to understand their solar, interplanetary, and geospace connections. This special section grew out of these CDAWs with additional contributions relevant to these storms. Here I provide a brief summary of the results presented in the special section.

Solar connections of geoeffective magnetic structures

Nat [Gopalswamy](#)

[Journal of Atmospheric and Solar-Terrestrial Physics](#)

[Volume 70, Issue 17](#), December 2008, Pages 2078-2100, File

Coronal mass ejections (CMEs) and high-speed solar wind streams (HSS) are two solar phenomena that produce large-scale structures in the interplanetary (IP) medium. CMEs evolve into interplanetary CMEs (ICMEs) and the HSS result in corotating interaction regions (CIRs) when they interact with preceding slow solar wind. This paper summarizes the properties of these structures and describes their geoeffectiveness. The primary focus is on the intense storms of solar cycle 23 because this is the first solar cycle during which simultaneous, extensive, and uniform data on solar, IP, and geospace phenomena exist. After presenting illustrative examples of coronal holes and CMEs, I discuss the internal structure of ICMEs, in particular the magnetic clouds (MCs). I then discuss how the magnetic field and speed correlate in the sheath and cloud portions of ICMEs. CME speed measured near the Sun also has significant correlations with the speed and magnetic field strengths measured at 1 AU. The dependence of storm intensity on MC, sheath, and CME properties is discussed pointing to the close connection between solar and IP phenomena. I compare the delay time between MC arrival at 1AU and the peak time of storms for the cloud and sheath portions and show that the internal structure of MCs leads to the variations in the observed delay times.

Finally, we examine the variation of solar-source latitudes of IP structures as a function of the solar cycle and find that they have to be very close to the disk center.

Comment on “Prediction of the 1-AU arrival times of CME associated interplanetary shocks: Evaluation of an empirical interplanetary shock propagation model” by K.-H. Kim et al.

N. [Gopalswamy](#)¹ and H. Xie²

JOURNAL OF GEOPHYSICAL RESEARCH, VOL. 113, A10105, doi:10.1029/2008JA013030, 2008, File

Table 1. List of Events With Solar Sources Used for Testing the ESA Model

Recently, Kim et al. [2007] (hereinafter referred to as KMC) have evaluated the empirical shock arrival (ESA) model and found only about 60% of the observed shocks arrived within ± 112 h of the model prediction. They also found the deviations of shock travel times from the ESA model strongly correlate with the CME initial speeds (VCME), suggesting that the constant interplanetary (IP) acceleration used in the ESA model may not be applicable to all CMEs. KMC further concluded that faster CMEs decelerate and slower CMEs accelerate more than that what is considered in the ESA model. We point out that such systematic deviations in arrival time arise owing to projection effects.

Solar Sources and Geospace Consequences of Interplanetary Magnetic Clouds Observed During Solar Cycle 23

Solar sources and geospace consequences of interplanetary magnetic clouds observed during solar cycle 23

N. [Gopalswamy](#), S. Akiyama, S. Yashiro, G. Michalek, and R. P. Lepping

J. of Atmospheric and Solar-Terrestrial Physics, Vol. 70, pp. 245-253, 2008, File

(see <http://cdaw.gsfc.nasa.gov/publications/>,

http://cdaw.gsfc.nasa.gov/publications/gopal2007.jastp_table.pdf Table)

A preprint of this paper can be downloaded as a [pdf file](#) ([an online supplement table](#)).

We present results of a statistical investigation of 99 magnetic clouds (MCs) observed during 1995-2005. The MC-associated coronal mass ejections (CMEs) are faster and wider on the average and originate within ± 30 deg from the Sun center. The solar sources of MCs also followed the butterfly diagram. The correlation between the magnetic field strength

and speed of MCs was found to be valid over a much wider range of speeds. The number of south-north (SN) MCs was dominant and decreased with solar cycle, while the number of north-south (NS) MCs increased confirming the odd-cycle behavior. Two-thirds of MCs were geoeffective; the Dst index was highly correlated with speed and magnetic field in MC as well as their product. Many (55%) fully northward (FN) MCs were geoeffective solely due to their sheaths. The non-geoeffective MCs were slower (average speed 382 km/s), had a weaker southward magnetic field (average -5.2 nT), and occurred mostly during the rise phase of the solar activity cycle.

Erratum to “Solar sources and geospace consequences of interplanetary magnetic clouds observed during solar cycle 23”(Paper 1) [J. Atmos. Sol.-Terr. Phys. 70(2?4) (2008) 245-253]

E-print, July 2009

Journal of Atmospheric and Solar-Terrestrial Physics, Volume 71, Issue 8-9, p. 1005-1009, 2009

One of the figures (Fig. 4) in “Solar sources and geospace consequences of interplanetary magnetic clouds observed during solar cycle 23” Paper 1?? by Gopalswamy et al.(2008, JASTP, Vol.70, Issues 2?4, February 2008, pp. 245-253) is incorrect because of a software error in the routine that was used to make the plot. The source positions of various magnetic cloud (MC) types are therefore not plotted correctly. Fig. 1 replaces Fig.4 in Paper 1 and is now plotted correctly.

Energetic Phenomena on the Sun

Nat [Gopalswamy](#)

E-print, Nov. 2007

AIP Conf. Proc. , Kodai School on Solar Physics, edited by S. S. Hasan and D. Banerjee, V. 919, pp. 275-313, 2007; **File**

Solar flares, coronal mass ejections (CMEs), solar energetic particles (SEPs), and fast solar wind represent the energetic phenomena on the Sun.

This paper provides an **over view** of the energetic phenomena on the Sun including their origin interplanetary propagation and space weather consequences.

Geoeffectiveness of halo coronal mass ejections

N. [Gopalswamy](#), S. Yashiro, and S. Akiyama

JGR, Vol. 112, No. A6, A06112, 2007, **File**

We studied the geoeffectiveness, speed, solar source, and flare association of a set of 378 halo coronal mass ejections (CMEs) of cycle 23 (1996-2005, inclusive). We compiled the minimum Dst values occurring within 1-5 days after the CME onset.

(See [Yermolaev, 2008](#))

PROPERTIES OF INTERPLANETARY CORONAL MASS EJECTIONS

Review

NAT [GOPALSWAMY](#)

Space Science Reviews (2006), Volume 124, Number 1-4, 145 – 168, **File**

Coronal mass ejections and space weather due to extreme events

N. [Gopalswamy](#), S. Yashiro and S. Akiyama

in "Solar Influence on the Heliosphere and Earth's Environment: Recent Progress and Prospects", ed. N. Gopalswamy and A. Battacharyya, Quest Publications, Mumbai, p. 79, 2006.

This paper summarizes the extreme solar activity and its space weather implications during the declining phase of the solar cycle 23: October-November 2003 (AR 486), November 2004 (AR 696), January 2005 (AR 720), and September 2005 (AR 808). We have compiled and compared the properties of eruptions and the underlying active regions. All these are super active regions, but the flare and CME productivity varied significantly. While the CMEs from all the regions kept the level of solar energetic particles (SEPs) at storm level for several days, their geoeffectiveness (the ability to produce geomagnetic storms) was significantly different, probably due to the location of the eruptions on the Sun.

Solar source of the largest geomagnetic storm of cycle 23

N. [Gopalswamy](#)¹, S. Yashiro^{1,2}, G. Michalek, H. Xie^{1,2}, R. P. Lepping¹, and R. A. Howard³

Geophys. Res. Lett. 32, 12, **2005**, [File](#)

The largest geomagnetic storm of solar cycle 23 occurred on 2003 November 20 with a Dst index of -472 nT, due to a coronal mass ejection (CME) from active region 0501. The CME near the Sun had a sky-plane speed of ~1660 km/s, but the associated magnetic cloud (MC) arrived with a speed of only 730 km/s. The MC at 1 AU (ACE Observations) had a high magnetic field (~56 nT) and high inclination to the ecliptic plane. The southward component of the MC's magnetic field was made up almost entirely of its axial field because of its east-south-west (ESW) chirality. We suggest that the southward pointing strong axial field of the MC reconnected with Earth's front-side magnetic field, resulting in the largest storm of the solar cycle 23.

An empirical model to predict the 1 - AU arrival of interplanetary shocks,

[Gopalswamy](#), N., A. Lara, P. K. Manoharan, and R. Howard,

Adv. Space Res., 36, 2289–2294, **(2005)**.

We extend the empirical coronal mass ejection (CME) arrival model of Gopalswamy et al. [Gopalswamy, N. et al. Predicting the 1-AU arrival times of coronal mass ejections, J. Geophys. Res. 106, 29207, 2001] to predict the 1-AU arrival of interplanetary (IP) shocks. A set of 29 IP shocks and the associated magnetic clouds observed by the Wind spacecraft are used for this study. The primary input to this empirical shock arrival model is the initial speed of white-light CMEs obtained using coronagraphs. We use the gas dynamic piston–shock relationship to derive the ESA model which provides a simple means of obtaining the 1-AU speed and arrival times of interplanetary shocks using CME speeds.

Predicting the 1-AU Arrival Times of Coronal Mass Ejections

N. [Gopalswamy](#), A. Lara, S. Yashiro, M. L. Kaiser, and R. A. Howard

Journal of Geophysical Research, Vol. 106 , No. A12 , p. 29,207 **(2001)** ; [File](#)

We describe an empirical model to predict the 1-AU arrival of coronal mass ejections (CMEs). This model is based on an effective interplanetary (IP) acceleration described in Gopalswamy et al. [2000b] that the CMEs are subject to, as they propagate from the Sun to 1 AU. We have improved this model (i) by minimizing the projection effects (using data from spacecraft in quadrature) in determining the initial speed of CMEs, and (ii) by allowing for the cessation of the interplanetary acceleration before 1 AU. The resulting effective IP acceleration was higher in magnitude than what was obtained from CME measurements from spacecraft along the Sun-Earth line. We evaluated the predictive capability of the CME arrival model using recent two-point measurements from the Solar and Heliospheric Observatory (SOHO), Wind and ACE spacecraft. We found that an acceleration cessation distance of 0.76 AU is in reasonable agreement with the observations. The new prediction model reduces the average prediction error from 15.4 to 10.7 hrs. The model is in good agreement with the observations for high speed CMEs. For slow CMEs, the model as well as observations show a flat arrival time of ~4.3 days. Use of quadrature observations minimized the projection effects naturally without the need to assume the width of the CMEs. However, there is no simple way of estimating the projection effects based on the surface location of the Earth-directed CMEs observed by a spacecraft (such as SOHO) located along the Sun-Earth line because it is impossible to measure the width of these CMEs. The standard assumption that the CME is a rigid cone may not be correct. In fact, the predicted arrival times have a better agreement with the observed arrival times when no projection correction is applied to the SOHO CME measurements. The results presented in this work suggest that CMEs expand and accelerate near the Sun (inside 0.7 AU) more than our model supposes; these aspects will have to be included in future models.

Interplanetary acceleration of coronal mass ejections.

[Gopalswamy](#), N.; Lara, A.; Lepping, R. P.; Kaiser, M. L.; Berdichevsky, D.; St. Cyr, O. C.

Geophys. Res. Lett. 27, 145–148 **(2000)**.

<http://onlinelibrary.wiley.com/doi/10.1029/1999GL003639/pdf>

Using an observed relation between speeds of CMEs near the Sun and in the solar wind, we determine an “effective” acceleration acting on the CMEs. We found a linear relation between this effective acceleration and the initial speed of the CMEs. The acceleration is similar to that of the slow solar wind in magnitude. The average solar wind speed naturally divides CMEs into fast and slow ones. Based on the relation between the acceleration and initial speed, we derive an empirical model to predict the arrival of CMEs at 1 AU.

Identification of Hot Plasma Anomalies in Solar Wind Using Fe Ion Charge Distributions

Farid F. **Goryaev**, Vladimir Slemzin, and Denis Rodkin

2020 ApJL 905 L17

<https://doi.org/10.3847/2041-8213/abcc76>

A presence of high Fe charge states in the ionic charge state distributions of the solar wind (SW) plasma, commonly characterized by the mean charge Q_{Fe} , provides valuable information on heating processes in the SW sources. We study the relationship between the parameter Q_{Fe} and the charge state distributions of Fe ions using the Solar TERrestrial Relations Observatory/PLASMA and SupraThermal Ion Composition data on the beginning of the 24th Cycle (2010 January–2011 July). We find that the Fe charge state distributions related to SW with $Q_{\text{Fe}} \approx 8\text{--}10$ have a uni-modal shape peaked around Fe⁸⁺–Fe⁹⁺. When the Q_{Fe} value increases, the distributions change: at first, the profile extends to higher charge states and then transforms into a bi-modal shape with a second maximum around Fe¹⁶⁺ and a minimum around Fe¹²⁺. We discuss possible reasons for such bi-modality through the example of the interplanetary coronal mass ejection (ICME) event on **2011 February 24–26**, where it was related to the heating of an eruptive prominence. For such an analysis, it is informative to have a special measure of the fraction of highly charged ions for the Fe ion charge distribution in SW. In addition to Q_{Fe} , we introduce a parameter q_{12} equal to a fraction of Fe ions with charges $Q \geq 12$ and show that this parameter can be applied for identifying both the large-scale hot plasma enhancements associated with ICMEs and small hot fragments of SW plasma, which may be associated with small-scale solar activity in various coronal structures.

Magnetic reconnection in the heliosphere: new insights from observations in the solar wind

J. T. **Gosling**

Proceedings of the International Astronomical Union / Volume 4 / Symposium S257, pp 367 – 377,

Published online: 16 May 2009

<http://journals.cambridge.org/action/displayIssue?iid=4866212>

Magnetic reconnection plays a central role in the interpretation of a wide variety of observed solar, space, astrophysical, and laboratory plasma phenomena. The relatively recent discovery that reconnection is common at thin current sheets in the solar wind opens up a new laboratory for studying this fundamental plasma process and its after-effects. Here we provide a brief overview of some of the new insights on reconnection derived from observations of reconnection exhaust jets in the solar wind.

Multiple magnetic reconnection sites associated with a coronal mass ejection in the solar wind

Gosling, J. T.; Eriksson, S.; McComas, D. J.; Phan, T. D.; Skoug, R. M.

J. Geophys. Res., Vol. 112, No. A8, A08106, 2007

<http://dx.doi.org/10.1029/2007JA012418>

Occasionally, an exhaust is observed at the interface between ambient solar wind and the leading edge of an ICME where reconnection serves to erode away some of the magnetic flux carried by the ICME. More often the exhausts are observed at thin current sheets within the interiors of ICMEs or near their trailing edges. We have examined an unusually large set of seven reconnection exhausts, including both sunward and antisunward directed events, observed within the interior of and near the trailing edge of an ICME.

Formation and evolution of corotating interaction regions and their three dimensional structure. **Review**

Gosling, J.T., Pizzo, V.J.:

1999, Space Sci. Rev. 89, 21.

sci-hub.se/10.1023/A:1005291711900

Corotating interaction regions are a consequence of spatial variability in the coronal expansion and solar rotation, which cause solar wind flows of different speeds to become radially aligned. Compressive interaction regions are produced where high-speed wind runs into slower plasma ahead. When the flow pattern emanating from the Sun is roughly time-stationary these compression regions form spirals in the solar equatorial plane that corotate with the Sun, hence the name corotating interaction regions, or CIRs. The leading edge of a CIR is a forward pressure wave that propagates into the slower plasma ahead, while the trailing edge is a reverse pressure wave that propagates back into the trailing high-speed flow. At large heliocentric distances the pressure waves bounding a CIR commonly steepen into forward and reverse shocks. Spatial variation in the solar wind outflow from the Sun is a consequence of the solar magnetic field, which modulates the coronal expansion. Because the magnetic equator of the Sun is commonly both warped and tilted with respect to the heliographic equator, CIRs commonly have substantial north-south tilts that are opposed in the northern

and southern hemispheres. Thus, with increasing heliocentric distance the forward waves in both hemispheres propagate toward and eventually across the solar equatorial plane, while the reverse shocks propagate poleward to higher latitudes. This paper provides an overview of observations and numerical models that describe the physical origin and radial evolution of these complex three-dimensional (3-D) heliospheric structures.

The solar flare myth.

Gosling, J.T.,

1993. J. Geophys. Res. 98, 18937–18950. **File**

<https://sci-hub.ru/10.1029/93JA01896>

Many years of research have demonstrated that large, nonrecurrent geomagnetic storms, shock wave disturbances in the solar wind, and energetic particle events in interplanetary space often occur in close association with large solar flares. This result has led to a paradigm of cause and effect - that large solar flares are the fundamental cause of these events in the near-Earth space environment. This paradigm, which I call "the solar flare myth," dominates the popular perception of the relationship between solar activity and interplanetary and geomagnetic events and has provided much of the pragmatic rationale for the study of the solar flare phenomenon. Yet there is good evidence that this paradigm is wrong and that flares do not generally play a central role in producing major transient disturbances in the near-Earth space environment. In this paper I outline a different paradigm of cause and effect that removes solar flares from their central position in the chain of events leading from the Sun to near-Earth space. Instead, this central role is given to events known as coronal mass ejections

Difference in the parameters of ICMEs in Ejecta and Sheath region and their impact on Dst index during 1997–2014

A.Goswami

[Advances in Space Research](#) **Volume 62, Issue 3**, 1 August 2018, Pages 692-706

<https://reader.elsevier.com/reader/sd/A2E30781C7C222DE3DCD5CBF00E17585D5634341A3EB75BA96844FB1E60B83753DBD8508EE05ACA454D926ADDCE9675F>

The comparisons in respect of mean parameters in [ejecta](#) and sheath region during 1997–2014 have been studied here. The results from statistical analysis indicate that all the parameters, are more powerful (in respect of amplitude) in the sheath region than that of ejecta, whether there is magnetic cloud (MC) structure or not. Probably, a shock plays the key role to such increases. The inter-relation of parameters in the sheath is higher than that of ejecta. In addition, I also discuss the nature of storm influence parameters variation in the sheath and ejecta separately for MC or non MC. The results in respect of t-test and correlations confirm that, associated with the shock, the [magnetic field](#) in the sheath region are opened up and sheath parameters are more energetic for producing geomagnetic storm. I have proposed multiple linear regression model for the prediction of response variable (Dst index) by using mean of the total magnetic field, southward magnetic field, velocity of the [solar wind](#). About 61% of the observed value can be predicted using this model for MC. The correlation becomes strong in case of addition and multiplication functions from the dependent components of [multiple regression](#) line equation with Dst index than that of individual parameters of MC and non MC with Dst index. Thus it is preferable to investigate accumulated effect of ICMEs causing successive geomagnetic storms as compared to their isolated effects. One ultimate finding is that, there is a higher correlation between Dst index and solar wind parameters (individually or combined) in the sheath than the ones in the ejecta, for both MCs and non-MCs.

Properties and Geoeffectiveness of Solar Wind High-Speed Streams and Stream Interaction Regions During Solar Cycles 23 and 24

Maxime [Grandin](#), [Anita T. Aikio](#), [Alexander Kozlovsky](#)

JGR [Volume124, Issue6](#) June 2019 Pages 3871-3892

sci-hub.se/10.1029/2018JA026396

We study the properties and geoeffectiveness of solar wind high-speed streams (HSSs) emanating from coronal holes and associated with stream interaction regions (SIRs). This paper presents a statistical study of 588 SIR/HSS events with solar wind speed at 1 AU exceeding 500 km/s during 1995–2017, encompassing the decline of solar cycle 22 to the decline of cycle 24. Events are detected using measurements of the solar wind speed and the interplanetary magnetic field. Events misidentified as or interacting with interplanetary coronal mass ejections are removed by comparison with an existing interplanetary coronal mass ejection list. Using this SIR/HSS event catalog (list given in the [supporting information](#)), a superposed epoch analysis of key solar wind parameters is carried out. It is found that the number of SIR/HSSs peaks during the late declining phase of solar cycle (SC) 23, as does their velocity, but that their geoeffectiveness in terms of the AE and SYM-H indices is low. This can be explained by the anomalously low values of

magnetic field during the extended solar minimum. Within SC23 and SC24, the highest geoeffectiveness of SIR/HSSs takes place during the early declining phases. Geoeffectiveness of SIR/HSSs continues to be up to 40% lower during SC24 than SC23, which can be explained by the solar wind properties. **6-24 June 2008**

• **Supporting Information** •

Table S1 List of SIR/HSS events during 1995-2017

https://agupubs.onlinelibrary.wiley.com/action/downloadSupplement?doi=10.1029%2F2018JA026396&file=jgra54960-sup-0009-Table_SI-S01.txt

A Geoeffective CME Caused by the Eruption of a Quiescent Prominence on 29 September 2013

V. V. [Grechnev](#) & [I. V. Kuzmenko](#)

[Solar Physics](#) volume 295, Article number: 55 (2020) **File**

<https://link.springer.com/content/pdf/10.1007/s11207-020-01619-x.pdf>

The eruption of a large prominence that occurred away of active regions in the SOL**2013-09-29** event produced a fast coronal mass ejection (CME) and a shock wave. The event caused considerable geospace disturbances, including a proton enhancement that have been addressed in previous studies. Continuing with the analysis of this event, we focus on the development of the CME and shock wave, assess an expected geospace impact using simplest considerations, and compare the expectations with in situ measurements near Earth. The high CME speed in this non-flare-associated event was determined by a considerable reconnected flux that corresponds to a pattern established by different authors. Estimations based on a few approaches showed the reconnection flux in this event to be comparable with a typical value in flare-associated eruptions. The shock wave was most likely impulsively excited by the erupting prominence in the same way as in flare-associated events and changed to the bow-shock regime later. The trajectory calculated for this scenario reproduces the Type II emission observed from 30 MHz to 70 kHz; its interruptions were probably caused by propagation effects. Properties of the near-Earth proton enhancement are discussed considering the results of recent studies

A Challenging Solar Eruptive Event of 18 November 2003 and the Causes of the 20 November Geomagnetic Superstorm. IV. Unusual Magnetic Cloud and Overall Scenario

V. V. [Grechnev](#), A. M. Uralov, I. M. Chertok, A. V. Belov, B. P. Filippov, V. A. Slemzin, B. V. Jackson

[Solar Phys](#) (2014) 289:4653–4673

<http://arxiv.org/pdf/1409.0283v1.pdf>

The geomagnetic superstorm of 20 November 2003 with Dst = -422 nT, one of the most intense in history, is not well understood. The superstorm was caused by a moderate solar eruptive event on 18 November, comprehensively studied in our preceding Papers I-III. The analysis has shown a number of unusual and extremely complex features, which presumably led to the formation of an isolated right-handed magnetic-field configuration. Here we analyze the interplanetary disturbance responsible for the 20 November superstorm, compare some of its properties with the extreme 28-29 October event, and reveal a compact size of the magnetic cloud (MC) and its disconnection from the Sun. Most likely, the MC had a spheromak configuration and expanded in a narrow angle of < 14 degree. A very strong magnetic field in the MC up to 56 nT was due to the unusually weak expansion of the disconnected spheromak in an enhanced-density environment constituted by the tails of the preceding ICMEs. Additional circumstances favoring the superstorm were (i) the exact impact of the spheromak on the Earth's magnetosphere and (ii) the almost exact southward orientation of the magnetic field, corresponding to the original orientation in its probable source region near the solar disk center.

A Challenging Solar Eruptive Event of 18 November 2003 and the Causes of the 20 November Geomagnetic Superstorm.

II. CMEs, Shock Waves, and Drifting Radio Bursts

V.V. [Grechnev](#), A.M. Uralov, I.M. Chertok, V.A. Slemzin, B.P. Filippov, Ya.I. Egorov, V.G. Fainshtein, A.N. Afanasyev, N.P. Prestage, M. Temmer

E-print, Aug **2013**; [Solar Phys.](#), April **2014**, Volume 289, Issue 4, pp 1279-1312

<http://arxiv.org/pdf/1308.3010v1.pdf>

We continue our study (Grechnev et al. (2013), doi:10.1007/s11207-013-0316-6; Paper I) on the 18 November 2003 geoeffective event. To understand possible impact on geospace of coronal transients observed on that day, we investigated their properties from solar near-surface manifestations in extreme ultraviolet, LASCO white-light images, and dynamic radio spectra. We reconcile near-surface activity with the expansion of coronal mass ejections (CMEs) and determine their orientation relative to the earthward direction. The kinematic measurements, dynamic radio spectra, and

microwave and X-ray light curves all contribute to the overall picture of the complex event and confirm an additional eruption at 08:07-08:20 UT close to the solar disk center presumed in Paper I. Unusual characteristics of the ejection appear to match those expected for a source of the 20 November superstorm but make its detection in LASCO images hopeless. On the other hand, none of the CMEs observed by LASCO seem to be a promising candidate for a source of the superstorm being able to produce, at most, a glancing blow on the Earth's magnetosphere. Our analysis confirms free propagation of shock waves revealed in the event and reconciles their kinematics with "EUV waves" and dynamic radio spectra up to decameters.

Paper III see Uralov et al. , 2014

A Challenging Solar Eruptive Event of 18 November 2003 and the Causes of the 20 November Geomagnetic Superstorm.

I. Unusual History of an Eruptive Filament

V. V. **Grechnev**, A. M. Uralov, V. A. Slemzin, I. M. Chertok, B. P. Filippov, G. V. Rudenko, M. Temmer
E-print, May **2013**; Solar Phys., (**2014**) 289, Issue 1, 289–318

<http://arxiv.org/pdf/1304.7950v1.pdf>

This is the first of four companion papers, which analyze a complex eruptive event of 18 November 2003 in AR 10501 and the causes of the largest Solar Cycle 23 geomagnetic storm on 20 November 2003. Analysis of a complete data set, not considered before, reveals a chain of eruptions to which hard X-ray and microwave bursts responded. A filament in AR 10501 was not a passive part of a larger flux rope, as usually considered. The filament erupted and gave origin to a CME. The chain of events was as follows: i) an eruption at 07:29 accompanied by a not reported M1.2 class flare associated with the onset of a first southeastern CME1, which is not responsible for the superstorm; ii) a confined eruption at 07:41 (M3.2 flare) that destabilized the filament; iii) the filament acceleration (07:56); iv) the bifurcation of the eruptive filament that transformed into a large cloud; v) an M3.9 flare in AR 10501 associated to this transformation. The transformation of the filament could be due to its interaction with the magnetic field in the neighborhood of a null point, located at a height of about 100 Mm above the complex formed by ARs 10501, 10503, and their environment. The CORONAS-F/SPIRIT telescope observed the cloud in 304 Å as a large Y-shaped darkening, which moved from the bifurcation region to the limb. The masses and kinematics of the cloud and the filament were similar. Remnants of the filament were not observed in the second southwestern CME2, previously regarded as a source of the 20 November superstorm. These facts do not support a simple scenario, in which the interplanetary magnetic cloud is considered as a flux rope formed from a structure initially associated with the pre-eruption filament in AR 10501. Observations suggest a possible additional eruption above the bifurcation region close to solar disk center between 08:07 and 08:17 that could be the source of the superstorm.

Comparative Study of MHD Modeling of the Background Solar Wind

C. **Gressl**, A. M. Veronig, M. Temmer, D. Odstrčil, J. A. Linker, Z. Mikić, P. Riley
Solar Physics, May **2014**, Volume 289, Issue 5, pp 1783-1801

Knowledge about the background solar wind plays a crucial role in the framework of space-weather forecasting. In-situ measurements of the background solar wind are only available for a few points in the heliosphere where spacecraft are located, therefore we have to rely on heliospheric models to derive the distribution of solar-wind parameters in interplanetary space. We test the performance of different solar-wind models, namely Magnetohydrodynamic Algorithm outside a Sphere/ENLIL (MAS/ENLIL), Wang–Sheeley–Arge/ENLIL (WSA/ENLIL), and MAS/MAS, by comparing model results with in-situ measurements from spacecraft located at 1 AU distance to the Sun (ACE, Wind). To exclude the influence of interplanetary coronal mass ejections (ICMEs), we chose **the year 2007** as a time period with low solar activity for our comparison. We found that the general structure of the background solar wind is well reproduced by all models. The best model results were obtained for the parameter solar-wind speed. However, the predicted arrival times of high-speed solar-wind streams have typical uncertainties of the order of about one day. Comparison of model runs with synoptic magnetic maps from different observatories revealed that the choice of the synoptic map significantly affects the model performance.

Recurrent Galactic Cosmic-Ray Flux Modulation in L1 and Geomagnetic Activity during the Declining Phase of the Solar Cycle 24

Catia **Grimani**^{1,2}, Andrea Cesarini², Michele Fabi^{1,2}, Federico Sabbatini³, Daniele Telloni⁴, and Mattia Villani^{1,2}

2020 ApJ 904 64

<https://doi.org/10.3847/1538-4357/abbb90>

<https://arxiv.org/pdf/2012.01152.pdf>

Short-term variations (<1 month) of the galactic cosmic-ray (GCR) flux in the inner heliosphere are mainly associated with the passage of high-speed solar wind streams (HSS) and interplanetary (IP) counterparts of coronal mass ejections (ICMEs). Data gathered with a particle detector flown on board the ESA LISA Pathfinder (LPF) spacecraft, during the declining part of solar cycle 24 (2016 February–2017 July) around the Lagrange point L1, have allowed us to study the characteristics of recurrent cosmic-ray flux modulations above 70 MeV n^{-1} . It is shown that the amplitude and evolution of individual modulations depend in a unique way on both IP plasma parameters and particle flux intensity before HSS and ICME transit. By comparing the LPF data with those gathered contemporaneously with the magnetic spectrometer experiment AMS-02 on board the International Space Station and with those of Earth's polar neutron monitors, the GCR flux modulation was studied at different energies during recurrent short-term variations. It is also aimed to set the near real-time particle observation requirements to disentangle the role of long- and short-term variations of the GCR flux to evaluate the performance of high-sensitivity instruments in space such as the future interferometers for gravitational wave detection. Finally, the association between recurrent GCR flux variation observations in L1 and weak to moderate geomagnetic activity in 2016–2017 is discussed. Short-term recurrent GCR flux variations are good proxies of recurrent geomagnetic activity when the B z component of the IP magnetic field is directed north.

Shock deceleration in interplanetary coronal mass ejections (ICMEs) beyond Mercury's orbit until one AU

Benjamin **Griton**^{1*}, Jan Souček¹, Vratislav Krupar^{2,3,1}, David Piša¹, Ondrej Santolík^{1,4}, Ulrich Taubenschuss¹ and František Němec⁴

J. Space Weather Space Clim. **2018**, 8, A54

<https://www.swsc-journal.org/articles/swsc/pdf/2018/01/swsc180026.pdf>

The CDPP propagation tool is used to propagate interplanetary coronal mass ejections (ICMEs) observed at Mercury by MESSENGER to various targets in the inner solar system (VEX, ACE, STEREO-A and B). The deceleration of ICME shock fronts between the orbit of Mercury and 1 AU is studied on the basis of a large dataset. We focus on the interplanetary medium far from the solar corona, to avoid the region where ICME propagation modifications in velocity and direction are the most drastic. Starting with a catalog of 61 ICMEs recorded by MESSENGER, the propagation tool predicts 36 ICME impacts with targets. ICME in situ signatures are investigated close to predicted encounter times based on velocities estimated at MESSENGER and on the default propagation tool velocity (500 km s⁻¹). ICMEs are observed at the targets in 26 cases and interplanetary shocks (not followed by magnetic ejecta) in two cases. Comparing transit velocities between the Sun and MESSENGER (\bar{v}_{SunMess}) and between MESSENGER and the targets (\bar{v}_{MessTar}), we find an average deceleration of 170 km s⁻¹ (28 cases). Comparing \bar{v}_{MessTar} to the velocities at the targets (v_{Tar}), average ICME deceleration is about 160 km s⁻¹ (13 cases). Our results show that the ICME shock deceleration is significant beyond Mercury's orbit. ICME shock arrival times are predicted with an average accuracy of about six hours with a standard deviation of eleven hours. Focusing on two ICMEs detected first at MESSENGER and later on by two targets illustrates our results and the variability in ICME propagations. The shock velocity of an ICME observed at MESSENGER, then at VEX and finally at STEREO-B decreases all the way. Predicting arrivals of potentially effective ICMEs is an important space weather issue. The CDPP propagation tool, in association with in situ measurements between the Sun and the Earth, can permit to update alert status of such arrivals.

Table 2. Details of the 36 pairs (2011-2014).

Source-dependent properties of two slow solar wind states

Léa **Griton**, Alexis P. Rouillard, Nicolas Poirier, Karine Issautier, Michel Moncuquet, Rui Pinto

ApJ **910** 63 **2021**

<https://arxiv.org/pdf/2102.06568.pdf>

<https://doi.org/10.3847/1538-4357/abe309>

Two states of the slow solar wind are identified from in-situ measurements by Parker Solar Probe (PSP) inside 50 solar radii from the Sun. At such distances the wind measured at PSP has not yet undergone significant transformation related to the expansion and propagation of the wind. We focus in this study on the properties of the quiet solar wind with no magnetic switchbacks. The two states differ by their plasma beta, flux and magnetic pressure. PSP's magnetic connectivity established with Potential Field Source Surface (PFSS) reconstructions, tested against extreme ultraviolet (EUV) and white-light imaging, reveals the two states correspond to a transition from a streamer to an equatorial coronal hole. The expansion factors of magnetic field lines in the streamer are 20 times greater than those rooted near the center of the coronal hole. The very different expansion rates of the magnetic field result in different magnetic pressures

measured by PSP in the two plasma states. Solar wind simulations run along these differing flux tubes reproduce the slower and denser wind measured in the streamer and the more tenuous wind measured in the coronal hole. Plasma heating is more intense at the base of the streamer field lines rooted near the boundary of the equatorial hole than those rooted closer to the center of the hole. This results in a higher wind flux driven inside the streamer than deeper inside the equatorial hole. **March 31, 2019-April 5, 2019**

TWO-PLASMA MODEL FOR LOW CHARGE STATE INTERPLANETARY CORONAL MASS EJECTION OBSERVATIONS

Jacob R. [Gruesbeck](#), Susan T. Lepri, and Thomas H. Zurbuchen

2012 ApJ 760 141

Recent ACE/SWICS observations have revealed that ~5% of all in situ observed interplanetary coronal mass ejections include time periods with very low charge state ions found to be associated with prominence eruptions. It was also shown that these low charge state ions are often observed concurrently with very high charge state ions. But, the physical process leading to these mixed charge states is not known and could be caused by either the mixing of plasmas of different temperatures or by non-local freeze-in effects as discussed by Gruesbeck. We provide a detailed and multi-stage analysis that excludes this latter option. We therefore conclude that time periods of very low charge states are the heliospheric remnants of plasmas born in prominences. We further conclude that the contemporaneously observed low and very high charge states are an indication of mixing of plasmas of different temperatures along magnetic field lines, suggesting that silicon and iron are depleted over carbon and oxygen in the cold, prominence-associated plasma. This represents the first experimental determination of elemental composition of prominence-associated plasma.

CONSTRAINTS ON CORONAL MASS EJECTION EVOLUTION FROM IN SITU OBSERVATIONS OF IONIC CHARGE STATES

Jacob R. [Gruesbeck](#)¹, Susan T. Lepri¹, Thomas H. Zurbuchen¹, and Spiro K. Antiochos²

Astrophysical Journal, 730:103 (9pp), **2011 April**; **File**

We present a novel procedure for deriving the physical properties of coronal mass ejections (CMEs) in the corona. Our methodology uses in situ measurements of ionic charge states of C, O, Si, and Fe in the heliosphere and interprets them in the context of a model for the early evolution of interplanetary CME (ICME) plasma, between 2 and 5R_⊙. We find that the data are best fit by an evolution that consists of an initial heating of the plasma, followed by an expansion that ultimately results in cooling. The heating profile is consistent with a compression of coronal plasma due to flare reconnection jets and an expansion cooling due to the ejection, as expected from the standard CME/flare model. The observed frozen-in ionic charge states reflect this time history and, therefore, provide important constraints for the heating and expansion timescales, as well as the maximum temperature the CME plasma is heated to during its eruption. Furthermore, our analysis places severe limits on the possible density of CME plasma in the corona. We discuss the implications of our results for CME models and for future analysis of ICME plasma composition.

Multiple-Hour-Ahead Forecast of the Dst Index Using a Combination of Long Short-Term Memory Neural Network and Gaussian Process

M. A. [Gruet](#), [M. Chandorkar](#), [A. Sicard](#), [E. Camporeale](#)

Space Weather **2018**

In this study, we present a method that combines a Long Short-Term Memory (LSTM) recurrent neural network with a Gaussian process (GP) model to provide up to 6-hr-ahead probabilistic forecasts of the Dst geomagnetic index. The proposed approach brings together the sequence modeling capabilities of a recurrent neural network with the error bars and confidence bounds provided by a GP. Our model is trained using the hourly OMNI and Global Positioning System (GPS) databases, both of which are publicly available. We first develop a LSTM network to get a single-point prediction of Dst. This model yields great accuracy in forecasting the Dst index from 1 to 6 hr ahead, with a correlation coefficient always higher than 0.873 and a root-mean-square error lower than 9.86. However, even if global metrics show excellent performance, it remains poor in predicting intense storms (Dst < -250 nT) 6 hr in advance. To improve it and to obtain probabilistic forecasts, we combine the LSTM model obtained with a GP and evaluate the hybrid predictor using the receiver operating characteristic curve and the reliability diagram. We conclude that this hybrid methodology provides improvements in the forecast of geomagnetic storms, from 1 to 6 hr ahead.

Detailed composition of iron ions in interplanetary coronal mass ejections based on a multipopulation approach*

Chaoran Gu¹, Verena Heidrich-Meisner¹, Robert F. Wimmer-Schweingruber¹ and Shuo Yao²
A&A 671, A63 (2023)

<https://www.aanda.org/articles/aa/pdf/2023/03/aa45500-22.pdf>

Context. Coronal mass ejections (CMEs) are extremely dynamical, large-scale events in which plasma – but not only the coronal plasma – is ejected into interplanetary space. If a CME is detected in situ by a spacecraft located in the interplanetary medium, it is then called an interplanetary coronal mass ejection (ICME). This solar activity has been studied widely since coronagraphs were first flown into space in the early 1970s.

Aims. Charge states of heavy ions reflect important information about the coronal temperature profile due to the freeze-in effect and it is estimated that iron ions freeze in at heights of ~ 5 solar radii. However, the measured charge-state distribution of iron ions cannot be composed of only one single group of plasma. To identify the different populations of iron charge-state composition of ICMEs and determine their sources, we developed a model that independently uses two, three, and four populations of iron ions to fit the measured charge-state distribution in ICMEs detected by the Advanced Composition Explorer (ACE) at 1 AU.

Methods. Three parameters are used to identify a certain population, namely freeze-in temperature, relative abundance, and kappa value (κ), which together describe the potential non-Maxwellian kappa distributions of coronal electrons. Our method chooses the reduced chi-squared to describe the goodness of fit of the model to the observations. The parameters of our model are optimized with the covariance-matrix-adaptation evolution strategy (CMA-ES).

Results. Two major types of ICMEs are identified according to the existence of hot material, and both, that is, the cool type and the hot type, have two main subtypes. Different populations in those types have their own features related to freeze-in temperature and κ . The electron velocity distribution function usually contains a significant hot tail in typical coronal material and hot material, while the Maxwellian distribution appears more frequently in mid-temperature material. Our model is also suitable for all types of solar wind and the existence of hot populations as well as the change of temperatures of individual populations may indicate boundaries between ICMEs and individual solar wind streams.

Abundances and Charge States of Heavy Ions in ICMEs Highly Related to Speed and Solar Activity

Chaoran Gu¹, Shuo Yao¹, and Lei Dai²

2020 ApJ 900 123

<https://doi.org/10.3847/1538-4357/aba7b8>

This statistical work studies the abundances and the charge states of the carbon, oxygen, and iron ions in 281 interplanetary coronal mass ejections (ICMEs) measured at 1 au by ACE spacecraft from 1998 to 2011. The Gaussian distribution test is applied, and the analysis of variance is used to quantify the similarity between two distributions of ionic charge states and abundances. The correlation coefficient is calculated to reveal the dependence of the abundances and the mean charge of heavy ions on the solar activity. The results show that the mean charge, the abundance, and the speed at 1 au are highly related to the sunspot number (SN). The O⁷⁺/O⁶⁺ shows statistical difference between the high speed and the low speed groups of ICMEs. Different from the cold materials inside ICMEs, the mean charge of carbon ions shows a positive relation to that of oxygen ions. The Mg/O in the studied ICMEs are much higher than that in the solar wind. Three types of charge distribution of C, O, and Fe ions are summarized. The fraction of each of the three types is related to the solar minimum or the solar maximum. The mean charge and the flux of oxygen ions show quasi-linear relations to the SN during solar minimum, and show fluctuations during maximum. The results reveal that the solar activity, which represents the solar magnetic field status by nature, controls the composition of heavy ions in ICMEs.

Forecasting Geoeffective Events from Solar Wind Data and Evaluating the Most Predictive Features through Machine Learning Approaches

Sabrina Guastavino, Katsiaryna Bahamazava, Emma Perracchione, Fabiana Camattari, Gianluca Audone, Daniele Telloni, Roberto Susino, Gianalfredo Nicolini, Silvano Fineschi, Michele Piana, Anna Maria Massone

ApJ 971 94 2024

<https://arxiv.org/pdf/2403.09847.pdf>

<https://iopscience.iop.org/article/10.3847/1538-4357/ad5b57/pdf>

This study addresses the prediction of geomagnetic disturbances by exploiting machine learning techniques. Specifically, the Long-Short Term Memory recurrent neural network, which is particularly suited for application over long time series, is employed in the analysis of in-situ measurements of solar wind plasma and magnetic field acquired over more than one solar cycle, from 2005 to 2019, at the Lagrangian point L1. The problem is approached as a binary classification aiming to predict one hour in advance a decrease in the SYM-H geomagnetic activity index below the threshold of -50 nT, which is generally regarded as indicative of magnetospheric perturbations. The strong class imbalance issue is tackled by using an appropriate loss function tailored to optimize appropriate skill scores in the training phase of the neural network. Beside classical skill scores, value-weighted skill scores are then employed to evaluate predictions, suitable in the study of problems, such as the one faced here, characterized by strong temporal variability. For the first time, the content of magnetic helicity and energy carried by solar transients, associated with their detection and likelihood of geo-effectiveness, were considered as input features of the network architecture. Their predictive capabilities are demonstrated through a correlation-driven feature selection method to rank the most relevant characteristics involved in the neural network prediction model. The optimal performance of the adopted neural network in properly forecasting the onset of geomagnetic storms, which is a crucial point for giving real warnings in an operational setting, is finally showed. **2005 July 24-August 2**

Physics-driven machine learning for the prediction of coronal mass ejections' travel times

Sabrina **Guastavino**, [Valentina Candiani](#), [Alessandro Bemporad](#), [Francesco Marchetti](#), [Federico Benvenuto](#), [Anna Maria Massone](#), [Roberto Susino](#), [Daniele Telloni](#), [Silvano Fineschi](#), [Michele Piana](#)

ApJ **954** 151 **2023**

<https://arxiv.org/pdf/2305.10057.pdf>

<https://iopscience.iop.org/article/10.3847/1538-4357/ace62d/pdf>

Coronal Mass Ejections (CMEs) correspond to dramatic expulsions of plasma and magnetic field from the solar corona into the heliosphere. CMEs are scientifically relevant because they are involved in the physical mechanisms characterizing the active Sun. However, more recently CMEs have attracted attention for their impact on space weather, as they are correlated to geomagnetic storms and may induce the generation of Solar Energetic Particles streams. In this space weather framework, the present paper introduces a physics-driven artificial intelligence (AI) approach to the prediction of CMEs travel time, in which the deterministic drag-based model is exploited to improve the training phase of a cascade of two neural networks fed with both remote sensing and in-situ data. This study shows that the use of physical information in the AI architecture significantly improves both the accuracy and the robustness of the travel time prediction.

Coronal Mass Ejections during Geomagnetic Storms on Earth.

Guido, R.M.D.

(2016). International Journal of Astronomy. (5) 2. DOI: 10.5923/j.astronomy/20160502.02

Expansion of magnetic clouds in the outer heliosphere

A.M. **Gulisano**, P. Demoulin, S. Dasso, L. Rodriguez

E-print, April, **2012**; A&A 543, A107 (**2012**)

A large amount of magnetized plasma are frequently ejected from the Sun as Coronal Mass Ejections (CMEs). A part of these ejections are detected in the solar wind as magnetic clouds (MCs) which have flux rope signatures. MCs are typically expanding structures in the inner heliosphere. The aim of this work is to derive the expansion properties of MCs in the outer heliosphere from 1 to 5 AU and to compare them to the ones in the inner heliosphere. We analyze MCs observed by the Ulysses spacecraft using in situ magnetic field and plasma measurements. The MC boundaries are defined in the MC frame after defining the MC axis with a minimum variance method applied only to the flux rope structure. As in the inner heliosphere, a large fraction of the velocity profile within MCs is close to a linear function of time. This implies a self-similar expansion and a MC size that locally follows a power-law of the solar distance with an exponent called zeta. We derive the value of zeta from the in situ velocity data. We analyze separately the non-perturbed MCs (cases presenting a linear velocity profile almost for the full event), and perturbed MCs (cases presenting a strongly distorted velocity profile). We find that non-perturbed MCs expand with a similar non-dimensional expansion rate ($\text{zeta} = 1.05 \pm 0.34$), i.e. slightly faster than the solar distance and than in the inner heliosphere ($\text{zeta} = 0.91 \pm 0.23$). The subset of perturbed MCs expands, as in the inner heliosphere, with a significant lower rate and with a larger dispersion ($\text{zeta} = 0.28 \pm 0.52$) as expected from the temporal evolution found in numerical simulations. This local measure of the expansion is also in agreement with the distribution with distance of MC size, mean magnetic field and plasma

parameters. The MCs in interaction with a strong field region, e.g. another MC, have the most variable expansion rate (ranging from compression to over-expansion).

Global and local expansion of magnetic clouds in the inner heliosphere

A. M. [Gulisano](#), P. Démoulin, S. Dasso, M. E. Ruiz and E. Marsch

A&A 509, A39 (2010)

Context. Observations of magnetic clouds (MCs) are consistent with the presence of flux ropes detected in the solar wind (SW) a few days after their expulsion from the Sun as coronal mass ejections (CMEs).

Aims. Both the in situ observations of plasma velocity profiles and the increase of their size with solar distance show that MCs are typically expanding structures. The aim of this work is to derive the expansion properties of MCs in the inner heliosphere from 0.3 to 1 AU.

Methods. We analyze MCs observed by the two Helios spacecraft using in situ magnetic field and velocity measurements. We split the sample in two subsets: those MCs with a velocity profile that is significantly perturbed from the expected linear profile and those that are not. From the slope of the in situ measured bulk velocity along the Sun-Earth direction, we compute an expansion speed with respect to the cloud center for each of the analyzed MCs.

Results. We analyze how the expansion speed depends on the MC size, the translation velocity, and the heliocentric distance, finding that all MCs in the subset of non-perturbed MCs expand with almost the same non-dimensional expansion rate (ζ). We find departures from this general rule for ζ only for perturbed MCs, and we interpret the departures as the consequence of a local and strong SW perturbation by SW fast streams, affecting the MC even inside its interior, in addition to the direct interaction region between the SW and the MC. We also compute the dependence of the mean total SW pressure on the solar distance and we confirm that the decrease of the total SW pressure with distance is the main origin of the observed MC expansion rate. We found that ζ was 0.91 ± 0.23 for non-perturbed MCs while ζ was 0.48 ± 0.79 for perturbed MCs, the larger spread in the last ones being due to the influence of the solar wind local environment conditions on the expansion.

Ranking ICME's efficiency for geomagnetic and ionospheric storms and risk of false alarms

T.L. [Gulyaeva](#)

Journal of Atmospheric and Solar-Terrestrial Physics Volume 164, November 2017, Pages 39-47

<https://www.sciencedirect.com/science/article/pii/S1364682617300135/pdf?md5=a2eda581d63b2bedcd51945229805b4e&pid=1-s2.0-S1364682617300135-main.pdf>

A statistical analysis is undertaken on ICME's efficiency in producing the geomagnetic and ionospheric storms. The mutually-consistent thresholds for the intense, moderate and weak space weather storms and quiet conditions are introduced with an analytical model based on relations between the equatorial Dst index and geomagnetic indices AE, aa, ap, ap(τ) and the ionospheric $V\sigma$ indices. The ionosphere variability $V\sigma$ index is expressed in terms of the total electron content (TEC) deviation from the -15-day sliding median normalized by the standard deviation for the 15 preceding days. The intensity of global positive ionospheric storm, $V\sigma_p$, and negative storm, $V\sigma_n$, is represented by the relative density of anomalous $\pm V\sigma$ index occurrence derived from the global ionospheric maps GIM-TEC for 1999–2016. An impact of total 421 ICME events for 1999–2016 on the geomagnetic and ionospheric storms expressed by AE, Dst, aa, ap, ap(τ), $V\sigma_p$, $V\sigma_n$ indices and their superposition is analyzed using ICME catalogue by Richardson and Cane (2010) during 24 h after the ICME start time t_0 . Hierarchy of efficiency of ICME \rightarrow storm relation is established. The ICMEs have a higher probability (22–25%) to be followed by the intense ionospheric and auroral electrojet storms at global and high latitudes as compared to the intense storms at middle and low latitudes (18–20%) and to moderate and weak storms at high latitudes (5–17%). At the same time ICMEs are more effective in producing the moderate storms (24–28%) at the middle and low latitudes as compared to the intense and weak storms at these latitudes (13–22%) and to moderate storms at high latitudes (8–17%). The remaining cases when quiet conditions are observed after ICMEs present higher chance for a false alarm. The risk factor for a false alarm can vary from 18% if the superposition of all indices is considered, to 51–64% for individual AE, $V\sigma_p$ and $V\sigma_n$ indices. The analysis indicates that the mutually-consistent thresholds can be successfully applied to the external sources of the geomagnetic and ionospheric storms other than ICME which present challenge for the further investigation.

Modelling the propagation of coronal mass ejections with COCONUT: implementation of the Regularized Biot-Savart Laws flux rope model

[Jinhan Guo](#), [L. Linan](#), [S. Poedts](#), [Y. Guo](#), [A. Lani](#), [B. Schmieder](#), [M. Brchneleva](#), [B. Perri](#), [T. Baratashvili](#), [Y. W. Ni](#), [P. F. Chen](#)

A&A 2023

<https://arxiv.org/pdf/2311.13432.pdf>

Context: Coronal mass ejections (CMEs) are rapid eruptions of magnetized plasma that occur on the Sun, which are known as the main drivers of adverse space weather. Accurately tracking their evolution in the heliosphere in numerical models is of utmost importance for space weather forecasting. Aims: The main objective of this paper is to implement the Regularized Biot-Savart Laws (RBSL) method in a new global corona model COCONUT. This approach has the capability to construct the magnetic flux rope with an axis of arbitrary shape. Methods: We present the implementation process of the RBSL flux rope model in COCONUT, which is superposed onto a realistic solar wind reconstructed from the observed magnetogram around the minimum of solar activity. Based on this, we simulate the propagation of an S-shaped flux rope from the solar surface to a distance of 25 solar radii. Results: Our simulation successfully reproduces the birth process of a CME originating from a sigmoid in a self-consistent way. The model effectively captures various physical processes and retrieves the prominent features of the CMEs in observations. In addition, the simulation results indicate that the magnetic topology of the CME flux rope at around 20 solar radii deviates from a coherent structure, and manifests as a mix of open and closed field lines with diverse footprints. Conclusions: This work demonstrates the potential of the RBSL flux rope model in reproducing CME events that are more consistent with observations. Moreover, our findings strongly suggest that magnetic reconnection during the CME propagation plays a critical role in destroying the coherent characteristic of a CME flux rope. **2007-02-11, 2011-03-08**

Advancing Theory and Modeling Efforts in Heliophysics

Review

Fan **Guo**, [Spiro Antiochos](#), [Paul Cassak](#), [Bin Chen](#), [Xiaohang Chen](#), [Chuanfei Dong](#), [Cooper Downs](#), [Joe Giacalone](#), [Colby C. Haggerty](#), [Hantao Ji](#), [Judith Karpen](#), [James Klimchuk](#), [Wen Li](#), [Xiaocan Li](#), [Mitsuo Oka](#), [Katharine K. Reeves](#), [Marc Swisdak](#), [Weichao Tu](#)

White paper submitted to Heliophysics 2024 Decadal Survey

2022

<https://arxiv.org/pdf/2209.03611.pdf>

Heliophysics theory and modeling build understanding from fundamental principles to motivate, interpret, and predict observations. Together with observational analysis, they constitute a comprehensive scientific program in heliophysics. As observations and data analysis become increasingly detailed, it is critical that theory and modeling develop more quantitative predictions and iterate with observations. Advanced theory and modeling can inspire and greatly improve the design of new instruments and increase their chance of success. In addition, in order to build physics-based space weather forecast models, it is important to keep developing and testing new theories, and maintaining constant communications with theory and modeling. Maintaining a sustainable effort in theory and modeling is critically important to heliophysics. We recommend that all funding agencies join forces and consider expanding current and creating new theory and modeling programs--especially, 1. NASA should restore the HTMS program to its original support level to meet the critical needs of heliophysics science; 2. a Strategic Research Model program needs to be created to support model development for next-generation basic research codes; 3. new programs must be created for addressing mission-critical theory and modeling needs; and 4. enhanced programs are urgently required for training the next generation of theorists and modelers.

A Global MHD Simulation of Outer Heliosphere Including Anomalous Cosmic-Rays

Xiaocheng **Guo**^{1,2}, Vladimir Florinski³, and Chi Wang^{1,2}

APJ 879:87 (10pp), **2019**

<https://iopscience.iop.org/article/10.3847/1538-4357/ab262b/pdf>

A global MHD-neutrals-cosmic-rays simulation is conducted to investigate the effects of anomalous cosmic-rays (ACRs) on the large-scale structure of the outer heliosphere. In the model, the cosmic-rays are treated as a massless fluid that only contribute their pressure to the dynamics of the system. The diffusion of cosmic-rays in the interstellar medium is assumed to be much faster than inside the heliosphere, where it depends on the strength of the magnetic field. The results show that the influence of the cosmic-rays on the structure of the outer heliosphere depends on momentum and energy transfer from the solar wind plasma to the ACRs, accomplished through diffusive shock acceleration at the termination shock, and the subsequent loss of ACRs across the heliopause and their rapid escape into the interstellar medium. Under favorable conditions characterized by a large fraction of energy conversion and a high enough diffusion coefficient in the solar wind, the ACRs were found to reduce the width of the heliosheath by up to ~18 au.

Consequently, these results indicate that the effect of cosmic-rays is a potential key factor for the global structure of the outer heliosphere in a computer model that could partially explain the timing of the heliopause encounters of the two Voyager probes.

Modeling the Evolution and Propagation of 10 September 2017 CMEs and SEPs Arriving at Mars Constrained by Remote Sensing and In Situ Measurement

Jingnan [Guo](#), [Mateja Dumbović](#), [Robert F. Wimmer-Schweingruber](#), [Manuela Temmer](#), [Henning Lohf](#), [Yuming Wang](#), [Astrid Veronig](#), [Donald M. Hassler](#) ...
Space Weather [Volume16, Issue8](#) August 2018 Pages 1156-1169
<http://sci-hub.tw/10.1029/2018SW001973>

On 10 September 2017, solar energetic particles originating from the active region 12673 produced a ground level enhancement at Earth. The ground level enhancement on the surface of Mars, 160 longitudinally east of Earth, observed by the Radiation Assessment Detector (RAD) was the largest since the landing of the Curiosity rover in August 2012. Based on multipoint coronagraph images and the Graduated Cylindrical Shell model, we identify the initial 3-D kinematics of an extremely fast coronal mass ejection (CME) and its shock front, as well as another two CMEs launched hours earlier with moderate speeds. The three CMEs interacted as they propagated outward into the heliosphere and merged into a complex interplanetary CME (ICME). The arrival of the shock and ICME at Mars caused a very significant Forbush decrease seen by RAD only a few hours later than that at Earth, which was about 0.5 AU closer to the Sun. We investigate the propagation of the three CMEs and the merged ICME together with the shock, using the drag-based model and the WSA-ENLIL plus cone model constrained by the in situ observations. The synergistic study of the ICME and solar energetic particle arrivals at Earth and Mars suggests that to better predict potentially hazardous space weather impacts at Earth and other heliospheric locations for human exploration missions, it is essential to analyze (1) the eruption of the flare and CME at the Sun, (2) the CME kinematics, especially during their interactions, and (3) the spatially and temporally varying heliospheric conditions, such as the evolution and propagation of the stream interaction regions.

GALACTIC COSMIC-RAY INTENSITY MODULATION BY COROTATING INTERACTION REGION STREAM INTERFACES AT 1 au

X. [Guo](#)^{1,2} and V. Florinski

2016 ApJ 826 65

We present a new model that couples galactic cosmic-ray (GCR) propagation with magnetic turbulence transport and the MHD background evolution in the heliosphere. The model is applied to the problem of the formation of corotating interaction regions (CIRs) during the last solar minimum from the period between 2007 and 2009. The numerical model simultaneously calculates the large-scale supersonic solar wind properties and its small-scale turbulent content from 0.3 au to the termination shock. Cosmic rays are then transported through the background, and thus computed, with diffusion coefficients derived from the solar wind turbulent properties, using a stochastic Parker approach. Our results demonstrate that GCR variations depend on the ratio of diffusion coefficients in the fast and slow solar winds. Stream interfaces inside the CIRs always lead to depressions of the GCR intensity. On the other hand, heliospheric current sheet (HCS) crossings do not appreciably affect GCR intensities in the model, which is consistent with the two observations under quiet solar wind conditions. Therefore, variations in diffusion coefficients associated with CIR stream interfaces are more important for GCR propagation than the drift effects of the HCS during a negative solar minimum.

Corotating interaction regions and the 27 day variation of galactic cosmic rays intensity at 1 AU during the cycle 23/24 solar minimum

X. [Guo](#)^{1,*} and V. Florinski

JGR, 119, Issue 4, pages 2411–2429, April 2014

We investigate the formation and evolution of corotating interaction regions (CIRs) in the solar wind and their effects on galactic cosmic rays (GCR) during the recent solar cycle 23/24 solar minimum. The output from a three-dimensional MHD model serves as background for kinetic time-dependent simulations of GCR transport based on the Parker equation. The results show that the CIR forward/reverse shock pairs or compression/rarefaction regions play important roles in the transport of GCR particles and directly control the observed 27 day periodic intensity variations. We find that stream interfaces (SIs) in CIRs and the heliospheric current sheet (HCS) are both closely associated with the GCR depression onset, in agreement with the observations at 1 AU. The HCS is more important when its tilt angle becomes small during the declining phase of the solar minimum, while the passages of SIs control the onset of GCR depressions for larger HCS tilt angles. The mechanism of GCR intensity variation near 1 AU can be explained through an interplay between the effects of particle drift and diffusion. The simulated plasma background and GCR intensity are compared with the observations from spacecraft and a neutron monitor on the ground, to find good qualitative agreement. Evidently, CIRs had a substantial modulational effect on GCR during the recent solar minimum.

Energy transfer during intense geomagnetic storms driven by interplanetary coronal mass ejections and their sheath regions

Guo, Jianpeng; Feng, Xueshang; Emery, Barbara A.; **Zhang, Jie**; Xiang, Changqing; Shen, Fang; Song, Wenbin

J. Geophys. Res., Vol. 116, No. A5, A05106, **2011**, **File**

<http://dx.doi.org/10.1029/2011JA016490>

The interaction of the solar wind and Earth's magnetosphere is complex, and the phenomenology of the interaction is very different for interplanetary coronal mass ejections (ICMEs) compared to their sheath regions. In this paper, a total of 71 intense ($Dst \leq -100$ nT) geomagnetic storm events in 1996–2006, of which 51 are driven by ICMEs and 20 by sheath regions, are examined to demonstrate similarities and differences in the energy transfer. Using superposed epoch analysis, the evolution of solar wind energy input and dissipation is investigated. The solar wind-magnetosphere coupling functions and geomagnetic indices show a more gradual increase and recovery during the ICME-driven storms than they do during the sheath-driven storms. However, the sheath-driven storms have larger peak values. In general, solar wind energy input (the epsilon parameter) and dissipation show similar trends as the coupling functions. The trends of ion precipitation and the ratio of ion precipitation to the total (ion and electron) are quite different for both classes of events. There are more precipitating ions during the peak of sheath-driven storms. However, a quantitative assessment of the relative importance of the different energy dissipation branches shows that the means of input energy and auroral precipitation are significantly different for both classes of events, whereas Joule heating, ring current, and total output energy display no distinguishable differences. The means of electron precipitation are significantly different for both classes of events. However, ion precipitation exhibits no distinguishable differences. The energy efficiency bears no distinguishable difference between these two classes of events. Ionospheric processes account for the vast majority of the energy, with the ring current only being 12%–14% of the total. Moreover, the energy partitioning for both classes of events is similar.

Interplanetary drivers of ionospheric prompt penetration electric fields

Jianpeng **Guo** a,n, XueshangFeng a, PingbingZuo a, JieZhang b, YongWei c, QiugangZong c

Journal of Atmospheric and Solar-Terrestrial Physics 73 (2011) 130–136, **File**

In this paper we discussed the penetration effects of common interplanetary magnetic cloud (MC) structures like sheath region, both sheath and magnetic cloud boundary layer (MCBL), MC body, and shock-running into a preceding MC on the equatorial ionosphere during intense ($SYM-H \leq -100$ nT) geomagnetic storms. Using solar wind data obtained from the ACE and WIND spacecraft, we have identified these four types of MC structures responsible for the electric field penetration events detected by Jicamarca incoherent scatter radar. After elimination of the propagation delay, the observations show that the equatorial electric field (EEF) was changed immediately following the arrival of solar wind disturbance. Moreover, the duration of EEF corresponded well with that of the corresponding MC structure interval. We suggest that identifying the solar wind structures associated with penetration electric field may shed light on the understanding of the penetration processes and further help exploring their effects on the ionospheric plasma.

Statistical properties and geoefficiency of interplanetary coronal mass ejections and their sheaths during intense geomagnetic storms,

Guo, J., X. Feng, J. Zhang, P. Zuo, and C. Xiang

J. Geophys. Res., 115, A09107, doi:10.1029/2009JA015140, (2010), **File**.

In this paper, we examine and compare the statistical properties of interplanetary coronal mass ejections (ICMEs) and their sheath regions in the near-Earth space, mainly focusing on the distributions of various physical parameters and their geoefficiency. The 53 events studied are a subset of events responsible for intense ($Dst \leq -100$ nT) geomagnetic storms during the time period from 1996 to 2005. These events all fall into the single-type category in which each of the geomagnetic storms was caused by a well-isolated single ICME, free of the complexity of the interaction of multiple ICMEs. For both sheaths and ICMEs, we find that the distributions of the magnetic field strength, the solar-wind speed, the density, the proton temperature, the dynamic pressure, the plasma beta, and the Alfvén Mach number are approximately lognormal, while those of the B_z component and the Y component of the electric field are approximately Gaussian. On the average, the magnetic field strengths, the B_z components, the speeds, the densities, the proton temperatures, the dynamic pressures, the plasma betas, and the Mach numbers for the sheaths are 15, 80, 4, 60, 70, 62, 67, and 30% higher than the corresponding values for ICMEs, respectively, whereas the Y component of the electric field for the sheaths is almost 1 s of that for ICMEs. The two structures have almost equal energy transfer efficiency and comparable Newell functions, whereas they show statistically meaningful differences in the dayside reconnection rate, according to the Borovsky function.

High-Speed Solar Wind Streams during 1996 – 2007: Sources, Statistical Distribution, and Plasma/Field Properties

V. **Gupta** · Badruddin

Solar Phys (2010) 264: 165–188, **File**

We present **a catalog of high-speed streams, along with their solar sources for solar cycle 23**. We study their distribution during different years and different phases of solar cycle after classifying them into different groups based on their source(s), duration, and speed. We also study the average plasma/field properties of streams after dividing them into suitable groups on the basis of their source(s), duration and speed. It is expected that the catalog and statistical results presented in this work will further stimulate the space weather and solar-terrestrial studies involving high-speed streams.

We have listed streams of solar cycle 23 (1996 – 2007) satisfying the above criteria

in Table 1 (electronic supplementary material). See [Gupta_Catalogue of high-speed solar wind streams.doc](#)

Identifying the Coronal Source Regions of Solar Wind Streams from Total Solar Eclipse Observations and in situ Measurements Extending Over a Solar Cycle

Shadia R. **Habbal**, [Miloslav Druckmüller](#), [Nathalia Alzate](#), [Adalbert Ding](#), [Judd Johnson](#), [Pavel Starha](#), [Jana Hoderova](#), [Benjamin Boe](#), [Sage Constantinou](#), [Martina Arndt](#)

ApJL **911** L4 **2021**

<https://arxiv.org/pdf/2103.02128.pdf>

<https://iopscience.iop.org/article/10.3847/2041-8213/abe775/pdf>

<https://doi.org/10.3847/2041-8213/abe775>

This Letter capitalizes on a unique set of total solar eclipse observations, acquired between **2006 and 2020**, in white light, Fe XI 789.2 nm ($T_{\text{FeXI}} = 1.2 \pm 0.1$ MK) and Fe XIV 530.3 nm ($T_{\text{FeXIV}} = 1.8 \pm 0.1$ MK) emission, complemented by in situ Fe charge state and proton speed measurements from ACE/SWEPAM-SWICS, to identify the source regions of different solar wind streams. The eclipse observations reveal the ubiquity of open structures, invariably associated with Fe XI emission from Fe10+, hence a constant electron temperature, $T_e = T_{\text{FeXI}}$, in the expanding corona. The in situ Fe charge states are found to cluster around Fe10+, independently of the 300 to 700 km s⁻¹ stream speeds, referred to as the continual solar wind. Fe10+ thus yields the fiducial link between the continual solar wind and its T_{FeXI} sources at the Sun. While the spatial distribution of Fe XIV emission, from Fe13+, associated with streamers, changes throughout the solar cycle, the sporadic appearance of charge states $> \text{Fe11+}$, in situ, exhibits no cycle dependence regardless of speed. These latter streams are conjectured to be released from hot coronal plasmas at temperatures $\geq T_{\text{FeXIV}}$ within the bulge of streamers and from active regions, driven by the dynamic behavior of prominences magnetically linked to them. The discovery of continual streams of slow, intermediate and fast solar wind, characterized by the same T_{FeXI} in the expanding corona, places new constraints on the physical processes shaping the solar wind.

Table 1. Eclipse dates with corresponding observing sites

Forecasting Occurrence and Intensity of Geomagnetic Activity with Pattern-Matching Approaches

C. **Haines**, [M.J. Owens](#), [L. Barnard](#), [M. Lockwood](#), [A. Ruffenach](#), [K. Boykin](#), [R. McGranaghan](#)

Space Weather **Volume19, Issue6** e2020SW002624 **2021**

<https://agupubs.onlinelibrary.wiley.com/doi/10.1029/2020SW002624>

<https://agupubs.onlinelibrary.wiley.com/doi/epdf/10.1029/2020SW002624>

<https://doi.org/10.1029/2020SW002624>

Variability in near-Earth solar wind conditions gives rise to space weather which can have adverse effects on space- and ground-based technologies. Enhanced and sustained solar wind coupling with the Earth's magnetosphere can lead to a geomagnetic storm. The resulting effects can interfere with power transmission grids, potentially affecting today's technology-centred society to great cost. It is therefore important to forecast the intensity and duration of geomagnetic storms to improve decision making capabilities of infrastructure operators. The 150-year aaH geomagnetic index gives a substantial history of observations from which empirical predictive schemes can be built. Here we investigate the forecasting of geomagnetic activity with two pattern-matching forecast techniques, using the long aaH record. The

techniques we investigate are an Analogue Ensemble Forecast (AnEn), and a Support Vector Machine (SVM). AnEn produces a probabilistic forecast by explicitly identifying analogues for recent conditions in the historical data. The SVM produces a deterministic forecast through dependencies identified by an interpretable machine learning approach. As a third comparative forecast, we use the 27-day recurrence model, based on the synodic solar rotation period. The methods are analysed using several forecast metrics and compared. All forecasts outperform climatology on the considered metrics and AnEn and SVM outperform 27-day recurrence. A Cost/Loss analysis reveals the potential economic value is maximised using the AnEn, but the SVM is shown as superior by the true skill score. It is likely that the best method for a user will depend on their need for probabilistic information and tolerance of false alarms.

The Variation of Geomagnetic Storm Duration with Intensity

C. [Haines](#), M. J. Owens, L. Barnard, M. Lockwood, A. Ruffenach

[Solar Physics](#) November 2019, 294:154

[sci-hub.se/10.1007/s11207-019-1546-z](https://doi.org/10.1007/s11207-019-1546-z)

Variability in the near-Earth solar wind conditions can adversely affect a number of ground- and space-based technologies. Such space-weather impacts on ground infrastructure are expected to increase primarily with geomagnetic storm intensity, but also storm duration, through time-integrated effects. Forecasting storm duration is also necessary for scheduling the resumption of safe operating of affected infrastructure. It is therefore important to understand the degree to which storm intensity and duration are correlated. The long-running, global geomagnetic disturbance index, *aa*, has recently been recalibrated to account for the geographic distribution of the component stations. We use this *aaHaaH* index to analyse the relationship between geomagnetic storm intensity and storm duration over the past 150 years, further adding to our understanding of the climatology of geomagnetic activity. Defining storms using a peak-above-threshold approach, we find that more intense storms have longer durations, as expected, though the relationship is nonlinear. The distribution of durations for a given intensity is found to be approximately log-normal. On this basis, we provide a method to probabilistically predict storm duration given peak intensity, and test this against the *aaHaaH* dataset. By considering the average profile of storms with a superposed-epoch analysis, we show that activity becomes less recurrent on the 27-day timescale with increasing intensity. This change in the dominant physical driver, and hence average profile, of geomagnetic activity with increasing threshold is likely the reason for the nonlinear behaviour of storm duration. **1870-09-24, 1988-04-04**

The April 2023 SYM-H = -233 nT Geomagnetic Storm: A Classical Event

Rajkumar [Hajra](#), [Bruce Tsatnam Tsurutani](#), [Quanming Lu](#), [Richard B. Horne](#), [Gurbax Singh Lakhina](#), [Xu Yang](#), [Pierre Henri](#), [Aimin Du](#), [Xingliang Gao](#), [Rongsheng Wang](#), [San Lu](#)

JGR 2024

<https://arxiv.org/pdf/2409.08118>

The **23-24 April 2023** double-peak (SYM-H intensities of -179 and -233 nT) intense geomagnetic storm was caused by interplanetary magnetic field southward component B_s associated with an interplanetary fast-forward shock-preceded sheath (B_s of 25 nT), followed by a magnetic cloud (MC) (B_s of 33 nT), respectively. At the center of the MC, the plasma density exhibited an order of magnitude decrease, leading to a sub-Alfvénic solar wind interval for ~2.1 hr. Ionospheric Joule heating accounted for a significant part (~81%) of the magnetospheric energy dissipation during the storm main phase. Equal amount of Joule heating in the dayside and nightside ionosphere is consistent with the observed intense and global-scale DP2 (disturbance polar) currents during the storm main phase. The sub-Alfvénic solar wind is associated with disappearance of substorms, a sharp decrease in Joule heating dissipation, and reduction in electromagnetic ion cyclotron wave amplitude. The shock/sheath compression of the magnetosphere led to relativistic electron flux losses in the outer radiation belt between $L^* = 3.5$ and 5.5. Relativistic electron flux enhancements were detected in the lower $L^* < 3.5$ region during the storm main and recovery phases. Equatorial ionospheric plasma anomaly structures are found to be modulated by the prompt penetration electric fields. Around the anomaly crests, plasma density at ~470 km altitude and altitude-integrated ionospheric total electron content are found to increase by ~60% and ~80%, with ~33% and ~67% increases in their latitudinal extents compared to their quiet-time values, respectively.

Interplanetary Causes and Impacts of the 2024 May Superstorm on the Geosphere: An Overview

Rajkumar [Hajra](#), [Bruce Tsatnam Tsurutani](#), [Gurbax Singh Lakhina](#), [Quanming Lu](#), [Aimin Du](#)

ApJ 2024

<https://arxiv.org/pdf/2408.14799>

The recent superstorm of **2024 May 10-11** is the second largest geomagnetic storm in the space age and the only one that has simultaneous interplanetary data (there were no interplanetary data for the 1989 March storm). The May superstorm was characterized by a sudden impulse (SI+) amplitude of +88 nT, followed by a three-step storm main phase development which had a total duration of ~9 hr. The cause of the first storm main phase with a peak SYM-H intensity of -183 nT was a fast forward interplanetary shock (magnetosonic Mach number $M_{ms} \sim 7.2$) and an interplanetary sheath with southward interplanetary magnetic field component B_s of ~40 nT. The cause of the second storm main phase with a SYM-H intensity of -354 nT was a deepening of the sheath B_s to ~43 nT. A magnetosonic wave ($M_{ms} \sim 0.6$) compressed the sheath to a high magnetic field strength of ~71 nT. Intensified B_s of ~48 nT was the cause of the third and most intense storm main phase with a SYM-H intensity of -518 nT. Three magnetic cloud events with B_s fields of ~25-40 nT occurred in the storm recovery phase, lengthening the recovery to ~2.8 days. At geosynchronous orbit, ~76 keV to ~1.5 MeV electrons exhibited ~1-3 orders of magnitude flux decreases following the shock/sheath impingement onto the magnetosphere. The cosmic ray decreases at Dome C, Antarctica (effective vertical cutoff rigidity <0.01 GV) and Oulu, Finland (rigidity ~0.8 GV) were ~17% and ~11%, respectively relative to quiet time values. Strong ionospheric current flows resulted in extreme geomagnetically induced currents of ~30-40 A in the sub-auroral region. The storm period is characterized by strong polar region field-aligned currents, with ~10 times intensification during the main phase, and equatorward expansion down to ~50 deg geomagnetic (altitude-adjusted) latitude.

Interplanetary Shocks between 0.3 and 1.0 au: Helios 1 and 2 Observations

Rajkumar **Hajra**¹, Bruce T. Tsurutani², Gurbax S. Lakhina³, Quanming Lu^{1,4}, Aimin Du^{5,6}, and Lican Shan^{6,7}

2023 ApJ 951 75

<https://iopscience.iop.org/article/10.3847/1538-4357/acd370/pdf>

The Helios 1 (H1) and Helios 2 (H2) spacecraft measured the solar winds at a distance between ~0.3 and 1.0 au from the Sun. With increasing heliocentric distance (r_h), the plasma speed is found to increase at ~34–40 km s⁻¹ au⁻¹ and the density exhibits a sharper fall (r_h^{-2}) compared to the magnetic field magnitude ($r_h^{-1.5}$) and the temperature ($r_h^{-0.8}$). Using all available solar wind plasma and magnetic field measurements, we identified 68 and 39 fast interplanetary shocks encountered by H1 and H2, respectively. The overwhelming majority (85%) of the shocks are found to be driven by interplanetary coronal mass ejections (ICMEs). While the two spacecraft encountered more than 73 solar wind high-speed streams (HSSs), only ~22% had shocks at the boundaries of corotating interaction regions (CIRs) formed by the HSSs. All of the ICME shocks were found to be fast forward (FF) shocks; only four of the CIR shocks were fast reverse shocks. Among all ICME FF shocks (CIR FF shocks), 60% (75%) are quasi-perpendicular with shock normal angles (θ_{Bn}) $\geq 45^\circ$ relative to the upstream ambient magnetic field, and 40% (25%) are quasi-parallel ($\theta_{Bn} < 45^\circ$). No radial dependences were found in FF shock normal angle and speed. The FF shock Mach number (M_{ms}), magnetic field, and plasma compression ratios are found to increase with increasing r_h at the rates of 0.72, 0.89, and 0.98 au⁻¹, respectively. On average, ICME FF shocks are found to be considerably faster (~20%) and stronger (with ~28% higher M_{ms}) than CIR FF shocks.

Near-Earth High-Speed and Slow Solar Winds: A Statistical Study on Their Characteristics and Geomagnetic Impacts

Rajkumar **Hajra**

Solar Physics volume 298, Article number: 53 (2023)

<https://doi.org/10.1007/s11207-023-02141-6>

Near-Earth solar winds are separated into two groups: slow solar wind (SSW) with plasma speed [V_{sw}] <500 km s⁻¹ and high-speed solar wind (HSW) with V_{sw} >700 km s⁻¹. A comparative study is performed on the plasma and interplanetary magnetic field (IMF) properties of the near-Earth SSW and HSW, using solar wind measurements propagated to Earth's bow shock nose from 1963 through 2022. On average, HSW is characterized by higher alpha-to-proton density ratio [N_a/N_p] (67%), ram pressure [P_{sw}] (95%), proton temperature [T_p] (370%), reconnection electric field [V_B s] (141%), Alfvén speed [V_A] (76%), magnetosonic speed [V_{ms}] (65%), and lower proton density [N_p] (52%) and plasma- β (54%) than SSW. In V_B s, $V = V_{sw}$, B_s is the southward component of IMF. $V_A = B_0 / \mu_0 \rho$, $V_{ms} = \sqrt{V_A^2 + V_S^2}$, where B_0 is the IMF magnitude, μ_0 is the free space permeability, ρ is the solar wind mass density, and V_S is the sound speed. β is defined as the plasma pressure to the magnetic-pressure ratio. The geomagnetic activity is found to be enhanced during HSW, as reflected in higher average auroral electrojet index [AE] (213%) and stronger geomagnetic Dst index (367%) compared to those during SSW. The SSW characteristic parameters N_a/N_p , T_p , B_0 , V_A , and V_{ms} exhibit medium to strong

correlations (correlation coefficients $r=0.51$ to 0.87) with the F10.7 solar flux, while β and Mach numbers exhibit strong anti-correlations ($r=-0.82$ to -0.90) with F10.7. The associations are weaker or insignificant for HSW.

Interplanetary Sheaths and Corotating Interaction Regions: A Comparative Statistical Study on Their Characteristics and Geoeffectiveness

Rajkumar Hajra, Jibin V. Sunny, Megha Babu & Archana Giri Nair

Solar Physics volume 297, Article number: 97 (2022)

<https://doi.org/10.1007/s11207-022-02020-6>

Interplanetary sheaths and corotating interaction regions (CIRs), while having different solar sources, represent turbulent solar-wind plasma and magnetic field that can perturb the Earth's magnetosphere. We explore long-term solar-wind measurements upstream of the Earth during Solar Cycle 24, from January 2008 to December 2019, to compare their solar-cycle variation, characteristic features, and geoeffectiveness. Earth is found to be encountered by ≈ 2.6 times more CIRs (290) than sheaths (110) during this period. The sheath occurrence follows the F10.7 solar radio-flux variation, with a cross-correlation coefficient (ccrcc) of $+0.71$ at zero-year time lag. However, the CIR occurrence is more prominent during the solar cycle descending to minimum phases, reflected in ccrcc values of -0.53 and $+0.50$ at time lags of -2 and $+4$ years, respectively, between the CIR occurrence and the F10.7 solar flux. Both sheath and CIR are characterized by identical average plasma density and interplanetary magnetic-field (IMF) magnitude, and their fluctuations characterized by enhanced variance, and periodic variations of a few minutes to an hour. However, on average, the CIR has $\approx 12\%$ higher plasma speed, $\approx 33\%$ higher temperature, $\approx 20\%$ stronger southward IMF component, $\approx 131\%$ longer duration, and $\approx 158\%$ longer radial extent than the sheath. The intensities of the auroral electrojet index [AE] and the symmetric ring-current index [SYM-H] are, respectively, $\approx 38\%$ and $\approx 55\%$ stronger during the CIR than the sheath, on average. The geoeffectiveness of the CIR is found to be significantly higher than the sheath. Among all CIRs (sheaths), $\approx 25\%$ ($\approx 14\%$) caused moderate storms ($-50 \text{ nT} \geq \text{SYM-H} > -100 \text{ nT}$), and $\approx 5\%$ ($\approx 4\%$) caused intense storms ($\text{SYM-H} \leq -100 \text{ nT}$).

Corotating Interaction Regions during Solar Cycle 24: A Study on Characteristics and Geoeffectiveness

Rajkumar Hajra & Jibin V. Sunny

Solar Physics volume 297, Article number: 30 (2022)

<https://link.springer.com/content/pdf/10.1007/s11207-022-01962-1.pdf>

Corotating interaction regions (CIRs) form in the interaction region between the solar-wind high-speed streams and slow streams, leading to compressed plasma and magnetic fields. Using solar-wind measurements upstream of Earth, we identified 290 CIRs encountered by Earth during January 2008 through December 2019 (Solar Cycle 24). The occurrence rate is the maximum during the solar-cycle descending phase (≈ 33 year $^{-1}$), followed by occurrences during solar minimum (≈ 24 year $^{-1}$), the ascending phase (≈ 22 year $^{-1}$), and solar maximum (≈ 11 year $^{-1}$). At 1 AU, CIRs are found to be large-scale interplanetary structures with an average (median) duration of ≈ 26 hours (≈ 24 hours) and radial extent of ≈ 0.31 AU (≈ 0.27 AU). CIRs are characterized by average (median) plasma density of ≈ 29 cm $^{-3}$ (≈ 26 cm $^{-3}$), ram pressure of ≈ 11 nPa (≈ 9 nPa), temperature of $\approx 5 \times 10^5$ K ($\approx 4 \times 10^5$ K), and magnetic-field magnitude of ≈ 15 nT (≈ 14 nT). The CIR characteristic features exhibit no clear solar-cycle phase dependence. About 30% of the CIRs are found to be geoeffective, causing geomagnetic storms with the peak SYM-H ≤ -50 nT; 25% caused moderate storms ($-50 \text{ nT} \geq \text{SYM-H} > -100 \text{ nT}$), and 5% caused intense storms ($\text{SYM-H} \leq -100 \text{ nT}$). The geoeffectiveness is found to decrease with the decreasing solar flux. CIRs during equinoxes are found to be more geoeffective compared to those during solstices. On average, SYM-H is strongly associated with the CIR plasma characteristic parameters (anti-correlation coefficient $r=-0.65$ to -0.89), while the association is weaker for the AE-index ($r=0.41$ to 0.67). 17 – 18 January 2017, 26 – 27 March 2017

Table 3 Catalog of all CIRs under this study. 2008-2009

Near-Earth Sub-Alfvénic Solar Winds: Interplanetary Origins and Geomagnetic Impacts

Rajkumar Hajra¹ and Bruce T. Tsurutani²

2022 ApJ 926 135

<https://iopscience.iop.org/article/10.3847/1538-4357/ac4471/pdf>

The near-Earth solar wind is in general super-Alfvénic and supermagnetosonic. Using all available near-Earth solar wind measurements between 1973 and 2020, we identified 30 intervals with sub-Alfvénic solar winds. The majority (83%) of the events occurred within interplanetary coronal mass ejection magnetic clouds (MCs)/driver gases. These MC sub-Alfvénic events are characterized by exceptionally low plasma densities (N_{sw}) of ~ 0.04 – 1.20 cm $^{-3}$, low temperatures

(T_{sw}) of $\sim 0.08 \times 10^5$ K to 12.46×10^5 K, enhanced magnetic field intensities (B_0) of ~ 8.3 – 53.9 nT, and speeds (V_{sw}) of ~ 328 – 949 km s $^{-1}$. The resultant high Alfvén wave speeds (VA) ranged from ~ 410 to 1471 km s $^{-1}$. This is consistent with a mechanism of the MC expansions as they propagate radially outward, causing small pockets of sub-Alfvénic wind regions within the MCs. The remainder of the sub-Alfvénic intervals (17%) occurred within the extreme trailing portions of solar wind high-speed streams (HSSs). These HSS sub-Alfvénic winds had low N_{sw} of ~ 0.04 – 0.97 cm $^{-3}$, low T_{sw} of $\sim 0.06 \times 10^5$ K to 0.46×10^5 K, B_0 of ~ 6.3 – 18.2 nT, V_{sw} of ~ 234 – 388 km s $^{-1}$, and a VA range of ~ 364 – 626 km s $^{-1}$. This is consistent with a mechanism of solar wind super-radial expansions in the trailing HSS regions. During sub-Alfvénic solar wind intervals, Earth's bow shock nose exhibited rapid evanescence, and the estimated geocentric magnetopause distance increased by $\sim 33\%$ – 86% . The inner magnetosphere was more or less unaffected by the sub-Alfvénic solar winds. No significant impact was observed in the outer radiation belt relativistic electrons, and no geomagnetic storms or substorms were triggered during the sub-Alfvénic solar wind events. **18–21**

Mar 2002, 12–14 Sep 2004

Table 1 The Sub-Alfvénic Solar Winds under This Study 1992–2016

September 2017 Space-Weather Events: A Study on Magnetic Reconnection and Geoeffectiveness

Rajkumar **Hajra**

[Solar Physics](#) volume 296, Article number: 50 (2021)

<https://doi.org/10.1007/s11207-021-01803-7>

<https://link.springer.com/content/pdf/10.1007/s11207-021-01803-7.pdf>

September 2017 was an extremely active space-weather period with multiple events leading to varying impacts on the Earth's magnetosphere. The geoeffectiveness of a space-weather event largely depends on the magnetic reconnection between the southward interplanetary magnetic field and the day-side northward geomagnetic field. In this work, we estimate the reconnection rates during two intense (SYM-H peak $\leq -100 \leq -100$ nT) and two moderate (-50 nT \geq SYM-H $> -100 > -100$ nT) geomagnetic storms, and a high-intensity long-duration continuous auroral electrojet (AE) activity (HILDCAA) event in order to assess the contribution of the reconnection to resultant geomagnetic effects. Strong reconnection rates led to intense geomagnetic storms, while moderate-intensity geomagnetic storms were associated with discrete and weaker reconnection events. Comparatively weak magnetic reconnection continuing for a long interval of time led to the HILDCAA event. On average, a significant correlation was observed between the reconnection rates and geomagnetic-activity indices. However, the relationships are found to be more complex on shorter time-scales, varying from event to event. The importance of a quantitative study of the reconnection process for the prediction of geomagnetic activity is demonstrated. **7 – 8 September 2017, 12 – 13 September 2017, 14 – 17 September 2017, 27 – 28 September 2017**

The Complex Space Weather Events of 2017 September

Rajkumar **Hajra**¹, Bruce T. Tsurutani², and Gurbax S. Lakhina³

2020 ApJ 899 3 File

<https://doi.org/10.3847/1538-4357/aba2c5>

Interplanetary coronal mass ejections (ICMEs), magnetic clouds (MCs), sheaths, corotating interaction regions (CIRs), solar wind high-speed streams (HSSs), fast forward shocks (FSs), reverse waves (RWs), stream interfaces, and heliospheric current sheet crossings detected upstream of the Earth and their geoeffectiveness are studied during 2017 September. The most intense geomagnetic storm (SYM-H peak = -146 nT) starting on September 7 had a three-step main phase. A compound interplanetary structure resulting from an FS encountering and compressing the upstream MC southward interplanetary magnetic fields (IMFs) caused the first two steps of the storm. A magnetospheric supersubstorm (SSS; SML peak = -3712 nT) led to the third and most intense step. An MC portion of an ICME created an intense storm (SYM-H peak = -115 nT) on September 8. A second SSS (SML peak = -2642 nT) occurred during the main phase of this storm. Intense geomagnetically induced currents (GICs) occurred during the SSSs. Two moderate magnetic storms with peak SYM-H indices of -65 and -74 nT occurring on September 13 and 27 were caused by sheath and CIR southward IMFs, respectively. Six FSs and their associated sheaths caused sudden impulses (SI+s) of magnitude ranging from $+11$ to $+56$ nT. The shocks/sheaths led to magnetospheric relativistic electron flux decreases. The RWs caused SI–s and substorm recoveries by reducing southward IMFs. The high-intensity long-duration continuous AE activities (HILDCAAs) caused by the HSSs were related to the increase/acceleration of relativistic electron fluxes.

Interplanetary Shocks Inducing Magnetospheric Supersubstorms (SML < -2500 nT): Unusual Auroral Morphologies and Energy Flow

Rajkumar [Hajra](#)¹ and Bruce T. Tsurutani²

2018 ApJ 858 123

<http://sci-hub.tw/10.3847/1538-4357/aabaed>

We present case studies of two interplanetary shock-induced supersubstorms (SSSs) with extremely high intensities (peak SML -4418 and -2668 nT) and long durations (~ 1.7 and ~ 3.1 hr). The events occurred on **2005 January 21** and **2010 April 5**, respectively. It is shown that these SSSs have a different auroral evolution than a nominal Akasofu-type substorm. The auroras associated with the SSSs did not have the standard midnight onset and following expansion. Instead, at the time of the SML index peak, the midnight sector was generally devoid of intense auroras, while the most intense auroras were located in the pre-midnight and post-midnight magnetic local times. Precursor energy input through magnetic reconnection was insufficient to balance the large ionospheric energy dissipation during the SSSs. It is argued that besides the release of stored magnetotail energy during the SSSs, these were powered by additional direct driving through both dayside magnetic reconnection and solar wind ram energy.

Supersubstorms (SML < -2500 nT): Magnetic Storm and Solar Cycle Dependences[†]

Rajkumar [Hajra](#), Bruce T. Tsurutani, Ezequiel Echer, Walter D. Gonzalez, Jesper W. Gjerloev

JGR 2016

We study extremely intense substorms with SuperMAG AL (SML) peak intensities < -2500 nT (“supersubstorms”/SSSs) for the period from 1981 through 2012. The SSS events were often found to be isolated SML peaks and not statistical fluctuations of the indices. The SSSs occur during all phases of the solar cycle with the highest occurrence (3.8 year⁻¹) in the descending phase. The SSSs exhibited an annual variation with equinoctial maximum altering between spring in solar cycle 22 and fall in solar cycle 23. The occurrence rate and strength of the SSSs did not show any strong relationship with the intensity of the associated geomagnetic storms. All SSS events were associated with strong southward interplanetary magnetic field B_s component. The B_s fields were part of interplanetary magnetic clouds in 46% and of interplanetary sheath fields in 54% of the cases. About 77% of the SSSs were associated with small regions of very high density solar wind plasma parcels or pressure pulses impinging upon the magnetosphere. Comments on how SSS events may cause power outages at Earth are discussed at the end of the paper.

Superposed epoch analyses of HILDCAAs and their interplanetary drivers: Solar cycle and seasonal dependences

Rajkumar [Hajra](#), Ezequiel Echer, Bruce T. Tsurutani, Walter D. Gonzalez

JASTP, Volume 121, Part A, December 2014, Pages 24–31

We study the solar cycle and seasonal dependences of high-intensity, long-duration, continuous AE activity (HILDCAA) events and associated solar wind/interplanetary external drivers for $\sim 3, 1/2$ solar cycle period, from 1975 to 2011. 99 HILDCAAs which had simultaneous solar wind/interplanetary data are considered in the present analyses. The peak occurrence frequency of HILDCAAs was found to be in the descending phase of the solar cycle. These events had the strongest time-integrated AE intensities and were coincident with peak occurrences of high-speed solar wind streams. The event initiations were statistically coincident with high-to-slow speed stream interactions, compressions in the solar wind plasma and interplanetary magnetic field (IMF). The latter were corotating interaction regions (CIRs). The signatures of related CIRs were most prominent for the events occurring during the descending and solar minimum phases of the solar cycles. For these events, the solar wind speed increased by $\sim 41\%$ and $\sim 57\%$ across the CIRs, respectively. There was weak or no stream–stream interaction or CIR structure during the ascending and solar maximum phases. HILDCAAs occurring during spring and fall seasons were found to occur preferentially in negative and positive IMF sector regions (toward and away from the Sun), respectively.

Relativistic electron acceleration during high-intensity, long-duration, continuous AE activity (HILDCAA) events: Solar cycle phase dependences.

[Hajra](#) R, Tsurutani BT, Echer E, Gonzalez WD

(2014), GRL 41:1876

Solar wind-magnetosphere energy coupling efficiency and partitioning: HILDCAAs and preceding CIR storms during solar cycle 23

Rajkumar [Hajra](#)^{1,*}, Ezequiel Echer¹, Bruce T. Tsurutani² and Walter D. Gonzalez

JGR, Volume 119, Issue 4, pages 2675–2690, April 2014

A quantitative study on the energetics of the solar wind-magnetosphere-ionosphere system during High-Intensity, Long-Duration, Continuous AE Activity (HILDCAA) events for solar cycle 23 (from 1995 through 2008) is presented. For all

HILDCAAs, the average energy transferred to the magnetospheric/ionospheric system was $\sim 6.3 \times 10^{16}$ J, and the ram kinetic energy of the incident solar wind was $\sim 7.1 \times 10^{18}$ J. For individual HILDCAA events the coupling efficiency, defined as the ratio of the solar wind energy input to the solar wind kinetic energy, varied between 0.3% and 2.8%, with an average value of $\sim 0.9\%$. The solar wind coupling efficiency for corotating interaction region (CIR)-driven storms prior to the HILDCAA events was found to vary from $\sim 1\%$ to 5%, with an average value of $\sim 2\%$. Both of these values are lower than the $> 5\%$ coupling efficiency noted for interplanetary coronal mass ejection (and sheath)-driven magnetic storms. During HILDCAAs, $\sim 67\%$ of the solar wind energy input went into Joule heating, $\sim 22\%$ into auroral precipitation, and $\sim 11\%$ into the ring current energy. The CIR-storm Joule heating ($\sim 49\%$) was noticeably less than that during HILDCAAs, while the ring current energies were comparable for the two. Joule dissipation was higher for HILDCAAs that followed CIR-storms (88%) than for isolated HILDCAAs ($\sim 60\%$). Possible physical interpretations for the statistical results obtained in this paper are discussed.

Electrons in the Young Solar Wind: First Results from the Parker Solar Probe

J. S. [Halekas](#), [P. Whittlesey](#), [D. E. Larson](#), [D. McGinnis](#), [M. Maksimovic](#), [M. Berthomier](#), [J. C. Kasper](#), [A. W. Case](#), [K. E. Korreck](#), [M. L. Stevens](#), [K. G. Klein](#), [S. D. Bale](#), [R. J. MacDowall](#), [M. P. Pulupa](#), [D. M. Malaspina](#), [K. Goetz](#), [P. R. Harvey](#)

ApJ 2019

<https://arxiv.org/pdf/1912.02216.pdf>

The Solar Wind Electrons Alphas and Protons experiment on the Parker Solar Probe (PSP) mission measures the three-dimensional electron velocity distribution function. We derive the parameters of the core, halo, and strahl populations utilizing a combination of fitting to model distributions and numerical integration for $\sim 100,000$ electron distributions measured near the Sun on the first two PSP orbits, which reached heliocentric distances as small as ~ 0.17 AU. As expected, the electron core density and temperature increase with decreasing heliocentric distance, while the ratio of electron thermal pressure to magnetic pressure (β_e) decreases. These quantities have radial scaling consistent with previous observations farther from the Sun, with superposed variations associated with different solar wind streams. The density in the strahl also increases; however, the density of the halo plateaus and even decreases at perihelion, leading to a large strahl/halo ratio near the Sun. As at greater heliocentric distances, the core has a sunward drift relative to the proton frame, which balances the current carried by the strahl, satisfying the zero-current condition necessary to maintain quasi-neutrality. Many characteristics of the electron distributions near perihelion have trends with solar wind flow speed, β_e , and/or collisional age. Near the Sun, some trends not clearly seen at 1 AU become apparent, including anti-correlations between wind speed and both electron temperature and heat flux. These trends help us understand the mechanisms that shape the solar wind electron distributions at an early stage of their evolution.

Dependence of the Interplanetary Magnetic Field on Heliocentric Distance at 0.3–1.7 AU: A Six-Spacecraft Study

Cedar [Hanneson](#), [Catherine L. Johnson](#), [Anna Mittelholz](#), [Manar M. Al Asad](#), [Colin Goldblatt](#)

JGR Volume 125, Issue 3 March 2020 e2019JA027139

<https://doi.org/10.1029/2019JA027139>

We use magnetometer data taken simultaneously by MESSENGER, VEX, STEREO and ACE to characterize the variation of the interplanetary magnetic field (IMF) with heliocentric distance, r , for $r > 1$ AU. Power law fits ($\propto r^{-\alpha}$) to the individual IMF components and magnitude indicate that, on average, the IMF is more tightly wound and its strength decreases less rapidly with r than the Parker spiral prediction. During Solar Cycle 24, temporal changes in α were insignificant, but changes in amplitude, B , were correlated with sunspot number, up to sunspot number 84. MAVEN data taken at 1.4–1.7 AU since late 2014 broadly confirm and extend these results in space and time. Our study demonstrates the importance of simultaneous observations from multiple spacecraft to separate heliocentric distance and temporal variations in the IMF and provides a modern benchmark for comparison with data from the Parker Solar Probe Mission.

The Great Storm of May 1921: An Exemplar of a Dangerous Space Weather Event

Mike [Hapgood](#)

Space Weather Volume 17, Issue 7 Pages 950-975 2019

[sci-hub.se/10.1029/2019SW002195](https://doi.org/10.1029/2019SW002195)

We reconstruct the timeline of the extreme space weather event of May 1921, reviewing a wealth of reports from scientific literature, databases, newspaper reports, and reports by historians and astronomers. A series of coronal mass ejections (CMEs) bombarded Earth between 13 and 16 May, as shown by a series of sudden commencements observed across the global network of magnetometers. These CMEs produced three major periods of geomagnetic activity. The first period followed the arrival of two CMEs on 13 May. These may have cleared much density from the inner

heliosphere, enabling a subsequent CME to travel quickly to Earth and cause intense activity. Continuing moderate magnetic activity following the first period may also have preconditioned the magnetosphere so it responded strongly to that later CME. This arrived late on 14 May, driving a short period of very intense activity early on 15 May, including technological impacts indicative of strong geoelectric fields. Another CME arrived early on 16 May, driving intense activity similar to that on 13 May. We show how these impacts fit with scientific observations to give a timeline that can be used in worst-case studies/benchmarks. We also show that some impacts were probably coincidental with the storm, but due to more prosaic faults. This sequence of preconditioning, intense geoelectric fields, and their impacts, plus coincidental faults, makes the 1921 event an excellent basis for building space weather scenarios. Such scenarios are vital scientific input to the development and implementation of policies for mitigation of severe space weather.

The Solar Source of a Magnetic Cloud Using a Velocity Difference Technique

L.K. [Harra](#), · C.H. Mandrini, · S. Dasso, A.M. Gulisano, · K. Steed, · S. Imada

E-print, Nov 2010; Solar Phys. (2011) 268: 213–230, [File](#)

For large eruptions on the Sun, it is often a problem that the **core dimming region** cannot be observed due to the bright emission from the flare itself. However, spectroscopic data can provide the missing information through the measurement of Doppler velocities. In this paper we analyse the well-studied flare and coronal mass ejection that erupted on the Sun on **13 December 2006** and reached the Earth on 14 December 2006. In this example, although the imaging data were saturated at the flare site itself, we could extract information on the core dimming region through velocity measurements, as well as on the remote dimmings. The purpose of this paper is to determine more accurately the magnetic flux of the solar source region, potentially involved in the ejection, through a new technique. The results of its application are compared to the flux in the magnetic cloud observed at 1AU, as a way to check the reliability of this technique. We analysed data from the {it Hinode} EUV Imaging Spectrometer to estimate the Doppler velocity in the active region and its surroundings before and after the event. This allowed us to determine a Doppler velocity 'difference' image. We used the velocity difference image overlaid on a Michelson Doppler Imager magnetogram to identify the regions in which the blue-shifts were more prominent after the event; the magnetic flux in these regions was used as a proxy for the ejected flux and compared to the magnetic cloud flux. This new method provides a more accurate flux determination in the solar source region.

How Does Large Flaring Activity from the Same Active Region Produce Oppositely Directed Magnetic Clouds?

Louise K. [Harra](#) · Nancy U. Crooker · Cristina H. Mandrini · Lidia van Driel-Gesztelyi · Sergio Dasso · Jingxiu Wang · Heather Elliott · Gemma Attrill · Bernard V. Jackson · Mario M. Bisi

Solar Phys, 244: 95–114, **2007**, DOI 10.1007/s11207-007-9002-x

We describe the interplanetary coronal mass ejections (ICMEs) that occurred as a result of a series of solar flares and eruptions from 4 to 8 November 2004. Two ICMEs/magnetic clouds occurring from these events had opposite magnetic orientations. This was despite the fact that the major flares related to these events occurred within the same active region that maintained the same magnetic configuration.

L1 and off Sun-Earth line visible-light imaging of Earth-directed CMEs: An analysis of inconsistent observations

Richard A. [Harrison](#), [Jackie A. Davies](#), [David Barnes](#), [Christian Möstl](#)

Space Weather [Volume21, Issue4](#) e2022SW003358 **2023**

<https://arxiv.org/ftp/arxiv/papers/2304/2304.05264.pdf>

<https://agupubs.onlinelibrary.wiley.com/doi/epdf/10.1029/2022SW003358>

The efficacy of coronal mass ejection (CME) observations as a key input to space weather forecasting is explored by comparing on and off Sun-Earth line observations from the ESA/NASA SOHO and NASA STEREO spacecraft. A comparison is made of CME catalogues based on L1 coronagraph imagery and off Sun-Earth line coronagraph and heliospheric imager (HI) observations, for the year 2011. Analysis reveals inconsistencies in the identification of a number of potentially Earth-directed CMEs. The catalogues reflect our ability to identify and characterise CMEs, so any discrepancies can impact our prediction of Earth-directed CMEs. We show that 15 CMEs, which were observed by STEREO, that had estimated directions compatible with Earth-directed events, had no identified halo/partial halo counterpart listed in the L1 coronagraph CME catalogue. In-situ data confirms that for 9 of these there was a consistent

L1 Interplanetary CME (ICME). The number of such "discrepant" events is significant compared to the number of ICMEs recorded at L1 in 2011, stressing the need to address space weather monitoring capabilities, particularly with the inclusion of off Sun-Earth line observation. While the study provides evidence that some halo CMEs are simply not visible in near-Earth coronagraph imagery, there is evidence that some halo CMEs viewed from L1 are compromised by preceding CME remnants or the presence of multiple-CMEs. This underlines (1) the value of multiple vantage point CME observation, and (2) the benefit of off Sun-Earth line platform heliospheric imaging, and coronagraph imaging, for the efficient identification and tracking of Earth-directed events. **2011: 24 Jan, 14 Feb, 25 May, 23 Jun, 03 Jul, 11 Jul, 05 Oct, 26 Oct, 29 Oct, 01 Nov, 29 Nov**

Table 1. Key parameters of the HIGeoCAT (SSEF30) and CDAW-listed CMEs

CMEs in the Heliosphere: I. A Statistical Analysis of the Observational Properties of CMEs Detected in the Heliosphere from 2007 to 2017 by STEREO/HI-1

R. A. **Harrison**, **J. A. Davies**, **D. Barnes**, **J. P. Byrne**, **C. H. Perry**, **V. Bothmer**, **J. P. Eastwood**, **P. T. Gallagher**, **E. K. J. Kilpua**, **C. Möstl**, **L. Rodriguez**, **A. P. Rouillard**, **D. Odstrcil**

Solar Phys. 293:77 2018

<https://arxiv.org/ftp/arxiv/papers/1804/1804.02320.pdf>

<https://link.springer.com/content/pdf/10.1007%2Fs11207-018-1297-2.pdf>

We present a statistical analysis of coronal mass ejections (CMEs) imaged by the Heliospheric Imager (HI) instruments aboard NASA's twin-spacecraft STEREO mission between April 2007 and August 2017 for STEREO-A and between April 2007 and September 2014 for STEREO-B. The analysis exploits a catalogue that was generated within the FP7 HELCATS project. Here, we focus on the observational characteristics of CMEs imaged in the heliosphere by the inner (HI-1) cameras. More specifically, in this paper we present distributions of the basic observational parameters - namely occurrence frequency, central position angle (PA) and PA span - derived from nearly 2000 detections of CMEs in the heliosphere by HI-1 on STEREO-A or STEREO-B from the minimum between Solar Cycles 23 and 24 to the maximum of Cycle 24; STEREO-A analysis includes a further 158 CME detections from the descending phase of Cycle 24, by which time communication with STEREO-B had been lost. We compare heliospheric CME characteristics with properties of CMEs observed at coronal altitudes, and with sunspot number. As expected, heliospheric CME rates correlate with sunspot number, and are not inconsistent with coronal rates once instrumental factors/differences in cataloguing philosophy are considered. As well as being more abundant, heliospheric CMEs, like their coronal counterparts, tend to be wider during solar maximum. Our results confirm previous coronagraph analyses suggesting that CME launch sites don't simply migrate to higher latitudes with increasing solar activity. At solar minimum, CMEs tend to be launched from equatorial latitudes while, at maximum, CMEs appear to be launched over a much wider latitude range; this has implications for understanding the CME/solar source association. Our analysis provides some supporting evidence for the systematic dragging of CMEs to lower latitude as they propagate outwards. **2008-12-13, 2009-09-01, 2010-06-02, 2011-07-03, 2011-12-01, 2013-12-15**

HELIOSPHERIC IMAGER CME CATALOGUE HTTPS://WWW.HELCCATS-FP7.EU/CATALOGUES/WP2_CAT.HTML

The application of heliospheric imaging to space weather operations: Lessons learned from published studies

Review

Richard A. **Harrison**, Jackie A. Davies, Doug Biesecker, Mark Gibbs

Space Weather Volume 15, Issue 8 August 2017 Pages 985–1003

<http://onlinelibrary.wiley.com/doi/10.1002/2017SW001633/full>

<http://onlinelibrary.wiley.com/doi/10.1002/2017SW001633/epdf>

The field of heliospheric imaging has matured significantly over the last 10 years—corresponding, in particular, to the launch of NASA's STEREO mission and the successful operation of the heliospheric imager (HI) instruments thereon. In parallel, this decade has borne witness to a marked increase in concern over the potentially damaging effects of space weather on space and ground-based technological assets, and the corresponding potential threat to human health, such that it is now under serious consideration at governmental level in many countries worldwide. Hence, in a political climate that recognizes the pressing need for enhanced operational space weather monitoring capabilities most appropriately stationed, it is widely accepted, at the Lagrangian L1 and L5 points, it is timely to assess the value of heliospheric imaging observations in the context of space weather operations. To this end, we review a cross section of the scientific analyses that have exploited heliospheric imagery—particularly from STEREO/HI—and discuss their relevance to operational predictions of, in particular, coronal mass ejection (CME) arrival at Earth and elsewhere. We believe that the potential benefit of heliospheric images to the provision of accurate CME arrival predictions on an operational basis, although as yet not fully realized, is significant and we assert that heliospheric imagery is central to

any credible space weather mission, particularly one located at a vantage point off the Sun-Earth line. **1 August 2010, 15 Feb 2011, 8 March 2012, 5 March 2013, 20-27 May 2017**

AN ANALYSIS OF THE ORIGIN AND PROPAGATION OF THE MULTIPLE CORONAL MASS EJECTIONS OF 2010 AUGUST 1

R. A. [Harrison](#)¹, J. A. Davies¹, C. Möstl^{2,3,4}, Y. Liu^{4,5}, M. Temmer^{2,3}, M. M. Bisi^{6,7}, J. P. Eastwood⁸, C. A. de Koning⁹, N. Nitta¹⁰, T. Rollett^{2,3}, C. J. Farrugia¹¹, R. J. Forsyth⁸, B. V. Jackson⁷, E. A. Jensen¹², E. K. J. Kilpua¹³, D. Odstrčil¹⁴, and D. F. Webb

2012 ApJ 750 45

On **2010 August 1**, the northern solar hemisphere underwent significant activity that involved a complex set of active regions near central meridian with, nearby, two large prominences and other more distant active regions. This activity culminated in the eruption of four major coronal mass ejections (CMEs), effects of which were detected at Earth and other solar system bodies. Recognizing the unprecedented wealth of data from the wide range of spacecraft that were available—providing the potential for us to explore methods for CME identification and tracking, and to assess issues regarding onset and planetary impact—we present a comprehensive analysis of this sequence of CMEs. We show that, for three of the four major CMEs, onset is associated with prominence eruption, while the remaining CME appears to be closely associated with a flare. Using instrumentation on board the Solar Terrestrial Relations Observatory spacecraft, three of the CMEs could be tracked out to elongations beyond 50°; their directions and speeds have been determined by various methods, not least to assess their potential for Earth impact. The analysis techniques that can be applied to the other CME, the first to erupt, are more limited since that CME was obscured by the subsequent, much faster event before it had propagated far from the Sun; we discuss the speculation that these two CMEs interact. The consistency of the results, derived from the wide variety of methods applied to such an extraordinarily complete data set, has allowed us to converge on robust interpretations of the CME onsets and their arrivals at 1 AU.

Two Years of the STEREO Heliospheric Imagers [Invited Review](#)

Richard A. [Harrison](#) · Jackie A. Davies · Alexis P. Rouillard · Christopher J. Davis · Christopher J. Eyles · Danielle Bewsher · Steve R. Crothers · Russell A. Howard · Neil R. Sheeley · Angelos Vourlidas · David F. Webb · Daniel S. Brown · Gareth D. Dorrian

Solar Phys (2009) 256: 219–237, DOI 10.1007/s11207-009-9352-7, **2009, File**

STEREO SCIENCE RESULTS AT SOLAR MINIMUM

Imaging of the heliosphere is a burgeoning area of research. As a result, it is awash with new results, using novel applications, and is demonstrating great potential for future research in a wide range of topical areas. The STEREO (*Solar TERrestrial Relations Observatory*) Heliospheric Imager (HI) instruments are at the heart of this new development, building on the pioneering observations of the SMEI (Solar Mass Ejection Imager) instrument aboard the *Coriolis* spacecraft. Other earlier heliospheric imaging systems have included ground-based interplanetary scintillation (IPS) facilities and the photometers on the *Helios* spacecraft. With the HI instruments, we now have routine wide-angle imaging of the inner heliosphere, from vantage points outside the Sun-Earth line. HI has been used to investigate the development of coronal mass ejections (CMEs) as they pass through the heliosphere to 1 AU and beyond. Synoptic mapping has also allowed us to see graphic illustrations of the nature of mass outflow as a function of distance from the Sun – in particular, stressing the complexity of the near-Sun solar wind. The instruments have also been used to image co-rotating interaction regions (CIRs), to study the interaction of comets with the solar wind and CMEs, and to witness the impact of CMEs and CIRs on planets. The very nature of this area of research – which brings together aspects of solar physics, space-environment physics, and solar-terrestrial physics – means that the research papers are spread among a wide range of journals from different disciplines. Thus, in this special issue, it is timely and appropriate to provide a review of the results of the first two years of the HI investigations.

Reconstruction of an evolving magnetic flux rope in the solar wind: Decomposing spatial and temporal variations from single-spacecraft data

Hiroshi [Hasegawa](#), Bengt U. Ö. Sonnerup, Qiang Hu and Takuma Nakamura

JGR, Volume 119, Issue 1, pages 97–114, January **2014**

<http://onlinelibrary.wiley.com/doi/10.1002/2013JA019180/pdf>

We present a novel single-spacecraft method for decomposing spatial and temporal variations of physical quantities at points along the path of a spacecraft in space-time. The method is designed for use in the reconstruction of evolving two-dimensional, approximately magnetohydrostatic structures in a space plasma. It is an extension of the one developed by Sonnerup and Hasegawa (2010) and Hasegawa et al. (2010), in which it was assumed that variations in the time series of data, recorded as the structures move past the spacecraft, are all due to spatial effects. In reality, some of the observed variations are usually caused by temporal evolution of the structure during the time it moves past the observing spacecraft; the information in the data about the spatial structure is aliased by temporal effects. The purpose here is to remove this time aliasing from the reconstructed maps of field and plasma properties. Benchmark tests are performed by use of synthetic data taken by a virtual spacecraft as it traverses, at a constant velocity, a magnetic flux rope growing sufficiently slowly (relative to the Alfvén speed) in a two-dimensional magnetohydrodynamic simulation of magnetic reconnection. These tests show that the new method can better recover the space-time behavior of the flux rope than does the original version, in which time-aliasing effects had not been removed. An application of the new method to a solar wind flux rope, observed by the ACE spacecraft, suggests that the cross-sectional shape of the core part of the flux rope was varying. **25–27 March 1998**

Occurrence of Great Magnetic Storms on 6-8 March 1582

Kentaro [Hattori](#), [Hisashi Hayakawa](#), [Yusuke Ebihara](#)

MNRAS Volume 487, Issue 3, Pages 3550–3559 2019

<https://arxiv.org/ftp/arxiv/papers/1905/1905.08017.pdf>

Although knowing the occurrence frequency of severe space weather events is important for a modern society, it is insufficiently known due to the lack of magnetic or sunspot observations, before the Carrington event in 1859 known as one of the largest events during the last two centuries. Here, we show that a severe magnetic storm occurred on 8 March 1582 based on auroral records in East Asia. The equatorward boundary of auroral visibility reached 28.8° magnetic latitude. The equatorward boundary of the auroral oval is estimated to be 33.0° invariant latitude (ILAT), which is comparable to the storms on 25/26 September 1909 (~31.6° ILAT, minimum Dst of -595 nT), 28/29 August 1859 (~36.5° ILAT), and 13/14 March 1989 (~40° ILAT, minimum Dst of -589 nT). Assuming that the equatorward boundary is a proxy for the scale of magnetic storms, we presume that the storm on March 1582 was severe. We also found that the storm on March 1582 lasted, at least, for three days by combining European records. The auroral oval stayed at mid-latitude for the first two days and moved to low-latitude (in East Asia) for the last day. It is plausible that the storm was caused by a series of ICMEs (interplanetary coronal mass ejections). We can reasonably speculate that a first ICME could have cleaned up interplanetary space to make the following ICMEs more geo-effective, as probably occurred in the Carrington and Halloween storms.

The Solar and Geomagnetic Storms in May 2024: A Flash Data Report

Hisashi [Hayakawa](#), [Yusuke Ebihara](#), [Alexander Mishev](#), [Sergey Koldobskiy](#), [Kanya Kusano](#), [Sabrina Bechet](#), [Seiji Yashiro](#), [Kazumasa Iwai](#), [Atsuki Shinbori](#), [Kalevi Mursula](#), [Fusa Miyake](#), [Daikou Shiota](#), [Marcos V. D. Silveira](#), [Robert Stuart](#), [Denny M. Oliveira](#), [Sachiko Akiyama](#), [Kouji Ohnishi](#), [Yoshizumi Miyoshi](#)

2024

<https://arxiv.org/pdf/2407.07665>

In May 2024, the scientific community observed intense solar eruptions that resulted in an extreme geomagnetic storm and auroral extension, highlighting the need to document and quantify these events. This study mainly focuses on their quantification. The source active region (AR 13664) evolved from 113 to 2761 millionths of the solar hemisphere between **4 May and 14 May 2024**. AR 13664's magnetic free energy surpassed 1033 erg on 7 May 2024, triggering 12 X-class flares. Multiple interplanetary coronal mass ejections (ICMEs) came out from this AR, accelerating solar energetic particles toward Earth. At least four ICMEs seemingly piled up to disturb the interplanetary space, according to the satellite data and interplanetary scintillation data. The shock arrival at 17:05 UT on 10 May 2024 significantly compressed the magnetosphere down to ~ 5.04 R_E, and triggered a deep Forbush decrease. GOES satellite data and ground-based neutron monitors confirmed a ground-level enhancement from 2 UT to 10 UT on 11 May 2024. The ICMEs induced extreme geomagnetic storms, peaking at a Dst index of -412 nT at 2 UT on 11 May 2024, marking the sixth-largest storm since 1957. The AE and AL indices showed extreme auroral extensions that located the AE/AL stations into the polar cap. We gathered auroral records at that time and reconstructed the equatorward boundary of the visual auroral oval to 29.8° invariant latitude. We compared naked-eye and camera auroral visibility, providing critical caveats on their difference. We also confirmed global enhancements of storm-enhanced density of the ionosphere.

Table 1: Summary of the X-class flare produced by the AR 13664

Table 2: Major CMEs observed in the Large Angle Spectroscopic Coronagraph (LASCO) from the AR 13664

The Extreme Space Weather Event of 1872 February: Sunspots, Magnetic Disturbance, and Auroral Displays

Hisashi [Hayakawa](#)^{1,2}, Edward W. Cliver³, Frédéric Clette⁴, Yusuke Ebihara^{5,6} ⁺⁺⁺
2023 ApJ 959 23

<https://iopscience.iop.org/article/10.3847/1538-4357/acc6cc/pdf>

We review observations of solar activity, geomagnetic variation, and auroral visibility for the extreme geomagnetic storm on **1872 February 4**. The extreme storm (referred to here as the Chapman–Silverman storm) apparently originated from a complex active region of moderate area ($\approx 500 \mu\text{sh}$) that was favorably situated near disk center ($S19^\circ E05^\circ$). There is circumstantial evidence for an eruption from this region at 9–10 UT on 1872 February 3, based on the location, complexity, and evolution of the region, and on reports of prominence activations, which yields a plausible transit time of ≈ 29 hr to Earth. Magnetograms show that the storm began with a sudden commencement at $\approx 14:27$ UT and allow a minimum Dst estimate of ≤ -834 nT. Overhead aurorae were credibly reported at Jacobabad (British India) and Shanghai (China), both at $19^\circ 9'$ in magnetic latitude (MLAT) and $24^\circ 2'$ in invariant latitude (ILAT). Auroral visibility was reported from 13 locations with MLAT below $|20|^\circ$ for the 1872 storm (ranging from $|10^\circ 0'|$ – $|19^\circ 9'|$ MLAT) versus one each for the 1859 storm ($|17^\circ 3'|$ MLAT) and the 1921 storm ($|16^\circ 2'|$ MLAT). The auroral extension and conservative storm intensity indicate a magnetic storm of comparable strength to the extreme storms of 1859 September ($25^\circ 1' \pm 0^\circ 5'$ ILAT and -949 ± 31 nT) and 1921 May ($27^\circ 1'$ ILAT and -907 ± 132 nT), which places the 1872 storm among the three largest magnetic storms yet observed.

The extreme solar and geomagnetic storms on 1940 March 20–25

Hisashi [Hayakawa](#), [Denny M Oliveira](#), [Margaret A Shea](#), [Don F Smart](#), [Seán P Blake](#), [Kentaro Hattori](#), [Ankush T Bhaskar](#), [Juan J Curto](#), [Daniel R Franco](#), [Yusuke Ebihara](#)

MNRAS, Volume 517, Issue 2, December 2022, Pages 1709–1723,

<https://doi.org/10.1093/mnras/stab3615>

<https://academic.oup.com/mnras/article-pdf/517/2/1709/46495872/stab3615.pdf>

In late 1940 March, at least five significant solar flares were reported. They likely launched interplanetary coronal mass ejections (ICMEs), and were associated with one of the largest storm sudden commencements (SSCs) since 1868, resulting in space weather hazards that would have significant societal impacts should it occur today. The initial solar activity is associated with a solar proton event. Afterwards, another flare was reported in the eastern solar quadrant (N12 E37–38) at 11:30–12:30 UT on March 23, with significant magnetic crochets (up to $\approx |80|$ nT at Eskdalemuir) during 11:07–11:40 UT. On their basis, we conservatively estimate the required energy flux of the source solar flare as $X35 \pm 1$ in soft X-ray class. The resultant ICMEs caused enormous SSCs (up to >425 nT recorded at Tucson) and allowed us to estimate an extremely inward magnetopause position (estimated magnetopause stand-off position ≈ 3.4 RE). The time series of the resultant geomagnetic storm is reconstructed using a Dst estimate, which peaked at 20 UT on March 24 at ≈ -389 nT. Around the storm main phase, the equatorward boundary of the auroral oval extended $\leq 46.3^\circ$ in invariant latitudes. This sequence also caused a solar proton event and Forbush decrease (≈ 3 per cent). These sequences indicate pile-up of multiple ICMEs, which even achieved a record value of inward magnetopause position. Our analyses of this historical pioneer event bring more insights into possible serious space weather hazards and provide a quantitative basis for future analyses and predictions.

A Review for Japanese auroral records on the three extreme space weather events around the International Geophysical Year (1957 -- 1958)

Hisashi [Hayakawa](#), [Yusuke Ebihara](#), [Hidetoshi Hata](#)

Geoscience Data Journal, 2021

<https://arxiv.org/ftp/arxiv/papers/2112/2112.09432.pdf>

DOI: 10.1002/GDJ3.140

Solar Cycle 19 was probably the greatest solar cycle over the last four centuries and significantly disrupted the solar-terrestrial environments with a number of solar eruptions and resultant geomagnetic storms. At its peak, the International Geophysical Year (IGY: 1957 -- 1958) was organised by international collaborations and benefitted scientific developments, capturing multiple unique extreme space weather events including the third and fourth greatest geomagnetic storms in the space age. In this article, we review and analyse original records of Japanese auroral observations around the IGY. These observations were organised by Masaaki Huruhashi in collaboration with professional observatories and citizen contributors. We have digitised and documented these source documents, which comprise significant auroral displays in March 1957 (minimum Dst = -255 nT), September 1957 (minimum Dst = -427 nT), and February 1958 (minimum Dst = -426 nT). These records allow us to visualise temporal and spatial evolutions

of these auroral displays, reconstruct their equatorward auroral boundaries down to 41.4° , 38.3° , and 33.3° in invariant latitudes, and contextualise their occurrences following contemporary geomagnetic disturbances. Our results have been compared with significant auroral displays during other extreme space weather events. These aurorae generally showed reddish colourations occasionally with yellowish rays. Their colourations are attributed to reddish oxygen emission and its mixture with greenish oxygen emission. Overall, these archival records provide the references for future discussions on the auroral activities during the uniquely intense and extreme space weather events. **2/3 March 1957, 13/14 September 1957, 11/12 February 1958**

Temporal Variations of the Three Geomagnetic Field Components at Colaba Observatory around the Carrington Storm in 1859

Hisashi **Hayakawa**, [Heikki Nevanlinna](#), [Séan P. Blake](#), [Yusuke Ebihara](#), [Ankush T. Bhaskar](#), [Yoshizumi Miyoshi](#)

ApJ **2021**

<https://arxiv.org/pdf/2109.13020>

The Carrington storm in 1859 September has been arguably identified as the greatest geomagnetic storm ever recorded. However, its exact magnitude and chronology remain controversial, while their source data have been derived from the Colaba H magnetometer. Here, we have located the Colaba 1859 yearbook, containing hourly measurements and spot measurements. We have reconstructed the Colaba geomagnetic disturbances in the horizontal component (ΔH), the eastward component (ΔY), and the vertical component (ΔZ) around the time of the Carrington storm. On their basis, we have chronologically revised the ICME transit time as ≤ 17.1 hrs and located the ΔH peak at 06:20 -- 06:25 UT, revealing a magnitude discrepancy between the hourly and spot measurements (-1691 nT vs. -1263 nT). Furthermore, we have newly derived the time series of ΔY and ΔZ , which peaked at $\Delta Y \sim 378$ nT (05:50 UT) and 377 nT (06:25 UT), and $\Delta Z \sim -173$ nT (06:40 UT). We have also computed the hourly averages and removed the solar quiet (Sq) field variations from each geomagnetic component to derive their hourly variations with latitudinal weighting. Our calculations have resulted in the disturbance variations (Dist) with latitudinal weighting of Dist Y ~ 328 nT and Dist Z ~ -36 nT, and three scenarios of Dist H $\sim -918, -979,$ and -949 nT, which also approximate the minimum Dst. These data may suggest preconditioning of the geomagnetic field after the August storm ($\Delta H \leq -570$ nT), which made the September storm even more geoeffective.

The Extreme Space Weather Event in 1941 February/March

Hisashi **Hayakawa**^{1,2,3,4}, Sean P. Blake^{5,6}, Ankush Bhaskar^{5,6,7}, Kentaro Hattori⁸, Denny M. Oliveira^{5,9}, and Yusuke Ebihara¹

2021 ApJ 908 209

<https://arxiv.org/ftp/arxiv/papers/2010/2010.00452.pdf>

<https://doi.org/10.3847/1538-4357/abb772>

Given the infrequency of extreme geomagnetic storms, it is significant to note the concentration of three extreme geomagnetic storms in 1941, whose intensities ranked fourth, twelfth, and fifth within the aa index between 1868–2010. Among them, the geomagnetic storm on 1941 March 1 was so intense that three of the four Dst station magnetograms went off scale. Herein, we reconstruct its time series and measure the storm intensity with an alternative Dst estimate (Dst*). The source solar eruption at 09:29–09:38 GMT on February 28 was located at RGO AR 13814 and its significant intensity is confirmed by large magnetic crochets of 135 nT measured at Abinger. This solar eruption most likely released a fast interplanetary coronal mass ejection with estimated speed 2260 km s^{-1} . After its impact at 03:57–03:59 GMT on March 1, an extreme magnetic storm was recorded worldwide. Comparative analyses on the contemporary magnetograms show the storm peak intensity of minimum $\text{Dst}^* \leq -464$ nT at 16 GMT, comparable to the most and the second most extreme magnetic storms within the standard Dst index since 1957. This storm triggered significant low-latitude aurorae in the East Asian sector and their equatorward boundary has been reconstructed as $38^\circ 5'$ in invariant latitude. This result agrees with British magnetograms, which indicate an auroral oval moving above Abinger at $53^\circ 0'$ in magnetic latitude. The storm amplitude was even more enhanced in equatorial stations and consequently casts caveats on their usage for measurements of the storm intensity in Dst estimates. **February 28-March 1 1941**

The intensity and evolution of the extreme storms in January 1938

Hisashi **Hayakawa**, [Kentaro Hattori](#), [Alexei A. Pevtsov](#), [Yusuke Ebihara](#), [Margaret A. Shea](#), [Ken G. McCracken](#), [Ioannis A. Daglis](#), [Ankush Bhaskar](#), [Paulo Ribeiro](#), [Delores J. Knipp](#)

ApJ **909** 197 **2021**

<https://arxiv.org/ftp/arxiv/papers/2010/2010.15762.pdf>

<https://doi.org/10.3847/1538-4357/abc427>

Major solar eruptions occasionally direct interplanetary coronal mass ejections (ICMEs) to Earth and cause significant geomagnetic storms and low-latitude aurorae. While single extreme storms are of significant threats to the modern civilization, storms occasionally appear in sequence and, acting synergistically, cause 'perfect storms' at Earth. The stormy interval in January 1938 was one of such cases. Here, we analyze the contemporary records to reveal its time series on their source active regions, solar eruptions, ICMEs, geomagnetic storms, low-latitude aurorae, and cosmic-ray (CR) variations. Geomagnetic records show that three storms occurred successively on **17/18 January** ($D_{cx} \sim -171$ nT) on **21/22 January** ($D_{cx} \sim -328$ nT) and on **25/26 January** ($D_{cx} \sim -336$ nT). The amplitudes of the cosmic-ray variations and sudden storm commencements show the impact of the first ICME as the largest ($\sim 6\%$ decrease in CR and 72 nT in SSC) and the ICME associated with the storms that followed as more moderate ($\sim 3\%$ decrease in CR and 63 nT in SSC; $\sim 2\%$ decrease in CR and 63 nT in SSC). Interestingly, a significant solar proton event occurred on 16/17 January and the Cheltenham ionization chamber showed a possible ground level enhancement. During the first storm, aurorae were less visible at mid-latitudes, whereas during the second and third storms, the equatorward boundaries of the auroral oval were extended down to 40.3° and 40.0° in invariant latitude. This contrast shows that the initial ICME was probably faster, with a higher total magnitude but a smaller southward component.

Intensity and time series of extreme solar-terrestrial storm in 1946 March

Hisashi [Hayakawa](#), [Yusuke Ebihara](#), [Alexei A Pevtsov](#), [Ankush Bhaskar](#), [Nina Karachik](#), [Denny M Oliveira](#)
Monthly Notices of the Royal Astronomical Society, Volume 497, Issue 4, **2020**, Pages 5507–5517,

<https://doi.org/10.1093/mnras/staa1508>

<https://sci-hub.st/10.1093/mnras/staa1508>

Major solar eruptions occasionally cause magnetic superstorms on the Earth. Despite their serious consequences, the low frequency of their occurrence provides us with only limited cases through modern instrumental observations, and the intensities of historical storms before the coverage of the Dst index have been only sporadically estimated. Herein, we examine a solar-terrestrial storm that occurred in 1946 March and quantitatively evaluate its parameters. During the ascending phase of Solar Cycle 18, two moderate sunspot groups caused a major flare. The $H\alpha$ flaring area was recorded to be ≥ 600 – 1200 millionths of solar hemisphere, suggesting that this was an M- or X-class flare in soft X-ray intensity. Upon this eruption, a rapid interplanetary coronal mass ejection (ICME) with an average speed of ≈ 1590 km s $^{-1}$ was launched. Based on measurements in four known mid-latitude and relatively complete magnetograms, the arrival of this extreme ICME caused a magnetic superstorm, which caused an initial phase with the H-component amplitude of ≥ 80 nT, followed by a main phase whose intensity was reconstructed as ≤ -512 nT using most negative Dst* estimates. Meanwhile, the equatorial boundary of the auroral oval extended down to $\leq 41.0^\circ$ in invariant latitude and formed a corona aurora in Watheroo, Australia. Interestingly, during this magnetic superstorm, larger magnetic disturbances were recorded at dusk and near the dip equator on the dayside. Its cause may be associated with a strong westward equatorial electrojet and field-aligned current, in addition to the contribution from the storm-time ring current.

Candidate Auroral Observations during the Major Solar-Terrestrial Storm in May 1680: Implication for Space Weather Events during the Maunder Minimum

Hisashi [Hayakawa](#), [Kristian Schlegel](#), [Bruno P. Besser](#), [Yusuke Ebihara](#)

ApJ **2020**

<https://arxiv.org/ftp/arxiv/papers/2008/2008.13739.pdf>

The Maunder Minimum (1645-1715) is currently considered the only grand minimum within telescopic sunspot observations since 1610. During this epoch, the Sun was extremely quiet and unusually free from sunspots. However, despite reduced frequency, candidate aurorae were reported in the mid-European sector during this period and have been associated with occurrences of interplanetary coronal mass ejections (ICMEs), whereas some of them have been identified as misinterpretations. Here, we have analysed reports of candidate aurorae on 1 June 1680 with simultaneous observations in mid-Europe, and compared their descriptions with visual accounts of early modern aurorae. Most contemporary sunspot drawings from 22, 24, and 27 May 1680 have shown that this apparent sunspot may have been a source of ICMEs, which caused the reported candidate aurorae. On the other hand, its intensity estimate shows that the magnetic storm during this candidate aurora was probably within the capability of the storms derived from the corotating interaction region (CIR). Therefore, we accommodate both ICMEs and CIRs as their possible origin. This interpretation is probably applicable to the candidate aurorae in the often-cited Hungarian catalogue, on the basis of the reconstructed margin of their equatorward auroral boundary. Moreover, this catalogue itself has clarified that the considerable candidates during the MM were probably misinterpretations. Therefore, frequency of the auroral visibility in Hungary

was probably lower than previously considered and agree more with the generally slow solar wind in the existing reconstructions, whereas sporadic occurrences of sunspots and coronal holes still caused occasional geomagnetic storms.

The Extreme Space Weather Event in 1903 October/November: An Outburst from the Quiet Sun

Hisashi [Hayakawa](#), [Paulo Ribeiro](#), [José M. Vaquero](#), [María Cruz Gallego](#), [Delores J. Knipp](#), [Florian Mekhaldi](#), [Ankush Bhaskar](#), [Denny M. Oliveira](#), [Yuta Notsu](#), [V́ctor M. S. Carrasco](#), [Ana Caccavari](#), [Bhaskara Veenadhari](#), [Shyamoli Mukherjee](#), [Yusuke Ebihara](#)

ApJL 897 L10 2020

<https://arxiv.org/ftp/arxiv/papers/2001/2001.04575.pdf>
sci-hub.tw/10.3847/2041-8213/ab6a18

While the Sun is generally more eruptive during its maximum and declining phases, observational evidence shows certain cases of powerful solar eruptions during the quiet phase of the solar activity. Occurring in the weak Solar Cycle 14 just after its minimum, the extreme space weather event in 1903 October -- November was one of these cases. Here, we reconstruct the time series of geomagnetic activity based on contemporary observational records. With the mid-latitude magnetograms, the 1903 magnetic storm is thought to be caused by a fast coronal mass ejection (~1500 km/s) and is regarded as an intense event with an estimated minimum Dst' of ~-513 nT. The reconstructed time series has been compared with the equatorward extension of auroral oval (~44.1° in invariant latitude) and the time series of telegraphic disturbances. This case study shows that potential threats posed by extreme space weather events exist even during weak solar cycles or near their minima. **Source 30 Nov, 06 UT, Dst ~-513 nT, 31 Nov, 14 UT**

A WARNING FROM HISTORY--THE CARRINGTON EVENT WAS NOT UNIQUE

[Hayakawa](#) 2020

See <https://www.spaceweather.com> 01.09.2020

South American auroral reports during the Carrington storm

Hisashi [Hayakawa](#), [José R. Ribeiro](#), [Yusuke Ebihara](#), [Ana P. Correia](#), [Mitsuru Sôma](#)

Earth, Planets and Space, 72, 122, 2020

<https://arxiv.org/ftp/arxiv/papers/2008/2008.13180.pdf>

The importance of the investigation of magnetic superstorms is not limited to academic interest, because these superstorms can cause catastrophic impact on the modern civilisation due to our increasing dependency on technological infrastructure. In this context, the Carrington storm in September 1859 is considered as a benchmark of observational history owing to its magnetic disturbance and equatorial extent of the auroral oval. So far, several recent auroral reports at that time have been published but those reports are mainly derived from the Northern Hemisphere. In this study, we analyse datable auroral reports from South America and its vicinity, assess the auroral extent using philological and astrometric approaches, identify the auroral visibility at - 17.3° magnetic latitude and further poleward and reconstruct the equatorial boundary of the auroral oval to be 25.1° +/- 0.5° in invariant latitude. Interestingly, brighter and more colourful auroral displays were reported in the South American sector than in the Northern Hemisphere. This north-south asymmetry is presumably associated with variations of their magnetic longitude and the weaker magnetic field over South America compared to the magnetic conjugate point and the increased amount of magnetospheric electron precipitation into the upper atmosphere. These results attest that the magnitude of the Carrington storm indicates that its extent falls within the range of other superstorms, such as those that occurred in May 1921 and February 1872, in terms of the equatorial boundary of the auroral oval.

Temporal and Spatial Evolutions of a Large Sunspot Group and Great Auroral Storms around the Carrington Event in 1859

Hisashi [Hayakawa](#), [Yusuke Ebihara](#), [David M. Willis](#), [Shin Toriumi](#), [Tomoya Iju](#), [Kentaro Hattori](#), [Matthew N. Wild](#), [Denny M. Oliveira](#), [Iaria Ermolli](#), [José R. Ribeiro](#), [Ana P. Correia](#), [Ana I. Ribeiro](#), [Delores J. Knipp](#)

Space Weather v. 17, # 11, 1553-1569, 2019

<https://arxiv.org/ftp/arxiv/papers/1908/1908.10326.pdf>
<https://doi.org/10.1029/2019SW002269>

The Carrington event is considered to be one of the most extreme space weather events in observational history within a series of magnetic storms caused by extreme interplanetary coronal mass ejections (ICMEs) from a large and complex active region (AR) emerged on the solar disk. In this article, we study the temporal and spatial evolutions of the source sunspot active region and visual aurorae, and compare this storm with other extreme space weather events on the basis

of their spatial evolution. Sunspot drawings by Schwabe, Secchi, and Carrington describe the position and morphology of the source AR at that time. Visual auroral reports from the Russian Empire, Iberia, Ireland, Oceania, and Japan fill the spatial gap of auroral visibility and revise the time series of auroral visibility in mid to low magnetic latitudes (MLATs). The reconstructed time series is compared with magnetic measurements and shows the correspondence between low to mid latitude aurorae and the phase of magnetic storms. The spatial evolution of the auroral oval is compared with those of other extreme space weather events in 1872, 1909, 1921, and 1989 as well as their storm intensity, and contextualizes the Carrington event, as one of the most extreme space weather events, but likely not unique. **28/29 Aug 1859, 1/2 Sept 1859, 4 Feb 1872, 25 Sept 1909, 14/15 May 1921, 13/14 March 1989**

Long-Lasting Extreme Magnetic Storm Activities in 1770 Found in Historical Documents

Hisashi [Hayakawa](#), [Kiyomi Iwahashi](#), [Yusuke Ebihara](#), [Harufumi Tamazawa](#), [Kazunari Shibata](#), [Delores J. Knipp](#), [Akito Davis Kawamura](#), [Kentaro Hattori](#), [Kumiko Mase](#), [Ichiro Nakanishi](#), [Hiroaki Isobe](#)

ApJL **850** L31 **2017**

<https://arxiv.org/ftp/arxiv/papers/1711/1711.00690.pdf>

Dim red aurora at low magnetic latitudes is a visual and recognized manifestation of geomagnetic storms. The great low-latitude auroral displays seen throughout East Asia on **16-18 September 1770** are considered to manifest one of the greatest storms. Recently found 111 historical documents in East Asia attest that these low-latitude auroral displays were succeeding for almost 9 nights during 10-19 September 1770 in the lowest magnetic latitude areas ($< 30^{\circ}$). This suggests that the duration of the great magnetic storm is much longer than usual. Sunspot drawings from 1770 reveals the fact that sunspots area was twice as large as those observed in another great storm of 1859, which substantiates this unusual storm activities in 1770. These spots likely ejected several huge, sequential magnetic structures in short duration into interplanetary space, resulting in spectacular world-wide aurorae in mid-September 1770. These findings provide new insights about the history, duration, and effects of extreme magnetic storms that may be valuable for those who need to mitigate against extreme events.

Boundary Treatment for the Subsonic/Alfvénic Inner Boundary at $2.5 R_{\odot}$ in a Time-dependent 3D Magnetohydrodynamics Solar Wind Simulation Model

Keiji [Hayashi](#)¹, Chin-Chun Wu², and Kan Liou³

2023 ApJS 268 39

<https://iopscience.iop.org/article/10.3847/1538-4365/acecf7/pdf>

A new magnetohydrodynamics (MHD) simulation model of the global solar corona and solar wind is presented. The model covers the range of heliocentric distance from 2.5 solar radii, so that coronal mass ejections at the earliest phase near the Sun can be treated in the future. This model is constructed by introducing a characteristics-based boundary treatment to an existing heliosphere 3D MHD model. In tailoring a set of characteristic equations for this new model, we assume that the coronal magnetic field is open to interplanetary space and that the solar coronal plasma is flowing outward everywhere at 2.5 solar radii. The characteristic equations for the subsonic/Alfvénic inner boundary surface are satisfied by altering the plasma density and/or temperature to maintain a polytropic relationship. In this article, the details of the characteristics-based boundary treatment for the middle of the corona (named CharM) are provided. The quasi-steady states of the solar wind derived from simulations with various choices of a parameter in the boundary treatments are compared and examined. Although further improvements are needed, we apply the new boundary treatment to simulations for three Carrington rotation periods from the minimum to maximum phase of the solar activity cycle, and show that an optimal choice yields a reasonable quasi-steady state of the transonic/Alfvénic solar wind matching the specified subsonic/Alfvénic plasma speed at $2.5 R_{\odot}$.

Coupling a Global Heliospheric Magnetohydrodynamic Model to a Magnetofrictional Model of the Low Corona

Keiji [Hayashi](#)¹, William P. Abbett², Mark C. M. Cheung³, and George H. Fisher²

2021 ApJS 254 1

<https://doi.org/10.3847/1538-4365/abe9b5>

Recent efforts coupling our Sun-to-Earth magnetohydrodynamics (MHD) model and lower-corona magnetofrictional (MF) model are described. Our Global Heliospheric MHD (GHM) model uses time-dependent three-component magnetic field data from the lower-corona MF model as time-dependent boundary values. The MF model uses data-assimilation techniques to introduce the vector magnetic field data from the Solar Dynamics Observatory/HelioSeismic and Magnetic Imager, hence as a whole this simulation coupling structure is driven with actual observations. The GHM model employs a newly developed interface boundary treatment that is based on the concept of characteristics, and it properly treats the interface boundary sphere set at a height of the sub-Alfvénic lower corona ($1.15 R_{\odot}$ in this work).

The coupled model framework numerically produces twisted nonpotential magnetic features and consequent eruption events in the solar corona in response to the time-dependent boundary values. The combination of our two originally independently developed models presented here is a model framework toward achieving further capabilities of modeling the nonlinear time-dependent nature of magnetic field and plasma, from small-scale solar active regions to large-scale solar wind structures. This work is a part of the Coronal Global Evolutionary Model project for enhancing our understanding of Sun–Earth physics to help improve space weather capabilities.

CME-related Large Decreases in the Differential Phase Delay of Tianwen-1 DOR Signals

Qingbao He¹, Zhichao Wang^{2,3}, Qinghui Liu², Kaijun Liu¹, and Li Guo²

2022 ApJL 940 L45

<https://iopscience.iop.org/article/10.3847/2041-8213/aca2a8/pdf>

Differential phase delay is calculated for the differential one-way range (DOR) signals transmitted by Tianwen-1, the first Chinese Mars spacecraft that entered into the Mars orbit on 2021 February 10. Large decreases in the differential phase delay are identified in the DOR signals received by ground stations on **2021 March 23 and June 18**. The decreases indicate sizable increases of the total electron content (TEC) along the DOR signal path between Tianwen-1 and the ground stations. The TEC increases are estimated to be 85 and 175 TEC units on 2021 March 23 and June 18, respectively. Evidence shows that they are caused by the sheath regions ahead of the coronal mass ejections (CMEs) that traversed the signal path on both days. The results represent the first observations of CME-related structures by the DOR signals and demonstrate the potential of DOR signals in remote sensing the interplanetary plasma structures in the solar wind.

Growth of Outward Propagating Fast-Magnetosonic/Whistler Waves in the Inner Heliosphere Observed by Parker Solar Probe

Jiansen He, Ying Wang, Xingyu Zhu, Die Duan, Daniel Verscharen, Guoqing Zhao

ApJ 2021

<https://arxiv.org/pdf/2109.12768.pdf>

The solar wind in the inner heliosphere has been observed by Parker Solar Probe (PSP) to exhibit abundant wave activities. The cyclotron wave modes in the sense of ions or electrons are among the most crucial wave components. However, their origin and evolution in the inner heliosphere close to the Sun remain mysteries. Specifically, it remains unknown whether it is an emitted signal from the solar atmosphere or an eigenmode growing locally in the heliosphere due to plasma instability. To address and resolve this controversy, we must investigate the key quantity of the energy change rate of the wave mode. We develop a new technique to measure the energy change rate of plasma waves, and apply this technique to the wave electromagnetic fields measured by PSP. We provide the wave Poynting flux in the solar wind frame, identify the wave nature to be the outward propagating fast-magnetosonic/whistler wave mode instead of the sunward propagating waves. We provide the first evidence for growth of the fast-magnetosonic/whistler wave mode in the inner heliosphere based on the derived spectra of the real and imaginary parts of the wave frequencies. The energy change rate rises and stays at a positive level in the same wavenumber range as the bumps of the electromagnetic field power spectral densities, clearly manifesting that the observed fast-magnetosonic/whistler waves are locally growing to a large amplitude. **Nov 4, 2018**

Solar Origin of Compressive Alfvénic Spikes/Kinks as Observed by Parker Solar Probe

Jiansen He¹, Xingyu Zhu¹, Liping Yang², Chuanpeng Hou¹, Die Duan¹, Lei Zhang³, and Ying Wang¹

2021 ApJL 913 L14

<https://doi.org/10.3847/2041-8213/abf83d>

The solar wind is found by the Parker Solar Probe to be abundant with Alfvénic velocity spikes and magnetic field kinks. Temperature enhancement is another remarkable feature associated with the Alfvénic spikes. How the prototype of these coincident phenomena is generated intermittently in the source region is an important and wide-ranging subject. Here we propose a new model introducing guide-field discontinuity into the interchange magnetic reconnection between open funnels and closed loops with different magnetic helicities. The modified interchange reconnection model not only can accelerate jet flows from the newly opening closed loop but also can excite and launch Alfvénic wave pulses along the newly reconnected and post-reconnected open flux tubes. We find that the modeling results can reproduce the following observational features: (1) Alfvén disturbance is pulsive in time and asymmetric in space; (2) Alfvénic pulse is compressive with temperature enhancement and density variation inside the pulse. We point out that three physical processes co-happening with Alfvén wave propagation can be responsible for the temperature enhancement: (a) convection of heated jet flow plasmas (decrease in density), (b) propagation of compressive slow-mode waves (increase in density), and (c) conduction of heat flux (weak change in density). We also suggest that the radial nonlinear evolution of the Alfvénic pulses should be taken into account to explain the formation of magnetic switchback geometry.

Encounter of Parker Solar Probe and a Comet-like Object During Their Perihelia: Model Predictions and Measurements

Jiansen He, Bo Cui, Liping Yang, Chuanpeng Hou, Lei Zhang, Wing-Huen Ip, Yingdong Jia, Chuanfei Dong, Die Duan, Qiugang Zong, Stuart D. Bale, Marc Pulupa, John W. Bonnell, Thierry Dudok de Wit, Keith Goetz, Peter R. Harvey, Robert J. MacDowall, David M. Malaspina

2021 *ApJ* **910** 7

<https://arxiv.org/pdf/2012.00005.pdf>

<https://doi.org/10.3847/1538-4357/abdf4a>

Parker Solar Probe (PSP) aims at exploring the nascent solar wind close to the Sun. Meanwhile, PSP is also expected to encounter small objects like comets and asteroids. In this work, we survey the ephemerides to find a chance of recent encounter, and then model the interaction between released dusty plasmas and solar wind plasmas. On **2019 September 2**, a comet-like object 322P/SOHO just passed its perihelion flying to a heliocentric distance of 0.12 au, and swept by PSP at a relative distance as close as 0.025 au. We present the dynamics of dust particles released from 322P, forming a curved dust tail. Along the PSP path in the simulated inner heliosphere, the states of plasma and magnetic field are sampled and illustrated, with the magnetic field sequences from simulation results being compared directly with the in-situ measurements from PSP. Through comparison, we suggest that 322P might be at a deficient activity level releasing limited dusty plasmas during its way to becoming a "rock comet". We also present images of solar wind streamers as recorded by WISPR, showing an indication of dust bombardment for the images superposed with messy trails. We observe from LASCO coronagraph that 322P was transiting from a dimming region to a relatively bright streamer during its perihelion passage, and simulate to confirm that 322P was flying from relatively faster to slower solar wind streams, modifying local plasma states of the streams.

A Stealth CME Bracketed between Slow and Fast Wind Producing Unexpected Geoeffectiveness

Wen He, Ying D.Liu, Huidong Hu, Rui Wang, Xiaowei Zhao

ApJ **860** 78 **2018**

<https://arxiv.org/pdf/1805.03128.pdf>

<https://iopscience.iop.org/article/10.3847/1538-4357/aac381/pdf>

We investigate how a weak coronal mass ejection (CME) launched on **2016 October 8** without obvious signatures in the low corona produced a relatively intense geomagnetic storm. Remote sensing observations from SDO, STEREO and SOHO and in situ measurements from WIND are employed to track the CME from the Sun to the Earth. Using a graduated cylindrical shell (GCS) model, we estimate the propagation direction and the morphology of the CME near the Sun. CME kinematics are determined from the wide-angle imaging observations of STEREO A and are used to predict the CME arrival time and speed at the Earth. We compare ENLIL MHD simulation results with in situ measurements to illustrate the background solar wind where the CME was propagating. We also apply a Grad-Shafranov technique to reconstruct the flux rope structure from in situ measurements in order to understand the geoeffectiveness associated with the CME magnetic field structure. Key results are obtained concerning how a weak CME can generate a relatively intense geomagnetic storm: (1) there were coronal holes at low latitudes, which could produce high speed streams (HSSs) to interact with the CME in interplanetary space; (2) the CME was bracketed between a slow wind ahead and a HSS behind, which enhanced the southward magnetic field inside the CME and gave rise to the unexpected geomagnetic storm.

Forbush decreases associated to Stealth Coronal Mass Ejections.

Heber B., Wallmann C., Galsdorf D., et al.

Cent. Eur. Astrophys. Bull. V. 39, PP. 75–82. **2015**

Установлено, что когда стелс-КВМ достигают орбиты Земли, могут возникать Форбуш-пониженияю.

Classification of Enhanced Geoeffectiveness Resulting from High-Speed Solar Wind Streams Compressing Slower Interplanetary Coronal Mass Ejections

Stephan G. Heinemann, Chaitanya Sishla, Simon Good, Maxime Grandin, Jens Pomoell

ApJ **963** L25 **2024**

<https://arxiv.org/pdf/2402.08065.pdf>

<https://iopscience.iop.org/article/10.3847/2041-8213/ad283a/pdf>

High-speed solar wind streams (HSSs) interact with the preceding ambient solar wind to form Stream Interaction Regions (SIRs), which are a primary source of recurrent geomagnetic storms. However, HSSs may also encounter and subsequently interact with Interplanetary Coronal Mass Ejections (ICMEs). In particular, the impact of the interaction between slower ICMEs and faster HSSs, represents an unexplored area that requires further in-depth investigation. This specific interaction can give rise to unexpected geomagnetic storm signatures, diverging from the conventional expectations of individual SIR events sharing similar HSS properties. Our study presents a comprehensive analysis of solar wind data spanning from 1996 to 2020, capturing 23 instances where such encounters led to geomagnetic storms ($SymH < -30$ nT). We determined that interaction events between preceding slower ICMEs and faster HSSs possess the potential to induce substantial storm activity, statistically nearly doubling the geoeffective impact in comparison to SIR storm events. The increase in the amplitude of the SymH index appears to result from heightened dynamic pressure, often coupled with the concurrent amplification of the CMEs rearward $|B|$ and/or B_z components. **4-6 Feb 2011**
Table 2. Summary of ICME - HSS interaction events 1999-2016

A statistical study of the long-term evolution of coronal hole properties as observed by SDO

S. G. **Heinemann**¹, V. Jerčić^{1,2}, M. Temmer¹, S. J. Hofmeister¹, M. Dumbović^{1,3}, S. Vennerstrom⁴, G. Verbanac⁵ and A. M. Veronig^{1,6}
A&A 638, A68 (2020)

<https://www.aanda.org/articles/aa/pdf/2020/06/aa37613-20.pdf>

Context. Understanding the evolution of coronal holes is especially important when studying the high-speed solar wind streams that emanate from them. Slow- and high-speed stream interaction regions may deliver large amounts of energy into the Earth's magnetosphere-ionosphere system, cause geomagnetic storms, and shape interplanetary space.

Aims. By statistically investigating the long-term evolution of well-observed coronal holes we aim to reveal processes that drive the observed changes in the coronal hole parameters. By analyzing 16 long-living coronal holes observed by the Solar Dynamic Observatory, we focus on coronal, morphological, and underlying photospheric magnetic field characteristics, and investigate the evolution of the associated high-speed streams.

Methods. We use the Collection of Analysis Tools for Coronal Holes to extract and analyze coronal holes using 193 Å EUV observations taken by the Atmospheric Imaging Assembly as well as line-of-sight magnetograms observed by the Helioseismic and Magnetic Imager. We derive changes in the coronal hole properties and look for correlations with coronal hole evolution. Further, we analyze the properties of the high-speed stream signatures near 1AU from OMNI data by manually extracting the peak bulk velocity of the solar wind plasma.

Results. We find that the area evolution of coronal holes shows a general trend of growing to a maximum followed by a decay. We did not find any correlation between the area evolution and the evolution of the signed magnetic flux or signed magnetic flux density enclosed in the projected coronal hole area. From this we conclude that the magnetic flux within the extracted coronal hole boundaries is not the main cause for its area evolution. We derive coronal hole area change rates (growth and decay) of $(14.2 \pm 15.0) \times 10^8$ km² per day showing a reasonable anti-correlation ($ccPearson = -0.48$) to the solar activity, approximated by the sunspot number. The change rates of the signed mean magnetic flux density (27.3 ± 32.2 mG day⁻¹) and the signed magnetic flux (30.3 ± 31.5 10¹⁸ Mx day⁻¹) were also found to be dependent on solar activity ($ccPearson = 0.50$ and $ccPearson = 0.69$ respectively) rather than on the individual coronal hole evolutions. Further we find that the relation between coronal hole area and high-speed stream peak velocity is valid for each coronal hole over its evolution, but we see significant variations in the slopes of the regression lines. **May 29, 2013**

2.2. Coronal hole detection and extraction

CME–HSS Interaction and Characteristics Tracked from Sun to Earth

Stephan G. **Heinemann**, Manuela Temmer, Charles J. Farrugia, Karin Dissauer, Christina Kay, Thomas Wiegmann, Mateja Dumbović, Astrid M. Veronig, Tatiana Podladchikova, Stefan J. Hofmeister, Noé Lugaz, Fernando Carcaboso

Solar Physics September 2019, 294:121

[sci-hub.se/10.1007/s11207-019-1515-6](https://doi.org/10.1007/s11207-019-1515-6)

<https://arxiv.org/pdf/1908.10161.pdf>

In a thorough study, we investigate the origin of a remarkable plasma and magnetic field configuration observed in situ on **June 22, 2011**, near L1, which appears to be a magnetic ejecta (ME) and a shock signature engulfed by a solar wind high-speed stream (HSS). We identify the signatures as an Earth-directed coronal mass ejection (CME), associated with a C7.7 flare on **June 21, 2011**, and its interaction with a HSS, which emanates from a coronal hole (CH) close to the launch site of the CME. The results indicate that the major interaction between the CME and the HSS starts at a

height of $1.3 R_{\odot}$ up to $3 R_{\odot}$. Over that distance range, the CME undergoes a strong north-eastward deflection of at least 30° due to the open magnetic field configuration of the CH. We perform a comprehensive analysis for the CME–HSS event using multi-viewpoint data (from the Solar TERrestrial RELations Observatories, the Solar and Heliospheric Observatory and the Solar Dynamics Observatory), and combined modeling efforts (nonlinear force-free field modeling, Graduated Cylindrical Shell CME modeling, and the Forecasting a CME’s Altered Trajectory – ForeCAT model). We aim at better understanding its early evolution and interaction process as well as its interplanetary propagation and related in situ signatures, and finally the resulting impact on the Earth’s magnetosphere.

Impact of Switchbacks on Turbulent Cascade and Energy Transfer Rate in the Inner Heliosphere

Carlos S. **Hernández**¹, Luca Sorriso-Valvo^{2,3}, Riddhi Bandyopadhyay⁴, Alexandros Chasapis⁵, Christian L. Vásconez¹, Raffaele Marino⁶, and Oreste Pezzi³

2021 ApJL 922 L11

<https://iopscience.iop.org/article/10.3847/2041-8213/ac36d1/pdf>

<https://doi.org/10.3847/2041-8213/ac36d1>

Recent Parker Solar Probe (PSP) observations of inner heliospheric plasma have shown an abundant presence of Alfvénic polarity reversal of the magnetic field, known as "switchbacks." While their origin is still debated, their role in driving the solar wind turbulence has been suggested through analysis of the spectral properties of magnetic fluctuations. Here, we provide a complementary assessment of their role in the turbulent cascade. The validation of the third-order linear scaling of velocity and magnetic fluctuations in intervals characterized by a high occurrence of switchbacks suggests that, irrespective of their local or remote origin, these structures are actively embedded in the turbulent cascade, at least at the radial distances sampled by PSP during its first perihelion. The stronger positive energy transfer rate observed in periods with a predominance of switchbacks indicates that they act as a mechanism injecting additional energy in the turbulence cascade. **3-9 Nov 2018**

SoloHI observations of coronal mass ejections observed by multiple spacecraft*

P. **Hess**¹, R. C. Colaninno¹, A. Vourlidis², R. A. Howard² and G. Stenborg²

A&A 679, A149 (2023)

<https://www.aanda.org/articles/aa/pdf/2023/11/aa46907-23.pdf>

Context. The Solar Orbiter Heliospheric Imager (SoloHI) instrument of the Solar Orbiter mission is a next-generation heliospheric imager. New observations from SoloHI demonstrate the improved spatial and temporal resolution compared to previous observations of the heliosphere and corona. At perihelion, the field of view (FoV) of SoloHI covers the transition between the coronagraph (COR2) and heliospheric imager (HI1) Sun-Earth Connection Coronal and Heliospheric Investigation (SECCHI) suite. In this paper, we focus on an active solar period following the first Solar Orbiter science perihelion that resulted in a number of well-observed large coronal mass ejections (CMEs) in SoloHI data in **March and April 2022**. Specifically, we highlight a series of events produced by AR12795 between **28 March and 2 April** and show overlapping observations with SECCHI/COR2 and HI1 and LASCO/C3.

Aims. We compare the performance of the SoloHI instrument against similar observations from 1 au imagers. We describe CME observations, highlighting the unique structural features captured within the SoloHI FoV. These observations demonstrate that SoloHI will provide new insights into CME morphology and evolution from a unique vantage point.

Methods. To provide a direct and relevant comparison, images from all the telescopes we used in the paper are presented in FoVs common to each and with minimal processing applied. The J-maps we used to highlight outflowing features are also presented to show that the CME kinematics can be tracked through the SoloHI FoV, and also to report how the rest of the Heliophysics Systems Observatory (HSO) can be used to support the SoloHI data.

Results. The high-resolution SoloHI images of these eruptions, taken from ~ 0.3 au, reveal a number of detailed structural CME features, including internal cavities or cores of the CME flux rope(s). They also show the surrounding material and associated sheath region of the compressed upstream solar wind plasma. Many features that could not have been observed by other instruments are highlighted and discussed.

Conclusions. The SoloHI instrument is performing well and has already provided detailed observations of CMEs that can help us understand the details of the internal structure and magnetic field of CMEs. These new observations in combination with synoptic observations from 1 au offer new opportunities for CME propagation from the corona to the heliosphere.

HIGH-RESOLUTION IMAGING OF CORONAL MASS EJECTIONS FROM SOLOHI

Phil **Hess**¹, R.C. Colaninno¹, A. Vourlidis², R.A. Howard², G. Stenborg² and the Solo/Hi team)

Solar Orbiter nugget #8 2023

<https://www.cosmos.esa.int/web/solar-orbiter/solar-nuggets/high-resolution-imaging-from-solohi>

2 Apr 2022

WISPR Imaging of a Pristine CME

Phillip [Hess](#), [Alexis Rouillard](#), [Athanasios Kouloumvakos](#), [Paulett C. Liewer](#), [Jie Zhang](#), [Suman Dhakal](#), [Guillermo Stenborg](#), [Robin C. Colaninno](#), [Russell A. Howard](#)

ApJS 246 25 2020

<https://arxiv.org/pdf/1912.02255.pdf>

<https://doi.org/10.3847/1538-4365/ab4ff0>

The Wide-field Imager for Solar Probe (WISPR) on board the Parker Solar Probe (PSP) observed a CME on **2018 November 01**, the first day of the initial PSP encounter. The speed of the CME, approximately 200-300 km s⁻¹ in the WISPR field of view, is typical of slow, streamer blowout CMEs. This event was also observed by the LASCO coronagraphs. WISPR and LASCO view remarkably similar structures that enable useful cross-comparison between the two data sets as well as stereoscopic imaging of the CME. Analysis is extended to lower heights by linking the white-light observations to EUV data from AIA, which reveal a structure that erupts more than a full day earlier before the CME finally gathers enough velocity to propagate outward. This EUV feature appears as a brightness enhancement in cooler temperatures such as 171 Å, but as a cavity in nominal coronal temperatures such as 193 Å. By comparing this circular, dark feature in 193 Å to the dark, white-light cavity at the center of the eruption in WISPR and LASCO, it can be seen that this is one coherent structure that exists prior to the eruption in the low corona before entering the heliosphere and likely corresponds to the core of the magnetic flux rope. It is also believed that the relative weakness of the event contributed to the clarity of the flux rope in WISPR, as the CME did not experience impulsive forces or strong interaction with external structures that can lead to more complex structural evolution.

A Study of the Earth-Affecting CMEs of Solar Cycle 24

Phillip [Hess](#), [Jie Zhang](#)

[Solar Physics](#) June 2017, 292:80 [File](#)

Using in situ observations from the Advanced Composition Explorer (ACE), we have identified 70 Earth-affecting interplanetary coronal mass ejections (ICMEs) in Solar Cycle 24. Because of the unprecedented extent of heliospheric observations in Cycle 24 that has been achieved thanks to the Sun Earth Connection Coronal and Heliospheric Investigation (SECCHI) instruments onboard the Solar Terrestrial Relations Observatory (STEREO), we observe these events throughout the heliosphere from the Sun to the Earth, and we can relate these in situ signatures to remote sensing data. This allows us to completely track the event back to the source of the eruption in the low corona. We present a summary of the Earth-affecting CMEs in Solar Cycle 24 and a statistical study of the properties of these events including the source region. We examine the characteristics of CMEs that are more likely to be strongly geoeffective and examine the effect of the flare strength on in situ properties. We find that Earth-affecting CMEs in the first half of Cycle 24 are more likely to come from the northern hemisphere, but after April 2012, this reverses, and these events are more likely to originate in the southern hemisphere, following the observed magnetic asymmetry in the two hemispheres. We also find that as in past solar cycles, CMEs from the western hemisphere are more likely to reach Earth. We find that Cycle 24 lacks in events driving extreme geomagnetic storms compared to past solar cycles.

Table 1 The catalog of Earth-affecting ICME events from 2007 to 2015.

PREDICTING CME EJECTA AND SHEATH FRONT ARRIVAL AT L1 WITH A DATA-CONSTRAINED PHYSICAL MODEL

Phillip [Hess](#) and [Jie Zhang](#)

2015 ApJ 812 144

We present a method for predicting the arrival of a coronal mass ejection (CME) flux rope in situ, as well as the sheath of solar wind plasma accumulated ahead of the driver. For faster CMEs, the front of this sheath will be a shock. The method is based upon geometrical separate measurement of the CME ejecta and sheath. These measurements are used to constrain a drag-based model, improved by including both a height dependence and accurate de-projected velocities. We also constrain the geometry of the model to determine the error introduced as a function of the deviation of the CME nose from the Sun–Earth line. The CME standoff-distance in the heliosphere fit is also calculated, fit, and combined with the ejecta model to determine sheath arrival. Combining these factors allows us to create predictions for both fronts at the L1 point and compare them against observations. We demonstrate an ability to predict the sheath arrival with an average error of under 3.5 hr, with an rms error of about 1.58 hr. For the ejecta the error is less than 1.5 hr, with an rms

error within 0.76 hr. We also discuss the physical implications of our model for CME expansion and density evolution. We show the power of our method with ideal data and demonstrate the practical implications of having a permanent L5 observer with space weather forecasting capabilities, while also discussing the limitations of the method that will have to be addressed in order to create a real-time forecasting tool.

Stereoscopic Study of the Kinematic Evolution of a Coronal Mass Ejection and Its Driven Shock from the Sun to the Earth and the Prediction of Their Arrival Times

Phillip [Hess](#) and Jie Zhang

2014 ApJ 792 49

<http://iopscience.iop.org/article/10.1088/0004-637X/792/1/49/pdf>

We present a detailed study of the complete evolution of a coronal mass ejection (CME). We have tracked the evolution of both the ejecta and its shock, and further fit the evolution of the fronts to a simple but physics-based analytical model. This study focuses on the CME initiated on the Sun on 2012 July 12 and arriving at the Earth on **2012 July 14**. Shock and ejecta fronts were observed by white light images, as well as in situ by the Advanced Composition Explorer satellite. We find that the propagation of the two fronts is not completely dependent upon one another, but can each be modeled in the heliosphere with a drag model that assumes the dominant force of affecting CME evolution to be the aerodynamic drag force of the ambient solar wind. Results indicate that the CME ejecta front undergoes a more rapid deceleration than the shock front within 50 R_{\odot} and therefore the propagation of the two fronts is not completely coupled in the heliosphere. Using the graduated cylindrical shell model, as well as data from time-elongation stack plots and in situ signatures, we show that the drag model can accurately describe the behavior of each front, but is more effective with the ejecta. We also show that without the in situ data, based on measurements out to 80 R_{\odot} combined with the general values for drag model parameters, the arrival of both the shock and ejecta can be predicted within four hours of arrival.

On the Flux-Rope Topology of Ejecta Observed in the Period 1997 – 2006

M. A. [Hidalgo](#), T. Nieves-Chinchilla, J. J. Blanco

Solar Physics, May 2013, Volume 284, Issue 1, pp 151-166

In the following study our aim is to analyse the magnetic flux-rope topology of some events observed in the interplanetary medium related to ejecta. The magnetic field structures associated with interplanetary coronal mass ejections are globally classified in magnetic clouds and ejecta. One of the main questions regarding these phenomena concerns their flux-rope or non-flux-rope magnetic field line configuration. From the experimental measurements the only way to elucidate such a question is analysing the corresponding data by means of a flux-rope physical model. After selecting the ejecta events observed during the period 1997 – 2006, we have analysed them in light of an analytical model with that topology for the magnetic field components, initially developed for magnetic clouds, and with a non-force-free character; then, incorporating the expansion of the magnetic structure during their evolution in the interplanetary medium. Different parameters obtained from the fitting of the model are related to the orientation of the axis of the magnetic flux-rope structure and, additionally, the closest distance approach of the spacecraft to its axis. One of the main conclusions achieved concerns the fact that the axes of most of those structures are close to the Sun–Earth line, which implies that the passage of the spacecraft through the corresponding ejecta event is by its flank. In general, we show a rough procedure for the analysis and classification of ejecta in terms of their magnetic field topology. **Tables.**

A Global Magnetic Topology Model for Magnetic Clouds. III

M. A. [Hidalgo](#)

2014 ApJ 784 67

In two previous papers, we presented a global model for the analysis of magnetic clouds (MCs), where the three components of the magnetic field were fitted to the corresponding Geocentric Solar Ecliptic experimental data, obtaining reliable information, for example, about the orientation of these events in the interplanetary medium. That model, due to its non-force-free character, ($\nabla p \neq 0$), could be extended to determine the plasma behavior. In the present work, we develop that extension, now including the plasma behavior inside the cloud through the analysis of the plasma pressure, and define a fitting procedure where the pressure and the magnetic field components are fitted simultaneously. After deducing the magnetic field topology and the current density components of the model, we calculate the expression of the pressure tensor and, in particular, its trace. In light of the results, we conclude that incorporating the plasma behavior in the analysis of the MCs can give us a better scenario in which to understand the physical mechanisms involved in the evolution of such magnetic structures in the interplanetary medium.

A GLOBAL MAGNETIC TOPOLOGY MODEL FOR MAGNETIC CLOUDS. II.

M. A. [Hidalgo](#)

2013 ApJ 766 125

In the present work, we extensively used our analytical approach to the global magnetic field topology of magnetic clouds (MCs), introduced in a previous paper, in order to show its potential and to study its physical consistency. The model assumes toroidal topology with a non-uniform (variable maximum radius) cross-section along them. Moreover, it has a non-force-free character and also includes the expansion of its cross-section. As is shown, the model allows us, first, to analyze MC magnetic structures—determining their physical parameters—with a variety of magnetic field shapes, and second, to reconstruct their relative orientation in the interplanetary medium from the observations obtained by several spacecraft. Therefore, multipoint spacecraft observations give the opportunity to infer the structure of this large-scale magnetic flux rope structure in the solar wind. For these tasks, we use data from Helios (A and B), STEREO (A and B), and Advanced Composition Explorer. We show that the proposed analytical model can explain quite well the topology of several MCs in the interplanetary medium and is a good starting point for understanding the physical mechanisms under these phenomena.

A GLOBAL MAGNETIC TOPOLOGY MODEL FOR MAGNETIC CLOUDS. I.

M. A. [Hidalgo](#)¹ and T. Nieves-Chinchilla

2012 ApJ 748 109

We present an analytical approach to the global magnetic field topology of magnetic clouds (MCs) that considers them like close magnetic structures with torus geometry and with a non-uniform (variable maximum radius) cross section along them. Following our previous approach to the problem of MCs (Hidalgo 2003, 2011), we establish an intrinsic coordinate system for that topology, and then we analytically solve the Maxwell equations in terms of it. The purpose of the present work is to present this model, which will lead us to understand in a more realistic way the physical mechanisms inside MCs. The model has a non-force-free character and also takes into account the time evolution of the cross sections of the MCs in their movement through the interplanetary medium. In this first paper, we obtain the expressions for the components of the magnetic field and the plasma current density imposing a large mean radius of the torus, and imposing a circular cross section with a variable maximum radius. Eventually, we fit the model to data related to four well-known MCs measurements at 1 AU, (three of them with circular cross sections and without expansion, as it is deduced from the experimental data). We compare the results of this toroidal model with those obtained with our previous cylindrical circular cross section model, also with a non-force-free character.

On the relationship between magnetic clouds and the great geomagnetic storms associated with the period 1995–2006

M.A. [Hidalgo](#) , J.J. Blancoa, F.J. Alvarezb and T. Nieves-Chinchilla

Journal of Atmospheric and Solar-Terrestrial Physics, Volume 73, Issues 11-12, **2011**, Pages 1372-1379

The fact that magnetic clouds are one of the main sources causing geomagnetic storms is a well-established fact. One of the issues is to establish those features of magnetic clouds determinant in the intensity of the Dst corresponding to geomagnetic storms. We examine measurements of geoeffective magnetic clouds during the period 1995–2006 providing geomagnetic storms with Dst indexes lower than -100 nT. These involve 46 geomagnetic storm events. After establishing the different characteristics of the magnetic clouds (plasma velocity, maximum magnetic intensity, etc.) we show some results about the correlations found among them and the storms intensity, finding that maximum magnetic field magnitude is a determinant factor to establish the importance of magnetic clouds in generating geomagnetic storms, having a correlation as good as the electric convective field.

Structured Slow Solar Wind Variability: Streamer-blob Flux Ropes and Torsional Alfvén Waves

A. K. [Higginson](#)¹ and B. J. Lynch

2018 ApJ 859 6

The slow solar wind exhibits strong variability on timescales from minutes to days, likely related to magnetic reconnection processes in the extended solar corona. Higginson et al. presented a numerical magnetohydrodynamic simulation that showed interchange magnetic reconnection is ubiquitous and most likely responsible for releasing much of the slow solar wind, in particular along topological features known as the Separatrix-Web (S-Web). Here, we continue our analysis, focusing on two specific aspects of structured slow solar wind variability. The first type is present in the slow solar wind found near the heliospheric current sheet (HCS), and the second we predict should be present

everywhere S-Web slow solar wind is observed. For the first type, we examine the evolution of three-dimensional magnetic flux ropes formed at the top of the helmet streamer belt by reconnection in the HCS. For the second, we examine the simulated remote and in situ signatures of the large-scale torsional Alfvén wave (TAW), which propagates along an S-Web arc to high latitudes. We describe the similarities and differences between the reconnection-generated flux ropes in the HCS, which resemble the well-known "streamer blob" observations, and the similarly structured TAW. We discuss the implications of our results for the complexity of the HCS and surrounding plasma sheet and the potential for particle acceleration, as well as the interchange reconnection scenarios that may generate TAWs in the solar corona. We discuss predictions from our simulation results for the dynamic slow solar wind in the extended corona and inner heliosphere.

Formation of Heliospheric Arcs of Slow Solar Wind

A. K. [Higginson](#)¹, S. K. Antiochos², C. R. DeVore², P. F. Wyper³, and T. H. Zurbuchen
2017 ApJL 840 L10

A major challenge in solar and heliospheric physics is understanding the origin and nature of the so-called slow solar wind. The Sun's atmosphere is divided into magnetically open regions, known as coronal holes, where the plasma streams out freely and fills the solar system, and closed regions, where the plasma is confined to coronal loops. The boundary between these regions extends outward as the heliospheric current sheet (HCS). Measurements of plasma composition strongly imply that much of the slow wind consists of plasma from the closed corona that escapes onto open field lines, presumably by field-line opening or by interchange reconnection. Both of these processes are expected to release closed-field plasma into the solar wind within and immediately adjacent to the HCS. Mysteriously, however, slow wind with closed-field plasma composition is often observed in situ far from the HCS. We use high-resolution, three-dimensional, magnetohydrodynamic simulations to calculate the dynamics of a coronal hole with a geometry that includes a narrow corridor flanked by closed field and is driven by supergranule-like flows at the coronal-hole boundary. These dynamics produce giant arcs of closed-field plasma that originate at the open-closed boundary in the corona, but extend far from the HCS and span tens of degrees in latitude and longitude at Earth. We conclude that such structures can account for the long-puzzling slow-wind observations.

Influence of Solar Disturbances on Galactic Cosmic Rays in the Solar Wind, Heliosheath, and Local Interstellar Medium: Advanced Composition Explorer, New Horizons, and Voyager Observations

M. E. [Hill](#)¹, R. C. Allen¹, P. Kollmann¹, L. E. Brown¹, R. B. Decker¹, R. L. McNutt Jr.¹, S. M. Krimigis^{1,2}, G. B. Andrews¹, F. Bagenal³, G. Clark¹, +
2020 ApJ 905 69

<https://iopscience.iop.org/article/10.3847/1538-4357/abb408/pdf>

We augment the heliospheric network of galactic cosmic ray (GCR) monitors using 2012–2017 penetrating radiation measurements from the New Horizons (NH) Pluto Energetic Particle Spectrometer Science Investigation (PEPSSI), obtaining intensities of $\gtrsim 75$ MeV particles. The new, predominantly GCR observations provide critical links between the Sun and Voyager 2 and Voyager 1 (V2 and V1), in the heliosheath and local interstellar medium (LISM), respectively. We provide NH, Advanced Composition Explorer (ACE), V2, and V1 GCR observations, using them to track solar cycle variations and short-term Forbush decreases from the Sun to the LISM, and to examine the interaction that results in the surprising, previously reported V1 LISM anisotropy episodes. To investigate these episodes and the hitherto unexplained lagging of associated in situ shock features at V1, propagating disturbances seen at ACE, NH, and V2 were compared to V1. We conclude that the region where LISM magnetic field lines drape around the heliopause is likely critical for communicating solar disturbance signals upstream of the heliosheath to V1. We propose that the anisotropy-causing physical process that suppresses intensities at $\sim 90^\circ$ pitch angles relies on GCRs escaping from a single compression in the draping region, not on GCRs trapped between two compressions. We also show that NH suprathermal and energetic particle data from PEPSSI are consistent with the interpretation that traveling shocks and corotating interaction region (CIR) remnants can be distinguished by the existence or lack of Forbush decreases, respectively, because turbulent magnetic fields at local shocks inhibit GCR transport while older CIR structures reaching the outer heliosphere do not.

Type II solar radio bursts: Modeling and extraction of shock parameters

[Hillan](#), D. S.; Cairns, I. H.; Robinson, P. A.

J. Geophys. Res., Vol. 117, No. A3, A03104, **2012**

<http://dx.doi.org/10.1029/2011JA016754>

This first paper in a two part series summarizes the current theory and the data-driven solar wind model for simulating dynamic spectra of type II radio bursts. It also introduces performance metrics and techniques for extraction of model shock parameters from these dynamic spectra. We use an iterative downhill simplex method which compares two dynamic spectra and quantitatively assesses and improves the agreement using two figures of merit: the first is based on the correlation function and the second is based on a normalized differences over the data set. By maximizing the agreement we are able to extract the input model shock parameters to within 30% or better when using model solar winds of increasing complexity. The effects on the spectra predicted and on the figures of merit from changing the model shock parameters and solar wind model are also investigated. The iterative downhill extraction method is then applied to the type II dynamic spectrum predicted using a realistic model solar wind and a shock model estimated for an observed type II event. The shock parameters are recovered to within 10% of the correct solution.

Drag-based CME modeling with heliospheric images incorporating frontal deformation: ELEvoHI 2.0

J. [Hinterreiter](#), [T. Amerstorfer](#), [M. Temmer](#), [M. A. Reiss](#), [A. J. Weiss](#), [C. Möstl](#), [L. A. Barnard](#), [J. Pomoell](#), [M. Bauer](#), [U. V. Amerstorfer](#)

Space Weather **Volume19, Issue10** e2021SW002836 2021

<https://arxiv.org/pdf/2108.08075.pdf>

<https://agupubs.onlinelibrary.wiley.com/doi/epdf/10.1029/2021SW002836>

<https://doi.org/10.1029/2021SW002836>

The evolution and propagation of coronal mass ejections (CMEs) in interplanetary space is still not well understood. As a consequence, accurate arrival time and arrival speed forecasts are an unsolved problem in space weather research. In this study, we present the ELLipse Evolution model based on HI observations (ELEvoHI) and introduce a deformable front to this model. ELEvoHI relies on heliospheric imagers (HI) observations to obtain the kinematics of a CME. With the newly developed deformable front, the model is able to react to the ambient solar wind conditions during the entire propagation and along the whole front of the CME. To get an estimate of the ambient solar wind conditions, we make use of three different models: Heliospheric Upwind eXtrapolation model (HUX), Heliospheric Upwind eXtrapolation with time dependence model (HUXt), and EUropean Heliospheric FORecasting Information Asset (EUHFORIA). We test the deformable front on a CME first observed in STEREO-A/HI on **February 3, 2010** 14:49 UT. For this case study, the deformable front provides better estimates of the arrival time and arrival speed than the original version of ELEvoHI using an elliptical front. The new implementation enables us to study the parameters influencing the propagation of the CME not only for the apex, but for the entire front. The evolution of the CME front, especially at the flanks, is highly dependent on the ambient solar wind model used. An additional advantage of the new implementation is given by the possibility to provide estimates of the CME mass. **February 6 – 9, 2010**

Why are ELEvoHI CME arrival predictions different if based on STEREO-A or STEREO-B heliospheric imager observations?

Jürgen [Hinterreiter](#) , [Tanja Amerstorfer](#) , [Martin A. Reiss](#) , [Christian Möstl](#) , [Manuela Temmer](#) , [Maike Bauer](#) , [Ute V. Amerstorfer](#) , [Rachel L. Bailey](#)

Space Weather e2020SW002674 **Volume19, Issue3** 2021

<https://agupubs.onlinelibrary.wiley.com/doi/epdf/10.1029/2020SW002674>

<https://doi.org/10.1029/2020SW002674>

<https://arxiv.org/pdf/2102.07478.pdf>

Accurate forecasting of the arrival time and arrival speed of coronal mass ejections (CMEs) is a unsolved problem in space weather research. In this study, a comparison of the predicted arrival times and speeds for each CME based, independently, on the inputs from the two STEREO vantage points is carried out. We perform hindcasts using ELLipse Evolution model based on Heliospheric Imager observations (ELEvoHI) ensemble modelling. An estimate of the ambient solar wind conditions is obtained by the Wang-Sheeley-Arge/Heliospheric Upwind eXtrapolation (WSA/HUX) model combination that serves as input to ELEvoHI. We carefully select 12 CMEs between February 2010 and July 2012 that show clear signatures in both STEREO-A and STEREO-B HI time-elongation maps, that propagate close to the ecliptic plane, and that have corresponding in situ signatures at Earth. We find a mean arrival time difference of 6.5 hrs between predictions from the two different viewpoints, which can reach up to 9.5 hrs for individual CMEs, while the mean arrival speed difference is 63 km s⁻¹. An ambient solar wind with a large speed variance leads to larger differences in the STEREO-A and STEREO-B CME arrival time predictions (cc = 0.92). Additionally, we compare the predicted arrivals, from both spacecraft, to the actual in situ arrivals at Earth and find a mean absolute error of 7.5 ± 9.5 hrs for the arrival time and 87 ± 111 km s⁻¹ for the arrival speed. There is no tendency for one spacecraft to provide more accurate arrival predictions than the other. **2010 May 23-28**

Table 1: List of selected CMEs. (2010-2012)

Testing the background solar wind modelled by EUHFORIA

J. [Hinterreiter](#) (1,2), [J. Magdalenic](#) (3), [M. Temmer](#) (2), [C. Verbeke](#) (4), [I.C. Jeberaj](#) (3,4), [E. Samara](#) (3,4), [E. Asvestari](#) (2,5), [S. Poedts](#) (4), [J. Pomoell](#) (5), [E. Kilpua](#) (5), [L. Rodriguez](#) (3), [C. Scolini](#) (3,4), [A. Isavnin](#) (4)

Solar Phys. 294:170 2019

<https://arxiv.org/pdf/1907.07461.pdf>

<https://link.springer.com/content/pdf/10.1007%2Fs11207-019-1558-8.pdf>

In order to address the growing need for the more accurate space weather predictions, a new model named EUHFORIA (EUropean Heliospheric FORecasting Information Asset) was recently developed (Pomoell and Poedts, 2018). We present the first results of the solar wind modeling with EUHFORIA and identify possible limitation of its present set up. Using the basic EUHFORIA 1.0.4. model setup with the default input parameters, we modeled background solar wind (no coronal mass ejections) and compared obtained results with ACE, in situ observations. For the need of statistical study we developed a technique of combining daily EUHFORIA runs into continuous time series. Using the combined time series we performed statistical study of the solar wind for years 2008 (low solar activity) and 2012 (high solar activity) with the focus on the in situ speed and density. We find for the low activity phase a better match between model results and observations compared to the considered high activity time interval. The quality of the modeled solar wind parameters is found to be very variable. Therefore, to better understand obtained results we also qualitatively inspected characteristics of coronal holes, sources of the studied fast streams. We discuss how different characteristics of the coronal holes and input parameters to EUHFORIA influence the modeled fast solar wind, and suggest the possibilities for the improvements of the model. 2012 May 7

On the Origin of an F-corona decrease revealed by the Parker Solar Probe

Thiem [Hoang](#), [Alex Lazarian](#), [Hyeseung Lee](#), [Kyungsuk Cho](#), [Pin-Gao Gu](#), [Chi-Hang Ng](#)

ApJ 2020

<https://arxiv.org/pdf/2004.06265.pdf>

The first-year results from the Parker Solar Probe (PSP) reveal a gradual decrease of F-coronal dust from distances of $D=0.166-0.336$ AU (or the inner elongations of $\sim 9.22-18.69 R_{\odot}$) to the Sun, which cannot be explained by the dust sublimation scenario that predicts a dust-free-zone $\leq 4-5 R_{\odot}$. In this paper, we attempt to explain this puzzle using our newly introduced mechanism of dust destruction so-called Radiative Torque Disruption (RATD) mechanism. We demonstrate that RATD rapidly breaks large grains into nanoparticles so that they can be efficiently destroyed by nonthermal sputtering induced by bombardment of energetic protons from slow solar winds. This joint effect extends the dust-free-zone established by thermal sublimation to $R_{dfz} \sim 8 R_{\odot}$, which is called a new dust-free-zone. Beyond this new dust-free-zone, we find that the dust mass decreases gradually from $R \sim 42 R_{\odot}$ toward the Sun due to partial removal of nanodust by nonthermal sputtering. This feature can successfully reproduce the gradual decrease of the F-corona between $19-9 R_{\odot}$ observed by the PSP. Finally, the RATD mechanism can efficiently produce nanoparticles usually observed in the inner solar system.

Application of the Electromotive Force as a Shock Front Indicator in the Inner Heliosphere

Bernhard [Hofer](#)^{1,2} and Philippe-A. Bourdin

2019 ApJ 878 30

[sci-hub.se/10.3847/1538-4357/ab1e48](https://arxiv.org/abs/1908.04488)

The electromotive force (EMF) describes how the evolution and generation of a large-scale magnetic field is influenced by small-scale turbulence. Recent studies of in situ measurements have shown a significant peak in the EMF while a coronal mass ejection (CME) shock front passes by the spacecraft. The goal of this study is to use the EMF as an indicator for the arrival of CME shock fronts. With Helios spacecraft measurements we carry out a statistical study on the EMF during CMEs in the inner heliosphere. We develop an automated shock front detection algorithm using the EMF as the main detection criterion and compare the results to an existing CME database. The properties of the EMF during the recorded events are discussed as a function of the heliocentric distance. Our algorithm reproduces most of the events from Kilpua et al. and finds many additional CME-like events, which proves that the EMF is a good shock front indicator. The largest peaks in the EMF are found from 0 to 50 minutes after the initial shock. We find a power law of -1.54 and -2.18 for two different formulations of the EMF with the heliocentric distance.

How the area of solar coronal holes affects the properties of high-speed solar wind streams near Earth: An analytical model

Stefan J. **Hofmeister**^{1,2,3}, Eleanna Asvestari⁴, Jingnan Guo^{5,6}, Verena Heidrich-Meisner⁵, Stephan G. Heinemann⁷, Jasmina Magdalenic^{8,9}, Stefaan Poedts^{8,10}, Evangelia Samara^{8,9}, Manuela Temmer¹, Susanne Vennerstrom¹¹, Astrid Veronig^{1,12}, Bojan Vršnak¹³ and Robert Wimmer-Schweingruber⁵

A&A 659, A190 (2022)

<https://www.aanda.org/articles/aa/pdf/2022/03/aa41919-21.pdf>

<https://doi.org/10.1051/0004-6361/202141919>

Since the 1970s it has been empirically known that the area of solar coronal holes affects the properties of high-speed solar wind streams (HSSs) at Earth. We derive a simple analytical model for the propagation of HSSs from the Sun to Earth and thereby show how the area of coronal holes and the size of their boundary regions affect the HSS velocity, temperature, and density near Earth. We assume that velocity, temperature, and density profiles form across the HSS cross section close to the Sun and that these spatial profiles translate into corresponding temporal profiles in a given radial direction due to the solar rotation. These temporal distributions drive the stream interface to the preceding slow solar wind plasma and disperse with distance from the Sun. The HSS properties at 1 AU are then given by all HSS plasma parcels launched from the Sun that did not run into the stream interface at Earth distance. We show that the velocity plateau region of HSSs as seen at 1 AU, if apparent, originates from the center region of the HSS close to the Sun, whereas the velocity tail at 1 AU originates from the trailing boundary region. Small HSSs can be described to entirely consist of boundary region plasma, which intrinsically results in smaller peak velocities. The peak velocity of HSSs at Earth further depends on the longitudinal width of the HSS close to the Sun. The shorter the longitudinal width of an HSS close to the Sun, the more of its “fastest” HSS plasma parcels from the HSS core and trailing boundary region have impinged upon the stream interface with the preceding slow solar wind, and the smaller is the peak velocity of the HSS at Earth. As the longitudinal width is statistically correlated to the area of coronal holes, this also explains the well-known empirical relationship between coronal hole areas and HSS peak velocities. Further, the temperature and density of HSS plasma parcels at Earth depend on their radial expansion from the Sun to Earth. The radial expansion is determined by the velocity gradient across the HSS boundary region close to the Sun and gives the velocity-temperature and density-temperature relationships at Earth their specific shape. When considering a large number of HSSs, the assumed correlation between the HSS velocities and temperatures close to the Sun degrades only slightly up to 1 AU, but the correlation between the velocities and densities is strongly disrupted up to 1 AU due to the radial expansion. Finally, we show how the number of particles of the piled-up slow solar wind in the stream interaction region depends on the velocities and densities of the HSS and preceding slow solar wind plasma.

On the Dependency between the Peak Velocity of High-speed Solar Wind Streams near Earth and the Area of Their Solar Source Coronal Holes

Stefan J. **Hofmeister**¹, Astrid M. Veronig^{1,2}, Stefaan Poedts^{3,4}, Evangelia Samara^{3,5}, and Jasmina Magdalenic⁵

2020 ApJL 897 L17

<https://sci-hub.tw/https://iopscience.iop.org/article/10.3847/2041-8213/ab9d19>

<https://arxiv.org/pdf/2007.02625>

The relationship between the peak velocities of high-speed solar wind streams near Earth and the areas of their solar source regions, i.e., coronal holes, has been known since the 1970s, but it is still physically not well understood. We perform 3D magnetohydrodynamic (MHD) simulations using the European Heliospheric Forecasting Information Asset (EUHFORIA) code to show that this empirical relationship forms during the propagation phase of high-speed streams from the Sun to Earth. For this purpose, we neglect the acceleration phase of high-speed streams, and project the areas of coronal holes to a sphere at 0.1 au. We then vary only the areas and latitudes of the coronal holes. The velocity, temperature, and density in the cross section of the corresponding high-speed streams at 0.1 au are set to constant, homogeneous values. Finally, we propagate the associated high-speed streams through the inner heliosphere using the EUHFORIA code. The simulated high-speed stream peak velocities at Earth reveal a linear dependence on the area of their source coronal holes. The slopes of the relationship decrease with increasing latitudes of the coronal holes, and the peak velocities saturate at a value of about 730 km s⁻¹, similar to the observations. These findings imply that the empirical relationship between the coronal hole areas and high-speed stream peak velocities does not describe the acceleration phase of high-speed streams, but is a result of the high-speed stream propagation from the Sun to Earth.

The Dependence of the Peak Velocity of High-Speed Solar Wind Streams as Measured in the Ecliptic by ACE and the STEREO satellites on the Area and Co-latitude of Their Solar Source Coronal Holes

Stefan J. [Hofmeister](#), Astrid Veronig, Manuela Temmer, Susanne Vennerstrom, Bernd Heber and Bojan Vršnak

JGR [Volume123, Issue3](#) March 2018 Pages 1738-1753

We study the properties of **115 coronal holes** in the time range from August 2010 to March 2017, the peak velocities of the corresponding high-speed streams as measured in the ecliptic at 1 AU, and the corresponding changes of the Kp index as marker of their geoeffectiveness. We find that the peak velocities of high-speed streams depend strongly on both the areas and the co-latitudes of their solar source coronal holes with regard to the heliospheric latitude of the satellites. Therefore, the co-latitude of their source coronal hole is an important parameter for the prediction of the high-speed stream properties near the Earth. We derive the largest solar wind peak velocities normalized to the coronal hole areas for coronal holes located near the solar equator and that they linearly decrease with increasing latitudes of the coronal holes. For coronal holes located at latitudes $\gtrsim 60^\circ$, they turn statistically to zero, indicating that the associated high-speed streams have a high chance to miss the Earth. Similarly, the Kp index per coronal hole area is highest for the coronal holes located near the solar equator and strongly decreases with increasing latitudes of the coronal holes. We interpret these results as an effect of the three-dimensional propagation of high-speed streams in the heliosphere; that is, high-speed streams arising from coronal holes near the solar equator propagate in direction toward and directly hit the Earth, whereas solar wind streams arising from coronal holes at higher solar latitudes only graze or even miss the Earth.

Toward more reliable long-term indices of geomagnetic activity: Correcting a new inhomogeneity problem in early geomagnetic data

L. [Holappa](#) and K. Mursula

JGR Volume 120, Issue 10 October 2015 Pages 8288–8297

For the time before the space era, our knowledge of the centennial evolution of solar wind (SW) and interplanetary magnetic field (IMF) is based on proxies derived from geomagnetic indices. The reliability of these proxies is dependent on the homogeneity of magnetic field data. In this paper, we study the interhourly (IHV) and interdiurnal (IDV1d) variability indices calculated from the data of two British observatories, Eskdalemuir and Lerwick, and compare them to the corresponding indices of the German Niemeck observatory. We find an excess of about $14 \pm 4\%$ ($5.8 \pm 2\%$) and $27 \pm 10\%$ ($15 \pm 6\%$) in the IHV (IDV1d) in the indices of Eskdalemuir and Lerwick in 1935–1969. The timing of this excess accurately coincides with instrument changes made in these observatories, strongly supporting the interpretation that the excess is indeed caused by instrument related inhomogeneities in the data of Eskdalemuir and Lerwick. We show that the detected excess notably modifies the long-term trend of geomagnetic activity and the centennial evolution of IMF strength and solar wind speed estimated using these indices. We note that the detected inhomogeneity problem may not be limited to the data of the two studied observatories but may be quite common to long series of geomagnetic measurements. These results question the reliability of the present measures of the centennial change in solar wind speed and IMF.

A new method to estimate annual solar wind parameters and contributions of different solar wind structures to geomagnetic activity†

L. [Holappa*](#), K. Mursula and T. Asikainen

JGR, Volume 119, Issue 12, pages 9407–9418, December 2014

<http://onlinelibrary.wiley.com/doi/10.1002/2014JA020599/pdf>

<http://arxiv.org/pdf/1501.03716v1.pdf>

In this paper, we study two sets of local geomagnetic indices from 26 stations using the principal component (PC) and the independent component (IC) analysis methods. We demonstrate that the annually averaged indices can be accurately represented as linear combinations of two first components with weights systematically depending on latitude. We show that the annual contributions of coronal mass ejections (CMEs) and high speed streams (HSSs) to geomagnetic activity are highly correlated with the first and second IC. The first and second ICs are also found to be very highly correlated with the strength of the interplanetary magnetic field (IMF) and the solar wind speed, respectively, because solar wind

speed is the most important parameter driving geomagnetic activity during HSSs while IMF strength dominates during CMEs. These results help in better understanding the long-term driving of geomagnetic activity and in gaining information about the long-term evolution of solar wind parameters and the different solar wind structures.

Signatures of coronal hole substructure in the solar wind: combined Solar Orbiter remote sensing and in situ measurements

T. S. [Horbury](#), [R. Laker](#), [L. Rodriguez](#), [K. Steinvall](#), [M. Maksimovic](#), [S. Livi](#), [D. Berghmans](#), [F. Auchere](#), [A. N. Zhukov](#), [Yu. V. Khotyaintsev](#), [L. Woodham](#), [L. Matteini](#), [J. Stawarz](#), [T. Woolley](#), [S. D. Bale](#), [A. Rouillard](#), [H. O'Brien](#), [V. Evans](#), [V. Angelini](#), [C. Owen](#), [S. K. Solanki](#), [B. Nicula](#), [D. Muller](#), [I. Zouganelis](#)
A&A 2021

<https://arxiv.org/pdf/2104.14960.pdf>

Context. The Sun's complex corona is the source of the solar wind and interplanetary magnetic field. While the large scale morphology is well understood, the impact of variations in coronal properties on the scale of a few degrees on properties of the interplanetary medium is not known. Solar Orbiter, carrying both remote sensing and in situ instruments into the inner solar system, is intended to make these connections better than ever before. Aims. We combine remote sensing and in situ measurements from Solar Orbiter's first perihelion at 0.5 AU to study the fine scale structure of the solar wind from the equatorward edge of a polar coronal hole with the aim of identifying characteristics of the corona which can explain the in situ variations. Methods. We use in situ measurements of the magnetic field, density and solar wind speed to identify structures on scales of hours at the spacecraft. Using Potential Field Source Surface mapping we estimate the source locations of the measured solar wind as a function of time and use EUVI images to characterise these solar sources. Results. We identify small scale stream interactions in the solar wind with compressed magnetic field and density along with speed variations which are associated with corrugations in the edge of the coronal hole on scales of several degrees, demonstrating that fine scale coronal structure can directly influence solar wind properties and drive variations within individual streams. Conclusions. This early analysis already demonstrates the power of Solar Orbiter's combined remote sensing and in situ payload and shows that with future, closer perihelia it will be possible dramatically to improve our knowledge of the coronal sources of fine scale solar wind structure, which is important both for understanding the phenomena driving the solar wind and predicting its impacts at the Earth and elsewhere. **19-24 June 2020**

Short, large-amplitude speed enhancements in the near-Sun fast solar wind

T S [Horbury](#) [L Matteini](#) [D Stansby](#)

MNRoyal Astronomical Society, Volume 478, Issue 2, 1 August 2018, Pages 1980–1986

<https://doi.org/10.1093/mnras/sty953>

sci-hub.tw/10.1093/mnras/sty953

We report the presence of intermittent, short discrete enhancements in plasma speed in the near-Sun high-speed solar wind. Lasting tens of seconds to minutes in spacecraft measurements at 0.3 au, speeds inside these enhancements can reach 1000 km s⁻¹, corresponding to a kinetic energy up to twice that of the bulk high-speed solar wind. These events, which occur around 5 per cent of the time, are Alfvénic in nature with large magnetic field deflections and are the same temperature as the surrounding plasma, in contrast to the bulk fast wind which has a well-established positive speed–temperature correlation. The origin of these speed enhancements is unclear but they may be signatures of discrete jets associated with transient events in the chromosphere or corona. Such large short velocity changes represent a measurement and analysis challenge for the upcoming Parker Solar Probe and Solar Orbiter missions.

UKSP Nuggets #94 September 2018 www.uksolphys.org/?p=14829

Analysis of Voyager 1 and Voyager 2 in situ CME observations

Skralan [Hosteaux](#), [Luciano Rodriguez](#), [Stefaan Poedts](#)

Advances in Space Research 2022

<https://arxiv.org/pdf/2207.00471.pdf>

This paper studies ICMEs detected by both Voyager spacecraft during propagation from 1 to 10 AU, with observations from 1977 to 1980. ICMEs are detected by using several signatures in the in-situ data, the primary one being the low measured to expected proton temperature ratio. We found 21 events common to both spacecraft and study their internal structure in terms of plasma and magnetic field properties. We find that ICMEs are expanding as they propagate outwards, with decreasing density and magnetic field intensities, in agreement with previous studies. We first carry out a statistical study and then a detailed analysis of each case. Furthermore, we analyse one case in which a shock can be clearly detected by both spacecraft. The methods described here can be interesting for other studies combining data sets from heliospheric missions. Furthermore, they highlight the importance of exploiting useful data from past missions.

Effect of the solar wind density on the evolution of normal and inverse coronal mass ejections

S. Hosteaux, E. Chané, S. Poedts

A&A 632, A89 2019

<https://arxiv.org/pdf/1910.04680.pdf>

We investigate the evolution of both normal and inverse CMEs ejected at different initial velocities, and observe the effect of the background wind density and their magnetic polarity on their evolution up to 1 AU. We performed 2.5D simulations by solving the magnetohydrodynamic equations on a radially stretched grid, employing a block-based adaptive mesh refinement scheme based on a density threshold to achieve high resolution following the evolution of the magnetic clouds and the leading bow shocks. All the simulations discussed in the present paper were performed using the same initial grid and numerical methods. The polarity of the internal magnetic field of the CME has a substantial effect on its propagation velocity and on its deformation and erosion during its evolution towards Earth. We quantified the effects of the polarity of the internal magnetic field of the CMEs and of the density of the background solar wind on the arrival times of the shock front and the magnetic cloud. We determined the positions and propagation velocities of the magnetic clouds and thus also the stand-off distance of the leading shock fronts (i.e. the thickness of the magnetic sheath region) and the deformation and erosion of the magnetic clouds during their evolution from the Sun to the Earth. Inverse CMEs were found to be faster than normal CMEs ejected in the same initial conditions, but with smaller stand-off distances. They also have a higher magnetic cloud length, opening angle, and mass. Synthetic satellite time series showed that the shock magnitude is not affected by the polarity of the CME. However, the density peak of the magnetic cloud is dependent on the polarity and, in case of inverse CMEs, also on the background wind density. The magnitude of the z-component of the magnetic field was not influenced by either the polarity or the wind density.

Connecting Solar Wind Velocity Spikes Measured by Solar Orbiter and Coronal Brightenings Observed by SDO

Chuanpeng Hou^{1,2}, Alexis P. Rouillard², Jiansen He¹, Bahaeddine Gannouni², Victor Réville², Philippe Louarn², Andrey Fedorov², Lubomír Přech³, Christopher J. Owen⁴, Daniel Verscharen⁴ Show full author list
2024 ApJL 968 L28

<https://iopscience.iop.org/article/10.3847/2041-8213/ad4eda/pdf>

The Parker Solar Probe's discovery that magnetic switchbacks and velocity spikes in the young solar wind are abundant has prompted intensive research into their origin(s) and formation mechanism(s) in the solar atmosphere. Recent studies, based on in situ measurements and numerical simulations, argue that velocity spikes are produced through interchange magnetic reconnection. Our work studies the relationship between interplanetary velocity spikes and coronal brightenings induced by changes in the photospheric magnetic field. Our analysis focuses on the characteristic periodicities of velocity spikes detected by the Proton Alpha Sensor on the Solar Orbiter during its fifth perihelion pass. Throughout the time period analyzed here, we estimate their origin along the boundary of a coronal hole. Around the boundary region, we identify periodic variations in coronal brightening activity observed by the Atmospheric Imaging Assembly onboard the Solar Dynamics Observatory. The spectral characteristics of the time series of in situ velocity spikes, remote coronal brightenings, and remote photospheric magnetic flux exhibit correspondence in their periodicities. Therefore, we suggest that the localized small-scale magnetic flux within coronal holes fuels a magnetic reconnection process that can be observed as slight brightness augmentations and outward fluctuations or jets. These dynamic elements may act as mediators, bonding magnetic reconnection with the genesis of velocity spikes and magnetic switchbacks. 2022-10-22-23

Nature, Generation, and Dissipation of Alfvénic Kinks/Switchbacks Observed by Parker Solar Probe and WIND

Chuanpeng Hou¹, Xingyu Zhu¹, Rui Zhuo¹, Jiansen He^{3,1}, Daniel Verscharen², and Die Duan¹
2023 ApJ 950 157

<https://iopscience.iop.org/article/10.3847/1538-4357/accf94/pdf>

The discovery of very prominent magnetic kinks/switchbacks in the solar wind within 0.3 au has become a scientific highlight of the Parker Solar Probe (PSP) mission. This discovery points at the promising impact of small-scale solar activity on the inner heliosphere. To address the nature, generation, and dissipation of these kinks, we perform a statistical analysis of the plasma and boundary properties of the kinks using PSP multi-encounter observations and WIND measurements at 1 au. The kinks show strong Alfvénicity and velocity fluctuations of the order of the local Alfvén speed. These findings suggest that the nature of the kinks is consistent with large-amplitude Alfvén pulses, and the steepening of these Alfvén pulses is likely the formation mechanism of these kinks. Based on the angle between the normal direction of the kinks' boundaries and the background magnetic field vector, PSP kinks and WIND kinks can be

divided into two groups: quasi-parallel and quasi-perpendicular kinks. We speculate that quasi-parallel kinks form through the coupling of Alfvén and fast waves as launched from coronal interchange magnetic reconnection. In contrast, quasi-perpendicular kinks may come from the steepening of Alfvén waves launched from both coronal interchange magnetic reconnection and from the more inhomogeneous lower solar atmosphere. We find that the kink velocity perturbation gradually decreases during outward propagation and is much lower than expected from WKB theory, suggesting a progressive dissipation of the kinks. Comparing PSP kinks and WIND kinks, we conjecture that the kinks dissipate through merging with the turbulent energy cascade within 0.25 au.

Overview of the remote sensing observations from PSP solar encounter 10 with perihelion at 13.3 R_{sun}

[Russell A. Howard](#), [Guillermo Stenborg](#), [Angelos Vourlidis](#), [Brendan M. Gallagher](#), [Mark G. Linton](#), [Phillip Hess](#), [Nathan B. Rich](#), [Paulett C. Liewer](#)

ApJ **936** 43 **2022**

<https://arxiv.org/pdf/2207.12175.pdf>

<https://iopscience.iop.org/article/10.3847/1538-4357/ac7ff5/pdf>

The closest perihelion pass of Parker Solar Probe (PSP), so far, occurred between **16 and 26 of November 2021** and reached ~13.29 R_{sun} from Sun center. This pass resulted in very unique observations of the solar corona by the Wide-field Instrument for Solar PRobe (WISPR). WISPR observed at least ten CMEs, some of which were so close that the structures appear distorted. All of the CMEs appeared to have a magnetic flux rope (MFR) structure and most were oriented such that the view was along the axis orientation, revealing very complex interiors. Two CMEs had a small MFR develop in the interior, with a bright circular boundary surrounding a very dark interior. Trailing the larger CMEs were substantial outflows of small blobs and flux-rope like structures within striated ribbons, lasting for many hours. When the heliophysics plasma sheet (HPS) was inclined, as it was during the days around perihelion on November 21, 2021, the outflow was over a very wide latitude range. One CME was overtaken by a faster one, with a resultant compression of the rear of the leading CME and an unusual expansion in the trailing CME. The small Thomson Surface creates brightness variations of structures as they pass through the field of view. In addition to this dynamic activity, a brightness band from excess dust along the orbit of asteroid/comet 3200 Phaethon is also seen for several days. **16, 19, 20-21, 22-23, 24-26 Nov 2021**

Measuring an Eruptive Prominence at Large Distances from the Sun. II. Approaching 1 AU

T. A. [Howard](#)

2015 ApJ 806 176

The physical properties of eruptive prominences are unknown at large distances from the Sun. They are rarely, if ever, measured by in situ spacecraft and until recently our ability to measure them beyond the fields of view of solar imagers has been severely limited. The data quality of heliospheric imaging has reached a point where some quantitative measurements of prominences are now possible. I present the first such measurements of a bright prominence continually out to distances of around 1 AU from the Sun. This work follows on from the preparatory work presented in an accompanying paper, which showed that the brightness of a prominence can be safely assumed to arise entirely from Thomson scattering in the STEREO/HI fields of view. Measurements of distance, speed, and mass are provided along with those from its accompanying coronal mass ejection (CME) to demonstrate their geometric, kinematic, and mass relationships. I find that the prominence travels with a slower speed than that of the CME, but its location relative to the CME structure does not conform to the expected location for basic geometric expansion. Further, the mass of the prominence was found to decrease by around an order of magnitude while that of the CME increased by an order of magnitude across the same distance.

Measuring an Eruptive Prominence at Large Distances from the Sun. I. Ionization and Early Evolution

T. A. [Howard](#)

2015 ApJ 806 175

Measurements of H α emission within an eruptive solar prominence are presented, using white light polarization properties as a proxy for the presence of H α in the STEREO COR1 and COR2 coronagraphs. The transition from H α emission to Thomson scattering radiance serves as an indicator of the ionization of the prominence, and I discuss the physical implications regarding the behavior of the neutrals and ions, and also for the measurement of coronal mass ejection properties using the Thomson scattering assumption. I find that the prominence has a high concentration of neutrals at around two solar radii that gradually exhibit ionization characteristics as it moves away from the Sun. The

prominence reaches complete ionization, or at least a state where the Thomson-scattered brightness dominates, by the time it reaches around seven solar radii. This is consistent with predictions inferred from direct H α measurements made from earlier studies in the 1980s and with the predicted ionization rate of neutral hydrogen near solar maximum. These results pave the way for an accompanying paper that reports on measurements of the prominence at large distances from the Sun using the assumptions verified here.

The Solar Mass Ejection Imager and Its Heliospheric Imaging Legacy

Review

T. A. **Howard**, M. M. Bisi, A. Buffington, J. M. Clover, M. P. Cooke, C. J. Eyles, P. P. Hick, P. E. Holladay, B. V. Jackson, J. C. Johnston, S.W. Kahler · T.A. Kuchar · D.R. Mizuno · A.J. Penny · S.D. Price · R.R. Radick · G.M. Simnett · S.J. Tappin, N.R. Waltham · D.F. Webb

Space Science Reviews, **2013**, 180: Issue 1-4, 1–38; **File**

The Solar Mass Ejection Imager (SMEI) was the first of a new class of heliospheric and astronomical white-light imager. A heliospheric imager operates in a fashion similar to coronagraphs, in that it observes solar photospheric white light that has been Thomson scattered by free electrons in the solar wind plasma. Compared with traditional coronagraphs, this imager differs in that it observes at much larger angles from the Sun. This in turn requires a much higher sensitivity and wider dynamic range for the measured intensity. SMEI was launched on the Coriolis spacecraft in January 2003 and was deactivated in September 2011, thus operating almost continuously for nearly nine years. Its primary objective was the observation of interplanetary transients, typically coronal mass ejections (CMEs), and tracking them continuously throughout the inner heliosphere. Towards this goal it was immediately effective, observing and tracking several CMEs in the first month of mission operations, with some 400 detections to follow. Along with this primary science objective, SMEI also contributed to many and varied scientific fields, including studies of corotating interaction regions (CIRs), the high-altitude aurora, zodiacal light, Gegenschein, comet tail disconnections and motions, and variable stars. It was also able to detect and track Earth-orbiting satellites and space debris. Along with its scientific advancements, SMEI also demonstrated a significantly improved accuracy of space weather prediction, thereby establishing the feasibility and usefulness of operational heliospheric imagers. In this paper we review the scientific and operational achievements of SMEI, discuss lessons learned, and present our view of potential next steps in future heliospheric imaging.

WHITE-LIGHT OBSERVATIONS OF SOLAR WIND TRANSIENTS AND COMPARISON WITH AUXILIARY DATA SETS

T. A. **Howard**¹, C. E. DeForest¹, and A. A. Reinard

2012 ApJ 754 102

This paper presents results utilizing a new data processing pipeline for STEREO/SECCHI. The pipeline is used to identify and track 24 large- and small-scale solar wind transients from the Sun out to 1 AU. This comparison was performed during a few weeks around the minimum at the end of Solar Cycle 23 and the start of Cycle 24 (**2008 December to 2009 January**). We use coronagraph data to identify features near the Sun, track them through HI-2A, and identify their signatures with in situ data at the Earth and STEREO-B. We provide measurements and preliminary analysis of the in situ signatures of these features near 1 AU. Along with the demonstration of the utility of heliospheric imagers for tracking even small-scale structures, we identify and discuss an important limitation in using geometric triangulation for determining three-dimensional properties.

INNER HELIOSPHERIC FLUX ROPE EVOLUTION VIA IMAGING OF CORONAL MASS EJECTIONS

T. A. **Howard** and C. E. DeForest

2012 ApJ 746 64, **File**

Understanding the evolution of flux ropes in coronal mass ejections (CMEs) is of importance both to the scientific and technological communities. Scientifically their presence is critical to models describing CME launch and they likely play a role in CME evolution. Technologically they are the major contributor to severe geomagnetic storms. Using a new processing technique on the STEREO/SECCHI heliospheric imaging data, we have tracked a magnetic flux rope observed by the Wind spacecraft in **December 2008** to its origins observed by coronagraphs. We thereby establish that the cavity in the classic three-part coronagraph CME is the feature that becomes the magnetic cloud. This implies that the bright material ahead of the cavity is piled-up coronal or solar wind material. We track the evolution of the cavity en-route and find that its structure transforms from concave inward (curving away from the Sun) to concave outward

(toward the Sun) around 0.065 AU from the Sun. The pileup was tracked and its leading edge remained concave inward throughout its journey. Two other CMEs in **January 2009** are also inspected and a similar cavity is observed in each, suggesting that they too each contained a flux rope. The results presented here are the first direct observation, through continuous tracking, associating a particular flux rope observed in situ with the same flux rope before ejection from the corona. We speculate that detailed heliospheric imagery of CMEs may lead to a means by which flux ropes can be identified remotely in the heliosphere.

Three-dimensional reconstruction of coronal mass ejections using heliospheric imager data

Timothy A. [Howard](#)

Journal of Atmospheric and Solar-Terrestrial Physics, Volume 73, Issue 10, **2011**, Pages 1242-1253, **File**
Innovative techniques have been developed to extract three-dimensional (3-D) information on coronal mass ejections. Some techniques have only been available since the launch of the STEREO spacecraft, where geometry can be applied to white light observations from three different viewpoints. Another technique not necessarily requiring the multiple-viewpoint capabilities of STEREO involves heliospheric imaging. With heliospheric imagers, we may take advantage of the breakdown in geometrical and Thomson scattering linearity and, with careful analysis of the data, extract 3-D parameters from CME images. In this review we discuss the various techniques that are being developed and used to reconstruct the 3-D structure and kinematic evolution of CMEs, with a particular emphasis on the work of the author and colleagues. Following a brief review of multiple-viewpoint coronagraph analysis, we focus on techniques involving heliospheric images, which can be used to achieve the reconstruction with a good degree of accuracy without the need for auxiliary data.

Application of a new phenomenological coronal mass ejection model to space weather forecasting,

[Howard](#), T. A., and S. J. Tappin

Space Weather, 8, S07004, doi:10.1029/2009SW000531 (**2010**), **File**.

Recent work by the authors has produced a new phenomenological model for coronal mass ejections (CMEs). This model, called the Tappin-Howard (TH) Model, takes advantage of the breakdown of geometrical linearity when CMEs are observed by white-light imagers at large distances from the Sun. The model extracts 3-D structure and kinematic information on the CME using heliospheric image data. This can estimate arrival times of the CME at 1 AU and impact likelihood with the Earth. Hence the model can be used for space weather forecasting. We present a preliminary evaluation of this potential with three mock trial forecasts performed using the TH Model. These are already-studied events from 2003, 2004 and 2007 but we performed the trials assuming that they were observed for the first time. The earliest prediction was made 17 hours before impact and predicted arrival times reached differences within one hour for at least one forecast for all three events. The most accurate predicted arrival time was 15 min from the actual, and all three events reach accuracies of the order of 30 min. Arrival speeds were predicted to be very similar to the bulk plasma speed within the CME near 1 AU for each event, with the largest difference around 300 km/s and the least 40 km/s. The model showed great potential and we aspire to fully validate it for integration with existing tools for space weather forecasting.

Interplanetary Coronal Mass Ejections Observed in the Heliosphere:

3. Physical Implications

Timothy A. [Howard](#) · S. James Tappin

Space Sci Rev (**2009**) 147: 89–110; **File**

We conclude the heliospheric image series with this third and final instalment, where we consider the physical implications of our reconstruction of interplanetary coronal mass ejections from heliospheric imagers. In Paper 1 a review of the theoretical framework for the appearance of ICMEs in the heliosphere was presented and in Paper 2 a model was developed that extracted the three-dimensional structure and kinematics of interplanetary coronal mass ejections directly from SMEI images. Here we extend the model to include STEREO Heliospheric Imager data and reproduce the three-dimensional structure and kinematic evolution of a single Earth-directed interplanetary coronal mass ejection that was

observed in November 2007. These measurements were made with each spacecraft independently using leading edge measurements obtained from each instrument. We found that when data from the three instruments was treated as a single collective, we were able to reproduce an estimate of the ICME structure and trajectory. There were some disparities between the modelled ICME and the *in situ* data, and we interpret this as a combination of a slightly more than spherically curved ICME structure and a corotating interaction region brought about by the creation of a coronal hole from the CME eruption. This is the first time evidence for such a structure has been presented and we believe that it is likely that many ICMEs are of this nature.

Part 2: see Tappin (2009)

Interplanetary Coronal Mass Ejections Observed in the Heliosphere:

1. Review of Theory

Timothy A. Howard · S. James Tappin

Space Sci Rev (2009) 147: 31–54; **File**

With the recent advancements in interplanetary coronal mass ejection (ICME) imaging it is necessary to understand how heliospheric images may be interpreted, particularly at large elongation angles. Of crucial importance is how the current methods used for coronal mass ejection measurement in coronagraph images must be changed to account for the large elongations involved in the heliosphere. In this review of theory we build up a picture of ICME appearance and evolution at large elongations in terms of how it would appear to an observer near 1 AU from the Sun. We begin by revisiting the basics of Thomson scattering describing how ICMEs are detected, in this we attempt to clarify a number of common misconceptions. We then build up from a single electron to an integrated line of sight, consider the ICME as a collection of lines of sight and describe how a map of ICME appearance may be developed based on its appearance relative to each line of sight. Finally, we discuss how the topology of the ICME affects its observed geometry and kinematic properties, particularly at large elongations. This review is the first of a three-part series of papers, where a review of theory is presented here and a model is developed and used in subsequent papers.

Interplanetary coronal mass ejections that are undetected by solar coronagraphs,

Howard, T. A., and G. M. Simnett

J. Geophys. Res., 113, A08102, 2008

<http://dx.doi.org/10.1029/2007JA012920>

From February 2003 to September 2005 the Solar Mass Ejection Imager on the Coriolis spacecraft detected 207 interplanetary coronal mass ejections (ICME) in the inner heliosphere. We have examined the data from the Large Angle Spectroscopic Coronagraph (LASCO) on the SOHO spacecraft for evidence of coronal transient activity that might have been the solar progenitor of the Solar Mass Ejection Imager (SMEI) events, taking into account the projected speed of the SMEI event and its position angle in the plane of the sky. We found a significant number of SMEI events where there is either only a weak or unlikely coronal mass ejection (CME) detected by LASCO or no event at all. A discussion of the effects of projection across large distances on the ICME measurements is made, along with a new technique called the Cube-Fit procedure that was designed to model the ICME trajectory more accurately than simple linear fits to elongation-time plots. Of the 207 SMEI events, 189 occurred during periods of full LASCO data coverage. Of these, 32 or 17% were found to have a weak or unlikely LASCO counterpart, and 14 or 7% had no apparent LASCO transient association. Using solar X-ray, EUV and $H\alpha$ data we investigated three main physical possibilities for ICME occurrence with no LASCO counterpart: (1) Corotating interaction regions (CIRs), (2) erupting magnetic structures (EMS), and (3) flare blast waves. We find that only one event may possibly be a CIR and that flare blast waves can be ruled out. *The most likely phenomenon is investigated and discussed, that of EMS. Here, the transient erupts in the same manner as a typical CME, except that they do not have sufficient mass to be detected by LASCO. As the structure moves outward, it accumulates and concentrates solar wind material until it is bright enough to be detected by SMEI.*

ON THE EVOLUTION OF CORONAL MASS EJECTIONS IN THE INTERPLANETARY MEDIUM

T. A. **Howard**, C. D. Fry, J. C. Johnston, and D. F. Webb

The Astrophysical Journal, 667:610-625, **2007**

<https://iopscience.iop.org/article/10.1086/519758/pdf>

Two coronal mass ejections (CMEs) are presented which were tracked through the LASCO field of view (FOV) within 30 R_☉ and later as interplanetary CMEs (ICMEs) through the SMEI FOV from 80 to 150 R_☉. They were also associated with erupting filaments observed by EIT, providing information on trajectory of propagation. This allowed three-dimensional reconstructions of CME/ICME geometry, along with corrected (not sky plane projected) measurements

of distance-time (DT) plots for each event to 0.5 AU. An investigation of morphology was conducted. The results suggest that fine structures of the CMEs are eroded by the solar wind, and curvature becomes more sharply convex outward, suggesting that ICME footpoints remain fixed to the Sun even at 0.5 AU. We also present two models describing the evolution of CMEs/ICMEs at large distances from the Sun (far from the launch mechanism and effects of gravity and solar pressure) and consider two drag models: aerodynamic drag and snowplow. There was little difference between these, and their DT profiles matched well with the SMEI data for event 1. Event 2 showed a net acceleration between the LASCO and SMEI FOVs and we could match the data for this event well by introducing a driving Lorentz force. ICME mass almost doubled as a result of swept-up solar wind material from the snowplow model. Finally, we compared the geometry and kinematics of the ICME with that produced by the HAFv2 model and found that the model reasonably matched the geometry, but overestimated the ICME speed.

Tracking halo coronal mass ejections from 0 -- 1 AU and space weather forecasting using the Solar Mass Ejection Imager (SMEI),

Howard, T. A., D. F. Webb, S. J. Tappin, D. R. Mizuno, and J. C. Johnston

J. Geophys. Res., 111, A04105, doi:10.1029/2005JA011349, (**2006**).

Howard et al. [2006] studied 20 ICMEs observed by SMEI over its first 19 months that were associated with LASCO halo CMEs and shocks observed by ACE at the L1 point. Their study focused on computing distance-time profiles using both the LASCO CME and SMEI ICME data to determine ICME speed, and then to predict its time of arrival at Earth. They used the shock arrival time (AT) at L1 as the indicator for ICME arrival, thus ignoring the shock standoff distance (time) from the ejecta. They then compared the predicted ICME AT with the actual shock ATs at ACE at L1.

Statistical survey of earthbound interplanetary shocks, associated coronal mass ejections and their space weather consequences

Howard, T. A.; Tappin, S. J.

Astronomy and Astrophysics, Volume 440, Issue 1, September II **2005**, pp.373-383; **File**

A comprehensive statistical analysis of events relevant to space weather over the 80 month period from January 1998 to August 2004 is presented. A database has been constructed using data from instruments from the SOHO, ACE, WIND and GOES spacecraft, as well as ground magnetometer data. Parameters investigated include times and epochs of halo and partial halo coronal mass ejections (HCMEs) along with details of the interplanetary shock at L1 (0.99 AU), namely the changes in the interplanetary magnetic field and solar wind density, and shock speed. Transit time to the Earth and average transient speed have also been determined, along with the projected speed and angular width of the HCME at the Sun. An estimate is made of the acceleration of the transients on their passage from the Sun to the Earth, and associated solar flare data are considered. Finally, the geoeffectiveness of the events are analysed using A_p, Dst and sudden commencement data. We found that just over a quarter of the 938 HCMEs observed by LASCO were associated with a forward shock near L1, suggesting that around half of the Earthbound HCMEs are either deflected away from the Sun-Earth line or do not form a shock. Around half of the shocks went on to cause a geomagnetic storm, consistent with a southward B_z IMF occurring 50% of the time. There was a general tendency for HCME and shock speeds to be more varied (with more events at higher speeds) around solar maximum, and most events decelerated in transit to the Earth, implying a speed "equalisation" between the HCME shock and surrounding solar wind, although an assumption of a constant acceleration appears to be invalid. Only around 40% of the shock/storms were associated with an X or M class flare, and there appears to be no relationship between flare intensity and any physical parameter close to the Earth, except in extreme cases. There was a tendency for HCME speed near the Sun to increase with flare intensity. This casts doubt on the validity of using flare data alone as an effective space weather forecaster.

Multi-Hour-Ahead Dst Index Prediction Using Multi-Fidelity Boosted Neural Networks

A. Hu, E. Camporeale, B. Swiger

Space Weather [Volume 21, Issue 4](#) e2022SW003286 2023

<https://doi.org/10.1029/2022SW003286>

<https://agupubs.onlinelibrary.wiley.com/doi/epdf/10.1029/2022SW003286>

The Disturbance storm time (Dst) index has been widely used as a proxy for the ring current intensity, and therefore as a measure of geomagnetic activity. It is derived by measurements from four ground magnetometers in the geomagnetic equatorial region. We present a new model for predicting Dst with a lead time between 1 and 6 hr. The model is first developed using a Gated Recurrent Unit (GRU) network that is trained using solar wind parameters. The uncertainty of the Dst model is then estimated by using the Accurate and Reliable Uncertainty Estimate method (Camporeale & Carè, 2021, <https://doi.org/10.1615/int.j.uncertaintyquantification.2021034623>). Finally, a multi-fidelity boosting method is developed in order to enhance the accuracy of the model and reduce its associated uncertainty. It is shown that the developed model can predict Dst 6 hr ahead with a root-mean-square-error of 13.54 nT. This is significantly better than a persistence model or a single GRU model. **20-21 Nov 2003, 07 Nov 2022,**

Table 2 List of First 66 Storm Events 2000-2003

A Magnetic Flux Rope Configuration Derived by Optimization of Two-Spacecraft In-situ Measurements

Qiang Hu, Wen He, and Yu Chen

Front. Phys. 10: 960315. 2022

doi: 10.3389/fphy.2022.960315

<https://www.frontiersin.org/articles/10.3389/fphy.2022.960315/pdf>

Increasingly one interplanetary coronal mass ejection (ICME) structure can propagate across more than one spacecraft in the solar wind. This usually happens when two or more spacecraft are nearly radially aligned with a relatively small longitudinal separation angle from one another. This provides multi-point measurements of the same structure and enables better characterization and validation of modeling results of the structures embedded in these ICMEs. We report such an event during **October 13-14, 2019** when the Solar TERrestrial RELations Observatory Ahead (STA) spacecraft and the Parker Solar Probe (PSP) crossed one ICME structure at two different locations with nominal separations in both heliocentric distances and the longitudinal angles. We first perform an optimal fitting to the STA in-situ measurements, based on an analytic quasi-three dimensional (3D) model, yielding a minimum reduced $\chi^2 = 0.468$. Then we further apply the optimization approach by combining the magnetic field measurements from both spacecraft along their separate paths across the ICME structure. We find that the output based on the optimization (with the minimum reduced $\chi^2 = 3.15$) of the combined two-spacecraft dataset yields a more consistent result, given the much improved agreement of the model output with PSP data. The result demonstrates a magnetic flux rope configuration with clear 3D spatial variations.

Validation and interpretation of three-dimensional configuration of a magnetic cloud flux rope

Qiang Hu, Chunming Zhu, Wen He, Jiong Qiu, Lan K. Jian, Avijeet Prasad

ApJ 934 50 2022

<https://arxiv.org/pdf/2204.03457>

<https://iopscience.iop.org/article/10.3847/1538-4357/ac7803/pdf>

One "strong" magnetic cloud (MC) with the magnetic field magnitude reaching ~ 40 nT at 1 au during **2012 June 16-17** is examined in association with a pre-existing magnetic flux rope (MFR) identified on the Sun. The MC is characterized by a quasi-three dimensional (3D) flux rope model based on in situ measurements from the Wind spacecraft. The magnetic flux contents and other parameters are quantified. In addition, a correlative study with the corresponding measurements of the same structure crossed by the Venus Express (VEX) spacecraft at a heliocentric distance 0.7 au and with an angular separation $\sim 6^\circ$ in longitude is performed to validate the MC modeling results. The spatial variation between the Wind and VEX magnetic field measurements is attributed to the 3D configuration of the structure as featured by a knotted bundle of flux. The comparison of the magnetic flux contents between the MC and the source region on the Sun indicates that the 3D reconnection process accompanying an M1.9 flare may correspond to the magnetic reconnection between the field lines of the pre-existing MFR rooted in the opposite polarity footpoints. Such a process reduces the amount of the axial magnetic flux in the erupted flux rope, by approximately 50%, in this case.

Probabilistic prediction of Dst storms one-day-ahead using Full-Disk SoHO Images

A. Hu, C. Shneider, A. Tiwari, E. Camporeale

Space Weather e2022SW003064 **Volume20, Issue8 2022**

<https://arxiv.org/pdf/2203.11001.pdf>

<https://doi.org/10.1029/2022SW003064>

<https://agupubs.onlinelibrary.wiley.com/doi/epdf/10.1029/2022SW003064>

We present a new model for the probability that the Disturbance storm time (Dst) index exceeds **-100 nT**, with a lead time between 1 and 3 days. Dst provides essential information about the strength of the ring current around the Earth caused by the protons and electrons from the solar wind, and it is routinely used as a proxy for geomagnetic storms. The model is developed using an ensemble of Convolutional Neural Networks (CNNs) that are trained using SoHO images (MDI, EIT and LASCO). The relationship between the SoHO images and the solar wind has been investigated by many researchers, but these studies have not explicitly considered using SoHO images to predict the Dst index.

This work presents a novel methodology to train the individual models and to learn the optimal ensemble weights iteratively, by using a customized class-balanced mean square error (CB-MSE) loss function tied to a least-squares (LS) based ensemble.

The proposed model can predict the probability that $Dst < -100$ nT 24 hours ahead with a True Skill Statistic (TSS) of 0.62 and Matthews Correlation Coefficient (MCC) of 0.37. The weighted TSS and MCC from Guastavino et al. (2021) is 0.68 and 0.47, respectively. An additional validation during non-Earth-directed CME periods is also conducted which yields a good TSS and MCC score.

Table 1: List of selected 51 Storm Events. 2001-2010

Configuration of a Magnetic Cloud from Solar Orbiter and Wind Spacecraft In-situ Measurements

Qiang Hu, Wen He, Lingling Zhao, Edward Lu

Frontiers in Physics 9:706056 2021

<https://arxiv.org/pdf/2107.01728.pdf>

<https://www.frontiersin.org/articles/10.3389/fphy.2021.706056/full>

<https://doi.org/10.3389/fphy.2021.706056>

Coronal mass ejections (CMEs) represent one type of the major eruption from the Sun. Their interplanetary counterparts, the interplanetary CMEs (ICMEs), are the direct manifestations of these structures when they propagate into the heliosphere and encounter one or more observing spacecraft. The ICMEs generally exhibit a set of distinctive signatures from the in-situ spacecraft measurements. A particular subset of ICMEs, the so-called Magnetic Clouds (MCs), is more uniquely defined and has been studied for decades, based on in-situ magnetic field and plasma measurements. By utilizing the latest multiple spacecraft measurements and analysis tools, we report a detailed study of the internal magnetic field configuration of an MC event observed by both the Solar Orbiter (SO) and Wind spacecraft in the solar wind near the Sun-Earth line. Both two-dimensional (2D) and three-dimensional (3D) models are applied to reveal the flux rope configurations of the MC. Various geometrical as well as physical parameters are derived and found to be similar within error estimates for the two methods. These results quantitatively characterize the coherent MC flux rope structure crossed by the two spacecraft along different paths. The implication for the radial evolution of this MC event is also discussed. **19 April 2020**

Optimal Fitting of the Freidberg Solution to In Situ Spacecraft Measurements of Magnetic Clouds

Qiang Hu

Solar Physics volume 296, Article number: 101 (2021)

<https://link.springer.com/content/pdf/10.1007/s11207-021-01843-z.pdf>

<https://doi.org/10.1007/s11207-021-01843-z>

We report, in detail, an optimization approach for fitting a three-dimensional (3D) magnetic cloud (MC) model to in situ spacecraft measurements. The model, dubbed the Freidberg solution, encompasses 3D spatial variations in a generally cylindrical geometry, as derived from a linear force-free formulation. The approach involves a least-squares minimization implementation with uncertainty estimates from magnetic field measurements. We present one case study of the MC event on **22 May 2007** to illustrate the method and demonstrate the satisfying result of the minimum reduced $\chi^2 \lesssim 1$, obtained from the Solar and TERrestrial RELations Observatory (STEREO) Behind spacecraft measurements. In addition, since the Advanced Composition Explorer (ACE) spacecraft at Earth crossed the STEREO Behind solution domain with an appropriate separation distance, the result from the optimally fitted Freidberg solution along the ACE

spacecraft path is compared with the actual measurements of magnetic field components. A correlation coefficient of 0.89 is obtained between the two sets of data.

On the quasi-three dimensional configuration of magnetic clouds

Qiang [Hu](#), [Wen He](#), [Jiong Qiu](#), [A. Vourlidas](#), [Chunming Zhu](#)

GRL 2020

<https://arxiv.org/pdf/2010.11889.pdf>

We develop an optimization approach to model the magnetic field configuration of magnetic clouds, based on a linear-force free formulation in three dimensions. Such a solution, dubbed the Freidberg solution, is kin to the axi-symmetric Lundquist solution, but with more general "helical symmetry". The merit of our approach is demonstrated via its application to two case studies of in-situ measured magnetic clouds. Both yield results of reduced $\chi^2 \approx 1$. Case 1 shows a winding flux rope configuration with one major polarity. Case 2 exhibits a double-helix configuration with two flux bundles winding around each other and rooted on regions of mixed polarities. This study demonstrates the three-dimensional complexity of the magnetic cloud structures. **15 July 2012, 14-15 Apr 2013**

Automated Detection of Small-scale Magnetic Flux Ropes in the Solar Wind: First Results from the Wind Spacecraft Measurements

Qiang [Hu](#)¹, Jinlei Zheng², Yu Chen², Jakobus le Roux¹, and Lulu Zhao³

2018 ApJS 239 12

sci-hub.tw/10.3847/1538-4365/aae57d

We have developed a new automated small-scale magnetic flux rope (SSMFR) detection algorithm based on the Grad-Shafranov (GS) reconstruction technique. We have applied this detection algorithm to the Wind spacecraft in situ measurements during 1996–2016, covering two solar cycles, and successfully detected a total number of 74,241 small-scale magnetic flux rope events with duration from 9 to 361 minutes. This large number of small-scale magnetic flux ropes has not been discovered by any other previous studies through this unique approach. We perform statistical analysis of the small-scale magnetic flux rope events based on our newly developed database, and summarize the main findings as follows. (1) The occurrence of small-scale flux ropes has strong solar-cycle dependency with a rate of a few hundred per month on average. (2) The small-scale magnetic flux ropes in the ecliptic plane tend to align along the Parker spiral. (3) In low-speed ($<400 \text{ km s}^{-1}$) solar wind, the flux ropes tend to have lower proton temperature and higher proton number density, while in high-speed ($\geq 400 \text{ km s}^{-1}$) solar wind, they tend to have higher proton temperature and lower proton number density. (4) Both the duration and scale size distributions of the small-scale magnetic flux ropes obey a power law. (5) The waiting time distribution of small-scale magnetic flux ropes can be fitted by an exponential function (for shorter waiting times) and a power-law function (for longer waiting times). (6) The wall-to-wall time distribution obeys double power laws with the break point at 60 minutes (corresponding to the correlation length). (7) The small-scale magnetic flux ropes tend to accumulate near the heliospheric current sheet (HCS). The entire database is available at <http://fluxrope.info> and in machine-readable format in this article.

The Grad-Shafranov Reconstruction of Toroidal Magnetic Flux Ropes: First Applications

Qiang [Hu](#), [M. G. Linton](#), [B. E. Wood](#), [P. Riley](#), [T. Nieves-Chinchilla](#)

Solar Phys. 292:171 2017

<https://arxiv.org/pdf/1707.09454.pdf>

This article completes and extends a recent study of the Grad-Shafranov (GS) reconstruction in toroidal geometry, as applied to a two and a half dimensional configurations in space plasmas with rotational symmetry. A further application to the benchmark study of an analytic solution to the toroidal GS equation with added noise shows deviations in the reconstructed geometry of the flux rope configuration, characterized by the orientation of the rotation axis, the major radius, and the impact parameter. On the other hand, the physical properties of the flux rope, including the axial field strength, and the toroidal and poloidal magnetic flux, agree between the numerical and exact GS solutions. We also present a real event study of a magnetic cloud flux rope from *in situ* spacecraft measurements. The devised procedures for toroidal GS reconstruction are successfully executed. Various geometrical and physical parameters are obtained with associated uncertainty estimates. The overall configuration of the flux rope from the GS reconstruction is compared with the corresponding morphological reconstruction based on white-light images. The results show overall consistency, but also discrepancy in that the inclination angle of the flux rope central axis with respect to the ecliptic plane differs by about 20-30 degrees in the plane of the sky. We also compare the results with the original straight-cylinder GS reconstruction and discuss our findings. **06-07-Jun-2008**

The Grad-Shafranov Reconstruction of Toroidal Magnetic Flux Ropes: Method Development and Benchmark Studies

Qiang **Hu**

Solar Phys. 292:116 2017

<https://www.dropbox.com/sh/wd5btkbldu5xvga/AABHQjCRRUH1NpEprmnKsccOa?dl=0>

<https://arxiv.org/pdf/1706.02732.pdf>

The underlying theory is the GS equation that describes two-dimensional magnetohydrostatic equilibrium as widely applied in fusion plasmas. The geometry is such that the arbitrary cross section of the torus has rotational symmetry about the rotation axis Z , with a major radius r_0 . The magnetic field configuration is thus determined by a scalar flux function Ψ and a functional F that is a single-variable function of Ψ . The algorithm is implemented through a two-step approach: i) a trial-and-error process by minimizing the residue of the functional $F(\Psi)$ to determine an optimal Z axis orientation, and ii) for the chosen Z , a χ^2 minimization process resulting in the range of r_0 . Benchmark studies of known analytic solutions to the toroidal GS equation with noise additions are presented to illustrate the two-step procedures and to demonstrate the performance of the numerical GS solver, separately. For the cases presented, the errors in Z and r_0 are 9° and 22%, respectively, and the relative percent error in the numerical GS solutions is less than 10%. We also make public the computer codes for these implementations and benchmark studies.

Sun-to-Earth Characteristics of the 2012 July 12 Coronal Mass Ejection and Associated Geo-effectiveness

Huidong **Hu**, Ying D. Liu, Rui Wang, [Christian Möstl](#), [Zhongwei Yang](#)

ApJ 829 97 2016

<http://arxiv.org/pdf/1607.06287v1.pdf> File

<https://iopscience.iop.org/article/10.3847/0004-637X/829/2/97/pdf>

We analyze multi-spacecraft observations associated with the 2012 July 12 Coronal Mass Ejection (CME), covering the source region on the Sun from SDO, stereoscopic imaging observations from STEREO, magnetic field characteristics at MESSENGER, and type II radio burst and in situ measurements from Wind. A triangulation method based on STEREO stereoscopic observations is employed to determine the kinematics of the CME, and the outcome is compared with the result derived from the type II radio burst with a solar wind electron density model. A Grad-Shafranov technique is applied to Wind in situ data to reconstruct the flux-rope structure and compare it with the observation of the solar source region, which helps understand the geo-effectiveness associated with the CME structure. Conclusions are as follows: (1) the CME undergoes an impulsive acceleration, a rapid deceleration before reaching MESSENGER, and then a gradual deceleration out to 1 AU, which should be noticed in CME kinematics models; (2) the type II radio burst was probably produced from a high-density interaction region between the CME-driven shock and a nearby streamer or from the shock flank with lower heights, which implies uncertainties in the determination of CME kinematics using solely type II radio bursts; (3) the flux-rope orientation and chirality deduced from in situ reconstruction at Wind agree with those obtained from solar source observations; (4) the prolonged southward magnetic field near the Earth is mainly from the axial component of the largely southward inclined flux rope, which indicates the importance of predicting both the flux-rope orientation and magnetic field components in geomagnetic activity forecasting.

Magnetic field-line lengths inside interplanetary magnetic flux ropes

Qiang **Hu**, Jiong Qiu, Sam Krucker

JGR Special Section: VarSITI, [Volume 120, Issue 7](#) Pages 5266–5283 2015

<http://arxiv.org/pdf/1502.05284v1.pdf>

We report on the detailed and systematic study of field-line twist and length distributions within magnetic flux ropes embedded in Interplanetary Coronal Mass Ejections (ICMEs). The Grad-Shafranov reconstruction method is utilized together with a constant-twist nonlinear force-free (Gold-Hoyle) flux rope model to reveal the close relation between the field-line twist and length in cylindrical flux ropes, based on in-situ Wind spacecraft measurements. We show that the field-line twist distributions within interplanetary flux ropes are inconsistent with the Lundquist model. In particular we utilize the unique measurements of magnetic field-line lengths within selected ICME events as provided by Kahler et al. (2011) based on energetic electron burst observations at 1 AU and the associated type III radio emissions detected by the Wind spacecraft. These direct measurements are compared with our model calculations to help assess the flux-rope interpretation of the embedded magnetic structures. By using the different flux-rope models, we show that the in-situ direct measurements of field-line lengths are consistent with a flux-rope structure with spiral field lines of constant and

low twist, largely different from that of the Lundquist model, especially for relatively large-scale flux ropes. **18 October 1995, 18 September 1997, 30 August 2004**

Structures of Interplanetary Magnetic Flux Ropes and Comparison with Their Solar Sources

Qiang **Hu**, Jiong Qiu, B. Dasgupta, A. Khare, and G. M. Webb

ApJ 793 53, **2014**; **File**

https://dl.dropboxusercontent.com/u/96898685/ms_fr_v4.pdf

<http://arxiv.org/pdf/1408.1470v1.pdf>

During the process of magnetic flux rope ejection, magnetic reconnection is essential to release the flux rope. the question remains: how does the magnetic reconnection change the flux rope structure? In this work, we continue with the original study by Qiu et al. (2007) by using a larger sample of flare-CME-ICME events to compare properties of ICME/MC flux ropes measured at 1 AU and properties of associated solar progenitors including flares, filaments, and CMEs. In particular, the magnetic field-line twist distribution within interplanetary magnetic flux ropes is systematically derived and examined. Our analysis shows that, similar to what was found before, for most of these events, the amount of twisted flux per AU in MCs is comparable with the total reconnection flux on the Sun, and the sign of the MC helicity is consistent with the sign of helicity of the solar source region judged from the geometry of postflare loops.

Remarkably, we find that about one half of the 18 magnetic flux ropes, most of them being associated with erupting filaments, have a nearly uniform and relatively low twist distribution from the axis to the edge, and the majority of the other flux ropes exhibit very high twist near the axis, of up to ≥ 5 turns per AU, which decreases toward the edge. The flux ropes are therefore not linear force free. We also conduct detailed case studies showing the contrast of two events with distinct twist distribution in MCs as well as different flare and dimming characteristics in solar source regions, and discuss how reconnection geometry reflected in flare morphology may be related to the structure of the flux rope formed on the Sun. 03/08/2008, 05/28/2010, 08/04/2010, 03/30/2011, 06/05/2011, 08/05/2011, 09/09/2011, 09/17/2011, **2011 September 13-17**, 10/24/2011

Effect of Electron Pressure on the Grad–Shafranov Reconstruction of Interplanetary Coronal Mass Ejections

Qiang **Hu**, C. J. Farrugia, V. A. Osherovich, C. Möstl, A. Szabo, K. W. Ogilvie, R. P. Lepping

Solar Physics, May **2013**, Volume 284, Issue 1, pp 275-291

We investigate the effect of electron pressure on the Grad–Shafranov (GS) reconstruction of Interplanetary Coronal Mass Ejection (ICME) structures. The GS method uses in situ magnetic field and plasma measurements to solve for a magnetohydrostatic quasi-equilibrium state of space plasmas. For some events, a magnetic flux-rope structure embedded within the ICME can be reconstructed. The electron temperature contributes directly to the calculation of the total plasma pressure, and in ICMEs its contribution often substantially exceeds that of proton temperature. We selected ICME events observed with the Wind spacecraft at 1 AU and applied the GS reconstruction method to each event for cases with and without electron temperature measurements. We sorted them according to the proton plasma β (the ratio of proton plasma pressure to magnetic pressure) and the electron-to-proton temperature ratio. We present case studies of three representative events, show the cross sections of GS reconstructed flux-rope structure, and discuss the electron pressure contribution to key quantities in the numerical reconstruction procedure. We summarize and compare the geometrical and physical parameters derived from the GS reconstruction results for cases with and without electron temperature contribution. We conclude that overall the electron pressure effect on the GS reconstruction results contributes to a 10–20 % discrepancy in some key physical quantities, such as the magnetic flux content of the ICME flux rope observed at 1 AU.

On the magnetic topology of October/November 2003 events

Hu, Q., C. W. Smith, N. F. Ness, and R. M. Skoug

J. Geophys. Res., 110, A09S03, doi:10.1029/2004JA010886, **2005**, **File**.

We examine the topology of several magnetic ejecta events during October–November 2003. The Grad-Shafranov reconstruction results from ACE magnetic and plasma data show magnetic flux rope configurations. Some are large scale, with sizes of tenths of an AU, typical of magnetic clouds. Some are of sizes hundredths of an AU. Their characteristic parameters are reported. Magnetic field data from Wind spacecraft are utilized to compare the prediction from numerical modeling with the actual measurement. Poor to good agreement is achieved. The deviations are discussed, particularly in the context of extremely high-speed solar wind flows.

Ensemble Modeling of Radiation Belt Electron Flux Decay Following a Geomagnetic Storm: Dependence on Key Input Parameters

Man [Hua](#), [Jacob Bortnik](#), [Adam C. Kellerman](#), [Enrico Camporeale](#), [Qianli Ma](#)

Space Weather 2022

<https://doi.org/10.1029/2022SW003051>

<https://agupubs.onlinelibrary.wiley.com/doi/epdf/10.1029/2022SW003051>

We perform an ensemble of quasi-linear diffusion simulations of the radiation belt electron flux decay for ~6 days at $L = 3.5$ during the recovery phase of the storm on **7 November 2015**, where plasmaspheric hiss dominantly drives the electron flux decay process. Based on Van Allen Probes measurements, we use percentiles to sample the distributions of the four key input parameters, which are the hiss wave amplitude B_w , hiss wave peak frequency f_m , background magnetic field B_0 and electron density N_e , with 11 points representing that range of each input, leading to 114 (~14,600) ensemble members. By developing a Lookup Table method to rapidly calculate the time-dependent diffusion coefficients, the changing wave environment at every time step is incorporated in our ensemble simulations. The comparison between the ensemble simulations and observation reveals the influence of uncertainties in the input parameters on the simulated electron fluxes. Our results demonstrate that the perturbations in B_w are the primary contributor for discrepancies between modeled and observed electron fluxes, while the simulation errors caused by variations in f_m and N_e are strongly energy-dependent. The simulated electron flux using the wave parameters observed at the 50th percentile agrees with observations, and most of the simulation errors increase with decreasing observational probability density of the parameters, with the largest log accuracy ratio of ~14. Our physics-based ensemble modeling provides the essential information about the robustness of radiation belt simulation and forecast considering the uncertainties in the plasma wave measurement or parameterization.

Solar Wind Driven from GONG Magnetograms in the Last Solar Cycle

Zhenguang [Huang](#)¹, Gábor Tóth¹, Nishtha Sachdeva¹, and Bart van der Holst¹

2024 ApJ 965 1

<https://iopscience.iop.org/article/10.3847/1538-4357/ad32ca/pdf>

In a previous study, Huang et al. used the Alfvén Wave Solar atmosphere Model, one of the widely used solar wind models in the community, driven by ADAPT-GONG magnetograms to simulate the solar wind in the last solar cycle and found that the optimal Poynting flux parameter can be estimated from either the open field area or the average unsigned radial component of the magnetic field in the open field regions. It was also found that the average energy deposition rate (Poynting flux) in the open field regions is approximately constant. In the current study, we expand the previous work by using GONG magnetograms to simulate the solar wind for the same Carrington rotations and determine if the results are similar to the ones obtained with ADAPT-GONG magnetograms. Our results indicate that similar correlations can be obtained from the GONG maps. Moreover, we report that ADAPT-GONG magnetograms can consistently provide better comparisons with 1 au solar wind observations than GONG magnetograms, based on the best simulations selected by the minimum of the average curve distance for the solar wind speed and density.

Interaction between a Coronal Mass Ejection and Comet 67P/Churyumov-Gerasimenko

Zhenguang [Huang](#), [Gabor Toth](#), [Tamas I. Gombosi](#), [Michael R. Combi](#), [Xianzhe Jia](#), [Yinsi Shou](#), [Valeriy Tenishev](#), [Kathrin Altwegg](#), [Martin Rubin](#)

ApJ 967 43 2024

<https://arxiv.org/pdf/2403.05779.pdf>

<https://iopscience.iop.org/article/10.3847/1538-4357/ad3c42/pdf>

The interaction between a Coronal Mass Ejection (CME) and a comet has been observed several times by in-situ observations from the Rosetta Plasma Consortium (RPC), which is designed to investigate the cometary magnetosphere of comet 67P/Churyumov-Gerasimenko (CG). Goetz et al. (2019) reported a magnetic field of up to 300 nT measured in the inner coma, which is among the largest interplanetary magnetic fields observed in the solar system. They suggested the large magnetic field observations in the inner coma come from magnetic field pile-up regions, which are generated by the interaction between a CME and/or corotating interaction region and the cometary magnetosphere. However, the detailed interaction between a CME and the cometary magnetosphere of comet CG in the inner coma has not been investigated by numerical simulations yet. In this manuscript, we will use a numerical model to simulate the interaction between comet CG and a Halloween class CME and investigate its magnetospheric response to the CME. We find that the plasma structures change significantly during the CME event, and the maximum value of the magnetic field strength is more than 500nT close to the nucleus. Virtual satellites at similar distances as Rosetta show that the magnetic field strength can be as large as 250nT, which is slightly less than what Goetz et al. (2019) reported. **29 Oct 2003**

The Structure and Origin of Switchbacks: Parker Solar Probe Observations

Jia **Huang**¹, J. C. Kasper^{2,3}, L. A. Fisk³, Davin E. Larson¹, Michael D. McManus¹ +++

2023 ApJ 952 33

<https://iopscience.iop.org/article/10.3847/1538-4357/acd17e/pdf>

Switchbacks are rapid magnetic field reversals that last from seconds to hours. Current Parker Solar Probe (PSP) observations pose many open questions in regard to the nature of switchbacks. For example, are they stable as they propagate through the inner heliosphere, and how are they formed? In this work, we aim to investigate the structure and origin of switchbacks. In order to study the stability of switchbacks, we suppose the small-scale current sheets therein are generated by magnetic braiding, and they should work to stabilize the switchbacks. With more than 1000 switchbacks identified with PSP observations in seven encounters, we find many more current sheets inside than outside switchbacks, indicating that these microstructures should work to stabilize the S-shape structures of switchbacks. Additionally, we study the helium variations to trace the switchbacks to their origins. We find both helium-rich and helium-poor populations in switchbacks, implying that the switchbacks could originate from both closed and open magnetic field regions in the Sun. Moreover, we observe that the alpha-proton differential speeds also show complex variations as compared to the local Alfvén speed. The joint distributions of both parameters show that low helium abundance together with low differential speed is the dominant state in switchbacks. The presence of small-scale current sheets in switchbacks along with the helium features are in line with the hypothesis that switchbacks could originate from the Sun via interchange reconnection process. However, other formation mechanisms are not excluded. **27 Apr 2021**

Table 1 The Distributions of Current Sheets in Different Regions of Switchbacks

Statistical Study of Ejections in Coronal Hole Regions As Possible Sources of Solar Wind Switchbacks and Small-scale Magnetic Flux Ropes

Nengyi **Huang**^{1,2}, Sophia D'Anna¹, and Haimin Wang^{1,2}

2023 ApJL 946 L17

<https://iopscience.iop.org/article/10.3847/2041-8213/acc0f1/pdf>

The omnipresence of transient fluctuations in the solar wind, such as switchbacks (SBs) and small-scale magnetic flux ropes (SMFRs), have been well observed by the in situ observation of Parker Solar Probe (PSP), yet their sources are not clear. Possible candidates fall into two categories: solar origin and in situ generation in the solar wind. Among the solar-origin scenarios, the small-scale activities (such as ejections and eruptions) in coronal hole (CH) regions, where solar wind originates, are suggested as candidates. Using full-disk extreme ultraviolet images from Atmospheric Imaging Assembly on board the Solar Dynamic Observatory, we identify small-scale ejections in CH regions during PSP Encounters 5, 7, and 8, and study their statistical properties. These ejections belong to two categories: standard jets and blowout jets. With 27,832 ejections identified in 24 days (about 2/3 of them are blowout jets), we updated the expected frequency for PSP to detect their counterparts in the heliospace. The ejections we identified are comparable to the frequency of PSP-detected SMFRs, but they are insufficient to serve as the only producer of SBs or SB patches. Certain smaller events missed by this study, such as jetlets, may fill the gap. **2020-01-23, 2020-06-09-10, 2021-04-29**

Modeling the Solar Wind During Different Phases of the Last Solar Cycle

Zhenguang **Huang**, [Gabor Toth](#), [Nishtha Sachdeva](#), [Lulu Zhao](#), [Bartholomeus van der Holst](#), [Igor](#)

[Sokolov](#), [Ward Manchester](#), [Tamas Gombosi](#)

ApJ **2022**

<https://arxiv.org/pdf/2210.02501.pdf>

We describe our first attempt to systematically simulate the solar wind during different phases of the last solar cycle with the Alfvén Wave Solar atmosphere Model (AWSoM) developed at the University of Michigan. Key to this study is the determination of the optimal values of one of the most important input parameter of the model, the Poynting flux, which prescribes the energy flux passing through the chromospheric boundary of the model in form of Alfvén wave turbulence. It is found that the optimal value of the Poynting flux parameter is correlated with: 1) the open magnetic flux with the linear correlation coefficient of 0.913; 2) the area of the open magnetic field regions with the linear correlation coefficient of 0.946. These highly linear correlations could shed light on understanding how Alfvén wave turbulence accelerates the solar wind during different phases of the solar cycle and estimating the Poynting flux parameter for real-time solar wind predictions with AWSoM.

Comparative Analyses of Plasma Properties and Composition in Two Types of Small-Scale Interplanetary Flux-ropes

Jin [Huang](#), [Yu Liu](#), [Jihong Liu](#), [Yuandeng Shen](#)

ApJL 899 L29 2020

<https://arxiv.org/pdf/2008.02256.pdf>

<https://doi.org/10.3847/2041-8213/abac18>

The origin of small-scale interplanetary magnetic flux-ropes (SIMFRs) and the relationship between SIMFRs and magnetic clouds (MCs) are still controversial. In this study, two populations of SIMFRs were collected, i.e., SIMFRs originating from the Sun (SIMFR-SUN) and those originating from the solar wind (SIMFR-SW). We defined the SIMFR-SUN (SIMFR-SW) as the SIMFRs that include (exclude) the counter-streaming suprathermal electrons and stay away from (close to) the heliospheric current sheet. After fitting with force-free flux-rope model, 52 SIMFR-SUN and 57 SIMFR-SW events observed by Advanced Composition Explorer (ACE) from 1998 February to 2011 August were qualified. Using the approach of relating the measurements to their spatial position within the flux-ropes, a comparative survey of plasma and composition characteristics inside the two populations of SIMFRs is presented. Results show that the two populations of SIMFRs have apparent differences. Compared with SIMFR-SW, SIMFR-SUN are MC-like, featuring lower central proton density, higher V_{rad} , higher low-FIP element abundances, higher and more fluctuate average ion charge-states and the ion charge-state ratios which are related to the heating in low corona. In addition, for the ion charge-state distributions inside SIMFR-SUN, the sunward side is higher than earthward, which might be caused by the flare heating during eruption. Moreover, both SIMFR-SUN and MCs show anti-correlation between plasma beta and He/P trend. These characteristics indicate that SIMFR-SUN and MCs are very likely to have the identical origination. This study supports the two-source origin of SIMFRs, i.e., the solar corona and the solar wind.

Alfvénic Slow Solar Wind Observed in the Inner Heliosphere by Parker Solar Probe

Jia [Huang](#), [J. C. Kasper](#), [M. Stevens](#), [D. Vech](#), [K. G. Klein](#), et al.

ApJS 2020

<https://arxiv.org/pdf/2005.12372>

The slow solar wind is typically characterized as having low Alfvénicity. However, Parker Solar Probe (PSP) observed predominately Alfvénic slow solar wind during several of its initial encounters. From its first encounter observations, about 55.3% of the slow solar wind inside 0.25 au is highly Alfvénic ($|\sigma_C| > 0.7$) at current solar minimum, which is much higher than the fraction of quiet-Sun-associated highly Alfvénic slow wind observed at solar maximum at 1 au. Intervals of slow solar wind with different Alfvénicities seem to show similar plasma characteristics and temperature anisotropy distributions. Some low Alfvénicity slow wind intervals even show high temperature anisotropies, because the slow wind may experience perpendicular heating as fast wind does when close to the Sun. This signature is confirmed by Wind spacecraft measurements as we track PSP observations to 1 au. Further, with nearly 15 years of Wind measurements, we find that the distributions of plasma characteristics, temperature anisotropy and helium abundance ratio (N_{α}/N_p) are similar in slow winds with different Alfvénicities, but the distributions are different from those in the fast solar wind. Highly Alfvénic slow solar wind contains both helium-rich ($N_{\alpha}/N_p \sim 0.045$) and helium-poor ($N_{\alpha}/N_p \sim 0.015$) populations, implying it may originate from multiple source regions. These results suggest that highly Alfvénic slow solar wind shares similar temperature anisotropy and helium abundance properties with regular slow solar winds, and they thus should have multiple origins.

A Statistical Study of the Plasma and Composition Distribution inside Magnetic Clouds: 1998–2011

Jin [Huang](#)^{1,2,3}, [Yu Liu](#)^{1,2,3}, [Hengqiang Feng](#)⁴, [Ake Zhao](#)⁵, [Z. Z. Abidin](#)⁶, [Yuandeng Shen](#)¹, and [Oloketuyi Jacob](#)^{1,3}

2020 ApJ 893 136

[sci-hub.tw/10.3847/1538-4357/ab7a28](https://arxiv.org/abs/2008.02256)

A comprehensive analysis of plasma and composition characteristics inside magnetic clouds (MCs) observed by the Advanced Composition Explorer spacecraft from **1998 February to 2011 August** is presented. The results show that MCs have specific interior structures, and MCs of different speeds show differences in composition and structure. Compared with the slow MCs, fast MCs have enhanced mean charge states of iron, oxygen, silicon, magnesium, , , , and values. For ionic species in fast MCs, a higher atomic number represents a greater enhancement of mean charge state than slow MCs. We also find that both the fast and slow MCs display bimodal structure distribution in the mean iron charge state ($\langle Z \rangle$), which suggests that the existence of flux rope prior to the eruption is common. Furthermore, the , , and ratio distribution inside fast MCs have the feature that the posterior peak is higher than the anterior one. This result agrees with the "standard model" for coronal mass ejection/flares, by which magnetic reconnection occurs beneath the flux rope, thereby ionizing the ions of the posterior part of the flux rope sufficiently by high-energy electron collisions or by direct heating in the reconnection region.

Table 1 ACE MC Events and Model Fit Parameters

A multispacecraft study of a small flux rope entrained by rolling back magnetic field lines

Jia **Huang**, Yong C.-M. Liu, Jun Peng, Hui Li, Berndt Klecker, Charles J. Farrugia, Wenyuan Yu, Antoinette B. Galvin, Liang Zhao, Jiansen He

JGR Volume 122, Issue 7 July 2017 Pages 6927–6939

<http://sci-hub.cc/10.1002/2017JA023906>

We present a small flux rope (SFR) with smooth magnetic field rotations entrained by rolling back magnetic field lines around 1 AU. Such SFRs have only been seldom reported in the literature. This SFR was adjacent to a heliospheric plasma sheet (HPS), which is defined as a high plasma beta region in the vicinity of a heliospheric current sheet. Even though the SFR and HPS have different plasma beta, they possess similar plasma signatures (such as temperature, density, and bulk speed), density ratio of alpha particle-to-proton (N_{α}/N_p), and heavy ion ionization states, which imply that they may have a similar origin in the corona. The composition and the configuration of the rolling back magnetic field lines suggested that the SFR originated from the streamer belt through interchange reconnection. The origin processes of the SFR are presented here. Combining the observations of STEREO and ACE, the SFR was shown to have an axis tilted to the ecliptic plane and the radius may vary with different spatial positions. In this study, we suggest that interchange reconnection can play an important role for the origin of, at least, some SFRs and slow solar wind. **26-27 Apr 2007**

A multievent study of the coincidence of heliospheric current sheet and stream interface

Jia **Huang**, Yong C.-M. Liu, Zhaohui Qi, Berndt Klecker, Octav Marghitu, Antoinette B. Galvin, Charles J. Farrugia, Xiaoyu Li

JGR Vol: 121, Pages: 10,768–10,782 2016

Generally, the heliospheric current sheet (HCS) is separated from the stream interface (SI) at about 1 AU. A recent study found an event where the HCS coincides with the SI, and in which the HCS is separated from the true sector boundary (TSB), defined by the switch of suprathermal electron pitch angle distributions. We present a multievent study by using STEREO, ACE, and Wind data during 2007 to 2010 to investigate whether other classes of such coincidence cases exist, as well as their stability. We find coincidence cases related to ideal HCSs, separated TSB and HCS, or heat flux dropouts in the vicinity; therefore, we define them as types I, II, and III. Among the nine coincidence cases, there are seven type I, one type II, and one type III. For each type, a possible schematic origin is presented. We also compared the observations on different spacecraft. Only two out of nine cases are observed by several spacecraft with a large separation, indicating that the coincidence structures are usually unstable. The study also shows that the coincidence cases have a variable connection with pseudostreamers. Interchange reconnection and pseudostreamers could play a role in forming these coincidence cases and lead to different configurations in different situations.

Coincidence of heliospheric current sheet and stream interface: Implications for the origin and evolution of the solar wind

Jia **Huang**, Yong C.-M. Liu, Berndt Klecker, Yao Chen

JGR Volume 121, Issue 1 January 2016 Pages 19–29 2016

In general, the heliospheric current sheet (HCS), which defines the boundary of sunward and antisunward magnetic field, is encased by the slow solar wind. The stream interface (SI) represents the boundary between the solar wind plasmas of different origin and/or characteristics. According to earlier studies using data of low time resolution, the SI and HCS get closer further away from the Sun, and the two structures coincide with each other around 5 AU. In this study, we use STEREO data of a much higher time resolution to reveal an unusual case where the SI and HCS are coincident near 1 AU and separated from the so-called true sector boundary (TSB) at which the suprathermal electrons change their relative propagation directions. Preliminary analysis suggests that the closed loops in pseudostreamers continually have interchange reconnection with the open-field lines that lead them, resulting not only in the coincidence of HCS and SI but also in the separation of the TSB from the HCS/SI. We therefore conclude that the interchange reconnection plays an important role in the evolution of slow solar wind.

Analysis of the Forbush Decreases and Ground-Level Enhancement on September 2017 Using Neutron Spectrometers Operated in Antarctic and Midlatitude Stations

G. [Hubert](#), [M. T. Pазianotto](#) [C. A. Federico](#) [P. Ricaud](#)

JGR [Volume 124, Issue 1](#) January 2019 Pages 661-673

[sci-hub.tw/10.1029/2018JA025834](https://doi.org/10.1029/2018JA025834)

This work investigates solar events occurred in September 2017 characterized by a series of Forbush decreases and a ground level enhancement (GLE). Forbush decreases is a rapid decrease in the observed https://en.wikipedia.org/wiki/Galactic_cosmic_ray intensity following a coronal mass ejection while GLE is induced by a strong solar event for which the flux of high-energy solar particles is sufficient to enhance the radiation level on the ground. These investigations were performed using data recorded by a neutron spectrometer network composed of a Bonner sphere system. Two instruments located at Pic-du-Midi Observatory (+2,885 m above sea level) and at Concordia station (Antarctica, +3,233 m) record simultaneously and continuously the neutron spectra, allowing to consider short-term variations during solar events. The main objective is to analyze neutron spectral properties including their energy distributions and dynamics. This paper presents cosmic ray-induced neutron spectra during active solar event leading to changes in the local cosmic ray spectrum (Forbush decreases and a GLE). Concerning the GLE, analyses show that neutrons in the evaporation domain are particularly amplified during the GLE, while other energetic domains increase uniformly.

An impulsive geomagnetic effect from an early-impulsive flare

Hugh S. [Hudson](#), [Edward. W. Cliver](#), [Lyndsay Fletcher](#), [Declan A. Diver](#), [Peter T. Gallagher](#), [Ying Li](#), [Christopher M.J. Osborne](#), [Craig Stark](#), [Yang Su](#)

MNRAS **2024**

<https://arxiv.org/abs/2407.09233>

The geomagnetic "solar flare effect" (SFE) results from excess ionization in the Earth's ionosphere, famously first detected at the time of the Carrington flare in 1859. This indirect detection of a flare constituted one of the first cases of "multimessenger astronomy," whereby solar ionizing radiation stimulates ionospheric currents. Well-observed SFEs have few-minute time scales and perturbations of >10 nT, with the greatest events reaching above 100 nT. In previously reported cases the SFE time profiles tend to resemble those of solar soft X-ray emission, which ionizes the D-region; there is also a less-well-studied contribution from Lyman-alpha. We report here a specific case, from flare SOL2024-03-10 (M7.4), in which an impulsive SFE deviated from this pattern. This flare contained an "early impulsive" component of exceptionally hard radiation, extending up to gamma-ray energies above 1 MeV, distinctly before the bulk of the flare soft X-ray emission. We can characterize the spectral distribution of this early-impulsive component in detail, thanks to the modern extensive wavelength coverage. A more typical gradual SFE occurred during the flare's main phase. We suggest that events of this type warrant exploration of the solar physics in the "impulse response" limit of very short time scales.

Carrington events.

[Hudson HS](#)

(2021) *Annu Rev Astron Astrophys* 59:445.

<https://doi.org/10.1146/annurev-astro-112420-023324>

The Carrington event in 1859, a solar flare with an associated geomagnetic storm, has served as a prototype of possible superflare occurrence on the Sun. Recent geophysical (^{14}C signatures in tree rings) and precise time-series photometry [the bolometric total solar irradiance (TSI) for the Sun, and the broadband photometry from *Kepler* and *Transiting Exoplanet Survey Satellite*, for the stars] have broadened our perspective on extreme events and the threats that they pose for Earth and for Earth-like exoplanets. This review assesses the mutual solar and/or stellar lessons learned and the status of our theoretical understanding of the new data, both stellar and solar, as they relate to the physics of the Carrington event. The discussion includes the event's implied coronal mass ejection, its potential "solar cosmic ray" production, and the observed geomagnetic disturbances based on the multimessenger information already available in that era. Taking the Carrington event as an exemplar of the most extreme solar event, and in the context of our rich modern knowledge of solar flare and/or coronal mass ejection events, we discuss the aspects of these processes that might be relevant to activity on solar-type stars, and in particular their superflares.

MHD-Test Particles Simulations of Moderate CME and CIR-Driven Geomagnetic Storms at Solar Minimum

Mary K. [Hudson](#), [Scot R. Elkington](#), [Zhao Li](#), [Maulik Patel](#), [Kevin Pham](#), [Kareem Sorathia](#), [Alex Boyd](#), [Allison Jaynes](#), [Alexis Leali](#)

Space Weather e2021SW002882 2021

<https://agupubs.onlinelibrary.wiley.com/doi/epdf/10.1029/2021SW002882>

<https://doi.org/10.1029/2021SW002882>

As part of the Whole Heliosphere and Planetary Interactions initiative, contrasting drivers of radiation belt electron response at solar minimum have been investigated with MHD-test particle simulations for the **May 13–14, 2019** Coronal Mass Ejection (CME)-shock event and the **August 30–September 3, 2019** high speed solar wind interval. Both solar wind drivers produced moderate geomagnetic storms characterized by a minimum Dst = −65 nT and −52 nT, respectively, with the August - September event accompanied by prolonged substorm activity. The latter, with characteristic features of a Corotating Interaction Region (CIR)-driven storm, produced the hardest relativistic electron spectrum observed by Van Allen Probes during the last two years of the mission, ending in October 2019. MHD simulations were performed using both the Lyon-Fedder-Mobarry global MHD code and recently developed GAMERA model coupled to the Rice Convection Model, run with measured L1 solar wind input for both events studied, and coupled with test particle simulations, including an initial trapped and injected population. Initial electron Phase Space Density (PSD) profiles used measurements from the Relativistic Electron Proton Telescope and MagEIS energetic particle instruments on Van Allen Probes for test particle weighting and updating of the injected population at apogee. Results were compared directly with measurements and found to reproduce magnetopause loss for the CME-shock event and increased PSD for the CIR event. The two classes of events are contrasted for their impact on outer zone relativistic electrons near the end of Solar Cycle 24.

Solar Sector Structure

Review

Hugh S. [Hudson](#), Leif Svalgaard, Iain G. Hannah

[Space Science Reviews](#), December 2014, Volume 186, [Issue 1-4](#), pp 17-34

The interplanetary magnetic field near 1 AU has a characteristic “sector” structure that reflects its polarity relative to the solar direction. Typically we observe large-scale coherence in these directions, with two or four “away” or “towards” sectors per solar rotation, from any platform in deep space and near the ecliptic plane. In a simple picture, this morphology simply reflects the idea that the sources of the interplanetary field lie mainly in or near the Sun, and that the solar-wind flow enforces a radial component in this field. The sector boundaries are sharply defined in the interplanetary field near one AU, but have more complicated sources within the Sun itself. Recent evidence confirms that the origins of this pattern also appear statistically at the level of the photosphere, with signatures found in the highly concentrated fields of sunspots and even solar flares. This complements the associations already known between the interplanetary sectors and large-scale coronal structures (i.e., the streamers). This association with small-scale fields strengthens at the Hale sector boundary, defining the Hale boundary as the one for which the polarity switch matches that of the leading-to-following polarity alternation in the sunspots of a given hemisphere. Surface features that appear 4.5 days prior to the sector crossings observed at 1 AU correlate with this sense of polarity reversal.

Geomagnetic storms over the last solar cycle: A superposed epoch analysis

[Hutchinson](#), J. A.; Wright, D. M.; Milan, S. E.

J. Geophys. Res., Vol. 116, No. A9, A09211, 2011

<http://dx.doi.org/10.1029/2011JA016463>

<https://agupubs.onlinelibrary.wiley.com/doi/pdf/10.1029/2011JA016463>

Presented here is a discussion of the results of a superposed epoch analysis of geomagnetic storms over the last solar cycle. Storms, identified by means of their characteristic SYM-H evolution, are separated by size into weak ($-150 < \text{SYM-H} \leq -80$) nT, moderate ($-300 < \text{SYM-H} \leq -150$) nT, and intense ($\text{SYM-H} \leq -300$) nT categories. Where possible, the corresponding solar wind (SW) onset mechanisms were located by means of 1 min ACE OMNI data. Intense storms were observed to be driven solely by coronal mass ejections (CMEs); moderate storms were dominated by CME onset, while only weak storms were driven by both CMEs and corotating interaction regions (CIRs) at a ratio of ~2:1, respectively. As might be expected, more intense storms resulted from the largest SW enhancements. Individual storm phase durations for different storm sizes were investigated, revealing that the duration of the main phase increases with storm size to a critical point, then decreases for more intense storms, contrary to the findings of a previous study by Yokoyama and Kamide (1997). Various SW-magnetosphere coupling functions were investigated for this data set in an attempt to estimate storm size from SW conditions.

Interplanetary Coronal Mass Ejections During Solar Cycles 23 and 24: Sun–Earth Propagation Characteristics and Consequences at the Near-Earth Region

M. Syed [Ibrahim](#), Bhuwan Joshi, K.-S. Cho, R.-S. Kim, Y.-J. Moon

[Solar Physics](#) May 2019, 294:54 [File](#)

sci-hub.se/10.1007/s11207-019-1443-5

In this article, we present a statistical study probing the relation between interplanetary coronal mass ejections (ICMEs) observed at 1 AU and their corresponding coronal mass ejections at the near-Sun region. The work encompasses the ICME activity that occurred during Solar Cycles 23 and 24 (1996 – 2017) while presenting an overall picture of ICME events during the complete Solar Cycle 24 for the first time. The importance of this study further lies in comparing two subsets of ICMEs, i.e. magnetic clouds (MCs) and ejecta (EJ), to explore how the observed structures of ICMEs at 1 AU could be associated with the properties of CMEs during their launch at the Sun. We find that, although Solar Cycle 24 saw a significant reduction in the number of ICME events compared to the previous cycle, the fraction of MCs was much higher during Cycle 24 than Cycle 23 (60% versus 41%). In general, the ICME transit-time decreases with the increase in the CME initial speed, although a broad range of transit times were observed for a given CME speed. We also find that the high-speed ICMEs ($\geq 500 \text{ km s}^{-1}$) form a distinct group in terms of the deficit in their transit times when compared with low-speed events ($\leq 500 \text{ km s}^{-1}$), which means that high-speed ICMEs acquire a much higher internal energy from the source active regions during the initiation process that effectively overcomes the aerodynamic drag force while they transit in the interplanetary medium. The CME propagation from the Sun to the near-Earth environment shows both an overall positive and negative acceleration (i.e. deceleration), although the acceleration is limited to only low-speed CMEs that are launched with a speed comparable with or less than the mean solar wind speed ($\approx 400\text{--}450 \text{ km s}^{-1}$). Within a given cycle, the similarities of MC and EJ profiles with respect to the CME–ICME speed relation as well as interplanetary acceleration support the hypothesis that all CMEs have a flux rope structure and that the trajectory of the CMEs essentially determines the observed ICME structure at 1 AU. **13 December 2006, 22 June 2015**

Propagation of Coronal Mass Ejections Observed During the Rising Phase of Solar Cycle 24

M. Syed [Ibrahim](#), P. K. Manoharan, A. Shanmugaraju

[Solar Physics](#) September 2017, 292:133 [File](#)

In this study, we investigate the interplanetary consequences and travel time details of 58 coronal mass ejections (CMEs) in the Sun–Earth distance. The CMEs considered are halo and partial halo events of width $>120^\circ$. These CMEs occurred during 2009 – 2013, in the ascending phase of the Solar Cycle 24. Moreover, they are Earth-directed events that originated close to the centre of the solar disk (within about $\pm 30^\circ$ from the Sun’s centre) and propagated approximately along the Sun–Earth line. For each CME, the onset time and the initial speed have been estimated from the white-light images observed by the LASCO coronagraphs onboard the SOHO space mission. These CMEs cover an initial speed range of $\sim 260\text{--}2700 \text{ km s}^{-1}$. For these CMEs, the associated interplanetary shocks (IP shocks) and interplanetary CMEs (ICMEs) at the near-Earth environment have been identified from *in-situ* solar wind measurements available at the OMNI data base. Most of these events have been associated with moderate to intense IP shocks. However, these events have caused only weak to moderate geomagnetic storms in the Earth’s magnetosphere. The relationship of the travel time with the initial speed of the CME has been compared with the observations made in the previous Cycle 23, during 1996 – 2004. In the present study, for a given initial speed of the CME, the travel time and the speed at 1 AU suggest that the CME was most likely not much affected by the drag caused by the slow-speed dominated heliosphere. Additionally, the weak geomagnetic storms and moderate IP shocks associated with the current set of Earth-directed CMEs indicate magnetically weak CME events of Cycle 24. The magnetic energy that is available to propagate CME and cause geomagnetic storm could be significantly low. **15 March 2013.**

Table 1 Observational parameters of 58 CME events (eight interacting CMEs are marked with asterisk symbols).

Transit time of CME/shock associated with four major geo-effective CMEs in solar cycle 24

M. Syed [Ibrahim](#), A. Shanmugaraju, M. Benedict Lawrance

Advances in Space Research, Volume 55, Issue 1, 1 January 2015, Pages 407–415

<http://www.sciencedirect.com/science/article/pii/S0273117714006139>

The kinematics of coronal mass ejection (CME) in the interplanetary medium is very important in the concept of space-weather. Main aim of this paper is to study the propagation of four major geo-effective CMEs and their associated shocks observed in solar cycle 24. The arrival of interplanetary shocks and CMEs of these events near the Earth is seen

from the ACE/wind in situ data available in OMNI data base. The CMEs considered in this study have a wide range of initial speeds 500–1900 km/s in the LASCO field of view, comprising of two slow CMEs ($V \sim 500$ km/s), one fast CME ($V \sim 1800$ km/s) and one moderate speed CME ($V \sim 800$ km/s). The observed transit time of these events are compared with transit time estimated using the empirical shock arrival model (ESA). Especially, we utilize (i) different acceleration – speed equations reported in the literature from the observations made in the last few decades and (ii) various acceleration cessation distances (Ac_d) In addition, we compared the estimated and observed transit time with that from the Drag Based Model (DBM). From the result of this analysis, we demonstrated that each CME behaves in its own way in the interplanetary medium and their propagation is governed by the CME initial speed, interplanetary acceleration and acceleration cessation distances. In the present paper, we found (i) which acceleration equation is better for the transit time calculations (ii) importance of the CME acceleration cessation distances (iii) reducing the transit time error in CME forecasting. Based on these results and on Zhao and Dryer (2014) review (that included physics-based models), the realistic statistics should be based on real-time studies, not on post-mortem case studies.

2011/10/22, 2012/03/07, 2012/04/19, 2012/07/12

The effects of solar wind on galactic cosmic ray flux at Earth

G. D. **Ihongo**, C. H.-T. Wang

[Astrophysics and Space Science](#) January 2016, 361:44 **Open Access**

The amount of solar wind produced continuously by the sun is not constant due to changes in solar activity. This unsteady nature of the solar wind seems to be responsible for galactic cosmic ray flux modulation, hence the flux of incoming galactic cosmic rays observed at the top of the Earth's atmosphere varies with the solar wind reflecting the solar activity. The aforementioned reasons have lead to attempts by several researchers to study correlations between galactic cosmic rays and the solar wind. However, most of the correlation studies carried out by authors earlier are based on the analyses of observational data from neutron monitors. In this context, we study the effects of solar wind on galactic cosmic ray flux observed at $r \approx 1$ AU, using a theoretical approach and found that the solar wind causes significant decreases in galactic cosmic ray flux at $r \approx 1$ AU. A short time variation of the calculated flux is also checked and the result is reflected by exposing a negative correlation of the solar wind with the corresponding galactic cosmic ray flux. This means that the higher the solar wind the lower the galactic cosmic rays flux and vice-versa. To obtain a better understanding, the calculated flux and its short time variation at 1 AU are compared to data that shows a good fit to the model making it possible to establish a statistically significant negative correlation of -0.988 ± 0.001 between solar wind variation and galactic cosmic rays flux variation theoretically.

Kinematic Properties of Slow ICMEs and an Interpretation of a Modified Drag Equation for Fast and Moderate ICMEs

T. **Iju**, M. Tokumaru, K. Fujiki

Solar Physics, June 2014, Volume 289, Issue 6, pp 2157-2175

<http://arxiv.org/pdf/1401.1724v1.pdf>

We report kinematic properties of slow interplanetary coronal mass ejections (ICMEs) identified by SOHO/LASCO, interplanetary scintillation, and in situ observations and propose a modified equation for the ICME motion. We identified seven ICMEs between 2010 and 2011 and compared them with 39 events reported in our previous work. We examined 15 fast ($V_{\text{SOHO}} - V_{\text{bg}} > 500$ km s⁻¹), 25 moderate ($0 \text{ km s}^{-1} \leq V_{\text{SOHO}} - V_{\text{bg}} \leq 500$ km s⁻¹), and 6 slow ($V_{\text{SOHO}} - V_{\text{bg}} < 0$ km s⁻¹) ICMEs, where V_{SOHO} and V_{bg} are the initial speed of ICMEs and the speed of the background solar wind. For slow ICMEs, we found the following results: i) They accelerate toward the speed of the background solar wind during their propagation and reach their final speed by 0.34 ± 0.03 AU. ii) The acceleration ends when they reach 479 ± 126 km s⁻¹; this is close to the typical speed of the solar wind during the period of this study. iii) When γ_1 and γ_2 are assumed to be constants, a quadratic equation for the acceleration $a = -\gamma_2 (V - V_{\text{bg}}) |V - V_{\text{bg}}|$ is more appropriate than a linear one $a = -\gamma_1 (V - V_{\text{bg}})$, where V is the propagation speed of ICMEs, while the latter gives a smaller χ^2 value than the former. For the motion of the fast and moderate ICMEs, we found a modified drag equation $a = -2.07 \times 10^{-12} (V - V_{\text{bg}}) |V - V_{\text{bg}}| - 4.84 \times 10^{-6} (V - V_{\text{bg}})$. From the viewpoint of fluid dynamics, we interpret this equation as indicating that ICMEs with $0 \text{ km s}^{-1} \leq V - V_{\text{bg}} \leq 2300$ km s⁻¹ are controlled mainly by the hydrodynamic Stokes drag force, while the aerodynamic drag force is a predominant factor for the propagation of ICME with $V - V_{\text{bg}} > 2300$ km s⁻¹.

Radial Speed Evolution of Interplanetary Coronal Mass Ejections During Solar Cycle 23

T. **Iju**, M. Tokumaru, K. Fujiki

Solar Physics, November 2013, Volume 288, Issue 1, pp 331-353

<http://arxiv.org/pdf/1303.5154v3.pdf>

We report radial-speed evolution of interplanetary coronal mass ejections (ICMEs) detected by the Large Angle and Spectrometric Coronagraph onboard the Solar and Heliospheric Observatory (SOHO/LASCO), interplanetary scintillation (IPS) at 327 MHz, and in-situ observations. We analyze solar-wind disturbance factor (g -value) data derived from IPS observations during 1997–2009 covering nearly the whole period of Solar Cycle 23. By comparing observations from SOHO/LASCO, IPS, and in situ, we identify 39 ICMEs that could be analyzed carefully. Here, we define two speeds [V SOHO and V bg], which are the initial speed of the ICME and the speed of the background solar wind, respectively. Examinations of these speeds yield the following results: i) Fast ICMEs (with V SOHO– V bg > 500 km s $^{-1}$) rapidly decelerate, moderate ICMEs (with 0 km s $^{-1}$ \leq V SOHO– V bg ≤ 500 km s $^{-1}$) show either gradually decelerating or uniform motion, and slow ICMEs (with V SOHO– V bg < 0 km s $^{-1}$) accelerate. The radial speeds converge on the speed of the background solar wind during their outward propagation. We subsequently find; ii) both the acceleration and the deceleration are nearly complete by 0.79 ± 0.04 AU, and those are ended when the ICMEs reach a 480 ± 21 km s $^{-1}$. iii) For ICMEs with $(V$ SOHO– V bg) ≥ 0 km s $^{-1}$, i.e. fast and moderate ICMEs, a linear equation $a = -\gamma_1(V - V_{bg})$ with $\gamma_1 = 6.58 \pm 0.23 \times 10^{-6}$ s $^{-1}$ is more appropriate than a quadratic equation $a = -\gamma_2(V - V_{bg})|V - V_{bg}|$ to describe their kinematics, where γ_1 and γ_2 are coefficients, and a and V are the acceleration and speed of ICMEs, respectively, because the χ^2 for the linear equation satisfies the statistical significance level of 0.05, while the quadratic one does not. These results support the assumption that the radial motion of ICMEs is governed by a drag force due to interaction with the background solar wind. These findings also suggest that ICMEs propagating faster than the background solar wind are controlled mainly by the hydrodynamic Stokes drag.

Table 1. Properties derived from SOHO/LASCO observations and those in the SOHO–IPS region derived from IPS observations for 39 ICMEs during 1997–2009.

Table 2. Properties in the IPS–Earth region derived from IPS observations, detection dates, times, and speeds obtained by in-situ observations at 1 AU, fitting parameters and speeds of the background solar wind for 39 ICMEs during 1997–2009.

Beyond the mini-solar maximum of solar cycle 24: Declining solar magnetic fields and the response of the terrestrial magnetosphere

M. Ingale, P. Janardhan, S. K. Bisoi

JGR **Volume 124, Issue 8** Pages 6363-6383 2019

<https://arxiv.org/pdf/1908.02576.pdf>

<https://agupubs.onlinelibrary.wiley.com/doi/epdf/10.1029/2019JA026616>

The present study examines the response of the terrestrial magnetosphere to the long-term steady declining trends observed in solar magnetic fields and solar wind micro-turbulence levels since mid-1990's that has been continuing beyond the mini-solar maximum of cycle 24. A detailed analysis of the response of the terrestrial magnetosphere has been carried out by studying the extent and shape of the Earth's magnetopause and bow shock over the past four solar cycles. We estimate sub-solar stand-off distance of the magnetopause and bow shock, and the shape of the magnetopause using numerical as well as empirical models. The computed magnetopause and bow shock stand-off distances have been found to be increasing steadily since around mid-1990's, consistent with the steady declining trend seen in solar magnetic fields and solar wind micro-turbulence levels. Similarly, we find an expansion in the shape of the magnetopause since 1996. The implications of the increasing trend seen in the magnetopause and bow shock stand-off distances are discussed and a forecast of the shape of the magnetopause in 2020, the minimum of cycle 24, has been made. Importantly, we also find two instances between 1968 and 1991 when the magnetopause stand-off distance dropped to values close to 6.6 earth radii, the geostationary orbit, for duration ranging from 9–11 hours and one event in 2005, post 1995 when the decline in photospheric fields began. Though there have been no such events since 2005, it represents a clear and present danger to our satellite systems.

Recent Voyager Evidence for Rapid Transport of Flare-Generated Disturbances by Polar Coronal Hole Streams

D S Intriligator¹, W D Miller¹, J Intriligator^{1,2}, W Webber³, W Sun⁴, T Detman¹, M Dwyer¹ and C Deehr⁴

Journal of Physics: Conference Series, Volume 900, Number 1 012010 2017

<http://iopscience.iop.org/article/10.1088/1742-6596/900/1/012010/pdf>

Disturbances observed by Voyagers 1 and 2 during the past five years or more may have been transported by plasma emitted from polar coronal holes, thereby having travelled much faster from the Sun to the termination shock than previously recognized. Estimating the average speed to the shock as 750 km/s has produced consistently good

associations between solar flares, or groups of them, and dynamic pressure increases at Voyager 2 and plasma wave events at Voyager 1. Furthermore, magnetograph observations confirm that polar coronal holes were present around the times of the flares to which the events at the Voyagers have been attributed. These calculations also provide revised estimates of the transport of heliospheric current sheet fluctuations. We discuss the possibilities that extrapolations from past observations and simulations based on them may provide insight into currently challenging issues and possible future developments. **Aug. 9, 2011 Sept. 6, 2011, Mar. 10, 2012, Jul. 12, 2012 Jul. 23, 2012, Dec. 14, 2012, Jun. 10, 2014, Dec. 13, 2014 Dec. 17, 2014, Feb. 21, 2015**

Did the July 2012 solar events cause a “tsunami” throughout the heliosphere, heliosheath, and into the interstellar medium?†

Devrie [Intriligator](#)^{1,*}, Wei Sun^{1,2}, Murray Dryer¹, James Intriligator^{1,3}, Charles Deehr², Thomas Detman¹ and William R. Webbe

JGR Volume 120, Issue 10 Volume 120, Issue 10 Oct 2015

The July 2012 major solar events gave rise to manifestations observed at many longitudes/latitudes/radial locations throughout the heliosphere, heliosheath, and into the interstellar medium. For these solar events we present our initial results at 1 AU from our HAFSS (HAF Source Surface) three-dimensional time-dependent kinematic modeling. Our simulations, using WSA maps and solar event observations, start at 2.5 Rs from the center of the Sun. We use both the quiescent background solar conditions and the solar events (e.g., coronal mass ejections (CMEs)) as inputs and propagate outward. We compare HAFSS predictions with in-situ spacecraft measurements and conclude that the July 2012 solar events caused a metaphorical “tsunami” in the plasma and magnetic field throughout the heliosphere/heliosheath/interstellar medium. The simulations show evidence of shocks, interaction regions, and rarefaction regions in the inner heliosphere (1 AU) and shocks, Global Merged Interaction Regions (GMIRs), and rarefaction regions in the heliosheath. The shocks/interaction regions/GMIRs and the rarefaction regions are, respectively, analogous to the “tsunami” “crests” and “troughs”. To provide important insights into 3D processes we simulated 1 AU observations (STEREO A and ACE) and observations at Voyager 2 (V2) and Voyager 1 (V1) far off the ecliptic plane: V2 at ~30° South, 217° longitude, and 102 AU; V1 at 34° North, 174° longitude, and 124 AU. HAFSS successfully predicted observed CME arrival times at 1 AU. Our results for this “tsunami” are the first simulations for these events in the distant V2/V1 radial/latitudinal/longitudinal regions based on 3D time-dependent modeling originating at the Sun.

An Investigation of Properties of the Coronal Holes Producing HSSs InProCH

D. Beşliu [Ionescu](#)^{1, 2} and G. Mariş Muntean¹

SCOSTEP/PRESTO NEWSLETTER Vol. 39, April 2024

https://scostep.org/wp-content/uploads/2024/04/SCOSTEP_PRESTO_Newsletter_Vol39_high_reso.pdf

We have prepared a database that is available online at <http://observer.astro.ro/inproch/>. This database contains coronal holes (CHs) observed during the descending phase of solar cycle 24 (SC24), specifically the period from Apr 2015 to Jul 2017, extended by three months before and after this interval.

FRiED: A NOVEL THREE-DIMENSIONAL MODEL OF CORONAL MASS EJECTIONS

A. [Isavnin](#)

2016 ApJ 833 267

<http://sci-hub.cc/10.3847/1538-4357/833/2/267>

We present a novel three-dimensional (3D) model of coronal mass ejections (CMEs) that unifies all key evolutionary aspects of CMEs and encapsulates their 3D magnetic field configuration. This fully analytic model is capable of reproducing the global geometrical shape of a CME with all major deformations taken into account, i.e., deflection, rotation, expansion, “pancaking,” front flattening, and rotational skew. Encapsulation of 3D magnetic structure allows the model to reproduce in-situ measurements of magnetic field for trajectories of spacecraft-CME encounters of any degree of complexity. As such, the model can be used single-handedly for the consistent analysis of both remote and in-situ observations of CMEs at any heliocentric distance. We demonstrate the latter by successfully applying the model for the analysis of two CMEs. **2010 December 12, 2011 October 1**

Three-Dimensional Evolution of Flux-Rope CMEs and Its Relation to the Local Orientation of the Heliospheric Current Sheet

A. [Isavnin](#), A. Vourlidas, E. K. J. Kilpua

Solar Phys., 2014, File

Flux ropes ejected from the Sun may change their geometrical orientation during their evolution, which directly affects their geoeffectiveness. Therefore, it is crucial to understand how solar flux ropes evolve in the heliosphere to improve our space-weather forecasting tools. We present a follow-up study of the concepts described by Isavnin, Vourlidas, and Kilpua (Solar Phys. 284, 203, 2013). We analyze 14 coronal mass ejections (CMEs), with clear flux-rope signatures, observed during the decay of Solar Cycle 23 and rise of Solar Cycle 24. First, we estimate initial orientations of the flux ropes at the origin using extreme-ultraviolet observations of post-eruption arcades and/or eruptive prominences. Then we reconstruct multi-viewpoint coronagraph observations of the CMEs from ≈ 2 to $30 R_{\odot}$ with a three-dimensional geometric representation of a flux rope to determine their geometrical parameters. Finally, we propagate the flux ropes from $\approx 30 R_{\odot}$ to 1 AU through MHD-simulated background solar wind while using in-situ measurements at 1 AU of the associated magnetic cloud as a constraint for the propagation technique. This methodology allows us to estimate the flux-rope orientation all the way from the Sun to 1 AU. We find that while the flux-ropes' deflection occurs predominantly below $30 R_{\odot}$, a significant amount of deflection and rotation happens between $30 R_{\odot}$ and 1 AU. We compare the flux-rope orientation to the local orientation of the heliospheric current sheet (HCS). We find that slow flux ropes tend to align with the streams of slow solar wind in the inner heliosphere. During the solar-cycle minimum the slow solar-wind channel as well as the HCS usually occupy the area in the vicinity of the solar equatorial plane, which in the past led researchers to the hypothesis that flux ropes align with the HCS. Our results show that exceptions from this rule are explained by interaction with the Parker-spiraled background magnetic field, which dominates over the magnetic interaction with the HCS in the inner heliosphere at least during solar-minimum conditions.

Three-Dimensional Evolution of Erupted Flux Ropes from the Sun ($2 - 20 R_{\odot}$) to 1 AU

A. [Isavnin](#), A. Vourlidas, E. K. J. Kilpua

Solar Physics

May **2013**, Volume 284, Issue 1, pp 203-215; **File**

Studying the evolution of magnetic clouds entrained in coronal mass ejections using in-situ data is a difficult task, since only a limited number of observational points is available at large heliocentric distances. Remote sensing observations can, however, provide important information for events close to the Sun. In this work we estimate the flux rope orientation first in the close vicinity of the Sun ($2 - 20 R_{\odot}$) using forward modeling of STEREO/SECCHI and SOHO/LASCO coronagraph images of coronal mass ejections and then in situ using Grad-Shafranov reconstruction of the magnetic cloud. Thus, we are able to measure changes in the orientation of the erupted flux ropes as they propagate from the Sun to 1 AU. We present both techniques and use them to study 15 magnetic clouds observed during the minimum following Solar Cycle 23 and the rise of Solar Cycle 24. This is the first multievent study to compare the three-dimensional parameters of CMEs from imaging and in-situ reconstructions. The results of our analysis confirm earlier studies showing that the flux ropes tend to deflect towards the solar equatorial plane. We also find evidence of rotation on their travel from the Sun to 1 AU. In contrast to past studies, our method allows one to deduce the evolution of the three-dimensional orientation of individual flux ropes rather than on a statistical basis.

Grad-Shafranov Reconstruction of Magnetic Clouds: Overview and Improvements

A. [Isavnin](#), E. K. J. Kilpua and H. E. J. Koskinen

Solar Physics, Volume 273, Number 1, 205-219, **2011**,

The Grad-Shafranov reconstruction is a method of estimating the orientation (invariant axis) and cross section of magnetic flux ropes using the data from a single spacecraft. It can be applied to various magnetic structures such as magnetic clouds (MCs) and flux ropes embedded in the magnetopause and in the solar wind. We develop a number of improvements of this technique and show some examples of the reconstruction procedure of interplanetary coronal mass ejections (ICMEs) observed at 1 AU by the STEREO, Wind, and ACE spacecraft during the minimum following Solar Cycle 23. The analysis is conducted not only for ideal localized ICME events but also for non-trivial cases of magnetic clouds in fast solar wind. The Grad-Shafranov reconstruction gives reasonable results for the sample events, although it possesses certain limitations, which need to be taken into account during the interpretation of the model results.

7 November 2008, 9 November 2004, 11 July 2009:

Suzaku detection of enigmatic geocoronal solar wind charge exchange event associated with coronal mass ejection

[Daiki Ishi](#), [Kumi Ishikawa](#), [Masaki Numazawa](#), [Yoshizumi Miyoshi](#), [Naoki Terada](#), [Kazuhiisa Mitsuda](#), [Takaya Ohashi](#), [Yuichiro Ezoe](#)

PASJ 2019

<https://arxiv.org/pdf/1902.07652.pdf>

Suzaku detected an enhancement of soft X-ray background associated with solar eruptions on **2013 April 14-15**. The solar eruptions were accompanied by an M6.5 solar flare and a coronal mass ejection with magnetic flux ropes. The enhanced soft X-ray background showed a slight variation in half a day and then a clear one in a few hours. The former spectrum was composed of oxygen emission lines, while the later one was characterized by a series of emission lines from highly ionized carbon to silicon. The soft X-ray enhancement originated from geocoronal solar wind charge exchange. However, there appeared to be no significant time correlation with the solar wind proton flux measured by the ACE and WIND satellites. From other solar wind signatures, we considered that an interplanetary shock associated with the coronal mass ejection and a turbulent sheath immediately behind the shock compressed the ambient solar wind ions and then resulted in the soft X-ray enhancement. Furthermore, the enriched emission lines were presumed to be due to an unusual set of ion abundances and ionization states within the coronal mass ejection. We found a better time correlation with the solar wind alpha flux rather than the solar wind proton flux. Our results suggest that the solar wind proton flux is not always a good indicator of geocoronal solar wind charge exchange, especially associated with coronal mass ejections. Instead, the solar wind alpha flux should be investigated when such a soft X-ray enhancement is detected in astronomical observations.

Intense geomagnetic storm during Maunder minimum possibly by a quiescent filament eruption

[Hiroaki Isobe](#), [Yusuke Ebihara](#), [Akito D. Kawamura](#), [Harufumi Tamazawa](#), [Hisashi Hayakawa](#)

ApJ 887 7 2019

<https://arxiv.org/pdf/1903.08466.pdf>

<https://doi.org/10.3847/1538-4357/ab107e>

<https://sci-hub.st/10.3847/1538-4357/ab107e>

The sun occasionally undergoes the so-called grand minima, in which its magnetic activity, measured by the number of sunspots, is suppressed for decades. The most prominent grand minima, since the beginning of telescopic observations of sunspots, is the Maunder minimum (1645-1715), when the sunspots became rather scarce. The mechanism underlying the grand minima remains poorly understood as there is little observational information of the solar magnetic field at that time. In this study, we examine the records of one candidate aurora display in China and Japan during the Maunder minimum. The presence of auroras in such mid magnetic latitudes indicates the occurrence of great geomagnetic storms that are usually produced by strong solar flares. However, the records of contemporary sunspot observations from Europe suggest that, at least for the likely aurora event, there was no large sunspot that could produce a strong flare. Through simple theoretical arguments, we show that this geomagnetic storm could have been generated by an eruption giant quiescent filament, or a series of such events. **March 2, 1653**

Solar-terrestrial storm of November 18 20, 2003. 1. Near-Earth disturbances in the solar wind

[Ivanov](#), K. G.; [Romashets](#), E. P.; [Kharshiladze](#), A. F.

Geomagnetism and Aeronomy, Volume 46, Issue 3, pp.275-293, 2006, File

Geomagnetizm i Aeronomiya, 2006, Vol. 46, No. 3, pp. 291–309.

The structure, configuration, dynamics, and solar sources of the near-Earth MHD disturbance of the solar wind on November 20, 2003, is considered. The disturbances of October 24 and November 22 after flares from the same AR 10484 (10501) are compared. The velocity field in the leading part of the sporadic disturbance is for the first time studied in the coordinate system stationary relative to the bow shock. A possible scenario of the physical processes in the course of this solar-terrestrial storm is discussed in comparison with the previously developed scenario for the storm of July 15, 2000. It has been indicated that (1) the near-Earth disturbance was observed at the sector boundary (HCS) and in its vicinities and (2) the disturbance MHD structure included: the complicated bow shock, wide boundary layer with reconnecting fields at a transition from the shock to the magnetic cloud, magnetic cloud with a magnetic cavity including packed substance of an active filament, and return shock layer (supposedly). It has been found out that the shock front configuration and the velocity field are reproduced at an identical position of AR and HCS relative to the Earth on November 20 and 24. It has been indicated that the maximal magnetic induction in the cloud satisfied the condition $B_m = (8\pi n l m p)^{1/2} (D - NV1)$, i.e., depended on the dynamic impact on the cloud during all three storms [Ivanov et al., 1974]. When the disturbance was related to solar sources, the attention has been paid to the parallelism of the axes of symmetry of the active filament, transient coronal hole, coronal mass ejection, zero line of the open coronal

field (HCS), and the axis of the near-Earth magnetic cloud: the regularity previously established in the scenario of the storm of July 15, 2000 [Ivanov et al., 2005]. It has been indicated that the extremely large B_m value in the cloud of October 20 was caused by a strong suppression of the series of postflare shocks reflected from the heliospheric streamer.

Interplanetary hydromagnetic clouds as flare-generated spheromaks

Ivanov, K.G., Kharshiladze, A.F.:

1985, Sol. Phys. 98, 379, **File**.

Solar flare-generated interplanetary clouds are proposed to be treated as oblate spheromaks (oblamaks) with predominantly force-free magnetic field. The solution found for a force-free field equation in spheroidal coordinates makes it possible to describe the spheromak magnetic fields by a series of spheroidal wave functions. Comparison between theoretical and experimental results is shown in the case of the hydromagnetic cloud from the November 22, 1977 flare (STIP Interval IV).

Magnetohydrodynamic simulation of coronal mass ejections using interplanetary scintillation data observed from radio sites ISEE and LOFAR

Kazumasa **Iwai**, [Richard A. Fallows](#), [Mario M. Bisi](#), [Daikou Shiota](#), [Bernard V. Jackson](#), [Munetoshi Tokumaru](#), [Ken'ichi Fujiki](#)

Advances in Space Research **2022**

<https://arxiv.org/ftp/arxiv/papers/2209/2209.12486.pdf>

Interplanetary scintillation (IPS) is a useful tool for detecting coronal mass ejections (CMEs) throughout interplanetary space. Global magnetohydrodynamic (MHD) simulations of the heliosphere, which are usually used to predict the arrival and geo-effectiveness of CMEs, can be improved using IPS data. In this study, we demonstrate an MHD simulation that includes IPS data from multiple stations to improve CME modelling. The CMEs, which occurred on 09-10 September 2017, were observed over the period 10-12 September 2017 using the Low-Frequency Array (LOFAR) and IPS array of the Institute for Space-Earth Environmental Research (ISEE), Nagoya University, as they tracked through the inner heliosphere. We simulated CME propagation using a global MHD simulation, SUSANOO-CME, in which CMEs were modeled as spheromaks, and the IPS data were synthesised from the simulation results. The MHD simulation suggests that the CMEs merged in interplanetary space, forming complicated IPS g-level distributions in the sky map. We found that the MHD simulation that best fits both LOFAR and ISEE data provided a better reconstruction of the CMEs and a better forecast of their arrival at Earth than from measurements when these simulations were fit from the ISEE site alone. More IPS data observed from multiple stations at different local times in this study can help reconstruct the global structure of the CME, thus improving and evaluating the CME modelling. **9-12 Sep 2017**

Development of a coronal mass ejection arrival time forecasting system using interplanetary scintillation observations

Kazumasa **Iwai**, [Daikou Shiota](#), [Munetoshi Tokumaru](#), [Kenichi Fujiki](#), [Mitsue Den](#), [Yūki Kubo](#)

Earth, Planets and Space **71:39 2019**

<https://arxiv.org/ftp/arxiv/papers/1903/1903.11769.pdf>

<https://arxiv.org/ftp/arxiv/papers/2012/2012.12635.pdf>

[sci-hub.se/10.1186/s40623-019-1019-5](https://doi.org/10.1186/s40623-019-1019-5)

Coronal mass ejections (CMEs) cause disturbances in the environment of the Earth when they arrive at the Earth. However, the prediction of the arrival of CMEs still remains a challenge. We have developed an interplanetary scintillation (IPS) estimation system based on a global magnetohydrodynamic (MHD) simulation of the inner heliosphere to predict the arrival time of CMEs. In this system, the initial speed of a CME is roughly derived from white light coronagraph observations. Then, the propagation of the CME is calculated by a global MHD simulation. The IPS response is estimated by the three-dimensional density distribution of the inner heliosphere derived from the MHD simulation. The simulated IPS response is compared with the actual IPS observations made by the Institute for Space-Earth Environmental Research, Nagoya University, and shows good agreement with that observed. We demonstrated how the simulation system works using a halo CME event generated by a X9.3 flare observed on **September 6, 2017**. We find that the CME simulation that best estimates the IPS observation can more accurately predict the time of arrival of the CME at the Earth. These results suggest that the accuracy of the CME arrival time can be improved if our current MHD simulations include IPS data.

Table 1. CME characteristics investigated in this study and their observed and forecasted arrival times.

PSTEP Science Nuggets # 23 Apr 2019

http://www.pstep.jp/news_en/nuggets23en.html

Forecasting Heliospheric CME Solar-Wind Parameters Using the UCSD Time-Dependent Tomography and ISEE Interplanetary Scintillation Data: The 10 March 2022 CME

Bernard V. Jackson, Munetoshi Tokumaru, Kazumasa Iwai, Matthew T. Bracamontes, +++
Solar Physics volume 298, Article number: 74 (2023)

<https://link.springer.com/content/pdf/10.1007/s11207-023-02169-8.pdf>

Remotely sensed interplanetary scintillation (IPS) data from the Institute for Space-Earth Environmental Research (ISEE), Japan, allows a determination of solar-wind parameters throughout the inner heliosphere. We show the 3D analysis technique developed for these data sets that forecast plasma velocity, density, and component magnetic fields at Earth, as well at the other inner heliospheric planets and spacecraft. One excellent coronal mass ejection (CME) example that occurred on the **10 March 2022** was viewed not only in the ISEE IPS analyses, but also by the spacecraft near Earth that measured the CME arrival at one AU. Solar Orbiter, that was nearly aligned along the Earth radial at 0.45 AU, also measured the CME in plasma density, velocity, and magnetic field. BepiColombo at 0.42 AU was also aligned with the STEREO A spacecraft, and viewed this CME. The instruments used here from BepiColombo include: 1) the European-Space-Agency Mercury-Planetary-Orbiter magnetic field measurements; 2) the Japan Aerospace Exploration Agency Mio spacecraft Solar Particle Monitor that viewed the CME Forbush decrease, and the Mercury Plasma Experiment/Mercury Electron Analyzer instruments that measured particles and solar-wind density from below the spacecraft protective sunshield covering. This article summarizes the analysis using ISEE, Japan real-time data for these forecasts: it provides a synopsis of the results and confirmation of the CME event morphology after its arrival, and discusses how future IPS analyses can augment these results.

Iterative Tomography: A Key to Providing Time- dependent 3-D Reconstructions of the Inner Heliosphere and the Unification of Space Weather Forecasting Techniques

Bernard Jackson^{1*}, Andrew Buffington¹, Lucas Cotal¹, Dusan Odstrcil², Mario M. Bisi³, Richard Fallows⁴ and Munetoshi Tokumaru

Front. Astron. Space Sci. Volume 7, id.76 2020

<https://doi.org/10.3389/fspas.2020.568429>

<https://www.frontiersin.org/articles/10.3389/fspas.2020.568429/full>

Over several decades UCSD has developed and continually updated a time dependent iterative three-dimensional (3-D) reconstruction technique to provide global heliospheric parameters – density, velocity, and component magnetic fields. For expediency, this has used a kinematic model as a kernel to provide a fit to either interplanetary scintillation (IPS) or Thomson-scattering observations. This technique has been used in near real time over this period, employing Institute for Space-Earth Environmental Research (ISEE), Japan IPS data to predict the propagation of these parameters throughout the inner heliosphere.

We have extended the 3-D reconstruction analysis to include other IPS Stations around the Globe in a Worldwide Interplanetary Scintillation Stations (WIPSS) Network. In addition, we also plan to resurrect the Solar Mass Ejection Imager (SMEI) Thomson-scattering analysis as a basis for 3-D analysis to be used by the latest NASA Small Explorer heliospheric imagers of the Polarimeter to Unify the Corona and Heliosphere (PUNCH) mission, the All Sky Heliospheric Imager (ASHI), and other modern wide-field imagers. Better data require improved Heliospheric modeling that incorporates non-radial transport of heliospheric flows, and shock processes. Looking ahead to this, we have constructed an interface between the 3-D reconstruction tomography and 3-D MHD models, and currently include the ENLIL model as a kernel in the reconstructions to provide this fit. In short, we are now poised to provide all of these innovations in a next step: to include them for planned ground-based and spacecraft instruments, all to be combined into a truly global 3-D heliospheric system which utilizes these aspects in their data and modeling.

A DAILY DETERMINATION OF BZ USING THE RUSSELL-MCPHERRON EFFECT TO FORECAST GEOMAGNETIC ACTIVITY

B.V. Jackson, H.-S. Yu, A. Buffington, P.P. Hick, M. Tokumaru, K. Fujiki, J. Kim, J. Yun

Space Weather Volume17, Issue4 Pages 639-652 2019

[sci-hub.se/10.1029/2018SW002098](https://doi.org/10.1029/2018SW002098)

Since the middle of the last decade, UCSD has incorporated magnetic field data in its Institute for Space-Earth Environmental Research interplanetary scintillation tomographic analysis. These data are extrapolated upward from the solar surface using the Current Sheet Source Surface model (Zhao & Hoeksema, 1995, <https://doi.org/10.1029/94JA02266>) to provide predictions of the interplanetary field in RTN coordinates. Over the years this technique has become ever more sophisticated, and allows different types of magnetogram data (SOLIS, Global Oscillation Network Group, etc.,) to be incorporated in the field extrapolations. At Earth, these fields can be displayed in a variety of ways, including Geocentric Solar Magnetospheric (GSM) Bx, By, and Bz coordinates.

Displayed daily, the Current Sheet Source Surface model-derived GSM Bz shows a significant positive correlation with the low-resolution (few day variation) in situ measurements of the Bz field. The nano-Tesla variations of Bz maximize in spring and fall as Russell and McPherron (1973, <https://doi.org/10.1029/JA078i001p00092>) have shown. More significantly, we find that the daily variations are correlated with geomagnetic Kp and Dst index variations, and that a decrease from positive to negative Bz has a high correlation with minor-to-moderate geomagnetic storm activity, as defined by NOAA Space Weather Prediction Center planetary Kp values. Here we provide an 11-year study of the predicted Bz field, from the extrapolation of the Global Oscillation Network Group-magnetograms. We provide a skill-score analysis of the technique's geomagnetic storm prediction capability, which allows forecasts of moderate enhanced geomagnetic storm activity. UCSD and the Korean Space Weather Center currently operate a website that predicts this low-resolution GSM Bz field component variation several days in advance. **2007/04/21; 2017/03/01**

A Determination of the North–South Heliospheric Magnetic Field Component from Inner Corona Closed-loop Propagation

B. V. **Jackson**¹, P. P. Hick¹, A. Buffington¹, H.-S. Yu¹, M. M. Bisi², M. Tokumaru³, and X. Zhao
2015 ApJ 803 L1

A component of the magnetic field measured in situ near the Earth in the solar wind is present from north–south fields from the low solar corona. Using the Current-sheet Source Surface model, these fields can be extrapolated upward from near the solar surface to 1 AU. Global velocities inferred from a combination of interplanetary scintillation observations matched to in situ velocities and densities provide the extrapolation to 1 AU assuming mass and mass flux conservation. The north–south field component is compared with the same ACE in situ magnetic field component—the Normal (Radial Tangential Normal) Bn coordinate—for three years throughout the solar minimum of the current solar cycle. We find a significant positive correlation throughout this period between this method of determining the Bn field compared with in situ measurements. Given this result from a study during the latest solar minimum, this indicates that a small fraction of the low-coronal Bn component flux regularly escapes from closed field regions. The prospects for Space Weather, where the knowledge of a Bz field at Earth is important for its geomagnetic field effects, is also now enhanced. This is because the Bn field provides the major portion of the Geocentric Solar Magnetospheric Bz field coordinate that couples most closely to the Earth's geomagnetic field.

The UCSD kinematic IPS solar wind boundary and its use in the ENLIL 3-D MHD prediction model

B. V. **Jackson**^{1,*}, D. Odstrcil^{2,3}, H.-S. Yu¹, P. P. Hick¹, A. Buffington¹, J. C. Mejia-Ambriz^{1,4}, J. Kim⁵, S. Hong⁵, Y. Kim⁵, J. Han⁵ and M. Tokumaru
Space Weather [Volume 13, Issue 2](#), pages 104–115, February **2015**

The University of California, San Diego interplanetary scintillation (IPS) time-dependent kinematic 3-D reconstruction technique has been used and expanded upon for over a decade to provide predictions of heliospheric solar wind parameters. These parameters include global reconstructions of velocity, density, and (through potential field modeling and extrapolation upward from the solar surface) radial and tangential interplanetary magnetic fields. Time-dependent results can be extracted at any solar distance within the reconstructed volume and are now being exploited as inner boundary values to drive the ENLIL 3-D MHD model in near real time. The advantage of this coupled system is that it uses the more complete physics of 3-D MHD modeling to provide an automatic prediction of coronal mass ejections and solar wind stream structures several days prior to their arrival at Earth without employing coronagraph observations. Here we explore, with several examples, the current differences between the IPS real-time kinematic analyses and those from the ENLIL 3-D MHD modeling using IPS-derived real-time boundaries. Future possibilities for this system include incorporating many different worldwide IPS stations as input to the remote sensing analysis using ENLIL as a kernel in the iterative 3-D reconstructions.

- Tomographic inner-boundaries are used to drive ENLIL in real-time
- CMEs, shocks, and other interplanetary structures are predicted
- Several comparisons and a successful prediction are shown

2011-09-02, 2014 Apr 18-20

Inclusion of Real-Time In-Situ Measurements into the UCSD Time-Dependent Tomography and Its Use as a Forecast Algorithm

B. V. **Jackson**, J. M. Clover, P. P. Hick, A. Buffington, M. M. Bisi and M. Tokumaru
Solar Physics, July **2013**, Volume 285, Issue 1-2, pp 151-165

The University of California, San Diego (UCSD) three-dimensional (3D) time-dependent tomography program, used for over a decade to reconstruct and forecast coronal mass ejections (CMEs), does so from observations of interplanetary scintillation (IPS) taken using the Solar-Terrestrial Environment Laboratory (STELab) radio arrays in Japan. An earlier article (Jackson et al. in *Solar Phys.* 265, 245, 2010) demonstrated how in-situ velocity measurements from the Advanced Composition Explorer (ACE) space-borne instrumentation can be used in addition to remote-sensing data to constrain a time-dependent tomographic velocity solution. Here we extend this in-situ inclusion to density measurements, and show how this constrains the tomographic density solution. Supplementing remote-sensing observations with in-situ measurements provides additional information to construct an iterated solar-wind parameter that is propagated outward from near the solar surface past the measurement location, and throughout the volume. As in the case of velocity when this is done, the largest changes within the volume are close to the radial directions around Earth that incorporate the in-situ measurements; the inclusion significantly reduces the uncertainty in extending these measurements to global 3D reconstructions that are distant in time and space from the spacecraft. At Earth, this analysis provides a finely tuned real-time result up to the latest time for which in-situ measurements are available, and enables more-accurate extension of these results near Earth to those remotely sensed. We show examples of this new algorithm using real-time STELab IPS data that were used in our forecasts throughout Carrington rotations 2010 through 2016, and we provide one metric prescription that we have used to determine the forecasting accuracy one, two, and three days in advance of the time data become available to analyze from STELab. We show that the accuracy is considerably better than assuming persistence of the same signal over one to two days in advance of when the data are available.

09-11 November 2011;

Forecasting transient heliospheric solar wind parameters at the location of the inner planets

B.V. **Jackson**, P.P. Hick, A. Buffington, J.M. Clover and M. Tokumaru

Advances in Geosciences: Solar and Terrestrial Science 30, 93–115, November **2012**

Remotely-sensed interplanetary scintillation (IPS) from the solar-terrestrial environment laboratory (STELab) system, and Thomson-scattering observations from the U.S. Air Force/NASA Solar Mass Ejection Imager (SMEI) allow the determination of solar wind parameters at the locations of the inner planets. We show a 3D analysis technique developed to provide daily-cadence transient solar wind forecasts of velocity and density at Earth and the inner planets. These now include in-situ measurements near Earth available in real time. Where in-situ measurements are available these real-time analyses are compared with the predicted values. Using the global velocity measurements available from IPS analysis and daily updated magnetograms from the National Solar Observatory, we are also able to project outward solar-surface magnetic fields in order to provide reasonable global in-situ magnetic-field component trends from one day to the next. This paper summarizes the analysis available and current progress in using the STELab, Japan real-time data for validating these forecasts. A discussion is also provided as to how we can derive more meaningful future information from these remotely-sensed heliospheric measurements.

The 3D analysis of the heliosphere using interplanetary scintillation and Thomson-scattering observations

B.V. **Jackson**

Adv. in Geosciences, Volume 30: Planetary Science (PS) and Solar & Terrestrial Science (ST), 69-91, **2012**

Both interplanetary scintillation (IPS) and Thomson-scattering observations from the U.S. Air Force/NASA Solar Mass Ejection Imager (SMEI) allow a determination of velocity and density in the inner heliosphere and its forecast from remote-sensing heliospheric observations. Recent solar missions, such as Hinode, STEREO, and SDO, and resultant modeling analysis using these data enhance our ability to measure detailed aspects of specific solar events, including their outflow and three-dimensional structure. Current success in this 3D heliospheric endeavor includes the analysis of heliospheric structures that are also measured in situ: interplanetary Coronal Mass Ejections (CMEs), shocks, solar co-rotating structures, and the energy transport provided by solar wind plasma throughout the heliosphere. This report highlights a portion of the work on this multi-faceted topic.

Solar Mass Ejection Imager (SMEI) 3-D reconstruction of density enhancements behind interplanetary shocks: In-situ comparison near Earth and at STEREO

B.V. **Jackson**, , M.S. Hamiltona, P.P. Hicka, b, A. Buffingtona, M.M. Bisia, c, J.M. Clovera, M. Tokumaru and K. Fujiki

Journal of Atmospheric and Solar-Terrestrial Physics, Volume 73, Issues 11-12, **2011**, Pages 1317-1329

SMEI and IPS remotely observe increased brightness and velocity enhancements behind interplanetary shocks that are also seen in situ. We use the UCSD time-dependent 3-D reconstruction technique to map these enhancements, and compare them with measurements at the SOHO, Wind, ACE, and STEREO spacecraft. The analyses of these shocks from hour-averaged in-situ data show that the enhanced density column associated with the shock response varies considerably between different instruments, even for in-situ instruments located at L1 near Earth. The relatively-low-resolution SMEI 3-D reconstructions generally show density enhancements, and within errors, the column excesses match those observed in situ. In these SMEI 3-D reconstructions from remotely-sensed data, the shock density enhancements appear not as continuous broad fronts, but as segmented structures. This may provide part of the explanation for the observed discrepancies between the various in-situ measurements at Earth and STEREO, but not between individual instruments near L1.

Three-dimensional reconstruction of heliospheric structure using iterative tomography: A review

B.V. Jackson, P.P. Hick, A. Buffington, M.M. Bisi, J.M. Clover, M. Tokumaru, M. Kojima, K. Fujiki
Journal of Atmospheric and Solar-Terrestrial Physics, Volume 73, Issue 10, 2011, Pages 1214-1227
Current perspective and in-situ analyses using data from NASA's twin Solar Terrestrial Relations Observatory (STEREO) spacecraft have focused studies on ways to provide three-dimensional (3-D) reconstructions of coronal and heliospheric structure. Data from STEREO are preceded by and contemporaneous with many other types of data and analysis techniques; most of the latter have provided 3-D information by relying on remote-sensing information beyond those of the near corona (outside 10 RS). These include combinations of past data from the Helios spacecraft and the Solwind coronagraphs and, continuing from the past to the present, from observations of interplanetary scintillation (IPS) and the Solar Mass Ejection Imager (SMEI) instrument. In this article we review past and ongoing analyses that have led to a current great wealth of 3-D information. When properly utilized, these analyses can provide not only shapes of CME/ICMEs but also a characterization of any solar wind structure or global outflow.

Research highlights

► Helios spacecraft photometer data began heliospheric Thomson-scattering analyses. ► SMEI Thomson-scattering data now allows a 3-D analysis of the heliosphere. ► UCSD and Japanese tomography of heliospheric data sets provides their 3-D structure. ► These techniques allow 3-D reconstruction of transient and co-rotating structure.

SMEI 3D RECONSTRUCTION OF A CORONAL MASS EJECTION INTERACTING WITH A COROTATING SOLAR WIND DENSITY ENHANCEMENT: THE 2008 APRIL 26 CME

B. V. Jackson¹, A. Buffington¹, P. P. Hick^{1,2}, J. M. Clover¹, M. M. Bisi^{1,3}, and D. F. Webb⁴
Astrophysical Journal, 724:829–834, 2010

The Solar Mass Ejection Imager (SMEI) has recorded the brightness responses of hundreds of interplanetary coronal mass ejections (CMEs) in the interplanetary medium. Using a three-dimensional (3D) reconstruction technique that derives its perspective views from outward-flowing solar wind, analysis of SMEI data has revealed the shapes, extents, and masses of CMEs. Here, for the first time, and using SMEI data, we report on the 3D reconstruction of a CME that intersects a corotating region marked by a curved density enhancement in the ecliptic. Both the CME and the corotating region are reconstructed and demonstrate that the CME disrupts the otherwise regular density pattern of the corotating material. Most of the dense CME material passes north of the ecliptic and east of the Sun–Earth line: thus, in situ measurements in the ecliptic near Earth and at the *Solar-Terrestrial Relations Observatory Behind* spacecraft show the CME as a minor density increase in the solar wind. The mass of the dense portion of the CME is consistent with that measured by the Large Angle Spectrometric Coronagraph on board the *Solar and Heliospheric Observatory* spacecraft, and is comparable to the masses of many other three-dimensionally reconstructed solar wind features at 1 AU observed in SMEI 3D reconstructions.

SMEI direct, 3-D-reconstruction sky maps, and volumetric analyses, and their comparison with SOHO and STEREO observations

B. V. Jackson, P. P. Hick, A. Buffington, M. M. Bisi, and J. M. Clover
Ann. Geophys., 27, 4097–4104, 2009; File

In this paper we present the results of the analysis of the late January 2007 Coronal Mass Ejection (CME) events recorded by the Solar Mass Ejection Imager (SMEI), the Solar Terrestrial Relations Observatory (STEREO), and the Solar and Heliospheric Observatory (SOHO) spacecraft. This period occurs when the two STEREO spacecraft views

are from close to Earth, and thus the views from both SMEI and the STEREO outer Heliospheric Imagers (HI-2s) coincide. Three-dimensional (3-D) analyses derived from SMEI data show many CMEs that have also been studied by others using short-term image subtractions (image-differencing techniques). During this interval we map several CME structures that are observed in both SMEI and the STEREO-A HI instruments. SMEI brightness analyses provided by short-term image subtractions ("difference images") and, alternatively, subtractions of a mean-brightness fit over a long-time duration, both show the extents of the CMEs travelling outward above the East limb that erupted from the Sun on **24 and 25 January 2007**. The SMEI 3-D-reconstructions not only enhance distinct features within the CME events, but also reconcile difference-imaging results with those where a long-term base has been removed. In the January 2007 example the structure as mapped by CME difference images traces the sharp intensity gradients at the front of the CMEs; generally brighter ejected material follows behind the location of the CME front, but shows poorly in these because of its larger angular extent. Using the long-duration background removal enables SMEI's 3-D analysis to determine a mass for this CME sequence North of the ecliptic.

Solar Mass Ejection Imager 3-D reconstruction of the 27–28 May 2003 coronal mass ejection sequence,

Jackson, B. V., M. M. Bisi, P. P. Hick, A. Buffington, J. M. Clover, and W. Sun, *J. Geophys. Res.*, 113, A00A15, doi:10.1029/2008JA013224, (2008).

<http://www.agu.org/pubs/crossref/2008/2008JA013224.shtml>

The Solar Mass Ejection Imager (SMEI) has recorded the inner-heliospheric response in white-light Thomson scattering for many hundreds of interplanetary coronal mass ejections (ICMEs). Some of these have been observed by the Solar and Heliospheric Observatory (SOHO) Large-Angle Spectroscopic Coronagraph (LASCO) instruments and also in situ by near-Earth spacecraft. This article presents a low-resolution three-dimensional (3-D) reconstruction of the 27–28 May 2003 halo CME event sequence observed by LASCO and later using SMEI observations; this sequence was also observed by all in situ monitors near Earth. The reconstruction derives its perspective views from outward flowing solar wind. Analysis results reveal the shape, extent, and mass of this ICME sequence as it reaches the vicinity of Earth. The extended shape has considerable detail that is compared with LASCO images and masses for this event. The 3-D reconstructed density, derived from the remote-sensed Thomson scattered brightness, is also compared with the Advanced Composition Explorer (ACE) and Wind spacecraft in situ plasma measurements. These agree well in peak and integrated total value for this ICME event sequence when an appropriately enhanced (~20%) electron number density is assumed to account for elements heavier than hydrogen in the ionized plasma.

SMEI observations in the STEREO era,

Jackson, B. V., P. P. Hick, A. Buffington, M. M. Bisi, and E. A. Jensen *Proc. SPIE Int. Soc. Opt. Eng.*, 6689, 66890G, 1 -14, doi:10.1117/12.734870, **2007, File**.

White-light Thomson scattering observations from the Solar Mass Ejection Imager (SMEI) have recorded the inner heliospheric response to many CMEs. Some of these are also observed from the LASCO instrumentation and, most recently, the STEREO spacecraft. Here, we detail several CME events in SMEI observations that have also been observed by the LASCO instrumentation and STEREO spacecrafts. We show how SMEI is able to measure CME events from their first observations as close as 20° from the solar disk until they fade away in the SMEI 180° field of view. We employ a 3D reconstruction technique that provides perspective views as observed from Earth, from outward-flowing solar wind. This is accomplished by iteratively fitting the parameters of a kinematic solar wind density model to the SMEI white-light observations and, where possible, including interplanetary scintillation (IPS) velocity data. This 3D modeling technique enables separating the true heliospheric response in SMEI from background noise, and reconstructing the 3D heliospheric structure as a function of time. These reconstructions allow both separation of CME structure from other nearby heliospheric features and a determination of CME mass. Comparisons with LASCO and STEREO images for individual CMEs or portions of them allow a detailed view of changes to the CME shape and mass as they propagate outward.

2003.05.28-29, 2003.10.28-30

Comparison of the extent and mass of CME events in the interplanetary medium using IPS and SMEI Thomson scattering observations

B. V. **JACKSON***†, P. P. **HICK**†, A. **BUFFINGTON**†, M. M. **BISI**†, M. **KOJIMA**‡,

and M. TOKUMARU[‡]

Astronomical and Astrophysical Transactions, Vol. 26, No. 6, December **2007**, 477–487, **File**
The Solar-Terrestrial Environment Laboratory (STELab), Japan, interplanetary scintillation (IPS) *g*-level and velocity measurements can be used to give the extent of CME disturbances in the interplanetary medium arising from the scattering of the radio waves from distant point-like natural sources through the intervening medium. In addition, white-light Thomson-scattering observations from the Solar Mass Ejection Imager (SMEI) have recorded the inner heliospheric response to several hundred CMEs. The work described here compares and details the difference in three-dimensional (3D) reconstructions for these two data sets for the well-observed **28 October 2003** halo CME seen in LASCO; this passed Earth on 29 October in the SMEI data at the same elongations as IPS *g*-level observations. The SMEI data analysis employs a 3D tomographic reconstruction technique that obtains perspective views from outward-flowing solar wind as observed from Earth, iteratively fitting a kinematic solar wind density model, and when available, including IPS velocity data. This technique improves the separation of the heliospheric response in SMEI from other sources of background noise, and also provides the 3D structure of the CME and its mass. The analysis shows and tracks outward the northward portion of a loop structure of this halo CME. We determine an excess mass for this structure of 6.74×10^{16} g and a total mass of 8.34×10^{16} g in the SMEI analysis, and these are comparable to values obtained using IPS *g*-level data and a 3D reconstruction technique developed for these data and applied to this event. We also extend further the application for these analyses.

Analysis of Solar Wind Events Using Interplanetary Scintillation Remote Sensing 3D Reconstructions and Their Comparison at Mars

B.V. **Jackson** · J.A. Boyer · P.P. Hick · A. Buffington · M.M. Bisi · D.H. Crider
Solar Phys (**2007**) 241: 385–396

Interplanetary Scintillation (IPS) allows observation of the inner heliospheric response to corotating solar structures and coronal mass ejections (CMEs) in scintillation level and velocity. With colleagues at STELab, Nagoya University, Japan, we have developed near-real-time access of STELab IPS data for use in space-weather forecasting. We use a 3D reconstruction technique that produces perspective views from solar corotating plasma and outward-flowing solar wind as observed from Earth by iteratively fitting a kinematic solar wind model to IPS observations. This 3D modeling technique permits reconstruction of the density and velocity structure of CMEs and other interplanetary transients at a relatively coarse resolution: a solar rotational cadence and 10° latitudinal and longitudinal resolution for the corotational model and a one-day cadence and 20° latitudinal and longitudinal heliographic resolution for the time-dependent model. This technique is used to determine solar-wind pressure (“ram” pressure) at Mars. Results are compared with rampressure observations derived from *Mars Global Surveyor* magnetometer data (Crider *et al.*, **2003**, *J. Geophys. Res.* **108**(A12), 1461) for the years 1999 through 2004. We identified 47 independent *in situ* pressure-pulse events above 3.5 nPa in the *Mars Global Surveyor* data in this time period where sufficient IPS data were available. We detail the large pressure pulse observed at Mars in association with a CME that erupted from the Sun on 27 May 2003, which was a halo CME as viewed from Earth. We also detail the response of a series of West-limb CME events and compare their response observed at Mars about 160° west of the Sun – Earth line by the *Mars Global Surveyor* with the response derived from the IPS 3D reconstructions.

Preliminary three-dimensional analysis of the heliospheric response to the 28 October 2003 CME using SMEI white-light observations,

B. V. **Jackson**, A. Buffington, P. P. Hick, X. Wang, D. Webb

JOURNAL OF GEOPHYSICAL RESEARCH, VOL. 111, A04S91, doi:10.1029/2004JA010942, **2006**, **File**.

The Solar Mass Ejection Imager (SMEI) has recorded the inner heliospheric response in white-light Thomson scattering to the 28 October 2003 coronal mass ejection (CME). This preliminary report shows the evolution of this particular event in SMEI observations, as we track it from a first measurement at approximately 20° elongation (angular distance) from the solar disk until it fades in the antisolar hemisphere in the SMEI 180° field of view. The large angle and

spectrometric coronagraph (LASCO) images show a CME and an underlying bright ejection of coronal material that is associated with an erupting prominence. Both of these are seen by SMEI in the interplanetary medium. We employ a three-dimensional (3-D) reconstruction technique that derives its perspective views from outward flowing solar wind to reveal the shape and extent of the CME. This is accomplished by iteratively fitting the parameters of a kinematic solar wind density model to both SMEI white-light observations and Solar-Terrestrial Environment Laboratory (STELab), interplanetary scintillation (IPS) velocity data. This modeling technique separates the true heliospheric signal in SMEI observations from background noise and reconstructs the 3-D heliospheric structure as a function of time. These reconstructions allow separation of the 28 October CME from other nearby heliospheric structure and a determination of its mass. The present results are the first utilizing this type of 3-D reconstruction with the SMEI data. We determine an excess-over-ambient mass for the southward moving ejecta associated with the prominence material of 7.1×10^{16} g and a total mass of 8.9×10^{16} g. Preliminary SMEI white-light calibration indicates that the total mass of this CME including possible associated nearby structures may have been as much as $\sim 2.0 \times 10^{17}$ g spread over much of the earthward facing hemisphere.

The Solar Mass Ejection Imager (SMEI): The mission,

Jackson, B. V., A. Buffington, P. P. Hick, R. C. Altrrock, S. Figueroa, P. E. Holladay, J. C. Johnston, S. W. Kahler, J. B. Mozer and S. Price, et al. (2004), *Sol. Phys.*, 225, 177-- 207

We have launched into near-Earth orbit a solar mass-ejection imager (SMEI) that is capable of measuring sunlight Thomson-scattered from heliospheric electrons from elongations to as close as 18 to greater than 90 from the Sun. SMEI is designed to observe time-varying heliospheric brightness of objects such as coronal mass ejections, co-rotating structures and shock waves. The instrument evolved from the heliospheric imaging capability demonstrated by the zodiacal light photometers of the Helios spacecraft. A near-Earth imager can provide up to three days warning of the arrival of a mass ejection from the Sun. In combination with other imaging instruments in deep space, or alone by making some simple assumptions about the outward flow of the solar wind, SMEI can provide a three-dimensional reconstruction of the surrounding heliospheric density structures.

Models for coronal mass ejections Review

Carla **Jacobsa**, b and Stefaan Poedtsa

Journal of Atmospheric and Solar-Terrestrial Physics, Volume 73, Issue 10, **2011**, Pages 1148-1155

Coronal mass ejections (CMEs) play a key role in space weather. The mathematical modelling of these violent solar phenomena can contribute to a better understanding of their origin and evolution and as such improve space weather predictions. We **review** the state-of-the-art in CME simulations, including a brief overview of current models for the background solar wind as it has been shown that the background solar wind affects the onset and initial evolution of CMEs quite substantially. We mainly focus on the attempt to retrieve the initiation and propagation of CMEs in the framework of computational magnetofluid dynamics (CMFD). Advanced numerical techniques and large computer resources are indispensable when attempting to reconstruct an event from Sun to Earth. Especially the simulations developed in dedicated event studies yield very realistic results, comparable with the observations. However, there are still a lot of free parameters in these models and ad hoc source terms are often added to the equations, mimicking the physics that is not really understood yet in detail.

Research highlights

► New insights in the origin and dynamics of coronal mass ejections. ► New developments in the numerical modelling of CMEs. ► State-of-the-art solar wind models. ► New pieces of the space weather puzzle.

The Internal Structure of Coronal Mass Ejections: Are all Regular Magnetic Clouds Flux Ropes?

C. **Jacobs**, I. I. Roussev, N. Lugaz, and S. Poedts

ApJL, 695, L171-L175, **2009**; doi: [10.1088/0004-637X/695/2/L171](https://doi.org/10.1088/0004-637X/695/2/L171)

In this Letter, we investigate the internal structure of a coronal mass ejection (CME) and its dynamics by invoking a realistic initiation mechanism in a quadrupolar magnetic setting. The study comprises a compressible three-dimensional magnetohydrodynamics simulation. We use an idealized model of the solar corona, into which we superimpose a

quadrupolar magnetic source region. By applying shearing motions resembling flux emergence at the solar boundary, the initial equilibrium field is energized and it eventually erupts, yielding a fast CME. The simulated CME shows the typical characteristics of a magnetic cloud (MC) as it propagates away from the Sun and interacts with a bimodal solar wind. However, no distinct flux rope structure is present in the associated interplanetary ejection. In our model, a series of reconnection events between the eruptive magnetic field and the ambient field results in the creation of significant writhe in the CME's magnetic field, yielding the observed rotation of the magnetic field vector, characteristic of an MC. We demonstrate that the magnetic field lines of the CME may suffer discontinuous changes in their mapping on the solar surface, with footpoints subject to meandering over the course of the eruption due to magnetic reconnection. We argue that CMEs with internal magnetic structure such as that described here should also be considered while attempting to explain in situ observations of regular MCs at L1 and elsewhere in the heliosphere.

Turbulence dynamics and flow speeds in the inner solar corona: Results from radio-sounding experiments by the Akatsuki spacecraft

Richa N. [Jain](#), [R. K. Choudhary](#), [Anil Bhardwaj](#), [T. Imamura](#), [Anshuman Sharma](#), [Umang M. Parikh](#)

MNRAS **2023**

<https://arxiv.org/pdf/2308.12596.pdf>

The solar inner corona is a region that plays a critical role in energizing the solar wind and propelling it to supersonic and supra-Alfvenic velocities. Despite its importance, this region remains poorly understood because of being least explored due to observational limitations. The coronal radio sounding technique in this context becomes useful as it helps in providing information in parts of this least explored region. To shed light on the dynamics of the solar wind in the inner corona, we conducted a study using data obtained from coronal radio-sounding experiments carried out by the Akatsuki spacecraft during the 2021 Venus-solar conjunction event. By analyzing X-band radio signals recorded at two ground stations (IDSN in Bangalore and UDSC in Japan), we investigated plasma turbulence characteristics and estimated flow speed measurements based on isotropic quasi-static turbulence models. Our analysis revealed that the speed of the solar wind in the inner corona (at heliocentric distances from 5 to 13 solar radii), ranging from 220-550 km/sec, was higher than the expected average flow speeds in this region. By integrating our radio-sounding results with EUV images of the solar disk, we gained a unique perspective on the properties and energization of high-velocity plasma streams originating from coronal holes. We tracked the evolution of fast solar wind streams emanating from an extended coronal hole as they propagated to increasing heliocentric distances. Our study provides unique insights into the least-explored inner coronal region by corroborating radio sounding results with EUV observations of the corona. **14 Mar-2 Apr 2021**

Sensitivity of Model Estimates of CME Propagation and Arrival Time to Inner Boundary Conditions

Lauren A. [James](#), [Christopher J. Scott](#), [Luke A. Barnard](#), [Mathew J. Owens](#), [Matthew S. Lang](#), [Shannon R. Jones](#)

Space Weather [Volume21, Issue4](#) e2022SW003289 **2023**

<https://doi.org/10.1029/2022SW003289>

<https://agupubs.onlinelibrary.wiley.com/doi/epdf/10.1029/2022SW003289>

Accurately forecasting the arrival of coronal mass ejections (CMEs) at Earth is important to enabling mitigation of the associated space weather risks to society. This is only possible with accurate modeling of the event. To do so, we must understand the propagation of a CME through the heliosphere and quantify the performance of models through comparison with spacecraft observations. For the **12 December 2008** Earth-directed CME event, we compute ensembles using the HUXt solar wind model to analyze CME distortion with a structured solar wind and explore hindcast arrival time error (ATE). By highlighting the impact CME shape has on Root-Mean-Square-Error (RMSE) values, we show that time-elongation profiles of fronts captured by the Heliospheric Imager (HI) instruments onboard NASA's STEREO mission match those of the modeled CME nose and flank and can therefore be used to infer details of the longitudinal extent of the CME. We then show that accounting for CME distortion is important to enable accurate estimates of the CME arrival at Earth. This can be achieved by either using observations of multiple features in HI data to infer CME evolution or mapping the solar wind back to a lower inner boundary to allow CMEs to be distorted close to the Sun. For the event studied we show that these approaches resulted in reduced RMSEs of 0.73° and 0.64° with an ATE of 1 hour and 3 hours respectively.

Comparison of ICME arrival times and solar wind parameters based on the WSA-ENLIL model with three cone types and observations†

Soojeong **Jang**, Y.-J. Moon*, Jae-Ok Lee and Hyeonock Na
JGR, Volume 119, Issue 9, pages 7120–7127, **2014**

We have made a comparison between CME-associated shock propagations based on the WSA-ENLIL model using three cone types and in-situ observations. For this we use 28 full-halo CMEs, whose cone parameters are determined and their corresponding interplanetary shocks were observed at the Earth, from 2001 to 2002. We consider three different cone types (an asymmetric cone model, an ice-cream cone model, and an elliptical cone model) to determine 3-D CME cone parameters (radial velocity, angular width and source location), which are the input values of the WSA-ENLIL model. The mean absolute error (MAE) of the CME-associated shock travel times for the WSA-ENLIL model using the ice-cream cone model is 9.9 hours, which is about 1 hour smaller than those of the other models. We compare the peak values and profiles of solar wind parameters (speed and density) with in-situ observations. We find that the root mean square (RMS) errors of solar wind peak speed and density for the ice-cream and asymmetric cone model are about 190 km/s and 24 /cm³, respectively. We estimate the cross correlations between the models and observations within the time lag of ± 2 days from the shock travel time. The correlation coefficients between the solar wind speeds from the WSA-ENLIL model using three cone types and in-situ observations are approximately 0.7, which is larger than those of solar wind density (~ 0.6). Our preliminary investigations show that the ice-cream cone model seems to be better than the other cone models in terms of the input parameters of the WSA-ENLIL model. **7 Sept 2002**

The two-step Forbush decrease: a tale of two substructures modulating galactic cosmic rays within coronal mass ejections

Miho **Janvier**, [Pascal Démoulin](#), [Jingnan Guo](#), [Sergio Dasso](#), [Florian Regnault](#), [Sofia Topsis-Moutesidou](#), [Christian Gutierrez](#), [Barbara Perri](#)

ApJ **922** 216 **2021**

<https://arxiv.org/pdf/2109.14469.pdf>

<https://doi.org/10.3847/1538-4357/ac2b9b>

Interplanetary Coronal Mass Ejections (ICMEs) are known to modify the structure of the solar wind as well as interact with the space environment of planetary systems. Their large magnetic structures have been shown to interact with galactic cosmic rays, leading to the Forbush decrease (FD) phenomenon. We revisit in the present article the 17 years of Advanced Composition Explorer spacecraft ICME detection along with two neutron monitors (McMurdo and Oulu) with a superposed epoch analysis to further analyze the role of the magnetic ejecta in driving FDs. We investigate in the following the role of the sheath and the magnetic ejecta in driving FDs, and we further show that for ICMEs without a sheath, a magnetic ejecta only is able to drive significant FDs of comparable intensities. Furthermore, a comparison of samples with and without a sheath with similar speed profiles enable us to show that the magnetic field intensity, rather than its fluctuations, is the main driver for the FD. Finally, the recovery phase of the FD for isolated magnetic ejecta shows an anisotropy in the level of the GCRs. We relate this finding at 1 au to the gradient of the GCR flux found at different heliospheric distances from several interplanetary missions.

Generic Magnetic Field Intensity Profiles of Interplanetary Coronal Mass Ejections at Mercury, Venus, and Earth From Superposed Epoch Analyses

Miho **Janvier**, [Reka M. Winslow](#), [Simon Good](#), [Elise Bonhomme](#), [Pascal Démoulin](#), [Sergio Dasso](#), [Christian Möstl](#), [Noé Lugaz](#), [Tanja Amerstorfer](#), [Elie Soubrié](#), [Peter D. Boakes](#)

JGR [Volume 124, Issue 2](#), February **2019**, Pages 812-836

[sci-hub.tw/10.1029/2018JA025949](https://doi.org/10.1029/2018JA025949)

<https://arxiv.org/pdf/1901.09921.pdf>

We study interplanetary coronal mass ejections (ICMEs) measured by probes at different heliocentric distances (0.3–1 AU) to investigate the propagation of ICMEs in the inner heliosphere and determine how the generic features of ICMEs change with heliospheric distance. Using data from the Mercury Surface, Space ENvironment, GEochemistry, and Ranging (MESSENGER), Venus Express and ACE spacecraft, we analyze with the superposed epoch technique the profiles of ICME substructures, namely, the sheath and the magnetic ejecta. We determine that the median magnetic field magnitude in the sheath correlates well with ICME speeds at 1 AU, and we use this proxy to order the ICMEs at all spacecraft. We then investigate the typical ICME profiles for three categories equivalent to slow, intermediate, and fast ICMEs. Contrary to fast ICMEs, slow ICMEs have a weaker solar wind field at the front and a more symmetric magnetic field profile. We find the asymmetry to be less pronounced at Earth than at Mercury, indicating a relaxation taking place as ICMEs propagate. We also find that the magnetic field intensities in the wake region of the ICMEs do not go back to the pre-ICME solar wind intensities, suggesting that the effects of ICMEs on the ambient solar wind last longer than the duration of the transient event. Such results provide an indication of physical processes that need to be

reproduced by numerical simulations of ICME propagation. The samples studied here will be greatly improved by future missions dedicated to the exploration of the inner heliosphere, such as Parker Solar Probe and Solar Orbiter.

5 Nov 2010, 8 Jan 2013

Table 2011-2015

Comparing generic models for interplanetary shocks and magnetic clouds axis configurations at 1 AU

Miho **Janvier**, Sergio Dasso, Pascal Demoulin, Jimmy Masias-Meza, Noe Lugaz

JGR Volume 120, Issue 5 Pages i - vi, pages 3328–3349 2015

<http://arxiv.org/pdf/1503.06128v1.pdf>

Interplanetary Coronal Mass Ejections are the manifestation of solar transient eruptions, which can significantly modify the plasma and magnetic conditions in the heliosphere. They are often preceded by a shock, and a magnetic flux rope is detected in situ in a third to half of them. The main aim of this study is to obtain the best quantitative shape for the flux rope axis and for the shock surface from in situ data obtained during spacecraft crossings of these structures. We first compare the orientation of the flux ropes axes and shock normals obtained from independent data analyses of the same events, observed in situ at 1AU from the Sun. Then, we carry out an original statistical analysis of axes/shock normals by deriving the statistical distributions of their orientations. We fit the observed distributions using the distributions derived from several synthetic models describing these shapes. We show that the distributions of axis/shock orientations are very sensitive to their respective shape. One classical model, used to analyze interplanetary imager data, is incompatible with the in situ data. Two other models are introduced, for which the results for axis and shock normals lead to very similar shapes; the fact that the data for MCs and shocks are independent strengthen this result. The model which best fit all the data sets has an ellipsoidal shape with similar aspect ratio values for all the data sets. These derived shapes for the flux rope axis and shock surface have several potential applications. First, these shapes can be used to construct a consistent ICME model. Second, these generic shapes can be used to develop a quantitative model to analyze imager data, as well as constraining the output of numerical simulations of ICMEs. Finally, they will have implications for space weather forecasting, in particular for forecasting the time arrival of ICMEs at the Earth.

In Situ Properties of Small and Large Flux Ropes in the Solar Wind

M. **Janvier**, P. Demoulin, S. Dasso

JGR, Volume 119, Issue 9, pages 7088–7107, 2014

<http://arxiv.org/pdf/1408.5520v1.pdf> ; File

Two populations of twisted magnetic field tubes, or flux ropes (hereafter, FRs), are detected by in situ measurements in the solar wind. While small FRs are crossed by the observing spacecraft within few hours, with a radius typically less than 0.1AU, larger FRs, or magnetic clouds (hereafter, MCs), have durations of about half a day.

The main aim of this study is to compare the properties of both populations of FRs observed by the Wind spacecraft at 1 AU.

To do so, we use standard correlation techniques for the FR parameters, as well as histograms and more refined statistical methods. Although several properties seem at first different for small FRs and MCs, we show that they are actually governed by the same propagation physics. For example, we observe no in situ signatures of expansion for small FRs, contrary to MCs. We demonstrate that this result is in fact expected: small FRs expand similarly to MCs, as a consequence of a total pressure balance with the surrounding medium, but the expansion signature is well hidden by velocity fluctuations.

Next, we find that the FR radius, velocity and magnetic field strength are all positively correlated, with correlation factors than can reach a value >0.5 . This result indicates a remnant trace of the FR ejection process from the corona. We also find a larger FR radius at the apex than at the legs (up to three times larger at the apex), for FR observed at 1 AU.

Finally, assuming that the detected FRs have a large-scale configuration in the heliosphere, we derived the mean axis shape from the probability distribution of the axis orientation. We therefore interpret the small FR and MC properties in a common framework of FRs interacting with the solar wind, and we disentangle the physics present behind their common and different features.

Mean shape of interplanetary shocks deduced from in situ observations and its relation with interplanetary CMEs

M. **Janvier**, P. Démoulin and S. Dasso

A&A 565, A99 (2014)

Context. Shocks are frequently detected by spacecraft in the interplanetary space. However, the in situ data of a shock do not provide direct information on its overall properties even when a following interplanetary coronal mass ejection (ICME) is detected.

Aims. The main aim of this study is to constrain the general shape of ICME shocks with a statistical study of shock orientations.

Methods. We first associated a set of shocks detected near Earth over 10 years with a sample of ICMEs over the same period. We then analyzed the correlations between shock and ICME parameters and studied the statistical distributions of the local shock normal orientation. Supposing that shocks are uniformly detected all over their surface projected on the 1 AU sphere, we compared the shock normal distribution with synthetic distributions derived from an analytical shock shape model. Inversely, we derived a direct method to compute the typical general shape of ICME shocks by integrating observed distributions of the shock normal.

Results. We found very similar properties between shocks with and without an in situ detected ICME, so that most of the shocks detected at 1 AU are ICME-driven even when no ICME is detected. The statistical orientation of shock normals is compatible with a mean shape having a rotation symmetry around the Sun-apex line. The analytically modeled shape captures the main characteristics of the observed shock normal distribution. Next, by directly integrating the observed distribution, we derived the mean shock shape, which is found to be comparable for shocks with and without a detected ICME and weakly affected by the limited statistics of the observed distribution. We finally found a close correspondence between this statistical result and the leading edge of the ICME sheath that is observed with STEREO imagers.

Conclusions. We have derived a mean shock shape that only depends on one free parameter. This mean shape can be used in various contexts, such as studies for high-energy particles or space weather forecasts.

New approach to unveil the shape of interplanetary structures

M. **Janvier**, P. Demoulin, S. Dasso

New UKSP Nugget: 45, March 2014.

<http://www.uksolphys.org/uksp-nugget/45-a-new-approach-to-unveil-the-shape-of-interplanetary-structures/>

How local in situ data can still reveal the mean shape of interplanetary structures

Are There Different Populations of Flux Ropes in the Solar Wind?

M. **Janvier**, P. Demoulin, S. Dasso

E-print, Feb 2014, Solar Physics July 2014, Volume 289, Issue 7, pp 2633-2652

<http://arxiv.org/pdf/1401.6812v1.pdf>

Flux ropes are twisted magnetic structures, which can be detected by in situ measurements in the solar wind. However, different properties of detected flux ropes suggest different types of flux-rope population. As such, are there different populations of flux ropes? The answer is positive, and is the result of the analysis of four lists of flux ropes, including magnetic clouds (MCs), observed at 1 AU. The in situ data for the four lists have been fitted with the same cylindrical force-free field model, which provides an estimation of the local flux-rope parameters such as its radius and orientation. Since the flux-rope distributions have a large dynamic range, we go beyond a simple histogram analysis by developing a partition technique that uniformly distributes the statistical fluctuations over the radius range. By doing so, we find that small flux ropes with radius $R < 0.1$ AU have a steep power-law distribution in contrast to the larger flux ropes (identified as MCs), which have a Gaussian-like distribution. Next, from four CME catalogs, we estimate the expected flux-rope frequency per year at 1 AU. We find that the predicted numbers are similar to the frequencies of MCs observed in situ. However, we also find that small flux ropes are at least ten times too abundant to correspond to CMEs, even to narrow ones. Investigating the different possible scenarios for the origin of those small flux ropes, we conclude that these twisted structures can be formed by blowout jets in the low corona or in coronal streamers.

Global axis shape of magnetic clouds deduced from the distribution of their local axis orientation

Janvier M., Demoulin P., Dasso S.

E-print, May 2013, A&A 556, A50 (2013)

Context. Coronal mass ejections (CMEs) are routinely tracked with imagers in the interplanetary space, while magnetic clouds (MCs) properties are measured locally by spacecraft. However, both imager and in situ data do not provide any direct estimation of the general flux rope properties.

Aims. The main aim of this study is to constrain the global shape of the flux rope axis from local measurements and to compare the results from in-situ data with imager observations.

Methods. We performed a statistical analysis of the set of MCs observed by WIND spacecraft over 15 years in the vicinity of Earth. We analyzed the correlation between different MC parameters and studied the statistical distributions of the angles defining the local axis orientation. With the hypothesis of having a sample of MCs with a uniform distribution of spacecraft crossing along their axis, we show that a mean axis shape can be derived from the distribution of the axis orientation. As a complement, while heliospheric imagers do not typically observe MCs but only their sheath region, we analyze one event where the flux rope axis can be estimated from the STEREO imagers.

Results. From the analysis of a set of theoretical models, we show that the distribution of the local axis orientation is strongly affected by the overall axis shape. Next, we derive the mean axis shape from the integration of the observed orientation distribution. This shape is robust because it is mostly determined from the overall shape of the distribution. Moreover, we find no dependence on the flux rope inclination on the ecliptic. Finally, the derived shape is fully consistent with the one derived from heliospheric imager observations of the June 2008 event.

Conclusions. We have derived a mean shape of MC axis that only depends on one free parameter, the angular separation of the legs (as viewed from the Sun). This mean shape can be used in various contexts, such as studies of high-energy particles or space weather forecasts. **2008-06-03**

Direct Measurements of Synchrotron-emitting Electrons at Near-Sun Shocks

I. C. **Jebaraj**¹, O. V. Agapitov^{2,3}, M. Gedalin⁴, L. Vuorinen^{1,5}, M. Miceli⁶, C. M. S. Cohen⁷, A. Voshchepnyets^{2,8}, A. Kouloumvakos⁹, N. Dresing¹, A. Marmyleva¹⁰Show full author list

2024 ApJL 976 L7

<https://iopscience.iop.org/article/10.3847/2041-8213/ad8eb8/pdf>

In this study, we present the first-ever direct measurements of synchrotron-emitting heliospheric traveling shocks, intercepted by the Parker Solar Probe (PSP) during its close encounters. Given that much of our understanding of powerful astrophysical shocks is derived from synchrotron radiation, these observations by PSP provide an unprecedented opportunity to explore how shocks accelerate relativistic electrons and the conditions under which they emit radiation. The probe's unparalleled capabilities to measure both electromagnetic fields and energetic particles with high precision in the near-Sun environment has allowed us to directly correlate the distribution of relativistic electrons with the resulting photon emissions. Our findings reveal that strong quasi-parallel shocks emit radiation at significantly higher intensities than quasi-perpendicular shocks due to the efficient acceleration of ultrarelativistic electrons. These experimental results are consistent with theory and recent observations of supernova remnant shocks and advance our understanding of shock physics across diverse space environments. **2022 September 5, 2023 March 13**

Acceleration of electrons and ions by an "almost" astrophysical shock in the heliosphere

Immanuel Christopher **Jebaraj**, [Oleksiy Agapitov](#), [Vladimir Krasnoselskikh](#), [Laura Vuorinen](#), [Michael Gedalin](#), +++

ApJ **2024**

<https://arxiv.org/pdf/2405.07074>

Collisionless shock waves, ubiquitous in the universe, are crucial for particle acceleration in various astrophysical systems. Currently, the heliosphere is the only natural environment available for their in situ study. In this work, we showcase the collective acceleration of electrons and ions by one of the fastest in situ shocks ever recorded, observed by the pioneering Parker Solar Probe at only 34.5 million kilometers from the Sun. Our analysis of this unprecedented, near-parallel shock shows electron acceleration up to 6 MeV amidst intense multi-scale electromagnetic wave emissions. We also present evidence of a variable shock structure capable of injecting and accelerating ions from the solar wind to high energies through a self-consistent process. The exceptional capability of the probe's instruments to measure electromagnetic fields in a shock traveling at 1% the speed of light has enabled us, for the first time, to confirm that the structure of a strong heliospheric shock aligns with theoretical models of strong shocks observed in astrophysical environments. This alignment offers viable avenues for understanding astrophysical shock processes and the acceleration of charged particles. **13 Mar 2023**

The Faraday Effect Tracker of Coronal and Heliospheric Structures (FETCH) Instrument

Elizabeth **Jensen**, Nat Gopalswamy, Lynn Wilson III, Lan Jian, Shing Fung, +++

Front. Astron. Space Sci., 10:1064069. **2023**

<https://www.frontiersin.org/articles/10.3389/fspas.2023.1064069/pdf>

There continue to be open questions regarding the solar wind and coronal mass ejections (CMEs). For example: how do magnetic fields within CMEs and corotating/stream interaction regions (CIRs/SIRs) evolve in the inner heliosphere? What is the radially distributed magnetic profile of shock-driving CMEs? What is the internal magnetic structure of CMEs that cause magnetic storms? It is clear that these questions involve the magnetic configurations of solar wind and transient interplanetary plasma structures, for which we have limited knowledge. In order to better understand the origin of the magnetic field variability in steady-state structures and transient events, it is necessary to probe the magnetic field in Earth-directed structures/disturbances. This is the goal of the Multiview Observatory for Solar Terrestrial Science (MOST) mission ([Gopalswamy et al., 2022](#)). For MOST to answer the aforementioned questions, we propose the instrument concept of the Faraday Effect Tracker of Coronal and Heliospheric structures (FETCH), a simultaneous quad-line-of-sight polarization radio remote-sensing instrument. With FETCH, spacecraft radio beams passing through the Sun–Earth line offer the possibility of obtaining information of plasma conditions via analysis of radio propagation effects such as Faraday rotation and wave dispersion, which provide information of the magnetic field and total electron content (TEC). This is the goal of the FETCH instrument, one of ten instruments proposed to be hosted on the MOST mission. The MOST mission will provide an unprecedented opportunity to achieve NASA’s heliophysics science goal to “explore and characterize the physical processes in the space environment from the Sun” ([Gopalswamy et al., 2022](#)).

Novel Magnetic Field and Electron Density Measurements of CMEs (within AU) with the Proposed Multiview Observatory for Solar Terrestrial Science (MOST) Mission

Jensen, P. E., C. S. P., Elizabeth ; [Manchester, Ward](#) ; [Fung, Shing](#) ; [Gopalswamy, Nat](#) et al.

AGU Fall Meeting 2021, held in New Orleans, LA, 13-17 December 2021, id. SH33A-08. **2021**

The Multiview Observatory for Solar Terrestrial Science (MOST) mission concept will be the most advanced solar observatory to date (Gopalswamy et al, SH0001, 2021). Comprising four spacecraft, two located in the L4 and ahead of L4 position and two located in the L5 and behind of the L5 position, the four lines-of-sight (LOSs) form the basis for the unique Faraday Effect Tracker of Coronal and Heliospheric Structures (FETCH) instrument (Wexler et al, SH0019, 2021). We report on our modeling into the expected Faraday rotation (FR) caused by an Earth-directed CME crossing the MOST/FETCH radio-sensing paths using a heliospheric 3-D MHD model to obtain the necessary LOS data on electron density and magnetic field components (see example image). Specifically, we utilized simulation data of the 2005 May 13 CME (Manchester IV et al., 2014, Plasma Phys. Control. Fusion), which erupted from the north-south polarity inversion line of AR 10759 at 16:03 UT, reaching speeds around 2000 km/s in the corona. The trajectory of the CME at an acute angle to the Earth-Sun line crosses each FETCH LOS at a different time. Two LOSs are at different viewing angles with little overlap between the CME sheath and magnetic flux rope core. A blind test fitting of the Faraday rotation functions (Figures 6 and 7 in Jensen et al., 2010, Sol. Phys.) to the simulated FETCH observations reproduced the orientation of the CME for its handedness as well as its associated complementary degenerate solution. In conclusion, one of the four LOSs will be more sensitive to observing CME flux rope structure of Earthward CMEs, depending on their trajectory. We find that two of the four LOSs enable analyzing CME evolution, whereas the other two LOSs enable analyzing the average magnetic field vector in the corresponding high density regions dominating the measurements at that time. For example, the average sheath magnetic field vector can be partially measured in the plane of the ecliptic due to the angular differences between 2 LOSs. We discuss future work as this effort develops.

Modeling FETCH Observations of 2005 May 13 CME

Elizabeth A. **Jensen**, [Ward B. Manchester IV](#), [David B. Wexler](#), [Jason E. Kooi](#), [Teresa Nieves-Chinchilla](#), [Lan K. Jian](#), [Alexei Pevtsov](#), [Shing Fung](#)

ApJ **2022**

<https://arxiv.org/pdf/2209.03350.pdf>

This paper evaluates the quality of CME analysis that has been undertaken with the rare Faraday rotation observation of an eruption. Exploring the capability of the FETCH instrument hosted on the MOST mission, a four-satellite Faraday rotation radio sounding instrument deployed between the Earth and the Sun, we discuss the opportunities and challenges to improving the current analysis approaches.

Plasma Interactions with the Space Environment in the Acceleration Region: Indications of CME-trailing Reconnection Regions

Elizabeth A. **Jensen**^{1,2}, Carl Heiles³, David Wexler⁴, Amanda A. Kepley⁵, Thomas Kuiper⁶, Mario M. Bisi⁷, Deborah Domingue Lorin¹, Elizabeth V. Kuiper⁸, and Faith Vilas¹,

Astrophysical Journal, 861:118 (12pp), **2018** July 10

<http://sci-hub.tw/http://iopscience.iop.org/0004-637X/861/2/118/>

Coronal mass ejections (CMEs) are sources of major geomagnetic disturbances. On **2013 May 10**, a CME crossed the signal path between the MErcury Surface, Space ENvironment, GEOchemistry, and Ranging (MESSENGER) spacecraft and Earth. Using the MESSENGER signal, characteristics of the density, velocity, and magnetic field properties of the crossing plasma were measured. An anomalously strong event occurred in the plasma trailing the CME's passage that correlated with a wave mode conversion, indicating a potential reconnection region. We determine that the plasma following CMEs should be considered when studying how CMEs evolve in interplanetary space and the severity of their geomagnetic impact.

Faraday Rotation Response to Coronal Mass Ejection Structure

E.A. **Jensen** · P.P. Hick · M.M. Bisi · B.V. Jackson · J. Clover · T. Mulligan

Solar Phys (2010) 265: 31–48

We present the results from modeling the coronal mass ejection (CME) properties that have an effect on the Faraday rotation (FR) signatures that may be measured with an imaging radio antenna array such as the Murchison Widefield Array (MWA). These include the magnetic flux rope orientation, handedness, magnetic-field magnitude, velocity, radius, expansion rate, electron density, and the presence of a shock/sheath region. We find that simultaneous multiple radio source observations (FR imaging) can be used to uniquely determine the orientation of the magnetic field in a CME, increase the advance warning time on the geoeffectiveness of a CME by an order of magnitude from the warning time possible from *in-situ* observations at L_1 , and investigate the extent and structure of the shock/sheath region at the leading edge of fast CMEs. The magnetic field of the heliosphere is largely “invisible” with only a fraction of the interplanetary magnetic-field lines convecting past the Earth; remote sensing the heliospheric magnetic field through FR imaging from the MWA will advance solar physics investigations into CME evolution and dynamics.

Faraday rotation observations of CMEs.

Jensen EA, Russell CT.

Geophys. Res. Lett. 35, 2008 L02103.

<https://agupubs.onlinelibrary.wiley.com/doi/full/10.1029/2007GL031038>
sci-hub.se/10.1029/2007GL031038

Simultaneous observations obtained by the Solwind coronagraph and Faraday rotation of the Helios radio frequency carrier signal in 1979 showed that CMEs produce characteristic ‘W’ or sigmoid transients in Faraday rotation observations similar to those observed by Pioneer 6 and 9 in 1968 and 1970. We demonstrate that a relaxed flux-rope model is capable of reproducing these observations. Through fitting the model to the observations, we can obtain information on the flux rope orientation, position, size, velocity, rate of change of rope radius and pitch angle. With electron density measurements, we can also obtain a measure of the magnetic field strength. These fits demonstrate that Faraday rotation observations can provide information on the magnetic field of a CME shortly after it erupts.

Comparison of Dst forecast models for intense geomagnetic storms

Ji, Eun-Young; Moon, Y.-J.; Gopalswamy, N.; Lee, D.-H.

J. Geophys. Res., Vol. 117, No. A3, A03209, 2012, **File**

We have compared six Dst forecast models using 63 intense geomagnetic storms ($Dst \leq -100$ nT) that occurred from 1998 to 2006. For comparison, we estimated linear correlation coefficients and RMS errors between the observed Dst data and the predicted Dst during the geomagnetic storm period as well as the difference of the value of minimum Dst (ΔDst_{min}) and the difference in the absolute value of Dst minimum time (Δt_{Dst}) between the observed and the predicted. As a result, we found that the model by Temerin and Li (2002, 2006) gives the best prediction for all parameters when all 63 events are considered. The model gives the average values: the linear correlation coefficient of 0.94, the RMS error of 14.8 nT, the ΔDst_{min} of 7.7 nT, and the absolute value of Δt_{Dst} of 1.5 hour. For further comparison, we classified the storm events into two groups according to the magnitude of Dst. We found that the model of Temerin and Lee (2002, 2006) is better than the other models for the events having $-100 \leq Dst < -200$ nT, and three recent models (the model of Wang et al. (2003), the model of Temerin and Li (2002, 2006), and the model of Boynton et al. (2011b)) are better than the other three models for the events having $Dst \leq -200$ nT.

Statistical comparison of interplanetary conditions causing intense geomagnetic storms (Dst

=< -100 nT)

Ji, Eun-Young; Moon, Y.-J.; Kim, K.-H.; Lee, D.-H.

J. Geophys. Res., Vol. 115, No. A10, A10232, 2010, **File**

It is well known that intense southward magnetic field and convection electric field ($V \times B$) in the interplanetary medium are key parameters that control the magnitude of geomagnetic storms. By investigating the interplanetary conditions of 82 intense geomagnetic storms from 1998 to 2006, we have compared many different criteria of interplanetary conditions for the occurrence of the intense geomagnetic storms ($Dst \leq -100$ nT). In order to examine if the magnetosphere always favors such interplanetary conditions for the occurrence of large geomagnetic storms, we applied these conditions to all the interplanetary data during the same period. For this study, we consider three types of interplanetary conditions as follows: B_z conditions, E_y conditions, and their combination. As a result, we present contingency tables between the number of events satisfying the condition and the number of observed geomagnetic storms. Then we obtain their statistical parameters for evaluation such as probability of detection yes, false alarm ratio, bias, and critical success index. From a comparison of these statistical parameters, we suggest that three conditions are promising candidates to trigger an intense storm: $B_z \leq -10$ nT for >3 h, $E_y \geq 5$ mV/m for >2 h, and $B_z \leq -15$ nT or $E_y \geq 5$ mV/m for >2 h. Also, we found that more than half of the “miss” events, when an intense storm occurs that was not expected, are associated with sheath field structures or corotating interacting regions. Our conditions can be used for not only the real-time forecast of geomagnetic storms but also the survey of interplanetary data to identify candidate events for producing intense geomagnetic storms.

STUDY OF THE 2007 APRIL 20 CME-COMET INTERACTION EVENT WITH AN MHD MODEL

Y. D. **Jia**¹, C. T. Russell¹, L. K. Jian¹, W. B. Manchester², O. Cohen², A. Vourlidas³, K. C. Hansen², M. R. Combi², and T. I. Gombosi²

Astrophysical Journal, 696:L56–L60, 2009 May

<http://arxiv.org/pdf/0903.4942v1.pdf>

This study examines the tail disconnection event on 2007 April 20 on comet 2P/Encke, caused by a coronal mass ejection (CME) at a heliocentric distance of 0.34 AU. During their interaction, both the CME and the comet are visible with high temporal and spatial resolution by the STEREO-A spacecraft. Previously, only current sheets or shocks have been accepted as possible reasons for comet tail disconnections, so it is puzzling that the CME caused this event. The MHD simulation presented in this work reproduces the interaction process and demonstrates how the CME triggered a tail disconnection in the April 20 event. It is found that the CME disturbs the comet with a combination of a 180° sudden rotation of the interplanetary magnetic field (IMF), followed by a 90° gradual rotation. Such an interpretation applies our understanding of solar wind-comet interactions to determine the in situ IMF orientation of the CME encountering Encke.

Solar Terrestrial Relations Observatory (STEREO) Observations of Stream Interaction Regions in 2007 – 2016: Relationship with Heliospheric Current Sheets, Solar Cycle Variations, and Dual Observations

L. K. **Jian**, [J. G. Luhmann](#), [C. T. Russell](#), [A. B. Galvin](#)

[Solar Physics](#) March 2019, 294:31

<http://sci-hub.tw/https://link.springer.com/article/10.1007/s11207-019-1416-8>

We have conducted a survey of 575 slow-to-fast stream interaction regions (SIRs) using Solar Terrestrial Relations Observatory (STEREO) A and B data, analyzing their properties while extending a Level-3 data product through 2016. Among 518 pristine SIRs, 54% are associated with heliospheric current sheet (HCS) crossings, and 34% are without any HCS crossing. The other 12% of the SIRs often occur in association with magnetic sectors shorter than three days. The SIRs with HCS crossings have slightly slower speeds but higher maximum number densities, magnetic-field strengths, dynamic pressures, and total pressures than the SIRs without an HCS. The iron charge state is higher throughout the SIRs with an HCS than the SIRs without an HCS, by about 1/31/3 charge unit. In contrast with the comparable phases of Solar Cycle 23, slightly more SIRs and higher recurrence rates are observed in the years 2009 – 2016 of Cycle 24, with a lower HCS association rate, possibly attributed to persistent equatorial coronal holes and more pseudo-streamers in this recent cycle. The solar-wind speed, peak magnetic field, and peak pressures of SIRs are all lower in this cycle, but the weakening is less than for the comparable background solar-wind parameters. Before STEREO-B lost contact in October 2014, 151 SIR pairs were observed by the twin spacecraft. Of the dual observations, the maximum speed is the best correlated of the plasma parameters. We have obtained a sample of plasma-parameter differences analogous to those that would be observed by a mission at Lagrange points 4 or 5. By studying several cases with large discrepancies between the dual observations, we investigate the effects of HCS relative location, tilt of stream interface, and small

transients on the SIR properties. To resolve the physical reasons for the variability of SIR structures, mesoscale multi-point observations and time-dependent solar-wind modeling are ultimately required.

STEREO Observations of Interplanetary Coronal Mass Ejections in 2007–2016

L. K. **Jian**^{1,2}, C. T. Russell^{3,4}, J. G. Luhmann⁵, and A. B. Galvin^{6,7}

2018 ApJ 855 114

<http://sci-hub.se/http://iopscience.iop.org/0004-637X/855/2/114/>

sci-hub.se/10.3847/1538-4357/aab189

We have conducted a survey of 341 interplanetary coronal mass ejections (ICMEs) using STEREO A/B data, analyzing their properties while extending a Level 3 product through 2016. Among the 192 ICMEs with distinguishable sheath region and magnetic obstacle, the magnetic field maxima in the two regions are comparable, and the dynamic pressure peaks mostly in the sheath. The north/south direction of the magnetic field does not present any clear relationship between the sheath region and the magnetic obstacle. About 71% of ICMEs are expanding at 1 au, and their expansion speed varies roughly linearly with their maximum speed except for ICMEs faster than 700 km s⁻¹. The total pressure generally peaks near the middle of the well-defined magnetic cloud (MC) passage, while it often declines along with the non-MC ICME passage, consistent with our previous interpretation concerning the effects of sampling geometry on what is observed. The hourly average iron charge state reaches above 12+ ~31% of the time for MCs, ~16% of the time for non-MC ICMEs, and ~1% of the time for non-ICME solar wind. In four ICMEs abrupt deviations of the magnetic field from the nominal field rotations occur in the magnetic obstacles, coincident with a brief drop or increase in field strength—features could be related to the interaction with dust. In comparison with the similar phases of solar cycle 23, the STEREO ICMEs in this cycle occur less often and are generally weaker and slower, although their field and pressure compressions weaken less than the background solar wind. **2006 Dec 14-15, 2009 Nov 1-3, 2010 Feb 5-6, 2011 Apr 5-6, 2012 Jan 1-2, 2013 December 1-4**

Validation for global solar wind prediction using Ulysses comparison: Multiple coronal and heliospheric models installed at the Community Coordinated Modeling Center

L. K. **Jian**, P. J. MacNeice, M. L. Mays, A. Taktakishvili, D. Odstrcil, B. Jackson, H.-S. Yu, P. Riley, I. V. Sokolov

Space Weather Volume 14, Issue 8 August 2016 Pages 592–611

The prediction of the background global solar wind is a necessary part of space weather forecasting. Several coronal and heliospheric models have been installed and/or recently upgraded at the Community Coordinated Modeling Center (CCMC), including the Wang-Sheely-Arge (WSA)-Enlil model, MHD-Around-a-Sphere (MAS)-Enlil model, Space Weather Modeling Framework (SWMF), and heliospheric tomography using interplanetary scintillation data. Ulysses recorded the last fast latitudinal scan from southern to northern poles in 2007. By comparing the modeling results with Ulysses observations over seven Carrington rotations, we have extended our third-party validation from the previous near-Earth solar wind to middle to high latitudes, in the same late declining phase of solar cycle 23. Besides visual comparison, we have quantitatively assessed the models' capabilities in reproducing the time series, statistics, and latitudinal variations of solar wind parameters for a specific range of model parameter settings, inputs, and grid configurations available at CCMC. The WSA-Enlil model results vary with three different magnetogram inputs. The MAS-Enlil model captures the solar wind parameters well, despite its underestimation of the speed at middle to high latitudes. The new version of SWMF misses many solar wind variations probably because it uses lower grid resolution than other models. The interplanetary scintillation-tomography cannot capture the latitudinal variations of solar wind well yet. Because the model performance varies with parameter settings which are optimized for different epochs or flow states, the performance metric study provided here can serve as a template that researchers can use to validate the models for the time periods and conditions of interest to them.

Validation for solar wind prediction at Earth: Comparison of coronal and heliospheric models installed at the CCMC

L. K. **Jian**, P. J. MacNeice, A. Taktakishvili, D. Odstrcil, B. Jackson, H.-S. Yu, P. Riley, I. V. Sokolov, R. M. Evans

Space Weather [Volume 13, Issue 5](#) May 2015 Pages 316–338

Multiple coronal and heliospheric models have been recently upgraded at the Community Coordinated Modeling Center (CCMC), including the Wang-Sheely-Arge (WSA)-Enlil model, MHD-Around-a-Sphere (MAS)-Enlil model, Space Weather Modeling Framework (SWMF), and heliospheric tomography using interplanetary scintillation data. To investigate the effects of photospheric magnetograms from different sources, different coronal models, and different

model versions on the model performance, we run these models in 10 combinations. Choosing seven Carrington rotations in 2007 as the time window, we compare the modeling results with the Operating Mission as Nodes on the Internet data for near-Earth space environment during the late declining phase of solar cycle 23. Visual comparison is proved to be a necessary addition to the quantitative assessment of the models' capabilities in reproducing the time series and statistics of solar wind parameters. The MAS-Enlil model captures the time patterns of solar wind parameters better, while the WSA-Enlil model matches with the time series of normalized solar wind parameters better. Models generally overestimate slow wind temperature and underestimate fast wind temperature and magnetic field. Using improved algorithms, we have identified magnetic field sector boundaries (SBs) and slow-to-fast stream interaction regions (SIRs) as focused structures. The success rate of capturing them and the time offset vary largely with models. For this quiet period, the new version of MAS-Enlil model works best for SBs, while heliospheric tomography works best for SIRs. The new version of SWMF with more physics added needs more development. General strengths and weaknesses for each model are diagnosed to provide an unbiased reference to model developers and users.

Electromagnetic Waves near the Proton Cyclotron Frequency: STEREO Observations

L. K. [Jian](#)^{1,2}, H. Y. Wei³, C. T. Russell³, J. G. Luhmann⁴, B. Klecker⁵, N. Omid⁶, P. A. Isenberg⁷, M. L. Goldstein², A. Figueroa-Viñas², and X. Blanco-Cano
2014 ApJ 786 123

Transverse, near-circularly polarized, parallel-propagating electromagnetic waves around the proton cyclotron frequency were found sporadically in the solar wind throughout the inner heliosphere. They could play an important role in heating and accelerating the solar wind. These low-frequency waves (LFWs) are intermittent but often occur in prolonged bursts lasting over 10 minutes, named "LFW storms." Through a comprehensive survey of them from Solar Terrestrial Relations Observatory A using dynamic spectral wave analysis, we have identified 241 LFW storms in 2008, present 0.9% of the time. They are left-hand (LH) or right-hand (RH) polarized in the spacecraft frame with similar characteristics, probably due to Doppler shift of the same type of waves or waves of intrinsically different polarities. In rare cases, the opposite polarities are observed closely in time or even simultaneously. Having ruled out interplanetary coronal mass ejections, shocks, energetic particles, comets, planets, and interstellar ions as LFW sources, we discuss the remaining generation scenarios: LH ion cyclotron instability driven by greater perpendicular temperature than parallel temperature or by ring-beam distribution, and RH ion fire hose instability driven by inverse temperature anisotropy or by cool ion beams. The investigation of solar wind conditions is compromised by the bias of the one-dimensional Maxwellian fit used for plasma data calibration. However, the LFW storms are preferentially detected in rarefaction regions following fast winds and when the magnetic field is radial. This preference may be related to the ion cyclotron anisotropy instability in fast wind and the minimum in damping along the radial field.

A Disconnection Event of Comet Lulin†

[Jian](#)-chun, Shi; Chi-sheng, Lin; Zhong-wei, Hu; Hai-bin, Zhao; Yue-hua, Ma
Chinese Astronomy and Astrophysics, Volume 35, Issue 3, p. 295-303. **2011**

The cometary disconnection event (DE) is the separation of the entire cometary tail or a part of it from the cometary head. It is one of the most spectacular phenomena of comets. The driving mechanism remains unclear, and at present there are many competitive theories to explain the onset of DE. However, the variable solar wind is suspected to play a major role. Comet Lulin exhibited a DE on 4th Feb. 2009. The data around this date are analyzed, and it is found that the comet Lulin had already endured a DE on 3rd Feb. 2009. By comparing the morphologies of the plasma tails in these two DEs, it is concluded that the DE which occurred on 3rd Feb. 2009 is another DE, which is distinct from that of 4th Feb. 2009. In this paper, we describe the results of analysis on the DE dated 3rd Feb. 2009. The measured velocity of disconnection motion is about 68 km/s, and the calculated onset time of this DE is 3.635 ± 0.215 Feb. 2009 in UT decimal date. Combining the orbital characteristics of Comet Lulin before and after the DE occurrence and the solar-wind data measured by the STEREO-A spacecraft, it is concluded that the DE which occurred on 3rd Feb. 2009 was probably caused by the magnetic reconnection due to the interaction between the comet and a coronal mass ejection (CME).

Multi-Spacecraft Observations: Stream Interactions and Associated Structures

L.K. [Jian](#) · C.T. Russell · J.G. Luhmann · A.B. Galvin · P.J. MacNeice
Solar Phys (2009) 259: 345–360

The stream interaction region (SIR), formed when a fast stream overtakes a preceding slow stream, is the predominant large-scale solar wind structure at this early phase of the STEREO mission. Using multi-spacecraft observations from STEREO A and B, ACE, *Wind*, and *Ulysses* in 2007, we analyze three stream interaction events in depth in May, August, and November of 2007, respectively, when the spacecraft had quite different spatial separations. We attempt to determine the causes of the differences in the SIR properties, whether they are spatial or temporal variations, and also to examine the steepening or widening of the SIR during its radial evolution. The presence and characteristics of associated shocks, the relation to the heliospheric current sheet, and other structures are also studied.

Stream Interactions and Interplanetary Coronal Mass Ejections at 0.72 AU

L.K. **Jian** · C.T. Russell · J.G. Luhmann · R.M. Skoug · J.T. Steinberg

Solar Phys (2008) 249: 85–101

<http://www.springerlink.com/content/q86841161156n644/fulltext.pdf>

We present comprehensive surveys of 203 stream interaction regions (SIRs) and 124 interplanetary CMEs (ICMEs) during 1979 – 1988 using *Pioneer Venus Orbiter* (PVO) *in situ* solar-wind observations at 0.72 AU and examine the solar-cycle variations of the occurrence rate, shock association rate, duration, width, maximum total perpendicular pressure (P_t), maximum dynamic pressure, maximum magnetic field intensity, and maximum velocity change of these two large-scale solar-wind structures. The medians, averages, and histogram distributions of these parameters are also reported. Furthermore, we sort ICMEs into three groups based on the temporal profiles of P_t , and we investigate the variations of the fractional occurrence rate of three groups of ICMEs with solar activity. We find that the fractional occurrence rate of magnetic-cloud-like ICMEs declined with solar activity, consistent with our former 1-AU results. This study at 0.72 AU provides a point of comparison in the inner heliosphere for examining the radial evolution of SIRs and ICMEs. The width of SIRs and ICMEs increases by 0.04 and 0.1 AU, respectively, and the maximum P_t decreases to about 1/3 from Venus to Earth orbit. In addition, our work establishes the statistical properties of the solar-wind conditions at 0.72 AU that control the solar-wind interaction with Venus and its atmosphere loss by related processes.

PROPERTIES OF INTERPLANETARY CORONAL MASS EJECTIONS AT ONE AU DURING 1995 – 2004

L. **JIAN**, C.T. RUSSELL, J.G. LUHMANN, and R.M. SKOUG

Solar Physics (2006) 239: 393–436, **File**

We present a comprehensive survey of 230 interplanetary CMEs (ICMEs) during 1995 – 2004 using *Wind* and ACE *in situ* observations near one AU, and examine the solar-cycle variation of the occurrence rate, shock association rate, scale size, velocity change, and other properties of ICMEs. The ICME occurrence rate increases (from 5 in 1996 to 40 in 2001) with solar activity; and 66% of all ICMEs occurred with shock(s). A compound parameter, the total pressure perpendicular to the magnetic field (P_t), *i.e.*, the sum of magnetic and perpendicular plasma thermal pressures, assists us in effectively distinguishing ICMEs from other solar-wind structures such as stream interactions, and in quantifying the interaction strength. We interpret the characteristic signatures of the P_t temporal variation in terms of the inferred distance perpendicular to the flow to the center of the obstacle. Group 1 includes events that appear to be traversed near the ICME center, showing an apparent enhanced central P_t ; Group 3 represents ICMEs passed far away from the center, displaying a rapid rise and then gradual decay in P_t ; and Group 2 includes events with intermediate signatures. About 36% of 198 classifiable ICMEs are Group 1 events, consistent with the conventional wisdom that at one AU a magnetic cloud is found during crossings of only ~1/3 of ICMEs. Our set of Group 1 ICMEs and the set of magnetic clouds from other researchers have significant overlap and a similar solar-cycle dependence. The rough decline of the Group 1 fraction as solar activity increases, is consistent with rough increases of scale size, shock percentage, and peak P_t . These results call into question the need to have different mechanisms to create differently appearing ICMEs. Rather it is possible that all ICMEs have a central flux rope that is traversed about 33% of the time, but in the majority of cases is missed by the spacecraft.

[List of ICMEs for 1995-2004](#)

A New Scenario of Solar Modulation Model during the Polarity Reversing

Jieteng **Jiang**, [Sujie Lin](#), [Lili Yang](#)

ApJ **2023**

<https://arxiv.org/pdf/2303.04460.pdf>

When the Galactic Cosmic Rays (GCRs) entering the heliosphere, they encounter the solar wind plasma, and their intensity is reduced, so-called solar modulation. The modulation is caused by the combination of a few factors, such as particle energies, solar activity and solar disturbance. In this work, a 2D numerical method is adopted to simulate the propagation of GCRs in the heliosphere with SOLARPROP, and to overcome the time-consuming issue, the machine learning technique is also applied. With the obtained proton local interstellar spectra (LIS) based on the observation from Voyager 1 and AMS-02, the solar modulation parameters during the solar maximum activity of cycle 24 have been found. It shows the normalization and index of the diffusion coefficient indeed reach a maximal value in February 2014. However, after taking into account the travel time of particles with different energies, the peak time was found postponed to November 2014 as expected. The nine-month late is so-called time lag.

During Two Steps of Energy Conversion in Magnetic Reconnection Exhaust Region of Solar Wind

He **Jiansen**¹, Zhu Xingyu¹, Chen Yajie¹, Salem Chadi², Stevens Michael³, Li Hui⁴, Ruan Wenzhi^{1,5}, Zhang Lei⁴, and Tu Chuanyi¹

2018 ApJ 856 148

<http://sci-hub.tw/http://iopscience.iop.org/0004-637X/856/2/148/>

The magnetic reconnection exhaust is a pivotal region with enormous magnetic energy being continuously released and converted. The physical processes of energy conversion involved are so complicated that an all-round understanding based on in situ measurements is still lacking. We present the evidence of plasma heating by illustrating the broadening of proton and electron velocity distributions, which are extended mainly along the magnetic field, in an exhaust of interchange reconnection between two interplanetary magnetic flux tubes of the same polarity on the Sun. The exhaust is asymmetric across an interface, with both sides being bounded by a pair of compound discontinuities consisting of rotational discontinuity and slow shock. The energized plasmas are found to be firehose unstable, and responsible for the emanation of Alfvén waves during the second step of energy conversion. It is realized that the energy conversion in the exhaust can be a two-step process involving both plasma energization and wave emission. **1997 November 23**

Properties of Steady Sub-Alfvénic Solar Wind in Comparison with Super-Alfvénic Wind from Measurements of Parker Solar Probe

Yiming **Jiao**, [Ying D. Liu](#), [Hao Ran](#), [Wenshuai Cheng](#)

ApJ **960** 42 **2023**

<https://arxiv.org/pdf/2311.15622.pdf>

<https://iopscience.iop.org/article/10.3847/1538-4357/ad0dfe/pdf>

We identify more than ten steady sub-Alfvénic solar wind intervals from the measurements of the Parker Solar Probe (PSP) from encounter 8 to encounter 14. An analysis of these sub-Alfvénic intervals reveals similar properties and similar origins. In situ measurements show that these intervals feature a decreased radial Alfvén Mach number resulting from a reduced density and a relatively low velocity, and that switchbacks are suppressed in these intervals. Magnetic source tracing indicates that these sub-Alfvénic streams generally originate from the boundaries inside coronal holes, or narrow/small regions of open magnetic fields. Such properties and origins suggest that these streams are low Mach-number boundary layers (LMBLs), which is a special component of the pristine solar wind proposed by Liu et al. (2023). We find that the LMBL wind, the fast wind from deep inside coronal holes, and the slow streamer wind constitute three typical components of the young solar wind near the Sun. In these sub-Alfvénic intervals, the Alfvén radius varies between 15 and 25 solar radii, in contrast with a typical 12 radii for the Alfvén radius of the super-Alfvénic wind. These results give a self-consistent picture interpreting the PSP measurements in the vicinity of the Sun.

Relation between Latitude-dependent Sunspot Data and Near-Earth Solar Wind Speed

Qirong **Jiao**^{1,2}, Wenlong Liu^{1,2}, Dianjun Zhang^{1,2}, and Jinbin Cao^{1,2}

2023 ApJ 958 70

<https://iopscience.iop.org/article/10.3847/1538-4357/acfc21/pdf>

Solar wind is important for the space environment between the Sun and the Earth and varies with the sunspot cycle, which is influenced by solar internal dynamics. We study the impact of latitude-dependent sunspot data on solar wind speed using the Granger causality test method and a machine-learning prediction approach. The results show that the low-latitude sunspot number has a larger effect on the solar wind speed. The time delay between the annual average solar wind speed and sunspot number decreases as the latitude range decreases. A machine-learning model is developed for the prediction of solar wind speed considering latitude and time effects. It is found that the model performs differently with latitude-dependent sunspot data. It is revealed that the timescale of the solar wind speed is more strongly influenced by low-latitude sunspots and that sunspot data have a greater impact on the 30 day average solar wind speed than on a daily basis. With the addition of sunspot data below $7^{\circ}2$ latitude, the prediction of the daily and 30 day averages is improved by 0.23% and 12%, respectively. The best correlation coefficient is 0.787 for the daily solar wind prediction model.

Assessing the Influence of Input Magnetic Maps on Global Modeling of the Solar Wind and CME-driven Shock in the 2013 April 11 Event

Meng [Jin](#), [Nariaki V. Nitta](#), [Christina M. S. Cohen](#)

Space Weather **Volume20, Issue3** e2021SW002894 2022

<https://arxiv.org/pdf/2202.07214.pdf>

<https://agupubs.onlinelibrary.wiley.com/doi/epdf/10.1029/2021SW002894>

In the past decade, significant efforts have been made in developing physics-based solar wind and coronal mass ejection (CME) models, which have been or are being transferred to national centers (e.g., SWPC, CCMC) to enable space weather predictive capability. However, the input data coverage for space weather forecasting is extremely limited. One major limitation is the solar magnetic field measurements, which are used to specify the inner boundary conditions of the global magnetohydrodynamic (MHD) models. In this study, using the Alfvén wave solar model (AWSoM), we quantitatively assess the influence of the magnetic field map input (synoptic/diachronic vs. synchronic magnetic maps) on the global modeling of the solar wind and the CME-driven shock in the **2013 April 11** solar energetic particle (SEP) event. Our study shows that due to the inhomogeneous background solar wind and dynamical evolution of the CME, the CME-driven shock parameters change significantly both spatially and temporally as the CME propagates through the heliosphere. The input magnetic map has a great impact on the shock connectivity and shock properties in the global MHD simulation. Therefore this study illustrates the importance of taking into account the model uncertainty due to the imperfect magnetic field measurements when using the model to provide space weather predictions.

Chromosphere to 1 AU Simulation of the 2011 March 7th Event: A Comprehensive Study of Coronal Mass Ejection Propagation

M. [Jin](#), W. B. Manchester, B. van der Holst, I. Sokolov, G. Toth, A. Vourlidas, C. A. de Koning, T. I. Gombosi

ApJ **834** 172 2016

<https://arxiv.org/pdf/1611.08897v1.pdf>

http://www.lmsal.com/~jinmeng/papers/mjin17a_apj.pdf

We perform and analyze results of a global magnetohydrodynamic (MHD) simulation of the fast coronal mass ejection (CME) that occurred on **2011 March 7**. The simulation is made using the newly developed Alfvén Wave Solar Model (AWSoM), which describes the background solar wind starting from the upper chromosphere and extends to $24 R_{\odot}$. Coupling AWSoM to an inner heliosphere (IH) model with the Space Weather Modeling Framework (SWMF) extends the total domain beyond the orbit of Earth. Physical processes included in the model are multi-species thermodynamics, electron heat conduction (both collisional and collisionless formulations), optically thin radiative cooling, and Alfvén-wave turbulence that accelerates and heats the solar wind. The Alfvén-wave description is physically self-consistent, including non-Wentzel-Kramers-Brillouin (WKB) reflection and physics-based apportioning of turbulent dissipative heating to both electrons and protons. Within this model, we initiate the CME by using the Gibson-Low (GL) analytical flux rope model and follow its evolution for days, in which time it propagates beyond STEREO A. A detailed comparison study is performed using remote as well as *in situ* observations. Although the flux rope structure is not compared directly due to lack of relevant ejecta observation at 1 AU in this event, our results show that the new model can reproduce many of the observed features near the Sun (e.g., CME-driven extreme ultraviolet (EUV) waves, deflection of the flux rope from the coronal hole, "double-front" in the white light images) and in the heliosphere (e.g., shock propagation direction, shock properties at STEREO A).

Data Constrained Coronal Mass Ejections in A Global Magnetohydrodynamics Model

M. **Jin**, W. B. Manchester, B. van der Holst, I. Sokolov, G. Toth, R. E. Mullinix, A. Taktakishvili, A. Chulaki, T. I. Gombosi

ApJ **834** 173 **2017**

<http://arxiv.org/pdf/1605.05360v1.pdf>

http://www.lmsal.com/~jinmeng/papers/mjin17b_apj.pdf

We present a first-principles-based coronal mass ejection (CME) model suitable for both scientific and operational purposes by combining a global magnetohydrodynamics (MHD) solar wind model with a flux rope-driven CME model. Realistic CME events are simulated self-consistently with high fidelity and forecasting capability by constraining initial flux rope parameters with observational data from GONG, SOHO/LASCO, and STEREO/COR. We automate this process so that minimum manual intervention is required in specifying the CME initial state. With the newly developed data-driven Eruptive Event Generator Gibson-Low (EEGGL), we present a method to derive Gibson-Low (GL) flux rope parameters through a handful of observational quantities so that the modeled CMEs can propagate with the desired CME speeds near the Sun. A test result with CMEs launched with different Carrington rotation magnetograms are shown. Our study shows a promising result for using the first-principles-based MHD global model as a forecasting tool, which is capable of predicting the CME direction of propagation, arrival time, and ICME magnetic field at 1 AU (see companion paper by Jin et al. 2016b).

See **Introduction** about three different categories of the CME models

Intense Flare-CME Event of the Year 2015: Propagation and Interaction Effects between Sun and Earth's Orbit

Abhishek **Johri**, P.K. Manoharan

Solar Phys. Volume 291, Issue 5, pp 1433-1446

2016

<http://arxiv.org/pdf/1603.04555v1.pdf>

sci-hub.tw/10.1007/s11207-016-0900-7

In this paper, We report the interplanetary effects of a fast coronal mass ejection (CME) associated with the intense X2.7 flare that occurred on **05 May 2015**. The near-Sun signatures of the CME at low-coronal heights $< 2 \{R_{\odot}\}$ are obtained from the EUV images at 171 $\{AA\}$ and metric radio observations. The intensity and duration of the CME-driven radio bursts in the near-Sun and interplanetary medium indicate this CME event to be an energetic one. The interplanetary scintillation data, along with the low-frequency radio spectrum, played a crucial role in understanding the radial evolution of the speed and expansion of the CME in the inner heliosphere as well as its interaction with a preceding slow CME. The estimation of the speed of the CME at several points along the Sun to 1 AU shows that i) the CME went through a rapid acceleration as well as expansion up to a height of $\approx 6 \{R_{\odot}\}$, and ii) the CME continued to propagate at speed $\geq 800 \text{ kms}^{-1}$ between the Sun and 1 AU. These results show that the CME likely overcame the drag exerted by the ambient/background solar-wind with the support of its internal magnetic energy. When the CME interacted with a slow preceding CME, the turbulence level associated with the CME-driven disturbance increased significantly.

The visual complexity of coronal mass ejections follows the solar cycle

S. R. Jones, **C. J. Scott**, **L. A. Barnard**, **R. Highfield**, **C. J. Lintott**, **E. Baeten**

Space Weather e2020SW002556 **2020**

<https://doi.org/10.1029/2020SW002556>

<https://agupubs.onlinelibrary.wiley.com/doi/epdf/10.1029/2020SW002556>

The Heliospheric Imagers on board NASA's twin STEREO spacecraft show that coronal mass ejections (CMEs) can be visually complex structures. To explore this complexity, we created a citizen science project with the UK Science Museum, in which participants were shown pairs of CME images and asked to decide which image in each pair appeared the most 'complicated'. A Bradley-Terry model was then applied to these data to rank the CMEs by their 'complicatedness', or 'visual complexity'. This complexity ranking revealed that the annual average visual complexity values follow the solar activity cycle, with a higher level of complexity being observed at the peak of the cycle. The average complexity of CMEs observed by STEREO-A was also found to be significantly higher than those observed by STEREO-B. Visual complexity was found to be associated with CME size and brightness, but our results suggest that complexity may be influenced by the scale-sizes of structure in the CMEs. **15 June 2011**

The Science of Sungrazers, Sunskirters, and Other Near-Sun Comets

Review

Geraint H. **Jones**, **Matthew M. Knight**, **Karl Battams**, **Daniel C. Boice**...

Space Science Reviews February **2018**, 214:20–86 pp.

<https://link.springer.com/content/pdf/10.1007%2Fs11214-017-0446-5.pdf>

This review addresses our current understanding of comets that venture close to the Sun, and are hence exposed to much more extreme conditions than comets that are typically studied from Earth. The extreme solar heating and plasma environments that these objects encounter change many aspects of their behaviour, thus yielding valuable information on both the comets themselves that complements other data we have on primitive solar system bodies, as well as on the near-solar environment which they traverse. We propose clear definitions for these comets: We use the term near-Sun comets to encompass all objects that pass sunward of the perihelion distance of planet Mercury (0.307 AU). Sunskirters are defined as objects that pass within 33 solar radii of the Sun's centre, equal to half of Mercury's perihelion distance, and the commonly-used phrase sungrazers to be objects that reach perihelion within 3.45 solar radii, i.e. the fluid Roche limit. Finally, comets with orbits that intersect the solar photosphere are termed sundivers. We summarize past studies of these objects, as well as the instruments and facilities used to study them, including space-based platforms that have led to a recent revolution in the quantity and quality of relevant observations. Relevant comet populations are described, including the Kreutz, Marsden, Kracht, and Meyer groups, near-Sun asteroids, and a brief discussion of their origins. The importance of light curves and the clues they provide on cometary composition are emphasized, together with what information has been gleaned about nucleus parameters, including the sizes and masses of objects and their families, and their tensile strengths. The physical processes occurring at these objects are considered in some detail, including the disruption of nuclei, sublimation, and ionisation, and we consider the mass, momentum, and energy loss of comets in the corona and those that venture to lower altitudes. The different components of comae and tails are described, including dust, neutral and ionised gases, their chemical reactions, and their contributions to the near-Sun environment. Comet-solar wind interactions are discussed, including the use of comets as probes of solar wind and coronal conditions in their vicinities. We address the relevance of work on comets near the Sun to similar objects orbiting other stars, and conclude with a discussion of future directions for the field and the planned ground- and space-based facilities that will allow us to address those science topics.

Interaction between coronal mass ejections and the solar wind

Jones, R. A.; Breen, A. R.; Fallows, R. A.; Canals, A.; Bisi, M. M.; Lawrence, G.
J. Geophys. Res., Vol. 112, No. A8, A08107

Interplanetary scintillation measurements (IPS).

The European Incoherent Scatter Radar and the Multi Element Radio Linked Interferometer Network systems, with a field of view covering 10–120 solar radii, can provide information on iCMEs in the inner regions of the solar wind. The results provide additional confirmation that iCMEs converge toward the velocity of the solar wind ahead of the event and that most of the resulting acceleration or deceleration occurs in the innermost regions of the solar wind.

The interaction of comet 153P/Ikeya-Zhang with interplanetary coronal mass ejections: Identification of fast ICME signatures

Geraint H. **Jones**¹ and John C. Brandt

Geophysical Research Letters, Volume 31, Issue 20, CiteID L20805, **2004**

The active comet 153P/Ikeya-Zhang possessed a highly-variable plasma tail. Favorable circumstances allowed the identification of the impact of fast ICMEs with the comet. The impact produces a specific morphology including a characteristic scalloped appearance which suggests that the ICME magnetic field drapes around preexisting tail density enhancements. This appears to be the first direct association between fast ICMEs and plasma tail structure and the specific structure should permit the identification of fast ICME locations in the heliosphere.

Revisiting two-step Forbush decreases

Jordan, A. P.; Spence, H. E.; Blake, J. B.; Shaul, D. N. A.

J. Geophys. Res., Vol. 116, No. A11, A11103, **2011**

<http://dx.doi.org/10.1029/2011JA016791>

Interplanetary coronal mass ejections (ICMEs) and their shocks can sweep out galactic cosmic rays (GCRs), thus creating Forbush decreases (FDs). The traditional model of FDs predicts that an ICME and its shock decrease the GCR intensity in a two-step profile. This model, however, has been the focus of little testing. Thus, our goal is to discover whether a passing ICME and its shock inevitably lead to a two-step FD, as predicted by the model. We use cosmic ray data from 14 neutron monitors and, when possible, high time resolution GCR data from the spacecraft International Gamma Ray Astrophysical Laboratory (INTEGRAL). We analyze 233 ICMEs that should have created two-step FDs. Of these, only 80 created FDs, and only 13 created two-step FDs. FDs are thus less common than predicted by the model. The majority of events indicates that profiles of FDs are more complicated, particularly within the ICME sheath, than predicted by the model. We conclude that the traditional model of FDs as having one or two steps should be

discarded. We also conclude that generally ignored small-scale interplanetary magnetic field structure can contribute to the observed variety of FD profiles.

Multipoint, high time resolution galactic cosmic ray observations associated with two interplanetary coronal mass ejections

Jordan, A. P.; Spence, H. E.; Blake, J. B.; Mulligan, T.; Shaul, D. N. A.; Galametz, M. J. *Geophys. Res.*, Vol. 114, No. A7, A07107, **2009**

<http://dx.doi.org/10.1029/2008JA013891>

Galactic cosmic rays (GCRs) play an important role in our understanding of the interplanetary medium (IPM). The causes of their short timescale variations, however, remain largely unexplored. In this paper, we compare high time resolution, multipoint space-based GCR data to explore structures in the IPM that cause these variations. To ensure that features we see in these data actually relate to conditions in the IPM, we look for correlations between the GCR time series from two instruments onboard the Polar and INTEGRAL (International Gamma Ray Astrophysical Laboratory) satellites, respectively inside and outside Earth's magnetosphere. We analyze the period of 18–24 August 2006 during which two interplanetary coronal mass ejections (ICMEs) passed Earth and produced a Forbush decrease (Fd) in the GCR flux. We find two periods, for a total of 10 h, of clear correlation between small-scale variations in the two GCR time series during these 7 days, thus demonstrating that such variations are observable using space-based instruments. The first period of correlation lasted 6 h and began 2 h before the shock of the first ICME passed the two spacecraft. The second period occurred during the initial decrease of the Fd, an event that did not conform to the typical one- or two-step classification of Fds. We propose that two planar magnetic structures preceding the first ICME played a role in both periods: one structure in driving the first correlation and the other in initiating the Fd.

A Major Geoeffective CME from NOAA 12371: Initiation, CME–CME Interactions, and Interplanetary Consequences

Bhuwan **Joshi**, M. Syed Ibrahim, A. Shanmugaraju, D. Chakrabarty

Solar Physics July **2018**, 293:107

<http://sci-hub.tw/http://link.springer.com/10.1007/s11207-018-1325-2>

In this article, we present a multi-wavelength and multi-instrument investigation of a halo coronal mass ejection (CME) from active region NOAA 12371 on **21 June 2015** that led to a major geomagnetic storm of minimum $Dst = -204$ nT. The observations from the Atmospheric Imaging Assembly onboard the Solar Dynamics Observatory in the hot EUV channel of 94 Å confirm the CME to be associated with a coronal sigmoid that displayed an intense emission ($T \sim 6$ MK) from its core before the onset of the eruption. Multi-wavelength observations of the source active region suggest tether-cutting reconnection to be the primary triggering mechanism of the flux rope eruption. Interestingly, the flux rope eruption exhibited a two-phase evolution during which the “standard” large-scale flare reconnection process originated two composite M-class flares. The eruption of the flux rope is followed by the coronagraphic observation of a fast, halo CME with linear projected speed of 1366 km s⁻¹. The dynamic radio spectrum in the decameter-hectometer frequency range reveals multiple continuum-like enhancements in type II radio emission which imply the interaction of the CME with other preceding slow speed CMEs in the corona within ≈ 10 –90 R_{\odot} . The scenario of CME–CME interaction in the corona and interplanetary medium is further confirmed by the height–time plots of the CMEs occurring during 19–21 June. In situ measurements of solar wind magnetic field and plasma parameters at 1 AU exhibit two distinct magnetic clouds, separated by a magnetic hole. Synthesis of near-Sun observations, interplanetary radio emissions, and in situ measurements at 1 AU reveal complex processes of CME–CME interactions right from the source active region to the corona and interplanetary medium that have played a crucial role towards the large enhancement of the geoeffectiveness of the halo CME on 21 June 2015.

Energetic particle evolution during coronal mass ejection passage from 0.3 to 1 AU

C. J. **Joyce**¹, D. J. McComas^{1,2}, N. A. Schwadron^{1,2}, A. Vourlidas³,

A&A 651, A2 (**2021**)

<https://www.aanda.org/articles/aa/pdf/2021/07/aa39933-20.pdf>

<https://doi.org/10.1051/0004-6361/202039933>

We provide analysis of a coronal mass ejection (CME) that passed over Parker Solar Probe (PSP) on January 20, 2020 when the spacecraft was at just 0.32 AU. The Integrated Science Investigation of the Sun instrument suite measures energetic particle populations associated with the CME before, during, and after its passage over the spacecraft. We observe a complex evolution of energetic particles, including a brief ~ 2 h period where the energetic particle fluxes are enhanced and the nominal orientation of the energetic particle streaming outward from the Sun (from 30 to 100 keV

nuc-1) abruptly reverses inward toward the Sun. This transient and punctuated evolution highlights the importance of magnetic field structures that connect the spacecraft to different acceleration sites, one of which is likely more distant from the Sun than PSP during the evolution of the CME. We discuss these characteristics and what they tell us about the source of the energetic particles. During this period, PSP was radially aligned with the Solar Terrestrial Relations Observatory A (STEREO-A), which measured the same CME when it passed 1 AU. The magnetic field measurements at both spacecraft are remarkably similar, indicating that the spacecraft are likely encountering the same portion of the magnetic structure that has not evolved significantly in transit. The energetic particle observations on the other hand, are quite different at STEREO-A, showing how transport effects have acted on the energetic particle populations and obscured the detailed properties present earlier in the development of the CME. This event provides a unique case study in how energetic particle populations evolve as CMEs propagate through the heliosphere.

MAGNETIC FIELD-LINE LENGTHS IN INTERPLANETARY CORONAL MASS EJECTIONS INFERRED FROM ENERGETIC ELECTRON EVENTS

S. W. [Kahler](#)¹, D. K. Haggerty² and I. G. Richardson

2011 ApJ 736 106

About one quarter of the observed interplanetary coronal mass ejections (ICMEs) are characterized by enhanced magnetic fields that smoothly rotate in direction over timescales of about 10-50 hr. These ICMEs have the appearance of magnetic flux ropes and are known as "magnetic clouds" (MCs). The total lengths of MC field lines can be determined using solar energetic particles of known speeds when the solar release times and the 1 AU onset times of the particles are known. A recent examination of about 30 near-relativistic (NR) electron events in and near 8 MCs showed no obvious indication that the field-line lengths were longest near the MC boundaries and shortest at the MC axes or outside the MCs, contrary to the expectations for a flux rope. Here we use the impulsive beamed NR electron events observed with the Electron Proton and Alpha Monitor instrument on the Advanced Composition Explorer spacecraft and type III radio bursts observed on the Wind spacecraft to determine the field-line lengths inside ICMEs included in the catalog of Richardson & Cane. In particular, we extend this technique to ICMEs that are not MCs and compare the field-line lengths inside MCs and non-MC ICMEs with those in the ambient solar wind outside the ICMEs. No significant differences of field-line lengths are found among MCs, ICMEs, and the ambient solar wind. The estimated number of ICME field-line turns is generally smaller than those deduced for flux-rope model fits to MCs. We also find cases in which the electron injections occur in solar active regions (ARs) distant from the source ARs of the ICMEs, supporting CME models that require extensive coronal magnetic reconnection with surrounding fields. The field-line lengths are found to be statistically longer for the NR electron events classified as ramps and interpreted as shock injections somewhat delayed from the type III bursts. The path lengths of the remaining spike and pulse electron events are compared with model calculations of solar wind field-line lengths resulting from turbulence and found to be in good agreement.

Solar energetic electron probes of magnetic cloud field line lengths

[Kahler](#), S. W.; Krucker, S.; Szabo, A.

J. Geophys. Res., Vol. 116, No. A1, A01104, 2011

Magnetic clouds (MCs) are large interplanetary coronal mass ejections of enhanced and low-variance fields with rotations indicative of magnetic flux ropes originally connected to the Sun. The MC flux rope models require field lines with larger pitch angles and longer lengths with increasing distance from the MC axis. While the models can provide good fits to the in situ solar wind observations, there have not been definitive observational tests of the global magnetic field geometry, particularly for the field line lengths. However, impulsive solar energetic ($E > 10$ keV) electron events occasionally occur within an MC, and the electron onsets can be used to infer L_e , the magnetic field line lengths traveled by the electrons from the Sun to the points in the MC where the electron onsets occur. We selected 8 MCs in and near which 30 solar electron events were observed by the 3DP instrument on the Wind spacecraft. We compared the corresponding L_e values with calculated model field line lengths to test two MC models. Some limitations on the technique are imposed by variations of the models and uncertainty about MC boundary locations. We found generally poor correlations between the computed electron path lengths and the model field line lengths. Only one value of L_e inside an MC, that of 18 October 1995, exceeded 3.2 AU, indicating an absence of the long path lengths expected in the highly wound outer regions of MC models. We briefly consider the implications for MC models.

V arc interplanetary coronal mass ejections observed with the Solar Mass Ejection Imager

Kahler, S. W.; Webb, D. F.

J. Geophys. Res., Vol. 112, No. A9, A09103, 2007

<http://dx.doi.org/10.1029/2007JA012358>

Since February 2003, the Solar Mass Ejection Imager (SMEI) has been observing interplanetary coronal mass ejections (ICMEs) at solar elongation angles $> 20^\circ$. The ICMEs generally appear as loops or arcs in the sky, but five show distinct outward concave shapes that we call V arcs. We expect to observe some V arcs, formed by trailing edges of ICME flux ropes or by leading ICME edges sheared by solar wind (SW) speed gradients at the heliospheric current sheet. We characterize the properties of these V arcs and compare them with average properties of all SMEI ICMEs. The typical V arc speeds argue against a slow MHD shock interpretation for their structures. We estimate the V arc solar source locations and their opening angle dynamics as tests for SW shearing. The first test contradicts but the second supports the SW shearing explanation. The implications of the small number of V arcs observed with SMEI is considered. The point P approximation used to determine the V arc locations and inferred solar source regions is critically examined in Appendix A.

Imaging Interplanetary Disturbances Causing Forbush Decreases

Kahler, S.W. and G.M. Simnett,

in Proc. of the 29th Intl. Cosmic Ray Conference, Pune, India, 2, 267-270 (2005), **File**

Forbush decreases (FDs) in neutron monitor (NM) counting rates are caused by enhanced magnetic fields in interplanetary shocks and solar ejecta that shield the Earth from galactic cosmic rays (GCRs). The solar origins of those ejecta can be observed as coronal mass ejections (CMEs) in coronagraphs, but their propagation through interplanetary space near or past the Earth has not been previously observable. The Solar Mass Ejection Imager (SMEI), launched into polar Earth orbit in January 2003, now allows us to search for the white light signatures of interplanetary CMEs (ICMEs) responsible for FDs. SMEI is unique in that it can monitor the progress of CMEs through the inner heliosphere out to distances beyond 1 AU and distinguish those which hit the Earth from those that do not. For comparison with SMEI observations, we selected all FDs of $\geq 2\%$ observed with the Oulu, Finland, NM. We find an excellent association of SMEI CMEs with those FDs and for each of the associated SMEI CMEs a good candidate associated LASCO CME was also found. The SMEI observations provide information on the approximate spatial locations and trajectories of large ICMEs that may result in FDs and hence can be useful as a space weather tool.

Solar flares and coronal mass ejections. (Review)

Kahler, S.W.,

1992. Ann Rev. Astron. Astrophys. 30, 113–141.

<http://sci-hub.ru/10.1146/annurev.aa.30.090192.000553>

This review addresses two basic questions. First, how did we form such a fundamentally incorrect view of the effects of flares after so much observational and theoretical work? Second, what is the observational and theoretical evidence to support a primary role for CMEs, and what can we say about the relationship between flares and CMEs? In Section 2 we present flare and CME observations in a historical context to show the changing perspective between the two phenomena. In Section 3 we discuss the coronal phenomena that bear on the relationship between flares and CMEs. Interplanetary effects are discussed in Section 4.

Transient Upstream Mesoscale Structures: Drivers of Solar-Quiet Space Weather

Primož **Kajdič**, [Xóchitl Blanco-Cano](#), [Lucile Turc](#), [Martin Archer](#), [Savvas Raptis](#), [Terry Z. Liu](#), [Yann Pfau-Kempf](#), [Adrian T. LaMoury](#), [Yufei Hao](#), [Philippe C. Escoubet](#), [Nojan Omid](#), [David G. Sibeck](#), [Boyi Wang](#), [Hui Zhang](#), [Yu Lin](#)

Front. Astron. Space Sci., (2024), Sec. Space Physics, Volume 11 - 2024

<https://arxiv.org/pdf/2411.07145>

In recent years, it has become increasingly clear that space weather disturbances can be triggered by transient upstream mesoscale structures (TUMS), independently of the occurrence of large-scale solar wind (SW) structures, such as interplanetary coronal mass ejections and stream interaction regions. Different types of magnetospheric pulsations, transient perturbations of the geomagnetic field and auroral structures are often observed during times when SW monitors indicate quiet conditions, and have been found to be associated to TUMS. In this mini-review we describe the space weather phenomena that have been associated with four of the largest-scale and the most energetic TUMS, namely hot flow anomalies, foreshock bubbles, travelling foreshocks and foreshock compressional boundaries. The space weather phenomena associated with TUMS tend to be more localized and less intense compared to geomagnetic storms.

However, the quiet time space weather may occur more often since, especially during solar minima, quiet SW periods prevail over the perturbed times. **14 Aug 2007, 14 Jul 2008**

Waves upstream and downstream of interplanetary shocks driven by coronal mass ejections

Kajdic, P.; Blanco-Cano, X.; Aguilar-Rodriguez, E.; Russell, C. T.; Jian, L. K.; Luhmann, J. G.

J. Geophys. Res., Vol. 117, No. A6, A06103, **2012**

<http://dx.doi.org/10.1029/2011JA017381>

In this work we study the waves in regions adjacent to ten interplanetary (IP) shocks formed by the interactions between interplanetary coronal mass ejections and the solar wind. We analyze the STEREO data for the years 2007–2010. Shocks in our sample have low magnetosonic Mach numbers ($M_{ms} \leq 2.3$), their criticality ratios range between 0.8 and 2.3 and θ_{Bn} are between 38° and 85° . We find ultra-low frequency (ULF, 0.01 Hz–0.05 Hz) waves and higher-frequency (HF, ≥ 1 Hz) whistler precursors upstream of these shocks. Downstream of them we observe irregular ULF fluctuations and regular HF waves with similar frequencies as in the upstream case. We find that IP shocks with relatively small M_{ms} can excite waves in large regions in front of them (2.2×10^{-3} AU– 4.6×10^{-3} AU), thereby forming large ULF wave foreshocks. We do not find any evidence for the steepening of these waves. We do observe suprathermal ($E \leq 30$ keV) proton foreshocks upstream of some of the shocks in the sample. The extensions of suprathermal proton foreshocks range between 0.02 AU and 0.1 AU. However, not all foreshocks with suprathermal ions show ULF waves or vice versa. The extensions of ULF and proton foreshocks can be very different. Enhanced ULF waves and suprathermal protons can be observed upstream of local quasi-perpendicular shocks. We propose that the observed discordance between the shock geometries and the presence of the foreshock phenomena may be explained in terms of temporal and spatial variations of the local geometry of the IP shocks.

The Earth's magnetosphere response to interplanetary medium conditions on January 21–22, 2005 and on December 14–15, 2006

V.V. **Kalegaev**, N.A. Vlasova

Advances in Space Research, **2014**

The Earth's magnetosphere response to interplanetary medium conditions on January 21–22, 2005 and on December 14–15, 2006 has been studied. The analysis of solar wind parameters measured by ACE spacecraft, of geomagnetic indices variations, of geomagnetic field measured by GOES 11, 12 satellites, and of energetic particle fluxes measured by POES 15, 16, 17 satellites was performed together with magnetospheric modeling based in terms of A2000 paraboloid model. We found the similar dynamics of three particle populations (trapped, quasi-trapped, and precipitating) during storms of different intensities developed under different external conditions: the maximal values of particle fluxes and the latitudinal positions of the isotropic boundaries were approximately the same. The main sources caused RC build-up have been determined for both magnetic storms. Global magnetospheric convection controlled by IMF and substorm activity driven magnetic storm on December 14–15, 2006. Extreme solar wind pressure pulse was mainly responsible for RC particle injection and unusual January 21, 2005 magnetic storm development under northward IMF during the main phase.

An analysis of large Forbush decrease events using phase diagrams of view channels of the Nagoya multidirectional muon telescope

G. **Kalugin**, K. Kabin

Journal of Atmospheric and Solar-Terrestrial Physics, Volume 123, February **2015**, Pages 124–136

Large Forbush decrease (FD) events are analysed using data recorded by the ground-based Nagoya multi-directional muon telescope in Japan. As a part of the analysis we introduce a phase diagram for the channels of telescope, which provides more robust information about characteristics of events. Specifically, the slope of the regression line in the phase diagram represents the FD amplitude which can be computed for different channels. This allows us to analyze the dependence of the FD amplitude on the rigidity of CR particles. Two models for this dependence are considered, a power law and exponential and the former is found to be more suitable for the considered events. In terms of the power-law index and the FD amplitude the events are split into two groups. It is shown that the larger events are characterized by smaller power-law index than the smaller ones.

No Major Solar Flares but the Largest Geomagnetic Storm in the Present Solar Cycle

Y. **Kamide**, K. Kusano

Space Weather Volume 13, Issue 6 June **2015** Pages 365–367

<http://onlinelibrary.wiley.com/doi/10.1002/2015SW001213/full>

A severe geomagnetic storm, and the largest in solar cycle 24, occurred on **17–18 March 2015** without significant precursor X- or M-type solar flares.

In summary, we suggest that the most recent case of a severe geomagnetic storm, which is the largest to date in solar cycle 24, represents a distinct class of two-step main phase storms. It is crucial to realize that instead of the simple assumption that an intense storm be generated by an intense solar/interplanetary disturbance, our suggestion indicates that an intense storm can result from the superposition of two successive, moderate storms, driven by two successive, southward IMF structures.

Evolution of Cosmic-Ray Intensities While the Earth Was Engulfed by the Interplanetary Storm (Blob) of 1–3 October 2013

R. P. [Kane](#)

Solar Phys., **2014**, Volume 289, Issue 7, pp 2669-2675 July 2014, Volume 289, Issue 7, pp 2669-2675

When a Coronal Mass Ejection (CME) is ejected by the Sun, it reaches the Earth orbit in a modified state and is called an ICME (Interplanetary CME). When an ICME blob engulfs the Earth, short-scale cosmic-ray (CR) storms (Forbush decreases, FDs) occur, sometimes accompanied by geomagnetic Dst storms, if the B_z component in the blob is negative. Generally, this is a sudden process that causes abrupt changes. However, sometimes before this abrupt change (FD) due to strong ICME blobs, there are slow, small changes in interplanetary parameters such as steady increases in solar wind speed V , which are small, but can last for several hours. In the present communication, CR changes in such an event are illustrated in the period 1–3 October 2013, when V increased steadily from $\sim 200 \text{ km s}^{-1}$ to $\sim 400 \text{ km s}^{-1}$ during 24 hours on 1 October 2013. The CR intensities decreased by 1–2 % during some hours of this 24-hour interval, indicating that CR intensities do respond to these weak but long-lasting increases in interplanetary solar wind speed.

Interplanetary and geomagnetic parameters during January 16-26, 2005

R. P. [Kane](#)

Planetary and Space Science, Volume 62, Issue 1, p. 97-99, **2012**

The interplanetary $B_z(\text{min})$ and geomagnetic $\text{Dst}(\text{min})$ are well related. There is no large negative B_z without causing large negative Dst. Similarly, large negative Dst is not expected to occur without a large negative B_z ; but recently, Du et al. (2008) reported that the Dst storm of Jan. 21-22, 2005 was anomalous because the Dst storm main phase developed during northward interplanetary magnetic field (positive B_z). Here, we examined this event (storm 3) and compared it with earlier events of Jan. 16-20, 2005 (storms 1 and 2, in quick succession). It was noticed that storms 1 and 2 had large negative Dst deviations (-121 nT and -93 nT, separated by 26 hours) but the B_z fluctuated between +21 nT and -17 nT. For storm 3 where negative Dst deviations were large (-105 nT), the B_z was not completely positive (northward) as mentioned by Du et al. (2008) but had negative values (-7 nT) for an hour, followed by positive values (13 nT). Thus, the need of a negative B_z (albeit small) was satisfied.

Relationship between Dst(min) magnitudes and characteristics of ICMEs

R. P. [Kane](#)

Indian Journal of Radio & Space Physics, V. 39, No. 4, p. 177-183, **2010**, [File](#)

[Новый PDF формат](#); см. [File](#)

Severe geomagnetic storms and Forbush decreases: interplanetary relationships reexamined

R. P. [Kane](#)

Ann. Geophys., 28, 479–489, **2010**, [File](#)

Severe storms (Dst) and Forbush decreases (FD) during cycle 23 showed that maximum negative Dst magnitudes usually occurred almost simultaneously with the maximum negative values of the B_z component of interplanetary magnetic field B , but the maximum magnitudes of negative Dst and B_z were poorly correlated (+0.28). A parameter $B_z(\text{CP})$ was calculated (cumulative partial B_z) as sum of the hourly negative values of B_z from the time of start to the maximum negative value. The correlation of negative Dst maximum with $B_z(\text{CP})$ was higher (+0.59) as compared to that of Dst with B_z alone (+0.28). When the product of B_z with the solar wind speed V (at the hour of negative B_z maximum) was considered, the correlation of negative Dst maximum with VB_z was +0.59 and with $VB_z(\text{CP})$, 0.71. Thus, including V improved the correlations. However, ground-based Dst values have a considerable contribution from magnetopause

currents (several tens of nT, even exceeding 100 nT in very severe storms). When their contribution is subtracted from Dst(nT), the residue Dst* representing true ring current effect is much better correlated with B_z and $B_z(\text{CP})$, but not with VB_z or $VB_z(\text{CP})$, indicating that these are unimportant parameters and the effect of V is seen only through the solar wind ram pressure causing magnetopause currents. Maximum negative Dst (or Dst*) did not occur at the same hour as maximum FD. The time evolutions of Dst and FD were very different. The correlations were almost zero. Basically, negative Dst (or Dst*) and FDs are uncorrelated, indicating altogether different mechanism.

Coronal mass ejection geoeffectiveness depending on field orientation and interplanetary coronal mass ejection classification

Seung-Mi [Kang](#),^{1,2} Y.-J. Moon,³ K.-S. Cho,³ Yeon-Han Kim,³ Y. D. Park,³ Ji-Hye Baek,³ and Heon-Young Chang¹

JOURNAL OF GEOPHYSICAL RESEARCH, VOL. 111, A05102, doi:10.1029/2005JA011445, **2006, File**
In this study, we have examined the coronal mass ejection (CME) geoeffectiveness characterized by $\text{Dst} \leq -50$ nT according to the field orientation (N or S) in a CME source region and its dependence on interplanetary CME (ICME) classification (magnetic clouds or ejecta). We first considered 133 CME-ICME pairs (1996 to 2001) whose CME source locations are identified by SOHO Large-Angle Spectrometric Coronagraph (SOHO/LASCO) and extreme ultraviolet imaging telescope (SOHO/EIT) data. Then we identified the shapes (S or Inverse-S) of the X-ray sigmoids associated with 63 of these CMEs using Yohkoh/Soft X-Ray Telescope (SXT) data. To determine the field orientation in the sigmoids, we applied the coronal flux rope (CFR) model and the force-free field (FFF) model to these 63 sigmoids using SOHO/Michelson Doppler Imager (MDI) images. We present the results in contingency tables, classified according to solar field orientation and geomagnetic storm strength/occurrence. We found that (1) the prediction of geomagnetic storms ($\text{Dst} \leq -50$ nT) based on the CFR model is much better than that on the FFF model, (2) the prediction for magnetic clouds (MCs) is much better than that for ejecta (EJ), which implies that the field orientation of the MCs is well conserved through the heliosphere, and (3) for about 86% of the magnetic clouds, the directions of their leading fields are consistent with those in the CME source regions. Our results support the findings that the southward orientations of the magnetic field in the CME source regions plays an important role in the production of geomagnetic storms.

Murchison Widefield Array Observations of Anomalous Variability: A Serendipitous Night-time Detection of Interplanetary Scintillation

D. L. [Kaplan](#), S. J. Tingay, P. K. Manoharan, J.-P. Macquart, P. Hancock, J. Morgan, D. A. Mitchell, R. D. Ekers, R. B. Wayth, C. Trott, T. Murphy, D. Oberoi, I. H. Cairns, L. Feng, N. Kudryavtseva, G. Bernardi, J. D. Bowman, F. Briggs, R. J. Cappallo, A. A. Deshpande, B. M. Gaensler, L. J. Greenhill, N. Hurley-Walker, B. J. Hazelton, M. Johnston-Hollitt, C. J. Lonsdale, S. R. McWhirter, E. Morgan, S. M. Ord, T. Prabu, N. Udaya Shankar, K. S. Srivani, R. Subrahmanyam, R. L. Webster, A. Williams, C. L. Williams
ApJL **2015**

<http://arxiv.org/pdf/1507.08236v1.pdf>

We present observations of high-amplitude rapid (2 s) variability toward two bright, compact extragalactic radio sources out of several hundred of the brightest radio sources in one of the 30x30 deg MWA Epoch of Reionization fields using the Murchison Widefield Array (MWA) at 155 MHz. After rejecting intrinsic, instrumental, and ionospheric origins we consider the most likely explanation for this variability to be interplanetary scintillation (IPS), likely the result of a large coronal mass ejection propagating from the Sun. This is confirmed by roughly contemporaneous observations with the Ooty Radio Telescope. We see evidence for structure on spatial scales ranging from <1000 km to $>1e6$ km. The serendipitous night-time nature of these detections illustrates the new regime that the MWA has opened for IPS studies with sensitive night-time, wide-field, low-frequency observations. This regime complements traditional dedicated strategies for observing IPS and can be utilized in real-time to facilitate dedicated follow-up observations. At the same time, it allows large-scale surveys for compact (arcsec) structures in low-frequency radio sources despite the 2 arcmin resolution of the array. **2014 November 06**

Alfvénic velocity spikes and rotational flows in the near-Sun solar wind

J. C. [Kasper](#), [S. D. Bale](#), [...] [N. A. Schwadron](#)

[Nature](#) volume 576, pages228–231 (2019)

<https://www.nature.com/articles/s41586-019-1813-z.pdf>

The prediction of a supersonic solar wind¹ was first confirmed by spacecraft near Earth^{2,3} and later by spacecraft at heliocentric distances as small as 62 solar radii⁴. These missions showed that plasma accelerates as it emerges from the corona, aided by unidentified processes that transport energy outwards from the Sun before depositing it in the wind. Alfvénic fluctuations are a promising candidate for such a process because they are seen in the corona and solar wind and contain considerable energy^{5,6,7}. Magnetic tension forces the corona to co-rotate with the Sun, but any residual rotation far from the Sun reported until now has been much smaller than the amplitude of waves and deflections from interacting wind streams⁸. Here we report observations of solar-wind plasma at heliocentric distances of about 35 solar radii^{9,10,11}, well within the distance at which stream interactions become important. We find that Alfvén waves organize into structured velocity spikes with duration of up to minutes, which are associated with propagating S-like bends in the magnetic-field lines. We detect an increasing rotational component to the flow velocity of the solar wind around the Sun, peaking at 35 to 50 kilometres per second—considerably above the amplitude of the waves. These flows exceed classical velocity predictions of a few kilometres per second, challenging models of circulation in the corona and calling into question our understanding of how stars lose angular momentum and spin down as they age^{12,13,14}.

A Zone of Preferential Ion Heating Extends Tens of Solar Radii from the Sun

J. C. **Kasper**^{1,7}, K. G. Klein^{1,8}, T. Weber², M. Maksimovic³, A. Zaslavsky³, S. D. Bale⁴, B. A. Maruca⁵, M. L. Stevens⁶, and A. W. Case⁶

2017 ApJ 849 126

<http://iopscience.iop.org/article/10.3847/1538-4357/aa84b1/pdf>

The extreme temperatures and nonthermal nature of the solar corona and solar wind arise from an unidentified physical mechanism that preferentially heats certain ion species relative to others. Spectroscopic indicators of unequal temperatures commence within a fraction of a solar radius above the surface of the Sun, but the outer reach of this mechanism has yet to be determined. Here we present an empirical procedure for combining interplanetary solar wind measurements and a modeled energy equation including Coulomb relaxation to solve for the typical outer boundary of this zone of preferential heating. Applied to two decades of observations by the Wind spacecraft, our results are consistent with preferential heating being active in a zone extending from the transition region in the lower corona to an outer boundary 20–40 solar radii from the Sun, producing a steady-state super-mass-proportional α -to-proton temperature ratio of 5.2–5.3. Preferential ion heating continues far beyond the transition region and is important for the evolution of both the outer corona and the solar wind. The outer boundary of this zone is well below the orbits of spacecraft at 1 au and even closer missions such as Helios and MESSENGER, meaning it is likely that no existing mission has directly observed intense preferential heating, just residual signatures. We predict that the Parker Solar Probe will be the first spacecraft with a perihelion sufficiently close to the Sun to pass through the outer boundary, enter the zone of preferential heating, and directly observe the physical mechanism in action.

Pileup accident hypothesis of magnetic storm on 17 March 2015

Kataoka, Ryuho ; [Shiota, Daikou](#) ; [Kilpua, Emilia](#) ; [Keika, Kunihiro](#)

Geophysical Research Letters, Volume 42, Issue 13, pp. 5155-5161, 2015

<https://agupubs.onlinelibrary.wiley.com/doi/epdf/10.1002/2015GL064816>

We propose a "pileup accident" hypothesis, based on the solar wind data analysis and magnetohydrodynamics modeling, to explain unexpectedly geoeffective solar wind structure which caused the largest magnetic storm so far during the solar cycle 24 on **17 March 2015**: First, a fast coronal mass ejection with strong southward magnetic fields both in the sheath and in the ejecta was followed by a high-speed stream from a nearby coronal hole. This combination resulted in less adiabatic expansion than usual to keep the high speed, strong magnetic field, and high density within the coronal mass ejection. Second, preceding slow and high-density solar wind was piled up ahead of the coronal mass ejection just before the arrival at the Earth to further enhance its magnetic field and density. Finally, the enhanced solar wind speed, magnetic field, and density worked all together to drive the major magnetic storm.

Probability of occurrence of extreme magnetic storms†

Ryuho **Kataoka**

Space Weather, 2013, VOL. 11, 214–218,

<http://onlinelibrary.wiley.com/doi/10.1002/swe.20044/pdf>

To calculate the probability of extreme magnetic storms in the solar cycle 24, cumulative distribution functions are investigated using an 89 year list of magnetic storms recorded at Kakioka Magnetic Observatory. It is found that the probability of occurrence of extreme magnetic storms can be modeled as a function of maximum sunspot number of a solar cycle, and the probability of another Carrington storm occurring within the next decade is estimated to be 4–6%.

Three-dimensional MHD modeling of the solar wind structures associated with 13 December 2006 coronal mass ejection

Kataoka, R.; Ebisuzaki, T.; Kusano, K.; Shiota, D.; Inoue, S.; Yamamoto, T. T.; Tokumaru, M
J. Geophys. Res., Vol. 114, No. A10, A10102, **2009**
<http://dx.doi.org/10.1029/2009JA014167>

A 3-D magnetohydrodynamic (MHD) simulation is performed to reconstruct the interplanetary propagation of a coronal mass ejection (CME) that occurred on **13 December 2006**. A spheromak-type magnetic field is superposed on a realistic ambient solar wind to reproduce the large-scale interplanetary magnetic field (IMF) associated with the CME. Here we show that a westward and southward directed spheromak CME with reasonable geometric, dynamic, and magnetic parameters reproduces the magnetic cloud, interplanetary shock, and sheath profiles as observed by in situ spacecraft. We suggest that the simple solar wind model developed in this study is topologically complex enough to be consistent with in situ observations, such as southward IMF associated with CMEs.

A Wavelet Based Approach to Solar-Terrestrial Coupling

Ch. **Katsavriasis**, A. Hillaris, P. Preka-Papadema
Advances in Space Research, Volume 57, Issue 10, p. 2234-2244. **2016**
<https://arxiv.org/pdf/1605.04005.pdf>

Transient and recurrent solar activity drive geomagnetic disturbances; these are quantified (amongst others) by DST, AE indices time-series. Transient disturbances are related to the Interplanetary Coronal Mass Ejections (ICMEs) while recurrent disturbances are related to corotating interaction regions (CIR). We study the relationship of the geomagnetic disturbances to the solar wind drivers within solar cycle 23 where the drivers are represented by ICMEs and CIRs occurrence rate and compared to the DST and AE as follows: terms with common periodicity in both the geomagnetic disturbances and the solar drivers are, firstly, detected using continuous wavelet transform (CWT). Then, common power and phase coherence of these periodic terms are calculated from the cross-wavelet spectra (XWT) and wavelet-coherence (WTC) respectively. In time-scales of ≈ 27 days our results indicate an anti-correlation of the effects of ICMEs and CIRs on the geomagnetic disturbances. The former modulates the DST and AE time series during the cycle maximum the latter during periods of reduced solar activity. The phase relationship of these modulation is highly non-linear. Only the annual frequency component of the ICMEs is phase-locked with DST and AE. In time-scales of ≈ 1.3 -1.7 years the CIR seem to be the dominant driver for both geomagnetic indices throughout the whole solar cycle 23.

Wavelet Analysis on Solar Wind Parameters and Geomagnetic Indices

C. **Katsavriasis**, P. Preka-Papadema, X. Moussas
Solar Physics, October **2012**, Volume 280, Issue 2, pp 623-640

The geomagnetic activity is the result of the solar wind-magnetosphere interaction. It varies following the basic 11-year solar cycle; yet shorter time-scale variations appear intermittently. We study the quasi-periodic behavior of the characteristics of solar wind (speed, temperature, pressure, density) and the interplanetary magnetic field (B_x , B_y , B_z , β , Alfvén Mach number) and the variations of the geomagnetic activity indices (DST, AE, Ap and Kp). In the analysis of the corresponding 14 time series, which span four solar cycles (1966–2010), we use both a wavelet expansion and the Lomb/Scargle periodograms. Our results verify intermittent periodicities in our time-series data, which correspond to already known solar activity variations on timescales shorter than the sunspot cycle; some of these are shared between the solar wind parameters and geomagnetic indices.

Statistical analysis of the geomagnetic response to different solar wind drivers and the dependence on storm intensity

R. M. **Katus**^{1,2,*}, M. W. Liemohn¹, E. L. Ionides¹, R. Ilie¹, D. Welling¹ and L. K. Sarno-Smith
JGR Volume 120, Issue 1, pages 310–327, January **2015**

Geomagnetic storms start with activity on the Sun that causes propagation of magnetized plasma structures in the solar wind. The type of solar activity is used to classify the plasma structures as being either interplanetary coronal mass ejection (ICME) or corotating interaction region (CIR) driven. The ICME-driven events are further classified as either

magnetic cloud (MC) driven or sheath (SH) driven by the geoeffective structure responsible for the peak of the storm. The geoeffective solar wind flow then interacts with the magnetosphere producing a disturbance in near-Earth space. It is commonly believed that a SH-driven event behaves more like a CIR-driven event than a MC-driven event; however, in our analysis this is not the case. In this study, geomagnetic storms are investigated statistically with respect to the solar wind driver and the intensity of the events. We use the Hot Electron and Ion Drift Integrator (HEIDI) model to simulate the inner magnetospheric hot ion population during all of the storms classified as intense ($Dst_{min} \leq -100$ nT) within solar cycle 23 (1996–2005). HEIDI is configured four different ways using either the Volland-Stern or self-consistent electric field and either event-based Los Alamos National Laboratory (LANL) magnetospheric plasma analyzer (MPA) data or a reanalyzed lower resolution version of the data that provides spatial resolution. Presenting the simulation results, geomagnetic data, and solar wind data along a normalized epoch timeline shows the average behavior throughout a typical storm of each classification. The error along the epoch timeline for each HEIDI configuration is used to rate the model's performance. We also subgrouped the storms based on the magnitude of the minimum Dst. We found that typically the LANL MPA data provide the best outer boundary condition. Additionally, the self-consistent electric field better reproduces SH- and MC-driven events throughout most of the storm timeline, but the Volland-Stern electric field better reproduces CIR-driven events. Contrary to what we expect, examination of the HEIDI model results and solar wind data shows that SH-driven events behave more like MC-driven events than CIR-driven storms.

Similarities and differences in low- to middle-latitude geomagnetic indices

R. M. [Katus*](#), M. W. Liemohn

Volume 118, Issue 8, pages 5149–5156, August 2013

[1] Several versions of low- to middle-latitude geomagnetic indices are examined throughout a 24 year interval and during storm time with respect to a normalized epoch timeline based on several key storm features. In particular, we conduct a quantitative comparison of the storm time superpositioning of the Dst, SYM-H, and 1 min U.S. Geological Survey Dst indices using error analysis and employing descriptive statistics to assess the similarities and differences between them. The events are then categorized by storm intensity and examined as a function of the storm phase. While the indices are highly correlated with each other, dramatic deviation between the indices exists at certain storm epoch times. In particular, the error increases at storm peak and especially for more intense storms. The differences at storm peak are, on average, 20% of the peak value of the indices. These differences arise from the choice of magnetometer stations to include in each index and the various methodologies used to compile the individual perturbation measurements into a global value. The conclusions are that multiple indices should be considered when determining low- to middle-latitude magnetic perturbations and that the difference between the indices should be considered as an error estimate on these values.

Unexpected Behavior of the Solar Wind Mass Flux During Solar Maxima: Two Peaks at Middle Heliolatitudes

Olga [Katushkina](#), Vladislav Izmodenov, Dimitra Koutroumpa, Eric Quémerais, Lan K. Jian

[Solar Physics](#) January 2019, 294:17

<https://link.springer.com/content/pdf/10.1007%2Fs11207-018-1391-5.pdf>

In this work we study the temporal and latitudinal variations of the solar wind mass flux at 1 AU derived from SOHO/SWAN data on backscattered solar Lyman- α radiation in 1996 – 2018. Previously Katushkina et al. (*J. Geophys. Res.* 118, 2800, 2013) have shown that the latitudinal profiles of the solar wind mass flux during the solar maximum 2001 – 2003 have two separate peaks at middle heliolatitudes. In this work we provide the data for the last solar maximum in 2014 – 2016 and show that the specific latitudinal distribution appears again. However, in 2014 – 2016 the two peaks are less separated and sometimes merged to one peak. For several years we have performed a comparison of SWAN observations with the results of the WSA-Enlil model, which is a coupled 3D time-dependent model of the solar wind propagation from the solar corona to the heliosphere. It is shown that the WSA-Enlil model confirms qualitatively the latitudinal distribution of the solar wind found from the SWAN data, although there are some quantitative differences. Physical reasons for the formation of this latitudinal structure at the solar maxima are discussed. Further investigation is needed and could provide new links between the solar corona and the heliospheric environment.

On the Usage of Geomagnetic Indices for Data Selection in Internal Field Modelling

K. [Kauristie](#), A. Morschhauser, N. Olsen, C. C. Finlay, R. L. McPherron, J. W. Gjerloev, H. J. Opgenoorth
Space Science Reviews 2017

We present a review on geomagnetic indices describing global geomagnetic storm activity (K_p , a_m , Dst and $dDst/dt$) and on indices designed to characterize high latitude currents and substorms (PC and AE-indices and their variants). The focus in our discussion is in main field modelling, where indices are primarily used in data selection criteria for weak magnetic activity. The publicly available extensive data bases of index values are used to derive joint conditional Probability Distribution Functions (PDFs) for different pairs of indices in order to investigate their mutual consistency in describing quiet conditions. This exercise reveals that Dst and its time derivative yield a similar picture as K_p on quiet conditions as determined with the conditions typically used in internal field modelling. Magnetic quiescence at high latitudes is typically searched with the help of Merging Electric Field (MEF) as derived from solar wind observations. We use in our PDF analysis the PC-index as a proxy for MEF and estimate the magnetic activity level at auroral latitudes with the AL-index. With these boundary conditions we conclude that the quiet time conditions that are typically used in main field modelling ($\mathit{PC} < 0.8$), ($\mathit{Kp} < 2$) and ($\mathit{Dst} < 30 \sim \text{nT}$) correspond to weak auroral electrojet activity quite well: Standard size substorms are unlikely to happen, but other types of activations (e.g. pseudo breakups ($\mathit{AL} > -300 \sim \text{nT}$)) can take place, when these criteria prevail. Although AE-indices have been designed to probe electrojet activity only in average conditions and thus their performance is not optimal during weak activity, we note that careful data selection with advanced AE-variants may appear to be the most practical way to lower the elevated RMS-values which still exist in the residuals between modeled and observed values at high latitudes. Recent initiatives to upgrade the AE-indices, either with a better coverage of observing stations and improved baseline corrections (the SuperMAG concept) or with higher accuracy in pinpointing substorm activity (the Midlatitude Positive Bay-index) will most likely be helpful in these efforts.

Updating Measures of CME Arrival Time Errors

C. Kay, E. Palmerio, P. Riley, M. L. Mays, T. Nieves-Chinchilla, M. Romano, Y. M. Collado-Vega, C. Wiegand, A. Chulaki

Space Weather [Volume22, Issue7](#) e2024SW003951 2024

<https://doi.org/10.1029/2024SW003951>

<https://agupubs.onlinelibrary.wiley.com/doi/epdf/10.1029/2024SW003951>

Coronal mass ejections (CMEs) drive space weather effects at Earth and the heliosphere. Predicting their arrival is a major part of space weather forecasting. In 2013, the Community Coordinated Modeling Center started collecting predictions from the community, developing an Arrival Time Scoreboard (ATSB). Riley et al. (2018, <https://doi.org/10.1029/2018sw001962>) analyzed the first 5 years of the ATSB, finding a bias of a few hours and uncertainty of order 15 hr. These metrics have been routinely quoted since 2018, but have not been updated despite continued predictions. We revise analysis of the ATSB using a sample 3.5 times the size of that in the original study. We find generally the same overall metrics, a bias of -2.5 hr, mean absolute error of 13.2 hr, and standard deviation of 17.4 hr, with only a slight improvement comparing between the previously-used and new sets. The most well-established, frequently-submitted model results tend to outperform those from seldomly-contributed models. These “best” models show a slight improvement over the 11 year span, with more scatter between the models during early times and a convergence toward the same error metrics in recent years. We find little evidence of any correlations between the arrival time errors and any other properties. The one noticeable exception is a tendency for late predictions for short transit times and vice versa. We propose that any model-driven systematic errors may be washed out by the uncertainties in CME reconstructions in characterization of the background solar wind, and suggest that improving these may be the key to better predictions.

A Series of Advances in Analytic Interplanetary CME Modeling

C. Kay, T. Nieves-Chinchilla, S. J. Hofmeister, E. Palmerio, V. E. Ledvina

Space Weather [Volume21, Issue11](#) November 2023 e2023SW003647

<https://agupubs.onlinelibrary.wiley.com/doi/epdf/10.1029/2023SW003647>

Coronal mass ejections (CMEs) and high speed streams (HSSs) are large-scale transient structures that routinely propagate away from the Sun. Individually, they can cause space weather effects at the Earth, or elsewhere in space, but many of the largest events occur when these structures interact during their interplanetary propagation. We present the initial coupling of Open Solar Physics Rapid Ensemble Information (OSPREDI), a model for CME evolution, with Mostly Empirical Operational Wind with a High Speed Stream, a time-dependent HSS model that can serve as a background for the OSPREDI CME. We present several improvements made to OSPREDI in order to take advantage of the new time-dependent, higher-dimension background. This includes an update in the drag calculation and the ability to determine the rotation of a yaw-like angle. We present several theoretical case studies, describing the difference in the CME behavior between a HSS background and a quiescent one. This behavior includes interplanetary CME propagation, expansion, deformation, and rotation, as well as the formation of a CME-driven sheath. We also determine how the

CME behavior changes with the HSS size and initial front distance. Generally, for a fast CME, we see that the drag is greatly reduced within the HSS, leading to faster CMEs and shorter travel times. The drag reappears stronger if the CME reaches the stream interaction region or upstream solar wind, leading to a stronger shock with more compression until the CME sufficiently decelerates. We model a CME–HSS interaction event observed by Parker Solar Probe in January 2022. The model improvements create a better match to the observed in situ profiles. **26 Jan 2022**

Beyond Basic Drag in Interplanetary CME Modeling: Effects of Solar Wind Pile-Up and High Speed Streams

C. Kay, [T. Nieves-Chinchilla](#), [S. J. Hofmeister](#), [E. Palmerio](#)

Space Weather e2022SW003165 **Volume20, Issue9** 2022

<https://doi.org/10.1029/2022SW003165>

<https://agupubs.onlinelibrary.wiley.com/doi/epdf/10.1029/2022SW003165>

Coronal mass ejections (CMEs) cause severe space weather effects throughout our solar system. As a fast CME propagates through interplanetary space it accumulates solar wind material at its front. This pile-up of material, or CME-driven sheath, can be important in determining the geoeffectiveness of a CME. We take an existing arrival time model that includes expansion and deformation of the CME flux rope (ANTEATR; Kay & Gopalswamy, 2018; Kay & Nieves-Chinchilla, 2021a) and add a pile-up procedure (PUP) as a physics-based approach to modeling the CME-driven sheath. ANTEATR-PUP solves the Rankine–Hugoniot equations for an oblique shock to determine the shock speed and sheath density, magnetic field, temperature. The extra sheath mass affects the background drag calculation. Additionally, ANTEATR can now use any 1D profile for the background solar wind, as opposed to the simple empirical models it previously relied upon. We present initial results from ANTEATR-PUP and compare with previous ANTEATR findings. Using results from an MHD simulation, we explore the effects of interactions with a static high speed stream (HSS) on the CME's and sheath's interplanetary evolution. The drag forces essentially disappear while a CME remains within the HSS, but reappear stronger once the CME exits. The HSS–CME interaction produces the largest changes in the CME and sheath properties at 1 au when it occurs either close to the Sun near the inner simulation boundary at 0.1 au) or right before the CME reaches 1 au. We estimate that these changes could significantly affect the geoeffectiveness.

OSPREDI: A Coupled Approach to Modeling CME-Driven Space Weather with Automatically-Generated, User-Friendly Outputs

C. Kay, [M. L. May](#), [Y. M. Collado-Vega](#)

Space Weather e2021SW002914 2022

<https://arxiv.org/pdf/2109.06960.pdf>

<https://agupubs.onlinelibrary.wiley.com/doi/epdf/10.1029/2021SW002914>

<https://doi.org/10.1029/2021SW002914>

Coronal Mass Ejections (CMEs) drive space weather activity at Earth and throughout the solar system. Current CME-related space weather predictions rely on information reconstructed from coronagraphs, sometimes from only a single viewpoint, to drive a simple interplanetary propagation model, which only gives the arrival time or limited additional information. We present the coupling of three established models into OSPREDI (Open Solar Physics Rapid Ensemble Information), a new tool that describes Sun-to-Earth CME behavior, including the location, orientation, size, shape, speed, arrival time, and internal thermal and magnetic properties, on the timescale needed for forecasts. First, ForeCAT describes the trajectory that a CME takes through the solar corona. Second, ANTEATR simulates the propagation, including expansion and deformation, of a CME in interplanetary space and determines the evolution of internal properties via conservation laws. Finally, FIDO produces in situ profiles for a CME's interaction with a synthetic spacecraft. OSPREDI includes ensemble modeling by varying each input parameter to probe any uncertainty in their values, yielding probabilities for all outputs. Standardized visualizations are automatically generated, providing easily-accessible, essential information for space weather forecasting. We show OSPREDI results for a CME observed in the corona on **2021 April 22** and at Earth on **2021 April 25**. We approach this CME as a forecasting proof-of-concept, using information analogous to what would be available in real time rather than fine-tuning input parameters to achieve a best fit for a detailed scientific study. The OSPREDI prediction shows good agreement with the arrival time and in situ properties. **9 May 2021**

Modeling Interplanetary Expansion and Deformation of Coronal Mass Ejections With ANTEATR-PARADE: Sensitivity to Input Parameters

C. Kay, [T. Nieves-Chinchilla](#)

JGR **Volume126, Issue6** June 2021 e2020JA028966

<https://agupubs.onlinelibrary.wiley.com/doi/epdf/10.1029/2020JA028966> <https://doi.org/10.1029/2020JA028966>

Space weather predictions related to coronal mass ejections (CMEs) requires understanding how a CME is initiated and how its properties change as it propagates. Most predictions have been limited to the arrival time of a CME and include little to no information about the CME's internal properties. ANother Type of Ensemble Arrival Time Results-Physics-driven Approach to Realistic Axis Deformation and Expansion (ANTEATR-PARADE) represents the most thorough description of the interplanetary evolution of CMEs in a highly computationally-efficient model (Kay & Nieves-Chinchilla, 2020, <https://doi.org/10.1029/2020JA028911>). presents the derivation of this model, where we have added an elliptical cross section to the original arrival time model ANTEATR and introduced internal magnetic and thermal forces that, combined with the drag, can alter the shape of the central axis and cross section. ANTEATR-PARADE results include the transit time of CMEs, as well as the shape and size, propagation and expansion velocities, density, and magnetic field properties upon impact. We determine the dependence of each output on each of the ANTEATR-PARADE input parameters. For a fast CME, we see that the parameterization of our thermal and magnetic models tends to be more important than the actual initial temperature or magnetic field strength. We extend to other CMEs and find that the sensitivities change with CME scale with thermal forces being more important for a weaker CME and magnetic forces being more important for a stronger CME. The most critical parameters for space weather predictions are the CME mass, the initial magnetic field strength, the adiabatic index, and the profile of the axial magnetic field strength.

Modeling Interplanetary Expansion and Deformation of CMEs with ANTEATR-PARADE I: Relative Contribution of Different Forces

C. Kay, T. Nieves-Chinchilla

JGR [Volume126, Issue5](#) May 2021 e2020JA028911

<https://agupubs.onlinelibrary.wiley.com/doi/epdf/10.1029/2020JA028911>

<https://doi.org/10.1029/2020JA028911>

<https://arxiv.org/pdf/2011.06030.pdf>

Coronal Mass Ejections (CMEs) are key drivers of space weather activity but most predictions have been limited to the expected arrival time of a CME, rather than the internal properties that affect the severity of an impact. Many properties, such as the magnetic field density and mass density, follow conservation laws and vary systematically with changes in the size of a CME. We present ANTEATR-PARADE, the newest version of the ANTEATR arrival time model, which now includes physics-driven changes in the size and shape of both the CME's central axis and its cross section. Internal magnetic and external drag forces affect the acceleration of the CME in different directions, inducing asymmetries between the radial and perpendicular directions. These improvements should lead to more realistic CME velocities, both bulk and expansion, sizes and shapes, and internal properties. ANTEATR-PARADE is the first model of its kind that provides this level of detail on the time scales needed for future space weather predictions. We present the model details, an initial illustration of the general behavior, and a study of the relative importance of the different forces. The model shows a pancaking of both the cross section and central axis of the CME so that their radial extent becomes smaller than their extent in the perpendicular direction. For a single parameterization of our magnetic field model we find that the drag forces tend to exceed the magnetic forces and the results are very sensitive to the initial velocities of the CME.

FIDO-SIT: The First Forward Model for the In Situ Magnetic Field of CME-Driven Sheaths

C. Kay, T. Nieves-Chinchilla, L. K. Jian

JGR [Volume125, Issue2](#) February 2020 e2019JA027423

<https://agupubs.onlinelibrary.wiley.com/doi/pdf/10.1029/2019JA027423>

We have shown previously that the in situ magnetic field of coronal mass ejections (CMEs) can be well reproduced by simple, physics-driven flux rope models using the ForeCAT In situ Data Observer (FIDO, Kay et al., 2017). Here, we show that a similar approach can be taken to forward model the shock and sheath of a CME (Sheath Induced by Transient [SIT]). We develop a relation between the downstream density and magnetic field strength that only depends on the upstream properties and downstream speed. Next, we establish a set of well-observed CME-driven shocks combining results from several online catalogs. We establish a baseline using the observed downstream speed and show that the mean absolute errors only increase slightly to 3.4 cm⁻³ and 3.8 nT when using a predicted downstream velocity. We also develop a model for the sheath duration or the standoff distance of the CME-driven shock. While there is certainly room for improvement, our model does perform better than those currently available, reducing the error from 7.0 to 4.6 hr. We couple our flux rope and sheath models as FIDO-SIT and present results for four observed cases. For three of the four cases, FIDO-SIT reproduces the sheath magnetic field with an error of one third the total magnitude for each individual vector component.

Identifying Critical Input Parameters for Improving Drag-Based CME Arrival Time Predictions

C. Kay , [M.L. Mays](#) , [C. Verbeke](#)

Space Weather **Volume18, Issue1** January 2020 e2019SW002382 **File**

sci-hub.se/10.1029/2019SW002382

<https://agupubs.onlinelibrary.wiley.com/doi/epdf/10.1029/2019SW002382>

Coronal mass ejections (CMEs) typically cause the strongest geomagnetic storms so a major focus of space weather research has been predicting the arrival time of CMEs. Most arrival time models fall into two categories: (1) drag-based models that integrate the drag force between a simplified CME structure and the background solar wind and (2) full magnetohydrodynamic (MHD) models. Drag-based models typically are much more computationally efficient than MHD models, allowing for ensemble modeling. While arrival time predictions have improved since the earliest attempts, both types of models currently have difficulty achieving mean absolute errors below 10 hours. Here we use a drag-based model ANTEATR (Another Type of Ensemble Arrival Time Results, Kay & Gopal-swamy, 2018) to explore the sensitivity of arrival times to various input parameters. We consider CMEs of different strengths from average to extreme size, speed, and mass (kinetic energies between 9×10^{29} and 6×10^{32} erg). For each scale CME we vary the input parameters to reflect the current observational uncertainty in each and determine how accurately each must be known to achieve predictions that are accurate within 5 hours. We find that different scale CMEs are the most sensitive to different parameters. The transit time of average strength CMEs depends most strongly on the CME speed whereas an extreme strength CME is the most sensitive to the angular width. A precise CME direction is critical for impacts near the flanks, but not near the CME nose. We also show that the Drag Based Model (Vršnak et al., 2013) has similar sensitivities, suggesting that these results are representative for all drag-based models.

Frequency of Coronal Mass Ejection Impacts with Early Terrestrial Planets and Exoplanets around Active Solar-like Stars

Christina Kay, Vladimir S. Airapetian, Theresa Lüftinger, and Oleg Kochukhov
2019 ApJL 886 L37

<https://iopscience.iop.org/article/10.3847/2041-8213/ab551f/pdf>

Energetic flares and associated coronal mass ejections (CMEs) from young magnetically active solar-like stars can play a critical role in setting conditions for atmospheric escape as well as penetration of accelerated particles into their atmospheres that promotes formation of biologically relevant molecules. We have used the observationally reconstructed magnetic field of the 0.7 Gyr young Sun's twin, κ 1 Ceti, to study the effects of CME deflections in the magnetic corona of the young Sun and their effects on the impact frequency on the early Venus, Earth, and Mars. We find that the coronal magnetic field deflects the CMEs toward the astrospheric current sheet. This effect suggests that CMEs tend to propagate within a small cone about the ecliptic plane increasing the impact frequency of CMEs with planetary magnetospheres near this plane to $\sim 30\%$ or by a factor of 6 as compared to previous estimate by Airapetian et al. Our model has important implications for the rise of prebiotic chemistry on early terrestrial planets as well as terrestrial-type exoplanets around young G-K dwarfs.

The Effects of Uncertainty in Initial CME Input Parameters on Deflection, Rotation, Bz, and Arrival Time Predictions

C. Kay , [N. Gopalswamy](#)

JGR v. 123 September 2018 Pages 7220-7240

sci-hub.tw/10.1029/2018JA025780

Understanding the effects of coronal mass ejections (CMEs) requires knowing if and when they will impact and their properties upon impact. Of particular importance is the strength of a CME's southward magnetic field component (B_z). Kay et al. (2013, <https://doi:10.1088/0004-637X/775/1/5>, 2015, <https://doi:10.1088/9480004-637X/805/2/168>) have shown that the simplified analytic model Forecasting a CME's Altered Trajectory (ForeCAT) can reproduce the deflection and rotation of CMEs. Kay, Gopalswamy, Reinard, and Opher (2017, <https://doi.org/10.3847/1538-4357/835/2/117>) introduced ForeCAT In situ Data Observer, which uses ForeCAT results to simulate magnetic field profiles. ForeCAT In situ Data Observer reproduces the in situ observations on roughly hourly time scales, suggesting that these models could be extremely useful for predictions of B_z . However, as with all models, both models are sensitive to their input parameters, which may not be precisely known for predictions. We explore this sensitivity using ensembles having small changes in the initial latitude, longitude, and orientation of the erupting CME. We explore the effects of different background magnetic field models and find that the changes in deflection and rotation resulting from the uncertainty in the initial parameters tend to exceed the changes from different magnetic backgrounds. The range in

the in situ profiles tends to scale with the range in the deflection and rotation. We also consider a simple arrival time model using ForeCAT results and find an average absolute error of only 3 hr. We show that an uncertainty in the CME position of $8.1^\circ \pm 6.9^\circ$ leads to variations of 6 hr in the arrival time. This measure depends strongly on the location of impact within the CME with the arrival time changing less for impacts near the nose. **06 September 2011, 12 July 2012, 28 September 2012, 23 November 2012, 29 September 2013, 12 February 2014**

Using the Coronal Evolution to Successfully Forward Model CMEs' In Situ Magnetic Profiles

C. Kay, N. Gopalswamy

JGR Volume 122, Issue 12 December 2017 Pages 11,810–11,834

[\[hub.tw/http://onlineibrary.wiley.com/doi/10.1002/2017JA024541/abstract;jsessionid=2DF604EC239663BA90D09F3C3BE44317.f01t04\]\(http://onlineibrary.wiley.com/doi/10.1002/2017JA024541/abstract;jsessionid=2DF604EC239663BA90D09F3C3BE44317.f01t04\)](http://sci-</p></div><div data-bbox=)

Predicting the effects of a coronal mass ejection (CME) impact requires knowing if impact will occur, which part of the CME impacts, and its magnetic properties. We explore the relation between CME deflections and rotations, which change the position and orientation of a CME, and the resulting magnetic profiles at 1 AU. For 45 STEREO-era, Earth-impacting CMEs, we determine the solar source of each CME, reconstruct its coronal position and orientation, and perform a ForeCAT (Forecasting a CME's Altered Trajectory) simulation of the coronal deflection and rotation. From the reconstructed and modeled CME deflections and rotations, we determine the solar cycle variation and correlations with CME properties. We assume no evolution between the outer corona and 1 AU and use the ForeCAT results to drive the ForeCAT In situ Data Observer (FIDO) in situ magnetic field model, allowing for comparisons with ACE and Wind observations. We do not attempt to reproduce the arrival time. On average FIDO reproduces the in situ magnetic field for each vector component with an error equivalent to 35% of the average total magnetic field strength when the total modeled magnetic field is scaled to match the average observed value. Random walk best fits distinguish between ForeCAT's ability to determine FIDO's input parameters and the limitations of the simple flux rope model. These best fits reduce the average error to 30%. The FIDO results are sensitive to changes of order a degree in the CME latitude, longitude, and tilt, suggesting that accurate space weather predictions require accurate measurements of a CME's position and orientation. **24 May 2010.**

Predicting the Magnetic Field of Earth-impacting CMEs

C. Kay¹, N. Gopalswamy¹, A. Reinard², and M. Opher³

2017 ApJ 835 117 **File**

<http://sci-hub.cc/doi/10.3847/1538-4357/835/2/117>

Predicting the impact of coronal mass ejections (CMEs) and the southward component of their magnetic field is one of the key goals of space weather forecasting. We present a new model, the ForeCAT In situ Data Observer (FIDO), for predicting the in situ magnetic field of CMEs. We first simulate a CME using ForeCAT, a model for CME deflection and rotation resulting from the background solar magnetic forces. Using the CME position and orientation from ForeCAT, we then determine the passage of the CME over a simulated spacecraft. We model the CME's magnetic field using a force-free flux rope and we determine the in situ magnetic profile at the synthetic spacecraft. We show that FIDO can reproduce the general behavior of four observed CMEs. FIDO results are very sensitive to the CME's position and orientation, and we show that the uncertainty in a CME's position and orientation from coronagraph images corresponds to a wide range of in situ magnitudes and even polarities. This small range of positions and orientations also includes CMEs that entirely miss the satellite. We show that two derived parameters (the normalized angular distance between the CME nose and satellite position and the angular difference between the CME tilt and the position angle of the satellite with respect to the CME nose) can be used to reliably determine whether an impact or miss occurs. We find that the same criteria separate the impacts and misses for cases representing all four observed CMEs. **2010 April 3, 2011 Feb 15, 2012 Jul 12, 2014 Sep 10**

Forecasting a coronal mass ejection's altered trajectory: ForeCAT.

Kay C, Opher M, Evans RM.

2013 *Astrophys. J.* 775, 5. (doi:10.1088/0004-637X/775/1/5)

Invited **Review**: Short-term Variability with the Observations from the Helioseismic and Magnetic Imager (HMI) Onboard the Solar Dynamics Observatory (SDO): Insights into Flare Magnetism

Maria D. [Kazachenko](#), Marcel F. [Albelo-Corchado](#), Cole A. [Tamburri](#) & Brian T. [Welsch](#)

[Solar Physics](#) volume 297, Article number: 59 (2022)

<https://link.springer.com/content/pdf/10.1007/s11207-022-01987-6.pdf> **File**

Continuous vector magnetic-field measurements by the Helioseismic and Magnetic Imager (HMI) onboard the Solar Dynamics Observatory (SDO) allow us to study magnetic-field properties of many flares. Here, we review new observational aspects of flare magnetism described using SDO data, including statistical properties of magnetic-reconnection fluxes and their rates, magnetic fluxes of flare dimmings, and magnetic-field changes during flares. We summarize how these results, along with statistical studies of coronal mass ejections (CMEs), have improved our understanding of flares and the flare/CME feedback relationship. Finally, we highlight future directions to improve the current state of understanding of solar-flare magnetism using observations. **14 Sep 2011, 7 March 2012, Sep 2014**

2. Flare Ribbons: Footpoints of Reconnected Fields
3. Coronal Dimmings: Footpoints of Expanding Coronal Structures
4. Flare-Associated Magnetic-Field Changes (FAMCs)
5. Relating CMEs and ICMEs to Their Source Regions

Predictions of Energy and Helicity in Four Major Eruptive Solar Flares

Maria D. [Kazachenko](#), Richard C. Canfield, Dana W. Longcope and Jiong Qiu

[Solar Physics](#), Volume 277, Number 1, 165-183, **2012**, **File**

In order to better understand the solar genesis of interplanetary magnetic clouds (MCs), we model the magnetic and topological properties of four large eruptive solar flares and relate them to observations. We use the three-dimensional Minimum Current Corona model (Longcope, 1996, *Solar Phys.* 169, 91) and observations of pre-flare photospheric magnetic field and flare ribbons to derive values of reconnected magnetic flux, flare energy, flux rope helicity, and orientation of the flux-rope poloidal field. We compare model predictions of those quantities to flare and MC observations, and within the estimated uncertainties of the methods used find the following: The predicted model reconnection fluxes are equal to or lower than the reconnection fluxes inferred from the observed ribbon motions. Both observed and model reconnection fluxes match the MC poloidal fluxes. The predicted flux-rope helicities match the MC helicities. The predicted free energies lie between the observed energies and the estimated total flare luminosities. The direction of the leading edge of the MC's poloidal field is aligned with the poloidal field of the flux rope in the AR rather than the global dipole field. These findings compel us to believe that magnetic clouds associated with these four solar flares are formed by low-corona magnetic reconnection during the eruption, rather than eruption of pre-existing structures in the corona or formation in the upper corona with participation of the global magnetic field. We also note that since all four flares occurred in active regions without significant pre-flare flux emergence and cancellation, the energy and helicity that we find are stored by shearing and rotating motions, which are sufficient to account for the observed radiative flare energy and MC helicity.

On the azimuthal evolution and geoeffectiveness of the SIR-associated stream interface[†]

A. C. [Kellerman](#), R. L. McPherron and J. M. Weygand

[JGR](#) [Volume 120, Issue 3](#) March 2015 Pages 1489–1508 **2015**

In this study, the azimuthal evolution of stream interaction regions are investigated, with the goal of predicting the time of arrival of an interface at some later position near 1 AU. A new SIR dataset is constructed from ACE, STEREO A and STEREO B in situ measurements, and it is demonstrated that the magnetic pressure and azimuthal flow angle provide the most simple robust estimation of the interface time. This dataset was applied in the investigation. In the analysis, the geometric effects of the magnetic spiral angle, and the tilt angle of stream interfaces are considered, and it is demonstrated how they may be used to improve forecasts of the arrival time of stream interaction regions from a spacecraft located at 1 AU. The polarity of the interplanetary magnetic field, towards or away from the Sun, observed by consecutive spacecraft measurements is considered for the slow and fast streams straddling a stream interface, in order to investigate whether the geoeffectiveness of the two streams may also be forecast from 1 AU. It is found that the polarity of the magnetic field, associated with a given stream interface, is conserved when observed by two separate spacecraft at azimuthal separations of 20° or less and while in the fast wind, however, the field polarity was not always conserved when observed in the slow wind ahead of the interface. An analysis of tilt angles evolution during 2008 showed that while the azimuthal tilt angles were generally similar between observations in the same Carrington rotation and in consecutive rotations of the same CIR, the meridional tilt angles may differ significantly. The forecast analysis showed that the azimuthal evolution of a SIR at 1 AU may be predicted to within a day or two of the actual evolution

time, while any discrepancy was most likely caused by changes at the coronal hole on the solar surface, leading azimuthal and radial evolution of the SIR.

Heating of the Solar Wind by Ion Acoustic Waves

Paul J. Kellogg

2020 ApJ 891 51

<https://doi.org/10.3847/1538-4357/ab7003>

Calculations are made of the energy supplied to the solar wind by the rapid decay of density fluctuations, identified as ion acoustic waves. It is shown that this process supplies an appreciable fraction, perhaps nearly all, of the observed heating of the solar wind. This process may be an important step in the conversion of magnetic turbulence to particle energy.

Inherent Length Scales of Periodic Mesoscale Density Structures in the Solar Wind Over Two Solar Cycles

L. Kepko [N. M. Viall](#) [K. Wolfinger](#)

JGR [Volume 125, Issue 8](#) August 2020 e2020JA028037

<https://agupubs.onlinelibrary.wiley.com/doi/10.1029/2020JA028037>

It is now well established through multiple event and statistical studies that the solar wind at 1 AU contains periodic, mesoscale ($L \sim 100\text{--}1,000$ Mm) structures in the proton density. Composition variations observed within these structures and remote sensing observations of similar structures in the young solar wind indicate that at least some of these periodic structures originate in the solar atmosphere as a part of solar wind formation. Viall et al. (2008, <https://doi.org/10.1029/2007JA012881>) analyzed 11 years of data from the Wind spacecraft near L1 and demonstrated a recurrence to the observed length scales of periodic structures in the solar wind proton density. In the time since that study, Wind has collected 14 additional years of solar wind data, new moment analysis of the Wind SWE data is available, and new methods for spectral background approximation have been developed. In this study, we analyze 25 years of Wind data collected near L1 and produce occurrence distributions of statistically significant periodic length scales in proton density. The results significantly expand upon the Viall et al. (2008, <https://doi.org/10.1029/2007JA012881>) study and further show a possible relation of the length scales to solar “termination” events.

Implications of L1 observations for slow solar wind formation by solar reconnection

L. Kepko, N. M. Viall, S. K. Antiochos, S. T. Lepri, J. C. Kasper, M. Weberg

Geophys. Res. Lett. 2016

<http://onlinelibrary.wiley.com/doi/10.1002/2016GL068607/full>

While the source of the fast solar wind is known to be coronal holes, the source of the slow solar wind has remained a mystery. Long time scale trends in the composition and charge states show strong correlations between solar wind velocity and plasma parameters, yet these correlations have proved ineffective in determining the slow wind source. We take advantage of new high time resolution (12 min) measurements of solar wind composition and charge state abundances at L1 and previously identified 90 min quasiperiodic structures to probe the fundamental timescales of slow wind variability. The combination of new high temporal resolution composition measurements and the clearly identified boundaries of the periodic structures allows us to utilize these distinct solar wind parcels as tracers of slow wind origin and acceleration. We find that each 90 min (2000 Mm) parcel of slow wind has near-constant speed yet exhibits repeatable, systematic charge state and composition variations that span the entire range of statistically determined slow solar wind values. The classic composition-velocity correlations do not hold on short, approximately hourlong, time scales. Furthermore, the data demonstrate that these structures were created by magnetic reconnection. Our results impose severe new constraints on slow solar wind origin and provide new, compelling evidence that *the slow wind results from the sporadic release of closed field plasma via magnetic reconnection at the boundary between open and closed flux in the Sun's atmosphere.*

See Wheeling, K. (2016), Spotting the source of slow solar wind, *Eos*, 97, doi:10.1029/2016EO057945. Published on 24 August 2016.

Reviews in Space Physics: Multi-Scale Processes in the Heliosphere

Editorial on the Research Topic

Olga Khabarova, Georgios Balasis, Radoslav Bučik, Jonathan Eastwood, Philip Erickson, and Rudolf Treumann

Front. Astron. Space Sci., 10: 1254235. 2023

<https://www.frontiersin.org/articles/10.3389/fspas.2023.1254235/pdf>

The present Research Topic opens the series of “Reviews in space physics” with a Research Topic comprising a limited number of submissions discussing the current state of research in the wide domain of Space Physics. Within the framework of this Research Topic, Frontiers will publish reviews, covering diverse aspects of heliospheric, solar, magnetospheric, and ionospheric physics. Reviews included in this Research Topic are aimed at covering processes from the upper terrestrial atmosphere to distant astronomical space, critically discussing past and future developments in theory, observation, analysis, and instrumentation.

This first 2023 Research Topic of Reviews in Space Physics contains six articles written by 60 authors. Its Research Topic focus on 1) space weather, its geo-effective mechanisms and possible threats to civilization, including radiation hazards; 2) studies of dynamical structures in the small- and large-scale solar wind and the consequences of their interaction with the terrestrial magnetosphere, with special focus on processes in Earth’s magnetosheath (MSH); 3) observations and modelling of MSH plasma jets, and 4) acceleration and propagation of solar energetic particles (SEPs) and cosmic rays (CRs) in the heliosphere and beyond.

Current sheets, plasmoids and flux ropes in the heliosphere.

Part I. General and observational aspects: 2-d or not 2-d?

Review

Khabarova OV, Malandraki O, Malova H, Kislov R, Greco A, Bruno R, Pezzi O, Servidio S, Li G, Matthaeus WH, le Roux J, Engelbrecht N, Pecora F, Zelenyi L, Obridko V, Kuznetsov V

Space Science Reviews 217, Article number: 38 2021

See Part II Pezzi et al. (2021)

<https://link.springer.com/content/pdf/10.1007/s11214-021-00814-x.pdf>

<https://doi.org/10.1007/s11214-021-00814-x>

Recent accumulation of a critical mass of observational material from different spacecraft complete with the enhanced abilities of numerical methods have led to a boom of studies revealing the high complexity of processes occurring in the heliosphere. Views on the solar wind filling the interplanetary medium have dramatically developed from the beginning of the space era. A 2-D picture of the freely expanding solar corona and non-interacting solar wind structures described as planar or spherically-symmetric objects has dominated for decades. Meanwhile, the scientific community gradually moved to a modern understanding of the importance of the 3-D nature of heliospheric processes and their studies via MHD/kinetic simulations, as well as observations of large-scale flows and streams both in situ and remotely, in white light and/or via interplanetary scintillations. The new 3-D approach has provided an opportunity to understand the dynamics of heliospheric structures and processes that could not even be imagined before within the 2-D paradigm. In this review, we highlight a piece of the puzzle, showing the evolution of views on processes related to current sheets, plasmoids, blobs and flux ropes of various scales and origins in the heliosphere. The first part of the review focuses on introducing these plasma structures, discussing their key properties, and paying special attention to their observations in different space plasmas. 29 May 1995, 30 Oct 2003, 24-26 Jun 2004, February 24, 2011 ...

Counterstreaming Strahls and Heat Flux Dropouts as Possible Signatures of Local Particle Acceleration in the Solar Wind

O. **Khabarova**¹, V. Zharkova², Q. Xia², and O. E. Malandraki³

2020 ApJL 894 L12

<https://iopscience.iop.org/article/10.3847/2041-8213/ab8cb8/pdf>

Suprathermal electrons with energies of ~70 eV and above are observed at 1 au as dispersionless halo electrons and magnetic field-aligned beams of strahls. For a long time, it has been thought that both populations originate only from the solar corona, and that the only active process impacting their properties in the solar wind is scattering. This view has consequently impacted the interpretation of typical patterns of pitch-angle distributions (PADs) of suprathermal electrons. Meanwhile, recent observational studies supported by numerical simulations have shown that there is an unaccounted population of electrons accelerated to suprathermal energies at reconnecting current sheets (RCSs) and 3D dynamical plasmoids (or 2D magnetic islands (MIs)) directly in the heliosphere. We present multispacecraft observations of counterstreaming strahls and heat flux dropouts in PADs within a region filled with plasmoids and RCSs unaffected by interplanetary shocks, comparing observed PAD features with those predicted by particle-in-cell simulations. We show typical PAD patterns determined by local acceleration of thermal-core electrons up to hundreds of electron volts. Resulting PAD views depend on properties and topology of particular RCSs, MIs, and plasma/magnetic field parameters. Our study suggests that solar wind-borne suprathermal electrons coexist with those of solar origin. Therefore, some of heat flux dropout and bidirectional strahl events can be explained by local dynamical processes involving magnetic reconnection. Possible implications of the results for the interpretation of the actively debated

decrease in the strahl/halo relative density with heliocentric distance and puzzling features of suprathermal electrons observed at crossings of the heliospheric current sheet and cometary comas are also discussed.

Observational evidence for local particle acceleration associated with magnetically confined magnetic islands in the heliosphere – a review

Olga V. [Khabarova](#) 1 , Gary P. Zank 2,3, Olga E. Malandraki 4 , Gang Li 2, 3 , Jakobus A. le Roux 2,3, Gary M. Webb

Sun and Geosphere, **2017**; 12/1: 23 -30

http://newserver.stil.bas.bg/SUNGEO//00SGArhiv/SG_v12_No1_2017-pp-23-30.pdf

The occurrence of unusual energetic particle enhancements up to several MeV/nuc at leading edges of corotating interaction regions (CIRs), near the heliospheric current sheet and downstream of interplanetary shocks at 1AU has puzzled observers for a long time. Commonly accepted mechanisms of particle energization, such as a classical diffusive shock acceleration mechanism or magnetic reconnection at current sheets, are unable to explain these phenomena. We present a review of recently obtained observational results that attribute these atypical energetic particle events to local acceleration of particles in regions filled with small-scale magnetic islands confined by currents sheets of various origins. The observations are in very good accordance with the theory of stochastic particle energization in the supersonic solar wind via a sea of small-scale flux-ropes interacting dynamically (Zank et al., 2014, 2015; le Roux et al., 2015, 2016). **07-09-1999, March 1st, 2006 , August 24-26, 2007**

SMALL-SCALE MAGNETIC ISLANDS IN THE SOLAR WIND AND THEIR ROLE IN PARTICLE ACCELERATION. II. PARTICLE ENERGIZATION INSIDE MAGNETICALLY CONFINED CAVITIES

Olga V. [Khabarova](#)1, Gary P. Zank2,3, Gang Li2,3, Olga E. Malandraki4, Jakobus A. le Roux2,3, and Gary M. Webb2

2016 ApJ 827 122

We explore the role of heliospheric magnetic field configurations and conditions that favor the generation and confinement of small-scale magnetic islands associated with atypical energetic particle events (AEPEs) in the solar wind. Some AEPEs do not align with standard particle acceleration mechanisms, such as flare-related or simple diffusive shock acceleration processes related to interplanetary coronal mass ejections (ICMEs) and corotating interaction regions (CIRs). As we have shown recently, energetic particle flux enhancements may well originate locally and can be explained by particle acceleration in regions filled with small-scale magnetic islands with a typical width of ~ 0.01 au or less, which is often observed near the heliospheric current sheet (HCS). The particle energization is a consequence of magnetic reconnection-related processes in islands experiencing either merging or contraction, observed, for example, in HCS ripples. Here we provide more observations that support the idea and the theory of particle energization produced by small-scale-flux-rope dynamics (Zank et al. and Le Roux et al.). If the particles are pre-accelerated to keV energies via classical mechanisms, they may be additionally accelerated up to 1–1.5 MeV inside magnetically confined cavities of various origins. The magnetic cavities, formed by current sheets, may occur at the interface of different streams such as CIRs and ICMEs or ICMEs and coronal hole flows. They may also form during the HCS interaction with interplanetary shocks (ISs) or CIRs/ICMEs. Particle acceleration inside magnetic cavities may explain puzzling AEPEs occurring far beyond ISs, within ICMEs, before approaching CIRs as well as between CIRs.

Dynamical small-scale magnetic islands as a source of local acceleration of particles in the solar wind

O. V. [Khabarova](#), G. P. Zank, G. Li, J. A. le Roux, G. M. Webb, A. Dosch, O. E. Malandraki, Zharkova V.V. Journal of Physics: Conference Series (JPCS), 642, 012033, **2015**

http://computing.unn.ac.uk/staff/slmv5/kinetics/Tampa15_Olga_v2.pdf

We present observations of energetic particle flux increases up to 1 MeV at 1 AU, which cannot be associated with ordinary mechanisms of particle acceleration, such as acceleration at shocks or at the Sun. Such unusual energetic particle events very likely have a local origin. Multi-spacecraft observations show that numerous cases of energetic particle flux enhancements and spikes correspond to passages of spacecraft through areas filled with magnetic islands with a typical width $\sim 0.01 \square 0.001$ AU that experience dynamical merging or/and contraction. The presence of magnetic islands inside magnetically confined cavities in the solar wind may lead to local particle energization, especially in the case when the particles have already been pre-accelerated to keV energies, for example, at shocks or due to magnetic reconnection at the heliospheric current sheet. We consider different magnetic configurations that provide favourable conditions for both the appearance of small-scale magnetic islands and their confinement.

Study of cosmic ray intensity and geomagnetic storms with solar wind parameters during the period 1998–2005

Hema [Kharayat](#), Lalan Prasad

[Astrophysics and Space Science](#) January 2017, 362:20

<http://sci-hub.cc/10.1007/s10509-016-2996-5>

The aim of this paper is to study the effect of solar wind parameters (solar wind speed VV , plasma flow pressure, and plasma density) on cosmic ray intensity and on geomagnetic storms for the period 1998–2005 (solar cycle 23). A Chree analysis by the superposed epoch method has been done for the study. From the present study we have found that the solar wind speed is a highly effective parameter in producing cosmic ray intensity decreases and geomagnetic storms. No time lag is found between cosmic ray intensity decreases, geomagnetic storms, and peak value of solar wind speed. Further, we have found that the plasma flow pressure is effectively correlated with geomagnetic storms but it is weakly correlated with cosmic ray intensity. The cosmic ray intensity and geomagnetic storms are found to be weakly correlated with plasma density. The decrease in cosmic ray intensity and geomagnetic storms takes place one day after the peak values of plasma flow pressure and plasma density. There is a time lag of one day between solar wind parameters (plasma flow pressure and plasma density) and cosmic ray intensity decrease, geomagnetic storms. Also, we have found a high correlation of cosmic ray intensity and geomagnetic storms with the product of interplanetary magnetic field BB and solar wind speed VV i.e. $B \cdot VB \cdot V$. This study may be useful in predicting the space-weather phenomena.

Table 1 Ground Level Enhancements during the period 1998–2005

Table 2 The largest FDs during 1998–2005

Study of Cosmic Ray Intensity in Relation to the Interplanetary Magnetic Field and Geomagnetic Storms for Solar Cycle 23

Hema [Kharayat](#), Lalan Prasad, Rajesh Mathpal, Suman Garia, Beena Bhatt

Solar Phys. Vol. 291, Issue 2 2016

We investigate the association of the cosmic-ray intensity (CRI) with the interplanetary magnetic field (IMF, B) and geomagnetic storms (GS) for the period 1997–2006 (Solar Cycle 23). To do this, we conducted a Chree analysis by the superposed-epoch method. A transient decrease in CRI is found on the occurrence days of GS, and this decrease shows a similar pattern to that of the disturbance storm-time index (Dst). In addition, we show that the CRI decreases with the increase in IMF. The time lag between the decrease in CRI and increase in IMF is about one day or less. Furthermore, an increase in IMF B is found with the decrease in Dst index. IMF and Dst index are highly anti-correlated to each other, while the sunspot number is not found to be correlated with IMF, Dst index, or CRI for the period studied. The IMF is found to be an effective parameter combination for producing GS and Forbush decrease. We also found two types of decrease in CRI for Solar Cycle 23: i) symmetric and ii) asymmetric decreases. The study of CRI decreases may be useful for studying space-weather effects.

Radar detection of interplanetary shocks: Scattering by anisotropic Langmuir turbulence

Mykola V. [Khotyaintsev](#), Valentin N. Mel'nik, Bo Thidé, Yuri V. Khotyaintsev

[Advances in Space Research](#), Volume 45, Issue 6, 15 March 2010, Pages 804-811

Earth-directed interplanetary shocks associated with coronal mass ejections (CMEs) are known to have a severe impact on the magnetosphere, causing strong geomagnetic storms and substorms. Hence, early detection of such shocks is important. Here we study the feasibility of radar detection of interplanetary shocks. We consider a scattering mechanism, which is based on the induced scattering $t+l \leftrightarrow t$ of a radar wave by anisotropic Langmuir turbulence, being generated by the shock-accelerated electrons. The problem is studied for an arbitrary angle between the electron beam and the incident radar wave, $\mathbf{v}_b \wedge \mathbf{k}_t$, and special emphasis is put on the study of a dependence of the scattering process on this angle. We obtain and analyze analytical expressions for the frequency shift, scattering cross-section of the turbulence, coefficient of absorption (due to scattering), and the optical depth. We show that the detection of such shocks is possible if the turbulence energy density exceeds $W = 10^{-5} nT$ (nT is the thermal energy density of a plasma), which is quite realistic according to our estimations. The altitudes in the solar corona where reflections may occur depend on the angle $\mathbf{v}_b \wedge \mathbf{k}_t$. If expressed in local plasma frequencies, ω_p , the altitudes span is $\omega_t/8 \lesssim \omega_p \lesssim \omega_t$ for $\mathbf{v}_b \wedge \mathbf{k}_t = \pi$ and $\omega_t/120 \lesssim \omega_p \lesssim \omega_t$ for $\mathbf{v}_b \wedge \mathbf{k}_t = \pi/2$, where ω_t is a frequency of the transmitted radar wave. Thus the scattering occurs much closer to the radar in the second case than in the first. Detection of the scattered signal, in the general case, requires a remote receiver, since the radar wave backscatters only for $\mathbf{v}_b \wedge \mathbf{k}_t = \pi$.

Physics-based model of solar wind stream interaction regions: Interfacing between Multi-VP and 1D MHD for operational forecasting at L1

R. Kieokaew, R. F. Pinto, E. Samara, C. Tao, M. Indurain, B. Lavraud, A. Brunet, V. Génot, A. Rouillard, N. André, S. Bourdarie, C. Katsavrias, F. Darrouzet, B. Grison, I. Daglis

2023

<https://arxiv.org/pdf/2303.09221.pdf>

Our current capability of space weather prediction in the Earth's radiation belts is limited to only an hour in advance using the real-time solar wind monitoring at the Lagrangian L1 point. To mitigate the impacts of space weather on telecommunication satellites, several frameworks were proposed to advance the lead time of the prediction. We develop a prototype pipeline called "Helio1D" to forecast ambient solar wind conditions (speed, density, temperature, tangential magnetic field) at L1 with a lead time of 4 days. This pipeline predicts Corotating Interaction Regions (CIRs) and high-speed streams that can increase high-energy fluxes in the radiation belts. The Helio1D pipeline connects the Multi-VP model, which provides real-time solar wind emergence at 0.14 AU, and a 1D MHD model of solar wind propagation. We benchmark the Helio1D pipeline for solar wind speed against observations for the intervals in 2004 - 2013 and 2017 - 2018. We developed a framework based on the Fast Dynamic Time Warping technique that allows us to continuously compare time-series outputs containing CIRs to observations to measure the pipeline's performance. In particular, we use this framework to calibrate and improve the pipeline's performance for operational forecasting. To provide timing and magnitude uncertainties, we model several solar wind conditions in parallel, for a total of 21 profiles corresponding to the various virtual targets including the Earth. This pipeline can be used to feed real-time, daily solar wind forecasting that aims to predict the dynamics of the inner magnetosphere and the radiation belts.

A Peculiar ICME Event in August 2018 Observed with the Global Muon Detector Network

W. Kihara, K. Munakata, C. Kato, R. Kataoka, A. Kadokura, S. Miyake, M. Kozai, T. Kuwabara, M. Tokumaru, R. R. S. Mendonça, E. Echer, A. Dal Lago, M. Rockenbach, N. J. Schuch, J. V. Bageston, C. R. Braga, H. K. Al Jassar, M. M. Sharma, M. L. Duldig, J. E. Humble, P. Evenson, I. Sabbah, J. Kóta

Space Weather e2020SW002531 **Volume19, Issue3** 2021

<https://arxiv.org/pdf/2101.12009.pdf>

<https://doi.org/10.1029/2020SW002531>

<https://agupubs.onlinelibrary.wiley.com/doi/epdf/10.1029/2020SW002531>

We demonstrate that global observations of high-energy cosmic rays contribute to understanding unique characteristics of a large-scale magnetic flux rope causing a magnetic storm in August 2018. Following a weak interplanetary shock on 25 August 2018, a magnetic flux rope caused an unexpectedly large geomagnetic storm. It is likely that this event became geoeffective because the flux rope was accompanied by a corotating interaction region and compressed by high-speed solar wind following the flux rope. In fact, a Forbush decrease was observed in cosmic-ray data inside the flux rope as expected, and a significant cosmic-ray density increase exceeding the unmodulated level before the shock was also observed near the trailing edge of the flux rope. The cosmic-ray density increase can be interpreted in terms of the adiabatic heating of cosmic rays near the trailing edge of the flux rope, as the corotating interaction region prevents free expansion of the flux rope and results in the compression near the trailing edge. A northeast-directed spatial gradient in the cosmic-ray density was also derived during the cosmic-ray density increase, suggesting that the center of the heating near the trailing edge is located northeast of Earth. This is one of the best examples demonstrating that the observation of high-energy cosmic rays provides us with information that can only be derived from the cosmic ray measurements to observationally constrain the three-dimensional macroscopic picture of the interaction between coronal mass ejections and the ambient solar wind, which is essential for prediction of large magnetic storms. **25-26 Aug 2018**

Solar and Geomagnetic Activity Relation for the Last two Solar Cycles

A. Kilcik¹, E. Yiğit², V. Yurchyshyn^{3,4}, A. Ozguc⁵, J.P. Rozelot⁶

Sun and Geosphere, **2017**; 12/1: 31-39

http://newserver.stil.bas.bg/SUNGEO/00SGArhiv/SG_v12_No1_2017-pp-31-39.pdf

The long-term relationship between solar (sunspot counts in different Zurich sunspot groups, International Sunspot Number (ISSN), solar wind, and X-Ray solar flare index and geomagnetic indices (Ap and Dst) is investigated. Data sets used in this study cover a time period from January 1996 to March 2014. Our main findings are as follows: 1) The best correlation between the sunspot counts and the Ap index are obtained for the large group time series, while the other categories exhibited lower (final and medium) or no correlation at all (small). It is interesting to note that Ap index is

delayed by about 13 months relatively to all sunspot count series and ISSN data. 2) The best correlation between the sunspot counts and the Dst index was as well obtained for the large AR time series. The Dst index delays with respect to the large group by about 2 months. 3) The highest correlation between the solar and geomagnetic indices were obtained between the solar wind speed and Ap and Dst indices with zero time delays ($r = 0.76$, $r = 0.52$, respectively). 4) The correlation coefficients between the geomagnetic indices (Ap, Dst) and X-Ray solar flare index ($r = 0.59$, $r = -0.48$, respectively) are a little higher than the correlation coefficients between these geomagnetic indices and ISSN ($r = 0.57$, $r = -0.43$, respectively). 5) The magnitude of all solar and geomagnetic indices (except the solar wind speed) has significantly decreased during the current solar cycle as compared to the same phase of the previous cycle.

Maximum CME speed as an indicator of solar and geomagnetic activities

A. [Kilcik](#)¹, V.B. Yurchyshyn¹, V. Abramenko¹, P.R. Goode¹, N. Gopalswamy², A. Ozguc³, J.P. Rozelot⁴
BBSO Preprint #1456, 2010; Ap. J. 727:44 (6pp), 2011 January, **File**

We investigate the relationship between the monthly averaged maximal speeds of coronal mass ejections (CMEs), international sunspot number (ISSN) and the geomagnetic Dst and Ap indices covering the 1996-2008 time interval (solar cycle 23). Our new findings are as follows. i) There is a noteworthy relationship between monthly averaged maximum CME speeds and sunspot numbers, Ap and Dst indices. Various peculiarities in the monthly Dst index are better correlated with the fine structures in the CME speed profile than that in the ISSN data. ii) Unlike the sunspot numbers, the CME speed index does not exhibit a double peak maximum. Instead, the CME speed profile peaks during the declining phase of solar cycle 23. Similar to the Ap index, both CME speed and the Dst indices lag behind the sunspot numbers by several months. iii) CME number shows a double peak similar to that seen in the sunspot numbers. The CME occurrence rate remained very high even near the minimum of the solar cycle 23, when both sunspot number and the CME average maximum speed were reaching their minimum values. iv) A well defined peak of the Ap index between May 2002 and August 2004 was co-temporal with the excess of the mid-latitude coronal holes during solar cycle 23. The above findings suggest that the CME speed index may be a useful indicator of both solar and geomagnetic activity. It may have advantages over the sunspot numbers, because it better reflects the intensity of Earth directed solar eruptions.

A Statistical Study of the Relationship Between the Sunspot Number, Maximum CME Speed and Geomagnetic Indices

A [Kilcik](#), V.B. Yurchyshyn, V. Abramenko, P.R. Goode, N. Gopalswamy, A. Ozguc and J.P. Rozelot
BBSO Preprint #1424, 2010; **File**

We investigated the relationship between the monthly averaged maximal speeds of coronal mass ejections (CMEs), sunspot number (SSN) and the geomagnetic Dst and Ap indices covering the 1996-2008 time interval. The study was carried out using frequency and correlation analyses. Frequency analysis of the maximum speed of CMEs (or CME speed index) shows a cyclic behavior similar to that found for SSN and the Ap index. Our new findings are as follows. 1) Unlike the SSN, the CME speed index does not exhibit a double peak maximum. 2) The CME speed index has a correlative relationship with SSN and Dst and Ap indices (correlation coefficients are 0.76, -0.53, 0.68 respectively). Various peculiarities in the monthly Dst index are better correlated with the fine structures in the CME speed profile than that in the SSN data. 3) Similar to the Ap index, both CME speed and the Dst indices lag behind the sunspot numbers by several months. We thus conclude that CME speed index may be a good parameter to describe the geo-effectiveness of solar activity.

Structure and fluctuations of a slow ICME sheath observed at 0.5 au by the Parker Solar Probe

E. K. J. [Kilpua](#), [S. W. Good](#), [M. Ala-Lahti](#), [A. Osmane](#), [S. Pal](#), [J. E. Soljento](#), [L. L. Zhao](#), [S. Bale](#)
A&A 663, A108 2022

<https://arxiv.org/pdf/2204.13058.pdf>

<https://www.aanda.org/articles/aa/pdf/2022/07/aa42191-21.pdf>

Sheaths ahead of interplanetary coronal mass ejections (ICMEs) are turbulent heliospheric structures. Knowledge of their structure and fluctuations is important for understanding their geoeffectiveness, their role in accelerating particles, and the interaction of ICMEs with the solar wind. We studied observations from the Parker Solar Probe of a sheath observed at 0.5 au in March 2019, ahead of a slow streamer blowout CME. To examine the MHD-scale turbulent properties, we calculated fluctuation amplitudes, magnetic compressibility, partial variance of increments (PVI), cross helicity (σ_c), residual energy (σ_r), and the Jensen-Shannon permutation entropy and complexity. The sheath consisted of

slow and fast flows separated by a 15-min change in magnetic sector that coincided with current sheet crossings and a velocity shear zone. Fluctuation amplitudes and PVI were greater through the sheath than upstream. Fluctuations had mostly negative σ_r and positive σ_c in the sheath, the latter indicating an anti-sunward sense of propagation. The velocity shear region marked an increase in temperature and specific entropy, and the faster flow behind had local patches of positive σ_r as well as higher fluctuation amplitudes and PVI. Fluctuations in the preceding wind and sheath were stochastic, with the sheath fluctuations showing lower entropy and higher complexity than upstream. The two-part sheath structure likely resulted from a warp in the heliospheric current sheet (HCS) being swept up and compressed. The ejecta accelerated and heated the wind at the sheath rear, which then interacted with the slower wind ahead of the HCS warp. This caused differences in fluctuation properties across the sheath. Sheaths of slow ICMEs can thus have complex structure where fluctuation properties are not just downstream shock properties, but are generated within the sheath.

March 15, 2019

Multi-spacecraft observations of the structure of the sheath of an interplanetary coronal mass ejection and related energetic ion enhancement

E. K. J. Kilpua, S. W. Good, N. Dresing, R. Vainio, + + +

Astronomy & Astrophysics, Solar Orbiter First Results (Cruise Phase) special issue 2021

<https://arxiv.org/pdf/2112.09472.pdf>

Sheaths ahead of coronal mass ejections (CMEs) are large heliospheric structures that form with CME expansion and propagation. Turbulent and compressed sheaths contribute to the acceleration of particles in the corona and in interplanetary space, but the relation of their internal structures to particle energization is still relatively little studied. In particular, the role of sheaths in accelerating particles when the shock Mach number is low is a significant open problem. This work seeks to provide new insights on the internal structure of CME sheaths with regard to energetic particle enhancements. A good opportunity to achieve this aim was provided by observations of a sheath made by radially aligned spacecraft at 0.8 and ~ 1 AU (Solar Orbiter, Wind, ACE and BepiColombo) on **19-21 April 2020**. The sheath was preceded by a weak shock. Energetic ion enhancements occurred at different locations within the sheath structure at Solar Orbiter and L1. Magnetic fluctuation amplitudes at inertial-range scales increased in the sheath relative to the upstream wind. However, when normalised to the local mean field, fluctuation amplitudes did not increase significantly; magnetic compressibility of fluctuation also did not increase. Various substructures were embedded within the sheath at the different spacecraft, including multiple heliospheric current sheet (HCS) crossings and a small-scale flux rope. At L1, the ion flux enhancement was associated with the HCS crossings, while at Solar Orbiter, the enhancement occurred within the rope. Substructures that are swept from the upstream solar wind and compressed in the sheath can act as particularly effective acceleration sites. A possible acceleration mechanism is betatron acceleration associated with the small-scale flux rope and the warped HCS in the sheath.

Statistical Analysis of Magnetic Field Fluctuations in Coronal Mass Ejection-Driven Sheath Regions

E. K. J. Kilpua^{1*}, S. W. Good¹, M. Ala-Lahti¹, A. Osmane¹, D. Fontaine², L. Hadid², M. Janvier³ and E. Yordanova⁴

Front. Astron. Space Sci., 04 February 2021 |

<https://doi.org/10.3389/fspas.2020.610278>

<https://www.frontiersin.org/articles/10.3389/fspas.2020.610278/full>

We report a statistical analysis of magnetic field fluctuations in 79 coronal mass ejection- (CME-) driven sheath regions that were observed in the near-Earth solar wind. Wind high-resolution magnetic field data were used to investigate 2 h regions adjacent to the shock and ejecta leading edge (Near-Shock and Near-LE regions, respectively), and the results were compared with a 2 h region upstream of the shock. The inertial-range spectral indices in the sheaths are found to be mostly steeper than the Kolmogorov $-5/3$ index and steeper than in the solar wind ahead. We did not find indications of an $f^{-1}f^{-1}$ spectrum, implying that magnetic fluctuation properties in CME sheaths differ significantly from planetary magnetosheaths and that CME-driven shocks do not reset the solar wind turbulence, as appears to happen downstream of planetary bow shocks. However, our study suggests that new compressible fluctuations are generated in the sheath for a wide variety of shock/upstream conditions. Fluctuation properties particularly differed between the Near-Shock region and the solar wind ahead. A strong positive correlation in the mean magnetic compressibility was found between the upstream and downstream regions, but the compressibility values in the sheaths were similar to those in the slow solar wind (<0.2), regardless of the value in the preceding wind. However, we did not find clear correlations between the inertial-range spectral indices in the sheaths and shock/preceding solar wind properties, nor with the mean normalized fluctuation amplitudes. Correlations were also considerably lower in the Near-LE region than in the Near-Shock region. Intermittency was also considerably higher in the sheath than in the upstream wind according to several proxies,

particularly so in the Near-Shock region. Fluctuations in the sheath exhibit larger rotations than upstream, implying the presence of strong current sheets in the sheath that can add to intermittency. **September 12, 2014**

Multipoint Observations of the June 2012 Interacting Interplanetary Flux Ropes

Emilia K. J. [Kilpua](#), [Simon W. Good](#), [Erika Palmerio](#), [Eleanna Asvestari](#), [Erkka Lumme](#), Matti Ala-Lahti, [Milla M. H. Kalliokoski](#), Diana E. Morosan, Jens Pomoell, [Daniel J. Price](#), Jasmina

Front. Astron. Space Sci. 6:50. **2019**

sci-hub.ru/10.3389/fspas.2019.00050

<https://www.frontiersin.org/articles/10.3389/fspas.2019.00050/full>

<https://doi.org/10.3389/fspas.2019.00050>

We report a detailed analysis of interplanetary flux ropes observed at Venus and subsequently at Earth's Lagrange L1 point between **June 15 and 17, 2012**. The observation points were separated by about 0.28 AU in radial distance and 5° in heliographic longitude at this time. The flux ropes were associated with three coronal mass ejections (CMEs) that erupted from the Sun on **June 12–14, 2012** (SOL2012-06-12, SOL2012-06-13, and SOL2012-06-14). We examine the CME–CME interactions using in-situ observations from the almost radially aligned spacecraft at Venus and Earth, as well as using heliospheric modeling and imagery. The June 14 CME reached the June 13 CME near the orbit of Venus and significant interaction occurred before they both reached Earth. The shock driven by the June 14 CME propagated through the June 13 CME and the two CMEs coalesced, creating the signatures of one large, coherent flux rope at L1. We discuss the origin of the strong interplanetary magnetic fields related to this sequence of events, the complexity of interpreting solar wind observations in the case of multiple interacting CMEs, and the coherence of the flux ropes at different observation points.

Solar wind properties and geospace impact of coronal mass ejection-driven sheath regions: variation and driver dependence

E.K.J. [Kilpua](#), [D. Fontaine](#), [C. Moissard](#), [M. Ala-Lahti](#), [E. Palmerio](#), [E. Yordanova](#), [S.W. Good](#), [M.M.H. Kalliokoski](#), [E. Lumme](#), [A. Osmane](#), [M. Palmroth](#), [L. Turc](#)

Space Weather [Volume17, Issue8](#) Pages 1257-1280 **2019**

sci-hub.se/10.1029/2019SW002217

We present a statistical study of interplanetary conditions and geospace response to 89 coronal mass ejection (CME)-driven sheaths observed during Solar Cycles 23 and 24. We investigate in particular the dependencies on the driver properties and variations across the sheath. We find that the ejecta speed principally controls the sheath geoeffectiveness and shows the highest correlations with sheath parameters, in particular in the region closest to the shock. Sheaths of fast ejecta have on average high solar wind speeds, magnetic (B)-field magnitudes, and fluctuations and they generate efficiently strong out-of-ecliptic fields. Slow-ejecta sheaths are considerably slower, have weaker fields and field fluctuations and therefore they cause primarily moderate geospace activity. Sheaths of weak and strong B-field ejecta have distinct properties but differences in their geoeffectiveness are less drastic. Sheaths of fast and strong ejecta push the subsolar magnetopause significantly earthward, often even beyond geostationary orbit. Slow-ejecta sheaths also compress the magnetopause significantly due to their large densities that likely result of their relatively long propagation times and source near the streamer belt. We find the regions near the shock and ejecta leading edge to be the most geoeffective parts of the sheath. These regions are also associated with the largest B-field magnitudes, out-of-ecliptic fields, and field fluctuations as well as largest speeds and densities. The variations, however, depend on driver properties. Forecasting sheath properties is challenging due to their variable nature, but the dependence on ejecta properties determined in this work could help to estimate sheath geoeffectiveness through remote-sensing CME observations. **April 13-14, 2013,**

Outer Van Allen Radiation Belt Response to Interacting Interplanetary Coronal Mass Ejections

E. K. J. [Kilpua](#), [D. L. Turner](#), [A. N. Jaynes](#), [H. Hietala](#), [H. E. J. Koskinen](#), [A. Osmane](#), [M. Palmroth](#), [T. I. Pulkkinen](#), [R. Vainio](#), [D. Baker](#), [S. G. Claudepierre](#)

JGR [Volume124, Issue3](#) March **2019** Pages 1927-1947

sci-hub.se/10.1029/2018JA026238

We study the response of the outer Van Allen radiation belt during an intense magnetic storm on **15–22 February 2014**. Four interplanetary coronal mass ejections (ICMEs) arrived at Earth, of which the three last ones were interacting. Using data from the Van Allen Probes, we report the first detailed investigation of electron fluxes from source (tens of kiloelectron volts) to core (megaelectron volts) energies and possible loss and acceleration mechanisms as a response to

substructures (shock, sheath and ejecta, and regions of shock-compressed ejecta) in multiple interacting ICMEs. After an initial enhancement induced by a shock compression of the magnetosphere, core fluxes strongly depleted and stayed low for 4 days. This sustained depletion can be related to a sequence of ICME substructures and their conditions that influenced the Earth's magnetosphere. In particular, the main depletions occurred during a high-dynamic pressure sheath and shock-compressed southward ejecta fields. These structures compressed/eroded the magnetopause close to geostationary orbit and induced intense and diverse wave activity in the inner magnetosphere (ULF Pc5, electromagnetic ion cyclotron, and hiss) facilitating both effective magnetopause shadowing and precipitation losses. Seed and source electrons in turn experienced stronger variations throughout the studied interval. The core fluxes recovered during the last ICME that made a glancing blow to Earth. This period was characterized by a concurrent lack of losses and sustained acceleration by chorus and Pc5 waves. Our study highlights that the seemingly complex behavior of the outer belt during interacting ICMEs can be understood by the knowledge of electron dynamics during different substructures.

Forecasting the Structure and Orientation of Earthbound Coronal Mass Ejections

E. K. J. [Kilpua](#) [N. Lugaz](#) [L. Mays](#) [M. Temmer](#)

Space Weather 17 [Issue 4](#) Pages 498-526 2019

Space Weather Quarterly 16, issue 1, 6-30 2019

<https://agupubs.onlinelibrary.wiley.com/doi/epdf/10.1002/swq.21>

[sci-hub.se/10.1029/2018SW001944](https://doi.org/10.1029/2018SW001944)

Coronal Mass Ejections (CMEs) are the key drivers of strong to extreme space weather storms at the Earth that can have drastic consequences for technological systems in space and on ground. The ability of a CME to drive geomagnetic disturbances depends crucially on the magnetic structure of the embedded flux rope, which is thus essential to predict. The current capabilities in forecasting in advance (at least half-a-day before) the geoeffectiveness of a given CME is however severely hampered by the lack of remote-sensing measurements of the magnetic field in the corona and adequate tools to predict how CMEs deform, rotate and deflect during their travel through the coronal and interplanetary space as they interact with the ambient solar wind and other CMEs. These problems can lead not only to over- or underestimation of the severity of a storm, but also to forecasting “misses” and “false alarms” that are particularly difficult for the end-users. In this paper, we discuss the current status and future challenges and prospects related to forecasting of the magnetic structure and orientation of CMEs. We focus both on observational and modeling (first-principle and semi-empirical) based approaches, and discuss the space- and ground-based observations that would be the most optimal for making accurate space weather predictions. We also cover the gaps in our current understanding related to the formation and eruption of the CME flux rope and physical processes that govern its evolution in the variable ambient solar wind background that complicate the forecasting. **27–31 October 2013, 19–20 November 2007, 24–29 May 2010, 16 June 2010, 2010-12-12, 2013-04-11-13**

Coronal mass ejections and their sheath regions in interplanetary space

Review

Emilia [Kilpua](#), Hannu E. J. Koskinen & Tuija I. Pulkkinen

Living Reviews in Solar Physics December 2017, 14:5 **File**

<https://link.springer.com/content/pdf/10.1007%2Fs41116-017-0009-6.pdf>

Interplanetary coronal mass ejections (ICMEs) are large-scale heliospheric transients that originate from the Sun. When an ICME is sufficiently faster than the preceding solar wind, a shock wave develops ahead of the ICME. The turbulent region between the shock and the ICME is called the sheath region. ICMEs and their sheaths and shocks are all interesting structures from the fundamental plasma physics viewpoint. They are also key drivers of space weather disturbances in the heliosphere and planetary environments. ICME-driven shock waves can accelerate charged particles to high energies. Sheaths and ICMEs drive practically all intense geospace storms at the Earth, and they can also affect dramatically the planetary radiation environments and atmospheres. This review focuses on the current understanding of observational signatures and properties of ICMEs and the associated sheath regions based on five decades of studies. In addition, we discuss modelling of ICMEs and many fundamental outstanding questions on their origin, evolution and effects, largely due to the limitations of single spacecraft observations of these macro-scale structures. We also present current understanding of space weather consequences of these large-scale solar wind structures, including effects at the other Solar System planets and exoplanets. We specially emphasize the different origin, properties and consequences of the sheaths and ICMEs. **February 7, 1981 , 5 Dec 1981, 13-14 July 1982, 14 Aug 1982, February 27, 2000 , June 10, 2000 , 16–22 Sept 2000. , 4-5 Apr 2004, 20-21 May 2005, 27-29 Dec 2004, 14–15 December, 2006 , 28 May 2010, 15 Sept 2010, 9 July 2013, 19-20 Aug 2014**

See comments of Yermolaev

https://www.researchgate.net/publication/321282888_Coronal_mass_ejections_and_their_sheath_regions_in_interplanetary_space?focusedCommentId=5a26cf564cde266d58787f4c

Geoeffective Properties of Solar Transients and Stream Interaction Regions Review

E. K. J. **Kilpua**, A. Balogh, R. von Steiger, Y. D. Liu

[Space Science Reviews](#) 212, 1271 **2017**

<https://link.springer.com/content/pdf/10.1007%2Fs11214-017-0411-3.pdf>

Interplanetary Coronal Mass Ejections (ICMEs), their possible shocks and sheaths, and co-rotating interaction regions (CIRs) are the primary large-scale heliospheric structures driving geospace disturbances at the Earth. CIRs are followed by a faster stream where Alfvénic fluctuations may drive prolonged high-latitude activity. In this paper we highlight that these structures have all different origins, solar wind conditions and as a consequence, different geomagnetic responses. We discuss general solar wind properties of sheaths, ICMEs (in particular those showing the flux rope signatures), CIRs and fast streams and how they affect their solar wind coupling efficiency and the resulting magnetospheric activity. We show that there are two different solar wind driving modes: (1) Sheath-like with turbulent magnetic fields, and large Alfvén Mach (MAMA) numbers and dynamic pressure, and (2) flux rope-like with smoothly varying magnetic field direction, and lower MAMA numbers and dynamic pressure. We also summarize the key properties of interplanetary shocks for space weather and how they depend on solar cycle and the driver.

Sources of The Slow Solar wind During the Solar Cycle 23/24 Minimum

E.K.J. **Kilpua**, M. S. Madjarska, N. Karna, T. Wiegelmann, C. Farrugia, W. Yu, K. Andreeova

Solar Phys. **2016**

<http://arxiv.org/pdf/1606.05142v1.pdf>

We investigate the characteristics and the sources of the slow (< 450 km/s) solar wind during the four years (2006-2009) of low solar activity between Solar Cycles 23 and 24. We use a comprehensive set of in-situ observations in the near-Earth solar wind (Wind and ACE) and remove the periods when large-scale interplanetary coronal mass ejections were present. The investigated period features significant variations in the global coronal structure, including the frequent presence of low-latitude active regions in 2006-2007, long-lived low- and mid-latitude coronal holes in 2006 - mid-2008 and mostly the quiet Sun in 2009. We examine both Carrington Rotation averages of selected solar plasma, charge state and compositional parameters and distributions of these parameters related to Quiet Sun, Active Region Sun and the Coronal Hole Sun. While some of the investigated parameters (e.g., speed, the C^{+6}/C^{+4} and He/H ratio) show clear variations over our study period and with solar wind source type, some (Fe/O) exhibit very little changes. Our results highlight the difficulty in distinguishing between the slow solar wind sources based on the inspection of the solar wind conditions.

Statistical Study of Strong and Extreme Geomagnetic Disturbances and Solar Cycle Characteristics

E. K. J. **Kilpua**¹, N. Olsper², A. Grigorievskiy², M. J. Käpylä², E. I. Tanskanen², H. Miyahara³, R. Kataoka^{4,5}, J. Pelt^{2,6}, and Y. D. Liu

2015 *ApJ* 806 272

<https://iopscience.iop.org/article/10.1088/0004-637X/806/2/272/pdf>

We study the relation between strong and extreme geomagnetic storms and solar cycle characteristics. The analysis uses an extensive geomagnetic index AA data set spanning over 150 yr complemented by the Kakioka magnetometer recordings. We apply Pearson correlation statistics and estimate the significance of the correlation with a bootstrapping technique. We show that the correlation between the storm occurrence and the strength of the solar cycle decreases from a clear positive correlation with increasing storm magnitude toward a negligible relationship. Hence, the quieter Sun can also launch superstorms that may lead to significant societal and economic impact. Our results show that while weaker storms occur most frequently in the declining phase, the stronger storms have the tendency to occur near solar maximum. Our analysis suggests that the most extreme solar eruptions do not have a direct connection between the solar large-scale dynamo-generated magnetic field, but are rather associated with smaller-scale dynamo and resulting turbulent magnetic fields. The phase distributions of sunspots and storms becoming increasingly in phase with increasing storm strength, on the other hand, may indicate that the extreme storms are related to the toroidal component of the solar large-scale field.

Properties and drivers of fast interplanetary shocks near the orbit of the Earth (1995-2013)

E. K. J. **Kilpua**, E. Lumme, K. Andreeova, A. Isavnin and H.E.J. Koskinen

JGR [Volume 120, Issue 6](#) Pages 4112–4125 **2015**

We present a comprehensive statistical analysis spanning over a solar cycle of the properties and drivers of traveling fast forward and fast reverse interplanetary shocks. We combine statistics of 679 shocks between 1995–2013 identified from the near-Earth (Wind and ACE) and STEREO-A observations. We find that fast forward shocks dominate over fast reverse shocks in all solar cycle phases except during solar minimum. Nearly all fast reverse shocks are driven by slow-fast stream interaction regions (SIRs), while coronal mass ejections (CMEs) are the principal drivers of fast forward shocks in all phases except at solar minimum. The occurrence rate and median speeds of CME-driven fast forward shocks follow the sunspot cycle, while SIR-associated shocks do not show such correspondence. The strength of the shock (characterized by the magnetosonic Mach number and by the upstream to downstream magnetic field and density ratio) shows relatively little variations over solar cycle. However, the shocks were slightly stronger during the ascending phase of a relatively weak solar cycle 24 than during the previous ascending phase. The CME- and SIR-driven fast forward shocks and reverse shocks have distinct upstream solar wind conditions, which reflect to their relative strengths. We found that CME-driven shocks are on average stronger and faster, and they show broader distributions of shock parameters than the shocks driven by SIRs.

Solar Sources of Interplanetary Coronal Mass Ejections During the Solar Cycle 23/24 Minimum

E. K. J. [Kilpua](#), M. Mierla, A. N. Zhukov, L. Rodriguez, A. Vourlidas, B. Wood
Solar Phys., Volume 289, Issue 10, pp 3773-3797, 2014

We examine solar sources for 20 interplanetary coronal mass ejections (ICMEs) observed in 2009 in the near-Earth solar wind. We performed a detailed analysis of coronagraph and extreme ultraviolet (EUV) observations from the Solar Terrestrial Relations Observatory (STEREO) and Solar and Heliospheric Observatory (SOHO). Our study shows that the coronagraph observations from viewpoints away from the Sun–Earth line are paramount to locate the solar sources of Earth-bound ICMEs during solar minimum. SOHO/LASCO detected only six CMEs in our sample, and only one of these CMEs was wider than 120° . This demonstrates that observing a full or partial halo CME is not necessary to observe the ICME arrival. Although the two STEREO spacecraft had the best possible configuration for observing Earth-bound CMEs in 2009, we failed to find the associated CME for four ICMEs, and identifying the correct CME was not straightforward even for some clear ICMEs. Ten out of 16 (63 %) of the associated CMEs in our study were “stealth” CMEs, i.e. no obvious EUV on-disk activity was associated with them. Most of our stealth CMEs also lacked on-limb EUV signatures. We found that stealth CMEs generally lack the leading bright front in coronagraph images. This is in accordance with previous studies that argued that stealth CMEs form more slowly and at higher coronal altitudes than non-stealth CMEs. We suggest that at solar minimum the slow-rising CMEs do not draw enough coronal plasma around them. These CMEs are hence difficult to discern in the coronagraphic data, even when viewed close to the plane of the sky. The weak ICMEs in our study were related to both intrinsically narrow CMEs and the non-central encounters of larger CMEs. We also demonstrate that narrow CMEs (angular widths $\leq 20^\circ$) can arrive at Earth and that an unstructured CME may result in a flux rope-type ICME.

Why have geomagnetic storms been so weak during the recent solar minimum and the rising phase of cycle 24?

E.K.J. [Kilpua](#), J.G. Luhmann, L.K. Jian, C.T. Russell, Y. Li
JASTP, Volume 107, January 2014, Pages 12–19, 2013

The minimum following solar cycle 23 was the deepest and longest since the dawn of the space age. In this paper we examine geomagnetic activity using Dst and AE indices, interplanetary magnetic field (IMF) and plasma conditions, and the properties and occurrence rate of interplanetary coronal mass ejections (ICMEs) during two periods around the last two solar minima and rising phases (Period 1: 1995–1999 and Period 2: 2006–2012). The data is obtained from the 1-h OMNI database. Geomagnetic activity was considerably weaker during Period 2 than during Period 1, in particular in terms of Dst. We show that the responses of AE and Dst depend on whether it is solar wind speed or the southward IMF component (BS) that controls the variations in solar wind driving electric field (EY). We conclude that weak Dst activity during Period 2 was primarily a consequence of weak BS and presumably further weakened due to low solar wind densities. In contrast, solar wind speed did not show significant differences between our two study periods and the high-speed solar wind during Period 2 maintained AE activity despite of weak BS. The weakness of BS during Period 2 was attributed in particular to the lack of strong and long-duration ICMEs. We show that for our study periods there was a clear annual north–south IMF asymmetry, which affected in particular the intense Dst activity. This implies that the annual amount of intense Dst activity may rather be determined by the coincidence of what magnetic structure the strong ICMEs encountering the Earth have than by the solar cycle size.

On the relationship between interplanetary coronal mass ejections and magnetic clouds

E.K.J. [Kilpua](#), A. Isavnin, A. Vourlidas, H.E.J Koskinen, and L. Rodriguez
Ann. Geophys., 31, 1251-1265, 2013, [File](#)

The relationship of magnetic clouds (MCs) to interplanetary coronal mass ejections (ICMEs) is still an open issue in space research. The view that all ICMEs would originate as magnetic flux ropes has received increasing attention, although near the orbit of the Earth only about one-third of ICMEs show clear MC signatures and often the MC occupies only a portion of the more extended region showing ICME signatures. In this work we analyze 79 events between 1996 and 2009 reported in existing ICME/MC catalogs (Wind magnetic cloud list and the Richardson and Cane ICME list) using near-Earth observations by ACE (Advanced Composition Explorer) and Wind. We perform a systematic comparison of cases where ICME and MC signatures coincided and where ICME signatures extended significantly beyond the MC boundaries. We find clear differences in the characteristics of these two event types. In particular, the events where ICME signatures continued more than 6 h past the MC rear boundary had 2.7 times larger speed difference between the ICME's leading edge and the preceding solar wind, 1.4 times higher magnetic fields, 2.1 times larger widths and they experienced three times more often strong expansion than the events for which the rear boundaries coincided. The events with significant mismatch in MC and ICME boundary times were also embedded in a faster solar wind and the majority of them were observed close to the solar maximum. Our analysis shows that the sheath, the MC and the regions of ICME-related plasma in front and behind the MC have different magnetic field, plasma and charge state characteristics, thus suggesting that these regions separate already close to the Sun. Our study shows that the geometrical effect (the encounter through the CME leg and/or far from the flux rope center) does not contribute much to the observed mismatch in the MC and ICME boundary times.

Observations of ICMEs and ICME-like Solar Wind Structures from 2007 – 2010 Using Near-Earth and STEREO Observations

E. K. J. [Kilpua](#), L. K. Jian, Y. Li, J. G. Luhmann, C. T. Russell
Solar Physics, November 2012, Volume 281, Issue 1, pp 391-409, [File](#)

The generally low interplanetary magnetic field magnitude around the minimum between Solar Cycles 23 and 24 (SC 23/24 minimum) allows us to identify weak and small solar wind structures. We use observations from near-Earth and twin STEREO spacecraft to study solar wind conditions from January 2007 through December 2010. In addition to 84 clear interplanetary coronal mass ejections (ICMEs), we identified 58 ICME-like transients, which exhibit some classical ICME signatures but have weak magnetic fields (<7 nT) and/or short durations (<10 hours). The number of ICME-like transients peaked during the SC 23/24 minimum, while the ICME rate increased with increasing solar activity. The magnetic structures of flux rope type ICMEs and transients show similar solar cycle variation trends, suggesting that ICMEs and transients originate from similar polarity regions at the Sun. We observed a gradual transition from ICME-like structures to ICMEs. The identified events display continuous distributions in duration and magnetic field magnitude ranging from a few hours to several days and from a few nanoteslas to a few tens of nanoteslas, respectively. Our ICME-like transient rate (less than one event/month) is considerably smaller than that suggested by solar observations of narrow CMEs. This implies that the majority of small coronal ejections are merged as a part of the solar wind by the time they reach 1 AU. We found that ICME-like transients generally occur closer to stream interaction regions (SIRs) than ICMEs, and the majority of the events we identified in declining parts of fast solar wind streams were ICME-like structures. This suggests that ICME-like transients tend to arise close to coronal hole boundaries and thus may have an important role in coronal hole dynamics. Diverse solar wind transients presumably manifest the variation of solar eruptions from small-scale blobs to wide CMEs. [Tables](#).

On the relationship between magnetic cloud field polarity and geoeffectiveness,

[Kilpua](#), E. K. J., Li, Y., Luhmann, J. G., Jian, L. K., and Russell, C. T.:
Ann. Geophys., 30, 1037-1050, 2012

In this paper, we have investigated geoeffectivity of near-Earth magnetic clouds during two periods concentrated around the last two solar minima. The studied magnetic clouds were categorised according to the behaviour of the Z-component of the interplanetary magnetic field (BZ) into bipolar (BZ changes sign) and unipolar (BZ maintains its sign) clouds. The magnetic structure of bipolar clouds followed the solar cycle rule deduced from observations over three previous solar cycles, except during the early rising phase of cycle 24 when both BZ polarities were identified almost with the same frequency. We found a clear difference in the number of unipolar clouds whose axial field points south (S-type) between our two study periods. In particular, it seems that the lack of S-type unipolar clouds contributed to relatively low geomagnetic activity in the early rising phase of cycle 24. We estimated the level of magnetospheric activity using a Dst prediction formula with the measured BZ and by reversing the sign of BZ. We found that bipolar clouds with fields

rotating south-to-north (SN) and north-to-south (NS) were equally geoeffective, but their geoeffectiveness was clearly modified by the ambient solar wind structure. Geoeffectivity of NS-polarity clouds was enhanced when they were followed by a higher-speed solar wind, while the majority of geoeffective SN-polarity clouds lacked the trailing faster wind. A leading shock increased the geoeffectiveness of both NS- and SN-polarity clouds, in particular, in the case of an intense storm. We found that in 1995–1998, SN-polarity clouds were more geoeffective, while in 2006–2011 NS-polarity clouds produced more storms. A considerably larger fraction of events were trailed by a higher-speed solar wind during our latter study period, which presumably increased geoeffectivity of NS-polarity. Thus, our study demonstrates that during low and moderate solar activity, geoeffectivity of opposite polarity bipolar clouds may depend significantly on the surrounding solar wind structure. In addition, different polarities also give different temporal storm evolutions: a storm from an SN-polarity cloud is expected to occur, on average, half-a-day earlier than a storm from an NS-polarity cloud.

Estimating Travel Times of Coronal Mass Ejections to 1 AU Using Multi-spacecraft Coronagraph Data

E. K. J. [Kilpua](#), M. Mierla, L. Rodriguez, A. N. Zhukov, N. Srivastava and M. J. West
Solar Physics, **2012**, Volume 279, Number 2, 477-496

We study the relationship between the speeds of coronal mass ejections (CMEs) obtained close to the Sun and in the interplanetary medium during the low solar-activity period from 2008 to 2010. We use a multi-spacecraft forward-modeling technique to fit a flux-rope-like model to white-light coronagraph images from the STEREO and SOHO spacecraft to estimate the geometrical configuration, propagation in three-dimensions (3D), and the radial speeds of the observed CMEs. The 3D speeds obtained in this way are used in existing CME travel-time prediction models. The results are compared to the actual CME transit times from the Sun to STEREO, ACE, and Wind spacecraft as well as to the transit times calculated using projected CME speeds. CME 3D speeds give slightly better predictions than projected CME speeds, but a large scatter is observed between the predicted and observed travel times, even when 3D speeds are used. We estimate the possible sources of errors and find a weak tendency for large interplanetary CMEs (ICMEs) with high magnetic fields to arrive faster than predicted and small, low-magnetic-field ICMEs to arrive later than predicted. The observed CME transit times from the Sun to 1 AU show a particularly good correlation with the upstream solar-wind speed. Similar trends have not been observed in previous studies using data sets near solar maximum. We suggest that near solar minimum a relatively narrow range of CME initial speeds, sizes, and magnetic-field magnitudes led to a situation where aerodynamic drag between CMEs and ambient solar wind was the primary cause of variations in CME arrival times from the Sun to 1 AU.

Multipoint ICME encounters: Pre-STEREO and STEREO observations

E.K.J. [Kilpua](#), , , L.K. Jianb, Y. Lic, J.G. Luhmannc and C.T. Russellb

Journal of Atmospheric and Solar-Terrestrial Physics, Volume 73, Issue 10, **2011**, Pages 1228-1241

The knowledge of the global properties of interplanetary coronal mass ejections (ICMEs) is of great interest for heliospheric research and space weather forecasting. Due to the large dimensions of ICMEs and the lack of systematic multipoint measurements the true three-dimensional configuration of ICMEs is still poorly understood. The launch of the STEREO twin observatory in October 2006 opened important new opportunities for ICME research. One of the scientific goals of the STEREO mission is to study the large-scale structure of ICMEs. In this paper we [review](#) the multi-spacecraft ICME observations conducted before the STEREO era and discuss the ICME properties that were identified at least by one of the STEREO spacecraft and those at the Lagrangian point L1 (Wind/ACE) from April 2007 through March 2008. The multi-spacecraft observations emphasize that ICMEs cannot be explained in terms of a simple flux rope model. The characteristics of ICMEs and the structure of the solar wind in which they were embedded varied significantly from event to event. The observations show that ICMEs can have cross-sectional shapes from almost circular to significantly distended. In the ecliptic plane ICMEs may span at least up to 40° in longitude, consistent with the angular span of the average CME close to the Sun. However, the association between the ICME observations at different spacecraft is not straightforward as significant differences were observed even when the spacecraft were separated by only a few degrees in longitude. In addition, multipoint observations confirm that the identification of the flux rope structure is modified by the spacecraft crossing distance from the center of the ICME. We show examples of the events where one spacecraft crosses the central flux rope, but the other spacecraft traverses the ICME close to the edge where the flux rope structure is no longer obvious.

Research Highlights

► We examine multi-spacecraft observations of interplanetary coronal mass ejections (ICMEs). ► We review the events during the pre-STEREO era and analyze STEREO observations. ► Observations emphasize that ICMEs cannot be

explained by simple flux rope model. ► ICMEs span at least 40° in longitude and their cross-sectional shapes can vary drastically. ► Flux rope signature depends strongly on the spacecraft crossing distance from the ICME center.

STEREO observations of interplanetary coronal mass ejections and prominence deflection during solar minimum period

E. K. J. **Kilpua**¹, J. Pomoell¹, A. Vourlidas³, R. Vainio¹, J. Luhmann², Y. Li², P. Schroeder², A. B. Galvin⁴, and K. Simunac

Ann. Geophys., 27, 4491-4503, 2009, **File**

www.ann-geophys.net/27/4491/2009/

In this paper we study the occurrence rate and solar origin of interplanetary coronal mass ejections (ICMEs) using data from the two Solar TERrestrial RELation Observatory (STEREO) and the Wind spacecraft. We perform a statistical survey of ICMEs during the late declining phase of solar cycle 23. Observations by multiple, well-separated spacecraft show that even at the time of extremely weak solar activity a considerable number of ICMEs were present in the interplanetary medium. Soon after the beginning of the STEREO science mission in January 2007 the number of ICMEs declined to less than one ICME per month, but in late 2008 the ICME rate clearly increased at each spacecraft although no apparent increase in the number of coronal mass ejections (CMEs) occurred. We suggest that the near-ecliptic ICME rate can increase due to CMEs that have been guided towards the equator from their high-latitude source regions by the magnetic fields in the polar coronal holes.

We consider two case studies to highlight the effects of the polar magnetic fields and CME deflection taking advantage of STEREO observations when the two spacecraft were in the quadrature configuration (i.e. separated by about 90 degrees). We study in detail the solar and interplanetary consequences of two CMEs that both originated from high-latitude source regions on **2 November 2008**. The first CME was slow (radial speed 298 km/s) and associated with a huge polar crown prominence eruption. The CME was guided by polar coronal hole fields to the equator and it produced a clear flux rope ICME in the near-ecliptic solar wind. The second CME (radial speed 438 km/s) originated from an active region 11007 at latitude 35° N. This CME propagated clearly north of the first CME and no interplanetary consequences were identified. The two case studies suggest that slow and elongated CMEs have difficulties overcoming the straining effect of the overlying field and as a consequence they are guided by the polar coronal fields and cause in-situ effects close to the ecliptic plane. The 3-D propagation directions and CME widths obtained by using the forward modelling technique were consistent with the solar and in-situ observations.

Table 1. ICMEs identified from the solar wind measurements by STA (A), STB (B) and Wind (W).

Multispacecraft Observations of Magnetic Clouds and Their Solar Origins between 19 and 23 May 2007

E. K. J. **Kilpua**, P. C. Liewer, C. Farrugia, J. G. Luhmann, C. Möstl, Y. Li, Y. Liu, B. J. Lynch, C. T. Russell, A. Vourlidas, M. H. Acuna, A. B. Galvin, D. Larson, J. A. Sauvaud

Solar Phys (2009) 254: 325–344

We analyze a series of complex interplanetary events and their solar origins that occurred between **19 and 23 May 2007** using observations by the STEREO and *Wind* satellites. The analyses demonstrate the new opportunities offered by the STEREO multispacecraft configuration for diagnosing the structure of *in situ* events and relating them to their solar sources. The investigated period was characterized by two high-speed solar wind streams and magnetic clouds observed in the vicinity of the sector boundary. The observing satellites were separated by a longitudinal distance comparable to the typical radial extent of magnetic clouds at 1 AU (fraction of an AU), and, indeed, clear differences were evident in the records from these spacecraft. Two partial-halo coronal mass ejections (CMEs) were launched from the same active region less than a day apart, the first on 19 May and the second on 20 May 2007. The clear signatures of the magnetic cloud associated with the first CME were observed by STEREO B and *Wind* while only STEREO A recorded clear signatures of the magnetic cloud associated with the latter CME. Both magnetic clouds appeared to have interacted strongly with the ambient solar wind and the data showed evidence that they were a part of the coronal streamer belt. *Wind* and STEREO B also recorded a shocklike disturbance propagating inside a magnetic cloud that compressed the field and plasma at the cloud's trailing portion. The results illustrate how distant multisatellite observations can reveal the complex structure of the extension of the coronal streamer into interplanetary space even during the solar activity minimum.

Electronic Supplementary Material The online version of this article ([10.1007/s11207-008-9300-y](https://doi.org/10.1007/s11207-008-9300-y)) contains supplementary material, which is available to authorized users.

Two-step forecast of geomagnetic storm using coronal mass ejection and solar wind condition†

R.-S. Kim^{1,*}, Y.-J. Moon², N. Gopalswamy³, Y.-D. Park¹ and Y.-H. Kim
Space Weather, Volume 12, Issue 4, pages 246–256, April 2014

To forecast geomagnetic storms we had examined initially-observed parameters of coronal mass ejections (CMEs) and introduced an empirical storm forecast model in a previous study (Kim et al. 2010). Now, we suggest a two-step forecast considering not only CME parameters observed in the solar vicinity, but also solar wind conditions near Earth to improve the forecast capability. We consider the empirical solar wind criteria derived in this study ($B_z \leq -5$ nT or $E_y \geq 3$ mV/m for $t \geq 2$ hr for moderate storms with minimum Dst less than -50 nT) and a Dst model developed by Temerin and Li (TL model, 2002; 2006).

Using 55 CME-Dst pairs during 1997 to 2003, our solar wind criteria produces slightly better forecasts for 31 storm events (90%) than the forecasts based on the TL model (87%). However, the latter produces better forecasts for 24 non-storm events (88%), while the former correctly forecasts only 71% of them.

We then performed the two-step forecast. The results are as follows: i) for 15 events that are incorrectly forecasted using CME parameters, 12 cases (80%) can be properly predicted based on solar wind conditions; ii) if we forecast a storm when both CME and solar wind conditions are satisfied (\cap), the critical success index (CSI) becomes higher than that from the forecast using CME parameters alone, however, only 25 storm events (81%) are correctly forecasted; iii) if we forecast a storm when either set of these conditions is satisfied (\cup), all geomagnetic storms are correctly forecasted.

Propagation Characteristics of CMEs Associated with Magnetic Clouds and Ejecta

R.-S. Kim, N. Gopalswamy, K.-S. Cho, Y.-J. Moon, S. Yashiro
Solar Phys., Volume 284, Issue 1, pp 77-88, 2013, File online first

We have investigated the characteristics of magnetic cloud (MC) and ejecta (EJ) associated coronal mass ejections (CMEs) based on the assumption that all CMEs have a flux rope structure. For this, we used 54 CMEs and their interplanetary counterparts (interplanetary CMEs: ICMEs) that constitute the list of events used by the NASA/LWS Coordinated Data Analysis Workshop (CDAW) on CME flux ropes. We considered the location, angular width, and speed as well as the direction parameter, D . The direction parameter quantifies the degree of asymmetry of the CME shape in coronagraph images, and shows how closely the CME propagation is directed to Earth. For the 54 CDAW events, we found the following properties of the CMEs: i) the average value of D for the 23 MCs (0.62) is larger than that for the 31 EJs (0.49), which indicates that the MC-associated CMEs propagate more directly toward the Earth than the EJ-associated CMEs; ii) comparison between the direction parameter and the source location shows that the majority of the MC-associated CMEs are ejected along the radial direction, while many of the EJ-associated CMEs are ejected non-radially; iii) the mean speed of MC-associated CMEs (946 km s⁻¹) is faster than that of EJ-associated CMEs (771 km s⁻¹). For seven very fast CMEs (≥ 1500 km s⁻¹), all CMEs with large D (≥ 0.4) are associated with MCs and the CMEs with small D are associated with EJs. From the statistical analysis of CME parameters, we found the superiority of the direction parameter. Based on these results, we suggest that the CME trajectory essentially determines the observed ICME structure.

Table List of shock-driving ICMEs during Solar Cycle 23 ($E15^\circ \leq l \leq W15^\circ$).

An Empirical Model for the Prediction of Geomagnetic Storms Using Initially Observed CME Parameters at the Sun

R.-S. Kim, K.S. Cho, Y.-J. Moon, M. Dryer, J. Lee, Y. Yi, K.-H. Kim, H. Wang and Y.-D. Park
BBSO preprint #1439, 2010; JGR VOL. 115, A12108, 9 PP., 2010, File

In this study, we discuss the general behaviors of geomagnetic storm strength associated with observed parameters of coronal mass ejection (CME) such as speed (V) and earthward direction (D) of CMEs and the longitude (L) and magnetic field orientation (M) of over laying potential fields of the CME source region and we develop an empirical model to predict the geomagnetic storm occurrence with its strength (gauged by the Dst index) in terms of these CME parameters. For this we select 66 halo or partial halo CMEs associated with M and X class solar flares, which have clearly identifiable source regions from 1997 to 2003. After examining how each of these CME parameters correlates with the geoeffectiveness of the CMEs, we find several properties as follows: (1) it is the parameter, D , that best correlates with the storm strength, Dst; (2) the majority of geoeffective CMEs have been originated from the solar longitude $W15^\circ$, and CMEs originated away from this longitude tend to produce weaker storms; (3) correlations between Dst and the CME parameters improve if CMEs are separated into two groups depending on whether their magnetic fields are oriented southward or northward in their source regions. Based on these observations, we present two empirical expressions for the Dst in terms of L , V , and D for the two groups of CMEs, respectively. This is a new attempt to predict not only the occurrence of geomagnetic storms but also the storm strength (Dst) solely based on the CME parameters.

CME Earthward Direction as an Important Geoeffectiveness Indicator

R.-S. **Kim**, K.-S. Cho, K.-H. Kim, Y.-D. Park, Y.-J. Moon, Y. Yi, J. Lee, H. Wang, H. Song, and M. Dryer

The Astrophysical Journal, Vol. 677, No. 2: 1378-1384, **2008**.

<http://www.journals.uchicago.edu/doi/pdf/10.1086/528928>

Recently Moon et al.

suggested that the degree of CME asymmetries, as defined by the ratio of the shortest to the longest distances of the CME front measured from the solar center, be used as a parameter for predicting their geoeffectiveness. They called this quantity a direction parameter, D , as it suggests how much CME propagation is directed to Earth, and examined its forecasting capability using 12 fast halo CMEs. In this paper, we extend this test by using a much larger database (486 frontside halo CMEs from 1997 to 2003) and more robust statistical tools (contingency table and statistical parameters).

We compared the forecast capability of this direction parameter to those of other CME parameters, such as location and speed. We found the following results: (1) The CMEs with large direction parameters ($D \geq 0.4$) are highly associated with geomagnetic storms. (2) If the direction parameter increases from 0.4 to 1.0, the geoeffective probability rises from 52% to 84%. (3) All CMEs associated with strong geomagnetic storms ($Dst \leq -200$ nT) are found to have large direction parameters ($D \geq 0.6$). (4) CMEs causing strong geomagnetic storms ($Dst \leq -100$ nT), in spite of their northward magnetic field, have large direction parameters ($D \geq 0.6$). (5) Forecasting capability improves when statistical parameters (e.g., “probability of detection—yes” and “critical success index”) are employed, in comparison with the forecast solely based on the location and speed of CMEs. *These results indicate that the CME direction parameter can be an important indicator for forecasting CME geoeffectiveness.*

Prediction of the 1-AU arrival times of CME-associated interplanetary shocks: Evaluation of an empirical interplanetary shock propagation model

Kim, K.-H.; Moon, Y.-J.; Cho, K.-S.

J. Geophys. Res., Vol. 112, No. A5, A05104, **2007**

<http://dx.doi.org/10.1029/2006JA011904>

(See Comment on “Prediction of the 1-AU arrival times of CME associated interplanetary shocks: Evaluation of an empirical interplanetary shock propagation model” by K.-H. Kim et al.

N. Gopalswamy¹ and H. Xie

JOURNAL OF GEOPHYSICAL RESEARCH, VOL. 113, A10105, doi:10.1029/2008JA013030, **2008**)

Forecast evaluation of the coronal mass ejection (CME) geoeffectiveness using halo CMEs from 1997 to 2003

R.-S. **Kim**, K.-S. Cho,³ Y.-J. Moon,³ Y.-H. Kim,³ Y. Yi,¹ M. Dryer,^{4,5} Su-Chan Bong,³ and Y.-D. Park³

JOURNAL OF GEOPHYSICAL RESEARCH, VOL. 110, A11104, doi:10.1029/2005JA011218, **2005**, File

In this study we have made a forecast evaluation of geoeffective coronal mass ejections (CMEs) by using frontside halo CMEs and the magnetospheric ring current index, Dst . This is the first time, to our knowledge, that an attempt has been made to construct contingency tables depending on the geoeffectiveness criteria as well as to estimate the probability of CME geoeffectiveness depending on CME location and/or speed. For this, we consider 7742 CMEs observed by SOHO/LASCO and select 305 frontside halo CMEs with their locational information from 1997 to 2003 using SOHO/EIT images and GOES data. To select CME-geomagnetic storm ($Dst < -50$ nT) pairs, we adopt a CME propagation model for estimating the arrival time of each CME at the Earth and then choose the nearest Dst minimum value within the window of ± 24 hours. For forecast evaluation, we present contingency tables to estimate statistical parameters such as probability of detection yes (PODy) and false alarm ratio (FAR). We examine the probabilities of CME geoeffectiveness according to their locations, speeds, and their combination. From these studies, we find that (1) the total probability of geoeffectiveness for frontside halo CMEs is 40% (121/305); (2) PODys for the location ($L < 50^\circ$) and the speed (> 400 km s⁻¹) are estimated to be larger than 80% but their FARs are about

60%; (3) the most probable areas (or coverage combinations) whose geoeffectiveness fraction is larger than the mean probability (~40%), are $0_ < L < +30_$ for slower speed CMEs ($< 800 \text{ km s}^{-1}$), and $_{30} < L < +60_$ for faster CMEs ($> 800 \text{ km s}^{-1}$); (4) when the most probable area is adopted as the new criteria, the PODy becomes slightly lower, but all other statistical parameters such as FAR and bias are significantly improved. Our results can give us some criteria to select geoeffective CMEs with the probability of geoeffectiveness depending on the location, speed, and their combination.

Nonlinear Analysis of Radial Evolution of Solar Wind in the Inner Heliosphere

K. Kiran, K. C. Ajithprasad, V. M. Ananda Kumar & K. P. Harikrishnan

Solar Physics volume 296, Article number: 23 (2021)

<https://link.springer.com/content/pdf/10.1007/s11207-021-01761-0.pdf>

We analyzed the radial evolution of solar wind in the inner heliosphere using nonlinear time series tools such as correlation dimension D2D2, correlation entropy K2K2 and multifractal analysis, to get information regarding the inherent nonlinearity associated with the solar wind data and to know how it is affected by the radial distance from the Sun. Our study provides some detailed information regarding the change of dynamics of the fast solar wind with radial distance in the inner heliosphere, apart from confirming the previous observation about the chaotic nature in the dynamics of the slow solar wind. Also we found that the fast wind in the inner heliosphere is dominated by stochastic fluctuations. As the wind is flowing radially away from the Sun, stochastic fluctuation in the fast wind decreases. The stochastic fluctuation present in the data is a clear indication of the Alfvénic fluctuation associated with the solar wind. Finally, our analysis suggests that Alfvénic fluctuation strongly influences the solar wind as it flows radially outwards to mask the nonlinear component associated with the fast wind.

On the Interaction of Galactic Cosmic Rays with Heliospheric Shocks During Forbush Decreases

Anamarija Kirin, Bojan Vršnak, Mateja Dumbović, Bernd Heber

Solar Physics February 2020, 295:28

<https://doi.org/10.1007/s11207-020-1593-5>

<https://arxiv.org/pdf/2002.09454.pdf>

Forbush decreases (FDs) are depletions in the galactic cosmic ray (GCR) count rate that last typically for about a week and can be caused by coronal mass ejections (CMEs) or corotating interacting regions (CIRs). Fast CMEs that drive shocks cause large FDs that often show a two-step decrease where the first step is attributed to the shock/sheath region, while the second step is attributed to the closed magnetic structure. Since the difference in size of shock and sheath region is significant, and since there are observed effects that can be related to shocks and not necessarily to the sheath region we expect that the physical mechanisms governing the interaction with GCRs in these two regions are different. We therefore aim to analyze interaction of GCRs with heliospheric shocks only. We approximate the shock by a structure where the magnetic field linearly changes with position within this structure. We assume protons of different energy, different pitch angle and different incoming direction. We also vary the shock parameters such as the magnetic field strength and orientation, as well as the shock thickness. The results demonstrate that protons with higher energies are less likely to be reflected. Also, thicker shocks and shocks with stronger field reflect protons more efficiently.

Combining STEREO SECCHI COR2 and HI1 images for automatic CME front edge tracking

Vladimir Kirnosov^{1*}, Lin-Ching Chang¹ and Antti Pulkkinen

J. Space Weather Space Clim., 6, A41 (2016)

<http://www.swsc-journal.org/articles/swsc/pdf/2016/01/swsc150079.pdf>

COR2 coronagraph images are the most commonly used data for coronal mass ejection (CME) analysis among the various types of data provided by the STEREO (Solar Terrestrial Relations Observatory) SECCHI (Sun-Earth Connection Coronal and Heliospheric Investigation) suite of instruments. The field of view (FOV) in COR2 images covers 2–15 solar radii (Rs) that allow for tracking the front edge of a CME in its initial stage to forecast the lead-time of a CME and its chances of reaching the Earth. However, estimating the lead-time of a CME using COR2 images gives a larger lead-time, which may be associated with greater uncertainty. To reduce this uncertainty, CME front edge tracking should be continued beyond the FOV of COR2 images. Therefore, heliospheric imager (HI1) data that covers 15–90 Rs FOV must be included. In this paper, we propose a novel automatic method that takes both COR2 and HI1 images into account and combine the results to track the front edges of a CME continuously. The method consists of two modules: pre-processing and tracking. The pre-processing module produces a set of segmented images, which contain the

signature of a CME, for both COR2 and HI1 separately. In addition, the HI1 images are resized and padded, so that the center of the Sun is the central coordinate of the resized HI1 images. The resulting COR2 and HI1 image set is then fed into the tracking module to estimate the position angle (PA) and track the front edge of a CME. The detected front edge is then used to produce a height-time profile that is used to estimate the speed of a CME. The method was validated using 15 CME events observed in the period from January 1, 2008 to August 31, 2009. The results demonstrate that the proposed method is effective for CME front edge tracking in both COR2 and HI1 images. Using this method, the CME front edge can now be tracked automatically and continuously in a much larger range, i.e., from 2 to 90 Rs, for the first time. These improvements can greatly help in making the quantitative CME analysis more accurate and have the potential to assist in space weather forecasting. **2008.04.26-27**

Table 1. The selected CME events used for the validation. 2008.02 – 2009.08

Long-term variations of geomagnetic activity and their solar sources

Kirov, B., Obridko, V. N., Georgieva, K., Nepomnyashtaya, E. V., & Shelting, B. D.

2013, *Geomagnetism and Aeronomy*, 53, 813

Quasi-stationary current sheets of the solar origin in the heliosphere

Roman **Kislov**

EGU2020-466 May **2020**

<https://meetingorganizer.copernicus.org/EGU2020/displays/36057>

The solar magnetic field (SMF) has historically been considered as dipole in order to build models of the radially expanding corona, that is, the solar wind in the solar minimum. The simplified approach suggests the existence of only one quasi-stationary current sheet (QCS) of solar origin in the heliosphere, namely, the heliospheric current sheet (HCS). However, the SMF becomes more complicated over the solar cycle, comprising higher-order components. The overlapping of the dipole and multipole components of the SMF suggests a formation of more than one QCS in the corona, which may expand further to the heliosphere. We study the impact of the quadrupole and octupole harmonics of the SMF on the formation and spatial characteristics of QCSs, building a stationary axisymmetric MHD model of QCSs in the heliosphere. It is shown that if the dipole component dominates, a single QCS appears in the solar wind at low heliolatitudes as the classic HCS. In other cases, the number of QCSs varies from one to three, depending on the relative input of the quadrupole and octupole components. QCSs possess a conic form and may occur at a wide variety of heliolatitudes. The existence of QCSs opens wide opportunities for explanations of puzzling observations of cosmic rays and energetic particles in the heliosphere and, at the same time, raises a risk of misinterpretation of in situ crossings of QCSs because of mixing up the HCS and higher-heliolatitude QCSs, which can be significantly disturbed in the dynamical solar wind.

Quasi-stationary Current Sheets of the Solar Origin in the Heliosphere

Roman A. **Kislov**^{1,2}, Olga V. Khabarova², and Helmi V. Malova^{1,3}

2019 *ApJ* 875 28

[sci-hub.se/10.3847/1538-4357/ab0dff](https://doi.org/10.3847/1538-4357/ab0dff)

The solar magnetic field (SMF) has historically been considered as dipole in order to build models of the radially expanding corona, that is, the solar wind in the solar minimum. The simplified approach suggests the existence of only one quasi-stationary current sheet (QCS) of solar origin in the heliosphere, namely, the heliospheric current sheet (HCS). However, the SMF becomes more complicated over the solar cycle, comprising higher-order components. The overlapping of the dipole and multipole components of the SMF suggests a formation of more than one QCS in the corona, which may expand further to the heliosphere. We study the impact of the quadrupole and octupole harmonics of the SMF on the formation and spatial characteristics of QCSs, building a stationary axisymmetric MHD model of QCSs in the heliosphere. It is shown that if the dipole component dominates, a single QCS appears in the solar wind at low heliolatitudes as the classic HCS. In other cases, the number of QCSs varies from one to three, depending on the relative input of the quadrupole and octupole components. QCSs possess a conic form and may occur at a wide variety of heliolatitudes. The existence of QCSs opens wide opportunities for explanations of puzzling observations of cosmic rays and energetic particles in the heliosphere and, at the same time, raises a risk of misinterpretation of in situ crossings of QCSs because of mixing up the HCS and higher-heliolatitude QCSs, which can be significantly disturbed in the dynamical solar wind.

A new stationary analytical model of the heliospheric current sheet and the plasma sheet

Roman A. **Kislov**, Olga V. Khabarova, Helmi V. Malova

We develop a single-fluid 2-D analytical model of the axially symmetric thin heliospheric current sheet (HCS) embedded into the heliospheric plasma sheet (HPS). A HCS-HPS system has a shape of a relatively thin plasma disk limited by separatrices that also represent current sheets, which is in agreement with Ulysses observations in the aphelion, when it crossed the HCS perpendicular to its plane. Our model employs a differential rotation of the solar photosphere that leads to unipolar induction in the corona. Three components of the interplanetary magnetic field (IMF), the solar wind speed, and the thermal pressure are taken into account. Solar corona conditions and a HCS-HPS system state are tied by boundary conditions and the “frozen-in” equation. The model allows finding spatial distributions of the magnetic field, the speed within the HPS, and electric currents within the HCS. An angular plasma speed is low within the HPS due to the angular momentum conservation (there is no significant corotation with the Sun), which is consistent with observations. We found that the HPS thickness L decreases with distance r , becoming a constant far from the Sun ($L \sim 2.5$ solar radii (R_0) at 1 AU). Above the separatrices and at large heliocentric distances, the solar wind behavior obeys Parker's model, but the magnetic field spiral form may be different from Parker's one inside the HPS. At $r \leq 245 R_0$, the IMF spiral may undergo a turn simultaneously with a change of the poloidal current direction (from sunward to antisunward).

4pi Models of CMEs and ICMEs **A Review**

Jens **Kleimann**

E-print, 11 Apr 2012, **File**; Solar Phys.

Coronal mass ejections (CMEs), which dynamically connect the solar surface to the far reaches of interplanetary space, represent a major manifestation of solar activity. They are not only of principal interest but also play a pivotal role in the context of space weather predictions. The steady improvement of both numerical methods and computational resources during recent years has allowed for the creation of increasingly realistic models of interplanetary CMEs (ICMEs), which can now be compared to high-quality observational data from various space-bound missions. This review discusses existing models of CMEs, characterizing them by scientific aim and scope, CME initiation method, and physical effects included, thereby stressing the importance of fully 3-D ('4pi') spatial coverage.

Timelines as a tool for learning about space weather storms

Delores J. **Knipp**^{1,2*}, Valerie Bernstein¹, Kaiya Wahl³ and Hisashi Hayakawa^{4,5,6}

J. Space Weather Space Clim. 2021, 11, 29

<https://www.swsc-journal.org/articles/swsc/pdf/2021/01/swsc200106.pdf>

<https://doi.org/10.1051/swsc/2021011>

Space weather storms typically have solar, interplanetary, geophysical and societal-effect components that overlap in time, making it hard for students and novices to determine cause-and-effect relationships and relative timing. To address this issue, we use timelines to provide context for space weather storms of different intensities. First, we present a timeline and tabular description for the great auroral storms of the last 500 years as an example for space climate. The graphical summary for these 14 events suggests that they occur about every 40–60 years, although the distribution of such events is far from even. One outstanding event in **1770** may qualify as a one-in-500-year auroral event, based on duration. Additionally, we present two examples that describe space weather storms using solar, geospace and effects categories. The first of these is for the prolonged storm sequence of late **January 1938** that produced low-latitude auroras and space weather impacts on mature technology (telegraphs) and on high frequency radio communication for aviation, which was a developing technology. To illustrate storm effects in the space-age, we produce a detailed timeline for the strong **December 2006** geomagnetic storm that impacted numerous space-based technologies for monitoring space weather and for communication and navigation. During this event there were numerous navigation system disturbances and hardware disruptions. We adopt terminology developed in many previous space weather studies and blend it with historical accounts to create graphical timelines to help organize and disentangle the events presented herein.

The May 1967 Great Storm and Radio Disruption Event:

Extreme Space Weather and Extraordinary Responses

D. J. **Knipp**^{1,2}, A. C. Ramsay³, E. D. Beard³, A. L. Boright³, W. B. Cade⁴, I. M. Hewins⁵,

R. McFadden⁵, W. F. Denig⁶, L. M. Kilcommons¹, M. A. Shea⁷ and D. F. Smart⁷

Space Weather 2016 doi: 10.1002/2016SW001423 **File**

<https://agupubs.onlinelibrary.wiley.com/doi/epdf/10.1002/2016SW001423>

Although listed as one of the most significant events of the last 80 years, the space weather storm of late May 1967 has been of mostly fading academic interest. The storm made its initial mark with a colossal solar radio burst causing radio

interference at frequencies between 0.01-9.0 GHz and near-simultaneous disruptions of dayside radio communication by intense fluxes of ionizing solar X-rays. Aspects of military control and communication were immediately challenged. Within hours a solar energetic particle event disrupted high frequency communication in the polar cap. Subsequently record-setting geomagnetic and ionospheric storms compounded the disruptions. We explain how the May 1967 storm was nearly one with ultimate societal impact, were it not for the nascent efforts of the United States Air Force in expanding its terrestrial weather monitoring-analysis-warning-prediction efforts into the realm of space weather forecasting. An important and long-lasting outcome of this storm was more formal Department of Defense support for current-day space weather forecasting. This story develops during the rapid rise of solar cycle 20 and the intense Cold War in the latter half of the 20th Century. We detail the events of late May 1967 in the intersecting categories of solar-terrestrial interactions and the political-military backdrop of the Cold War. This was one of the —Great Storms|| of the 20th century, despite the lack of large geomagnetically-induced currents. Radio disruptions like those discussed here warrant the attention of today's radio-reliant, cellular-phone and satellite-navigation enabled world. **May 23 1967**

Advances in Space Weather Ensemble Forecasting

Knipp, Delores J.

Space Weather, Volume 14, Issue 2, pp. 52-53, **2016** DOI: 10.1002/2016SW001366

At many space weather-related meetings I hear that space weather (SW) forecasting is several decades behind terrestrial weather forecasting. Some attribute the lag to the dearth of space environment observations. Occasionally, the relative youth of our science and the corresponding lack of sophistication in forecasting methodologies are mentioned. Ours will always be the “younger science.” Nonetheless, our community is making significant progress in the latter category, especially with respect to “ensemble forecasting.”

Waves and Magnetism in the Solar Atmosphere (WAMIS)

Yuan-Kuen **Ko**^{1*}, John D. Moses², John M. Laming¹, 1, Samuel Tun Beltran¹, Steven Tomczyk³, et al.

Front. Astron. Space Sci., **3**, 1. **2016**

sci-hub.se/10.3389/fspas.2016.00001

Comprehensive measurements of magnetic fields in the solar corona have a long history as an important scientific goal. Besides being crucial to understanding coronal structures and the Sun's generation of space weather, direct measurements of their strength and direction are also crucial steps in understanding observed wave motions. In this regard, the remote sensing instrumentation used to make coronal magnetic field measurements is well suited to measuring the Doppler signature of waves in the solar structures. In this paper, we describe the design and scientific values of the Waves and Magnetism in the Solar Atmosphere (WAMIS) investigation. WAMIS, taking advantage of greatly improved infrared filters and detectors, forward models, advanced diagnostic tools and inversion codes, is a long-duration high-altitude balloon payload designed to obtain a breakthrough in the measurement of coronal magnetic fields and in advancing the understanding of the interaction of these fields with space plasmas. It consists of a 20 cm aperture coronagraph with a visible-IR spectro-polarimeter focal plane assembly. The balloon altitude would provide minimum sky background and atmospheric scattering at the wavelengths in which these observations are made. It would also enable continuous measurements of the strength and direction of coronal magnetic fields without interruptions from the day-night cycle and weather. These measurements will be made over a large field-of-view allowing one to distinguish the magnetic signatures of different coronal structures, and at the spatial and temporal resolutions required to address outstanding problems in coronal physics. Additionally, WAMIS could obtain near simultaneous observations of the electron scattered K-corona for context and to obtain the electron density. These comprehensive observations are not provided by any current single ground-based or space observatory. The fundamental advancements achieved by the near-space observations of WAMIS on coronal field would point the way for future ground based and orbital instrumentation.

ANATOMY OF DEPLETED INTERPLANETARY CORONAL MASS EJECTIONS

M. **Kocher**, S. T. Lepri, E. Landi, L. Zhao, and W. B. Manchester IV

2017 ApJ 834 147

We report a subset of interplanetary coronal mass ejections (ICMEs) containing distinct periods of anomalous heavy-ion charge state composition and peculiar ion thermal properties measured by ACE/SWICS from 1998 to 2011. We label them “depleted ICMEs,” identified by the presence of intervals where C6+/C5+ and O7+/O6+ depart from the direct correlation expected after their freeze-in heights. These anomalous intervals within the depleted ICMEs are referred to

as "Depletion Regions." We find that a depleted ICME would be indistinguishable from all other ICMEs in the absence of the Depletion Region, which has the defining property of significantly low abundances of fully charged species of helium, carbon, oxygen, and nitrogen. Similar anomalies in the slow solar wind were discussed by Zhao et al. We explore two possibilities for the source of the Depletion Region associated with magnetic reconnection in the tail of a CME, using CME simulations of the evolution of two Earth-bound CMEs described by Manchester et al.

Successive interacting coronal mass ejections: How to create a perfect storm?

Gordon J. **Koehn**, [Ravindra T. Desai](#), [Emma E. Davies](#), [Robert J. Forsyth](#), [Jonathan P. Eastwood](#), [Stefaan Poedts](#)

ApJ **941** 139 **2022**

<https://arxiv.org/pdf/2211.05899.pdf>

<https://iopscience.iop.org/article/10.3847/1538-4357/aca28c/pdf>

Coronal mass ejections (CMEs) are the largest type of eruptions on the Sun and the main driver of severe space weather at the Earth. In this study, we implement a force-free spheromak CME description within 3-D magnetohydrodynamic simulations to parametrically evaluate successive interacting CMEs within a representative heliosphere. We explore CME-CME interactions for a range of orientations, launch time variations and CME handedness and quantify their geoeffectiveness via the primary solar wind variables and empirical measures of the disturbance storm time index and subsolar magnetopause standoff distance. We show how the interaction of two moderate CMEs between the Sun and the Earth can translate into extreme conditions at the Earth and how CME-CME interactions at different radial distances can maximise different solar wind variables that induce different geophysical impacts. In particular, we demonstrate how the orientation and handedness of a given CME can have a significant impact on the conservation and loss of magnetic flux, and consequently Bz, due to magnetic reconnection with the interplanetary magnetic field. This study thus implicates identification of CME chirality in the solar corona as an early diagnostic for forecasting geomagnetic storms involving multiple CMEs. **13-14 July 2012.**

PUNCH: Polarimeter to UNify the Corona and Heliosphere

Kolinski, Don ; [Deforest, Craig](#) ; [Gibson, Sarah](#) ; [Morrow, Cherilynn](#) ; [Colaninno, Robin](#) ; et al.

The Third Triennial Earth-Sun Summit (TESS), held 8-11 August, **2022** in Bellevue/Seattle, WA. Bulletin of the AAS, Volume 54, Issue 7, article id. 2022n7i125p22

<https://baas.aas.org/pub/2022n7i125p22/release/1>

PUNCH is a NASA Small Explorer mission to better understand how the mass and energy of the Sun's corona become the solar wind that fills the solar system. The mission consists of a constellation of four small satellites in Sun-synchronous, low Earth orbit that together will produce deep-field, continuous, 3D images of the solar corona as it makes a transition to the young solar wind from the outermost solar atmosphere to the inner heliosphere. PUNCH's science goal is to comprehend cross-scale physical processes of heliophysics, from micro scale turbulence to the evolution of global scale structures. There are six science objectives that span the quiescent and dynamic young solar wind, which will be achieved by activities of six working groups. Through a series of workshops, PUNCH has been engaging the broader solar and heliospheric community to develop tools in anticipation of the data and to grow a broad community of PUNCH users to realize its maximum benefit. An undergraduate student collaboration to search for X-ray signatures of coronal heating mechanisms includes development of another instrument, the Student Thermal Energetic Activity Module (STEAM). Moreover, PUNCH engages interested heliophysicists in a mission-embedded outreach program with an Ancient & Modern Sun Watching theme that is collaborating with underserved and underrepresented populations and connecting to the broader public in the US Southwest and beyond. PUNCH is scheduled to launch in April of 2025. See our website (<https://punch.spaceops.swri.org>) for more information.

Magnetosheath jet occurrence rate in relation to CMEs and SIRs

Florian **Koller**, Manuela Temmer, Luis Preisser, Ferdinand Plaschke, Paul Geyer, Lan K Jian, Owen Wyn Roberts, Heli Hietala, Adrian T. LaMoury

JGR **Volume127, Issue4** e2021JA030124 **2022**

<https://www.essoar.org/doi/abs/10.1002/essoar.10508761.2>

<https://doi.org/10.1029/2021JA030124>

<https://agupubs.onlinelibrary.wiley.com/doi/epdf/10.1029/2021JA030124>

Magnetosheath jets constitute a significant coupling effect between the solar wind (SW) and the magnetosphere of the Earth. In order to investigate the effects and forecasting of these jets, we present the first-ever statistical study of the jet production during large-scale SW structures like coronal mass ejections (CMEs), stream interaction regions (SIRs) and high speed streams (HSSs). Magnetosheath data from Time History of Events and Macroscale Interactions during

Substorms (THEMIS) spacecraft between January 2008 to December 2020 serve as measurement source for jet detection. Two different jet definitions were used to rule out statistical biases induced by our jet detection method. For the CME and SIR+HSS lists, we used lists provided by literature and expanded on incomplete lists using OMNI data to cover the time range of May 1996 to December 2020. We find that the number and total time of observed jets decrease when CME-sheaths hit the Earth. The number of jets is lower throughout the passing of the CME-magnetic ejecta (ME) and recovers quickly afterwards. On the other hand, the number of jets increases during SIR and HSS phases. We discuss a few possibilities to explain these statistical results. **6 Feb 2013, 15 Feb 2013, 19-31 Jul 2016**

Suprathermal Electron Acceleration by a Quasi-perpendicular Shock: Simulations and Observations

F.-J. Kong and G. Qin

2020 ApJ 896 20

<https://sci-hub.tw/https://iopscience.iop.org/article/10.3847/1538-4357/ab8e32>

The acceleration of suprathermal electrons in the solar wind is mainly associated with shocks driven by interplanetary coronal mass ejections (ICMEs). It is well known that the acceleration of electrons is much more efficient at quasi-perpendicular shocks than at quasi-parallel ones. Yang et al. studied the acceleration of suprathermal electrons with observations at a quasi-perpendicular ICME-driven shock event to claim the important role of shock-drift acceleration (SDA). Here, we perform test-particle simulations to study the acceleration of electrons in this event, by calculating the downstream electron intensity distribution for all energy channels assuming an initial distribution based on the average upstream intensities. Using simulations, we obtain the results similar to the observations from Yang et al. as follows. It is shown that the ratio of downstream to upstream intensities peaks at about 90° pitch angle. In addition, in each pitch angle direction the downstream electron energy spectral index is much larger than the theoretical index of diffusive shock acceleration. Furthermore, the estimated drift length is proportional to the electron energy but the drift time is almost energy independent. Finally, we use a theoretical model based on SDA to describe the drift length and drift time especially, to explain their energy dependence. These results indicate the importance of SDA in the acceleration of electrons by quasi-perpendicular shocks.

An Anisotropic Density Turbulence Model from the Sun to 1 au Derived From Radio Observations

Eduard P. Kontar, A. Gordon Emslie, Daniel L. Clarkson, Xingyao Chen, Nicolina Chrysaphi, Francesco Azzollini, Natasha L. S. Jeffrey, Mykola Gordovskyy

ApJ 2023

<https://arxiv.org/pdf/2308.05839.pdf>

Solar radio bursts are strongly affected by radio-wave scattering on density inhomogeneities, changing their observed time characteristics, sizes, and positions. The same turbulence causes angular broadening and scintillation of galactic and extra-galactic compact radio sources observed through the solar atmosphere. Using large-scale simulations of radio-wave transport, the characteristics of anisotropic density turbulence from $0.1R_\odot$ to 1 au are explored. For the first time, a profile of heliospheric density fluctuations is deduced that accounts for the properties of extra-solar radio sources, solar radio bursts, and in-situ density fluctuation measurements in the solar wind at 1 au. The radial profile of the spectrum-weighted mean wavenumber of density fluctuations (a quantity proportional to the scattering rate of radio-waves) is found to have a broad maximum at around $(4-7)R_\odot$, where the slow solar wind becomes supersonic. The level of density fluctuations at the inner scale (which is consistent with the proton resonance scale) decreases with heliocentric distance as $\langle \delta n^2 \rangle(r) \approx 2 \times 10^7 (r/R_\odot - 1)^{-3.7} \text{ cm}^{-6}$. Due to scattering, the apparent positions of solar burst sources observed at frequencies between 0.1 and 300 MHz are computed to be essentially co-spatial and to have comparable sizes, for both fundamental and harmonic emission. Anisotropic scattering is found to account for the shortest solar radio burst decay times observed, and the required wavenumber anisotropy is $q_{\parallel}/q_{\perp} = 0.25-0.4$, depending on whether fundamental or harmonic emission is involved. The deduced radio-wave scattering rate paves the way to quantify intrinsic solar radio burst characteristics.

Modern Faraday Rotation Studies to Probe the Solar Wind

Jason Kooi, David Wexler, Elizabeth Jensen, Megan Kenny, Teresa Nieves-Chinchilla, Lynn Wilson III, Brian Wood, Lan Jian, Shing Fung, Alexei Pevtsov, Nat Gopalswamy, and Ward Manchester

Front. Astron. Space Sci., 9:841866. 2022 |

<https://doi.org/10.3389/fspas.2022.841866>

<https://www.frontiersin.org/articles/10.3389/fspas.2022.841866/full>
<https://www.frontiersin.org/articles/10.3389/fspas.2022.841866/pdf>

For decades, observations of Faraday rotation have provided unique insights into the plasma density and magnetic field structure of the solar wind. Faraday rotation (FR) is the rotation of the plane of polarization when linearly polarized radiation propagates through a magnetized plasma, such as the solar corona, coronal mass ejection (CME), or stream interaction region. FR measurements are very versatile: they provide a deeper understanding of the large-scale coronal magnetic field over a range of heliocentric distances (especially $\approx 1.5 \approx 1.5$ to $20 R_{\odot}$) not typically accessible to in situ spacecraft observations; detection of small-timescale variations in FR can provide information on magnetic field fluctuations and magnetohydrodynamic wave activity; and measurement of differential FR can be used to detect electric currents. FR depends on the integrated product of the plasma density and the magnetic field component along the line of sight to the observer; historically, models have been used to distinguish between their contributions to FR. In the last two decades, though, new methods have been developed to complement FR observations with independent measurements of the plasma density based on the choice of background radio source: calculation of the dispersion measure (pulsars), measurement of Thomson scattering brightness (radio galaxies), and application of radio ranging and apparent-Doppler tracking (spacecraft). New methods and new technology now make it possible for FR observations of solar wind structures to return not only the magnitude of the magnetic field, but also the full vector orientation. In the case of a CME, discerning the internal magnetic flux rope structure is critical for space weather applications. **2003 October 28 , 2011 August 17 , 2012 August 2, 2013 May 10, 2015 July 31, 2015 August 21,**

Cosmic-Ray Transport in Heliospheric Magnetic Structures. III. Implications of Solar Magnetograms for the Drifts of Cosmic Rays

Andreas **Kopp**^{1,2}, Jan Louis Raath², Horst Fichtner^{1,3}, Marius S. Potgieter⁴, Stefan E. S. Ferreira², and Bernd Heber⁴

2021 ApJ 922 124

<https://doi.org/10.3847/1538-4357/ac23e0>

The transport of energetic particles in the heliosphere is reviewed regarding the treatment of their drifts over an entire solar cycle including the periods around solar maximum, when the tilt angles of the heliospheric current sheet increase to large values and the sign of the magnetic polarity changes. While gradient and curvature drifts are well-established elements of the propagation of cosmic rays in the heliospheric magnetic field, their perturbation by the solar-activity-induced large-scale distortions of dipole-like field configurations and by magnetic turbulence is an open problem. Various empirical or phenomenological approaches have been suggested, but either lack a theory-based motivation or have been shown to be incompatible with measurements. We propose a new approach of more closely investigating solar magnetograms obtained from GONG maps, leading to a new definition of (i) tilt angles that may exceed those provided by the Wilcox Solar Observatory during high activity and of (ii) a "noninteger sign" that can be used to reduce the drifts during these periods as well as to provide a refinement of the magnetic field polarity. The change of sign from $A < 0$ to $A > 0$ of solar cycle 24 can be in this way localized to occur between Carrington Rotations 2139 and 2140 in mid 2013. This treatment is fully consistent in the sense that the transport modeling uses the same input data to formulate the boundary conditions at the heliobase as do the magnetohydrodynamic models of the solar wind and the embedded heliospheric magnetic field that exploit solar magnetograms as inner boundary conditions.

Source and Propagation of a Streamer Blowout Coronal Mass Ejection Observed by the Parker Solar Probe

Kelly E. **Korreck**, Adam Szabo, Teresa Nieves Chinchilla, Benoit Lavraud, Janet Luhmann, Tatiana Niembro,

2020 ApJS 246 69

<https://sci-hub.si/https://iopscience.iop.org/article/10.3847/1538-4365/ab6ff9>

In the first orbit of the Parker Solar Probe (PSP), in situ thermal plasma and magnetic field measurements were collected as close as 35 R Sun from the Sun, an environment that had not been previously explored. During the first orbit of PSP, the spacecraft flew through a streamer blowout coronal mass ejection (SBO-CME) on **2018 November 11** at 23:50 UT as it exited the science encounter. The SBO-CME on November 11 was directed away from the Earth and was not visible by L1 or Earth-based telescopes due to this geometric configuration. However, PSP and the STEREO - A spacecraft were able to make observations of this slow ($v \approx 380 \text{ km s}^{-1}$) SBO-CME. Using the PSP data, STEREO - A images, and Wang–Sheeley–Arge model, the source region of the CME is found to be a helmet streamer formed between the northern polar coronal hole and a mid-latitude coronal hole. Using the YGUAZU-A model, the propagation of the CME is traced from the source at the Sun to PSP. This model predicts the travel time of the flux rope to the PSP spacecraft as 30 hr, which is within 0.33 hr of the actual measured arrival time. The in situ Solar Wind Electrons

Alphas and Protons data were examined to determine that no shock was associated with this SBO-CME. Modeling of the SBO-CME shows that no shock was present at PSP; however, at other positions along the SBO-CME front, a shock could have formed. The geometry of the event requires in situ and remote sensing observations to characterize the SBO-CME and further understand its role in space weather.

Physics of Space Storms: From the Solar Surface to the Earth

Hannu **Koskinen**

Read online:

<http://www.springerlink.com/content/978-3-642-00310-3/#section=845487&page=1&locus=49>

This **book** can be interpreted to consist of three parts. The long Chapter 1 forms the first part. It contains a phenomenological introduction to the scene, from the Sun to the Earth, where space weather plays are performed. A reader familiar with basic physics of the Sun, solar wind, magnetosphere and ionosphere can jump over this chapter and only return to it when there is a need to check definitions or concepts introduced there. The second part of the book consists of several chapters on fundamental space plasma physics. While this part is written in a self-consistent way, it is aimed at readers who already have been exposed to basic plasma physics. Chapter 2 briefly introduces the fundamental concepts and tools of plasma physics inherited from both electrodynamics and statistical physics. Chapter 3 reviews the classical guiding center approach to single particle motion and adiabatic invariants, including motion in the dipole field, near a current sheet, and in a time-dependent electric field.

GEOEFFECTIVITY OF CORONAL MASS EJECTIONS

H. E. J. **KOSKINEN**^{1,*} and K. E. J. **HUTTUNEN**[†]

Space Science Reviews (2006) 124: 169–181, **File**

Coronal mass ejections and post-shock streams driven by them are the most efficient drivers of strong magnetospheric activity, magnetic storms. For this reason there is considerable interest in trying to make reliable forecasts for the effects of CMEs as much in advance as possible. To succeed this requires understanding of all aspects related to CMEs, starting from their emergence on the Sun to their propagation to the vicinity of the Earth and to effects within the magnetosphere. In this article we discuss some recent results on the geoeffectivity of different types of CME/shock structures. A particularly intriguing observation is that smoothly rotating magnetic fields within CMEs are most efficient in driving storm activity seen in the inner magnetosphere due to enhanced ring current, whereas the sheath regions between the shock and the ejecta tend to favour high-latitude activity.

Behaviour of 27-Day and 13.5-Day Periodicities in Galactic Cosmic Particles as Observed by Spacecraft and Neutron Monitors During Different Solar Polarity Cycles

Pieter **Kotzé**

Solar Physics 298, Article number: 107 (2023)

<https://link.springer.com/content/pdf/10.1007/s11207-023-02203-9.pdf>

An analysis has been made of the behaviour of the 27-day and 13.5-day periodicities in proton, C, and O galactic-cosmic-ray (GCR) particles at different energies as observed by the Advanced Composition Explorer (ACE) and SOHO (Solar and Heliospheric Observatory) spacecraft during both Solar Cycles 23 and 24. In addition, the behaviour of the 27-day and 13.5-day periods in the solar-wind-modulation parameter $\zeta = \text{BIMF} \times \text{VSW}$ has been investigated during the same time interval to determine the existence of a possible solar-polarity dependence. Ground-based neutron-monitor (NM) observations, corresponding to different rigidity cutoff [RC] parameters, were also studied to determine the temporal behaviour of both the 27-day and 13.5-day periods during Cycles 23 and 24, revealing a statistically significant solar-polarity correlation. The Lomb–Scargle periodogram technique has been employed to extract spectral information from the above-mentioned observations for each individual year from 2001 – 2009 (Cycle 23) and 2010 – 2019 (Cycle 24). Daily mean energetic ACE and SOHO particle measurements are used to identify how both the 27-day and 13.5-day periodicities vary during each individual year during these cycles as a function of particle mean energy. This spectral analysis of proton, C, and O galactic-cosmic-particle data at different energies revealed that both the 27-day and 13.5-day periods are stronger during the minimum of Solar Cycle 24/25 when $A > 0$ (solar dipole pointing North) in comparison to the minimum of Cycle 23/24 when $A < 0$ (solar dipole pointing South) at certain energy levels. This showed a particularly strong energy-dependent behaviour for both periodicities. This article reports for the first time an annual time- and energy-dependent behaviour of both the 27-day and 13.5-day periodicities in daily-mean galactic cosmic particles observed by spacecraft and ground-based neutron monitors during consecutive Solar Cycles 23 and 24,

corresponding to opposite solar-magnetic-field orientations. Periodicity behaviour in heliospheric solar-wind data corroborate these results in general.

Spectral Analysis of Rieger Periodicity Behaviour in O and Fe Galactic Cosmic Particles Observed by ACE in Solar Cycles 23 and 24

Pieter **Kotzé**

[Solar Physics](#) volume 296, Article number: 177 (2021)

<https://link.springer.com/content/pdf/10.1007/s11207-021-01925-y.pdf>

<https://doi.org/10.1007/s11207-021-01925-y>

The behaviour of the Rieger periodicity at 152 – 156 days in O and Fe galactic cosmic ray (GCR) particles, at different energies as observed by the Advanced Composition Explorer (ACE) satellite, has been studied. Energetic particle data between 2000 and 2019 have been analysed using the Lomb-Scargle periodogram and Morlet wavelet spectral analysis techniques. Daily mean energetic particle measurements are used to identify how the Rieger periodicity varies in each individual year as a function of the mean particle energy. In particular, spectral analysis of galactic cosmic particle data at different energies revealed that the Rieger period occurs exceptionally strong during Solar Cycle 23 when $A < 0$ (solar dipole pointing south) compared to Cycle 24 when $A > 0$ (solar dipole pointing north). This article reports for the first time the time-dependence of the Rieger (152 – 156 days) periodicity in O and Fe GCR particles at various energies ranging from ≈ 70 MeV/n to ≈ 471 MeV/n.

Variation Spectra and Anisotropy of Cosmic Rays during Forbush Effects in March 2023

Kovalev, II ; Kravtsova, MV ; Olemskoy, SV ; Sdobnov, VE

COSMIC RESEARCH Volume 62 Issue 6 Page 533-539 2024

DOI 10.1134/S001095252460032X

Based on ground-based observations of cosmic rays (CRs) on the global network of neutron monitors, the Yakutsk complex of muon telescopes, and the URAGAN muon hodoscope (Moscow), the spectra of CR variations and anisotropy during the Forbush effects of **March 15 and 23, 2023** were calculated using the spectrographic global survey method. It is shown that the spectrum of CR variations during these periods is not described by a power function in a wide range of rigidities. It was found that the Earth was in a loop-shaped structure of the interplanetary magnetic field on March 15 and that it entered a magnetic cloud with closed field lines on March 23.

Spectra and Anisotropy of Cosmic Rays during GLE64.

Kovalev, I.I., Kravtsova, M.V., Olemskoy, S.V. et al.

Geomagn. Aeron. 64, 44–48 (2024).

<https://doi.org/10.1134/S0016793223600893>

Ground-based observations of cosmic rays by the spectrographic global survey method were used to study the ground-level enhancement in cosmic ray intensity on **August 24, 2002**. Spectra of variations of primary cosmic rays and their anisotropy were obtained. Based on measurements from the GOES spacecraft and global network of cosmic ray stations, the differential rigidity spectra of accelerated particles in the vicinity of the Sun were calculated. The maximum rigidity to which solar particles were accelerated was estimated.

Assessment of the near-Sun magnetic field of the 10 March 2022 coronal mass ejection observed by Solar Orbiter

Shifana **Koya**, [Spiros Patsourakos](#), [Manolis K. Georgoulis](#), [Alexander Nindos](#)

A&A 2024

<https://arxiv.org/pdf/2408.01142>

Aims. We estimate the near-Sun axial magnetic field of a coronal mass ejection (CME) on **10 March 2022**. Solar Orbiter's in situ measurements, 7.8 degrees east of the Sun-Earth line at 0.43 AU, provided a unique vantage point, along with the WIND measurements at 0.99 AU. We determine a single power-law index from near-Sun to L1, including in situ measurements from both vantage points. **Methods.** We tracked the temporal evolution of the instantaneous relative magnetic helicity of the source active region (AR), NOAA AR 12962. By estimating the helicity budget of the pre-and post-eruption AR, we estimated the helicity transported to the CME. Assuming a Lundquist flux-rope model and geometrical parameters obtained through the graduated cylindrical shell (GCS) CME forward modelling, we determined the CME axial magnetic field at a GCS-fitted height. Assuming a power-law variation of the axial magnetic field with heliocentric distance, we extrapolated the estimated near-Sun axial magnetic field to in situ measurements at 0.43 AU and 0.99 AU. **Results.** The net helicity difference between the post-and pre-eruption AR is

$(-7.1 \pm 1.2) \times 1041 \text{ Mx}^2$, which is assumed to be bodily transported to the CME. The estimated CME axial magnetic field at a near-Sun heliocentric distance of 0.03 AU is 2067 ± 405 nT. From 0.03 AU to L1, a single power-law falloff, including both vantage points at 0.43 AU and 0.99 AU, gives an index -1.23 ± 0.18 . Conclusions. We observed a significant decrease in the pre-eruptive AR helicity budget. Extending previous studies on innerheliospheric intervals from 0.3 AU to ~ 1 AU, referring to estimates from 0.03 AU to measurements at ~ 1 AU. Our findings indicate a less steep decline in the magnetic field strength with distance compared to previous studies, but they align with studies that include near-Sun in situ magnetic field measurements, such as from Parker Solar Probe.

Cosmic ray north-south anisotropy: rigidity spectrum and solar cycle variations observed by ground-based muon detectors

M. Kozai, Y. Hayashi, K. Fujii, K. Munakata, C. Kato, N. Miyashita, A. Kadokura, R. Kataoka, S. Miyake, M.L. Duldig, J.E. Humble, K. Iwai

ApJ 977 160 2024

<https://arxiv.org/pdf/2409.03182>

<https://iopscience.iop.org/article/10.3847/1538-4357/ad8577/pdf>

The north-south (NS) anisotropy of galactic cosmic rays (GCRs) is dominated by a diamagnetic drift flow of GCRs in the interplanetary magnetic field (IMF), allowing us to derive key parameters of cosmic-ray propagation, such as the density gradient and diffusion coefficient. We propose a new method to analyze the rigidity spectrum of GCR anisotropy and reveal a solar cycle variation of the NS anisotropy's spectrum using ground-based muon detectors in Nagoya, Japan, and Hobart, Australia. The physics-based correction method for the atmospheric temperature effect on muons is used to combine the different-site detectors free from local atmospheric effects. NS channel pairs in the multi-directional muon detectors are formed to enhance sensitivity to the NS anisotropy, and in this process, general graph matching in graph theory is introduced to survey optimized pairs. Moreover, Bayesian estimation with the Gaussian process allows us to unfold the rigidity spectrum without supposing any analytical function for the spectral shape. Thanks to these novel approaches, it has been discovered that the rigidity spectrum of the NS anisotropy is dynamically varying with solar activity every year. It is attributed to a rigidity-dependent variation of the radial density gradient of GCRs based on the nature of the diamagnetic drift in the IMF. The diffusion coefficient and mean-free-path length of GCRs as functions of the rigidity are also derived from the diffusion-convection flow balance. This analysis expands the estimation limit of the mean-free-path length into ≤ 200 GV rigidity region from < 10 GV region achieved by solar energetic particle observations.

Average spatial distribution of cosmic rays behind the interplanetary shock -Global Muon Detector Network observations-

M. Kozai, K. Munakata, C. Kato, T. Kuwabara, M. Rockenbach, A. Dal Lago, N. J. Schuch, C. R. Braga, R. R. S. Mendonça, H. K. Al Jassar, M. M. Sharma, M. L. Duldig, J. E. Humble, P. Evenson, I. Sabbah, M. Tokumaru

ApJ 825 100 2016

<http://arxiv.org/pdf/1605.06591v1.pdf>

We analyze the galactic cosmic ray (GCR) density and its spatial gradient in Forbush Decreases (FDs) observed with the Global Muon Detector Network (GMDN) and neutron monitors (NMs). By superposing the GCR density and density gradient observed in FDs following 45 interplanetary shocks (IP-shocks), each associated with an identified eruption on the sun, we infer the average spatial distribution of GCRs behind IP-shocks. We find two distinct modulations of GCR density in FDs, one in the magnetic sheath and the other in the coronal mass ejection (CME) behind the sheath. The density modulation in the sheath is dominant in the western flank of the shock, while the modulation in the CME ejecta stands out in the eastern flank. This east-west asymmetry is more prominent in GMDN data responding to ~ 60 GV GCRs than in NM data responding to ~ 10 GV GCRs, because of softer rigidity spectrum of the modulation in the CME ejecta than in the sheath. The GSE-y component of the density gradient, G_y shows a negative (positive) enhancement in FDs caused by the eastern (western) eruptions, while G_z shows a negative (positive) enhancement in FDs by the northern (southern) eruptions. This implies the GCR density minimum being located behind the central flank of IP-shock and propagating radially outward from location of the solar eruption. We also confirmed the average G_z changing its sign above and below the heliospheric current sheet, in accord with the prediction of the drift model for the large-scale GCR transport in the heliosphere. **2006 Dec 14, 2012 Jun 16, 2013 Apr 13**

Table 1. List of SSC events associated with solar eruptions

Solar filament impact on 21 January 2005: Geospace consequences

J. U. [Kozyra](#)^{1,*}, M. W. Liemohn¹, C. Cattell², D. De Zeeuw¹, C. P. Escoubet³, D. S. Evans⁴, X. Fang⁵, M.-C. Fok⁶, H. U. Frey⁷, W. D. Gonzalez⁸, M. Hairston⁹, R. Heelis⁹, G. Lu¹⁰, W. B. Manchester IV¹, S. Mende⁷, L. J. Paxton¹¹, L. Rastaetter¹², A. Ridley¹, M. Sandanger¹³, F. Soraas¹³, T. Sotirelis¹¹, M. W. Thomsen¹⁴, B. T. Tsurutani¹⁵ and O. Verkhoglyadova

JGR, Volume 119, Issue 7, pages 5401–5448, July 2014

On **21 January 2005**, a moderate magnetic storm produced a number of anomalous features, some seen more typically during superstorms. The aim of this study is to establish the differences in the space environment from what we expect (and normally observe) for a storm of this intensity, which make it behave in some ways like a superstorm. The storm was driven by one of the fastest interplanetary coronal mass ejections in solar cycle 23, containing a piece of the dense erupting solar filament material. The momentum of the massive solar filament caused it to push its way through the flux rope as the interplanetary coronal mass ejection decelerated moving toward 1 AU creating the appearance of an eroded flux rope (see companion paper by Manchester et al. (2014)) and, in this case, limiting the intensity of the resulting geomagnetic storm. On impact, the solar filament further disrupted the partial ring current shielding in existence at the time, creating a brief superfountain in the equatorial ionosphere—an unusual occurrence for a moderate storm. Within 1 h after impact, a cold dense plasma sheet (CDPS) formed out of the filament material. As the interplanetary magnetic field (IMF) rotated from obliquely to more purely northward, the magnetotail transformed from an open to a closed configuration and the CDPS evolved from warmer to cooler temperatures. Plasma sheet densities reached tens per cubic centimeter along the flanks—high enough to inflate the magnetotail in the simulation under northward IMF conditions despite the cool temperatures. Observational evidence for this stretching was provided by a corresponding expansion and intensification of both the auroral oval and ring current precipitation zones linked to magnetotail stretching by field line curvature scattering. Strong Joule heating in the cusps, a by-product of the CDPS formation process, contributed to an equatorward neutral wind surge that reached low latitudes within 1–2 h and intensified the equatorial ionization anomaly. Understanding the geospace consequences of extremes in density and pressure is important because some of the largest and most damaging space weather events ever observed contained similar intervals of dense solar material.

Earth's collision with a solar filament on 21 January 2005: Overview†

J. U. [Kozyra](#)^{1,*}, W. B. Manchester IV, ¹, C. P. Escoubet², S. T. Lepri, ¹, M. W. Liemohn, ¹, W. D. Gonzalez³, M. W. Thomsen, ⁴, B. T. Tsurutani

JGR, 2013

On **21 January 2005**, one of the fastest interplanetary coronal mass ejections (ICME) of solar cycle 23, containing exceptionally dense plasma directly behind the sheath, hit the magnetosphere. We show from charge-state analysis that this material was a piece of the erupting solar filament, and further, based on comparisons to the simulation of a fast CME, that the unusual location of the filament material was a consequence of three processes. As the ICME decelerated, the momentum of the dense filament material caused it to push through the flux rope towards the nose. Diverging non-radial flows in front of the filament moved magnetic flux to the sides of the ICME. At the same time reconnection between the leading edge of the ICME and the sheath magnetic fields worked to peel away the outer layers of the flux rope creating a remnant flux rope and a trailing region of newly opened magnetic field lines. These processes combined to move the filament material into direct contact with the ICME sheath region. Within one hour after impact and under northward IMF conditions, a cold dense plasma sheet formed within the magnetosphere from the filament material. Dense plasma sheet material continued to move through the magnetosphere for more than 6 hours as the filament passed by the Earth. Densities were high enough to produce strong diamagnetic stretching of the magnetotail despite the northward IMF conditions and low levels of magnetic activity. The disruptions from the filament collision are linked to an array of unusual features throughout the magnetosphere, ionosphere and atmosphere. These results raise questions about whether rare collisions with solar filaments may, under the right conditions, be a factor in producing even more extreme events.

Flux Rope Model of the 2003 October 28-30 Coronal Mass Ejection and Interplanetary Coronal Mass Ejection

[Krall](#), J.; Yurchyshyn, V. B.; Slinker, S.; Skoug, R. M.; Chen, J.

Astrophysical Journal, 642:541–553, 2006

the erupting flux rope (EFR) model (Chen and Garren 1993; Chen 1996; Krall,

Chen, and Santoro 2000) was able to reproduce many details of the CME/ICME event on October 28-30, 2003.

Ion kinetics of plasma interchange reconnection in the lower solar corona

Vladimir [Krasnoselskikh](#) (1,2), [Arnaud Zaslavsky](#) (3), [Anton Artemyev](#) (4), [Clara Froment](#) (1), [Thierry Dudok de Wit](#) (1,5), [Nour E. Raouafi](#) (6), [Oleksiy V. Agapitov](#) (2), [Stuart D. Bale](#) (2, 7), [Jaye L. Verniero](#) (8)
ApJ **959** 15 **2023**

<https://arxiv.org/pdf/2310.12093.pdf>

<https://iopscience.iop.org/article/10.3847/1538-4357/ad046b/pdf>

The exploration of the inner heliosphere by Parker Solar Probe has revealed a highly structured solar wind with ubiquitous deflections from the Parker spiral, known as switchbacks. Interchange reconnection (IR) may play an important role in generating these switchbacks by forming unstable particle distributions that generate wave activity that in turn may evolve to such structures. IR occurs in very low beta plasmas and in the presence of strong guiding fields. Although IR is unlikely to release enough energy to provide an important contribution to the heating and acceleration of the solar wind, it affects the way the solar wind is connected to its sources, connecting open field lines to regions of closed fields. This "switching on" provides a mechanism by which plasma near coronal hole boundaries can mix with that trapped inside the closed loops. This mixing can lead to a new energy balance. It may significantly change the characteristics of the solar wind because this plasma is already pre-heated and can potentially have quite different density and particle distributions. It not only replenishes the solar wind, but also affects the electric field, which in turn affects the energy balance. This interpenetration is manifested by the formation of a bimodal ion distribution, with a core and a beam-like population. Such distributions are indeed frequently observed by the Parker Solar Probe. Here we provide a first step towards assessing the role of such processes in accelerating and heating the solar wind.

Localized magnetic field structures and their boundaries in the near-Sun solar wind from Parker Solar Probe measurements

V. [Krasnoselskikh](#) (1 and 2), [A. Larosa](#) (1), [O. Agapitov](#) (2), [T. Dudok de Wit](#) (1), [M. Moncuquet](#) (3), [F. S. Mozer](#) (2 and 4), [M. Stevens](#) (5), [S. D. Bale](#) (2 and 4 and 6 and 7), [J. Bonnell](#) (2), [C. Froment](#) (1), [K. Goetz](#) (8), [K. Goodrich](#) (2), [P. Harvey](#) (2), [J. Kasper](#) (5 and 9), [R. MacDowall](#) (10), [D. Malaspina](#) (11), [M. Pulupa](#) (2), [N. Raouafi](#) (12), [C. Revillet](#) (1), [M. Velli](#) (13), [J. Wygant](#) (8)

ApJS **893** 93 **2020**

<https://arxiv.org/pdf/2003.05409.pdf>

<https://doi.org/10.3847/1538-4357/ab7f2d>

One of the discoveries made by Parker Solar Probe during first encounters with the Sun is the ubiquitous presence of relatively small-scale structures standing out as sudden deflections of the magnetic field. They were called switchbacks as some of them show up the full reversal of the radial component of the magnetic field and then return to regular conditions. Analyzing the magnetic field and plasma perturbations associated with switchbacks we identify three types of structures with slightly different characteristics: 1. Alfvénic structures, where the variations of the magnetic field components take place while the magnitude of the field remains constant; 2. Compressional, the field magnitude varies together with changes of the components; 3. Structures manifesting full reversal of the magnetic field (extremal class of Alfvénic structures). Processing of structures boundaries and plasma bulk velocity perturbations lead to the conclusion that they represent localized magnetic field tubes with enhanced parallel plasma velocity and ion beta moving together with respect to surrounding plasma. The magnetic field deflections before and after the switchbacks reveal the existence of total axial current. The electric currents are concentrated on the relatively narrow boundary layers on the surface of the tubes and determine the magnetic field perturbations inside the tube. These currents are closed on the structure surface, and typically have comparable azimuthal and the axial components. The surface of the structure may also accommodate an electromagnetic wave, that assists to particles in carrying currents. We suggest that the two types of structures we analyzed here may represent the local manifestations of the tube deformations corresponding to a saturated stage of the Firehose instability development.

Thermosphere and geomagnetic response to interplanetary coronal mass ejections observed by ACE and GRACE: Statistical results

S. [Krauss](#), M. Temmer, A.M. Veronig, O. Baur, H. Lammer

JGR **2015**

<http://arxiv.org/pdf/1510.03549v1.pdf>

For the period July 2003 to August 2010, the interplanetary coronal mass ejection (ICME) catalogue maintained by Richardson and Cane lists 106 Earth-directed events, which have been measured in-situ by plasma and field instruments onboard the ACE satellite. We present a statistical investigation of the Earth's thermospheric neutral density response by

means of accelerometer measurements collected by the GRACE satellites, which are available for 104 ICMEs in the data set, and its relation to various geomagnetic indices and characteristic ICME parameters such as the impact speed, southward magnetic field strength (B_z). The majority of ICMEs causes a distinct density enhancement in the thermosphere, with up to a factor of eight compared to the pre-event level. We find high correlations between ICME B_z and thermospheric density enhancements (~ 0.9), while the correlation with the ICME impact speed is somewhat smaller (~ 0.7). The geomagnetic indices revealing the highest correlations are Dst and SYM-H (~ 0.9), the lowest correlations are obtained for k_p and AE (~ 0.7), which show a nonlinear relation with the thermospheric density enhancements. Separating the response for the shock sheath region and the magnetic structure of the ICME, we find that the Dst and SYM-H reveal a tighter relation to the B_z minimum in the magnetic structure of the ICME, whereas the polar cap indices show higher correlations with the B_z minimum in the shock sheath region. Since the strength of the B_z component - either in the sheath or the magnetic structure of the ICME - is highly correlated (~ 0.9) with the neutral density enhancement, we discuss the possibility of satellite orbital decay estimates based on magnetic field measurements at L1, i.e. before the ICME hits the Earth's magnetosphere. This will further stimulate progress in space weather understanding and applications regarding satellite operations.

Solar energetic particle cutoff variations during the 29-31 October 2003 geomagnetic storm

Kress, B. T.; Mertens, C. J.; Wiltberger, M.
Space Weather, Vol. 8, No. 5, S05001, 2010

<http://dx.doi.org/10.1029/2009SW000488>

At low latitudes to midlatitudes the Earth's magnetic field usually shields the upper atmosphere and spacecraft in low Earth orbit from solar energetic particles (SEPs). During severe geomagnetic storms, distortion of the Earth's field suppresses geomagnetic shielding, allowing SEPs access to the midlatitudes. A case study of the 26–31 October 2003 solar-geomagnetic event is used to examine how a severe geomagnetic storm affects SEP access to the Earth. Geomagnetic cutoffs are numerically determined in model geomagnetic fields using code developed by the Center for Integrated Space Weather Modeling (CISM) at Dartmouth College. The CISM-Dartmouth geomagnetic cutoff model is being used in conjunction with the High Energy and Charge Transport code (HZETRN) at the NASA Langley Research Center to develop a real-time data-driven prediction of radiation exposure at commercial airline altitudes. In this work, cutoff rigidities are computed on global grids and along several high-latitude flight routes before and during the geomagnetic storm. It is found that significant variations in SEP access to the midlatitudes and high latitudes can occur on time scales of an hour or less in response to changes in the solar wind dynamic pressure and interplanetary magnetic field. The maximum suppression of the cutoff is ~ 1 GV occurring in the midlatitudes during the main phase of the storm. The cutoff is also significantly suppressed by the arrival of an interplanetary shock. The maximum suppression of the cutoff due to the shock is approximately one half of the maximum suppression during the main phase of the storm.

Density Fluctuations in the Solar Wind Based on Type III Radio Bursts Observed by Parker Solar Probe

Vratislav **Krupar**, [Adam Szabo](#), [Milan Maksimovic](#), [Oksana Kruparova](#), [Eduard P. Kontar](#), [Laura A. Balmaceda](#), [Xavier Bonnin](#), [Stuart D. Bale](#), [Marc Pulupa](#), [David M. Malaspina](#), [John W. Bonnell](#), [Peter R. Harvey](#), [Keith Goetz](#), [Thierry Dudok de Wit](#), [Robert J. MacDowall](#), [Justin C. Kasper](#), [Anthony W. Case](#), [Kelly E. Korreck](#), [Davin E. Larson](#), [Roberto Livi](#), [Michael L. Stevens](#), [Phyllis L. Whittlesey](#), [Alexander M. Hegedus](#)

ApJS 2020

<https://arxiv.org/pdf/2001.03476.pdf>

Radio waves are strongly scattered in the solar wind, so that their apparent sources seem to be considerably larger and shifted than the actual ones. Since the scattering depends on the spectrum of density turbulence, better understanding of the radio wave propagation provides indirect information on the relative density fluctuations $\epsilon = \langle \delta n \rangle / \langle n \rangle$ at the effective turbulence scale length. Here, we have analyzed 30 type III bursts detected by Parker Solar Probe (PSP). For the first time, we have retrieved type III burst decay times τ_d between 1 MHz and 10 MHz thanks to an unparalleled temporal resolution of PSP. We observed a significant deviation in a power-law slope for frequencies above 1 MHz when compared to previous measurements below 1 MHz by the twin-spacecraft Solar TERrestrial RELations Observatory (STEREO) mission. We note that altitudes of radio bursts generated at 1 MHz roughly coincide with an expected location of the Alfvén point, where the solar wind becomes super-Alfvénic. By comparing PSP observations and Monte Carlo simulations, we predict relative density fluctuations ϵ at the effective turbulence scale length at radial distances between $2.5R_\odot$ and $14R_\odot$ to range from 0.22 and 0.09. Finally, we calculated relative density fluctuations ϵ measured

in situ by PSP at a radial distance from the Sun of $35.7 \sim R_{\odot}$ during the perihelion \#1, and the perihelion \#2 to be 0.07 and 0.06, respectively. It is in a very good agreement with previous STEREO predictions ($\epsilon=0.06-0.07$) obtained by remote measurements of radio sources generated at this radial distance. **2019 April 1–10; 2019-04-03 Table 1.** The list of type III burst time-frequency intervals

Statistical Survey of Coronal Mass Ejections and Interplanetary Type II Bursts

V. **Krupar**^{1,2,3}, J. Magdalenic⁴, J. P. Eastwood⁵, N. Gopalswamy², O. Kruparova³, A. Szabo², and F. Neme^c

2019 ApJ 882 92

<https://iopscience.iop.org/article/10.3847/1538-4357/ab3345/pdf>

Coronal mass ejections (CMEs) are responsible for most severe space weather events, such as solar energetic particle events and geomagnetic storms at Earth. Type II radio bursts are slow drifting emissions produced by beams of suprathermal electrons accelerated at CME-driven shock waves propagating through the corona and interplanetary medium. Here, we report a statistical study of 153 interplanetary type II radio bursts observed by the two STEREO spacecraft between 2008 March and 2014 August. The shock associated radio emission was compared with CME parameters included in the Heliospheric Cataloguing, Analysis and Techniques Service catalog. We found that faster CMEs are statistically more likely to be associated with the interplanetary type II radio bursts. We correlate frequency drifts of interplanetary type II bursts with white-light observations to localize radio sources with respect to CMEs. Our results suggest that interplanetary type II bursts are more likely to have a source region situated closer to CME flanks than CME leading edge regions. **2012 October 22**

AN ANALYSIS OF INTERPLANETARY SOLAR RADIO EMISSIONS ASSOCIATED WITH A CORONAL MASS EJECTION

V. **Krupar**^{1,2}, J. P. Eastwood¹, O. Kruparova², O. Santolik^{2,3}, J. Soucek², J. Magdalenic⁴, A. Vourlidas⁵, M. Maksimovic⁶, X. Bonnin⁶, V. Bothmer⁷, N. Mrotzek⁷, A. Pluta⁷, D. Barnes⁸, J. A. Davies⁸, J. C. Martínez Oliveros⁹, and S. D. Bale^{9,10}

2016 ApJ 823 L5

Coronal mass ejections (CMEs) are large-scale eruptions of magnetized plasma that may cause severe geomagnetic storms if Earth directed. Here, we report a rare instance with comprehensive in situ and remote sensing observations of a CME combining white-light, radio, and plasma measurements from four different vantage points. For the first time, we have successfully applied a radio direction-finding technique to an interplanetary type II burst detected by two identical widely separated radio receivers. The derived locations of the type II and type III bursts are in general agreement with the white-light CME reconstruction. We find that the radio emission arises from the flanks of the CME and are most likely associated with the CME-driven shock. Our work demonstrates the complementarity between radio triangulation and 3D reconstruction techniques for space weather applications.

Quasi-thermal Noise Spectroscopy Analysis of Parker Solar Probe Data: Improved Electron Density Model for Solar Wind

Oksana **Kruparova**^{1,2}, Vratislav Krupar^{1,2}, Adam Szabo², Marc Pulupa³, and Stuart D. Bale^{3,4}

2023 ApJ 957 13

<https://iopscience.iop.org/article/10.3847/1538-4357/acf572/pdf>

We present a comprehensive analysis of electron density measurements in the solar wind using quasi-thermal noise (QTN) spectroscopy applied to data from the first 15 encounters of the Parker Solar Probe mission (2018 November–2023 March). Our methodology involves the identification of the plasma line frequency and the calculation of plasma density based on in situ measurements. By analyzing over 2.1 million data points, we derive a power-law model for electron density as a function of radial distance from the Sun in the range of 13 to $50 R_{\odot}$: $n_e(r) = (343,466 \pm 19921) \times r^{(-1.87 \pm 0.11)}$. This model provides improved estimates for localizing interplanetary solar radio bursts. Moreover, obtained electron densities can be used for calibrating particle instruments on board the Parker Solar Probe. We discuss its limitations and potential for further refinement with additional Parker Solar Probe encounters.

Average characteristics of high-energy magnetospheric electron flux enhancements and the parameters of near-Earth and interplanetary medium in 1987–2021

O N Kryakunova, A V Belov, A F Yakovets, A A Abunin, I L Tsepakina, B B Seifullina, M A Abunina, N F Nikolayevskiy, N S Shlyk, A B Andreyev

MNRAS Volume 516, Issue 4, November 2022, Pages 4782–4791,

<https://doi.org/10.1093/mnras/stac2382>

Based on the data of 35-yr (1987–2021) measurements of magnetospheric electron fluxes with energy >2 MeV in geostationary orbits, solar wind speed, and geomagnetic activity, a catalogue of electron flux enhancements was compiled in which the electron fluence exceeds $108 \text{ cm}^{-2} \text{ sr}^{-1} \text{ d}^{-1}$. The epoch superposition method performed using the GOES-13 spacecraft data shows that large electron flux enhancements are preceded by a significant increase in the solar wind velocity and the Ap index of geomagnetic activity, and immediately before the increase the relativistic electron flux decreases. For the events of the catalogue, the average characteristics of electron flux enhancements and parameters of the interplanetary and near-Earth medium were calculated: the mean values of the diurnal and total fluxes during an event and the average duration of electron enhancements. The average duration of the electron flux enhancement is 5 d, and the maximum duration is 24 d. Based on the calculated mean values of the electron fluxes, solar wind velocity, and Ap-index of geomagnetic activity on the day of electron enhancement and on previous days, a typical behaviour of these parameters during and before an electron flux enhancement was obtained. The average characteristics of electron flux enhancements and the parameters of interplanetary and near-Earth medium are calculated before large electron flux enhancements, when the fluence exceeds 3×10^8 , 5×10^8 , and 10^9 particles $\text{cm}^{-2} \text{ sr}^{-1} \text{ d}^{-1}$, respectively. It is shown that the greater the increase in solar wind velocity and geomagnetic activity the larger the subsequent electron flux enhancement.

Recurrent and sporadic Forbush-effects in deep solar minimum

O Kryakunova¹, A Belov², A Abunin², M Abunina², E Eroshenko², A Malimbayev¹, I Tsepakina¹, V Yanke

Journal of Physics: Conference Series 632 (2015) 012062

<http://spaceweather.izmiran.ru/papers/kryakunova2015.pdf>

The effects of high-speed solar wind streams from low-latitude coronal holes and coronal mass ejections (CMEs) on cosmic ray intensity in 2007 are studied. The database on Forbush effects created at IZMIRAN, with cosmic ray density and anisotropy calculated by the Global Survey Method (GSM) on the basis of Neutron Monitor network data has been used. The behaviour of the mean characteristics by all the Forbush-effects in 2007 caused by coronal holes (interplanetary magnetic field intensity and solar wind velocity, 10 GV cosmic ray density and equatorial component of the cosmic ray anisotropy) is calculated by the epoch method. Features of the Forbush-effects caused by high-speed solar wind streams from lowlatitude coronal holes and coronal mass ejections are described.

Influence of high-speed streams from coronal holes on cosmic ray intensity in 2007

O Kryakunova, I Tsepakina, N Nikolayevskiy, A Malimbayev, A Belov, A Abunin, M Abunina, E Eroshenko, V Oleneva, V Yanke

ECRS-2012, sh_526.

In this work we study the effect of high-speed solar wind streams from low-latitude coronal holes on cosmic ray intensity. We used Forbush effect database created at IZMIRAN with calculations of the cosmic ray density and anisotropy performed by the Global Survey Method (GSM) using Neutron Monitor network data for the entire 2007. The essential growths of the solar wind plasma density and interplanetary magnetic field intensity are observed before arrival of high-speed solar wind streams from low-latitude coronal holes. From the analysis of events in 2007 we found that relationship of the Forbush effect magnitude and solar wind speed is much weaker than with the magnitude of the interplanetary magnetic field. One of the typical signs of the impact of high-speed streams from coronal holes on cosmic ray intensity is a gradual onset of the Forbush effect. As a rule, the direction of the equatorial vector component of anisotropy changed before the Forbush effect.

Prediction of Geomagnetic Storm Strength from Inner Heliospheric In Situ Observations

M. Kubicka, C. Möstl, T. Amerstorfer, P. D. Boakes, L. Feng, J. P. Eastwood, O. Tormanen

2016 ApJ 833 255

<https://arxiv.org/pdf/1610.06713v1.pdf>

Prediction of the effects of coronal mass ejections (CMEs) on Earth strongly depends on knowledge of the interplanetary magnetic field southward component, Bz. Predicting the strength and duration of Bz inside a CME with sufficient

accuracy is currently impossible, which forms the so-called Bz problem. Here, we provide a proof-of-concept of a new method for predicting the CME arrival time, speed, Bz and the resulting Dst index at Earth based only on magnetic field data, measured in situ in the inner heliosphere (< 1AU). On **2012 June 12-16**, three approximately Earthward-directed and interacting CMEs were observed by the STEREO imagers, and by Venus Express (VEX) in situ at 0.72 AU, 6 degree away from the Sun Earth line. The CME kinematics are calculated using the drag-based and WSA-Enlil models, constrained by the arrival time at VEX, resulting in the CME arrival time and speed at Earth. The CME magnetic field strength is scaled with a power law from VEX to Wind. Our investigation shows promising results for the Dst forecast (predicted: -96 and -114 nT (from 2 Dst models), observed: -71 nT), for the arrival speed (predicted: 531 +- 23 km s⁻¹, observed: 488 +- 30 km s⁻¹) and timing (6 +- 1 hours after actual arrival time). The prediction lead time is 21 hours. The method may be applied to vector magnetic field data from a spacecraft at an artificial Lagrange point between the Sun and Earth, or to data taken by any spacecraft temporarily crossing the Sun--Earth line.

Observations of a comet tail disruption induced by the passage of a CME

Kuchar, T. A.; Buffington, A.; Arge, C. N.; Hick, P. P.; Howard, T. A.; Jackson, B. V.; Johnston, J. C.; Mizuno, D. R.; Tappin, S. J.; Webb, D. F.

Journal of Geophysical Research: Space Physics, Volume 113, Issue A4, CiteID A04101, **2008**

The Solar Mass Ejection Imager observed an extremely faint interplanetary coronal mass ejection (ICME) as it passed Comet C/2001 Q4 (NEAT) on 5 May 2004, apparently causing a disruption of its plasma tail. This is the first time that an ICME has been directly observed interacting with a comet. SMEI's nearly all-sky coverage and image cadence afforded unprecedented coverage of this rarely observed event. The onset first appeared as a "kink" moving antisunward that eventually developed knots within the disturbed tail. These knots appeared to be swept up in the solar wind flow. We present the SMEI observations as well as identify a likely SOHO/LASCO progenitor of the CME. SMEI observed two other comets (C/2002 T7 [LINEAR] and C/2004 F4 [Bradfield]) and at least five similar events during a 35-d period encompassing this observation. Although these had similar morphologies to the 5 May NEAT event, SMEI did not observe any ICMEs in these cases. Three of these were observed close to the heliospheric current sheet indicating that a magnetic boundary crossing may have contributed to the disruptions. However, there are no discernable causes in the SMEI observations for the remaining two events.

Variability of Low Energy Cosmic Rays Near Earth

A Review

Karel **Kudela**

In: Exploring the Solar Wind, Ed. Marian Lazar, **2012**, File

<http://www.intechopen.com/books/exploring-the-solar-wind>

On The Influence Of The Solar Wind On The Propagation Of Earth-impacting Coronal Mass Ejections

Sandeep **Kumar**, [Nandita Srivastava](#), [Nat Gopalswamy](#), [Ashutosh Dash](#)

ApJ **977** 57 **2024**

<https://arxiv.org/pdf/2411.01165>

<https://iopscience.iop.org/article/10.3847/1538-4357/ad8e63/pdf>

Coronal Mass Ejections (CMEs) are subject to changes in their direction of propagation, tilt, and other properties as they interact with the variable solar wind. We investigated the heliospheric propagation of 15 Earth-impacting CMEs observed during April 2010 to August 2018 in the field of view (FOV) of the Heliospheric Imager (HI) onboard the STEREO. About half of the 15 events followed self-similar expansion up to 40 R_☉. The remaining events showed deflection either in latitude, longitude, or a tilt change. Only two events showed significant rotation in the HI1 FOV. We also use toroidal and cylindrical flux rope fitting on the in situ observations of interplanetary magnetic field (IMF) and solar wind parameters to estimate the tilt at L1 for these two events. Although the sample size is small, this study suggests that CME rotation is not very common in the heliosphere. We attributed the observed deflections and rotations of CMEs to a combination of factors, including their interaction with the ambient solar wind and the influence of the ambient magnetic field. These findings contribute to our understanding of the complex dynamics involved in CME propagation and highlight the need for comprehensive modeling and observational studies to improve space weather prediction. In particular, HI observations help us to connect observations near the Sun and near Earth, improving our understanding of how CMEs move through the heliosphere. **May 23, 2010, September 7, 2011, May 23-27, 2017, Table 1.** List of 15 Earth-impacting events selected for our study 2010-2018

Rotation of a Stealth CME on 2012 October 5 Observed in the Inner Heliosphere

Sandeep Kumar, [Dinesha V. Hegde](#), [Nandita Srivastava](#), [Nikolai V. Pogorelov](#), [Nat Gopalswamy](#), [Seiji Yashiro](#)

ApJ **958** 103 **2023**

<https://arxiv.org/pdf/2310.04023.pdf>

<https://iopscience.iop.org/article/10.3847/1538-4357/ad011f/pdf>

Coronal Mass Ejections (CMEs) are subject to changes in their direction of propagation, tilt, and other properties. This is because CMEs interact with the ambient solar wind and other large-scale magnetic field structures. In this work, we report on the observations of the **2012 October 5** stealth CME using coronagraphic and heliospheric images. We find clear evidence of a continuous rotation of the CME, i.e., an increase in the tilt angle, estimated using the Graduated Cylindrical Shell (GCS) reconstruction at different heliocentric distances, up to 58 solar radii. We find a further increase in the tilt at L1 estimated from the toroidal and cylindrical flux rope fitting on the in situ observations of IMF and solar wind parameters. This study highlights the importance of observations of Heliospheric Imager (HI), onboard the Solar TERrestrial RELations Observatory (STEREO). In particular, the GCS reconstruction of CMEs in HI field-of-view promises to bridge the gap between the near-Sun and in-situ observations at the L1. The changes in the CME tilt has significant implications for the space weather impact of stealth CMEs.

New Evidence on the Origin of Solar Wind Microstreams/Switchbacks

Pankaj Kumar, [Judith T. Karpen](#), [Vadim M. Uritsky](#), [Craig E. Deforest](#), [Nour E. Raouafi](#), [C. Richard DeVore](#), [Spiro K. Antiochos](#)

ApJL **951** L15 **2023**

<https://arxiv.org/pdf/2305.06914.pdf>

<https://iopscience.iop.org/article/10.3847/2041-8213/acd54e/pdf>

Microstreams are fluctuations in the solar wind speed and density associated with polarity-reversing folds in the magnetic field (also denoted switchbacks). Despite their long heritage, the origin of these microstreams/switchbacks remains poorly understood. For the first time, we investigated periodicities in microstreams during Parker Solar Probe (PSP) Encounter 10 to understand their origin. Our analysis was focused on the inbound corotation interval on **2021 November 19-21**, while the spacecraft dove toward a small area within a coronal hole (CH). Solar Dynamics Observatory remote-sensing observations provide rich context for understanding the PSP in-situ data. Extreme ultraviolet images from the Atmospheric Imaging Assembly reveal numerous recurrent jets occurring within the region that was magnetically connected to PSP during intervals that contained microstreams. The periods derived from the fluctuating radial velocities in the microstreams (approximately 3, 5, 10, and 20 minutes) are consistent with the periods measured in the emission intensity of the jetlets at the base of the CH plumes, as well as in larger coronal jets and in the plume fine structures. Helioseismic and Magnetic Imager magnetograms reveal the presence of myriad embedded bipoles, which are known sources of reconnection-driven jets on all scales. Simultaneous enhancements in the PSP proton flux and ionic (3He, 4He, Fe, O) composition during the microstreams further support the connection with jetlets and jets. In keeping with prior observational and numerical studies of impulsive coronal activity, we conclude that quasiperiodic jets generated by interchange/breakout reconnection at CH bright points and plume bases are the most likely sources of the microstreams/switchbacks observed in the solar wind.

A parametric study of performance of two solar wind velocity forecasting models during 2006 to 2011

Sandeep Kumar, [Nandita Srivastava](#)

Space Weather e2022SW003069 [Volume20, Issue9](#) **2022**

<https://doi.org/10.1029/2022SW003069>

<https://agupubs.onlinelibrary.wiley.com/doi/epdf/10.1029/2022SW003069>

There is an increasing need for the development of a robust space weather forecasting framework. State-of-the-art MHD space weather forecasting frameworks are based upon the Potential Field Source Surface and Schatten Current Sheet extrapolation models for the magnetic field using synoptic magnetograms. These models create a solar wind background for the simulations using empirical relations of Wang, Sheeley and Arge, at the inner boundary of heliosphere and have been used to simulate CMEs for specific cases in previous studies. Besides these MHD frameworks, the Heliospheric Upwind eXtrapolation technique can extrapolate solar wind from inner heliospheric boundaries to L1 and can give a reliable estimate of the solar wind velocity at L1 comparable to MHD models but in a short computational time. We carried out an extensive parametric study of the performance of the Model1 and Model2 for solar wind velocity prediction at L1. We implemented this framework on 60 Carrington Rotations from CR2047 to CR2107 during 2006 to 2011, covering the descending and deep minimum phase of solar cycle (SC) 23, and the ascending phase of SC 24. Our results show an unexpected decrease in the performance of the framework during the deep minimum phase of cycle 23,

which is attributed to the decrease in the observed coronal hole area. As SC 24 began, this decreasing trend vanished due to an increase in the coronal hole area at the low and mid-latitudes, suggesting a correlation between the performance of the framework and the variation in the coronal hole area.

A comparison study of extrapolation models and empirical relations in forecasting solar wind

Sandeep Kumar, Arghyadeep Paul, Bhargav Vaidya

Frontiers Astron. Space Sci. Volume 7, id.92 2020

<https://arxiv.org/pdf/2010.13793.pdf>

<https://www.frontiersin.org/articles/10.3389/fspas.2020.572084/full>

<https://doi.org/10.3389/fspas.2020.572084>

Coronal mass ejections (CMEs) and high speed solar streams serve as perturbations to the background solar wind that have major implications in space weather dynamics. Therefore, a robust framework for accurate predictions of the background wind properties is a fundamental step towards the development of any space weather prediction toolbox. In this pilot study, we focus on the implementation and comparison of various models that are critical for a steady state, solar wind forecasting framework. Specifically, we perform case studies on Carrington rotations 2053, 2082 and 2104, and compare the performance of magnetic field extrapolation models in conjunction with velocity empirical formulations to predict solar wind properties at Lagrangian point L1. Two different models to extrapolate the solar wind from the coronal domain to the inner-heliospheric domain are presented, namely, (a) Kinematics based (Heliospheric Upwind eXtrapolation [HUX]) model and (b) Physics based model. The physics based model solves a set of conservative equations of hydrodynamics using the PLUTO code and can additionally predict the thermal properties of solar wind. The assessment in predicting solar wind parameters of the different models is quantified through statistical measures. We further extend this developed framework to also assess the polarity of inter-planetary magnetic field at L1. Our best models for the case of CR2053 gives a very high correlation coefficient ($\sim 0.73-0.81$) and has an root mean square error of ($\sim 75-90$ kms $^{-1}$). Additionally, the physics based model has a standard deviation comparable with that obtained from the hourly OMNI solar wind data and also produces a considerable match with observed solar wind proton temperatures measured at L1 from the same database.

Passage of ICMEs, Their Associated Shock Structure, and Transient Modulation of Galactic Cosmic Rays

Anand Kumar, Badruddin, Moncef Derouich

Solar Physics November 2017, 292:166

<https://link.springer.com/content/pdf/10.1007%2Fs11207-017-1190-4.pdf>

Coronal mass ejections (CMEs) from the Sun propagate into interplanetary space and evolve to form a structure. When this structure is observed in near-Earth space, it consists in many cases of the CME ejecta and an extended shock region. Thus, while passing a point of observation (Earth/spacecraft), the interplanetary CME (ICME) structure may cross it from its near-central, intermediate, or near-end location. Therefore, galactic cosmic rays (GCRs) arriving at the Earth-based/space-borne detector may encounter solar plasma and field regimes of different strength, topology, and duration. We analyse the GCR intensity and the solar plasma/field parameters in three different situations when the ICME structure passes the detector from the central, intermediate, and the near-end portions of its extended structure. We study the behaviour of transient depressions in the GCR intensity in these three situations. Simultaneous changes in the solar plasma and field parameters are also studied. The differences in the amplitudes of the depression and the recovery characteristics during the passage of three groups of ICMEs are analysed and discussed.

Study of solar transients causing GMSs with Dst ≤ -100 nT during the period 1999-2010

Rajiv Kumar, N.K. Pandey, Gajendra Singh

Proc. of 35th International Cosmic Ray Conference - ICRC2017 10-20 July, 2017 Bexco, Busan, Korea

<https://pos.sissa.it/301/069/pdf>

The effect of solar features on geospheric conditions leading to geomagnetic storms(GMSs)with Dst index $Dst \leq -100$ nT has been investigated using interplanetary magnetic field(IMF),solar wind data(SWP) and solar geophysical data with CMEs that erupted between 1999 and 2010, we considered all 51 events .The study investigated *the relationship coronal mass ejection (CME) and their influence on Earth's geomagnetic field*, i.e. storms and sub storms .The study is performed mainly considering intense geomagnetic storms that occurred during Solar Cycle 23 and ascending phase of 24 Solar Cycle . It has been analysed and estimated by cross correlation method that there is a delay of 17 to 96 hours in happening GMSs on the Earth after the happening of the CME on the sun.

Estimation of interplanetary electric field conditions for historical geomagnetic storms

Sandeep **Kumar**, B. Veenadhari, S. Tulasi Ram, R. Selvakumaran, Shyamoli Mukherjee, Rajesh Singh, B. D. Kadam

JGR Volume 120, Issue 9 September 2015 Pages 7307–7317

Ground magnetic measurements provide a unique database in understanding space weather. The continuous geomagnetic records from Colaba-Alibag observatories in India contain historically longest and continuous observations from 1847 to present date. Some of the super intense geomagnetic storms that occurred prior to 1900 have been revisited and investigated in order to understand the probable interplanetary conditions associated with intense storms. Following Burton et al. (1975), an empirical relationship is derived for estimation of interplanetary electric field (IEFy) from the variations of *Dst* index and ΔH at Colaba-Alibag observatories. The estimated IEFy values using *Dst* and ΔH_{ABG} variations agree well with the observed IEFy, calculated using Advanced Composition Explorer (ACE) satellite observations for intense geomagnetic storms in solar cycle 23. This study will provide the uniqueness of each event and provide important insights into possible interplanetary conditions for intense geomagnetic storms and probable frequency of their occurrence.

Cosmic-Ray Modulation due to High-Speed Solar-Wind Streams of Different Sources, Speed, and Duration

Anand **Kumar**, Badruddin

Solar Physics, Volume 289, Issue 11, pp 4267-4296 2014

We study the modulation of galactic cosmic rays (GCR) due to high-speed streams (HSS) identified in the solar wind. We compare the GCR modulation due to i) streams with different speed, ii) streams of different duration, and iii) streams from different solar sources. We apply the method of superposed-epoch analysis to analyze the interplanetary plasma and field parameters during the passage of streams with distinct plasma and field characteristics. We use the plasma/field characteristics to distinguish various features of solar sources and interplanetary structures, and discuss the observed differences in the cosmic-ray response. We study the influence of speed, duration, and solar sources of the streams on the GCR modulation. We discuss the relative importance of different solar-wind parameters in the modulation process.

Interplanetary Coronal Mass Ejections, Associated Features, and Transient Modulation of Galactic Cosmic Rays

Review

Anand **Kumar**, Badruddin

Solar Phys., Volume 289, Issue 6, pp 2177-2205, 2014, **File**

Interplanetary structures such as shocks, sheaths, interplanetary counterparts of coronal mass ejections (ICMEs), magnetic clouds, and corotating interaction regions (CIRs) are of special interest for the study of the transient modulation of galactic cosmic rays (GCRs). These structures modulate the GCR intensity with varying amplitudes and recovery-time profiles. It is known that ICMEs are mainly responsible for Forbush decreases in the GCR intensity. However, not all of the ICMEs produce such decreases in GCR intensity. We utilize GCR intensity data recorded by neutron monitors and solar-wind plasma/field data during the passage of ICMEs with different features and structures, and we perform a superposed-epoch analysis of the data. We also adopt the best-fit approach with suitable functions to interpret the observed similarities and differences in various parameters. Using the GCR-effectiveness as a measure of the cosmic-ray response to the passage of ICMEs, about half of the ICMEs identified during 1996–2009 are found to produce moderate to very large intensity depressions in GCR intensity. The ICMEs associated with halo CMEs, magnetic-cloud (MC) structures, bidirectional superthermal electron (BDE) signatures, and those driving shocks are 1.5 to 4 times more GCR effective than the ICMEs not associated with these structures/features. Further, the characteristic recovery time of GCR intensity due to shock/BDE/MC/halo-CME-associated ICMEs is larger than those due to ICMEs not associated with these structures/features.

Solar Wind: Origin, Properties and Impact on Earth

Review

U.L. Visakh **Kumar** and P.J. Kurian

In: *Exploring the Solar Wind*, Ed. Marian Lazar, 2012, **File**

<http://www.intechopen.com/books/exploring-the-solar-wind>

Multiwavelength Study on Solar and Interplanetary Origins of the Strongest Geomagnetic Storm of Solar Cycle 23

Pankaj [Kumar](#), P. K. Manoharan and Wahab Uddin

Solar Physics, Volume 271, Numbers 1-2, 149-167, **2011**, [File](#)

We study the solar sources of an intense geomagnetic storm of solar cycle 23 that occurred on **20 November 2003**, based on ground- and space-based multiwavelength observations. The coronal mass ejections (CMEs) responsible for the above geomagnetic storm originated from the super-active region NOAA 10501. We investigate the H α observations of the flare events made with a 15 cm solar tower telescope at ARIES, Nainital, India. The propagation characteristics of the CMEs have been derived from the three-dimensional images of the solar wind (i.e., density and speed) obtained from the interplanetary scintillation data, supplemented with other ground- and space-based measurements. The TRACE, SXI and H α observations revealed two successive ejections (of speeds ≈ 350 and ≈ 100 km s $^{-1}$), originating from the same filament channel, which were associated with two high speed CMEs (≈ 1223 and ≈ 1660 km s $^{-1}$, respectively). These two ejections generated propagating fast shock waves (i.e., fast-drifting type II radio bursts) in the corona. The interaction of these CMEs along the Sun–Earth line has led to the severity of the storm. According to our investigation, the interplanetary medium consisted of two merging magnetic clouds (MCs) that preserved their identity during their propagation. These magnetic clouds made the interplanetary magnetic field (IMF) southward for a long time, which reconnected with the geomagnetic field, resulting the super-storm (Dst peak = -472 nT) on the Earth.

Observation of Kinetic Alfvén Waves inside an Interplanetary Coronal Mass Ejection Magnetic Cloud at 1 au

Kishor [Kumbhar](#)^{1,2}, Anil Raghav¹, Omkar Dhamane¹, Kalpesh Ghag¹, Vinit Pawaskar¹, Zubair Shaikh³, Ankush Bhaskar⁴, Raffaella D'Amicis⁵, and Daniele Telloni⁶

2024 ApJ 965 139

<https://iopscience.iop.org/article/10.3847/1538-4357/ad323c/pdf>

Recent advancements have significantly enhanced our grasp of interplanetary coronal mass ejections (ICMEs) in the heliosphere. These observations have uncovered complex kinematics and structural deformations in ICMEs, hinting at the possible generation of magnetohydrodynamic (MHD) and kinetic-scale waves. While MHD-scale waves in magnetic clouds have been explored, understanding the dynamics of kinetic-scale mode waves remains challenging. This article demonstrates the first in situ observation of kinetic Alfvén waves (KAWs) within an ICME's magnetic cloud, notably near the heliospheric current sheet–ICME interaction region, close to the reconnection exhaust. Analysis indicates a distinctive negative bump in the estimated normalized magnetic helicity ($\sigma_m = -0.38$) around the gyrofrequency spread, indicating a right-handed polarization of the wave. Furthermore, examination across flow angle (θ_{VB}) within the frequency domain reveals a specific zone (90° – 135°) showcasing negative helicity fluctuations, confirming the presence of KAWs. Moreover, we noted a significant rise in temperature anisotropy in the vicinity, indicating the role of KAWs in plasma heating. Identifying KAW challenges established notions about ordered magnetic clouds and raises questions about energy transfer processes within these structures. This finding opens the door to a deeper understanding of energy transfer mechanisms within traditionally nondissipative regions and invites further exploration of low-beta plasma heating and the interactions between waves and particles in magnetic clouds.

EVOLUTION OF A CORONAL MASS EJECTION AND ITS MAGNETIC FIELD IN INTERPLANETARY SPACE

V. [Kunkell](#)^{1,2} and J. Chen³

Astrophysical Journal Letters, 715:L80–L83, **2010** June

This Letter presents the first theoretical study of the dynamics of a coronal mass ejection (CME) observed by *STEREO-A/B*. The CME was continuously tracked by SECCHI-A, providing position-time data from eruption to 1 AU. The ejecta was intersected by *STEREO-B* at 1 AU, where the magnetic field and plasma parameters were measured. The observed CME trajectory and the evolution of the CME magnetic field are modeled using the semianalytic erupting flux-rope model. It is shown that the best-fit theoretical solution is in good agreement—within 1% of the measured CME trajectory in the 1 AU field of view—and is consistent with the in situ magnetic field and plasma data at 1 AU. **2007** December 24

Determination of interplanetary coronal mass ejection geometry and orientation from ground-based observations of galactic cosmic rays

Kuwabara, T.; Bieber, J. W.; Evenson, P.; Munakata, K.; Yasue, S.; Kato, C.; Fushishita, A.; Tokumaru, M.; Duldig, M. L.; Humble, J. E.; Silva, M. R.; Dal Lago, A.; Schuch, N. J.

J. Geophys. Res., Vol. 114, No. A5, A05109, 2009 **File**

<http://dx.doi.org/10.1029/2008JA013717>

We have developed a method for determining interplanetary coronal mass ejection (ICME) geometry from galactic cosmic ray data recorded by the ground-based muon detector network. The cosmic ray density depression inside the ICME, which is associated with a Forbush decrease, is represented by an expanding cylinder that is based on a theoretical model of the cosmic ray particle diffusion. ICME geometry and orientation are deduced from observed time variations of cosmic ray density and density gradient and are compared with those deduced from a magnetic flux rope model. From March 2001 to May 2005, 11 ICME events that produced Forbush decreases >2% were observed, and clear variations of the density gradient due to ICME passage were observed in 8 of 11 events. In five of the eight events, signatures of magnetic flux rope structure (large, smooth rotation of magnetic field) were also seen, and the ICME geometry and orientation deduced from the two methods were very similar in three events. This suggests that the cosmic ray-based method can be used as a complementary method for deducing ICME geometry especially for events where a large Forbush decrease is observed.

Study of Forbush Decrease Recovery Times by the Payload for Antimatter Matter Exploration and Light-Nuclei Astrophysics (PAMELA) Experiment

I. A. **Lagoida**, [S. A. Voronov](#), [V. V. Mikhailov](#), [M. Boezio](#), [R. Munini](#), [G. C. Barbarino](#), [G. A.](#)

[Bazilevskaya](#), [R. Bellotti](#), [E. A. Bogomolov](#), +++

[Solar Physics](#) volume 298, Article number: 9 (2023)

<https://doi.org/10.1007/s11207-022-02097-z>

A Forbush decrease (FD) is a sudden drop of cosmic-ray intensity arising as an effect of coronal mass ejection (CME) propagation in interplanetary space. The different physical properties of each CME cause variability in the FDs observed by scientific instruments. A comprehensive study of both phenomena is required to properly understand the processes involved in FDs. Most of the current studies in this field use experimental data obtained by ground-based apparatus that measure the flux of cosmic rays via their interaction with Earth's atmosphere. Direct measurements in space of FDs are rather rare. In this work, we present the results obtained by the spacecraft-borne experiment Payload for Antimatter Matter Exploration and Light-nuclei Astrophysics (PAMELA). The experiment took data from 15 June 2006 until January 2016. A series of FDs during the period 2006 – 2013 were studied. Only significant events with amplitude $\geq 10\%$ for the proton flux $R=1.1 - 2.9$ GV were taken into account. The dependencies of the recovery times on the particle rigidity were obtained for FD events generated by halo-type CMEs.

Interplanetary Consequences of a Large CME

M. **Lahkar**, P. K. Manoharan², K. Mahalakshmi², K. Prabhu², G. Agalya², S. Shaheda Begum², and P. Revathi

To appear in "Magnetic Coupling between the Interior and the Atmosphere of the Sun", eds. S.S. Hasan and R.J. Rutten, Astrophysics and Space Science Proceedings, Springer-Verlag, Heidelberg, Berlin, 2009, **File**

We analyze a coronal mass ejection (CME) which resulted from an intense flare in active region AR486 on **November 4, 2003**. The CME propagation and speed are studied with interplanetary scintillation images, near-Earth space mission data, and Ulysses measurements. Together, these diverse diagnostics suggest that the internal magnetic energy of the CME determines its interplanetary consequences.

The Radial Variation of Interplanetary Shocks in the Inner Heliosphere: Observations by Helios, MESSENGER, and STEREO

H. R. **Lai**, C. T. Russell, L. K. Jian, X. Blanco-Cano, B. J. Anderson, J. G. Luhmann and A. Wennmacher
[Solar Physics](#), Volume 278, Number 2 (2012), 421-433

The two major sources of collisionless shocks in the solar wind are interplanetary coronal mass ejections (ICMEs) and stream interaction regions (SIRs). Previous studies show that some SIR-associated shocks form between Venus and

Earth while most form beyond 1 AU. Here we examine the high-resolution magnetometer records from Helios 1 and 2 obtained between 0.28 and 1 AU and from MESSENGER obtained between 0.3 and 0.7 AU to further refine our understanding as to where, and in what context, shocks are formed in the inner solar system. From Helios data (Helios 1 from 1974 to 1981 and Helios 2 from 1976 to 1980), we find there were only a few shocks observed inside the orbit of Venus with the closest shock to the Sun at 0.29 AU. We find that there is a strong correlation between shock occurrence and solar activity as measured by the sunspot number. Most of the shocks inside of the orbit of Venus appear to be associated with ICMEs. Even the ICME-associated shocks are quite weak inside the orbit of Venus. By comparing MESSENGER and STEREO results, from 2007 to 2009, we find that in the deep solar minimum, SIR-driven shocks began to form at about 0.4 AU and increased in number with heliocentric distance.

Access of Energetic Particles to a Magnetic Flux Rope from External Magnetic Field Lines

T. Laitinen and S. Dalla

2021 ApJ 906 9

<https://doi.org/10.3847/1538-4357/abc622>

Cosmic-ray (CR) fluxes in the heliosphere are affected by the transient interplanetary coronal mass ejections (ICMEs), causing so-called Forbush decreases (FDs), characterized by a decline of up to 25% in the neutron monitor counts at the Earth's surface, lasting up to over a week. FDs are thought to be caused by the ICME shock wave or the magnetic flux rope embedded in the ICME inhibiting CR propagation through the ICME structure. FDs are typically modeled as enhanced diffusion within the ICME structure. However, so far modeling has not considered the access of the CRs from the interplanetary field lines into the isolated magnetic field lines of the ICME flux rope. We study the effect of an ICME flux rope on particle propagation by using full-orbit particle simulations, with the interface between the external interplanetary magnetic field and the isolated flux rope field lines modeled analytically. We find that the particles can access the flux rope through the x-point region, where the external magnetic fields cancel the azimuthal component of the rope field. The transport through this region is fast compared to diffusive radial propagation within the rope. As a result, the propagation of CRs into the flux rope can be modeled as diffusion into a cylinder. The density cavity within the rope is asymmetric, and limited to the magnetic field lines isolated from the external field. Thus, in order to evaluate the role of the flux rope in FDs, one must analyze the extent of the region where the flux rope magnetic field lines are separated from the interplanetary magnetic fields.

Using Solar Orbiter as an Upstream Solar Wind Monitor for Real Time Space Weather Predictions

R. Laker, T. S. Horbury, H. O'Brien, E. J. Fauchon-Jones, V. Angelini, N. Fargette, T. Amerstorfer, M. Bauer, C. Möstl, E. E. Davies, J. A. Davies, R. Harrison, D. Barnes, M. Dumbović

Space Weather Volume22, Issue2 February 2024 e2023SW003628

<https://doi.org/10.1029/2023SW003628>

<https://agupubs.onlinelibrary.wiley.com/doi/epdf/10.1029/2023SW003628>

Coronal mass ejections (CMEs) can create significant disruption to human activities and systems on Earth, much of which can be mitigated with prior warning of the upstream solar wind conditions. However, it is currently extremely challenging to accurately predict the arrival time and internal structure of a CME from coronagraph images alone. In this study, we take advantage of a rare opportunity to use Solar Orbiter, at 0.5 au upstream of Earth, as an upstream solar wind monitor. In combination with low-latency images from STEREO-A, we successfully predicted the arrival time of two CME events before they reached Earth. Measurements at Solar Orbiter were used to constrain an ensemble of simulation runs from the ELEvoHI model, reducing the uncertainty in arrival time from 10.4 to 2.5 hr in the first case study. There was also an excellent agreement in the Bz profile between Solar Orbiter and Wind spacecraft for the second case study, despite being separated by 0.5 au and 10° longitude. The opportunity to use Solar Orbiter as an upstream solar wind monitor will repeat once a year, which should further help assess the efficacy upstream in-situ measurements in real time space weather forecasting. Coronal mass ejections (CMEs) can create significant disruption to human activities and systems on Earth, much of which can be mitigated with prior warning of the upstream solar wind conditions. However, it is currently extremely challenging to accurately predict the arrival time and internal structure of a CME from coronagraph images alone. In this study, we take advantage of a rare opportunity to use Solar Orbiter, at 0.5 au upstream of Earth, as an upstream solar wind monitor. In combination with low-latency images from STEREO-A, we successfully predicted the arrival time of two CME events before they reached Earth. Measurements at Solar Orbiter were used to constrain an ensemble of simulation runs from the ELEvoHI model, reducing the uncertainty in arrival time from 10.4 to 2.5 hr in the first case study. There was also an excellent agreement in the Bz profile between Solar Orbiter and Wind spacecraft for the second case study, despite being separated by 0.5 au and 10° longitude. The opportunity to

use Solar Orbiter as an upstream solar wind monitor will repeat once a year, which should further help assess the efficacy upstream in-situ measurements in real time space weather forecasting. **10-11 Mar 2022, 12-14 Mar 2022 SO Nugget #29 May 2024** <https://www.cosmos.esa.int/web/solar-orbiter/-/science-nugget-real-time-space-weather-prediction-with-solar-orbiter>

Switchback deflections beyond the early parker solar probe encounters

R **Laker**, [T S Horbury](#), [L Matteini](#), [S D Bale](#), [J E Stawarz](#), [L D Woodham](#), [T Woolley](#)

MNRAS, Volume 517, Issue 1, November **2022**, Pages 1001–1005,

<https://doi.org/10.1093/mnras/stac2477>

Switchbacks are Alfvénic fluctuations in the solar wind, which exhibit large rotations in the magnetic field direction. Observations from Parker Solar Probe’s (PSP’s) first two solar encounters have formed the basis for many of the described switchback properties and generation mechanisms. However, this early data may not be representative of the typical near-Sun solar wind, biasing our current understanding of these phenomena. One defining switchback property is the magnetic deflection direction. During the first solar encounter, this was primarily in the tangential direction for the longest switchbacks, which has since been discussed as evidence, and a testable prediction, of several switchback generation methods. In this study, we re-examine the deflection direction of switchbacks during the first eight PSP encounters to confirm the existence of a systematic deflection direction. We first identify switchbacks exceeding a threshold deflection in the magnetic field and confirm a previous finding that they are arc-polarized. In agreement with earlier results from PSP’s first encounter, we find that groups of longer switchbacks tend to deflect in the same direction for several hours. However, in contrast to earlier studies, we find that there is no unique direction for these deflections, although several solar encounters showed a non-uniform distribution in deflection direction with a slight preference for the tangential direction. This result suggests a systematic magnetic configuration for switchback generation, which is consistent with interchange reconnection as a source mechanism, although this new evidence does not rule out other mechanisms, such as the expansion of wave modes.

Multi-spacecraft study of the solar wind at solar minimum: Dependence on latitude and transient outflows

R. **Laker**¹, T. S. Horbury¹, S. D. Bale^{1,2,3}, L. Matteini¹, T. Woolley¹, L. D. Woodham¹, J. E. Stawarz¹, E. E. Davies¹, J. P. Eastwood¹, M. J. Owens⁴, H. O’Brien¹, V. Evans¹, V. Angelini¹, I. Richter⁵, D. Heyner⁵, C. J. Owen⁶, P. Louarn⁷ and A. Fedorov⁷

A&A 652, A105 (**2021**)

<https://www.aanda.org/articles/aa/pdf/2021/08/aa40679-21.pdf>

<https://doi.org/10.1051/0004-6361/202140679>

Context. The recent launches of Parker Solar Probe, Solar Orbiter (SO), and BepiColombo, along with several older spacecraft, have provided the opportunity to study the solar wind at multiple latitudes and distances from the Sun simultaneously.

Aims. We take advantage of this unique spacecraft constellation, along with low solar activity across two solar rotations between May and July 2020, to investigate how the solar wind structure, including the heliospheric current sheet (HCS), varies with latitude.

Methods. We visualise the sector structure of the inner heliosphere by ballistically mapping the polarity and solar wind speed from several spacecraft onto the Sun’s source surface. We then assess the HCS morphology and orientation with the in situ data and compare this with a predicted HCS shape.

Results. We resolve ripples in the HCS on scales of a few degrees in longitude and latitude, finding that the local orientations of sector boundaries were broadly consistent with the shape of the HCS but were steepened with respect to a modelled HCS at the Sun. We investigate how several CIRs varied with latitude, finding evidence for the compression region affecting slow solar wind outside the latitude extent of the faster stream. We also identified several transient structures associated with HCS crossings and speculate that one such transient may have disrupted the local HCS orientation up to five days after its passage.

Conclusions. We have shown that the solar wind structure varies significantly with latitude, with this constellation providing context for solar wind measurements that would not be possible with a single spacecraft. These measurements provide an accurate representation of the solar wind within $\pm 10^\circ$ latitude, which could be used as a more rigorous constraint on solar wind models and space weather predictions. In the future, this range of latitudes will increase as SO’s orbit becomes more inclined.

Statistical analysis of orientation, shape, and size of solar wind switchbacks

Ronan [Laker](#), [Timothy S. Horbury](#), [Stuart D. Bale](#), [Lorenzo Matteini](#), [Thomas Woolley](#), [Lloyd D. Woodham](#), [Samuel T. Badman](#), [Marc Pulupa](#), [Justin C. Kasper](#), [Michael Stevens](#), [Anthony W. Case](#), [Kelly E. Korreck](#)

A&A 650, A1 2021

<https://arxiv.org/pdf/2010.10211.pdf>

<https://www.aanda.org/articles/aa/pdf/2021/06/aa39354-20.pdf>

<https://doi.org/10.1051/0004-6361/202039354>

One of the main discoveries from the first two orbits of Parker Solar Probe (PSP) was the presence of magnetic switchbacks, whose deflections dominated the magnetic field measurements. Determining their shape and size could provide evidence of their origin, which is still unclear. Previous work with a single solar wind stream has indicated that these are long, thin structures although the direction of their major axis could not be determined. We investigate if this long, thin nature extends to other solar wind streams, while determining the direction along which the switchbacks within a stream were aligned. We try to understand how the size and orientation of the switchbacks, along with the flow velocity and spacecraft trajectory, combine to produce the observed structure durations for past and future orbits. We searched for the alignment direction that produced a combination of a spacecraft cutting direction and switchback duration that was most consistent with long, thin structures. The expected form of a long, thin structure was fitted to the results of the best alignment direction, which determined the width and aspect ratio of the switchbacks for that stream. The switchbacks had a mean width of 50,000km, with an aspect ratio of the order of 10. We find that switchbacks are not aligned along the background flow direction, but instead aligned along the local Parker spiral, perhaps suggesting that they propagate along the magnetic field. Since the observed switchback duration depends on how the spacecraft cuts through the structure, the duration alone cannot be used to determine the size or influence of an individual event. For future PSP orbits, a larger spacecraft transverse component combined with more radially aligned switchbacks will lead to long duration switchbacks becoming less common.

Chapter 7 - Supergeomagnetic Storms: Past, Present, and Future

Review

Gurbax S. [Lakhina](#) [Bruce T. Tsurutani](#)

In: Extreme Events in Geospace

Origins, Predictability, and Consequences

Book

Editor: Natalia [Buzulukova](#), Elsevier, 2018, 798 p. **File**

Pages 157-185 **File**

<http://sci-hub.se/10.1016/B978-0-12-812700-1.00007-8>

Geomagnetic storms are large-scale disturbances in the Earth's magnetic field due to orders of magnitude increases in trapped energetic $\sim 10\text{--}300$ keV particle fluxes in the magnetosphere. During geomagnetic storms, the horizontal component of the low-latitude magnetic fields is significantly depressed over a time span of one to a few hours from the diamagnetic effect from the enhanced ring current fluxes. This is known as the main phase of the storm, and is followed by the recovery phase where the particles are lost. This latter phase may extend over several days. The strength of magnetic storms is measured by the Disturbance Storm Time (Dst) index. Superintense magnetic storms (defined here as those with $\text{Dst} < -500$ nT), although relatively rare in occurrence, have the largest societal and technological impacts. Such storms can cause life-threatening power outages, satellite damage, satellite communication failures, navigational problems, and loss of satellites in low Earth orbit (LEO). In this chapter, we shall first review the present knowledge about supermagnetic storms. Then, we discuss the superstorms that have occurred in the past, and consider the case history of the Carrington storm as a representative example. This will be followed by the consideration of supermagnetic storms of present (the space-age era). Next, we explore supermagnetic storms that can occur in the future with an emphasis on the maximum possible intensity of an event. The occurrence probability of superstorms having intensities equal to the Carrington storm or higher will be discussed. Finally, we discuss the status of nowcasting (~ 1 h) and short-time scale forecasting (\sim a few hours to a few days) of supermagnetic storms. **September 1–2, 1859, March 13–16, 1989**

Table 1 A List of Intense and Superintense Magnetic Storms From Colaba and Alibag Magnetic Observatories (1847-2005)

Coronal mass ejections and solar wind mass fluxes over the heliosphere during solar cycles 23 and 24 (1996–2014)†

P. [Lamy](#), O. Floyd, E. Quémerais, B. Boclet, S. Ferron Ferro

JGR Volume 122, Issue 1 January 2017 Pages 50–62

doi: 10.1002/2016ja022970

Coronal mass ejections (CMEs) play a major role in the heliosphere and their contribution to the solar wind mass flux, already considered in the Skylab and Solwind eras with conflicting results, is re-examined in the light of 19 years (1996-

2014) of SOHO observations with the Large Angle and Spectroscopic Coronagraph “LASCO-C2” for the CMEs and extended for the first time to all latitudes thanks to the whole-heliosphere data from the Solar Wind ANisotropies “SWAN” instrument supplemented by in-situ data aggregated in the OMNI database. First, several mass estimates reported in the ARTEMIS catalog of LASCO CMEs are compared with determinations based on the combined observations with the twin STEREO/SECCHI coronagraphs in order to ascertain their validity. A simple geometric model of the CMEs is introduced to generate Carrington maps of their mass flux and then to produce annualized synoptic maps. The Lyman- α SWAN data are inverted to similarly produce synoptic maps to be compared with those of the CME flux. The ratio of the annualized CME to solar wind mass flux is found to closely track the solar cycle over the heliosphere. In the near-ecliptic region and at latitudes up to $\sim 55^\circ$, this ratio was negligibly small during the solar minima of cycles 22/23 and 23/24 and rose to 6% and 5% respectively at the maximum of solar cycles 23 and 24. These maximum ratios increased at higher latitudes but this result is likely biased by the inherent limitation of determining the true latitude of CMEs.

A robust estimation of the twist distribution in magnetic clouds

V. Lanabere, P. Démoulin, S. Dasso

A&A 668, A160 2022

<https://arxiv.org/pdf/2211.08758.pdf>

<https://www.aanda.org/articles/aa/pdf/2022/12/aa45062-22.pdf>

Magnetic clouds (MCs) are observed in situ by spacecraft. The rotation of their magnetic field is typically interpreted as the crossing of a twisted magnetic flux tube, or flux rope, which was launched from the solar corona. The detailed magnetic measurements across MCs permit us to infer the flux rope characteristics. Still, the precise spatial distribution of the magnetic twist is challenging, and thus is debated. In order to improve the robustness of the results, we performed a superposed epoch analysis (SEA) of a set of well observed MCs at 1 au. While previous work was done using the MC central time, we here used the result of a fitted flux rope model to select the time of the closest approach to the flux rope axis. This implies a precise separation of the in- and outbound regions to coherently phase the observed signals. We also searched for and minimised the possible biases such as magnetic asymmetry and a finite impact parameter. We applied the SEA to derive the median profiles both for the flux rope remaining when crossed by the spacecraft and to recover the one present before erosion. In particular, the median azimuthal B component is nearly a linear function of the radius. More generally, the results confirm our previous results realised without such a deep analysis. The twist profile is nearly uniform in the flux rope core, with a steep increase at the border of the flux rope and with similar profiles in the in- and outbound regions. The main difference with our previous study is a larger twist by $\sim 20\%$. **22 August 1995, 24 July 2004**

Magnetic twist profile inside magnetic clouds derived with a superposed epoch analysis

V. Lanabere¹, S. Dasso^{1,2,3}, P. Démoulin⁴, M. Janvier⁵, L. Rodriguez⁶ and J. J. Masías-Meza³

A&A 635, A85 (2020)

<https://doi.org/10.1051/0004-6361/201937404>

https://lesia.obspm.fr/perso/pascal-demoulin/20/Lanabere20_twist_profile_SEA.pdf

Context. Magnetic clouds (MCs) are large-scale interplanetary transient structures in the heliosphere that travel from the Sun into the interplanetary medium. The internal magnetic field lines inside the MCs are twisted, forming a flux rope (FR). This magnetic field structuring is determined by its initial solar configuration, by the processes involved during its eruption from the Sun, and by the dynamical evolution during its interaction with the ambient solar wind.

Aims. One of the most important properties of the magnetic structure inside MCs is the twist of the field lines forming the FR (the number of turns per unit length). The detailed internal distribution of twist is under debate mainly because the magnetic field (B) in MCs is observed only along the spacecraft trajectory, and thus it is necessary to complete observations with theoretical assumptions. Estimating the twist from the study of a single event is difficult because the field fluctuations significantly increase the noise of the observed B time series and thus the bias of the deduced twist.

Methods. The superposed epoch applied to MCs has proven to be a powerful technique, permitting the extraction of their common features, and removing the peculiarity of individual cases. We apply a superposed epoch technique to analyse the magnetic components in the local FR frame of a significant sample of moderately asymmetric MCs observed at 1 au. **Results.** From the superposed profile of B components in the FR frame, we determine the typical twist distribution in MCs. The twist is nearly uniform in the FR core (central half part), and it increases moderately, up to a factor two, towards the MC boundaries. This profile is close to the Lundquist field model limited to the FR core where the axial field component is above about one-third of its central value.

Improving solar wind forecasting using Data Assimilation

Matthew **Lang**, [Jake Witherington](#), [Harriet Turner](#), [Matt Owens](#), [Pete Riley](#)
Space Weather **Volume19, Issue7** e2020SW002698 2021
<https://arxiv.org/pdf/2012.06362.pdf>
<https://agupubs.onlinelibrary.wiley.com/doi/epdf/10.1029/2020SW002698>

Data Assimilation (DA) has enabled huge improvements in the skill of terrestrial operational weather forecasting. In this study, we use a variational DA scheme with a computationally efficient solar wind model and in situ observations from STEREO A, STEREO B and ACE. This scheme enables solar-wind observations far from the Sun, such as at 1 AU, to update and improve the inner boundary conditions of the solar wind model (at 30 solar radii). In this way, observational information can be used to improve estimates of the near-Earth solar wind, even when the observations are not directly downstream of the Earth. This allows improved initial conditions of the solar wind to be passed into forecasting models. To this effect we employ the HUXt solar wind model to produce 27-day forecasts of the solar wind during the operational time of STEREO B (01/11/2007–30/09/2014). At ACE, we compare these DA forecasts to the corotation of STEREO B observations and find that 27-day RMSE for STEREO-B corotation and DA forecasts are comparable. However, the DA forecast is shown to improve solar wind forecasts when STEREO-B's latitude is offset from Earth. And the DA scheme enables the representation of the solar wind in the whole model domain between the Sun and the Earth to be improved, which will enable improved forecasting of CME arrival time and speed.

A Variational Approach to Data Assimilation in the Solar Wind

Matthew **Lang** [Mathew J. Owens](#)
Space Weather 17(1) Pages: 59-83 2019
sci-hub.se/10.1029/2018SW001857

Variational data assimilation (DA) has enabled huge improvements in the skill of operational weather forecasting. In this study, we use a simple solar-wind propagation model to develop the first solar-wind variational DA scheme. This scheme enables solar-wind observations far from the Sun, such as at 1 AU, to update and improve the inner-boundary conditions of the solar wind model (at 30 solar radii). In this way, observational information can be used to improve estimates of the near-Earth solar wind, even when the observations are not directly downstream of the Earth. Using controlled experiments with synthetic observations, we demonstrate this method's potential to improve solar wind forecasts, though the best results are achieved in conjunction with accurate initial estimates of the solar wind. The variational DA scheme is also applied to Solar-Terrestrial Relations Observatory (STEREO) in situ observations using initial solar wind conditions supplied by a coronal model of the observed photospheric magnetic field. We consider the period October 2010 to October 2011, when the STEREO spacecraft were approximately 80° ahead/behind Earth in its orbit. For 12 of 13 Carrington Rotations, assimilation of STEREO data improves the near-Earth solar wind estimate over the nonassimilated state, with a 18.4% reduction in the root mean square error. The largest gains are made by the DA during times when the steady-state assumption of the coronal models breaks down. While applying this pure variational approach to complex solar-wind models is technically challenging, we discuss hybrid DA approaches which are simpler to implement and may retain many of the advantages demonstrated here.

Dynamic Time Warping as a New Evaluation for Dst Forecast With Machine Learning

Brecht **Laperre***, Jorge Amaya and Giovanni Lapenta
Front. Astron. Space Sci. 7:39. 2020
<https://www.frontiersin.org/articles/10.3389/fspas.2020.00039/full>
<https://doi.org/10.3389/fspas.2020.00039>

Models based on neural networks and machine learning are seeing a rise in popularity in space physics. In particular, the forecasting of geomagnetic indices with neural network models is becoming a popular field of study. These models are evaluated with metrics such as the root-mean-square error (RMSE) and Pearson correlation coefficient. However, these classical metrics sometimes fail to capture crucial behavior. To show where the classical metrics are lacking, we trained a neural network, using a long short-term memory network, to make a forecast of the disturbance storm time index at origin time t with a forecasting horizon of 1 up to 6 h, trained on OMNIWeb data. Inspection of the model's results with the correlation coefficient and RMSE indicated a performance comparable to the latest publications. However, visual inspection showed that the predictions made by the neural network were behaving similarly to the persistence model. In this work, a new method is proposed to measure whether two time series are shifted in time with respect to each other, such as the persistence model output versus the observation. The new measure, based on Dynamical Time Warping, is capable of identifying results made by the persistence model and shows promising results in confirming the visual observations of the neural network's output. Finally, different methodologies for training the neural network are explored in order to remove the persistence behavior from the results.

Editorial: Solar Wind at the Dawn of the Parker Solar Probe and Solar Orbiter Era Review

Giovanni [Lapenta](#), [Andrei Zhukov](#) & [Lidia van Driel-Gesztelyi](#)

[Solar Physics](#) volume 295, Article number: 103 (2020)

<https://link.springer.com/content/pdf/10.1007/s11207-020-01670-8.pdf>

Solar Wind 15 (18 to 22 June 2018) brought together almost 250 experts from all continents of the world to discuss the current trends and future perspectives of the research on the Sun and its solar wind. The present article collection recaptures some of the highlights of their contributions.

Interaction of Cosmic Rays With Magnetic Flux Ropes

Alejandro [Lara](#), [A. Borgazzi](#), [Eduardo Guennam](#), [Tatiana Niembro](#), [K. P. Arunbabu](#)

JGR [Volume 129, Issue 8](#) August 2024 e2024JA032478

<https://agupubs.onlinelibrary.wiley.com/doi/epdf/10.1029/2024JA032478>

<https://doi.org/10.1029/2024JA032478>

The heliosphere is full of galactic cosmic rays (GCR), high-energy charged particles coming isotropically from the galaxy. The GCR interact with the solar wind blown by the Sun carrying out plasma, magnetic fields and transient structures such as interplanetary coronal mass ejections (ICMEs) and their associated magnetic flux ropes (MFR). The GCR interaction with ICMEs has been extensively studied particularly the GCR flux attenuation (known as Forbush decreases) as a result of interacting with the ICME sheath and magnetic field. In this work, we investigate the opposite effect: the MFR's ability to generate GCR anisotropies which an observer may detect as an increase in the GCR flux. To achieve this, we simulated a flux of protons with energies in the 10–160 GeV range arriving from all directions to a cylindrical MFR (with and without sheath) with plasma, magnetic field, and spatial dimensions found in average ICMEs observed at 1 au. By following the individual trajectories of the injected particles we found that the MFR deviates the charged particles preferentially in one direction parallel to the MFR-axis. We also found that the peak of this anisotropic GCR flux depends on: the angle between the MFR and ambient magnetic fields; the presence or not of the sheath region; the energy of the incident particles and the observer location inside the MFR.

Galactic Cosmic Ray Sun Shadow during the declining phase of cycle 24 observed by HAWC

Alejandro [Lara](#), [Paulina Colin](#), [K.P. Arunbabu](#), [James Ryan](#)

PoS(ICRC2019)1104 **2019**

<https://arxiv.org/pdf/1908.07509.pdf>

The High Altitude Water Cherenkov (HAWC) array is sensitive to high energy Cosmic Rays (CR) in the ~ 10 to ~ 200 TeV energy range, making it possible to construct maps of the so called "Sun Shadow" (SS), i. e. of the deficit of CR coming from the direction of the Sun. In this work, we present the variation of the Relative Intensity of the deficit (SSRI) for three years of HAWC observations from 2016 to 2018 in which we found a clear decreasing trend of the (SSRI) over the studied period, corresponding to the declining phase of the solar cycle 24. By comparing the SSRI with the photospheric magnetic field evolution, we show that there is a linear relationship between the SSRI and the median photospheric magnetic field of the Active Region belt ($-40^\circ \leq \text{lat} \leq 40^\circ$) and an inverse linear relationship with the polar photospheric magnetic field ($\text{lat} \geq \pm 60^\circ$). The former relationship is due to the magnetic field causing a deviation of the CR, whereas the latter reflects the change of the heliospheric field topology from multipolar to dipolar configurations. These relationships are valid only when the median magnetic field is lower than 8 G, during the declining and minimum phases of the solar cycle 24. Finally, we show that relativistic charged particles, in the 10 to 200 TeV energy range, are deflected a few degrees.

Velocity profile of interplanetary coronal mass ejections beyond 1 AU

[Lara](#), A.; [Flandes](#), A.; [Borgazzi](#), A.; [Subramanian](#), P.

J. Geophys. Res., Vol. 116, No. A12, A12102, 2011

<http://onlinelibrary.wiley.com/doi/10.1029/2011JA016807/pdf>

We analyze the dynamics of interplanetary coronal mass ejections (ICMEs) through the interplanetary medium from the lower solar corona to ~ 5.3 AU. Our analysis uses a one-dimensional hydrodynamical model derived from the fluid equation of motion that considers an effective drag force under both the laminar and turbulent hypotheses (low and high Reynolds number, respectively). The model has three sets of input parameters. The first set is related to the ICME itself, i. e., initial speed and mass; the second set of parameters is related to the ambient solar wind: density and velocity; and the final set corresponds to the ambient solar wind-ICME interaction: an ICME expansion factor and a viscosity or drag parameter. We use this model to explain the radial dynamics of a particular ICME detected at three different locations:

close to the Sun, where the ICME was ejected on **20 January 2004**, and detected by the SOHO/LASCO coronagraphs; two days later, at Earth's L1 by the ACE spacecraft (~ 1.0 AU), and finally, ~ 14 days later, at ~ 5.3 AU by the Ulysses spacecraft near Jupiter's orbit. The model is then compared to a general set of ICMEs data from Ulysses that cover distances from ~ 1.3 AU to ~ 5.3 AU. Our model successfully reproduces the dynamical behavior of ICMEs at distances near Earth's orbit and works reasonably well at larger distances ≈ 5.3 AU. Therefore, our analysis shows that the ICME - solar wind interaction may be treated as a drag interaction with the appropriate drag factors, not only at distances ≤ 1 AU, but at larger distances. Finally, we show that our model is useful in identifying ICMEs at different heliocentric distances.

Dynamics of interplanetary CMEs and associated type II bursts

Alejandro **Lara** and Andrea I. Borgazzi

Proceedings of the International Astronomical Union / Volume 4 / Symposium S257, pp 287 – 290,

Published online: 16 Март **2009**, **File**

Coronal mass ejections (CMEs) are large scale structures of plasma ($\sim 10^{16}$ g) and magnetic field expelled from the solar corona to the interplanetary medium. During their travel in the inner heliosphere, these “interplanetary CMEs” (ICMEs), suffer acceleration due to the interaction with the ambient solar wind. Based on hydrodynamic theory, we have developed an analytical model for the ICME transport which reproduce well the observed deceleration of fast ICMEs. In this work we present the results of the model and its application to the CME observed on **May 13, 2005** and the associated interplanetary type II burst.

The Extended Field-aligned Suprathermal Proton Beam and Long-lasting Trapped Energetic Particle Population Observed Upstream of a Transient Interplanetary Shock

D. **Lario**¹, I. G. Richardson^{1,2}, L. B. Wilson III¹, L. Berger¹, L. K. Jian¹, and D. Trotta³

2022 ApJ 925 198

<https://iopscience.iop.org/article/10.3847/1538-4357/ac3c47/pdf>

The properties of the suprathermal particle distributions observed upstream of interplanetary shocks depend not only on the properties of the shocks but also on the transport conditions encountered by the particles as they propagate away from the shocks. The confinement of particles in close proximity to the shocks, as well as particle scattering processes during propagation to the spacecraft, lead to the common observation of upstream diffuse particle distributions. We present observations of a rare extended anisotropic low-energy ($\lesssim 30$ keV) proton beam together with a trapped $\gtrsim 500$ keV proton population observed in association with the arrival of an oblique interplanetary shock at the Advanced Composition Explorer, the Interplanetary Monitoring Platform-8, and the Wind spacecraft on **2001 January 31**. Continuous injection of particles by the traveling shock into a smooth radial magnetic field region formed in the tail of a modest high-speed solar wind stream produced an extended foreshock region of energetic particles. The absence of enhanced magnetic field fluctuations upstream of the shock results in the observation of a prolonged anisotropic field-aligned beam of $\lesssim 30$ keV protons as well as a population of higher-energy ($\gtrsim 500$ keV) protons with small pitch-angle cosine ($\mu \sim 0$) extending far from the shock.

The Streamer Blowout Origin of a Flux Rope and Energetic Particle Event Observed by Parker Solar Probe at 0.5 au

D. **Lario**¹, L. Balmaceda^{1,2}, N. Alzate^{1,3}, M. L. Mays¹, I. G. Richardson^{1,4}, R. C. Allen⁵, M. Florido-Llinas⁶, T. Nieves-Chinchilla¹, A. Koval^{1,7}, N. Lugaz

2020 ApJ 897 134

<https://doi.org/10.3847/1538-4357/ab9942>

The distribution of spacecraft in the inner heliosphere during 2019 March enabled comprehensive observations of an interplanetary coronal mass ejection (ICME) that encountered Parker Solar Probe (PSP) at 0.547 au from the Sun. This ICME originated as a slow (~ 311 km s⁻¹) streamer blowout (SBO) on the Sun as measured by the white-light coronagraphs on board the Solar TERrestrial RELations Observatory-A and the Solar and Heliospheric Observatory.

Despite its low initial speed, the passage of the ICME at PSP was preceded by an anisotropic, energetic (≈ 100 keV/n) ion enhancement and by two interplanetary shocks. The ICME was embedded between slow (~ 300 km s⁻¹) solar wind and a following, relatively high-speed (~ 500 km s⁻¹), stream that most likely was responsible for the unexpectedly short (based on the SBO speed) ICME transit time of less than ~ 56 hr between the Sun and PSP, and for the formation of the preceding shocks. By assuming a graduated cylindrical shell (GCS) model for the SBO that expands self-similarly with time, we estimate the propagation direction and morphology of the SBO near the Sun. We reconstruct the flux-rope structure of the in situ ICME assuming an elliptic-cylindrical topology and compare it with the portion of the 3D flux-

rope GCS morphology intercepted by PSP. ADAPT-WSA-ENLIL-Cone magnetohydrodynamic simulations are used to illustrate the ICME propagation in a structured background solar wind and estimate the time when PSP established magnetic connection with the compressed region that formed in front of the ICME. This time is consistent with the arrival at PSP of energetic particles accelerated upstream of the ICME.

Evolution of the magnetic field rotation distributions in the inner heliosphere

A. [Larosa](#)^{1,2}, C. H. K. Chen², J. R. McIntyre², V. K. Jagarlamudi³ and L. Sorriso-Valvo^{1,4}

A&A, 686, A238 (2024)

<https://www.aanda.org/articles/aa/pdf/2024/06/aa50030-24.pdf>

Context. The nature and evolution of the solar wind magnetic field rotations is studied in data from the Parker Solar Probe.

Aims. We investigated the magnetic field deflections in the inner heliosphere below 0.5 au in a distance- and scale-dependent manner to shed some light on the mechanism behind their evolution.

Methods. We used the magnetic field data from the FIELDS instrument suite to study the evolution of the magnetic field vector increment and rotation distributions that contain switchbacks.

Results. We find that the rotation distributions evolve in a scale-dependent fashion. They have the same shape at small scales regardless of the radial distance, in contrast to larger scales, where the shape evolves with distance. The increments are shown to evolve towards a log-normal shape with increasing radial distance, even though the log-normal fit works quite well at all distances, especially at small scales. The rotation distributions are shown to evolve towards a previously developed rotation model moving away from the Sun.

Conclusions. Our results suggest a scenario in which the evolution of the rotation distributions is primarily the result of the expansion-driven growth of the fluctuations, which are reshaped into a log-normal distribution by the solar wind turbulence.

Switchbacks: statistical properties and deviations from alfvénicity

A. [Larosa](#), [V. Krasnoselskikh](#), [T. Dudok de Wit](#)^{1,2},

A&A 2020

<https://arxiv.org/pdf/2012.10420.pdf>

{Parker Solar Probe's first solar encounter has revealed the presence of sudden magnetic field deflections that are called switchbacks and are associated with proton velocity enhancements in the slow alfvénic solar wind.} {We study their statistical properties with a special focus on their boundaries.} {Using data from SWEAP and FIELDS we investigate particle and wavefield properties. The magnetic boundaries are analyzed with the minimum variance technique.} {Switchbacks are found to be alfvénic in 73% of the cases and compressible in 27%. The correlations between magnetic field magnitude and density fluctuations reveal the existence of both positive and negative correlations, and the absence of perturbations of the magnetic field magnitude. Switchbacks do not lead to a magnetic shear in the ambient field. Their boundaries can be interpreted in terms of rotational or tangential discontinuities. The former are more frequent.} {Our findings provide constraints on the possible generation mechanisms of switchbacks, which has to be able to account also for structures that are not purely alfvénic. One of the possible candidates, among others, manifesting the described characteristics is the firehose instability.} 4-8 Nov 2018

Evolution of coronal mass ejections with and without sheaths from the inner to the outer heliosphere: Statistical investigation for 1975 to 2022

C. [Larrodera](#)^{1,2} and M. Temmer²

A&A, 685, A89 (2024)

<https://arxiv.org/pdf/2402.16653.pdf>

<https://www.aanda.org/articles/aa/pdf/2024/05/aa48641-23.pdf>

Aims. This study covers a thorough statistical investigation of the evolution of interplanetary coronal mass ejections (ICMEs) with and without sheaths through a broad heliocentric distance and temporal range. The analysis treats the sheath and magnetic obstacle (MO) separately in order to gain more insight on their physical properties. In detail, we aim to unravel different characteristics of these structures occurring over the inner and outer heliosphere.

Methods. The method is based on a large statistical sample of ICMEs probed over different distances in the heliosphere. For this, information about detection times for the sheath and MO from 13 individual ICME catalogs was collected and crosschecked. The time information was then combined into a main catalog that was used as the basis for the statistical investigation. The data analysis based on this catalog covers a large number of spacecraft missions, enabling in situ solar wind measurements from 1975 to 2022. This allowed us to study the differences between solar cycles.

Results. All the structures under study (sheath, MO with and without sheath) show the biggest increase in size together with the largest decrease in density at a distance of ~ 0.75 AU. At 1 AU, we found different sizes for MOs with and without a sheath, with the former being larger. Up to 1 AU, the upstream solar wind shows the strongest pileup close to the interface with the sheath. For larger distances, the pileup region seems to shift, and it recedes from that interface further into the upstream solar wind. This might refer to a change in the sheath formation mechanism (driven versus non-driven) with heliocentric distance, suggesting the relevance of the CME propagation and the expansion behavior in the outer heliosphere. A comparison to previous studies showed inconsistencies over the solar cycle, which makes more detailed studies necessary in order to fully understand the evolution of ICME structures.

Appendix A: Description of catalogs Table A.1. References of the individual catalogs used.

Estimation of the solar wind extreme events

C. Larrodera, L. Nikitina, C. Cid

Space Weather. **Volume19, Issue12** e2021SW002902 2021

<https://arxiv.org/pdf/2112.00005.pdf>

<https://agupubs.onlinelibrary.wiley.com/doi/epdf/10.1029/2021SW002902>

<https://doi.org/10.1029/2021SW002902>

This research provides an analysis of extreme events in the solar wind and in the magnetosphere due to disturbances of the solar wind. Extreme value theory has been applied to a 20 year data set from the Advanced Composition Explorer (ACE) spacecraft for the period 1998-2017. The solar proton speed, solar proton temperature, solar proton density and magnetic field have been analyzed to characterize extreme events in the solar wind. The solar wind electric field, vB_z has been analyzed to characterize the impact from extreme disturbances in the solar wind to the magnetosphere. These extreme values were estimated for one-in-40 and one-in-80 years events, which represent two and four times the range of the original data set. The estimated values were verified by comparison with measured values of extreme events recorded in previous years. Finally, our research also suggests the presence of an upper boundary in the magnitudes under study.

The distribution function of the average iron charge state at 1 AU: from a bimodal wind to ICME identification

C. Larrodera, C. Cid

Solar Phys. **295**, Article number: 156 2020

<https://arxiv.org/pdf/2009.07596.pdf>

<https://link.springer.com/content/pdf/10.1007/s11207-020-01727-8.pdf>

We aim to investigate the distribution function of $\langle Q_{Fe} \rangle$ at 1AU to check if it corresponds to a bimodal wind. We use data from SWICS instrument on board the ACE spacecraft along 20 years. We propose the bi-Gaussian function as the probability distribution function that fits the $\langle Q_{Fe} \rangle$ distribution. We study the evolution of the parameters of the bimodal distribution with the solar cycle. We compare the outliers of the sample with the existing catalogues of ICMEs and identify new ICMEs. The $\langle Q_{Fe} \rangle$ at 1 AU shows a bimodal distribution related to the solar cycle. Our results confirm that $\langle Q_{Fe} \rangle > 12$ is a trustworthy proxy for ICME identification and a reliable signature in the ICME boundary definition.

26 April-2 May 2003 , 16-23 February 2011

Table 1. List of outlier events (1999-2016)

Coronal shocks associated with CMEs and flares and their space weather consequences

Marina Laskari¹, Panagiota Preka-Papadema¹, Constantine Caroubalos², George Pothitakis², Xenophon Moussas¹, Eleftheria Mitsakou¹ and A. Hillaris¹

Universal Heliophysical Processes Proceedings IAU Symposium No. 257, 2008, N. Gopalswamy & D.F. Webb, eds., 2009

<http://journals.cambridge.org/action/displayIssue?iid=4866212>

We study the geoeffectiveness of a sample of complex events; each includes a coronal type II burst, accompanied by a GOES SXR flare and LASCO CME. The radio bursts were recorded by the ARTEMIS-IV radio spectrograph, in the 100-650 MHz range; the GOES SXR flares and SOHO/LASCO CMEs, were obtained from the Solar Geophysical Data (SGD) and the LASCO catalogue respectively. These are compared with changes of solar wind parameters and geomagnetic indices in order to establish a relationship between solar energetic events and their effects on geomagnetic activity.

Magnetic reconnection as a mechanism to produce multiple proton populations and beams locally in the solar wind

B. Lavraud, R. Kieokaew, N. Fargette, P. Louarn, A. Fedorov, N. André, G. Fruit, V. Génot, V. Réville, A. P. Rouillard, I. Plotnikov, E. Penou, A. Barthe, L. Prech, C. J. Owen, R. Bruno, F. Allegrini, M. Berthomier, D. Kataria, S. Livi, J. M. Raines, R. D'Amicis, J. P. Eastwood, C. Froment, R. Laker, M. Maksimovic, F. Marcucci, S. Perri, D. Perrone, T. D. Phan, D. Stansby, J. Stawarz, S. Toledo Redondo, A. Vaivads, D. Verscharen, I. Zouganelis, V. Angelini, V. Evans, T. S. Horbury, H. O'Brien

A&A 2021

<https://arxiv.org/pdf/2109.11232.pdf>

Context. Spacecraft observations early revealed frequent multiple proton populations in the solar wind. Decades of research on their origin have focused on processes such as magnetic reconnection in the low corona and wave-particle interactions in the corona and locally in the solar wind.

Aims. This study aims to highlight that multiple proton populations and beams are also produced by magnetic reconnection occurring locally in the solar wind.

Methods. We use high resolution **Solar Orbiter** proton velocity distribution function measurements, complemented by electron and magnetic field data, to analyze the association of multiple proton populations and beams with magnetic reconnection during a period of slow Alfvénic solar wind on **16 July 2020**.

Results. At least 6 reconnecting current sheets with associated multiple proton populations and beams, including a case of magnetic reconnection at a switchback boundary, are found during this day. This represents 2% of the measured distribution functions. We discuss how this proportion may be underestimated, and how it may depend on solar wind type and distance from the Sun. Conclusions. Although suggesting a likely small contribution, but which remains to be quantitatively assessed, Solar Orbiter observations show that magnetic reconnection must be considered as one of the mechanisms that produce multiple proton populations and beams locally in the solar wind.

The Heliospheric Current Sheet and Plasma Sheet during Parker Solar Probe's First Orbit

B. Lavraud¹, N. Fargette¹, V. Réville¹, A. Szabo², J. Huang ...

2020 ApJL 894 L19

<https://doi.org/10.3847/2041-8213/ab8d2d>

We present heliospheric current sheet (HCS) and plasma sheet (HPS) observations during Parker Solar Probe's (PSP) first orbit around the Sun. We focus on the eight intervals that display a true sector boundary (TSB; based on suprathermal electron pitch angle distributions) with one or several associated current sheets. The analysis shows that (1) the main density enhancements in the vicinity of the TSB and HCS are typically associated with electron strahl dropouts, implying magnetic disconnection from the Sun, (2) the density enhancements are just about twice that in the surrounding regions, suggesting mixing of plasmas from each side of the HCS, (3) the velocity changes at the main boundaries are either correlated or anticorrelated with magnetic field changes, consistent with magnetic reconnection, (4) there often exists a layer of disconnected magnetic field just outside the high-density regions, in agreement with a reconnected topology, (5) while a few cases consist of short-lived density and velocity changes, compatible with short-duration reconnection exhausts, most events are much longer and show the presence of flux ropes interleaved with higher- β regions. These findings are consistent with the transient release of density blobs and flux ropes through sequential magnetic reconnection at the tip of the helmet streamer. The data also demonstrate that, at least during PSP's first orbit, the only structure that may be defined as the HPS is the density structure that results from magnetic reconnection, and its byproducts, likely released near the tip of the helmet streamer.

Geo-effectiveness and radial dependence of magnetic cloud erosion by magnetic reconnection

Benoit Lavraud, Alexis Ruffenach, Alexis P. Rouillard, Primoz Kajdic, Ward B. Manchester and Noé Lugaz
JGR, Volume 119, Issue 1, pages 26–35, January 2014

<http://onlinelibrary.wiley.com/doi/10.1002/2013JA019154/pdf>

Magnetic flux erosion by magnetic reconnection occurs at the front of at least some magnetic clouds (MCs). We first investigate how erosion influences the geo-effectiveness of MCs in a general sense and using a south-north magnetic polarity MC observed on **18–20 October 1995**. Although the magnetic shear at its front may not be known during propagation, measurements at 1 AU show signatures of local reconnection. Using a standard MC model, an empirical model of the geomagnetic response (Dst), and an observational estimate of the magnetic flux erosion, we find that the strength of the observed ensuing storm was ~30% lower than if no erosion had occurred. We then discuss the interplay between adiabatic compression and magnetic erosion at the front of MCs. We conclude that the most geo-effective configuration for a south-north polarity MC is to be preceded by a solar wind with southward IMF. This stems not only from the formation of a geo-effective sheath ahead of it but also from the adiabatic compression and reduced (or lack

thereof) magnetic erosion which constructively conspire for the structure to be more geo-effective. Finally, assuming simple semiempirical and theoretical Alfvén speed profiles expected from expansion to 1 AU, we provide first-order estimates of the erosion process radial evolution. We find that the expected reconnection rates during propagation allow for significant erosion, on the order of those reported. Calculations also suggest that most of the erosion should occur in the inner heliosphere, and up to ~50% may yet occur beyond Mercury's orbit.

Statistics of counter-streaming solar wind suprathermal electrons at solar minimum: STEREO observations

B. [Lavraud](#), A. Opitz, J. Gosling, A. Rouillard, K. Meziane, J. Sauvaud, A. Fedorov, I. Dandouras, V. Genot, C. Jacquy, P. Louarn, C. Mazelle, E. Penou, D. Larson, J. Luhmann, P. Schroeder, L. Jian, C. Russell, C. Foullon, R. Skoug, J. Steinberg, K. Simunac, and A. Galvin
Ann. Geophys., 28, 233-246, 2010

Previous work has shown that solar wind suprathermal electrons can display a number of features in terms of their anisotropy. Of importance is the occurrence of counter-streaming electron patterns, i.e., with "beams" both parallel and anti-parallel to the local magnetic field, which is believed to shed light on the heliospheric magnetic field topology. In the present study, we use STEREO data to obtain the statistical properties of counter-streaming suprathermal electrons (CSEs) in the vicinity of corotating interaction regions (CIRs) during the period March–December 2007. Because this period corresponds to a minimum of solar activity, the results are unrelated to the sampling of large-scale coronal mass ejections, which can lead to CSE owing to their closed magnetic field topology. The present study statistically confirms that CSEs are primarily the result of suprathermal electron leakage from the compressed CIR into the upstream regions with the combined occurrence of halo depletion at 90° pitch angle. The occurrence rate of CSE is found to be about 15–20% on average during the period analyzed (depending on the criteria used), but superposed epoch analysis demonstrates that CSEs are preferentially observed both before and after the passage of the stream interface (with peak occurrence rate >35% in the trailing high speed stream), as well as both inside and outside CIRs. The results quantitatively show that CSEs are common in the solar wind during solar minimum, but yet they suggest that such distributions would be much more common if pitch angle scattering were absent. We further argue that (1) the formation of shocks contributes to the occurrence of enhanced counter-streaming sunward-directed fluxes, but does not appear to be a necessary condition, and (2) that the presence of small-scale transients with closed-field topologies likely also contributes to the occurrence of counter-streaming patterns, but only in the slow solar wind prior to CIRs.

Relationships between Interplanetary Coronal Mass Ejection Characteristics and Geoeffectiveness in the Declining Phase of Solar Cycles 23 and 24

M. Benedict [Lawrance](#), [Y.-J. Moon](#) & [A. Shanmugaraju](#)

[Solar Physics](#) volume 295, Article number: 62 (2020)

<https://link.springer.com/content/pdf/10.1007%2Fs11207-020-01623-1.pdf>

In this paper, we have examined the relationships between the characteristics of interplanetary coronal mass ejections (ICMEs) and geoeffectiveness in the declining phase of Solar Cycles 23 and 24. We discuss the results in comparison with those of the rising phase. Major results of this study are as follows: The ICMEs in the declining phase of Cycle 23 have generated higher storm strength than those in Cycle 24. The mean storm strength of the sheath and ICME for each cycle in the declining phase is greater than in the rising phase. This indicates that the declining phase is more geoeffective than the rising phase. Cycle 24 events seem to be slightly more geoeffective towards the second half of the cycle even though the cycle is weak in the rising phase. The mean radial size of ICMEs is ~ 0.36 AU in Cycle 23 and ~0.32 AU in Cycle 24. Around 25% of the ICMEs in Cycle 23 and 15% in Cycle 24 exceed ~0.5 AU in size at 1 AU. The correlation between the southward magnetic component (BsBs) and the storm strength they cause is decisive in both cycles. This substantiates that the storm strength of the ICMEs strongly relies on the ICME BsBs in both cycles. The correlation between the storm strength/BsBs and the size of sheath/ICME seems insignificant, which suggests that the storm strength is independent of the size of the ICMEs. Almost 80% of geomagnetic storm peaks occurred in the ICME duration of the declining phase of Cycles 23 and 24, which is substantially identical to the rising phase. Summing up, this sort of study will be eminent to emphasize the variations in the rising and declining phases of solar cycles. The ICMEs are dominant in generating storms both in the rising and declining phases of a solar although in the declining phase they seem to generate more geoeffectiveness than in the rising phase.

Table 1 List of ICME and sheath parameters for the declining phase of Cycle 23 (2002 – 2008).

Table 2 List of ICME and sheath parameters for the declining phase of Cycle 24 (2014 – 2018).

Relationships Between Interplanetary Coronal Mass Ejection Characteristics and Geoeffectiveness in the Rising Phase of Solar Cycles 23 and 24

M. Benedict [Lawrance](#), A. Shanmugaraju, Y.-J. Moon, M. Syed Ibrahim, S. Umapathy
Solar Physics, Volume 291, Issue 5, pp 1547-1560 2016

The characteristics and geoeffectiveness of interplanetary coronal mass ejections (ICMEs) are derived and their relationships are investigated. The results are compared for a set of events in the rising phase of Solar Cycles 23 and 24. These events are considered from the reported list of Cane and Richardson (Geophys. Res. Lett. 27, 3591, [2000](#)). The geoeffectiveness is studied independently for ICME and sheath. The results obtained are that i) CMEs of Cycle 23 have generated a higher Dst index than Cycle 24 CMEs and that ii) the southward magnetic component (BsBs) and the Dst index of ICMEs correlate well for both Cycles 23 and 24 in their rising phase. These findings agree with the literature, which has described Cycle 24 to be weaker than Cycle 23 and where the ICME/sheath regions of Cycle 23 are found to have a greater BsBs that results in stronger storms. In addition, other results obtained are as follows: i) The relation between ICME size and the related Dst index gives a weak correlation for the rising phases of both Cycles 23 and 24. ii) The correlation between sheath size and Dst index is higher in the rising phase of Cycle 24 than in the rising phase of Cycle 23. iii) The average ICME size of the rising phase of Cycle 23 (84 R_☉) is greater than that of the rising phase of Cycle 24 (58 R_☉). However, the average sheath size is 24 R_☉, which is nearly equal to that of Cycle 24 (26 R_☉). Thus the differences between the properties of ICME and sheath in both the cycles are demonstrated. Nearly 75 % of geomagnetic storm peaks occurred in the ICME duration in the rising phase of Cycles 23 and 24. This shows that the ICMEs are more important in generating the storms than the sheaths in the rising phase of a solar cycle.

Solar Wind Electron Strahls Associated with a High-Latitude CME: **\emph{Ulysses}** Observations

M. [Lazar](#), J. Pomoell, S. Poedts, C. Dumitrache, N.A. Popescu
Solar Phys., Volume 289, Issue 11, pp 4239-4266 2014

<http://arxiv.org/pdf/1405.5690v1.pdf>

Counterstreaming beams of electrons are ubiquitous in coronal mass ejections (CMEs) - although their existence is not unanimously accepted as a necessary and/or sufficient signature of these events. We continue the investigations of a high-latitude CME registered by the **\emph{Ulysses}** spacecraft on **January 18--19, 2002** (Dumitrache, Popescu, and Oncica, Solar Phys. **{\bf 272}**, 137, 2011), by surveying the solar wind electron distributions associated with this event. The temporal-evolution of the pitch-angle distributions reveal populations of electrons distinguishable through their anisotropy, with clear signatures of i) electron strahls, ii) counter-streaming in the magnetic clouds and their precursors, and iii) unidirectional in the fast wind preceding the CME. The analysis of the counter-streams inside the CME allows us to elucidate the complexity of the magnetic-cloud structures embedded in the CME and to refine the borders of the event. Identifying such strahls in CMEs, which preserve properties of the low $\beta < 1$ coronal plasma, gives more support to the hypothesis that these populations are remnants of the hot coronal electrons that escape from the electrostatic potential of the Sun into the heliosphere.

Dst index forecast based on ground-level data aided by bio-inspired algorithms

J. A. [Lazzús](#) , [P. Vega-Jorquera](#) , [L. Palma-Chilla](#) , [M. V. Stepanova](#),
[N. V. Romanova](#)

Space Weather [Volume 17, Issue 10](#) Pages 1487-1506 2019

<https://doi.org/10.1029/2019SW002215>

<https://agupubs.onlinelibrary.wiley.com/doi/epdf/10.1029/2019SW002215>

In this study, different hybridized techniques that combine an artificial neural network (ANN) with bio-inspired optimization algorithms such as particle swarm optimization (PSO), genetic algorithm (GA), and a hybridized PSO+GA were applied to update the ANN connection weights and so forecast the disturbance storm time (Dst) index. The past values of Dst index time series were used as input parameters to forecast its variation from 1 to 6 hours ahead. The database collected considers 233,760 hourly data from 01 January 1990 to 31 August 2016, containing storms and quiet period, grouped into three data sets: learning set (116,880 hourly data points), validation set (58,440 data points), and testing set (58,440 data points). Several ANN configurations were studied and optimized during the training process by evaluating the root mean square error (RMSE) and the correlation coefficient (R). An analysis of the predictive capability of each method was made year per year, and according to the levels of the geomagnetic storm. Also, an additional test was applied to the proposed method using 17 intense geomagnetic storms reported during solar cycle 24, including the St. Patrick's Day storm of 2015. Results show that the hybridized ANN+PSO method can forecast the Dst index quite accurately from 1 to 3 h in advance (with $RMSE \leq 5$ nT and $R \geq 0.9$), while the ANN+PSO+GA method can forecast the Dst index quite accurately from 4 to 6 h ahead ($RMSE \leq 7$ nT and $R \geq 0.8$)

Source Locations and Solar-Cycle Distribution of the Major Geomagnetic Storms ($Dst \leq -100$ nT) from 1932 to 2018

Gui-Ming Le, [Ming-Xian Zhao](#), [Wen-Tao Zhang](#) & [Gui-Ang Liu](#)

[Solar Physics](#) volume 296, Article number: 187 (2021)

<https://link.springer.com/content/pdf/10.1007/s11207-021-01927-w.pdf>

<https://doi.org/10.1007/s11207-021-01927-w>

We studied the source locations and solar-cycle (SC) distribution of the major geomagnetic storms (MGSs) that occurred from 1932 to 2018. We divided the MGSs into two groups: the intense geomagnetic storms (IGSs) ($-200 \text{ nT} < Dst \leq -100 \text{ nT}$) and the great geomagnetic storms (GGSs) ($Dst \leq -200 \text{ nT}$). The GGSs were split into three subgroups: GGSs-I ($-300 \text{ nT} < Dst \leq -200 \text{ nT}$), GGSs-II ($-400 \text{ nT} < Dst \leq -300 \text{ nT}$) and GGSs-III ($-600 \text{ nT} < Dst \leq -400 \text{ nT}$). The source locations of the GGSs-I and GGSs-II were distributed in the longitudinal range of [E84, W73], while the GGSs-III were distributed in the range of [E22, W14]. 90% of the GGSs were distributed in the longitudinal area of [E45, W45]. The statistical results show that 38.6%, 61.4% and 86% of the GGSs occurred in the ascending phase, the descending phase, and the period from two years before to three years after the solar maximum, respectively. 33.3%, 66.7% and 76% of the IGSs appeared in the ascending phase, the descending phase, and the period from two years to three years after the solar maximum, respectively. The number of MGSs in a SC has a good correlation with the SC size. However, the largest storm intensity in a SC has almost no relationship with the SC size, implying that the number of MGSs in a weak SC will be small. However, we cannot rule out the possibility that a weak SC may have a very strong extreme geomagnetic storm.

Table 1 The largest storm intensity for each SC from 1932 to 2016

Table 4 The GGSs during SCs 17 – 24 ($Dst \leq -200$ nT).

Dependence of Major Geomagnetic Storm Intensity ($Dst \leq -100$ nT) on Associated Solar Wind Parameters

Gui-Ming Le, [Gui-Ang Liu](#) & [Ming-Xian Zhao](#)

[Solar Physics](#) volume 295, Article number: 108 (2020)

<https://link.springer.com/content/pdf/10.1007/s11207-020-01675-3.pdf>

We investigate the influence of various solar wind parameters on the intensity of the associated major geomagnetic storm. SYM-Hmin was used to indicate the intensity of major geomagnetic storms, while $I(B_s)$, $I(E_y)$ and $I(Q)$ were used to indicate the time integrals of the southward interplanetary magnetic field component (B_s), the solar wind electric field (E_y), and Q , which is the combination of E_y and the solar wind dynamic pressure, during the main phase of a major geomagnetic storm, respectively. We have found that the correlation coefficient (CC) between the time integral of solar wind parameters and the intensity of an associated major geomagnetic storm has a physical meaning, while the CC between the peak value of a given solar wind parameter and the intensity of an associated major geomagnetic storm has no physical meaning. We used 67 major geomagnetic storms that occurred between 1998 and 2006 to calculate the CC between SYM-Hmin and $I(B_s)$, the CC between SYM-Hmin and $I(E_y)$, and the CC between SYM-Hmin and $I(Q)$. The derived CC between $I(B_s)$ and SYM-Hmin is 0.33, while the CC between $I(E_y)$ and SYM-Hmin is 0.57, and the CC between $I(Q)$ and SYM-Hmin is 0.86, respectively. These values indicate that $I(B_s)$, $I(E_y)$ and $I(Q)$ contribute in a small, moderate, and crucial way to the intensity of a major geomagnetic storm, respectively. For the solar wind to have a strong geoeffectiveness B_s plays a role, together the solar wind speed and density, but also the dynamic pressure > 3 nPa. Large and long duration B_s or E_y cannot ensure a major geomagnetic storm, if the solar wind dynamic pressure is much lower than 3 nPa. **18–19, October 1998**

Geoeffectiveness of the coronal mass ejections associated with solar proton events

Gui-Ming Le, Chuan Li, Yu-Hua Tang, Liu-Guan Ding, Zhi-Qiang Yin, Yu-Lin Chen, Yang-Ping Lu, Min-Hao Chen, Zhong-Yi Li

Research in Astronomy and Astrophysics (RAA) [Vol 16, No 1 \(2016\)](#) paper 14, **File**

The intensity-time profiles of solar proton events (SPEs) are grouped into three types in the present study. The Type-I means that the intensity-time profile of an SPE has one peak, which occurs shortly after the associated solar flare and coronal mass ejection (CME). The Type-II means that the SPE profile has two peaks: the first peak occurs shortly after the solar eruption, the second peak occurs at the time when the CME-driven shock reaches the Earth, and the intensity of the second peak is lower than the first one. If the intensity of the second peak is higher than the first one, or the SPE intensity increases continuously until the CME-driven shock reaches the Earth, this kind of intensity-time profile is defined as Type-III. It is found that most CMEs associated with Type-I SPEs have no geoeffectiveness and only a small part of CMEs associated with Type-I SPEs can produce minor ($-50 \text{ nT} \leq Dst \leq -30 \text{ nT}$) or moderate geomagnetic storms

($-100 \text{ nT} \leq \text{Dst} \leq -50 \text{ nT}$), but never an intense geomagnetic storm ($-200 \text{ nT} \leq \text{Dst} < -100 \text{ nT}$). However, most of the CMEs associated with Type-II and Type-III SPEs can produce intense or great geomagnetic storms ($\text{Dst} \leq -200 \text{ nT}$). The solar wind structures responsible for the geomagnetic storms associated with SPEs with different intensity-time profiles have also been investigated and discussed. **1998 May 2, 1998 May 6, 2001 January 28, 2003 October 28, 2004 July 25, 2006 December 13**

Table 1 Geoeffectiveness of CMEs Associated with Type-I SPEs during Solar Cycle 23

Table 2 Geoeffectiveness of CMEs Associated with Type-II SPEs during Solar Cycle 23

Modeling Energetic Particle Acceleration and Transport in a Solar Wind Region with Contracting and Reconnecting Small-scale Flux Ropes at Earth Orbit

J. A. **Le Roux**^{1,2}, G. M. Webb², O. V. Khabarova³, L.-L. Zhao², and L. Adhikari²

2019 ApJ 887 77

[sci-hub.se/10.3847/1538-4357/ab521f](https://doi.org/10.3847/1538-4357/ab521f)

New analytical steady-state and time-dependent solutions for the acceleration of energetic particles by contracting and reconnecting small-scale flux ropes (SMFRs) in the solar wind are presented. For this purpose, a telegrapher-type Parker transport equation was derived from the existing underlying focused transport equation. The solutions unify all SMFR acceleration mechanisms present in the transport equation, showing that SMFR acceleration by the reconnection electric field in the mixed-derivative transport term is constrained by and requires the presence of second-order Fermi SMFR acceleration. We explore the potential of these solutions in reproducing energetic proton flux enhancements and spectral evolution between $\sim 50 \text{ keV}$ and 5 MeV in dynamic SMFR regions near large-scale reconnecting current sheets in the solar wind at Earth orbit. It is shown that second-order Fermi SMFR acceleration involving the variance in SMFR compression and incompressible parallel shear flow and confirmed that first-order SMFR Fermi acceleration, due to mean SMFR compression (successfully used before in data fits), are both workable options in reproducing observed flux amplification factors when using reasonable SMFR parameters. However, the predicted substantial quantitative differences in the spatial evolution of the accelerated spectra through the SMFR region might provide a way to distinguish between first- and second-order Fermi SMFR acceleration in observations. It is concluded that more detailed data analysis of SMFR parameters in SMFR acceleration events is needed before the relative role of first- and second-order SMFR acceleration mechanisms can be determined.

HOW THE SOLAR WIND TIES TO ITS PHOTOSPHERIC ORIGINS

Robert J. Leamon¹ and Scott W. McIntosh²

2009 ApJ 697 L28-L32 doi: [10.1088/0004-637X/697/1/L28](https://doi.org/10.1088/0004-637X/697/1/L28)

We present a new method of visualizing the solar photospheric magnetic field based on the "Magnetic Range of Influence" (MRoI). The MRoI is a simple realization of the magnetic environment in the photosphere, reflecting the distance required to balance the integrated magnetic field contained in any magnetogram pixel. It provides a new perspective on where subterrestrial field lines in a Potential Field Source Surface (PFSS) model connect to the photosphere, and thus the source of Earth-directed solar wind (within the limitations of PFSS models), something that is not usually obvious from a regular synoptic magnetogram. In each of three sample solar rotations, at different phases of the solar cycle, the PFSS footpoint either jumps between isolated areas of high MRoI or moves slowly within one such area. Footpoint motions are consistent with Fisk's interchange reconnection model.

Helicity of magnetic clouds and their associated active regions

Leamon, R.J., Canfield, R.C., Jones, S.L., Lambkin, K., Lundberg, B.J., Pevtsov, A.A.:

2004, *J. Geophys. Res.* **109**, 5106. **File**

<http://onlinelibrary.wiley.com/doi/10.1029/2003JA010324/pdf>

In this work we relate the magnetic and topological parameters of twelve interplanetary magnetic clouds to associated solar active regions. We use a cylindrically symmetric constant- α force-free model to derive field line twist, total current, and total magnetic flux from in situ observations of magnetic clouds. We compare these properties with those of the associated solar active regions, which we infer from solar vector magnetograms. Our comparison of fluxes and currents reveals: (1) the total flux ratios $\Phi_{\text{MC}}/\Phi_{\text{AR}}$ tend to be of order unity, (2) the total current ratios $I_{\text{MC}}/I_{\text{AR}}$ are orders of magnitude smaller, and (3) there is a statistically significant proportionality between them. Our key findings in comparing total twists αL are that (1) the values of $(\alpha L)_{\text{MC}}$ are typically an order of magnitude greater than those of $(\alpha L)_{\text{AR}}$ and (2) **there is no statistically significant sign or amplitude relationship between them. These findings compel us to believe that magnetic clouds associated with active region eruptions are formed by magnetic**

reconnection between these regions and their larger-scale surroundings, rather than simple eruption of preexisting structures in the corona or chromosphere.

Leamon *et al.* (2004) performed such fits to 12 MCs and found that their inferred axial fluxes roughly matched the flux of the entire active region (AR) whose CME had ejected it.

We note that the solar observations are ambiguous, and that in an active region a left-handed flux rope in the low corona may also be associated with a right-handed MC, as in some cases reported by Leamon *et al.* (2004).

Modeling CME encounters at Parker Solar Probe with OSPREI: Dependence on photospheric and coronal conditions*

Vincent E. **Ledvina**^{1,★★}, Erika Palmerio¹, Christina Kay^{2,3}, Nada Al-Haddad⁴ and Pete Riley¹
A&A 673, A96 (2023)

<https://doi.org/10.1051/0004-6361/202245445>

<https://www.aanda.org/articles/aa/pdf/2023/05/aa45445-22.pdf>

Context. Coronal mass ejections (CMEs) are eruptions of plasma from the Sun that travel through interplanetary space and may encounter Earth. CMEs often enclose a magnetic flux rope (MFR), the orientation of which largely determines the CMEs' geoeffectiveness. Current operational CME models do not model MFRs, but a number of research ones do, including the Open Solar Physics Rapid Ensemble Information (OSPREI) model.

Aims. We report the sensitivity of OSPREI to a range of user-selected photospheric and coronal conditions.

Methods. We modeled four separate CMEs observed in situ by Parker Solar Probe (PSP). We varied the input photospheric conditions using four input magnetograms (HMI Synchronic, HMI Synoptic, GONG Synoptic Zero-Point Corrected, and GONG ADAPT). To vary the coronal field reconstruction, we employed the Potential Field Source Surface (PFSS) model and varied its source-surface height in the range 1.5–3.0 R_{\odot} with 0.1 R_{\odot} increments.

Results. We find that both the input magnetogram and PFSS source surface often affect the evolution of the CME as it propagates through the Sun's corona into interplanetary space, and therefore the accuracy of the MFR prediction compared to in situ data at PSP. There is no obvious best combination of input magnetogram and PFSS source surface height.

Conclusions. The OSPREI model is moderately sensitive to the input photospheric and coronal conditions. Based on where the source region of the CME is located on the Sun, there may be best practices when selecting an input magnetogram to use. **21 Jun 2020, 9 Jun 2021, 7 Nov 2021, 26 Jan 2022**

Solar Chromospheric Network as a Source for Solar Wind Switchbacks

Jeongwoo **Lee**, Vasyli Yurchyshyn, Haimin Wang, Xu Yang, Wenda Cao, Juan Carlos Martínez Oliveros
ApJL , 935:L27 2022

<https://iopscience.iop.org/article/10.3847/2041-8213/ac86bf/pdf>

Recent studies suggest that the magnetic switchbacks (SBs) detected by the Parker Solar Probe carry information on the scales of solar supergranulation (large scale) and granulation (medium scale). We test this claim using high-resolution $H\alpha$ images obtained with the visible spectropolarimeters of the Goode Solar Telescope in Big Bear Solar Observatory. As possible solar sources, we count all the spicule-like features standing along the chromospheric networks near the coronal hole boundary visible in the $H\alpha$ blue-wing but absent in the red-wing images and measure the geometric parameters of dense sections of individual flux tubes. Intervals between adjacent spicules located along the chromospheric networks are found in the range of 0.4–1.5 Mm ($0^{\circ}.03$ – $0^{\circ}.12$) tending to be smaller than the medium scale of SBs. Interdistances between all pairs of the flux tubes are also counted and they appear in a single peak distribution around 0.7 Mm ($0^{\circ}.06$) unlike the waiting-time distribution of SBs in a scale-free single power-law form. The length-to-diameter ratio of the dense section of flux tubes is as high as 6–40, similar to the aspect ratio of SBs. The number of spicules along a network can be as high as 40–100, consistent with numerous SBs within a patch. With these numbers, it is argued that the medium scale of SBs can be understood as an equilibrium distance resulting from a random walk within each diverging magnetic field funnel connected to the chromospheric networks. **2020 June 17**

Effects of Geometries and Substructures of ICMEs on Geomagnetic Storms

Jae-Ok **Lee**, Kyung-Suk Cho, Rok-Soon Kim, Soojeong Jang, Katsuhide Marubashi

Solar Physics September 2018, 293:129 **File**

<https://link.springer.com/content/pdf/10.1007%2Fs11207-018-1344-z.pdf>

To better understand geomagnetic storm generations by ICMEs, we consider the effect of substructures (magnetic cloud, MC, and sheath) and geometries (impact location of flux-rope at the Earth) of the ICMEs. We apply the toroidal magnetic flux-rope model to 59 CDAW CME–ICME pairs to identify their substructures and geometries, and select 20 MC-associated and five sheath-associated storm events. We investigate the relationship between the storm strength indicated by minimum Dst index (D_{stmin}) and solar wind conditions related to a southward magnetic field. We find that all slopes of linear regression lines for sheath-storm events are steeper (≥ 1.4) than those of the MC-storm events in the relationship between D_{stmin} and solar wind conditions, implying that the efficiency of sheath for the process of geomagnetic storm generations is higher than that of MC. These results suggest that different general solar wind conditions (sheaths have a higher density, dynamic and thermal pressures with a higher fluctuation of the parameters and higher magnetic fields than MCs) have different impact on storm generation. Regarding the geometric encounter of ICMEs, 100% (2/2) of major storms ($D_{stmin} \leq -100$ nT) occur in the regions at negative PYPY (relative position of the Earth trajectory from the ICME axis in the YY component of the GSE coordinate) when the eastern flanks of ICMEs encounter the Earth. We find similar statistical trends in solar wind conditions, suggesting that the dependence of geomagnetic storms on 3D ICME–Earth impact geometries is caused by asymmetric distributions of the geoeffective solar wind conditions. For western flank events, 80% (4/5) of the major storms occur in positive PYPY regions, while intense geoeffective solar wind conditions are not located in the positive PYPY. These results suggest that the strength of geomagnetic storms depends on ICME–Earth impact geometries as they determine the solar wind conditions at Earth. **10 December 1997, 22 January 2000, 11 – 13 April 2001, 18 – 20 May 2002**

Table 1 Observational solar wind conditions of 25 ICMEs and their associated geomagnetic storm (1997-2006)

Are 3-D coronal mass ejection parameters from single-view observations consistent with multiview ones?

Harim Lee, Y.-J. Moon, Hyeonock Na, Soojeong Jang, Jae-Ok Lee

JGR December 2015 Vol: 120, Pages: 10,237–10,249

<http://onlinelibrary.wiley.com/doi/10.1002/2015JA021118/pdf>

To prepare for when only single-view observations are available, we have made a test whether the 3-D parameters (radial velocity, angular width, and source location) of halo coronal mass ejections (HCMEs) from single-view observations are consistent with those from multiview observations. For this test, we select 44 HCMEs from December 2010 to June 2011 with the following conditions: partial and full HCMEs by SOHO and limb CMEs by twin STEREO spacecraft when they were approximately in quadrature. In this study, we compare the 3-D parameters of the HCMEs from three different methods: (1) a geometrical triangulation method, the STEREO CAT tool developed by NASA/CCMC, for multiview observations using STEREO/SECCHI and SOHO/LASCO data, (2) the graduated cylindrical shell (GCS) flux rope model for multiview observations using STEREO/SECCHI data, and (3) an ice cream cone model for single-view observations using SOHO/LASCO data. We find that the radial velocities and the source locations of the HCMEs from three methods are well consistent with one another with high correlation coefficients (≥ 0.9). However, the angular widths by the ice cream cone model are noticeably underestimated for broad CMEs larger than 100° and several partial HCMEs. A comparison between the 3-D CME parameters directly measured from twin STEREO spacecraft and the above 3-D parameters shows that the parameters from multiview are more consistent with the STEREO measurements than those from single view.

2011-02-15

Table 1. Three-Dimensional CME Parameters of 44 Events Using Several Different Methods

Ensemble Modeling of Successive Halo CMEs: A Case Study

C. O. Lee, C. N. Arge, D. Odstrcil, G. Millward, V. Pizzo, N. Lugaz

Solar Phys., **2015**

The Wang–Sheeley–Arge (WSA)–Enlil cone modeling system is used for making routine arrival-time forecasts of Earth-directed halo coronal mass ejections (CMEs), since they typically produce the most geoeffective events. A major objective of this work is to better understand the sensitivity of the WSA–Enlil modeling results to input model parameters and how these parameters contribute to the overall model uncertainty and performance. In this study, ensemble-modeling results for a succession of three halo CME events that occurred on **2 – 4 August 2011** are presented. We investigate the sensitivity of the modeled CME arrival times to small variations in the input-cone properties by creating ensemble sets of numerical simulations for each CME event, based on multiple sets of cone parameters. We find that the accuracy of the modeled CME arrival times not only depends on the small variations to the initial input geometry, but also on the reliable specification of the background solar wind, which is driven by the input maps of the photospheric magnetic field. The accuracy in the arrival-time predictions also depends on whether the cone parameters

for all three CMEs are specified in a single WSA–Enlil simulation. The inclusion or exclusion of one or two of the preceding CMEs affects the solar-wind conditions through which the succeeding CME propagates. Although the accuracy of the modeled arrival times is sensitive to the input maps that are used to drive the background solar wind, the spread in the modeling ensemble remains mostly unchanged when different input maps are used.

Dependence of Geomagnetic Storms on Their Associated Halo CME Parameters

Jae-Ok [Lee](#)¹, Y.-J. Moon^{1, 2}, Kyoung-Sun Lee³ and R.-S. Kim

Solar Phys, Volume 289, Issue 6, pp 2233-2245, **2014, File**

We compare the geoeffective parameters of halo coronal mass ejections (CMEs). We consider **50 front-side full-halo CMEs (FFH CMEs)**, which are from the list of Michalek, Gopalswamy, and Yashiro (Solar Phys. 246, 399, 2007), whose asymmetric-cone model parameters and earthward-direction parameter were available. For each CME we use its projected velocity [V p], radial velocity [V r], angle between cone axis and sky plane [γ] from the cone model, earthward-direction parameter [D], source longitude [L], and magnetic-field orientation [M] of its CME source region. We make a simple linear-regression analysis to find out the relationship between CME parameters and Dst index. The main results are as follows: i) The combined parameters [(V r D)^{1/2} and V r γ] have higher correlation coefficients [cc] with the Dst index than the other parameters [V p and V r]: cc=0.76 for (V r D)^{1/2}, cc=0.70 for V r γ , cc=0.55 for V r, and cc=0.17 for V p. ii) Correlation coefficients between V r γ and Dst index depend on L and M; cc=0.59 for 21 eastern events [E], cc=0.80 for 29 western events [W], cc=0.49 for 17 northward magnetic-field events [N], and cc=0.69 for 33 southward magnetic-field events [S]. iii) Super geomagnetic storms (Dst \leq -200 nT) only appear in the western and southward magnetic-field events. The mean absolute Dst values of geomagnetic storms (Dst \leq -50 nT) increase with an order of E+N, E+S, W+N, and W+S events; the mean absolute Dst value (169 nT) of W+S events is significantly larger than that (75 nT) of E+N events. Our results demonstrate that not only do the cone-model parameters together with the earthward-direction parameter improve the relationship between CME parameters and Dst index, but also the longitude and the magnetic-field orientation of a FFH CME source region play a significant role in predicting geomagnetic storms.

Table 1 Front-side full-halo CMEs (2001 – 2002).

Ensemble Modeling of CME Propagation

C. O. [Lee](#)¹, C. N. Arge¹, D. Odstrčil², G. Millward³, V. Pizzo³, J. M. Quinn¹ and C. J. Henney

Solar Phys. July **2013**, Volume 285, Issue 1-2, pp 349-368; **File, 2012**,

The current progression toward solar maximum provides a unique opportunity to use multi-perspective spacecraft observations together with numerical models to better understand the evolution and propagation of coronal mass ejections (CMEs). Of interest to both the scientific and forecasting communities are the Earth-directed “halo” CMEs, since they typically produce the most geoeffective events. However, determining the actual initial geometries of halo CMEs is a challenge due to the plane-of-sky projection effects. Thus the recent **15 February 2011** halo CME event has been selected for this study. During this event the Solar TERrestrial Relations Observatory (STEREO) A and B spacecraft were fortuitously located $\sim 90^\circ$ away from the Sun–Earth line such that the CME was viewed as a limb event from these two spacecraft, thereby providing a more reliable constraint on the initial CME geometry. These multi-perspective observations were utilized to provide a simple geometrical description that assumes a cone shape for a CME to calculate its angular width and central position. The event was simulated using the coupled Wang–Sheeley–Arge (WSA)-Enlil 3D numerical solar corona-solar wind model. Daily updated global photospheric magnetic field maps were used to drive the background solar wind. To improve our modeling techniques, the sensitivity of the modeled CME arrival times to the initial input CME geometry was assessed by creating an ensemble of numerical simulations based on multiple sets of cone parameters for this event. It was found that the accuracy of the modeled arrival times not only depends on the initial input CME geometry, but also on the accuracy of the modeled solar wind background, which is driven by the input maps of the photospheric field. To improve the modeling of the background solar wind, the recently developed data-assimilated magnetic field synoptic maps produced by the Air Force Data Assimilative Photospheric flux Transport (ADAPT) model were used. The ADAPT maps provide a more instantaneous snapshot of the global photospheric field distribution than that provided by traditional daily updated synoptic maps. Using ADAPT to drive the background solar wind, an ensemble set of eight different CME arrival times was generated, where the spread in the predictions was ~ 13 hours and was nearly centered on the observed CME shock arrival time.

Simultaneity of Forbush decrease events observed at middle-latitude neutron monitors

Seongsuk [Lee](#), Suyeon Oh, Yu Yi

JGR, Volume 118, Issue 2, pages 608–614, February 2013

<http://onlinelibrary.wiley.com/doi/10.1002/jgra.50159/abstract>

Ground neutron monitors (NMs) sometimes observe a sudden reduction in galactic cosmic ray intensity—the so-called Forbush decrease (FD) event. Such events are mainly associated with interplanetary coronal mass ejections passing around the Earth and corotating interaction regions in the heliosphere. Some FD events are observed globally, either simultaneously or nonsimultaneously, at different NM stations in the case that the simultaneity is determined by the overlapping of the FD main phase, with the period of the cosmic ray intensity decreasing before returning to a steady state. Previous studies have identified two types of FD events with statistically significant differences in the distributions of the main phase onset time. It has been hypothesized that simultaneous FD events occur when a strong magnetic cloud passes by the Earth through the central part of the magnetic barrier, whereas nonsimultaneous events occur if a weaker magnetic cloud passes on the duskside of the magnetosphere. However, the previous statistical analyses were performed using only data from high geomagnetic latitude NM stations in the Northern Hemisphere. To address this shortcoming and to further test the above hypothesis, we repeated the analysis using data from NM stations located at middle latitudes (Jungfrauoch, Irkutsk, and Climax), employing cutoff rigidities 3–6 GV for the last solar maximum period (1998–2002), spanning the same time period as Oh et al. (2008) that employed high-latitude NM stations. The results of the present statistical analysis support the above hypothesis with high confidence levels. **Table (1998-2002).**

Organization of Energetic Particles by the SolarWind Structure During the Declining to Minimum Phase of Solar Cycle 23

C.O. Lee · J.G. Luhmann · I. de Pater · G.M. Mason · D. Haggerty · I.G. Richardson · H.V. Cane · L.K. Jian · C.T. Russell · M.I. Desai

Solar Phys (2010) 263: 239–261, DOI 10.1007/s11207-010-9556-x

We investigate the organization of the low energy energetic particles ($\leq 1\text{MeV}$) by solar wind structures, in particular corotating interaction regions (CIRs) and shocks driven by interplanetary coronal mass ejections, during the declining-to-minimum phase of Solar Cycle 23 from Carrington rotation 1999 to 2088 (January 2003 to October 2009). Because CIR-associated particles are very prominent during the solar minimum, the unusually long solar minimum period of this current cycle provides an opportunity to examine the overall organization of CIR energetic particles for a much longer period than during any other minimum since the dawn of the Space Age. We find that the particle enhancements associated with CIRs this minimum period recurred for many solar rotations, up to 30 at times, due to several high-speed solar wind streams that persisted. However, very few significant CIR-related energetic particle enhancements were observed towards the end of our study period, reflecting the overall weak high-speed streams that occurred at this time. We also contrast the solar minimum observations with the declining phase when a number of solar energetic particle events occurred, producing a mixed particle population. In addition, we compare the observations from this minimum period with those from the previous solar cycle. One of the main differences we find is the shorter recurrence rate of the high-speed solar wind streams (~ 10 solar rotations) and the related CIR energetic particle enhancements for the Solar Cycle 22 minimum period. Overall our study provides insight into the coexistence of different populations of energetic particles, as well as an overview of the large-scale organization of the energetic particle populations approaching the beginning of Solar Cycle 24.

Detailed Analysis of Solar Data Related to Historical Extreme Geomagnetic Storms: 1868 – 2010

Laure Lefèvre, Susanne Vennerstrøm, Mateja Dumbović, Bojan Vršnak, Davor Sudar, Rainer Arlt, Frédéric Clette, Norma Crosby

Solar Phys. Volume 291, Issue 5, pp 1483-1531 2016 File

An analysis of historical Sun–Earth connection events in the context of the most extreme space weather events of the last ~ 150 years is presented. To identify the key factors leading to these extreme events, a sample of the most important geomagnetic storms was selected based mainly on the well-known aa index and on geomagnetic parameters described in the accompanying paper (Vennerstrøm et al., Solar Phys. in this issue, 2016, hereafter Paper I). This part of the analysis

focuses on associating and characterizing the active regions (sunspot groups) that are most likely linked to these major geomagnetic storms.

For this purpose, we used detailed sunspot catalogs as well as solar images and drawings from 1868 to 2010. We have systematically collected the most pertinent sunspot parameters back to 1868, gathering and digitizing solar drawings from different sources such as the Greenwich archives, and extracting the missing sunspot parameters. We present a detailed statistical analysis of the active region parameters (sunspots, flares) relative to the geomagnetic parameters developed in Paper I.

In accordance with previous studies, but focusing on a much larger statistical sample, we find that the level of the geomagnetic storm is highly correlated to the size of the active regions at the time of the flare and correlated with the size of the flare itself. We also show that the origin at the Sun is most often a complex active region that is also most of the time close to the central meridian when the event is identified at the Sun. Because we are dealing with extremely severe storms, and not the usual severe storm sample, there is also a strong correlation between the size of the linked active region, the estimated transit speed, and the level of the geomagnetic event. In addition, we confirm that the geomagnetic events studied here and the associated events at the Sun present a low probability of occurring at low sunspot number value and are associated mainly with the maximum and descending part of the solar cycle.

Model Fitting of Wind Magnetic Clouds for the Period 2004 – 2006

R. P. [Lepping](#), [C.-C. Wu](#), [D. B. Berdichevsky](#) & [A. Szabo](#)

[Solar Physics](#) volume 295, Article number: 83 (2020)

<https://link.springer.com/content/pdf/10.1007/s11207-020-01630-2.pdf>

We give the results of parameter fitting of the magnetic clouds (MCs) observed by the Wind spacecraft for the three year period – 2004 to the end of 2006 (the “Present period”) using the force-free MC model of Lepping, Jones, and Burlaga (J. Geophys. Res.95, 11957, [1990](#)). There were 19 MCs identified in the Present period, which was mainly in the declining phase of the solar cycle. The long-term occurrence rate of MCs is 10.3/year (1995-2015), whereas the occurrence rate for the Present period is only 6.3/year, similar to that for the period 2007-2009. Hence, the MC occurrence rate has had an appreciable decrease for the six years 2004-2009. The MC modeling gives such basic MC quantities as size, axial orientation, field handedness, axial magnetic field strength, center time, and closest approach vector. A statistically based modification of the modeled field intensity is tested. Also calculated are derived quantities, such as axial magnetic flux, axial current density, and axial current. Quality (Q0Q0) estimates are assigned representing excellent (1), good/fair (2), and poor (3). We provide error estimates on the specific fit parameters for the individual MCs for the Q0=1,2,Q0=1,2 cases, and give a distribution of MC types (i.e. N ⇒ S, S ⇒ N, All N, All S, etc., ten categories in all). There is an inordinately large percentage of the N ⇒ S type in the Present period (32%). The Present period basic model fitting results are compared to the results of the full Wind mission and other 3-year periods. First, we notice that during the Present period the MCs are, on average, significantly faster (by 21%), distinctly stronger in axial magnetic field (by 37%), and smaller in diameter (by 5.5%), than those in the Long-term period. The quality of the MCs in the Present period is significantly better than that of the Long-term period, where the ratio $N(Q0=1,2)/N(Q0=1,2,3)N(Q0=1,2)/N(Q0=1,2,3)$ for each is 0.79 and 0.58, respectively. The Present period is quite different from the Long-term period (1995-2015), it is from the other three 3-year periods between 2006 and the end of 2015. In the Present period upstream shocks occur for the first 12 MCs of the 19 cases (63%); for comparison the Long-term rate is 56%.

Table 1, MCs 2004-2006

Magnetic Field Magnitude Modification for a Force-free Magnetic Cloud Model

R. P. [Lepping](#), [C.-C. Wu](#), [D. B. Berdichevsky](#), [C. Kay](#)

[Solar Phys.](#) 293:162 2018

<https://arxiv.org/ftp/arxiv/papers/1811/1811.07978.pdf>

A scheme was developed by Lepping, Berdichevsky, and Wu (Solar Phys., doi.10. 1007/ s11207-016-1040-9, 2017) [called the LBW article here] to approximate the average magnetic field magnitude (B-) profile of a "typical" magnetic cloud (MC) at/near 1AU. It was based on actual Wind MC data, taken over 21 years, that was used to modify a time shifted Bessel function (force-free) magnetic field, where shifted refers to a field that was adjusted for typical MC self-similar expansion. This was developed in the context of the Lepping, Jones, and Burlaga (J. Geophys. Res. vol. 95, p.11957, 1990) [called LJB here] MC parameter fitting model and should provide more realistic future representations of the MC's B-profile in most cases. In the LBW article, through testing, it was shown that on average it can be expected that in about 80% of the MC cases (but it varies according to the spacecrafts' actual closest approach distances) the modified model's B-profile of the MC should be significantly improved by use of this scheme. We describe how this scheme can be

employed practically in modifying the LJB MC fitting model, and we test a new and slightly better (and less unwieldy) version of the scheme, the non-shifted (of Bessel functions) version, which is the one actually used in the LJB model modification. The new scheme is based on modification formulae that are slightly more accurate than the old scheme, and it is expected to improve the B-profile in approximately 83% of the cases on average. The schemes are applicable for use with data originating only at/near 1 AU, since the magnetic field and plasma data used in the development of the associated formulae were from only the Wind spacecraft, which was and is at 1 AU.

Wind Magnetic Clouds for the Period 2013–2015: Model Fitting, Types, Associated Shock Waves, and Comparisons to Other Periods

R. P. Lepping, C.-C. Wu, D. B. Berdichevsky, A. Szabo

Solar Physics April 2018, 293:65

<https://link.springer.com/content/pdf/10.1007%2Fs11207-018-1273-x.pdf>

We give the results of parameter fitting of the magnetic clouds (MCs) observed by the Wind spacecraft for the three-year period 2013 to the end of 2015 (called the “Present” period) using the MC model of Lepping, Jones, and Burlaga (J. Geophys. Res.95, 11957, 1990). The Present period is almost coincident with the solar maximum of the sunspot number, which has a broad peak starting in about 2012 and extending to almost 2015. There were 49 MCs identified in the Present period. The modeling gives MC quantities such as size, axial attitude, field handedness, axial magnetic-field strength, center time, and closest-approach vector. Derived quantities are also estimated, such as axial magnetic flux, axial current density, and total axial current. Quality estimates are assigned representing excellent, fair/good, and poor. We provide error estimates on the specific fit parameters for the individual MCs, where the poor cases are excluded. Model-fitting results that are based on the Present period are compared to the results of the full Wind mission from 1995 to the end of 2015 (Long-term period), and compared to the results of two other recent studies that encompassed the periods 2007–2009 and 2010–2012, inclusive. We see that during the Present period, the MCs are, on average, slightly slower, slightly weaker in axial magnetic field (by 8.7%), and larger in diameter (by 6.5%) than those in the Long-term period. However, in most respects, the MCs in the Present period are significantly closer in characteristics to those of the Long-term period than to those of the two recent three-year periods. However, the rate of occurrence of MCs for the Long-term period is 10.3 year⁻¹–110.3 year⁻¹, whereas this rate for the Present period is 16.3 year⁻¹–116.3 year⁻¹, similar to that of the period 2010–2012. Hence, the MC occurrence rate has increased appreciably in the last six years. MC Type (N–S, S–N, All N, All S, etc.) is assigned to each MC; there is an inordinately large percentage of All S, by about a factor of two compared to that of the Long-term period, indicating many strongly tipped MCs. In 2005, there was a distinct change in variability and average value (viewed at 1/21/2 year averages) of the duration, MC speed, axial magnetic field strength, axial magnetic flux, and total current to lower values. In the Present period, upstream shocks occur for 43% of the 49 cases; for comparison, the Long-term rate is 56%.

Table 49 MCs

Average Magnetic Field Magnitude Profiles of Wind Magnetic Clouds as a Function of Closest Approach to the Clouds’ Axes and Comparison to Model

R. P. Lepping, D. B. Berdichevsky, C.-C. Wu

Solar Physics February 2017, 292:27

We examine the average magnetic field magnitude ($|\mathbf{B}| \equiv B$) within magnetic clouds (MCs) observed by the Wind spacecraft from 1995 to July 2015 to understand the difference between this B and the ideal B -profiles expected from using the static, constant- α , force-free, cylindrically symmetric model for MCs of Lepping, Jones, and Burlaga (J. Geophys. Res.95, 11957, 1990, denoted here as the LJB model). We classify all MCs according to an assigned quality, Q_0 ($= 1, 2, 3$), for excellent, good, and poor). There are a total of 209 MCs and 124 when only $Q_0 = 1$, 2 cases are considered. The average normalized field with respect to the closest approach (CA) is stressed, where we separate cases into four CA sets centered at 12.5 %, 37.5 %, 62.5 %, and 87.5 % of the average radius; the averaging is done on a percentage-duration basis to treat all cases the same. Normalized B means that before averaging, the B for each MC at each point is divided by the LJB model-estimated B for the MC axis, B_0 . The actual averages for the 209 and 124 MC sets are compared to the LJB model, after an adjustment for MC expansion (e.g. Lepping et al. in Ann. Geophys.26, 1919, 2008). This provides four separate difference-relationships, each fitted with a quadratic (Quad) curve of very small σ . Interpreting these Quad formulae should provide a comprehensive view of the variation in normalized B throughout the average MC, where we expect external front and rear compression to be part of its explanation. These formulae are also being considered for modifying the LJB model. This modification will be used in a scheme for forecasting the timing and

magnitude of magnetic storms caused by MCs. Extensive testing of the Quad formulae shows that the formulae are quite useful in correcting individual MC B_z -profiles, especially for the first $\approx 1/3$ of these MCs. However, the use of this type of B_z correction constitutes a (slight) violation of the force-free assumption used in the original LJB MC model.

Table 3 Examples of magnetic clouds used for checking the B/B_0 -correction with expansion* considered.

Wind Magnetic Clouds for 2010 – 2012: Model Parameter Fittings, Associated Shock Waves, and Comparisons to Earlier Periods

R. P. [Lepping](#), C.-C. Wu, D. B. Berdichevsky, A. Szabo

Solar Phys. Volume 290, Issue 8, pp 2265-2290 **2015**

We fitted the parameters of magnetic clouds (MCs) as identified in the Wind spacecraft data from early 2010 to the end of 2012 using the model of Lepping, Jones, and Burlaga (J. Geophys. Res. 95, 1195, [1990](#)). The interval contains 48 MCs and 39 magnetic cloud-like (MCL) events. This work is a continuation of MC model fittings of the earlier Wind sets, including those in a recent publication, which covers 2007 to 2009. This period (2010 – 2012) mainly covers the maximum portion of Solar Cycle 24. Between the previous and current interval, we document 5.7 years of MCs observations. For this interval, the occurrence frequency of MCs markedly increased in the last third of the time. In addition, over approximately the last six years, the MC type (i.e. the profile of the magnetic-field direction within an MC, such as North-to-South, South-to-North, all South) dramatically evolved to mainly North-to-South types when compared to earlier years. Furthermore, this evolution of MC type is consistent with global solar magnetic-field changes predicted by Bothmer and Rust (Coronal Mass Ejections, 139, [1997](#)). Model fit parameters for the MCs are listed for 2010 – 2012. For the 5.7 year interval, the observed MCs are found to be slower, weaker in estimated axial magnetic-field intensity, and shorter in duration than those of the earlier 12.3 years, yielding much lower axial magnetic-field fluxes. For about the first half of this 5.7 year period, i.e. up to the end of 2009, there were very few associated MC-driven shock waves (distinctly fewer than the long-term average of about 50 % of MCs). But since 2010, such driven shocks have increased markedly, reflecting similar statistics as the long-term averages. We estimate that 56 % of the total observed MCs have upstream shocks when the full interval of 1995 – 2012 is considered. However, only 28 % of the total number of MCLs have driven shocks over the same period. Some interplanetary shocks during the 2010 – 2012 interval are seen to apparently occur without an obvious MC-driver, probably indicating an encounter with a distant flank of a MC-driven shock. Some of these may be driven by a different kind of structure, however.

Yearly Comparison of Magnetic Cloud Parameters, Sunspot Number, and Interplanetary Quantities for the First 18 Years of the Wind Mission

R. P. [Lepping](#), C.-C. Wu, D. B. Berdichevsky

Solar Phys., February **2015**, Volume 290, [Issue 2](#), pp 553-578

In the scalar part of this study, we determine various statistical relationships between estimated magnetic cloud (MC) model fit-parameters and sunspot number (SSN) for the interval defined by the Wind mission, i.e., early 1995 until the end of 2012, all in terms of yearly averages. The MC-fitting model used is that of Lepping, Jones, and Burlaga (J. Geophys. Res. 95, 11957 – 11965, 1990). We also statistically compare the MC fit-parameters and other derived MC quantities [e.g., axial magnetic flux (Φ_0) and total axial current density (J_{O})] with some associated ambient interplanetary quantities (including the interplanetary magnetic field (B IMF), proton number density (N P), and others). Some of the main findings are that the minimum SSN is nearly simultaneous with the minimum in the number of MCs per year (N MC), which occurs in 2008. There are various fluctuations in N MC and the MC model-fit quality (Q') throughout the mission, but the last four years (2009 – 2012) are markedly different from the others; Q' is low and N MC is large over these four years. N MC is especially large for 2012. The linear correlation coefficient (c.c. ≈ 0.75) between the SSN and each of the three quantities J_{O} , MC diameter ($2R_{\text{O}}$), and B IMF, is moderately high, but none of the MC parameters track the SSN well in the sense defined in this article. However, there is good statistical tracking among the following: MC axial field, B IMF, $2R_{\text{O}}$, average MC speed (V_{MC}), and yearly average solar wind speed (V_{SW}) with relatively high c.c.s among most of these. From the start of the mission until late 2005, J_{O} gradually increases, with a slight violation in 2003, but then a dramatic decrease (by more than a factor of five) occurs to an almost steady and low value of $\approx 3 \mu\text{A km}^{-2}$ until the end of the interval of interest, i.e., lasting for at least seven years. This tends to split the overall 18-year interval into two phases with a separator at the end of 2005. There is good tracking between $2R_{\text{O}}$ and the total axial current density, as expected. The MC duration is also correlated well with these two quantities. Φ_0 shows marked variations throughout the mission, but has no obvious trend. N P, B IMF, V_{MC} , Q' , and V_{SW} are all quite steady over the full 18 years and have markedly low relative variation. Concerning vector quantities, we examine the distribution of MC type for the 18 years, where type refers to the field directional change through a given MC starting at first encounter (i.e., North-to-South, or South-to-North, All South, All North, etc.). Combining all 18 years of MC types

shows that the occurrence rate varies strongly across the various MC types, with N-to-S being most prevalent, with a 27 % occurrence rate (of all MCs), and S-to-N being second, with a 23 % occurrence. Then All N and All S come next at 16 % and 10 % occurrence rate, respectively. All others are at 7 % or lower. For the variation of MC types with time, the southern types (i.e., those that start with a southern magnetic field, a negative B Z in geocentric-solar-ecliptic coordinates) decrease, as the northern types (i.e., those that start with a northern field) increase, apparently consistent with the specific timing of the polarity change of the solar magnetic field, as predicted by Bothmer and Rust (in Crooker, N., Joselyn, J., Feynman J. (eds), Geophys. Monogr., 139 – 146, 1997).

Selection effects in identifying magnetic clouds and the importance of the closest approach parameter,

Lepping, R. P. and Wu, C.-C.:

Ann. Geophys., 28, 1539-1552, doi:10.5194/angeo-28-1539-2010, **2010**.

This study is motivated by the unusually low number of magnetic clouds (MCs) that are strictly identified within interplanetary coronal mass ejections (ICMEs), as observed at 1 AU; this is usually estimated to be around 30% or lower. But a looser definition of MCs may significantly increase this percentage. Another motivation is the unexpected shape of the occurrence distribution of the observers' "closest approach distances" (measured from a MC's axis, and called CA) which drops off somewhat rapidly as |CA| (in % of MC radius) approaches 100%, based on earlier studies. We suggest, for various geometrical and physical reasons, that the |CA|-distribution should be somewhere between a uniform one and the one actually observed, and therefore the 30% estimate should be higher. So we ask, When there is a failure to identify a MC within an ICME, is it occasionally due to a large |CA| passage, making MC identification more difficult, i.e., is it due to an event selection effect? In attempting to answer this question we examine WIND data to obtain an accurate distribution of the number of MCs vs. |CA| distance, whether the event is ICME-related or not, where initially a large number of cases (N=98) are considered. This gives a frequency distribution that is far from uniform, confirming earlier studies. This along with the fact that there are many ICME identification-parameters that do not depend on |CA| suggest that, indeed an MC event selection effect may explain at least part of the low ratio of (No. MCs)/(No. ICMEs). We also show that there is an acceptable geometrical and physical consistency in the relationships for both average "normalized" magnetic field intensity change and field direction change vs. |CA| within a MC, suggesting that our estimates of |CA|, BO (magnetic field intensity on the axis), and choice of a proper "cloud coordinate" system (all needed in the analysis) are acceptably accurate. Therefore, the MC fitting model (Lepping et al., 1990) is adequate, on average, for our analysis. However, this selection effect is not likely to completely answer our original question, on the unexpected ratio of MCs to ICMEs, so we must look for other factors, such as peculiarities of CME birth conditions. As a by-product of this analysis, we determine that the first order structural effects within a MC due to its interaction with the solar wind, plus the MC's usual expansion at 1 AU (i.e., the non-force free components of the MC's field) are, on average, weakly dependent on radial distance from the MC's axis; that is, in the outer reaches of a typical MC the non-force free effects show up, but even there they are rather weak. Finally, we show that it is not likely that a MC's size distribution statistically controls the occurrence distribution of the estimated |CA|s.

Average Thickness of Magnetosheath Upstream of Magnetic Clouds at 1 AU versus Solar Longitude of Source

R.P. **Lepping** · C.-C.Wu · N. Gopalswamy · D.B. Berdichevsky

Solar Phys (2008) 248: 125–139

<http://www.springerlink.com/content/e01848h71hm75634/fulltext.pdf>

Starting with a large number ($N = 100$) of *Wind* magnetic clouds (MCs) and applying necessary restrictions, we find a proper set of $N = 29$ to investigate the average ecliptic plane projection of the upstream magnetosheath thickness as a function of the longitude of the solar source of the MCs, for those cases of MCs having upstream shock waves.

Table

On the variation of interplanetary magnetic cloud type through solar cycle 23: Wind events,

Lepping, R. P., and C. Wu (2007),

J. Geophys. Res., 112, A10103, <http://dx.doi.org/10.1029/2006JA012140>, 2007

This statistical study examines the change in interplanetary magnetic cloud (MC) type, based on Wind observations of 100 MCs, taken during solar cycle 23 and split into three intervals: the minimum and rising phase of the cycle (over the years 1995–1998), the maximum phase (1999–2001), and the declining phase (2002 to early 2006).

The Wind magnetic cloud and events of October 18–20, 1995: Interplanetary properties and as triggers for geomagnetic activity

R. P. **Lepping**, L. F. Burlaga, A. Szabo, K. W. Ogilvie, W. H. Mish, D. Vassiliadis, A. J. Lazarus, J. T. Steinberg, C. J. Farrugia, L. Janoo, F. Mariani

JGR, Volume 102, Issue A7, pages 14049–14063, January 1997

<http://onlinelibrary.wiley.com/doi/10.1029/97JA00272/pdf>

Late on **October 18, 1995**, a magnetic cloud arrived at the Wind spacecraft ≈ 175 RE upstream of the Earth. The cloud had an intense interplanetary magnetic field that varied slowly in direction, from being strongly southward to strongly northward during its ≈ 30 hours duration, and a low proton temperature throughout. From a linear force free field model the cloud was shown to have a flux rope magnetic field line geometry, an estimated diameter of about 0.27 AU, and an axis that was aligned with the Y axis(GSE) within about 25° . A corotating stream, in which large amplitude Alfvén waves of about 0.5 hour period were observed, was overtaking the cloud and intensifying the fields in the rear of the cloud. The prolonged southward magnetic field observed in the early part of the cloud produced a geomagnetic storm of $K_p = 7$ and considerable auroral activity late on October 18. About 8 hours in front of the cloud an interplanetary shock occurred. About three-fourths the way into the cloud another apparent interplanetary shock was observed. It had an unusual propagation direction, differing by only 21° from alignment with the cloud axis. It may have been the result of the interaction with the postcloud stream, compressing the cloud, or was possibly due to an independent solar event. It is shown that the front and rear boundaries of the cloud and the upstream driven shock had surface normals in good agreement with the cloud axis in the ecliptic plane. The integrated Poynting flux into the magnetosphere, which correlated well with geomagnetic indices, jumped abruptly to a high value upon entry into the magnetic cloud, slowly decreased to zero near its middle, and again reached substantial but sporadic values in the cloud-stream interface region. This report aims to support a variety of ISTP studies ranging from the solar origins of these events to resulting magnetospheric responses.

Elemental Abundances of Prominence Material inside ICMEs

Susan T. **Lepri**¹ and Yeimy J. Rivera^{1,2}

2021 ApJ 912 51

<https://doi.org/10.3847/1538-4357/abea9f>

A small number of interplanetary coronal mass ejections (ICMEs) have been identified that contain measurable contributions from prominence plasma. In situ measurements from during these events are marked by the presence of unusually low-charge states of C, O, and Fe, representing ionization equilibrium formation temperatures of ~ 104 – 105 K, consistent with prominence material observed at the Sun. We present a thorough analysis of the elemental abundances of a wide variety of heavy ions, measured by Advanced Composition Explorer/SWICS, in prominence material observed in the solar wind. We find that prominence material observed in situ tends to be more enriched in heavy ions than the surrounding ICME plasma and the fast and slow solar wind. We also find that the material is on average moderately enhanced in low first ionization potential elements compared to photospheric abundances, with values that lie between fast and slow solar wind. In rare instances, where in situ prominence material is observed to have clear, persistent, low-charge states over longer periods of time, it exhibits elemental abundances that are photospheric in nature. However, in most prominence events we see indications that the associated material contains a mixture of prominence and adjacent ICME plasma. The anomalous behavior of the elemental and ionic composition in ICMEs with and without prominence material can be used to study physical processes that occur during CME initiation and release.

SPATIALLY DEPENDENT HEATING AND IONIZATION IN AN ICME OBSERVED BY BOTH ACE AND ULYSSES

Susan T. **Lepri**¹, J. Martin Laming², Cara E. Rakowski², and Rudolf von Steiger

2012 ApJ 760 105

The **2005 January 21** interplanetary coronal mass ejection (ICME) observed by multiple spacecraft at L1 was also observed from January 21–February 4 at Ulysses (5.3 AU). Previous studies of this ICME have found evidence suggesting that the flanks of a magnetic cloud like structure associated with this ICME were observed at L1 while a more central cut through the associated magnetic cloud was observed at Ulysses. This event allows us to study spatial variation across the ICME and relate it to the eruption at the Sun. In order to examine the spatial dependence of the heating in this ICME, we present an analysis and comparison of the heavy ion composition observed during the passage of the ICME at L1 and at Ulysses. Using SWICS, we compare the heavy ion composition across the two different observation cuts through the ICME and compare it with predictions for heating during the eruption based on models of the time-dependent ionization balance throughout the event.

DIRECT OBSERVATIONAL EVIDENCE OF FILAMENT MATERIAL WITHIN INTERPLANETARY CORONAL MASS EJECTIONS

S. T. [Lepri](#) and T. H. Zurbuchen

The Astrophysical Journal Letters, 723:L22–L27, 2010

Coronal mass ejections (CMEs) are explosive events that escape the Sun's corona carrying solar material and energy into the heliosphere. The classic picture of a CME observed in the corona presents a "three-part structure," including a bright front at the leading edge indicating dense plasma, a low-density cavity, the possible signature of an embedded magnetic flux rope, and the so-called core, a high-density region observed to be associated with an erupting filament. Although there are experimental analogs to the first two parts of the CME when observed in situ, there are only a handful of in situ observations of cold, filament-type plasma. This has been a source of major uncertainty and qualitative disagreement between remote and in situ observations of these ejecta. We present the first comprehensive and long-term survey of such low charge states observed by the *Advanced Composition Explorer* SolarWind Ion Composition Spectrometer, using a novel data analysis process developed to identify ions with low ionic charge states. Using a very stringent set of observational signatures, we find that more than 4% of detected interplanetary CMEs have significant contributions of ions with low charge states. These time periods of low-charge ions often occur concurrent with some of the hottest ions, previously interpreted to be affected by flare heating during the CME initiation.

Prediction of the Dst Index and Analysis of Its Dependence on Solar Wind Parameters Using Neural Network

Ahmed [Lethy](#), [Mohamed A. El-Eraki](#), [Aalaa Samy](#), [Hanafy A. Deebes](#)

Space Weather [Volume16, Issue9](#) Pages 1277-1290 2018

<http://sci-hub.tw/10.1029/2018SW001863>

In this work, we propose an artificial neural network (ANN) with seven input parameters for the prediction of disturbance storm time (Dst) index 1 to 12 hr ahead. The ANN uses past near-Earth solar wind parameter values to forecast the Dst. The input parameters are the solar wind interplanetary magnetic field, north-south component of interplanetary magnetic field, temperature, density, speed, pressure, and electric field. The ANN was trained on the data period from 1 January 2007 to 31 December 2015, which contains 78,888 hourly data samples. While the period from 1 January 2016 to 31 May 2017 was used to test the prediction capabilities of the ANN. Several ANN structures were tested and the best results were determined using the correlation coefficient (R) during the training and prediction phases. The results indicate an adequate accuracy of $R = 0.876$ for prediction 2 hr in advance and $R = 0.857$ for prediction 12 hr in advance. The power of the proposed ANN was illustrated using the strongest six storms recorded during the prediction period. Generally, the duration and number of the input parameters significantly affect the training and prediction performance of the applied ANN. The results are outstanding in term of accuracy when considering a medium-term prediction of 12 hr in advance and in terms of timing of the Dst minimum occurrence. In addition, the results show a strong dependence on the solar wind electric current.

Monitoring the daily variation of Sun-Earth magnetic fields using galactic cosmic rays

The [LHAASO Collaboration](#)

The Innovation 5(6): 100695, November 4, 2024

<https://arxiv.org/pdf/2410.09064>

The interplanetary magnetic field (IMF) between the Sun and Earth is an extension of the solar magnetic field carried by the solar wind into interplanetary space. Monitoring variations in the IMF upstream of the Earth would provide very important information for the prediction of space weather effects, such as effects of solar storms and the solar wind, on human activity. In this study, the IMF between the Sun and Earth was measured daily for the first time using a cosmic-ray observatory. Cosmic rays mainly consist of charged particles that are deflected as they pass through a magnetic [this http URL](#), the cosmic-ray Sun shadow, caused by high-energy charged cosmic rays blocked by the Sun and deflected by the magnetic field, can be used to explore the transverse IMF between the Sun and Earth. By employing the powerful kilometer-square array at the Large High Altitude Air Shower Observatory, the cosmic-ray Sun shadows were observed daily with high significance for the first time. The displacement of the Sun shadow measured in 2021 correlates well with the transverse IMF component measured in situ by spacecraft near the Earth, with a time lag of $3:31 \pm 0:12$ days. The displacement of the Sun shadow was also simulated using Parker's classic IMF model, yielding a time lag of $2:06 \pm 0:04$ days. This deviation may provide valuable insights into the magnetic field structure, which can improve space weather research.

CME Arrival Time Prediction Based on Coronagraph Observations and Machine-learning Techniques

Yucong Li^{1,2}, Yi Yang^{1,2}, Fang Shen^{1,2}, Bofeng Tang¹, and Rongpei Lin^{1,2}
2024 ApJ 976 141

<https://iopscience.iop.org/article/10.3847/1538-4357/ad82e5/pdf>

The timely and precise prediction of the arrival time of coronal mass ejections (CMEs) is crucial in mitigating their potential adverse effects. In this study, we present a novel prediction method utilizing a deep-learning framework coupled with physical characteristics of CMEs and background solar wind. Time series images from synchronized solar white-light and EUV observations of 156 geoeffective CME events during 2000–2020 are collected for this study, according to the Richardson and Cane interplanetary CME directory and the SOHO/LASCO CME catalog of NASA/CDAW. The CME parameters are obtained from the CDAW website and the solar wind parameters are from OMNI2 website. The observational images are first fed into a convolutional neural network (CNN) to train a regression model as Model A. The results generated by the original CNN are then integrated with 11 selected physical parameters in additional neural network layers of Model B to improve the predictions. Under optimal configurations, Model A achieves a minimum mean absolute error (MAE) of 7.87 hr, whereas Model B yields a minimum MAE of 5.12 hr. During model training, we employed tenfold cross validation to reduce the occasionality of biased data. The average MAE of Model B on 10 folds is 33% lower than that of model A. The results demonstrate that combining the imaging observations with the physical properties of CMEs and background solar wind to train a machine-learning model can benefit the forecasting of CME arrival times.

Predicting the Arrival Time of an Interplanetary Shock Based on DSRT Spectrum Observations for the Corresponding Type II Radio Burst and a Blast Wave Theory

Ran Li^{1,2}, Xinhua Zhao^{1,3}, Jingye Yan^{1,3}, Lin Wu^{1,3}, Yang Yang^{1,3}, +++
2024 ApJ 962 178

<https://iopscience.iop.org/article/10.3847/1538-4357/ad150f/pdf>

Since fast head-on coronal mass ejections and their associated shocks represent potential hazards to the space environment of the Earth and even other planets, forecasting the arrival time of the corresponding interplanetary shock is a priority in space weather research and prediction. Based on the radio spectrum observations of the 16-element array of the Daocheng Solar Radio Telescope (DSRT), the flagship instrument of the Meridian Project of China, during its construction, this study determines the initial shock speed of a type II solar radio burst on 2022 April 17 from its drifting speed in the spectrum. Assuming that the shock travels at a steady speed during the piston-driven phase (determined from the X-ray flux of the associated flare) and then propagates through interplanetary space as a blast wave, we estimate the propagation and arrival time of the corresponding shock at the orbit of the Solar Terrestrial Relations Observatory-A (STEREO-A). The prediction shows that the shock will reach STEREO-A at 14:31:57 UT on 2022 April 19. The STEREO-A satellite detected an interplanetary shock at 13:52:12 UT on the same day. The discrepancy between the predicted and observed arrival time of the shock is only 0.66 hr. The purpose of this paper is to establish a general method for predicting the shock's propagation and arrival time from this example, which will be utilized to predict more events in the future based on the observations of ground-based solar radio spectrometers or telescopes like DSRT. **2022-04-17-19**

Comparison of the Composition of ICMEs from Active Regions and Quiet-Sun Regions

Jinrong Li, Hongqiang Song, Qi Lv, Hui Fu, Leping Li, Ruisheng Zheng, Yao Chen

ApJ 945 163 2023

<https://arxiv.org/pdf/2302.03804.pdf>

<https://iopscience.iop.org/article/10.3847/1538-4357/acba90/pdf>

The composition, including the ionic charge states and elemental abundances of heavy elements, within interplanetary coronal mass ejections (ICMEs) has tight correlations with their source regions and eruption processes. This can help analyze the eruption mechanisms and plasma origins of CMEs, and deepen our understanding of energetic solar activities. The active regions and quiet-Sun regions have different physical properties, thus from a statistical point of view, ICMEs originating from the two types of regions should exhibit different compositional characteristics. To demonstrate the differences comprehensively, we conduct survey studies on the ionic charge states of five elements (Mg, Fe, Si, C, and O) and the relative abundances of six elements (Mg/O, Fe/O, Si/O, C/O, Ne/O, and He/O) within ICMEs from 1998 February to 2011 August through the data of advanced composition explorer. The results show that ICMEs from active regions have higher ionic charge states and relative abundances than those from quiet-Sun regions. For the active-region ICMEs, we further analyze the relations between their composition and flare class, and find a positive relationship between them, i.e., the higher classes of the associated flares, the larger means of ionic charge states and

relative abundances (except the C/O) within ICMEs. As more (less) fractions of ICMEs originate from active regions around solar maximum (minimum), and active-region ICMEs usually are associated with higher-class flares, our studies might answer why ICME composition measured near 1 au exhibits the solar cycle dependence.

Table 1. The information of 96 ICMEs (CMEs) with identified source regions 1998-2011

Galactic Cosmic-Ray Propagation in the Inner Heliosphere: Improved Force-Field Model

Jung-Tsung Li, [John F. Beacom](#), [Annika H. G. Peter](#)

ApJ **937** 27 **2022**

<https://arxiv.org/pdf/2206.14815.pdf>

<https://iopscience.iop.org/article/10.3847/1538-4357/ac8cf3/pdf>

A key goal of heliophysics is to understand how cosmic rays propagate in the solar system's complex, dynamic environment. One observable is solar modulation, i.e., how the flux and spectrum of cosmic rays changes as they propagate inward. We construct an improved force-field model, taking advantage of new measurements of magnetic power spectral density by Parker Solar Probe to predict solar modulation within the Earth's orbit. We find that modulation of cosmic rays between the Earth and Sun is modest, at least at solar minimum and in the ecliptic plane. Our results agree much better with the limited data on cosmic-ray radial gradients within Earth's orbit than past treatments of the force-field model. Our predictions can be tested with forthcoming direct cosmic-ray measurements in the inner heliosphere by Parker Solar Probe and Solar Orbiter. They are also important for interpreting the gamma-ray emission from the Sun due to scattering of cosmic rays with solar matter and photons.

Radial velocity map of solar wind transients in the field of view of STEREO/HI1 on 3 and 4 April 2010

Xiaolei Li, [Yuming Wang](#), [Jingnan Guo](#), [Rui Liu](#)¹, [Bin Zhuang](#)

A&A **649**, A58 **2021**

<https://arxiv.org/pdf/2103.04740.pdf>

<https://www.aanda.org/articles/aa/pdf/2021/05/aa39766-20.pdf>

<https://doi.org/10.1051/0004-6361/202039766>

The solar wind transients propagating out in the inner heliosphere can be observed in white-light images from Heliospheric Imager-1 (HI1), an instrument of the Sun Earth Connection Coronal and Heliospheric Investigation (SECCHI) on board the Solar Terrestrial Relations Observatory (STEREO), from two perspectives. The spatial velocity distribution inside solar wind transients is key to understanding their dynamic evolution processes. We generated a velocity map of transients in 3D space based on 2D white-light images and used it to estimate the expansion rate as well as some kinematic properties of solar wind transients. Based on the recently developed correlation-aided reconstruction (CORAR) method in our previous work, which can recognize and locate 3D solar wind transients from STEREO/HI1 image data, we further developed a new technique for deriving the spatial distribution of the radial velocities of the most pronounced features inside solar wind transients. The technique was applied to events including a coronal mass ejection (CME) and three small-scale transients, so-called blobs, observed by HI1 on 3-4 April 2010 to reconstruct their radial velocity maps. The results match the forward-modeling results, simulations, and in situ observations at 1 AU fairly well. According to the obtained spatial distributions of height and radial velocity of the CME, we analyzed the self-similarity of the radial expansion of the CME ejecta. The dimensionless radial expansion rate of the northern and middle parts of the CME ejecta varies in the range of 0.7 - 1.0 at heliocentric distance between 25 Rs and 55Rs and the rate of the southern part in the range of 0.3 - 0.5, suggesting that the CME structure was distorted and shaped by the ambient solar wind. The technique we developed is expected to be applied to more events.

Simulation of the Interplanetary B z Using a Data-driven Heliospheric Solar Wind Model

Huichao Li^{1,2}, Xueshang Feng^{1,2}, Pingbing Zuo¹, and Fengsi Wei^{1,2}

2020 ApJ **900** 76

<https://doi.org/10.3847/1538-4357/aba61f>

Aimed to be ready for the transition from research to operation, we have developed a solar wind model by coupling a data-driven empirical coronal model with a magnetohydrodynamics heliospheric model. We performed a data-driven simulation of the solar wind for a two-year period during the declining and minimum phases of solar cycle 23. Comparisons with OMNI and Ulysses spacecraft data show that the model can reproduce the large-scale variations of the solar wind plasma parameters. The evolution of geocentric solar magnetospheric (GSM) B x and B z components are also reasonably duplicated by the model in terms of polarity and strength. Apparent signatures of the Russell–McPherron (R-M) effect are found from both observed data and simulated results, indicating that during the investigated

interval the R-M effect is the dominant mechanism that controls the large-scale evolution of the north–south component of the interplanetary magnetic field in the GSM frame. The results demonstrate that the established model can provide valuable space weather information about the solar wind.

Reconstructing solar wind inhomogeneous structures from stereoscopic observations in white-light: Solar wind transients in 3D

Xiaolei Li, [Yuming Wang](#), [Rui Liu](#), [Chenglong Shen](#), [Quanhao Zhang](#), [Shaoyu Lyu](#), [Bin Zhuang](#), [Fang Shen](#), [Jiajia Liu](#), [Yutian Chi](#)

JGR **Volume125, Issue7** e2019JA027513 2020

<https://arxiv.org/ftp/arxiv/papers/2005/2005.01238.pdf>

<https://agupubs.onlinelibrary.wiley.com/doi/pdf/10.1029/2019JA027513>

White-light images from Heliospheric Imager-1 (HI1) onboard the Solar Terrestrial Relations Observatory (STEREO) provide 2-dimensional (2D) global views of solar wind transients traveling in the inner heliosphere from two perspectives. How to retrieve the hidden three-dimensional (3D) features of the transients from these 2D images is intriguing but challenging. In our previous work (Li et al., 2018), a 'correlation-aided' method is developed to recognize the solar wind transients propagating along the Sun-Earth line based on simultaneous HI1 images from two STEREO spacecraft. Here the method is extended from the Sun-Earth line to the whole 3D space to reconstruct the solar wind transients in the common field of view of STEREO HI1 cameras. We demonstrate the capability of the method by showing the 3D shapes and propagation directions of a coronal mass ejection (CME) and three small-scale blobs during **3-4 April 2010**. Comparing with some forward modeling methods, we found our method reliable in terms of the position, angular width and propagation direction. Based on our 3D reconstruction result, an angular distorted, nearly North-South oriented CME on 3 April 2010 is revealed, manifesting the complexity of a CME's 3D structure.

Spatial Distribution of Electromagnetic Waves near the Proton Cyclotron Frequency in ICME Sheath Regions Associated with Quasi-perpendicular Shocks: Wind Observations

Q. H. Li^{1,2}, L. Yang^{1,3}, L. Xiang⁴, and D. J. Wu¹

2020 ApJ 892 98

<https://doi.org/10.3847/1538-4357/ab7cde>

Electromagnetic waves (EMWs) near the proton cyclotron frequency f_{cp} are transverse left-handed (LH) or right-handed (RH) polarized waves, and are ubiquitous in the solar wind. However, the characteristics of these waves in the sheath regions of interplanetary coronal mass ejections (ICMEs) are poorly understood. Through a comprehensive survey of Wind magnetic field and plasma data using dynamic spectra and repeated filtering analyses, 700 EMW events (7.1% of the analysis time) are identified in the 62 ICME sheath regions associated with quasi-perpendicular shocks involved with a low shock Mach number M_f and low upstream β_1 . In the ICME sheath regions, outward (inward)-propagating LH (RH) EMWs have relatively higher counts and longer duration than inward (outward)-propagating LH (RH) EMWs in the plasma frame, consistent with previous STEREO observations. The spatial distributions of the magnetic field, plasma, and frequency parameters of EMWs are also presented in both spacecraft and plasma frames, especially the proton (alpha) temperature anisotropy, α abundance N_α/N_p , and normalized differential alpha-proton speed V_d/V_A . After removing the Doppler shift, 81.1% (59%) of all outward (inward)-propagating LH EMWs have a frequency below (above) $0.5f_{cp}$, while 68.3% (64%) of all outward (inward)-propagating RH EMWs have a frequency smaller (greater) than $0.5f_{cp}$. Further investigations of local plasma parameters reveal that different excitation mechanisms for EMWs are in different subregions of the ICME sheath regions. These results are helpful in understanding the important role of EMWs in the solar wind–ICME coupling process with different sheath regions.

Stronger Southward Magnetic Field and Geoeffectiveness of ICMEs Containing Prominence Materials Measured from 1998 to 2011

Dongni Li and Shuo Yao¹

2020 ApJ 891 79

<https://iopscience.iop.org/article/10.3847/1538-4357/ab7197/pdf>

Interplanetary coronal mass ejections (ICMEs) could be classified into magnetic clouds (MCs) and non-MCs according to their magnetic field signatures, and into prominence-inside ICMEs (PIs) and non-PIs based on whether they contain colder and higher helium abundance plasmas than the solar wind. It is known that the MCs often lead to magnetic storms. However, whether or not the PIs have significant geoeffectiveness is unclear. This statistical work studies the southward interplanetary magnetic field (IMF) magnitude of the PIs, and the related magnetic storms' level. The data include the IMF and plasma moments measured by ACE and WIND, and the Dst index from 1998 to 2011. The

hypothesis test based on the proportions of two groups is used to analyze 95 ICMEs related to single storms (SSs). The results show that the magnetic storms caused by the PIs mostly distribute at a strong level, while that caused by the non-PIs and by all the 95 ICMEs mostly distribute at a moderate level. The PIs have a significantly higher probability of generating SSs than the non-PIs. Moreover, the MCs containing carbon-cold and helium-enhanced materials (MC&PIs) have the highest fraction of minimum B_z , less than -11 nT. Since the MC&PIs have large-scale magnetic flux rope and prominence material, the stronger southward IMF is probably provided by the prominence. It is in accordance with the observed injection of enhanced twisted flux ropes to prominence. Therefore, the detailed eruption and propagation processes of the three-part coronal mass ejections deserve more concern from a space weather perspective. **2000.07.27-29, 2000-10-29, 2001.06.26-27, 2005-09-11**

Table 2. 95 Single Storms and the Related ICMEs Selected from Feng et al. (2018)

Characteristics of solar wind rotation

Kejun Li, W. Feng

MNRAS Volume 489, Issue 3, Pages 3427–3435, 2019

<https://arxiv.org/pdf/1908.11021.pdf>

<https://doi.org/10.1093/mnras/stz2407>

Over 54 years of hourly mean value of solar wind velocity from 27 Nov. 1963 to 31 Dec. 2017 are used to investigate characteristics of the rotation period of solar wind through auto-correlation analysis. Solar wind of high velocity is found to rotate faster than low-velocity wind, while its rotation rate increases with velocity increasing, but in contrast for solar wind of low velocity, its rotation rate decreases with velocity increasing. Our analysis shows that solar wind of a higher velocity statistically possesses a faster rotation rate for the entire solar wind. The yearly rotation rate of solar wind velocity does not follow the Schwabe cycle, but it is significantly negatively correlated to yearly sunspot number when it leads by 3 years. Physical explanations are proposed to these findings.

Electromagnetic Waves around the Proton Cyclotron Frequency in the Sheath Regions of Interplanetary Magnetic Clouds: STEREO Observations

Q. H. Li^{1,2}, L. Yang^{1,3}, D. J. Wu¹, and T. Y. Wang⁴

2019 ApJ 874 55

sci-hub.se/10.3847/1538-4357/ab06f7

The compressed and turbulent sheath regions of interplanetary magnetic clouds (IMCs) provide a natural laboratory to study electromagnetic waves (EMWs) around the proton cyclotron frequency f_{cp} . Based on the Morlet wavelet spectral analysis, the repeated filtering analysis and the minimum variance analysis of high-resolution magnetic field data from the STEREO spacecraft, 81 EMW events are identified in the sheath regions of six IMCs. These EMWs are all transverse, almost circularly polarized, and quasi-parallel propagating along the background magnetic field. They can be left-handed (LH) or right-handed (RH) polarized in the spacecraft frame, where the occurrence rate of the LH-polarized EMWs is higher than that of RH-polarized ones, consistent with previous observations in the solar wind. Also, a comparative analysis of polarization sense of these EMWs has been made in the spacecraft and plasma frames. Our results show that more than half of EMW events suffer a polarization reversal from the spacecraft to plasma frames, which are deduced to propagate inward relative to the solar wind flow. Others are outward-propagating waves. In the plasma frame, the outward-propagating LH-EMWs and inward-propagating RH-EMWs have relatively higher occurrence rates than the inward-propagating LH-EMWs and outward-propagating RH-EMWs, respectively. Furthermore, in the plasma frame all the frequencies of LH-EMWs are below f_{cp} , but the RH-EMW frequencies can exceed f_{cp} . These results are helpful in understanding the physical properties of EMWs and their roles in the sheath regions of IMCs.

Magnetic Clouds: Solar Cycle Dependence, Sources, and Geomagnetic Impacts

Y. Li, J. G. Luhmann, B. J. Lynch

Solar Physics October 2018, 293:135

<https://link.springer.com/content/pdf/10.1007%2Fs11207-018-1356-8.pdf>

Magnetic clouds (MCs) are transient magnetic structures giving the strongest southward magnetic field (B_z south) in the solar wind. The sheath regions of MCs may also carry a southward magnetic field. The southward magnetic field is responsible for space-weather disturbances. We report a comprehensive analysis of MCs and B_z components in their sheath regions for 1995 to 2017. 85% of 303 MCs contain a south B_z up to 50 nT. Sheath B_z during the 23 years may reach as high as 40 nT. MCs of the strongest magnetic magnitude and B_z south occur in the declining phase of the solar cycle. Bipolar MCs depend on the solar cycle in their polarity, but not in the occurrence frequency. Unipolar MCs show solar-cycle dependence in their occurrence frequency, but not in their polarity. MCs with the highest speeds, the largest

total-BB magnitudes, and sheath Bz south originate from source regions closer to the solar disk center. About 80% of large Dst storms are caused by MC events. Combinations of a south Bz in the sheath and south-first MCs in close succession have caused the largest storms. The solar-cycle dependence of bipolar MCs is extended to 2017 and now spans 42 years. We find that the bipolar MC Bz polarity solar-cycle dependence is given by MCs that originated from quiescent filaments in decayed active regions and a group of weak MCs of unclear sources, while the polarity of bipolar MCs with active-region flares always has a mixed Bz polarity without solar-cycle dependence and is therefore the least predictable for Bz forecasting. **17 March 2015, 20 Dec 2015**

Reconstructing solar wind inhomogeneous structures from stereoscopic observations in white-light: Small transients along the Sun-Earth line

Xiaolei Li, [Yuming Wang](#), [Rui Liu](#), [Chenglong Shen](#), [Quanhao Zhang](#), [Bin Zhuang](#), [Jiajia Liu](#), [Yutian Chi](#)
JGR 2018

<https://arxiv.org/ftp/arxiv/papers/1809/1809.03651.pdf>

The Heliospheric Imagers (HI) on board the two spacecraft of the Solar Terrestrial Relations Observatory (STEREO) provided white-light images of transients in the solar wind from dual perspectives from 2007 to 2014. In this paper, we develop a new method to identify and locate the transients automatically from simultaneous images from the two inner telescopes, known as HI-1, based on a correlation analysis. Correlation coefficient (cc) maps along the Sun-Earth line are constructed for the period from 1 Jan 2010 to 28 Feb 2011. From the maps, transients propagating along the Sun-Earth line are identified, and a 27-day periodic pattern is revealed, especially for small-scale transients. Such a periodicity in the transient pattern is consistent with the rotation of the Sun's global magnetic structure and the periodic crossing of the streamer structures and slow solar wind across the Sun-Earth line, and this substantiates the reliability of our method and the high degree of association between the small-scale transients of the slow solar wind and the coronal streamers. Besides, it is suggested by the cc map that small-scale transients along the Sun-Earth line are more frequent than large-scale transients by a factor of at least 2, and that they quickly diffused into background solar wind within about 40 Rs in terms of the signal-to-noise ratio of white-light emissions. The method provides a new tool to reconstruct inhomogeneous structures in the heliosphere from multiple perspectives.

Magnetic Clouds: Solar Cycle Dependence, Sources, and Geomagnetic Impacts

Y. Li, [J. G. Luhmann](#), [B. J. Lynch](#)

Solar Phys. 293:135 2018

<https://arxiv.org/ftp/arxiv/papers/1808/1808.04078.pdf>

<https://link.springer.com/content/pdf/10.1007%2Fs11207-018-1356-8.pdf>

Magnetic clouds (MCs) are transient magnetic structures giving the strongest southward magnetic field (Bz south) in the solar wind. The sheath regions of MCs may also carry southward magnetic field. Southward magnetic field is responsible for causing space weather disturbances. We report a comprehensive analysis of MCs and Bz components in their sheath regions during 1995-2017. Eighty-five percent of 303 MCs contain a south Bz up to 50 nT. Sheath Bz during the 23 years may reach as high as 40 nT. The MCs of strongest magnetic magnitude and Bz south occur in the declining phase of the solar cycle. The bipolar MCs have solar cycle dependence in their polarity, but not in the occurrence frequency. Unipolar MCs show solar cycle dependence in their occurrence frequency but not in their polarity. MCs with the highest speeds, largest total B magnitudes and sheath Bz south are from source regions closer to the solar disk center. About 80% of large Dst storms are caused by MC events. The combinations of south Bz in the sheath and the south-first MCs in close succession have given the largest storms. The solar cycle dependence of bipolar MCs is extended to 2017, spanning 42 years. We find that the bipolar MC Bz polarity solar cycle dependence is given by MCs originated from quiescent filaments in decayed active regions and a group of weak MCs of unclear sources, while the polarity of bipolar MCs with active region flares always has mixed Bz polarity without solar cycle dependence and therefore the least predictable for Bz forecasting. **15-20 March 2015, 19-23 Dec 2015**

PLASMA HEATING INSIDE INTERPLANETARY CORONAL MASS EJECTIONS BY ALFVÉNIC FLUCTUATIONS DISSIPATION

Hui Li¹, Chi Wang¹, Jiansen He², Lingqian Zhang¹, John D. Richardson³, John W. Belcher³, and Cui Tu⁴
2016 ApJL 831 L13

Nonlinear cascade of low-frequency Alfvénic fluctuations (AFs) is regarded as one of the candidate energy sources that heat plasma during the non-adiabatic expansion of interplanetary coronal mass ejections (ICMEs). However, AFs inside ICMEs were seldom reported in the literature. In this study, we investigate AFs inside ICMEs using observations from Voyager 2 between 1 and 6 au. It has been found that AFs with a high degree of Alfvénicity frequently occurred

inside ICMEs for almost all of the identified ICMEs (30 out of 33 ICMEs) and for 12.6% of the ICME time interval. As ICMEs expand and move outward, the percentage of AF duration decays linearly in general. The occurrence rate of AFs inside ICMEs is much less than that in ambient solar wind, especially within 4.75 au. AFs inside ICMEs are more frequently presented in the center and at the boundaries of ICMEs. In addition, the proton temperature inside ICME has a similar "W"-shaped distribution. These findings suggest significant contribution of AFs on local plasma heating inside ICMEs.

Mapping magnetic field lines between the Sun and Earth†

B. Li, Iver H. Cairns, J.T. Gosling, G. Steward, M. Francis, D. Neudegg, H. Schulte in den Bäumen, P.R. Player, A.R. Milne

JGR 2016

Magnetic field topologies between the Sun and Earth are important for the connectivity to Earth of solar suprathermal particles, e.g., solar energetic particles and beam electrons in type III solar radio bursts. An approach is developed for mapping large-scale magnetic field lines near the solar equatorial plane, using near-Earth observations and a solar wind model with nonzero azimuthal magnetic field at the source surface. Unlike Parker's spiral model, which restricts the in-ecliptic angle Φ_B in the Geocentric Solar Ecliptic coordinates to $(90^\circ - 180^\circ, 270^\circ - 360^\circ)$, and so is unable to predict field configurations for the other Φ_B values frequently observed in the solar wind, our approach can account for all the observed Φ_B values. A set of predicted maps show that near both minimal and maximal solar activity the field lines are typically open and that loops with both ends either connected to or disconnected from the Sun are relatively rare. The open field lines, nonetheless, often do not closely follow the Parker spiral, being less or more tightly wound, or strongly azimuthally or radially oriented, or inverted. The time-varying classes, e.g., bidirectional electrons, of suprathermal electron pitch angle distributions (PADs) at 1 AU are predicted from the mapped field line configurations and compared with Wind observations for two solar rotations, one each near solar minimum and solar maximum. PAD predictions by our approach agree quantitatively ($\approx 90\%$) with the PAD observations and outperform (by $\approx 20\%$) PAD predictions using Parker's model.

Magnetic Clouds and Origins in STEREO Era†

Yan Li^{1,*}, J. G. Luhmann¹, B. J. Lynch¹ and E. K. J. Kilpua

JGR, Volume 119, Issue 5, pages 3237–3246, May 2014; File

When a CME encounters the Earth, the Earth's electromagnetic environment is disturbed, especially when it is a Magnetic Cloud (MC) with enhanced, steady and long lasting southward field. The speed and the magnetic field of an MC are the two important properties for its geoeffectiveness. The correspondence between a CME and its resulting MC is not straight forward, partly due to the CME velocity and the complications during propagation through corona and the solar wind. From 2007 to 2012, we have three observing points at 1 AU near the ecliptic plane (ACE, STEREO A and B). We search for MC events encountered at one of the three observers and study the statistics independently and in comparison. We found that the annual number of MCs at each receiver vary significantly, and the temporal variation at each receiver does not always follow the solar activity level. The speed and the magnetic field strength of the MCs do vary with the solar activity level. The polarity of MC magnetic field at ACE and STEREO also shows large fluctuations. We have also identified the CME and solar activity sources for the L1 MC events. STEREO SECCHI images served critical roles in the determination of the CMEs both in solar quiet times and active times. We found that halo CMEs are not necessarily good indicators for receiving MCs. Further studies of CME initial velocity and the propagation through the heliosphere are needed in order to improve our space weather forecasting capability.

Table 1. L1 Magnetic Clouds and Origins in 2007–2012: 47 MCs from ACE,

New approach for solving the inverse boundary value problem of Laplace's equation on a circle: Technique renovation of the Grad-Shafranov (GS) reconstruction

H. J. Li^{1,2}, X. S. Feng, ^{2,*}, J. Xiang, ¹, P. B. Zuo

JGR, Volume 118, Issue 6, pages 2876–2881, June 2013

In this paper, the essential technique of Grad-Shafranov (GS) reconstruction is reformulated into an inverse boundary value problems (IBVPs) for Laplace's equation on a circle by introducing a Hilbert transform between the normal and tangent component of the boundary gradients. It is proved that the specified IBVPs have unique solution, given the known Dirichlet and Neumann conditions on certain arc. Even when the arc is reduced to only one point on the circle, it can be inferred logically that the unique solution still exists there on the remaining circle. New solution approach for the specified IBVP is suggested with the help of the introduced Hilbert transform. An iterated Tikhonov regularization scheme is applied to deal with the ill-posed linear operators appearing in the discretization of the new approach.

Numerical experiments highlight the efficiency and robustness of the proposed method. According to linearity of the elliptic operator in GS equation, its solution can be divided into two parts. One is solved from a semilinear elliptic equation with an homogeneous Dirichlet boundary condition. The other is solved from the IBVP of Laplace's equation. It is concluded that there exists a unique solution for the so-called elliptic Cauchy problem for the essential technique of GS reconstruction.

Cyclic Reversal of Magnetic Cloud Poloidal Field

Y. [Li](#), J. G. Luhmann, B. J. Lynch and E. K. J. Kilpua

Solar Physics, Volume 270, Number 1, 331-346, 2011

Coronal mass ejections (CMEs) carry magnetic structure from the low corona into the heliosphere. The interplanetary CMEs (ICMEs) that exhibit the topology of helical magnetic fluxropes are traditionally called magnetic clouds (MCs). MC fluxropes with axis of low (high) inclination with respect to the ecliptic plane have been referred to as bipolar (unipolar) MCs. The poloidal field of bipolar MCs has a solar cycle dependence. We report a cyclic reversal of the poloidal field of low inclination MC fluxropes during 1976 to 2009. The MC poloidal field cyclic reversal on the same time scale of the solar magnetic cycle is evident over three sunspot cycles. Approximately 48% of ICMEs are MCs, and 40% of IMCs are bipolar MCs during solar cycle 23. The speed of the bipolar MCs has essentially the same distribution as all ICMEs, which implies that they are not from any special type of CMEs in terms of the solar origin. Although CME fluxropes may undergo a number of complications during the eruption and propagation, a significant group of MCs retains sufficient similarity to the source region magnetic field to possess the same cyclic periodicity in polarity reversal. The poloidal field of bipolar MCs gives the out-of-ecliptic-plane field or B_z component in the IMF time series. MCs with southward B_z field are particularly effective in causing geomagnetic disturbances. During the solar minima, the B_z field IMF sequence within MCs at the leading portion of a bipolar MC is the same with the solar global dipole field. Our finding shows that MCs preferentially remove the like polarity of the solar dipole field, and it supports the participation of CMEs in the solar magnetic cycle.

Table 1. Magnetic Clouds in 1996 - 2009 (Electronic attachment to Li et al. 2011)

On improvement to the Shock Propagation Model (SPM) applied to interplanetary shock transit time forecasting,

[Li](#), H. J., F. S. Wei, X. S. Feng, and Y. Q. Xie

J. Geophys. Res., 113, A09101, (2008),

<http://dx.doi.org/10.1029/2008JA013167>

This paper investigates methods to improve the predictions of Shock Arrival Time (SAT) of the original Shock Propagation Model (SPM). According to the classical blast wave theory adopted in the SPM, the shock propagating speed is determined by the total energy of the original explosion together with the background solar wind speed. Noting that there exists an intrinsic limit to the transit times computed by the SPM predictions for a specified ambient solar wind, we present a statistical analysis on the forecasting capability of the SPM using this intrinsic property. Two facts about SPM are found: (1) the error in shock energy estimation is not the only cause of the prediction errors and we should not expect that the accuracy of SPM to be improved drastically by an exact shock energy input; and (2) there are systematic differences in prediction results both for the strong shocks propagating into a slow ambient solar wind and for the weak shocks into a fast medium. Statistical analyses indicate the physical details of shock propagation and thus clearly point out directions of the future improvement of the SPM. A simple modification is presented here, which shows that there is room for improvement of SPM and thus that the original SPM is worthy of further development.

Visualizing CMEs and Predicting Geomagnetic Storms from Solar Magnetic Fields

Yan [Li](#), [Janet G. Luhmann](#), [J. Todd. Hoeksema](#), [Xuepu Zhao](#), [C. Nick Arge](#)

Space Weather Geophysical Monograph 125 2001

<https://agupubs.onlinelibrary.wiley.com/doi/pdf/10.1029/GM125p0177>

Because solar photospheric magnetic fields are the main source of the magnetic field in the corona and interplanetary space, changes in the photospheric field may be expected to drive transients in both regions. However, because the solar field is both complex and influenced by the solar wind, it is difficult to determine whether specific photospheric field features underlie the important transients called Coronal Mass Ejections (CMEs). Models enable us to link the photospheric field to coronal field changes and visualize the response. The potential field source surface (PFSS) model is known for its combination of relative simplicity and ability to approximate coronal hole geometry and eclipse images.

We utilize PFSS models and specialized synoptic maps of the solar magnetic field to study the relationship between coronal field changes and CMEs, and to attempt to visualize CMEs and predict geomagnetic storms. For prediction purposes, updated synoptic maps in real time are needed. Several solar observatories and SOHO/MDI are currently providing such maps on a roughly daily basis, although the potential exists for hourly updates. Our results to date suggest that the combination of photospheric field observations and coronal models can provide a useful addition to the collection of space weather forecast tools.

Predicting Arrival Times of the CCMC CME/Shock Events Based on the SPM3 Model

Yidan **Liang** (梁一丹)^{1,2}, Xinhua Zhao (赵新华)^{1,2,3}, Nanbin Xiang (向南彬)⁴, Shiwei

Feng (冯士伟)⁵, Fuyu Li (李富羽)⁶, Linhua Deng (邓林华)⁷, Miao Wan (万苗)⁷, and Ran Li (李冉)^{1,2}

2024 ApJ 976 235

<https://iopscience.iop.org/article/10.3847/1538-4357/ad84f0/pdf>

Coronal mass ejection (CME) is a powerful solar phenomenon that can lead to severe space weather events. Forecasting whether and when the corresponding interplanetary coronal mass ejection (ICME) will reach the Earth is very important in space weather study and forecast. At present, many different kinds of models use the near-Sun CME observations as model inputs to predict its propagation with similar prediction accuracies for large sample events. Among a series of physics-based models, the best-performing version of the shock propagation model (SPM) for large sample events, i.e., SPM3, had achieved a good forecast effect for the 23rd Solar Cycle events (1997.02–2006.12). To further evaluate SPM3, we collected CME events from 2013 January to 2023 July from the Community Coordinated Modeling Center (CCMC) CME scoreboard as a new data set. SPM3 achieved a total prediction success rate of 57% for these new events with a mean absolute error of 8.93 hr and a rms error of 10.86 hr for the shock's arrival time. Interestingly, SPM3 provided better predictions for the CME/shock events during high solar activity years than low solar activity years. We also analyzed the influence of input parameters on CME propagation and found that the larger the angular width of the CME event, the higher the probability of the corresponding IP shock's reaching the Earth. Source latitude had little effect on the arrival probability of the corresponding shock, while source longitude did. The CMEs originating from around W15° had the largest probability of hitting the Earth.

Model Evaluation Guidelines for Geomagnetic Index Predictions

Michael W. **Liemohn**, [James P. McCollough](#), [Vania K. Jordanova](#), [Chigomezoyo M. Ngwira](#), [Steven K. Morley](#), [Consuelo Cid](#), [W. Kent Tobiska](#), [Peter Wintoft](#) ...

Space Weather 16?, 12, 2079-2102 **2018**

<http://sci-hub.tw/10.1029/2018SW002067>

Geomagnetic indices are convenient quantities that distill the complicated physics of some region or aspect of near-Earth space into a single parameter. Most of the best-known indices are calculated from ground-based magnetometer data sets, such as Dst, SYM-H, Kp, AE, AL, and PC. Many models have been created that predict the values of these indices, often using solar wind measurements upstream from Earth as the input variables to the calculation. This document reviews the current state of models that predict geomagnetic indices and the methods used to assess their ability to reproduce the target index time series. These existing methods are synthesized into a baseline collection of metrics for benchmarking a new or updated geomagnetic index prediction model. These methods fall into two categories: (1) fit performance metrics such as root-mean-square error and mean absolute error that are applied to a time series comparison of model output and observations and (2) event detection performance metrics such as Heidke Skill Score and probability of detection that are derived from a contingency table that compares model and observation values exceeding (or not) a threshold value. A few examples of codes being used with this set of metrics are presented, and other aspects of metrics assessment best practices, limitations, and uncertainties are discussed, including several caveats to consider when using geomagnetic indices.

Structure of the Plasma near the Heliospheric Current Sheet as Seen by WISPR/Parker Solar Probe from inside the Streamer Belt

Paulett C. **Liewer**¹, Angelos Vourlidas², Guillermo Stenborg², Russell A. Howard², Jiong Qiu³, Paulo

Penteado¹, Olga Panasenco⁴, and Carlos R. Braga⁵

2023 ApJ 948 24

<https://iopscience.iop.org/article/10.3847/1538-4357/acc8c7/pdf>

Parker Solar Probe (PSP) crossed the heliospheric current sheet (HCS) near the perihelion on encounters E8 and E11, enabling the Wide-field Imager for Solar Probe (WISPR) to image the streamer belt plasma in high resolution while flying through it. With perihelia of 16 R_☉ and 13 R_☉ for E8 and E11, respectively, WISPR images enable

investigation of the structure of density encasing the HCS at much higher resolution than reported previously. As PSP flies closer to the Sun, fine-scale structures are resolved within the coronal rays of the streamer belt. Near the HCS, WISPR observes a fan of rays of various sizes and brightnesses, indicating large density variations in the HCS plasma sheet transverse to the radial direction. Near the perihelion, when PSP's speed exceeds the solar corotation speed, some rays exhibit large changes in apparent latitude as the HCS is encountered, and rays pass over and under the spacecraft. The multiple viewpoints provided during the HCS crossing enable us to extract the coordinates of a few rays in a heliocentric frame. The rays were found to lie near the HCS from a PFSS model. We compare their locations to the location of the streamers as seen in synoptic maps from the Large Angle and Spectrometric Coronagraph, and find that the rays generally fall within the bright streamer bands seen in these maps, which confirms that they are features of the streamer belt plasma. We speculate that the density variations in the helmet streamer plasma result from continuous interchange reconnection along the coronal hole boundaries. **26 Apr-3 May 2021, 28-29 Apr 2021, 22-28 Feb 2022**

Trajectory Determination for Coronal Ejecta Observed by WISPR/Parker Solar Probe

[P. C. Liewer](#), [J. Qiu](#), [P. Penteadó](#), [J. R. Hall](#), [A. Vourlidas](#), [R. A. Howard](#)

Solar Phys. **295**, Article number: 140 **2020**

<https://arxiv.org/pdf/2009.09323.pdf>

<https://link.springer.com/content/pdf/10.1007/s11207-020-01715-y.pdf>

The *Wide-field Imager for Solar Probe* (WISPR) on the *Parker Solar Probe* (PSP), observing in white light, has a fixed angular field of view, extending from 13.5° to 108° from the Sun and approximately 50° in the transverse directions. Because of the highly elliptical orbit of PSP, the physical extent of the imaged coronal region varies directly as the distance from the Sun, requiring new techniques for analysis of the motions of observed density features. Here, we present a technique for determining the 3D trajectory of CMEs and other coronal ejecta moving radially at a constant velocity by first tracking the motion in a sequence of images and then applying a curve-fitting procedure to determine the trajectory parameters (distance vs. time, velocity, longitude and latitude). To validate the technique, we have determined the trajectory of two CMEs observed by WISPR that were also observed by another white-light imager, either LASCO/C3 or STEREO-A/HI1. The second viewpoint was used to verify the trajectory results from this new technique and help determine its uncertainty. **2018 November 1-2, 2019 April 2-3**

Stereoscopic Analysis of STEREO/SECCHI Data for CME Trajectory Determination

P. C. [Liewer](#), J. R. Hall, R. A. Howard, E. M. De Jong, W. T. Thompson, A. Thernisien

E-print, 6 Oct **2010**, File ; JASTP, Volume 73, Issue 10, 20 June **2011**, Pages 1173-1186

The Sun Earth Connection Coronal and Heliospheric Investigation (SECCHI) coronagraphs on the twin Solar Terrestrial Relations Observatory (STEREO) spacecraft provide simultaneous views of the corona and coronal mass ejections from two view points. Here, we analyze simultaneous image pairs using the technique of tie-pointing and triangulation (T&T) to determine the three-dimensional trajectory of seven coronal mass ejections (CMEs). The bright leading edge of a CME seen in coronagraph images results from line-of-sight integration through the CME front; the two STEREO coronagraphs see different apparent leading edges, leading to a systematic error in its three-dimensional reconstruction. We analyze this systematic error using a simple geometric model of a CME front. We validate the technique and analysis by comparing T&T trajectory determinations for seven CMEs with trajectories determined by Thernisien, Vourlidas and Howard (2009) using a forward modeling technique not susceptible to this systematic effect. We find that, for the range of spacecraft separation studied ($\leq 50^\circ$), T&T gives reliable trajectories (uncertainty $< 10^\circ$ in direction and $< 15\%$ velocity) for CME propagating within approximately 40° of perpendicular to Sun-Earth line. For CMEs close to the Sun-Earth or Sun-Spacecraft lines, T&T is subject to larger errors, especially in the velocity.

Research highlights

► The coronagraphs on the twin Solar Terrestrial Relations Observatory (STEREO) spacecraft allow stereoscopic viewing of coronal mass ejections (CMEs). ► The technique of tie-pointing and triangulation is used to determine the trajectories (velocity and propagation angle) of CMEs. ► CMEs are optically thin and the images from the two spacecraft show different apparent leading edges and the error cause by this is analyzed. ► The ranges where the technique is reliable and where it is not are discussed.

Interplanetary Coronal Mass Ejection Associated Forbush Decreases in Neutron Monitors

Christopher [Light](#), Veronica Bindi, Cristina Consolandi, Claudio Corti, Christopher Freeman, Andrew Kuhlman, Matteo Palermo, and Siqi Wang

2020 ApJ 896 133

[C](#)

Interplanetary coronal mass ejections (ICMEs) are eruptions of plasma that propagate outward through the heliosphere. ICMEs, and the shocks they drive, cause a sudden decrease in the cosmic-ray flux in their local area of the heliosphere, called a Forbush decrease (FD). A method of defining FDs is established, and an automated process for identifying FDs in neutron monitor (NM) data is created. The correlation between ICME properties and FD magnitude in 12 different NMs is examined for 91 ICME-associated FD events occurring from 2001 through 2019 August. A number of ICME properties show positive correlation with FD magnitude, with decreasing correlation strength as NM cutoff rigidity increases. **7-8 Mar 2012**

Table 2 Forbush-decrease Events Marked in at Least Four Neutron Monitors (2001)

Table 3 Dip Size for ICME-associated Forbush-decrease Events (2001)

Prediction of Solar Wind Speed Through Machine Learning From Extrapolated Solar Coronal Magnetic Field

Prediction of solar wind speed by applying convolutional neural network to potential field source surface (PFSS) magnetograms

Rong [Lin](#), [Zhekai Luo](#), [Jiansen He](#), [Lun Xie](#), [Chuanpeng Hou](#), [Shuwei Chen](#)

Space Weather [Volume 22, Issue 6](#) June 2024 e2023SW003561

<https://arxiv.org/pdf/2304.01234.pdf>

<https://doi.org/10.1029/2023SW003561>

<https://agupubs.onlinelibrary.wiley.com/doi/epdf/10.1029/2023SW003561>

An accurate solar wind speed model is important for space weather predictions, catastrophic event warnings, and other issues concerning solar wind - magnetosphere interaction. In this work, we construct a model based on convolutional neural network (CNN) and Potential Field Source Surface (PFSS) magnetograms, considering a solar wind source surface of $R_{SS}=2.5R_{\odot}$, aiming to predict the solar wind speed at the Lagrange 1 (L1) point of the Sun-Earth system. The input of our model consists of four Potential Field Source Surface (PFSS) magnetograms at R_{SS} , which are 7, 6, 5, and 4 days before the target epoch. Reduced magnetograms are used to promote the model's efficiency. We use the Global Oscillation Network Group (GONG) photospheric magnetograms and the potential field extrapolation model to generate PFSS magnetograms at the source surface. The model provides predictions of the continuous test dataset with an averaged correlation coefficient (CC) of 0.52 and a root mean square error (RMSE) of 80.8 km/s in an eight-fold validation training scheme with the time resolution of the data as small as one hour. The model also has the potential to forecast high speed streams of the solar wind, which can be quantified with a general threat score of 0.39.

Drag Force on Coronal Mass Ejections (CMEs)

Chia-Hsien [Lin](#), [James Chen](#)

JGR [Volume 127, Issue 6](#) 2022 e2020JA028744

<https://doi.org/10.1029/2020JA028744>

The drag force experienced by coronal mass ejections (CMEs) plays an important role in determining the dynamics of CMEs. Numerous empirical studies have attempted to estimate the drag coefficient (cd) using the assumption that the observed deceleration of CMEs is primarily caused by drag alone. The observed CME motion, however, is determined by the net force—the sum of all the forces, and data contain no information to allow one to separately determine the individual forces. In the present work, we revisit the forces acting on CMEs using the erupting flux rope (EFR) model, making no assumptions on the magnitude of any force. Calculating the individual forces for four observed CME trajectories, it is shown that drag is generally not the dominant retarding force and that drag, magnetic tension, and pressure gradient can yield comparable deceleration. No force can be assumed negligible. It is further shown that the EFR equations can qualitatively replicate the observed deceleration with zero drag, contradicting the assertion that deceleration of CMEs necessarily implies the dominance of drag. A theoretical derivation of the drag coefficient cd for flux-rope CMEs is given for a range of idealized flows including the so-called “snow plow” effect. We show that $cd \sim 0-1$ unless the snow-plow effect is significant or the solar wind flows are specularly reflected, in which case $cd \sim 2-3$. The values of cd predicted by the EFR model for the observed trajectories are $cd \approx 1.1-1.2$ for three events and $cd \approx 0.4$ for one.

Understanding Magnetic Cloud Structure from Shock/Discontinuity Analysis

P. H. [Lin](#), [Y. H. Yang](#), [J. K. Chao](#), [H. Q. Feng](#), [J. Y. Liu](#)

JGR 2018

<http://sci-hub.tw/https://agupubs.onlinelibrary.wiley.com/doi/abs/10.1029/2018JA025225>

We reexamine the magnetic cloud (MC) event during the period of **21-23 May 2007**. In this event, the axis of the MC has a high inclination to the ecliptic plane and the heliospheric current sheet (HCS) happens to be on the ecliptic plane.

Therefore, we can use the feature of zero north-south component of interplanetary magnetic field to identify the MC boundaries. Inside the MC, there is an enhanced pressure/density region enclosed by two discontinuities. We verified these discontinuities through multiple spacecraft in-situ observations. The front one is a forward fast shock, which is a quasi-perpendicular shock at STEREO B but a quasi-parallel shock at Wind location. The discontinuity at the rear part of the enhanced pressure region resembles a reverse slow shock. However, we verify it is a tangential discontinuity (TD) using multi-spacecraft observations. Furthermore, we analyze the successive TDs inside the MC based on the TD signature of no normal magnetic field component to estimate the magnetic field morphology along the spacecraft trajectories. A novel method to evaluate the uncertainties of those TDs in this study has been given. It is found that the errors of the TD normal are much smaller than that calculated by conventional methods.

CME propagation in the dynamically coupled space weather tool: COCONUT + EUHFORIA

L. Linan, T. Baratashvili, A. Lani, B. Schmieder, M. Brchneleva, J. H. Guo, S. Poedts

A&A 2024

<https://arxiv.org/pdf/2411.19340>

This paper aims to present the time-dependent coupling between the coronal model COolfluid COroNal UnsTructured (COCONUT) and the heliospheric forecasting tool EUHFORIA.

We perform six COCONUT simulations where a flux rope is implemented at the solar surface using either the Titov-Démoulin CME model or the Regularized Biot-Savart Laws (RBSL) CME model. At regular intervals, the magnetic field, velocity, temperature, and density of the 2D surface $R_b=21.5 R_\odot$ are saved in boundary files. This series of coupling files is read in a modified version of EUHFORIA to update progressively its inner boundary. After presenting the early stage of the propagation in COCONUT, we examine how the disturbance of the solar corona created by the propagation of flux ropes is transmitted into EUHFORIA. In particular, we consider the thermodynamic and magnetic profiles at L1 and compare them with those obtained at the interface between the two models.

We demonstrate that the properties of the heliospheric solar wind in EUHFORIA are consistent with those in COCONUT, acting as a direct extension of the coronal domain. Moreover, the disturbances initially created from the propagation of flux ropes in COCONUT continue evolving from the corona in the heliosphere to Earth with a smooth transition at the interface between the two simulations. Looking at the profile of magnetic field components at Earth and different distances from the Sun, we also find that the transient magnetic structures have a self-similar expansion in COCONUT and EUHFORIA. However, the amplitude of the profiles depends on the flux rope model used and its properties, thus emphasizing the important role of the initial properties in solar source regions for accurately predicting the impact of CMEs.

Toroidal Miller-Turner and Soloviev CME models in EUHFORIA: I. Implementation

L. Linan, A. Maharana, S. Poedts, B. Schmieder, R. Keppens

A&A 2023

<https://arxiv.org/pdf/2310.17239.pdf>

The aim of this paper is to present the implementation of two new CME models in the space weather forecasting tool, EUHFORIA. We introduce the two toroidal CME models analytically, along with their numerical implementation in EUHFORIA. One model is based on the modified Miller-Turner (mMT) solution, while the other is derived from the Soloviev equilibrium, a specific solution of the Grad-Shafranov equation. The magnetic field distribution in both models is provided in analytic formulae, enabling a swift numerical computation. After detailing the differences between the two models, we present a collection of thermodynamic and magnetic profiles obtained at Earth using these CME solutions in EUHFORIA with a realistic solar wind background. Subsequently, we explore the influence of their initial parameters on the time profiles at L1. In particular, we examine the impact of the initial density, magnetic field strength, velocity, and minor radius. In EUHFORIA, we obtained different thermodynamic and magnetic profiles depending on the CME model used. We found that changing the initial parameters affects both the amplitude and the trend of the time profiles. For example, using a high initial speed results in a fast evolving and compressed magnetic structure. The speed of the CME is also linked to the strength of the initial magnetic field due to the contribution of the Lorentz force on the CME expansion. However, increasing the initial magnetic field also increases the computation time. Finally, the expansion and integrity of the magnetic structure can be controlled via the initial density of the CME. Both toroidal CME models are successfully implemented in EUHFORIA and can be utilized to predict the geo-effectiveness of the impact of real CME events. Moreover, the current implementation could be easily modified to model other toroidal magnetic configurations. **4, 6 November 2015**

Self-consistent propagation of flux ropes in realistic coronal simulations

L. Linan, F. Regnault, B. Perri, M. Brchneleva, B. Kuzma, A. Lani, S. Poedts, B. Schmieder

A&A 2023

<https://arxiv.org/pdf/2305.02089.pdf>

The aim of this paper is to demonstrate the possible use of the new coronal model COCONUT to compute a detailed representation of a numerical CME at 0.1~AU, after its injection at the solar surface and propagation in a realistic solar wind, as derived from observed magnetograms. We present the implementation and propagation of modified Titov-Démoulin (TDm) flux ropes in the COCONUT 3D MHD coronal model. The background solar wind is reconstructed in order to model two opposite configurations representing a solar activity maximum and minimum respectively. Both were derived from magnetograms which were obtained by the Helioseismic and Magnetic Imager (HMI) onboard the Solar Dynamic Observatory (SDO) satellite. We track the propagation of 24 flux ropes, which differ only by their initial magnetic flux. We especially investigate the geometry of the flux rope during the early stages of the propagation as well as the influence of its initial parameters and solar wind configuration on 1D profiles derived at 0.1~AU. At the beginning of the propagation, the shape of the flux ropes varies between simulations during low and high solar activity. We find dynamics that are consistent with the standard CME model, such as the pinching of the legs and the appearance of post-flare loops. Despite the differences in geometry, the synthetic density and magnetic field time profiles at 0.1~AU are very similar in both solar wind configurations. These profiles are similar to those observed further in the heliosphere and suggest the presence of a magnetic ejecta composed of the initially implemented flux rope and a sheath ahead of it. Finally, we uncover relationships between the properties of the magnetic ejecta, such as density or speed and the initial magnetic flux of our flux ropes. **20 March 2015, 2 July 2019**

Precursory Signals of Forbush Decreases Not Connected with Shock Waves

D. [Lingri](#), [H. Mavromichalaki](#), [M. Abunina](#), [A. Belov](#), [E. Eroshenko](#), [I. Daglis](#) & [A. Abunin](#)

[Solar Physics](#) volume 297, Article number: 24 (2022)

<https://link.springer.com/content/pdf/10.1007/s11207-022-01951-4.pdf>

Forbush decreases (FDs) are sharp reductions of the cosmic-ray (CR) intensity, following intense solar activity such as coronal mass ejections (CMEs) and their corresponding interplanetary shocks. In some cases, shocks create sudden storm commencements (SSCs) at the Earth's magnetosphere with significant interest for space-weather studies. Preincreases and/or predecreases of CR intensity before the onset of FDs, known as precursory signals, have been widely examined by many authors. In this work, an attempt to define precursory signals that are not related to SSCs is presented. For the present analysis, CR data recorded by the ground-based Neutron Monitor Network as well as data on solar flares, CMEs, solar-wind speed, interplanetary magnetic field, and geomagnetic indices for the years 1969 – 2019 are used. To identify FDs that present precursors, the adopted criteria are mainly the FD amplitude (> 2%) and the equatorial CR anisotropy before the onset time (> 0.8%). The analysis of FDs and the study of their asymptotic-longitude CR distribution for precursors are based on the Global Survey Method and the Ring of Stations Method, respectively. Precursory signals are identified in 17 out of 27 events without SSCs. **10 October 1980, 22-24 May 1999, 27-28 Jan 2002, 05 April 2014**

Table 2 FDs studied in this work that presented precursor signals. 1971-2016

An Extended Study of the Precursory Signs of Forbush Decreases: New Findings over the Years 2008 – 2016

D. [Lingri](#), [H. Mavromichalaki](#), [A. Belov](#), [M. Abunina](#), [E. Eroshenko](#), [A. Abunin](#)

[Solar Physics](#) June 2019, 294:70

sci-hub.se/10.1007/s11207-019-1461-3

In spite of the fact that the current Solar Cycle 24 is close to its end now, it is a less active Solar Cycle, during its time period (2008 – 2016) and a lot of Forbush decreases of cosmic ray intensity with rigidity 10 GV and amplitude greater than 2% were recorded by the ground-based neutron monitors. Among these events, the ones associated with sudden geomagnetic storm commencements (SSCs) and presenting a first harmonic of cosmic ray anisotropy greater than 0.8% were examined. Cosmic ray data recorded at the neutron monitor stations were obtained from the European high resolution neutron monitor database, while the Forbush decreases, accompanied by their characteristics were accessed from the updated Database of the Institute of Terrestrial Magnetism, Ionosphere and Radio Wave Propagation (IZMIRAN). Solar, interplanetary and geomagnetic characteristic parameters of each event separately have been studied in detail and analyzed. It was shown through the usage of the “ring of neutron monitor stations” method that, in some cases, precursory signals before the main phase of the event appeared. After an extended study of the Forbush decreases precursors during the examined period, the appearance of pre-decreases and/or pre-increases of the cosmic ray intensity before the beginning of the events, acting as precursory signals, were identified in almost half of the cases studied. In combination with other parameters, their common features are discussed, with the purpose of monitoring and possibly forecasting the space-weather conditions. **14-17 July 2012, 6-8 May 2015, 20-22 July 2016**

Table

Forbush Decreases during the DeepMin and MiniMax of Solar Cycle 24

D. **Lingri**, H. Mavromichalaki, A. Belov, E. Eroshenko, V. Yanke, A. Abunin, M. Abunina

XXV European Cosmic Ray Symposium, Turin, Sept. 4-9 2016

2016

<https://arxiv.org/pdf/1612.08900v1.pdf>

After a prolong and deep solar minimum at the end of solar cycle 23, the current cycle 24 is one of the lowest cycles. The two periods of deep minimum and mini-maximum of the cycle 24 are connected by a period of increasing solar activity. In this work, the Forbush decreases of cosmic ray intensity during the period from January 2008 to December 2014 are studied. A statistical analysis of 749 events using the IZMIRAN database of Forbush effects obtained by processing the data of the worldwide neutron monitor network using the global survey method is performed. A further study of the events that happened on the Sun and affected the interplanetary space, and finally provoked the decreases of the galactic cosmic rays near Earth is performed. A statistical analysis of the amplitude of the cosmic ray decreases with solar and geomagnetic parameters is carried out. The results will be useful for space weather studies and especially for Forbush decreases forecasting.

TABLE I: List of FDs with amplitude greater than 5%

Solar Activity Parameters and Associated Forbush Decreases During the Minimum Between Cycles 23 and 24 and the Ascending Phase of Cycle 24

D. **Lingri**, H. Mavromichalaki, A. Belov, E. Eroshenko, V. Yanke, A. Abunin, M. Abunina

Solar Phys. Volume 291, [Issue 3](#), pp 1025-1041 **2016**

<http://cosray.phys.uoa.gr/publications/D110.pdf>

We study the Forbush decreases in cosmic-ray intensity from January 2008 to December 2013, covering the minimum between Solar Cycles 23 and 24 and the ascending phase of Cycle 24. We performed a statistical analysis of 617 events and concentrated on three of the most important ones. We used the IZMIRAN database of Forbush effects obtained by processing the data of the worldwide neutron monitor network using the global survey method. The first event occurred on **18 February 2011** with a $\sim 5\%$ decrease of cosmic rays with 10 GV rigidity, the second on **8 March 2012** with an amplitude of $\sim 12\%$, and the third on **14 July 2012** with an amplitude of $\sim 6\%$. For these three events, we also studied the events that occurred on the Sun and the way that these affected the interplanetary space, and finally provoked the decreases of the galactic cosmic rays near Earth. We found that each neutron monitor records these decreases, which depend on the cut-off rigidity of the station. We carried out a statistical analysis of the amplitude of the cosmic-ray decreases with solar and geomagnetic parameters.

Table 1 The selected FDs of the cosmic-ray intensity with their characteristics during 2008 – 2013.

Magnetohydrodynamic Simulations of Interplanetary Coronal Mass Ejections

Roberto **Lionello**, Cooper Downs, Jon A. Linker, Tibor Török, Pete Riley, and Zoran Mikić

2013 ApJ 777 76

We describe a new MHD model for the propagation of interplanetary coronal mass ejections (ICMEs) in the solar wind. Accurately following the propagation of ICMEs is important for determining space weather conditions. Our model solves the MHD equations in spherical coordinates from a lower boundary above the critical point to Earth and beyond. On this spherical surface, we prescribe the magnetic field, velocity, density, and temperature calculated typically directly from a coronal MHD model as time-dependent boundary conditions. However, any model that can provide such quantities either in the inertial or rotating frame of the Sun is suitable. We present two validations of the technique employed in our new model and a more realistic simulation of the propagation of an ICME from the Sun to Earth.

Global simulation of extremely fast coronal mass ejection on 23 July 2012

Kan **Liou**, Chin-Chun Wu, Murray Dryer, Shi-Tsan Wu, Nathan Rich, Simon Plunkett, Lynn Simpson, Craig D. Fry, Kevin Schenk

JASTP, Volume 121, Part A, December **2014**, Pages 32–41

<http://www.sciencedirect.com/science/article/pii/S1364682614002247> **File**

The July 23, 2012 CME was an extremely fast backside event, reaching ~ 1 AU (STEREO-A) within 20 h as compared to ~ 3 – 6 days for typical CME events. Here, we present results from a simulation study of the CME and its driven shock using a combined kinematic and magnetohydrodynamic (MHD) simulation model, H3DMHD. In general, the model results match well with in situ measurements in the arrival time of the CME-driven shock and the total magnetic field

strength, assuming an initial CME speed of 3100 km/s. Based on extrapolation of an empirical model, the fast CME and its large magnetic field ($|B| \sim 120$ nT) are capable of producing an extremely large geomagnetic storm ($Dst \sim -545$ nT), comparable to the well-known Halloween storm in 2003, if the CME had made a direct impact to the Earth. We investigated the effect of the adiabatic index (γ). It is found that the shock tends to arrive slightly later for a smaller γ value, and $\gamma=5/3$ provides the best agreement for the shock arrival time. We also demonstrate that the strength (the Mach number) of the CME-driven fast-mode shock is not the largest at the “nose” of the CME. This is mainly due to the manifestation of fast-mode wave speed upstream of the shock.

A Pileup of Coronal Mass Ejections Produced the Largest Geomagnetic Storm in Two Decades

Ying D. Liu, [Huidong Hu](#), [Xiaowei Zhao](#), [Chong Chen](#), [Rui Wang](#)

ApJL **974** L8 **2024**

<https://arxiv.org/pdf/2409.11492>

<https://iopscience.iop.org/article/10.3847/2041-8213/ad7ba4/pdf>

The largest geomagnetic storm in two decades occurred in 2024 May with a minimum Dst of -412 nT. We examine its solar and interplanetary origins by combining multipoint imaging and in situ observations. The source active region, NOAA AR 13664, exhibited extraordinary activity and produced successive halo eruptions, which were responsible for two complex ejecta observed at the Earth. In situ measurements from STEREO A, which was 12.6° apart, allow us to compare the “geo-effectiveness” at the Earth and STEREO A. We obtain key findings concerning the formation of solar superstorms and how mesoscale variations of coronal mass ejections affect geo-effectiveness: (1) the 2024 May storm supports the hypothesis that solar superstorms are “perfect storms” in nature, i.e., a combination of circumstances resulting in an event of an unusual magnitude; (2) the first complex ejecta, which caused the geomagnetic superstorm, shows considerable differences in the magnetic field and associated “geo-effectiveness” between the Earth and STEREO A, despite a mesoscale separation; and (3) two contrasting cases of complex ejecta are found in terms of the geo-effectiveness at the Earth, which is largely due to different magnetic field configurations within the same active region. **10-11 May 2024**

Table 1. Information about the Full Halo CMEs Impacting the Earth **8-13 May 2024**

Forecasting the Dst Index with Temporal Convolutional Network and Integrated Gradients.

Liu, J., Shen, C., Wang, Y. et al.

Sol Phys 299, 98 (2024).

<https://doi.org/10.1007/s11207-024-02340-9>

The Disturbance Storm Time (Dst) Index stands as a crucial geomagnetic metric, serving to quantify the intensity of geomagnetic disturbances. The accurate prediction of the Dst index plays a pivotal role in mitigating the detrimental effects caused by severe space-weather events. Therefore, Dst prediction has been a long-standing focal point within the realms of space physics and space-weather forecasting. In this study, a Temporal Convolutional Network (TCN) is deployed in tandem with the Integrated Gradient (IG) algorithm to predict the Dst index and scrutinize its associated physical processes. With these two components, our model can give the contribution of each input parameter to the outcome along with the forecast. The TCN component of our model utilizes interplanetary observational data, encompassing the vector magnetic field, solar-wind velocity, proton temperature, proton density, interplanetary electric field, and other relevant parameters for forecasting Dst indices. Despite the disparity in test sets, our model’s forecast accuracy approximates the error levels of the prior models. Remarkably, the prediction error of these machine-learning models has become comparable to the inherent error between the Dst index itself and the actual ring-current strength.

To understand the physical process behind the forecasting model, the IG algorithm was applied in our prediction model, in an attempt to analyze the underlying physical process of the machine-learning black box. In the temporal dimension, it is evident that the more recent the time, the more substantial the influence on the final prediction. Regarding the physical parameters, besides the historical Dst index itself, the flow pressure, the z-component of the magnetic field, and the proton density all significantly contribute to the final prediction. Additionally, IG attributions were analyzed for subsets of data, including different Dst-index ranges, different observation times, and different interplanetary structures. Most of the subsets exhibit an IG matrix with deviations from the mean distribution, which

indicates a complex nonlinear system and sensitivity of the prediction to input values. These analyses align with physical reasoning and are in good agreement with previous research. The results affirm that the TCN+IG technique not only enhances space-weather forecast accuracy but also advances our comprehension of the underlying physical processes in space weather.

Direct In Situ Measurements of a Fast Coronal Mass Ejection and Associated Structures in the Corona

Ying D. [Liu](#), [Bei Zhu](#), [Hao Ran](#), [Huidong Hu](#), [Mingzhe Liu](#), [Xiaowei Zhao](#), [Rui Wang](#), [Michael L. Stevens](#), [Stuart D. Bale](#)

ApJ **963** 85 **2024**

<https://arxiv.org/pdf/2401.06449.pdf>

<https://iopscience.iop.org/article/10.3847/1538-4357/ad1e56/pdf>

We report on the first direct in situ measurements of a fast coronal mass ejection (CME) and shock in the corona, which occurred on **2022 September 5**. In situ measurements from the Parker Solar Probe (PSP) spacecraft near perihelion suggest two shocks with the second one decayed, which is consistent with more than one eruptions in coronagraph images. Despite a flank crossing, the measurements indicate unique features of the young ejecta: a plasma much hotter than the ambient medium suggestive of a hot solar source, and a large plasma β implying a highly non-force-free state and the importance of thermal pressure gradient for CME acceleration and expansion. Reconstruction of the global coronal magnetic fields shows a long-duration change in the heliospheric current sheet (HCS), and the observed field polarity reversals agree with a more warped HCS configuration. Reconnection signatures are observed inside an HCS crossing as deep as the sonic critical point. As the reconnection occurs in the sub-Alfvénic wind, the reconnected flux sunward of the reconnection site can close back to the Sun, which helps balance magnetic flux in the heliosphere. The nature of the sub-Alfvénic wind after the HCS crossing as a low Mach-number boundary layer (LMBL) leads to in situ measurements of the near subsonic plasma at a surprisingly large distance. Specifically, an LMBL may provide favorable conditions for the crossings of the sonic critical point in addition to the Alfvén surface.

On the Generation and Evolution of Switchbacks and the Morphology of the Alfvénic Transition: Low Mach-number Boundary Layers

Ying D. [Liu](#)^{1,2}, [Hao Ran](#)^{1,2}, [Huidong Hu](#)¹, and [Stuart D. Bale](#)³

2023 ApJ 944 116

<https://iopscience.iop.org/article/10.3847/1538-4357/acb345/pdf>

We investigate the generation and evolution of switchbacks (SBs), the nature of the sub-Alfvénic wind observed by the Parker Solar Probe (PSP), and the morphology of the Alfvénic transition, all of which are key issues in solar wind research. First we highlight a special structure in the pristine solar wind, termed a low Mach-number boundary layer (LMBL). An increased Alfvén radius and suppressed SBs are observed within an LMBL. A probable source on the Sun for an LMBL is the peripheral region inside a coronal hole with rapidly diverging open fields. The sub-Alfvénic wind detected by PSP is an LMBL flow by nature. The similar origin and similar properties of the sub-Alfvénic intervals favor a wrinkled surface for the morphology of the Alfvénic transition. We find that a larger deflection angle tends to be associated with a higher Alfvén Mach number. The magnetic deflections have an origin well below the Alfvén critical point, and deflection angles larger than 90° seem to occur only when $MA \gtrsim 2$. The velocity enhancement in units of the local Alfvén speed generally increases with the deflection angle, which is explained by a simple model. A nonlinearly evolved, saturated state is revealed for SBs, where the local Alfvén speed is roughly an upper bound for the velocity enhancement. In the context of these results, the most promising theory on the origin of SBs is the model of expanding waves and turbulence, and the patchy distribution of SBs is attributed to modulation by reductions in the Alfvén Mach number. Finally, a picture of the generation and evolution of SBs is created based on the results.

Total electron temperature derived from quasi-thermal noise spectroscopy in the pristine solar wind from Parker Solar Probe observations

M. [Liu](#)¹, [K. Issautier](#)¹, [M. Moncuquet](#)¹, [N. Meyer-Vernet](#)¹, [M. Maksimovic](#)¹, + + +

A&A 674, A49 (2023)

<https://www.aanda.org/articles/aa/pdf/2023/06/aa45450-22.pdf>

Aims. We applied the quasi-thermal noise (QTN) method to Parker Solar Probe (PSP) observations to derive the total electron temperature (T_e). We combined a set of encounters to make up a 12-day period of observations around each

perihelion from encounter one (E01) to ten (E10), with E08 not included. Here, the heliocentric distance varies from about 13 to 60 solar radii (R_{\odot}).

Methods. The QTN technique is a reliable tool to yield accurate measurements of the electron parameters in the solar wind. We obtained T_e from the linear fit of the high-frequency part of the QTN spectra acquired by the RFS/FIELDS instrument. Then, we provided the mean radial electron temperature profile, and examined the electron temperature gradients for different solar wind populations (i.e. classified by the proton bulk speed, V_p , and the solar wind mass flux). **Results.** We find that the total electron temperature decreases with the distance as $\sim R^{-0.66}$, which is much slower than adiabatic. The extrapolated T_e based on PSP observations is consistent with the exospheric solar wind model prediction at $\sim 10 R_{\odot}$, Helios observations at ~ 0.3 AU, and Wind observations at 1 AU. Also, T_e , extrapolated back to $10 R_{\odot}$, is almost the same as the Strahl electron temperature, T_s (measured by SPAN-E), which is considered to be closely related to or even almost equal to the coronal electron temperature. Furthermore, the radial T_e profiles in the slower solar wind (or flux tube with larger mass flux) are steeper than those in the faster solar wind (or flux tube with smaller mass flux). The more pronounced anticorrelation of V_p - T_e is observed when the solar wind is slower and located closer to the Sun.

Numerical Research on the Effect of the Initial Parameters of CME Flux-rope Model on Simulation Results. III. Different Initial Energy of CMEs

Yousheng Liu^{1,2}, Fang Shen^{1,2}, Yi Yang^{1,2}, and Mengxuan Ma^{1,2}
2022 ApJ 940 11

<https://iopscience.iop.org/article/10.3847/1538-4357/ac9b16/pdf>

In numerical studies, the initial parameters of coronal mass ejections (CMEs) have great influence on the simulation results. In our previous work, it has been proved that when the initial velocity is constant, the initial total mass mainly determines the propagation of the CME. On this basis, we carry out further research from the perspective of CME initial energy. We introduced a graduated cylindrical shell model into a 3D interplanetary total variation diminishing magnetohydrodynamic model to study the effect of different parameters of CMEs on simulation results. In this paper, we simulate several CME cases with different initial parameters and study the simulation results with a different initial energy composition. Actually, in interplanetary space, the kinetic energy of the CME always plays a dominant role. In order to study the effect of the initial thermal energy and magnetic energy on the propagation process of the CME, in this simulation, we adjust the initial parameters to make the thermal energy and magnetic energy reach the same level as the kinetic energy or an even higher level. Our results show that the initial total energy of the CME basically determines its arrival time at Earth, which indicates that the kinetic energy, thermal energy, and magnetic energy have similar effects on the propagation of the CMEs. Moreover, when the total energy keeps constant, the decrease of initial density will lead to the enhancement of CME expansion, which may make the front of the CME reach Earth earlier.

Statistical Study of Small-Scale Interplanetary Magnetic Flux Ropes in the Vicinity of the Heliospheric Current Sheet.

Liu Q, Zhao Y and Zhao G
(2021) Front. Phys. 9:745152.

<https://www.frontiersin.org/articles/10.3389/fphy.2021.745152/full>

<https://doi.org/10.3389/fphy.2021.745152>

The small-scale interplanetary magnetic flux ropes (SIMFRs) are common magnetic structures in the interplanetary space, yet their origination is still an open question. In this article, we surveyed 63 SIMFRs found within 6-day window around the heliospheric current sheet (HCS) and investigated their axial direction, as well as the local normal direction of the HCS. Results showed that the majority (48/63) of the SIMFRs were quasi-parallel to the associated HCS (i.e., the axial direction of SIMFRs was quasi-perpendicular to the normal direction of the associated HCS). They also showed that the SIMFRs quasi-parallel to the associated HCS statistically had shorter duration than the cases quasi-perpendicular. The results indicate that most of these SIMFRs may be generated in the nearby HCSs.

Investigation on the Spatiotemporal Structures of Supra-Arcade Spikes

Rui Liu, Yuming Wang

A&A 653, A51 2021

<https://arxiv.org/pdf/2106.04752.pdf>

<https://www.aanda.org/articles/aa/pdf/2021/09/aa40847-21.pdf>

<https://doi.org/10.1051/0004-6361/202140847>

The vertical current sheet (VCS) trailing coronal mass ejections (CMEs) is the key place where the flare energy release and the CME buildup take place through magnetic reconnection. It is often studied from the edge-on perspective for the

morphological similarity with the two-dimensional "standard" picture, but its three dimensional structure can only be revealed when the flare arcade is observed side on. The structure and dynamics in the so-called supra-arcade region thus contain important clues to the physical processes in flares and CMEs. Here we focus on the supra-arcade spikes (SASs), interpreted as the VCS viewed side-on, to study their spatiotemporal structures. By identifying each individual spike during the decay phase of four selected flares, in which the associated CME is traversed by a near-Earth spacecraft, we found that the widths of spikes are log-normal distributed, while the Fourier power spectra of the overall supra-arcade EUV emission, including bright spikes and dark downflows as well as the diffuse background, are power-law distributed, in terms of either spatial frequency k or temporal frequency ν , which reflects the fragmentation of the VCS. We demonstrate that coronal emission-line intensity observations dominated by Kolmogorov turbulence would exhibit a power spectrum of $E(k) \sim k^{-13/3}$ or $E(\nu) \sim \nu^{-7/2}$, which is consistent with our observations. By comparing the number of SASs and the turns of field lines as derived from the ICMEs, we found a consistent axial length of ~ 3.5 AU for three events with a CME speed of ~ 1000 km/s in the inner heliosphere, but a much longer axial length (~ 8 AU) for the fourth event with an exceptionally fast CME speed of ~ 1500 km/s, suggesting that this ICME is flattened and its "nose" has well passed the Earth when the spacecraft traversed its leg. **2011-Oct-22, 2013-Apr-11, 2013-Nov-07, 2014-Apr-02**

Solar wind energy flux observations in the inner heliosphere: First results from Parker Solar Probe

M. Liu, K. Issautier, N. Meyer-Vernet, M. Moncuquet, M. Maksimovic, J. S. Halekas, J. Huang, L. Griton, S. Bale, J. W. Bonnell, A. W. Case, K. Goetz, P. R. Harvey, J. C. Kasper, R. J. MacDowall, D. M. Malaspina, M. Pulupa, M. L. Stevens

A&A **2021**

<https://arxiv.org/pdf/2101.03121.pdf>

We investigate the solar wind energy flux in the inner heliosphere using 12-day observations around each perihelion of Encounter One (E01), Two (E02), Four (E04), and Five (E05) of Parker Solar Probe (PSP), respectively, with a minimum heliocentric distance of 27.8 solar radii (R_{\odot}). Energy flux was calculated based on electron parameters (density n_e , core electron temperature T_c , and suprathermal electron temperature T_h) obtained from the simplified analysis of the plasma quasi-thermal noise (QTN) spectrum measured by RFS/FIELDS and the bulk proton parameters (bulk speed V_p and temperature T_p) measured by the Faraday Cup onboard PSP, SPC/SWEAP. Combining observations from E01, E02, E04, and E05, the averaged energy flux value normalized to 1 R_{\odot} plus the energy necessary to overcome the solar gravitation (WR_{\odot}) is about 70 ± 14 Wm^{-2} , which is similar to the average value (79 ± 18 Wm^{-2}) derived by Le Chat et al from 24-year observations by Helios, Ulysses, and Wind at various distances and heliolatitudes. It is remarkable that the distributions of WR_{\odot} are nearly symmetrical and well fitted by Gaussians, much more so than at 1 AU, which may imply that the small heliocentric distance limits the interactions with transient plasma structures.

A Pilot Study of Interplanetary Scintillation with FAST

Li-Jia Liu, Bo Peng, Lei Yu, Ye-Zhao Yu, Ji-Guang Lu, Bin Liu, O. Chang, M. M. Bisi, FAST Collaboration

MNRAS **2021**

<https://arxiv.org/pdf/2105.02783.pdf>

Observations of Interplanetary Scintillation (IPS) are an efficient remote-sensing method to study the solar wind and inner heliosphere. From 2016 to 2018, some distinctive observations of IPS sources like 3C 286 and 3C 279 were accomplished with the Five-hundred-meter Aperture Spherical radio Telescope (FAST), the largest single-dish telescope in the world. Due to the 270-1620 MHz wide frequency coverage of the Ultra-Wideband (UWB) receiver, one can use both single-frequency and dual-frequency analyses to determine the projected velocity of the solar wind. Moreover, based on the extraordinary sensitivity owing to the large collecting surface area of FAST, we can observe weak IPS signals. With the advantages of both the wider frequency coverage and high sensitivity, also with our radio frequency interference (RFI) mitigation strategy and an optimized model-fitting method developed, in this paper, we analyze the fitting confidence intervals of the solar wind velocity, and present some preliminary results achieved using FAST, which points to the current FAST system being highly capable of carrying out observations of IPS.

Editorial: Magnetic Flux Ropes: From the Sun to the Earth and Beyond

Rui Liu^{1,2,3*}, Jie Zhang⁴, Yuming Wang^{1,2} and Hongqiang Song⁵

Front. Astron. Space Sci., 16 November 2020 |

<https://doi.org/10.3389/fspas.2020.605957>

The purpose of this Frontiers Research Topic on magnetic flux ropes is to provide a forum to bring together multi-wavelength remote sensing and in-situ diagnostics, to integrate observation and numerical modeling, and to confront

established models with new observations. The articles published in this Topic represent the most active fronts of research on a few important questions, namely, how flux ropes originate and evolve toward destabilization and beyond, how they are structured, and how they interact with each other and with surrounding magnetic fields and plasma. Below we briefly summarize the major results achieved by these articles.

Electron Energization and Energy Dissipation in Microscale Electromagnetic Environments

J. Liu^{1,2,3}, S. T. Yao², Q. Q. Shi², X. G. Wang⁴, Q. G. Zong⁵, Y. Y. Feng¹, H. Liu⁵, R. L. Guo⁶, Z. H. Yao⁷, I. J. Rae⁸Show full author list

2020 ApJL 899 L31

<https://doi.org/10.3847/2041-8213/abab92>

<https://iopscience.iop.org/article/10.3847/2041-8213/abab92/pdf>

Particle energization and energy dissipation in electromagnetic environments are longstanding topics of intensive research in space, laboratory, and astrophysical plasmas. One challenge is to understand these conversion processes at smaller and smaller spatial/temporal scales. In this Letter, with very high cadence measurements of particle distributions from the Magnetospheric Multiscale spacecraft, we report evidence of evolution of an identified microscale (i.e., electron gyro-scale) magnetic cavity structure and reveal within it a unique energization process that does not adhere to prevailing adiabatic invariance theory. Our finding indicates that this process is largely energy dependent, and can accelerate/decelerate charged particles inside the trapping region during their gyromotion, clearly altering the particle distribution.

Unusually low density regions in the compressed slow wind: Solar wind transients of small coronal hole origin

Yong C.-M. Liu¹, Zhaohui Qi^{1,2}, Jia Huang³, Chi Wang^{1,2}, Hui Fu⁴, Berndt Klecker⁵, Linghua Wang⁶ and Charles J. Farrugia⁷

A&A 635, A49 (2020)

<https://doi.org/10.1051/0004-6361/201935884>

We report on two small solar wind transients embedded in the corotating interaction region, characterized by surprisingly lower proton density compared with their surrounding regions. In addition to lower density, these two small solar wind transients showed other interesting features like higher proton temperature, higher alpha-proton ratios, and lower charge states (C+6/C+5 and O+7/O+6). A synthesized picture for event One combining the observations by STEREO B, ACE, and Wind showed that this small solar transient has an independent magnetic field. Back-mapping links the origin of the small solar transient to a small coronal hole on the surface of the Sun. Considering these special features and the back-mapping, we conclude that such small solar wind transients may have originated from a small coronal hole at low latitudes.

Characteristics and Importance of "ICME-in-Sheath" Phenomenon and Upper Limit for Geomagnetic Storm Activity

Ying D. Liu, Chong Chen, Xiaowei Zhao

ApJL 897 L11 2020

<https://arxiv.org/pdf/2006.09699.pdf>

<https://doi.org/10.3847/2041-8213/ab9d25>

As an important source for large geomagnetic storms, an "ICME-in-sheath" is a completely shocked interplanetary coronal mass ejection (ICME) stuck in the sheath between a shock and host ejecta. Typical characteristics are identified from coordinated multi-sets of observations: (1) it is usually short in duration and lasts a few hours at 1 AU; (2) its solar wind parameters, in particular the magnetic field, seem to keep enhanced for a large range of distances; and (3) common ICME signatures are often lost. The host ejecta could be a single ICME or a complex ejecta, being fast enough to drive a shock. These results clarify previous misinterpretations of this phenomenon as a normal part of a sheath region. The "ICME-in-sheath" phenomenon, together with a preconditioning effect, produced an extreme set of the magnetic field, speed and density near 1 AU in the **2012 July 23** case, all around their upper limits at the same time. This is probably the most extreme solar wind driving at 1 AU and enables us to estimate the plausible upper limit for geomagnetic storm activity. With an appropriate modification in the southward field, we suggest that a geomagnetic storm with a minimum Dst of about -2000 nT could occur in principle. The magnetopause would be compressed to about 3.3 Earth radii from the Earth's center, well inside the geosynchronous orbit. **2001 Nov 24**, **2012 July 23**, **2011 February 18**

Numerical Simulation on the Propagation and Deflection of Fast Coronal Mass Ejections (CMEs) Interacting with a Corotating Interaction Region in Interplanetary Space

Yousheng Liu^{1,2}, Fang Shen^{1,2,3}, and Yi Yang^{1,2}

2019 ApJ 887 150

<https://iopscience.iop.org/article/10.3847/1538-4357/ab543e/pdf>

Previous research has shown that the deflection of coronal mass ejections (CMEs) in interplanetary space, especially fast CMEs, is a common phenomenon. The deflection caused by the interaction with background solar wind is an important factor to determine whether CMEs could hit Earth or not. As the Sun rotates, there will be interactions between solar wind flows with different speeds. When faster solar wind runs into slower solar wind ahead, it will form a compressive area corotating with the Sun, which is called a corotating interaction region (CIR). These compression regions always have a higher density than the common background solar wind. When interacting with CME, will this make a difference in the deflection process of CME? In this research, first, a three-dimensional (3D) flux-rope CME initialization model is established based on the graduated cylindrical shell (GCS) model. Then this CME model is introduced into the background solar wind, which is obtained using a 3D IN (INterplanetary) -TV D-MHD model. The Carrington Rotation (CR) 2154 is selected as an example to simulate the propagation and deflection of fast CME when it interacts with background solar wind, especially with the CIR structure. The simulation results show that: (1) the fast CME will deflect eastward when it propagates into the background solar wind without the CIR; (2) when the fast CME hits the CIR on its west side, it will also deflect eastward, and the deflection angle will increase compared with the situation without CIR.

A Comparative Study of 2017 July and 2012 July Complex Eruptions: Are Solar Superstorms "Perfect Storms" in Nature?

Ying D. Liu, Xiaowei Zhao, Huidong Hu, Angelos Vourlidas, Bei Zhu

ApJ 2019

<https://arxiv.org/pdf/1902.03416.pdf>

It is paramount from both scientific and societal perspectives to understand the generation of extreme space weather. We discuss the formation of solar superstorms based on a comparative study of the **2012 July 23 and 2017 July 23** eruptions. The first one is Carrington-class, and the second could rival the 1989 March event that caused the most intense geomagnetic storm of the space age. Observations of these events in the historically weak solar cycle 24 indicate that a solar superstorm can occur in any solar cycle and at any phase of the cycle. Recurrent patterns are identified in both cases, including the long-lived eruptive nature of the active region, a complex event composed of successive eruptions from the same active region, and in-transit interaction between the successive eruptions resulting in exceptionally strong ejecta magnetic fields at 1 AU. Each case also shows unique characteristics. Preconditioning of the upstream solar wind leading to unusually high solar wind speeds at 1 AU is observed in the first case whereas not in the latter. This may suggest that the concept of "preconditioning" appears to be necessary for making a Carrington-class storm. We find a considerable deflection by nearby coronal holes in the second case but not in the first. On the basis of these results, we propose a hypothesis for further investigation that superstorms are "perfect storms" in nature, i.e., a combination of circumstances that results in an event of unusual magnitude. Historical records of some extreme events seem to support our hypothesis.

Geometry, Kinematics and Heliospheric Impact of a Large CME-driven Shock in 2017 September

Ying D. Liu, Bei Zhu, Xiaowei Zhao

ApJ 871 8 2019

<https://arxiv.org/pdf/1811.10162.pdf>

sci-hub.tw/10.3847/1538-4357/aaf425

A powerful coronal mass ejection (CME) occurred on 2017 September 10 near the end of the declining phase of the historically weak solar cycle 24. We obtain new insights concerning the geometry and kinematics of CME-driven shocks in relation to their heliospheric impacts from the optimal, multi-spacecraft observations of the eruption. The shock, which together with the CME driver can be tracked from the early stage to the outer corona, shows a large oblate structure produced by the vast expansion of the ejecta. The expansion speeds of the shock along the radial and lateral directions are much larger than the translational speed of the shock center, all of which increase during the flare rise phase, peak slightly after the flare maximum and then decrease. The near simultaneous arrival of the CME-driven shock at the Earth and Mars, which are separated by 156.6° in longitude, is consistent with the dominance of expansion over translation observed near the Sun. The shock decayed and failed to reach STEREO A around the backward direction. Comparison between ENLIL MHD simulations and the multi-point in situ measurements indicates that the shock expansion near the Sun is crucial for determining the arrival or non-arrival and space weather impact at certain

heliospheric locations. The large shock geometry and kinematics have to be taken into account and properly treated for accurate predictions of the arrival time and space weather impact of CMEs. **10 Sept 2017**

Kinetic Properties of an Interplanetary Shock Propagating inside a Coronal Mass Ejection

Mingzhe [Liu](#)^{1,2}, Ying D. Liu^{1,2}, Zhongwei Yang¹, L. B. Wilson III³, and Huidong Hu

2018 ApJL 859 L4

<https://arxiv.org/pdf/1805.11528.pdf>

We investigate the kinetic properties of a typical fast-mode shock inside an interplanetary coronal mass ejection (ICME) observed on **1998 August 6** at 1 au, including particle distributions and wave analysis with the in situ measurements from Wind. Key results are obtained concerning the shock and the shock–ICME interaction at kinetic scales: (1) gyrating ions, which may provide energy dissipation at the shock in addition to wave–particle interactions, are observed around the shock ramp; (2) despite the enhanced proton temperature anisotropy of the shocked plasma, the low plasma β inside the ICME constrains the shocked plasma under the thresholds of the ion cyclotron and mirror-mode instabilities; (3) whistler heat flux instabilities, which can pitch-angle scatter halo electrons through a cyclotron resonance, are observed around the shock, and can explain the disappearance of bi-directional electrons (BDEs) inside the ICME together with normal betatron acceleration; (4) whistler waves near the shock are likely associated with the whistler heat flux instabilities excited at the shock ramp, which is consistent with the result that the waves may originate from the shock ramp; (5) the whistlers share a similar characteristic with the shocklet whistlers observed by Wilson et al., providing possible evidence that the shock is decaying because of the strong magnetic field inside the ICME.

A New Tool for CME Arrival Time Prediction Using Machine Learning Algorithms: CAT-PUMA

Jiajia [Liu](#), [Yudong Ye](#), [Chenlong Shen](#), [Yuming Wang](#), [Robert Erdélyi](#)

ApJ 855 109 **2018**

<https://arxiv.org/pdf/1802.02803.pdf> File

<http://sci-hub.tw/10.3847/1538-4357/aaae69>

Coronal Mass Ejections (CMEs) are arguably the most violent eruptions in the Solar System. CMEs can cause severe disturbances in the interplanetary space and even affect human activities in many respects, causing damages to infrastructure and losses of revenue. Fast and accurate prediction of CME arrival time is then vital to minimize the disruption CMEs may cause when interacting with geospace. In this paper, we propose a new approach for partial-/full-halo CME Arrival Time Prediction Using Machine learning Algorithms (CAT-PUMA). Via detailed analysis of the CME features and solar wind parameters, we build a prediction engine taking advantage of 182 previously observed geo-effective partial-/full-halo CMEs and using algorithms of the Support Vector Machine (SVM). We demonstrate that CAT-PUMA is accurate and fast. In particular, predictions after applying CAT-PUMA to a test set, that is unknown to the engine, show a mean absolute prediction error ~ 5.9 hours of the CME arrival time, with 54% of the predictions having absolute errors less than 5.9 hours. Comparison with other models reveals that CAT-PUMA has a more accurate prediction for 77% of the events investigated; and can be carried out very fast, i.e. within minutes after providing the necessary input parameters of a CME. A practical guide containing the CAT-PUMA engine and the source code of two examples are available in the Appendix, allowing the community to perform their own applications for prediction using CAT-PUMA. **2015-12-28**

Multi-Spacecraft Observations of the Rotation and Non-Radial Motion of a CME Flux Rope causing an intense geomagnetic storm

Yi A. [Liu](#), [Ying D. Liu](#), [Huidong Hu](#), [Rui Wang](#), [Xiaowei Zhao](#)

ApJ 854 126 **2018**

<https://arxiv.org/pdf/1801.07457.pdf>

<http://sci-hub.tw/http://iopscience.iop.org/0004-637X/854/2/126/>

We present an investigation of the rotation and non-radial motion of a coronal mass ejection (CME) from AR 12468 on **2015 December 16** using observations from SDO, SOHO, STEREO A and Wind. The EUV and HMI observations of the source region show that the associated magnetic flux rope (MFR) axis pointed to the east before the eruption. We use a nonlinear force-free field (NLFFF) extrapolation to determine the configuration of the coronal magnetic field and calculate the magnetic energy density distributions at different heights. The distribution of the magnetic energy density shows a strong gradient toward the northeast. The propagation direction of the CME from a Graduated Cylindrical Shell (GCS) modeling deviates from the radial direction of the source region by about 45 deg in longitude and about 30 deg

in latitude, which is consistent with the gradient of the magnetic energy distribution around the AR. The MFR axis determined by the GCS modeling points southward, which has rotated counterclockwise by about 95 deg compared with the orientation of the MFR in the low corona. The MFR reconstructed by a Grad-Shafranov (GS) method at 1 AU has almost the same orientation as the MFR from the GCS modeling, which indicates that the MFR rotation occurred in the low corona. It is the rotation of the MFR that caused the intense geomagnetic storm with the minimum Dst of -155 nT. These results suggest that the coronal magnetic field surrounding the MFR plays a crucial role in the MFR rotation and propagation direction.

Propagation and Interaction Properties of Successive Coronal Mass Ejections in Relation to a Complex Type II Radio Burst

Ying D. [Liu](#)^{1,2}, Xiaowei Zhao^{1,2}, and Bei Zhu

2017 ApJ 849 112

<http://sci-hub.cc/10.3847/1538-4357/aa9075>

We examine the propagation and interaction properties of three successive coronal mass ejections (CMEs) from **2001 November 21–22**, with a focus on their connection with the behaviors of the associated long-duration complex type II radio burst. In combination with coronagraph and multi-point in situ observations, the long-duration type II burst provides key features for resolving the propagation and interaction complexities of the three CMEs. The two CMEs from November 22 interacted first and then overtook the November 21 CME at a distance of about 0.85 au from the Sun. The timescale for the shock originally driven by the last CME to propagate through the preceding two CMEs is estimated to be about 14 and 6 hr, respectively. We present a simple analytical model without any free parameters to characterize the whole Sun-to-Earth propagation of the shock, which shows a remarkable consistency with all the available data and MHD simulations even out to the distance of Ulysses (2.34 au). The coordination of in situ measurements at the Earth and Ulysses, which were separated by about 71° in latitude, gives important clues for the understanding of shock structure and the interpretation of in situ signatures. The results also indicate a means by which to increase geo-effectiveness with multiple CMEs, which can be considered as another manifestation of the "perfect storm" scenario proposed by Liu et al., although the current case is not "super" in the same sense as the 2012 July 23 event.

Structure, Propagation and Expansion of a CME-Driven Shock in the Heliosphere: A Revisit of the 2012 July 23 Extreme Storm

Ying D. [Liu](#), Huidong Hu, Bei Zhu, Janet G. Luhmann, Angelos Vourlidis

ApJ 834 158 2017

<https://arxiv.org/pdf/1611.04239v1.pdf>

We examine the structure, propagation and expansion of the shock associated with the **2012 July 23** extreme coronal mass ejection (CME). Characteristics of the shock determined from multi-point imaging observations are compared to in situ measurements at different locations and a complex radio type II burst, which according to our definition has multiple branches that may not all be fundamental-harmonic related. The white-light shock signature can be modeled reasonably well by a spherical structure and was expanding backward even on the opposite side of the Sun. The expansion of the shock, which was roughly self-similar after the first ~1.5 hours from launch, largely dominated over the translation of the shock center for the time period of interest. Our study also suggests a bow-shock morphology around the nose at later times due to the outward motion in combination with the expansion of the ejecta. The shock decayed and failed to reach Mercury in the backward direction and STEREO B and Venus in the lateral directions, as indicated by the imaging and in situ observations. The shock in the nose direction, however, may persist to the far outer heliosphere, with predicted impact on Dawn around 06 UT on July 25 and on Jupiter around 23:30 UT on July 27 by an MHD model. The type II burst shows properties generally consistent with the spatial/temporal variations of the shock deduced from imaging and in situ observations. In particular, the low-frequency bands agree well with the in situ measurements of a very low density ahead of the shock at STEREO A.

On Sun-to-Earth Propagation of Coronal Mass Ejections: 2. Slow Events and Comparison with Others

Ying D. [Liu](#), Huidong Hu, Chi Wang, Janet G. Luhmann, John D. Richardson, Zhongwei Yang, Rui Wang

ApJ Supplement 2016

<http://arxiv.org/pdf/1512.07949v1.pdf>

As a follow-up study on Sun-to-Earth propagation of fast coronal mass ejections (CMEs), we examine the Sun-to-Earth characteristics of slow CMEs combining heliospheric imaging and in situ observations. Three events of particular interest, the **2010 June 16, 2011 March 25 and 2012 September 25** CMEs, are selected for this study. We compare slow CMEs with fast and intermediate-speed events, and obtain key results complementing the attempt of \cite{liu13} to create a general picture of CME Sun-to-Earth propagation: (1) the Sun-to-Earth propagation of a typical slow CME can be approximately described by two phases, a gradual acceleration out to about 20-30 solar radii, followed by a nearly invariant speed around the average solar wind level, (2) comparison between different types of CMEs indicates that faster CMEs tend to accelerate and decelerate more rapidly and have shorter cessation distances for the acceleration and deceleration, (3) both intermediate-speed and slow CMEs would have a speed comparable to the average solar wind level before reaching 1 AU, (4) slow CMEs have a high potential to interact with other solar wind structures in the Sun-Earth space due to their slow motion, providing critical ingredients to enhance space weather, and (5) the slow CMEs studied here lack strong magnetic fields at the Earth but tend to preserve a flux-rope structure with axis generally perpendicular to the radial direction from the Sun. We also suggest a "best" strategy for the application of a triangulation concept in determining CME Sun-to-Earth kinematics, which helps to clarify confusions about CME geometry assumptions in the triangulation and to improve CME analysis and observations.

Plasma and Magnetic Field Characteristics of Solar Coronal Mass Ejections in Relation to Geomagnetic Storm Intensity and Variability

Ying D. [Liu](#), [Huidong Hu](#), [Rui Wang](#), [Zhongwei Yang](#), [Bei Zhu](#), [Yi A. Liu](#), [Janet G. Luhmann](#), [John D. Richardson](#)

ApJL 809 L34 2015

<http://arxiv.org/pdf/1508.01267v1.pdf>

The largest geomagnetic storms of solar cycle 24 so far occurred on **2015 March 17 and June 22 with Dst minima of -223 and -195 nT**, respectively. Both of the geomagnetic storms show a multi-step development. We examine the plasma and magnetic field characteristics of the driving coronal mass ejections (CMEs) in connection with the development of the geomagnetic storms. A particular effort is to reconstruct the in situ structure using a Grad-Shafranov technique and compare the reconstruction results with solar observations, which gives a larger spatial perspective of the source conditions than one-dimensional in situ measurements. Key results are obtained concerning how the plasma and magnetic field characteristics of CMEs control the geomagnetic storm intensity and variability: (1) a sheath-ejecta-ejecta mechanism and a sheath-sheath-ejecta scenario are proposed for the multi-step development of the 2015 March 17 and June 22 geomagnetic storms, respectively; (2) two contrasting cases of how the CME flux-rope characteristics generate intense geomagnetic storms are found, which indicates that a southward flux-rope orientation is not a necessity for a strong geomagnetic storm; and (3) the unexpected 2015 March 17 intense geomagnetic storm resulted from the interaction between two successive CMEs plus the compression by a high-speed stream from behind, which is essentially the "perfect storm" scenario proposed by \cite{liu14a}, so the "perfect storm" scenario may not be as rare as the phrase implies.

Improvements of the shock arrival times at the Earth model STOA

H.-L. [Liu](#), G. Qin

JGR [Volume 120, Issue 7](#) Pages 5290–5297 2015

<http://arxiv.org/pdf/1502.01069v1.pdf>

Prediction of the shocks' arrival times (SATs) at the Earth is very important for space weather forecast. There is a well-known SAT model, STOA, which is widely used in the space weather forecast. However, the shock transit time from STOA model usually has a relative large error compared to the real measurements. In addition, STOA tends to yield too much 'yes' prediction, which causes a large number of false alarms. Therefore, in this work, we work on the modification of STOA model. First, we give a new method to calculate the shock transit time by modifying the way to use the solar wind speed in STOA model. Second, we develop new criteria for deciding whether the shock will arrive at the Earth with the help of the sunspot numbers and the angle distances of the flare events. It is shown that our work can improve the SATs prediction significantly, especially the prediction of flare events without shocks arriving at the Earth.

A Statistical Analysis of Heliospheric Plasma Sheets, Heliospheric Current Sheets and Sector Boundaries Observed in situ by STEREO†

Y. C.-M. [Liu](#)^{1,*}, J. Huang¹, C. Wang¹, B. Klecker², A.B. Galvin³, K.D.C. Simunac³, M.A. Popecki³, L. Kistler³, C. Farrugia³, M. A. Lee³, H Kucharek³, A. Opitz⁴, J.G. Luhmann⁵ and Lan Jian
JGR, Volume 119, Issue 11, pages 8721–8732 **2014**

The heliocentric orbits of STEREO A and B with a separation in longitude increasing by about 45° per year provide the unique opportunity to study the evolution of the heliospheric plasma sheet (HPS) on a time scale of up to ~2 days and to investigate the relative locations of HPSs and heliospheric current sheets (HCSs). Previous work usually determined the HCS locations based only on the interplanetary magnetic field. A recent study showed that a HCS can be taken as a global structure only when it matches with a sector boundary (SB). Using magnetic field and suprathermal electron data it was also shown that the relative location of HCS and HPS can be classified into five different types of configurations. However, only for two out of these five configurations the HCS and HPS are located at the same position and only these will therefore be used for our study of the HCS/HPS relative location. We find out of 37 SBs in our dataset 10 suitable HPS/HCS event pairs. We find that an HPS can either straddle or border the related HCS. Comparing the corresponding HPS observations between STEREO A and B, we find that the relative HCS/HPS locations are mostly similar. In addition, the time difference of the HPSs observations between STEREO A and B match well with the predicted time delay for the solar wind coming out of a similar region of the sun. We therefore conclude that HPSs are stationary structures originating at the sun.

Sun-to-Earth Characteristics of Two Coronal Mass Ejections Interacting near 1 AU: Formation of a Complex Ejecta and Generation of a Two-Step Geomagnetic Storm

Ying D. [Liu](#), Zhongwei Yang, Rui Wang, Janet G. Luhmann, John D. Richardson, Noé Lugaz
ApJL, 793 L41 **2014**

<http://arxiv.org/pdf/1409.2954v1.pdf>

On **2012 September 30 - October 1** the Earth underwent a two-step geomagnetic storm. We examine the Sun-to-Earth characteristics of the coronal mass ejections (CMEs) responsible for the geomagnetic storm with combined heliospheric imaging and in situ observations. The first CME, which occurred on **2012 September 25**, is a slow event and shows an acceleration followed by a nearly invariant speed in the whole Sun-Earth space. The second event, launched from the Sun on **2012 September 27**, exhibits a quick acceleration, then a rapid deceleration and finally a nearly constant speed, a typical Sun-to-Earth propagation profile for fast CMEs \citep{liu13}. These two CMEs interacted near 1 AU as predicted by the heliospheric imaging observations and formed a complex ejecta observed at Wind, with a shock inside that enhanced the pre-existing southward magnetic field. Reconstruction of the complex ejecta with the in situ data indicates an overall left-handed flux rope-like configuration, with an embedded concave-outward shock front, a maximum magnetic field strength deviating from the flux rope axis and convex-outward field lines ahead of the shock. While the reconstruction results are consistent with the picture of CME-CME interactions, a magnetic cloud-like structure without clear signs of CME interactions \citep{lugaz14} is anticipated when the merging process is finished.

Propagation of the 2012 March Coronal Mass Ejections from the Sun to Heliopause

Ying D. [Liu](#), John D. Richardson, Chi Wang, Janet G. Luhmann
ApJL, 788 L28 **2014**

<http://arxiv.org/pdf/1405.6086v1.pdf>

In 2012 March the Sun exhibited extraordinary activities. In particular, the active region NOAA AR 11429 emitted a series of large coronal mass ejections (CMEs) which were imaged by STEREO as it rotated with the Sun from the east to west. These sustained eruptions are expected to generate a global shell of disturbed material sweeping through the heliosphere. A cluster of shocks and interplanetary CMEs (ICMEs) were observed near the Earth, and are propagated outward from 1 AU using an MHD model. The transient streams interact with each other, which erases memory of the source and results in a large merged interaction region (MIR) with a preceding shock. The MHD model predicts that the shock and MIR would reach 120 AU around 2013 April 22, which agrees well with the period of radio emissions and the time of a transient disturbance in galactic cosmic rays detected by Voyager 1. These results are important for understanding the "fate" of CMEs in the outer heliosphere and provide confidence that the heliopause is located around 120 AU from the Sun. **5-13 March 2012**

Observations of an extreme storm in interplanetary space caused by successive coronal mass ejections

Ying D. **Liu**, Janet G. Luhmann, Primož Kajdič, Emilia K.J. Kilpua, Noé Lugaz, Nariaki V. Nitta, Christian Möstl, Benoit Lavraud, Stuart D. Bale, Charles J. Farrugia & Antoinette B. Galvin

Nature Communications 5, Article number: 3481, 2014, **File**

<http://arxiv.org/pdf/1405.6088v1.pdf>

Space weather refers to dynamic conditions on the Sun and in the space environment of the Earth, which are often driven by solar eruptions and their subsequent interplanetary disturbances. It has been unclear how an extreme space weather storm forms and how severe it can be. Here we report and investigate an extreme event with multi-point remote-sensing and in situ observations. The formation of the extreme storm showed striking novel features. We suggest that the in-transit interaction between two closely launched coronal mass ejections resulted in the extreme enhancement of the ejecta magnetic field observed near 1 AU at STEREO A. The **fast transit to STEREO A (in only 18.6 h)**, or the unusually weak deceleration of the event, was caused by the preconditioning of the upstream solar wind by an earlier solar eruption. These results provide a new view crucial to solar physics and space weather as to how an extreme space weather event can arise from a combination of solar eruptions.

Spaceweather.com (20 March 2014): An intense solar storm that narrowly missed Earth almost two years ago.

On **July 23, 2012**, a CME rocketed away from the sun at 2000 km/s, almost four times faster than a typical eruption. The storm tore through Earth orbit, but fortunately Earth wasn't there. Instead it hit the STEREO-A spacecraft, which experienced the most intense solar proton storm since 1976. Researchers have been analyzing the data ever since, and they have concluded that the storm was akin to the Carrington Event of 1859.

<http://www.youtube.com/watch?v=vQvsFjse9yw>

ON SUN-TO-EARTH PROPAGATION OF CORONAL MASS EJECTIONS

Ying D. **Liu**^{1,2}, Janet G. Luhmann², Noé Lugaz³, Christian Möstl^{2,4}, Jackie A. Davies⁵, Stuart D. Bale², and Robert P. Lin

2013 ApJ 769 45, **File**

http://sprg.ssl.berkeley.edu/~liuxying/pubs/2013_apj_prop.pdf

<http://arxiv.org/pdf/1304.3777v1.pdf>

We investigate how coronal mass ejections (CMEs) propagate through, and interact with, the inner heliosphere between the Sun and Earth, a key question in CME research and space weather forecasting. CME Sun-to-Earth kinematics are constrained by combining wide-angle heliospheric imaging observations, interplanetary radio type II bursts, and in situ measurements from multiple vantage points. We select three events for this study, the **2012 January 19, 23, and March 7 CMEs**. Different from previous event studies, this work attempts to create a general picture for CME Sun-to-Earth propagation and compare different techniques for determining CME interplanetary kinematics. Key results are obtained concerning CME Sun-to-Earth propagation: (1) the Sun-to-Earth propagation of fast CMEs can be approximately formulated into three phases: an impulsive acceleration, then a rapid deceleration, and finally a nearly constant speed propagation (or gradual deceleration); (2) the CMEs studied here are still accelerating even after the flare maximum, so energy must be continuously fed into the CME even after the time of the maximum heating and radiation has elapsed in the corona; (3) the rapid deceleration, presumably due to interactions with the ambient medium, mainly occurs over a relatively short timescale following the acceleration phase; and (4) CME-CME interactions seem a common phenomenon close to solar maximum. Our comparison between different techniques (and data sets) has important implications for CME observations and their interpretations: (1) for the current cases, triangulation assuming a compact CME geometry is more reliable than triangulation assuming a spherical front attached to the Sun for distances below 50-70 solar radii from the Sun, but beyond about 100 solar radii we would trust the latter more; (2) a proper treatment of CME geometry must be performed in determining CME Sun-to-Earth kinematics, especially when the CME propagation direction is far away from the observer; and (3) our approach to comparing wide-angle heliospheric imaging observations with interplanetary radio type II bursts provides a novel tool in investigating CME propagation characteristics. Future CME observations and space weather forecasting are discussed based on these results.

2012 January 19, January 23, March 7,

Using soft X-ray observations to help the prediction of flare related interplanetary shocks arrival times at the Earth

Liu, H.-L.; Qin, G.

J. Geophys. Res., Vol. 117, No. A4, A04108, **2012, File**

It is very important to predict the shock arrival times (SATs) at Earth for space weather practice. In this paper we use the energy of soft X-ray during solar flare events to help predict the SATs at Earth. We combine the soft X-ray energy and SAT prediction models previously developed by researchers to obtain two new methods. By testing the methods with the total of 585 solar flare events following the generation of a metric type II radio burst during the Solar Cycle 23 from September 1997 to December 2006, we find that the predictions of SATs at Earth could be improved by significantly increasing PODn, the proportion of events without shock detection that were correctly forecast. PODn represents a method's ability in forecasting the solar flare events without shocks arriving at the Earth, which is important for operational predictions.

SOLAR SOURCE AND HELIOSPHERIC CONSEQUENCES OF THE 2010 APRIL 3 CORONAL MASS EJECTION: A COMPREHENSIVE VIEW

Ying **Liu**¹, Janet G. Luhmann¹, Stuart D. Bale¹ and Robert P. Lin

2011 ApJ 734 84, File

We study the solar source and heliospheric consequences of the 2010 April 3 coronal mass ejection (CME) in the frame of the Sun-Earth connection using observations from a fleet of spacecraft. The CME is accompanied by a B7.4 long-duration flare, dramatic coronal dimming, and EUV waves. It causes significant heliospheric consequences and space weather effects such as radio bursts, a prominent shock wave, the largest/fastest interplanetary CME at 1 AU since the 2006 December 13 CME, the first gradual solar energetic particle (SEP) events in solar cycle 24, and a prolonged geomagnetic storm resulting in a breakdown of the Galaxy 15 satellite. This event, together with several following periods of intense solar activities, indicates awakening of the Sun from a long minimum. The CME EUV loop begins to rise at least 10 minutes before the flare impulsive phase. The associated coronal wave forms an envelope around the CME, a large-scale three-dimensional structure that can only be explained by a pressure wave. The CME and its preceding shock are imaged by both STEREO A and B almost throughout the whole Sun-Earth space. CME kinematics in the ecliptic plane are obtained as a function of distance out to 0.75 AU by a geometric triangulation technique. The CME has a propagation direction near the Sun-Earth line and a speed that first increases to 1000-1100 km s⁻¹ and then decreases to about 800 km s⁻¹. Both the predicted arrival time and speed at the Earth are well confirmed by the in situ measurements. The gradual SEP events observed by three widely separated spacecraft show time profiles much more complicated than suggested by the standard conceptual picture of SEP event heliolongitude distribution. Evolving shock properties, the realistic time-dependent connection between the observer and shock source, and a possible role of particle perpendicular diffusion may be needed to interpret this SEP event spatial distribution.

Grad-Shafranov Reconstruction of Magnetic Flux Ropes in the Near-Earth Space

A.T.Y. **Liu**

Space Sci Rev (**2011**) 158: 43–68, **File**

Electric currents permeate space plasmas and often have a significant component along the magnetic field to form magnetic flux ropes. A larger spatial perspective of these structures than from the direct observation along the satellite path is crucial in visualizing their role in plasma dynamics. For magnetic flux ropes that are approximately two-dimensional equilibrium structures on a certain plane, Grad-Shafranov reconstruction technique, developed by Bengt Sonnerup and his colleagues (see Sonnerup et al. in J. Geophys. Res. 111:A09204, **2006**), can be used to reveal two-dimensional maps of associated plasma and field parameters. This review gives a brief account of the technique and its application to magnetic flux ropes near the Earth's magnetopause, in the solar wind, and in the magnetotail. From this brief survey, the ranges of the total field-aligned current and the total magnetic flux content for these magnetic flux ropes are assessed. The total field-aligned current is found to range from ~0.14 to ~9.74104 MA, a range of nearly six orders of magnitude.

The total magnetic flux content is found to range from ~0.25 to ~2.34106 MWb, a range of nearly seven orders of magnitude. To the best of our knowledge, this review reports the largest range of both the total field-aligned current and the total magnetic flux content

for magnetic flux ropes in space plasmas.

20 Nov 2003

RECONSTRUCTING CORONAL MASS EJECTIONS WITH COORDINATED IMAGING AND IN SITU OBSERVATIONS: GLOBAL STRUCTURE, KINEMATICS, AND IMPLICATIONS FOR SPACE WEATHER FORECASTING

Ying Liu¹, Arnaud Thernisien², Janet G. Luhmann¹, Angelos Vourlidas³, Jackie A. Davies⁴, Robert P. Lin^{1,5}, and Stuart D. Bale¹

The Astrophysical Journal, 722:1762–1777, 2010, **File**

We reconstruct the global structure and kinematics of coronal mass ejections (CMEs) using coordinated imaging and in situ observations from multiple vantage points. A forward modeling technique, which assumes a rope-like morphology for CMEs, is used to determine the global structure (including orientation and propagation direction) from coronagraph observations. We reconstruct the corresponding structure from in situ measurements at 1 AU with the Grad–Shafranov method, which gives the flux-rope orientation, cross section, and a rough knowledge of the propagation direction. CME kinematics (propagation direction and radial distance) during the transit from the Sun to 1 AU are studied with a geometric triangulation technique, which provides an unambiguous association between solar observations and in situ signatures; a track fitting approach is invoked when data are available from only one spacecraft. We show how the results obtained from imaging and in situ data can be compared by applying these methods to the **2007 November 14–16 and 2008 December 12 CMEs**. This merged imaging and in situ study shows important consequences and implications for CME research as well as space weather forecasting: (1) CME propagation directions can be determined to a relatively good precision as shown by the consistency between different methods; (2) the geometric triangulation technique shows a promising capability to link solar observations with corresponding in situ signatures at 1 AU and to predict CME arrival at the Earth; (3) the flux rope within CMEs, which has the most hazardous southward magnetic field, cannot be imaged at large distances due to expansion; (4) the flux-rope orientation derived from in situ measurements at 1 AU may have a large deviation from that determined by coronagraph image modeling; and (5) we find, for the first time, that CMEs undergo a westward migration with respect to the Sun–Earth line at their acceleration phase, which we suggest is a universal feature produced by the magnetic field connecting the Sun and ejecta. The importance of having dedicated spacecraft at L4 and L5, which are well situated for the triangulation concept, is also discussed based on the results.

GEOMETRIC TRIANGULATION OF IMAGING OBSERVATIONS TO TRACK CORONAL MASS EJECTIONS CONTINUOUSLY OUT TO 1 AU

Ying Liu¹, Jackie A. Davies², Janet G. Luhmann¹, Angelos Vourlidas³, Stuart D. Bale¹, and Robert P. Lin^{1,4}

Astrophysical Journal Letters, 710:L82–L87, 2010 February; **File**

We describe a geometric triangulation technique, based on time–elongation maps constructed from imaging observations, to track coronal mass ejections (CMEs) continuously in the heliosphere and predict their impact on the Earth. Taking advantage of stereoscopic imaging observations from the Solar Terrestrial Relations Observatory, this technique can determine the propagation direction and radial distance of CMEs from their birth in the corona all the way to 1 AU. The efficacy of the method is demonstrated by its application to the **2008 December 12 CME**, which manifests as a magnetic cloud (MC) from in situ measurements at the Earth. The predicted arrival time and radial velocity at the Earth are well confirmed by the in situ observations around the MC. Our method reveals non-radial motions and velocity changes of the CME over large distances in the heliosphere. It also associates the flux-rope structure measured in situ with the dark cavity of the CME in imaging observations. Implementation of the technique, which is expected to be a routine possibility in the future, may indicate a substantial advance in CME studies as well as space weather forecasting.

A Comprehensive View of the 2006 December 13 CME: From the Sun to Interplanetary Space

Y. **Liu**, J. G. Luhmann, R. Muller-Mellin, P. C. Schroeder, L. Wang, R. P. Lin, S. D. Bale, Y. Li, M. H. Acuna, and J.-A. Sauvaud

The Astrophysical Journal, Vol. 689, No. 1: 563-571, **2008**, File.

<http://www.journals.uchicago.edu/doi/abs/10.1086/592031>

The biggest halo coronal mass ejection (CME) since the Halloween storm in 2003, which occurred on 2006 December 13, is studied in terms of its solar source and heliospheric consequences. The CME was accompanied by an X3.4 flare, EUV dimmings, and coronal waves. It generated significant space weather effects such as an interplanetary shock, radio bursts, major solar energetic particle (SEP) events, and a magnetic cloud (MC) that were detected by a fleet of spacecraft including **STEREO**, ACE, WIND, and Ulysses. Reconstruction of the MC with the Grad-Shafranov (GS) method yields an axis orientation oblique to the flare ribbons. Observations of the SEP intensities and anisotropies show that the particles can be trapped, deflected, and reaccelerated by the large-scale transient structures. The CME-driven shock was observed at both the Earth and Ulysses when they were separated by 74° in latitude and 117° in longitude, which is the largest shock extent ever detected. The ejecta seem to have been missed at Ulysses. The shock arrival time at Ulysses is well predicted by an MHD model that can propagate the 1 AU data outward. The CME/shock is tracked remarkably well from the Sun all the way to Ulysses by coronagraph images, type II frequency drift, in situ measurements, and the MHD model. These results reveal a technique that combines MHD propagation of the solar wind and type II emissions to predict the shock arrival time at the Earth, which is a significant advance for space weather forecasting, especially when in situ data become available from the Solar Orbiter and Solar Sentinels.

Deflection Flows Ahead of ICMEs as an Indicator of Curvature and Geoeffectiveness

Y. **Liu**, W. B. Manchester IV, J. D. Richardson, J. G. Luhmann, R. P. Lin, and S. D. Bale

E-print, April **2008**; JGR

We examine the upstream meridional deflection flows of interplanetary coronal mass ejections (ICMEs) in an effort to investigate their cross-sectional shape and the magnetic field orientation in their sheath regions. Eight out of 11 magnetic clouds (MCs) near solar minimum identified for the curvature study are concave outward as indicated by the elevation angle of the MC normal with respect to the solar equatorial plane; an inverse correlation is observed between the meridional deflection flow and the spacecraft latitude for these concave-outward MCs, which suggests that the upstream plasma is deflected toward the equatorial plane. MHD simulations, however, show that the meridional deflection flow moves poleward for a concave-outward CME. The poleward flow deflection is observed only ahead of convex-outward MCs. Possibilities leading to this discrepancy are discussed. The deflection flow speed in sheath regions of ICMEs increases with the ICME speed relative to the ambient solar wind, which together with the coupling between the meridional magnetic field and deflection flow yields a positive linear correlation between the sheath meridional field and the ICME relative speed. This empirical relationship could predict the sheath meridional field based on the observed CME speed, which may be useful for space weather forecasting as ICME sheaths are often geoeffective. Implications of the deflection flows and ICME curvature are also discussed in terms of magnetic reconnection and particle acceleration in ICME sheaths.

RECONSTRUCTION OF THE 2007 MAY 22 MAGNETIC CLOUD: HOW MUCH CAN WE TRUST THE FLUX-ROPE GEOMETRY OF CMES?

Y. **Liu**, G. Luhmann,¹ K. E. J. Huttunen,¹ R. P. Lin,¹ S. D. Bale,¹ C. T. Russell,³ and A. B. Galvin⁴

The Astrophysical Journal, 677:L133–L136, **2008**

<http://www.journals.uchicago.edu/doi/pdf/10.1086/587839>

Coronal mass ejections (CMEs) are often assumed to be magnetic flux ropes, but direct proof has been lacking. A key feature, resulting from the translational symmetry of a flux rope, is that the total transverse pressure as well as the axial magnetic field has the same functional form over the vector potential along any crossing of the flux rope. We test this feature (and hence the flux-rope structure) by reconstructing the **2007 May 22** magnetic cloud (MC) observed at *STEREO B*, *Wind/ACE*, and possibly *STEREO A* with the Grad-Shafranov (GS) method. The model output from reconstruction at *STEREO B* agrees fairly well with the magnetic field and thermal pressure observed at *ACE/Wind*; the separation between *STEREO B* and *ACE/Wind* is about 0.06 AU, almost half of the MC radial width. For the first time, we reproduce observations at one spacecraft with data from another well separated spacecraft, which provides compelling evidence for the flux-rope geometry and is of importance for understanding CME initiation and propagation. We also discuss the global configuration of the MC at different

spacecraft on the basis of the reconstruction results.

DETERMINING THE MAGNETIC FIELD ORIENTATION OF CORONAL MASS EJECTIONS FROM FARADAY ROTATION

Y. **Liu**,^{1,2} W. B. Manchester IV,³ J. C. Kasper,¹ J. D. Richardson,^{1,2} and J. W. Belcher¹

The Astrophysical Journal, 665:1439–1447, 2007

<http://www.journals.uchicago.edu/doi/pdf/10.1086/520038>

We describe a method with which to measure the magnetic field orientation of coronal mass ejections (CMEs) using Faraday rotation (FR). Two basic FR profiles, Gaussian-shaped with a single polarity or N-shaped with polarity reversals, are produced by a radio source occulted by a moving flux rope, depending on its orientation. These curves are consistent with Helios observations, providing evidence for the flux rope geometry of CMEs. Many background radio sources can map CMEs in FR onto the sky. We demonstrate with a simple flux rope that the magnetic field orientation and helicity of the flux rope can be determined 2–3 days before it reaches the Earth, which is of crucial importance for space weather forecasting. An FR calculation based on global magnetohydrodynamic (MHD) simulations of CMEs in a background heliosphere shows that FR mapping can also resolve a CME geometry that curves back to the Sun. We discuss implementation of the method using data from the Mileura Widefield Array (MWA).

MAGNETIC STRUCTURES OF SOLAR ACTIVE REGIONS, FULL-HALO CORONAL MASS EJECTIONS, AND GEOMAGNETIC STORMS

Y. **Liu**, D. F. Webb,^{2, 3} and X. P. Zhao¹

The Astrophysical Journal, 646:000Y000, 2006, **File**

In this study, we seek correlation between speed of the active region-related halo Coronal Mass Ejections (CMEs) and configuration of the ambient magnetic fields. Having studied 99 halo CMEs in the period from 2000 to 2004, we find that CMEs under the heliospheric current sheet are significantly slower than CMEs situated under unidirectional open field structures. The average speed of the former is 883 km/s, while the latter is 1388 km/s. The effect is not biased by the flare importance. This implies that the ambient magnetic field structure plays a role in determining speed of the halo CMEs.

A statistical study of the properties of interplanetary coronal mass ejections from 0.3 to 5.4AU.

Liu, Y., Richardson, J. D. & Belcher, J. W.

Plan. Space Sci. 53, 3–17 (2005).

Spectral Analysis of Forbush Decreases Using a New Yield Function

M. **Livada** & **H. Mavromichalaki**

Solar Physics volume 295, Article number: 115 (2020)

<https://link.springer.com/content/pdf/10.1007/s11207-020-01679-z.pdf>

The Forbush decreases of the cosmic ray intensity observed on **24 December 2014** and on **8 September 2017** were chosen for cosmic ray spectral analysis. At first an analytical study of the solar and geomagnetic parameters of these events was carried out due to the fact that both are typical cosmic ray events. Hourly cosmic ray data of the neutron monitor stations obtained from the high-resolution neutron monitor database were used for calculating the cosmic ray density and anisotropy variations. Following the method of the coupling coefficients, the galactic cosmic ray spectral index was calculated using the technique of Wawrzynczak and Alania (Adv. Space Res. 45, 622, 2010). A newly presented yield function by Mishev, Usoskin, and Kovaltsov (J. Geophys. Res. 118, 2783, 2013) including a geometrical correction factor, already used in the spectral analysis of the cosmic ray ground level enhancements, was applied for the first time to the case of Forbush decreases. A comparison of these results during the events is performed by using two other coupling functions: the function presented in the work of Clem and Dorman (Space Sci. Rev. 93, 335, 2000) and the one in the work of Belov and Struminsky (Proc. 25th Int. Cosmic Ray Conf. 1, 201, 1997). The latter includes an extension for neutron monitor stations with rigidity $1 \text{ GV} < R < 2.78 \text{ GV}$. The obtained spectral index and the calculated cosmic ray intensity in the heliosphere during the two Forbush decreases after the coupling by these three functions are presented and discussed.

Table 2 Values of the spectral index for the time period 21 December 2014 till 14 January 2015.

Galactic cosmic ray spectral index: the case of Forbush decreases of March 2012

M. Livada, H. Mavromichalaki, C. Plainaki

Astrophysics and Space Science January 2018, 363:8

<http://sci-hub.tw/10.1007/s10509-017-3230-9>

<http://cosray.phys.uoa.gr/publications/D117.pdf>

During the burst of solar activity in March 2012, close to the maximum of solar cycle 24, a number of X-class and M-class flares and halo CMEs with velocity up to 2684 km/s were recorded. During a relatively short period (7–21 March 2012) two Forbush decreases were registered in the ground-level neutron monitor data. In this work, after a short description of the solar and geomagnetic background of these Forbush decreases, we deduce the cosmic ray density and anisotropy variations based on the daily cosmic ray data of the neutron monitor network

(<http://www.nmdb.eu>; <http://cosray.phys.uoa.gr>). Applying to our data two different coupling functions methods, the spectral index of these Forbush decreases was calculated following the technique of Wawrzynczak and Alania (*Adv. Space Res.* 45:622–631, 2010). We pointed out that the estimated values of the spectral index γ of these events are almost similar for both cases following the fluctuation of the Forbush decrease. The study and the calculation of the cosmic ray spectrum during such cosmic ray events are very important for Space Weather applications. **7-13 March 2012**

Coronal Mass Ejections in July 2005 and an Unusual Heliospheric Event

M. A. Livshitsa, A. V. Belova, A. I. Shakhovskaya, E. A. Eroshenko,

A. R. Osokinc, and L. K. Kashapova

Cosmic Research, 2013, Vol. 51, No. 5, pp. 326–334.

Kosmicheskie Issledovaniya, 2013, Vol. 51, No. 5, pp. 363–371.

Using the events in July 2005 as an example, the causes and peculiarities of Forbush effects produced by solar sources remote from the central zone are discussed. The event in question differs from other effects observed at the periphery of interplanetary disturbances by strong variations in cosmic rays on the background of weak disturbances in the solar wind and magnetic field of the Earth. The cloud of magnetized plasma ejected from the Sun was large and fast, but it passed to the west from the Sun-Earth line. According to performed estimates, the mass of the ejected substance was close to the upper boundary of mass for coronal mass ejections (CMEs). Anomalous parameters and high modulation capability of the formed solar wind disturbance are explained, in particular, by the fact that it combined several CMEs and that the last fast disturbance was prepared by a series of impulsive events in the active region of the Sun. Usually, such a great mass is ejected directly after the main energy release in strong solar flares. In the given case, a powerful MHD disturbance occurred approximately half an hour after a maximum of hard X-ray burst under the conditions when gas pressure in the flare loops became close to magnetic pressure, which was just a premise of the largescale ejection.

Reconstruction of Carrington Rotation Means of Open Solar Flux over the Past 154 Years.

Lockwood, M., Owens, M.

Sol Phys 299, 28 (2024).

<https://doi.org/10.1007/s11207-024-02268-0>

<https://link.springer.com/content/pdf/10.1007/s11207-024-02268-0.pdf>

We generate reconstructions of signed open solar flux (OSF) for the past 154 years using observations of geomagnetic activity. Previous reconstructions have been limited to annual resolution, but this is here increased by a factor of more than 13 by using averages over Carrington rotation (CR) intervals. We use two indices of geomagnetic activity, the homogeneous aa index, aaH, and the IDV(1d) index; a combination of the two is fitted to OSF estimates from near-Earth interplanetary satellite data. For 1995–2022, these are corrected for excess flux (i.e. orthogardenhose flux and switchbacks) using strahl electrons. For 1970–2022, we also use the absolute values of the radial component of the near-Earth interplanetary magnetic field $|B_{\text{r}}|_{\text{CR}}$, where the excess flux is allowed for by adopting the optimum averaging interval τ of 20 h. However, in the interval 1970–1995, data gaps in the interplanetary data are a serious problem. The errors that these missing data cause in CR averages of OSF are evaluated by synthetically masking data for CRs that have a full complement, using the same number and time series of data gaps as for the CR in question. Given the potential for missing data to generate large errors, we use the near-continuous 1995–2022 data to derive the best-fit combination of the geomagnetic data and employ the 1970–1995 data for testing in which we can readily allow for the errors caused by data gaps. Errors caused by inaccuracies in the geomagnetic data are shown to be considerably smaller than the uncertainties due to the polynomial fitting. It is shown that the new reconstructions are consistent with the previous annual estimates and that there is considerable variability in the OSF values from one CR to the next; in

particular, in high-activity solar cycles, there can be individual CRs in which the OSF exceeds that for adjacent CRs by a factor as large as two.

On the Origin of Ortho-Gardenhose Heliospheric Flux

Mike **Lockwood**, Mathew J. Owens, Allan Macneil

[Solar Physics](#) June 2019, 294:85

[sci-hub.se/10.1007/s11207-019-1478-7](https://doi.org/10.1007/s11207-019-1478-7)

Parker-spiral theory predicts that the heliospheric magnetic field (HMF) will have components of opposite polarity radially toward the Sun and tangentially antiparallel to the solar rotation direction (i.e., in Geocentric Solar Ecliptic (GSE) coordinates, with $B_X/B_Y < 0$ and $B_Z/B_Y < 0$). This theory explains the average orientation of the HMF very well indeed but does not predict the so-called “ortho-gardenhose” (hereafter OGH) flux with $B_X/B_Y > 0$ and $B_Z/B_Y > 0$ which is frequently observed. We here study the occurrence and structure of OGH flux, as seen in near-Earth space (heliocentric distance $r = 1$ AU) by the Wind and Advanced Composition Explorer (ACE) spacecraft (for 1995 – 2017, inclusive) and by the Helios-1 and -2 spacecraft at $0.29 \text{ AU} < r \leq 1 \text{ AU}$ (for December 1974 to August 1981), in order to evaluate the contributions to OGH flux generation of the various mechanisms and factors that are not accounted for by Parker-spiral theory. We study the loss of OGH flux with increasing averaging timescale $[\tau]$ between 16 seconds and 100 hours and so determine its spectrum of spatial/temporal scale sizes. OGH flux at Earth at sunspot minimum is shown to be more common than at sunspot maximum and caused by smaller-scale structure in the HMF (with a mode temporal scale at a fixed point of $\tau_{mp} \approx 10$ hours compared to $\tau_{mp} \approx 40$ hours for sunspot maximum, corresponding to about 5.5° and 22° (respectively) of heliocentric angular width for corotational motion or $21 R_\odot$ and $84 R_\odot$ for radial solar-wind flow (where R_\odot is the mean solar radius). OGH field generated by rotating the HMF through the radial direction is also shown to differ in its spectrum of scale sizes from that generated by rotating the HMF through the tangential direction – the former does not contribute to the “excess” open heliospheric flux at a given r but the latter does. We show that roughly half of the HMF deflection from the ideal Parker-spiral needed to give the observed occurrence of OGH flux at Earth occurs at r below 0.3 AU. By comparing the Helios and near-Earth data we highlight some questions that can be addressed by the Parker Solar Probe mission, which will study the HMF down to $r = 0.046$ AU. We suggest that with decreasing heliocentric distance, Probewill detect decreased OGH field due to draping around transient ejecta, such as blobs and coronal mass ejections, but increasing structure in the radial field within traditional HMF sectors that are remnant Alfvénic disturbances in outflow regions from coronal reconnection sites.

Time-of-day/timeof-year response functions of planetary geomagnetic indices.

Lockwood, M., Chambodut, A., Finch, I.D., Barnard, L.A., Owens, M.J., Haines, C.:

2019, *J. Space Weather Space Clim.* 9, A20.

<https://www.swsc-journal.org/articles/swsc/pdf/2019/01/swsc190002.pdf>

Aims: To elucidate differences between commonly-used mid-latitude geomagnetic indices and study quantitatively the differences in their responses to solar forcing as a function of Universal Time (UT), time-of-year (F), and solar-terrestrial activity level. To identify the strengths, weaknesses and applicability of each index and investigate ways to correct for any weaknesses without damaging their strengths.

Methods: We model how the location of a geomagnetic observatory influences its sensitivity to solar forcing. This modelling for a single station can then be applied to indices that employ analytic algorithms to combine data from different stations and thereby we derive the patterns of response of the indices as a function of UT, F and activity level. The model allows for effects of solar zenith angle on ionospheric conductivity and of the station’s proximity to the midnight-sector auroral oval: it employs coefficients that are derived iteratively by comparing data from the current aa index stations (Hartland and Canberra) to simultaneous values of the am index, constructed from chains of stations in both hemispheres. This is done separately for eight overlapping bands of activity level, as quantified by the am index. Initial estimates were obtained by assuming the am response is independent of both F and UT and the coefficients so derived were then used to compute a corrected F-UT response pattern for am. This cycle was repeated until it resulted in changes in predicted values that were below the adopted uncertainty level (0.001%). The ideal response pattern of an index would be uniform and linear (i.e., independent of both UT and F and the same at all activity levels). We quantify the response uniformity using the percentage variation at any activity level, $V = 100 (\sigma_S / \langle S \rangle)$, where S is the index’s sensitivity at that activity level and σ_S is the standard deviation of S : both S and σ_S were computed using the eight UT ranges of the 3-hourly indices and 20 equal-width ranges of F. As an overall metric of index performance, we take an occurrence-weighted mean of V , V_{av} , over the eight activity-level bins. This metric would ideally be zero and a large value shows that the index compilation is introducing large spurious UT and/or F variations into the data. We also study index performance by comparisons with

the SME and SML indices, compiled from a very large number of stations, and with an optimum solar wind “coupling function”, derived from simultaneous interplanetary observations.

Results: It is shown that a station’s response patterns depend strongly on the level of geomagnetic activity because at low activity levels the effect of solar zenith angle on ionospheric conductivity dominates over the effect of station proximity to the midnight-sector auroral oval, whereas the converse applies at high activity levels. The metric V_{av} for the two-station aa index is modelled to be 8.95%, whereas for the multi-station am index it is 0.65%. The ap (and hence Kp) index cannot be analyzed directly this way because its construction employs tabular conversions, but the very low V_{av} for am allows us to use $\langle ap \rangle / \langle am \rangle$ to evaluate the UT-F response patterns for ap. This yields $V_{av} = 11.20\%$ for ap. The same empirical test applied to the classical aa index and the new “homogenous” aa index, aaH (derived from aa using the station sensitivity model), yields V_{av} of, respectively, 10.62% (i.e., slightly higher than the modelled value) and 5.54%. The ap index value of V_{av} is shown to be high because it exaggerates the average semi-annual variation and has an annual variation giving a lower average response in northern hemisphere winter. It also contains a strong artefact UT variation. We derive an algorithm for correcting for this uneven response which gives a corrected ap value, apC, for which V_{av} is reduced to 1.78%. The unevenness of the ap response arises from the dominance of European stations in the network used and the fact that all data are referred to a European station (Niemegek). However, in other contexts, this is a strength of ap, because averaging similar data gives increased sensitivity and more accurate values on annual timescales, for which the UT-F response pattern is averaged out.

A homogeneous aa index: 2. Hemispheric asymmetries and the equinoctial variation.

Lockwood, M., Finch, I.D., Chambodut, A., Barnard, L.A., Owens, M.J., Clarke, E.:

2018b, J. Space Weather Space Clim. 8, A58. DOI.

<https://www.swsc-journal.org/articles/swsc/pdf/2018/01/swsc180022.pdf>

Paper 1 ([Lockwood et al., 2018](#)) generated annual means of a new version of the aa geomagnetic activity index which includes corrections for secular drift in the geographic coordinates of the auroral oval, thereby resolving the difference between the centennial-scale change in the northern and southern hemisphere indices, aaN and aaS. However, other hemispheric asymmetries in the aa index remain: in particular, the distributions of 3-hourly aaN and aaS values are different and the correlation between them is not high on this timescale ($r = 0.66$). In the present paper, a location-dependant station sensitivity model is developed using the am index (derived from a much more extensive network of stations in both hemispheres) and used to reduce the difference between the hemispheric aa indices and improve their correlation (to $r = 0.79$) by generating corrected 3-hourly hemispheric indices, aaHN and aaHS, which also include the secular drift corrections detailed in Paper 1. These are combined into a new, “homogeneous” aa index, aaH. It is shown that aaH, unlike aa, reveals the “equinoctial”-like time-of-day/time-of-year pattern that is found for the am index.

A homogeneous aa index: 1. Secular variation.

Lockwood, M., Chambodut, A., Barnard, L.A., Owens, M.J., Mendel, V.:

2018, J. Space Weather Space Clim. 8, A53. DOI

<https://www.swsc-journal.org/articles/swsc/pdf/2018/01/swsc180020.pdf>

Originally compiled for 1868–1967 and subsequently continued so that it now covers 150 years, the aa index has become a vital resource for studying space climate change. However, there have been debates about the inter-calibration of data from the different stations. In addition, the effects of secular change in the geomagnetic field have not previously been allowed for. As a result, the components of the “classical” aa index for the southern and northern hemispheres (aa_S and aa_N) have drifted apart. We here separately correct both aa_S and aa_N for both these effects using the same method as used to generate the classic aa values but allowing δ , the minimum angular separation of each station from a nominal auroral oval, to vary as calculated using the IGRF-12 and gufm1 models of the intrinsic geomagnetic field. Our approach is to correct the quantized a_K -values for each station, originally scaled on the assumption that δ values are constant, with time-dependent scale factors that allow for the drift in δ . This requires revisiting the intercalibration of successive stations used in making the aa_S and aa_N composites. These intercalibrations are defined using independent data and daily averages from 11 years before and after each station change and it is shown that they depend on the time of year. This procedure produces new homogenized hemispheric aa indices, aa_{HS} and aa_{HN} , which show centennial-scale changes that are in very close agreement. Calibration problems with the classic aa index are shown to have arisen from drifts in δ combined with simpler corrections which gave an incorrect temporal variation and underestimate the rise in aa during the 20th century by about 15%.

Space climate and space weather over the past 400 years: 2. Proxy indicators of geomagnetic storm and substorm occurrence

Mike **Lockwood**, Mathew J. Owens, Luke A. Barnard, Chris J. Scott, Clare E. Watt and Sarah Bentley
J. Space Weather Space Clim. **2018**, 8, A12

<https://www.swsc-journal.org/articles/swsc/pdf/2018/01/swsc170036.pdf>

Using the reconstruction of power input to the magnetosphere presented in Paper 1 Lockwood et al. [J Space Weather Space Clim 7 (2017a)], we reconstruct annual means of the geomagnetic Ap and AE indices over the past 400 years to within a 1-sigma error of $\pm 20\%$. In addition, we study the behaviour of the lognormal distribution of daily and hourly values about these annual means and show that we can also reconstruct the fraction of geomagnetically-active (storm-like) days and (substorm-like) hours in each year to accuracies of to accuracies of $\sim 50\%$, including the large percentage uncertainties in near-zero values. The results are the first physics-based quantification of the space weather conditions in both the Dalton and Maunder minima. Looking to the future, the weakening of Earth's magnetic moment means that the terrestrial disturbance levels during a future repeats of the solar Dalton and Maunder minima will be weaker and we here quantify this effect for the first time.

On the origins and timescales of geoeffective IMF

Mike **Lockwood**, Mathew J. Owens, Luke A. Barnard, Sarah Bentley, Chris J. Scott, Clare E. Watt
Space Weather **2016** Vol: 14, Pages: 406–432

<http://onlinelibrary.wiley.com/doi/10.1002/2016SW001375/epdf>

<https://agupubs.onlinelibrary.wiley.com/doi/epdf/10.1002/2016SW001375>

Southward interplanetary magnetic field (IMF) in the geocentric solar magnetospheric (GSM) reference frame is the key element that controls the level of space weather disturbance in Earth's magnetosphere, ionosphere, and thermosphere. We discuss the relation of this geoeffective IMF component to the IMF in the geocentric solar ecliptic (GSE) frame, and using the almost continuous interplanetary data for 1996–2015 (inclusive), we show that large geomagnetic storms are always associated with strong southward, out-of-ecliptic field in the GSE frame: Dipole tilt effects, which cause the difference between the southward field in the GSM and GSE frames, generally make only a minor contribution to these strongest storms. The time-of-day/time-of-year response patterns of geomagnetic indices and the optimum solar wind coupling function are both influenced by the timescale of the index response. We also study the occurrence spectrum of large out-of-ecliptic field and show that for 1 h averages it is, surprisingly, almost identical in ICMEs (interplanetary coronal mass ejections), around CIRs/SIRs (corotating and stream interaction regions) and in the “quiet” solar wind (which is shown to be consistent with the effect of weak SIRs). However, differences emerge when the timescale over which the field remains southward is considered: for longer averaging timescales the spectrum is broader inside ICMEs, showing that these events generate longer intervals of strongly southward average IMF and consequently stronger geomagnetic storms. The behavior of out-of-ecliptic field with timescale is shown to be very similar to that of deviations from the predicted Parker spiral orientation, suggesting the two share common origins.

Reconstruction of geomagnetic activity and near-Earth interplanetary conditions over the past 167 yr – Part 4: Near-Earth solar wind speed, IMF, and open solar flux

M. **Lockwood**, H. Nevanlinna, L. Barnard, M.J. Owens, R.G. Harrison, A.P. Rouillard, and C.J. Scott
Ann. Geophys., 32, 367–381, **2014**

<http://www.ann-geophys.net/32/367/2014/angeo-32-367-2014.pdf>

Svalgaard (2014) has recently pointed out that the calibration of the Helsinki magnetic observatory's H component variometer was probably in error in published data for the years 1866–1874.5 and that this makes the interdiurnal variation index based on daily means, IDV(1d), (Lockwood et al., 2013a), and the interplanetary magnetic field strength derived from it (Lockwood et al., 2013b), too low around the peak of solar cycle 11. We use data from the modern Nurmijarvi station, relatively close to the site of the original Helsinki Observatory, to confirm a 30% underestimation in this interval and hence our results are fully consistent with the correction derived by Svalgaard. We show that the best method for recalibration uses the Helsinki Ak (H) and aa indices and is accurate to $\pm 10\%$. This makes it preferable to recalibration using either the sunspot number or the diurnal range of geomagnetic activity which we find to be accurate to $\pm 20\%$. In the case of Helsinki data during cycle 11, the two recalibration methods produce very similar corrections which are here confirmed using newly digitised data from the nearby St Petersburg observatory and also using declination data from Helsinki. However, we show that the IDV index is, compared to later years, too similar to sunspot number before 1872, revealing independence of the two data series has been lost; either because the geomagnetic data used to compile IDV has been corrected using sunspot numbers, or vice versa, or both. We present corrected data sequences for both the IDV(1d) index and the reconstructed IMF (interplanetary magnetic field). We also analyse the

relationship between the derived near-Earth IMF and the sunspot number and point out the relevance of the prior history of solar activity, in addition to the contemporaneous value, to estimating any "floor" value of the near-Earth interplanetary field.

Reconstruction of geomagnetic activity and near-Earth interplanetary conditions over the past 167 yr – Part 3: Improved representation of solar cycle 11

M. **Lockwood**, H. Nevanlinna, M. Vokhmyanin, D. Ponyavin, S. Sokolov, L. Barnard, M.J. Owens, R.G. Harrison, A.P. Rouillard, and C.J. Scott
Ann. Geophys., 32, 383-399, 2014

<http://www.ann-geophys.net/32/383/2014/angeo-32-383-2014.pdf>

In the concluding paper of this tetralogy, we here use the different geomagnetic activity indices to reconstruct the near-Earth interplanetary magnetic field (IMF) and solar wind flow speed, as well as the open solar flux (OSF) from 1845 to the present day. The differences in how the various indices vary with near-Earth interplanetary parameters, which are here exploited to separate the effects of the IMF and solar wind speed, are shown to be statistically significant at the 93% level or above. Reconstructions are made using four combinations of different indices, compiled using different data and different algorithms, and the results are almost identical for all parameters. The correction to the aa index required is discussed by comparison with the Ap index from a more extensive network of mid-latitude stations. Data from the Helsinki magnetometer station is used to extend the aa index back to 1845 and the results confirmed by comparison with the nearby St Petersburg observatory. The optimum variations, using all available long-term geomagnetic indices, of the near-Earth IMF and solar wind speed, and of the open solar flux, are presented; all with $\pm 2\sigma$ uncertainties computed using the Monte Carlo technique outlined in the earlier papers. The open solar flux variation derived is shown to be very similar indeed to that obtained using the method of Lockwood et al. (1999).

Reconstruction of geomagnetic activity and near-Earth interplanetary conditions over the past 167 yr – Part 2: A new reconstruction of the interplanetary magnetic field

M. **Lockwood**¹, L. Barnard¹, H. Nevanlinna², M. J. Owens¹, R. G. Harrison¹, A. P. Rouillard³, and C. J. Davis

Ann. Geophys., 31, 1979-1992, doi:10.5194/angeo-31-1979-2013, 2013.

<http://www.ann-geophys.net/31/1979/2013/angeo-31-1979-2013.pdf>

We present a new reconstruction of the interplanetary magnetic field (IMF, B) for 1846–2012 with a full analysis of errors, based on the homogeneously constructed IDV(1d) composite of geomagnetic activity presented in Part 1 (Lockwood et al., 2013a). Analysis of the dependence of the commonly used geomagnetic indices on solar wind parameters is presented which helps explain why annual means of interdiurnal range data, such as the new composite, depend only on the IMF with only a very weak influence of the solar wind flow speed. The best results are obtained using a polynomial (rather than a linear) fit of the form $B = \chi \cdot (\text{IDV}(1d) - \beta)\alpha$ with best-fit coefficients $\chi = 3.469$, $\beta = 1.393$ nT, and $\alpha = 0.420$. The results are contrasted with the reconstruction of the IMF since 1835 by Svalgaard and Cliver (2010).

Reconstruction of geomagnetic activity and near-Earth interplanetary conditions over the past 167 yr – Part 1: A new geomagnetic data composite

M. **Lockwood**¹, L. Barnard¹, H. Nevanlinna², M. J. Owens¹, R. G. Harrison¹, A. P. Rouillard³, and C. J. Davis

Ann. Geophys., 31, 1957-1977, doi:10.5194/angeo-31-1957-2013, 2013.

<http://www.ann-geophys.net/31/1957/2013/angeo-31-1957-2013.pdf>

We present a new composite of geomagnetic activity which is designed to be as homogeneous in its construction as possible. This is done by only combining data that, by virtue of the locations of the source observatories used, have similar responses to solar wind and IMF (interplanetary magnetic field) variations. This will enable us (in Part 2, Lockwood et al., 2013a) to use the new index to reconstruct the interplanetary magnetic field, B, back to 1846 with a full analysis of errors. Allowance is made for the effects of secular change in the geomagnetic field. The composite uses interdiurnal variation data from Helsinki for 1845–1890 (inclusive) and 1893–1896 and from Eskdalemuir from 1911 to the present. The gaps are filled using data from the Potsdam (1891–1892 and 1897–1907) and the nearby Seddin observatories (1908–1910) and intercalibration achieved using the Potsdam–Seddin sequence. The new index is termed IDV(1d) because it employs many of the principles of the IDV index derived by Svalgaard and Cliver (2010), inspired by the u index of Bartels (1932); however, we revert to using one-day (1d) means, as employed by Bartels, because the

use of near-midnight values in IDV introduces contamination by the substorm current wedge auroral electrojet, giving noise and a dependence on solar wind speed that varies with latitude. The composite is compared with independent, early data from European-sector stations, Greenwich, St Petersburg, Parc St Maur, and Ekaterinburg, as well as the composite u index, compiled from 2–6 stations by Bartels, and the IDV index of Svalgaard and Cliver. Agreement is found to be extremely good in all cases, except two. Firstly, the Greenwich data are shown to have gradually degraded in quality until new instrumentation was installed in 1915. Secondly, we infer that the Bartels u index is increasingly unreliable before about 1886 and overestimates the solar cycle amplitude between 1872 and 1883 and this is amplified in the proxy data used before 1872. This is therefore also true of the IDV index which makes direct use of the u index values.

Reconstruction and Prediction of Variations in the Open Solar Magnetic Flux and Interplanetary Conditions

Review

Mike **Lockwood**

Living Rev. Solar Phys. 10 (2013), 4

<http://www.livingreviews.org/lrsp-2013-4>

Historic geomagnetic activity observations have been used to reveal centennial variations in the open solar flux and the near-Earth heliospheric conditions (the interplanetary magnetic field and the solar wind speed). The various methods are in very good agreement for the past 135 years when there were sufficient reliable magnetic observatories in operation to eliminate problems due to site-specific errors and calibration drifts. This review underlines the physical principles that allow these reconstructions to be made, as well as the details of the various algorithms employed and the results obtained. Discussion is included of: the importance of the averaging timescale; the key differences between "range" and "interdiurnal variability" geomagnetic data; the need to distinguish source field sector structure from heliospherically-imposed field structure; the importance of ensuring that regressions used are statistically robust; and uncertainty analysis. The reconstructions are exceedingly useful as they provide calibration between the in-situ spacecraft measurements from the past five decades and the millennial records of heliospheric behaviour deduced from measured abundances of cosmogenic radionuclides found in terrestrial reservoirs. Continuity of open solar flux, using sunspot number to quantify the emergence rate, is the basis of a number of models that have been very successful in reproducing the variation derived from geomagnetic activity. These models allow us to extend the reconstructions back to before the development of the magnetometer and to cover the Maunder minimum. Allied to the radionuclide data, the models are revealing much about how the Sun and heliosphere behaved outside of grand solar maxima and are providing a means of predicting how solar activity is likely to evolve now that the recent grand maximum (that had prevailed throughout the space age) has come to an end.

Forbush Decreases in the Cosmic Radiation

Review

Lockwood, John A.

Space Science Reviews, Volume 12, Issue 5, pp.658-715, 1971

sci-hub.tw/10.1007/BF00173346

The experimental observations of Forbush decreases in recent years are reviewed and related to different theoretical models which have been proposed. The observational data from both ground-based and spacecraft experiments were selected to illustrate the important characteristics of Forbush decreases. The form of the rigidity dependence of the cosmic-ray modulation during the decreases and effects of the geomagnetic field upon the magnitude of the decreases are discussed. Recent results to deduce the cosmic-ray flow patterns from the observed anisotropies during the decreases are presented. Other features such as differences in onset times, recovery times, precursory increases are discussed. In considering the theoretical models particular emphasis is placed upon the agreement of the predictions of the model with the experimental observations. A theoretical model is suggested which is not original but represents a synthesis of several models previously proposed. Future important measurements and analyses necessary to an understanding of Forbush decreases are outlined.

New Findings from Explainable SYM-H Forecasting using Gradient Boosting Machines

Daniel **Iong**, **Yang Chen**, **Gabor Toth**, **Shasha Zou**, **Tuija Pulkkinen**, **Jiaen Ren**, **Enrico Camporeale**, **Tamas Gombosi**

Space Weather e2021SW002928 2022

<https://agupubs.onlinelibrary.wiley.com/doi/epdf/10.1029/2021SW002928>

<https://doi.org/10.1029/2021SW002928>

In this work, we develop gradient boosting machines (GBMs) for forecasting the SYM-H index multiple hours ahead using different combinations of solar wind and interplanetary magnetic field (IMF) parameters, derived parameters, and

past SYM-H values. Using Shapley Additive Explanation (SHAP) values to quantify the contributions from each input to predictions of the SYM-H index from GBMs, we show that our predictions are consistent with physical understanding while also providing insight into the complex relationship between the solar wind and Earth's ring current. In particular, we found that feature contributions vary depending on the storm phase. We also perform a direct comparison between GBMs and neural networks presented in prior publications for forecasting the SYM-H index by training, validating, and testing them on the same data. We find that the GBMs yield a statistically significant improvement in root mean squared error over the best published black-box neural network schemes and the Burton equation. **6-8 Apr 2000, 31 Mar 2001, 22 Jan 2004, 7-8 Nov 2004**

Table 1. Storms used to train GBMs. These storms are identical to the ones used to train and validate models in Collado-Villaverde et al. (2021), 1998-2017

Table 2. Storms used to test GBMs.

Study of the Relationship Between Sunspot Number and the Duration of the $\approx 1.6 - 2.2$ Year Period in Neutron Monitor Counting Rates

A. López-Comazzi & J. J. Blanco

[Solar Physics](#) volume 298, Article number: 67 (2023)

<https://link.springer.com/content/pdf/10.1007/s11207-023-02153-2.pdf>

Neutron monitor counting rates show periodicities in the $\approx 1.6 - 2.2$ -year range. These periodicities have been associated with a solar origin affecting the cosmic ray propagation conditions through the heliosphere. Our hypothesis is that the periodicities in the $\approx 1.6 - 2.2$ -years range correspond to a single periodicity that changes its duration over time.

López-Comazzi and Blanco (Astrophys. J. 927(2), 155, 2022) found that the duration of the $\approx 1.6 - 2.2$ -year period (τ) is linearly related to the average sunspot number (SSNa) in each solar cycle. The relationship shows that shorter $\approx 1.6 - 2.2$ -year periods occur during stronger cycles when SSNa is higher. Therefore, the duration of this period varies from one solar cycle to another. This study focuses on this relation. For obtaining this relation, the values of the duration of the $\approx 1.6 - 2.2$ -year period in global neutron monitor counting rates (a virtual station determined by averaging of the different neutron monitor counting rates along the world) along the Solar Cycles 20 – 24 have been used. We extend the sample by adding the duration of the $\approx 1.6 - 2.2$ -year period in Huancayo neutron monitor counting rates along Solar Cycle 19 to this linear relationship. Once the linear relationship is extended, τ for the current Solar Cycle 25 is computed giving ≈ 2.24 years. Drawing on this more accurate relationship given by $SSNa = (-120 \pm 10)\tau + (320 \pm 20)$, we computed τ for the cycles previous to the existence of neutron monitors (Solar Cycles 7 – 18).

These $\approx 1.6 - 2.2$ -year periodicities in neutron monitor counting rates could be produced by variations in the solar magnetic field due to an internal mechanism of the solar dynamo called Rossby waves. Concretely, the harmonic of fast Rossby waves with $m=1$ and $n=8$ fit with the detected $\approx 1.6 - 2.2$ -year periodicity. In addition, the variation of the solar magnetic-field strength from weaker to stronger solar cycles could explain the different periods detected in each cycle. Based on the detected periodicities using the dispersion relation for fast Rossby waves, a solar tachocline magnetic-field strength of $\approx 7 - 25$ kG has been estimated.

Kinetic-scale current sheets in near-Sun solar wind: properties, scale-dependent features and reconnection onset

A. Lotekar, I.Y. Vasko, T. Phan, S.D. Bale, T.A. Bowen, J. Halekas, A.V. Artemyev, Yu. Khotyaintsev, F.S. Mozer

ApJ 2022

<https://arxiv.org/pdf/2202.12341.pdf>

We present statistical analysis of 11,200 proton kinetic-scale current sheets (CS) observed by Parker Solar Probe during 10 days around the first perihelion. The CS thickness λ is in the range from a few to 200 km with the typical value around 30 km, while current densities are in the range from 0.1 to $10 \mu\text{A}/\text{m}^2$ with the typical value around $0.7 \mu\text{A}/\text{m}^2$. These CSs are resolved thanks to magnetic field measurements at 73--290 Samples/s resolution. In terms of proton inertial length λ_p , the CS thickness λ is in the range from about 0.1 to $10\lambda_p$ with the typical value around $2\lambda_p$. The magnetic field magnitude does not substantially vary across the CSs and, accordingly, the current density is dominated by the magnetic field-aligned component. The CSs are typically asymmetric with statistically different magnetic field magnitudes at the CS boundaries. The current density is larger for smaller-scale CSs, $J_0 \approx 0.15 \cdot (\lambda/100\text{km}) - 0.76 \mu\text{A}/\text{m}^2$, but does not statistically exceed the Alfvén current density J_A corresponding to the ion-electron drift of local Alfvén speed. The CSs exhibit remarkable scale-dependent current density and magnetic shear angles, $J_0/J_A \approx 0.17 \cdot (\lambda/\lambda_p) - 0.67$ and $\Delta\theta \approx 21 \cdot (\lambda/\lambda_p) - 0.32$. Based on these observations and comparison to recent studies at 1 AU, we conclude that proton kinetic-scale CSs in the near-Sun solar wind are produced by turbulence cascade and

they are automatically in the parameter range, where reconnection is not suppressed by the diamagnetic mechanism, due to their geometry dictated by turbulence cascade. **1-10 Nov 2018**

Validation of the DSCOVR Spacecraft Mission Space Weather Solar Wind Products

Paul T. M. [Loto'aniu](#), [K. Romich](#), [W. Rowland](#), [S. Codrescu](#), [D. Biesecker](#), [J. Johnson](#), [H.J. Singer](#), [A. Szabo](#), [M. Stevens](#)

Space Weather e2022SW003085 **Volume20, Issue10 2022**

<https://doi.org/10.1029/2022SW003085>

<https://agupubs.onlinelibrary.wiley.com/doi/epdf/10.1029/2022SW003085>

In this paper, we present a statistical validation of the DSCOVR solar wind data in the operational space weather archive. The DSCOVR observations of the interplanetary magnetic field (IMF), solar wind velocity, density, and temperature were hourly averaged and compared to measurements from NASA's ACE and Wind spacecraft. Hourly averages, in general, show good correlations between the satellites for the IMF, solar wind velocity GSE vx-component, and density. During the period covered by this study (spanning from late July 2016, when DSCOVR went operational, to the end of 2020), the DSCOVR products show no clear evidence of permanent degradation. However, for plasma parameters there were periods of disagreement with ACE and Wind. The correlation coefficients (Pearson's r) calculated over the entire study period were similar or the same between DSCOVR versus Wind and DSCOVR versus ACE. For comparisons between DSCOVR and Wind, the IMF Bx and By GSE r were 0.94 and 0.96, respectively, while r for the IMF GSE Bz-component was 0.88. For solar wind velocity, r was found to be 0.96 for the GSE vx-component, compared with 0.30 for vy and 0.33 for vz. For density, r was found to be 0.84. DSCOVR density observations tend to overestimate compared to Wind values when the solar wind densities are low (below ~ 5 /cc), while agreement between the two spacecraft on IMF measurements tend to increase with decreasing spatial separation.

The GOES-16 Spacecraft Science Magnetometer

T. M. [Loto'aniu](#), [R. J. Redmon](#), [S. Califf](#), [H. J. Singer](#), [W. Rowland](#)...

[Space Science Reviews](#) June 2019, 215:32

<https://link.springer.com/content/pdf/10.1007%2Fs11214-019-0600-3.pdf>

Since their inception in the 1970s, the NOAA Geostationary Operational Environmental Satellite (GOES) system has monitored the sources of space weather on the sun and the effects of space weather at Earth. These observations are important for providing forecasts, warnings and alerts to many customers, including satellite operators, the power utilities, and NASA's human activities in space. The GOES magnetometer provides observations of the geomagnetic field, which can be the first indication that significant space weather has reached Earth. In addition, the magnetic field observations are used to identify and forecast the severity of the space weather activity. This paper reviews the capabilities of the GOES-16 magnetometer (MAG) and presents initial post-launch calibration/validation results including issues found in the data. The GOES-16 MAG requirements and capabilities are similar to those for previously flown instruments, measuring three components of the geomagnetic field but with an improved sampling rate of 10 samples/second. The MAG data are low-pass filtered with a 2.5 Hz cutoff compared to the 0.5 Hz cutoff of previous GOES magnetometers. The MAG is composed of two magnetometers, an inboard (closer to spacecraft bus) and outboard (on tip of boom) magnetometer. Presented are the science and instrument requirements, ground and initial on-orbit instrument calibration and data validation. The on-orbit analysis found magnetic contamination along with temperature dependency effects that resulted in unexpected instrument noise and decreased accuracy, with the issues generally more significant on the inboard magnetometer. The outboard sensor was used for initial analysis of MAG performance. Preliminary comparison, excluding arcjet firing periods, between the outboard magnetometer and the GOES-14 magnetometer found a statistical difference of 5 nT at 3σ for the total field. This comparison does not consider inaccuracies in the GOES-14 magnetometer. Future studies will focus on optimizing the outboard sensor performance.

On the uncertain intensity estimate of the 1859 Carrington storm

Jeffrey J. [Love](#)^{1*}, E. Joshua [Rigler](#)¹, Hisashi [Hayakawa](#)^{2,3,4} and Kalevi [Mursula](#)⁵

J. Space Weather Space Clim. **2024**, 14, 21

<https://doi.org/10.1051/swsc/2024015>

<https://www.swsc-journal.org/articles/swsc/pdf/2024/01/swsc230032.pdf>

A study is made of the intensity of the Carrington magnetic storm of September 1859 as inferred from visual measurements of horizontal-component geomagnetic disturbance made at the Colaba observatory in India. Using data from modern observatories, a lognormal statistical model of storm intensity is developed, to characterize the maximum-negative value of the storm-time disturbance index (maximum $-Dst$) versus geomagnetic disturbance recorded at low-

latitude observatories during magnetic storms. With this model and a recently published presentation of the Colaba data, the most likely maximum $-Dst$ of the Carrington storm and its credibility interval are estimated. A related model is used to examine individual Colaba disturbance values reported for the Carrington storm. Results indicate that only about one in a million storms with maximum $-Dst$ like the Carrington storm would result in local disturbance greater than that reported from Colaba. This indicates that either the Colaba data were affected by magnetospheric-ionospheric current systems in addition to the ring current, or there might be something wrong with the Colaba data. If the most extreme Colaba disturbance value is included in the analysis, then, of all hypothetical storms generating the hourly average disturbance recorded at Colaba during the Carrington storm, the median maximum $-Dst = 964$ nT, with a 68% credibility interval of [855,1087] nT. If the most extreme Colaba disturbance value is excluded from the analysis, then the median maximum $-Dst = 866$ nT, with a 68% credibility interval of [768,977] nT. The widths of these intervals indicate that estimates of the occurrence frequency of Carrington-class storms are very uncertain, as are related estimates of risk for modern technological systems.

Extreme-event magnetic storm probabilities derived from rank statistics of historical Dst intensities for solar cycles 14-24

Jeffrey J. Love

Space Weather [Volume19, Issue4](#) e2020SW002579 2021

<https://doi.org/10.1029/2020SW002579>

<https://agupubs.onlinelibrary.wiley.com/doi/epdf/10.1029/2020SW002579>

A compilation is made of the largest and second-largest magnetic storm-maximum intensities, $-Dst_1$ and $-Dst_2$, for solar cycles 14-24 (1902-2016) by sampling Oulu Dcx for cycles 19-24, using published $-Dst_m$ values for four intense storms in cycles 14, 15, and 18 (1903, 1909, 1921, 1946), and calculating fifteen new storm-maximum $-Dst_m$ values (reported here) for cycles 14-18. Three different models are fitted to the cycle-ranked $-Dst_1$ and $-Dst_2$ values using a maximum-likelihood algorithm: A Gumbel model, an unconstrained Generalized-Extreme-Value model, and a Weibull model constrained to have a physically justified maximum storm intensity of $-Dst_m = 2500$ nT. All three models are good descriptions of the data. Since the best model is not clearly revealed with standard statistical tests, inference is precluded of the source process giving rise to storm-maximum $-Dst_m$ values. Of the three candidate models, the constrained Weibull gives the lowest superstorm occurrence probabilities. Using the compiled data and the constrained Weibull model, a once-per-century storm intensity is estimated to be $-Dst_1 = 663$ nT, with a bootstrap 68% confidence interval of [497, 694] nT. Similarly, the probability that a future storm will have an intensity exceeding that of the March 1989 superstorm, $-Dst_m > 565$ nT, is 0.246 per cycle with a 68% confidence interval of [0.140, 0.311] per cycle. Noting (possibly slight) ambiguity in the rankings of storm intensities, using the same methods, but storms more intense than those identified for cycles 14-16, would yield a higher once-per-century intensity and a higher probability for a $-Dst_m > 565$ nT storm.

Table 1: Summary of magnetic storm intensities $-Dst_m$ and related factors (1903-2015)

Some Experiments in Extreme-Value Statistical Modeling of Magnetic Superstorm Intensities

Jeffrey J. Love

Space Weather [Volume18, Issue1](#) January 2020 e2019SW002255

<https://doi.org/10.1029/2019SW002255>

<https://agupubs.onlinelibrary.wiley.com/doi/epdf/10.1029/2019SW002255>

In support of projects for forecasting and mitigating the deleterious effects of extreme space weather storms, an examination is made of the intensities of magnetic superstorms recorded in the Dst index time series (1957–2016). Modified peak-over-threshold and solar cycle, block-maximum samplings of the Dst time series are performed to obtain compilations of storm maximum $-Dst_m$ intensity values. Lognormal, upper limit lognormal, generalized Pareto, and generalized extreme-value model distributions are fitted to the $-Dst_m$ data using a maximum-likelihood algorithm. All four candidate models provide good representations of the data. Comparisons of the statistical significance and goodness of fits of the various models give no clear indication as to which model is best. The statistical models are used to extrapolate to extreme-value intensities, such as would be expected (on average) to occur once per century. An upper limit lognormal fit to peak-over-threshold $-Dst_m$ data above a superstorm threshold of 283 nT gives a 100-year extrapolated intensity of 542 nT and a 68% confidence interval (obtained by bootstrap resampling) of [466, 583] nT. A generalized extreme-value distribution fit to solar cycle, block-maximum $-Dst_m^{BM}$ data gives a nine-solar cycle (approximately 100-year) extrapolated intensity of 591 nT. The Dst data are found to be insufficient for providing

usefully accurate estimates of a statistically theoretical upper limit for magnetic storm intensity. Secular change in storm intensities is noted, as is a need for improved estimates of pre-1957 magnetic storm intensities.

On the Intensity of the Magnetic Superstorm of September 1909

Jeffrey J. [Love](#), [Hisashi Hayakawa](#), [Edward W. Cliver](#)

Space Weather 17(1) Pages: 37-45 2019

<https://agupubs.onlinelibrary.wiley.com/doi/epdf/10.1029/2018SW002079>
[sci-hub.se/10.1029/2018SW002079](https://doi.org/10.1029/2018SW002079)

Analysis is made of solar observations and ground-based magnetometer data recording space weather before and during the magnetic superstorm of **25 September 1909**. From these data, it is inferred that the storm was initiated by an interplanetary coronal-mass ejection having a mean Sun-to-Earth velocity of ~1,679 km/s. The commencement pressure on the magnetopause was ~32.4 nPa, sufficient to compress the subsolar magnetopause radius to ~5.9 Earth radii. Early on in the evolution of the storm, low-latitude geomagnetic disturbance exhibited extreme longitudinal asymmetry, something that can be attributed to substorm activity extending to low latitudes. For this storm, Dst attained a minimum of -595 nT, comparable to that of the great magnetic storm of March 1989 (-589 nT; the most intense storm in terms of Dst of the space age). These results inform projects focused on understanding and mitigating the deleterious effects of extreme space-weather events.

Real-time geomagnetic monitoring for space weather-related applications: Opportunities and challenges

Jeffrey J. [Love](#), Carol A. Finn

Space Weather Volume 15, Issue 7 July 2017 Pages 820–827

<http://sci-hub.cc/10.1002/2017SW001665>

An examination is made of opportunities and challenges for enhancing global, real-time geomagnetic monitoring that would be beneficial for a variety of operational projects. This enhancement in geomagnetic monitoring can be attained by expanding the geographic distribution of magnetometer stations, improving the quality of magnetometer data, increasing acquisition sampling rates, increasing the promptness of data transmission, and facilitating access to and use of the data. Progress will benefit from new partnerships to leverage existing capacities and harness multisector, cross-disciplinary, and international interests.

The Geomagnetic Blitz of September 1941

[Love](#), J. J., and P. Coïsson

(2016), Eos, 97,doi:10.1029/2016EO059319.

https://eos.org/features/the-geomagnetic-blitz-of-september-1941?utm_source=eos&utm_medium=email&utm_campaign=EosBuzz091616

At 08:38 universal time (UT) on **17 September 1941**, the Greenwich Observatory spectroheliograph recorded a solar flare above this sunspot group

Less than 20 hours after the flare was reported by Greenwich, a magnetic storm commenced at **0412 UT on 18 September** with the arrival at Earth of a coronal mass ejection.

Solar Cell Degradation Due to Proton Belt Enhancements During Electric Orbit Raising to GEO

Alexander R. [Lozinski](#), [Richard B. Horne](#), [Sarah A. Glauert](#), [Giulio Del Zanna](#), [Daniel Heynderickx](#), [Hugh D. R. Evans](#)

Space Weather [Volume 17, Issue 7](#) July 2019 Pages 1059-1072

<https://agupubs.onlinelibrary.wiley.com/doi/epdf/10.1029/2019SW002213>

The recent introduction of all-electric propulsion on geosynchronous satellites enables lower-cost access to space by replacing chemical propellant. However, the time period required to initially raise the satellite to geostationary orbit (GEO) is around 200 days. During this time the satellite can be exposed to dynamic increases in trapped flux, which are challenging to model. To understand the potential penalty of this new technique in terms of radiation exposure, the influence of several key parameters on solar cell degradation during the electric orbit raising period has been investigated. This is achieved by calculating the accumulation of nonionizing dose through time for a range of approaches. We demonstrate the changes in degradation caused by launching during a long-lived (hundreds of days)

enhancement in megaelectron volt trapped proton flux for three different electric orbit raising scenarios and three different thicknesses of coverglass. Results show that launching in an active environment can increase solar cell degradation due to trapped protons by ~5% before start of service compared with a quiet environment. The crucial energy range for such enhancements in proton flux is 3–10 MeV (depending on shielding). Further changes of a few percent can occur between different trajectories, or when a 50- μm change in coverglass thickness is applied.

Full velocities and propagation directions of coronal mass ejections inferred from simultaneous full-disk imaging and Sun-as-a-star spectroscopic observations

[Hong-peng Lu](#), [Hui Tian](#), [He-chao Chen](#), [Yu Xu](#), [Zhen-yong Hou](#), [Xian-yong Bai](#), [Guang-yu Tan](#), [Zi-hao Yang](#), [Jie Ren](#)

ApJ 2023

<https://arxiv.org/pdf/2305.08765.pdf>

Coronal mass ejections (CMEs) are violent ejections of magnetized plasma from the Sun, which can trigger geomagnetic storms, endanger satellite operations and destroy electrical infrastructures on the Earth. After systematically searching Sun-as-a-star spectra observed by the Extreme-ultraviolet Variability Experiment (EVE) onboard the Solar Dynamics Observatory (SDO) from May 2010 to May 2022, we identified eight CMEs associated with flares and filament eruptions by analyzing the blue-wing asymmetry of the O III 52.58 nm line profiles. Combined with images simultaneously taken by the 30.4 nm channel of the Atmospheric Imaging Assembly onboard SDO, the full velocity and propagation direction for each of the eight CMEs are derived. We find a strong correlation between geomagnetic indices (Kp and Dst) and the angle between the CME propagation direction and the Sun-Earth line, suggesting that Sun-as-a-star spectroscopic observations at EUV wavelengths can potentially help to improve the prediction accuracy of the geoeffectiveness of CMEs. Moreover, an analysis of synthesized long-exposure Sun-as-a-star spectra implies that it is possible to detect CMEs from other stars through blue-wing asymmetries or blueshifts of spectral lines. **20110214, 20120702, 20141115, 20150311, 20150625, 20151104, 20170906, 20211028**

Table 1. Information of eight CMEs

Two-dimensional Particle-in-cell Simulation of Magnetic Reconnection in the Downstream of a Quasi-perpendicular Shock

Quanming [Lu](#)^{1,2}, Zhongwei [Yang](#)³, Huanyu [Wang](#)^{1,2}, Rongsheng [Wang](#)^{1,2}, Kai [Huang](#)^{1,2}, San [Lu](#)^{1,2}, and Shui [Wang](#)^{1,2}

2021 ApJ 919 28

<https://doi.org/10.3847/1538-4357/ac18c0>

In this paper, by performing a two-dimensional particle-in-cell simulation, we investigate magnetic reconnection in the downstream of a quasi-perpendicular shock. The shock is nonstationary, and experiences cyclic reformation. At the beginning of the reformation process, the shock front is relatively flat, and part of the upstream ions are reflected by the shock front. The reflected ions move upward in the action of the Lorentz force, which leads to the upward bending of the magnetic field lines at the foot of the shock front, and then a current sheet is formed due to the squeezing of the bending magnetic field lines. The formed current sheet is brought toward the shock front by the solar wind, and the shock front becomes irregular after interacting with the current sheet. Both the current sheet carried by the solar wind and the current sheet associated with the shock front are then fragmented into many small filamentary current sheets. Electron-scale magnetic reconnection may occur in several of these filamentary current sheets when they are convected into the downstream, and magnetic islands are generated. A strong reconnection electric field and energy dissipation are also generated around the X line, and a high-speed electron outflow is also formed.

Generalized Additive Modeling combined with Multiple Collinear for ICME velocity forecasting

J.Y. [Lu](#), C.Q. [Jin](#), M. [Wang](#), H.S. [Ji](#), K. [Iluore](#), H.Y. [Guan](#), J.F. [Li](#), J.Y. [Li](#)

Space Weather **Volume17, Issue4** Pages 567-585 2019

sci-hub.se/10.1029/2018SW002135

One of the main issues of space weather is the timely prediction of disturbed solar wind parameters at L1, especially caused by Coronal Mass Ejection (CME). Using the data from 170 front-halo, flare-associated CMEs, and in-site solar wind data, an analysis of the ICME peak velocity at L1 related to associated coronal parameters is performed. The statistical methods including the Generalized Additive Modeling (GAM) and Multiple Collinear (MC) have been applied to explain the underlying physical reasons and set up a new prediction model. Our results indicate that (1) X-flare integral flux, CME linear velocity, and Acceleration observed on corona play key roles in ICME velocity, while other coronal parameters only present a weak correlation, such as the CME Mass and Angular Width, (2) the relationship

between ICME velocity and CME Acceleration, as well as CME linear velocity, is non-stationary, and the ICME velocity will increase with the increasing CME Acceleration or linear velocity until saturation, and (3) MC is an effective method to improve the forecast model performance. Compared with 0.52 for only GAM, the correlation coefficient using GAM+MC reaches to 0.71. To further testify the prediction ability, the GAM+MC model results are compared with the Back Propagation (BP) network model and a typically empirical statistic relation proposed by Manoharan et al. [2006] (their correlation coefficients and root mean squared errors are both roughly 0.6 and 100 km/s, respectively). It is found that the MC+GAM can upgrade the forecast at least over 10%.

Geomagnetic and auroral activity driven by corotating interaction regions during the declining phase of Solar Cycle 23 (pages 1255–1269)

Xiaoli Luan, Wenbin Wang, Jiuhou Lei, Alan Burns, Xiankang Dou and Jiyao Xu
JGR, 118, Issue 3, pages 1255–1269, March 2013

A superposed epoch analysis is performed to investigate the relative impact of the solar wind/interplanetary magnetic field (IMF) on geomagnetic activity, auroral hemispheric power, and auroral morphology during corotating interaction regions (CIRs) events between 2002 and 2007, when auroral images from Thermosphere Ionosphere Mesosphere Energetics and Dynamics/Global Ultraviolet Imager were available. Four categories of CIRs have been compared. These were classified by the averaged IMF Bz and the time of maximum solar wind dynamic pressure around the CIR stream interface or onset time. It is found that during CIR events: (1) The peaks of auroral power and Kp were largely associated with dominant southward Bz, whereas auroral activity also became stronger with increases of solar wind speed, density, and dynamic pressure. (2) The percentage and absolute increases of auroral hemispheric power with solar wind speed were much greater under dominantly northward Bz conditions than under dominantly southward Bz conditions. (3) The enhancement of the auroral power and Kp with increasing solar wind speed followed the same pattern, for both dominantly southward and northward Bz conditions, regardless of the behavior of solar wind density and dynamic pressure. These results suggest that, during CIR events, southward Bz played the most critical role in determining geomagnetic and auroral activity, whereas solar wind speed was the next most important contributor. The solar wind dynamic pressure was the less important factor, as compared with Bz and solar wind speed. Relatively strong auroral precipitation energy flux ($> \sim 3$ mW/m²) occurred in a wider auroral oval region after the stream interface than before it for both dominantly northward and southward Bz conditions. These conditions enhanced the auroral hemispheric power after the stream interface. Intense auroral precipitation ($> \sim 4$ mW/m²) generally occurred widely at night under dominantly southward Bz conditions, but the location of this precipitation in the auroral oval was different when it was associated with different solar wind density and speed conditions.

The Need for Near-Earth Multi-Spacecraft Heliospheric Measurements and an Explorer Mission to Investigate Interplanetary Structures and Transients in the Near-Earth Heliosphere.

Review

Lugaz, N., Lee, C.O., Al-Haddad, N. et al.
Space Sci Rev 220, 73 (2024).

<https://doi.org/10.1007/s11214-024-01108-8>

<https://link.springer.com/content/pdf/10.1007/s11214-024-01108-8.pdf>

Based on decades of single-spacecraft measurements near 1 au as well as data from heliospheric and planetary missions, multi-spacecraft simultaneous measurements in the inner heliosphere on separations of 0.05–0.2 au are required to close existing gaps in our knowledge of solar wind structures, transients, and energetic particles, especially coronal mass ejections (CMEs), stream interaction regions (SIRs), high speed solar wind streams (HSS), and energetic storm particle (ESP) events. The Mission to Investigate Interplanetary Structures and Transients (MIIST) is a concept for a small multi-spacecraft mission to explore the near-Earth heliosphere on these critical scales. It is designed to advance two goals: (a) to determine the spatiotemporal variations and the variability of solar wind structures, transients, and energetic particle fluxes in near-Earth interplanetary (IP) space, and (b) to advance our fundamental knowledge necessary to improve space weather forecasting from in situ data. We present the scientific rationale for this proposed mission, the science requirements, payload, implementation, and concept of mission operation that address a key gap in our knowledge of IP structures and transients within the cost, launch, and schedule limitations of the NASA Heliophysics Small Explorers program.

The Width of Magnetic Ejecta Measured near 1 au: Lessons from STEREO-A Measurements in 2021–2022

Noé **Lugaz**^{4,1}, Bin Zhuang¹, Camilla Scolini^{1,2}, Nada Al-Haddad¹, Charles J. Farrugia¹, Réka M. Winslow¹, Florian Regnault¹, Christian Möstl³, Emma E. Davies³, and Antoinette B. Galvin¹
2024 ApJ 962 193

<https://iopscience.iop.org/article/10.3847/1538-4357/ad17b9/pdf>

<https://doi.org/10.3847/1538-4357/ad17b9/pdf>

Coronal mass ejections (CMEs) are large-scale eruptions with a typical radial size at 1 au of 0.21 au but their angular width in interplanetary space is still mostly unknown, especially for the magnetic ejecta (ME) part of the CME. We take advantage of STEREO-A angular separation of 20°–60° from the Sun–Earth line from 2020 October to 2022 August, and perform a two-part study to constrain the angular width of MEs in the ecliptic plane: (a) we study all CMEs that are observed remotely to propagate between the Sun–STEREO-A and the Sun–Earth lines and determine how many impact one or both spacecraft in situ, and (b) we investigate all in situ measurements at STEREO-A or at L1 of CMEs during the same time period to quantify how many are measured by the two spacecraft. A key finding is that out of 21 CMEs propagating within 30° of either spacecraft only four impacted both spacecraft and none provided clean magnetic cloud-like signatures at both spacecraft. Combining the two approaches, we conclude that the typical angular width of an ME at 1 au is ~20°–30°, or 2–3 times less than often assumed and consistent with a 2:1 elliptical cross section of an ellipsoidal ME. We discuss the consequences of this finding for future multi-spacecraft mission designs and for the coherence of CMEs. **2021 May 22, 2021 August 26, 2021, 2021 October 12, October 28, 2021 November 2, 2022 January 29, 2022 March 25, 2022 August 15**

Table 1 Overview of the 21 Cat I CMEs Studied Here Dec 2020-Aug 2022

A Coronal Mass Ejection and Magnetic Ejecta Observed In Situ by STEREO-A and Wind at 55° Angular Separation

Noé **Lugaz**, [Tarik M. Salman](#), [Charles J. Farrugia](#), [Wenyuan Yu](#), [Bin Zhuang](#), [Nada Al-Haddad](#), [Camilla Scolini](#), [Réka M. Winslow](#), [Christian Möstl](#), [Emma E. Davies](#), [Antoinette B. Galvin](#)

ApJ **929** 149 **2022**

<https://arxiv.org/pdf/2203.16477>

<https://doi.org/10.3847/1538-4357/ac602f>

<https://iopscience.iop.org/article/10.3847/1538-4357/ac602f/pdf>

We present an analysis of *in situ* and remote-sensing measurements of a coronal mass ejection (CME) that erupted on **2021 February 20** and impacted both the Solar TERrestrial RELations Observatory (STEREO)-A and the *Wind* spacecraft, which were separated longitudinally by 55°. Measurements on **2021 February 24** at both spacecraft are consistent with the passage of a magnetic ejecta (ME), making this one of the widest reported multi-spacecraft ME detections. The CME is associated with a low-inclined and wide filament eruption from the Sun's southern hemisphere, which propagates between STEREO-A and *Wind* around E34. At STEREO-A, the measurements indicate the passage of a moderately fast (~425 km s⁻¹) shock-driving ME, occurring 2–3 days after the end of a high speed stream (HSS). At *Wind*, the measurements show a faster (~490 km s⁻¹) and much shorter ME, not preceded by a shock nor a sheath, and occurring inside the back portion of the HSS. The ME orientation measured at both spacecraft is consistent with a passage close to the legs of a curved flux rope. The short duration of the ME observed at *Wind* and the difference in the suprathermal electron pitch-angle data between the two spacecraft are the only results that do not satisfy common expectations. We discuss the consequence of these measurements on our understanding of the CME shape and extent and the lack of clear signatures of the interaction between the CME and the HSS.

Inconsistencies Between Local and Global Measures of CME Radial Expansion as Revealed by Spacecraft Conjunctions

Noé **Lugaz**, [Tarik M. Salman](#), [Réka M. Winslow](#), [Nada Al-Haddad](#), [Charles J. Farrugia](#), [Bin Zhuang](#), and [Antoinette B. Galvin](#)

2020 ApJ 899 119

<https://doi.org/10.3847/1538-4357/aba26b>

The radial expansion of coronal mass ejections (CMEs) is known to occur from remote observations, from the variation of their properties with radial distance, and from local *in situ* plasma measurements showing a decreasing speed profile throughout the magnetic ejecta (ME). However, little is known on how local measurements compare to global measurements of expansion. Here, we present results from the analysis of 42 CMEs measured in the inner heliosphere by two spacecraft in radial conjunction. The magnetic-field decrease with distance provides a measure of their global expansion. Near 1 au, the decrease in their bulk speed provides a measure of their local expansion. We find that these two measures have little relation with each other. We also investigate the relation between characteristics of CME expansion and CME properties. We find that the expansion depends on the initial magnetic-field strength inside the ME,

but not significantly on the magnetic field inside the ME measured near 1 au. This is indirect evidence that CME expansion in the innermost heliosphere is driven by the high magnetic pressure inside the ME, while by the time the MEs reach 1 au, they are expanding due to the decrease in the solar-wind dynamic pressure with distance. We also determine the evolution of the ME tangential and normal magnetic-field components with distance, revealing significant deviations as compared to the expectations from force-free field configurations as well as some evidence that the front half of MEs expand at a faster rate than the back half.

Future Interplanetary Space Weather Assets

Review

Noe **Lugaz**

Space Weather **Volume 18, Issue 6**, e2020 SW002518 **2020**

<https://doi.org/10.1029/2020SW002518>

<https://agupubs.onlinelibrary.wiley.com/doi/pdf/10.1029/2020SW002518>

Late 2019 and early 2020 have witnessed numerous developments regarding future interplanetary space weather missions in Europe and in the United States of America. In parallel, space weather related legislation is being considered in the USA. A summary of these developments is presented and two related topical issues of Space Weather are introduced.

Evolution of a Long-Duration Coronal Mass Ejection and Its Sheath Region Between Mercury and Earth on 9–14 July 2013

N. **Lugaz**, [R. M. Winslow](#), [C. J. Farrugia](#)

JGR **Volume 125, Issue 1** January **2020** A027213

<https://doi.org/10.1029/2019JA027213>

Using in situ measurements and remote-sensing observations, we study a coronal mass ejection (CME) that left the Sun on 9 July 2013 and impacted both Mercury and Earth while the planets were in radial alignment (within $\sim 10^\circ$). The CME had an initial speed as measured by coronagraphs of 580 ± 20 km/s, an inferred speed at Mercury of 580 ± 30 km/s, and a measured maximum speed at Earth of 530 km/s, indicating that it did not decelerate substantially in the inner heliosphere. The magnetic field measurements made by MESSENGER and Wind reveal a very similar magnetic ejecta at both planets. We consider the CME expansion as measured by the ejecta duration and the decrease of the magnetic field strength between Mercury and Earth and the velocity profile measured in situ by Wind. The long-duration magnetic ejecta (20 and 42 hr at Mercury and Earth, respectively) is found to be associated with a relatively slowly expanding ejecta at 1 AU, revealing that the large size of the ejecta is due to the CME itself or its expansion in the corona or innermost heliosphere and not due to a rapid expansion between Mercury at 0.45 AU and Earth at 1 AU. We also find evidence that the CME sheath is composed of compressed material accumulated before the shock formed, as well as more recently shocked material.

On the Spatial Coherence of Magnetic Ejecta: Measurements of Coronal Mass Ejections by Multiple Spacecraft Longitudinally Separated by 0.01 au

Noé **Lugaz**^{1,2}, Charles J. Farrugia^{1,2}, Reka M. Winslow¹, Nada Al-Haddad³, Antoinette B.

Galvin^{1,2}, Teresa Nieves-Chinchilla^{3,4}, Christina O. Lee⁵, and Miho Janvier⁶

2018 ApJL 864 L7

<https://sci-hub.tw/10.3847/2041-8213/aad9f4>

Measurements of coronal mass ejections (CMEs) by multiple spacecraft at small radial separations but larger longitudinal separations is one of the ways to learn about the three-dimensional structure of CMEs. Here, we take advantage of the orbit of the Wind spacecraft that ventured to distances of up to 0.012 au from the Sun–Earth line during 2000–2002. Combined with measurements from the Advanced Composition Experiment, which is in a tight halo orbit around L1, the multipoint measurements allow us to investigate how the magnetic field inside magnetic ejecta (MEs) changes on scales of 0.005–0.012 au. We identify 21 CMEs measured by these two spacecraft for longitudinal separations of 0.007 au or more. We find that the time-shifted correlation between 30 minute averages of the non-radial magnetic field components measured at the two spacecraft is systematically above 0.97 when the separation is 0.008 au or less, but is on average 0.89 for greater separations. Overall, these newly analyzed measurements, combined with 14 additional ones when the spacecraft separation is smaller, point toward a scale length of longitudinal magnetic coherence inside MEs of 0.25–0.35 au for the magnitude of the magnetic field, but 0.06–0.12 au for the magnetic field components. This finding raises questions about the very nature of MEs. It also highlights the need for additional "mesoscale" multipoint measurements of CMEs with longitudinal separations of 0.01–0.2 au. **2002 May 19**

The Interaction of Successive Coronal Mass Ejections: A Review

Noé **Lugaz**, Manuela Temmer, Yuming Wang, Charles J. Farrugia

Sol Phys (2017) 292: 64. doi:10.1007/s11207-017-1091-6

<https://link.springer.com/content/pdf/10.1007/s11207-017-1091-6.pdf>

We present a review of the different aspects associated with the interaction of successive coronal mass ejections (CMEs) in the corona and inner heliosphere, focusing on the initiation of series of CMEs, their interaction in the heliosphere, the particle acceleration associated with successive CMEs, and the effect of compound events on Earth's magnetosphere. The two main mechanisms resulting in the eruption of series of CMEs are sympathetic eruptions, when one eruption triggers another, and homologous eruptions, when a series of similar eruptions originates from one active region. CME – CME interaction may also be associated with two unrelated eruptions. The interaction of successive CMEs has been observed remotely in coronagraphs (with the Large Angle and Spectrometric Coronagraph Experiment – LASCO – since the early 2000s) and heliospheric imagers (since the late 2000s), and inferred from in situ measurements, starting with early measurements in the 1970s. The interaction of two or more CMEs is associated with complex phenomena, including magnetic reconnection, momentum exchange, the propagation of a fast magnetosonic shock through a magnetic ejecta, and changes in the CME expansion. The presence of a preceding CME a few hours before a fast eruption has been found to be connected with higher fluxes of solar energetic particles (SEPs), while CME – CME interaction occurring in the corona is often associated with unusual radio bursts, indicating electron acceleration. Higher suprathermal population, enhanced turbulence and wave activity, stronger shocks, and shock – shock or shock – CME interaction have been proposed as potential physical mechanisms to explain the observed associated SEP events. When measured in situ, CME – CME interaction may be associated with relatively well organized multiple-magnetic cloud events, instances of shocks propagating through a previous magnetic ejecta or more complex ejecta, when the characteristics of the individual eruptions cannot be easily distinguished. CME – CME interaction is associated with some of the most intense recorded geomagnetic storms. The compression of a CME by another and the propagation of a shock inside a magnetic ejecta can lead to extreme values of the southward magnetic field component, sometimes associated with high values of the dynamic pressure. This can result in intense geomagnetic storms, but can also trigger substorms and large earthward motions of the magnetopause, potentially associated with changes in the outer radiation belts. Future in situ measurements in the inner heliosphere by Solar Probe+ and Solar Orbiter may shed light on the evolution of CMEs as they interact, by providing opportunities for conjunction and evolutionary studies.

Factors affecting the geoeffectiveness of shocks and sheaths at 1 AU

N. **Lugaz**, C. J. Farrugia, R. M. Winslow, N. Al-Haddad, E. K. J. Kilpua, P. Riley

JGR Vol: 121, Pages: 10,861–10,879 2016

We identify all fast-mode forward shocks, whose sheath regions resulted in a moderate (56 cases) or intense (38 cases) geomagnetic storm during 18.5 years from January 1997 to June 2015. We study their main properties, interplanetary causes, and geoeffects. We find that half (49/94) such shocks are associated with interacting coronal mass ejections (CMEs), as they are either shocks propagating into a preceding CME (35 cases) or a shock propagating into the sheath region of a preceding shock (14 cases). About half (22/45) of the shocks driven by isolated transients and which have geoeffective sheaths compress preexisting southward Bz. Most of the remaining sheaths appear to have planar structures with southward magnetic fields, including some with planar structures consistent with field line draping ahead of the magnetic ejecta. A typical (median) geoeffective shock-sheath structure drives a geomagnetic storm with peak Dst of -88 nT pushes the subsolar magnetopause location to 6.3 RE, i.e., below geosynchronous orbit and is associated with substorms with a peak AL index of -1350 nT. There are some important differences between sheaths associated with CME-CME interaction (stronger storms) and those associated with isolated CMEs (stronger compression of the magnetosphere). We detail six case studies of different types of geoeffective shock-sheaths, as well as two events for which there was no geomagnetic storm but other magnetospheric effects. Finally, we discuss our results in terms of space weather forecasting and potential effects on Earth's radiation belts.

Shocks inside CMEs: A Survey of Properties from 1997 to 2006†

N. **Lugaz***, C. J. Farrugia, C. W. Smith and K. Paulson

JGR 2015

We report on 49 fast-mode forward shocks propagating inside coronal mass ejections (CMEs) as measured by Wind and ACE at 1 AU from 1997 to 2006. Compared to typical CME-driven shocks, these shocks propagate in different upstream conditions, where the median upstream Alfvén speed is 85 km s^{-1} , the proton $\beta = 0.08$ and the magnetic field strength is 8 nT . These shocks are fast with a median speed of 590 km s^{-1} but weak with a median Alfvénic Mach number of 1.9.

They typically compress the magnetic field and density by a factor of 2–3. The most extreme upstream conditions found were a fast magnetosonic speed of 230 km s^{-1} , a plasma β of 0.02, upstream solar wind speed of 740 km s^{-1} and density of 0.5 cm^{-3} . Nineteen of these complex events were associated with an intense geomagnetic storm (peak Dst under -100 nT) within 12 hours of the shock detection at Wind, and fifteen were associated with a drop of the storm-time Dst index of more than 50 nT between 3 and 9 hours after shock detection. We also compare them to a sample of 45 shocks propagating in more typical upstream conditions. We show the average property of these shocks through a superposed epoch analysis, and we present some analytical considerations regarding the compression ratios of shocks in low β regimes. As most of these shocks are measured in the back half of a CME, we conclude that about half the shocks may not remain fast-mode shocks as they propagate through an entire CME due to the large upstream and magnetosonic speeds.

Eruptive Prominences and Their Impact on the Earth and Our Life

Review

Noé **Lugaz**

Solar Prominences

Astrophysics and Space Science Library Volume 415, **2015**, pp 433-453

http://link.springer.com/chapter/10.1007/978-3-319-10416-4_17

Following prominence eruptions (see Chap. 16: Webb, Solar prominences. New York: Springer, 2014), the associated coronal mass ejections (CMEs) propagate into the solar wind and interplanetary medium. While the complex interactions with the magnetic field and plasma in the corona (see Chaps. 15 and 16: Gopalswamy, Solar prominences. New York: Springer, 2014; Webb, Solar prominences. New York: Springer, 2014) have been observed for decades, it has only been in the last decade that the interaction of CMEs with the interplanetary medium can be directly imaged. As CMEs and prominences impact Earth, Earth's magnetosphere may be disrupted through reconnection and/or compression, resulting in geomagnetic storms. In the most extreme cases, CMEs and prominences may have a global effect on man-made technologies and human beings, especially if they are in space. The conditions in the near-Earth environment directly affected by the Sun and the solar activity are known as space weather and will be discussed here. In this chapter, we review different types of measurements and observations of prominences and CMEs as they propagate between the Sun and the Earth, as well as recent advances in numerical modeling and theoretical ideas related to CME propagation. We also discuss the potential effects of CMEs and prominences on Earth's magnetosphere and atmosphere and the very direct impact it may exert on our lives.

The Interaction of Two Coronal Mass Ejections: Influence of Relative Orientation

N. **Lugaz**¹, C. J. Farrugia¹, W. B. Manchester IV², and N. Schwadron

2013 ApJ 778 20

<http://arxiv.org/pdf/1309.2210v1.pdf>

We report on a numerical investigation of two coronal mass ejections (CMEs) that interact as they propagate in the inner heliosphere. We focus on the effect of the orientation of the CMEs relative to each other by performing four different simulations with the axis of the second CME rotated by 90° from one simulation to the next. Each magnetohydrodynamic simulation is performed in three dimensions with the Space Weather Modeling Framework in an idealized setting reminiscent of solar minimum conditions. We extract synthetic satellite measurements during and after the interaction and compare the different cases. We also analyze the kinematics of the two CMEs, including the evolution of their widths and aspect ratios. We find that the first CME contracts radially as a result of the interaction in all cases, but the amount of subsequent radial expansion depends on the relative orientation of the two CMEs. Reconnection between the two ejecta and between the ejecta and the interplanetary magnetic field determines the type of structure resulting from the interaction. When a CME with a high inclination with respect to the ecliptic overtakes one with a low inclination, it is possible to create a compound event with a smooth rotation in the magnetic field vector over more than 180° . Due to reconnection, the second CME only appears as an extended "tail," and the event may be mistaken for a glancing encounter with an isolated CME. This configuration differs significantly from the one usually studied of a multiple-magnetic-cloud event, which we found to be associated with the interaction of two CMEs with the same orientation.

Effect of Solar Wind Drag on the Determination of the Properties of Coronal Mass Ejections from Heliospheric Images

N. **Lugaz**¹ and P. Kintner

Solar Phys. July **2013**, Volume 285, Issue 1-2, pp 281-294

The Fixed- Φ (F Φ) and Harmonic Mean (HM) fitting methods are two methods to determine the “average” direction and velocity of coronal mass ejections (CMEs) from time–elongation tracks produced by Heliospheric Imagers (HIs), such as the HIs onboard the STEREO spacecraft. Both methods assume a constant velocity in their descriptions of the time–elongation profiles of CMEs, which are used to fit the observed time–elongation data. Here, we analyze the effect of aerodynamic drag on CMEs propagating through interplanetary space, and how this drag affects the result of the F Φ and HM fitting methods. A simple drag model is used to analytically construct time–elongation profiles which are then fitted with the two methods. It is found that higher angles and velocities give rise to greater error in both methods, reaching errors in the direction of propagation of up to 15° and 30° for the F Φ and HM fitting methods, respectively. This is due to the physical accelerations of the CMEs being interpreted as geometrical accelerations by the fitting methods. Because of the geometrical definition of the HM fitting method, it is more affected by the acceleration than the F Φ fitting method. Overall, we find that both techniques overestimate the initial (and final) velocity and direction for fast CMEs propagating beyond 90° from the Sun–spacecraft line, meaning that arrival times at 1 AU would be predicted early (by up to 12 hours). We also find that the direction and arrival time of a wide and decelerating CME can be better reproduced by the F Φ due to the cancelation of two errors: neglecting the CME width and neglecting the CME deceleration. Overall, the inaccuracies of the two fitting methods are expected to play an important role in the prediction of CME hit and arrival times as we head towards solar maximum and the STEREO spacecraft further move behind the Sun.

THE DEFLECTION OF THE TWO INTERACTING CORONAL MASS EJECTIONS OF 2010 MAY 23-24 AS REVEALED BY COMBINED IN SITU MEASUREMENTS AND HELIOSPHERIC IMAGING

N. [Lugaz](#)¹, C. J. Farrugia¹, J. A. Davies², C. Möstl^{3,4,5}, C. J. Davis^{2,6}, I. I. Roussev^{7,8}, and M. Temmer
2012 ApJ 759 68, File

In **2010 May 23-24**, Solar Dynamics Observatory (SDO) observed the launch of two successive coronal mass ejections (CMEs), which were subsequently tracked by the SECCHI suite on board STEREO. Using the COR2 coronagraphs and the heliospheric imagers (HIs), the initial direction of both CMEs is determined to be slightly west of the Sun-Earth line. We derive the CME kinematics, including the evolution of the CME expansion until 0.4 AU. We find that, during the interaction, the second CME decelerates from a speed above 500 km s⁻¹ to 380 km s⁻¹, the speed of the leading edge of the first CME. STEREO observes a complex structure composed of two different bright tracks in HI2-A but only one bright track in HI2-B. In situ measurements from Wind show an "isolated" interplanetary CME, with the geometry of a flux rope preceded by a shock. Measurements in the sheath are consistent with draping around the transient. By combining remote-sensing and in situ measurements, we determine that this event shows a clear instance of deflection of two CMEs after their collision, and we estimate the deflection of the first CME to be about 10° toward the Sun-Earth line. The arrival time, arrival speed, and radius at Earth of the first CME are best predicted from remote-sensing observations taken before the collision of the CMEs. Due to the over-expansion of the CME after the collision, there are few, if any, signs of interaction in in situ measurements. This study illustrates that complex interactions during the Sun-to-Earth propagation may not be revealed by in situ measurements alone.

Heliospheric Observations of STEREO-Directed Coronal Mass Ejections in 2008 – 2010: Lessons for Future Observations of Earth-Directed CMEs

N. [Lugaz](#), P. Kintner, C. Möstl, L. K. Jian, C. J. Davis and C. J. Farrugia
Solar Physics, **2012**, Volume 279, Number 2, 497-515

We present a study of coronal mass ejections (CMEs) which impacted one of the STEREO spacecraft between January 2008 and early 2010. We focus our study on 20 CMEs which were observed remotely by the Heliospheric Imagers (HIs) onboard the other STEREO spacecraft up to large heliocentric distances. We compare the predictions of the Fixed- Φ and Harmonic Mean (HM) fitting methods, which only differ by the assumed geometry of the CME. It is possible to use these techniques to determine from remote-sensing observations the CME direction of propagation, arrival time and final speed which are compared to in-situ measurements. We find evidence that for large viewing angles, the HM fitting method predicts the CME direction better. However, this may be due to the fact that only wide CMEs can be successfully observed when the CME propagates more than 100° from the observing spacecraft. Overall eight CMEs, originating from behind the limb as seen by one of the STEREO spacecraft can be tracked and their arrival time at the other STEREO spacecraft can be successfully predicted. This includes CMEs, such as the events **on 4 December 2009 and 9 April 2010**, which were viewed 130° away from their direction of propagation. Therefore, we predict that some

Earth-directed CMEs will be observed by the HIs until early 2013, when the separation between Earth and one of the STEREO spacecraft will be similar to the separation of the two STEREO spacecraft in 2009–2010.

Determining CME parameters by fitting heliospheric observations: Numerical investigation of the accuracy of the methods

Noé [Lugaz](#), , , Iliia I. Rousseva, and Tamas I. Gombosib,

Advances in Space Research, Volume 48, Issue 2, 15 July 2011, Pages 292-299

Transients in the heliosphere, including coronal mass ejections (CMEs) and corotating interaction regions can be imaged to large heliocentric distances by heliospheric imagers (HIs), such as the HIs onboard STEREO and SMEI onboard Coriolis. These observations can be analyzed using different techniques to derive the CME speed and direction. In this paper, we use a three-dimensional (3-D) magneto-hydrodynamic (MHD) numerical simulation to investigate one of these methods, the fitting method of (Sheeley et al., 1999) and (Rouillard et al., 2008). Because we use a 3-D simulation, we can determine with great accuracy the CME initial speed, its speed at 1 AU and its average transit speed as well as its size and direction of propagation. We are able to compare the results of the fitting method with the values from the simulation for different viewing angles between the CME direction of propagation and the Sun-spacecraft line. We focus on one simulation of a wide (120–140°) CME, whose initial speed is about 800 km s⁻¹. For this case, we find that the best-fit speed is in good agreement with the speed of the CME at 1 AU, and this, independently of the viewing angle. The fitted direction of propagation is not in good agreement with the viewing angle in the simulation, although smaller viewing angles result in smaller fitted directions. This is due to the extremely wide nature of the ejection. A new fitting method, proposed to take into account the CME width, results in better agreement between fitted and actual directions for directions close to the Sun–Earth line. For other directions, it gives results comparable to the fitting method of Sheeley et al. (1999). The CME deceleration has only a small effect on the fitted direction, resulting in fitted values about 1–4° higher than the actual values.

Numerical modeling of interplanetary coronal mass ejections and comparison with heliospheric images

N. [Lugaz](#), a, and I.I. Roussev

Journal of Atmospheric and Solar-Terrestrial Physics, Volume 73, Issue 10, 2011, Pages 1187-1200

Interplanetary coronal mass ejections (ICMEs) have complex magnetic and density structures, which are the result of their interaction with the structured solar wind and with previous eruptions. ICMEs are revealed by in situ measurements and in the past five years, through remote-sensing observations by heliospheric imagers. However, to understand and analyze these observations often requires the use of numerical modeling. It is because no instruments can yet provide a simple view of ICMEs in two or three dimensions. Numerical simulations can be used to determine the origin of a complex ejecta observed near Earth, or to analyze the origin, speed and extent of density structures observed remotely. Here, we [review](#) and discuss recent efforts to use numerical simulations of ICMEs to investigate the magnetic topology, density structure, energetics and kinematics of ICMEs in the interplanetary space.

After reviewing existing numerical models of ICMEs, we first focus on numerical modeling in support of the SMEI and STEREO observations. 3-D simulations can help determining the origins of the fronts observed by SECCHI and SMEI, especially for complex events such as the **January 24–25, 2007** CMEs. They can also be used to test different methods to derive ICME properties from remote observations, to predict and explain observational effects, and to understand the deceleration and deformation of ICMEs. In the last part, we focus on the numerical investigation of non-magnetic cloud ejecta. We discuss how simulations are crucial to understand the formation of non-twisted ejecta and the formation of complex ejecta due to the interaction of multiple ICMEs.

Research Highlights

► Simulations are used in support of observations of ICMEs, such as these done by STEREO. ► Simulations are used to test analysis methods for in situ and remote observations of ICMEs. ► Simulations can reveal the physical processes during ICME-ICME interaction. ► Ejecta with low twist but large writhe may be mistaken for twisted flux rope.

Accuracy and Limitations of Fitting and Stereoscopic Methods to Determine the Direction of Coronal Mass Ejections from Heliospheric Imagers Observations

N. [Lugaz](#)

Solar Phys (2010) 267: 411–429; **File**

Using data from the Heliospheric Imagers (HIs) onboard STEREO, it is possible to derive the direction of propagation of coronal mass ejections (CMEs) in addition to their speed with a variety of methods. For CMEs observed by both STEREO spacecraft, it is possible to derive their direction using simultaneous observations from the twin spacecraft and also, using observations from only one spacecraft with fitting methods. This makes it possible to test and compare different analysis techniques. In this article, we propose a new fitting method based on observations from one spacecraft, which we compare to the commonly used fitting method of Sheeley *et al.* (*J. Geophys. Res.* **104**, 24739, 1999). We also compare the results from these two fitting methods with those from two stereoscopic methods, focusing on 12 CMEs observed simultaneously by the two STEREO spacecraft in 2008 and 2009. We find evidence that the fitting method of Sheeley *et al.* (*J. Geophys. Res.* **104**, 24739, 1999) may result in significant errors in the determination of the CME direction when the CME propagates outside of $60^\circ \pm 20^\circ$ from the Sun – spacecraft line. We expect our new fitting method to be better adapted to the analysis of halo or limb CMEs with respect to the observing spacecraft. We also find some evidence that direct triangulation in the HI fields-of-view should only be applied to CMEs propagating approximately toward Earth ($\pm 20^\circ$ from the Sun – Earth line). Last, we address one of the possible sources of errors of fitting methods: the assumption of radial propagation. Using stereoscopic methods, we find that at least seven of the 12 studied CMEs had a heliospheric deflection of less than 20° as they propagated in the HI fields-of-view, which, we believe, validates this approximation.

DETERMINING THE AZIMUTHAL PROPERTIES OF CORONAL MASS EJECTIONS FROM MULTI-SPACECRAFT REMOTE-SENSING OBSERVATIONS WITH STEREO SECCHI

N. [Lugaz](#)¹, J. N. Hernandez-Charpak², I. I. Roussev¹, C. J. Davis³, A. Vourlidas⁴, and J. A. Davies³
Astrophysical Journal, 715:493–499, 2010 May; **File**

We discuss how simultaneous observations by multiple heliospheric imagers (HIs) can provide some important information about the azimuthal properties of coronal mass ejections (CMEs) in the heliosphere. We propose two simple models of CME geometry that can be used to derive information about the azimuthal deflection and the azimuthal expansion of CMEs from SECCHI/HI observations. We apply these two models to four CMEs well observed by both STEREO spacecraft during the year 2008. We find that in three cases, the joint STEREO-A and B observations are consistent with CMEs moving radially outward. In some cases, we are able to derive the azimuthal cross section of the CME fronts, and we are able to measure the deviation from self-similar evolution. The results from this analysis show the importance of having multiple satellites dedicated to space weather forecasting, for example, in orbits at the Lagrangian L4 and L5 points.

Deriving the radial distances of wide coronal mass ejections from elongation measurements in the heliosphere – application to CME-CME interaction

N. [Lugaz](#)¹, A. Vourlidas², and I. I. Roussev¹

Ann. Geophys., 27, 3479–3488, 2009, **File**

www.ann-geophys.net/27/3479/2009/

We present general considerations regarding the derivation of the radial distances of coronal mass ejections (CMEs) from elongation angle measurements such as those provided by SECCHI and SMEI, focusing on measurements in the Heliospheric Imager 2 (HI-2) field of view (i.e. past 0.3 AU). This study is based on a three-dimensional (3-D) magneto-hydrodynamics (MHD) simulation of two CMEs observed by SECCHI on **24–27 January 2007**. Having a 3-D simulation with synthetic HI images, we are able to compare the two basic methods used to derive CME positions from elongation angles, the so-called "Point-P" and "Fixed- ϕ " approximations. We confirm, following similar works, that both methods, while valid in the most inner heliosphere, yield increasingly large errors in HI-2 field of view for fast and wide CMEs. Using a simple model of a CME as an expanding self-similar sphere, we derive an analytical relationship between elongation angles and radial distances for wide CMEs. This relationship is simply the harmonic mean of the "Point-P" and "Fixed- ϕ " approximations and it is aimed at complementing 3-D fitting of CMEs by cone models or flux rope shapes. It proves better at getting the kinematics of the simulated CME right when we compare the results of our line-of-sights to the MHD simulation. Based on this approximation, we re-analyze the J-maps (time-elongation maps) in

26–27 January 2007 and present the first observational evidence that *the merging of CMEs is associated with a momentum exchange from the faster ejection to the slower one due to the propagation of the shock wave associated with the fast eruption through the slow eruption.* **STEREO**

Solar – Terrestrial Simulation in the STEREO Era: The 24 – 25 January 2007 Eruptions

N. [Lugaz](#) · A. Vourlidas · I.I. Roussev · H. Morgan

Solar Phys (2009) 256: 269–284, DOI 10.1007/s11207-009-9339-4, **2009, File**

STEREO SCIENCE RESULTS AT SOLAR MINIMUM

The SECCHI instruments aboard the recently launched STEREO spacecraft enable for the first time the continuous tracking of coronal mass ejections (CMEs) from the Sun to 1 AU. We analyze line-of-sight observations of the 24 – 25 January 2007 CMEs and fill the 20-hour gap in SECCHI coverage in 25 January by performing a numerical simulation using a three-dimensional magneto-hydrodynamic (MHD) code, the Space Weather Modeling Framework (SWMF). We show how the observations reflect the interaction of the two successive CMEs with each other and with the structured solar wind. We make a detailed comparison between the observations and synthetic images from our model, including time-elongation maps for several position angles. Having numerical simulations to disentangle observational from physical effects, we are able to study the three-dimensional nature of the ejections and their evolution in the inner heliosphere. This study reflects the start of a new era where, on one hand, models of CME propagation and interaction can be fully tested by using heliospheric observations and, on the other hand, observations can be better interpreted by using global numerical models.

The August 24, 2002 Coronal Mass Ejection: When a Western Limb Event Connects to Earth

Notes [Lugaz](#)¹, Ilia I. Roussev¹ and Igor V. Sokolov²

Universal Heliophysical Processes

Proceedings IAU Symposium No. IAU257, **2008; File**

N. Gopalswamy, D. Webb & A. Nindos, eds.

Abstract. We discuss how some coronal mass ejections (CMEs) originating from the western limb of the Sun are associated with space weather effects such as solar energetic particles (SEPs), shock or geo-effective ejecta at Earth. We focus on the August 24, 2002 coronal mass ejection, a fast (~ 2000 km s⁻¹) eruption originating from W81. Using a three-dimensional magneto-hydrodynamic simulation of this ejection with the Space Weather Modeling Framework (SWMF), we show how a realistic initiation mechanism enables us to study the deflection of the CME in the corona and the heliosphere. Reconnection of the erupting magnetic field with that of neighboring streamers and active regions modify the solar connectivity of the field lines connecting to Earth and can also partly explain the deflection of the eruption during the first tens of minutes. Comparing the results at 1 AU of our simulation with observations by the ACE spacecraft, we find that the simulated shock does not reach Earth, but has a maximum angular span of about 120°, and reaches 35° West of Earth in 58 hours. We find no significant deflection of the CME and its associated shock wave in the heliosphere, and we discuss the consequences for the shock angular span.

Solar-terrestrial Simulations in the STEREO Era

[Lugaz](#), N.¹; Roussev, I.¹; Vourlidas, A.²

Freiburg ESP Meeting **2008, Presentation**

Due to the scarcity of heliospheric observations, over the past decade global 3-D numerical simulations have become increasingly important in studying the propagation of coronal mass ejections (CMEs) from the Sun to the Earth. Since the launch of STEREO in November 2006, continuous white-light observations of solar transients on their way to the Earth in near-real time have become possible.

In this talk, we will discuss the significance of 3-D simulations in the interpretation of observations taken by the Heliospheric Imagers. We will focus on a series of two ejections in **January, 24-25, 2007**, which have been simulated with the Space Weather Modeling Framework (SWMF). We will present detailed comparisons between real and simulated time-elongation plots and discuss the appearance of CME-CME interaction in real and synthetic observations.

THE BRIGHTNESS OF DENSITY STRUCTURES AT LARGE SOLAR ELONGATION ANGLES: WHAT IS BEING OBSERVED BY *STEREO SECCHI*?

N. [Lugaz](#),¹ A. Vourlidas,² I. I. Roussev,¹ C. Jacobs,³ W. B. Manchester IV,⁴ and O. Cohen⁴
Astrophysical Journal, 684: L111–L114, **2008** September

<http://www.journals.uchicago.edu/toc/apjl/2008/684/2>

We discuss features of coronal mass ejections (CMEs) that are specific to heliospheric observations at large elongation angles. Our analysis is focused on a series of two eruptions that occurred on **2007 January 24–25**, which were tracked by the Heliospheric Imagers (HIs) on board *STEREO*. Using a three-dimensional (3D) magnetohydrodynamic simulation of these ejections with the **Space Weather Modeling Framework (SWMF)**, we illustrate how the combination of the 3D nature of CMEs, solar rotation, and geometry associated with the Thomson sphere results in complex effects in the brightness observed by the HIs. Our results demonstrate that these effects make any in-depth analysis of CME observations without 3D simulations challenging. In particular, the association of bright features seen by the HIs with fronts of CME-driven shocks is far from trivial. In this Letter, we argue that, on 2007 January 26, the HIs observed not only two CMEs, but also a dense corotating stream compressed by the CME-driven shocks.

NUMERICAL SIMULATION OF THE INTERACTION OF TWO CORONAL MASS EJECTIONS FROM SUN TO EARTH

N. [Lugaz](#), W. B. Manchester IV, and T. I. Gombosi

The Astrophysical Journal, 634:651–662, **2005**

We present a three-dimensional compressible magnetohydrodynamics (MHD) model of the interaction of two coronal mass ejections (CMEs). Two identical CMEs are launched in the exact same direction into a preexisting solar wind, the second one 10 hr after the first one.

ICME Evolution in the Inner Heliosphere

Invited Review

J. G. [Luhmann](#), [N. Gopalswamy](#), [L. K. Jian](#) & [N. Lugaz](#)

[Solar Physics](#) volume 295, Article number: 61 (**2020**) **File**

<https://link.springer.com/content/pdf/10.1007%2Fs11207-020-01624-0.pdf>

ICMEs (interplanetary coronal mass ejections), the heliospheric counterparts of what is observed with coronagraphs at the Sun as CMEs, have been the subject of intense interest since their close association with geomagnetic storms was established in the 1980s. These major interplanetary plasma and magnetic field transients, often preceded and accompanied by solar energetic particles (SEPs), interact with planetary magnetospheres, ionospheres, and upper atmospheres in now fairly well-understood ways, although their details and context affect their overall impacts. The term ICME as it is used here refers to the complete solar-wind plasma and field disturbance, including the leading shock (if present), the compressed, deflected solar-wind plasma and the field behind the shock (“sheath”), and the coronal ejecta (the “driver”) – often called a magnetic cloud. Many uncertainties remain in understanding both the relationship to what is observed at the Sun and the variety of local outcomes suggested by in-situ observations. This impacts our abilities to interpret events and to forecast effects based on solar observations. Here, we briefly consider what is known about ICMEs and their evolution en route from the Sun from the combination of available observations and interpretive models that have been developed up to now. The included references are only representative of the large body of work that has been published on this subject. Our aim is to provide the reader with an updated synthesis of research results in this still active area of heliophysics at the dawn of the Parker Solar Probe (PSP) and Solar Orbiter (SO) mission era. **3 Aug 2010, 15 Feb 2011, 2 Dec 2013, 21 June 2015**

SolarWind Sources in the Late Declining Phase of Cycle 23: Effects of the Weak Solar Polar Field on High Speed Streams

J.G. [Luhmann](#) · C.O. Lee · Yan Li · C.N. Arge · A.B. Galvin · K. Simunac · C.T. Russell · R.A. Howard · G. Petrie

Solar Phys (**2009**) 256: 285–305, DOI 10.1007/s11207-009-9354-5

STEREO SCIENCE RESULTS AT SOLAR MINIMUM

The declining phases of solar cycles are known for their high speed solar wind streams that dominate the geomagnetic responses during this period. Outstanding questions about these streams, which can provide the fastest winds of the solar cycle, concern their solar origins, persistence, and predictability. The declining phase of cycle 23 has lasted significantly longer than

the corresponding phases of the previous two cycles. Solar magnetograph observations suggest that the solar polar magnetic field is also $\sim 2 - 3$ times weaker. The launch of STEREO in late 2006 provided additional incentive to examine the origins of what is observed at 1 AU in the recent cycle, with the OMNI data base at the NSSDC available as an Earth/L1 baseline for comparisons. Here we focus on the year 2007 when the solar corona exhibited large, long-lived mid-to-low latitude coronal holes and polar hole extensions observed by both SOHO and STEREO imagers. STEREO provides *in situ* measurements consistent with rigidly corotating solar wind stream structure at up to $\sim 45^\circ$ heliolongitude separation by late 2007. This stability justifies the use of magnetogram-based steady 3D solar wind models to map the observed high speed winds back to their coronal sources. We apply the WSA solar wind model currently running at the NOAA Space Weather Prediction Center with the expectation that it should perform its best at this quiet time. The model comparisons confirm the origins of the observed high speed streams expected from the solar images, but also reveal uncertainties in the solar wind source mapping associated with this cycle's weaker solar polar fields. Overall, the results illustrate the importance of having accurate polar fields in synoptic maps used in solar wind forecast models. At the most fundamental level, they demonstrate the control of the solar polar fields over the high speed wind sources, and thus one specific connection between the solar dynamo and the solar wind character.

Grad-Shafranov Reconstruction of Magnetic Flux Ropes in the Near-Earth Space

A.T.Y. **Lui**

Space Science Reviews, Volume 158, Number 1 (2011), 43-68,

Electric currents permeate space plasmas and often have a significant component along the magnetic field to form magnetic flux ropes. A larger spatial perspective of these structures than from the direct observation along the satellite path is crucial in visualizing their role in plasma dynamics. For magnetic flux ropes that are approximately two-dimensional equilibrium structures on a certain plane, Grad-Shafranov reconstruction technique, developed by Bengt Sonnerup and his colleagues (see Sonnerup et al. in J. Geophys. Res. 111:A09204, 2006), can be used to reveal two-dimensional maps of associated plasma and field parameters. This review gives a brief account of the technique and its application to magnetic flux ropes near the Earth's magnetopause, in the solar wind, and in the magnetotail. From this brief survey, the ranges of the total field-aligned current and the total magnetic flux content for these magnetic flux ropes are assessed. The total field-aligned current is found to range from ~ 0.14 to $\sim 9.7 \times 10^4$ MA, a range of nearly six orders of magnitude. The total magnetic flux content is found to range from ~ 0.25 to $\sim 2.3 \times 10^6$ MWb, a range of nearly seven orders of magnitude. To the best of our knowledge, this review reports the largest range of both the total field-aligned current and the total magnetic flux content for magnetic flux ropes in space plasmas.

The extreme solar storm of May 1921: observations and a complex topological model

H. **Lundstedt**¹, T. Persson², and V. Andersson

Ann. Geophys., 33, 109-116, 2015

www.ann-geophys.net/33/109/2015/

A complex solid torus model was developed in order to be able to study an extreme solar storm, the so-called "Great Storm" or "New York Railroad Storm" of May 1921, when neither high spatial and time resolution magnetic field measurements, solar flare nor coronal mass ejection observations were available. We suggest that a topological change happened in connection with the occurrence of the extreme solar storm. The solar storm caused one of the most severe space weather effects ever.

A Numerical Study of the Effects of a Corotating Interaction Region on Cosmic-Ray Transport. II. Features of Cosmic-Ray Composition and Rigidity

Xi **Luo**¹, Marius S. Potgieter^{1,2}, Ming Zhang³, and Fang Shen⁴

2024 ApJ 961 21

<https://iopscience.iop.org/article/10.3847/1538-4357/ad0cb6/pdf>

We continue the numerical modeling of a corotating interaction region (CIR) and the effects it has on solar-rotational recurrent variations of galactic cosmic rays (GCRs). A magnetohydrodynamic model is adapted to simulate the background solar wind plasma with a CIR structure in the inner heliosphere, which is incorporated into a comprehensive Parker-type transport model. The focus is on the simulation of the effects of a CIR on GCR protons and the two helium isotopes as a function of heliolongitude. This is to establish whether the difference in composition affects how they are modulated by the CIR in terms of their distribution in longitude. It is demonstrated that particle diffusion and drift influence the effects of the CIR with increasing rigidity from 100 MV up to 15 GV. It is found that protons and helium isotopes are modulated differently with longitude by the CIR and that particle drift influences the modulation effects in longitude. These differences dissipate with increasing rigidity. The final results are focused on the simulated amplitude of these GCR flux variations as a function of rigidity. The amplitude displays a power-law behavior above ~ 1 GV with

an index similar to the power index of the rigidity dependence of the assumed diffusion coefficients. The simulations further show that below this rigidity, the amplitude at first flattens off, displaying a plateau-like profile, but it then increases systematically with decreasing rigidity below ~ 0.3 GV. Again, a power-law behavior is displayed, but it is completely different from that above 1 GV.

Statistical Study of Anisotropic Proton Heating in Interplanetary Magnetic Switchbacks Measured by Parker Solar Probe

Qiaowen **Luo**^{1,2}, Die Duan², Jiansen He², Xingyu Zhu², Daniel Verscharen³, Jun Cui¹, and Hairong Lai¹
2023 ApJL 952 L40

<https://iopscience.iop.org/article/10.3847/2041-8213/acce9f/pdf>

Magnetic switchbacks, which are large angular deflections of the interplanetary magnetic field, are frequently observed by Parker Solar Probe (PSP) in the inner heliosphere. Magnetic switchbacks are believed to play an important role in the heating of the solar corona and the solar wind as well as the acceleration of the solar wind in the inner heliosphere. Here, we analyze magnetic field data and plasma data measured by PSP during its second and fourth encounters, and select 71 switchback events with reversals of the radial component of the magnetic field at times of unchanged electron-strahl pitch angles. We investigate the anisotropic thermal kinetic properties of plasma during switchbacks in a statistical study of the measured proton temperatures in the parallel and perpendicular directions as well as proton density and specific proton fluid entropy. We apply the "genetic algorithm" method to directly fit the measured velocity distribution functions in field-aligned coordinates using a two-component bi-Maxwellian distribution function. We find that the protons in most switchback events are hotter than the ambient plasma outside the switchbacks, with characteristics of parallel and perpendicular heating. Specifically, significant parallel and perpendicular temperature increases are seen for 45 and 62 of the 71 events, respectively. We find that the density of most switchback events decreases rather than increases, which indicates that proton heating inside the switchbacks is not caused by adiabatic compression, but is probably generated by nonadiabatic heating caused by field-particle interactions. Accordingly, the proton fluid entropy is greater inside the switchbacks than in the ambient solar wind.

A Study of Electron Forbush Decreases with a 3D SDE Numerical Model

Xi **Luo**^{1,2}, Marius S. Potgieter², Ming Zhang³, and Xueshang Feng¹

2018 ApJ 860 160 DOI [10.3847/1538-4357/aac5f2](https://doi.org/10.3847/1538-4357/aac5f2)

Because of the precise measurements of the cosmic ray electron flux by the PAMELA and AMS02, Electron Forbush decreases (Fd) have recently been observed for the first time. This serves as motivation to perform a numerical study of electron Forbush decreases with an advanced time-dependent, three-dimensional (3D) stochastic differential equation model, developed earlier to study proton Fd. The model includes a realistic interstellar electron spectrum reconstructed from Voyager observations, and diffusion and drift coefficients to reproduce the modulated spectrum observed by PAMELA in 2009. On the basis of this numerical model, electron Fd profiles for a range of rigidities are simulated. In addition, a systematic comparison between electron and proton Fd during different solar polarity epochs is performed. This approach gives insight into the rigidity dependence of the heliospheric diffusion coefficients and of drift effects over two magnetic field polarity cycles. We find that during an $A > 0$ epoch, the recovery time of a 1 GV proton Fd is remarkably shorter than the 1 GV electrons, whereas the electron Fd display a faster recovery during an $A < 0$ epoch. This model clearly predicts a charge-sign dependent effect in the recovery time of Fd but less so for their magnitude.

Two empirical models for short-term forecast of Kp

B. **Luo**, S. Liu, J. Go

Space Weather March **2017** Vol: 15, Pages: 503–516 DOI: 10.1002/2016SW001585

In this paper, two empirical models are developed for short-term forecast of the Kp index, taking advantage of solar wind-magnetosphere coupling functions proposed by the research community. Both models are based on the data for years 1995 to 2004. Model 1 mainly uses solar wind parameters as the inputs, while model 2 also utilizes the previous measured Kp value. Finally, model 1 predicts Kp with a linear correlation coefficient (r) of 0.91, a prediction efficiency (PE) of 0.81, and a root-mean-square (RMS) error of 0.59. Model 2 gives an r of 0.92, a PE of 0.84, and an RMS error of 0.57. The two models are validated through out-of-sample test for years 2005 to 2013, which also yields high forecast accuracy. Unlike in the other models reported in the literature, we are taking the response time of the magnetosphere to external solar wind at the Earth explicitly in the modeling. Statistically, the time delay in the models turns out to be about 30 min. By introducing this term, both the accuracy and lead time of the model forecast are improved. Through verification and validation, the models can be used in operational geomagnetic storm warnings with reliable performance.

A Numerical Study of Forbush Decreases with a 3D Cosmic-Ray Modulation Model Based on an SDE Approach

Xi [Luo](#)^{1,2}, Marius S. Potgieter², Ming Zhang³, and Xueshang Feng ¹
2017 ApJ 839 53

<http://sci-hub.cc/10.3847/1538-4357/aa6974>

Based on the reduced diffusion mechanism for producing Forbush decreases (Fds) in the heliosphere, we constructed a three-dimensional (3D) diffusion barrier, and by incorporating it into a stochastic differential equation (SDE) based time-dependent, cosmic-ray transport model, a 3D numerical model for simulating Fds is built and applied to a period of relatively quiet solar activity. This SDE model generally corroborates previous Fd simulations concerning the effects of the solar magnetic polarity, the tilt angle of the heliospheric current sheet (HCS), and cosmic-ray particle energy. Because the modulation processes in this 3D model are multi-directional, the barrier's geometrical features affect the intensity profiles of Fds differently. We find that both the latitudinal and longitudinal extent of the barrier have relatively fewer effects on these profiles than its radial extent and the level of decreased diffusion inside the disturbance. We find, with the 3D approach, that the HCS rotational motion causes the relative location from the observation point to the HCS to vary, so that a periodic pattern appears in the cosmic-ray intensity at the observing location. Correspondingly, the magnitude and recovery time of an Fd change, and the recovering intensity profile contains oscillation as well. Investigating the Fd magnitude variation with heliocentric radial distance, we find that the magnitude decreases overall and, additionally, that the Fd magnitude exhibits an oscillating pattern as the radial distance increases, which coincides well with the wavy profile of the HCS under quiet solar modulation conditions.

On the utility of flux rope models for CME magnetic structure below 30R_⊙

[Benjamin Lynch](#), [Nada Al-Haddad](#), [Wenyuan Yu](#), [Erika Palmerio](#), [Noé Lugaz](#)

Adv. Space Res 2022

<https://arxiv.org/pdf/2205.02144.pdf>

We present a comprehensive analysis of the three-dimensional magnetic flux rope structure generated during the Lynch et al. (2019) magnetohydrodynamic (MHD) simulation of a global-scale, 360 degree-wide streamer blowout coronal mass ejection (CME) eruption. We create both fixed and moving synthetic spacecraft to generate time series of the MHD variables through different regions of the flux rope CME. Our moving spacecraft trajectories are derived from the spatial coordinates of Parker Solar Probe's past encounters 7 and 9 and future encounter 23. Each synthetic time series through the simulation flux rope ejecta is fit with three different in-situ flux rope models commonly used to characterize the large-scale, coherent magnetic field rotations observed in a significant fraction of interplanetary CMEs (ICMEs). We present each of the in-situ flux rope model fits to the simulation data and discuss the similarities and differences between the model fits and the MHD simulation's flux rope spatial orientations, field strengths and rotations, expansion profiles, and magnetic flux content. We compare in-situ model properties to those calculated with the MHD data for both classic bipolar and unipolar ICME flux rope configurations as well as more problematic profiles such as those with a significant radial component to the flux rope axis orientation or profiles obtained with large impact parameters. We find general agreement among the in-situ flux rope fitting results for the classic profiles and much more variation among results for the problematic profiles. We also examine the force-free assumption for a subset of the flux rope models and quantify properties of the Lorentz force within MHD ejecta intervals. We conclude that the in-situ flux rope models are generally a decent approximation to the field structure, but all the caveats associated with in-situ flux rope models will still apply...

Sun to 1 AU propagation and evolution of a slow streamer-blowout coronal mass ejection

B. J. [Lynch](#), Y. Li, A. F. R. Thernisien, E. Robbrecht, G. H. Fisher, J. G. Luhmann, and A. Vourlidas
2010, JGR VOL. 115, A07106,

sci-hub.se/10.1029/2009JA015099

We present a comprehensive analysis of the evolution of the classic, slow streamer-blowout CME of **1 June 2008** observed by the STEREO twin spacecraft to infer relevant properties of the pre-eruption source region which includes a substantial portion of the coronal helmet streamer belt. The CME was directed $\sim 40^\circ$ East of the Sun-Earth line and the Heliospheric Imager observations are consistent with the CME propagating essentially radially to 1 AU. The elongation-time J-map constructed from the STEREO-A HI images tracks the arrival of two density peaks that bound the magnetic flux rope ICME seen at STEREO-B on 6 June 2008. From the STEREO-A elongation-time plots we measure the ICME flux rope radial size $R_c(t)$ and find it well approximated by the constant expansion value $V_{exp} = 24.5$ km/s obtained from the STEREO-B declining velocity profile within the magnetic cloud. The flux rope spatial orientation, determined by forward modeling fits to the STEREO COR2 and HI1 data, approaches the observed 1 AU flux rope orientation and suggests large-scale rotation during propagation, as predicted by recent numerical simulations. We compare the ICME

flux content to the PFSS model coronal field for Carrington Rotation 2070 and find sufficient streamer belt flux to account for the observed ICME poloidal/twist flux if reconnection during CME initiation process is responsible for the conversion of overlying field into the flux rope twist component in the standard fashion. However, the PFSS model field cannot account for the ICME toroidal/axial flux component. We estimate the field strength of the pre-eruption sheared/axial component in the low corona and the timescales required to accumulate this energized pre-eruption configuration via differential rotation and flux cancellation by supergranular diffusion at the polarity inversion line. We show that both mechanisms are capable of generating the desired shear component over time periods of roughly 1–2 months. We discuss the implications for slow streamer-blowout CMEs arising as a natural consequence of the corona's re-adjustment to the long term evolutionary driving of the photospheric fields.

Rotation of Coronal Mass Ejections During Eruption

B. J. **Lynch**, S. K. Antiochos, Y. Li, J. G. Luhmann, C. R. DeVore

E-print, March 2009; File; ApJ 697 1918-1927 doi: [10.1088/0004-637X/697/2/1918](https://doi.org/10.1088/0004-637X/697/2/1918)

<http://www.iop.org/EJ/toc/-alert=43190/0004-637X/697/2>

Understanding the connection between coronal mass ejections (CMEs) and their interplanetary counterparts (ICMEs) is one of the most important problems in solar-terrestrial physics. We calculate the rotation of erupting field structures predicted by numerical simulations of CME initiation via the magnetic breakout model. In this model the initial potential magnetic field has a multipolar topology and the system is driven by imposing a shear flow at the photospheric boundary. Our results yield insight on how to connect solar observations of the orientation of the filament or polarity inversion line (PIL) in the CME source region, the orientation of the CME axis as inferred from coronagraph images, and the ICME flux rope orientation obtained from in-situ measurements. We present the results of two numerical simulations that differ only in the direction of the applied shearing motions (i.e., the handedness of the sheared arcade systems and their resulting CME fields). In both simulations, eruptive flare reconnection occurs underneath the rapidly expanding sheared fields transforming the ejecta fields into 3-dimensional flux rope structures. As the erupting flux ropes propagate through the low corona (from 2–4 R_{\odot}) the right-handed breakout flux rope rotates clockwise and the left-handed breakout flux rope rotates counterclockwise, in agreement with recent observations of the rotation of erupting filaments. We find that by 3.5 R_{\odot} the average rotation angle between the flux rope axes and the active region PIL is approximately 50 degrees. We discuss the implications of these results for predicting, from the observed chirality of the pre-eruption filament and/or other properties of the CME source region, the direction and amount of rotation that magnetic flux rope structures will experience during eruption. We also discuss the implications of our results for CME initiation models.

Inferring the Solar Wind Velocity in the Outer Corona Based on Multiview Observations of Small-scale Transients by STEREO/COR2

Shaoyu **Lyu**^{1,2}, Yuming Wang^{1,2,3}, Xiaolei Li^{1,2}, Quanhao Zhang^{1,2,4}, and Jiajia Liu^{1,2,4}

2024 ApJ 962 170

<https://iopscience.iop.org/article/10.3847/1538-4357/ad1dd5/pdf>

Based on the Heliospheric Imager-1 images of the STEREO twin spacecraft, we established the CORrelation-Aided Reconstruction (CORAR) technique to locate and reconstruct the 3D structures of solar wind transients in interplanetary space. Here, we extend the CORAR method to images of COR2 on board STEREO to study the evolution of small-scale transients in the outer corona from 2010 January to May. We confirm that the transients can be located and reconstructed well by comparing the results with those of a self-similar expanding model. The speed distribution of the reconstructed transients generally shows the typical characteristics of the slow solar wind. We further study the sources of the transients on the Sun, and find that most reconstructed transients are located near the top of streamer belts or the heliospheric current sheet and can be tracked back to the boundaries of the closed-field and open-field regions along the field lines extrapolated by corona models. The formation mechanisms of these transients in the slow solar wind are also discussed. 2010/02/26, 2010 March 9

Coronal mass ejections as expanding force-free structures

Maxim **Lyutikov** and Konstantinos N. Gourgouliatos

Solar Physics, Online First, May 2011, File

We model solar coronal mass ejections (CMEs) as expanding force-free magnetic structures and study the self-similar dynamics of configurations with spatially constant α , where $J = \alpha B$, in spherical and cylindrical geometries, expanding spheromaks and Lundquist fields respectively. The field structures remain force-free, under the conventional non-relativistic assumption that the dynamical ef-

fects of the inductive electric fields can be neglected. While keeping the internal magnetic field structure of the stationary solutions, expansion leads to complicated internal velocities and rotation, caused by inductive electric fields. The structure depends only on overall radius $R(t)$ and rate of expansion $\dot{R}(t)$ measured at a given moment, and thus is applicable to arbitrary expansion laws. In case of cylindrical Lundquist fields, magnetic flux conservation requires that both axial and radial expansion proceed with equal rates. In accordance with observations, the model predicts that the maximum magnetic field is reached before the spacecraft reaches the geometric center of a CME.

Interplanetary Rotation of 2021 December 4 Coronal Mass Ejection on Its Journey to Mars

Mengxuan Ma, Liping Yang, Fang Shen, Chenglong Shen, Yutian Chi, Yuming Wang, Yufen Zhou, Man Zhang, Daniel Heyner, Uli Auster, Ingo Richter, Beatriz Sanchez-Cano

ApJ 976 183 2024

<https://arxiv.org/pdf/2410.20803>

<https://iopscience.iop.org/article/10.3847/1538-4357/ad8a5a/pdf>

The magnetic orientation of coronal mass ejections (CMEs) is of great importance to understand their space weather effects. Although many evidences suggest that CMEs can undergo significant rotation during the early phases of evolution in the solar corona, there are few reports that CMEs rotate in the interplanetary space. In this work, we use multi-spacecraft observations and a numerical simulation starting from the lower corona close to the solar surface to understand the CME event on **2021 December 4**, with an emphatic investigation of its rotation. This event is observed as a partial halo CME from the back side of the Sun by coronagraphs, and reaches the BepiColombo spacecraft and the MAVEN/Tianwen-1 as a magnetic flux rope-like structure. The simulation discloses that in the solar corona the CME is approximately a translational motion, while the interplanetary propagation process evidences a gradual change of axis orientation of the CME's flux rope-like structure. It is also found that the downside and the right flank of the CME moves with the fast solar wind, and the upside does in the slow-speed stream. The different parts of the CME with different speeds generate the nonidentical displacements of its magnetic structure, resulting in the rotation of the CME in the interplanetary space. Furthermore, at the right flank of the CME exists a corotating interaction region (CIR), which makes the orientation of the CME alter, and also deviates from its route due to the CIR. These results provide new insight on interpreting CMEs' dynamics and structures during their travelling through the heliosphere.

Magnetic Field Structure, Doppler Shift, and Intensity of Active Regions and Their Connections with the Solar Wind

Chi Ma¹, Hui Fu¹, Zhenghua Huang¹, Lidong Xia¹, Jinmei Zheng¹, Xinzheng Shi¹, and Bo Li¹
2022 ApJ 939 20

<https://iopscience.iop.org/article/10.3847/1538-4357/ac960f/pdf>

The properties of active regions and their connections with the solar wind are important issues. In this study, nine isolated active regions near the solar disk center were chosen. The relationships between blueshift, intensity, magnetic concentrated areas (MCAs), and the potential-field source-surface (PFSS) open magnetic field of active regions were analyzed. Whether an active region contributes to the solar wind was identified only based on the relationship between the properties of in situ solar wind and the large structure of the corona. Then the two phenomena (blueshift and PFSS open magnetic field) for inferring whether an active region contributes to the solar wind were tested. We find that the blueshift areas appear in all cases and the average Doppler speed ranges from -6 to -23 km s⁻¹. The blueshift areas generally root inside MCAs and are far from the neutral lines. The intensity of blueshift areas negatively correlates with the blueshift speed. Statistically, 10 of 16 blueshift areas are associated with the PFSS open magnetic field lines, and all 10 PFSS open magnetic field areas are accompanied by blueshift. We demonstrate that a polarity of an active region generally contributes to the solar wind if it is associated with a PFSS open magnetic field. There are 9 of 10 (13 of 16) PFSS open magnetic field areas (blueshift regions) associated with the solar wind. The results of this study should help determine the observation target of SPICE on board the Solar Orbiter whose scientific goal is connecting the Sun and the heliosphere.

Detecting the oscillation and propagation of the nascent dynamic solar wind structure at 2.6 solar radii using VLBI radio telescopes

Maoli Ma, Guifre Molera Calves, Giuseppe Cimo, Ming Xiong, +++

ApJ 2022

<https://arxiv.org/pdf/2210.10324.pdf>

Probing the solar corona is crucial to study the coronal heating and solar wind acceleration. However, the transient and inhomogeneous solar wind flows carry large-amplitude inherent Alfvén waves and turbulence, which make detection more difficult. We report the oscillation and propagation of the solar wind at 2.6 solar radii (R_s) by observation of China Tianwen and ESA Mars Express with radio telescopes. The observations were carried out on **Oct.9 2021**, when one coronal mass ejection (CME) passed across the ray paths of the telescope beams. We obtain the frequency fluctuations (FF) of the spacecraft signals from each individual telescope. Firstly, we visually identify the drift of the frequency spikes at a high spatial resolution of thousands of kilometers along the projected baselines. They are used as traces to estimate the solar wind velocity. Then we perform the cross-correlation analysis on the time series of FF from different telescopes. The velocity variations of solar wind structure along radial and tangential directions during the CME passage are obtained. The oscillation of tangential velocity confirms the detection of streamer wave. Moreover, at the tail of the CME, we detect the propagation of an accelerating fast field-aligned density structure indicating the presence of magnetohydrodynamic waves. This study confirms that the ground station-pairs are able to form particular spatial projection baselines with high resolution and sensitivity to study the detailed propagation of the nascent dynamic solar wind structure. **Oct.9 2021**

Coronal Mass Ejection Data Clustering and Visualization of Decision Trees

Ruizhe [Ma](#)¹, Rafal A. Angryk¹, Pete Riley², and Soukaina Filali Boubrahimi

2018 ApJS 236 14

<http://sci-hub.tw/10.3847/1538-4365/aab76f>

Coronal mass ejections (CMEs) can be categorized as either "magnetic clouds" (MCs) or non-MCs. Features such as a large magnetic field, low plasma-beta, and low proton temperature suggest that a CME event is also an MC event; however, so far there is neither a definitive method nor an automatic process to distinguish the two. Human labeling is time-consuming, and results can fluctuate owing to the imprecise definition of such events. In this study, we approach the problem of MC and non-MC distinction from a time series data analysis perspective and show how clustering can shed some light on this problem. Although many algorithms exist for traditional data clustering in the Euclidean space, they are not well suited for time series data. Problems such as inadequate distance measure, inaccurate cluster center description, and lack of intuitive cluster representations need to be addressed for effective time series clustering. Our data analysis in this work is twofold: clustering and visualization. For clustering we compared the results from the popular hierarchical agglomerative clustering technique to a distance density clustering heuristic we developed previously for time series data clustering. In both cases, dynamic time warping will be used for similarity measure. For classification as well as visualization, we use decision trees to aggregate single-dimensional clustering results to form a multidimensional time series decision tree, with averaged time series to present each decision. In this study, we achieved modest accuracy and, more importantly, an intuitive interpretation of how different parameters contribute to an MC event.

On the characteristic parameters of magnetic storms during two solar cycles

R. Monreal [MacMahon](#), C. Llop-Romero

JASTP, Volume 114, Pages 66–72, **2014**

Relationships between characteristic parameters of geomagnetic storms like the pressure corrected Dst index (Dst^*), the solar wind speed, the southward component of the interplanetary magnetic field B_S , and their associated times, were studied during two solar cycles and for approximately 300 storm events extracted from the OMNI database (1974–1996) to further analyze what drives Dst^* not only during storms but also during non-storm times.

Analyzing the whole data set, that is considering storm time and the less disturbed (non storm) times, we infer that outside the storm phases the dominant driver role is played by the solar wind speed and that its role during storms is usually not negligible. However, as expected, during the main and recovery phases of magnetic storms the driving parameter is the dawn-dusk component of the interplanetary electric field vB_S , where the main role is played by B_S . We found that the Dst^* peak grows monotonically with the peak of B_S . The duration time t_{BstB_S} that B_S remains over a certain threshold value grows linearly with the peak of Dst^* for weak, moderate and some intense storms. For more intense events the growth rate diminishes and probably vanishes. Significant differences appear when the correlation between the peaks of Dst^* and B_S is analyzed during the different solar cycle phases. That correlation and also the recurrence of our chosen storms have a periodic behavior, similar to the solar cycle. The most of storms are registered during the ascending phases of the solar cycle and sunspot maxima, however the higher correlations between the peaks of B_S and Dst^* are found during minima and ascending phases of the solar cycle.

Assessing the Quality of Models of the Ambient Solar Wind

Review

P. MacNeice, L. K. Jian, S. K. Antiochos, C. N. Arge, C. D. Bussy-Virat, M. L. DeRosa, B. V. Jackson, J. A. Linker, Z. Mikic, M. J. Owens, A. J. Ridley, P. Riley, N. Savani, I. Sokolov
Space Weather Volume 16, Issue 11, pp. 1644-1667 2018
<https://agupubs.onlinelibrary.wiley.com/doi/epdf/10.1029/2018SW002040>
<https://doi.org/10.1029/2018SW002040>

In this paper we present an assessment of the status of models of the global Solar Wind in the inner heliosphere. We limit our discussion to the class of models designed to provide solar wind forecasts, excluding those designed for the purpose of testing physical processes in idealized configurations. In addition, we limit our discussion to modeling of the ‘ambient’ wind in the absence of coronal mass ejections. In this assessment we cover use of the models both in forecast mode and as tools for scientific research. We present a brief history of the development of these models, discussing the range of physical approximations in use. We discuss the limitations of the data inputs available to these models and its impact on their quality. We also discuss current model development trends.

Validation of community models: 2. Development of a baseline using the Wang-Sheeley-Arge model

Peter MacNeice

Space Weather, 7, S12002, doi:10.1029/2009SW000489, 2009.

This paper is the second in a series providing independent validation of community models of the outer corona and inner heliosphere. Here I present a comprehensive validation of the Wang-Sheeley-Arge (WSA) model. These results will serve as a baseline against which to compare the next generation of comparable forecasting models. The WSA model is used by a number of agencies to predict Solar wind conditions at Earth up to 4 days into the future. Given its importance to both the research and forecasting communities, it is essential that its performance be measured systematically and independently. I offer just such an independent and systematic validation. I report skill scores for the model's predictions of wind speed and interplanetary magnetic field (IMF) polarity for a large set of Carrington rotations. The model was run in all its routinely used configurations. It ingests synoptic line of sight magnetograms. For this study I generated model results for monthly magnetograms from multiple observatories, spanning the Carrington rotation range from 1650 to 2074. I compare the influence of the different magnetogram sources and performance at quiet and active times. I also consider the ability of the WSA model to forecast both sharp transitions in wind speed from slow to fast wind and reversals in the polarity of the radial component of the IMF. These results will serve as a baseline against which to compare future versions of the model as well as the current and future generation of magnetohydrodynamic models under development for forecasting use.

Evolving solar wind flow properties of magnetic inversions observed by *Helios*

Allan R Macneil, Mathew J Owens, Robert T Wicks, Mike Lockwood

Monthly Notices of the Royal Astronomical Society, Volume 501, Issue 4, March 2021, Pages 5379–5392,
<https://doi.org/10.1093/mnras/staa3983>

In its first encounter at solar distances as close as $r = 0.16$ au, Parker Solar Probe observed numerous local reversals, or inversions, in the heliospheric magnetic field (HMF), which were accompanied by large spikes in solar wind speed. Both solar and in situ mechanisms have been suggested to explain the existence of HMF inversions in general. Previous work using *Helios 1*, covering 0.3–1 au, observed inverted HMF to become more common with increasing r , suggesting that some heliospheric driving process creates or amplifies inversions. This study expands upon these findings, by analysing inversion-associated changes in plasma properties for the same large data set, facilitated by observations of ‘strahl’ electrons to identify the unperturbed magnetic polarity. We find that many inversions exhibit anticorrelated field and velocity perturbations, and are thus characteristically Alfvénic, but many also depart strongly from this relationship over an apparent continuum of properties. Inversions depart further from the ‘ideal’ Alfvénic case with increasing r , as more energy is partitioned in the field, rather than the plasma, component of the perturbation. This departure is greatest for inversions with larger density and magnetic field strength changes, and characteristic slow solar wind properties. We find no evidence that inversions that stray further from ‘ideal’ Alfvénicity have different generation processes from those which are more Alfvénic. Instead, different inversion properties could be imprinted based on transport or formation within different solar wind streams.

Parker Solar Probe Observations of Suprathermal Electron Flux Enhancements Originating from Coronal Hole Boundaries

Allan R Macneil, Mathew J Owens, Laura Berčič, Adam J Finley

MNRAS Volume 498, Issue 4, Pages 5273–5283, 2020

<https://arxiv.org/pdf/2009.01558.pdf>
<https://doi.org/10.1093/mnras/staa2660>

Reconnection between pairs of solar magnetic flux elements, one open and the other a closed loop, is theorised to be a crucial process for both maintaining the structure of the corona and producing the solar wind. This 'interchange reconnection' is expected to be particularly active at the open-closed boundaries of coronal holes (CHs). Previous analysis of solar wind data at 1AU indicated that peaks in the flux of suprathermal electrons at slow-fast stream interfaces may arise from magnetic connection to the CH boundary, rather than dynamic effects such as compression. Further, offsets between the peak and stream interface locations are suggested to be the result of interchange reconnection at the source. As a preliminary test of these suggestions, we analyse two solar wind streams observed during the first Parker Solar Probe (PSP) perihelion encounter, each associated with equatorial CH boundaries (one leading and one trailing with respect to rotation). Each stream features a peak in suprathermal electron flux, the locations and associated plasma properties of which are indicative of a solar origin, in agreement with previous suggestions from 1AU observations. Discrepancies between locations of the flux peaks and other features suggest these peaks may too be shifted by source region interchange reconnection. Our interpretation of each event is compatible with a global pattern of open flux transport, although random footpoint motions or other explanations remain feasible. These exploratory results highlight future opportunities for statistical studies regarding interchange reconnection and flux transport at CH boundaries with modern near-Sun missions. **2018.11.05-13**

The Evolution of Inverted Magnetic Fields Through the Inner Heliosphere

Allan [Macneil](#), [Mathew Owens](#), [Robert Wicks](#), [Mike Lockwood](#), [Sarah Bentley](#), [Mathew Lang](#)

MNRAS Volume 494, Issue 3, May 2020, Pages 3642–3655, **2020**

<https://arxiv.org/pdf/2004.05449.pdf>

<https://doi.org/10.1093/mnras/staa951>

Local inversions are often observed in the heliospheric magnetic field (HMF), but their origins and evolution are not yet fully understood. Parker Solar Probe has recently observed rapid, Alfvénic, HMF inversions in the inner heliosphere, known as 'switchbacks', which have been interpreted as the possible remnants of coronal jets. It has also been suggested that inverted HMF may be produced by near-Sun interchange reconnection; a key process in mechanisms proposed for slow solar wind release. These cases suggest that the source of inverted HMF is near the Sun, and it follows that these inversions would gradually decay and straighten as they propagate out through the heliosphere. Alternatively, HMF inversions could form during solar wind transit, through phenomena such as velocity shears, draping over ejecta, or waves and turbulence. Such processes are expected to lead to a qualitatively radial evolution of inverted HMF structures. Using Helios measurements spanning 0.3-1 AU, we examine the occurrence rate of inverted HMF, as well as other magnetic field morphologies, as a function of radial distance A , and find that it continually increases. This trend may be explained by inverted HMF observed between 0.3-1 AU being primarily driven by one or more of the above in-transit processes, rather than created at the Sun. We make suggestions as to the relative importance of these different processes based on the evolution of the magnetic field properties associated with inverted HMF. We also explore alternative explanations outside of our suggested driving processes which may lead to the observed trend.

Radial Evolution of Sunward Strahl Electrons in the Inner Heliosphere

Allan R. [Macneil](#)¹ · Mathew J. Owens¹ · Mike Lockwood¹ · Štěpán Štverák^{2,3} · Christopher J. Owen⁴

Solar Physics volume **295**, Article number: 16 (**2020**)

<https://link.springer.com/content/pdf/10.1007/s11207-019-1579-3.pdf>

The heliospheric magnetic field (HMF) exhibits local inversions, in which the field apparently “bends back” upon itself. Candidate mechanisms to produce these inversions include various configurations of upstream interchange reconnection; either in the heliosphere, or in the corona where the solar wind is formed. Explaining the source of these inversions, and how they evolve in time and space, is thus an important step towards explaining the origins of the solar wind. Inverted heliospheric magnetic field lines can be identified by the anomalous sunward (i.e. inward) streaming of the typically anti-sunward propagating, field-aligned (or anti-aligned), beam of electrons known as the “strahl”. We test if the pitch angle distribution (PAD) properties of sunward-propagating strahl are different from those of outward strahl. We perform a statistical study of strahl observed by the Helios spacecraft, over heliocentric distances spanning $\approx 0.3 \approx 0.3 - 1$ AU. We find that sunward strahl PADs are broader and less intense than their outward directed counterparts; particularly at distances 0.3 – 0.75 AU. This is consistent with sunward strahl being subject to additional, path-length dependent, scattering in comparison to outward strahl. We conclude that the longer and more variable path from the Sun to the spacecraft, along inverted magnetic field, leads to this additional scattering. The results also suggest that the relative importance of scattering along this additional path length drops off with heliocentric distance. These results can be explained by a relatively simple, constant-rate, scattering process.

Active Region Modulation of Coronal Hole Solar Wind

Allan R. [Macneil](#)^{1,2}, Christopher J. Owen², Deborah Baker², David H. Brooks³, Louise K. Harra^{2,4,5}, David M. Long², and Robert T. Wicks^{2,6}

2019 ApJ 887 146

<https://doi.org/10.3847/1538-4357/ab5586>

Active regions (ARs) are a candidate source of the slow solar wind (SW), the origins of which are a topic of ongoing research. We present a case study that examines the processes by which SW is modulated in the presence of an AR in the vicinity of the SW source. We compare properties of SW associated with a coronal hole (CH)–quiet Sun boundary to SW associated with the same CH but one Carrington rotation later, when this region bordered the newly emerged NOAA AR 12532. Differences found in a range of in situ parameters are compared between these rotations in the context of source region mapping and remote sensing observations. Marked changes exist in the structure and composition of the SW, which we attribute to the influence of the AR on SW production from the CH boundary. These unique observations suggest that the features that emerge in the AR-associated wind are consistent with an increased occurrence of interchange reconnection during SW production, compared with the initial quiet Sun case. **21 Apr 2016 Hinode/ EIS Nugget, Mar 2020** http://solarb.mssl.ucl.ac.uk/SolarB/nuggets/nugget_2020apr.jsp
2016-03-24, 2016-04-20

Tests for coronal electron temperature signatures in suprathermal electron populations at 1 AU

Allan R. [Macneil](#), [Christopher J. Owen](#), [Robert T. Wicks](#)

Annales Geophysicae 2017

<https://arxiv.org/pdf/1711.02905.pdf>

The development of knowledge of how the coronal origin of the solar wind affects its in situ properties is one of the keys to understanding the relationship between the Sun and the heliosphere. In this paper, we analyse ACE/SWICS and WIND/3DP data spanning >12 years, and test properties of solar wind suprathermal electron distributions for the presence of signatures of the coronal temperature at their origin which may remain at 1AU. In particular we re-examine a previous suggestion that these properties correlate with the oxygen charge state ratio $O7+/O6+$; an established proxy for coronal electron temperature. We find only a very weak but variable correlation between measures of suprathermal electron energy content and $O7+/O6+$. The weak nature of the correlation leads us to conclude, in contrast to earlier results, that an initial relationship with core electron temperature has the possibility to exist in the corona, but that in most cases no strong signatures remain in the suprathermal electron distributions at 1AU. It can not yet be confirmed whether this is due to the effects of coronal conditions on the establishment of this relationship, or to the altering of the electron distributions by processing during transport in the solar wind en route to 1AU. Contrasting results for the halo and strahl population favours the latter interpretation. Confirmation of this will be possible using Solar Orbiter data (cruise and nominal mission phase) to test whether the weakness of the relationship persists over a range of heliocentric distances. If the correlation is found to strengthen when closer to the Sun, then this would indicate an initial relationship which is being degraded, perhaps by wave-particle interactions, en route to the observer.

Interaction of the Prominence Plasma within the Magnetic Cloud of an Interplanetary Coronal Mass Ejection with the Earth's Bow Shock

Hadi [Madanian](#)^{1,2}, Li-Jen Chen¹, Jonathan Ng^{1,3}, Michael J. Starkey⁴, Stephen A.

Fuselier⁴, Naoki Bessho^{1,3}, Daniel J. Gershman¹, and Terry Z. Liu⁵

2024 ApJ 976 219

<https://iopscience.iop.org/article/10.3847/1538-4357/ad8579/pdf>

The magnetic cloud within an interplanetary coronal mass ejection (ICME) is characterized by high magnetic field intensities. In this study, we investigate the interaction of a magnetic cloud carrying a density structure with the Earth's bow shock during the ICME event on **2023 April 24**. Elevated abundances of cold protons and heavier ions, namely, alpha particles and singly charged helium ions, associated with the prominence plasma are observed within this structure. The plasma downstream of the bow shock exhibits an irregular compression pattern, which could be due to the presence of heavy ions. Heavy ions carry a significant fraction of the upstream flow energy; however, due to their different mass-per-charge ratio and rigidity, they are less scattered by the electromagnetic and electrostatic waves at the shock. We find that downstream of the shock, while the ion thermal energy is only a small fraction of the background magnetic energy, nevertheless increased ion fluxes reduce the characteristic wave speeds in that region. As such, we observe a transition state of an unstable bow shock in which the plasma flow is super Alfvénic both upstream and downstream of the bow shock. Our findings help with the understanding of the intense space weather impacts of such events.

Could switchbacks originate in the lower solar atmosphere? II. Propagation of switchbacks in the solar corona

Norbert **Magyar**, [Dominik Utz](#), [Robertus Erdélyi](#), [Valery M. Nakariakov](#)

ApJ 2021

<https://arxiv.org/pdf/2104.10126.pdf>

The magnetic switchbacks observed recently by the Parker Solar Probe have raised the question about their nature and origin. One of the competing theories of their origin is the interchange reconnection in the solar corona. In this scenario, switchbacks are generated at the reconnection site between open and closed magnetic fields, and are either advected by an upflow or propagate as waves into the solar wind. In this paper we test the wave hypothesis, numerically modelling the propagation of a switchback, modelled as an embedded Alfvén wave packet of constant magnetic field magnitude, through the gravitationally stratified solar corona with different degrees of background magnetic field expansion. While switchbacks propagating in a uniform medium with no gravity are relatively stable, as reported previously, we find that gravitational stratification together with the expansion of the magnetic field act in multiple ways to deform the switchbacks. These include WKB effects, which depend on the degree of magnetic field expansion, and also finite-amplitude effects, such as the symmetry breaking between nonlinear advection and the Lorentz force. In a straight or radially expanding magnetic field the propagating switchbacks unfold into waves that cause minimal magnetic field deflections, while a super-radially expanding magnetic field aids in maintaining strong deflections. Other important effects are the mass uplift the propagating switchbacks induce and the reconnection and drainage of plasmoids contained within the switchbacks. In the Appendix, we examine a series of setups with different switchback configurations and parameters, which broaden the scope of our study.

Could switchbacks originate in the lower solar atmosphere? I. Formation mechanisms of switchbacks

Norbert **Magyar**, [Dominik Utz](#), [Robertus Erdélyi](#), [Valery M. Nakariakov](#)

ApJ 2021

<https://arxiv.org/pdf/2103.03726.pdf>

The recent rediscovery of magnetic field switchbacks or deflections embedded in the solar wind flow by the Parker Solar Probe mission lead to a huge interest in the modelling of the formation mechanisms and origin of these switchbacks. Several scenarios for their generation were put forth, ranging from lower solar atmospheric origins by reconnection, to being a manifestation of turbulence in the solar wind, and so on. Here we study some potential formation mechanisms of magnetic switchbacks in the lower solar atmosphere, using three-dimensional magneto-hydrodynamic (MHD) numerical simulations. The model is that of an intense flux tube in an open magnetic field region, aiming to represent a magnetic bright point opening up to an open coronal magnetic field structure, e.g. a coronal hole. The model is driven with different plasma flows in the photosphere, such as a fast up-shooting jet, as well as shearing flows generated by vortex motions or torsional oscillations. In all scenarios considered, we witness the formation of magnetic switchbacks in regions corresponding to chromospheric heights. Therefore, photospheric plasma flows around the foot-points of intense flux tubes appear to be suitable drivers for the formation of magnetic switchbacks in the lower solar atmosphere. Nevertheless, these switchbacks do not appear to be able to enter the coronal heights of the simulation in the present model. In conclusion, based on the presented simulations, switchbacks measured in the solar wind are unlikely to originate from photospheric or chromospheric dynamics.

Three-dimensional simulations of the inhomogeneous Low Solar Wind

N. **Magyar**, [V. M. Nakariakov](#)

ApJ 2020

<https://arxiv.org/pdf/2012.00811.pdf>

In the near future, Parker Solar Probe will put theories about the dynamics and nature of the transition between the solar corona and the solar wind to stringent tests. The most popular mechanism aimed to explain the dynamics of the nascent solar wind, including its heating and acceleration is magnetohydrodynamic (MHD) turbulence. Most of the previous models focus on nonlinear cascade induced by interactions of outgoing Alfvén waves and their reflections, ignoring effects that might be related to perpendicular structuring of the solar coronal plasma, despite overwhelming evidence for it. In this paper, for the first time, we analyse through 3D MHD numerical simulations the dynamics of the perpendicularly structured solar corona and solar wind, from the low corona to 15 R_{\odot} . We find that background structuring has a strong effect on the evolution of MHD turbulence, on much faster time scales than in the perpendicularly homogeneous case. On time scales shorter than nonlinear times, linear effects related to phase mixing

result in a $1/f$ perpendicular energy spectrum. As the turbulent cascade develops, we observe a perpendicular (parallel) energy spectrum with the power law index of $-3/2$ or $-5/3$ (-2), a steeper perpendicular magnetic field than velocity spectrum, and a strong build-up of negative residual energy. We conclude that the turbulence is most probably generated by the self-cascade of the driven transverse kink waves, referred to previously as 'uniturbulence', which might represent the dominant nonlinear energy cascade channel in the pristine solar wind.

Toroidal modified Miller-Turner CME model in EUHFORIA: II. Validation and comparison with flux rope and spheromak

Anwasha **Maharana**, [Luis Linan](#), [Stefaan Poedts](#), [Jasmina Magdalenic](#)

A&A 691, A146 2024

<https://arxiv.org/pdf/2408.03882>

<https://www.aanda.org/articles/aa/pdf/2024/11/aa50459-24.pdf>

<https://doi.org/10.1051/0004-6361/202450459>

Context. Rising concerns about the impact of space-weather-related disruptions demand modelling and reliable forecasting of coronal mass ejection (CME) impacts.

Aims. In this study, we demonstrate the application of the modified Miller-Turner (mMT) model implemented within European Heliospheric FORecasting Information Asset (EUHFORIA) in forecasting the geo-effectiveness of observed coronal mass ejection (CME) events in the heliosphere. Our goal is to develop a model that not only has a global geometry, in order to improve overall forecasting, but is also fast enough for operational space-weather forecasting.

Methods. We test the original full torus implementation and introduce a new three-fourths Torus version called the Horseshoe CME model. This new model has a more realistic CME geometry, and overcomes the inaccuracies of the full torus geometry. We constrain the torus geometrical and magnetic field parameters using observed signatures of the CMEs before, during, and after the eruption. We perform EUHFORIA simulations for two validation cases – the isolated CME event of **12 July 2012** and the CME–CME interaction event of **8–10 September 2014**. We performed an assessment of the model's capability to predict the most important B_z component using the advanced dynamic time-warping (DTW) technique.

Results. The Horseshoe model predictions of CME arrival time and geo-effectiveness for both validation events compare well with the observations and are weighed against the results obtained with the spheromak and FRi3D models, which were already available in EUHFORIA.

Conclusions. The runtime of the Horseshoe model simulations is close to that of the spheromak model, which is suitable for operational space weather forecasting. However, the capability of the magnetic field prediction at 1 AU of the Horseshoe model is close to that of the FRi3D model. In addition, we demonstrate that the Horseshoe CME model can be used for simulating successive CMEs in EUHFORIA, overcoming a limitation of the FRi3D model.

12-16 July 2012, 10-13 September 2014

Employing the coupled EUHFORIA-OpenGGCM model to predict CME geoeffectiveness

Anwasha **Maharana**, [W. Douglas Cramer](#), [Evangelia Samara](#), [Camilla Scolini](#), [Joachim Raeder](#), [Stefaan Poedts](#)

Space Weather 2024

<https://arxiv.org/pdf/2403.19873.pdf>

European Heliospheric FORecasting Information Asset (EUHFORIA) is a physics-based data-driven solar wind and CME propagation model designed for space weather forecasting and event analysis investigations. Although EUHFORIA can predict the solar wind plasma and magnetic field properties at Earth, it is not equipped to quantify the geoeffectiveness of the solar transients in terms of the geomagnetic indices like the disturbance storm time (Dst) index and the auroral indices that quantify the impact of the magnetized plasma encounters on Earth's magnetosphere. Therefore, we couple EUHFORIA with the Open Geospace General Circulation Model (OpenGGCM), a magnetohydrodynamic model of the response of Earth's magnetosphere, ionosphere, and thermosphere, to transient solar wind characteristics. In this coupling, OpenGGCM is driven by the solar wind and interplanetary magnetic field obtained from EUHFORIA simulations to produce the magnetospheric and ionospheric response to the CMEs. This coupling is validated with two observed geoeffective CME events driven with the spheromak flux-rope CME model. We compare these simulation results with the indices obtained from OpenGGCM simulations driven by the measured solar wind data from spacecraft. We further employ the dynamic time warping (DTW) technique to assess the model performance in predicting Dst. The main highlight of this study is to use EUHFORIA simulated time series to predict the Dst and auroral indices 1 to 2 days in advance, as compared to using the observed solar wind data at L1, which only provides predictions 1 to 2 hours before the actual impact. **2012-07-12-14, 2017-09-04-06**

Updates on the FRi3D CME model in EUHFORIA

Anwasha [Maharana](#), [Karel Plets](#), [Alexey Isavnin](#), [Stefaan Poedts](#)

A&A 2023

<https://arxiv.org/pdf/2310.11402.pdf>

A magnetised flux rope model, "Flux Rope in 3D" (FRi3D) is used in the framework of European Heliospheric Forecasting Information Asset (EUHFORIA) for studying the evolution and propagation of coronal mass ejections (CME). In this paper, we rectify the mistake in the mentioned magnetic field profile of the FRi3D model used in Maharana et al., 2022, and we clarify the actual profile used in that work. In addition, we provide the recent updates introduced to the FRi3D implementation in EUHFORIA like optimising the "ai.fri3d" python package to reduce computational time and exploring different CME leg disconnection methods to make the numerical implementation more stable.

Rotation and interaction of the September 8 and 10, 2014 CMEs tested with EUHFORIA

Anwasha [Maharana](#), [Camilla Scolini](#), [Brigitte Schmieder](#), [Stefaan Poedts](#)

A&A 675, A136 2023

<https://arxiv.org/pdf/2305.06881.pdf>

Aim: We aim to show how interactions undergone by a CME in the corona and heliosphere can play a significant role in altering its geoeffectiveness predicted at the time of its eruption. To do so, we consider a case study of two successive CMEs launched from the active region NOAA 12158 in early September 2014. The second CME was predicted to be extensively geoeffective based on the remote-sensing observations of the source region. However, in situ measurements at 1 au recorded only a short-lasting weak negative Bz component followed by a prolonged positive Bz component.

Methods: The European Heliosphere FORecasting Information Asset (EUHFORIA) is used to perform a self-consistent 3D MHD data-driven simulation of the two CMEs in the heliosphere. First, the ambient solar wind is modelled, followed by the time-dependent injection of CME1 with the LFF spheromak and CME2 with the "Flux Rope in 3D" (FRi3D) model. The initial conditions of the CMEs are determined by combining observational insights near the Sun, fine-tuned to match the in situ observations near 1 au, and additional numerical experiments of each individual CME.

Results: By introducing CME1 before CME2 in the EUHFORIA simulation, we modelled the negative Bz component in the sheath region ahead of CME2 whose formation can be attributed to the interaction between CME1 and CME2. To reproduce the positive Bz component in the magnetic ejecta of CME2, we had to initialise CME2 with an orientation determined at 0.1 au and consistent with the orientation interpreted at 1 au, instead of the orientation observed during its eruption.

Conclusions: EUHFORIA simulations suggest the possibility of a significant rotation of CME2 in the low corona in order to explain the in situ observations at 1 au. Coherent magnetic field rotations with enhanced strength (potentially geoeffective) can be formed in the sheath region as a result of interactions between two CMEs in the heliosphere even if the individual CMEs are not geoeffective. **8-10 Sep 2014, 10-11 Sep 2014**

Implementation and validation of the FRi3D flux rope model in EUHFORIA

[Anwasha Maharana](#), [Alexey Isavnin](#), [Camilla Scolini](#), [Nicolas Wijsen](#), [Luciano Rodriguez](#), [Marilena Mierla](#), [Jasmina Magdalenic](#), [Stefaan Poedts](#)

Advances in Space Research 70, 1641 (2022)

<https://arxiv.org/pdf/2207.06707.pdf>

The Flux Rope in 3D (FRi3D, Isavnin, 2016), a coronal mass ejection (CME) model with global three-dimensional (3D) geometry, has been implemented in the space weather forecasting tool EUHFORIA (Pomoell and Poedts, 2018). By incorporating this advanced flux rope model in EUHFORIA, we aim to improve the modelling of CME flank encounters and, most importantly, the magnetic field predictions at Earth. After using synthetic events to showcase FRi3D's capabilities of modelling CME flanks, we optimize the model to run robust simulations of real events and test its predictive capabilities. We perform observation-based modelling of the halo CME event that erupted on **12 July 2012**. The geometrical input parameters are constrained using the forward modelling tool included in FRi3D with additional flux rope geometry flexibilities as compared to the pre-existing models. The magnetic field input parameters are derived using the differential evolution algorithm to fit FRi3D parameters to the in situ data at 1 AU. An observation-based approach to constrain the density of CMEs is adopted, in order to achieve a better estimation of mass corresponding to the FRi3D geometry. The CME is evolved in EUHFORIA's heliospheric domain and a comparison of FRi3D's predictive performance with the previously implemented spheromak CME in EUHFORIA is presented. For this event, FRi3D improves the modelling of the total magnetic field magnitude and Bz at Earth by ~30% and ~70%, respectively. Moreover, we compute the expected geoeffectiveness of the storm at Earth using an empirical Dst model and find that

the FRi3D model improves the predictions of minimum Dst by ~20% as compared to the spheromak CME model. Finally, we discuss the limitations of the current implementation of FRi3D in EUHFORIA and propose possible improvements.

Tracking the CME-driven Shock Wave on 2012 March 5 and Radio Triangulation of Associated Radio Emission

J. **Magdaleníć**¹, C. Marqué¹, V. Krupar², M. Mierla^{1,3}, A. N. Zhukov^{1,4}, L. Rodriguez¹, M. Maksimović⁵, and B. Cecconi

2014 ApJ 791 115

We present a multiwavelength study of the **2012 March 5** solar eruptive event, with an emphasis on the radio triangulation of the associated radio bursts. The main points of the study are reconstruction of the propagation of shock waves driven by coronal mass ejections (CMEs) using radio observations and finding the relative positions of the CME, the CME-driven shock wave, and its radio signatures. For the first time, radio triangulation is applied to different types of radio bursts in the same event and performed in a detailed way using goniopolarimetric observations from STEREO/Waves and WIND/Waves spacecraft. The event on 2012 March 5 was associated with a X1.1 flare from the NOAA AR 1429 situated near the northeast limb, accompanied by a full halo CME and a radio event comprising long-lasting interplanetary type II radio bursts. The results of the three-dimensional reconstruction of the CME (using SOHO/LASCO, STEREO COR, and HI observations), and modeling with the ENLIL cone model suggest that the CME-driven shock wave arrived at 1 AU at about 12:00 UT on March 7 (as observed by SOHO/CELIAS). The results of radio triangulation show that the source of the type II radio burst was situated on the southern flank of the CME. We suggest that the interaction of the shock wave and a nearby coronal streamer resulted in the interplanetary type II radio emission.

Could Switchbacks Originate in the Lower Solar Atmosphere? II. Propagation of Switchbacks in the Solar Corona

Norbert **Magyar**^{1,2}, Dominik Utz^{3,4}, Robertus Erdélyi^{5,6,7}, and Valery M. Nakariakov^{1,8}

2021 ApJ 914 8

<https://iopscience.iop.org/article/10.3847/1538-4357/abfa98/pdf>

<https://doi.org/10.3847/1538-4357/abfa98>

The magnetic switchbacks observed recently by the Parker Solar Probe have raised the question about their nature and origin. One of the competing theories of their origin is the interchange reconnection in the solar corona. In this scenario, switchbacks are generated at the reconnection site between open and closed magnetic fields, and are either advected by an upflow or propagate as waves into the solar wind. In this paper we test the wave hypothesis, numerically modeling the propagation of a switchback, modeled as an embedded Alfvén wave packet of constant magnetic field magnitude, through the gravitationally stratified solar corona with different degrees of background magnetic field expansion. While switchbacks propagating in a uniform medium with no gravity are relatively stable, as reported previously, we find that gravitational stratification together with the expansion of the magnetic field act in multiple ways to deform the switchbacks. These include WKB effects, which depend on the degree of magnetic field expansion, and also finite-amplitude effects, such as the symmetry breaking between nonlinear advection and the Lorentz force. In a straight or radially expanding magnetic field the propagating switchbacks unfold into waves that cause minimal magnetic field deflections, while a super-radially expanding magnetic field aids in maintaining strong deflections. Other important effects are the mass uplift the propagating switchbacks induce and the reconnection and drainage of plasmoids contained within the switchbacks. In the Appendix, we examine a series of setups with different switchback configurations and parameters, which broaden the scope of our study.

Could Switchbacks Originate in the Lower Solar Atmosphere? I. Formation Mechanisms of Switchbacks

Norbert **Magyar**^{1,2}, Dominik Utz^{3,4}, Robertus Erdélyi^{5,6,7}, and Valery M. Nakariakov^{1,8}

2021 ApJ 911 75

<https://arxiv.org/pdf/2103.03726.pdf>

<https://doi.org/10.3847/1538-4357/abec49>

The recent rediscovery of magnetic field switchbacks or deflections embedded in the solar wind flow by the Parker Solar Probe mission lead to a huge interest in the modeling of the formation mechanisms and origin of these switchbacks. Several scenarios for their generation were put forth, ranging from lower solar atmospheric origins by reconnection, to being a manifestation of turbulence in the solar wind, and so on. Here we study some potential formation mechanisms of

magnetic switchbacks in the lower solar atmosphere, using three-dimensional magnetohydrodynamic (MHD) numerical simulations. The model is that of an intense flux tube in an open magnetic field region, aiming to represent a magnetic bright point opening up to an open coronal magnetic field structure, e.g., a coronal hole. The model is driven with different plasma flows in the photosphere, such as a fast up-shooting jet, as well as shearing flows generated by vortex motions or torsional oscillations. In all scenarios considered, we witness the formation of magnetic switchbacks in regions corresponding to chromospheric heights. Therefore, photospheric plasma flows around the foot-points of intense flux tubes appear to be suitable drivers for the formation of magnetic switchbacks in the lower solar atmosphere. Nevertheless, these switchbacks do not appear to be able to enter the coronal heights of the simulation in the present model. In conclusion, based on the presented simulations, switchbacks measured in the solar wind are unlikely to originate from photospheric or chromospheric dynamics.

Employing the Coupled EUHFORIA-OpenGGCM Model to Predict CME Geoeffectiveness

Anwsha Maharana, [W. Douglas Cramer](#), [Evangelia Samara](#), [Camilla Scolini](#), [Joachim Raeder](#), [Stefaan Poedts](#)

Space Weather [Volume22, Issue5](#) May 2024 e2023SW003715

<https://doi.org/10.1029/2023SW003715>

<https://agupubs.onlinelibrary.wiley.com/doi/epdf/10.1029/2023SW003715> File

EUropean Heliospheric FORecasting Information Asset (EUHFORIA) is a physics-based data-driven solar wind and coronal mass ejections (CMEs) propagation model designed for space weather forecasting and event analysis investigations. Although EUHFORIA can predict the solar wind plasma and magnetic field properties at Earth, it is not equipped to quantify the geo-effectiveness of the solar transients in terms of geomagnetic indices like the disturbance storm time (Dst) index and the auroral indices, that quantify the impact of the magnetized plasma encounters on Earth's magnetosphere. Therefore, we couple EUHFORIA with the Open Geospace General Circulation Model (OpenGGCM), a magnetohydrodynamic model of the response of Earth's magnetosphere, ionosphere, and thermosphere to transient solar wind characteristics. In this coupling, OpenGGCM is driven by the solar wind and interplanetary magnetic field obtained from EUHFORIA simulations to produce the magnetospheric and ionospheric response to the CMEs. This coupling is validated with two observed geo-effective CME events driven with the spheromak flux-rope CME model. We compare these simulation results with the indices obtained from OpenGGCM simulations driven by the measured solar wind data from spacecraft. We further employ the dynamic time warping (DTW) technique to assess the model performance in predicting Dst. The main highlight of this study is to use EUHFORIA simulated time series to predict the Dst and auroral indices 1–2 days in advance, as compared to using the observed solar wind data at L1, which only provides predictions 1–2 hr before the actual impact. **2 July 2012, 4–6 September 2017**

Magnetohydrodynamic Modeling of the Solar Wind Key Parameters and Current Sheets in the Heliosphere: Radial and Solar Cycle Evolution

E. V. [Maiewski](#)^{1,2}, R. A. Kislov^{2,3}, O. V. Khabarova³, H. V. Malova^{2,4}, V. Yu. Popov^{1,5}, A. A. Petrukovich², and L. M. Zelenyi²

2020 ApJ 892 12

<https://doi.org/10.3847/1538-4357/ab712c>

We develop an axisymmetric numerical MHD model that allows us to investigate the spatial characteristics of the interplanetary magnetic field (IMF) and key solar wind plasma parameters from 20 to 400 solar radii over all heliolatitudes. The study is aimed at an analysis of the evolution of the spatial structure of the heliosphere through the solar cycle. We consider various combinations of the relative input of the quadrupole and dipole harmonics of the solar magnetic field to imitate the solar cycle. Self-consistent solutions for the IMF, electric current, solar wind speed, density, thermal pressure, and temperature in the solar wind are obtained. The spatial evolution of the IMF and properties of quasi-stationary current sheets (QCSs) are analyzed during different phases of the solar cycle. It is shown that a classic low-latitude heliospheric current sheet is formed in the solar wind as a part of the system of longitudinal and latitudinal electric currents symmetric in the northern and southern hemispheres only during solar minimum. While the quadrupole magnetic field increases, the second QCS appears. The model successfully describes a smooth transition from the state of the fast solar wind at high heliolatitudes and the slow solar wind at low heliolatitudes at solar minimum to the solar wind speed of the same values in a wide range of heliolatitudes at solar maximum. It reproduces the actively debated phenomenon of the south–north asymmetry of the IMF in the heliosphere and shows the distribution of thermal plasma parameters consistent with observations.

The radial speed-expansion speed relation for Earth-directed CMEs

P. **Mäkelä**, N. Gopalswamy, S. Yashiro

Space Weather Volume 14, Issue 5 May 2016 Pages 368–378 **File**

<http://cdaw.gsfc.nasa.gov/publications/makela/makela2016SpaceWeather.pdf>

Earth-directed coronal mass ejections (CMEs) are the main drivers of major geomagnetic storms. Therefore, a good estimate of the disturbance arrival time at Earth is required for space weather predictions. The STEREO and SOHO spacecraft were viewing the Sun in near quadrature during January 2010 to September 2012, providing a unique opportunity to study the radial speed (Vrad)-expansion speed (Vexp) relationship of Earth-directed CMEs. This relationship is useful in estimating the Vrad of Earth-directed CMEs, when they are observed from Earth view only. We selected **19 Earth-directed CMEs** observed by the Large Angle and Spectrometric Coronagraph (LASCO)/C3 coronagraph on SOHO and the Sun Earth Connection Coronal and Heliospheric Investigation (SECCHI)/COR2 coronagraph on STEREO during January 2010 to September 2012. We found that of the three tested geometric CME models the full ice-cream cone model of the CME describes best the Vrad-Vexp relationship, as suggested by earlier investigations. We also tested the prediction accuracy of the empirical shock arrival (ESA) model proposed by Gopalswamy et al. (2005a), while estimating the CME propagation speeds from the CME expansion speeds. If we use STEREO observations to estimate the CME width required to calculate the Vrad from the Vexp measurements, the mean absolute error (MAE) of the shock arrival times of the ESA model is 8.4 h. If the LASCO measurements are used to estimate the CME width, the MAE still remains below 17 h. Therefore, by using the simple Vrad-Vexp relationship to estimate the Vrad of the Earth-directed CMEs, the ESA model is able to predict the shock arrival times with accuracy comparable to most other more complex models.

Table 1. List of 19 Earth-directed CMEs driving a shock (2010-2012).

Coronal Hole Influence on the Observed Structure of Interplanetary CMEs

Pertti **Makela**, Nat Gopalswamy, Hong Xie, Amaal A. Mohamed, Sachiko Akiyama, Seiji Yashiro

E-print, Jan 2013, **File**; Solar Phys. Volume 284, Issue 1, pp 59-75, 2013

We report on the coronal hole (CH) influence on the **54 magnetic cloud (MC) and non-MC associated coronal mass ejections (CMEs)** selected for studies during the Coordinated Data Analysis Workshops (CDAWs) focusing on the question if all CMEs are flux ropes. All selected CMEs originated from source regions located between longitudes 15E-15W. Xie, Gopalswamy, and St. Cyr (2013, Solar Phys., doi:10.1007/s11207-012-0209-0) found that these MC and non-MC associated CMEs are on average deflected towards and away from the Sun-Earth line respectively. We used a CH influence parameter (CHIP) that depends on the CH area, average magnetic field strength, and distance from the CME source region to describe the influence of all on-disk CHs on the erupting CME. We found that for CHIP values larger than 2.6 G the MC and non-MC events separate into two distinct groups where MCs (non-MCs) are deflected towards (away) from the disk center. Division into two groups was also observed when the distance to the nearest CH was less than 3.2×10^5 km. At CHIP values less than 2.6 G or at distances of the nearest CH larger than 3.2×10^5 km the deflection distributions of the MC and non-MCs started to overlap, indicating diminishing CH influence. These results give support to the idea that all CMEs are flux ropes, but those observed to be non-MCs at 1 AU could be deflected away from the Sun-Earth line by nearby CHs, making their flux rope structure unobservable at 1 AU.

Table; 18 October 1999, 6 December 1997, 9 April 2001, 12 May 1997, 13 April 1999, 17 February 2000, 25 July 2000 MC, 15 March 2002 MC

Convolutional Neural Networks for Predicting the Strength of the Near-Earth Magnetic Field Caused by Interplanetary Coronal Mass Ejections

Anna **Malanushenko**^{1*}, Natasha Flyer² and Sarah Gibson¹

Front. Astron. Space Sci., 2020

<https://doi.org/10.3389/fspas.2020.00062>

<https://www.frontiersin.org/articles/10.3389/fspas.2020.00062/full>

In this paper, we explore the potential of neural networks for making space weather predictions based on near-Sun observations. Our second goal is to determine the extent to which coronal polarimetric observations of erupting structures near the Sun encode sufficient information to predict the impact these structures will have on Earth. In particular, we focus on predicting the maximal southward component of the magnetic field (“-Bz”) inside an interplanetary coronal mass ejection (ICME) as it impacts the Earth. We use Gibson & Low (G&L) self-similarly expanding flux rope model ([Gibson and Low, 1998](#)) as a first test for the project, which allows to consider CMEs with varying location, orientation, size, and morphology. We vary 5 parameters of the model to alter these CME properties, and generate a large database of synthetic CMEs (over 36k synthetic events). For each model CME, we synthesize near-Sun observations, as seen from an observer in quadrature (assuming the CME is directed earthwards), of either three

components of the vector magnetic field, (B_x , B_y , B_z) (“Experiment 1”), or of synthetic Stokes images, (L/I , A_z , V/I) (“Experiment 2”). We then allow the flux rope to expand and record $\max\{-B_z\}$ as the ICME passes 1AU. We further conduct two separate machine learning experiments and develop two different regression-based deep convolutional neural networks (CNNs) to predict $\max\{-B_z\}$ based on these two kinds of the near-Sun input data. Experiment 1 is a test which we do as a proof of concept, to see if a 3-channel CNN (hereafter CNN1), similar to those used in RGB image recognition, can reproduce the results of the self-similar (i.e., scale-invariant) expansion of the G&L model. Experiment 2 is less trivial, as Stokes vector is not linearly related to B , and the line-of-sight integration in the optically thin corona presents additional difficulties for interpreting the signal. This second CNN (hereafter CNN2), although resembling CNN1 in Experiment 1, will have a different number of layers and set of hyperparameters due to a much more complicated mapping between the input and output data. We find that, given three components of B , CNN1 can predict $\max\{-B_z\}$ with 97% accuracy, and for three components of the Stokes vector as input, CNN2 can predict $\max\{-B_z\}$ with 95%, both measured in the relative root square error.

Electron Bernstein waves and narrowband plasma waves near the electron cyclotron frequency in the near-Sun solar wind

D. M. **Malaspina**^{1,2}, L. B. Wilson III³, R. E. Ergun^{1,2}, S. D. Bale^{4,5}, J. W. Bonnell⁴, K. Goodrich⁴, K. Goetz⁶, P. R. Harvey⁴, R. J. MacDowall³, M. Pulupa⁴, J. Halekas⁷, A. Case⁸, J. C. Kasper⁹, D. Larson⁴, M. Stevens⁸ and P. Whittlesey⁴

A&A 650, A97 (2021)

<https://doi.org/10.1051/0004-6361/202140449>

<https://www.aanda.org/articles/aa/pdf/2021/06/aa40449-21.pdf>

Context. Recent studies of the solar wind sunward of 0.25 AU reveal that it contains quiescent regions, with low-amplitude plasma and magnetic field fluctuations, and a magnetic field direction similar to the Parker spiral. The quiescent regions are thought to have a more direct magnetic connection to the solar corona than other types of solar wind, suggesting that waves or instabilities in the quiescent regions are indicative of the early evolution of the solar wind as it escapes the corona. The quiescent solar wind regions are highly unstable to the formation of plasma waves near the electron cyclotron frequency (f_{ce}).

Aims. We examine high time resolution observations of these waves in an effort to understand their impact on electron distribution functions of the quiescent near-Sun solar wind.

Methods. High time resolution waveform captures of near- f_{ce} waves were examined to determine variations of their amplitude and frequency in time as well as their polarization properties.

Results. We demonstrate that the near- f_{ce} wave intervals contain several distinct wave types, including electron Bernstein waves and extremely narrowband waves that are highly sensitive to the ambient magnetic field orientation. Using the properties of these waves, we suggest possible plasma wave mode classifications and possible instabilities that generate these waves. The results of this analysis indicate that these waves may modify the cold core of the electron distribution functions in the quiescent near-Sun solar wind.

Plasma Waves near the Electron Cyclotron Frequency in the near-Sun Solar Wind

David M. **Malaspina**, [Jasper Halekas](#), [Laura Bercic](#), [Davin Larson](#),

ApJ 2019

<https://arxiv.org/pdf/1912.06793.pdf>

Data from the first two orbits of the Sun by Parker Solar Probe reveal that the solar wind sunward of 50 solar radii is replete with plasma waves and instabilities. One of the most prominent plasma wave power enhancements in this region appears near the electron cyclotron frequency (f_{ce}). Most of this wave power is concentrated in electric field fluctuations near $0.7 f_{ce}$ and f_{ce} , with strong harmonics of both frequencies extending above f_{ce} . At least two distinct, often concurrent, wave modes are observed, preliminarily identified as electrostatic whistler-mode waves and electron Bernstein waves. Wave intervals range in duration from a few seconds to hours. Both the amplitudes and number of detections of these near- f_{ce} waves increase significantly with decreasing distance to the Sun, suggesting that they play an important role in the evolution of electron populations in the near-Sun solar wind. Correlations are found between the detection of these waves and properties of solar wind electron populations, including electron core drift, implying that these waves play a role in regulating the heat flux carried by solar wind electrons. Observation of these near- f_{ce} waves is found to be strongly correlated with near-radial solar wind magnetic field configurations with low levels of magnetic turbulence. A scenario for the growth of these waves is presented which implies that regions of low-turbulence near-radial magnetic field are a prominent feature of solar wind structure near the Sun. **2-18-11-07, 2019-04-04**

Evolution of Large-amplitude Alfvén Waves and Generation of Switchbacks in the Expanding Solar Wind

Alfred Mallet¹, Jonathan Squire², Benjamin D. G. Chandran³, Trevor Bowen¹, and Stuart D. Bale^{1,4}
2021 ApJ 918 62

<https://doi.org/10.3847/1538-4357/ac0c12>

Motivated by recent Parker Solar Probe (PSP) observations of "switchbacks" (abrupt, large-amplitude reversals in the radial magnetic field, which exhibit Alfvénic correlations), we examine the dynamics of large-amplitude Alfvén waves in the expanding solar wind. We develop an analytic model that makes several predictions: switchbacks should preferentially occur in regions where the solar wind plasma has undergone a greater expansion, the switchback fraction at radii comparable to PSP should be an increasing function of radius, and switchbacks should have their gradients preferentially perpendicular to the mean magnetic field direction. The expansion of the plasma generates small compressive components as part of the wave's nonlinear evolution: these are maximized when the normalized fluctuation amplitude is comparable to $\sin \theta$, where θ is the angle between the propagation direction and the mean magnetic field. These compressive components steepen the primary Alfvénic waveform, keeping the solution in a state of nearly constant magnetic field strength as its normalized amplitude $\delta B/B$ grows due to expansion. The small fluctuations in the magnetic field strength are minimized at a particular θ -dependent value of β , usually of order unity, and the density and magnetic-field-strength fluctuations can be correlated or anticorrelated depending on β and θ . Example solutions of our dynamical equation are presented; some do indeed form magnetic-field reversals. Our predictions appear to match some previously unexplained phenomena in observations and numerical simulations, providing evidence that the observed switchbacks result from the nonlinear evolution of the initially small-amplitude Alfvén waves already known to be present at the coronal base.

STEREO DIRECT IMAGING OF A CORONAL MASS EJECTION-DRIVEN SHOCK TO 0.5 AU

Shane A. Maloney and Peter T. Gallagher

E-print, June 2011, File ; 2011 ApJ 736 L5

Fast coronal mass ejections (CMEs) generate standing or bow shocks as they propagate through the corona and solar wind. Although CME shocks have previously been detected indirectly via their emission at radio frequencies, direct imaging has remained elusive due to their low contrast at optical wavelengths. Here we report the first images of a CME-driven shock as it propagates through interplanetary space from 8 R_{\odot} to 120 R_{\odot} (0.5 AU), using observations from the STEREO Heliospheric Imager. The CME was measured to have a velocity of ~ 1000 km s⁻¹ and a Mach number of 4.1 ± 1.2 , while the shock front standoff distance (Δ) was found to increase linearly to $\sim 20 R_{\odot}$ at 0.5 AU. The normalized standoff distance (Δ/DO) showed reasonable agreement with semi-empirical relations, where DO is the CME radius. However, when normalized using the radius of curvature, Δ/RO did not agree well with theory, implying that RO was underestimated by a factor of 3-8. This is most likely due to the difficulty in estimating the larger radius of curvature along the CME axis from the observations, which provide

Solar Wind Drag and the Kinematics of Interplanetary Coronal Mass Ejections

Shane A. Maloney and Peter T. Gallagher

E-print, Oct 2010; ApJL 724:L127–L132, 2010, File

Coronal mass ejections (CMEs) are large-scale ejections of plasma and magnetic field from the solar corona, which propagate through interplanetary space at velocities of ~ 100 – 2500 km s⁻¹. Although plane-of-sky coronagraph measurements have provided some insight into their kinematics near the Sun ($< 32 R_{\odot}$), it is still unclear what forces govern their evolution during both their early acceleration and later propagation. Here, we use the dual perspectives of the STEREO spacecraft to derive the three-dimensional kinematics of CMEs over a range of heliocentric distances (~ 2 – $250 R_{\odot}$). We find evidence for solar wind (SW) drag forces acting in interplanetary space, with a fast CME decelerated and a slow CME accelerated toward typical SW velocities. We also find that the fast CME showed linear ($\delta = 1$) dependence on the velocity difference between the CME and the SW, while the slow CME showed a quadratic ($\delta = 2$) dependence. The differing forms of drag for the two CMEs indicate the forces responsible for their acceleration may be different.

Reconstructing the 3-D Trajectories of CMEs in the Inner Heliosphere

Shane A. **Maloney**, Peter T. Gallagher and R. T. James McAteer¹

E-print, May 2009, *Solar Phys* (2009) 256: 149–166; **File**

A method for the full three-dimensional (3-D) reconstruction of the trajectories of coronal mass ejections (CMEs) using *Solar TERrestrial RELations Observatory* (STEREO) data is presented. Four CMEs that were simultaneously observed by the inner and outer coronagraphs (COR1 and 2) of the Ahead and Behind STEREO satellites were analysed. These observations were used to derive CME trajectories in 3-D out to $\sim 15 R_{\odot}$. The reconstructions using COR1/2 data support a radial propagation model. Assuming pseudo-radial propagation at large distances from the Sun ($15 - 240 R_{\odot}$), the CME positions were extrapolated into the Heliospheric Imager (HI) field-of-view. We estimated the CME velocities in the different fields-of-view. It was found that CMEs slower than the solar wind were accelerated, while CMEs faster than the solar wind were decelerated, with both tending to the solar wind velocity.

The Physical Processes of CME/ICME Evolution

Review

Ward **Manchester** IV, Emilia K. J. Kilpua, Ying D. Liu, Noé Lugaz, Pete Riley, Tibor Török, Bojan Vršnak
Space Science Reviews Volume 212, **Issue 3–4**, pp 1159–1219 **2017**

<https://link.springer.com/content/pdf/10.1007%2Fs11214-017-0394-0.pdf>

As observed in Thomson-scattered white light, coronal mass ejections (CMEs) are manifest as large-scale expulsions of plasma magnetically driven from the corona in the most energetic eruptions from the Sun. It remains a tantalizing mystery as to how these erupting magnetic fields evolve to form the complex structures we observe in the solar wind at Earth. Here, we strive to provide a fresh perspective on the post-eruption and interplanetary evolution of CMEs, focusing on the physical processes that define the many complex interactions of the ejected plasma with its surroundings as it departs the corona and propagates through the heliosphere. We summarize the ways CMEs and their interplanetary CMEs (ICMEs) are rotated, reconfigured, deformed, deflected, decelerated and disguised during their journey through the solar wind. This study then leads to consideration of how structures originating in coronal eruptions can be connected to their far removed interplanetary counterparts. Given that ICMEs are the drivers of most geomagnetic storms (and the sole driver of extreme storms), this work provides a guide to the processes that must be considered in making space weather forecasts from remote observations of the corona. **17-18 Apr 1999, 14 July 2000, 27 May 2002, 28 October 2003, 2 November 2008, 12 December 2008, 16 June 2010, 7 Mar 2012**

Simulation of magnetic cloud erosion during propagation

W. B. **Manchester** IV¹, J. U. Kozyra¹, S. T. Lepri¹ and B. Lavraud
JGR, Volume 119, Issue 7, pages 5449–5464, July **2014**

We examine a three-dimensional (3-D) numerical magnetohydrodynamic (MHD) simulation describing a very fast interplanetary coronal mass ejection (ICME) propagating from the solar corona to 1 AU. In conjunction with its high speed, the ICME evolves in ways that give it a unique appearance at 1 AU that does not resemble a typical ICME. First, as the ICME decelerates far from the Sun in the solar wind, filament material at the back of the flux rope pushes its way forward through the flux rope. Second, diverging nonradial flows in front of the filament transport poloidal flux of the rope to the sides of the ICME. Third, the magnetic flux rope reconnects with the interplanetary magnetic field (IMF). As a consequence of these processes, the flux rope partially unravels and appears to evolve to an entirely unbalanced configuration. At the same time, filament material at the base of the flux rope moves forward and comes in direct contact with the shocked plasma in the CME sheath. We find evidence that such remarkable behavior has actually occurred when we examine a very fast CME that erupted from the Sun on **2005 January 20**. In situ observations of this event near 1 AU show very dense cold material impacting the Earth following immediately behind the CME sheath. Charge state analysis shows this dense plasma is filament material. Consistent with the simulation, we find the poloidal flux (B_z) to be entirely unbalanced, giving the appearance that the flux rope has eroded. The dense solar filament material and unbalanced positive IMF B_z produced a number of anomalous features in a moderate magnetic storm already underway, which are described in a companion paper by Kozyra et al. (2014).

Flux rope evolution in interplanetary coronal mass ejections: the 13 May 2005 event

Manchester, W. B., IV; van der Holst, B.; Lavraud, B.

Plasma Physics and Controlled Fusion, Volume 56, Issue 6, article id. 064006 (2014).

http://iopscience.iop.org/0741-3335/56/6/064006/pdf/0741-3335_56_6_064006.pdf

Coronal mass ejections (CMEs) are a dramatic manifestation of solar activity that release vast amounts of plasma into the heliosphere, and have many effects on the interplanetary medium and on planetary atmospheres, and are the major driver of space weather. CMEs occur with the formation and expulsion of large-scale magnetic flux ropes from the solar corona, which are routinely observed in interplanetary space. Simulating and predicting the structure and dynamics of these interplanetary CME magnetic fields are essential to the progress of heliospheric science and space weather prediction. We discuss the simulation of the 13 May 2005 CME event in which we follow the propagation of a flux rope from the solar corona to beyond Earth orbit. In simulating this event, we find that the magnetic flux rope reconnects with the interplanetary magnetic field, to evolve to an open configuration and later reconnects to reform a twisted structure sunward of the original rope. Observations of the 13 May 2005 CME magnetic field near Earth suggest that such a rearrangement of magnetic flux by reconnection may have occurred.

THREE-DIMENSIONAL MHD SIMULATION OF THE 2003 OCTOBER 28 CORONAL MASS EJECTION: COMPARISON WITH LASCO CORONAGRAPH OBSERVATIONS

Ward B. **Manchester**¹, Angelos Vourlidas,² Ga'bor To'th,¹ Noe' Lugaz,³ Ilia I. Roussev,³ Igor V. Sokolov,¹ Tamas I. Gombosi,¹ Darren L. De Zeeuw,¹ and Merav Opher⁴

Astrophysical Journal, 684:1448-1460, **2008** September; **File**

<http://www.journals.uchicago.edu/toc/apj/2008/684/2>

We numerically model the coronal mass ejection (CME) event of 2003 October 28 that erupted from AR 10486 and propagated to Earth in less than 20 hr, causing severe geomagnetic storms. The magnetohydrodynamic (MHD) model is formulated by first arriving at a steady state corona and solar wind employing synoptic magnetograms. We initiate two CMEs from the same active region, one approximately a day earlier that preconditions the solar wind for the much faster CME on the 28th. This second CME travels through the corona at a rate of over 2500 km s⁻¹, driving a strong forward shock. We clearly identify this shock in an image produced by the Large Angle Spectrometric Coronagraph (LASCO) C3 and reproduce the shock and its appearance in synthetic white-light images from the simulation. We find excellent agreement with both the general morphology and the quantitative brightness of the model CME with LASCO observations. These results demonstrate that the CME shape is largely determined by its interaction with the ambient solarwind and may not be sensitive to the initiation process. We then show how the CME would appear as observed by wide-angle coronagraphs on board the Solar Terrestrial Relations Observatory (STEREO) spacecraft. We find complex time evolution of the white-light images as a result of the way in which the density structures pass through the Thomson sphere. **The simulation is performed with the SpaceWeatherModeling Framework (SWMF).**

The link between CME-associated dimmings and interplanetary magnetic clouds

Cristina H. **Mandrini**¹, Marria S. Nakwacki¹, Gemma Attrill^{2,6}, Lidia

van Driel-Gesztelyi^{2,3,4}, Sergio Dasso^{1,5} and Pascal Dremoulin³

Universal Heliophysical Processes, Proceedings IAU Symposium No. 257, 2008, N. Gopalswamy & D.F. Webb, eds., p. 265-270, 2009, File

Coronal dimmings often develop in the vicinity of erupting magnetic configurations. It has been suggested that they mark the location of the footpoints of ejected flux ropes and, thus, their magnetic flux can be used as a proxy for the ejected flux. If so, this quantity can be compared to the flux in the associated interplanetary magnetic cloud (MC) to find clues about the origin of the ejected flux rope. In the context of this interpretation, we present several events for which we have done a comparative solar-interplanetary analysis. We combine SOHO/Extreme Ultraviolet Imaging Telescope (EIT) data and Michelson Doppler Imager (MDI) magnetic maps to identify and measure the flux in the dimmed regions. We model the associated MCs and compute their magnetic flux using in situ observations. We find that the magnetic fluxes in the dimmings and MCs are compatible in some events; though this is not the case for large-scale and intense eruptions that occur in regions that are not isolated from others. We conclude that, in these particular cases, a fraction of the dimmed regions can be formed by reconnection between the erupting field and the surrounding magnetic structures, via a stepping process that can also explain other CME associated events.

Are CME-Related Dimmings Always a Simple Signature of Interplanetary Magnetic Cloud Footpoints?

C.H. **Mandrini** · M.S. Nakwacki · G. Attrill · L. van Driel-Gesztelyi · P. Démoulin · S. Dasso · H. Elliott
Solar Phys (2007) 244: 25–43; **File**

It has been suggested that dimmings mark the location of the footpoints of ejected flux ropes and, thus, their magnetic flux can be used as a proxy for the flux involved in the ejection.

28 October 2003

We find that the magnetic fluxes of the dimmings and magnetic cloud are incompatible, in contrast to what has been found in previous studies. We conclude that, in certain cases, especially in large-scale events and eruptions that occur in regions that are not isolated from other flux concentrations, the interpretation of dimmings requires a deeper analysis of the global magnetic configuration, since at least a fraction of the dimmed regions is formed by reconnection between the erupting field and the surrounding magnetic structures.

Interplanetary flux rope ejected from an X-ray bright point. The smallest magnetic cloud source-region ever observed

Mandrini, C. H.; Pohjolainen, S.; Dasso, S.; Green, L. M.; Démoulin, P.; van Driel-Gesztelyi, L.; Copperwheat, C.; Foley, C.

Astronomy and Astrophysics, Volume 434, Issue 2, May 2005, pp.725-740

<http://www.aanda.org/articles/aa/pdf/2005/17/aa1079.pdf>

Using multi-instrument and multi-wavelength observations (SOHO/MDI and EIT, TRACE and Yohkoh/SXT), as well as computing the coronal magnetic field of a tiny bipole combined with modelling of Wind in situ data, we provide evidences for the smallest event ever observed which links a sigmoid eruption to an interplanetary magnetic cloud (MC). The tiny bipole, which was observed very close to the solar disc centre, had a factor one hundred less flux than a classical active region (AR). In the corona it had a sigmoidal structure, observed mainly in EUV, and we found a very high level of non-potentiality in the modelled magnetic field, 10 times higher than we have ever found in any AR. From May 11, 1998, and until its disappearance, the sigmoid underwent three intense impulsive events. The largest of these events had extended EUV dimmings and a cusp. The Wind spacecraft detected 4.5 days later one of the smallest MC ever identified (about a factor one hundred times less magnetic flux in the axial component than that of an average MC). The link between this last eruption and the interplanetary magnetic cloud is supported by several pieces of evidence: good timing, same coronal loop and MC orientation, same magnetic field direction and magnetic helicity sign in the coronal loops and in the MC. We further quantify this link by estimating the magnetic flux (measured in the dimming regions and in the MC) and the magnetic helicity (pre- to post-event change in the solar corona and helicity content of the MC). Within the uncertainties, both magnetic fluxes and helicities are in reasonable agreement, which brings further evidences of their link. These observations show that the ejections of tiny magnetic flux ropes are indeed possible and put new constraints on CME models. **10-15 May 1998**

Impulsive increase of galactic cosmic ray flux observed by icetop.

Mangeard, P.-S., Muangha, P., Pyle, R., Ruffolo, D., Saiz, A., et al. (The IceCube collaboration): **2017**, In: Proc. 35th Internat. Cosmic Ray Conf. 35, 133.

A heliospheric density and magnetic field model*

G. **Mann**¹, A. Warmuth¹, C. Vocks¹ and A. P. Rouillard^{2,3}

A&A 679, A64 (2023)

<https://www.aanda.org/articles/aa/pdf/2023/11/aa45050-22.pdf>

Context. The radial evolution of the density of the plasma and the magnetic field in the heliosphere, especially in the region between the solar corona and the Earth's orbit, has been a topic of active research for several decades. Both remote-sensing observations and in situ measurements by spacecraft such as HELIOS, Ulysses, and WIND have provided critical data on this subject. The NASA space mission Parker Solar Probe (PSP), which will approach the Sun down to a distance of 9.9 solar radii on December 24, 2024, gives new insights into the structure of the plasma density and magnetic field in the heliosphere, especially in the near-Sun interplanetary space. This region is of particular interest because the launch and evolution of coronal mass ejections (CMEs), which can influence the environment of our Earth (usually called space weather), takes place there.

Aims. Because of the new data from PSP, it is time to revisit the subject of the radial evolution of the plasma density and magnetic field in the heliosphere. To do this, we derive a radial heliospheric density and magnetic field model in the vicinity of the ecliptic plane above quiet equatorial regions. The model agrees well with the measurements in the sense of a global long-term average.

Methods. The radial evolution of the density and solar wind velocity is described in terms of Parker's wind equation. A special solution of this equation includes two integration constants that are fitted by the measurements. For the magnetic field, we employed a previous model in which the magnetic field is describe by a superposition of the magnetic fields of a dipole and a quadrupole of the quiet Sun and a current sheet in the heliosphere.

Results. We find the radial evolution of the electron and proton number density as well as the radial component of the magnetic field and the total field strength in the heliosphere from the bottom of the corona up to a heliocentric distance of 250 solar radii. The modelled values are consistent with coronal observations, measurements at 1 AU, and with the recent data from the inner heliosphere provided by PSP.

Conclusions. With the knowledge of the radial evolution of the plasma density and the magnetic field in the heliosphere the radial behaviour of the local Alfvén speed can be calculated. It can reach a local maximum of 392 km s⁻¹ at a distance of approximately 4 solar radii, and it exceeds the local solar wind speed at distances in the range of 3.6–13.7 solar radii from the centre of the Sun.

Current State of Reduced Solar Activity: Intense Space Weather Events in the Inner Heliosphere

P.K. **Manoharan**, K. Mahalakshmi, A. Johri, B.V. Jackson, D. Ravikumar,
K. Kalyanasundaram, S.P. Subramanian, A. K. Mittal
SUN and GEOSPHERE Vol.13, No.2 – **2018**, 135-144

http://newserver.stil.bas.bg/SUNGEO//00SGArhiv/SG_v13_No2_2018-pp-135-143.pdf

We present a study of 21 geomagnetic storms, occurred during 2011–2017 in association with the propagation of coronal mass ejections (CMEs). These storms are selected with the minimum storm disturbance index (SYM-H) intensity of -100 nT or less and are distributed from the maximum to the minimum of the weak solar cycle 24. We identify and investigate these storm-driving CMEs (halo and partial halo CMEs) by combining EUV and white-light images in the nearSun region, interplanetary scintillation images in between the Sun and the Earth, and in-situ measurements at the nearEarth orbit. These CMEs cover a wide range of initial speeds, ~180 to 2680 km/s. For about 50% of the CMEs, the fast initial speed at the near-Sun region does not correlate with the final speed at the near-Earth orbit. The storm indexes range between -100 and -233 nT and they are associated with minimum Bz values in the range of -12 to -38 nT. The Forbush decrease (FD) levels associated with these storms vary in the range of about -2% to -10%. A comparison of travel times of CMEs to 1 AU with the observed initial/final speeds and estimated initial speed suggests that a large fraction of fast initial speeds could possibly be due to the sudden expansion of the CME into a relatively low pressure interplanetary medium. Most of the geomagnetic storms (i.e., 19 storms) have been caused by the strong intrinsic magnetic field of the CME and only 2 storms are produced by the sheath region between the arrival times of interplanetary shock and CME. The geomagnetic storm index is compared with the possible reconnection electric field component, BzVICME. It suggests an empirical relationship for the likely lower level of storm index, SYM-H = -70 - 0.003·BzVICME. (nT), in which Bz and VICME are respectively given in units of nT and km/s. **21 June 2015**

Space Weather and Solar Wind Studies with OWFA

Review

P. K. **Manoharan**, C. R. Subrahmanya, J. N. Chengalur

J. Astrophysics and Astronomy **2017**

<https://arxiv.org/pdf/1703.00631.pdf>

In this paper, we review the results of interplanetary scintillation (IPS) observations made with the legacy system of the Ooty Radio Telescope (ORT) and compare them with the possibilities opened by the upgraded ORT, the Ooty Wide Field Array (OWFA). The stability and the sensitivity of the legacy system of ORT allowed the regular monitoring of IPS on a grid of large number of radio sources and the results of these studies have been useful to understand the physical processes in the heliosphere and space weather events, such as coronal mass ejections, interaction regions and their propagation effects. In the case of OWFA, its wide bandwidth of 38 MHz, the large field of view of ~27° and increased sensitivity provide a unique capability for the heliospheric science at 326.5 MHz. IPS observations with the OWFA would allow one to monitor more than 5000 sources per day. This, in turn, will lead to much improved studies of space weather events and solar wind plasma, overcoming the limitations faced with the legacy system. We also highlight some of the specific aspects of the OWFA, potentially relevant for the studies of coronal plasma and its turbulence characteristics.

Interplanetary Consequences of Coronal Mass Ejection Events occurred during 18--25 June 2015

P.K. **Manoharan**, D. Maia, A. Johri, M.S. Induja

Ground-based Solar Observations in the Space Instrumentation Era

ASP Conference Series, Vol. 504, p. 59 **2016**

<http://arxiv.org/pdf/1603.03562v1.pdf>

<http://aspbooks.org/publications/504/059.pdf>

In this paper, we review the preliminary results on the propagation effects and interplanetary consequences of fast and wide coronal mass ejection (CME) events, occurred during **18--25 June 2015**, in the Sun-Earth distance range. The interplanetary scintillation (IPS) images reveal that the large-scale structures of CME-driven disturbances filled nearly the entire inner heliosphere with a range of speeds, $\sim 300\text{--}1000$ {kmps}. The comparison of speed data sets, from IPS technique results in the inner heliosphere and {it in-situ} measurements at 1 AU, indicates that the drag force imposed by the low-speed wind dominated heliosphere on the propagation of CMEs may not be effective. The arrival of shocks at 1 AU suggests that a shock can be driven in the interplanetary medium by the central part of the moving CME and also by a different part away from its centre. The increased flux of proton at energies >10 MeV is consistent with the acceleration of particles by the shock ahead of the CME.

THREE-DIMENSIONAL EVOLUTION OF SOLAR WIND DURING SOLAR CYCLES 22–24

P. K. Manoharan

2012 ApJ 751 128

This paper presents an analysis of three-dimensional evolution of solar wind density turbulence and speed at various levels of solar activity between solar cycles 22 and 24. The solar wind data used in this study have been obtained from the interplanetary scintillation (IPS) measurements made at the Ooty Radio Telescope, operating at 327 MHz. Results show that (1) on average, there was a downward trend in density turbulence from the maximum of cycle 22 to the deep minimum phase of cycle 23; (2) the scattering diameter of the corona around the Sun shrunk steadily toward the Sun, starting from 2003 to the smallest size at the deepest minimum, and it corresponded to a reduction of $\sim 50\%$ in the density turbulence between the maximum and minimum phases of cycle 23; (3) the latitudinal distribution of the solar wind speed was significantly different between the minima of cycles 22 and 23. At the minimum phase of solar cycle 22, when the underlying solar magnetic field was simple and nearly dipole in nature, the high-speed streams were observed from the poles to $\sim 30^\circ$ latitudes in both hemispheres. In contrast, in the long-decay phase of cycle 23, the sources of the high-speed wind at both poles, in accordance with the weak polar fields, occupied narrow latitude belts from poles to $\sim 60^\circ$ latitudes. Moreover, in agreement with the large amplitude of the heliospheric current sheet, the low-speed wind prevailed in the low- and mid-latitude regions of the heliosphere. (4) At the transition phase between cycles 23 and 24, the high levels of density and density turbulence were observed close to the heliospheric equator and the low-speed solar wind extended from the equatorial-to-mid-latitude regions. The above results in comparison with Ulysses and other in situ measurements suggest that the source of the solar wind has changed globally, with the important implication that the supply of mass and energy from the Sun to the interplanetary space has been significantly reduced in the prolonged period of low solar activity. The IPS results are consistent with the onset and growth of the current solar cycle 24, starting from the middle of 2009. However, the width of the high-speed wind at the northern high latitudes has almost disappeared and indicates that the ascending phase of the current cycle has almost reached the maximum phase in the northern hemisphere of the Sun. However, in the southern part of the hemisphere, the solar activity has yet to develop and/or increase.

ERRATUM: 2012 ApJ 753 93

Coronal mass ejections—Propagation time and associated internal energy

P.K. Manoharan a,_, A. Mujiber Rahman

Journal of Atmospheric and Solar-Terrestrial Physics 73 (2011) 671–677, File

In this paper, we analyze 91 coronal mass ejection (CME) events studied by Manoharan et al. (2004) and Gopalswamy and Xie (2008). These earth-directed CMEs are large (width $>160^\circ$) and cover a wide range of speeds ($\sim 1202\text{--}2400$ km s⁻¹) in the LASCO field of view. This set of events also includes interacting CMEs and some of them take longer time to reach 1 AU than the travel time inferred from their speeds at 1 AU. We study the link between the travel time of the CME to 1 AU (combined with its final speed at the Earth) and the effective acceleration in the Sun–Earth distance. Results indicate that (1) for almost all the events (85 out of 91 events), the speed of the CME at 1 AU is always less than or equal to its initial speed measured at the near-Sun region, (2) the distributions of initial speeds, CME-driven shock and CME speeds at 1 AU clearly show the effects of aero-dynamical drag between the CME and the solar wind and in consequence, the speed of the CME tends to equalize to that of the background solar wind, (3) for a large fraction of CMEs (for $\sim 50\%$ of the events), the inferred effective acceleration along the Sun–Earth line dominates the above drag force. The net acceleration suggests an average dissipation of energy $\sim 10^{31\text{--}32}$ ergs, which is likely provided by the Lorentz force associated with the internal magnetic energy carried by the CME.

Ooty Interplanetary Scintillation – Remote-Sensing Observations and Analysis of Coronal Mass Ejections in the Heliosphere

P.K. Manoharan

Solar Phys, 265: 137–157, 2010, [File](#)

In this paper, I investigate the three-dimensional evolution of solar wind density and speed distributions associated with coronal mass ejections (CMEs). The primary solar wind data used in this study has been obtained from the interplanetary scintillation (IPS) measurements made at the Ooty Radio Telescope, which is capable of measuring scintillation of a large number of radio sources per day and solar wind estimates along different cuts of the heliosphere that allow the reconstruction of three-dimensional structures of propagating transients in the inner heliosphere. The results of this study are: *i*) three-dimensional IPS images possibly show evidence for the flux-rope structure associated with the CME and its radial size evolution; the overall size and features within the CME are largely determined by the magnetic energy carried by the CME. Such a magnetically energetic CME can cause an intense geomagnetic storm, even if the trailing part of the CME passes through the Earth; *ii*) IPS measurements along the radial direction of a CME at $\sim 120 R_{\odot}$ show density turbulence enhancements linked to the shock ahead of the CME and the core of the CME. The density of the core decreases with distance, suggesting the expansion of the CME. However, the density associated with the shock increases with distance from the Sun, indicating the development of a strong compression at the leading edge of the CME. The increase of stand-off distance between $\sim 120 R_{\odot}$ and 1 AU is consistent with the deceleration of the CME and the continued outward expansion of the shock. The key point in this study is that the magnetic energy possessed by the transient determines its radial evolution.

7-13 Sept 2005, 13-16 Dec 2006

Evolution of Coronal Mass Ejections in the Inner Heliosphere: A Study Using White-Light and Scintillation Images

Manoharan, P.K.: 2006, Solar Phys. 235, 345, [File](#).

Knowledge of the radial evolution of the coronal mass ejection (CME) is important for the understanding of its arrival at the near-Earth space and of its interaction with the disturbed/ambient solar wind in the course of its travel to 1AU and further. In this paper, the radial evolution of 30 large CMEs (angular width $>150^{\circ}$, i.e., halo and partial halo CMEs) has been investigated between the Sun and the Earth using (i) the white-light images of the near-Sun region from the *Large Angle Spectroscopic Coronagraph* (LASCO) onboard SOHO mission and (ii) the *interplanetary scintillation* (IPS) images of the inner heliosphere obtained from the Ooty Radio Telescope (ORT). In the LASCO field of view at heliocentric distances $R \leq 30$ solar radii (R_{\odot}), these CMEs cover an order of magnitude range of initial speeds, $V_{CME} \approx 260\text{--}2600$ km s $^{-1}$. Following results have been obtained from the speed evolution of these CMEs in the Sun–Earth distance range: (1) the speed profile of the CME shows dependence on its initial speed; (2) the propagation of the CME goes through continuous changes, which depend on the interaction of the CME with the surrounding solar wind encountered on the way; (3) the radial-speed profiles obtained by combining the LASCO and IPS images yield the factual view of the propagation of CMEs in the inner heliosphere and transit times and speeds at 1AU computed from these profiles are in good agreement with the actual measurements; (4) the mean travel time curve for different initial speeds and the shape of the radial-speed profiles suggest that up to a distance of $\sim 80 R_{\odot}$, the internal energy of the CME (or the expansion of the CME) dominates and however, at larger distances, the CME's interaction with the solar wind controls the propagation; (5) most of the CMEs tend to attain the speed of the ambient flow at 1AU or further out of the Earth's orbit. The results of this study are useful to quantify the drag force imposed on a CME by the interaction with the ambient solar wind and it is essential in modeling the CME propagation. This study also has a great importance in understanding the prediction of CME-associated space weather at the near-Earth environment.

In the present study, the multi-point IPS measurements of CMEs under investigation in the Sun-Earth space have been obtained with the Ooty Radio Telescope, which is operated by the Radio Astronomy Centre, Tata Institute of

Fundamental Research, India. The description of Ooty IPS observations and the method of data reduction procedure have been given by Manoharan (2006) and references therein.

Influence of coronal mass ejection interaction on propagation of interplanetary shocks,

Manoharan, P. K., N. Gopalswamy, S. Yashiro, A. Lara, G. Michales, and R. A. Howard
J. Geophys. Res., 109, A06109, doi:10.1029/2003JA010300, **2004**.

Coronal mass ejection of 2000 July 14 flare event: imaging from near-Sun to Earth environment,

Manoharan, P.K. M. Tokumaru, M. Pick, P. Subramanian, F.M. Ipavich, K. Schenk, M.L. Kaiser, R.P. Lepping, and A. Vourlidis
Astrophys. J., 559, 1,180, **2001**.

Double Superposed Epoch Analysis of Geomagnetic Storms and Corresponding Solar Wind and IMF in Solar Cycles 23 and 24

V. **Manu**, **N. Balan**, **Qing-He Zhang**, **Zan-Yang Xing**
Space Weather [Volume21, Issue3](#) e2022SW003314 **2023**
<https://doi.org/10.1029/2022SW003314>

<https://agupubs.onlinelibrary.wiley.com/doi/epdf/10.1029/2022SW003314>

The weakest solar cycle 24 (SC24, 2010–2019) in 100 years was 1/3rd less active compared to the previous solar cycle 23 (SC23, 1996–2009). We identify 135 and 61 ICME (interplanetary coronal mass ejection) driven clear geomagnetic storms ($Dst_{Min} \leq -50$ nT) in SC23 and SC24, respectively, giving a reduction of 55% storms in SC24, and present the double superposed epoch analysis (DSEA) of the storms/activities in SC23 and SC24 using the Dst, symmetric H (SymH), Kp and AE indices. The DSEA method for the corresponding solar wind velocity V, north-south component of the interplanetary magnetic field (IMF Bz) and the product VBz are also presented. Compared to SC23, the maximum storm/activity intensity in SC24 reduces by 52%, 12%, and 45% at low, mid and high latitudes and the corresponding maxima in -VBz, V, and -Bz reduce by 39%, 17%, and 38%, respectively. The epoch average storm/activity intensity reduces by 27%, 11%, and 4% at low, mid and high latitudes and average maxima in -VBz, V, and -Bz reduce by 24%, 14%, and 13%, respectively. The results seem to reveal that the average reduction in the main driver -VBz (~24%) might have caused nearly the same and equal average storm/activity intensity reductions in all latitudes (~25%), though the irregular nature of the AE index makes the reduction very small (4%) at high latitudes, and small (~11%) at mid latitudes mainly due to the small (0–9) quasi logarithmic scale of the Kp index. **20 Nov 2003, 17 Mar 2015**

Numerical Study of Erosion, Heating, and Acceleration of the Magnetic Cloud as Impacted by Fast Shock

Shoudi **Mao**¹, Jiansen He¹, Lei Zhang², Liping Yang^{1,2}, and Linghua Wang¹
2017 *ApJ* 842 109

The impact of an overtaking fast shock on a magnetic cloud (MC) is a pivotal process in CME–CME (CME: coronal mass ejection) interactions and CME–SIR (SIR: stream interaction region) interactions. MC with a strong and rotating magnetic field is usually deemed a crucial part of CMEs. To study the impact of a fast shock on an MC, we perform a 2.5 dimensional numerical magnetohydrodynamic simulation. Two cases are run in this study: without and with impact by fast shock. In the former case, the MC expands gradually from its initial state and drives a relatively slow magnetic reconnection with the ambient magnetic field. Analyses of forces near the core of the MC as a whole body indicates that the solar gravity is quite small compared to the Lorentz force and the pressure gradient force. In the second run, a fast shock propagates, relative to the background plasma, at a speed twice that of the perpendicular fast magnetosonic speed, catches up with and takes over the MC. Due to the penetration of the fast shock, the MC is highly compressed and heated, with the temperature growth rate enhanced by a factor of about 10 and the velocity increased to about half of the shock speed. The magnetic reconnection with ambient magnetic field is also sped up by a factor of two to four in reconnection rate as a result of the enhanced density of the current sheet, which is squeezed by the forward motion of the shocked MC.

Helium fluxes measured by the PAMELA experiment from the minimum to the maximum solar activity for solar cycle 24

N. Marcelli, M. Boezio, A. Lenni, W. Menn, R. Munini, O. P. M. Aslam, et al.

ApJ 2022

<https://arxiv.org/pdf/2201.01045.pdf>

Time-dependent energy spectra of galactic cosmic rays (GCRs) carry fundamental information regarding their origin and propagation. When observed at the Earth, these spectra are significantly affected by the solar wind and the embedded solar magnetic field that permeates the heliosphere, changing significantly over an 11-year solar cycle. Energy spectra of GCRs measured during different epochs of solar activity provide crucial information for a thorough understanding of solar and heliospheric phenomena. The PAMELA experiment had collected data for almost ten years (15th June 2006 - 23rd January 2016), including the minimum phase of solar cycle 23 and the maximum phase of solar cycle 24. In this paper, we present new spectra for helium nuclei measured by the PAMELA instrument from January 2010 to September 2014 over a three Carrington rotation time basis. These data are compared to the PAMELA spectra measured during the previous solar minimum providing a picture of the time dependence of the helium nuclei fluxes over a nearly full solar cycle. Time and rigidity dependencies are observed in the proton-to-helium flux ratios. The force-field approximation of the solar modulation was used to relate these dependencies to the shapes of the local interstellar proton and helium-nuclei spectra.

Time Dependence of the Flux of Helium Nuclei in Cosmic Rays Measured by the PAMELA Experiment between 2006 July and 2009 December

N. Marcelli^{1,2}, M. Boezio^{3,4}, A. Lenni^{3,4,5}, W. Menn⁶, R. Munini^{3,4}

2020 ApJ 893 145

<https://doi.org/10.3847/1538-4357/ab80c2>

Precise time-dependent measurements of the $Z = 2$ component in the cosmic radiation provide crucial information about the propagation of charged particles through the heliosphere. The PAMELA experiment, with its long flight duration (2006 June 15–2016 January 23) and the low energy threshold (80 MeV/n) is an ideal detector for cosmic-ray solar modulation studies. In this paper, the helium nuclei spectra measured by the PAMELA instrument from 2006 July to 2009 December over a Carrington rotation time basis are presented. A state-of-the-art three-dimensional model for cosmic-ray propagation inside the heliosphere was used to interpret the time-dependent measured fluxes. Proton-to-helium flux ratio time profiles at various rigidities are also presented in order to study any features that could result from the different masses and local interstellar spectra shapes.

Probing coronal mass ejections inclination effects with EUHFORIA

Karmen Martinić, Eleanna Asvestari, Mateja Dumbović, Tobias Rindlisbacher, Manuela Temmer, Bojan Vršnak

ApJ 974 203 2024

<https://arxiv.org/pdf/2408.14971>

<https://iopscience.iop.org/article/10.3847/1538-4357/ad7392/pdf>

Coronal mass ejections (CMEs) are complex magnetized plasma structures in which the magnetic field spirals around a central axis, forming what is known as a flux rope (FR). The central FR axis can be oriented at any angle to the ecliptic. Throughout its journey, a CME will encounter interplanetary magnetic field and solar wind which are neither homogeneous nor isotropic. Consequently, CMEs with different orientations will encounter different ambient medium conditions and, thus, the interaction of a CME with its surrounding environment will vary depending on the orientation of its FR axis, among other factors. This study aims to understand the effect of inclination on CME propagation. We performed simulations with the EUHFORIA 3D magnetohydrodynamic model. This study focuses on two CMEs modelled as spheromaks with nearly identical properties, differing only by their inclination. We show the effects of CME orientation on sheath evolution, MHD drag, and non-radial flows by analyzing the model data from a swarm of 81 virtual spacecraft scattered across the inner heliospheric. We have found that the sheath duration increases with radial distance from the Sun and that the rate of increase is greater on the flanks of the CME. Non-radial flows within the studied sheath region appear larger outside the ecliptic plane, indicating a "sliding" of the IMF in the out-of ecliptic plane. We found that the calculated drag parameter does not remain constant with radial distance and that the inclination dependence of the drag parameter can not be resolved with our numerical setup.

Effects of coronal mass ejection orientation on its propagation in the heliosphere

K. Martinić¹, M. Dumbović¹, J. Čalogović¹, B. Vršnak¹, N. Al-Haddad³ and M. Temmer²

A&A 679, A97 (2023)

<https://www.aanda.org/articles/aa/pdf/2023/11/aa46858-23.pdf>

<https://arxiv.org/pdf/2309.15475.pdf>

Context. In the scope of space weather forecasting, it is crucial to be able to more reliably predict the arrival time, speed, and magnetic field configuration of coronal mass ejections (CMEs). From the time a CME is launched, the dominant factor influencing all of the above is the interaction of the interplanetary CME (ICME) with the ambient plasma and interplanetary magnetic field.

Aims. Due to a generally anisotropic heliosphere, differently oriented ICMEs may interact differently with the ambient plasma and interplanetary magnetic field, even when the initial eruption conditions are similar. For this, we examined the possible link between the orientation of an ICME and its propagation in the heliosphere (up to 1 AU).

Methods. We investigated 31 CME-ICME associations in the period from 1997 to 2018. The CME orientation in the near-Sun environment was determined using an ellipse-fitting technique applied to single-spacecraft data from SOHO/LASCO C2 and C3 coronagraphs. In the near-Earth environment, we obtained the orientation of the corresponding ICME using in situ plasma and magnetic field data. The shock orientation and nonradial flows in the sheath region for differently oriented ICMEs were investigated. In addition, we calculated the ICME transit time to Earth and drag parameter to probe the overall drag force for differently oriented ICMEs. The drag parameter was calculated using the reverse modeling procedure with the drag-based model.

Results. We found a significant difference in nonradial flows for differently oriented ICMEs, whereas a significant difference in drag for differently oriented ICMEs was not found. **10 January 1997, 3 November 2000, 15-16 March 2002**

Table 1. Remote features of the observed CMEs 1997-2018

Sun-to-Earth Observations and Characteristics of Isolated Earth-Impacting Interplanetary Coronal Mass Ejections During 2008 – 2014

D. [Maričić](#), [B. Vršnak](#), [A. M. Veronig](#), [M. Dumbović](#), [F. Šterc](#), [D. Roša](#), [M. Karlica](#), [D. Hržina](#) & [I. Romštajn](#)

[Solar Physics](#) volume 295, Article number: 91 (2020)

<https://link.springer.com/content/pdf/10.1007/s11207-020-01658-4.pdf>

<https://arxiv.org/ftp/arxiv/papers/2008/2008.10265.pdf>

A sample of isolated Earth-impacting interplanetary coronal mass ejections (ICMEs) that occurred in the period January 2008 to August 2014 is analyzed to study in detail the ICME in situ signatures, with respect to the type of filament eruption related to the corresponding CME. Observations from different vantage points provided by the Solar and Heliospheric Observatory (SOHO) and the Solar Terrestrial Relations Observatory Ahead and Behind (STEREO-A and B) are used to determine whether each CME under study is Earth directed or not. For Earth-directed CMEs, a kinematical study was performed using the STEREO-A and B COR1 and COR2 coronagraphs and the Heliospheric Imagers (HI1), to estimate the CME arrival time at 1 AU and to link the CMEs with the corresponding in situ solar wind counterparts. Based on the extrapolated CME kinematics, we identified interacting CMEs, which were excluded from further analysis. Applying this approach, a set of 31 isolated Earth-impacting CMEs was unambiguously identified and related to the in situ measurements recorded by the Wind spacecraft. ***We classified the events into subsets with respect to the CME source location, as well as with respect to the type of the associated filament eruption. Hence, the events are divided into three subsamples: active region (AR) CMEs, disappearing filament (DSF) CMEs, and stealthy CMEs.*** The related three groups of ICMEs were further divided into two subsets: magnetic obstacle (MO) events (out of which four were stealthy), covering ICMEs that at least partly showed characteristics of flux ropes, and ejecta (EJ) events, not showing such characteristics. In this way, 14 MO-ICMEs and 17 EJ-ICMEs were identified. The solar source regions of the non-stealthy MO-ICMEs are found to be located predominantly (9/10, 90%) within $\pm 30^\circ \pm 30^\circ$ from the solar central meridian, whereas EJ-ICMEs originate predominantly (16/17, 94%) from source regions that are outside $\pm 30^\circ \pm 30^\circ$. In the next step, MO-events were analyzed in more detail, considering the magnetic field strength and the plasma characteristics in three different segments, defined as the turbulent sheath (TS), the frontal region (FR), and the MO itself. The analysis revealed various well-defined correlations for AR, DSF, and stealthy ICMEs, which we interpreted considering basic physical concepts. Our results support the hypothesis that ICMEs show different signatures depending on the in situ spacecraft trajectory, in terms of apex versus flank hits. **26 October 2010, 15 February 2011, 7 June 2011, 27-31 January 2012, 12-14 June 2012, 12-13 July 2012**

Table 2 Parameters of the isolated Earth-impacting ICMEs during the period from January 2008 to August 2014.

Kinematics of Interacting ICMEs and Related Forbush Decrease: Case Study

D. [Maričić](#) · [B. Vršnak](#) · [M. Dumbović](#) · [T. Žić](#) · [D. Roša](#) · [D. Hržina](#) · [S. Lulić](#) · [I. Romštajn](#) · [I. Bušić](#) · [K. Salamon](#) · [M. Temmer](#) · [T. Rollett](#) · [A. Veronig](#) · [N. Bostanjyan](#) · [A. Chilingarian](#) · [B. Mailyan](#) · [K. Arakelyan](#) · [A. Hovhannysyan](#) · [N. Mujić](#)

Solar Phys., 2013, File

We study heliospheric propagation and some space weather aspects of three Earth-directed interplanetary coronal mass ejections (ICMEs), successively launched from the active region AR 11158 in the period **13 – 15 February 2011**. From the analysis of the ICME kinematics, morphological evolution, and in situ observations, we infer that the three ICMEs interacted on their way to Earth, arriving together at 1 AU as a single interplanetary disturbance. Detailed analysis of the in situ data reveals complex internal structure of the disturbance, where signatures of the three initially independent ICMEs could be recognized. The analysis also reveals compression and heating of the middle ICME, as well as ongoing magnetic reconnection between the leading and the middle ICME. We present evidence showing that the propagation of these two, initially slower ICMEs, was boosted by the fastest, third ICME. Finally, we employ the ground-based cosmic ray observations, to show that this complex disturbance produced a single cosmic ray event, i.e., a simple Forbush decrease (FD). The results presented provide a better understanding of the ICME interactions and reveal effects that should be taken into account in forecasting of the arrival of such compound structures.

The Successive CME on 13th; 14th and 15th February 2011 and Forbush decrease on 18 February 2011

D [Maričić](#)¹, N Bostasyan², M Dumbović³, A Chilingarian², B Mailyan², H Rostomyan², K Arakelyan², B Vršnak³, D Roša¹, D Hržina¹, I Romštajn¹ and A Veronig

2013 J. Phys.: Conf. Ser. 409 012158

Aims. We analyze the kinematics of three interplanetary coronal mass ejections (ICMEs) that occurred on 13th, 14th and 15th February 2011 in the active region AR 11155 and have shown that they appeared at the Earth orbit on February, 18th and caused Forbush decrease (FD). **Methods.** The solar coordinates of flares are (S19W03), (S20W14) and (S21W18). The kinematic curves were obtained using STEREO (A&B) data. Additionally, we explore the possibility of the CME-CME interaction for these three events. We compare obtained estimates of ICME arrival with the in-situ measurements from WIND satellite at L1 point and with ground-based cosmic ray data obtained from SEVAN network. **Results.** The acceleration of each CME is highly correlated with the associated SXR flares energy release. CMEs that erupted at 13 and 14 Feb 2011 are not associated with prominence eruption; maximum velocity was $v_{\max} 550 \pm 50$ km/s and $v_{\max} 400 \pm 50$ km/s, respectively. However, 15 Feb 2011 CME is connected with much more violent eruption associated with a prominence, with maximum velocity of $v_{\max} 1400 \pm 50$ km/s. The last overtakes 13th and 14th Feb CMEs at distances of 32 and 160 R_{\odot} , respectively. **13-18 Feb 2011**

HIGH - SPEED STREAMS CATALOGUE (1996 – 2008)

O. [Maris](#) and G. [Maris](#)

http://www.spacescience.ro/new1/HSS_Catalogue.html

Effects of coronal mass ejection orientation on its propagation in the heliosphere

K. [Martinic](#), M. [Dumbovic](#), J. [Calogovic](#), B. [Vrsnak](#), N. [Al-Haddad](#), M. [Temmer](#)

A&A 2023

<https://arxiv.org/pdf/2309.15475.pdf>

Context. In the scope of space weather forecasting, it is crucial to be able to more reliably predict the arrival time, speed, and magnetic field configuration of coronal mass ejections (CMEs). From the time a CME is launched, the dominant factor influencing all of the above is the interaction of the interplanetary CME (ICME) with the ambient plasma and interplanetary magnetic field.

Aims. Due to a generally anisotropic heliosphere, differently oriented ICMEs may interact differently with the ambient plasma and interplanetary magnetic field, even when the initial eruption conditions are similar. For this, we examined the possible link between the orientation of an ICME and its propagation in the heliosphere (up to 1 AU).

Methods. We investigated 31 CME-ICME associations in the period from 1997 to 2018. The CME orientation in the near-Sun environment was determined using an ellipse-fitting technique applied to single-spacecraft data from SOHO/LASCO C2 and C3 coronagraphs. In the near-Earth environment, we obtained the orientation of the corresponding ICME using in situ plasma and magnetic field data. The shock orientation and nonradial flows in the sheath region for differently oriented ICMEs were investigated. In addition, we calculated the ICME transit time to Earth and drag parameter to probe the overall drag force for differently oriented ICMEs. The drag parameter was calculated using the reverse modeling procedure with the drag-based model.

Results. We found a significant difference in nonradial flows for differently oriented ICMEs, whereas a significant difference in drag for differently oriented ICMEs was not found. **10 January 1997, 3 November 2000, 15-16 March 2002**

Table 1. Remote features of the observed CMEs 1997-2018

Determination of CME orientation and consequences for their propagation

[Karmen Martinic](#), [Mateja Dumbovic](#), [Manula Temmer](#), [Astrid Veronig](#), [Bojan Vršnak](#)

A&A 2022

<https://arxiv.org/pdf/2204.10112.pdf>

The configuration of the interplanetary magnetic field and features of the related ambient solar wind in the ecliptic and meridional plane are different. Therefore, one can expect that the orientation of the flux-rope axis of a coronal mass ejection (CME) influences the propagation of the CME itself. However, the determination of the CME orientation, especially from image data, remains a challenging task to perform. This study aims to provide a reference to different CME orientation determination methods in the near-Sun environment. Also, it aims to investigate the non-radial flow in the sheath region of the interplanetary CME (ICME) in order to provide the first proxy to relate the ICME orientation with its propagation. We investigated 22 isolated CME-ICME events in the period 2008-2015. We determined the CME orientation in the near-Sun environment using the following: 1) a 3D reconstruction of the CME with the graduated cylindrical shell (GCS) model applied to coronagraphic images provided by the STEREO and SOHO missions and; 2) an ellipse fitting applied to single spacecraft data from SOHO/LASCO C2 and C3 coronagraphs. In the near-Earth environment, we obtained the orientation of the corresponding ICME using in situ plasma and field data and also investigated the non-radial flow (NRF) in its sheath region. The ability of GCS and ellipse fitting to determine the CME orientation is found to be limited to reliably distinguish only between the high or low inclination of the events. Most of the CME-ICME pairs under investigation were found to be characterized by a low inclination. For the majority of CME-ICME pairs, we obtain consistent estimations of the tilt from remote and in situ data. The observed NRFs in the sheath region show a greater y direction to z direction flow ratio for high-inclination events, indicating that the CME orientation could have an impact on the CME propagation. **3-5 April 2010**

Table 1. Results of the GCS modeling 2008-2016

Time Dependence of 50–250 MeV Galactic Cosmic-Ray Protons between Solar Cycles 24 and 25, Measured by the High-energy Particle Detector on board the CSES-01 Satellite

M. [Martucci](#)¹, R. Ammendola¹, D. Badoni¹, S. Bartocci¹, R. Battiston^{2,3}, S. Beolè^{4,5}, W. J. Burger², D. Campana⁶, G. Castellini⁷, P. Cipollone¹Show full author list

2023 ApJL 945 L39

<https://iopscience.iop.org/article/10.3847/2041-8213/acbea7/pdf>

Time-dependent energy spectra of galactic cosmic rays (GCRs) carry crucial information regarding their origin and propagation throughout the interstellar environment. When observed at the Earth, after traversing the interplanetary medium, such spectra are heavily affected by the solar wind and the embedded solar magnetic field permeating the inner sectors of the heliosphere. The activity of the Sun changes significantly over an 11 yr solar cycle—and so does the effect on cosmic particles; this translates into a phenomenon called solar modulation. Moreover, GCR spectra during different epochs of solar activity provide invaluable information for a complete understanding of the plethora of mechanisms taking place in various layers of the Sun's atmosphere and how they evolve over time. The High-Energy Particle Detector (HEPD-01) has been continuously collecting data since 2018 August, during the quiet phase between solar cycles 24 and 25; the activity of the Sun is slowly but steadily rising and is expected to peak around 2025/2026. In this paper, we present the first spectra for ~50–250 MeV galactic protons measured by the HEPD-01 instrument—placed on board the CSES-01 satellite—from 2018 August to 2022 March over a one-Carrington-rotation time basis. Such data are compared to the ones from other spaceborne experiments, present (e.g., EPHIN, Parker Solar Probe) and past (PAMELA), and to a state-of-the-art three-dimensional model describing the GCRs propagation through the heliosphere.

Interplanetary Magnetic Flux Ropes as Agents Connecting Solar Eruptions and Geomagnetic Activities

K. [Marubashi](#), K.-S. Cho, H. Ishibashi

[Solar Physics](#) December 2017, 292:189

<https://link.springer.com/content/pdf/10.1007%2Fs11207-017-1204-2.pdf>

We investigate the solar wind structure for 11 cases that were selected for the campaign study promoted by the International Study of Earth-affecting Solar Transients (ISEST) MiniMax24 Working Group 4. We can identify clear flux rope signatures in nine cases. The geometries of the nine interplanetary magnetic flux ropes (IFRs) are examined with a model-fitting analysis with cylindrical and toroidal force-free flux rope models. For seven cases in which magnetic fields in the solar source regions were observed, we compare the IFR geometries with magnetic structures in their solar source regions. As a result, we can confirm the coincidence between the IFR orientation and the orientation of

the magnetic polarity inversion line (PIL) for six cases, as well as the so-called helicity rule as regards the handedness of the magnetic chirality of the IFR, depending on which hemisphere of the Sun the IFR originated from, the northern or southern hemisphere; namely, the IFR has right-handed (left-handed) magnetic chirality when it is formed in the southern (northern) hemisphere of the Sun. The relationship between the orientation of IFRs and PILs can be taken as evidence that the flux rope structure created in the corona is in most cases carried through interplanetary space with its orientation maintained. In order to predict magnetic field variations on Earth from observations of solar eruptions, further studies are needed about the propagation of IFRs because magnetic fields observed at Earth significantly change depending on which part of the IFR hits the Earth. **7 – 9 March 2012, 12 – 14 July 2012, 23 – 24 July 2012, 4 – 8 October 2012, 15 – 17 March 2013, 1 June 2013, 10 – 13 September 2014, 15 – 17 March 2015, 22 – 24 June 2015**

Geometrical Relationship Between Interplanetary Flux Ropes and Their Solar Sources

K. [Marubashi](#), S. Akiyama, S. Yashiro, N. Gopalswamy, K.-S. Cho, Y.-D. Park

Solar Phys. May 2015, Volume 290, [Issue 5](#), pp 1371-1397 **2015**

We investigated the physical connection between interplanetary flux ropes (IFRs) near Earth and coronal mass ejections (CMEs) by comparing the magnetic field structures of IFRs and CME source regions. The analysis is based on the list of 54 pairs of ICMEs (interplanetary coronal mass ejections) and CMEs that are taken to be the most probable solar source events. We first attempted to identify the flux rope structure in each of the 54 ICMEs by fitting models with a cylinder and torus magnetic field geometry, both with a force-free field structure. This analysis determined the possible geometries of the identified flux ropes. Then we compared the flux rope geometries with the magnetic field structure of the solar source regions. We obtained the following results: (1) Flux rope structures are seen in 51 ICMEs out of the 54. The result implies that all ICMEs have an intrinsic flux rope structure, if the three exceptional cases are attributed to unfavorable observation conditions. (2) It is possible to find flux rope geometries with the main axis orientation close to the orientation of the magnetic polarity inversion line (PIL) in the solar source regions, the differences being less than 25° . (3) The helicity sign of an IFR is strongly controlled by the location of the solar source: flux ropes with positive (negative) helicity are associated with sources in the southern (northern) hemisphere (six exceptions were found). (4) Over two-thirds of the sources in the northern hemisphere are concentrated along PILs with orientations of $45^\circ \pm 30^\circ$ (measured clockwise from the east), and over two-thirds in the southern hemisphere along PILs with orientations of $135^\circ \pm 30^\circ$, both corresponding to the Hale boundaries. *These results strongly support the idea that a flux rope with the main axis parallel to the PIL erupts in a CME and that the erupted flux rope propagates through the interplanetary space with its orientation maintained and is observed as an IFR.*

Geometry of the 20 November 2003 Magnetic Cloud

Katsuhide [Marubashi](#), Kyung-Suk Cho, Yeon-Han Kim, Yong-Deuk Park, and Sung-Hong Park

J. Geophys. Res., Vol. 117, No. A1, A01101, **2012**, [File](#)

This study is an attempt to find a coherent interpretation of the link between the 20 November 2003 magnetic cloud (MC) and its solar source. Most previous studies agree on the orientation of the MC, but the orientation is nearly perpendicular to the axis of the post-eruption arcade (PEA) or the orientation of the neutral line in the solar source region. We first determine the geometry of this MC by fitting methods with both torus and cylinder models. Three possible geometries are obtained, which can reproduce the observed magnetic field variations associated with the MC, one from the cylinder fit and two from the torus fit. The cylinder fit gives the MC orientation with a tilt of a large angle ($\sim 60^\circ$) from the ecliptic plane and nearly perpendicular to the PEA axis, being similar to those from previous studies. In contrast, two torus fit results give the MC axis with tilt angles less than 20° from the ecliptic plane. The two torus results correspond to the spacecraft encounter with the eastern flank of the flux rope loop (model A) and the western flank of the loop (model B), respectively. In either case, the orientation of the loop around the apex is nearly parallel to the PEA as observed by the SOHO/extreme ultraviolet imaging telescope instrument in the most plausible solar source region of a halo coronal mass ejection (CME), which appeared in the field of view of Large Angle and Spectrometric Coronagraph (LASCO) C2 at 08:50 UT, 18 November 2003. The magnetic helicity of the PEA region is positive in agreement with the helicity of the MC. The 3-D reconstruction from the Solar Mass Ejection Imager data shows that the main part of the ejected plasma expands mainly to the west of the Sun-Earth line. Thus, we reach the most straightforward interpretation of the link between the MC and its solar source as follows. The MC was created in association with the launch of the CME that was first observed by the LASCO C2 at 08:50 UT, 18 November 2003, and propagated through interplanetary space with its orientation almost unchanged. The spacecraft encountered the eastern flank of the loop as described by model A.

Superposed epoch study of ICME sub-structures near Earth and their effects on Galactic cosmic rays

J. J. **Masías-Meza**¹, S. Dasso^{2,3}, P. Démoulin⁴, L. Rodríguez⁵ and M. Janvier⁶
A&A 592, A118 (2016)

Context. Interplanetary coronal mass ejections (ICMEs) are the interplanetary manifestations of solar eruptions. The overtaken solar wind forms a sheath of compressed plasma at the front of ICMEs. Magnetic clouds (MCs) are a subset of ICMEs with specific properties (e.g. the presence of a flux rope). When ICMEs pass near Earth, ground observations indicate that the flux of Galactic cosmic rays (GCRs) decreases.

Aims. The main aims of this paper are to find common plasma and magnetic properties of different ICME sub-structures and which ICME properties affect the flux of GCRs near Earth.

Methods. We used a superposed epoch method applied to a large set of ICMEs observed in situ by the spacecraft ACE, between 1998 and 2006. We also applied a superposed epoch analysis on GCRs time series observed with the McMurdo neutron monitors.

Results. We find that slow MCs at 1 AU have on average more massive sheaths. We conclude that this is because they are more effectively slowed down by drag during their travel from the Sun. Slow MCs also have a more symmetric magnetic field and sheaths expanding similarly as their following MC, while in contrast, fast MCs have an asymmetric magnetic profile and a sheath in compression. In all types of MCs, we find that the proton density and the temperature and the magnetic fluctuations can diffuse within the front of the MC due to 3D reconnection. Finally, we derive a quantitative model that describes the decrease in cosmic rays as a function of the amount of magnetic fluctuations and field strength.

Conclusions. The obtained typical profiles of sheath, MC and GCR properties corresponding to slow, middle, and fast ICMEs, can be used for forecasting or modelling these events, and to better understand the transport of energetic particles in ICMEs. They are also useful for improving future operative space weather activities.

Microwave radio emissions as a proxy for coronal mass ejection speed in arrival predictions of interplanetary coronal mass ejections at 1 AU

Carolina Salas **Matamoros**^{1,2*}, Karl Ludwig Klein¹ and Gerard Trottet
J. Space Weather Space Clim., 7, A2 (2017)

<http://www.swsc-journal.org/articles/swsc/pdf/2017/01/swsc160027.pdf>

The propagation of a coronal mass ejection (CME) to the Earth takes between about 15 h and several days. We explore whether observations of non-thermal microwave bursts, produced by near-relativistic electrons via the gyrosynchrotron process, can be used to predict travel times of interplanetary coronal mass ejections (ICMEs) from the Sun to the Earth. In a first step, a relationship is established between the CME speed measured by the Solar and Heliospheric Observatory/Large Angle and Spectrometric Coronagraph (SoHO/LASCO) near the solar limb and the fluence of the microwave burst. This relationship is then employed to estimate speeds in the corona of earthward-propagating CMEs. These speeds are fed into a simple empirical interplanetary acceleration model to predict the speed and arrival time of the ICMEs at Earth. The predictions are compared with observed arrival times and with the predictions based on other proxies, including soft X-rays (SXR) and coronagraphic measurements. We found that CME speeds estimated from microwaves and SXR predict the ICME arrival at the Earth with absolute errors of 11 ± 7 and 9 ± 7 h, respectively. A trend to underestimate the interplanetary travel times of ICMEs was noted for both techniques. This is consistent with the fact that in most cases of our test sample, ICMEs are detected on their flanks. Although this preliminary validation was carried out on a rather small sample of events (11), we conclude that microwave proxies can provide early estimates of ICME arrivals and ICME speeds in the interplanetary space. This method is limited by the fact that not all CMEs are accompanied by non-thermal microwave bursts. But its usefulness is enhanced by the relatively simple observational setup and the observation from ground, which makes the instrumentation less vulnerable to space weather hazards.

11 Apr 1997, 2002 Aug 23, 2003 Oct 24, 2004 Jun 16, 2008 Mar 25, 28 Oct 2011, 9 Mar 2012

Table 1. Table of events: event number (col. 1), date (col. 2), time of the first appearance of the CME in LASCO/C2 coronagraph (col. 3), CME speed in the plane of the sky reported in LASCO-CME (col. 4), SXR peak time (col. 5), times of onset (col. 6), end (col. 7), fluences at 3 GHz (col. 8), 9 GHz (col. 9), maximum (col. 10) of microwave bursts. Lower limits of the maximum fluence mean that the real maximum was outside the observed frequency range.

Table 3. Comparison between ICME arrival times measured at Wind spacecraft and predicted based on 9 GHz fluence: See CESRA highlight #1336 May 2017 <http://cesra.net/?p=1336>

Microwave emission as a proxy of CME speed in ICME arrival time predictions

Carolina Salas **Matamoros**^{1,2}, Karl-Ludwig Klein^{3,4}, and Gerard Trottet³
CESRA 2016, p.82

http://cesra2016.sciencesconf.org/conference/cesra2016/pages/CESRA2016_prog_abs_book_v3.pdf

The propagation of a coronal mass ejection (CME) to the Earth takes between about 13 hours and several days. Observations of early radiative signatures of CMEs therefore provide a possible means to predict the arrival time of the CME near Earth. The fundamental tool to measure CME speeds in the corona is coronagraphy, but the Earth-directed speed of a CME cannot be measured by a coronagraph located on the Sun-Earth line. Various proxies have been devised, based on the coronagraphic measurement. As an alternative, we explore radiative proxies. In the present contribution we investigate if microwave observations can be employed as a proxy for CME propagation speed. Caroubalos (1964) had shown that the higher the uence of a solar radio burst near 3 GHz, the shorter is the time lapse between the solar event and the sudden commencement of a geomagnetic storm. We reconsider the relationship between CME speed and microwave uence for limb CMEs in cycle 23 and early cycle 24. Then we use the microwave uence as a proxy of CME speed of Earth-directed CMEs, together with the empirical interplanetary acceleration model devised by Gopalswamy et al. (2001), to predict the CME arrival time at Earth. These predictions are compared with observed arrival times and with the predictions based on other proxies, including soft X-rays and coronagraphic measurements.

Study of Moderate, Intense and Severe Geomagnetic Storms in Relation to the Interplanetary Magnetic Field for Solar Cycle 24

Chandni [Mathpal](#), Lalan Prasad, Meena Pokharia, Chandrasekhar Bhoj, Rajesh Mathpal and Hema Kharayat
[Journal of Pure Applied and Industrial Physics 2018](#)

Dependence of Geomagnetic Storms on Diverse Solar Wind Parameters, Interplanetary Magnetic Field, Interplanetary Conditions for Solar Cycle 23

Chandni [Mathpal](#) and Lalan Prasad

J. Pure Appl. & Ind. Phy. Vol.8 (8), 90 - 97 (2018)

<http://physics-journal.org/download/Chandni-Mathpal-and-Lalan-Prasad/PHYSICS-JOURNAL-PHSV08I08P0090.pdf>

In order to find the association of geomagnetic storm (GS) with various solar wind parameters, interplanetary magnetic field (IMF B), interplanetary conditions (such as B_y , B_z and E_y), we incorporate the analysis technique by superposed-epoch method. The current analysis depict that solar wind parameters (such as solar wind speed V and plasma proton temperature), interplanetary conditions (such as B_z and E_y) and IMF B are geo-effective parameters while B_y component is not a geo-effective parameter. By the comparison of different indices and finally we conclude that K_p index is a powerful indicator of geomagnetic activity.

Full compressible 3D magnetohydrodynamic simulation of solar wind

[Takuma Matsumoto](#)

MNRAS 2020

<https://arxiv.org/pdf/2009.03770>

Identifying the heating mechanisms of the solar corona and the driving mechanisms of solar wind are key challenges in understanding solar physics. A full three-dimensional compressible magnetohydrodynamic (MHD) simulation was conducted to distinguish between the heating mechanisms in the fast solar wind above the open field region. Our simulation describes the evolution of the Alfvénic waves, which includes the compressible effects from the photosphere to the heliospheric distance s of 27 solar radii (R_\odot). The hot corona and fast solar wind were reproduced simultaneously due to the dissipation of the Alfvén waves. The inclusion of the transition region and lower atmosphere enabled us to derive the solar mass loss rate for the first time by performing a full three-dimensional compressible MHD simulation. The Alfvén turbulence was determined to be the dominant heating mechanism in the solar wind acceleration region ($s > 1.3R_\odot$), as suggested by previous solar wind models. In addition, shock formation and phase mixing are important below the lower transition region ($s < 1.03R_\odot$) as well.

The essential role of multi-point measurements in investigations of turbulence, three-dimensional structure, and dynamics: the solar wind beyond single scale and the Taylor Hypothesis

W. H. [Matthaeus](#), [R. Bandyopadhyay](#), [M.R.Brown](#), [R.Bruno](#), [J. Borovsky](#), [V. Carbone](#), [D. Caprioli](#), et al.
White Paper submitted to: Decadal Survey for Solar and Space Physics (Heliophysics) 2024-2033. 2022

<https://arxiv.org/ftp/arxiv/papers/2211/2211.12676.pdf>

Space plasmas are three-dimensional dynamic entities. Except under very special circumstances, their structure in space and their behavior in time are not related in any simple way. Therefore, single spacecraft in situ measurements cannot unambiguously unravel the full space-time structure of the heliospheric plasmas of interest in the inner heliosphere, in the Geospace environment, or the outer heliosphere. This shortcoming leaves numerous central questions incompletely answered. Deficiencies remain in at least two important subjects, Space Weather and fundamental plasma turbulence theory, due to a lack of a more complete understanding of the space-time structure of dynamic plasmas. Only with multispacecraft measurements over suitable spans of spatial separation and temporal duration can these ambiguities be resolved. We note that these characterizations apply to turbulence across a wide range of scales, and also equally well to shocks, flux ropes, magnetic clouds, current sheets, stream interactions, etc. In the following, we will describe the basic requirements for resolving space-time structure in general, using turbulence' as both an example and a principal target of study. Several types of missions are suggested to resolve space-time structure throughout the Heliosphere.

The geomagnetic Kp index and derived indices of geomagnetic activity

J. Matzka , C. Stolle , Y. Yamazaki , O. Bronkalla , A. Morschhauser

Space Weather **Volume19, Issue5** e2020SW002641 2021

<https://agupubs.onlinelibrary.wiley.com/doi/epdf/10.1029/2020SW002641>

<https://doi.org/10.1029/2020SW002641>

The geomagnetic Kp index is one of the most extensively used indices of geomagnetic activity, both for scientific and operational purposes. This article reviews the properties of the Kp index and provides a reference for users of the Kp index and associated data products as derived and distributed by the GFZ German Research Centre for Geosciences. The near real-time production of the nowcast Kp index is of particular interest for space weather services and here we describe and evaluate its current setup.

Multi-Spacecraft Observations of an Interplanetary Coronal Mass Ejection Interacting with Two Solar-Wind Regimes Observed by the Ulysses and Twin-STEREO Spacecraft

Megan L. Maunder, Claire Foullon, Robert Forsyth, David Barnes & Jackie Davies

Solar Physics volume 297, Article number: 148 (2022)

<https://link.springer.com/content/pdf/10.1007/s11207-022-02077-3.pdf>

We present a combined study of a coronal mass ejection (CME), revealed in a unique orbital configuration that permits the analysis of remote-sensing observations on **27 June 2007** from the twin Solar Terrestrial Relations Observatory (STEREO)-A and -B spacecraft and of its subsequent in situ counterpart outside the ecliptic plane, the interplanetary coronal mass ejection (ICME) observed on **04 July 2007** by Ulysses at 1.5 AU and heliographic-Earth-ecliptic coordinates system (HEE) 33° latitude and 49° longitude. We apply a triangulation method to the STEREO Sun Earth Connection Coronal and Heliospheric Investigation (SECCHI) COR2 coronagraph images of the CME, and a self-similar expansion fitting method to STEREO/SECCHI Heliospheric Imager (HI)-B. At Ulysses we observe: a preceding forward shock, followed by a sheath region, a magnetic cloud, a rear forward shock, followed by a compression region due to a succeeding high-speed stream (HSS) interacting with the ICME. From a minimum variance analysis (MVA) and a length-scale analysis we infer that the magnetic cloud at Ulysses, with a duration of 24 h, has a west-north-east configuration, length scale of ≈ 0.2 AU, and mean expansion speed of 14.2 km s⁻¹. The relatively small size of this ICME is likely to be a result of its interaction with the succeeding HSS. This ICME differs from the previously known over-expanding types observed by Ulysses, in that it straddles a region between the slow and fast solar wind that in itself drives the rear shock. We describe the agreements and limitations of these observations in comparison with 3D magneto-hydrodynamic (MHD) heliospheric simulations of the ICME in the context of a complex solar-wind environment.

Study of Evolution and Geo-effectiveness of Coronal Mass Ejection–Coronal Mass Ejection Interactions Using Magnetohydrodynamic Simulations with SWASTi Framework

Prateek Mayank¹, Stefan Lotz², Bhargav Vaidya^{1,3}, Wageesh Mishra⁴, and D. Chakrabarty⁵

2024 ApJ 976 126

<https://iopscience.iop.org/article/10.3847/1538-4357/ad8084/pdf>

The geo-effectiveness of coronal mass ejections (CMEs) is a critical area of study in space weather, particularly in the lesser-explored domain of CME–CME interactions and their geomagnetic consequences. This study leverages the Space Weather Adaptive Simulation framework to perform 3D MHD simulation of a range of CME–CME interaction scenarios within realistic solar wind conditions. The focus is on the dynamics of the initial magnetic flux, speed, density,

and tilt of CMEs, and their individual and combined impacts on the disturbance storm time (Dst) index. Additionally, the kinematic, magnetic, and structural impacts on the leading CME, as well as the mixing of both CMEs, are analyzed. Time-series in situ studies are conducted through virtual spacecraft positioned along three different longitudes at 1 au. Our findings reveal that CME–CME interactions are nonuniform along different longitudes, due to the inhomogeneous ambient solar wind conditions. A significant increase in the momentum and kinetic energy of the leading CME is observed due to collisions with the trailing CME, along with the formation of reverse shocks in cases of strong interaction. These reverse shocks lead to complex wave patterns inside CME2, which can prolong the storm recovery phase. Furthermore, we observe that the minimum Dst value decreases with an increase in the initial density, tilt, and speed of the trailing CME. **2015-06-23, 2017-09-08, 2023-04-24, 2023 May 13-15**

Table 1 CME Initial Properties of All the Ensemble Cases

SWASTi-CME: A physics-based model to study CME evolution and its interaction with Solar Wind

Prateek **Mayank**, [Bhargav Vaidya](#), [Wageesh Mishra](#), [D. Chakrabarty](#)

2024 ApJS 270 10

<https://arxiv.org/pdf/2310.18219.pdf>

<https://iopscience.iop.org/article/10.3847/1538-4365/ad08c7/pdf>

Coronal mass ejections (CMEs) are primary drivers of space weather and studying their evolution in the inner heliosphere is vital to prepare for a timely response. Solar wind streams, acting as background, influence their propagation in the heliosphere and associated geomagnetic storm activity. This study introduces SWASTi-CME, a newly developed MHD-based CME model integrated into the Space Weather Adaptive SimulaTion (SWASTi) framework. It incorporates a non-magnetized elliptic cone and a magnetized flux rope CME model. To validate the model's performance with in-situ observation at L1, two Carrington rotations were chosen: one during solar maxima with multiple CMEs, and one during solar minima with a single CME. The study also presents a quantitative analysis of CME-solar wind interaction using this model. To account for ambient solar wind effects, two scenarios of different complexity in solar wind conditions were established. The results indicate that ambient conditions can significantly impact some of the CME properties in the inner heliosphere. We found that the drag force on the CME front exhibits a variable nature, resulting in asymmetric deformation of the CME leading edge. Additionally, the study reveals that the impact on the distribution of CME internal pressure primarily occurs during the initial stage, while the CME density distribution is affected throughout its propagation. Moreover, regardless of the ambient conditions, it was observed that after a certain propagation time (t), the CME volume follows a non-fractal power-law expansion ($\propto t^{3.03-3.33}$) due to the attainment of a balanced state with ambient. **2015-06-18-25, 07 Dec. 2020**

SWASTi-SW: Space Weather Adaptive SimulaTion framework for Solar Wind and its relevance to ADITYA-L1 mission

Prateek **Mayank**, [Bhargav Vaidya](#), [D. Chakrabarty](#)

ApJS 262 23 2022

<https://arxiv.org/pdf/2207.13708.pdf>

<https://iopscience.iop.org/article/10.3847/1538-4365/ac8551/pdf>

Solar wind streams, acting as background, govern the propagation of space weather drivers in the heliosphere, which induce geomagnetic storm activities. Therefore, predictions of the solar wind parameters are the core of space weather forecasts. This work presents an indigenous three-dimensional (3D) Solar Wind model (SWASTi-SW). This numerical framework for forecasting the ambient solar wind is based on a well-established scheme that uses a semi-empirical coronal model and a physics-based inner heliospheric model. This study demonstrates a more generalized version of Wang-Sheeley-Arge (WSA) relation, which provides a speed profile input to the heliospheric domain. Line-of-sight observations of GONG and HMI magnetograms are used as inputs for the coronal model, which in turn, provides the solar wind plasma properties at 0.1 AU. These results are then used as an initial boundary condition for the magnetohydrodynamics (MHD) model of the inner heliosphere to compute the solar wind properties up to 2.1 AU. Along with the validation run for multiple Carrington rotations, the effect of variation of specific heat ratio and study of stream interaction region (SIR) is also presented. This work showcases the multi-directional features of SIRs and provides synthetic measurements for potential observations from the Solar Wind Ion Spectrometer (SWIS) subsystem of Aditya Solar wind Particle EXperiment (ASPEX) payload on-board ISRO's upcoming solar mission Aditya-L1.

Propagation of the 7 January 2014 CME and Resulting Geomagnetic Non-Event

M. L. **Mays**, B. J. Thompson, L. K. Jian, R. C. Colaninno, D. Odstrcil, C. Möstl, M. Temmer, N. P. Savani, A. Taktakishvili, P. J. MacNeice, Y. Zheng

2015 ApJ 812 145

<http://arxiv.org/pdf/1509.06477v1.pdf>

On 7 January 2014 an X1.2 flare and CME with a radial speed ≈ 2500 km s⁻¹ was observed from near an active region close to disk center. This led many forecasters to estimate a rapid arrival at Earth (≈ 36 hours) and predict a strong geomagnetic storm. However, only a glancing CME arrival was observed at Earth with a transit time of ≈ 49 hours and a KP geomagnetic index of only 3-. We study the interplanetary propagation of this CME using the ensemble Wang-Sheeley-Argé (WSA)-ENLIL+Cone model, that allows a sampling of CME parameter uncertainties. We explore a series of simulations to isolate the effects of the background solar wind solution, CME shape, tilt, location, size, and speed, and the results are compared with observed in-situ arrivals at Venus, Earth, and Mars. Our results show that a tilted ellipsoid CME shape improves the initial real-time prediction to better reflect the observed in-situ signatures and the geomagnetic storm strength. CME parameters from the Graduated Cylindrical Shell model used as input to WSA-ENLIL+Cone, along with a tilted ellipsoid cloud shape, improve the arrival-time error by 14.5, 18.7, 23.4 hours for Venus, Earth, and Mars respectively. These results highlight that CME orientation and directionality with respect to observatories play an important role in understanding the propagation of this CME, and for forecasting other glancing CME arrivals. This study also demonstrates the importance of three-dimensional CME fitting made possible by multiple viewpoint imaging.

Ensemble Modeling of CMEs Using the WSA-ENLIL+Cone Model

M. L. Mays, A. Taktakishvili, A. Pulkkinen, [P. J. MacNeice](#), [L. Rastätter](#), [D. Odstrcil](#), [L. K. Jian](#), [I. G. Richardson](#), [J. A. LaSota](#), [Y. Zheng](#), ...

Solar Phys. Volume 290, Issue 6, pp 1775-1814 2015

<http://arxiv.org/pdf/1504.04402v2.pdf>

Ensemble modeling of coronal mass ejections (CMEs) provides a probabilistic forecast of CME arrival time that includes an estimation of arrival-time uncertainty from the spread and distribution of predictions and forecast confidence in the likelihood of CME arrival. The real-time ensemble modeling of CME propagation uses the Wang-Sheeley-Argé (WSA)-ENLIL+Cone model installed at the Community Coordinated Modeling Center (CCMC) and executed in real-time at the CCMC/[Space Weather](#) Research Center. The current implementation of this ensemble-modeling method evaluates the sensitivity of WSA-ENLIL+Cone model simulations of CME propagation to initial CME parameters. We discuss the results of real-time ensemble simulations for a total of 35 CME events that occurred between January 2013 – July 2014. For the 17 events where the CME was predicted to arrive at Earth, the mean absolute arrival-time prediction error was 12.3 hours, which is comparable to the errors reported in other studies. For predictions of CME arrival at Earth, the correct-rejection rate is 62 %, the false-alarm rate is 38 %, the correct-alarm ratio is 77 %, and the false-alarm ratio is 23 %. The arrival time was within the range of the ensemble arrival predictions for 8 out of 17 events. The Brier Score for CME arrival-predictions is 0.15 (where a score of 0 on a range of 0 to 1 is a perfect forecast), which indicates that on average, the predicted probability, or likelihood, of CME arrival is fairly accurate. The reliability of ensemble CME-arrival predictions is heavily dependent on the initial distribution of CME input parameters (e.g. speed, direction, and width), particularly the median and spread. Preliminary analysis of the probabilistic forecasts suggests undervariability, indicating that these ensembles do not sample a wide-enough spread in CME input parameters. Prediction errors can also arise from ambient-model parameters, the accuracy of the solar-wind background derived from coronal maps, or other model limitations. Finally, predictions of the K P geomagnetic index differ from observed values by less than one for 11 out of 17 of the ensembles and K P prediction errors computed from the mean predicted K P show a mean absolute error of 1.3. **11 April 2013, 18 April 2014**

Table 1.: Summary of the ensemble simulation results for 35 CME events (January 2013 - June 2014).

Observations of Switchback Chains in a Double Solar Proton Event

Emily McDougall, [Bala Poduval](#)

Solar Phys. 2024

<https://arxiv.org/abs/2407.01815>

Although recent research suggests a link in support of a model of switchback formation in the solar corona via interchange reconnection that is propagated outward with the solar wind and similarities in their ion composition to plasma instability produced plasmoids, these plasma instabilities have yet to be observationally linked to magnetic switchbacks. In this paper we aim to use the theoretical framework of a twin coronal mass ejection event which is known to include interchange reconnection processes and compare this model with experimental observations using Parker Solar Probe FIELDS and *is* instrumentation of an actual event containing two CMEs identified via the associated solar proton event in order to further test and refine the hypothesis of interchange reconnection as a possible

physical origin for the magnetic switchback phenomenon. We also intend to introduce a plasma model for the formation of the switchbacks noted within the CME event. **2022 17-18 August**

Correcting Parker Solar Probe Electron Measurements for Spacecraft Magnetic and Electric Fields

Daniel **McGinnis**, Jasper Halekas, Phyllis Whittlesey, Davin Larson, Justin Kasper

Space Weather [Volume 124, Issue 9](#) September 2019 Pages 7369-7384

[sci-hub.se/10.1029/2019ja026823](https://doi.org/10.1029/2019ja026823)

The spacecraft body of the Parker Solar Probe may interfere with electron measurements in two ways. The first is the presence of several permanent magnets near the Solar Probe Analyzers (SPAN) instruments. The second is the widely varying spacecraft potential. We estimate the effect of these interferences by performing particle tracing simulations on electrons of various energies using a simplified model of the spacecraft potential and measurements of the magnetic fields. From this we can (1) estimate the individual and combined fields of view of the SPAN-E instruments, (2) identify regions of phase space that may be highly distorted, and (3) simulate measurements of the velocity distribution function. We compute density, temperature, and bulk velocity moments of the measured distribution functions and find that a correction table derived from the particle tracing results can be incorporated in the computation to greatly decrease the errors caused by the spacecraft potential and magnetic fields. Similar tables could be computed for a wide range of spacecraft potentials and applied during the processing of actual SPAN data.

Properties Underlying the Variation of the Magnetic Field Spectral Index in the Inner Solar Wind

R. **McIntyre**¹, C. H. K. Chen¹, and A. Larosa¹

2023 ApJ 957 111

<https://iopscience.iop.org/article/10.3847/1538-4357/acf3dd/pdf>

Using data from orbits 1–11 of the Parker Solar Probe mission, the magnetic field spectral index was measured across a range of heliocentric distances. The previously observed transition between a value of $-5/3$ far from the Sun and a value of $-3/2$ close to the Sun was recovered, with the transition occurring at around $50 R_{\odot}$ and the index saturating at $-3/2$ as the Sun is approached. A statistical analysis was performed to separate the variation of the index on distance from its dependence on other parameters of the solar wind that are plausibly responsible for the transition, including the cross helicity, residual energy, turbulence age, and magnitude of magnetic fluctuations. Of all parameters considered, the cross helicity was found to be by far the strongest candidate for the underlying variable responsible. The velocity spectral index was also measured and found to be consistent with $-3/2$ over the range of values of cross helicity measured. Possible explanations for the behavior of the indices are discussed, including the theorized different behavior of imbalanced, compared to balanced, turbulence.

Near real-time predictions of the arrival at Earth of flare-related shocks during Solar Cycle 23

S. M. P. **McKenna-Lawlor**, M. Dryer et al.

JOURNAL OF GEOPHYSICAL RESEARCH, VOL. 111, A11103, doi:10.1029/2005JA011162, **2006**

Predicting interplanetary shock arrivals at Earth, Mars, and Venus: A real-time modeling experiment following the solar flares of 5-14 December 2006

McKenna-Lawlor, S. M. P., M. Dryer, C. D. Fry, Z. K. Smith, D. S. Intriligator, W. R. Courtney, C. S. Deehr, W. Sun, K. Kecskemety, K. Kudela, J. Balaz, S. Barabash, Y. Futaana, M. Yamauchi, and R. Lundin (2008),

J. Geophys. Res., 113, A06101, 3 June **2008**

<http://dx.doi.org/10.1029/2007JA012577>

A 3-D, kinematic, solar wind model (Hakamada-Akasofu-Fry version 2 (HAFv.2)) is used to predict interplanetary shock arrivals at Venus, Earth, and Mars during a sequence of significant solar events that occurred in the interval 5–14 December 2006. Mars and Venus were on the opposite side of the Sun from Earth during this period. The shocks from the first two east limb events (5 and 6 December) were predicted to interact to form a single disturbance before reaching Earth and Venus. A single shock was indeed recorded at Earth only about 3 h earlier than had been predicted. The composite shock was predicted by HAFv.2 to arrive at Venus on 8 December at ~ 0500 UT. Solar energetic particles (SEPs) were detected in Venus Express Analyzer of Space Plasmas and Energetic Atoms-4 data for some 3 d (from <0530 UT on 6 December), and an energetic storm particle (ESP) event signaled the arrival of a single shock wave at 0900 UT on 7 December. SEPs were correspondingly recorded at Mars. However, the eastern flank of the composite

shock was predicted to decay to an MHD wave prior to reaching this location, and no shock signature was observed in the available data. The shocks generated in association with two flare events that occurred closer to the West Limb on 13 and 14 December were predicted by HAFv.2 to remain separate when they arrived at Earth but to combine thereafter before reaching Mars. Each was expected to decay to MHD waves before reaching Venus, which was at that time located behind the Sun. Separated shocks were observed to arrive at L1 (ACE) only 8 min earlier than and 5.3 h later than their predicted times. The western flank of the combined shocks was predicted to arrive at Mars early on 20 December 2006. An indication of the passage of this shock was provided by a signature of ion heating in Mars Express IMA (ion mass-resolving analyzer) data from <0424 UT on 20 December. The predictions of the HAFv.2 model for Earth were each well within the ± 11 h. RMS error earlier found, on the basis of significant statistics, to apply at 1 AU during the rise and maximum phases of solar cycle 23. Overall, the model is demonstrated to be capable of predicting the effects produced by shocks and by the background solar wind at Venus, Earth, and Mars. It is suggested that the continuous presence of solar wind monitors (plasma and interplanetary magnetic field observations) at “benchmark planets” can constitute a necessary and valuable component of ongoing and future space weather programs for the validation of solar wind models such as HAFv.2.

Validation of community models: 2. Development of a baseline using the Wang-Sheeley-Arge model

Near realtime predictions of the arrival at Earth of flare - related shocks during Solar Cycle 23,

McKenna - Lawlor, S. M. P., M. Dryer, M. D. Kartalev, Z. Smith, C. D. Fry, W. Sun, C. S. Deehr, K. Kecskemety, and K. Kudela (2006), *J. Geophys. Res.*, 111, A11103, doi:10.1029/2005JA011162.

The arrival times at Earth of 166 flare-related shocks identified exiting the Sun (using metric radio drift data) during the maximum phase of Solar Cycle 23, were forecast in near-real time using the Shock Time of Arrival Model (STOA), the Interplanetary Shock Propagation Model (ISPM) and the Hakamada-Akasofu-Fry Model (version 2, HAFv.2). These predictions are compared with the arrival at L1 of shocks recorded in plasma and magnetic data aboard the ACE spacecraft. The resulting correspondences are graded following standard statistical methods. Among other parameters, a representative reference metric defined by $\{(\text{“hits”} + \text{“correct nulls”}) \times 100\} / (\text{total number of predictions})$ is used to describe the success rates of the predictions relative to the measurements. Resulting values for STOA, ISPM, and HAFv.2 were 50%, 57%, and 51%, respectively, for a hit window of ± 24 hours. On increasing the statistical sample by 173 events recorded during the rise phase of the same cycle, corresponding success rates of 54%, 60%, and 52%, respectively, were obtained. A χ^2 test shows these results to be statistically significant at better than the 0.05 level. The effect of decreasing/increasing the size of the hit window is explored and the practical utility of shock predictions considered. Circumstances under which the models perform well/poorly are investigated through the formation, and statistical analysis, of various event subsets, within which the constituent shocks display common characteristics. The results thereby obtained are discussed in detail in the context of the limitations that affect some aspects of the data utilized in the models.

Early Studies in Solar Wind Coupling and Substorms

Historical **Review**

Robert L. **McPherron**

JGR **Volume 125, Issue 5** May 2020 2019JA027615

https://agupubs.onlinelibrary.wiley.com/doi/pdf/10.1029/2019JA027615?casa_token=qtLH6w8E-icAAAAA:GncaFsXY_-xWlqdScdUr5JBObWpq709xWWHQbL1aJbEkqj00Chwc74_YpMHLyof9dIYqZiPyrj11Q

The space age began while I was a Physics student at Berkeley. NASA stimulated space research by the creation of eight centers of excellence each with a new building and very large grants. These centers became the nucleus of research activities that continue 55 years later. Data from new instruments and spacecraft provided unique opportunities for young people to make significant discoveries. In my case the concept of the auroral substorm was crucial, as later were data from the first instrumented synchronous satellite ATS-1, and one of the first eccentric orbiters OGO-5. In this account I describe my early experiences and the difficulties of completing my undergraduate degree. I then describe graduate work at Berkeley and multiple trips to the auroral zone. On completion of my PhD I began work at University of California, Los Angeles (UCLA) and soon became a professor. My graduate work and early research as a professor enabled me to introduce important concepts including the substorm growth phase, the concept of a magnetospheric substorm, the substorm current wedge, the near-Earth neutral line, the dipolarization of the synchronous magnetic field during substorms, the semiannual variation in geomagnetic activity, and algorithms to predict the Dst index and AL

index. I also did extensive work in investigations of ULF waves, magnetic storms, and the interaction of the solar wind with the magnetosphere, but these occurred later and are not discussed. I end with the question of whether it is possible today for young people with a background similar to mine to achieve similar success.

Data Assimilative Optimization of WSA Source Surface and Interface Radii using Particle Filtering

Grant David [Meadors](#) , [Shaela I. Jones](#) , [Kyle S. Hickmann](#) et al.

Space Weather **2020** e2020SW002464

<https://doi.org/10.1029/2020SW002464>

The Wang-Sheeley-Argge (WSA) model estimates solar wind speed and interplanetary magnetic field polarity in the inner heliosphere using global photospheric magnetic field maps. WSA employs the Potential Field Source Surface (PFSS) and Schatten Current Sheet (SCS) models to determine the Sun's global coronal magnetic field. The PFSS and SCS models are connected through two radial parameters, the source surface and interface radii, which specify the overlap region between the inner SCS and outer PFSS model. Though both radii values are adjustable, they have typically been fixed to 2.5 solar radii. Our work highlights how solar wind predictions improve when the radii are allowed to vary over time. Data assimilation using particle filtering (sequential Monte Carlo) is used to infer optimal values over a fixed time window. Solar wind model predictions and satellite observations are compared with a newly-developed quality-of-agreement prediction metric. The agreement metric between the model and observations is assumed to correspond to the probability of the two key WSA model parameters, the source surface and interface radii, where the highest metric value implies the optimal radii. We find that the optimal particle filter values of solar radii can perform twice as well as standard values for an exploratory period during Carrington Rotation 1901, with these values also reducing nonphysical kinking effects seen in solar magnetic field lines. Data assimilation choices of input realization and time frame have implications for variation in the solar wind over time. We present this work's theoretical context and practical applications for prediction accuracy.

Remote-Sensing of Solar Wind Speeds from IPS Observations at 140 and 327 MHz Using MEXART and STEL

J. C. [Mejia-Ambriz](#), B. V. Jackson, J. A. Gonzalez-Esparza, [A. Buffington](#), [M. Tokumaru](#), [E. Aguilar-Rodriguez](#)

Solar Phys. Volume 290, Issue 9, pp 2539-2552 **2015**

Interplanetary scintillation (IPS) is used to probe solar wind speeds in the inner heliosphere by applying either of two generalized data-analysis techniques: model fitting to power spectra (MFPS) from a single station, or cross-correlation functions (CCF) produced by cross-correlating two simultaneous IPS time series from separate stations. The MEXican Array Radio Telescope (MEXART), observing at 140 MHz, is starting to use an MFPS technique. Here we report the first successful solar wind speed determinations with IPS observations by MEXART. Three stations of the Solar-Terrestrial Environment Laboratory (STEL), observing at 327 MHz, use a CCF, and an MFPS technique is also used at one of these sites. We here analyze data from MEXART and from one antenna of STEL to obtain solar wind speeds using an MFPS technique from a single station. The IPS observations were carried out with radio source 3C48 during [Solar Cycle](#) 24. The MFPS method we describe here is tested by comparing its obtained speeds with those from the STEL CCF technique. We find that the speeds from the two techniques generally agree within the estimated errors.

Forbush Decreases and Associated Geomagnetic Storms: Statistical Comparison in Solar Cycles 23 and 24.

[Melkumyan](#), A.A., Belov, A.V., Shlyk, N.S., M.A. Abunina, A.A. Abunin, V.A. Oleneva & V.G. Yanke

Sol Phys 299, 40 (**2024**).

<https://doi.org/10.1007/s11207-024-02281-3>

Statistical relations between the geomagnetic Dst index, cosmic ray variations, and solar wind characteristics are compared for Forbush decreases associated with: (i) coronal mass ejections from active regions (AR-CMEs) accompanied by solar flares, (ii) filament eruptions outside active regions, (iii) corotating interaction regions (CIRs) caused by high-speed streams from coronal holes, (iv) mixed events induced by two or more solar sources. Relationships of geomagnetic indices and parameters of cosmic rays and the solar wind are also compared between sporadic events with or without magnetic clouds (MCs) and between Solar Cycles (SCs) 23 and 24. The results reveal that interplanetary disturbances originated by AR-CMEs associated with an MC are most geoeffective and cause powerful geomagnetic

storms, while CIRs create only moderate and weak storms. Sporadic and recurrent events differ in values of the Dst index and southward component of the magnetic field, as well as in the relationship between them. For sporadic events, geomagnetic activity is more affected by the presence or absence of an MC than by the type of solar source. Interplanetary disturbances associated with AR-CMEs are more effective in SC 23 while those associated with other types of solar sources have approximately the same geoeffectiveness in both SCs.

Statistical comparison of time profiles of Forbush decreases associated with coronal mass ejections and streams from coronal holes in solar cycles 23–24

A A [Melkumyan](#), A V [Belov](#), N S [Shlyk](#), M A [Abunina](#), A A [Abunin](#), V A [Oleneva](#), V G [Yanke](#)

Monthly Notices of the Royal Astronomical Society, Volume 521, Issue 3, May 2023, Pages 4544–4560, <https://doi.org/10.1093/mnras/stad772>

In this paper, Forbush decrease (FD) profiles are compared for events associated with (i) coronal mass ejections from active regions accompanied by solar flares (AR CMEs), (ii) filament eruptions away from active regions (non-AR CMEs), and (iii) high-speed streams (HSSs) from coronal holes (CHs). FD profiles are described by time parameters that are delayed from an FD onset to the registration of maximum values of cosmic ray (CR) density variations, CR density hourly decrease, CR equatorial anisotropy, solar wind (SW) speed, interplanetary magnetic field (IMF) strength and minimum *Dst* index. Distributions of these parameters from 1997 to 2020 and within maxima and minima of the last solar cycles (SCs) were compared by statistical methods. The results obtained reveal that statistical properties of the time parameters depend both on the FD source and on the solar activity period. FDs associated with AR CMEs develop even at close values of SW parameters faster than those associated with non-AR CMEs and HSS from CHs. Differences between typical FD profiles for events associated with AR and non-AR CMEs are more significant when the interplanetary disturbance contains a magnetic cloud. The difference between FD profiles for events associated with AR and non-AR CMEs is less distinguishable within maximum SC 24 than within maximum SC 23. For FDs associated with HSS from CHs, the main phase durations and the time delays of maximal SW speed are longer within SC 23–24 minimum, while the time delays of maximal IMF strength differ insignificantly between 23–24 and 24–25 minima.

Forbush Decreases and Geomagnetic Disturbances: 2. Comparison of Solar Cycles 23–24 and Events with Sudden and Gradual Commencement.

[Melkumyan](#), A.A., [Belov](#), A.V., [Shlyk](#), N.S. et al.

Geomagn. Aeron. 64, 32–43 (2024).

<https://doi.org/10.1134/S0016793223600911>

The article investigates the statistical relations between the values of geomagnetic indices and the characteristics of cosmic rays and interplanetary disturbances for Forbush decreases with a sudden and gradual commencement associated with different types of solar sources: (a) coronal mass ejections from active regions accompanied by solar flares; (b) filament eruptions outside active regions; (c) high-speed streams from coronal holes; and (d) multiple sources. Using statistical methods, we also compare the dependence of geomagnetic indices on cosmic ray and solar wind parameters for Forbush decreases in solar cycles 23 and 24. The results show that (a) interplanetary disturbances associated with coronal mass ejections from active regions cause mainly magnetic storms with a sudden commencement, (b) interplanetary disturbances associated with high-speed streams from coronal holes cause mainly storms with a gradual commencement, and (c) interplanetary disturbances associated with filament eruptions outside active regions cause equally likely storms with a sudden and gradual commencement. For sporadic Forbush decreases, the cosmic ray and geomagnetic activity parameters are, on average, larger for sudden commencement events; for recurrent Forbush decreases, the nature of the event commencement does not affect the magnitude of these parameters. For all types of solar sources, the disturbed solar wind parameters are, on average, larger in events with sudden commencement. The geoeffectiveness of interplanetary disturbances is significantly higher in cycle 23 for events associated with ejections from active regions; for other types of disturbances, the difference between cycles is weak.

Forbush decreases associated with coronal mass ejections from active and non-active regions: statistical comparison

A A [Melkumyan](#), A V [Belov](#), M A [Abunina](#), A A [Abunin](#), N S [Shlyk](#), V A [Oleneva](#), V G [Yanke](#)

MNRAS Volume 515, Issue 3, September 2022, Pages 4430–4444,

<https://doi.org/10.1093/mnras/stac2017>

In this paper, Forbush decreases (FDs) from 1997 to 2020 associated with coronal mass ejections from active and non-active regions are compared between themselves and to FDs caused by high-speed streams from coronal holes. The two

types of sporadic FDs are also compared when corresponding solar wind (SW) disturbances contain, or do not contain, magnetic clouds (MCs) near Earth. Cosmic ray density and anisotropy variations, SW speed, interplanetary magnetic field (IMF) strength, and geomagnetic indices have been examined using statistical methods. The results reveal that these parameters are larger for FDs associated with active region (AR) ejections and have highly skewed distributions for both types of sporadic events. In the same ranges of SW parameters, FD magnitude is larger for flare-associated events; more efficient modulation occurs in FDs associated with AR ejections. Differences between FDs associated with AR and non-AR ejections are more pronounced when an MC is registered. For IMF strength and geomagnetic indices, differences between the distributions depend more upon MC presence or absence than on the type of solar source. Correlation of IMF strength and SW speed differs slightly between FDs caused by AR and non-AR ejections regardless of the presence or absence of an MC, akin to the partial correlation between FD magnitude and IMF strength. Difference between the speeds of disturbed and background SW is larger for FDs associated with AR ejections especially when an MC is registered; the interaction region of different-speed SW streams occurs more frequently in interplanetary disturbances induced by AR ejections.

Solar wind temperature–velocity relationship over the last five solar cycles and Forbush decreases associated with different types of interplanetary disturbance

A A [Melkumyan](#), [A V Belov](#), [M A Abunina](#), [A A Abunin](#), [E A Eroshenko](#), [V G Yanke](#), [V A Oleneva](#)
Monthly Notices of the Royal Astronomical Society, Volume 500, Issue 3, January 2021, Pages 2786–2797,
<https://doi.org/10.1093/mnras/staa3366>

The behaviour of the solar wind (SW) proton temperature and velocity and their relationship during Forbush decreases (FDs) associated with various types of solar source – coronal mass ejections (CMEs) and coronal holes (CHs) – have been studied. Analysis of cosmic ray variations, SW temperature, velocity, density, plasma beta, and magnetic field (from 1965–2019) is carried out using three databases: the OMNI database, Variations of Cosmic Rays database (IZMIRAN) and Forbush Effects & Interplanetary Disturbances database (IZMIRAN). Comparison of the observed SW temperature (T) and velocity (V) for the undisturbed SW allows us to derive a formula for the expected SW temperature (T_{exp} , the temperature given by a T–V formula, if V is the observed SW speed). The results reveal a power-law T–V dependence with a steeper slope for low speeds ($V < 425 \text{ km s}^{-1}$, exponent = 3.29 ± 0.02) and flatter slope for high speeds ($V > 425 \text{ km s}^{-1}$, exponent = 2.25 ± 0.02). A study of changes in the T–V dependence over the last five solar cycles finds that this dependence varies with solar activity. The calculated temperature index $K_T = T/T_{exp}$ can be used as an indicator of interplanetary and solar sources of FDs. It usually has abnormally large values in interaction regions of different-speed SW streams and abnormally low values inside magnetic clouds (MCs). The results obtained help us to identify the different kinds of interplanetary disturbance: interplanetary CMEs, sheaths, MCs, corotating interaction regions, high-speed streams from CHs, and mixed events.

Power Law Distribution of Forbush Decrease Magnitude

A. A. [Melkumyan](#)¹, A. V. [Belov](#)², M. A. [Abunina](#)², A. A. [Abunin](#)², E. A. [Eroshenko](#)², V. G. [Yanke](#)², and V. A. [Oleneva](#)

[Research Notes of the AAS](#), Volume 2, Number 2 ID 49 2018

Accordingly, based on a comparison between FD magnitude power law slope and the above values of various solar–terrestrial phenomena we conclude that: (i) solar flares and solar energetic particles have flatter slopes than FDs; (ii) geomagnetic storms have steeper slopes than FDs; (iii) the power law slope for FD magnitude distribution is close to the power law slopes for CMEs parameters.

Trajectories of Coronal Mass Ejection from Solar-type Stars

Fabian [Menezes](#), [Adriana Valio](#), [Yuri Netto](#), [Alexandre Araújo](#), [Christina Kay](#), [Merav Opher](#)

Monthly Notices of the Royal Astronomical Society, Volume 522, Issue 3, July 2023, Pages 4392–4403

<https://doi.org/10.1093/mnras/stad1078>

<https://arxiv.org/pdf/2305.07159.pdf>

The Sun and other solar-type stars have magnetic fields that permeate their interior and surface, extends through the interplanetary medium, and is the main driver of stellar activity. Stellar magnetic activity affects physical processes and conditions of the interplanetary medium and orbiting planets. Coronal mass ejections (CMEs) are the most impacting of these phenomena in near-Earth space weather, and consist of plasma clouds, with magnetic field, ejected from the solar corona. Precisely predicting the trajectory of CMEs is crucial in determining whether a CME will hit a planet and impact its magnetosphere and atmosphere. Despite the rapid developments in the search for stellar CMEs, their detection is still very incipient. In this work we aim to better understand the propagation of CMEs by analysing the influence of initial parameters on CME trajectories, such as position, velocities, and stellar magnetic field's configuration. We reconstruct

magnetograms for Kepler-63 (KIC 11554435) and Kepler-411 (KIC 11551692) from spot transit mapping, and use a CME deflection model, ForeCAT, to simulate trajectories of hypothetical CMEs launched into the interplanetary medium from Kepler-63 and Kepler-411. We apply the same methodology to the Sun, for comparison. Our results show that in general, deflections and rotations of CMEs decrease with their radial velocity, and increase with ejection latitude. Moreover, magnetic fields stronger than the Sun's, such as Kepler-63's, tend to cause greater CME deflections.

The Solar and Interplanetary Causes of Superstorms (Minimum Dst ≤ -250 nT) During the Space Age

Xing [Meng](#), [Bruce T. Tsurutani](#), [Anthony J. Mannucci](#)

JGR [Volume 124, Issue 6](#) June 2019 Pages 3926-3948 **File**

[sci-hub.se/10.1029/2018JA026425](https://doi.org/10.1029/2018JA026425)

<https://agupubs.onlinelibrary.wiley.com/doi/epdf/10.1029/2018JA026425>

A comprehensive study of all superstorms (minimum Dst ≤ -250 nT) occurring during the space age (after 1957) and their interplanetary and solar causes has been performed. Most superstorms were driven solely by the sheath preceding an interplanetary coronal mass ejection (ICME) or by a combination of the sheath and an ICME magnetic cloud. Only one superstorm was driven solely by a magnetic cloud. There were two superstorms caused by “compound events” with two ICMEs. No superstorms in this study were induced by corotating interaction regions. For the interplanetary shocks antisunward of the ICMEs, the shock normal angles were almost all quasi-perpendicular. Quasi-perpendicular shocks theoretically cause greater sheath magnetic field intensities than do quasi-parallel shocks. Larger shock normal angles statistically corresponded to greater superstorm intensities. Ninety percent of the superstorms occurred either near solar maximum or during the declining phase, 8% of the superstorms occurred during the ascending phase, and 2% of the superstorms occurred during solar minimum. Fifty-four percent of the superstorms were associated with X-class solar flares, 36% were associated with M-class flares, and 5% with C-class flares. All solar flares related to superstorms occurred in active regions, indicating the importance of active regions to superstorms. Most flares were located in the central meridian or slightly west of it as expected. Two superstorms were caused by limb flares, one on the west limb (confirmed) and the other on the east limb (unconfirmed). The confirmed event was a sheath event led by a Mach 4.1 shock. **21 Jan 1957, 23 Sept 1957, 30 Apr 1960, 31 March 2001**

Table 1 Geomagnetic Storms With Dst ≤ -250 nT (Superstorms) Ranked by the Minimum Dst, 1957–2018

See comment in Tsurutani et al. (2024)

A preliminary investigation of the empirical relationship between small-amplitude Forbush Decreases and solar wind disturbances

F M [Menteso](#), [A E Chukwude](#), [O Okike](#), [J A Alhassan](#)

Monthly Notices of the Royal Astronomical Society, Volume 521, Issue 4, June 2023, Pages 6330–6353,

<https://doi.org/10.1093/mnras/stad783>

High-magnitude (amplitude ≤ -3 per cent) Forbush decreases (FDs) are generally employed by researchers investigating the solar-terrestrial connection mechanisms. Although it has been observed that small-amplitude FDs are relatively important as they may be the outcome of the response of cosmic ray time-intensity variations to solar ejections that generate interplanetary and solar wind plasma disturbances, empirical relations between weak FDs and solar-terrestrial parameters are rarely tested. In an attempt to analyse the suggested strong connections between weak FDs and solar-terrestrial phenomena, we employed some comparatively more efficient, accurate, and highly sensitive versions of the recently developed computer FD event selection software. Large catalogues of low-amplitude (FD(per cent) ≥ -3) Forbush events were selected from Apatity, Moscow, Newark, and Oulu NMs. These catalogues allow us to test, for the first time, the empirical relations between small-amplitude FDs and solar wind data. We find significant negative correlations between solar wind speed (SWS) and the small FDs at OULU, NWRK, and MOSC stations. While the relation at OULU is strong and statistically significant at 95 per cent confidence level, the weak correlation at NWRK and MOSC is only significant at a 90 per cent level. The negative correlation between the small events at OULU and the interplanetary magnetic field (IMF) is also significant at the a 95 per cent level. The relation between SWS and IMF and high-amplitude FDs were also tested, and the correlation coefficients were negative, strong, and statistically significant at a 99.9 per cent level of significance.

Strong Relativistic Electron Flux Events in GPS Orbit

Nigel P. [Meredith](#), [Thomas E. Cayton](#), [Michael D. Cayton](#), [Richard B. Horne](#)

Space Weather [Volume 22, Issue 12](#) December 2024 e2024SW004042

<https://doi.org/10.1029/2024SW004042>

<https://agupubs.onlinelibrary.wiley.com/doi/epdf/10.1029/2024SW004042>

Relativistic electrons cause internal charging on satellites and are a significant space weather hazard. In this study we analyze approximately 20 years of data from the US Global Positioning System (GPS) satellite NS41 to determine the conditions associated with the largest daily averaged fluxes of $E = 2.0$ MeV relativistic electrons. The largest flux events at $L = 4.5$ and $L = 6.5$ were associated with moderate to strong CME-driven geomagnetic storms. However, the majority of the 50 largest flux events at $L = 4.5$ (30 out of 50) and $L = 6.5$ (37 out of 50) were associated with high speed solar wind streams from coronal holes. Both solar drivers are thus very important for relativistic electron flux enhancements in GPS orbit. The 1 in 3 year flux level was not exceeded following any of the 15 largest geomagnetic storms as monitored by the D_{st} index, showing that the largest geomagnetic storms, most often associated with extreme space weather, do not result in significantly larger relativistic electron flux events in GPS orbit. **20 November 2003, 5 April 2010**

Table A1. The fifty largest $E = 2.0$ MeV relativistic electron flux events at $L = 4.5$ 2002-2019

Table B1. The fifty largest $E = 2.0$ MeV relativistic electron flux events at $L = 6.5$

Table C1. The peak $E = 2.0$ MeV relativistic electron fluxes at $L = 4.5$ and $L = 6.5$ associated with the fifteen largest geomagnetic storms

Predicting magnetospheric dynamics with a coupled Sun-to-Earth model: Challenges and first results

V. G. **Merkin**, M. J. Owens, H. E. Spence, W. J. Hughes, J. M. Quinn

SPACE WEATHER, VOL. 5, S12001, doi:10.1029/2007SW000335, 2007

Results from the first Sun-to-Earth coupled numerical model developed at the Center for Integrated Space Weather Modeling are presented. The model simulates physical processes occurring in space spanning from the corona of the Sun to the Earth's ionosphere, and it represents the first step toward creating a physics-based numerical tool for predicting space weather conditions in the near-Earth environment. Two 6- to 7-d intervals, representing different heliospheric conditions in terms of the three-dimensional configuration of the heliospheric current sheet, are chosen for simulations. These conditions lead to drastically different responses of the simulated magnetosphere-ionosphere system, emphasizing, on the one hand, challenges one encounters in building such forecasting tools, and on the other hand, emphasizing successes that can already be achieved even at this initial stage of Sun-to-Earth modeling.

Study of the Mass-loss Rate from the Sun

Grzegorz **Michalek**¹, Nat Gopalswamy², and Seiji Yashiro^{2,3}

The Astrophysical Journal, 930:74 (16pp), **2022** May 1

<https://iopscience.iop.org/article/10.3847/1538-4357/ac4fcb/pdf>

We investigate the temporal evolution of the yearly total mass-loss rate (YTMLR) from the Sun through coronal mass ejections (CMEs) over solar cycles 23 and 24. The mass determination of CMEs can be subject to significant uncertainty. To minimize this problem, we have used extensive statistical analysis. For this purpose, we employed data included in the Coordinated Data Analysis Workshop (CDAW) catalog. We estimated the contributions to mass loss from the Sun from different subsamples of CMEs (selected on the basis of their masses, angular widths, and position angles). The temporal variations of the YTMLR were compared to those of the sunspot number (SSN), X-ray flare flux, and the Disturbance Storm Time (Dst) index. We show that the CME mass included in the CDAW catalog reflects with high accuracy the actual mass-loss rate from the Sun through CMEs. Additionally, it is shown that the CME mass distribution in the log-lin representation reflects the Gaussian distribution very well. This means that the CMEs included in the CDAW catalog form one coherent population of ejections that have been correctly identified. Unlike the CME occurrence rate, it turns out that the YTMLR is a very good indicator of solar activity (e.g., SSN) and space weather (e.g., Dst index) consequences. These results are very important, since the YTMLR, unlike the mass loss through solar wind, significantly depends on solar cycles.

Space Weather Application Using Projected Velocity Asymmetry of Halo CMEs

G. **Michalek** · N. Gopalswamy · S. Yashiro

Solar Phys (**2008**) 248: 113–123, **File**

<http://www.springerlink.com/content/1576772m28w324t5/fulltext.pdf>

Halo coronal mass ejections (HCMEs) originating from regions close to the center of the Sun are likely to be responsible for severe geomagnetic storms. It is important to predict geoeffectiveness of HCMEs by using observations when they are still near the Sun. Unfortunately, coronagraphic observations do not provide true speeds of CMEs because of projection effects. In the present paper, we present a new technique to allow estimates of the space speed and approximate source location using

projected speeds measured at different position angles for a given HCME (velocity asymmetry). We apply this technique to HCMEs observed during 2001 – 2002 and find that the improved speeds are better correlated with the travel times of HCMEs to Earth and with the magnitudes of ensuing geomagnetic storms. **Table**

4.2. Magnitudes of Geomagnetic Disturbances

Prediction of SpaceWeather Using an Asymmetric Cone Model for Halo CMEs

G. Michalek · N. Gopalswamy · S. Yashiro

Solar Phys (2007) 246: 399–408, File

Halo coronal mass ejections (HCMEs) are responsible of the most severe geomagnetic storms. A prediction of their geoeffectiveness and travel time to Earth's vicinity is crucial to forecast space weather. Unfortunately, coronagraphic observations are subjected to projection effects and do not provide true characteristics of CMEs. Recently, Michalek (*Solar Phys.* **237**, 101, 2006) developed an asymmetric cone model to obtain **the space speed, width, and source location of HCMEs**. We applied this technique to obtain the parameters of all front-sided HCMEs observed by the SOHO/LASCO experiment during a period from the beginning of 2001 until the end of 2002 (solar cycle 23). These parameters were applied for space weather forecasting. **Our study finds that the space speeds are strongly correlated with the travel times of HCMEs to Earth's vicinity and with the magnitudes related to geomagnetic disturbances.**

Studies of Coronal Mass Ejections That Have Produced Major Geomagnetic Storms

M. Mierla, D. Besliu-Ionescu, O. Chiricuta, C. Oprea, G. Maris

SUN and GEOSPHERE, Vol.7 - No.1 – 2012, File

Twenty five major geomagnetic storms ($Dst < -150$ nT) associated with clear coronal mass ejections (CMEs) at the Sun were produced in the period 1996 - 2008. There were 57 possible coronal mass ejections (CMEs) which could have produced these storms. We are studying these CMEs in order to see their propagation and possible interaction into the interplanetary space. We will also investigate possible connection between CMEs and solar seismic signatures. Their in situ signatures and their correlation with geomagnetic indexes are also analyzed.

Using Cosmic Rays Detected by HST as Geophysical Markers. I. Detection and Characterization of Cosmic Rays

Nathan D. Miles^{1,2}, Susana E. Deustua¹, Gonzalo Tancredi³, Germán Schnyder³, Sergio Nesmachnow³, and Geoffrey Cromwell^{5,4}

2021 ApJ 918 86

<https://doi.org/10.3847/1538-4357/abfa9b>

The Hubble Space Telescope (HST) has been operational for over 30 years, and throughout that time it has been bombarded by high-energy charged particles colloquially referred to as cosmic rays. In this paper, we present a comprehensive study of more than 1.2 billion cosmic rays observed with HST using a custom-written Python package, HSTcosmicrays, that is available to the astronomical community. We analyzed 75,908 dark calibration files taken as part of routine calibration programs for five different CCD imagers with operational coverage of Solar Cycle 23 and 24. We observe the expected modulation of galactic cosmic rays by solar activity. We model the observed energy-loss distributions to derive an estimate of 534 ± 117 MeV for the kinetic energy of the typical cosmic ray impacting HST. For the three imagers with the largest nonuniformity in thickness, we independently confirm the overall structure produced by fringing analyses by analyzing cosmic ray strikes across the detector field of view. We analyze STIS/CCD observations taken as HST crosses over the South Atlantic Anomaly and find a peak cosmic ray particle flux of ~ 1100 particle $s^{-1} cm^{-2}$. We find strong evidence for two spatially confined regions over North America and Australia that exhibit increased cosmic ray particle fluxes at the 5σ level.

Distribution and recovery phase of geomagnetic storms during solar cycles 23 and 24

Wageesh Mishra, Preity Sukla Sahani, Soumyaranjan Khuntia, Dibyendu Chakrabarty

MNRAS, Volume 530, Issue 3, May 2024, Pages 3171–3182,

<https://doi.org/10.1093/mnras/stae1045>

<https://watermark.silverchair.com/stae1045.pdf>

Coronal mass ejections (CMEs) and Stream Interaction Regions (SIRs) are the main drivers of intense geomagnetic storms. We study the distribution of geomagnetic storms associated with different drivers during solar cycles 23 and 24 (1996–2019). Although the annual occurrence rate of geomagnetic storms in both cycles tracks the sunspot cycle, the second peak in storm activity lags the second sunspot peak. SIRs contribute significantly to the second peak in storm numbers in both cycles, particularly for moderate to stronger-than-moderate storms. We note semiannual peaks in storm

numbers much closer to equinoxes for moderate storms, and slightly shifted from equinoxes for intense and stronger-than-intense storms. We note a significant fraction of multiple-peak storms in both cycles due to isolated ICMEs/SIRs, while single-peak storms from multiple interacting drivers, suggesting a complex relationship between storm steps and their drivers. Our study focuses on investigating the recovery phases of geomagnetic storms and examining their dependencies on various storm parameters. Multiple-peak storms in both cycles have recovery phase duration strongly influenced by slow and fast decay phases with no correlation with the main phase build-up rate and Dst peak. However, the recovery phase in single-peak storms for both cycles depends to some extent on the main phase build-up rate and Dst peak, in addition to slow and fast decay phases. Future research should explore recovery phases of single and multiple-peak storms incorporating in situ solar wind observations for a deeper understanding of storm evolution and decay processes.

Wavelet Analysis of Forbush Decreases at High-Latitude Stations During Geomagnetic Disturbances

Roshan Kumar [Mishra](#), [Ashok Silwal](#), [Rabin Baral](#), [Binod Adhikari](#), [Carlos Roberto Braga](#), [Sujan Prasad Gautam](#), [Priyanka Kumari Das](#) & [Yenca Migoya-Orue](#)

Solar Physics volume 297, Article number: 26 (2022)

<https://link.springer.com/content/pdf/10.1007/s11207-022-01948-z.pdf>

We analyzed the behavior of Cosmic-Ray (CR) intensity during five geomagnetic events over 9-day periods of varying disturbance, using ground-based CR measurements from the Bartol Research Institute neutron-monitor program that occurred on **25th October – 2nd November 2003, 23rd – 31st July 2004, 13th – 21st May 2005, 13th – 21st Mar 2015, and 19th – 27th June 2015**. A nine-day time frame gives us a reasonable time interval for data analysis before, during, and after the main event(s). These events have been deliberately chosen, intending to track Forbush Decreases (FDs) at high-latitude stations following geomagnetic storms of different intensity and duration from the perspectives of their origin and geoeffectiveness. FDs are observed when the magnetic fields entangled in and around a Coronal Mass Ejection (CME) exert a deflecting effect on galactic cosmic radiation, resulting in a sudden reduction in their intensities. The results revealed that the CR intensity dropped by 4 – 17% in the chosen events. The FDs examined were not typical, with multistage decrement during the event period. Furthermore, we have used the Discrete Wavelet Transform (DWT) technique to detect a singularity on the CR intensity at the stations described. The first three decomposition levels have proved sufficient to isolate the transients in CR intensity in conjunction with varying nature and intensities, ranging from intense to superintense geomagnetic storms to a high-intensity long-duration continuous auroral electrojet activity (HILDCAA) event. Finally, the findings of the detrended crosscorrelation technique showed a good association of percentage decrease in cosmic-ray intensity with the Dst index during the process. No noticeable lag has been found between the parameters discussed, which indicates a strong correlation between the IMF-Bz and the Dst index and the FD.

Domain of Influence analysis: implications for Data Assimilation in space weather forecasting Review

[Dimitrios Millas](#), [Maria Elena Innocenti](#), [Brecht Laperre](#), [Joachim Raeder](#), [Stefaan Poedts](#), [Giovanni Lapenta](#)

Frontiers in Astronomy and Space Sciences 2020

<https://arxiv.org/pdf/2009.04211.pdf>

Solar activity, ranging from the background solar wind to energetic coronal mass ejections (CMEs), is the main driver of the conditions in the interplanetary space and in the terrestrial space environment, known as space weather. A better understanding of the Sun-Earth connection carries enormous potential to mitigate negative space weather effects with economic and social benefits. Effective space weather forecasting relies on data and models. In this paper, we discuss some of the most used space weather models, and propose suitable locations for data gathering with space weather purposes. We report on the application of *Representative analysis (RA)* and *Domain of Influence (DOI) analysis* to three models simulating different stages of the Sun-Earth connection: the OpenGGCM and Tsyanenko models, focusing on solar wind - magnetosphere interaction, and the PLUTO model, used to simulate CME propagation in interplanetary space. Our analysis is promising for space weather purposes for several reasons. First, we obtain quantitative information about the most useful locations of observation points, such as solar wind monitors. For example, we find that the absolute values of the DOI are extremely low in the magnetospheric plasma sheet. Since knowledge of that particular sub-system is crucial for space weather, enhanced monitoring of the region would be most beneficial. Second, we are able to better characterize the models. Although the current analysis focuses on spatial rather than temporal correlations, we find that time-independent models are less useful for Data Assimilation activities than time-dependent models. Third, we take the first steps towards the ambitious goal of identifying the most relevant heliospheric parameters for modelling CME propagation in the heliosphere, their arrival time, and their geoeffectiveness at Earth.

Improvements to the Empirical Solar Wind Forecast (ESWF) model

D. Milošić, M. Temmer, S. G. Heinemann, T. Podladchikova, A. Veronig & B. Vršnak
Solar Physics volume 298, Article number: 45 (2023)

<https://link.springer.com/content/pdf/10.1007/s11207-022-02102-5.pdf>

The empirical solar wind forecast (ESWF) model in its current version 2.0 runs as a space-safety service in the frame of ESA's Heliospheric Weather Expert Service Centre. The ESWF model forecasts the solar-wind speed at Earth with a lead time of 4 days. The algorithm uses an empirical relation found between the area of solar coronal-holes (CHs), as observed in EUV within a $15^\circ \times 15^\circ$ meridional slice, and the in-situ measured solar-wind speed at 1 AU. This relation however, forecasts Gaussian type speed profiles, as the CH rotates in and out of the meridional slice, causing some discrepancy in the timing between forecasted and observed solar-wind speed. With adaptations to the ESWF 2.0 algorithm we improve the precision and accuracy of the ESWF speed profiles. For that we implement compression and rarefaction effects occurring between solar-wind streams of different velocities in interplanetary space. By considering the propagation times for plasma parcels between the Sun and Earth and their interactions, we achieve the asymmetrical shape of the speed profile that is characteristic of high-speed streams (HSS). By further implementing CH segmentation, co-latitude information and dynamic thresholding, we find that the newly developed ESWF 3.2 performs significantly better than ESWF 2.0. For a sample of 294 different HSSs, we derive a relative increase in hits of the timing and peak velocity by 13.9%. The Pearson correlation coefficient increases by 14.3% from 0.35 to 0.40. **2015-02-12**

Distribution and Recovery Phase of Geomagnetic Storms During Solar Cycles 23 and 24

Wageesh Mishra, Preity Sukla Sahani, Soumyaranjan Khuntia, Dibyendu Chakrabarty
MNRAS 2024

<https://arxiv.org/pdf/2404.09234.pdf>

Coronal mass ejections (CMEs) and Stream Interaction Regions (SIRs) are the main drivers of intense geomagnetic storms. We study the distribution of geomagnetic storms associated with different drivers during solar cycles 23 and 24 (1996-2019). Although the annual occurrence rate of geomagnetic storms in both cycles tracks the sunspot cycle, the second peak in storm activity lags the second sunspot peak. SIRs contribute significantly to the second peak in storm numbers in both cycles, particularly for moderate to stronger-than-moderate storms. We note semiannual peaks in storm numbers much closer to equinoxes for moderate storms, and slightly shifted from equinoxes for intense and stronger-than-intense storms. We note a significant fraction of multiple-peak storms in both cycles due to isolated ICMEs/SIRs, while single-peak storms from multiple interacting drivers, suggesting a complex relationship between storm steps and their drivers. Our study focuses on investigating the recovery phases of geomagnetic storms and examining their dependencies on various storm parameters. Multiple-peak storms in both cycles have recovery phase duration strongly influenced by slow and fast decay phases with no correlation with the main phase buildup rate and Dst peak. However, the recovery phase in single-peak storms for both cycles depends to some extent on the main phase buildup rate and Dst peak, in addition to slow and fast decay phases. Future research should explore recovery phases of single and multiple-peak storms incorporating in-situ solar wind observations for a deeper understanding of storm evolution and decay processes. **18 Nov 2003, 6-7 Sep 2017**

Propagation of Coronal Mass Ejections from the Sun to Earth

Review

Wageesh Mishra, Luca Teriaca

Journal of Astrophysics and Astronomy 2022

<https://arxiv.org/pdf/2210.02782.pdf>

Coronal Mass Ejections (CMEs), as they can inject a large amounts of mass and magnetic flux into the interplanetary space, are the primary source of space weather phenomena on the Earth. The present review first briefly introduces the solar surface signatures of the origins of CMEs and then focuses on the attempts to understand the kinematic evolution of CMEs from the Sun to the Earth. CMEs have been observed in the solar corona in white-light from a series of space missions over the last five decades. In particular, LASCO/SOHO has provided almost continuous coverage of CMEs for more than two solar cycles until today. However, the observations from LASCO suffered from projection effects and limited field of view (within 30 Rs from the Sun). The launch in 2006 of the twin STEREO spacecraft made possible multiple viewpoints imaging observations, which enabled us to assess the projection effects on CMEs. Moreover, heliospheric imagers (HIS) onboard STEREO continuously observed the large and unexplored distance gap between the Sun and Earth. Finally, the Earth-directed CMEs that before have been routinely identified only near the Earth at 1 AU in in situ observations from ACE and WIND, could also be identified at longitudes away from the Sun-Earth line using the in situ instruments onboard STEREO. Our review presents the frequently used methods for estimation of the kinematics of CMEs and their arrival time at 1 AU using primarily SOHO and STEREO observations. We emphasize the need of deriving the three-dimensional (3D) properties of Earth-directed CMEs from the locations away from the

Sun-Earth line. The results improving the CME arrival time prediction at Earth and the open issues holding back progress are also discussed. Finally, we summarize the importance of heliospheric imaging and discuss the path forward to achieve improved space weather forecasting. **2011-02-14-17**

Wavelet Analysis of Forbush Decreases at High-Latitude Stations During Geomagnetic Disturbances

Roshan Kumar **Mishra**, [Ashok Silwal](#), [Rabin Baral](#), [Binod Adhikari](#), [Carlos Roberto Braga](#), [Sujan Prasad Gautam](#), [Priyanka Kumari Das](#) & [Yenca Migoya-Orue](#)

[Solar Physics](#) volume 297, Article number: 26 (2022)

<https://doi.org/10.1007/s11207-022-01948-z>

<https://link.springer.com/content/pdf/10.1007/s11207-022-01948-z.pdf>

We analyzed the behavior of Cosmic-Ray (CR) intensity during five geomagnetic events over 9-day periods of varying disturbance, using ground-based CR measurements from the Bartol Research Institute neutron-monitor program that occurred on **25th October – 2nd November 2003**, **23rd – 31st July 2004**, **13th – 21st May 2005**, **13th – 21st Mar 2015**, and **19th – 27th June 2015**. A nine-day time frame gives us a reasonable time interval for data analysis before, during, and after the main event(s). These events have been deliberately chosen, intending to track Forbush Decreases (FDs) at high-latitude stations following geomagnetic storms of different intensity and duration from the perspectives of their origin and geoeffectiveness. FDs are observed when the magnetic fields entangled in and around a Coronal Mass Ejection (CME) exert a deflecting effect on galactic cosmic radiation, resulting in a sudden reduction in their intensities. The results revealed that the CR intensity dropped by 4 – 17% in the chosen events. The FDs examined were not typical, with multistage decrement during the event period. Furthermore, we have used the Discrete Wavelet Transform (DWT) technique to detect a singularity on the CR intensity at the stations described. The first three decomposition levels have proved sufficient to isolate the transients in CR intensity in conjunction with varying nature and intensities, ranging from intense to superintense geomagnetic storms to a high-intensity long-duration continuous auroral electrojet activity (HILDCAA) event. Finally, the findings of the detrended crosscorrelation technique showed a good association of percentage decrease in cosmic-ray intensity with the Dst index during the process. No noticeable lag has been found between the parameters discussed, which indicates a strong correlation between the IMF-Bz and the Dst index and the FD.

Correction: [Solar Physics](#) volume 297, Article number: 60 (2022)

<https://link.springer.com/content/pdf/10.1007/s11207-022-02000-w.pdf>

Radial sizes and expansion behavior of ICMEs in solar cycles 23 and 24

As a Review

Wageesh **Mishra**, Urmi Doshi, and Nandita Srivastava

Front. Astron. Space Sci., 8:713999. **2021** |

<https://doi.org/10.3389/fspas.2021.713999>

<https://www.frontiersin.org/articles/10.3389/fspas.2021.713999/full>

<https://www.frontiersin.org/articles/10.3389/fspas.2021.713999/pdf>

We attempt to understand the influence of the heliospheric state on the expansion behavior of coronal mass ejections (CMEs) and their interplanetary counterparts (ICMEs) in solar cycles 23 and 24. Our study focuses on the distributions of the radial sizes and duration of ICMEs, their sheaths, and magnetic clouds (MCs). We find that the average radial size of ICMEs (MCs) at 1 AU in cycle 24 is decreased by ~33% (~24%) of its value in cycle 23. This is unexpected as the reduced total pressure in cycle 24 should have allowed the ICMEs in cycle 24 to expand considerably to larger sizes at 1 AU. To understand this, we study the evolution of radial expansion speeds of CME-MC pairs between the Sun and Earth based on their remote and in situ observations. We find that radial expansion speeds of MCs at 1 AU in solar cycles 23 and 24 are only 9 and 6%, respectively, of their radial propagation speeds. Also, the fraction of radial propagation speeds as expansion speeds of CMEs close to the Sun are not considerably different between solar cycles 23 and 24. We also find a constant (0.63 ± 0.1) dimensionless expansion parameter of MCs at 1 AU for both solar cycles 23 and 24. We suggest that the reduced heliospheric pressure in cycle 24 is compensated by the reduced magnetic content inside CMEs/MCs, which did not allow the CMEs/MCs to expand enough in the later phase of their propagation. Furthermore, the average radial sizes of sheaths are the same in both cycles, which is unexpected, given the weaker CMEs/ICMEs in cycle 24. We discuss the possible causes and consequences of our findings relevant for future studies.

Probing the Thermodynamic State of a Coronal Mass Ejection (CME) Up to 1 AU

Wageesh **Mishra**, Yuming Wang, Luca Teriaca, Jie Zhang, and Yutian Chi

Front. Astron. Space Sci., 7:1 2020 |

<https://doi.org/10.3389/fspas.2020.00001>

<https://www.frontiersin.org/articles/10.3389/fspas.2020.00001/pdf>

Several earlier studies have attempted to estimate some of the thermodynamic properties of Coronal Mass Ejections (CMEs) either very close to the Sun or at 1 AU. In the present study, we attempt to extrapolate the internal thermodynamic properties of **2010 April 3** flux rope CME from near the Sun to 1 AU. For this purpose, we use the flux rope internal state (FRIS) model which is constrained by the kinematics of the CME. The kinematics of the CME is estimated using the STEREO/COR and HI observations in combination with drag based model (DBM) of CME propagation. Using the FRIS model, we focus on estimating the polytropic index of the CME plasma, heating/cooling rate, entropy changing rate, Lorentz force and thermal pressure force acting inside the CME. Our study finds that the polytropic index of the selected CME ranges between 1.7 and 1.9. This implies that the CME is in the heat-releasing state (i.e., entropy loss) throughout its journey from the Sun to Earth. The hindering role of Lorentz force and contributing role of thermal pressure force in governing the expansion of the CME is also identified. On comparing the estimated properties of the CME flux rope from the FRIS model with the in situ observations of the CME taken at 1 AU, we find relevant discrepancies between the results predicted by the model and the observations. We outline the approximations made in our study of probing the internal state of the CME during its heliospheric evolution and discuss the possible causes of the observed discrepancies.

[THIS ARTICLE IS PART OF THE RESEARCH TOPIC](#)

[Magnetic Flux Ropes: From the Sun to the Earth and Beyond View all 9 Articles](#)

Linkage of Geoeffective Stealth CMEs Associated with the Eruption of Coronal Plasma channel and Jet-Like Structure

Sudheer K. [Mishra](#), [A.K. Srivastava](#)

Solar Phys. 294:169 2019

<https://arxiv.org/pdf/1911.07134.pdf>

<https://link.springer.com/content/pdf/10.1007%2Fs11207-019-1560-1.pdf>

<https://doi.org/10.1007/s11207-019-1560-1>

We analyze the eruption of a coronal plasma channel (CPC) and an overlying flux rope using \textit{Atmospheric Imaging Assembly/Solar Dynamic Observatory} (AIA/SDO) and \textit{Solar TERrestrial Relations Observatory} (STEREO)-A spacecraft data. The CPC erupted first with its low and very faint coronal signature. Later, above the CPC, a diffuse and thin flux rope also developed and erupted. The spreading CPC further triggered a rotating jet-like structure from the coronal hole lying to its northward end. This jet-like eruption may have evolved due to the interaction between spreading CPC and the open field lines of the coronal hole lying towards its northward foot-point. The CPC connected two small trans-equatorial coronal holes lying respectively in the northern and southern hemisphere on either side of the Equator. These eruptions were collectively associated with the stealth-type CMEs and CME associated with a jet-like eruption. The source region of the stealth CMEs lay between two coronal holes connected by a coronal plasma channel. Another CME was also associated with a jet-like eruption that occurred from the coronal hole in the northern hemisphere. These CMEs evolved without any low coronal signature and yet were responsible for the third strongest geomagnetic storm of Solar cycle 24. These stealth CMEs further merged and collectively passed through the interplanetary space. The compound CME further produced an intense geomagnetic storm (GMS) with Dst index = -176 nT. The z-component of the interplanetary magnetic field [Bz] switched to negative (-18 nT) during this interaction, and simultaneous measurement of the disturbance in the Earth's magnetic field (Kp=7) indicates the onset of the geomagnetic storm. **20-28 Aug 2018**

Long-Term Modulation of Cosmic-Ray Intensity and Correlation Analysis Using Solar and Heliospheric Parameters

V. K. [Mishra](#), [A. P. Mishra](#)

[Solar Physics](#) October 2018, 293:141

<https://link.springer.com/content/pdf/10.1007%2Fs11207-018-1357-7.pdf>

Based on the monthly sunspot numbers (SSNs), the solar-flare index (SFI), grouped solar flares (GSFs), the tilt angle of heliospheric current sheet (HCS), and cosmic-ray intensity (CRI) for Solar Cycles 21 – 24, a detailed correlation study has been performed using the cycle-wise average correlation (with and without time lag) method as well as by the “running cross-correlation” method. It is found that the slope of regression lines between SSN and SFI, as well as between SSN and GSF, is continuously decreasing from Solar Cycle 21 to 24. The length of regression lines has significantly decreased during Cycles 23 and 24 in comparison to Cycles 21 and 22. The cross-correlation coefficient (without time lag) between SSN–CRI, SFI–CRI, and GSF–CRI has been found to be almost the same during Cycles 21

and 22, while during Cycles 23 and 24 it is significantly higher between SSN–CRI and HCS–CRI than for SFI–CRI and GSF–CRI. Considering time lags of 1 to 20 months, the maximum correlation coefficient (negative) amongst all of the sets of solar parameters is observed with almost the same time lags during Cycles 21 – 23, whereas exceptional behaviour of the time lag has been observed during Cycle 24, as the correlation coefficient attains its maximum value with two time lags (four and ten months) in the case of the SSN–CRI relationship. A remarkably large time lag (22 months) between HCS and CRI has been observed during the odd-numbered Cycle 21, whereas during another odd cycle, Cycle 23, the lag is small (nine months) in comparison to that for other solar/flare parameters (13 – 15 months). On the other hand, the time lag between SSN–CRI and HCS–CRI has been found to be almost the same during even-numbered Solar Cycles 22 and 24. A similar analysis has been performed between SFI and CRI, and it is found that the correlation coefficient is maximum at zero time lag during the present solar cycle. The GSFs have shown better maximum correlation with CRI as compared to SFI during Cycles 21 to 23, indicating that GSF could also be used as a significant solar parameter to study the cosmic-ray modulation. Furthermore, the running cross-correlation coefficient between SSN–CRI and HCS–CRI, as well as between solar-flare activity parameters (SFI and GSF) and CRI is observed to be strong during the ascending and descending phases of solar cycles. The level of cosmic-ray modulation during the period of investigation shows the appropriateness of different parameters in different cycles, and even during the different phases of a particular solar cycle. We have also studied the galactic cosmic-ray modulation in relation to combined solar and heliospheric parameters using the empirical model suggested by Paouris et al. (Solar Phys.280, 255, 2012). The proposed model for the calculation of the modulated cosmic-ray intensity obtained from the combination of solar and heliospheric parameter gives a very satisfactory value of standard deviation as well as R2R2 (the coefficient of determination) for Solar Cycles 21 – 24.

Modeling the thermodynamic evolution of Coronal Mass Ejections (CMEs) using their kinematics

Wageesh [Mishra](#), [Yuming Wang](#)

ApJ **2018**

<https://arxiv.org/pdf/1808.06794.pdf>

Earlier studies on Coronal Mass Ejections (CMEs), using remote sensing and in situ observations, have attempted to determine some of the internal properties of CMEs, which were limited to a certain position or a certain time. For understanding the evolution of the internal thermodynamic state of CMEs during their heliospheric propagation, we improve the self-similar flux rope internal state (FRIS) model, which is constrained by measured propagation and expansion speed profiles of a CME. We implement the model to a CME erupted on **2008 December 12** and probe the internal state of the CME. It is found that the polytropic index of the CME plasma decreased continuously from 1.8 to 1.35 as the CME moved away from the Sun, implying that the CME released heat before it reached adiabatic state and then absorbed heat. We further estimate the entropy changing and heating rate of the CME. We also find that the thermal force inside the CME is the internal driver of CME expansion while Lorentz force prevented the CME from expanding. It is noted that centrifugal force due to poloidal motion decreased with the fastest rate and Lorentz force decreased slightly faster than thermal pressure force as CME moved away from the Sun. We also discuss the limitations of the model and approximations made in the study.

Solar cycle variation of coronal mass ejections contribution to solar wind mass flux

[Wageesh Mishra](#), [Nandita Srivastava](#), [Zavkiddin Mirtoshev](#), [Yuming Wang](#)

Proceedings IAU Symposium No. 340, **2018**

<https://arxiv.org/pdf/1805.07593.pdf>

Coronal Mass Ejections (CMEs) contributes to the perturbation of solar wind in the heliosphere. Thus, depending on the different phases of the solar cycle and the rate of CME occurrence, contribution of CMEs to solar wind parameters near the Earth changes. In the present study, we examine the long term occurrence rate of CMEs, their speeds, angular widths and masses. We attempt to find correlation between near sun parameters, determined using white light images from coronagraphs, with solar wind measurements near the Earth from in-situ instruments. Importantly, we attempt to find what fraction of the averaged solar wind mass near the Earth is provided by the CMEs during different phases of the solar cycles.

Assessing the collision nature of coronal mass ejections in the inner heliosphere

Wageesh [Mishra](#), [Yuming Wang](#), [Nandita Srivastava](#), [Chenglong Shen](#)

ApJ Supplement Series Volume 232, Issue 1, article id. 5 **2017**

<https://arxiv.org/pdf/1707.08299.pdf>

<https://iopscience.iop.org/article/10.3847/1538-4365/aa8139/pdf>

There have been few attempts in the past to understand the collision of individual cases of interacting Coronal Mass Ejections (CMEs). We selected 8 cases of interacting CMEs and estimated their propagation and expansion speeds, direction of impact and masses exploiting coronagraphic and heliospheric imaging observations. Using these estimates with ignoring the errors therein, we find that the nature of collision is perfectly inelastic for 2 cases (e.g., 2012 March and November), inelastic for 2 cases (e.g., 2012 June and 2011 August), elastic for 1 case (e.g., 2013 October) and super-elastic for 3 cases (e.g., 2011 February, 2010 May and 2012 September). Admitting large uncertainties in the estimated directions, angular widths and pre-collision speeds; the probability of perfectly inelastic collision for 2012 March and November cases diverge from 98%-60% and 100%-40%, respectively, reserving some probability for other nature of collision. Similarly, the probability of inelastic collision diverge from 95%-50% for 2012 June case, 85%-50% for 2011 August case, and 75%-15% for 2013 October case. We note that probability of super-elastic collision for 2011 February, 2010 May and 2012 September CMEs diverge from 90%-75%, 60%-45% and 90%-50%, respectively. Although the sample size is small, we find a good dependence of nature of collision on CMEs parameters. The crucial pre-collision parameters of the CMEs responsible for increasing the probability of super-elastic collision, in descending order of priority, are their lower approaching speed, higher expansion speed of the following CME over the preceding one, and longer duration of collision phase. **2010 May 23-24 , 2011 February 14-15, 2011 August 3-4 , 2012 March 4-5 , 2012 June 13-14, 2012 September 25-28 , 2012 November 9-10, 2013 October 25**
Table 1. Selected CMEs Events

Evolution and Consequences of Coronal Mass Ejections in the Heliosphere

Wageesh Mishra

The **thesis** was submitted in Mar **2015** to MLS university, Udaipur, for which the university granted the degree in Jan 2016

<https://arxiv.org/pdf/2204.09879.pdf>

Investigating the heliospheric evolution and consequences of Coronal mass ejections (CMEs) is critical to understanding the solar-terrestrial relationship. For the first time, Heliospheric Imagers (HIs) onboard STEREO, providing multiple views of CMEs in the heliosphere, observed the vast and crucial observational gap between the Sun and the Earth. Using J-maps constructed from coronagraphs (CORs) and HIs observations, we continuously tracked different density enhanced features of CMEs. We implemented several reconstruction methods to estimate the three-dimensional (3D) kinematics of CMEs during their evolution from the Sun to Earth. Our study provides evidence that the 3D speeds of CMEs near the Sun are not reasonably sufficient for understanding the propagation and accurate forecasting of the arrival time at the Earth of a majority of CMEs. This finding can be due to many factors that significantly change the CME kinematics beyond the COR field of view, such as the interaction/collision of two or more CMEs or the interaction of CMEs with the ambient solar wind medium. We attempted to understand the evolution and consequences of the interacting/colliding CMEs in the heliosphere using STEREO/Hi, WIND, and ACE observations. The study found a significant change in the dynamics of the CMEs after their collision and interaction. The in situ observations show the signatures of CME-CME interaction as heating and compression, formation of magnetic holes (MHs), and interaction region (IR). We also noticed that long-lasting IR, formed at the rear edge of preceding CME, is responsible for large geomagnetic perturbations. Our study highlights the significance of using HIs observations in studying heliospheric evolution of CMEs, CME-CME collision, identifying and associating the three-part structure of CMEs in their remote and in situ observations, and hence for improved space weather forecasting. **2008 December 12, 2010 February 7, 2010 February 12, 2010 March 14, 2010 April 3, 2010 April 6, 2010 April 8, 2010 October 6, 2010 October 10, 2010 October 26, 2011 February 13-15, 2012 November 9-10**

Kinematics of Interacting CMEs of September 25 and 28, 2012

Wageesh Mishra, Nandita Srivastava, Talwinder Singh

JGR Volume 120, Issue 12 Pages 10,221–10,236 **2015**

<http://arxiv.org/pdf/1511.06970v1.pdf>

<http://onlinelibrary.wiley.com/doi/10.1002/2015JA021415/pdf>

We have studied two Coronal Mass Ejections (CMEs) that occurred on **September 25 and 28, 2012** and interacted near the Earth. By fitting the Graduated Cylindrical Shell (GCS) model on the SECCHI/COR2 images and applying the Stereoscopic Self-Similar Expansion (SSSE) method on the SECCHI/Hi images, the initial direction of both the CMEs is estimated to be west of the Sun-Earth line. Further, the three-dimensional (3D) heliospheric kinematics of these CMEs have been estimated using Self-Similar Expansion (SSE) reconstruction method. We show that use of SSE method with different values of angular extent of the CMEs, leads to significantly different kinematics estimates for the CMEs propagating away from the observer. Using the estimated kinematics and true masses of the CMEs, we have derived the coefficient of restitution for the collision which is found to be close to elastic. The in situ measurements at 1 AU show

two distinct structures of interplanetary CMEs, heating of the following CME, as well as ongoing interaction between the preceding and the following CME. We highlight the signatures of interaction in remote and in situ observations of these CMEs and the role of interaction in producing a major geomagnetic storm.

Heliospheric tracking of enhanced density structures of the 6 October 2010 CME

Wageesh **Mishra**, Nandita Srivastava

J. Space Weather Space Clim., 5, A20 2015

<http://arxiv.org/pdf/1505.04871v1.pdf>

<http://www.swsc-journal.org/articles/swsc/pdf/2015/01/swsc140047.pdf>

A Coronal Mass Ejection (CME) is an inhomogeneous structure consisting of different features which evolve differently with the propagation of the CME. Simultaneous heliospheric tracking of different observed features of a CME can improve our understanding about relative forces acting on them. It also helps to estimate accurately their arrival times at the Earth and identify them in in-situ data. This also enables to find association between remotely observed features and in-situ observations near the Earth. In this paper, we attempt to continuously track two density enhanced features, one at the front and another at the rear edge of the 6 October 2010 CME. This is achieved by using time-elongation maps constructed from STEREO/SECCHI observations. We derive the kinematics of the tracked features using various reconstruction methods. The estimated kinematics are used as inputs in the Drag Based Model (DBM) to estimate the arrival time of the tracked features of the CME at L1. On comparing the estimated kinematics as well as the arrival times of the remotely observed features with in-situ observations by ACE and Wind, we find that the tracked bright feature in the J-map at the rear edge of 6 October 2010 CME corresponds most probably to the enhanced density structure after the magnetic cloud detected by ACE and Wind. In-situ plasma and compositional parameters provide evidence that the rear edge density structure may correspond to a filament associated with the CME while the density enhancement at the front corresponds to the leading edge of the CME. Based on this single event study, we discuss the relevance and significance of heliospheric imager (HI) observations in identification of the three-part structure of the CME.

Morphological and Kinematic Evolution of Three Interacting Coronal Mass Ejections of 2011 February 13-15

Wageesh **Mishra**, Nandita Srivastava

ApJ, 794 64 2014

<http://arxiv.org/pdf/1408.4604v1.pdf>

During 2011 February 13 to 15, three Earth-directed CMEs launched in successively were recorded as limb CMEs by coronagraphs (COR) of STEREO. These CMEs provided an opportunity to study their geometrical and kinematic evolution from multiple vantage points. In this paper, we examine the differences in geometrical evolution of slow and fast speed CMEs during their propagation in the heliosphere. We also study their interaction and collision using STEREO/SECCHI COR and Heliospheric Imager (HI) observations. We have found evidence of interaction and collision between the CMEs of February 15 and 14 in COR2 and HI1 FOV, respectively, while the CME of February 14 caught the CME of February 13 in HI2 FOV. By estimating the true mass of these CMEs and using their pre and post-collision dynamics, the momentum and energy exchange between them during collision phase are studied. We classify the nature of observed collision between CME of February 14 and 15 as inelastic, reaching close to elastic regime. Relating imaging observations with the in situ measurements, we find that the CMEs move adjacent to each other after their collision in the heliosphere and are recognized as distinct structures in in situ observations by WIND spacecraft at L1. Our results highlight the significance of HI observations in studying CME-CME collision for the purpose of improved space weather forecasting.

Evolution and Consequences of Interacting CMEs of 2012 November 9-10 using STEREO/SECCHI and In Situ Observations

Wageesh **Mishra**, Nandita Srivastava, D. Chakrabarty

Solar Phys., February 2015, Volume 290, Issue 2, pp 527-552

<http://arxiv.org/pdf/1408.0352v1.pdf>

Understanding of the kinematic evolution of Coronal Mass Ejections (CMEs) in the heliosphere is important to estimate their arrival time at the Earth. It is found that kinematics of CMEs can change when they interact or collide with each other as they propagate in the heliosphere. In this paper, we analyze the collision and post-interaction characteristics of two Earth-directed CMEs, launched successively on 2012 November 9 and 10, using white light imaging observations from STEREO/SECCHI and in situ observations taken from WIND spacecraft. We tracked two density enhanced features associated with leading and trailing edge of November 9 CME and one density enhanced feature associated with

leading edge of November 10 CME by constructing J-maps. We found that the leading edge of November 10 CME interacted with the trailing edge of November 9 CME. We also estimated the kinematics of these features of the CMEs and found a significant change in their dynamics after interaction. In situ observations, we identified distinct structures associated with interacted CMEs and also noticed their heating and compression as signatures of CME-CME interaction. Our analysis shows an improvement in arrival time prediction of CMEs using their post-collision dynamics than using pre-collision dynamics. Estimating the true masses and speeds of these colliding CMEs, we investigated the nature of observed collision which is found to be close to perfectly inelastic. The investigation also places in perspective the geomagnetic consequences of the two CMEs and their interaction in terms of occurrence of geomagnetic storm and triggering of magnetospheric substorms.

A Comparison of Reconstruction Methods for the Estimation of Coronal Mass Ejections Kinematics Based on SECCHI/HI Observations

Wageesh [Mishra](#), Nandita Srivastava, and Jackie A. Davies

2014 ApJ 784 135

<http://arxiv.org/pdf/1407.8446v1.pdf>

A study of the kinematics and arrival times of coronal mass ejections (CMEs) at Earth, derived from time-elongation maps (J-maps) constructed from STEREO/heliospheric imager (HI) observations, provides an opportunity to understand the heliospheric evolution of CMEs in general. We implement various reconstruction techniques, based on the use of time-elongation profiles of propagating CMEs viewed from single or multiple vantage points, to estimate the dynamics of three geo-effective CMEs. We use the kinematic properties, derived from analysis of the elongation profiles, as inputs to the Drag Based Model for the distance beyond which the CMEs cannot be tracked unambiguously in the J-maps. The ambient solar wind into which these CMEs, which travel with different speeds, are launched, is different. Therefore, these CMEs will evolve differently throughout their journey from the Sun to 1 AU. We associate the CMEs, identified and tracked in the J-maps, with signatures observed in situ near 1 AU by the WIND spacecraft. By deriving the kinematic properties of each CME, using a variety of existing methods, we assess the relative performance of each method for the purpose of space weather forecasting. We discuss the limitations of each method, and identify the major constraints in predicting the arrival time of CMEs near 1 AU using HI observations. **2010 October 6, 2010 April 3, 2010 February 12**

Estimating the Arrival Time of Earth-directed Coronal Mass Ejections at in Situ Spacecraft Using COR and HI Observations from STEREO

Wageesh [Mishra](#) and Nandita Srivastava

2013 ApJ 772 70

<http://arxiv.org/pdf/1306.1397v1.pdf>

Predicting the arrival time and transit speed of coronal mass ejections (CMEs) near the Earth is critical to understanding the solar-terrestrial relationship. Even though STEREO observations now provide multiple views of CMEs in the heliosphere, the true speeds derived from stereoscopic reconstruction of SECCHI coronagraph data are not quite sufficient for accurate forecasting of the arrival time at Earth of a majority of CMEs. This uncertainty is due to many factors that change CME kinematics, such as the interaction of two or more CMEs or the interaction of CMEs with the pervading solar wind. In order to understand the propagation of CMEs, we have used the three-dimensional triangulation method on SECCHI coronagraph (COR2) images and geometric triangulation on the J-maps constructed from Heliospheric Imagers HI1 and HI2 data for eight Earth-directed CMEs observed during 2008-2010. Based on the reconstruction, and implementing the drag-based model for the distance where the CMEs could not be tracked unambiguously in the interplanetary (IP) medium, the arrival time of these CMEs have been estimated. These arrival times have also been compared with the actual arrival times as observed by in situ instruments. The analysis reveals the importance of heliospheric imaging for improved forecasting of the arrival time and direction of propagation of CMEs in the IP medium.

Statistical Study of ICMEs and Their Sheaths During Solar Cycle 23 (1996–2008)

E. [Mitsakou](#), X. Moussas

Solar Physics, Volume 289, Issue 8, pp 3137-3157 **2014**

We have created a **new catalog of 325 interplanetary coronal mass ejections (ICMEs)** using their in-situ plasma signatures from 1996 to 2008; this time period includes Solar Cycle 23. The data set came from the OMNI near-Earth database. The one-minute resolution data that we used include magnetic-field strength, solar-wind speed, proton density, proton temperature, and plasma β . We compared this new catalog with other published catalogs. For every event, we indicated the presence of an ICME-driven shock. We identified the boundaries of ICMEs and their sheaths, and examined the statistical properties of characteristic parameters. We derived the duration and radial width of ICMEs and sheaths in the region near Earth. The statistical analysis of all events shows that, on average, sheaths travel faster than ICMEs, which indicates the expansion of CMEs in the interplanetary medium. They have higher mean magnetic-field strength values than ICMEs, and they are denser. They have higher mean proton temperature and plasma β than ICMEs, but they are smaller than ICMEs and last for a shorter time. The events were divided into different categories according to whether they included a shock and according to the phase of Solar Cycle 23 in which they are observed, i.e. ascending, maximum, or descending phase. We compared the different categories. We present a catalog of events available to the scientific community that studies ICMEs, and show the distribution and statistical properties of various parameters during these phenomena that govern the solar wind, the interplanetary medium, and space weather.

Erratum to: Solar Phys (2014) 289:3137–3157 DOI10.1007/s11207-014-0505-y

The Appendix (Table 6) and the downloadable version available as Electronic Supplementary Material should be replaced with those given here. We regret the inconvenience.

Solar Physics, Volume 289, Issue 11, pp 4413-4421, 2014

Interplanetary coronal mass ejections during the descending cycle 23: Sheath and ejecta properties comparison

Adv. Space Res. **Volume 43, Issue 4, Pages 495-498, 2009**

E. [Mitsakou](#), G. Babasidis, X. Moussas

We have used Omniweb data in order to identify the sheath and the ejecta boundaries of 67 shock-driving interplanetary coronal mass ejections during the time period 2003–2006. We examine and compare their statistical properties (speed, magnetic field strength, proton density and temperature, proton plasma beta), with those of the typical solar wind. We also calculate their passage time and radial width. We study the correlation between the ejecta and sheath characteristics.

On the Predictive Ability of Geomagnetic Disturbances from Solar Wind Measurements at Separated Solar Longitude

Wataru [Miyake](#), [Tsutomu Nagatsuma](#)

[International Journal of Astronomy and Astrophysic...](#) (IJAA) Vol.2 No.2, June 2012 PP. 63-73

http://file.scirp.org/pdf/IJAA20120200007_71512007.pdf

In-situ solar wind measurement at a solar longitude separated from the earth in interplanetary space is expected to provide a great progress in practical space weather forecast, which has been confirmed by some recent studies. We introduce geoeffective solar wind conditions in correlation analysis between STEREO and ACE measurements. We sort solar wind data of ACE by using geomagnetic condition, and evaluate actual ability for predicting geoeffective solar wind arrival at ACE from STEREO-A and B solar wind measurement, by assuming simple corotating structures in interplanetary space. The results show that geomagnetic disturbances are more difficult to be predicted than quiet intervals, suggesting that the simple correlation method of solar wind measurement at separated solar longitude is not enough for accurately predicting geomagnetic disturbances, even though the correlation seems generally high. Although in-situ solar wind monitoring at a vantage point trailing behind the earth would definitely improve the prediction capability of solar wind structure arriving at the terrestrial plasma environment, we emphasize that the predictive ability of geoeffective disturbances would still remain low. We suggest that more sophisticated prediction schemes should be developed.

Scaling Features of Diurnal Variation of Galactic Cosmic Rays

Renata [Modzelewska](#), [Agata Krasińska](#), [Anna Wawrzaszek](#) & [Agnieszka Gil](#)

[Solar Physics](#) volume 296, Article number: 125 (2021)

<https://link.springer.com/content/pdf/10.1007/s11207-021-01866-6.pdf>

<https://doi.org/10.1007/s11207-021-01866-6>

We analyze the scaling properties of the diurnal variation of galactic cosmic rays (GCRs) in Solar Cycle 24 and the solar minima between Solar Cycles 23/24 and 24/25 for 2007 – 2019 based on the count rates of the Oulu, Newark, Hermanus, and Potchefstroom neutron monitors. The scaling features of the GCR diurnal variation are studied by

evaluating the Hurst exponent, a quantitative parameter used as an indicator of the state of the randomness of a time series. We estimate the Hurst exponents for GCR diurnal-variation parameters amplitude and phase using structure-function and detrended-fluctuation-analysis methods. Results show that the Hurst exponents for the GCR diurnal variation vary in the range from $\approx 0.3 \approx 0.3$ to $\approx 0.9 \approx 0.9$, with a general tendency of being systematically above 0.5. It suggests that the GCR diurnal variation reveals a more persistent structure than Brownian motion. However, the time series of GCR diurnal-variation amplitude and phase evolve from a more persistent structure in the solar minimum between Solar Cycles 23/24 in 2007–2009 to a more random character in and near the solar maximum 2012–2014. This observation seems to be in agreement with the general configuration of the heliosphere through the 11-year solar-activity cycle. Moreover, the temporal profile of the Hurst exponent for GCR diurnal amplitude and phase around the beginning of the solar minimum between Solar Cycles 24/25 (2018–2019) differs from the solar minimum between Solar Cycles 23/24 in 2007–2009, suggesting a dependence on solar-magnetic polarity. These findings could shed more light on GCR particle transport in the turbulent heliosphere over the solar cycle.

Recurrence of galactic cosmic-ray intensity and anisotropy in solar minima 23/24 and 24/25 observed by ACE/CRIS, STEREO, SOHO/EPHIN and neutron monitors

Fourier and wavelet analysis★

R. **Modzelewska**¹ and A. Gill^{1,2}

A&A 646, A128 (2021)

<https://doi.org/10.1051/0004-6361/202039651>

<https://www.aanda.org/articles/aa/pdf/2021/02/aa39651-20.pdf>

Aims. We studied the 27-day variations of galactic cosmic rays (GCRs) based on neutron monitor (NM), ACE/CRIS, STEREO, and SOHO/EPHIN measurements in the solar minima 23/24 and 24/25, which are characterized by the opposite polarities of solar magnetic cycle. We used the opportunity to reanalyze the polarity dependence of the amplitudes of the recurrent GCR variations in 2007–2009 for the negative $A < 0$ solar magnetic polarity and to compare it with the clear periodic variations related to solar rotation in 2017–2019 for positive $A > 0$.

Methods. We used the Fourier analysis method to study the periodicity in the GCR fluxes. Because the GCR recurrence is a consequence of solar rotation, we analyzed not only GCR fluxes, but also solar and heliospheric parameters to examine the relations of the 27-day GCR variations and heliospheric as well as solar wind parameters.

Results. We find that the polarity dependence of the amplitudes of the 27-day variations of the GCR intensity and anisotropy for NMs data is kept for the last two solar minima: 23/24 (2007–2009) and 24/25 (2017–2019), with greater amplitudes in the positive $A > 0$ solar magnetic polarity. ACE/CRIS, SOHO/EPHIN, and STEREO measurements are not governed by this principle of greater amplitudes in the positive $A > 0$ polarity. The GCR recurrence caused by the solar rotation for low-energy (< 1 GeV) cosmic rays is more sensitive to the enhanced diffusion effects, resulting in the same level in 27-day amplitudes for the positive and negative polarities. In contrast, the high-energy (> 1 GeV) cosmic rays that are registered by NMs are more sensitive to the large-scale drift effect, which leads to the 22-year Hale cycle in the 27-day GCR variation, with the larger amplitudes in the $A > 0$ polarity than in $A < 0$.

Study of the 27 Day Variations in GCR Fluxes during 2007–2008 Based on PAMELA and ARINA Observations

R. **Modzelewska**¹, G. A. Bazilevskaya², M. Boezio^{3,4}, S. V. Koldashov⁵, M. B. Krainev², N.

Marcelli^{6,7}, A. G. Mayorov⁵, M. A. Mayorova⁵, R. Munini^{3,4}, I. K. Troitskaya⁵

2020 ApJ 904 3

<https://doi.org/10.3847/1538-4357/abbdac>

Using measurements from the PAMELA and ARINA spectrometers on board the Resurs-DK1 satellite, we have examined the 27 day intensity variations in galactic cosmic ray (GCR) proton fluxes in 2007–2008. The PAMELA and ARINA data allow for the first time a study of time profiles and the rigidity dependence of the 27 day variations observed directly in space in a wide rigidity range from ~ 300 MV to several gigavolts. We find that the rigidity dependence of the amplitude of the 27 day GCR variations cannot be described by the same power law at both low and high energies. A flat interval occurs at rigidity $R = (0.6-1.0)$ GV with a power-law index $\gamma = -0.13 \pm 0.44$ for PAMELA, whereas for $R \geq 1$ GV, the power-law dependence is evident with index $\gamma = -0.51 \pm 0.11$. We describe the rigidity dependence of the 27 day GCR variations for PAMELA and ARINA data in the framework of the modulation potential concept using the force-field approximation for GCR transport. For a physical interpretation, we have considered the relationship between the 27 day GCR variations and solar wind plasma and other heliospheric

parameters. Moreover, we have discussed possible implications of MHD modeling of the solar wind plasma together with a stochastic GCR transport model concerning the effects of corotating interaction regions.

On the 27-day Variations of Cosmic Ray Intensity in Recent Solar Minimum 23/24

R. **Modzelewska**, M.V. Alania

Solar Phys. **2013**

<http://arxiv.org/pdf/1504.00180v1.pdf>

We have studied the 27-day variations and their harmonics of the galactic cosmic ray (GCR) intensity, solar wind velocity, and interplanetary magnetic field (IMF) components in the recent prolonged solar minimum 23 24. The time evolution of the quasi-periodicity in these parameters connected with the Sun's rotation reveals that their synodic period is stable and is approx 26-27 days. This means that the changes in the solar wind speed and IMF are related to the Sun's near equatorial regions in considering the differential rotation of the Sun. However, the solar wind parameters observed near the Earth's orbit provide only the conditions in the limited local vicinity of the equatorial region in the heliosphere (within in latitude). We also demonstrate that the observed period of the GCR intensity connected with the Sun's rotation increased up to approx 33-36 days in 2009. This means that the process driving the 27-day variations of the GCR intensity takes place not only in the limited local surroundings of the equatorial region but in the global 3-D space of the heliosphere, covering also higher latitude regions. A relatively long period (approx 34 days) found for 2009 in the GCR intensity gives possible evidence of the onset of cycle 24 due to active regions at higher latitudes and rotating slowly because of the Sun's differential rotation. We also discuss the effect of differential rotation on the theoretical model of the 27-day variations of the GCR intensity.

The relation between coronal holes and coronal mass ejections during the rise, maximum, and declining phases of Solar Cycle 23

Mohamed, A. A.; Gopalswamy, N.; Yashiro, S.; Akiyama, S.; Мджелд, P.; Xie, H.; Jung, H.

J. Geophys. Res., Vol. 117, No. A1, A01103, **2012**

<http://dx.doi.org/10.1029/2011JA016589>

We study the interaction between coronal holes (CHs) and coronal mass ejections (CMEs) using a resultant force exerted by all the coronal holes present on the disk and is defined as the coronal hole influence parameter (CHIP). The CHIP magnitude for each CH depends on the CH area, the distance between the CH centroid and the eruption region, and the average magnetic field within the CH at the photospheric level. The CHIP direction for each CH points from the CH centroid to the eruption region. We focus on Solar Cycle 23 CMEs originating from the disk center of the Sun (central meridian distance $\leq 15^\circ$) and resulting in magnetic clouds (MCs) and non-MCs in the solar wind. The CHIP is found to be the smallest during the rise phase for MCs and non-MCs. The maximum phase has the largest CHIP value (2.9 G) for non-MCs. The CHIP is the largest (5.8 G) for driverless (DL) shocks, which are shocks at 1 AU with no discernible MC or non-MC. These results suggest that the behavior of non-MCs is similar to that of the DL shocks and different from that of MCs. In other words, the CHs may deflect the CMEs away from the Sun-Earth line and force them to behave like limb CMEs with DL shocks. This finding supports the idea that all CMEs may be flux ropes if viewed from an appropriate vantage point.

Was the cosmic ray burst detected by the GRAPES-3 on 22 June 2015 caused by transient weakening of geomagnetic field or by an interplanetary anisotropy?

P.K. Mohanty, **K.P. Arunbabu**, **T. Aziz**, **S.R. Dugad**, **S.K. Gupta**, **B. Hariharan**, **P. Jagadeesan**, **A. Jain**, **S.D. Morris**, **P.K. Nayak**, **P.S. Rakshe**, **K. Ramesh**, **B.S. Rao**, **M. Zuberi**, **Y. Hayashi**, **S. Kawakami**, **P. Subramanian**, **S. Raha**, **S. Ahmad**, **A. Oshima**, **S. Shibata**, **H. Kojima**

Physical Review D **2018**

<https://arxiv.org/pdf/1803.10499.pdf>

The GRAPES-3 muon telescope in Ooty, India had claimed detection of a 2 hour (h) high-energy (~ 20 GeV) burst of galactic cosmic-rays (GCRs) through a $>50\sigma$ surge in GeV muons, was caused by reconnection of the interplanetary magnetic field (IMF) in the magnetosphere that led to transient weakening of Earth's magnetic shield. This burst had occurred during a G4-class geomagnetic storm (storm) with a delay of 12h relative to the coronal mass ejection (CME) of 22 June 2015 (Mohanty et al., 2016). However, recently a group interpreted the occurrence of the same burst in a subset of 31 neutron monitors (NMs) to have been the result of an anisotropy in interplanetary space (Evenson et al., 2017) in contrast to the claim in (Mohanty et al., 2016). A new analysis of the GRAPES-3 data with a fine 10.6° angular segmentation shows the speculation of interplanetary anisotropy to be incorrect, and offers a possible explanation of the

NM observations. The observed 28 minutes (min) delay of the burst relative to the CME can be explained by the movement of the reconnection front from the bow shock to the surface of Earth at an average speed of 35 km/s, much lower than the CME speed of 700 km/s. This measurement may provide a more accurate estimate of the start of the storm.

Transient Weakening of Earth's Magnetic Shield Probed by a Cosmic Ray Burst

P. K. **Mohanty**, K. P. Arunbabu, T. Aziz, S. R. Dugad, S. K. Gupta, B. Hariharan, P. Jagadeesan, A. Jain, S. D. Morris, B. S. Rao, Y. Hayashi, S. Kawakami, A. Oshima, S. Shibata, S. Raha, P. Subramanian, and H. Kojima

Phys. Rev. Lett. 117, 171101 – Published 20 October 2016

[sci-hub.tw/10.1103/PhysRevLett.117.171101](https://doi.org/10.1103/PhysRevLett.117.171101)

The GRAPES-3 tracking muon telescope in Ooty, India measures muon intensity at high cutoff rigidities (15–24 GV) along nine independent directions covering 2.3 sr. The arrival of a coronal mass ejection on **22 June 2015** 18:40 UT had triggered a severe G4-class geomagnetic storm (storm). Starting 19:00 UT, the GRAPES-3 muon telescope recorded a 2 h high-energy (~20 GeV) burst of galactic cosmic rays (GCRs) that was strongly correlated with a 40 nT surge in the interplanetary magnetic field (IMF). Simulations have shown that a large (17×) compression of the IMF to 680 nT, followed by reconnection with the geomagnetic field (GMF) leading to lower cutoff rigidities could generate this burst. Here, 680 nT represents a short-term change in GMF around Earth, averaged over 7 times its volume. The GCRs, due to lowering of cutoff rigidities, were deflected from Earth's day side by ~210° in longitude, offering a natural explanation of its night-time detection by the GRAPES-3. The simultaneous occurrence of the burst in all nine directions suggests its origin close to Earth. It also indicates a transient weakening of Earth's magnetic shield, and may hold clues for a better understanding of future superstorms that could cripple modern technological infrastructure on Earth, and endanger the lives of the astronauts in space.

A Study of Fluctuations in Magnetic Cloud-Driven Sheaths

C. **Moissard**, [D. Fontaine](#), [P. Savoini](#)

JGR [Volume124, Issue11](#) November 2019 Pages 8208-8226

<https://doi.org/10.1029/2019JA026952>

Interplanetary coronal mass ejections are at the center of the research on geomagnetic activity. Sheaths, highly fluctuating structures, which can be found in front of fast interplanetary coronal mass ejections, are some of the least known geoeffective solar transients. Using Morlet transforms, we analyzed the magnetic fluctuations in a list of 42 well-identified and isolated magnetic clouds driving a sheath and shock (Masias-Meza et al., 2016, <https://doi.org/10.1051/0004-6361/201628571>). We studied the fluctuations inside sheaths by defining two quantities: the power and the anisotropy. With a simple statistical approach we found that sheaths, in particular, those driven by a fast magnetic cloud, encountering a highly turbulent solar wind, and forming a high Alfvén Mach number shock have high levels of turbulent energy (~10 times compared with the solar wind) as well as a low anisotropy (approximately halved compared with the solar wind) of their fluctuations. On the other hand, the effect of the shock angle and plasma beta in the solar wind are less straightforward: If the shock is quasi-parallel or the beta in the solar wind is high, both the turbulent energy in the sheaths and the anisotropy of the fluctuations are reduced; but for quasi-perpendicular shocks or low beta solar wind the turbulent energy and anisotropy can take any value.

Consequences of a Solar Wind Stream Interaction Region on the Low Latitude Ionosphere: Event of 7 October 2015

M. G. **Molina**, [S. Dasso](#), [G. Mansilla](#), [J. H. Namour](#), [M. A. Cabrera](#) & [E. Zuccheretti](#)

[Solar Physics](#) volume 295, Article number: 173 (2020)

<https://link.springer.com/content/pdf/10.1007/s11207-020-01728-7.pdf>

In this article, we present a study of the perturbations occurring in the Earth's environment on 7 October 2015. We use a multi-instrument approach, including space and ground observations.

In particular, we study the ionospheric conditions at low latitudes. Two ionospheric storms are observed at the low latitude station of Tucumán (26°26' 51.51" S, 65°65' 12.12" W). We observe a negative ionospheric storm followed by a positive one. These ionospheric perturbations were triggered by two sudden storm commencements (SSCs) of a strong geomagnetic storm. Preliminary results show that the main mechanism involved in both ionospheric storms is the prompt penetration of electric fields (PPEFs) from the magnetosphere. Furthermore, in the positive storm, disturbed dynamo electric fields are observed acting in combination with the PPEFs. The impact of the solar wind on the Earth's

environment is analyzed using geomagnetic data and proxies, combined with data acquired in the Tucumán Low Latitude Observatory for the Upper Atmosphere.

We also investigate the solar and interplanetary drivers of this intense perturbation. We find that, although typically interplanetary coronal mass ejections (ICMEs) are the most geoeffective transient interplanetary events, in this case, a corotating interaction region (CIR) is responsible for these strong perturbations to the geospace.

First in-situ Measurements of Electron Density and Temperature from Quasi-Thermal Noise Spectroscopy with Parker Solar Probe/FIELDS

Michel [Moncuquet](#), [Nicole Meyer-Vernet](#), [Karine Issautier](#), [Marc Pulupa](#), [J. W. Bonnell](#), [Stuart D. Bale](#), [Thierry Dudok de Wit](#), [Keith Goetz](#), [Léa Griton](#), [Peter R. Harvey](#), [Robert J. MacDowall](#), [Milan Maksimovic](#), [David M. Malaspina](#)

ApJS 2019

<https://arxiv.org/pdf/1912.02518.pdf>

Heat transport in the solar corona and wind is still a major unsolved astrophysical problem. Because of the key role played by electrons, the electron density and temperature(s) are important prerequisites for understanding these plasmas. We present such in situ measurements along the two first solar encounters of Parker Solar Probe (PSP), between 0.5 and 0.17 AU from the Sun, revealing different states of the emerging solar wind near solar activity minimum. These preliminary results are obtained from a simplified analysis of the plasma quasi-thermal noise (QTN) spectrum measured by the Radio Frequency Spectrometer (RFS/FIELDS). The local electron density is deduced from the tracking of the plasma line, which enables accurate measurements, independent of calibrations and spacecraft perturbations, whereas the temperatures of the thermal and supra-thermal components of the velocity distribution, as well as the average kinetic temperature are deduced from the shape of the plasma line. The temperature of the weakly collisional thermal population, similar for both encounters, decreases with distance as $R^{-0.74}$, much slower than adiabatic. In contrast, the temperature of the nearly collisionless suprathermal population exhibits a virtually flat radial variation. The 7-second resolution of the density measurements enables us to deduce the low-frequency spectrum of compressive fluctuations around perihelion, varying as $f^{-1.4}$. This is the first time that QTN spectroscopy is implemented with an electric antenna length not exceeding the plasma Debye length. As PSP will approach the Sun, the decrease in Debye length is expected to considerably improve the accuracy of the temperature measurements.

Acceleration of Solar Energetic Particles by the shock of Interplanetary Coronal Mass Ejection

Shanlee Sow [Mondal](#), [Aveek Sarkar](#), [Bhargav Vaidya](#), [Andrea Mignone](#)

ApJ 923 80 2021

<https://arxiv.org/pdf/2110.01828.pdf>

<https://doi.org/10.3847/1538-4357/ac2c7a>

Interplanetary Coronal Mass Ejection (ICME) shocks are known to accelerate particles and contribute significantly to Solar Energetic Particle (SEP) events. We have performed Magnetohydrodynamic-Particle in Cell (MHD-PIC) simulations of ICME shocks to understand the acceleration mechanism. These shocks vary in Alfvénic Mach numbers as well as in magnetic field orientations (parallel & quasi-perpendicular). We find that Diffusive Shock Acceleration (DSA) plays a significant role in accelerating particles in a parallel ICME shock. In contrast, Shock Drift Acceleration (SDA) plays a pivotal role in a quasi-perpendicular shock. High-Mach shocks are seen to accelerate particles more efficiently. Our simulations suggest that background turbulence and local particle velocity distribution around the shock can indirectly hint at the acceleration mechanism. Our results also point towards a few possible *in situ* observations that could validate our understanding of the topic.

Variability of Interplanetary Shock and Associated Energetic Particle Properties as a Function of the Time Window Around the Shock

K. [Moreland](#)^{1,2}, M. A. Dayeh^{1,2}, G. Li³, A. Farahat⁴, R. W. Ebert^{1,2}, and M. I. Desai^{1,2}

2023 ApJ 956 107

<https://iopscience.iop.org/article/10.3847/1538-4357/accec6c/pdf>

We study the effect of sampling windows on derived shock and associated energetic storm particle (ESP) properties in 296 fast-forward interplanetary shocks using Advanced Composition Explorer measurements at 1 au between 1998 February and 2013 August. We vary the time windows from 2 minutes to 20 minutes for the shock properties and from 2 minutes to 540 minutes for ESP properties. Variability is quantified by the median absolute deviation statistic. We find that the magnetic, density, and temperature compression ratios vary from their median values by 17.03%, 20.05%, and

25.91%, respectively; shock speed by 16.26%; speed jump by 45.46%; Alfvénic Mach number by 31.53%; and shock obliquity by 24.25%. Spectral indices in the 2 minute–540 minute windows downstream of the shock vary from the median value of 1.79 by 26.05% and by 30.53% from the 1.70 median value upstream of the shock. Similarity of ESP spectral indices upstream and downstream of the shock suggest that these ESP populations are likely locally accelerated at the shock. Furthermore, we find that for a moving sampling window around the shock, values for the density ratio hold for ~10 minutes; the magnetic ratio and shock speed jump hold for ~30 minutes and ~60 minutes, respectively. Fixing the upstream window to 2 minutes and moving only in the downstream direction, the density ratio holds for ~60 minutes downstream, magnetic ratio holds for ~30 minutes, and the shock speed jump holds for ~110 minutes. Beyond these time windows, derived shock properties are no longer representative of shock properties. These results provide constraints for modeling and forecasting efforts of shock and ESP-associated properties. 1998-08-26

Detection and Characterisation of a Coronal Mass Ejection using Interplanetary Scintillation measurements from the Murchison Widefield Array

J. Morgan, P. I. McCauley, A. Waszewski, R. Ekers, R. Chhetri

Space Weather **Volume21, Issue5** e2022SW003396 2023

<https://arxiv.org/pdf/2303.09134.pdf>

<https://doi.org/10.1029/2022SW003396>

<https://agupubs.onlinelibrary.wiley.com/doi/epdf/10.1029/2022SW003396>

We have shown previously that the Murchison Widefield Array (MWA), can detect hundreds of Interplanetary Scintillation (IPS) sources simultaneously across a field of view ~30° in extent. To test if we can use this capability to track heliospheric structures, we undertook a search of 88 hours of MWA IPS data, and identified an observation likely to have a significant Coronal Mass Ejection (CME) in the field of view. We demonstrate that in a single 5-minute MWA observation we are able to localise and image a CME ~33 hours after launch at an elongation of ~37° from the Sun. We use IPS observables to constrain the kinematics of the CME, and describe how MWA IPS observations can be used in the future to make a unique contribution to heliospheric modelling efforts. 2016-05-15

Daily Variations of Plasma Density in the Solar Streamer Belt

Huw Morgan

2021 ApJ 922 165

<https://iopscience.iop.org/article/10.3847/1538-4357/ac1799/pdf>

<https://doi.org/10.3847/1538-4357/ac1799>

Improved space weather diagnostics depend critically on improving our understanding of the evolution of the slow solar wind in the streamer belts near the Sun. Recent innovations in tomography techniques are opening a new window on this complex environment. In this work, a new time-dependent technique is applied to COR2A/Solar Terrestrial Relations Observatory observations from a period near solar minimum (2018 November 11) for heliocentric distances of 4–8 R_⊙. For the first time, we find density variations of large amplitude throughout the quiescent streamer belt, ranging between 50% and 150% of the mean density, on timescales of tens of hours to days. Good agreement is found with Parker Solar Probe measurements at perihelion; thus, the variations revealed by tomography must form a major component of the slow solar wind variability, distinct from coronal mass ejections or smaller transients. A comparison of time series at different heights reveals a consistent time lag, so that changes at 4 R_⊙ occur later at increasing height, corresponding to an outward propagation speed of around 100 km s⁻¹. This speed may correspond to either the plasma sound speed or the bulk outflow speed depending on an important question: are the density variations caused by the spatial movement of a narrow streamer belt (moving magnetic field, constant plasma density), or changes in plasma density within a nonmoving streamer belt (rigid magnetic field, variable density), or a combination of both? 2018 November 04-07

The width, density and outflow of solar coronal streamers

Huw Morgan, Anthony C. Cook

2020

<https://arxiv.org/pdf/2003.04809.pdf>

Characterising the large-scale structure and plasma properties of the inner corona is crucial to understand the source and subsequent expansion of the solar wind and related space weather effects. Here we apply a new coronal rotational tomography method, along with a method to narrow streamers and refine the density estimate, to COR2A/STEREO observations from a period near solar minimum and maximum, gaining density maps for heights between 4 and 8 R_s. The coronal structure is highly radial at these heights, and the streamers are very narrow, in some regions only a few degrees in width. The mean densities of streamers is almost identical between solar minimum and maximum. However,

streamers at solar maximum contain around 50% more total mass due to their larger area. By assuming a constant mass flux, and constraints on proton flux measured by Parker Solar Probe (PSP), we estimate an outflow speed within solar minimum streamers of 50-120 km/s at 4 R_s, increasing to 90-250 km/s at 8 R_s. Accelerations of around 6 m/s² are found for streamers at a height of 4 R_s, decreasing with height. The solar maximum slow wind shows a higher acceleration to extended distances compared to solar minimum. To satisfy the solar wind speeds measured by PSP, there must be a mean residual acceleration of around 1-2 m/s² between 8 and 40 R_s. Several aspects of this study strongly suggest that the coronal streamer belt density is highly variable on small scales, and that the tomography can only reveal a local spatial and temporal average.

The Impact of Geometry on Observations of CME Brightness and Propagation

J.S. [Morrill](#) · R.A. Howard · A. Vourlidas · D.F. Webb · V. Kunkel

Solar Phys (2009) 259: 179–197, [File](#)

Coronal mass ejections (CMEs) have a significant impact on space weather and geomagnetic storms and so have been the subject of numerous studies. Most CME observations have been made while these events are near the Sun (*e.g.*, SOHO/LASCO). Recent data from the *Coriolis*/SMEI and STEREO/SECCHI-HI instruments have imaged CMEs farther into the heliosphere. Analyses of CME observations near the Sun measure the properties of these events by assuming that the emission is in the plane of the sky and hence the speed and mass are lower limits to the true values. However, this assumption cannot be used to analyze optical observations of CMEs far from the Sun, such as observations from SMEI and SECCHI-HI, since the CME source is likely to be far from the limb. In this paper we consider the geometry of observations made by LASCO, SMEI, and SECCHI. We also present results that estimate both CME speed and trajectory by fitting the CME elongations observed by these instruments. Using a constant CME speed does not generally produce profiles that fit observations at both large and small elongation, simultaneously. We include the results of a simple empirical model that alters the CME speed to an estimated value of the solar wind speed to simulate the effect of drag on the propagating CME. This change in speed improves the fit between the model and observations over a broad range of elongations.

Interfacing MHD Single Fluid and Kinetic Exospheric Solar Wind Models and Comparing Their Energetics

Sofia-Paraskevi [Moschou](#), Viviane Pierrard, Rony Keppens, Jens Pomoell

[Solar Physics](#) September 2017, 292:139

An exospheric kinetic solar wind model is interfaced with an observation-driven single-fluid magnetohydrodynamic (MHD) model. Initially, a photospheric magnetogram serves as observational input in the fluid approach to extrapolate the heliospheric magnetic field. Then semi-empirical coronal models are used for estimating the plasma characteristics up to a heliocentric distance of 0.1 AU. From there on, a full MHD model that computes the three-dimensional time-dependent evolution of the solar wind macroscopic variables up to the orbit of Earth is used. After interfacing the density and velocity at the inner MHD boundary, we compare our results with those of a kinetic exospheric solar wind model based on the assumption of Maxwell and Kappa velocity distribution functions for protons and electrons, respectively, as well as with in situ observations at 1 AU. This provides insight into more physically detailed processes, such as coronal heating and solar wind acceleration, which naturally arise from including suprathermal electrons in the model. We are interested in the profile of the solar wind speed and density at 1 AU, in characterizing the slow and fast source regions of the wind, and in comparing MHD with exospheric models in similar conditions. We calculate the energetics of both models from low to high heliocentric distances.

See [Mostl](#) and [Moestl](#)

Multipoint ICME events during the first year of combined Solar Orbiter, BepiColombo, Parker Solar Probe, Wind and STEREO-A observations

C. [Möstl](#), [A. J. Weiss](#), [M. A. Reiss](#), [T. Amerstorfer](#), [R. L. Bailey](#), [J. Hinterreiter](#), [M. Bauer](#), [D. Barnes](#), [J. A. Davies](#), [R. A. Harrison](#), [J. L. Freiherr von Forstner](#), [E. E. Davies](#), [D. Heyner](#), [T. Horbury](#), [S. D. Bale](#)

ApJL 924 L6 2022

<https://arxiv.org/pdf/2109.07200.pdf>
<https://iopscience.iop.org/article/10.3847/2041-8213/ac42d0/pdf>
<https://doi.org/10.3847/2041-8213/ac42d0>

We report the result of the first search for multipoint in situ and imaging observations of interplanetary coronal mass ejections (ICMEs) starting with the first Solar Orbiter data in April 2020 to April 2021. A data exploration analysis is performed including visualizations of the magnetic field and plasma observations made by the five spacecraft Solar Orbiter, BepiColombo, Parker Solar Probe, Wind and STEREO-A, in connection with coronagraph and heliospheric imaging observations from STEREO-Ahead/SECCHI and SOHO/LASCO. We identify ICME events that could be unambiguously followed with the STEREO-A heliospheric imagers during their interplanetary propagation to their impact at the aforementioned spacecraft, and look for events where the same ICME is seen in situ by widely separated spacecraft. We highlight two events: (1) a small streamer blowout CME on **2020 June 23** observed with a triple lineup by Parker Solar Probe, BepiColombo and Wind, guided by imaging with STEREO-A, and (2) the first fast CME of solar cycle 25 ($\approx 1600 \text{ km s}^{-1}$) on **2020 Nov 29** observed in situ by Parker Solar Probe and STEREO-A. These results are useful for modeling the magnetic structure of ICMEs, the interplanetary evolution and global shape of their flux ropes and shocks, and for studying the propagation of solar energetic particles. The combined data from these missions is already turning out to be a treasure trove for space weather research and is expected to become even more valuable with an increasing number of ICME events expected during the rise and maximum of solar cycle 25.

Table 1. Multipoint imaging and in situ CME events

Prediction of the in situ coronal mass ejection rate for solar cycle 25: Implications for Parker Solar Probe in situ observations

Christian [Möstl](#), [Andreas J. Weiss](#), [Rachel L. Bailey](#), [Martin A. Reiss](#), [Ute V. Amerstorfer](#), [Tanja Amerstorfer](#), [Jürgen Hinterreiter](#), [Maike Bauer](#), [Scott W. McIntosh](#), [Noé Lugaz](#), [David Stansby](#)

ApJ **903** 92 **2020**

arxiv.org/pdf/2007.14743.pdf

<https://iopscience.iop.org/article/10.3847/1538-4357/abb9a1/pdf>

The Parker Solar Probe (PSP) and Solar Orbiter missions are designed to make groundbreaking observations of the Sun and interplanetary space within this decade. We show that a particularly interesting in situ observation of an interplanetary coronal mass ejection (ICME) by PSP may arise during close solar flybys ($<0.1 \text{ AU}$). During these times, the same magnetic flux rope inside an ICME could be observed in situ by PSP twice, by impacting its frontal part as well as its leg. Investigating the odds of this situation, we forecast the ICME rate in solar cycle 25 based on 2 models for the sunspot number (SSN): (1) the consensus prediction of an expert panel in 2019 (maximum SSN = 115), and (2) a prediction by McIntosh et al. (2020, maximum SSN = 232). We link the SSN to the observed ICME rates in solar cycles 23 and 24 with the Richardson and Cane list and our own ICME catalog with a linear fit. We calculate that between 2 and 7 ICMEs will be observed by PSP at heliocentric distances $<0.1 \text{ AU}$ until 2025, including 1σ uncertainties. We then model the potential flux rope signatures of such a double-crossing event with the semi-empirical 3DCORE flux rope model, showing a telltale elevation of the radial magnetic field component BR and a sign reversal in the component BN normal to the solar equator, which is in contrast to the classic field rotation in the first encounter. This holds considerable promise to determine the structure of CMEs close to their origin in the solar corona.

Forward modeling of coronal mass ejection flux ropes in the inner heliosphere with 3DCORE

Christian [Möstl](#), [Tanja Amerstorfer](#), [Erika Palmerio](#), [Alexey Isavnin](#), [Charles J. Farrugia](#), [Chris Lowder](#), [Reka M. Winslow](#), [Julia Donnerer](#), [Emilia K. J. Kilpua](#), [Peter D. Boakes](#)

Space Weather v.16 no. 3, p. 216-229 **2018**

<https://arxiv.org/ftp/arxiv/papers/1710/1710.00587.pdf>

<https://agupubs.onlinelibrary.wiley.com/doi/epdf/10.1002/2017SW001735>

Forecasting the geomagnetic effects of solar storms, known as coronal mass ejections (CMEs), is currently severely limited by our inability to predict the magnetic field configuration in the CME magnetic core and by the observational effects of a single spacecraft trajectory through its 3D structure. CME magnetic flux ropes lead to continuous forcing of the energy input to the Earth's magnetosphere by strong and steady southward-pointing magnetic fields. Here, we demonstrate in a proof-of-concept way a new approach to predict the southward field B_z in a CME flux rope. It combines a novel semi-empirical model of CME flux rope magnetic fields (3-Dimensional Coronal ROpe Ejection or 3DCORE) with solar observations and in situ magnetic field data from along the Sun-Earth line. These are provided here by the MESSENGER spacecraft for a CME event on **2013 July 9-13**. 3DCORE is the first such model that contains the interplanetary propagation and evolution of a 3D flux rope magnetic field, the observation by a synthetic spacecraft and the prediction of an index of geomagnetic activity. A counterclockwise rotation of the left-handed erupting CME flux

rope in the corona of 30 degree and a deflection angle of 20 degree is evident from comparison of solar and coronal observations. The calculated Dst matches reasonably the observed Dst minimum and its time evolution, but the results are highly sensitive to the CME axis orientation. We discuss assumptions and limitations of the method prototype and its potential for real time space weather forecasting and heliospheric data interpretation.

Modeling observations of solar coronal mass ejections with heliospheric imagers verified with the Heliophysics System Observatory

C. **Möstl**, A. Isavnin, P. D. Boakes, E. K. J. Kilpua, J. A. Davies, R. A. Harrison, D. Barnes, V. Krupar, J. P. Eastwood, S. W. Good, et al

Space Weather Volume 15, Issue 7 July 2017 Pages 955–970

<http://sci-hub.cc/10.1002/2017SW001614>

[https://tuhat.helsinki.fi/portal/en/publications/modeling-observatio\(8499e6f5-fe34-4659-81d6-2eb4d293700e\).html](https://tuhat.helsinki.fi/portal/en/publications/modeling-observatio(8499e6f5-fe34-4659-81d6-2eb4d293700e).html)

We present an advance toward accurately predicting the arrivals of coronal mass ejections (CMEs) at the terrestrial planets, including Earth. For the first time, we are able to assess a CME prediction model using data over two thirds of a solar cycle of observations with the Heliophysics System Observatory. We validate modeling results of 1337 CMEs observed with the Solar Terrestrial Relations Observatory (STEREO) heliospheric imagers (HI) (science data) from 8 years of observations by five in situ observing spacecraft. We use the self-similar expansion model for CME fronts assuming 60° longitudinal width, constant speed, and constant propagation direction. With these assumptions we find that 23%–35% of all CMEs that were predicted to hit a certain spacecraft lead to clear in situ signatures, so that for one correct prediction, two to three false alarms would have been issued. In addition, we find that the prediction accuracy does not degrade with the HI longitudinal separation from Earth. Predicted arrival times are on average within 2.6 ± 16.6 h difference of the in situ arrival time, similar to analytical and numerical modeling, and a true skill statistic of 0.21. We also discuss various factors that may improve the accuracy of space weather forecasting using wide-angle heliospheric imager observations. These results form a first-order approximated baseline of the prediction accuracy that is possible with HI and other methods used for data by an operational space weather mission at the Sun-Earth L5 point.

Strong coronal channelling and interplanetary evolution of a solar storm up to Earth and Mars

Christian **Möstl**, Tanja Rollett, Rudy A. Frahm, Ying D. Liu, David M. Long, Robin C. Colaninno, Martin A. Reiss, Manuela Temmer, Charles J. Farrugia, Arik Posner, Mateja Dumbović, Miho Janvier, Pascal Démoulin, Peter Boakes, Andy Devos, Emil Kraaikamp, Mona L. Mays, Bojan Vrsnak

Nature Communications 2015

<http://arxiv.org/pdf/1506.02842v1.pdf>

The severe geomagnetic effects of solar storms or coronal mass ejections (CMEs) are to a large degree determined by their propagation direction with respect to Earth. There is a lack of understanding of the processes that determine their non-radial propagation. Here we present a synthesis of data from seven different space missions of a fast CME, which originated in an active region near the disk centre and, hence, a significant geomagnetic impact was forecasted. However, the CME is demonstrated to be channelled during eruption into a direction $+37^\circ \pm 10^\circ$ (longitude) away from its source region, leading only to minimal geomagnetic effects. In situ observations near Earth and Mars confirm the channelled CME motion, and are consistent with an ellipse shape of the CME-driven shock provided by the new Ellipse Evolution model, presented here. The results enhance our understanding of CME propagation and shape, which can help to improve space weather forecasts. **7 January 2014**

Connecting speeds, directions and arrival times of 22 coronal mass ejections from the Sun to 1 AU

C. **Möstl**, K. Amla, J. R. Hall, P. C. Liewer, E. M. De Jong, R. C. Colaninno, A. M. Veronig, T. Rollett, M. Temmer, V. Peinhart, J. A. Davies, N. Lugaz, Y. D. Liu, C.J. Farrugia, J. G. Luhmann, B. Vršnak, R. A. Harrison, A. B. Galvin

ApJ, 787 119, 2014

<http://arxiv.org/pdf/1404.3579v1.pdf>

<https://iopscience.iop.org/article/10.1088/0004-637X/787/2/119/pdf>

Forecasting the in situ properties of coronal mass ejections (CMEs) from remote images is expected to strongly enhance predictions of space weather, and is of general interest for studying the interaction of CMEs with planetary environments. We study the feasibility of using a single heliospheric imager (HI) instrument, imaging the solar wind density from the Sun to 1 AU, for connecting remote images to in situ observations of CMEs. We compare the

predictions of speed and arrival time for 22 CMEs (in 2008–2012) to the corresponding interplanetary coronal mass ejection (ICME) parameters at in situ observatories (STEREO PLASTIC/IMPACT, Wind SWE/MFI). The list consists of front- and back-sided, slow and fast CMEs (up to 2700km s^{-1}). We track the CMEs to 34.9 ± 7.1 degrees elongation from the Sun with J-maps constructed using the SATPLOT tool, resulting in prediction lead times of -26.4 ± 15.3 hours. The geometrical models we use assume different CME front shapes (Fixed- Φ , Harmonic Mean, Self-Similar Expansion), and constant CME speed and direction. We find no significant superiority in the predictive capability of any of the three methods. The absolute difference between predicted and observed ICME arrival times is 8.1 ± 6.3 hours (rms value of 10.9h). Speeds are consistent to within $284 \pm 288\text{km s}^{-1}$. Empirical corrections to the predictions enhance their performance for the arrival times to 6.1 ± 5.0 hours (rms value of 7.9h), and for the speeds to $53 \pm 50\text{km s}^{-1}$. These results are important for Solar Orbiter and a space weather mission positioned away from the Sun-Earth line.

TABLE 1 Imaging: Croissant and geometrical modeling (SSEF) results

TABLE 2 In situ ICME parameters

Speeds and Arrival Times of Solar Transients Approximated by Self-similar Expanding Circular Fronts

C. Möstl · J.A. Davies

Solar Phys, July 2013, Volume 285, Issue 1-2, pp 411-423

The NASA Solar TERrestrial RELations Observatory (STEREO) mission offered the possibility to forecast the arrival times, speeds, and directions of solar transients from outside the Sun-Earth line. In particular, we are interested in predicting potentially geoeffective interplanetary coronal mass ejections (ICMEs) from observations of density structures at large observation angles from the Sun (with the STEREO Heliospheric Imager instrument). We contribute to this endeavor by deriving analytical formulas concerning a geometric correction for the ICME speed and arrival time for the technique introduced by Davies et al. (Astrophys. J., 2012, in press), called self-similar expansion fitting (SSEF). This model assumes that a circle propagates outward, along a plane specified by a position angle (e.g., the ecliptic), with constant angular half-width (λ). This is an extension to earlier, more simple models: fixed- Φ fitting ($\lambda=0^\circ$) and harmonic mean fitting ($\lambda=90^\circ$). In contrast to previous models, this approach has the advantage of allowing one to assess clearly if a particular location in the heliosphere, such as a planet or spacecraft, might be expected to be hit by the ICME front. Our correction formulas are especially significant for glancing hits, where small differences in the direction greatly influence the expected speeds (up to 100 - 200 km s⁻¹) and arrival times (up to two days later than the apex). For very wide ICMEs ($2\lambda > 120^\circ$), the geometric correction becomes very similar to the one derived by Möstl et al. (Astrophys. J. 741, 34, 2011) for the harmonic mean model. These analytic expressions can also be used for empirical or analytical models to predict the 1 AU arrival time of an ICME by correcting for effects of hits by the flank rather than the apex, if the width and direction of the ICME in a plane are known and a circular geometry of the ICME front is assumed.

Multi-point Shock and Flux Rope Analysis of Multiple Interplanetary Coronal Mass Ejections around 2010 August 1 in the Inner Heliosphere

Möstl, C., Farrugia, C. J., Kilpua, E. K. J., et al. 2012, ApJ, 758, 10 <http://arxiv.org/pdf/1209.2866v1.pdf>
<http://arxiv.org/pdf/1404.3579v1.pdf>

We present multi-point in situ observations of a complex sequence of coronal mass ejections (CMEs) which may serve as a benchmark event for numerical and empirical space weather prediction models. On **2010 August 1**, instruments on various space missions, Solar Dynamics Observatory/Solar and Heliospheric Observatory/Solar-TERrestrial-Relations-Observatory (SDO/SOHO/STEREO), monitored several CMEs originating within tens of degrees from the solar disk center. We compare their imprints on four widely separated locations, spanning 120° in heliospheric longitude, with radial distances from the Sun ranging from MESSENGER (0.38 AU) to Venus Express (VEX, at 0.72 AU) to Wind, ACE, and ARTEMIS near Earth and STEREO-B close to 1 AU. Calculating shock and flux rope parameters at each location points to a non-spherical shape of the shock, and shows the global configuration of the interplanetary coronal mass ejections (ICMEs), which have interacted, but do not seem to have merged. VEX and STEREO-B observed similar magnetic flux ropes (MFRs), in contrast to structures at Wind. The geomagnetic storm was intense, reaching two minima in the Dst index (-100 nT), and was caused by the sheath region behind the shock and one of two observed MFRs. MESSENGER received a glancing blow of the ICMEs, and the events missed STEREO-A entirely. The observations demonstrate how sympathetic solar eruptions may immerse at least 1/3 of the heliosphere in the ecliptic with their distinct plasma and magnetic field signatures. We also emphasize the difficulties in linking the local views derived from single-spacecraft observations to a consistent global picture, pointing to possible alterations from the classical picture of ICMEs.

Speeds and arrival times of solar transients approximated by self-similar expanding circular fronts

Christian [Mostl](#) and Jackie A. Davies

E-print, Feb 2012, [File](#); Solar Phys.

The NASA STEREO mission opened up the possibility to forecast the arrival times, speeds and directions of solar transients from outside the Sun-Earth line. In particular, we are interested in predicting potentially geo-effective Interplanetary Coronal Mass Ejections (ICMEs) from observations of density structures at large observation angles from the Sun (with the STEREO Heliospheric Imager instrument). We contribute to this endeavor by deriving analytical formulas concerning a geometric correction for the ICME speed and arrival time for the technique introduced by Davies et al. (2012, submitted to ApJ) called Self-Similar Expansion Fitting (SSEF). This model assumes that a circle propagates outward, along a plane specified by a position angle (e.g. the ecliptic), with constant angular half width (λ). This is an extension to earlier, more simple models: Fixed-Phi Fitting ($\lambda = 0$ degree) and Harmonic Mean Fitting ($\lambda = 90$ degree). This approach has the advantage that it is possible to assess clearly, in contrast to previous models, if a particular location in the heliosphere, such as a planet or spacecraft, might be expected to be hit by the ICME front. Our correction formulas are especially significant for glancing hits, where small differences in the direction greatly influence the expected speeds (up to 100-200 km/s) and arrival times (up to two days later than the apex). For very wide ICMEs ($\lambda > 120$ degree), the geometric correction becomes very similar to the one derived by Mostl et al. (2011, ApJ) for the Harmonic Mean model. These analytic expressions can also be used for empirical or analytical models to predict the 1 AU arrival time of an ICME by correcting for effects of hits by the flank rather than the apex, if the width and direction of the ICME in a plane are known and a circular geometry of the ICME front is assumed.

Arrival time calculation for interplanetary coronal mass ejections with circular fronts and application to STEREO observations of the 2009 February 13 eruption

C. [Mostl](#), T. Rollett, N. Lugaz, C. J. Farrugia, J. A. Davies, M. Temmer, A. M. Veronig, R. Harrison, S. Crothers, J. G. Luhmann, A. B. Galvin, T. L. Zhang, W. Baumjohann, H. K. Biernat

E-print, 2 Aug, 2011, ApJ, 741 34, 2011, [File](#)

A goal of the NASA STEREO mission is to study the feasibility of forecasting the direction, arrival time and internal structure of solar coronal mass ejections (CMEs) from a vantage point outside the Sun-Earth line. Through a case study, we discuss the arrival time calculation of interplanetary CMEs (ICMEs) in the ecliptic plane using data from STEREO/SECCHI at large elongations from the Sun in combination with different geometric assumptions about the ICME front shape (Fixed- Φ (FP): a point and harmonic Mean (HM): a circle). These forecasting techniques use single-spacecraft imaging data and are based on the assumptions of constant velocity and direction. We show that for the slow (350 km/s) ICME on 2009 February 13-18, observed at quadrature by the two STEREO spacecraft, the results for the arrival time given by the HM approximation are more accurate by 12 hours than those for FP in comparison to in situ observations of solar wind plasma and magnetic field parameters by STEREO/IMPACT/PLASTIC, and by 6 hours for the arrival time at Venus Express (MAG). We propose that the improvement is directly related to the ICME front shape being more accurately described by HM for an ICME with a low inclination of its symmetry axis to the ecliptic. In this case the ICME has to be tracked to $> 30^\circ$ elongation to get arrival time errors $< \pm 5$ hours. A newly derived formula for calculating arrival times with the HM method is also useful for a triangulation technique assuming the same geometry.

STEREO and Wind observations of a fast ICME flank triggering a prolonged geomagnetic storm on 5-7 April 2010

[Mostl](#), C., M. Temmer, T. Rollett, C.J. Farrugia, Y. Liu, A. Veronig, M. Leitner, A.B. Galvin, H.K. Biernat
E-print, Oct 2010, [File](#), Geophys. Res. Lett., 37, L24103, doi:10.1029/2010GL045175, 2010.

On 5 April 2010 an interplanetary (IP) shock was detected by the Wind spacecraft ahead of Earth, followed by a fast (average speed 650 km/s) IP coronal mass ejection (ICME). During the subsequent moderate geomagnetic storm (minimum Dst = -72 nT, maximum Kp = 8-), communication with the Galaxy 15 satellite was lost. We link images from STEREO/ SECCHI to the near-Earth in situ observations and show that the ICME did not decelerate much between Sun and Earth. The ICME flank was responsible for a long storm growth phase. This type of glancing collision was for the first time directly observed with the STEREO Heliospheric Imagers. The magnetic cloud (MC) inside the ICME cannot be modeled with approaches assuming an invariant direction. These observations confirm the hypotheses that parts of ICMEs classified as (1) long-duration MCs or (2) magnetic cloud-like (MCL) structures can be a consequence of a spacecraft trajectory through the ICME flank.

Linking remote imagery of a coronal mass ejection to its in situ signatures at 1 AU

Christian Möstl, Charles J. Farrugia, Manuela Temmer, Christiane Miklenic, Astrid M. Veronig, Antoinette B. Galvin, Martin Leitner, Helfried K. Biernat

E-print, Oct 2009, File

In a case study (**June 6-7, 2008**) we report on how the internal structure of a coronal mass ejection (CME) at 1 AU can be anticipated from remote observations of white-light images of the heliosphere. Favorable circumstances are the absence of fast equatorial solar wind streams and a low CME velocity which allow us to relate the imaging and in-situ data in a straightforward way. The STEREO-B spacecraft encountered typical signatures of a magnetic flux rope inside an interplanetary CME (ICME) whose axis was inclined at 45 degree to the solar equatorial plane. Various CME direction-finding techniques yield consistent results to within 15 degree. Further, remote images from STEREO-A show that (1) the CME is unambiguously connected to the ICME and can be tracked all the way to 1 AU, (2) the particular arc-like morphology of the CME points to an inclined axis, and (3) the three-part structure of the CME may be plausibly related to the in situ data. This is a first step in predicting both the direction of travel and the internal structure of CMEs from complete remote observations between the Sun and 1 AU, which is one of the main requirements for forecasting the geo-effectiveness of CMEs.

Optimized Grad – Shafranov Reconstruction of a Magnetic Cloud Using STEREO-Wind Observations

C. Möstl · C.J. Farrugia · H.K. Biernat · M. Leitner · E.K.J. Kilpua · A.B. Galvin · J.G. Luhmann

Solar Phys (2009) 256: 427–441, DOI 10.1007/s11207-009-9360-7

STEREO SCIENCE RESULTS AT SOLAR MINIMUM

We present results on the geometry of a magnetic cloud (MC) on **23 May 2007** from a comprehensive analysis of *Wind* and STEREO observations. We first apply a Grad – Shafranov reconstruction to the STEREO-A plasma and magnetic field data, delivered by the PLASTIC and IMPACT instruments. We then optimize the resulting field map with the aid of observations by *Wind*, which were made at the very outer boundary of the cloud, at a spacecraft angular separation of 6°. For the correct choice of reconstruction parameters such as axis orientation, interval and grid size, we find both a very good match between the predicted magnetic field at the position of *Wind* and the actual observations as well as consistent timing. We argue that the reconstruction captures almost the full extent of the cross-section of the cloud. The resulting shape transverse to the invariant axis consists of distorted ellipses and is slightly flattened in the direction of motion. The MC axis is inclined at -58° to the ecliptic with an axial field strength of 12 nT. We derive integrated axial fluxes and currents with increased precision, which we contrast with the results from linear force-free fitting. The helical geometry of the MC with almost constant twist (≈ 1.5 turns AU $^{-1}$) is not consistent with the linear force-free Lundquist model. We also find that the cloud is non-force-free ($|J_\perp|/|J_\parallel| > 0.3$) in about a quarter of the cloud cross sectional area, particularly in the back part which is interacting with the trailing high speed stream. Based on the optimized reconstruction we put forward preliminary guidelines for the improved use of single-spacecraft Grad – Shafranov reconstruction. The results also give us the opportunity to compare the CME direction inferred from STEREO/SECCHI observations by Mierla *et al.* (*Solar Phys.* **252**, 385, 2008) with the three-dimensional configuration of the MC at 1 AU. This yields an almost radial CME propagation from the Sun to the Earth.

Multi-spacecraft recovery of a magnetic cloud and its origin from magnetic reconnection on the Sun

C. Möstl, C.J. Farrugia, C. Miklenic, M. Temmer, A.B. Galvin, J.G. Luhmann, E.K.J. Kilpua, M. Leitner, T. Nieves-Chinchilla, A. Veronig, H.K. Biernat

E-print, Jan 2009, JGR Vol. 114, No. A4, A04102, 2009

Multi-point spacecraft observations of a magnetic cloud on **May 22, 2007** has given us the opportunity to apply a multi-spacecraft technique to infer the structure of this large-scale magnetic flux rope in the solar wind. Combining WIND and STEREO-B magnetic field and plasma measurements we construct a combined magnetic field map by integrating the Grad-Shafranov equation, this being one of the very first applications of this technique in the interplanetary context. From this we obtain robust results on the shape of the cross-section, the orientation and magnetic fluxes of the cloud. The only slightly flattened shape is discussed with respect to its heliospheric environment and theoretical expectations. We also relate these results to observations of the solar source region and its associated two-ribbon flare on **May 19, 2007**, using H-alpha images from the Kanzelhöhe observatory, SOHO/MDI magnetograms and SECCHI/EUVI 171 Å images. We find a close correspondence between the magnetic flux reconnected in the flare and the poloidal flux of the

magnetic cloud. The axial flux of the cloud agrees with the prediction of a recent 3D finite sheared arcade model to within a factor of 2, which is evidence for formation of at least half of the magnetic flux of the ejected flux rope during the eruption. We outline the relevance of this result to models of coronal mass ejection initiation, and find that to explain the solar and interplanetary observations elements from sheared-arcade as well as erupting-flux-rope models are needed.

Two-spacecraft reconstruction of a magnetic cloud and comparison to its solar source

C. **Mostl**^{1,2}, C. Miklenic¹, C.J. Farrugia³, M. Temmer^{2,4}, A. Veronig¹, A.B. Galvin³,
B. Vrsnak⁴, and H.K. Biernat^{1,2}

E-print, Jan 2008; Ann. Geophys..., 26, 3139–3152, 2008, File

www.ann-geophys.net/26/3139/2008/

This paper compares properties of the source region with those inferred from satellite observations near Earth of the magnetic cloud which reached 1 AU on 20 November 2003. We use observations from space missions SOHO and TRACE together with ground-based data to study the magnetic structure of the active region NOAA 10501 containing a highly curved filament, and determine the reconnection rates and fluxes in an M4 flare on **18 November 2003** which is associated with a fast halo CME. This event has been linked before to the magnetic cloud on 20 November 2003. We model the near-Earth observations with the Grad-Shafranov reconstruction technique using a novel approach in which we optimize the results with two-spacecraft measurements of the solar wind plasma and magnetic field made by ACE and WIND. The two probes were separated by hundreds of Earth radii. They pass through the axis of the cloud which is inclined -50 degree to the ecliptic. The magnetic cloud orientation at 1 AU is consistent with an encounter with the heliospheric current sheet. We estimate that 50 % of its poloidal flux has been lost through reconnection in interplanetary space. By comparing the flare ribbon flux with the original cloud fluxes we infer a flux rope formation during the eruption, though uncertainties are still significant. The multi-spacecraft Grad-Shafranov method opens new vistas in probing of the spatial structure of magnetic clouds in STEREO-WIND/ACE coordinated studies.

NEW GEOEFFECTIVE PARAMETERS OF VERY FAST HALO CORONAL MASS EJECTIONS

Y.-J. **Moon**, K.-S. Cho,¹ M. Dryer,^{2,3} Y.-H. Kim,¹ Su-chan Bong,¹ Jongchul Chae,⁴ and Y. D. Park

The Astrophysical Journal, 624:414–419, 2005, File

b/a – direction parameter

See **Mostl** and **Moestl**

Singular Spectral Analysis of the aa and Dst Geomagnetic Indices

J. L. Le **Mouël**, **F. Lopes**, **V. Courtillot**

JGR [Volume 124, Issue 8](#) Pages: 6403-6417 2019

<https://agupubs.onlinelibrary.wiley.com/doi/epdf/10.1029/2019JA027040>

We apply singular spectrum analysis in order to identify trends and quasi-periodic oscillations in the aa and Dst series of geomagnetic activity. We also analyze the sunspot number International SunSpot Number (ISSN) and the number of polar faculae Polar Faculae (PF). Singular spectrum analysis provides the eigenvalues and therefore trends and oscillatory components of the four series. ISSN is dominated by a trend (the Gleissberg cycle), followed by 10.6, 35.5 years, two ~8-year components, 21.4 and 5.3 year. aa shows the same trend, a ~47-year component, then 10.8, 32.3, 21.8, and a series of three close components at 10.6, 12.2, and 9.2 years, followed by a 6 month seasonal component. PF is dominated by the 20.7-year period, followed by 10.2, 8.3, 41, and 31 years, then a 5.2 year component. Dst is dominated by a trend, then a strong 6-month component; next are found a 47-year component, the 10.6 years and a second seasonal line at 1 year. The ~22-, ~11-, and ~5.5-year components are common to the four indices. These “pseudo harmonic” components are evidence of solar activity. Singular spectrum analysis identifies components that vary in frequency and amplitude. The phase relationships of any two components over time can be studied in detail. An illustration is given by the remarkable phase coherency of the 5.3-year component. But the components are neither truly periodical nor exact multiples of each other. These differences reflect the complex mechanisms that govern solar-terrestrial relationships.

Statistics of extreme time-integrated geomagnetic activity.

Mourenas, D., Artemyev, A.V., Zhang, X.J.:

2018, Geophys. Res. Lett. 45, 502.

sci-hub.se/10.1002/2017GL076828

A statistical analysis of the time-integrated Dst index is performed over 1958–2007. The tail of the probability distribution of extreme time-integrated Dst events, which occur during strong geomagnetic storms, can be precisely fitted by a power law function with upper cutoff, apparently not exceeded even by the 1859 Carrington event. This time-integrated Dst is expected to be a reasonable proxy for maximum densities of MeV electrons in the heart of the outer radiation belt, which are known to pose a serious threat to satellites. During such strong events, a correlation is found between the time-integrated levels of various physical quantities, such as interplanetary magnetic field B_z , particle energy fluxes measured during injections in the magnetotail, geosynchronous ULF wave index, and geomagnetic activity in the inner magnetosphere, suggesting cumulative effects from successive disturbances.

On the Effect of Geomagnetic Storms on Relativistic Electrons in the Outer Radiation Belt: Van Allen Probes Observations

Pablo S. Moya, Víctor A. Pinto, David G. Sibeck, Shrikanth G. Kanekal, Daniel N. Baker

JGR November 2017 Vol: 122, Pages: 11,100–11,108

<http://sci-hub.tw/10.1002/2017JA024735>

[http://sci-](http://sci-hub.cc/http://onlinelibrary.wiley.com/doi/10.1002/2017JA024735/abstract;jsessionid=48E043E86C22084A1908FD5A8AEDAF03t01)

[hub.cc/http://onlinelibrary.wiley.com/doi/10.1002/2017JA024735/abstract;jsessionid=48E043E86C22084A1908FD5A8AEDAF03t01](http://sci-hub.cc/http://onlinelibrary.wiley.com/doi/10.1002/2017JA024735/abstract;jsessionid=48E043E86C22084A1908FD5A8AEDAF03t01)

Using Van Allen Probes ECT-REPT observations we performed a statistical study on the effect of geomagnetic storms on relativistic electrons fluxes in the outer radiation belt for 78 storms between September 2012 and June 2016. We found that the probability of enhancement, depletion and no change in flux values depends strongly on L and energy. Enhancement events are more common for ~ 2 MeV electrons at $L \sim 5$, and the number of enhancement events decreases with increasing energy at any given L shell. However, considering the percentage of occurrence of each kind of event, enhancements are more probable at higher energies, and the probability of enhancement tends to increase with increasing L shell. Depletion are more probable for 4–5 MeV electrons at the heart of the outer radiation belt, and no change events are more frequent at $L < 3.5$ for $E \sim 3$ MeV particles. Moreover, for $L > 4.5$ the probability of enhancement, depletion or no-change response presents little variation for all energies. Because these probabilities remain relatively constant as a function of radial distance in the outer radiation belt, measurements obtained at Geosynchronous orbit may be used as a proxy to monitor $E \geq 1.8$ MeV electrons in the outer belt. **14 Nov 2012, 1 June 2013, 8 May 2016**

On the origin of switchbacks observed in the solar wind

Forrest S. Mozer, [Stuart Bale](#), [John Bonnell](#), [James Drake](#), [Elizabeth Hanson](#), [Michael C. Mozer](#)

2021 *ApJ* **919** 60

<https://arxiv.org/ftp/arxiv/papers/2105/2105.07601.pdf>

<https://iopscience.iop.org/article/10.3847/1538-4357/ac110d/pdf>

<https://doi.org/10.3847/1538-4357/ac110d>

The origin of switchbacks in the solar wind is discussed in two classes of theory that differ in the location of the source being either in the transition region near the Sun or in the solar wind, itself. The two classes of theory differ in their predictions of the switchback rate as a function of distance from the Sun. To test these theories, one-hour averages of Parker Solar Probe data were summed over orbits three through seven. It is found that:

1. The average switchback rate was independent of distance from the Sun.
2. The average switchback rate increased with solar wind speed.
3. The switchback size perpendicular to the flow increased as R , the distance from the Sun, while the radial size increased as R^2 , resulting in a large and increasing switchback aspect ratio with distance from the Sun.
4. The switchback rotation angle did not depend on either the solar wind speed or the distance from the Sun.

These results are consistent with switchback formation in the transition region because their increase of tangential size with radius compensates for the radial falloff of their equatorial density to produce switchback rates that are independent of distance from the Sun. This constant observed switchback rate is inconsistent with an in situ source. Once formed, the switchback size and aspect ratio, but not the rotation angle, increased with radial distance to at least 100 solar radii. In addition, quiet intervals between switchback patches occurred at the lowest solar wind speeds. **22 Aug-14 Sep 2019**

Time domain structures and dust in the solar vicinity: Parker Solar Probe observations

F.S. Mozer, O.V. Agapitov, S.D. Bale, J.W. Bonnell, K. Goetz, K.A. Goodrich,

First results from the Parker Solar Probe 2020

<https://arxiv.org/ftp/arxiv/papers/1912/1912.09234.pdf>

On April 5, 2019, while the Parker Solar Probe was at its 35 solar radius perihelion, the data set collected at 293 samples/sec contained more than 10,000 examples of spiky electric-field-like structures having durations less than 200 milliseconds and amplitudes greater than 10 mV/m. The vast majority of these events was caused by plasma turbulence. Defining dust events as those having similar, narrowly peaked, positive, single-ended signatures, resulted in finding 135 clear dust events, which, after correcting for the low detection efficiency, resulted in an estimate consistent with the 1000 dust events expected from other techniques. Defining time domain structures (TDS) as those having opposite polarity signals in the opposite antennas resulted in finding 238 clear TDS events which, after correcting for the detection efficiency, resulted in an estimated 500-1000 TDS events on this day. The TDS electric fields were bipolar, as expected for electron holes. Several events were found at times when the magnetic field was in the plane of the two measured components of the electric field such that the component of the electric field parallel to the magnetic field was measured. One example of significant parallel electric fields shows the negative potential that classified them as electron holes. Because the TDS observation rate was not uniform with time, it is likely that there were local regions below the spacecraft with field-aligned currents that generated the TDS.

Switchbacks in the solar magnetic field: their evolution, their content, and their effects on the plasma, V2

F.S. Mozer¹, O.V. Agapitov¹, S.D. Bale¹, J.W. Bonnell¹, T. Case⁴,

First results from the Parker Solar Probe

2020 *ApJS* 246 68

<https://arxiv.org/ftp/arxiv/papers/1912/1912.09252.pdf>

<https://iopscience.iop.org/article/10.3847/1538-4365/ab7196/pdf>

Switchbacks (rotations of the magnetic field) are observed on the Parker Solar Probe. Their evolution, content, and plasma effects are studied in this paper. The solar wind does not receive a net acceleration from switchbacks that it encountered upstream of the observation point. The typical switchback rotation angle increased with radial distance. Significant Poynting fluxes existed inside, but not outside, switchbacks and they are related to the increased EXB/B² flow caused by the magnetic field rotating to become more perpendicular to the flow direction. (Outside the switchbacks, the magnetic field and solar wind flow were generally radial.) The solar wind flow inside switchbacks was faster than that outside due to the frozen-in ions moving with the magnetic structure at the Alfvén speed. This energy gain results from the divergence of the Poynting flux from outside to inside the switchback, which produces a loss of electromagnetic energy on switchback entry and recovery of that energy on exit, with the lost energy appearing in the plasma flow. Switchbacks contain 0.3-10 Hz waves that may result from currents and the Kelvin-Helmholtz instability that occurs at the switchback boundaries. These waves may combine with lower frequency MHD waves to heat the plasma. The radial decreases of the Poynting flux and solar wind speed inside switchbacks are due to a geometrical effect. April 2019

A catalogue of observed geo-effective CME/ICME characteristics

R. Mugatwala, S. Chierichini, G. Francisco, G. Napolitano, R. Foldes, L. Giovannelli, G. De Gasperis, E. Camporeale, R. Erdélyi, D. Del Moro

Journal of Space Weather and Space Climate 14, 6 2024

<https://arxiv.org/pdf/2311.13429.pdf>

<https://www.swsc-journal.org/articles/swsc/pdf/2024/01/swsc230027.pdf>

One of the goals of Space Weather studies is to achieve a better understanding of impulsive phenomena, such as Coronal Mass Ejections (CMEs), to improve our ability to forecast their propagation characteristics and mitigate the risks to our technologically driven society. The essential part of achieving this goal is to assess the performance of forecasting models. To this end, the quality and availability of suitable data are of paramount importance. In this work, we merged publicly available data of CMEs from both in-situ and remote observations in order to build a dataset of CME properties. To evaluate the accuracy of the dataset and confirm the relationship between in-situ and remote observations, we have employed the Drag-Based Model (DBM) due to its simplicity and modest consumption of computational resources. In this study, we have also explored the parameter space for the drag parameter and solar wind speed using a Monte Carlo approach to evaluate how efficiently the DBM determines the propagation of CMEs for the events in the dataset. The geoeffective CMEs selected as a result of this work are compliant with the hypothesis of DBM (isolated CME, constant solar wind speed beyond 20 R_☉) and also yield further insight into CME features such as arrival time and arrival speed

at L1 point, lift-off time, speed at 20 R_{\odot} and other similar quantities. Our analysis based on the acceptance rate in the DBM inversion procedure shows that almost 50% of the CME events in the dataset are well described by DBM as they propagate in the heliosphere. The dataset includes statistical metrics for the DBM model parameters. The probability distribution functions (PDFs) for the free parameters of DBM have been derived through a Monte Carlo-like inversion procedure. Probability distribution functions obtained from this work are comparable to PDFs employed in previous works. The analysis showed that there exist two different most probable values (median values) of solar wind speed for DBM input based on slow ($w_{\text{slow}} \approx 386$ km/s) and fast ($w_{\text{fast}} \approx 547$ km/s) solar wind type. The most probable value for the drag parameter ($\gamma \approx 0.687 \times 10^{-7}$ km $^{-1}$) in our study is somewhat higher than the values reported in previous studies. Using a data-driven approach, this procedure allows us to present a homogeneous, reliable, and robust dataset for the investigation of CME propagation. Additionally, possible CME events are identified where the DBM prediction is not valid due to model limitations and higher uncertainties in the input parameters. These events require further thorough investigation in the future.

See <https://zenodo.org/records/8063404>

A statistical study on the stand-off distances of interplanetary coronal mass ejections

Mujiber Rahman, A.; Shanmugaraju, A.; Umapathy, S.; Moon, Y.-J.

Journal of Atmospheric and Solar-Terrestrial Physics, Volume 105, p. 181-190. 2013

We have analyzed the stand-off distance values of 101 interplanetary CMEs (ICMEs) observed during the period 1997-2005. Main aim of the present work is to study the stand-off distance and its dependence on various parameters of CMEs, ICMEs and IP shocks, Alfvénic Mach numbers and transit time. From the distribution, the stand-off time and stand-off distance values of many of the events are found to be in the range between ~ 2 -20 h and ~ 1 -40 R_{\odot} (R_{\odot} =Solar radius). From the correlation between speed of CMEs and stand-off distance, we noted smaller stand-off distance for energetic CMEs, which indicated that the driver CME (CME which is generating the shock) and its shock travel closely together. From the correlation plot between CME acceleration and stand-off distance, we found that the highly decelerated events and highly accelerated events have lower stand-off distance range (i.e., 10-40 R_{\odot}) than the other events. The events with longer travel time to reach 1 AU (>70 h) show stand-off times ≤ 20 h and for those faster events ($V_{\text{CME}} > 2200$ km/s) with smaller travel time (≤ 40 h), stand-off time is extremely low (≤ 10 h). A wide range of stand-off distance is seen for a particular value of CME and ICME parameters. The poor correlations of stand-off distance with all the above parameters confirm that the stand-off distance does not strongly depend on CME, ICME and IP shock parameters, but depends on a combination of all these parameters. On the other hand, the faster CMEs having lower stand-off distance and/or stand-off time imply that as long as the CMEs are energetic, the CMEs and shocks travel closely together. Also, it can be noted that the stand-off distance is not only dependent on gamma, but it is related to other parameters.

Propagation of normal and faster CMEs in the interplanetary medium

Mujiber Rahman, A.; Shanmugaraju, A.; Umapathy, S.

Advances in Space Research, Volume 52, Issue 6, p. 1168-1177. 2013

We have analyzed 101 Coronal Mass Ejection (CME) events and their associated interplanetary CMEs (ICMEs) and interplanetary (IP) shocks observed during the period 1997-2005 from the list given by Mujiber Rahman et al. (2012). The aim of the present work is to correlate the interplanetary parameters such as, the speeds of IP shocks and ICMEs, CME transit time and their relation with CME parameters near the Sun. Mainly, a group of 10 faster CME events ($V_{\text{INT}} > 2200$ km/s) are compared with a list of 91 normal events of Manoharan et al. (2004). From the distribution diagrams of CME, ICME and IP shock speeds, we note that a large number of events tends to narrow towards the ambient (i.e., background) solar wind speed (~ 500 km/s) in agreement with the literature. Also, we found that the IP shock speed and the average ICME speed measured at 1 AU are well correlated. In addition, the IP shock speed is found to be slightly higher than the ICME speed. While the normal events show CME travel time in the range of ~ 40 -80 h with a mean value of 65 h, the faster events have lower transit time with a mean value of 40 h. The effect of solar wind drag is studied using the correlation of CME acceleration with interplanetary (IP) acceleration and with other parameters of ICMEs. While the mean acceleration values of normal and faster CMEs in the LASCO FOV are 1 m/s 2 , 18 m/s 2 , they are -1.5 m/s 2 and -14 m/s 2 in the interplanetary medium, respectively. The relation between CME speed and IP acceleration for normal and faster events are found to agree with that of Lindsay et al. (1999) and Gopalswamy et al. (2001) except slight deviations for the faster events. It is also seen that the faster events with less travel time face higher negative acceleration (> -10 m/s 2) in the interplanetary medium up to 1 AU.

The Solar Orbiter mission -- Science overview

Review

[D. Müller](#), [O.C. St. Cyr](#), [I. Zouganelis](#), [H.R. Gilbert](#), [R. Marsden](#), [T. Nieves-Chinchilla](#), [E. Antonucci](#), [F. Auchère](#), [D. Berghmans](#), [T. Horbury](#), [R.A. Howard](#), [S. Krucker](#), [M. Maksimovic](#), [C.J. Owen](#), [P. Rochus](#), [J. Rodriguez-Pacheco](#), [M. Romoli](#), [S.K. Solanki](#), [R. Bruno](#), [M. Carlsson](#), [A. Fludra](#), [L. Harra](#), [D.M. Hassler](#), [S. Livi](#), [P. Louarn](#), [H. Peter](#), [U. Schühle](#), [L. Teriaca](#), [J.C. del Toro Iniesta](#), [R.F. Wimmer-Schweingruber](#), [E. Marsch](#), [M. Velli](#), [A. De Groof](#), [A. Walsh](#), [D. Williams](#)

A&A 642, A1 2020

<https://arxiv.org/pdf/2009.00861.pdf> **File**

<https://www.aanda.org/articles/aa/pdf/2020/10/aa38467-20.pdf>

Solar Orbiter, the first mission of ESA's Cosmic Vision 2015-2025 programme and a mission of international collaboration between ESA and NASA, will explore the Sun and heliosphere from close up and out of the ecliptic plane. It was launched on 10 February 2020 04:03 UTC from Cape Canaveral and aims to address key questions of solar and heliospheric physics pertaining to how the Sun creates and controls the Heliosphere, and why solar activity changes with time. To answer these, the mission carries six remote-sensing instruments to observe the Sun and the solar corona, and four in-situ instruments to measure the solar wind, energetic particles, and electromagnetic fields. In this paper, we describe the science objectives of the mission, and how these will be addressed by the joint observations of the instruments onboard. The paper first summarises the mission-level science objectives, followed by an overview of the spacecraft and payload. We report the observables and performance figures of each instrument, as well as the trajectory design. This is followed by a summary of the science operations concept. The paper concludes with a more detailed description of the science objectives. Solar Orbiter will combine in-situ measurements in the heliosphere with high-resolution remote-sensing observations of the Sun to address fundamental questions of solar and heliospheric physics. The performance of the Solar Orbiter payload meets the requirements derived from the mission's science objectives. Its science return will be augmented further by coordinated observations with other space missions and ground-based observatories.

Europe's next mission to the Sun.

[Müller](#), D., [Zouganelis](#), I., [St. Cyr](#), O.C., [Gilbert](#), H.R., [Nieves-Chinchilla](#), T.:

2020, Nature Astron. 4, 205.

<https://www.nature.com/articles/s41550-020-1015-5.pdf>

As the **Solar Orbiter** spacecraft is scheduled for launch this month, European Space Agency (ESA) and NASA Project Scientists provide an overview of this major ESA–NASA mission to the Sun.

Solar Orbiter. Exploring the Sun-heliosphere connection

[Müller](#), D., [Marsden](#), R.G., [St. Cyr](#), O.C., [Gilbert](#), H.R.:

2013, Solar Phys. 285, 25. 2013

Advancing in situ modeling of ICMEs: New techniques for New observations†

T. [Mulligan](#)^{1,*}, [Alysha A. Reinard](#)², [Benjamin J. Lynch](#)

JGR, Volume 118, Issue 4, pages 1410–1427, 2013

It is generally known that multi-spacecraft observations of interplanetary coronal mass ejections (ICMEs) are more likely to reveal their three-dimensional structure than single-spacecraft observations. The launch of STEREO in October 2006 has greatly increased the number of multipoint ICME studies, but the field is still in its infancy. To date, many studies still use flux rope models that rely on single track observations through a vast, multi-faceted structure, which oversimplifies the problem and hinders interpretation of the large-scale geometry. This oversimplification is especially problematic for multispacecraft ICME observations in which only one spacecraft observes a flux rope structure. In order to tackle these complex problems we describe two new techniques and combine them to analyze two ICMEs observed at the twin STEREO spacecraft on 22–23 May 2007, when the spacecraft were separated by $\sim 9^\circ$. We find a combination of non-force-free flux rope multi-spacecraft modeling, together with a new non-flux rope ICME plasma flow deflection model, better constrains the large-scale structure of these ICMEs. We also introduce a new spatial mapping technique that allows us to put multispacecraft observations and the new ICME model results in context with the convecting solar wind. What is distinctly different about this analysis is that it reveals aspects of ICME geometry and dynamics in a far more visually intuitive way than previously accomplished. In the case of the 22–23 May ICMEs, the analysis facilitates a more physical understanding of ICME large-scale structure, the location and geometry of flux rope sub-structures within these ICMEs, and their dynamic interaction with the ambient solar wind.

Short-period variability in the galactic cosmic ray intensity: High statistical resolution observations and interpretation around the time of a Forbush decrease in August 2006

Mulligan, T.; Blake, J. B.; Shaul, D.; Quenby, J. J.; Leske, R. A.; Mewaldt, R. A.; Galametz, M.

J. Geophys. Res., Vol. 114, No. A7, A07105, 2009

<http://dx.doi.org/10.1029/2008JA013783>

On 20 August 2006 a Forbush decrease observed at Polar in the Earth's magnetosphere was also seen at the INTEGRAL spacecraft outside the magnetosphere during a very active time in the solar wind. High-resolution energetic particle data from ACE SIS, the Polar high-sensitivity telescope, and INTEGRAL's Ge detector saturation rate, which measures the galactic cosmic ray (GCR) background with a threshold of ~ 200 MeV, show similar, short-period GCR variations in and around the Forbush decrease. Focusing upon the GCR intensity within a 3-day interval from 19 August 2006 to 21 August 2006 reveals many intensity variations in the GCR on a variety of time scales and amplitudes. These intensity variations are greater than the 3σ error in all the data sets used. The fine structures in the GCR intensities along with the Forbush decrease are propagated outward from ACE to the Earth with very little change. The solar wind speed stays relatively constant during these periods, indicating that parcels of solar wind are transporting the GCR population outward in the heliosphere. This solar wind convection of GCR fine structure is observed for both increases and decreases in GCR intensity, and the fine structure increases and decreases are bracketed by solar wind magnetic field discontinuities associated with interplanetary coronal mass ejection (ICME) magnetosheath regions, clearly seen as discontinuous rotations of the field components at ACE and at Wind. Interestingly, the electron heat flux shows different flux tube connectivity also associated with the different regions of the ICME and magnetosheath. Gosling et al. (2004) first discussed the idea that solar energetic particle intensities commonly undergo dispersionless modulation in direct association with discontinuous changes in the solar wind electron strahl. The observations show that the intensity levels in the GCR flux may undergo a similar partitioning, possibly because of the different magnetic field regions having differing magnetic topologies.

Magnetic flux rope model geometry constraints and their relationship to the SMEI 3D density reconstruction analyses for the October 29, 2003 ICME,

T. **Mulligan**, E.A. Jensen, and B.V. Jackson,

Geophys. Res. Letts., 2007 (submitted).

Global analysis of the extended cosmic-ray decreases observed with world-wide networks of neutron monitors and muon detectors; temporal variation of the rigidity spectrum and its implication

K. Munakata, **Y. Hayashi**, **M. Kozai**, **C. Kato**, **N. Miyashita**, **R. Kataoka**, **A. Kadokura**, **S. Miyake**, **K. Iwai**, **E. Echer**, **A. Dal Lago**, **M. Rockenbach**, **N. J. Schuch**, **J. V. Bageston**, **C. R. Braga**, **H. K. Al Jassar**, **M. M. Sharma**, **M. L. Duldig**, **J. E. Humble**, **I. Sabbah**, **P. Evenson**, **T. Kuwabara**, **J. Kóta**

ApJ **774** 283 2024

<https://arxiv.org/pdf/2408.14696>

<https://iopscience.iop.org/article/10.3847/1538-4357/ad7466/pdf>

This paper presents the global analysis of two extended decreases of the galactic cosmic ray intensity observed by world-wide networks of ground-based detectors in 2012. This analysis is capable of separately deriving the cosmic ray density (or omnidirectional intensity) and anisotropy each as a function of time and rigidity. A simple diffusion model along the spiral field line between Earth and a cosmic-ray barrier indicates the long duration of these events resulting from about 190° eastern extension of a barrier such as an IP-shock followed by the sheath region and/or the corotating interaction region (CIR). It is suggested that the coronal mass ejection merging and compressing the preexisting CIR at its flank can produce such the extended barrier. The derived rigidity spectra of the density and anisotropy both vary in time during each event period. In particular we find that the temporal feature of the "phantom Forbush decrease" reported in an analyzed period is dependent on rigidity, looking quite different at different rigidities. From these rigidity spectra of the density and anisotropy, we derive the rigidity spectrum of the average parallel mean-free-path of pitch angle scattering along the spiral field line and infer the power spectrum of the magnetic fluctuation and its temporal variation. Possible physical cause of the strong rigidity dependence of the "phantom Forbush decrease" is also discussed. These results demonstrate the high-energy cosmic rays observed at Earth responding to remote space weather.

13 Jul. - 9 Aug., 2012, . 17 Jan - 13 Feb., 2012

A Peculiar ICME Event in August 2018 Observed with the Global Muon Detector Network

K. [Munakata](#) and on behalf of the GMDN Collaboration

[PoS\(ICRC2021\)1265](#) 2022

<https://pos.sissa.it/395/1265/pdf>

We demonstrate that global observations of high-energy cosmic rays contribute to understanding unique characteristics of a large-scale magnetic flux rope (MFR) causing a magnetic storm in August 2018. Following a weak interplanetary shock on 25 August 2018, a MFR caused an unexpectedly large geomagnetic storm. It is likely that this event became geoeffective because the MFR was accompanied by a corotating interaction region (CIR) and compressed by high-speed solar wind following the MFR. In fact, a Forbush decrease was observed in cosmic-ray data inside the MFR as expected, and a significant cosmic-ray density increase exceeding the unmodulated level before the shock was also observed near the trailing edge of the MFR. The cosmic-ray density increase can be interpreted in terms of the adiabatic heating of cosmic rays near the trailing edge of the MFR, as the corotating interaction region prevents free expansion of the MFR and results in the compression near the trailing edge. A northeast-directed spatial gradient in the cosmic-ray density was also derived during the cosmic-ray density increase, suggesting that the center of the heating near the trailing edge is located northeast of Earth. The second order anisotropy is observed during the density increase clearly representing an intensity enhancement of cosmic rays with approximately 90 degree pitch angle, possibly indicating the betatron acceleration of CRs during the cosmic-ray density increase and/or accelerated CRs leaking along the magnetic field from the density increase region toward the south where lower CR population is expected. This is one of the best examples demonstrating that the observation of high energy cosmic rays provides us with information of the three-dimensional macroscopic picture of the interaction between coronal mass ejections and the ambient solar wind, which is essential for prediction of large magnetic storms.

Large amplitude bidirectional anisotropy of cosmic-ray intensity observed with world-wide networks of ground-based neutron monitors and muon detectors in November, 2021

K. [Munakata](#), [M. Kozai](#), [C. Kato](#), [Y. Hayashi](#), [R. Kataoka](#), + + +

ApJ 938 30 2022

<https://arxiv.org/pdf/2209.05743.pdf>

<https://iopscience.iop.org/article/10.3847/1538-4357/ac91c5/pdf>

We analyze the cosmic-ray variations during a significant Forbush decrease observed with world-wide networks of ground-based neutron monitors and muon detectors during November 3-5, 2021. Utilizing the difference between primary cosmic-ray rigidities monitored by neutron monitors and muon detectors, we deduce the rigidity spectra of the cosmic-ray density (or omnidirectional intensity) and the first- and second-order anisotropies separately, for each hour of data. A clear two-step decrease is seen in the cosmic-ray density with the first $\sim 2\%$ decrease after the interplanetary shock arrival followed by the second $\sim 5\%$ decrease inside the magnetic flux rope (MFR) at 15 GV. Most strikingly, a large bidirectional streaming along the magnetic field is observed in the MFR with a peak amplitude of $\sim 5\%$ at 15 GV which is comparable to the total density decrease inside the MFR. The bidirectional streaming could be explained by adiabatic deceleration and/or focusing in the expanding MFR, which have stronger effects for pitch angles near 90° , or by selective entry of GCRs along a leg of the MFR. The peak anisotropy and density depression in the flux rope both decrease with increasing rigidity. The spectra vary dynamically indicating that the temporal variations of density and anisotropy appear different in neutron monitor and muon detector data. **November 3-5, 2021**

Cosmic-Ray Short Burst Observed with the Global Muon Detector Network (GMDN) on 2015 June 22

K. [Munakata](#)¹, [M. Kozai](#)², [P. Evenson](#)³, [T. Kuwabara](#)³, [C. Kato](#)¹, [M. Tokumaru](#)⁴, [M. Rockenbach](#)⁵, [A. Dal Lago](#)⁵, [R. R. S. de Mendonca](#)^{5,6}, [C. R. Braga](#)^{5...}

2018 ApJ 862 170

<http://sci-hub.tw/http://iopscience.iop.org/article/10.3847/1538-4357/aacdf/meta>

We analyze the short cosmic-ray intensity increase ("cosmic-ray burst": CRB) on **2015 June 22** utilizing a global network of muon detectors and derive the global anisotropy of cosmic-ray intensity and the density (i.e., the omnidirectional intensity) with 10 minute time resolution. We find that the CRB was caused by a local density maximum and an enhanced anisotropy of cosmic rays, both of which appeared in association with Earth's crossing of the heliospheric current sheet (HCS). This enhanced anisotropy was normal to the HCS and consistent with a diamagnetic drift arising from the spatial gradient of cosmic-ray density, which indicates that cosmic rays were drifting along the HCS from the north of Earth. We also find a significant anisotropy along the HCS, lasting a few hours after the HCS crossing, indicating that cosmic rays penetrated

into the inner heliosphere along the HCS. Based on the latest geomagnetic field model, we quantitatively evaluate the reduction of the geomagnetic cutoff rigidity and the variation of the asymptotic viewing direction of cosmic rays due to a major geomagnetic storm that occurred during the CRB and conclude that the CRB is not caused by the geomagnetic storm, but by a rapid change in the cosmic-ray anisotropy and density outside the magnetosphere.

Using CME Progenitors to Assess CME Geoeffectiveness

Kashvi **Mundra**^{3,1}, V. Aparna², and Petrus Martens²

2021 ApJS 257 33

<https://iopscience.iop.org/article/10.3847/1538-4365/ac3136/pdf>

<https://doi.org/10.3847/1538-4365/ac3136>

There have been a few previous studies claiming that the effects of geomagnetic storms strongly depend on the orientation of the magnetic cloud portion of coronal mass ejections (CMEs). Aparna & Martens, using halo-CME data from 2007 to 2017, showed that the magnetic field orientation of filaments at the location where CMEs originate on the Sun can be used to credibly predict the geoeffectiveness of the CMEs being studied. The purpose of this study is to extend their survey by analyzing the halo-CME data for 1996–2006. The correlation of filament axial direction on the solar surface and the corresponding Bz signatures at L1 are used to form a more extensive analysis for the results previously presented by Aparna & Martens. This study utilizes Solar and Heliospheric Observatory Extreme-ultraviolet Imaging Telescope 195 Å, Michelson Doppler Imager magnetogram images, and Kanzelhöhe Solar Observatory and Big Bear Solar Observatory H α images for each particular time period, along with ACE data for interplanetary magnetic field signatures. Utilizing all these, we have found that the trend in Aparna & Martens' study of a high likelihood of correlation between the axial field direction on the solar surface and Bz orientation persists for the data between 1996 and 2006, for which we find a match percentage of 65%. **1997 May 12, 2000 November 1, 2001 September 2**

Table 3. The Bz Analysis for the Determined Set of the Data 1996–2006

Analysis of the Coronal Mass Ejections through Axial Field Direction of Solar Filaments and IMF Bz

Kashvi **Mundra**, [V. Aparna](#), [Petrus C. H. Martens](#)

ApJ 2020

<https://arxiv.org/pdf/2011.02123.pdf>

In the past, there have been many studies claiming that the effects of geomagnetic storms strongly depends on the orientation of the magnetic-cloud part of the Coronal Mass Ejections (CMEs). Aparna & Martens (2020), using Halo-CME data from 2007-2017, have shown that the magnetic field orientation of filaments at the location where CMEs originate can be effectively used for predicting the onset of geo-magnetic storms. The purpose of this study is to extend their survey by analyzing the halo-CME data for 1996-2006. The correlation of filament axial direction and their corresponding Bz signatures are used to form a more extensive reasoning for the claims presented by Aparna & Martens before. This study utilizes SOHO EIT 195 Å, MDI magnetogram images, KSO and BBSO H α images for the time period, along with ACE data for inter-planetary magnetic field signatures. Correlating all these, we have found that the trend in Aparna & Martens' study of a high likelihood of the correlation between the axial field direction and Bz orientation, persists for the data between 1996-2006 as well. **September 16th, 2000, 02/09/2001, 2000-11-01**

Evidence of Energy and Charge Sign Dependence of the Recovery Time for the 2006 December Forbush Event Measured by the PAMELA Experiment

R. **Munini**¹, M. Boezio¹, A. Bruno², E. C. Christian³, G. A. de Nolfo³, V. Di Felice^{4,5}, M. Martucci^{6,7}, M. Merge^{4,6}, I. G. Richardson^{3,8}, J. M. Ryan⁹

2018 ApJ 853 76

DOI [10.3847/1538-4357/aaa0c8](https://doi.org/10.3847/1538-4357/aaa0c8)

New results on the short-term galactic cosmic-ray (GCR) intensity variation (Forbush decrease) in 2006 December measured by the PAMELA instrument are presented. Forbush decreases are sudden suppressions of the GCR intensities, which are associated with the passage of interplanetary transients such as shocks and interplanetary coronal mass ejections (ICMEs). Most of the past measurements of this phenomenon were carried out with ground-based detectors such as neutron monitors or muon telescopes. These techniques allow only the indirect detection of the overall GCR intensity over an integrated energy range. For the first time, thanks to the unique features of the PAMELA magnetic spectrometer, the Forbush decrease, commencing on **2006 December 14** and following a CME at the Sun on 2006 December 13, was studied in a wide rigidity range (0.4–20 GV) and for different species of GCRs detected directly in space. The daily averaged GCR proton intensity was used to investigate the rigidity dependence of the amplitude and the recovery time of the Forbush decrease. Additionally, for the first time, the temporal variations in the helium and electron

intensities during a Forbush decrease were studied. Interestingly, the temporal evolutions of the helium and proton intensities during the Forbush decrease were found to be in good agreement, while the low rigidity electrons (<2 GV) displayed a faster recovery. This difference in the electron recovery is interpreted as a charge sign dependence introduced by drift motions experienced by the GCRs during their propagation through the heliosphere.

Complex catalogue of high speed streams and geomagnetic storms during solar cycle 24 (2009 – 2016)

G. M. [Muntean](#)¹, D. Besliu-Ionescu^{1,2}, V. Dobrica

http://newserver.stil.bas.bg/varsiti/newsL/VarSITI_Newsletter_Vol17.pdf

Connection Between Solar Hemispheric Toroidal Cycles and Geomagnetic Variations

Judit [Muraközy](#)

[Solar Physics](#) April 2019, 294:46

[sci-hub.se/10.1007/s11207-019-1438-2](https://doi.org/10.1007/s11207-019-1438-2)

<https://link.springer.com/content/pdf/10.1007%2Fs11207-019-1438-2.pdf>

The solar activity has hemispheric asymmetries. The levels of activity are different on the two hemispheres on intermediate and longer time scales. During four Schwabe cycles the progress of the northern hemispheric activity precedes the southern one, while in the next four cycles the southern cycle takes over the preceding role (Muraközy and Ludmány, Mon. Not. Roy. Astron. Soc. 419, 3624, [2012](#); Muraközy, Astrophys. J. 826, 145, [2016](#)). The interplanetary magnetic field is formed by the distribution of the solar magnetic fields and the outward-streaming solar wind. The present study intends to show how the solar-hemispheric predominance affects the interplanetary and geophysical magnetic field. The interplanetary and geophysical data sets have been chosen from various sources such as the components of the interplanetary magnetic field [BB], cosmic-ray data, Ap, aa, and Dst geomagnetic indices, while the solar-hemispheric asymmetry has been examined by using sunspot data from Greenwich Photoheliographic Results (GPR) and Debrecen Photoheliographic Data (DPD).

A framework for understanding and quantifying the loss and acceleration of relativistic electrons in the outer radiation belt during geomagnetic storms

Kyle R. [Murphy](#), [Ian R. Mann](#), [David G. Sibeck](#), [I. Jonathan Rae](#), [C.E.J. Watt](#), [Louis G. Ozeke](#), [Shri G. Kaneka](#), [Daniel N. Baker](#)

Space Weather **Volume 18, Issue 5** 2020 e2020SW002477

<https://agupubs.onlinelibrary.wiley.com/doi/pdf/10.1029/2020SW002477>

We present detailed analysis of the global relativistic electron dynamics as measured by total radiation belt content (RBC) during coronal mass ejection (CME) and co-rotating interaction region (CIR) driven geomagnetic storms. Recent work has demonstrated that the response of the outer radiation belt is consistent and repeatable during geomagnetic storms. Here we build on this work to show that radiation belt dynamics can be divided into two sequential phases which have different solar wind dependencies, and which when analysed separately reveal that the radiation belt responds more predictably than if the overall storm response is analyzed as a whole. In terms of RBC, in every storm we analyzed, a phase dominated by loss is followed by a phase dominated by acceleration. Analysis of the RBC during each of these phases demonstrates that they both respond coherently to solar wind and magnetospheric driving. However, the response is independent whether the of the storm response is associated with either a coronal mass ejection or corotating interaction region. Our analysis shows that during the initial phase, radiation belt loss is organized by the location of the magnetopause and the strength of Dst and ultralow frequency wave power. During the second phase, radiation belt enhancements are well-organized by the amplitude of ultra-low frequency waves, the auroral electrojet index, and solar wind energy input. Overall, our results demonstrate that storm-time dynamics of the RBC is repeatable and well-characterized by solar wind and geomagnetic driving, albeit with different dependencies during the two phases of a storm.

Magnetic storms during the space age: Occurrence and relation to varying solar activity

Kalevi [Mursula](#), [Timo Qvick](#), [Lauri Holappa](#), [Timo Asikainen](#)

JGR 2022

<https://arxiv.org/pdf/2212.00510.pdf>

We study the occurrence of magnetic storms in space age (1957-2021) using Dst and Dxt indices. We find 2526/2743 magnetic storms in the Dxt/Dst index, out of which 45% are weak, 40% moderate, 12% intense and 3% major storms. Occurrence of storms in space age follows the slow decrease of sunspot activity and the related change in solar magnetic structure. We quantify the sunspot - CME storm relation in the five cycles of space age. We explain how the varying solar activity changes the structure of the heliospheric current sheet (HCS), and how this affects the HSS/CIR storms. Space age started with a record number of storms in 1957-1960, with roughly one storm per week. Solar polar fields attained their maximum in cycle 22, which led to an exceptionally thin HCS, and a space age record of large HSS/CIR storms in 1990s. In the minimum of cycle 23, for the only time in space age, CME storm occurrence reduced below that predicted by sunspots. Weak sunspot activity since cycle 23 has weakened solar polar fields and widened the HCS, which has decreased the occurrence of large and moderate HSS/CIR storms. Because of a wide HCS, the Earth has spent 50% of its time in slow solar wind since cycle 23. The wide HCS has also made large and moderate HSS/CIR storms occur in the early declining phase in recent cycles, while in the more active cycles 20-22 they occurred in the late declining phase.

Occurrence of high-speed solar wind streams over the Grand Modern Maximum

Kalevi **Mursula**, Renata Lukianova, Lauri Holappa

2015 *ApJ* **801** 30

<http://arxiv.org/pdf/1501.05010v1.pdf> In the declining phase of the solar cycle, when the new-polarity fields of the solar poles are strengthened by the transport of same-signed magnetic flux from lower latitudes, the polar coronal holes expand and form non-axisymmetric extensions toward the solar equator. These extensions enhance the occurrence of high-speed solar wind streams (HSS) and related co-rotating interaction regions in the low-latitude heliosphere, and cause moderate, recurrent geomagnetic activity in the near-Earth space. Here, using a novel definition of geomagnetic activity at high (polar cap) latitudes and the longest record of magnetic observations at a polar cap station, we calculate the annually averaged solar wind speeds as proxies for the effective annual occurrence of HSS over the whole Grand Modern Maximum (GMM) from 1920s onwards. We find that a period of high annual speeds (frequent occurrence of HSS) occurs in the declining phase of each solar cycle 16-23. For most cycles the HSS activity clearly maximizes during one year, suggesting that typically only one strong activation leading to a coronal hole extension is responsible for the HSS maximum. We find that the most persistent HSS activity occurred in the declining phase of solar cycle 18. This suggests that cycle 19, which marks the sunspot maximum period of the GMM, was preceded by exceptionally strong polar fields during the previous sunspot minimum. This gives interesting support for the validity of solar dynamo theory during this dramatic period of solar magnetism.

Correct normalization of the Dst index

K. **Mursula**¹, L. Holappa¹, and A. Karinen¹,

Astrophys. Space Sci. Trans., 4, 41-45, **2008**

www.astrophys-space-sci-trans.net/4/41/2008/

doi:10.5194/astra-4-41-2008

<http://www.astrophys-space-sci-trans.net/4/41/2008/astra-4-41-2008.pdf>

The Dst index has been one of the most important solar-terrestrial indices for decades, and it is used in numerous studies as a measure of the temporal development and intensity of magnetic storms and the ring current. Here we discuss two issues related to the relative and absolute normalization that are problematic to the Dst index. We show for the first time quantitatively that the magnetic disturbances at the four Dst stations are ordered according to the latitudinal projection of an equatorial disturbance upon the local horizontal component of the geomagnetic field. Therefore, the disturbances observed at each station should be first normalized by the cosine of the geomagnetic latitude of the station before they are averaged to form the Dst index. Perhaps surprisingly, the recipe to calculate the Dst index does not include this normalization and, therefore, must be revised on this part. We also discuss the effects of correcting the quiet-time seasonal variation, the so called "non-storm component" in the Dst index. This correction is seasonally varying, being largest around equinoxes and smallest at solstices, leading to an average correction (increase) of about 6 nT, i.e. about 25–30%, for annual averages of the Dst index. This increase also leads to significantly improved correlations between the corrected Dst index, the so called Dcx index, and many other indices of solar-terrestrial disturbance. We show here in detail that the correlation between the geomagnetic Ap index and the Dcx index ($cc = 0.83$) is much higher than between Ap and Dst ($cc = 0.60$). These results give further evidence that the Dcx index is a more truthful measure of magnetic storminess than the original Dst index.

Variations of interplanetary magnetic field on various long time-scales

Yury A **Nagovitsyn**, [Aleksandra A Osipova](#)

Monthly Notices of the Royal Astronomical Society, Volume 492, Issue 2, February 2020, Pages 1914–1918,

<https://doi.org/10.1093/mnras/stz3594>

The IDV index of geomagnetic activity is used by many researchers as a proxy of the interplanetary magnetic field (IMF) strength B . Using the original multiscale regression (MSR) method based on wavelet transformation, we obtained a long series of B values starting from 1845. Then, based on the new 2.0 versions of the sunspot number and group sunspot number and using MSR method and this series as a reference, we reconstructed IMF strength B starting from 1610. Further extension of the reconstruction is associated with radiocarbon reconstructions of solar activity at a time-scale of up to several millennia. It is shown that in the last 3200 yr the IMF strength has been experiencing a downward trend of $-(0.39 \pm 0.17) \cdot 10^{-3} \text{ nT} \cdot \text{yr}^{-1}$.

MagNet—A Data-Science Competition to Predict Disturbance Storm-Time Index (Dst) From Solar Wind Data

Manoj Nair, Rob Redmon, Li-Yin Young, Arnaud Chulliat, Belinda Trotta, Christine Chung, Greg Lipstein, Isaac Slavitt

Space Weather [Volume21, Issue10](#) October 2023 e2023SW003514

<https://doi.org/10.1029/2023SW003514>

<https://agupubs.onlinelibrary.wiley.com/doi/epdf/10.1029/2023SW003514>

Enhanced interaction between solar-wind and Earth's magnetosphere can cause space weather and geomagnetic storms that have the potential to damage critical technologies, such as magnetic navigation, radio communications, and power grids. The severity of a geomagnetic storm is measured using the disturbance-storm-time (Dst) index. The Dst index is calculated by averaging the horizontal component of the magnetic field observed at four near-equatorial observatories and is used to drive geomagnetic disturbance models. As a key specification of the magnetospheric dynamics, the Dst index is used to drive geomagnetic disturbance models such as the High Definition Geomagnetic Model—Real Time. Since 1975, forecasting models have been proposed to forecast Dst solely from solar wind observations at the Lagrangian-1 position. However, while the recent Machine-Learning (ML) models generally perform better than other approaches, many are unsuitable for operational use. Recent exponential growth in data-science research and the democratization of ML tools have opened up the possibility of crowd-sourcing specific problem-solving tasks with clear constraints and evaluation metrics. To this end, National Oceanic and Atmospheric Administration (NOAA)'s National Centers for Environmental Information and the University of Colorado's Cooperative Institute for Research in Environmental Sciences conducted an open data-science challenge called “MagNet: Model the Geomagnetic Field.” The challenge attracted 622 participants, resulting in 1,197 model submissions that used various ML approaches. The top models that met the evaluation criteria are operationally viable and retrainable and suitable for NOAA's operational needs. The paper summarizes the competition results and lessons learned.

Development of the 3-D MHD model of the solar corona-solar wind combining system

Nakamizo, A.; Tanaka, T.; Kubo, Y.; Kamei, S.; Shimazu, H.; Shinagawa, H.

J. Geophys. Res., Vol. 114, No. A7, A07109, 2009

<http://dx.doi.org/10.1029/2008JA013844>

In the framework of integrated numerical space weather prediction, we have developed a 3-D MHD simulation model of the solar surface-solar wind system. We report the construction method of the model and its first results. By implementing a grid system with angularly unstructured and increasing radial spacing, we realized a spherical grid that has no pole singularity and realized a fine grid size around the inner boundary and a wide-range grid up to a size of 1 AU simultaneously. The magnetic field at the inner boundary is specified by the observational data. In order to obtain the supersonic solar wind speed, parameterized source functions are introduced into the momentum and energy equations. These source functions decay exponentially in altitude as widely used in previous studies. The absolute values of the source functions are controlled so as to reflect the topology of the coronal magnetic field. They are increased inside the magnetic flux tube with subradial expansion and reduced inside the magnetic flux tube with overradial expansion. This adjustment aims to reproduce the variation of the solar wind speed according to the coronal magnetic structure. The simulation simultaneously reproduces the plasma-exit structure, the high- and low-temperature regions, the open and closed magnetic field regions in the corona, the fast and slow solar wind, and the sector structure in interplanetary space. It is confirmed from the comparison with observations that the MHD model successfully reproduces many features of both the fine solar coronal structure and the global solar wind structure.

Dynamical evolution of a magnetic cloud from the Sun to 5.4 AU

M. S. [Nakwacki](#)^{1,2}, S. Dasso^{2,3}, P. Démoulin⁴, C. H. Mandrini^{2,5} and A. M. Gulisano
A&A 535, A52 (2011)

Context. Significant quantities of magnetized plasma are transported from the Sun to the interstellar medium via interplanetary coronal mass ejections (ICMEs). Magnetic clouds (MCs) are a particular subset of ICMEs, forming large-scale magnetic flux ropes. Their evolution in the solar wind is complex and mainly determined by their own magnetic forces and the interaction with the surrounding solar wind.

Aims. Magnetic clouds are strongly affected by the surrounding environment as they evolve in the solar wind. We study expansion of MCs, its consequent decrease in magnetic field intensity and mass density, and the possible evolution of the so-called global ideal-MHD invariants.

Methods. In this work we analyze the evolution of a particular MC (observed in March 1998) using in situ observations made by two spacecraft approximately aligned with the Sun, the first one at 1 AU from the Sun and the second one at 5.4 AU. We describe the magnetic configuration of the MC using different models and compute relevant global quantities (magnetic fluxes, helicity, and energy) at both heliodistances. We also tracked this structure back to the Sun, to find out its solar source.

Results. We find that the flux rope is significantly distorted at 5.4 AU. From the observed decay of magnetic field and mass density, we quantify how anisotropic is the expansion and the consequent deformation of the flux rope in favor of a cross section with an aspect ratio at 5.4 AU of ≈ 1.6 (larger in the direction perpendicular to the radial direction from the Sun). We quantify the ideal-MHD invariants and magnetic energy at both locations, and find that invariants are almost conserved, while the magnetic energy decays as expected with the expansion rate found.

Conclusions. The use of MHD invariants to link structures at the Sun and the interplanetary medium is supported by the results of this multi-spacecraft study. We also conclude that the local dimensionless expansion rate, which is computed from the velocity profile observed by a single-spacecraft, is very accurate for predicting the evolution of flux ropes in the solar wind.

Nature and Variability of the Electron Velocity Distribution Functions and the Nonequilibrium Boltzmann Entropy in the Solar Wind at the First Lagrangian (L1) Point During the Halo CME Event on 25 July 2004

Govind G. [Nampoothiri](#), [R. Satheesh Thampi](#), [Smitha V. Thampi](#), [Tarun K. Pant](#) & [Abhishek J.K.](#)
[Solar Physics](#) volume 296, Article number: 159 (2021)

<https://link.springer.com/content/pdf/10.1007/s11207-021-01900-7.pdf>

<https://doi.org/10.1007/s11207-021-01900-7>

In this paper, using the measurements at the Sun–Earth first Lagrangian point (L1), the kinetic properties of the electron velocity distribution functions (EVDs) during the passage of a typical halo coronal mass ejection (CME) has been analyzed. This CME was a front-sided, full halo CME, which erupted on **25 July 2004** (Carrington rotation 2019) from the active region NOAA AR 10652 (N04W30), and the CME reached at the L1 point ≈ 31 hours after the eruption. Solar wind electron measurements from the three-dimensional plasma (3DP) instrument onboard the WIND spacecraft and CME observations from the Large Angle and Spectroscopic Coronagraph (LASCO) onboard the Solar and Heliospheric Observatory (SOHO) have been used for performing the present study. The velocity distributions of the electrons observed at the L1 point show distinct features representing the passage of the CME plasma and the associated magnetic cloud (MC). The relative enhancements in the core and the suprathermal electron populations were delineated from the EVDF measurements. This study shows that, relative to the ambient solar wind condition, the suprathermal electron population enhanced more than the core electron population during the CME passage at the spacecraft location. Following the CME sheath-shock plasma, a bidirectional electron streaming (BDE) representing a closed magnetic flux rope was observed. The Boltzmann entropy analysis of the event shows that the magnetic cloud held the largest share of the nonequilibrium Boltzmann entropy among all the CME sectors.

Differences in the response to CME and CIR drivers of geomagnetic disturbances.

[Namuun B.](#), [Tsegmed B.](#), [Li L. Y.](#), [Leghari G.M.](#)

[СОЛНЕЧНО-ЗЕМНАЯ ФИЗИКА Том 9 № 2 , 2023](#) С. 35–40.

<https://naukaru.ru/ru/storage/viewWindow/124487>

Используя 1-минутные данные геомагнитных индексов SYM-H, AE, параметров солнечного ветра (скорость V_{sw} и плотность N_p и z-компоненту B_z межпланетного магнитного поля (ММП)) во время 23-го и 24-го циклов солнечной активности, мы статистически проанализировали корреляции между геомагнитной активностью (бури и суббури), V_{sw} , N_p , B_z и функциями передачи энергии из солнечного ветра в магнитосферу Земли. Для выбранной 131 бури, вызванной КВМ, SYM-H имеет более сильную зависимость от V_{sw} и B_z , чем другие параметры, тогда как выбранная 161 буря, вызванная CIR, имеет почти такие же зависимости от электрического

поля солнечного ветра, скорости открытого магнитного потока $d\phi/dt$ и электрического поля пересоединения Ekl. Таким образом, электрическое поле солнечного ветра и дневное магнитное пересоединение, возможно, вносят разный вклад бури двух типов. Во время бурь различных типов интенсивность суббури АЕ зависит в основном от B_z ММП, скорости открытого магнитного потока и электрического поля пересоединения.

Parameter Distributions for the Drag-Based Modeling of CME Propagation

Gianluca [Napoletano](#), [Raffaello Foldes](#), [Enrico Camporeale](#), [Giancarlo de Gasperis](#), [Luca Giovannelli](#), [Evangelos Paouris](#), [Ermanno Pietropaolo](#), [Jannis Teunissen](#) ... [See all authors](#)

Space Weather e2021SW002925 **Volume20, Issue9** 2022

<https://agupubs.onlinelibrary.wiley.com/doi/epdf/10.1029/2021SW002925>

<https://doi.org/10.1029/2021SW002925>

<https://arxiv.org/pdf/2201.12049.pdf>

In recent years, ensemble modeling has been widely employed in space weather to estimate uncertainties in forecasts. We here focus on the ensemble modeling of CME arrival times and arrival velocities using a drag-based model, which is well-suited for this purpose due to its simplicity and low computational cost. Although ensemble techniques have previously been applied to the drag-based model, it is still not clear how to best determine distributions for its input parameters, namely the drag parameter and the solar wind speed. The aim of this work is to evaluate statistical distributions for these model parameters starting from a list of past CME-ICME events. We employ LASCO coronagraph observations to measure initial CME position and speed, and in situ data to associate them with an arrival date and arrival speed. For each event we ran a statistical procedure to invert the model equations, producing parameters distributions as output. Our results indicate that the distributions employed in previous works were appropriately selected, even though they were based on restricted samples and heuristic considerations. On the other hand, possible refinements to the current method are also identified, such as the dependence of the drag parameter distribution on the CME being accelerated or decelerated by the solar wind, which deserve further investigation.

A Probabilistic Approach to the Drag-Based Model

Gianluca [Napoletano](#), [Roberta Forte](#), [Dario Del Moro](#), [Ermanno Pietropaolo](#), [Luca Giovannelli](#), [Francesco Berrilli](#)

Journal of Space Weather and Space Climate 2018, 8, A11

<https://arxiv.org/pdf/1801.04201.pdf>

<https://www.swsc-journal.org/articles/swsc/pdf/2018/01/swsc170019.pdf>

The forecast of the time of arrival of a coronal mass ejection (CME) to Earth is of critical importance for our high-technology society and for any future manned exploration of the Solar System. As critical as the forecast accuracy is the knowledge of its precision, i.e. the error associated to the estimate. We propose a statistical approach for the computation of the time of arrival using the drag-based model by introducing the probability distributions, rather than exact values, as input parameters, thus allowing the evaluation of the uncertainty on the forecast. We test this approach using a set of CMEs whose transit times are known, and obtain extremely promising results: the average value of the absolute differences between measure and forecast is 9.1h, and half of these residuals are within the estimated errors.

These results suggest that this approach deserves further investigation. We are working to realize a real-time implementation which ingests the outputs of automated CME tracking algorithms as inputs to create a database of events useful for a further validation of the approach.

Table 1. Sample of events from Shi et al. (2015) employed to test the P-DBM.

Space–time structure and wavevector anisotropy in space plasma turbulence

Review

Yasuhiro [Narita](#)

[Living Reviews in Solar Physics](#) December 2018, 15:2

<https://link.springer.com/content/pdf/10.1007%2Fs41116-017-0010-0.pdf>

Space and astrophysical plasmas often develop into a turbulent state and exhibit nearly random and stochastic motions. While earlier studies emphasize more on understanding the energy spectrum of turbulence in the one-dimensional context (either in the frequency or the wavenumber domain), recent achievements in plasma turbulence studies provide an increasing amount of evidence that plasma turbulence is essentially a spatially and temporally evolving phenomenon. This review presents various models for the space–time structure and anisotropy of the turbulent fields in space plasmas, or equivalently the energy spectra in the wavenumber–frequency domain for the space–time structures and that in the wavevector domain for the anisotropies. The turbulence energy spectra are evaluated in different one-dimensional spectral domains; one speaks of the frequency spectra in the spacecraft observations and the wavenumber spectra in the numerical simulation studies. The notion of the wavenumber–frequency spectrum offers a more comprehensive picture

of the turbulent fields, and good models can explain the one-dimensional spectra in the both domains at the same time. To achieve this goal, the Doppler shift, the Doppler broadening, linear-mode dispersion relations, and sideband waves are reviewed. The energy spectra are then extended to the wavevector domain spanning the directions parallel and perpendicular to the large-scale magnetic field. By doing so, the change in the spectral index at different projections onto the one-dimensional spectral domain can be explained in a simpler way.

Relation of Microstreams in the Polar Solar Wind to Switchbacks and Coronal X-ray Jets

Marcia Neugebauer, [Alphonse C. Sterling](#)

2021

<https://arxiv.org/ftp/arxiv/papers/2110/2110.00079.pdf>

Ulysses data obtained at high solar latitudes during periods of minimum solar activity in 1994 and 2007 are examined to determine the relation between velocity structures called microstreams and folds in the magnetic field called switchbacks. A high correlation is found. The possibility of velocity peaks in microstreams originating from coronal X-ray jets is re-examined; we now suggest that microstreams are the consequence of the alternation of patches of switchbacks and quiet periods, where the switchbacks could be generated by minifilament/flux rope eruptions that cause coronal jets. **3 Dec 2007, 19 Dec 2007**

Solar wind transient currents: statistical properties and impact on Earth's magnetosphere

Robert Newman, [Dmitri Vainchtein](#) & [Anton Artemyev](#)

[Solar Physics](#) volume 295, Article number: 129 (2020)

<https://link.springer.com/content/pdf/10.1007/s11207-020-01695-z.pdf>

Solar wind discontinuities carry intense transient currents and significantly contribute to the turbulent spectrum and plasma heating. The most-investigated characteristics of these discontinuities are the magnetic field configuration and the current density, whereas plasma characteristics attract less attention. In this study, we utilize eight years of ARTEMIS spacecraft observations in the solar wind to investigate plasma density, velocity, and temperature variations across discontinuities. We also consider the role of discontinuities in the development of Earth's magnetospheric perturbations. We show that observed discontinuities can be separated into two groups: (i) discontinuities with weak plasma density variations and a significant correlation between the solar wind and Alfvén velocities, (ii) discontinuities with significant variations of plasma density and temperature. For most discontinuities, observed density variations anti-correlate with temperature variations, but larger density/temperature variations correspond to stronger current densities. Time intervals characterized by increased occurrence rate of solar wind discontinuities correspond to enhanced geomagnetic activity in the Earth's magnetosphere as characterized by geomagnetic indices.

Coronal Mass Ejections, Solar Cycles and Magnetic Poles Reversal,

Kim Kwee [Ng](#),

American Journal of Astronomy and Astrophysics. Vol. 7, No. 1, **2019**, pp. 10-17.

[10.11648.j.ajaa.20190701.12.pdf](https://doi.org/10.11648/j.ajaa.20190701.12.pdf)

The magnitude of the measured geomagnetic index increases when the Coronal Mass Ejections occur on the Sun's surface. The abrupt increase in the geomagnetic index has seriously impacted the accuracy in the forecast of the activity of the next solar cycle. A method is proposed to filter the effect from the Coronal Mass Ejections. The correlation between the geomagnetic index and the activity of the subsequent solar cycle is found to have drastically improved with the proposed scheme. A strong correlation between the maximum amplitude R_N of a solar cycle N and its pre-cycle coronal mass ejections adjusted monthly geomagnetic activity index has been qualitatively determined, as illustrated by an impressive correlation coefficient of $0.91 \pm 0.09 - 0.12$, with its statistical significance estimated at 4.3σ . The corrected data have significantly improved the correlation between the observed variables from their original un-corrected case of 0.63 ± 0.23 . Our result indicates that the upcoming solar cycle, estimated at $R_{25} = 147 \pm 30$, would be stronger than the current waning solar cycle 24. In a related calculation, the magnetic poles reversals occurring in the solar cycles 21 and 22 are reproduced numerically from Maxwell's electromagnetic equations.

Automatic detection of Interplanetary Coronal Mass Ejections from in-situ data: a deep learning approach

Gautier [Nguyen](#), [Nicolas Aunaj](#), [Dominique Fontaine](#), [Erwan Le Pennec](#), [Joris Van den Bossche](#), [Alexis Jeandet](#), [Brice Bakkali](#), [Louis Vignoli](#), [Bruno Regaldo-Saint Blancar](#)

2019

<https://arxiv.org/pdf/1903.10780.pdf>

<https://iopscience.iop.org/article/10.3847/1538-4357/ab0d24/pdf>

Decades of studies have suggested several criteria to detect Interplanetary coronal mass ejections (ICME) in time series from in-situ spacecraft measurements. Among them the most common are an enhanced and smoothly rotating magnetic field, a low proton temperature and a low plasma beta. However, these features are not all observed for each ICME due to their strong variability. Visual detection is time-consuming and biased by the observer interpretation leading to non exhaustive, subjective and thus hardly reproducible catalogs. Using convolutional neural networks on sliding windows and peak detection, we provide a fast, automatic and multi-scale detection of ICMEs. The method has been tested on the in-situ data from WIND between 1997 and 2015 and on the 657 ICMEs that were recorded during this period. The method offers an unambiguous visual proxy of ICMEs that gives an interpretation of the data similar to what an expert observer would give. We found at a maximum 197 of the 232 ICMEs of the 2010-2015 period (recall $84 \pm 4.5\%$ including 90% of the ICMEs present in the lists of Nieves-Chinchilla et al. (2015) and Chi et al. (2016)). The minimal number of False Positives was 25 out of 158 predicted ICMEs (precision $84 \pm 2.6\%$). Although less accurate, the method also works with one or several missing input parameters. The method has the advantage of improving its performance by just increasing the amount of input data. The generality of the method paves the way for automatic detection of many different event signatures in spacecraft in-situ measurements. **2011-03-30, 3 July 2012, 17 July 2012.**

Modeling extreme ‘Carrington-type’ space weather events using three-dimensional global MHD simulations†

Chigomezyo M. **Ngwira**^{1,2,*}, Antti Pulkkinen², Maria M. Kuznetsova² and Alex Gloer

JGR, 119, 4456-4474, **2014**

<http://sci-hub.tw/10.1002/2013JA019661>

There is a growing concern over possible severe societal consequences related to adverse space weather impacts on man-made technological infrastructure. In the last two decades, significant progress has been made towards the first-principles modeling of space weather events, and three-dimensional (3-D) global magnetohydrodynamics (MHD) models have been at the forefront of this transition, thereby playing a critical role in advancing our understanding of space weather. However, the modeling of extreme space weather events is still a major challenge even for the modern global MHD models. In this study, we introduce a specially adapted University of Michigan 3-D global MHD model for simulating extreme space weather events with a Dst footprint comparable to the Carrington superstorm of September 1859 based on the estimate by Tsurutani et. al., (2003). Results are presented for a simulation run with “very extreme” constructed/idealized solar wind boundary conditions driving the magnetosphere. In particular, we describe the reaction of the magnetosphere-ionosphere system and the associated induced geoelectric field on the ground to such extreme driving conditions. The model set-up is further tested using input data for an observed space weather event of Halloween storm October 2003 to verify the MHD model consistence and to draw additional guidance for future work. This extreme space weather MHD model set-up is designed specifically for practical application to the modeling of extreme geomagnetically induced electric fields, which can drive large currents in ground-based conductor systems such as power transmission grids. Therefore, our ultimate goal is to explore the level of geoelectric fields that can be induced from an assumed storm of the reported magnitude, i.e., $Dst \sim -1600$ nT.

See

Comment on “Modeling extreme “Carrington-type” space weather events using three-dimensional global MHD simulations” by C.M. Ngwira, A. Pulkkinen, M.M. Kuznetsova and A. Gloer

Bruce T. **Tsurutani**, Gurbax S. Lakhina, Ezequiel Echer, Chinmaya Nayak, Anthony J. Mannucci, Xing Meng

JGR **Volume123, Issue2** Pages 1388-1392 **2018**

<http://onlinelibrary.wiley.com/doi/10.1002/2017JA024779/epdf>

Reply to Comments JGR [Volume123, Issue2](http://onlinelibrary.wiley.com/doi/10.1002/2017JA024779/epdf) February **2018** Pages 1393-1395

Simulation of the 23 July 2012 extreme space weather event: What if this extremely rare CME was Earth directed?

Chigomezyo M. **Ngwira**, Antti Pulkkinen, M. Leila Mays, Maria M. Kuznetsova, A. B. Galvin, Kristin Simunac, Daniel N. Baker, Xinlin Li, Yihua Zheng and Alex Gloer

Space Weather, Volume 11, Issue 12, pages 671–679, December **2013**

<http://onlinelibrary.wiley.com/doi/10.1002/2013SW000990/pdf>

Extreme space weather events are known to cause adverse impacts on critical modern day technological infrastructure such as high-voltage electric power transmission grids. On 23 July 2012, NASA's Solar Terrestrial Relations Observatory-Ahead (STEREO-A) spacecraft observed in situ an extremely fast coronal mass ejection (CME) that traveled 0.96 astronomical units (~ 1 AU) in about 19 h. Here we use the Space Weather Modeling Framework (SWMF)

to perform a simulation of this rare CME. We consider STEREO-A in situ observations to represent the upstream L1 solar wind boundary conditions. The goal of this study is to examine what would have happened if this Rare-type CME was Earth-bound. Global SWMF-generated ground geomagnetic field perturbations are used to compute the simulated induced geoelectric field at specific ground-based active INTERMAGNET magnetometer sites. Simulation results show that while modeled global SYM-H index, a high-resolution equivalent of the Dst index, was comparable to previously observed severe geomagnetic storms such as the Halloween 2003 storm, the 23 July CME would have produced some of the largest geomagnetically induced electric fields, making it very geoeffective. These results have important practical applications for risk management of electrical power grids.

Coronal Mass Ejection Image Edge Detection In Heliospheric Imager STEREO SECCHI Data

Marc [Nichitiu](#)

2022

<https://arxiv.org/pdf/2202.07678.pdf>

We present an algorithm to detect the outer edges of Coronal Mass Ejection (CME) events as seen in differences of Heliospheric Imager STEREO SECCHI HI-1 images from either A or B spacecraft, as well as its implementation in Python. 2008-12-12, 2011-01-31

Evaluating the performance of a plasma analyzer for a space weather monitor mission concept

G. [Nicolau](#), [R. T. Wicks](#), [I. J. Rae](#), [D. O. Kataria](#)

Space Weather e2020SW002559 2020

<https://doi.org/10.1029/2020SW002559>

<https://agupubs.onlinelibrary.wiley.com/doi/epdf/10.1029/2020SW002559>

We use historical analysis of solar wind plasma and Coronal Mass Ejections to define the range of performance required for an ion analyzer for future space weather monitoring missions. We adopt the design of a top-hat electrostatic analyzer, capable of measuring the plasma protons and constructing their three-dimensional distribution functions. The design is based on previous heritage instruments and allows monitoring of extreme space weather events. In order to evaluate the future observations and their analysis methods, we model the expected response of the instrument in simulated plasma conditions. We evaluate a novel analysis method which can determine on-board the plasma bulk properties, such as density, velocity and temperature from the statistical moments of the observed velocity distribution functions of the plasma particles. We quantify the accuracy of the derived parameters critical for space weather purposes, by comparing them with the corresponding input solar wind parameters. In order to validate the instrument design, we examine the accuracy over the entire range of the input parameters we expect to observe in solar wind, from benign to extreme space weather conditions. We also use realistic parameters of fast solar wind streams and Interplanetary Coronal Mass Ejections as measured by the Advanced Composition Explorer spacecraft, to investigate the performance of the example instrument and the accuracy of the analysis. We discuss the achieved accuracy and its relevance to space weather monitoring concepts. We address sources of significant errors and we demonstrate potential improvements by using a fitting analysis method to derive the results.

Long-term observation of magnetic pulsations through the ELF Hylaty station located in the Bieszczady Mountains (south-eastern Poland)

Zenon [Nieckarz](#)^{1*} and Grzegorz Michalek²

J. Space Weather Space Clim. 2020, 10, 59

<https://www.swsc-journal.org/articles/swsc/pdf/2020/01/swsc200024.pdf>

Ground-based measurements of ultra- and extremely low-frequency waves (ULF/ELF) carried out in 2005–2016 (the 23rd and 24th solar cycle) at the ELF Hylaty station in Bieszczady Mountains (south-eastern Poland) were used to identify the days (360 days) in which magnetic pulsation events (MPEs) occurred. To reveal sources of MPEs at the Sun we considered their correlation with the basic indices describing solar activity. Our analysis, like earlier studies, did not reveal a significant positive correlation between the MPE detection rate and the sunspot numbers (SSN). On the other hand, we showed that MPEs are strongly correlated (correlation coefficient ≈ 0.70) with moderate ($Dst < -70$ nT) and intense ($Dst < -100$ nT) geomagnetic disturbances expressed by the Disturbance Storm Index (Dst). We recognized all sources of these geomagnetic storms associated with the considered MPEs. Only 44% of the MPEs were associated with storms caused by CMEs listed in the CDAW LASCO CME catalog. 56% of the MPEs were associated with storms caused by other phenomena including corotating interaction regions (CIRs), slow solar wind or CMEs not detected by LASCO. We also demonstrated that the CMEs associated with the MPEs were very energetic, i.e. they were extremely wide (partial and halo events) and fast (with the average speed above 1100 km s⁻¹). CMEs and CIRs generally appear in different phases of solar cycles. Because MPEs are strongly related to both of these phenomena they cannot be

associated with any phase of a solar cycle or with any indicator characterizing a 11-year solar activity. We also suggested that the low number of MPEs associated with CMEs is due to the anomalous 24 solar cycle. During this cycle, due to low density of the interplanetary medium, CMEs could easily eject and expand, but they were not geoeffective.

Following a prominence eruption from the Sun to Parker Solar Probe with multi-spacecraft observations

Tatiana **Niembro**, Daniel Seaton, Phillip Hess, David Berghmans, +++

Front. Astron. Space Sci. 10 :1191294. **2023**

doi: 10.3389/fspas.2023.1191294

<https://www.frontiersin.org/articles/10.3389/fspas.2023.1191294/pdf>

In the early hours of **2021 April 25**, the Solar Probe Cup on board Parker Solar Probe registered the passage of a solar wind structure characterized by a clear and constant He²⁺/H⁺ density ratio above 6% during three hours. The He²⁺ contribution remained present but fainting and intermittent within a twelve-hour window. Solar Orbiter and Parker Solar Probe were in nearly perfect quadrature, allowing for optimal observing configuration in which the material impacting the Parker Solar Probe was in the Solar Orbiter plane of the sky and visible off the limb. In this work, we report the journey of the helium-enriched plasma structure from the Sun to the Parker Solar Probe by combining multi-spacecraft remote-sensing and in situ measurements. We identify an erupting prominence as the likely source, behind the Sun relative to the Earth, but visible to multiple instruments on both the Solar-Terrestrial Relations Observatory-A and Solar Orbiter. The associated CME was also observed by coronagraphs and heliospheric imagers from both spacecrafts before reaching the Parker Solar Probe at 46 R_☉, 8 h after the spacecraft registered a crossing of the heliospheric current sheet. Except for extraordinary helium enhancement, the CME showed ordinary plasma signatures and a complex magnetic field with an overall strength enhancement. The images from the Wide-field Imager for Solar Probe (WISPR) aboard Parker Solar Probe show a structure entering the field of view a few hours before the in situ crossing, followed by repetitive transient structures that may be the result of flying through the CME body. We believe this to be the first example of a CME being imaged by WISPR directly before and during being detected in situ. This study highlights the potential of combining the Parker Solar Probe in situ measurements in the inner heliosphere with simultaneous remote-sensing observations in (near) quadrature from other spacecrafts.

Numerical simulations of ICME-ICME interactions

Tatiana **Niembro**, [Alejandro Lara](#), [Ricardo F. González](#), [J. Cantó](#)

J. Space Weather Space Clim. **2019** 9, A4

<https://arxiv.org/pdf/1801.03136.pdf>

<https://www.swsc-journal.org/articles/swsc/pdf/2019/01/swsc170072.pdf>

We present hydrodynamical simulations of interacting Coronal Mass Ejections in the Interplanetary medium (ICMEs). In these events, two consecutive CMEs are launched from the Sun in similar directions within an interval of time of a few hours. In our numerical model, we assume that the ambient solar wind is characterized by its velocity and mass-loss rate. Then, the CMEs are generated when the flow velocity and mass-loss rate suddenly change, with respect to the ambient solar wind conditions during two intervals of time, which correspond to the durations of the CMEs. After their interaction, a merged region is formed and evolve as a single structure into the interplanetary medium. In this work, we are interested in the general morphology of this merged region, which depends on the initial parameters of the ambient solar wind and each of the CMEs involved. In order to understand this morphology, we have performed a parametric study in which we characterize the effects of the initial parameters variations on the density and velocity profiles at 1 AU, using as reference the well-documented event of **July 25th, 2004**. Based on this parametrization we were able to reproduce with a high accuracy the observed profiles. Then, we apply the parametrization results to the interaction events of **May 23, 2010; August 1, 2010; and November 9, 2012**. With this approach and using values for the input parameters within the CME observational errors, our simulated profiles reproduce the main features observed at 1 AU. Even though we do not take into account the magnetic field, our models give a physical insight into the propagation and interaction of ICMEs.

AN ANALYTICAL MODEL OF INTERPLANETARY CORONAL MASS EJECTION INTERACTIONS

T. **Niembro**^{1,3}, J. Cantó², A. Lara³, and R. F. González

2015 ApJ 811 69

We present an analytical model that describes the evolution of two consecutive interplanetary coronal mass ejections (ICMEs), their interaction, and the evolution of the merged region. In this model, the coronal mass ejections (CMEs) are seen as velocity and density (mass loss rate) fluctuations of the solar wind that result in the formation of shocks traveling

into the ambient solar wind (ASW). The dynamical evolution of these structures depends on both the CME parameters such as the initial velocity, density, and the duration of the eruption as well as the solar wind conditions (ejection velocity and mass loss rate). The probability of an interaction of two consecutive CMEs launched in the same direction is high, basically depending on their speeds and the interval of time between the CMEs. As a result of the interaction, a merged region is formed. Its dynamical evolution is also addressed by the present model. Given a set of initial CMEs and ASW conditions, our model is able to predict the time and distance of the interaction between the ICMEs and the velocity of the merged region as a function of the heliospheric distance. These are fundamental parameters of space weather predictions. Also, the model is able to predict the arrival time and velocity of the merged region at 1 AU. In this work, we validate the model through its application to well documented interaction events observed on **2007 January 24, 2010 May 23, 2010 August 01, and 2012 November 09.**

Advancing interplanetary magnetohydrodynamic models through solar energetic particle modelling

Insights from the 2013 March 15 SEP event*

A. Niemela^{1,2}, N. Wijsen^{3,4}, A. Aran^{5,6}, L. Rodriguez², J. Magdalenic^{1,2} and S. Poedts^{1,7}
A&A 679, A93 (2023)

<https://www.aanda.org/articles/aa/pdf/2023/11/aa47116-23.pdf>

Aims. This study utilises a modelling approach to investigate the impact of perturbed solar wind conditions caused by multiple interplanetary coronal mass ejections (ICMEs) on the evolution of solar energetic particle (SEP) distributions. Furthermore, we demonstrate the utility of SEP models in evaluating the performance of solar wind and coronal mass ejection (CME) models. To illustrate these concepts, we focussed on modelling the gradual SEP event that occurred on **2023 March 15.**

Methods. We utilised the 3D magnetohydrodynamic model EUHFORIA (EUropean Heliospheric FORecasting Information Asset) to simulate the various ICMEs that caused the highly perturbed solar wind conditions observed during the March 15 event. We conducted three separate EUHFORIA simulations, employing both non-magnetised and magnetised models for these ICMEs. To analyse the behaviour of energetic particles in the simulated solar wind environments, we employed the energetic particle transport and acceleration model PARADISE (PARTicle Radiation Asset Directed at Interplanetary Space Exploration).

Results. In the vicinity of Earth, the three EUHFORIA simulations exhibit strong similarities and closely match the observed in situ data. Nevertheless, when incorporating these distinct solar wind configurations into PARADISE, notable disparities emerge in the simulated SEP intensities. This discrepancy can be attributed to the different magnetic enhancements and closed magnetic structures introduced by the different CME models within the EUHFORIA simulations. These variations strongly impact the transport mechanisms of SEPs, leading to significant deviations in the particle intensities simulated by PARADISE. Furthermore, our findings highlight the significance of cross-field diffusion even in scenarios with reduced perpendicular mean free path. This effect becomes particularly prominent when SEPs are trapped within the inner heliosphere due to the presence of ICMEs. In these scenarios, the extended duration of confinement allows the slower cross-field diffusion process to become more pronounced and exert a greater influence on the spatial distribution of SEPs, especially near and within the boundaries of ICMEs.

Redefining Flux Ropes in Heliophysics

Review

Teresa Nieves-Chinchilla, Sanchita Pal, Tarik Salman, Fernando Carcaboso, et al.
Front. Astron. Space Sci. 10: 1114838 2023

<https://www.frontiersin.org/articles/10.3389/fspas.2023.1114838/full>

<https://www.frontiersin.org/articles/10.3389/fspas.2023.1114838/pdf>

Magnetic flux ropes manifest as twisted bundles of magnetic field lines. They carry significant amounts of solar mass in the heliosphere. This paper underlines the need to advance our understanding of the fundamental physics of heliospheric flux ropes and provides the motivation to significantly improve the status quo of flux rope research through novel and requisite approaches. It briefly discusses the current understanding of flux rope formation and evolution, and summarizes the strategies that have been undertaken to understand the dynamics of heliospheric structures. The challenges and recommendations put forward to address them are expected to broaden the in-depth knowledge of our nearest star, its dynamics, and its role in its region of influence, the heliosphere.

Direct First PSP Observation of the Interaction of Two Successive Interplanetary Coronal Mass Ejections in November 2020

Teresa Nieves-Chinchilla, [Nathalia Alzate](#), [Hebe Cremades](#), [Laura Rodriguez-Garcia](#), et al.

ApJ 2022

<https://arxiv.org/pdf/2201.11212.pdf>

We investigate the effects of the evolutionary processes in the internal magnetic structure of two interplanetary coronal mass ejections (ICMEs) detected in situ between **2020 November 29 and December 1** by Parker Solar Probe (PSP). The sources of the ICMEs were observed remotely at the Sun in EUV and subsequently tracked to their coronal counterparts in white light. This period is of particular interest to the community since it has been identified as the first widespread solar energetic particle event of Solar Cycle 25. The distribution of various solar and heliospheric-dedicated spacecraft throughout the inner heliosphere during PSP observations of these large-scale magnetic structures enables a comprehensive analysis of the internal evolution and topology of such structures. By assembling different models and techniques, we identify the signatures of interaction between the two consecutive ICMEs and the implications for their internal structure. We use multispacecraft observations in combination with a remote-sensing forward modeling technique, numerical propagation models, and in-situ reconstruction techniques. The outcome, from the full reconciliations, demonstrates that the two CMEs are interacting in the vicinity of PSP. Thus, we identify the in-situ observations based on the physical processes that are associated with the interaction and collision of both CMEs. We also expand the flux rope modeling and in-situ reconstruction technique to incorporate the aging and expansion effects in a distorted internal magnetic structure and explore the implications of both effects in the magnetic configuration of the ICMEs.

Unraveling the Internal Magnetic Field Structure of the Earth-directed Interplanetary Coronal Mass Ejections During 1995 – 2015

Teresa [Nieves-Chinchilla](#), Lan K. Jian, Laura Balmaceda, Angelos Vourlidas, Luiz F. G. dos Santos, Adam Szabo

[Solar Physics](#) July 2019, 294:89

[sci-hub.se/10.1007/s11207-019-1477-8](https://doi.org/10.1007/s11207-019-1477-8)

<https://link.springer.com/content/pdf/10.1007%2Fs11207-019-1477-8.pdf>

The magnetic field configurations associated with interplanetary coronal mass ejections (ICMEs) are the in situ manifestations of the entrained magnetic structure associated with coronal mass ejections (CMEs). We present a comprehensive study of the internal magnetic field configurations of ICMEs observed at 1 AU by the Wind mission during 1995 – 2015. The goal is to unravel the internal magnetic structure associated with the ICMEs and establish the signatures that validate a flux-rope structure. We examine the expected magnetic field signatures by simulating spacecraft trajectories within a simple flux rope, i.e., with circular–cylindrical (CC) helical magnetic field geometry. By comparing the synthetic configurations with the 353 ICME in situ observations, we find that only 152 events (FrFr) display the clear signatures of an expected axial-symmetric flux rope. Two more populations exhibit possible signatures of flux rope; 58 cases (F–F–) display a small rotation ($<90^\circ < 90^\circ$) of the magnetic field direction, interpreted as a large separation of the spacecraft from the center, and, 62 cases (F+F+) exhibit larger rotations, possibly arising from more complex configuration. The categories, CxCx (14%) and EE events (9%), reveal signatures of complexity possibly related with evolutionary processes. We then reconstruct the flux ropes assuming CC geometry. We examine the orientation and geometrical properties during the solar activity levels at the end of Solar Cycle 22 (SC22), SC23 and part of SC24. The orientation exhibits solar cycle trends and follow the heliospheric current sheet orientation. We confirm previous studies that found a Hale cycle dependence of the poloidal field reversal. By comparing our results with the occurrence of CMEs with large angular width ($AW > 60^\circ$ $AW > 60^\circ$) we find a broad correlation suggesting that such events are highly inclined CMEs. The solar cycle distribution of bipolar vs. unipolar BzBz configuration confirms that the CMEs may remove solar cycle magnetic field and helicity.

Table 5 Catalog of ICMEs observed by Wind from 1995 to 2015.

Understanding the Internal Magnetic Field Configurations of ICMEs Using More than 20 Years of Wind Observations

T. [Nieves-Chinchilla](#), A. Vourlidas, J. C. Raymond, M. G. Linton, N. Al-haddad, N. P. Savani, A. Szabo, M. A. Hidalgo

[Solar Physics](#) February 2018, 293:25

<https://link.springer.com/content/pdf/10.1007%2Fs11207-018-1247-z.pdf>

The magnetic topology, structure, and geometry of the magnetic obstacles embedded within interplanetary coronal mass ejections (ICMEs) are not yet fully and consistently described by in situ models and reconstruction techniques. The main goal of this work is to better understand the status of the internal magnetic field of ICMEs and to explore in situ signatures to identify clues to develop a more accurate and reliable in situ analytical models. We take advantage of

more than 20 years of Wind observations of transients at 1 AU to compile a comprehensive database of ICMEs through three solar cycles, from 1995 to 2015. **The catalog is publicly available at wind.gsfc.nasa.gov and is fully described in this article.** We identify and collect the properties of 337 ICMEs, of which 298 show organized magnetic field signatures. To allow for departures from idealized magnetic configurations, we introduce the term “magnetic obstacle” (MO) to signify the possibility of more complex configurations. To quantify the asymmetry of the magnetic field strength profile within these events, we introduce the distortion parameter (DiP) and calculate the expansion velocity within the magnetic obstacle. Circular-cylindrical geometry is assumed when the magnetic field strength displays a symmetric profile. We perform a statistical study of these two parameters and find that only 35% of the events show symmetric magnetic profiles and a low enough expansion velocity to be compatible with the assumption of an idealized cylindrical static flux rope, and that 41% of the events do not show the expected relationship between expansion and magnetic field compression in the front, with the maximum magnetic field closer to the first encounter of the spacecraft with the magnetic obstacle; 18% show contractions (i.e. apparent negative expansion velocity), and 30% show magnetic field compression in the back. We derive an empirical relation between DiP and expansion velocity that is the first step toward improving reconstructions with possible applications to space weather studies. In summary, our main results demonstrate that the assumed correlation between expanding structure and asymmetric magnetic field is not always valid. Although 59% of the cases could be described by circular-cylindrical geometry, with or without expansion, the remaining cases show significant in situ signatures of departures from circular-cylindrical geometry. These results will aid in the development of more accurate in situ models to reconcile image. **February 7, 1995., October 18, 1995, February 10, 1997, May 15, 1997, November 6, 2000, May 18, 2002, May 15, 2005, September 30, 2006**
Table 1 Catalog of ICMEs observed by Wind from 1995 to 2015.

Inner Heliospheric Evolution of a "Stealth" CME Derived from Multi-view Imaging and Multipoint in Situ observations. I. Propagation to 1 AU

T. [Nieves-Chinchilla](#)^{1,2}, A. Vourlidas³, G. Stenborg⁴, N. P. Savani^{2,5}, A. Koval^{2,6}, A. Szabo², and L. K. Jian

2013 ApJ 779 55

Coronal mass ejections (CMEs) are the main driver of space weather. Therefore, a precise forecasting of their likely geoeffectiveness relies on an accurate tracking of their morphological and kinematical evolution throughout the interplanetary medium. However, single viewpoint observations require many assumptions to model the development of the features of CMEs. The most common hypotheses were those of radial propagation and self-similar expansion. The use of different viewpoints shows that, at least for some cases, those assumptions are no longer valid. From radial propagation, typical attributes that can now be confirmed to exist are over-expansion and/or rotation along the propagation axis. Understanding the 3D development and evolution of the CME features will help to establish the connection between remote and in situ observations, and hence help forecast space weather. We present an analysis of the morphological and kinematical evolution of a STEREO-B-directed CME on **2009 August 25-27**. By means of a comprehensive analysis of remote imaging observations provided by the SOHO, STEREO, and SDO missions, and in situ measurements recorded by Wind, ACE, and MESSENGER, we prove in this paper that the event exhibits signatures of deflection, which are usually associated with changes in the direction of propagation and/or also with rotation. The interaction with other magnetic obstacles could act as a catalyst of deflection or rotation effects. We also propose a method to investigate the change of the CME tilt from the analysis of height-time direct measurements. If this method is validated in further work, it may have important implications for space weather studies because it will allow for inference of the interplanetary counterpart of the CME's orientation.

Remote and in situ observations of an unusual Earth-directed coronal mass ejection from multiple viewpoints

[Nieves-Chinchilla](#), T.; Colaninno, R.; Vourlidas, A.; Szabo, A.; Lepping, R. P.; Boardsen, S. A.; Anderson, B. J.; Korth, H.

J. Geophys. Res., Vol. 117, No. A6, A06106, **2012**

<http://dx.doi.org/10.1029/2011JA017243>

During **June 16–21, 2010**, an Earth-directed coronal mass ejection (CME) event was observed by instruments onboard STEREO, SOHO, MESSENGER and Wind. This event was the first direct detection of a rotating CME in the middle and outer corona. Here, we carry out a comprehensive analysis of the evolution of the CME in the interplanetary medium comparing in situ and remote observations, with analytical models and three-dimensional reconstructions. In particular, we investigate the parallel and perpendicular cross section expansion of the CME from the corona through the

heliosphere up to 1 AU. We use height-time measurements and the Gradual Cylindrical Shell (GCS) technique to model the imaging observations, remove the projection effects, and derive the 3-dimensional extent of the event. Then, we compare the results with in situ analytical Magnetic Cloud (MC) models, and with geometrical predictions from past works. We find that the parallel (along the propagation plane) cross section expansion agrees well with the in situ model and with the Bothmer and Schwenn (1998) empirical relationship based on in situ observations between 0.3 and 1 AU. Our results effectively extend this empirical relationship to about 5 solar radii. The expansion of the perpendicular diameter agrees very well with the in situ results at MESSENGER (~ 0.5 AU) but not at 1 AU. We also find a slightly different, from Bothmer and Schwenn (1998), empirical relationship for the perpendicular expansion. More importantly, we find no evidence that the CME undergoes a significant latitudinal over-expansion as it is commonly assumed. Instead, we find evidence that effects due to CME rotation and expansion can be easily confused in the images leading to a severe overestimation of the proper 3D size of the event. Finally, we find that the reconstructions of the CME morphology from the in situ observations at 1 AU are in agreement with the remote sensing observations but they show a big discrepancy at MESSENGER. We attribute this discrepancy to the ambiguity of selecting the proper boundaries due to the lack of accompanying plasma measurements.

Analysis and study of the in situ observation of the June 1st 2008 CME by STEREO

T. [Nieves-Chinchilla](#)^{a, b, ,}, R. Gómez-Herrero^c, A.F. Viñas^b, O. Malandrakid, N. Dresing^c, M.A. Hidalgo^e, A. Opitz^f, J.-A. Sauvaud^f, B. Lavraud^f and J.M. Davilab

Journal of Atmospheric and Solar-Terrestrial Physics, Volume 73, Issues 11-12, **2011**, Pages 1348-1360

In this work we present a combined study of the counterpart of the coronal mass ejection (CME) of **June 1st of 2008** in the interplanetary medium. This event has been largely studied because of its peculiar initiation and its possible forecasting consequences for space weather. We show an in situ analysis (on days June 6th–7th of 2008) of the CME in the interplanetary medium in order to shed some light on the propagation and evolution mechanisms of the interplanetary CME (ICME). The goals of this work are twofold: gathering the whole in situ data from PLASTIC and IMPACT onboard STEREO B in order to provide a complete characterization of the ICME, and to present a model where the thermal plasma pressure is included. The isolated ICME features show a clear forward shock which we identify as an oblique forward fast shock accelerating ions to a few-hundred keV during its passage. Following the shock, a flux rope is easily defined as a magnetic cloud (MC) by the magnetic field components and magnitude, and the low proton plasma- β . During the spacecraft passage through the MC, the energetic ion intensity shows a pronounced decrease, suggesting a closed magnetic topology, and the suprathermal electron population shows a density and temperature increase, demonstrating the importance of the electrons in the MC description. The in situ evidence suggests that there is no direct magnetic connection between the forward shock and the MC, and the characteristics of the reverse shock determined suggest that the shock pair is a consequence of the propagation of the ICME in the interplanetary medium. The energetic ions measured by the SEPT instrument suggest that their enhancement is not related to any solar event, but is solely due to the interplanetary shock consistent with the fact that no flares are observed on the Sun. The changes in the polarity of the interplanetary magnetic field in the vicinity of the ICME observed by electron PADs from SWEA are in accordance with the idea that the CME originated along a neutral line over the quiet Sun. The magnetic cloud model presented in this work provides the plasma pressure as a new factor to consider in the study of the expansion and evolution of CMEs in the interplanetary medium. This model could provide a new understanding of the Sun–Earth connection because of the important role that the plasma plays in the eruption of the CME in the solar corona and the reconnection process carried out with the Earth’s magnetosphere

MAGNETIC CLOUDS OBSERVED AT 1 AU DURING THE PERIOD 2000–2003

T. [NIEVES-CHINCHILLA](#), M. A. HIDALGO and J. SEQUEIROS

Solar Physics (**2005**) 232: 105–126, [File](#)

AN ANALYTICAL MODEL OF INTERPLANETARY CORONAL MASS EJECTION INTERACTIONS

T. [Niembro](#)^{1,3}, J. Cantó², A. Lara³, and R. F. González

2015 ApJ 811 69

We present an analytical model that describes the evolution of two consecutive interplanetary coronal mass ejections (ICMEs), their interaction, and the evolution of the merged region. In this model, the coronal mass ejections (CMEs) are

seen as velocity and density (mass loss rate) fluctuations of the solar wind that result in the formation of shocks traveling into the ambient solar wind (ASW). The dynamical evolution of these structures depends on both the CME parameters such as the initial velocity, density, and the duration of the eruption as well as the solar wind conditions (ejection velocity and mass loss rate). The probability of an interaction of two consecutive CMEs launched in the same direction is high, basically depending on their speeds and the interval of time between the CMEs. As a result of the interaction, a merged region is formed. Its dynamical evolution is also addressed by the present model. Given a set of initial CMEs and ASW conditions, our model is able to predict the time and distance of the interaction between the ICMEs and the velocity of the merged region as a function of the heliospheric distance. These are fundamental parameters of space weather predictions. Also, the model is able to predict the arrival time and velocity of the merged region at 1 AU. In this work, we validate the model through its application to well documented interaction events observed on **2007 January 24, 2010 May 23, 2010 August 01, and 2012 November 09.**

Distorted-Toroidal Flux Rope model for Heliospheric Flux Ropes

Teresa **Nieves-Chinchilla**, [Miguel Angel Hidalgo](#), [Hebe Cremades](#)

ApJ **2022**

<https://arxiv.org/pdf/2210.15705.pdf>

The three-dimensional characterization of magnetic flux-rope observed in the heliosphere has been a challenging task for decades. This is mainly due to the limitation to infer the 3D global topology and the physical properties from the 1D time series from any spacecraft. To advance our understanding of magnetic flux-rope whose configuration departs from the typical stiff geometries, here we present the analytical solution for a 3D flux-rope model with an arbitrary cross-section and a toroidal global shape. This constitutes the next level of complexity following the elliptic-cylindrical (EC) geometry. The mathematical framework was established by Nieves-Chinchilla et al. (2018) ApJ, with the EC flux-rope model that describes the magnetic topology with elliptical cross-section as a first approach to changes in the cross-section. In the distorted-toroidal flux rope model, the cross-section is described by a general function. The model is completely described by a non-orthogonal geometry and the Maxwell equations can be consistently solved to obtain the magnetic field and relevant physical quantities. As a proof of concept, this model is generalized in terms of the radial dependence of current density components. The last part of this paper is dedicated to a specific function, $F(\varphi)=\delta(1-\lambda\cos\varphi)$, to illustrate possibilities of the model. This model paves the way to investigate complex distortions of the magnetic structures in the solar wind. Future investigations will in-depth explore these distortions by analyzing specific events, the implications in the physical quantities, such as magnetic fluxes, helicity or energy, and evaluating the force balance with the ambient solar wind that allows such distortions.

Direct First Parker Solar Probe Observation of the Interaction of Two Successive Interplanetary Coronal Mass Ejections in 2020 November

Teresa **Nieves-Chinchilla**¹, Nathalia Alzate^{1,2}, Hebe Cremades³, Laura Rodríguez-García⁴, Luiz F. G. Dos Santos⁵, Ayris Narock^{1,2}, Hong Xie^{1,6}, Adam Szabo¹, Erika Palmerio^{7,8}, Vratislav Krupar^{1,9}Show full author list

2022 ApJ 930 88

<https://iopscience.iop.org/article/10.3847/1538-4357/ac590b/pdf>

We investigate the effects of the evolutionary processes in the internal magnetic structure of two interplanetary coronal mass ejections (ICMEs) detected in situ between 2020 November 29 and December 1 by the Parker Solar Probe (PSP). The sources of the ICMEs were observed remotely at the Sun in EUV and subsequently tracked to their coronal counterparts in white light. This period is of particular interest to the community as it has been identified as the first widespread solar energetic particle event of solar cycle 25. The distribution of various solar and heliospheric-dedicated spacecraft throughout the inner heliosphere during PSP observations of these large-scale magnetic structures enables a comprehensive analysis of the internal evolution and topology of such structures. By assembling different models and techniques, we identify the signatures of interaction between the two consecutive ICMEs and the implications for their internal structure. We use multispacecraft observations in combination with a remote-sensing forward modeling technique, numerical propagation models, and in situ reconstruction techniques. The outcome, from the full reconciliations, demonstrates that the two coronal mass ejections (CMEs) are interacting in the vicinity of the PSP. Thus, we identify the in situ observations based on the physical processes that are associated with the interaction and collision of both CMEs. We also expand the flux rope modeling and in situ reconstruction technique to incorporate the aging and expansion effects in a distorted internal magnetic structure and explore the implications of both effects in the magnetic configuration of the ICMEs. **26 Nov, 29 Nov-1 Dec 2020**

Elliptic-cylindrical Analytical Flux Rope Model for Magnetic Clouds

T. Nieves-Chinchilla^{1,2}, M. G. Linton³, M. A. Hidalgo⁴, and A. Vourlidas⁵
2018 ApJ 861 139

<http://sci-hub.tw/10.3847/1538-4357/aac951>

In this paper, we present the elliptic-cylindrical analytical flux rope model, which constitutes the first level of complexity above that of a circular-cylindrical geometry. The framework of this series of models was established by Nieves-Chinchilla et al. with the circular-cylindrical analytical flux rope model. The model describes the magnetic flux rope topology with distorted cross section as a possible consequence of the flux rope interaction with the solar wind. In this model, for the first time, a flux rope is completely described by a nonorthogonal geometry. The Maxwell equations can be consistently solved using tensorial analysis, and relevant physical quantities can be derived, such as magnetic fluxes, number of turns, or Lorentz force distribution. The model is generalized in terms of the radial dependence of the poloidal and axial current density components. The circular-cylindrical reconstruction technique has been adapted to the new geometry for a specific case of the model and tested against an interplanetary coronal mass ejection observed by the Wind spacecraft on **2005 June 12**. In this specific case, from the comparative analysis between the circular-cylindrical and elliptic-cylindrical models, the inclusion of the cross-section distortion in the 3D reconstruction results in significant changes in the derived axis orientation, size, central magnetic field, magnetic fluxes, and force-freeness. The case studied in this paper exemplifies the use of the model and reconstruction technique developed. Furthermore, the novel mathematical formulation to model flux ropes in heliophysics paves the way to the inclusion of more complex magnetic field configurations.

Modeling of the corrected D_{st}^* index temporal profile on the main phase of the magnetic storms generated by different types of solar wind

N. S. Nikolaeva, Yu. I. Yermolaev, I. G. Lodkina

Cosmic Research, March 2015, Volume 53, Issue 2, pp 119-127

Kosmicheskie Issledovaniya, 2015, Vol. 53, No. 2, pp. 126–135.

A modeling of the corrected (taking into account the magnetopause currents [9]) D_{st}^* index during the main phase of magnetic storms generated by four types of the solar wind (SW), namely MC (10 storms), CIR (28 storms), Sheath (21 storms), and Ejecta (31 storms), is performed similarly to our previous work on the simple D_{st} index [8]. The “Catalog of large-scale solar wind phenomena during 1976–2000” ([1], <ftp://ftp.iki.rssi.ru/pub/omni/>) prepared on the basis of the OMNI database, was used for the identification of SW types. The time behavior of D_{st}^* is approximated by a linear dependence on the integral electric field ($\sum E_y$), dynamic pressure (P_d), and fluctuation level (s_B) of the interplanetary magnetic field (IMF). Three types of D_{st}^* modeling are performed: (1) by individual values of the approximation coefficients; (2) by approximation coefficients averaged over SW type, and (3) in the same way as in (2) but with allowance for the D_{st}^* -index values preceding the beginning of the main phase of the magnetic storm. The results of modeling the corrected D_{st}^* index are compared to modeling of the usual D_{st} index. In the conditions of a strong statistical scatter of the approximation coefficients, the use of D_{st} instead of D_{st}^* insignificantly influences the accuracy of the modeling and correlation coefficient.

Forecasting Geomagnetic activity (Dst Index) using the ensemble kalman filter

B Nilam, S Tulasi Ram

MNRAS, Volume 511, Issue 1, March 2022, Pages 723–731,

<https://doi.org/10.1093/mnras/stac099>

A novel Ensemble Kalman Filter (EnKF) method is adopted to make reliable forecasts of geomagnetic activity (Dst index) for real-time applications. In this method, an educated estimate (forecast) of Disturbance storm time (Dst) is made based on the ring current dynamics like injection and decay rates. This estimated Dst is further updated with the assimilation of real-time Dst values or ΔH values from a single ground based magnetometer observations. The forecasted Dst values by this EnKF method are validated with the true Dst during the severely disturbed period that consists of 2 super (Dst < -250 nT), 8 intense (Dst < -100 nT), and 13 moderate geomagnetic storms (Dst < -50 nT). It is found that the EnKF method implemented in this work offers the best accurate forecast of Dst with a root mean square error (RMSE) and regression coefficient (R) of 4.3 nT and 0.99, respectively.

Tracking solar wind flows from rapidly varying viewpoints by the Wide-field Imager for Parker Solar Probe

A. Nindos, S. Patsourakos, A. Vourlidas, P. C. Liewer, P. Penteado, J. R. Hall

A&A 2020

<https://arxiv.org/pdf/2010.13140.pdf>

Aims: Our goal is to develop methodologies to seamlessly track transient solar wind flows viewed by coronagraphs or heliospheric imagers from rapidly varying viewpoints.

Methods: We constructed maps of intensity versus time and elongation (J-maps) from Parker Solar Probe (PSP) Wide-field Imager (WISPR) observations during the fourth encounter of PSP. From the J-map, we built an intensity on impact-radius-on-Thomson-surface map (R-map). Finally, we constructed a latitudinal intensity versus time map (Lat-map). Our methodology satisfactorily addresses the challenges associated with the construction of such maps from data taken from rapidly varying viewpoint observations.

Results: Our WISPR J-map exhibits several tracks, corresponding to transient solar wind flows ranging from a coronal mass ejection (CME) down to streamer blobs. The latter occurrence rate is about 4-5 per day, which is similar to the occurrence rate in a J-map made from ~ 1 AU data obtained with the Heliospheric Imager-1 (HI-1) on board the Solar Terrestrial Relations Observatory Ahead spacecraft (STEREO-A). STEREO-A was radially aligned with PSP during the study period. The WISPR J-map tracks correspond to angular speeds of $2.28 \pm 0.7^\circ/\text{hour}$ ($2.49 \pm 0.95^\circ/\text{hour}$), for linear (quadratic) time-elongation fittings, and radial speeds of about 150-300 km s^{-1} . The analysis of the Lat-map reveals a bifurcating streamer, which implies that PSP was flying through a slightly folded streamer during perihelion.

Conclusions: We developed a framework to systematically capture and characterize transient solar wind flows from space platforms with rapidly varying vantage points. The methodology can be applied to PSP WISPR observations as well as to upcoming observations from instruments on board the Solar Orbiter mission.

Comparison of Toroidal Interplanetary Flux-rope Model Fitting with Different Boundary Pitch-angle Treatments

N. Nishimura, K. Marubashi & M. Tokumaru

Solar Physics volume 295, Article number: 40 (2020)

<https://link.springer.com/content/pdf/10.1007/s11207-020-01607-1.pdf>

<https://doi.org/10.1007/s11207-020-01607-1>

We developed a new fitting method of a toroidal model for the analysis of interplanetary flux ropes (IFRs). The pitch angle of the magnetic field at the IFR boundary [$\alpha_{\text{p}}\alpha_{\text{p}}$] is fixed to $90^\circ 90^\circ$ in the toroidal model of Romashets and Vandas (Geophys. Res. Lett. 30, 2065, 2003) (conventional method). To relax this condition for our method, the pitch angle was made one of the free parameters (generalized method). In this paper, we examine the difference between the results of these two toroidal IFR model fitting methods by applying them to magnetic-obstacle (MO) events observed by the Wind and Solar Terrestrial Relations Observatory (STEREO) spacecraft. We found that the generalized method gives an $\alpha_{\text{p}}\alpha_{\text{p}}$ near $90^\circ 90^\circ$ (within the range of $90^\circ \pm 30^\circ 90^\circ \pm 30^\circ$) for approximately 60% of events. Thus, the assumption in the conventional method that $\alpha_{\text{p}}\alpha_{\text{p}}$ is $90^\circ 90^\circ$ is valid for many cases. This also implies that many flanks of IFR have a magnetic field line nearly perpendicular to the IFR axis. We also found that the generalized method gives a similar normal direction of the torus plane and poloidal magnetic flux as the conventional method. However, the generalized method gives a toroidal magnetic flux that is significantly different from that given by the conventional method for a non-negligible number of events. Thus, we concluded that it is better to use the generalized method than the conventional method in order to get more accurate estimation of the toroidal magnetic flux of IFRs.

Comparison of Cylindrical Interplanetary Flux-Rope Model Fitting with Different Boundary Pitch-Angle Treatments

N. Nishimura, K. Marubashi, M. Tokumaru

Solar Physics April 2019, 294:49

<https://link.springer.com/content/pdf/10.1007%2Fs11207-019-1435-5.pdf>

Interplanetary flux ropes (IFRs) observed in the solar wind have been investigated through application of the Lundquist model, which is a cylindrical flux-rope model with a constant- α force-free magnetic-field model. This study evaluated two Lundquist-model fitting methods by applying them to magnetic-obstacle (MO) events observed by the Wind and Solar TERrestrial RELations Observatory (STEREO) spacecraft and by comparing the results. In one method, the pitch angle of the magnetic field at the IFR boundary is assumed to be $90^\circ 90^\circ$, whereas in the other method this restriction is relaxed and the pitch angle is handled as a free parameter [$\alpha_{\text{p}}\alpha_{\text{p}}$]. We found that the angle between the axial and radial directions in radial tangential normal (RTN) coordinates (cone angle) and the magnetic flux of the IFR were significantly different for approximately 30% of these events. However, both methods yielded similar values for the direction of the IFR axis projected onto the T-N plane in the RTN coordinates (tilt angle). We also found that the statistical distribution of $\alpha_{\text{p}}\alpha_{\text{p}}$, which was estimated using the generalized method, shows a spread of $34^\circ 34^\circ$ centered at $82^\circ 82^\circ$, implying that a highly twisted magnetic-field line surrounds the surface of the IFR for approximately 60% of the events. On the other hand, it was noted that a significant number of events (approximately 25%) have a small $\alpha_{\text{p}}\alpha_{\text{p}}$ ($< 60^\circ < 60^\circ$). These results prove that it is better to use the generalized method than the conventional method

for solving the cone angle, magnetic flux, or pitch angle of the flux rope, which would lead to a more accurate derivation of the properties of IFRs. 6-7 Jun 2008, 16-17 Jan 2011, 20-21 June 2013

Table 1995-2016

Simulating White-Light Images of Coronal Structures for Parker Solar Probe/WISPR: Study of the Total Brightness Profiles

Giuseppe [Nisticò](#), [Volker Bothmer](#), [Angelos Vourlidas](#), [Paulett C. Liewer](#), [Arnaud F. Thernisien](#), [Guillermo Stenborg](#) & [Russell A. Howard](#)

[Solar Physics](#) volume 295, Article number: 63 (2020)

<https://link.springer.com/content/pdf/10.1007/s11207-020-01626-y.pdf>

The Wide-field Imager for Parker Solar Probe (WISPR) captures unprecedented white-light images of the solar corona and inner heliosphere. Thanks to the uniqueness of the Parker Solar Probe's (PSP) orbit, WISPR is able to image "locally" coronal structures at high spatial and time resolutions. The observed plane of sky, however, rapidly changes because of the PSP's high orbital speed. Therefore, the interpretation of the dynamics of the coronal structures recorded by WISPR is not straightforward. A first study, undertaken by Liewer et al. (*Solar Phys.* 294, 93, [2019](#)), shows how different coronal features (e.g., streamers, flux ropes) appear in the field-of-view of WISPR by means of raytracing simulations. In particular, they analyze the effects of the spatial resolution changes on both the images and the associated height-time maps, and introduce the fundamentals for geometric triangulation. In this follow-up paper, we focus on the study of the total brightness of a simple, spherical, plasma density structure, to understand how the analysis of Thomson-scattered emission by the electrons in a coronal feature can shed light into the determination of its kinematic properties. We investigate two cases: (i) a density sphere at a constant distance from the Sun for different heliographic longitudes; (ii) a density sphere moving outwardly with constant speed. The study allows us to characterize the effects of the varying heliocentric distance of the observer and scattering angle on the total brightness observed, which we exploit to contribute to a better determination of the position and speed of the coronal features observed by WISPR.

Understanding the Origins of Problem Geomagnetic Storms Associated With "Stealth" Coronal Mass Ejections Review

Nariaki V. [Nitta](#), [Tamitha Mulligan](#), [Emilia K. J. Kilpua](#), [Benjamin J. Lynch](#), [Marilena Mierla](#), [Jennifer O'Kane](#), [Paolo Pagano](#), [Erika Palmerio](#), [Jens Pomoell](#), [Ian G. Richardson](#), [Luciano Rodriguez](#), [Alexis P. Rouillard](#), [Suvadip Sinha](#), [Nandita Srivastava](#), [Dana-Camelia Talpeanu](#), [Stephanie L. Yardley](#), [Andrei N. Zhukov](#)

Space Science Reviews 217, Article number: 82 2021

<https://link.springer.com/content/pdf/10.1007/s11214-021-00857-0.pdf> File

<https://arxiv.org/pdf/2110.08408.pdf>

<https://doi.org/10.1007/s11214-021-00857-0>

Geomagnetic storms are an important aspect of space weather and can result in significant impacts on space- and ground-based assets. The majority of strong storms are associated with the passage of interplanetary coronal mass ejections (ICMEs) in the near-Earth environment. In many cases, these ICMEs can be traced back unambiguously to a specific coronal mass ejection (CME) and solar activity on the frontside of the Sun. Hence, predicting the arrival of ICMEs at Earth from routine observations of CMEs and solar activity currently makes a major contribution to the forecasting of geomagnetic storms. However, it is clear that some ICMEs, which may also cause enhanced geomagnetic activity, cannot be traced back to an observed CME, or, if the CME is identified, its origin may be elusive or ambiguous in coronal images. Such CMEs have been termed "stealth CMEs." In this review, we focus on these "problem" geomagnetic storms in the sense that the solar/CME precursors are enigmatic and stealthy. We start by reviewing evidence for stealth CMEs discussed in past studies. We then identify several moderate to strong geomagnetic storms (minimum Dst < -50 nT) in solar cycle 24 for which the related solar sources and/or CMEs are unclear and apparently stealthy. We discuss the solar and in situ circumstances of these events and identify several scenarios that may account for their elusive solar signatures. These range from observational limitations (e.g., a coronagraph near Earth may not detect an incoming CME if it is diffuse and not wide enough) to the possibility that there is a class of mass ejections from the Sun that have only weak or hard-to-observe coronal signatures. In particular, some of these sources are only clearly revealed by considering the evolution of coronal structures over longer time intervals than is usually considered. We also review a variety of numerical modelling approaches that attempt to advance our understanding of the origins and consequences of stealthy solar eruptions with geoeffective potential. Specifically, we discuss magnetofrictional modelling of the energisation of stealth CME source regions and magnetohydrodynamic modelling of the physical processes that generate stealth CME or CME-like eruptions, typically from higher altitudes in the solar corona than

CMEs from active regions or extended filament channels. **2 June 2008, 12 July 2012, 2013-11-05-09, 2014-04-06-12, 3-7 January, 2015, 5-11 May 2015, 2016-10-09-13, 2018-08-19-26**

Table 1 List of Selected ICMEs With Dst ≤ -50 nT Geomagnetic Storms (2011-2018)

Table 2 CMEs and Low Coronal Signatures Associated With the Events in Table 1

Earth-Affecting Coronal Mass Ejections Without Obvious Low Coronal Signatures

Nariaki V. [Nitta](#), Tamitha Mulligan

[Solar Physics](#) September **2017**, 292:125 **File**

We present a study of the origin of coronal mass ejections (CMEs) that were not accompanied by obvious low coronal signatures (LCSs) and yet were responsible for appreciable disturbances at 1 AU. These CMEs characteristically start slowly. In several examples, extreme ultraviolet (EUV) images taken by the Atmospheric Imaging Assembly onboard the Solar Dynamics Observatory reveal coronal dimming and a post-eruption arcade when we make difference images with long enough temporal separations, which are commensurate with the slow initial development of the CME. Data from the EUV imager and COR coronagraphs of the Sun Earth Connection Coronal and Heliospheric Investigation onboard the Solar Terrestrial Relations Observatory, which provide limb views of Earth-bound CMEs, greatly help us limit the time interval in which the CME forms and undergoes initial acceleration. For other CMEs, we find similar dimming, although only with lower confidence as to its link to the CME. It is noted that even these unclear events result in unambiguous flux rope signatures in in situ data at 1 AU. There is a tendency that the CME source regions are located near coronal holes or open field regions. This may have implications for both the initiation of the stealthy CME in the corona and its outcome in the heliosphere. **16-20 June 2010, 23-28 Dec 2010, 19-24 Jan 2011, 30 Jan-4 Feb 2011, 3-6 March 2011, 25-29 March 2011, 25-28 May 2011, 4-5-8 October 2012, 27-31 May 2013, 2-6 June 2013, 23-27 June 2013, 30 June-5 July 2013, 3-7 Jan 2015, 8-12 Oct 2016**

Table 1 Partial list of stealthy events (solar)

Table 2 Partial list of stealthy events (1 AU)

Geomagnetic storm forecasting from solar coronal holes

Simona [Nitti](#), [Tatiana Podladchikova](#), [Stefan J. Hofmeister](#), [Astrid M. Veronig](#), [Giuliana Verbanac](#), [Mario Bandić](#)

MNRAS Volume 519, Issue 2, February **2023**, Pages 3182–3193,

<https://arxiv.org/pdf/2211.16572.pdf>

<https://doi.org/10.1093/mnras/stac3533>

Coronal holes (CHs) are the source of high-speed streams (HSSs) in the solar wind, whose interaction with the slow solar wind creates corotating interaction regions (CIRs) in the heliosphere. Whenever the CIRs hit the Earth, they can cause geomagnetic storms. We develop a method to predict the strength of CIR/HSS-driven geomagnetic storms directly from solar observations using the CH areas and associated magnetic field polarity. First, we build a dataset comprising the properties of CHs on the Sun, the associated HSSs, CIRs, and orientation of the interplanetary magnetic field (IMF) at L1, and the strength of the associated geomagnetic storms by the geomagnetic indices Dst and Kp. Then, we predict the Dst and Kp indices using a Gaussian Process model, which accounts for the annual variation of the orientation of Earth's magnetic field axis. We demonstrate that the polarity of the IMF at L1 associated with CIRs is preserved in around 83% of cases when compared to the polarity of their CH sources. Testing our model over the period 2010–2020, we obtained a correlation coefficient between the predicted and observed Dst index of $R = 0.63/0.73$, and Kp index of $R = 0.65/0.67$, for HSSs having a polarity towards/away from the Sun. These findings demonstrate the possibility of predicting CIR/HSS-driven geomagnetic storms directly from solar observations and extending the forecasting lead time up to several days, which is relevant for enhancing space weather predictions. **2017 June 13**

Correction: Volume 520, Issue 1, March 2023, Page 612, <https://doi.org/10.1093/mnras/stad292>

Energetic seed particles in self-consistent particle acceleration modeling at interplanetary shock waves

S. [Nyberg](#)^{1,*}, L. Vuorinen¹, A. Afanasiev¹, D. Trotta² and R. Vainio¹

A&A 690, A287 (**2024**)

<https://www.aanda.org/articles/aa/pdf/2024/10/aa51279-24.pdf>

Aims. The study investigates the relevance of the seed particle population in the results of particle acceleration in interplanetary shock waves, when wave–particle interactions are treated self-consistently.

Methods. We employed the SOLar Particle Acceleration in Coronal Shocks (SOLPACS) model, which is a proton acceleration simulation in shocks with self-consistent nonlinear wave–particle interactions. We compared a suprathermal monoenergetic injection with a two-component injection, including the suprathermal monoenergetic component and a broad-spectrum energetic component corresponding to the observed background particle spectrum. Energetic particles in

the beginning of the simulation could increase the local wave intensities sufficiently to increase the rate of acceleration for injected particles and even reshape the resulting particle energy spectra and spatial distributions. The resulting particle energy spectra, particle spatial distributions, and wave intensity spectra are compared to observations made by Solar Orbiter's instrument suite of the **2021 October 30** energetic storm particle (ESP) event to evaluate the relevance of the seed particle population in the acceleration model.

Results. The energetic component of the seed particle population shortens the needed acceleration time for particles and enhances the tail of the spectrum to a level that matches the observations. The highest compared energies (> 1 MeV) match only when an energetic component is included in the seed particle population. The wave intensities and spatial distributions, on the other hand, showed no significant differences with the monoenergetic and two-component injection. While the simulated and observed wave intensities match within five minutes before the shock passing, the simulated wave field is too intense farther out from the shock, probably due to a lack of wave damping and/or decay processes in the simulation, leading to particles being slightly overtrapped to regions closer to the shock.

Prediction of shock arrival times from CME and flare data

Marlon **Núñez**, Teresa Nieves-Chinchilla, Antti Pulkkinen

Space Weather Volume 14, Issue 8 August 2016 Pages 544–562

<https://agupubs.onlinelibrary.wiley.com/doi/pdf/10.1002/2016SW001361>

This paper presents the Shock Arrival Model (SARM) for predicting shock arrival times for distances from 0.72 AU to 8.7 AU by using coronal mass ejections (CME) and flare data. SARM is an aerodynamic drag model described by a differential equation that has been calibrated with a data set of 120 shocks observed from 1997 to 2010 by minimizing the mean absolute error (MAE), normalized to 1 AU. SARM should be used with CME data (radial, earthward, or plane-of-sky speeds) and flare data (peak flux, duration, and location). In the case of 1 AU, the MAE and the median of absolute errors were 7.0 h and 5.0 h, respectively, using the available CME/flare data. The best results for 1 AU (an MAE of 5.8 h) were obtained using both CME data, either radial or cone model-estimated speeds, and flare data. For the prediction of shock arrivals at distances from 0.72 AU to 8.7 AU, the normalized MAE and the median were 7.1 h and 5.1 h, respectively, using the available CME/flare data. SARM was also calibrated to be used with CME data alone or flare data alone, obtaining normalized MAE errors of 8.9 h and 8.6 h, respectively, for all shock events. The model verification was carried out with an additional data set of 20 shocks observed from 2010 to 2012 with radial CME speeds to compare SARM with the empirical ESA model and the numerical MHD-based ENLIL model. The results show that the ENLIL's MAE was lower than the SARM's MAE, which was lower than the ESA's MAE. The SARM's best results were obtained when both flare and true CME speeds were used.

Can Smartphones Detect Geomagnetic Storms?

S. F. **Odenwald**

Space Weather e2020SW002669 2021

<https://agupubs.onlinelibrary.wiley.com/doi/epdf/10.1029/2020SW002669>

Several smartphone models on the Android and iOS platforms have been investigated for their ability to detect geomagnetic storms. Although this capability could have scientific application, there is a growing commercial interest in using smartphones for precision location applications not involving the GPS system. Under these circumstances, geomagnetic storms could in principle interfere with navigation accuracy. The ability of smartphones to detect geomagnetic disturbances has been tested by developing synthetic magnetometer data for two historical storm events: **October 29, 2003** (G5) and **July 15, 2012** (G2). These were created by combining typical sensor noise profiles with actual magnetic observatory data, and also by using a Helmholtz coil to calibrate the magnetometer responsivity near 1 microTesla. A comparison of the iPhone 6S, Samsung Note 5, Galaxy S8 and S9 responses based upon their actual ambient noise measurements reveals that for the high and mid-latitude simulations, storms stronger than G2 (Kp=6) provided indications of detectability, with the strongest detections occurring for the high-latitude simulations. The low-latitude simulated observations near North American latitudes of +38° tended to register storm events at about G4 (Kp=8) or above. The degree to which geomagnetic storms interfere with precision position measurement applications can be significant at high latitudes for the occasional strong storm events during the peak of the sunspot cycle, but are probably not a significant source of error at other times for most low-latitude conditions.

Heliospheric 3-D MHD ENLIL simulations of multi-CME and multi-spacecraft events

Dusan **Odstreil**

<https://www.frontiersin.org/articles/10.3389/fspas.2023.1226992/pdf>

Front. Astron. Space Sci. 10: 1226992. 2023

doi: 10.3389/fspas.2023.1226992

<https://www.frontiersin.org/articles/10.3389/fspas.2023.1226992/pdf>

Interpreting multi-spacecraft heliospheric observations of the evolving solar wind (SW) streams with propagating and interacting coronal mass ejections (CMEs) is challenging. Numerical simulations can provide global context and suggest what may and may not be observed. The heliospheric three-dimensional (3D) magnetohydrodynamic (MHD) ENLIL model can provide a near-real-time prediction of heliospheric space weather, and it is used at NASA Community Coordinated Modeling Center (CCMC), NOAA Space Weather Prediction Center (SWPC), and UK Meteorological Office (MetOffice). However, this version does not show its full potential, especially in the case of multi-CME events observed by various spacecraft. We describe tools developed to interpret remote observations and in-situ measurements better and apply them to multi-CME events observed by ACE, STEREO-A, Parker Solar Probe (PSP), BepiColombo, and Solar Orbiter. We present some results on 1) global structures of the SW speed and density at the ecliptic, 2) the evolution of SW parameters at the spacecraft, 3) magnetic field connectivity at the spacecraft, 4) automatic detection of shock parameters and alert plots, and 5) synthetic white-light (WL) imaging. This paper is not on model initialization or analyzing specific CME events, but it describes features not used at space weather prediction centers and provided by NASA/CCMC Run-On-Request service. This paper advertises new tools and shows their benefits when applied to selected heliospheric space weather events observed at near-Earth, PSP, Solar Orbiter, and STEREO-A spacecraft. **1-31 Dec 2014, 2021-04-17-22, 28 Mar-3 Apr 2022, 14-18 Aug 2022**

Numerical Heliospheric Simulations as Assisting Tool for Interpretation of Observations by STEREO Heliospheric Imagers

Dusan **Odstrcil** · Victor J. Pizzo

Solar Phys (2009) 259: 297–309, **File**

The interpretation of multi-spacecraft heliospheric observations and three-dimensional reconstruction of structured and evolving solar wind is challenging. This is especially true for the interpretation of white-light structures observed by the Heliospheric Imagers (HI) onboard STEREO spacecraft since their appearance depends on three-dimensional geometric factors. Numerical simulations can provide global context and suggest what may and may not be observed. We use the heliospheric code ENLIL to simulate various scenarios of well-defined corotating solar wind streams and ejected transient density structures, and we generate from the solutions synthetic white-light images at various locations. We illustrate that corotating interaction regions (CIRs) show up differently in HI-2A and HI-2B and that they may appear as transient structures in HI-2A but not in HI-2B. This asymmetry is caused by differing Thomson scattering responses. Further, we illustrate that a given interplanetary coronal mass ejection (ICME) may exhibit drastically different white-light brightness depending on the observing position and that some ICMEs can eventually reach Earth without being detected by the imagers. Finally, we demonstrate application of the modeling system through simulation of the **24 – 25 January 2007, 31 December 2007 and 26 April 2008 CMEs.**

Propagation of the **12 May 1997** interplanetary coronal mass ejection in evolving solar wind structures,

Odstrcil, D., Pizzo, V.J., Arge, C.N.

(2005), J. Geophys. Res., 110, 2004JA010745.

Nonlinear Evolution of Ion Kinetic Instabilities in the Solar Wind

Leon **Ofman**

Solar Phys. 294:51 **2019**

[sci-hub.se/10.1007/s11207-019-1440-8](https://doi.org/10.1007/s11207-019-1440-8)

In-situ observations of the solar wind (SW) plasma from 0.29 to 1AU show that the protons and α particles are often non-Maxwellian, with evidence of kinetic instabilities, temperature anisotropies, differential ion streaming, and associated magnetic fluctuations spectra. The kinetic instabilities in the SW multi-ion plasma can lead to preferential heating of α particles and the dissipation of magnetic fluctuation energy, affecting the kinetic and global properties of the SW. Using for the first time a three-dimensional hybrid model, where ions are modeled as particle using the Particle-In-Cell (PIC) method and electrons are treated as fluid, we study the onset, nonlinear evolution and dissipation of ion kinetic instabilities. The Alfvén/ion-cyclotron, and the ion drift instabilities are modeled in the region close to the Sun

(~ 10Rs). Solar wind expansion is incorporated in the model. The model produces self-consistent non-Maxwellian velocity distribution functions (VDFs) of unstable ion populations, the associated temperature anisotropies, and wave spectra for several typical SW instability cases in the nonlinear growth and saturation stage of the instabilities. The 3D hybrid modeling of the multi-ion SW plasma could be used to study the SW acceleration region close to the Sun that will be explored by the Parker Solar Probe mission.

Solar polar magnetic field dependency of geomagnetic activity semiannual variation indicated in the Aa index

Suyeon **Oh**, YuYi

[Advances in Space Research](#) Volume 61, Issue 1, 1 January 2018, Pages 530-539

https://ac.els-cdn.com/S0273117717306415/1-s2.0-S0273117717306415-main.pdf?_tid=2b77af76-de42-11e7-8448-00000aab0f26&acdnat=1512976324_9b95fc7d592cd9a94cb855bbef4b60bb

Three major hypotheses have been proposed to explain the well-known semiannual variation of geomagnetic activity, maxima at equinoxes and minima at solstices. This study examined whether the seasonal variation of equinoctial geomagnetic activity is different in periods of opposite solar magnetic polarity in order to understand the contribution of the interplanetary magnetic field (IMF) in the Sun-Earth connection. Solar magnetic polarity is parallel to the Earth's polarity in solar minimum years of odd/even cycles but antiparallel in solar minimum years of even/odd cycles. The daily mean of the aa, Aa indices during each solar minimum was compared for periods when the solar magnetic polarity remained in opposite dipole conditions. The Aa index values were used for each of the three years surrounding the solar minimum years of the 14 solar cycles recorded since 1856. The Aa index reflects seasonal variation in geomagnetic activity, which is greater at the equinoxes than at the solstices. The Aa index reveals solar magnetic polarity dependency in which the geomagnetic activity is stronger in the antiparallel solar magnetic polarity condition than in the parallel one. The periodicity in semiannual variation of the Aa index is stronger in the antiparallel solar polar magnetic field period than in the parallel period. Additionally, we suggest the favorable IMF condition of the semiannual variation in geomagnetic activity. The orientation of IMF toward the Sun in spring and away from the Sun in fall mainly contributes to the semiannual variation of geomagnetic activity in both antiparallel and parallel solar minimum years.

A Simultaneous Forbush Decrease Associated with an Earthward Coronal Mass Ejection Observed by STEREO

S. Y. **Oh** and Y. Yi

Solar Physics, 2012, DOI: 10.1007/s11207-012-0053-2, **File**, Volume 280, Number 1, Pages 197-20

The intensity–time profile of Forbush decrease (FD) events observed by neutron monitors (NMs) looks like that of a geomagnetic storm as defined by the Dst index. Oh, Yi, and Kim (*J. Geophys. Res.* 113, A01103, 2008) and Oh and Yi (*J. Geophys. Res.* 114, A11102, 2009) classified FD events based on the amount of overlap and simultaneity of their main phase in Universal Time (UT). Oh and Yi define an FD event as simultaneous if the main phases observed by NMs distributed evenly around the Earth overlap in UT, and nonsimultaneous if they overlap only in the local time of some stations. They suggested that the occurrence mechanisms of two types of FD events may be related to interplanetary (IP) magnetic structures such as IP shocks and magnetic clouds. In their model, the simultaneity of FD events depends on the strength and propagation direction of magnetic structures overtaking the Earth. Recently, the Solar Terrestrial Relations Observatory (STEREO) mission has been able to visualize the emergence and propagation direction of coronal mass ejections (CMEs) in three dimensions in the heliosphere; thus, it is now possible to test the suggested mechanisms. One simultaneous FD event observed on **18 February 2011** may have been caused by a CME heading directly toward the Earth, which was observed on **15 February 2011** by the STEREO mission. Therefore, the simultaneity of FD events is proven to be a useful analysis tool in understanding the geoeffectiveness of solar events such as interplanetary CMEs and IP shocks.

Solar magnetic polarity dependency of geomagnetic storm seasonal occurrence

Oh, S. Y.; Yi, Y.

J. Geophys. Res., Vol. 116, No. A6, A06101, 2011

For nearly a century it has been known that the tendency for geomagnetic activity is, on average, higher at the equinoxes than at the solstices. Previous studies on semiannual geomagnetic activity were performed mainly for geomagnetic indices such as am, aa, U, and AL. Thus, we need to understand the seasonal variation of geomagnetic activity defined by the Dst index over the long term. It is also necessary to test the solar magnetic polarity dependence of geomagnetic activity. This paper is a statistical analysis of the geomagnetic storms defined by the Dst index. Our storm data consists of two sets of storm data for 5 years at each solar minimum during the four solar cycles (19–22) from 1962 through 1998 for two of each solar magnetic polarity. The storms are divided into two groups defined by Dst index ($Dst(\min) < -50$

nT, $|Dst| > 70$ nT; $Dst(\min) < -50$ nT, $|Dst| > 90$ nT). Monthly occurrences of these storms are compared. Storms of $|Dst| > 90$ nT and of $|Dst| > 70$ nT occurred 153 and 238 times, respectively, during the testing periods. Storms occurred more frequently during the spring and fall seasons for all solar cycle minima, regardless of solar magnetic polarity.

Characterization of the Complex Ejecta Measured In Situ on 19 – 22 March 2001 by Six Different Methods

Arian [Ojeda-González](#), Virginia Klausner, Odim Mendes, Margarete Oliveira Domingues, Alan Prestes [Solar Physics](#) November 2017, 292:160

This article proposes some traditional and newly developed methods to evaluate the properties of the magnetic cloud (MC) observed on 19 – 22 March 2001. We used physical and mathematical approaches to analyze the time series of solar wind plasma and interplanetary magnetic field data. Two methods that are commonly used to derive the MC properties, the minimum variance analysis and the Grad–Shafranov reconstruction, were applied to derive the properties of the MCs by fitting in situ measurements in the corresponding time intervals, as discussed in previous studies. Other methods developed by us (a travel time analysis of the interplanetary coronal mass ejection, spatio-temporal entropy, nonlinear fluctuation analysis, and wavelet analysis) are used as auxiliary tools to help identify whether the event consists of one or possibly two MCs. Our results suggest that the 19 – 22 March 2001 event was composed by two MCs. Our results agree with those of other researchers who used various fitting methods and identified the solar origin of this event as two CMEs.

An Alternative Method for Identifying Interplanetary Magnetic Cloud Regions

A. [Ojeda-Gonzalez](#)^{1,5,6}, O. Mendes², A. Calzadilla³, M. O. Domingues⁴, A. Prestes¹, and V. Klausner 2017 ApJ 837 156

Spatio-temporal entropy (STE) analysis is used as an alternative mathematical tool to identify possible magnetic cloud (MC) candidates. We analyze Interplanetary Magnetic Field (IMF) data using a time interval of only 10 days. We select a convenient data interval of 2500 records moving forward by 200 record steps until the end of the time series. For every data segment, the STE is calculated at each step. During an MC event, the STE reaches values close to zero. This extremely low value of STE is due to MC structure features. However, not all of the magnetic components in MCs have STE values close to zero at the same time. For this reason, we create a standardization index (the so-called Interplanetary Entropy, IE, index). This index is a worthwhile effort to develop new tools to help diagnose ICME structures. The IE was calculated using a time window of one year (1999), and it has a success rate of 70% over other identifiers of MCs. The unsuccessful cases (30%) are caused by small and weak MCs. The results show that the IE methodology identified 9 of 13 MCs, and emitted nine false alarm cases. In 1999, a total of 788 windows of 2500 values existed, meaning that the percentage of false alarms was 1.14%, which can be considered a good result. In addition, four time windows, each of 10 days, are studied, where the IE method was effective in finding MC candidates. As a novel result, two new MCs are identified in these time windows.

Spatio-temporal entropy analysis of the magnetic field to help magnetic cloud characterization†

G. A. [Ojeda](#)^{1,2,*}, O. Mendes, ¹, M. A. Calzadilla², M. O. Domingues *JGR*, Volume 118, Issue 9, pages 5403–5414, 2013

<http://onlinelibrary.wiley.com/doi/10.1002/jgra.50504/pdf>

The aim of this work is to create a methodology to characterize the dynamics of magnetic clouds (MCs) from signals measured by satellites in the interplanetary medium. We have tested Spatio-Temporal Entropy (STE) technique to study 41 MCs identified by other authors, where the plasma sheath region has been identified. The STE was implemented in Visual Recurrence Analysis (VRA) software to quantify the order in the recurrence plot. Some tests using synthetic time series were performed to validate the method. In particular, we worked with IMF components Bx, By, Bz of 16 s. Time windows from March 1998 to December 2003 for some MCs were selected. We found higher STE values in the sheaths and zero STE values in some of the three components in most of the MCs (30 among 41 events). The trend is the principal cause of the lower STE values in the MCs. Also, MCs have magnetic field more structured than sheath and quiet solar wind. We have done a test considering the magnetic components of a cylindrically symmetric force-free constructed analytically, with the result of zero STE value. It agrees with the physical assumption of finding zero STE values when studying experimental data in MC periods. The new feature just examined here adds to the usual features, as described in Burlaga et al. (1981), for the characterization of MCs. The STE calculation can be an auxiliary objective tool to identify flux-ropes associated with MCs, mainly during events with no available plasma data but only with IMF.

Table

Amplitude of the Observational Forbush Decreases in the Presence of Cosmic Ray Diurnal Anisotropy During High Solar Activity in 1972

O. Okike & J. A. Alhassan

Solar Physics volume 296, Article number: 112 (2021)

<https://link.springer.com/content/pdf/10.1007/s11207-021-01855-9.pdf>

<https://doi.org/10.1007/s11207-021-01855-9>

The short-term rapid depressions in cosmic-ray (CR) flux intensity, historically referred to as Forbush decreases (FDs), are useful tools for testing some of the numerous hypotheses on space weather. Due to their long-term reliability and automated data acquisition, ground-based CR measurements by neutron monitors (NMs) provide the best direct means of comparing CR intensity variations during FDs with solar-wind disturbances in the vicinity of the Earth.

Unfortunately, there is a mixture of high-magnitude FDs and CR diurnal anisotropies of enhanced amplitude during periods of high solar activity. The difficulties of isolating FDs from the superposed effects of diurnal anisotropies cast some doubt on the usefulness of FDs in space-weather studies. Using numerical filtering techniques over two isolated NMs' data (Apatity and Mount Washington) during high solar activity in 1972, we attempt to show that the slowly varying component of CR flux containing the CR anisotropies may be separated from the high-frequency part that contains the FDs. Subsequently, the rapidly varying component is passed to an FD location algorithm for accurate event timing as well as precise quantitative predictions, where the day-to-day amplitudes of the CR diurnal anisotropies are estimated from the slowly varying frequency component of the raw CR data. For effective comparison of event amplitudes and timing, the magnitudes of FDs from raw CR data are also estimated using an FD selection technique. **6 June 1972 and 10 June 1972, 4 – 5 August 1972, 1 November 1972**

Amplitude of the Usual Cosmic Ray Diurnal and Enhanced Anisotropies: Implications for the Observed Magnitude, Timing, and Ranking of Forbush Decreases

O. Okike¹

2021 ApJ 915 60

<https://doi.org/10.3847/1538-4357/abfe60>

Cosmic ray (CR) diurnal anisotropy and Forbush decreases (FDs), as well as the relationship between them, have received considerable study. Several astrophysicists have focused on the speculated impact of FDs on the amplitude of the diurnal CR variations on different timescales. In an attempt to disentangle the contribution of FDs, days of Forbush events are traditionally excluded while calculating the diurnal amplitude in individual neutron monitor (NM) data. But the implications of CR diurnal anisotropy on the magnitude of FDs are rarely investigated in detail. Recently, an effort was made, using a combination of Fast Fourier transform and FD-location algorithms, to account for the contribution of CR diurnal anisotropy on the number, magnitude, and timing of FDs. With some technical advancements, the efficiency of the software is tested in the current work using CR data measured by the oldest CR observatory (Climax) from 1953 to 2006. We find strong and statistically significant correlations between FD magnitude calculated from raw and Fourier transformed CR data and the amplitude of diurnal anisotropy. The relationship is stronger in the case of the Fourier transformed signal, lending credence to the idea that CR anisotropy is a part of Forbush events. In order to validate the observed relationship between the amplitude of CR diurnal variations, magnitude, and timing of FDs, large volumes of data from the Moscow, McMurdo, and Potchefstroom NMs were also analyzed. The significant CR intensity decreases (FD magnitude >5%) at the four stations were ranked according to their magnitudes.

A comparison of catalogues of Forbush decreases identified from individual and a network of neutron monitors: a critical perspective

O Okike, J A Alhassan, E U Iyida, A E Chukwude

Monthly Notices of the Royal Astronomical Society, Volume 503, Issue 4, June 2021, Pages 5675–5691,

<https://doi.org/10.1093/mnras/stab680>

Short-term rapid depressions in Galactic cosmic ray (GCR) flux, historically referred to as Forbush decreases (FDs), have long been recognized as important events in the observation of cosmic ray (CR) activity. Although theories and empirical results on the causes, characteristics, and varieties of FDs have been well established, detection of FDs, from either isolated detectors' or arrays of neutron monitor data, remains a subject of interest. Efforts to create large catalogues of FDs began in the 1990s and have continued to the present. In an attempt to test some of the proposed CR theories, several analyses have been conducted based on the available lists. Nevertheless, the results obtained depend on the FD catalogues used. This suggests a need for an examination of consistency between FD catalogues. This is the aim of the present study. Some existing lists of FDs, as well as FD catalogues developed in the current work, were compared,

with an emphasis on the FD catalogues selected by the global survey method (GSM). The Forbush effects and interplanetary disturbances database (FEID), created by the Pushkov Institute of Terrestrial Magnetism, Ionosphere and Radiowave Propagation Russian Academy of Sciences (IZMIRAN), is the only available comprehensive and up to date FD catalogue. While there are significant disparities between the IZMIRAN FD and other event lists, there is a beautiful agreement between FDs identified in the current work and those in the FEID. This may be a pointer to the efficiency of the GSM and the automated approach to FD event detection presented here.

Testing the impact of coronal mass ejections on cosmic-ray intensity modulation with algorithm selected Forbush decreases

Okike, O.; [Nwuzor, O. C.;](#) [Odo, F. C.;](#) [Iyida, E. U.;](#) [Ekpe, J. E.;](#) [Chukwude, A. E.](#)

Monthly Notices of the Royal Astronomical Society, Volume 502, Issue 1, pp.300-312, **2021**

DOI: [10.1093/mnras/staa4002](https://doi.org/10.1093/mnras/staa4002)

The relationship between coronal mass ejections (CMEs) and Forbush decreases (FDs) has been investigated in the past. But the selection of both solar events are difficult. Researchers have developed manual and automated methods in efforts to identify CMEs as well as FDs. While scientists investigating CMEs have made significant advancement, leading to several CME catalogues, including manual and automated events catalogues, those analyzing FDs have recorded relatively less progress. Till date, there are no comprehensive manual FD catalogues, for example. There are also paucity of automated FD lists. Many investigators, therefore, attempt to manually select FDs which are subsequently used in the analysis of the impact of CMEs on galactic cosmic-ray (GCR) flux depressions. However, some of the CME versus FD correlation results might be biased since manual event identification is usually subjective, unable to account for the presence of solar-diurnal anisotropy which characterizes GCR flux variations. The current paper investigates the relation between CMEs and FDs with emphasis on accurate and careful Forbush event selection.

What determines the observational magnitudes of Forbush events on Earth: A critique of the traditional manual method

O Okike

Mon Not R Astron Soc, Volume 491, Issue 3, January **2020**, Pages 3793–3804,

[sci-hub.se/10.1093/mnras/stz3123](https://doi.org/10.1093/mnras/stz3123)

Forbush decreases (FDs) seem to be the compass for researchers searching for Sun–Earth weather relationships. Thus, a wide range of the solar-terrestrial literature is dominated by FD-based analyses. While the results of such investigations are often questioned on the basis of small FD sample sizes, statistical significance tests and inappropriate methodological approaches, the efficiency and the validity of manual FD event selection are yet to be examined in detail. Because the results obtained depend on the Forbush event location on Earth, and on timing and magnitude estimation, this paper emphasizes the need for the correct acquisition of FD data prior to composition or correlation/regression analyses.

Investigation of the rigidity and sensitivity dependence of neutron monitors for cosmic ray modulation using algorithm-selected Forbush decreases

O Okike, O C Nwuzor

Mon Not R Astron Soc, Volume 493, Issue 2, April **2020**, Pages 1948–1959,

[sci-hub.si/10.1093/mnras/staa370](https://doi.org/10.1093/mnras/staa370)

We emphasize the need for a careful and rigorous timing of Forbush decreases (FDs) as well as a correct calculation of FD magnitudes in studies related to cosmic ray (CR) modulation. We have employed Fourier and *R*-based algorithms for FD event selection, timing and magnitude estimation. The large number of Forbush events that have been identified were employed in correlation and regression analyses to investigate the rigidity and sensitivity dependence of neutron monitors (NMs). It was found that there is a significant difference between the number of FDs identified manually and those selected by the automated method. While the minimum number (238) of FDs occurred at Irkutsk NM, the Novosibirsk CR station observed the largest number (386) of Forbush events. However, within the north high-latitude band ($39^{\circ}\text{N} \leq \text{latitude} \leq 90^{\circ}\text{N}$), only 29 FDs have been simultaneously identified using the data from some NMs in the region, including Irkutsk and Novosibirsk. The result obtained using a large number of FDs differs significantly from those employing manual identification of Forbush events. We conclude, among other things, that the automation of FD event selection is essential for understanding the dependence of CR modulation on NM rigidity and altitude, as well as on the contribution from terrestrial modulation agents.

Investigation of Forbush Decreases and Other Solar/Geophysical Agents Associated With Lightning Over the U.S. Latitude Band and the Continental Africa

O. Okike

JGR [Volume124, Issue6](#) June 2019 Pages 3910-3925

[sci-hub.se/10.1029/2018JA026456](https://doi.org/10.1029/2018JA026456)

Regardless of the numerous significant contributions in the field (e.g., Svensmark, H. & Svensmark, J., 2009, <https://doi.org/10.1029/2009GL038429>; Svensmark, J., et al, 2012, <https://doi.org/10.5194/acpd-12-3595-2012>), the impact of cosmic rays on Earth's weather is still a source of misunderstanding among scientists. Chree method of analysis (Chree, 1912, <https://doi.org/10.1098/rsta.1913.0003>) is one of the commonest tool used in the investigation. But the method has been queried by some publications. Greater number of these critiques (Forbush et al., 1983, <https://doi.org/10.1007/BF00145551>; Prager & Hoenig, 1989, [https://doi.org/10.1577/1548-8659\(1989\)118<0608:SEAART>2.3.CO;2](https://doi.org/10.1577/1548-8659(1989)118<0608:SEAART>2.3.CO;2)) (Forbush et al., 1983; Prager & Hoenig, 1989) point to the test of significance of epoch superposition results. Forbush events are the most widely key event time used in solar Earth's weather investigation. Despite the early indications of Marcz (1997, [https://doi.org/10.1016/S1364-6826\(96\)00076-4](https://doi.org/10.1016/S1364-6826(96)00076-4)) that the result of compositing analysis depends on the Forbush event selection criteria and timing, various conflicting methods of event selection still dominate articles documenting Forbush decrease (FD)-related correlations. The present submission calls the attention of researchers to the need for a systematic FD event identification with respect to timing and magnitude estimation prior to compositing/correlation/regression analyses. The relationship between program-selected FDs, World Wide Lightning Location Network (WWLLN) data, and solar/geophysical parameters is tested at different regions of the world. Significant correlations between WWLLN and other parameters were observed at the U.S. latitude band and within the African region.

The Empirical Implication of Conducting a Chree Analysis Using Data from Isolated Neutron Monitors

O. Okike, A. E. Umahi

[Solar Physics](#) January 2019, 294:16

[sci-hub.tw/10.1007/s11207-019-1405-y](https://doi.org/10.1007/s11207-019-1405-y)

The analysis method developed by Chree has received several critical reviews since its introduction in geophysical studies (Chree in Philos. Trans. Roy. Soc. London, Ser. A, Contain. Pap. Math. Phys. Character 212, 75, 1912). Several of these critiques, such as those by Forbush et al. (Solar Phys. 82, 113, 1983), point to the test of significance of epoch superposition results. Forbush events are a key event time used in space weather investigations. Despite the early indications of Marz (J. Atmos. Solar-Terr. Phys. 59, 957, 1997) that the result of a compositing analysis depends on the method of Forbush decrease (FD) date selection, the various conflicting methods of key event date selection appearing in the publications that document an FD-based epoch analysis are yet to be cross-examined in detail. This is the goal of the present submission.

Table 3 Date of FD events seen by NMs that are close in longitude in 2005.

A multivariate study of Forbush decrease simultaneity

O. Okike and A.B. Colliera

Journal of Atmospheric and Solar-Terrestrial Physics

Volume 73, Issues 7-8, May 2011, Pages 796-804

The distribution of the cosmic ray flux over the Earth is not uniform, but the result of complex phenomena within the Sun–Earth environment. A Forbush decrease (Fd) is a rapid decrease in the intensity of cosmic rays. A given Fd can appear in different forms at different locations of the Earth. An investigation of simultaneous observations of Fd events by a selection of cosmic ray stations remains a subject of interest among researchers and numerous methods of analysis can be found in literature. Although these studies have contributed significantly to our knowledge, the variability in the manifestations of Fds demonstrates that there are still open questions in this field. The present work suggests that multivariate analysis is a simple method that can be used to discriminate between globally simultaneous and non-simultaneous Fds.

Predicting Interplanetary Shock Occurrence for Solar Cycle 25: Opportunities and Challenges in Space Weather Research

Denny M. Oliveira, Robert C. Allen, Livia R. Alves, Séan P. Blake, Brett A. Carter, Dibyendu Chakrabarty, Giulia D'Angelo, Kevin Delano, Ezequiel Echer ... [See all authors](#)

Space Weather [Volume22, Issue8](#) August 2024 e2024SW003964

<https://agupubs.onlinelibrary.wiley.com/doi/epdf/10.1029/2024SW003964>

Interplanetary (IP) shocks are perturbations observed in the solar wind. IP shocks correlate well with solar activity, being more numerous during times of high sunspot numbers. Earth-bound IP shocks cause many space weather effects that are promptly observed in geospace and on the ground. Such effects can pose considerable threats to human assets in space and on the ground, including satellites in the upper atmosphere and power infrastructure. Thus, it is of great interest to the space weather community to (a) keep an accurate catalog of shocks observed near Earth, and (b) be able to forecast shock occurrence as a function of the solar cycle (SC). In this work, we use a supervised machine learning regression model to predict the number of shocks expected in SC25 using three previously published sunspot predictions for the same cycle. We predict shock counts to be around 275 ± 10 , which is $\sim 47\%$ higher than the shock occurrence in SC24 (187 ± 8), but still smaller than the shock occurrence in SC23 (343 ± 12). With the perspective of having more IP shocks on the horizon for SC25, we briefly discuss many opportunities in space weather research for the remainder years of SC25. The next decade or so will bring unprecedented opportunities for research and forecasting effects in the solar wind, magnetosphere, ionosphere, and on the ground. As a result, we predict SC25 will offer excellent opportunities for shock occurrences and data availability for conducting space weather research and forecasting.

Interplanetary shock data base

Denny **Oliveira**

Front. Astron. Space Sci. 10: 1240323 2023

<https://www.frontiersin.org/articles/10.3389/fspas.2023.1240323/pdf>

The main goal of this short report is to release an expanded version of an IP shock data base that was published before ([Oliveira and Raeder, 2015](#); [Oliveira et al., 2018](#)). A major component of this new shock data base is a revision of the methodology used to calculate shock impact angles and speeds with respect to past versions of this list. Additionally, more shock and solar wind parameters before and after shock impacts and geomagnetic activity information were included in the list. 23 June 2000

Geoeffectiveness of Interplanetary Shocks Controlled by Impact Angles: Past Research, Recent Advancements, and Future Work

miniReview

Denny **Oliveira**

Front. Astron. Space Sci. 10: 1179279. doi: 10.3389 2023

<https://www.frontiersin.org/articles/10.3389/fspas.2023.1179279/pdf>

<https://doi.org/10.3389/fspas.2023.1179279>

Interplanetary shocks are disturbances commonly observed in the solar wind. IP shock impacts can cause a myriad of space weather effects in the Earth's magnetopause, inner magnetosphere, ionosphere, thermosphere, and ground magnetic field. The shock impact angle, measured as the angle the shock normal vector performs with the Sun-Earth line, has been shown to be a very important parameter that controls shock geoeffectiveness. An extensive review provided by [Oliveira and Samsonov \(2018\)](#) summarized all the work known at the time with respect to shock impact angles and geomagnetic activity; however, this topic has had some progress since [Oliveira and Samsonov \(2018\)](#) and the main goal of this mini review is to summarize all achievements to date in the topic to the knowledge of the author. Finally, this mini review also brings a few suggestions and ideas for future research in the area of IP shock impact angle geoeffectiveness.

Resolving the Ambiguity of a Magnetic Cloud's Orientation Caused by Minimum Variance Analysis Comparing it with a Force-Free Model

Rosemeire Aparecida Rosa **Oliveira**, [Marcos William da Silva Oliveira](#), [Arian Ojeda-González](#), [Valdir Gil Pillat](#), [Ezequiel Echer](#) & [Teresa Nieves-Chinchilla](#)

Solar Physics volume 296, Article number: 182 (2021)

<https://link.springer.com/content/pdf/10.1007/s11207-021-01921-2.pdf>

<https://doi.org/10.1007/s11207-021-01921-2>

This study aims to incorporate an algebraic and computational method for calculating the angles of the magnetic clouds' (MC) axis from the minimum variance analysis (MVA) and correcting them compared to a simulated model from the linear, force-free approximation. Consequently, it determines the type of flux-rope consistently and automatically. In general, MCs measured in situ at 1 Astronomical Unit (AU) may be approximated to have a cylindrical geometry, and the internal magnetic-field topology is traditionally described by a force-free equilibrium flux-rope model. Based on the BzBz-rotation, the flux-rope configuration can be classified in eight groups. This classification is obtained from the angle of rotation of the magnetic-field vector and inclination of the flux-rope axis (ϕ, θ) in relation to the plane of the Ecliptic. The MVA is applied to interplanetary magnetic-field (IMF) observations to obtain the direction of the cylinder

axis. However, MVA estimates may have an ambiguity of 180° in this direction. This is directly affected by the eigenvector signal since eigenvalues in MVA are always positive. To apply the methodology, a sample of 50 MC events measured by the Advance Composition Explorer (ACE) spacecraft was investigated in the period from 1998 to 2003. 83.72% of the analysed events achieved a satisfactory match between the maximum- and minimum-variance planes (from MVA) with the model (force-free) and (ϕ, θ) angles consistent with the MC geometry. Moreover, automatic classification of the MC or flux-rope tube type related to the MC-axis was consistent for 100% of the events studied. This processing is organized in a computational tool described in this publication. We discuss the results and implications of our analysis of six magnetic cloud events in 2018 during the solar minimum. **21-22 Feb 2000, 29 April 2001, 28 Feb-1 Mar 2002, 9-11 Mar 2018, 13 May 2018, 6-7 Jun 2018, 25-26 Jun 2018, 30 Jun-2 Jul 2018, 10-11 Jul 2018, 25-26 Aug 2018**

Table 11 Correction of the incoherence obtained by the program. (2000-2003)

Table 12 Result of the analysis of the events (2018)

Table 14 Result of the analysis of the events (1998-2003)

Estimating satellite orbital drag during historical magnetic superstorms

Denny M. [Oliveira](#), [Eftyhia Zesta](#), [Hisashi Hayakawa](#), [Ankush Bhaskar](#)

Space Weather **Volume18, Issue11** e2020SW002472 2020

<https://doi.org/10.1029/2020SW002472>

<https://agupubs.onlinelibrary.wiley.com/doi/epdf/10.1029/2020SW002472>

Understanding extreme space weather events is of paramount importance in efforts to protect technological systems in space and on the ground. Particularly in the thermosphere, the subsequent extreme magnetic storms can pose serious threats to low-Earth orbit (LEO) spacecraft by intensifying errors in orbit predictions. Extreme magnetic storms (minimum Dst \leq ---250 nT) are extremely rare: only 7 events occurred during the era of spacecraft with high-level accelerometers such as CHAMP (CHALLENGE Mini-satellite Payload) and GRACE (Gravity Recovery And Climate experiment), and none with minimum Dst \leq --- 500 nT, here termed magnetic superstorms. Therefore, current knowledge of thermospheric mass density response to superstorms is very limited. Thus, in order to advance this knowledge, four known magnetic superstorms in history, i.e., events occurring before CHAMP's and GRACE's commission times, with complete datasets, are used to empirically estimate density enhancements and subsequent orbital drag. The November 2003 magnetic storm (minimum Dst = --- 422 nT), the most extreme event observed by both satellites, is used as the benchmark event. Results show that, as expected, orbital degradation is more severe for the most intense storms. Additionally, results clearly point out that the time duration of the storm is strongly associated with storm-time orbital drag effects, being as important as or even more important than storm intensity itself. The most extreme storm-time decays during CHAMP/GRACE-like sample satellite orbits estimated for the March 1989 magnetic superstorm show that long-lasting superstorms can have highly detrimental consequences for the orbital dynamics of satellites in LEO. **25 Sep 1909, 14-15 May 1921, 30 Oct-1 Nov 2003, 20 Nov 2003, 13 Mar 2009**

New Metric for Minimum Variance Analysis Validation in the Study of Interplanetary Magnetic Clouds

Rosemeire Aparecida Rosa [Oliveira](#), [Marcos William da Silva Oliveira](#), [Arian Ojeda-González](#) & [Victor De La Luz](#)

[Solar Physics](#) volume 295, Article number: 45 (2020)

<https://doi.org/10.1007/s11207-020-01610-6>

The aim of this article is to study the minimum variance analysis (MVA) degeneration problem based on the variance space geometry. We propose a mathematical metric to evaluate the separation of the eigenvalues. In the MVA method, a variance space is obtained geometrically using an ellipsoid where the axes are equal to the square root of the eigenvalues of the covariance matrix. The metric is defined as the product between the geometric flattening of the ellipsoid with respect to the three axes. In this article, we present a statistical analysis applied to the distribution of the eigenvalue ratios and the mathematical metric focussed on the study of several interplanetary coronal mass ejections with and without magnetic clouds (MCs). The results show the non-applicability of the ratio between the intermediate and minimum eigenvalues, as well as that around 90% of MC events have values in the [4.5,19.5] range for the defined metric. Our metric is compared with others and we show its robustness in indicating the usefulness of the MVA method to identify the axes of MCs.

Geoeffectiveness of interplanetary shocks controlled by impact angles: A **review**

D.M. [Oliveira](#), [A.A. Samsonov](#)

[Advances in Space Research](#) **Volume 61, Issue 1**, 1 January 2018, Pages 1-44

https://ac.els-cdn.com/S0273117717307275/1-s2.0-S0273117717307275-main.pdf?_tid=bba606ae-de3f-11e7-b55e-00000aacb35e&acdnat=1512975277_eb1699c52c6f97d7ff8493d1fe7e47bb
<https://sci-hub.se/10.1016/j.asr.2017.10.006>

The high variability of the Sun's magnetic field is responsible for the generation of perturbations that propagate throughout the heliosphere. Such disturbances often drive interplanetary shocks in front of their leading regions. Strong shocks transfer momentum and energy into the solar wind ahead of them which in turn enhance the solar wind interaction with magnetic fields in its way. Shocks then eventually strike the Earth's magnetosphere and trigger a myriad of geomagnetic effects observed not only by spacecraft in space, but also by magnetometers on the ground. Recently, it has been revealed that shocks can show different geoeffectiveness depending closely on the angle of impact. Generally, frontal shocks are more geoeffective than inclined shocks, even if the former are comparatively weaker than the latter. This review is focused on results obtained from modeling and experimental efforts in the last 15 years. Some theoretical and observational background are also provided. **1995-12-15, 1997-11-01, 14 July 2012, 30 January 2017**

Large-scale structure of solar wind and geomagnetic phenomena

M.R. **Olyak**

JASTP, 86, 34-40, **2012**

In this work I propose a method for determining the solar wind parameters at distances from the Sun more than 1 AU. The method is based on formulas for the scintillation indices and spectra for the interplanetary plasma with the large-scale flow structure. According to the results of observations of scintillations performed at the Ukrainian decameter radio telescope UTR-2, I analyzed the structure of the solar wind flows at different periods of the 23–24th solar cycles. The results of the work reveal that the speed of solar wind flows, which cause moderate geomagnetic storms with $A_p \leq 66$, was 590 ± 40 km/s. This is on average lower than that for the quasi-stationary fast solar wind, but higher than that for the slow solar wind. Solar wind disturbances which triggered geomagnetic storms showed a noticeable growth of solar wind velocity within a wider range of helio-latitudes comparing with disturbances which did not trigger geomagnetic storms. These results can be used to improve methods of forecasting magnetic storms on Earth.

Impact angle control of interplanetary shock geoeffectiveness: A statistical study

Denny M. **Oliveira**, Joachim Raeder

JGR Volume 120, Issue 6 June **2015** Pages 4313–4323

We present a survey of interplanetary (IP) shocks using Wind and ACE satellite data from January 1995 to December 2013 to study how IP shock geoeffectiveness is controlled by IP shock impact angles. A shock list covering one and a half solar cycle is compiled. The yearly number of IP shocks is found to correlate well with the monthly sunspot number. We use data from SuperMAG, a large chain with more than 300 geomagnetic stations, to study geoeffectiveness triggered impacts on the Earth's magnetosphere are investigated in terms of IP shock orientation and speed. We find that, in general, strong (high speed) and almost frontal (small impact angle) shocks by IP shocks. The SuperMAG SML index, an enhanced version of the familiar AL index, is used in our statistical analysis. The jumps of the SML index triggered by IP shock are more geoeffective than inclined shocks with low speed. The strongest correlation (correlation coefficient $R = 0.78$) occurs for fixed IP shock speed and for varied IP shock impact angle. We attribute this result, predicted previously with simulations, to the fact that frontal shocks compress the magnetosphere symmetrically from all sides, which is a favorable condition for the release of magnetic energy stored in the magnetotail, which in turn can produce moderate to strong auroral substorms, which are then observed by ground-based magnetometers.

Geomagnetic storms caused by shocks and ICMEs

Ontiveros, Veronica; Gonzalez-Esparza, J. Americo

J. Geophys. Res., Vol. 115, No. A10, A10244, **2010**; **File**

We performed an event-by-event study of 47 geomagnetic storms (GSs) that occurred during the ascending phase of solar cycle 23. All the GSs are associated with the passage of a shock and an interplanetary coronal mass ejection (ICME). For each event, we identified the section in the interplanetary (IP) medium causing the GS (the sheath behind the shock, the main body of the ICME or the combination of both). On average, the most intense GSs are caused by sheaths, followed by sheath-ICME combinations and by ICMEs. We obtained the correlation coefficients between the intensity of each GS (minimum Dst) and several solar wind parameters. We found that the well-known correlation between the GS intensity and the solar wind convected electric field, E_y , stands for the GSs caused by ICMEs ($CC =$

-0.88) and sheath-ICME combinations ($CC = -0.95$), but it is very low for the GSs caused by sheaths ($CC = -0.44$). In contrast, we found a very good correlation between the GSs caused by sheaths and the total convected electric field (ΣE_y) ($CC = -0.89$). On the other hand, we estimated the total perpendicular pressure (P_t) for each IP event associated with the GSs and identified the three different types of P_t profiles. The most intense GSs are related with IP events with $P_t = 1$, but moderate and less intense storms are associated with the three P_t profiles. The correlations between the Dst and the solar wind parameters results that the CCs decrease significantly for IP events having a P_t profile of 3.

INTERVALS OF RADIAL INTERPLANETARY MAGNETIC FIELDS AT 1 AU, THEIR ASSOCIATION WITH RAREFACTION REGIONS, AND THEIR APPARENT MAGNETIC FOOT POINTS AT THE SUN

Steven T. [Orlove](#)¹, Charles W. Smith¹, Bernard J. Vasquez¹, Nathan A. Schwadron¹, Ruth M. Skoug², Thomas H. Zurbuchen³, and Liang Zhao

2013 ApJ 774 15

We have examined 226 intervals of nearly radial interplanetary magnetic field orientations at 1 AU lasting in excess of 6 hr. They are found within rarefaction regions as are the previously reported high-latitude observations. We show that these rarefactions typically do not involve high-speed wind such as that seen by Ulysses at high latitudes during solar minimum. We have examined both the wind speeds and the thermal ion composition before, during and after the rarefaction in an effort to establish the source of the flow that leads to the formation of the rarefaction. We find that the bulk of the measurements, both fast- and slow-wind intervals, possess both wind speeds and thermal ion compositions that suggest they come from typical low-latitude sources that are nominally considered slow-wind sources. In other words, we find relatively little evidence of polar coronal hole sources even when we examine the faster wind ahead of the rarefaction regions. While this is in contrast to high-latitude observations, we argue that this is to be expected of low-latitude observations where polar coronal hole sources are less prevalent. As with the previous high-latitude observations, we contend that the best explanation for these periods of radial magnetic field is interchange reconnection between two sources of different wind speed.

Observational Evidence for a Double-Helix Structure in CMEs and Magnetic Clouds

Vladimir [Osherovich](#), Joseph Fainberg, Alla Webb

Solar Physics, May **2013**, Volume 284, Issue 1, pp 261-274

We compare recent observations of a solar eruptive prominence as seen in extreme-UV light on **30 March 2010** by the Solar Dynamics Observatory (SDO) with the multi-tube model for interplanetary magnetic clouds (Osherovich, Fainberg, Stone, Geophys. Res. Lett. 26, 2597, 1999). Our model is based on an exact analytical solution of the plasma equilibrium with magnetic force balanced by a gradient of scalar gas pressure. Topologically, this solution describes two magnetic helices with opposite magnetic polarity embedded in a cylindrical magnetic flux tube that creates magnetic flux inequality between the two helices by enhancing one helix and suppressing the other. The magnetic field in this model is continuous everywhere and has a finite magnetic energy per unit length of the tube. These configurations have been introduced as MHD bounded states (Osherovich, Soln. Dannye 5, 70, 1975). Apparently, the SDO observations depict two non-equal magnetically interacting helices described by this analytical model. We consider magnetic and thermodynamic signatures of multiple magnetic flux ropes inside the same magnetic cloud, using in situ observations. The ratio of magnetic energy density to bulk speed solar wind energy density has been defined as a solar wind quasi-invariant (QI). We analyze the structure of the QI profile to probe the topology of the internal structure of magnetic clouds. From the superposition of 12 magnetically isolated clouds observed by Ulysses, we have found that the corresponding QI is consistent with our double helix model.

A Geomagnetic Estimate of Heliospheric Modulation Potential over the Last 175 Years.

[Owens](#), M.J., Barnard, L.A., Muscheler, R. *et al.*

Sol Phys **299**, 84 (2024).

<https://doi.org/10.1007/s11207-024-02316-9>

<https://link.springer.com/content/pdf/10.1007/s11207-024-02316-9.pdf>

Galactic cosmic rays (GCRs) interact with the Earth's atmosphere to produce energetic neutrons and cosmogenic radionuclides, such as ^{14}C . The atmosphere is partially shielded from the interstellar GCR spectrum by both the geomagnetic and solar magnetic fields. Solar shielding is often expressed as the heliospheric modulation potential ϕ , which consolidates information about the strength and structure of the solar magnetic field into a single parameter. For

the period 1951 to today, ϕ can be estimated from ground-based neutron monitor data. Prior to 1950, ^{14}C in tree rings can be used to estimate ϕ and hence the solar magnetic field, back centuries or millennia. Bridging the gap in the ϕ record is therefore of vital importance for long-term solar reconstructions. One method is to model ϕ using the sunspot number (SN) record. However, the SN record is only an indirect measure of the Sun's magnetic field, introducing uncertainty, and the record suffers from calibration issues. Here we present a new reconstruction of ϕ based on geomagnetic data, which spans both the entire duration of the neutron monitor record and stretches back to 1845, providing a significant overlap with the ^{14}C data. We first modify and test the existing model of ϕ based on a number of heliospheric parameters, namely the open solar flux FS , the heliospheric current sheet tilt angle α , and the global heliospheric magnetic polarity p . This modified model is applied to recently updated geomagnetic estimates of FS and cyclic variations of α and p . This approach is shown to produce an annual estimate of ϕ in excellent agreement with that obtained from neutron monitors over 1951 – 2023. It also suggests that ionisation chamber estimates of ϕ – which have previously been used to extend the instrumental estimate back from 1951 to 1933 – are not well calibrated. Comparison of the new geomagnetic ϕ with ^{14}C estimates of ϕ suggests that the long-term trend is overestimated in the most recent ^{14}C data, possibly due to hemispheric differences in the Suess effect, related to the release of carbon by the burning of fossil fuels. We suggest that the new geomagnetic estimate of ϕ will provide an improved basis for future calibration of long-term solar activity reconstructions.

Rate of Change of Large-Scale Solar-Wind Structure

Mathew J. Owens, [Nachiketa Chakraborty](#), [Harriet Turner](#), [Matthew Lang](#), [Pete Riley](#), [Mike Lockwood](#), [Luke A. Barnard](#) & [Yutian Chi](#)

[Solar Physics](#) volume 297, Article number: 83 (2022)

<https://link.springer.com/content/pdf/10.1007/s11207-022-02006-4.pdf>

Quantifying the rate at which the large-scale solar-wind structure evolves is important for both understanding the physical processes occurring in the corona and for space-weather forecast improvement. Models of the global corona and heliosphere typically assume that the ambient solar-wind structure is steady and corotates with the Sun, which is generally expected to be more valid at solar minimum than solar maximum, but this has not been well tested. Similarly, assimilation of solar-wind observations into models requires quantitative knowledge of how the reliability of the observations changes with age. In this study we examine 25 years of near-Earth in situ solar-wind observations and 45 years of observation-constrained solar-wind simulations to determine how much the 1-AU solar-wind speed, VV, and radial magnetic-field component, BRBR, vary between consecutive Carrington rotations (CRs). For the in situ spacecraft observations, we find the rate of change of VV and BRBR is similar during solar maximum and minimum, particularly when transient interplanetary coronal mass ejections are removed from the data. This is somewhat counter to expectations. Conversely, the rate of change in VV and BRBR obtained from global heliospheric simulations is strongly correlated with the solar cycle, with the corona and heliosphere being more variable at solar maximum, as expected. Limiting the analysis of the simulations to the solar equatorial region, however, strongly reduces the difference between solar maximum and minimum, bringing the result into close agreement with the in situ observations. This latitudinal sensitivity is explained in terms of the global solar-wind structure over the solar cycle. For the purposes of assimilating in-ecliptic solar-wind observations, we suggest the uncertainty in VV should increase by around 3 km s⁻¹ per day since the observation was made and 0.1 nT per day for BRBR. For observations made at higher latitude, the effect of observation age will be solar-cycle dependent.

Coherence of Coronal Mass Ejections in Near-Earth Space

Mathew J. Owens

[Solar Physics](#) volume 295, Article number: 148 (2020)

<https://link.springer.com/content/pdf/10.1007/s11207-020-01721-0.pdf>

Interplanetary coronal mass ejections (ICMEs) primarily move radially as they propagate away from the Sun, maintaining approximately constant angular width with respect to the Sun. As ICMEs have typical angular widths of around 60°–60°, plasma elements on opposite flanks of an ICME separate in the non-radial direction at a speed, v_{GvG} , roughly equal to the ICME radial speed. This rapid expansion is a limiting factor on the propagation of information across an ICME at the local Alfvén speed, v_{AvA} . In this study, the 1-AU properties of ICMEs are used to compute two measures of ICME coherence. The first is the angular separation for which v_{GvG} exceeds the local v_{AvA} . The second measure is the angular extent over which a wavefront can propagate as an ICME travels from a given heliocentric distance to 1 AU. For both measures, ICMEs containing magnetic clouds show greater coherence than non-cloud ICMEs. However, even for magnetic clouds, information is unable to propagate across the full span of the structure. Thus interactions of ICMEs with other solar wind structures in the heliosphere are likely to lead to localised distortion, rather than solid-body like deflection. For magnetic clouds, the coherence length scale is significantly greater near the centre of the spacecraft encounter than at the leading or trailing edges. This suggests that magnetic clouds may be more

coherent, and thus less prone to distortion, along the direction of the magnetic flux-rope axis than in directions perpendicular to the axis.

The value of CME arrival-time forecasts for space weather mitigation

M. J. [Owens](#), [M. Lockwood](#), [L. A. Barnard](#),

Space Weather **Volume18, Issue9** e2020SW002507 2020

<https://agupubs.onlinelibrary.wiley.com/doi/pdf/10.1029/2020SW002507>

Severe geomagnetic storms are driven by the coronal mass ejections (CMEs). Consequently, there has been a great deal of focus on predicting if and when a CME will arrive in near-Earth space. However, it is useful to step back and ask, “How value is this information, in isolation, useful for making decisions to mitigate against the adverse effects of space weather?” While all severe geomagnetic storms are triggered by CMEs, not all CMEs trigger severe storms. Thus even perfect knowledge of CME arrival time will provide ‘actionable’ forecast information only in operational situations where false alarms can be tolerated. Of course, any CME transit model used to predict CME arrival time must also produce an estimate of CME speed at Earth. This can help discriminate between geoeffective and non-geoeffective CMEs, reducing false alarms and expanding the range of operational scenarios under which a forecast provides value. Thus, from an end-user perspective, CME arrival speed should form part of the standard metric by which CME transit models are evaluated. Looking to the future, even coarse information about the CME magnetic properties would likely provide even greater forecast value. These points are illustrated by a simple analysis of solar wind data.

Signatures of Coronal Loop Opening via Interchange Reconnection in the Slow Solar Wind at 1 AU

Mathew [Owens](#), [Mike Lockwood](#), [Allan Macneil](#) & [David Stansby](#)

[Solar Physics](#) volume 295, Article number: 37 (2020)

<https://link.springer.com/content/pdf/10.1007/s11207-020-01601-7.pdf>

The opening of closed magnetic loops via reconnection with open solar flux, so called “interchange reconnection”, is invoked in a number of models of slow solar wind release. In the heliosphere, this is expected to result in local switchbacks or inversions in heliospheric magnetic flux (HMF). When observed at 1 AU, inverted HMF has previously been shown to exhibit high ion charge states, suggestive of hot coronal loops, and to map to the locations of coronal magnetic separatrices. However, simulations show that inverted HMF produced directly by reconnection in the low corona is unlikely to survive to 1 AU without the amplification by solar wind speed shear. By considering the surrounding solar wind, we show that inverted HMF is preferably associated with regions of solar wind shear at 1 AU. Compared with the surrounding solar wind, inverted HMF intervals have lower magnetic field intensity and show intermediate speed and density values between the faster, more tenuous wind ahead and the slower, denser wind behind. There is no coherent signature in iron charge states, but oxygen and carbon charge states within the inverted HMF are in agreement with the higher values in the slow wind behind. Conversely, the iron-to-oxygen abundance ratio is in better agreement with the lower values in the solar wind ahead, while the alpha-to-proton abundance ratio shows no variation. One possible explanation for these observations is that the interchange reconnection (and subsequent solar wind shear) that is responsible for generation of inverted HMF involves very small, quiet-Sun loops of approximately photospheric composition, which are impulsively heated in the low corona, rather than large-scale active region loops with enhanced first-ionisation potential elements. Whether signatures of such small loops could be detected in situ at 1 AU still remains to be determined.

Towards Construction of a Solar Wind “Reanalysis” Dataset: Application to the First Perihelion Pass of Parker Solar Probe

Mathew J. [Owens](#), Matthew Lang, Pete Riley, David Stansby

[Solar Physics](#) June 2019, 294:83

sci-hub.se/10.1007/s11207-019-1479-6

Accurate reconstruction of global solar-wind structure is essential for connecting remote and in situ observations of solar plasma, and hence understanding formation and release of solar wind. Information can routinely be obtained from photospheric magnetograms, via coronal and solar-wind modelling, and directly from in situ observations, typically at large heliocentric distances (most commonly near 1 AU). Magnetogram-constrained modelling has the benefit of reconstructing global solar-wind structure, but with relatively large spatial and/or temporal errors. In situ observations, on the other hand, make accurate temporal measurements of solar-wind structure, but are highly localised. We here use a data assimilative (DA) approach to combine these two sources of information as a first step towards producing a solar-wind “reanalysis” dataset that optimally combines model and observation. The physics of solar wind stream interaction

is used to extrapolate in heliocentric distance, while the assumption of steady-state solar-wind structure enables extrapolation in longitude. The major challenge is extrapolating in latitude. Using solar-wind speed during the interval of the first perihelion pass of Parker Solar Probe (PSP) in November 2018 as a test bed, we investigate two approaches. The first is to assume the solar wind is two-dimensional and thus has no latitudinal structure within the $\pm 7^\circ \pm 7^\circ$ bounded by the heliographic equatorial and ecliptic planes. The second assumes in situ solar-wind observations are representative of some (small) latitudinal range. We show how observations of the inner heliosphere, such as will be provided by PSP, can be exploited to constrain the latitudinal representivity of solar-wind observations to improve future solar-wind reconstruction and space-weather forecasting.

Near-Earth solar wind forecasting using corotation from L5: The error introduced by heliographic latitude offset

M.J. Owens, P. Riley, M. Lang, M. Lockwood

Space Weather **Volume17, Issue7** Pages 1105-1113 2019

[sci-hub.se/10.1029/2019SW002204](https://doi.org/10.1029/2019SW002204)

Routine in-situ solar wind observations from L5, located 60° behind Earth in its orbit, would provide a valuable input to space-weather forecasting. One way to utilise such observations is to assume that the solar wind is in perfect steady state over the 4.5 days it takes the Sun to rotate 60° and thus near-Earth solar wind in 4.5-days time would be identical to that at L5 today. This corotation approximation is most valid at solar minimum when the solar wind is slowly evolving. Using STEREO data, it has been possible to test L5-corotation forecasting for a few months at solar minimum, but the various contributions to forecast error cannot be disentangled. This study uses 40+ years of magnetogram-constrained solar wind simulations to isolate the effect of latitudinal offset between L5 and Earth due to the inclination of the ecliptic plane to the solar rotational equator. Latitudinal offset error is found to be largest at solar minimum, due to the latitudinal ordering of solar wind structure. It is also a strong function of time of year; maximum at the solstices and very low at equinoxes. At solstice, the latitudinal offset alone means L5-corotation forecasting is expected to be less accurate than numerical solar wind models, even before accounting for time-dependent solar wind structures. Thus, a combination of L5-corotation and numerical solar wind modelling may provide the best forecast. These results also highlight that three-dimensional solar wind structure must be accounted for when performing solar wind data assimilation.

Time-Window Approaches to Space-Weather Forecast Metrics: A Solar Wind Case Study

Mathew J. Owens

Review

Space Weather 2018

[sci-hub.tw/10.1029/2018sw002059](https://doi.org/10.1029/2018sw002059)

Metrics are an objective, quantitative assessment of forecast (or model) agreement with observations. They are essential for assessing forecast accuracy and reliability and consequently act as a diagnostic for forecast development. Partly as a result of limited spatial sampling of observations, much of space-weather forecasting is focused on the time domain rather than inherent spatial variability. Thus, metrics are primarily point-by-point approaches, in which observed conditions at time t are compared directly (and only) with the forecast conditions at time t . Such metrics are undoubtedly useful. But in lacking an explicit consideration of timing uncertainties, they have limitations as diagnostic tools and can, under certain conditions, be misleading. Using a near-Earth solar wind speed forecast as an illustrative example, this study briefly reviews the most commonly used point-by-point metrics and advocates for complementary time window approaches. In particular, a scale-selective approach, originally developed in numerical weather prediction for validation of spatially patchy rainfall forecasts, is adapted to the time domain for space-weather purposes. This simple approach readily determines the time scales over which a forecast is and is not valuable, allowing the results of point-by-point metrics to be put in greater context.

Generation of Inverted Heliospheric Magnetic Flux by Coronal Loop Opening and Slow Solar Wind Release

Mathew J. Owens, Mike Lockwood, Luke A. Barnard, and Allan R. MacNeil

2018 ApJL 868 L14

[sci-hub.tw/10.3847/2041-8213/aace82](https://doi.org/10.3847/2041-8213/aace82)

In situ spacecraft observations provide much-needed constraints on theories of solar wind formation and release, particularly the highly variable slow solar wind, which dominates near-Earth space. Previous studies have shown an association between local inversions in the heliospheric magnetic field (HMF) and solar wind released from the vicinity of magnetically closed coronal structures. We here show that in situ properties of inverted HMF are consistent with the

same hot coronal source regions as the slow solar wind. We propose that inverted HMF is produced by solar wind speed shear, which results from interchange reconnection between a coronal loop and open flux tube, and introduces a pattern of fast–slow–fast wind along a given HMF flux tube. This same loop-opening process is thought to be central to slow solar wind formation. The upcoming Parker Solar Probe and Solar Orbiter missions provide a unique opportunity to directly observe these processes and thus determine the origin of the slow solar wind.

Solar Wind and Heavy Ion Properties of Interplanetary Coronal Mass Ejections

M. J. Owens

[Solar Physics](#) August 2018, 293:122

<https://link.springer.com/content/pdf/10.1007%2Fs11207-018-1343-0.pdf>

Magnetic field and plasma properties of the solar wind measured in near-Earth space are a convolution of coronal source conditions and in-transit processes which take place between the corona and near-Earth space. Elemental composition and heavy ion charge states, however, are not significantly altered during transit to Earth and thus such properties can be used to diagnose the coronal source conditions of the solar wind observed in situ. We use data from the Advanced Composition Explorer (ACE) spacecraft to statistically quantify differences in the coronal source properties of interplanetary coronal mass ejections (ICMEs). Magnetic clouds, ICMEs which contain a magnetic flux-rope signature, display heavy ion properties consistent with significantly hotter coronal source regions than non-cloud ICMEs. Specifically, magnetic clouds display significantly elevated ion charge states, suggesting they receive greater heating in the low corona. Further dividing ICMEs by speed, however, shows this effect is primarily limited to fast magnetic clouds and that in terms of heavy ion properties, slow magnetic clouds are far more similar to non-cloud ICMEs. As such, fast magnetic clouds appear distinct from other ICME types in terms of both ion charge states and elemental composition. ICME speed, rather ICME type, correlates with helium abundance and iron charge state, consistent with fast ICMEs being heated through the more extended corona. Fast ICMEs also tend to be embedded within faster ambient solar wind than slow ICMEs, though this could be partly the result of in-transit drag effects. These signatures are discussed in terms of spatial sampling of ICMEs and from fundamentally different coronal formation and release processes.

Ion Charge States and Potential Geoeffectiveness: The Role of Coronal Spectroscopy for Space-Weather Forecasting

M. J. Owens [M. Lockwood](#) [L. A. Barnard](#)

Space Weather Volume 16, Issue 6 June 2018 Pages 694-703

<http://sci-hub.tw/10.1029/2018SW001855>

Severe space weather is driven by interplanetary coronal mass ejections (ICMEs), episodic eruptions of solar plasma, and magnetic flux that travel out through the heliosphere and can perturb the Earth's magnetosphere and ionosphere. In order for space-weather forecasts to allow effective mitigating action, forecasts must be made as early as possible, necessitating identification of potentially “geoeffective” ICMEs close to the Sun. This presents two challenges. First, geoeffectiveness is primarily determined by the magnetic field intensity and orientation, both of which are difficult to measure close to the Sun. Second, the magnetic field evolves in transit between the Sun and the Earth, sometimes in a highly nonlinear way. Conversely, solar wind ion charge states, such as the ratio of O7+ to O6+, are fixed by the electron temperature at the coronal height where ion-electron collisions are last possible as the ICME erupts. After this point, they are said to be “frozen in” as they do not evolve further as the ICME propagates through the solar wind. In this study we show that ion charge states, while not geoeffective in and of themselves, act as strong markers for the geoeffectiveness of the ICME. The probability of severe space weather is around 7 times higher in “hot” ICMEs than “cold” ICMEs, as defined by O7+/O6+. We suggest that coronal spectroscopy of ICMEs could complement current forecasting techniques, providing valuable additional information about potential geoeffectiveness.

Propagation of information within coronal mass ejections

Matthew Owens (Reading)

UK Solar Physics (UKSP) – Nuggets # 82 2017 www.uksolphys.org/?p=13322

Communication by Alfvén waves sets a basic limit to the coherence of propagating CMEs.

Coronal mass ejections are not coherent magnetohydrodynamic structures

M. J. Owens, [M. Lockwood](#) & [L. A. Barnard](#)

Scientific Reports 7, Article number: 4152(2017)

<https://www.nature.com/articles/s41598-017-04546-3.pdf>

Coronal mass ejections (CMEs) are episodic eruptions of solar plasma and magnetic flux that travel out through the solar system, driving extreme space weather. Interpretation of CME observations and their interaction with the solar wind typically assumes CMEs are coherent, almost solid-like objects. We show that supersonic radial propagation of CMEs away from the Sun results in geometric expansion of CME plasma parcels at a speed faster than the local wave speed. Thus information cannot propagate across the CME. Comparing our results with observed properties of over 400 CMEs, we show that CMEs cease to be coherent magnetohydrodynamic structures within 0.3 AU of the Sun. This suggests Earth-directed CMEs are less like billiard balls and more like dust clouds, with apparent coherence only due to similar initial conditions and quasi homogeneity of the medium through which they travel. The incoherence of CMEs suggests interpretation of CME observations requires accurate reconstruction of the ambient solar wind with which they interact, and that simple assumptions about the shape of the CMEs are likely to be invalid when significant spatial/temporal gradients in ambient solar wind conditions are present.

Probabilistic Solar Wind and Geomagnetic Forecasting Using an Analogue Ensemble or “Similar Day” Approach

M. J. Owens, P. Riley, T. S. Horbury

Solar Physics May 2017, 292:69

<http://link.springer.com/content/pdf/10.1007%2Fs11207-017-1090-7.pdf>

Effective space-weather prediction and mitigation requires accurate forecasting of near-Earth solar-wind conditions. Numerical magnetohydrodynamic models of the solar wind, driven by remote solar observations, are gaining skill at forecasting the large-scale solar-wind features that give rise to near-Earth variations over days and weeks. There remains a need for accurate short-term (hours to days) solar-wind forecasts, however. In this study we investigate the analogue ensemble (AnEn), or “similar day”, approach that was developed for atmospheric weather forecasting. The central premise of the AnEn is that past variations that are analogous or similar to current conditions can be used to provide a good estimate of future variations. By considering an ensemble of past analogues, the AnEn forecast is inherently probabilistic and provides a measure of the forecast uncertainty. We show that forecasts of solar-wind speed can be improved by considering both speed and density when determining past analogues, whereas forecasts of the out-of-ecliptic magnetic field [(B_{N})] are improved by also considering the in-ecliptic magnetic-field components. In general, the best forecasts are found by considering only the previous 6 – 12 hours of observations. Using these parameters, the AnEn provides a valuable probabilistic forecast for solar-wind speed, density, and in-ecliptic magnetic field over lead times from a few hours to around four days. For (B_{N}) , which is central to space-weather disturbance, the AnEn only provides a valuable forecast out to around six to seven hours. As the inherent predictability of this parameter is low, this is still likely a marked improvement over other forecast methods. We also investigate the use of the AnEn in forecasting geomagnetic indices Dst and Kp. The AnEn provides a valuable probabilistic forecast of both indices out to around four days. We outline a number of future improvements to AnEn forecasts of near-Earth solar-wind and geomagnetic conditions.

DO THE LEGS OF MAGNETIC CLOUDS CONTAIN TWISTED FLUX-ROPE MAGNETIC FIELDS?

M. J. Owens

2016 ApJ 818 197

Magnetic clouds (MCs) are a subset of interplanetary coronal mass ejections (ICMEs) characterized primarily by a smooth rotation in the magnetic field direction indicative of the presence of a magnetic flux rope. Energetic particle signatures suggest MC flux ropes remain magnetically connected to the Sun at both ends, leading to widely used model of global MC structure as an extended flux rope, with a loop-like axis stretching out from the Sun into the heliosphere and back to the Sun. The time of flight of energetic particles, however, suggests shorter magnetic field line lengths than such a continuous twisted flux rope would produce. In this study, two simple models are compared with observed flux rope axis orientations of 196 MCs to show that the flux rope structure is confined to the MC leading edge. The MC “legs,” which magnetically connect the flux rope to the Sun, are not recognizable as MCs and thus are unlikely to contain twisted flux rope fields. Spacecraft encounters with these non-flux rope legs may provide an explanation for the frequent observation of non-MC ICMEs.

The source of the slow solar wind

Matt **Owens**

New UKSP Nugget: 46, **2014**.

<http://www.uksolphys.org/?p=7936>

Heliospheric magnetic flux topology and connectivity deduced from suprathermal electrons sheds light on the slow wind formation.

Pseudostreamers are an additional source of slow solar wind. This explains a long-standing mystery about the early Ulysses observations.

Solar cycle evolution of dipolar and pseudostreamer belts and their relation to the slow solar wind†

M.J. **Owens**^{1,*}, N.U. Crooker², M. Lockwood

JGR, Volume 119, Issue 1, pages 36–46, January **2014**

Dipolar streamers are coronal structures formed by open solar flux converging from coronal holes of opposite polarity. Thus the dipolar streamer belt traces the coronal foot print of the heliospheric current sheet (HCS), and it is strongly associated with the origin of slow solar wind. Pseudostreamers, on the other hand, separate converging regions of open solar flux from coronal holes of the same polarity and do not contain current sheets. They have recently received a great deal of interest as a possible additional source of slow solar wind. Here we add to that growing body of work by using the potential-field source-surface model to determine the occurrence and location of dipolar and pseudostreamers over the last three solar cycles. In addition to providing new information about pseudostreamer morphology, the results help explain why the observations taken during the first Ulysses perihelion pass in 1995 showed noncoincidence between dipolar streamer belt and the locus of slowest flow. We find that Carrington rotation averages of the heliographic latitudes of dipolar and pseudostreamer belts are systematically shifted away from the equator, alternately in opposite directions, with a weak solar cycle periodicity, thus keeping slow wind from the web of combined streamer belts approximately symmetric about the equator. The largest separation of dipolar and pseudostreamer belts occurred close to the Ulysses pass, allowing a unique opportunity to see that slow wind from pseudostreamer belts north of the southward-displaced dipolar belt was responsible for the noncoincident pattern.

Solar origin of heliospheric magnetic field inversions: Evidence for coronal loop opening within Pseudostreamers†

M. J. **Owens**^{1,*}, N. U. Crooker, ², M. Lockwood

JGR, **2013**

The orientation of the heliospheric magnetic field (HMF) in near-Earth space is generally a good indicator of the polarity of HMF foot points at the photosphere. There are times, however, when the HMF folds back on itself (is inverted), as indicated by suprathermal electrons locally moving sunward, even though they must ultimately be carrying the heat flux away from the Sun. Analysis of the near-Earth solar wind during the period 1998–2011 reveals that inverted HMF is present approximately 5.5% of the time and is generally associated with slow, dense solar wind and relatively weak HMF intensity. Inverted HMF is mapped to the coronal source surface, where a new method is used to estimate coronal structure from the potential-field source-surface model. We find a strong association with bipolar streamers containing the heliospheric current sheet, as expected, but also with unipolar or pseudostreamers, which contain no current sheet. Because large-scale inverted HMF is a widely-accepted signature of interchange reconnection at the Sun, this finding provides strong evidence for models of the slow solar wind which involve coronal loop opening by reconnection within pseudostreamer belts as well as the bipolar streamer belt. Occurrence rates of bipolar- and pseudostreamers suggest that they are equally likely to result in inverted HMF and, therefore, presumably undergo interchange reconnection at approximately the same rate. Given the different magnetic topologies involved, this suggests the rate of reconnection is set externally, possibly by the differential rotation rate which governs the circulation of open solar flux.

Implications of Non-cylindrical Flux Ropes for Magnetic Cloud Reconstruction Techniques and the Interpretation of Double Flux Rope Events

M.J. **Owens**, P. D?moulin, N.P. Savani, B. Lavraud, A. Ruffenach

E-print, Feb **2012**, Solar Physics Volume 278, Number 2 (**2012**), 435-44

Magnetic clouds (MCs) are a subset of interplanetary coronal mass ejections (ICMEs) which exhibit signatures consistent with a magnetic flux rope structure. Techniques for reconstructing flux rope orientation from single-point in

situ observations typically assume the flux rope is locally cylindrical, e.g., minimum variance analysis (MVA) and forcefree flux rope (FFFR) fitting. In this study, we outline a non-cylindrical magnetic flux rope model, in which the flux rope radius and axial curvature can both vary along the length of the axis. This model is not necessarily intended to represent the global structure of MCs, but it can be used to quantify the error in MC reconstruction resulting from the cylindrical approximation. When the local flux rope axis is approximately perpendicular to the heliocentric radial direction, which is also the effective spacecraft trajectory through a magnetic cloud, the error in using cylindrical reconstruction methods is relatively small (approx 10 deg). However, as the local axis orientation becomes increasingly aligned with the radial direction, the spacecraft trajectory may pass close to the axis at two separate locations. This results in a magnetic field time series which deviates significantly from encounters with a force-free flux rope, and consequently the error in the axis orientation derived from cylindrical reconstructions can be as much as 90 deg. Such two-axis encounters can result in an apparent 'double flux rope' signature in the magnetic field time series, sometimes observed in spacecraft data. Analysing each axis encounter independently produces reasonably accurate axis orientations with MVA, but larger errors with FFR fitting.

Magnetic Discontinuities in the Near-Earth Solar Wind: Evidence of In-Transit Turbulence or Remnants of Coronal Structure?<<<<

M. J. [Owens](#), R. T. Wicks & T. S. Horbury

Solar Physics Volume 269, Number 2, 401-410, 2011

Fluctuations in the solar wind plasma and magnetic field are well described by the sum of two power law distributions. It has been postulated that these distributions are the result of two independent processes: turbulence, which contributes mainly to the smaller fluctuations, and crossing the boundaries of flux tubes of coronal origin, which dominates the larger variations. In this study we explore the correspondence between changes in the magnetic field with changes in other solar wind properties. Changes in density and temperature may result from either turbulence or coronal structures, whereas changes in composition, such as the alpha-to-proton ratio are unlikely to arise from in-transit effects. Observations spanning the entire ACE dataset are compared with a null hypothesis of no correlation between magnetic field discontinuities and changes in other solar wind parameters. Evidence for coronal structuring is weaker than for in-transit turbulence, with only ~ 25% of large magnetic field discontinuities associated with a significant change in the alpha-to-proton ratio, compared to ~ 40% for significant density and temperature changes. However, note that a lack of detectable alpha-to-proton signature is not sufficient to discount a structure as having a solar origin.

The expected imprint of flux rope geometry on suprathermal electrons in magnetic clouds

M. J. [Owens](#), N. U. Crooker, and T. S. Horbury

Ann. Geophys., 27, 4057-4067, 2009

[Abstract](#) [Full Article](#) (PDF, 2146 KB)

Magnetic clouds are a subset of interplanetary coronal mass ejections characterized by a smooth rotation in the magnetic field direction, which is interpreted as a signature of a magnetic flux rope. Suprathermal electron observations indicate that one or both ends of a magnetic cloud typically remain connected to the Sun as it moves out through the heliosphere. With distance from the axis of the flux rope, out toward its edge, the magnetic field winds more tightly about the axis and electrons must traverse longer magnetic field lines to reach the same heliocentric distance. This increased time of flight allows greater pitch-angle scattering to occur, meaning suprathermal electron pitch-angle distributions should be systematically broader at the edges of the flux rope than at the axis. We model this effect with an analytical magnetic flux rope model and a numerical scheme for suprathermal electron pitch-angle scattering and find that the signature of a magnetic flux rope should be observable with the typical pitch-angle resolution of suprathermal electron data provided ACE's SWEPAM instrument. Evidence of this signature in the observations, however, is weak, possibly because reconnection of magnetic fields within the flux rope acts to intermix flux tubes.

The Formation of Large-Scale Current Sheets within Magnetic Clouds

M.J. [Owens](#)

Solar Phys (2009) 260: 207–217

Magnetic clouds are a class of interplanetary coronal mass ejections (CME) predominantly characterised by a smooth rotation in the magnetic field direction, indicative of a magnetic flux rope structure. Many magnetic clouds, however, also contain sharp discontinuities within the smoothly varying magnetic field, suggestive of narrow current sheets. In this study we present observations and modelling of magnetic clouds with strong current sheet signatures close to the centre of the apparent flux rope structure. Using an analytical

magnetic flux rope model, we demonstrate how such current sheets can form as a result of a cloud's kinematic propagation from the Sun to the Earth, without any external forces or influences. This model is shown to match observations of four particular magnetic clouds remarkably well. The model predicts that current sheet intensity increases for increasing CME angular extent and decreasing CME radial expansion speed. Assuming such current sheets facilitate magnetic reconnection, the process of current sheet formation could ultimately lead a single flux rope becoming fragmented into multiple flux ropes. This change in topology has consequences for magnetic clouds as barriers to energetic particle propagation.

Conservation of open solar magnetic flux and the floor in the heliospheric magnetic field

M. J. Owens,¹ N. U. Crooker,² N. A. Schwadron,² T. S. Horbury,¹ S. Yashiro,³ H. Xie,³ O. C. St. Cyr,⁴ and N. Gopalswamy⁴

GEOPHYSICAL RESEARCH LETTERS, VOL. 35, L20108, doi:10.1029/2008GL035813, 2008, File

The near-Earth heliospheric magnetic field intensity, $|B|$, exhibits a strong solar cycle variation, but returns to the same "floor" value each solar minimum. The current minimum, however, has seen $|B|$ drop below previous minima, bringing in to question the existence of a floor, or at the very least requiring a re-assessment of its value. In this study we assume heliospheric flux consists of a constant open flux component and a time-varying contribution from CMEs. In this scenario, the true floor is $|B|$ with zero CME contribution. Using observed CME rates over the solar cycle, we estimate the "no-CME" $|B|$ floor at 4.0 ± 0.3 nT, lower than previous floor estimates and below $|B|$ observed this solar minimum. We speculate that the drop in $|B|$ observed this minimum may be due to a persistently lower CME rate than the previous minimum, though there are large uncertainties in the supporting observational data.

Combining remote and in situ observations of coronal mass ejections to better constrain magnetic cloud reconstruction,

Owens, M. J.

J. Geophys. Res., 113, A12102, (2008), <http://dx.doi.org/10.1029/2008JA013589>

Determination of the nonradial extent of magnetic clouds (MCs) is vital for two key reasons. First, it affects the amount of "drag" a fast MC experiences and therefore controls the travel time from the Sun to 1-AU, a critical parameter for space-weather prediction. Second, it is vital to estimating the flux content of MCs, which in turn is important for understanding both the formation and eruption of the magnetic flux rope and for determining the role of coronal mass ejections in the heliospheric flux budget and the evolution of heliospheric flux over the solar cycle. In this study, it is demonstrated that the cross-sectional elongation of MCs is poorly constrained by in situ observations of the magnetic field alone. A method for combining remote and in situ observations of ejecta to better determine MC cross-sectional elongation is then outlined and applied to a previously studied event which occurred during the SOHO-Ulysses quadrature of late 1996. The new technique reveals an axial magnetic flux content ~ 4 times higher than that inferred by a force-free flux rope model fit to the same in situ observations of the magnetic cloud. This event also shows evidence of axial distortion by the structured ambient solar wind.

Characteristic magnetic field and speed properties of interplanetary coronal mass ejections and their sheath regions

Owens, M. J., Cargill, P. J., Pagel, C., Siscoe, G. L., and Crooker, N. U.:

2005, *JGR* 110, A01105, doi:10.1029/2004JA010814.

Prediction of the solar wind conditions in near-Earth space, arising from both quasi-steady and transient structures, is essential for space weather forecasting. To achieve forecast lead times of a day or more, such predictions must be made on the basis of remote solar observations. A number of empirical prediction schemes have been proposed to forecast the transit time and speed of coronal mass ejections (CMEs) at 1 AU. However, the current lack of magnetic field measurements in the corona severely limits our ability to forecast the 1 AU magnetic field strengths resulting from interplanetary CMEs (ICMEs). In this study we investigate the relation between the characteristic magnetic field strengths and speeds of both magnetic cloud and noncloud ICMEs at 1 AU. Correlation between field and speed is found to be significant only in the sheath region ahead of magnetic clouds, not within the clouds themselves. The lack of such a relation in the sheaths ahead of noncloud ICMEs is consistent with such ICMEs being skimming encounters of magnetic clouds, though other explanations are also put forward. Linear fits to the radial speed profiles of ejecta reveal that faster-traveling ICMEs are also expanding more at 1 AU. We combine these empirical relations to form a prediction

scheme for the magnetic field strength in the sheaths ahead of magnetic clouds and also suggest a method for predicting the radial speed profile through an ICME on the basis of upstream measurements.

Predictions of the arrival time of Coronal Mass Ejections at 1AU: an analysis of the causes of errors

M. Owens and P. Cargill. *Annales Geophysicae* (2004) 22: 661–671

Three existing models of Interplanetary Coronal Mass Ejection (ICME) transit between the Sun and the Earth are compared to coronagraph and in situ observations: all three models are found to perform with a similar level of accuracy (i.e. an average error between observed and predicted 1AU transit times of approximately 11h). To improve long-term space weather prediction, factors influencing CME transit are investigated. Both the removal of the plane of sky projection (as suffered by coronagraph derived speeds of Earth directed CMEs) and the use of observed values of solar wind speed, fail to significantly improve transit time prediction. However, a correlation is found to exist between the late/early arrival of an ICME and the width of the preceding sheath region, suggesting that the error is a geometrical effect that can only be removed by a more accurate determination of a CME trajectory and expansion. The correlation between magnetic field intensity and speed of ejecta at 1AU is also investigated. It is found to be weak in the body of the ICME, but strong in the sheath, if the upstream solar wind conditions are taken into account.

Coronal mass ejections and magnetic flux buildup in the heliosphere

Owens, M. J.; Crooker, N. U.

J. Geophys. Res., Vol. 111, No. A10, A10104

<http://dx.doi.org/10.1029/2006JA011641>

Temporal and Periodic Variations of the Solar Flare Index During the Last Four Solar Cycles and Their Association with Selected Geomagnetic-Activity Parameters

Atila Özgüç, Ali Kilcik & Vasyl Yurchyshyn

Solar Physics volume 297, Article number: 112 (2022)

<https://doi.org/10.1007/s11207-022-02049-7>

We studied the temporal and periodic variations of the monthly solar flare index (FI) and selected geomagnetic-activity parameters (Ap, Dst, Scalar B, and aa) measured during Solar Cycles 21 – 24 (from January 1, 1975 to December 31, 2020) and report the following findings: 1) all data sets except the FI peak values gradually decreased after 1992, while the FI peak values began their gradual decrease in 1982; 2) all data sets show double or multiple peaks during the maximum phase of solar cycles; 3) the FI shows meaningful correlations with the investigated geomagnetic-activity parameters; 4) the 11-year sunspot-cycle periodicity and periodicities lower than 3.9 months were observed in all data sets without exception; 5) the FI time series exhibits a unique period of 4.8 – 5.2 months that is not present in all the other indices, while geomagnetic aa, Ap, and Dst indices show a unique 6 – 6.1 months periodicity that does not appear in the scalar B and FI; 6) crosswavelet transform (XWT) spectra between FI and other parameters generally show phase mixing in the short (2 – 8 months) period range, while all parameters used in this study were found to be inphase and highly correlated with the 11-year solar-activity period. All these results show that the FI variations are one of the main drivers of the geomagnetic activity.

Temporal Offsets between Maximum CME Speed Index and Solar, Geomagnetic, and Interplanetary Indicators during Solar Cycle 23 and the Ascending Phase of Cycle 24

A. Özgüç, A. Kilcik, K. Georgieva, B. Kirov

Solar Phys. 2016

<https://arxiv.org/ftp/arxiv/papers/1604/1604.05941.pdf>

On the basis of morphological analysis of yearly values of the maximum CME (coronal mass ejection) speed index, the sunspot number and total sunspot area, sunspot magnetic field, and solar flare index, the solar wind speed and interplanetary magnetic field strength, and the geomagnetic Ap and Dst indices, we point out the particularities of solar and geomagnetic activity during the last cycle 23, the long minimum which followed it and the ascending branch of cycle 24. We also analyze temporal offset between the maximum CME speed index and the above-mentioned solar, geomagnetic, and interplanetary indices. It is found that this solar activity index, analyzed jointly with other solar activity, interplanetary parameters, and geomagnetic activity indices, shows a hysteresis phenomenon. It is observed that these parameters follow different paths for the ascending and the descending phases of solar cycle 23. It is noticed that

the hysteresis phenomenon represents a clue in the search for physical processes responsible for linking the solar activity to the near-Earth and geomagnetic responses.

Searching for a Solar Source of Magnetic-Field Switchbacks in Parker Solar Probe's First Encounter

D. de Pablos, [T. Samanta](#), [S. T. Badman](#), [C. Schwanitz](#), [S. M. Bahaouddin](#), [L. K. Harra](#), [G. Petrie](#), [C. Mac Cormack](#), [C. H. Mandrini](#), [N. E. Raouafi](#), [V. Martinez Pillet](#) & [M. Velli](#)
[Solar Physics](#) volume 297, Article number: 90 (2022)

<https://link.springer.com/content/pdf/10.1007/s11207-022-02022-4.pdf>

Parker Solar Probe observations show ubiquitous magnetic-field reversals closer to the Sun, often referred to as “switchbacks”. The switchbacks have been observed before in the solar wind near 1 AU and beyond, but their occurrence was historically rare. PSP measurements below ~ 0.2 AU show that switchbacks are, however, the most prominent structures in the “young” solar wind. In this work, we analyze remote-sensing observations of a small equatorial coronal hole to which PSP was connected during the perihelion of Encounter 1. We investigate whether some of the switchbacks captured during the encounter were of coronal origin by correlating common switchback in situ signatures with remote observations of their expected coronal footpoint. We find strong evidence that timescales present in the corona are relevant to the outflowing, switchback-filled solar wind, as illustrated by strong linear correlation. We also determine that spatial analysis of the observed region is optimal, as the implied average solar-wind speed more closely matches that observed by PSP at the time. We observe that hemispherical structures are strongly correlated with the radial proton velocity and the mass flux in the solar wind. The above findings suggest that a subpopulation of the switchbacks are seeded at the corona and travel into interplanetary space. **29 Oct-2 Nov 2018**

Matching temporal signatures of solar features to their corresponding solar wind outflows

[Diego de Pablos](#), [David M. Long](#), [Christopher J. Owen](#), [Gherardo Valori](#), [Georgios Nicolaou](#), [Louise K. Harra](#)

[Solar Phys.](#) **296**, Article number: 68 2021

<https://arxiv.org/pdf/2103.09077.pdf>

<https://doi.org/10.1007/s11207-021-01813-5>

<https://link.springer.com/content/pdf/10.1007/s11207-021-01813-5.pdf>

The role of small-scale coronal eruptive phenomena in the generation and heating of the solar wind remains an open question. Here, we investigate the role played by coronal jets in forming the solar wind by testing whether temporal variations associated with jetting in EUV intensity can be identified in the outflowing solar wind plasma. This type of comparison is challenging due to inherent differences between remote-sensing observations of the source and in situ observations of the outflowing plasma, as well as travel time and evolution of the solar wind throughout the heliosphere. To overcome these, we propose a novel algorithm combining signal filtering, two-step solar wind ballistic backmapping, window shifting, and Empirical Mode Decomposition. We first validate the method using synthetic data, before applying it to measurements from the Solar Dynamics Observatory, and Wind spacecraft. The algorithm enables the direct comparison of remote sensing observations of eruptive phenomena in the corona to in situ measurements of solar wind parameters, among other potential uses. After application to these datasets, we find several time windows where signatures of dynamics found in the corona are embedded in the solar wind stream, at a time significantly earlier than expected from simple ballistic backmapping, with the best performing in situ parameter being the solar wind mass flux. **9-14 Nov 2016**

Automatic detection of large-scale flux ropes and their geoeffectiveness with a machine learning approach

[Sanchita Pal](#), [Luiz F. G. dos Santos](#), [Andreas J. Weiss](#), [Thomas Narock](#), [Ayrís Narock](#), [Teresa Nieves-Chinchilla](#), [Lan K. Jian](#), [Simon W. Good](#)

[ApJ](#) **972** 94 2024

<https://arxiv.org/pdf/2406.07798>

<https://iopscience.iop.org/article/10.3847/1538-4357/ad54c3/pdf>

Detecting large-scale flux ropes (FRs) embedded in interplanetary coronal mass ejections (ICMEs) and assessing their geoeffectiveness are essential since they can drive severe space weather. At 1 au, these FRs have an average duration of 1 day. Their most common magnetic features are large, smoothly rotating magnetic fields. Their manual detection has become a relatively common practice over decades, although visual detection can be time-consuming and subject to observer bias. Our study proposes a pipeline that utilizes two supervised binary-classification machine learning (ML)

models trained with solar wind magnetic properties to automatically detect large-scale FRs and additionally determine their geoeffectiveness. The first model is used to generate a list of auto-detected FRs. Using the properties of southward magnetic field the second model determines the geoeffectiveness of FRs. Our method identifies 88.6% and 80% large-scale ICMEs (duration ≥ 1 day) observed at 1 au by Wind and Sun Earth Connection Coronal and Heliospheric Investigation (STEREO) mission, respectively. While testing with a continuous solar wind data obtained from Wind, our pipeline detected 56 of the 64 large-scale ICMEs during 2008 - 2014 period (recall= 0.875) but many false positives (precision= 0.56) as we do not take into account any additional solar wind properties than the magnetic properties. We found an accuracy of 0.88 when estimating the geoeffectiveness of the auto-detected FRs using our method. Thus, in space weather now-casting and forecasting at L1 or any planetary missions, our pipeline can be utilized to offer a first-order detection of large-scale FRs and geoeffectiveness. **2012-07-15, 2013/01/16-19**

Eruption and Interplanetary Evolution of a Stealthy Streamer-Blowout CME Observed by PSP at ~ 0.5 -AU

[Sanchita Pal](#), [Benjamin J. Lynch](#), [Simon W. Good](#), [Erika Palmerio](#), [Eleanna Asvestari](#), [Jens Pomoell](#), [Michael L. Stevens](#), [Emilia K. J. Kilpua](#)
Front. Astron. Space Sci. 9: 903676 **2022**
<https://arxiv.org/pdf/2205.07713.pdf>
<https://www.frontiersin.org/articles/10.3389/fspas.2022.903676/full>
<https://doi.org/10.3389/fspas.2022.903676>

Streamer-blowout coronal mass ejections (SBO-CMEs) are the dominant CME population during solar minimum. Although they are typically slow and lack clear low-coronal signatures, they can cause geomagnetic storms. With the aid of extrapolated coronal fields and remote observations of the off-limb low corona, we study the initiation of an SBO-CME preceded by consecutive CME eruptions consistent with a multi-stage sympathetic breakout scenario. From inner-heliospheric Parker Solar Probe (PSP) observations, it is evident that the SBO-CME is interacting with the heliospheric magnetic field and plasma sheet structures draped about the CME flux rope. We estimate that $18 \pm 11\%$ of the CME's azimuthal magnetic flux has been eroded through magnetic reconnection and that this erosion began after a heliospheric distance of ~ 0.35 AU from the Sun was reached. This observational study has important implications for understanding the initiation of SBO-CMEs and their interaction with the heliospheric surroundings. **22 June 2020**

A magnetic cloud prediction model for forecasting space weather relevant properties of Earth-directed coronal mass ejections

[Sanchita Pal](#), [Dibyendu Nandy](#), [Emilia K J Kilpua](#)
A&A 665, A110 **2022**
<https://arxiv.org/pdf/2203.05231.pdf>
<https://www.aanda.org/articles/aa/pdf/2022/09/aa43513-22.pdf>

Coronal Mass Ejections (CMEs) are energetic storms in the Sun that result in the ejection of large-scale magnetic clouds (MCs) in interplanetary space that contain enhanced magnetic fields with coherently changing field direction. The severity of geomagnetic perturbations depends on the direction and strength of the interplanetary magnetic field (IMF), as well as the speed and duration of passage of the storm. The coupling between the heliospheric environment and Earth's magnetosphere is the strongest when the IMF direction is persistently southward for a prolonged period. Predicting the magnetic profile of such Earth-directed CMEs is crucial for estimating their geomagnetic impact. We aim to build upon and integrate diverse techniques towards development of a comprehensive magnetic cloud prediction (MCP) model that can forecast the magnetic field vectors, Earth-impact time, speed and duration of passage of solar storms. A novelty of our scheme is the ability to predict the passage duration of the storm without recourse to computationally intensive, time-dependent dynamical equations. Our methodology is validated by comparing the MCP model output with observations of ten MCs at 1 AU. In our sample, we find that eight MCs show a root mean square deviation of less than 0.1 between predicted and observed magnetic profiles and the passage duration of seven MCs fall within the predicted range. Based on the success of this approach, we conclude that predicting the near-Earth properties of MCs based on analysis and modelling of near-Sun CME observations is a viable endeavor with potential benefits for space weather assessment. **24 May 2010, 2 Jun 2011, 04 Jun 2011, 10 Feb 2012, 14 Jun 2012, 12 Jul 2012, 9 Nov 2012, 2013-03-15, 2013-04-11, 2 Jun 2013, 9 Jul 2013**

Table 1. Near-Sun observations of CME latitude (θ_{HG}), longitude (ϕ_{HG}), tilt (η), aspect ratio (κ), height (hl) of the CME leading edges and the angular width (AW), their initiation time (CMEstart), and associated MCs' start (MCstart) and end times (MCend). 2010-2013

Uncovering Erosion Effects on Magnetic Flux Rope Twist

Sanchita **Pal**, [Emilia Kilpua](#), [Simon Good](#), [Jens Pomoell](#), [Daniel J. Price](#)

A&A 650, A176 2021

<https://arxiv.org/pdf/2104.03569.pdf>

<https://www.aanda.org/articles/aa/pdf/2021/06/aa40070-20.pdf>

<https://doi.org/10.1051/0004-6361/202040070>

Magnetic clouds (MCs) are transient structures containing large-scale magnetic flux ropes from solar eruptions. The twist of magnetic field lines around the rope axis reveals information about flux rope formation processes and geoeffectivity. During propagation, MC flux ropes may erode via reconnection with the ambient solar wind. Any erosion reduces the magnetic flux and helicity of the ropes, and changes their cross-sectional twist profiles. This study relates twist profiles in MC flux ropes observed at 1 AU to the amount of erosion undergone by the MCs in interplanetary space. The twist profiles of two well-identified MC flux ropes associated with the clear appearance of post eruption arcades in the solar corona are analysed. To infer the amount of erosion, the magnetic flux content of the ropes in the solar atmosphere is estimated, and compared to estimates at 1 AU. The first MC shows a monotonically decreasing twist from the axis to periphery, while the second displays high twist at the axis, rising twist near the edges, and lower twist in between. The first MC displays a larger reduction in magnetic flux between the Sun and 1 AU, suggesting more erosion, than that seen in the second MC. In the second cloud, rising twist at the rope edges may have been due to an envelope of overlying coronal field lines with relatively high twist, formed by reconnection beneath the erupting flux rope in the low corona. This high-twist envelope remained almost intact from the Sun to 1 AU due to the low erosion levels. In contrast, the high-twist envelope of the first cloud may have been entirely peeled away via erosion by the time it reaches 1 AU.

April 3-5-6, 2010, July 9-13-14, 2013

Flux erosion of magnetic clouds by reconnection with the Sun's open flux

Sanchita **Pal**, [Soumyaranjan Dash](#), [Dibyendu Nandy](#)

Geophysical Research Letters, 47, Issue 8, e2019GL086372, 2020

<https://arxiv.org/pdf/2103.05990.pdf>

<https://doi.org/10.1029/2019GL086372>

Magnetic clouds (MCs) are flux-rope magnetic structures forming a subset of solar coronal mass ejections which have significant space weather impacts. The geoeffectiveness of MCs depends on their properties which evolve during their interplanetary passage. Based on an analysis of observations spanning two solar cycles we establish that MCs interacting with the ambient solar wind magnetic field (i.e., heliospheric open flux) lose a substantial amount of their initial magnetic flux via magnetic reconnection, which in some cases, reduce their geoeffectiveness. We find a linear correlation between the eroded flux of MCs and solar open flux which is consistent with the scenario that MC erosion is mediated via the local heliospheric magnetic field draping around an MC during its interplanetary propagation. The solar open flux is governed by the sunspot cycle. This work therefore uncovers a hitherto unknown pathway for solar cycle modulation of the properties of MCs. 30 Sep 2002, 29 Jun 2014

Comparison between the magnetic properties of magnetic clouds and those of associated coronal flux ropes

Sanchita **Pal**

VarSITI Newsletter Vol. 21 p.11-13, 2019

http://newserver.stil.bas.bg/varsiti/newsL/VarSITI_Newsletter_Vol21.pdf

9-13 July 2013

Dependence of coronal mass ejection properties on their solar source active region characteristics and associated flare reconnection flux

Sanchita **Pal**, [Dibyendu Nandy](#), [Nandita Srivastava](#), [Nat Gopalswamy](#), [Suman Panda](#)

2018 Astrophysical Journal, Volume 865, Issue 1, article id. 4

<https://arxiv.org/pdf/1808.04144.pdf> File

<https://iopscience.iop.org/article/10.3847/1538-4357/aada10/pdf>

The near-Sun kinematics of coronal mass ejections (CMEs) determine the severity and arrival time of associated geomagnetic storms. We investigate the relationship between the deprojected speed and kinetic energy of CMEs and magnetic measures of their solar sources, reconnection flux of associated eruptive events and intrinsic flux rope characteristics. Our data covers the period 2010-2014 in solar cycle 24. Using vector magnetograms of source active regions we estimate the size and nonpotentiality. We compute the total magnetic reconnection flux at the source regions of CMEs using the post-eruption arcade method. By forward modeling the CMEs we find their deprojected geometric parameters and constrain their kinematics and magnetic properties. Based on an analysis of this database we report that the correlation between CME speed and their source active region size and global nonpotentiality is weak, but not negligible. We find the near-Sun velocity and kinetic energy of CMEs to be well correlated with the associated magnetic reconnection flux. We establish a statistically significant empirical relationship between the CME speed and reconnection flux that may be utilized for prediction purposes. Furthermore, we find CME kinematics to be related with the axial magnetic field intensity and relative magnetic helicity of their intrinsic flux ropes. The amount of coronal magnetic helicity shed by CMEs is found to be well correlated with their near-Sun speeds. The kinetic energy of CMEs is well correlated with their intrinsic magnetic energy density. Our results constrain processes related to the origin and propagation of CMEs and may lead to better empirical forecasting of their arrival and geoeffectiveness. **14 June, 2012**
Table 1. Properties of selected CMEs and associated source region information (2010-2014)

A Sun-to-Earth analysis of magnetic helicity of the 17-18 March 2013 interplanetary coronal mass ejection

Sanchita [Pal](#), [Nat Gopalswamy](#), [Dibyendu Nandy](#), [Sachiko Akiyama](#), [Seiji Yashiro](#), [Pertti Makela](#), [Hong Xie](#)
2017

<https://arxiv.org/pdf/1712.01114.pdf>

We compare the magnetic helicity in the 17-18 March 2013 interplanetary coronal mass ejection (ICME) flux-rope at 1 AU and in its solar counterpart. The progenitor coronal mass ejection (CME) erupted on **15 March 2013** from NOAA active region 11692 and associated with an M1.1 flare. We derive the source region reconnection flux using post-eruption arcade (PEA) method (Gopalswamy et al. 2017a) that uses the photospheric magnetogram and the area under the PEA. The geometrical properties of the near-Sun flux rope is obtained by forward-modeling of white-light CME observations. Combining the geometrical properties and the reconnection flux we extract the magnetic properties of the CME flux rope (Gopalswamy et al. 2017b). We derive the magnetic helicity of the flux rope using its magnetic and geometric properties obtained near the Sun and at 1 AU. We use a constant- α force-free cylindrical flux rope model fit to the in situ observations in order to derive the magnetic and geometric information of the 1-AU ICME. We find a good correspondence in both amplitude and sign of the helicity between the ICME and the CME assuming a semi-circular (half torus) ICME flux rope with a length of π AU. We find that about 83% of the total flux rope helicity at 1 AU is injected by the magnetic reconnection in the low corona. We discuss the effect of assuming flux rope length in the derived value of the magnetic helicity. This study connecting the helicity of magnetic flux ropes through the Sun-Earth system has important implications for the origin of helicity in the interplanetary medium and the topology of ICME flux ropes at 1 AU and hence their space weather consequences.

A coronal mass ejection encountered by four spacecraft within 1 au from the Sun: ensemble modelling of propagation and magnetic structure

Erika [Palmerio](#), Christina Kay, Nada Al-Haddad, Benjamin J Lynch, Domenico Trotta, Wenjuan Yu, Vincent E Ledvina, Beatriz Sánchez-Cano, Pete Riley, Daniel Heyner ++
MNRAS Volume 536, Issue 1, January **2025**, Pages 203–222,

<https://arxiv.org/pdf/2411.12706>

<https://doi.org/10.1093/mnras/stae2606>

<https://watermark.silverchair.com/stae2606.pdf>

Understanding and predicting the structure and evolution of coronal mass ejections (CMEs) in the heliosphere remains one of the most sought-after goals in heliophysics and space weather research. A powerful tool for improving current knowledge and capabilities consists of multispacecraft observations of the same event, which take place when two or more spacecraft fortuitously find themselves in the path of a single CME. Multiprobe events can not only supply useful data to evaluate the large-scale of CMEs from 1D in situ trajectories, but also provide additional constraints and validation opportunities for CME propagation models. In this work, we analyse and simulate the coronal and heliospheric evolution of a slow, streamer-blowout CME that erupted on **2021 September 23** and was encountered in situ by four spacecraft approximately equally distributed in heliocentric distance between 0.4 and 1 au. We employ the Open Solar Physics Rapid Ensemble Information modelling suite in ensemble mode to predict the CME arrival and structure in a hindcast fashion and to compute the ‘best-fitting’ solutions at the different spacecraft individually and

together. We find that the spread in the predicted quantities increases with heliocentric distance, suggesting that there may be a maximum (angular and radial) separation between an inner and an outer probe beyond which estimates of the in situ magnetic field orientation (parametrized by flux rope model geometry) increasingly diverge. We discuss the importance of these exceptional observations and the results of our investigation in the context of advancing our understanding of CME structure and evolution as well as improving space weather forecasts.

On the Mesoscale Structure of Coronal Mass Ejections at Mercury's Orbit: BepiColombo and Parker Solar Probe Observations

Erika **Palmerio**¹, Fernando Carcaboso², Leng Ying Khoo³, Tarik M. Salman^{4,5}, Beatriz Sánchez-Cano⁶, Benjamin J. Lynch^{7,8}, Yeimy J. Rivera⁹, Sanchita Pal², Teresa Nieves-Chinchilla⁴, Andreas J. Weiss²Show full author list

2024 ApJ 963 108

<https://iopscience.iop.org/article/10.3847/1538-4357/ad1ab4/pdf>

<https://arxiv.org/pdf/2401.01875.pdf>

On **2022 February 15**, an impressive filament eruption was observed off the solar eastern limb from three remote-sensing viewpoints, namely, Earth, STEREO-A, and Solar Orbiter. In addition to representing the most-distant observed filament at extreme ultraviolet wavelengths—captured by Solar Orbiter's field of view extending to above $6 R_{\odot}$ —this event was also associated with the release of a fast ($\sim 2200 \text{ km s}^{-1}$) coronal mass ejection (CME) that was directed toward BepiColombo and Parker Solar Probe. These two probes were separated by 2° in latitude, 4° in longitude, and 0.03 au in radial distance around the time of the CME-driven shock arrival in situ. The relative proximity of the two probes to each other and the Sun ($\sim 0.35 \text{ au}$) allows us to study the mesoscale structure of CMEs at Mercury's orbit for the first time. We analyze similarities and differences in the main CME-related structures measured at the two locations, namely, the interplanetary shock, the sheath region, and the magnetic ejecta. We find that, despite the separation between the two spacecraft being well within the typical uncertainties associated with determination of CME geometric parameters from remote-sensing observations, the two sets of in situ measurements display some profound differences that make understanding the overall 3D CME structure particularly challenging. Finally, we discuss our findings within the context of space weather at Mercury's distance and in terms of the need to investigate solar transients via spacecraft constellations with small separations, which has been gaining significant attention during recent years.

Modeling a Coronal Mass Ejection from an Extended Filament Channel. II. Interplanetary Propagation to 1 au

Erika **Palmerio**, [Anwsha Maharana](#), [Benjamin J. Lynch](#), [Camilla Scolini](#), [Simon W. Good](#), [Jens Pomoell](#), [Alexey Isavnin](#), [Emilia K. J. Kilpua](#)

ApJ 2023

<https://arxiv.org/pdf/2310.05846.pdf>

We present observations and modeling results of the propagation and impact at Earth of a high-latitude, extended filament channel eruption that commenced on **2015 July 9**. The coronal mass ejection (CME) that resulted from the filament eruption was associated with a moderate disturbance at Earth. This event could be classified as a so-called "problem storm" because it lacked the usual solar signatures that are characteristic of large, energetic, Earth-directed CMEs that often result in significant geoeffective impacts. We use solar observations to constrain the initial parameters and therefore to model the propagation of the **2015 July 9** eruption from the solar corona up to Earth using 3D magnetohydrodynamic heliospheric simulations with three different configurations of the modeled CME. We find the best match between observed and modeled arrival at Earth for the simulation run that features a toroidal flux rope structure of the CME ejecta, but caution that different approaches may be more or less useful depending on the CME-observer geometry when evaluating the space weather impact of eruptions that are extreme in terms of their large size and high degree of asymmetry. We discuss our results in the context of both advancing our understanding of the physics of CME evolution and future improvements to space weather forecasting.

CME Evolution in the Structured Heliosphere and Effects at Earth and Mars During Solar Minimum

Erika **Palmerio**, [Christina O. Lee](#), [Ian G. Richardson](#), [Teresa Nieves-Chinchilla](#), [Luiz F. G. Dos Santos](#), [Jacob R. Gruesbeck](#), [Nariaki V. Nitta](#), [M. Leila Mays](#), [Jasper S. Halekas](#), [Cary Zeitlin](#), [Shaosui Xu](#), [Mats Holmström](#), [Yoshifumi Futaana](#), [Tamitha Mulligan](#), [Benjamin J. Lynch](#), [Janet G. Luhmann](#)

Space Weather e2022SW003215 Volume 20 Issue 9 2022

<https://arxiv.org/pdf/2209.05760.pdf>

<https://agupubs.onlinelibrary.wiley.com/doi/epdf/10.1029/2022SW003215>

The activity of the Sun alternates between a solar minimum and a solar maximum, the former corresponding to a period of "quieter" status of the heliosphere. During solar minimum, it is in principle more straightforward to follow eruptive events and solar wind structures from their birth at the Sun throughout their interplanetary journey. In this paper, we report analysis of the origin, evolution, and heliospheric impact of a series of solar transient events that took place during the second half of August 2018, i.e. in the midst of the late declining phase of Solar Cycle 24. In particular, we focus on two successive coronal mass ejections (CMEs) and a following high-speed stream (HSS) on their way towards Earth and Mars. We find that the first CME impacted both planets, whilst the second caused a strong magnetic storm at Earth and went on to miss Mars, which nevertheless experienced space weather effects from the stream interacting region (SIR) preceding the HSS. Analysis of remote-sensing and in-situ data supported by heliospheric modelling suggests that CME--HSS interaction resulted in the second CME rotating and deflecting in interplanetary space, highlighting that accurately reproducing the ambient solar wind is crucial even during "simpler" solar minimum periods. Lastly, we discuss the upstream solar wind conditions and transient structures responsible for driving space weather effects at Earth and Mars. **20 August 2018**

Magnetic Structure and Propagation of Two Interacting CMEs from the Sun to Saturn

Erika **Palmerio**, [Teresa Nieves-Chinchilla](#), [Emilia K. J. Kilpua](#), [David Barnes](#), [Andrei N. Zhukov](#), [Lan K. Jian](#), [Olivier Witasse](#), [Gabrielle Provan](#), [Chihiro Tao](#), [Laurent Lamy](#), [Thomas J. Bradley](#), [M. Leila Mays](#), [Christian Möstl](#), [Elias Roussos](#), [Yoshifumi Futaana](#), [Adam Masters](#), [Beatriz Sánchez-Cano](#)
JGR **Volume126, Issue11** e2021JA029770 **2021**

<https://arxiv.org/pdf/2110.02190.pdf>

<https://agupubs.onlinelibrary.wiley.com/doi/epdf/10.1029/2021JA029770>

<https://doi.org/10.1029/2021JA029770>

One of the grand challenges in heliophysics is the characterisation of coronal mass ejection (CME) magnetic structure and evolution from eruption at the Sun through heliospheric propagation. At present, the main difficulties are related to the lack of direct measurements of the coronal magnetic fields and the lack of 3D in-situ measurements of the CME body in interplanetary space. Nevertheless, the evolution of a CME magnetic structure can be followed using a combination of multi-point remote-sensing observations and multi-spacecraft in-situ measurements as well as modelling. Accordingly, we present in this work the analysis of two CMEs that erupted from the Sun on **28 April 2012**. We follow their eruption and early evolution using remote-sensing data, finding indications of CME--CME interaction, and then analyse their interplanetary counterpart(s) using in-situ measurements at Venus, Earth, and Saturn. We observe a seemingly single flux rope at all locations, but find possible signatures of interaction at Earth, where high-cadence plasma data are available. Reconstructions of the in-situ flux ropes provide almost identical results at Venus and Earth but show greater discrepancies at Saturn, suggesting that the CME was highly distorted and/or that further interaction with nearby solar wind structures took place before 10 AU. This work highlights the difficulties in connecting structures from the Sun to the outer heliosphere and demonstrates the importance of multi-spacecraft studies to achieve a deeper understanding of the magnetic configuration of CMEs.

Predicting the Magnetic Fields of a Stealth CME Detected by Parker Solar Probe at 0.5 AU

Erika **Palmerio**, [Christina Kay](#), [Nada Al-Haddad](#), [Benjamin J. Lynch](#), [Wenyuan Yu](#), [Michael L. Stevens](#), [Sanchita Pal](#), [Christina O. Lee](#)

ApJ **920** 65 **2021**

<https://arxiv.org/pdf/2109.04933.pdf>

<https://iopscience.iop.org/article/10.3847/1538-4357/ac25f4/pdf>

<https://doi.org/10.3847/1538-4357/ac25f4>

Stealth coronal mass ejection (CMEs) are eruptions from the Sun that are not associated with appreciable low-coronal signatures. Because they often cannot be linked to a well-defined source region on the Sun, analysis of their initial magnetic configuration and eruption dynamics is particularly problematic. In this manuscript, we address this issue by undertaking the first attempt at predicting the magnetic fields of a stealth CME that erupted in 2020 June from the Earth-facing Sun. We estimate its source region with the aid of off-limb observations from a secondary viewpoint and photospheric magnetic field extrapolations. We then employ the Open Solar Physics Rapid Ensemble Information (OSPREDI) modelling suite to evaluate its early evolution and forward-model its magnetic fields up to Parker Solar Probe, which detected the CME in situ at a heliocentric distance of 0.5 AU. We compare our hindcast prediction with in-situ measurements and a set of flux rope reconstructions, obtaining encouraging agreement on arrival time, spacecraft crossing location, and magnetic field profiles. This work represents a first step towards reliable understanding and forecasting of the magnetic configuration of stealth CMEs and slow, streamer-blowout events. **2020 June 21-26**

CME Magnetic Structure and IMF Preconditioning Affecting SEP Transport

Erika **Palmerio**, [Emilia K. J. Kilpua](#), [Olivier Witasse](#), [David Barnes](#), [Beatriz Sánchez-Cano](#), [Andreas J. Weiss](#), [Teresa Nieves-Chinchilla](#), [Christian Möstl](#), [Lan K. Jian](#), ... See all authors

Space Weather [Volume19, Issue4](#), April 2021, e2020SW002654

<https://agupubs.onlinelibrary.wiley.com/doi/epdf/10.1029/2020SW002654> <https://doi.org/10.1029/2020SW002654>

Coronal mass ejections (CMEs) and solar energetic particles (SEPs) are two phenomena that can cause severe space weather effects throughout the heliosphere. The evolution of CMEs, especially in terms of their magnetic structure, and the configuration of the interplanetary magnetic field (IMF) that influences the transport of SEPs are currently areas of active research. These two aspects are not necessarily independent of each other, especially during solar maximum when multiple eruptive events can occur close in time. Accordingly, we present the analysis of a CME that erupted on **May 11, 2012** (SOL2012-05-11) and an SEP event following an eruption that took place on **May 17, 2012** (SOL2012-05-17). After observing the May 11 CME using remote-sensing data from three viewpoints, we evaluate its propagation through interplanetary space using several models. Then, we analyze in-situ measurements from five predicted impact locations (Venus, Earth, the Spitzer Space Telescope, the Mars Science Laboratory en route to Mars, and Mars) in order to search for CME signatures. We find that all in-situ locations detect signatures of an SEP event, which we trace back to the May 17 eruption. These findings suggest that the May 11 CME provided a direct magnetic connectivity for the efficient transport of SEPs. We discuss the space weather implications of CME evolution, regarding in particular its magnetic structure, and CME-driven IMF preconditioning that facilitates SEP transport. Finally, this work remarks the importance of using data from multiple spacecraft, even those that do not include space weather research as their primary objective.

Multipoint study of successive coronal mass ejections driving moderate disturbances at 1 AU

Erika **Palmerio**, [Camilla Scolini](#), [David Barnes](#), [Jasmina Magdalenić](#), [Matthew J. West](#), [Andrei N. Zhukov](#), [Luciano Rodriguez](#), [Marilena Mierla](#), [Simon W. Good](#), [Diana E. Morosan](#), [Emilia K. J. Kilpua](#), [Jens Pomoell](#), [Stefaan Poedts](#)

ApJ **878** 37 **2019**

<https://arxiv.org/pdf/1906.01353.pdf>

sci-hub.se/10.3847/1538-4357/ab1850

We analyse in this work the propagation and geoeffectiveness of four successive coronal mass ejections (CMEs) that erupted from the Sun during **21--23 May 2013** and that were detected in interplanetary space by the Wind and/or STEREO-A spacecraft. All these CMEs featured critical aspects for understanding so-called "problem space weather storms" at Earth. In the first three events a limb CMEs resulted in moderately geoeffective in-situ structures at their target location in terms of the disturbance storm time (Dst) index (either measured or estimated). The fourth CME, which also caused a moderate geomagnetic response, erupted from close to the disc centre as seen from Earth, but it was not visible in coronagraph images from the spacecraft along the Sun--Earth line and appeared narrow and faint from off-angle viewpoints. Making the correct connection between CMEs at the Sun and their in-situ counterparts is often difficult for problem storms. We investigate these four CMEs using multiwavelength and multipoint remote-sensing observations (extreme ultraviolet, white light, and radio), aided by 3D heliospheric modelling, in order to follow their propagation in the corona and in interplanetary space and to assess their impact at 1 AU. Finally, we emphasise the difficulties in forecasting moderate space weather effects provoked by problematic and ambiguous events and the importance of multispacecraft data for observing and modelling problem storms.

Coronal Magnetic Structure of Earthbound CMEs and In situ Comparison

Erika **Palmerio**, [Emilia K. J. Kilpua](#), [Christian Möstl](#), [Volker Bothmer](#), [Alexander W. James](#), [Lucie M. Green](#), [Alexey Isavnin](#), [Jackie A. Davies](#), [Richard A. Harrison](#)

Space Weather [Volume16, Issue5](#) Pages 442-460 **2018**

<https://arxiv.org/pdf/1803.04769.pdf> **File**

<http://sci-hub.tw/10.1002/2017SW001767>

Predicting the magnetic field within an Earth-directed coronal mass ejection (CME) well before its arrival at Earth is one of the most important issues in space weather research. In this article, we compare the intrinsic flux rope type, i.e. the CME orientation and handedness during eruption, with the in situ flux rope type for 20 CME events that have been uniquely linked from Sun to Earth through heliospheric imaging. Our study shows that the intrinsic flux rope type can be estimated for CMEs originating from different source regions using a combination of indirect proxies. We find that only 20% of the events studied match strictly between the intrinsic and in situ flux rope types. The percentage rises to 55% when intermediate cases (where the orientation at the Sun and/or in situ is close to 45{deg}) are considered as a match.

We also determine the change in the flux rope tilt angle between the Sun and Earth. For the majority of the cases, the rotation is several tens of degrees, whilst 35% of the events change by more than 90°. While occasionally the intrinsic flux rope type is a good proxy for the magnetic structure impacting Earth, our study highlights the importance of capturing the CME evolution for space weather forecasting purposes. Moreover, we emphasize that determination of the intrinsic flux rope type is a crucial input for CME forecasting models. **2012.06.14-17, 2013.04.11-14, 2013.07.09-13**
Table 1. A summary of the chirality and shear determinations used for each of the CMEs studied (2010-2015).

Planar magnetic structures in coronal mass ejection-driven sheath regions

Erika **Palmerio**¹, Emilia K. J. Kilpua¹, and Neel P. Savani

Ann. Geophys., 34, 313-322, **2016**

<http://www.ann-geophys.net/34/313/2016/angeo-34-313-2016.pdf>

<https://arxiv.org/pdf/1701.08739v1.pdf>

Planar magnetic structures (PMSs) are periods in the solar wind during which interplanetary magnetic field vectors are nearly parallel to a single plane. One of the specific regions where PMSs have been reported are coronal mass ejection (CME)-driven sheaths. We use here an automated method to identify PMSs in 95 CME sheath regions observed in situ by the Wind and ACE spacecraft between 1997 and 2015. The occurrence and location of the PMSs are related to various shock, sheath, and CME properties. We find that PMSs are ubiquitous in CME sheaths; 85 % of the studied sheath regions had PMSs with the mean duration of 6 h. In about one-third of the cases the magnetic field vectors followed a single PMS plane that covered a significant part (at least 67 %) of the sheath region. Our analysis gives strong support for two suggested PMS formation mechanisms: the amplification and alignment of solar wind discontinuities near the CME-driven shock and the draping of the magnetic field lines around the CME ejecta. For example, we found that the shock and PMS plane normals generally coincided for the events where the PMSs occurred near the shock (68 % of the PMS plane normals near the shock were separated by less than 20° from the shock normal), while deviations were clearly larger when PMSs occurred close to the ejecta leading edge. In addition, PMSs near the shock were generally associated with lower upstream plasma beta than the cases where PMSs occurred near the leading edge of the CME. We also demonstrate that the planar parts of the sheath contain a higher amount of strong southward magnetic field than the non-planar parts, suggesting that planar sheaths are more likely to drive magnetospheric activity.
18 May 2002

Automated Detection of Coronal Mass Ejections in STEREO Heliospheric Imager data

V. **Pant**, S. Willems, L. Rodriguez, M. Mierla, D. Banerjee, J. A. Davies

ApJ **2016**

<https://arxiv.org/pdf/1610.01904v1.pdf>

We have performed, for the first time, the successful automated detection of Coronal Mass Ejections (CMEs) in data from the inner heliospheric imager (HI-1) cameras on the STEREO A spacecraft. Detection of CMEs is done in time-height maps based on the application of the Hough transform, using a modified version of the CACTus software package, conventionally applied to coronagraph data. In this paper we describe the method of detection. We present the result of the application of the technique to a few CMEs that are well detected in the HI-1 imagery, and compare these results with those based on manual cataloging methodologies. We discuss in detail the advantages and disadvantages of this method. **2010-04-03**

SOLOHI'S VIEWPOINT ADVANTAGE: TRACKING THE FIRST MAJOR GEO-EFFECTIVE CORONAL MASS EJECTION OF THE CURRENT SOLAR CYCLE

E. **Paouris**^{1,2}, A. Vourlidis², P. Hess³, M. Georgoulis², G. Stenborg²

Solar Orbiter Nugget #30 May **2024**

<https://www.cosmos.esa.int/web/solar-orbiter/-/science-nugget-tracking-the-first-major-geo-effective-coronal-mass-ejection-of-the-current-solar-cycle>

On **April 23-24, 2023**, Earth experienced its first severe geomagnetic storm in eight years, marked by the Dst index reaching -213 nT and the K_p index exceeding 8,

The storm on April 23, 2023, was triggered by the arrival of an Earth-directed Coronal Mass Ejection (CME) detected in the corona on **April 21**, at around 18:00 UT. Originally the CME, associated with a filament eruption and a GOES M1.7 class solar flare, did not appear to be of particular concern. The low magnetic complexity of the active region (AR), as expressed through the calculation of the effective connected magnetic field strength [2] [Georgoulis and Rust, 2007] in the photosphere, further indicated that the solar signatures were not suggesting an impending major event. The CME characteristics -neither extreme in terms of speed nor of flare levels (see e.g. [3] [Paouris et al. 2023]) - did not suggest

that it could trigger the severe G4 geomagnetic storm that actually occurred taking the space weather community by surprise. This was certainly an extraordinary space weather event.

The Space Weather Context of the First Extreme Event of Solar Cycle 25, on 2022 September 5

Paouris, Evangelos ; [Vourlidas, Angelos](#) ; [Kouloumvakos, Athanasios](#) ; [Papaioannou, Athanasios](#) ;

[Jagarlamudi, Vamsee Krishna](#) ; [Horbury, Timothy](#)

The Astrophysical Journal, Volume 956, Issue 1, id.58, 13 pp. **2023**

<https://iopscience.iop.org/article/10.3847/1538-4357/acf30f/pdf>

The coronal mass ejection (CME) on 2022 September 5 was the fastest CME yet observed and measured in situ by a spacecraft inside the corona (0.06 au for the Parker Solar Probe). Here we assess the significance of this event for space weather studies by analyzing the source region characteristics and its temporal evolution via a magnetic complexity index. We also examine the kinematics and energetics of the CME. We find that it was a very fast and massive event, with a speed greater than 2200 km s⁻¹ and a mass of 2×10^{16} g. Consequently, this is within the top 1% of all CMEs observed by SOHO/LASCO since 1996. It is therefore natural to ask, "What if this CME was an Earth-directed one?" To answer this question, we put the CME and the associated flare properties in the context of similar previous extreme events (namely, the 2012 July 23 and 2012 March 7 eruptions), discussing the possibility that these trigger a solar energetic particle (SEP) event. We find that 2022 September 5 could have resulted in a high-energy SEP event. We also estimate the transit time and speed of the CME and calculate the likely Dst variations if this was an Earth-directed event.

Time-of-Arrival of Coronal Mass Ejections: A Two-Phase Kinematics Approach Based on Heliospheric Imaging Observations

Paouris Evangelos, [Vourlidas Angelos](#)

Space Weather e2022SW003070 **Volume20, Issue7 2022**

<https://doi.org/10.1029/2022SW003070>

<https://agupubs.onlinelibrary.wiley.com/doi/epdf/10.1029/2022SW003070>

The forecasting of the Time-of-Arrival (ToA) of coronal mass ejections (CMEs) to Earth does not yet meet most Space Weather users' requirements. The main physical reason is our incomplete understanding of CME propagation in the inner heliosphere. Therefore, many ToA forecasting algorithms rely on simple empirical relations to represent the interplanetary propagation phase using, mostly, kinematic information from coronagraphic observations below 30 solar radii (Rs) and a couple rather simplifying assumptions of constant direction and speed for the transient. We replace the assumption of constant speed in the inner heliosphere with a two-phase behavior consisting of a decelerating (or accelerating) phase from 20 Rs to some distance, followed by a coasting phase to Earth. In a nod towards a forecasting scheme, we consider Earth-directed CMEs, use kinematic measurements only from the Heliospheric Imagers aboard both STEREO spacecraft, treat each spacecraft separately to increase the event statistics, analyze the measurements in a data-assimilative fashion, and intercompare them against three localization schemes for single viewpoint observations (fixed- ϕ , harmonic mean and self-similar expansion). For the 21 cases, we obtain the best mean absolute error (MAE) of 6.4 ± 1.9 hours. In fact, the difference between calculated and observed ToA is < 52 minutes for 42% of the cases that return plausible ToA estimates. We find that some CMEs continue to decelerate beyond even 0.7 AU but reasonable forecasts should be possible with 31-hour lead time. This work is a proof-of-concept and an analysis of a larger event sample is required to fully validate this technique. **August 4, 2011, December 7, 2020**

Table 1. The sample of 13 CMEs/ICMEs and their associated solar flares used in our study 2010-2014, 2020

Propagating Conditions and the Time of ICME Arrival: A Comparison of the Effective Acceleration Model with ENLIL and DBEM Models

Evangelos **Paouris**, [Jaša Čalogović](#), [Mateja Dumbović](#), [M. Leila Mays](#), [Angelos Vourlidas](#), [Athanasios Papaioannou](#), [Anastasios Anastasiadis](#) & [Georgios Balasis](#)

Solar Physics volume 296, Article number: 12 (**2021**)

<https://link.springer.com/content/pdf/10.1007/s11207-020-01747-4.pdf>

The Effective Acceleration Model (EAM) predicts the Time-of-Arrival (ToA) of the Coronal Mass Ejection (CME) driven shock and the average speed within the sheath at 1 AU. The model is based on the assumption that the ambient solar wind interacts with the interplanetary CME (ICME) resulting in constant acceleration or deceleration. The upgraded version of the model (EAMv3), presented here, incorporates two basic improvements: (i) a new technique for the calculation of the acceleration (or deceleration) of the ICME from the Sun to 1 AU and (ii) a correction for the CME

plane-of-sky speed. A validation of the upgraded EAM model is performed via comparisons to predictions from the ensemble version of the Drag-Based model (DBEM) and the WSA-ENLIL+Cone ensemble model. A common sample of 16 CMEs/ICMEs, in 2013 – 2014, is used for the comparison. Basic performance metrics such as the mean absolute error (MAE), mean error (ME) and root mean squared error (RMSE) between observed and predicted values of ToA are presented. MAE for EAM model was 8.7 ± 1.68 hours while for DBEM and ENLIL was 14.3 ± 2.2 and 12.8 ± 1.7 hours, respectively. ME for EAM was -1.4 ± 2.7 hours in contrast with -9.7 ± 3.4 and -6.1 ± 3.3 hours from DBEM and ENLIL. We also study the hypothesis of stronger deceleration in the interplanetary (IP) space utilizing the EAMv3 and DBEM models. In particular, the DBEM model perform better when a greater value of drag parameter, of order of a factor of 3, is used in contrast to previous studies. EAMv3 model shows a deceleration of ICMEs at greater distances, with a mean value of 0.72 AU.

Table 2 Details for the 16 common CMEs/ICMEs and the calculated metrics for ENLIL, DBEMv1 and EAMv3 models. (2013-2014)

Assessing the projection correction of Coronal Mass Ejection speeds on Time-of-Arrival prediction performance using the Effective Acceleration Model

Evangoulos **Paouris**, [Angelos Vourlidas](#), [Athanasios Papaioannou](#), [Anastasios Anastasiadis](#)

Space Weather e2020SW002617 **Volume 19, Issue 2** 2021

<https://arxiv.org/ftp/arxiv/papers/2012/2012.04703.pdf>

<https://agupubs.onlinelibrary.wiley.com/doi/epdf/10.1029/2020SW002617>

<https://doi.org/10.1029/2020SW002617>

White light images of Coronal Mass Ejections (CMEs) are projections on the plane-of-sky (POS). As a result, CME kinematics are subject to projection effects. The error in the true (deprojected) speed of CMEs is one of the main causes of uncertainty to Space Weather forecasts, since all estimates of the CME Time-of-Arrival (ToA) at a certain location within the heliosphere require, as input, the CME speed. We use single viewpoint observations for 1037 flare-CME events between 1996-2017 and propose a new approach for the correction of the CME speed assuming radial propagation from the flare site. Our method is uniquely capable to produce physically reasonable deprojected speeds across the full range of source longitudes. We bound the uncertainty in the deprojected speed estimates via limits in the true angular width of a CME based on multiview-point observations. Our corrections range up to 1.37-2.86 for CMEs originating from the center of the disk. On average, the deprojected speeds are 12.8% greater than their POS speeds. For slow CMEs (VPOS < 400 km/s) the full ice-cream cone model performs better while for fast and very fast CMEs (VPOS > 700 km/s) the shallow ice-cream model gives much better results. CMEs with 691-878 km/s POS speeds have a minimum ToA mean absolute error (MAE) of 11.6 hours. This method, is robust, easy to use, and has immediate applicability to Space Weather forecasting applications. Moreover, regarding the speed of CMEs, our work suggests that single viewpoint observations are generally reliable.

Effective Acceleration Model for the Arrival Time of Interplanetary Shocks driven by Coronal Mass Ejections

Evangoulos **Paouris**, Helen Mavromichalaki

[Solar Physics](#) December 2017, 292:180

<https://link.springer.com/content/pdf/10.1007%2Fs11207-017-1212-2.pdf>

In a previous work (Paouris and Mavromichalaki in *Solar Phys.* 292, 30, 2017), we presented a total of 266 interplanetary coronal mass ejections (ICMEs) with as much information as possible. We developed a new empirical model for estimating the acceleration of these events in the interplanetary medium from this analysis. In this work, we present a new approach on the effective acceleration model (EAM) for predicting the arrival time of the shock that precedes a CME, using data of a total of 214 ICMEs. For the first time, the projection effects of the linear speed of CMEs are taken into account in this empirical model, which significantly improves the prediction of the arrival time of the shock. In particular, the mean value of the time difference between the observed time of the shock and the predicted time was equal to +3.03 hours with a mean absolute error (MAE) of 18.58 hours and a root mean squared error (RMSE) of 22.47 hours. After the improvement of this model, the mean value of the time difference is decreased to -0.28 hours with an MAE of 17.65 hours and an RMSE of 21.55 hours. This improved version was applied to a set of three recent Earth-directed CMEs reported in May, June, and July of 2017, and we compare our results with the values predicted by other related models. **23 May, 28 June, and 14 July 2017**

Interplanetary Coronal Mass Ejections Resulting from Earth-Directed CMEs Using SOHO and ACE Combined Data During Solar Cycle 23

Evangelos **Paouris**, Helen Mavromichalaki
Solar Physics February 2017, 292:30 **File**
<http://cosray.phys.uoa.gr/publications/D115.pdf>

In this work a total of 266 interplanetary coronal mass ejections observed by the Solar and Heliospheric Observatory/Large Angle and Spectrometric Coronagraph (SOHO/LASCO) and then studied by in situ observations from Advanced Composition Explorer (ACE) spacecraft, are presented in a new catalog for the time interval 1996 – 2009 covering Solar Cycle 23. Specifically, we determine the characteristics of the CME which is responsible for the upcoming ICME and the associated solar flare, the initial/background solar wind plasma and magnetic field conditions before the arrival of the CME, the conditions in the sheath of the ICME, the main part of the ICME, the geomagnetic conditions of the ICME's impact at Earth and finally we remark on the visual examination for each event. Interesting results revealed from this study include the high correlation coefficient values of the magnetic field (B_z) component against the Ap index ($r = 0.84$), as well as against the Dst index ($r = 0.80$) and of the effective acceleration against the CME linear speed ($r = 0.98$). We also identify a north–south asymmetry for X-class solar flares and an east–west asymmetry for CMEs associated with strong solar flares (magnitude $\geq M1.0$) which finally triggered intense geomagnetic storms (with $\text{Ap} \geq 179$). The majority of the geomagnetic storms are determined to be due to the ICME main part and not to the extreme conditions which dominate inside the sheath. For the intense geomagnetic storms the maximum value of the Ap index is observed almost 4 hours before the minimum Dst index. The amount of information makes this new catalog the most comprehensive ICME catalog for Solar Cycle 23. **6 November 2000**

There are many **ICME catalogs** which contain useful information as regards these events, such as those by Jian *et al.* (2006), Richardson and Cane (2010), Gopalswamy *et al.* (2010), Mitsakou and Moussas (2014) or more recently Chi *et al.* (2016). A comprehensive list of different ICME catalogs can be found at http://solar.gmu.edu/heliophysics/index.php/The_ISEST_ICME%5CCME_Lists or the ISEST Master CME list at http://solar.gmu.edu/heliophysics/index.php/The_ISEST_Master_CME_List.

Using the CME-index for short-term estimation of Ap geomagnetic index

Evangelos **Paouris**

The 11th Hellenic Astronomical Conference, held 8-12 September, 2013 in Athens, Greece.

Online at <http://www.helas.gr/conf/2013/>

Using the CME-index for short-term estimation of Ap geomagnetic index E. Paouris, M. Gerontidou and H. Mavromichalaki Faculty of Physics, University of Athens It is known that the long-term cosmic ray modulation is very well anticorrelated with the coronal mass ejections emitted from the Sun. For this reason a CME-index has introduced to these studies and improved very well the reproduced cosmic ray intensity (Mavromichalaki and Paouris, 2013). In this work this index is examined from a new perspective applied to the short-term estimation of geomagnetic index Ap with daily or weekly duration. The characteristics of CMEs as the number per day, the angular width and the linear velocity through a new relation for this daily index show a good approximation to the geomagnetic conditions after extreme events associated with CMEs and energetic solar flares. This study will be useful for the estimation of the geomagnetic Ap index and it is a first effort for short prediction of the geomagnetic conditions based on CMEs.

Ineffectiveness of Narrow CMEs for Cosmic Ray Modulation

Forbush

Evangelos **Paouris**

Solar Phys., June 2013, Volume 284, Issue 2, pp 589-597, 2013, **File**

Monthly coronal mass ejection (CME) counts, – for all CMEs and CMEs with widths $> 30^\circ$, – and monthly averaged speeds for the events in these two groups were compared with both the monthly averaged cosmic ray intensity and the monthly sunspot number. The monthly P i-index, which is a linear combination of monthly CME count rate and average speed, was also compared with the cosmic ray intensity and sunspot number. The main finding is that narrow CMEs, which were numerous during 2007 – 2009, are ineffective for modulation. A cross-correlation analysis, calculating both the Pearson (r) product–moment correlation coefficient and the Spearman (ρ) rank correlation coefficient, has been used. Between all CMEs and cosmic ray intensity we found correlation coefficients $r = -0.49$ and $\rho = -0.46$, while between CMEs with widths $> 30^\circ$ and cosmic ray intensity we found $r = -0.75$ and $\rho = -0.77$, which implies a significant increase. Finally, the best expression for the P i-index for the examined period was analyzed. The highly anticorrelated behavior among this CME index, the cosmic ray intensity ($r = -0.84$ and $\rho = -0.83$), and the sunspot number ($r = +0.82$ and $\rho = +0.89$) suggests that the first one is a very useful solar–heliospheric parameter for heliospheric and space weather models in general..

Large Forbush Decreases and their Solar Sources: Features and Characteristics

M. **Papailiou**, M. **Abunina**, A. **Belov**, E. **Eroshenko**, V. **Yanke** & H. **Mavromichalaki**
[Solar Physics](#) volume 295, Article number: 164 (2020)

<https://link.springer.com/content/pdf/10.1007/s11207-020-01735-8.pdf>

One of the factors responsible for the wide variety of Forbush decreases is the different solar sources related to them. In this investigation the different features and characteristics of Forbush decreases, with emphasis on large Forbush decreases and their association with solar sources, are examined. Initially, a wider selection of events from the Pushkov Institute of Terrestrial Magnetism, Ionosphere and Radiowave Propagation of the Russian Academy of Sciences Forbush decreases database served as a starting point for this study, which was then narrowed down to a group of large Forbush decreases. According to the helio-longitude of the solar source, the events under study were separated into three subcategories: western ($21^\circ \leq \text{helio-longitude} \leq 60^\circ$), eastern ($-60^\circ \leq \text{helio-longitude} \leq -21^\circ$), and central ($-20^\circ \leq \text{helio-longitude} \leq 20^\circ$). The selected events cover the period 1967–2017. The “Global Survey Method” was used for analyzing the aforementioned Forbush decreases, along with data on solar flares, solar-wind speed, geomagnetic indices (Kp and Dst), and interplanetary magnetic field. The superimposed epoch method was applied to display the temporal profiles for the selected events. This detailed analysis reveals interesting results concerning the features of cosmic-ray decreases in relation to the helio-longitude of the solar sources. Specifically, Forbush decreases related to central or eastern solar sources are more often observed, have a greater magnitude, and present a slower development than Forbush decreases related to western sources, which are rarer, have a smaller magnitude, and have a shorter lifespan. Nevertheless, regardless of the helio-longitude of the solar source, large Forbush decreases are accompanied by increased geomagnetic activity and increased anisotropy, including anisotropy before the events, which can serve as a typical precursor of Forbush decreases. **17 August 2001, 07 September 2002, 22 January 2004**

Interplanetary Coronal Mass Ejections as the Driver of Non-recurrent Forbush Decreases

Athanasios **Papaioannou**¹, Anatoly Belov², Maria Abunina², Eugenia Eroshenko², Artem Abunin², Anastasios Anastasiadis¹, Spiros Patsourakos³, and Helen Mavromichalaki⁴
2020 ApJ 890 101

<https://sci-hub.si/10.3847/1538-4357/ab6bd1>

Interplanetary coronal mass ejections (ICMEs) are the counterparts of coronal mass ejections (CMEs) that extend in the interplanetary (IP) space and interact with the underlying solar wind (SW). ICMEs and their corresponding shocks can sweep out galactic cosmic rays (GCRs) and thus modulate their intensity, resulting in non-recurrent Forbush decreases (FDs). In this work, we selected all FDs that were associated with a sudden storm commencement (SSC) at Earth, and a solar driver (e.g., CME) was clearly identified as the ICME's source. We introduce and employ the t_H parameter, which is the time delay (in hours) of the maximum strength of the interplanetary magnetic field from the FD onset (as is marked via the SSC), and consequently derive three groups of FD events (i.e., the early, medium, and late ones). For each of these we examine the mean characteristics of the FDs and the associated IP variations per group, as well as the resulting correlations. In addition, we demonstrate the outputs of a superposed epoch analysis, which led to an average time profile of the resulting FDs and the corresponding IP variations, per group. Finally, we interpret our results based on the theoretical expectations for the FD phenomenon. We find that both the shock sheath and the ejecta are necessary for deep GCR depressions and that the FD amplitude (A_0) is larger for faster-propagating ICMEs. Additionally, we note the importance of the turbulent shock-sheath region across all groups. Finally, we present empirical relations connecting A_0 to SW properties. **2000 February 20–22, 2001 May 27–29, 2002 April 17–20, 2006 December 13–16**
Table 5 List of the 42 Forbush Decreases Used in This Study (1997–2016)

Satellite Drag Analysis During the May 2024 Geomagnetic Storm

William E. **Parker**¹ and Richard Linares ²

JGR **2024**

<https://arxiv.org/html/2406.08617v1>

Between May 10–12, 2024, Earth saw its largest geomagnetic storm in over 20 years. Since the last major storm in 2003, the population of satellites in low Earth orbit has surged following the commercialization of space services and the ongoing establishment of proliferated LEO constellations. In this note, we investigate the various impacts of the geomagnetic storm on satellite operations. A forecast performance assessment of the geomagnetic index $a_{\text{p}}^{\text{[X]}}$ shows that the magnitude and duration of the storm were poorly predicted, even one day in advance. Total mass density enhancements in the thermosphere are identified by tracking satellite drag decay characteristics. A history of two-line element (TLE) data from the entire NORAD catalog in LEO is used to observe large-scale trends. Better understanding how geomagnetic storms impact satellite operations is critical for maintaining satellite safety and ensuring long-term robust sustainability in LEO.

See <https://www.spaceweather.com> for 12 Jul 2024

Forbush decreases at a middle latitude neutron monitor: relations to geomagnetic activity and to interplanetary plasma structures

I. [Parnahaj](#) , K. Kudela

[Astrophysics and Space Science](#) September 2015, 359:35 **File**

Results of statistical study on relations between Forbush decreases (FDs) as observed at a middle-latitude, high mountain cosmic ray (CR) neutron monitor (NM), and the geomagnetic storms (GS), as well as on connections of FDs to interplanetary plasma structures, are presented. Study confirms and extends (until 2014) earlier results based on NM data from different geomagnetic cut-off positions and covering earlier periods, namely that FDs associated with halo coronal mass ejections (CMEs) and those related with the shocks correspond to higher amplitudes of FDs than those without the mentioned features.

Magnetospheric transmissivity for cosmic rays during selected recent events with interplanetary/geomagnetic disturbances

[Parnahaj](#), I. ; [Bobík](#), P. ; [Kudela](#), K.

Journal of Physics: Conference Series, Volume 632, Issue 1, article id. 012064 (2015).

The variability of cosmic rays (CRs) observed at selected European neutron monitors (NMs) around moderate geomagnetic disturbances, namely during the intervals (a) **DOY 49-51 in 2014**, (b) **DOY 58-59 in 2014**, (c) **DOY 238-240 in 2014** and (d) **DOY 6-8 in 2015** is discussed. Assuming the primary spectra of the CREME96 model, the yield function and geomagnetic transmissivity changes provided by the Tsyganenko96 model, the expected increases at the mid-latitude station Lomnický štít are compared with the observed ones. The examples stress the importance of including anisotropy of the CR flux in interplanetary space, the use of other geomagnetic field models and other yield functions to the computations in future analysis.

Precursory Signs of Large Forbush Decreases: The Criterion of Anisotropy.

[Papailiou](#), M., [Abunina](#), M., [Mavromichalaki](#), H. et al.

Sol Phys 299, 154 (2024).

<https://doi.org/10.1007/s11207-024-02391-y>

The study of precursors preceding Forbush decreases belongs to the applied side of space research and to a relatively new area of modern science, that of Space Weather. Moreover, it is a pioneering and innovative research field with interesting results. In the framework of the above, the Athens Cosmic Ray Group of the National and Kapodistrian University of Athens (NKUA) and the Cosmic Ray Group of the Pushkov Institute of Terrestrial Magnetism, Ionosphere and Radiowave Propagation of the Russian Academy of Sciences (IZMIRAN) have collaborated in investigating predecreases and/or preincreases of the cosmic-ray intensity before the development of a Forbush decrease, that could serve as precursory signs of the upcoming event and consequently play a significant role in the prediction of cosmic-ray and geomagnetic activity. In this work, the criterion of the increased anisotropy one hour before the onset of the event (A_{xyb} , %) is being examined for large Forbush decreases. Specifically, Forbush decreases with magnitude greater than 5%, accompanied with geomagnetic storms (i.e., geomagnetic index $Dst < -100$ nT and $5 \leq Kp\text{-index} \leq 9$) and characterized by $A_{xyb} \geq 0.8\%$ were analyzed. The catalog of Forbush Effects and Interplanetary Disturbances of IZMIRAN was used for analyzing the solar, interplanetary, and geomagnetic conditions during each event. Additionally, for a visual inspection of the precursory signs in each event the Ring of Stations method (i.e., asymptotic longitude–time diagram) was applied. Results revealed that the increased anisotropy one hour before the main phase of the Forbush decrease is a valid and reliable criterion of precursors that can be eventually used in the development of a Forbush decrease prognosis application tool.

Precursory Signs of Large Forbush Decreases

M. [Papailiou](#), [M. Abunina](#), [H. Mavromichalaki](#), [A. Belov](#), [A. Abunin](#), [E. Eroshenko](#) & [V. Yanke](#)

[Solar Physics](#) volume 296, Article number: 100 (2021)

<https://link.springer.com/content/pdf/10.1007/s11207-021-01844-y.pdf>

<https://doi.org/10.1007/s11207-021-01844-y>

The study of space-weather effects and more specifically Forbush decreases of the cosmic-ray intensity depends on space and ground measurements. Very often Forbush decreases and geomagnetic storms are accompanied by pre-increases and/or pre-decreases manifested in cosmic-ray behavior, known as precursory signs. These cosmic-ray intensity variations do not coincide with the shock arrival but begin well before (up to 24 hours) the onset of the main event. In this study a group of large Forbush decreases with amplitude $\geq 4\%$ was examined for precursors. According to the helio-longitude of the solar source, the events were separated into three categories: western ($21^\circ \leq$ helio-longitude

$\leq 60^\circ$), eastern ($-60^\circ \leq$ helio-longitude $\leq -21^\circ$), and central ($-20^\circ \leq$ helio-longitude $\leq 20^\circ$). The selected events cover 1967 – 2017. The analysis of the Forbush decreases and the plotting of the asymptotic longitudinal cosmic-ray distribution diagrams were based on the “Global Survey Method” and the “Ring of Stations” method, respectively. Data on solar flares, solar-wind speed, interplanetary magnetic field, and geomagnetic indices (Kp and Dst) were also used. The results show the clear signs of precursors in a significant number of events. **6-7 Jun 1979, 2-4 Sep 1981, 1-2 Oct 1991, 3-5 Nov 2003, 26-27 Jul 2004, 14-15 May 2005, 15-16 May 2005, 12-15 Apr 2013, 15-19 Mar 2015, 5-7 Nov 2015,**

Table 1 Classification of Forbush decreases, revealing precursory signals according to their solar sources.

Large Forbush Decreases and their Solar Sources: Features and Characteristics

M. [Papailiou](#), [M. Abunina](#), [A. Belov](#), [E. Eroshenko](#), [V. Yanke](#) & [H. Mavromichalaki](#)

[Solar Physics](#) volume 295, Article number: 164 (2020)

<https://link.springer.com/content/pdf/10.1007/s11207-020-01735-8.pdf>

One of the factors responsible for the wide variety of Forbush decreases is the different solar sources related to them. In this investigation the different features and characteristics of Forbush decreases, with emphasis on large Forbush decreases and their association with solar sources, are examined. Initially, a wider selection of events from the Pushkov Institute of Terrestrial Magnetism, Ionosphere and Radiowave Propagation of the Russian Academy of Sciences Forbush decreases database served as a starting point for this study, which was then narrowed down to a group of large Forbush decreases. According to the helio-longitude of the solar source, the events under study were separated into three subcategories: western ($21^\circ \leq$ helio-longitude $\leq 60^\circ$), eastern ($-60^\circ \leq$ helio-longitude $\leq -21^\circ$), and central ($-20^\circ \leq$ helio-longitude $\leq 20^\circ$). The selected events cover the period 1967 – 2017. The “Global Survey Method” was used for analyzing the aforementioned Forbush decreases, along with data on solar flares, solar-wind speed, geomagnetic indices (Kp and Dst), and interplanetary magnetic field. The superimposed epoch method was applied to display the temporal profiles for the selected events. This detailed analysis reveals interesting results concerning the features of cosmic-ray decreases in relation to the helio-longitude of the solar sources. Specifically, Forbush decreases related to central or eastern solar sources are more often observed, have a greater magnitude, and present a slower development than Forbush decreases related to western sources, which are rarer, have a smaller magnitude, and have a shorter lifespan. Nevertheless, regardless of the helio-longitude of the solar source, large Forbush decreases are accompanied by increased geomagnetic activity and increased anisotropy, including anisotropy before the events, which can serve as a typical precursor of Forbush decreases. **17 August 2001, 07 September 2002, 22 January 2004**

Forbush Decreases Associated with Western Solar Sources and Geomagnetic Storms: A Study on Precursors

M. [Papailiou](#), [H. Mavromichalaki](#), [M. Abunina](#), [A. Belov](#), [E. Eroshenko](#), [V. Yanke](#), [O. Kryakunova](#)

[Solar Physics](#), April 2013, Volume 283, Issue 2, pp 557-563

<http://cosray.phys.uoa.gr/Publications/D97.pdf>

As suggested in many studies the pre-increases or pre-decreases of the cosmic ray intensity (known as precursors), which usually precede a Forbush decrease, could serve as a useful tool for studying space weather effects. The events in this study were chosen based on two criteria. Firstly, the heliolongitude of the solar flare associated with each cosmic ray intensity decrease was in the $50^\circ - 70^\circ$ W sector and, secondly, the values of the geomagnetic activity index, Kp max, were ≥ 5 . Twenty five events were selected from 1967 to 2006. We have used data on solar flares, solar wind speed, geomagnetic indices (Kp and Dst), and interplanetary magnetic field in our detailed analysis. The asymptotic longitudinal cosmic ray distribution diagrams were plotted using the “Ring of Stations” method for all the events. The results reveal clear signs of precursors in 60 % of selected events.

Table

The Asymptotic Longitudinal Cosmic Ray Intensity Distribution as a Precursor of Forbush Decreases

M. [Papailiou](#), [H. Mavromichalaki](#), [A. Belov](#), [E. Eroshenko](#), [V. Yanke](#)

[Solar Physics](#), October 2012, Volume 280, Issue 2, pp 641-650

Identifying the precursors (pre-increases or pre-decreases) of a geomagnetic storm or a Forbush decrease is of great importance since they can forecast and warn of oncoming space weather effects. A wide investigation using 93 events which occurred in the period from 1967 to 2006 with an anisotropy $A_{xy} > 1.2\%$ has been conducted. Twenty-seven of the events revealed clear signs of precursors and were classified into three categories. Here we present one of the aforementioned groups, including five Forbush decreases (**24 June 1980, 28 October 2000, 17 August 2001, 23 April**

2002, and 10 May 2002). Apart from hourly cosmic ray intensity data, provided by the worldwide network of neutron monitor stations, data on solar flares, solar wind speed, geomagnetic indices (Kp and Dst), and interplanetary magnetic field were used for the analysis of the examined cosmic ray intensity decreases. The asymptotic longitudinal cosmic ray distribution diagrams were plotted using the “ring of stations” method. Results reveal a long pre-decrease up to 24 hours before the shock arrival in a narrow longitudinal zone from 90° to 180°.

Precursor Effects in Different Cases of Forbush Decreases

M. [Papailiou](#), H. Mavromichalaki, A. Belov, E. Eroshenko and V. Yanke

Solar Physics, Volume 276, Numbers 1-2, 337-350, **2012**

Over the last few years, the pre-decreases or pre-increases of the cosmic-ray intensity observed before a Forbush decrease, called the precursor effect and registered by the worldwide neutron monitor network, have been investigated for different cases of intense events. The Forbush decreases presented in this particular study were chosen from a list of events that occurred in the time period 1967–2006 and were characterized by an enhanced first harmonic of cosmic-ray anisotropy prior to the interplanetary disturbance arrival. The asymptotic longitudinal cosmic-ray distribution diagrams for the events under consideration were studied using the “Ring of Stations” method, and data on solar flares, solar-wind speed, geomagnetic indices, and interplanetary magnetic field were analyzed in detail. The results revealed that the use of this method allowed the selection of a large number of events with well-defined precursors, which could be separated into at least three categories, according to duration and longitudinal zone. Finally, this analysis showed that the first harmonic of cosmic-ray anisotropy could serve as an adequate tool in the search for precursors and could also be evidence for them.

A Catalogue of Forbush Decreases Recorded on the Surface of Mars from 2012 Until 2016: Comparison with Terrestrial FDs

A. [Papaioannou](#), [A. Belov](#), [M. Abunina](#), [J. Guo](#), [A. Anastasiadis](#)...

[Solar Physics](#) June **2019**, 294:66

[sci-hub.se/10.1007/s11207-019-1454-2](https://doi.org/10.1007/s11207-019-1454-2)

<https://link.springer.com/content/pdf/10.1007%2Fs11207-019-1454-2.pdf>

Forbush decreases (FDs) in galactic cosmic rays (GCRs) have been recorded by neutron monitors (NMs) at Earth for more than 60 years. For the past five years, with the establishment of the Radiation Assessment Detector (RAD) onboard the Mars Science Laboratory (MSL) rover Curiosity at Mars, it is possible to continuously detect, for the first time, FDs at another planet: Mars. In this work, we have compiled a catalogue of 424 FDs at Mars using RAD dose rate data, from 2012 to 2016. Furthermore, we applied, for the first time, a comparative statistical analysis of the FDs measured at Mars, by RAD, and at Earth, by NMs, for the same time span. A carefully chosen sample of FDs at Earth and at Mars, driven by the same ICME, led to a significant correlation ($cc=0.71$) and a linear regression between the sizes of the FDs at the different observing points at the respective energies at Mars and Earth. We show that the amplitude of the FD at Mars (AMAM), for an energy of $E>150$ MeV, is higher by a factor of 1.5–2 compared to the size of the FD at Earth (AEAE), for a definite rigidity of 10 GV. Finally, almost identical regressions were obtained for both Earth and Mars as concerns the dependence of the maximum hourly decrease of the CR density (DMin/DMin) to the size of the FD.

2014.01.09, 2014.02.14-20, 2014.02.21-27

Table 2012 to 2016

On the Analysis of the Complex Forbush Decreases of January 2005

[Papaioannou](#), A.; [Malandraki](#), O.; [Belov](#), A.; [Skoug](#), R.; [Mavromichalaki](#), H.; [Eroshenko](#), E.; [Abunin](#), A.; [Lepri](#), S.

Solar Physics, Volume 266, Issue 1, pp.181-193, **2010; File**

In this work an analysis of a series of complex cosmic ray events that occurred between **17 January 2005 and 23 January 2005** using solar, interplanetary and ground based cosmic ray data is being performed. The investigated period was characterized both by significant galactic cosmic ray (GCR) and solar cosmic ray (SCR) variations with highlighted cases such as the noticeable series of Forbush effects (FEs) from 17 January 2005 to 20 January 2005, the Forbush decrease (FD) on 21 January 2005 and the ground level enhancement (GLE) of the cosmic ray counter measurements on 20 January 2005. The analysis is focusing on the aforementioned FE cases, with special attention drawn on the 21 January 2005, FD event, which demonstrated several exceptional features testifying its uniqueness. Data from the ACE spacecraft, together with GOES X-ray recordings and LASCO CME coronagraph images were used in conjunction to the ground based recordings of the Worldwide Neutron Monitor Network, the interplanetary data of OMNI database and the geomagnetic activity manifestations denoted by K p and D st indices. More than that, cosmic ray characteristics as density, anisotropy and density gradients were also calculated. The results illustrate the state of the interplanetary space

that cosmic rays crossed and their corresponding modulation with respect to the multiple extreme solar events of this period. In addition, the western location of the 21 January 2005 solar source indicates a new cosmic ray feature, which connects the position of the solar source to the cosmic ray anisotropy variations. In the future, this feature could serve as an indicator of the solar source and can prove to be a valuable asset, especially when satellite data are unavailable.

The unusual cosmic ray variations in July 2005 resulted from western and behind the limb solar activity

A. [Papaioannou](#), A. Belovb, , H. Mavromichalakia, , , E. Eroshenkob, and V. Olenevab
Advances in Space Research, Volume 43, Issue 4, 16 February 2009, Pages 582-588, **File**

One of the most interesting and unusual periods of the recent solar activity was July 2005. Despite the fact that it was a late declining phase of the 23rd solar cycle, generally a time of solar quiescence, that period was marked by extreme activity. The main events occurred at the invisible side of the Sun and did not reveal significant consequences in the Earth or near the Earth. However, cosmic ray variations testify to the high power of these events. A rather unusual Forbush effect was observed starting from July 16, 2005. It was characterized by very large cosmic ray anisotropy, the magnitude and direction of which are in accordance with a western powerful source. Usually in such a case when the main interplanetary disturbance is far in the west, the Forbush effect is absent or it is very small and short lasting. In July 2005 a rare exclusion was observed which may testify to the giant decrease of 10 GV cosmic ray density (quite possible $\geq 30\%$, indicating an unusually high cosmic ray gradient) to the west from the Sun-Earth line. In this work, a description of the July 2005 situation as well as the results of the convection- diffusion treatment with space cosmic ray gradients is presented. Some general remarks concerning extreme western solar events and their impact on cosmic rays are also discussed.

See ESA Space Weather Week 2, November 2005

<http://esa-spaceweather.net/spweather/workshops/eswwII/proc/Session1/SESWW-Papaioannou-Poster-pdf.pdf>

The burst of solar and geomagnetic activity in August–September 2005

A. [Papaioannou](#)¹, H. Mavromichalaki¹, E. Eroshenko², A. Belov², and V. Oleneva²
Ann. Geophys., 27, 1019–1026, 2009, **File**

During the August–September 2005 burst of solar activity, close to the current solar cycle minimum, a significant number of powerful X-ray flares were recorded, among which was the outstanding X17.0 flare of 7 September 2005. Within a relatively short period (from 22 August to 17 September) two severe magnetic storms were also recorded as well as several Forbush effects. These events are studied in this work, using hourly mean variations of cosmic ray density and anisotropy, derived from data of the neutron monitor network. During these Forbush effects the behavior of high energy cosmic ray characteristics (density and anisotropy) is analyzed together with interplanetary disturbances and their solar sources, and is compared to the variations observed in geomagnetic activity. A big and long lasting (~6 h) cosmic ray pre-decrease (~2%) is defined before the shock arrival on 15 September 2005. The calculated cosmic ray gradients for September 2005 are also discussed.

Measures of Scale Dependent Alfvénicity in the First PSP Solar Encounter

T. N. [Parashar](#), [M. L. Goldstein](#), [B. A. Maruca](#), [W. H. Matthaeus](#),

ApJ 2019

<https://arxiv.org/pdf/1912.07181.pdf>

The solar wind shows periods of highly Alfvénic activity, where velocity fluctuations and magnetic fluctuations are aligned or anti-aligned with each other. It is generally agreed that solar wind plasma velocity and magnetic field fluctuations observed by Parker Solar Probe (PSP) during the first encounter are mostly highly Alfvénic. However, quantitative measures of Alfvénicity are needed to understand how the characterization of these fluctuations compares with standard measures from prior missions in the inner and outer heliosphere, in fast wind and slow wind, and at high and low latitudes. To investigate this issue, we employ several measures to quantify the extent of Alfvénicity -- the Alfvén ratio r_A , {normalized} cross helicity σ_c , {normalized} residual energy σ_r , and the cosine of angle between velocity and magnetic fluctuations $\cos\theta_{vb}$. We show that despite the overall impression that the Alfvénicity is large in the solar wind sampled by PSP during the first encounter, during some intervals the cross helicity starts decreasing at very large scales. These length-scales (often $>1000d_i$) are well inside inertial range, and therefore, the suppression of cross helicity at these scales cannot be attributed to kinetic physics. This drop at large scales could potentially be

explained by large-scale shears present in the inner heliosphere sampled by PSP. In some cases, despite the cross helicity being constant down to the noise floor, the residual energy decreases with scale in the inertial range. These results suggest that it is important to consider all these measures to quantify Alfvénicity. **3-10 Nov 2018**

Linking the Sun to the Heliosphere Using Composition Data and Modelling. A Test Case with a Coronal Jet

Susanna **Parenti**, [Julia Chifu](#), [Giulio Del Zanna](#), [Justin Edmondson](#), [Alessandra Giunta](#), [Viggo H. Hansteen](#), [Aleida Higginson](#), [J. Martin Laming](#), [Susan T. Lepri](#), [Benjamin J. Lynch](#), [Yeimy J. Rivera](#), [Rudolf von Steiger](#), [Thomas Wiegmann](#), [Robert F. Wimmer-Schweingruber](#), [Natalia Zambrana Prado](#), [Gabriel Pelouze](#)

Space Science Reviews **2021**

<https://arxiv.org/pdf/2110.06111.pdf>

Our understanding of the formation and evolution of the corona and the heliosphere is linked to our capability of properly interpreting the data from remote sensing and in-situ observations. In this respect, being able to correctly connect in-situ observations with their source regions on the Sun is the key for solving this problem. In this work we aim at testing a diagnostics method for this connectivity. This paper makes use of a coronal jet observed on **2010 August 2nd** in active region 11092 as a test for our connectivity method. This combines solar EUV and in-situ data together with magnetic field extrapolation, large scale MHD modeling and FIP (First Ionization Potential) bias modeling to provide a global picture from the source region of the jet to its possible signatures at 1AU. Our data analysis reveals the presence of outflow areas near the jet which are within open magnetic flux regions and which present FIP bias consistent with the FIP model results. In our picture, one of these open areas is the candidate jet source. Using a back-mapping technique we identified the arrival time of this solar plasma at the ACE spacecraft. The in-situ data show signatures of changes in the plasma and magnetic field parameters, with FIP bias consistent with the possible passage of the jet material. Our results highlight the importance of remote sensing and in-situ coordinated observations as a key to solve the connectivity problem. We discuss our results in view of the recent Solar Orbiter launch which is currently providing such unique data. **2-5 Aug 2010**

Near-Earth Interplanetary Coronal Mass Ejections and Their Association with DH Type II Radio Bursts During Solar Cycles 23 and 24

Binal D. **Patel**, [Bhuwan Joshi](#), [Kyung-Suk Cho](#), [Rok-Soon Kim](#) & [Yong-Jae Moon](#)

[Solar Physics](#) volume 297, Article number: 139 (**2022**)

<https://doi.org/10.1007/s11207-022-02073-7>

<https://arxiv.org/pdf/2210.14535.pdf>

We analyse the characteristics of interplanetary coronal mass ejections (ICMEs) during Solar Cycles 23 and 24. The present analysis is primarily based on the near-Earth ICME catalogue (Richardson and Cane, [2010](#)). An important aspect of this study is to understand the near-Earth and geoeffective aspects of ICMEs in terms of their association (type II ICMEs) versus absence (non-type II ICMEs) of decameter-hectometer (DH) type II radio bursts, detected by Wind/WAVES and STEREO/WAVES. Notably, DH type II radio bursts driven by a CME indicate powerful MHD shocks leaving the inner corona and entering the interplanetary medium. We find a drastic reduction in the occurrence of ICMEs by 56% in Solar Cycle 24 compared to the previous cycle (64 versus 147 events). Interestingly, despite a significant decrease in ICME/CME counts, both cycles contain almost the same fraction of type II ICMEs ($\approx 47\%$). Our analysis reveals that, even at a large distance of 1 AU, type II CMEs maintain significantly higher speeds compared to non-type II events (523 km s^{-1} versus 440 km s^{-1}). While there is an obvious trend of decrease in ICME transit times with increase in the CME initial speed, there also exists a noticeable wide range of transit times for a given CME speed. Contextually, Cycle 23 exhibits 10 events with shorter transit times ranging between 20 – 40 hours of predominantly type II categories while, interestingly, Cycle 24 almost completely lacks such “fast” events. We find a significant reduction in the parameter $\text{VICME} \times \text{Bz}_{\text{VICME} \times \text{Bz}}$, the dawn to dusk electric field, by 39% during Solar Cycle 24 in comparison with the previous cycle. Further, $\text{VICME} \times \text{Bz}_{\text{VICME} \times \text{Bz}}$ shows a strong correlation with Dst index, which even surpasses the consideration of BzBz and $\text{VICME}_{\text{VICME}}$ alone. The above results imply the crucial role of $\text{VICME} \times \text{Bz}_{\text{VICME} \times \text{Bz}}$ toward effectively modulating the geoeffectiveness of ICMEs.

A LOW FREE-PARAMETER STOCHASTIC MODEL OF DAILY FORBUSH DECREASE INDICES

Sankar Narayan **Patra**, Gautam Bhattacharyab, , Subhash Chandra Panjac, , Koushik Ghosh
Journal of Atmospheric and Solar-Terrestrial Physics, Volume 107, January **2014**, Pages 30–35

Forbush decrease is a rapid decrease in the observed galactic cosmic ray intensity pattern occurring after a coronal mass ejection. In the present paper we have analyzed the daily Forbush decrease indices from January, 1967 to December, 2003 generated in IZMIRAN, Russia. First the entire indices have been smoothed and next we have made an attempt to fit a suitable stochastic model for the present time series by means of a necessary number of process parameters. The study reveals that the present time series is governed by a stationary autoregressive process of order 2 with a trace of white noise. Under the consideration of the present model we have shown that chaos is not expected in the present time series which opens up the possibility of validation of its forecasting (both short-term and long-term) as well as its multi-periodic behaviour.

Constraints on the variable nature of the slow solar wind with the Wide-Field Imager on board the Parker Solar Probe

Spiros **Patsourakos**, [Angelos Vourlidas](#), [Alexander Nindos](#)

A&A 2023

<https://arxiv.org/pdf/2307.10336>

In a previous work we analysed the white-light coronal brightness as a function of elongation and time from Wide-Field Imager (WISPR) observations on board the Parker Solar Probe (PSP) mission when PSP reached a minimum heliocentric distance of ~ 28 Rs. We found 4-5 transient outflows per day over a narrow wedge in the PSP orbital plane, which is close to the solar equatorial plane. However, the elongation versus time map (J-map) analysis supplied only lower limits on the number of released density structures due to the small spatial-scales of the transient outflows and line-of-sight integration effects. In this work we place constraints on the properties of slow solar wind transient mass release from the entire solar equatorial plane. We simulated the release and propagation of transient density structures in the solar equatorial plane for four scenarios: (1) periodic release in time and longitude with random speeds; (2) corotating release in longitude, periodic release in time with random speeds; (3) random release in longitude, periodic release in time and speed; and (4) random release in longitude, time, and speed. The simulations were used in the construction of synthetic J-maps, which are similar to the observed J-map. The four considered scenarios have similar ranges (35-45 for the minimum values and 96-127 for the maximum values) of released density structures per day from the solar equatorial plane and consequently from the streamer belt, given its proximity to the solar equatorial plane during the WISPR observation. Our results also predict that density structures with sizes in the range 2-8 Rs, covering 1-20 % of the perihelion could have been detectable by PSP in situ observations during that interval.

ISEST Working Group 5: Bs Challenge

Spiros **Patsourakos**

VarSITI Newsletter Vol. 16, January 2018 Article 2

http://newsserver.stil.bas.bg/varsiti/newsL/VarSITI_Newsletter_Vol16.pdf

Near-Sun and 1 AU magnetic field of coronal mass ejections: A parametric study

S. **Patsourakos**, M. K. Georgoulis

A&A 595, A121 2016

<http://arxiv.org/pdf/1609.00134v1.pdf>

<http://www.aanda.org/sci-hub/cc/articles/aa/pdf/2016/11/aa28277-16.pdf>

Aims. The magnetic field of coronal mass ejections (CMEs) determines their structure, evolution, and energetics, as well as their geoeffectiveness. However, we currently lack routine diagnostics of the near-Sun CME magnetic field, which is crucial for determining the subsequent evolution of CMEs.

Methods. We recently presented a method to infer the near-Sun magnetic field magnitude of CMEs and then extrapolate it to 1 AU. This method uses relatively easy to deduce observational estimates of the magnetic helicity in CME-source regions along with geometrical CME fits enabled by coronagraph observations. We hereby perform a parametric study of this method aiming to assess its robustness. We use statistics of active region (AR) helicities and CME geometrical parameters to determine a matrix of plausible near-Sun CME magnetic field magnitudes. In addition, we extrapolate this matrix to 1 AU and determine the anticipated range of CME magnetic fields at 1 AU representing the radial falloff of the magnetic field in the CME out to interplanetary (IP) space by a power law with index a_B .

Results. The resulting distribution of the near-Sun (at 10 Rs) CME magnetic fields varies in the range [0.004, 0.02] G, comparable to, or higher than, a few existing observational inferences of the magnetic field in the quiescent corona at the same distance. We also find that a theoretically and observationally motivated range exists around $a_B = -1.6 \pm 0.2$, thereby leading to a ballpark agreement between our estimates and observationally inferred field magnitudes of magnetic clouds (MCs) at L1.

Conclusions. In a statistical sense, our method provides results that are consistent with observations.

THE MAJOR GEOEFFECTIVE SOLAR ERUPTIONS OF 2012 MARCH 7: COMPREHENSIVE SUN-TO-EARTH ANALYSIS

S. [Patsourakos](#)¹, M. K. Georgoulis², A. Vourlidas³, A. Nindos¹,

2016 ApJ 817 14

During the interval **2012 March 7–11** the geospace experienced a barrage of intense space weather phenomena including the second largest geomagnetic storm of solar cycle 24 so far. Significant ultra-low-frequency wave enhancements and relativistic-electron dropouts in the radiation belts, as well as strong energetic-electron injection events in the magnetosphere were observed. These phenomena were ultimately associated with two ultra-fast (>2000 km s⁻¹) coronal mass ejections (CMEs), linked to two X-class flares launched on early 2012 March 7. Given that both powerful events originated from solar active region NOAA 11429 and their onsets were separated by less than an hour, the analysis of the two events and the determination of solar causes and geospace effects are rather challenging. Using satellite data from a flotilla of solar, heliospheric and magnetospheric missions a synergistic Sun-to-Earth study of diverse observational solar, interplanetary and magnetospheric data sets was performed. It was found that only the second CME was Earth-directed. Using a novel method, we estimated its near-Sun magnetic field at 13 R_⊙ to be in the range [0.01, 0.16] G. Steep radial fall-offs of the near-Sun CME magnetic field are required to match the magnetic fields of the corresponding interplanetary CME (ICME) at 1 AU. Perturbed upstream solar-wind conditions, as resulting from the shock associated with the Earth-directed CME, offer a decent description of its kinematics. The magnetospheric compression caused by the arrival at 1 AU of the shock associated with the ICME was a key factor for radiation-belt dynamics.

Sun-to-Earth Analysis of a Major Geoeffective Solar Eruption within the Framework of the Hellenic National Space Weather Research Network

[Patsourakos](#) S.

2013

http://www.helas.gr/conf/2013/talks/S_1/patsourakos.pdf

<http://proteus.space.noaa.gov/~hnswrn/>

7-8 March 2012

Advance warning of high-speed ejecta based on real-time shock analyses: When fast-moving ejecta appear to be overtaking slow-moving shocks

[Paulson](#), Kristoff W.; Taylor, David K.; Smith, Charles W.; Vasquez, Bernard J.; Hu, Q.

Space Weather, Vol. 10, No. 12, S12002, **2012**

<http://dx.doi.org/10.1029/2012SW000855>

Interplanetary shocks propagating into the magnetosphere can have significant space weather consequences. However, for many purposes it is the ejecta behind the shock that is the greater threat. The ejecta can be fast moving, impart significant momentum upon the magnetopause, and may contain a flux rope with strong southward magnetic fields. When transient solar wind activity strikes the magnetosphere, it can lead to enhanced magnetospheric currents and elevated radiation levels in the near-Earth environment. It is therefore desirable to use the observed shocks ahead of ejecta to predict any aspects of the approaching ejecta that can be predicted. We have examined 39 shocks observed by the Advanced Composition Explorer spacecraft in the years 1998 to 2003. Within the selection are shocks that were chosen because they appear to propagate significantly more slowly than the speed of the ejecta behind it. While appearing at first to be a contradiction, we show that the shocks are propagating across the radial direction and at significant angles to the velocity of the ejecta. These slow-moving shocks are actually precursors of fast-moving and potentially significant ejecta. Reversing the analysis, we are able to predict the peak speed of the ejecta well in advance of their observation, up to or in excess of 10 h following the shock crossing, when slow-moving shocks are seen, and we have incorporated this feature into our real-time shock analysis.

Parker Solar Probe Observations of Helical Structures as Boundaries for Energetic Particles

F. [Pecora](#), [S. Servidio](#), [A. Greco](#), [W. H. Matthaeus](#), [D. J. McComas](#), [J. Giacalone](#), [C. J. Joyce](#), [T. Getachew](#), [C. M. S. Cohen](#), [R. A. Leske](#), [M. E. Wiedenbeck](#), [R. L. McNutt Jr.](#), [M. E. Hill](#), [D. G. Mitchell](#), [E. R. Christian](#), [E. C. Roelof](#), [N. A. Schwadron](#), [S. D. Bale](#)

MNRAS 2021

<https://arxiv.org/pdf/2109.04571.pdf>

<https://arxiv.org/pdf/2109.04571.pdf>

Energetic particle transport in the interplanetary medium is known to be affected by magnetic structures. It has been demonstrated for solar energetic particles in near-Earth orbit studies, and also for the more energetic cosmic rays. In this paper, we show observational evidence that intensity variations of solar energetic particles can be correlated with the occurrence of helical magnetic flux tubes and their boundaries. The analysis is carried out using data from Parker Solar Probe orbit 5, in the period **2020 May 24 to June 2**. We use FIELDS magnetic field data and energetic particle measurements from the Integrated Science Investigation of the Sun (iSois) suite on the Parker Solar Probe. We identify magnetic flux ropes by employing a real-space evaluation of magnetic helicity, and their potential boundaries using the Partial Variance of Increments method. We find that energetic particles are either confined within or localized outside of helical flux tubes, suggesting that the latter act as transport boundaries for particles, consistent with previously developed viewpoints.

Single-spacecraft Identification of Flux Tubes and Current Sheets in the Solar Wind

Francesco **Pecora**¹, Antonella Greco¹, Qiang Hu², Sergio Servidio¹, Alexandros G. Chasapis³, and William H. Matthaeus³

2019 ApJL 881 L11

[sci-hub.se/10.3847/2041-8213/ab32d9](https://arxiv.org/abs/1905.08133)

A novel technique is presented for describing and visualizing the local topology of the magnetic field using single-spacecraft data in the solar wind. The approach merges two established techniques: the Grad-Shafranov (GS) reconstruction method, which provides a plausible regional two-dimensional magnetic field surrounding the spacecraft trajectory, and the Partial Variance of Increments (PVI) technique that identifies coherent magnetic structures, such as current sheets. When applied to one month of Wind magnetic field data at 1 minute resolution, we find that the quasi-two-dimensional turbulence emerges as a sea of magnetic islands and current sheets. Statistical analysis confirms that current sheets associated with high values of PVI are mostly located between and within the GS magnetic islands, corresponding to X points and internal boundaries. The method shows great promise for visualizing and analyzing single-spacecraft data from missions such as Parker Solar Probe and Solar Orbiter, as well as 1 au Space Weather monitors such as ACE, Wind, and IMAP. **2016 Jan 11-12**

Origin of the solar wind: A novel approach to link in situ and remote observations - A study for SPICE and SWA on the upcoming Solar Orbiter mission A24

Thies **Peleikis**, Martin Kruse, Lars Berger and Robert Wimmer-Schweingruber

A&A 602, A24 (2017)

<https://www.aanda.org/articles/aa/pdf/2017/06/aa29727-16.pdf>

Context. During the last decades great progress has been achieved in understanding the properties and the origin of the solar wind. While the sources for the fast solar wind are well understood, the sources for the slow solar wind remain elusive.

Aims. The upcoming Solar Orbiter mission aims to improve our understanding of the sources of the solar wind by establishing the link between in situ and remote sensing observations. In this paper we aim to address the problem of linking in situ and remote observations in general and in particular with respect to ESA's Solar Orbiter mission.

Methods. We have used a combination of ballistic back mapping and a potential field source surface model to identify the solar wind source regions at the Sun. As an input we use in situ measurements from the Advanced Composition Explorer and magnetograms obtained from the Michelson Doppler Interferometer on board the Solar Heliospheric Observatory. For the first time we have accounted for the travel time of the solar wind above and also below the source surface.

Results. We find that a prediction scheme for the pointing of any remote sensing instrumentation is required to capture a source region not only in space but also in time. An ideal remote-sensing instrument would cover up to $\approx 50\%$ of all source regions at the right time. In the case of the Spectral Imaging of the Coronal Environment instrument on Solar Orbiter we find that $\approx 25\%$ of all source regions would be covered.

Conclusions. To successfully establish a link between in situ and remote observations the effects of the travel time of the solar wind as well as the magnetic displacement inside the corona cannot be neglected. The predictions needed cannot be based solely on a model, nor on observations alone, only the combination of both is sufficient.

Evolution of CIR storm on 22 July 2009

Perez, J. D., E. W. Grimes, J. Goldstein, D. J. McComas, P. Valek, and N. Billor
J. Geophys. Res., 117, A09221, doi:10.1029/2012JA017572, 2012

Global images of ion intensities are deconvolved from TWINS ENA images during the main and recovery phase of a CIR storm on 22 July 2009. The global spatial ion images taken at different times, along with solar wind data, geomagnetic activity indices, geosynchronous orbit observations, and in situ measurements from the THEMIS mission provide a picture of the evolution of the ring current during both the main phase and early recovery phase of the storm. Major features of the evolution are consistent with expectations based upon time dependent geomagnetic indices, e.g., SYM/H and ASY/H, and geosynchronous orbit detection of dipolarizations from GOES 11 and 12. Direct comparisons are made with in situ THEMIS ESA and SST spectral measurements. The peak energy of the ion spectrum in the ring current is seen to decrease in the recovery phase. The time evolution of the ion energy spectra over the range from 2.5 to 97.5 keV at the spatial peaks of the ring current in the inner magnetosphere obtained from ENA images is presented for the first time.

Statistical Analysis of Interplanetary Shocks from Mercury to Jupiter

Carlos **Pérez-Alanis**, [Miho Janvier](#), [Teresa Nieves-Chinchilla](#), [Ernesto Aguilar-Rodríguez](#), [Pascal Démoulin](#), [Pedro Corona-Romero](#)

Solar Phys. 298, Article number: 60 2023

<https://arxiv.org/pdf/2304.05733>

<https://link.springer.com/content/pdf/10.1007/s11207-023-02152-3.pdf>

In situ observations of interplanetary (IP) coronal mass ejections (ICMEs) and IP shocks are important to study as they are the main components of the solar activity. Hundreds of IP shocks have been detected by various space missions at different times and heliocentric distances. Some of these are followed by clearly identified drivers, while some others are not. In this study, we carry out a statistical analysis of the distributions of plasma and magnetic parameters of the IP shocks recorded at various distances to the Sun. We classify the shocks according to the heliocentric distance, namely from 0.29 to 0.99 AU (Helios-1/2); near 1 AU (Wind, ACE and STEREO-A/B); and from 1.35 to 5.4 AU (Ulysses). We also differentiate the IP shocks into two populations, those with a detected ICME and those without one. We find, as expected, that there are no significant differences in the results from spacecraft positioned at 1 AU. Moreover, the distributions of shock parameters, as well as the shock normal have no significant variations with the heliocentric distance. Additionally, we investigate how the number of shocks associated to stream-interaction regions (SIRs) increases with distance in proportion of ICME/shocks. From 1 to 5 AU, SIRs/ shock occurrence increases slightly from 21% to 34%, in contrast ICME/shocks occurrence decreases from 47% to 17%. We find also indication of an asymmetry induced by the Parker spiral for SIRs and none for ICMEs.

Impact of the solar activity on the propagation of ICMEs: Simulations of hydro, magnetic and median ICMEs at minimum and maximum of activity

Barbara **Perri**, [Brigitte Schmieder](#), [Pascal Démoulin](#), [Stefaan Poedts](#), [Florian Regnault](#)

ApJ 955 50 2023

<https://arxiv.org/pdf/2306.15560.pdf>

<https://iopscience.iop.org/article/10.3847/1538-4357/acec6f/pdf>

The propagation of Interplanetary Coronal Mass Ejections (ICMEs) in the heliosphere is influenced by many physical phenomena, related to the internal structure of the ICME and its interaction with the ambient solar wind and magnetic field. As the solar magnetic field is modulated by the 11-year dynamo cycle, our goal is to perform a theoretical exploratory study to assess the difference of propagation of an ICME in typical minimum and maximum activity backgrounds. We define a median representative CME at 0.1~au, using both observations and numerical simulations, and describe it using a spheromak model. We use the heliospheric propagator European Heliospheric FORecasting Information Asset (EUHFORIA) to inject the same ICME in two different background wind environments. We then study how the environment and the internal CME structure impact the propagation of the ICME towards Earth, by comparison with an unmagnetized CME. At minimum of activity, the structure of the heliosphere around the ecliptic causes the ICME to slow down, creating a delay with the polar parts of the ejecta. This delay is more important if the ICME is faster. At maximum of activity, a southern coronal hole causes a northward deflection. For these cases, we always find that the ICME at maximum of activity arrives first, while the ICME at minimum of activity is actually more geo-effective. The helicity sign of the ICME is also a crucial parameter but at minimum of activity only, since it affects the magnetic profile and the arrival time of up to 8 hours.

COCONUT, a Novel Fast-converging MHD Model for Solar Corona Simulations:

I. Benchmarking and Optimization of Polytropic Solutions et al.

Barbara Perri^{4,1}, Peter Leitner^{4,1,2}, Michaela Brčnelova¹
2022 ApJ 936 19

<https://iopscience.iop.org/article/10.3847/1538-4357/ac7237/pdf>

We present a novel global 3D coronal MHD model called COCONUT, polytropic in its first stage and based on a time-implicit backward Euler scheme. Our model boosts run-time performance in comparison with contemporary MHD-solvers based on explicit schemes, which is particularly important when later employed in an operational setting for space-weather forecasting. It is data-driven in the sense that we use synoptic maps as inner boundary inputs for our potential-field initialization as well as an inner boundary condition in the further MHD time evolution. The coronal model is developed as part of the European Heliospheric Forecasting Information Asset (EUHFORIA) and will replace the currently employed, more simplistic, empirical Wang–Sheeley–Arge (WSA) model. At $21.5 R_{\odot}$ where the solar wind is already supersonic, it is coupled to EUHFORIA's heliospheric model. We validate and benchmark our coronal simulation results with the explicit-scheme Wind-Predict model and find good agreement for idealized limit cases as well as real magnetograms, while obtaining a computational time reduction of up to a factor 3 for simple idealized cases, and up to 35 for realistic configurations, and we demonstrate that the time gained increases with the spatial resolution of the input synoptic map. We also use observations to constrain the model and show that it recovers relevant features such as the position and shape of the streamers (by comparison with eclipse white-light images), the coronal holes (by comparison with EUV images), and the current sheet (by comparison with WSA model at 0.1 au).

Evolution of coronal hole solar wind in the inner heliosphere: Combined observations by Solar Orbiter and Parker Solar Probe

D. Perrone¹, S. Perri², R. Bruno³, D. Stansby⁴, R. D'Amicis³, + + +
A&A 668, A189 (2022)

<https://doi.org/10.1051/0004-6361/202243989>

<https://www.aanda.org/articles/aa/pdf/2022/12/aa43989-22.pdf>

We study the radial evolution, from 0.1 AU to the Earth, of a homogeneous recurrent fast wind, coming from the same source on the Sun, by means of new measurements by both Solar Orbiter and Parker Solar Probe. With respect to previous radial studies, we extend, for the first time, the analysis of a recurrent fast stream at distances never reached prior to the Parker Solar Probe mission. Confirming previous findings, the observations show: (i) a decrease in the radial trend of the proton density that is slower than the one expected for a radially expanding plasma, due to the possible presence of a secondary beam in the velocity distribution function; (ii) a deviation for the magnetic field from the Parker prediction, supported by the strong Alfvénicity of the stream at all distances; and (iii) a slower decrease in the proton temperature with respect to the adiabatic prediction, suggesting the local presence of external heating mechanisms. Focusing on the radial evolution of the turbulence, from the inertial to the kinetic range along the turbulent cascade, we find that the slopes, in both frequency ranges, strongly depend on the different turbulence observed by the two spacecraft, namely a mostly parallel turbulence in the Parker Solar Probe data and a mostly perpendicular turbulence in the Solar Orbiter intervals. Moreover, we observe a decrease in the level of intermittency for the magnetic field during the expansion of the stream. Furthermore, we perform, for the first time, a statistical analysis of coherent structures around proton scales at 0.1 AU and we study how some of their statistical properties change from the Sun to the Earth. As expected, we find a higher occurrence of events in the Parker Solar Probe measurements than in the Solar Orbiter data, considering the ratio between the intervals length and the proton characteristic scales at the two radial distances. Finally, we complement this statistical analysis with two case studies of current sheets and vortex-like structures detected at the two radial distances, and we find that structures that belong to the same family have similar characteristics at different radial distances. This work provides an insight into the radial evolution of the turbulent character of solar wind plasma coming from coronal holes.

Coherent events at ion scales in the inner Heliosphere: \textit{Parker Solar Probe} observations during the first Encounter

Denise Perrone, Roberto Bruno, Raffaella D'Amicis, Daniele Telloni, Rossana De Marco, Marco Stangalini, Silvia Perri, Oreste Pezzi, Olga Alexandrova, Stuart D. Bale

ApJ 905 142 2020

<https://arxiv.org/pdf/2010.02578.pdf>

<https://doi.org/10.3847/1538-4357/abc480>

The Parker Solar Probe mission has shown the ubiquitous presence of strong magnetic field deflections, namely switchbacks, during its first perihelion where it was embedded in a highly Alfvénic slow stream. Here, we study the turbulent magnetic fluctuations around ion scales in three intervals characterized by a different switchback activity, identified by the behavior of the magnetic field radial component, B_r . *Quiet* (B_r does not show significant

fluctuations), *weakly disturbed* ($B r$ has strong fluctuations but no reversals), and *highly disturbed* ($B r$ has full reversals) periods also show different behavior for ion quantities. However, the spectral analysis shows that each stream is characterized by the typical Kolmogorov/Kraichnan power law in the inertial range, followed by a break around the characteristic ion scales. This frequency range is characterized by strong intermittent activity, with the presence of noncompressive coherent events, such as current sheets, vortex-like structures, and wave packets identified as ion cyclotron modes. Although all these events have been detected in the three periods, they have different influences in each of them. Current sheets are dominant in the *highly disturbed* period, wave packets are the most common in the *quiet* interval; while, in the *weakly disturbed* period, a mixture of vortices and wave packets is observed. This work provides an insight into the heating problem in collisionless plasmas, fitting in the context of the new solar missions, and, especially for Solar Orbiter, which will allow an accurate magnetic connectivity analysis to link the presence of different intermittent events to the source region.

Highly Alfvénic slow solar wind at 0.3 au during a solar minimum: Helios insights for Parker Solar Probe and Solar Orbiter

D. **Perrone**^{1,2}, R. D'Amicis², R. De Marco², L. Matteini^{3,4}, D. Stansby^{4,5}, R. Bruno² and T. S. Horbury
A&A 633, A166 (2020)

<https://doi.org/10.1051/0004-6361/201937064>

Alfvénic fluctuations in solar wind are an intrinsic property of fast streams, while slow intervals typically have a very low degree of Alfvénicity, with much more variable parameters. However, sometimes a slow wind can be highly Alfvénic. Here we compare three different regimes of solar wind, in terms of Alfvénic content and spectral properties, during a minimum phase of the solar activity and at 0.3 au. We show that fast and Alfvénic slow intervals share some common characteristics. This would suggest a similar solar origin, with the latter coming from over-expanded magnetic field lines, in agreement with observations at 1 au and at the maximum of the solar cycle. Due to the Alfvénic nature of the fluctuations in both fast and Alfvénic slow winds, we observe a well-defined correlation between the flow speed and the angle between magnetic field vector and radial direction. The high level of Alfvénicity is also responsible of intermittent enhancements (i.e. spikes), in plasma speed. Moreover, only for the Alfvénic intervals do we observe a break between the inertial range and large scales, on about the timescale typical of the Alfvénic fluctuations and where the magnetic fluctuations saturate, limited by the magnitude of the local magnetic field. In agreement with this, we recover a characteristic low-frequency $1/f$ scaling, as expected for fluctuations that are scale-independent. This work is directly relevant for the next solar missions, Parker Solar Probe and Solar Orbiter. One of the goals of these two missions is to study the origin and evolution of slow solar wind. In particular, Parker Solar Probe will give information about the Alfvénic slow wind in the unexplored region much closer to the Sun and Solar Orbiter will allow us to connect the observed physics to the source of the plasma.

Forbush Decrease Characteristics in a Magnetic Cloud

A. S. **Petukhova**, I. S. **Petukhov**, S. I. **Petukhov**

Space Weather **Volume 18, Issue 12** e2020SW002616 2020

<https://doi.org/10.1029/2020SW002616>

<https://agupubs.onlinelibrary.wiley.com/doi/epdf/10.1029/2020SW002616>

Based on the new mechanism, the Forbush decrease characteristics are calculated for eight magnetic cloud types. It is shown that the Forbush decrease amplitude does not depend on the magnetic cloud type, while the anisotropy strongly does. The Forbush decrease spectrum for (2-150) GV rigidities is calculated for the first time. The Forbush decrease amplitude for low rigidities is $\sim 100\%$, which can be explained by a large number of forbidden particle trajectories. The Forbush decrease amplitude rapidly decreases for high rigidities due to the geometric condition. Comparing the calculated Forbush decrease characteristics with measurements for two events shows that the Forbush decrease amplitudes agree with the measurements quantitatively, and the anisotropies do qualitatively. **2000 July 16, 2004 July 2**

Theory of the Formation of Forbush Decrease in a Magnetic Cloud: Dependence of Forbush Decrease Characteristics on Magnetic Cloud Parameters

A. S. **Petukhova**, I. S. **Petukhov**, and S. I. **Petukhov**

2019 ApJ 880 17

[sci-hub.se/10.3847/1538-4357/ab2889](https://doi.org/10.3847/1538-4357/ab2889)

A theory of the formation of Forbush decrease in a magnetic cloud is presented. It is found that the formation mechanism is the energy loss of cosmic rays in a magnetic cloud represented as a moving magnetic loop with a helical field. The Forbush decrease amplitude, the components of the vector, and tensor anisotropies are calculated along the path of the magnetic cloud passing Earth. It is shown that the Forbush decrease characteristics depend on the following

magnetic cloud parameters: magnetic field strength, the helical field structure, velocity and the velocity gradient, and geometric dimensions. It is found that the Forbush decrease characteristics mainly depend on the magnetic field strength and the state of the global helical structure of the field.

Image of Forbush Decrease in a Magnetic Cloud by Three Moments of Cosmic Ray Distribution Function

A. S. [Petukhova](#) [I. S. Petukhov](#) [S. I. Petukhov](#)

JGR [Volume124, Issue1](#) Pages: 19-31 **2019**

sci-hub.tw/10.1029/2018JA025964

The time dynamics of the cosmic ray distribution function in a magnetic cloud is calculated. The magnetic cloud has the form of a torus segment with the force-free magnetic field structure at the initial moment. The subsequent propagation of the magnetic cloud in interplanetary space is determined by inertial description. The magnetic field is determined by the frozen-in condition. When calculating the particle distribution function, the electromagnetic field of the magnetic cloud is taken into account, with the scattering of particles not being taken into account. Relations between the particle distribution function and its three moments (particle density and unidirectional and bidirectional anisotropies) are derived. It is established that cosmic ray losses at the regions connecting the magnetic cloud with the Sun determine the amplitude of the second step of Forbush decrease. The time dependence of the Forbush decrease characteristics on magnetic cloud type is determined. The calculation results of the particle density and unidirectional anisotropy generally correspond to measurements. The referred results show a prominent role of the magnetic field structure in the time dynamics of the Forbush decrease.

Effect of additional magnetograph observations from different Lagrangian points in Sun-Earth system on predicted properties of quasi-steady solar wind at 1 AU

A. A. [Pevtsov](#) , [G. Petrie](#) , [P. MacNeice](#) , [I. I. Virtanen](#)

Space Weather [Volume18, Issue7](#) e2020SW002448 **2020**

<https://agupubs.onlinelibrary.wiley.com/doi/epdf/10.1029/2020SW002480>

<https://doi.org/10.1029/2020SW002448>

Modeling the space weather conditions for a near-Earth environment depends on a proper representation of magnetic fields on the Sun. There are discussions in the community with respect to the value of observations taken at several Lagrangian points (L1-L5) in the Sun-Earth system. Observations from a single (e.g., Earth/L1) vantage point are insufficient to characterize rapid changes in magnetic field on the far side of the Sun. Nor can they represent well the magnetic fields near the solar poles. However, if the changes in sunspot activity were moderate, how well would our predictions of the solar wind based on a single viewing point work? How much improvement could we see by adding magnetograph observations from L5, L4, and even L3? Here, we present the results of our recent modeling, which shows the level of improvement in forecasting the properties of the solar wind at Earth made possible by using additional observations from different vantage points during a period of moderate evolution of sunspot activity. As an example, we also show the improvements to the solar wind forecast from adding a single observation of the southern polar area from out-of-ecliptic spacecraft at -30° heliographic latitude vantage point. **23 to 30 August 2018**

Effect of uncertainties in solar synoptic magnetic flux maps in modeling of solar wind

Alexei A. [Pevtsov](#), Luca Bertellob, , Peter MacNeice

Advances in Space Research Volume 56, Issue 12, 15 December **2015**, Pages 2719–2726

<http://www.sciencedirect.com/science/article/pii/S0273117715004007>

Recently, the NSO/SOLIS team developed variance (error) maps that represent uncertainties in magnetic flux synoptic charts. These uncertainties are determined by the spatial variances of the magnetic flux distribution from full disk magnetograms that contribute to each bin in the synoptic chart. Here we present a study of the effects of variances on solar wind parameters (wind speed, density, magnetic field, and temperature) derived using the WSA–ENLIL model and ensemble modeling approach. We compare the results of the modeling with near-Earth solar wind magnetic field and plasma data as extracted from NASA/GSFC's OMNI data set. We show that analysis of uncertainties may be useful for understanding the sensitivity of the model predictions to short-term evolution of magnetic field and noise in the synoptic magnetograms.

Current sheets, plasmoids and flux ropes in the heliosphere.

Part II: Theoretical aspects

Review

O. [Pezzi](#), [F. Pecora](#), [J. le Roux](#), [N.E. Engelbrecht](#), [A. Greco](#), [S. Servidio](#), [H.V. Malova](#), [O.V. Khabarova](#), [O. Malandraki](#), [R. Bruno](#), [W.H. Matthaeus](#), [G. Li](#), [L.M. Zelenyi](#), [R.A. Kislov](#), [V.N. Obridko](#), [V.D. Kuznetsov](#)
Space Science Reviews 217, 39 2021

See Part I [Khabarova et al. \(2021\)](#)

<https://arxiv.org/pdf/2101.05007.pdf>

<https://link.springer.com/content/pdf/10.1007/s11214-021-00799-7.pdf>

<https://doi.org/10.1007/s11214-021-00799-7>

Our understanding of processes occurring in the heliosphere historically began with reduced dimensionality - one-dimensional (1D) and two-dimensional (2D) sketches and models, which aimed to illustrate views on large-scale structures in the solar wind. However, any reduced dimensionality vision of the heliosphere limits the possible interpretations of in-situ observations. Accounting for non-planar structures, e.g. current sheets, magnetic islands, flux ropes as well as plasma bubbles, is decisive to shed the light on a variety of phenomena, such as particle acceleration and energy dissipation. In part I of this review, we have described in detail the ubiquitous and multi-scale observations of these magnetic structures in the solar wind and their significance for the acceleration of charged particles. Here, in part II, we elucidate existing theoretical paradigms of the structure of the solar wind and the interplanetary magnetic field, with particular attention to the fine structure and stability of current sheets. Differences in 2D and 3D views of processes associated with current sheets, magnetic islands, and flux ropes are discussed. We finally review the results of numerical simulations and in-situ observations, pointing out the complex nature of magnetic reconnection and particle acceleration in a strongly turbulent environment.

Fully Kinetic Simulations of Proton-Beam-Driven Instabilities from Parker Solar Probe Observations

Luca [Pezzini](#), [Andrei N. Zhukov](#), [Fabio Bacchini](#), [Giuseppe Arrò](#), [Rodrigo A. López](#), [Alfredo Micera](#), [Maria Elena Innocenti](#), [Giovanni Lapenta](#)

ApJ 2024

<https://arxiv.org/pdf/2405.08196>

The expanding solar wind plasma ubiquitously exhibits anisotropic non-thermal particle velocity distributions. Typically, proton Velocity Distribution Functions (VDFs) show the presence of a core and a field-aligned beam. Novel observations made by Parker Solar Probe (PSP) in the innermost heliosphere have revealed new complex features in the proton VDFs, namely anisotropic beams that sometimes experience perpendicular diffusion. This phenomenon gives rise to VDFs that resemble a "hammerhead". In this study, we use a 2.5D fully kinetic simulation to investigate the stability of proton VDFs with anisotropic beams observed by PSP. Our setup consists of a core and an anisotropic beam populations that drift with respect to each other. This configuration triggers a proton-beam instability from which nearly parallel fast magnetosonic modes develop. Our results demonstrate that before this instability reaches saturation, the waves resonantly interact with the beam protons, causing significant perpendicular heating at the expense of the parallel temperature. Furthermore, the proton perpendicular heating induces a hammerhead-like shape in the resulting VDF. Our results suggest that this mechanism probably contributes to producing the observed hammerhead distributions.

Parker Solar Probe In-Situ Observations of Magnetic Reconnection Exhausts During Encounter 1

T. D. [Phan](#), [S. D. Bale](#), [J. P. Eastwood](#), [B. Lavraud](#), [J. F. Drake](#), [M. Oieroset](#), [M. A. Shay](#), [M. Pulupa](#), [M. Stevens](#), [R. J. MacDowall](#), [A. W. Case](#), [D. Larson](#), [J. Kasper](#), [P. Whittlesey](#), [A. Szabo](#), [K. E. Korreck](#), [J. W. Bonnell](#), [T. Dudok de Wit](#), [K. Goetz](#), [P. R. Harvey](#), [T. S. Horbury](#), [R. Livi](#), [D. Malaspina](#), [K. Paulson](#), [N. E. Raouafi](#), [M. Velli](#)

ApJS 2020

<https://arxiv.org/ftp/arxiv/papers/2001/2001.06048.pdf>

Magnetic reconnection in current sheets converts magnetic energy into particle energy. The process may play an important role in the acceleration and heating of the solar wind close to the Sun. Observations from Parker Solar Probe provide a new opportunity to study this problem, as it measures the solar wind at unprecedented close distances to the Sun. During the 1st orbit, PSP encountered a large number of current sheets in the solar wind through perihelion at 35.7 solar radii. We performed a comprehensive survey of these current sheets and found evidence for 21 reconnection exhausts. These exhausts were observed in heliospheric current sheets, coronal mass ejections, and regular solar wind. However, we find that the majority of current sheets encountered around perihelion, where the magnetic field was strongest and plasma beta was lowest, were Alfvénic structures associated with bursty radial jets and these current sheets did not appear to be undergoing local reconnection. We examined conditions around current sheets to address why some current sheets reconnected, while others did not. A key difference appears to be the degree of plasma velocity shear

across the current sheets: The median velocity shear for the 21 reconnection exhausts was 24% of the Alfvén velocity shear, whereas the median shear across 43 Alfvénic current sheets examined was 71% of the Alfvén velocity shear. This finding could suggest that large, albeit sub-Alfvénic, velocity shears suppress reconnection. An alternative interpretation is that the Alfvénic current sheets are isolated rotational discontinuities which do not undergo local reconnection.

A “Space Weather Buoy” Operated by Citizen Scientists

Phillips, T., et al.

(2016), *Space Weather Ballooning*, *Space Weather*, 14, 697–703

<http://onlinelibrary.wiley.com/doi/10.1002/swq.12/pdf>

We have developed a “Space Weather Buoy” for measuring upper atmospheric radiation from cosmic rays and solar storms. The Buoy, which is carried to the stratosphere by helium balloons, is relatively inexpensive and uses off-the-shelf technology accessible to small colleges and high schools. Using this device, we have measured two Forbush Decreases and a small surge in atmospheric radiation during the St. Patrick’s Day geomagnetic storm of March 2015. **12 September 2014, 21–22 December 2014, 17 March 2015**

Long- and Short-Term Evolutions of Magnetic Field Fluctuations in High-Speed Streams

Gilbert **Pi**, [Alexander Pitňa](#), [Zdenek Němeček](#), [Jana Šafránková](#), [Jih-Hong Shue](#) & [Ya-Hui Yang](#)

Solar Physics volume 295, Article number: 84 (2020)

<https://link.springer.com/content/pdf/10.1007/s11207-020-01646-8.pdf>

High-speed streams (HSSs) are believed to be only slightly affected by different interactions on their path from the Sun to Earth and thus the analysis of their observations can provide information on the structure and temporal variations of the magnetic field and plasma parameters at the source region. We have chosen three coronal holes supplying 14 HSSs recorded by Wind in 2008. For each HSS, we have calculated the average magnetic field and plasma parameters as well as power spectral densities (PSDs) of magnetic field fluctuations in the MHD and kinetic ranges to investigate their long- and short-term variations. We suggest that long-term variations are connected with a time evolution of the source region on the time scale of solar rotations. On the other hand, the short-term variations would reflect a longitudinal structure of the coronal hole. Our study reveals that coronal holes are very stable source of HSSs and their temporal evolution on short- and long-time scales is negligible. This is true for the average parameters as well as for the fluctuation power and PSDs. Observed correlations between bulk and/or thermal velocity and PSD parameters are consistent with already published results. We suggest that they do not originate in the source region but they can be mostly attributed to interaction with the ambient slow wind that affects even the HSS core. **4–12 January 2008**

Table 1 List of HSS events and the related CHs (2008)

Role of the Coronal Environment in the Formation of Four Shocks Observed without Coronal Mass Ejections at Earth's Lagrangian Point L1

M. **Pick**¹, J. Magdalenic², N. Cornilleau-Wehrin^{1,3}, B. Grison⁴, B. Schmieder^{1,5}, and K. Bocchialini⁶

2020 *ApJ* 895 144

<https://sci-hub.tw/https://iopscience.iop.org/article/10.3847/1538-4357/ab8fae>

The main goal of this study is to determine the solar origin of four single shocks observed at the Lagrange point L1 and followed by storm sudden commencements (SSCs) during 2002. We look for associated coronal mass ejections (CMEs), starting from estimates of the transit time from Sun to Earth. For each CME, we investigate its association with a radio type II burst, an indicator of the presence of a shock wave. For three of the events, the type II burst is shown to propagate along the same, or a similar, direction as the fastest segment of the CME leading edge. We analyze for each event the role of the coronal environment in the CME development, the shock formation, and their propagation, to finally identify its complex evolution. The ballistic velocity of these shocks during their propagation from the corona to L1 is compared to the shock velocity at L1. Based on a detailed analysis of the shock propagation and possible interactions up to 30 solar radii, we find a coherent velocity evolution for each event, in particular for one event, the **2002 April 14** SSC, for which a previous study did not find a satisfactory CME source. For the other three events, we observe the formation of a white-light shock overlying the different sources associated with those events. The localization of the event sources over the poles, together with an origin of the shocks being due to encounters of CMEs, can explain why at L1 we observe only single shocks and not interplanetary CMEs. **11-14 Apr 2002, 18-21 May 2002, 27-30 May 2002, 26-29 July 2002**

Evolution of Large-Scale Magnetic Fields From Near-Earth Space During the Last 11 Solar Cycles

Leonie **Pick**, Monika Korte, Yannik Thomas, Natalie Krivova, Chi-Ju Wu

We use hourly mean magnetic field measurements from 34 midlatitude geomagnetic observatories between 1900 and 2015 to investigate the long-term evolution and driving mechanism of the large-scale external magnetic field at ground. The Hourly Magnetospheric Currents index (HMC) is derived as a refinement of the Annual Magnetospheric Currents index (AMC, Pick & Korte, 2017, <https://doi.org/10.1093/gji/ggx367>). HMC requires an extensive revision of the observatory hourly means. It depends on three third party geomagnetic field models used to eliminate the core, the crustal, and the ionospheric solar-quiet field contributions. We mitigate the dependency of HMC on the core field model by subtracting only nondipolar components of the model from the data. The separation of the residual (dipolar) signal into internal and external (HMC) parts is the main methodological challenge. Observatory crustal biases are updated with respect to AMC, and the solar-quiet field estimation is extended to the past based on a reconstruction of solar radio flux (F10.7). We find that HMC has more power at low frequencies (periods ≥ 1 year) than the Dcx index, especially at periods relevant to the solar cycle. Most of the slow variations in HMC can be explained by the open solar magnetic flux. There is a weakly decreasing linear trend in absolute HMC from 1900 to present, which depends sensitively on the data rejection criteria at early years. HMC is well suited for studying long-term variations of the geomagnetic field.

CME development in the corona and interplanetary medium: A multi-wavelength approach

M. Pick, B. Kliem

EAS Publications Ser. 55, 299, 2012, File

<http://arxiv.org/pdf/1407.2271v1.pdf>

This **review** focuses on the so called three-part CMEs which essentially represent the standard picture of a CME eruption. It is shown how the multi-wavelength observations obtained in the last decade, especially those with high cadence, have validated the early models and contributed to their evolution. These observations cover a broad spectral range including the EUV, white-light, and radio domains. **02 June 2002, 29 January 2008, 2008-06-03-05, 2010 November 3,**

Comprehensive Analysis of the Geoeffective Solar Event of 21 June 2015: Effects on the Magnetosphere, Plasmasphere, and Ionosphere Systems

Mirko [Piersanti](#), Tommaso Alberti, Alessandro Bemporad ...

[Solar Physics](#) November 2017, 292:169

<https://link.springer.com/content/pdf/10.1007%2Fs11207-017-1186-0.pdf>

A full-halo coronal mass ejection (CME) left the Sun on 21 June 2015 from active region (AR) NOAA 12371. It encountered Earth on 22 June 2015 and generated a strong geomagnetic storm whose minimum Dst value was -204 nT. The CME was associated with an M2-class flare observed at 01:42 UT, located near disk center (N12 E16). Using satellite data from solar, heliospheric, and magnetospheric missions and ground-based instruments, we performed a comprehensive Sun-to-Earth analysis. In particular, we analyzed the active region evolution using ground-based and satellite instruments (Big Bear Solar Observatory (BBSO), Interface Region Imaging Spectrograph (IRIS), Hinode, Atmospheric Imaging Assembly (AIA) onboard the Solar Dynamics Observatory (SDO), Reuven Ramaty High Energy Solar Spectroscopic Imager (RHESSI), covering H α , EUV, UV, and X-ray data); the AR magnetograms, using data from SDO/Heliographic and Magnetic Imager (HMI); the high-energy particle data, using the Payload for Antimatter Matter Exploration and Light-nuclei Astrophysics (PAMELA) instrument; and the Rome neutron monitor measurements to assess the effects of the interplanetary perturbation on cosmic-ray intensity. We also evaluated the 1–8 Å soft X-ray data and the ~ 1 –1 MHz type III radio burst time-integrated intensity (or fluence) of the flare in order to predict the associated solar energetic particle (SEP) event using the model developed by Laurenza et al. (Space Weather 7(4), 2009). In addition, using ground-based observations from lower to higher latitudes (International Real-time Magnetic Observatory Network (INTERMAGNET) and European Quasi-Meridional Magnetometer Array (EMMA)), we reconstructed the ionospheric current system associated with the geomagnetic sudden impulse (SI). Furthermore, Super Dual Auroral Radar Network (SuperDARN) measurements were used to image the global ionospheric polar convection during the SI and during the principal phases of the geomagnetic storm. In addition, to investigate the influence of the disturbed electric field on the low-latitude ionosphere induced by geomagnetic storms, we focused on the morphology of the crests of the equatorial ionospheric anomaly by the simultaneous use of the Global Navigation Satellite System (GNSS) receivers, ionosondes, and Langmuir probes onboard the Swarm constellation satellites. Moreover, we investigated the dynamics of the plasmasphere during the different phases of the geomagnetic storm by examining the time evolution of the radial profiles of the equatorial plasma mass density derived from field line resonances detected at the EMMA network ($1.5 < L < 6.5$). Finally, we present the general features of the geomagnetic response to the

CME by applying innovative data analysis tools that allow us to investigate the time variation of ground-based observations of the Earth's magnetic field during the associated geomagnetic storm.

Solar Wind Plasma Particles Organized by the Flow Speed

Viviane [Pierrard](#), [Marian Lazar](#) & [Stepan Štverák](#)

[Solar Physics](#) volume 295, Article number: 151 (2020)

<https://link.springer.com/content/pdf/10.1007/s11207-020-01730-z.pdf>

Recent reports of the first data from Parker Solar Probe (PSP) have pointed to a series of links, correlations or anti-correlations between the solar wind bulk speed (VSWVSW) and physical properties of plasma particles from less than 0.25 AU in the corona. In the present paper, we describe corresponding and additional links of solar wind properties, at 0.4 AU and 1.0 AU, in an attempt to complement the PSP data and understand their evolution. A detailed analysis is carried out for the main electron populations, comparing the low-energy (thermal) core and the collisionless suprathermal halo. We show that the anti-correlation observed at 0.4 AU between VSWVSW and the number density (average value) is maintained also at 1 AU for both the core and halo electrons. On the contrary, only the core electrons manifest a clear anti-correlation of the temperature with VSWVSW, while the halo temperature does not vary much. We also describe the ions, protons and helium, which have a more reduced mobility and their properties exhibit different variations with the solar wind speed. The results are used to shed more light on the mechanisms leading to a differential acceleration of these species and the origin of slow and fast wind modulation.

Solar physics in the 2020s: DKIST, parker solar probe, and solar orbiter as a multi-messenger constellation

Review

V. Martinez [Pillet](#), [A. Tritschler](#), [L. Harra](#), [V. Andretta](#), [A. Vourlidas](#) ...

2020

<https://arxiv.org/ftp/arxiv/papers/2004/2004.08632.pdf>

The National Science Foundation (NSF) Daniel K. Inouye Solar Telescope (DKIST) is about to start operations at the summit of Haleakala (Hawaii). DKIST will join the early science phases of the NASA and ESA Parker Solar Probe and Solar Orbiter encounter missions. By combining in-situ measurements of the near-sun plasma environment and detail remote observations of multiple layers of the Sun, the three observatories form an unprecedented multi-messenger constellation to study the magnetic connectivity inside the solar system. This white paper outlines the synergistic science that this multi-messenger suite enables.

Solar wind rotation rate and shear at coronal hole boundaries, possible consequences for magnetic field inversions

R. F. [Pinto](#), [N. Poirier](#), [A. P. Rouillard](#), [A. Kouloumvakos](#), [L. Griton](#), [N. Fargette](#), [R. Kieokaew](#), [B. Lavraud](#), [A. S. Brun](#)

A&A 2021

<https://arxiv.org/pdf/2104.08393.pdf>

In-situ measurements by several spacecraft have revealed that the solar wind is frequently perturbed by transient structures (magnetic folds, jets, waves, flux-ropes) that propagate rapidly away from the Sun over large distances. Parker Solar Probe has detected frequent rotations of the magnetic field vector at small heliocentric distances, accompanied by surprisingly large solar wind rotation rates. The physical origin of such magnetic field bends, the conditions for their survival across the interplanetary space, and their relation to solar wind rotation are yet to be clearly understood. We traced measured solar wind flows from the spacecraft position down to the surface of the Sun to identify their potential source regions and used a global MHD model of the corona and solar wind to relate them to the rotational state of the low solar corona. We identified regions of the solar corona for which solar wind speed and rotational shear are important and long-lived, that can be favourable to the development of magnetic deflections and to their propagation across extended heights in the solar wind. We show that coronal rotation is highly structured and that enhanced flow shear develops near the boundaries between coronal holes and streamers, around and above pseudo-streamers, even when such boundaries are aligned with the direction of solar rotation. A large fraction of the switchbacks identified by PSP map back to these regions, both in terms of instantaneous magnetic field connectivity and of the trajectories of wind streams that reach the spacecraft. These regions of strong shears are likely to leave an imprint on the solar wind over large distances and to increase the transverse speed variability in the slow solar wind. The simulations and connectivity analysis suggest they can be a source of the switchbacks and spikes observed by Parker Solar Probe.

Interplanetary Parameters Leading to Relativistic Electron Enhancement and Persistent Depletion Events at Geosynchronous Orbit and Potential for Prediction

Victor A. [Pinto](#), [Hee-Jeong Kim](#), [Larry R. Lyons](#), [Jacob Bortnik](#)

JGR [Volume 123](#), [Issue 2](#) February 2018 Pages 1134-1145

<http://sci-hub.tw/10.1002/2017JA024902>

We have identified 61 relativistic electron enhancement events and 21 relativistic electron persistent depletion events during 1996 to 2006 from the Geostationary Operational Environmental Satellite (GOES) 8 and 10 using data from the Energetic Particle Sensor (EPS) >2 MeV fluxes. We then performed a superposed epoch time analysis of the events to find the characteristic solar wind parameters that determine the occurrence of such events, using the OMNI database. We found that there are clear differences between the enhancement events and the persistent depletion events, and we used these to establish a set of threshold values in solar wind speed, proton density and interplanetary magnetic field (IMF) B_z that can potentially be useful to predict sudden increases in flux. Persistent depletion events are characterized by a low solar wind speed, a sudden increase in proton density that remains elevated for a few days, and a northward turning of IMF B_z shortly after the depletion starts. We have also found that all relativistic electron enhancement or persistent depletion events occur when some geomagnetic disturbance is present, either a coronal mass ejection or a corotational interaction region; however, the storm index, SYM-H, does not show a strong connection with relativistic electron enhancement events or persistent depletion events. We have tested a simple threshold method for predictability of relativistic electron enhancement events using data from GOES 11 for the years 2007–2010 and found that around 90% of large increases in electron fluxes can be identified with this method.

A Multiple Flux-tube Solar Wind Model

Rui F. [Pinto](#) and Alexis P. Rouillard

2017 ApJ 838 89

<http://iopscience.iop.org/article/10.3847/1538-4357/aa6398/pdf>

We present a new model, MULTI-VP, which computes the three-dimensional structure of the solar wind and includes the chromosphere, the transition region, and the corona and low heliosphere. MULTI-VP calculates a large ensemble of wind profiles flowing along open magnetic field lines that sample the entire three-dimensional atmosphere or, alternatively, a given region of interest. The radial domain starts from the photosphere and typically extends to about . The elementary uni-dimensional wind solutions are based on a mature numerical scheme that was adapted in order to accept any flux-tube geometry. We discuss here the first results obtained with this model. We use Potential Field Source-surface extrapolations of magnetograms from the Wilcox Solar Observatory to determine the structure of the background magnetic field. Our results support the hypothesis that the geometry of the magnetic flux-tubes in the lower corona controls the distribution of slow and fast wind flows. The inverse correlation between density and speed far away from the Sun is a global effect resulting from small readjustments of the flux-tube cross-sections in the high corona (necessary to achieve global pressure balance and a uniform open flux distribution). In comparison to current global MHD models, MULTI-VP performs much faster and does not suffer from spurious cross-field diffusion effects. We show that MULTI-VP has the capability to predict correctly the dynamical and thermal properties of the background solar wind (wind speed, density, temperature, magnetic field amplitude, and other derived quantities) and to approach real-time operation requirements.

Flux-tube geometry and solar wind speed during an activity cycle

R. F. [Pinto](#)^{1,2}, A. S. Brun³ and A. P. Rouillard

A&A 592, A65 (2016)

<http://www.aanda.org/articles/aa/pdf/2016/08/aa28599-16.pdf>

Context. The solar wind speed at 1 AU shows cyclic variations in latitude and in time which reflect the evolution of the global background magnetic field during the activity cycle. It is commonly accepted that the terminal (asymptotic) wind speed in a given magnetic flux-tube is generally anti-correlated with its total expansion ratio, which motivated the definition of widely used semi-empirical scaling laws relating one to the other. In practice, such scaling laws require ad hoc corrections (especially for the slow wind in the vicinities of streamer/coronal hole boundaries) and empirical fits to in situ spacecraft data. A predictive law based solely on physical principles is still missing.

Aims. We test whether the flux-tube expansion is the controlling factor of the wind speed at all phases of the cycle and at all latitudes (close to and far from streamer boundaries) using a very large sample of wind-carrying open magnetic flux-tubes. We furthermore search for additional physical parameters based on the geometry of the coronal magnetic field which have an influence on the terminal wind flow speed.

Methods. We use numerical magneto-hydrodynamical simulations of the corona and wind coupled to a dynamo model to determine the properties of the coronal magnetic field and of the wind velocity (as a function of time and latitude) during a whole 11-yr activity cycle. These simulations provide a large statistical ensemble of open flux-tubes which we analyse conjointly in order to identify relations of dependence between the wind speed and geometrical parameters of the flux-tubes which are valid globally (for all latitudes and moments of the cycle).

Results. Our study confirms that the terminal (asymptotic) speed of the solar wind depends very strongly on the geometry of the open magnetic flux-tubes through which it flows. The total flux-tube expansion is more clearly anti-correlated with the wind speed for fast rather than for slow wind flows, and effectively controls the locations of these flows during solar minima. Overall, the actual asymptotic wind speeds attained – especially those of the slow wind – are also strongly dependent on field-line inclination and magnetic field amplitude at the foot-points. We suggest ways of including these parameters in future predictive scaling laws for the solar wind speed.

DENSITY FLUCTUATIONS UPSTREAM AND DOWNSTREAM OF INTERPLANETARY SHOCKS

A. **Pitňa**¹, J. Šafránková¹, Z. Němeček¹, O. Goncharov¹, F. Němec¹, L. Přech¹, C. H. K. Chen², and G. N. Zastenker³

2016 ApJ 819 41

Interplanetary (IP) shocks as typical large-scale disturbances arising from processes such as stream–stream interactions or Interplanetary Coronal Mass Ejection (ICME) launching play a significant role in the energy redistribution, dissipation, particle heating, acceleration, etc. They can change the properties of the turbulent cascade on shorter scales. We focus on changes of the level and spectral properties of ion flux fluctuations upstream and downstream of fast forward oblique shocks. Although the fluctuation level increases by an order of magnitude across the shock, the spectral slope in the magnetohydrodynamic range is conserved. The frequency spectra upstream of IP shocks are the same as those in the solar wind (if not spoiled by foreshock waves). The spectral slopes downstream are roughly proportional to the corresponding slopes upstream, suggesting that the properties of the turbulent cascade are conserved across the shock; thus, the shock does not destroy the shape of the spectrum as turbulence passes through it. Frequency spectra downstream of IP shocks often exhibit "an exponential decay" in the ion kinetic range that was earlier reported at electron scales in the solar wind or at ion scales in the interstellar medium. We suggest that the exponential shape of ion flux spectra in this range is caused by stronger damping of the fluctuations in the downstream region.

Theoretical basis for operational ensemble forecasting of coronal mass ejections

V. J. **Pizzo**, C. de Koning, M. Cash, G. Millward, D. A. Biesecker, L. Puga, M. Codrescu and D. Odstrcil
Space Weather v.13, No. 10 (pages 676–697) **2015** DOI: 10.1002/2015SW001221
SWQuarterly Vol. 13, Issue 1, **2016**

<http://onlinelibrary.wiley.com/doi/10.1002/SWQv13i001/epdf>

We lay out the theoretical underpinnings for the application of the Wang-Sheeley-Arge-Enlil modeling system to ensemble forecasting of coronal mass ejections (CMEs) in an operational environment. In such models, there is no magnetic cloud component, so our results pertain only to CME front properties, such as transit time to Earth. Within this framework, we find no evidence that the propagation is chaotic, and therefore, CME forecasting calls for different tactics than employed for terrestrial weather or hurricane forecasting. We explore a broad range of CME cone inputs and ambient states to flesh out differing CME evolutionary behavior in the various dynamical domains (e.g., large, fast CMEs launched into a slow ambient, and the converse; plus numerous permutations in between). CME propagation in both uniform and highly structured ambient flows is considered to assess how much the solar wind background affects the CME front properties at 1 AU. Graphical and analytic tools pertinent to an ensemble approach are developed to enable uncertainties in forecasting CME impact at Earth to be realistically estimated. We discuss how uncertainties in CME pointing relative to the Sun-Earth line affects the reliability of a forecast and how glancing blows become an issue for CME off-points greater than about the half width of the estimated input CME. While the basic results appear consistent with established impressions of CME behavior, the next step is to use existing records of well-observed CMEs at both Sun and Earth to verify that real events appear to follow the systematic tendencies presented in this study.

Wang-Sheeley-Arge-Enlil Cone Model Transitions to Operations

Vic **Pizzo**, George Millward, Annette Parsons, Douglas Biesecker, Steve Hill, Dusan Odstrcil
SPACE WEATHER, VOL. 9, S03004, 2 PP., 2011, **File**

The National Weather Service's (NWS) Space Weather Prediction Center (SWPC) is transitioning the first large-scale, physics-based space weather prediction model into operations on the NWS National Centers for Environmental Prediction (NCEP) supercomputing system (see also C. Schultz, Space weather model moves into prime time, Space Weather, 9, S03005, doi:10.1029/2011SW000669, 2011). The model is intended to provide 1- to 4-day advance warning of geomagnetic storms from quasi-recurrent solar wind structures and Earth-directed coronal mass ejections (CMEs). A team has been put together at SWPC to bring an advanced numerical model—developed with broad participation of the research community—into operational status. The modeling system consists of two main parts: (1) a semiempirical near-Sun module (Wang-Sheeley-Arge (WSA)) that approximates the outflow at the base of the solar wind; and (2) a sophisticated three-dimensional magnetohydrodynamic numerical model (Enlil) that simulates the resulting flow evolution out to Earth. The former module is driven by observations of the solar surface magnetic field accumulated over a solar rotation and composited into a synoptic map; this input is used to drive a parameterized model of the near-Sun expansion of the solar corona, which provides input for the interplanetary module to compute the quasi-steady (ambient) solar wind outflow. Finally, when an Earth-directed CME is detected in coronagraph images from NASA spacecraft, these images are used to characterize the basic properties of the CME, including speed, direction, and size. This input “cone” representation is injected into the preexisting ambient flow, and the subsequent transient evolution forms the basis for the prediction of the CME's arrival time at Earth, its intensity, and its duration (Figure 1).

See a voice presentation at

<http://ams.confex.com/ams/91Annual/flvgateway.cgi/id/17355?recordingid=17355>

http://www.swpc.noaa.gov/sww/SWW_2011_Presentations/Thur_300/SWW_2011/SWW_WSA_Enlil_2011.ppt

The National Weather Service's (NWS's) Space Weather Prediction Center (SWPC) is transitioning the first large-scale, physics-based space weather prediction model into operations on the NWS National Centers for Environmental Prediction supercomputing system. The model is intended to provide 1-4 day advance warning of quasi-recurrent solar wind structures and Earth-directed coronal mass ejections (CMEs). Travelling solar disturbances have long been known to disrupt communications, wreak havoc with geomagnetic systems, and to pose dangers for satellite operations. A team has been put together at SWPC to bring an advanced numerical model, well-developed within the research community, to bear upon forecasting these space weather hazards.

The modeling system consists of two main parts: 1) a semi-empirical near-Sun module that approximates the outflow at the base of the solar wind; and 2) a sophisticated 3-D magnetohydrodynamic numerical model that simulates the resulting flow evolution out to Earth. The former module is driven by observations of the solar surface magnetic field, as taken over a solar rotation and composited into a synoptic map; this input is used to drive a parameterized near-Sun expansion of the solar corona, which is subsequently input into the second, interplanetary module to compute the quasi-steady (ambient) solar wind outflow. Finally, when an Earth-directed CME is detected, coronagraph images from NASA spacecraft are used to characterize the basic properties of the CME, including timing, location, direction, and speed. This input (the “cone” model) is injected into the pre-existing ambient conditions, and the subsequent transient evolution forms the basis for the prediction of the CME arrival time at Earth, its intensity, and its duration.

Steps necessary to acquire and test the models, to assure robust access to the observational inputs, and to develop the requisite computational, communications, and archival infrastructure are well underway. SWPC forecasters are being trained in the full process of creating CME inputs, interpreting the standard and specialized outputs from the model, and melding them into a coherent and informative forecast product. The initial version of the full system is on schedule to enter operational evaluation at the end of FY11.

<http://ams.confex.com/ams/91Annual/webprogram/Paper187467.html>

See also:

<http://ccmc.gsfc.nasa.gov/models/modelinfo.php?model=ENLIL%20with%20Cone%20Model>

Long-Term Tracking of Corotating Density Structures using Heliospheric Imaging

I. **Plotnikov**, A.P. Rouillard, J.A. Davies, V. Bothmer, J.P. Eastwood, P. Gallagher, R.A. Harrison, E. Kilpua, C. Möstl, C.H. Perry, L. Rodriguez, B. Lavraud, V. Génot, R.F. Pinto, E. Sanchez-Diaz
Solar Phys. 2016

<http://arxiv.org/pdf/1606.01127v1.pdf>

The systematic monitoring of the solar wind in high-cadence and high-resolution heliospheric images taken by the Solar-Terrestrial Relation Observatory (STEREO) spacecraft permits the study of the spatial and temporal evolution of variable solar wind flows from the Sun out to 1~AU, and beyond. As part of the EU Framework 7 (FP7) Heliospheric Cataloguing, Analysis and Techniques Service (HELCASTS) project, we have generated a **catalogue listing the**

properties of 190 corotating structures well-observed in images taken by the Heliospheric Imager instruments on-board STEREO-A. We present here one of very few long-term analyses of solar wind structures advected by the background solar wind. This analysis confirms that most of the corotating density structures detected by the heliospheric imagers comprises a series of density inhomogeneities advected by the slow solar wind that eventually become entrained by stream interaction regions. We have derived the spatial-temporal evolution of each of these corotating density structures by using a well-established fitting technique. The mean radial propagation speed of the corotating structures is found to be $311 \pm 31 \text{ km} \cdot \text{s}^{-1}$. We predicted the arrival time of each corotating density structure at different probes. We show that the speeds of the corotating density structures derived using our fitting technique track well the long-term variation of the radial speed of the slow solar wind during solar minimum years (2007--2008). Furthermore, we demonstrate that these features originate near the coronal neutral line that eventually becomes the heliospheric current sheet. July 25 to August 14 2008

The first catalogue of CDSs derived from white-light imagery <http://www.helcats-fp7.eu>

Geomagnetic storm forecasting service StormFocus: 5 years online

Tatiana **Podladchikova**, Anatoly Petrukovich and Yuri Yermolaev

J. Space Weather Space Clim. **2018**, 8, A22

<https://www.swsc-journal.org/articles/swsc/pdf/2018/01/swsc170027.pdf>

Forecasting geomagnetic storms is highly important for many space weather applications. In this study, we review performance of the geomagnetic storm forecasting service StormFocus during 2011–2016. The service was implemented in 2011 at SpaceWeather.Ru and predicts the expected strength of geomagnetic storms as measured by Dst index several hours ahead. The forecast is based on L1 solar wind and IMF measurements and is updated every hour. The solar maximum of cycle 24 is weak, so most of the statistics are on rather moderate storms. We verify quality of selection criteria, as well as reliability of real-time input data in comparison with the final values, available in archives. In real-time operation 87% of storms were correctly predicted while the reanalysis running on final OMNI data predicts successfully 97% of storms. Thus the main reasons for prediction errors are discrepancies between real-time and final data (Dst, solar wind and IMF) due to processing errors, specifics of datasets. **6 August 2011, 10-11 Sept 2011, 1-2 Nov 2011, 27-28 Aug 2015**

Extended geomagnetic storm forecast ahead of available solar wind measurements,

Podladchikova, T., and A. A. Petrukovich

Space Weather, Vol. 10, No. 0, S07001, (2012)

<http://dx.doi.org/10.1029/2012SW000786>

We develop a technique to predict geomagnetic storm magnitudes (peak Dst values) several hours in advance using the first indications of extreme solar wind conditions, as well as an assumption of constant driving function VBs. For larger storms with clear VBs jump we predict lower and upper limits of expected peak Dst. For smaller storms and storms with gradually increasing VBs we predict Dst several hours ahead. The data from 1995-2010 were used to design the technique. The actual advance time of reliable forecasts (before the peak value is reached) is on average 5-6 hours, illustrating the realistic horizon of such "constant input" assumption. Larger storms are developing faster and thus are better predicted. False warnings (predictions more than 25% larger than the actual peak) occur in about 10% of events. The algorithm is implemented in real-time in Space Research Institute, Moscow (www.spaceweather.ru).

Uncertainty Estimates of Solar Wind Prediction using HMI Photospheric Vector and Spatial Standard Deviation Synoptic Maps

Bala **Poduval**, **Gordon Petrie**, **Luca Bertello**

Solar Phys. **295**, Article number: 138 **2020**

<https://arxiv.org/pdf/2008.06538.pdf>

Current solar wind prediction is based on the Wang & Sheeley empirical relationship between the solar wind speed observed at 1 AU and the rate of magnetic flux tube expansion (FTE) between the photosphere and the inner corona, where FTE is computed by coronal models that take the photospheric flux density synoptic maps as their inner boundary conditions to extrapolate the photospheric magnetic fields to deduce the coronal and the heliospheric magnetic field configuration. Since these synoptic maps are among the most widely-used of all solar magnetic data products, the uncertainties in the model predictions that are caused by the uncertainties in the synoptic maps are worthy of study. However, such an estimate related to synoptic map construction was not available until Bertello et al. (Solar Physics, 289, 2014) obtained the spatial standard deviation synoptic maps; 98 Monte-Carlo realizations of the spatial standard deviation maps for each photospheric synoptic maps. In this paper, we present an estimate of uncertainties in the solar wind speed predicted at 1 AU by the CSSS model due to the uncertainties in the photospheric synoptic maps. We also

present a comparison of the coronal hole locations predicted by the models with the STEREO/SECCHI EUV synoptic maps. In order to quantify the extent of the uncertainties involved, we compared the predicted speeds with the OMNI solar wind data during the same period (taking the solar wind transit time into account) and obtained the root mean square error between them. To illustrate the significance of the uncertainty estimate in the solar wind prediction, we carried out the analysis for three Carrington rotations, CR 2102, CR 2137 and CR 2160 at different phases of the solar cycle. The uncertainty estimate is critical information necessary for the current and future efforts of improving the solar wind prediction accuracies. **3 – 30 October 2010, 14 May – 11 June, 2013, 1 – 28 February, 2015**

CONTROLLING INFLUENCE OF MAGNETIC FIELD ON SOLAR WIND OUTFLOW: AN INVESTIGATION USING CURRENT SHEET SOURCE SURFACE MODEL

B. Poduval

2016 ApJ 827 L6

This Letter presents the results of an investigation into the controlling influence of large-scale magnetic field of the Sun in determining the solar wind outflow using two magnetostatic coronal models: current sheet source surface (CSSS) and potential field source surface. For this, we made use of the Wang and Sheeley inverse correlation between magnetic flux expansion rate (FTE) and observed solar wind speed (SWS) at 1 au. During the period of study, extended over solar cycle 23 and beginning of solar cycle 24, we found that the coefficients of the fitted quadratic equation representing the FTE–SWS inverse relation exhibited significant temporal variation, implying the changing pattern of the influence of FTE on SWS over time. A particularly noteworthy feature is an anomaly in the behavior of the fitted coefficients during the extended minimum, 2008–2010 (CRs 2073–2092), which is considered due to the particularly complex nature of the solar magnetic field during this period. However, this variation was significant only for the CSSS model, though not a systematic dependence on the phase of the solar cycle. Further, we noticed that the CSSS model demonstrated better solar wind prediction during the period of study, which we attribute to the treatment of volume and sheet currents throughout the corona and the more accurate tracing of footpoint locations resulting from the geometry of the model.

Validating Solar Wind Prediction Using the Current Sheet Source Surface Model

B. Poduval and X. P. Zhao

2014 ApJ 782 L22

We have carried out a comparative study of the predicted solar wind based on the flux tube expansion factor computed using the current sheet source surface (CSSS) model and the potential field source surface (PFSS) model, with the aim of determining whether the CSSS model represents the solar wind sources better than the PFSS model. For this, we obtained the root mean square errors (RMSEs) and the correlation coefficients between the observed solar wind speed and that predicted by the models, the ratio of RMSEs between the two models, and a skill score. On average, the CSSS predictions are more accurate than the PFSS predictions by a factor of 1.6, taking RMSE as the metric of accuracy. The RMSEs increased as the solar cycle progressed toward maximum, indicating the difficulty in modeling the corona as the global field becomes more complex. We also compared the WSA/ENLIL predictions for a few Carrington rotations; the Wang-Sheeley-Argé (WSA) model makes use of the PFSS extrapolations to model the wind source. We found that the average value of RMSE ratio between the CSSS and the WSA/ENLIL predictions was about 1.9, implying that the CSSS predictions are nearly twice better than the WSA/ENLIL predictions, despite the simplicity of the CSSS model compared to ENLIL. We conclude, based on the present analysis, that the CSSS model is a valid proxy for solar wind measurements and that it improves upon existing commonly used methods of wind prediction or proxy analysis.

Heliosheath Processes and the Structure of the Heliopause: Modeling Energetic Particles, Cosmic Rays, and Magnetic Fields

N. V. Pogorelov, H. Fichtner, A. Czechowski, A. Lazarian...

Space Science Reviews 2017

<http://link.springer.com/content/pdf/10.1007%2Fs11214-017-0354-8.pdf>

This paper summarizes the results obtained by the team “Heliosheath Processes and the Structure of the Heliopause: Modeling Energetic Particles, Cosmic Rays, and Magnetic Fields” supported by the International Space Science Institute (ISSI) in Bern, Switzerland. We focus on the physical processes occurring in the outer heliosphere, especially at its boundary called the heliopause, and in the local interstellar medium. The importance of magnetic field, charge exchange between neutral atoms and ions, and solar cycle on the heliopause topology and observed heliocentric distances to different heliospheric discontinuities are discussed. It is shown that time-dependent, data-driven boundary conditions are necessary to describe the heliospheric asymmetries detected by the Voyager spacecraft. We also discuss the structure of the heliopause, especially due to its instability and magnetic reconnection. It is demonstrated that the Rayleigh–Taylor instability of the nose of the heliopause creates consecutive layers of the interstellar and heliospheric plasma which are

magnetically connected to different sources. This may be a possible explanation of abrupt changes in the galactic and anomalous cosmic ray fluxes observed by Voyager 1 when it was crossing the heliopause structure for a period of about one month in the summer of 2012. This paper also discusses the plausibility of fitting simulation results to a number of observational data sets obtained by in situ and remote measurements. The distribution of magnetic field in the vicinity of the heliopause is discussed in the context of Voyager measurements. It is argued that a classical heliospheric current sheet formed due to the Sun's rotation is not observed by in situ measurements and should not be expected to exist in numerical simulations extending to the boundary of the heliosphere. Furthermore, we discuss the transport of energetic particles in the inner and outer heliosheath, concentrating on the anisotropic spatial diffusion tensor and the pitch-angle dependence of perpendicular diffusion and demonstrate that the latter can explain the observed pitch-angle anisotropies of both the anomalous and galactic cosmic rays in the outer heliosheath.

Interplanetary radio type II and type IV bursts as indicators of propagating solar transients

[Silja Pohjolainen](#), [Nasrin Talebpour Sheshvan](#)

Proceedings of 2nd URSI AT-RASC Meeting in Gran Canaria, 28 May - 1 June 2018 **2018**

<https://arxiv.org/ftp/arxiv/papers/1806/1806.05065.pdf>

Recent studies of interplanetary radio type II bursts and their source locations are reviewed. As these bursts are due to propagating shock waves, driven by coronal mass ejections, they can be followed to near-Earth distances and can be used to predict the arrival times of geo-effective disturbances. Radio type IV bursts, on the other hand, are usually due to moving magnetic structures in the low corona and trapped particles form at least part of the emission. The observed directivity of type IV emission may also be used for space weather purposes. **22 September 2011**

Variability of the slow solar wind: New insights from modelling and PSP-WISPR observations★

Nicolas [Poirier](#)^{1,2}, Victor Réville³, Alexis P. Rouillard³, Athanasios Kouloumvakos⁴ and Emeline Valette³

A&A 677, A108 (2023)

<https://www.aanda.org/articles/aa/pdf/2023/09/aa47146-23.pdf>

Aims. We analyse the signature and origin of transient structures embedded in the slow solar wind, and observed by the Wide-Field Imager for Parker Solar Probe (WISPR) during its first ten passages close to the Sun. WISPR provides a new in-depth vision on these structures, which have long been speculated to be a remnant of the pinch-off magnetic reconnection occurring at the tip of helmet streamers.

Methods. We pursued the previous modelling works of Réville et al. (2020, *ApJ*, 895, L20; 2022, *A&A*, 659, A110) that simulate the dynamic release of quasi-periodic density structures into the slow wind through a tearing-induced magnetic reconnection at the tip of helmet streamers. Synthetic WISPR white-light (WL) images are produced using a newly developed advanced forward modelling algorithm that includes an adaptive grid refinement to resolve the smallest transient structures in the simulations. We analysed the aspect and properties of the simulated WL signatures in several case studies that are typical of solar minimum and near-maximum configurations.

Results. Quasi-periodic density structures associated with small-scale magnetic flux ropes are formed by tearing-induced magnetic reconnection at the heliospheric current sheet and within $3 - 7 R_{\odot}$. Their appearance in WL images is greatly affected by the shape of the streamer belt and the presence of pseudo-streamers. The simulations show periodicities on $\approx 90 - 180$ min, $\approx 7 - 10$ h, and $\approx 25 - 50$ h timescales, which are compatible with WISPR and past observations.

Conclusions. This work shows strong evidence for a tearing-induced magnetic reconnection contributing to the long-observed high variability of the slow solar wind. **April 26-30, 2021, 8-10 Aug 2021, 1 Mar 2022**

Confined plasma transition from the solar atmosphere to the interplanetary medium

Nicolas [Poirier](#), [Alexis Rouillard](#), [Pierre-Louis Blelly](#)

Thesis **2022**

<https://arxiv.org/pdf/2208.11637.pdf>

The last 60 years of space exploration have shown that the interplanetary medium is continually perturbed by a myriad of different solar winds and storms that transport solar material across the whole heliosphere. If there is a consensus on the source of the fast solar wind that is known to originate in coronal holes, the question is still largely debated on the origin of the slow solar wind (SSW). The recent observations from the Parker Solar Probe mission provide new insights on the nascent solar wind. And a great challenge remains to explain both the composition and bulk properties of the SSW in a self-consistent manner. For this purpose we exploit and develop models with various degrees of complexity. This context constitutes the backbone of this thesis which is structured as follows: we exploit the first images taken by the Wide-Field Imager for Solar PRobe (WISPR) from inside the solar corona to test our global models at smaller scales,

because WISPR offers an unprecedented close-up view of the fine structure of the nascent SSW. This work provides further evidence for the transient release of plasma trapped in coronal loops into the solar wind, that we interpret by exploiting high-resolution magneto-hydrodynamics simulations. Finally we develop and exploit a new multi-specie model of coronal loops called the Irap Solar Atmosphere Model (ISAM) to provide an in-depth analysis of the plasma transport mechanisms at play between the chromosphere and the corona. ISAM solves for the coupled transport of the main constituents of the solar wind with minor ions through a comprehensive treatment of collisions as well as partial ionization and radiative cooling/heating mechanisms near the top of the chromosphere. We use this model to study the different mechanisms that can preferentially extract ions according to their first ionization potential (FIP) from the chromosphere to the corona. **2013 May 29, 21 August 2017, 2018 November 1-10, April 3, 2019, 2020-06-07-08, April 25-27, 2021, 2021-08-09, August 14 2021**

Exploiting White-Light Observations to Improve Estimates of Magnetic Connectivity

Nicolas **Poirier**^{1*}, Alexis P. Rouillard¹, Athanasios Kouloumvakos¹, Alexis Przybylak¹, Naïs Fargette¹, Raphaël Pobeda¹, Victor Réville¹, Rui F. Pinto^{1,2}, Mikel Indurain¹ and Matthieu Alexandre¹

Front. Astron. Space Sci., May **2021** |

<https://www.frontiersin.org/articles/10.3389/fspas.2021.684734/full>

<https://doi.org/10.3389/fspas.2021.684734>

The Solar Orbiter (SoLO) and Parker Solar Probe missions have opened up new challenges for the heliospheric scientific community. Their proximity to the Sun and their high quality measurements allow us to investigate, for the first time, potential sources for the solar wind plasma measured in situ. More accurate estimates of magnetic connectivities from spacecraft to the Sun are required to support science and operations for these missions. We present a methodology to systematically compare coronal and heliospheric models against white-light (WL) observations. WL images from the SOLar and Heliospheric Observatory (SoHO) are processed to unveil the faint structures of the K-corona. Images are then concatenated over time and are projected into a Carrington synoptic map. Features of interest such as the Streamer Belt (SB) are reduced to simplified geometric objects. Finally, a metric is defined to rank models according to their performance against WL observations. The method has been exploited to reproduce magnetic sectors from WL observations. We tested our results against one year of in situ magnetic polarity measurements taken at near one AU from the Advanced Composition Explorer (ACE) and the Solar TERrestrial Relations Observatory (STEREO-A). We obtained a good correlation that emphasizes the relevance of using WL observations to infer the shape of the sector structure. We show that WL observations provide additional constraints to better select model parameters such as the input photospheric magnetic map. We highlight the capability of this technique to systematically optimize coronal and heliospheric models using continuous and near-real-time WL observations. Several relevant practical applications are discussed, which should allow us to improve connectivity estimates.

A comparative study of geomagnetic storms for solar cycles 23 and 24

Pokharia, Meena; [Prasad, Lalan](#); [Bhoj, Chandrasekhar](#); [Mathpal, Chandni](#)

Journal of Astrophysics and Astronomy, Volume 39, Issue 5, article id. 53, 9 pp. **2018**

<https://link.springer.com/article/10.1007%2Fs12036-018-9538-1>

The aim of this paper is to investigate the association of the geomagnetic storms with the magnitude of interplanetary magnetic field IMF (B), solar wind speed (V), product of IMF and wind speed ($V \cdot B$), Ap index and solar wind plasma density (np) for solar cycles 23 and 24. A Chree analysis by the superposed epoch method has been done for the study. The results of the present analysis showed that $V \cdot B$ is more geoeffective when compared to V or B alone. Further the high and equal anti-correlation coefficient is found between Dst and Ap index (- 0.7) for both the solar cycles. We have also discussed the relationship between solar wind plasma density (np) and Dst and found that both these parameters are weakly correlated with each other. We have found that the occurrence of geomagnetic storms happens on the same day when IMF, V , Ap and $V \cdot B$ reach their maximum value while 1 day time lag is noticed in case of solar wind plasma density with few exceptions. The study of geomagnetic storms with various solar-interplanetary parameters is useful for the study of space weather phenomenon.

Study of Geomagnetic Storms and Solar and Interplanetary Parameters for Solar Cycles 22 and 24

Meena **Pokharia**, Lalan Prasad, Chandrashekhar Bhoj, Chandni Mathpal

[Solar Physics](#) September **2018**, 293:126

<https://link.springer.com/article/10.1007/s11207-018-1345-y>

<http://sci-hub.tw/https://link.springer.com/article/10.1007/s11207-018-1345-y>

The aim of this paper is to investigate the association of geomagnetic storms with the component of the interplanetary magnetic field (IMF) perpendicular to the ecliptic (BzBz), the solar wind speed (VV), the product of solar wind speed and BzBz (VBz), the Kp index, and the sunspot number (SSN) for two consecutive even solar cycles, Solar Cycles 22 (1986 – 1995) and 24 (2009 – 2017). A comparative study has been done using the superposed epoch method (Chree analysis). The results of the present analysis show that BzBz is a geoeffective parameter. The correlation coefficient between Dst and BzBz is found to be 0.8 for both Solar Cycles 22 and 24, which indicates that these two parameters are highly correlated. Statistical relationships between Dst and Kp are established and it is shown that for the two consecutive even solar cycles, Solar Cycles 22 and 24, the patterns are strikingly similar. The correlation coefficient between Dst and Kp is found to be the same for the two solar cycles (–0.8), which clearly indicates that these parameters are well anti-correlated. For the same studied period we found that the SSN does not show any relationship with Dst and Kp, while there exists an inverse relation between Dst and the solar wind speed, with some time lag. We have also found that VBz is a more relevant parameter for the production of geomagnetic storms, as compared to VV and BzBz separately. In addition, we have found that in Solar Cycles 22 and 24 this combined parameter is more relevant during the descending phase as compared to the ascending phase.

DETERMINATION OF THE HELIOSPHERIC RADIAL MAGNETIC FIELD FROM THE STANDOFF DISTANCE OF A CME-DRIVEN SHOCK OBSERVED BY THE STEREO SPACECRAFT

Watanachak [Poomvises](#)^{1,2}, Nat Gopalswamy¹, Seiji Yashiro^{1,2}, Ryun-Young Kwon^{1,2}, and Oscar Olmedo **2012** ApJ 758 118, [File](#)

We report on the determination of radial magnetic field strength in the heliocentric distance range from 6 to 120 solar radii (R_{\odot}) using data from Coronagraph 2 (COR2) and Heliospheric Imager I (HI1) instruments on board the Solar Terrestrial Relations Observatory spacecraft following the standoff-distance method of Gopalswamy & Yashiro. We measured the shock standoff distance of the **2008 April 5** coronal mass ejection (CME) and determined the flux-rope curvature by fitting the three-dimensional shape of the CME using the Graduated Cylindrical Shell model. The radial magnetic field strength is computed from the Alfvén speed and the density of the ambient medium. We also compare the derived magnetic field strength with in situ measurements made by the Helios spacecraft, which measured the magnetic field at the heliocentric distance range from 60 to 215 R_{\odot} . We found that the radial magnetic field strength decreases from 28 mG at 6 R_{\odot} to 0.17 mG at 120 R_{\odot} . In addition, we found that the radial profile can be described by a power law.

CORONAL MASS EJECTION PROPAGATION AND EXPANSION IN THREE-DIMENSIONAL SPACE IN THE HELIOSPHERE BASED ON STEREO/SECCHI OBSERVATIONS

[Poomvises](#), W., Zhang, J., & Olmedo, O. **2010**, ApJ, 717, L159, [File](#)

We report on several new findings regarding the kinematic and morphological evolution of coronal mass ejections (CMEs) in the inner heliosphere using the unprecedented STEREO/SECCHI observations. The CME tracking is based on the three-dimensional Raytrace model, which is free of the projection effect, resulting in true CME velocities. We also measure the cross section size of the CME and hence its expansion velocity. For the four major CME events investigated, we find that their leading edge (LE) velocity converges from an initial range between 400 km s⁻¹ and 1500 km s⁻¹ at 5-10 R_{\odot} to a narrow range between 500 km s⁻¹ and 750 km s⁻¹ at 50 R_{\odot} . The expansion velocity is also found to converge into a narrow range between 75 km s⁻¹ and 175 km s⁻¹. Both LE and expansion velocities are nearly constant after 50 R_{\odot} . We further find that the acceleration of CMEs in the inner heliosphere from ~10 to 90 R_{\odot} can be described by an exponential function, with an initial value as large as ~80 m s⁻² but exponentially decreasing to almost zero (more precisely, less than ± 5 m s⁻² considering the uncertainty of measurements). These results provide important observational constraints on understanding CME dynamics in interplanetary space

A new 3D solar wind speed and density model based on interplanetary scintillation

C. [Porowski](#) (1), [M. Bzowski](#) (1), [M. Tokumaru](#) (2)

ApJS **2021**

<https://arxiv.org/pdf/2110.15847.pdf>

The solar wind (SW) is an outflow of the solar coronal plasma, expanding supersonically throughout the heliosphere. SW particles interact by charge exchange with interstellar neutral atoms and on one hand, they modify the distribution of this gas in interplanetary space, and on the other hand they are seed population for heliospheric pickup ions and energetic neutral atoms (ENAs). The heliolatitudinal profiles of the SW speed and density evolve during the cycle of solar activity. A model of evolution of the SW speed and density is needed to interpret observations of ENAs, pickup ions, the heliospheric backscatter glow, etc. We derive the Warsaw Heliospheric Ionization Model 3DSW (WawHelIon 3DSW) based on interplanetary scintillation (IPS) tomography maps of the SW speed. We take the IPS tomography data from 1985 until 2020, compiled by \cite{tokumaru_etal:21a}. We derive a novel statistical method of filtering these data against outliers, we present a flexible analytic formula for the latitudinal profiles of the SW speed based on Legendre polynomials of varying order with additional restraining conditions at the poles, fit this formula to the yearly filtered data, and calculate the yearly SW density profiles using the latitudinally invariant SW energy flux, observed in the ecliptic plane. Despite application of refined IPS data set, a more sophisticated data filtering method, and a more flexible analytic model, the present results mostly agree with those obtained previously, which demonstrates the robustness of IPS studies of the SW structure.

A Multi-purpose Heliophysics L4 Mission

A. Posner, C. N. Arge, J. Staub, O. C. StCyr, D. Folta, S. K. Solanki, R. D. T. Strauss, F. Effenberger, A. Gandorfer, B. Heber, C. J. Henney, J. Hirschberger, S. I. Jones ... See all authors

Space Weather e2021SW002777 **Volume19, Issue9 2021**

<https://agupubs.onlinelibrary.wiley.com/doi/epdf/10.1029/2021SW002777>

<https://doi.org/10.1029/2021SW002777>

The Earth-Sun Lagrangian point 4 is a meta-stable location at 1 au from the Sun, 60° ahead of Earth's orbit. It has an uninterrupted view of the solar photosphere centered on W60, the Earth's nominal magnetic field connection to the Sun. Such a mission on its own would serve as a solar remote sensing observatory that would oversee the entire solar radiation hemisphere with significant relevance for protecting Moon and Mars explorers from radiation exposure. In combination with appropriately planned observatories at L1 and L5, the three spacecraft would provide 300° longitude coverage of photospheric magnetic field structure, and allow continuous viewing of both solar poles, with >3.6° elevation. Ideally, the L4 and L5 missions would orbit the Sun with a 7.2° inclination out of the heliographic equator, 14.5° out of the ecliptic plane. We discuss the impact of extending solar magnetic field observations in both longitude and latitude to improve global solar wind modeling and, with the development of local helioseismology, the potential for long-term solar activity forecasting. Such a mission would provide a unique opportunity for interplanetary and interstellar dust science. It would significantly add to reliability of operational observations on fast coronal mass ejections directed at Earth and for human Mars explorers on their round-trip journey. The L4 mission concept is technically feasible, and is scientifically compelling.

The main pillar: Assessment of space weather observational asset performance supporting nowcasting, forecasting, and research to operations

A. Posner, M. Hesse and O. C. St. Cyr

Space Weather, Volume 12, Issue 4, pages 257–276, April 2014

Space weather forecasting critically depends upon availability of timely and reliable observational data. It is therefore particularly important to understand how existing and newly planned observational assets perform during periods of severe space weather. Extreme space weather creates challenging conditions under which instrumentation and spacecraft may be impeded or in which parameters reach values that are outside the nominal observational range. This paper analyzes existing and upcoming observational capabilities for forecasting, and discusses how the findings may impact space weather research and its transition to operations. A single limitation to the assessment is lack of information provided to us on radiation monitor performance, which caused us not to fully assess (i.e., not assess short term) radiation storm forecasting. The assessment finds that at least two widely spaced coronagraphs including L4 would provide reliability for Earth-bound CMEs. Furthermore, all magnetic field measurements assessed fully meet requirements. However, with current or even with near term new assets in place, in the worst-case scenario there could be a near-complete lack of key near-real-time solar wind plasma data of severe disturbances heading toward and impacting Earth's magnetosphere. Models that attempt to simulate the effects of these disturbances in near real time or with archival data require solar wind plasma observations as input. Moreover, the study finds that near-future observational assets will be less capable of advancing the understanding of extreme geomagnetic disturbances at Earth, which might make the resulting space weather models unsuitable for transition to operations.

Current and high- β sheets in CIR streams: statistics and interaction with the HCS and the magnetosphere

A. S. **Potapov**

Astrophysics and Space Science April 2018, 363:81

<https://link.springer.com/content/pdf/10.1007%2Fs10509-018-3304-3.pdf>

Thirty events of CIR streams (corotating interaction regions between fast and slow solar wind) were analyzed in order to study statistically plasma structure within the CIR shear zones and to examine the interaction of the CIRs with the heliospheric current sheet (HCS) and the Earth's magnetosphere. The occurrence of current layers and high-beta plasma sheets in the CIR structure has been estimated. It was found that on average, each of the CIR streams had four current layers in its structure with a current density of more than 0.12 A/m² and about one and a half high-beta plasma regions with a beta value of more than five. Then we traced how and how often the high-speed stream associated with the CIR can catch up with the heliospheric current sheet (HCS) and connect to it. The interface of each fourth CIR stream coincided in time within an hour with the HCS, but in two thirds of cases, the CIR connection with the HCS was completely absent. One event of the simultaneous observation of the CIR stream in front of the magnetosphere by the ACE satellite in the vicinity of the L1 libration point and the Wind satellite in the remote geomagnetic tail was considered in detail. Measurements of the components of the interplanetary magnetic field and plasma parameters showed that the overall structure of the stream is conserved. Moreover, some details of the fine structure are also transferred through the magnetosphere. In particular, the so-called "magnetic hole" almost does not change its shape when moving from L1 point to a neighborhood of L2 point.

Properties of Supersonic Evershed Downflows

Sara Esteban **Pozuelo**, Luis R. Bellot Rubio, Jaime de la Cruz Rodriguez

ApJ 2016

<http://arxiv.org/pdf/1609.01106v1.pdf>

We study supersonic Evershed downflows in a sunspot penumbra by means of high spatial resolution spectropolarimetric data acquired in the Fe I 617.3 nm line with the CRISP instrument at the Swedish 1-m Solar Telescope. Physical observables, such as Dopplergrams calculated from line bisectors and Stokes V zero-crossing wavelengths, and Stokes V maps in the far red wing, are used to find regions where supersonic Evershed downflows may exist. We retrieve the LOS velocity and the magnetic field vector in these regions using two-component inversions of the observed Stokes profiles with the help of the SIR code. We follow these regions during their lifetime to study their temporal behavior. Finally, we carry out a statistical analysis of the detected supersonic downflows to characterize their physical properties. Supersonic downflows are contained in compact patches moving outward, which are located in the mid and outer penumbra. They are observed as bright, roundish structures at the outer end of penumbral filaments that resemble penumbral grains. The patches may undergo fragmentations and mergings during their lifetime, even some of them are recurrent. Supersonic downflows are associated with strong and rather vertical magnetic fields with a reversed polarity compared to that of the sunspot. Our results suggest that downflows returning back to the solar surface with supersonic velocities are abruptly stopped in dense deep layers and produce a shock. Consequently, this shock enhances the temperature and is detected as a bright grain in the continuum filtergrams, which could explain the existence of outward moving grains in the mid and outer penumbra. 28 September 2011

Geoeffectiveness and flare properties of radio-loud CMEs

Prakash, O.; Shanmugaraju, A.; Michalek, G.; Umapathy, S.

Astrophysics and Space Science, Volume 350, Issue 1, pp.33-45, 2014

A detailed investigation on geoeffective CMEs associated with meter to Deca-Hectometer (herein after m- and DH-type-II) wavelengths range type-II radio bursts observed during the period 1997-2005 is presented. The study consists of three steps: i) the characteristics of m- and DH-type-II bursts associated with flares and geoeffective CMEs; ii) characteristics of geo and non-geoeffective radio-loud and quiet CMEs, iii) the relationships between the geoeffective CMEs and flare properties. Interestingly, we found that 92 % of DH-type-II bursts are extension of m-type-II burst which are associated with faster and wider geoeffective DH-CMEs and also associated with longer/stronger flares. The geoeffective CME-associated m-type-II bursts have higher starting frequency, lower ending frequency and larger bandwidth compared to the general population of m-type-II bursts. The geoeffective CME-associated DH-type-II bursts have longer duration ($P < 1\%$), lower ending frequency ($P = 2\%$) and lower drift rates ($P = 2\%$) than that of DH-type-IIs associated with non-geoeffective CMEs. The differences in mean speed of geoeffective DH-CMEs and non-geoeffective DH-CMEs (1327 km s⁻¹ and 1191 km s⁻¹, respectively) is statistically insignificant ($P = 20\%$). However, the mean difference in width

(339° and 251°, respectively) is high statistical significant ($P=0.8\%$). The geo-effective general populations of LASCO CMEs speeds (545 km s⁻¹ and 450 km s⁻¹, respectively) and widths (252° and 60°, respectively) is higher than the non geo-effective general populations of LASCO CMEs ($P=3\%$ and $P=0.02\%$, respectively). The geoeffective CMEs associated flares have longer duration, and strong flares than non-geoeffective DH-CMEs associated flares ($P=0.8\%$ and $P=1\%$, respectively). We have found a good correlation between the geo-effective flare and DH-CMEs properties: i) CMEs speed—acceleration ($R=-0.78$, where R is a linear correlation coefficient), ii) acceleration—flare peak flux ($R=-0.73$) and, iii) acceleration—Dst index intensity ($R=0.75$). The radio-rich CMEs (DH-CMEs) produced more energetic storm than the radio-quiet CMEs (general populations of LASCO CMEs). The above results indicate that the DH-type-II bursts tend to be related with flares and geoeffective CMEs, although there is no physical explanation for the result. If the DH-type-II burst is a continuation of m-type-II burst, it could be a good indicator of geoeffective storms, which has important implications for space weather studies.

EUHFORIA modelling of the Sun-Earth chain of the magnetic cloud of 28 June 2013

G. Prete^{1,★}, A. Niemela^{3,4,★}, B. Schmieder^{3,5}, N. Al-Haddad⁶, B. Zhuang⁶, F. Lepreti^{1,2}, V.

Carbone^{1,2} and S. Poedts^{3,7}

A&A 683, A28 (2024)

<https://www.aanda.org/articles/aa/pdf/2024/03/aa46906-23.pdf>

Context. Predicting geomagnetic events starts with an understanding of the Sun-Earth chain phenomena in which (interplanetary) coronal mass ejections (CMEs) play an important role in bringing about intense geomagnetic storms. It is not always straightforward to determine the solar source of an interplanetary coronal mass ejection (ICME) detected at 1 au.

Aims. The aim of this study is to test by a magnetohydrodynamic (MHD) simulation the chain of a series of CME events detected from L1 back to the Sun in order to determine the relationship between remote and in situ CMEs.

Methods. We analysed both remote-sensing observations and in situ measurements of a well-defined magnetic cloud (MC) detected at L1 occurring on 28 June 2013. The MHD modelling is provided by the 3D MHD European Heliospheric FORecasting Information Asset (EUHFORIA) simulation model.

Results. After computing the background solar wind, we tested the trajectories of six CMEs occurring in a time window of five days before a well-defined MC at L1 that may act as the candidate of the MC. We modelled each CME using the cone model. The test involving all the CMEs indicated that the main driver of the well-defined, long-duration MC was a slow CME. For the corresponding MC, we retrieved the arrival time and the observed proton density.

Conclusions. EUHFORIA confirms the results obtained in the George Mason data catalogue concerning this chain of events. However, their proposed solar source of the CME is disputable. The slow CME at the origin of the MC could have its solar source in a small, emerging region at the border of a filament channel at latitude and longitude equal to +14 degrees. **23-28-30 Jun 2013**

Predicting the Geoeffectiveness of CMEs Using Machine Learning

[Andreea-Clara Pricopi](#), [Alin Razvan Paraschiv](#), [Diana Besliu-Ionescu](#), [Anca-Nicoleta Marginean](#)

ApJ 934 176 2022

<https://arxiv.org/pdf/2206.11472.pdf>

<https://iopscience.iop.org/article/10.3847/1538-4357/ac7962/pdf>

Coronal mass ejections (CMEs) are the most geoeffective space weather phenomena, being associated with large geomagnetic storms, having the potential to cause disturbances to telecommunication, satellite network disruptions, power grid damages and failures. Thus, considering these storms' potential effects on human activities, accurate forecasts of the geoeffectiveness of CMEs are paramount. This work focuses on experimenting with different machine learning methods trained on white-light coronagraph datasets of close to sun CMEs, to estimate whether such a newly erupting ejection has the potential to induce geomagnetic activity. We developed binary classification models using logistic regression, K-Nearest Neighbors, Support Vector Machines, feed forward artificial neural networks, as well as ensemble models. At this time, we limited our forecast to exclusively use solar onset parameters, to ensure extended warning times. We discuss the main challenges of this task, namely the extreme imbalance between the number of geoeffective and ineffective events in our dataset, along with their numerous similarities and the limited number of available variables. We show that even in such conditions, adequate hit rates can be achieved with these models. **1997-01-20, 2006-07-09, 2010-12-21, 2012-05-21, 2014-04-01**

Table 1. A sample of the aggregated dataset used for this work

Table 8. Example false negatives predicted by the ensemble model on the test set

Analysis of a coronal mass ejection and co-rotating interaction region as they travel from the Sun passing Venus, Earth, Mars and Saturn†

A. J. **Prise**^{1,*}, L. K. Harra¹, S. A. Matthews¹, C. S. Arridge² and N. Achilleos

JGR Volume 120, Issue 3 Pages 1566–1588 **2015**

<http://www.mssl.ucl.ac.uk/~ajp2/Prise2015.pdf>

During June 2010 a good alignment in the solar system between Venus, STEREO-B, Mars and Saturn provided an excellent opportunity to study the propagation of a Coronal Mass Ejection (CME) and closely occurring Co-rotating Interaction Region (CIR) from the Sun to Saturn. The CME erupted from the Sun at 01:30 UT on **20 June 2010**, with $v \approx 600$ km s⁻¹, as observed by STEREO-B, SDO and SOHO/LASCO. It arrived at Venus over 2 days later, some 3.5 days after a CIR is also detected here. The CIR was also observed at STEREO-B and Mars, prior to the arrival of the CME. The CME is not directed Earthward, but the CIR is detected here less than 2 days after its arrival at Mars. Around a month later, a strong compression of the Saturn magnetosphere is observed by Cassini, consistent with the scenario that the CME and CIR have merged into a single solar transient. The arrival times of both the CME and the CIR at different locations were predicted using the ENLIL with cone model. The arrival time of the CME at Venus, STEREO-B and Mars is predicted to within 20 hours of its actual detection, but the predictions for the CIR showed greater differences from observations, all over 1.5 days early. More accurate predictions for the CIR were found by extrapolating the travel time between different locations using the arrival times and speeds detected by STEREO-B and ACE. We discuss the implications of these results for understanding the propagation of solar transients.

MHD modeling of a geoeffective interplanetary CME with the magnetic topology informed by in-situ observations

E. **Provornikova**, V.G. Merkin, A. Vourlidas, A. Malanushenko, S.E. Gibson, E. Winter, N. Arge

ApJ **977** 106 **2024**

<https://arxiv.org/pdf/2405.13069>

<https://iopscience.iop.org/article/10.3847/1538-4357/ad83b1/pdf>

Variations of the magnetic field within solar coronal mass ejections (CMEs) in the heliosphere depend on the CME's magnetic structure as it leaves the solar corona and its subsequent evolution through interplanetary space. To account for this evolution, we developed a new numerical model of the inner heliosphere that simulates the propagation of a CME through a realistic background solar wind and allows various CME magnetic topologies. To this end, we incorporate the Gibson-Low CME model within our global MHD model of the inner heliosphere, GAMERA-Helio. We apply the model to study the propagation of the geoeffective CME that erupted on **3 April, 2010** with the aim to reproduce the temporal variations of the magnetic field vector during the CME passage by Earth. Parameters of the Gibson-Low CME are informed by STEREO white-light observations near the Sun. The magnetic topology for this CME - the tethered flux rope - is informed by in-situ magnetic field observations near Earth. We performed two simulations testing different CME propagation directions. For an in-ecliptic direction, the simulation shows a rotation of all three magnetic field components within the CME, as seen at Earth, similar to that observed. With a southward propagation direction, suggested by coronal imaging observations, the modeled B_y and B_z components are consistent with the ACE data, but the B_x component lacks the observed change from negative to positive. In both cases, the model favors the East-West orientation of the CME flux rope, consistent with the orientation previously inferred from the STEREO/HI heliospheric images.

Propagation into the heliosheath of a large-scale solar wind disturbance bounded by a pair of shocks★

E. **Provornikova**^{1,2}, M. Opher¹, V. Izmodenov^{2,3,4} and G. Toth

A&A **552**, A99 (**2013**)

Context. After the termination shock (TS) crossing, the Voyager 2 spacecraft has been observing strong variations of the magnetic field and solar wind parameters in the heliosheath. Anomalous cosmic rays, electrons, and galactic cosmic rays present strong intensity fluctuations. Several works suggested that the fluctuations might be attributed to spatial variations within the heliosheath. Additionally, the variability of the solar wind in this region is caused by different temporal events that occur near the Sun and propagate to the outer heliosphere.

Aims. To understand the spatial and temporal effects in the heliosheath, it is important to study these effects separately. In this work we explore the role of shocks as one type of temporal effects in the dynamics of the heliosheath. Although

currently plasma in the heliosheath is dominated by solar minima conditions, with increasing solar cycle shocks associated with transients will play an important role.

Methods. We used a 3D MHD multi-fluid model of the interaction between the solar wind and the local interstellar medium to study the propagation of a pair of forward-reverse shocks in the supersonic solar wind, interaction with the TS, and propagation to the heliosheath.

Results. We found that in the supersonic solar wind the interaction region between the shocks expands, the shocks weaken and decelerate. The fluctuation amplitudes of the plasma parameters vary with heliocentric distance. The interaction of the pair of shocks with the TS creates a variety of new waves and discontinuities in the heliosheath, which produce a highly variable solar wind flow. The collision of the forward shock with the heliopause causes a reflection of fast magnetosonic waves inside the heliosheath.

Solar Storm GIC (Geomagnetically Induced Current) Forecasting: Solar Shield Extension—Development of the End-User Forecasting System Requirements

A. [Pulkkinen](#), S. Mahmood, C. Ngwira, C. Balch, R. Lordan, D. Fugate, W. Jacobs, I. Honkonen
Space Weather Volume 13, Issue 9 September 2015 Pages 531–532

Full text <http://www.dhs.gov/sites/default/files/publications/Solar%20Storm%20GIC%20Forecasting-Solar%20Shield%20Extension%20-%20GIC%20Forecasting%20System%20Requirements-508.pdf>

A NASA Goddard Space Flight Center Heliophysics Science Division-lead team that includes NOAA Space Weather Prediction Center, Electric Power Research Institute, and Electric Research and Management, Inc. participants has recently partnered with the Department of Homeland Security Science and Technology Directorate to better understand the impact of Geomagnetically Induced Current (GIC) on the electric power industry. As a part of the process to improve resiliency of the system, better understanding of the power industry user requirements is needed. The ultimate goal in our work is to improve forecasting capability that will support operational decisions about proactive GIC mitigation actions. This report is based on communications with representatives of the US electric power transmission industry and documents the findings as part of the team's requirements development work.

Automatic Determination of the Conic Coronal Mass Ejection Model Parameters

A. [Pulkkinen](#), T. Oates & A. Taktakishvili

Solar Physics, Volume 261, Number 1, Page: 115 – 126, 2010, **FILE**

Characterization of the three-dimensional structure of solar transients using incomplete plane of sky data is a difficult problem whose solutions have potential for societal benefit in terms of space weather applications. In this paper transients are characterized in three dimensions by means of conic coronal mass ejection (CME) approximation. A novel method for the automatic determination of cone model parameters from observed halo CMEs is introduced. The method uses both standard image processing techniques to extract the CME mass from white-light coronagraph images and a novel inversion routine providing the final cone parameters. A bootstrap technique is used to provide model parameter distributions. When combined with heliospheric modeling, the cone model parameter distributions will provide direct means for ensemble predictions of transient propagation in the heliosphere.

An initial validation of the automatic method is carried by comparison to manually determined cone model parameters. It is shown using 14 halo CME events that there is reasonable agreement, especially between the heliocentric locations of the cones derived with the two methods. It is argued that both the heliocentric locations and the opening half-angles of the automatically determined cones may be more realistic than those obtained from the manual analysis.

Novel approach to geomagnetically induced current forecasts based on remote solar observations

[Pulkkinen](#), A.; Taktakishvili, A.; Odstrcil, D.; Jacobs, W.

Space Weather, Vol. 7, No. 8, S08005, 2009

<http://dx.doi.org/10.1029/2008SW000447>

In this paper, a novel approach that uses remote solar observations to forecast geomagnetically induced currents (GIC) is introduced. The approach utilizes first-principles-based propagation of the observed coronal mass ejections in the heliosphere and uses the modeled transient properties at the Earth to make site-specific statistical estimates of GIC. The approach provides unprecedented forecast lead time of 1–2 days. The approach is validated for two nodes of the North American power transmission system by means of 14 coronal mass ejection events for which GIC observations are available. It is shown that the mean of the absolute value of the error in the GIC event start time prediction is about 5 h

while the length of the events is underestimated on average by 17 h. The success rate, i.e., hits versus the total number of events, of the predictions are 12/14 and 7/14 for the two GIC stations, respectively. The implications of the new approach and the accuracy of the approach are discussed and possible avenues for future improvements are outlined.

Differences in geomagnetic storms driven by magnetic clouds and ICME sheath regions

T. I. [Pulkkinen](#), N. Partamies, K. E. J. Huttunen, G. D. Reeves, H. E. J. Koskinen

GEOPHYSICAL RESEARCH LETTERS, VOL. 34, L02105, doi:10.1029/2006GL027775, 2007

Twenty-eight geomagnetic storms driven by magnetic clouds or by sheath regions ahead of interplanetary coronal mass ejections are examined to address the dependence of the driver properties on the storm evolution and storm-substorm relationship. A superposed epoch analysis shows that the sheath-driven storms have stronger auroral activity, stronger magnetotail field stretching, and larger asymmetry in the inner magnetosphere field configuration. We suggest that the strong stretching during the sheath-driven storms leaves ions drifting Earthward from the plasma sheet on open drift paths, which limits the symmetric ring current growth. This decouples the substorm injections from the ring current enhancement, and can in part explain why there is no direct relationship between the auroral electrojet AL index and the midlatitude ring current Dst index.

On the Correlation of Cosmic-Ray Intensity with Solar Activity and Interplanetary Parameters.

[Putri](#), A.N.I., Herdiwijaya, D. & Hidayat, T.

Sol Phys 299, 12 (2024).

<https://doi.org/10.1007/s11207-023-02249-9>

We investigated correlations between cosmic-ray intensity and 14 solar and interplanetary parameters, which were classified into four cases. We used the modulation of cosmic-ray intensity observed at six distinct stations with different latitudes and cut-off rigidities. We used the partial least-squares (PLS) method to rank the parameters. In the first case, we employed 11 parameters without considering halo-type coronal mass ejections (CMEs) and solar proton events (SPEs). In addition, we considered energetic phenomena associated with halo CMEs for the second case and SPEs in the third case. In the fourth case, we combined all of the parameters. The results based on the magnitude of the first principal component show that the sunspot number (SN), interplanetary magnetic field (IMF), heliospheric current sheet (HCS), and plasma velocity are the parameters with the strongest influence on the modulation of the cosmic-ray intensity at all six stations and in the first case we considered. For a halo-type CME (second case), SN, IMF, HCS, CME speed, and proton density were identified as the most significant parameters, which is identical to the results obtained in the fourth case. During an SPE (third case), the most significant parameters were SN, IMF, HCS, SPEs, and plasma velocity. The INVK and OULU stations, with nearly the same latitude and altitude, exhibit similar results. Our analysis of the results from the low-latitude stations (PSNM and TSMB) yielded different results from the other three stations at higher latitude. For the PSNM and TSMB stations, α , β , γ , and the cone angle are the parameters that most strongly influence the modulation of the cosmic-ray intensity. This occurs because the influence of these parameters on cosmic-ray modulation depends on the latitude.

Magnetic Cloud and Sheath in the Ground-level Enhancement Event of 2000 July 14.

II. Effects on the Forbush Decrease

G. [Qin](#)¹ and S.-S. Wu¹

2021 ApJ 908 236

<https://doi.org/10.3847/1538-4357/abd77c>

<https://iopscience.iop.org/article/10.3847/1538-4357/abd77c/pdf>

Forbush decreases (Fds) in galactic cosmic ray intensity are related to interplanetary coronal mass ejections (ICMEs). The parallel diffusion of particles is reduced because the magnetic turbulence level in the sheath region bounded by the ICME's leading edge and shock is high. In the sheath and magnetic cloud (MC) energetic particles would feel an enhanced magnetic focusing effect caused by the strong inhomogeneity of the background magnetic field. Therefore, particles would be partially blocked in the sheath–MC structure. Here, we study two-step Fds by considering the magnetic turbulence and background magnetic field in the sheath–MC structure with diffusion coefficients calculated using theoretical models, to reproduce the Fd associated with the ground-level enhancement event on 2000 July 14 by solving the focused transport equation. The sheath and MC are set to spherical caps that are portions of spherical shells with enhanced background magnetic field. The magnetic turbulence levels in the sheath and MC are set to higher and lower than those in ambient solar wind, respectively. In general, the simulation result conforms to the main characteristics of the Fd observation, such as the pre-increase precursor, amplitude, total recovery time, and two-step decrease of the flux at the arrival of the sheath and MC. It is suggested that the sheath plays an important role in the

amplitude of the Fd while the MC contributes to the formation of the second-step decrease and prolonged recovery time. It is also inferred that both magnetic turbulence and background magnetic field in the sheath–MC structure are important for reproducing the observed two-step Fd.

The efficiency of electron acceleration by ICME-driven shocks

G. [Qin](#), [F.-J. Kong](#), [S.-S. Wu](#)

ApJ 2020

<https://arxiv.org/pdf/2012.10905.pdf>

We present a study of the acceleration efficiency of suprathermal electrons at collisionless shock waves driven by interplanetary coronal mass ejections (ICMEs), with the data analysis from both the spacecraft observations and test-particle simulations. The observations are from the 3DP/EESA instrument onboard *Wind* during the 74 shock events listed in Yang et al. 2019, ApJ, and the test-particle simulations are carried out through 315 cases with different shock parameters. It is shown that a large shock-normal angle, upstream Alfvén Mach number, and shock compression ratio would enhance the shock acceleration efficiency. In addition, we develop a theoretical model of the critical shock normal angle for efficient shock acceleration by assuming the shock drift acceleration to be efficient. We also obtain models for the critical values of Mach number and compression ratio with efficient shock acceleration, based on the suggestion of Drury 1983 about the average momentum change of particle crossing of shock. It is shown that the theories have similar trends of the observations and simulations. Therefore, our results suggest that the shock drift acceleration is efficient in the electron acceleration by ICME-driven shocks, which confirms the findings of Yang et al.

Prediction of the shock arrival time with SEP observations

G. [Qin](#), M. Zhang, H. K. Rassoul

J. Geophys. Res., Vol. 114, No. A9, A09104, 2009

Real-time prediction of the arrival times at Earth of shocks is very important for space weather research. Recently, various models for shock propagation are used to forecast the shock arriving times (SATs) with information of initial coronal shock and flare from near real-time radio and X-ray data. In this paper, we add the use of solar energetic particles (SEP) observation to improve the shock arrival time (SAT) prediction. High-energy SEPs originating from flares move to the Earth much faster than the shocks related to the same flares. We develop an SAT prediction model by combining a well-known shock propagation model, STOA, and the analysis of SEPs detected at Earth. We demonstrate that the SAT predictions are improved by the new model with the help of 38–53 keV electron SEP observations. In particular, the correct prediction to false alarm ratio is improved significantly.

ON THE MAGNETIC FLUX BUDGET IN LOW-CORONA MAGNETIC RECONNECTION AND INTERPLANETARY CORONAL MASS EJECTIONS

Jiong [Qiu](#),¹ Qiang Hu,² Timothy A. Howard,¹ and Vasyl B. Yurchyshyn³

The Astrophysical Journal, 659:758-772, 2007, File

We present the first quantitative comparison between the total magnetic reconnection flux in the low corona in the wake of coronal mass ejections (CMEs) and the magnetic flux in magnetic clouds (MCs) that reach 1 AU 2Y3 days after CME onset. The total reconnection flux is measured from flare ribbons, and the MC flux is computed using in situ observations at 1 AU, all ranging from 10^{20} to 10^{22} Mx. It is found that for the nine studied events in which the association between flares, CMEs, and MCs is identified, the MC flux is correlated with the total reconnection flux Φ_r . Further, the poloidal (azimuthal) MC flux Φ_p is comparable with the reconnection flux Φ_r , and the toroidal (axial) MC flux Φ_t is a fraction of Φ_r . Events associated with filament eruption do not exhibit a different Φ_t - Φ_r relation from events not accompanied by erupting filaments. The relations revealed between these independently measured physical quantities suggest that for the studied samples, the magnetic flux and twist of interplanetary magnetic flux ropes, reflected by MCs, are highly relevant to low-corona magnetic reconnection during the eruption. We discuss the implications of this result for the formation mechanism of twisted magnetic flux ropes, namely, whether the helical structure of the magnetic flux rope is largely pre-existing or formed in situ by low-corona magnetic reconnection. **We also measure magnetic flux encompassed in coronal dimming regions (Φ_d) and discuss its relation to the reconnection flux inferred from flare ribbons and MC flux.**

The Efficiency of Electron Acceleration by ICME-driven Shocks

G. Qin¹, F.-J. Kong^{1,2}, and S.-S. Wu¹

2023 ApJ 942 63

<https://iopscience.iop.org/article/10.3847/1538-4357/aca60e/pdf>

We present a study of the efficiency of the acceleration of suprathermal electrons at collisionless shock waves driven by interplanetary coronal mass ejections (ICMEs), with the data analysis from both the spacecraft observations and test-particle simulations. The observations are from the 3DP/EESA instrument on board Wind during the 74 shock events listed in Yang et al., and the test-particle simulations are carried out through 315 cases with different shock parameters. A total of seven energy channels ranging from 0.428–4.161 keV are selected. In the simulations, using a backward-in-time method, we calculate the average downstream flux in the 90° pitch angle. On the other hand, the average downstream and upstream fluxes in the 90° pitch angle can also be directly obtained from the 74 observational shock events. In addition, the variation in the event number ratio with the downstream to upstream flux ratio above a threshold value in terms of the shock angle (the angle between the shock normal and upstream magnetic field), upstream Alfvén Mach number, and shock compression ratio is statistically obtained. It is shown from both the observations and simulations that a large shock angle, upstream Alfvén Mach number, and shock compression ratio can enhance the efficiency of the shock acceleration. Our results suggest that shock drift acceleration is more efficient in the electron acceleration by ICME-driven shocks, which confirms the findings of Yang et al.

Magnetic Cloud and Sheath in the Ground-level Enhancement Event of 2000 July 14.

II. Effects on the Forbush Decrease

G. Qin¹ and S.-S. Wu¹

2021 ApJ 908 236

<https://doi.org/10.3847/1538-4357/abd77c>

<https://iopscience.iop.org/article/10.3847/1538-4357/abd77c/pdf>

Forbush decreases (Fds) in galactic cosmic ray intensity are related to interplanetary coronal mass ejections (ICMEs). The parallel diffusion of particles is reduced because the magnetic turbulence level in the sheath region bounded by the ICME's leading edge and shock is high. In the sheath and magnetic cloud (MC) energetic particles would feel an enhanced magnetic focusing effect caused by the strong inhomogeneity of the background magnetic field. Therefore, particles would be partially blocked in the sheath–MC structure. Here, we study two-step Fds by considering the magnetic turbulence and background magnetic field in the sheath–MC structure with diffusion coefficients calculated using theoretical models, to reproduce the Fd associated with the ground-level enhancement event on **2000 July 14** by solving the focused transport equation. The sheath and MC are set to spherical caps that are portions of spherical shells with enhanced background magnetic field. The magnetic turbulence levels in the sheath and MC are set to higher and lower than those in ambient solar wind, respectively. In general, the simulation result conforms to the main characteristics of the Fd observation, such as the pre-increase precursor, amplitude, total recovery time, and two-step decrease of the flux at the arrival of the sheath and MC. It is suggested that the sheath plays an important role in the amplitude of the Fd while the MC contributes to the formation of the second-step decrease and prolonged recovery time. It is also inferred that both magnetic turbulence and background magnetic field in the sheath–MC structure are important for reproducing the observed two-step Fd.

Three-dimensional inversion of corona structure and simulation of solar wind parameters based on the photospheric magnetic field deduced from Global Oscillation Network Group (GONG)

Shican Qiu, Xiao Zhang, Willie Soon, and Hamad Yousof

Front. Astron. Space Sci. 10: 1234391. 2023

<https://www.frontiersin.org/articles/10.3389/fspas.2023.1234391/pdf>

In this research, the Potential Field Source Surface–Wang–Sheeley–Arge (PFSS–WSA) solar wind model is used. This model consists of the Potential Field Source Surface (PFSS) coronal magnetic field extrapolation module and the Wang–Sheeley–Arge (WSA) solar wind velocity module. PFSS is implemented by the POT3D package deployed on Tianhe 1A supercomputer system. In order to obtain the three-dimensional (3D) distribution of the coronal magnetic field at different source surface radii (R_{ss}), the model utilizes the Global Oscillation Network Group (GONG) photospheric magnetic field profiles for two Carrington rotations (CRs), CR2069 (in 2008) and CR2217 (in 2019), as the input data, with the source surface at $R_{ss} = 2R_s$, $R_{ss} = 2.5R_s$ and $R_{ss} = 3R_s$, respectively. Then the solar wind velocity, the coronal magnetic field expansion factor, and the minimum angular distance of the open magnetic field lines from the coronal hole boundary are estimated within the WSA module. The simulated solar wind speed is compared with the value for the corona extrapolated from the data observed near 1 AU, through the calculations of the mean square error (MSE), root mean square error (RMSE) and correlation coefficient (CC). Here we extrapolate the solar wind velocity at 1 AU back to

the source surface via the Parker spiral. By comparing the evaluation metrics of the three source surface heights, we concluded that the solar source surface should be properly decreased with respect to $R_{ss} = 2.5R_s$ during the low solar activity phase of solar cycle 23.

Local and nonlocal geometry of interplanetary coronal mass ejections: Galactic cosmic ray (GCR) short-period variations and magnetic field modeling,

Quenby, J. J., T. Mulligan, J. B. Blake, J. E. Mazur, and D. Shaul

J. Geophys. Res., 113, A10102, (2008),

<http://dx.doi.org/10.1029/2007JA012849>

We examined the temporal history of the integral GCR fluence (≥ 100 MeV) measured by the high-sensitivity telescope (HIST) aboard the Polar spacecraft, along with the solar wind magnetic field and plasma data from the ACE spacecraft during a 40-day period encompassing the 25 September 1998 Forbush decrease. We also examined the Forbush and (energetic storm particles) ESP event on 28 October 2003.

Part I: S.-S. **Wu** and G. Qin¹

2020 ApJ 904 151

<https://doi.org/10.3847/1538-4357/abc0f2>

<https://iopscience.iop.org/article/10.3847/1538-4357/abc0f2/pdf>

The effect and properties of drifts in the heliosphere

J. L. **Raath**¹, S. E. S. Ferreira¹ and A. Kopp^{1,2}

A&A 665, A4 (2022)

<https://www.aanda.org/articles/aa/pdf/2022/09/aa40406-21.pdf>

We investigate the properties of drifts and their effect on cosmic ray modulation in the heliosphere using a numerical modulation model based on the solution of a set of stochastic differential equations that was derived from the Parker transport equation. The illustrative capabilities of the numerical model are exploited to yield a better understanding of the physical modulation processes involved. Various studies have indicated that drifts need to be scaled down towards solar maximum conditions and the present study looks at how this can be achieved. Drifts are scaled down directly by multiplying the drift coefficient by a factor of less than unity as well as indirectly through the drift–diffusion relation, that is, by modifying the diffusion coefficient so as to cause a change in the drift effects through altered gradients in particle intensity. Contour plots of particle exit positions and exit energies are presented for both of these cases, and it is illustrated that drifts in the model lead to larger energy losses. This is explained with the aid of figures indicating the relative amount of time spent by pseudo-particles in different regions of the heliosphere during the modulation process. These figures also indicate that an increase in diffusion leads to a suppression or reduction of drift effects. Finally, the figures also show that drift effects are reduced as a function of increasing particle energy; even though the drift coefficient increases with particle energy, the total drift effect, taking into account the contribution from the increased diffusion associated with larger energies, causes drift effects to be reduced with an increase in energy.

The Possible Cause of Most Intense Geomagnetic Superstorm of the 21st Century on 20 November 2003

Anil **Raghav**, [Zubair Shaikh](#), [P. Vemareddy](#), [Ankush Bhaskar](#), [Omkar Dhamane](#), [Kalpesh Ghag](#), [Prathmesh Tari](#), [Baiju Dayanandan](#) & [Badar Mohammed Al Suti](#)

Solar Physics volume 298, Article number: 64 (2023)

<https://doi.org/10.1007/s11207-023-02157-y>

An extreme geomagnetic storm has the potential to affect various technologies and activities in space and on the ground, e.g., power grids, oil and gas industries, communications, ground transportation, satellite infrastructure, global navigation satellite systems, aviation, etc. Therefore, it is considered a major source of risk by various governmental agencies and corporations at the international level. All notable space weather events (superstorms) are caused by interplanetary coronal mass ejections (ICMEs). But not every ICME leads to an extreme storm. Moreover, how does an extreme storm form? Or which explicit characteristic of ICME actually is responsible for inducing a superstorm? Here, we re-investigate the ICME characteristics that contribute to the most intense storm of the current century that occurred on **20 November 2003**. Interestingly, the studied ICME magnetic cloud shows characteristics of extremely flattened (pancaked) structure i.e. quasi-planar magnetic structure (PMS). The pancaked ICME shows less adiabatic expansion than usual in the compressed direction, which leads to strong magnetic field strength, high plasma density, high solar wind speed, high dynamic pressure, and a high eastward interplanetary electric field. Here, we propose that the ICME

that transformed into a quasi-PMS has the aforementioned enhanced features with strong southward magnetic field component that contributes to efficiently transferring plasma and energy into the Earth's magnetosphere to cause the observed superstorm.

First in-situ observation of surface Alfvén waves in ICME flux rope

Anil [Raghav](#), [Omkar Dhamane](#), [Zubair shaikh](#), [Naba Azmi](#), [Ankita Manjrekar](#), [Utsav Panchal](#), [Kalpesh Ghag](#), [Daniele Telloni](#), [Raffaella D'Amicis](#), [Prathmesh Tari](#), [Akshata Gurav](#)

2023 *ApJ* **945** 64

<https://arxiv.org/pdf/2211.16972.pdf>

<https://iopscience.iop.org/article/10.3847/1538-4357/acb93c/pdf>

Alfvén waves (AWs) are inevitable in space and astrophysical plasma. Their crucial role in various physical processes, occurring in plasma, has triggered intense research in solar-terrestrial physics. Simulation studies have proposed the generation of AWs along the surface of a cylindrical flux rope, referred to as Surface AWs (SAWs); however the observational verification of this distinct wave has been elusive to date. We report the first *in-situ* observation of SAWs in an interplanetary coronal mass ejection flux rope. We apply the Walén test to identify them. The Elsasser variables are used to estimate the characterization of these SAWs. They may be excited by the movement of the flux rope's foot points or by instabilities along the plasma magnetic cloud's boundaries. Here, the change in plasma density or field strength in the surface-aligned magnetic field may trigger SAWs. **2005 September 2**

In-situ Observation Of Alfv'en Waves In Icm Shock-Sheath Indicates Existence Of Alfv'enic Turbulence

Anil [Raghav](#), [Zubair Shaikh](#), [Omkar Dhamane](#), [Kalpesh Ghag](#), [Prathmesh Tari](#), [Utsav Panchal](#)

2022

<https://arxiv.org/pdf/2209.05037.pdf>

The dynamic evolution of coronal mass ejection (CME) in interplanetary space generates highly turbulent, compressed, and heated shock-sheath. This region furnishes a unique environment to study the turbulent fluctuations at the small scales and serve an opportunity for unfolding the physical mechanisms by which the turbulence is dissipated and plasma is heated. How does the turbulence in the magnetized plasma control the energy transport process in space and astrophysical plasmas is an attractive and challenging open problem of the 21st century. For this, the literature discusses three types of magnetohydrodynamics (MHD) waves/ fluctuations in magnetized plasma as the magnetosonic (fast), Alfv'enic (intermediate), and sonic (slow). The magnetosonic type is most common in the interplanetary medium. However, Alfv'enic waves/fluctuations have not been identified to date in the ICME sheath. The steepening of the Alfv'en wave can form a rotational discontinuity that leads to an Alfv'enic shock. But, the questions were raised on their existence based on the theoretical ground. Here, we demonstrate the observable in-situ evidence of Alfv'en waves inside turbulent shock-sheath at 1 AU using three different methods described in the literature. We also estimate Els'asser variables, normalized cross helicity, normalized residual energy and which indicate outward flow of Alfv'en waves. Power spectrum analysis of IMF indicates the existence of Alfv'enic turbulence in ICME shock-sheath. The study has strong implications in the domain of interplanetary space plasma, its interaction with planetary plasma, and astrophysical plasma. **6 Nov 2000**

The role of extreme geomagnetic storms in the Forbush decrease profile

Anil [Raghav](#), [Prathmesh Tari](#), [Kalpesh Ghag](#), [Zubair Shaikh](#), [Omkar Dhamane](#), [Utsav Panchal](#), [Mayuri Katvankar](#), [Komal Chorgha](#), [Digvijay Mishra](#), [Kishor Kumbhar](#)

MNRAS **2021**

<https://arxiv.org/pdf/2112.09918.pdf>

The Forbush decrease (FD) and Geomagnetic storm (GS) are the two distinct space weather events having common causing agents like interplanetary coronal mass ejection (ICME) or corotating interacting region (CIR). Generally, an ICME causes high amplitude FDs and extreme GSs. However, the interlinks between extreme GS and strong FDs are poorly studied. Here, we demonstrate five ICME induced extreme storms and their effects on respective FD profiles. We observed the sudden storm commencement of the GS coincides with the FD onset. Interestingly, we also noted a gradual increase in neutron counts during the main and recovery phases of GS. The maximum enhancement in neutron counts coincides with the minimum value of the Sym-H index. The enhancement is visible primarily in all the neutron monitors but significantly pronounced in high-energy neutrons compared to low-energy neutrons. The weakening of Earth's magnetic shield due to ICME-Magnetosphere interaction allows more cosmic rays to reach the ground. Thus, we conclude that the geomagnetic storm conditions highly influence the FD profile along with the external causing agent.

Therefore, it is essential to include the effect of geomagnetic field variation in the models that are used to reproduce the FD profile. **26 August, 2018; 20 November, 2003; 24 November, 2001 ; 10 May, 1992 and 13 July, 1991**

Study of flux-rope characteristics at sub-astronomical-unit distances using the Helios 1 and 2 spacecraft

Anil **Raghav**, [Sandesh Gaikwad](#), [Yuming Wang](#), [Zubair I Shaikh](#), [Wageesh Mishra](#), [Ake Zao](#)

Monthly Notices of the Royal Astronomical Society, Volume 495, Issue 2, June 2020, Pages 1566–1576, **2020**

<https://doi.org/10.1093/mnras/staa1189>

Magnetic flux ropes observed as magnetic clouds near 1 au have been extensively studied in the literature and their distinct features are derived using numerous models. These studies summarize the general characteristics of flux ropes at 1 au without providing an understanding of the continuous evolution of the flux ropes from near the Sun to 1 au. In the present study, we investigate 26 flux ropes observed by the Helios 1 and 2 spacecraft (from 0.3 to 1 au) using the velocity-modified Gold–Hoyle model. The correlation and regression analyses suggest that the expansion speed, poloidal speed, total magnetic helicity and twist per au of the flux rope are independent of heliospheric distance. The study implies that the aforementioned features are more strongly influenced by their internal properties compared with external conditions in the ambient medium. Moreover, the poloidal magnetic flux and magnetic energy of the studied flux ropes exhibit power-law dependence on heliospheric distance. A better understanding of the underlying physics and corroboration of these results is expected from the Parker Solar Probe measurements in the near future.

The pancaking of coronal mass ejections: an *in situ* attestation

Anil N **Raghav**, [Zubair I Shaikh](#)

Monthly Notices of the Royal Astronomical Society: Letters, Volume 493, Issue 1, March **2020**, Pages L16–L21,

[sci-hub.si/10.1093/mnrasl/slz187](https://doi.org/10.1093/mnrasl/slz187)

The interplanetary counterparts of coronal mass ejections (ICMEs) are the leading driver of severe space weather. Their morphological evolution in interplanetary space and the prediction of their arrival time at Earth are the ultimate focus of space weather studies, because of their scientific and technological effects. Several investigations in the last couple of decades have assumed that ICMEs have a circular cross-section. Moreover, various models have also been developed to understand the morphology of ICMEs based on their deformed cross-section. In fact, simulation studies have suggested that the initial circular cross-section flattens significantly during their propagation in the solar wind and this is referred to as ‘pancaking’. However, an observational verification of this phenomenon is still pending and it will eventually be the primary concern of several morphological models. Here, we report the first unambiguous observational evidence of extreme flattening of the cross-section of ICMEs, similar to pancaking, based on *in situ* measurements of 30 ICME events. In fact, we conclude that the cross-section of ICME flux ropes transformed into a two-dimensional planar magnetic structure. Such a deformed morphological feature not only alters the prediction of their arrival time but also has significant implications in solar-terrestrial physics, the energy budget of the heliosphere, charged particle energization, turbulence dissipation and enhanced geo-effectiveness, etc. **20 Nov 2003**

Table A1. List of ICME flux rope events transformed to PMS (1998-2016)

Torsional Alfvén Wave Embedded ICME Magnetic Cloud and Corresponding Geomagnetic Storm

Anil N. **Raghav**¹, Ankita Kule¹, Ankush Bhaskar^{2,3}, Wageesh Mishra⁴, Geeta Vichare⁵, and Shobha Surve⁶

2018 ApJ 860 26

DOI [10.3847/1538-4357/aabba3](https://doi.org/10.3847/1538-4357/aabba3)

Energy transfer during the interaction of large-scale solar wind structure and the Earth's magnetosphere is a chronic issue in space-weather studies. To understand this, researchers widely studied the geomagnetic storm and substorm phenomena. The present understanding suggests that the long duration of the southward interplanetary magnetic field component is the most important parameter for the geomagnetic storm. Such a long duration strong southward magnetic field is often associated with ICMEs, torsional Alfvén fluctuations superposed corotating interacting regions (CIRs), and fast solar wind streams. Torsional Alfvén fluctuations embedded CIRs have been known of for a long time; however, magnetic clouds embedded with such fluctuations are rarely observed. The presence of Alfvén waves in the ICME/MC and the influence of these waves on the storm evolution remains an interesting topic of study. The present work confirms the torsional Alfvén waves in a magnetic cloud associated with a CME launched on **2011 February 15**, which impacted the Earth's magnetosphere on **2011 February 18**. Furthermore, observations indicate that these waves inject energy into

the magnetosphere during the storm and contribute to the long recovery time of geomagnetic storms. Our study suggests that the presence of torsional Alfvén waves significantly controls the storm dynamics.

The energy exchange mechanism in large-scale magnetic plasmoids collision

Anil [Raghav](#), [Ankita Kule](#)

2017

<https://arxiv.org/pdf/1710.05755.pdf>

Recently, a super-elastic collision of large-scale plasmoids i.e. solar coronal mass ejections (CMEs) has been observed and further supported by numerical simulations. However, the energy gain by the system in the collision process is not clear. In-fact during plasmoids collision process, the energy exchange mechanism is still a chronic issue. Here, we present conclusive in situ evidence of sunward torsional Alfvén waves in the magnetic cloud after the super-elastic collision of the largest plasmoids in the heliosphere. We conclude that magnetic reconnection and Alfvén waves are the possible energy exchange mechanism during plasmoids interaction.

Forbush Decrease: A New Perspective with Classification

Anil [Raghav](#), Zubair Shaikh, Ankush Bhaskar, Gauri Datar, Geeta Vichare

[Solar Physics](#) August 2017, 292:99

<http://sci-hub.cc/10.1007/s11207-017-1121-4>

Sudden short-duration decreases in cosmic ray flux, known as Forbush decreases (FDs), are mainly caused by interplanetary disturbances. A generally accepted view is that the first step of an FD is caused by a shock sheath and the second step is due to the magnetic cloud (MC) of the interplanetary coronal mass ejection (ICME). This simplistic picture does not consider several physical aspects, such as whether the complete shock sheath or MC (or only part of these) contributes to the decrease or the effect of internal structure within the shock-sheath region or MC. We present an analysis of 16 large ($\geq 8\%$) FD events and the associated ICMEs, a majority of which show multiple steps in the FD profile. We propose a reclassification of FD events according to the number of steps observed in their respective profiles and according to the physical origin of these steps. This study determines that 13 out of 16 major events ($\sim 81\%$) can be explained completely or partially on the basis of the classic FD model. However, it cannot explain all the steps observed in these events. Our analysis clearly indicates that not only broad regions (shock sheath and MC), but also localized structures within the shock sheath and MC have a significant role in influencing the FD profile. The detailed analysis in the present work is expected to contribute toward a better understanding of the relationship between FD and ICME parameters. **24 September 1998, 13 July 2000, 17 September 2000, 24 November 2001, 9 November 2004, Table 1** List of analyzed Forbush decrease events classified on the basis of the number of steps observed in cosmic ray flux.

Understanding Forbush decrease drivers based on shock-only and CME-only models using global signature of February 14, 1978 event

Anil [Raghav](#), Ankush Bhaskar, Ajay Lotekar, Geeta Vichare, Virendra Yadav

2014

<http://arxiv.org/pdf/1406.4608v1.pdf>

We have studied Forbush decrease (FD) event occurred on February 14, 1978 using 43 neutron monitor observatories to understand the global signature of FD. We have studied rigidity dependence of shock amplitude and total FD amplitude. We have found almost the same power law index for both shock phase amplitude and total FD amplitude. Local time variation of shock phase amplitude and maximum depression time of FD have been investigated which indicate possible effect of shock/CME orientation. We have analyzed rigidity dependence of time constants of two phase recovery. Time constants of slow component of recovery phase show rigidity dependence and implies possible effect of diffusion. Solar wind speed was observed to be well correlated with slow component of FD recovery phase. This indicates solar wind speed as possible driver of recovery phase. To investigate the contribution of interplanetary drivers, shock and CME in FD, we have used shock-only and CME-only models. We have applied these models separately to shock phase and main phase amplitudes respectively. **This confirms present accepted physical scenario that the first step of FD is due to propagating shock barrier and second step is due to flux rope of CME/magnetic cloud.**

Flow-line Wandering in the Turbulent Solar Wind and Space Environment Forecasts

B. R. [Ragot](#)

2018 ApJ 868 35

<https://doi.org/10.3847/1538-4357/aae47e>

Space environment forecasts are based on ab initio modeling of the solar wind (SW) wherein solar magnetic fields and plasmas are propagated from an initial/boundary model source surface in the lower solar corona out to 1 au. Testing of these space environment forecasts relative to in situ measurements at 1 au typically shows uncertainties in the arrival times of fast SW streams of the order of a day, with broad distributions, means/medians of the order of half a day, and large variations between models but no definite winner. Here the effect of flow-line (FL) wandering due to the higher frequency velocity fluctuations within the turbulent SW on the arrival-time statistics of parcels of SW plasma transiting through the inner heliosphere out to 1 au is evaluated for a range of cutoff timescales in the velocity fluctuations. Used for this evaluation are in situ SW velocity measurements onboard Wind at 1 au, detailed spectral analysis of these measurements, WKB extrapolations to the inner heliosphere and simple application of a newly extended theoretical calculation of the mean SWFL cross-flow and "flow-aligned" displacements from the measured spectra. It is found that the velocity fluctuations near 1 au have little effect on the arrival times. The effect of the velocity fluctuations increases sunward, however, to a level sufficient to explain the large and broadly distributed "uncertainties" found in the testing of the forecasts.

A Statistical Study on the Stand-off Distances of Interplanetary Coronal Mass Ejections

A. Mujiber **Rahman**, b, , , A. Shanmugarajuc, S. Umaphya, Y.-J. Moond

Journal of Atmospheric and Solar-Terrestrial Physics, **2013, Volumes 105–106, December 2013, Pages 181–190**

<http://www.sciencedirect.com/science/article/pii/S1364682613002587>

We have analyzed the stand-off distance values of 101 interplanetary CMEs (ICMEs) observed during the period 1997–2005. Main aim of the present work is to study the stand-off distance and its dependence on various parameters of CMEs, ICMEs and IP shocks, Alfvénic Mach numbers and transit time. From the distribution, the stand-off time and stand-off distance values of many of the events are found to be in the range between ~2–20 hours and ~1–40 R_{\odot} (R_{\odot} =Solar radius). From the correlation between speed of CMEs and stand-off distance, we noted smaller stand-off distance for energetic CMEs, which indicated that the driver CME (CME which is generating the shock) and its shock travel closely together. From the correlation plot between CME acceleration and stand-off distance, we found that the highly decelerated events and highly accelerated events have lower stand-off distance range (i.e., 10 R_{\odot} to 40 R_{\odot}) than the other events. The events with longer travel time to reach 1 AU (> 70 h) show stand-off times ≤ 20 h and for those faster events ($V_{CME} > 2200$ km/s) with smaller travel time (≤ 40 h), stand-off time is extremely low (≤ 10 h). A wide range of stand-off distance is seen for a particular value of CME and ICME parameters. The poor correlations of stand-off distance with all the above parameters confirm that the stand-off distance does not strongly depend on CME, ICME and IP shock parameters, but depends on a combination of all these parameters. On the other hand, the faster CMEs having lower stand-off distance and/or stand-off time imply that as long as the CMEs are energetic, the CMEs and shocks travel closely together. Also, it can be noted that the stand-off distance is not only dependent on gamma, but it is related to other parameters.

Table 1. List of CMEs associated with ICMEs, IP Shocks, stand-off time and stand-off distance.

Propagation of normal and faster CMEs in the interplanetary medium

A. Mujiber **Rahman**, , , A. Shanmugarajub, 1, , S. Umaphya

Advances in Space Research, Volume 52, Issue 6, 15 September 2013, Pages 1168–1177, **2013; File**

We have analyzed 101 Coronal Mass Ejection (CME) events and their associated interplanetary CMEs (ICMEs) and interplanetary (IP) shocks observed during the period 1997–2005 from the **list given by Mujiber Rahman et al. (2012)**.

The aim of the present work is to correlate the interplanetary parameters such as, the speeds of IP shocks and ICMEs, CME transit time and their relation with CME parameters near the Sun. Mainly, a group of 10 faster CME events ($V_{INT} > 2200$ km/s) are compared with a list of 91 normal events of Manoharan et al. (2004). From the distribution diagrams of CME, ICME and IP shock speeds, we note that a large number of events tends to narrow towards the ambient (i.e., background) solar wind speed (~500 km/s) in agreement with the literature. Also, we found that the IP shock speed and the average ICME speed measured at 1 AU are well correlated. In addition, the IP shock speed is found to be slightly higher than the ICME speed. While the normal events show CME travel time in the range of ~40–80 h with a mean value of 65 h, the faster events have lower transit time with a mean value of 40 h. The effect of solar wind drag is studied using the correlation of CME acceleration with interplanetary (IP) acceleration and with other parameters of ICMEs. While the mean acceleration values of normal and faster CMEs in the LASCO FOV are 1 m/s², 18 m/s², they are -1.5 m/s² and -14 m/s² in the interplanetary medium, respectively. The relation between CME speed and IP acceleration for normal and faster events are found to agree with that of Lindsay et al., 1999 and Gopalswamy et al.,

2001 except slight deviations for the faster events. It is also seen that the faster events with less travel time face higher negative acceleration (>-10 m/s²) in the interplanetary medium up to 1 AU.

Table 1: List of IP shocks, ICMEs and associated CMEs.

Evidence from Galactic Cosmic Rays That the Sun Has Likely Entered A Secular Minimum in Solar Activity

[F. Rahmanifard](#), [A. P. Jordan](#), [W. C. de Wet](#), [N. A. Schwadron](#), [J. K. Wilson](#), [M. J. Owens](#), [H. E. Spence](#), [P. Riley](#)

Space weather **Volume20, Issue2** e2021SW002796 **2022**

<https://agupubs.onlinelibrary.wiley.com/doi/epdf/10.1029/2021SW002796>

<https://doi.org/10.1029/2021SW002796>

Since the beginning of the space age, the Sun has been in a multi-cycle period of elevated activity (secular maximum). This secular maximum is the longest in the last 9300 years. Since the end of solar cycle 21 (SC21), however, the Sun has shown a decline in overall activity, which has remarkably increased the fluxes of galactic cosmic rays (GCRs). Here, we investigate the correlation between the modulation of GCRs, the heliospheric magnetic field, and solar wind speed for the last 24 solar cycles to find trends that can potentially be used to predict future solar activity. Specifically, we develop a tool for predicting future magnetic field intensity, based on the hysteresis in the GCR variation, during the last phases of the current cycle. This method estimates that SC25 will be as weak as or weaker than SC24. This would mean that the Sun has likely entered a secular minimum, which, according to historical records, should last for another two cycles (SC25 and SC26).

CNN-Based Deep Learning in Solar Wind Forecasting

Hemapriya [Raju](#), [Saurabh Das](#)

Solar Phys. **296**, Article number: 134 **2021**

<https://arxiv.org/pdf/2108.09114.pdf>

<https://link.springer.com/content/pdf/10.1007/s11207-021-01874-6.pdf>

<https://doi.org/10.1007/s11207-021-01874-6>

This article implements a Convolutional Neural Network (CNN)-based deep learning model for solar-wind prediction. Images from the Atmospheric Imaging Assembly (AIA) at 193Å wavelength are used for training. Solar-wind speed is taken from the Advanced Composition Explorer (ACE) located at the Lagrangian L1 point. The proposed CNN architecture is designed from scratch for training with four years' data. The solar-wind has been ballistically traced back to the Sun assuming a constant speed during propagation, to obtain the corresponding coronal intensity data from AIA images. This forecasting scheme can predict the solar-wind speed well with a RMSE of 76.3 km/s and an overall correlation coefficient of 0.57 for the year 2018, while significantly outperforming benchmark models. The threat score for the model is around 0.46 in identifying the HSEs with zero false alarms. **19-24 Jun 2017**

Dissipation scale lengths of density turbulence in the inner solar wind

K. Sasikumar [Raja](#), [Prasad Subramanian](#), [Madhusudan Ingale](#), [R. Ramesh](#)

ApJ **2019**

<https://arxiv.org/pdf/1901.02297.pdf>

Knowing the lengthscales at which turbulent fluctuations dissipate is key to understanding the nature of weakly compressible magnetohydrodynamic turbulence. We use radio wavelength interferometric imaging observations which measure the extent to which distant cosmic sources observed against the inner solar wind are scatter-broadened. We interpret these observations to determine that the dissipation scales of solar wind density turbulence at heliocentric distances of 2.5 -- 20.27 R_⊙ range from ≈ 13500 to 520 m. Our estimates from ≈ 10 --20 R_⊙ suggest that the dissipation scale corresponds to the proton gyroradius. They are relevant to in-situ observations to be made by the Parker Solar Probe, and are expected to enhance our understanding of solar wind acceleration.

IN SITU HEATING OF THE 2007 MAY 19 CME EJECTA DETECTED BY STEREO/PLASTIC AND ACE

Cara E. [Rakowski](#)¹, J. Martin Laming² and Maxim Lyutikov³

2011 ApJ 730 30, [File](#)

In situ measurements of ion charge states can provide unique insight into the heating and evolution of coronal mass ejections (CMEs) when tested against realistic non-equilibrium ionization modeling. In this work, **we investigate the representation of the CME magnetic field as an expanding spheromak configuration**, where the plasma heating is

prescribed by the choice of anomalous resistivity and the spheromak dynamics. We chose as a test case the 2007 May 19 CME observed by STEREO and ACE. The spheromak is an appealing physical model, because the location and degree of heating are fixed by the choice of anomalous resistivity and the spheromak expansion rate which we constrain with observations. This model can provide the heating required between 1.1R and Earth's orbit to produce charge states observed in the CME flux rope. However, this source of heating in the spheromak alone has difficulty accounting for the rapid heating to Fe8-Fe11+ at lower heights, as observed in STEREO EUVI due to the rapid radiative cooling that occurs at the high densities involved. Episodes of heating and cooling clearly unrelated to spheromak expansion are observed prior to the eruption, and presumably still play a role during the eruption itself. Spheromak heating is also not capable of reproducing the high Fe charge states (Fe16+ and higher) seen in situ exterior to the flux rope in this CME. Thus, while the spheromak configuration may be a valid model for the magnetic topology, other means of energization are still required to provide much of the rapid heating observed.

The pancaking of coronal mass ejections: an in situ attestation

Anil N. **Raghav** ¹ and Zubair I. Shaikh ²

MNRAS 493, L16–L21 (2020)

<https://sci-hub.ru/10.1093/mnras/slz187>

The interplanetary counterparts of coronal mass ejections (ICMEs) are the leading driver of severe space weather. Their morphological evolution in interplanetary space and the prediction of their arrival time at Earth are the ultimate focus of space weather studies, because of their scientific and technological effects. Several investigations in the last couple of decades have assumed that ICMEs have a circular cross-section. Moreover, various models have also been developed to understand the morphology of ICMEs based on their deformed cross-section. In fact, simulation studies have suggested that the initial circular cross-section flattens significantly during their propagation in the solar wind and this is referred to as ‘pancaking’. However, an observational verification of this phenomenon is still pending and it will eventually be the primary concern of several morphological models. Here, we report the first unambiguous observational evidence of extreme flattening of the cross-section of ICMEs, similar to pancaking, based on in situ measurements of 30 ICME events. In fact, we conclude that the cross-section of ICME flux ropes transformed into a two-dimensional planar magnetic structure. Such a deformed morphological feature not only alters the prediction of their arrival time but also has significant implications in solar-terrestrial physics, the energy budget of the heliosphere, charged particle energization, turbulence dissipation and enhanced geo-effectiveness, etc. **20 Nov 2003**

Super-Intense Geomagnetic Storm on 10–11 May 2024: Possible Mechanisms and Impacts

S. Tulasi **Ram**, [B. Veenadhari](#), [A. P. Dimri](#), [J. Bulusu](#), [M. Bagiya](#), [S. Gurubaran](#), [N. Parihar](#), [B.](#)

[Remya](#), [G. Seemala](#), [Rajesh Singh](#), [S. Sripathi](#), [S. V. Singh](#), [G. Vichare](#)

Space Weather [Volume22, Issue12](#) December **2024** e2024SW004126

<https://doi.org/10.1029/2024SW004126>

<https://agupubs.onlinelibrary.wiley.com/doi/epdf/10.1029/2024SW004126>

One of the most intense geomagnetic storms of recent times occurred on 10–11 May 2024. With a peak negative excursion of Sym-H below -500 nT, this storm is the second largest of the space era. Solar wind energy transferred through radiation and mass coupling affected the entire Geospace. Our study revealed that the dayside magnetopause was compressed below the geostationary orbit (6.6 RE) for continuously ~ 6 hr due to strong Solar Wind Dynamic Pressure (SWDP). Tremendous compression pushed the bow-shock also to below the geostationary orbit for a few minutes. Magnetohydrodynamic models suggest that the magnetopause location could be as low as 3.3RE. We show that a unique combination of high SWDP (≥ 15 nPa) with an intense eastward interplanetary electric field (IEFY ≥ 2.5 mV/m) within a super-dense Interplanetary Coronal Mass Ejection lasted for 409 min—is the key factor that led to the strong ring current at much closer to the Earth causing such an intense storm. Severe electrodynamic disturbances led to a strong positive ionospheric storm with more than 100% increase in dayside ionospheric Total Electron Content (TEC), affecting GPS positioning/navigation. Further, an HF radio blackout was found to occur in the 2–12 MHz frequency band due to strong D- and E-region ionization resulting from a solar flare prior to this storm.

How comets reveal structure of the inner heliosphere

[Ramanjooloo](#), Yudish

Astronomy & Geophysics (A&G) **2014** Volume 55, Issue 1, p.1.32-1.35

how the interaction between comets and the solar wind can help to understand the inner heliosphere structure.

Galactic Cosmic Rays Throughout the Heliosphere and in the Very Local Interstellar Medium Review

Jamie S. [Rankin](#), [Veronica Bindi](#), [Andrei M. Bykov](#), [Alan C. Cummings](#), [Stefano Della Torre](#), [Vladimir Florinski](#), [Bernd Heber](#), [Marius S. Potgieter](#), [Edward C. Stone](#) & [Ming Zhang](#)
Space Science Reviews volume 218, Article number: 42 (2022)

<https://link.springer.com/content/pdf/10.1007/s11214-022-00912-4.pdf>

We review recent observations and modeling developments on the subject of galactic cosmic rays through the heliosphere and in the Very Local Interstellar Medium, emphasizing knowledge that has accumulated over the past decade. We begin by highlighting key measurements of cosmic-ray spectra by Voyager, PAMELA, and AMS and discuss advances in global models of solar modulation. Next, we survey recent works related to large-scale, long-term spatial and temporal variations of cosmic rays in different regimes of the solar wind. Then we highlight new discoveries from beyond the heliopause and link these to the short-term evolution of transients caused by solar activity. Lastly, we visit new results that yield interesting insights from a broader astrophysical perspective.

First Observations of Anomalous Cosmic Rays in to 36 Solar Radii

J. S. [Rankin](#)¹, D. J. McComas¹, R. A. Leske², E. R. Christian³, C. M. S. Cohen², A. C. Cummings², C. J. Joyce¹, A. W. Labrador², R. A. Mewaldt², A. Posner⁴Show full author list
2021 ApJ 912 139

<https://doi.org/10.3847/1538-4357/abec7e>

NASA's Parker Solar Probe mission continues to travel closer to the Sun than any prior human-made object, with an expected closest approach of <10 solar radii (<0.046 au) by 2024. On board, the Integrated Science Investigation of the Sun instrument suite makes unprecedented in situ measurements of energetic particles in the near-Sun environment. The current low level of solar activity offers a prime opportunity to measure cosmic rays closer to the Sun than ever before. We present the first observations of anomalous cosmic rays in to 36 solar radii (0.166 au), focusing specifically on helium. Our results indicate a strong radial intensity gradient of $\sim 25 \pm 5\%$ /au over energies of ~ 4 to ~ 45 MeV/nuc. These values are larger than prior observations, further out in the heliosphere, and come at a unique time in our understanding and modeling of particle transport and acceleration, particularly as both Voyagers have crossed the heliopause and IBEX has accumulated a full solar cycle of observations. Thus, continued measurements of cosmic rays by Parker Solar Probe will play a critical role in linking past observations with our present knowledge and significantly advancing our understanding of cosmic ray transport in the heliosphere.

Heliosheath Properties Measured from a Voyager 2 to Voyager 1 Transient

Jamie S. [Rankin](#), [David J. McComas](#), [John D. Richardson](#), [Nathan A. Schwadron](#)
Astrophysical Journal, 883:101, 2019

<https://arxiv.org/ftp/arxiv/papers/1910/1910.00676.pdf>

In mid-2012, a GMIR observed by Voyager 2 crossed through the heliosheath and collided with the heliopause, generating a pressure pulse that propagated into the very local interstellar medium. The effects of the transmitted wave were seen by Voyager 1 just 93 days after its own heliopause crossing. The passage of the transient was accompanied by long-lasting decreases in galactic cosmic ray intensities that occurred from ~ 2012.55 to ~ 2013.35 and ~ 2012.91 to ~ 2013.70 at Voyager 2 and Voyager 1, respectively. Omnidirectional (>20 MeV) proton-dominated measurements from each spacecraft's Cosmic Ray Subsystem reveal a remarkable similarity between these causally-related events, with a correlation coefficient of 91.2% and a time-lag of 130 days. Knowing the locations of the two spacecraft, we use the observed time-delay to calculate the GMIR's average speed through the heliosheath (inside the heliopause) as a function of temperature in the very local interstellar medium. This, combined with particle, field, and plasma observations enables us to infer previously unmeasured properties of the heliosheath, including a range of sound speeds and total effective pressures. For a nominal temperature of $\sim 20,000$ K just outside the heliopause, we find a sound speed of 314 (+/-) 32 km/s and total effective pressure of 267 (+/-) 55 fPa inside the heliopause. We compare these results with the Interstellar Boundary Explorer's data-driven models of heliosheath pressures derived from energetic neutral atom fluxes (the globally distributed flux) and present them as additional evidence that the heliosheath's dynamics are driven by suprathermal energetic processes.

Magnetic Reconnection as the Driver of the Solar Wind

Nour E. [Raouafi](#)¹, G. Stenborg¹, D. B. Seaton², H. Wang^{3,4,5}, J. Wang^{3,4,5}, C. E. DeForest², S. D. Bale^{6,7}, J. F. Drake⁸, V. M. Uritsky^{9,10}, J. T. Karpen¹⁰Show full author list
2023 ApJ 945 28

<https://iopscience.iop.org/article/10.3847/1538-4357/acaf6c/pdf>
<https://arxiv.org/pdf/2301.00903.pdf>

We present EUV solar observations showing evidence for omnipresent jetting activity driven by small-scale magnetic reconnection at the base of the solar corona. We argue that the physical mechanism that heats and drives the solar wind at its source is ubiquitous magnetic reconnection in the form of small-scale jetting activity (a.k.a. jetlets). This jetting activity, like the solar wind and the heating of the coronal plasma, is ubiquitous regardless of the solar cycle phase. Each event arises from small-scale reconnection of opposite-polarity magnetic fields producing a short-lived jet of hot plasma and Alfvén waves into the corona. The discrete nature of these jetlet events leads to intermittent outflows from the corona, which homogenize as they propagate away from the Sun and form the solar wind. This discovery establishes the importance of small-scale magnetic reconnection in solar and stellar atmospheres in understanding ubiquitous phenomena such as coronal heating and solar wind acceleration. Based on previous analyses linking the switchbacks to the magnetic network, we also argue that these new observations might provide the link between the magnetic activity at the base of the corona and the switchback solar wind phenomenon. These new observations need to be put in the bigger picture of the role of magnetic reconnection and the diverse form of jetting in the solar atmosphere. **2019-07-29, 2021-04-28**

Parker Solar Probe: Four Years of Discoveries at Solar Cycle Minimum

Review

[N. E. Raouafi](#), [L. Matteini](#), [J. Squire](#), [S. T. Badman](#), [M. Velli](#), +++

Space Science Reviews **2023** 157 pages, 65 figures

<https://arxiv.org/pdf/2301.02727.pdf>

Launched on 12 Aug. 2018, NASA's Parker Solar Probe had completed 13 of its scheduled 24 orbits around the Sun by Nov. 2022. The mission's primary science goal is to determine the structure and dynamics of the Sun's coronal magnetic field, understand how the solar corona and wind are heated and accelerated, and determine what processes accelerate energetic particles. Parker Solar Probe returned a treasure trove of science data that far exceeded quality, significance, and quantity expectations, leading to a significant number of discoveries reported in nearly 700 peer-reviewed publications. The first four years of the 7-year primary mission duration have been mostly during solar minimum conditions with few major solar events. Starting with orbit 8 (i.e., 28 Apr. 2021), Parker flew through the magnetically dominated corona, i.e., sub-Alfvénic solar wind, which is one of the mission's primary objectives. In this paper, we present an overview of the scientific advances made mainly during the first four years of the Parker Solar Probe mission, which go well beyond the three science objectives that are: (1) Trace the flow of energy that heats and accelerates the solar corona and solar wind; (2) Determine the structure and dynamics of the plasma and magnetic fields at the sources of the solar wind; and (3) Explore mechanisms that accelerate and transport energetic particles. **1 Nov. 2018, 5 Nov. 2018, 11-12 Nov. 2018, 15 Mar. 2019, 2 and 4 Apr. 2019, 20-21 Apr. 2019, 13 Oct. 2019, 20 Jan. 2020, 26-27 Jan. 2020, 25 Jun. 2020, 19 Nov. 2020, 29 Nov. 2020**

1 Introduction	3
2 Historical Context: Mariner 2 , Helios, and Ulysses	5
3 Mission Status	7
4 Magnetic Field Switchbacks	10
5 Solar Wind Sources and Associated Signatures	34
6 Kinetic Physics and Instabilities in the Young Solar Wind	43
7 Turbulence	54
8 Large-Scale Structures in the Solar Wind	72
9 Solar Radio Emission	91
10 Energetic Particles	92
11 Dust	118
12 Venus	133
13 Summary and Conclusions	135
14 List of Abbreviations	141

Magnetic Reconnection as the Driver of the Solar Wind

[Nour E. Raouafi](#), [G. Stenborg](#), [D. B. Seaton](#), [H. Wang](#), [J. Wang](#), [C. E. DeForest](#), [S. D. Bale](#), [J. F. Drake](#), [V. M. Uritsky](#), [J. T. Karpen](#), [C. R. DeVore](#), [A. C. Sterling](#), [T. S. Horbury](#), [L. K. Harra](#), [S. Bourouaine](#), [J. C. Kasper](#), [P. Kumar](#), [T. D. Phan](#), [M. Velli](#)

ApJ **2023**

<https://arxiv.org/pdf/2301.00903.pdf>

We present EUV solar observations showing evidence for omnipresent jetting activity driven by small-scale magnetic reconnection at the base of the solar corona. We argue that the physical mechanism that heats and drives the solar wind

at its source is ubiquitous magnetic reconnection in the form of small-scale jetting activity (i.e., a.k.a. jetlets). This jetting activity, like the solar wind and the heating of the coronal plasma, are ubiquitous regardless of the solar cycle phase. Each event arises from small-scale reconnection of opposite polarity magnetic fields producing a short-lived jet of hot plasma and Alfvén waves into the corona. The discrete nature of these jetlet events leads to intermittent outflows from the corona, which homogenize as they propagate away from the Sun and form the solar wind. This discovery establishes the importance of small-scale magnetic reconnection in solar and stellar atmospheres in understanding ubiquitous phenomena such as coronal heating and solar wind acceleration. Based on previous analyses linking the switchbacks to the magnetic network, we also argue that these new observations might provide the link between the magnetic activity at the base of the corona and the switchback solar wind phenomenon. These new observations need to be put in the bigger picture of the role of magnetic reconnection and the diverse form of jetting in the solar atmosphere.
2018-07-29, 2021-04-28

Switchbacks and Associated Magnetic Holes Observed near the Alfvén Critical Surface

Anthony P. **Rasca**^{1,2}, William M. Farrell³, Jacob R. Gruesbeck⁴, Robert J. MacDowall⁴, Stuart D. Bale^{5,6}, and Justin C. Kasper^{7,8}

2023 ApJ 959 10

<https://iopscience.iop.org/article/10.3847/1538-4357/ad06b4/pdf>

During recent solar encounters, the Parker Solar Probe (PSP) began its initial dips below the Alfvén critical surface to measure in situ the sub-Alfvénic coronal wind. While the near-Sun super-Alfvénic solar wind is shown to be dominated by impulsive magnetic switchbacks (short magnetic field reversals), these brief encounters with the sub-Alfvénic coronal wind show switchbacks and associated magnetic holes (MHs) to still be present but different in character. In this work, we compare and contrast specific features of the switchbacks, including the change in B_r and V_r and associated boundary B-field dropouts (MHs) at locations when PSP was both above and below the Alfvén critical surface. We use observations from the PSP perihelion Encounters 8 (E8) and 12 (E12) in the analysis. We first perform a superposed epoch analysis to identify common features in the switchback boundaries, including the formation of the associated $|B|$ dropouts/MHs in slow and fast flows. We then examine the presence of B-field dropouts/MHs as a function of Alfvén Mach number, MA . From E12, we find that the switchbacks have a systematic reduction in rotation (and reduction in B_r deflection) with decreasing MA . Further, the $|B|$ dropouts/MHs associated with the boundaries were also found to decrease in strength and occurrence with MA (with no or few $|B|$ dropouts at $MA < 0.7$). The results suggest that the switchback rotation and boundary-associated MHs are connected, possibly consistent with diamagnetic effects at the boundary that require large rotations to be initiated.

Magnetic Field Dropouts and Associated Plasma Wave Emission near the Electron Plasma Frequency at Switchback Boundaries as Observed by the Parker Solar Probe

Anthony P. **Rasca**¹, William M. Farrell¹, Phyllis L. Whittlesey², Robert J. MacDowall¹, Stuart D. Bale^{2,3}, and Justin C. Kasper^{4,5}

2022 ApJ 935 81

<https://iopscience.iop.org/article/10.3847/1538-4357/ac80c3/pdf>

The first solar encounters by the Parker Solar Probe revealed the magnetic field to be dominated by short field reversals in the radial direction, referred to as "switchbacks." While radial velocity and proton temperature were shown to increase inside the switchbacks, $|B|$ exhibits very brief dropouts only at the switchback boundaries. Brief intensifications in spectral density measurements near the electron plasma frequency, f_{pe} , were also observed at these boundaries, indicating the presence of plasma waves triggered by current systems in the form of electron beams. We perform a correlative study using observations from the Parker FIELDS Radio Frequency Spectrometer and Fluxgate Magnetometer to compare occurrences of spectral density intensifications at the electron plasma frequency (f_{pe} emissions) and $|B|$ dropouts at switchback boundaries during Parker's first and second solar encounters. We find that only a small fraction of minor $|B|$ dropouts are associated with f_{pe} emissions. This fraction increases with $|B|$ dropout size until all dropouts are associated with f_{pe} emissions. Brief spikes in the differential electron flux measured by the SWEAP Solar Probe Analyzer for Electron sensors also occur in conjunction with nearly all f_{pe} emissions. This suggests that in the presence of strong $|B|$ dropouts, electron currents that create the perturbation in $|B|$ along the boundaries are also stimulating plasma waves such as Langmuir waves. **5, 6-7, 10 Nov 2018**

Estimation of Arrival Time of Coronal Mass Ejections in the Vicinity of the Earth Using Solar and Heliospheric Observatory and Solar TERrestrial RELations Observatory Observations

Anitha [Ravishankar](#), Grzegorz Michalek

[Solar Physics](#) September 2019, 294:125

<https://arxiv.org/pdf/1910.02797.pdf>

<https://link.springer.com/content/pdf/10.1007%2Fs11207-019-1470-2.pdf>

<https://doi.org/10.1007/s11207-019-1470-2>

The arrival time of coronal mass ejections (CMEs) in the vicinity of the Earth is one of the most important parameters in determining space weather. We have used a new approach to predicting this parameter. First, in our study, we have introduced a new definition of the speed of ejection. It can be considered as the maximum speed that the CME achieves during the expansion into the interplanetary medium. Additionally, in our research we have used not only observations from the SOLar and Heliospheric Observatory (SOHO) spacecraft but also from Solar TERrestrial RELations Observatory (STEREO) spacecrafts. We focus on halo and partial-halo CMEs during the ascending phase of Solar Cycle 24. During this period the STEREO spacecraft were in quadrature position in relation to the Earth. We demonstrated that these conditions of the STEREO observations can be crucial for an accurate determination of the transit times (TTs) of CMEs to the Earth. In our research we defined a new initial velocity of the CME, the maximum velocity determined from the velocity profiles obtained from a moving linear fit to five consecutive height–time points. This new approach can be important from the point of view of space weather as the new parameter is highly correlated with the final velocity of ICMEs. It allows one to predict the TTs with the same accuracy as previous models. However, what is more important is the fact that the new approach has radically reduced the maximum TT estimation errors to 29 hours. Previous studies determined the TT with a maximum error equal to 50 hours.

Table 1 Observational parameters of 51 ICMEs in the period 2009 – 2013.

Remote Sensing of Magnetic-Cloud Topology

Donald V. [Reames](#)

[Solar Phys](#) (2010) 265: 187–195, [File](#)

We investigate the topology of magnetic clouds using energetic particles from a variety of sources outside the clouds as probes to remotely sense the interconnections of the magnetic field. We find that only a small percentage of field lines in magnetic clouds are truly closed directly to the Sun, so as to exclude particles from an external source. Field lines that are open to the outer heliosphere must be mixed with closed field lines on a fine spatial scale in the clouds to explain the simultaneous observation of anomalous cosmic rays from the outer heliosphere and of counter-streaming suprathermal electrons from the corona. The results of this paper show that, given sufficient time, particles accelerated at shock waves outside magnetic clouds have access to the interior and to a wide region of solar longitude in interplanetary space surrounding the clouds.

ANOMALOUS COSMIC RAYS AS PROBES OF MAGNETIC CLOUDS

D. V. [Reames](#)¹, S. W. Kahler², and A. J. Tylka³

[Astrophysical Journal](#), 700:L196–L199, 2009

We report, for the first time, the observation near the Earth of anomalous cosmic ray (ACR) particles throughout the interiors of interplanetary magnetic clouds (MCs) at the same intensity as outside the MCs. ACRs, accelerated in the outer heliosphere, have unique elemental abundances making their identity unambiguous as they probe these clouds from the outside. Thus, MCs, carried out from the Sun by coronal mass ejections (CMEs), are seen to contain no structures that are magnetically closed to the penetration of ions with energies above a few MeV amu⁻¹. As the MCs expand outward, they must fill their increasing volume with ACRs dynamically, to the same degree as neighboring “open” field lines. These observations cast doubt on conventional ideas about the closed field topologies of MCs and the cross-field transport of energetic particles. The ACR observations conflict with some reports of significant exclusion from MCs of solar energetic particles (SEPs) of comparable energy and rigidity. A process that allows cross-field transport of ACRs may also allow similar transport of SEPs late in events, causing the large spatial extent and uniformity of SEPs in “invariant spectral regions” extending far behind CME-driven shock waves.

On the time lag between solar wind dynamic parameters and solar activity UV proxies

R. Reda a b, L. Giovannelli a, T. Alberti b

[Advances in Space Research](#) Volume 71, Issue 4, 15 February 2023, Pages 2038-2047

<https://doi.org/10.1016/j.asr.2022.10.011>

The solar activity displays variability and periodic behaviours over a wide range of timescales, with the presence of a most prominent cycle with a mean length of 11 years. Such variability is transported within the [heliosphere](#) by solar wind, radiation and other processes, affecting the properties of the [interplanetary medium](#). The presence of solar activity-related periodicities is well visible in different solar wind and geomagnetic indices, although their time lags with respect to the solar cycle lead to [hysteresis](#) cycles. Here, we investigate the time lag behaviour between a physical proxy of the solar activity, the Ca II K index, and two solar wind parameters (speed and dynamic pressure), studying how their pairwise relative lags vary over almost five solar cycles. We find that the lag between Ca II K index and solar [wind speed](#) is not constant over the whole time interval investigated, with values ranging from 6 years to ~1 year (average 3.2 years). A similar behaviour is found also for the solar wind dynamic pressure. Then, by using a Lomb-Scargle periodogram analysis we obtain a 10.21-year mean periodicity for the speed and 10.30-year for the dynamic pressure. We speculate that the different periodicities of the solar wind parameters with respect to the solar 11-year cycle may be related to the overall observed [temporal evolution](#) of the time lags. Finally, by accounting for them, we obtain empirical relations that link the amplitude of the Ca II K index to the two solar wind parameters.

Defining Radiation Belt Enhancement Events Based on Probability Distributions

Geoffrey D. [Reeves](#), [Elizabeth M. Vandegriff](#), [Jonathan T. Niehof](#), [Steven K. Morley](#), [Gregory S. Cunningham](#), [Michael G. Henderson](#), [Brian A. Larsen](#)

Space Weather e2020SW002528 2020

<https://agupubs.onlinelibrary.wiley.com/doi/epdf/10.1029/2020SW002528>

We present a methodology to define moderate, strong, and intense space weather events based on probability distributions. We have illustrated this methodology using a long-duration, uniform data set of 1.8-3.5 MeV electron fluxes from multiple LANL geosynchronous satellite instruments but a strength of this methodology is that it can be applied uniformly to heterogeneous data sets. It allows quantitative comparison of data sets with different energies, units, orbits, etc. The methodology identifies a range of times, “events”, using variable flux thresholds to determine average event occurrence in arbitrary 11-year intervals (“cycles”). We define moderate, strong, and intense events as those that occur 100, 10, and 1 time per cycle and identify the flux thresholds that produce those occurrence frequencies. The methodology does not depend on any ancillary data set (e.g. solar wind or geomagnetic conditions). We show event probabilities using GOES > 2 MeV fluxes and compare them against event probabilities using LANL 1.8-3.5 MeV fluxes. We present some examples of how the methodology picks out moderate, strong, and intense events and how those events are distributed in time: 1989 through 2018, which includes the declining phases of solar cycles 22, 23, and 24. We also provide an illustrative comparison of moderate and strong events identified in the geosynchronous data with Van Allen Probes observations across all L-shells. We also provide a catalog of start and stop times of moderate, strong, and intense events that can be used for future studies.

Exploring the Impact of the Aging Effect on Inferred Properties of Solar Coronal Mass Ejections

F. [Regnault](#)¹, N. Al-Haddad¹, N. Lugaz¹, C. J. Farrugia¹, B. Zhuang¹, W. Yu¹, and A. Strugarek²

2024 ApJL 966 L17

<https://iopscience.iop.org/article/10.3847/2041-8213/ad3806/pdf>

In situ measurements of coronal mass ejections (CMEs) when they pass over an interplanetary probe are one of the main ways we directly measure their properties. However, such in situ profiles are subject to several observational constraints that are still poorly understood. This work aims at quantifying one of them, namely, the aging effect, using a CME simulated with a three-dimensional magnetohydrodynamical code. The synthetic in situ profile and the instantaneous profile of the magnetic field strength differ more from each other when taken close to the Sun than far from it. Moreover, out of three properties we compute in this study (i.e., size, distortion parameter, and expansion speed), only the expansion speed shows a dependence of the aging as a function of distance. It is also the property that is the most impacted by the aging effect as it can amount to more than 100 km s⁻¹ for CMEs observed closer than 0.15 au. This work calls for caution when deducing the expansion speed from CME profiles when they still are that close to the Sun since the aging effect can significantly impact the derived properties.

Discrepancies in the Properties of a Coronal Mass Ejection on Scales of 0.03~au as Revealed by Simultaneous Measurements at Solar Orbiter and Wind: The 2021 November 3--5 Event

[F. Regnault](#), [N. Al-Haddad](#), [N. Lugaz](#), [C. J. Farrugia](#), [W. Yu](#), [B. Zhuang](#), [E. E. Davies](#)

ApJ 962 190 2023

<https://arxiv.org/pdf/2311.14046.pdf>

<https://iopscience.iop.org/article/10.3847/1538-4357/ad1883/pdf>

Simultaneous in situ measurements of coronal mass ejections (CMEs), including both plasma and magnetic field, by two spacecraft in radial alignment have been extremely rare. Here, we report on one such CME measured by Solar Orbiter (SolO) and Wind on **2021 November 3--5**, while the spacecraft were radially separated by a heliocentric distance of 0.13 au and angularly by only 2.2°. We focus on the magnetic cloud (MC) part of the CME. We find notable changes in the R and N magnetic field components and in the speed profiles inside the MC between SolO and Wind. We observe a greater speed at the spacecraft further away from the Sun without any clear compression signatures. Since spacecraft are close to each other and computing fast magnetosonic wave speed inside the MC we rule out temporal evolution as the reason on the observed differences suggesting that spatial variations over 2.2° of the MC structure are at the heart of the observed discrepancies. Moreover, using shock properties at SolO, we forecast an arrival time 2h30 too late for a shock that is just 5h31 away hours from Wind. Predicting the north-south component of the magnetic field at Wind from SolO measurements leads to a relative error of 55 %. These results show that even angular separations as low as 2.2° (or 0.03 au in arclength) between spacecraft can have a large impact on the observed CME properties, rising up the issue of the resolutions of current CME models and potentially affecting our forecasting capabilities.

Investigating the Magnetic Structure of Interplanetary Coronal Mass Ejections using Simultaneous Multi-Spacecraft In situ Measurements

[F. Regnault](#), [N. Al-Haddad](#), [N. Lugaz](#), [C. J. Farrugia](#), [W. Yu](#), [E. E. Davies](#), [A. B. Galvin](#), [B. Zhuang](#)

ApJ 957 49 2023

<https://arxiv.org/pdf/2309.10582.pdf>

<https://iopscience.iop.org/article/10.3847/1538-4357/acef16/pdf>

In situ measurements from spacecraft typically provide a time series at a single location through coronal mass ejections (CMEs) and they have been one of the main methods to investigate CMEs. CME properties derived from these in situ measurements are affected by temporal changes that occur as the CME passes over the spacecraft, such as radial expansion and ageing, as well as spatial variations within a CME. This study uses multi-spacecraft measurements of the same CME at close separations to investigate both the spatial variability (how different a CME profile is when probed by two spacecraft close to each other) and the so-called ageing effect (the effect of the time evolution on in situ properties). We compile a database of 19 events from the past four decades measured by two spacecraft with a radial separation <0.2 au and an angular separation <10°. We find that the average magnetic field strength measured by the two spacecraft differs by 18% of the typical average value, which highlights non-negligible spatial or temporal variations. For one particular event, measurements taken by the two spacecraft allow us to quantify and significantly reduce the ageing effect to estimate the asymmetry of the magnetic field strength profile. This study reveals that single-spacecraft time series near 1 au can be strongly affected by ageing and that correcting for self-similar expansion does not capture the whole ageing effect. **1997-12-10-11, 2011 September 17**

Table 1. Catalog of the 19 events with simultaneous spacecraft measurements.

Eruption and propagation of twisted flux ropes from the base of the solar corona to 1 au

[F. Regnault](#), [A. Strugarek](#), [M. Janvier](#), [F. Auchère](#), [N. Lugaz](#), [N. Al-Haddad](#)

A&A 2022

<https://arxiv.org/pdf/2211.02569.pdf>

Interplanetary Coronal Mass Ejections (ICMEs) originate from the eruption of complex magnetic structures occurring in our star's atmosphere. Determining the general properties of ICMEs and the physical processes at the heart of their interactions with the solar wind is a hard task, in particular using only unidimensional in situ profiles. Thus, these phenomena are still not well understood. In this study we simulate the propagation of a set of flux ropes in order to understand some of the physical processes occurring during the propagation of an ICME such as their growth or their rotation. We present simulations of the propagation of a set of flux ropes in a simplified solar wind. We consider different magnetic field strengths and sizes at the initiation of the eruption, and characterize their influence on the properties of the flux ropes during their propagation. We use the 3D MHD module of the PLUTO code on an Adaptive Mesh Refinement grid. The evolution of the magnetic field of the flux rope during the propagation matches evolution law deduced from in situ observations. We also simulate in situ profiles that spacecraft would have measured at the Earth, and we compare with the results of statistical studies. We find a good match between simulated in situ profiles and typical profiles obtained in these studies. During their propagation, flux ropes interact with the magnetic field of the wind but still show realistic signatures of ICMEs when analyzed with synthetic satellite crossings. We also show that

flux ropes with different shapes and orientations can lead to similar unidimensional crossings. This warrants some care when extracting magnetic topology of ICMEs using unidimensional crossings.

20 Years of ACE Data: How Superposed Epoch Analyses Reveal Generic Features in Interplanetary CME Profiles Review

F. [Regnault](#), [M. Janvier](#), [P. Démoulin](#), [F. Auchère](#), [A. Strugarek](#), [S. Dasso](#), [C. Noûs](#)

JGR [Volume125, Issue11](#) e2020JA028150 2020

<https://arxiv.org/pdf/2011.05050.pdf>

<https://doi.org/10.1029/2020JA028150>

Interplanetary coronal mass ejections (ICMEs) are magnetic structures propagating from the Sun's corona to the interplanetary medium. With over 20 years of observations at the L1 libration point, ACE offers hundreds of ICMEs detected at different times during several solar cycles and with different features such as the propagation speed. We investigate a revisited catalog of more than 400 ICMEs using the superposed epoch method on the mean, median, and the most probable values of the distribution of magnetic and plasma parameters. We also investigate the effects of the speed of ICMEs relative to the solar wind, the solar cycle, and the existence of a magnetic cloud on the generic ICME profile. We find that fast-propagating ICMEs (relatively to the solar wind in front) still show signs of compression at 1 au, as seen by the compressed sheath and the asymmetric profile of the magnetic field. While the solar cycle evolution does not impact the generic features of ICMEs, there are more extreme events during the active part of the cycle, widening the distributions of all parameters. Finally, we find that ICMEs with or without a detected magnetic cloud show similar profiles, which confirms the hypothesis that ICMEs with no detected magnetic clouds are crossed further away from the flux rope core. Such a study provides a generic understanding of processes that shape the overall features of ICMEs in the solar wind and can be extended with future missions at different locations in the solar system. **2015-11-06**

The revisited catalog is at https://idoc.ias.u-psud.fr/sites/idoc/files/CME_catalog/html/ACE-ICMEs-list-dates-quality-nosheath-forweb.html

COMPOSITION STRUCTURE OF INTERPLANETARY CORONAL MASS EJECTIONS FROM MULTISPACECRAFT OBSERVATIONS, MODELING, AND COMPARISON WITH NUMERICAL SIMULATIONS

Alysha A. [Reinard](#)¹, Benjamin J. Lynch², and Tamitha Mulligan

2012 ApJ 761 175

We present an analysis of the ionic composition of iron for two interplanetary coronal mass ejections (ICMEs) observed on **2007 May 21-23** by the ACE and STEREO spacecraft in the context of the magnetic structure of the ejecta flux rope, sheath region, and surrounding solar wind flow. This analysis is made possible due to recent advances in multispacecraft data interpolation, reconstruction, and visualization as well as results from recent modeling of ionic charge states in MHD simulations of magnetic breakout and flux cancellation coronal mass ejection (CME) initiation. We use these advances to interpret specific features of the ICME plasma composition resulting from the magnetic topology and evolution of the CME. We find that, in both the data and our MHD simulations, the flux ropes centers are relatively cool, while charge state enhancements surround and trail the flux ropes. The magnetic orientations of the ICMEs are suggestive of magnetic breakout-like reconnection during the eruption process, which could explain the spatial location of the observed iron enhancements just outside the traditional flux rope magnetic signatures and between the two ICMEs. Detailed comparisons between the simulations and data were more complicated, but a sharp increase in high iron charge states in the ACE and STEREO-A data during the second flux rope corresponds well to similar features in the flux cancellation results. We discuss the prospects of this integrated in situ data analysis and modeling approach to advancing our understanding of the unified CME-to-ICME evolution.

ANALYSIS OF INTERPLANETARY CORONAL MASS EJECTION PARAMETERS AS A FUNCTION OF ENERGETICS, SOURCE LOCATION, AND MAGNETIC STRUCTURE

A. A. [Reinard](#)

Astrophysical Journal, 682:1289Y1305, 2008

<http://www.journals.uchicago.edu/toc/apj/2008/682/2>

We describe a study of how ICME parameters vary as function of source location, associated flare magnitude, and magnetic structure. The strongest compositional enhancements are found to occur in events originating in central longitudes of the Sun, those with large associated flares, and those that are identified as magnetic clouds. In situ

velocity is highest for events associated with large flares. Density has a strong negative correlation with associated flare size, but no strong trend with source longitude or magnetic cloud structure. Temperature is lower than expected for events originating in central longitudes, events associated with large flares, and for magnetic clouds. Total magnetic field is highest for events originating in central longitudes and for magnetic clouds. Combining these results, we suggest that ICMEs may have a basic structure consisting of a core (or cores) of magnetic cloud plasma and compositional signatures that are modulated by CME energetics, surrounded by an envelope with weaker signatures. If this core/envelope scenario is proven to be valid, that suggests that a larger percentage of energetic ICMEs may contain enhanced composition that is not detected by the current single track observations.

Machine learning for predicting the Bz magnetic field component from upstream in situ observations of solar coronal mass ejections

M. A. Reiss, C. Möstl, R. L. Bailey, H. T. Rüdiger, U. V. Amerstorfer, T. Amerstorfer, A. J. Weiss, J. Hinterreiter, A. Windisch

Space Weather **Volume 19, Issue 12** e2021SW002859 **2021**

<https://agupubs.onlinelibrary.wiley.com/doi/epdf/10.1029/2021SW002859>

<https://doi.org/10.1029/2021SW002859>

Predicting the Bz magnetic field embedded within ICMEs, also known as the Bz problem, is a key challenge in space weather forecasting. We study the hypothesis that upstream in situ measurements of the sheath region and the first few hours of the magnetic obstacle provide sufficient information for predicting the downstream Bz component.

To do so, we develop a predictive tool based on machine learning that is trained and tested on 348 ICMEs from Wind, STEREO-A, and STEREO-B measurements. We train the machine learning models to predict the minimum value of the Bz component and the maximum value of the total magnetic field Bt in the magnetic obstacle. To validate the tool, we let the ICMEs sweep over the spacecraft and assess how continually feeding in situ measurements into the tool improves the Bz prediction.

We specifically find that the predictive tool can predict the minimum value of the Bz component in the magnetic obstacle with a mean absolute error of 3.12 nT and a Pearson correlation coefficient of 0.71 when the sheath region and the first 4 hours of the magnetic obstacle are observed. While the underlying hypothesis is unlikely to solve the Bz problem, the tool shows promise for ICMEs that have a recognizable magnetic flux rope signature. Transitioning the tool to operations could lead to improved space weather forecasting. **29-31 Mar 2011, 14-17 Apr 2013, 27-29 Jun 2013**

Forecasting the Ambient Solar Wind with Numerical Models. II. An Adaptive Prediction System for Specifying Solar Wind Speed near the Sun

Martin A. Reiss^{1,2}, Peter J. MacNeice¹, Karin Muglach^{1,3}, Charles N. Arge¹, Christian Möstl², Pete Riley⁴, Jürgen Hinterreiter², Rachel L. Bailey², Andreas J. Weiss², Mathew J. Owens⁵

2020 ApJ 891 165

<https://doi.org/10.3847/1538-4357/ab78a0>

The ambient solar wind flows and fields influence the complex propagation dynamics of coronal mass ejections in the interplanetary medium and play an essential role in shaping Earth's space weather environment. A critical scientific goal in the space weather research and prediction community is to develop, implement, and optimize numerical models for specifying the large-scale properties of solar wind conditions at the inner boundary of the heliospheric domain. Here we present an adaptive prediction system that fuses information from in situ measurements of the solar wind into numerical models to better match the global solar wind model solutions near the Sun with prevailing physical conditions in the vicinity of Earth. In this way, we attempt to advance the predictive capabilities of well-established solar wind models for specifying solar wind speed, including the Wang–Sheeley–Arge model. In particular, we use the Heliospheric Upwind eXtrapolation (HUX) model for mapping the solar wind solutions from the near-Sun environment to the vicinity of Earth. In addition, we present the newly developed Tunable HUX (THUX) model, which solves the viscous form of the underlying Burgers equation. We perform a statistical analysis of the resulting solar wind predictions for the period 2006–2015. The proposed prediction scheme improves all the investigated coronal/heliospheric model combinations and produces better estimates of the solar wind state at Earth than our reference baseline model. We discuss why this is the case and conclude that our findings have important implications for future practice in applied space weather research and prediction.

Forecasting the Ambient Solar Wind with Numerical Models. I. On the Implementation of an Operational Framework

Martin A. [Reiss](#)¹, Peter J. MacNeice¹, Leila M. Mays¹, Charles N. Arge¹, Christian Möstl², Ljubomir Nikolic³, and Tanja Amerstorfer²

2019 ApJS 240 35

The ambient solar wind conditions in interplanetary space and in the near-Earth environment are determined by activity on the Sun. Steady solar wind streams modulate the propagation behavior of interplanetary coronal mass ejections and are themselves an important driver of recurrent geomagnetic storm activity. The knowledge of the ambient solar wind flows and fields is thus an essential component of successful space weather forecasting. Here, we present an implementation of an operational framework for operating, validating, and optimizing models of the ambient solar wind flow on the example of Carrington Rotation 2077. We reconstruct the global topology of the coronal magnetic field using the potential field source surface model (PFSS) and the Schatten current sheet model (SCS) and discuss three empirical relationships for specifying the solar wind conditions near the Sun, namely the Wang–Sheeley (WS) model, the distance from the coronal hole boundary model (DCHB), and the Wang–Sheeley–Arge (WSA) model. By adding uncertainty in the latitude about the sub-Earth point, we select an ensemble of initial conditions and map the solutions to Earth by the Heliospheric Upwind eXtrapolation (HUX) model. We assess the forecasting performance from a continuous variable validation and find that the WSA model most accurately predicts the solar wind speed time series (RMSE ≈ 83 km s⁻¹). We note that the process of ensemble forecasting slightly improves the forecasting performance of all solar wind models investigated. We conclude that the implemented framework is well suited for studying the relationship between coronal magnetic fields and the properties of the ambient solar wind flow in the near-Earth environment.

Verification of high-speed solar wind stream forecasts using operational solar wind models

Martin A. [Reiss](#), Manuela Temmer, Astrid M. Veronig, Ljubomir Nikolic, Susanne Vennerstrom, Florian Schöngassner, Stefan J. Hofmeister

Space Weather Volume 14, Issue 7 July 2016 Pages 495–510

High-speed solar wind streams emanating from coronal holes are frequently impinging on the Earth's magnetosphere causing recurrent, medium-level geomagnetic storm activity. Modeling high-speed solar wind streams is thus an essential element of successful space weather forecasting. Here we evaluate high-speed stream forecasts made by the empirical solar wind forecast (ESWF) and the semiempirical Wang-Sheeley-Arge (WSA) model based on the in situ plasma measurements from the Advanced Composition Explorer (ACE) spacecraft for the years 2011 to 2014. While the ESWF makes use of an empirical relation between the coronal hole area observed in Solar Dynamics Observatory (SDO)/Atmospheric Imaging Assembly (AIA) images and solar wind properties at the near-Earth environment, the WSA model establishes a link between properties of the open magnetic field lines extending from the photosphere to the corona and the background solar wind conditions. We found that both solar wind models are capable of predicting the large-scale features of the observed solar wind speed (root-mean-square error, RMSE ≈ 100 km/s) but tend to either overestimate (ESWF) or underestimate (WSA) the number of high-speed solar wind streams (threat score, TS ≈ 0.37). The predicted high-speed streams show typical uncertainties in the arrival time of about 1 day and uncertainties in the speed of about 100 km/s. General advantages and disadvantages of the investigated solar wind models are diagnosed and outlined.

Deriving the interaction point between a Coronal Mass Ejection and High Speed Stream: A case study

Akshay Kumar [Remeshan](#), [Mateja Dumbovic](#), [Manuela Temmer](#)

ApJ 974 140 2024

<https://arxiv.org/pdf/2410.00615>

<https://iopscience.iop.org/article/10.3847/1538-4357/ad6c43/pdf>

We analyze the interaction between an Interplanetary Coronal Mass Ejection (ICME) detected in situ at the L1 Lagrange point on **2016 October 12** with a trailing High-Speed Stream (HSS). We aim to estimate the region in the interplanetary (IP) space where the interaction happened/started using a combined observational-modeling approach. We use Minimum Variance Analysis and the Walen test to analyze possible reconnection exhaust at the interface of ICME and HSS. We perform a Graduated Cylindrical Shell reconstruction of the CME to estimate the geometry and source location of the CME. Finally, we use a two-step Drag Based Model (DBM) model to estimate the region in IP space where the interaction took place. The magnetic obstacle (MO) observed in situ shows a fairly symmetric and undisturbed structure and shows the magnetic flux, helicity, and expansion profile/speed of a typical ICME. The MVA together with the Walen test, however, confirms reconnection exhaust at the ICME HSS boundary. Thus, in situ signatures are in favor of

a scenario where the interaction is fairly recent. The trailing HSS shows a distinct velocity profile which first reaches a semi-saturated plateau with an average velocity of 500 km/s and then saturates at a maximum speed of 710 km/s. We find that the HSS interaction with the ICME is influenced only by this initial plateau. The results of the two-step DBM suggest that the ICME has started interacting with the HSS close to Earth (approx 0.81 au), which compares well with the deductions from in situ signatures.

Global Ionospheric TEC Forecasting for Geomagnetic Storm Time Using a Deep Learning-Based Multi-Model Ensemble Method

Xiaodong Ren, [Pengxin Yang](#), [Dengkui Mei](#), [Hang Liu](#), [Guozhen Xu](#), [Yue Dong](#)

Space Weather: [Volume 21, Issue 3](#) e2022SW003231 2023

<https://doi.org/10.1029/2022SW003231>

<https://agupubs.onlinelibrary.wiley.com/doi/epdf/10.1029/2022SW003231>

In recent years, deep learning has been extensively used for ionospheric total electron content (TEC) prediction, and many models can yield promising prediction results, particularly under quiet conditions. Owing to the ionosphere's intricate and dramatic changes during geomagnetic storms, the high-reliable prediction of the storm-time ionospheric TEC remains a challenging problem. In this study, we developed a new deep learning-based multi-model ensemble method (DLMEM) to forecast geomagnetic storm-time ionospheric TEC that combines the Random Forest (RF) model, the Extreme Gradient Boosting (XGBoost) algorithm, and the Gated Recurrent Unit (GRU) network with the attention mechanism. Seven features in 170 geomagnetic storm events, including the three components Bx, By and Bz of interplanetary magnetic field (IMF), the Kp and Dst indices of geomagnetic activity data, the F10.7 index of solar activity data and global TEC data, were used for modeling. The test set results showed that the DLMEM model can reduce the root mean square errors (RMSE) by an average of 43.6% in comparison to our previously presented model Ion-LSTM, especially during the recovery period of geomagnetic storms. Furthermore, compared to Ion-LSTM, the RMSE values of the low-, middle- and high-latitude single-station forecast TEC can be greatly decreased by 33%, 53% and 59%, respectively. It was shown that the new model allows for more precise short-term global ionospheric forecasting during geomagnetic storms, enabling real-time monitoring of ionospheric changes.

A neural network Dst index model driven by input time histories of the solar wind-magnetosphere interaction

M. [Revallo](#), , F. Valachb, , P. Hejdac, , J. Bochničekc,

JASTP, Volumes 110–111, April 2014, Pages 9–14, 2014

<http://www.sciencedirect.com/science/article/pii/S1364682614000248>

A model to forecast one-hour lead Dst index is proposed. Our approach is based on artificial neural networks (ANN) combined with an analytical model of the solar wind-magnetosphere interaction. Previously, the hourly solar wind parameters have been considered in the analytical model, all of them provided by registration of the ACE satellite. They were the solar wind magnetic field component Bz, velocity V, particle density n and temperature T. The solar wind parameters have been used to compute analytically the discontinuity in magnetic field across the magnetopause, denoted as [Bt][Bt]. This quantity has been shown to be important in connection with ground magnetic field variations. The method was published, in which the weighted sum of a sequence of [Bt][Bt] was proposed to produce the value of Dst index. The maximum term in the sum, possessing the maximum weight, is the one denoting the contribution of the current state of the near-Earth solar wind. The role of the older states is less important – the weights exponentially decay. Moreover, the terms turn to zero if $Bz \approx 0$ or $Bz \approx 0$. In this study, we set up a more comprehensive model on the basis of the ANNs. The model is driven by input time histories of the discontinuity in magnetic field [Bt][Bt], which are provided by the analytical model. At the output of such revised model, the Dst index is obtained and compared with the real data records. In this way we replaced those exponential weights in the published method with another set of weights determined by the neural networks. We retrospectively tested our models with real data from solar cycle 23. The ANN approach provided better results than a simple method based on exponentially decaying weights. Moreover, we have shown that our ANN model could be used to predict Dst one hour ahead. We assessed the predictive capability of the model with a set of independent events and found correlation coefficient $CC=0.74 \pm 0.13$ and prediction efficiency $PE=0.44 \pm 0.15$. We also compared our model with the so called Dst-specification models. In those models, the Dst index was derived directly through an analytic or iterative formula or a neural network-based algorithm. We showed that the performance of our model was comparable to that of Dst-specification models.

HelioCast: heliospheric forecasting based on white-light observations of the solar corona. I. Solar minimum conditions

Victor [Réville](#), [Nicolas Poirier](#), [Athanasios Kouloumvakos](#), [Alexis P. Rouillard](#), [Rui F. Pinto](#), [Naïs Fargette](#), [Mikel Indurain](#), [Raphaël Fournon](#), [Théo James](#), [Raphaël Pobeda](#), [Cyril Scoul](#)

Journal of Space Weather and Space Climate **13**, 11 **2023**

<https://arxiv.org/pdf/2303.14972.pdf>

<https://www.swsc-journal.org/articles/swsc/pdf/2023/01/swsc220066.pdf>

We present a new 3D MHD heliospheric model for space-weather forecasting driven by boundary conditions defined from white-light observations of the solar corona. The model is based on the MHD code PLUTO, constrained by an empirical derivation of the solar wind background properties at 0.1au. This empirical method uses white-light observations to estimate the position of the heliospheric current sheet. The boundary conditions necessary to run HelioCast are then defined from pre-defined relations between the necessary MHD properties (speed, density and temperature) and the distance to the current sheet. We assess the accuracy of the model over six Carrington rotations during the first semester of 2018. Using point-by-point metrics and event based analysis, we evaluate the performances of our model varying the angular width of the slow solar wind layer surrounding the heliospheric current sheet. We also compare our empirical technique with two well tested models of the corona: Multi-VP and WindPredict-AW. We find that our method is well suited to reproduce high speed streams, and does -- for well chosen parameters -- better than full MHD models. The model shows, nonetheless, limitations that could worsen for rising and maximum solar activity.

Flux ropes and dynamics of the heliospheric current sheet

Study of the Parker Solar Probe and Solar Orbiter conjunction of June 2020

V. [Réville](#), [N. Fargette](#), [A.P. Rouillard](#), [B. Lavraud](#), [M. Velli](#), [A. Strugarek](#), [S. Parenti](#), [A.S. Brun](#), [C. Shi](#), [A. Kouloumvakos](#), [N. Poirier](#), [R.F. Pinto](#), [P. Louarn](#), [A. Fedorov](#), [C.J. Owen](#), [V. Génot](#), [T.S. Horbury](#), [R. Laker](#), [H. O'Brien](#), [V. Angelini](#), [E. Fauchon-Jones](#), [J.C. Kasper](#)

A&A 659, A110 **2022**

<https://arxiv.org/pdf/2112.07445.pdf>

<https://www.aanda.org/articles/aa/pdf/2022/03/aa42381-21.pdf>

Context. Solar Orbiter and PSP jointly observed the solar wind for the first time in **June 2020**, capturing data from very different solar wind streams, calm and Alfvénic wind as well as many dynamic structures. Aims. The aim here is to understand the origin and characteristics of the highly dynamic solar wind observed by the two probes, in particular in the vicinity of the heliospheric current sheet (HCS). Methods. We analyse the plasma data obtained by PSP and Solar Orbiter in situ during the month of **June 2020**. We use the Alfvén-wave turbulence MHD solar wind model WindPredict-AW, and perform two 3D simulations based on ADAPT solar magnetograms for this period. Results. We show that the dynamic regions measured by both spacecraft are pervaded with flux ropes close to the HCS. These flux ropes are also present in the simulations, forming at the tip of helmet streamers, i.e. at the base of the heliospheric current sheet. The formation mechanism involves a pressure driven instability followed by a fast tearing reconnection process, consistent with the picture of Réville et al. (2020a). We further characterize the 3D spatial structure of helmet streamer born flux ropes, which seems, in the simulations, to be related to the network of quasi-separatrices.

The role of Alfvén wave dynamics on the large scale properties of the solar wind: comparing a MHD simulation with PSP E1 data

Victor [Réville](#), [Marco Velli](#), [Olga Panasenco](#), [Anna Tenerani](#), [Chen Shi](#), [Samuel T. Badman](#), [Stuart D. Bale](#), [J. C. Kasper](#), [Michael L. Stevens](#), [Kelly E. Korreck](#), [J. W. Bonnell](#), [Anthony W. Case](#), [Thierry Dudok de Wit](#), [Keith Goetz](#), [Peter R. Harvey](#), [Davin E. Larson](#), [Roberto Livi](#), [David M. Malaspina](#), [Robert J. MacDowall](#), [Marc Pulupa](#), [Phyllis L. Whittlesey](#)

the Parker Solar Probe ApJ Special Issue

2019

<https://arxiv.org/pdf/1912.03777.pdf>

During Parker Solar Probe's first orbit, the solar wind plasma has been observed in situ closer than ever before, the perihelion on **November 6th 2018** revealing a flow that is constantly permeated by large amplitude Alfvénic fluctuations. These include radial magnetic field reversals, or switchbacks, that seem to be a persistent feature of the young solar wind. The measurements also reveal a very strong, unexpected, azimuthal velocity component. In this work, we numerically model the solar corona during this first encounter, solving the MHD equations and accounting for Alfvén wave transport and dissipation. We find that the large scale plasma parameters are well reproduced, allowing the computation of the solar wind sources at Probe with confidence. We try to understand the dynamical nature of the solar wind to explain both the amplitude of the observed radial magnetic field and of the azimuthal velocities.

Global solar magnetic field organization in the outer corona: influence on the solar wind speed and mass flux over the cycle

Victor Réville, Allan Sacha Brun

ApJ 2017

<https://arxiv.org/pdf/1710.02908.pdf>

The dynamics of the solar wind depends intrinsically on the structure of the global solar magnetic field, which undergoes fundamental changes over the 11-yr solar cycle. For instance, the wind terminal velocity is thought to be anti-correlated with the expansion factor, a measure of how the magnetic field varies with height in the solar corona, usually computed at a fixed height ($\approx 2.5R_{\odot}$, the source surface radius which approximates the distance at which all magnetic field lines become open). However, the magnetic field expansion affects the solar wind in a more detailed way, its influence on the solar wind properties remaining significant well beyond the source surface. We demonstrate this using 3D global MHD simulations of the solar corona, constrained by surface magnetograms over half a solar cycle (1989–2001). A self-consistent expansion beyond the solar wind critical point (even up to $10R_{\odot}$) makes our model comply with observed characteristics of the solar wind, namely, that the radial magnetic field intensity becomes latitude independent at some distance from the Sun, and that the mass flux is mostly independent of the terminal wind speed. We also show that near activity minimum, the expansion in the higher corona has more influence on the wind speed than the expansion below $2.5R_{\odot}$.

Geomagnetic Storm Occurrence and Their Relation With Solar Cycle Phases

Paula Reyes, Victor A. Pinto, Pablo S. Moya

Space Weather e2021SW002766 Volume19, Issue9 2021

<https://agupubs.onlinelibrary.wiley.com/doi/epdf/10.1029/2021SW002766>

<https://doi.org/10.1029/2021SW002766>

Using a time series of geomagnetic storm events between 1957 and 2019, obtained by selecting storms where $D_{st} < -50$ nT, we have analyzed the probability of occurrence of moderate, intense and severe events. Considering that geomagnetic storms can be modeled as stochastic processes with a log-normal probability distribution over their minimum D_{st} index, the dataset was separated according to solar cycle and solar cycle phases, and the distributions of events were fitted through maximum likelihood method in order to characterize the occurrence of storms in each cycle and phase, and then compare those occurrences to the solar cycle 24 (SC24). Our results show that there is a strong dependence between the occurrence of intense storms, with $D_{st} < -100$ nT, and the strength of the solar cycle measured by the sunspot numbers. In particular, SC24 is very similar to SC20. However, when comparing the occurrence of storms by solar cycle phases, events tend to show similar activity towards the minimum phase and have significant differences in the maximum phases. By looking at the σ value – the fit log-normal distribution “width” parameter – characteristic of the occurrence rate of storms, we have found that the σ_{des} (the sigma value in the descending phase of one cycle) shows the highest correlation ($r = -0.76$) with σ_{max} (the sigma value in the maximum phase of the next cycle) which allows us to estimate the occurrence rate of storms for SC25 to be similar to those of SC21 and SC22, suggesting a more intense cycle than the one that just ended.

Characteristics of turbulence in transition regions near large-scale boundaries in the solar wind.

Maria Riazantseva, Liudmila Rakhmanova, Georgy Zastenker, Yuri Yermolaev, Irina Lodkina, Jana Safrankova, Zdenek Nemecek, and Lubomir Prech

EGU2020-7605 May 2020

<https://meetingorganizer.copernicus.org/EGU2020/displays/36057>

Fluctuations of solar wind parameters can be strongly affected by the presence of sharp boundaries between different large-scale structures. Turbulence cannot develop freely across such boundaries, just as it could in the undisturbed solar wind. It can lead the growing of fluctuation level and changes in shape and properties of turbulent cascade too. The compression regions, for example Sheath regions before magnetic clouds, and CIR regions (the compression areas between fast solar wind from coronal holes and slow solar wind from coronal streamers), are typical examples of such transitions. Here we present the analysis of turbulence spectrum changes during crossings of Sheath and CIR regions. We use unique high time resolution plasma measurements by BMSW instrument at Spektr-R spacecraft in order to consider both MHD and kinetic scales of turbulent cascade. We analyze the base properties of turbulence spectra: spectral power and slopes at corresponding scales, break frequency between scales, and also shape of spectra. We began by examining of the case study crossings of the transition regions and then compared statistically the spectral properties in such regions with the same ones in the undisturbed solar wind. We have shown that spectra fall nonlinearly at kinetic scales and become steeper with growing of fluctuation level in transition regions, at the same time the slope of spectra at

MHD scale remains almost Kolmogorov. Withal some interesting features can be observed in the vicinity of the break between characteristic scales during crossing of transition regions. The given results reveal the lack of energy balance between MHD and kinetic scales, and can indicate the intensification of dissipation processes and the additional plasma heating in the transition regions. The work is supported by Russian Science Foundation grant 16-12-10062.

Presentation #7605 <https://presentations.copernicus.org/EGU2020/presentations-ST1.7.zip>

Global Coronal Equilibria with Solar Wind Outflow

[Oliver E. K. Rice](#), [Anthony R. Yeates](#)

ApJ 2021

<https://arxiv.org/pdf/2110.01319.pdf>

Given a known radial magnetic field distribution on the Sun's photospheric surface, there exist well-established methods for computing a potential magnetic field in the corona above. Such potential fields are routinely used as input to solar wind models, and to initialize magneto-frictional or full magnetohydrodynamic simulations of the coronal and heliospheric magnetic fields. We describe an improved magnetic field model which calculates a magneto-frictional equilibrium with an imposed solar wind profile (which can be Parker's solar wind solution, or any reasonable equivalent). These 'outflow fields' appear to approximate the real coronal magnetic field more closely than a potential field, take a similar time to compute, and avoid the need to impose an artificial source surface. Thus they provide a practical alternative to the potential field model for initializing time-evolving simulations or modeling the heliospheric magnetic field. We give an open-source Python implementation in spherical coordinates and apply the model to data from Solar Cycle 24. The outflow tends to increase the open magnetic flux compared to the potential field model, reducing the well known discrepancy with in situ observations.

Probabilistic hazard assessment: Application to geomagnetic activity

Gemma S. [Richardson](#)* and Alan W. P. Thomson

J. Space Weather Space Clim. 2022, 12, 4

<https://doi.org/10.1051/swsc/2022001>

<https://www.swsc-journal.org/articles/swsc/pdf/2022/01/swsc210005.pdf>

Probabilistic Hazard Assessment (PHA) provides an appropriate methodology for assessing space weather hazards and their impact on technology. PHA is widely used in geosciences to determine the probability of exceedance of critical thresholds, caused by one or more hazard sources. PHA has proved useful with limited historical data to estimate the likelihood of specific impacts. PHA has also driven the development of empirical and physical models, or ensembles of models, to replace measured data. Here we aim to highlight the PHA method to the space weather community and provide an example of how it could be used. In terms of space weather impact, the critical hazard thresholds might include the Geomagnetically Induced Current in a specific high voltage power transformer neutral, or the local pipe-to-soil potential in a particular metal pipe. We illustrate PHA in the space weather context by applying it to a twelve-year dataset of Earth-directed solar Coronal Mass Ejections (CME), which we relate to the probability that the global three-hourly geomagnetic activity index K_p exceeds specific thresholds. We call this a "Probabilistic Geomagnetic Hazard Assessment", or PGHA. This provides a simple but concrete example of the method. We find that the cumulative probability of $K_p > 6-$, $> 7-$, $> 8-$ and $K_p = 9_0$ is 0.359, 0.227, 0.090, 0.011, respectively, following observation of an Earth-directed CME, summed over all CME launch speeds and solar source locations. According to the historical K_p distribution, this represents an order of magnitude increase in the a priori probability of exceeding these thresholds. For the lower K_p thresholds, the results are somewhat distorted by our exclusion of coronal hole high-speed stream effects. The PHGA also reveals useful probabilistic associations between solar source location and subsequent maximum K_p for operational forecasters.

Solar wind stream interaction regions throughout the heliosphere

Review

Ian G. [Richardson](#)

Living Reviews in Solar Physics 2018, 15:1

<https://link.springer.com/content/pdf/10.1007%2Fs41116-017-0011-z.pdf>

<https://doi.org/10.1007/s41116-017-0011-z>.

This paper focuses on the interactions between the fast solar wind from coronal holes and the intervening slower solar wind, leading to the creation of stream interaction regions that corotate with the Sun and may persist for many solar rotations. Stream interaction regions have been observed near 1 AU, in the inner heliosphere (at ~ 0.3 – 0.3 – 1 AU) by the Helios spacecraft, in the outer and distant heliosphere by the Pioneer 10 and 11 and Voyager 1 and 2 spacecraft, and out of the ecliptic by Ulysses, and these observations are reviewed. Stream interaction regions accelerate energetic particles, modulate the intensity of Galactic cosmic rays and generate enhanced geomagnetic activity. The remote detection of

interaction regions using interplanetary scintillation and white-light imaging, and MHD modeling of interaction regions will also be discussed.

Near-Earth Interplanetary Coronal Mass Ejections Since January 1996 (to June 2019)

Compiled by Ian [Richardson](#)(1) and Hilary [Cane](#)(2),
<http://www.srl.caltech.edu/ACE/ASC/DATA/level3/icmetable2.htm>

Identification of Interplanetary Coronal Mass Ejections at Ulysses Using Multiple Solar Wind Signatures

I. G. [Richardson](#)

Solar Phys., Volume 289, Issue 10, pp 3843-3894, 2014

Previous studies have discussed the identification of interplanetary coronal mass ejections (ICMEs) near the Earth based on various solar wind signatures. In particular, methods have been developed of identifying regions of anomalously low solar wind proton temperatures (T_p) and plasma compositional anomalies relative to the composition of the ambient solar wind that are frequently indicative of ICMEs. In this study, similar methods are applied to observations from the Ulysses spacecraft that was launched in 1990 and placed in a heliocentric orbit over the poles of the Sun. **Some 279 probable ICMEs are identified during the spacecraft mission, which ended in 2009.** The identifications complement those found independently in other studies of the Ulysses data, but a number of additional events are identified. The properties of the ICMEs detected at Ulysses and those observed near the Earth and in the inner heliosphere are compared.

Geomagnetic activity during the rising phase of solar cycle 24

Ian G. [Richardson](#)

J. Space Weather Space Clim. 3 (2013) A08

<https://www.swsc-journal.org/articles/swsc/pdf/2013/01/swsc130001.pdf>

As previous studies have shown, geomagnetic activity during the solar minimum following solar cycle 23 was at low levels unprecedented during the space era, and even since the beginning of the K_p index in 1932. Here, we summarize the characteristics of geomagnetic activity during the first 4 years of cycle 24 following smoothed sunspot minimum in December, 2008, and compare these with those of similar periods during earlier cycles going back to the start of K_p (cycles 17–23). The most outstanding feature is the continuing low levels of geomagnetic activity that are well below those observed during the rising phases of the other cycles studied. Even 4 years into cycle 24, geomagnetic storm rates are still only comparable to or below the rates observed during activity minima in previous cycles. We note that the storm rate during the rising phases of cycles 17–23 was correlated with the peak sunspot number (SSN) in the cycle. Extrapolating these results to the low storm rates in cycle 24 suggests values of the peak SSN in cycle 24 that are consistent with the NOAA Space Weather Prediction Center prediction of 90 ± 10 , indicating that cycle 24 is likely to be the weakest cycle since at least 1932. No severe ($Dst < -200$ nT) storms have been observed during the first 4 years of cycle 24 compared with 4 in the comparable interval of cycle 23, and only 10 intense ($Dst < -100$ nT) storms, compared with 21 in cycle 23. These storms were all associated with the passage of Interplanetary Coronal Mass Ejections (ICMEs) and/or their associated sheaths. The lack of strong southward magnetic fields in ICMEs and their sheaths, their lower speeds close to the average solar wind speed, a ~20% reduction in the number of ICMEs passing the Earth, and weaker than normal fields in corotating high-speed streams, contribute to the low levels of geomagnetic storm activity in the rise phase of cycle 24. However, the observation of an ICME with strong southward fields at the STEREO A spacecraft on July 24, 2012, which would have been highly geoeffective had it encountered the Earth, demonstrates that strong geomagnetic storms may still occur during weak solar cycles.

Near-earth solar wind flows and related geomagnetic activity during more than four solar cycles (1963–2011)

Ian G. [Richardson](#)^{1,2,*}, and Hilary V. Cane³

J. Space Weather Space Clim. 2 (2012) A02

<http://www.swsc-journal.org/articles/swsc/pdf/2012/01/swsc120017.pdf>

In past studies, we classified the near-Earth solar wind into three basic flow types based on inspection of solar wind plasma and magnetic field parameters in the OMNI database and additional data (e.g., geomagnetic indices, energetic particle, and cosmic ray observations). These flow types are: (1) High-speed streams associated with coronal holes at the Sun, (2) Slow, interstream solar wind, and (3) Transient flows originating with coronal mass ejections at the Sun, including interplanetary coronal mass ejections and the associated upstream shocks and post-shock regions. The solar wind classification in these previous studies commenced with observations in 1972. In the present study, as well as

updating this classification to the end of 2011, we have extended the classification back to 1963, the beginning of near-Earth solar wind observations, thereby encompassing the complete solar cycles 20 to 23 and the ascending phase of cycle 24. We discuss the cycle-to-cycle variations in near-Earth solar wind structures and the related geomagnetic activity over more than four solar cycles, updating some of the results of our earlier studies.

Solar wind drivers of geomagnetic storms during more than four solar cycles

Ian G. [Richardson](#)^{1,2,*}, and Hilary V. Cane³

J. Space Weather Space Clim. 2 (2012) A01

<http://www.swsc-journal.org/articles/swsc/pdf/2012/01/swsc120012.pdf>

Using a classification of the near-Earth solar wind into three basic flow types: (1) High-speed streams associated with coronal holes at the Sun; (2) Slow, interstream solar wind; and (3) Transient flows originating with coronal mass ejections (CMEs) at the Sun, including interplanetary CMEs and the associated upstream shocks and post-shock regions, we determine the drivers of geomagnetic storms of various size ranges based on the Kp index and the NOAA “G” criteria since 1964, close to the beginning of the space era, to 2011, encompassing more than four solar cycles (20–23). We also briefly discuss the occurrence of storms since the beginning of the Kp index in 1932, in the minimum before cycle 17. We note that the extended low level of storm activity during the minimum following cycle 23 is without precedent in this 80-year interval. Furthermore, the “typical” numbers of storm days/cycle quoted in the standard NOAA G storm table appear to be significantly higher than those obtained from our analysis, except for the strongest (G5) storms, suggesting that they should be revised downward.

Geoeffectiveness (Dst and Kp) of interplanetary coronal mass ejections during 1995-2009 and implications for storm forecasting

[Richardson](#), I. G.; Cane, H. V.

Space Weather, Vol. 9, No. 7, S07005, 2011, **File**

<http://dx.doi.org/10.1029/2011SW000670>

We summarize the geoeffectiveness (based on the Dst and Kp indices) of the more than 300 interplanetary coronal mass ejections (ICMEs) that passed the Earth during 1996–2009, encompassing solar cycle 23. We subsequently estimate the probability that an ICME will generate geomagnetic activity that exceeds certain thresholds of Dst or Kp, including the NOAA “G” storm scale, based on maximum values of the southward magnetic field component (Bs), the solar wind speed (V), and the y component (Ey) of the solar wind convective electric field $E = -V \times B$, in the ICME or sheath ahead of the ICME. Consistent with previous studies, the geoeffectiveness of an ICME is correlated with Bs or $Ey \approx VB$ in the ICME or sheath, indicating that observations from a solar wind monitor upstream of the Earth are likely to provide the most reliable forecasts of the activity associated with an approaching ICME. There is also a general increase in geoeffectiveness with ICME speed, though the overall event-to-event correlation is weaker than for Bs and Ey. Nevertheless, using these results, we suggest that the speed of an ICME approaching the Earth inferred, for example, from routine remote sensing by coronagraphs on spacecraft well separated from the Earth or by all-sky imagers, could be used to estimate the likely geoeffectiveness of the ICME (our “comprehensive” ICME database provides a proxy for ICMEs identified in this way) with a longer lead time than may be possible using an upstream monitor.

Galactic Cosmic Ray Intensity Response to Interplanetary Coronal Mass Ejections/Magnetic Clouds in 1995 – 2009

I.G. [Richardson](#) · H.V. Cane

Solar Phys., 2011, **File**;

Solar Physics, Volume 270, Number 2, 609-627, 2011

We summarize the response of the galactic cosmic ray (GCR) intensity to the passage of the more than 300 interplanetary coronal mass ejections (ICMEs) and their associated shocks that passed the Earth during 1995 – 2009, a period that encompasses the whole of Solar Cycle 23. In ~80% of cases, the GCR intensity decreased during the passage of these structures, *i.e.*, a “**Forbush decrease**” occurred, while in ~10% there was no significant change. In the remaining cases, the GCR intensity increased. Where there was an intensity decrease, minimum intensity was observed inside the ICME in ~90% of these events. The observations confirm the role of both post-shock regions and ICMEs in the generation of these decreases, consistent with many previous studies, but contrary to the conclusion of Reames,

Kahler, and Tylka (*Astrophys. J. Lett.* **700**, L199, 2009) who, from examining a subset of ICMEs with flux-rope-like magnetic fields (magnetic clouds) argued that these are “open structures” that allow free access of particles including GCRs to their interior. In fact, we find that magnetic clouds are more likely to participate in the deepest GCR decreases than ICMEs that are not magnetic clouds.

Interplanetary circumstances of quasi-perpendicular interplanetary shocks in 1996-2005

Richardson, I. G.; Cane, H. V.

J. Geophys. Res., Vol. 115, No. A7, A07103, 2010

The angle (B_n) between the normal to an interplanetary shock front and the upstream magnetic field direction, though often thought of as a property “of the shock,” is also determined by the configuration of the magnetic field immediately upstream of the shock. We investigate the interplanetary circumstances of 105 near-Earth quasi-perpendicular shocks during 1996–2005 identified by $B_n \geq 80^\circ$ and/or by evidence of shock drift particle acceleration. Around 87% of these shocks were driven by interplanetary coronal mass ejections (ICMEs); the remainder were probably the forward shocks of corotating interaction regions. For around half of the shocks, the upstream field was approximately perpendicular to the radial direction, either east-west or west-east or highly inclined to the ecliptic. Such field directions will give quasi-perpendicular configurations for radially propagating shocks. Around 30% of the shocks were propagating through, or closely followed, ICMEs at the time of observation. Another quarter were propagating through the heliospheric plasma sheet (HPS), and a further quarter occurred in slow solar wind that did not have characteristics of the HPS. Around 11% were observed in high-speed streams, and 7% in the sheaths following other shocks. The fraction of shocks found in high-speed streams is around a third of that expected based on the fraction of the time when such streams were observed at Earth. Quasi-perpendicular shocks are found traveling through ICMEs around 2–3 times more frequently than expected. In addition, shocks propagating through ICMEs are more likely to have larger values of B_n than shocks outside ICMEs.

Near-Earth Interplanetary Coronal Mass Ejections During Solar Cycle 23 (1996 – 2009): Catalog and Summary of Properties

I.G. **Richardson** · H.V. Cane

Solar Phys (2010) 264: 189–237, **File**

<https://link.springer.com/content/pdf/10.1007/s11207-010-9568-6.pdf>

In a previous study (Cane and Richardson, *J. Geophys. Res.* **108**(A4), SSH6-1, 2003), we investigated the occurrence of interplanetary coronal mass ejections in the near-Earth solar wind during 1996 – 2002, corresponding to the increasing and maximum phases of solar cycle 23, and provided a “comprehensive” catalog of these events. In this paper, we present a revised and updated catalog of the ≈ 300 near-Earth ICMEs in 1996 – 2009, encompassing the complete cycle 23, and summarize their basic properties and geomagnetic effects. In particular, solar wind composition and charge state observations are now considered when identifying the ICMEs. In general, these additional data confirm the earlier identifications based predominantly on other solar wind plasma and magnetic field parameters. However, the boundaries of ICME-like plasma based on charge state/composition data may deviate significantly from those based on conventional plasma/magnetic field parameters. Furthermore, the much studied “magnetic clouds”, with flux-rope-like magnetic field configurations, may form just a substructure of the total ICME interval.

Table

Multiple-step geomagnetic storms and their interplanetary drivers

Richardson, I. G.; Zhang, J.

Geophysical Research Letters, Volume 35, Issue 6, CiteID L06S07, 2008, **File**

While the classic picture of a geomagnetic storm is of a main phase eventually reaching maximum intensity, followed by a recovery, the profile can often be more complex. This has been recognized in past studies that have classified storms as having “one” or “two” “steps” during the main phase. However, the intense ($Dst \leq -100$ nT) storms studied during the LWS CDAW Workshop may be more complicated. We discuss the variety of interplanetary circumstances that gave rise to several storms of varying complexity.

Major geomagnetic storms ($Dst < -100$ nT) generated by corotating interaction regions

I. G. [Richardson](#), D. F. Webb,³ J. Zhang,⁴ D. B. Berdichevsky,^{1,5} D. A. Biesecker,⁶
J. C. Kasper,⁷ R. Kataoka,¹ J. T. Steinberg,⁸ B. J. Thompson,¹ C.-C. Wu,^{1,9}
and A. N. Zhukov^{10,11}

JGR, VOL. 111, A07S09, doi:10.1029/2005JA011476, 2006, **File**

Seventy-nine major geomagnetic storms (minimum $Dst \leq -100$ nT) observed in 1996 to 2004 were the focus of a “Living with a Star” Coordinated Data Analysis Workshop (CDAW) in March 2005. In nine cases, the storm driver appears to have been purely a corotating interaction region (CIR) without any contribution from coronal mass ejection-related material (interplanetary coronal mass ejections (ICMEs)). These storms were generated by structures within CIRs located both before and/or after the stream interface that included persistently southward magnetic fields for intervals of several hours. We compare their geomagnetic effects with those of 159 CIRs observed during 1996–2005. The major storms form the extreme tail of a continuous distribution of CIR geoeffectiveness which peaks at $Dst \sim -40$ nT but is subject to a prominent seasonal variation of ~ 40 nT which is ordered by the spring and fall equinoxes and the solar wind magnetic field direction toward or away from the Sun. The O'Brien and McPherron (2000) equations, which estimate Dst by integrating the incident solar wind electric field and incorporating a ring current loss term, largely account for the variation in storm size. They tend to underestimate the size of the larger CIR-associated storms by $Dst \sim 20$ nT. This suggests that injection into the ring current may be more efficient than expected in such storms. Four of the nine major storms in 1996–2004 occurred during a period of less than three solar rotations in September to November 2002, also the time of maximum mean IMF and solar magnetic field intensity during the current solar cycle. The maximum CIR-storm strength found in our sample of events, plus additional 23 probable CIR-associated $Dst \leq -100$ nT storms in 1972–1995, is ($Dst = -161$ nT). This is consistent with the maximum storm strength ($Dst \sim -180$ nT) expected from the O'Brien and McPherron equations for the typical range of solar wind electric fields associated with CIRs. This suggests that CIRs alone are unlikely to generate geomagnetic storms that exceed these levels.

Table 1. CIR-Associated $Dst \leq -100$ nT Storms in 1996–2004

Correction to Major geomagnetic storms ($Dst = -100$ nT) generated by corotating interaction regions,

[Richardson](#), I. G. et al.

J. Geophys. Res., 112, A12105, <http://dx.doi.org/10.1029/2007JA012332>, (2007); **File (2006)**

In Figures 1, 2, 3, 4, and 7, the y component of the solar wind electric field (E_y) is plotted with the incorrect sign. Signed values of E_y referred to in the text and given in Table 1 also have the incorrect sign. As stated in the second paragraph of section 2, the “ E_y ” panel shows the value of $-V_x B_z$. However, this is equal to $-E_y$, not E_y (assuming that $V_x B_z = -V_z B_x$ in the solar wind).

A SURVEY OF INTERPLANETARY CORONAL MASS EJECTIONS IN THE NEAR-EARTH SOLAR WIND DURING 1996 - 2005

Ian G. Richardson^(1,2) & Hilary V. Cane^(1,3)

⁽¹⁾Code 661, NASA Goddard Space Flight Center, Greenbelt, Maryland, 20771, USA,
Email: Ian.Richardson@gssc.nasa.gov

⁽²⁾Also at the Department of Astronomy, University of Maryland, College Park, 20742, USA.

⁽³⁾Also at the School of Mathematics and Physics, University of Tasmania, Hobart, Tasmania 7005, Australia,
Email: hilary.cane@utas.edu.au

ABSTRACT

We have extended our comprehensive survey of interplanetary coronal mass ejections (ICMEs) in the near-Earth solar wind since 1996 up to near-present, and have incorporated solar wind compositional data from ACE/SWICS into the identification of these events. We discuss the variations in the ICME occurrence rate, including evidence for a ~160 day periodicity, the average properties of the ICMEs, the fraction that are magnetic clouds, and the relationship between ICME properties and geomagnetic storms.

Klein and Burlaga, 1982). Thus, ~70-80% of the SWICS observations inside the CR03 ICMEs show enhanced O^7/O^6 or Fe charge states. Lower occurrence rates are found for enhanced Mg/O and Ne/O . The occurrence rates tend to increase in the vicinity of the ICME leading edge, and decrease near the trailing edge, indicating that the regions identified by CR03 do closely correspond to CME-associated source material that has been heated near the Sun. In some events, charge states remain high for a short distance after the trailing edge.

Non-Cloud ICMEs

Magnetic Clouds

*Proc. Solar Wind 11 – SOHO 16 “Connecting Sun and Heliosphere”, Whistler, Canada
12 – 17 June 2005 (ESA SP-592, September 2005)*

File

Energetic particles and corotating interaction regions in the solar wind.

Review

Richardson, I.G.:

2004, Space Sci. Rev. 111(3 – 4), 267

sci-hub.se/10.1023/B:SPAC.0000032689.52830

This paper reviews three important effects on energetic particles of corotating interaction regions (CIRs) in the solar wind that are formed at the leading edges of high-speed solar wind streams originating in coronal holes. A brief overview of CIRs and their important features is followed by a discussion of CIR-associated modulations in the galactic cosmic ray intensity, with an emphasis on observations made by spacecraft particle telescope ‘anti-coincidence’ guards. Such guards combine high counting rates (hundreds of counts/s) and a lower rigidity response than neutron monitors to provide detailed information on the relationship between cosmic ray modulations and CIR structure. The modulation of Jovian electrons by CIRs is then described. Finally, the acceleration of ions to energies of ~20 MeV/n in the vicinity of CIRs is reviewed.

Sources of geomagnetic storms for solar minimum and maximum conditions during 1972 – 2000.

Richardson, I.G., Cliver, E.W., Cane, H.V.:

2001, Geophys. Res. Lett. 28(13), 2569. DOI.

<https://agupubs.onlinelibrary.wiley.com/doi/pdf/10.1029/2001GL013052>

We determine the solar wind structures (coronal mass ejection (CME)-related, corotating high-speed streams, and slow solar wind) driving geomagnetic storms of various strength over nearly three solar cycles (1972–2000). The most intense storms (defined by K_p) at both solar minimum and solar maximum are almost all (~97%) generated by transient structures associated with CMEs. Weaker storms are preferentially associated with streams at solar minimum and with CMEs at solar maximum, reflecting the change in the structure of the solar wind between these phases of the solar cycle. Slow solar wind generates a small fraction of the weaker storms at solar minimum and maximum. We also determine the size distributions of K_p for each solar wind component.

Which Upstream Solar Wind Conditions Matter Most in Predicting Bz Within Coronal Mass Ejections

Pete [Riley](#), [M. A. Reiss](#), [C. Möstl](#)

Space Weather [Volume 21, Issue 4](#) e2022SW003327 2023

<https://arxiv.org/pdf/2303.17682.pdf>

<https://doi.org/10.1029/2022SW003327>

<https://agupubs.onlinelibrary.wiley.com/doi/epdf/10.1029/2022SW003327>

Accurately predicting the z-component of the interplanetary magnetic field, particularly during the passage of an interplanetary coronal mass ejection (ICME), is a crucial objective for space weather predictions. Currently, only a handful of techniques have been proposed and they remain limited in scope and accuracy. Recently, a robust machine learning technique was developed for predicting the minimum value of Bz within ICMEs based on a set of 42 “features,” that is, variables calculated from measured quantities upstream of the ICME and within its sheath region. In this study, we investigate these so-called explanatory variables in more detail, focusing on those that were (a) statistically significant and (b) most important. We find that number density and magnetic field strength accounted for a large proportion of the variability. These features capture the degree to which the ICME compresses the ambient solar wind ahead. Intuitively, this makes sense: Energy made available to coronal mass ejections (CMEs) as they erupt is partitioned into magnetic and kinetic energy. Thus, more powerful CMEs are launched with larger flux-rope fields (larger Bz), at greater speeds, resulting in more sheath compression (increased number density and total field strength).

On the Sources and Sizes of Uncertainty in Predicting the Arrival Time of Interplanetary Coronal Mass Ejections using Global MHD Models

Pete [Riley](#), [Michal Ben-Nun](#)

Space Weather [Volume 19, Issue 6](#) e2021SW002775 May 2021

<https://agupubs.onlinelibrary.wiley.com/doi/epdf/10.1029/2021SW002775>

<https://doi.org/10.1029/2021SW002775>

Accurate predictions of the properties of interplanetary coronal mass ejection (ICME)-driven disturbances are a key objective for space weather forecasts. The ICME’s time of arrival (ToA) at Earth is an important parameter, and one that is amenable to a variety of modeling approaches. Previous studies suggest that the best models can predict the arrival time to within an absolute uncertainty of 10-15 hours. Here, we investigate the main sources of uncertainty in predicting a CME’s ToA at Earth. These can be broken into two main categories: (1) the initial properties of the ejecta, including its speed, mass, and direction of propagation; and (2) the properties of the ambient solar wind into which it propagates. To estimate the relative contribution to ToA uncertainties, we construct a set of numerical experiments of cone-model CMEs, where we vary the initial speed, mass, and direction at the inner radial boundary. Additionally, we build an ensemble of 12 ambient solar wind solutions using realizations from the ADAPT model. We find that each component in the chain contributes between ± 2.5 and ± 7 hours of uncertainty to the estimate of the CME’s ToA. Importantly, different realizations of the synoptic produce the largest uncertainties. This suggests that estimates of ToA will continue to be plagued with intrinsic uncertainties of ± 10 hours until tighter constraints can be found for these boundary conditions. Our results suggest that there are clear benefits to focused investigations aimed at reducing the uncertainties in CME speed, mass, direction, and input boundary magnetic fields.

Predicting the Structure of the Solar Corona and Inner Heliosphere during Parker Solar Probe's First Perihelion Pass

Pete [Riley](#), Cooper Downs, Jon A. Linker, Zoran Mikic, Roberto Lionello, and Ronald M. Caplan

2019 ApJL 874 L15

sci-hub.se/10.3847/2041-8213/ab0ec3

NASA’s Parker Solar Probe (PSP) spacecraft reached its first perihelion of 35.7 solar radii on 2018 November 5. To aid in mission planning, and in anticipation of the unprecedented measurements to be returned, in late October, we developed a three-dimensional magnetohydrodynamic (MHD) solution for the solar corona and inner heliosphere, driven by the then available observations of the Sun’s photospheric magnetic field. Our model incorporates a wave-turbulence-driven model to heat the corona. Here, we present our predictions for the structure of the solar corona and the likely in situ measurements that PSP will be returning over the next few months. We infer that, in the days prior to first encounter, PSP was immersed in wind emanating from a well-established, positive-polarity northern polar coronal hole. During the encounter, however, field lines from the spacecraft mapped to a negative-polarity equatorial coronal hole, within which it remained for the entire encounter, before becoming magnetically connected to a positive-polarity equatorial coronal hole. When the PSP data become available, these model results can be used to assist in their

calibration and interpretation, and, additionally, provide a global context for interpreting the localized in situ measurements. In particular, we can identify what types of solar wind PSP encountered, what the underlying magnetic structure was, and how complexities in the orbital trajectory can be interpreted within a global, inertial frame. Ultimately, the measurements returned by PSP can be used to constrain current theories for heating the solar corona and accelerating the solar wind.

Forecasting the Arrival Time of Coronal Mass Ejections: Analysis of the CCMC CME Scoreboard

Pete [Riley](#), [M. Leila Mays](#), [Jesse Andries](#), [Tanja Amerstorfer](#), [Douglas Biesecker](#), [Veronique Delouille](#), [Mateja Dumbović](#), [Xueshang Feng](#), [Edmund Henley](#), [Jon A. Linker](#), [Christian Möstl](#), [Marlon Nuñez](#), [Vic Pizzo](#), [Manuela Temmer](#), [W. K. Tobiska](#), [C. Verbeke](#), [Matthew J West](#), [Xinhua Zhao](#)

Space Weather **Volume16, Issue9** Pages 1245-1260 **2018**

Space Weather Quarterly v 15 No. 3 **2018**

<http://sci-hub.tw/10.1029/2018SW001962>

<https://agupubs.onlinelibrary.wiley.com/doi/epdf/10.1002/swq.19>

Accurate forecasting of the properties of coronal mass ejections (CMEs) as they approach Earth is now recognized as an important strategic objective for both NOAA and NASA. The time of arrival of such events is a key parameter, one that had been anticipated to be relatively straightforward to constrain. In this study, we analyze forecasts submitted to the Community Coordinated Modeling Center at NASA's Goddard Space Flight Center over the last 6 years to answer the following questions: (1) How well do these models forecast the arrival time of CME-driven shocks? (2) What are the uncertainties associated with these forecasts? (3) Which model(s) perform best? (4) Have the models become more accurate during the past 6 years? We analyze all forecasts made by 32 models from 2013 through mid-2018, and additionally focus on 28 events, all of which were forecasted by six models. We find that the models are generally able to predict CME-shock arrival times—in an average sense—to within ± 10 hr, but with standard deviations often exceeding 20 hr. The best performers, on the other hand, maintained a mean error (bias) of -1 hr, a mean absolute error of 13 hr, and a precision (standard deviation) of 15 hr. Finally, there is no evidence that the forecasts have become more accurate during this interval. We discuss the intrinsic simplifications of the various models analyzed, the limitations of this investigation, and suggest possible paths to improve these forecasts in the future.

Extreme geomagnetic storms: Probabilistic forecasts and their uncertainties

Pete [Riley](#), Jeffrey J. Love

Space Weather Volume 15, Issue 1 January **2017** Pages 53–64

sci-hub.se/10.1002/2016SW001470

Extreme space weather events are low-frequency, high-risk phenomena. Estimating their rates of occurrence, as well as their associated uncertainties, is difficult. In this study, we derive statistical estimates and uncertainties for the occurrence rate of an extreme geomagnetic storm on the scale of the Carrington event (or worse) occurring within the next decade. We model the distribution of events as either a power law or lognormal distribution and use (1) Kolmogorov-Smirnov statistic to estimate goodness of fit, (2) bootstrapping to quantify the uncertainty in the estimates, and (3) likelihood ratio tests to assess whether one distribution is preferred over another. Our best estimate for the probability of another extreme geomagnetic event comparable to the Carrington event occurring within the next 10 years is 10.3% 95% confidence interval (CI) [0.9,18.7] for a power law distribution but only 3.0% 95% CI [0.6,9.0] for a lognormal distribution. However, our results depend crucially on (1) how we define an extreme event, (2) the statistical model used to describe how the events are distributed in intensity, (3) the techniques used to infer the model parameters, and (4) the data and duration used for the analysis. We test a major assumption that the data represent time stationary processes and discuss the implications. If the current trends persist, suggesting that we are entering a period of lower activity, our forecasts may represent upper limits rather than best estimates.

PROPERTIES OF THE FAST FORWARD SHOCK DRIVEN BY THE 2012 JULY 23 EXTREME CORONAL MASS EJECTION

Pete [Riley](#)¹, Ronald M. Caplan¹, Joe Giacalone², David Lario³, and Ying Liu

2016 ApJ 819 57

Late on **2012 July 23**, the STEREO-A spacecraft encountered a fast forward shock driven by a coronal mass ejection (CME) launched from the Sun earlier that same day. The estimated travel time of the disturbance (~ 20 hr), together with the massive magnetic field strengths measured within the ejecta (>100 nT), made it one of the most extreme events observed during the space era. In this study, we examine the properties of the shock wave. Because of an instrument malfunction, plasma measurements during the interval surrounding the CME were limited, and our approach has been

modified to capitalize on the available measurements and suitable proxies, where possible. We were able to infer the following properties. First, the shock normal was pointing predominantly in the radial direction (\hat{n}). Second, the angle between \hat{n} and the upstream magnetic field, θ_{Bn} , was estimated to be $\approx 34^\circ$, making the shock "quasi-parallel," and supporting the idea of an earlier "preconditioning" ICME. Third, the shock speed was estimated to be $\approx 3300 \text{ km s}^{-1}$. Fourth, the sonic Mach number, M_s , for this shock was ~ 28 . We support these results with an idealized numerical simulation of the ICME. Finally, we estimated the change in ram pressure upstream of the shock to be ~ 5 times larger than the pressure from the energetic particles, suggesting that this cosmic-ray modified shock had not reached steady-state, but instead, had been caught in an early, transient phase in its evolution.

Using Statistical Multivariable Models to Understand the Relationship Between Interplanetary Coronal Mass Ejecta and Magnetic Flux Ropes

P. Riley and I. G. Richardson

Solar Physics, Volume 284, Issue 1, pp 217-233, 2013, DOI: 10.1007/s11207-012-0006-9

In-situ measurements of interplanetary coronal mass ejections (ICMEs) display a wide range of properties. A distinct subset, "magnetic clouds" (MCs), are readily identifiable by a smooth rotation in an enhanced magnetic field, together with an unusually low solar wind proton temperature. In this study, we analyze Ulysses spacecraft measurements to systematically investigate five possible explanations for why some ICMEs are observed to be MCs and others are not: i) An observational selection effect; that is, all ICMEs do in fact contain MCs, but the trajectory of the spacecraft through the ICME determines whether the MC is actually encountered; ii) interactions of an erupting flux rope (FR) with itself or between neighboring FRs, which produce complex structures in which the coherent magnetic structure has been destroyed; iii) an evolutionary process, such as relaxation to a low plasma- β state that leads to the formation of an MC; iv) the existence of two (or more) intrinsic initiation mechanisms, some of which produce MCs and some that do not; or v) MCs are just an easily identifiable limit in an otherwise continuous spectrum of structures. We apply quantitative statistical models to assess these ideas. In particular, we use the Akaike information criterion (AIC) to rank the candidate models and a Gaussian mixture model (GMM) to uncover any intrinsic clustering of the data. Using a logistic regression, we find that plasma- β , CME width, and the ratio O^{7+}/O^{6+} are the most significant predictor variables for the presence of an MC. Moreover, the propensity for an event to be identified as an MC decreases with heliocentric distance. These results tend to refute ideas ii) and iii). GMM clustering analysis further identifies three distinct groups of ICMEs; two of which match (at the 86 % level) with events independently identified as MCs, and a third that matches with non-MCs (68 % overlap). Thus, idea v) is not supported. Choosing between ideas i) and iv) is more challenging, since they may effectively be indistinguishable from one another by a single in-situ spacecraft. We offer some suggestions on how future studies may address this.

Interpreting some properties of CIRs and their associated shocks during the last two solar minima using global MHD simulations

Pete Riley, , Jon A. Linker, J. Americo Gonzalez Esparzab, L.K. Jianc, C.T. Russellc, J.G. Luhmannnd
JASTP, Volume 83, July 2012, Pages 11–2

In this study, we investigate some properties of corotating interaction regions (CIRs) during the recent solar minimum (December 2008), and compare them to CIRs observed during the previous minimum (September 1996). In particular, we focus on the orientation of stream interfaces (SIs), which separate wind that was originally slow and dense from wind that was originally fast and tenuous. We find that while the east–west flow deflections imply a systematic tilt of CIRs such that they are aligned with the nominal Parker spiral direction, the north–south flow deflections are much more irregular and show no discernible patterns. Comparison with global MHD model results suggest that this is a consequence of the spacecraft intercepting the equatorward flanks of the CIRs. We also study the solar-cycle variations of CIR-associated shocks over the last cycle, finding that forward (F) shocks tended to occur approximately three times more frequently than reverse (R) shocks, and, moreover, during the recent minimum, there were approximately 3–4 times more R shocks than during the previous minimum. We show that this too is likely due to the orientation of CIRs and Earth's limited vantage point in the ecliptic plane.

Extreme geomagnetic storms: Probabilistic forecasts and their uncertainties

Pete Riley¹ and Jeffrey J. Love

Space Weather Quarterly v. 14 No. 1 p. 16-27 2017

<http://onlinelibrary.wiley.com/doi/10.1002/swq.13/pdf>

Extreme space weather events are low-frequency, high-risk phenomena. Estimating their rates of occurrence, as well as their associated uncertainties, is difficult. In this study, we derive statistical estimates and uncertainties for the occurrence rate of an extreme geomagnetic storm on the scale of the Carrington event (or worse) occurring within the next decade. We model the distribution of events as either a power law or lognormal distribution and use (1) Kolmogorov-Smirnov statistic to estimate goodness of fit, (2) bootstrapping to quantify the uncertainty in the estimates, and (3) likelihood ratio tests to assess whether one distribution is preferred over another. Our best estimate for the probability of another extreme geomagnetic event comparable to the Carrington event occurring within the next 10 years is 10.3% 95% confidence interval (CI) [0.9,18.7] for a power law distribution but only 3.0% 95% CI [0.6,9.0] for a lognormal distribution. However, our results depend crucially on (1) how we define an extreme event, (2) the statistical model used to describe how the events are distributed in intensity, (3) the techniques used to infer the model parameters, and (4) the data and duration used for the analysis. We test a major assumption that the data represent time stationary processes and discuss the implications. If the current trends persist, suggesting that we are entering a period of lower activity, our forecasts may represent upper limits rather than best estimates.

Properties of the Fast Forward Shock Driven by the July 23 2012 Extreme Coronal Mass Ejection

Pete [Riley](#), Ronald M. Caplan, Joe Giacalone, David Lario, Ying Liu
2015

<http://arxiv.org/pdf/1510.06088v1.pdf>

Late on July 23, 2012, the STEREO-A spacecraft encountered a fast forward shock driven by a coronal mass ejection launched from the Sun earlier that same day. The estimated travel time of the disturbance (~ 20 hrs), together with the massive magnetic field strengths measured within the ejecta (>100 nT), made it one of the most extreme events observed during the space era. In this study, we examine the properties of the shock wave. Because of an instrument malfunction, plasma measurements during the interval surrounding the CME were limited, and our approach has been modified to capitalize on the available measurements and suitable proxies, where possible. We were able to infer the following properties. First, the shock normal was pointing predominantly in the radial direction ($n=0.97e^{-0.09t}-0.23en$). Second, the angle between n and the upstream magnetic field, θ_{Bn} , was estimated to be $\approx 34^\circ$, making the shock "quasi-parallel," and supporting the idea of an earlier "preconditioning" ICME. Third, the shock speed was estimated to be ≈ 3300 km s $^{-1}$. Fourth, the sonic Mach number, M_s , for this shock was ~ 28 . We support these results with an idealized numerical simulation of the ICME. Finally, we estimated the change in ram pressure upstream of the shock to be ~ 5 times larger than the pressure from the energetic particles, suggesting that this was not a standard "steady-state" cosmic-ray modified shock (CRMS). Instead it might represent an early, transient phase in the evolution of the CRMS.

On the probability of occurrence of extreme space weather events

Pete [Riley](#)

Space Weather, Volume 10, Issue 2, February 2012

By virtue of their rarity, extreme space weather events, such as the Carrington event of 1859, are difficult to study, their rates of occurrence are difficult to estimate, and prediction of a specific future event is virtually impossible. Additionally, events may be extreme relative to one parameter but normal relative to others. In this study, we analyze several measures of the severity of space weather events (flare intensity, coronal mass ejection speeds, Dst, and >30 MeV proton fluences as inferred from nitrate records) to estimate the probability of occurrence of extreme events. By showing that the frequency of occurrence scales as an inverse power of the severity of the event, and assuming that this relationship holds at higher magnitudes, we are able to estimate the probability that an event larger than some criteria will occur within a certain interval of time in the future. For example, the probability of another Carrington event (based on $Dst < -850$ nT) occurring within the next decade is $\sim 12\%$. We also identify and address several limitations with this approach. In particular, we assume time stationarity, and thus, the effects of long-term space climate change are not considered. While this technique cannot be used to predict specific events, it may ultimately be useful for probabilistic forecasting.

Corotating interaction regions during the recent solar minimum: The power and limitations of global MHD modeling

Pete [Riley](#), , Jon A. Linker, R. Lionello, Z. Mikic
JASTP, Volume 83, July 2012, Pages 1–10

The declining phase of solar activity cycle 23 has provided an unprecedented opportunity to study the evolution and properties of corotating interaction regions (CIRs) during unique and relatively steady conditions. The absence of significant transient activity has allowed modelers to test ambient solar wind models, but has also challenged them to reproduce structure that was qualitatively different than had been observed previously (at least within the space era). In this study, we present and analyze global magnetohydrodynamic (MHD) solutions of the inner heliosphere (from 1RS to 1 AU) for several intervals defined as part of a Center for Integrated Space weather Modeling (CISM) interdisciplinary campaign study, and, in particular, Carrington rotation 2060. We compare in situ measurements from ACE and STEREO A and B with the model results to illustrate both the capabilities and limitations of current numerical techniques. We show that, overall, the models do capture the essential structural features of the solar wind for specific time periods; however, there are times when the models and observations diverge. We describe, and, to some extent assess the sources of error in the modeling chain from the input photospheric magnetograms to the numerical schemes used to propagate structure through the heliosphere, and speculate on how they may be resolved, or at least mitigated in the future.

Modeling interplanetary coronal mass ejections

Pete [Riley](#), J.A. Linker, Z. Mikic and Dusan Odstrcil

[Advances in Space Research, Volume 38, Issue 3](#), pp. 535-546, 2006, preprint file

Derivation of fluid conservation relations to infer near-Sun properties of coronal mass ejections from in situ measurements,

[Riley](#), P., and D. J. McComas

J. Geophys. Res., 114, A09102, (2009), doi:10.1029/2009JA014436.

Coronal mass ejections (CMEs) are observed both near the Sun using remote solar measurements, as well as in the solar wind using in situ measurements. While many relationships have been made between these relatively disparate data sets, a number of connections remain poorly known. In this study, we use mass, momentum, and energy conservation to derive a set of conservation relations based on the observed in situ properties of CMEs and the ambient environment into which they propagate. We focus on fast CMEs that drive shocks and produce sheath regions. These relations allow us to infer the plasma and magnetic field properties of the ejecta close to the Sun based primarily on in situ observations. In this first paper, we consider the limit where both magnetic and thermal plasma pressure can be neglected and derive an equation for the initial speed of the ejecta. We apply this result to (1) a simulated fast CMEs (for which the true initial speed is known) to verify that the approach produces reasonable results and (2) an observed CME for which several other empirical techniques for inferring initial speed have been applied. Finally, using these results, we derive an estimate for the transit time of a CME from the Sun to 1 AU. Our results are promising, yet tentative. More extensive studies will be necessary to either support or refute this technique.

ON THE RATES OF CORONAL MASS EJECTIONS: REMOTE SOLAR AND IN SITU OBSERVATIONS

P. [Riley](#), C. Schatzman, H. V. Cane, I. G. Richardson, and N. Gopalswamy

The Astrophysical Journal, 647:648Y653, 2006, [File](#)

Galactic cosmic rays at 0.7 AU with Venus Express housekeeping data

[Rimbot](#), T ; [Witasse](#), O ; [Pinto](#), M ; [Knutsen](#), EW et al.

[PLANETARY AND SPACE SCIENCE](#)

Volume 242 Article Number 105867 2024

DOI 10.1016/j.pss.2024.105867

We apply a previously developed procedure to characterize galactic cosmic rays (GCRs) at 0.7 A.U. with engineering data coming from the Venus Express mission. The engineering parameters are the Error Detection and Correction EDAC cumulative counters, used for detection and correction of memory errors induced by highly energetic particles. It has already been demonstrated that the slope of this counter measures GCR fluxes using data from Mars Express (1.5 A.U.) and Rosetta (up to 4 A.U.) data. Here, we reproduce these methods using Venus Express EDAC data in order to understand the behavior of GCRs closer to the Sun. We again witness the anti-correlation of EDAC slope with the solar activity and further investigate this procedure. The resulting time-lag between maximum sunspot number and minimum

GCRs intensity at Venus is close to one day instead of the expected several months. This work represents one of the first characterization of galactic cosmic rays at small distances to the Sun over a long period of time and further cements the value of using EDAC counters as scientific information.

Particle Dynamics in the Earth's Radiation Belts: **Review** of Current Research and Open Questions

J.-F. **Ripoll** , [S. G. Claudepierre](#) , [A. Y. Ukhorskiy](#) , [C. Colpitts](#) , [X. Li](#) , [J. F. Fennell](#) , [C. Crabtree](#)

JGR [Volume125, Issue5](#) May 2020 e2019JA026735

https://agupubs.onlinelibrary.wiley.com/doi/pdf/10.1029/2019JA026735?casa_token=my0tfqaY9KUAAAAA:0ISqoN34ZJquVmaHFXUMha46OGvmnwGgdWowLAd9Mzn5_WzPmO4AIx5LSXGFaLqCy0RzmUrI-HiNGw

The past decade transformed our observational understanding of energetic particle processes in near-Earth space. An unprecedented suite of observational systems was in operation including the Van Allen Probes, Arase, Magnetospheric Multiscale, Time History of Events and Macroscale Interactions during Substorms, Cluster, GPS, GOES, and Los Alamos National Laboratory-GEO magnetospheric missions. They were supported by conjugate low-altitude measurements on spacecraft, balloons, and ground-based arrays. Together, these significantly improved our ability to determine and quantify the mechanisms that control the buildup and subsequent variability of energetic particle intensities in the inner magnetosphere. The high-quality data from National Aeronautics and Space Administration's Van Allen Probes are the most comprehensive in situ measurements ever taken in the near-Earth space radiation environment. These observations, coupled with recent advances in radiation belt theory and modeling, including dramatic increases in computational power, have ushered in a new era, perhaps a “golden era,” in radiation belt research. We have edited a Journal of Geophysical Research: Space Science Special Collection dedicated to Particle Dynamics in the Earth's Radiation Belts in which we gather the most recent scientific findings and understanding of this important region of geospace. This collection includes the results presented at the American Geophysical Union Chapman International Conference in Cascais, Portugal (March 2018) and many other recent and relevant contributions. The present article introduces and review the context, current research, and main questions that motivate modern radiation belt research divided into the following topics: (1) particle acceleration and transport, (2) particle loss, (3) the role of nonlinear processes, (4) new radiation belt modeling capabilities and the quantification of model uncertainties, and (5) laboratory plasma experiments.

Manifestation of Gravitational Settling in Coronal Mass Ejections Measured in the Heliosphere

Yeimy J. **Rivera**¹, John C. Raymond¹, Enrico Landi², Susan T. Lepri², Katharine K. Reeves¹, Michael L. Stevens¹, and B. L. Alterman³

2022 ApJ 936 83

<https://iopscience.iop.org/article/10.3847/1538-4357/ac8873/pdf>

Elemental composition in the solar wind reflects the fractionation processes at the Sun. In coronal mass ejections (CMEs) measured in the heliosphere, the elemental composition can vary between plasma of high and low ionization states as indicated by the average Fe charge state, $\langle Q_{Fe} \rangle$. It is found that CMEs with higher ionized plasma, $\langle Q_{Fe} \rangle$ greater than 12, are significantly more enriched in low first ionization potential (FIP) elements compared to their less ionized, $\langle Q_{Fe} \rangle$ less than 12, counterparts. In addition, the CME elemental composition has been shown to vary along the solar cycle. However, the processes driving changes in elemental composition in the plasma are not well understood. To gain insight into this variation, this work investigates the effects of gravitational settling in the ejecta to examine how that process can modify signatures of the FIP effect found in CMEs. We examine the absolute abundances of C, N, O, Ne, Mg, Si, S, and Fe in CMEs between 1998 and 2011. Results show that the ejecta exhibits some gravitational settling effects in approximately 33% of all CME periods in plasma where the Fe abundance of the ejecta compared to the solar wind (Fe/HCME:Fe/HSW) is depleted compared to the C abundance (C/HCME:C/HSW). We also find gravitational settling is most prominent in CMEs during solar minimum; however, it occurs throughout the solar cycle. This study indicates that gravitational settling, along with the FIP effect, can become important in governing the compositional makeup of CME source regions.

Solar Origin of Bare Ion Anomalies in the Solar Wind and Interplanetary Coronal Mass Ejections

Yeimy J. **Rivera**¹, Susan T. Lepri², John C. Raymond¹, Katharine K. Reeves¹, Michael L. Stevens¹, and Liang Zhao²

2021 ApJ 921 93

<https://doi.org/10.3847/1538-4357/ac1676>

Previous studies of the solar wind and interplanetary coronal mass ejections (ICMEs) have shown periods throughout solar cycle 23 when heliospheric measurements of ion composition appear anomalous. In these cases, C6+ and other bare ion densities, i.e., fully stripped ions, are unusually low, leading it to be classified as the Outlier solar wind. However, its origin and solar source(s) remain largely uncertain. In this work, we further characterize the Outlier wind to connect its heliospheric structure to its solar source to constrain the conditions of its formation. Through an analysis of the plasma and magnetic field properties of each occurrence between 1998 and 2011, we find that the Outlier plasma occurs in the slow solar wind or interplanetary mass ejections ($\sim 460 \text{ km s}^{-1}$), and comprises distinct, high density events lasting less than 10 hr. The number of events is correlated with the solar cycle, indicating the process leading to the depletion of bare ions is strongly governed by the magnetic field. Additionally, the events exhibit a bi- or unidirectional suprathermal electron strahl that is concurrent with changes in the magnetic field direction. Moreover, the Outlier wind's composition, entropy, Alfvén speed, and proton temperature suggest a helmet streamer or active region origin. Together, the properties exhibited by the Outlier wind suggest a strong connection to the heliospheric current sheet and that the solar wind events are smaller scale versions of those seen in ICMEs, such as small magnetic flux ropes. However, more work is necessary to determine the source and creation process in the vicinity of the Sun.

Empirical Modeling of CME Evolution Constrained to ACE/SWICS Charge State Distributions

Yeimy J. **Rivera**, Enrico Landi, Susan T. Lepri, and Jason A. Gilbert

2019 ApJ 874 164

sci-hub.se/10.3847/1538-4357/ab0e11

It is generally accepted that coronal mass ejections (CMEs) undergo rapid heating as they are released from the Sun. However, to date, the heating mechanism remains an open question. To gain insight into the plasma heating, we derive the density, temperature, and velocity evolution of the **2005 January 9** interplanetary CME event from launch to ion freeze-in distance by examining ion distributions collected within the ejecta near the Earth. We use the Michigan Ionization Code to simulate the ion evolution and determine thermodynamic properties through an extensive iterative search that finds agreement between simulated and observed ion populations. The final results show that the ion distributions can be effectively reconstructed using a combination of ions generated within four distinct plasma structures traveling together. Three of the modeled plasma components derived originate from the prominence and the prominence–corona transition region (PCTR) structures, while a fourth plasma shares features common to the ambient corona. The absolute abundances computed for each plasma reveal that the prominence material contains photospheric composition, while the remaining PCTR and warmer plasma have coronal abundances. Furthermore, we computed an energy release rate for each plasma structure that includes the kinetic, potential, and thermal energy rates, along with the radiative cooling, thermal conduction, and adiabatic cooling rates. We found the prominence material's energy release rate to be consistently larger compared to the other components. In future work, the energy results will be used to investigate the feasibility of a proposed heating mechanism in an effort to gain a more comprehensive understanding of the eruption process.

Current Space Weather Forecasting

Review

E. **Robbrecht**

ESPM Presentation, 2011, File

Big flare forecasting; CMEs, Are halo CMEs special? geoeffectiveness of CMEs; CME travel times; Predicting “Bz”; CMEs can rotate

Хорошие ссылки

Global Muon Detector Network Used for Space Weather Applications

Review

M. **Rockenbach**, A. Dal Lago, N. J. Schuch, K. Munakata, T. Kuwabara, A. G. Oliveira, E. Echer, C. R. Braga, R. R. S. Mendonça, C. Kato, ... show all 19

Space Science Reviews, August 2014, Volume 182, Issue 1-4, pp 1-18

<https://link.springer.com/content/pdf/10.1007%2Fs11214-014-0048-4.pdf>

In this work, we summarize the development and current status of the Global Muon Detector Network (GMDN). The GMDN started in 1992 with only two muon detectors. It has consisted of four detectors since the Kuwait-city muon hodoscope detector was installed in March 2006. The present network has a total of 60 directional channels with an improved coverage of the sunward Interplanetary Magnetic Field (IMF) orientation, making it possible to continuously

monitor cosmic ray precursors of geomagnetic storms. The data analysis methods developed also permit precise calculation of the three dimensional cosmic ray anisotropy on an hourly basis free from the atmospheric temperature effect and analysis of the cosmic ray precursors free from the diurnal anisotropy of the cosmic ray intensity.

Hybrid Simulation of Solar-Wind-Like Turbulence

D. Aaron [Roberts](#), Leon Ofman

[Solar Physics](#) November 2019, 294:153

<https://link.springer.com/content/pdf/10.1007%2Fs11207-019-1548-x.pdf>

We present 2.5D hybrid simulations of the spectral and thermodynamic evolution of an initial state of magnetic field and plasma variables that in many ways represents solar wind fluctuations. In accordance with Helios near-Sun high-speed stream observations, we start with Alfvénic fluctuations along a mean magnetic field in which the fluctuations in the magnitude of the magnetic field are minimized. Since fluctuations in the radial flow speed are the dominant free energy in the observed fluctuations, we include a field-aligned $v_{\parallel}(k_{\perp})v_{\perp}(k_{\perp})$ with an $k^{-1}k^{-1}$ spectrum of velocity fluctuations to drive the turbulent evolution. The flow rapidly distorts the Alfvénic fluctuations, yielding spectra (determined by spacecraft-like cuts) transverse to the field that become comparable to the $k_{\parallel}|k|$ fluctuations, as in spacecraft observations. The initial near constancy of the magnetic field is lost during the evolution; we show this also takes place observationally. We find some evolution in the anisotropy of the thermal fluctuations, consistent with expectations based on Helios data. We present 2D spectra of the fluctuations, showing the evolution of the power spectrum and cross-helicity. Despite simplifying assumptions, many aspects of simulations and observations agree. The greatly faster evolution in the simulations is at least in part due to the small scales being simulated, but also to the non-equilibrium initial conditions and the relatively low overall Alfvénicity of the initial fluctuations.

3D Reconstruction and Interplanetary Expansion of the 2010 April 3rd CME

Martina [Rodari](#), [Mateja Dumbović](#), [Manuela Temmer](#), [Lukas M. Holzknecht](#), [Astrid Veronig](#)

Central European Astrophysical Bulletin 2019

<https://arxiv.org/pdf/1904.05611.pdf>

We analyse the 2010 April 3rd CME using spacecraft coronagraphic images at different vantage points (SOHO, STEREO-A and STEREO-B). We perform a 3D reconstruction of both the flux rope and shock using the Graduated Cylindrical Shell (GCS) model to calculate CME kinematic and morphologic parameters (e.g. velocity, acceleration, radius). The obtained results are fitted with empirical models describing the expansion of the CME radius in the heliosphere and compared with in situ measurements from Wind spacecraft: the CME is found to expand linearly towards Earth. Finally, we relate the event with decreases in the Galactic Cosmic Ray (GCR) Flux, known as Forbush decreases (FD), detected by EPHIN instrument onboard SOHO spacecraft. We use the analytical diffusion-expansion model (ForbMod) to calculate the magnetic field power law index, obtaining a value of approximately 1.6, thus estimating a starting magnetic field of around 0.01 G and an axial magnetic flux of around 5×10^{20} Mx at 15.6 Rsun.

Prediction of Geomagnetic Storms Associated with Interplanetary Coronal Mass Ejections

[Rodkin](#), D.G., [Slemzin](#), V.A.

Astronomy Reports. Volume: 68. Issue: 2. 192–199, 2024

<https://doi.org/10.1134/S1063772924700185>

Geomagnetic storms have a significant impact on the performance of technical systems both in space and on Earth. The sources of strong geomagnetic storms are most often interplanetary coronal mass ejections (ICMEs), generated by coronal mass ejections (CMEs) in the solar corona. The ICME forecast is based on regular optical observations of the Sun, which make it possible to detect CMEs at the formation stage. It is known that the intensity of geomagnetic storms correlates with the magnitude of the southern component of the magnetic field (B_z) of the ICME. However, it is not possible yet to predict the sign and magnitude of B_z from solar observations for the operational forecast of an arbitrary CME. Under these conditions, a preliminary forecast of the magnetic storm probability can be obtained under the assumption that the strength of the storm is related to the magnitude of the magnetic flux from the eruption region, observed as dimming. In this paper, we examine the relationship between the integral magnetic flux from the dimming region and the probability that CMEs associated with them will cause geomagnetic storms, using a series of 37 eruptive events in 2010–2012. It is shown that there is a general trend toward an increase in the ICMEs geoefficiency with an increase in the magnitude of the magnetic flux from the dimming region. It has been demonstrated that the frequency of moderate and severe storms observation increases in cases of complex events associated with the interaction of CMEs with other solar wind streams in the heliosphere.

Single ICMEs and Complex Transient Structures in the Solar Wind in 2010 – 2011

D. [Rodkin](#), V. [Slemzin](#), A. N. [Zhukov](#), F. [Goryaev](#), Y. [Shugay](#), I. [Veselovsky](#)

[Solar Physics](#) May 2018, 293:78

<https://link.springer.com/content/pdf/10.1007%2Fs11207-018-1295-4.pdf>

We analyze the statistics, solar sources, and properties of interplanetary coronal mass ejections (ICMEs) in the solar wind. The total number of coronal mass ejections (CMEs) registered in the Coordinated Data Analysis Workshops catalog (CDAW) during the first eight years of Cycle 24 was 61% larger than in the same period of Cycle 23, but the number of X-ray flares registered by the Geostationary Operational Environmental Satellite (GOES) was 20 % smaller because the solar activity was lower. The total number of ICMEs in the given period of Cycle 24 in the Richardson and Cane list was 29% smaller than in Cycle 23, which may be explained by a noticeable number of non-classified ICME-like events in the beginning of Cycle 24. For the period January 2010 – August 2011, we identify solar sources of the ICMEs that are included in the Richardson and Cane list. The solar sources of ICME were determined from coronagraph observations of the Earth-directed CMEs, supplemented by modeling of their propagation in the heliosphere using kinematic models (a ballistic and drag-based model). A detailed analysis of the ICME solar sources in the period under study showed that in 11 cases out of 23 (48%), the observed ICME could be associated with two or more sources. For multiple-source events, the resulting solar wind disturbances can be described as complex (merged) structures that are caused by stream interactions, with properties depending on the type of the participating streams. As a reliable marker to identify interacting streams and their sources, we used the plasma ion composition because it freezes in the low corona and remains unchanged in the heliosphere. According to the ion composition signatures, we classify these cases into three types: complex ejecta originating from weak and strong CME–CME interactions, as well as merged interaction regions (MIRs) originating from the CME high-speed stream (HSS) interactions. We describe temporal profiles of the ion composition for the single-source and multi-source solar wind structures and compared them with the ICME signatures determined from the kinematic and magnetic field parameters of the solar wind. In single-source events, the ion charge state, as a rule, has a one-peak enhancement with an average duration of about oneabout one day, which is similar to the mean ICME duration of 1.12 days derived from the Richardson and Cane list. In the multi-source events, the total profile of the ion charge state consists of a sequence of enhancements that is associated with the interaction between the participating streams. On average, the total duration of the complex structures that appear as a result of the CME–CME and CME–HSS interactions as determined from their ion composition is 2.4 days, which is more than twice longer than that of the single-source events. **11 February 2010, 5 April 2010, 4 February 2011, 6 August 2011**

Table 2 ICMEs from the RC list detected in 2010 and parameters of their possible solar sources.

Table 3 ICMEs from the RC list detected in 2011 and parameters of their possible solar sources.

Quantifying Extreme Values in Geomagnetic Perturbations Using Ground Magnetic Records

J. [Rodríguez-Zuluaga](#), J. [Gjerloev](#), S. [Ohtani](#), Y. [Zou](#), B. [Anderson](#)

Space Weather [Volume22, Issue7](#) July 2024 e2024SW003991

<https://doi.org/10.1029/2024SW003991>

<https://agupubs.onlinelibrary.wiley.com/doi/epdf/10.1029/2024SW003991>

We comprehensively analyzed geomagnetic perturbations using ground magnetic records from over 400 stations spanning four solar cycles, from 1976 to 2023. We assess the perturbations in the three magnetic components separately. Our study covers low, middle, and high magnetic latitudes in the northern magnetic hemisphere, with the primary objective of quantifying extreme values and evaluating their variability on magnetic latitude, local time, and solar cycle phases “minimum, ascending, maximum, and declining.” Our findings reveal spatial patterns to be less discernible as perturbations intensify, with distinct responses at middle and high latitudes. The extreme values, defined as percentiles 0 and 100, were observed to be localized and randomly distributed in local time, especially in the east magnetic component. Additionally, we observed dusk-dawn asymmetries in the magnitude of perturbations related to the auroral electrojets, indicating complex interactions between the magnetosphere and ionosphere. Furthermore, the results reveal a preference for the most significant extreme values to occur in the declining phase of the solar cycle. These insights deepen our understanding of geomagnetic perturbations and their variability, contributing to space weather forecasting and mitigation strategies.

Validation of EUHFORIA cone and spheromak Coronal Mass Ejection Models

L. [Rodriguez](#), D. [Shukhobodskaya](#), A. [Niemela](#), A. [Maharana](#), E. [Samara](#), C. [Verbeke](#), J. [Magdalenic](#), R.

[Vansintjan](#), M. [Mierla](#), C. [Scolini](#), R. [Sarkar](#), E. [Kilpua](#), E. [Asvestari](#), K. [Herbst](#), G. [Lapenta](#), A.D.

[Chaduteau](#), J. [Pomoell](#), S. [Poedts](#)

A&A 689, A187 2024

<https://arxiv.org/pdf/2405.04637>

<https://www.aanda.org/articles/aa/pdf/2024/09/aa49530-24.pdf>

Aims. We present the validation results for arrival times and geomagnetic impact of Coronal Mass Ejections (CMEs), using the cone and spheromak CME models implemented in European Heliospheric FORecasting Information Asset (EUHFORIA). Validating numerical models is crucial in ensuring their accuracy and performance with respect to real data.

Methods. We compare CME plasma and magnetic field signatures, measured in situ by satellites at the L1 point, with the simulation output of EUHFORIA. The validation of this model was carried out by using two datasets in order to ensure a comprehensive evaluation. The first dataset focuses on 16 CMEs that arrived at the Earth, offering specific insights into the model's accuracy in predicting arrival time and geomagnetic impact. Meanwhile, the second dataset encompasses all CMEs observed over eight months within Solar Cycle 24, regardless of whether they arrived at Earth, covering periods of both solar minimum and maximum activity. This second dataset enables a more comprehensive evaluation of the model's predictive precision in terms of CME arrivals and misses.

Results. Our results show that EUHFORIA provides good estimates in terms of arrival times, with root mean square errors (RMSE) values of 9 hours. Regarding the number of correctly predicted ICME arrivals and misses, we find a 75% probability of detection in a 12 hours time window and 100% probability of detection in a 24 hours time window. The geomagnetic impact forecasts, measured by the Kp index, provide different degrees of accuracy, ranging from 31% to 69%. These results validate the use of cone and spheromak CMEs for real-time space weather forecasting. **29**

September 2013

Table 1. The table includes a list of CME–ICME pairs used in this study 2010-2017

Turbulence, intermittency and cross-scale energy transfer in an interplanetary coronal mass ejection

Roque Márquez [Rodríguez](#), [Luca Sorriso-Valvo](#), [Emiliya Yordanova](#)

Solar Phys. **298**, Article number: 54 (2023)

<https://arxiv.org/pdf/2212.06871.pdf>

<https://link.springer.com/content/pdf/10.1007/s11207-023-02146-1.pdf>

Solar wind measurements carried out by NASA's Wind spacecraft before, during and after the passing of an interplanetary coronal mass ejection (ICME) detected on **12-14 September 2014** have been used in order to examine several properties of magnetohydrodynamic (MHD) turbulence. Spectral indices and flatness scaling exponents of magnetic field, velocity and proton density measurements were obtained, and provided a standard description of the characteristics of turbulence within different sub-regions of the ICME and its surroundings. This analysis was followed by the validation of the third-order moment scaling law for isotropic, incompressible MHD turbulence in the same sub-regions, which confirmed the fully developed nature of turbulence in the ICME plasma. The energy transfer rate was also estimated in each ICME sub-region and in the surrounding solar wind. An exceptionally high value was found within the ICME sheath, accompanied by enhanced intermittency, possibly related to the powerful energy injection associated with the arrival of the ICME.

Space weather monitor at the L5 point: a case study of a CME observed with STEREO B

L. [Rodríguez](#), [C. Scolini](#), [M. Mierla](#), [A. N. Zhukov](#), [M. J. West](#)

Space Weather **Volume18, Issue10** e2020SW002533 **2020**

<https://doi.org/10.1029/2020SW002533>

<https://agupubs.onlinelibrary.wiley.com/doi/epdf/10.1029/2020SW002533>

An important location for future space weather monitoring is the Lagrange point 5 (L5) of the Sun–Earth system. We test the performance of L5 for space weather monitoring using STEREO–B observations of an Earth-directed Coronal Mass Ejection (CME), seen as a partial halo by SOHO at L1. STEREO–B (located close to L5) continuously tracked the CME. By using these data in combination with methods to calculate the CME arrival time at the Earth (extrapolation, drag-based model, and a magnetohydrodynamic model), we demonstrate that the estimation of the CME arrival time can be drastically improved by adding L5 data. Based on the L1 data alone, one could predict that the CME would arrive at the Earth. Using only the L5 data, one would not expect an arrival, as the estimations of the CME 3D configuration is uncertain. The combination of L1 and L5 data leads to an ambiguous prediction of the CME arrival due to low CME brightness in L1 data. To obtain an unambiguous prediction, one needs its 3D configuration, from observing the CME material close to the plane of the sky from at least two viewpoints (in this case L5 and, coincidentally, L4). This event demonstrates that L1 observations may be better to determine CME arrival, but L5 observations are superior for constraining arrival time. In this work the advantages and caveats of using data from a space weather monitor at L5

for predicting interplanetary propagation of CMEs are discussed and demonstrated in a direct case study. **October 17-21, 2009**

Typical Profiles and Distributions of Plasma and Magnetic Field Parameters in Magnetic Clouds at 1 AU

L. [Rodríguez](#), J. J. Masías-

Meza, S. Dasso, P. Démoulin, A. N. Zhukov, A. M. Gulisano, M. Mierla, E. Kilpua, M. West and [3 more](#)
Solar Phys. Volume 291, [Issue 7](#), pp 2145–2163 **2016**

Magnetic clouds (MCs) are a subset of interplanetary coronal mass ejections (ICMEs). They are important because of their simple internal magnetic field configuration, which resembles a magnetic flux rope, and because they represent one of the most geoeffective types of solar transients. In this study, we analyze their internal structure using a superposed epoch method on 63 events observed at L1 by the *Advance Composition Explorer* (ACE), between 1998 and 2006. In this way, we obtain an average profile for each plasma and magnetic field parameter at each point of the cloud. Furthermore, we take a fixed time-window upstream and downstream from the MC to also sample the regions preceding the cloud and the wake trailing it. We then perform a detailed analysis of the internal characteristics of the clouds and their surrounding solar wind environments. We find that the parameters studied are compatible with log-normal distribution functions. The plasma β and the level of fluctuations in the magnetic field vector are the best parameters to define the boundaries of MCs. We find that one third of the events shows a peak in plasma density close to the trailing edge of the flux ropes. We provide several possible explanations for this result and investigate if the density peak is of a solar origin (*e.g.* erupting prominence material) or formed during the magnetic cloud travel from the Sun to 1 AU. The most plausible explanation is the compression due to a fast overtaking flow, coming from a coronal hole located to the east of the solar source region of the magnetic cloud.

Linking Remote-Sensing and In Situ Observations of Coronal Mass Ejections Using STEREO

L. [Rodríguez](#), M. Mierla, A. N. Zhukov, M. West and E. Kilpua

Solar Physics, Volume 270, Number 2, 561-573, **2011**

The twin STEREO spacecraft have been observing the Sun since 2006. Even though STEREO has only been active during solar minimum conditions so far, an important number of coronal mass ejections (CMEs) and their interplanetary counterparts (ICMEs) have been observed. Many of the ICMEs can be linked back to the corresponding CMEs on the Sun through the combination of remote-sensing and in situ observations. This paper aims to answer the question whether a CME observed by a coronagraph will be detected in situ by a spacecraft in a specific location in the heliosphere. We use a flux-rope-like model fit to the STEREO SECCHI/COR2 data to obtain the direction of CME propagation and its geometrical configuration in three dimensions. Based on model parameters, we then calculate their angular widths and determine whether they should have been detected by STEREO-A, STEREO-B, Wind or ACE. We compare the results with corresponding in situ observations of ICMEs. We find that predictions of ICME detections on the base of COR2 data generally match well the actual in situ observations.

Three frontside full halo coronal mass ejections with a nontypical geomagnetic response

[Rodríguez](#), L.; Zhukov, A. N.; Cid, C.; Cerrato, Y.; Saiz, E.; Cremades, H.; Dasso, S.; Menvielle, M.; Aran, A.; Mandrini, C.; Poedts, S.; Schmieder, B.

Space Weather, Vol. 7, No. 6, S06003, **2009**

<http://dx.doi.org/10.1029/2008SW000453>

Forecasting potential geoeffectiveness of solar disturbances (in particular, of frontside full halo coronal mass ejections) is important for various practical purposes, *e.g.*, for satellite operations, radio communications, global positioning system applications, power grid, and pipeline maintenance. We analyze **three frontside full halo coronal mass ejections (CMEs) that occurred in the year 2000** (close to the activity maximum of solar cycle 23), together with associated solar and heliospheric phenomena as well as their impact on the Earth's magnetosphere. Even though all three were fast full halos (with plane of the sky speeds higher than 1100 km/s), the geomagnetic response was very different for each case. After analyzing the source regions of these halo CMEs, it was found that the halo associated with the strongest geomagnetic disturbance was the one that initiated farther away from disk center (source region at **W66**); while the other two CMEs originated closer to the central meridian but had weaker geomagnetic responses. Therefore, these three events do not fit into the general statistical trends that relate the location of the solar source and the corresponding geoeffectivity. We investigate possible causes of such a behavior. Nonradial direction of eruption, passage of the Earth through a leg of an interplanetary flux rope, and strong compression at the eastern flank of a

propagating interplanetary CME during its interaction with the ambient solar wind are found to be important factors that have a direct influence on the resulting north-south interplanetary magnetic field (IMF) component and thus on the CME geoeffectiveness. We also find indications that interaction of two CMEs could help in producing a long-lasting southward IMF component. Finally, we are able to explain successfully the geomagnetic response using plasma and magnetic field in situ measurements at the L1 point. We discuss the implications of our results for operational space weather forecasting and stress the difficulties of making accurate predictions with the current knowledge and tools at hand.

Magnetic clouds seen at different locations in the Heliosphere

L. [Rodríguez](#)¹, A. N. Zhukov^{1,2}, S. Dasso^{3,4}, C. H. Mandrini³, H. Cremades⁵, C. Cid⁶, Y. Cerrato⁶, E. Saiz⁶, A. Aran⁷, M. Menvielle⁸, S. Poedts⁹, and B. Schmieder¹⁰
Ann. Geophys., 25, 1–17, 2007, www.ann-geophys.net/25/1/2007/

We analyze two magnetic clouds (MCs) observed in different points of the heliosphere. The main aim of the present study is to provide a link between the different aspects of this phenomenon, starting with information on the origins of the MCs at the Sun and following by the analysis of in-situ observations at 1AU and at Ulysses. The candidate source regions were identified in SOHO/EIT and SOHO/MDI observations. They were correlated with H_α images that were obtained from ground-based observatories. Hints on the internal magnetic field configuration of the associated coronal mass ejections are obtained from LASCO C2 images. In interplanetary space, magnetic and plasma moments of the distribution function of plasma species (ACE/Ulysses) were analyzed together with information on the plasma composition, and the results were compared between both spacecraft in order to understand how these structures interact and evolve in their cruise from the Sun to 5AU. Additionally, estimates of global magnitudes of magnetic fluxes and helicity were obtained from magnetic field models applied to the data in interplanetary space. We have found that these magnetic characteristics were well kept from their solar source, up to 5AU where Ulysses provided valuable information which, together with that obtained from ACE, can help to reinforce the correct matching of solar events and their interplanetary counterparts.

21-22 Nov 2001, 20 Jan 2005

Evidence of a complex structure within the 2013 August 19 coronal mass ejection

Radial and longitudinal evolution in the inner heliosphere*

L. [Rodríguez-García](#)¹, T. Nieves-Chinchilla², R. Gómez-Herrero¹, I. Zouganelis³, A. Vourlidas⁴, L. A. Balmaceda^{2,5}, M. Dumbović⁶, L. K. Jian², L. Mays², F. Carcaboso^{1,2,7}, L. F. G. dos Santos⁸ and J. Rodríguez-Pacheco¹
A&A 662, A45 (2022)

<https://arxiv.org/pdf/2203.02713.pdf>

<https://www.aanda.org/articles/aa/pdf/2022/06/aa42966-21.pdf>

Context. Late on **2013 August 19**, a coronal mass ejection (CME) erupted from an active region located near the far-side central meridian from Earth's perspective. The event and its accompanying shock were remotely observed by the STEREO-A, STEREO-B, and SOHO spacecraft. The interplanetary counterpart (ICME) was intercepted by MESSENGER near 0.3 au and by both STEREO-A and STEREO-B near 1 au, which were separated from each other by 78° in heliolongitude.

Aims. The main objective of this study is to follow the radial and longitudinal evolution of the ICME throughout the inner heliosphere and to examine possible scenarios for the different magnetic flux-rope configuration observed on the solar disk and measured in situ at the locations of MESSENGER and STEREO-A, separated by 15° in heliolongitude, and at STEREO-B, which detected the ICME flank.

Methods. Solar disk observations are used to estimate the “magnetic flux-rope type”, namely, the magnetic helicity, axis orientation, and axial magnetic field direction of the flux rope. The graduated cylindrical shell model is used to reconstruct the CME in the corona. The analysis of in situ data, specifically the plasma and magnetic field, is used to estimate the global interplanetary shock geometry and to derive the magnetic flux-rope type at different in situ locations, which is compared to the type estimated from solar disk observations. The elliptical cylindrical analytical model is used for the in situ magnetic flux-rope reconstruction.

Results. Based on the CME geometry and on the spacecraft configuration, we find that the magnetic flux-rope structure detected at STEREO-B belongs to the same ICME detected at MESSENGER and STEREO-A. The opposite helicity deduced at STEREO-B might be due to that fact that it intercepted one of the legs of the structure far from the flux-rope axis, in contrast to STEREO-A and MESSENGER, which were crossing through the core of the magnetic flux rope. The different flux-rope orientations measured at MESSENGER and STEREO-A probably arise because the two spacecraft

measure a curved, highly distorted, and rather complex magnetic flux-rope topology. The ICME may have suffered additional distortion in its evolution in the inner heliosphere, such as the west flank propagating faster than the east flank when arriving near 1 au.

Conclusions. This work illustrates how a wide, curved, highly distorted, and rather complex CME showed different orientations as observed on the solar disk and measured in situ at 0.3 au and near 1 au. Furthermore, the work shows how the ambient conditions can significantly affect the expansion and propagation of the CME and ICME, introducing additional irregularities to the already asymmetric eruption. The study also manifests how these complex structures cannot be directly reconstructed with the currently available models and that multi-point analysis is of the utmost importance in such complex events.

EIEvoHI: a novel CME prediction tool for heliospheric imaging combining an elliptical front with drag-based model fitting

Tanja [Rollett](#), Christian Möstl, Alexey Isavnin, [Jackie A. Davies](#), [Manuel Kubicka](#), [Ute V. Amerstorfer](#), [Richard A. Harrison](#)

ApJ 824 131 2016

<http://arxiv.org/pdf/1605.00510v1.pdf>

In this study, we present a new method for forecasting arrival times and speeds of coronal mass ejections (CMEs) at any location in the inner heliosphere. This new approach enables the adoption of a highly flexible geometrical shape for the CME front with an adjustable CME angular width and an adjustable radius of curvature of its leading edge, i.e. the assumed geometry is elliptical. Using, as input, STEREO heliospheric imager (HI) observations, a new elliptic conversion (EICon) method is introduced and combined with the use of drag-based model (DBM) fitting to quantify the deceleration or acceleration experienced by CMEs during propagation. The result is then used as input for the Ellipse Evolution Model (EIEvo). Together, EICon, DBM fitting, and EIEvo form the novel EIEvoHI forecasting utility. To demonstrate the applicability of EIEvoHI, we forecast the arrival times and speeds of 21 CMEs remotely observed from STEREO/HI and compare them to in situ arrival times and speeds at 1 AU. Compared to the commonly used STEREO/HI fitting techniques (Fixed- Φ , Harmonic Mean, and Self-similar Expansion fitting), EIEvoHI improves the arrival time forecast by about 2 hours to ± 6.5 hours and the arrival speed forecast by ≈ 250 km s⁻¹ to ± 53 km s⁻¹, depending on the ellipse aspect ratio assumed. In particular, the remarkable improvement of the arrival speed prediction is potentially beneficial for predicting geomagnetic storm strength at Earth.

Table 1 Differences between EIEvoHI predictions and in situ arrival time and speed

Table 3 List of input parameters obtained from EICon and DBM fitting, which are used for EIEvo.

ERRATUM to Table 1 and Table 3: T. [Amerstorfer](#) et al. 2016 ApJ 831 210

<http://iopscience.iop.org/article/10.3847/0004-637X/831/2/210>

Assessing the Constrained Harmonic Mean Method for Deriving the Kinematics of ICMEs with a Numerical Simulation

T. [Rollett](#), M. Temmer, C. Möstl, N. Lugaz, A. M. Veronig, U. V. Möstl

Solar Physics April 2013, Volume 283, Issue 2, pp 541-556

In this study we use a numerical simulation of an artificial coronal mass ejection (CME) to validate a method for calculating propagation directions and kinematical profiles of interplanetary CMEs (ICMEs). In this method observations from heliospheric images are constrained with in-situ plasma and field data at 1 AU. These data are used to convert measured ICME elongations into distance by applying the harmonic mean approach, which assumes a spherical shape of the ICME front. We used synthetic white-light images, similar to those observed by STEREO-A/HI, for three different separation angles between remote and in-situ spacecraft of 30°, 60°, and 90°. To validate the results of the method, the images were compared to the apex speed profile of the modeled ICME, as obtained from a top view. This profile reflects the “true” apex kinematics because it is not affected by scattering or projection effects. In this way it is possible to determine the accuracy of the method for revealing ICME propagation directions and kinematics. We found that the direction obtained by the constrained harmonic mean method is not very sensitive to the separation angle (30° sep: $\phi=W7$; 60° sep: $\phi=W12$; 90° sep: $\phi=W15$; true dir.: E0/W0). For all three cases the derived kinematics agree relatively well with the real kinematics. The best consistency is obtained for the 30° case, while with growing separation angle the ICME speed at 1 AU is increasingly overestimated (30° sep: $\Delta V_{arr} \approx -50$ km s⁻¹, 60° sep: $\Delta V_{arr} \approx +75$ km s⁻¹, 90° sep: $\Delta V_{arr} \approx +125$ km s⁻¹). Especially for future L4/L5 missions, the 60° separation case is highly interesting in order to improve space-weather forecasts. **15-17 February 2011**

Constraining the Kinematics of Coronal Mass Ejections in the Inner Heliosphere with In-Situ Signatures

T. **Rollett**, C. Möstl, M. Temmer, A. M. Veronig, C. J. Farrugia and H. K. Biernat

Solar Physics, Volume 276, Numbers 1-2, 293-314, **2012**, **File**

We present a new approach to combine remote observations and in-situ data by STEREO/HI and Wind, respectively, to derive the kinematics and propagation directions of interplanetary coronal mass ejections (ICMEs). We use two methods, Fixed- φ (F φ) and Harmonic Mean (HM), to convert ICME elongations into distance, and constrain the ICME direction such that the ICME distance–time and velocity–time profiles are most consistent with in-situ measurements of the arrival time and velocity. The derived velocity–time functions from the Sun to 1 AU for the three events under study (**1–6 June 2008, 13–18 February 2009, 3–5 April 2010**) do not show strong differences for the two extreme geometrical assumptions of a wide ICME with a circular front (HM) or an ICME of small spatial extent in the ecliptic (F φ). Due to the geometrical assumptions, HM delivers the propagation direction further away from the observing spacecraft with a mean difference of $\approx 25^\circ$.

Charge sign dependence of recurrent Forbush decreases in 2016–2017

L. **Romanehsen**,^{*} B. Heber and J. Marquardt

A&A, 690, A31 (**2024**)

<https://www.aanda.org/articles/aa/pdf/2024/10/aa49836-24.pdf>

Context. This study investigates the periodicities of galactic cosmic ray flux attributed to corotating interaction regions (CIRs) using Alpha Magnetic Spectrometer (AMS-02) data from late 2016 to early 2017.

Aims. We determine the rigidity dependence of recurrent Forbush decrease (RFD) amplitudes induced by CIRs for different particles with a focus on charge sign.

Methods. We carried out a frequency analysis using a Lomb-Scargle algorithm and superposed epoch analysis for all particles. For protons and helium, we compared the results with a single Forbush decrease (FD) analysis.

Results. Our results reveal that the rigidity dependence of proton amplitudes attributed to the northern coronal hole is in qualitative agreement with previous findings. In contrast, the amplitudes attributed to the southern coronal hole show no rigidity dependence. Furthermore, the amplitude of the helium modulation exceeds that of protons, in line with the observation for long-term modulation. For positrons, statistical limitations stand in the way of any definitive conclusions. In comparison to the positively charged particles, the modulation behavior of electrons reveals a different pattern. **2016.09-2017.01, 2016.11.17-12.13**

Modeling Irregularities in Solar Flux Ropes

E. **Romashets**, M. Vandas

Solar Physics, May **2013**, Volume 284, Issue 1, pp 235-243

To model irregularities in the magnetic structure of solar flux ropes or in interplanetary magnetic clouds, we propose the following approach. A local irregularity in the form of a compact toroid is added into a cylindrical linear force-free magnetic structure. The radius of the cylinder and the small radius of the toroid are the same, since the force-free parameter α is constant, that is, we have in total a linear force-free configuration, too. Meanwhile, the large radius of the toroid can be smaller. The effect of such modeling depends on the aspect ratio of the compact toroid, its location and orientation, and on its magnetic field magnitude in comparison with that of the cylinder.

Near-Sun In Situ and Remote-sensing Observations of a Coronal Mass Ejection and its Effect on the Heliospheric Current Sheet

O. M. **Romeo**^{1,2}, C. R. Braga³, S. T. Badman⁴, D. E. Larson¹, M. L. Stevens⁴, J. Huang¹

2023 ApJ 954 168

<https://iopscience.iop.org/article/10.3847/1538-4357/ace62e/pdf>

During the thirteenth encounter of the Parker Solar Probe (PSP) mission, the spacecraft traveled through a topologically complex interplanetary coronal mass ejection (ICME) beginning on **2022 September 5**. PSP traversed through the flank and wake of the ICME while observing the event for nearly two days. The Solar Probe ANalyzer and FIELDS instruments collected in situ measurements of the plasma particles and magnetic field at ~ 13.3 RS from the Sun. We observe classical ICME signatures, such as a fast-forward shock, bidirectional electrons, low proton temperatures, low plasma β , and high alpha particle to proton number density ratios. In addition, PSP traveled through two magnetic

inversion lines, a magnetic reconnection exhaust, and multiple sub-Alfvénic regions. We compare these in situ measurements to remote-sensing observations from the Wide-field Imager for Solar PRobe Plus instrument on board PSP and the Sun Earth Connection Coronal and Heliospheric Investigation on the Solar Terrestrial Relations Observatory. Based on white-light coronagraphs, two CMEs are forward modeled to best fit the extent of the event. Furthermore, Air Force Data Assimilative Flux Transport magnetograms modeled from Global Oscillation Network Group magnetograms and Potential Field Source Surface modeling portray a global reconfiguration of the heliospheric current sheet (HCS) after the CME event, suggesting that these eruptions play a significant role in the evolution of the HCS. **5-7 Sep 2022**

A Semi-empirical Approach to the Dynamic Coupling of CMEs and Solar Wind

P. **Romero-Corona**^{1,2,3}, J. J. **González-Avilés**^{1,2,3}, and P. **Riley**⁴

2022 ApJ 937 24

<https://iopscience.iop.org/article/10.3847/1538-4357/ac8b03/pdf>

Coronal mass ejections (CMEs) are one of the most relevant phenomena for space weather. Moreover, CMEs can negatively affect essential services and facilities. Therefore, to protect society, we require well-grounded knowledge of the physics that governs the propagation of CMEs from near the Sun to the orbit of Earth. In this work, we deduce expressions to approximate the main forces that affect the dynamic coupling between CMEs and the surrounding solar wind. Therefore, we explore the CME–solar wind dynamic coupling from a magnetohydrodynamic perspective, which, combined with a few reasonable assumptions, allows us to obtain expressions for the thermal and magnetic pressure forces, viscous and dynamic drag, and gravity. We simultaneously use our expressions to compute the trajectories of 34 Earth-directed CMEs. Our results, which are compared with in situ data, show significant quantitative consistency; our synthetic transits closely mimic their in situ observed counterparts. We conclude from our results that magnetic, thermal, and dynamic drag significantly surpass the other forces such as dynamic agents of CMEs in the interplanetary medium. In addition, we find that the initial relative speed of CMEs and solar wind is a determinant factor for the dynamic behavior of CMEs. In other words, subsonic CMEs are initially mostly affected by magnetic and thermal pressure forces, whereas super-magnetosonic CMEs are initially governed by inertial drag. **2000.06.06, 2004-12-03, 2013-07-09**
Table 1 Study Cases and the General Results from Our Analysis **1997-2018**

Detection of Solar Wind Disturbances: Mexican Array Radio Telescope IPS Observations at 140 MHz

E. **Romero-Hernandez**, J. A. **Gonzalez-Esparza**, E. **Aguilar-Rodriguez**, V. **Ontiveros-Hernandez**, P. **Villanueva-Hernandez**

Solar Phys. Volume 290, Issue 9, pp 2553-2566 **2015**

The interplanetary scintillation (IPS) technique is a remote-sensing method for monitoring solar-wind perturbations. The Mexican Array Radio Telescope (MEXART) is a single-station instrument operating at 140 MHz, fully dedicated to performing solar-wind studies employing the IPS technique. We report MEXART solar-wind measurements (scintillation indices and solar-wind velocities) using data obtained during the 2013 and 2014 campaigns. These solar-wind measurements were calculated employing a new methodology based on the wavelet transform (WT) function. We report the variation of the scintillation indices versus the heliocentric distance for two IPS sources (3C48 and 3C147). We found different average conditions of the solar-wind density fluctuations in 2013 and 2014. We used the fittings of the radial dependence of the scintillation index to calculate g-indices. Based on the g-index value, we identified 17 events that could be associated with strong compression regions in the solar wind. We present the first ICME identifications in our data. We associated 14 IPS events with preceding CME counterparts by employing white-light observations from the Large Angle and Spectrometric Coronagraph (LASCO) onboard the Solar and Heliospheric Observatory (SOHO) spacecraft. We found that most of the IPS events, detected during the solar maximum of Cycle 24 were associated with complex CME events. For the IPS events associated with single CME counterparts, we found a deceleration tendency of the CMEs as they propagate in the interplanetary medium. These results show that the instrument detects solar-wind disturbances, and the WT methodology provides solar-wind information with good accuracy. The MEXART observations will complement solar-wind IPS studies using other frequencies, and the tracking of solar-wind disturbances by other stations located at different longitudes. **23 May 2013, 22-25 July 2014**

Table List of CME–IPS events (2013-2014)

First light observations of the solar wind in the outer corona with the Metis coronagraph

M. **Romoli** (1 and 2), **E. Antonucci** (3), **V. Andretta** (3), **G.E. Capuano** (4 and 5), **V. Da Deppo** (6)

A&A **2021**

<https://arxiv.org/pdf/2106.13344.pdf>

The investigation of the wind in the solar corona initiated with the observations of the resonantly scattered UV emission of the coronal plasma obtained with UVCS-SOHO, designed to measure the wind outflow speed by applying the Doppler dimming diagnostics. Metis on Solar Orbiter complements the UVCS spectroscopic observations, performed during solar activity cycle 23, by simultaneously imaging the polarized visible light and the HI Ly-alpha corona in order to obtain high-spatial and temporal resolution maps of the outward velocity of the continuously expanding solar atmosphere. The Metis observations, on **May 15, 2020**, provide the first HI Ly-alpha images of the extended corona and the first instantaneous map of the speed of the coronal plasma outflows during the minimum of solar activity and allow us to identify the layer where the slow wind flow is observed. The polarized visible light (580-640 nm), and the UV HI Ly-alpha (121.6 nm) coronal emissions, obtained with the two Metis channels, are combined in order to measure the dimming of the UV emission relative to a static corona. This effect is caused by the outward motion of the coronal plasma along the direction of incidence of the chromospheric photons on the coronal neutral hydrogen. The plasma outflow velocity is then derived as a function of the measured Doppler dimming. The static corona UV emission is simulated on the basis of the plasma electron density inferred from the polarized visible light. This study leads to the identification, in the velocity maps of the solar corona, of the high-density layer about +/-10 deg wide, centered on the extension of a quiet equatorial streamer present at the East limb where the slowest wind flows at about (160 +/- 18) km/s from 4 Rs to 6 Rs. Beyond the boundaries of the high-density layer, the wind velocity rapidly increases, marking the transition between slow and fast wind in the corona.

Extended Drag-Based Model for better predicting the evolution of Coronal Mass Ejections

Mattia **Rossi**, [Sabrina Guastavino](#), [Michele Piana](#), [Anna Maria Massone](#)

2024

<https://arxiv.org/pdf/2409.03281>

The solar wind drag-based model is a widely used framework for predicting the propagation of Coronal Mass Ejections (CMEs) through interplanetary space. This model primarily considers the aerodynamic drag exerted by the solar wind on CMEs. However, factors like magnetic forces, pressure gradients, and the internal dynamics within CMEs justify the need of introducing an additional small-scale acceleration term in the game. Indeed, by accounting for this extra acceleration, the extended drag-based model is shown to offer improved accuracy in describing the evolution of CMEs through the heliosphere and, in turn, in forecasting CME trajectories and arrival times at Earth. This enhancement is crucial for better predicting Space Weather events and mitigating their potential impacts on space-based and terrestrial technologies.

Modeling the Early Evolution of a Slow Coronal Mass Ejection Imaged by the Parker Solar Probe

Alexis P. **Rouillard**, [Nicolas Poirier](#), [Michael Lavarra](#), [Antony Bourdelle](#), [Kévin Dalmasse](#), [Athanasios Kouloumvakos](#), [Angelos Vourlidas](#), [Valbona Kunkel](#), [Phillip Hess](#), [Russ A. Howard](#), [Guillermo Stenborg](#), [Nour E. Raouafi](#)

ApJS **2020**

<https://arxiv.org/pdf/2002.08756.pdf>

During its first solar encounter, the Parker Solar Probe (PSP) acquired unprecedented up-close imaging of a small Coronal Mass Ejection (CME) propagating in the forming slow solar wind. The CME originated as a cavity imaged in extreme ultraviolet that moved very slowly (<50 km/s) to the 3-5 solar radii (R_{\odot}) where it then accelerated to supersonic speeds. We present a new model of an erupting Flux Rope (FR) that computes the forces acting on its expansion with a computation of its internal magnetic field in three dimensions. The latter is accomplished by solving the Grad-Shafranov equation inside two-dimensional cross sections of the FR. We use this model to interpret the kinematic evolution and morphology of the CME imaged by PSP. We investigate the relative role of toroidal forces, momentum coupling, and buoyancy for different assumptions on the initial properties of the CME. The best agreement between the dynamic evolution of the observed and simulated FR is obtained by modeling the two-phase eruption process as the result of two episodes of poloidal flux injection. Each episode, possibly induced by magnetic reconnection, boosted the toroidal forces accelerating the FR out of the corona. We also find that the drag induced by the accelerating solar wind could account for about half of the acceleration experienced by the FR. We use the model to interpret the presence of a small dark cavity, clearly imaged by PSP deep inside the CME, as a low-density region dominated by its strong axial magnetic fields. **2018 November 1-3**

Relating streamer flows to density and magnetic structures at the Parker Solar Probe

Alexis P. **Rouillard**, [Athanasios Kouloumvakos](#), [Angelos Vourlidas](#), [Justin Kasper](#), [Stuart Bale](#), [Nour-Edine Raouafi](#), ...

ApJ **2020**

<https://arxiv.org/pdf/2001.01993.pdf>

The physical mechanisms that produce the slow solar wind are still highly debated. Parker Solar Probe's (PSP's) second solar encounter provided a new opportunity to relate in situ measurements of the nascent slow solar wind with white-light images of streamer flows. We exploit data taken by the Solar and Heliospheric Observatory (SOHO), the Solar TERrestrial RELations Observatory (STEREO) and the Wide Imager on Solar Probe to reveal for the first time a close link between imaged streamer flows and the high-density plasma measured by the Solar Wind Electrons Alphas and Protons (SWEAP) experiment. We identify different types of slow winds measured by PSP that we relate to the spacecraft's magnetic connectivity (or not) to streamer flows. SWEAP measured high-density and highly variable plasma when PSP was well connected to streamers but more tenuous wind with much weaker density variations when it exited streamer flows. STEREO imaging of the release and propagation of small transients from the Sun to PSP reveals that the spacecraft was continually impacted by the southern edge of streamer transients. The impact of specific density structures is marked by a higher occurrence of magnetic field reversals measured by the FIELDS magnetometers. Magnetic reversals originating from the streamers are associated with larger density variations compared with reversals originating outside streamers. We tentatively interpret these findings in terms of magnetic reconnection between open magnetic fields and coronal loops with different properties, providing support for the formation of a subset of the slow wind by magnetic reconnection. **2019 March 30 - April 10**

A propagation tool to connect remote-sensing observations with in-situ measurements of heliospheric structures

A.P. **Rouillard**, B. Lavraud, V. Genot, M. Bouchemit, N. Dufourg, I. Plotnikov, R.F. Pinto, E. Sanchez-Diaz, M. Lavarra, M. Penou, C. Jacquy, N. Andre, S. Caussarieu, J.-P. Toniutti, D. Popescu, E. Buchlin, S. Caminade, P. Alingery, J.A. Davies, D. Odstrcil, L. Mays
Planetary and Space Science **2017**

<https://arxiv.org/pdf/1702.00399v1.pdf>

The remoteness of the Sun and the harsh conditions prevailing in the solar corona have so far limited the observational data used in the study of solar physics to remote-sensing observations taken either from the ground or from space. In contrast, the 'solar wind laboratory' is directly measured in situ by a fleet of spacecraft measuring the properties of the plasma and magnetic fields at specific points in space. Since 2007, the solar-terrestrial relations observatory (STEREO) has been providing images of the solar wind that flows between the solar corona and spacecraft making in-situ measurements. This has allowed scientists to directly connect processes imaged near the Sun with the subsequent effects measured in the solar wind. This new capability prompted the development of a series of tools and techniques to track heliospheric structures through space. This article presents one of these tools, a web-based interface called the 'Propagation Tool' that offers an integrated research environment to study the evolution of coronal and solar wind structures, such as Coronal Mass Ejections (CMEs), Corotating Interaction Regions (CIRs) and Solar Energetic Particles (SEPs). These structures can be propagated from the Sun outwards to or alternatively inwards from planets and spacecraft situated in the inner and outer heliosphere. In this paper, we present the global architecture of the tool, discuss some of the assumptions made to simulate the evolution of the structures and show how the tool connects to different databases. **2010-04-05, 13 May 2012, 2012-05-17, 2013-06-01**

Relating white light and in situ observations of coronal mass ejections: A review

A.P. **Rouillard**

Journal of Atmospheric and Solar-Terrestrial Physics, Volume 73, Issue 10, **2011**, Pages 1201-1213, **File**

This paper provides a short review of some of the basic concepts related to the observations of coronal mass ejections (CMEs) in white light images and at large distances from the Sun. We review the various ideas which have been put forward to explain the dramatic changes in CME appearance in white light images from the Sun to 1 AU, focusing on results obtained by comparing white light observations of CMEs to the in situ measurements of Interplanetary CMEs (or ICMEs). We start with a list of definitions for the various in situ structures that form an ICME. A few representative examples of the formation of sheath regions and other interaction regions as well as the expansion of magnetic flux ropes are used to illustrate the basic phenomena which induce significant brightness variations during a CME's propagation to 1 AU and beyond. The white light signatures of a number of CMEs observed by the coronagraphs have been successfully simulated numerically by assuming that most of the coronal plasma observed in white light images is located on the surface of a croissant-shaped structure reminiscent of a magnetic flux rope. At large distances from the Sun, white light imagers show that the appearance of CMEs changes dramatically due to the changing position of the CME relative to the Thomson sphere, the expansion of the ejecta and the interaction of the ejecta with the ambient solar wind.

Research Highlights

► Review of white light observations made by STEREO. ► Direct links between white light observations of CMEs and in situ measurements of magnetic flux ropes near 1 AU. ► Discussion of the various types of ejecta observed simultaneously in white light and in situ.

THE SOLAR ORIGIN OF SMALL INTERPLANETARY TRANSIENTS

A. P. [Rouillard](#)^{1,2}, N. R. Sheeley, Jr.³, T. J. Cooper³, J. A. Davies⁴, B. Lavraud^{5,6}, E. K. J. Kilpua⁷, R. M. Skoug⁸, J. T. Steinberg⁸, A. Szabo², A. Opitz^{5,6} and J.-A. Sauvaud

2011 ApJ 734 7, File

In this paper, we present evidence for magnetic transients with small radial extents ranging from 0.025 to 0.118 AU measured in situ by the Solar-Terrestrial Relations Observatory (STEREO) and the near-Earth Advanced Composition Explorer (ACE) and Wind spacecraft. The transients considered in this study are much smaller (<0.12 AU) than the typical sizes of magnetic clouds measured near 1 AU (~ 0.23 AU). They are marked by low plasma beta values, generally lower magnetic field variance, short timescale magnetic field rotations, and are all entrained by high-speed streams by the time they reach 1 AU. We use this entrainment to trace the origin of these small interplanetary transients in coronagraph images. We demonstrate that these magnetic field structures originate as either small or large mass ejecta. The small mass ejecta often appear from the tip of helmet streamers as arch-like structures and other poorly defined white-light features (the so-called blobs). However, we have found a case of a small magnetic transient tracing back to a small and narrow mass ejection erupting from below helmet streamers. Surprisingly, one of the small magnetic structures traces back to a large mass ejection; in this case, we show that the central axis of the coronal mass ejection is along a different latitude and longitude to that of the in situ spacecraft. The small size of the transient is related to the in situ measurements being taken on the edges or periphery of a larger magnetic structure. In the last part of the paper, an ejection with an arch-like aspect is tracked continuously to 1 AU in the STEREO images. The associated in situ signature is not that of a magnetic field rotation but rather of a temporary reversal of the magnetic field direction. Due to its "open-field topology," we speculate that this structure is partly formed near helmet streamers due to reconnection between closed and open magnetic field lines. The implications of these observations for our understanding of the variability of the slow solar wind are discussed.

Solar Wind Structures Seen in Heliospheric Imagers

A. P. [Rouillard](#), N. R. Sheeley, [Russ A. Howard](#), B. Lavraud, J. A. Davies

COSPAR meeting, Bremen, July **2010**, **Presentation**

<http://solphys.nrl.navy.mil/users/howard/cospar-10/>

I'll be presenting results obtained by comparing white-light observations of solar wind structures with their in situ signatures. The results were obtained with the data taken over the last three and half years by new generation of white light imagers onboard the STEREO spacecraft. I'll be first presenting some general features about white light observations and the angular coordinate system used to measure the outward propagation of white light structures as move from the Sun to 1 AU. I will review the basic physical processes which we think are at play when plasma density is increased on the surface of transient ejecta as they propagate to 1 AU. I'll then present the simple techniques used to derive the 3-D trajectory of these white light structures which allow us to relate the white light structures detected along a line of sight to a particular in situ measurements. Finally I will present some recent STEREO results on the formation and nature of the slow solar wind.

Intermittent release of transients in the slow solar wind: 1. Remote sensing observations.

[Rouillard](#), A.P., Davies, J.A., Lavraud, B., Forsyth, R.J., Savani, N.P., Bewsher, D., Brown, D.S., Sheeley, N.R., Davis, C.J., Harrison, R.A., Howard, R.A., Vourlidas, A., Lockwood, M., Crothers, S.R., Eyles, C.J.: **2010**, J. Geophys. Res. 115 A04103. DOI.

White Light and In Situ Comparison of a Forming Merged Interaction Region

A. P. [Rouillard](#), B. Lavraud, N. R. Sheeley, J. A. Davies, L. F., Burlaga, N. P. Savani, C. Jacquy, and R. J. Forsyth

2010 ApJ 719 1385-1392, File

The images taken by the Heliospheric Imager (HI) instruments, part of the *SECCHI* imaging package on board the pair of *STEREO* spacecraft, provide information on the radial and latitudinal evolution of the plasma transported by coronal mass ejections (CMEs). In this case study, a CME, appearing near 15 UT on **2007 November 15** in

SECCHI coronagraph images, leads to the formation of two out-flowing density structures (DSs) in the heliosphere. The analysis of time-elongation maps constructed from images obtained by the HI instruments shows that these DSs were propagating along the Sun–Earth line. A direct comparison of HI images and in situ measurements taken near Earth could therefore be performed. These two DSs are separated by a cavity associated with little brightness variation or equivalently little electron density variation. In situ measurements made in the solar wind near Earth on 2007 November 20 show that this cavity corresponds to a magnetic cloud (MC). While the leading DS is related to the sheath in front of the MC, the second DS is located on the sunward side of the MC where high-speed solar wind from a coronal hole catches up and interacts with the MC. We conclude that HI observes the sub-structures of a merged interaction region (MIR), a region of the interplanetary medium where the total solar wind pressure is greatly enhanced by the interaction of an MC with the ambient solar wind. This MIR caused the largest geomagnetic storm in 2007.

A multispacecraft analysis of a small-scale transient entrained by solar wind streams.

Rouillard, A.P., Savani, N.P., Davies, J.A., Lavraud, B., Forsyth, R.J., Morley, S.K., Opitz, A., Sheeley, N.R., Burlaga, L.F., Sauvaud, J.-A., Simunac, K.D.C., Luhmann, J.G., Galvin, A.B., Crothers, S.R., Davis, C.J., Harrison, R.A., Lockwood, M., Eyles, C.J., Bewsher, D., Brown, D.S.: *Solar Phys.* 256(1–2), 307, **2009**. DOI.

A solar storm observed from the Sun to Venus using the STEREO, Venus Express, and MESSENGER spacecraft

Rouillard, A. P.; Davies, J. A.; Forsyth, R. J.; Savani, N. P.; Sheeley, N. R.; Thernisien, A.; Zhang, T.-L.; Howard, R. A.; Anderson, B.; Carr, C. M.; Tsang, S.; Lockwood, M.; Davis, C. J.; Harrison, R. A.; Bewsher, D.; Fränz, M.; Crothers, S. R.; Eyles, C. J.; Brown, D. S.; Whittaker, I.; Hapgood, M.; Coates, A. J.; Jones, G. H.; Grande, M.; Frahm, R. A.; Winningham, J. D.

J. Geophys. Res., Vol. 114, No. A7, A07106, **2009**

<http://dx.doi.org/10.1029/2008JA014034>

The suite of SECCHI optical imaging instruments on the STEREO-A spacecraft is used to track a solar storm, consisting of several coronal mass ejections (CMEs) and other coronal loops, as it propagates from the Sun into the heliosphere during May 2007. The 3-D propagation path of the largest interplanetary CME (ICME) is determined from the observations made by the SECCHI Heliospheric Imager (HI) on STEREO-A (HI-1/2A). Two parts of the CME are tracked through the SECCHI images, a bright loop and a V-shaped feature located at the rear of the event. We show that these two structures could be the result of line-of-sight integration of the light scattered by electrons located on a single flux rope. In addition to being imaged by HI, the CME is observed simultaneously by the plasma and magnetic field experiments on the Venus Express and MESSENGER spacecraft. The imaged loop and V-shaped structure bound, as expected, the flux rope observed in situ. The SECCHI images reveal that the leading loop-like structure propagated faster than the V-shaped structure, and a decrease in in situ CME speed occurred during the passage of the flux rope. We interpret this as the result of the continuous radial expansion of the flux rope as it progressed outward through the interplanetary medium. An expansion speed in the radial direction of $\sim 30 \text{ km s}^{-1}$ is obtained directly from the SECCHI-HI images and is in agreement with the difference in speed of the two structures observed in situ. This paper shows that the flux rope location can be determined from white light images, which could have important space weather applications.

Eruptive events in the solar atmosphere: new insights from theory and 3-D numerical modelling

Ilia I. **Roussev**

2008, *J. Contemp. Phys.*, 49, 237

Ejections of magnetised plasma from the Sun, commonly known as coronal mass ejections (CMEs), are one of the most stunning manifestations of solar activity. These ejections play a leading role in the Sun–Earth connection, because of their large-scale, energetics and direct impact on the space environment near the Earth. As CMEs evolve in the solar corona and interplanetary space they drive shock waves, which act as powerful accelerators of charged particles in the inner solar system. Some of these particles, known as solar energetic particles (SEPs), can strike our planet, and in doing so they

can disrupt satellites and knock out power systems on the ground, among other effects. These particles, along with the intensive X-ray radiation from solar flares, also endanger human life in outer space. That is why it is important for space scientists to understand and predict the ever changing environmental conditions in outer space due to solar eruptive events - the so-called space weather. To enable the development of accurate space weather forecast, in the past three decades solar scientists have been challenged to provide an improved understanding of the physical causes of the CME phenomenon and its numerous effects. **This paper summarises the most recent advances from theory and modelling in understanding the origin and evolution of solar eruptive events and related phenomena.**

The Growth of Ring Current/SYM-H Under Northward IMF Bz Conditions Present During the 21–22 January 2005 Geomagnetic Storm

Diptiranjana [Rout](#), [S. Patra](#), [S. Kumar](#), [D. Chakrabarty](#), [G. D. Reeves](#), [C. Stolle](#), [K. Pandey](#), [S. Chakraborty](#), [E. A. Spencer](#)

Space Weather [Volume 21, Issue 10](#) e2023SW003489 **2023**

<https://agupubs.onlinelibrary.wiley.com/doi/epdf/10.1029/2023SW003489>

The total energy transfer from the solar wind to the magnetosphere is governed by the reconnection rate at the magnetosphere edges as the Z-component of interplanetary magnetic field (IMF Bz) turns southward. The geomagnetic storm on **21–22 January 2005** is considered to be anomalous as the SYM-H index that signifies the strength of ring current, decreases and had a sustained trough value of -101 nT lasting more than 6 hr under northward IMF Bz conditions. In this work, the standard WINDMI model is utilized to estimate the growth and decay of magnetospheric currents by using several solar wind-magnetosphere coupling functions. However, it is found that the WINDMI model driven by any of these coupling functions is not fully able to explain the decrease of SYM-H under northward IMF Bz. A dense plasma sheet along with signatures of a highly stretched magnetosphere was observed during this storm. The SYM-H variations during the entire duration of the storm were only reproduced after modifying the WINDMI model to account for the effects of the dense plasma sheet. The limitations of directly driven models relying purely on the solar wind parameters and not accounting for the state of the magnetosphere are highlighted by this work.

The Origin of Extremely Nonradial Solar Wind Outflows

Diptiranjana [Rout](#)¹, Janardhan P.², Fujiki K.³, Chakrabarty D.⁴, and Bisoi S. K.⁵

2023 ApJ 950 1

<https://iopscience.iop.org/article/10.3847/1538-4357/acd000/pdf>

The origin of nonradial solar wind flows and their effect on space weather are poorly understood. Here we present a detailed investigation of 12 nonradial solar wind events during solar cycles 23–24, covering the period 1995–2017. In all these events the azimuthal flow angles of the solar wind exceed 6° as measured at the L1 Lagrangian point of the Sun–Earth system, for periods of 24 hr. In addition, all the events were selected during periods when coronal mass ejections (CMEs) and/or corotating interaction regions (CIRs) were absent. For most of the events, the near-Earth solar wind density was <5 cm $^{-3}$ for periods exceeding 24 hr, similar to the well-known "solar wind disappearance events" wherein near-Earth solar wind densities dropped by two orders of magnitude for periods exceeding 24 hr. The solar source regions determined for all the cases were found to be associated with active region–coronal hole (AR–CH) pairs located around the central meridian. Further, the dynamical evolution of the source regions, studied using both the Extreme-ultraviolet Imaging Telescope and the Michelson Doppler Imager, showed a clear reduction in the CH area accompanied by the emergence of new magnetic flux regions. This dynamic evolution in the AR–CH source regions eventually disturbed the stable CH configurations, thereby giving rise to the extremely nonradial solar wind outflows. We discuss, based on our results, a possible causative mechanism for the origin of these highly nonradial flows that were not associated with either CMEs or CIRs. **1999 May 5–6, 10–12, 2000 March 22–24, 27–30; 2004 February 13–14, 15–18, Table 1** Details of Extremely Nonradial Flow Events 1998–2011

Solar wind flow angle and geo-effectiveness of corotating interaction regions: First results

Diptiranjana [Rout](#)¹, [D. Chakrabarty](#)¹, [P. Janardhan](#)¹, [R. Sekar](#)¹, [Vrunda](#)

[Maniyal](#), [Kuldeep Pandey](#)¹

Geophys. Res. Lett., **2017**

[https://onlinelibrary.wiley.com/sci-](https://onlinelibrary.wiley.com/sci-hub/doi/10.1002/2017GL073038/abstract;jsessionid=81CDFA9E47491A9DB3F194AB19EA9F36.f04t01)

[hub.cc/doi/10.1002/2017GL073038/abstract;jsessionid=81CDFA9E47491A9DB3F194AB19EA9F36.f04t01](https://onlinelibrary.wiley.com/sci-hub/doi/10.1002/2017GL073038/abstract;jsessionid=81CDFA9E47491A9DB3F194AB19EA9F36.f04t01)

A total of 43 CIR-induced geomagnetic storms during the unusually deep solar minimum of solar cycle 23 (2006-2010) were identified using a superposed epoch analysis technique. Of these 43 events, a detailed cross spectrum analyses, between the variations in the Z-component of the interplanetary magnetic field (IMF Bz) and the equatorial electrojet (EEJ) strength, were performed for 22 events when the daytime EEJ strengths from Jicamarca were available. The analyses revealed that the ~30 and ~60 min periodic components in IMF Bz were causally related to the EEJ strength subject to the average solar wind flow being radial to within 6° at L1 during the interval for which EEJ strengths were considered. This investigation elicits the important role of average solar wind azimuthal flow angle in determining the geo-effectiveness of CIR events. **Table 1.**

A Time-Efficient, Data Driven Modelling Approach To Predict The Geomagnetic Impact of Coronal Mass Ejections

Souvik **Roy**, [Dibyendu Nandy](#)

2023 *ApJL* **950** L11

<https://arxiv.org/pdf/2210.00071.pdf>

<https://iopscience.iop.org/article/10.3847/2041-8213/acd77c/pdf>

To understand the global-scale physical processes behind coronal mass ejection (CME)–driven geomagnetic storms and predict their intensity as a space weather forecasting measure, we develop an interplanetary CME flux rope–magnetosphere interaction module using 3D magnetohydrodynamics. The simulations adequately describe CME-forced dynamics of the magnetosphere including the imposed magnetotail torsion. These interactions also result in induced currents, which are used to calculate the geomagnetic perturbation. Through a suitable calibration, we estimate a proxy of geoeffectiveness—the Storm Intensity index (STORMI)—that compares well with the Dst/ SYM-H index. Simulated impacts of two contrasting CMEs quantified by the STORMI index exhibit a high linear correlation with the corresponding Dst and SYM-H indices. Our approach is relatively simple, has fewer parameters to be fine-tuned, and is time efficient compared to complex fluid-kinetic methods. Furthermore, we demonstrate that flux rope erosion does not significantly affect our results. Thus our method has the potential to significantly extend the time window for predictability—an outstanding challenge in geospace environment forecasting—if early predictions of near-Earth CME flux rope structures based on near-Sun observations are available as inputs. This study paves the way for early warnings based on operational predictions of CME-driven geomagnetic storms. **20 Nov 2003, 13-14 Apr 2006**

Planar Magnetic Structures Downstream of Coronal Mass Ejection–driven Shocks in the Inner Heliosphere

Mengsi **Ruan**^{1,2}, Pingbing Zuo^{1,2}, Xueshang Feng^{1,2}, Qi Xu^{1,2}, Zilu Zhou³, Jiayun Wei^{1,2}, Chaowei Jiang^{1,2}, Yi Wang^{1,2}, Xiaojun Xu³, and Zhenning Shen³

2023 *ApJ* **951** 47

<https://iopscience.iop.org/article/10.3847/1538-4357/acd245/pdf>

Planar magnetic structures (PMSs), characterized by interplanetary magnetic field vectors remaining parallel to a specific plane, are commonly observed in the solar wind, especially in the sheath region of interplanetary coronal mass ejections (ICMEs). In this study, PMS events in the 2 hr regions downstream of ICME-driven shocks were investigated to reveal the relationship between PMS formation and shock environment using data collected by the Parker Solar Probe, Solar Orbiter, and Venus Express spacecraft in the inner heliosphere. PMS events are identified in the majority (around 93%) of the postshock 2 hr regions, with transit times ranging from 10 to 120 minutes, which demonstrates their common occurrence associated with ICME-driven shocks. About 33% of the detected PMS events cover the whole 2 hr intervals, called full PMS events. Most of the full PMS events are observed in the downstream region of quasi-perpendicular shocks. In addition, statistical results show that full PMS events occurring in the downstream region of quasi-perpendicular shocks are generally associated with higher magnetic compression ratios, which implies that full PMS events are more likely to be formed in the downstream region of strong quasi-perpendicular shocks. **2019 March 15, 2020 August 21**

Table 1 List of the Investigated 55 Interplanetary Shocks and the Information of the Identified Planar Magnetic Structures 2006-2022

Understanding the effects of spacecraft trajectories through solar coronal mass ejection flux ropes using 3DCOREweb

Hannah Theresa **Rüdiger**, [Andreas Jeffrey Weiss](#), [Justin Le Louëdec](#), [Ute V. Amerstorfer](#), [Christian Möstl](#), [Emma E. Davies](#), [Helmut Lammer](#)

ApJ **973** 150 **2024**

<https://arxiv.org/pdf/2405.03271>

<https://iopscience.iop.org/article/10.3847/1538-4357/ad660a/pdf>

This study investigates the impact of spacecraft positioning and trajectory on in situ signatures of coronal mass ejections (CMEs). Employing the 3DCORE model, a 3D flux rope model that can generate in situ profiles for any given point in space and time, we conduct forward modeling to analyze such signatures for various latitudinal and longitudinal positions, with respect to the flux rope apex, at 0.8au. Using this approach, we explore the appearance of the resulting in situ profiles for different flux rope types, with different handedness and inclination angles, for both high and low twist CMEs. Our findings reveal that even high twist CMEs exhibit distinct differences in signatures between apex hits and flank encounters, with the latter displaying stretched-out profiles with reduced rotation. Notably, constant, non-rotating in situ signatures are only observed for flank encounters of low twist CMEs, suggesting implications for the magnetic field structure within CME legs. Additionally, our study confirms the unambiguous appearance of different flux rope types in in situ signatures, contributing to the broader understanding and interpretation of observational data. Given the model assumptions, this may refute trajectory effects to be the cause for mismatching flux rope types as identified in solar signatures. While acknowledging limitations inherent in our model, such as the assumption of constant twist and non-deformable torus-like shape, we still draw relevant conclusions within the context of global magnetic field structures of CMEs and the potential for distinguishing flux rope types based on in situ observations.

Automatic Detection of Interplanetary Coronal Mass Ejections in Solar Wind In Situ Data

Hannah T. Rüdiger, [Andreas Windisch](#), [Ute V. Amerstorfer](#), [Christian Möstl](#), [Tanja Amerstorfer](#), [Rachel L. Bailey](#), [Martin A. Reiss](#)

Space Weather e2022SW003149 [Volume20, Issue10](#) 2022

<https://arxiv.org/pdf/2205.03578.pdf>

<https://doi.org/10.1029/2022SW003149>

<https://agupubs.onlinelibrary.wiley.com/doi/epdf/10.1029/2022SW003149>

Interplanetary coronal mass ejections (ICMEs) are one of the main drivers for space weather disturbances. In the past, different approaches have been used to automatically detect events in existing time series resulting from solar wind in situ observations. However, accurate and fast detection still remains a challenge when facing the large amount of data from different instruments. For the automatic detection of ICMEs we propose a pipeline using a method that has recently proven successful in medical image segmentation. Comparing it to an existing method, we find that while achieving similar results, our model outperforms the baseline regarding training time by a factor of approximately 20, thus making it more applicable for other datasets. The method has been tested on in situ data from the Wind spacecraft between 1997 and 2015 with a True Skill Statistic (TSS) of 0.64. Out of the 640 ICMEs, 466 were detected correctly by our algorithm, producing a total of 254 False Positives. Additionally, it produced reasonable results on datasets with fewer features and smaller training sets from Wind, STEREO-A and STEREO-B with True Skill Statistics of 0.56, 0.57 and 0.53, respectively. Our pipeline manages to find the start of an ICME with a mean absolute error (MAE) of around 2 hours and 56 minutes, and the end time with a MAE of 3 hours and 20 minutes. The relatively fast training allows straightforward tuning of hyperparameters and could therefore easily be used to detect other structures and phenomena in solar wind data, such as corotating interaction regions. **2 Jan 2009, 29 Mar 2011, 5 Oct 2011, 26 Jan 2012, 8 Jun 2012, 13 Nov 2012**

Statistical study of magnetic cloud erosion by magnetic reconnection†

A. [Ruffenach](#)^{1,2,*}, B. Lavraud^{1,2}, C. J. Farrugia³, P. Démoulin⁴, S. Dasso^{5,6}, M. J. Owens⁷, J.-A.

Sauvaud^{1,2}, A. P. Rouillard^{1,2}, A. Lynnyk^{1,2}, C. Foullon⁸, N. P. Savani^{9,10}, J. G. Luhmann¹¹ and A. B. Galvin

JGR Volume 120, Issue 1, pages 43–60, 2015

<http://onlinelibrary.wiley.com/doi/10.1002/2014JA020628/pdf>

Several recent studies suggest that magnetic reconnection is able to erode substantial amounts of the outer magnetic flux of interplanetary magnetic clouds (MCs) as they propagate in the heliosphere. We quantify and provide a broader context to this process, starting from 263 tabulated interplanetary coronal mass ejections (ICMEs), including MCs, observed over a time period covering 17 years and at a distance of 1 AU from the Sun with Wind (1995-2008) and the two STEREO (2009-2012) spacecraft. Based on several quality factors, including careful determination of the MC boundaries and main magnetic flux rope axes, an analysis of the azimuthal flux imbalance expected from erosion by magnetic reconnection was performed on a subset of 50 MCs. The results suggest that MCs may be eroded at the front or at rear and in similar proportions, with a significant average erosion of about 40 % of the total azimuthal magnetic flux. We also searched for in situ signatures of magnetic reconnection causing erosion at the front and rear boundaries of these MCs. Nearly ~30 % of the selected MC boundaries show reconnection signatures. Given that observations were

acquired only at 1 AU and that MCs are large-scale structures, this finding is also consistent with the idea that erosion is a common process. Finally, we studied potential correlations between the amount of eroded azimuthal magnetic flux and various parameters such as local magnetic shear, Alfvén speed, and leading and trailing ambient solar wind speeds. However, no significant correlations were found, suggesting that the locally observed parameters at 1 AU are not likely to be representative of the conditions that prevailed during the erosion which occurred during propagation from the Sun to 1 AU. Future heliospheric missions, and in particular Solar Orbiter or Solar Probe Plus, will be fully geared to answer such questions.

Multispacecraft observation of magnetic cloud erosion by magnetic reconnection during propagation

Ruffenach, A.; Lavraud, B.; Owens, M. J.; Sauvaud, J.-A.; Savani, N. P.; Rouillard, A. P.; Demoulin, P.; Foullon, C.; Opitz, A.; Fedorov, A.; Jacquy, C. J.; GИnot, V.; Louarn, P.; Luhmann, J. G.; Russell, C. T.; Farrugia, C. J.; Galvin, A. B.

J. Geophys. Res., Vol. 117, No. A9, A09101, **2012**

<http://dx.doi.org/10.1029/2012JA017624>

During propagation, Magnetic Clouds (MC) interact with their environment and, in particular, may reconnect with the solar wind around it, eroding away part of its initial magnetic flux. Here we quantitatively analyze such an interaction using combined, multipoint observations of the same MC flux rope by STEREO A, B, ACE, WIND and THEMIS on **November 19–20, 2007**. Observation of azimuthal magnetic flux imbalance inside a MC flux rope has been argued to stem from erosion due to magnetic reconnection at its front boundary. The present study adds to such analysis a large set of signatures expected from this erosion process. (1) Comparison of azimuthal flux imbalance for the same MC at widely separated points precludes the crossing of the MC leg as a source of bias in flux imbalance estimates. (2) The use of different methods, associated errors and parametric analyses show that only an unexpectedly large error in MC axis orientation could explain the azimuthal flux imbalance. (3) Reconnection signatures are observed at the MC front at all spacecraft, consistent with an ongoing erosion process. (4) Signatures in suprathermal electrons suggest that the trailing part of the MC has a different large-scale magnetic topology, as expected. The azimuthal magnetic flux erosion estimated at ACE and STEREO A corresponds respectively to 44% and 49% of the inferred initial azimuthal magnetic flux before MC erosion upon propagation. The corresponding average reconnection rate during transit is estimated to be in the range 0.12–0.22 mV/m, suggesting most of the erosion occurs in the inner parts of the heliosphere. Future studies ought to quantify the influence of such an erosion process on geo-effectiveness.

Small-scale flux ropes in ICME sheaths

J. **Ruohotie**, **E. K. J. Kilpua**, **S. W. Good**, **M. Ala-Lahti**

Frontiers in Astronomy and Space Sciences 9: 943247. **2022**

<https://arxiv.org/pdf/2208.07662.pdf>

<https://www.frontiersin.org/articles/10.3389/fspas.2022.943247/pdf>

Sheath regions of interplanetary coronal mass ejections (ICMEs) are formed when the upstream solar wind is deflected and compressed due to the propagation and expansion of the ICME. Small-scale flux ropes found in the solar wind can thus be swept into ICME-driven sheath regions. They may also be generated locally within the sheaths through a range of processes. This work applies wavelet analysis to obtain the normalized reduced magnetic helicity, normalized cross helicity, and normalized residual energy, and uses them to identify small-scale flux ropes and Alfvén waves in 55 ICME-driven sheath regions observed by the Wind spacecraft in the near-Earth solar wind. Their occurrence is investigated separately for three different frequency ranges between 10–2–10–4 Hz. We find that small scale flux ropes are more common in ICME sheaths than in the upstream wind, implying that they are at least to some extent actively generated in the sheath and not just compressed from the upstream wind. Alfvén waves occur more evenly in the upstream wind and in the sheath. This study also reveals that while the highest frequency (smallest scale) flux ropes occur relatively evenly across the sheath, the lower frequency (largest scale) flux ropes peak near the ICME leading edge. This suggests that they could have different physical origins, and that processes near the ICME leading edge are important for generating the larger scale population. **July 14–15, 2012, September 12, 2014**

Comment on: “Origin and Characteristics of the Southward Component of the Interplanetary Magnetic Field” by G. Verbanac and M. Bandić

Christopher T. Russell,

[Solar Physics](#) volume 297, Article number: 119 (2022)

<https://doi.org/10.1007/s11207-022-02043-z>

THE VERY UNUSUAL INTERPLANETARY CORONAL MASS EJECTION OF 2012 JULY 23: A BLAST WAVE MEDIATED BY SOLAR ENERGETIC PARTICLES

C. T. Russell¹, R. A. Mewaldt², J. G. Luhmann³, G. M. Mason⁴, T. T. von Rosenvinge⁵, C. M. S. Cohen², R. A. Leske², R. Gomez-Herrero⁶, A. Klassen⁷, A. B. Galvin⁸, and K. D. C. Simunac

2013 ApJ 770 38; **File**

The giant, superfast, interplanetary coronal mass ejection, detected by STEREO A on **2012 July 23**, well away from Earth, appears to have reached 1 AU with an unusual set of leading bow waves resembling in some ways a subsonic interaction, possibly due to the high pressures present in the very energetic particles produced in this event. Eventually, a front of record high-speed flow reached STEREO. The unusual behavior of this event is illustrated using the magnetic field, plasma, and energetic ion observations obtained by STEREO. Had the Earth been at the location of STEREO, the large southward-oriented magnetic field component in the event, combined with its high speed, would have produced a record storm.

Flows and obstacles in the solar wind

C.T. Russell and L. Jian

[Advances in Space Research](#), Volume 41, Issue 8, 2008, Pages 1177-1187

Understanding the physics of the various disturbances in the solar wind is critical to successful forecasts of space weather. The STEREO mission promises to bring us new and deeper understanding of these disturbances. As we stand on the threshold of the first results from this mission, it is appropriate to review what we know about solar wind disturbances. Because of their complementary nature we discuss both the disturbances that arise within the solar wind due to the stream structure and coronal mass ejecta and the disturbances that arise when the solar wind collides with planetary obstacles, such as magnetospheres.

Semiannual Variation of Geomagnetic Activity

C.T. RUSSELL AND R. L. MCPHERRON

J. Geophys. Res., 78(1), page 92-108, 1973.

<http://www-ssc.igpp.ucla.edu/personnel/russell/papers/40/>

<https://doi.org/10.1029/JA078i001p00092>

<https://sci-hub.ru/10.1029/JA078i001p00092>

The semiannual variation in geomagnetic activity is well established in geomagnetic data. Its explanation has remained elusive, however. We propose, simply, that it is caused by a semiannual variation in the effective southward component of the interplanetary field. The southward field arises because the interplanetary field is ordered in the solar equatorial coordinate system, whereas the interaction with the magnetosphere is controlled by a magnetospheric system. Several simple models utilizing this effective modulation of the southward component of the interplanetary field are examined. One of these closely predicts the observed phase and amplitude of the semiannual variation. This model assumes that northward interplanetary fields are noninteracting and that the interaction with southward fields is ordered in solar magnetospheric coordinates. The prediction of the diurnal variation of the strength of the interaction at the magnetopause by this model, does not, however, match the diurnal -variation of geomagnetic activity as derived from ground-based data. However, predictions of the dependence of geomagnetic activity on the polarity of the interplanetary magnetic field and a 22-year cycle in geomagnetic activity are confined by studies of ground-based data. It appears that the mechanism controlling the semiannual variation of geomagnetic activity has been identified but that a quantitative model must await further refinements in our knowledge of the solar wind-magnetosphere coupling.

H-alpha features with hot onsets III. Fibrils in Lyman-alpha and with ALMA

Robert J. Rutten

A&A 2016

<http://arxiv.org/pdf/1609.01122v1.pdf>

In H-alpha most of the solar surface is covered by a dense canopy of long opaque fibrils, but predictions for quiet-Sun observations with ALMA have ignored this fact. Comparison with Ly-alpha suggests that the large opacity of H-alpha fibrils is caused by hot precursor events. Application of a recipe that assumes momentary Saha-Boltzmann extinction during their hot onset to millimeter wavelengths suggests that ALMA will observe the H-alpha fibril canopy, not acoustic shocks underneath, and will yield data more interesting than if this canopy were transparent.

Simulating Solar Maximum Conditions Using the Alfvén Wave Solar Atmosphere Model (AWSoM)

Nishtha **Sachdeva**¹, Gábor Tóth¹, Ward B. Manchester¹, Bart van der Holst¹, Zhenguang Huang¹, Igor V. Sokolov¹, Lulu Zhao¹, Qusai Al Shidi¹, Yuxi Chen¹, Tamas I. Gombosi¹Show full author list

2021 ApJ 923 176

<https://iopscience.iop.org/article/10.3847/1538-4357/ac307c/pdf>

<https://doi.org/10.3847/1538-4357/ac307c>

To simulate solar coronal mass ejections (CMEs) and predict their time of arrival and geomagnetic impact, it is important to accurately model the background solar wind conditions in which CMEs propagate. We use the Alfvén Wave Solar atmosphere Model (AWSoM) within the the Space Weather Modeling Framework to simulate solar maximum conditions during two Carrington rotations and produce solar wind background conditions comparable to the observations. We describe the inner boundary conditions for AWSoM using the ADAPT global magnetic maps and validate the simulated results with EUV observations in the low corona and measured plasma parameters at L1 as well as at the position of the Solar Terrestrial Relations Observatory spacecraft. This work complements our prior AWSoM validation study for solar minimum conditions and shows that during periods of higher magnetic activity, AWSoM can reproduce the solar plasma conditions (using properly adjusted photospheric Poynting flux) suitable for providing proper initial conditions for launching CMEs. **28 Apr-25 May 2012, 28 Jun-25 Jul 2014**

CME propagation: Where does the solar wind drag “take over”?

Nishtha **Sachdeva**, Prasad Subramanian, Robin Colaninno, Angelos Vourlidis

ApJ **809** 158 **2015**

<http://arxiv.org/pdf/1507.05199v1.pdf>

We investigate the Sun-Earth dynamics of a set of eight well observed solar coronal mass ejections (CMEs) using data from the STEREO spacecraft. We seek to quantify the extent to which momentum coupling between these CMEs and the ambient solar wind (i.e., the aerodynamic drag) influences their dynamics. To this end, we use results from a 3D flux rope model fit to the CME data. We find that solar wind aerodynamic drag adequately accounts for the dynamics of the fastest CME in our sample. For the relatively slower CMEs, we find that drag-based models initiated below heliocentric distances ranging from 15 to 50 R_{\odot} cannot account for the observed CME trajectories. This is at variance with the general perception that the dynamics of slow CMEs are influenced primarily by solar wind drag from a few R_{\odot} onwards. Several slow CMEs propagate at roughly constant speeds above 15--50 R_{\odot} . Drag-based models initiated above these heights therefore require negligible aerodynamic drag to explain their observed trajectories.

2010 Mar 19-23, 2010 Apr 03 -05, 2010 Apr 08-11, 2010 Jun 16-20, 2010 Sep 11-14, 2010 Oct 26-31, 2011 Feb 15-18, 2011 Mar 25-29

See CESRA Highlight #897 Oct **2016** <http://www.astro.gla.ac.uk/users/eduard/cesra/?p=897>

Formation of current sheets and plasmoids within corotating/stream interaction regions

Timofey **Sagitov** and Roman Kislov

EGU2020-2102 May **2020**

<https://meetingorganizer.copernicus.org/EGU2020/displays/36057>

High speed streams originating from coronal holes are long-lived plasma structures that form corotating interaction regions (CIRs) or stream interface regions (SIRs) in the solar wind. The term CIR is used for streams existing for at least one solar rotation period, and the SIR stands for streams with a shorter lifetime. Since the plasma flows from coronal holes quasi-continuously, CIRs/SIRs simultaneously expand and rotate around the Sun, approximately following the Parker spiral shape up to the Earth's orbit.

Coronal hole streams rotate not only around the Sun but also around their own axis of symmetry, resembling a screw. This effect may occur because of the following mechanisms: (1) the existence of a difference between the solar wind speed at different sides of the stream, (2) twisting of the magnetic field frozen into the plasma, and (3) a vortex-like motion of the edge of the mothering coronal hole at the Sun. The screw type of the rotation of a CIR/SIR can lead to centrifugal instability if CIR/SIR inner layers have a larger angular velocity than the outer. Furthermore, the rotational plasma movement and the stream distortion can twist magnetic field lines. The latter contributes to the pinch effect in

accordance with a well-known criterion of Suydam instability (Newcomb, 1960, doi: 10.1016/0003-4916(60)90023-3). Owing to the presence of a cylindrical current sheet at the boundary of a coronal hole, conditions for tearing instability can also appear at the CIR/SIR boundary. Regardless of their geometry, large scale current sheets are subject to various instabilities generating plasmoids. Altogether, these effects can lead to the formation of a turbulent region within CIRs/SIRs, making them filled with current sheets and plasmoids.

We study a substructure of CIRs/SIRs, characteristics of their rotation in the solar wind, and give qualitative estimations of possible mechanisms which lead to splitting of the leading edge a coronal hole flow and consequent formation of current sheets within CIRs/SIRs.

Transequatorial magnetic flux loops on the Sun as a possible new source of geomagnetic storms

Saito, Takao; Sun, W.; Deehr, C. S.; Akasofu, S.-I.
J. Geophys. Res., Vol. 112, No. A5, A05102, 2007
<http://dx.doi.org/10.1029/2006JA011941>

The relevance of local magnetic records when using extreme space weather events as benchmarks

Elena **Saiz***, Consuelo Cid and Antonio Guerrero
J. Space Weather Space Clim. 2021, 11, 35
<https://www.swsc-journal.org/articles/swsc/pdf/2021/01/swsc200104.pdf>
<https://doi.org/10.1051/swsc/2021018>

Space weather indices introduced for scientific purposes are commonly used to quantify operational nowcast of the geospace state during extreme space weather events. Some indices, such as the Disturbance storm time (Dst) index, have been applied to situations for which they are not originally intended. This raises a question about suitability as a space weather benchmark. In analysing historical records for different magnetometers at low- and mid-latitude, we find periods with longitudinal asymmetry in magnetic response that suggest important signals from individual magnetometers are being averaged out of the Dst record. This asymmetry develops as a double spike in the H-component: one negative in the observatories in the day sector and one positive in the observatories in the night sector. These spikes develop in short-time (about 2 h) and pose a potential hazardous effect for users affected by space weather. The results from historical events have been reinforced with the systematic study of magnetic records during extreme events ($Dst \leq -200$ nT and $AL \leq -2000$ nT) in the period 1998–2017 from six magnetic observatories at about 40° magnetic latitude. Moreover, we show that the largest asymmetries take place during the early main phase and are recorded in narrow local time sectors. An important outcome of these results is that space weather benchmarks should be based on local records instead of the commonly used global indices. This action improves two important aspects of space weather: the assessment of historical extreme events and that of the needs of users. **1859 Sep, 1870 Oct 24, 1903 Oct 31, 1909 Sep 25, 1918 Mar 07, 1921 May 14, 1940 Mar 24, 1958 Feb 11, 1959 Jul 15, 4–5 August 1972, 13–14 July 1982, 1991 Jul 08**

Searching for Carrington-like events and their signatures and triggers

Elena **Saiz***, Antonio Guerrero, Consuelo Cid, Judith Palacios and Yolanda Cerrato
J. Space Weather Space Clim., 6, A6 (2016) **Open Access**
<http://www.swsc-journal.org/articles/swsc/pdf/2016/01/swsc150040.pdf>

The Carrington storm in 1859 is considered to be the major geomagnetic disturbance related to solar activity. In a recent paper, Cid et al. (2015) discovered a geomagnetic disturbance case with a profile extraordinarily similar to the disturbance of the Carrington event at Colaba, but at a mid-latitude observatory, leading to a reinterpretation of the 1859 event. Based on those results, this paper performs a deep search for other “Carrington-like” events and analyses interplanetary observations leading to the ground disturbances which emerged from the systematic analysis. The results of this study based on two Carrington-like events (1) reinforce the awareness about the possibility of missing hazardous space weather events as the large H-spike recorded at Colaba by using global geomagnetic indices, (2) argue against the role of the ring current as the major current involved in Carrington-like events, leaving field-aligned currents (FACs) as the main current involved and (3) propose abrupt southward reversals of IMF along with high solar wind pressure as the interplanetary trigger of a Carrington-like event. **18 June 2003, 29 Oct 2003, 21 Jan 2005**

Geomagnetic response to solar and interplanetary disturbances

Review

E. Saiz¹, Y. Cerrato¹, C. Cid¹, V. Dobrica², P. Hejda³, P. Nenovski⁴, P. Stauning⁵, J. Bochnicek³, D. Danov⁶, C. Demetrescu², W. D. Gonzalez⁷, G. Maris², D. Teodosiev⁶, F. Valach⁸

Journal of Space Weather and Space Climate · July 2013 3 A26

<http://sci-hub.tw/10.1051/swsc/2013048>

The space weather discipline involves different physical scenarios, which are characterized by very different physical conditions, ranging from the Sun to the terrestrial magnetosphere and ionosphere. Therefore, development of a comprehensive model to explain the entire Sun–Earth chain is presently still far from completion. However, the effects of solar activity on our modern technological infrastructure have clearly demonstrated the need for accurate space weather services to address a broad spectrum of user needs. A key element for completion of this task is to push for advances in our knowledge of solar–terrestrial physics. This review paper focuses on the geomagnetic response to solar and interplanetary disturbances. Following a description of their long-term evolution, we discuss short-term responses, where we distinguish between responses of the terrestrial environment to solar activity (and specifically to solar energetic events) and to the solar wind. Geomagnetic responses at low and high latitudes are considered separately. At low latitudes, the evolution of the ring current in both the main and recovery phases is discussed. At high latitudes, achievements in modelling the coupling between magnetospheric and ionospheric processes are described, with special attention to the polar caps and field-aligned currents.

Forecasting intense geomagnetic activity using interplanetary magnetic field data.

Saiz, E., Cid, C., Cerrato, Y.,

2008. Ann. Geophys. 26, 3989–3998.

Continuous Plasma Outflows from the Edge of a Solar Active Region as a Possible Source of Solar Wind.

Sakao, T., Kano, R., Narukage, N., Kotoku, J., Bando, T., DeLuca, E.E., Lundquist, L.L., Tsuneta, S., Harra, L.K., Katsukawa, Y., Kubo, M., Hara, H., Matsuzaki, K., Shimojo, M., Bookbinder, J.A., Golub, L., Korreck, K.E., Su, Y., Shibasaki, K., Shimizu, T., Nakatani, I.,

2007. Science 318, 1585–1588.

Nonlinear Alfvén Wave Model of Stellar Coronae and Winds from the Sun to M dwarfs

Takahito Sakaue, Kazunari Shibata

ApJL 2020

<https://arxiv.org/pdf/2012.10868.pdf>

M dwarf's atmosphere and wind is expected to be highly magnetized. The nonlinear propagation of Alfvén wave could play a key role in both heating the stellar atmosphere and driving the stellar wind. Along this Alfvén wave scenario, we carried out the one-dimensional compressive magnetohydrodynamic (MHD) simulation about the nonlinear propagation of Alfvén wave from the M dwarf's photosphere, chromosphere to the corona and interplanetary space. Based on the simulation results, we develop the semi-empirical method describing the solar and M dwarf's coronal temperature, stellar wind velocity, and wind's mass loss rate. We find that M dwarfs' coronae tend to be cooler than solar corona, and that M dwarfs' stellar winds would be characterized with faster velocity and much smaller mass loss rate compared to those of the solar wind.

A geometrical description for interplanetary propagation of Earth-directed CMEs based on radiative proxies

C Salas-Matamoros, J Sanchez-Guevara

Monthly Notices of the Royal Astronomical Society, Volume 504, Issue 4, July 2021, Pages 5899–5906,

<https://doi.org/10.1093/mnras/stab1232>

We present a 3D geometrical model to describe the propagation and expansion of coronal mass ejections (CMEs) in the interplanetary space based on radiative proxies to be implemented in previous procedures that use SXR and microwave emissions to estimate the Earth-directed CME propagation speed. We carefully selected a sample of 45 well-defined CME-ICME events to evaluate our model. We computed this 3D geometrical model for each event as a tool to improve

the arrival time predictions based on radiative proxies. We conducted a different analysis for each radiative proxy: SXR emission and microwave emission at 9 GHz, and we compared the results separately with the observations by the Wind spacecraft. In general, the results showed that the implementation of our 3D geometrical model improves the predictions and provides an important complement to the arrival time prediction method based on radiative proxies, especially for CME events whose source origin were located at helio longitudes far from the central meridian at least 10° . Improvements for this tool based on observations by Parker Solar Probe and Solar Orbiter must be developed in the future work.

On the Statistical Relationship between CME Speed and Soft X-ray Flux and Fluence of the Associated Flare

C. [Salas-Matamoros](#), K.-L. Klein

Solar Phys. Volume 290, Issue 5, pp.1337-1353 2015

<http://arxiv.org/pdf/1503.08613v1.pdf>

<https://link.springer.com/content/pdf/10.1007/s11207-015-0677-0.pdf>

Both observation and theory reveal a close relationship between the kinematics of coronal mass ejections (CMEs) and the thermal energy release traced by the related soft X-ray (SXR) emission. The major problem of empirical studies of this relationship is the distortion of the CME speed by the projection effect in the coronagraphic measurements. We present a re-assessment of the statistical relationship between CME velocities and SXR parameters, using the SOHO/LASCO catalog and GOES whole Sun observations during the period 1996 to 2008. 49 events were identified where CMEs originated near the limb, at central meridian distances between 70° and 85° , and had a reliably identified SXR burst, the parameters of which - peak flux and fluence - could be determined with some confidence. We find similar correlations between the logarithms of CME speed and of SXR peak flux and fluence as several earlier studies, with correlation coefficients of 0.48 and 0.58, respectively. Correlations are slightly improved over an unrestricted CME sample when only limb events are used. However, a broad scatter persists. We derive the parameters of the CME-SXR relationship and use them to predict ICME arrival times at Earth. *We show that the CME speed inferred from SXR fluence measurements tends to perform better than SoHO/LASCO measurements in the prediction of ICME arrival times near 1 AU. The estimation of the CME speed from SXR observations can therefore make a valuable contribution to space weather predictions.*

Table 1. Table of events:

Table 2.: Comparison of travel time of CMEs

A Survey of Coronal Mass Ejections Measured In Situ by Parker Solar Probe During 2018-2022

Tarik M. [Salman](#) (1 and 2), [Teresa Nieves-Chinchilla](#) (2), [Lan K. Jian](#) (2), [Noé Lugaz](#) (3), [Fernando Carcaboso](#) (4), [Emma E. Davies](#) (5), [Yaireska M. Collado-Vega](#) (2)

ApJ 966 118 2024

<https://arxiv.org/pdf/2403.02594.pdf>

<https://iopscience.iop.org/article/10.3847/1538-4357/ad320c/pdf>

We present a statistical investigation of the radial evolution of 28 interplanetary coronal mass ejections (ICMEs), measured in situ by the Parker Solar Probe (PSP) spacecraft from 2018 October to 2022 August. First, by analyzing the radial distribution of ICME classification based on magnetic hodograms, we find that coherent configurations are more likely to be observed close to the Sun. In contrast, more complex configurations are observed farther out. We also notice that the post-ICME magnetic field is more impacted following an ICME passage at larger heliocentric distances. Second, with a multi-linear robust regression, we derive a slower magnetic ejecta (ME) expansion rate within 1-au compared to previous statistical estimates. Then, investigating the magnetic field fluctuations within ICME sheaths, we see that these fluctuations are strongly coupled to the relative magnetic field strength gradient from the upstream solar wind to the ME. Third, we identify ME expansion as an important factor in forming sheaths. Finally, we determine the distortion parameter (DiP) which is a measure of magnetic field asymmetry in an ME. We discover lower overall asymmetries within MEs. We reveal that even for expanding MEs, the time duration over which an ME is sampled does not correlate with DiP values, indicating that the aging effect is not the sole contributor to the observed ME asymmetries. **2022 Jan 29**

Table 1. The PSP ICME list. 2018.10-2022.08

Categorization of Coronal Mass Ejection Driven Sheath Regions: Characteristics of STEREO Events

T. M. [Salman](#), [N. Lugaz](#), [R. M. Winslow](#), [C. J. Farrugia](#), [L. K. Jian](#), [A. B. Galvin](#)

ApJ **921** 57 **2021**

<https://arxiv.org/pdf/2106.12076.pdf>

<https://doi.org/10.3847/1538-4357/ac11f3>

We present a comprehensive statistical analysis of 106 sheath regions driven by coronal mass ejections (CMEs) and measured near 1 AU. Using data from the STEREO probes, this extended analysis focuses on two discrete categorizations. In the first categorization, we investigate how the generic features of sheaths change with their potential formation mechanisms (propagation and expansion sheaths), namely, their associations with magnetic ejectas (MEs) which are primarily expanding or propagating in the solar wind. We find propagation sheaths to be denser and driven by stronger MEs, whereas expansion sheaths are faster. Exploring the temporal profiles of these sheaths with a superposed epoch technique, we observe that most of the magnetic field and plasma signatures are more elevated in propagation sheaths relative to expansion sheaths. The second categorization is based on speed variations across sheaths. Employing linear least squares regression, we categorize four distinct speed profiles of the sheath plasma. We find that the associated shock properties and solar cycle phase do not impact the occurrence of such variations. Our results also highlight that the properties of the driving MEs are a major source of variability in the sheath properties. Through logistic regression, we conclude that the magnetic field strength and the ME speed in the frame of the solar wind are likely drivers of these speed variations. **2011 January 17 , 2012 October 5 , 2014 January 29, 2014 February 25**

Properties of the Sheath Regions of Coronal Mass Ejections with or without Shocks from STEREO in situ Observations near 1 AU

T. M. [Salman](#), [N. Lugaz](#), [C. J. Farrugia](#), [R. M. Winslow](#), [L. K. Jian](#), [A. B. Galvin](#)

ApJ **904** 177 **2020**

<https://arxiv.org/pdf/2011.06632.pdf>

<https://doi.org/10.3847/1538-4357/abbd5>

We examine 188 coronal mass ejections (CMEs) measured by the twin STEREO spacecraft during 2007-2016 to investigate the generic features of the CME sheath and the magnetic ejecta (ME) and dependencies of average physical parameters of the sheath on the ME. We classify the MEs into three categories, focusing on whether a ME drives both a shock and sheath, or only a sheath, or neither, near 1 AU. We also reevaluate our initial classification through an automated algorithm and visual inspection. We observe that even for leading edge speeds greater than 500 km/s, 1 out of 4 MEs do not drive shocks near 1 AU. MEs driving both shocks and sheaths are the fastest and propagate in high magnetosonic solar wind, whereas MEs driving only sheaths are the slowest and propagate in low magnetosonic solar wind. Our statistical and superposed epoch analyses indicate that all physical parameters are more enhanced in the sheath regions following shocks than in sheaths without shocks. However, differences within sheaths become statistically less significant for similar driving MEs. We also find that the radial thickness of ME-driven sheaths apparently has no clear linear correlation with the speed profile and associated Mach numbers of the driver. **28-29 April 2011, 29 October 2011, 12 April 2014**

Radial Evolution of Coronal Mass Ejections Between MESSENGER, Venus Express, STEREO, and L1: Catalog and Analysis

T. M. [Salman](#), [R. M. Winslow](#), [N. Lugaz](#)

JGR [Volume 125, Issue 1](#) January **2020** A027084

[sci-hub.si/10.1029/2019JA027084](https://doi.org/10.1029/2019JA027084)

Our knowledge of the properties of coronal mass ejections (CMEs) in the inner heliosphere is constrained by the relative lack of plasma observations between the Sun and 1 AU. In this work, we present a comprehensive catalog of 47 CMEs measured in situ measurements by two or more radially aligned spacecraft (MESSENGER, Venus Express, STEREO, Wind/ACE). We estimate the CME impact speeds at Mercury and Venus using a drag-based model and present an average propagation profile of CMEs (speed and deceleration/acceleration) in the inner heliosphere. We find that CME deceleration continues past Mercury's orbit but most of the deceleration occurs between the Sun and Mercury. We examine the exponential decrease of the maximum magnetic field strength in the CME with heliocentric distance using two approaches: a modified statistical method and analysis from individual conjunction events. Findings from both the approaches are on average consistent with previous studies but show significant event-to-event variability. We also find the expansion of the CME sheath to be well fit by a linear function. However, we observe the average sheath duration and its increase to be fairly independent of the initial CME speed, contradicting commonly held knowledge that slower CMEs drive larger sheaths. We also present an analysis of the **3 November 2011** CME observed in longitudinal conjunction between MESSENGER, Venus Express, and STEREO-B focusing on the expansion of the CME and its correlation with the exponential falloff of the maximum magnetic field strength in the ejecta.

Calibrating the WSA Model in EUHFORIA Based on Parker Solar Probe Observations

E. Samara¹, C. N. Arge¹, R. F. Pinto^{2,3}, J. Magdalenic^{4,5}, N. Wijsen⁵, M. L. Stevens⁶, L. Rodriguez⁴, and S. Poedts^{5,7}

2024 ApJ 971 83

<https://iopscience.iop.org/article/10.3847/1538-4357/ad53c6/pdf>

We employ Parker Solar Probe (PSP) observations during the latest solar minimum period (years 2018–2021) to calibrate the version of the Wang–Sheeley–Arge (WSA) coronal model used in the European Heliospheric Forecasting Information Asset (EUHFORIA). WSA provides a set of boundary conditions at 0.1 au necessary to initiate the heliospheric part of EUHFORIA, namely, the domain extending beyond the solar Alfvénic point. To calibrate WSA, we observationally constrain four constants in the WSA semiempirical formula based on PSP observations. We show how the updated (after the calibration) WSA boundary conditions at 0.1 au are compared to PSP observations at similar distances, and we further propagate these conditions in the heliosphere according to EUHFORIA's magnetohydrodynamic (MHD) approach. We assess the predictions at Earth based on the dynamic time-warping technique. Our findings suggest that, for the period of interest, the WSA configurations that resembled optimally the PSP observations close to the Sun were different from the ones needed to provide better predictions at Earth. One reason for this discrepancy can be attributed to the scarcity of fast solar wind velocities recorded by PSP. The calibration of the model was performed based on unexpectedly slow velocities that did not allow us to achieve generally and globally improved solar wind predictions compared to older studies. Other reasons can be attributed to missing physical processes from the heliospheric part of EUHFORIA but also the fact that the currently employed WSA relationship, as coupled to the heliospheric MHD domain, may need a global reformulation beyond that of just updating the four constant factors that were taken into account in this study.

Influence of coronal hole morphology on the solar wind speed at Earth

Evangelia Samara, [Jasmina Magdalenic](#), [Luciano Rodriguez](#), [Stephan G. Heinemann](#), [Manolis K. Georgoulis](#), [Stefan J. Hofmeister](#), [Stefaan Poedts](#)

A&A 2022

<https://arxiv.org/pdf/2204.00368.pdf>

It has long been known that the high-speed stream (HSS) peak velocity at Earth directly depends on the area of the coronal hole (CH) on the Sun. Different degrees of association between the two parameters have been shown by many authors. In this study, we revisit this association in greater detail for a sample of 45 nonpolar CHs during the minimum phase of solar cycle 24. The aim is to understand how CHs of different properties influence the HSS peak speeds observed at Earth and draw from this to improve solar wind modeling. The characteristics of the CHs of our sample were extracted based on the Collection of Analysis Tools for Coronal Holes (CATCH) which employs an intensity threshold technique applied to extreme-ultraviolet (EUV) filtergrams. We first examined all the correlations between the geometric characteristics of the CHs and the HSS peak speed and duration at Earth, for the entire sample. The CHs were then categorized in different groups based on morphological criteria, such as the aspect ratio, the orientation angle and the geometric complexity, a parameter which is often neglected when the formation of the fast solar wind at Earth is studied. Our results, confirmed also by the bootstrapping technique, show that all three aforementioned morphological criteria play a major role in determining the HSS peak speed at 1 AU. Therefore, they need to be taken into consideration for empirical models that aim to forecast the fast solar wind at Earth based on the observed CH solar sources.

Calibrating the WSA model in EUHFORIA based on PSP observations

Evangelia Samara, [Charles N. Arge](#), [Rui F. Pinto](#), [Jasmina Magdalenic](#), [Nicolas Wijsen](#), [Michael L. Stevens](#), [Luciano Rodriguez](#), [Stefaan Poedts](#)

ApJ 2024

<https://arxiv.org/pdf/2405.09693>

We employ Parker Solar Probe (PSP) observations during the latest solar minimum period (years 2018 -2021) to calibrate the version of the Wang-Sheeley-Arge (WSA) coronal model used in the European space weather forecasting tool EUHFORIA. WSA provides a set of boundary conditions at 0.1 au necessary to initiate the heliospheric part of EUHFORIA, namely, the domain extending beyond the solar Alfvénic point. To calibrate WSA, we observationally constrain four constants in the WSA semi-empirical formula based on PSP observations. We show how the updated (after the calibration) WSA boundary conditions at 0.1 au are compared to PSP observations at similar distances, and we further propagate these conditions in the heliosphere according to EUHFORIA's magnetohydrodynamic (MHD) approach. We assess the predictions at Earth based on the Dynamic Time Warping technique. Our findings suggest that, for the period of interest, the WSA configurations which resembled optimally the PSP observations close to the Sun,

were different than the ones needed to provide better predictions at Earth. One reason for this discrepancy can be attributed to the scarcity of fast solar wind velocities recorded by PSP. The calibration of the model was performed based on unexpectedly slow velocities that did not allow us to achieve generally and globally improved solar wind predictions, compared to older studies. Other reasons can be attributed to missing physical processes from the heliospheric part of EUHFORIA but also the fact that the currently employed WSA relationship, as coupled to the heliospheric MHD domain, may need a global reformulation beyond that of just updating the four constant factors that were taken into account in this study.

Unusual Cosmic Ray Variations During the Forbush Decreases of June 2015

E. [Samara](#), A. Smponias, I. Lytrosyngounis, D. Lingri, H. Mavromichalaki, C. Sgouropoulos

[Solar Physics](#) April 2018, 293:67

<https://link.springer.com/content/pdf/10.1007%2Fs11207-018-1290-9.pdf>

<http://cosray.phys.uoa.gr/publications/D119.pdf>

Although the current Solar Cycle 24 is characterized by low solar activity, an intense geomagnetic storm (G4) was recorded in June 2015. It was a complex phenomenon that began on 22 June 2015 as the result of intense solar activity, accompanied by several flares and coronal mass ejections that interacted with the Earth's magnetic field. A Forbush decrease was also recorded at the neutron monitors of the worldwide network, with an amplitude of 8.4%, and in its recovery phase, a second Forbush decrease followed, with an amplitude of 4.0% for cosmic rays of 10 GV obtained with the global survey method. The Dst index reached a minimum value of -204 nT that was detected on **23 June 2015** at 05:00–06:00 UT, while the Kp index reached the value eight. For our analysis, we used hourly cosmic-ray intensity data recorded by polar, mid-, and high-latitude neutron monitor stations obtained from the High Resolution Neutron Monitor Database. The cosmic-ray anisotropy variation at the ecliptic plane was also estimated and was found to be highly complex. We study and discuss the unusual and complex cosmic-ray and geomagnetic response to these solar events.

In situ measurements of the variable slow solar wind near sector boundaries

E. [Sanchez-Diaz](#) (IRAP), [A. Rouillard](#), [B. Lavraud](#) (IRAP), [E. Kilpua](#) (FMI), [J. Davies](#)

[ApJ](#) 2019

<https://arxiv.org/ftp/arxiv/papers/1911/1911.09683.pdf>

The release of density structures at the tip of the coronal helmet streamers, likely as a consequence of magnetic reconnection, contributes to the mass flux of the slow solar wind. In situ measurements in the vicinity of the heliospheric plasma sheet of the magnetic field, protons and suprathermal electrons reveal details of the processes at play during the formation of density structures near the Sun. In a previous article, we exploited remote-sensing observations to derive a 3-D picture of the dynamic evolution of a streamer. We found evidence of the recurrent and continual release of dense blobs from the tip of the streamers. In the present paper, we interpret in situ measurements of the slow solar wind during solar maximum. Through both case and statistical analysis, we show that in situ signatures (magnetic field magnitude, smoothness and rotation, proton density and suprathermal electrons, in the first place) are consistent with the helmet streamers producing, in alternation, high-density regions (mostly disconnected) separated by magnetic flux ropes (mostly connected to the Sun). This sequence of emission of dense blobs and flux ropes also seems repeated at smaller scales inside each of the high-density regions. These properties are further confirmed with in situ measurements much closer to the Sun using Helios observations. We conclude on a model for the formation of dense blobs and flux ropes that explains both the in situ measurements and the remote-sensing observations presented in our previous studies. **2010 January 30, 2011 April 27, 2011 May 19, 2013 July 08**

Table 1. List of crossings of highly-tilted HCSs not contaminated by CMEs during solar cycle 24

The temporal and spatial scales of density structures released in the slow solar wind during solar activity maximum

Eduardo [Sanchez-Diaz](#), [Alexis P. Rouillard](#), [Jackie A. Davies](#), [Benoit Lavraud](#), [Rui F. Pinto](#), [Emilia Kilpua](#)

[ApJ](#) 851, 32 2017

<https://arxiv.org/ftp/arxiv/papers/1711/1711.02486.pdf>

In a recent study, we took advantage of a highly tilted coronal neutral sheet to show that density structures, extending radially over several solar radii (R_s), are released in the forming slow solar wind approximately 4-5 R_s above the solar surface (Sanchez-Diaz et al. 2017). We related the signatures of this formation process to intermittent magnetic reconnection occurring continuously above helmet streamers. We now exploit the heliospheric imagery from the Solar

Terrestrial Relation Observatory (STEREO) to map the spatial and temporal distribution of the ejected structures. We demonstrate that streamers experience quasi-periodic bursts of activity with the simultaneous outpouring of small transients over a large range of latitudes in the corona. This cyclic activity leads to the emergence of well-defined and broad structures. Derivation of the trajectories and kinematic properties of the individual small transients that make up these large-scale structures confirms their association with the forming Slow Solar Wind (SSW). We find that these transients are released, on average, every 19.5 hours, simultaneously at all latitudes with a typical radial size of 12 Rs. Their spatial distribution, release rate and three-dimensional extent are used to estimate the contribution of this cyclic activity to the mass flux carried outward by the SSW. Our results suggest that, in interplanetary space, the global structure of the heliospheric current sheet is dominated by a succession of blobs and associated flux ropes. We demonstrated this with an example event using STEREO-A in-situ measurements. **2013 June 3, 2013 May 28 to June 06, 2013 July 08-10**

Identifying Flux Rope Signatures Using a Deep Neural Network

Luiz F. G. dos [Santos](#), [Ayrís Narock](#), [Teresa Nieves-Chinchilla](#), [Marlon Nuñez](#), [Michael Kirk](#)

Solar Phys. **295**, Article number: 131 **2020**

<https://arxiv.org/pdf/2008.13294.pdf>

<https://link.springer.com/content/pdf/10.1007/s11207-020-01697-x.pdf>

Among the current challenges in Space Weather, one of the main ones is to forecast the internal magnetic configuration within Interplanetary Coronal Mass Ejections (ICMEs). Currently, a monotonic and coherent magnetic configuration observed is associated with the result of a spacecraft crossing a large flux rope with helical magnetic field lines topology. The classification of such an arrangement is essential to predict geomagnetic disturbance. Thus, the classification relies on the assumption that the ICME's internal structure is a well organized magnetic flux rope. This paper applies machine learning and a current physical flux rope analytical model to identify and further understand the internal structures of ICMEs. We trained an image recognition artificial neural network with analytical flux rope data, generated from the range of many possible trajectories within a cylindrical (circular and elliptical cross-section) model. The trained network was then evaluated against the observed ICMEs from WIND during 1995-2015.

The methodology developed in this paper can classify 84% of simple real cases correctly and has a 76% success rate when extended to a broader set with 5% noise applied, although it does exhibit a bias in favor of positive flux rope classification. As a first step towards a generalizable classification and parameterization tool, these results show promise. With further tuning and refinement, our model presents a strong potential to evolve into a robust tool for identifying flux rope configurations from in situ data. **May 13th, 1995, 21-27 June 2000, 12-15 Apr 2006, January 24th, 2011, October 2nd, 2013, August 26th, 2014**

A Revised 27-day Recurrence Index

[H. H. Sargent](#)

2021

<https://arxiv.org/ftp/arxiv/papers/2101/2101.02155.pdf>

The original 110 year long 27-day Recurrence Index (original R27) was published more than forty years ago. That index, based on the autocorrelation of consecutive 27-day sets of the geomagnetic aa-index, is a measure of the cycle-to-cycle stability of high speed solar wind structure. During an effort to extend the index, it was discovered that the index could be significantly strengthened by pre-smoothing the geomagnetic aa-index listing used as input. A revised index (revised R27) is presented which clearly shows periods of long term stable solar wind structure toward the end of every sunspot cycle over the last 150 years. The extension of R27 over an interval including the greater part of the space age enables the updating of various studies of long-term solar wind variability based on R27, as well as comparison of R27 with more recently-developed solar-terrestrial parameters.

Modelling the magnetic vectors of ICMEs at different heliocentric distances with INFROS

Ranadeep [Sarkar](#), [Nandita Srivastava](#), [Nat Gopalswamy](#), [Emilia Kilpua](#)

ApLS **273** 36 **2024**

<https://arxiv.org/pdf/2406.09247>

<https://iopscience.iop.org/article/10.3847/1538-4365/ad5835/pdf>

The INterplanetary Flux ROpe Simulator (INFROS) is an observationally constrained analytical model dedicated for forecasting the strength of the southward component (B_z) of the magnetic field embedded in interplanetary coronal mass ejections (ICMEs). In this work, we validate the model for six ICMEs sequentially observed by two radially-aligned spacecraft positioned at different heliocentric distances. The six selected ICMEs in this study comprise of cases associated with isolated CME evolution as well as those interacting with high-speed streams (HSS) and high-density

streams (HDS). For the isolated CMEs, our results show that the model outputs at both the spacecraft are in good agreement with in-situ observations. However, for most of the interacting events, the model correctly captures the CME evolution only at the inner spacecraft. Due to the interaction with HSS and HDS, which in most cases occurred at heliocentric distances beyond the inner spacecraft, the ICME evolution no longer remains self-similar. Consequently, the model underestimates the field strength at the outer spacecraft. Our findings indicate that constraining the INFROS model with inner spacecraft observations significantly enhances the prediction accuracy at the outer spacecraft for the three events undergoing self-similar expansion, achieving a 90 % correlation between observed and predicted Bz profiles. This work also presents a quantitative estimation of the ICME magnetic field enhancement due to interaction which may lead to severe space weather. We conclude that the assumption of self-similar expansion provides a lower limit to the magnetic field strength estimated at any heliocentric distance, based on the remote sensing observations. **2008-12-27, 2010-11-04, 2011-10-14, 2011-11-03, 2013-01-06, 2013-07-09**

Studying the spheromak rotation in data-constrained CME modelling with EUHFORIA and assessing its effect on the Bz prediction

Ranadeep [Sarkar](#), [Jens Pomoell](#), [Emilia Kilpua](#), [Eleanna Asvestari](#), [Nicolas Wijsen](#), [Anwasha Maharana](#), [Stefaan Poedts](#)

ApJS **270** 18 **2024**

<https://arxiv.org/pdf/2311.15616.pdf>

<https://iopscience.iop.org/article/10.3847/1538-4365/ad0df4/pdf>

A key challenge in space weather forecasting is accurately predicting the magnetic field topology of interplanetary coronal mass ejections (ICMEs), specifically the north-south magnetic field component (Bz) for Earth-directed CMEs. Heliospheric MHD models typically use spheromaks to represent the magnetic structure of CMEs. However, when inserted into the ambient interplanetary magnetic field, spheromaks can experience a phenomenon reminiscent of the condition known as the "spheromak tilting instability", causing its magnetic axis to rotate. From the perspective of space weather forecasting, it is crucial to understand the effect of this rotation on predicting Bz at 1 au while implementing the spheromak model for realistic event studies. In this work, we study this by modelling a CME event on **2013 April 11** using the "EUropean Heliospheric FORecasting Information Asset" (EUHFORIA). Our results show that a significant spheromak rotation up to 90 degrees has occurred by the time it reaches 1 au, while the majority of this rotation occurs below 0.3 au. This total rotation resulted in poor predicted magnetic field topology of the ICME at 1 au. To address this issue, we further investigated the influence of spheromak density on mitigating rotation. The results show that the spheromak rotation is less for higher densities. Importantly, we observe a substantial reduction in the uncertainties associated with predicting Bz when there is minimal spheromak rotation. Therefore, we conclude that spheromak rotation adversely affects Bz prediction in the analyzed event, emphasizing the need for caution when employing spheromaks in global MHD models for space weather forecasting.

An Observationally Constrained Analytical Model for Predicting the Magnetic Field Vectors of ICMEs at 1 AU

Ranadeep [Sarkar](#), [Nat Gopalswamy](#), [Nandita Srivastava](#)

2020 ApJ **888** 121

<https://arxiv.org/pdf/1912.03494.pdf>

<https://doi.org/10.3847/1538-4357/ab5fd7>

sci-hub.si/10.3847/1538-4357/ab5fd7

We report on an observationally constrained analytical model, the INterplanetary Flux ROpe Simulator (INFROS), for predicting the magnetic-field vectors of coronal mass ejections (CMEs) in the interplanetary medium. The main architecture of INFROS involves using the near-Sun flux rope properties obtained from the observational parameters that are evolved through the model in order to estimate the magnetic field vectors of interplanetary CMEs (ICMEs) at any heliocentric distance. We have formulated a new approach in INFROS to incorporate the expanding nature and the time-varying axial magnetic field-strength of the flux rope during its passage over the spacecraft. As a proof of concept, we present the case study of an Earth-impacting CME which occurred on **2013 April 11**. Using the near-Sun properties of the CME flux rope, we have estimated the magnetic vectors of the ICME as intersected by the spacecraft at 1 AU. The predicted magnetic field profiles of the ICME show good agreement with those observed by the in-situ spacecraft. Importantly, the maximum strength (10.5 ± 2.5 nT) of the southward component of the magnetic field (Bz) obtained from the model prediction, is in agreement with the observed value (11 nT). Although our model does not include the prediction of the ICME plasma parameters, as a first order approximation it shows promising results in forecasting of Bz in near real time which is critical for predicting the severity of the associated geomagnetic storms. This could prove to

be a simple space-weather forecasting tool compared to the time-consuming and computationally expensive MHD models.

Chaos and periodicity in solar wind speed: cycle 23

Tushnik **Sarkar**, Rajdeep Ray, Mofazzal H. Khondekar, Koushik Ghosh, Subrata Banerjee

Astrophysics and Space Science May **2015**, 357:128

The solar wind speed time series data from 1st January, 1997 to 28th October, 2003 has been pre-processed using simple exponential smoothing, discrete wavelet transform for denoising to investigate the underneath dynamics of it.

Recurrence plot and recurrence quantification analysis has revealed that the time series is non-stationary one with deterministic chaotic behavior. The Hilbert-Huang Transform has been used in search of the underlying periods of the data series. Present investigation has revealed the periods of 21 days, 32.5 days, 43.6 days, 148.86 days, 180.7 days, 355.5 days, 403.2 days, 413.6 days, 490.72 days, 729.6 days, 1086.76 days, 1599.4 days and 1892.6 days.

Predicting the magnetic vectors within coronal mass ejections arriving at Earth:

2. Geomagnetic response: BZ VALIDATION

N. P. **Savani**,^{1, 2} A. Vourlidas,³ I. G. Richardson,^{4, 2} A. Szabo,² B. J. Thompson,² A. Pulkkinen,² M. L. Mays,^{5, 2} T. Nieves-Chinchilla,^{5, 2} V. Bothmer⁶

Space Weather 15, 441–461 **2017**

<http://sci-hub.tw/10.1002/2016SW001458>

This is a companion to [Savani et al., 2015] that discussed how a first-order prediction of the internal magnetic field of a coronal mass ejection (CME) may be made from observations of its initial state at the Sun for space weather forecasting purposes (BSS model). For eight CME events, we investigate how uncertainties in their predicted magnetic structure influence predictions of the geomagnetic activity. We use an empirical relationship between the solar wind plasma drivers and Kp index together with the inferred magnetic vectors, to make a prediction of the time variation of Kp (Kp(BSS)). We find a 2σ uncertainty range on the magnetic field magnitude (jB_j) provides a practical and convenient solution for predicting the uncertainty in geomagnetic storm strength. We also find the estimated CME velocity is a major source of error in the predicted maximum Kp. The time variation of Kp(BSS) is important for predicting periods of enhanced and maximum geomagnetic activity, driven by southerly-directed magnetic fields, and periods of lower activity driven by northerly directed magnetic field. We compare the skill score of our model to a number of other forecasting models, including the NOAA/SWPC and CCMC/SWRC estimates. The BSS model was the most unbiased prediction model while the other models predominately tended to significantly over-forecast. The True skill score of the BSS prediction model (TSS = 0:43 _ 0:06) exceeds the results of 2 baseline models and the NOAA/SWPC forecast. The BSS model prediction performed equally with CCMC/SWRC predictions while demonstrating a lower uncertainty. . **3 Apr 2010, 25 Mar 2011, 10 Mar 2012, 14 Jun 2012, 12 Jul 2012, 27 Sep 2012, 7 Jan 2014, 10 Sep 2014**

Predicting the magnetic vectors within coronal mass ejections arriving at Earth: 2.

Geomagnetic response

N. P. **Savani**, A. Vourlidas, I. G. Richardson, A. Szabo, B. J. Thompson, A. Pulkkinen, M. L. Mays, T. Nieves-Chinchilla, V. Bothmer

Space Weather Volume 15, Issue 2 February **2017** Pages 441–461 DOI: 10.1002/2016SW001458

<http://onlinelibrary.wiley.com/doi/10.1002/2016SW001458/full>

<http://sci-hub.cc/10.1002/2016SW001458>

This is a companion to Savani et al. (2015) that discussed how a first-order prediction of the internal magnetic field of a coronal mass ejection (CME) may be made from observations of its initial state at the Sun for space weather forecasting purposes (Bothmer-Schwenn scheme (BSS) model). For eight CME events, we investigate how uncertainties in their predicted magnetic structure influence predictions of the geomagnetic activity. We use an empirical relationship between the solar wind plasma drivers and Kp index together with the inferred magnetic vectors, to make a prediction of the time variation of Kp (Kp(BSS)). We find a 2σ uncertainty range on the magnetic field magnitude ($|B|$) provides a practical and convenient solution for predicting the uncertainty in geomagnetic storm strength. We also find the estimated CME velocity is a major source of error in the predicted maximum Kp. The time variation of Kp(BSS) is important for predicting periods of enhanced and maximum geomagnetic activity, driven by southerly directed magnetic fields, and periods of lower activity driven by northerly directed magnetic field. We compare the skill score of our model to a number of other forecasting models, including the NOAA/Space Weather Prediction Center (SWPC) and Community Coordinated Modeling Center (CCMC)/SWRC estimates. The BSS model was the most unbiased prediction model, while the other models predominately tended to significantly overforecast. The True skill score of the BSS

prediction model ($TSS = 0.43 \pm 0.06$) exceeds the results of two baseline models and the NOAA/SWPC forecast. The BSS model prediction performed equally with CCMC/SWRC predictions while demonstrating a lower uncertainty.

3 Apr 2010, 25 Mar 2011, 10 Mar 2012, 14 Jun 2012, 12 Jul 2012, 27 Sep 2012, 7 Jan 2014, 10 Sep 2014

Хороший справочник

Predicting the magnetic vectors within coronal mass ejections arriving at Earth

1. Initial architecture

Savani, N. P.; Vourlidas, A.; Szabo, A.; Mays, M. L.; Thompson, B. J.; Richardson, I. G.; Evans, R.; Pulkkinen, A.; Nieves-Chinchilla, T.

Space Weather, Volume 13, Issue 6 June 2015 Pages 374–385,

<http://arxiv.org/pdf/1502.02067v1.pdf> **File**

<http://onlinelibrary.wiley.com/doi/10.1002/2015SW001171/full>

The process by which the Sun affects the terrestrial environment on short timescales is predominately driven by the amount of magnetic reconnection between the solar wind and Earth's magnetosphere. Reconnection occurs most efficiently when the solar wind magnetic field has a southward component. The most severe impacts are during the arrival of a coronal mass ejection (CME) when the magnetosphere is both compressed and magnetically connected to the heliospheric environment. Unfortunately, forecasting magnetic vectors within coronal mass ejections remain elusive. Here we report how, by combining a statistically robust helicity rule for a CME's solar origin with a simplified flux rope topology, the magnetic vectors within the Earth-directed segment of a CME can be predicted. In order to test the validity of this proof-of-concept architecture for estimating the magnetic vectors within CMEs, a total of eight CME events (between 2010 and 2014) have been investigated. With a focus on the large false alarm of **January 2014**, this work highlights the importance of including the early evolutionary effects of a CME for forecasting purposes. The angular rotation in the predicted magnetic field closely follows the broad rotational structure seen within the in situ data. This time-varying field estimate is implemented into a process to quantitatively predict a time-varying K_p index that is described in detail in paper II. Future statistical work, quantifying the uncertainties in this process, may improve the more heuristic approach used by early forecasting systems.

Tracking the momentum flux of a CME and quantifying its influence on geomagnetically induced currents at Earth

N. P. **Savani**, A. Vourlidas, A. Pulkkinen, T. Nieves-Chinchilla, B. Lavraud and M. J. Owens
SPACE WEATHER, VOL. 11, 245–261, doi:10.1002/swe.20038, 2013

<http://onlinelibrary.wiley.com/doi/10.1002/swe.20038/pdf>

We investigate a coronal mass ejection (CME) propagating toward Earth on **29 March 2011**. This event is specifically chosen for its predominately northward directed magnetic field, so that the influence from the momentum flux onto Earth can be isolated. We focus our study on understanding how a small Earth-directed segment propagates. Mass images are created from the white-light cameras onboard STEREO which are also converted into mass height-time maps (mass J-maps). The mass tracks on these J-maps correspond to the sheath region between the CME and its associated shock front as detected by in situ measurements at L1. A time series of mass measurements from the STEREO COR-2A instrument is made along the Earth propagation direction. Qualitatively, this mass time series shows a remarkable resemblance to the L1 in situ density series. The in situ measurements are used as inputs into a three-dimensional (3-D) magnetospheric space weather simulation from the Community Coordinated Modeling Center. These simulations display a sudden compression of the magnetosphere from the large momentum flux at the leading edge of the CME, and predictions are made for the time derivative of the magnetic field (dB/dt) on the ground. The predicted dB/dt values were then compared with the observations from specific equatorially located ground stations and showed notable similarity. This study of the momentum of a CME from the Sun down to its influence on magnetic ground stations on Earth is presented as a preliminary proof of concept, such that future attempts may try to use remote sensing to create density and velocity time series as inputs to magnetospheric simulations.

A STUDY OF THE HELIOCENTRIC DEPENDENCE OF SHOCK STANDOFF DISTANCE AND GEOMETRY USING 2.5D MAGNETOHYDRODYNAMIC SIMULATIONS OF CORONAL MASS EJECTION DRIVEN SHOCKS

N. P. **Savani**^{1,2}, D. Shiota³, K. Kusano^{4,5}, A. Vourlidas⁶, and N. Lugaz
2012 ApJ 759 103

We perform four numerical magnetohydrodynamic simulations in 2.5 dimensions (2.5D) of fast coronal mass ejections (CMEs) and their associated shock fronts between 10 Rs and 300 Rs. We investigate the relative change in the shock standoff distance, Δ , as a fraction of the CME radial half-width, D_{OB} (i.e., Δ/D_{OB}). Previous hydrodynamic studies have related the shock standoff distance for Earth's magnetosphere to the density compression ratio (DR; ρ_u/ρ_d) measured across the bow shock. The DR coefficient, k_{dr} , which is the proportionality constant between the relative standoff distance (Δ/D_{OB}) and the compression ratio, was semi-empirically estimated as 1.1. For CMEs, we show that this value varies linearly as a function of heliocentric distance and changes significantly for different radii of curvature of the CME's leading edge. We find that a value of 0.8 ± 0.1 is more appropriate for small heliocentric distances (<30 Rs) which corresponds to the spherical geometry of a magnetosphere presented by Seiff. As the CME propagates its cross section becomes more oblate and the k_{dr} value increases linearly with heliocentric distance, such that $k_{dr} = 1.1$ is most appropriate at a heliocentric distance of about 80 Rs. For terrestrial distances (215 Rs) we estimate $k_{dr} = 1.8 \pm 0.3$, which also indicates that the CME cross-sectional structure is generally more oblate than that of Earth's magnetosphere. These alterations to the proportionality coefficients may serve to improve investigations into the estimates of the magnetic field in the corona upstream of a CME as well as the aspect ratio of CMEs as measured in situ.

Observational Tracking of the 2D Structure of Coronal Mass Ejections Between the Sun and 1 AU

N. P. **Savani**, J. A. Davies, C. J. Davis, D. Shiota, A. P. Rouillard, M. J. Owens, K. Kusano, V. Bothmer, S. P. Bamford and C. J. Lintott, et al.

Solar Physics, Volume 279, Number 2 (2012), 517-53

<http://arxiv.org/pdf/1503.08774v1.pdf>

The Solar TERrestrial RELations Observatory (STEREO) provides high cadence and high resolution images of the structure and morphology of coronal mass ejections (CMEs) in the inner heliosphere. CME directions and propagation speeds have often been estimated through the use of time-elongation maps obtained from the STEREO Heliospheric Imager (HI) data. Many of these CMEs have been identified by citizen scientists working within the SolarStormWatch project (www.solarstormwatch.com) as they work towards providing robust real-time identification of Earth-directed CMEs. The wide field of view of HI allows scientists to directly observe the two-dimensional (2D) structures, while the relative simplicity of time-elongation analysis means that it can be easily applied to many such events, thereby enabling a much deeper understanding of how CMEs evolve between the Sun and the Earth. For events with certain orientations, both the rear and front edges of the CME can be monitored at varying heliocentric distances (R) between the Sun and 1 AU. Here we take four example events with measurable position angle widths and identified by the citizen scientists. These events were chosen for the clarity of their structure within the HI cameras and their long track lengths in the time-elongation maps. We show a linear dependency with R for the growth of the radial width (W) and the 2D aspect ratio (χ) of these CMEs, which are measured out to ≈ 0.7 AU. We estimated the radial width from a linear best fit for the average of the four CMEs. We obtained the relationships $W=0.14R+0.04$ for the width and $\chi=2.5R+0.86$ for the aspect ratio (W and R in units of AU).

EVOLUTION OF CORONAL MASS EJECTION MORPHOLOGY WITH INCREASING HELIOCENTRIC DISTANCE. II. IN SITU OBSERVATIONS

N. P. **Savani**¹, M. J. Owens^{2,3}, A. P. Rouillard^{4,5}, R. J. Forsyth³, K. Kusano^{1,6}, D. Shiota⁷, R. Kataoka⁸, L. Jian⁹ and V. Bothmer

2011 ApJ 732 117, **File**

Interplanetary coronal mass ejections (ICMEs) are often observed to travel much faster than the ambient solar wind. If the relative speed between the two exceeds the fast magnetosonic velocity, then a shock wave will form. The Mach number and the shock standoff distance ahead of the ICME leading edge is measured to infer the vertical size of an ICME in a direction that is perpendicular to the solar wind flow. We analyze the shock standoff distance for 45 events varying between 0.5 AU and 5.5 AU in order to infer their physical dimensions. We find that the average ratio of the inferred vertical size to measured radial width, referred to as the aspect ratio, of an ICME is 2.8 ± 0.5 . We also compare these results to the geometrical predictions from Paper I that forecast an aspect ratio between 3 and 6. The geometrical solution varies with heliocentric distance and appears to provide a theoretical maximum for the aspect ratio of ICMEs. The minimum aspect ratio appears to remain constant at 1 (i.e., a circular cross section) for all distances. These results suggest that possible distortions to the leading edge of ICMEs are frequent. But, these results may also indicate that the

constants calculated in the empirical relationship correlating the different shock front need to be modified; or perhaps both distortions and a change in the empirical formulae are required.

EVOLUTION OF CORONAL MASS EJECTION MORPHOLOGY WITH INCREASING HELIOCENTRIC DISTANCE. I. GEOMETRICAL ANALYSIS

N. P. [Savani](#)¹, M. J. Owens^{2,3}, A. P. Rouillard^{4,5}, R. J. Forsyth³, K. Kusano^{1,6}, D. Shiota⁷ and R. Kataoka
2011 ApJ 731 109

At launch, coronal mass ejections (CMEs) are often approximated as locally cylindrical objects with circular cross sections. However, CMEs have long been known to propagate almost radially away from the Sun along with the bulk solar wind. This has important consequences for the structure of CMEs; an initially circular cross section will be severely flattened by this radial motion. Yet calculations of total flux and helicity transport by CMEs based on in situ observations still use the assumption of a locally cylindrical object. In this paper, we investigate the morphology of an interplanetary CME based upon geometric arguments. By radially propagating an initial cylindrical object that maintains a constant ratio between its expansion speed and bulk flow, A , we show that the flattening, or "pancaking," of the two-dimensional cross section effectively ceases; the aspect ratios of these CMEs converge to a fixed value as they propagate further into the heliosphere. Thereafter the CME morphology is scale invariant. We predict aspect ratios of 5 ± 1 at terrestrial distances. By correlating a planetary shock with an interplanetary shock linked to a CME, these aspect ratios are estimated using in situ measurements in Paper II. These estimates are made at various heliocentric distances.

OBSERVATIONAL EVIDENCE OF A CORONAL MASS EJECTION DISTORTION DIRECTLY ATTRIBUTABLE TO A STRUCTURED SOLAR WIND

N. P. [Savani](#)¹, M. J. Owens^{1,5}, A. P. Rouillard^{2,3}, R. J. Forsyth¹, and J. A. Davies⁴
Astrophysical Journal Letters, 714:L128–L132, **2010 May**; **File**

We present the first observational evidence of the near-Sun distortion of the leading edge of a coronal mass ejection (CME) by the ambient solar wind into a concave structure. On **2007 November 14**, a CME was observed by coronagraphs onboard the *STEREO-B* spacecraft, possessing a circular cross section. Subsequently the CME passed through the field of view of the *STEREO-B* Heliospheric Imagers where the leading edge was observed to distort into an increasingly concave structure. The CME observations are compared to an analytical flux rope model constrained by a magnetohydrodynamic solar wind solution. The resultant bimodal speed profile is used to kinematically distort a circular structure that replicates the initial shape of the CME. The CME morphology is found to change rapidly over a relatively short distance. This indicates an approximate radial distance in the heliosphere where the solar wind forces begin to dominate over the magnetic forces of the CME influencing the shape of the CME.

The radial width of a Coronal Mass Ejection between 0.1 and 0.4 AU estimated from the Heliospheric Imager on STEREO

N.P. [Savani](#), A.P. Rouillard, J.A. Davies, M.J. Owens, R.J. Forsyth, C.J. Davis, and R.A. Harrison
Ann. Geophys., 27, 4349-4358, **2009**
www.ann-geophys.net/27/4349/2009/

On **15–17 February 2008**, a CME with an approximately circular cross section was tracked through successive images obtained by the Heliospheric Imager (HI) instrument onboard the *STEREO-A* spacecraft. Reasoning that an idealised flux rope is cylindrical in shape with a circular cross-section, best fit circles are used to determine the radial width of the CME. As part of the process the radial velocity and longitude of propagation are determined by fits to elongation-time maps as 252 ± 5 km/s and $70 \pm 5^\circ$ respectively. With the longitude known, the radial size is calculated from the images, taking projection effects into account. The radial width of the CME, S (AU), obeys a power law with heliocentric distance, R , as the CME travels between 0.1 and 0.4 AU, such that $S = 0.26 R^{0.6 \pm 0.1}$. The exponent value obtained is compared to published studies based on statistical surveys of in situ spacecraft observations of ICMEs between 0.3 and 1.0 AU, and general agreement is found. This paper demonstrates the new opportunities provided by HI to track the radial width of CMEs through the previously unobservable zone between the LASCO field of view and Helios in situ measurements.

New insights from cross-correlation studies between solar activity indices and cosmic-ray flux during Forbush decrease events

Mihailo **Savić**, Nikola Veselinović, Aleksandar Dragić, Dimitrije Maletić, Dejan Joković, Vladimir Udovičić, Radomir Banjanac, David Knežević

[Advances in Space Research](#) **Volume 71, Issue 4**, 15 February 2023, Pages 2006-2016

<https://doi.org/10.1016/j.asr.2022.09.057>

Observed [galactic cosmic ray](#) intensity can be subjected to a transient decrease. These so-called [Forbush decreases](#) are driven by [coronal mass ejection](#) induced shockwaves in the [heliosphere](#). By combining [in situ measurements](#) by space borne instruments with ground-based cosmic ray observations, we investigate the relationship between [solar energetic particle](#) flux, various solar activity indices, and intensity measurements of cosmic rays during such an event. We present cross-correlation study done using proton flux data from the SOHO/ERNE instrument, as well as data collected during some of the strongest Forbush decreases over the last two completed solar cycles by the network of neutron monitor detectors and different [solar observatories](#). We have demonstrated connection between the shape of solar energetic particles [fluence](#) spectra and selected coronal mass ejection and Forbush decrease parameters, indicating that power exponents used to model these fluence spectra could be valuable new parameters in similar analysis of mentioned phenomena. They appear to be better predictor variables of Forbush decrease magnitude in [interplanetary magnetic field](#) than coronal mass ejection velocities.

Rigidity dependence of Forbush decreases in the energy region exceeding the sensitivity of neutron monitors

M.**Savić** [N.Veselinović](#) [A.Dragić](#) [D.Maletić](#) [D.Joković](#) [R.Banjanac](#) [V.Udovičić](#)

[Advances in Space Research](#) **Volume 63, Issue 4**, 15 February 2019, Pages 1483-1489

<https://sci-hub.ru/10.1016/j.asr.2018.09.034>

Applicability of our present setup for solar [modulation](#) studies in a shallow underground laboratory is tested on four prominent examples of Forbush decrease during [solar cycle](#)24. Forbush decreases are of interest in [space weather](#) application and study of energy-dependent solar modulation, and they have been studied extensively. The characteristics of these events, as recorded by various neutron monitors and our detectors, were compared, and rigidity spectrum was found. Linear regression was performed to find power indices that correspond to each event. As expected, a steeper spectrum during more intense extreme solar events with strong X-flares shows a greater modulation of [galactic cosmic rays](#). Presented comparative analysis illustrates the applicability of our setup for studies of solar modulation in the energy region exceeding the sensitivity of neutron monitors. **March 8, 2012, September 12, 2014, June 22, 2015, Sept 06-08, 2017**

Hit or Miss, Arrival Time, and Bz Orientation Predictions of BATS-R-US CME Simulations at 1 AU

J. M. **Schmidt**, [Iver H. Cairns](#)

Space Weather **2019**

<https://arxiv.org/pdf/1905.08961.pdf>

Using a refined setup process, we simulated the propagation of six observed Coronal Mass Ejections (CMEs) with the 2012 Block-Adaptive-Tree-Solarwind-Roe-Upwind-Scheme (BATS-R-US) code from the Sun to the Earth or STEREO A and compared the outputs with observations. A linear relation between the average CME speed below 6 solar radii and the flux rope current is demonstrated and used to tune the simulations. The simulations correctly predict if and when an observable CME shock reaches one astronomical unit (AU). The arrival time predictions of the CME shocks at 1 AU have an accuracy of 0.9 ± 1.9 hours. The simulated initial CME speeds and average accelerations are close to the model and data of Gopalswamy et al., 2000. The approach shows promise for predicting the sense of the predominant shock-associated change in the magnetic field component Bz. However, the magnetic fields and plasma conditions in the solar wind and CME are not predicted well quantitatively.

See:

Can One Predict Coronal Mass Ejection Arrival Times With Thirty-Minute Accuracy?

Gábor **Tóth**, [Bart van der Holst](#), [Ward Manchester IV](#)

Space Weather e2023SW003463 [Volume21, Issue5](#) **2023**

<https://agupubs.onlinelibrary.wiley.com/doi/epdf/10.1029/2023SW003463>

Type II solar radio bursts predicted by 3D MHD CME and kinetic radio emission simulations†

J. M. [Schmidt*](#), Iver H. Cairns
JGR, 2014

Impending space weather events at Earth are often signalled by type II solar radio bursts. These bursts are generated upstream of shock waves driven by coronal mass ejections (CMEs) that move away from the Sun. We combine elaborate three-dimensional (3D) magnetohydrodynamic (MHD) predictions of realistic CMEs near the Sun with a recent analytic kinetic radiation theory in order to simulate two type II bursts. Magnetograms of the Sun are used to reconstruct initial solar magnetic and active region fields for the modeling. STEREO spacecraft data are used to dimension the flux rope of the initial CME, launched into an empirical data driven corona and solar wind. We demonstrate impressive accuracy in time, frequency, and intensity for the two type II bursts observed by the WIND spacecraft on **15 February 2011 and 7 March 2012**. Propagation of the simulated CME-driven shocks through coronal plasmas containing pre-existing density and magnetic field structures that stem from the coronal setup and CME initiation closely reproduce the isolated islands of type II emission observed. These islands form because of a competition between the growth of the radio source due to spherical expansion, and a fragmentation of the radio source due to increasingly radial fields in the nose region of the shock and interactions with streamers in the flank regions of the shock. Our study provides strong support for this theory for type II bursts and implies that the physical processes involved are understood. It also supports a near-term capability to predict and track these events for space weather predictions.

Low geo-effectiveness of fast halo CMEs related to the 12 X-class flares in 2002

B. [Schmieder](#), [R.S. Kim](#), [B. Grison](#), [K. Bocchialini](#), [R.Y. Kwon](#), [S. Poedts](#), [P. Démoulin](#)

JGR [Volume125, Issue6](#) e2019JA027529 2020

<https://arxiv.org/pdf/2003.10777.pdf>

https://agupubs.onlinelibrary.wiley.com/doi/pdf/10.1029/2019JA027529?casa_token=qNyoJvbrF9EAAAAA:Ov2NI1dg sV-48ml5iYKPeVMo8rzYNjcTdotpY2DvAZMmhzG4xKlxInv7r3iXohm6XiKTrqXwz6Gvz087
sci-hub.tw/10.1029/2019JA027529

It is generally accepted that extreme space weather events tend to be related to strong flares and fast halo coronal mass ejections CMEs. In the present paper, we carefully identify the chain of events from the Sun to the Earth induced by all 12 X-class flares that occurred in 2002. In this small sample, we find an unusual high rate (58%) of solar sources with a longitude larger than 74 degrees. Yet, all 12 X-class flares are associated with at least one CME. The fast halo CMEs (50%) are related to interplanetary CMEs (ICMEs) at L1 and weak Dst minimum values (>-51 nT); while 5 (41%) of the 12 X-class flares are related to solar proton events (SPE). We conclude that: (i) All twelve analyzed solar events, even those associated with fast halo CMEs originating from the central disk region, and those ICMEs and SPEs were not very geo-effective. This unexpected result demonstrates that the suggested events in the chain (fast halo CME, X-class flares, central disk region, ICME, SPE) are not infallible proxies for geo-effectiveness. (ii) The low value of integrated and normalized southward component of the IMF (B^*z) may explain the low geo-effectiveness for this small sample. In fact, B^*z is well correlated to the weak Dst and low auroral electrojet (AE) activity. Hence, the only space weather impact at Earth in 2002 we can explain is based on B^*z at L1. **2002: Apr-21, May-20, Jul-03, Jul-15, Jul-18, Jul-20, Jul-23, Aug-03, Aug-21, Aug-24, Aug-30, Oct-31**

Table 1. Properties of the 12 X-class ares in 2002 and their related phenomena.

Extreme solar storms based on solar magnetic field

Brigitte [Schmieder](#)

Varsiti Conference in Varna June 2016

2017

<https://arxiv.org/pdf/1708.01790.pdf>

File

Many questions have to be answered before understanding the relationship between the emerging magnetic flux through the solar surface and the extreme geoeffective events. Which threshold determines the onset of the eruption? What is the upper limit in energy for a flare? Is the size of sunspot the only criteria to get extreme solar events?

Based on observations of previous solar cycles, and theory, the main ingredients for getting X ray class flares and large Interplanetary Corona Mass Ejections e.g. the built up of the electric current in the corona, are presented such as the existence of magnetic free energy, magnetic helicity, twist and stress in active regions. The upper limit of solar flare energy in space research era and the possible chances to get super-flares and extreme solar events can be predicted using MHD simulation of coronal mass ejections. **September 1, 1859, July 25 1946, April 4-5, 1947, August 1972, October 28 2003, October 28, October 29 and November 4, November 17 2003, October 2014.**

Actors of the main activity in large complex centres during the 23 solar cycle maximum

B. [Schmieder](#) ^{a,*}, P. Dermoulin ^a, E. Pariat ^a, T. ToËroËk ^{a,1}, G. Molodij ^a, C.H. Mandrini ^b, S. Dasso ^b, R. Chandra ^c, W. Uddin ^d, P. Kumar ^d, P.K. Manoharan ^e, P. Venkatakrishnan ^f, N. Srivastava
Advances in Space Research 47 (2011) 2081–2091, [File](#)

During the maximum of Solar Cycle 23, large active regions had a long life, spanning several solar rotations, and produced large numbers of X-class flares and CMEs, some of them associated to magnetic clouds (MCs). This is the case for the Halloween active regions in 2003. The most geoeffective MC of the cycle (Dst = -457) had its source during the disk passage of one of these active regions (NOAA 10501) on 18 November 2003. Such an activity was presumably due to continuous emerging magnetic flux that was observed during this passage. Moreover, the region exhibited a complex topology with multiple domains of different magnetic helicities. The complexity was observed to reach such unprecedented levels that a detailed multi-wavelength analysis is necessary to precisely identify the solar sources of CMEs and MCs. Magnetic clouds are identified using in situ measurements and interplanetary scintillation (IPS) data. Results from these two different sets of data are also compared.

Using an Ellipsoid Model to Track and Predict the Evolution and Propagation of Coronal Mass Ejections

S. [Schreiner](#) ¹, C. Cattell ¹, K. Kersten ¹ and A. Hupach
Solar Phys., 2013, Volume 288, Issue 1, pp 291-309

We present a method for tracking and predicting the propagation and evolution of coronal mass ejections (CMEs) using the imagers on the STEREO and SOHO satellites. By empirically modeling the material between the inner core and leading edge of a CME as an expanding, outward propagating ellipsoid, we track its evolution in three-dimensional space. Though more complex empirical CME models have been developed, we examine the accuracy of this relatively simple geometric model, which incorporates relatively few physical assumptions, including i) a constant propagation angle and ii) an azimuthally symmetric structure. Testing our ellipsoid model developed herein on three separate CMEs, we find that it is an effective tool for predicting the arrival of density enhancements and the duration of each event near 1 AU. For each CME studied, the trends in the trajectory, as well as the radial and transverse expansion are studied from 0 to ~0.3 AU to create predictions at 1 AU with an average accuracy of 2.9 hours.

Erratum: *Solar Physics*, November 2013, Volume 288, Issue 1, p 311

Space Weather From Explosions on the Sun: How Bad Could It Be?

Carolus J. [Schrijver](#) ¹ and Jürg Beer

Eos, Transactions American Geophysical Union, Volume 95, Issue 24, pages 201–202, 17 June 2014
<http://onlinelibrary.wiley.com/doi/10.1002/2014EO240001/pdf>

The variable conditions in geospace driven by the Sun's magnetic activity, known as space weather, pose an increasing threat to society [National Research Council, 2008]. Of particular concern are the infrequent and poorly known extremes.

Estimating the frequency of extremely energetic solar events, based on solar, stellar, lunar, and terrestrial records

[Schrijver](#), C. J.; Beer, J.; Baltensperger, U.; Cliver, E. W.; GÖdel, M.; Hudson, H. S.; McCracken, K. G.; Osten, R. A.; Peter, T.; Soderblom, D. R.; Usoskin, I. G.; Wolff, E. W.
J. Geophys. Res., Vol. 117, No. A8, A08103, 2012

<http://dx.doi.org/10.1029/2012JA017706>

The most powerful explosions on the Sun – in the form of bright flares, intense storms of solar energetic particles (SEPs), and fast coronal mass ejections (CMEs) – drive the most severe space-weather storms. Proxy records of flare energies based on SEPs in principle may offer the longest time base to study infrequent large events. We conclude that one suggested proxy, nitrate concentrations in polar ice cores, does not map reliably to SEP events. Concentrations of select radionuclides measured in natural archives may prove useful in extending the time interval of direct observations up to ten millennia, but as their calibration to solar flare fluences depends on multiple poorly known properties and processes, these proxies cannot presently be used to help determine the flare energy frequency distribution. Being thus limited to the use of direct flare observations, we evaluate the probabilities of large-energy solar events by combining solar flare observations with an ensemble of stellar flare observations. We conclude that solar flare energies form a relatively smooth distribution from small events to large flares, while flares on magnetically active, young Sun-like stars have energies and frequencies markedly in excess of strong solar flares, even after an empirical scaling with the mean coronal activity level of these stars. In order to empirically quantify the frequency of uncommonly large solar flares

extensive surveys of stars of near-solar age need to be obtained, such as is feasible with the Kepler satellite. Because the likelihood of flares larger than approximately X30 remains empirically unconstrained, we present indirect arguments, based on records of sunspots and on statistical arguments, that solar flares in the past four centuries have likely not substantially exceeded the level of the largest flares observed in the space era, and that there is at most about a 10% chance of a flare larger than about X30 in the next 30 years.

Space Weather model moves into prime time.

Schultz C.

Space Weather 9, S03005, 2011.

When category 5 Tropical Cyclone Yasi struck the northeastern coast of Australia in early February, it left hundreds of thousands of people without power but none dead or seriously injured, possibly thanks to the detailed forecasting efforts that warned Australians, tens of thousands of whom then sought emergency shelter. But as society increases its dependence on space-based technology, it may be vulnerable to space weather that forecasters cannot predict with current capabilities. "We've recognized terrestrial weather as a hazard for millennia," said Jeffrey Hughes, director of the Center for Integrated Space Weather Modeling (CISM). "Space weather," on the other hand, "has only been recognized as a hazard relatively recently."

Seed Population Pre-Conditioning and Acceleration Observed by Parker Solar Probe

N. A. [Schwadron](#), [S. Bale](#), [J. Bonnell](#), [A. Case](#), [E. R. Christian](#), [C. M. S. Cohen](#),

ApJ 2019

<https://arxiv.org/pdf/1912.02888.pdf>

A series of solar energetic particle (SEP) events were observed at Parker Solar Probe (PSP) by the Integrated Science Investigation of the Sun (ISOIS) during the period from **April 18, 2019 through April 24, 2019**. The PSP spacecraft was located near 0.48 au from the Sun on Parker spiral field lines that projected out to 1 au within $\sim 25^\circ$ of near Earth spacecraft. These SEP events, though small compared to historically large SEP events, were amongst the largest observed thus far in the PSP mission and provide critical information about the space environment inside 1 au during SEP events. During this period the Sun released multiple coronal mass ejections (CMEs). One of these CMEs observed was initiated on **April 20, 2019** at 01:25 UTC, and the interplanetary CME (ICME) propagated out and passed over the PSP spacecraft. Observations by the Electromagnetic Fields Investigation (FIELDS) show that the magnetic field structure was mostly radial throughout the passage of the compression region and the plasma that followed, indicating that PSP did not directly observe a flux rope internal to the ICME, consistent with the location of PSP on the ICME flank. Analysis using relativistic electrons observed near Earth by the Electron, Proton and Alpha Monitor (EPAM) on the Advanced Composition Explorer (ACE) demonstrates the presence of electron seed populations (40--300 keV) during the events observed. The energy spectrum of the ISOIS-observed proton seed population below 1 MeV is close to the limit of possible stationary state plasma distributions out of equilibrium. ISOIS-observations reveal the \backslash revise{enhancement} of seed populations during the passage of the ICME, which \backslash revise{likely indicates a key part} of the pre-acceleration process that occurs close to the Sun.

THE SOLAR WIND POWER FROM MAGNETIC FLUX

N. A. [Schwadron](#)^{1,2} and D. J. McComas²

Astrophysical Journal, 686: L33–L36, 2008 October

<http://www.journals.uchicago.edu/doi/pdf/10.1086/592877>

Observations of the fast, high-latitude solar wind throughout *Ulysses*' three orbits show that solar wind power correlates remarkably well with the Sun's total open magnetic flux. These observations support a recent model of the solar wind energy and particle sources, where magnetic flux emergence naturally leads to an energy flux proportional to the strength of the large-scale magnetic field. This model has also been shown to be consistent with X-ray observations of the Sun and a variety of other stars over 12 decades of magnetic flux. The observations reported here show that the Sun delivers ~ 600 kW Wb_{\perp} to power the solar wind, and that this power to magnetic flux relation has been extremely stable over the last 15 years. Thus, the same law that governs energy released in the corona and from other stars also applies to the total energy in the solar wind.

The association of coronal mass ejections with their effects near the Earth

R. [Schwenn](#)¹, A. Dal Lago², E. Huttunen³, and W. D. Gonzalez

Ann. Geophys., 23, 1033-1059, 2005, File

www.ann-geophys.net/23/1033/2005/

To this day, the prediction of space weather effects near the Earth suffers from a fundamental problem: The radial propagation speed of "halo" CMEs (i.e. CMEs pointed along the Sun-Earth-line that are known to be the main drivers of space weather disturbances) towards the Earth cannot be measured directly because of the unfavorable geometry. From inspecting many limb CMEs observed by the LASCO coronagraphs on SOHO we found that there is usually a good correlation between the radial speed and the lateral expansion speed V_{exp} of CME clouds. This latter quantity can also be determined for earthward-pointed halo CMEs. Thus, V_{exp} may serve as a proxy for the otherwise inaccessible radial speed of halo CMEs. We studied this connection using data from both ends: solar data and interplanetary data obtained near the Earth, for a period from January 1997 to 15 April 2001. The data were primarily provided by the LASCO coronagraphs, plus additional information from the EIT instrument on SOHO. Solar wind data from the plasma instruments on the SOHO, ACE and Wind spacecraft were used to identify the arrivals of ICME signatures. Here, we use "ICME" as a generic term for all CME effects in interplanetary space, thus comprising not only ejecta themselves but also shocks as well. Among 181 front side or limb full or partial halo CMEs recorded by LASCO, on the one hand, and 187 ICME events registered near the Earth, on the other hand, we found 91 cases where CMEs were uniquely associated with ICME signatures in front of the Earth. Eighty ICMEs were associated with a shock, and for 75 of them both the halo expansion speed V_{exp} and the travel time T_{tr} of the shock could be determined. The function $T_{\text{tr}}=203-20.77*\ln(V_{\text{exp}})$ fits the data best. This empirical formula can be used for predicting further ICME arrivals, with a 95% error margin of about one day. Note, though, that in 15% of comparable cases, a full or partial halo CME does not cause any ICME signature at Earth at all; every fourth partial halo CME and every sixth limb halo CME does not hit the Earth (false alarms). Furthermore, every fifth transient shock or ICME or isolated geomagnetic storm is not caused by an identifiable partial or full halo CME on the front side (missing alarms)

On the Role of Alfvénic Fluctuations as Mediators of Coherence within Interplanetary Coronal Mass Ejections: Investigation of Multi-spacecraft Measurements at 1 au

Camilla [Scolini](#), [Noe Lugaz](#), [Reka M. Winslow](#), [Charles J. Farrugia](#), [Norbert Magyar](#), [Fabio Bacchini](#)

ApJ 961 135 2024

<https://arxiv.org/pdf/2312.04480.pdf>

<https://iopscience.iop.org/article/10.3847/1538-4357/ad0ed1/pdf>

<https://arxiv.org/pdf/2412.08008>

Interplanetary coronal mass ejections (ICMEs) are defined as "coherent" if they are capable of responding to external perturbations in a collective manner. This implies that information must be able to propagate across ICME structures, and if this is not the case, single-point in-situ measurements cannot be considered as indicative of global ICME properties. Here, we investigate the role of Alfvénic fluctuations (AFs) as mediators of ICME coherence. We consider multi-point magnetic field and plasma measurements of 10 ICMEs observed by the ACE and Wind spacecraft at 1 au at longitudinal separations of 0.5° - 0.7° . For each event, we analyze the Alfvénicity in terms of the residual energy and cross helicity of fluctuations, and the coherence in terms of the magnetic correlation between Wind and ACE. We find that ~65% and 90% of ICME sheaths and magnetic ejecta (MEs), respectively, present extended AFs covering at least 20% of the structure. Cross helicity suggests AFs of solar and interplanetary origin may co-exist in the ICME population at 1 au. AFs are mainly concentrated downstream of shocks and in the back of MEs. The magnetic field is poorly correlated within sheaths, while the correlation decreases from the front to the back of the MEs for most magnetic field components. AFs are also associated with lower magnetic field correlations. This suggests either that ICME coherence is not mediated by Alfvén waves, implying that the coherence scale may be smaller than previously predicted, or that the magnetic field correlation is not a measure of coherence. 2001 Dec 29-30

Table 1. Summary of the ICME times at ACE and Wind 2000-2002

Characteristic Scales of Complexity and Coherence within Interplanetary Coronal Mass Ejections: Insights from Spacecraft Swarms in Global Heliospheric Simulations

Camilla [Scolini](#), [Reka M. Winslow](#), [Noé Lugaz](#), [Stefaan Poedts](#)

ApJ 944 46 2023

<https://arxiv.org/pdf/2212.01308>

<https://iopscience.iop.org/article/10.3847/1538-4357/aca893/pdf>

Many aspects of the three-dimensional (3-D) structure and evolution of interplanetary coronal mass ejections (ICMEs) remain unexplained. Here, we investigate two main topics: (1) the coherence scale of magnetic fields inside ICMEs, and (2) the dynamic nature of ICME magnetic complexity. We simulate ICMEs interacting with different solar winds using the linear force-free spheromak model incorporated into the EUHFORIA model. We place a swarm of ~20000

spacecraft in the 3-D simulation domain and characterize ICME magnetic complexity and coherence at each spacecraft based on simulated time series. Our simulations suggest that ICMEs retain a lower complexity and higher coherence along their magnetic axis, but that a characterization of their global complexity requires crossings along both the axial and perpendicular directions. For an ICME of initial half angular width of 45° that does not interact with other large-scale solar wind structures, global complexity can be characterized by as little as 7-12 spacecraft separated by 25° , but the minimum number of spacecraft rises to 50-65 (separated by 10°) if interactions occur. Without interactions, ICME coherence extends for 45° , 20° - 30° , 15° - 30° , and 0° - 10° for B, B_ϕ , B_θ , and Br, respectively. Coherence is also lower in the ICME west flank compared to the east flank due to Parker spiral effects. Moreover, coherence is reduced by a factor of 3-6 by interactions with solar wind structures. Our findings help constrain some of the critical scales that control the evolution of ICMEs and aid in the planning of future dedicated multi-spacecraft missions.

Causes and Consequences of Magnetic Complexity Changes within Interplanetary Coronal Mass Ejections: a Statistical Study

Camilla Scolini, [Réka M. Winslow](#), [Noé Lugaz](#), [Tarik M. Salman](#), [Emma E. Davies](#), [Antoinette B. Galvin](#)

ApJ 927 102 2021

<https://arxiv.org/pdf/2111.12637.pdf>

<https://iopscience.iop.org/article/10.3847/1538-4357/ac3e60/pdf>

We present the first statistical analysis of complexity changes affecting the magnetic structure of interplanetary coronal mass ejections (ICMEs), with the aim of answering the questions: How frequently do ICMEs undergo magnetic complexity changes during propagation? What are the causes of such changes? Do the in situ properties of ICMEs differ depending on whether they exhibit complexity changes? We consider multi-spacecraft observations of 31 ICMEs by MESSENGER, Venus Express, ACE, and STEREO between 2008 and 2014 while radially aligned. By analyzing their magnetic properties at the inner and outer spacecraft, we identify complexity changes which manifest as fundamental alterations or significant re-orientations of the ICME. Plasma and suprathermal electron data at 1 au, and simulations of the solar wind enable us to reconstruct the propagation scenario for each event, and to identify critical factors controlling their evolution. Results show that ~65% of ICMEs change their complexity between Mercury and 1 au and that interaction with multiple large-scale solar wind structures is the driver of these changes. Furthermore, 71% of ICMEs observed at large radial (>0.4 au) but small longitudinal (<15 degrees) separations exhibit complexity changes, indicating that propagation over large distances strongly affects ICMEs. Results also suggest ICMEs may be magnetically coherent over angular scales of at least 15 degrees, supporting earlier theoretical and observational estimates. This work presents statistical evidence that magnetic complexity changes are consequences of ICME interactions with large-scale solar wind structures, rather than intrinsic to ICME evolution, and that such changes are only partly identifiable from in situ measurements at 1 au. **June 2-3, 2009**,

Table 1. Sample of the ICMEs considered in this work

Evolution of interplanetary coronal mass ejection complexity: a numerical study through a swarm of simulated spacecraft

Camilla Scolini, [Reka M. Winslow](#), [Noé Lugaz](#), [Stefaan Poedts](#)

ApJL 916 L15 2021

<https://arxiv.org/pdf/2106.10554.pdf>

<https://doi.org/10.3847/2041-8213/ac0d58>

In-situ measurements carried out by spacecraft in radial alignment are critical to advance our knowledge on the evolutionary behavior of coronal mass ejections (CMEs) and their magnetic structures during propagation through interplanetary space. Yet, the scarcity of radially aligned CME crossings restricts investigations on the evolution of CME magnetic structures to a few case studies, preventing a comprehensive understanding of CME complexity changes during propagation. In this paper, we perform numerical simulations of CMEs interacting with different solar wind streams using the linear force-free spheromak CME model incorporated into the EUropean Heliospheric FOrecasting Information Asset (EUHFORIA) model. The novelty of our approach lies in the investigation of the evolution of CME complexity using a swarm of radially aligned, simulated spacecraft. Our scope is to determine under which conditions, and to what extent, CMEs exhibit variations of their magnetic structure and complexity during propagation, as measured by spacecraft that are radially aligned. Results indicate that the interaction with large-scale solar wind structures, and particularly with stream interaction regions, doubles the probability to detect an increase of the CME magnetic complexity between two spacecraft in radial alignment, compared to cases without such interactions. This work represents the first attempt to quantify the probability of detecting complexity changes in CME magnetic structures by spacecraft in radial alignment using numerical simulations, and it provides support to the interpretation of multi-point

CME observations involving past, current (such as Parker Solar Probe and Solar Orbiter), and future missions. **2020-01-03**

Exploring the radial evolution of interplanetary coronal mass ejections using EUHFORIA

C. [Scolini](#)^{1,2}, S. Dasso^{3,4}, L. Rodriguez², A. N. Zhukov^{2,5} and S. Poedts

A&A 649, A69 (2021)

<https://arxiv.org/pdf/2102.07569.pdf>

<https://doi.org/10.1051/0004-6361/202040226>

Context. Coronal mass ejections (CMEs) are large-scale eruptions coming from the Sun and transiting into interplanetary space. While it is widely known that they are major drivers of space weather, further knowledge of CME properties in the inner heliosphere is limited by the scarcity of observations at heliocentric distances other than 1 au. In addition, most CMEs are observed in situ by a single spacecraft and in-depth studies require numerical models to complement the few available observations.

Aims. We aim to assess the ability of the linear force-free spheromak CME model of the EUropean Heliospheric FORecasting Information Asset (EUHFORIA) to describe the radial evolution of interplanetary CMEs in order to yield new contexts for observational studies.

Methods. We modelled one well-studied CME with EUHFORIA, investigating its radial evolution by placing virtual spacecraft along the Sun–Earth line in the simulation domain. To directly compare observational and modelling results, we characterised the interplanetary CME signatures between 0.2 and 1.9 au from modelled time series, exploiting techniques that are traditionally employed to analyse real in situ data.

Results. Our results show that the modelled radial evolution of the mean solar wind and CME values is consistent with the observational and theoretical expectations. The CME expands as a consequence of the decaying pressure in the surrounding solar wind: the expansion is rapid within 0.4 au and moderate at larger distances. The early rapid expansion was not sufficient to explain the overestimated CME radial size in our simulation, suggesting this is an intrinsic limitation of the spheromak geometry applied in this case. The magnetic field profile indicates a relaxation on the part of the CME structure during propagation, while CME ageing is most probably not a substantial source of magnetic asymmetry beyond 0.4 au. Finally, we report a CME wake that is significantly shorter than what has been suggested by observations.

Conclusions. Overall, EUHFORIA provides a consistent description of the radial evolution of solar wind and CMEs, at least close to their centres. Nevertheless, improvements are required to better reproduce the CME radial extension.

12 July 2012

Improving predictions of high-latitude Coronal Mass Ejections throughout the heliosphere

C. [Scolini](#), [E. Chané](#), [J. Pomoell](#), [L. Rodriguez](#), [S. Poedts](#)

Space Weather **2020**

<https://agupubs.onlinelibrary.wiley.com/doi/pdf/10.1029/2019SW002246>

Predictions of the impact of Coronal Mass Ejections (CMEs) in the heliosphere mostly rely on cone CME models, whose performances are optimised for locations in the ecliptic plane and at 1 AU (e.g. at Earth). Progresses in the exploration of the inner heliosphere, however, advocate the need to assess their performances at both higher latitudes and smaller heliocentric distances. In this work, we perform 3-D MHD simulations of artificial cone CMEs using the EUropean Heliospheric FORecasting Information Asset (EUHFORIA), investigating the performances of cone models in the case of CMEs launched at high latitudes. We compare results obtained initialising CMEs using a commonly-applied approximated (Euclidean) distance relation and using a proper (great-circle) distance relation.

Results show that initialising high-latitude CMEs using the Euclidean approximation results in a teardrop-shaped CME cross section at the model inner boundary that fails in reproducing the initial shape of high-latitude cone CMEs as a circular cross section. Modelling errors arising from the use of an inappropriate distance relation at the inner boundary eventually propagate to the heliospheric domain. Errors are most prominent in simulations of high-latitude CMEs and at the location of spacecraft at high latitudes and/or small distances from the Sun, with locations impacted by the CME flanks being the most error-sensitive. This work shows that the low-latitude approximations commonly employed in cone models, if not corrected, may significantly affect CME predictions at various locations compatible with the orbit of space missions such as Parker Solar Probe, Ulysses and Solar Orbiter.

CME-CME Interactions as Sources of CME Geo-effectiveness: The Formation of the Complex Ejecta and Intense Geomagnetic Storm in Early September 2017

Camilla [Scolini](#), [Emmanuel Chané](#), [Manuela Temmer](#), [Emilia K. J. Kilpua](#), [Karin Dissauer](#), [Astrid M. Veronig](#), [Erika Palmerio](#), [Jens Pomoell](#), [Mateja Dumbović](#), [Jingnan Guo](#), [Luciano Rodriguez](#), [Stefaan Poedts](#)
ApJS 247 21 2020

<https://arxiv.org/pdf/1911.10817.pdf>

<https://sci-hub.si/10.3847/1538-4365/ab6216>

Coronal mass ejections (CMEs) are the primary sources of intense disturbances at Earth, where their geo-effectiveness is largely determined by their dynamic pressure and internal magnetic field, which can be significantly altered during interactions with other CMEs in interplanetary space. We analyse three successive CMEs that erupted from the Sun during September 4-6, 2017, investigating the role of CME-CME interactions as source of the associated intense geomagnetic storm ($Dst_{min} = -142$ nT on September 7). To quantify the impact of interactions on the (geo-)effectiveness of individual CMEs, we perform global heliospheric simulations with the EUHFORIA model, using observation-based initial parameters with the additional purpose of validating the predictive capabilities of the model for complex CME events. The simulations show that around 0.45 AU, the shock driven by the September 6 CME started compressing a preceding magnetic ejecta formed by the merging of two CMEs launched on September 4, significantly amplifying its B_z until a maximum factor of 2.8 around 0.9 AU. The following gradual conversion of magnetic energy into kinetic and thermal components reduced the B_z amplification until its almost complete disappearance around 1.8 AU. We conclude that a key factor at the origin of the intense storm triggered by the **September 4-6, 2017** CMEs was their arrival at Earth during the phase of maximum B_z amplification. Our analysis highlights how the amplification of the magnetic field of individual CMEs in space-time due to interaction processes can be characterised by a growth, a maximum, and a decay phase, suggesting that the time interval between the CME eruptions and their relative speeds are critical factors in determining the resulting impact of complex CMEs at various heliocentric distances (heliogeo-effectiveness).

EGU2020 presentation # 1777 File

Effect of the Initial Shape of Coronal Mass Ejections on 3-D MHD Simulations and Geoeffectiveness Predictions

C. [Scolini](#) C. [Verbeke](#) S. [Poedts](#) E. [Chané](#) J. [Pomoell](#) F. P. [Zuccarello](#)

Space Weather Volume 16, Issue 6 June 2018 Pages 754-771

<http://sci-hub.tw/https://onlinelibrary.wiley.com/doi/abs/10.1029/2018SW001806>

Coronal mass ejections (CMEs) are the major space weather drivers, and an accurate modeling of their onset and propagation up to 1 AU represents a key issue for more reliable space weather forecasts. In this paper we use the newly developed European Heliospheric FORecasting Information Asset (EUHFORIA) heliospheric model to test the effect of different CME shapes on simulation outputs. In particular, we investigate the notion of “spherical” CME shape, with the aim of bringing to the attention of the space weather community the great implications of the CME shape implementation details for simulation results and geoeffectiveness predictions. We take as case study an artificial Earth-directed CME launched on **6 June 2008**, corresponding to a period of quiet solar wind conditions near Earth. We discuss the implementation of the cone model used to inject the CME into the modeled ambient solar wind, running several simulations of the event and investigating the outputs in interplanetary space and at different spacecraft and planetary locations. We apply empirical relations to simulation outputs at L1 to estimate the expected CME geoeffectiveness in terms of the magnetopause stand-off distance and the induced K_p index. Our analysis shows that talking about spherical CMEs is ambiguous unless one has detailed information on the implementation of the CME shape in the model. All the parameters specifying the CME shape in the model significantly affect simulation results at 1 AU as well as the predicted CME geoeffectiveness, confirming the pivotal role played by the shape implementation details in space weather forecasts.

Halo Coronal Mass Ejections during Solar Cycle 24: reconstruction of the global scenario and geoeffectiveness

Camilla [Scolini](#), [Mauro Messerotti](#), [Stefaan Poedts](#), [Luciano Rodriguez](#)

Journal of Space Weather and Space Climate 2018, 8, A09

<https://arxiv.org/pdf/1712.05847.pdf>

<https://www.swsc-journal.org/articles/swsc/pdf/2018/01/swsc170032.pdf> **File**

Coronal mass ejections (CMEs), in particular Earth-directed ones, are regarded as the main drivers of geomagnetic activity. In this study, we present a statistical analysis of a set of 53 fast ($V \geq 1000 \text{ km}\cdot\text{s}^{-1}$) Earth-directed halo CMEs observed by the SOHO/LASCO instrument during the period Jan. 2009–Sep. 2015, and we then use this CME sample to test the forecasting capabilities of a new Sun-to-Earth prediction scheme for the geoeffectiveness of Earth-directed halo CMEs. First, we investigate the CME association with other solar activity features such as solar flares, active regions, and others, by means of multi-instrument observations of the solar magnetic and plasma properties, with the final aim of identifying recurrent peculiar features that can be used as precursors of CME-driven geomagnetic storms. Second, using coronagraphic images to derive the CME kinematical properties at 0.1 AU, we propagate the events to 1 AU by means of 3D global MHD simulations. In particular, we use the WSA-ENLIL+Cone model to reconstruct the propagation and global evolution of each event up to their arrival at Earth, where simulation results are compared with interplanetary CME (ICME) in-situ signatures. We then use simulation outputs upstream of Earth to predict their impact on geospace. By applying the pressure balance condition at the magnetopause and the coupling function proposed by Newell et al. [J Geophys Res: Space Phys 113 (2008)] to link upstream solar wind properties to the global Kp index, we estimate the expected magnetospheric compression and geomagnetic activity level, and compare our predictions with global data records. The analysis indicates that 82% of the fast Earth-directed halo CMEs arrived at Earth within the next 4 days. Almost the totality of them compressed the magnetopause below geosynchronous orbits and triggered a minor or major geomagnetic storm afterwards. Among them, complex sunspot-rich active regions associated with X- and M-class flares are the most favourable configurations from which geoeffective CMEs originate. The analysis of related Solar Energetic Particle (SEP) events shows that 74% of the CMEs associated with major SEPs were geoeffective, i.e. they triggered a minor to intense geomagnetic storm ($K_p \geq 5$). Moreover, the SEP production is enhanced in the case of fast and interacting CMEs. In this work we present a first attempt at applying a Sun-to-Earth geoeffectiveness prediction scheme – based on 3D simulations and solar wind-geomagnetic activity coupling functions – to a statistical set of fast Earth-directed, potentially geoeffective halo CMEs. The results of the prediction scheme are promising and in good agreement with the actual data records for geomagnetic activity. However, we point out the need for future studies performing a fine-tuning of the prediction scheme, in particular in terms of the evaluation of the CME input parameters and the modelling of their internal magnetic structure. **5-13 March 2012, 18-27 June 2015,**
Table 1. Complete list of the selected CME events.

Exploring the radial evolution of Interplanetary Coronal Mass Ejections using EUHFORIA

Camilla [Scolini](#), [Sergio Dasso](#), [Luciano Rodriguez](#), [Andrei N. Zhukov](#), [Stefaan Poedts](#)

A&A **2015**

<https://arxiv.org/pdf/2102.07569.pdf>

Coronal Mass Ejections (CMEs) are large-scale eruptions from the Sun into interplanetary space. Despite being major space weather drivers, our knowledge of the CME properties in the inner heliosphere remains constrained by the scarcity of observations at distances other than 1 au. Furthermore, most CMEs are observed in situ by single spacecraft, requiring numerical models to complement the sparse observations available. We aim to assess the ability of the linear force-free spheromak CME model in EUHFORIA to describe the radial evolution of interplanetary CMEs, yielding new context for observational studies. We model one well-studied CME, and investigate its radial evolution by placing virtual spacecraft along the Sun-Earth line in the simulation domain. To directly compare observational and modelling results, we characterise the interplanetary CME signatures between 0.2 and 1.9 au from modelled time series, exploiting techniques traditionally employed to analyse real in situ data. Results show that the modelled radial evolution of the mean solar wind and CME values is consistent with observational and theoretical expectations. The CME expands as a consequence of the decaying pressure in the surrounding wind: the expansion is rapid within 0.4 au, and moderate at larger distances. The early rapid expansion could not explain the overestimated CME radial size in our simulation, suggesting this is an intrinsic limitation of the spheromak geometry used. The magnetic field profile indicates a relaxation of the CME during propagation, while ageing is most probably not a substantial source of magnetic asymmetry beyond 0.4 au. We also report a CME wake that is significantly shorter than suggested by observations. Overall, EUHFORIA provides a consistent description of the radial evolution of solar wind and CMEs; nevertheless, improvements are required to better reproduce the CME radial extension. **12 July 2012**

Using Ghost fronts within STEREO Heliospheric Imager data to infer the evolution in longitudinal structure of a Coronal Mass Ejection

C.J. [Scott](#), [M.J. Owens](#), [C.A. de Koning](#), [L.A. Barnard](#), [S.R. Jones](#), [J. Wilkinson](#)

Space Weather **Volume17, Issue4** Pages 539-552 **2019**

[sci-hub.se/10.1029/2018SW002093](https://doi.org/10.1029/2018SW002093)

Images of coronal mass ejections (CMEs) from the Heliospheric Imager (HI) instruments on board the STEREO spacecraft frequently contain rich structure. Here, we present analysis of the Earth-directed CME launched on **12 December 2008** in which we interpret the revealed structure as projections of separate discrete sections of the physical boundary of the CME. By comparing the relative position of the outer and inner 'ghost' fronts seen in the STEREO HI1 cameras with the positions of features determined from three CME models we show that the two fronts seen in the images correspond to the expected position of the flank and nose of the CME where the background solar wind is uniform. In contrast, the flank of the CME observed expanding into a structured background solar wind results in the elongation between the two fronts being greater than expected. This is consistent with the CME flank distorting in the presence of a high-speed solar wind stream. Further work is required to consolidate these results. The presence of a shock for this event was ruled out by consideration of the low CME speed and by studying in-situ spacecraft data. The CME flank crossing the Thomson sphere was also ruled out as a cause of the ghost fronts. Ghost fronts could provide information about the longitudinal shape of the CME independent of geometric models. This technique could subsequently be used to improve space weather forecast models through techniques such as data assimilation.

The role of interplanetary shock orientation on SC/SI rise time and geoeffectiveness

R. [Selvakumaran](#), , B. Veenadharia, , Y. Ebiharab, , Sandeep Kumara, , D.S.V.V.D. Prasad
Advances in Space Research Volume 59, Issue 5, 1 March **2017**, Pages 1425–1434

Interplanetary (IP) shocks interact with the Earth's magnetosphere, resulting in compression of the magnetosphere which in turn increases the Earth's magnetic field termed as Sudden commencement/Sudden impulse (SC/SI). Apart from IP shock speed and solar wind dynamic pressure, IP shock orientation angle also plays a major role in deciding the SC rise time. In the present study, the IP shock orientation angle and SC/SI rise time for 179 IP shocks are estimated which occurred during solar cycle 23. More than 50% of the Shock orientations are in the range of 140° – 160° . The SC/SI rise time decreases with the increase in the orientation angle and IP shock speed. In this work, the type of IP shocks i.e., Radio loud (RL) and Radio quiet (RQ) are examined in connection with SC/SI rise time. The RL associated IP shock speeds show a better correlation than RQ shocks with SC/SI rise time irrespective of the orientation angle. Magnetic Cloud (MC) associated shocks dominate in producing less rise time when compared to Ejecta (EJ) shocks. Magneto hydrodynamic (MHD) simulations are used for three different IP shock orientation categories to see the importance of orientation angle in determining the geoeffectiveness. Simulations results reveal that shocks hitting parallel to the magnetosphere are more geoeffective as compared to oblique shocks by means of change in magnetic field, pressure and Field Aligned Current (FAC).

On the reduced geoeffectiveness of solar cycle 24: a moderate storm perspective

R. [Selvakumaran](#), B. Veenadhari, S. Akiyama, Megha Pandya, N. Gopalswamy, S. Yashiro, Sandeep Kumar, P. Mäkelä, H. Xie

JGR **2016** DOI: 10.1002/2016JA022885 [File](#)

The moderate and intense geomagnetic storms are identified for the first 77 months of solar cycle 23 and 24. The solar sources responsible for the moderate geomagnetic storms are identified during the same epoch for both the cycles. Solar cycle 24 has shown nearly 80 % reduction in the occurrence of intense storms where as it is only 40 % in case of moderate storms when compared to previous cycle. The solar and interplanetary characteristics of the moderate storms driven by CME are compared for solar cycle 23 and 24 in order to see reduction in geoeffectiveness has anything to do with the occurrence of moderate storm. Though there is reduction in the occurrence of moderate storms, the Dst distribution does not show much difference. Similarly the solar source parameters like CME speed, mass and width did not show any significant variation in the average values as well as the distribution. The correlation between VBz and Dst is determined and it is found to be moderate with value of 0.68 for cycle 23 and 0.61 for cycle 24. The magnetospheric energy flux parameter epsilon (ϵ) is estimated during the main phase of all moderate storms during solar cycles 23 and 24. The energy transfer decreased in solar cycle 24 when compared to cycle 23. These results are significantly different when all geomagnetic storms are taken in to consideration for both the solar cycles.

Anisotropic Heating and Cooling within Interplanetary Coronal Mass Ejection Sheath Plasma

Zubair I. [Shaikh](#)¹, Daniel Verscharen², Ivan Y. Vasko³, Bennett A. Maruca⁴, Dibyendu Chakrabarty⁵, and Anil N. Raghav⁶

2024 ApJ 974 249

<https://iopscience.iop.org/article/10.3847/1538-4357/ad782b/pdf>

This study presents the first comprehensive investigation of the relationship between heating and cooling, temperature anisotropy, turbulence level, and collisional age within interplanetary coronal mass ejection (ICME) sheaths, which are

highly compressed, heated, and turbulent. Using Wind spacecraft data, we analyze 333 ICME sheaths observed at 1 au from 1995 to 2015. The proton temperature within the ICME sheaths has a log-normal probability distribution. Irrespective of instability growth rates, plasma unstable to proton-cyclotron (PC) and firehose instabilities appear to be statistically hotter, at least by a factor of 5 to 10, compared to stable plasma. We also observe relatively enhanced magnetic fluctuations and low collisional age, especially in regimes unstable to PC and firehose instabilities at low proton betas $\beta_p \leq 2$. In the case of high beta $\beta_p \geq 2$, we observe high magnetic fluctuations close to the instabilities and less collisional age to the plasma unstable to firehose instability rather than near the mirror mode and PC threshold. Our findings suggest that heating processes dominate over cooling processes in producing proton temperature anisotropy in the ICME sheath region. Moreover, collisional age and magnetic fluctuations are critical in maintaining anisotropic and isotropic conditions.

Statistical Plasma Properties of the Planar and Nonplanar ICME Magnetic Clouds during Solar Cycles 23 and 24

Zubair I. [Shaikh](#)¹ and Anil N. Raghav²

2022 ApJ 938 146

<https://iopscience.iop.org/article/10.3847/1538-4357/ac8f2b/pdf>

Various remote and in situ observations, along with several models, simulations, and kinetic studies, have been proposed in recent years, suggesting that the morphology of an interplanetary coronal mass ejection (ICME) magnetic cloud can vary from cylindrical, elliptical, toroidal, flattened, pancaked, etc. Recently, Raghav et al. proposed for the first time a unique morphological characteristic of an ICME magnetic cloud at 1 au that showed characteristics of a planar magnetic structure, using in situ data from the ACE spacecraft. In this study, we statistically investigate the plasma properties of planar and nonplanar ICMEs from 1998–2017 at 1 au. The detailed study of 469 ICMEs suggests that 136 (~29%) ICMEs are planar, whereas 333 (~71%) are nonplanar. Furthermore, total interplanetary magnetic field strength, average plasma parameters, i.e., plasma density, beta, thermal pressure, and magnetic pressure in planar ICME, are significantly higher than in the nonplanar ICME. Also, we noticed that the thickness of planar ICMEs is less compared to nonplanar ICMEs. This analysis demonstrates that planar ICMEs are formed due to the high compression of ICME. Moreover, we also observed the southward/northward magnetic field component's double strength during planar ICMEs compared to nonplanar ICMEs. It implies that planar ICMEs are more geoeffective than nonplanar ICMEs. **5-6 Apr 2010, 12-17 Jul 2013, 19-21 Aug 2014**

Table 1 List of Planar ICME MC/N-MCs from 1998–2017

Table 2 List of Nonplanar ICME MC/N-MCs from 1998–2017

CMEchaser, Detecting Line-of-Sight Occultations Due to Coronal Mass Ejections

Golam [Shaifullah](#), [Caterina Tiburzi](#) & [Pietro Zucca](#)

[Solar Physics](#) volume 295, Article number: 136 (2020)

<https://arxiv.org/pdf/2008.12153.pdf>

<https://link.springer.com/content/pdf/10.1007/s11207-020-01705-0.pdf>

We present a python-based tool to detect the occultation of back-ground sources by foreground solar coronal mass ejections. The tool takes as input standard celestial coordinates of the source and translates those to the helioprojective plane, and is thus well suited for use with a wide variety of background astronomical sources. This tool provides an easy means to search through a large archival dataset for such crossings and relies on the well-tested AstroPy and SunPy modules. **August 15, 2012, April 20, 2014, August 13 to 28, 2015**

Turbulence properties of interplanetary coronal mass ejection flux ropes at 1 au

Zubair I [Shaikh](#)

MNRAS, Volume 530, Issue 3, May 2024, Pages 3005–3012,

<https://doi.org/10.1093/mnras/stae897>

<https://watermark.silverchair.com/stae897.pdf>

Interplanetary coronal mass ejection (ICME) is a massive, coherent magnetic structure emitting from the Sun in interplanetary space and plays an essential role in space weather processes. Here, we focus on determining the turbulent characteristics of magnetic field fluctuations in 358 ICMEs magnetic flux ropes (MFR) at 1 au using Wind spacecraft data. We observed that during injection, inertial, and dissipation scales, the average spectral index of the analysed MFRs is -1.70 ± 0.26 , -1.64 ± 0.06 , and -2.31 ± 0.40 , respectively. It implies that overall the turbulence inside the ICME MFR has a Kolmogorow ($f^{-5/3}$) type spectrum. We observe the nature of the spectral index to be unaffected by the MFR boundary and the presence of a background magnetic field. Thus, coherent MFRs show some turbulent characteristics. The low compressibility value during injection and the inertial scale indicate that Alfvénic fluctuations

may dominate at these scales. We observe spectral break at the dissipation scale, but low normalized magnetic helicity denied the role of wave activity. Therefore, thorough research of the causes of a spectral break during the ICME MFR is necessary. Our results are relevant to exploring the energy cascade process, plasma heating, and energetic particle modulation in low plasma beta structures. **2001 November 24**

Proton Temperature Anisotropy within the Interplanetary Coronal Mass Ejections Sheath at 1 au

Zubair I. [Shaikh](#)¹, Anil N. Raghav², and Ivan Y. Vasko^{1,3}

2023 ApJL 955 L5

<https://iopscience.iop.org/article/10.3847/2041-8213/acf575/pdf>

The sheath plasma of interplanetary coronal mass ejections (ICMEs) is highly compressed, heated, turbulent, and magnetically intense relative to the ambient solar wind. In this Letter, we perform a detailed study of proton temperature anisotropy within the 333 ICME sheath regions observed on board the Wind spacecraft spanning the years 1995–2015. Our observations show that marginal stability thresholds of mirror mode and firehose instabilities predominantly constrain the proton temperature anisotropy within these sheath regions regardless of ICME sheath plasma speed. This is true even when the plasma beta values are less than 2, a parameter space that should have favored the prevalence of parallel firehose and proton cyclotron instabilities according to linear stability analysis. This investigation demonstrates the critical role played by distinct plasma instabilities in shaping the evolution of ICME sheath plasma compared to the broader solar wind environment.

Concurrent effect of Alfvén waves and planar magnetic structure on geomagnetic storms

Zubair I. [Shaikh](#), [Anil Raghav](#), [Geeta Vichare](#), [Ankush Bhaskar](#), [Wageesh Mishra](#), [Komal Choraghe](#)

MNRAS Volume 490, Issue 3, December **2019**, Pages 3440–3447,

sci-hub.se/10.1093/mnras/stz2806

Generally, interplanetary coronal mass ejection (ICME) triggers intense and strong geomagnetic storms. It has been established that the ICME sheath-moulded planar magnetic structure enhances the amplitude of the storms. Alfvén waves embedded in ICME magnetic clouds or high solar streams including corotating interacting regions (CIRs) in turn extend the recovery phase of the storm. Here, we investigate a geomagnetic storm with a very complex temporal profile with multiple decreasing and recovery phases. We examine the role of planar magnetic structure (PMS) and Alfvén waves in the various phases of the storm. We find that fast decrease and fast recovery phases are evident during transit of PMS regions, whereas a slight decrease or recovery is found during the transit of regions embedded with Alfvénic fluctuations. **2000 October 12**

The Identification of a Planar Magnetic Structure within the ICME Shock Sheath and Its influence on Galactic Cosmic-Ray Flux

Zubair I. [Shaikh](#)¹, Anil N. Raghav², Geeta Vichare¹, Ankush Bhaskar³, and Wageesh Mishra⁴

2018 ApJ 866 118

<http://iopscience.iop.org/article/10.3847/1538-4357/aae1b1/pdf>

A Forbush decrease is a sudden decrease in cosmic-ray intensity caused by transient interplanetary disturbances. The substructure of an interplanetary counterpart of a coronal mass ejection (ICME) such as a shock sheath and/or a magnetic cloud independently contributes to cosmic-ray decrease, which is evident as a two-step decrease. Our earlier work has shown multistep decrease and recovery within the ICME-driven shock-sheath region. Further, we have suggested that the presence of a small-scale flux rope within the shock-sheath region causes a steady/gradual recovery in cosmic-ray intensity. Here, we demonstrate the presence of a planar magnetic structure (PMS) and small-scale flux rope within a single shock sheath of an ICME. The plot of the elevation (θ) versus azimuthal (ϕ) angle of the interplanetary magnetic field (IMF) is used for the identification of the PMS. The planarity, efficiency, and a plane-normal vector are estimated by employing a minimum variance analysis (MVA) technique, which confirmed the presence of the PMS. In addition, a 2D-hodogram method in conjunction with the MVA technique is utilized to identify the flux-rope structure and turbulent conditions in the corresponding ICME region. The observation in the visible suggests that the PMS region within the ICME shock sheath caused the decrease in the cosmic-ray flux observed at Earth. It has also been observed that the sharp variations in the IMF (i.e., turbulence) cause a decrease, whereas the flux-rope structure is responsible for the recovery of the CR flux. Further studies are needed to investigate their origins and to confirm their effects on space weather. **2015 December 31**

The Presence of Turbulent and Ordered Local Structure within the ICME Shock-sheath and Its Contribution to Forbush Decrease

Zubair [Shaikh](#)^{1,2}, Anil Raghav^{2,3}, and Ankush Bhaskar

2017 ApJ 844 121

<http://sci-hub.cc/10.3847/1538-4357/aa729f>

The transient interplanetary disturbances evoke short-time cosmic-ray flux decrease, which is known as Forbush decrease. The traditional model and understanding of Forbush decrease suggest that the sub-structure of an interplanetary counterpart of coronal mass ejection (ICME) independently contributes to cosmic-ray flux decrease. These sub-structures, shock-sheath, and magnetic cloud (MC) manifest as classical two-step Forbush decrease. The recent work by Raghav et al. has shown multi-step decreases and recoveries within the shock-sheath. However, this cannot be explained by the ideal shock-sheath barrier model. Furthermore, they suggested that local structures within the ICME's sub-structure (MC and shock-sheath) could explain this deviation of the FD profile from the classical FD. Therefore, the present study attempts to investigate the cause of multi-step cosmic-ray flux decrease and respective recovery within the shock-sheath in detail. A 3D-histogram method is utilized to obtain more details regarding the local structures within the shock-sheath. This method unambiguously suggests the formation of small-scale local structures within the ICME (shock-sheath and even in MC). Moreover, the method could differentiate the turbulent and ordered interplanetary magnetic field (IMF) regions within the sub-structures of ICME. The study explicitly suggests that the turbulent and ordered IMF regions within the shock-sheath do influence cosmic-ray variations differently. **1998 September 24, 2000 September 17,**

Arrival time of solar eruptive CMEs associated with ICMEs of magnetic cloud and ejecta

A. [Shanmugaraju](#), M. Syed Ibrahim, Y.-J. Moon, K. Kasro Lourdhina, M. Dharanya

Astrophysics and Space Science April **2015**, 357:69

The Coronal Mass Ejection (CME) is an eruptive event in which magnetic plasma is ejected from the Sun into space through the solar corona. We considered a set of 51 Interplanetary Coronal Mass Ejections (ICMEs) listed by Kim et al. (Solar Phys. 184:77, 2013) from Coordinated Data Analysis Workshop (CDAW, Gopalswamy et al. in Astrophys. J. 710:1111, 2010). Among the 51 events, 22 events are classified as Magnetic Clouds (MC) and 29 events are classified as Ejecta (EJ) where the MC and EJ are subsets of ICMEs. We have analyzed the physical properties of CMEs and ICMEs associated with MC and EJ, and correlated them with the CME's transit time/arrival time from the Sun to the Earth. Main aims of the present study are to examine (a) dependence of transit time on the properties of CMEs and ICMEs, and (b) differences between MC and EJ. It is found that CME's initial speed decides the transit time which is in support of the known results in literature. Apart from this, some important results from the present study are: (i) transit time predicted using an empirical relation obtained in the present work is found comparable with the observations (correlation coefficient=0.70). (ii) The transit time of MC and EJ-associated CMEs ranges from 20 to 120 hours and IP acceleration lies between -10 m/s² to 5 m/s². (iii) There are certain differences between MC and EJ such as: (a) Ejecta takes slightly more time to travel and only 30 % of them are accelerated in the interplanetary medium. Whereas, MC takes less time to travel and nearly 50 % of them are accelerated, (b) The correlations of IP acceleration and speed with transit time are higher for MC than that of EJ, (c) A weak relationship between the deflection and transit time is found for MC, but it is absent in the case of EJ and (d) Only EJ-type CMEs have wider range of direction parameter and acceleration. Further, we checked the solar wind speed as another parameter has any influence on CME acceleration and it shows that there is no clear dependence between the two parameters. While it is observed that the average acceleration of MC-associated CME is larger for lower direction parameter values (<0.2), it is larger for EJ-associated CME for higher direction parameter values (>0.6).

Empirical Relationship Between CME Parameters and Geo-effectiveness of Halo CMEs in the Rising Phase of Solar Cycle 24 (2011 – 2013)

A. [Shanmugaraju](#), M. Syed Ibrahim, Y.-J. Moon, A. Mujiber Rahman, S. Umapathy

Solar Phys. May 2015, Volume 290, [Issue 5](#), pp 1417-1427 **2015; File**

We analyzed the physical characteristics of 40 halo coronal mass ejections (CMEs) and their geo-effective parameters observed during the period 2011 to 2013 in the rising phase of [Solar Cycle](#) 24. Out of all halo CMEs observed by [SOHO](#)/LASCO, we selected 40 halo CMEs and investigated their geomagnetic effects. In particular, we estimated

the CME direction parameter (DP) from coronagraph observations, and we obtained the geomagnetic storm disturbance index (Dst) value corresponding to each event by following certain criteria. We studied the correlation between near-Sun parameters of CMEs such as speed and DP with Dst. For this new set of events in the current solar cycle, the relations are found to be consistent with those of previous studies. When the direction parameter increases, the Dst value also increases for symmetrical halo CME ejections. If $DP > 0.6$, these events produce high Dst values. In addition, the intensity of geomagnetic storm calculated using an empirical model with the near-Sun parameters is nearly equal to the observed values. More importantly, we find that the geo-effectiveness in the rising phase of [Solar Cycle 24](#) is much weaker than that in Cycle 23. **Table 1** The details of 40 halo CME events and their geo-effectiveness.

Transit Time of Coronal Mass Ejections under Different Ambient Solar Wind Conditions

A. [Shanmugaraju](#), Bojan Vršnak

Solar Phys., 2013, File

The speed $[v(R)]$ of coronal mass ejections (CMEs) at various distances from the Sun is modeled (as proposed by Vršnak and Gopalswamy in J. Geophys. Res. 107, 2002, doi: 10.1029/2001JA000120) by using the equation of motion $a_{\text{drag}} = \gamma(v-w)$ and its quadratic form $a_{\text{drag}} = \gamma(v-w)|v-w|$, where v and w are the speeds of the CME and solar wind, respectively. We assume that the parameter γ can be expressed as $\gamma = \alpha R^{-\beta}$, where R is the heliocentric distance, and α and β are constants. We extend the analysis of Vršnak and Gopalswamy to obtain a more detailed insight into the dependence of the CME Sun–Earth transit time on the CME speed and the ambient solar-wind speed, for different combinations of α and β . In such a parameter-space analysis, the results obtained confirm that the CME transit time depends strongly on the state of the ambient solar wind. Specifically, we found that: i) for a particular set of values of α and β , a difference in the solar-wind speed causes larger transit-time differences at low CME speeds $[v \rightarrow 0]$, than at high $v \rightarrow 0$; ii) the difference between transit times of slow and fast CMEs is larger at low solar-wind speed $[w \rightarrow 0]$ than at high $w \rightarrow 0$; iii) transit times of fast CMEs are only slightly influenced by the solar-wind speed. The last item is especially important for space-weather forecasting, since it reduces the number of key parameters that determine the arrival time of fast CMEs, which tend to be more geo-effective than the slow ones. Finally, we compared the drag-based model results with the observational data for two CME samples, consisting of non-interacting and interacting CMEs (Manoharan et al. in J. Geophys. Res. 109, 2004). The comparison reveals that the model results are in better agreement with the observations for non-interacting events than for the interacting events. It was also found that for slow CMEs ($v < 500 \text{ km s}^{-1}$), there is a deviation between the observations and the model if slow-wind speeds ($\approx 300\text{--}400 \text{ km s}^{-1}$) are taken for the model input. On the other hand, the model values and the observed data agree for both the slow and the fast CMEs if higher solar-wind speeds are assumed. It is also found that the quadratic form of the drag equation reproduces the observed transit times of fast CMEs better than the linear drag model.

Interplanetary and geomagnetic consequences of 5 January 2005, CMEs associated with eruptive filaments†

Rahul [Sharma](#), Nandita Srivastava, D. Chakrabarty, Christian Möstl, Qiang Hu

JGR, 2013, Volume 118, Issue 7, pages 3954–3967

On **5 January 2005**, SoHO/LASCO observed launch of two successive coronal mass ejections (CMEs) associated with the filament (active region and quiescent) structures. The eruptions resulted in two distinct magnetic clouds whose embedded flux rope topology is modeled by the Grad-Shafranov (G-S) reconstruction technique. Filament plasma remnants in these magnetic clouds were identified using a combination of in-situ plasma, magnetic and composition signatures. In-situ spacecraft (ACE & Wind) measurements suggest interaction between two magnetic clouds with complex magnetic structures at interface region; separated by magnetic holes. These features impacted the Earth's terrestrial magnetosphere - ionosphere system and resulted in a moderate geomagnetic storm (peak Dst $\approx -96 \text{ nT}$). During the main phase of this storm on **7 January 2005**, polarity reversals in the Y-component (dawn-to-dusk) of interplanetary electric field triggered two major auroral substorms with concomitant changes in the polar ionospheric electric field. However, similar polarity reversal on 8 January 2005 during the recovery phase of the storm did not trigger any auroral substorm activity. The results provide clues for the interplanetary interaction of the two CMEs and its possible role in the development of the geomagnetic storm and substorms.

Presence of solar filament plasma detected in interplanetary coronal mass ejections by in situ spacecraft

Rahul [Sharma](#)^{1,*} and Nandita Srivastava²

J. Space Weather Space Clim. 2 (2012) A10

<http://www.swsc-journal.org/articles/swsc/pdf/2012/01/swsc120018.pdf>

Aims: To identify the solar filament plasma at 1 AU by using in situ spacecraft data.

Methods: We used magnetic, plasma and compositional parameters to identify the presence of filamentary material within and outside magnetic clouds.

Results: We report two cases of observed filament plasma embedded in interplanetary coronal mass ejections (ICMEs) related to a flare-associated eruptive filament and a quiescent filament eruption at different phases of solar cycle by using magnetic, plasma, and compositional parameters.

Conclusions: Analysis of in situ multi-spacecraft observations of ICME structures and substructures confirms the presence of solar filament material.

The study of variations of low energy cosmic helium's flux (up to 6 MeV) due to solar activity

M. **Shayan**, P. Davoudifar, Z. Bagheri

Advances in Space Research Volume 59, Issue 8, 15 April 2017, Pages 2186–2191

In General, the flux of low energy cosmic rays varies with time due to solar activities. The cosmic particle fluxes were studied using data of satellites near the Earth. In this work, first we studied the variations of particle fluxes from 1 Jan to 31 Dec 2000 and 35 events were selected. Then we proposed a relation for cosmic particle flux as a function of time and rigidity in the time of approaching ejecta to the Earth. The coefficients of the relation were calculated using experimental data of particle fluxes from ACE satellite. Finally, we compare time variations of these coefficients for different events.

An Optical Analysis of Sunspots as Predictors of Geomagnetic Storms

Matthew **Shelby**, [Scott Scharlach](#), [Petar Matejic](#), [RJ Everett](#), [Colton Morgan](#)

2023

<https://arxiv.org/pdf/2308.09848.pdf>

Although a variety of phenomena may create a geomagnetic storm on Earth, the most severe geomagnetic storms arise from solar activity, and in particular, coronal mass ejections (CMEs) and solar flares. CMEs and flares originate primarily from sunspots. The "aa index" is a metric which ranks all of the strongest geomagnetic storms between 1868 and 2010 based on a variety of characteristics taken from several sources. This paper examines correlations between the aa index of the most severe geomagnetic storms and the intrinsic characteristics of the sunspots from which they originated. We find a correlation between the total rank of the aa index of the storms and the "total intensity" of the sunspot, where total intensity is defined as the sunspot's mean intensity multiplied by its area. The correlation has an R-Squared = 0.690 and R-Squared = 0.855 when a potentially corrupted data point is removed. **18 Jan 1938**

Origination of Extremely Intense South Component of Magnetic Field ($B_{s,s}$) in the ICME

Chenglong **Shen**, Yutian Chi, Mengjiao Xu, and Yuming Wang

Front. Phys., 2021 |

<https://www.frontiersin.org/articles/10.3389/fphy.2021.762488/full>

<https://doi.org/10.3389/fphy.2021.762488>

The intensity of the southward component of the magnetic field (B_s) carried by Interplanetary Coronal Mass Ejections (ICMEs) is one of the most critical parameters in causing extreme space weather events, such as intense geomagnetic storms. In this work, we investigate three typical ICME events with extremely intense B_s in detail and present a statistical analysis of the origins of intense B_s in different types of ICMEs based on the ICME catalogue from 1995 to 2020. According to the in-situ characteristics, the ICME events with extremely high B_s are classified into three types: isolated ICMEs, multiple ICMEs, and shock-ICME interaction events with shocks inside ICMEs or shocks passing through ICMEs. By analyzing all ICME events with $B_{s,mean} \geq 10\text{nT}$ and $B_{s,mean} \geq 20\text{nT}$, we find that 39.6% of $B_{s,mean} \geq 10\text{nT}$ events and 50% of $B_{s,mean} \geq 20\text{nT}$ events are associated with shock-ICME events. Approximately 35.7% of shock-ICME events have $B_{s,mean} \geq 10\text{nT}$, which is much higher than the other two types (isolated ICMEs: 7.2% and multiple ICMEs: 12.1%). Those results confirm that the ICMEs interaction events are more likely to carry extreme intense B_s and cause intense geomagnetic storms. Only based on the in-situ observations at Earth, some interaction ICME events, such as shock-ICME interaction events with shocks passing through the preceding ICME or ICME cannibalism, could be classified as isolated ICME events. This may lead to an overestimate of the probability of ICME carrying extremely intense B_s . To further investigate such events, direct and multi-point observations of the CME propagation in the inner heliosphere from the Solar Ring Mission could be crucial in the future. **31 Mar 2001, 5-6 Nov 2001, 20 Nov 2003, 2012 June 16**

Solar Modulation of Galactic Cosmic-Ray Protons Based on a Modified Force-field Approach

Zhenning **Shen**^{1,2}, Hao Yang¹, Pingbing Zuo^{1,2}, Gang Qin³, Fengsi Wei¹, Xiaojun Xu², and Yanqiong Xie⁴

2021 ApJ 921 109

<https://doi.org/10.3847/1538-4357/ac1fe8>

In this work, a modified force-field approach is established to investigate the long-term solar modulation of galactic cosmic-ray (GCR) protons. In this approach, the solar modulation potential ϕ is assumed to be energy dependent. As ϕ also depends on the local interstellar spectrum (LIS), a new proton LIS model is first presented based on data from Voyager 1 and 2, PAMELA, and AMS-02. Then, a double power-law expression is proposed to model ϕ as a function of proton energy. By fitting to the selected GCR measurements, the solar cycle variation characteristics of parameters in the expression of ϕ are obtained, and these parameters are reconstructed using the sunspot number, the heliospheric current sheet tilt angle, and the polarity of heliospheric magnetic field. Finally, a new analytical predictive model for GCR protons is established. It is shown that the 11 and 22 yr cyclic variations of GCRs are reproduced, and the computed proton intensities are in good agreement with GCR measurements at various energies since 1954.

Numerical Research on the Effect of the Initial Parameters of a CME Flux-rope Model on Simulation Results

Fang **Shen**^{4,1,2,3}, Yousheng Liu^{1,2}, and Yi Yang^{1,2}

2021 ApJS 253 12

<https://doi.org/10.3847/1538-4365/abd4d2>

<https://iopscience.iop.org/article/10.3847/1538-4365/abd4d2/pdf>

Coronal mass ejections (CMEs) are the major drivers of space weather, and an accurate modeling of their initialization and propagation up to 1 au and beyond is an important issue for space weather research and forecasts. In this research, we use the newly developed three-dimensional (3D) flux-rope CME initialization model and 3D IN (interplanetary)-TVD MHD model to study the effect of different CME initial parameters on simulation outputs. The initial CME flux model is established based on the graduated cylindrical shell model. In order to test the influence of the CME initial parameters on the simulation results, we try to run several simulations with different CME initial parameters, then investigate the outputs in interplanetary space. Here, we focus only on cases in which observers are located in the same initial direction of propagation of the CME. Our analysis shows that the parameters specifying the CME initialization in the model, including the initial density, the thickness of CME flux tube, initial mass, and initial magnetic field, have different effects on the simulation results for observers near the Earth and Mars, and on the process of propagation of the CME in interplanetary space. This confirms the important role played by details of the initial implementation of geometric and physical parameters on space weather research and forecasts.

Why the Shock-ICME Complex Structure is Important: Learning From the Early 2017 September CMEs

Chenglong **Shen**, [Mengjiao Xu](#), [Yuming Wang](#), [Yutian Chi](#), [Bingxian Luo](#)

2018 ApJ 861 28

<https://doi.org/10.3847/1538-4357/aac204>

<https://arxiv.org/pdf/1805.05763.pdf>

<http://sci-hub.tw/10.3847/1538-4357/aac204> **File**

In the early days of 2017 September, an exceptionally energetic solar active region AR12673 aroused great interest in the solar physics community. It produced four X class flares, more than 20 CMEs and an intense geomagnetic storm, for which the peak value of the Dst index reached up to -142nT at 2017 September 8 02:00 UT. In this work, we check the interplanetary and solar source of this intense geomagnetic storm. We find that this geomagnetic storm was mainly caused by a shock-ICME complex structure, which was formed by a shock driven by the **2017 September 6** CME propagating into a previous ICME which was the interplanetary counterpart of the **2017 September 4** CME. To better understand the role of this structure, we conduct the quantitative analysis about the enhancement of ICME's geoeffectiveness induced by the shock compression. The analysis shows that the shock compression enhanced the intensity of this geomagnetic storm by a factor of two. Without shock compression, there would be only a moderate geomagnetic storm with a peak Dst value of -79 nT. In addition, the analysis of the proton flux signature inside the shock-ICME complex structure shows that this structure also enhanced the solar energetic particles (SEPs) intensity by a factor of ~ 5 . These findings illustrate that the shock-ICME complex structure is a very important factor in solar physics study and space weather forecast.

See STEP Team at USTC (University of Science and Technology of China) <http://space.ustc.edu.cn/dreams/>

Statistical comparison of the ICME's geoeffectiveness of different types and different solar phases from 1995 to 2014

Chenglong [Shen](#), Yutian Chi, Yuming Wang, Mengjiao Xu, Shui Wang
JGR Volume 122, Issue 6 June 2017 Pages 5931–5948

<http://sci-hub.cc/10.1002/2016JA023768>

The geoeffectiveness of interplanetary coronal mass ejections (ICMEs) is an important issue in space weather research and forecasting. Based on the ICME catalog that we recently established and the Dst indices from the World Data Center, we study and compare the geoeffectiveness of ICMEs of different in situ signatures and different solar phases from 1995 to 2014. According to different in situ signatures, all ICMEs are divided into three types: isolated ICMEs (I-ICMEs), multiple ICMEs (M-ICMEs), and shock-embedded ICMEs (S-ICMEs), resulting in a total of 363 group events. The main findings of this work are as follows: (1) Fifty-eight percent of ICMEs caused geomagnetic storms with $Dst_{min} \leq -30$ nT. Further, large fraction (87%) of intense geomagnetic storms are caused by ICME groups and their sheath regions. (2) Numbers of ICME groups and the probabilities of ICME groups in causing geomagnetic storms varied in pace with the solar cycle. Meanwhile, the ICME groups and the probabilities of them in causing geomagnetic storms in Solar Cycle 24 are much lower than those in Solar Cycle 23. (3) The maximum value of the intensity of the magnetic field (B), south component of the magnetic field (B_s), and dawn-dusk electric field vB_s are well correlated with the intensity of the magnetic storms. (4) Shock-embedded ICMEs have a high probability in causing geomagnetic storms, especially intense geomagnetic storms. (5) The compression of shock on the south component of magnetic field is an important factor to enhance the geoeffectiveness of S-ICMEs structures. 24–26 September 1998, 3 March 2001, 2000-02-11, 25-29 September 2001, 2002-05-18, 15 February 2010,

Evolution of the 2012 July 12 CME from the Sun to the Earth: Data-Constrained Three-Dimensional MHD Simulations†

Fang [Shen](#)^{1,*}, Chenglong Shen², Jie Zhang³, Phillip Hess³, Yuming Wang², Xueshang Feng¹, Hongze Cheng² and Yi Yang

JGR, 2014

<http://arxiv.org/ftp/arxiv/papers/1501/1501.01704.pdf>

The dynamic process of coronal mass ejections (CMEs) in the heliosphere provides us the key information for evaluating CMEs' geo-effectiveness and improving the accurate prediction of CME-induced Shock Arrival Time (SAT) at the Earth. We present a data-constrained three-dimensional (3D) magnetohydrodynamic (MHD) simulation of the evolution of the CME in a realistic ambient solar wind for the **July 12-16, 2012** event by using the 3D COIN-TVD MHD code. A detailed comparison of the kinematic evolution of the CME between the observations and the simulation is carried out, including the usage of the time-elongation maps from the perspectives of both Stereo A and Stereo B. In this case study, we find that our 3D COIN-TVD MHD model, with the magnetized plasma blob as the driver, is able to re-produce relatively well the real 3D nature of the CME in morphology and their evolution from the Sun to Earth. The simulation also provides a relatively satisfactory comparison with the in-situ plasma data from the Wind spacecraft.

Full Halo Coronal Mass Ejections: Arrival at the Earth

Chenglong [Shen](#), Yuming Wang, Zonghao Pan, Bin Miao, Pinzhong Ye, S. Wang
JGR, Volume 119, Issue 7, pages 5107–5116, 2014

<http://arxiv.org/pdf/1406.4589v1.pdf>

A geomagnetic storm is mainly caused by a front-side coronal mass ejection (CME) hitting the Earth and then interacting with the magnetosphere. However, not all front-side CMEs can hit the Earth. Thus, which CMEs hit the Earth and when they do so are important issues in the study and forecasting of space weather. In our previous work (Shen et al., 2013), the de-projected parameters of the full-halo coronal mass ejections (FHCMEs) that occurred from 2007 March 1 to 2012 May 31 were estimated, and there are 39 front-side events could be fitted by the Graduated Cylindrical Shell (GCS) model. In this work, we continue to study whether and when these front-side FHCMEs (FFHCMEs) hit the Earth. It is found that 59% of these FFHCMEs hit the Earth, and for central events, whose deviation angles ϵ , which are the angles between the propagation direction and the Sun-Earth line, are smaller than 45 degrees, the fraction increases to 75%. After checking the deprojected angular widths of the CMEs, we found that all of the Earth-encountered CMEs satisfy a simple criterion that the angular width (ω) is larger than twice the deviation angle (ϵ). This result suggests that some simple criteria can be used to forecast whether a CME could hit the Earth. Furthermore, for Earth-encountered CMEs, the transit time is found to be roughly anti-correlated with the de-projected velocity, but some

events significantly deviate from the linearity. For CMEs with similar velocities, the differences of their transit times can be up to several days. Such deviation is further demonstrated to be mainly caused by the CME geometry and propagation direction, which are essential in the forecasting of CME arrival. 2010 April 7-9

Table 1: The GCS model's parameters and the times of the associated ICMEs of the FFHCMEs occurred from 2007 to 2012 May 31

Could the collision of CMEs in the heliosphere be super-elastic? --- Validation through three-dimensional simulations

Fang **Shen**, Chenglong Shen, Yuming Wang, Xueshang Feng, Changqing Xiang

Geophys. Res. Lett., 40, 1457-1461, **2013**

<http://arxiv.org/pdf/1412.7374v1.pdf>

Though coronal mass ejections (CMEs) are magnetized fully-ionized gases, a recent observational study of a CME collision event in 2008 November has suggested that their behavior in the heliosphere is like elastic balls, and their collision is probably super-elastic (Shen et al. 2012). If this is true, this finding has an obvious impact on the space weather forecasting because the direction and velocity of CMEs may change. To verify it, we numerically study the event through three-dimensional MHD simulations. The nature of CMEs' collision is examined by comparing two cases. In one case the two CMEs collide as observed, but in the other, they do not. Results show that the collision leads to extra kinetic energy gain by 3%--4% of the initial kinetic energy of the two CMEs. It firmly proves that the collision of CMEs could be super-elastic. **November 2--8, 2008**

Super-elastic collision of large-scale magnetized plasmoids in the heliosphere

Chenglong **Shen**¹, Yuming Wang^{1*}, Shui Wang¹, Ying Liu^{2,3}, Rui Liu¹, Angelos Vourlidas⁴, Bin Miao¹, Pinzhong Ye¹, Jijia Liu¹ and Zhenjun Zhou¹

2012, Nature Phys., 8, 923

http://sprg.ssl.berkeley.edu/~liuxying/pubs/2012_nphys_shen.pdf

<http://arxiv.org/pdf/1412.7375v1.pdf>

A super-elastic collision is an unusual process in which some mechanism causes the kinetic energy of the system to increase. Most studies have focused on solid-like objects, and have rarely considered gases or liquids, as the collision of these is primarily a mixing process. However, magnetized plasmoids are different from ordinary gases—as cross-field diffusion is effectively prohibited—but it remains unclear how they behave during a collision. Here we present a comprehensive picture of a unique collision between two coronal mass ejections in the heliosphere, which are the largest magnetized plasmoids erupting from the Sun. Our analysis reveals that these two magnetized plasmoids collided as if they were solid-like objects, with a likelihood of 73% that the collision was super-elastic. The total kinetic energy of the plasmoid system increased by about 6.6% through the collision, significantly influencing its dynamics.

2008-11-04

Acceleration and deceleration of coronal mass ejections during propagation and interaction

Shen, F., S. T. Wu, X. Feng, and C.-C. Wu

J. Geophys. Res., 117, A11101, doi:10.1029/2012JA017776, **2012**, File

A major challenge to the space weather forecasting community is accurate prediction of Coronal Mass Ejections (CMEs) induced Shock Arrival Time (SAT) at Earth's environment. In order to improve the current accuracy, one of the steps is to understand the physical processes of the acceleration and deceleration of a CME's propagation in the heliosphere. We employ our previous study of a three-dimensional (3D) magnetohydrodynamic (MHD) simulation for the evolution of two interacting CMEs in a realistic ambient solar wind during the period **28--31 March 2001** event to illustrate these acceleration and deceleration processes. The forces which caused the acceleration and deceleration are analyzed in detail. The forces which caused the acceleration are the magnetic pressure term of Lorentz force and pressure gradient. On the other hand, the forces which caused the deceleration are aerodynamic drag, the Sun's gravity and the tension of magnetic field. In addition the momentum exchange between the solar wind and the moving CMEs can cause acceleration and deceleration of the CME which are now analyzed. In this specific CME event 28--31 March 2001 we have analyzed those forces which cause acceleration and deceleration of CME with and without interaction with another CME. It shows that there are significant momentum changes between these two interacting CMEs to cause the acceleration and deceleration.

Three-dimensional MHD simulation of two coronal mass ejections' propagation and interaction using a successive magnetized plasma blobs model

Shen, F.; Feng, X. S.; Wang, Yuming; Wu, S. T.; Song, W. B.; Guo, J. P.; Zhou, Y. F.

J. Geophys. Res., Vol. 116, No. A9, A09103, **2011**, **File**

A three-dimensional (3-D), time-dependent, numerical magnetohydrodynamic (MHD) model is used to investigate the evolution and interaction of two coronal mass ejections (CMEs) in the nonhomogeneous ambient solar wind. The background solar wind is constructed on the basis of the self-consistent source surface with observed line of sight of magnetic field and density from the source surface of 2.5 Rs to Earth's orbit (215 Rs) and beyond. The two successive CMEs occurring on **28 March 2001** and forming a multiple magnetic cloud in interplanetary space are chosen as a test case, in which they are simulated by means of a two high-density, high-velocity, and high-temperature magnetized plasma blobs model, and are successively ejected into the nonhomogeneous background solar wind medium along different initial launch directions. The dynamical propagation and interaction of the two CMEs between 2.5 and 220 Rs are investigated. Our simulation results show that, although the two CMEs are separated by 10 h, the second CME is able to overtake the first one and cause compound interactions and an obvious acceleration of the shock. At the L1 point near Earth the two resultant magnetic clouds in our simulation are consistent with the observations by ACE. In this validation study we find that this 3-D MHD model, with the self-consistent source surface as the initial boundary condition and the magnetized plasma blob as the CME model, is able to reproduce and explain some of the general characters of the multiple magnetic clouds observed by satellite.

Three-dimensional MHD simulation of the evolution of the April 2000 CME event and its induced shocks using a magnetized plasma blob model

Shen, F.; Feng, X. S.; Wu, S. T.; Xiang, C. Q.; Song, W. B.

J. Geophys. Res., Vol. 116, No. A4, A04102, **2011**

A three-dimensional (3-D) time-dependent, numerical magnetohydrodynamic (MHD) model with asynchronous and parallel time-marching method is used to investigate the propagation of coronal mass ejections (CMEs) in the nonhomogenous background solar wind flow. The background solar wind is constructed based on the self-consistent source surface with observed line-of-sight of magnetic field and density from the source surface of 2.5 Rs to the Earth's orbit (215 Rs) and beyond. The CMEs are simulated by means of a very simple flux rope model: a high-density, high-velocity, and high-temperature magnetized plasma blob is superimposed on a steady state background solar wind with an initial launch direction. The dynamical interaction of a CME with the background solar wind flow between 2.5 and 220 Rs is investigated. The evolution of the physical parameters at the cobpoint, which is located at the shock front region magnetically connected to ACE spacecraft, is also investigated. We have chosen the well-defined halo-CME event of **4–6 April 2000** as a test case. In this validation study we find that this 3-D MHD model, with the asynchronous and parallel time-marching method, the self-consistent source surface as initial boundary conditions, and the simple flux rope as CME model, provide a relatively satisfactory comparison with the ACE spacecraft observations at the L1 point.

The differences in the origination and properties of the near-Earth solar wind between solar cycles 23 and 24

Xinzheng **Shi**, [Hui Fu](#), [Zhenghua Huang](#), [Limei Yan](#), [Chi Ma](#), [Chenxi Huangfu](#), [Hongqiang Song](#), [Lidong Xia](#)

ApJ **2024**

<https://arxiv.org/pdf/2407.00915>

The dependence of the sources and properties of the near-Earth solar wind on solar cycle activity is an important issue in solar and space physics. We use the improved two-step mapping procedure that takes into account the initial acceleration processes to trace the near-Earth solar winds back to their source regions from 1999 to 2020, covering solar cycles (SCs) 23 and 24. Then the solar wind is categorized into coronal hole (CH), active region (AR), and quiet Sun (QS) solar wind based on the source region types. We find that the proportions of CH and AR (QS) wind during SC 23 are higher (lower) than those during SC 24. During solar maximum and declining phases, the magnetic field strength, speed, helium abundance (AHe), and charge states of all three types of solar wind during SC 23 are generally higher than those during SC 24. During solar minimum, these parameters of solar wind are generally lower during SC 23 than those during SC 24. There is a significant decrease in the charge states of all three types of solar wind during the solar minimum of SC 23. The present statistical results demonstrate that the sources and properties of the solar wind are both influenced by solar cycle amplitude. The temperatures of AR, QS, and CH regions exhibit significant difference at low altitudes, whereas they are almost uniform at high altitudes.

The Solar Cycle Dependence of In Situ Properties of Two Types of Interplanetary CMEs during 1999–2020

Xinzheng Shi¹, Hui Fu¹, Zhenghua Huang¹, Chi Ma¹, and Lidong Xia¹
2022 ApJ 940 103

<https://iopscience.iop.org/article/10.3847/1538-4357/ac9b20/pdf>

Generally, in situ parameters of interplanetary coronal mass ejections (ICMEs) are analyzed as a whole, or ICMEs are classified by speed or whether they are with and without magnetic clouds. Zhai and colleagues found that ICMEs with and without flares can be extracted only by the average charge states of iron (QFe). In the present study, the ICMEs are categorized into two types, flare CMEs (FCs) and nonflare CMEs (NFCs) by the QFe. We find that the occurrence rates of FCs and NFCs are both decreased from solar maximum to minimum. The occurrence rates and proportions of FCs are both higher in solar cycle 23 than in solar cycle 24. In contrast, the occurrence rates of NFCs are almost the same during the two solar cycles. The durations of FCs are longer than those of NFCs. The fractions of FCs and NFCs that are associated with magnetic clouds (MCs) or magnetic field direction rotation evidence are 73% and 69%, respectively. The speed, QFe, O⁷⁺/O⁶⁺, helium abundance (AHe), and first ionization potential bias are all higher for FCs than for NFCs. The above parameters inside NFCs and solar wind are almost the same. The solar cycle dependence of the parameters inside NFCs is more clear than that inside FCs. The statistical results demonstrate that the material sources of FCs are not completely the same as those of NFCs. Part of the material inside FCs should come from the lower atmosphere where the AHe is higher. The statistical results indicate that all CMEs are associated with flux ropes on the Sun.

Table 1 The Occurrences, Durations, and Properties of Two Types of ICMEs from 1999 to 2020

Patches of Magnetic Switchbacks and Their Origins

Chen Shi¹, Olga Panasenco², Marco Velli¹, Anna Tenerani³, Jaye L. Verniero⁴, Nikos Sioulas et al.
2022 ApJ 934 152

<https://iopscience.iop.org/article/10.3847/1538-4357/ac7c11/pdf>

Parker Solar Probe (PSP) has shown that the solar wind in the inner heliosphere is characterized by the quasi omnipresence of magnetic switchbacks ("switchback" hereinafter), local backward bends of magnetic field lines. Switchbacks also tend to come in patches, with a large-scale modulation that appears to have a spatial scale size comparable to supergranulation on the Sun. Here we inspect data from the first 10 encounters of PSP focusing on different time intervals when clear switchback patches were observed by PSP. We show that the switchbacks modulation, on a timescale of several hours, seems to be independent of whether PSP is near perihelion, when it rapidly traverses large swaths of longitude remaining at the same heliocentric distance, or near the radial-scan part of its orbit, when PSP hovers over the same longitude on the Sun while rapidly moving radially inwards or outwards. This implies that switchback patches must also have an intrinsically temporal modulation most probably originating at the Sun. Between two consecutive patches, the magnetic field is usually very quiescent with weak fluctuations. We compare various parameters between the quiescent intervals and the switchback intervals. The results show that the quiescent intervals are typically less Alfvénic than switchback intervals, and the magnetic power spectrum is usually shallower in quiescent intervals. We propose that the temporal modulation of switchback patches may be related to the "breathing" of emerging flux that appears in images as the formation of "bubbles" below prominences in the Hinode/SOT observations. **16 Aug 2007, 2-3 Nov 2018, 26-28 Jan 2020, 25-27 Sep 2020, 12-16 Jan 2021, 18-19 Nov 2021,**

Multiband Electrostatic Waves below and above the Electron Cyclotron Frequency in the Near-Sun Solar Wind

Chen Shi^{1,2}, Jinsong Zhao^{1,2}, David M. Malaspina^{3,4}, Stuart D. Bale^{5,6}, Xiangcheng Dong⁷, Tieyan Wang⁸, and Dejin Wu¹

2022 ApJL 926 L3

<https://iopscience.iop.org/article/10.3847/2041-8213/ac4d37/pdf>

Using the Parker Solar Probe measurements, this Letter reports two new types of multiband electrostatic waves in and near the heliospheric current sheet. They are classified into the $f < f_{ce}$ and $f > f_{ce}$ multiband electrostatic waves, in which most (or all) of the bands in the former type are lower than f_{ce} , and all of the bands in the latter type are higher than f_{ce} , where f and f_{ce} denotes the wave frequency and the electron cyclotron frequency, respectively. This Letter also exhibits observational evidence of the existence of nonlinear wave-wave interactions of both types of electrostatic waves. In particular, the $f > f_{ce}$ multiband electrostatic waves are found to be modulated in the presence of low-frequency oblique ion-scale waves. According to the observed frequency distribution, this Letter proposes that the mode nature of the $f < f_{ce}$ multiband electrostatic waves could be the oblique ion acoustic wave or the lower-hybrid wave, and the $f > f_{ce}$ multiband electrostatic waves are the electron Bernstein mode wave. These findings provide a challenge to understand the complex electron and ion dynamical processes in and near the heliospheric current sheet.

Parker Solar Probe Observations of Alfvénic Waves and Ion-cyclotron Waves in a Small-scale Flux Rope

Chen [Shi](#)^{1,2}, Jinsong Zhao^{1,2}, Jia Huang³, Tieyan Wang⁴, Dejin Wu¹, Yu Chen⁵, Qiang Hu^{5,6}, Justin C. Kasper^{3,7}, and Stuart D. Bale^{8,9,10,11}

2021 ApJL 908 L19

<https://doi.org/10.3847/2041-8213/abdd28>

Small-scale flux ropes (SFRs) are common in the interplanetary environment. However, previous identification procedures generally discard SFRs with medium and high Alfvénicity, which are thought to be Alfvénic waves or Alfvénic structures. This paper first identifies an SFR event with medium Alfvénicity in the inner heliosphere (at ~ 0.2 au) using Parker Solar Probe measurements. We find Alfvénic waves that arise inside SFR based on high correlations between the magnetic field and velocity fluctuations. We also observe quasi-monochromatic electromagnetic waves with frequencies f that are usually larger than the local proton cyclotron frequency at the leading and trailing edges of this SFR. These waves are well explained by the outward-propagating ion-cyclotron waves, which have wave frequencies ~ 0.03 – 0.3 Hz and wavelengths ~ 60 – 2000 km in the plasma frame. Moreover, we show that the power spectral density of the magnetic field in SFR middle region follows the power-law distribution, where the spectral index changes from -1.5 ($f \lesssim 1$ Hz) to -3.3 ($f \gtrsim 1$ Hz). These findings would motivate developing an automated program to identify SFRs with medium and high Alfvénicity from Alfvénic waves/structures.

The Dynamics of the Inner Boundary of the Outer Radiation Belt During Geomagnetic Storms

Xiaofei [Shi](#), [Jie Ren](#), [Q. G. Zong](#)

JGR [Volume 125, Issue 5](#) May 2020 e2019JA027309

<https://agupubs.onlinelibrary.wiley.com/doi/epdf/10.1029/2019JA027309>

We investigate the shapes of the inner boundary of the outer radiation belt during different geomagnetic storm phases using energetic electron observations from Van Allen Probes. The case of two consecutive but isolated storms in April 2016 shows that (a) the inner boundary, as a function of L shell and energy, exhibits a “V-shaped” form with the energetic electrons showing a kappa-like energy spectrum (electron flux steeply falling with increasing energies), whereas it is in a “S-shaped” form as the energetic electrons show a reversed energy spectrum (electron flux going up with increasing energies from hundreds of keV to ~ 1 MeV); (b) the boundary is abruptly transformed from S to V shape during the storm main phase and retains in V shape for several days until it evolves into S shape during the late recovery phase. The main statistical results from 37 isolated geomagnetic storms between 2013 and 2017 present that (a) the more SYM-H drops, the closer to Earth the transition from V to S shape starts, with a linear correlation coefficient of ~ 0.7 ; (b) the minimum energy at which the transition starts is between 100 and 550 keV (typically, less than 250 keV); (c) the transition from V to S shape typically occurs in the plasmasphere. **Apr 2016**

Predicting the Arrival Time of Coronal Mass Ejections with the Graduated Cylindrical Shell and Drag Force Model

Tong [Shi](#), Yikang Wang, Linfeng Wan, Xin Cheng, Mingde Ding, Jie Zhang

ApJ **806** 271 **2015**

<http://arxiv.org/pdf/1505.00884v1.pdf>

Accurately predicting the arrival of coronal mass ejections (CMEs) at the Earth based on remote images is of critical significance in the study of space weather. In this paper, we make a statistical study of 21 Earth directed CMEs, exploring in particular the relationship between CME initial speeds and transit times. The initial speed of a CME is obtained by fitting the CME with the Graduated Cylindrical Shell model and is thus free of projection effects. We then use the drag force model to fit results of the transit time versus the initial speed. By adopting different drag regimes, i.e., the viscous, aerodynamics, and hybrid regimes, we get similar results, with the least mean estimation error of the hybrid model of 12.9 hours. CMEs with a propagation angle (the angle between the propagation direction and the Sun-Earth line) larger than its half angular width arrive at the Earth with an angular deviation caused by factors other than the radial solar wind drag. The drag force model cannot be well applied to such events. If we exclude these events in the sample, the prediction accuracy can be improved, i.e., the estimation error reduces to 6.8 hours. This work suggests that it is viable to predict the arrival time of CMEs at the Earth based on the initial parameters with a fairly good accuracy. Thus, it provides a method of space weather forecast of 1–5 days following the occurrence of CMEs.

TABLE 1 List of the CME events studied in this work **2008-2012**

Basic Study of Space Weather Predictions: A New Project in Japan

Kazunari [Shibata](#) and Yohsuke Kamide

SPACE WEATHER, VOL. 5, S12006, doi:10.1029/2006SW000306, 2007

In order to have successful space weather predictions, scientists must have a good physical model of solar-terrestrial phenomena. This model should deal with the key processes, spanning from solar flares and coronal mass ejections on the Sun to geomagnetic storms and their effects in the upper atmosphere of Earth. To reach this goal, a number of fundamental questions must first be solved. For example: What is the triggering condition of solar flares? How do coronal mass ejections form? What is the mechanism of particle acceleration? What are the mechanisms of geomagnetic storms and substorms? Solving these basic questions is equivalent to understanding multiscale coupling of various physical processes occurring on different scales. This is partly what space weather research aims to accomplish, because finding empirical formulas without understanding physical processes will not lead to successful predictions of all space weather events.

Magnetohydrodynamic simulation of interplanetary propagation of multiple coronal mass ejections with internal magnetic flux rope (SUSANOO-CME)

D. [Shiota](#), R. Kataoka

Space Weather Volume 14, Issue 2 Pages 56–75 2016

<https://agupubs.onlinelibrary.wiley.com/doi/epdf/10.1002/2015SW001308>

Coronal mass ejections (CMEs) are the most important drivers of various types of space weather disturbance. Here we report a newly developed magnetohydrodynamic (MHD) simulation of the solar wind, including a series of multiple CMEs with internal spheromak-type magnetic fields. First, the polarity of the spheromak magnetic field is set as determined automatically according to the Hale-Nicholson law and the chirality law of Bothmer and Schwenn. The MHD simulation is therefore capable of predicting the time profile of the southward interplanetary magnetic field at the Earth, in relation to the passage of a magnetic cloud within a CME. This profile is the most important parameter for space weather forecasts of magnetic storms. In order to evaluate the current ability of our simulation, we demonstrate a test case: the propagation and interaction process of multiple CMEs associated with the highly complex active region **NOAA 10486 in October to November 2003**, and present the result of a simulation of the solar wind parameters at the Earth during the 2003 Halloween storms. We succeeded in reproducing the arrival at the Earth's position of a large amount of southward magnetic flux, which is capable of causing an intense magnetic storm. We find that the observed complex time profile of the solar wind parameters at the Earth could be reasonably well understood by the interaction of a few specific CMEs.

Analysis of Differences between ICME catalogues and Construction of a Unified Catalogue

Anton [Shiryaev](#) (1 and 2), [Ksenia Kaportseva](#) (1 and 3)

Ученые записки физического факультета МГУ (in Russian) 2024

<https://arxiv.org/pdf/2406.14363>

Multiple magnetic and kinetic solar wind plasma parameters are used to detect coronal mass ejections (CMEs) as they travel through the heliosphere. There are various interplanetary CME (ICME) catalogues, but due to differences between their ICME identification criteria they can significantly vary. In this paper we analyze Richardson and Cane and CCMC CME Scoreboard ICME catalogues and the SRI RAS solar wind types catalogue, and propose an algorithm of merging them. A unified catalogue is constructed for 2010 to 2022. The resulting catalogue is completed with data from the OMNI database. Analysis of the unified catalogue demonstrated high accuracy when merging events present in multiple catalogues and a tendency of events defined in all three initial catalogues to demonstrate greater duration, speed and geoeffectiveness. The catalog is presented on the SINP MSU Space Weather Exchange website: [this https URL](https://arxiv.org/pdf/2406.14363)

Abnormal Quasi-Recurrent Variations of Cosmic Rays in September 2014–February 2015

[Shlyk](#), N.S., Belov, A.V., Obridko, V.N. et al.

Geomagn. Aeron. 64, 211–223 (2024).

<https://doi.org/10.1134/S0016793223601096>

An anomaly in the behavior of galactic cosmic rays in September 2014–February 2015 was studied, which manifested itself as significant modulation of their flux with a period close to the Sun's rotation. The state of the solar magnetic field and changes in the parameters of the solar wind and interplanetary magnetic field during the specified period are analyzed. The reasons for the longitudinal asymmetry in the distribution of galactic cosmic rays in the inner heliosphere are discussed. It has been established that the studied period is divided into two parts with different physical conditions on the Sun. Conclusions are drawn on the decisive joint influence of sporadic and recurrent events: repeatedly renewed “magnetic traps” created by successive coronal mass ejections from the same longitudinal zone, and anomalously expanded polar coronal holes with an enhanced magnetic field.

Forbush decreases caused by paired interacting solar wind disturbances

N S Shlyk, [A V Belov](#), [M A Abunina](#), [A A Abunin](#), [V A Oleneva](#) [V G Yanke](#)

MNRAS, Volume 511, Issue 4, April 2022, Pages 5897–5908,

<https://doi.org/10.1093/mnras/stac478>

The paper discusses changes in various characteristics of the solar wind, interplanetary magnetic field, geomagnetic activity, and cosmic rays during the registration of paired interacting solar wind disturbances on the Earth using the data base of Forbush effects and interplanetary disturbances – FEID. The cases of pair interaction are considered for 1995–2020: (i) successive coronal mass ejections; (ii) coronal mass ejections and high-speed streams from coronal holes; (iii) successive high-speed streams from coronal holes. It is shown that for the first events from a pair, the times for reaching the maximum values of the interplanetary magnetic field and solar wind velocity are significantly reduced, and the amplitudes of the recorded Forbush decreases decline. It is also found that the presence of interaction enriches the second event at the expense of the resources of the first, increasing geomagnetic efficiency and the degree of cosmic ray modulation for the second event in comparison with isolated events, which is especially pronounced for a pair of interacting coronal mass ejections. The existence of the described effects can be explained by the observed increase in the interplanetary magnetic field magnitude in the second events due to the presence of interaction.

Turbulent generation of magnetic switchbacks in the Alfvénic solar wind

Munehito [Shoda](#), [Benjamin D. G. Chandran](#), [Steven R. Cranmer](#)

ApJ 915 52 2021

<https://arxiv.org/pdf/2101.09529.pdf>

<https://doi.org/10.3847/1538-4357/abfdbc>

One of the most important early results from the Parker Solar Probe (PSP) is the ubiquitous presence of magnetic switchbacks, whose origin is under debate. Using a three-dimensional direct numerical simulation of the equations of compressible magnetohydrodynamics from the corona to 40 solar radii, we investigate whether magnetic switchbacks emerge from granulation-driven Alfvén waves and turbulence in the solar wind. The simulated solar wind is an Alfvénic slow-solar-wind stream with a radial profile consistent with various observations, including observations from PSP. As a natural consequence of Alfvén-wave turbulence, the simulation reproduced magnetic switchbacks with many of the same properties as observed switchbacks, including Alfvénic v-b correlation, spherical polarization (low magnetic compressibility), and a volume filling fraction that increases with radial distance. The analysis of propagation speed and scale length shows that the magnetic switchbacks are large-amplitude (nonlinear) Alfvén waves with discontinuities in the magnetic field direction. We directly compare our simulation with observations using a virtual flyby of PSP in our simulation domain. We conclude that at least some of the switchbacks observed by PSP are a natural consequence of the growth in amplitude of spherically polarized Alfvén waves as they propagate away from the Sun. **2018 November 5-6**

Three-dimensional simulation of the fast solar wind driven by compressible MHD turbulence

Munehito [Shoda](#), [Takeru Ken Suzuki](#), [Mahboubeh Asgari-Targhi](#), [Takaaki Yokoyama](#)

ApJL 2019

<https://arxiv.org/pdf/1905.11685.pdf>

Using a three-dimensional compressible magnetohydrodynamic (MHD) simulation, we have reproduced the fast solar wind in a direct and self-consistent manner, based on the wave/turbulence driven scenario. As a natural consequence of Alfvénic perturbations at its base, highly compressional and turbulent fluctuations are generated, leading to heating and acceleration of the solar wind. The analysis of power spectra and structure functions reveals that the turbulence is characterized by its imbalanced (in the sense of outward Alfvénic fluctuations) and anisotropic nature. The density fluctuation originates from the parametric decay instability of outwardly propagating Alfvén waves and plays a significant role in the Alfvén wave reflection that triggers turbulence. Our conclusion is that the fast solar wind is heated and accelerated by compressible MHD turbulence driven by parametric decay instability and resultant Alfvén wave reflection.

Now-casting and Predicting the Kp index Using Historical Values and Real-time Observations

Yuri Y. [Shprits](#), [Ruggero Vasile](#), [Irina S. Zhelavskaya](#)

Space Weather **2019**

[sci-hub.se/10.1029/2018SW002141](https://doi.org/10.1029/2018SW002141)

Current algorithms for the real-time prediction of the Kp index use a combination of models empirically driven by solar wind measurements at the L1 Lagrange point and historical values of the index. In this study, we explore the limitations of this approach, examining the forecast for short and long lead times using measurements at L1 and Kp time series as input to artificial neural networks. We explore the relative efficiency of the solar wind-based predictions, predictions based on recurrence, and based on persistence. Our modeling results show that for short-term forecasts of approximately half a day, the addition of the historical values of Kp to the measured solar wind values provides a barely noticeable improvement. For a longer-term forecast of more than two days, predictions can be made using recurrence only, while solar wind measurements provide very little improvement for a forecast with long horizon times. We also examine predictions for disturbed and quiet geomagnetic activity conditions. Our results show that the paucity of historical measurements of the solar wind for high Kp results in a lower accuracy of predictions during disturbed conditions. Rebalancing of input data can help tailor the predictions for more disturbed conditions.

Longitudinal Distribution of Solar Flares and Their Association with Coronal Mass Ejections and Forbush Decreases<<<

Pankaj K. [Shrivastava](#), Mukesh K. Jothe & Mahendra Singh

Solar Physics, Volume 269, Number 2, 401-410, **2011**, **File**

Major H α solar-flare events of high optical importance have been employed to study their heliographic distribution in longitude around the Sun for the period of 2001 to 2006. A statistical analysis was performed to obtain their relationship with halo/partial-halo CMEs and Forbush decreases (Fds) of cosmic-ray intensity. Our analysis indicates that 63% of the solar flares associated with halo CMEs and Fds occur in the western hemisphere and of 37% of such flares occur in the eastern hemisphere. Similarly, we found that nearly 60% of the solar flares associated with partial-halo CMEs and Fds occur in the western hemisphere and the rest (40%) occur in the eastern hemisphere. Finally, we conclude that the flares in association with CMEs and located in the western hemisphere of the solar disk are more effective in producing Fds. The magnitudes of Fds are observed to be higher when in association of halo CMEs. A slight excess in the eastern hemisphere is found for both the halo and partial-halo CMEs.

Modeling of Solar Wind Disturbances Associated with Coronal Mass Ejections and Verification of the Forecast Results

Yulia [Shugay](#) 1,* , Vladimir Kalegaev 1, Ksenia Kaportseva 1, Vladimir Slemzin 2, Denis Rodkin 2 and Valeriy Ereemeev 1

Universe **2022**, 8(11), 565;

<https://doi.org/10.3390/universe8110565>

<https://www.mdpi.com/2218-1997/8/11/565>

Solar wind (SW) disturbances associated with coronal mass ejections (CMEs) cause significant geomagnetic storms, which may lead to the malfunction or damage of sensitive on-ground and space-based critical infrastructure. CMEs are formed in the solar corona, and then propagate to the Earth through the heliosphere as Interplanetary CME (ICME) structures. We describe the main principles in development with the online, semi-empirical system known as the Space Monitoring Data Center (SMDC) of the Moscow State University, which forecasts arrival of ICMEs to Earth. The initial parameters of CMEs (speeds, startup times, location of the source) are determined using data from publicly available catalogs based on solar images from space telescopes and coronagraphs. After selecting the events directed to Earth, the expected arrival time and speed of ICMEs at the L1 point are defined using the Drag-Based model (DBM), which describes propagation of CMEs through the heliosphere under interaction with the modeled quasi-stationary SW. We present the test results of the ICME forecast in the falling phase of Cycle 24 obtained with the basic version of SMDC in comparison with results of other models, its optimization and estimations of the confidence intervals, and probabilities of a successful forecast. **7-25 Aug 2022**

Table 5. Identification of solar origins for the selected ICMEs in the period 2013–2015 by RDBM.

Table 6. Parameters of the CME sources identified from the CACTus and CDAW databases.

Influence of coronal mass ejections on parameters of high-speed solar wind: a case study

Yulia [Shugay](#), Vladimir Slemzin, Denis Rodkin, Yuri Yermolaev and Igor Veselovsky

J. Space Weather Space Clim. **2018**, 8, A28

<https://www.swsc-journal.org/articles/swsc/pdf/2018/01/swsc170045.pdf>

We investigate the case of disagreement between predicted and observed in-situ parameters of the recurrent high-speed solar wind streams (HSSs) existing for Carrington rotation (CR) 2118 (December 2011) in comparison with CRs 2117 and 2119. The HSSs originated at the Sun from a recurrent polar coronal hole (CH) expanding to mid-latitudes, and its area in the central part of the solar disk increased with the rotation number. This part of the CH was responsible for the equatorial flank of the HSS directed to the Earth. The time and speed of arrival for this part of the HSS to the Earth were predicted by the hierarchical empirical model based on EUV-imaging and the Wang-Sheeley-Argé ENLIL semi-empirical replace model and compared with the parameters measured in-situ by model. The predicted parameters were compared with those measured in-situ. It was found, that for CR 2117 and CR 2119, the predicted HSS speed values agreed with the measured ones within the typical accuracy of $\pm 100 \text{ km s}^{-1}$. During CR 2118, the measured speed was on 217 km s^{-1} less than the value predicted in accordance with the increased area of the CH. We suppose that at CR 2118, the HSS overtook and interacted with complex ejecta formed from three merged coronal mass ejections (CMEs) with a mean speed about 400 km s^{-1} . According to simulations of the Drag-based model, this complex ejecta might be created by several CMEs starting from the Sun in the period between **25 and 27 December 2011** and arriving to the Earth simultaneously with the HSS. Due to its higher density and magnetic field strength, the complex ejecta became an obstacle for the equatorial flank of the HSS and slowed it down. During CR 2117 and CR 2119, the CMEs appeared before the arrival of the HSSs, so the CMEs did not influence on the HSSs kinematics.

Magnetic field sector structure and origins of solar wind streams in 2012

Yulia [Shugay](#), Vladimir Slemzin and Igor Veselovsky

J. Space Weather Space Clim. 4 (2014) A24

The origins of the solar wind and the interplanetary magnetic field sector structure in the beginning of the magnetic polarity reversal of 24th solar cycle were investigated using the Wilcox Solar Observatory magnetic field measurements and their products as well as the solar wind data from ACE and the SDO/AIA EUV images. The dominance of the quadrupole harmonics in the solar magnetic field in this period resulted in a four-sector structure of the interplanetary magnetic field. The dominating source of recurrent high-speed solar wind stream was a large trans-equatorial coronal hole of negative polarity evolving in the course of the polarity reversal process. The contribution of ICMEs to the high-speed solar wind did not exceed 17% of the total flux. The solar wind density flux averaged over the year amounted to $1 \times 10^8 \text{ cm}^{-2} \text{ s}^{-1}$ which is considerably lower than the typical long-term value ($2-4 \times 10^8 \text{ cm}^{-2} \text{ s}^{-1}$). The slow-speed component of solar wind density flux constituted in average more than 68% of the total flux, the high-speed component was about 10%, reaching the maximum of 32% in some Carrington rotations.

Forecasting SYM-H Index: A Comparison Between Long Short-Term Memory and Convolutional Neural Networks

[F. Siciliano](#) , [G. Consolini](#) , [R. Tozzi](#) , [M. Gentili](#) , [F. Giannattasio](#), [P. De Michelis](#)

Space Weather e2020SW002589 [Volume19, Issue2](#) 2021

<https://doi.org/10.1029/2020SW002589>

<https://agupubs.onlinelibrary.wiley.com/doi/epdf/10.1029/2020SW002589>

<https://doi.org/10.1029/2020SW002589>

Forecasting geomagnetic indices represents a key point to develop warning systems for the mitigation of possible effects of severe geomagnetic storms on critical ground infrastructures. Here we focus on SYM-H index, a proxy of the axially symmetric magnetic field disturbance at low and middle latitudes on the Earth's surface. To forecast SYM-H we built two artificial neural network (ANN) models and trained both of them on two different sets of input parameters including interplanetary magnetic field components and magnitude, and differing for the presence or not of previous SYM-H values. These ANN models differ in architecture being based on two conceptually different neural networks: the Long Short-Term Memory (LSTM) and the Convolutional Neural Network (CNN). Both networks are trained, validated and tested on a total of 42 geomagnetic storms among the most intense occurred between 1998 and 2018. Performance comparison of the two ANN models shows that: 1) both are able to well forecast SYM-H index 1 hour in advance, with an accuracy of more than 95% in terms of the coefficient of determination R^2 ; 2) the model based on LSTM is slightly more accurate than that based on CNN when including SYM-H index at previous steps among the inputs; 3) the model based on CNN has interesting potentialities being more accurate than that based on LSTM when not including SYM-H index among the inputs. Predictions made including SYM-H index among the inputs provide a root mean squared error on average 42% lower than that of predictions made without SYM-H. **02/11/1998, 02/04/2000, 04/11/2004, 10/09/2012**

Table 1. Details of the storms used to develop the ANN model 1998-2018.

A multifractal approach to understanding Forbush Decrease events: Correlations with geomagnetic storms and space weather phenomena

Sierra-Porta, D

CHAOS SOLITONS & FRACTALS, Volume 185, Article Number 115089, 2024

DOI 10.1016/j.chaos.2024.115089

The Forbush decrease phenomenon has significant impacts on several environmental conditions, including interference in radio communications, satellite navigation systems, and the health of astronauts in space, among others. It is characterized by a temporary and noticeable reduction in the observed flux of galactic cosmic rays recorded at the Earth's surface. This decrease occurs due to the modulation of cosmic rays through their interaction with shock waves generated by coronal mass ejections. As these shock waves traverse the interplanetary medium, which includes the solar wind and galactic cosmic rays, they exert compression forces on the cosmic ray flux, leading to a reduction in observed flux levels at Earth. This study investigates Forbush Decrease events across different solar cycles and explores their correlation with geomagnetic storm conditions using multifractal detrended fluctuation analysis. The findings indicate variations in the multifractal spectra for series under different geomagnetic storm conditions compared to the full Forbush decrease series. Moreover, it is observed that the amplitude of the multifractal spectrum is greater in the series that include events with a maximum Kp index exceeding 6, suggesting a significant influence of geomagnetic storm conditions on the fractality and variability of Forbush Decrease magnitudes.

Cross correlation and time-lag between cosmic ray intensity and solar activity during solar cycles 21, 22 and 23

Review

D. Sierra-Porta

[Astrophysics and Space Science](#) July 2018, 363:137

<http://sci-hub.tw/10.1007/s10509-018-3360-8>

In the present paper a systematic study is carried out to validate the similarity or co-variability between daily terrestrial cosmic-ray intensity and three parameters of the solar corona evolution, i.e., the number of sunspots and flare index observed in the solar corona and the Ap index for regular magnetic field variations caused by regular solar radiation changes. The study is made for a period including three solar cycles starting with cycle 21 (year 1976) and ending on cycle 23 (year 2008). A cross-correlation analysis was used to establish patterns and dependence of the variables. This study focused on the time lag calculation for these variables and found a maximum of negative correlation over $CC1 \approx 0.85$, $CC2 \approx 0.75$ and $CC3 \approx 0.63$ with an estimation of 181, 156 and 2 days of deviation between maximum/minimum of peaks for the intensity of cosmic rays related with sunspot number, flare index and Ap index regression, respectively.

Ensemble Forecasts of Solar Wind Connectivity to 1 Rs using ADAPT-WSA

D. E. da Silva, S. Wallace, C. N. Arge, S. Jones

Space Weather 2023

<https://arxiv.org/ftp/arxiv/papers/2309/2309.08734.pdf>

The solar wind which arrives at any location in the solar system is, in principle, relatable to the outflow of solar plasma from a single source location. This source location, itself usually being part of a larger coronal hole, is traceable to 1 Rs along the Sun's magnetic field, in which the entire path from 1 Rs to a location in the heliosphere is referred to as the solar wind connectivity. While not directly measurable, the connectivity between the near-Earth solar wind is of particular importance to space weather. The solar wind solar source region can be obtained by leveraging near-sun magnetic field models and a model of the interplanetary solar wind. In this article we present a method for making an ensemble forecast of the connectivity presented as a probability distribution obtained from a weighted collection of individual forecasts from the combined Air Force Data Assimilative Photospheric Flux Transport - Wang Sheeley Arge (ADAPT-WSA) model. The ADAPT model derives the photospheric magnetic field from synchronic magnetogram data, using flux transport physics and ongoing data assimilation processes. The WSA model uses a coupled set of potential field type models to derive the coronal magnetic field, and an empirical relationship to derive the terminal solar wind speed observed at Earth. Our method produces an arbitrary 2D probability distribution capable of reflecting complex source configurations with minimal assumptions about the distribution structure, prepared in a computationally efficient manner.

Multispecies Energetic Particle Acceleration Associated with CIR and ICME-driven Shocks

Ashok **Silwal**¹, Lingling Zhao^{1,2}, Gary P. Zank^{1,2}, Bingbing Wang², Alexander Pitña³, Sujan Prasad Gautam¹, Byeongseon Park³, Masaru Nakanotani², and Xingyu Zhu²

2024 ApJ 972 168

<https://iopscience.iop.org/article/10.3847/1538-4357/ad614e/pdf>

A multispecies energetic particle intensity enhancement event at 1 au is analyzed. We identify this event as a corotating interaction region (CIR) structure that includes a stream interface (SI), a forward-reverse shock pair, and an embedded heliospheric current sheet (HCS). The distinct feature of this CIR event is that (1) the high-energy (>1 MeV) ions show significant flux enhancement at the reverse wave (RW)/shock of the CIR structure, following their passage through the SI and HCS. The flux amplification appears to depend on the energy per nucleon. (2) Electrons in the energy range of 40.5–520 keV are accelerated immediately after passing through the SI and HCS regions, and the flux quickly reaches a peak for low-energy electrons. At the RW, only high-energy electrons (~520 keV) show significant local flux enhancement. The CIR structure is followed by a fast-forward perpendicular shock driven by a coronal mass ejection (CME), and we observed a significant flux enhancement of low-energy protons and high-energy electrons. Specifically, the 210–330 keV proton and 180–520 keV electron fluxes are enhanced by approximately 2 orders of magnitude. This suggests that the later ICME-driven shock may accelerate particles out of the suprathermal pool. In this paper, we further present that for CIR-accelerated particles, the increase in turbulence power at SI and RWs may be an important factor for the observed flux enhancement in different species. The presence of ion-scale waves near the RW, as indicated by the spectral bump near the proton gyrofrequency, suggests that the resonant wave–particle interaction may act as an efficient energy transfer between energetic protons and ion-scale waves.

The Dalton Minimum and John Dalton's Auroral Observations

[Sam M. Silverman](#), [Hisashi Hayakawa](#)

Journal of Space Weather and Space Climate, 2021

<https://arxiv.org/ftp/arxiv/papers/2012/2012.13713.pdf>

In addition to the regular Schwabe cycles of approximately 11 y, "prolonged solar activity minima" have been identified through the direct observation of sunspots and aurorae, as well as proxy data of cosmogenic isotopes. Some of these minima have been regarded as grand solar minima, which are arguably associated with the special state of the solar dynamo and have attracted significant scientific interest. In this paper, we review how these prolonged solar activity minima have been identified. In particular, we focus on the Dalton Minimum, which is named after John Dalton. We review Dalton's scientific achievements, particularly in geophysics. Special emphasis is placed on his lifelong observations of auroral displays over approximately five decades in Great Britain. Dalton's observations for the auroral frequency allowed him to notice the scarcity of auroral displays in the early 19th century. We analyze temporal variations in the annual frequency of such displays from a modern perspective. The contemporary geomagnetic positions of Dalton's observational site make his dataset extremely valuable because his site is located in the sub-auroral zone and is relatively sensitive to minor enhancements in solar eruptions and solar wind streams. His data indicate clear solar cycles in the early 19th century and their significant depression from 1798 to 1824. Additionally, his data reveal a significant spike in auroral frequency in 1797, which chronologically coincides with the "lost cycle" that is believed to have occurred at the end of Solar Cycle 4. Therefore, John Dalton's achievements can still benefit modern science and help us improve our understanding of the Dalton Minimum.

In situ observations from STEREO/PLASTIC: a test for L5 space weather monitors

K. D. C. [Simunac](#), L. M. Kistler, A. B. Galvin, M. A. Popecki, and C. J. Farrugia

Ann. Geophys., 27, 3805-3809, 2009

[Abstract](#) [Full Article](#) (PDF, 1634 KB)

Stream interaction regions (SIRs) that corotate with the Sun (corotating interaction regions, or CIRs) are known to cause recurrent geomagnetic storms. The Earth's L5 Lagrange point, separated from the Earth by 60 degrees in heliographic longitude, is a logical location for a solar wind monitor – nearly all SIRs/CIRs will be observed at L5 several days prior to their arrival at Earth. Because the Sun's heliographic equator is tilted about 7 degrees with respect to the ecliptic plane, the separation in heliographic latitude between L5 and Earth can be more than 5 degrees. In July 2008, during the period of minimal solar activity at the end of solar cycle 23, the two STEREO observatories were separated by about 60 degrees in longitude and more than 4 degrees in heliographic latitude. This time period affords a timely test for the practical application of a solar wind monitor at L5. We compare in situ observations from PLASTIC/AHEAD and PLASTIC/BEHIND, and report on how well the BEHIND data can be used as a forecasting tool for in situ conditions at the AHEAD spacecraft with the assumptions of ideal corotation and minimal source evolution. Preliminary results show the bulk proton parameters (density and bulk speed) are not in quantitative agreement from one observatory to the next, but the qualitative profiles are similar.

***In Situ* Observations of Solar Wind Stream Interface Evolution**

K.D.C. [Simunac](#) · L.M. Kistler · A.B. Galvin · M.A. Lee · M.A. Popecki · C. Farrugia · E. Moebius · L.M. Blush · P. Bochslers · P. Wurz · B. Klecker · R.F. Wimmer-Schweingruber · B. Thompson · J.G. Luhmann · C.T. Russell · R.A. Howard

Solar Phys (2009) 259: 323–344

The heliocentric orbits of the two STEREO satellites are similar in radius and ecliptic latitude, with separation in longitude increasing by about 45° per year. This arrangement provides a unique opportunity to study the evolution of stream interfaces near 1 AU over time scales of hours to a few days, much less than the period of a Carrington rotation. Assuming nonevolving solar wind sources that corotate with the Sun, we calculated the expected time and longitude of arrival of stream interfaces at the Ahead observatory based on the *in situ* solar wind speeds measured at the Behind observatory. We find agreement to within 5° between the expected and actual arrival longitude until the spacecraft are separated by more than 20° in heliocentric inertial longitude. This corresponds to about one day between the measurement times. Much larger deviations, up to 25° in longitude, are observed after 20° separation. Some of the deviations can be explained by a latitude difference between the spacecraft, but other deviations most likely result from evolution of the source region. Both remote and *in situ* measurements show that changes at the source boundary can occur on a time scale much shorter than one solar rotation. In 32 of 41 cases, the interface was observed earlier than expected at STEREO/Ahead.

Modeling a Coronal Mass Ejection as a Magnetized Structure with EUHFORIA

G. [Sindhuja](#)¹, Jagdev Singh¹, E. Asvestari², and B. Raghavendra Prasad¹

2022 *ApJ* 925 25

<https://iopscience.iop.org/article/10.3847/1538-4357/ac3bd2/pdf>

We studied an Earth-directed coronal mass ejection (CME) that erupted on **2015 March 15**. Our aim was to model the CME flux rope as a magnetized structure using the European Heliospheric Forecasting Information Asset (EUHFORIA). The flux rope from eruption data (FRED) output was applied to the EUHFORIA spheromak CME model. In addition to the geometrical properties of the CME flux rope, we needed to input the parameters that determine the CME internal magnetic field like the helicity, tilt angle, and toroidal flux of the CME flux rope. According to the FRED technique geometrical properties of the CME flux rope are obtained by applying a graduated cylindrical shell fitting of the CME flux rope on the coronagraph images. The poloidal field magnetic properties can be estimated from the reconnection flux in the source region utilizing the post-eruption arcade method, which uses the Heliospheric Magnetic Imager magnetogram together with the Atmospheric Imaging Assembly (AIA) 193 Å images. We set up two EUHFORIA runs with RUN-1 using the toroidal flux obtained from the FRED technique and RUN-2 using the toroidal flux that was measured from the core dimming regions identified from the AIA 211 Å images. We found that the EUHFORIA simulation outputs from RUN-1 and RUN-2 are comparable to each other. Overall using the EUHFORIA spheromak model, we successfully obtained the magnetic field rotation of the flux rope, while the arrival time near Earth and the strength of the interplanetary CME magnetic field at Earth are not as accurately modeled.

Improving the Arrival Time Estimates of Coronal Mass Ejections by Using Magnetohydrodynamic Ensemble Modeling, Heliospheric Imager data, and Machine Learning

Talwinder [Singh](#), [Bernard Benson](#), [Syed A. Z. Raza](#), [Tae K. Kim](#), [Nikolai V. Pogorelov](#), [William P. Smith](#), [Charles N. Arge](#)

2023 *ApJ* 948 78

<https://arxiv.org/pdf/2302.05588.pdf>

<https://iopscience.iop.org/article/10.3847/1538-4357/acc10a/pdf>

The arrival time prediction of Coronal mass ejections (CMEs) is an area of active research. Many methods with varying levels of complexity have been developed to predict CME arrival. However, the mean absolute error (MAE) of predictions remains above 12 hours, even with the increasing complexity of methods. In this work we develop a new method for CME arrival time prediction that uses magnetohydrodynamic simulations involving data-constrained flux-rope-based CMEs, which are introduced in a data-driven solar wind background. We found that, for 6 CMEs studied in this work, the MAE in arrival time was ~8 hours. We further improved our arrival time predictions by using ensemble modeling and comparing the ensemble solutions with STEREO-A&B heliospheric imager data. This was done by using

our simulations to create synthetic J-maps. A machine learning (ML) method called the lasso regression was used for this comparison. Using this approach, we could reduce the MAE to ~4 hours. Another ML method based on the neural networks (NNs) made it possible to reduce the MAE to ~5 hours for the cases when HI data from both STEREO-A&B were available. NNs are capable of providing similar MAE when only the STEREO-A data is used. Our methods also resulted in very encouraging values of standard deviation (precision) of arrival time. The methods discussed in this paper demonstrate significant improvements in the CME arrival time predictions. Our work highlights the importance of using ML techniques in combination with data-constrained magnetohydrodynamic modeling to improve space weather predictions. **2010/08/01, 2011/09/06, 2011/09/13, 2012/01/19, 2012/07/12, 2012/09/28**

Ensemble simulations of the 12 July 2012 Coronal Mass Ejection with the Constant Turn Flux Rope Model

[Talwinder Singh](#), [Tae K. Kim](#), [Nikolai V. Pogorelov](#), [Charles N. Arge](#)

2022 *ApJ* **933** 123

<https://arxiv.org/pdf/2205.13009.pdf>

<https://iopscience.iop.org/article/10.3847/1538-4357/ac73f3/pdf>

Flux-rope-based magnetohydrodynamic modeling of coronal mass ejections (CMEs) is a promising tool for the prediction of the CME arrival time and magnetic field at Earth. In this work, we introduce a constant-turn flux rope model and use it to simulate the **12-July-2012** 16:48 CME in the inner heliosphere. We constrain the initial parameters of this CME using the graduated cylindrical shell (GCS) model and the reconnected flux in post-eruption arcades. We correctly reproduce all the magnetic field components of the CME at Earth, with an arrival time error of approximately 1 hour. We further estimate the average subjective uncertainties in the GCS fittings, by comparing the GCS parameters of 56 CMEs reported in multiple studies and catalogs. We determined that the GCS estimates of the CME latitude, longitude, tilt, and speed have average uncertainties of 5.74 degrees, 11.23 degrees, 24.71 degrees, and 11.4% respectively. Using these, we have created 77 ensemble members for the 12-July-2012 CME. We found that 55% of our ensemble members correctly reproduce the sign of the magnetic field components at Earth. We also determined that the uncertainties in GCS fitting can widen the CME arrival time prediction window to about 12 hours for the 12-July-2012 CME. On investigating the forecast accuracy introduced by the uncertainties in individual GCS parameters, we conclude that the half-angle and aspect ratio have little impact on the predicted magnetic field of the 12-July-2012 CME, whereas the uncertainties in longitude and tilt can introduce a relatively large spread in the magnetic field predicted at Earth.

Application of a Modified Spheromak Model to Simulations of Coronal Mass Ejection in the Inner Heliosphere

[Talwinder Singh](#), [Tae K. Kim](#), [Nikolai V. Pogorelov](#), [Charles N. Arge](#)

Space Weather **2020** e2019SW002405

<https://doi.org/10.1029/2019SW002405>

The magnetic fields of interplanetary coronal mass ejections (ICMEs), which originate close to the Sun in the form of a flux rope, determine their geoeffectiveness. Therefore, robust flux rope-based models of CMEs are required to perform magnetohydrodynamic (MHD) simulations aimed at space weather predictions. We propose a modified spheromak model and demonstrate its applicability to CME simulations. In this model, such properties of a simulated CME as the poloidal and toroidal magnetic fluxes, and the helicity sign can be controlled with a set of input parameters. We propose a robust technique for introducing CMEs with an appropriate speed into a background, MHD solution describing the solar wind in the inner heliosphere. Through a parametric study, we find that the speed of a CME is much more dependent on its poloidal flux than on the toroidal flux. We also show that the CME speed increases with its total energy, giving us control over its initial speed. We further demonstrate the applicability of this model to simulations of CME-CME collisions. Finally, we use this model to simulate the **12 July 2012** CME and compare the plasma properties at 1 AU with observations. The predicted CME properties agree reasonably with observational data.

PreMeV Update: Forecasting Ultra-relativistic Electrons inside Earth's Outer Radiation Belt

[Saurabh Sinha](#), [Yue Chen](#), [Youzuo Lin](#), [Rafael Pires de Lima](#)

Space Weather **2021**

<https://agupubs.onlinelibrary.wiley.com/doi/10.1029/2021SW002773>

<https://doi.org/10.1029/2021SW002773>

Energetic electrons inside Earth's Van Allen belts pose a major radiation threat to space-borne electronics that often play vital roles in modern society. Ultra-relativistic electrons with energies greater than or equal to two Megaelectron-volt (MeV) are of particular interest, and thus forecasting these ≥ 2 MeV electrons has significant meaning to all space sectors. Here we update the latest development of the predictive model for MeV electrons in the outer radiation belt. The

new version, called PreMeV-2E, forecasts ultra-relativistic electron flux distributions across the outer belt, with no need for in-situ measurements of the trapped MeV electron population except at geosynchronous (GEO) orbit. Model inputs include precipitating electrons observed in low-Earth-orbits by NOAA satellites, upstream solar wind speeds and densities from solar wind monitors, as well as ultra-relativistic electrons measured by one Los Alamos GEO satellite. We evaluated 32 supervised machine learning models that fall into four different classes of linear and neural network architectures, and successfully tested ensemble forecasting by using groups of top-performing models. All models are individually trained, validated, and tested by in-situ electron data from NASA's Van Allen Probes mission. It is shown that the final ensemble model outperforms individual models at most L-shells, and this PreMeV-2E model can provide 25-hr (~1-day) and 50-hr (~2-day) forecasts with high mean performance efficiency and correlation values. Our results also suggest this new model is dominated by nonlinear components at L-shells $< \sim 4$ for ultra-relativistic electrons, different from the dominance of linear components for 1 MeV electrons as previously discovered.

Magnetic field spectral evolution in the inner heliosphere

Nikos [Sioulas](#), [Zesen Huang](#), [Chen Shi](#), [Marco Velli](#), [Anna Tenerani](#), [Loukas Vlahos](#), [Trevor A. Bowen](#), [Stuart D. Bale](#), [J.W. Bonnell](#), [P. R. Harvey](#), [Davin Larson](#), [arc Pulupa](#), [Roberto Livi](#), [L. D. Woodham](#), [T. S. Horbury](#), [Michael L. Stevens](#), [T. Dudok de Wit](#), [R. J. MacDowall](#), [David M. Malaspina](#), [K. Goetz](#), [Jia Huang](#), [Justin Kasper](#), [Christopher J. Owen](#), [Milan Maksimović](#), [P. Louarn](#), [A. Fedorov](#)

PRL **2022**

<https://arxiv.org/pdf/2209.02451.pdf>

The radial evolution of the magnetic field fluctuations spectral index and its dependence on plasma parameters is investigated using a merged Parker Solar Probe (PSP) and Solar Orbiter (SO) dataset covering heliocentric distances between $0.06 \lesssim R \lesssim 1$ au. The spectrum is studied as a function of scale, normalized to the radially dependent ion inertial scale d_i . In the vicinity of the Sun, the magnetic spectrum inertial range is limited with a power law exponent α_B consistent with the Iroshnikov-Kraichman phenomenology of Alfvénic turbulence, $\alpha_B = -3/2$, independent of plasma parameters. The inertial range of turbulence grows with distance from the Sun, progressively extending to larger spatial scales, while at the same time steepening towards a Kolomogorov scaling, with a mean value of $\alpha_B = -5/3$. Highly alfvénic intervals seem to retain their near-Sun scaling and only show a minor steepening with distance. In contrast, intervals, where turbulence is characterized by large magnetic energy excess and no dominance of outwardly propagating Alfvénic fluctuations, appear to have spectra that steepen significantly with distance from the Sun, resulting in slightly anomalously steep inertial range slopes at 1 au. Though generically slower solar wind streams exhibit steeper spectra, the correlation can be attributed to the underlying positive correlation between solar wind speed and alfvénicity, i.e. to the relatively rare occurrence of highly Alfvénic slow wind.

Dst of the Carrington storm of 1859

G. [Siscoe](#), N.U. Crooker, C.R. Clauer

Advances in Space Research, Volume 38, Issue 2, **2006**, Pages 173–179, **File**

The super-storm of 1859 gives an opportunity to apply models to predict Dst that have been exercised mostly on non-extreme cases. The exercise gains significance through a Bombay magnetogram that Tsurutani et al. (2003) recently published showing a negative H excursion of ~ 1600 nT, which is unprecedented for the latitude of the station, and which presents difficulties of interpretation if the negative excursion is taken to be equivalent to Dst. Following a suggestion by Li et al. (2006), we have replaced the original Bombay magnetogram, which has many points per hour during the interesting phase of the storm, by hourly averages, thereby constructing a time profile that is closer to a Dst profile as it is usually calculated. Then, the maximum H-depression is ~ -850 nT, which lies not so astonishingly outside the officially observed range. The Bombay magnetogram exhibits two major H-depressions, which we interpret to mean that the event was caused by a geoeffective ICME-sheath followed by a magnetic cloud across which the magnetic field rotated from north to south. On this interpretation, the ICME-sheath caused the extraordinary -1600 nT excursion in H. Then, the issue is whether this large excursion was produced by ionospheric currents (in which case it is not so exceptional) or by magnetospheric currents (in which case it is unprecedented)? To explore the second possibility, we use empirical models that relate the measured shock transit time to the ICME speed and peak magnetic field strength at 1 AU together with average pre-shock interplanetary conditions to construct geoeffective parameters throughout the ICME-sheath. We use the Burton et al. equation as modified by O'Brien and McPherron to calculate Dst. The resulting Dst profile lies reasonably close to hourly averaged Bombay magnetogram, especially if one uses the upper limit allowed for field strength in the ICME-sheath or if one discards the most extreme outlier of the Bombay measurements. We conclude that it is possible to interpret the Bombay magnetogram as having been produced by the magnetospheric currents.

CME DISTURBANCE FORECASTING

G. [SISCOE](#)^{1,*} and R. SCHWENN²

Space Science Reviews (2006) 123: 453–470, **File**,

CME disturbances at Earth arise from the sheath that arrives in front of the ICME and from the ICME itself. The geoeffective environment is qualitatively different in the sheath than within the ICME. Consequently two types of forecast procedures using solar observations of phenomena associated with the release of the CME as input parameters have been developed to treat the two types of environment. This chapter surveys efforts that have resulted in implementable (at least in principle) forecast algorithms for sheath and ICME disturbances and discusses uncertainties associated with both.

East-west asymmetry in coronal mass ejection geoeffectiveness

[Siscoe](#), George L.; [MacNeice](#), Peter J.; [Odstrcil](#), Dusan

Space Weather, Vol. 5, No. 4, S04002

Previous theories on the relationship between geomagnetic storm production and the geometry of the interplanetary magnetic field around coronal mass ejections are refined to show that the twisted shape of the Sun's extended magnetic field concentrates activity to the east side of the coronal mass ejection sheath.

<http://dx.doi.org/10.1029/2006SW000286>

Validity of using Elsässer variables to study the interaction of compressible solar wind fluctuations with a coronal mass ejection

Chaitanya Prasad [Sishtla](#), [Jens Pomoell](#), [Norbert Magyar](#), [Emilia Kilpua](#), [Simon Good](#)

A&A 2024

<https://arxiv.org/pdf/2402.09250.pdf>

Alfvénic fluctuations, as modelled by the non-linear interactions of Alfvén waves of various scales, are seen to dominate solar wind turbulence. However, there is also a non-negligible component of non-Alfvénic fluctuations. The Elsässer formalism, which is central to the study of Alfvénic turbulence due to its ability to differentiate between parallel and anti-parallel Alfvén waves, cannot strictly separate wavemodes in the presence of compressive magnetoacoustic waves. In this study, we analyse the deviations generated in the Elsässer formalism as density fluctuations are naturally generated through the propagation of a linearly polarised Alfvén wave. The study was performed in the context of a coronal mass ejection (CME) propagating through the solar wind, which enables the creation of two solar wind regimes, pristine wind and a shocked CME sheath, where the Elsässer formalism can be evaluated. In these two regimes we studied the deviations of the Elsässer formalism in separating parallel and anti-parallel components of Alfvénic solar wind perturbations generated by small-amplitude density fluctuations. We used an ideal 2.5D magnetohydrodynamic (MHD) model with an adiabatic equation of state. An Alfvén pump wave was injected into the quiet solar wind by

perturbing the transverse magnetic field and velocity components. This wave subsequently generates density fluctuations through the ponderomotive force. A CME was injected by inserting a flux-rope modelled as a magnetic island into the quasi-steady solar wind. The presence of density perturbations creates an approximately 10% deviation in the Elsässer variables and reflection coefficient for the Alfvén waves as well as a deviation of approximately 0.1 in the cross helicity in regions containing both parallel and anti-parallel fluctuations.

Flux-tube-dependent propagation of Alfvén waves in the solar corona

Chaitanya Prasad [Sishtla](#), Jens Pomoell, Emilia Kilpua, Simon Good, Farhad Daei and Minna Palmroth
A&A 661, A58 (2022)

<https://www.aanda.org/articles/aa/pdf/2022/05/aa42999-21.pdf>

Context. Alfvén-wave turbulence has emerged as an important heating mechanism to accelerate the solar wind. The generation of this turbulent heating is dependent on the presence and subsequent interaction of counter-propagating Alfvén waves. This requires us to understand the propagation and evolution of Alfvén waves in the solar wind in order to develop an understanding of the relationship between turbulent heating and solar-wind parameters.

Aims. We aim to study the response of the solar wind upon injecting monochromatic single-frequency Alfvén waves at the base of the corona for various magnetic flux-tube geometries.

Methods. We used an ideal magnetohydrodynamic model using an adiabatic equation of state. An Alfvén pump wave was injected into the quiet solar wind by perturbing the transverse magnetic field and velocity components.

Results. Alfvén waves were found to be reflected due to the development of the parametric decay instability (PDI).

Further investigation revealed that the PDI was suppressed both by efficient reflections at low frequencies as well as magnetic flux-tube geometries.

Reconstruction of extreme geomagnetic storms: Breaking the data paucity curse

M. I. [Sitnov](#), [G. K. Stephens](#), [N. A. Tsyganenko](#), [H. Korth](#), [E. C. Roelof](#), [P. C. Brandt](#), [V. G. Merkin](#), [A. Y. Ukhorskiy](#)

Space Weather e2020SW002561 2020

<https://doi.org/10.1029/2020SW002561>

Reconstruction of the magnetic field, electric current and plasma pressure is provided using a new data mining (DM) method with weighted nearest neighbors (NN) for strong storms with the storm activity index Sym-H < -300 nT, the Bastille Day event (14 July 2000) and the 20 November 2003 superstorm. It is shown that the new method significantly reduces the statistical bias of the original NN algorithm toward weaker storms. In the DM approach the magnetic field is reconstructed using a small NN subset of the large historical database, with the subset number KNN \gg 1 being still much larger than any simultaneous multi-probe observation number. This allows one to fit with observations a very flexible magnetic field model using basis function expansions for equatorial and field-aligned currents, and at the same time, to keep the model sensitive to storm variability. This also allows one to calculate the plasma pressure by integrating the quasi-static force balance equation with the isotropic plasma approximation. For strong storms of particular importance becomes the resolution of the eastward current, which prevents the divergence of the pressure integral. It is shown that in spite of the strong reduction of the dominant NN number in the new weighted NN algorithm to capture strong storm features, it is still possible to resolve the eastward current and to retrieve plasma pressure distributions. It is found that the pressure peak for strong storms may be as close as \approx 2.1RE to Earth and its value may exceed 300 nPa.

Low-frequency-waves within isolated magnetic clouds and complex structures: STEREO observations.[†]

A. [Siu-Tapia](#)^{1,2,*}, X. Blanco-Cano¹, P. Kajdic¹, E. Aguilar-Rodriguez³, C. T. Russell⁴, L. K. Jian^{5,6} and J. G. Luhmann

JGR 2015

Complex Structures (CSs) formed by the interaction of Magnetic Cloud (MC)-like structures with other transients (e. g. another MC, a stream interaction region or a fast stream of solar wind) were frequently observed in the interplanetary space by STEREO spacecraft during the solar minimum 23 and the rising phase of the solar cycle 24. Here we report the presence of low frequency waves (LFWs) inside some Isolated MCs (IMCs) and inside the CSs observed by STEREO during such period (2007-2011). It is important to study in detail the properties of waves in space plasmas since particle distribution functions can be modified by wave-particle interactions. We compare wave characteristics within IMCs with those waves observed inside CSs. Both, left-handed (LH) and right-handed (RH), near-circularly polarized, transverse and almost parallel-propagating LFWs (around the proton cyclotron frequency) were sporadically observed inside both, IMCs and CSs. In contrast, compressive mirrormode waves (MMs) were observed only within CSs. We studied local

plasma conditions inside the IMCs and CSs to gain insight about wave origin: most of the MMs within CSs were observed in regions with enhanced plasma beta ($\beta > 1$); the majority of the LH waves were found in low-beta plasmas ($\beta > 1$) and the RH waves were predominantly observed at moderate betas ($0.4 < \beta \leq 2$). These observations are in agreement with linear kinetic theory predictions for the growth of the mirror, the LH ion cyclotron and the RH ion firehose instability, respectively. It is possible that the waves were generated locally inside the IMCs and CSs via temperature anisotropies. The plasma beta enhancements that were frequently observed inside the CSs may be the result of compressions and heating taking place inside the interacting structures.

Formation of Coronal Mass Ejection and Post-eruption Flow of Solar Wind on 2010 August 18 event

Vladimir [Slemzin](#), [Farid Goryaev](#), [Denis Rodkin](#)

ApJ **929** 146 **2022**

<https://arxiv.org/pdf/2203.06976.pdf>

<https://iopscience.iop.org/article/10.3847/1538-4357/ac5901/pdf>

The state of the space environment plays a significant role for forecasting of geomagnetic storms produced by disturbances of the solar wind (SW). Coronal mass ejections (CMEs) passing through the heliosphere often have a prolonged (up to several days) trail with declining speed, which affects propagation of the subsequent SW streams. We studied the CME and the post-eruption plasma flows behind the CME rear in the event on **2010 August 18** observed in quadrature by several space-based instruments. Observations of the eruption in the corona with EUV telescopes and coronagraphs revealed several discrete outflows followed by a continuous structureless post-eruption stream. The interplanetary coronal mass ejection (ICME), associated with this CME, was registered by PLASMA and SupraThermal Ion Composition (PLASTIC) instrument aboard the Solar TERrestrial RELations Observatory (STEREO-A) between **August 20, 16:14 UT and August 21, 13:14 UT**, after which the SW disturbance was present over 3 days. Kinematic consideration with the use of the gravitational and Drag-Based models has shown that the discrete plasma flows can be associated with the ICME, whereas the post-eruption outflow was arrived in the declining part of the SW transient. We simulated the Fe-ion charge distributions of the ICME and post-CME parts of SW using the plasma temperature and density in the ejection region derived from the Differential Emission Measure analysis. The results demonstrate that in the studied event the post-ICME trailing region was associated with the post-eruption flow from the corona, rather than with the ambient SW entrained by the CME.

Medium Energy Electron Flux in Earth's Outer Radiation Belt (MERLIN): A Machine Learning Model

A. G. [Smirnov](#), [M. Berrendorf](#), [Y. Y. Shprits](#), [E. A. Kronberg](#), [H. J. Allison](#) et al.

Space Weather **e2020SW002532** **2020**

<https://doi.org/10.1029/2020SW002532>

<https://agupubs.onlinelibrary.wiley.com/doi/epdf/10.1029/2020SW002532>

The radiation belts of the Earth, filled with energetic electrons, comprise complex and dynamic systems that pose a significant threat to satellite systems. While various models of electron flux both for low and relativistic energies have been developed, the behaviour of medium energy (120-600 keV) electrons, especially in the MEO region remains poorly quantified. At these energies, electrons are driven by both convective and diffusive transport, and their prediction usually requires sophisticated 4D modeling codes. In this paper we present an alternative approach using the Light Gradient Boosting (LightGBM) machine learning algorithm. The Medium Energy electRON fLUX In Earth's outer radiationN belt (MERLIN) model takes as input the satellite position, a combination of geomagnetic indices and solar wind parameters including the time history of velocity, and does not use persistence. MERLIN is trained on >15 years of the GPS electron flux data, and tested on more than 1.5 years of measurements. 10-fold cross validation yields that the model predicts the MEO radiation environment well, both in terms of dynamics and amplitudes of flux. Evaluation on the test set yields high correlation between the predicted and observed electron flux (0.8) and low values of absolute error. The MERLIN model can have wide space weather applications, providing information for the scientific community in the form of radiation belts reconstructions, as well as industry for satellite mission design, nowcast of the MEO environment and surface charging analysis.

Probabilistic Forecasts of Storm Sudden Commencements from Interplanetary Shocks using Machine Learning

A. W. [Smith](#), [I. J. Rae](#), [C. Forsyth](#), [D. M. Oliveira](#), [M. P. Freeman](#), [D. R. Jackson](#)

Space Weather **Volume18, Issue11** e2020SW002603 **2020**

<https://doi.org/10.1029/2020SW002603>

<https://agupubs.onlinelibrary.wiley.com/doi/epdf/10.1029/2020SW002603>

In this study we investigate the ability of several different machine learning models to provide probabilistic predictions as to whether interplanetary shocks observed upstream of the Earth at L1 will lead to immediate (Sudden Commencements, SCs) or longer lasting magnetospheric activity (Storm Sudden Commencements, SSCs).

Four models are tested including linear (Logistic Regression), non-linear (Naive Bayes and Gaussian Process) and ensemble (Random Forest) models, and are shown to provide skillful and reliable forecasts of SCs with Brier Skill Scores (BSSs) of ~ 0.3 and ROC scores > 0.8 . The most powerful predictive parameter is found to be the range in the interplanetary magnetic field. The models also produce skillful forecasts of SSCs, though with less reliability than was found for SCs. The BSSs and ROC scores returned are ~ 0.21 and 0.82 respectively. The most important parameter for these predictions was found to be the minimum observed BZ.

The simple parameterization of the shock was tested by including additional features related to magnetospheric indices and their changes during shock impact, resulting in moderate increases in reliability. Several parameters, such as velocity and density, may be able to be more accurately predicted at a longer lead time, e.g. from heliospheric imagery. When the input was limited to the velocity and density the models were found to perform well at forecasting SSCs, though with lower reliability than previously (BSSs ~ 0.16 , ROC Scores ~ 0.8). Finally, the models were tested with hypothetical extreme data beyond current observations, showing dramatically different extrapolations.

Predictions of interplanetary shock arrivals at Earth: Dependence of forecast outcome on the input parameters

Smith, Z. K.; Steenburgh, R.; Fry, C. D.; Dryer, M.

Space Weather, Vol. 7, No. 12, S12005, 2009

<http://dx.doi.org/10.1029/2009SW000500>

Predictions of interplanetary shock arrivals at Earth are important to space weather because they are often followed by geomagnetic disturbances that disrupt human technologies. The success of numerical simulation predictions depends on the codes and on the inputs obtained from solar observations. The inputs are usually divided into the more slowly varying background solar wind, onto which short-duration solar transient events are superposed. This paper examines the dependence of the prediction success on the range of values of the solar transient inputs. These input parameters are common to many 3-D MHD codes. The predictions of the Hakamada-Akasofu-Fry version 2 (HAFv2) model were used because its predictions of shock arrivals were tested, informally in the operational environment, from 1997 to 2006. The events list and HAFv2's performance were published in a series of three papers. The third event set is used to investigate the success and accuracy of the predictions in terms of the input parameter ranges (considered individually). By defining three thresholds for the input speed, duration, and X-ray class, it is possible to categorize the prediction outcomes by these input ranges. The X-ray class gives the most successful classification. Above the highest threshold, 89% of the predictions were successful while below the lowest threshold, only 40% were successful. The accuracy, measured in terms of the time differences between the observed and predicted shock arrivals, also shows largest improvement for the X-ray class. Guidelines are presented for space weather forecasters using the HAFv2 or other interplanetary simulation models.

Modeling the arrival at Earth of the interplanetary shock following the 12 May 1997 solar event using HAFv2 and 3-D MHD HHMS models

Smith, Z. K.; Detman, T. R.; Sun, W.; Dryer, M.; Deehr, C. S.; Fry, C. D.

Space Weather, Vol. 6, No. 5, S05006, 2008

<http://dx.doi.org/10.1029/2007SW000356>

Using data from a 1997 solar event, scientists show how recent improvements have been made in predicting the time of arrival at Earth of solar-caused interplanetary shocks.

The Hakamada-Akasofu-Fry model (version 2: HAFv2) near-real-time prediction gave an error of 31 h. Because the accuracy of predicted Sun-to-Earth transit times of such shocks depends both on the model and our ability to determine the proper inputs from available observations, we reexamined the predictions made for the 12 May event using inputs that could have been available in near-real-time, both with HAFv2 and a second, ensemble-partnered solar wind prediction model, the 3-D MHD Hybrid Heliospheric Model System (HHMS). We use updated methods of estimating the initial shock velocity (from Smith et al., 2005b) and examine the influence of the background solar wind. This reexamination reduced the error from the original 31 h to less than 4 h. Achieving near-real-time accuracies to this level would greatly enhance operations of technologies such as electrical power grids, satellite systems, and polar flight communications.

Energetic Particle Perpendicular Diffusion: Simulations and Theory in Noisy Reduced Magnetohydrodynamic Turbulence

P. **Snodin**^{1,2,3}, T. Jitsuk^{3,5}, D. Ruffolo³, and W. H. Matthaeus⁴

Astrophysical Journal, 932:127 (12pp), 2022

<https://iopscience.iop.org/article/10.3847/1538-4357/ac6e6d/pdf>

The transport of energetic charged particles (e.g., cosmic rays) in turbulent magnetic fields is usually characterized in terms of the diffusion parallel and perpendicular to a large-scale (or mean) magnetic field. The nonlinear guiding center theory has been a prominent perpendicular diffusion theory. A recent version of this theory, based on the random ballistic spreading of magnetic field lines and a backtracking correction (RBD/BC), has shown good agreement with test particle simulations for a two-component magnetic turbulence model. The aim of the present study is to test the generality of the improved theory by applying it to the noisy reduced magnetohydrodynamic (NRMHD) turbulence model, determining perpendicular diffusion coefficients that are compared with those from the field line random walk (FLRW) and unified nonlinear (UNLT) theories and our test particle simulations. The synthetic NRMHD turbulence model creates special conditions for energetic particle transport, with no magnetic fluctuations at higher parallel wavenumbers so there is no resonant parallel scattering if the particle Larmor radius RL is even slightly smaller than the minimum resonant scale. This leads to nonmonotonic variation in the parallel mean free path λ_{\parallel} with RL . Among the theories considered, only RBD/BC matches simulations within a factor of 2 over the range of parameters considered. This accuracy is obtained even though the theory depends on λ_{\parallel} and has no explicit dependence on RL . In addition, the UNLT theory often provides accurate results, and even the FLRW limit provides a very simple and reasonable approximation in many cases.

Numerical simulations of homologous coronal mass ejections in the solar wind:

A. **Soenen**, F. P. Zuccarello, C. Jacobs, S. Poedts, R. Keppens and B. van der Holst

A&A 501 (2009) 1123-1130

<http://www.aanda.org/10.1051/0004-6361/200911877>

Context. Coronal mass ejections (CMEs) are enormous expulsions of magnetic flux and plasma from the solar corona. Most scientists agree that a coronal mass ejection is the sudden release of magnetic free energy stored in a strongly stressed field. However, the exact reason for this sudden release is still highly debated.

Aims. In an initial multflux system in steady state equilibrium, containing a pre-eruptive region consisting of three arcades with alternating magnetic flux polarity, we study the initiation and early evolution properties of a sequence of CMEs by shearing a region slightly larger than the central arcade.

Methods. We solve the ideal magnetohydrodynamics (MHD) equations in an axisymmetrical domain from the

solar surface up to $30 R_{\odot}$. The ideal MHD equations are advanced in time over a non uniform grid using a modified version of the Versatile Advection Code (VAC).

Results. By applying shearing motions on the solar surface, the magnetic field is energised and multiple eruptions are obtained. Magnetic reconnection first opens the overlying field and two new reconnections sites set in on either side of the central arcade. After the disconnection of the large helmet top, the system starts to restore itself but cannot return to its original configuration as a new arcade has already started to erupt. This process then repeats itself as we continue shearing.

Conclusions. The simulations reported in the present paper, demonstrate the ability to obtain a sequence of CMEs by shearing a large region of the central arcade or by shearing a region that is only slightly larger than the central arcade. We show, be it in an axisymmetric configuration, that the breakout model can not only lead to confined eruptions but also to actual coronal mass ejections provided the model includes a realistic solar wind model.

Reconstruction of Helio-latitudinal Structure of the Solar Wind Proton Speed and Density

Justyna M. **Sokół**, Paweł Swaczyna, Maciej Bzowski, Munetoshi Tokumaru

Solar Phys. Volume 290, Issue 9, pp 2589-2615 2015

<http://link.springer.com/article/10.1007/s11207-015-0800-2>

The modeling of the heliosphere requires continuous three-dimensional solar wind data. The in-situ out-of-ecliptic measurements are very rare, so that other methods of solar wind detection are needed. We use the remote sensing data of the solar wind speed from observations of interplanetary scintillation (IPS) to reconstruct spatial and temporal structures of the solar wind proton speed from 1985 to 2013. We developed a method of filling the data gaps in the IPS observations to obtain continuous and homogeneous solar wind speed records. We also present a method to retrieve the

solar wind density from the solar wind speed, utilizing the invariance of the solar wind dynamic pressure and energy flux with latitude. To construct the synoptic maps of solar wind speed we use the decomposition into spherical harmonics of each of the Carrington rotation map. To fill the gaps in time we apply the singular spectrum analysis to the time series of the coefficients of spherical harmonics. We obtained helio-latitudinal profiles of the solar wind proton speed and density over almost three recent solar cycles. The accuracy in the reconstruction is, due to computational limitations, about 20%. The proposed methods allow us to improve the spatial and temporal resolution of the model of the solar wind parameters presented in our previous paper (Sokół et al. 2013) and give a better insight into the time variations of the solar wind structure. Additionally, the solar wind density is reconstructed more accurately and it fits better to the in-situ measurements from Ulysses.

Heliolatitude and Time Variations of Solar Wind Structure from in situ Measurements and Interplanetary Scintillation Observations

J. M. Sokół, M. Bzowski, M. Tokumaru, K. Fujiki and D. J. McComas

Solar Phys. 2012

<http://arxiv.org/pdf/1510.04092v1.pdf>

The 3D structure of the solar wind and its evolution in time are needed for heliospheric modeling and interpretation of energetic neutral atoms observations. We present a model to retrieve the solar wind structure in heliolatitude and time using all available and complementary data sources. We determine the heliolatitude structure of solar wind speed on a yearly time grid over the past 1.5 solar cycles based on remote-sensing observations of interplanetary scintillations, in situ out-of-ecliptic measurements from Ulysses, and in situ in-ecliptic measurements from the OMNI 2 database. Since in situ out-of-ecliptic information on the solar wind density structure is not available apart from the Ulysses data, we derive correlation formulae between the solar wind speed and density and use the information on the solar wind speed from interplanetary scintillation observations to retrieve the 3D structure of the solar wind density. With the variations of solar wind density and speed in time and heliolatitude available, we calculate variations in solar wind flux, dynamic pressure, and charge-exchange rate in the approximation of stationary H atoms.

Three-day Forecasting of Solar Wind Speed Using SDO/AIA Extreme-ultraviolet Images by a Deep-learning Model

Jihyeon Son¹, Suk-Kyung Sung², Yong-Jae Moon^{1,2}, Harim Lee², and Hyun-Jin Jeong²

2023 ApJS 267 45

<https://iopscience.iop.org/article/10.3847/1538-4365/ace59a/pdf>

In this study, we forecast solar wind speed for the next 3 days with a 6 hr cadence using a deep-learning model. For this we use Solar Dynamics Observatory/Atmospheric Imaging Assembly 211 and 193 Å images together with solar wind speeds for the last 5 days as input data. The total period of the data is from 2010 May to 2020 December. We divide them into a training set (January–August), validation set (September), and test set (October–December), to consider the solar cycle effect. The deep-learning model consists of two networks: a convolutional layer-based network for images and a dense layer-based network for solar wind speeds. Our main results are as follows. First, our model successfully predicts the solar wind speed for the next 3 days. The rms error (RMSE) of our model is from 37.4 km s⁻¹ (for the 6 hr prediction) to 68.2 km s⁻¹ (for the 72 hr prediction), and the correlation coefficient is from 0.92 to 0.67. These results are much better than those of previous studies. Second, the model can predict sudden increase of solar wind speeds caused by large equatorial coronal holes. Third, solar wind speeds predicted by our model are more consistent with observations than those by the Wang–Sheely–Arge–ENLIL model, especially in high-speed-stream regions. It is also noted that our model cannot predict solar wind speed enhancement by coronal mass ejections. Our study demonstrates the effectiveness of deep learning for solar wind speed prediction, with potential applications in space weather forecasting. 2013-09-26-30, 2016-11-08-13, 2017-11-06-13, 2018-10-01-05, 2019-10-19-23

Inspect the Time Lag in Galactic Cosmic-Ray Solar Modulation

Xiaojian Song¹, Xi Luo¹, and Zhaomin Wang¹

2024 ApJ 975 273

<https://iopscience.iop.org/article/10.3847/1538-4357/ad8443/pdf>

It is well known that there is a time lag between the solar activity and the galactic cosmic-ray flux. How to accurately describe this delay is the key problem in making precise predictions of cosmic-ray flux. In this work, a response function in convolution is first used to describe the relative contribution of the solar wind blowout at earlier times to the current

flux (the origin of time lag), and its explicit profile is obtained by our 3D time-dependent numerical model. It is found that our response function is superior to other functions in accounting for the time lag effect, and its rigidity and physical process dependence are studied thoroughly. At last, this description is partly demonstrated by a simplified derivation based on the underlying physical processes.

A Numerical Study of the Solar Modulation of Galactic Protons and Helium from 2006 to 2017

Xiaojian **Song**¹, Xi Luo¹, Marius S. Potgieter², XinMing Liu^{1,3}, and Zekun Geng^{1,3}

2021 ApJS 257 48

<https://doi.org/10.3847/1538-4365/ac281c>

With continuous measurements from space-borne cosmic-ray detectors such as AMS-02 and PAMELA, precise spectra of galactic cosmic rays over the 11 yr solar cycle have become available. For this study, we utilize proton and helium spectra below 10 GV from these missions from 2006 to 2017 to construct a cosmic-ray transport model for a quantitative study of the processes of solar modulation. This numerical model is based on Parker's transport equation, which includes four major transport processes. The Markov Chain Monte Carlo method is utilized to search the relevant parameter space related to the drift and the diffusion coefficients by reproducing and fitting the mentioned observed spectra. The resulting best-fit normalized χ^2 is mainly less than 1. It is found that (1) when reproducing these observations the parameters required for the drift and diffusion coefficients exhibit a clear time dependence, with the magnitude of the diffusion coefficients anticorrelated with solar activity; (2) the rigidity dependence of the resulting mean free paths varies with time, and their rigidity dependence at lower rigidity can even have a larger slope than at higher rigidity; (3) using a single set of modulation parameters for each pair of observed proton and helium spectra, most spectra are reproduced within observational uncertainty; and (4) the simulated proton-to-helium flux ratio agrees with the observed values in terms of its long-term time dependence, although some discrepancy exists, and the difference is mostly coming from the underestimation of proton flux.

Comparison of Helium Abundance between ICMEs and Solar Wind near 1 AU

Hongqiang **Song**, [Xin Cheng](#), [Leping Li](#), [Jie Zhang](#), [Yao Chen](#)

ApJ 925 137 2022

<https://arxiv.org/pdf/2111.10503.pdf>

<https://iopscience.iop.org/article/10.3847/1538-4357/ac3bbf/pdf>

The Helium abundance, defined as $A_{\text{He}} = n_{\text{He}}/n_{\text{H}} \times 100$, is ~ 8.5 in the photosphere and seldom exceeds 5 in fast solar wind. Previous statistics have demonstrated that A_{He} in slow solar wind correlates tightly with sunspot number. However, less attention is paid to the solar cycle dependence of A_{He} within interplanetary coronal mass ejections (ICMEs) and comparing the A_{He} characteristics of ICMEs and solar wind. In this paper we conduct a statistical comparison of Helium abundance between ICMEs and solar wind near 1 AU with observations of *Advanced Composition Explorer* from 1998 to 2019, and find that the ICME A_{He} also exhibits the obvious solar cycle dependence. Meanwhile, we find that the A_{He} is obviously higher within ICMEs compared to solar wind, and the means within 37% and 12% of ICMEs exceed 5 and 8.5, respectively. It is interesting to answer where and how the high Helium abundance originates. Our statistics demonstrate that 21% (3%) of ICME (slow wind) A_{He} data points exceed 8.5 around solar maximum, which decreases dramatically near minimum, while no such high A_{He} values appear in the fast wind throughout the whole solar cycle. This indicates that the high A_{He} (e.g., >8.5) emanates from active regions as more ICMEs and slow wind originates from active regions around maximum, and supports that both active regions and quiet-Sun regions are the sources of slow wind. We suggest that the high A_{He} from active regions could be explained by means of the magnetic loop confinement model and/or photoionization effect.

The Inhomogeneity of Composition Along the Magnetic Cloud Axis

Hongqiang **Song**^{1,2*}, Qiang Hu³, Xin Cheng⁴, Jie Zhang⁵, Leping Li², Ake Zhao⁶, Bing Wang¹,

Ruisheng Zheng¹ and Yao Chen¹

Front. Phys., 9:684345 2021 |

<https://www.frontiersin.org/articles/10.3389/fphy.2021.684345/full>

<https://doi.org/10.3389/fphy.2021.684345>

Coronal mass ejections (CMEs) are one of the most energetic explosions in the solar system. It is generally accepted that CMEs result from eruptions of magnetic flux ropes, which are dubbed as magnetic clouds (MCs) in interplanetary space. The composition (including the ionic charge states and elemental abundances) is determined prior to and/or during CME eruptions in the solar atmosphere and does not alter during MC propagation to 1 AU and beyond. It has been known that the composition is not uniform within a cross section perpendicular to the MC axis, and the distribution of ionic charge states within a cross section provides us an important clue to investigate the formation and eruption processes of flux

ropes due to the freeze-in effect. The flux rope is a three-dimensional magnetic structure intrinsically, and it remains unclear whether the composition is uniform along the flux rope axis as most MCs are only detected by one spacecraft. In this study, we report an MC that was observed by Advanced Composition Explorer at ~ 1 AU during **March 4–6, 1998**, and Ulysses at ~ 5.4 AU during **March 24–28, 1998**, sequentially. At these times, both spacecraft were located around the ecliptic plane, and the latitudinal and longitudinal separations between them were $\sim 2.2^\circ$ and $\sim 5.5^\circ$, respectively. It provides us an excellent opportunity to explore the axial inhomogeneity of flux rope composition, as both spacecraft almost intersected the cloud center at different sites along its axis. Our study shows that the average values of ionic charge states exhibit significant difference along the axis for carbon, and the differences are relatively slight but still obvious for charge states of oxygen and iron as well as the elemental abundances of iron and helium. Besides the means, the composition profiles within the cloud measured by both spacecraft also exhibit some discrepancies. We conclude that the inhomogeneity of composition exists along the cloud axis.

Solar Cycle Dependence of ICME Composition

Hongqiang Song, [Leping Li](#), [Yanyan Sun](#), [Qi Lv](#), [Ruisheng Zheng](#), [Yao Chen](#)

Solar Phys. **296**, Article number: 111 **2021**

<https://link.springer.com/content/pdf/10.1007/s11207-021-01852-y.pdf>

<https://arxiv.org/pdf/2106.03003.pdf>

Coronal mass ejections (CMEs) are one of the most energetic explosions in the solar atmosphere, and their occurrence rates exhibit obvious solar cycle dependence with more events taking place around solar maximum. Composition of interplanetary CMEs (ICMEs), referring to the charge states and elemental abundances of ions, opens an important avenue to investigate CMEs. In this paper, we conduct a statistical study on the charge states of five elements (Mg, Fe, Si, C, and O) and the relative abundances of six elements (Mg/O, Fe/O, Si/O, C/O, Ne/O, and He/O) within ICMEs from 1998 to 2011, and find that all the ICME compositions possess the solar cycle dependence. All of the ionic charge states and most of the relative elemental abundances are positively correlated with sunspot numbers (SSNs), and only the C/O ratios are inversely correlated with the SSNs. The compositions (except the C/O) increase with the SSNs during the ascending phase (1998--2000 and 2009--2011) and remain elevated during solar maximum and descending phase (2000--2005) compared to solar minimum (2007--2009). The charge states of low-FIP (first ionization potential) elements (Mg, Fe, and Si) and their relative abundances are correlated well, while no clear correlation is observed between the $C6+/C5+$ or $C6+/C4+$ and C/O. Most interestingly, we find that the Ne/O ratios of ICMEs and slow solar wind have the opposite solar cycle dependence.

Do All Interplanetary Coronal Mass Ejections Have A Magnetic Flux Rope Structure Near 1 AU?

Hongqiang Song, [Jie Zhang](#), [Xin Cheng](#), [Gang Li](#), [Qiang Hu](#), [Leping Li](#), [Shujun Chen](#), [Ruisheng Zheng](#), [Yao Chen](#)

ApJL **901** L21 **2020**

<https://arxiv.org/pdf/2009.05212.pdf>

<https://iopscience.iop.org/article/10.3847/2041-8213/abb6ec/pdf>

Interplanetary coronal mass ejections (ICMEs) often consist of a shock wave, sheath region, and ejecta region. The ejecta regions are divided into two broad classes: magnetic clouds (MC) that exhibit the characteristics of magnetic flux ropes and non-magnetic clouds (NMC) that do not. As CMEs result from eruption of magnetic flux ropes, it is important to answer why NMCs do not have the flux rope features. One claims that NMCs lose their original flux rope features due to the interactions between ICMEs or ICMEs and other large scale structures during their transit in the heliosphere. The other attributes this phenomenon to the geometric selection effect, i.e., when an ICME has its nose (flank, including leg and non-leg flanks) pass through the observing spacecraft, the MC (NMC) features will be detected along the spacecraft trajectory within the ejecta. In this Letter, we examine which explanation is more reasonable through the geometric properties of ICMEs. If the selection effect leads to different ejecta types, MCs should have narrower sheath region compared to NMCs from the statistical point of view, which is confirmed by our statistics. Besides, we find that NMCs have the similar size in solar cycles 23 and 24, and NMCs are smaller than MCs in cycle 23 but larger than MCs in cycle 24. This suggests that most NMCs have their leg flank pass through the spacecraft. Our geometric analyses support that all ICMEs should have a magnetic flux rope structure near 1 AU.

Table 1: Information on the 76 MCs and 73 NMCs (1995-1915)

Characteristics and applications of interplanetary coronal mass ejection composition **Review**

[Hongqiang Song](#), [Shuo Yao](#)

<https://arxiv.org/pdf/2006.11473.pdf>

In situ measurements of interplanetary coronal mass ejection (ICME) composition, including elemental abundances and charge states of heavy ions, open a new avenue to study coronal mass ejections (CMEs) besides remote-sensing observations. The ratios between different elemental abundances can diagnose the plasma origin of CMEs (e.g., from the corona or chromosphere/photosphere) due to the first ionization potential (FIP) effect, which means elements with different FIP get fractionated between the photosphere and corona. The ratios between different charge states of a specific element can provide the electron temperature of CMEs in the corona due to the freeze-in effect, which can be used to investigate their eruption process. In this review, we first give an overview of the ICME composition and then demonstrate their applications in investigating some important subjects related to CMEs, such as the origin of filament plasma and the eruption process of magnetic flux ropes. Finally, we point out several important questions that should be addressed further for better utilizing the ICME composition to study CMEs. **01-May-98**

A Statistical Study of the Average Iron Charge Distributions inside Magnetic Clouds for Solar Cycle 23

Hongqiang [Song](#), Ze Zhong, Yao Chen, Jie Zhang, Xin Cheng, Liang Zhao, Qiang Hu, Gang Li

ApJ 2016

<http://arxiv.org/pdf/1604.03205v1.pdf>

Magnetic clouds (MCs) are the interplanetary counterpart of coronal magnetic flux ropes. They can provide valuable information to reveal the flux rope characteristics at their eruption stage in the corona, which are unable to be explored in situ at present. In this paper, we make a comprehensive survey of the average iron charge state ($\langle Q \rangle_{\text{Fe}}$) distributions inside 96 MCs for solar cycle 23 using ACE (Advanced Composition Explorer) data. As the $\langle Q \rangle_{\text{Fe}}$ in the solar wind are typically around 9+ to 11+, the Fe charge state is defined as high when the $\langle Q \rangle_{\text{Fe}}$ is larger than 12+, which implies the existence of a considerable amount of Fe ions with high charge states (e.g., $\geq 16+$). The statistical results show that the $\langle Q \rangle_{\text{Fe}}$ distributions of 92 (~ 96%) MCs can be classified into four groups with different characteristics. In group A (11 MCs), the $\langle Q \rangle_{\text{Fe}}$ shows a bimodal distribution with both peaks higher than 12+. Group B (4 MCs) presents a unimodal distribution of $\langle Q \rangle_{\text{Fe}}$ with its peak higher than 12+. In groups C (29 MCs) and D (48 MCs), the $\langle Q \rangle_{\text{Fe}}$ remains higher and lower than 12+ throughout ACE passage through the MC, respectively. Possible explanations to these distributions are discussed.

Evidence of the Solar EUV hot channel as a magnetic flux rope from remote-sensing and in-situ observations

Hongqiang [Song](#), [Yao Chen](#), [Jie Zhang](#), [Xin Cheng](#), [Bing Wang](#), [Qiang Hu](#), [Gang Li](#), [Yuming Wang](#)

ApJL 2015

<http://arxiv.org/pdf/1507.00078v1.pdf>

Hot channels (HCs), high temperature erupting structures in the lower corona of the Sun, have been proposed as a proxy of magnetic flux ropes (MFRs) since their initial discovery. However, it is difficult to make definitive proof given the fact that there is no direct measurement of magnetic field in the corona. An alternative way is to use the magnetic field measurement in the solar wind from in-situ instruments. On **2012 July 12**, an HC was observed prior to and during a coronal mass ejection (CME) by the AIA high-temperature images. The HC is invisible in the EUVI low-temperature images, which only show the cooler leading front (LF). However, both the LF and an ejecta can be observed in the coronagraphic images. These are consistent with the high temperature and high density of the HC and support that the ejecta is the erupted HC. In the meanwhile, the associated CME shock was identified ahead of the ejecta and the sheath through the COR2 images, and the corresponding ICME was detected by \textit{ACE}, showing the shock, sheath and magnetic cloud (MC) sequentially, which agrees with the coronagraphic observations. Further, the MC contained a low-ionization-state center and a high-ionization-state shell, consistent with the pre-existing HC observation and its growth through magnetic reconnection. All of these observations support that the MC detected near the Earth is the counterpart of the erupted HC in the corona for this event. Therefore, our study provides strong observational evidence of the HC as an MFR.

First Taste of Hot Channel in Interplanetary Space

H. Q. [Song](#)¹, J. Zhang², Y. Chen¹, X. Cheng³, G. Li⁴, and Y. M. Wang

2015 ApJ 803 96

<http://arxiv.org/pdf/1502.04408v1.pdf>

A hot channel (HC) is a high temperature (~10 MK) structure in the inner corona first revealed by the Atmospheric Imaging Assembly on board the Solar Dynamics Observatory. Eruptions of HCs are often associated with flares and coronal mass ejections (CMEs). Results of previous studies have suggested that an HC is a good proxy for a magnetic flux rope (MFR) in the inner corona as well as another well known MFR candidate, the prominence-cavity structure, which has a normal coronal temperature (~1–2 MK). In this paper, we report a high temperature structure (HTS, ~1.5 MK) contained in an interplanetary CME induced by an HC eruption. According to the observations of bidirectional electrons, high temperature and density, strong magnetic field, and its association with the shock, sheath, and plasma pile-up region, we suggest that the HTS is the interplanetary counterpart of the HC. The scale of the measured HTS is around 14 R_☉, and it maintained a much higher temperature than the background solar wind even at 1 AU. It is significantly different from the typical magnetic clouds, which usually have a much lower temperature. Our study suggests that the existence of a corotating interaction region ahead of the HC formed a magnetic container to inhibit expansion of the HC and cool it down to a low temperature. **2012 January 27,**

Visualizing CMEs and Predicting Geomagnetic Storms from Solar Magnetic Fields

Paul **Song**, Howard J. Singer and George L. Siscoe

Yan Li¹, Janet G. Luhmann, ¹, J. Todd. Hoeksema², Xuepu Zhao, and C. Nick Arge
Space Weather **2013**

<http://onlinelibrary.wiley.com/doi/10.1029/GM125p0177/pdf>

An Analytical Model to Predict the Arrival Time of Interplanetary CMEs

W. B. **Song**

Solar Phys., 261(2), 311-320, **2010**

Referring to the aerodynamic drag force, we present an analytical model to predict the arrival time of coronal mass ejections (CMEs). All related calculations are based on the expression for the deceleration of fast CMEs in the

$$\dot{v} = -\frac{1}{15700}(v - V_{sw})^2$$

interplanetary medium (ICMEs), where V_{sw} is the solar wind speed. The results can reproduce well the observations of three typical parameters: the initial speed of the CME, the speed of the ICME at 1 AU and the transit time. Our simple model reveals that the drag acceleration should be really the essential feature of the interplanetary motion of CMEs, as suggested by Vršnak and Gopalswamy (*J. Geophys. Res.* **107**, 1019, 2002).

The Automatic Predictability of Super Geomagnetic Storms from halo CMEs associated with Large Solar Flares,

Hui **Song**, Vasyl Yurchyshyn, Guo Yang, Changyi Tan, Weizhong Chen and Haimin Wang,
Solar Physics, Volume 238 Number 1, p. 141-165, **2006. File.**

We investigate the relationship between magnetic structures of coronal mass ejection (CME) source regions and geomagnetic storms, in particular, the super storms when the D_{st} index decreases below -200 nT. By examining all full halo CMEs that erupted between 1996 and 2004, we selected 73 events associated with M-class and X-class solar flares, which have a clearly identifiable source region. By analyzing daily full-disk MDI magnetograms, we found that the horizontal gradient of the line-of-sight magnetic field is a viable parameter to identify a flaring magnetic neutral line and thus can be used to predict the possible source region of CMEs. The accuracy of this prediction is about 75%, especially for those associated with X-class flares (up to 89%). The mean orientation of the magnetic structures of source regions was derived and characterized by the orientation angle θ , which is defined to be $\leq 90^\circ$ in the case of the southward orientation and $\geq 90^\circ$, when the magnetic structure is northwardly oriented. The orientation angle was calculated as the median orientation angle of extrapolated field lines relative to the flaring neutral line. We report that for about 92% of super storms (12 out of 13 events) the orientation angle was found to be southward. In the case of intense and moderate storms ($D_{st} \geq -200$ nT), the relationship is less pronounced (70%, 21 out of 30 events). Our findings demonstrate that the approach presented in this paper can be used to perform an automatic prediction of the occurrence of large X-class flares and super geomagnetic storms.

CMEs evolve in the interplanetary medium to double their predicted geo-effectiveness

Shirsh Lata **Soni**^{1,2}, Anwasha Maharana³, Antonio Guerrero⁴, Wageesh Mishra⁵, Stefaan Poedts^{3,6}, Smitha Thampi² and Mojtaba Akhavan-Tafti¹
A&A, 686, A23 (**2024**)

<https://doi.org/10.1051/0004-6361/202347552>
<https://www.aanda.org/articles/aa/pdf/2024/06/aa47552-23.pdf>

Context. We explore the impact of interactions between coronal mass ejections (CMEs) – known as CME–CME interactions – on Earth using remote-sensing and in situ observations and estimate the amplification of the geo-effectiveness of the individual CMEs by a factor of ~ 2 due to CME–CME interactions.

Aims. We present 3D reconstructions of interacting CMEs, which provide essential information on the orientation and interaction of the events. Additionally, we analysed coronal evolution of CMEs and their in situ characteristics at 1 AU to explore the impact of interactions between CMEs on their geo-effectiveness.

Methods. We analysed CME interaction using white light data from LASCO and STEREO COR-A. The reported CMEs were reconstructed using the gradual cylindrical shell (GCS) model and simulated self-consistently with the physics-based 3D MHD model EUHFORIA (EUropean Heliosphere FORecasting Information Asset). By running different simulations, we estimated the geo-effectiveness of both individual and interacting CMEs using an empirical relationship method for the disturbance storm index.

Results. The SOHO/LASCO spacecraft observed three CMEs erupting from the Sun within an interval of 10 h during a very active period in early November 2021. There were two partial halo CMEs that occurred on **1 Nov. 2021** at 19:00 UT and 22:00 UT, respectively, from the active region 12887 (S28W58), and a third halo CME occurred from AR 12891 (N17E03) on **2 Nov. 2021** at 02:48 UT. By combining remote observations close to the Sun, in situ data at 1 AU, and further numerical analyses of each individual CME, we are able to identify the initial and interplanetary evolution of the CMEs.

Conclusions. (i) White light observations and a 3D reconstruction of the CMEs show cannibalism by CME-2 on CME-1 and a flank interaction of CME-3 with the merged CME-1 and CME-2 at 45–50 Rs. (ii) Interacting CMEs exhibit an increase in geo-effectiveness compared to an individual CME.

Switchback Patches Evolve into Microstreams via Magnetic Relaxation

Shirsh Lata [Soni](#), [Mojtaba Akhavan-Tafti](#), [Gabriel Ho Hin Suen](#), [Justin Kasper](#), [Marco Velli](#), [Rossana De Marco](#), [Christopher Owen](#)

2024

<https://arxiv.org/pdf/2402.13964.pdf>

Magnetic switchbacks are distinct magnetic structures characterized by their abrupt reversal in the radial component of the magnetic field within the pristine solar wind. Switchbacks are believed to lose magnetic energy with heliocentric distance. To investigate this switchbacks originating from similar solar source regions are identified during a radial alignment of the Parker Solar Probe (PSP; 25.8 solar radii) and Solar Orbiter (SolO; 152 solar radii). We found that 1) the dynamic and thermal pressures decrease at the switchback boundaries by up to 20% at PSP and relatively unchanged at SolO and magnetic pressure jump across the boundary remains negligible at both distances, and 2) bundles of switchbacks are often observed in switchback patches near the Sun, and in microstreams farther away. Background proton velocity (v_p) is 10% greater than the pristine solar wind (v_{sw}) in microstreams, whereas $v_p \sim v_{sw}$ in switchback patches. Microstreams contain an average of 30% fewer switchbacks than switchback patches. It is concluded that switchbacks likely relax magnetically and equilibrate their plasma with the surrounding environment with heliocentric distance. Switchback relaxation can, in turn, accelerate the surrounding plasma. Therefore, it is hypothesized that magnetic relaxation of switchbacks may cause switchback patches to evolve into microstreams with heliocentric distance. Statistical analysis of PSP and SolO switchbacks is underway to further test our hypothesis. **August 11-12, 2021**

Table:1 Radial alignment durations of PSP and SolO, their distance from Sun. 2020-2022

Assessment of the arrival signatures of the March 2012 CME–CME interaction event with respect to Mercury, Venus, Earth, STEREO-B, and Mars locations

[Soni](#), Shirsh Lata ; [Selvakumaran, R.](#) ; [Thampi, R. Satheesh](#)

Frontiers in Astronomy and Space Sciences, Volume 9, id.441 (2022)

<https://doi.org/10.3389/fspas.2022.1049906>

<https://www.frontiersin.org/articles/10.3389/fspas.2022.1049906/full>

In March 2012, favourable positions of Mercury, Venus, Earth, Mars, and STEREO-B in the inner solar system provided an opportunity to understand the global structure and the propagation of a CME across the inner solar system. On March 7, 2012, the Sun ejected two very fast CMEs from solar active region NOAA AR11489, which were accompanied by two X-class flares. Initialization and subsequent fast expansion from lower coronal heights of flux rope structures were detected as their early eruption signatures in SDO observations. White light observations have been imaged by SOHO/LASCO and followed from 00:24 UT on **March 7, 2012**. We examined the kinematics of the reported CMEs and

found a significant exchange of momentum and kinetic energy during the interaction, indicating that the collision was close to inelastic. Further, we observed the arrival of this merged CME event at different distances in the inner solar system and compared the arrival time with other models. The reported event arrived at Mercury at 04:30 UT, Venus at 13:28 UT on March 7, 2012, and it took roughly 36 hours to reach STEREO-B. The arrivals at Mercury and Venus are observed in the magnetometer measurements onboard Messenger and VEx, respectively. A powerful Interplanetary shock was observed at 1 AU around 34 hours after the two X-class flares and CMEs eruption. Subsequently, a south-directed interplanetary magnetic field (IMF) was observed at Earth, indicating the arrival of an ICME. This event caused the sudden storm commencement and development of one of the major intense geomagnetic storms of SC 24, with a minimum Dst value of -148nT. The observations by the Mars Express (MEX) mission indicated the arrival of a merged CME ~2.5 days after its initial observation at Sun. We have analysed the evolution of these CMEs as well as their propagation in the inner heliosphere and arrival signatures at four planetary locations. The propagation and arrival signatures are compared to simulations using the WSA ENLIL+Cone model and the Drag Based Model at various vantage points. The study showcases the importance of multi-vantage point observations in understanding the propagation of CMEs and their interactions.

Turbulent Cascade and Energy Transfer Rate in a Solar Coronal Mass Ejection

Luca **Sorriso-Valvo**^{1,2}, Emiliya Yordanova¹, Andrew P. Dimmock¹, and Daniele Telloni³

2021 ApJL 919 L30

<https://arxiv.org/pdf/2110.02664.pdf>

<https://doi.org/10.3847/2041-8213/ac26c5>

Turbulence properties are examined before, during, and after a coronal mass ejection (CME) detected by the Wind spacecraft in 2012 July. The power-law scaling of the structure functions, providing information on the power spectral density and flatness of the velocity, magnetic field, and density fluctuations, were examined. The third-order moment scaling law for incompressible, isotropic magnetohydrodynamic turbulence was observed in the preceding and trailing solar wind, as well as in the CME sheath and magnetic cloud. This suggests that the turbulence could develop sufficiently after the shock, or that turbulence in the sheath and cloud regions was robustly preserved even during the mixing with the solar wind plasma. The turbulent energy transfer rate was thus evaluated in each of the regions. The CME sheath shows an increase of energy transfer rate, as expected from the lower level of Alfvénic fluctuations and suggesting the role of the shock-wind interaction as an additional source of energy for the turbulent cascade. **12-15 Jul 2012**

On the Statistical Properties of Turbulent Energy Transfer Rate in the Inner Heliosphere

Luca **Sorriso-Valvo**, Francesco Carbone, Silvia Perri, Antonella Greco, Raffaele Marino, Roberto Bruno

Solar Physics January **2018**, 293:10

<https://link.springer.com/content/pdf/10.1007%2Fs11207-017-1229-6.pdf>

The transfer of energy from large to small scales in solar wind turbulence is an important ingredient of the long-standing question of the mechanism of the interplanetary plasma heating. Previous studies have shown that magnetohydrodynamic (MHD) turbulence is statistically compatible with the observed solar wind heating as it expands in the heliosphere. However, in order to understand which processes contribute to the plasma heating, it is necessary to have a local description of the energy flux across scales. To this aim, it is customary to use indicators such as the magnetic field partial variance of increments (PVI), which is associated with the local, relative, scale-dependent magnetic energy. A more complete evaluation of the energy transfer should also include other terms, related to velocity and cross-helicity. This is achieved here by introducing a proxy for the local, scale-dependent turbulent energy transfer rate $\epsilon\Delta t(t)\epsilon\Delta t(t)$, based on the third-order moment scaling law for MHD turbulence. Data from Helios 2 are used to determine the statistical properties of such a proxy in comparison with the magnetic and velocity fields PVI, and the correlation with local solar wind heating is computed. PVI and $\epsilon\Delta t(t)\epsilon\Delta t(t)$ are generally well correlated; however, $\epsilon\Delta t(t)\epsilon\Delta t(t)$ is a very sensitive proxy that can exhibit large amplitude values, both positive and negative, even for low amplitude peaks in the PVI. Furthermore, $\epsilon\Delta t(t)\epsilon\Delta t(t)$ is very well correlated with local increases of the temperature when large amplitude bursts of energy transfer are localized, thus suggesting an important role played by this proxy in the study of plasma energy dissipation.

MEASURING THE NASCENT SOLAR WIND OUTFLOW VELOCITIES VIA THE DOPPLER DIMMING TECHNIQUE

Daniele **Spadaro**¹, Daniele Telloni² and the METIS team

Solar Orbiter nugget #7 **2023**

<https://www.cosmos.esa.int/web/solar-orbiter/solar-nuggets/measuring-the-solar-wind-via-the-doppler-dimming-technique>

15 May 2020

Comparison of Radioastronomical Estimates of the Coronal and Solar Wind Magnetic Field with Measurements from Parker Solar Probe

Steven R. [Spangler](#)

2020 Res. Notes AAS 4 147

<https://iopscience.iop.org/article/10.3847/2515-5172/abb29a>

<https://doi.org/10.3847/2515-5172/abb29a>

The Parker Solar Probe (PSP) spacecraft is measuring plasma properties of the solar wind to heliocentric distances as small as 0.125 au or 26.9 solar radii. One of the most important plasma parameters is the strength of the magnetic field. A variety of radioastronomical remote sensing measurements also provide information on the magnetic field, from the solar surface to heliocentric distances of about 10 solar radii. In this paper, we compare radioastronomical estimates from one technique, Faraday rotation of background radio sources, with the PSP measurements. The extrapolated radioastronomical values are in good agreement with the measurements at the first and second perihelion passages in 2018 and 2019. Future radio measurements could therefore complement PSP measurements as it approaches the ultimate perihelion of 9.8 solar radii.

Radio Propagation Studies of the Solar Wind in the Era of Parker Solar Probe

Review

Steven R. [Spangler](#)

2020 Res. Notes AAS 4 102

<https://iopscience.iop.org/article/10.3847/2515-5172/aba35d>

The NASA Parker Solar Probe mission is providing unprecedented measurements of solar wind plasma and plasma turbulence at heliocentric distances as small as 0.125 au, or 26.9 solar radii. Radioastronomical remote sensing measurements of the coronal and solar wind plasma have been made since the 1960s over a heliocentric distance range that overlaps with and extends that of Parker Solar Probe. This paper will compare radio scintillation and Parker Solar Probe results on the heliocentric-distance-dependence of the plasma density variance (where there may be an inconsistency between the two techniques), the speed at which turbulence density irregularities move radially with respect to the Sun, and other topics.

In-situ switchback formation in the expanding solar wind

Jonathan [Squire](#), [Benjamin D. G. Chandran](#), [Romain Meyrand](#)

2020 *ApJL* 891 L2

<https://arxiv.org/pdf/2001.08422.pdf>

<https://doi.org/10.3847/2041-8213/ab74e1>

Recent near-sun solar-wind observations from Parker Solar Probe have found a highly dynamic magnetic environment, permeated by abrupt radial-field reversals, or "switchbacks." We show that many features of the observed turbulence are reproduced by a spectrum of Alfvénic fluctuations advected by a radially expanding flow. Starting from simple superpositions of low-amplitude outward-propagating waves, our expanding-box compressible MHD simulations naturally develop switchbacks due to (i) wave growth caused by expansion and (ii) the fluctuations' evolution towards spherical polarization (i.e., nearly constant field strength). These results suggest that switchbacks form in-situ in the expanding solar wind and are not indicative of impulsive processes in the chromosphere or corona.

Investigating the Variations in Compositions and Heating of Interacting ICMEs

Nandita [Srivastava](#), Zavkiddin Mirtoshev, and Wageesh Mishra

Front. Astron. Space Sci., 10 :1154612 2023

<https://doi.org/10.3389/fspas.2023.1154612>

<https://www.frontiersin.org/articles/10.3389/fspas.2023.1154612/pdf>

Interacting coronal mass ejections (CMEs) have been commonly reported during the STEREO era. With the interaction of CMEs in the heliosphere, it is expected that the participating CMEs will either merge to form a single interplanetary CME (ICME) or will arrive as distinct entities or ICMEs at 1 AU. Previous studies have focused on in situ observations of solar wind, i.e., plasma and magnetic field properties to understand the nature of the CME–CME interaction and its impact. In this study, we examine the observations of composition parameters of those ICMEs that resulted due to the interaction of two CMEs during their propagation between the Sun and the Earth. We report two events of the CME–

CME interaction observed in 2012, of which one led to a merged structure after the interaction, as observed at 1 AU. The second interaction event was reported to arrive at L1 as two distinct structures. Our analysis reveals distinct composition signatures in the form of ion charge state enhancements. The results improve our understanding of the signatures of ICMEs and different complex structures formed after the interaction. The study reveals that compression can occur due to the passage of the shock associated with the following CME through the preceding CME and not due to the CME–CME interaction. The results also highlight the importance of the comparison of solar wind proton velocity data with the expected temperature data, in particular, to understand the ICME–ICME interaction processes. **13–14 June 2012 , 9–10 November 2012**

Interplanetary and Geomagnetic Consequences of Interacting CMEs of 13-14 June 2012

Nandita [Srivastava](#), [Wageesh Mishra](#), [D. Chakrabarty](#)

Solar Phys. 2018, 293:5

<https://arxiv.org/pdf/1712.08408.pdf>

We report on the kinematics of two interacting CMEs observed on **13 and 14 June 2012**. Both CMEs originated from the same active region NOAA 11504. After their launches which were separated by several hours, they were observed to interact at a distance of 100 Rs from the Sun. The interaction led to a moderate geomagnetic storm at the Earth with Dst index of approximately, -86 nT. The kinematics of the two CMEs is estimated using data from the Sun Earth Connection Coronal and Heliospheric Investigation (SECCHI) onboard the Solar Terrestrial Relations Observatory (STEREO). Assuming a head-on collision scenario, we find that the collision is inelastic in nature. Further, the signatures of their interaction are examined using the in situ observations obtained by Wind and the Advance Composition Explorer (ACE) spacecraft. It is also found that this interaction event led to the strongest sudden storm commencement (SSC) (approximately 150 nT) of the present Solar Cycle 24. The SSC was of long duration, approximately 20 hours. The role of interacting CMEs in enhancing the geoeffectiveness is examined.

On three-dimensional aspects of CMEs, their source regions and interplanetary manifestations: [Introduction to special issue](#) [Review](#)

Nandita [Srivastava](#), Marilena Mierlab, c, d and Luciano Rodriguez

Journal of Atmospheric and Solar-Terrestrial Physics, Volume 73, Issue 10, **2011**, Pages 1077-1081, **File Article Outline**

1. Introduction

1.1. CMEs source regions: 3D observations and models

1.2. CMEs: 3D observations and models

1.3. Interplanetary CMEs: 3D observations and models

Source region of the 18 November 2003 coronal mass ejection that led to the strongest magnetic storm of cycle 23

[Srivastava](#), Nandita; Mathew, Shibu K.; Louis, Rohan E.; Wiegelmann, Thomas

J. Geophys. Res., Vol. 114, No. A3, A03107, **2009**; **File**

<http://dx.doi.org/10.1029/2008JA013845>

The superstorm of **20 November 2003** was associated with a high-speed coronal mass ejection (CME) which originated in the NOAA AR 10501 on 18 November. This coronal mass ejection had severe terrestrial consequences leading to a geomagnetic storm with *Dst* index of -472 nT, the strongest of the current solar cycle. In this paper, we attempt to understand the factors that led to the coronal mass ejection on 18 November. We have also studied the evolution of the photospheric magnetic field of NOAA AR 10501, the source region of this coronal mass ejection. For this purpose, the Michelson Doppler Imager line-of-sight magnetograms and vector magnetograms from Solar Flare Telescope, Mitaka, obtained during 17–19 November 2003 were analyzed. In particular, quantitative estimates of the temporal variation in magnetic flux, energy, and magnetic field gradient were estimated for the source active region. The evolution of these quantities was studied for the 3-day period with an objective to understand the preflare configuration leading up to the moderate flare which was associated with the geoeffective coronal mass ejection. We also examined the chromospheric images recorded in H_{α} from Udaipur Solar Observatory to compare the flare location with regions of different magnetic field and energy. Our observations provide evidence that the flare associated with the CME occurred at a location marked by high magnetic field gradient which led to release of free energy stored in the active region.

Predicting the occurrence of super-storms

N. [Srivastava](#)

Annales Geophysicae, 23, 2989–2995, 2005, [File](#)

A comparative study of five super-storms ($D_{st} < -300$ nT) of the current solar cycle after the launch of SoHO, to identify solar and interplanetary variables that influence the magnitude of resulting geomagnetic storms, is described. Amongst solar variables, the initial speed of a CME is considered the most reliable predictor of the strength of the associated geomagnetic storm because fast mass ejections are responsible for building up the ram pressure at the Earth's magnetosphere. However, although most of the super-storms studied were associated with high speed CMEs, the D_{st} index of the resulting geomagnetic storms varied between -300 to -472 nT. The most intense storm of 20 November 2003, ($D_{st} -472$ nT) had its source in a comparatively smaller active region and was associated with a relatively weaker, M-class flare while all other super-storms had their origins in large active regions and were associated with strong X-class flares. However, this superstorm did not show any associated extraordinary solar and interplanetary characteristics. The study also reveals the challenge in the reliable prediction of the magnitude of a geomagnetic storm from solar and interplanetary variables.

A logistic regression model for predicting the occurrence of intense geomagnetic storms

N. [Srivastava](#)

Annales Geophysicae, 23, 2969–2974, 2005, [File](#)

A logistic regression model is implemented for predicting the occurrence of intense/super-intense geomagnetic storms. A binary dependent variable, indicating the occurrence of intense/super-intense geomagnetic storms, is regressed against a series of independent model variables that define a number of solar and interplanetary properties of geo-effective CMEs. The model parameters (regression coefficients) are estimated from a training data set which was extracted from a dataset of 64 geo-effective CMEs observed during 1996–2002. The trained model is validated by predicting the occurrence of geomagnetic storms from a validation dataset, also extracted from the same data set of 64 geoeffective CMEs, recorded during 1996–2002, but not used for training the model. The model predicts 78% of the geomagnetic storms from the validation data set. In addition, the model predicts 85% of the geomagnetic storms from the training data set. These results indicate that logistic regression models can be effectively used for predicting the occurrence of intense geomagnetic storms from a set of solar and interplanetary factors.

Solar and interplanetary sources of major geomagnetic storms during 1996–2002,

[Srivastava](#), N., and P. Venkatakrishnan

J. Geophys. Res., 109, A10103, doi:10.1029/2003JA010175, (2004).

sci-hub.se/10.1029/2003JA010175

Srivastava and Venkatakrishnan [2004] showed that CME speeds in the Large Angle and Spectrometric Coronagraph (LASCO) field of view **were roughly correlated with the strength of geomagnetic storms** and that a large percentage (62%) of the geoeffective CMEs are faster than 700 km s^{-1} .

Abstract During the 7-year period of the current solar cycle, 64 geoeffective coronal mass ejections (CMEs) were found to produce major geomagnetic storms ($DST < 100$ nT) at the Earth. In this paper we examine solar and interplanetary properties of these geoeffective coronal mass ejections (CMEs). The observations reveal that full-halo CMEs are potential sources of intense geomagnetic activity at the Earth. However, not all fullhalo CMEs give rise to major geomagnetic storms, which complicates the task of space weather forecasting. We examine solar origins of the geoeffective CMEs and their interplanetary effects, namely, solar wind speed, interplanetary shocks, and the southward component of the interplanetary magnetic field, in order to investigate the relationship between the solar and interplanetary parameters. In particular, the present study aims at ascertaining solar parameters that govern important interplanetary parameters responsible for producing major geomagnetic storms. Our investigation shows that fast full-halo CMEs associated with strong flares and originating from a favorable location, i.e., close to the central meridian and low and middle latitudes, are the most potential candidates for producing strong ram pressure at the Earth's magnetosphere and hence intense geomagnetic storms. The results also show that the intensity of geomagnetic storms depends most strongly on the southward component of the interplanetary magnetic field, followed by the initial speed of the CME and the ram pressure.

Relation between CME speed and geomagnetic storm intensity

Srivastava, N., and P. Venkatakrisnan
(2002), , Geophys. Res. Lett., 29(9), 1287,
[sci-hub.se/10.1029/2001GL013597](https://doi.org/10.1029/2001GL013597)

In this paper, we discuss the solar origin and interplanetary consequences of the coronal mass ejection of March 29, 2001 that was responsible for the most intense geomagnetic storm (DST ~ -377 nT) of the current solar cycle to date. A comparison of the CME of **March 29, 2001**, with a set of geo-effective halo CMEs associated with X-class flares showed that the strength of the geomagnetic storm at the earth is well correlated with the speed of the halo. Our study shows that the fast ejection is responsible for building up the ram pressure at the earth's magnetosphere. This may serve as a useful tool in the forecasting of intense geomagnetic storms.

ON SOLAR WIND ORIGIN AND ACCELERATION: MEASUREMENTS FROM ACE

Mark **Stakhiv**, Susan T. Lepri, Enrico Landi, Patrick Tracy, and Thomas H. Zurbuchen
2016 ApJ 829 117

The origin and acceleration of the solar wind are still debated. In this paper, we search for signatures of the source region and acceleration mechanism of the solar wind in the plasma properties measured in situ by the Advanced Composition Explorer spacecraft. Using the elemental abundances as a proxy for the source region and the differential velocity and ion temperature ratios as a proxy for the acceleration mechanism, we are able to identify signatures pointing toward possible source regions and acceleration mechanisms. We find that the fast solar wind in the ecliptic plane is the same as that observed from the polar regions and is consistent with wave acceleration and coronal-hole origin. We also find that the slow wind is composed of two components: one similar to the fast solar wind (with slower velocity) and the other likely originating from closed magnetic loops. Both components of the slow solar wind show signatures of wave acceleration. From these findings, we draw a scenario that envisions two types of wind, with different source regions and release mechanisms, but the same wave acceleration mechanism.

On the Origin of Mid-latitude Fast Wind: Challenging the Two-state Solar Wind Paradigm

Mark **Stakhiv**¹, Enrico Landi², Susan T. Lepri³, Rona Oran^{4,5}, and Thomas H. Zurbuchen
2015 ApJ 801 100

The bimodal paradigm of solar wind describes a slow solar wind situated near the heliospheric current sheet while a fast wind overexpands from the poles to fill in the remainder of the heliosphere. In this paper, we challenge this paradigm and focus here on mid-latitude wind using three fast-latitude passes completed by the Ulysses spacecraft. Based on its composition and dynamic properties, we discuss how this wind differs from both the fast, polar coronal hole wind and the low latitude, streamer-associated slow solar wind. Using a detailed analysis of ionic and elemental abundances, as well as solar wind dynamic properties, we conclude that there is a third quasi-stationary solar wind state, called the boundary wind. This boundary wind is characterized by a charge-state distribution that is similar to slow wind, but with an elemental composition that is coronal hole like. Based on these data, we present arguments for the location of the origin of this wind. We conclude that the boundary wind is a subset of the fast wind emanating from regions close to the boundaries of coronal holes and is accelerated by a similar process.

How Magnetic Erosion Affects the Drag-Based Kinematics of Fast Coronal Mass Ejections

Sotiris **Stamkos**, [Spiros Patsourakos](#), [Angelos Vourlidas](#) & [Ioannis A. Daglis](#)

[Solar Physics](#) volume 298, Article number: 88 (2023)

<https://link.springer.com/content/pdf/10.1007/s11207-023-02178-7.pdf>

<https://arxiv.org/pdf/2307.12370.pdf>

In order to advance our understanding of the dynamic interactions between coronal mass ejections (CMEs) and the magnetized solar wind, we investigate the impact of magnetic erosion on the well-known aerodynamic drag force acting on CMEs traveling faster than the ambient solar wind. In particular, we start by generating empirical relationships for the basic physical parameters of CMEs that conserve their mass and magnetic flux. Furthermore, we examine the impact of the virtual mass on the equation of motion by studying a variable-mass system. We next implement magnetic reconnection into CME propagation, which erodes part of the CME magnetic flux and outer-shell mass, on the drag acting on CMEs, and we determine its impact on their time and speed of arrival at 1 AU. Depending on the strength of the magnetic erosion, the leading edge of the magnetic structure can reach near-Earth space up to \approx three hours later, compared to the non-eroded case. Therefore, magnetic erosion may have a significant impact on the propagation of fast CMEs and on predictions of their arrivals at 1 AU. Finally, the modeling indicates that eroded CMEs may experience a significant mass decrease. Since such a decrease is not observed in the corona, the initiation distance of erosion may lie beyond the field-of-view of coronagraphs (i.e. $30 R_{\odot}$).

Active region contributions to the solar wind over multiple solar cycles

D. Stansby, [L. M. Green](#), [L. van Driel-Gesztelyi](#), [T. S. Horbury](#)

Solar Phys. 296, Article number: 116 2021

<https://arxiv.org/pdf/2104.04417.pdf>

<https://link.springer.com/content/pdf/10.1007/s11207-021-01861-x.pdf>

<https://doi.org/10.1007/s11207-021-01861-x>

Both coronal holes and active regions are source regions of the solar wind. The distribution of these coronal structures across both space and time is well known, but it is unclear how much each source contributes to the solar wind. In this study we use photospheric magnetic field maps observed over the past four solar cycles to estimate what fraction of magnetic open solar flux is rooted in active regions, a proxy for the fraction of all solar wind originating in active regions. We find that the fractional contribution of active regions to the solar wind varies between 30% to 80% at any one time during solar maximum and is negligible at solar minimum, showing a strong correlation with sunspot number. While active regions are typically confined to latitudes $\pm 30^\circ$ in the corona, the solar wind they produce can reach latitudes up to $\pm 60^\circ$. Their fractional contribution to the solar wind also correlates with coronal mass ejection rate, and is highly variable, changing by $\pm 20\%$ on monthly timescales within individual solar maxima. We speculate that these variations are primarily driven by coronal mass ejections causing global reconfigurations of the coronal magnetic field on sub-monthly timescales.

Sensitivity of solar wind mass flux to coronal temperature

D. Stansby, [L. Berčič](#), [L. Matteini](#), [C. J. Owen](#), [R. French](#), [D. Baker](#), [S. T. Badman](#)

MNRAS 2020

<https://arxiv.org/pdf/2009.13918.pdf>

Solar wind models predict that the mass flux carried away from the Sun in the solar wind should be extremely sensitive to the temperature in the corona, where the solar wind is accelerated. We perform a direct test of this prediction in coronal holes and active regions, using a combination of in-situ and remote sensing observations. For coronal holes, a 50% increase in temperature from 0.8 MK to 1.2 MK is associated with a tripling of the coronal mass flux. At temperatures over 2 MK, within active regions, this trend is maintained, with a four-fold increase in temperature corresponding to a 200-fold increase in coronal mass flux.

Directly comparing coronal and solar wind elemental fractionation A28

D. Stansby, D. Baker, D. H. Brooks and C. J. Owen

A&A 640, A28 (2020)

<https://www.aanda.org/articles/aa/pdf/2020/08/aa38319-20.pdf>

Context. As the solar wind propagates through the heliosphere, dynamical processes irreversibly erase the signatures of the near-Sun heating and acceleration processes. The elemental fractionation of the solar wind should not change during transit, however, making it an ideal tracer of these processes.

Aims. We aim to verify directly if the solar wind elemental fractionation is reflective of the coronal source region fractionation, both within and across different solar wind source regions.

Methods. A backmapping scheme was used to predict where solar wind measured by the Advanced Composition Explorer (ACE) originated in the corona. The coronal composition measured by the Hinode Extreme ultraviolet Imaging Spectrometer (EIS) at the source regions was then compared with the in situ solar wind composition.

Results. On hourly timescales, there is no apparent correlation between coronal and solar wind composition. In contrast, the distribution of fractionation values within individual source regions is similar in both the corona and solar wind, but distributions between different sources have a significant overlap.

Conclusions. The matching distributions directly verify that elemental composition is conserved as the plasma travels from the corona to the solar wind, further validating it as a tracer of heating and acceleration processes. The overlap of fractionation values between sources means it is not possible to identify solar wind source regions solely by comparing solar wind and coronal composition measurements, but a comparison can be used to verify consistency with predicted spacecraft-corona connections.

Hinode/EIS Nuggets Nov 2020

http://solarb.mssl.ucl.ac.uk/SolarB/nuggets/nugget_2020nov.jsp

The origin of slow Alfvénic solar wind at solar minimum

D. Stansby, [L. Matteini](#), [T. S. Horbury](#), [D. Perrone](#), [R. D'Amicis](#), [L. Berčič](#)

MNRAS 2019

<https://arxiv.org/pdf/1907.02646.pdf>

Although the origins of slow solar wind are unclear, there is increasing evidence that at least some of it is released in a steady state on over-expanded coronal hole magnetic field lines. This type of slow wind has similar properties to the fast solar wind, including a high degree of Alfvénicity. In this study a combination of proton, alpha particle, and electron measurements are used to investigate the kinetic properties of a single interval of slow Alfvénic wind at 0.35 AU. It is shown that this slow Alfvénic interval is characterised by high alpha particle abundances, pronounced alpha-proton differential streaming, strong proton beams, and large alpha to proton temperature ratios. These are all features observed consistently in the fast solar wind, adding evidence that at least some Alfvénic slow solar wind also originates in coronal holes. Observed differences between speed, mass flux, and electron temperature between slow Alfvénic and fast winds are explained by differing magnetic field geometry in the lower corona.

Predicting Large-scale Coronal Structure for Parker Solar Probe Using Open Source Software

David [Stansby](#)¹, Timothy S. Horbury¹, Samantha Wallace^{2,3}, and C. Nick Arge³

2019 Res. Notes AAS 3 57

<https://iopscience.iop.org/article/10.3847/2515-5172/ab13b7>

NASA's Parker Solar Probe (PSP) was launched in 2018 August, and in November had its first perihelion at 0.165 au. In this note several open source software packages are combined to predict the large scale structure of the solar wind that PSP will encounter on its second perihelion pass, using a Potential Field Source Surface (PFSS) and ballistic propagation model (e.g., Neugebauer et al. [1998](#)).

Diagnosing solar wind origins using *in situ* measurements in the inner heliosphere

D [Stansby](#) [T S Horbury](#) [L Matteini](#)

MNRAS 482, Issue 2, 11 January 2019, Pages 1706–1714,

<http://sci-hub.tw/10.1093/mnras/sty2814>

Robustly identifying the solar sources of individual packets of solar wind measured in interplanetary space remains an open problem. We set out to see if this problem is easier to tackle using solar wind measurements closer to the Sun than 1 au, where the mixing and dynamical interaction of different solar wind streams is reduced. Using measurements from the Helios mission, we examined how the proton core temperature anisotropy and cross-helicity varied with distance. At 0.3 au there are two clearly separated anisotropic and isotropic populations of solar wind that are not distinguishable at 1 au. The anisotropic population is always Alfvénic and spans a wide range of speeds. In contrast the isotropic population has slow speeds, and contains a mix of Alfvénic wind with constant mass fluxes and non-Alfvénic wind with large and highly varying mass fluxes. We split the *in situ* measurements into three categories according to these observations, and suggest that these categories correspond to wind that originated in the core of coronal holes, in or near active regions or the edges of coronal holes, and as small transients form streamers or pseudo-streamers. Although our method by itself is simplistic, it provides a new tool that can be used in combination with other methods for identifying the sources of solar wind measured by Parker Solar Probe and Solar Orbiter.

A new inner heliosphere proton parameter data set from the Helios mission

D. [Stansby](#), [C. S. Salem](#), [L. Matteini](#), [T. S. Horbury](#)

Solar Phys. 2018

<https://arxiv.org/pdf/1807.04376.pdf>

In the near future, Parker Solar Probe and Solar Orbiter will provide the first comprehensive *in-situ* measurements of the solar wind in the inner heliosphere since the Helios mission in the 1970s. We describe a reprocessing of the original Helios ion distribution functions to provide reliable and reproducible data to characterise the proton core population of the solar wind in the inner heliosphere. A systematic fitting of bi-Maxwellian distribution functions was performed to the raw Helios ion distribution function data to extract the proton core number density, velocity, and temperatures parallel and perpendicular to the magnetic field. We present radial trends of these derived proton parameters, forming a benchmark from which new measurements in the inner heliosphere will be compared to. The new dataset has been made openly available for other researchers to use, along with the source code used to generate it.

Number density structures in the inner heliosphere

D. [Stansby](#) and T. S. Horbury

A&A 613, A62 (2018)

<https://www.aanda.org/articles/aa/pdf/2018/05/aa32567-17.pdf>

Aims. The origins and generation mechanisms of the slow solar wind are still unclear. Part of the slow solar wind is populated by number density structures, discrete patches of increased number density that are frozen in to and move with the bulk solar wind. In this paper we aimed to provide the first in-situ statistical study of number density structures in the inner heliosphere.

Methods. We reprocessed in-situ ion distribution functions measured by Helios in the inner heliosphere to provide a new reliable set of proton plasma moments for the entire mission. From this new data set we looked for number density structures measured within 0.5 AU of the Sun and studied their properties.

Results. We identified 140 discrete areas of enhanced number density. The structures occurred exclusively in the slow solar wind and spanned a wide range of length scales from 50 Mm to 2000 Mm, which includes smaller scales than have been previously observed. They were also consistently denser and hotter than the surrounding plasma, but had lower magnetic field strengths, and therefore remained in pressure balance.

Conclusions. Our observations show that these structures are present in the slow solar wind at a wide range of scales, some of which are too small to be detected by remote sensing instruments. These structures are rare, accounting for only 1% of the slow solar wind measured by Helios, and are not a significant contribution to the mass flux of the solar wind.

PMI: The Photospheric Magnetic Field Imager

Jan **Staub**^{1*}, German Fernandez-Rico¹, Achim Gandorfer¹, Laurent Gizon^{1,4,5}, Johann Hirzberger¹, Stefan Kraft³, Andreas Lagg¹, Jesper Schou¹, Sami K. Solanki^{1,6}, Jose Carlos del Toro Iniesta², Thomas Wiegmann¹ and Joachim Woch¹

J. Space Weather Space Clim. **2020**, 10, 54

<https://www.swsc-journal.org/articles/swsc/pdf/2020/01/swsc200066.pdf>

We describe the design and the capabilities of the Photospheric Magnetic field Imager (PMI), a compact and lightweight vector magnetograph, which is being developed for ESA's Lagrange mission to the **Lagrange L5 point**. After listing the design requirements and give a scientific justification for them, we describe the technical implementation and the design solution capable of fulfilling these requirements. This is followed by a description of the hardware architecture as well as the operations principle. An outlook on the expected performance concludes the paper.

Modified manuscript 8 March 2022/PSI Revision of manuscript 30 September 2021/PSI submitted to AGU Space Weather journal. The polar cap (PC) index: PCS version based on Dome-C data

Peter **Stauning**

Space Weather e2021SW002941 **2022**

<https://agupubs.onlinelibrary.wiley.com/doi/epdf/10.1029/2021SW002941>

<https://doi.org/10.1029/2021SW002941>

The standard Polar Cap (PC) indices, PCN (North) based on magnetic data from Qaanaaq in Greenland and PCS (South) based on data from Vostok in Antarctica, have been submitted from the Arctic and Antarctic Research Institute (AARI) in St. Petersburg, Russia, the Danish Meteorological Institute (DMI), and the Danish Space Research Institute (DTU Space) in different versions. In order to consolidate PCS indices based on Vostok data or replace poor or missing index data, derivation procedures have been developed to generate alternative PCS index values based on data from Dome Concordia (Dome-C) magnetic observations from epoch 2009-2020 of solar cycle 24. The reference levels and calibration parameters needed for calculations of Dome-C-based PCS values in post-event and real-time versions are defined and explained in the present work. Assessments of the new PCS index have shown its unprecedented high relevance. Part of the methods used here, such as the quiet reference level construction and the correlation and regression procedures used for calculations of scaling parameters, deviate from corresponding features considered inadequate of the IAGA-endorsed PC index derivation methods.

The Polar Cap (PC) index combination, PCC: relations to solar wind properties and global magnetic disturbances

Peter **Stauning**

J. Space Weather Space Clim. **2021**, 11, 19

<https://doi.org/10.1051/swsc/2020074>

<https://www.swsc-journal.org/articles/swsc/pdf/2021/01/swsc200030.pdf>

The non-negative Polar Cap PCC index built from PCN (North) and PCS (South) indices correlates better with the solar wind merging electric field and is more representative for the total energy input from the solar wind to the magnetosphere and for the development of geomagnetic disturbances represented by the Kp index and ring current

indices than either of the hemispheric indices. The present work shows that the ring current index, Dst, to a high degree of accuracy can be derived from a source function built from PCC indices. The integration of the PCC-based source function throughout the interval from 1992 to 2018 without attachment to the real Dst indices based on low latitude magnetic observations has generated equivalent Dst values that correlate very well ($R = 0.86$) with the real Dst index values, which are represented with a mean deviation less than 1 nT and an overall RMS deviation less than 13 nT. The precise correlation between the real and equivalent Dst values has been used to correct the PCC indices for saturation effects at high intensity disturbance conditions where the Dst index may take values beyond -100 nT. The relations between PCC and the ring current indices, Dst and ASY-H have been used, in addition, to derive the precise timing between polar cap convection processes reflected in the polar cap indices and the formation of the partial and total ring current systems. Building the ring current is considered to represent the energy input from the solar wind, which also powers auroral disturbance processes such as substorms and upper atmosphere heating. With current available PC indices, detailed and accurate SYM-H or Dst index values could be derived up to nearly one hour ahead of actual time by integration of the PCC-based source function from any previous quiet state. Thus, the PCC indices enabling accurate estimates of the energy input from the solar wind are powerful tools for space weather monitoring and for solar-terrestrial research.

Reliable real-time Polar Cap (PC) indices for space weather monitoring and forecasts

Peter **Stauning**

J. Space Weather Space Clim. Volume 8, A49 **2018**

<https://www.swsc-journal.org/articles/swsc/pdf/2018/01/swsc180039.pdf>

The Polar Cap (PC) indices were approved by the International Association for Geomagnetism and Aeronomy (IAGA) by Resolution No. 3 (2013) noting that “IAGA ... recommends use of the PC index by the international scientific community in its near-real time and definitive forms”. PC indices were made available in 2014 at the web portal <http://pcindex.org> holding near-real time as well as final index values. The near-real time PC index values are not permanently available. However, analyses of indices on basis of occasional downloads have detected differences between near-real time and final PC indices of up to 3.65 mV/m ([Stauning, 2018b](#), Ann Geophys, 36, 621–631). At such differences, one or the other index may indicate (or hide) strong geomagnetic activity without justification in the actual conditions. The present work has disclosed the cause of observed large differences between real-time and final PC index values in the IAGA-endorsed versions. In addition, anticipated differences are derived on a general basis from the available basic magnetic data by using the index calculation procedures and calibration constants provided by the PC index suppliers. It is shown that corresponding or even larger anomalies are expected to be common during moderate to strong magnetic activity where the near-real time PC indices might otherwise prove very useful for space weather monitoring, e.g., for power grid protection. An alternative real-time PC index derivation scheme described here reduces the excessive differences between real-time and final PC index values by an order of magnitude.

Investigating the observational signatures of magnetic cloud substructure

Steed, K.; Owen, C. J.; D’Imoulin, P.; Dasso, S.

J. Geophys. Res., Vol. 116, No. A1, A01106, **2011**, File

Magnetic clouds (MCs) represent a subset of interplanetary coronal mass ejections (ICMEs) that exhibit a magnetic flux rope structure. They are primarily identified by smooth, large-scale rotations of the magnetic field. However, both small- and large-scale fluctuations of the magnetic field are observed within some magnetic clouds. We analyzed the magnetic field in the frames of the flux ropes, approximated using a minimum variance analysis (MVA), and have identified a small number of MCs within which multiple reversals of the gradient of the azimuthal magnetic field are observed. We herein use the term “substructure” to refer to regions that exhibit this signature. We examine, in detail, one such MC observed on 13 April 2006 by the ACE and WIND spacecraft and show that substructure has distinct signatures in both the magnetic field and plasma observations. We identify two thin current sheets within the substructure and find that they bound the region in which the observations deviate most significantly from those typically expected in MCs. The majority of these clouds are followed by fast solar wind streams, and a comparison of the properties of this magnetic cloud with five similar events reveals that they have lower nondimensional expansion rates than nonovertaken magnetic clouds. We discuss and evaluate several possible explanations for this type of substructure, including the presence of multiple flux ropes and warping of the MC structure, but we conclude that none of these scenarios is able to fully explain all of the aspects of the substructure observations.

Multi-scale image preprocessing and feature tracking for remote CME characterization

Oleg **Stepanyuk***, Kamen Kozarev and Mohamed Nedal

J. Space Weather Space Clim. **2022**, 12, 20

<https://www.swsc-journal.org/articles/swsc/pdf/2022/01/swsc210084.pdf>

Coronal Mass Ejections (CMEs) influence the interplanetary environment over vast distances in the solar system by injecting huge clouds of fast solar plasma and energetic particles (SEPs). A number of fundamental questions remain about how SEPs are produced, but current understanding points to CME-driven shocks and compressions in the solar corona. At the same time, unprecedented remote and in situ (Parker Solar Probe, Solar Orbiter) solar observations are becoming available to constrain existing theories. Here we present a general method for recognition and tracking solar images of objects such as CME shock waves and filaments. The calculation scheme is based on a multi-scale data representation concept à trous wavelet transform, and a set of image filtering techniques. We showcase its performance on a small set of CME-related phenomena observed with the SDO/AIA telescope. With the data represented hierarchically on different decomposition and intensity levels, our method allows extracting certain objects and their masks from the imaging observations in order to track their evolution in time. The method presented here is general and applicable to detecting and tracking various solar and heliospheric phenomena in imaging observations. It holds the potential to prepare large training data sets for deep learning. We have implemented this method into a freely available Python library.

Possible Evolution of Minifilament-Eruption-Produced Solar Coronal Jets, Jetlets, and Spicules, into Magnetic-Twist-Wave "Switchbacks" Observed by the Parker Solar Probe (PSP)

Alphonse C. [Sterling](#), [Ronald L. Moore](#), [Navdeep K. Panesar](#), [Tanmoy Samanta](#)

2020

<https://arxiv.org/pdf/2010.12991.pdf>

Many solar coronal jets result from erupting miniature-filament ("minifilament") magnetic flux ropes that reconnect with encountered surrounding far-reaching field. Many of those minifilament flux ropes are apparently built and triggered to erupt by magnetic flux cancellation. If that cancellation (or some other process) results in the flux rope's field having twist, then the reconnection with the far-reaching field transfers much of that twist to that reconnected far-reaching field. In cases where that surrounding field is open, the twist can propagate to far distances from the Sun as a magnetic-twist Alfvénic pulse. We argue that such pulses from jets could be the kinked-magnetic-field structures known as "switchbacks," detected in the solar wind during perihelion passages of the Parker Solar Probe (PSP). For typical coronal-jet-generated Alfvénic pulses, we expect that the switchbacks would flow past PSP with a duration of several tens of minutes; larger coronal jets might produce switchbacks with passage durations ~1hr. Smaller-scale jet-like features on the Sun known as "jetlets" may be small-scale versions of coronal jets, produced in a similar manner as the coronal jets. We estimate that switchbacks from jetlets would flow past PSP with a duration of a few minutes. Chromospheric spicules are jet-like features that are even smaller than jetlets. If some portion of their population are indeed very-small-scale versions of coronal jets, then we speculate that the same processes could result in switchbacks that pass PSP with durations ranging from about ~2 min down to tens of seconds.

A Generalized Fisk-type HMF: Implications of Spatially Dependent Photospheric Differential Rotation

P. J. [Steyn](#) and R. A. Burger

2020 ApJ 902 33

<https://doi.org/10.3847/1538-4357/abb2a5>

The existence of a Fisk-type heliospheric magnetic field (HMF) has been debated ever since Fisk proposed an alternative to the traditional view of the HMF first proposed by Parker. Several modifications of the original Fisk field model have been published in the past, for example, the Schwadron field and the Fisk–Parker hybrid HMF model. This study presents a new generalized Fisk HMF model that implements for the first time a spatially dependent differential rotation rate of the photosphere, by mapping magnetic field lines from the solar wind source surface to the photosphere. Data analysis methods of Forsyth et al. are used to search for a signature of a Fisk-type field during solar minimum conditions, using the magnetic field data from the first solar orbit of the Ulysses spacecraft. The new generalized Fisk field agrees better with the observed magnetic field winding angle than a standard Parker field during the majority of intervals scanned by Ulysses.

On the Performance of a Real-Time Electron Radiation Belt Specification Model

Frances [Staples](#), [Adam Kellerman](#), [Janet Green](#)

Space Weather [Volume22, Issue12](#) December 2024 e2024SW003950

<https://doi.org/10.1029/2024SW003950>

<https://agupubs.onlinelibrary.wiley.com/doi/epdf/10.1029/2024SW003950>

Maintaining accurate real-time hindcast and forecast specification of the radiation environment is essential for operators to monitor and mitigate the effects of hazardous radiation on satellite components. The Radiation Belt Forecasting Model and Framework (RBFMF) provides real-time forecasts and hindcasts of the electron radiation belt environment, which are used as inputs for the Satellite Charging Assessment Tool. We evaluated the long-term statistical error and bias of the RBFMF by comparing the 10-hr hindcast of electron phase space densities (PSD) to a multi-mission data set of PSD observations. We found that, between the years 2016–2018, the RBFMF reproduced the radiation belt environment to within a factor of 1.5. While the error and bias of assimilated observations were found to influence the error and bias of the hindcast, data assimilation resulted in more accurate specification of the radiation belt state than real-time Van Allen Probe observations alone. Furthermore, when real-time Van Allen Probe observations were no longer available, the hindcast errors increased by an order of magnitude. This highlights two needs; (a) the development of physics-based modeling incorporated into this framework, and (b) the need for real-time observations which span the entire outer radiation belt.

Multispacecraft Energetic Particle Enhancements Associated with a Single Corotating Interaction Region

M. J. [Starkey](#)¹, M. A. Dayeh^{1,2}, M. I. Desai^{1,2}, R. Bučik¹, S. T. Hart^{1,2}, and H. A. Elliott^{1,2}
2024 ApJ 962 160

<https://iopscience.iop.org/article/10.3847/1538-4357/ad1cea/pdf>

The radial evolution of particles accelerated at corotating interaction regions (CIRs) is not fully understood, particularly the distance range over which this particle acceleration occurs and how the energy spectra are modulated by transport through the inner heliosphere. Here, we present observations of energetic proton enhancements associated with a CIR observed by Parker Solar Probe on 2021 April 25 during the inbound leg of its orbit near ~ 46 Rs (~ 0.21 au). The CIR is identified at additional spacecraft (Solar Terrestrial Relations Observatory, STEREO-A; Solar Orbiter, SoHO; and Advanced Composition Explorer, ACE) using a corotation time delay estimation, and energetic proton spectra from each spacecraft are compared. We find that (1) energetic protons are observed near 46 Rs streaming sunward ahead of the CIR; (2) the CIR persists for at least one solar rotation and the corresponding energetic proton enhancements are observed at STEREO-A, SoHO, and ACE; and (3) the proton energy spectrum is steeper near the Sun and hardens near 1 au. This observation presents the closest in situ energetic particle observation of a CIR to the Sun ever recorded. Results presented here suggest that particles can be accelerated by CIR structures within 1 au and these particles can penetrate very deep into the inner heliosphere. 0.05–0.20 MeV

Forecast of the arrival of interplanetary shocks by measuring cosmic ray fluctuations in the interplanetary medium

S A [Starodubtsev](#)¹, V G Grigoryev¹ and I G Usoskin
2013 J. Phys.: Conf. Ser. 409 012180

Here we present a method to forecast the arrival of an interplanetary shock to the Earth's orbit in advance of up to one day, using cosmic ray fluctuations and solar wind parameters measured onboard the ACE spacecraft. The method is based on our previous results [1]. By means of continuous monitoring of the interplanetary space state since April 2010, we conclude that not all shocks can be reliably forecasted by the method. Only those interplanetary shocks, for which a large flux of low-energy particles (10 keV – 10 MeV) of solar or interplanetary origin exists in the upstream region, can be forecasted. This is typically related to quasi-parallel shocks. In the absence of such particles, a forecast cannot be made. This is a typical situation for quasi-perpendicular shocks. Our analysis shows that, on average, an interplanetary shock can be forecasted for several hours up to one day, with the probability about 70%.

From Predicting Solar Activity to Forecasting Space Weather: Practical Examples of Research-to-Operations and Operations-to-Research

R. A. [Steenburgh](#), D. A. Biesecker, G. H. Millward
Solar Physics, February **2014**, Volume 289, Issue 2, pp 675-690; **File**

The successful transition of research to operations (R2O) and operations to research (O2R) requires, above all, interaction between the two communities. We explore the role that close interaction and ongoing communication played in the successful fielding of three separate developments: an observation platform, a numerical model, and a visualization and specification tool. Additionally, we will examine how these three pieces came together to revolutionize interplanetary coronal mass ejection (ICME) arrival forecasts. A discussion of the importance of education and training in ensuring a positive outcome from R2O activity follows. We describe efforts by the meteorological community to make research results more accessible to forecasters and the applicability of these efforts to the transfer of space-weather

research. We end with a forecaster “wish list” for R2O transitions. Ongoing, two-way communication between the research and operations communities is the thread connecting it all.

3.1 The STEREO Mission

3.2 The WSA–Enlil Model

3.3 The CME Analysis Tool (CAT)

The Solar Origin of an Intense Geomagnetic Storm on 2023 December 1st: Successive Slipping and Eruption of Multiple Magnetic Flux Ropes

[Zheng Sun](#), [Ting Li](#), [Yijun Hou](#), [Hui Tian](#), [Ziqi Wu](#), [Ke Li](#), [Yining Zhang](#), [Zhentong Li](#), [Xianyong Bai](#), [Li Feng](#), [Chuan Li](#), [Zhenyong Hou](#), [Qiao Song](#), [Jingsong Wang](#), [Guiping Zhou](#)

Solar Phys. **299**, 93 **2024**

<https://arxiv.org/pdf/2405.14983>

<https://doi.org/10.1007/s11207-024-02329-4>

The solar eruption that occurred on **2023 November 28** (SOL2023-11-28) triggered an intense geomagnetic storm on Earth on **2023 December 1**. The associated Earth's auroras manifested at the most southern latitudes in the northern hemisphere observed in the past two decades. In order to explore the profound geoeffectiveness of this event, we conducted a comprehensive analysis of its solar origin to offer potential factors contributing to its impact. Magnetic flux ropes (MFRs) are twisted magnetic structures recognized as significant contributors to coronal mass ejections (CMEs), thereby impacting space weather greatly. In this event, we identified multiple MFRs in the solar active region and observed distinct slipping processes of the three MFRs: MFR1, MFR2, and MFR3. All three MFRs exhibit slipping motions at a speed of 40--137 km s⁻¹, extending beyond their original locations. Notably, the slipping of MFR2 extends to ~30 Mm and initiate the eruption of MFR3. Ultimately, MFR1's eruption results in an M3.4-class flare and a CME, while MFR2 and MFR3 collectively produce an M9.8-class flare and another halo CME. This study shows the slipping process in a multi-MFR system, showing how one MFR's slipping can trigger the eruption of another MFR. We propose that the CME--CME interactions caused by multiple MFR eruptions may contribute to the significant geoeffectiveness.

Coronal-Jet-Producing Minifilament Eruptions as a Possible Source of Parker Solar Probe (PSP) Switchbacks

[Alphonse C. Sterling](#), [Ronald L. Moore](#)

ApJ **896** L18 **2020**

<https://arxiv.org/pdf/2006.04990.pdf>

<https://doi.org/10.3847/2041-8213/ab96be>

The Parker Solar Probe (PSP) has observed copious rapid magnetic field direction changes in the near-Sun solar wind. These features have been called "switchbacks," and their origin is a mystery. But their widespread nature suggests that they may be generated by a frequently occurring process in the Sun's atmosphere. We examine the possibility that the switchbacks originate from coronal jets. Recent work suggests that many coronal jets result when photospheric magnetic flux cancels, and forms a small-scale "minifilament" flux rope that erupts and reconnects with coronal field. We argue that the reconnected erupting minifilament flux rope can manifest as an outward propagating Alfvénic fluctuation that steepens into an increasingly compact disturbance as it moves through the solar wind. Using previous observed properties of coronal jets that connect to coronagraph-observed white-light jets (a.k.a. "narrow CMEs"), along with typical solar wind speed values, we expect the coronal-jet-produced disturbances to traverse near-perihelion PSP in ~<25 min, with a velocity of ~400 km/s. To consider further the plausibility of this idea, we show that a previously studied series of equatorial latitude coronal jets, originating from the periphery of an active region, generate white-light jets in the outer corona (seen in STEREO/COR2 coronagraph images; 2.5---15 R_{sun}), and into the inner heliosphere (seen in STEREO/Hi1 heliospheric imager images; 15---84 R_{sun}). Thus it is tenable that disturbances put onto open coronal magnetic field lines by coronal-jet-producing erupting minifilament flux ropes can propagate out to PSP space and appear as switchbacks. **30 June 2012**

The Modulation of Anomalous and Galactic Cosmic-Ray Oxygen over Successive Solar Cycle Minima

R. D. [Strauss](#)¹, R. A. [Leske](#)², and J. S. [Rankin](#)³

2023 ApJ 944 114

<https://iopscience.iop.org/article/10.3847/1538-4357/acb53d/pdf>

Both the recent 2009 and 2020 solar minima were classified as unusually quiet and characterized with unusually high galactic cosmic-ray (GCR) levels. However, unlike the trends from previous decades, in which anomalous cosmic-ray

(ACR) and GCR levels strongly agreed, the ACR intensities did not reach such high, record-setting levels. This discrepancy between the behavior of GCRs and ACRs is investigated in this work by simulating the acceleration and transport of GCR and ACR oxygen under different transport conditions. After using recent observations to constrain any remaining free parameters present in the model, we show that less turbulent conditions are characterized by higher GCR fluxes and lower ACR fluxes, due to less efficient ACR acceleration at the solar wind termination shock. We offer this as an explanation for the ACR/GCR discrepancy observed during 2009 and 2020, when compared to previous solar cycles.

Cosmic-Ray Transport near the Sun

R. D. **Strauss**^{3,1}, J. P. van den Berg^{4,1}, and J. S Rankin²

2022 ApJ 928 22

<https://iopscience.iop.org/article/10.3847/1538-4357/ac582a/pdf>

The strongly diverging magnetic field lines in the very inner heliosphere, through the associated magnetic focusing/mirroring forces, can, potentially, lead to highly anisotropic galactic cosmic-ray distributions close to the Sun. Using a simplified analytical approach, validated by numerical simulations, we study the behavior of the galactic cosmic-ray distribution in this newly explored region of the heliosphere and find that significant anisotropies can be expected inside 0.2 au.

A Space Weather Mission Concept: Observatories of the Solar Corona and Active Regions

(OSCAR)

Antoine **Strugarek**, Nils Janitzek, Arrow Lee, Philipp Löschl, Bernhard Seifert, Sanni Hoilijoki, Emil Kraaikamp, Alankrita Isha Mrigakshi, Thomas Philippe, Sheila Spina, Malte Bröse, Sonny Massahi, Liam O'Halloran, Victor Pereira Blanco, Christoffer Stausland, Philippe Escoubet, Günter Kargl

Space Weather and Space Climate, 5, A4 2015;

<http://arxiv.org/pdf/1409.0458v1.pdf>

<http://www.swsc-journal.org/articles/swsc/pdf/2015/01/swsc140008.pdf> , File

Coronal Mass Ejections (CMEs) and Corotating Interaction Regions (CIRs) are major sources of magnetic storms on Earth and are therefore considered to be the most dangerous space weather events. The Observatories of Solar Corona and Active Regions (OSCAR) mission is designed to identify the 3D structure of coronal loops and to study the trigger mechanisms of CMEs in solar Active Regions (ARs) as well as their evolution and propagation processes in the inner heliosphere. It also aims to provide monitoring and forecasting of geo-effective CMEs and CIRs. OSCAR would contribute to significant advancements in the field of solar physics, improvements of the current CME prediction models, and provide data for reliable space weather forecasting. These objectives are achieved by utilising two spacecraft with identical instrumentation, located at a heliocentric orbital distance of 1~AU from the Sun. **The spacecraft will be separated by an angle of 68° to provide optimum stereoscopic view of the solar corona. We study the feasibility of such a mission and propose a preliminary design for OSCAR.**

Erratum J. Space Weather Space Clim., 7, A1 (2017)

Can solar wind viscous drag account for CME deceleration?

Prasad **Subramanian**, Alejandro Lara, Andrea Borgazzi

E-print, Sept, 2012, Geophysical Research Letters

The forces acting on solar Coronal Mass Ejections (CMEs) in the interplanetary medium have been evaluated so far in terms of an empirical drag coefficient $C_m D \sim 1$ that quantifies the role of the aerodynamic drag experienced by a typical CME due to its interaction with the ambient solar wind. We use a microphysical prescription for viscosity in the turbulent solar wind to obtain an analytical model for the drag coefficient $C_m D$. This is the first physical characterization of the aerodynamic drag experienced by CMEs. We use this physically motivated prescription for $C_m D$ in a simple, 1D model for CME propagation to obtain velocity profiles and travel times that agree well with observations of deceleration experienced by fast CMEs.

Forbush decreases and turbulence levels at CME fronts

Prasad **Subramanian**, H. M. Antia, S. R. Dugad, U. D. Goswami, S. K. Gupta, Y. Hayashi, N. Ito, S.

Kawakami, H. Kojima, P. K. Mohanty, P. K. Nayak, T. Nonaka, A. Oshima, K. Sivaprasad, H. Tanaka, S. C. Tonwar

A&A Volume 494, Issue 3, 2009, pp.1107-1118

<https://www.aanda.org/articles/aa/pdf/2009/06/aa09551-08.pdf> **File**

<http://solar.physics.montana.edu/cgi-bin/eprint/index.pl?entry=8571>

We seek to estimate the average level of MHD turbulence near coronal mass ejection (CME) fronts as they propagate from the Sun to the Earth. We examine the cosmic ray data from the GRAPES-3 tracking muon telescope at Ooty, together with the data from other sources for three well observed Forbush decrease events. Each of these events are associated with frontside halo Coronal Mass Ejections (CMEs) and near-Earth magnetic clouds. In each case, we estimate the magnitude of the Forbush decrease using a simple model for the diffusion of high energy protons through the largely closed field lines enclosing the CME as it expands and propagates from the Sun to the Earth. We use estimates of the cross-field diffusion coefficient D_{\perp} derived from published results of extensive Monte Carlo simulations of cosmic rays propagating through turbulent magnetic fields. Our method helps constrain the ratio of energy density in the turbulent magnetic fields to that in the mean magnetic fields near the CME fronts. This ratio is found to be $\sim 2\%$ for the **11 April 2001** Forbush decrease event, $\sim 6\%$ for the **20 November 2003** Forbush decrease event and $\sim 249\%$ for the much more energetic event of **29 October 2003**.

Influence of the drag force on the leading edge of a coronal mass ejection

D. Sudar¹, B. Vršnak¹, M. Dumbović¹, M. Temmer² and J. Čalogović¹

A&A 665, A142 (2022)

<https://www.aanda.org/articles/aa/pdf/2022/09/aa44114-22.pdf>

Context. The drag based model (DBM) is frequently used to analyse the kinematics of coronal mass ejections (CMEs) in interplanetary space. The DBM incorporates a 2D solution with the leading edge of the CME.

Aims. Certain aspects of the evolution of the CME leading edge in the DBM have not been fully and accurately described previously. The main goal of this paper is to clarify these issues.

Methods. We analysed the behaviour of the leading edge according to the DBM equations by studying the dependence of the radial distance of each segment of the leading edge on the angular coordinate, ϕ , and observed the limits as time goes to infinity. We also analysed the behaviour of the velocity profile, $v(\phi)$.

Results. We showed that for isotropic solar wind conditions, the distance between the apex and the flank is a monotonically increasing function of time that converges at infinity to a constant value. The leading edge never becomes fully circular. The analysis of the $v(\phi)$ profile shows that the speed of all CME leading-edge segments converges towards the solar wind speed, w , but the speed of the CME flank never exceeds that of the apex.

Conclusions. The drag force alone cannot flatten the leading edge of a CME in isotropic solar wind conditions. This also holds for any model that uses the drag as a description of the CME kinematics if the typical initial assumption that the flank is slower and farther behind than the apex is used. On the other hand, non-isotropic solar wind conditions can change this conclusion and even introduce a deformation of the leading edge. A similar effect can be obtained with temporal variations in solar wind conditions along the path of the CME, or by introducing other forces.

Predicting Coronal Mass Ejections transit times to Earth with neural network

D. Sudar, B. Vršnak, M. Dumbović

MNRAS 2015

<http://arxiv.org/pdf/1511.07620v1.pdf>

Predicting transit times of Coronal Mass Ejections (CMEs) from their initial parameters is a very important subject, not only from the scientific perspective, but also because CMEs represent a hazard for human technology. We used a neural network to analyse transit times for 153 events with only two input parameters: initial velocity of the CME, v , and Central Meridian Distance, CMD, of its associated flare. We found that transit time dependence on v is showing a typical drag-like pattern in the solar wind. The results show that the speed at which acceleration by drag changes to deceleration is $\sim 500 \text{ km s}^{-1}$. Transit times are also found to be shorter for CMEs associated with flares on the western hemisphere than those originating on the eastern side of the Sun. We attribute this difference to the eastward deflection of CMEs on their path to 1 AU. The average error of the NN prediction in comparison to observations is ~ 12 hours which is comparable to other studies on the same subject. **1996 Dec 19, 1997 Jan 6, 1997 Feb 7, 1997 Apr 7, 1997 May 12**

Magnetic reconnection as an erosion mechanism for magnetic switchbacks

G.H.H. Suen, C.J. Owen, D. Verscharen, T.S. Horbury, P. Louarn, R. De Marco

A&A 675, A128 2023

<https://arxiv.org/pdf/2305.06035.pdf>

<https://www.aanda.org/articles/aa/pdf/2023/07/aa45922-23.pdf>

Magnetic switchbacks are localised polarity reversals in the radial component of the heliospheric magnetic field. Observations from Parker Solar Probe (PSP) have shown that they are a prevalent feature of the near-Sun solar wind. However, observations of switchbacks at 1 au and beyond are less frequent, suggesting that these structures evolve and potentially erode through yet-to-be identified mechanisms as they propagate away from the Sun. We analyse magnetic field and plasma data from the Magnetometer and Solar Wind Analyser instruments aboard Solar Orbiter between 10 August and 30 August 2021. During this period, the spacecraft was 0.6 to 0.7 au from the Sun. We identify three instances of reconnection occurring at the trailing edge of magnetic switchbacks, with properties consistent with existing models describing reconnection in the solar wind. Using hodographs and Walen analysis methods, we test for rotational discontinuities (RDs) in the magnetic field and reconnection-associated outflows at the boundaries of the identified switchback structures. Based on these observations, we propose a scenario through which reconnection can erode a switchback and we estimate the timescales over which this occurs. For our events, the erosion timescales are much shorter than the expansion timescale and thus, the complete erosion of all three observed switchbacks would occur well before they reach 1 au. Furthermore, we find that the spatial scale of these switchbacks would be considerably larger than is typically observed in the inner heliosphere if the onset of reconnection occurs close to the Sun. Hence, our results suggest that the onset of reconnection must occur during transport in the solar wind in our cases. These results suggest that reconnection can contribute to the erosion of switchbacks and may explain the relative rarity of switchback observations at 1 au. **10 Aug 2021, 30 Aug 2021**

Solar Wind Speed Prediction via Graph Attention Network

Yanru Sun, Zongxia Xie, Haocheng Wang, Xin Huang, Qinghua Hu

Space Weather e2022SW003128 **Volume20, Issue7 2022**

<https://doi.org/10.1029/2022SW003128>

<https://agupubs.onlinelibrary.wiley.com/doi/epdf/10.1029/2022SW003128>

The solar wind is a plasma flow formed by the expansion of the high-temperature corona and propagates in the interplanetary space with speeds between 200 km/s and 900 km/s. Accurate solar wind speed prediction and longer lead time will help mitigate the impact of solar storms on aerospace equipment and the Earth's magnetic field. Recently, most approaches do not explicitly capture the relationships between different solar wind features, and the prediction accuracy of 96-hours is still not good enough. This paper elaborately designs an end-to-end model: Graph-Temporal-AR model (GTA) for solar wind speed prediction. Firstly, our framework considers each feature as the node to construct the graph structure and adopts the graph attention module to learn the complex dependencies among features. Secondly, our approach employs the dilated causal convolution to extend the receptive field and prolong the prediction time. Furthermore, we leverage the autoregressive model to solve the scale insensitive problem of the neural network, making our model more robust. Specifically, we combine the OMNI data measured at Lagrangian Point 1 (L1) with the extreme ultraviolet (EUV) images observed by the Solar Dynamics Observatory (SDO) satellite to predict the solar wind speed at L1. Compared with the baseline models, GTA obtains significant performance improvements. Through visualization, we find GTA excavates the relationships between multiply variables without domain prior knowledge, which may help us find other unknown associations in heliophysics data sets. The data and code are available from <https://github.com/syrGitHub/GTA>.

Solar Wind Speed Prediction With Two-Dimensional Attention Mechanism

Yanru Sun, Zongxia Xie, Yanhong Chen, Xin Huang, Qinghua Hu

Space Weather **Volume19, Issue7 e2020SW002707 2021**

<https://agupubs.onlinelibrary.wiley.com/doi/epdf/10.1029/2020SW002707>

<https://doi.org/10.1029/2020SW002707>

As more and more high-technical systems are exposed to the space environment, extreme space weather becomes a great threat to human society. In the solar system, space weather is influenced by the solar wind, such that reliable prediction of solar wind conditions in the near-Earth environment effectively reduces the impact of space weather on human society. Solar wind speed prediction is improved by making full use of OMNI data measured at Lagrangian Point 1 (L1) by the National Aeronautics and Space Administration (NASA) and image data observed by the Solar Dynamics Observatory (SDO) satellite in this work. Specifically, we propose a model based on the “**two-dimensional attention mechanism**” (TDAM) to predict solar wind speed. In this study, we first analyze and preprocess data from 2011 to 2017. Second, considering the characteristics of time series data, we adopt the gated recurrent units (GRU) model which can deal with long-term dependence as the prediction part of our model. Third, we design a TDAM, which enables our prediction network to focus on important parts. Three performance indices are used: root-mean-square error (RMSE), mean absolute error (MAE), and correlation coefficient (CC). By comparing TDAM with other models, we find that the TDAM model achieves the best prediction results, with RMSE of 62.8 km/s, MAE of 47.8 km/s, and CC of 0.789 24 h

in advance. The experimental results show that the proposed TDAM model can improve the prediction accuracy of solar wind speed.

Simulated Solar Mass Ejection Imager and "Solar Terrestrial Relations Observatory-like" views of the solar wind following the solar flares of 27-29 May 2003

Sun, W.; Deehr, C. S.; Dryer, M.; Fry, C. D.; Smith, Z. K.; Akasofu, S.-I.

Space Weather, Vol. 6, No. 3, S03006, 2008

<http://www.agu.org/pubs/crossref/2008/2006SW000298.shtml>

Scientists show how a three-dimensional kinematic solar wind model can be extended to predict what the Solar Terrestrial Relations Observatory (STEREO) spacecraft might expect in observing large-scale plasma clouds ejected from the Sun

A COMPARISON OF THE INITIAL SPEED OF CORONAL MASS EJECTIONS WITH THE MAGNETIC FLUX AND MAGNETIC HELICITY OF MAGNETIC CLOUDS

S.-K. [Sung](#)^{1,2,3}, K. Marubashi¹, K.-S. Cho¹, Y.-H. Kim¹, K.-H. Kim^{1,3}, J. Chae², Y.-J. Moon³, and I.-H. Kim³

Astrophysical Journal, 699:298–304, 2009, [File](#)

To investigate the relationship between the speed of a coronal mass ejection (CME) and the magnetic energy released during its eruption, we have compared the initial speed of CMEs (V_{CME}) and the two parameters of their associated magnetic clouds (MC), magnetic flux (F_{MC}), and magnetic helicity per unit length ($|H_{MC}|/L$), for 34 pairs of CMEs and MCs. The values of these parameters in each MC have been determined by fitting the magnetic data of the MC to the linear force-free cylindrical model. As a result, we found that there are positive correlations between V_{CME}^2 and F_{MC} , and between V_{CME}^2 and $|H_{MC}|/L$. It is also found that the kinetic energy of CMEs (E_{CME}) is correlated with F_{MC} and $|H_{MC}|/L$ of the associated MC. In contrast, we found no significant correlation between V_{CME}^2 and F_{MC} , nor between V_{CME}^2 and $|H_{MC}|/L$. Our results support the notion that the eruption of a CME is related to the magnetic helicity of the source active region.

Arrival Time Estimates of Earth-Directed CME-Driven Shocks

K. [Suresh](#), [N. Gopalswamy](#) & [A. Shanmugaraju](#)

[Solar Physics](#) volume 297, Article number: 3 (2022)

<https://doi.org/10.1007/s11207-021-01914-1>

<https://link.springer.com/content/pdf/10.1007/s11207-021-01914-1.pdf>

We report on the travel times of 19 interplanetary (IP) shocks driven by Earth-directed coronal mass ejections (CMEs) that occurred from 2010 to 2017. We track the shocks ahead of CMEs using the graduated cylindrical shell (GCS) model constructed from multiple-view observations from the Solar TERrestrial RELations Observatory (STEREO) and Solar and Heliospheric Observatory (SOHO) coronagraphs. We calculate the Earthward speed of the shocks from the height–time data obtained from the GCS fit that we use as input to the Empirical Shock Arrival (ESA) model to predict the shock travel times to 1 AU. We find that the mean absolute deviation (MAD) of the predicted IP shock travel time from the observed travel time is about 6.1 hours. The prediction error ranges from -14.3 hours to $+13.1$ hours with a standard deviation of 7.5 hours. The MAD and RMS errors are significantly smaller than those in the previous report ([Gopalswamy et al., Space Weather 11, 661, 2013](#)), which used SOHO–STEREO quadrature observations to obtain the Earthward speed of halo CMEs. The χ^2 -test confirms the high consistency level between predicted and observed travel times. These results suggest that the three-dimensional speeds of shocks can be derived using the GCS model outside of quadrature intervals and can be used in the determination of shock travel times. **03 April 2010, 02 August 2011, 07 March 2012, 14 June 2012**

Table 1 List of 19 Earth-directed CMEs, their travel times, and the deviation from observed travel times.

Study of Interplanetary CMEs/Shocks During Solar Cycle 24 Using Drag-Based Model: The Role of Solar Wind

K. [Suresh](#), S. Prasanna Subramanian, A. Shanmugaraju, Bojan Vršnak, S. Umapathy

[Solar Physics](#) April 2019, 294:47

[sci-hub.se/10.1007/s11207-019-1432-8](https://doi.org/10.1007/s11207-019-1432-8)

In this paper we analyze a set of 27 fast interplanetary coronal mass ejections (ICMEs) observed during the period January 2010 – December 2013 in Solar Cycle 24. The arrivals of interplanetary shocks and CMEs at 1 AU are found from OMNI spacecraft high resolution data and their travel times are compared with Empirical Shock Arrival (ESA);

Gopalswamy et al. in *Adv. Space Res.*36, 2289, [2005](#)) and Drag Based Model (DBM; Vršnak et al. in *Solar Phys.*285, 295, [2013](#)). The analysis of the transit time, deceleration, and drag parameter is used to examine the role of the solar-wind characteristics in the dynamics of ICMEs. The obtained ICME parameters (deceleration, drag parameter) are compared with the decelerated events (34 of 91 events in Solar Cycle 23) from the study of Manoharan et al. (*J. Geophys. Res.*109, A06109, [2004](#)). The interplanetary (IP) deceleration shows similar trend between the cycles. Though the Cycle 24 has weak solar wind, it does not affect the arrival time behavior. It is concluded that the solar-wind behavior is considered to be the same in Cycles 23 and 24 for ICMEs. The IP drag parameter is linearly correlated with CME initial speed. The p-value between CME speed and drag parameter suggests that they are highly significant. The important result of the study is that the solar wind showed a similar kind of drag effect for the propagating CMEs in both cycles. **Table 1** Characteristics of CMEs and X-ray flares, and observed and estimated IP shock transit times.(2010-2013)

Transit time of CME/shock associated with four major geo-effective CMEs in solar cycle 24

Syed Ibrahim, M.; Shanmugaraju, A.; Bendict Lawrance, M.

Advances in Space Research, Volume 55, Issue 1, p. 407-415. **2015**

The kinematics of coronal mass ejection (CME) in the interplanetary medium is very important in the concept of space-weather. Main aim of this paper is to study the propagation of four major geo-effective CMEs and their associated shocks observed in solar cycle 24. The arrival of interplanetary shocks and CMEs of these events near the Earth is seen from the ACE/wind in situ data available in OMNI data base. The CMEs considered in this study have a wide range of initial speeds 500-1900 km/s in the LASCO field of view, comprising of two slow CMEs ($V \sim 500$ km/s), one fast CME ($V \sim 1800$ km/s) and one moderate speed CME ($V \sim 800$ km/s). The observed transit time of these events are compared with transit time estimated using the empirical shock arrival model (ESA). Especially, we utilize (i) different acceleration - speed equations reported in the literature from the observations made in the last few decades and (ii) various acceleration cessation distances (Ac_d) In addition, we compared the estimated and observed transit time with that from the Drag Based Model (DBM). From the result of this analysis, we demonstrated that each CME behaves in its own way in the interplanetary medium and their propagation is governed by the CME initial speed, interplanetary acceleration and acceleration cessation distances. In the present paper, we found (i) which acceleration equation is better for the transit time calculations (ii) importance of the CME acceleration cessation distances (iii) reducing the transit time error in CME forecasting. Based on these results and on Zhao and Dryer (2014) review (that included physics-based models), the realistic statistics should be based on real-time studies, not on post-mortem case studies.

Sheath-Accumulating Propagation of Interplanetary Coronal Mass Ejection

Takuya **Takahashi**, Kazunari Shibata

ApJL **837** L17 **2017**

<https://arxiv.org/pdf/1702.06607.pdf>

Fast interplanetary coronal mass ejections (interplanetary CMEs, or ICMEs) are the drivers of strongest space weather storms such as solar energetic particle events and geomagnetic storms. The connection between space weather impacting solar wind disturbances associated with fast ICMEs at Earth and the characteristics of causative energetic CMEs observed near the Sun is a key question in the study of space weather storms as well as in the development of practical space weather prediction. Such shock-driving fast ICMEs usually expand at supersonic speed during the propagation, resulting in the continuous accumulation of shocked sheath plasma ahead. In this paper, we propose the "sheath-accumulating propagation" (SAP) model that describe the coevolution of the interplanetary sheath and decelerating ICME ejecta by taking into account the process of upstream solar wind plasma accumulation within the sheath region. Based on the SAP model, we discussed (1) ICME deceleration characteristics, (2) the fundamental condition for fast ICME at Earth, (3) thickness of interplanetary sheath, (4) arrival time prediction and (5) the super-intense geomagnetic storms associated with huge solar flares. We quantitatively show that not only speed but also mass of the CME are crucial in discussing the above five points. The similarities and differences among the SAP model, the drag-based model and the 'snow-plough' model proposed by [Tappin2006](#) are also discussed.

The Instantaneous Response of the Geomagnetic Field, Near-Earth IMF, and Cosmic-Ray Intensity to Solar Flares.

Takalo, J.

Sol Phys 299, 16 (2024).

<https://doi.org/10.1007/s11207-024-02257-3>

<https://link.springer.com/content/pdf/10.1007/s11207-024-02257-3.pdf>

We show using superposed epoch analysis (SEA) that the most energetic protons (>60 MeV) in the near-Earth interplanetary magnetic field (IMF) have a peak almost immediately (less than a day) after the peak in solar-flare index (SFI), while protons greater than 10 MeV peak one day after the SFI and protons greater than 1 MeV peak two days after the SFI.

The geomagnetic indices AU, -AL, PC, Ap, and -Dst peak after two to three days in SEAs after the peak in SFI. The auroral electrojet indices AU and -AL, however, have only low peaks. In particular, the response of the eastward electrojet, AU, to SFI is negligible compared to other geomagnetic indices.

The SEAs of the SFI and cosmic-ray counts (CR) show that the deepest decline in the CR intensity also follows with a 2 – 3-day lag the maximum of the SFI for Solar Cycles 20 – 24. The depths of the declines are related to the SFI strength of each cycle, i.e., the average decline is about 5% for Cycles 21 and 22, but only 3% for Cycle 24. The strongest Cycle 19, however, differs from the other cycles such that it has a double-peaked decline and lasts longer than the decline of the other cycles.

The double-superposed epoch analyses show that the response of IMF Bv2, which is about two days, and CR to SFI are quite simultaneous, but sometimes Bv2 may peak somewhat earlier than the decline existing in CR.

Separating aa-index into Solar and Hale Cycle Related Components Using Principal Component Analysis

Jouni Takalo

Solar Phys. 2021

<https://arxiv.org/pdf/2103.16862.pdf>

We decompose the monthly aa-index of cycles 10-23 using principal component analysis (PCA). We show that the first component (PC1) is related to solar cycle, and accounts for 41.5 % of the variance of the data. The second component (PC2) is related to 22-year Hale cycle, and explains 23.6% of the variance of the data. The PC1 time series of aa cycles 10-23 has only one peak in its power spectrum at the period 10.95 years, which is the average solar cycle period for the interval SC10-SC23. The PC2 time series of the same cycles has a clear peak at period 21.90 (Hale cycle) and a smaller peak at 3/4 of that period. We also study the principal component of sunspot numbers (SSN) for cycles 10-23, and compare mutual behavior of the PC2 components of aa-index and SSN PCA analyses. We note that they are in the same phase in all other cycles than Solar Cycles 15 and 20. The aa cycle 20 also differs from other even aa cycles in its shape, especially in anomalously high peaks during its descending phase. Even though there is a coherence in the PC2 time series phases of aa-index and sunspot number, this effect is too small to cause all of the difference of the shape of even and odd aa cycles. We estimate that 30% of the shape of the PC2 component of aa-index is due to sunspot number and the rest to other recurrent events in Sun/solar-wind. The first maximum of aa-data (typical to odd cycles), during sunspot maximum, has been shown to be related to coronal mass ejections (CME), while the second maximum (typical to even cycles) in the declining phase of cycle, is probably related to high-speed streams (HSS). The last events increase the activity level such that the minimum between even-odd cycle-pair is always higher than the minimum between succeeding odd-even cycle pair.

Comparison of geomagnetic indices during even and odd solar cycles SC17-SC24: Signatures of Gnevyshev gap in geomagnetic activity

Jouni J. Takalo

Solar Phys. 296, Article number: 19 (2021)

<https://arxiv.org/pdf/2012.05061.pdf>

<https://link.springer.com/content/pdf/10.1007/s11207-021-01765-w.pdf>

We show that the time series of sunspot group areas has a gap, so-called Gnevyshev gap (GG), between ascending and descending phases of the cycle and especially so for the even cycles. For the odd cycles this gap is less obvious, and is only a small decline after the maximum of the cycle. We resample the cycles to have same length of 3945 days (about 10.8 years), and show that the decline is between 1445-1567 days after the start of the cycle for the even cycles, and extending sometimes until 1725 days from the start of the cycle. For the odd cycles the gap is a little earlier 1332-1445 days after the start of the cycles with no extension. We analyze geomagnetic disturbances for solar cycles 17-24 using Dst-index, related Dxt- and Dcx-indices and Ap-index. In all of these time series there is a decline at the time or somewhat after the GG in the solar indices, and as deepest between 1567-1725. The declines are significant at 99 % level for both even and odd cycles of the Dst-index and for Dxt-, Dcx- and Ap-indices for even cycles. For odd cycles of Dxt-index the significance is 95 %, but insignificant for odd cycles of Dcx- and Ap indices. We, however, show that for the cycles 21 and 23, for which Dst exists, the GG is more intense than for the earlier odd cycles. The analyzes of OMNI2 data for 1964-2020 (SC20-SC24) show that these gaps during the maxima of the solar cycles can be seen also in the near-Earth solar wind velocity and IMF magnetic field intensity, and the energy function BV^2 .

Modeling of coronal mass ejections that caused particularly large geomagnetic storms using ENLIL heliosphere cone model

Taktakishvili, A.; Pulkkinen, A.; MacNeice, P.; Kuznetsova, M.; Hesse, M.; Odstrcil, D.
Space Weather, Vol. 9, No. 6, S06002, **2011**, **File**

In our previous paper we reported the results of modeling of 14 selected well-observed strong halo coronal mass ejection (CME) events using the WSA-ENLIL cone model combination. Cone model input parameters were obtained from white light coronagraph images of the CME events using the analytical method developed by Xie et al. (2004). This work verified that coronagraph input gives reasonably good results for the CME arrival time prediction. In contrast to Taktakishvili et al. (2009), where we started the analysis by looking for clear CME signatures in the data and then proceeded to model the interplanetary consequences at 1 AU, in the present paper we start by generating a list of observed geomagnetic storm events and then work our way back to remote solar observations and carry out the corresponding CME modeling. The approach used in this study is addressing space weather forecasting and operational needs. We analyzed 36 particularly strong geomagnetic storms, then tried to associate them with particular CMEs using SOHO/LASCO catalogue, and finally modeled these CMEs using WSA-ENLIL cone model. Recently, Pulkkinen et al. (2010) developed a novel method for automatic determination of cone model parameters. We employed both analytical and automatic methods to determine cone model input parameters. We examined the CME arrival times and magnitude of impact at 1 AU for both techniques. The results of the simulations are compared with the ACE satellite observations. This comparison demonstrated that WSA-ENLIL model combination with coronagraph input gives reasonably good results for the CME arrival times for this set of “geoeffective” CME events as well.

Model uncertainties in predictions of arrival of coronal mass ejections at Earth orbit,

Taktakishvili, A., P. MacNeice, and D. Odstrcil,
Space Weather, 8, S06007, doi:10.1029/2009SW000543. **(2010)**, **File**

It is very important, both for research and forecasting application, to be aware of uncertainty estimation of a scientific model, i.e., to know how model performance depends on the uncertainty in the input parameters. Scientific models are becoming more important as tools for space weather operators' applications and for space weather forecasting. It is essential that operational users, forecasters, model developers, and the scientific community are aware of model capabilities and limitations. In our previous study we validated the performance of the WSA/ENLIL cone model combination in simulating the propagation of 14 events of coronal mass ejections (CMEs) to the L1 point using the cone model approach for halo CMEs. In this short report we present the results of the uncertainty estimation for the WSA/ENLIL cone model combination studying the dependence of the arrival time of the CME shock and the magnitude of the CME impact on the magnetosphere on the uncertainty in the CME input parameters using three events from the previously reported 14 event list.

Validation of the coronal mass ejection predictions at the Earth orbit estimated by ENLIL heliosphere cone model

Taktakishvili, A.; Kuznetsova, M.; MacNeice, P.; Hesse, M.; RastDttter, L.; Pulkkinen, A.; Chulaki, A.; Odstrcil, D.

Space Weather, Vol. 7, No. 3, S03004, **2009**, **File**

<http://dx.doi.org/10.1029/2008SW000448>

Modeling is an important tool in understanding physical processes in the space weather. Model performance studies evaluate the quality of model operation by comparing its output to a measurable parameter of interest. In this paper we studied the performance of the combination of the halo coronal mass ejection (CME) analytical cone model and ENLIL three-dimensional MHD heliosphere model. We examined the CME arrival time and magnitude of impact at 1 AU for different geoeffective events, including the **October 2003 Halloween Storm** and the **14 December 2006 storm CMEs**. The results of the simulation are compared with the ACE satellite observations. The comparison of the simulation results with the observations demonstrates that ENLIL cone model performs better compared to reference mean velocity and empirical models.

See presentation [MacNeice_ Validation of ICME models.pdf](#) (2010)

Dynamic and Thermal Disappearance of Prominences and Their Geoeffectiveness

Lela [Taliashvili](#) · Zadig Mouradian · Jorge Páez

Solar Phys (2009) 258: 277–295

<https://link.springer.com/content/pdf/10.1007%2Fs11207-009-9414-x.pdf>

This paper is a qualitative study of 42 events of solar filament/prominence sudden disappearances (“disparitions brusques”; henceforth DBs) around two solar minima, 1985 – 1986 and 1994. The studied events were classified as 17 thermal and 25 dynamic disappearances. Associated events, *i.e.* coronal mass ejections (CMEs), type II bursts, evolution of nearby coronal holes, as well as solar wind speed, and geomagnetic disturbances are discussed. We have found that about 50% of the thermal DBs with adjacent (within 15° from the DB) coronal holes were associated with CMEs within a selected time window. All the studied thermal disappearances with adjacent coronal holes or accompanied by dynamic disappearances were associated with weak and medium geomagnetic storms. Also, nearly 64% of dynamic DBs were associated with CMEs. Ten (40%) dynamic disappearances were associated with intense geomagnetic storms, even when no CMEs was reported, six (24%) dynamic disappearances corresponded to extreme storms, and five (20%) corresponded to medium geomagnetic storms. The extreme geomagnetic storms appeared to be related to combined events, involving dynamic disappearances with adjacent coronal holes or including thermal disappearances. Furthermore, the geomagnetic activity (Dst index) increased if the source was close to the central meridian ($\pm 30^\circ$). The highest interplanetary magnetic field (B), longest duration, lowest southward direction B_z component, and lowest Dst were highly correlated for all studied events. The Sun – Earth transit time computed from the starting time of the sudden disappearance and the time its effect was measured at Earth was about 4.3 days and was mainly well correlated with the solar wind speed measured *in situ* (daily value).

Interaction of coronal mass ejections and the solar wind. A force analysis

Dana-Camelia [Talpeanu](#) (1 and 2), [Stefaan Poedts](#) (1 and 3), [Elke D’Huys](#) (2), [Marilena Mierla](#) (2 and 4), [Ian G. Richardson](#)

A&A 663, A32 2022

<https://arxiv.org/pdf/2203.09393.pdf>

<https://www.aanda.org/articles/aa/pdf/2022/07/aa43150-22.pdf>

Aims. Our goal is to thoroughly analyse the dynamics of single and multiple solar eruptions, as well as a stealth ejecta. The data were obtained through self-consistent numerical simulations performed in a previous study. We also assess the effect of a different background solar wind on the propagation of these ejecta to Earth.

Methods. We calculated all the components of the forces contributing to the evolution of the numerically modelled consecutive coronal mass ejections (CMEs) obtained with the 2.5D magnetohydrodynamics (MHD) module of the code MPI-AMRVAC. We analysed the thermal and magnetic pressure gradients and the magnetic tension dictating the formation of several flux ropes in different locations in the aftermath of the eruptions. These three components were tracked in the equatorial plane during the propagation of the CMEs to Earth. Their interaction with other CMEs and with the background solar wind was also studied.

Results. We explain the formation of the stealth ejecta and the plasma blobs (or plasmoids) occurring in the aftermath of solar eruptions. We also address the faster eruption of a CME in one case with a different background wind, even when the same triggering boundary motions were applied, and attribute this to the slightly different magnetic configuration and the large neighbouring arcade. The thermal pressure gradient revealed a shock in front of these slow eruptions, formed during their propagation to 1 AU. The double-peaked magnetic pressure gradient indicates that the triggering method affects the structure of the CMEs and that a part of the adjacent streamer is ejected along with the CME.

Study of the propagation, in situ signatures, and geoeffectiveness of shear-induced coronal mass ejections in different solar winds

Dana-Camelia [Talpeanu](#) (1 and 2), [Stefaan Poedts](#) (1 and 3), [Elke D’Huys](#) (2), [Marilena Mierla](#) (2 and 4)

A&A 658, A56 2022

<https://arxiv.org/pdf/2111.14909.pdf>

<https://doi.org/10.1051/0004-6361/202141977>

<https://www.aanda.org/articles/aa/pdf/2022/02/aa41977-21.pdf>

Aims: Our goal is to propagate multiple eruptions - obtained through numerical simulations performed in a previous study - to 1 AU and to analyse the effects of different background solar winds on their dynamics and structure at Earth.

We also aim to improve the understanding of why some consecutive eruptions do not result in the expected geoeffectiveness, and how a secondary coronal mass ejection (CME) can affect the configuration of the preceding one.

Methods: Using the 2.5D magnetohydrodynamics (MHD) package of the code MPI-AMRVAC, we numerically modeled consecutive CMEs inserted in two different solar winds by imposing shearing motions onto the inner boundary.

The initial magnetic configuration depicts a triple arcade structure shifted southward, and embedded into a bimodal solar wind. We compared our simulated signatures with those of a multiple CME event in Sept 2009 using data from spacecraft around Mercury and Earth. We computed and analysed the Dst index for all the simulations performed. Results: The observed event fits well at 1 AU with two of our simulations, one with a stealth CME and the other without. This highlights the difficulty of attempting to use in situ observations to distinguish whether or not the second eruption was stealthy, because of the processes the flux ropes undergo during their propagation in the interplanetary space. We simulate the CMEs propagated in two different solar winds, one slow and another faster one. Only in the first case, plasma blobs arise in the trail of eruptions. Interestingly, the Dst computation results in a reduced geoeffectiveness in the case of consecutive CMEs when the flux ropes arrive with a leading positive Bz. When the Bz component is reversed, the geoeffectiveness increases, meaning that the magnetic reconnections with the trailing blobs and eruptions strongly affect the impact of the arriving interplanetary CME. **21-22 Sept 2009**

Correlation of Electron Path Lengths Observed in the Highly Wound Outer Region of Magnetic Clouds with the Slab Fraction of Magnetic Turbulence in the Dissipation Range

Lun C. [Tan](#)^{1,2}, Donald V. Reames³, Chee K. Ng⁴, Xi Shao^{1,2}, and Linghua Wang
2014 ApJ 786 122.

Three magnetic cloud events, in which solar impulsive electron events occurred in their outer region, are employed to investigate the difference of path lengths L_{0eIII} traveled by non-relativistic electrons from their release site near the Sun to the observer at 1 AU, where $L_{0eIII} = v_l \times (t_l - t_{III})$, v_l and t_l being the velocity and arrival time of electrons in the lowest energy channel (~ 27 keV) of the Wind/3DP/SST sensor, respectively, and t_{III} being the onset time of type III radio bursts. The deduced L_{0eIII} value ranges from 1.3 to 3.3 AU. Since a negligible interplanetary scattering level can be seen in both $L_{0eIII} > 3$ AU and ~ 1.2 AU events, the difference in L_{0eIII} could be linked to the turbulence geometry (slab or two-dimensional) in the solar wind. By using the Wind/MFI magnetic field data with a time resolution of 92 ms, we examine the turbulence geometry in the dissipation range. In our examination, ~ 6 minutes of sampled subintervals are used in order to improve time resolution. We have found that, in the transverse turbulence, the observed slab fraction is increased with an increasing L_{0eIII} value, reaching $\sim 100\%$ in the $L_{0eIII} > 3$ AU event. Our observation implies that when only the slab spectral component exists, magnetic flux tubes (magnetic surfaces) are closed and regular for a very long distance along the transport route of particles.

USE OF INCIDENT AND REFLECTED SOLAR PARTICLE BEAMS TO TRACE THE TOPOLOGY OF MAGNETIC CLOUDS

Lun C. [Tan](#)^{1,2}, Olga E. Malandraki², Donald V. Reames³, Chee K. Ng⁴, Linghua Wang⁵, and Gareth Dorrian
2012 ApJ 750 146

Occasionally, large solar energetic particle (SEP) events occur inside magnetic clouds (MCs). In this work, the onset time analysis, the peak intensity analysis, and the decay phase analysis of SEPs are used to investigate two large SEP events inside MCs: the **1998 May 2** and **2002 April 21** events. The onset time analysis of non-relativistic electrons and \sim MeV nucleon $^{-1}$ heavy ions shows the stability of the magnetic loop structure during a period of a few hours in the events examined. The joint analysis of pitch-angle distributions and peak intensities of electrons exhibits that, depending on the particle pitch angle observed at 1 AU, in the April event the reflection point of particles may be distributed along a wide spatial range, implying that the magnetic loop is a magnetic bottle connected to the Sun with both legs. In contrast, in the May event particle reflection occurs abruptly at the magnetic mirror formed by a compressed field enhancement behind the interplanetary shock, consistent with its open field line topology.

Seasonal Variation of High-Latitude Geomagnetic Activity in Individual Years

E. I. [Tanskanen](#), R. Hynönen, K. Mursula

JGR Volume 122, Issue 10 October **2017** Pages 10,058–10,071

<http://sci-hub.cc/10.1002/2017JA024276>

We study the seasonal variation of high-latitude geomagnetic activity in individual years in 1966–2014 (solar cycles 20–24) by identifying the most active and the second most active season based on westward electrojet indices AL (1966–2014) and IL (1995–2014). The annual maximum is found at either equinox in two thirds and at either solstice in one third of the years examined. The traditional two-equinox maximum pattern is found in roughly one fourth of the years. We found that the seasonal variation of high-latitude geomagnetic activity closely follows the solar wind speed. While the mechanisms leading to the two-equinox maxima pattern are in operation, the long-term change of solar wind speed

tends to mask the effect of these mechanisms for individual years. Large cycle-to-cycle variation is found in the seasonal pattern: equinox maxima are more common during cycles 21 and 22 than in cycles 23 or 24. Exceptionally long winter dominance in high-latitude activity and solar wind speed is seen in the declining phase of cycle 23, after the appearance of the long-lasting low-latitude coronal hole.

From space weather toward space climate time scales: Substorm analysis from 1993 to 2008

Tanskanen, E. I.; Pulkkinen, T. I.; Viljanen, A.; Mursula, K.; Partamies, N.; Slavin, J. A.

J. Geophys. Res., Vol. 116, No. null, A00I34, **2011**

Magnetic activity in the Northern Hemisphere auroral region was examined during solar cycles 22 and 23 (1993–2008). Substorms were identified from ground-based magnetic field measurements by an automated search engine. On average, 550 substorms were observed per year, which gives in total about 9000 substorms. The interannual, seasonal and solar cycle-to-cycle variations of the substorm number (Rss), substorm duration (Tss), and peak amplitude (Ass) were examined. The declining phases of both solar cycles 22 and 23 were more active than the other solar cycle phases due to the enhanced solar wind speed. The spring substorms during the declining solar cycle phase ($|Ass,decl| = 500$ nT) were 25% larger than the spring substorms during the ascending solar cycle years ($|Ass,acsl| = 400$ nT). The following seasonal variation was found: the most intense substorms occurred during spring and fall, the largest substorm frequency in the Northern Hemisphere winter, and the longest-duration substorms in summer. Furthermore, we found a winter-summer asymmetry in the substorm number and duration, which is speculated to be due to the variations in the ionospheric conductivity. The solar cycle-to-cycle variation was found in the yearly substorm number and peak amplitude. The decline from the peak substorm activity in 1994 and 2003 to the following minima took 3 years during solar cycle 22, while it took 6 years during solar cycle 23.

Modeling energetic proton transport in a corotating interaction region - An energetic particle event observed by STEREO-A from 21 to 24 August 2016

Xinyi **Tao**, Fang Shen, Wenwen Wei, Yuji Zhu, Xi Luo and XueShang Feng

A&A 682, A82 (**2024**)

<https://www.aanda.org/articles/aa/pdf/2024/02/aa47248-23.pdf>

Aims. An energetic particle event related to a corotating interaction region (CIR) structure was observed by the Solar-Terrestrial Relations Observatory-A (STEREO-A) from **21 to 24 August 2016**. Based on an analysis of measurement data, we suggest that instead of being accelerated by distant shocks, a local mechanism similar to diffusive shock acceleration (DSA) acting in the compression region could explain the flux enhancements of 1.8–10.0 MeV nucleon⁻¹ protons. We created simulations to verify our hypothesis.

Methods. We developed a coupled model composed of a data-driven analytical background model providing solar wind configuration and a particle transport model represented by the focused transport equation (FTE). We simulated particle transport in the CIR region of interest in order to obtain the evolution of proton fluxes and derive the spectra.

Results. We find that the simulation is well correlated with the observation. The mechanism of particle scattering back and forth between the trap-like structure of interplanetary magnetic field (IMF) in the compression region is the major factor responsible for the flux enhancements in this energetic particle event, and perpendicular diffusion identified by a ratio of $\kappa_{\perp}/\kappa_{\parallel} \sim 10^{-2}$ plays an important role in the temporal evolution of proton fluxes.

A Post-Conjunction Re-Evaluation of the Calibration and Long-term Evolution of the STEREO-A Heliospheric Imagers

S. J. **Tappin**, [C. J. Eyles](#) & [J. A. Davies](#)

[Solar Physics](#) volume 297, Article number: 37 (**2022**)

<https://link.springer.com/content/pdf/10.1007/s11207-022-01966-x.pdf>

In two earlier articles (Tappin, Eyles and Davies in Solar Phys. 290, 2143, [2015](#), and Solar Phys. 292, 28, [2017](#)), we used the stellar photometry to determine the calibration parameters and long-term trends of the Heliospheric Imagers (HI) on board the Solar Terrestrial Relations Observatory (STEREO). In this article we provide an update on these determinations for the ahead spacecraft (STEREO-A) to incorporate the interval after solar superior conjunction (when STEREO-B was non-operational). We describe the modifications needed to our photometry procedures to accommodate the reduced pointing stability following the switch-off of the spacecraft gyros shortly prior to conjunction. We find a small revision to the absolute levels is required. We also show that the very low rates of degradation (less than 0.2% per year) found in the earlier determinations have continued beyond solar conjunction.

On the Long-Term Evolution of the Sensitivity of the STEREO HI-1 Cameras

S. J. [Tappin](#), C. J. Eyles, J. A. Davies

Solar Physics February **2017**, 292:28

The Heliospheric Imagers (HI) on the Solar TERrestrial RELations Observatory (STEREO) observe the solar wind and disturbances therein as it propagates from close to the Sun to 1 AU and beyond. In this article we use stellar photometry over much of the mission to date to make a determination of the long-term evolution of the photometric response of the inner (HI-1) cameras. We find very slow degradation rates of the order of 0.1 % per year, similar to those found for HI-2 by Tappin, Eyles and Davies (Solar Phys.290, 2143, 2015) and significantly slower than rates found for other comparable instruments. We also find that it is necessary to make a small ($\sim 1\%$) revision to the photometric calibration parameters used to convert instrument units into physical units. Finally, we briefly discuss the effects of pointing instabilities on the measurement of stellar count rates.

Determination of the Photometric Calibration and Large-Scale Flatfield of the STEREO Heliospheric Imagers : II. HI-2

S. J. [Tappin](#), C. J. Eyles, J. A. Davies

Solar Phys. Volume 290, [Issue 7](#), pp 2143-2170 **2015**

In this article we describe the methods used to determine the photometric calibration parameters for the outer Heliospheric Imagers (HI-2) onboard the Solar Terrestrial Relations Observatory (STEREO) spacecraft from measurements of background stars, and we present those values that represent small corrections to the values predicted from pre-launch calibrations. Conversion factors to physical units are also derived. We determine the degradation of these instruments over the course of the mission to date; this is found to be around an order of magnitude slower than for white-light instruments on other spacecraft. We compute a correction to the large-scale flatfield for HI-2A, allowing for vignetting in the outer parts of the images. In addition, we consider the effects of pixel saturation and the implications for the use of the HI-2 instruments for stellar photometry. We also discuss the limitations of the currently employed geometrical projection assumptions.

On the autonomous detection of coronal mass ejections in heliospheric imager data

[Tappin](#), S. J.; Howard, T. A.; Hampson, M. M.; Thompson, R. N.; Burns, C. E.

J. Geophys. Res., Vol. 117, No. A5, A05103, **2012**

http://www.boulder.swri.edu/~howard/Papers/2012_Tappin_AICMED.pdf - **File**

We report on the development of an Automatic Coronal Mass Ejection (CME) Detection tool (AICMED) for the **Solar Mass Ejection Imager (SMEI)**. CMEs observed with heliospheric imagers are much more difficult to detect than those observed by coronagraphs as they have a lower contrast compared with the background light, have a larger range of intensity variation and are easily confused with other transient activity. CMEs appear in SMEI images as very faint often-fragmented arcs amongst a much brighter and often variable background. AICMED operates along the same lines as Computer Aided CME Tracking (CACTus), using the Hough Transform on elongation-time J-maps to extract straight lines from the data set. We compare AICMED results with manually measured CMEs on almost three years of data from early in SMEI operations. AICMED identified 83 verifiable events. Of these 46 could be matched with manually identified events, the majority of the non-detections can be explained. The remaining 37 AICMED events were newly discovered CMEs. The proportion of false identification was high, at 71% of the autonomously detected events. We find that AICMED is very effective as a region of interest highlighter, and is a promising first step in autonomous heliospheric imager CME detection, but the SMEI data are too noisy for the tool to be completely automated.

Reconstructing CME Structures from IPS Observations Using a Phenomenological Model

S.J. [Tappin](#) · T.A. Howard

Solar Phys (**2010**) 265: 159–186, **File**

We present an extension of the Tappin – Howard (TH) phenomenological model (Tappin and Howard, *Space Sci. Rev.* **147**, 55, [2009](#)) for coronal mass ejection reconstruction to use interplanetary scintillation *g*-map data. The necessary changes to the model are discussed. We then use the modified model to reconstruct two major interplanetary disturbances observed using the Cambridge 3.6 ha Array in September 1980. We find that despite the lower cadence of IPS observations compared with white-light imagers, a consistent reconstruction can be generated which is in agreement with *in-situ* measurements and solar observations.

Interplanetary Coronal Mass Ejections Observed in the Heliosphere: 2. Model and Data Comparison

S. James [Tappin](#) · Timothy A. Howard

Space Sci Rev (2009) 147: 55–87, [File](#)

With the recent advancements in interplanetary coronal mass ejection (ICME) imaging it is necessary to understand how heliospheric images may be interpreted, particularly at large elongation angles. Of crucial importance is how the current methods used for coronal mass ejection measurement in coronagraph images must be changed to account for the large elongations involved in the heliosphere. We present results comparing a new model of interplanetary disturbances with heliospheric image data, from the Solar Mass Ejection Imager. A database containing a range of ICMEs simulated with varying parameters describing its topology, orientation, location and speed was produced and compared with two ICMEs observed in February and December 2004. We identify the simulated ICME that best matches the data, and use the parameters required to identify their three-dimensional leading-edge structure, orientation and kinematics. By constant comparison with the data we are able to keep track of small changes to the ICME topology and kinematic properties, thus for the first time are able to monitor how the dynamic interaction between the ICME and the interplanetary medium affects ICME evolution. This is the second part of a series of three papers, where the theory behind the model is presented in an accompanying paper and the physical implications are discussed in the third part. The first part considers the effects of Thomson scattering across the entire span of the disturbance and includes its apparent geometry at large elongations. We find that the model converges reliably to a solution for both events, although we identify four separate structures during the December period. Comparing the 3-D trajectory and source location with known associated features identified with other spacecraft, we find a remarkable agreement between the model and data. We conclude with a brief discussion of the physical implications of the model.

[Parts 1 and 3: see Howard \(2009\)](#)

DIRECT OBSERVATION OF A COROTATING INTERACTION REGION BY THREE SPACECRAFT

S. J. [Tappin](#) and T. A. Howard

Astrophysical Journal, 702:862–870, 2009 September

White-light observations of interplanetary disturbances have been dominated by interplanetary coronal mass ejections (ICMEs). This is because the other type of disturbance, the corotating interaction region (CIR), has proved difficult to detect using white-light imagers. Recently, a number of papers have appeared presenting CIR observations using the *Solar Terrestrial Relations Observatory (STEREO)* Heliospheric Imagers (HIs), but have mostly only focused on a single spacecraft and imager. In this paper, we present observations of a single CIR that was observed by all three current white-light heliospheric imagers (SMEI and both *STEREO* HIs), as well as the in situ instruments on both *STEREO* satellites and *ACE*. We begin with a discussion of the geometry of the CIR structure, and show how the apparent leading edge structure is expected to change as it corotates relative to the observer. We use these calculations to predict elongation–time profiles for CIRs of different speeds for each of the imagers, and also to predict the arrival times at the in situ instruments. We show that although all three measured different parts, they combine to produce a self-consistent picture of the CIR. Finally, we offer some thoughts on why CIRs have proved so difficult to detect in white-light heliospheric images.

THE DECELERATION OF AN INTERPLANETARY TRANSIENT FROM THE SUN TO 5 AU

S. J. [TAPPIN](#)

Solar Physics (2006) 233: 233–248; [File](#)

A CME which was first seen in LASCO is tracked through SMEI and on out to *Ulysses*. These measurements allow us to determine the deceleration and compare different models of the deceleration process. It is found that both a simple “snow plough” model and an aerodynamic drag model predict a much more rapid deceleration in the lower solar wind than is observed. Therefore

some driving force is needed over an extended range of distances to account for the motion of the transient. It is conjectured that at least part of this driving force may be provided by one of two low-latitude coronal holes which were close to the site of the CME.

Tracking a major interplanetary disturbance with SMEI,

Tappin, S. J.; Buffington, A.; Cooke, M. P.; Eyles, C. J.; Hick, P. P.; Holladay, P. E.; Jackson, B. V.; Johnston, J. C.; Kuchar, T.; Mizuno, D.; and 7 coauthors

Geophys. Res. Lett., 31, L02802, doi:10.1029/2003GL018766, 2004.

We present the first clear observations of an Earth-directed interplanetary disturbance tracked by the Solar Mass Ejection Imager (SMEI). We find that this event can be related to two halo CMEs seen at the Sun about 2 days earlier, and which merged in transit to 1 AU. The disturbance was seen about 16 hours before it reached Earth, and caused a severe geomagnetic storm at the time which would have been predicted had SMEI been operating as a real-time monitor. It is concluded that SMEI is capable of giving many hours advance warning of the possible arrival of interplanetary disturbances.

Mapping Magnetic Field Lines for an Accelerating Solar Wind

S. **Tasnim**, Iver H. Cairns, B. Li, M. S. Wheatland

Solar Physics November 2019, 294:155

<https://link.springer.com/content/pdf/10.1007%2Fs11207-019-1541-4.pdf>

Mapping of magnetic field lines is important for studies of the solar wind and the sources and propagation of energetic particles between the Sun and observers. A recently developed mapping approach is generalized to use a more advanced solar wind model that includes the effects of solar wind acceleration, non-radial intrinsic magnetic fields and flows at the source surface/inner boundary, and conservation of angular momentum. The field lines are mapped by stepping along BB and via a Runge–Kutta algorithm, leading to essentially identical maps. The new model's maps for Carrington rotation CR 1895 near solar minimum (19 April to 15 May 1995) and a solar rotation between CR 2145 and CR 2146 near solar maximum (14 January to 9 February 2014) are compared with the published maps for a constant solar wind model. The two maps are very similar on a large scale near both solar minimum and solar maximum, meaning that the field-line orientations, winding angles, and connectivity generally agree very well. However, close inspection shows that the field lines have notable small-scale structural differences. An interpretation is that inclusion of the acceleration and intrinsic azimuthal velocity has significant effects on the local structure of the magnetic field lines. Interestingly, the field lines are more azimuthal for the accelerating solar wind model for both intervals. In addition, predictions for the pitch angle distributions (PADs) for suprathermal electrons agree at the 90 – 95% level with observations for both solar wind models for both intervals.

The Independence of Magnetic Turbulent Power Spectra to the Presence of Switchbacks in the Inner Heliosphere

Peter **Tatum**, [David Malaspina](#), [Alexandros Chasapis](#), [Benjamin Short](#)

ApJ 2024

<https://arxiv.org/pdf/2404.03075.pdf>

An outstanding gap in our knowledge of the solar wind is the relationship between switchbacks and solar wind turbulence. Switchbacks are large fluctuations, even reversals, of the background magnetic field embedded in the solar wind flow. It has been proposed that switchbacks may form as a product of turbulence and decay via coupling with the turbulent cascade. In this work, we examine how properties of solar wind magnetic field turbulence vary in the presence or absence of switchbacks. Specifically, we use in-situ particle and fields measurements from Parker Solar Probe to measure magnetic field turbulent wave power, separately in the inertial and kinetic ranges, as a function of switchback magnetic deflection angle. We demonstrate that the angle between the background magnetic field and the solar wind velocity in the spacecraft frame (θ_{vB}) strongly determines whether Parker Solar Probe samples wave power parallel or perpendicular to the background magnetic field. Further, we show that θ_{vB} is strongly modulated by the switchback magnetic deflection angle. In this analysis, we demonstrate that switchback deflection angle does not correspond to any significant increase in wave power in either the inertial range or at kinetic scales. This result implies that switchbacks do not strongly couple to the turbulent cascade in the inertial or kinetic ranges via turbulent wave-particle interactions. Therefore, we do not expect switchbacks to contribute significantly to solar wind heating through this type of energy conversion pathway, although contributions via other mechanisms, such as magnetic reconnection may still be significant. 2018-11-06

The role of magnetic handedness in magnetic cloud propagation,

Taubenschuss, U., Erkaev, N. V., Biernat, H. K., Farrugia, C. J., Möstl, C., and Amerstorfer, U. V.: *Ann. Geophys.*, 28, 1075-1100, **2010**.

We investigate the propagation of magnetic clouds (MCs) through the inner heliosphere using 2.5-D ideal magnetohydrodynamic (MHD) simulations. A numerical solution is obtained on a spherical grid, either in a meridional plane or in an equatorial plane, by using a Roe-type approximate Riemann solver in the frame of a finite volume approach. The structured background solar wind is simulated for a solar activity minimum phase. In the frame of MC propagation, special emphasis is placed on the role of the initial magnetic handedness of the MC's force-free magnetic field because this parameter strongly influences the efficiency of magnetic reconnection between the MC's magnetic field and the interplanetary magnetic field. Magnetic clouds with an axis oriented perpendicular to the equatorial plane develop into an elliptic shape, and the ellipse drifts into azimuthal direction. A new feature seen in our simulations is an additional tilt of the ellipse with respect to the direction of propagation as a direct consequence of magnetic reconnection. During propagation in a meridional plane, the initial circular cross section develops a concave-outward shape. Depending on the initial handedness, the cloud's magnetic field may reconnect along its backside flanks to the ambient interplanetary magnetic field (IMF), thereby losing magnetic flux to the IMF. Such a process in combination with a structured ambient solar wind has never been analyzed in detail before. Furthermore, we address the topics of force-free magnetic field conservation and the development of equatorward flows ahead of a concave-outward shaped MC. Detailed profiles are presented for the radial evolution of magnetoplasma and geometrical parameters. The principal features seen in our MHD simulations are in good agreement with in-situ measurements performed by spacecraft. The 2.5-D studies presented here may serve as a basis under more simple geometrical conditions to understand more complicated effects seen in 3-D simulations.

A New Estimate for the Orientation of Underlying Heliospheric Magnetic Field Associated with Alfvénic Fluctuations

W.-L. **Teh**¹ and J. T. Gosling²

2020 *ApJ* 896 52

<https://doi.org/10.3847/1538-4357/ab8fa4>

In the solar wind Alfvénic fluctuations are coupled fluctuations in the transverse components of plasma velocity, \mathbf{v}_\perp , and magnetic field, \mathbf{B}_\perp , in which B_\parallel remains nearly constant. Consequently, the fluctuations in the component of \mathbf{v}_\perp and \mathbf{B}_\perp along the direction of the underlying magnetic field, \mathbf{B}_\parallel , are always one-sided relative to base values rather than mean values. This paper proposes a new method for estimating \mathbf{B}_\parallel and verifies it using simulation data. The new approach is to find a consistent minimum variance direction of magnetic field for two different data subsets divided by a threshold angle from the original data set. Simulation results show that (1) the direction of \mathbf{B}_\parallel predicted by the new method is generally more accurate than the average magnetic field, \mathbf{B}_\perp , and that (2) \mathbf{B}_\parallel does not correspond to \mathbf{B}_\perp when the averages of the transverse field fluctuations are nonzero. Two events of one-sided Alfvénic fluctuations in the solar wind observed at 0.36 and 1 au, where a small but significant mean \mathbf{B}_\parallel appears in the transverse field fluctuation, are demonstrated for the new method. Results show that the new estimate is more radial than \mathbf{B}_\perp and also different from that predicted by Parker's model of the heliospheric magnetic field (HMF). This new technique will be useful for comparing solar wind observations with the global HMF model and for determining the fluctuation \mathbf{k} -vector, which is presumably directed along \mathbf{B}_\parallel .

Prediction Capability of Geomagnetic Events from Solar Wind Data Using Neural Networks

Daniele **Telloni**^{4,1}, Maurizio Lo Schiavo^{4,2}, Enrico Magli², Silvano Fineschi¹ +++

2023 *ApJ* 952 111

<https://iopscience.iop.org/article/10.3847/1538-4357/acdeea/pdf>

Multiple neural network architectures, with different structural composition and complexity, are implemented in this study with the aim of providing multi-hour-ahead warnings of severe geomagnetic disturbances, based on in situ measurements of the solar wind plasma and magnetic field acquired at the Lagrangian point L1. First, a statistical analysis of the interplanetary data was performed to point out which are the most relevant parameters to be provided as input to the neural networks, and a preprocessing of the data set was implemented to face its heavy imbalance (the Earth's magnetosphere is in fact mostly at rest). Then, neural networks were tested to evaluate their performance. It turned out that, in a binary classification problem, recurrent approaches are best at predicting critical events both 1 and 8 hr in advance, achieving a balanced accuracy of 94% and 70%, respectively. Finally, in an attempt at multistep prediction of the criticality of future geomagnetic events from 1–8 hr ahead, more complex neural networks, built by merging the different types of basic convolutional and recurrent architectures, have been shown to outperform single-

step and state-of-the-art approaches with a balanced accuracy of at least 70%. Interestingly, the accuracy peaks at 4 hr, corresponding to the waiting time between the detection of solar drivers at L1 and the onset of the geomagnetic storm (as previously obtained by statistical investigations), suggesting that on average this is the time the Earth's magnetosphere takes to react to the solar event.

Does Turbulence along the Coronal Current Sheet Drive Ion Cyclotron Waves?

Daniele **Telloni**, [Gary P. Zank](#), [Laxman Adhikari](#), [Lingling Zhao](#), et al.

ApJ **2023**

<https://arxiv.org/pdf/2302.10545>

Evidence for the presence of ion cyclotron waves, driven by turbulence, at the boundaries of the current sheet is reported in this paper. By exploiting the full potential of the joint observations performed by Parker Solar Probe and the Metis coronagraph on board Solar Orbiter, local measurements of the solar wind can be linked with the large-scale structures of the solar corona. The results suggest that the dynamics of the current sheet layers generates turbulence, which in turn creates a sufficiently strong temperature anisotropy to make the solar-wind plasma unstable to anisotropy-driven instabilities such as the Alfvén ion-cyclotron, mirror-mode, and firehose instabilities. The study of the polarization state of high-frequency magnetic fluctuations reveals that ion cyclotron waves are indeed present along the current sheet, thus linking the magnetic topology of the remotely imaged coronal source regions with the wave bursts observed in situ. The present results may allow improvement of state-of-the-art models based on the ion cyclotron mechanism, providing new insights into the processes involved in coronal heating. **14-17 Jan 2021**

Daniele **Telloni**¹, Gary P. Zank^{2,3}, Luca Sorriso-Valvo^{4,5}, Raffaella D'Amicis⁶, Olga Panasenco⁷, Roberto Susino¹, Roberto Bruno⁶, Denise Perrone⁸, Laxman Adhikari², Haoming Liang²Show full author list
2022 ApJ 935 112

<https://iopscience.iop.org/article/10.3847/1538-4357/ac8103/pdf>

The solar wind measured in situ by Parker Solar Probe in the very inner heliosphere is studied in combination with the remote-sensing observation of the coronal source region provided by the METIS coronagraph aboard Solar Orbiter. The coronal outflows observed near the ecliptic by Metis on **2021 January 17** at 16:30 UT, between 3.5 and 6.3 R_{\odot} above the eastern solar limb, can be associated with the streams sampled by PSP at 0.11 and 0.26 au from the Sun, in two time intervals almost 5 days apart. The two plasma flows come from two distinct source regions, characterized by different magnetic field polarity and intensity at the coronal base. It follows that both the global and local properties of the two streams are different. Specifically, the solar wind emanating from the stronger magnetic field region has a lower bulk flux density, as expected, and is in a state of well-developed Alfvénic turbulence, with low intermittency. This is interpreted in terms of slab turbulence in the context of nearly incompressible magnetohydrodynamics. Conversely, the highly intermittent and poorly developed turbulent behavior of the solar wind from the weaker magnetic field region is presumably due to large magnetic deflections most likely attributed to the presence of switchbacks of interchange reconnection origin.

Observation of Magnetic Switchback in the Solar Corona

Daniele **Telloni**, [Gary P. Zank](#), [Marco Stangalini](#), [Cooper Downs](#), et al.

ApJL **936** L25 **2022**

<https://arxiv.org/pdf/2206.03090.pdf>

<https://iopscience.iop.org/article/10.3847/2041-8213/ac8104/pdf>

Switchbacks are sudden, large radial deflections of the solar wind magnetic field, widely revealed in interplanetary space by the Parker Solar Probe. The switchbacks' formation mechanism and sources are still unresolved, although candidate mechanisms include Alfvénic turbulence, shear-driven Kelvin-Helmholtz instabilities, interchange reconnection, and geometrical effects related to the Parker spiral. This Letter presents observations from the Metis coronagraph onboard Solar Orbiter of a single large propagating S-shaped vortex, interpreted as first evidence of a switchback in the solar corona. It originated above an active region with the related loop system bounded by open-field regions to the East and West. Observations, modeling, and theory provide strong arguments in favor of the interchange reconnection origin of switchbacks. Metis measurements suggest that the initiation of the switchback may also be an indicator of the origin of slow solar wind. **March 25, 2022**

Statistical Methods Applied to Space Weather Science

Daniele **Telloni**

Front. Astron. Space Sci., 9: 865880 **2022** |

<https://doi.org/10.3389/fspas.2022.865880>

<https://www.frontiersin.org/articles/10.3389/fspas.2022.865880/full>
<https://www.frontiersin.org/articles/10.3389/fspas.2022.865880/pdf>

Space Weather is receiving more and more attention from the heliophysical scientific community, as it is now well established that an adequate capability of monitoring any Earth-directed heliospheric event and forecasting the most severe perturbations produced by solar activity and their impact on the geo-spatial environment is crucial, given the human increasing reliance on space-related technologies and infrastructures. Predicting how the Sun affects life on Earth and human activities in the short term relies on establishing empirical laws to forecast not only the arrival time on Earth of potentially geo-effective solar drivers, but also, and more importantly, the intensity of induced geomagnetic disturbance (if any). Scientific studies performed on a statistical basis are the key to providing such empirical laws and analytically relating solar-wind properties to geomagnetic indices. This paper summarizes the results achieved by the author in the last few years in the context of Space Weather science, and based on statistical analyses of interplanetary and geomagnetic data.

Exploring the Solar Wind from Its Source on the Corona into the Inner Heliosphere during the First Solar Orbiter–Parker Solar Probe Quadrature

Daniele **Telloni**¹, Vincenzo Andretta², Ester Antonucci¹, Alessandro Bemporad¹, Giuseppe E. Capuano^{3,4}, Silvano Fineschi¹, Silvio Giordano¹, Shadia Habbal⁵, Denise Perrone⁶, Rui F. Pinto^{7,8}Show full author list

2021 ApJL 920 L14

<https://arxiv.org/pdf/2110.11031.pdf>
<https://doi.org/10.3847/2041-8213/ac282f>

This Letter addresses the first Solar Orbiter (SO)–Parker Solar Probe (PSP) quadrature, occurring on **2021 January 18** to investigate the evolution of solar wind from the extended corona to the inner heliosphere. Assuming ballistic propagation, the same plasma volume observed remotely in the corona at altitudes between 3.5 and 6.3 solar radii above the solar limb with the Metis coronagraph on SO can be tracked to PSP, orbiting at 0.1 au, thus allowing the local properties of the solar wind to be linked to the coronal source region from where it originated. Thanks to the close approach of PSP to the Sun and the simultaneous Metis observation of the solar corona, the flow-aligned magnetic field and the bulk kinetic energy flux density can be empirically inferred along the coronal current sheet with an unprecedented accuracy, allowing in particular estimation of the Alfvén radius at 8.7 solar radii during the time of this event. This is thus the very first study of the same solar wind plasma as it expands from the sub-Alfvénic solar corona to just above the Alfvén surface.

Alfvénicity-related Long Recovery Phases of Geomagnetic Storms: A Space Weather Perspective

Daniele **Telloni**¹, Raffaella D'Amicis², Roberto Bruno², Denise Perrone³, Luca Sorriso-Valvo^{4,5}, Anil N. Raghav⁶, and Komal Choraghe⁶

2021 ApJ 916 64

<https://doi.org/10.3847/1538-4357/ac071f>

This paper reports, for the first time on a statistical basis, on the key role played by the Alfvénic fluctuations in modulating the recovery phase of the geomagnetic storms, slowing down the restoration of the magnetosphere toward its pre-storm equilibrium state. Using interplanetary and geomagnetic measurements collected over more than one solar cycle, a high correlation between the durations of Alfvénic streams and concurrent recovery phases is found, pointing to a clear coupling between Alfvénic turbulence and magnetospheric ring current dynamics. By exploiting current solar wind models, these observations also provide space weather opportunities of predicting the total duration of any geomagnetic storm induced by any solar driver provided that it is followed by an Alfvénic stream, a crucial piece of information for ground technologies and infrastructures that are affected by time-integrated effects throughout the duration of the storm.

Evolution of Solar Wind Turbulence from 0.1 to 1 au during the First Parker Solar Probe–Solar Orbiter Radial Alignment

Daniele **Telloni**¹, Luca Sorriso-Valvo^{2,3}, Lloyd D. Woodham⁴, Olga Panasenco⁵, Marco Velli⁶, Francesco Carbone⁷, Gary P. Zank^{8,9}, Roberto Bruno¹⁰, Denise Perrone¹¹, Masaru Nakanotani⁸

2021 ApJL 912 L21

<https://doi.org/10.3847/2041-8213/abf7d1>

The first radial alignment between Parker Solar Probe and Solar Orbiter spacecraft is used to investigate the evolution of solar wind turbulence in the inner heliosphere. Assuming ballistic propagation, two 1.5 hr intervals are tentatively identified as providing measurements of the same plasma parcels traveling from 0.1 to 1 au. Using magnetic field measurements from both spacecraft, the properties of turbulence in the two intervals are assessed. Magnetic spectral density, flatness, and high-order moment scaling laws are calculated. The Hilbert–Huang transform is additionally used to mitigate short sample and poor stationarity effects. Results show that the plasma evolves from a highly Alfvénic, less-developed turbulence state near the Sun, to fully developed and intermittent turbulence at 1 au. These observations provide strong evidence for the radial evolution of solar wind turbulence.

Magnetohydrodynamic Turbulent Evolution of a Magnetic Cloud in the Outer Heliosphere

Daniele **Telloni**¹, Lingling Zhao², Gary P. Zank^{2,3}, Haoming Liang², Masaru Nakanotani², Laxman Adhikari², Francesco Carbone⁴, Raffaella D'Amicis⁵, Denise Perrone⁶, Roberto Bruno⁵

2020 ApJL 905 L12

<https://doi.org/10.3847/2041-8213/abcb03>

This Letter exploits joint observations of the same interplanetary coronal mass ejection by widely separated spacecraft to study, for the first time, the turbulent evolution of the magnetohydrodynamic (MHD) properties of the embedded magnetic cloud, during its propagation throughout interplanetary space. Specifically, the event was observed by Wind at 1 au on **1998 March 4–6** and tracked to the location of Ulysses at 5.4 au 18 days later, when the two spacecraft were radially aligned with the Sun. The analysis of the MHD invariants within the magnetic cloud, along with its energy budget, provides compelling evidence of magnetic erosion of the structure thanks to its interaction with a trailing magnetic cloud. The helical configuration is thus largely deformed and degraded, and the initial dominance of magnetic over kinetic energy is observed to evolve toward a less imbalanced condition. This is consistent with the expected conversion of magnetic energy into kinetic energy due to magnetic reconnection processes. Local interaction of the magnetic cloud's (MC) outer layers with the solar wind acts to generate larger amplitude Alfvénic fluctuations in the downstream region, leading the MC to turbulently evolve toward a more complex cross-helicity configuration in the outer heliosphere. Finally, evidence of a flux rope locally generated by magnetic reconnection events at 1 au that likely decays by the time it reaches Ulysses is also reported.

Detection Capability of Flux Ropes during the Solar Orbiter Mission

Daniele **Telloni**¹, Raffaella D'Amicis², Roberto Bruno², Francesco Carbone³, Denise Perrone⁴, Gary P. Zank^{5,6}, Lingling Zhao⁵, Masaru Nakanotani⁵, and Laxman Adhikari⁵

2020 ApJL 899 L25

<https://doi.org/10.3847/2041-8213/abacc4>

Flux ropes are interplanetary magnetic helical structures that are receiving increasing attention because of their likely role in magnetohydrodynamic (MHD) processes as well as their impact on space weather science. A very promising and powerful approach to address their investigation and characterization is based on wavelet spectrograms of the invariants of the ideal MHD equations. The accuracy of this method to infer flux rope properties depends on the proper evaluation of the direction of propagation of the flux rope itself, which is often difficult to assess. We present a numerical test of the reliability of this diagnostic technique, by simulating a synthetic flux rope of fixed size and propagation direction along the Solar Orbiter orbit, that is very elongated and inclined with respect to the orbital plane. We find that when the flux rope is crossed for less than 50% of its width, the procedure becomes unreliable. Quantitative information on how to properly recover the flux-rope intrinsic properties is provided.

Study of the Influence of the Solar Wind Energy on the Geomagnetic Activity for Space Weather Science

Daniele **Telloni**¹, Francesco Carbone², Ester Antonucci¹, Roberto Bruno³, Catia Grimani^{4,5}, Umberto Villante⁶, Silvio Giordano¹, Salvatore Mancuso¹, and Luca Zangrilli¹

2020 ApJ 896 149

<https://iopscience.iop.org/article/10.3847/1538-4357/ab91b9/pdf>

<https://sci-hub.tw/10.3847/1538-4357/ab91b9>

This paper addresses the investigation of the interaction of the solar wind energy with the Earth's magnetosphere, by studying its correlation with the disturbance storm time (Dst) index, a proxy of the geomagnetic activity. Some relevant parameters of the solar wind (the bulk speed and the z-component of the interplanetary magnetic field) are explored in the energy–Dst space. It results that (i) the solar wind energy and the geomagnetic activity are strictly related, with the coronal mass ejections representing the most energetic and geoeffective driver; (ii) the slow solar wind has negligible effects on Earth regardless of its energy content, whereas high-speed streams may induce severe geomagnetic storming

depending on the advected energy; and (iii) while at low and mid energies, geomagnetic disturbances are induced provided the magnetic reconnection between the interplanetary and terrestrial magnetic fields occurs, high-energy solar wind plasma can impact Earth even without reconnecting with the geomagnetic field at the dayside magnetopause. The most significant result in the framework of space weather science resides in the observational evidence that the Earth's magnetosphere has a maximum response to the energetic content of the solar wind, which leads to the derivation of an empirical law allowing the proper forecast of the upper limit of the intensity of any geomagnetic disturbance on the basis of the solar wind energy derived in situ at the Lagrangian point L1.

Detection of Coronal Mass Ejections at L1 and Forecast of Their Geoeffectiveness

Daniele **Telloni**¹, Ester Antonucci¹, Alessandro Bemporad¹, Tiziano Bianchi², Roberto Bruno³, Silvano Fineschi¹, Enrico Magli², Gianalfredo Nicolini¹, and Roberto Susino¹

2019 ApJ 885 120

[sci-hub.se/10.3847/1538-4357/ab48e9](https://doi.org/10.3847/1538-4357/ab48e9)

A novel tool aimed to detect solar coronal mass ejections (CMEs) at the Lagrangian point L1 and to forecast their geoeffectiveness is presented in this paper. This approach is based on the analysis of in situ magnetic field and plasma measurements to compute some important magnetohydrodynamic quantities of the solar wind (the total pressure, the magnetic helicity, and the magnetic and kinetic energy), which are used to identify the CME events, that is their arrival and transit times, and to assess their likelihood for impacting the Earth's magnetosphere. The method is essentially based on the comparison of the topological properties of the CME magnetic field configuration and of the CME energetic budget with those of the quasi-steady ambient solar wind. The algorithm performances are estimated by testing the tool on solar wind data collected in situ by the Wind spacecraft from 2005 to 2016. In the scanned 12 yr time interval, it results that (i) the procedure efficiency is of 86% for the weakest magnetospheric disturbances, increasing with the level of the geomagnetic storming, up to 100% for the most intense geomagnetic events, (ii) zero false positive predictions are produced by the algorithm, and (iii) the mean delay between the potentially geoeffective CME detection and the geomagnetic storm onset is of 4 hr, with a 98% 2–8 hr confidence interval. Hence, this new technique appears to be very promising in forecasting space weather phenomena associated to CMEs. **15 May 2005**

On the Fast Solar Wind Heating and Acceleration Processes: A Statistical Study Based on the UVCS Survey Data

Daniele **Telloni**, Silvio Giordano, and Ester Antonucci

2019 ApJL 881 L36

[sci-hub.se/10.3847/2041-8213/ab3731](https://doi.org/10.3847/2041-8213/ab3731)

The UltraViolet Coronagraph Spectrometer (UVCS) on board the SOlar and Heliospheric Observatory has almost continuously observed, throughout the whole solar cycle 23, the UV solar corona. This work addresses the first-ever statistical analysis of the daily UVCS observations, performed in the O vi channel, of the northern polar coronal hole, between 1.5 and 3 R_☉, during the period of low solar activity from 1996 April to 1997 December. The study is based on the investigation, at different heights, of the correlation between the variance of the O vi 1031.92 Å spectral line and the O vi 1031.92, 1037.61 Å doublet intensity ratio, which are proxies of the kinetic temperature of the O⁵⁺ ions and of the speed of the oxygen component of the fast solar wind, respectively. This analysis allows the clear identification of the sonic point in polar coronal holes at the distance of 1.9 R_☉. The results show that heat addition below the sonic point does not lead to an increase of the outflow speed. As a matter of fact, the coronal plasma is heated more efficiently in the subsonic region, while its acceleration occurs more effectively in the region of supersonic flow. So, within the panorama of the Parker Solar Probe and Solar Orbiter missions, the statistical analysis of the historical UVCS data appears to be very promising in providing unique clues to some still unsolved problems, as the coronal heating, in the solar corona.

RELAXATION PROCESSES WITHIN FLUX ROPES IN SOLAR WIND

D. **Telloni**¹, V. Carbone^{2,3}, S. Perri², R. Bruno⁴, F. Lepreti², and P. Veltri

2016 ApJ 826 205

Flux ropes are localized structures in space plasma whose tube-like organized magnetic configuration can be well approximated by a force-free field model. Both numerical simulations and simple models suggest that the ideal magnetohydrodynamics (MHD) can relax toward a minimum energy state, where magnetic helicity is conserved, characterized by force-free magnetic fields (Taylor relaxation). In this paper, we evaluate MHD rugged invariants within more than 100 flux ropes identified in the solar wind at 1 AU, showing that the magnetic and cross-helicity content carried out by these structures tend to be "attracted" toward a particular subphase in the parameter plane. The final configuration of the MHD rugged invariants in the parameter plane suggests indeed that flux ropes represent well-

organized structures coming from the dynamical evolution of MHD turbulent cascade. These observational results, along with a simple model based on a truncated set of nonlinear ordinary differential equations for both the velocity and magnetic field Fourier coefficients, thus, support a scenario in which the flux ropes naturally come out from the ideal MHD decay to large-scale magnetic field in space plasmas, probably governed by relaxation processes similar to those observed in laboratory plasmas.

An Analysis of Magnetohydrodynamic Invariants of Magnetic Fluctuations within Interplanetary Flux Ropes

D. [Telloni](#)¹, S. Perri², R. Bruno³, V. Carbone^{2,4}, and R. D Amicis

2013 ApJ 776 3

A statistical analysis of magnetic flux ropes, identified by large-amplitude, smooth rotations of the magnetic field vector and a low level of both proton density and temperature, has been performed by computing the invariants of the ideal magnetohydrodynamic (MHD) equations, namely the magnetic helicity, the cross-helicity, and the total energy, via magnetic field and plasma fluctuations in the interplanetary medium. A technique based on the wavelet spectrograms of the MHD invariants allows the localization and characterization of those structures in both scales and time: it has been observed that flux ropes show, as expected, high magnetic helicity states ($|\sigma_m| [0.6: 1]$), but extremely variable cross-helicity states ($|\sigma_c| [0: 0.8]$), which, however, are not independent of the magnetic helicity content of the flux rope itself. The two normalized MHD invariants observed within the flux ropes tend indeed to distribute, neither trivially nor automatically, along the curve, thus suggesting that some constraint should exist between the magnetic and cross-helicity content of the structures. The analysis carried out has further showed that the flux rope properties are totally independent of their time duration and that they are detected either as a sort of interface between different portions of solar wind or as isolated structures embedded in the same stream.

WAVELET ANALYSIS AS A TOOL TO LOCALIZE MAGNETIC AND CROSS-HELICITY EVENTS IN THE SOLAR WIND

D. [Telloni](#)¹, R. Bruno², R. D'Amicis², E. Pietropaolo³, and V. Carbone

2012 ApJ 751 19

In this paper, we adopt the use of the wavelet transform as a new tool to investigate the time behavior at different scales of reduced magnetic helicity, cross-helicity, and residual energy in space plasmas. The main goal is a better characterization of the fluctuations in which interplanetary flux ropes are embedded. This kind of information is still missing in the present literature, and our tool can represent the basis for a new treatment of in situ measurements of this kind of event. There is a debate about the origins of small-scale flux ropes. It has been suggested that they are formed through magnetic reconnection in the solar wind, such as across the heliospheric current sheet. On the other hand, it has also been suggested that they are formed in the corona, similar to magnetic clouds. Thus, it looks like that there are two populations, one originating in the solar wind via magnetic reconnection across the current sheet in the inner heliosphere and the other originating in the corona. Small-scale flux ropes might be the remnants of the streamer belt blobs formed from disconnection; however, a one-to-one observation of a blob and a small-scale flux rope in the solar wind has yet to be found. Within this panorama of possibilities, this new technique appears to be very promising in investigating the origins of these objects advected by the solar wind.

The Dst Index Underestimates the Solar Cycle Variation of Geomagnetic Activity†

Michael [Temerin](#), Xinlin Li

JGR 2015

<http://onlinelibrary.wiley.com/doi/10.1002/2015JA021467/pdf>

It is known that the correction of the Kyoto Dst index for the secular variation of the Earth's internal field produces a discontinuity in the Kyoto Dst index at the end of each year. We show that this secular correction also introduces a significant baseline error to the Kyoto Dst index that leads to an underestimate of the solar cycle variation of geomagnetic activity and of the strength of the ring current as measured by the Kyoto Dst index. Thus the average value of the Kyoto Dst index would be approximately 13 nT more negative for the active year 2003 compared to quiet years 2006 and 2009 if the Kyoto Dst index properly measured the effects of the ring current and other currents that influence the Dst observatories. Discontinuities in the Kyoto Dst index at the end of each year have an average value of about 5 nT but the discontinuity at the end of year 2002 was approximately 12 nT and the discontinuity at the end of year 1982 may have been as large as 20 nT.

Dst model for 1995-2002

M. [Temerin](#), Xinlin Li

Journal of Geophysical Research, Volume 111, Issue A4, CiteID A04221, **2006**

The Dst index is predicted on the basis of the solar wind for the years 1995-2002 using an update of the previous Temerin and Li [2002] prediction model for Dst. The updated model is based on additional data from the years 2000-2002 corresponding to the maximum of the solar cycle and includes several large magnetic storms. For this 8-year period, the linear correlation between the model and the Dst index is 0.956, the prediction efficiency is 0.914, and the RMS error of the prediction is 6.65 nT (nanoTesla). An analysis of some of the error in the model indicates that at least 25% of the remaining error is due to the effect on the Dst index of a portion of the Sq ionospheric current system and that close to 99% of the variance of Dst index due to magnetospheric currents is predictable. An examination of 10-day intervals around the six largest magnetic storms for which there is good solar wind data shows prediction efficiencies between 0.93 and 0.98 and linear correlation coefficients between 0.96 and 0.99. It is suggested that the annual variation in the Dst index is mainly due to magnetopause and ring currents and the location of the magnetometer stations used to calculate the Dst index. The dependence of the model on the solar wind implies that magnetospheric activity depends on the solar wind approximately in proportion to the square root of the density, square of the velocity, and linearly with the interplanetary magnetic field (IMF). In addition, there is strong dependence on the direction of IMF such that magnetic activity depends approximately on the sixth power of the sine of half the IMF clock angle, where the IMF clock angle is angle of the IMF in the plane perpendicular to the solar wind velocity measured from the northward direction. The model has also strong dependence on the angle between the dipole axis and the solar wind velocity which explains, in part, the seasonal dependence of magnetospheric activity. Overall, the updated model further demonstrates that the large-scale currents that affect the Dst index are well controlled by solar wind variations.

A new model for the prediction of Dst on the basis of the solar wind

M. [Temerin](#), Xinlin Li

JOURNAL OF GEOPHYSICAL RESEARCH, VOL. 107, 1472, 8 PP., **2002**

An explicit model for predicting Dst based on solar wind data for the years 1995–1999 gives a good fit with a prediction efficiency of 88%, a linear correlation coefficient between the Dst index and the model of 0.94, and a RMS error of 6.4 nT. The same model applied to the first half of 2000 gave a prediction efficiency of 91%, a linear correlation coefficient of 0.95, and a RMS error of 7.9 nT. The modeled Dst is a sum of three terms that have growth and decay, a dynamic pressure term, an interplanetary magnetic field term, and some offset terms. The main innovations are that the decay terms have different time constants ranging from 5 days to 1 hour and that all the terms except the offsets depend on the angle of the Earth's dipole with respect to the solar wind velocity. This result shows that the magnetosphere is highly predictable and that chaotic behavior within the magnetosphere has little influence on the large-scale currents that determine Dst.

Dipole Tilt Effects on the Dst index

M. [Temerin](#), Xinlin Li

American Geophysical Union, Fall Meeting **2002**, abstract #SM22B-03

The Dst index shows a large variation with season with larger negative values occurring at the equinoxes. As is well known, larger magnetic storms occur more often near the equinoxes but the average baseline value of Dst also shows the same seasonal periodicity. We have been able to model Dst using the solar wind as an input. The modeled Dst index is sum of several driver terms with different decay constants and a pressure term. All terms have a significant equinoctial variation. The equinoctial terms were introduced into the model with arbitrary phases and best phase was found through minimizing the least square error. The phase agrees with and thus confirms the equinoctial effect. Much of the baseline seasonal variation in Dst is the result of the varying effect of the pressure term. The diurnal variation in Dst is substantially smaller than one would expect given the seasonal variation. This may be due to the removal of the diurnal variation from the Dst index. Some of the diurnal variation, which is mostly due to the Sq ionospheric current, is in fact due to magnetospheric currents and may also be removed in forming the Dst index. The removal of the Sq current system is not perfect and there is on average 9 nT peak-to-peak residual diurnal signal of varying phase remaining in the Dst index. The modeled Dst confirms the dominance of the equinoctial effect on the seasonal dependence of Dst index and thus on magnetospheric activity despite many minor inconsistencies in the behavior of the individual terms that make up the modeled Dst.

CME Propagation Through the Heliosphere: Status and Future of Observations and Model Development

Review

M. Temmer, C. Scolini, I. G. Richardson, S. G. Heinemann, +++

Advances in Space Research 2023

<https://arxiv.org/pdf/2308.04851.pdf>

The ISWAT clusters H1+H2 have a focus on interplanetary space and its characteristics, especially on the large-scale co-rotating and transient structures impacting Earth. SIRs, generated by the interaction between high-speed solar wind originating in large-scale open coronal magnetic fields and slower solar wind from closed magnetic fields, are regions of compressed plasma and magnetic field followed by high-speed streams that recur at the ca. 27 day solar rotation period. Short-term reconfigurations of the lower coronal magnetic field generate flare emissions and provide the energy to accelerate enormous amounts of magnetised plasma and particles in the form of CMEs into interplanetary space. The dynamic interplay between these phenomena changes the configuration of interplanetary space on various temporal and spatial scales which in turn influences the propagation of individual structures. While considerable efforts have been made to model the solar wind, we outline the limitations arising from the rather large uncertainties in parameters inferred from observations that make reliable predictions of the structures impacting Earth difficult. Moreover, the increased complexity of interplanetary space as solar activity rises in cycle 25 is likely to pose a challenge to these models. Combining observational and modeling expertise will extend our knowledge of the relationship between these different phenomena and the underlying physical processes, leading to improved models and scientific understanding and more-reliable space-weather forecasting. The current paper summarizes the efforts and progress achieved in recent years, identifies open questions, and gives an outlook for the next 5-10 years. It acts as basis for updating the existing COSPAR roadmap by Schrijver+ (2015), as well as providing a useful and practical guide for peer-users and the next generation of space weather scientists. **May 29th, 2013, November 8 th, 2018**

Evolution of sheath and leading edge structures of interplanetary coronal mass ejections in the inner heliosphere based on Helios and Parker Solar Probe observations

Manuela Temmer, Volker Bothmer

A&A 665, A70 2022

<https://arxiv.org/pdf/2202.04391.pdf>

<https://www.aanda.org/articles/aa/pdf/2022/09/aa43291-22.pdf>

Context: We investigate the evolution of the sheath and leading edge (LE) structure of interplanetary coronal mass ejections (ICMEs) as function of distance in the inner heliosphere. Results are related both to the magnetic ejecta (ME) and to the ambient solar wind (SW). Aims: From a sample of 40 well-observed Helios 1/2 events, we derive the average density separately for sheath, LE, and ME. The results are placed into comparison with the upstream SW to investigate at which distance the sheath is formed. Methods: We use plasma and magnetic field measurements from Helios 1/2 data in the distance range 0.3-1 au from the ICME list by Bothmer and Schwenn (1998). For comparison, we add a sample of four ICMEs observed with PSP in 2019-2021 covering 0.32-0.62 au. Results. At the distance of ~13 Rs, the CME sheath becomes denser than the ambient SW density. At ~38 Rs the sheath structure density starts to dominate over the density within the ME. The ME density falls below the ambient SW density at ~230 Rs. Besides the well-known expansion of the ME, the sheath size shows a weak positive correlation with distance, while the LE does not expand. We find a moderate anti-correlation between sheath density and local SW plasma speed upstream of the ICME shock. An empirical relation is derived connecting the ambient SW speed with sheath and LE density. Conclusions: The average starting distance for actual sheath formation is found to be located at ~13 Rs. The ME expansion changes strongly at ~38 Rs, leading to a density dominance of the sheath structure. The LE can be understood as a structure isolated from the ambient SW flow. The results allow for better interpretation of ICME evolution and possibly mass increase due to sheath enlargement. The empirical results between sheath and LE density and ambient SW speed can be used for more detailed modeling of ICME evolution in the inner heliosphere. **19 Jun 1980, 15 Mar 2019**

Deriving CME Density From Remote Sensing Data and Comparison to In-Situ Measurements

M. Temmer, L. Holzkecht, M. Dumbović, B. Vršnak, N. Sachdeva, S. G. Heinemann, K. Dissauer, C. Scolini, E. Asvestari, A. M. Veronig, S. J. Hofmeister

JGR Volume 126, Issue 1 January 2021 e2020JA028380

<https://doi.org/10.1029/2020JA028380>

<https://agupubs.onlinelibrary.wiley.com/doi/epdf/10.1029/2020JA028380>

https://indico.ict.inaf.it/event/794/contributions/9518/attachments/4858/9952/ESPM16_Temmer.pdf

We determine the three-dimensional geometry and deprojected mass of 29 well-observed coronal mass ejections (CMEs) and their interplanetary counterparts (ICMEs) using combined Solar Terrestrial Relations Observatory - Solar and Heliospheric Observatory white-light data. From the geometry parameters, we calculate the volume of the CME for the magnetic ejecta (flux-rope type geometry) and sheath structure (shell-like geometry resembling the (I)CME frontal rim). Working under the assumption that the CME mass is roughly equally distributed within a specific volume, we expand the CME self-similarly and calculate the CME density for distances close to the Sun (15–30 Rs) and at 1 AU. Specific trends are derived comparing calculated and in-situ measured proton densities at 1 AU, though large uncertainties are revealed due to the unknown mass and geometry evolution: (1) a moderate correlation for the magnetic structure having a mass that stays rather constant ($cc \approx 0.56 - 0.59$), and (2) a weak correlation for the sheath density ($cc \approx 0.26$) by assuming the sheath region is an extra mass—as expected for a mass pile-up process—that is in its amount comparable to the initial CME deprojected mass. High correlations are derived between in-situ measured sheath density and the solar wind density ($cc \approx -0.73$) and solar wind speed ($cc \approx 0.56$) as measured 24 h ahead of the arrival of the disturbance. This gives additional confirmation that the sheath-plasma indeed stems from piled-up solar wind material. While the CME interplanetary propagation speed is not related to the sheath density, the size of the CME may play some role in how much material could be piled up. **4 Aug 2011, 15-16 Mar 2012**

Table A1 Parameters of 29CMEs/ICMEs under study (2008-2014)

On Flare-CME Characteristics from Sun to Earth Combining Remote-Sensing Image Data with In Situ Measurements Supported by Modeling

Manuela **Temmer**, Julia K. Thalmann, Karin Dissauer, Astrid M. Veronig, Johannes Tschernitz, Jürgen Hinterreiter, Luciano Rodriguez

Solar Physics July 2017, 292:93

<https://link.springer.com/content/pdf/10.1007%2Fs11207-017-1112-5.pdf>

<https://arxiv.org/pdf/1703.00694.pdf>

We analyze the well-observed flare and coronal mass ejection (CME) from **1 October 2011** (SOL2011-10-01T09:18) covering the complete chain of effects – from Sun to Earth – to better understand the dynamic evolution of the CME and its embedded magnetic field. We study in detail the solar surface and atmosphere associated with the flare and CME using the Solar Dynamics Observatory (SDO) and ground-based instruments. We also track the CME signature off-limb with combined extreme ultraviolet (EUV) and white-light data from the Solar Terrestrial Relations Observatory (STEREO). By applying the graduated cylindrical shell (GCS) reconstruction method and total mass to stereoscopic STEREO-SOHO (Solar and Heliospheric Observatory) coronagraph data, we track the temporal and spatial evolution of the CME in the interplanetary space and derive its geometry and 3D mass. We combine the GCS and Lundquist model results to derive the axial flux and helicity of the magnetic cloud (MC) from in situ measurements from Wind. This is compared to nonlinear force-free (NLFF) model results, as well as to the reconnected magnetic flux derived from the flare ribbons (flare reconnection flux) and the magnetic flux encompassed by the associated dimming (dimming flux). We find that magnetic reconnection processes were already ongoing before the start of the impulsive flare phase, adding magnetic flux to the flux rope before its final eruption. The dimming flux increases by more than 25% after the end of the flare, indicating that magnetic flux is still added to the flux rope after eruption. Hence, the derived flare reconnection flux is most probably a lower limit for estimating the magnetic flux within the flux rope. We find that the magnetic helicity and axial magnetic flux are lower in the interplanetary space by $\sim 50\%$ and 75% , respectively, possibly indicating an erosion process. A CME mass increase of 10% is observed over a range of $\sim 4-20 R_{\odot}$. The temporal evolution of the CME-associated core-dimming regions supports the scenario that fast outflows might supply additional mass to the rear part of the CME.

Preconditioning of interplanetary space due to transient CME disturbances

Manuela **Temmer**, Martin A. Reiss, Ljubomir Nikolic, Stefan J. Hofmeister, Astrid M. Veronig
2017 ApJ 835 141

<https://arxiv.org/pdf/1612.06080v1.pdf>

Interplanetary space is characteristically structured mainly by high-speed solar wind streams emanating from coronal holes and transient disturbances such as coronal mass ejections (CMEs). While high-speed solar wind streams pose a continuous outflow, CMEs abruptly disrupt the rather steady structure causing large deviations from the quiet solar wind conditions. For the first time, we give a quantification of the duration of disturbed conditions (preconditioning) for interplanetary space caused by CMEs. To this aim, we investigate the plasma speed component of the solar wind and the impact of in situ detected CMEs (ICMEs), compared to different background solar wind models (ESWF, WSA, persistence model) for the time range 2011-2015. We quantify in terms of standard error measures the deviations between modeled background solar wind speed and observed solar wind speed. Using the mean absolute error, we

obtain an average deviation for quiet solar activity within a range of 75.1-83.1 km/s. Compared to this baseline level, periods within the ICME interval showed an increase of 18-32% above the expected background and the period of 2 days after the ICME displayed an increase of 9-24%. We obtain a total duration of enhanced deviations over about 3 and up to 6 days after the ICME start, which is much longer than the average duration of an ICME disturbance itself (~1.3 days), concluding that interplanetary space needs ~2-5 days to recover from the impact of ICMEs. The obtained results have strong implications for studying CME propagation behavior and also for space weather forecasting.

Kinematical properties of coronal mass ejections

Review

Manuela **Temmer**

Astronomische Nachrichten **2016 File**

<http://arxiv.org/pdf/1603.01398v1.pdf>

Coronal mass ejections (CMEs) are the most dynamic phenomena in our solar system. They abruptly disrupt the continuous outflow of solar wind by expelling huge clouds of magnetized plasma into interplanetary space with velocities enabling to cross the Sun-Earth distance within a few days. Earth-directed CMEs may cause severe geomagnetic storms when their embedded magnetic fields and the shocks ahead compress and reconnect with the Earth's magnetic field. The transit times and impacts in detail depend on the initial CME velocity, size, and mass, as well as on the conditions and coupling processes with the ambient solar wind flow in interplanetary space. The observed CME parameters may be severely affected by projection effects and the constant changing environmental conditions are hard to derive. This makes it difficult to fully understand the physics behind CME evolution, preventing to do a reliable forecast of Earth-directed events. This short review focusing on observational data, shows recent methods which were developed to derive the CME kinematical profile for the entire Sun-Earth distance range as well as studies which were performed to shed light on the physical processes that CMEs encounter when propagating from Sun to Earth.

23 July 2012

Interplanetary Propagation Behavior of the Fast Coronal Mass Ejection from 23 July 2012

Manuela **Temmer** and Nariaki Nitta

Solar Phys. Volume 290, [Issue 3](#), pp 919-932 **2015**

<http://arxiv.org/pdf/1411.6559v1.pdf> **File**

The fast coronal mass ejection (CME) from **23 July 2012** raised attention due to its extremely short transit time from Sun to 1 AU of less than 21 h. In-situ data from STEREO-A revealed the arrival of a fast forward shock with a speed of more than 2200 km s⁻¹ followed by a magnetic structure moving with almost 1900 km s⁻¹. We investigate the propagation behavior of the CME shock and magnetic structure with the aim to reproduce the short transit time and high impact speed as derived from in-situ data. We carefully measure the 3D kinematics of the CME using the graduated cylindrical shell model, and obtain a maximum speed of 2580±280 km s⁻¹ for the CME shock and of 2270±420 km s⁻¹ for its magnetic structure. Based on the 3D kinematics, the drag-based model (DBM) reproduces the observational data reasonably well. To successfully simulate the CME shock, we find that the ambient flow speed should be of average value close to the slow solar wind speed (450 km s⁻¹), and the initial shock speed at a distance of 30 Rs should not exceed ≈2300 km s⁻¹, otherwise it would arrive much too early at STEREO-A. The model results indicate that an extremely low aerodynamic drag force is exerted on the shock, smaller by one order of magnitude compared to the average. As a consequence, the CME hardly decelerates in interplanetary space and maintains its high initial speed. The low aerodynamic drag can only be reproduced when reducing the density of the ambient solar wind flow, in which the massive CME propagates, to $\rho_{sw}=1-2 \text{ cm}^{-3}$ at the distance of 1 AU. This result is consistent with the preconditioning of interplanetary space owing to a previous CME.

INFLUENCE OF THE AMBIENT SOLAR WIND FLOW ON THE PROPAGATION BEHAVIOR OF INTERPLANETARY CORONAL MASS EJECTIONS

Manuela **Temmer**¹, Tanja Rollett^{1,2}, Christian Möstl^{1,2}, Astrid M. Veronig¹, Bojan Vršnak³ and Dusan Odstrčil

2011 ApJ 743 101, File

We study three coronal mass ejection (CME)/interplanetary coronal mass ejection (ICME) events (**2008 June 1-6**, **2009 February 13-18**, and **2010 April 3-5**) tracked from Sun to 1 AU in remote-sensing observations of Solar Terrestrial Relations Observatory Heliospheric Imagers and in situ plasma and magnetic field measurements. We focus on the ICME propagation in interplanetary (IP) space that is governed by two forces: the propelling Lorentz force and the drag force. We address the question: which heliospheric distance range does the drag become dominant and the CME adjust

to the solar wind flow. To this end, we analyze speed differences between ICMEs and the ambient solar wind flow as a function of distance. The evolution of the ambient solar wind flow is derived from ENLIL three-dimensional MHD model runs using different solar wind models, namely, Wang-Sheeley-Arge and MHD-Around-A-Sphere. Comparing the measured CME kinematics with the solar wind models, we find that the CME speed becomes adjusted to the solar wind speed at very different heliospheric distances in the three events under study: from below $30 R_{\odot}$, to beyond 1 AU, depending on the CME and ambient solar wind characteristics. ENLIL can be used to derive important information about the overall structure of the background solar wind, providing more reliable results during times of low solar activity than during times of high solar activity. The results from this study enable us to obtain greater insight into the forces acting on CMEs over the IP space distance range, which is an important prerequisite for predicting their 1 AU transit times.

Evolution of Switchbacks in the Inner Heliosphere

Anna **Tenerani**¹, Nikos Sioulas², Lorenzo Matteini³, Olga Panasenco⁴, Chen Shi², and Marco Velli²
2021 ApJL 919 L31

<https://doi.org/10.3847/2041-8213/ac2606>

We analyze magnetic field data from the first six encounters of Parker Solar Probe, three Helios fast streams and two Ulysses south polar passes covering heliocentric distances $0.1 \lesssim R \lesssim 3$ au. We use this data set to statistically determine the evolution of switchbacks of different periods and amplitudes with distance from the Sun. We compare the radial evolution of magnetic field variances with that of the mean square amplitudes of switchbacks, and quantify the radial evolution of the cumulative counts of switchbacks per kilometer. We find that the amplitudes of switchbacks decrease faster than the overall turbulent fluctuations, in a way consistent with the radial decrease of the mean magnetic field. This could be the result of a saturation of amplitudes and may be a signature of decay processes of large amplitude Alfvénic fluctuations in the solar wind. We find that the evolution of switchback occurrence in the solar wind is scale dependent: the fraction of longer-duration switchbacks increases with radial distance, whereas it decreases for shorter switchbacks. This implies that switchback dynamics is a complex process involving both decay and in situ generation in the inner heliosphere. We confirm that switchbacks can be generated by the expansion, although other types of switchbacks generated closer to the Sun cannot be ruled out.

Magnetic field kinks and folds in the solar wind

Anna **Tenerani**, [Marco Velli](#), [Lorenzo Matteini](#), [Victor Réville](#), [Chen Shi](#), [Stuart D. Bale](#), [Justin Kasper](#), [J. W. Bonnell](#), [Anthony W. Case](#), [Thierry Dudok de Wit](#), [Keith Goetz](#), [Peter R. Harvey](#), [Kristopher G. Klein](#), [Kelly Korreck](#), [Davin Larson](#), [Roberto Livi](#), [Robert J. MacDowall](#), [David M. Malaspina](#), [Marc Pulupa](#), [Michael Stevens](#), [Phyllis Whittlesey](#)

ApJ PSP special issue **2020**

<https://arxiv.org/pdf/1912.03240.pdf>

Parker Solar Probe (PSP) observations during its **first encounter** at $35.7 R_{\odot}$ have shown the presence of magnetic field lines which are strongly perturbed to the point that they produce local inversions of the radial magnetic field, known as switchbacks. Their counterparts in the solar wind velocity field are local enhancements in the radial speed, or jets, displaying (in all components) the velocity-magnetic field correlation typical of large amplitude Alfvén waves propagating away from the Sun. Switchbacks and radial jets have previously been observed over a wide range of heliocentric distances by Helios, WIND and Ulysses, although they were prevalent in significantly faster streams than seen at PSP. Here we study via numerical MHD simulations the evolution of such large amplitude Alfvénic fluctuations by including, in agreement with observations, both a radial magnetic field inversion and an initially constant total magnetic pressure. Despite the extremely large excursion of magnetic and velocity fields, switchbacks are seen to persist for up to hundreds of Alfvén crossing times before eventually decaying due to the parametric decay instability. Our results suggest that such switchback/jet configurations might indeed originate in the lower corona and survive out to PSP distances, provided the background solar wind is sufficiently calm, in the sense of not being pervaded by strong density fluctuations or other gradients, such as stream or magnetic field shears, that might destabilize or destroy them over shorter timescales.

INWARD MOTIONS IN THE OUTER SOLAR CORONA BETWEEN 7 AND 12 R_{\odot} : EVIDENCE FOR WAVES OR MAGNETIC RECONNECTION JETS?

Anna **Tenerani**¹, Marco Velli¹, and Craig DeForest

2016 ApJ 825 L3

DeForest et al. used synoptic visible-light image sequences from the COR2 coronagraph on board the STEREO-A spacecraft to identify inbound wave motions in the outer corona beyond 7 solar radii and inferred, from the observation,

that the Alfvén surface separating the magnetically dominated corona from the flow dominated wind must be located beyond at least 12 solar radii from the Sun over polar coronal holes and beyond 15 solar radii in the streamer belt. Here, we attempt identification of the observed inward signal by theoretically reconstructing height-speed diagrams and comparing them to the observed profiles. Interpretation in terms of Alfvén waves or Alfvénic turbulence appears to be ruled out by the fact that the observed signal shows a deceleration of inward motion when approaching the Sun. Fast magnetoacoustic waves are not directly ruled out in this way, as it is possible for inward waves observed in quadrature, but not propagating exactly radially, to suffer total reflection as the Alfvén speed rises close to the Sun. However, the reconstructed signal in the height-speed diagram has the wrong concavity. A final possibility is decelerating reconnection jets, most probably from component reconnection, in the accelerating wind: the profile in this case appears to match the observations very well. This interpretation does not alter the conclusion that the Alfvén surface must be at least 12 solar radii from the photosphere. Further observations should help constrain this process, never identified previously in this way, in the distance range from 7 to 12 solar radii.

Unexpected major geomagnetic storm caused by faint eruption of a solar trans-equatorial flux rope

Teng, WL (Teng, Weilin) ; **Su, YN** (Su, Yingna) ; **Ji, HS** (Ji, Haisheng) ; **Zhang, QM** (Zhang, Qingmin)
Nature Communication Volume 15 Issue 1 Article Number 9198 **2024**
DOI 10.1038/s41467-024-53538-1

Some geomagnetic storms' solar origins are ambiguous, making them hard to predict. On **March 23, 2023**, a severe geomagnetic storm occurred, however, forecasts based on remote-sensing observations failed to predict it. Here, we show clear evidence that this storm originates from the eruption of a trans-equatorial, longitudinal and low-density magnetic flux rope (FR) with weaker coronal emission and no chromospheric signs. The FR's gentle eruption results in a faint full-halo coronal mass ejection (CME), which is missed by forecasters and not included in CME catalogs. Combining magnetic field modeling and in-situ measurements, we reveal the FR's southward axial magnetic field as the main cause of the geomagnetic storm. This CME is the stealthiest one reported causing a severe geomagnetic storm. Our study highlights that erupting trans-equatorial FRs can generate major geomagnetic storms in a stealthy way. Characteristic observational signatures of similar eruptions are proposed to help in future forecasts. Geomagnetic storms are common, and a strong one occurred on **23 March 2023**. Here, the authors show that it was due to a stealthy solar coronal mass ejection originated from the faint eruption of a trans-equatorial magnetic flux rope.

Studying the Temporal Variation of the Cosmic-Ray Sun Shadow Using IceCube Data

Frederik **Tenholt**, [Julia Becker Tjus](#), [Paolo Desiati](#) (for the IceCube Collaboration)
the 36th International Cosmic Ray Conference (ICRC 2019). See [arXiv:1907.11699](#) for all IceCube contributions **2019**
<https://arxiv.org/pdf/1908.10148.pdf>

The shadowing effect of the Moon and Sun in TeV cosmic rays has been measured with high statistical significance by several experiments. Unlike particles from directions close to the Moon, however, charged particles passing by the neighborhood of the Sun are affected not only by the geomagnetic but also by the solar near- and interplanetary-magnetic field. Since the latter undergoes a well-known 11-year cycle -- during which it can become highly disordered -- the cosmic-ray shadow cast by the Sun as observed on Earth is expected to change over time. We present an update of the analysis of the cosmic-ray Moon and Sun shadows using data taken with the IceCube Neutrino Observatory. With a median energy after quality cuts of approximately 50–60 TeV, depending on the cosmic-ray flux model used, primary cosmic rays inducing events which pass IceCube's Sun shadow filter have a comparatively high energy. While the results for the Moon shadow confirm the stability of the IceCube observatory, the results for the Sun shadow exhibit a clear variation correlating with solar activity and theoretical models of the solar magnetic field.

The Cosmic-Ray Shadow and Coronal Magnetism

Frederik **Tenholt**
RHESI Nuggets #351 May 2019
http://sprg.ssl.berkeley.edu/~tohban/wiki/index.php/The_Cosmic-Ray_Shadow_and_Coronal_Magnetism

The cosmic-ray shadow of the Sun as measured by several experiments is a relatively new, but powerful diagnostic tool for evaluating different models of the coronal magnetic field close to the Sun. An energy-dependent measurement of the shadow even further enhances the possibilities for quantitative studies.

Tracking magnetic flux and helicity from Sun to Earth -- Multi-spacecraft analysis of a magnetic cloud and its solar source

J. K. **Thalmann**, [M. Dumbovic](#), [K. Dissauer](#), [T. Podladchikova](#), [G. Chikunova](#), [M. Temmer](#), [E. Dickson](#), [A. M. Veronig](#)

A&A 669, A72 (2023)

<https://arxiv.org/pdf/2210.02228.pdf>

<https://www.aanda.org/articles/aa/pdf/2023/01/aa44248-22.pdf>

We analyze the complete chain of effects caused by a solar eruptive event in order to better understand the dynamic evolution of magnetic-field related quantities in interplanetary space, in particular that of magnetic flux and helicity. We study a series of connected events (a confined C4.5 flare, a flare-less filament eruption and a double-peak M-class flare) that originated in NOAA active region (AR) 12891 on **2021 November 1 and November 2**. We deduce the magnetic structure of AR 12891 using stereoscopy and nonlinear force-free (NLFF) magnetic field modeling, allowing us to identify a coronal flux rope and to estimate its axial flux and helicity. Additionally, we compute reconnection fluxes based on flare ribbon and coronal dimming signatures from remote sensing imagery. Comparison to corresponding quantities of the associated magnetic cloud (MC), deduced from in-situ measurements from Solar Orbiter and near-Earth spacecraft, allows us to draw conclusions on the evolution of the associated interplanetary coronal mass ejection (ICME). The latter are aided through the application of geometric fitting techniques (graduated cylindrical shell modeling; GCS) and interplanetary propagation models (drag based ensemble modeling; DBEM) to the ICME. NLFF modeling suggests the host AR's magnetic structure in the form of a left-handed (negative-helicity) sheared arcade/flux rope reaching to altitudes of 8-10 Mm above photospheric levels, in close agreement with the corresponding stereoscopic estimate. Revealed from GCS and DBEM modeling, the ejected flux rope propagated in a self-similar expanding manner through interplanetary space. Comparison of magnetic fluxes and helicities processed by magnetic reconnection in the solar source region and the respective budgets of the MC indicate a considerable contribution from the eruptive process, though the pre-eruptive budgets appear of relevance too.

The Impact of a Stealth CME on the Martian Topside Ionosphere

Smitha V. **Thampi**, [C. Krishnaprasad](#), [Govind G. Nampoothiri](#), [Tarun K. Pant](#)

MNRAS Volume 503, Issue 1, Pages 625–632, 2021

<https://arxiv.org/pdf/2102.09304.pdf>

<https://doi.org/10.1093/mnras/stab494>

Solar cycle 24 is one of the weakest solar cycles recorded, but surprisingly the declining phase of it had a slow CME which evolved without any low coronal signature and is classified as a stealth CME which was responsible for an intense geomagnetic storm at Earth ($Dst = -176$ nT). The impact of this space weather event on the terrestrial ionosphere has been reported. However, the propagation of this CME beyond 1 au and the impact of this CME on other planetary environments have not been studied so far. In this paper, we analyse the data from Sun-Earth L1 point as well as from the Martian orbit (near 1.5 au) to understand the characteristics of the stealth CME as observed beyond 1 au. The observations near Earth are using data from the Solar Dynamics Observatory (SDO) and the Advanced Composition Explorer (ACE) satellite located at L1 point whereas those near Mars are from the instruments for plasma and magnetic field measurements on board Mars Atmosphere and Volatile Evolution (MAVEN) mission. The observations show that the stealth CME has reached 1.5 au after 7 days of its initial observations at the Sun and caused depletion in the nightside topside ionosphere of Mars, as observed during the inbound phase measurements of the Langmuir Probe and Waves (LPW) instrument on board MAVEN. These observations have implications on the ion escape rates from the Martian upper atmosphere. **2018-08-20-28**

Near-Earth Cosmic Ray Decreases Associated with Remote Coronal Mass Ejections

S. R. **Thomas**^{1,2}, M. J. Owens², M. Lockwood², L. Barnard², and C. J. Scott

2015 ApJ 801 5

Galactic cosmic ray (GCR) flux is modulated by both particle drift patterns and solar wind structures on a range of timescales. Over solar cycles, GCR flux varies as a function of the total open solar magnetic flux and the latitudinal extent of the heliospheric current sheet. Over hours, drops of a few percent in near-Earth GCR flux (Forbush decreases, FDs) are well known to be associated with the near-Earth passage of solar wind structures resulting from corotating interaction regions (CIRs) and transient coronal mass ejections (CMEs). *We report on four FDs seen at ground-based*

neutron monitors which cannot be immediately associated with significant structures in the local solar wind. Similarly, there are significant near-Earth structures which do not produce any corresponding GCR variation. Three of the FDs are during the STEREO era, enabling in situ and remote observations from three well-separated heliospheric locations. Extremely large CMEs passed the STEREO-A spacecraft, which was behind the West limb of the Sun, approximately 2-3 days before each near-Earth FD. Solar wind simulations suggest that the CMEs combined with pre-existing CIRs, enhancing the pre-existing barriers to GCR propagation. Thus these observations provide strong evidence for the modulation of GCR flux by remote solar wind structures.

Galactic Cosmic Ray Modulation near the Heliospheric Current Sheet

S. R. [Thomas](#), M. J. Owens, M. Lockwood, C. J. Scott
Solar Phys., 2014

Galactic cosmic rays (GCRs) are modulated by the heliospheric magnetic field (HMF) both over decadal time scales (due to long-term, global HMF variations), and over time scales of a few hours (associated with solar wind structures such as coronal mass ejections or the heliospheric current sheet, HCS). Due to the close association between the HCS, the streamer belt, and the band of slow solar wind, HCS crossings are often associated with corotating interaction regions where fast solar wind catches up and compresses slow solar wind ahead of it. However, not all HCS crossings are associated with strong compressions. In this study we categorize HCS crossings in two ways: Firstly, using the change in magnetic polarity, as either away-to-toward (AT) or toward-to-away (TA) magnetic field directions relative to the Sun and, secondly, using the strength of the associated solar wind compression, determined from the observed plasma density enhancement. For each category, we use superposed epoch analyses to show differences in both solar wind parameters and GCR flux inferred from neutron monitors. For strong-compression HCS crossings, we observe a peak in neutron counts preceding the HCS crossing, followed by a large drop after the crossing, attributable to the so-called 'snow-plough' effect. For weak-compression HCS crossings, where magnetic field polarity effects are more readily observable, we instead observe that the neutron counts have a tendency to peak in the away magnetic field sector. By splitting the data by the dominant polarity at each solar polar region, we find that the increase in GCR flux prior to the HCS crossing is primarily from strong compressions in cycles with negative north polar fields due to GCR drift effects. Finally, we report on unexpected differences in GCR behavior between TA weak compressions during opposing polarity cycles.

Current STEREO Status on the Far Side of the Sun

[Thompson](#), William T.; [Gurman](#), Joseph; [Ossing](#), Daniel; [Luhmann](#), Janet; [Curtis](#), David; [Schroeder](#), Peter; [Mewaldt](#), Richard; [Davis](#), Andrew; [Wortman](#), Kristin; [Russell](#), Christopher; [Galvin](#), Antoinette; [Kistler](#), Lynn; [Ellis](#), Lorna; [Howard](#), Russell; [Vourlidis](#), Angelos; [Rich](#), Nathan; [Hutting](#), Lynn; [Maksimovic](#), Milan; [Bale](#), Stuart D.; [Goetz](#), Keith

Joint American Astronomical Society/American Geophysical Union Triennial Earth-Sun Summit, meeting #1, #402.05, 04/2015

The current positions of the two STEREO spacecraft on the opposite side of the Sun from Earth (superior solar conjunction) has forced some significant changes in the spacecraft and instrument operations. No communications are possible when the spacecraft is within 2 degrees of the Sun, requiring that the spacecraft be put into safe mode until communications can be restored. Unfortunately, communications were lost with the STEREO Behind spacecraft on October 1, 2014, during testing for superior solar conjunction operations. We will discuss what is known about the causes of loss of contact, the steps being taken to try to recover the Behind spacecraft, and what has been done to prevent a similar occurrence on STEREO Ahead. We will also discuss the effect of being on the far side of the Sun on the science operations of STEREO Ahead. Starting on August 20, 2014, the telemetry rate from the STEREO Ahead spacecraft has been tremendously reduced due to the need to keep the temperature of the feed horn on the high gain antenna below acceptable limits. However, the amount of telemetry that can be brought down has been highly reduced. Even so, significant science is still possible from STEREO's unique position on the solar far side. We will discuss the science and space weather products that are, or will be, available from each STEREO instrument, when those products will be available, and how they will be used. Some data, including the regular space weather beacon products, are brought down for an average of a few hours each day during the daily real-time passes, while the in situ and radio beacon data are being stored on the onboard recorder to provide a continuous 24-hour coverage for eventual downlink once the spacecraft is back to normal operations.

Quantifying extreme behavior in geomagnetic activity

[Thomson](#), Alan W. P.; [Dawson](#), Ewan B.; [Reay](#), Sarah J.

Space Weather, Vol. 9, No. 10, S10001, 2011

<http://dx.doi.org/10.1029/2011SW000696>

Understanding the extremes in geomagnetic activity is an important component in understanding just how severe conditions can become in the terrestrial space environment. Extreme activity also has consequences for technological systems. On the ground, extreme geomagnetic behavior has an impact on navigation and position accuracy and the operation of power grids and pipeline networks. We therefore use a number of decades of one-minute mean magnetic data from magnetic observatories in Europe, together with the technique of extreme value statistics, to provide a preliminary exploration of the extremes in magnetic field variations and their one-minute rates of change. These extremes are expressed in terms of the variations that might be observed every 100 and 200 years in the horizontal strength and in the declination of the field. We find that both measured and extrapolated extreme values generally increase with geomagnetic latitude (as might be expected), though there is a marked maximum in estimated extreme levels between about 53 and 62 degrees north. At typical midlatitude European observatories (55–60 degrees geomagnetic latitude), compass variations may reach approximately 3–8 degrees/minute, and horizontal field changes may reach 1000–4000 nT/minute, in one magnetic storm once every 100 years. For storm return periods of 200 years the equivalent figures are 4–11 degrees/minute and 1000–6000 nT/minute.

A Snapshot of the Sun Near Solar Minimum: The Whole Heliosphere Interval Review

Barbara J. **Thompson** Sarah E. Gibson Peter C. Schroeder David F. Webb Show all 25 authors

Solar Phys (2011) 274:29–56

https://www.researchgate.net/publication/226068880_A_Snapshot_of_the_Sun_Near_Solar_Minimum_The_Whole_Heliosphere_Interval

We present an overview of the data and models collected for the Whole Heliosphere Interval, an international campaign to study the three-dimensional solar–heliospheric–planetary connected system near solar minimum. The data and models correspond to solar Carrington Rotation 2068 (20March – 16April 2008) extending from below the solar photosphere, through interplanetary space, and down to Earth’s mesosphere. Nearly 200 people participated in aspects of WHI studies, analyzing and interpreting data from nearly 100 instruments and models in order to elucidate the physics of fundamental heliophysical processes. The solar and inner heliospheric data showed structure consistent with the declining phase of the solar cycle. A closely spaced cluster of low-latitude active regions was responsible for an increased level of magnetic activity, while a highly warped current sheet dominated heliospheric structure. The geospace data revealed an unusually high level of activity, driven primarily by the periodic impingement of high-speed streams. The WHI studies traced the solar activity and structure into the heliosphere and geospace, and provided new insight into the nature of the interconnected heliophysical system near solar minimum.

SOHO/EIT observations of an Earth-directed coronal mass ejection on May 12, 1997.

Thompson, B.J., Plunkett, S.P., Gurman, J.B., Newmark, J.S., St. Cyr, O.C., Michels, D.J., Delaboudini`ere, J.P.,

1998. Geophys. Res. Lett. 25, 2461–2464.

Upflows in the upper solar atmosphere

Review

[Hui Tian](#), [Louise Harra](#), [Deborah Baker](#), [David H. Brooks](#), [Lidong Xia](#)

Solar Phys. 2021

<https://arxiv.org/pdf/2102.02429.pdf>

Spectroscopic observations at extreme and far ultraviolet wavelengths have revealed systematic upflows in the solar transition region and corona. These upflows are best seen in the network structures of the quiet Sun and coronal holes, boundaries of active regions, and dimming regions associated with coronal mass ejections. They have been intensively studied in the past two decades because they are highly likely to be closely related to the formation of the solar wind and heating of the upper solar atmosphere. We present an overview of the characteristics of these upflows, introduce their possible formation mechanisms, and discuss their potential roles in the mass and energy transport in the solar atmosphere. Though past investigations have greatly improved our understanding of these upflows, they have left us with several outstanding questions and unresolved issues that should be addressed in the future. New observations from the Solar Orbiter mission, the Daniel K. Inouye Solar Telescope and the Parker Solar Probe will likely provide critical information to advance our understanding of the generation, propagation and energization of these upflows.

3.4. Connection to the solar wind

4. Upflows from CME-induced dimming

The impact of solar wind variability on pulsar timing

C. **Tiburzi**¹, G. M. Shaifullah^{1,2}, C. G. Bassa¹, P. Zucca¹, J. P. W. Verbiest^{3,4}, N. K. Porayko⁴, E. van der Wateren^{1,5}, R. A. Fallows¹, R. A. Main⁴, G. H. Janssen^{1,5}, J. M. Anderson^{6,7}, A.-S. Bak Nielsen^{4,3}, J. Y. Donner^{4,3}, E. F. Keane⁸, J. Künsemöller³, S. Osłowski^{9,10}, J.-M. Grießmeier^{11,12}, M. Serylak^{13,14}, M. Brügggen¹⁵, B. Ciardi¹⁶, R.-J. Dettmar¹⁷, M. Hoeft¹⁸, M. Kramer^{4,19}, G. Mann²⁰ and C. Vocks²⁰
A&A 647, A84 (2021)

<https://doi.org/10.1051/0004-6361/202039846>

<https://www.aanda.org/articles/aa/pdf/2021/03/aa39846-20.pdf>

Context. High-precision pulsar timing requires accurate corrections for dispersive delays of radio waves, parametrized by the dispersion measure (DM), particularly if these delays are variable in time. In a previous paper, we studied the solar wind (SW) models used in pulsar timing to mitigate the excess of DM that is annually induced by the SW and found these to be insufficient for high-precision pulsar timing. Here we analyze additional pulsar datasets to further investigate which aspects of the SW models currently used in pulsar timing can be readily improved, and at what levels of timing precision SW mitigation is possible.

Aims. Our goals are to verify: (a) whether the data are better described by a spherical model of the SW with a time-variable amplitude, rather than a time-invariant one as suggested in literature, and (b) whether a temporal trend of such a model's amplitudes can be detected.

Methods. We use the pulsar timing technique on low-frequency pulsar observations to estimate the DM and quantify how this value changes as the Earth moves around the Sun. Specifically, we monitor the DM in weekly to monthly observations of 14 pulsars taken with parts of the LOw-Frequency ARray (LOFAR) across time spans of up to 6 years. We develop an informed algorithm to separate the interstellar variations in the DM from those caused by the SW and demonstrate the functionality of this algorithm with extensive simulations. Assuming a spherically symmetric model for the SW density, we derive the amplitude of this model for each year of observations.

Results. We show that a spherical model with a time-variable amplitude models the observations better than a spherical model with a constant amplitude, but that both approaches leave significant SW-induced delays uncorrected in a number of pulsars in the sample. The amplitude of the spherical model is found to be variable in time, as opposed to what has been previously suggested.

Parker Solar Probe Observations of Near-fCe Harmonic Emissions in the Near-Sun Solar Wind and Their Dependence on the Magnetic Field Direction

Sabrina F. **Tigik**¹, Andris Vaivads¹, David M. Malaspina^{2,3}, and Stuart D. Bale^{4,5}

2022 ApJ 936 7

<https://iopscience.iop.org/article/10.3847/1538-4357/ac8473/pdf>

Wave emissions at frequencies near electron gyrofrequency harmonics are observed at small heliocentric distances below about $40 R_{\odot}$ and are known to occur in regions with quiescent magnetic fields. We show the close connection of these waves to the large-scale properties of the magnetic field. Near electron gyrofrequency harmonic emissions occur only when the ambient magnetic field points to a narrow range of directions bounded by polar and azimuthal angular ranges in the RTN coordinate system of correspondingly $80^{\circ} \lesssim \theta_B \lesssim 100^{\circ}$ and $10^{\circ} \lesssim \phi_B \lesssim 30^{\circ}$. We show that the amplitudes of wave emissions are highest when both angles are close to the center of their respective angular interval favorable to wave emissions. The intensity of wave emissions correlates with the magnetic field angular changes at both large and small timescales. Wave emissions intervals correlate with intervals of decreases in the amplitudes of broadband magnetic fluctuations at low frequencies of 10–100 Hz. We discuss possible generation mechanisms of the waves.

Solar Wind Reconnection Exhausts in the Inner Heliosphere Observed by Helios and Detected via Machine Learning

H. **Tilquin**¹, J. P. Eastwood¹, and T. D. Phan²

2020 ApJ 895 68

<https://doi.org/10.3847/1538-4357/ab8812>

Reconnecting current sheets in the solar wind play an important role in the dynamics of the heliosphere and offer an opportunity to study magnetic reconnection exhausts under a wide variety of inflow and magnetic shear conditions. However, progress in understanding reconnection can be frustrated by the difficulty of finding events in long time-series data. Here we describe a new method to detect magnetic reconnection events in the solar wind based on machine learning, and apply it to Helios data in the inner heliosphere. The method searches for known solar wind reconnection exhaust features, and parameters in the algorithm are optimized to maximize the Matthews Correlation Coefficient using a training set of events and non-events. Applied to the whole Helios data set, the trained algorithm generated a candidate set of events that were subsequently verified by hand, resulting in a database of 88 events. This approach offers a

significant reduction in construction time for event databases compared to purely manual approaches. The database contains events covering a range of heliospheric distances from ~0.3 to ~1 au, and a wide variety of magnetic shear angles, but is limited by the relatively coarse time resolution of the Helios data. Analysis of these events suggests that proton heating by reconnection in the inner heliosphere depends on the available magnetic energy in a manner consistent with observations in other regimes such as at the Earth's magnetopause, suggesting this may be a universal feature of reconnection.

The Anemomilos prediction methodology for Dst

W. K. **Tobiska**^{1,*}, D. Knipp^{1,2,3}, W. J. Burke¹, D. Bouwer¹, J. Bailey¹, D. Odstrcil¹, M. P. Hagan¹, J. Gannon⁴, B. R. Bowman

Space Weather, Volume 11, Issue 9, pages 490–508, September 2013

This paper describes new capabilities for operational geomagnetic Disturbance storm time (Dst) index forecasts. We present a data-driven, deterministic algorithm called Anemomilos for forecasting Dst out to a maximum of 6 days for large, medium, and small storms, depending upon transit time to the Earth. This capability is used for operational satellite management and debris avoidance in Low Earth Orbit (LEO). Anemomilos has a 15 min cadence, 1 h time granularity, 144 h prediction window (+6 days), and up to 1 h latency. A new finding is that nearly all flare events above a certain irradiance threshold, occurring within a defined solar longitude/latitude region and having sufficient estimated liftoff velocity of ejected material, will produce a geoeffective Dst perturbation. Three solar observables are used for operational Dst forecasting: flare magnitude, integrated flare irradiance through time, and event location. Magnitude is a proxy for ejecta quantity or mass and, combined with speed derived from the integrated flare irradiance, represents the kinetic energy. Speed is estimated as the line-of-sight velocity for events within 45° radial of solar disk center. Storms resulting from high-speed streams emanating from coronal holes are not modeled or predicted. A new result is that solar disk, not limb, observable features are used for predictive techniques. Comparisons between Anemomilos predicted and measured Dst for every hour over 25 months in three continuous time frames between 2001 (high solar activity), 2005 (low solar activity), and 2012 (rising solar activity) are shown. The Anemomilos operational algorithm was developed for a specific customer use related to thermospheric mass density forecasting. It is an operational space weather technology breakthrough using solar disk observables to predict geomagnetically effective Dst up to several days at 1 h time granularity. Real-time forecasts are presented at http://sol.spacenvironment.net/~sam_ops/index.html?

East–West Asymmetry in Interplanetary-Scintillation-Level Variation Associated with Solar-Wind Disturbances

Munetoshi **Tokumaru**, Miho Nagai, Kazumasa Iwai

Solar Phys. 298, Article number: 127 (2023)

<https://doi.org/10.1007/s11207-023-02220-8>

Interplanetary-scintillation (IPS) observations provide useful information on large-scale solar-wind disturbances, such as interplanetary coronal mass ejections (ICMEs) and stream interaction regions (SIRs), which impact the Earth and drive space weather. In the present study, we derived the $\langle \delta I^2 \rangle_{\text{ave}}$ -index, which represents daily variations in the density-fluctuation level of the inner heliosphere, based on IPS observations at the Institute for Space-Earth Environmental Research of Nagoya University between 1997 and 2019, and investigated the response of $\langle \delta I^2 \rangle_{\text{ave}}$ to ICME and SIR events. A clear difference was observed in the temporal profile of $\langle \delta I^2 \rangle_{\text{ave}}$ obtained from the superposed-epoch analysis between ICME and SIR events. The $\langle \delta I^2 \rangle_{\text{ave}}$ -values for the east and west sides of the sky plane for ICME events increased simultaneously and peaked at the ICME start time, which is consistent with the analysis of ICMEs directed toward the Earth. In contrast, the analysis of SIR events showed an asymmetric response between eastern and western $\langle \delta I^2 \rangle_{\text{ave}}$, with a distinct increase in $\langle \delta I^2 \rangle_{\text{ave}}$ observed on the west side after the SIR start time and higher $\langle \delta I^2 \rangle_{\text{ave}}$ -values observed on the east side before the start time. These findings were explained by the effect of the spiral-shaped structure of the SIR. Significant positive correlations were found between $\langle \delta I^2 \rangle_{\text{ave}}$ and solar-wind density and speed, which also showed east–west asymmetry. These phenomena were ascribed to the effect of SIR events, while the occurrence of peak correlations between $\langle \delta I^2 \rangle_{\text{ave}}$ and density at zero delay time for Cycle 23 was ascribed to the effect of ICMEs. The difference in correlations between Cycles 23 and 24 was ascribed to the weakening of activity in Cycle 24. The occurrence of a correlation peak for a positive delay time suggests that eastern and western $\langle \delta I^2 \rangle_{\text{ave}}$ data are useful for predicting the arrival of the solar wind with increased density and speed, respectively, although the correlation magnitudes were weak.

Interplanetary Scintillation Observations of Solar-Wind Disturbances During Cycles 23 and 24

[Munetoshi Tokumaru](#), [Ken'ichi Fujiki](#) & [Kazumasa Iwai](#)

[Solar Physics](#) volume 298, Article number: 22 (2023)

<https://doi.org/10.1007/s11207-023-02116-7>

Interplanetary scintillation (IPS) analysis is an effective technique for remotely sensing solar-wind disturbances, such as stream-interaction regions (SIRs) and coronal mass ejections (CMEs), which are the main drivers of space weather. Here, we employed 327-MHz IPS observations conducted at the Institute of Space–Earth Environmental Research, Nagoya University for the period of 1997 – 2019 to determine IPS indices that represent the density-fluctuation level of the inner heliosphere. We then compared these indices with the solar-wind density and speed measured near the Earth. Consequently, we found weak but significant positive correlations between the IPS indices and both the solar-wind density and speed gradient at a time lag of 0 days. This suggests that an increase in IPS indices corresponds to the arrival of the compression region associated with SIR or CME at the Earth, which is consistent with model calculations. Significant negative correlations were observed between the IPS and disturbance storm time (Dst) indices at a time lag of a few days; however, the correlations were too weak to enable reliable predictions of space weather. Possible reasons for these weak correlations are also discussed. Using the IPS indices, we determined the solar-cycle variation in the occurrence rate of solar-wind disturbances for the analysis period. The occurrence rates exhibited two maxima corresponding to the solar maximum and minimum, which are generally consistent with the combined effects of CME and SIR. The lower occurrence rates in Cycle 24 than in Cycle 23 reflect a weaker solar activity. These results suggest that the proposed IPS indices are useful for studying the long-term characteristics of solar-wind disturbances.

Correction [Solar Physics](#) volume 298, Article number: 79 (2023)

<https://link.springer.com/content/pdf/10.1007/s11207-023-02182-x.pdf>

Global Distribution of the Solar Wind Speed Reconstructed from Improved Tomographic Analysis of Interplanetary Scintillation Observations between 1985 and 2019

Munetoshi **Tokumaru**¹, Ken'ichi Fujiki¹, Masayoshi Kojima¹, and Kazumasa Iwai¹

2021 ApJ 922 73

<https://doi.org/10.3847/1538-4357/ac1862>

Computer-assisted tomography (CAT) for interplanetary scintillation (IPS) observations enables the determination of the global distribution of solar wind speed. We compared solar wind speeds derived from the CAT analysis of IPS observations between 1985 and 2019 with in situ observations conducted by the near-Earth and Ulysses spacecraft. From this comparison, we found that solar wind speeds from the IPS observations for 2009–2019 were systematically higher than the in situ observations, whereas those for the period until 2008 were in good agreement with the in situ observations. Further, we found that the discrepancy between IPS and the in situ observations is improved by changing the power index of the empirical relation between the solar wind speed and density fluctuations. The CAT analysis using an optimal value for the power index determined from the comparison between IPS and in situ observations revealed long-term variations in the solar wind speed distribution over three cycles, leading to a better understanding of the time-varying global heliosphere. We found that polar solar winds become highly anisotropic at the Cycle 24/25 minimum, which is a peculiar aspect of this minimum. The IPS observations showed general agreement with the Parker Solar Probe observations around the perihelion of Orbit 1; this supports the reliability of the CAT analysis. The results of this study suggest that the physical properties of solar wind microturbulence may vary with a long-term decline in the solar activity, which provides important implication on the solar wind acceleration.

Coordinated Interplanetary Scintillation Observations in Japan and Russia for Coronal Mass Ejection Events in Early September 2017

Munetoshi **Tokumaru**, Ken'ichi Fujiki, Kazumasa Iwai, Sergey Tyul'bashev, Igor Chashei

[Solar Physics](#) July 2019, 294:87

<https://link.springer.com/content/pdf/10.1007%2Fs11207-019-1487-6.pdf>

Interplanetary (IP) shocks traveling between the Sun and the Earth's orbit were clearly detected in interplanetary scintillation (IPS) observations made at Toyokawa (Japan) and Pushchino (Russia), in association with two halo coronal mass ejections (CMEs) that occurred on 04 and 06 September 2017. Since the observation times at Toyokawa and Pushchino differ by about six hours, a combined analysis of the IPS data obtained at these sites enabled high-cadence tracking of the IP shock for one of the CME events. The plane-of-sky locations where the IP disturbances were observed at Toyokawa were generally consistent with those at Pushchino. The propagation speeds of IP shocks inferred from IPS observations were higher than the average speeds derived from the occurrence time of IP shocks at Earth. This difference was ascribed to the deceleration of the CME-driven shocks during propagation. The east–west asymmetry of the propagation speed of IP shocks was also revealed from IPS observations. Solar-wind disturbances moving at a speed significantly slower than the average speed of the IP shock were identified from the IPS observations of the 06 September 2017 halo CME event. A wide longitudinal extent of these slow disturbances was suggested by the fact they

were observed not only west but also east of the Sun; i.e. the opposite side to the flare/CME site. The origin of the slow disturbances is considered to represent either wing portions of the highly warped IP shock or the post-shock dense materials.

Relation Between Coronal Hole Areas and Solar Wind Speeds Derived from Interplanetary Scintillation Measurements

Munetoshi **Tokumar**, Daiki Satonaka, Ken'ichi Fujiki, Keiji Hayashi, Kazuyuki Hakamada

Solar Physics March 2017, 292:41

<http://link.springer.com/article/10.1007/s11207-017-1066-7>

We investigate the relation between coronal hole (CH) areas and solar wind speeds during 1995–2011 using the potential field (PF) model analysis of magnetograph observations and interplanetary scintillation (IPS) observations by the Institute for Space–Earth Environmental Research (formerly Solar–Terrestrial Environment Laboratory) of Nagoya University. We obtained a significant positive correlation between the CH areas (AA) derived from the PF model calculations and solar wind speeds (VV) derived from the IPS observations. The correlation coefficients between them are usually high, but they drop significantly in solar maxima. The slopes of the AA–VV relation are roughly constant except for the period around solar maximum, when flatter or steeper slopes are observed. The excursion of the correlation coefficients and slopes at solar maxima is ascribed partly to the effect of rapid structural changes in the coronal magnetic field and solar wind, and partly to the predominance of small CHs. It is also demonstrated that VV is inversely related to the flux expansion factor (ff) and that ff is closely related to $A^{-1/2}A^{1/2}$; hence, $V \propto A^{1/2}V \propto A^{1/2}$. A better correlation coefficient is obtained from the $A^{1/2}A^{1/2}$ –VV relation, and this fact is useful for improving space weather predictions. We compare the CH areas derived from the PF model calculations with He I 1083 nm observations and show that the PF model calculations provide reliable estimates of the CH area, particularly for large AA.

North–south Asymmetry in Global Distribution of the Solar Wind Speed During 1985–2013†

Munetoshi **Tokumar***, Ken'ichi Fujiki and Tomoya Iju

JGR 2015

Interplanetary scintillation (IPS) observations made between 1985 and 2013 are used to investigate the north–south (N–S) asymmetry in global distribution of the solar wind speed. The IPS observations clearly demonstrate that the global distribution of the solar wind speed systematically changes with the solar activity. This change is found to closely correlate with that in polar magnetic fields of the Sun, while fast wind data at solar minima systematically deviate from this correlation. The IPS observations show that notable N–S asymmetry of polar solar winds occurs at the solar maxima, and small but significant N–S asymmetry exists at the solar minima. The observed asymmetry at the solar maxima is consistent with the time lag in the reversal of polar magnetic fields between north and south hemispheres. We also find that significant N–S asymmetry of the polar fast wind lasts for the period between Cycle 23 and 24 solar maxima, starting from predominance of the fast wind over the north pole and ending with that over the south pole. The N–S asymmetry revealed from IPS observations is found to be generally consistent with Ulysses observations. We compare IPS observations with magnetic field data of the Sun, and find that the ratio of the quadrupole to dipole coefficients exhibits a similar time variation to that of the N–S asymmetry revealed from IPS observations. This suggests that higher-order multipole moments play an important role in determining the N–S asymmetry of the solar wind when the dipole moment weakens.

The source and propagation of the interplanetary disturbance associated with the full-halo coronal mass ejection on 28 October 2003

Tokumar, Munetoshi; Kojima, Masayoshi; Fujiki, Ken'ichi; Yamashita, Masahiro; Jackson, Bernard V. *J. Geophys. Res.*, Vol. 112, No. A5, A05106, 2007; **File**

<http://dx.doi.org/10.1029/2006JA012043>

Observations of interplanetary scintillations made with the 327-MHz four-station system of the Solar–Terrestrial Environment Laboratory of Nagoya University were analyzed to study the three-dimensional properties of a transient solar wind stream associated with the 28 October 2003 full-halo coronal mass ejection (CME). A loop-shaped high-density region propagating at a significantly slower speed than the CME-driven shock was identified. This feature appeared approximately the same as the structure seen in white-light observations made simultaneously. The orientation of the loop structure was found in general agreement with the inclination of the magnetic flux rope observed at 1 AU. Therefore we propose that the origin of this loop structure included the high-density plasma ejected from the corona in

association with the 28 October 2003 CME. By comparing this loop structure with solar wind speed data, we find that the loop structure had a solar source aligned with a slow-speed solar wind region.

Reconstructed global feature of an interplanetary disturbance for the full-halo coronal mass ejection event on 1999 September 20 •

M. [Tokumar](#), M. Yamashita, M. Kojima, K. Fujiki and T. Nakagawa
Adv. Space Res., v. 38(3), p. 547-551, **2006**.

[Tokumar](#), M., Kojima M., Fujiki, K., Yamashita, M., Yokobe, A.:
J. Geophys. Res., 108, 1220, **2003**.

Present-day IPS measurements at higher frequencies provide CMEs' size, speed, turbulence level, and mass also closer to the Sun, at distances $r > 50 R_{\odot}$ (e.g., Manoharan et al., 1995; Tokumar et al., 2003).

Data driven analysis of cosmic rays in the heliosphere: diffusion of cosmic protons

N. [Tomassetti](#), [E. Fiandrini](#), [B. Bertucci](#), [F. Donnini](#), [M. Graziani](#), [B. Khiali](#), [A. Reina Conde](#)
2023

<https://arxiv.org/pdf/2303.12239.pdf>

Understanding the time-dependent relationship between the Sun's variability and cosmic rays (GCR) is essential for developing predictive models of energetic radiation in space. When traveling inside the heliosphere, GCRs are affected by magnetic turbulence and solar wind disturbances which result in the so-called solar modulation effect. To investigate this phenomenon, we have performed a data-driven analysis of the temporal dependence of the GCR flux over the solar cycle. With a global statistical inference of GCR data collected in space by AMS-02 and PAMELA on monthly basis, we have determined the rigidity and time dependence of the GCR diffusion mean free path. Here we present our results for GCR protons, we discuss their interpretation in terms of basic processes of particle transport and their relations with the dynamics of the heliospheric plasma.

New insights from cross-correlation studies between Solar activity and Cosmic-ray fluxes

Nicola [Tomassetti](#), [Bruna Bertucci](#), [Emanuele Fiandrini](#)

Proceedings of the ICRC-2021 conference.

Journal reference: PoS (ICRC2021) 1324 (**2021**)

<https://arxiv.org/pdf/2210.05701.pdf>

The observed variability of the cosmic-ray intensity in the interplanetary space is driven by the evolution of the Sun's magnetic activity over its 11-year quasiperiodical cycle. Investigating the relationship between solar activity indices and cosmic-ray intensity measurements is then essential for understanding the fundamental processes of particle transport in the heliosphere. Here we have performed a global characterization the solar modulation of cosmic rays over the solar activity cycle and for different energies of the cosmic particles. We present our cross-correlation studies using data from space experiments, neutron monitors and solar observatories collected over several solar cycles.

Solar Modulation of Galactic Cosmic Rays: Physics Challenges for AMS-02

Nicola [Tomassetti](#)

Proceedings of the 18th Lomonosov Conference - 2017, Moscow **2017**

<https://arxiv.org/pdf/1712.03178.pdf>

The Alpha Magnetic Spectrometer (AMS) is a new generation high-energy physics experiment installed on the International Space Station in May 2011 and operating continuously since then. Using an unprecedentedly large collection of particles and antiparticles detected in space, AMS is performing precision measurements of cosmic ray energy spectra and composition. In this paper, we discuss the physics of solar modulation in Galactic cosmic rays that can be investigated with AMS by means of dedicated measurements on the time-dependence of cosmic-ray proton, helium, electron and positron fluxes.

Results on Solar Physics from AMS-02

S. Della [Torre](#), AMS-02 Collaboration

XXV ECRS 2016 Proceedings - eConf C16-09-04.3 **2016**

<https://arxiv.org/pdf/1612.08441v1.pdf>

AMS-02 is a wide acceptance high-energy physics experiment installed on the International Space Station in May 2011 and operating continuously since then. Using the largest number of detected particles in space of any space-borne experiment, it performs precision measurements of galactic cosmic rays fluxes. Detailed time variation studies of Protons, Heliums, Electron and Positron fluxes were presented. The low-rigidity range exhibits a decreasing general trend strongly related to the increase of solar activity, as well local decreases associated with strong solar events. **March 7th, 2012.**

Sun-to-Earth MHD Simulation of the 14 July 2000 "Bastille Day" Eruption

Tibor [Török](#), [Cooper Downs](#), [Jon A. Linker](#), [Roberto Lionello](#), [Viacheslav S. Titov](#), [Zoran Mikić](#), [Pete Riley](#), [Ron M. Caplan](#), [Janvier Wijaya](#)

ApJ 856 75 2018

<https://arxiv.org/pdf/1801.05903.pdf>

<http://sci-hub.tw/http://iopscience.iop.org/0004-637X/856/1/75/>

Solar eruptions are the main driver of space-weather disturbances at the Earth. Extreme events are of particular interest, not only because of the scientific challenges they pose, but also because of their possible societal consequences. Here we present a magnetohydrodynamic (MHD) simulation of the **14 July 2000** Bastille Day eruption, which produced a very strong geomagnetic storm. After constructing a thermodynamic MHD model of the corona and solar wind, we insert a magnetically stable flux rope along the polarity inversion line of the eruption's source region and initiate the eruption by boundary flows. More than 10^{33} ergs of magnetic energy are released in the eruption within a few minutes, driving a flare, an EUV wave, and a coronal mass ejection (CME) that travels in the outer corona at about 1500 km/s, close to the observed speed. We then propagate the CME to Earth, using a heliospheric MHD code. Our simulation thus provides the opportunity to test how well in situ observations of extreme events are matched if the eruption is initiated from a stable magnetic-equilibrium state. We find that the flux-rope center is very similar in character to the observed magnetic cloud, but arrives about 8.5 hours later and about 15 degrees too far to the North, with field strengths that are too weak by a factor of about 1.6. The front of the flux rope is highly distorted, exhibiting localized magnetic-field concentrations as it passes 1 AU. We discuss these properties with regard to the development of space-weather predictions based on MHD simulations of solar eruptions.

Galactic Cosmic-Ray Anisotropy During the Forbush Decrease Starting 2013 April 13

U. [Tortermun](#)¹, D. Ruffolo¹, and J. W. Bieber

2018 ApJL 852 L26

<http://iopscience.iop.org/sci-hub.tw/2041-8205/852/2/L26/>

The flux of Galactic cosmic rays (GCRs) can undergo a Forbush decrease (FD) during the passage of a shock, sheath region, or magnetic flux rope associated with a coronal mass ejection (CME). Cosmic-ray observations during FDs can provide information complementary to in situ observations of the local plasma and magnetic field, because cosmic-ray distributions allow remote sensing of distant conditions. Here we develop techniques to determine the GCR anisotropy before and during an FD using data from the worldwide network of neutron monitors, for a case study of the FD starting on **2013 April 13**. We find that at times with strong magnetic fluctuations and strong cosmic-ray scattering, there were spikes of high perpendicular anisotropy and weak parallel anisotropy. In contrast, within the CME flux rope there was a strong parallel anisotropy in the direction predicted from a theory of drift motions into one leg of the magnetic flux rope and out the other, confirming that the anisotropy can remotely sense a large-scale flow of GCRs through a magnetic flux structure.

Can One Predict Coronal Mass Ejection Arrival Times With Thirty-Minute Accuracy?

Gábor [Tóth](#), [Bart van der Holst](#), [Ward Manchester IV](#)

Space Weather e2023SW003463 [Volume21, Issue5](#) 2023

<https://agupubs.onlinelibrary.wiley.com/doi/epdf/10.1029/2023SW003463>

J. Schmidt and Cairns (2019, <https://doi.org/10.48550/arXiv.1905.08961>) have recently claimed that they can predict Coronal Mass Ejection (CME) arrival times with an accuracy of 0.9 ± 1.9 hr for four separate events. They also stated that the accuracy gets better with increased grid resolution. Here, we show that combining their results with the Richardson extrapolation (Richardson & Gaunt, 1927, <https://doi.org/10.1098/rsta.1927.0008>), which is a standard technique in computational fluid dynamics, could predict the CME arrival time with 0.2 ± 0.26 hr accuracy. The CME

arrival time errors of this model would lie in a 95% confidence interval $[-0.21, 0.61]$ hr. We also show that the probability of getting these accurate arrival time predictions with a model with a standard deviation exceeding 2 hr is less than 0.1%, indicating that these results cannot be due to random chance. This unprecedented accuracy is about 20 times better than the current state-of-the-art prediction of CME arrival times with an average error of about ± 10 hr. Based on our analysis there are only two possibilities: the results shown by J. Schmidt and Cairns (2019, <https://doi.org/10.48550/arXiv.1905.08961>) were not obtained from reproducible numerical simulations, or their method combined by the Richardson extrapolation is in fact providing CME arrival times with half an hour accuracy. We believe that this latter interpretation is very unlikely to hold true. We also discuss how the peer-review process apparently failed to even question the validity of the results presented by J. Schmidt and Cairns (2019, <https://doi.org/10.48550/arXiv.1905.08961>). **29 Nov 2013, 4 and 6 Sep 2017, 12 Feb 2018,**

Theory of Magnetic Switchbacks Fully Supported by Parker Solar Probe Observations

Gabor **Toth**¹, Marco Velli^{2,3}, and Bart van der Holst¹

2023 ApJ 957 95

<https://iopscience.iop.org/article/10.3847/1538-4357/acfd91/pdf>

Magnetic switchbacks are rapid high-amplitude reversals of the radial magnetic field in the solar wind that do not involve a heliospheric current sheet crossing. First seen sporadically in the 1970s in Mariner and Helios data, switchbacks were later observed by the Ulysses spacecraft beyond 1 au and have been recently discovered to be a typical component of solar wind fluctuations in the inner heliosphere by the Parker Solar Probe spacecraft. While switchbacks are now well understood to be spherically polarized Alfvén waves thanks to Parker Solar Probe observations, their formation has been an intriguing and unsolved puzzle. Here we provide a simple yet predictive theory for the formation of these magnetic reversals: the switchbacks are produced by the distortion and twisting of circularly polarized Alfvén waves by a transversely varying radial wave propagation velocity. We provide an analytic expression for the magnetic field variation, establish the necessary and sufficient conditions for the formation of switchbacks, and show that the proposed mechanism works in a realistic solar wind scenario. We also show that the theoretical predictions are in excellent agreement with observations, and the high-amplitude radial oscillations are strongly correlated with the shear of the wave propagation speed. The correlation coefficient is around 0.3–0.5 for both encounter 1 and encounter 12. The probability of this being a lucky coincidence is essentially zero with p-values below 0.1%.

Formation of Magnetic Switchbacks Observed by Parker Solar Probe

Gabor **Toth**, [Marco Velli](#), [Bart van der Holst](#)

Nature **2023**

<https://arxiv.org/pdf/2301.02572.pdf>

Magnetic switchbacks are rapid high amplitude reversals of the radial magnetic field in the solar wind that do not involve a heliospheric current sheet crossing. First seen sporadically in the seventies in Mariner and Helios data, switchbacks were later observed by the Ulysses spacecraft beyond 1 au and have been recently identified as a typical component of solar wind fluctuations in the inner heliosphere by the Parker Solar Probe spacecraft. Here we provide a simple yet predictive theory for the formation of these magnetic reversals: the switchbacks are produced by the shear of circularly polarized Alfvén waves by a transversely varying radial wave propagation velocity. We provide an analytic expression for the magnetic field variation, establish the necessary and sufficient conditions and show that the mechanism works in a realistic solar wind scenario.

Propagation of untwisting solar jets from the low-beta corona into the super-Alfvénic wind: Testing a solar origin scenario for switchbacks

[Jade Touresse](#), [Etienne Pariat](#), [Clara Froment](#), [Valentin Aslanyan](#), [Peter F. Wyper](#), [Louis Seyfritz](#)

A&A **2024**

<https://arxiv.org/pdf/2412.15930>

Parker Solar Probe's (PSP) discovery of the prevalence of switchbacks (SBs), localised magnetic deflections in the nascent solar wind, has sparked interest in uncovering their origins. A prominent theory suggests these SBs originate in the lower corona through magnetic reconnection processes, closely linked to solar jet phenomena. Jets are impulsive events, observed across scales and solar atmosphere layers, associated with the release of magnetic twist and helicity. This study examines whether self-consistent jets can form and propagate into the super-Alfvénic wind, assesses the impact of distinct Parker solar wind profiles on jet dynamics, and determines if jet-induced magnetic untwisting waves display signatures typical of SBs. We employed parametric 3D numerical MHD simulations using the ARMS code to model the self-consistent generation of solar jets. Our study focuses on the propagation of solar jets in distinct atmospheric plasma β and Alfvén velocity profiles, including a Parker solar wind. Our findings show that self-consistent

coronal jets can form and propagate into the super-Alfvénic wind. Notable structures such as the leading Alfvénic wave and trailing dense-jet region were consistently observed across diverse plasma β atmospheres. The jet propagation dynamics are significantly influenced by atmospheric variations, with changes in Alfvén velocity profiles affecting the group velocity and propagation ratio of the leading and trailing structures. U-loops, prevalent at jet onset, do not persist in the low- β corona, but magnetic untwisting waves associated with jets show SB-like signatures. However, full-reversal SBs were not observed. These findings may explain the absence of full reversal SBs in the sub-Alfvénic wind and illustrate the propagation of magnetic deflections through jet-like events, shedding light on possible SB formation processes.

Occurrence of severe geomagnetic storms and their association with solar–interplanetary features

R. **Tripathi** and A. P. Mishra

ILWS WORKSHOP 2006, GOA, FEBRUARY 19-24, 2006, **File**

Severe geomagnetic storms are observed to be the largest 2% of all large geomagnetic storms. Here great geomagnetic storms **with Dst magnitude < -200 nT** are considered. In this paper all severe geomagnetic storms have been selected which have occurred during year 1996 to 2005. We have found 16 severe geomagnetic storms during this period. These storms are significant not only because of the extremely high magnetic activity but also due to their great impact on the magnetosphere. The relationship of severe geomagnetic storms with different interplanetary parameters and their solar source origin is presented. We have found that 95% severe geomagnetic storms are associated with halo coronal mass ejections.

Properties of HALO CME in relation to large geomagnetic storms

Roopali **Tripathi** and A.P. Mishra

29th International Cosmic Ray Conference Pune (2005) 1, 161-164, **File**

Based on the observations from the Large Angle and Spectrometric Coronagraph (LASCO) on board the Solar and Heliospheric Observatory (SOHO) spacecraft we have studied the coronal mass ejections. Coronal mass ejections (CME) are dynamic large-scale event during which large amounts of plasma expel from the sun's outer atmosphere. When these ejections directed towards the earth (or conversely, directed away from the earth) it looks like roughly circular "HALO" surrounding the sun. The CME originates interplanetary shocks, which impinging the magnetosphere results the geomagnetic storms. In the presents paper we have analyzed 314 HALO CMEs, which have occurred during the current solar cycle 23. It is found that HALO CME is much faster and more energetic than the other CME. The occurrence of HALO CME increases during solar maximum. The maximum speed of HALO CME is found to be as large as 4000 km/sec., where as minimum speed of HALO CME is some time of the order of 100 km/sec. We have also found that HALO CME is the main cause to produce large geomagnetic storms.

Ground-Based Monitoring of the Solar Wind Geoefficiency

A review

Oleg **Troshichev**

In: Exploring the Solar Wind, Ed. Marian Lazar, 2012,

<http://www.intechopen.com/books/exploring-the-solar-wind>

An Overview of Solar Orbiter Observations of Interplanetary Shocks in Solar Cycle 25

Review

D. **Trotta**, [A. Dimmock](#), [H. Hietala](#), [X. Blanco-Cano](#), [T. S. Horbury](#), + + +

ApJ 2024

<https://arxiv.org/pdf/2410.24007>

Interplanetary shocks are fundamental constituents of the heliosphere, where they form as a result of solar activity. We use previously unavailable measurements of interplanetary shocks in the inner heliosphere provided by Solar Orbiter, and present a survey of the first 100 shocks observed in situ at different heliocentric distances during the rising phase of solar cycle 25. The fundamental shock parameters (shock normals, shock normal angles, shock speeds, compression ratios, Mach numbers) have been estimated and studied as a function of heliocentric distance, revealing a rich scenario of configurations. Comparison with large surveys of shocks at 1~au show that shocks in the quasi-parallel regime and with high speed are more commonly observed in the inner heliosphere. The wave environment of the shocks has also been addressed, with about 50% of the events exhibiting clear shock-induced upstream fluctuations. We characterize

energetic particle responses to the passage of IP shocks at different energies, often revealing complex features arising from the interaction between IP shocks and pre-existing fluctuations, including solar wind structures being processed upon shock crossing. Finally, we give details and guidance on the access use of the present survey, available on the EU-project "solar energetic particle analysis platform for the inner heliosphere" (SERPENTINE) website. The algorithm used to identify shocks in large datasets, now publicly available, is also described. **2021-07-19, Nov 03, 2021, Aug 31, 2022, 2022-03-08,11; 2023-02-21,**

Observation of a Fully-formed Forward--Reverse Shock Pair Due to the Interaction Between Two Coronal Mass Ejections at 0.5 au

D. Trotta, [A. Dimmock](#), [X. Blanco-Cano](#), [R. Forsyth](#), [H. Hietala](#), +++

ApJ **971** L35 **2024**

<https://arxiv.org/pdf/2404.17315>

<https://iopscience.iop.org/article/10.3847/2041-8213/ad68fa/pdf>

We report direct observations of a fast magnetosonic forward--reverse shock pair observed by Solar Orbiter on **March 8, 2022** at the short heliocentric distance of 0.5 au. The structure, sharing some features with fully-formed stream interaction regions (SIRs), is due to the interaction between two successive coronal mass ejections (CMEs), never previously observed to give rise to a forward--reverse shock pair. The scenario is supported by remote observations from the STEREO-A coronagraphs, where two candidate eruptions compatible with the in-situ signatures have been found. In the interaction region, we find enhanced energetic particle activity, strong non-radial flow deflections and evidence of magnetic reconnection. At 1~au, well radially-aligned \textit{Wind} observations reveal a complex event, with characteristic observational signatures of both SIR and CME--CME interaction, thus demonstrating the importance of investigating the complex dynamics governing solar eruptive phenomena.

Properties of an interplanetary shock observed at 0.07 and 0.7 Astronomical Units by Parker Solar Probe and Solar Orbiter

D. Trotta, [A. Larosa](#), [G. Nicolaou](#), [T. S. Horbury](#), [L. Matteini](#), +++

ApJ **962** 147 **2024**

<https://arxiv.org/pdf/2312.05983.pdf>

<https://iopscience.iop.org/article/10.3847/1538-4357/ad187d/pdf>

The Parker Solar Probe (PSP) and Solar Orbiter (SolO) missions opened a new observational window in the inner heliosphere, which is finally accessible to direct measurements. On **September 05, 2022**, a coronal mass ejection (CME)-driven interplanetary (IP) shock has been observed as close as 0.07 au by PSP. The CME then reached SolO, which was well radially-aligned at 0.7 au, thus providing us with the opportunity to study the shock properties at so different heliocentric distances. We characterize the shock, investigate its typical parameters and compare its small-scale features at both locations. Using the PSP observations, we investigate how magnetic switchbacks and ion cyclotron waves are processed upon shock crossing. We find that switchbacks preserve their V--B correlation while compressed upon the shock passage, and that the signature of ion cyclotron waves disappears downstream of the shock. By contrast, the SolO observations reveal a very structured shock transition, with a population of shock-accelerated protons of up to about 2 MeV, showing irregularities in the shock downstream, which we correlate with solar wind structures propagating across the shock. At SolO, we also report the presence of low-energy (~ 100 eV) electrons scattering due to upstream shocklets. This study elucidates how the local features of IP shocks and their environments can be very different as they propagate through the heliosphere.

Multi-spacecraft observations of shocklets at an interplanetary shock

D Trotta, [H Hietala](#), [T Horbury](#), [N Dresing](#), [R Vainio](#), [L Wilson, III](#), [I Plotnikov](#), [E Kilpua](#)

MNRAS, Volume 520, Issue 1, March **2023**, Pages 437--445,

<https://doi.org/10.1093/mnras/stad104>

<https://watermark.silverchair.com/stad104.pdf>

Interplanetary (IP) shocks are fundamental building blocks of the heliosphere, and the possibility to observe them in situ is crucial to address important aspects of energy conversion for a variety of astrophysical systems. Steepened waves known as shocklets are known to be important structures of planetary bow shocks, but they are very rarely observed related to IP shocks. We present here the first multi-spacecraft observations of shocklets observed by upstream of an unusually strong IP shock observed on 3 November 2021 by several spacecraft at L1 and near-Earth solar wind. The same shock was detected also by radially aligned Solar Orbiter at 0.8 AU from the Sun, but no shocklets were identified

from its data, introducing the possibility to study the environment in which shocklets developed. The Wind spacecraft has been used to characterize the shocklets, associated with pre-conditioning of the shock upstream by decelerating incoming plasma in the shock normal direction. Finally, using the Wind observations together with ACE and DSCOVR spacecraft at L1, as well as THEMIS B and THEMIS C in the near-Earth solar wind, the portion of interplanetary space filled with shocklets is addressed, and a lower limit for its extent is estimated to be of about 110RE in the shock normal direction and 25RE in the directions transverse to the shock normal. Using multiple spacecraft also reveals that for this strong IP shock, shocklets are observed for a large range of local obliquity estimates (9° – 64°). **3 Nov 2021**

AN INTERESTING INTERPLANETARY SHOCK

Solar Orbiter nugget #10 2023

<https://www.cosmos.esa.int/web/solar-orbiter/solar-nuggets/an-interesting-interplanetary-shock>

Spectral Analysis of Solar and Geomagnetic Parameters in Relation to Cosmic-ray Intensity for the Time Period 1965 – 2018

M. **Tsichla** M. Gerontidou H. Mavromichalaki

Solar Physics January 2019, 294:15

sci-hub.tw/10.1007/s11207-019-1403-0

<https://link.springer.com/content/pdf/10.1007%2Fs11207-019-1403-0.pdf>

Spectral analysis of solar and geomagnetic parameters as well as of cosmic-ray intensity was performed aiming to identify possible new periodicities and confirm the well-known ones. Specifically, short-, mid-, and long-term periodicities of these parameters such as sunspot number, Bz-component of the interplanetary magnetic field, geomagnetic Ap index, and cosmic-ray intensity over the time period 1965 – 2018, covering five solar cycles from Cycles 20 to 24, are presented. For this purpose, two different techniques, fast Fourier transformation and wavelet analysis, have been used in order to ensure accuracy in the frequency values and also their localization in the time series. The periodicities resulting from our comprehensive study, including the well-known 11-year and 27-day periods, the harmonics of the 5.5-year and of the 6-, 9-, and 13.9-day periods, respectively, and the ≈ 1.3 -year and 1.7-year periods, were found in all of the above parameters except for the Bz-component of the interplanetary magnetic field. New periodicities such as the ≈ 10 -month period for sunspot number and cosmic-ray intensity and the ≈ 3 -year period for sunspot number, Ap index, and cosmic-ray intensity, were also determined. Furthermore, the newly introduced splitting of the 27-day periodicity into two adjacent peaks was confirmed in the Fourier spectra of the interplanetary magnetic field and the geomagnetic Ap index. It was concluded that several common periodicities appear in solar activity: the Ap index, and the cosmic-ray intensity. This result, in association with the fact that the spectral behavior of geomagnetic-activity parameters, provides invaluable information about the physical processes involved, and indicates that the Ap index might be used as a suitable index for space-weather forecasting.

Long-term occurrence probabilities of intense geomagnetic storm events

K. **Tsubouchi** and Y. Omura

SPACE WEATHER, VOL. 5, S12003, doi:10.1029/2007SW000329, 2007

A quantitative assessment of the occurrence probability of intense geomagnetic storms (peak $Dst < -100$ nT) has been investigated by analyzing the Dst index time series database from 1957 to 2001. The main purpose was to derive two parameters, the probable intensity S_T and the occurrence frequency λ_T , that can act as proxies for long-term space weather quantities. The intensity S_T represents the expected maximum storm level with an occurrence rate of $1/T$ (a^{-1} , where a is years) and has been derived from the probability density function (PDF) of extreme ($|Dst| > 280$ nT) storms. The mathematical tool to determine this type of PDF is the extreme value modeling, which exhibits more accurate statistics for extreme behavior. Our results estimate $S_{60} \approx 589$, indicating that the March 1989 storm (the event with the largest $|Dst|$ in the database) corresponds to an event expected to occur only once every 60 a. The other parameter λ_T gives the average occurrence rate of storm events. We have tested the null hypothesis that the storm occurrence pattern can be modeled as a Poisson process represented by λ_T , where different λ_T exist for the active and quiet periods of the solar cycle. Ordinary χ^2 tests of goodness of fit can not reject this hypothesis, except within the periods that include extremely frequent occurrences. The rate λ_T is approximately 2.3 (0.7) per 3 months in the active (quiet) period. A future practical application of this work is that the resultant Poisson probability will enable us to calculate the expected damage due to storms, which represent potential risks in space activities.

Revisiting the Superstorm on 6–7 April 2000 Caused by an Extraordinary Corotating Interaction Region (With an Embedded Coronal Jet?)

Bruce T. Tsurutani, [Rajkumar Hajra](#), [Gurbax Lakhina](#), [Xing Meng](#)

JGR Volume 129, Issue 11 November 2024 e2024JA032989

<https://agupubs.onlinelibrary.wiley.com/doi/epdf/10.1029/2024JA032989>

The 6–7 April 2000 superstorm of SYM-H intensity = -319 nT discussed in Meng et al. (2019; <https://doi.org/10.1029/2018JA026425>) was misidentified as being due to an interplanetary coronal mass ejection associated with a solar flare. The interplanetary cause was a highly unusual corotating interaction region (CIR) bounded by a strong fast forward shock (FS) with magnetosonic Mach number $M_{ms} = 4.6$ and a fast reverse shock (RS) with $M_{ms} = 1.9$. The exceptionally strong FS caused a ~ 3 -factor interplanetary magnetic field (IMF) magnitude amplification in the leading half of the CIR with peak southward IMF $B_z = -27$ nT causing the superstorm. A plasma region between a tangential discontinuity and the stream interface had a scale size of ~ 0.096 AU. We hypothesize that this is the first detection of a coronal jet at 1 AU. The jet/Gold magnetic tongue (1959; <https://doi.org/10.1029/JZ064i011p01665>) was embedded within the CIR, contained the southward B_z and caused the magnetic storm. We hypothesize that a shrinking coronal hole and magnetic reconnection caused the formation and release of the jet.

Review of the August 1972 and March 1989 Space Weather Events: Can We Learn Anything New From Them?

Bruce T. Tsurutani, [Abhijit Sen](#), [Rajkumar Hajra](#), [Gurbax S. Lakhina](#), [Richard B. Horne](#), [Tohru Hada](#)

JGR volume : 129, number: e2024JA032622,

2024

<https://doi.org/10.1029/2024JA032622>

<https://arxiv.org/pdf/2409.00452>

Updated summaries of the August 1972 and March 1989 space weather events have been constructed. The features of these two events are compared to the Carrington 1859 event and a few other major space weather events. It is concluded that solar active regions release energy in a variety of forms (X-rays, EUV photons, visible light, coronal mass ejection (CME) plasmas and fields) and they in turn can produce other energetic effects (solar energetic particles (SEPs), magnetic storms) in a variety of ways. It is clear that there is no strong one-to-one relationship between these various energy sinks. The energy is often distributed differently from one space weather event to the next. Concerning SEPs accelerated at interplanetary CME (ICME) shocks, it is concluded that the Fermi mechanism associated with quasi-parallel shocks is relatively weak and that the gradient drift mechanism (electric fields) at quasi-perpendicular shocks will produce harder spectra and higher fluxes. If the 4 August 1972 intrinsic magnetic cloud condition (southward interplanetary magnetic field instead of northward) and the interplanetary Sun to 1 au conditions were different, a 4 August 1972 magnetic storm and magnetospheric dawn-to-dusk electric fields substantially larger than the Carrington event would have occurred. Under these special interplanetary conditions, a Miyake et al. (2012)-like extreme SEP event may have been formed. The long duration complex 1989 storm was probably greater than the Carrington storm in the sense that the total ring current particle energy was larger. **2-7 Aug 1972, 6–19 Mar 1989**

Energetics of Shock-triggered Supersubstorms (SML < -2500 nT)

Bruce T. Tsurutani¹ and Rajkumar Hajra²

2023 ApJ 946 17

<https://iopscience.iop.org/article/10.3847/1538-4357/acb143/pdf>

The solar wind energy input and dissipation in the magnetospheric–ionospheric systems of 17 supersubstorms (SSSs: SML < -2500 nT) triggered by interplanetary shocks during solar cycles 23 and 24 are studied in detail. The SSS events had durations ranging from ~ 42 minutes to ~ 6 hr, and SML intensities ranging from -2522 nT to -4143 nT. Shock compression greatly strengthens the upstream interplanetary magnetic field southward component (B_s), and thus, through magnetic reconnection at the Earth's dayside magnetopause, greatly enhances the solar wind energy input into the magnetosphere and ionosphere during the SSS events studied. The additional solar wind magnetic reconnection energy input supplements the ~ 1.5 hr precursor (growth-phase) energy input and both supply the necessary energy for the high-intensity, long-duration SSS events. Some of the solar wind energy is immediately deposited in the magnetosphere/ionosphere system, and some is stored in the magnetosphere/magnetotail system. During the SSS events,

the major part of the solar wind input energy is dissipated into Joule heating (~30%), with substantially less energy dissipation in auroral precipitation (~3%) and ring current energy (~2%). The remainder of the solar wind energy input is probably lost down the magnetotail. It is found that during the SSS events, the dayside Joule heating is comparable to that of the nightside Joule heating, giving a picture of the global energy dissipation in the magnetospheric/ionospheric system, not simply a nightside-sector substorm effect. Several cases are shown where an SSS is the only substorm that occurs during a magnetic storm, essentially equating the two phenomena for these cases.

Space Plasma Physics: A **Review**

Bruce T. [Tsurutani](#), [Gary P. Zank](#), [Veerle J. Sterken](#), [Kazunari Shibata](#), [Tsugunobu Nagai](#), [Anthony J. Mannucci](#), [David M. Malaspina](#), [Gurbax S. Lakhina](#), [Shrikanth G. Kanekal](#), [Keisuke Hosokawa](#), [Richard B. Horne](#), [Rajkumar Hajra](#), [Karl-Heinz Glassmeier](#), [C. Trevor Gaunt](#), [Peng-Fei Chen](#), [Syun-Ichi Akasofu](#)

IEEE Transactions on Plasma Science (2022)

<https://arxiv.org/ftp/arxiv/papers/2209/2209.14545.pdf>

Owing to the ever-present solar wind, our vast solar system is full of plasmas. The turbulent solar wind, together with sporadic solar eruptions, introduces various space plasma processes and phenomena in the solar atmosphere all the way to the Earth's ionosphere and atmosphere and outward to interact with the interstellar media to form the heliopause and termination shock. Remarkable progress has been made in space plasma physics in the last 65 years, mainly due to sophisticated in-situ measurements of plasmas, plasma waves, neutral particles, energetic particles, and dust via space-borne satellite instrumentation. Additionally high technology ground-based instrumentation has led to new and greater knowledge of solar and auroral features. As a result, a new branch of space physics, i.e., space weather, has emerged since many of the space physics processes have a direct or indirect influence on humankind. After briefly reviewing the major space physics discoveries before rockets and satellites, we aim to review all our updated understanding on coronal holes, solar flares and coronal mass ejections, which are central to space weather events at Earth, solar wind, storms and substorms, magnetotail and substorms, emphasizing the role of the magnetotail in substorm dynamics, radiation belts/energetic magnetospheric particles, structures and space weather dynamics in the ionosphere, plasma waves, instabilities, and wave-particle interactions, long-period geomagnetic pulsations, auroras, geomagnetically induced currents (GICs), planetary magnetospheres and solar/stellar wind interactions with comets, moons and asteroids, interplanetary discontinuities, shocks and waves, interplanetary dust, space dusty plasmas and solar energetic particles and shocks, including the heliospheric termination shock. This paper is aimed to provide a panoramic view of space physics and space weather.

Extremely Slow ($V_{sw} < 300 \text{ km s}^{-1}$) Solar Winds (ESSWs) at 1 au: Causes of Extreme Geomagnetic Quiet at Earth

Bruce T. [Tsurutani](#)¹ and [Rajkumar Hajra](#)²

2022 ApJ 936 155

<https://iopscience.iop.org/article/10.3847/1538-4357/ac7444/pdf>

A search for extremely slow ($V_{sw} < 300 \text{ km s}^{-1}$) solar winds (ESSWs) at 1 au has been conducted using hourly average solar wind data from 1963 through 2021. 297 ESSW events were identified with an average duration of $\sim 2.0 \pm 1.4$ days. The lowest speed detected was 156 km s^{-1} . Ten of the lowest-speed events were analyzed in detail. It was found that all 10 events were located at the ends of high-speed solar wind (HSSW) streams. The termination of the ESSWs was caused by high-density plasmas, either a corotating interaction region associated with the next HSSW stream or a heliospheric plasma sheet encounter. There was a greater occurrence of ESSW events in solar cycles 23 and 24 than in previous solar cycles. This phenomenon is associated with the much lower solar activity during these two cycles. The decrease in solar polar open magnetic fields was accompanied by an increase in low and midlatitude open magnetic fields. The ESSWs were accompanied by low interplanetary magnetic fields ($4.4 \pm 2.1 \text{ nT}$) and low negative interplanetary B_z fields ($-1.7 \pm 1.5 \text{ nT}$), which led to extreme geomagnetic quiet: $AE = 67 \pm 78 \text{ nT}$ and $Dst = 2.2 \pm 9.9 \text{ nT}$. We encourage magnetospheric researchers to use ESSW events to better understand the ground states of the magnetosphere and ionosphere.

The physics of space weather/solar-terrestrial physics (STP): what we know now and what the current and future challenges are. **Review**

[Tsurutani](#) BT, [Lakhina](#) GS, [Hajra](#) R

(2020) Nonlinear Proc Geophys [Volume 27, issue 1](#) NPG, 27, 75–119,

<https://doi.org/10.5194/npg-27-75-2020>

<https://npg.copernicus.org/articles/27/75/2020/>

<https://sci-hub.ru/10.5194/npg-27-75-2020>

Major geomagnetic storms are caused by unusually intense solar wind southward magnetic fields that impinge upon the Earth's magnetosphere (Dungey, 1961). How can we predict the occurrence of future interplanetary events? Do we currently know enough of the underlying physics and do we have sufficient observations of solar wind phenomena that will impinge upon the Earth's magnetosphere? We view this as the most important challenge in space weather. We discuss the case for magnetic clouds (MCs), interplanetary sheaths upstream of interplanetary coronal mass ejections (ICMEs), corotating interaction regions (CIRs) and solar wind high-speed streams (HSSs). The sheath- and CIR-related magnetic storms will be difficult to predict and will require better knowledge of the slow solar wind and modeling to solve. For interplanetary space weather, there are challenges for understanding the fluences and spectra of solar energetic particles (SEPs). This will require better knowledge of interplanetary shock properties as they propagate and evolve going from the Sun to 1 AU (and beyond), the upstream slow solar wind and energetic "seed" particles. Dayside aurora, triggering of nightside substorms, and formation of new radiation belts can all be caused by shock and interplanetary ram pressure impingements onto the Earth's magnetosphere. The acceleration and loss of relativistic magnetospheric "killer" electrons and prompt penetrating electric fields in terms of causing positive and negative ionospheric storms are reasonably well understood, but refinements are still needed. The forecasting of extreme events (extreme shocks, extreme solar energetic particle events, and extreme geomagnetic storms (Carrington events or greater)) are also discussed. Energetic particle precipitation into the atmosphere and ozone destruction are briefly discussed. For many of the studies, the Parker Solar Probe, Solar Orbiter, Magnetospheric Multiscale Mission (MMS), Arase, and SWARM data will be useful.

A Review of Alfvénic Turbulence in High-Speed Solar Wind Streams: Hints From Cometary Plasma Turbulence

Bruce T. [Tsurutani](#), [Gurbax S. Lakhina](#), [Abhijit Sen](#), [Petr Hellinger](#), [Karl-Heinz Glassmeier](#), [Anthony J. Mannucci](#)

JGR **Volume123, Issue4** Pages 2458-2492 **2018**

<http://sci-hub.tw/10.1002/2017JA024203>

Solar wind turbulence within high-speed streams is reviewed from the point of view of embedded single nonlinear Alfvén wave cycles, discontinuities, magnetic decreases (MDs), and shocks. For comparison and guidance, cometary plasma turbulence is also briefly reviewed. It is demonstrated that cometary nonlinear magnetosonic waves phase-steepen, with a right-hand circular polarized foreshortened front and an elongated, compressive trailing edge. The former part is a form of "wave breaking" and the latter that of "period doubling." Interplanetary nonlinear Alfvén waves, which are arc polarized, have a $\sim 180^\circ$ foreshortened front and with an elongated trailing edge. Alfvén waves have polarizations different from those of cometary magnetosonic waves, indicating that helicity is a durable feature of plasma turbulence. Interplanetary Alfvén waves are noted to be spherical waves, suggesting the possibility of additional local generation. They kinetically dissipate, forming MDs, indicating that the solar wind is partially "compressive" and static. The ~ 2 MeV protons can nonresonantly interact with MDs leading to rapid cross-field ($\sim 5.5\%$ Bohm) diffusion. The possibility of local (~ 1 AU) generation of Alfvén waves may make it difficult to forecast High-Intensity, Long-Duration AE Activity and relativistic magnetospheric electrons with great accuracy. The future Solar Orbiter and Solar Probe Plus missions should be able to not only test these ideas but to also extend our knowledge of plasma turbulence evolution.

Comment on "Modeling extreme "Carrington-type" space weather events using three-dimensional global MHD simulations" by C.M. Ngwira, A. Pulkkinen, M.M. Kuznetsova and A. Gloer"

Bruce T. [Tsurutani](#), [Gurbax S. Lakhina](#), [Ezequiel Echer](#), [Chinmaya Nayak](#), [Anthony J. Mannucci](#), [Xing Meng](#)

JGR **2018**

<http://onlinelibrary.wiley.com/doi/10.1002/2017JA024779/epdf>

An alternative scenario to the Ngwira et al. (2014) high sheath densities is proposed for modeling the Carrington magnetic storm. Typical slow solar wind densities (~ 5 cm $^{-3}$) and lower interplanetary magnetic cloud (MC) magnetic fields intensities (~ 90 nT) can be used to explain the observed initial and main phase storm features. A second point is that the fast storm recovery may be explained by ring current losses due to electromagnetic ion cyclotron (EMIC) wave scattering.

An extreme coronal mass ejection and consequences for the magnetosphere and Earth, [Tsurutani](#), B. T., and [G. S. Lakhina](#)

(2014), *Geophys. Res. Lett.*, 41, 287–292,
<http://onlinelibrary.wiley.com/doi/10.1002/2013GL058825/pdf>
<https://doi.org/10.1002/2013GL058825>
<https://agupubs.onlinelibrary.wiley.com/doi/epdf/10.1002/2013GL058825>

A "perfect" ICME could create a magnetic storm with intensity up to the saturation limit (Dst ~ -2500 nT), a value greater than the Carrington storm. Many of the other space weather effects will not be limited by saturation effects, however. The interplanetary shock would arrive at Earth within ~12 hrs with a magnetosonic Mach number ~45. The shock impingement onto the magnetosphere will create a SI+ of ~234 nT, the magnetic pulse duration in the magnetosphere will be ~22 s with a dB/dt of ~30 nT s⁻¹, and the magnetospheric electric field associated with the dB/dt ~1.9 V m⁻¹, creating a new relativistic electron radiation belt. The magnetopause location of 4 Re from the Earth's surface will allow expose of orbiting satellites to extreme levels of flare and ICME shock-accelerated particle radiation. The results of our calculations are compared with current observational records. Comments are made concerning further data analysis and numerical modeling needed for the field of space weather

The interplanetary causes of geomagnetic activity during the 7–17 March 2012 interval: a CAUSES II overview

Bruce T. **Tsurutani**^{1*}, Ezequiel Echer², Kazunari Shibata³, Olga P. Verkhoglyadova^{1,4}, Anthony J. Mannucci¹, Walter D. Gonzalez², Janet U. Kozyra⁵ and Martin Pätzold
J. Space Weather Space Clim. 4 (2014) A02

<http://www.swsc-journal.org/articles/swsc/pdf/2014/01/swsc130026.pdf>

This overview paper presents/discusses the major solar, interplanetary, magnetospheric, and ionospheric features of the CAUSES II interval of study: **7–17 March 2012**. Magnetic storms occurred on 7, 9, 12, and 15 March with peak SYM-H intensities of -98 nT, -148 nT, -75 nT (pressure corrected), and -79 nT, respectively. These are called the S1, S2, S3, and S4 events. Although three of the storm main phases (S1, S3, and S4) were caused by IMF B_{south} sheath fields and the S2 event was associated with a magnetic cloud (MC), the detailed scenario for all four storms were different. Two interplanetary features with unusually high temperatures and intense and quiet magnetic fields were identified located antisunward of the MCs (S2 and S3). These features are signatures of either coronal loops or coronal sheaths. A high speed stream (HSS) followed the S4 event where the presumably southward IMF B_z components of the Alfvén waves extended the storm "recovery phase" by several days. The ICME-associated shocks were particularly intense. The fast forward shock for the S2 event had a magnetosonic Mach number of ~9.4, the largest in recorded history. All of the shocks associated with the ICMEs created sudden impulses (SI+s) at Earth. The shocks preceding the S2 and S3 magnetic storms caused unusually high SI+ intensities of ~60 and 68 nT, respectively. Many further studies on various facets of this active interval are suggested for CAUSES II researchers and other interested parties.

CAUSES November 7 – 8, 2004, superstorm: Complex solar and interplanetary features in the post-solar maximum phase,

Tsurutani, B. T., E. Echer, F. L. Guarnieri, and J. U. Kozyra (2008),
Geophys. Res. Lett., doi:10.1029/2007GL031473, in press.

The complex interplanetary structures during 7 to 8 Nov 2004 are analyzed to identify their properties as well as resultant geomagnetic effects and the solar origins. Three fast forward shocks, three directional discontinuities and two reverse waves were detected and analyzed in detail. The three fast forward shocks "pump" up the interplanetary magnetic field from a value of ~4 nT to ~44 nT. However, the fields after the shocks were northward, and magnetic storms did not result. The three ram pressure increases were associated with major sudden impulses (SI + s) at Earth. A magnetic cloud followed the third forward shock and the southward B_z associated with the latter was responsible for the superstorm. Two reverse waves were detected, one at the edge and one near the center of the magnetic cloud (MC). It is suspected that these "waves" were once reverse shocks which were becoming evanescent when they propagated into the low plasma beta MC. The second reverse wave caused a decrease in the southward component of the IMF and initiated the storm recovery phase. It is determined that flares located at large longitudinal distances from the subsolar point were the most likely causes of the first two shocks without associated magnetic clouds. It is thus unlikely that the shocks were "blast waves" or that magnetic reconnection eroded away the two associated MCs. This interplanetary/solar event is an example of the extremely complex magnetic storms which can occur in the post-solar maximum phase.

(See **Eselevich et al., 2009**)

Corotating solar wind streams and recurrent geomagnetic activity: A **review.**

Tsurutani, B.T., Gonzalez, W.D., Gonzalez, A.L.C., Guarnieri, F.L., Gopalswamy, N., Grande, M., Kamide, Y., Kasahara, Y., Lu, G., Mann, I., McPherron, R., Soraas, F., Vasyliunas, V.:

2006, J. Geophys. Res. Space Phys. 111(7), 1.

sci-hub.se/10.1029/2005JA011273

<https://doi.org/10.1029/2005JA011273>

Solar wind fast streams emanating from solar coronal holes cause recurrent, moderate intensity geomagnetic activity at Earth. Intense magnetic field regions called Corotating Interaction Regions or CIRs are created by the interaction of fast streams with upstream slow streams. Because of the highly oscillatory nature of the GSM magnetic field z component within CIRs, the resultant magnetic storms are typically only weak to moderate in intensity. CIR-generated magnetic storm main phases of intensity $Dst < -100$ nT (major storms) are rare. The elongated storm “recovery” phases which are characterized by continuous AE activity that can last for up to 27 days (a solar rotation) are caused by nonlinear Alfvén waves within the high streams proper. Magnetic reconnection associated with the southward (GSM) components of the Alfvén waves is the solar wind energy transfer mechanism. The acceleration of relativistic electrons occurs during these magnetic storm “recovery” phases. The magnetic reconnection associated with the Alfvén waves cause continuous, shallow injections of plasma sheet plasma into the magnetosphere. The asymmetric plasma is unstable to wave (chorus and other modes) growth, a feature central to many theories of electron acceleration. It is noted that the continuous AE activity is not a series of substorm expansion phases. Arguments are also presented why these AE activity intervals are not convection bays. The auroras during these continuous AE activity intervals are less intense than substorm auroras and are global (both dayside and nightside) in nature. Owing to the continuous nature of this activity, it is possible that there is greater average energy input into the magnetosphere/ionosphere system during far declining phases of the solar cycle compared with those during solar maximum. The discontinuities and magnetic decreases (MDs) associated with interplanetary Alfvén waves may be important for geomagnetic activity. In conclusion, it will be shown that geomagnetic storms associated with high-speed streams/CIRs will have the same initial, main, and “recovery” phases as those associated with ICME-related magnetic storms but that the interplanetary causes are considerably different.

The extreme magnetic storm of 1-2 September 1859

Tsurutani, B. T., Gonzalez, W. D., Lakhina, G. S., and Alex, S.:

2003, J. Geophys. Res. 108(A7), 1268,

The 1-2 September 1859 magnetic storm was the most intense in recorded history on the basis of previously reported ground observations and on newly reduced ground-based magnetic field data. Using empirical results on the interplanetary magnetic field strengths of magnetic clouds versus velocities, we show that the 1 September 1859 Carrington solar flare most likely had an associated intense magnetic cloud ejection which led to a storm on Earth of $DST \sim -1760$ nT. This is consistent with the Colaba, India local noon magnetic response of $\Delta H = 1600 \pm 10$ nT. It is found that both the 1-2 September 1859 solar flare energy and the associated coronal mass ejection speed were extremely high but not unique. Other events with more intense properties have been detected; thus a storm of this or even greater intensity may occur again. Because the data for the high-energy tails of solar flares and magnetic storms are extremely sparse, the tail distributions and therefore the probabilities of occurrence cannot be assigned with any reasonable accuracy. A further complication is a lack of knowledge of the saturation mechanisms of flares and magnetic storms. These topics are discussed in some detail.

Validation of a priori CME Arrival Predictions Made Using Real-Time Heliospheric Imager Observations†

Kimberley **Tucker-Hood**^{1,*}, Chris Scott¹, Mathew Owens¹, David Jackson², Luke Barnard¹, Jackie A. Davies³, Steve Crothers³, Chris Lintott⁴, Robert Simpson⁴, Neel P. Savani⁵, J. Wilkinson⁶, B. Harder⁶, G.M. Eriksson⁶, E.M.L Baeten⁶ and Lily Lau Wan Wah

Space Weather, Volume 13, Issue 1, pages 35–48, **2015**

<http://onlinelibrary.wiley.com/doi/10.1002/2014SW001106/abstract>

Between December 2010 and March 2013, volunteers for the Solar Stormwatch (SSW) Citizen Science project have identified and analysed Coronal Mass Ejections (CMEs) in the near real-time STEREO HI observations, in order to make “Fearless Forecasts” of CME arrival times and speeds at Earth. Of the 60 predictions of Earth-directed CMEs, 20 resulted in an identifiable ICME at Earth within 1.5-6 days, with an average error in predicted transit time of 22 h, and average transit time of 82.3 h. The average error in predicting arrival speed is 151 km s^{-1} , with an average arrival speed of 425 km s^{-1} . In the same time period, there were 44 CMEs for which there are no corresponding SSW predictions, and there were 600 days on which there was neither a CME predicted nor observed. A number of metrics show that the SSW predictions do have useful forecast skill, however there is still much room for improvement. We investigate potential improvements by using SSW inputs in three models of ICME propagation: two of constant acceleration and one of

aerodynamic drag. We find that taking account of interplanetary acceleration can improve the average errors of transit time to 19 h and arrival speed to 77kms^{-1} .

Solar Wind Data Assimilation in an Operational Context: Use of Near-Real-Time Data and the Forecast Value of an L5 Monitor

Harriet **Turner**, [Matthew Lang](#), [Mathew Owens](#), [Andy Smith](#), [Pete Riley](#), [Mike Marsh](#), [Siegfried Gonzi](#)
Space Weather [Volume21, Issue5](#) e2023SW003457 **2023**

<https://doi.org/10.1029/2023SW003457>

<https://agupubs.onlinelibrary.wiley.com/doi/epdf/10.1029/2023SW003457>

For accurate and timely space weather forecasting, advanced knowledge of the ambient solar wind is required, both for its direct impact on the magnetosphere and for accurately forecasting the propagation of coronal mass ejections to Earth. Data assimilation (DA) combines model output and observations to form an optimum estimation of reality. Initial experiments with assimilation of in situ solar wind speed observations suggest the potential for significant improvement in the forecast skill of near-Earth solar wind conditions. However, these experiments have assimilated science-quality observations, rather than near-real-time (NRT) data that would be available to an operational forecast scheme. Here, we assimilate both NRT and science observations from the Solar Terrestrial Relations Observatory (STEREO) and near-Earth observations from the Advanced Composition Explorer and Deep Space Climate Observatory spacecraft. We show that solar wind speed forecasts using NRT data are comparable to those based on science-level data. This suggests that an operational solar wind DA scheme would provide significant forecast improvement, with reduction in the mean absolute error of solar wind speed around 46% over forecasts without DA. With a proposed space weather monitor planned for the L5 Lagrange point, we also quantify the solar wind forecast gain expected from L5 observations alongside existing observations from L1. This is achieved using configurations of the STEREO and L1 spacecraft. There is a 15% improvement for forecast lead times of less than 5 days when observations from L5 are assimilated alongside those from L1, compared to assimilation of L1 observations alone. **Apr 2012, Jul 2017**

Quantifying the effect of ICME removal and observation age for in situ solar wind data assimilation

Harriet **Turner**, [Mathew Owens](#), [Matthew Lang](#), [Siegfried Gonzi](#), [Pete Riley](#)

Space Weather e2022SW003109 [Volume20, Issue8](#) **2022**

<https://doi.org/10.1029/2022SW003109>

<https://agupubs.onlinelibrary.wiley.com/doi/epdf/10.1029/2022SW003109>

Accurate space weather forecasting requires advanced knowledge of the solar wind conditions in near-Earth space. Data assimilation (DA) combines model output and observations to find an optimum estimation of reality and has led to large advances in terrestrial weather forecasting. It is now being applied to space weather forecasting. Here, we use solar wind DA with in-situ observations to reconstruct solar wind speed in the ecliptic plane between 30 solar radii and Earth's orbit. This is used to provide solar wind speed hindcasts. Here, we assimilate observations from the Solar Terrestrial Relations Observatory (STEREO) and the near-Earth dataset, OMNI. Analysis of two periods of time, one in solar minimum and one in solar maximum, reveals that assimilating observations from multiple spacecraft provides a more accurate forecast than using any one spacecraft individually. The age of the observations also has a significant impact on forecast error, whereby the mean absolute error (MAE) sharply increases by up to 23% when the forecast lead time first exceeds the corotation time associated with the longitudinal separation between the observing spacecraft and the forecast location. It was also found that removing coronal mass ejections from the DA input and verification time series reduces the forecast MAE by up to 10% as it removes false streams from the forecast time series. This work highlights the importance of an L5 space weather monitoring mission for near-Earth solar wind forecasting and suggests that an additional mission to L4 would further improve future solar wind DA forecasting capabilities.

The Influence of Spacecraft Latitudinal Offset on the Accuracy of Corotation Forecasts

Harriet **Turner**, [Mathew J. Owens](#), [Matthew S. Lang](#), [Siegfried Gonzi](#)

Space Weather [Volume19, Issue8](#) e2021SW002802 **2021**

<https://doi.org/10.1029/2021SW002802>

<https://agupubs.onlinelibrary.wiley.com/doi/epdf/10.1029/2022SW003109>

Knowledge of the ambient solar wind is important for accurate space weather forecasting. A simple-but-effective method of forecasting near-Earth solar wind speed is "corotation," wherein solar wind structure is assumed to be fixed in the reference frame rotating with the Sun. Under this approximation, observations at a source spacecraft can be rotated to a target location, such as Earth. Forecast accuracy depends upon the rate of solar wind evolution, longitudinal and latitudinal separation between the source and target, and latitudinal structure in the solar wind itself. The time-evolution

rate and latitudinal structure of the solar wind are both strongly influenced by the solar cycle, though in opposing ways. A latitudinal separation (offset) between source and target spacecraft is typically present, introducing an error to corotation forecasts. In this study, we use observations from the Solar Terrestrial Relations Observatory (STEREO) and near-Earth spacecraft to quantify the latitudinal error. Aliasing between the solar cycle and STEREO orbits means that individual contributions to the forecast error are difficult to isolate. However, by considering an 18-month interval near the end of solar minimum, we find that the latitudinal-offset contribution to corotation forecast error cannot be directly detected for offsets $<6^\circ$, but is increasingly important as offsets increase. This result can be used to improve solar wind data assimilation, allowing representivity errors in solar wind observations to be correctly specified. Furthermore, as the maximum latitudinal offset between L5 and Earth is $\approx 5^\circ$, corotation forecasts from a future L5 spacecraft should not be greatly affected by latitudinal offset.

Commercial Space Tourism and Space Weather: An Update

Ronald E. [Turner](#)

Space Weather, 10, S11005, 2012

<http://www.agu.org/journals/sw/swa/feature/article/?id=2012SW000868>

A look at the effects radiation exposure could have on biological systems during flights

On the variation of small-amplitude Forbush decreases with solar-geomagnetic parameters

[Ugwu](#), CJ ; [Okike](#), O ; [Menteso](#), FM +++

ASTROPHYSICS AND SPACE SCIENCE 369 Issue 5 Article Number 45 2024

DOI 10.1007/s10509-024-04310-w

<https://www.webofscience.com/wos/woscc/full-record/WOS:001216147700001>

Detection of weak signals remains challenging in astrophysics. This is particularly applicable in the investigation of Forbush events. There is thus, a paucity of catalogs of small-amplitude Forbush decreases (FDs). Detail investigations of the space-weather implications of small FDs are, thus, lacking in the literature. Recently, large catalogs of weak FDs, for the first time, have been published. This work employs the newly created lists of small-amplitude FDs to investigate the statistical link between small FDs and solar-geomagnetic variables. The solar-geomagnetic variables were obtained from the OMNI database. A simple coincident R software code was employed in matching the related solar-geomagnetic variables with the weak Forbush events. The FD dates were taken as the input signal. Scatter plots of FDs against interplanetary magnetic field (IMF), solar wind speed (SWS), planetary K-index (Kp) and planetary A-index (Ap) reveal a negative relationship, while that of FDs against disturbance storm time index (Dst) shows a positive relationship. Statistical significance of these relations were tested. The small-amplitude FDs and solar-geomagnetic variables at Potchefstroom (PTFM) station register statistically significant relations. Non-statistically significant correlation between the small-amplitude FDs and solar-geomagnetic variables were obtained at South Pole (SOPO) station, with the exception of FD-SWS that reveals statistically significant correlation. The differences in the correlation results obtained at the two stations (PTFM and SOPO) could be attributed to the differences in the characteristics of the NM stations. These results suggest that geomagnetic storm indices play important role in the evolution of FDs.

Solar sources of interplanetary magnetic clouds leading to helicity prediction

Roger K. [Ulrich](#), [Pete Riley](#), [T. Tran](#)

Space Weather **Volume16, Issue11** Pages 1668-1685 2018

<https://arxiv.org/ftp/arxiv/papers/1811/1811.03560.pdf>

<http://sci-hub.se/10.1029/2018SW001912>

<https://agupubs.onlinelibrary.wiley.com/doi/epdf/10.1029/2018SW001912>

This study identifies the solar origins of magnetic clouds that are observed at 1 AU and predicts the helical handedness of these clouds from the solar surface magnetic fields. We started with the magnetic clouds listed by the Magnetic Field Investigation (MFI) team supporting NASA's WIND spacecraft in what is known as the MFI table and worked backwards in time to identify solar events that produced these clouds. Our methods utilize magnetograms from the Helioseismic and Magnetic Imager (HMI) instrument on the Solar Dynamics Observatory (SDO) spacecraft so that we could only analyze MFI entries after the beginning of 2011. This start date and the end date of the MFI table gave us 37 cases to study. Of these we were able to associate only eight surface events with clouds detected by WIND at 1 AU. We developed a simple algorithm for predicting the cloud helicity which gave the correct handedness in all eight cases. The algorithm is based on the conceptual model that an ejected flux tube has two magnetic origination points at the positions of the strongest radial magnetic field regions of opposite polarity near the places where the ejected arches end at the solar surface. We were unable to find events for the remaining 29 cases: lack of a halo or partial halo CME in an

appropriate time window, lack of magnetic and/or filament activity in the proper part of the solar disk, or the event was too far from disk center. The occurrence of a flare was not a requirement for making the identification but in fact flares, often weak, did occur for seven of the eight cases. **2011.02.15, 2011.06.01, 2011.06.02, 2011.09.13, 2012.06.06, 2012.06.14, 2012.09.02, 2012.11.10**

Generation of a North/South Magnetic Field Component from Variations in the Photospheric Magnetic Field

Roger K. **Ulrich**, Tham Tran

Solar Phys. **2016**

<http://arxiv.org/pdf/1603.02697v1.pdf>

We address the problem of calculating the transverse magnetic field in the solar wind outside of the hypothetical sphere called the source surface where the solar wind originates. This calculation must overcome a widely used fundamental assumption about the source surface -- the field is normally required to purely radial at the source surface. Our model rests on the fact that a change in the radial field strength at the source surface is a change in the field line density. Surrounding field lines must move laterally in order to accommodate this field line density change. As the outward wind velocity drags field lines past the source surface this lateral component of motion produces a tilt implying there is a transverse component to the field. An analytic method of calculating the lateral translation speed of the field lines is developed. We apply the technique to an interval of approximately two Carrington rotations at the beginning of 2011 using 2-h averages of data from the Helioseismic Magnetic Imager instrument on the Solar Dynamics Observatory spacecraft. We find that the value of the transverse magnetic field is dominated on a global scale by the effects of high latitude concentrations of field lines being buffeted by supergranular motions. **7 January - 2 March 2011**

On the formation of solar wind & switchbacks, and quiet Sun heating

Vishal **Upendran** (1), [Durgesh Tripathi](#) (1)

ApJ **2021**

<https://arxiv.org/pdf/2111.11668.pdf>

The solar coronal heating in quiet Sun (QS) and coronal holes (CH), including solar wind formation, are intimately tied by magnetic field dynamics. Thus, a detailed comparative study of these regions is needed to understand the underlying physical processes. CHs are known to have subdued intensity and larger blueshifts in the corona. This work investigates the similarities and differences between CHs and QS in the chromosphere using the Mg II h & k, C II lines, and transition region using Si IV line, for regions with identical absolute magnetic flux density ($|B|$). We find CHs to have subdued intensity in all the lines, with the difference increasing with line formation height and $|B|$. The chromospheric lines show excess upflows and downflows in CH, while Si IV shows excess upflows (downflows) in CHs (QS), where the flows increase with $|B|$. We further demonstrate that the upflows (downflows) in Si IV are correlated with both upflows and downflows (only downflows) in the chromospheric lines. CHs (QS) show larger Si IV upflows (downflows) for similar flows in the chromosphere, suggesting a common origin to these flows. These observations may be explained due to impulsive heating via interchange (closed-loop) reconnection in CHs (QS), resulting in bidirectional flows at different heights, due to differences in magnetic field topologies. Finally, the kinked field lines from interchange reconnection may be carried away as magnetic field rotations and observed as switchbacks. Thus, our results suggest a unified picture of solar wind emergence, coronal heating, and near-Sun switchback formation.

IRIS Nugget Feb 2022 <https://iris.lmsal.com/nugget>

Solar wind prediction using deep learning

Vishal **Upendran**, [M.C.M Cheung](#), [Shravan Hanasoge](#), [Ganapathi Krishnamurthi](#)

Space Weather e2020SW002478 **2020**

<https://arxiv.org/pdf/2006.05825.pdf>

<https://agupubs.onlinelibrary.wiley.com/doi/epdf/10.1029/2020SW002478>

Emanating from the base of the Sun's corona, the solar wind fills the interplanetary medium with a magnetized stream of charged particles whose interaction with the Earth's magnetosphere has space-weather consequences such as geomagnetic storms. Accurately predicting the solar wind through measurements of the spatio-temporally evolving conditions in the solar atmosphere is important but remains an unsolved problem in heliophysics and space-weather research.

In this work, we use deep learning for prediction of solar wind (SW) properties. We use Extreme Ultraviolet images of the solar corona from space based observations to predict the SW speed from the NASA OMNIWEB dataset, measured at Lagrangian point 1. We evaluate our model against autoregressive and naive models, and find that our model outperforms the benchmark models, obtaining a best-fit correlation of 0.55 ± 0.03 with the observed data.

Upon visualization and investigation of how the model uses data to make predictions, we find higher activation at the coronal holes for fast wind prediction (≈ 3 to 4 days prior to prediction), and at the active regions for slow wind prediction. These trends bear an uncanny similarity to the influence of regions potentially being the sources of fast and slow wind, as reported in literature. This suggests that our model was able to learn some of the salient associations between coronal and solar wind structure without built-in physics knowledge. Such an approach may help us discover hitherto unknown relationships in heliophysics datasets. **2012-05-27-30, 2016-01-26**

A Challenging Solar Eruptive Event of 18 November 2003 and the Causes of the 20 November Geomagnetic Superstorm. III. Catastrophe of the Eruptive Filament in a Magnetic Null Point and Formation of an Opposite-Handedness CME

A.M. [Uralov](#) (1), V.V. Grechnev (1), G.V. Rudenko (1), I.I. Myshyakov (1), I.M. Chertok (2), B.P. Filippov (2), V.A. Slemzin (3)

Solar Phys., Volume 289, Issue 10, pp 3747-3772, **2014**

<http://arxiv.org/pdf/1404.3515v1.pdf>

Our analysis in Papers I and II (Grechnev et al., 2014, Solar Phys. 289, 289 and 1279) of the 18 November 2003 solar event responsible for the 20 November geomagnetic superstorm has revealed a complex chain of eruptions. In particular, the eruptive filament encountered a topological discontinuity located near the solar disk center at a height of about 100 Mm, bifurcated, and transformed into a large cloud, which did not leave the Sun. Concurrently, an additional CME presumably erupted close to the bifurcation region. The conjectures about the responsibility of this compact CME for the superstorm and its disconnection from the Sun are confirmed in Paper IV (Grechnev et al., Solar Phys., submitted), which concludes about its probable spheromak-like structure. The present paper confirms the presence of a magnetic null point near the bifurcation region and addresses the origin of the magnetic helicity of the interplanetary magnetic clouds and their connection to the Sun. We find that the orientation of a magnetic dipole constituted by dimmed regions with the opposite magnetic polarities away from the parent active region corresponded to the direction of the axial field in the magnetic cloud, while the pre-eruptive filament mismatched it. To combine all of the listed findings, we come to an intrinsically three-dimensional scheme, in which a spheromak-like eruption originates via the interaction of the initially unconnected magnetic fluxes of the eruptive filament and pre-existing ones in the corona. Through a chain of magnetic reconnections their positive mutual helicity was transformed into the self-helicity of the spheromak-like magnetic cloud.

Force-field parameterization of the galactic cosmic ray spectrum: Validation for Forbush decreases

I.G. [Usoskin](#), [G.A. Kovaltsovc](#), [O. Adrianid](#), [e](#), [G.C. Barbarinof](#), [g](#), [G.A. Bazilevskayah](#), et al.

Advances in Space Research [Volume 55, Issue 12](#), 15 June **2015**, Pages 2940–2945

A useful parametrization of the energy spectrum of galactic cosmic rays (GCR) near Earth is offered by the so-called force-field model which describes the shape of the entire spectrum with a single parameter, the modulation potential. While the usefulness of the force-field approximation has been confirmed for regular periods of solar modulation, it was not tested explicitly for disturbed periods, when GCR are locally modulated by strong interplanetary transients. Here we use direct measurements of protons and α -particles performed by the PAMELA space-borne instrument during **December 2006**, including a major Forbush decrease, in order to directly test the validity of the force-field parameterization. We conclude that (1) The force-field parameterization works very well in describing the energy spectra of protons and α -particles directly measured by PAMELA outside the Earth's atmosphere; (2) The energy spectrum of GCR can be well parameterized by the force-field model also during a strong Forbush decrease; (3) The estimate of the GCR modulation parameter, obtained using data from the world-wide neutron monitor network, is in good agreement with the spectra directly measured by PAMELA during the studied interval. This result is obtained on the basis of a single event analysis, more events need to be analyzed.

Solar modulation parameter for cosmic rays since 1936 reconstructed from ground-based neutron monitors and ionization chambers,

[Usoskin](#), I. G., G. A. Bazilevskaya, and G. A. Kovaltsov
(2011), J. Geophys. Res., 116, A02104,

The differential energy spectrum of galactic cosmic rays near Earth is often parameterized by the force field model with the only time-dependent parameter, the modulation potential. Here we present a series of reconstructed monthly values of the modulation potential for the period from July 1936 through December 2009. This work extends our earlier study by employing new data and improving the reconstruction method. The presented series is a composite of three parts. The most reliable part is based on data from the world network of sea level neutron monitors and covers the period since April 1964. The part between February 1951 and March 1964 is based on data from one to two mountain neutron monitors of IGY type and is characterized by larger uncertainties and possible systematic error. The part related to the period before 1951 is based on data from Forbush ground-based ionization chambers and is characterized by large uncertainties and should be taken with caveats. The reconstructed series has been tested against long-term data of balloon-borne measurements of flux of cosmic ray ionizing radiation in the stratosphere performed by the Lebedev Institute since 1957. The comparison shows good agreement since 1964 but suggests that the result before 1964 may contain larger errors in that the NM-based reconstruction method may underestimate the low energy part of GCR spectrum.

Solar and interplanetary precursors of geomagnetic storms in solar cycle 23

J. **Uwamahoro**, L.-A. McKinnell

Adv. Space Res., V.51(3), Pages 395-410, 2013, File

<http://www.sciencedirect.com/science/article/pii/S0273117712006242>

Estimating the magnetic storm effectiveness of solar and associated interplanetary phenomena is of practical importance for space weather modelling and prediction. This article presents results of a qualitative and quantitative analysis of the probable causes of geomagnetic storms during the 11-year period of solar cycle 23: 1996–2006. Potential solar causes of 229 magnetic storms ($Dst \leq -50$ nT) were investigated with a particular focus on halo coronal mass ejections (CMEs). A 5-day time window prior to the storm onset was considered to track backward the Sun's eruptions of halo CMEs using the SOHO/LASCO CMEs catalogue list. Solar and interplanetary (IP) properties associated with halo CMEs were investigated and correlated to the resulting geomagnetic storms (GMS). In addition, a comparative analysis between full and partial halo CME-driven storms is established. The results obtained show that about 83% of intense storms ($Dst \leq -100$ nT) were associated with halo CMEs. For moderate storms (-100 nT $< Dst \leq -50$ nT), only 54% had halo CME background, while the remaining 46% were assumed to be associated with corotating interaction regions (CIRs) or undetected frontside CMEs. It was observed in this study that intense storms were mostly associated with full halo CMEs, while partial halo CMEs were generally followed by moderate storms. This analysis indicates that up to 86% of intense storms were associated with interplanetary coronal mass ejections (ICMEs) at 1 AU, as compared to moderate storms with only 44% of ICME association. Many other quantitative results are presented in this paper, providing an estimate of solar and IP precursor properties of GMS within an average 11-year solar activity cycle. The results of this study constitute a key step towards improving space weather modelling and prediction.

Tables

Revised Reconstruction of the Heliospheric Modulation Potential for 1964–2022

Pauli **Väisänen**, [Ilya Usoskin](#), [Riikka Kähkönen](#), [Sergey Koldobskiy](#), [Kalevi Mursula](#)

JGR [Volume128, Issue41](#) e2023JA031352 2023

<https://doi.org/10.1029/2023JA031352>

<https://agupubs.onlinelibrary.wiley.com/doi/epdf/10.1029/2023JA031352>

Galactic cosmic rays (GCRs) impinge on the Earth's atmosphere and generate showers of secondary particles in nuclear collisions with the atmospheric constituents. The flux of GCR near Earth is subjected to heliospheric modulation driven by solar magnetic activity and to geomagnetic shielding. Variability of the GCR flux is continuously monitored by the worldwide network of ground-based neutron monitors (NMs) since the 1950s. Solar modulation is often quantified via the force-field approximation parameterized by the modulation potential ϕ , which can be evaluated from the global NM data set. Here we revisit the methodology and provide an updated and extended reconstruction of the heliospheric modulation potential for 1964–2022, using a recent NM yield function and the measurements of the 10 most stable high-latitude NMs. A key improvement in the reconstructed heliospheric modulation potential is the new daily resolution, which provides new opportunities for further research. Reconstruction uses the root-mean square error (RMSE) minimization to find the optimum daily and monthly scaling factors for individual NMs. The stability of the reconstruction is analyzed and the errors are estimated. The mean level of uncertainty is low, generally within $\pm 1\%$, but it is found to depict marginal variability at the 11-year, annual and 27-day timescales at the $< 1\%$ level, indicating that a very small systematic uncertainty is still present.

Seven Decades of Neutron Monitors (1951–2019): Overview and Evaluation of Data Sources

Pauli Väisänen, Ilya Usoskin, Kalevi Mursula

JGR [Volume126, Issue5](#) May 2021 e2020JA028941

<https://agupubs.onlinelibrary.wiley.com/doi/epdf/10.1029/2020JA028941>

<https://doi.org/10.1029/2020JA028941>

The worldwide network of neutron monitors (NMs) is the primary instrument to study cosmic-ray variability on time scales of up to 70 yr. Since the 1950s, 147 NMs with publicly available data have been in operation, and their records are archived in and distributed through different repositories and data sources. A comprehensive analysis of all available NM data sets (300 data sets from 147 NMs) is performed here to check the quality and consistency of the data. The data sources include World Data Center for Cosmic Rays, the Neutron Monitor Database, the Pushkov Institute of Terrestrial Magnetism, Ionosphere, and Radiowave Propagation (IZMIRAN) and individual station/institution databases. It was found that the data from the same NM can be nonidentical and of different quality in different sources. We give and tabulate here a recommendation for the optimal data source of each NM. We also present here a list of 29 “prime” stations with the longest and most reliable data. Verified data sets for these prime stations are provided as supplementary information.

Modeling Arrival Time of Coronal Mass Ejections to Near-Earth Orbit Using Coronal Dimming Parameters

Vakhrusheva, AA ; Kaportseva, KB ; Shugay, YS ; Ereemeev, VE ; Kalegaev, VV

COSMIC RESEARCH Volume 62 Issue 4 Page 350-358 APR 2024

DOI 10.1134/S0010952524600422

The paper demonstrates results of modeling arrival time of coronal mass ejections (CME) to near-Earth space with parameters of coronal dimmings in 2010-2018. We use drag-based model (DBM) for CME propagation and empirical model for quasi-stationary solar wind streams. We compared the ICME arrival time and speed forecast for events with coronal source in the central region of the solar disk based on the CME initial speed using (1) CACTus database; (2) dimming maximum intensity drop from Solar Demon database to calculate the initial speed of the CME. Results show that the methods result in similar errors. To study the possibility of predicting ICME, for which a CME may not be observed in the coronagraph for some reason, modeling of ICME was carried out using dimming parameters. In 43% of cases, ICME arrival time were forecasted with an accuracy of 24 h using parameters of dimmings in the central region of solar disk that could not be associated with any CMEs.

Strong geomagnetic activity forecast by neural networks under dominant southern orientation of the interplanetary magnetic field

Fridrich Valacha, , Josef Bochníček, , Pavel Hejdab, , Miloš Revalloc,

Advances in Space Research, 2014

The paper deals with the relation of the southern orientation of the north-south component B_z of the interplanetary magnetic field to geomagnetic activity (GA) and subsequently a method is suggested of using the found facts to forecast potentially dangerous high GA. We have found that on a day with very high GA hourly averages of B_z with a negative sign occur at least 16 times in typical cases. Since it is very difficult to estimate the orientation of B_z in the immediate vicinity of the Earth one day or even a few days in advance, we have suggested using a neural-network model, which assumes the worse of the possibilities to forecast the danger of high GA - the dominant southern orientation of the interplanetary magnetic field. The input quantities of the proposed model were information about X-ray flares, type II and IV radio bursts as well as information about coronal mass ejections (CME). In comparing the GA forecasts with observations, we obtain values of the Hanssen-Kuiper skill score ranging from 0.463 to 0.727, which are usual values for similar forecasts of space weather. The proposed model provides forecasts of potentially dangerous high geomagnetic activity should the interplanetary CME (ICME), the originator of geomagnetic storms, hit the Earth under the most unfavorable configuration of cosmic magnetic fields. We cannot know in advance whether the unfavorable configuration is going to occur or not; we just know that it will occur with the probability of 31%.

Solar energetic particle flux enhancement as a predictor of geomagnetic activity in a neural network - based model,

Valach, F., M. Revallo, J. Bochníček, and P. Hejda (2009),

Space Weather, 7, S04004, doi:10.1029/2008SW000421.

<http://www.agu.org/pubs/crossref/2009/2008SW000421.shtml>

Coronal mass ejections (CMEs) are believed to be the principal cause of increased geomagnetic activity. They are regarded as being in context of a series of related solar energetic events, such as X-ray flares (XRAs) accompanied by solar radio bursts (RSPs) and also by solar energetic particle (SEP) flux. Two types of the RSP events are known to be geoeffective, namely, the RSP of type II, interpreted as the signature of shock initiation in the solar corona, and type IV, representing material moving upward in the corona. The SEP events causing geomagnetic response are known to be produced by CME-driven shocks. In this paper, we use the method of the artificial neural network in order to quantify the geomagnetic response of particular solar events. The data concerning XRAs and RSPs II and/or IV together with their heliographic positions are taken as the input for the neural network. There is a key question posed in our study: can the successfulness of the neural network prediction scheme based solely on the solar disc observations (XRA and RSP) be improved by additional information concerning the SEP flux? To resolve this problem, we chose the SEP events possessing significant enhancement in the 10-h window, commencing 12 h after the generation of XRAs. In particular, we consider the flux of high-energy protons with energies over 10 MeV. We have used a chi-square test to demonstrate that supplying such extra input data improves the neural network prediction scheme.

Improving the Alfvén Wave Solar Atmosphere Model Based on Parker Solar Probe Data

B. [van der Holst](#)¹, J. Huang¹, N. Sachdeva¹, J. C. Kasper¹, W. B. Manchester IV¹, D. Borovikov², B. D. G. Chandran², A. W. Case³, K. E. Korreck³, D. Larson⁴

2022 ApJ 925 146

<https://iopscience.iop.org/article/10.3847/1538-4357/ac3d34/pdf>

In van der Holst et al. (2019), we modeled the solar corona and inner heliosphere of the first encounter of NASA's Parker Solar Probe (PSP) using the Alfvén Wave Solar atmosphere Model (AWSoM) with Air Force Data Assimilative Photospheric flux Transport–Global Oscillation Network Group magnetograms, and made predictions of the state of the solar wind plasma for the first encounter. AWSoM uses low-frequency Alfvén wave turbulence to address the coronal heating and acceleration. Here, we revise our simulations, by introducing improvements in the energy partitioning of the wave dissipation to the electron and anisotropic proton heating and using a better grid design. We compare the new AWSoM results with the PSP data and find improved agreement with the magnetic field, turbulence level, and parallel proton plasma beta. To deduce the sources of the solar wind observed by PSP, we use the AWSoM model to determine the field line connectivity between PSP locations near the perihelion at **2018 November 6 UT 03:27** and the solar surface. Close to the perihelion, the field lines trace back to a negative-polarity region about the equator.

Predictions for the First Parker Solar Probe Encounter

B. [van der Holst](#), [W.B. Manchester](#), [K.G. Klein](#), [J.C. Kasper](#)

ApJL Volume 872, Issue 2, article id. L18, 2019

<https://arxiv.org/pdf/1902.03921.pdf>

<https://iopscience.iop.org/article/10.3847/2041-8213/ab04a5/pdf>

We examine Alfvén Wave Solar atmosphere Model (AWSoM) predictions of the first Parker Solar Probe (PSP) encounter. We focus on the 12-day closest approach centered on the 1st perihelion. AWSoM (van der Holst et al., 2014) allows us to interpret the PSP data in the context of coronal heating via Alfvén wave turbulence. The coronal heating and acceleration is addressed via outward-propagating low-frequency Alfvén waves that are partially reflected by Alfvén speed gradients. The nonlinear interaction of these counter-propagating waves results in a turbulent energy cascade. To apportion the wave dissipation to the electron and anisotropic proton temperatures, we employ the results of the theories of linear wave damping and nonlinear stochastic heating as described by Chandran et al. (2011). We find that during the first encounter, PSP was in close proximity to the heliospheric current sheet (HCS) and in the slow wind. PSP crossed the HCS two times, namely at **2018/11/03 UT 01:02** and **2018/11/08 UT 19:09** with perihelion occurring on the south of side of the HCS. We predict the plasma state along the PSP trajectory, which shows a dominant proton parallel temperature causing the plasma to be firehose unstable.

Magnetic Flux Emergence, Activity, Eruptions and Magnetic Clouds: Following Magnetic Field from the Sun to the Heliosphere A review

L. [van Driel-Gesztelyi](#) · J.L. Culhane

Space Sci Rev (2009) 144: 351–381, **File**

We present an [overview](#) of how the principal physical properties of magnetic flux which emerges from the toroidal fields in the tachocline through the turbulent convection zone to the solar surface are linked to solar activity events, emphasizing the effects of magnetic field evolution and interaction with other magnetic structures on the latter. We compare the results of different approaches using various magnetic observables to evaluate the probability of flare and coronal mass ejection (CME) activity and forecast eruptive activity on the short term (i.e. days). Then, after a brief

overview of the observed properties of CMEs and their theoretical models, we discuss the ejecta properties and describe some typical magnetic and composition characteristics of magnetic clouds (MCs) and interplanetary CMEs (ICMEs). We review some individual examples to clarify the link between eruptions from the Sun and the properties of the resulting ejecta. The importance of a synthetic approach to solar and interplanetary magnetic fields and activity is emphasized.

Interplanetary flux ropes of any twist distribution

M. [Vandas](#)¹ and E. P. Romashets²

A&A 627, A90 (2019)

DOI: 10.1051/0004-6361/201935216

Context. Recent investigations indicate that the magnetic field configuration in interplanetary flux ropes is in contrast with the common magnetic field models that are used to fit them, namely constant-alpha force-free fields, whose twist increases without limits toward the flux-rope boundary. Therefore, magnetic field configurations with a constant twist are now being employed in fits.

Aims. Real flux ropes have varying twist. Therefore, analytical magnetic field configurations with prescribed twist distributions are searched for in cylindrical geometry.

Methods. Equations for the field solenoidality and for the force-free condition are solved for case when a twist profile is prescribed.

Results. A model of a force-free magnetic field configuration with an arbitrarily given twist distribution in a cylinder and its relative helicity per unit length are presented. It is applied to a core-envelope model recently suggested in studies of twist in magnetic clouds.

Magnetic cloud fit by uniform-twist toroidal flux ropes

M. [Vandas](#)¹ and E. Romashets

A&A 608, A118 (2017)

<https://www.aanda.org/articles/aa/pdf/2017/12/aa31412-17.pdf>

Context. Detailed studies of magnetic cloud observations in the solar wind in recent years indicate that magnetic clouds are interplanetary flux ropes with a low twist. Commonly, their magnetic fields are fit by the axially symmetric linear force-free field in a cylinder (Lundquist field), which in contrast has a strong and increasing twist toward the boundary of the flux rope. Therefore another field, the axially symmetric uniform-twist force-free field in a cylinder (Gold-Hoyle field) has become employed to analyze magnetic clouds.

Aims. Magnetic clouds are bent, and for some observations, a toroidal rather than a cylindrical flux rope is needed for a local approximation of the cloud fields. We therefore try to derive an axially symmetric uniform-twist force-free field in a toroid, either exactly, or approximately, and to compare it with observations.

Methods. Equations following from the conditions of solenoidality and force-freeness in toroidally curved cylindrical coordinates were solved analytically. The magnetic field and velocity observations of a magnetic cloud were compared with solutions obtained using a nonlinear least-squares method.

Results. Three solutions of (nearly) uniform-twist magnetic fields in a toroid were obtained. All are exactly solenoidal, and in the limit of high aspect ratios, they tend to the Gold-Hoyle field. The first solution has an exactly uniform twist, the other two solutions have a nearly uniform twist and approximate force-free fields. The analysis of a magnetic cloud observation showed that these fields may fit the observed field equally well as the already known approximately linear force-free (Miller-Turner) field, but it also revealed that the geometric parameters of the toroid might not be reliably determined from fits, when (nearly) uniform-twist model fields are used. Sets of parameters largely differing in the size of the toroid and its aspect ratio yield fits of a comparable quality. **April 22, 2001**

Toroidal Flux Ropes with Elliptical Cross Sections and Their Magnetic Helicity

M. [Vandas](#), E. Romashets

[Solar Physics](#) September 2017, 292:129

Axially symmetric constant-alpha force-free magnetic fields in toroidal flux ropes with elliptical cross sections are constructed in order to investigate how their alphas and magnetic helicities depend on parameters of the flux ropes. Magnetic configurations are found numerically using a general solution of a constant-alpha force-free field with an axial symmetry in cylindrical coordinates for a wide range of oblatenesses and aspect ratios. Resulting alphas and magnetic helicities are approximated by polynomial expansions in parameters related to oblateness and aspect ratio. These approximations hold for toroidal as well as cylindrical flux ropes with an accuracy better than or of about 1%. Using

these formulae, we calculate relative helicities per unit length of two (probably very oblate) magnetic clouds and show that they are very sensitive to the assumed magnetic cloud shapes (circular versus elliptical cross sections).

Modeling of magnetic cloud expansion

M. [Vandas](#)¹, E. Romashets² and A. Geranios

A&A 583, A78 (2015)

Aims. Magnetic clouds are large interplanetary flux ropes that propagate in the solar wind from the Sun and that expand during their propagation. We check how magnetic cloud models, represented by cylindrical magnetic flux ropes, which include expansion, correspond to in situ observations.

Methods. Spacecraft measurements of magnetic field and velocity components inside magnetic clouds with clearly expressed expansion are studied in detail and fit by models. The models include expanding cylindrical linear force-free flux ropes with circular or elliptic cross sections.

Results. From the period of 1995–2009, 26 magnetic clouds were fit by the force-free model of an expanding circular cylindrical flux rope. Expansion velocity profiles qualitatively correspond to model ones in the majority of cases (81%) and quantitatively in more than half of them (58%). In four cases an elliptic cross section significantly improved a match between observed and modeled expansion velocity profiles.

Conclusions. Analysis of velocity components tests magnetic cloud models more strictly and may reveal information on magnetic cloud shapes.

How do fits of simulated magnetic clouds correspond to their real shapes in 3-D?

M. [Vandas](#)¹, E. Romashets^{2,3}, and A. Geranios⁴

Ann. Geophys., 28, 1581-1588, 2010

Magnetic clouds are important objects for space weather forecasters due to their impact on the Earth's magnetosphere and their consequences during geomagnetic storms. Being considered as cylindrical or toroidal flux ropes, their size, velocity, magnetic field strength, and axis orientation determine its impact on Earth. Above mentioned parameters are usually extracted from model fits using measurements from one-spacecraft crossings of these structures. In order to relate solar events with these spacecraft observations, the parameters are then compared to situation at the Sun around a most probable source region with a goal to correlate them with near-Sun observed quantities for prediction purposes. In the past we performed three-dimensional simulations of magnetic cloud propagation in the inner heliosphere. Simulated spacecraft measurements are fitted by models of magnetic clouds and resulting parameters are compared with real shapes of magnetic clouds which can be directly obtained from our simulations. The comparison shows that cloud parameters are determined quite reliably for spacecraft crossings near the cloud axis.

Investigation of the Geoeffectiveness of CMEs Associated with IP Type II Radio Bursts

V. [Vasanth](#), Y. Chen, X. L. Kong, B. Wang

Solar Phys. Volume 290, [Issue 6](#), pp 1815-1826 2015

We perform a statistical analysis of the geoeffectiveness of coronal mass ejections (CMEs) that are associated with interplanetary (IP) type II bursts in Solar Cycle 23 during the period 1997 – 2008. About 47 % (109 out of 232) of IP type II bursts are found to be associated with geomagnetic storms. Of these 47 %, 27 % are associated with moderate, 14 % with intense, and 6 % with severe geomagnetic storms. We find that the IP type II bursts and their corresponding end frequencies can be used as indicators of CME geoeffectiveness: the lower the type II burst end frequency, the higher the possibility of having a stronger storm. In addition, we show that various combinations of CME remote-sensing and IP type II parameters can be used to improve geomagnetic storm forecasting.

The largest imaginable magnetic storm

Vytenis M. [Vasyliūnas](#)

Journal of Atmospheric and Solar-Terrestrial Physics, Volume 73, Issues 11-12, 2011, Pages 1444-1446

The size of a magnetic storm is measured by the maximum depression of the horizontal magnetic field at the Earth's equator. The largest depression that could possibly occur can be estimated by noting that the geomagnetic field is inflated by plasma pressure in the magnetosphere that is enhanced above the effective pressure of the surrounding medium (magnetosheath and magnetotail), and that this pressure enhancement results largely from adiabatic compression as plasma is transported inward into dipolar flux tubes of decreasing volume. A rough but reasonable upper

limit can then be estimated by setting the effective plasma pressure equal to the magnetic pressure of the dipole field at the equator of each flux tube, and applying the Dessler–Parker–Scopke theorem. The upper limit thus obtained for the (negative) value of the Dst index is ; for comparison, the largest depression yet observed is estimated as .

Coronal mass ejection-driven shocks and the associated sudden commencements/sudden impulses

Veenadhari, B.; Selvakumaran, R.; Singh, Rajesh; Maurya, Ajeet K.; Gopalswamy, N.; Kumar, Sushil; Kikuchi, T.

J. Geophys. Res., Vol. 117, No. A4, A04210, **2012**

<http://dx.doi.org/10.1029/2011JA017216>

Interplanetary (IP) shocks are mainly responsible for the sudden compression of the magnetosphere, causing storm sudden commencement (SC) and sudden impulses (SIs) which are detected by ground-based magnetometers. On the basis of **the list of 222 IP shocks compiled by Gopalswamy et al. (2010)**, we have investigated the dependence of SC/SIs amplitudes on the speed of the coronal mass ejections (CMEs) that drive the shocks near the Sun as well as in the interplanetary medium. We find that about 91% of the IP shocks were associated with SC/SIs. The average speed of the SC/SI-associated CMEs is 1015 km/s, which is almost a factor of 2 higher than the general CME speed. When the shocks were grouped according to their ability to produce type II radio burst in the interplanetary medium, we find that the radio-loud (RL) shocks produce a much larger SC/SI amplitude (average ~32 nT) compared to the radio-quiet (RQ) shocks (average ~19 nT). Clearly, RL shocks are more effective in producing SC/SIs than the RQ shocks. We also divided the IP shocks according to the type of IP counterpart of interplanetary CMEs (ICMEs): magnetic clouds (MCs) and nonmagnetic clouds. We find that the MC-associated shock speeds are better correlated with SC/SI amplitudes than those associated with non-MC ejecta. The SC/SI amplitudes are also higher for MCs than ejecta. Our results show that RL and RQ type of shocks are important parameters in producing the SC/SI amplitude.

Origin and Characteristics of the Southward Component of the Interplanetary Magnetic Field

Giuliana **Verbanac** & [Mario Bandić](#)

[Solar Physics](#) volume 296, Article number: 183 (**2021**)

<https://doi.org/10.1007/s11207-021-01930-1>

We investigate the rectified interplanetary magnetic field (IMF) components in two coordinate systems, GSEQ and GSM, focusing on the southward pointing component (B_s in GSM within the period 1999 – 2017. The analysis is performed for different solar activity levels. The obtained results are valuable for the theoretical interpretation of IMF components variations and variations seen in geomagnetic indices. B_s ordered according to the polarity exhibits a “pair of spectacles” pattern. This reveals that B_s can also exist for toward/away field in fall/spring. The field is reduced, but it is not zero. Thus, in “unfavorable” seasons, geomagnetic activity can be due to reduced B_s and not because the field is northward pointing. We show that patterns of the experimental B_s fields are not in agreement with the Russell-McPherron model of B_s as widely assumed. The present study contributes in understanding the nature and behavior of B_s , which is the important element that controls the reconnection process and has a great influence on terrestrial space weather over the solar cycle.

Comparison of magnetic properties in a magnetic cloud and its solar source on

April 11-14 2013

P. **Vemareddy**, C. Möstl, T. Rollett, [W. Mishra](#), [C. Farrugia](#), [M. Leitner](#)

ApJ **828** 12 **2016**

<http://arxiv.org/pdf/1607.03811v1.pdf>

In the context of Sun-Earth connection of coronal mass ejections and magnetic flux ropes (MFRs), we studied the solar active region (AR) and the magnetic properties of magnetic cloud (MC) event during **April 14-15, 2013**. We use in-situ observations from the Advanced Composition Explorer and source AR measurements from the Solar Dynamic Observatory. The MCs magnetic structure is reconstructed from the Grad-Shafranov method which reveals a northern component of the axial field with left-handed helicity. The MC invariant axis is highly inclined to the ecliptic plane pointing northward and is rotated by 117° with respect to the source region PIL. The net axial flux and current in the MC are comparatively higher than from the source region. Linear force-free alpha distribution (10^{-7} – 10^{-6} m⁻¹) at the sigmoid leg matches the range of twist number in the MC of 1-2 AU MFR. The MFR is non-linear force-free with decreasing twist from the axis (9 turns/AU) towards the edge. Therefore Gold-Hoyle (GH) configuration, assuming a constant twist, is more consistent with the MC structure than the Lundquist configuration of increasing twist from the axis to boundary. As an indication to that, the GH configuration yields better fitting to the global trend of in-situ magnetic field components, in terms of rms, than the Lundquist model. These cylindrical configurations improved the

MC fitting results when considered the effect of self-similar expansion of MFR. For such twisting behaviour, this study suggests an alternative fitting procedure to better characterise the MC magnetic structure and its source region links.

A Full Study on the Sun-Earth Connection of an Earth-Directed CME Magnetic Flux Rope

P. **Vemareddy**, W. Mishra

ApJ **2015**

<http://arxiv.org/pdf/1510.01846v1.pdf>

We present an investigation of an eruption event of coronal mass ejection (CME) magnetic flux rope (MFR) from source active region (AR) NOAA 11719 on **11 April 2013** utilizing observations from SDO, STEREO, SOHO, and WIND spacecraft. The source AR consists of pre-existing sigmoidal structure stacked over a filament channel which is regarded as MFR system. EUV observations of low corona suggest a further development of this MFR system by added axial flux through tether-cutting reconnection of loops at the middle of sigmoid under the influence of continuous slow flux motions during past two days. Our study implies that the MFR system in the AR is initiated to upward motion by kink-instability and further driven by torus-instability. The CME morphology, captured in simultaneous three-point coronagraph observations, is fitted with Graduated Cylindrical Shell (GCS) model and discerns an MFR topology with orientation aligning with magnetic neutral line in the source AR. This MFR expands self-similarly and is found to have source AR twist signatures in the associated near Earth magnetic cloud (MC). We further derived kinematics of this CME propagation by employing a plethora of stereoscopic as well as single spacecraft reconstruction techniques. While stereoscopic methods perform relatively poorly compared to other methods, fitting methods worked best in estimating the arrival time of the CME compared to in-situ measurements. Supplied with values of constrained solar wind velocity, drag parameter and 3D kinematics from GCS fit, we construct CME kinematics from the drag based model consistent with in-situ MC arrival.

Relationship between CME velocity and active region magnetic energy

P. **Venkatakrishnan**, B. Ravindra

GEOPHYSICAL RESEARCH LETTERS, VOL. 30, NO. 23, 2181, **2003**; **File**

We find an empirical relationship between the initial speed of Coronal Mass Ejection (CME) and the potential magnetic field energy of the associated active region (AR) that closely resembles the Sedov relation between the speed of a blast wave and the blast energy. We conclude that it is the magnetic energy of an AR that drives the CME. The restructuring of the AR field lines in the corona which can push material with Alfvén speed and thus inject energy into the plasma on a time scale shorter than the dynamical time of the corona, is a likely process that can drive the CME. The empirical relationship allows the prediction of the maximum speed of a CME that can result from an AR of a given magnetic energy.

Extreme geomagnetic storms – 1868 – 2010

Vennerstrøm, S., Lefevre, L., Dumbovic, M., Crosby, N., Malandraki, O., Patsou, I., Clette, F., Veronig, A., Vrsnak, B., Leer, K., Moretto, T.:

2016, Solar Phys. Volume 291, Issue 5, pp 1447-1481, DOI: 10.1007/s11207-016-0897-y **File**

sci-hub.se/10.1007/s11207-016-0897-y

<https://link.springer.com/content/pdf/10.1007%2Fs11207-016-0897-y.pdf>

We present the first large statistical study of extreme geomagnetic storms based on historical data from the time period 1868 – 2010. This article is the first of two companion papers. Here we describe how the storms were selected and focus on their near-Earth characteristics. The second article presents our investigation of the corresponding solar events and their characteristics. The storms were selected based on their intensity in the aa index, which constitutes the longest existing continuous series of geomagnetic activity. They are analyzed statistically in the context of more well-known geomagnetic indices, such as the Kp and Dcx/Dst index. This reveals that neither Kp nor Dcx/Dst provide a comprehensive geomagnetic measure of the extreme storms. We rank the storms by including long series of single magnetic observatory data. The top storms on the rank list are the New York Railroad storm occurring in May 1921 and the Quebec storm from March 1989. We identify key characteristics of the storms by combining several different available data sources, lists of storm sudden commencements (SSCs) signifying occurrence of interplanetary shocks, solar wind in-situ measurements, neutron monitor data, and associated identifications of Forbush decreases as well as satellite measurements of energetic proton fluxes in the near-Earth space environment. From this we find, among other results, that the extreme storms are very strongly correlated with the occurrence of interplanetary shocks (91 – 100 %), Forbush decreases (100 %), and energetic solar proton events (70 %). A quantitative comparison of these associations relative to less intense storms is also presented. Most notably, we find that most often the extreme storms are characterized by a complexity that is associated with multiple, often interacting, solar wind disturbances and that they

frequently occur when the geomagnetic activity is already elevated. We also investigate the semiannual variation in storm occurrence and confirm previous findings that geomagnetic storms tend to occur less frequently near solstices and that this tendency increases with storm intensity. However, we find that the semiannual variation depends on both the solar wind source and the storm level. Storms associated with weak SSC do not show any semiannual variation, in contrast to weak storms without SSC.

Table 2 List of geomagnetic parameters for the 105 extreme storms

Table 5 Cosmic-ray and energetic particle characteristics of the extreme storms (FD)

Solar-wind predictions for the Parker Solar Probe orbit Near-Sun extrapolations derived from an empirical solar-wind model based on Helios and OMNI observations

M. S. [Venzmer](#) and V. Bothmer

A&A 611, A36 (2018)

<http://sci-hub.tw/https://www.aanda.org/articles/aa/abs/2018/03/aa31831-17/aa31831-17.html>

Context. The Parker Solar Probe (PSP; formerly Solar Probe Plus) mission will be humanity's first in situ exploration of the solar corona with closest perihelia at 9.86 solar radii (R_{\odot}) distance to the Sun. It will help answer hitherto unresolved questions on the heating of the solar corona and the source and acceleration of the solar wind and solar energetic particles. The scope of this study is to model the solar-wind environment for PSPs unprecedented distances in its prime mission phase during the years 2018 to 2025. The study is performed within the Coronagraphic German And US SolarProbePlus Survey (CGAUSS) which is the German contribution to the PSP mission as part of the Wide-field Imager for Solar PRobe.

Aim. We present an empirical solar-wind model for the inner heliosphere which is derived from OMNI and Helios data. The German-US space probes Helios 1 and Helios 2 flew in the 1970s and observed solar wind in the ecliptic within heliocentric distances of 0.29 au to 0.98 au. The OMNI database consists of multi-spacecraft intercalibrated in situ data obtained near 1 au over more than five solar cycles. The international sunspot number (SSN) and its predictions are used to derive dependencies of the major solar-wind parameters on solar activity and to forecast their properties for the PSP mission.

Methods. The frequency distributions for the solar-wind key parameters, magnetic field strength, proton velocity, density, and temperature, are represented by lognormal functions. In addition, we consider the velocity distributions bi-componental shape, consisting of a slower and a faster part. Functional relations to solar activity are compiled with use of the OMNI data by correlating and fitting the frequency distributions with the SSN. Further, based on the combined data set from both Helios probes, the parameters frequency distributions are fitted with respect to solar distance to obtain power law dependencies. Thus an empirical solar-wind model for the inner heliosphere confined to the ecliptic region is derived, accounting for solar activity and for solar distance through adequate shifts of the lognormal distributions. Finally, the inclusion of SSN predictions and the extrapolation down to PSPs perihelion region enables us to estimate the solar-wind environment for PSPs planned trajectory during its mission duration.

Results. The CGAUSS empirical solar-wind model for PSP yields dependencies on solar activity and solar distance for the solar-wind parameters' frequency distributions. The estimated solar-wind median values for PSPs first perihelion in 2018 at a solar distance of 0.16 au are 87 nT, 340 km s⁻¹, 214 cm⁻³, and 503 000 K. The estimates for PSPs first closest perihelion, occurring in 2024 at 0.046 au (9.86 R_{\odot}), are 943 nT, 290 km s⁻¹, 2951 cm⁻³, and 1 930 000 K. Since the modeled velocity and temperature values below approximately 20 R_{\odot} appear overestimated in comparison with existing observations, this suggests that PSP will directly measure solar-wind acceleration and heating processes below 20 R_{\odot} as planned.

Reply to Comment on “Origin and Characteristics of the Southward Component of the Interplanetary Magnetic Field”

Giuliana [Verbanac](#) & [Mario Bandić](#)

[Solar Physics](#) volume 297, Article number: 156 (2022)

<https://doi.org/10.1007/s11207-022-02086-2>

Dr. Christopher T. Russell (C.T.R.) recently made comments (Solar Phys. 297, 119, [2022](#)) on the paper of Verbanac and Bandić, hereinafter referred to as B.V.2021 (Solar Phys. 296, 183, [2021](#)). C.T.R. claimed that analyses of B.V.2021 was not performed in the proper coordinate system and that “Russell-McPherron effect” was not determined due to the employed 1-hour resolution of the interplanetary magnetic field (IMF) data. In this paper, we reply to these comments and explain why they are unfounded.

Origin and Characteristics of the Southward Component of the Interplanetary Magnetic Field

Giuliana Verbanac & Mario Bandić

Solar Physics volume 296, Article number: 183 (2021)

<https://link.springer.com/content/pdf/10.1007/s11207-021-01930-1.pdf>

We investigate the rectified interplanetary magnetic field (IMF) components in two coordinate systems, GSEQ and GSM, focusing on the southward pointing component (BsBs) in GSM within the period 1999 – 2017. The analysis is performed for different solar activity levels. The obtained results are valuable for the theoretical interpretation of IMF components variations and variations seen in geomagnetic indices. BsBs ordered according to the polarity exhibits a “pair of spectacles” pattern. This reveals that BsBs can also exist for toward/away field in fall/spring. The field is reduced, but it is not zero. Thus, in “unfavorable” seasons, geomagnetic activity can be due to reduced BsBs and not because the field is northward pointing. We show that patterns of the experimental BsBs fields are not in agreement with the Russell-McPherron model of BsBs as widely assumed. The present study contributes in understanding the nature and behavior of BsBs, which is the important element that controls the reconnection process and has a great influence on terrestrial space weather over the solar cycle.

Comments: by Christopher T. Russell, *Solar Physics* volume 297, Article number: 119 (2022)

<https://doi.org/10.1007/s11207-022-02043-z>

Comparison of geoeffectiveness of coronal mass ejections and corotating interaction regions

G. Verbanac¹, S. Živković¹, B. Vršnak², M. Bandić³ and T. Hojsak

A&A 558, A85 (2013); **File**

Context. A detailed comparison of the geomagnetic responses to interplanetary coronal mass ejection (ICMEs) and corotating interaction regions (CIRs) during solar cycle 23 was performed using geomagnetic indices Dst, Ap, and AE. **Aims.** We aim to find out if there are relative differences in the response of various magnetospheric current systems to the impact of ICMEs and CIRs. In addition, we are exploring the possibility of forecasting geomagnetic activity using the coronagraphic observations of the ICME take-off.

Methods. The peak values of the plasma characteristics of ICMEs and CIRs (velocity V , magnetic field B , and BV related to the electric field), and geomagnetic indices were investigated by applying the linear and power-law cross correlation analysis. The influence of the time-resolution on the results was performed for two time resolutions obtained by one-hour (three-hour for Ap) and six-hour data averaging.

Results. For ICMEs the power-law fits are found to be important only for the relationships between BV and geomagnetic indices. For Ap and Dst, there is no difference between the one-hour (three-hour for Ap) and six-hour option. For AE, the one-hour data distribution shows more clearly the non-linear dependence on BV . Our data set shows that below $BV \sim 5 \text{ mV m}^{-1}$ ICMEs have practically no geomagnetic effect at low and mid latitudes, but at high latitudes at least some geomagnetic activity will be triggered. For all HSS/CIRs dependencies, a power law is found to better describe the data than the linear fit. The data distributions show that BV has to reach $\sim 4 \text{ mV m}^{-1}$ in order to drive at least some geomagnetic activity at all latitudes. We observed that there are fast CMEs that have almost no geomagnetic effect at low and mid latitudes. On the other hand, at high latitudes, fast CMEs always trigger some geomagnetic activity. This might have implications for space weather forecasting.

Conclusions. Magnetospheric response to both solar drivers (ICMEs and CIRs) is different at various latitudes, thus results in different development of various current systems within the Earth’s magnetosphere and ionosphere.

Furthermore, we show that ICMEs and CIRs cause different geomagnetic activity. In the case of ICMEs equatorial current system responses in a linear manner, while the response of the polar-current system is likely to be non-linear. For HSS/CIRs, apparently all current systems respond in a non-linear way, especially the polar current system.

Solar wind high-speed streams and related geomagnetic activity in the declining phase of solar cycle 23

G. Verbanac¹, B. Vršnak², S. Živković¹, T. Hojsak¹, A. M. Veronig³ and M. Temmer

A&A 533, A49 (2011), **File**

Context. Coronal holes (CHs) are the source of high-speed streams (HSSs) in the solar wind, whose interaction with the slow solar wind creates corotating interaction regions (CIRs) in the heliosphere.

Aims. We investigate the magnetospheric activity caused by CIR/HSS structures, focusing on the declining phase of the solar cycle 23 (years 2005 and 2006), when the occurrence rate of coronal mass ejections (CMEs) was low. We aim to (i) perform a systematic analysis of the relationship between the CH characteristics, basic parameters of HSS/CIRs, and

the geomagnetic indices Dst, Ap and AE; (ii) study how the magnetospheric/ionospheric current systems behave when influenced by HSS/CIR; (iii) investigate if and how the evolution of the background solar wind from 2005 to 2006 affected the correlations between CH, CIR, and geomagnetic parameters.

Methods. The cross-correlation analysis was applied to the fractional CH area (CH) measured in the central meridian distance interval $\pm 10^\circ$, the solar wind velocity (V), the interplanetary magnetic field (B), and the geomagnetic indices Dst, Ap, and AE.

Results. The performed analysis shows that Ap and AE are better correlated with CH and solar wind parameters than Dst, and quantitatively demonstrates that the combination of solar wind parameters BV2 and BV plays the central role in the process of energy transfer from the solar wind to the magnetosphere.

Conclusions. We provide reliable relationships between CH properties, HSS/CIR parameters, and geomagnetic indices, which can be used in forecasting the geomagnetic activity in periods of low CME activity.

Evolution of Solar and Geomagnetic Activity Indices, and Their Relationship: 1960–2001

G. [Verbanac](#), M. Manda, B. Vršnak and S. Sentic
Solar Physics, Volume 271, Numbers 1-2, 183-195, 2011

We employ annually averaged solar and geomagnetic activity indices for the period 1960–2001 to analyze the relationship between different measures of solar activity as well as the relationship between solar activity and various aspects of geomagnetic activity. In particular, to quantify the solar activity we use the sunspot number R_s , group sunspot number R_g , cumulative sunspot area Cum, solar radio flux F10.7, and interplanetary magnetic field strength IMF. For the geomagnetic activity we employ global indices Ap, Dst and Dcx, as well as the regional geomagnetic index RES, specifically estimated for the European region. In the paper we present the relative evolution of these indices and quantify the correlations between them. Variations have been found in: i) time lag between the solar and geomagnetic indices; ii) relative amplitude of the geomagnetic and solar activity peaks; iii) dual-peak distribution in some of solar and geomagnetic indices. The behavior of geomagnetic indices is correlated the best with IMF variations. Interestingly, among geomagnetic indices, RES shows the highest degree of correlation with solar indices.

Equatorial coronal holes, solar wind high-speed streams, and their geoeffectiveness

G. [Verbanac](#)¹, B. Vršnak², A. Veronig³, and M. Temmer³
A&A 526, A20 (2011), [File](#)

Context. Solar wind high-speed streams (HSSs), originating in equatorial coronal holes (CHs), are the main driver of the geomagnetic activity in the late-declining phase of the solar cycle.

Aims. We analyze correlations between CH characteristics, HSSs parameters, and the geomagnetic activity indices, to establish empirical relationships that would provide forecasting of the solar wind characteristics, as well as the effect of HSSs on the geomagnetic activity in periods when the effect of coronal mass ejections is low.

Methods. We apply the cross-correlation analysis to the fractional CH area (CH) measured between central meridian distances $\pm 10^\circ$, solar wind parameters (flow velocity V , proton density n , temperature T , and the magnetic field B), and the geomagnetic indices Dst and Ap .

Results. The cross-correlation analysis reveals a high degree of correlation between all studied parameters. In particular, we show that the Ap index is considerably more sensitive to HSS and CH characteristics than Dst . The Ap and Dst indices are most tightly correlated with the solar wind parameter $BV2$.

Conclusions. From the point of view of space weather, the most important result is that the established empirical relationships provide a few-days-in-advance forecasting of the HSS characteristics and the related geomagnetic activity at the six-hour resolution.

Four decades of geomagnetic and solar activity: 1960-2001

[Verbanac](#), G., Vršnak, B., Temmer, M., Manda, M., & Korte, M.
2010, J. Atmos. Sol. Terr. Phys., 607

<http://www.sciencedirect.com/science/article/pii/S136468261000074X>

We analyze the relationship between some space weather indices (Dst, Ap, F10.7) and geomagnetic effects on the regional (European) scale, over the period 1960-2001. The remaining external field signal (RES) detected in the Northward magnetic component of the European observatory annual means are used as an indicator of the regional geomagnetic activity. Relationship RES-F10.7 suggests correction factors for getting the geomagnetic annual means of the Northern component less affected by the external sources. We have found some time lags among investigated

parameters. These delays may suggest that the Ap responds to the solar activity in a differently than Dst and RES, Ap being more sensitive to the high-speed streams (HSS) and the Alfvénic waves present in HSS, while Dst and RES being more influenced by the coronal mass ejections activity (CME).

The evolution of coronal mass ejections in the inner heliosphere: Implementing the spheromak model with EUHFORIA

C. [Verbeke](#), J. Pomoell and S. Poedts

A&A 627, A111 (2019)

[sci-hub.se/10.1051/0004-6361/201834702](https://doi.org/10.1051/0004-6361/201834702)

Aims. We introduce a new model for coronal mass ejections (CMEs) that has been implemented in the magnetohydrodynamics (MHD) inner heliosphere model EUHFORIA. Utilising a linear force-free spheromak (LFFS) solution, the model provides an intrinsic magnetic field structure for the CME. As a result, the new model has the potential to predict the magnetic components of CMEs at Earth. In this paper, we present the implementation of the new model and show the capability of the new model.

Methods. We present initial validation runs for the new magnetised CME model by considering the same set of events as used in the initial validation run of EUHFORIA that employed the Cone model. In particular, we have focused on modelling the CME that was responsible for creating the largest geomagnetic disturbance (Dst index). Two scenarios are discussed: one where a single magnetised CME is launched and another in which we launch all five Earth-directed CMEs that were observed during the considered time period. Four out of the five CMEs were modelled using the Cone model.

Results. In the first run, where the propagation of a single magnetized CME is considered, we find that the magnetic field components at Earth are well reproduced as compared to in-situ spacecraft data. Considering a virtual spacecraft that is separated approximately seven heliographic degrees from the position of Earth, we note that the centre of the magnetic cloud is missing Earth and a considerably larger magnetic field strength can be found when shifting to that location. For the second run, launching four Cone CMEs and one LFFS CME, we notice that the simulated magnetised CME is arriving at the same time as in the corresponding full Cone model run. We find that to achieve this, the speed of the CME needs to be reduced in order to compensate for the expansion of the CME due to the addition of the magnetic field inside the CME. The reduced initial speed of the CME and the added magnetic field structure give rise to a very similar propagation of the CME with approximately the same arrival time at 1 au. In contrast to the Cone model, however, the magnetised CME is able to predict the magnetic field components at Earth. However, due to the interaction between the Cone model CMEs and the magnetised CME, the magnetic field amplitude is significantly lower than for the run using a single magnetised CME.

Conclusions. We have presented the LFFS model that is able to simulate and predict the magnetic field components and the propagation of magnetised CMEs in the inner heliosphere and at Earth. We note that shifting towards a virtual spacecraft in the neighbourhood of Earth can give rise to much stronger magnetic field components. This gives the option of adding a grid of virtual spacecrafts to give a range of values for the magnetic field components.

2015-06-18, 2015-06-19, 2015-06-21, 2015-06-22, 2015-06-25

Benchmarking CME Arrival Time and Impact: Progress on Metadata, Metrics, and Events

C. [Verbeke](#), [M. L. Mays](#), [M. Temmer](#), [S. Bingham](#), [R. Steenburgh](#), [M. Dumbović](#), [M. Núñez](#), [L.K. Jian](#), [P. Hess](#), [C. Wiegand](#), [A. Taktakishvili](#), [J. Andries](#)

Space Weather special issue: Space Weather Capabilities Assessment 17(1) Pages: 6-26 2019

<https://arxiv.org/pdf/1811.10695.pdf>

<https://agupubs.onlinelibrary.wiley.com/doi/epdf/10.1029/2018SW002046>

Accurate forecasting of the arrival time and subsequent geomagnetic impacts of Coronal Mass Ejections (CMEs) at Earth is an important objective for space weather forecasting agencies. Recently, the CME Arrival and Impact working team has made significant progress towards defining community-agreed metrics and validation methods to assess the current state of CME modeling capabilities. This will allow the community to quantify our current capabilities and track progress in models over time. Firstly, it is crucial that the community focuses on the collection of the necessary metadata for transparency and reproducibility of results. Concerning CME arrival and impact we have identified 6 different metadata types: 3D CME measurement, model description, model input, CME (non-)arrival observation, model output data and metrics and validation methods. Secondly, the working team has also identified a validation time period, where all events within the following two periods will be considered: 1 January 2011-31 December 2012 and January 2015-31 December 2015. Those two periods amount to a total of about 100 hit events at Earth and a large amount of misses. Considering a time period will remove any bias in selecting events and the event set will represent a sample set that will

not be biased by user selection. Lastly, we have defined the basic metrics and skill scores that the CME Arrival and Impact working team will focus on. **2010-04-03, 2013-03-15, 2014-01-07, 2015-03-15**

Turbulent Heating in the Accelerating Region Using a Multishell Model

Andrea **Verdini**, Roland Grappin, Victor Montagué-Camps

[Solar Physics](#) May 2019, 294:65

<https://link.springer.com/content/pdf/10.1007%2Fs11207-019-1458-y.pdf>

Recent studies of turbulence-driven solar winds indicate that fast winds are obtained only at the price of unrealistic bottom boundary conditions: too large wave amplitudes and small frequencies. In this work, the incompressible turbulent dissipation is modeled with a large-scale von Karman–Howarth–Kolmogorov-like phenomenological expression (Q0K41QK410). An evaluation of the phenomenology is thus necessary to understand if unrealistic boundary conditions result from physical or model limitations. To assess the validity of the Kolmogorov-like expression, Q0K41QK410, one needs to compare it to exact heating, which requires describing the cascade in detail. This has been done in the case of homogeneous MHD turbulence, including expansion, but not in the critical accelerating region. To assess the standard incompressible turbulent heating in the accelerating region, we use a reduced MHD model (multishell model) in which the perpendicular turbulent cascade is described by a shell model, allowing to reach a Reynolds number of 106106. We first consider the homogeneous and expanding cases, and find that primitive MHD and multishell equations give remarkably similar results. We thus feel free to use the multishell model in the accelerating region. The results indicate that the large-scale phenomenology is inaccurate and it overestimates the heating by a factor at least 20, thus invalidating earlier studies of winds driven by incompressible turbulence. We conclude that realistic 1D wind models cannot be based solely on incompressible turbulence, but probably need an addition of compressible turbulence and shocks to increase the wave reflection and thus the heating.

PATCH: Particle Arrival Time Correlation for Heliophysics

J. L. **Verniero**, [G. G. Howes](#), [D. E. Stewart](#), [K. G. Klein](#)

JGR [Volume126, Issue5](#) May 2021 e2020JA028940

<https://agupubs.onlinelibrary.wiley.com/doi/epdf/10.1029/2020JA028940>

<https://doi.org/10.1029/2020JA028940>

The ability to understand the fundamental nature of the physics that governs the heliosphere requires spacecraft instrumentation to measure energy transfer at kinetic scales. This translates to a time cadence resolving the proton kinetic timescales, typically of the order of the proton gyrofrequency. The downlinked survey-mode data from modern spacecraft are often much lower resolution than this criterion, meaning that the higher resolution, burst-mode data must be captured to study an event at kinetic time scales. Telemetry restrictions, however, prohibit a sizable fraction of this burst-mode data from being downlinked to the ground. The field-particle correlation (FPC) technique can quantify kinetic-scale energy transfer between electromagnetic fields and charged particles and identify the mechanisms responsible for mediating the transfer. In this study, we adapt the FPC technique for calculating wave-particle energy transfer onboard modern spacecraft using time-tagged particle counts simultaneous with electromagnetic field measurements. The newly developed procedure, called Particle Arrival Time Correlation for Heliophysics (PATCH), is tested using synthetic spacecraft data, where output from a gyrokinetic plasma turbulence simulation was downsampled to Parker Solar Probe (PSP) energy-angle resolution. We assess the ability of the PATCH algorithm to recover the qualitative and quantitative features of the resulting velocity-space signatures, such as ion-Landau damping, that can be used to distinguish different kinetic mechanisms of particle energization. Ultimately, we demonstrate a proof-of-concept that the PATCH method could enable calculations of onboard wave-particle correlations, with the intent of enhancing spacecraft data return by several orders of magnitude.

The multi-scale nature of the solar wind

Review

Daniel **Verscharen** (UCL/MSSL, UNH), [Kristopher G. Klein](#) (UA), [Bennett A. Maruca](#) (UD)

Living Reviews in Solar Physics 16, Article number: 5 2019

<https://arxiv.org/pdf/1902.03448.pdf>

<https://link.springer.com/content/pdf/10.1007/s41116-019-0021-0.pdf>

The solar wind is a magnetized plasma and as such exhibits collective plasma behavior associated with its characteristic spatial and temporal scales. The characteristic length scales include the size of the heliosphere, the collisional mean free paths of all species, their inertial lengths, their gyration radii, and their Debye lengths. The characteristic timescales include the expansion time, the collision times, and the periods associated with gyration, waves, and oscillations. We review the past and present research into the multi-scale nature of the solar wind based on in-situ spacecraft measurements and plasma theory. We establish the notion that couplings of processes across scales are important for the

global dynamics and thermodynamics of the solar wind. We describe methods to measure in-situ properties of particles and fields. We then discuss the role of expansion effects, non-equilibrium distribution functions, collisions, waves and turbulence, and kinetic microinstabilities for the multi-scale plasma evolution.

Nine Outstanding Questions of Solar Wind Physics

Review

Nicholeen M. [Viall](#), [Joseph E. Borovsky](#)

JGR [Volume 125, Issue 7](#) July 2020 e2018JA026005

<https://agupubs.onlinelibrary.wiley.com/doi/pdfdirect/10.1029/2018JA026005>

In situ measurements of the solar wind have been available for almost 60 years, and in that time plasma physics simulation capabilities have commenced and ground-based solar observations have expanded into space-based solar observations. These observations and simulations have yielded an increasingly improved knowledge of fundamental physics and have delivered a remarkable understanding of the solar wind and its complexity. Yet there are longstanding major unsolved questions. Synthesizing inputs from the solar wind research community, nine outstanding questions of solar wind physics are developed and discussed in this commentary. These involve questions about the formation of the solar wind, about the inherent properties of the solar wind (and what the properties say about its formation), and about the evolution of the solar wind. The questions focus on (1) origin locations on the Sun, (2) plasma release, (3) acceleration, (4) heavy-ion abundances and charge states, (5) magnetic structure, (6) Alfvén waves, (7) turbulence, (8) distribution-function evolution, and (9) energetic-particle transport. On these nine questions we offer suggestions for future progress, forward looking on what is likely to be accomplished in near future with data from Parker Solar Probe, from Solar Orbiter, from the Daniel K. Inouye Solar Telescope (DKIST), and from Polarimeter to Unify the Corona and Heliosphere (PUNCH). Calls are made for improved measurements, for higher-resolution simulations, and for advances in plasma physics theory.

How has the solar wind evolved to become what it is today?

Review

A. A. [Vidotto](#)

Proceedings IAU Symposium 372. 2022

<https://arxiv.org/pdf/2211.15400.pdf>

In this contribution, I briefly review the long-term evolution of the solar wind (its mass-loss rate), including the evolution of observed properties that are intimately linked to the solar wind (rotation, magnetism and activity). I also briefly discuss implications of the evolution of the solar wind on the evolving Earth. I argue that studying exoplanetary systems could open up new avenues for progress to be made in our understanding of the evolution of the solar wind.

The evolution of the solar wind

Review

A. A. [Vidotto](#)

Living Reviews in Solar Physics, V. 18 Article number: 3 2021

<https://arxiv.org/pdf/2103.15748.pdf>

<https://link.springer.com/content/pdf/10.1007/s41116-021-00029-w.pdf>

<https://doi.org/10.1007/s41116-021-00029-w>

How has the solar wind evolved to reach what it is today? In this review, I discuss the long-term evolution of the solar wind, including the evolution of observed properties that are intimately linked to the solar wind: rotation, magnetism and activity. Given that we cannot access data from the solar wind 4 billion years ago, this review relies on stellar data, in an effort to better place the Sun and the solar wind in a stellar context. I overview some clever detection methods of winds of solar-like stars, and derive from these an observed evolutionary sequence of solar wind mass-loss rates. I then link these observational properties (including, rotation, magnetism and activity) with stellar wind models. I conclude this review then by discussing implications of the evolution of the solar wind on the evolving Earth and other solar system planets. I argue that studying exoplanetary systems could open up new avenues for progress to be made in our understanding of the evolution of the solar wind.

On long-term variations of solar wind parameters and solar activity

V.I. [Vlasov](#), [R.D. Dagkesamanskii](#), [V.A. Potapov](#), [S.A. Tyul'bashev](#), [I.V. Chashei](#)

Bulletin of the Lebedev Physics Institute, 2022, v.49, issue 1, pp.6-9

<https://arxiv.org/ftp/arxiv/papers/2208/2208.04158.pdf>

Comparison is carried out of the long term variation of the year averaged solar wind speed and interplanetary scintillation index with the variations of Wolf's numbers and A_P indexes of geomagnetic activity for the data of 20-24

solar activity cycles. It is shown that the slow non-monotonous trend in the scintillation parameters at middle and high heliolatitudes exists with the typical scale of order of century cycle. Correlation between the variations of Wolf's numbers and anomalies of the air temperature is analyzed for long data series from 1610 up to the present time. Possible application of the results to the global climate problem is discussed.

On the evaluation of data quality in the OMNI interplanetary magnetic field database

M. V. [Vokhmyanin](#) , [N. A. Stepanov](#) , [V. A. Sergeev](#)

Space Weather [Volume17, Issue3](#) Pages 476-486 **2019**

sci-hub.tw/10.1029/2018SW002113

The OMNI database is formed by propagating the solar wind measured at around Lagrange point L1, whose result may differ from the actual solar wind in the vicinity of the bow shock nose. To test the quality of the OMNI database we cross-correlate the 2-hr intervals of 1-min interplanetary magnetic field (IMF) data provided mostly by ACE and WIND spacecraft with Geotail measurements in front of the bow shock (10409 cases in 1997-2016). We used two metrics: Pearson correlation coefficient (CC) and prediction efficiency (PE). Confirming previous studies, we found that the prediction quality of actual IMF degrades continuously with increasing distance of OMNI spacecraft from the Sun-Earth line, with the amounts of poor and good predictions become nearly equal for $R_{YZ} \geq 65$ RE (they constitute ~12% of the entire data base). In roughly 20% of the analyzed data, low CC and PE values were the consequence of low IMF variability (a low signal to noise ratio). The remaining data set include 42% of very good data ($CC \geq 0.8$), 33% of relatively good data ($0.5 \leq CC < 0.8$ and $PE \geq 0$), 10% of data having correct variability but wrong absolute values ($0.5 \leq CC < 0.8$ and $PE < 0$), and 15% of poor data ($CC < 0.5$). We also discovered that the OMNI data are generally of a good quality when the PC index of geomagnetic activity correlates well with the solar wind-magnetosphere coupling factor suggested by Kan and Lee (1979).

Radial Evolution of the April 2020 Stealth Coronal Mass Ejection between 0.8 and 1 AU -- A Comparison of Forbush Decreases at Solar Orbiter and Earth

Johan L. Freiherr [von Forstner](#), [Mateja Dumbović](#), [Christian Möstl](#), [Jingnan Guo](#),

[Athanasios Papaioannou](#), Anatoly V. Belov, Maria A. Abunina

A&A **2021**

<https://arxiv.org/pdf/2102.12185.pdf>

Aims. We present observations of the first coronal mass ejection (CME) observed at the Solar Orbiter spacecraft on April 19, 2020, and the associated Forbush decrease (FD) measured by its High Energy Telescope (HET). This CME is a multispacecraft event also seen near Earth the next day.

Methods. We highlight the capabilities of HET for observing small short-term variations of the galactic cosmic ray count rate using its single detector counters. The analytical ForbMod model is applied to the FD measurements to reproduce the Forbush decrease at both locations. Input parameters for the model are derived from both in situ and remote-sensing observations of the CME.

Results. The very slow (~350 km/s) stealth CME caused a FD with an amplitude of 3 % in the low-energy cosmic ray measurements at HET and 2 % in a comparable channel of the Cosmic Ray Telescope for the Effects of Radiation (CRaTER) on the Lunar Reconnaissance Orbiter, as well as a 1 % decrease in neutron monitor measurements. Significant differences are observed in the expansion behavior of the CME at different locations, which may be related to influence of the following high speed solar wind stream. Under certain assumptions, ForbMod is able to reproduce the observed FDs in low-energy cosmic ray measurements from HET as well as CRaTER, but with the same input parameters, the results do not agree with the FD amplitudes at higher energies measured by neutron monitors on Earth. We study these discrepancies and provide possible explanations.

Conclusions. This study highlights that the novel measurements of the Solar Orbiter can be coordinated with other spacecraft to improve our understanding of space weather in the inner heliosphere. Multi-spacecraft observations combined with data-based modeling are also essential to understand the propagation and evolution of CMEs as well as their space weather impacts. **April 19-20, 2020**

Properties of ICME-Induced Forbush decreases at Earth and Mars

Freiherr [von Forstner](#), J.L., Guo, J., Wimmer-Schweingruber, R.F., Dumbovic, M., Janvier, M., Demoulin, P., Veronig, A., Temmer, M., Papaioannou, A., Dasso, S., Hassler, D.M., Zeitlin, C.J.,

JGR **2020**

https://lesia.obspm.fr/perso/pascal-demoulin/20/Freiherr_von_Forstner20_comparing_fds_earth_mars.pdf

Forbush decreases (FDs), which are short-term drops in the flux of galactic cosmic rays (GCR), are caused by the shielding from strong and/or turbulent magnetic structures in the solar wind, especially interplanetary coronal mass

ejections (ICMEs) and their associated shocks, as well as corotating interaction regions (CIRs). Such events can be observed at Earth, e.g. using neutron monitors, but also at many other locations in the solar system, such as on the surface of Mars with the Radiation Assessment Detector (RAD) instrument onboard Mars Science Laboratory (MSL). They are often used as a proxy for detecting the arrival of ICMEs or CIRs, especially when sufficient in situ solar wind measurements are not available. We compare the properties of FDs observed at Earth and Mars, focusing on events produced by ICMEs. We find that FDs at both locations show a correlation between their total amplitude and the maximum hourly decrease, but with different proportionality factors. We explain this difference using theoretical modelling approaches and suggest that it is related to the size increase of ICMEs, and in particular their sheath regions, en route from Earth to Mars. From the FD data, we can derive the sheath broadening factor to be between about 1.5 and 1.9, agreeing with our theoretical considerations. This factor is also in line with previous measurements of the sheath evolution closer to the Sun.

Tracking and validating ICMEs propagating towards Mars using STEREO Heliospheric Imagers combined with Forbush decreases detected by MSL/RAD

Johan L. Freiherr [von Forstner](#), [Jingnan Guo](#), [Robert F. Wimmer-Schweingruber](#), [Manuela Temmer](#), [Mateja Dumbovi](#), [Astrid Veronig](#), [Christian Möstl](#), [Donald M. Hassler](#), [Cary J. Zeitlin](#), [Bent Ehresmann](#)

Space Weather 2019

[sci-hub.se/10.1029/2018SW002138](https://doi.org/10.1029/2018SW002138)

The Radiation Assessment Detector (RAD) instrument onboard the Mars Science Laboratory (MSL) mission's Curiosity rover has been measuring galactic cosmic rays (GCR) as well as solar energetic particles (SEP) on the surface of Mars for more than 6 years since its landing in August 2012. The observations include a large number of Forbush decreases (FD) caused by interplanetary coronal mass ejections (ICMEs) and/or their associated shocks shielding away part of the GCR particles with their turbulent and enhanced magnetic fields while passing Mars.

This study combines MSL/RAD FD measurements and remote tracking of ICMEs using the STEREO Heliospheric Imager (HI) telescopes in a statistical study for the first time. The large dataset collected by HI makes it possible to analyze 149 ICMEs propagating towards MSL both during its 8-month cruise phase and after its landing on Mars. We link 45 of the events observed at STEREO-HI to their corresponding FDs at MSL/RAD and study the accuracy of the ICME arrival time at Mars predicted from HI data using different methods.

The mean differences between the predicted arrival times and those observed using FDs range from -11 h to 5 h for the different methods, with standard deviations between 17 and 20 hours. These values for predictions at Mars are very similar compared to other locations closer to the Sun, and also comparable to the precision of some other modeling approaches.

Using Forbush decreases to derive the transit time of ICMEs propagating from 1 AU to Mars

Johan L. Freiherr [von Forstner](#), [Jingnan Guo](#), [Robert F. Wimmer-Schweingruber](#), [Donald M. Hassler](#), [Manuela Temmer](#), [Mateja Dumbović](#), [Lan K. Jian](#), [Jan K. Appel](#), [Jaša Čalogović](#), [Bent Ehresmann](#), [Bernd Heber](#), [Henning Lohf](#), [Arik Posner](#), [Christian T. Steigies](#), [Bojan Vršnak](#), [Cary J. Zeitlin](#)

JGR Volume 123, Issue 1 January 2018 Pages 39–56

<https://arxiv.org/pdf/1712.07301.pdf>

The propagation of 15 interplanetary coronal mass ejections (ICMEs) from Earth's orbit (1 AU) to Mars (~ 1.5 AU) has been studied with their propagation speed estimated from both measurements and simulations. The enhancement of magnetic fields related to ICMEs and their shock fronts cause the so-called Forbush decrease, which can be detected as a reduction of galactic cosmic rays measured on-ground. We have used galactic cosmic ray (GCR) data from in-situ measurements at Earth, from both STEREO A and B as well as GCR measurements by the Radiation Assessment Detector (RAD) instrument onboard Mars Science Laboratory (MSL) on the surface of Mars. A set of ICME events has been selected during the periods when Earth (or STEREO A or B) and Mars locations were nearly aligned on the same side of the Sun in the ecliptic plane (so-called opposition phase). Such lineups allow us to estimate the ICMEs' transit times between 1 and 1.5 AU by estimating the delay time of the corresponding Forbush decreases measured at each location. We investigate the evolution of their propagation speeds before and after passing Earth's orbit and find that the deceleration of ICMEs due to their interaction with the ambient solar wind may continue beyond 1 AU. We also find a substantial variance of the speed evolution among different events revealing the dynamic and diverse nature of eruptive solar events. Furthermore, the results are compared to simulation data obtained from two CME propagation models, namely the Drag-Based Model and ENLIL plus cone model. **Table 2.** Table of all the ICMEs examined in this study

ICMES IN THE OUTER HELIOSPHERE AND AT HIGH LATITUDES:

AN INTRODUCTION

R. **VON STEIGER**^{1,*} and J. D. RICHARDSON²
Space Science Reviews (2006) 123: 111–126

Magnetic Reconnection within the Boundary Layer of a Magnetic Cloud in the Solar Wind

Zoltán Vörös, [Ali Varsani](#), [Emiliya Yordanova](#), [Yury L. Sasunov](#), [Owen W. Roberts](#), [Árpád Kis](#), [Rumi Nakamura](#), [Yasuhito Narita](#)

JGR **Volume 126, Issue 9** e2021JA029415 2021

<https://arxiv.org/pdf/2108.09049.pdf>

<https://agupubs.onlinelibrary.wiley.com/doi/epdf/10.1029/2021JA029415>

<https://doi.org/10.1029/2021JA029415>

The twisted local magnetic field at the front or rear regions of the magnetic clouds (MCs) associated with interplanetary coronal mass ejections (ICMEs) is often nearly opposite to the direction of the ambient interplanetary magnetic field (IMF). There is also observational evidence for magnetic reconnection (MR) outflows occurring within the boundary layers of MCs. In this paper a MR event located at the western flank of the MC occurring on **2000-10-03** is studied in detail. Both the large-scale geometry of the helical MC and the MR outflow structure are scrutinized in a detailed multi-point study. The ICME sheath is of hybrid propagation-expansion type. Here the freshly reconnected open field lines are expected to slip slowly over the MC resulting in plasma mixing at the same time. As for MR, the current sheet geometry and the vertical motion of the outflow channel between ACE-Geotail-WIND spacecraft was carefully studied and tested. The main findings on MR include: (1) First-time observation of non-Petschek-type slow-shock-like discontinuities in the inflow regions; (2) Observation of turbulent Hall magnetic field associated with a Lorentz force deflected electron jet; (3) Acceleration of protons by reconnection electric field and their back-scatter from the slow shock-like discontinuity; (4) Observation of relativistic electron near the MC inflow boundary/separatrix; these electron populations can presumably appear as a result of non-adiabatic acceleration, gradient B drift and via acceleration in the electrostatic potential well associated with the Hall current system; (5) Observation of Doppler shifted ion-acoustic and Langmuir waves in the MC inflow region.

Automated shock detection and analysis algorithm for space weather application

[Vorotnikov](#), Vasily S.; [Smith](#), Charles W.; [Hu](#), Qiang; [Szabo](#), Adam; [Skoug](#), Ruth M.;
[Cohen](#), Christina M. S.

Space Weather, Vol. 6, No. 3, S03002, 2008.

To help better monitor incoming solar disturbances, space weather researchers are developing a tool that can find and analyze shocks in interplanetary plasma data without operator intervention.

Space weather applications have grown steadily as real-time data have become increasingly available. Numerous industrial applications have arisen with safeguarding of the power distribution grids being a particular interest. NASA uses short-term and long-term space weather predictions in its launch facilities. Researchers studying ionospheric, auroral, and magnetospheric disturbances use real-time space weather services to determine launch times. Commercial airlines, communication companies, and the military use space weather measurements to manage their resources and activities. As the effects of solar transients upon the Earth's environment and society grow with the increasing complexity of technology, better tools are needed to monitor and evaluate the characteristics of the incoming disturbances. A need is for automated shock detection and analysis methods that are applicable to in situ measurements upstream of the Earth. Such tools can provide advance warning of approaching disturbances that have significant space weather impacts. Knowledge of the shock strength and speed can also provide insight into the nature of the approaching solar transient prior to arrival at the magnetopause. We report on efforts to develop a tool that can find and analyze shocks in interplanetary plasma data without operator intervention. This method will run with sufficient speed to be a practical space weather tool providing useful shock information within 1 min of having the necessary data to ground. The ability to run without human intervention frees space weather operators to perform other vital services. We describe ways of handling upstream data that minimize the frequency of false positive alerts while providing the most complete description of approaching disturbances that is reasonably possible.

The Science Case for the 4 π Perspective: A Polar/Global View for Studying the Evolution & Propagation of the Solar Wind and Solar Transients mini-Review

A. [Vourlidas](#), [S. Gibson](#), [D. Hassler](#), [T. Hoeksema](#), [M. Linton](#), [N. Lugaz](#), [J. Newmark](#)

White Paper submitted to the Heliophysics 2050 Workshop 2020

<https://arxiv.org/ftp/arxiv/papers/2009/2009.04880.pdf>

To make progress on the open questions on CME/CIR propagation, their interactions and the role and nature of the ambient solar wind, we need spatially resolved coverage of the inner heliosphere -- both in-situ and (critically) imaging - - at temporal scales matching the evolutionary timescales of these phenomena (tens of minutes to hours), and from multiple vantage points. The polar vantage is uniquely beneficial because of the wide coverage and unique perspective it provides. The ultimate goal is to achieve full 4π coverage of the solar surface and atmosphere by 2050.

Predicting the geoeffective properties of coronal mass ejections: current status, open issues and path forward

Review

A. [Vourlidas](#), [S. Patsourakos](#), and [N. P. Savani](#)

Philosophical Transactions of the Royal Society A v. 377 [Issue 2148](#) Article ID:20180096 **2019** File <https://royalsocietypublishing.org/doi/pdf/10.1098/rsta.2018.0096>

Much progress has been made in the study of coronal mass ejections (CMEs), the main drivers of terrestrial space weather thanks to the deployment of several missions in the last decade. The flow of energy required to power solar eruptions is beginning to be understood. The initiation of CMEs is routinely observed with cadences of tens of seconds with arc-second resolution. Their inner heliospheric evolution can now be imaged and followed routinely. Yet relatively little progress has been made in predicting the geoeffectiveness of a particular CME. Why is that? What are the issues holding back progress in medium-term forecasting of space weather? To answer these questions, we review, here, the measurements, status and open issues on the main CME geoeffective parameters; namely, their entrained magnetic field strength and configuration, their Earth arrival time and speed, and their mass (momentum). We offer strategies for improving the accuracy of the measurements and their forecasting in the near and mid-term future. To spark further discussion, we incorporate our suggestions into a top-level draft action plan that includes suggestions for sensor deployment, technology development and modelling/theory improvements.

2. Forecasting coronal mass ejection time of arrivals and speeds at 1 AU

(a) Empirical models (b) Drag-based models (c) Shock-based models (d) Magnetohydrodynamic models (e) Machine learning (f) Assessment of time-of-arrival studies (g) Hit/miss (h) What limits the accuracy of coronal mass ejection arrival prediction? (i) Path forward

3. Forecasting coronal mass ejection mass at 1 AU

(a) State-of-the-art (b) Issues and path forward

4. Forecasting coronal mass ejection size at 1 AU

(a) State-of-the-art (b) Issues and path forward

5. Forecasting coronal mass ejection magnetic fields at 1 AU

(a) Decomposing the B_z problem (b) The magnitude of the magnetic field (c) Empirical models (d) Why is difficult to predict B_z ? (e) Path forward

Mission to the Sun-Earth L5 Lagrangian Point: An Optimal Platform for Space Weather Research

Angelos [Vourlidas](#)

Space Weather [Volume 13, Issue 4](#) April **2015** Pages 197–201

Space Weather Quarterly Vol. 12, Issue 2, pp. 9-13, **2015**

<http://onlinelibrary.wiley.com/doi/10.1002/SWQv12i002/epdf>

The Sun-Earth Lagrangian L5 point is a uniquely advantageous location for space weather research and monitoring. It covers the “birth-to-impact” travel of solar transients; it enables imaging of solar activity at least 3 days prior to a terrestrial viewpoint and measures the solar wind conditions 4–5 days ahead of Earth impact. These observations, especially behind east limb magnetograms, will be a boon for background solar wind models, which are essential for coronal mass ejection (CME) and shock propagation forecasting. From an operational perspective, the L5 orbit is the space weather equivalent to the geosynchronous orbit for weather satellites. Optimal for both research and monitoring, an L5 mission is ideal for developing a Research-to-Operations capability in Heliophysics.

First Direct Observation of the Interaction between a Comet and a Coronal Mass Ejection Leading to a Complete Plasma Tail Disconnection

[Vourlidas](#), Angelos; Davis, Chris J.; Eyles, Chris J.; Crothers, Steve R.; Harrison, Richard A.; Howard, Russell A.; Moses, J. Daniel; Socker, Dennis G.

The Astrophysical Journal, Volume 668, Issue 1, pp. L79-L82, **2007**

This a discovery report of the first direct imaging of the interaction a comet with a coronal mass ejection (CME) in the inner heliosphere with high temporal and spatial resolution. The observations were obtained by the Sun-Earth Connection Coronal and Heliospheric Investigation (SECCHI) Heliospheric Imager-1 (HI-1) aboard the STEREO mission. They reveal the extent of the plasma tail of comet 2P/Encke to unprecedented lengths and allow us to examine the mechanism behind a spectacular tail disconnection event. Our preliminary analysis suggests that the disconnection is driven by magnetic reconnection between the magnetic field entrained in the CME and the interplanetary field draped around the comet and not by pressure effects. Further analysis is required before we can conclude whether the reconnection occurs on the day side or on the tail side of the comet. However, the observations offer strong support to the idea that large-scale tail disconnections are magnetic in origin. The online movie reveals a wealth of interactions between solar wind structures and the plasma tail beyond the collision with the CME. Future analyses of this data set should provide critical insights on the structure of the inner heliosphere.

Analytic modeling of recurrent Forbush decreases caused by corotating interaction regions

Bojan **Vršnak**, [Mateja Dumbovic](#), [Bernd Heber](#), [Anamarija Kirin](#)

A&A 658, A186 2022

<https://arxiv.org/pdf/2201.09619.pdf>

<https://doi.org/10.1051/0004-6361/202140846>

<https://www.aanda.org/articles/aa/pdf/2022/02/aa40846-21.pdf>

On scales of days, the galactic cosmic ray (GCR) flux is affected by coronal mass ejections and corotating interaction regions (CIRs), causing so-called Forbush decreases and recurrent Forbush decreases (RFDs), respectively. We explain the properties and behavior of RFDs recorded at about 1 au that are caused by CIRs generated by solar wind high-speed streams (HSSs) that emanate from coronal holes. We employed a convection-diffusion GCR propagation model based on the Fokker-Planck equation and applied it to solar wind and interplanetary magnetic field properties at 1 au. Our analysis shows that the only two effects that are relevant for a plausible overall explanation of the observations are the enhanced convection effect caused by the increased velocity of the HSS and the reduced diffusion effect caused by the enhanced magnetic field and its fluctuations within the CIR and HSS structure. These two effects that we considered in the model are sufficient to explain not only the main signatures of RFDs, but also the sometimes observed "over-recovery" and secondary dips in RFD profiles. The explanation in terms of the convection-diffusion GCR propagation hypothesis is tested by applying our model to the observations of a long-lived CIR that recurred over 27 rotations in 2007-2008. Our analysis demonstrates a very good match of the model results and observations.

Analytical and empirical modelling of the origin and heliospheric propagation of coronal mass ejections, and space weather applications

Review

Bojan **Vršnak***

J. Space Weather Space Clim. 2021, 11, 34

<https://www.swsc-journal.org/articles/swsc/pdf/2021/01/swsc200091.pdf>

<https://doi.org/10.1051/swsc/2021012>

The focus is on the physical background and comprehension of the origin and the heliospheric propagation of interplanetary coronal mass ejections (ICMEs), which can cause most severe geomagnetic disturbances. The paper considers mainly the analytical modelling, providing useful insight into the nature of ICMEs, complementary to that provided by numerical MHD models. It is concentrated on physical processes related to the origin of CMEs at the Sun, their heliospheric propagation, up to the effects causing geomagnetic perturbations. Finally, several analytical and statistical forecasting tools for space weather applications are described. **November 3, 1997**

Heliospheric Evolution of Magnetic Clouds

Bojan **Vršnak**, [Tanja Amerstorfer](#), [Mateja Dumbović](#), [Martin Leitner](#), [Astrid M. Veronig](#), [Manuela Temmer](#), [Christian Möstl](#), [Ute V. Amerstorfer](#), [Charles J. Farrugia](#), [Antoinette B. Galvin](#)

ApJ 877:77 2019

<https://arxiv.org/pdf/1904.08266.pdf>

sci-hub.se/10.3847/1538-4357/ab190a

Interplanetary evolution of eleven magnetic clouds (MCs) recorded by at least two radially aligned spacecraft is studied. The in situ magnetic field measurements are fitted to a cylindrically symmetric Gold-Hoyle force-free uniform-twist flux-rope configuration. The analysis reveals that in a statistical sense the expansion of studied MCs is compatible with self-similar behavior. However, individual events expose a large scatter of expansion rates, ranging from very weak to very strong expansion. Individually, only four events show an expansion rate compatible with the isotropic self-similar expansion. The results indicate that the expansion has to be much stronger when MCs are still close to the Sun than in

the studied 0.47 - 4.8 AU distance range. The evolution of the magnetic field strength shows a large deviation from the behavior expected for the case of an isotropic self-similar expansion. In the statistical sense, as well as in most of the individual events, the inferred magnetic field decreases much slower than expected. Only three events show a behavior compatible with a self-similar expansion. There is also a discrepancy between the magnetic field decrease and the increase of the MC size, indicating that magnetic reconnection and geometrical deformations play a significant role in the MC evolution. About half of the events show a decay of the electric current as expected for the self-similar expansion. Statistically, the inferred axial magnetic flux is broadly consistent with it remaining constant. However, events characterized by large magnetic flux show a clear tendency of decreasing flux. **2009 March 10-12, 2009 July 10-12, 2010 November 5-8, 2011 Dec 25-27, 2013 Jan 8-10, 2013 July 11-14**

Geomagnetic Effects of Corotating Interaction Regions

Bojan **Vršnak**, Mateja Dumbović, Jaša Čalogović, Giuliana Verbanac, Ivana Poljanić–Beljan
[Solar Physics](#) September **2017**, 292:140

We present an analysis of the geoeffectiveness of corotating interaction regions (CIRs), employing the data recorded from 25 January to 5 May 2005 and throughout 2008. These two intervals in the declining phase of Solar Cycle 23 are characterised by a particularly low number of interplanetary coronal mass ejections (ICMEs). We study in detail how four geomagnetic-activity parameters (the Dst, Ap, and AE indices, as well as the Dst time derivative, $dDst/dt$) are related to three CIR-related solar wind parameters (flow speed, VV, magnetic field, BB, and the convective electric field based on the southward Geocentric solar magnetospheric (GSM) magnetic field component, VBSVBs) on a three-hour time resolution. In addition, we quantify statistical relationships between the mentioned geomagnetic indices. It is found that Dst is correlated best to VV, with a correlation coefficient of $cc \approx 0.6$, whereas there is no correlation between $dDst/dt$ and VV. The Ap and AE indices attain peaks about half a day before the maximum of VV, with correlation coefficients ranging from $cc \approx 0.6$ to $cc \approx 0.7$, depending on the sample used. The best correlations of Ap and AE are found with VBSVBs with a delay of 3 h, being characterised by $cc \geq 0.6$. The Dst derivative $dDst/dt$ is also correlated with VBSVBs, but the correlation is significantly weaker $cc \approx 0.4 - 0.5$, with a delay of 0 – 3 h, depending on the employed sample. Such low values of correlation coefficients indicate that there are other significant effects that influence the relationship between the considered parameters. The correlation of all studied geomagnetic parameters with BB are characterised by considerably lower correlation coefficients, ranging from $cc = 0.3$ in the case of $dDst/dt$ up to $cc = 0.56$ in the case of Ap. It is also shown that peak values of geomagnetic indices depend on the duration of the CIR-related structures. The Dst is closely correlated with Ap and AE ($cc = 0.7$), Dst being delayed for about 3 h. On the other hand, $dDst/dt$ peaks simultaneously with Ap and AE, with correlation coefficients of 0.48 and 0.56, respectively. The highest correlation ($cc = 0.81$) is found for the relationship between Ap and AE.

Forecasting the Arrival of Coronal Mass Ejections: The Drag-Based Model

Vršnak, B.; Temmer, M.; Žic, T.; Dumbović, M.; Čalogović, J.
Ground-based Solar Observations in the Space Instrumentation Era
ASP Conference Series, Vol. 504, p. 209 **2016**
<http://aspbooks.org/publications/504/209.pdf>

Arrival-time predictions based on the numerical “WSA-ENLIL+Cone model” and the analytical “Drag-based model” (DBM) are analyzed, employing a sample of 50 well observed CMEs. The best match between the two models is obtained if the background solar-wind speed of $w = 400 \text{ km s}^{-1}$ is applied in DBM. It is also demonstrated that both models show similar prediction accuracy.

Propagation of Interplanetary Coronal Mass Ejections: The Drag-Based Model

B. **Vršnak**, T. Žic, D. Vrbanec, M. Temmer, T. Rollett, C. Möstl, A. Veronig, J. Čalogović, M. Dumbović and S. Lulić, et al.
[Solar Physics](#), July **2013**, Volume 285, Issue 1-2, pp 295-315
<http://iopscience.iop.org/1538-4357/668/1/L79/pdf/21977.web.pdf>

We present the “Drag-Based Model” (DBM) of heliospheric propagation of interplanetary coronal mass ejections (ICMEs). The DBM is based on the hypothesis that the driving Lorentz force, which launches a CME, ceases in the upper corona and that beyond a certain distance the dynamics becomes governed solely by the interaction of the ICME and the ambient solar wind. In particular, we consider the option where the drag acceleration has a quadratic dependence on the ICME relative speed, which is expected in a collisionless environment, where the drag is caused primarily by emission of magnetohydrodynamic (MHD) waves. In this paper we present the simplest version of DBM, where the

equation of motion can be solved analytically, providing explicit solutions for the Sun–Earth ICME transit time and impact speed. This offers easy handling and straightforward application to real-time space-weather forecasting. Beside presenting the model itself, we perform an analysis of DBM performances, applying a statistical and case-study approach, which provides insight into the advantages and drawbacks of DBM. Finally, we present a public, DBM-based, online forecast tool. **20 Apr 2007**

The role of aerodynamic drag in propagation of interplanetary coronal mass ejections

B. [Vršnak](#)¹, T. Žic¹, T. V. Falkenberg², C. Möstl^{3,4}, S. Vennerstrom², and D. Vrbanec¹

A&A 512, A43 (2010); **File**

Context. The propagation of interplanetary coronal mass ejections (ICMEs) and the forecast of their arrival on Earth is one of the central issues of space weather studies.

Aims. We investigate to which degree various ICME parameters (mass, size, take-off speed) and the ambient solar-wind parameters (density and velocity) affect the ICME Sun–Earth transit time.

Methods. We study solutions of a drag-based equation of motion by systematically varying the input parameters. The analysis is focused on ICME transit times and 1 AU velocities.

Results. The model results reveal that wide ICMEs of low masses adjust to the solar-wind speed already close to the sun, so the transit time is determined primarily by the solar-wind speed. The shortest transit times and accordingly the highest 1 AU velocities are related to narrow and massive ICMEs (i.e. high-density eruptions) propagating in high-speed solar wind streams. We apply the model to the Sun–Earth event associated with the CME of **25 July 2004** and compare the results with the outcome of the numerical MHD modeling.

Хорошая сводка литературы.

The role of aerodynamic drag in dynamics of coronal mass ejections

Bojan [Vršnak](#), Dijana Vrbanec, Jaša Čalogović and Tomislav Žic

Proceedings of the International Astronomical Union / Volume 4 / Symposium S257, pp 271 – 277,

Published online: 16 Mar 2009, **File**

Dynamics of coronal mass ejections (CMEs) is strongly affected by the interaction of the erupting structure with the ambient magnetoplasma: eruptions that are faster than solar wind transfer the momentum and energy to the wind and generally decelerate, whereas slower ones gain the momentum and accelerate. Such a behavior can be expressed in terms of “aerodynamic” drag. We employ a large sample of CMEs to analyze the relationship between kinematics of CMEs and drag-related parameters, such as ambient solar wind speed and the CME mass. Employing coronagraphic observations it is demonstrated that massive CMEs are less affected by the aerodynamic drag than light ones. On the other hand, in situ measurements are used to inspect the role of the solar wind speed and it is shown that the Sun–Earth transit time is more closely related to the wind speed than to take-off speed of CMEs. These findings are interpreted by analyzing solutions of a simple equation of motion based on the standard form for the drag acceleration. The results show that most of the acceleration/deceleration of CMEs on their way through the interplanetary space takes place close to the Sun, where the ambient plasma density is still high. Implications for the space weather forecasting of CME arrival-times are discussed.

Transit times of interplanetary coronal mass ejections and the solar wind speed:

B. [Vrsnak](#) and T. Zic

A&A 472 (2007) 937-943

Our aim is to find out to what degree the ICME transit time depends on the solar wind speed.

Since the ICME transit time is significantly influenced by the solar wind speed, this effect should be included in statistical and kinematical methods of the space weather forecast.

Coronal Holes and Solar Wind High-Speed Streams:

I. Forecasting the Solar Wind Parameters

II. Forecasting the Geomagnetic Effects

Bojan [Vrsnak](#), Manuela Temmer, Astrid M. Veronig

Solar Phys., 240 (2), Page: 315 – 330, 331 – 346, **2007**; **Files**

The relationship between the coronal hole (CH) area/position and physical characteristics of the associated corotating high-speed stream (HSS) in the solar wind at 1 AU

SuperDARN observations during geomagnetic storms, geomagnetically active times and enhanced solar wind driving.

Walach, M.-T., Grocott, A.:

2019, J. Geophys. Res. Space Phys. 124, 5828.

[sci-hub.se/10.1029/2019JA026816](https://doi.org/10.1029/2019JA026816)

The Super Dual Auroral Radar Network (SuperDARN) was built to study ionospheric convection at Earth and has in recent years been expanded to lower latitudes to observe ionospheric flows over a larger latitude range. This enables us to study extreme space weather events, such as geomagnetic storms, which are a global phenomenon, on a large scale (from the pole to magnetic latitudes of 40°). We study the backscatter observations from the SuperDARN radars during all geomagnetic storm phases from the most recent solar cycle and compare them to other active times to understand radar backscatter and ionospheric convection characteristics during extreme conditions and to discern differences specific to geomagnetic storms and other geomagnetically active times. We show that there are clear differences in the number of measurements the radars make, the maximum flow speeds observed, and the locations where they are observed during the initial, main, and recovery phase. We show that these differences are linked to different levels of solar wind driving. We also show that when studying ionospheric convection during geomagnetically active times, it is crucial to consider data at midlatitudes, as we find that during 19% of storm time the equatorward boundary of the convection is located below 50° of magnetic latitude.

On the Relationship between Magnetic Expansion Factor and Observed Speed of the Solar Wind from Coronal Pseudostreamers

Samantha **Wallace**^{1,2}, C. Nick Arge², Nicholeen Viall², and Ylva Pihlström^{1,3}

2020 ApJ 898 78

<https://doi.org/10.3847/1538-4357/ab98a0>

<https://arxiv.org/ftp/arxiv/papers/2007/2007.16168.pdf>

For the past 30+ yr, the magnetic expansion factor (f_s) has been used in empirical relationships to predict solar wind speed (v_{obs}) at 1 au based on an inverse relationship between these two quantities. Coronal unipolar streamers (i.e., pseudostreamers) undergo limited field line expansion, resulting in f_s -dependent relationships to predict the fast wind associated with these structures. However, case studies have shown that the in situ observed pseudostreamer solar wind was much slower than that derived with f_s . To investigate this further, we conduct a statistical analysis to determine if f_s and v_{obs} are inversely correlated for a large sample of periods when pseudostreamer wind was observed at multiple 1 au spacecraft (i.e., ACE, STEREO-A/B). We use the Wang–Sheeley–Arge model driven by Air Force Data Assimilative Photospheric Flux Transport (ADAPT) photospheric field maps to identify 38 periods when spacecraft observe pseudostreamer wind. We compare the expansion factor of the last open field lines on either side of a pseudostreamer cusp with the corresponding in situ measured solar wind speed. We find that only slow wind ($v_{\text{obs}} < 500 \text{ km s}^{-1}$) is associated with pseudostreamers and that there is not a significant correlation between f_s and v_{obs} for these field lines. This suggests that field lines near the open–closed boundary of pseudostreamers are not subject to the steady-state acceleration along continuously open flux tubes assumed in the $f_s - v_{\text{obs}}$ relationship. In general, dynamics at the boundary between open and closed field lines such as interchange reconnection will invalidate the steady-state assumptions of this relationship.

Estimating Total Open Heliospheric Magnetic Flux

S. **Wallace**, C. N. Arge, M. Pattichis, R. A. Hock-Mysliwiec, C. J. Henney

Solar Physics February **2019**, 294:19

[sci-hub.tw/10.1007/s11207-019-1402-1](https://doi.org/10.1007/s11207-019-1402-1)

Over the solar-activity cycle, there are extended periods where significant discrepancies occur between the spacecraft-observed total (unsigned) open magnetic flux and that determined from coronal models. In this article, the total open heliospheric magnetic flux is computed using two different methods and then compared with results obtained from in-situ interplanetary magnetic-field observations. The first method uses two different types of photospheric magnetic-field maps as input to the Wang–Sheeley–Arge (WSA) model: i) traditional Carrington or diachronic maps, and ii) Air Force Data Assimilative Photospheric Flux Transport model synchronic maps. The second method uses observationally derived helium and extreme-ultraviolet coronal-hole maps overlaid on the same magnetic-field maps in order to compute total open magnetic flux. The diachronic and synchronic maps are both constructed using magnetograms from the same

source, namely the National Solar Observatory Kitt Peak Vacuum Telescope and Vector Spectromagnetograph. The results of this work show that the total open flux obtained from observationally derived coronal holes agrees remarkably well with that derived from WSA, especially near solar minimum. This suggests that, on average, coronal models capture well the observed large-scale coronal-hole structure over most of the solar cycle. Both methods show considerable deviations from total open flux deduced from spacecraft data, especially near solar maximum, pointing to something other than poorly determined coronal-hole area specification as the source of these discrepancies.

Short-Term Prediction of the Dst Index and Estimation of Efficient Uncertainty Using a Hybrid Deep Learning Network

Ruyao Wang, Jianhui Wang, Tuo Liang, Huixiong Zhang

Space Weather [Volume22, Issue12](#) December 2024 e2024SW004002

<https://doi.org/10.1029/2024SW004002>

<https://agupubs.onlinelibrary.wiley.com/doi/epdf/10.1029/2024SW004002>

In this study, we developed a novel deep learning model to predict the disturbance storm time (Dst) index 1–4 hr ahead. We also employed the Monte Carlo (MC) dropout technique to estimate the uncertainty and provide the prediction interval by introducing a recalibration factor. The proposed model achieves excellent scalability by extracting representative embeddings from the Dst index time series through an encoder-decoder framework and integrating these with external solar wind parameters via a prediction network. We utilized magnetic storm data from 1998 to 2018 to evaluate the performance of the prediction model. Experimental results indicate that the proposed model reduces root mean square errors (RMSE) and improves the coefficient of determination (R²) compared to existing methods. Quantitative uncertainty analysis demonstrates that the prediction interval is reliable in most cases. The percent distribution across test storms by comparing the uncertainty-based prediction of the minimum peak with the mean prediction indicates the probabilistic forecast model is competitive. **Oct, 22–Sept 2, 2018**

Table 1. Storms Used to Train the Predicted Model

Table 2. Storms Used to Validate the Predicted Model

Table 3. Storms Used to Test the Predicted Model 1998-2018

Unveiling key factors in solar eruptions leading to the solar superstorm in 2024 May

Rui Wang^{1,2,3*}, Ying D. Liu^{1,2,3}, Xiaowei Zhao^{4,5} and Huidong Hu^{1,2}

A&A 692, A112 (2024)

<https://arxiv.org/pdf/2410.00891> **File**

<https://doi.org/10.1051/0004-6361/202452008>

<https://www.aanda.org/articles/aa/pdf/2024/12/aa52008-24.pdf>

NOAA active region (AR) 13664/8 produced the most intense geomagnetic effects since the Halloween event of 2003. The resulting extreme solar storm is thought to be the consequence of multiple interacting coronal mass ejections (CMEs). Notably, this AR exhibits exceptionally rapid magnetic flux emergence. The eruptions on which we focus all occurred along collisional polarity inversion lines (PILs) through collisional shearing during a three-day period of extraordinarily high flux emergence ($\sim 1021 \text{ Mx h}^{-1}$). Our key findings reveal how photospheric magnetic configurations in eruption sources influence solar superstorm formation and geomagnetic responses, and link exceptionally strong flux emergence to sequential homologous eruptions: (1) We identified the source regions of seven halo CMEs that were distributed primarily along two distinct PILs. This distribution suggests two groups of homologous CMEs. (2) The variations in the magnetic flux emergence rates in the source regions are correlated with the CME intensities. This might explain the two contrasting cases of complex ejecta that are observed at Earth. (3) Our calculations of the magnetic field gradients around the CME source regions show strong correlations with eruptions. This provides crucial insights into solar eruption mechanisms and enhances our prediction capabilities for future events. **May 2024: 4-12, 8, 9, 10,11**

Dynamic Responses of Outer Radiation Belt Electron Phase Space Densities to Geomagnetic Storms: A Statistical Analysis Based on Van Allen Probes Observations

Xiaoyu Wang, Binbin Ni, Xing Cao, Xin Ma, Yuan Lei, Xiankang Dou

Space Weather [Volume22, Issue11](#) November 2024 e2024SW004038

<https://doi.org/10.1029/2024SW004038>

<https://agupubs.onlinelibrary.wiley.com/doi/epdf/10.1029/2024SW004038>

Using Van Allen Probes observations from September 2012 to June 2019, we statistically investigate responses of the Earth's outer radiation belt electron phase space densities (PSDs) in the adiabatic invariant coordinates to isolated geomagnetic storms. Electron PSDs for $\mu = 50\text{--}5,000 \text{ MeV/G}$, covering energy range of seed, relativistic and ultra-

relativistic electrons, are calculated to evaluate three types of storm-time PSD responses (i.e., enhancement, depletion, and no change). In statistics, the seed PSD variations are dominated by enhancement-type events, the percentages of which increase from >50% for small storms ($-50 \text{ nT} < \text{SYM-Hmin} \leq -30 \text{ nT}$) to >70% for large storms ($\text{SYM-Hmin} \leq -50 \text{ nT}$). The relativistic and ultra-relativistic PSDs exhibit the three response types with comparable occurrence rates for small storms but present predominantly enhancement-type variations (>50%) for large storms. Enhanced storm activity increases the enhancement-type responses for seed PSDs at all L^* and for relativistic and ultra-relativistic PSDs at $L^* > 3.5$. It also results in the increased depletion-type response occurrence for relativistic and ultra-relativistic PSDs at lower L^* . Our results further indicate that the depletion-type responses manifest evident dependence on the level of solar and geomagnetic activity and the μ -value, implying complex physics accounting for outer zone electron losses. Improved knowledge of the storm-time dynamics of outer radiation belt electron PSDs is valuable to in-depth comprehension of various mechanisms responsible for the electron acceleration and loss. It has important implications for future simulations and forecasts of radiation belt electron variability, in particular, during geomagnetically disturbed periods.

The State of Solar Wind Heavy Ions in Interplanetary Coronal Mass Ejection–Driven Geomagnetic Storms

Cong Wang^{1,2,3}, Fei He⁴, and Xiaoxin Zhang^{2,3}

2024 ApJ 975 106

<https://iopscience.iop.org/article/10.3847/1538-4357/ad7b07/pdf>

During geomagnetic storms, which are the primary periods for heavy ions from the solar wind to enter Earth's magnetospheric space, the charge state of solar wind heavy ions during these storms has significant implications for studying the distribution and effects of heavy ions in the magnetosphere. We analyzed the states and variations of heavy ions during 158 interplanetary coronal mass ejection (ICME)–driven geomagnetic storm events using data from the Advanced Composition Explorer satellite and examined four of these events in detail. We found that the increase in the average charge state of heavy ions such as O, Mg, Si, and Fe is positively correlated with the intensity of the geomagnetic storm. Regarding the abundance ratio of heavy ions such as Ne, Mg, Si, and Fe relative to oxygen ions, the rate and magnitude of increase in abundance ratios during extreme geomagnetic storms ($K_p = 9$) triggered by ICME events are significantly higher than those during other levels of geomagnetic storms. Additionally, we observed that although the average charge states of heavy ions such as O and Fe are correlated with the geomagnetic storm intensity induced by ICMEs, there are significant individual differences in the charge state variations of heavy ions. **1998 May 4 and 2004 April 3, 2000 October 5 and 1999 September 22**

Global Effect of New Active Regions on Coronal Holes and Their Wind Streams

Y.-M. Wang¹, K. J. Knizhnik¹, I. Ugarte-Urra¹, and M. J. Weberg¹

2024 ApJ 972 107

<https://iopscience.iop.org/article/10.3847/1538-4357/ad5f87/pdf>

Solar wind prediction algorithms and simulations of coronal events often employ photospheric field maps that are assembled over a 27 day solar rotation. This has stimulated efforts to update and better synchronize the maps by applying flux transport and including observations of the back side of the Sun. Here, using potential-field source-surface extrapolations, we address the question of how the emergence of a large active region (AR) on the Sun's farside affects the coronal field and configuration of coronal holes on the Earth-facing side. We find that, if the new AR is located $\sim 135^\circ$ – 180° in longitude from Earth, the effect on the coronal field and solar wind near the central meridian will be almost negligible. This is because, when sunspot activity is relatively low, the outermost AR loops will become connected to the nearby polar fields; when sunspot activity is high, the newly emerged flux will connect to neighboring ARs. However, large ARs that emerge near the solar limb may sometimes have a significant effect on the field near the central meridian. In particular, a coronal hole having opposite polarity to that of the nearest sector of the AR may partially close down, resulting in slower wind; conversely, if the coronal hole has the same polarity as the facing AR sector, it will tend to increase in areal size, resulting in faster wind. In most cases, the main effect of a new AR will be to redistribute open flux between itself and neighboring coronal holes (including the polar holes) through interchange reconnection. **2021 January 22–February 18, 2012 April 28–May 25**

Coronal Holes, Footpoint Reconnection, and the Origin of the Slow (and Fast) Solar Wind.

Wang, Y.M.

Sol Phys 299, 54 (2024).

<https://doi.org/10.1007/s11207-024-02300-3>

<https://link.springer.com/content/pdf/10.1007/s11207-024-02300-3.pdf>

The tendency for low-speed solar wind to show greater spatiotemporal variability and different compositional properties from high-speed wind has led to the prevailing idea of a bimodal solar wind, in which fast wind comes from coronal holes and slow wind comes from coronal streamers. We present observational evidence that most of the slow wind originates from small coronal holes or from just inside the boundaries of large holes, with the rest leaking out from coronal streamers and confined to the immediate vicinity of the heliospheric current and plasma sheets. Although this conclusion was suggested earlier by extrapolations of photospheric field maps, additional support comes from (1) observations of slow wind at Earth following the central-meridian passage of small equatorial holes; (2) observations of slow wind with high Alfvénicity at 1 au by Wind, and more recently near the Sun by Parker Solar Probe and Solar Orbiter; and (3) the finding that 80% of the solar wind observed by Helios at 0.3 – 0.4 au during 1974 – 1978 was Alfvénic. We show that compositional properties such as charge-state ratios vary over the solar cycle and may depend on parameters such as the footpoint field strength B_0 , and thus cannot be used alone to distinguish between coronal hole and noncoronal-hole wind. Finally, we note that magnetograms greatly underestimate the amount of small-scale flux emerging inside coronal holes and other unipolar regions. If this rate is taken to be the same as in the quiet Sun, the energy flux density resulting from interchange reconnection with open field lines is on the order of $3 \times 10^5 \text{ erg cm}^{-2} \text{ s}^{-1}$ ($B_0/10 \text{ G}$), sufficient to drive the solar wind. The wind speed depends on the rate of flux-tube expansion, with slower expansion leading to more energy deposition at greater heights and faster wind.

The Effect of Solar Wind on Charged Particles' Diffusion Coefficients

J. F. Wang¹ and G. Qin

2024 ApJ 961 6

<https://iopscience.iop.org/article/10.3847/1538-4357/ad09b7/pdf>

The transport of energetic charged particles through magnetized plasmas is ubiquitous in interplanetary space and astrophysics, and the important physical quantities are the parallel and perpendicular diffusion coefficients of energetic charged particles. In this paper, the influence of solar wind on particle transport is investigated. Using the focusing equation, we obtain parallel and perpendicular diffusion coefficients, accounting for the solar wind effect. For different conditions, the relative importance of the solar wind effect to diffusion is investigated. It is shown that, when energetic charged particles are close to the Sun, for parallel diffusion, the solar wind effect needs to be taken into account. These results are important for studying energetic charged particle transport processes in the vicinity of the Sun.

Application of the Tianwen-1 DOR Signals Observed by Very Long Baseline Interferometry Radio Telescopes in the Study of Solar Wind Plasma and a Coronal Mass Ejection

Zhichao Wang^{1,2}, Maoli Ma¹, Qinghui Liu¹, Qingbao He³, Xin Zheng¹, Lijia Liu⁴, and Guifré Molera Calvés⁵

2023 ApJS 269 57

<https://iopscience.iop.org/article/10.3847/1538-4365/ad077f/pdf>

The Tianwen-1 (TW1) Mars probe experienced solar conjunction for the first time in 2021. The China VLBI Network (CVN) observes the differential one-way ranging (DOR) signals of TW1 throughout its phase. This paper explores the application of CVN observation data to study the solar wind plasma. First, the frequency and phase of the DOR carrier and sidetones at each station are calculated using the Doppler method. Then, the variations in both the differential phase delays (DPD) and the total electron content (TEC) are calculated using the phase of the sidetones. We also statistically analyze the fluctuations in the Delta-DOR (Δ DOR) group delay. The results indicate that the fluctuations of the frequency, phase, Δ DOR group delay, delay rate, and TEC variations of the TW1 signals increase with the decrease of the heliocentric distance. On **2021 November 2**, a coronal mass ejection (CME) passed across the ray paths of the telescope beams, when the heliocentric distance and heliographic latitude of the projected position of Mars were 30.6 Rs and 3° , respectively. Our data catch the impact of the CME on the DOR signals. The change of the DPD reaches 170 ps, which is equivalent to 986 TECU. We utilize the cross correlation to analyze the frequency fluctuations at multiple stations, and obtain the propagation direction and velocity variations of the CME. Our analysis indicates that multifrequency DOR signals observed by very long baseline interferometry stations have great application to characterize the electron density variations and propagation of the solar wind plasma.

A New Method for Predicting Non-Recurrent Geomagnetic Storms

Cong Wang, Qian Ye, Fei He, Bo Chen, Xiaoxin Zhang

Space Weather [Volume21, Issue8](#) August 2023 e2023SW003522

<https://agupubs.onlinelibrary.wiley.com/doi/epdf/10.1029/2023SW003522>

Predicting non-recurrent geomagnetic storms caused by Coronal Mass Ejection (CME) is important and necessary for space weather forecasting. Previous studies have shown that it is feasible to predict non-recurrent geomagnetic storms

by reconstructing precursors from cosmic ray intensity (CRI) in the frequency domain. However, the difficulty lies in predicting the minor storms, the moderate storms, and the storms accompanying ground level enhancement (GLE). This study proposes a new method that includes the spectral whitening method and CEEMDAN-CWT for predicting non-recurrent geomagnetic storms. The method was applied to 229 CME-driven events, including 166 events with $K_p \geq 5$ and 63 events with $K_p < 5$, during the solar cycles 23 and 24. This study analyzed 166 geomagnetic storm events and found that 129 of them were accurately predicted, resulting in a recall rate of 77.7%. Additionally, the study found that as the K_p index increased, the amplitude of the precursor detected by this method also increased, while the time interval between the onset of CME and the maximum amplitude of the precursor decreased. **2001-11-01-10, 2018-08-16-31**

Properties of Forbush Decreases with AMS-02 Daily Proton Flux Data

Siqi Wang¹, Veronica Bindi¹, Cristina Consolandi¹, Claudio Corti¹, Christopher Light¹, Nikolay Nikonov¹, and Andrew Kuhlman¹

2023 ApJ 950 23

<https://iopscience.iop.org/article/10.3847/1538-4357/acca1b/pdf>

A Forbush decrease (FD) is a sudden reduction of Galactic Cosmic Rays (GCRs) that is usually caused by intense solar wind transients, such as Interplanetary Coronal Mass Ejections (ICMEs) and Corotating Interaction Regions (CIRs). Using daily proton fluxes measured by AMS-02 between 2011 May and 2019 October, we identified 142 FD events with an automatic systematic analysis method. The properties of 47 FDs caused by ICMEs and of 54 FDs caused by CIRs were analyzed. We found that the rigidity dependence of the GCR flux decrease is generally better described by an exponential function for both ICME and CIR FDs. We also found that the FD Amplitude of ICME FDs has a moderate correlation with the minimum Dst index and a number of solar wind parameters, such as maximum temperature, pressure, and magnetic field. For CIR FD events, neither FD Amplitude nor Maximum Affected Rigidity had a significant correlation with solar wind parameters. **26 Sep 2011, 22-28 Jun 2015, 22-25 Nov 2016**

Table 3 List of FD Events Derived with AMS Daily Proton Data 2011-2019

Observation of the Hall Magnetic Reconnection As Close As 56 Solar Radii from the Sun

Rongsheng Wang^{1,2,3}, Xiancai Yu⁴, Yuming Wang^{1,2}, Quanming Lu^{1,2,3}, and San Lu^{1,2,3}

2023 ApJ 947 78

<https://iopscience.iop.org/article/10.3847/1538-4357/acbdf6/pdf>

A few thin current layers were detected in the rear boundary of an interplanetary coronal mass ejection (ICME) observed at 56 solar radii from the Sun as the Parker Solar Probe spacecraft approached the perihelion for the first time, and were caused by the interaction between the background solar wind and the rear boundary of the ICME. Among two of the current layers, the ion diffusion region of the Hall magnetic reconnection was directly detected, based on opposite ion jets, low-speed inflows, and the Hall effect. Both reconnection events were fast and occurred in the current layer with a small magnetic field shear angle and with significantly asymmetric magnetic field intensity as well as plasma between their two sides, i.e., an asymmetric magnetic reconnection with a strong guide field. A magnetic flux rope was detected inside one of the diffusion regions, indicating bursty reconnection. Additionally, multiple reconnection jets were detected inside the ICME and its rear boundary. Thus, we speculate that more ongoing reconnection events were occurring inside the ICME and its boundary. The observations suggested that fast Hall magnetic reconnection can occur as close as 56 solar radii from the Sun and plays a crucial role in ICME evolution. **31 Oct 2018**

A machine-learning-based model for the next 3-day Geomagnetic Index (K_p) Forecast

Jingjing Wang, Bingxian Luo, Siqing Liu, and Liqin Shi

Front. Astron. Space Sci. 10: 1082737 **2023**

<https://doi.org/10.3389/fspas.2023.1082737>

<https://www.frontiersin.org/articles/10.3389/fspas.2023.1082737/pdf>

<https://www.frontiersin.org/articles/10.3389/fspas.2023.1082737/full>

The 3-day K_p forecast product is important and necessary for space weather forecasts. There is some essential information that can be obtained from the 3-day K_p forecast product, such as the start time of the geomagnetic storm, the maximum storm level, and the storm duration. In this study, we aimed to predict the next 3-day K_p index based on the previous K_p time series and SDO/AIA 193 Å images. We prepared datasets from May 2010 to December 2019 for training and datasets from January 2020 to October 2022 for testing. The similarity parameters of the previous and current geomagnetic conditions between the samples are calculated and analyzed. We assumed that the paired samples with high-similarity parameters of the previous and current geomagnetic conditions would also have high-similarity parameters of the next 3-day geomagnetic conditions. Based on the assumption, we selected the three best similarity parameters through the feature selection process and adopted the scalable tree boosting system (XGBoost) to develop a prediction model. It took the similarity parameters of the previous and current geomagnetic conditions as input and

provided the best match sample from the training subset as a forecast. For the next 3-day non-storm (maximum $K_p \ll 5$) prediction period, our model reached an F1-score of 0.96. For the next 3-day storm (maximum $K_p \geq 5$) prediction period, our model reached an F1-score of 0.82, a recall of 0.70, and a precision of 0.98. **22 Oct 2019**

Upstream Solar Wind Prediction up to Mars by an Operational Solar Wind Prediction System

Jingjing Wang, Yurong Shi, Bingxian Luo, Siqing Liu, Linggao Kong, +++

Space Weather [Volume21, Issue1](#) **2023** e2022SW003281

<https://agupubs.onlinelibrary.wiley.com/doi/epdf/10.1029/2022SW003281>

Combining the upstream solar wind observations measured by Mars Atmosphere and Volatile Evolution (MAVEN), Advanced Composition Explorer(ACE) and Deep Space Climate Observatory (DSCOVR) from October 2014 to April 2021, we investigate the statistical properties of the background solar wind at Mars and Earth. By applying an operational solar wind prediction system (Wang et al., 2018, <https://doi.org/10.1051/swsc/2018025>) in Space Weather Prediction Center (SEPC), we simulate the solar wind conditions and carry out a comparative analysis with observations to study our model performance. We find that our model is able to simulate the solar wind conditions upstream of Earth and Mars, corresponding to the different heliocentric distances and different levels of solar activity. Furthermore, we apply an event-based evaluation by analyzing the high speed enhancements (HSEs), and find that the hit rate of HSEs is 70.38% and 66.37% for Earth and Mars, respectively. By predicting the HSEs at Earth (Mars), our model reaches a Mean Absolute Error (MAE) of 83.93 km/s (65.91 km/s) and 22.98 hr (21.65 hr) for maximum speed and arrival time prediction error, respectively. We also conduct a three-month case study, from November 2020 to January 2021, analyzing solar wind conditions upstream of Earth, Mars, and measured by Tianwen-1 (China's first Mars mission), for which our model is capable to predict the upstream solar wind conditions up to Mars.

Prompt Enhancements of Radiation Belt Electrons over a Wide Energy Range Based on Phase Space Density Variations: A Detailed Case Study

Xiaoyu Wang¹, Xing Cao¹, Xudong Gu¹, Binbin Ni^{1,2}, Xin Ma¹, Taorong Luo¹, and Deyu Guo¹

2023 ApJ 942 30

<https://iopscience.iop.org/article/10.3847/1538-4357/aca4c7/pdf>

Based on Van Allen Probes observations, we report a prompt enhancement event of radiation belt electrons over a wide energy range from tens of keV to multiple meV spanning **2013 January 13–15**. During this period, we also observe prolonged moderate substorm activities and intense whistler-mode chorus emissions. To differentiate the underlying mechanisms responsible for this prompt electron enhancement process, we investigate in detail the evolution of electron phase space densities (PSDs) for various values of the first and second adiabatic invariants (μ and K). The results show that tens to hundreds of keV electrons rapidly penetrated to $L^* < 4$ during the substorm period, with the corresponding PSDs increasing by more than 3 orders of magnitude within about 1 day. Comparatively, the PSD enhancements of higher energy electrons are less significant and shift to higher L^* . We find that the fast acceleration of hundreds of keV seed electrons to multi-meV electrons may be reasonably attributed to interactions with the concurrent chorus waves. Specifically, the electron PSD increases for $\mu \geq 300$ MeV G⁻¹ become less pronounced as K increases, consistent with the pitch angle dependence of chorus-induced electron energy diffusion at high energies. Our results therefore provide clear observational evidence for the combined effect of substorm-induced injection and chorus wave scattering on the prompt enhancements of radiation belt electrons over a wide energy range within a couple of days.

Solar Ring Mission: Building a Panorama of the Sun and Inner-heliosphere

Yuming Wang, Xianyong Bai, Changyong Chen, Linjie Chen, Xin Cheng, +++

Advances in Space Research **2022**

<https://arxiv.org/ftp/arxiv/papers/2210/2210.10402.pdf>

Solar Ring (SOR) is a proposed space science mission to monitor and study the Sun and inner heliosphere from a full 360° perspective in the ecliptic plane. It will deploy three 120°-separated spacecraft on the 1-AU orbit. The first spacecraft, S1, locates 30° upstream of the Earth, the second, S2, 90° downstream, and the third, S3, completes the configuration. This design with necessary science instruments, e.g., the Doppler-velocity and vector magnetic field imager, wide-angle coronagraph, and in-situ instruments, will allow us to establish many unprecedented capabilities: (1) provide simultaneous Doppler-velocity observations of the whole solar surface to understand the deep interior, (2) provide vector magnetograms of the whole photosphere - the inner boundary of the solar atmosphere and heliosphere, (3) provide the information of the whole lifetime evolution of solar featured structures, and (4) provide the whole view of solar transients and space weather in the inner heliosphere. With these capabilities, Solar Ring mission aims to address outstanding questions about the origin of solar cycle, the origin of solar eruptions and the origin of extreme

space weather events. The successful accomplishment of the mission will construct a panorama of the Sun and inner-heliosphere, and therefore advance our understanding of the star and the space environment that holds our life.

Predicting CME Arrival Time through Data Integration and Ensemble Learning

Jason **Wang**, Khalid Alobaid, Khalid Alobaid, Yasser Abdullallah, Yasser Abdullallah, Haimin Wang, Haodi Jiang, Yan Xu, Vasyi Yurchyshyn, Hongyang Zhang, Huseyin Cavus, and Ju Jing

Front. Astron. Space Sci. 9: 1013345. 2022

doi: 10.3389/fspas.2022.1013345

<https://www.frontiersin.org/articles/10.3389/fspas.2022.1013345/pdf>

The Sun constantly releases radiation and plasma into the heliosphere. Sporadically, the Sun launches solar eruptions such as flares and coronal mass ejections (CMEs). CMEs carry away a huge amount of mass and magnetic flux with them. An Earth-directed CME can cause serious consequences to the human system. It can destroy power grids/pipelines, satellites, and communications. Therefore, accurately monitoring and predicting CMEs is important to minimize damages to the human system. In this study we propose an ensemble learning approach, named CMETNet, for predicting the arrival time of CMEs from the Sun to the Earth. We collect and integrate eruptive events from two solar cycles, #23 and #24, from 1996 to 2021 with a total of 363 geoeffective CMEs. The data used for making predictions include CME features, solar wind parameters and CME images obtained from the SOHO/LASCO C2 coronagraph. Our ensemble learning framework comprises regression algorithms for numerical data analysis and a convolutional neural network for image processing. Experimental results show that CMETNet performs better than existing machine learning methods reported in the literature, with a Pearson product-moment correlation coefficient of 0.83 and a mean absolute error of 9.75 h.

Cosmic Ray Variation Lags behind Sunspot Number due to the Late Opening of Solar Magnetic Field

Yuming **Wang**, [Jingnan Guo](#), [Gang Li](#), [Elias Roussos](#), [Junwei Zhao](#)

ApJ 2022

<https://arxiv.org/pdf/2201.01908.pdf>

Galactic cosmic rays (GCRs), the highly energetic particles that may raise critical health issues of astronauts in space, are modulated by solar activity with their intensity lagging behind the sunspot number (SSN) variation by about one year. Previously, this lag has been attributed to result of outward convecting solar wind and inward propagating GCRs. However, the lag's amplitude and its solar-cycle dependence are still not fully understood (e.g., Ross & Chaplin 2019). By investigating the solar surface magnetic field, we find that the source of heliospheric magnetic field, i.e., the open magnetic flux on the Sun, already lags behind SSN before it convects into heliosphere along with the solar wind, and the delay during odd cycles is longer than that during sequential even cycles. Thus, we propose that the GCR lag is primarily due to the greatly late opening of the solar magnetic field with respect to SSN, though solar wind convection and particle transport in the heliosphere also matters. We further investigate the origin of the open flux from different latitudes of the Sun and found that the total open flux is significantly contributed by that from low latitudes where coronal mass ejections frequently occur and also show an odd-even cyclic pattern. Our findings challenge existing theories, and may serve as the physical basis of long-term forecasts radiation dose estimates for manned deep-space exploration missions.

Figure 6. The solar cycle variations of the CME numbers

Observations of a Quickly Flapping Interplanetary Magnetic Reconnection Exhaust

Jiemin **Wang**^{1,2} and Yan Zhao¹

Front. Phys., 2021 |

<https://www.frontiersin.org/articles/10.3389/fphy.2021.736319/full>

<https://doi.org/10.3389/fphy.2021.736319>

On the basis of the Petschek reconnection model and the characteristics of reconnection, hundreds of reconnection exhausts were reported in the solar wind. Many multi-spacecraft observations also indicated that interplanetary magnetic reconnection is a quasi-steady-state plasma process and the reconnection X-line can extend hundreds of Earth radii. In this study, we report an interplanetary flapping reconnection exhaust observed by Wind on April 1, 2003 at one AU. The magnetic reconnection event has two adjacent accelerated flows. We compared the plasma and magnetic characteristics of the two accelerated flows and found that the second accelerated flow was due to the back-and-forth movement of the

reconnection exhaust. Our observations reveal that not all interplanetary reconnections operate in a quasi-steady-state manner; some reconnection current sheets can move rapidly back and forth.

Interplanetary Shock Candidates Observed at Venus's Orbit

Can **Wang**^{1,2,3}, Mengjiao Xu^{1,2}, Chenglong Shen^{1,2}, Yutian Chi^{1,2,4}, and Yuming Wang^{1,2,5}
2021 ApJ 912 85

<https://doi.org/10.3847/1538-4357/abee7b>

The measurements from the Venus Express spacecraft are analyzed for the basic properties of fast forward interplanetary shocks at Venus's orbit (~0.72 au). A total of 143 fast forward interplanetary shock candidates during 2006–2014 are identified. The shock angle Θ_{Bn} , defined as the angle between the shock normal and the upstream magnetic field, and the magnetic compression ratio r_B , defined as the ratio of the magnetic field strength downstream to that upstream, of these shocks are determined based on the magnetic coplanarity method. The shock occurrence at Venus shows a correlated variation with the solar activity level measured by the number of sunspots, while the shock angle and magnetic compression ratio do not show such a correspondence. The shock angle spreads almost uniformly between 10° and 80° with its mean value at about 45° , and the magnetic compression ratio shows a unimodal distribution between 1.0 and 4.5 with a mean value of 2.1. In addition, we also analyze the properties of fast forward shocks driven by interplanetary coronal mass ejections (ICMEs). We found that interplanetary shocks with and without detected ICMEs showed no significant differences in terms of the shock strength and the shock angle. Further comparison with previous observational results at 1 au shows that fast forward shocks at 1 au are generally weaker than those at 0.72 au, and the shock angle Θ_{Bn} is more perpendicular at 1 au.

Aurora Sightings Observed in Chinese History Caused by CIRs or Great-storm CMEs

Guowei **Wang**^{1,2}, Shuo Yao¹, Yiqun Yu³, Dong Wei³, Fei Di¹, Xiujuan Bao¹, Shihong Zhang¹, and Jianjun Liu²
2021 ApJ 908 187

<https://doi.org/10.3847/1538-4357/abd0fe>

<https://iopscience.iop.org/article/10.3847/1538-4357/abd0fe/pdf>

Auroras observed at middle and low geographic latitudes are related to external inputs and varying geomagnetic fields. This work aims to exclude corotating interaction region (CIR) storms and identify strong coronal mass ejection (CME) storms according to historical auroral records when the geomagnetic field varies substantially. An existing catalog of the aurora records in Chinese history reported by Zeng & Jin from 193 B.C. to 1911 A.D. is used. Archaeomagnetic field models are adopted to estimate the variation of the dipole field. According to the empirical relation between the equatorward boundary of the auroral oval, Dst index, and geomagnetic field intensity, the auroras caused by CIRs can be excluded, and those caused by strong CMEs are identified. After 1500 A.D., China's magnetic latitude decreased substantially due to the pole shift. This shift provides a better opportunity to investigate the existence of great-level storms. These great-storm CMEs occurred in both solar maximum and minimum. The space weather modeling framework is used to calculate the cusp area and the downward ion flux through the cusp for varied geomagnetic field and solar wind. For the present solar wind condition and tilt angle $<15^\circ$, stronger geomagnetic field tends to generate a larger cusp area and higher ion flux through the cusp. For the weaker solar wind in the Maunder minimum, the ion flux is lower, but the cusp area is similar to that at present.

Table 1 Important Auroral Records in Maunder Minimum Selected for Simulation

Small-scale Flux Emergence, Coronal Hole Heating, and Flux-tube Expansion: A Hybrid Solar Wind Model

Y.-M. **Wang**

2020 ApJ 904 199

<https://doi.org/10.3847/1538-4357/abbd6>

Extreme-ultraviolet images from the Solar Dynamics Observatory often show loop-like fine structure to be present where no minority-polarity flux is visible in magnetograms, suggesting that the rate of ephemeral region (ER) emergence inside "unipolar" regions has been underestimated. Assuming that this rate is the same inside coronal holes as in the quiet Sun, we show that interchange reconnection between ERs and open field lines gives rise to a solar wind energy flux that exceeds $105 \text{ erg cm}^{-2} \text{ s}^{-1}$ and that scales as the field strength at the coronal base, consistent with observations. In addition to providing ohmic heating in the low corona, these reconnection events may be a source of Alfvén waves with periods ranging from the granular timescale of ~10 minutes to the supergranular/plume timescale of many hours, with some of the longer-period waves being reflected and dissipated in the outer corona. The asymptotic

wind speed depends on the radial distribution of the heating, which is largely controlled by the rate of flux-tube expansion. Along the rapidly diverging flux tubes associated with slow wind, heating is concentrated well inside the sonic point (1) because the outward conductive heat-flux density and thus the outer coronal temperatures are reduced, and (2) because the net wave energy flux is dissipated at a rate proportional to the local Alfvén speed. In this "hybrid" solar wind model, reconnection heats the lower corona and drives the mass flux, whereas waves impart energy and momentum to the outflow at greater distances.

Solar modulation of cosmic proton and helium with AMS-02

[Bing-Bing Wang](#), [Xiao-Jun Bi](#), [Kun Fang](#), [Sujie Lin](#), [Peng-Fei Yin](#)

2020

<https://arxiv.org/pdf/2011.12531.pdf>

We investigate the solar modulation effect with the long time cosmic ray proton and helium spectrum measured by AMS-02 on the time scale of a Bartels rotation (27 days) between May 2011 and May 2017. The time-span covers the negative heliospheric magnetic field polarity cycle, the polarity reversal period and the positive polarity cycle. The unprecedented accuracy of AMS-02 observation data provide a good opportunity to improve the understanding of the time dependent solar modulation effect. In this work, a two-dimensional solar modulation model is used to compute the propagation of cosmic rays in the heliosphere. Some important ingredients of the model which reflect the global heliospherical environment are taken from the observations. The propagation equation is numerically solved with the public Solarprop code. We find that the drift effect is suppressed during the high solar activity period but nearly recovered in the first half of 2017. The time-dependent rigidity dependence of the mean free path is critical to reproduce the observations between August 2012 and October 2015.

Concept of the Solar Ring Mission: An overview

YuMing Wang, [HaiSheng Ji](#), [YaMin Wang](#), [LiDong Xia](#), [ChengLong Shen](#), et al.

[Science China Technological Sciences](#) volume 63, pages1699–1713 (2020)

<https://arxiv.org/pdf/2003.12728.pdf>

<https://link.springer.com/content/pdf/10.1007/s11431-020-1603-2.pdf>

<https://doi.org/10.1007/s11431-020-1603-2>

The concept of the Solar Ring mission was gradually formed from L5/L4 mission concept, and the proposal of its pre-phase study was funded by the National Natural Science Foundation of China in November 2018 and then by the Strategic Priority Program of Chinese Academy of Sciences in space sciences in May 2019. Solar Ring mission will be the first attempt to routinely monitor and study the Sun and inner heliosphere from a full 360-degree perspective in the ecliptic plane. The current preliminary design of the Solar Ring mission is to deploy six spacecraft, grouped in three pairs, on a sub-AU orbit around the Sun. The two spacecraft in each group are separated by about 30° and every two groups by about 120°. This configuration with necessary science payloads will allow us to establish three unprecedented capabilities: (1) determine the photospheric vector magnetic field with unambiguity, (2) provide 360-degree maps of the Sun and the inner heliosphere routinely, and (3) resolve the solar wind structures at multiple scales and multiple longitudes. With these capabilities, the Solar Ring mission aims to address the origin of solar cycle, the origin of solar eruptions, the origin of solar wind structures and the origin of severe space weather events. The successful accomplishment of the mission will advance our understanding of the star and the space environment that hold our life and enhance our capability of expanding the next new territory of human. **3 April 2010, 1–2 August 2010, 2014-10-23, 10–16 September 2017**

Comparison of counterstreaming suprathermal electron signatures of ICMEs with and without magnetic cloud: are all ICMEs flux ropes?

Jiemin Wang, Yan Zhao, Hengqiang Feng, Qiang Liu, Zhanjun Tian, Hongbo Li, Ake Zhao and Guoqing Zhao

A&A 632, A129 (2019)

<https://www.aanda.org/articles/aa/pdf/2019/12/aa36733-19.pdf>

Context. Magnetic clouds (MCs), as in large-scale interplanetary magnetic flux ropes, are usually still connected to the Sun at both ends near 1 AU. Many researchers believe that all nonMC interplanetary coronal mass ejections (ICMEs) also have magnetic flux rope structures, which are inconspicuous because the observing spacecraft crosses the flanks of the rope structures. If so, the field lines of nonMC ICMEs should also usually be connected to the Sun at both ends. Aims. We want to know whether or not the field lines of most nonMC ICMEs are still connected to the Sun at both ends. Methods. This study examined the counterstreaming suprathermal electron (CSE) signatures of 272 ICMEs observed by the Advanced Composition Explorer (ACE) spacecraft from 1998 to 2008 and compared the CSE signatures of MCs and

nonMC ICMEs. Results show that only 10 of the 101 MC events (9.9%) and 75 of the 171 nonMC events (43.9%) have no CSEs. Moreover, 21 of the nonMC ICMEs have high CSE percentages (more than 70%) and show relatively stable magnetic field components with slight rotations, which are in line with the expectations that the observing spacecraft passes through the flank of magnetic flux ropes. Therefore, the 21 events may be magnetic flux ropes but the ACE spacecraft passes through their flanks of magnetic flux ropes. Conclusions. Considering that most other nonMC events have disordered magnetic fields, we suggest that some nonMC ICMEs inherently have disordered magnetic fields, and therefore no magnetic flux rope structures. **21 Oct 1999, 18-19 Feb 2005**

Table A.1. Percentage of counterstreaming suprathermal electrons in ICMEs (1998-2008)

Multispacecraft Observation of Unidirectional and Bidirectional Alfvén Waves within Large-scale Magnetic Clouds

Zehao [Wang](#)^{1,2}, Xueshang Feng¹, and Jianchuan Zheng

2019 ApJL 887 L18

[sci-hub.se/10.3847/2041-8213/ab595d](https://doi.org/10.3847/2041-8213/ab595d)

Recent years have seen growing evidence of the existence of Alfvén waves within interplanetary magnetic flux ropes, which are believed to be an important aspect of dynamics connecting the Sun and the heliosphere. Previous studies, due to localized observation by single spacecraft, focused on sunward or antisunward Alfvén waves propagating along with magnetic field lines. In this Letter, for the first time, we use multispacecraft observations to verify and analyze two large-scale magnetic clouds (MCs), when the spacecraft had quite different spatial separations. What surprises us is that not only unidirectional but bidirectional Alfvén waves exist in the large-scale MC, which is rooted to the Sun. We speculate that unidirectional Alfvén waves within an MC are generated by distortions produced within a preexisting flux rope, and bidirectional Alfvén waves are emitted from the center of reconnection and then travel outward along with two loop legs of an MC. **2011 October 22-25, 2013 November 7, 2013 November 11-13**

Table 1 List of MCs with Long-duration Alfvén Waves Observed by WIND during 1995–2015

CME Arrival Time Prediction Using Convolutional Neural Network

Yimin [Wang](#)^{1,2}, Jijia Liu¹, Ye Jiang³, and Robert Erdélyi^{1,4}

2019 ApJ 881 15

[sci-hub.se/10.3847/1538-4357/ab2b3e](https://doi.org/10.3847/1538-4357/ab2b3e)

Fast and accurate prediction of the arrival time of coronal mass ejections (CMEs) at Earth is vital to minimize hazards caused by CMEs. In this paper, we use a deep-learning framework, i.e., a convolutional neural network (CNN) regression model, to analyze transit times from the Sun to Earth of 223 geoeffective CME events observed in the past 30 yr. 90% of them were used to build the prediction model, and the rest 10% have been used for test purpose. Unlike previous studies on this topic, our proposed CNN regression model does not require manually selected features for model training, it does not need time spent on feature collection, and it can deliver predictions without deeper expert knowledge. The only input to our CNN regression model is the instances of the white-light observations of CMEs. The mean absolute error of the constructed CNN regression model is about 12.4 hr, which is comparable to the average performance of the previous studies on this subject. As more CME data become available, we expect the CNN regression model will reveal better results.

Observations of Slow Solar Wind from Equatorial Coronal Holes

Y.-M. [Wang](#) and Y.-K. Ko

2019 ApJ 880 146

[sci-hub.se/10.3847/1538-4357/ab2add](https://doi.org/10.3847/1538-4357/ab2add)

Because of its distinctive compositional properties and variability, low-speed (~ 450 km s⁻¹) solar wind is widely believed to originate from coronal streamers, unlike high-speed wind, which comes from coronal holes. An alternative scenario is that the bulk of the slow wind (excluding that in the immediate vicinity of the heliospheric current sheet) originates from rapidly diverging flux tubes rooted inside small coronal holes or just within the boundaries of large holes. This viewpoint is based largely on photospheric field extrapolations, which are subject to considerable uncertainties and do not include dynamical effects, making it difficult to be certain whether a source is located just inside or outside a hole boundary, or whether a high-latitude hole will be connected to Earth. To minimize the dependence on field-line extrapolations, we have searched for cases where equatorial coronal holes at central meridian are followed by low-speed streams at Earth. We describe 14 examples from the period 2014–2017, involving Fe xiv 21.1 nm coronal holes located near active regions and having equatorial widths of $\sim 3^\circ$ – 10° . The associated in situ wind was characterized by speeds $v \sim 300$ – 450 km s⁻¹ and by O7+/O6+ ratios of ~ 0.05 – 0.15 , with v showing the usual correlation with proton temperature. In addition, consistent with other recent studies, this slow wind had remarkably

high Alfvénicity, similar to that in high-speed streams. We conclude that small coronal holes are a major contributor to the slow solar wind during the maximum and early post-maximum phases of the solar cycle. **2014 Feb 11-Mar 11, 2014 Feb 26-28, 2014 Mar 11_Apr 7, 2014 May 4-31, 2014 June 28-July 25, 2014 Aug 21-Sep 17, 2015 May 21-June 17, 2015 July 14_Aug 11, 2016 Feb 18-Apr 16, 2016 June 6-July 3, 2017 Sep 12 –Oct 10**

Possible Cool Prominence Materials Detected within Interplanetary Small Magnetic Flux Ropes

J. M. Wang^{1,2}, H. Q. Feng¹, H. B. Li¹, A. K. Zhao¹, Z. J. Tian¹, G. Q. Zhao¹, Y. Zhao¹, and Q. Liu¹
2019 ApJ 876 57

[sci-hub.se/10.3847/1538-4357/ab148b](https://doi.org/10.3847/1538-4357/ab148b)

Previous studies indicate that interplanetary small magnetic flux ropes (SMFRs) are manifestations of microflare-associated small coronal mass ejections (CMEs), and the hot material with high-charge states heated by related microflares are found in SMFRs. Ordinary CMEs are frequently associated with prominence eruptions, and cool prominence materials are found within some magnetic clouds (MCs). Therefore, the predicted small CMEs may also be frequently associated with small prominence eruptions. In this work, we aim to search for cool prominence materials within SMFRs. We examined all the O5+ and Fe6+ fraction data obtained by the Advanced Composition Explorer (ACE) spacecraft during 1998–2008 and found that 13 SMFRs might exhibit low-charge-state signatures of unusual O5+ and/or Fe6+ abundances. One of the 13 SMFRs also exhibited signatures of high ionic charge states. We also reported a SMFR with high Fe6+ fraction, but the values of Fe6+ is a little lower than the threshold defining unusual Fe6+. However, the Solar Dynamics Observatory/ Atmospheric Imaging Assembly observations confirmed that the progenitor CME of this SMFR is associated with a small eruptive prominence, and the observations also supported the prominence materials were embedded in the CME. These observations are at the edge of the capabilities of ACE/Solar Wind Ion Composition Spectrometer and it cannot be ruled out that they are solely caused by instrumental effects. If these observations are real, they provide new evidence for the conjecture that SMFRs are small-scale MCs but also imply that the connected small CMEs could be associated with flares and prominence eruptions. **2002 July 19, 2006 September 21, 2011 May 28**

Table 1 The Cold Materials within Small Magnetic Flux Ropes (1998-2008)

Observations of Solar Wind from Earth-directed Coronal Pseudostreamers

Y.-M. Wang¹ and O. Panasenco

2019 ApJ 872 139

[sci-hub.se/10.3847/1538-4357/aaff5e](https://doi.org/10.3847/1538-4357/aaff5e)

Low-speed (~ 450 km s⁻¹) solar wind is widely considered to originate from streamer loops that intermittently release their contents into the heliosphere, in contrast to high-speed wind, which has its source in large coronal holes. To account for the presence of slow wind far from the heliospheric current sheet (HCS), it has been suggested that "pseudostreamers" rooted between coronal holes of the same polarity continually undergo interchange reconnection with the adjacent open flux, producing a wide band of slow wind centered on the separatrix/plasma sheet that extends outward from the pseudostreamer cusp. Employing extreme-ultraviolet images and potential-field source-surface extrapolations, we have identified 10 Earth-directed pseudostreamers during 2013–2016. In situ measurements show wind speeds ranging from ~ 320 to ~ 600 km s⁻¹ in the days immediately preceding and following the predicted pseudostreamer crossings, with the proton densities and O7+/O6+ ratios tending to be inversely correlated with the bulk speed. We also identify examples of coronal holes that straddle the solar equator and give rise to wind speeds of order 400 km s⁻¹. Our results support the idea that the bulk of the slow wind observed more than a few degrees from the HCS originates from just inside coronal holes.

The Merging of Two Stream Interaction Regions within 1 au: The Possible Role of Magnetic Reconnection

Zehao Wang^{1,2}, Jianpeng Guo^{3,4,5}, Xueshang Feng¹, Chaoxu Liu¹, Hui Huang³, Haibo Lin³, Chenming Tan⁵, Yihua Yan⁵, and Weixing Wan

2018 ApJL 869 L6

[sci-hub.tw/10.3847/2041-8213/aaf398](https://doi.org/10.3847/2041-8213/aaf398)

As the Sun rotates, a fast stream can overtake a preceding slow stream, leading to the formation of a stream interaction region (SIR). Two neighboring SIRs may eventually coalesce to produce a merged interaction region (MIR) en route to the outer heliosphere. However, instances of significant interaction and merging of two neighboring SIRs within 1 au are thought to be extremely rare. In this Letter, we present a case report of two interacting and merging SIRs observed near 1 au, which was associated with two adjacent low-latitude coronal holes. The two SIRs were filled with outward

propagating Alfvénic fluctuations associated with magnetohydrodynamic turbulence. A reconnection exhaust associated with a current sheet was identified. We suggest that magnetic reconnection represented a potentially important mechanism for the merging of two neighboring SIRs. This observation may shed light on the understanding of the structure and formation of a MIR within 1 au. **2011/07/08-12, 2011/07/14-18**

The responses of the earth's magnetopause and bow shock to the IMF Bz and the solar wind dynamic pressure: a parametric study using the AMR-CESE-MHD model

Juan **Wang**, Zhifang Guo, Yasong S. Ge, Aimin Du, Can Huang and Pengfei Qin

J. Space Weather Space Clim. **2018**, 8, A41

<https://www.swsc-journal.org/articles/swsc/pdf/2018/01/swsc180003.pdf>

We have used the AMR-CESE-MHD model to investigate the influences of the IMF Bz and the upstream solar wind dynamic pressure (Dp) on Earth's magnetopause and bow shock. Our results present that the earthward displacement of the magnetopause increases with the intensity of the IMF Bz. The increase of the northward IMF Bz also brings the magnetopause closer to the Earth even though with a small distance. Our simulation results show that the subsolar bow shock during the southward IMF is much closer to the Earth than during the northward IMF. As the intensity of IMF Bz increases (also the total field strength), the subsolar bow shock moves sunward as the solar wind magnetosonic Mach number decreases. The sunward movement of the subsolar bow shock during southward IMF are much smaller than that during northward IMF, which indicates that the decrease of solar wind magnetosonic Mach number hardly changes the subsolar bow shock location during southward IMF. Our simulations also show that the effects of upstream solar wind dynamic pressure (Dp) changes on both the subsolar magnetopause and bow shock locations are much more significant than those due to the IMF changes, which is consistent with previous studies. However, in our simulations the earthward displacement of the subsolar magnetopause during high solar wind Dp is greater than that predicted by the empirical models.

Cold prominence materials detected within magnetic clouds during 1998–2007

Jiemin **Wang** (王杰敏), Hengqiang Feng (冯恒强) and Guoqing Zhao (赵国清)

A&A 616, A41 (2018)

<http://sci-hub.tw/https://www.aanda.org/articles/aa/abs/2018/08/aa31807-17/aa31807-17.html>

Context. Coronal mass ejections (CMEs) are intense solar explosive eruptions, and they are frequently correlated with prominence eruptions. Previous observations show that about 70% of CMEs are associated with prominence eruptions. However, there are only a handful of reported observations of prominence plasma materials within interplanetary CMEs (ICMEs), which are the interplanetary manifestations of CMEs. Moreover, approximately 4% of ICMEs exhibit the presence of prominence materials, and approximately 12% of magnetic clouds (MCs) contain prominence materials. Aims. We aim to comprehensively search for cold prominence materials in MCs observed by the Advanced Composition Explorer (ACE) spacecraft during 1998–2007.

Methods. Using the criteria of unusual O5+ and (or) Fe6+ abundances, we examined 76 MCs observed by ACE during 1998–2007 to search for cold prominence materials.

Results. Our results revealed that out of the 76 MCs, 27 (36%) events contained prominence material regions with low-charge-state signatures.

Conclusions. Although the fraction is still lower than the approximately 70% of CMEs associated with prominence eruptions, it is much higher than 12%. The unusual O5+ and (or) Fe6+ abundances may be simple and reliable criteria to investigate prominence materials in the interplanetary medium. **4-6 March 1998, 9-10 Nov 2004, 19-21 May 2005**

Table 1. Cold material regions within magnetic clouds (1998-2007)

Magnetic Disconnections at the Boundary of a Small Interplanetary Magnetic Flux Rope Associated with a Reconnection Exhaust

JieMin **Wang**, Qiang Liu, Yan Zhao

[Solar Physics](#) August **2018**, 293:116

A local current sheet and a subsequent small interplanetary magnetic-flux rope were observed on **1 April 2003** by Wind and the Advanced Composition Explorer (ACE). A Petschek reconnection-like exhaust crossing of the local current sheet was identified using the Walén test. The Wind spacecraft re-entered the reconnection exhaust after the main exhaust encounter, and the reentry may be due to a spatial fold of the current-sheet surface itself. The absence of parallel strahls and the presence of antiparallel strahls on either side of the current sheet suggest that the magnetic-field

lines before the exhaust and in the subsequent small flux rope are all open. The 180° - 180° pitch-angle strahls were clearly absent, and halo-suprathermal electron pitch-angle distributions were observed in the exhaust. This finding means that the open field lines of the magnetic-flux rope were reconnecting to the adjacent open field lines to produce U-shaped field lines disconnected from the Sun. These observations provide direct evidence that the magnetic fields of the interplanetary small magnetic-flux rope were disconnecting from the Sun through magnetic reconnection. This type of disconnected event potentially has important implications for the magnetic-flux budget of the heliosphere.

A Solar Eruption with Relatively Strong Geo-effectiveness Originating from Active Region Peripheral Diffusive Polarities

Rui **Wang**, [Ying D. Liu](#), [Huidong Hu](#), [Xiaowei Zhao](#)

2018 *ApJ* 863 81

<https://arxiv.org/pdf/1807.03047.pdf>

<http://sci-hub.tw/http://iopscience.iop.org/article/10.3847/1538-4357/aad22d/meta>

We report the observations of a moderate but relatively intense geo-effective solar eruption on **2015 November 4** from the peripheral diffusive polarities of active region 12443. We use space-borne Solar Dynamics Observatory and ACE observations. EUV images identified helical pattern along a filament channel and we regard this channel as flux-rope structure. Flow velocity derived from tracked magnetograms infers converging motion along the polarity inversion line beneath the filament channel. An associated magnetic cancellation process was detected in the converging region. Further, the pre-eruptive EUV brightening was observed in the converging region, the most intense part of which appeared in the magnetic cancellation region. These observations imply that the converging and cancelling flux probably contributed to the formation of the helical magnetic fields associated with the flux rope. A filament-height estimation method suggests that the middle part of the filament probably lies at a low altitude and was consistent with the initial place of the eruption. A thick current channel associated with the flux rope is also determined. For an expanding thick current channel, the critical height of the decay index for torus instability lies in the range of 37 - 47 Mm. Southward magnetic fields in the sheath and the ejecta induced a geomagnetic storm with a Dst global minimum of ~ -90 nT.

Understanding the twist distribution inside magnetic flux ropes by anatomizing an interplanetary magnetic cloud

Yuming **Wang**, [Chenglong Shen](#), [Rui Liu](#), [Jiajia Liu](#), [Jingnan Guo](#), [Xiaolei Li](#), [Mengjiao Xu](#), [Qiang Hu](#), [Tielong Zhang](#)

JGR **Volume 123, Issue 5** Pages 3238-3261 **2018** <https://doi.org/10.1002/2017JA024971>

<https://arxiv.org/pdf/1803.01353.pdf>

Magnetic flux rope (MFR) is the core structure of the greatest eruptions, i.e., the coronal mass ejections (CMEs), on the Sun, and magnetic clouds are post-eruption MFRs in interplanetary space. There is a strong debate about whether or not a MFR exists prior to a CME and how the MFR forms/grows through magnetic reconnection during the eruption. Here we report a rare event, in which a magnetic cloud was observed sequentially by four spacecraft near Mercury, Venus, Earth and Mars, respectively. With the aids of a uniform-twist flux rope model and a newly developed method that can recover a shock-compressed structure, we find that the axial magnetic flux and helicity of the magnetic cloud decreased when it propagated outward but the twist increased. Our analysis suggests that the 'pancaking' effect and 'erosion' effect may jointly cause such variations. The significance of the 'pancaking' effect is difficult to be estimated, but the signature of the erosion can be found as the imbalance of the azimuthal flux of the cloud. The latter implies that the magnetic cloud was eroded significantly leaving its inner core exposed to the solar wind at far distance. The increase of the twist together with the presence of the erosion effect suggests that the post-eruption MFR may have a high-twist core enveloped by a less-twisted outer shell. These results pose a great challenge to the current understanding on the solar eruptions as well as the formation and instability of MFRs. **2014 February 15 – 16.**

Observations of a Small Interplanetary Magnetic Flux Rope Opening by Interchange Reconnection

J. M. **Wang**, H. Q. Feng, and G. Q. Zhao

2018 *ApJ* 853 94

<http://sci-hub.tw/http://iopscience.iop.org/0004-637X/853/1/94/>

Interchange reconnection, specifically magnetic reconnection between open magnetic fields and closed magnetic flux ropes, plays a major role in the heliospheric magnetic flux budget. It is generally accepted that closed magnetic field lines of interplanetary magnetic flux ropes (IMFRs) can gradually open through reconnection between one of its legs

and other open field lines until no closed field lines are left to contribute flux to the heliosphere. In this paper, we report an IMFR associated with a magnetic reconnection exhaust, whereby its closed field lines were opening by a magnetic reconnection event near 1 au. The reconnection exhaust and the following IMFR were observed on **2002 February 2** by both the Wind and ACE spacecraft. Observations on counterstreaming suprathermal electrons revealed that most magnetic field lines of the IMFR were closed, especially those after the front boundary of the IMFR, with both ends connected to the Sun. The unidirectional suprathermal electron strahls before the exhaust manifested the magnetic field lines observed before the exhaust was open. These observations provide direct evidence that closed field lines of IMFRs can be opened by interchange reconnection in interplanetary space. This is the first report of the closed field lines of IMFRs being opened by interchange reconnection in interplanetary space. This type of interplanetary interchange reconnection may pose important implications for balancing the heliospheric flux budget.

Small Coronal Holes Near Active Regions as Sources of Slow Solar Wind

Y.-M. **Wang**

2017 ApJ 841 94

<http://sci-hub.cc/10.3847/1538-4357/aa706e> **File**

We discuss the nature of the small areas of rapidly diverging, open magnetic flux that form in the strong unipolar fields at the peripheries of active regions (ARs), according to coronal extrapolations of photospheric field measurements. Because such regions usually have dark counterparts in extreme-ultraviolet (EUV) images, we refer to them as coronal holes, even when they appear as narrow lanes or contain sunspots. Revisiting previously identified "AR sources" of slow solar wind from 1998 and 1999, we find that they are all associated with EUV coronal holes; the absence of well-defined He I 1083.0 nm counterparts to some of these holes is attributed to the large flux of photoionizing radiation from neighboring AR loops. Examining a number of AR-associated EUV holes during the 2014 activity maximum, we confirm that they are characterized by wind speeds of $\sim 300\text{--}450\text{ km s}^{-1}$, O7+/O6+ ratios of $\sim 0.05\text{--}0.4$, and footpoint field strengths typically of order 30 G. The close spacing between ARs at sunspot maximum limits the widths of unipolar regions and their embedded holes, while the continual emergence of new flux leads to rapid changes in the hole boundaries. Because of the highly nonradial nature of AR fields, the smaller EUV holes are often masked by the overlying canopy of loops, and may be more visible toward one solar limb than at central meridian. As sunspot activity declines, the AR remnants merge to form much larger, weaker, and longer-lived unipolar regions, which harbor the "classical" coronal holes that produce recurrent high-speed streams.

Sympathetic Solar Filament Eruptions

Rui **Wang**, Ying D. Liu, Ivan Zimovets, Huidong Hu, Xinghua Dai, Zhongwei Yang

2016

<http://arxiv.org/pdf/1608.01067v1.pdf>

The **2015 March 15** coronal mass ejection as one of the two that together drove the largest geomagnetic storm of solar cycle 24 so far was associated with sympathetic filament eruptions. We investigate the relations between the different filaments involved in the eruption. A surge-like small-scale filament motion is confirmed as the trigger that initiated the erupting filament with multi-wavelength observations and using a forced magnetic field extrapolation method. When the erupting filament moved to an open magnetic field region, it experienced an obvious acceleration process and was accompanied by a C-class flare and the rise of another larger filament that eventually failed to erupt. We measure the decay index of the background magnetic field, which presents a critical height of 118 Mm. Combining with a potential field source surface extrapolation method, we analyze the distributions of the large-scale magnetic field, which indicates that the open magnetic field region may provide a favorable condition for F2 rapid acceleration and have some relation with the largest solar storm. The comparison between the successful and failed filament eruptions suggests that the confining magnetic field plays an important role in the preconditions for an eruption.

On the twists of interplanetary magnetic flux ropes observed at 1 AU

Yuming **Wang**, Bin Zhuang, Qiang Hu, [Rui Liu](#), [Chenglong Shen](#), [Yutian Chi](#)

JGR 2016

<http://arxiv.org/pdf/1608.05607v1.pdf>

Magnetic flux ropes (MFRs) are one kind of fundamental structures in the solar physics, and involved in various eruption phenomena. Twist, characterizing how the magnetic field lines wind around a main axis, is an intrinsic property of MFRs, closely related to the magnetic free energy and stableness. So far it is unclear how much amount of twist is carried by MFRs in the solar atmosphere and in heliosphere and what role the twist played in the eruptions of MFRs. Contrasting to the solar MFRs, there are lots of in-situ measurements of magnetic clouds (MCs), the large-scale MFRs in interplanetary space, providing some important information of the twist of MFRs. Thus, starting from MCs, we investigate the twist of interplanetary MFRs with the aid of a velocity-modified uniform-twist force-free flux rope

model. It is found that most of MCs can be roughly fitted by the model and nearly half of them can be fitted fairly well though the derived twist is probably over-estimated by a factor of 2.5. By applying the model to 115 MCs observed at 1 AU, we find that (1) the twist angles of interplanetary MFRs generally follow a trend of about $0.61R$ radians, where $1R$ is the aspect ratio of a MFR, with a cutoff at about 12π radians AU^{-1} , (2) most of them are significantly larger than 2.5π radians but well bounded by $21R$ radians, (3) strongly twisted magnetic field lines probably limit the expansion and size of MFRs, and (4) the magnetic field lines in the legs wind more tightly than those in the leading part of MFRs. These results not only advance our understanding of the properties and behavior of interplanetary MFRs, but also shed light on the formation and eruption of MFRs in the solar atmosphere. A discussion about the twist and stableness of solar MFRs are therefore given.

On the Propagation of a Geoeffective Coronal Mass Ejection during March 15 -- 17, 2015

Yuming Wang, Quanhao Zhang, Jijia Liu, [Chenglong Shen](#), [Fang Shen](#), [Zicai Yang](#), [T. Zic](#), [B. Vrsnak](#), [D. F. Webb](#), [Rui Liu](#), [S. Wang](#), [Jie Zhang](#), [Qiang Hu](#), [Bin Zhuang](#)

JGR 2016

<http://arxiv.org/pdf/1607.07750v1.pdf> File

The largest geomagnetic storm so far in the solar cycle 24 was produced by a fast coronal mass ejection (CME) originating on **2015 March 15**. It was an initially west-oriented CME and expected to only cause a weak geomagnetic disturbance. Why did this CME finally cause such a large geomagnetic storm? We try to find some clues by investigating its propagation from the Sun to 1 AU. First, we reconstruct the CME's kinematic properties in the corona from the SOHO and SDO imaging data with the aid of the graduated cylindrical shell (GCS) model. It is suggested that the CME propagated to the west $\sim 33^\circ \pm 10^\circ$ away from the Sun-Earth line with a speed of about 817 km s^{-1} before leaving the field of view of the SOHO/LASCO C3 camera. A magnetic cloud (MC) corresponding to this CME was measured in-situ by the Wind spacecraft two days later. By applying two MC reconstruction methods, we infer the configuration of the MC as well as some kinematic information, which implies that the CME possibly experienced an eastward deflection on its way to 1 AU. However, due to the lack of observations from the STEREO spacecraft, the CME's kinematic evolution in interplanetary space is not clear. In order to fill this gap, we utilize numerical MHD simulation, drag-based CME propagation model (DBM) and the model for CME deflection in interplanetary space (DIPS) to recover the propagation process, especially the trajectory, of the CME from 30RS to 1 AU. It is suggested that the trajectory of the CME was deflected toward the Earth by about 12° , consistent with the implication from the MC reconstruction at 1 AU. This eastward deflection probably contributed to the CME's unexpected geoeffectiveness by pushing the center of the initially west-oriented CME closer to the Earth.

On the propagation of a geoeffective coronal mass ejection during 15–17 March 2015

Yuming Wang, Quanhao Zhang, Jijia Liu, Chenglong Shen, Fang Shen, Zicai Yang, T. Zic, B. Vrsnak, D. F. Webb, Rui Liu, S. Wang, Jie Zhang, Qiang Hu, Bin Zhuang

JGR Volume 121, Issue 8 August 2016 Pages 7423–7434

<http://arxiv.org/pdf/1607.07750v1.pdf> File

The largest geomagnetic storm so far, called 2015 St. Patrick's Day event, in the solar cycle 24 was produced by a fast coronal mass ejection (CME) originating on 15 March 2015. It was an initially west-oriented CME and expected to only cause a weak geomagnetic disturbance. Why did this CME finally cause such a large geomagnetic storm? We try to find some clues by investigating its propagation from the Sun to 1 AU. First, we reconstruct the CME's kinematic properties in the corona from the SOHO and Solar Dynamics Observatory imaging data with the aid of the graduated cylindrical shell model. It is suggested that the CME propagated to the west $\sim 33^\circ \pm 10^\circ$ away from the Sun-Earth line with a speed of about 817 km s^{-1} before leaving the field of view of the SOHO/Large Angle and Spectrometric Coronagraph (LASCO) C3 camera. A magnetic cloud (MC) corresponding to this CME was measured in situ by the Wind spacecraft 2 days after the CME left LASCO's field of view. By applying two MC reconstruction methods, we infer the configuration of the MC as well as some kinematic information, which implies that the CME possibly experienced an eastward deflection on its way to 1 AU. However, due to the lack of observations from the STEREO spacecraft, the CME's kinematic evolution in interplanetary space is not clear. In order to fill this gap, we utilize numerical MHD simulation, drag-based CME propagation model (DBM) and the model for CME deflection in interplanetary space (DIPS) to recover the propagation process, especially the trajectory, of the CME from 30RS to 1 AU under the constraints of the derived CME's kinematics near the Sun and at 1 AU. It is suggested that the trajectory of the CME was deflected toward the Earth by about 12° , consistent with the implication from the MC reconstruction at 1 AU. This eastward deflection probably contributed to the CME's unexpected geoeffectiveness by pushing the center of the initially west-oriented CME closer to the Earth.

Toward an Understanding of Earth-Affecting Solar Eruptions

Yuming **Wang**

EOS 1 Apr 2016

Coronal mass ejection forecasting improves with technological developments and increasing availability of data.

Statistical analysis and verification of 3-hourly geomagnetic activity probability predictions

Jingjing **Wang**, Qiuzhen Zhong, Siqing Liu, Juan Miao, Fanghua Liu, Zhitao Li, Weiwei Tang

Space Weather Volume 13, Issue 12 December 2015 Pages 831–852

The Space Environment Prediction Center (SEPC) has classified geomagnetic activity into four levels: quiet to unsettled ($K_p < 4$), active ($K_p = 4$), minor to moderate storm ($K_p = 5$ or 6), and major to severe storm ($K_p > 6$). The 3-hourly K_p index prediction product provided by the SEPC is updated half hourly. In this study, the statistical conditional forecast models for the 3-hourly geomagnetic activity level were developed based on 10 years of data and applied to more than 3 years of data, using the previous K_p index, interplanetary magnetic field, and solar wind parameters measured by the Advanced Composition Explorer as conditional parameters. The quality of the forecast models was measured and compared against verifications of accuracy, reliability, discrimination capability, and skill of predicting all geomagnetic activity levels, especially the probability of reaching the storm level given a previous “calm” (nonstorm level) or “storm” (storm level) condition. It was found that the conditional models that used the previous K_p index, the peak value of BtV (the product of the total interplanetary magnetic field and speed), the average value of B_z (the southerly component of the interplanetary magnetic field), and BzV (the product of the southerly component of the interplanetary magnetic field and speed) over the last 6 h as conditional parameters provide a relative operating characteristic area of 0.64 and can be an appropriate predictor for the probability forecast of geomagnetic activity level.

Coronal Mass Ejections and the Solar Cycle Variation of the Sun's Open Flux

Y.-M. **Wang** and N. R. Sheeley, Jr.

2015 ApJ 809 L24

The strength of the radial component of the interplanetary magnetic field (IMF), which is a measure of the Sun's total open flux, is observed to vary by roughly a factor of two over the 11 year solar cycle. Several recent studies have proposed that the Sun's open flux consists of a constant or “floor” component that dominates at sunspot minimum, and a time-varying component due to coronal mass ejections (CMEs). Here, we point out that CMEs cannot account for the large peaks in the IMF strength which occurred in 2003 and late 2014, and which coincided with peaks in the Sun's equatorial dipole moment. We also show that near-Earth interplanetary CMEs, as identified in the catalog of Richardson and Cane, contribute at most ~30% of the average radial IMF strength even during sunspot maximum. We conclude that the long-term variation of the radial IMF strength is determined mainly by the Sun's total dipole moment, with the quadrupole moment and CMEs providing an additional boost near sunspot maximum. Most of the open flux is rooted in coronal holes, whose solar cycle evolution in turn reflects that of the Sun's lowest-order multipoles.

Investigating plasma motion of magnetic clouds at 1 AU through a velocity-modified cylindrical force-free flux rope model

Yuming **Wang**, Zhenjun Zhou, Chenglong Shen, Rui Liu, S. Wang

2015 JGR Volume 120, Issue 3 Pages 1543–1565

<http://arxiv.org/pdf/1502.05112v1.pdf>

Magnetic clouds (MCs) are the interplanetary counterparts of coronal mass ejections (CMEs), and usually modeled by a flux rope. By assuming the quasi-steady evolution and self-similar expansion, we introduce three types of global motion into a cylindrical force-free flux rope model, and developed a new velocity-modified model for MCs. The three types of the global motion are the linear propagating motion away from the Sun, the expanding and the poloidal motion with respect to the axis of the MC. The model is applied to 72 MCs observed by Wind spacecraft to investigate the properties of the plasma motion of MCs. First, we find that some MCs had a significant propagation velocity perpendicular to the radial direction, suggesting the direct evidence of the CME's deflected propagation and/or rotation in interplanetary space. Second, we confirm the previous results that the expansion speed is correlated with the radial propagation speed and most MCs did not expand self-similarly at 1 AU. In our statistics, about 62%/17% of MCs underwent a under/over-expansion at 1 AU and the expansion rate is about 0.6 on average. Third, most interestingly, we find that a significant poloidal motion did exist in some MCs. Three speculations about the cause of the poloidal motion are

therefore proposed. These findings advance our understanding of the MC's properties at 1 AU as well as the dynamic evolution of CMEs from the Sun to interplanetary space. **23 dec 1996, 25 Sept 1998**

Deflected propagation of a coronal mass ejection from the corona to interplanetary space

Yuming [Wang](#), Boyi Wang, Chenglong Shen, Fang Shen, Noe Lugaz

JGR, Volume 119, Issue 7, pages 5117–5132, 2014

<http://arxiv.org/pdf/1406.4684v1.pdf>

Among various factors affecting the space weather effects of a coronal mass ejection (CME), its propagation trajectory in the interplanetary space is an important one determining whether and when the CME will hit the Earth. Many direct observations have revealed that a CME may not propagate along a straight trajectory in the corona, but whether or not a CME also experiences a deflected propagation in the interplanetary space is a question, which has never been fully answered. Here by investigating the propagation process of an isolated CME from the corona to interplanetary space during **2008 September 12 -- 19**, we present solid evidence that the CME was deflected not only in the corona but also in the interplanetary space. The deflection angle in the interplanetary space is more than 20 degrees toward the west, resulting a significant change in the probability the CME encounters the Earth. A further modeling and simulation-based analysis suggest that the cause of the deflection in the interplanetary space is the interaction between the CME and the solar wind, which is different from that happening in the corona.

What Is a Solar Electromagnetic Storm?

[Wang](#), H., G. Ai, and J. Wang

(2012), Space Weather, 10, S09003, doi:10.1029/2012SW000847. **File**

In recent years, the expression “solar storm” has become popular in China, but many Chinese do not realize that solar storms are very different from storms on Earth. As solar physicists and members of the Regional Warning Center China (RWCC) of International Space Environment Services (ISES), we frequently encounter the question “What is a solar storm?” In order to properly respond to the customers of the RWCC, we investigated the historical evolution of the term “solar storm.”

An analytical model probing the internal state of coronal mass ejections based on observations of their expansions and propagations

[Wang](#), Yuming; Zhang, Jie; Shen, Chenglong

J. Geophys. Res., Vol. 114, No. A10, A10104, 2009

In this paper, a generic self-similar flux rope model is proposed to probe the internal state of CMEs in order to understand the thermodynamic process and expansion of CMEs in interplanetary space. Using this model, three physical parameters and their variations with heliocentric distance can be inferred based on coronagraph observations of CMEs' propagation and expansion. One is the polytropic index Γ of the CME plasma, and the other two are the average Lorentz force and the thermal pressure force inside CMEs. By applying the model to the **8 October 2007** CME observed by STEREO/SECCHI, we find that (1) the polytropic index of the CME plasma increased from initially 1.24 to more than 1.35 quickly and then slowly decreased to about 1.34; it suggests that there be continuously heat injected/converted into the CME plasma and the value of Γ tends to be $\frac{4}{3}$, a critical value inferred from the model for a force-free flux rope; (2) the Lorentz force directed inward while the thermal pressure force outward, and both of them decreased rapidly as the CME moved out; the direction of the two forces reveals that the thermal pressure force is the internal driver of the CME expansion, whereas the Lorentz force prevented the CME from expanding. Some limitations of the model and approximations are discussed meanwhile.

Large geomagnetic storms of extreme solar event periods in solar cycle 23

Ruiguang [Wang](#)

[Advances in Space Research](#)

[Volume 40, Issue 12, 2007](#), Pages 1835-1841

During extreme solar events such as big flares or/and energetic coronal mass ejections (CMEs) high energy particles are accelerated by the shocks formed in front of fast interplanetary coronal mass ejections (ICMEs). The ICMEs (and their sheaths) also give rise to large geomagnetic storms which have significant effects on the Earth's environment and human life. Around 14 solar cosmic ray ground level enhancement (GLE) events in solar cycle 23 we examined the cosmic ray

variation, solar wind speed, ions density, interplanetary magnetic field, and geomagnetic disturbance storm time index (Dst). We found that all but one of GLEs are always followed by a geomagnetic storm with $Dst \leq -50$ nT within 1–5 days later. Most(10/14) geomagnetic storms have Dst index ≤ -100 nT therefore generally belong to strong geomagnetic storms. This suggests that GLE event prediction of geomagnetic storms is 93% for moderate storms and 71% for large storms when geomagnetic storms preceded by GLEs. All Dst depressions are associated with cosmic ray decreases which occur nearly simultaneously with geomagnetic storms. We also investigated the interplanetary plasma features. Most geomagnetic storm correspond significant periods of southward Bz and in close to 80% of the cases that the Bz was first northward then turning southward after storm sudden commencement (SSC). Plasma flow speed, ion number density and interplanetary plasma temperature near 1 AU also have a peak at interplanetary shock arrival. Solar cause and energetic particle signatures of large geomagnetic storms and a possible prediction scheme are discussed.

The Dependence of the Geoeffectiveness of Interplanetary Flux Rope on Its Orientation, with Possible Application to Geomagnetic Storm Prediction

Yuming Wang, Pinzhong Ye, S. Wang

Solar Phys., 240 (2), Page: 373 – 386, 2007, File.

Interplanetary magnetic clouds (MCs) are one of the main sources of large nonrecurrent geomagnetic storms. With the aid of a force-free flux rope model, the dependence of the intensity of geomagnetic activity (indicated by *Dst* index) on the axial orientation (denoted by θ and φ in GSE coordinates) of the magnetic cloud is analyzed theoretically. The distribution of the *Dst* values in the (θ , φ) plane is calculated by changing the axial orientation for various cases. It is concluded that (i) geomagnetic storms tend to occur in the region of $\theta < 0^\circ$, especially in the region of $\theta \sim -45^\circ$, where larger geomagnetic activity could be created; (ii) the intensity of geomagnetic activity varies more strongly with θ than with φ ; (iii) when the parameters B_0 (the magnetic field strength at the flux rope axis), R_0 (the radius of the flux rope), or V (the bulk speed) increase, or $|D|$ (the shortest distance between the flux rope axis and the x -axis in GSE coordinates) decreases, a flux rope not only can increase the intensity of geomagnetic activity, but also is more likely to create a storm, however the variation of n (the density) only has a little effect on the intensity; (iv) the most efficient orientation (MEO) in which a flux rope can cause the largest geomagnetic activity appears at $\varphi \sim 0^\circ$ or $\sim 180^\circ$, and some value of θ which depends mainly on D ; (v) the minimum *Dst* value that could be caused by a flux rope is the most sensitive to changes in B_0 and V of the flux rope, and for a stronger and/or faster MC, a wider range of orientations will be geoeffective. Further, through analyzing 20 MC-caused moderate to large geomagnetic storms during 1998 – 2003, a long-term prediction of MC-caused geomagnetic storms on the basis of the flux rope model is proposed and assessed. The comparison between the theoretical results and the observations shows that there is a close linear correlation between the estimated and observed minimum *Dst* values. This suggests that using the ideal flux rope to predict practical MC-caused geomagnetic storms is applicable. The possibility of the long-term prediction of MC-caused geomagnetic storms is discussed briefly.

A Study of the Orientation of Interplanetary Magnetic Clouds and Solar Filaments

Yuming Wang, Guiping Zhou, Pinzhong Ye, S. Wang, and Jingxiu Wang

The Astrophysical Journal, 651:1245-1255, 2006; File

As a kind of eruptive phenomenon associated with coronal mass ejections (CMEs), solar eruptive filaments are thought to be parallel to the axis of surrounding arcade coronal magnetic fields that erupt and develop into interplanetary magnetic clouds (MCs). By investigating three events from 2000 August, 2003 October, and 2003 November, we estimate the axial orientations of the MCs and make a quantitative comparison with the filament orientations. By defining “tilt angle” as the angle between projected orientation on the plane of the sky and the ecliptic, we find that the tilt angles of these MCs are about 30° , 60° , and 55° , respectively. However, H_α images show that the associated filaments were all highly curved. The tilt angles of the long axes of these filaments prior to their eruption vary in a range that corresponds to tangents along the entire curved path of the filaments. Comparison between the MCs and filaments shows that for the first and third events, the estimated MC tilt angles are within the range of tilt angles of the associated filaments and almost parallel to the central parts of the filaments. But for the second event, the MC tilt angle is outside the

range. This work suggests that (1) the curvature of filaments should be considered in studying the relation between filament and MC orientations, (2) inconsistencies between them do occur, even if the filament curvature is taken into account, and (3) the largest deviation in the tilt angle between MCs and their associated filaments occurs for those MCs whose orientations are not perpendicular to the Earth-Sun line, indicating that the measured part of the MC is not its leading front. **2000 August 09-13, 2003 October, and 2003 November**

Orientation and Geoeffectiveness of Magnetic Clouds as Consequences of Filament Eruptions

Yuming Wang¹, Guiping Zhou², Pinzhong Ye¹, S. Wang¹ and Jingxiu Wang²

Coronal and Stellar Mass Ejections, Proceedings IAU Symposium No. 226, 2005, K. P. Dere, J. Wang & Y. Yan, eds., File

By investigating ten typical magnetic clouds (MCs) associated with large geomagnetic storms ($Dst \sim -100$ nT) from 2000 to 2003, the geoeffectiveness of MCs with various orientations is addressed. It is found that the Dst peak values during the geomagnetic storms are well estimated by applying flux rope model to these magnetic clouds. A high correlation between estimated and observed Dst values is obtained. Moreover, the effect of orientations of MCs on intensities of geomagnetic storms is studied. It is found that the favorable orientations of MCs are approximately at $\theta \sim 70^\circ$ and $\varphi \sim 40^\circ$ in GSE coordinates to cause large geomagnetic storms. Further, by analyzing solar observations of four associated erupted filaments, the question who determine the orientations of MCs is studied. The likelihood of predicting the intensities of a geomagnetic storms several tens hours before their occurrences is also discussed.

Deflection of coronal mass ejection in the interplanetary medium,

Wang, Y., Shen, C., Wang, S., and Ye, P.

(2004), *Solar Phys.*, 222, 329–343

<http://sci-hub.tw/10.1023/B:SOLA.0000043576.21942.aa>

<https://link.springer.com/content/pdf/10.1023%2FB%3ASOLA.0000043576.21942.aa.pdf>

A solar coronal mass ejection (CME) is a large-scale eruption of plasma and magnetic fields from the Sun. It is believed to be the main source of strong interplanetary disturbances that may cause intense geomagnetic storms. However, not all front-side halo CMEs can encounter the Earth and produce geomagnetic storms. The longitude distribution of the Earth-encountered frontside halo CMEs (EFHCMEs) has not only an east–west (E–W) asymmetry (Wang et al., 2002), but also depends on the EFHCMEs' transit speeds from the Sun to 1 AU. The faster the EFHCMEs are, the more westward does their distribution shift, and as a whole, the distribution shifts to the west. Combining the observational results and a simple kinetic analysis, we believe that such E–W asymmetry appearing in the source longitude distribution is due to the deflection of CMEs' propagation in the interplanetary medium. Under the effect of the Parker spiral magnetic field, a fast CME will be blocked by the background solar wind ahead and deflected to the east, whereas a slow CME will be pushed by the following background solar wind and deflected to the west. The deflection angle may be estimated according to the CMEs' transit speed by using a kinetic model. It is shown that slow CMEs can be deflected more easily than fast ones. This is consistent with the observational results obtained by Zhang et al. (2003), that all four Earth-encountered limb CMEs originated from the east. On the other hand, since the most of the EFHCMEs are fast events, the range of the longitude distribution given by the theoretical model is $E40^\circ, W70^\circ$, which is well consistent with the observational results ($E40^\circ, W75^\circ$).

TABLE I List of the Earth-encountered front-side halo CMEs during 1996 – 2002.

A statistical study on the geoeffectiveness of Earth - directed coronal mass ejections from March 1997 to December 2000,

Wang, Y. M., P. Z. Ye, S. Wang, G. P. Zhau, and J. Wang

(2002), *J. Geophys. Res.*, 107(A11), 1340, doi:10.1029/2002JA009244.

sci-hub.se/10.1029/2002ja009244

We have identified 132 Earth-directed coronal mass ejections (CMEs) based on the observations of the Large Angle Spectroscopic Coronagraph (LASCO) and Extreme Ultraviolet Imaging Telescope (EIT) on board of Solar and Heliospheric Observatory (SOHO) from March 1997 to December 2000 and carried out a statistical study on their geoeffectiveness. The following results are obtained: (1) Only 45% of the total 132 Earth-directed halo CMEs caused geomagnetic storms with $Kp \geq 5$; (2) The initial sites of these geoeffective halo CMEs are rather symmetrically distributed in the heliographic latitude of the visible solar disc, while asymmetrical in longitude with the majority located in the west side of the central meridian; (3) The frontside halo CMEs accompanied with solar flares (identified

from GOES-8 satellite observations) seem to be more geoeffective; (4) Only a weak correlation between the CME projected speed and the transit time is revealed. However, for the severe geomagnetic storms (with $K_p \geq 7$), a significant correlation at the confidence level of 99% is found.

Wang et al. [2002] found that 83% of the frontside halo CMEs that caused geomagnetic storms with $K_p \geq 5$ took place within $\pm 30^\circ$ of the central meridian and that their source locations are asymmetrical in longitude, with the majority located in the west side of the central meridian.

The application of radio diagnostics to the study of the solar drivers of space weather

Warmuth, A., & Mann, G.:

Springer Lecture Notes in Physics, Vol. 656, 49, **2005; File**

Intense Geomagnetic Storms Associated with Coronal Holes Under the Weak Solar-Wind Conditions of Cycle 24

S. Watari

[Solar Physics](#) February **2018**, 293:23

<https://link.springer.com/content/pdf/10.1007%2Fs11207-018-1248-y.pdf>

The activity of Solar Cycle 24 has been extraordinarily low. The yearly averaged solar-wind speed is also lower in Cycle 24 than in Cycles 22 and 23. The yearly averaged speed in the rising phase of Cycle 21 is as low as that of Cycle 24, although the solar activity of Cycle 21 is higher than that of Cycle 24. The relationship between the solar-wind temperature and its speed is preserved under the solar-wind conditions of Cycle 24. Previous studies have shown that only a few percent of intense geomagnetic storms (minimum $Dst < -100$ nT) were caused by high-speed solar-wind flows from coronal holes. We identify two geomagnetic storms associated with coronal holes within the 19 intense geomagnetic storms that took place in Cycle 24. **31 May 2013, 6-7 October 2015,**

Geomagnetic storms of cycle 24 and their solar sources

Shinichi Watari

Earth, Planets and Space **2017** 69:70

<https://doi.org/10.1186/s40623-017-0653-z>

<https://earth-planets-space.springeropen.com/track/pdf/10.1186/s40623-017-0653-z>

Solar activity of cycle 24 following the deep minimum between cycle 23 and cycle 24 is the weakest one since cycle 14 (1902–1913). Geomagnetic activity is also low in cycle 24. We show that this low geomagnetic activity is caused by the weak dawn-to-dusk solar wind electric field (E_{d-d}) and that the occurrence rate of $E_{d-d} > 5$ mV/m decreased in the interval from 2013 to 2014. We picked up seventeen geomagnetic storms with the minimum Dst index of less than -100 nT and identified their solar sources in cycle 24 (2009–2015). It is shown that the relatively slow coronal mass ejections contributed to the geomagnetic storms in cycle 24.

Forecast of recurrent geomagnetic storms

S. Watari

Advances in Space Research, Volume 47, Issue 12, 15 June **2011**, Pages 2162-2171

Long-term forecast of space weather allows in achieving a longer lead time for taking the necessary precautions against disturbances. Hence, there is a need for long-term forecasting of space weather. We studied the possibility for a long-term forecast of recurrent geomagnetic storms. Geomagnetic storms recur with an approximate 27-day period during the declining phase of a solar cycle. These disturbances are caused by the passage of corotating interaction regions, which are formed by interactions between the background slow-speed solar wind and high-speed solar wind streams from a coronal hole. In this study, we report on the performance of 27-day-ahead forecasts of the recurrent geomagnetic disturbances using K_p index. The methods of the forecasts are on the basis of persistence, autoregressive model, and categorical forecast using occurrence probability. The forecasts show better performance during the declining phase of a solar cycle than other phases. The categorical forecast shows the probability of detection (POD) more than 0.5 during the declining phase. Transition of the performance occurs sharply among the declining phases and other phases.

Webb_ISEST (International Study for Earth-Affecting Solar Transients) _MM WG4 Campaign Events_2014, File

See http://solar.gmu.edu/heliophysics/index.php/The_ISEST_Event_List

2007 November 14-20 , 2008 September 12-19, 2009 August 25, 2012 January 19 and January 23 , 2012 March 7-9, 2012 July 12-14, 2012 July 23-24 , 2012 September 28, 2012 October 4-8, 2013 March 15-17, 2013 June 1, 2014 January 6, 2014 January 7-9, 2014 September 10-13

An Ensemble Study of a January 2010 Coronal Mass Ejection (CME): Connecting a Non-obvious Solar Source with Its ICME/Magnetic Cloud

D. F. **Webb**, M. M. Bisi, C. A. de Koning, C. J. Farrugia, B. V. Jackson, L. K. Jian, N. Lugaz, K. Marubashi, C. Möstl, E. P. Romashets, ... show all 12

Solar Phys., 2014

A distinct magnetic cloud (MC) was observed in-situ at the Solar TERrestrial RELations Observatory (STEREO)-B on **20–21 January 2010**. About three days earlier, on **17 January**, a bright flare and coronal mass ejection (CME) were clearly observed by STEREO-B, which suggests that this was the progenitor of the MC. However, the in-situ speed of the event, several earlier weaker events, heliospheric imaging, and a longitude mismatch with the STEREO-B spacecraft made this interpretation unlikely. We searched for other possible solar eruptions that could have caused the MC and found a faint filament eruption and the associated CME on **14–15 January** as the likely solar source event. We were able to confirm this source by using coronal imaging from the Sun Earth Connection Coronal and Heliospheric Investigation (SECCHI)/EUVI and COR and Solar and Heliospheric Observatory (SOHO)/Large Angle and Spectrometric Coronagraph (LASCO) telescopes and heliospheric imaging from the Solar Mass Ejection Imager (SMEI) and the STEREO/Heliospheric Imager instruments. We use several empirical models to understand the three-dimensional geometry and propagation of the CME, analyze the in-situ characteristics of the associated ICME, and investigate the characteristics of the MC by comparing four independent flux-rope model fits with the launch observations and magnetic-field orientations. The geometry and orientations of the CME from the heliospheric-density reconstructions and the in-situ modeling are remarkably consistent. Lastly, this event demonstrates that a careful analysis of all aspects of the development and evolution of a CME is necessary to correctly identify the solar counterpart of an ICME/MC.

Heliospheric Imaging of 3D Density Structures During the Multiple Coronal Mass Ejections of Late July to Early August 2010

D. F. **Webb**, C. Möstl, B. V. Jackson, M. M. Bisi, T. A. Howard, T. Mulligan, E. A. Jensen, L. K. Jian, J. A. Davies, C. A. de Koning, ... show all 19

Solar Physics, July 2013, Volume 285, Issue 1-2, pp 317-348

http://sprg.ssl.berkeley.edu/~liuxying/pubs/2013_sp_webb.pdf

It is usually difficult to gain a consistent global understanding of a coronal mass ejection (CME) eruption and its propagation when only near-Sun imagery and the local measurements derived from single-spacecraft observations are available. Three-dimensional (3D) density reconstructions based on heliospheric imaging allow us to “fill in” the temporal and spatial gaps between the near-Sun and in situ data to provide a truly global picture of the propagation and interactions of the CME as it moves through the inner heliosphere. In recent years the heliospheric propagation of dense structures has been observed and measured by the heliospheric imagers of the Solar Mass Ejection Imager (SMEI) and on the twin Solar TERrestrial RELations Observatory (STEREO) spacecraft. We describe the use of several 3D reconstruction techniques based on these heliospheric imaging data sets to distinguish and track the propagation of multiple CMEs in the inner heliosphere during the very active period of solar activity in late July – early August 2010. We employ 3D reconstruction techniques used at the University of California, San Diego (UCSD) based on a kinematic solar wind model, and also the empirical Tappin–Howard model. We compare our results with those from other studies of this active period, in particular the heliospheric simulations made with the ENLIL model by Odstrcil et al. (J. Geophys. Res., 2013) and the in situ results from multiple spacecraft provided by Möstl et al. (Astrophys. J. 758, 10 – 28, 2012). We find that the SMEI results in particular provide an overall context for the multiple-density flows associated with these CMEs. For the first time we are able to intercompare the 3D reconstructed densities with the timing and magnitude of in situ density structures at five spacecraft spread over 150° in ecliptic longitude and from 0.4 to 1 AU in radial distance. We also model the magnetic flux-rope structures at three spacecraft using both force-free and non-force-free modelling, and compare their timing and spatial structure with the reconstructed density flows.

Solar Wind Quasi-invariant for Slow and Fast Magnetic Clouds

Alla **Webb**, Joseph Fainberg and Vladimir Osherovich

Solar Physics, Volume 277, Number 2, 375-388, **2012**

The solar wind quasi-invariant (QI) has been defined by Osherovich, Fainberg, and Stone (Geophys. Res. Lett. 26, 2597, 1999) as the ratio of magnetic energy density and the energy density of the solar wind flow. In the regular solar wind QI is a rather small number, since the energy of the flow is almost two orders of magnitude greater than the magnetic energy. However, in magnetic clouds, QI is the order of unity (less than 1) and thus magnetic clouds can be viewed as a great anomaly in comparison with its value in the background solar wind. We study the duration, extent, and amplitude of this anomaly for two groups of isolated magnetic clouds: slow clouds ($360 < v < 450 \text{ km s}^{-1}$) and fast clouds ($450 \leq v < 720 \text{ km s}^{-1}$). By applying the technique of superposition of epochs to 12 slow and 12 fast clouds from the catalog of Richardson and Cane (Solar Phys. 264, 189, 2010), we create an average slow cloud and an average fast cloud observed at 1 AU. From our analysis of these average clouds, we obtain cloud boundaries in both time and space as well as differences in QI amplitude and other parameters characterizing the solar wind state. Interplanetary magnetic clouds are known to cause major magnetic storms at the Earth, especially those clouds which travel from the sun to the Earth at high speeds. Characterizing each magnetic cloud by its QI value and extent may help in understanding the role of those disturbances in producing geomagnetic activity.

Studying geoeffective interplanetary coronal mass ejections between the Sun and Earth: Space weather implications of Solar Mass Ejection Imager observations

Webb, D. F.; Howard, T. A.; Fry, C. D.; Kuchar, T. A.; Mizuno, D. R.; Johnston, J. C.; Jackson, B. V.

Space Weather, Vol. 7, No. 5, S05002, **2009**, File; <http://dx.doi.org/10.1029/2008SW000409>

Interplanetary coronal mass ejections (ICMEs) are the primary cause of severe space weather at Earth because they drive shocks and trigger geomagnetic storms that can damage spacecraft and ground-based systems. The Solar Mass Ejection Imager (SMEI) is a U. S. Air Force experiment with the ability to track ICMEs in white light from near the Sun to Earth and beyond, thus providing an extended observational range for forecasting storms. We summarize several studies of SMEI's detection and tracking capability, especially of the ICMEs associated with the intense (peak $Dst \leq -100 \text{ nT}$) geomagnetic storms that were the focus of the NASA Living With a Star Geostorm Coordinated Data Analysis Workshop. We describe the SMEI observations and analyses for the 18 intense storms observed from May 2003–2007 with adequate SMEI coverage and identified solar and interplanetary source regions. SMEI observed the associated ICMEs for 89% of these intense storms. For each event we extracted the time differences between these sets of times at 1 AU for shock arrival time, predicted ICME arrival time, onset of high-altitude aurora observed by SMEI, and storm onset. The mean intervals between successive pairs of these data were found to each be ~ 4 hours. On average, SMEI first detected the geoeffective ICME about 1 day in advance, yielding a prediction lead time of ~ 18 hours. Finally, the RMS values for the ICME-shock and storm-ICME time differences were determined, and provide at least a 1-hour improvement compared to similar observational and model-dependent studies.

Study of CME Propagation in the Inner Heliosphere: SOHO LASCO, SMEI and STEREO HI Observations of the January 2007 Events

D.F. **Webb** · T.A. Howard · C.D. Fry · T.A. Kuchar · D. Odstrcil · B.V. Jackson · M.M. Bisi · R.A. Harrison · J.S. Morrill · R.A. Howard · J.C. Johnston

Solar Phys (2009) 256: 239–267, DOI 10.1007/s11207-009-9351-8, **2009**, File

STEREO SCIENCE RESULTS AT SOLAR MINIMUM

We are investigating the geometric and kinematic characteristics of interplanetary coronal mass ejections (ICMEs) using data obtained by the LASCO coronagraphs, the Solar Mass Ejection Imager (SMEI), and the SECCHI imaging experiments on the STEREO spacecraft. The early evolution of CMEs can be tracked by the LASCO C2 and C3 and SECCHI COR1 and COR2 coronagraphs, and the HI and SMEI instruments can track their ICME counterparts through

the inner heliosphere. The HI fields of view ($4 - 90^\circ$) overlap with the SMEI field of view ($>20^\circ$ to all sky) and, thus, both instrument sets can observe the same ICME. In this paper we present results for ICMEs observed on **24 – 29 January 2007**, when the STEREO spacecraft were still near Earth so that both the SMEI and STEREO views of large ICMEs in the inner heliosphere coincided. These results include measurements of the structural and kinematic evolution of two ICMEs and comparisons with drive/drag kinematic, 3D tomographic reconstruction, the HAFv2 kinematic, and the ENLIL MHD models. We find it encouraging that the four model runs generally were in agreement on both the kinematic evolution and appearance of the events. Because it is essential to understand the effects of projection across large distances, that are not generally crucial for events observed closer to the Sun, we discuss our analysis procedure in some detail.

Solar Mass Ejection Imager (SMEI) observations of coronal mass ejections (CMEs) in the heliosphere

Webb, D. F.; Mizuno, D. R.; Buffington, A.; Cooke, M. P.; Eyles, C. J.; Fry, C. D.; Gentile, L. C.; Hick, P. P.; Holladay, P. E.; Howard, T. A.; Hewitt, J. G.; Jackson, B. V.; Johnston, J. C.; Kuchar, T. A.; Mozer, J. B.; Price, S.; Radick, R. R.; Simnett, G. M.; Tappin, S. J.

J. Geophys. Res., Vol. 111, No. A12, A12101, **2006**, **File**

The Solar Mass Ejection Imager (SMEI) on the Coriolis spacecraft has been obtaining white light images of nearly the full sky every 102 minutes for three years. We present statistical results of analysis of the SMEI observations of coronal mass ejections (CMEs) traveling through the inner heliosphere; 139 CMEs were observed during the first 1.5 years of operations. At least 30 of these CMEs were observed by SMEI to propagate out to 1 AU and beyond and were associated with major geomagnetic storms at Earth. Most of these were observed as frontside halo events by the SOHO LASCO coronagraphs.

Coronal mass ejections and space weather

D. F. **Webb** and N. Gopalswamy

in "Solar Influence on the Heliosphere and Earth's Environment: Recent Progress and Prospects", ed. N. Gopalswamy and A. Battacharyya, Quest Publications, Mumbai, p. 71, **2006**. **File**

Coronal mass ejections (CMEs) are a key feature of coronal and interplanetary (IP) dynamics. Major CMEs inject large amounts of mass and magnetic fields into the heliosphere and, when aimed Earthward, can cause major geomagnetic storms and drive IP shocks, a key source of solar energetic particles. Studies over this solar cycle using the excellent data sets from the SOHO, TRACE, Yohkoh, Wind, ACE and other spacecraft and ground-based instruments have improved our knowledge of the origins and early development of CMEs at the Sun and how they affect space weather at Earth. A new heliospheric experiment, the Solar Mass Ejection Imager, has completed 3 years in orbit and has obtained results on the propagation of CMEs through the inner heliosphere and their geoeffectiveness. We review key coronal properties of CMEs, their source regions, their manifestations in the solar wind, and their geoeffectiveness. Halo-like CMEs are of special interest for space weather because they suggest the launch of a geoeffective disturbance toward Earth. However, not all halo CMEs are equally geoeffective and this relationship varies over the solar cycle. Although CMEs are involved with the largest storms at all phases of the cycle, recurrent features such as interaction regions and high speed wind streams can also be geoeffective.

Spacecraft and Ground Anomalies Related to the October-November 2003 Solar Activity,

Webb, D. and J. Allen,

Space Weather, 2, S03008, doi:10.1029/2004SW000075 (**2004**)

CMEs and the solar cycle variation in their geoeffectiveness,

Webb, D. F. (2002),

Proc. Sol. Heliospheric Obs. 11 Symp., **2002**, 409–419.

The Solar Sources of Geoeffective Structures

Review

D. F. **Webb**, 1 ' 2 N. U. Crooker, 3 S. P. Plunkett, 4 and 0 . C. St. Cyr 5

Space Weather Geophysical Monograph 125 **2001**

<https://agupubs.onlinelibrary.wiley.com/doi/pdf/10.1029/GM125p0123>

We review our current understanding of the solar sources of interplanetary structures that result in geomagnetic disturbances, especially storms. These sources have been broadly classified as: 1) transient or sporadic, or 2) recurrent, although we now know that these categories are not exclusive. Transients usually refer to coronal mass ejections (CMEs). Recurrence refers to disturbances that repeat with the 27-day synodic rotation period of the Sun. CMEs are expulsions of large quantities of plasma and magnetic field from the Sun's corona. The occurrence rate of CMEs approximately follows that of the solar (sunspot) activity cycle. Recurrent sources are usually attributed to high-speed solar wind streams emanating from coronal holes. However, compression at the leading edge of the stream as it runs into the higher-density slow flow surrounding the heliospheric current sheet leads to a corotating interaction region (CIR), and it is passage of the CIR, not the high speed flow, that results in enhanced recurrent geomagnetic disturbances. Moreover, the largest recurrent geomagnetic storms are actually caused by CMEs caught up in the CIRs.

The origin and development of the May 1997 magnetic cloud,

Webb, D. F., Lepping, R. P., Burlaga, L. F., et al.,

J. Geophys. Res. 105, 27251, 2000

<http://onlinelibrary.wiley.com/doi/10.1029/2000JA000021/pdf>

the axial flux in MCs seem to be related to the flux in the dimming region observed in coronal images
A complete halo coronal mass ejection (CME) was observed by the SOHO Large-Angle and Spectrometric Coronagraph (LASCO) coronagraphs on **May 12, 1997**. It was associated with activity near Sun center, implying that it was aimed earthward. Three days later on May 15 an interplanetary shock and magnetic cloud/flux rope transient was detected at the Wind spacecraft 190 RE upstream of Earth. The long enduring southward magnetic fields associated with these structures triggered a geomagnetic storm. The CME was associated with a small coronal arcade that formed over a filament eruption with expanding double ribbons in H α emission. The flare was accompanied by a circular EUV wave, and the arcade was flanked by adjacent dimming regions. We surmise that these latter regions marked the feet of a flux rope that expanded earthward into the solar wind and was observed as the magnetic cloud at Wind. To test this hypothesis we determined key parameters of the solar structures on May 12 and compared them with the modeled flux rope parameters at Wind on May 15. The measurements are consistent with the flux rope originating in a large coronal structure linked to the erupting filament, with the opposite-polarity feet of the rope terminating in the depleted regions. However, bidirectional electron streaming was not observed within the cloud itself, suggesting that there is not always a good correspondence between such flows and ejecta.

Solar wind density influence on geomagnetic storm intensity

Weigel, R. S.

J. Geophys. Res., Vol. 115, No. A9, A09201, 2010

Solar wind density has been argued to have a strong effect on geomagnetic storms. Elevated solar wind density tends to occur in time intervals when the solar wind electric field is large. This complicates the analysis required to identify a solar wind density influence because the solar wind electric field is the dominant driver of geomagnetic storms. Statistical studies have consistently shown that the independent correlation between solar wind density and geomagnetic storm intensity (via a proxy, such as the Dst index) is small. Modeling considerations predict a significant geomagnetic storm dependence on the plasma sheet density, which is indirectly connected to solar wind density. In this work, the solar wind density influence is quantified using two statistical measures: (1) data-derived impulse response functions and (2) the relationship between the integrated value of Dst to the integrated value of the solar wind electric field during geomagnetic storm intervals. Results from both approaches indicate that the solar wind density modifies the geoefficiency or the ability of a given value of the solar wind electric field to create a Dst disturbance. The impulse response method also predicts that solar wind density explains the difference in geoefficiency, as opposed to the solar wind dynamic pressure. Although the geoefficiency effect is large, its influence is shown to be small when only large storms are considered because large storms typically have large density.

Statistical maps of geomagnetic perturbations as a function of the interplanetary magnetic field,

Weimer, D. R., C. R. Clauer, M. J. Engebretson, T. L. Hansen, H. Gleisner, I. Mann, and K. Yumoto (2010), J. Geophys. Res., 115, A10320, doi:10.1029/2010JA015540.

Mappings of geomagnetic perturbations are shown for different combinations of the solar wind velocity, interplanetary magnetic field (IMF), and dipole tilt angle (season). Average maps were derived separately for the northward, eastward, and vertical (downward) components of the geomagnetic disturbances, using spherical cap harmonics in least error fits of sorted measurements. The source data are obtained from 104 ground-based magnetometer stations in the Northern

Hemisphere at geomagnetic latitudes over 40° during the years 1998 through 2001. Contour maps of statistical fits are shown along-side scatter plots of individual measurements in corrected geomagnetic apex coordinates. The patterns are consistent with previous mappings of ionospheric electric potential. Interestingly, the vertical component of the magnetic perturbations closely resembles maps of the overhead, field-aligned currents, including the Northward IMF configuration. The maximum and minimum values from the statistical mappings are graphed to show their changes as a function of southward IMF magnitude, solar wind velocity, and seasons. It is expected that this work will lead to better advance predictions of the geomagnetic perturbations that are based on real-time IMF measurements.

Impact of Non-potential Coronal Boundary Conditions on Solar Wind Prediction

Marion [Weinzierl](#), [Francois-X. Bocquet](#), [Anthony R. Yeates](#)

2017

<https://arxiv.org/pdf/1709.01730.pdf>

Predictions of the solar wind at Earth are a central aspect of space weather prediction. The outcome of such a prediction, however, is highly sensitive to the method used for computing the magnetic field in the corona. We analyze the impact of replacing the potential field coronal boundary conditions, as used in operational space weather prediction tools, by non-potential conditions. For this, we compare the predicted solar wind plasma parameters with observations at 1 AU for two six-months intervals, one at solar maximum and one in the descending phase of the current cycle. As a baseline, we compare with the operational Wang-Sheeley-Argue model. We find that for solar maximum, the non-potential coronal model and an adapted solar wind speed formula lead to the best solar wind predictions in a statistical sense. For the descending phase, the potential coronal model performs best. The Wang-Sheeley-Argue model outperforms the others in predicting high speed enhancements and streamer interactions. A better parameter fitting for the adapted wind speed formula is expected to improve the performance of the non-potential model here.

Distorted Magnetic Flux Ropes within Interplanetary Coronal Mass Ejections

[Andreas J. Weiss](#), [Teresa Nieves-Chinchilla](#), [Christian Möstl](#)

ApJ 975 169 2024

<https://arxiv.org/pdf/2406.13022>

<https://iopscience.iop.org/article/10.3847/1538-4357/ad7940/pdf>

Magnetic flux ropes within interplanetary coronal mass ejections are often characterized as simplistic cylindrical or toroidal tubes with field lines that twist around the cylinder or torus axis. Recent multi-point observations suggest that the overall geometry of these large-scale structures may be significantly more complex, so that the contemporary modeling approaches would be, in some cases, insufficient to properly understand the global structure of any interplanetary coronal mass ejection. In an attempt to partially rectify this issue, we have developed a novel magnetic flux rope model that allows for the description of arbitrary distortions of the cross-section or deformation of the magnetic axis. The distorted magnetic flux rope model is a fully analytic flux rope model, that can be used to describe significantly more complex geometries and is numerically efficient enough to be used for large ensemble simulations. To demonstrate the usefulness of our model, we focus on a specific implementation of our model and apply it to an ICME event that was observed *in situ* on **2023 April 23** at the L1 point by the Wind spacecraft and also by the STEREO-A spacecraft that was 10.2° further east and 0.9° south in heliographic coordinates. We demonstrate that our model can accurately reconstruct each observation individual and also gives a fair reconstruction of both events simultaneously using a multi-point reconstruction approach, which results in a geometry that is not fully consistent with a cylindrical or toroidal approximation.

Writhed Analytical Magnetic Flux Rope Model

[A. J. Weiss](#), [T. Nieves-Chinchilla](#), [C. Möstl](#), [M. A. Reiss](#), [T. Amerstorfer](#), [R. L. Bailey](#)

JGR e2022JA030898 [Volume127, Issue12](#) 2022

<https://doi.org/10.1029/2022JA030898>

<https://agupubs.onlinelibrary.wiley.com/doi/epdf/10.1029/2022JA030898>

Observations of magnetic clouds, within interplanetary coronal mass ejections (ICMEs), are often well described by flux rope models. Most of these assume either a cylindrical or toroidal geometry. In some cases, these models are also capable of accounting for non-axisymmetric cross-sections but they generally all assume axial invariance. It can be expected that any ICME, and its flux rope, will be deformed along its axis due to influences such as the solar wind. In this work, we aim to develop a writhed analytical magnetic flux rope model which would allow us to analytically describe a flux rope structure with varying curvature and torsion so that we are no longer constrained to a cylindrical or toroidal geometry. In this first iteration of our model we will solely focus on a circular cross-section of constant size. We describe our flux rope geometry in terms of a parametrized flux rope axis and a parallel transport frame. We derive

expressions for the axial and poloidal magnetic field components under the assumption that the total axial magnetic flux is conserved. We find an entire class of possible solutions, which differ by the choice of integration constants, and present the results for a specific example. In general, we find that the twist of the magnetic field locally changes when the geometry deviates from a cylinder or torus. This new approach also allows us to generate completely new types of in situ magnetic field profiles which strongly deviate from those generated by cylindrical or toroidal models.

Generally Curved Magnetic Flux Rope Structures

Andreas J. [Weiss](#), [Teresa Nieves-Chinchilla](#), [Christian Möstl](#), [Martin A. Reiss](#), [Tanja Amerstorfer](#), [Rachel L. Bailey](#)

ApJ 2022

<https://arxiv.org/pdf/2202.10096.pdf>

We present a new analytical approach with the aim to describe generally curved and twisted magnetic flux rope structures, that are embedded within interplanetary coronal mass ejections, under the constraint of invariant axial flux. In this paper we showcase the simplest case of a generally curved flux rope with a circular cross-section which can be described in terms of the curvature and the torsion of the Frenet-Serret equations. The magnetic field configuration, for the axial and poloidal field components, are described in terms of a radial expansion using a Legendre basis. We further derive equations that allow us to configure our model for any arbitrary magnetic twist and also evaluate the force distribution. We show the effects and differences of our proposed model compared to a purely cylindrical or toroidal geometry using an arbitrarily twisted exemplary flux rope structure with a uniformly twisted magnetic field configuration. In order to indirectly compare our model with real in-situ measurements we generate two synthetic in-situ profiles using virtual spacecraft trajectories, realistically simulating apex and flank encounters of an interplanetary coronal mass ejection. This proposed model presents an intermediate step towards describing more complex flux rope structures with arbitrary cross-section shapes.

Multi point analysis of coronal mass ejection flux ropes using combined data from Solar Orbiter, BepiColombo and Wind

A. J. [Weiss](#), [C. Moestl](#), [E. E. Davies](#), [T. Amerstorfer](#), [M. Bauer](#), [J. Hinterreiter](#), [M. Reiss](#), [R. L. Bailey](#), [T. S. Horbury](#), [H. O'Brien](#), [V. Evans](#), [V. Angelini](#), [D. Heiner](#), [I. Richter](#), [H-U. Auster](#), [W. Magnes](#), [D. Fischer](#), [W. Baumjohann](#)

A&A 2021

<https://arxiv.org/pdf/2103.16187.pdf>

The recent launch of Solar Orbiter and BepiColombo opened a brief window in which these two spacecraft were positioned in a constellation that allows for the detailed sampling of any Earth-directed CMEs. Fortunately, two such events occurred with in situ detections of an ICME by Solar Orbiter on the **19th of April and the 28th of May 2020**. These two events were subsequently also observed in situ by BepiColombo and Wind around a day later. We attempt to reconstruct the observed in situ magnetic field measurements for all three spacecraft simultaneously using an empirical magnetic flux rope model. This allows us to test the validity of our flux rope model on a larger and more global scale and allows for cross-validation of the analysis with different spacecraft combinations. Finally, we can also compare the results from the in situ modeling to remote observations obtained from the STEREO-A heliospheric imagers. We make use of the 3D coronal rope ejection model in order to simulate the ICME evolution. We adapt a previously developed ABC-SMC fitting algorithm for the application to multi point scenarios. We show that we are able to generally reconstruct the flux ropes signatures at three different spacecraft positions simultaneously using our model in combination with the flux rope fitting algorithm. For the well-behaved 19th of April ICME our approach works very well. The 28th of May ICME, on the other hand, shows the limitations of our approach. Unfortunately, the usage of multi point observations for these events does not appear to solve inherent issues, such as the estimation of the magnetic field twist or flux rope aspect-ratios due to the specific constellation of the spacecraft positions. As our general approach can be used for any fast forward simulation based model we give a blueprint for future studies using more advanced ICME models.

Analysis of coronal mass ejection flux rope signatures using 3DCORE and approximate Bayesian Computation

[Andreas J. Weiss](#), [Christian Möstl](#), [Tanja Amerstorfer](#), [Rachel L. Bailey](#), [Martin A. Reiss](#), [Jürgen Hinterreiter](#), [Ute A. Amerstorfer](#), [Maike Bauer](#)

ApJS 2020

<https://arxiv.org/pdf/2009.00327.pdf>

We present a major update to the 3D coronal rope ejection (3DCORE) technique for modeling coronal mass ejection flux ropes in conjunction with an Approximate Bayesian Computation (ABC) algorithm that is used for fitting the model to in situ magnetic field measurements. The model assumes an empirically motivated torus-like flux rope structure that expands self-similarly within the heliosphere, is influenced by a simplified interaction with the solar wind environment and carries along an embedded analytical magnetic field. The improved 3DCORE implementation allows us to generate extremely large ensemble simulations which we then use to find global best-fit model parameters using an ABC sequential Monte Carlo (SMC) algorithm. The usage of this algorithm, under some basic assumptions on the uncertainty of the magnetic field measurements, allows us to furthermore generate estimates on the uncertainty of model parameters using only a single in situ observation. We apply our model to synthetically generated measurements in order to prove the validity of our implementation for the fitting procedure. We also present a brief analysis of an event captured by Parker Solar Probe (PSP), within the scope of our model, shortly after its first fly-by of the Sun on 2018 November 12 at 0.25 AU. The presented tool set is easily extendable to the analysis of events captured by multiple spacecraft which will facilitate the study of such events. **12 Nov 2018**

Numerical simulations of the geospace response to the arrival of an idealized perfect interplanetary coronal mass ejection

Daniel T. [Welling](#) , [Jeffrey J. Love](#) , [E. Joshua Rigler](#) , [Denny M. Oliveira](#) , [Colin M. Komar](#) , [Steven K. Morley](#)

Space Weather e2020SW002489 **2021**

<https://doi.org/10.1029/2020SW002489>

<https://agupubs.onlinelibrary.wiley.com/doi/epdf/10.1029/2020SW002489>

Previously, Tsurutani & Lakhina (2014) created estimates for a “perfect” interplanetary coronal mass ejection and performed simple calculations for the response of geospace, including dB/dt . In this study, these estimates are used to drive a coupled magnetohydrodynamic-ring current-ionosphere model of geospace to obtain more physically accurate estimates of the geospace response to such an event. The sudden impulse phase is examined and compared to the estimations of Tsurutani & Lakhina (2014). The physics-based simulation yields similar estimates for Dst rise, magnetopause compression, and equatorial dB/dt values as the previous study. However, results diverge away from the equator. dB/dt values in excess of $30nT/s$ are found as low as 40° magnetic latitude. Under southward interplanetary magnetic field conditions, magnetopause erosion combines with strong region 1 Birkeland currents to intensify the dB/dt response. Values obtained here surpass those found in historically recorded events and set the upper threshold of extreme geomagnetically induced current activity at Earth.

Scientists get first glimpse of solar wind as it forms,

[Wendel, J.](#)

(2016), *Eos*, 97, doi:10.1029/2016EO059053.

Low heliosphere pressure drives wider CMEs in weaker solar cycles

JoAnna [Wendel](#)

Eos, Transactions American Geophysical Union, Volume 95, Issue 30, page 276, 29 July 2014

Every 11 years, the Sun cycles from a period where sunspot counts are high to one where counts are low. Individual cycles, however, are not created equal—the current solar cycle, 24, has been called the weakest (with the fewest sunspot counts) in 100 years. The weakness of the solar cycle could be the reason the massive ejections of charged plasma from the Sun's corona have been anomalously wider and thus more diffuse than in preceding cycles.

Modeling the multiple CME interaction event on 6-9 September 2017 with WSA-ENLIL+Cone

A. L. E. [Werner](#), [E. Yordanova](#), [A. P. Dimmock](#), [M. Temmer](#)

Space Weather **2019**

[sci-hub.tw/10.1029/2018SW001993](https://doi.org/10.1029/2018SW001993)

<https://doi.org/10.1029/2018SW001993>

A series of coronal mass ejections (CMEs) erupted from the same active region between 4–6 September 2017. Later, on 6–9 September, two interplanetary (IP) shocks reached L1, creating a complex and geoeffective plasma structure. To understand the processes leading up to the formation of the two shocks, we model the CMEs with the Wang-Sheeley-Arge (WSA)-ENLIL+Cone model. The first two CMEs merged already in the solar corona driving the

first IP shock. In IP space, another fast CME presumably interacted with the flank of the preceding CMEs and caused the second shock detected in situ. By introducing a customized density enhancement factor (dclld) in the WSA-ENLIL+Cone model based on coronagraph image observations, the predicted arrival time of the first IP shock was drastically improved. When the dclld factor was tested on a well-defined single CME event from 12 July 2012 the shock arrival time saw similar improvement. These results suggest that the proposed approach may be an alternative to improve the forecast for fast and simple CMEs. Further, the slowly decelerating kilometric type II radio burst confirms that the properties of the background solar wind have been preconditioned by the passage of the first IP shock. This likely caused the last CME to experience insignificant deceleration and led to the early arrival of the second IP shock. This result emphasizes the need to take preconditioning of the IP medium into account when making forecasts of CMEs erupting in quick succession.

LUCI onboard Lagrange, the Next Generation of EUV Space Weather Monitoring

M.J. West, C. Kintziger, M. Haberreiter, M. Gyo, D. Berghmans, S. Gissot, V Büchel, L. Golub, S. Shestov, J.A. Davies

Journal of Space Weather and Space Climate 2020

<https://arxiv.org/pdf/2009.04788.pdf>

LUCI (Lagrange eUv Coronal Imager) is a solar imager in the Extreme UltraViolet (EUV) that is being developed as part of the Lagrange mission, a mission designed to be positioned at the L5 Lagrangian point to monitor space weather from its source on the Sun, through the heliosphere, to the Earth. LUCI will use an off-axis two mirror design equipped with an EUV enhanced active pixel sensor. This type of detector has advantages that promise to be very beneficial for monitoring the source of space weather in the EUV. LUCI will also have a novel off-axis wide field-of-view, designed to observe the solar disk, the lower corona, and the extended solar atmosphere close to the Sun-Earth line. LUCI will provide solar coronal images at a 2-3 minute cadence in a pass-band centred on 19.5 nm. Observations made through this pass-band allow for the detection and monitoring of semi-static coronal structures such as coronal holes, prominences, and active regions; as well as transient phenomena such as solar flares, limb Coronal Mass Ejections (CMEs), EUV waves, and coronal dimmings. The LUCI data will complement EUV solar observations provided by instruments located along the Sun-Earth line such as PROBA2-SWAP, SUVI-GOES and SDO-AIA, as well as provide unique observations to improve space weather forecasts. Together with a suite of other remote-sensing and in-situ instruments onboard Lagrange, LUCI will provide science quality operational observations for space weather monitoring. **2014-Jan-01, 2017 Apr 01, 2020-Jan-01**

Investigating a Solar Wind Stream Interaction Region using Interplanetary Spacecraft Radio Signals: A Magnetohydrodynamic Simulation Study

David B. Wexler¹, Ward B. Manchester², Lan K. Jian³, Lynn B. Wilson III³, Natchimuthuk Gopalswamy³, Paul Song¹, Jason E. Kooi⁴, Bart van der Holst², and Elizabeth A. Jensen⁵

2023 ApJ 955 90

<https://iopscience.iop.org/article/10.3847/1538-4357/acedac/pdf>

Stream interaction regions (SIRs) are spiral heliospheric structures that arise at the interface between fast and preceding slow solar wind regions. SIR enhancements of density and magnetic field intensity, often with magnetic polarity inversion, are potentially geoeffective and therefore important in the analysis of space weather. We studied an MHD heliospheric simulation containing a well-defined SIR using a new instrument concept based on trans-heliospheric radio sensing: Faraday Effect Tracker of Coronal and Heliospheric structures (FETCH). FETCH uses line-of-sight radio propagation techniques to measure Faraday rotation and electron column density. Analysis of the simulated FETCH observations clearly demonstrated density and magnetic field enhancements, and magnetic polarity reversal, all of which were confirmed in Wind spacecraft measurements at 1 au. FETCH provided 4.5–5.7 days lead times for predicting the arrival of SIR features at Earth. The SIR radial speed was estimated to be 350–390 km s⁻¹. These initial results hold promise that FETCH will be valuable in detecting and characterizing the inner heliosphere SIR properties well ahead of their presentation in the local geospace environment.

Slow solar wind acceleration through the middle corona: Spacecraft radio studies.

Wexler DB, Kooi JE, Jensen EA and Song P

(2022) Front. Astron. Space Sci. 9: 1047875.

doi: 10.3389/fspas.2022.1047875

<https://www.frontiersin.org/articles/10.3389/fspas.2022.1047875/pdf>

The “Middle Corona”, defined by recent consensus as the region spanning 1.5–6 solar radii (R_☉, heliocentric), is an important zone through which several structural and dynamic changes occur in coronal streamer regions. Among these is

a regime change from high density, closed magnetic field structures to open field structures of much lower electron concentration. Along with this complex restructuring, the forming slow solar wind is channeled and accelerated through the middle corona. Solar wind (SW) outflow speeds can be estimated from trans-coronal radio observations. The method of radio frequency fluctuation (FF) analysis considers the frequency variations arising from density inhomogeneities crossing the sensing line-of-sight (LOS). Below $2 R_{\odot}$, where the SW is beginning to form and outflow speed is expected to be below the acoustic wave speed, the radio FF can be attributed to the density oscillations of acoustic waves crossing the radio sensing path. With increasing helioaltitudes through the middle corona, the FF are dominated by density disturbances advected across the sensing LOS. This property enables estimation of solar wind outflow speed at various heliodistances. The coronal plasma is believed to enter the middle corona in a subsonic state, then accelerate to exit the zone generally with supersonic, but sub-Alfvénic flows. Trans-coronal radio sensing complements imaging and other remote coronal observations, and helps bridge the observational gap across the full distance range of the middle corona. Radio techniques enrich the study of solar wind, and should be utilized in next-generation, multiwavelength campaigns that tackle the challenging physics of coronal plasma acceleration.

Alfvén Speed Transition Zone in the Solar Corona

David B. **Wexler**¹, Michael L. Stevens², Anthony W. Case², and Paul Song¹

2021 ApJL 919 L33

<https://doi.org/10.3847/2041-8213/ac25fa>

The Alfvén radius, r_A , at which solar wind radial outflow speed exceeds the Alfvén wave speed, is an important parameter in understanding solar wind evolution in the extended corona. The mean solar wind angular momentum scales with r_A^2 in the axisymmetric steady-state approximation, so the Alfvén radius is often referenced in the study of solar wind corotation and dynamics. Alfvén wave speed is derived from the magnetic-field intensity and plasma mass density. In the inner coronal regions, these parameters were previously estimated using empirical models based on remote sensing observations or from inverse-square scaling of measurements at 1 au. Parker Solar Probe (PSP) orbital encounters now provide in situ coronal plasma measurements to determine Alfvén speeds within 30 solar radii of the heliocenter. We combined the PSP solar-wind speed measurements and calculated Alfvén speeds with an inner corona wind speed profile from remote sensing studies. The zone of super-Alfvénic speed cross over is estimated to occur at mean heliocentric distance of $17.9 \pm 2.1 R_{\odot}$ for slow solar winds of the low heliolatitude corona in a near-minimum solar activity state. Our r_A values constrain the angular momentum flux to a mean of $3.5 \pm 1.01 \times 10^{22} \text{ N m sr}^{-1}$, reinforcing the recent PSP results by direct measurements of particle flows.

Locating the Alfvénic Speed Transition in the Solar Corona

David B. **Wexler**, Gavin M. Lawwhite, and Paul Song

2020 Res. Notes AAS 4 216

<https://doi.org/10.3847/2515-5172/abcf3a>

<https://iopscience.iop.org/article/10.3847/2515-5172/abcf3a>

Alfvén wave speed, which is the characteristic propagation speed of low-frequency MHD perturbations, is derived from the magnetic field intensity and plasma mass density. In the inner coronal regions, these parameters are often estimated using empirical models based on remote sensing observations. Parker Solar Probe (PSP) orbital encounter 4 provides, for the first time, in situ coronal plasma measurements to determine Alfvén speeds within 30 solar radii of the heliocenter. We combined the PSP SW speed measurements and calculated Alfvén speeds with inner corona wind speed results from remote sensing studies. The zone of super-Alfvénic speed cross-over is estimated to range $10\text{--}27 R_{\odot}$ for the near-equatorial corona. Future PSP data will constrain this estimate further.

Coronal Electron Density Fluctuations Inferred from Akatsuki Spacecraft Radio Observations

D. Wexler, **T. Imamura**, **A. Efimov**, **P. Song**, **L. Lukanina**, **H. Ando**, **E. Jensen**, **J. Vierinen** & **A. Coster**

Solar Physics volume 295, Article number: 111 (2020)

<https://link.springer.com/content/pdf/10.1007/s11207-020-01677-1.pdf>

Trans-coronal radio observations were taken during the 2011 observing campaign of the Akatsuki spacecraft through superior conjunction. The observed X-band (8.4 GHz) signals exhibit frequency fluctuations (FF) that are produced by temporal variations in electron density along the radio ray path. A two-component model for interpretation of the FF is proposed: FF scales largely with acoustic wave amplitude through the inner coronal regions where the sound speed dwarfs the solar wind outflow speed, while FF in the region of solar wind acceleration is dominated by the increased density oscillation frequency on the sensing path that results from bulk advection of the plasma inhomogeneities. An estimate of fractional electron density fluctuation is obtained from the mid-corona. A radial profile of slow solar wind

speed is determined in the extended corona using mass-flux continuity principles. The coronal sonic point for slow solar wind is estimated to range from 4 to 5 solar radii from the heliocenter. **2011-06-25**

Radio Occultation Observations of the Solar Corona Over 1.60–1.86 R_☉: Faraday Rotation and Frequency Shift Analysis

David. B. [Wexler](#), Joseph V. Hollweg, Anatoli I. Efimov, Paul Song, Elizabeth A. Jensen, Roberto Lionello, Juha Vierinen, Anthea J. Coster

JGR Volume 124, Issue 10 Pages: 7761-7777 **2019**

<https://doi.org/10.1029/2019JA026937>

The study of coronal energy transport, central to the solar wind acceleration problem, relies upon accurate representation of magnetic fields and plasma electron densities. This information is difficult to obtain in middle-to-lower coronal regions that may contain complex magnetic structures. Faraday rotation (FR) solar radio occultation observations, which reveal line-of-sight (LOS) integrated product of the coronal magnetic field and electron density, can help characterize the coronal environment and constrain magnetic field strengths. Global magnetohydrodynamic (MHD) models use specified synoptic solar surface magnetograms and may be used to facilitate FR interpretation by estimating detailed magnetic field properties along the radio LOS. We present a hybrid FR analysis incorporating magnetic field solutions from an MHD coronal model, and an electron density radial profile conforming to radio frequency shift observations. The FR modeled by the hybrid method is compared to MERcury Surface, Space ENvironment, GEOchemistry and Ranging spacecraft radio FR observations through a coronal region of low heliolatitudes and radial distance 1.60–1.86 R_☉ from the heliocenter, collected during a state of relative solar quiescence. The hybrid model reasonably reproduces the form, polarity, and magnitude of the observed FR. For this specific coronal region, the calculated radial profile of electron concentrations and varied magnetic field strengths indicate Alfvén wave speeds below 50 km/s close to the point of closest approach but near 400 km/s in adjacent regions along the sounding LOS. The new approach of combining MHD models with radio sounding observations supports study of MHD wave processes in the challenging middle-coronal magneto-ionic environment. **10 November 2009**

Spacecraft Radio Frequency Fluctuations in the Solar Corona: A MESSENGER–HELIOS Composite Study

David B. [Wexler](#)^{1,7}, Joseph V. Hollweg², Anatoli I. Efimov³, Liudmila A. Lukanina³, Anthea J. Coster⁴, Juha Vierinen⁵, and Elizabeth A. Jensen

2019 ApJ 871 202

Fluctuations in plasma electron density may play a role in solar coronal energy transport and the dissipation of wave energy. Transcoronal spacecraft radio sounding observations reveal frequency fluctuations (FFs) that encode the electron number density disturbances, allowing an exploration of the coronal compressive wave and advected inhomogeneity models. Primary FF observations from MESSENGER 2009 and published FF residuals from HELIOS 1975–1976 superior conjunctions were combined to produce a composite view of equatorial region FF near solar minimum over solar offset range 1.4–25R_☉. Methods to estimate the electron number density fluctuation variance from the observed FF were developed. We created a simple stacked, magnetically structured slab model that incorporated both propagating slow density waves and advected spatial density variations to explain the observed FF. Slow density waves accounted for most of the FF at low solar offset, while spatial density inhomogeneities advected at solar wind speed dominated above the sonic point at 6R_☉. Corresponding spatial scales ranged 1–38 Mm, with scales above 10 Mm contributing most to FF variance. Magnetic structuring of the model introduced radial elongation anisotropy at lower solar offsets, but geometric conditions for isotropy were achieved as the slab correlation scales increased further out in the corona. The model produced agreement with the FF observations up to 12R_☉. FF analysis provides information on electron density fluctuations in the solar corona, and should take into account the background compressive slow waves and solar wind-related advection of quasi-static spatial density variations.

Incorporation of Heliospheric Imagery into the CME Analysis Tool for improvement of CME Forecasting

S. J. [Wharton](#), [G. H. Millward](#), [S. Bingham](#), [E. M. Henley](#), [S. Gonzi](#), [D. R. Jackson](#)

Space Weather [Volume17, Issue8](#) Pages 1312-1328 **2019** **File**

sci-hub.se/10.1029/2019SW002166

Coronal Mass Ejections (CMEs) cause the largest geomagnetic disturbances at Earth which impact satellites, wired communication systems and power grids. The CME Analysis Tool (CAT) is used to determine a CME's initial longitude, latitude, angular width and radial speed from coronagraph images. These are the initial conditions for the Wang-Sheeley-Arge (WSA) Enlil solar wind model, along with the ambient solar wind properties derived from magnetograms. However, the coronagraph imagery is limited by field of view. We have incorporated heliospheric imagery (HI) from the Solar Terrestrial Relations Observatory (STEREO) into CAT to create the CME Analysis Tool with Heliospheric Imagery (CAT-HI). These HI images have a larger field of view, allowing tracking of CMEs to greater distances from the Sun. We have compared the performances of CAT and CAT-HI by examining the expected arrival times of CMEs at the L1 Lagrange point and found them to be consistent. However, CAT-HI is advantageous because it could be used to prune ensemble forecasts and issue routine updates for CME arrival time forecasts. Finally, we discuss CAT-HI in the context of an operational mission at the L4 or L5 Lagrange points.

Table 1. Initial parameters for CMEs analysed in this study. (2016-2017)

Table 2. Results of statistical test for acceleration/deceleration. For each CME,

The Solar Probe Analyzers -- Electrons on Parker Solar Probe

Phyllis L [Whittlesey](#) (1), [Davin E Larson](#) (1), [Justin C Kasper](#) (2) (3), [Jasper Halekas](#) (4), [Mamuda Abatcha](#) (1), [Robert Abiad](#) (1), [M. Berthomier](#) (5),

Astrophysical Journal Special issue for Parker Solar Probe 2020

<https://arxiv.org/pdf/2002.04080.pdf>

Electrostatic analyzers of different designs have been used since the earliest days of the space age, beginning with the very earliest solar wind measurements made by Mariner 2 en route to Venus in 1962. The Parker Solar Probe (PSP) mission, NASA's first dedicated mission to study the innermost reaches of the heliosphere, makes its thermal plasma measurements using a suite of instruments called the Solar Wind Electrons, Alphas, and Protons (SWEAP) investigation. SWEAP's electron Parker Solar Probe Analyzer (SPAN-E) instruments are a pair of top-hat electrostatic analyzers on PSP that are capable of measuring the electron distribution function in the solar wind from 2 eV to 30 keV. For the first time, in-situ measurements of thermal electrons provided by SPAN-E will help reveal the heating and acceleration mechanisms driving the evolution of the solar wind at the points of acceleration and heating, closer than ever before to the Sun. This paper details the design of the SPAN-E sensors and their operation, data formats, and measurement caveats from Parker Solar Probe's first two close encounters with the Sun.

Implementing turbulence transport in the CRONOS framework and application to the propagation of CMEs

Tobias [Wiengarten](#), Horst Fichtner, Jens Kleimann, Ralf Kissmann

2015 ApJ 805 155

<http://arxiv.org/pdf/1504.01858v1.pdf>

We present the implementation of turbulence transport equations in addition to the Reynolds-averaged MHD equations within the Cronos framework. The model is validated by comparisons with earlier findings before it is extended to be applicable to regions in the solar wind that are not highly super-Alfvénic. We find that the respective additional terms result in absolute normalized cross-helicity to decline more slowly, while a proper implementation of the mixing terms can even lead to increased cross-helicities in the inner heliosphere. The model extension allows to place the inner boundary of the simulations closer to the Sun, where we choose its location at 0.1 AU for future application to the Wang-Sheeley-Arge model. Here, we concentrate on effects on the turbulence evolution for transient events by injecting a coronal mass ejection (CME). We find that the steep gradients and shocks associated with these structures result in enhanced turbulence levels and reduced cross-helicity. Our results can now be used straightforwardly for studying the transport of charged energetic particles, where the elements of the diffusion tensor can now benefit from the self-consistently computed solar wind turbulence. Furthermore, we find that there is no strong back-reaction of the turbulence on the large-scale flow so that CME studies concentrating on the latter need not be extended to include turbulence transport effects.

A Self-consistent Simulation of Proton Acceleration and Transport Near a High-speed Solar Wind Stream

Nicolas [Wijzen](#), [Evangelia Samara](#), [Àngels Aran](#), [David Lario](#), [Jens Pomoell](#), [Stefaan Poedts](#)

ApJ 2021

<https://arxiv.org/pdf/2102.10950.pdf>

Solar wind stream interaction regions (SIRs) are often characterized by energetic ion enhancements. The mechanisms accelerating these particles, as well as the locations where the acceleration occurs, remain debated. Here, we report the

findings of a simulation of a SIR event observed by Parker Solar Probe at ~ 0.56 au and the Solar Terrestrial Relations Observatory-Ahead at ~ 0.95 au in 2019 September when both spacecraft were approximately radially aligned with the Sun. The simulation reproduces the solar wind configuration and the energetic particle enhancements observed by both spacecraft. Our results show that the energetic particles are produced at the compression waves associated with the SIR and that the suprathermal tail of the solar wind is a good candidate to provide the seed population for particle acceleration. The simulation confirms that the acceleration process does not require shock waves and can already commence within Earth's orbit, with an energy dependence on the precise location where particles are accelerated. The three-dimensional configuration of the solar wind streams strongly modulates the energetic particle distributions, illustrating the necessity of advanced models to understand these particle events. **19-23 Sep 2019**

Transport Near a High-speed Solar Wind Stream

Nicolas **Wijzen**¹, Evangelia Samara^{1,2}, Àngels Aran³, David Lario⁴, Jens Pomoell⁵, and Stefaan Poedts^{1,6}
2021 ApJL 908 L26

<https://doi.org/10.3847/2041-8213/abe1cb>

Solar wind stream interaction regions (SIRs) are often characterized by energetic ion enhancements. The mechanisms accelerating these particles, as well as the locations where the acceleration occurs, remain debated. Here, we report the findings of a simulation of a SIR event observed by Parker Solar Probe at ~ 0.56 au and the Solar Terrestrial Relations Observatory-Ahead at ~ 0.95 au in **2019 September** when both spacecraft were approximately radially aligned with the Sun. The simulation reproduces the solar wind configuration and the energetic particle enhancements observed by both spacecraft. Our results show that the energetic particles are produced at the compression waves associated with the SIR and that the suprathermal tail of the solar wind is a good candidate to provide the seed population for particle acceleration. The simulation confirms that the acceleration process does not require shock waves and can already commence within Earth's orbit, with an energy dependence on the precise location where particles are accelerated. The three-dimensional configuration of the solar wind streams strongly modulates the energetic particle distributions, illustrating the necessity of advanced models to understand these particle events.

Deriving solar transient characteristics from single spacecraft STEREO/HI elongation variations: a theoretical assessment of the technique

A. O. **Williams**¹, J. A. Davies², S. E. Milan¹, A. P. Rouillard^{2,3}, C. J. Davis², C. H. Perry², and R. A. Harrison²

Ann. Geophys., 27, 4359-4368, **2009**

www.ann-geophys.net/27/4359/2009/

Recently, a technique has been developed whereby the radial velocity, V_r , and longitude direction, β , of propagation of an outward-moving solar transient, such as a Coronal Mass Ejection (CME), can be estimated from its track in a time-elongation map produced using Heliospheric Imager (HI) observations from a single STEREO spacecraft. The method employed, which takes advantage of an artefact of projective geometry, is based on the evaluation of the best fit of the time-elongation profile of the transient, extracted from a time-elongation map, to a set of theoretical functions corresponding to known combinations of radial velocity and direction; here we present an initial theoretical assessment of the efficacy of this technique. As the method relies on the manual selection of points along the time-elongation profile, an assessment of the accuracy with which this is feasible, is initially made. The work then presented assesses theoretically this method of recovering the velocity and propagation direction of solar transients from their time-elongation profiles using a Monte-Carlo simulation approach. In particular, we assess the range of elongations over which it is necessary to make observations in order to accurately recover these parameters. Results of the Monte-Carlo simulations suggest that it is sufficient to track a solar transient out to around 40° elongation to provide accurate estimates of its associated radial velocity and direction; the accuracy to which these parameters can be estimated for a transient tracked over a particular elongation extent is, however, sensitive to its velocity and direction relative to the Sun-Spacecraft line. These initial results suggest that this technique based on single spacecraft STEREO/HI observations could prove extremely useful in terms of providing an early warning of a CME impact on the near-Earth environment.

Fifth Space Weather Enterprise Forum Reaches New Heights

Williamson, Samuel P.; Babcock, Michael R.; Bonadonna, Michael F.

Space Weather, Vol. 9, No. 9, S090026 **2011**

<http://dx.doi.org/10.1029/2011SW000719>

As the world's commercial infrastructure grows more dependent on sensitive electronics and space-based technologies, the global economy is becoming increasingly vulnerable to solar storms. Experts from the federal government,

academia, and the private sector met to discuss the societal effects of major solar storms and other space weather at the fifth annual Space Weather Enterprise Forum (SWEF), held on 21 June 2011 at the National Press Club in Washington, D. C. More than 200 members of the space weather community attended this year's SWEF, which focused on the consequences of severe space weather for national security, critical infrastructure, and human safety. Participants also addressed the question of how to prepare for and mitigate those consequences as the current solar cycle approaches and reaches its peak, expected in 2013. This year's forum included details of plans for a "Unified National Space Weather Capability," a new interagency initiative which will be implemented over the next two years, designed to improve forecasting, warning, and other services ahead of the coming solar maximum.

A Quarter Century of Wind Spacecraft Discoveries

Review

Wilson, Lynn B., III ; [Brosius, Alexandra L.](#) ; [Gopalswamy, Natchimuthuk](#) ; [Nieves-Chinchilla, Teresa](#) ; [Szabo, Adam](#) ; [Hurley, Kevin](#) ; [Phan, Tai](#) ; [Kasper, Justin C.](#) ; [Lugaz, No e](#) ; [Richardson, Ian G.](#) ; [Chen, Christopher H. K.](#) ; [Verscharen, Daniel](#) ; [Wicks, Robert T.](#) ; [TenBarge, Jason M.](#)

Reviews of Geophysics, Vol. 59, Issue 2, pp. e2020RG000714, **2021**, doi:10.1029/2020RG000714

<https://agupubs.onlinelibrary.wiley.com/doi/epdf/10.1029/2020RG000714> **File**

The Wind spacecraft, launched on November 1, 1994, is a critical element in NASA's Heliophysics System Observatory (HSO) - a fleet of spacecraft created to understand the dynamics of the Sun-Earth system. The combination of its longevity (>25 years in service), its diverse complement of instrumentation, and high resolution and accurate measurements has led to it becoming the "standard candle" of solar wind measurements. Wind has over 55 selectable public data products with over ~1,100 total data variables (including OMNI data products) on SPDF/CDAWeb alone. These data have led to paradigm shifting results in studies of statistical solar wind trends, magnetic reconnection, large-scale solar wind structures, kinetic physics, electromagnetic turbulence, the Van Allen radiation belts, coronal mass ejection topology, interplanetary and interstellar dust, the lunar wake, solar radio bursts, solar energetic particles, and extreme astrophysical phenomena such as gamma-ray bursts. This review introduces the mission and instrument suites then discusses examples of the contributions by Wind to these scientific topics that emphasize its importance to both the fields of heliophysics and astrophysics.

Electron energy partition across interplanetary shocks: I. Methodology and Data Product

Lynn B. [Wilson](#) III, [Li-Jen Chen](#), [Shan Wang](#), [Steven J. Schwartz](#), [Drew L. Turner](#), [Michael L. Stevens](#), [Justin C. Kasper](#), [Adnane Osmane](#), [Damiano Caprioli](#), [Stuart D. Bale](#), [Marc P. Pulupa](#), [Chadi S. Salem](#), [Katherine A. Goodrich](#)

Astrophys. J. Suppl **2019**

<https://arxiv.org/pdf/1902.01476.pdf>

Analysis of 15314 electron velocity distribution functions (VDFs) within ± 2 hours of 52 interplanetary (IP) shocks observed by the *Wind* spacecraft near 1 AU are introduced. The electron VDFs are fit to the sum of three model functions for the cold dense core, hot tenuous halo, and field-aligned beam/strahl component. The best results were found by modeling the core as either a bi-kappa or a symmetric (or asymmetric) bi-self-similar velocity distribution function, while both the halo and beam/strahl components were best fit to bi-kappa velocity distribution function. This is the first statistical study to show that the core electron distribution is better fit to a self-similar velocity distribution function than a bi-Maxwellian under all conditions. The self-similar distribution deviation from a Maxwellian is a measure of inelasticity in particle scattering from waves and/or turbulence. The range of values defined by the lower and upper quartiles for the kappa exponents are $\kappa_{ec} \sim 5.40\text{--}10.2$ for the core, $\kappa_{eh} \sim 3.58\text{--}5.34$ for the halo, and $\kappa_{eb} \sim 3.40\text{--}5.16$ for the beam/strahl. The lower-to-upper quartile range of symmetric bi-self-similar core exponents are $\kappa_{ec} \sim 2.00\text{--}2.04$, and asymmetric bi-self-similar core exponents are $\kappa_{ec} \sim 2.20\text{--}4.00$ for the parallel exponent, and $\kappa_{ec} \sim 2.00\text{--}2.46$ for the perpendicular exponent. The nuanced details of the fit procedure and description of resulting data product are also presented. The statistics and detailed analysis of the results are presented in Paper II and Paper III of this three-part study.

UNDERSTANDING INTERPLANETARY CORONAL MASS

EJECTION SIGNATURES

Report of Working Group B

R. F. [WIMMER-SCHWEINGRUBER](#)^{1,*}, N. U. CROOKER², A. BALOGH³, V. BOTHMER⁴, R. J. FORSYTH³, P. GAZIS⁵, J. T. GOSLING⁶, T. HORBURY³, A. KILCHENMANN⁷, I. G. RICHARDSON⁸, J. D. RICHARDSON⁹, P. RILEY¹⁰, L. RODRIGUEZ⁴, R. VON STEIGER⁷, P. WURZ¹¹, and T. H. ZURBUCHEN¹²

Space Science Reviews (2006) 123: 177–216

First simultaneous in situ measurements of a coronal mass ejection by Parker Solar Probe and STEREO-A

Reka M. Winslow, [Noé Lugaz](#), [Camilla Scolini](#), [Antoinette B. Galvin](#)

ApJ 2021

<https://arxiv.org/pdf/2106.04685.pdf>

We present the first PSP-observed CME that hits a second spacecraft before the end of the PSP encounter, providing an excellent opportunity to study short-term CME evolution. The CME was launched from the Sun on 10 October 2019 and was measured in situ at PSP on 13 October 2019 and at STEREO-A on 14 October 2019. The small, but not insignificant, radial (~0.15 au) and longitudinal (~8 deg) separation between PSP and STEREO-A at this time allows for observations of both short-term radial evolution as well as investigation of the global CME structure in longitude. Although initially a slow CME, magnetic field and plasma observations indicate that the CME drove a shock at STEREO-A and also exhibited an increasing speed profile through the CME (i.e. evidence for compression). We find that the presence of the shock and other compression signatures at 1 au are due to the CME having been overtaken and accelerated by a high speed solar wind stream (HSS). We estimate the minimum interaction time between the CME and the HSS to be about 2.5 days, indicating the interaction started well before the CME arrival at PSP and STEREO-A. Despite alterations of the CME by the HSS, we find that the CME magnetic field structure is similar between the vantage points, with overall the same flux rope classification and the same field distortions present. These observations are consistent with the fact that coherence in the magnetic structure is needed for steady and continued acceleration of the CME. **10-14 Oct 2019**

The effect of stream interaction regions on ICME structures observed in longitudinal conjunction

Reka M. Winslow, [Camilla Scolini](#), [Noé Lugaz](#), [Antoinette B. Galvin](#)

ApJ 2021

<https://arxiv.org/pdf/2105.10602.pdf>

We study two interplanetary coronal mass ejections (ICMEs) observed at Mercury and 1 AU by spacecraft in longitudinal conjunction, investigating the question: what causes the drastic alterations observed in some ICMEs during propagation, while other ICMEs remain relatively unchanged? Of the two ICMEs, the first one propagated relatively self-similarly, while the second one underwent significant changes in its properties. We focus on the presence or absence of large-scale corotating structures in the ICME propagation space between Mercury and 1 AU, that have been shown to influence the orientation of ICME magnetic structures and the properties of ICME sheaths. We determine the flux rope orientation at the two locations using force-free flux rope fits as well as the classification by Nieves-Chinchilla et al. (2019). We also use measurements of plasma properties at 1 AU, the size evolution of the sheaths and ME with heliocentric distance, and identification of structures in the propagation space based on in situ data, remote-sensing observations, and simulations of the steady-state solar wind, to complement our analysis. Results indicate that the changes observed in one ICME were likely caused by a stream interaction region, while the ICME exhibiting little change did not interact with any transients between Mercury and 1 AU. This work provides an example of how interactions with corotating structures in the solar wind can induce fundamental changes in ICMEs. Our findings can help lay the foundation for improved predictions of ICME properties at 1 AU. **9, 12-14 July 2013; 26, 28-30 December 2013**

Opening a Window on ICME-driven GCR Modulation in the Inner Solar System

Reka M. Winslow¹, Nathan A. Schwadron¹, Noé Lugaz¹, Jingnan Guo², Colin J. Joyce¹, Andrew P.

Jordan¹, Jody K. Wilson¹, Harlan E. Spence¹, David J. Lawrence³

2018 ApJ 856 139

<http://sci-hub.tw/http://iopscience.iop.org/0004-637X/856/2/139/>

Interplanetary coronal mass ejections (ICMEs) often cause Forbush decreases (Fds) in the flux of galactic cosmic rays (GCRs). We investigate how a single ICME, launched from the Sun on **2014 February 12**, affected GCR fluxes at Mercury, Earth, and Mars. We use GCR observations from MESSENGER at Mercury, ACE/LRO at the Earth/Moon, and MSL at Mars. We find that Fds are steeper and deeper closer to the Sun, and that the magnitude of the magnetic field in the ICME magnetic ejecta as well as the "strength" of the ICME sheath both play a large role in modulating the depth of the Fd. Based on our results, we hypothesize that (1) the Fd size decreases exponentially with heliocentric distance, and (2) that two-step Fds are more common closer to the Sun. Both hypotheses will be directly verifiable by the upcoming Parker Solar Probe and Solar Orbiter missions. This investigation provides the first systematic study of the changes in GCR modulation as a function of distance from the Sun using nearly contemporaneous observations at

Mercury, Earth/Moon, and Mars, which will be critical for validating our physical understanding of the modulation process throughout the heliosphere.

Longitudinal conjunction between MESSENGER and STEREO A: development of ICME complexity through stream interactions

Reka M. [Winslow](#), Noé Lugaz, Nathan A. Schwadron, Charles J. Farrugia, Wenyan Yu, Jim M. Raines, M. Leila Mays, Antoinette B. Galvin and Thomas H. Zurbuchen

JGR 121, #7 Pages: 6092–6106 2016

We use data on an interplanetary coronal mass ejection (ICME) seen by MESSENGER and STEREO A starting on **29 December 2011** in a near-perfect longitudinal conjunction (within 3°) to illustrate changes in its structure via interaction with the solar wind in less than 0.6 AU. From force-free field modeling we infer that the orientation of the underlying flux rope has undergone a rotation of $\sim 80^\circ$ in latitude and $\sim 65^\circ$ in longitude. Based on both spacecraft measurements as well as ENLIL model simulations of the steady state solar wind, we find that interaction involving magnetic reconnection with corotating structures in the solar wind dramatically alters the ICME magnetic field. In particular, we observed a highly turbulent region with distinct properties within the flux rope at STEREO A, not observed at MESSENGER, which we attribute to interaction between the ICME and a heliospheric plasma sheet/current sheet during propagation. Our case study is a concrete example of a sequence of events that can increase the complexity of ICMEs with heliocentric distance even in the inner heliosphere. The results highlight the need for large-scale statistical studies of ICME events observed in conjunction at different heliocentric distances to determine how frequently significant changes in flux rope orientation occur during propagation. These results also have significant implications for space weather forecasting and should serve as a caution on using very distant observations to predict the geoeffectiveness of large interplanetary transients.

Exploring three recurrent neural network architectures for geomagnetic predictions

Peter [Wintoft](#), and Magnus Wik

Front. Astron. Space Sci., 12 May 2021 |

<https://doi.org/10.3389/fspas.2021.664483>

<https://www.frontiersin.org/articles/10.3389/fspas.2021.664483/full>

Three different recurrent neural network (RNN) architectures are studied for the prediction of geomagnetic activity. The RNNs studied are the Elman, gated recurrent unit (GRU), and long short-term memory (LSTM). The RNNs take solar wind data as inputs to predict the Dst index. The Dst index summarizes complex geomagnetic processes into a single time series. The models are trained and tested using five-fold cross-validation based on the hourly resolution OMNI dataset using data from the years 1995–2015. The inputs are solar wind plasma (particle density and speed), vector magnetic fields, time of year, and time of day. The RNNs are regularized using early stopping and dropout. We find that both the gated recurrent unit and long short-term memory models perform better than the Elman model; however, we see no significant difference in performance between GRU and LSTM. RNNs with dropout require more weights to reach the same validation error as networks without dropout. However, the gap between training error and validation error becomes smaller when dropout is applied, reducing over-fitting and improving generalization. Another advantage in using dropout is that it can be applied during prediction to provide confidence limits on the predictions. The confidence limits increase with increasing Dst magnitude: a consequence of the less populated input-target space for events with large Dst values, thereby increasing the uncertainty in the estimates. The best RNNs have test set RMSE of 8.8 nT, bias close to zero, and linear correlation of 0.90. 2001-04-22, 2004-11-08

Evaluation of Kp and Dst Predictions Using ACE and DSCOVR Solar Wind DataP. [Wintoft](#) , [M. Wik](#)

Space Weather 16?, 12, 1972-1983, 2018

<https://doi.org/10.1029/2018SW001994>

Models that predict the Kp and Dst indices are evaluated using solar wind data at L1. The models consist of ensembles of neural networks that have been developed using ACE Level 2 data from the period 1998–2015. The use of ensembles is motivated by the difficulty of generating functions that generalize well in regions of the input-output space that are poorly sampled, which typically occurs during stronger events. Since the launch of the DSCOVR spacecraft, providing measurements from about August 2016, new and independent data have become available to test the models. ACE Level 2 data for almost the same period are also available, representing another independent set collected after 2015. We evaluate the models using plots and various statistical measures. We also study the performance of the predictions for lead times up to 3 hr. The results show that the models perform better when using ACE or cleaned DSCOVR data compared to the real-time DSCOVR data and that lead times of L1-Earth travel time plus a maximum of 1 hr are possible. As the models use only solar wind for their inputs, and the temporal dynamics of Kp and Dst are very different,

we see significant differences in the error distributions that we believe are related to long-term changes in Dst that are not captured by the Dst prediction model.

First Simultaneous In Situ Measurements of a Coronal Mass Ejection by Parker Solar Probe and STEREO-A

Reka M. Winslow¹, Noé Lugaz¹, Camilla Scolini^{1,2}, and Antoinette B. Galvin¹

2021 ApJ 916 94

<https://arxiv.org/pdf/2106.04685.pdf>

<https://doi.org/10.3847/1538-4357/ac0821>

We present the first Parker Solar Probe mission (PSP)-observed coronal mass ejection (CME) that hits a second spacecraft before the end of the PSP encounter, providing an excellent opportunity to study short-term CME evolution. The CME was launched from the Sun on **2019 October 10** and was measured in situ at PSP on **2019 October 13** and at STEREO-A on **2019 October 14**. The small, but not insignificant, radial (~0.15 au) and longitudinal (~8°) separation between PSP and STEREO-A at this time allows for both observations of short-term radial evolution as well as investigation of the global CME structure in longitude. Although initially a slow CME, magnetic field and plasma observations indicate that the CME drove a shock at STEREO-A and also exhibited an increasing speed profile through the CME (i.e., evidence for compression). We find that the presence of the shock and other compression signatures at 1 au are due to the CME having been overtaken and accelerated by a high speed solar wind stream (HSS). We estimate the minimum interaction time between the CME and the HSS to be ~2.5 days, indicating the interaction started well before the CME arrival at PSP and STEREO-A. Despite alterations of the CME by the HSS, we find that the CME magnetic field structure is similar between the vantage points, with overall the same flux rope classification and the same field distortions present. These observations are consistent with the fact that coherence in the magnetic structure is needed for steady and continued acceleration of the CME.

The Effect of Stream Interaction Regions on ICME Structures Observed in Longitudinal Conjunction

Reka M. Winslow¹, Camilla Scolini^{1,2}, Noé Lugaz¹, and Antoinette B. Galvin¹

2021 ApJ 916 40

<https://doi.org/10.3847/1538-4357/ac0439>

We study two interplanetary coronal mass ejections (ICMEs) observed at Mercury and at 1 au by spacecraft in longitudinal conjunction, investigating the question: what causes the drastic alterations observed in some ICMEs during propagation, while other ICMEs remain relatively unchanged? Of the two ICMEs, the first one propagated relatively self-similarly, while the second one underwent significant changes in its properties. We focus on the presence or absence of large-scale corotating structures in the ICME propagation space between Mercury and 1 au, which have been shown to influence the orientation of ICME magnetic structures and the properties of ICME sheaths. We determine the flux rope orientation at the two locations using force-free flux rope fits as well as the classification by Nieves-Chinchilla et al. We also use measurements of plasma properties at 1 au, the size evolution of the sheaths and magnetic ejecta with heliocentric distance, and identification of structures in the propagation space based on in situ data, remote-sensing observations, and simulations of the steady-state solar wind to complement our analysis. Results indicate that the changes observed in one ICME were likely caused by a stream interaction region, while the ICME exhibiting little change did not interact with any transients between Mercury and 1 au. This work provides an example of how interactions with corotating structures in the solar wind can induce fundamental changes in ICMEs. Our findings can help lay the foundation for improved predictions of ICME properties at 1 au.

Forecasting Kp from solar wind data: input parameter study using 3-hour averages and 3-hour range values

Peter Wintoft, Magnus Wik, Jürgen Matzka and Yuri Shprits

J. Space Weather Space Clim. 2017, 7, A29

<https://www.swsc-journal.org/articles/swsc/pdf/2017/01/swsc160051.pdf>

We have developed neural network models that predict Kp from upstream solar wind data. We study the importance of various input parameters, starting with the magnetic component Bz, particle density n, and velocity V and then adding total field B and the By component. As we also notice a seasonal and UT variation in average Kp we include functions of day-of-year and UT. Finally, as Kp is a global representation of the maximum range of geomagnetic variation over 3-hour UT intervals we conclude that sudden changes in the solar wind can have a big effect on Kp, even though it is a 3-hour value. Therefore, 3-hour solar wind averages will not always appropriately represent the solar wind condition, and we introduce 3-hour maxima and minima values to some degree address this problem. We find that introducing total

field B and 3-hour maxima and minima, derived from 1-minute solar wind data, have a great influence on the performance. Due to the low number of samples for high Kp values there can be considerable variation in predicted Kp for different networks with similar validation errors. We address this issue by using an ensemble of networks from which we use the median predicted Kp. The models (ensemble of networks) provide prediction lead times in the range 20–90 min given by the time it takes a solar wind structure to travel from L1 to Earth. Two models are implemented that can be run with real time data: (1) IRF-Kp-2017-h3 uses the 3-hour averages of the solar wind data and (2) IRF-Kp-2017 uses in addition to the averages, also the minima and maxima values. The IRF-Kp-2017 model has RMS error of 0.55 and linear correlation of 0.92 based on an independent test set with final Kp covering 2 years using ACE Level 2 data. The IRF-Kp-2017-h3 model has RMSE = 0.63 and correlation = 0.89. We also explore the errors when tested on another two-year period with real-time ACE data which gives RMSE = 0.59 for IRF-Kp-2017 and RMSE = 0.73 for IRF-Kp-2017-h3. The errors as function of Kp and for different years are also studied.

Interplanetary coronal mass ejection observed at STEREO-A, Mars, comet 67P/Churyumov-Gerasimenko, Saturn, and New Horizons en-route to Pluto. Comparison of its Forbush decreases at 1.4, 3.1 and 9.9 AU

O. [Witasse](#), B. Sánchez-Cano, M. L. Mays, P. Kajdič

JGR Volume 122, Issue 8 Pages 7865–7890 2017

<http://onlinelibrary.wiley.com/doi/10.1002/2017JA023884/pdf>

We discuss observations of the journey throughout the Solar System of a large interplanetary coronal mass ejection (ICME) that was ejected at the Sun on **14 October 2014**. The ICME hit Mars on 17 October, as observed by the Mars Express, MAVEN, Mars Odyssey and MSL missions, 44 hours before the encounter of the planet with the Siding-Spring comet, for which the space weather context is provided. It reached comet 67P/Churyumov-Gerasimenko, which was perfectly aligned with the Sun and Mars at 3.1 AU, as observed by Rosetta on 22 October. The ICME was also detected by STEREO-A on 16 October at 1 AU, and by Cassini in the solar wind around Saturn on the 12 November at 9.9 AU. Fortunately, the New Horizons spacecraft was also aligned with the direction of the ICME at 31.6 AU. We investigate whether this ICME has a non-ambiguous signature at New Horizons. A potential detection of this ICME by Voyager-2 at 110-111 AU is also discussed. The multi-spacecraft observations allow the derivation of certain properties of the ICME, such as its large angular extension of at least 116° , its speed as a function of distance, and its magnetic field structure at four locations from 1 to 10 AU. Observations of the speed data allow two different solar wind propagation models to be validated. Finally, we compare the Forbush decreases (transient decreases followed by gradual recoveries in the galactic cosmic ray intensity) due to the passage of this ICME at Mars, comet 67P and Saturn.

Two-fluid numerical simulations of the origin of the fast solar wind

D. [Wójcik](#), [B. Kuźma](#), [K. Murawski](#), [A.K. Srivastava](#)

2019

<https://arxiv.org/pdf/1906.01897.pdf>

With the use of our JOANNA code, which solves radiative equations for ion + electron and neutral fluids, we perform realistic 2.5D numerical simulations of plasma outflows associated with the solar granulation. These outflows exhibit physical quantities consistent to the order of magnitude with the observational findings for mass and energy losses in the upper chromosphere, transition region and inner corona, and they may originate the fast solar wind.

Verification of real-time WSA-ENLIL+Cone simulations of CME arrival-time at the CCMC from 2010-2016

A. M. [Wold](#), [M. L. Mays](#), [A. Taktakishvili](#), [L. K. Jian](#), [D. Odstrcil](#), [P. MacNeice](#)

Journal of Space Weather and Space Climate 8, A17 2018

<https://arxiv.org/pdf/1801.07818.pdf>

<https://www.swsc-journal.org/articles/swsc/pdf/2018/01/swsc170034.pdf>

The Wang-Sheeley-Argge (WSA)-ENLIL+Cone model is used extensively in space weather operations world-wide to model CME propagation. As such, it is important to assess its performance. We present validation results of the WSA-ENLIL+Cone model installed at the Community Coordinated Modeling Center (CCMC) and executed in real-time by the CCMC space weather team. CCMC uses the WSA-ENLIL+Cone model to predict CME arrivals at NASA missions throughout the inner heliosphere. In this work we compare model predicted CME arrival-times to in-situ ICME leading edge measurements at STEREO-A, STEREO-B, and Earth (Wind and ACE) for simulations completed between March 2010-December 2016 (over 1,800 CMEs). We report hit, miss, false alarm, and correct rejection statistics for all three locations. For all predicted CME arrivals, the hit rate is 0.5, and the false alarm rate is 0.1. For the 273 events where the CME was predicted to arrive at Earth, STEREO-A, or STEREO-B, and was actually observed (hit event), the mean

absolute arrival-time prediction error was 10.4 +/- 0.9 hours, with a tendency to early prediction error of -4.0 hours. We show the dependence of the arrival-time error on CME input parameters. We also explore the impact of the multi-spacecraft observations used to initialize the model CME inputs by comparing model verification results before and after the STEREO-B communication loss (since September 2014) and STEREO-A sidelobe operations (August 2014-December 2015). There is an increase of 1.7 hours in the CME arrival time error during single, or limited two-viewpoint periods, compared to the three-spacecraft viewpoint period. This trend would apply to a future space weather mission at L5 or L4 as another coronagraph viewpoint to reduce CME arrival time errors compared to a single L1 viewpoint.

Sequential Small Coronal Mass Ejections Observed In-situ and in White-Light Images by Parker Solar Probe

[Brian E. Wood](#), [Phillip Hess](#), [Yu Chen](#), [Qiang Hu](#)

ApJ **2023**

<https://arxiv.org/pdf/2308.01372.pdf>

We reconstruct the morphology and kinematics of a series of small transients that erupt from the Sun on **2021 April 24** using observations primarily from Parker Solar Probe (PSP). These sequential small coronal mass ejections (CMEs) may be the product of continuous reconnection at a current sheet, a macroscopic example of the more microscopic reconnection activity that has been proposed to accelerate the solar wind more generally. These particular CMEs are of interest because they are the first CMEs to hit PSP and be simultaneously imaged by it, using the Wide-field Imager for Solar Probe (WISPR) instrument. Based on imaging from WISPR and STEREO-A, we identify and model six discrete transients, and determine that it is the second of them (CME2) that first hits PSP, although PSP later more obliquely encounters the third transient as well. Signatures of these encounters are seen in the PSP in situ data. Within these data, we identify six candidate magnetic flux ropes (MFRs), all but one of which are associated with the second transient. The five CME2 MFRs have orientations roughly consistent with PSP encountering the right sides of roughly E-W oriented MFRs, which are sloping back towards the Sun.

Inferences About the Magnetic Field Structure of a CME with Both In Situ and Faraday Rotation Constraints

Brian E. [Wood](#)¹, Samuel Tun-Beltran¹, Jason E. Kooi², Emil J. Polisensky², and Teresa Nieves-Chinchilla³
2020 ApJ 896 99

<https://arxiv.org/pdf/2006.10794>

<https://sci-hub.tw/https://iopscience.iop.org/article/10.3847/1538-4357/ab93b8>

On 2012 August 2, two coronal mass ejections (CMEs; CME-1 and CME-2) erupted from the west limb of the Sun as viewed from Earth, and were observed in images from the white-light coronagraphs on the Solar and Heliospheric Observatory and Solar TERrestrial RELations Observatory (STEREO) spacecraft. These events were also observed by the Very Large Array (VLA), which was monitoring the Sun at radio wavelengths, allowing time-dependent Faraday rotation observations to be made of both events. We use the white-light imaging and radio data to model the 3D field geometry of both CMEs, assuming a magnetic flux rope geometry. For CME-2, we also consider 1 au in situ field measurements in the analysis, as this CME hits STEREO-A on August 6, making this the first CME with observational constraints from stereoscopic coronal imaging, radio Faraday rotation, and in situ plasma measurements combined. The imaging and in situ observations of CME-2 provide two clear predictions for the radio data: VLA should observe positive rotation measures (RMs) when the radio line of sight first encounters the CME, and the sign should reverse to negative within two hours. The initial positive RMs are in fact observed. The expected sign reversal is not, but the VLA data unfortunately end too soon to be sure of the significance of this discrepancy. We interpret an RM increase prior to the expected occultation time of the CME as a signature of a sheath region of deflected field ahead of the CME itself.

2012 August 2-6

Morphological Reconstruction of a Small Transient Observed by Parker Solar Probe on 2018 November 5

Brian E. [Wood](#), [Phillip Hess](#), [Russell A. Howard](#), [Guillermo Stenborg](#), [Yi-Ming Wang](#)

ApJS **246** 28 **2020**

<https://arxiv.org/pdf/2001.08716.pdf>

<https://doi.org/10.3847/1538-4365/ab5219>

On **2018 November 5**, about 24 hours before the first close perihelion passage of Parker Solar Probe (PSP), a *coronal mass ejection (CME)* entered the field of view of the inner detector of the Wide-field Imager for Solar PRobe (WISPR) instrument onboard PSP, with the northward component of its trajectory carrying the leading edge of the CME off the

top edge of the detector about four hours after its first appearance. We connect this event to a very small jet-like transient observed from 1 au by coronagraphs on both the Solar and Heliospheric Observatory (SOHO) and the A component of the Solar TERrestrial RELations Observatory mission (STEREO-A). This allows us to make the first three-dimensional reconstruction of a CME structure considering both observations made very close to the Sun and images from two observatories at 1 au. The CME may be small and jet-like as viewed from 1 au, but the close-in vantage point of PSP/WISPR demonstrates that it is not intrinsically jet-like, but instead has a structure consistent with a flux rope morphology. Based on its appearance in the SOHO and STEREO-A images, the event belongs in the "streamer blob" class of transients, but its kinematic behavior is very unusual, with a more impulsive acceleration than previously studied blobs.

A STEREO Survey of Magnetic Cloud Coronal Mass Ejections Observed at Earth in 2008--2012

Brian E. [Wood](#), Chin-Chun Wu, Ronald P. Lepping, [Teresa Nieves-Chinchilla](#), [Russell A. Howard](#), [Mark G. Linton](#), [Dennis G. Socker](#)

Astrophysical Journal Supplement **229:** 29 **2017**

<https://arxiv.org/pdf/1701.01682v1.pdf>

<https://iopscience.iop.org/article/10.3847/1538-4365/229/2/29/pdf>

We identify coronal mass ejections (CMEs) associated with magnetic clouds (MCs) observed near Earth by the Wind spacecraft from 2008 to mid-2012, a time period when the two STEREO spacecraft were well positioned to study Earth-directed CMEs. We find 31 out of 48 Wind MCs during this period can be clearly connected with a CME that is trackable in STEREO imagery all the way from the Sun to near 1 AU. For these events, we perform full 3-D reconstructions of the CME structure and kinematics, assuming a flux rope morphology for the CME shape, considering the full complement of STEREO and SOHO imaging constraints. We find that the flux rope orientations and sizes inferred from imaging are not well correlated with MC orientations and sizes inferred from the Wind data. However, velocities within the MC region are reproduced reasonably well by the image-based reconstruction. Our kinematic measurements are used to provide simple prescriptions for predicting CME arrival times at Earth, provided for a range of distances from the Sun where CME velocity measurements might be made. Finally, we discuss the differences in the morphology and kinematics of CME flux ropes associated with different surface phenomena (flares, filament eruptions, or no surface activity).

Table 1. CMEs Associated with Wind MCs (2008-2012)

Table 2. CME Measurements

Table 3. Relating CME Velocity to 1 AU Travel Time

Comparative ionospheric impacts and solar origins of nine strong geomagnetic storms in 2010 – 2015.

[Wood](#), B.E., [Lean](#), J.L., [McDonald](#), S.E., [Wang](#), Y.-M.:

2016, J. Geophys. Res. 121(6), 4938. DOI. ADS.

<https://agupubs.onlinelibrary.wiley.com/doi/epdf/10.1002/2015JA021953>

For nine of the strongest geomagnetic storms in solar cycle 24 we characterize, quantify, and compare the impacts on ionospheric total electron content (TEC) and the U.S. Wide Area Augmentation System (WAAS) with the heliospheric morphology and kinematics of the responsible coronal mass ejections (CMEs) and their solar source regions. Regional TEC responses to the events are similar in many respects, especially in the initial positive phase. For the subsequent negative phase, Dst is a better indicator than ap of the magnitude of the TEC decrease. The five events that arrive between 13:00 UT and 21:00 UT (local daytime in the U.S.) produce large WAAS degradations, and the four events that arrive outside this time of day produce lesser or no WAAS degradation. Our sample of geoeffective events includes CMEs with only modestly fast speeds, ones that only provided glancing impacts on Earth by their shock sheaths and ones not associated with any significant flare. While all of the CMEs traveled faster than the solar wind, they nevertheless have a wide range of velocities and produced a range of Bz values; neither speed nor Bz correlates significantly with ionospheric impact. Comparison with the locations of surface activity leads to estimates of deflection for the CMEs, with the average deflection being 19°. At least a few events may have missed Earth entirely in the absence of coronal deflection.

Imaging Prominence Eruptions Out to 1 AU

Brian E. [Wood](#), [Russell A. Howard](#), [Mark G. Linton](#)

ApJ **2015**

<http://arxiv.org/pdf/1512.06748v1.pdf>

Views of two bright prominence eruptions trackable all the way to 1AU are here presented, using the heliospheric imagers on the Solar TERrestrial RELations Observatory (STEREO) spacecraft. The two events first erupted from the Sun on **2011 June 7 and 2012 August 31**, respectively. Only these two examples of clear prominence eruptions observable this far from the Sun could be found in the STEREO image database, emphasizing the rarity of prominence eruptions this persistently bright. For the 2011 June event, a time-dependent 3-D reconstruction of the prominence structure is made using point-by-point triangulation. This is not possible for the August event due to a poor viewing geometry. Unlike the coronal mass ejection (CME) that accompanies it, the 2011 June prominence exhibits little deceleration from the Sun to 1 AU, as a consequence moving upwards within the CME. This demonstrates that prominences are not necessarily tied to the CME's magnetic structure far from the Sun. A mathematical framework is developed for describing the degree of self-similarity for the prominence's expansion away from the Sun. This analysis suggests only modest deviations from self-similar expansion, but close to the Sun the prominence expands radially somewhat more rapidly than self-similarity would predict.

Connecting Coronal Mass Ejections and Magnetic Clouds: A Case Study Using an Event from 22 June 2009

B. E. **Wood**, A. P. Rouillard, C. Möstl, K. Battams, N. P. Savani, K. Marubashi, R. A. Howard and D. G. Socker

Solar Physics, **2012**, Volume 281, Issue 1, pp 369-389

On 27 June 2009 the Wind and Advanced Composition Explorer (ACE) spacecraft near Earth detected a magnetic cloud (MC). The MC can be traced back to a slow coronal mass ejection (CME) launched from the Sun on **22 June 2009** but this connection relies entirely on heliospheric imaging of the Sun–Earth line from the two STEREO spacecraft, illustrating the value of such imaging. The STEREO and SOHO/LASCO views of this event collectively suggest strongly that the CME has the shape of a magnetic flux rope. The arrival times of two density peaks at ACE are consistent with the expected arrival times of the front and back of the flux rope observed in the images, and the velocity of the CME seen by ACE is also consistent with the STEREO measurements. However, the complex nature of the MC signature of this event complicates attempts to compare the flux rope orientations inferred from the imaging and in situ data. Various analyses of the in situ data, performed using both force-free and Grad–Shafranov approaches to MC modeling, yield a wide range of flux rope orientations depending on the type of analysis and on the exact time interval used. The best reproduction of the image-inferred orientation occurs when the first third of the MC time interval is ignored.

EMPIRICAL RECONSTRUCTION AND NUMERICAL MODELING OF THE FIRST GEOEFFECTIVE CORONAL MASS EJECTION OF SOLAR CYCLE 24

B. E. **Wood**¹, C.-C. Wu¹, R. A. Howard¹, D. G. Socker¹, and A. P. Rouillard²

Astrophysical Journal, 729:70 (10pp), **2011** March, **File**

We analyze the kinematics and morphology of a coronal mass ejection (CME) from **2010 April 3**, which was responsible for the first significant geomagnetic storm of solar cycle 24. The analysis utilizes coronagraphic and heliospheric images from the two *STEREO* spacecraft, and coronagraphic images from *SOHO/LASCO*. Using an empirical three-dimensional (3D) reconstruction technique, we demonstrate that the CME can be reproduced reasonably well at all times with a 3D flux rope shape, but the case for a flux rope being the correct interpretation is not as strong as some events studied with *STEREO* in the past, given that we are unable to infer a unique orientation for the flux rope. A model with an orientation angle of -80° from the ecliptic plane (i.e., nearly N–S) works best close to the Sun, but a model at 10° (i.e., nearly E–W) works better far from the Sun. Both interpretations require the cross section of the flux rope to be significantly elliptical rather than circular. In addition to our empirical modeling, we also present a fully 3D numerical MHD model of the CME. This physical model appears to effectively reproduce aspects of the shape and kinematics of the CME's leading edge. It is particularly encouraging that the model reproduces the amount of interplanetary deceleration observed for the CME during its journey from the Sun to 1AU.

THE THREE-DIMENSIONAL MORPHOLOGY OF A COROTATING INTERACTION REGION IN THE INNER HELIOSPHERE

[B. E. Wood](#), [R. A. Howard](#), [A. Thernisien](#) and [D. G. Socker](#)

ApJ **708** L89-L94, **2010**

In its three years of operation, the HI2 imagers on the two *Solar Terrestrial Relations Observatory (STEREO)* spacecraft have imaged many corotating interaction regions (CIRs) in the interplanetary medium, allowing the study of their three-dimensional (3D) morphology. Using an entirely empirical analysis technique, we construct a 3D model of one CIR, which is able to reproduce the general appearance and evolution of the CIR in HI2 images. The model CIR is also consistent with in situ data. Its curvature is compatible with the observed speed of the slow wind that is acting as the barrier for the fast wind piling up against it, and the width of the model CIR is consistent with the duration of the observed density pulse. Perpendicular to the equatorial plane, the model CIR has a parabolic shape that maps beautifully back to a bifurcated streamer observed at the Sun, which surrounds a coronal hole. This implies that this particular CIR is due to fast wind emanating from low latitudes that is impinging against slow wind in overlying streamers.

AN EMPIRICAL RECONSTRUCTION OF THE 2008 APRIL 26 CORONAL MASS EJECTION

B. E. [Wood](#) and R. A. Howard

Astrophysical Journal, 702:901–910, **2009** September

We present a three-dimensional model of the density distribution of a coronal mass ejection (CME) from **2008 April 26**. This CME was observed by the two spacecraft composing the Solar Terrestrial Relations Observatory (*STEREO*), which tracked the CME from near the Sun, into the interplanetary medium (IPM), and all the way to 1 AU. The CME was directed toward *STEREO-B* and hit that spacecraft on 2008 April 29. The *STEREO* images of the CME show an internal structure that can be interpreted as having a flux rope shape. The two different perspectives on the event provided by the two *STEREO* spacecraft allow us to make a particularly strong argument for the flux rope interpretation, and the *STEREO* data also allow us to study the evolution of the flux rope in the IPM. The flux rope is oriented close to the ecliptic plane, but with the western leg tilted northwards by about 20°. This implies an orientation roughly perpendicular to the neutral line of the active region at the event's point of origin, apparently an unusual geometry given that previous analyses have found that CME flux ropes are usually, but not always, oriented *parallel* to the neutral lines of their source regions. The CME model also consists of a front out ahead of the flux rope, possibly a shock launched by the flux rope driver. The model density distribution is reasonably successful at reproducing the CME appearance both close to the Sun in coronagraphic images, and far from the Sun in images of the IPM from *STEREO*'s heliospheric imagers. *This suggests that self-similar expansion is a reasonable first-order approximation for this particular CME, and also indicates that the flux rope's orientation does not change much during its journey through the IPM.*

Comprehensive Observations of a Solar Minimum Coronal Mass Ejection with the Solar Terrestrial Relations Observatory

B. E. [Wood](#), R. A. Howard, S. P. Plunkett, and D. G. Socker

Astrophysical Journal, 694:707–717, **2009**; **File**

We perform the first kinematic analysis of a coronal mass ejection (CME) observed by both imaging and in situ instruments on board the Solar Terrestrial Relations Observatory (**STEREO**). Launched on **2008 February 4**, the CME is tracked continuously from initiation to 1 AU using the imagers on both *STEREO* spacecraft, and is then detected by the particle and field detectors on board *STEREO-B* on February 7. The CME is also detected in situ by the Advanced Composition Explorer and Solar and Heliospheric Observatory at Earth's L1 Lagrangian point. This event provides a good example of just how different the same event can look when viewed from different perspectives. We also demonstrate many ways in which the comprehensive and continuous coverage of this CME by *STEREO* improves confidence in our assessment of its kinematic behavior, with potential ramifications for space weather forecasting. The observations provide several lines of evidence in favor of the observable part of the CME being narrow in angular extent, a determination crucial for deciding how best to convert observed CME elongation angles from Sun-center to actual Sun-center distances.

Proton Core Behaviour Inside Magnetic Field Switchbacks

Thomas [Woolley](#), [Lorenzo Matteini](#), [Timothy S. Horbury](#), [Stuart D. Bale](#), [Lloyd D. Woodham](#), [Ronan Laker](#), [Benjamin L. Alterman](#), [John W. Bonnell](#), [Anthony W. Case](#), [Justin C. Kasper](#), [Kristopher G. Klein](#), [Mihailo M. Martinović](#), [Michael Stevens](#)

MNRAS Volume 498, Issue 4, Pages 5524–5531 **2020**

<https://arxiv.org/pdf/2007.10906.pdf>

<https://doi.org/10.1093/mnras/staa2770>

During Parker Solar Probe's first two orbits there are widespread observations of rapid magnetic field reversals known as switchbacks. These switchbacks are extensively found in the near-Sun solar wind, appear to occur in patches, and have possible links to various phenomena such as magnetic reconnection near the solar surface. As switchbacks are associated with faster plasma flows, we questioned whether they are hotter than the background plasma and whether the microphysics inside a switchback is different to its surroundings. We have studied the reduced distribution functions from the Solar Probe Cup instrument and considered time periods with markedly large angular deflections, to compare parallel temperatures inside and outside switchbacks. We have shown that the reduced distribution functions inside switchbacks are consistent with a rigid phase space rotation of the background plasma. As such, we conclude that the proton core parallel temperature is the same inside and outside of switchbacks, implying that a T-V relationship does not hold for the proton core parallel temperature inside magnetic field switchbacks. We further conclude that switchbacks are consistent with Alfvénic pulses travelling along open magnetic field lines. The origin of these pulses, however, remains unknown. We also found that there is no obvious link between radial Poynting flux and kinetic energy enhancements suggesting that the radial Poynting flux is not important for the dynamics of switchbacks. **7 Nov 2018**

Solar wind modeling: a computational tool for the classroom

Lauren N. **Woolsey**

2015

<http://arxiv.org/pdf/1505.00727v1.pdf>

This article presents a Python model and library that can be used for student investigation of the application of fundamental physics on a specific problem: the role of magnetic field in solar wind acceleration. The paper begins with a short overview of the open questions in the study of the solar wind and how they relate to many commonly taught physics courses. The physics included in the model, The Efficient Modified Parker Equation Solving Tool (TEMPEST), is laid out for the reader. Results using TEMPEST on a magnetic field structure representative of the minimum phase of the Sun's activity cycle are presented and discussed. The paper suggests several ways to use TEMPEST in an educational environment and provides access to the current version of the code.

Analysis of Galactic Cosmic Ray Anisotropy During the Time Period from 1996 to 2020

Witold **Wozniak**, [Krzysztof Iskra](#), [Renata Modzelewska](#) & [Marek Siluszyk](#)

[Solar Physics](#) volume 298, Article number: 28 (**2023**)

<https://link.springer.com/content/pdf/10.1007/s11207-023-02120-x.pdf>

We study the influence of drift effects on the galactic cosmic ray anisotropy (GCRA) in different periods of solar activity (from 1996 to 2020) using data from the global network of neutron monitors. We analyze the GCRA in 1996, the last year of Solar Cycle 22 with positive polarity ($A > 0$), Solar Cycles 23 and 24 with both positive ($A > 0$) and negative polarities ($A < 0$), and the 2020 onset of Solar Cycle 25 with positive polarity ($A > 0$). We show that in positive polarity periods, a diffusion model with noticeably manifested drift is acceptable, whereas the diffusion-dominated model of galactic cosmic ray (GCR) transport is more acceptable in negative polarity periods.

We found that the average radial component of the drift vector for $A > 0$ practically points to 12 h, and for the $A < 0$ polarity to 24 h, respectively. These results are consistent with the drift theory of modulation of GCRs. According to theory, during positive or negative polarity periods, a drift stream of GCRs is directed away from or toward the Sun, respectively, thus giving rise to long-term changes of the radial component of the GCRA.

The calculated magnitudes of the radial and tangential components of the GCRA in different sectors of the heliospheric magnetic field were used to calculate the parameters that characterize the GCR modulation in interplanetary space.

Effects of background solar wind and drag force on the propagation of coronal mass ejection driven shock

Chin-Chun **Wu** (1), [Kan Liou](#) (2), [Brian E. Wood](#) (1), [Lynn Hutting](#) (1)

2024 *ApJ* 977 212

<https://arxiv.org/pdf/2411.00747>

<https://iopscience.iop.org/article/10.3847/1538-4357/ad88ee/pdf>

Propagation of interplanetary (IP) shocks, particularly those driven by coronal mass ejections (CMEs), is still an outstanding question in heliophysics and space weather forecasting. Here we address effects of the ambient solar wind on the propagation of two similar CME-driven shocks from the Sun to Earth. The two shock events (CME03: **April 3, 2010** and CME12: **July 12, 2012**) have the following properties: Both events (1) were driven by a halo CME (i.e., source location is near the Sun-Earth line), (2) had a CME source in the southern hemisphere, (3) had a similar transit time (~ 2 days) to Earth, (4) occurred in a non-quiet solar period, and (5) led to a severe geomagnetic storm. The initial (near the Sun) propagation speed, as measured by coronagraph images, was slower (by ~ 300 km/s) for CME03 than

CME12, but it took about the same amount of traveling time for both events to reach Earth. According to the in-situ solar wind observations from the Wind spacecraft, the CME03-driven shock was associated with a faster solar wind upstream of the shock than the CME12-driven shock. This is also demonstrated in our global MHD simulations. Analysis of our simulation result indicates that the drag force indirectly plays an important role in the shock propagation. The present study suggests that in addition to the initial CME propagation speed near the Sun the shock speed (in the inertial frame) and the ambient solar wind condition, in particular the solar wind speed, are the key to timing the arrival of CME-driven-shock events.

Magnetohydrodynamic simulation of the 2012-July-12 CME Event With the Fluxrope-G3DMHD Model

Chin-Chun **Wu** (1,a)[Kan Liou](#) (2,b)[Brian Wood](#) (1,c)[Keiji Hayashi](#) (3,d)

Phys Astron Int J. **2024**; 8(I):1-3.

DOI:<https://doi.org/10.15406/paij.2024.08.00324>

<https://arxiv.org/pdf/2406.13090>

Coronal mass ejections (CMEs) and their driven shocks are a major source of large geomagnetic storms due to their large and long-lasting, southward component of magnetic field in the sheath and the flux rope (e.g., magnetic cloud). Predicting the strength and arrival time of southward fields accurately thus plays a key role in space weather predictions. To address this problem, we have developed a new model, which combines the global three-dimensional, time-dependent, magnetohydrodynamic (MHD), data-driven model (G3DMHD) and a self-contained magnetic flux-rope model [1]. As a demonstration and validation, here we simulate the evolution of a Sun-Earth-directed CME that erupted on **2012-July-12**. The computational domain spans from 2.5 solar radii (R_s) from the surface of the Sun, where the flux rope is injected, to 245 R_s . We compare the time profiles of the simulated MHD parameters (Density, velocity, temperature, and magnetic field) with in situ solar wind observations acquired at ~ 1 AU by the Wind spacecraft and the result is encouraging. The model successfully reproduces the shock, sheath, and flux rope similar to those observed by Wind.

Magnetohydrodynamic Simulation of Multiple Coronal Mass Ejections: An Effect of "Pre-events"

Chin-Chun **Wu**¹, Kan Liou², Lynn Hutting¹, and Brian E. Wood¹

2022 ApJ 935 67

<https://iopscience.iop.org/article/10.3847/1538-4357/ac7f2a/pdf>

Coronal mass ejections (CMEs) are a major source of solar wind disturbances that affect the space plasma and magnetic field environment along their propagation path. Accurate prediction of the arrival of a CME at Earth or any point in the heliosphere is still a daunting task. In this study we explore an often overlooked factor—the effects of "pre-events" that can alter the propagation of a CME due to a preceding CME. A data-driven magnetohydrodynamic numerical model is used to simulate the propagation of multiple CMEs and their driven shocks that occurred in 2012 July. The simulation results are validated with in situ solar wind plasma and magnetic field measurements at 1 au, testing the appropriateness of our simulation results for interpreting the CME/shock evolution. By comparing the simulation results with and without preceding CMEs, we find that the trailing CME can be accelerated by the "wake" of a preceding CME. A detailed analysis suggests that the acceleration is caused partially by an increase in the background solar wind and partially by the so-called "snowplow" effect, with the latter being the major contributor for the 2012 July event. **13-27 Jul 2012**

Magnetic Field Intensity Modification to Force Free Model of Magnetic Clouds: Website of Wind Examples From Launch to July of 2015.

Wu C-C, Lepping RP and Berdichevsky DB

(**2021**) Front. Phys. 9:712599

<https://www.frontiersin.org/articles/10.3389/fphy.2021.712599/full>

<https://doi.org/10.3389/fphy.2021.712599>

We describe a new NASA website that shows normalized magnetic field (B) magnitude profiles within Wind magnetic clouds (MCs) (i.e., observations versus basic model versus modified model) for 209 MCs observed from launch in late 1994 to July of 2015, where model modification is based on the studies of Lepping et al. (Solar Phys, 2017, 292:27) and Lepping et al. (Solar Phys, 2018, 293:162); the basic force free magnetic cloud parameter fitting model employing Bessel functions (Lepping et al., J. Geophys. Res., 1990, 95:11957) is called the LJB model here. The fundamental principles should be applicable to the B -data from any spacecraft at 1 AU. Earlier (in the LJB study), we justified why the field magnitude can be thought of as decoupled from the field direction within an MC, and further, we justified this

idea in terms of actual observations seen over a few decades with examples of MCs from Wind data. The model modification is achieved by adding a correction (“Quad”) value to the LJB model (Bessel function) value in the following manner: $B(\text{est})/B_0 \approx [\text{LJB Model} + \text{Quad}(CA, u)]$, where B_0 is the LJB-estimated field magnitude value on the MC’s axis, CA is the relative closest approach (See [Supplementary Appendix A](#)), and u is the distance that the spacecraft travels through the MC from its entrance point. In an average sense, the Quad technique is shown to be successful for 82% of the past modeled MCs, when Quality (Q0) is good or excellent (see [Supplementary Appendix A](#)). The Quad technique is successful for 78% of MCs when all cases are considered. So Q0 of the MC LJB-fit is not a big factor when the success of the Quad scheme is considered. In addition, it is found that the Quad technique does not work better for MC events with higher solar wind speed. Yearly occurrence frequency of all MC events (N_{Yearly}) and those MC events with $\Delta\sigma N/\sigma N_2 \geq 0.5$ ($N\Delta\sigma N/\sigma N_2 \geq 0.5$) are well correlated, but there is no solar cycle dependence for normalizing $N\Delta\sigma N/\sigma N_2 \geq 0.5$ with N_{Yearly} .

Magnetic Cloud and Sheath in the Ground-level Enhancement Event of 2000 July 14.

I. Effects on the Solar Energetic Particles

S.-S. Wu and G. Qin¹

2020 ApJ 904 151

<https://doi.org/10.3847/1538-4357/abc0f2>

<https://iopscience.iop.org/article/10.3847/1538-4357/abc0f2/pdf>

Ground-level enhancements generally accompany fast interplanetary coronal mass ejections (ICMEs), and ICME-driven shocks are sources of solar energetic particles (SEPs). Observations of the GLE event of **2000 July 14** show that a very fast and strong magnetic cloud (MC) is behind the ICME shock and the proton intensity-time profiles observed at 1 au had a rapid two-step decrease near the sheath and MC. Therefore, we study the effect of sheath and MC on SEPs accelerated by an ICME shock by numerically solving the focused transport equation. The shock is regarded as a moving source of SEPs with an assumed particle distribution function. The sheath and MC are set to thick spherical caps with enhanced magnetic field, and the turbulence levels in the sheath and MC are set to be higher and lower than those of the ambient solar wind, respectively. The simulation results of proton intensity-time profiles agree well with the observations in energies ranging from ~ 1 to ~ 100 MeV, and the two-step decrease is reproduced when the sheath and MC arrived at the Earth. The simulation results show that the sheath-MC structure reduced the proton intensities for about 2 days after the shock passed through the Earth. It is found that the sheath contributed most of the decrease while the MC facilitated the formation of the second step decrease. The simulation also infers that the coordination of magnetic field and turbulence in sheath-MC structure can produce a stronger reduction of SEP intensities.

Energy Supply for Heating the Slow Solar Wind Observed by Parker Solar Probe between 0.17 and 0.7 au

Honghong Wu¹, Chuanyi Tu¹, Xin Wang², Jiansen He¹, and Liping Yang³

2020 ApJL 904 L8

<https://iopscience.iop.org/article/10.3847/2041-8213/abc5b6/pdf>

<https://doi.org/10.3847/2041-8213/abc5b6>

The Parker Solar Probe (PSP) mission provides a good opportunity to study this issue. Recently, PSP observations have found that the slow solar wind experiences stronger heating inside 0.24 au. Here for the first time we measure in the slow solar wind the radial gradient of the low-frequency breaks on the magnetic trace power spectra and evaluate the associated energy supply rate. We find that the energy supply rate is consistent with the observed perpendicular heating rate calculated based on the gradient of the magnetic moment. Based on this finding, one could explain why the slow solar wind is strongly heated inside 0.25 au but expands nearly adiabatically outside 0.25 au. This finding supports the concept that the energy added from the energy-containing range is transferred by an energy cascade process to the dissipation range, and then dissipates to heat the slow solar wind. The related issues for further study are discussed. **the first three orbits of PSP from 2018 October 31 to 2019 October 13**

The 04 – 10 September 2017 Sun–Earth Connection Events: Solar Flares, Coronal Mass Ejections/Magnetic Clouds, and Geomagnetic Storms

Chin-Chun Wu, Kan Liou, Ronald P. Lepping, Lynn Hutting

[Solar Physics](#) August 2019, 294:110

[sci-hub.se/10.1007/s11207-019-1446-2](https://doi.org/10.1007/s11207-019-1446-2)

In early September 2017, a series of solar flares and coronal mass ejections (CMEs) erupted from the Sun. The Cor2a coronagraph, a unit of the Sun Earth Connection Coronal and Heliospheric Investigation (SECCHI), onboard the Solar Terrestrial Relations Observatory (STEREO)-A spacecraft recorded two Sun–Earth-directed CMEs on

4 September (referred to as CME04) and **6 September** (referred to as CME06). A few days later, the Wind spacecraft ($\approx 212.4 \approx 212.4$ solar radii: R_{\odot}) recorded two interplanetary shocks, presumably driven by CME04 and CME06, at $\approx 22:41$ UT $\approx 22:41$ UT on 06 September 2017 (referred to as Shock06) and at $\approx 22:48$ UT $\approx 22:48$ UT on 07 September 2017 (referred to as Shock07), respectively. The travel time of the CME04/Shock06 [$\Delta t_{\text{shock-CME@18}R_{\odot}}$] and CME06/Shock07 from $18 R_{\odot}$ to the Wind spacecraft was 41.52 hours and 32.47 hours, respectively. The propagating speed [V_{CME}] of the CME04 and CME06 at $\approx 18 R_{\odot}$ was determined with SECCHI/Cor2a as $\approx 886 \text{ km s}^{-1}$ and $\approx 1368 \text{ km s}^{-1}$, respectively. Assuming a constant velocity after $18 R_{\odot}$, the estimated $\Delta t_{\text{shock-CME@18}R_{\odot}}$ is 42.45 and 27.5 hours for CME04 and CME06, respectively. This simple estimate of the CME propagation speed provides a satisfactory result for the CME04 event (error $\approx 2.3\%$) but not for the CME06 event (error $\approx 15.3\%$). The second event, CME06, was delayed further due to an interaction with the preceding event (CME04). It is suggested that the CME speed estimated near the Sun with coronagraph images can be a good estimator for the interplanetary CME (ICME) transit time when there is no pre-event. A three-dimensional magnetohydrodynamic simulation is performed to address this issue by providing a panoramic view of the entire process not available from the observations. A southward interplanetary magnetic field [B_s] increased sharply to -31.6 nT on 7 September at Wind, followed by a severe geomagnetic storm ($D_{\text{st}} = -124$ nT). The sharp increase of the IMF [B_s] was a result of the interaction between Shock07 and the driver of Shock06 (CME04). This study suggests that a severe geomagnetic storm can be caused by the interaction between a MC, with an impinging IP shock from behind, and the Earth's magnetosphere. The intensity of a geomagnetic storm will likely be stronger for an event associated with ICME-ICME interaction than for a geomagnetic event caused by only a single ICME.

Modeling Inner Boundary Values at 18 Solar Radii During Solar Quiet time for Global Three-dimensional Time-Dependent Magnetohydrodynamic Numerical Simulation

Chin-Chun [Wu](#), [Kan Liou](#), [Simon Plunkett](#), [Dennis Socker](#), [Y.M. Wang](#), [Brian Wood](#), [S. T. Wu](#), [Murray Dryer](#), [Christopher Kung](#)

2018

<https://arxiv.org/ftp/arxiv/papers/1810/1810.01755.pdf>

The solar wind speed plays a key role in the transport of CME out of the Sun and ultimately determines the arrival time of CME-driven shocks in the heliosphere. Here, we develop an empirical model of the solar wind parameters at the inner boundary (18 solar radii, R_s) used in our global, 3D MHD model (G3DMHD) or other equivalent ones. The model takes solar magnetic field maps at $2.5 R_s$ (which is based on the Potential Field Source Surface, PFSS model) and interpolates the solar wind plasma and field out to $18 R_s$ using the algorithm of Wang and Sheeley [1990a]. A formula $V_{18R_s} = V_1 + V_2 fs^{\alpha}$ is used to calculate the solar wind speed at $18 R_s$, where V_1 is in a range of 150-350 km/s, V_2 is in the range of 250-500 km/s, and fs is an expansion factor, which was derived from the Wang and Sheeley (WS) algorithm at $2.5 R_s$. To estimate the solar wind density and temperature at $18 R_s$, we assume an incompressible solar wind and a constant total pressure. The three free parameters are obtained by adjusting simulation results to match in-situ observations (Wind) for more than 54 combination of V_1 , V_2 and α during a quiet solar wind interval, CR2082. We found $V_{18R_s} = (150 \pm 50) + (500 \pm 100) fs^{-0.4}$ km/s performs reasonably well in predicting solar wind parameters at 1 AU not just for CR 2082 but other quiet solar period. Comparing results from the present study with those from WSA [Arge et al. 2000; 2004] we conclude that i) Results of using V_{18R_s} with the full rotation data (FR) as input to drive G3DMHD model is better than the results of WSA using FR, or daily updated. ii) When using a modified daily updated 4-day-advanced solar wind speed predictions WSA performs slightly better than our G3DMHD. iii) When using V_{18R_s} as input, G3DMHD model performs much better than the WSA formula. We argue the necessity of the extra angular width (θ_b) parameter used in WSA. **4 April 2009, 2017-09-04, 2017-09-06**

Observation of an Extremely Large-Density Heliospheric Plasma Sheet Compressed by an Interplanetary Shock at 1 AU

Chin-Chun [Wu](#), [Kan Liou](#), [R. P. Lepping](#), [Angelos Vourlidas](#), [Simon Plunkett](#), [Dennis Socker](#), [S. T. Wu](#)
[Solar Physics](#) August 2017, 292:109

At 11:46 UT on **9 September 2011**, the Wind spacecraft encountered an interplanetary (IP) fast-forward shock. The shock was followed almost immediately by a short-duration (~ 35 minutes) extremely dense pulse (with a peak $\sim 94 \text{ cm}^{-3}$). The pulse induced an extremely large positive impulse ($S_{\text{YM-H}} = 74$ nT and $D_{\text{st}} = 48$ nT) on the ground. A close examination of other in situ parameters from Wind shows that the density pulse was associated with i) a spike in the plasma β (ratio of thermal to magnetic pressure), ii) multiple sign changes in the azimuthal component of the magnetic field (B_{ϕ}), iii) a depressed magnetic field magnitude, iv) a small radial component of the magnetic field, and v) a large ($> 90^\circ$) change in the suprathermal (~ 255 eV) electron pitch angle across the density pulse. We conclude

that the density pulse is associated with the heliospheric plasma sheet (HPS). The thickness of the HPS is estimated to be $\sim 8.2 \times 10^5$ km $\sim 8.2 \times 10^5$ km. The HPS density peak is about five times the value of a medium-sized density peak inside the HPS (~ 18 cm $^{-3}$) at 1 AU. Our global three-dimensional magnetohydrodynamic simulation results (Wu et al. in J. Geophys. Res. 212, 1839, 2016) suggest that the extremely large density pulse may be the result of the compression of the HPS by an IP shock crossing or an interaction between an interplanetary shock and a corotating interaction region.

A comparison between the geoeffectiveness of north-south and south-north magnetic clouds and an associated prediction

Chin-Chun **Wu**, Ronald P. Lepping, Daniel Benjamin Berdichevsky, Kan Liou

Space Weather March 2017 Vol: 15, Pages: 517–525 DOI: 10.1002/2016SW001520

[http://onlinelibrary.wiley.com/sci-](http://onlinelibrary.wiley.com/sci-hub/doi/10.1002/2016SW001520/abstract;jsessionid=16411D446AA0F8A36F824BFA3A190E6C.f03t02)

[hub.cc/doi/10.1002/2016SW001520/abstract;jsessionid=16411D446AA0F8A36F824BFA3A190E6C.f03t02](http://onlinelibrary.wiley.com/sci-hub/doi/10.1002/2016SW001520/abstract;jsessionid=16411D446AA0F8A36F824BFA3A190E6C.f03t02)

Using 1995–2015 Wind in situ solar wind plasma and magnetic field data, 217 magnetic clouds (MCs) were identified. The following pertinent results were found: (i) 120 MCs were N-S type (northward \rightarrow southward, magnetic field, B rotated from northward to southward), and 97 MCs are S-N type. (ii) S-N MCS-N dominated N-S MCN-S in the periods of 1995–1999, 2001–2002, and 2014–2015. In contrast, N-S MCN-S dominated S-N MCS-N in the periods of 2000 and 2003–2013. (iii) The averages of storm intensity ($\langle \text{Dstmin} \rangle$) were -69 , -57 , and -84 nT for “all 217 MCs,” “120 N-S MCs,” and “97 S-N MCs” types, respectively. (iv) Confirmed with observations, MC type depends on the phase of the magnetic solar cycle. Hence, on average, the S-N types trigger more severe storms (i.e., $\text{Dstmin} < -100$ nT). Also, from 1995 to 2009, the percentage of N-S types of MCs keeps increasing and the percentage of S-N types decreasing. The percentage of S-N MCs starts increasing in the interval of 2010–2015. Therefore, we expect to see a predominance of the S-N types of MC for the coming few years. This means on average that more severe geomagnetic storms are expected in the near future. This is an interesting solar wind feature and is going to be stressed in its application to “space weather predictions.” 16-06-2012, 17-03-2015

Table 1. List of MC That Occurred During 2013–2015

MCs for January 1995 to December 2012, is listed on the Wind-MFI website

(http://lepmfi.gsfc.nasa.gov/mfi/mag_cloud_pub1.html), and the 2013–2015

MCs are listed in Table 1

Wind data <http://cdaweb.gsfc.nasa.gov/pub/data/wind/>.

Numerical Simulation of Multiple CME-Driven Shocks in the Month of 2011 September†

Chin-Chun **Wu**, Kan Liou, Angelos Vourlidas, Simon Plunkett, Murray Dryer, S. T. Wu, Dennis Socker, Brian E. Wood, Lynn Hutting, Russell A. Howar

JGR Volume 121, Issue 3 Pages 1839–1856 2016

A global, three-dimensional (3-D) numerical simulation model has been employed to study the Sun-to-Earth propagation of multiple (12) coronal mass ejections (CMEs) and their associated shocks in **September 2011**. The inputs to the simulation are based on actual solar observations, which include the CME speeds, source locations, and photospheric magnetic fields. The simulation result is fine tuned with in situ solar wind data observations at 1 AU by matching the arrival time of CME-driven shocks. During this period three CME-driven interplanetary (IP) shocks induced three sizable geomagnetic storms on **September 9, 17, and 26**, with Dst values reaching -69 , -70 , and -101 nT respectively. These storm events signify the commencement of geomagnetic activity in the solar cycle 24. The CME propagation speed near the Sun (e.g., < 30 R_{Sun}) has been widely used to estimate the ICME/Shock arrival time at 1 AU (c.f., the review by Zhao and Dryer, 2014). Our simulation indicates that the background solar wind speed, as expected, is an important controlling parameter in the propagation of IP shocks and CMEs. Prediction of the ICME/Shock arrival time at 1 AU can be more problematic for slow (e.g., < 500 km s $^{-1}$) than fast CMEs (> 1000 km s $^{-1}$). This is because the effect of the background solar wind is more pronounced for slow CMEs. Here we demonstrate this difficulty with a slow (400 km s $^{-1}$) CME event that arrived at the Earth in 3 days instead of the predicted 4.3 days. Our results also demonstrate that a long period (a month in this case) of simulation may be necessary to make meaningful solar source-geomagnetic storm associations.

Relationships Among Geomagnetic Storms, Interplanetary Shocks, Magnetic Clouds, and Sunspot Number During 1995 – 2012

Chin-Chun **Wu**, Ronald P. Lepping

Solar Phys. January 2016, Volume 291, [Issue 1](#), pp 265-284

During 1995 – 2012, the Wind spacecraft has recorded 168 magnetic clouds (MCs), 197 magnetic cloud-like structures (MCLs), and 358 interplanetary (IP) shocks. Ninety-four MCs and 56 MCLs had upstream shock waves. The following features are found: i) The averages of the solar wind speed, interplanetary magnetic field (IMF), duration ($\langle \Delta t \rangle$), the minimum of B_{\min} , and intensity of the associated geomagnetic storm/activity ($\langle Dst_{\min} \rangle$) for MCs with upstream shock waves (MCshock) are higher (or stronger) than those averages for the MCs without upstream shock waves (MCno-shock). ii) The average $\langle \Delta t \rangle$ of MCshock events (≈ 19.8 h) is 9 % longer than that for MCno-shock events (≈ 17.6 h). iii) For the MCshock events, the average duration of the sheath ($\langle \Delta t_{\text{sheath}} \rangle$) is 12.1 h. These findings could be very useful for space weather predictions, i.e. IP shocks driven by MCs are expected to arrive at Wind (or at 1 AU) about 12 h ahead of the front of the MCs on average. iv) The occurrence frequency of IP shocks is well associated with sunspot number (SSN). The average intensity of geomagnetic storms measured by $\langle Dst_{\min} \rangle$ for MCshock and MCno-shock events is -102 and -31 nT, respectively. The average values $\langle Dst_{\min} \rangle$ are -78 , -70 , and -35 nT for the 358 IP shocks, 168 MCs, and 197 MCLs, respectively. These results imply that IP shocks, when they occur with MCs/MCLs, must play an important role in the strength of geomagnetic storms. We speculate about the reason for this. Yearly occurrence frequencies of MC shock and IP shocks are well correlated with solar activity (e.g., SSN). Choosing the correct Dst_{\min} estimating formula for predicting the intensity of MC-associated geomagnetic storms is crucial for space weather predictions.

Comparisons of Characteristics of Magnetic Clouds and Cloud-Like Structures During 1995 – 2012

Chin-Chun Wu, Ronald P. Lepping

Solar Phys. Volume 290, [Issue 4](#), pp 1243-1269 2015

Using eighteen years (1995 – 2012) of solar wind plasma and magnetic field data (observed by the *Wind* spacecraft), solar activity (e.g. sunspot number: SSN), and the geomagnetic-activity index (Dst), we have identified 168 magnetic clouds (MCs) and 197 magnetic-cloud-like structures (MCLs), and we have made relevant comparisons. The following features are found during seven different periods (TP: total period during 1995 – 2012, P1 and P2: first and second half-period during 1995 – 2003 and 2004 – 2012, Q1 and Q2: quiet periods during 1995 – 1997 and 2007 – 2009, A1 and A2: active periods during 1998 – 2006 and 2010 – 2012). (1) During the total period, the yearly occurrence frequency is 9.3 for MCs and 10.9 for MCLs. (2) In the quiet periods $\langle N_{MCs} \rangle_{Q1} > \langle N_{MCLs} \rangle_{Q1}$ and $\langle N_{MCs} \rangle_{Q2} > \langle N_{MCLs} \rangle_{Q2}$, but in the active periods $\langle N_{MCs} \rangle_{A1} < \langle N_{MCLs} \rangle_{A1}$ and $\langle N_{MCs} \rangle_{A2} < \langle N_{MCLs} \rangle_{A2}$. (3) The minimum B_z ($B_{z_{\min}}$) inside of an MC is well correlated with the intensity of geomagnetic activity, Dst_{\min} (minimum Dst found within a storm event) for MCs (with a Pearson correlation coefficient, c.c.=0.75, and the fitting function is $Dst_{\min} = 0.90 + 7.78 B_{z_{\min}}$), but $B_{z_{\min}}$ for MCLs is not well correlated with the Dst index (c.c.=0.56, and the fitting function is $Dst_{\min} = -9.40 + 4.58 B_{z_{\min}}$). (4) MCs play a major role in producing geomagnetic storms: the absolute value of the average Dst_{\min} ($\langle Dst_{\min} \rangle_{MC} = -70$ nT) for MCs associated geomagnetic storms is twice as strong as that for MCLs ($\langle Dst_{\min} \rangle_{MCL} = -35$ nT) because of the difference in the IMF (interplanetary magnetic field) strength. (5) The SSN is uncorrelated with MCs ($\langle N_{MCs} \rangle_{TP, c.c.} = 0.27$), but is well associated with MCLs ($\langle N_{MCLs} \rangle_{TP, c.c.} = 0.85$). Note that the c.c. for SSN vs. $\langle N_{MCs} \rangle_{P2}$ is higher than that for SSN vs. $\langle N_{MCLs} \rangle_{P2}$. (6) Averages of IMF, solar wind speed, and density inside of the MCs are higher than those inside of the MCLs. (7) The average of MC duration (≈ 18.82 hours) is ≈ 20 % longer than the average of MCL duration (≈ 15.69 hours). (8) There are more MCs than MCLs in the quiet solar period and more MCLs than MCs in the active solar period, probably as a result of the interaction between an MC and another significant interplanetary disturbance (including another MC), which could obviously change the character of an MC, but we speculate that some MCLs are no doubt due to other factors such as complex birth conditions at the Sun.

Analyses of the Evolution and Interaction of Multiple Coronal Mass Ejections and Their Shocks in July 2012

Wu, S. T.; Wu, C.; Liou, K.; Plunkett, S.; Dryer, M.; Fry, C. D.

Outstanding Problems in Heliophysics: From Coronal Heating to the Edge of the Heliosphere. Proceedings of a conference held 14-19 April 2013 at Myrtle Beach, South Carolina, USA. Edited by Qiang Hu and Gary P. Zank. **ASP Conference Series**, Vol. 484, 2014, p.241

The Sun has become more active since 2010 after a long-lasting solar minimum (2007-2009) between Cycle 23 and 24. Many Coronal Mass Ejections (CMEs) have been detected by current orbiting instruments on-board SOHO/LASCO and

STEREO-A and B. During the period of July 2012 three consecutive CMEs were observed on **July 17 (~13:54UT), July 18 (~06:24UT) and July 19 (~05:39UT)** from three different source regions on the solar surface located at S23W61, N18W180 and S17W92. Their corresponding average speeds were 802, 713, and 1160 km s⁻¹, respectively. Multiple interplanetary (IP) shocks and CMEs arrived at the twin STEREO-A/B, SOHO/LASCO, ACE and WIND spacecraft where STEREO-A and STEREO-B were orbiting near 121 degrees West and 114 degrees East of the Sun-Earth line. The orbit of ACE and SOHO/LASCO were at L1 and WIND was near the Sun-Earth line. This unique line-up gave us opportunity to test the simulation of CMEs propagation and its induced IP shocks. Thus, we have used a well-developed global three-dimensional magnetohydrodynamic (MHD) model (Wu et al. 2007a) to perform forward MHD modeling to investigate the evolution of these CMEs and IP shocks. Using simulation results together with observations we found that an IP shock driven by the July 18 CME arrived at STEREO-B first, another IP shock driven by the July 19 CME arrived at STEREO-A, then the flank of an IP shock driven by the July 17 CME arrived at Earth. The observations from both coronal images and in-situ solar wind measurements are used to assess the reality of the IP shock arrival time from the simulation.

Observations of Energetic Particles between a Pair of Corotating Interaction Regions

Z. **Wu**¹, Y. Chen¹, G. Li², L. L. Zhao², R. W. Ebert³, M. I. Desai^{3,4}, G. M. Mason⁵, B. Lavraud⁶, L. Zhao⁷, Y. C.-M. Liu⁸, F. Guo⁹, C. L. Tang¹, E. Landi⁷, and J. Sauvaud

2014 ApJ 781 17

We report observations of the acceleration and trapping of energetic ions and electrons between a pair of corotating interaction regions (CIRs). The event occurred in Carrington Rotation 2060. Observed by the STEREO-B spacecraft, the two CIRs were separated by less than 5 days. In contrast to other CIR events, the fluxes of the energetic ions and electrons in this event reached their maxima between the trailing edge of the first CIR and the leading edge of the second CIR. The radial magnetic field (B_r) reversed its sense and the anisotropy of the flux also changed from Sunward to anti-Sunward between the two CIRs. Furthermore, there was an extended period of counterstreaming suprathermal electrons between the two CIRs. Similar observations for this event were also obtained with the Advanced Composition Explorer and STEREO-A. We conjecture that these observations were due to a U-shaped, large-scale magnetic field topology connecting the reverse shock of the first CIR and the forward shock of the second CIR. Such a disconnected U-shaped magnetic field topology may have formed due to magnetic reconnection in the upper corona.

Global three-dimensional simulation of the interplanetary evolution of the observed geoeffective coronal mass ejection during the epoch 1-4 August 2010

Wu, Chin-Chun; Dryer, Murray; Wu, S. T.; Wood, Brian E.; Fry, Craig D.; Liou, Kan; Plunkett, Simon J. *Geophys. Res.*, Vol. 116, No. A12, A12103, **2011**

<http://onlinelibrary.wiley.com/doi/10.1029/2011JA016947/pdf>

Several coronal mass ejections (CMEs) were observed during **1-4 August 2010**. At ~17:12 UT on 3 August 2010, the Wind spacecraft detected an interplanetary shock followed by two magnetic cloud-like (MCL) structures that induced geomagnetic activity. The geomagnetic index, Dst, dropped to -65 nT while one of the MCLs passed through the magnetosphere. A global, three-dimensional magnetohydrodynamic (MHD) numerical model and a kinematic model (HAFv.2), with inputs based on actual solar observations, were used to simulate the response of the three-dimensional heliosphere. HAFv.2 and MHD models were used to simulate regions from 2.5 to 18 solar radii (Rs) and 18 to 285 Rs, respectively. A velocity pulse was used to simulate the major CME on 1 August 2010. The solar disturbances were injected into the lower boundary at 2.5 Rs. It is found that the background solar wind plays an important role in the evolution of this CME on its way to Earth. We compared the derived solar wind parameters (density, velocity, magnetic field, and temperature) with in situ observations from Wind near Earth. The simulation demonstrates a useful tool to link the general case of ICME at 1 AU to their solar sources. Simulation results also show that adiabatic value of $\gamma = 5/3$ seems to be appropriate for ideal MHD simulation studies of solar wind at 1 AU.

Imaging interplanetary CMEs at radio frequency from solar polar orbit

Ji **Wu**, Weiyang Sun, Jianhua Zheng, Cheng Zhang, Hao Liu, Jingye Yan, Chi Wang, Chuanbing Wang and Shui Wang

Advances in Space Research, Volume 48, Issue 5, 1 September **2011**, Pages 943-954

https://ac.els-cdn.com/S0273117711003115/1-s2.0-S0273117711003115-main.pdf?_tid=978179cb-4883-4c23-9058-85abe16f054d&acdnat=1527596765_9d0080a91ff0ab39de21aa6fabcedffb

Coronal mass ejections (CMEs) represent a great concentration of mass and energy input into the lower corona. They have come to be recognized as the major driver of physical conditions change in the Sun-Earth system. Consequently, observations of CMEs are important for understanding and ultimately predicting space weather conditions. This paper

discusses a proposed mission, the Solar Polar Orbit Radio Telescope (**SPORT**) mission, which will observe the propagation of interplanetary CMEs to distances of near 0.35 AU from the Sun. The orbit of SPORT is an elliptical solar polar orbit. The inclination angle between the orbit and ecliptic plane should be about 90°. The main payload on board SPORT will be an imaging radiometer working at the meter wavelength band (radio telescope), which can follow the propagation of interplanetary CMEs. The images that are obtained by the radio telescope embody the brightness temperature of the objectives. Due to the very large size required for the antenna aperture of the radio telescope, we adopt interferometric imaging technology to reduce it. Interferometric imaging technology is based on indirect spatial frequency domain measurements plus Fourier transformation. The SPORT spacecraft will also be equipped with a set of optical and in situ measurement instruments such as a EUV solar telescope, a solar wind ion instrument, an energetic particle detector, a magnetometer, a wave detector and a solar radio burst spectrometer.

Statistical Comparison of Magnetic Clouds with Interplanetary Coronal Mass Ejections for Solar Cycle 23

Chin-Chun **Wu** · R.P. Lepping

Solar Phys (2011) 269: 141–153, **File**

We compare the number and characteristics of interplanetary coronal mass ejections (ICMEs) to those of magnetic clouds (MCs) by using *in-situ* solar wind plasma and magnetic field observations made at 1 AU during solar cycle 23.

We found that $\approx 28\%$ of ICMEs appear to contain MCs, since 103 magnetic clouds (MCs) occurred during 1995 – 2006, and 307 ICMEs occurred during 1996 – 2006. For the period between 1996 and 2006, 85 MCs are identified as part of ICMEs, and six MCs are not associated with ICMEs, which conflicts with the idea that MCs are usually a subset of ICMEs. It was also found that solar wind conditions inside MCs and ICMEs are usually similar, but the linear correlation between geomagnetic storm intensity (Dst_{min}) and relevant solar wind parameters is better for MCs than for ICMEs. The differences between average event duration ($\langle t \rangle$) and average proton plasma β ($\langle \beta \rangle$) are two of the major differences between MCs and ICMEs: *i*) the average duration of ICMEs (29.6 h) is 44% longer than for MCs (20.6 hours), and *ii*) the average of $\langle \beta \rangle$ is 0.01 for MCs and 0.24 for ICMEs. The difference between the definition of a MC and that for an ICME is one of the major reasons for these average characteristics being different (*i.e.*, listed above as items *i*) and *ii*)), and it is the reason for the frequency of their occurrences being different.

Comparison of the Characteristics of Magnetic Clouds and Magnetic Cloud-Like Structures for the Events of 1995-2003

Chin-Chun **Wu**, R. P. Lepping

Solar Phys., 242(1-2), Page: 159 – 165, **2007**

Three-dimensional global simulation of interplanetary coronal mass ejection propagation from the Sun to the heliosphere: Solar event of 12 May 1997,

Wu, C., C. D. Fry, S. T. Wu, M. Dryer, and K. Liou (2007)

J. Geophys. Res., 112, A09104, **2007**

<http://dx.doi.org/10.1029/2006JA012211>

RELATIONSHIPS AMONG MAGNETIC CLOUDS, CMES, AND GEOMAGNETIC STORMS

C.C. **WU**, R.P. LEPPING and N. GOPALSWAMY

Solar Physics (2006) 239: 449–460, **File**

During solar cycle 23, 82 interplanetary magnetic clouds (MCs) were identified by the Magnetic Field Investigation (MFI) team using *Wind* (1995 – 2003) solar wind plasma and magnetic field data from solar minimum through the maximum of cycle 23. The average occurrence rate is 9.5 MCs per year for the overall period. It is found that some of the anomalies in the frequency of occurrence were during the early part of solar cycle 23: (i) only four MCs were observed in 1999, and (ii) an unusually large number of MCs (17 events) were observed in 1997, just after solar minimum. We also discuss the relationship between MCs, coronal mass ejections (CMEs), and geomagnetic storms. During the period 1996 – 2003, almost 8000 CMEs were observed

by SOHO-LASCO. The occurrence frequency of MCs appears to be related neither to the occurrence of CMEs as observed by SOHO LASCO nor to the sunspot number. When we included “magnetic cloud-like structures” (MCLs, defined by Lepping, Wu, and Berdichevsky, 2005), we found that the occurrence of the joint set (MCs+MCLs) is correlated with both sunspot number and the occurrence rate of CMEs. The average duration of the MCL structures is ~40% shorter than that of the MCs. The MCs are typically more geoeffective than the MCLs, because the average southward field component is generally stronger and longer lasting in MCs than in MCLs. In addition, most severe storms caused by MCs/MCLs with $Dst_{min} \leq -100$ nT occurred in the active solar period.

Relationships for predicting magnetic cloud-related geomagnetic storm intensity

Wu, C.-C.; Lepping, R. P.

Journal of Atmospheric and Solar-Terrestrial Physics, Volume 67, Issue 3, p. 283-291, **2005**.

Studying geomagnetic storm activity during 135 interplanetary magnetic cloud periods from 1965 to 1998, Wu and Lepping (J. Geophys. Res. 107 (2002b) 1346) found that the storm Dst index correlated well with both the interplanetary magnetic field z-component (Bz) and the “rectified” electric field VBs but did not correlate well with solar wind speed. It is shown that the role of magnetic cloud speed in predicting storm intensity is a minor one. It also was found that the correlation coefficient for Dst vs. Bz increases dramatically when the solar wind speed exceeds 600 km/s. This implies that solar wind speed is also important indirectly for predicting the storm intensity when using Bz (or VBs) as a direct predictor. Using the same data set of 135 magnetic cloud-associated storms, two Dst prediction-relationships were developed: one is velocity independent and the other is velocity dependent. In this study, (i) both Dst prediction-relationships will be presented and (ii) some recent storm events will be presented and discussed by (as examples) using both Dst prediction-relationships. The results of this study also show: (1) The intensity of a magnetic storm which is associated with a magnetic cloud is predictable. (2) The prediction relationships for storm intensity, Dst_{min} are: $Dst_{min} = 0.83 + 7.85 \times Bz_{min}$ and $Dst_{min} = -16.48 - 12.89 \times (VBs)_{max}$. (3) The velocity dependence of the Dst_{min} prediction relationship will improve the accuracy for a Bz-base prediction result. (4) For the $(VBs)_{max}$ -based prediction relationship, the prediction accuracy of Dst_{min} becomes worse when a velocity-dependent prediction relationship is used.

The Imprint of Intermittent Interchange Reconnection on the Solar Wind

Peter F. **Wyper**¹, C. R. DeVore², S. K. Antiochos², D. I. Pontin³, Aleida K. Higginson², Roger Scott⁴, Sophie Masson^{5,6}, and Theo Pelegrin-Frachon⁵

2022 ApJL 941 L29

<https://iopscience.iop.org/article/10.3847/2041-8213/aca8ae/pdf>

The solar wind is known to be highly structured in space and time. Observations from Parker Solar Probe have revealed an abundance of so-called magnetic switchbacks within the near-Sun solar wind. In this Letter, we use a high-resolution, adaptive-mesh, magnetohydrodynamics simulation to explore the disturbances launched into the solar wind by intermittent/bursty interchange reconnection and how they may be related to magnetic switchbacks. We find that repeated ejection of plasmoid flux ropes into the solar wind produces a curtain of propagating and interacting torsional Alfvénic waves. We demonstrate that this curtain forms when plasmoid flux ropes dynamically realign with the radial field as they are ejected from the current layer and that this is a robust effect of the 3D geometry of the interchange reconnection region. Simulated flythroughs of this curtain in the low corona reveal an Alfvénic patch that closely resembles observations of switchback patches, but with relatively small magnetic field deflections. Therefore, we suggest that switchbacks could be the solar wind imprint of intermittent interchange reconnection in the corona, provided an in situ process subsequently amplifies the disturbances to generate the large deflections or reversals of radial field that are typically observed. That is to say, our results indicate that a combination of low-coronal and inner-heliospheric mechanisms may be required to explain switchback observations.

First Application of a Theoretically Derived Coupling Function in Cosmic-Ray Intensity for the Case of the 10 September 2017 Ground-Level Enhancement (GLE 72)

L. **Xaplanteris**, [M. Gerontidou](#), [H. Mavromichalaki](#), [J. V. Rodriguez](#), [M. Livada](#), [M. K. Georgoulis](#), [T. E. Sarris](#), [V. Spanos](#) & [L. Dorman](#)

[Solar Physics](#) volume 297, Article number: 73 (2022)

<https://doi.org/10.1007/s11207-022-02009-1>

In this work we implement an analytically derived coupling function between ground-level and primary proton particles for the case of ground-level enhancement events (GLEs). The main motivation for this work is to determine whether this coupling function is suitable for the study of both major cases of cosmic-ray (CR) variation events, namely GLEs and

Forbush decreases. This version of the coupling function, which relies on formalism used in quantum field theory (QFT) computations, has already been applied to Forbush decreases yielding satisfactory results. In this study, it is applied to a GLE event that occurred on 10 September 2017. For the analytical derivations, normalized ground-level cosmic-ray data were used from seven neutron-monitor stations with low cutoff rigidities. To assess and evaluate the results for the normalized proton intensity, we benchmark them with the time series for the proton flux, as recorded by the GOES 13 spacecraft during the same time period. The theoretically calculated results for proton energy ≥ 1 GeV are in general agreement with the recorded data for protons with energy >700 MeV, presenting a least-squares linear best fit with slope 0.75 ± 0.17 and a Pearson correlation coefficient equal to 0.62. We conclude that the coupling function presented in this work is the first coupling function that is well applicable to both cases of cosmic-ray intensity events, namely GLEs and Forbush decreases.

Improved Approach in the Coupling Function Between Primary and Ground Level Cosmic Ray Particles Based on Neutron Monitor Data

L. Xaplanteris, M. Livada, H. Mavromichalaki, L. Dorman, M. K. Georgoulis & T. E. Sarris

Solar Physics volume 296, Article number: 91 (2021)

<https://link.springer.com/content/pdf/10.1007/s11207-021-01836-y.pdf>

<https://doi.org/10.1007/s11207-021-01836-y>

In this work an improved approach of existing approximations on the coupling function between primary and ground-level cosmic-ray particles is presented. The proposed coupling function is analytically derived based on a formalism used in Quantum Field Theory calculations. It is upgraded compared to previous versions with the inclusion of a wider energy spectrum that is extended to lower energies, as well as an altitude correction factor, also derived analytically. The improved approximations are applied to two cases of Forbush decreases detected in March 2012 and September 2017. In the analytical procedure for the derivation of the primary cosmic-ray spectrum during these events, we also consider the energy spectrum exponent γ to be varied with time. For the validation of the findings, we present a direct comparison between the primary spectrum and the amplitude values derived by the proposed method and the obtained time series of the cosmic-ray intensity at the rigidity of 10 GV obtained from the Global Survey Method. The two sets of results are found to be in very good agreement for both events as denoted by the Pearson correlation factors and slope values of their scatter plots. In such way we determine the validity and applicability of our method to Forbush decreases as well as to other cosmic-ray phenomena, thus introducing a new, alternative way of inferring the primary cosmic-ray intensity.
7-15 Mar 2012, 8-11 Sep 2017

Solar wind re-acceleration in local current sheets and their diagnostics from observations

Qian Xia and Valentina Zharkova

EGU2020-9446 May 2020

<https://meetingorganizer.copernicus.org/EGU2020/displays/36057>

We explore solar wind re-acceleration during their passage through reconnecting current sheets in the interplanetary space using the particle-in-cell approach. We investigate particle acceleration in 3D Harris-type reconnecting current sheets with a single or multiple X-nullpoints taking into account the ambient plasma feedback to the presence of accelerated particles. We also consider coalescent and squashed magnetic islands formed in the current sheets with different magnetic field topologies, thickness, ambient density, and mass ratios. With the PIC approach, we detected distinct populations of two groups of particles, transit and bounced ones, which have very different energy and asymmetric pitch-angle distributions associated with the magnetic field parameters. We present a few cross-sections of the simulated pitch-angle distributions of accelerated particles and compare them with the in-situ observations of solar wind particles. This comparison indicates that locally generated superthermal electrons can account for the counter-streaming 'strahls' often observed in pitch-angle distribution spectrograms of the satellites crossing heliospheric current sheets.

Presentation #9446 <https://presentations.copernicus.org/EGU2020/presentations-ST1.7.zip>

Temporal Evolution of the Rotation of the Interplanetary Magnetic Field B_x , B_y , and B_z Components

N. B. Xiang^{1,2,5}, Z. J. Ning², and F. Y. Li^{3,4}

2020 ApJ 896 12

<https://doi.org/10.3847/1538-4357/ab91bc>

The daily interplanetary magnetic field (IMF) B_x , B_y , and B_z components from 1967 January 1 to 2018 December 31 listed in the OMNI database are used to investigate their periodicity and study temporal variation of their rotation cycle lengths through continuous wavelet transform, autocorrelation, and cross-correlation analyses. The dominant

rotation period in each of the daily B_x , B_y , and B_z components is 27.4 days, implying the existence of rotational modulation in the three time series. The dependence of the rotation cycle lengths for both B_x and B_y components on solar cycle phase almost shows the same result. The rotation cycle lengths for both B_x and B_y components increase from the start to the first year of a new Schwabe cycle, then decrease gradually from the first to the fourth year, and finally fluctuate around the 27.4-day period within a small amplitude from the fourth year to the end of the Schwabe solar cycle. For the B_z component, its rotation cycle length does not show such a solar cycle variation. The significant periods in the variation of B_x rotation are 2.9, 3.4, 4.3, 4.9, 10.5, and 11.9 yr, and there exist significant periods of 3.4, 9.9, and 14.1 yr in the variation of B_y rotation. The relationship of solar activity with B_x and B_y components is complex. The possible mechanisms for the temporal variation of the rotation period of the three components are discussed.

Plasma and Magnetic-Field Characteristics of Magnetic Decreases in the Solar Wind at 1 AU: Cluster-C1 Observations

T. **Xiao**, Q. Q. Shi, A. M. Tian, W. J. Sun, H. Zhang, X. C. Shen, W. S. Shang, A. M. Du
Solar Physics, Volume 289, Issue 8, pp 3175-3195 2014

Magnetic decreases (MDs) are structures observed in interplanetary space with significant decreases in magnetic-field magnitude. Events with little or no change in the field direction are called linear magnetic decreases (LMDs), the others are called nonlinear MDs (NMDs). In this article we focus on LMD and NMD trains, where LMD trains are defined as at least three LMDs in a row and NMD trains as trains (\geq three MDs in a row) that are not all linear. If the temporal separation between two MDs was shorter than five minutes, they were considered as one train event. A total of 16 273 MD trains (including 897 LMD trains and 15 376 NMD trains) were identified and studied. The details of the background magnetic-field and plasma (e.g. ion-density and velocity) features were examined and compared with the average solar-wind properties. LMD trains are found to occur in regions with relatively low magnetic-field strengths, high ion-number densities, and large plasma β s (ratio of the plasma thermal pressure to the magnetic pressure). In sharp contrast, NMD trains have plasma properties similar to the average solar wind. Forty-three LMD trains are related to interplanetary coronal mass ejections (ICMEs) (including 19 events that occurred in ICME sheaths and 24 in the ICME proper), while 222 LMD trains occurred in corotating interaction regions (CIRs), and the remaining 632 events in the normal solar wind. The LMD trains that occurred in ICME sheaths are thought to be associated with the generation mechanism of the mirror-mode instability. Only 552 of the NMD trains are related to ICMEs (including 236 events in ICME sheaths and 316 in ICMEs proper), while 3889 (25 %) NMD trains occurred in CIRs, and the remaining 71 % occurred in the normal solar wind. Because the NMD trains have various plasma properties that differ from the LMD trains, we suggest that NMD trains may be generated by different mechanisms, for instance by a steepening of Alfvén waves.

The Structural Connection between Coronal Mass Ejection Flux Ropes near the Sun and at 1 au

H. **Xie**^{1,2}, N. Gopalswamy², and S. Akiyama^{1,2}
2021 ApJ 922 64

<https://doi.org/10.3847/1538-4357/ac23cc>

We have performed the first comprehensive statistical analysis comparing flux rope (FR) structures of coronal mass ejections (CMEs) near the Sun and at 1 au, using Solar and Heliospheric Observatory and Solar Terrestrial Relations Observatory measurements for the two full solar cycles 23 and 24. This study aims to investigate the physical connection of 102 magnetic FRs among solar source regions, CMEs in the extended corona, and magnetic clouds (MCs) near Earth. Our main results are as follows: (1) We confirmed that the hemispheric-helicity rule holds true for $\sim 87\%$ of our 102 events. For the 13 events that do not follow this rule, the FR axis directions and helicity signs can be inferred from soft X-ray and extreme ultraviolet images and magnetogram data in the source regions (e.g., coronal arcade skews, Fe xii stalks, sigmoids, and magnetic tongues). (2) Around 25% of the 102 events have rotations $>40^\circ$ between the MC and CME-FR axial orientations. (3) For $\sim 56\%$ of these rotational events, the FR rotations occurred within the COR2 field of view, which can be predicted from the CME tilts obtained from FR fitting models. In addition, we found that for 89% of the 19 stealth CMEs under study, we were able to use coronal neutral line locations and tilts to predict the FR helicity and its axial direction in the MCs. The above results should help improve the prediction of FR structures in situ. We discuss their implications on space weather forecasts.

Understanding shock dynamics in the inner heliosphere with modeling and type ii radio data: a statistical study†

H. **Xie**, O. C. St. Cyr, N. Gopalswamy, D. Odstrcil, H. Cremades

JGR, 2013, File

See <http://www.youtube.com/watch?v=QAs73yvZ7eY>

[1] We study two methods of predicting interplanetary (IP) shock location and strength in the inner heliosphere: 1) the ENLIL simulation and 2) the kilometric type II (kmTII) prediction. To evaluate differences in the performance of the first method, we apply two sets of CME parameters from the cone model fitting and flux-rope (FR) model fitting as input to the ENLIL model for 16 halo CMEs. The results show that the ENLIL model using the actual CME speeds from FR-fit provided an improved shock arrival time (SAT) prediction. The mean prediction errors for the FR and cone-model inputs are 4.90 ± 5.92 hr and 5.48 ± 6.11 hr, respectively. A deviation of 100 kms⁻¹ from the actual CME speed has resulted in a SAT error of 3.46 hr on average.

[2] The simulations show that the shock dynamics in the inner heliosphere agrees with the drag-based model. The shock acceleration can be divided as two phases: a faster deceleration phase within 50Rs and a slower deceleration phase at distances beyond 50Rs. The linear fit deceleration in phase 1 is about one order magnitude larger than that in phase 2. When applying the kmTII method to 14 DH-km CMEs, we found that combining the kmTII method with the ENLIL outputs improved the kmTII prediction. Due to a better modeling of plasma density upstream of shocks and the kmTII location, we are able to provide a more accurate shock time-distance and speed profiles.

[3] The mean kmTII prediction error using the ENLIL model density is 6.7 ± 6.4 hr; it is 8.4 ± 10.4 hr when the average solar wind plasma density is used. Applying the ENLIL density has reduced the mean kmTII prediction error by ~ 2 hr and the standard deviation by 4.0 hr. Especially, when we applied the combined approach to two interacting events, the kmTII prediction error was drastically reduced from 29.6 hr to -4.9 hr in one case and 10.6 hr to 4.2 hr in the other. Furthermore, the results derived from the kmTII method and the ENLIL simulation, together with white-light data, provide a valuable validation of shock formation location and strength. Such information has important implications for SEP acceleration.

Table 1. Summary of the Properties of the 16 Halo CME/Shocks and the ENLIL Predictions^a

Table 2. Summary of the Properties of the 14 DH-km CME/Shocks, ENLIL, and kmTII Predictions^a

Table 3. Summary of the Properties of CMEs for Interacting Events^a

Near-Sun Flux-Rope Structure of CMEs

H. Xie, N. Gopalswamy, O. C. St. Cyr

Solar Physics, May 2013, Volume 284, Issue 1, pp 47-58

We have used the Krall flux-rope model (Krall and St. Cyr, *Astrophys. J.* 2006, 657, 1740) (KFR) to fit 23 magnetic cloud (MC)-CMEs and 30 non-cloud ejecta (EJ)-CMEs in the Living With a Star (LWS) Coordinated Data Analysis Workshop (CDAW) 2011 list. The KFR-fit results shows that the CMEs associated with MCs (EJs) have been deflected closer to (away from) the solar disk center (DC), likely by both the intrinsic magnetic structures inside an active region (AR) and ambient magnetic structures (e.g. nearby ARs, coronal holes, and streamers, etc.). The mean absolute propagation latitudes and longitudes of the EJ-CMEs (18° , 11°) were larger than those of the MC-CMEs (11° , 6°) by 7° and 5° , respectively. Furthermore, the KFR-fit widths showed that the MC-CMEs are wider than the EJ-CMEs. The mean fitting face-on width and edge-on width of the MC-CMEs (EJ-CMEs) were 87 (85°) and 70 (63°), respectively. The deflection away from DC and narrower angular widths of the EJ-CMEs have caused the observing spacecraft to pass over only their flanks and miss the central flux-rope structures. The results of this work support the idea that all CMEs have a flux-rope structure.

Understanding shock dynamics in the inner heliosphere with modeling and Type II radio data: The 2010-04-03 event

Xie, H.; Odstrcil, D.; Mays, L.; St. Cyr, O. C.; Gopalswamy, N.; Cremades, H.

J. Geophys. Res., Vol. 117, No. A4, A04105, 2012, **preprint File**

<http://dx.doi.org/10.1029/2011JA017304>

The 2010 April 03 solar event was studied using observations from STEREO SECCHI, SOHO LASCO, and Wind kilometric Type II data (kmTII) combined with WSA-Cone-ENLIL model simulations performed at the Community Coordinated Modeling Center (CCMC). In particular, we identified the origin of the coronal mass ejection (CME) using STEREO EUVI and SOHO EIT images. A flux-rope model was fit to the SECCHI A and B, and LASCO images to determine the CME's direction, size, and actual speed. J-maps from STEREO COR2/HI-1/HI-2 and simulations from CCMC were used to study the formation and evolution of the shock in the inner heliosphere. In addition, we also studied the time-distance profile of the shock propagation from kmTII radio burst observations. The J-maps together with in-situ data from the Wind spacecraft provided an opportunity to validate the simulation results and the kmTII prediction. Here we report on a comparison of two methods of predicting interplanetary shock arrival time: the ENLIL model and the

kmTII method; and investigate whether or not using the ENLIL model density improves the kmTII prediction. We found that the ENLIL model predicted the kinematics of shock evolution well. The shock arrival times (SAT) and linear-fit shock velocities in the ENLIL model agreed well with those measurements in the J-maps along both the CME leading edge and the Sun-Earth line. The ENLIL model also reproduced most of the large scale structures of the shock propagation and gave the SAT prediction at Earth with an error of $\sim 1 \pm 7$ hours. The kmTII method predicted the SAT at Earth with an error of ~ 15 hours when using $n_0 = 4.16 \text{ cm}^{-3}$, the ENLIL model plasma density near Earth; but it improved to ~ 2 hours when using $n_0 = 6.64 \text{ cm}^{-3}$, the model density near the CME leading edge at 1 AU.

Modeling and prediction of fast CME/shocks associated with type II bursts

H. Xie, N. Gopalswamy² and O. C. St. Cyr

Proceedings of the International Astronomical Union / Volume 4 / Symposium S257, pp 489 – 491,

Published online: 16 Mar 2009

<http://journals.cambridge.org/action/displayIssue?iid=4866212>

A numerical simulation with ENLIL+Cone model was carried out to study the propagation of the shock driven by the **2005 May 13** CME. We then conducted a statistical analysis on a subset of similar events, where a decameter-hectometric (DH) type II radio burst and a counterpart kilometric type II have been observed to be associated with each CME (DHkm CME). The simulation results show that fast CME-driven shocks experienced a rapid deceleration as they propagated through the corona and then kept a nearly constant speed traveling out into the heliosphere. Two improved methods are proposed to predict the fast CME-driven shock arrival time, which give the prediction errors of 3.43 and 6.83 hrs, respectively.

Effects of solar wind dynamic pressure and preconditioning on large geomagnetic storms.

Xie, H., Gopalswamy, N., Cyr, O.C.S., Yashiro, S.:

2008, Geophys. Res. Lett. 35(6), 6. DOI.

<https://agupubs.onlinelibrary.wiley.com/doi/pdf/10.1029/2007GL032298>

We investigate the effects of solar wind dynamic pressure, P_{dyn} , and preconditioning in 88 large magnetic storms ($\text{Dst} < -100 \text{ nT}$) occurring during solar cycle 23. We have developed an improved model of the Dst profile, based on a modified Burton equation, where additional effects of P_{dyn} and diminished Dst pressure-correction have been taken into account. On the average, our model predicts the Dst peak values within 9% of observations and gives an overall RMS error of 11%, which is an improvement over those models whose injection functions only depend on the solar wind electric field. The results demonstrate that there is an increase in the Dst peak value when there is a large enhancement of P_{dyn} during the main phase of a storm. The average increase of the storm intensity is estimated to be 26% for 15 storms with the max ($P_{\text{dyn}} > 15 \text{ nPa}$). We find that the preconditioning in multi-step Dst storms plays no significant role in strengthening the storm intensity, but increases the storm duration.

THE EFFECT OF THE HELIOSPHERIC CURRENT SHEET ON INTERPLANETARY SHOCKS

YANQIONG XIE, FENGSI WEI, CHANGQING XIANG and XUESHANG FENG

Solar Physics (2006) 238: 377–390, **2006**, File

Long-lived geomagnetic storms and coronal mass ejections

H. Xie,^{1,2} N. Gopalswamy,³ P. K. Manoharan,⁴ A. Lara,⁵ S. Yashiro,^{1,2} and S. Lepri

JOURNAL OF GEOPHYSICAL RESEARCH, VOL. 111, A01103, doi:10.1029/2005JA011287, **2006**, File

Coronal mass ejections (CMEs) are major solar events that are known to cause large geomagnetic storms ($\text{Dst} < -100 \text{ nT}$). Isolated geomagnetic storms typically have a main phase of 3–12 hours and a recovery phase of around 1 day. However, there are some storms with main and recovery phases exceeding 3 days. We trace the origin of these long-lived geomagnetic storms (LLGMS) to frontside halo CMEs. We studied 37 LLGMS events with $\text{Dst} < -100 \text{ nT}$ and the associated CMEs which occurred during 1998–2002. It is found that LLGMS events are caused by (1) successive CMEs, accounting for 64.9% (24 of 37); (2) single CMEs, accounting for 21.6% (8 of 37); and (3) highspeed streams (HSS) in corotating interaction regions (CIRs) with no related CME, accounting for 13.5% (5 of 37). The long duration of the LLGMS events was found to be due to successive CMEs and HSS events; the high intensity of the LLGMS events was related to the interaction of CMEs with other CMEs and HSS events. We find that the duration of LLGMS is well correlated to the number of participating CMEs (correlation coefficient $r = 0.78$). We also find that the intensity of LLGMS has a good correlation with the degree of interaction (the number of CMEs interacting with a HSS event or with themselves) ($r = 0.67$). The role of preconditioning in LLGMS events, where the Dst development occurred in multiple

steps in the main and recovery phases, has been investigated. It is found that preconditioning does not affect the main phase of the LLGMS events, while it plays an important role during the recovery phase of the LLGMS events.

Interplanetary Scintillation Observation and Space Weather Modelling

Review

Ming Xiong, Xueshang Feng, Bo Li, Jiansen He, Wei Wang, +++

Front. Astron. Space Sci., 10: 1159166 2023

<https://www.frontiersin.org/articles/10.3389/fspas.2023.1159166/pdf>

Interplanetary scintillation (IPS) refers to random fluctuations in radio intensity of distant small-diameter celestial object, over time periods of the order of 1 s. The scattering and scintillation of emergent radio waves are ascribed to turbulent density irregularities transported by the ubiquitous solar wind streams. The spatial correlation length of density irregularities and the Fresnel radius of radio diffraction are two key parameters in determining the scintillation pattern. Such a scintillation pattern can be measured and correlated between multi-station radio telescopes on the Earth. Using the “phase-changing screen” scenario based on the Born approximation, the bulk-flow speed and turbulent spectrum of the solar wind streams can be extracted from the single-station power spectra fitting and the multi-station cross-correlation analysis. Moreover, a numerical computer-assisted tomography (CAT) model, iteratively fit to a large number of IPS measurements over one Carrington rotation, can be used to reconstruct the global velocity and density structures in the inner heliosphere for the purpose of space weather modelling and prediction. In this review, we interpret the underlying physics governing the IPS phenomenon caused by the solar wind turbulence, describe the power spectrum and cross correlation of IPS signals, highlight the space weather application of IPS-CAT models, and emphasize the significant benefits from international cooperation within the Worldwide IPS Stations (WIPSS) network. Stations (WIPSS) network.

Prospective White-light Imaging and In Situ Measurements of Quiescent Large-scale Solar-wind Streams from the Parker Solar Probe and Solar Orbiter

Ming Xiong^{1,2,3}, Jackie A. Davies⁴, Xueshang Feng^{1,2}, Bo Li⁵, Liping Yang^{1,2}, Lidong Xia⁵, Richard A. Harrison⁴, Keiji Hayashi^{1,6}, Huichao Li^{1,3}, and Yufen Zhou^{1,2}

2018 ApJ 868 137

Deep-space exploration of the inner heliosphere is in an unprecedented golden age, with the recent and forthcoming launches of the Parker Solar Probe (PSP) and Solar Orbiter (SolO) missions, respectively. In order to both predict and understand the prospective observations by PSP and SolO, we perform forward MHD modeling of the 3D inner heliosphere at solar minimum, and synthesize the white-light (WL) emission that would result from Thomson scattering of sunlight from the coronal and heliospheric plasmas. Both solar rotation and spacecraft trajectory should be considered when reconstructing quiescent large-scale solar-wind streams from PSP and SolO WL observations. When transformed from a static coordinate system into a corotating one, the elliptical orbit of PSP becomes a multiwinding spiral. The innermost spiral winding of this corotating PSP orbit takes the form of a closed “heart shape” within around $80 R_{\odot}$ of the Sun. PSP, when traveling along this “heart-shaped” trajectory, can cross a single corotating interaction region (CIR) twice. This enables in situ measurements of the same CIR to be made in both the corona and heliosphere. As PSP approaches perihelion, the WL radiance from the corona increases. Polarization can be used to localize the main WL scattering region in the corona. Large-scale structures around PSP can be further resolved in the longitudinal dimension, using additional WL imagery from the out-of-ecliptic perspective of SolO. Coordinated observations between PSP and SolO are very promising in the quest to differentiate background CIRs from transient ejecta.

Prospective Out-of-ecliptic White-light Imaging of Coronal Mass Ejections Traveling through the Corona and Heliosphere

Ming Xiong (熊明)^{1,2,3}, Jackie A. Davies⁴, Richard A. Harrison⁴, Yufen Zhou (周玉芬)^{1,2}, Xueshang

Feng (冯学尚)^{1,2}, Lidong Xia (夏利东)⁵, Bo Li (李波)⁵, Ying D. Liu (刘颖)^{1,3}, Keiji

Hayashi (林启志)^{1,6}, Huichao Li

2018 ApJ 852 111

<http://sci-hub.tw/10.3847/1538-4357/aaa028>

The in-flight performance of the Coriolis/SMEI and STEREO/HI instruments substantiates the high-technology readiness level of white-light (WL) imaging of coronal mass ejections (CMEs) in the inner heliosphere. The WL intensity of a propagating CME is jointly determined by its evolving mass distribution and the fixed Thomson-scattering geometry. From their in-ecliptic viewpoints, SMEI and HI, the only heliospheric imagers that have been flown to date, integrate the longitudinal dimension of CMEs. In this paper, using forward magnetohydrodynamic modeling, we synthesize the WL radiance pattern of a typical halo CME viewed from an out-of-ecliptic (OOE) vantage point. The

major anatomical elements of the CME identified in WL imagery are a leading sheath and a trailing ejecta; the ejecta-driven sheath is the brightest feature of the CME. The sheath, a three-dimensional (3D) dome-like density structure, occupies a wide angular extent ahead of the ejecta itself. The 2D radiance pattern of the sheath depends critically on viewpoint. For a CME modeled under solar minimum conditions, the WL radiance pattern of the sheath is generally a quasi-straight band when viewed from an in-ecliptic viewpoint and a semicircular arc from an OOE viewpoint. The dependence of the radiance pattern of the ejecta-driven sheath on viewpoint is attributed to the bimodal nature of the 3D background solar wind flow. Our forward-modeling results suggest that OOE imaging in WL radiance can enable (1) a near-ecliptic CME to be continuously tracked from its coronal initiation, (2) the longitudinal span of the CME to be readily charted, and (3) the transporting speed of the CME to be reliably determined. Additional WL polarization measurements can significantly limit the ambiguity of localizing CMEs. We assert that a panoramic OOE view in WL would be highly beneficial in revealing CME morphology and kinematics in the hitherto-unresolved longitudinal dimension and hence for monitoring the propagation and evolution of near-ecliptic CMEs for space weather operations.

Prospective Out-of-ecliptic White-light Imaging of Interplanetary Corotating Interaction Regions at Solar Maximum

Ming **Xiong**^{1,2,3}, Jackie A. Davies⁴, Bo Li⁵, Liping Yang^{1,2}, Ying D. Liu^{1,3}, Lidong Xia⁵, Richard A. Harrison⁴, Hayashi Keiji^{1,6}, and Huichao Li

2017 ApJ 844 76

<http://sci-hub.cc/10.3847/1538-4357/aa7aaa>

Interplanetary corotating interaction regions (CIRs) can be remotely imaged in white light (WL), as demonstrated by the Solar Mass Ejection Imager (SMEI) on board the Coriolis spacecraft and Heliospheric Imagers (HIs) on board the twin Solar TERrestrial RELations Observatory (STEREO) spacecraft. The interplanetary WL intensity, due to Thomson scattering of incident sunlight by free electrons, is jointly determined by the 3D distribution of electron number density and line-of-sight (LOS) weighting factors of the Thomson-scattering geometry. The 2D radiance patterns of CIRs in WL sky maps look very different from different 3D viewpoints. Because of the in-ecliptic locations of both the STEREO and Coriolis spacecraft, the longitudinal dimension of interplanetary CIRs has, up to now, always been integrated in WL imagery. To synthesize the WL radiance patterns of CIRs from an out-of-ecliptic (OOE) vantage point, we perform forward magnetohydrodynamic modeling of the 3D inner heliosphere during Carrington Rotation CR1967 at solar maximum. The mixing effects associated with viewing 3D CIRs are significantly minimized from an OOE viewpoint. Our forward modeling results demonstrate that OOE WL imaging from a latitude greater than 60° can (1) enable the garden-hose spiral morphology of CIRs to be readily resolved, (2) enable multiple coexisting CIRs to be differentiated, and (3) enable the continuous tracing of any interplanetary CIR back toward its coronal source. In particular, an OOE view in WL can reveal where nascent CIRs are formed in the extended corona and how these CIRs develop in interplanetary space. Therefore, a panoramic view from a suite of wide-field WL imagers in a solar polar orbit would be invaluable in unambiguously resolving the large-scale longitudinal structure of CIRs in the 3D inner heliosphere.

CR1967, in 2000 September

Responses of relativistic electron fluxes in the outer radiation belt to geomagnetic storms

Ying **Xiong**, Lun Xie, Zuyin Pu, Suiyan Fu, Lunjin Chen, Binbin Ni, Wen Li, Jinxing Li, Ruilong Guo, G. K. Parks

JGR Volume 120, Issue 11 November 2015 Pages 9513–9523

Geomagnetic storms can either increase or decrease relativistic electron fluxes in the outer radiation belt. A statistical survey of 84 isolated storms demonstrates that geomagnetic storms preferentially decrease relativistic electron fluxes at higher energies, while flux enhancements are more common at lower energies. In about 87% of the storms, 0.3–2.5 MeV electron fluxes show an increase, whereas 2.5–14 MeV electron fluxes increase in only 35% of the storms. Superposed epoch analyses suggest that such “energy-dependent” responses of electrons preferably occur during conditions of high solar wind density which is favorable to generate magnetospheric electromagnetic ion cyclotron (EMIC) waves, and these events are associated with relatively weaker chorus activities. We have examined one of the cases where observed EMIC waves can resonate effectively with >2.5 MeV electrons and scatter them into the atmosphere. The correlation study further illustrates that electron flux dropouts during storm main phases do not correlate well with the flux buildup during storm recovery phases. We suggest that a combination of efficient EMIC-induced scattering and weaker chorus-driven acceleration provides a viable candidate for the energy-dependent responses of outer radiation belt relativistic electrons to geomagnetic storms. These results are of great interest to both understanding of the radiation belt dynamics and applications in space weather. **23 Oct 1994, 23 Nov 1997, 6 Aug 1998**

Effects of Thomson-Scattering Geometry on White-Light Imaging of an Interplanetary Shock: Synthetic Observations from Forward Magnetohydrodynamic Modelling

Ming **Xiong**, J. A. Davies, M. M. Bisi, M. J. Owens, R. A. Fallows, G. D. Dorrian
Solar Physics, July 2013, Volume 285, Issue 1-2, pp 369-389

Stereoscopic white-light imaging of a large portion of the inner heliosphere has been used to track interplanetary coronal mass ejections. At large elongations from the Sun, the white-light brightness depends on both the local electron density and the efficiency of the Thomson-scattering process. To quantify the effects of the Thomson-scattering geometry, we study an interplanetary shock using forward magnetohydrodynamic simulation and synthetic white-light imaging. Identifiable as an inclined streak of enhanced brightness in a time–elongation map, the travelling shock can be readily imaged by an observer located within a wide range of longitudes in the ecliptic. Different parts of the shock front contribute to the imaged brightness pattern viewed by observers at different longitudes. Moreover, even for an observer located at a fixed longitude, a different part of the shock front will contribute to the imaged brightness at any given time. The observed brightness within each imaging pixel results from a weighted integral along its corresponding ray-path. It is possible to infer the longitudinal location of the shock from the brightness pattern in an optical sky map, based on the east–west asymmetry in its brightness and degree of polarisation. Therefore, measurement of the interplanetary polarised brightness could significantly reduce the ambiguity in performing three-dimensional reconstruction of local electron density from white-light imaging.

USING COORDINATED OBSERVATIONS IN POLARIZED WHITE LIGHT AND FARADAY ROTATION TO PROBE THE SPATIAL POSITION AND MAGNETIC FIELD OF AN INTERPLANETARY SHEATH

Ming **Xiong**^{1,2}, Jackie A. Davies³, Xueshang Feng¹, Mathew J. Owens⁴,
Richard A. Harrison³, Chris J. Davis⁴, and Ying D. Liu¹
Astrophysical Journal, 777:32 (14pp), 2013

http://sprg.ssl.berkeley.edu/~liuxying/pubs/2013_apj_xiong.pdf

Coronal mass ejections (CMEs) can be continuously tracked through a large portion of the inner heliosphere by direct imaging in visible and radio wavebands. White light (WL) signatures of solar wind transients, such as CMEs, result from Thomson scattering of sunlight by free electrons and therefore depend on both viewing geometry and electron density. The Faraday rotation (FR) of radio waves from extragalactic pulsars and quasars, which arises due to the presence of such solar wind features, depends on the line-of-sight magnetic field component B_{\parallel} and the electron density. To understand coordinated WL and FR observations of CMEs, we perform forward magnetohydrodynamic modeling of an Earth-directed shock and synthesize the signatures that would be remotely sensed at a number of widely distributed vantage points in the inner heliosphere. Removal of the background solar wind contribution reveals the shock-associated enhancements in WL and FR. While the efficiency of Thomson scattering depends on scattering angle, WL radiance I decreases with heliocentric distance r roughly according to the expression $I \propto r^{-3}$. The sheath region downstream of the Earth-directed shock is well viewed from the L4 and L5 Lagrangian points, demonstrating the benefits of these points in terms of space weather forecasting. The spatial position of the main scattering site r_{sheath} and the mass of plasma at that position M_{sheath} can be inferred from the polarization of the shock-associated enhancement in WL radiance. From the FR measurements, the local B_{\parallel} sheath at r_{sheath} can then be estimated. Simultaneous observations in polarized WL and FR can not only be used to detect CMEs, but also to diagnose their plasma and magnetic field properties.

Forward modelling to determine the observational signatures of white-light imaging and interplanetary scintillation for the propagation of an interplanetary shock in the ecliptic plane

Ming **Xiong**, , A.R. Breena, M.M. Bisia, M.J. Owensb, R.A. Fallowsa, G.D. Dorrianc, J.A. Daviesd and P. Thomasson

Journal of Atmospheric and Solar-Terrestrial Physics, Volume 73, Issue 10, 2011, Pages 1270-1280

Recent coordinated observations of interplanetary scintillation (IPS) from the EISCAT, MERLIN, and STELab, and stereoscopic white-light imaging from the two heliospheric imagers (HIs) onboard the twin STEREO spacecraft are significant to continuously track the propagation and evolution of solar eruptions throughout interplanetary space. In order to obtain a better understanding of the observational signatures in these two remote-sensing techniques, the magnetohydrodynamics of the macro-scale interplanetary disturbance and the radio-wave scattering of the micro-scale electron-density fluctuation are coupled and investigated using a newly constructed multi-scale numerical model. This model is then applied to a case of an interplanetary shock propagation within the ecliptic plane. The shock could be nearly invisible to an HI, once entering the Thomson-scattering sphere of the HI. The asymmetry in the optical images

between the western and eastern HIs suggests the shock propagation off the Sun–Earth line. Meanwhile, an IPS signal, strongly dependent on the local electron density, is insensitive to the density cavity far downstream of the shock front. When this cavity (or the shock nose) is cut through by an IPS ray-path, a single speed component at the flank (or the nose) of the shock can be recorded; when an IPS ray-path penetrates the sheath between the shock nose and this cavity, two speed components at the sheath and flank can be detected. Moreover, once a shock front touches an IPS ray-path, the derived position and speed at the irregularity source of this IPS signal, together with an assumption of a radial and constant propagation of the shock, can be used to estimate the later appearance of the shock front in the elongation of the HI field of view. The results of synthetic measurements from forward modelling are helpful in inferring the in-situ properties of coronal mass ejection from real observational data via an inverse approach.

Research highlights

► A new multi-scale model for coordinated white-light and IPS observations. ► Remote-sensing signatures of interplanetary shock propagation. ► Using this model to infer possible longitudinal deflection of CMEs.

Magnetohydrodynamic simulation of the interaction between two interplanetary magnetic clouds and its consequent geoeffectiveness: 2. Oblique collision

[Xiong](#), Ming; [Zheng](#), Huinan; [Wang](#), Shui

J. Geophys. Res., Vol. 114, No. A11, A11101, 2009; [File](#)

The numerical studies of the interplanetary coupling between multiple magnetic clouds (MCs) are continued by a 2.5-dimensional ideal magnetohydrodynamic (MHD) model in the heliospheric meridional plane. The interplanetary direct collision (DC)/oblique collision (OC) between both MCs results from their same/different initial propagation orientations. Here the OC is explored in contrast to the results of the DC. Both the slow MC1 and fast MC2 are consequently injected from the different heliospheric latitudes to form a compound stream during the interplanetary propagation. The MC1 and MC2 undergo contrary deflections during the process of oblique collision. Their deflection angles of $|\delta\Theta_1|$ and $|\delta\Theta_2|$ continuously increase until both MC-driven shock fronts are merged into a stronger compound one. The $|\delta\Theta_1|$, $|\delta\Theta_2|$, and total deflection angle $\Delta\Theta$ ($\Delta\Theta = |\delta\Theta_1| + |\delta\Theta_2|$) reach their corresponding maxima when the initial eruptions of both MCs are at an appropriate angular difference. Moreover, with the increase of MC2's initial speed, the OC becomes more intense, and the enhancement of $\delta\Theta_1$ is much more sensitive to $\delta\Theta_2$. The $|\delta\Theta_1|$ is generally far less than the $|\delta\Theta_2|$, and the unusual case of $|\delta\Theta_1| \simeq |\delta\Theta_2|$ only occurs for an extremely violent OC. But because of the elasticity of the MC body to buffer the collision, this deflection would gradually approach an asymptotic degree. As a result, the opposite deflection between the two MCs, together with the inherent magnetic elasticity of each MC, could efficiently relieve the external compression for the OC in the interplanetary space. Such a deflection effect for the OC case is essentially absent for the DC case. Therefore, besides the magnetic elasticity, magnetic helicity, and reciprocal compression, the deflection due to the OC should be considered for the evolution and ensuing geoeffectiveness of interplanetary interaction among successive coronal mass ejections.

Magnetohydrodynamic simulation of the interaction between two interplanetary magnetic clouds and its consequent geoeffectiveness

[Xiong](#), Ming; [Zheng](#), Huinan; [Wu](#), S. T.; [Wang](#), Yuming; [Wang](#), Shui

JGR, Volume 112, Issue A11, CiteID A11103, 2007; [File](#)

Numerical studies of the interplanetary "multiple magnetic clouds (Multi-MC)" are performed by a 2.5-dimensional ideal magnetohydrodynamic (MHD) model in the heliospheric meridional plane. Both slow MC1 and fast MC2 are initially emerged along the heliospheric equator, one after another with different time intervals. The coupling of two MCs could be considered as the comprehensive interaction between two systems, each comprising of an MC body and its driven shock. The MC2-driven shock and MC2 body are successively involved into interaction with MC1 body. The momentum is transferred from MC2 to MC1. After the passage of MC2-driven shock front, magnetic field lines in MC1 medium previously compressed by MC2-driven shock are prevented from being restored by the MC2 body pushing. MC1 body undergoes the most violent compression from the ambient solar wind ahead, continuous penetration of MC2-driven shock through MC1 body, and persistent pushing of MC2 body at MC1 tail boundary. As the evolution proceeds, the MC1 body suffers from larger and larger compression, and its original vulnerable magnetic elasticity becomes stiffer and stiffer. So there exists a maximum compressibility of Multi-MC when the accumulated elasticity can balance the external compression. This cutoff limit of compressibility mainly decides the maximally available geoeffectiveness of Multi-MC because the geoeffectiveness enhancement of MCs interacting is ascribed to the compression. Particularly, the greatest geoeffectiveness is excited among all combinations of each MC helicity, if magnetic field lines in the interacting region of Multi-MC are all southward. Multi-MC completes its final evolutionary stage when the MC2-driven shock is

merged with MC1-driven shock into a stronger compound shock. With respect to Multi-MC geoeffectiveness, the evolution stage is a dominant factor, whereas the collision intensity is a subordinate one. The magnetic elasticity, magnetic helicity of each MC, and compression between each other are the key physical factors for the formation, propagation, evolution, and resulting geoeffectiveness of interplanetary Multi-MC.

Magnetohydrodynamic Simulation of the Interaction between Interplanetary Strong Shock and Magnetic Cloud and its Consequent Geoeffectiveness 2:

Oblique Collision

Ming [Xiong](#), Huinan Zheng, Yuming Wang, and Shui Wang

Journal of Geophysical Research, Volume 111, Issue A11, CiteID A11102, **2006; File**

Numerical studies of the interplanetary "shock overtaking magnetic cloud (MC)" event are continued by a 2.5-dimensional magnetohydrodynamic (MHD) model in heliospheric meridional plane. Interplanetary direct collision (DC)/oblique collision (OC) between an MC and a shock results from their same/different initial propagation orientations. For radially erupted MC and shock in solar corona, the orientations are only determined respectively by their heliographic locations. OC is investigated in contrast with the results in DC (Xiong, 2006). The shock front behaves as a smooth arc. The cannibalized part of MC is highly compressed by the shock front along its normal. As the shock propagates gradually into the preceding MC body, the most violent interaction is transferred sideways with an accompanying significant narrowing of the MC's angular width. The opposite deflections of MC body and shock aphelion in OC occur simultaneously through the process of the shock penetrating the MC. After the shock's passage, the MC is restored to its oblate morphology. With the decrease of MC-shock commencement interval, the shock front at 1 AU traverses MC body and is responsible for the same change trend of the latitude of the greatest geoeffectiveness of MC-shock compound. Regardless of shock orientation, shock penetration location regarding the maximum geoeffectiveness is right at MC core on the condition of very strong shock intensity. An appropriate angular difference between the initial eruption of an MC and an overtaking shock leads to the maximum deflection of the MC body. The larger the shock intensity is, the greater is the deflection angle. The interaction of MCs with other disturbances could be a cause of deflected propagation of interplanetary coronal mass ejection (ICME).

Magnetohydrodynamic Simulation of the Interaction between Interplanetary Strong Shock and Magnetic Cloud and its Consequent Geoeffectiveness

Ming [Xiong](#), Huinan Zheng, Yuming Wang, and Shui Wang

Journal of Geophysical Research, Volume 111, Issue A8, CiteID A08105, **2006; File**

Numerical studies have been performed to interpret the observed "shock overtaking magnetic cloud (MC)" event by a 2.5 dimensional magnetohydrodynamic (MHD) model in the heliospheric meridional plane. Results of an individual MC simulation show that the MC travels with a constant bulk flow speed. The MC is injected with a very strong inherent magnetic field over that in the ambient flow and expands rapidly in size initially. Consequently, the diameter of the MC increases in an asymptotic speed while its angular width contracts gradually. Meanwhile, simulations of MC-shock interaction are also presented, in which both a typical MC and a strong fast shock emerge from the inner boundary and propagate along the heliospheric equator, separated by an appropriate interval. The results show that the shock first catches up with the preceding MC, then penetrates through the MC, and finally merges with the MC-driven shock into a stronger compound shock. The morphologies of shock front in interplanetary space and MC body behave as a central concave and a smooth arc, respectively. The compression and rotation of the magnetic field serve as an efficient mechanism to cause a large geomagnetic storm. The MC is highly compressed by the overtaking shock. Contrarily, the transport time of the incidental shock influenced by the MC depends on the interval between their commencements. Maximum geoeffectiveness results from when the shock enters the core of preceding MC, which is also substantiated to some extent by a corresponding simplified analytic model. Quantified by the Dst index, the specific result is that the geoeffectiveness of an individual MC is largely enhanced with 80% increment in maximum by an incidental shock.

Multipoint Analysis of the Interaction between a Shock and an ICME-like Structure around 2011 March 22

Mengjiao [Xu](#)^{1,2}, Chenglong Shen^{1,2}, Can Wang¹, Yutian Chi^{1,2}, Zhihui Zhong¹, and Yuming Wang^{1,2,3}

2022 ApJL 930 L11

<https://iopscience.iop.org/article/10.3847/2041-8213/ac6879/pdf>

This work reports on the interaction between a fast forward shock and an interplanetary coronal-mass-ejection-like structure (ICMELS) as observed by in situ observations of radially aligned spacecraft. Around **2011 March 22**, the Venus EXpress (VEX) and Solar TERrestrial RELations Observatory-A (STEREO-A) were nearly at the same longitude,

providing us with an excellent opportunity to study the formation and evolution of the complex structures. The shock and ICMEs investigated in this paper are isolated near Venus, but when they approach STEREO-A, the shock nearly approaches the front edge of the ICMEs and forms a shock–ICMEs complex structure. The maximal magnetic field in the ICMEs increased 2.3 times due to shock compression, according to the observation. The recovery model, which restores the shocked portion of the shock–ICMEs to its uncompressed condition, likewise confirms this improvement. The interaction with the ICMEs, on the other hand, weakens shock 2. The magnetic compression ratio falls from 2.4 at Venus to 2.0 at STEREO-A. This research enables us to have a better physical knowledge of the impacts of the interaction between a shock and an ICME (or ICMEs), which will aid future space weather predictions.

Whether Small Flux Ropes and Magnetic Clouds Have the Same Origin: A Statistical Study of Small Flux Ropes in Different Types of Solar Wind

Mengjiao **Xu**^{1,2}, Chenglong Shen^{1,2}, Qiang Hu³, Yuming Wang^{1,2,4}, and Yutian Chi^{1,2,5}

2020 ApJ 904 122

<https://doi.org/10.3847/1538-4357/abbe21>

According to the duration and size, magnetic flux ropes can be divided into large-scale flux ropes, namely, magnetic clouds, and small-scale flux ropes (SFRs). Whether SFRs have the same origin as magnetic clouds has been a hot topic for a long time. Based on the SFR database developed by Hu et al. and Chen et al., this paper analyzes the properties of SFRs in different types of solar wind, which are SFRs in interplanetary coronal mass ejections (ICMEs), SFRs in stream interaction regions, and SFRs in background solar wind. On the assumption that SFRs in ICMEs have the same origin as magnetic clouds, we compare the three types of SFRs from several aspects, attempting to shed some light on the dispute, i.e., whether SFRs are homologous to magnetic clouds. The results show that up to 91% of the SFRs are outside ICMEs. Unlike SFRs in ICMEs, SFRs outside ICMEs seldom have large magnetic field strength and apparent expansion signatures. In addition, 36% of the SFRs in ICMEs have enhanced iron charge states. This probability is much higher than the other two types of SFRs. By an automatic method, this paper also finds that counterstreaming electrons are more common in SFRs in ICMEs. Considering strong magnetic field, expansion signatures, large iron charge state, and counterstreaming electrons are important indicators of magnetic clouds, we believe that most of the SFRs near Earth have different origins from magnetic clouds.

Prediction of the Dst Index with Bagging Ensemble-learning Algorithm

S. B. **Xu**¹, S. Y. Huang¹, Z. G. Yuan¹, X. H. Deng², and K. Jiang¹

ApJS 248 14 2020

<https://iopscience.iop.org/article/10.3847/1538-4365/ab880e/pdf>

The Dst index is a commonly geomagnetic index used to measure the strength of geomagnetic activity. The accurate prediction of the Dst index is one of the main subjects of space weather studies. In this study, we use the Bagging ensemble-learning algorithm, which combines three algorithms—the artificial neural network, support vector regression, and long short-term memory network—to predict the Dst index 1–6 hr in advance. Taking solar wind parameters (including the interplanetary total magnetic field, magnetic field B_z component, total electric field, solar wind speed, plasma temperature, and proton pressure) as inputs, we establish the Dst index models and complete not only the point prediction but also the interval prediction in forecasting the Dst index. The results show that the root mean square error (rmse) of the point prediction is always lower than 8.0936 nT, the correlation coefficient (R) is always higher than 0.8572 and the accuracy of interval prediction is always higher than 90%, implying that our model can improve the accuracy of point prediction and significantly promote the accuracy of interval prediction. In addition, a new proposed metric shows that the Bagging algorithm brings better stability to the model. Our model was also used to predicate a magnetic storm event from 2016 October 12–17. The most accurate prediction of this storm event is the 1 hr ahead prediction, which holds a result with the rmse of 3.7327 nT, the correlation coefficient of 0.9928, and the interval prediction accuracy of 96.69%. Moreover, we also discuss the balance in the Bagging ensemble model in this paper.

Importance of Shock Compression in Enhancing ICME's Geoeffectiveness

Mengjiao **Xu**¹, Chenglong Shen^{1,2}, Yuming Wang^{1,2,3}, Bingxian Luo^{4,5}, and Yutian Chi¹

2019 ApJL 884 L30

<https://doi.org/10.3847/2041-8213/ab4717>

Shock embedded interplanetary coronal mass ejections (ICMEs) are of great interest in the solar and heliosphere physics community due to their high potential to cause intense geomagnetic storms. In this work, **18 moderate to intense geomagnetic storms** caused by shock-ICME complex structures are analyzed in order to show the importance of shock compression in enhancing ICMEs' geoeffectiveness. Based on the characteristics of the shocks inside ICMEs, including the shock velocity, shock normal direction, and the density compression ratio, we recover the shocked part in the ICME

to the uncompressed state by using a recovery model developed by Wang et al. according to the Rankine–Hugoniot relationship. Comparing the observational data and the recovered parameters, we find that the maximum southward magnetic field in the ICME is doubled and the dawn–dusk electric field is increased 2.2 times due to the shock compression. Then, the parameters of the observed and recovered solar wind and magnetic field are, respectively, introduced into various Dst prediction models. The prediction results show that, on average, the shock compression can enhance the intensity of the geomagnetic storm by a factor of 1.4. Without shock compression, the geoeffectiveness of these ICMEs would be markedly reduced. Moreover, there is a significant correlation between the shock density compression ratio and the shock's capacity of strengthening geomagnetic storms. The larger the shock density compression ratio is, the more obvious Dst index decrease is caused.

Angular Distribution of Solar Wind Magnetic Field Vector at 1 Au

F. Xu^{1,2}, G. Li², L. Zhao², Y. Zhang^{1,2}, O. Khabarova^{2,3}, B. Miao⁴, and J. le Roux
2015 ApJ 801 58.

We study the angular distribution of the solar wind magnetic field vector at 1 AU and its solar cycle dependence using ACE observations. A total of twelve 27.27 day (the duration of a solar rotation) intervals during the solar maximum, the solar minimum, as well as the ascending and descending phases of solar cycle 23 are examined. For all selected intervals, we obtain the angular distribution function $f_{\tau}(\alpha)$, where α is the angle between the instantaneous solar wind magnetic field vector and the average background magnetic field vector, and τ is the period length for the averaging. Our results show that in all periods $f_{\tau}(\alpha)$ has two populations, one at small angles and one at large angles. We suggest that the second population is due to the presence of current sheets in the solar wind. The solar-cycle dependence of $f_{\tau}(\alpha)$ and a τ -scaling property of the second population of $f_{\tau}(\alpha)$ are discussed. The τ scaling shows a clear dependence on the solar wind type. The implication of $f_{\tau}(\alpha)$ for particle acceleration at interplanetary shocks driven by coronal mass ejections, such as those in solar energetic particle events, is also discussed.

Observations of reconnection exhausts associated with large-scale current sheets within a complex ICME at 1 AU

Xu, X.; Wei, F.; Feng, X.

J. Geophys. Res., Vol. 116, No. A5, A05105, **2011**

<http://dx.doi.org/10.1029/2010JA016159>

During **26–27 November 2000** a complex interplanetary coronal mass ejection, composed of four flux ropes, was detected by Wind and ACE at 1 AU. We identify two Petschek-like exhaust events within the interiors of the second and third flux ropes, respectively. In the first event, Wind and ACE detected an exhaust at the same side from the reconnection site, which was associated with a large-scale bifurcated current sheet with a spatial width of $\sim 10,000$ ion inertial lengths and the magnetic shear was 155° . In the second event, the two spacecraft observed the oppositely directed exhausts from a single reconnection X line. The exhausts were also related to a large-scale current sheet with a spatial width of ~ 3000 ion inertial lengths and a shear angle of about 135° . The two exhaust events resulted from fast and quasi-stationary reconnection. The related current sheets were both flat on the scale of a few hundred Earth radii and located close to the centers of subflux ropes. The decrease of radial expansion speed of each flux rope might account for the formation of the two current sheets. Reconnections at the centers of flux ropes may change the entire topology of the flux ropes and may fragment them into smaller ones.

Analysis on the interplanetary causes of the great magnetic storms in solar maximum (2000–2001)

X.H. Xu[✉], Yuming Wang[✉], P.Z. Ye, S. Wang and M. Xiong

Planetary and Space Science, Volume 53, Issue 4, April **2005**, Pages 443-457

In this paper, we analyze the interplanetary causes of eight great geomagnetic storms ($D_{st} \leq -200$ nT) during the solar maximum (2000–2001). The result shows that the interplanetary causes were the intense southward magnetic field and the notable characteristic among the causal mechanism is compression. Six of eight great geomagnetic storms were associated with the compression of southward magnetic field, which can be classified into (1) the compression between ICMEs (2) the compression between ICMEs and interplanetary medium. It suggests that the compressed magnetic field would be more geoeffective. At the same time, we also find that half of all great storms were related to successive halo CMEs, most of which originated from the same active region. The interactions between successive halo CMEs usually can lead to greater geoeffectiveness by enhancing their southward field B_s interval either in the sheath region of the

ejecta or within magnetic clouds (MCs). The types of them included: the compression between the fast speed transient flow and the slow speed background flow, the multiple MCs, besides shock compression. Further, the linear fit of the Dst versus $(-\overline{VB_z})^\alpha(\Delta t)^\beta$ gives the weights of $-\overline{VB_z}$ and Δt as $\alpha=2.51$ and $\beta=0.75$, respectively. This may suggest that the compression mechanism, with associated intense B_z , rather than duration, is the main factor in causing a great geomagnetic storm.

A Complete Catalogue of High-Speed Solar Wind Streams during Solar Cycle 23

G. [Xystouris](#), E. Sigala, H. Mavromichalaki

Solar Physics, March 2014, Volume 289, Issue 3, pp 995-1012

High-speed solar wind streams (HSSWSs) are ejected from the Sun and travel into the interplanetary space. Because of their high speed, they carry out energetic particles such as protons and heavy ions, which leads to an increase in the mean interplanetary magnetic field (IMF). Since the Earth is in the path of those streams, Earth's magnetosphere interacts with the disturbed magnetic field, leading to a significant radiation-induced degradation of technological systems. These interactions provide an enhanced energy transfer from the solar wind/IMF system into the Earth's magnetosphere and initiate geomagnetic disturbances that may have a possible impact on human health. Solar cycle 23 was a particularly unusual cycle with many energetic phenomena during its descending phase and also had an extended minimum. We have identified and catalogued the HSSWSs of this cycle and determined their characteristics, such as their maximum velocity, beginning and ending time, duration, and possible sources. We identified 710 HSSWSs and compared them with the corresponding characteristics of the streams of previous solar cycles. For first time, we used the CME data to study the stream sources, which led to useful results for the monitoring and forecasting of space weather effects.

(See **HIGH - SPEED STREAMS CATALOGUE (1996 – 2008)**)

O. Maris and G. Maris

http://www.space-science.ro/new1/HSS_Catalogue.html)

Science objectives of the magnetic field experiment onboard Aditya-L1 spacecraft

Vipin K. [Yadav](#), [NanditaSrivastava](#), [S.S.Ghosh](#), [P.T.Srikard](#), [Krishnamoorthy](#), [Subhalakshmi](#)

[Advances in Space Research](#) Volume 61, Issue 2, 15 January 2018, Pages 749-758

The Aditya-L1 is first Indian solar mission scheduled to be placed in a halo orbit around the first Lagrangian point (L1) of Sun-Earth system in the year 2018–19. The approved scientific payloads onboard Aditya-L1 spacecraft includes a Fluxgate Digital Magnetometer (FGM) to measure the local magnetic field which is necessary to supplement the outcome of other scientific experiments onboard. The in-situ vector magnetic field data at L1 is essential for better understanding of the data provided by the particle and plasma analysis experiments, onboard Aditya-L1 mission. Also, the dynamics of Coronal Mass Ejections (CMEs) can be better understood with the help of in-situ magnetic field data at the L1 point region. This data will also serve as crucial input for the short lead-time space weather forecasting models. The proposed FGM is a dual range magnetic sensor on a 6 m long boom mounted on the Sun viewing panel deck and configured to deploy along the negative roll direction of the spacecraft. Two sets of sensors (tri-axial each) are proposed to be mounted, one at the tip of boom (6 m from the spacecraft) and other, midway (3 m from the spacecraft). The main science objective of this experiment is to measure the magnitude and nature of the interplanetary magnetic field (IMF) locally and to study the disturbed magnetic conditions and extreme solar events by detecting the CME from Sun as a transient event. The proposed secondary science objectives are to study the impact of interplanetary structures and shock solar wind interaction on geo-space environment and to detect low frequency plasma waves emanating from the solar corona at L1 point. This will provide a better understanding on how the Sun affects interplanetary space.

In this paper, we shall give the main scientific objectives of the magnetic field experiment and brief technical details of the FGM onboard Aditya-1 spacecraft.

Average properties of geomagnetic storms in 1932-2009

[Yakovchouk](#), O. S.; [Mursula](#), K.; [Holappa](#), L.; [Veselovsky](#), I. S.; [Karinen](#), A.

J. Geophys. Res., Vol. 117, No. A3, A03201, 2012

<http://dx.doi.org/10.1029/2011JA017093>

We investigate the average properties of geomagnetic storms using the global and local Dst indices at four Dst stations in 1932–2009. Imposing the condition of complete data availability during storms, our study includes 1268/362/134/59 storms with Dst minimum less than $-50/-100/-150/-200$ nT, respectively. The global Dst minima were, on an average, $-94/-156/-216/-275$ nT, while deepest storm-time local Dst minima were $-137/-214/-285/-350$ nT. Accordingly, the local Dst minima are typically 25–30% stronger than the global Dst minima. The distribution of largest storm-time

disturbances is strongly peaked at 18 local time (LT), challenging local midnight as the dominant ion source. Relative timing of local minima verifies that stations at earlier LT hour observe their minimum a couple of hours after the deepest minimum, in agreement with westward drift of ions. Storm-time maximum asymmetries were found to increase with storm intensity level from about 70 nT to 150 nT for -50 to -200 nT storms. However, strong storms are relatively more symmetric than weak storms when compared to the typical level of local disturbance. During individual storms the asymmetry can be more than 200 nT. The rate of evolution of storm-time asymmetry is found to be roughly twice as fast for large storms. We emphasize that the unique database of local Dxt indices proves to be very useful in studying the average spatial distribution and temporal evolution of storms.

Radio sounding of the solar wind acceleration region with spacecraft signals

Oleg I. [Yakovlev](#), Yuri V. [Pisanko](#)

[Advances in Space Research](#) Volume 61, Issue 1, 1 January 2018, Pages 552-566

https://ac.els-cdn.com/S0273117717307913/1-s2.0-S0273117717307913-main.pdf?_tid=3512c3f2-de44-11e7-be1a-00000aab0f6c&acdnat=1512977199_3ae49cbdfab783860b5adb1b09683268

Data from coronal radio-sounding experiments carried out on various interplanetary spacecraft are used to derive the empirical radial dependence of solar wind velocity and density at heliocentric distances from 3 to 60 solar radii for heliolatitudes below 60° and for low solar activity. The radial dependencies of solar wind power and acceleration are derived from these results. Summaries of the radial behavior of characteristic parameters of the solar wind turbulence (e.g., the spectral index and the inner and outer turbulence scales), as well as the fractional density fluctuation, are also presented. These radio-sounding results provide a benchmark for models of the solar wind in its acceleration region.

HELICAL LENGTHS OF MAGNETIC CLOUDS FROM THE MAGNETIC FLUX CONSERVATION

[Tetsuya T. Yamamoto](#)¹, [R. Kataoka](#)² and [S. Inoue](#)³

ApJ 710 456-461, 2010

We estimate axial lengths of helical parts in magnetic clouds (MCs) at 1 AU from the magnetic flux (magnetic helicity) conservation between solar active regions (ARs) and MCs with the event list of Leamon et al. Namely, considering poloidal magnetic flux (Φ_p) conservation between MCs and ARs, we estimated L_h in MCs, where L_h is the axial length of an MC where poloidal magnetic flux and magnetic twist exist. It is found that L_h is 0.01-1.25 AU in the MCs. If the cylinder flux rope picture is assumed, this result leads to a possible new picture of the cylinder model whose helical structure (namely, poloidal magnetic flux) localizes in a part of a MC.

Radial dependence of CME propagation speed in interplanetary space

M. [Yamashita](#), M. Tokumaru, M. Kojima, and K. Fujiki

JGR, Draft, 2005

We studied radial variation of coronal mass ejection (CME) speeds between the Sun and the Earth orbit using interplanetary scintillation (IPS) measurements at 327 MHz. We analyzed here nine Earth-directed CME events which occurred between 1997 and 2002. Using the enhancement factor of solar wind density fluctuation level (g -value), derived from IPS measurements, we performed a model-fitting analysis of three dimensional CME structure and estimated CME locations in the ambient solar wind. Combining the IPS measurements with coronagraph measurements and near-Earth in situ observations, CME speeds were derived at distances from the Sun to the Earth orbit. The results show that (1) a fast CME is significantly decelerated during the propagation while a slow CME is accelerated, (2) the acceleration and deceleration is mostly was completed by 0.7 AU, and the CME attains nearly the same speed as that of the ambient solar wind. *We found that the deceleration rate of the fast CME inversely correlated with the initial speed difference between CMEs and the ambient solar wind. This implies that propagation dynamics of fast CMEs is governed by retardation force caused by interaction with the ambient solar wind, and this supports the aerodynamic drag force model.*

Assessment of Geomagnetic Activity for the Kp=9 “Gannon Storm” in May 2024 Based on Version 3.0 Hpo Indices

Yosuke **Yamazaki**, Jürgen Matzka, Marcos Vinicius Siqueira da Silva, Guram N Kervalishvili, ++
ESS Open Archive . June 14, 2024.

<https://essopenarchive.org/doi/full/10.22541/essoar.171838396.68563140/v1>

DOI: [10.22541/essoar.171838396.68563140/v1](https://doi.org/10.22541/essoar.171838396.68563140/v1)

The geomagnetic storm of May 2024, which we call “Gannon storm” in memoriam of Jennifer L. Gannon, was such an intense event that the geomagnetic activity index Kp reached its upper limit value of 9 for the first time since October 2003. This paper introduces the new version (V. 3.0) of Hpo indices and evaluates geomagnetic activity during the Gannon storm. The Hpo indices, namely Hp30 and Hp60, are measures of geomagnetic activity, similar to the 3-hourly Kp index but with higher temporal resolutions of 30 min and 60 min, without an upper limit at 9, enabling them to assess geomagnetic activity during Kp=9 storms. In V. 3.0, an improved algorithm is implemented, and the indices are extended back to 1985. In the current dataset, the March 1989 storm is the strongest event by various measures based on the Hpo indices, while the Gannon storm ranks between 2nd to 5th.

Geomagnetic Activity Index Hpo

Y. **Yamazaki**, J. **Matzka**, C. **Stolle**, G. **Kervalishvili**, J. **Rauberg**, O. **Bronkalla**, A. **Morschhauser**, S. **Bruinsma**, Y. Y. **Shprits**, D. R. **Jackson**

Geophysical Research Letters, 49, e2022GL098860. (2022)

<https://doi.org/10.1029/2022GL098860>

<https://agupubs.onlinelibrary.wiley.com/doi/epdf/10.1029/2022GL098860>

The geomagnetic activity index Kp is widely used but is restricted by low time resolution (3-hourly) and an upper limit. To address this, new geomagnetic activity indices, Hpo, are introduced. Similar to Kp, Hpo expresses the level of planetary geomagnetic activity in units of thirds (0o, 0+, 1-, 1o, 1+, 2-, ...) based on the magnitude of geomagnetic disturbances observed at subauroral observatories. Hpo has a high time resolution than Kp. 30-min (Hp30) and 60-min (Hp60) indices are produced. The frequency distribution of Hpo is designed to be similar to that of Kp so that Hpo may be used as a higher time-resolution alternative to Kp. Unlike Kp, which is capped at 9o, Hpo is an open-ended index and thus can characterize severe geomagnetic storms more accurately. Hp30, Hp60 and corresponding linearly scaled ap30 and ap60 are available, in near real time, at the GFZ website (<https://www.gfz-potsdam.de/en/hpo-index>)

See <https://kp.gfz-potsdam.de/en/hp30-hp60>

New Interplanetary Scintillation Array in China for Space Weather

Yihua **Yan** 1,2, Wei Wang 1, Linjie Chen 1, Fei Liu 1, Lihong Geng 1, Zhijun Chen
Sun and Geosphere, 2018; 13/2: 153 -155

http://newserver.stil.bas.bg/SUNGEO/00SGArhiv/SG_v13_No2_2018-pp-153-155.pdf

Interplanetary Scintillation (IPS) is a useful ground-based method to investigate solar wind structure and its parameters through the scintillation of distant, compact radio sources at radio wavelengths. Current worldwide IPS facilities include both single-site systems (which are typically a large telescope or array), and multi-site systems (which are typically more varied telescope/array sizes). To combine the advantages of both of these system types, we propose a new design for the IPS telescope in China, implementing a large collecting area at one main site, with smaller collecting areas at the other sites. This new IPS telescope concept is a part of the Phase-II Meridian Space Weather Monitoring Project under the 2016-2020 National Infrastructure Program in China to be constructed in near future. Some specifications and basic considerations of this telescope are described in this paper.

How Switchbacks Can Maintain a Longer Time in the Interplanetary Space

Y. **Yang** 1,2, W. Su 3, and P. F. Chen 4,5

2024 ApJ 969 17

<https://iopscience.iop.org/article/10.3847/1538-4357/ad4b18/pdf>

Parker Solar Probe, the closest spacecraft to the Sun, has renewed our understanding of the solar corona and the interplanetary space. One of its important findings is the prevalence of switchbacks, which display localized magnetic reversals along the otherwise Parker spirals. While some switchbacks might disappear quickly, others can maintain for a long period of time, and there are indications that many switchbacks strengthen from the solar corona to the interplanetary space despite their magnetic tension force, which tends to straighten the magnetic field lines. Therefore, how these switchbacks could be maintained for a long period of time remains a mystery. In this paper, we employed a 3D data-driven global full magnetohydrodynamics numerical model to explore the evolution of switchbacks formed in

the dynamic corona. Our simulations indicate that two factors can affect the lifetime of a switchback. One factor is the combination of angle and leg length ensures that the switchback with greater curvature after reconnection can last longer, and the greater the angle, the more magnetic field lines that can be reconnected, and thus the longer the duration. We call this influencing factor flux tube shape factor. The other factor is the velocity shear, i.e., when the solar wind at the convex-outward turning of a switchback is faster than that at the concave-outward turning, the switchback becomes enhanced during propagation, and it weakens when the velocity difference is opposite.

Prediction of the Transit Time of Coronal Mass Ejections with an Ensemble Machine-learning Method

Y. **Yang**¹, J. J. Liu², X. S. Feng^{3,4}, P. F. Chen^{5,6}, and B. Zhang⁷

2023 ApJS 268 69

<https://iopscience.iop.org/article/10.3847/1538-4365/acf218/pdf>

Coronal mass ejections (CMEs), a kind of violent solar eruptive activity, can exert a significant impact on space weather. When arriving at the Earth, they interact with the geomagnetic field, which can boost the energy supply to the geomagnetic field and may further result in geomagnetic storms, thus having potentially catastrophic effects on human activities. Therefore, accurate forecasting of the transit time of CMEs from the Sun to the Earth is vital for mitigating the relevant losses brought by them. XGBoost, an ensemble model that has better performance in some other fields, is applied to the space weather forecast for the first time. During multiple tests with random data splits, the best mean absolute error (MAE) of ~ 5.72 hr was obtained, and in this test, 62% of the test CMEs had absolute arrival time error of less than 5.72 hr. The average MAE over all random tests was ~ 10 hr. It indicates that our method has a better predictive potential and baseline. Moreover, we introduce two effective feature importance ranking methods. One is the information gain method, a built-in method of ensemble models. The other is the permutation method. These two methods combine the learning process of the model and its performance to rank the CME features, respectively. Compared with the direct correlation analysis on the sample data set, they can help select the important features that closely match the model. These two methods can assist researchers to process large sample data sets, which often require feature selection in advance.

Global Morphology Distortion of the 2021 October 9 Coronal Mass Ejection from an Ellipsoid to a Concave Shape

Liping **Yang**¹, Chuanpeng Hou², Xueshang Feng^{1,3}, Jiansen He², Ming Xiong^{1,4}, Man Zhang¹, Yufen Zhou¹, Fang Shen^{1,4}, Xinhua Zhao¹, Huichao Li^{3,1}[Show full author list](#)

2023 ApJ 942 65

<https://iopscience.iop.org/article/10.3847/1538-4357/aca52d/pdf>

This paper presents a study of a **2021 October 9** coronal mass ejection (CME) with multipoint imaging and in situ observations. We also simulate this CME from the Sun to Earth with a passive tracer to tag the CME's motion. The coronagraphic images show that the CME is observed as a full halo by SOHO and as a partial halo by STEREO-A. The heliospheric images reveal that the propagation speed of the CME approaches about 1° hr^{-1} , suggesting a slow CME. With simulated results matching these observation results, the simulation discloses that as the CME ejects from the Sun out to interplanetary space, its global morphology is distorted from an ellipsoid to a concave shape owing to interactions with the bimodal solar wind. The cross section of the CME's flux rope structure transforms from a circular shape into a flat one. As a result of the deflection, the propagation direction of the CME is far away from the Sun–Earth line. This means that the CME flank (or the ICME leg) likely arrives at both Solar Orbiter and the L1 point. From the CME's eruption to 1 au, its volume and mass increase by about two orders and one order of magnitude, respectively. Its kinetic energy is about 100 times larger than its magnetic energy at 1 au. These results have important implications for our understanding of CMEs' morphology, as well as their space weather impacts.

The First Intense Geomagnetic Storm Event Recorded by the China Seismo-Electromagnetic Satellite

Y.-Y. **Yang** , [Z.-R. Zhima](#) , [X.-H. Shen](#) , [W. Chu](#) , [J.-P. Huang](#) , [Q. Wang](#) , [R. Yan](#) , [S. Xu](#) , [H.-X. Lu](#) , [D.-P. Liu](#)

Space Weather [Volume18, Issue1](#) January 2020 e2019SW002243

<https://agupubs.onlinelibrary.wiley.com/doi/pdf/10.1029/2019SW002243>

On 25 August 2018, the China Seismo-Electromagnetic Satellite (CSES) encountered the first intense geomagnetic storm event since its launch on 2 February 2018. The main purpose of this work is to check in-flight performance of the assembled payloads onboard CSES, as well as to investigate the ionosphere perturbations induced by this geomagnetic

storm. The study shows that all investigated parameters simultaneously respond to the different phases of the geomagnetic storm, verifying the measuring capabilities of the assembled payloads onboard CSES. Specifically, the magnetic field obtained from the high-precision magnetometer fits well with that obtained by the Swarm satellite, clearly demonstrating the development phase of the storm; joint analysis using the Langmuir probe, plasma analyzer, electric field detector, and GNSS occultation receiver data demonstrate that this is a positive storm event and that electric field penetration is the possible mechanism for the disturbance in the ionosphere. During this storm event, some significant ELF/VLF waves are also excited and there is enhancement of the energetic electron flux (of energy <1 MeV). These main features are consistent with results from previous works, indicating the excellent performance of the search coil magnetometer and high-energy particle detector.

Modeling the Global Distribution of Solar Wind Parameters on the Source Surface Using Multiple Observations and the Artificial Neural Network Technique

Yi **Yang**, Fang Shen

Solar Phys. August **2019**, 294:111

<https://link.springer.com/content/pdf/10.1007%2Fs11207-019-1496-5.pdf>
sci-hub.se/10.1007/s11207-019-1496-5

The global distribution of magnetic field and other plasma parameters on the source surface, which we set at 2.5 solar radii, is important for coronal and heliospheric modeling. In this article, we introduce a new data-driven self-consistent method to obtain the global distribution of different parameters. The magnetic and polarized brightness (pBpB) observations are used to derive the magnetic field and electron density on the source surface, respectively. Then, an artificial neural network (ANN) machine learning technique is applied to establish an empirical relation among the solar wind velocity, the magnetic field properties, and the electron density. The ANN is trained with global observational data, and is validated to be more reliable than the Wang–Sheeley–Arge (WSA) model for reconstructing the solar wind velocity, especially at high latitudes. The plasma temperature distribution is derived by solving a simplified one-dimensional (1D) magnetohydrodynamic (MHD) equation system on the source surface. Using the method in this study we can obtain the global distribution for all the parameters self-consistently based on magnetic and polarized brightness observations. The modeling results of four Carrington rotations from different solar cycle phases are presented to validate the method.

Prediction of Solar Wind Speed at 1 AU Using an Artificial Neural Network

Yi **Yang**, [Fang Shen](#), [Zicai Yang](#), [Xueshang Feng](#)

Space Weather **Volume16, Issue9** Pages 1227-1244 **2018**

<https://agupubs.onlinelibrary.wiley.com/doi/10.1029/2018SW001955>

A hybrid intelligent source surface model applying the artificial neural network tactic for solar wind speed prediction is presented in this paper. The model is a hybrid system merging various observational and theoretical information as input. Different inputs are tested including individual parameters and their combinations in order to select an optimum. Then, the optimal model is implemented for prediction. The prediction is validated by both error analysis and event-based analysis from 2007 to 2016. The overall correlation coefficient is 0.74, and the root-mean-square error is 68 km/s. The probability for detecting a high-speed-event is 0.68, the positive predicted value is 0.73, and the threat score is 0.55.

Correlation Between the Magnetic Field and Plasma Parameters at 1 AU

Zicai **Yang**, Fang Shen, Jie Zhang, Yi Yang, Xueshang Feng, Ian G. Richardson

[Solar Physics](#) February **2018**, 293:24

<https://link.springer.com/content/pdf/10.1007%2Fs11207-017-1238-5.pdf>

The physical parameters of the solar wind observed in-situ near 1 AU have been studied for several decades, and relationships between them, such as the positive correlation between the solar wind plasma temperature, T , and velocity, V , and the negative correlation between density, N , and velocity, V , are well known. However, the magnetic field intensity, B , does not appear to be well correlated with any individual plasma parameter. In this article, we discuss previously under-reported correlations between B and the combined plasma parameters $\sqrt{NV^2}$ as well as between B and \sqrt{NT} . These two correlations are strong during periods of corotating interaction regions and high-speed streams, and moderate during intervals of slow solar wind. The results indicate that the magnetic pressure in the solar wind is well correlated both with the plasma dynamic pressure and the thermal pressure.

A Self-consistent Numerical Study of the Global Solar Wind Driven by the Unified Nonlinear Alfvén Wave

L. P. **Yang**, X. S. Feng, J. S. He, L. Zhang, M. Zhang
Solar Phys. **2016**

The global solar wind has been revealed via in situ observations to consist of two populations, i.e. the tenuous fast solar wind and the dense slow solar wind. Here, we present a self-consistent modeling of the global solar wind driven by the unified nonlinear Alfvén wave. Considering polytropic closure of magnetohydrodynamics instead of isothermal assumption, the low-frequency Alfvén waves with a broadband spectrum are globally injected at the base of the corona, with the amplitude independent of latitude. In our 2.5 dimensional model, the presence of the Alfvén waves is identified overall in a region away from the equatorial plane, and the waves significantly accelerate the plasma therein to form the fast wind. Near the equatorial plane, a slow wind is generated, and the slowness can be attributed to the absence of Alfvén waves owing to the strong damping at lower altitude. The velocity ratio of both modes, if extrapolated to 1 AU, conforms to the measurements. Far from the Sun, however, the temperature of the fast wind is lower than that of its surroundings, indicating that shock-heating might be inadequate and other mechanisms are probably required to heat the fast wind, such as the dissipation of Alfvénic turbulence.

Forecast of Modulation of Cosmic Rays with Rigidity of 10 GV in the 25th Solar Activity Cycle.

Yanke, V.G., Belov, A.V., Gushchina, R.T. et al.
Geomagn. Aeron. 64, 201–210 (2024).

<https://doi.org/10.1134/S0016793223601072>

Based on a forecast of solar activity parameters and the model developed by the authors for modulation of Galactic cosmic rays, we forecasted cosmic ray variations in the 25th solar activity cycle. The cosmic ray flux forecast is based on correlation with the number of sunspots (single-parameter model) or with a set of solar (mainly magnetic) parameters (multiparameter model). The forecast for the number of sunspots was taken from published data; the forecast for other solar parameters was done in the study. It is shown that variations in cosmic rays over three years of the current 25th cycle, in general, do not contradict the forecasts and indicate that the 25th solar activity cycle is expected to be slightly more active compared to the 24th.

Identification of prominence ejecta by the proton distribution function and magnetic fine structure in interplanetary coronal mass ejections in the inner heliosphere

Yao, Shuo; Marsch, Eckart; Tu, Chuan-Yi; Schwenn, Rainer
J. Geophys. Res., Vol. 115, No. A5, A05103, 2010

<http://dx.doi.org/10.1029/2009JA014914>

This work presents in situ solar wind observations of three magnetic clouds (MCs) that contain cold high-density material when Helios 2 was located at 0.3 AU on 9 May 1979, 0.5 AU on 30 March 1976, and 0.7 AU on 24 December 1978. In the cold high-density regions embedded in the interplanetary coronal mass ejections we find (1) that the number density of protons is higher than in other regions inside the magnetic cloud, (2) the possible existence of He⁺, (3) that the thermal velocity distribution functions are more isotropic and appear to be colder than in the other regions of the MC, and the proton temperature is lower than that of the ambient plasma, and (4) that the associated magnetic field configuration can for all three MC events be identified as a flux rope. This cold high-density region is located at the polarity inversion line in the center of the bipolar structure of the MC magnetic field (consistent with previous solar observation work that found that a prominence lies over the neutral line of the related bipolar solar magnetic field). Specifically, for the first magnetic cloud event on 8 May 1979, a coronal mass ejection (CME) was related to an eruptive prominence previously reported as a result of the observation of Solwind (P78-1). Therefore, we identify the cold and dense region in the MC as the prominence material. It is the first time that prominence ejecta were identified by both the plasma and magnetic field features inside 1 AU, and it is also the first time that the thermal ion velocity distribution functions were used to investigate the microstate of the prominence material. Moreover, from our three cases, we also found that this material tended to fall behind the magnetic cloud and become smaller as it propagated farther away from the Sun, which confirms speculations in previous work. Overall, our in situ observations are consistent with three-part CME models.

Slow Solar Wind Connection Science during Solar Orbiter's First Close Perihelion Passage

Stephanie L. **Yardley**, [Christopher J. Owen](#), [David M. Long](#), [Deborah Baker](#), +++

ApJ **2023**

<https://arxiv.org/pdf/2304.09570.pdf>

The Slow Solar Wind Connection Solar Orbiter Observing Plan (Slow Wind SOOP) was developed to utilise the extensive suite of remote sensing and in situ instruments on board the ESA/NASA Solar Orbiter mission to answer

significant outstanding questions regarding the origin and formation of the slow solar wind. The Slow Wind SOOP was designed to link remote sensing and in situ measurements of slow wind originating at open-closed field boundaries. The SOOP ran just prior to Solar Orbiter's first close perihelion passage during two remote sensing windows (RSW1 and RSW2) between **2022 March 3-6** and **2022 March 17-22**, while Solar Orbiter was at a heliocentric distance of 0.55-0.51 and 0.38-0.34 au from the Sun, respectively. Coordinated observation campaigns were also conducted by Hinode and IRIS. The magnetic connectivity tool was used, along with low latency in situ data, and full-disk remote sensing observations, to guide the target pointing of Solar Orbiter. Solar Orbiter targeted an active region complex during RSW1, the boundary of a coronal hole, and the periphery of a decayed active region during RSW2. Post-observation analysis using the magnetic connectivity tool along with in situ measurements from MAG and SWA/PAS, show that slow solar wind, with velocities between 210 and 600 km/s, arrived at the spacecraft originating from two out of the three of the target regions. The Slow Wind SOOP, despite presenting many challenges, was very successful, providing a blueprint for planning future observation campaigns that rely on the magnetic connectivity of Solar Orbiter.

Solar Orbiter Nugget #35 Aug 2024 <https://www.cosmos.esa.int/web/solar-orbiter/-/science-nugget-multi-source-connectivity-drives-heliospheric-solar-wind-variability>

Post-Eruption Arcades and Interplanetary Coronal Mass Ejections

S. **Yashiro** · N. Gopalswamy · P. Makela · S. Akiyama

Solar Phys., Volume 284, Issue 1, pp 5-15, **2013**, **File**

We compare the temporal and spatial properties of posteruption arcades (PEAs) associated with coronal mass ejections (CMEs) at the Sun that end up as magnetic cloud (MC) and non-MC events in the solar wind. We investigate the length, width, area, tilt angle, and formation time of the PEAs associated with 22 MC and 29 non-MC events and we find no difference between the two populations. According to current ideas on the relation between flares and CMEs, the PEA is formed together with the CME flux-rope structure by magnetic reconnection. Our results indicate that at the Sun flux ropes form during CMEs in association with both MC and non-MC events; however, for non-MC events the fluxrope structure is not observed in the interplanetary space because of the geometry of the observation, *i.e.* the location of the spacecraft when the structure passes through it.

Table: 59 events. 2000-07-14, 2000-07-25, 2000-10-02, 2000-11-24, 2004-01-20, 2005-05-17

An Improved Halo Coronal Mass Ejection Geoeffectiveness Prediction Model Using Multiple Coronal Mass Ejection Features Based on the DC-PCA-KNN Method

Dalin **Ye**, Huimin Li, Lixin Guo, and Xiaoli Jiang

2025 ApJ 978 66

<https://iopscience.iop.org/article/10.3847/1538-4357/ad98f0/pdf>

Coronal mass ejections (CME) are regarded as the main drivers of geomagnetic storms (GSs). In the prediction of geoeffectiveness, various CME features have been introduced without adequately considering the geoeffectiveness of CMEs and strong correlations among the features. In this study, a feature dimension reduction method combining distance correlation (DC) and principal component analysis (PCA) was employed for the K-nearest neighbors (KNN) model to predict the geoeffectiveness of halo CME by using the multiple CME features. First, based on CME features and the Disturbance Storm Time index, there are 169 CME-related GS (CME-GS) pairs that were defined as positive samples during the entire phases of solar cycles 23 and 24. Next, DC was used to screen the eight original CME features. It was found that the three CME features, such as acceleration, kinetic energy, and measurement position angle, were weakly correlated with CME-GS pairs according to the performance of KNN prediction models and then were discarded. In order to further reduce the dimension of the input features for the KNN prediction model, PCA was subsequently applied. And the above remaining five principal components were reduced to one. Finally, the DC-PCA-KNN prediction model, achieving a mean true positive rate of 0.6519 and an accuracy of 0.6494, performed well in the prediction of halo CME geoeffectiveness and was superior to the DC or PCA model alone.

Table A1 The Entire CME-GS Pairs during Solar Cycles 23 and 24 **1997-2017**

Evaluating the Geoeffectiveness of Interplanetary Coronal Mass Ejections: Insights from a Support Vector Machine Approach with SHAP Value Analysis

Yudong **Ye**¹, Jiajia Liu^{2,3}, Yongqiang Hao¹, and Jun Cui¹

2024 ApJ 972 52

<https://iopscience.iop.org/article/10.3847/1538-4357/ad61d7/pdf>

In this study, we compiled a data set of 510 interplanetary coronal mass ejections (ICME) events from 1996–2023 and trained a radial basis function support vector machine (RBF-SVM) model to investigate the geoeffectiveness of ICMEs

and its dependence on the solar wind conditions observed at 1 au. The model demonstrates high performance in classifying geomagnetic storm intensities at specific Disturbance Storm Time thresholds and evaluating the geoeffectiveness of ICMEs. The model's output was assessed using precision, recall, F1 score, and true skill statistics (TSS), complemented by stratified k-folds cross-validation for robustness. At the -50 nT threshold, the model achieves precisions of 0.84 and 0.93, recalls of 0.94 and 0.82, and corresponding F1 scores of 0.89 and 0.87 for the categories separated by this threshold, respectively. Overall accuracy is noted at 0.88, with a TSS of 0.76. Despite challenges at the -100 nT threshold due to data set imbalance and limited samples, the model maintains an overall accuracy of 0.87, with a TSS of 0.69, demonstrating the model's ability to effectively handle imbalanced data. Physical insights were gained through model explanation with a SHapley Additive exPlanations (SHAP) value analysis, pinpointing the role of the southward magnetic field component in triggering geomagnetic storms, as well as the critical impact of shock-ICME combinations in intensifying these storms. The effective application of an SVM model with SHAP value analysis offers a way to understand and predict the geoeffectiveness of ICMEs. It also underscores the capability of a relatively simple machine learning model in predicting space weather and revealing the underlying physical mechanisms.

The Frequency-Domain Characterization of Cosmic Ray Intensity Variations Before Forbush Decreases Associated with Geomagnetic Storms

Qian Ye, [Cong Wang](#), [Fei He](#), [Bingsen Xue](#), [Xiaoxin Zhang](#)

Space Weather **Volume 20, Issue 3** e2021SW002863 2022

<https://agupubs.onlinelibrary.wiley.com/doi/epdf/10.1029/2021SW002863>

<https://doi.org/10.1029/2021SW002863>

Non-recurrent geomagnetic storms caused by Coronal Mass Ejection (CME) can induce serious impacts on space- and ground-based equipment. However, these non-recurrent geomagnetic storms are hard to predict since CMEs are not periodic. Previous studies have shown that the variations of Cosmic Ray Intensity (CRI) before non-recurrent storms may forebode the coming geomagnetic storm. But it is difficult to extract the variations since the cosmic ray flux is a complex signal. In order to identify the precursory signal in CRI variations triggered by CME, an ensemble self-adaptive time-frequency analysis method was proposed and applied to 65 non-recurrent geomagnetic storms occurred between 1998 and 2019. The results indicate that the precursory signals are successfully identified in 43 of 45 storms, after excluding 20 storms accompanied by ground level enhancement. In addition, it is also found that the spectral density of the precursory signal could reflect the active level of geomagnetic condition, which is lower during geomagnetic quiet period. **2003.08.14-18, 2005-01-20**

Table 1. The Properties of Strong Geo-effective CMEs during SolarCycle 23 & 24 and the corresponding ambient solar wind conditions 1998-2019

Effects of the Heliospheric Current Sheet on Trains of Enhanced Diurnal Variations in Galactic Cosmic Rays

T. [Yeeram](#), N. Saengdokmai

Solar Phys. Volume 290, Issue 8, pp 2311-2331 2015

We present recurrent trains of the enhanced diurnal anisotropy (DA) of Galactic cosmic rays (GCRs) during 2010 as observed by the Princess Sirindhorn Neutron Monitor at Doi Inthanon with a vertical cutoff rigidity of 16.8 GV. By investigating synoptic charts of the heliospheric current sheet (HCS) and the trains of enhanced DA, we found some consistency between them. During most time periods when recurrent trains of enhanced DA occurred, the DAs were noticeably enhanced more during the away sector than during the toward sector of the interplanetary magnetic field B. We interpret these temporal features in terms of a $B \times \nabla n$ gradient anisotropy, which is associated with latitudinal gradients of the GCR density (n) derived from the perpendicular component of DA in the solar wind frame. The gradual changes of DA in the trains in turn are associated with the gradual change in the latitudinal gradient of the GCR density along the HCS. We found that the north-south asymmetry (offset) of the HCS is responsible for the asymmetric recurrent modulation of the GCR intensity and suggest that particle drift along the wavy HCS and the adiabatic loss can cause the recurrent modulation, which is related to a local latitudinal gradient in the GCR density. The causes of the latitudinal gradient are discussed in light of current theories and observations.

Solar wind parameters in rising phase of solar cycle 25

[Yuri I. Yermolaev](#), [Irina G. Lodkina](#), [Alexander A. Khokhlachev](#), [Michael Yu. Yermolaev](#), [Maria O. Riazantseva](#), [Liudmila S. Rakhmanova](#), [Natalia L. Borodkova](#), [Olga V. Sapunova](#), [Anastasiia V. Moskaleva](#)
2023

<https://arxiv.org/ftp/arxiv/papers/2304/2304.14707.pdf>

Solar activity and solar wind parameters decreased significantly in solar cycles (SCs) 23-24. In this paper, we analyze solar wind measurements at the rising phase of SC 25 and compare them with similar data from the previous cycles. For this purpose, we simultaneously selected the OMNI database data for 1976-2022, both by phases of the 11-year solar cycle and by large-scale solar wind types (in accordance with IKI's catalog, see [this http URL](#)), and calculated the mean values of the parameters for the selected datasets. The obtained results testify in favor of the hypothesis that the continuation of this cycle will be similar to the previous cycle 24, i.e. SC 25 will be weaker than SCs 21 and 22.

Dynamics of Large Scale Solar Wind Streams Obtained by the Double Superposed Epoch Analysis: 5. Influence of the Solar Activity Decrease

Yuri I. [Yermolaev](#), [Irina G. Lodkina](#), [Alexander A. Khokhlachev](#), [Michael Yu. Yermolaev](#), [Maria O. Riazantseva](#), [Liudmila S. Rakhmanova](#), [Natalia L. Borodkova](#), [Olga V. Sapunova](#), [Anastasiia V. Moskaleva](#)
2022

<https://arxiv.org/ftp/arxiv/papers/2208/2208.04849.pdf>

In solar cycles 23-24, solar activity noticeably decreased, and, as a result, solar wind parameters decreased. Based on the measurements of the OMNI base for the period 1976-2019, the time profiles of the main solar wind parameters and magnetospheric indices for the main interplanetary drivers of magnetospheric disturbances (solar wind types CIR, Sheath, ejecta and MC) are studied using the double superposed epoch method. The main task of the research is to compare time profiles for the epoch of high solar activity at 21-22 solar cycles and the epoch of low activity at 23-24 solar cycles. The following results were obtained. (1) The analysis did not show a statistically significant change in driver durations during the epoch of minimum. (2) The time profiles of all parameters for all types of SW in the epoch of low activity have the same shape as in the epoch of high activity, but locate at lower values of the parameters. (3) In CIR events, the longitude angle of the solar wind flow has a characteristic S-shape, but in the epoch of low activity it varies in a larger range than in the previous epoch.

Drop of solar wind at the end of the 20th century

[Yuri I. Yermolaev](#), [Irina G. Lodkina](#), [Alexander A. Khokhlachev](#), [Michael Yu. Yermolaev](#), [Maria O. Riazantseva](#), [Liudmila S. Rakhmanova](#), [Natalia L. Borodkova](#), [Olga V. Sapunova](#), [Anastasiia V. Moskaleva](#)
JGR Volume126, Issue9 e2021JA029618 2021

<https://arxiv.org/ftp/arxiv/papers/2105/2105.10955.pdf>

<https://agupubs.onlinelibrary.wiley.com/doi/epdf/10.1029/2021JA029618>

<https://doi.org/10.1029/2021JA029618>

Variations in the solar wind (SW) parameters with scales of several years are an important characteristic of solar activity and the basis for a long-term space weather forecast. We examine the behavior of interplanetary parameters over 21-24 solar cycles (SCs) on the basis of OMNI database ([this https URL](#)). Since changes in parameters can be associated both with changes in the number of different large-scale types of SW, and with variations in the values of these parameters at different phases of the solar cycle and during the transition from one cycle to another, we select the entire study period in accordance with the Catalog of large-scale SW types for 1976-2019 (See the site [this http URL](#), [Yermolaev et al., 2009]), which covers the period from 21 to 24 SCs, and in accordance with the phases of the cycles, and averaging the parameters at selected intervals. In addition to a sharp drop in the number of ICMEs (and associated Sheath types), there is a noticeable drop in the value (by 20-40%) of plasma parameters and magnetic field in different types of solar wind at the end of the 20th century and a continuation of the fall or persistence at a low level in the 23-24 cycles. Such a drop in the solar wind is apparently associated with a decrease in solar activity and manifests itself in a noticeable decrease in space weather factors.

Statistic study of the geoeffectiveness of compression regions CIRs and Sheaths

[Yu I. Yermolaev](#), [I.G. Lodkina](#), [N.S. Nikolaeva](#), [M. Yu Yermolaev](#), [M.O. Riazantseva](#), [L.S. Rakhmanova](#)
Journal of Atmospheric and Solar-Terrestrial Physics

Volume 180, Pages 52-59, November **2018**

[sci-hub.tw/10.1016/j.jastp.2018.01.027](https://doi.org/10.1016/j.jastp.2018.01.027)

We statistically study the geoeffectiveness of two types of compression regions: corotating interaction regions (CIRs) before the [solar wind](#) high-speed streams (HSSs) from the coronal holes and Sheaths before the fast interplanetary CMEs (ICMEs) including flux-rope magnetic clouds (MCs) and non-MC [Ejecta](#) using the OMNI dataset (<http://omniweb.gsfc.nasa.gov> (King and Papitashvili, 2004)) and our Catalog of large-scale solar wind phenomena for 1976-2000 (<ftp://ftp.iki.rssi.ru/pub/omni/> (Yermolaev et al., 2009)). Our analysis shows that the magnitude of the [interplanetary magnetic field](#) B in CIRs and Sheaths increases with increasing speed of both types of pistons: HSS

and ICME; the increase of the piston speed results in the increase of geoeffectiveness of both compression regions. The value B in Sheaths before Ejecta is higher than B in Ejecta. The value B in Sheaths before MCs in the beginning of phenomena interval is lower than in MCs but in the end of interval it is close to B in MCs. The contribution of Sheath in storm generation can be significant for so-called "CME-induced" storms and Sheath-induced storms should be identified and analyzed separately.

Chapter 4 - Geoeffectiveness of Solar and Interplanetary Structures and Generation of Strong Geomagnetic Storms Review

Yuri I. Yermolaev, Irina G. Lodkina, Nadezhda S. Nikolaeva, Michael Yu. Yermolaev

In: Extreme Events in Geospace

Origins, Predictability, and Consequences Book

Editor: Natalia Buzulukova, Elsevier, 2018, 798 p. File

Pages 99-113

<http://sci-hub.st/10.1016/B978-0-12-812700-1.00004-2>

We study the large-scale phenomena of solar wind (SW), its source on the Sun, and its capability of generating magnetic storms on Earth. On the basis of the OMNI database, we identify the interplanetary drivers of magnetic storms as interplanetary coronal mass ejections (CMEs) (also interplanetary CMEs (ICMEs) including magnetic cloud (MC) and Ejecta), compression regions Sheath before fast ICMEs, and the co-rotating interaction region (CIR) before high-speed streams of solar wind. We approximate the tails of distribution functions of all storms and storms separately induced by four various drivers in the Dst range with large number of storms (-50 to -200 nT) and then extrapolate the approximating function in the range of extreme storms. Obtained results show that extreme storms with $Dst < -1700$ nT can be generated on Earth with a frequency not higher than one event during ~ 500 years with accuracy of this factor ~ 3 .

Dynamics of Large-Scale Solar-Wind Streams Obtained by the Double Superposed Epoch

Analysis: 3. Deflection of the Velocity Vector

Y. I. Yermolaev, I. G. Lodkina, M. Y. Yermolaev

Solar Physics June 2018, 293:91

<https://link.springer.com/content/pdf/10.1007%2Fs11207-018-1310-9.pdf>

This work is a continuation of our previous articles (Yermolaev et al. in J. Geophys. Res. 120, 7094, 2015 and Yermolaev et al. in Solar Phys. 292, 193, 2017), which describe the average temporal profiles of interplanetary plasma and field parameters in large-scale solar-wind (SW) streams: corotating interaction regions (CIRs), interplanetary coronal mass ejections (ICMEs, including both magnetic clouds (MCs) and ejecta), and sheaths as well as interplanetary shocks (ISs). Changes in the longitude angle, ϕ , in CIRs from -2 to 2 agree with earlier results (e.g. Gosling and Pizzo, 1999). We have also analyzed the average temporal profiles of the bulk velocity angles in sheaths and ICMEs. We have found that the angle ϕ in ICMEs changes from 2 to -2 , while in sheaths it changes from -2 to 2 (similar to the change in CIRs), i.e. the angle in CIRs and sheaths deflects in the opposite sense to ICMEs. When averaging the latitude angle θ on all the intervals of the chosen SW types, the angle θ is almost constant at ~ 1 . We made for the first time a selection of SW events with increasing and decreasing θ and found that the average θ temporal profiles in the selected events have the same "integral-like" shape as for ϕ . The difference in ϕ and θ average profiles is explained by the fact that most events have increasing profiles for the angle in the ecliptic plane as a result of solar rotation, while for the angle in the meridional plane, the numbers of events with increasing and decreasing profiles are equal.

Dynamics of Large-Scale Solar-Wind Streams Obtained by the Double Superposed Epoch

Analysis: 2. Comparisons of CIR vs . Sheath and MC vs . Ejecta

Y. I. Yermolaev, I. G. Lodkina, N. S. Nikolaeva, M. Y. Yermolaev

Solar Physics 292:193 2017 DOI 10.1007/s11207-017-1205-1

<https://link.springer.com/content/pdf/10.1007%2Fs11207-017-1205-1.pdf>

This work is a continuation of our previous article (Yermolaev et al. in J. Geophys. Res. 120, 7094, 2015), which describes the average temporal profiles of interplanetary plasma and field parameters in large-scale solar-wind (SW) streams: corotating interaction regions (CIRs), interplanetary coronal mass ejections (ICMEs including both magnetic clouds (MCs) and ejecta), and sheath as well as interplanetary shocks (ISs). As in the previous article, we use the data of the OMNI database, our catalog of large-scale solar-wind phenomena during 1976 – 2000 (Yermolaev et al. in Cosmic

Research, 47, 2, 81, 2009) and the method of double superposed epoch analysis (Yermolaev et al. in Ann. Geophys., 28, 2177, 2010a). We rescale the duration of all types of structures in such a way that the beginnings and endings for all of them coincide. We present new detailed results comparing pair phenomena: 1) both types of compression regions (i.e. CIRs vs. sheaths) and 2) both types of ICMEs (MCs vs. ejecta). The obtained data allow us to suggest that the formation of the two types of compression regions responds to the same physical mechanism, regardless of the type of piston (high-speed stream (HSS) or ICME); the differences are connected to the geometry (i.e. the angle between the speed gradient in front of the piston and the satellite trajectory) and the jumps in speed at the edges of the compression regions. In our opinion, one of the possible reasons behind the observed differences in the parameters in MCs and ejecta is that when ejecta are observed, the satellite passes farther from the nose of the area of ICME than when MCs are observed.

Some problems of identifying types of large-scale solar wind and their role in the physics of the magnetosphere

Y. I. [Yermolaev](#), I. G. Lodkina, N. S. Nikolaeva, M. Y. Yermolaev & M. O. Riazantseva

Cosmic Res (2017) 55: 178. doi:10.1134/S0010952517030029

Original Russian Text © Y.I. Yermolaev, I.G. Lodkina, N.S. Nikolaeva, M.Y. Yermolaev, M.O. Riazantseva, 2017, published in Kosmicheskie Issledovaniya, 2017, Vol. 55, No. 3, pp. 189–200.

This paper discusses the errors in analyzing solar-terrestrial relationships, which result from either disregarding the types of interplanetary drivers in studying the magnetosphere response on their effect or from the incorrect identification of the type of these drivers. In particular, it has been shown that the absence of selection between the Sheath and ICME (the study of so-called CME-induced storms, i.e., magnetic storms generated by CME) leads to errors in the studies of interplanetary conditions of magnetic storm generation, because the statistical analysis has shown that, in the Sheath + ICME sequences, the largest number of storm onsets fell on the Sheath, and the largest number of storms maxima fell at the end of the Sheath and the beginning of the ICME. That is, the situation is observed most frequently when at least the larger part of the main phase of storm generation falls on the Sheath and, in reality, Sheath-induced storms are observed. In addition, we consider several cases in which magnetic storms were generated by corotating interaction regions, whereas the authors attribute them to CME.

Dynamics of large-scale solar-wind streams obtained by the double superposed epoch analysis†

Yu. I. [Yermolaev](#), I. G. Lodkina, N. S. Nikolaeva, M. Yu. Yermolaev

JGR Volume 120, Issue 9 Pages 7094–7106 2015

Using the OMNI data for period 1976–2000 we investigate the temporal profiles of 20 plasma and field parameters in the disturbed large-scale types of solar wind (SW): CIR, ICME (both MC and Ejecta) and Sheath as well as the interplanetary shock (IS). To take into account the different durations of SW types we use the double superposed epoch analysis (DSEA) method: re-scaling the duration of the interval for all types in such a manner that, respectively, beginning and end for all intervals of selected type coincide. As the analyzed SW types can interact with each other and change parameters as a result of such interaction, we investigate separately 8 sequences of SW types: (1) CIR, (2) IS/CIR, (3) Ejecta, (4) Sheath/Ejecta, (5) IS/Sheath/Ejecta, (6) MC, (7) Sheath/MC, and (8) IS/Sheath/MC. The main conclusion is that the behavior of parameters in Sheath and in CIR are very similar both qualitatively and quantitatively. Both the high-speed stream (HSS) and the fast ICME play a role of pistons which push the plasma located ahead them. The increase of speed in HSS and ICME leads at first to formation of compression regions (CIR and Sheath, respectively), and then to IS. The occurrence of compression regions and IS increases the probability of growth of magnetospheric activity.

Influence of the interplanetary driver type on the durations of the main and recovery phases of magnetic storms†

Yu. I. [Yermolaev](#), I. G. Lodkina, N. S. Nikolaeva and M. Yu. Yermolaev

JGR, Volume 119, Issue 10, pages 8126–8136, October 2014

We study the durations of the main and recovery phases of magnetic storms induced by different types of large-scale solar-wind streams (Sheath, magnetic cloud (MC), Ejecta and CIR) on the basis of OMNI data for 1976–2000. The durations of both the main and recovery phases depend on the type of interplanetary drivers. On average, the duration of

the main phase of storms induced by compressed regions (CIR and Sheath) is shorter than for MC and Ejecta while the duration of the recovery phase of CIR- and Sheath-induced storms is longer. Analysis of the durations of individual storms shows that the durations of the main and recovery phases anti-correlate for CIR- and Sheath-induced storms and there is no dependence between them for (MC + Ejecta)-induced storms.

Occurrence rate of extreme magnetic storms

Yu I. **Yermolaev**, I. G. Lodkina, N. S. Nikolaeva and M. Yu. Yermolaev

JGR, Volume 118, Issue 8, pages 4760–4765, **2013**

<http://arxiv.org/abs/1211.4417>

Statistical analysis of occurrence rate of magnetic storms induced by different types of interplanetary drivers is made on the basis of OMNI data for period 1976–2000. Using our catalog of large scale types of solar wind streams we study storms induced by interplanetary coronal mass ejections (ICME) (separately magnetic clouds (MC) and Ejecta) and both types of compressed regions: corotating interaction regions (CIR) and Sheaths. For these types of drivers we calculate integral probabilities of storms with minimum Dst < -50, -70, -100, -150, and -200 nT. The highest probability in this interval of Dst is observed for MC, probabilities for other drivers are 3–10 times lower than for MC. Extrapolation of obtained results to extreme storms shows that such a magnetic storm as Carrington storm in 1859 with Dst = -1760 nT is observed on the Earth with frequency 1 event during ~500 year.

Recovery phase of magnetic storms induced by different interplanetary drivers

Yermolaev, Y. I., I. G. Lodkina, N. S. Nikolaeva, and M. Y. Yermolaev

J. Geophys. Res., 117, A08207, **2012**

Statistical analysis of Dst behavior during recovery phase of magnetic storms induced by different types of interplanetary drivers is made on the basis of OMNI data in period 1976–2000. We study storms induced by ICMEs (including magnetic clouds (MC) and Ejecta) and both types of compressed regions: corotating interaction regions (CIR) and Sheaths. The shortest, moderate and longest durations of recovery phase are observed in ICME-, CIR-, and Sheath-induced storms, respectively. Recovery phases of strong (Dstmin ≤ -100 nT) magnetic storms are well approximated by hyperbolic functions $Dst(t) = a/(1 + t/\tau_h)$ with constant τ_h times for each types of drivers while for moderate (-100 < Dstmin ≤ -50 nT) storms Dst profile can not be approximated by hyperbolic function with constant τ_h times because hyperbolic τ_h times increase with increasing time of recovery phase. Dependence of τ_h times on types of interplanetary drivers is the same as indicated above. Relation between duration and value Dstmin for storms induced by MC and Sheath has 2 parts: module of Dstmin and duration correlate at small durations while they anticorrelate at large durations. Obtained results show that recovery phase Dst variations depend on type of interplanetary drivers inducing magnetic storms.

Geoeffectiveness and efficiency of CIR, sheath, and ICME in generation of magnetic storms

Yermolaev, Y. I.; Nikolaeva, N. S.; Lodkina, I. G.; Yermolaev, M. Y.

J. Geophys. Res., Vol. 117, No. null, A00L07, **2012**

We investigate the relative role of various types of solar wind streams in generation of magnetic storms. On the basis of the OMNI data of interplanetary measurements for the period of 1976–2000, we analyze 798 geomagnetic storms with Dst ≤ -50 nT and five various types of solar wind streams as their interplanetary sources: corotating interaction regions (CIR), interplanetary coronal mass ejection (ICME) including magnetic clouds (MC) and ejecta, and a compression region sheath before both types of ICME (SHEMC and SHEEj, respectively). For various types of the solar wind we study the following relative characteristics: occurrence rate; mass, momentum, energy and magnetic fluxes; probability of generation of a magnetic storm (geoeffectiveness); efficiency of the process of this generation; and solar cycle variation of some of these parameters. Obtained results show that in spite of the fact that magnetic clouds have lower occurrence rates and lower efficiency than CIR and sheath, they play an essential role in generation of magnetic storms due to higher geoeffectiveness of storm generation (i.e., higher probability to contain large and long-term southward IMF Bz component). Geoeffectiveness for all drives has the smallest value during a solar cycle minimum and increases at other phases of the cycle.

Statistical study of interplanetary condition effect on geomagnetic storms: 2. Variations of parameters

Yu. I. [Yermolaev](#), I. G. Lodkina, N. S. Nikolaeva & M. Yu. Yermolaev
Cosmic Research, Vol. 49, Issue 1, 2011

Statistical study of interplanetary condition effect on geomagnetic storms

Yu. I. [Yermolaev](#), I. G. Lodkina, N. S. Nikolaeva & M. Yu. Yermolaev
Cosmic Research, Vol. 48, No. 6, pp. 485–500. 2010, File.

Original Russian Text: Kosmicheskie Issledovaniya, 2010, Vol. 48, No. 6, pp. 499–515.

Based on the archive OMNI data for the period 1976–2000 an analysis has been made of 798 geomagnetic storms with $Dst < -50$ nT and their interplanetary sources—large-scale types of the solar wind: CIR (145 magnetic storms), Sheath (96), magnetic clouds MC (62), and Ejecta (161). The remaining 334 magnetic storms have no well-defined sources. For the analysis, we applied the double method of superposed epoch analysis in which the instants of the magnetic storm beginning and minimum of Dst index are taken as reference times. The well-known fact that, independent of the interplanetary source type, the magnetic storm begins in 1–2 h after a southward turn of the IMF ($B_z < 0$) and both the end of the main phase of a storm and the beginning of its recovery phase are observed in 1–2 h after disappearance of the southward component of the IMF is confirmed. Also confirmed is the result obtained previously that the most efficient generation of magnetic storms is observed for Sheath before MC. On the average parameters B_z and E_y slightly vary between the beginning and end of the main phase of storms (minimum of Dst and indices), while Dst and indices decrease monotonically proportionally to integral of B_z and E_y over time. Such a behavior of the indices indicates that the used double method of superposed epoch analysis can be successfully applied in order to study dynamics of the parameters on the main phase of magnetic storms having different duration.

The “Floor” in the Interplanetary Magnetic Field: Estimation on the Basis of Relative Duration of ICME Observations in Solar Wind During 1976 – 2000

Y.I. [Yermolaev](#) · I.G. Lodkina · N.S. Nikolaeva · M.Y. Yermolaev

Solar Phys (2009) 260: 219–224

Measurement of the floor in the interplanetary magnetic field and estimation of the time-invariant open magnetic flux of the Sun require knowledge of closed magnetic flux carried away by coronal mass ejections (CMEs). In contrast with previous papers, we do not use global solar parameters to estimate such values: instead we identify different large-scale types of solar wind for the 1976 – 2000 interval to obtain the fraction of interplanetary CMEs (ICMEs). By calculating the magnitude of the interplanetary magnetic field B averaged over two Carrington rotations, the floor of the magnetic field can be estimated from the B value at a solar cycle minimum when the number of ICMEs is minimal. We find a value of 4.65 ± 0.6 nT, in good agreement with previous results.

Geomagnetic storm dependence on the solar flare class

Yu. I. [Yermolaev](#) and M. Yu. Yermolaev

A&A, 2009, File

Content. Solar flares are often used as precursors of geomagnetic storms. In particular, Howard and Tappin (2005) recently published in *A&A* a dependence between X-ray class of solar flares and A_p and Dst indexes of geomagnetic storms which contradicts to early published results.

Aims. We compare published results on flare-storm dependences and discuss possible sources of the discrepancy.

Methods. We analyze following sources of difference: (1) different intervals of observations, (2) different statistics and (3) different methods of event identification and comparison.

Catalog of Large-Scale Solar Wind Phenomena during 1976–2000

Yu. I. [Yermolaev](#), N. S. Nikolaeva, I. G. Lodkina, and M. Yu. Yermolaev
Cosmic Research, **2009**, Vol. 47, No. 2, pp. 81–94, [File](#).

Original Russian Text published in Kosmicheskie Issledovaniya, 2009, Vol. 47, No. 2, pp. 99–113.

The main goal of this paper is to compile a catalog of large-scale phenomena in the solar wind over the observation period of 1976–2000 using the measurement data presented in the OMNI database. This work included several stages. At first the original OMNI database was supplemented by certain key parameters of the solar wind that determine the type of the solar wind stream. The following parameters belong to this group: the plasma ratio β , thermal (NkT) and kinetic (mNV^2) pressures of the solar wind, the ratio T/T_{exp} of measured and expected temperatures, gradients of the plasma velocity and density, and the magnetic field gradient. The results of visualization of basic plasma parameters that determine the character of the solar wind stream are presented on the website of the Space Research Institute, Moscow. Preliminary identification of basic types of the solar wind stream (FAST and SLOW streams, Heliospheric Current Sheet (HCS), Corotating Interaction Region (CIR), EJECTA (or Interplanetary Coronal Mass Ejections), Magnetic Cloud (MC), SHEATH (compression region before EJECTA/MC), rarified region RARE, and interplanetary shock wave IS) had been made with the help of a preliminary identification program using the preset threshold criteria for plasma and interplanetary magnetic field parameters. Final identification was done by comparison with the results of visual analysis of the solar wind data. In conclusion, histograms of distributions and statistical characteristics are presented for some parameters of various large-scale types of the solar wind.

Comment on "Sizes and relative geoeffectiveness of interplanetary coronal mass ejections and the preceding shock sheaths during intense storms in 1996-2005" by J. Zhang et al.

Yu. I. [Yermolaev](#) and M. Yu. Yermolaev

GEOPHYSICAL RESEARCH LETTERS, **2009**, [File](#)

Recently *Zhang et al.* [2008] presented a statistical study of sizes and relative geoeffectiveness of ICMEs (bodies of magnetic clouds) and preceding sheaths for 46 events responsible for intense ($Dst < -100$ nT) geomagnetic storms in 1996-2005 in which only a single ICME was responsible for generating the storm. Here we would like to comment several results and conclusions of this paper.

Comment on "Source regions and storm effectiveness of frontside full halo coronal mass ejections" by X. P. Zhao and D. F. Webb

Yu. I. [Yermolaev](#)

2009?, [File](#)

Attention is drawn to the fact that the storm effectiveness of coronal mass ejections in paper by *Zhao and Webb* [2003] is in conflict with other results, including ones published in papers by *Wang et al.* [2002], *Yermolaev and Yermolaev* [2003a] analyzing the same data set and paper by *Cane and Richardson* [2003] analyzing CME possibility to generate interplanetary CME near the Earth. Our brief review of published results and methods of data processing shows that estimation of storm effectiveness of coronal mass ejections in paper by *Zhao and Webb* [2003] is likely to be overestimated and requires a further investigation.

Magnetic storm of November, 2004: Solar, interplanetary, and magnetospheric disturbances

Yu.I. [Yermolaev](#), L.M. Zeleniya, V.D. Kuznetsov, I.M. Chertok,

M.I. Panasyuk, I.N. Myagkov, I.A. Zhitnik, S.V. Kuzind, V.G. Eseleviche,

V.M. Bogodf, I.V. Arkhangelskajag, A.I. Arkhangelskyg, Yu.D. Kotov

Journal of Atmospheric and Solar-Terrestrial Physics 70 (**2008**) 334–341

We briefly review data on observations of the Sun, interplanetary medium, and magnetosphere, obtained by participants of the "Solar Extreme Events in 2004 (SEE'04)" collaboration before and during one of the strongest (4th in the 23rd solar cycle) magnetic storm of November 08, 2004 with Dst_{j_373} nT.

Comment on “Geoeffectiveness of Halo Coronal Mass Ejections” by N. Gopalswamy, S. Yashiro, and S. Akiyama (J. Geophys. Res. 2007, 112, doi:10.1029/2006JA012149)

Yu. I. [Yermolaev](#)

Cosmic Research, 2008, Vol. 46, No. 6, pp. 540-541, [File](#)

Comment on “Interplanetary origin of intense geomagnetic storms ($D_{st} < -100$ nT) during solar cycle 23” by W. D. Gonzalez et al.

Y. I. [Yermolaev](#)¹ and M. Y. Yermolaev¹

GEOPHYSICAL RESEARCH LETTERS, VOL. 35, L01101, doi:10.1029/2007GL030281, 2008, [File](#)

Statistical Investigation of Heliospheric Conditions Resulting in Magnetic Storms: 2

Yu. I. [Yermolaev](#), M. Yu. Yermolaev, I. G. Lodkina, and N. S. Nikolaeva

Cosmic Research, 2007, Vol. 45, No. 6, pp. 461–470, [File](#).

Original Russian Text published in Kosmicheskie Issledovaniya, 2007, Vol. 45, No. 6, pp. 489–498.

—This work is a continuation of investigation [1] of the behavior of the solar wind’s and interplanetary magnetic field’s parameters near the onset of geomagnetic storms for various types of solar wind streams. The data of the OMNI base for the 1976–2000 period are used in the analysis. The types of solar wind streams were determined, and the times of beginning (onsets) of magnetic storms were distributed in solar wind types as follows: CIR (121 storms), Sheath (22 storms), MC (113 storms), and “uncertain type” (367 storms). The growth of variations (hourly standard deviations) of the density and IMF magnitude was observed 5–10 hours before the onset only in the Sheath. For the CIR-, Sheath- and MC-induced storms the dependence between the minimum of the IMF B_z -component and the minimum of the D_{st} -index, as well as the dependence between the electric field E_y of solar wind and the minimum of the D_{st} -index are steeper than those for the “uncertain” solar wind type. The steepest D_{st} vs B_z dependence is observed in the Sheath, and the steepest D_{st} vs E_y dependence is observed in the MC.

Statistical Investigation of Heliospheric Conditions Resulting in Magnetic Storms

Yu. I. [Yermolaev](#), M. Yu. Yermolaev, I. G. Lodkina, and N. S. Nikolaeva

Cosmic Research, 2007, Vol. 45, No. 1, pp. 1–8, [File](#).

Original Russian Text published in Kosmicheskie Issledovaniya, 2007, Vol. 45, No. 1, pp. 3–11.

—Time behavior of the solar wind and interplanetary magnetic field parameters is investigated for 623 magnetic storms of the OMNI database for the period 1976–2000. The analysis is carried out by the superposed epoch technique (the magnetic storm onset time is taken to be the beginning of an epoch) for five various categories of storms induced by various types of solar wind: CIR (121 storms), Sheath (22 storms), MC (113 storms), and “uncertain type” (367 storms). In total, the analysis conducted for “all storms” included 623 storms. The obtained data, on one hand, confirm the results obtained earlier without selecting the intervals according to the solar wind types, and, on the other hand, they indicate the existence of distinctions in the time variation of parameters for various types of solar wind. Though the lowest values of the B_z -component of IMF are observed in the MC, the lowest values of the D_{st} -index are achieved in the Sheath. Thus, the strongest magnetic storms are induced, on average, during the Sheath rather than during the MC body passage, probably owing to higher pressure in the Sheath. Higher values of nkT , T/T_{exp} , and ® parameters are observed in the CIR and Sheath and lower ones in the MC, which corresponds to the physical essence of these solar wind types.

Statistic study on the geomagnetic storm effectiveness of solar and interplanetary events

Yu.I. [Yermolaev](#) *, M.Yu. Yermolaev

Advances in Space Research, Volume 37, Issue 6, p. 1175-1181, 2006, [File](#)

In the literature on the solar–terrestrial relations there are different estimations of storm effectiveness of solar and interplanetary events – from 30% up to 100%. We made a review of published results and found that different results arise due to differences in the methods used to analyze the data: (1) the directions in which the events are compared, (2) the pairs of compared events, and (3) the methods of the event classifications. We selected papers using: (1) the analysis on direct and back tracings of events, and (2) solar (coronal flares and CMEs), interplanetary (magnetic clouds, ejecta and CIR) and geomagnetic disturbances (storms on D_{st} and K_p indices). The classifications of magnetic storms by the

Kp and Dst indices, the solar flare classifications by optical and X-ray observations, and the classifications of different geoeffective interplanetary events are compared and discussed. Taking into account this selection, all published results on the geoeffectiveness agree to each other in each subset: “CME ! Storm” (40–50%), “CME ! MC, Ejecta” (60–80%), “MC, Ejecta ! Storm” (50–80%), “Storm! MC, Ejecta” (30–70%), “MC, Ejecta ! CME” (50–80%), “Storm !CME” (80–100%), “Flare! Storm” (30–40%) and “Storm! Flare” (50–80%).

Statistical studies of geomagnetic storm dependencies on solar and interplanetary events: a review

Y.I. [Yermolaev](#), M.Y. Yermolaeva, G.N. Zastenker, L.M. Zelenyia, A.A. Petrukovich, J.-A. Sauvaud
Planetary and Space Science, 53/1-3 pp. 189-196, **2005**, [File](#)

We present a brief review of published results on the geomagnetic storm effectiveness of CMEs and solar flares as well as of interplanetary events. Attention is drawn to the fact that the published values of storm effectiveness are in conflict with one another. Possible reasons of their differences are discussed. The presented comparison of methods and results of the analysis of the phenomena on the Sun, in the interplanetary space and in the Earth’s magnetosphere shows that in addition to different methods used in each of areas, a way of comparison of the phenomena in various space areas or for different direction of data tracing is of great importance for research of the entire chain of solar-terrestrial physics.

A holistic approach to understand Helium enrichment in Interplanetary coronal mass ejections: New insights

[Yogesh](#), [D. Chakrabarty](#), [N. Srivastava](#)

MNRAS Letters, Volume 513, Issue 1, pp.L106-L111 **2022**

<https://arxiv.org/pdf/2202.01722.pdf>

Despite helium abundance ($A_{He} = n_{H}/n_{He}$) is $\sim 8\%$ at the solar photospheric/chromospheric heights, A_{He} can be found to exceed 8% in interplanetary coronal mass ejections (ICMEs) on many occasions. Although various factors like interplanetary shocks, chromospheric evaporation and "sludge removal" have been separately invoked in the past to address the A_{He} enhancements in ICMEs, none of these processes could explain the variability of A_{He} in ICMEs comprehensively. Based on extensive analysis of 275 ICME events, we show that there is a solar activity variation of ICME averaged A_{He} values. The investigation also reveals that the first ionization potential effect as well as coronal temperature are not the major contributing factors for A_{He} enhancements in ICMEs. Investigation on concurrent solar flares and ICME events for 63 cases reveals that chromospheric evaporation in tandem with gravitational settling determine the A_{He} enhancements and variabilities beyond 8% in ICMEs. While chromospheric evaporation releases the helium from chromosphere into the corona, the gravitationally settled helium is thrown out during the ICMEs. We show that the intensity and timing of the preceding flares from the same active region from where the CME erupts are important factors to understand the A_{He} enhancements in ICMEs. **28–29 Mar 2001, 12-14 Sep 2004, 12 Feb 2014, 02 Apr 2014,**

Correction: Volume 520, Issue 1, March **2023**, Page L78, <https://doi.org/10.1093/mnrasl/slado11>

Statistical nature of geomagnetic storms.

[Yokoyama](#), N., Kamide, Y.:

1997, J. Geophys. Res. Space Phys. 102(A7), 14215.

<https://agupubs.onlinelibrary.wiley.com/doi/pdf/10.1029/97JA00903>

On the basis of geomagnetic activity indices and solar wind parameters, a superposed epoch analysis has been conducted for more than 300 geomagnetic storms. The intensity of magnetic storms is found to depend on the duration of the main phase; larger storms have longer timescales. For intense storms, however, not only the duration of energy injection into the ring current but also the strength of injection is important in determining their size. It is confirmed that the southward component of the interplanetary magnetic field plays a crucial role both in triggering the storm main phase and in determining the magnitude of magnetic storms. It is also found that the time profile of the energy injection rate during the main phase tends to have two peaks. This is particularly the case for intense magnetic storms, where the second peak is more intense than the first. Implications of our findings are discussed in terms of the existing concept of geomagnetic storms and recent observations of ring current particles and of interplanetary disturbances.

Refined Modeling of Geoeffective Fast Halo CMEs During Solar Cycle 24

E. [Yordanova](#), [M. Temmer](#), [M. Dumbović](#), [C. Scolini](#), [E. Paouris](#), [A. L. E. Werner](#), [A. P. Dimmock](#), [L. Sorriso-Valvo](#)

Space Weather [Volume22, Issue1](#) e2023SW003497 **2024**

<https://doi.org/10.1029/2023SW003497>

<https://agupubs.onlinelibrary.wiley.com/doi/epdf/10.1029/2023SW003497>

The propagation of geoeffective fast halo coronal mass ejections (CMEs) from solar cycle 24 has been investigated using the European Heliospheric Forecasting Information Asset (EUHFORIA), ENLIL, Drag-Based Model (DBM) and Effective Acceleration Model (EAM) models. For an objective comparison, a unified set of a small sample of CME events with similar characteristics has been selected. The same CME kinematic parameters have been used as input in the propagation models to compare their predicted arrival times and the speed of the interplanetary (IP) shocks associated with the CMEs. The performance assessment has been based on the application of an identical set of metrics. First, the modeling of the events has been done with default input concerning the background solar wind, as would be used in operations. The obtained CME arrival forecast deviates from the observations at L1, with a general underestimation of the arrival time and overestimation of the impact speed (mean absolute error [MAE]: 9.8 ± 1.8 – 14.6 ± 2.3 hr and 178 ± 22 – 376 ± 54 km/s). To address this discrepancy, we refine the models by simple changes of the density ratio (d_{cld}) between the CME and IP space in the numerical, and the IP drag (γ) in the analytical models. This approach resulted in a reduced MAE in the forecast for the arrival time of 8.6 ± 2.2 – 13.5 ± 2.2 hr and the impact speed of 51 ± 6 – 243 ± 45 km/s. In addition, we performed multi-CME runs to simulate potential interactions. This leads, to even larger uncertainties in the forecast. Based on this study we suggest simple adjustments in the operational settings for improving the forecast of fast halo CMEs. **2012-01-22-25, 2014-02-15-20, 2014-12-21-25**

Table 1 List of Halo Coronal Mass Ejection (CME) Events and Relevant Parameters 2011–2015

AN IMPROVED SOLAR WIND ELECTRON DENSITY MODEL FOR PULSAR TIMING

X. P. You,^{1, 2,3} G. B. Hobbs,² W. A. Coles,⁴ R. N. Manchester,² and J. L. Han¹

The Astrophysical Journal, 671:907Y911, 2007 December 10

<http://www.journals.uchicago.edu/doi/pdf/10.1086/522227>

The effects of the solar magnetic polarity and the solar wind velocity on Bz-component of the interplanetary magnetic field

M. Yousefa, A. Mahrousb, R. Mawadb, E. Ghamrya, b, M. Shaltouta, , , , M. El-Nawawyb, c, A. Fahim
Advances in Space Research, Volume 49, Issue 7, 1 April 2012, Pages 1198–1202

We have studied the effect of both solar magnetic polarity and the solar wind velocity on the Bz-component of the interplanetary magnetic field, IMFBz, for the minimum activity of the solar cycles 21, 22, 23 and 24. We made a statistical study of IMFBz in the first section which is considered as an extension of Lyatsky et al. (2003). They made a statistical study of IMFBz for two periods of minimum solar activity 22 and 23 related to 1985–1987 and 1995–1997 when the solar magnetic field had opposite polarity. Our results seem to be consistent with the results obtained by Lyatsky et al. (2003). We found that there is a dependence of IMFBz on the IMFBx and the solar magnetic polarity for the minimum periods of the selected four solar cycles. In addition, we found that there is a dependence of IMFBz on the solar wind velocity.

Small-Scale Magnetic Holes in the Solar Wind Observed by Parker Solar Probe

L. Yu,[S. Y. Huang](#),[Z. G. Yuan](#),[K. Jiang](#),[Y. Y. Wei](#),[J. Zhang](#),[S. B. Xu](#),[Q. Y. Xiong](#),[Z. Wang](#),[R. T. Lin](#),[Y. J. Li](#),[C. M. Wang](#),[G. J. Song](#)

JGR [Volume127, Issue8](#) e2022JA030505 2022

<https://doi.org/10.1029/2022JA030505>

<https://agupubs.onlinelibrary.wiley.com/doi/epdf/10.1029/2022JA030505>

The small-scale magnetic hole (SSMH), characterized by magnetic field depression, is a structure with the size in the order of proton gyro-radius. SSMHs near the Earth or other planets have been widely observed in recent years. However, SSMHs in the solar wind near the Sun are rarely investigated due to mission constraints. In the present study, SSMHs in the pristine solar wind within a wide heliocentric distance range are analyzed based on the Parker Solar Probe (PSP) Mission measurements. A total of 2,416 SSMHs are successfully identified during the orbits of PSP from 2nd October, 2018, to 31st December, 2020, with an average occurrence rate of ~ 5.8 events/day. The occurrence rate of SSMHs decreases from ~ 29.5 to ~ 0.6 events/day as the heliocentric distance R increases. The spatial scale of these SSMHs obeys a bi-log-normal distribution, with the median scale $L \sim 137$ km (~ 6 pp, proton gyro-radius). As interplanetary magnetic field B_{ave} increases or R decreases, the upper limit of the spatial scale L corresponding to each bin extends to a larger value. The L corresponding to the maximum occurrence rate also increases when B_{ave} increases and R decreases. Besides, the SSMHs tend to occur more frequently in the solar wind environment with weak B_{ave} and high thermal pressure P_t . Our results shed light on the characteristics and the origin of SSMHs in the pristine solar wind.

Investigating the Asymmetry of Magnetic Field Profiles of "Simple" Magnetic Ejecta through an Expansion-modified Flux Rope Model

Wenyuan **Yu**¹, Nada Al-Haddad¹, Charles J. Farrugia¹, Noé Lugaz¹, Florian Regnault¹, and Antoinette Galvin¹

2022 ApJ 937 86

<https://iopscience.iop.org/article/10.3847/1538-4357/ac88c3/pdf>

Magnetic clouds (MCs) are most often fitted with flux rope models that are static and have symmetric magnetic field profiles. However, spacecraft measurements near 1 au show that MCs usually expand when propagating away from the Sun and that their magnetic field profiles are asymmetric. Both effects are expected to be related, since expansion has been shown to result in a shift of the peak of the magnetic field toward the front of the MC. In this study, we investigate the effects of expansion on the asymmetry of the total magnetic field strength profile of MCs. We restrict our study to the simplest events, i.e., those that are crossed close to the nose of the MC. From a list of 25 such "simple" events, we compare the fitting results of a specific expanding Lundquist model with those of a classical force-free circular cross-sectional static Lundquist model. We quantify the goodness of the fits by the χ^2 of the total magnetic field and identify three types of MCs: (i) those with little expansion, which are well fitted by both models; (ii) those with moderate expansion, which are well fitted by the expanding model, but not by the static model; and (iii) those with expansion, whose asymmetry of the magnetic field cannot be explained. We find that the assumption of self-similar expansion cannot explain the measured asymmetry in the magnetic field profiles of some of these magnetic ejecta (MEs). We discuss our results in terms of our understanding of the magnetic fields of the MEs and their evolution from the Sun to Earth.

Table 1 MVA Results for the 25 MEs 2010-2015

Characteristics of Magnetic Holes in the Solar Wind Revealed by Parker Solar Probe

L. **Yu**, [S. Y. Huang](#), [Z. G. Yuan](#), [K. Jiang](#), [Q. Y. Xiong](#), [S. B. Xu](#), [Y. Y. Wei](#), [J. Zhang](#), [Z. H. Zhang](#)

ApJ 908 56 2021

<https://arxiv.org/ftp/arxiv/papers/2010/2010.14008.pdf>

<https://doi.org/10.3847/1538-4357/abb9a8>

We present a statistical analysis for the characteristics and radial evolution of linear magnetic holes (LMHs) in the solar wind from 0.166 to 0.82 AU using Parker Solar Probe observations of the first two orbits. It is found that the LMHs mainly have a duration less than 25 s and the depth is in the range from 0.25 to 0.7. The durations slightly increase and the depths become slightly deeper with the increasing heliocentric distance. Both the plasma temperature and the density for about 50% of all events inside the holes are higher than the ones surrounding the holes. The average occurrence rate is 8.7 events/day, much higher than that of the previous observations. The occurrence rate of the LMHs has no clear variation with the heliocentric distance (only a slight decreasing trend with the increasing heliocentric distance), and has several enhancements around ~ 0.525 AU and ~ 0.775 AU, implying that there may be new locally generated LMHs. All events are segmented into three parts (i.e., 0.27, 0.49 and 0.71 AU) to investigate the geometry evolution of the linear magnetic holes. The results show that the geometry of LMHs are prolonged both across and along the magnetic field direction from the Sun to the Earth, while the scales across the field extend a little faster than along the field. The present study could help us to understand the evolution and formation mechanism of the LMHs in the solar wind. **11 Oct 2018, 14 Apr 2019**

The Magnetic Field Geometry of Small Solar Wind Flux Ropes Inferred from Their Twist Distribution

W. **Yu**, C. J. Farrugia, N. Lugaz, A. B. Galvin, C. Möstl, K. Paulson, P. Vemareddy

[Solar Physics](#) December 2018, 293:165

<https://link.springer.com/content/pdf/10.1007%2Fs11207-018-1385-3.pdf>

This work extends recent efforts on the force-free modeling of large flux rope-type structures (magnetic clouds, MCs) to much smaller spatial scales. We first select small flux ropes (SFRs) by eye whose duration is unambiguous and which were observed by the Solar Terrestrial Relations Observatory (STEREO) or Wind spacecraft during solar maximum years. We inquire into which analytical technique is physically most appropriate, augmenting the numerical modeling with considerations of magnetic twist. The observational fact that these SFRs typically do not expand significantly into the solar wind makes static models appropriate for this study. SFRs can be modeled with force-free methods during the maximum phase of solar activity. We consider three models: (i) a linear force-free field ($\nabla \times \mathbf{B} = \alpha \mathbf{B}$) with a specific, prescribed constant α (Lundquist solution), and (ii) with α as a free constant parameter ("Lundquist-alpha" solution), and (iii) a uniform twist field (Gold-Hoyle solution). We retain only those cases where the impact parameter is less than

one-half the flux rope (FR) radius, R , so the results should be robust (29 cases). The SFR radii lie in the range $[\approx 0.003, 0.059]$ AU. Comparing results, we find that the Lundquist-alpha and uniform twist solutions yielded comparable and small normalized χ^2 values in most cases. This means that analytical modeling alone cannot distinguish which of these two is better in reproducing their magnetic field geometry. We then use Grad-Shafranov (GS) reconstruction to analyze these events further in a model-independent way. The orientations derived from GS are close to those obtained from the uniform twist field model. We then considered the twist per unit length, τ , both its profile through the FR and its absolute value, applying a graphic approach to obtain τ from the GS solution. The results are in better agreement with the uniform twist model. We find τ to lie in the range $[5.6, 34]$ turns/AU, i.e. much higher than typical values for MCs. The GH model-derived τ values are comparable to those obtained from GS reconstruction. We find that the twist per unit length, L , is inversely proportional to R , as $\tau \approx 0.17/R$. We combine MC and SFR results on $\tau(R)$ and give a relation that is approximately valid for both sets. Using this, we find that the axial and azimuthal fluxes, F_z and F_ϕ , vary as $\approx 2.1B_0R^2$ ($\times 10^{21}$ Mx) and $F_\phi/L \approx 0.36B_0R$ ($\times 10^{21}$ Mx/AU). The relative helicity per unit length is $H/L \approx 0.75B_0R^3$ ($\times 10^{42}$ Mx²/AU). Table

Suprathermal helium in corotating interaction regions: combined observations from SOHO/CELIAS/STOF and ACE/SWICS

J. Yu¹, L. Berger¹, R. Wimmer-Schweingruber¹, P. Bochsler², B. Klecker³, M. Hilchenbach⁴ and R. Kallenbach

A&A 599, A13 (2017) 10.1051/0004-6361/201628641

Context. Energetic particle enhancements that are associated with corotating interaction regions (CIRs) are typically believed to arise from the sunward propagation of particles that are accelerated by CIR-driven shocks beyond 1 AU. It is expected that these sunward-travelling particles will lose energy and scatter, resulting in a turnover of the energy spectra below ~ 0.5 MeV/nuc. However, the turnover has not been observed so far, suggesting that the CIR-associated low-energy suprathermal ions are accelerated locally close to the observer.

Aims. We investigate the variability of suprathermal particle spectra from CIR to CIR as well as their evolution and variation as the observer moves away from the rear shock or wave.

Methods. Helium data in the suprathermal energy range from the Solar and Heliospheric Observatory/Charge, Element, and Isotope Analysis System/Suprathermal Time-of-Flight (SOHO/CELIAS/STOF) were used for the spectral analysis and were combined with data from the Advanced Composition Explorer/ Solar Wind Ion Composition Spectrometer (ACE/SWICS) in the solar wind energies.

Results. We investigated sixteen events: nine clean CIR events, three CIR events with possible contamination from upstream ion events or solar energetic particles (SEPs), and four events that occurred during CIR periods that were dominated by SEPs. Six of the nine clean CIR events showed possible signs of a turnover between ~ 10 – 40 keV/nuc in the fast solar wind that trails the compression regions. Three of them even showed this behaviour inside the compressed fast wind. The turnover part of the spectra became flatter and shifted from lower to higher energies with increasing connection distance to the reverse shock. The remaining three clean events showed continuous power-law spectra in both the compressed fast wind and fast wind regions, that is, the same behaviour as reported from previous observations. The spectra of the seven remaining events are more variable, that is, they show power law, turnover, and a superposition of these two shapes.

Small Solar Wind Transients at 1 AU: STEREO Observations (2007–2014) and Comparison with Near-Earth Wind Results (1995–2014) †

W. Yu, C. J. Farrugia, A. B. Galvin, Noé Lugaz, J. G. Luhmann, K. D. C. Simunac, E. Kilpua
JGR 2016

This paper discusses small solar wind transients (STs) from 1995 to 2014. Using STEREO data, we have more sites from which to study STs near 1 AU. STEREO measurements are compared with Wind observations near the Sun-Earth line. We examined statistically the dependence of ST occurrence frequency on (i) solar cycle phase, as monitored by the sunspot number (SSN), and (ii) solar wind speed. We find dependencies on both: an anti-correlation with SSN, an opposite trend to that of ICMEs, and correlation with slow solar wind (over 80 % in the slow wind). We compare ST distributions during solar maximum year 2003, which had the lowest percentage of slow wind, and minimum year 2009, which had the highest percentage thereof, and show evidence of both dependencies. We give a statistical overview of ST parameters: field strength, B , Alfvén Mach number, MA , and proton beta, β_p . They show the same temporal trends as the ambient solar wind, but have twice (B) or one half (MA , β_p) of its average values. In STs, the proton temperature is not below the temperature expected from corotating solar wind expansion. Non-force free models should be used in solar minimum years where $\beta_{\text{plasma}} \approx 1$, while the force free models could be used in solar maximum when

$\beta_{\text{plasma}} \ll 1$. We find that only $\sim 5\%$ of STs show enhanced values of iron charge states. Our work further supports the 2-source origin of STs, i.e., the solar corona and the interplanetary medium.

A 17 June 2011 Polar Jet and its Presence in the Background Solar Wind

H.-S. Yu, B.V. Jackson, Y.-H. Yang, N.-H. Chen, A. Buffington, P.P. Hick

JGR 2016

High-speed jet responses in the polar solar wind are enigmatic. Here, we measure a jet response that emanates from the southern polar coronal hole on **17 June 2011** at the extreme speed of over 1200 km/s. This response was recorded from the Sun-Earth line in SDO/AIA and LASCO/C2 and both STEREO EUVI and COR2 coronagraphs when the three spacecraft were situated $\sim 90^\circ$ from one another. These certify the coronal 3D location of the response that is associated with an existing solar plume structure, and show its high speed to distances of over 14 Rs. This jetting is associated with magnetic flux changes in the polar region as measured by the SDO/HMI instrumentation over a period of several hours. The fastest coronal response observed can be tracked to a time near the period of greatest flux changes, and to the onset of the brightest flaring in AIA. This high-speed response can be tracked directly as a small patch of outward-moving brightness in coronal images as in Yu et al. [2014] where three slower events were followed from the perspective of Earth. This accumulated jet response has the largest mass and energy we have yet seen in 3D reconstructions from Solar Mass Ejection Imager (SMEI) observations, and its outward motion is certified for the first time using interplanetary scintillation (IPS) observations. This jet response is surrounded by similar high-speed patches but these are smoothed out in Ulysses polar measurements, we speculate about how these dynamic activities relate to solar wind acceleration.

3D Reconstruction of Interplanetary Scintillation (IPS) Remote-Sensing Data: Global Solar Wind Boundaries for Driving 3D-MHD Models

H.-S. Yu, B. V. Jackson, P. P. Hick, [A. Buffington](#), [D. Odstreil](#), [C.-C. Wu](#), [J. A. Davies](#), [M. M. Bisi](#), [M. Tokumaru](#)

Solar Phys. Volume 290, Issue 9, pp 2519-2538 2015

The University of California, San Diego, time-dependent analyses of the heliosphere provide three-dimensional (3D) reconstructions of solar wind velocities and densities from observations of interplanetary scintillation (IPS). Using data from the Solar-Terrestrial Environment Laboratory, Japan, these reconstructions provide a real-time prediction of the global solar-wind density and velocity throughout the whole heliosphere with a temporal cadence of about one day (ips.ucsd.edu). Updates to this modeling effort continue: in the present article, near-Sun results extracted from the time-dependent 3D reconstruction are used as inner boundary conditions to drive 3D-MHD models (e.g. ENLIL and H3D-MHD). This allows us to explore the differences between the IPS kinematic-model data-fitting procedure and current 3D-MHD modeling techniques. The differences in these techniques provide interesting insights into the physical principles governing the expulsion of coronal mass ejections (CMEs). Here we detail for the first time several specific CMEs and an induced shock that occurred in **September 2011** that demonstrate some of the issues resulting from these analyses.

Underlying scaling relationships between solar activity and geomagnetic activity revealed by multifractal analyses†

Zu-Guo Yu^{1,2,*}, Vo Anh² and Richard Eastes

JGR, Volume 119, Issue 9, pages 7577–7586, 2014

This paper identifies some scaling relationships between solar activity and geomagnetic activity. We examine the scaling properties of hourly data for two geomagnetic indices (ap and AE), two solar indices (solar X-rays XI and solar flux F10.7), and two inner heliospheric indices (ion density Ni and flow speed Vs) over the period 1995-2001 by the universal multifractal approach and the traditional multifractal analysis. We found that the universal multifractal model (UMM) provides a good fit to the empirical $K(q)$ and $\tau(q)$ curves of these time series. The estimated values of the Lévy index α in the UMM indicate that multifractality exists in the time series for ap, AE, XI and Ni, while those for F10.7 and Vs are monofractal. The estimated values of the non-conservation parameter H of this model confirm that these time are conservative which indicates the mean value of the process is constant for varying resolution.

Additionally, the multifractal $K(q)$ and $\tau(q)$ curves, and the estimated values of the sparseness parameter C1 of the UMM indicate that there are three pairs of indices displaying similar scaling properties, namely ap and XI, AE and Ni, F10.7 and Vs. The similarity in the scaling properties of pairs (ap, XI) and (AE, Ni) suggests that ap and XI, AE and Ni are better correlated — in terms of scaling — than previous thought, respectively. But our results still cannot be used to advance forecasting of ap and AE by XI and Ni, respectively, due to some reasons.

The Three-dimensional Analysis of Hinode Polar Jets using Images from LASCO C2, the Stereo COR2 Coronagraphs, and SMEI

H.-S. Yu¹, B. V. Jackson¹, A. Buffington¹, P. P. Hick¹, M. Shimojo², and N. Sako
2014 ApJ 784 166

Images recorded by the X-ray Telescope on board the Hinode spacecraft are used to provide high-cadence observations of solar jetting activity. A selection of the brightest of these polar jets shows a positive correlation with high-speed responses traced into the interplanetary medium. LASCO C2 and STEREO COR2 coronagraph images measure the coronal response to some of the largest jets, and also the nearby background solar wind velocity, thereby giving a determination of their speeds that we compare with Hinode observations. When using the full Solar Mass Ejection Imager (SMEI) data set, we track these same high-speed solar jet responses into the inner heliosphere and from these analyses determine their mass, flow energies, and the extent to which they retain their identity at large solar distances.

Influence of Magnetic Clouds on Variations of Cosmic Rays in November 2004

Xiao Xia Yu · Hong Lu · Gui Ming Le · Feng Shi

Solar Phys (2010) 263: 223–237, DOI 10.1007/s11207-010-9522-7; File

We investigate the effects of two magnetic clouds on hourly cosmic-ray intensity profiles in the Forbush decrease events in November 2004 observed by 47 ground-based neutron-monitor stations. By using a wavelet decomposition, the start time of the main phase in a Forbush decrease event can be defined, and then clearer definitions of initial phase, main phase, and recovery phase are proposed. Our analyses suggest that the main phase of this Fd event precedes the arrival time of the first magnetic cloud by about three hours, and the Fds observed at the majority (39/47) of the stations were found to originate from the sheath region as indicated by large fluctuations in magnetic field vectors at 19:00 UT on 7 November 2004, regardless of the station location. In addition, about 45% of the onset times of the recovery phase in the Forbush decreases took place at 04:00 UT on 10 November, independent of the station position. *The results presented here support the hypothesis that the sheath region between the shock and the magnetic cloud, especially the enhanced turbulent magnetic field, results in the scattering of cosmic-ray particles, and causes the following Forbush decreases.* Analysis of variation profiles from different neutron monitors reveals the global simultaneity of this Forbush decrease event. Moreover, we infer that the interplanetary disturbance was asymmetric when it reached the Earth, inclined to the southern hemisphere. These results provide several observational constraints for more detailed simulations of the Forbush decrease events with time-dependent cosmic-ray modulation models.

Multifractal analysis of geomagnetic storm and solar flare indices and their class dependence

Yu, Zu-Guo; Anh, Vo; Eastes, Richard

J. Geophys. Res., Vol. 114, No. A5, A05214, 2009

<http://dx.doi.org/10.1029/2008JA013854>

The multifractal properties of two indices of geomagnetic activity, D_{st} (representative of low latitudes) and a_p (representative of the global geomagnetic activity), with the solar X-ray brightness, X_{11} , during the period from 1 March 1995 to 17 June 2003 are examined using multifractal detrended fluctuation analysis (MF-DFA). The $h(q)$ curves of D_{st} and a_p in the MF-DFA are similar to each other, but they are different from that of X_{11} , indicating that the scaling properties of X_{11} are different from those of D_{st} and a_p . Hence, one should not predict the magnitude of magnetic storms directly from solar X-ray observations. However, a strong relationship exists between the classes of the solar X-ray irradiance (the classes being chosen to separate solar flares of class X-M, class C, and class B or less, including no flares) in hourly measurements and the geomagnetic disturbances (large to moderate, small, or quiet) seen in D_{st} and a_p during the active period.

The Efficiency of Coronal Mass Ejection With Different IMF Preconditions on the Production of Megaelectronvolt Electron Content in the Outer Radiation Belt

C.-J. Yuan Q.-G. Zong

Fifty-two coronal mass ejections (CMEs) from 2012 to 2017 are categorized into four types according to different interplanetary magnetic field (IMF) preconditions, and behaviors of 1.8-, 3.4-, 5.2-, and 7.7-MeV electrons are quantitatively investigated using an Radiation Belt Content (RBC) index improved for nondipolar geomagnetic field configuration due to interaction with CMEs. Statistical analyses show that CMEs with continuous southward IMF from upstream of shock front to CME leading edge are the most efficient in the production of megaelectronvolt electron content, with RBC five times larger after shock arrival for 1.8-MeV channel, seven times larger for 3.4-MeV channel, and three times larger for 5.2-MeV channel; the 7.7-MeV channel also experiences less pronounced enhancements. For CMEs with continuous northward IMF from upstream of shock front to CME leading edge, clear dropouts of RBC are revealed. The depletion is the most significant for 1.8 MeV, and the magnitude of depletion gradually decreases when the electron energy goes higher. It is suggested that the location of magnetopause and plasmopause, and thus magnetopause shadowing and magnetospheric waves like whistler mode chorus, contributes to the dynamics of megaelectronvolt electrons in the outer radiation belt, with energy dependence, in response to CMEs with different preconditions. **8 October 2012, 12 Sept 2014, 11-13 July 2015**

Geomagnetic activity triggered by interplanetary shocks

Yue, C.; Zong, Q. G.; Zhang, H.; Wang, Y. F.; Yuan, C. J.; Pu, Z. Y.; Fu, S. Y.; Lui, A. T. Y.; Yang, B.; Wang, C. R.

J. Geophys. Res., Vol. 115, A00I05, 13 PP., 2010

Interplanetary (IP) shocks can greatly disturb the Earth's magnetosphere, causing the global dynamic changes in the electromagnetic fields and the plasma. In order to investigate this, we have systematically analyzed 106 IP shock events based on OMNI data, GOES, and Los Alamos National Laboratory satellite observations during 1997–2007. It is revealed that the median value of IMF Bz keeps negative/positive prior to shock arrival and becomes more negative/positive following the shock arrival. The statistical analysis shows that IP shocks with southward interplanetary magnetic field (IMF) (46%) are likely to increase AE (AL, AU) and PC indices significantly. The amplitude of AE index increases from 200 to 600 nT, AU from 100 to 200 nT, AL from 50 to 400 nT, and PC from 1.5 to 3 approximately in 10 min, which could be a signature of geomagnetic activity/substorms onset (or substorm further intensification). Meanwhile, there is a strong injection of energetic electrons in the dawn region following the shock arrival and a strong depletion in the dusk region 30 min later, showing a clear dawn-dusk asymmetry. On the other hand, there is only the typical shock compression effect for IP shocks with northward IMF (54%). The median value of AE index increased from 80 to 150 nT, AU from 50 to 90 nT, AL index decreased from –30 to –40 nT, and PC index increased from 0.6 to 1.2 in ~10 min following the shock arrival. Both individual cases and statistical studies indicate that the magnetosphere-ionosphere system must be preconditioned for a substorm-like geomagnetic activity to be triggered by an IP shock with southward IMF impact, whereas IP shock with northward IMF precondition shows only compression effect.

Solar wind parameters and geomagnetic indices for four different interplanetary shock/ICME structures

Yue, Chao; Zong, Qiugang

J. Geophys. Res., Vol. 116, No. A12, A12201, 2011

<http://dx.doi.org/10.1029/2011JA017013>

<http://onlinelibrary.wiley.com/doi/10.1029/2011JA017013/pdf>

Interplanetary shocks associated with coronal mass ejections (CMEs) have very profound effects on geomagnetic storms. In order to investigate the role of the interplanetary shock properties and pre-conditions, we present a statistical study of 280 interplanetary shocks and their associated geomagnetic activities during 1998–2007. The results show that perpendicular shocks can cause more intense geomagnetic activities compared with parallel ones under the same IMF pre-condition. Through a southward IMF pre-condition, interplanetary shocks and driven ICMEs can intensify geomagnetic storms significantly. It is revealed that interplanetary shocks would intensify negative IMF Bz pre-condition by a factor of 3 to 6. This effect would enhance geomagnetic storms greatly. The result shows that there are 74% of intense ($Dst \leq -100$ nT) and 69% of super ($Dst \leq -200$ nT) geomagnetic storms related to a negative IMF Bz pre-condition.

Coronal Hole Analysis and Prediction using Computer Vision and LSTM Neural Network

Juyoung **Yun**

2023

<https://arxiv.org/pdf/2301.06732.pdf>

As humanity has begun to explore space, the significance of space weather has become apparent. It has been established that coronal holes, a type of space weather phenomenon, can impact the operation of aircraft and satellites. The coronal hole is an area on the sun characterized by open magnetic field lines and relatively low temperatures, which result in the emission of the solar wind at higher than average rates. In this study, To prepare for the impact of coronal holes on the Earth, we use computer vision to detect the coronal hole region and calculate its size based on images from the Solar Dynamics Observatory (SDO). We then implement deep learning techniques, specifically the Long Short-Term Memory (LSTM) method, to analyze trends in the coronal hole area data and predict its size for different sun regions over 7 days. By analyzing time series data on the coronal hole area, this study aims to identify patterns and trends in coronal hole behavior and understand how they may impact space weather events. This research represents an important step towards improving our ability to predict and prepare for space weather events that can affect Earth and technological systems.
23-26 Dec 2022

ROTATION OF WHITE LIGHT CME STRUCTURES AS INFERRED FROM LASCO CORONAGRAPH

Vasyl **Yurchyshyn**, Valentyna Abramenko, Durgesh Tripathi

BBSO Preprint #1404, **2009**, **File**; ApJ,

Understanding the connection between the magnetic configurations of a coronal mass ejection (CME) and their counterpart in the interplanetary medium is very important in terms of space weather predictions. Our previous findings indicate that the orientation of a halo CME elongation may correspond to the orientation of the underlying flux rope. Here we further explore these preliminary results by comparing orientation angles of elongated LASCO CMEs, both full and partial halos, to the EIT post eruption arcades (PEAs). By analyzing a sample of 100 events, we found that overwhelming majority of CMEs are elongated in the direction of the axial field of PEAs. During their evolution, CMEs appear to rotate by about 10 degree for most of the events (70%) with about 30-50 degrees for some events and the corresponding time profiles display regular and gradual changes. It seems that there is a slight preference for the CMEs to rotate toward the solar equator and heliospheric current sheet (59% of cases). We suggest that the rotation of the ejecta may be due to the presence of heliospheric magnetic field, and it could shed light on the problems related to connecting solar surface phenomena to their interplanetary counterparts.

RELATIONSHIP BETWEEN EARTH - DIRECTED SOLAR ERUPTIONS AND MAGNETIC CLOUDS AT 1AU: A BRIEF REVIEW

V. **YURCHYSHYN**, DURGESH TRIPATHI

E-print, May **2009**, **File**; Advances in Geosciences, Adv. Geoscience, **21**, p.51, **2009**

We review relationships between coronal mass ejections (CMEs), EIT post eruption arcades, and the coronal neutral line associated with global magnetic field and magnetic clouds near the Earth. Our previous findings indicate that the orientation of a halo CME elongation may correspond to the orientation of the underlying flux rope. Here we revisit these preliminary reports by comparing orientation angles of elongated LASCO CMEs, both full and partial halos, to the post eruption arcades. Based on 100 analysed events, it was found that the overwhelming majority of halo CMEs are elongated in the direction of the axial field of the post eruption arcades. Moreover, this conclusion also holds for partial halo CMEs as well as for events that originate further from the disk center. This suggests that the projection effect does not drastically change the appearance of full and partial halos and their images still bear reliable information about the underlying magnetic fields. We also compared orientations of the erupted fields near the Sun and in the interplanetary space and found that the local tilt of the coronal neutral line at 2.5 solar radii is well correlated with the magnetic cloud axis measured near the Earth. We suggest that the heliospheric magnetic fields significantly affect the propagating ejecta. Sometimes, the ejecta may even rotate so that its axis locally aligns itself with the heliospheric current sheet.

Relationships between EIT Post Eruption Arcades, Coronal Mass Ejections, Coronal Neutral Line and Magnetic Clouds

Vasyl **Yurchyshyn**

BBSO Preprint Number: 1350, Sept **2007**

<http://solar.njit.edu/preprints/yurchyshyn1350.pdf>

The Astrophysical Journal, 675: L49–L52, **2008** March 1, **File**

<http://www.journals.uchicago.edu/doi/pdf/10.1086/533413>

There is observational evidence that the elongation of an Earth directed coronal mass ejection (CME) may indicate the orientation of the underlying erupting flux rope. In this study, we compare orientations of CMEs, MCs, eruption arcades and coronal neutral line (CNL). We report on good correlations between i) the directions of the axial field in EIT arcades and the elongations of halo CMEs and ii) the tilt of the CNL and MC axis orientations. We found that majority of the eruptions that had EIT arcades, CMEs and MCs similarly oriented also had the CNL co-aligned with them. To the contrary, those events that showed no agreement between orientations of the EIT arcades, CMEs and MCs, had their MCs aligned with the coronal neutral line. We speculate that the axis of the ejecta may be rotated in such a way that it is locally aligns itself with the heliospheric current sheet.

Orientations of LASCO Halo CMEs and Their Connection to the Flux Rope Structure of Interplanetary CMEs

V. **Yurchyshyn**, Q. Hu, R.P. Lepping, B.J. Lynch and J. Krall

BBSO Preprint 1329, 2007, <http://solar.njit.edu/preprints/yurchyshyn1329.pdf>

[Advances in Space Research](#) **Volume 40, Issue 12, 2007**, Pages 1821-1826

we found a good correspondence between the CME and ICME (MC) orientation angles implying that for the majority of interplanetary ejecta their orientations do not change significantly (less than 45 deg rotation) while travelling from the Sun to the near Earth environment.

Orientations of Halo CMEs and MCs

V. **Yurchyshyn**

Presentation at 36th COSPAR Meeting (China), 2006, **ppt File**

The May 13, 2005 eruption: Observations, data analysis and interpretation,

Yurchyshyn, V., C. Liu, V. Abramenko, and J. Krall

Sol. Phys., 239, 317–335, (2006).

<http://solar.njit.edu/preprints/yurchyshyn1315.pdf>

persisting converging and shearing motions near the main neutral line could lead to the formation of twisted core fields and eventually their eruption via reconnection

Structure of magnetic fields in NOAA active regions 0486 and 0501 and in the associated interplanetary ejecta

Vasyl **Yurchyshyn**, Qiang Hu, Valentyna Abramenko

Space Weather v..3, No. 8, S08C02, 10.1029/2004SW000124, 2005; **File**.

Spectacular burst of solar activity in **October – November 2003**, when large solar spots and intense solar flares dominated the solar surface for many consecutive days, caused intense geomagnetic storms. In this paper we analyze solar and interplanetary magnetic fields associated with the storms in October – November 2003. We used space and ground based data in order to compare the orientations of the magnetic fields on the solar surface and at 1AU as well as to estimate parameters of geomagnetic storms during this violent period of geomagnetic activity. Our study further supports earlier reports on the correlation between the CME speed and the strength of the magnetic field in an interplanetary ejecta. A good correspondence was also found between directions of the helical magnetic fields in interplanetary ejecta and in the source active regions. These findings are quite significant in terms of their potential to predict the severity of geomagnetic activity 1 – 2 days in advance, immediately after an earth-directed solar eruption.

Early Diagnostics of Coronal Mass Ejections as a Potential Cause of Geomagnetic Activity

Vasyl **Yurchyshyn**

Poster presented at SSPVSE meeting on 16-29 October 2005. **PDF File**.

Correlation between speeds of coronal mass ejections and the intensity of geomagnetic storms

Yurchyshyn, Vasyl; Wang, Haimin; Abramenko, Valentyna

Space Weather, Volume 2, Issue 2, CiteID S02001, **2004**; [File](#)

We studied the relationship between the projected speed of coronal mass ejections (CMEs), determined from a sequence of Solar and Heliospheric Observatory/Large Angle and Spectrometric Coronagraph Experiment (SOHO/LASCO) images, and the hourly averaged magnitude of the Bz component of the magnetic field in an interplanetary ejecta, as measured by the Advanced Composition Explorer (ACE) magnetometer in the Geocentric Solar Magnetospheric Coordinate System (GSM). For CMEs that originate at the central part of the solar disk we found that the intensity of Bz is correlated with the projected speed of the CME, Vp. The relationship is more pronounced for very fast ejecta (Vp > 1200 km/s), while slower events display larger scatter. We also present data which support earlier conclusions about the correlation of Bz and the Dst index of geomagnetic activity. A possible application of the results to space weather forecasting is discussed.

Coronal and Interplanetary Magnetic Fields in October-November 2003 and November 7 2004 CMEs

Vasyl [Yurchyshyn](#)

Presentation at the [RST Workshop](#) in Sonoma, CA, Dec 8-11, 2004, [File](#)

How directions and helicity of erupted solar magnetic fields define geoeffectiveness of coronal mass ejections

Vasyl [Yurchyshyn](#)^{1, 2}, Haimin Wang¹ and Valentyna Abramenko^{1, 2}

Advances in Space Research, Volume 32, Issue 10, **2003**, Pages 1965-1970

In this study we report on the relationship between the projected speed of CMEs, measured at 20R from SOHO/LASCO images, and the hourly averaged magnitude of the southwardly directed magnetic field, Bz, at the leading edge of interplanetary ejecta, as measured by the ACE magnetometer. We found that those CMEs that originate at the central part of the solar disk ($r < 0.6R$) are the most geoeffective and the intensity of Bz is an exponential function of the CME's speeds. We propose an approach to estimate the strength of the southward IMF at least one day in advance, immediately after a CME started. The predicted value of the Bz component can be then used to estimate the intensity of a geomagnetic storm caused by the eruption. The prediction method is based on the correlation between the speeds of CMEs and magnitudes of the southward IMF as well as the fact that the orientation and chirality of the erupted solar filaments correspond to the orientation and chirality of interplanetary ejecta.

Effects of solar flares and coronal mass ejections on Earth's horizontal magnetic field and solar wind parameters during the minimum solar cycle 24

S N A Syed [Zafar](#), [R Umar](#), [N H Sabri](#), [M H Jusoh](#), [A N Dagang](#), [A Yoshikawa](#)

Monthly Notices of the Royal Astronomical Society, Volume 504, Issue 3, July **2021**, Pages 3812–3822, <https://doi.org/10.1093/mnras/stab1161>

Previous studies have reported that coronal mass ejections (CMEs) and solar flares lead to the development of huge storms and high-speed streams. Our aim in this paper is to investigate the response of the geomagnetic index SYM/H to the solar wind parameters, such as solar wind speed V, dynamic pressure P, input energy IE and the interplanetary magnetic field (IMF) Bz component, associated with solar flares and CME events. The response of the ground geomagnetic field (H-component) to the solar wind parameters and the IMF Bz component at three low-latitude stations has also been analysed. Our findings show that the delay of the solar wind changes in the Earth's magnetosphere in response to the weak geomagnetic storm (SYM/H = -30 nT) at the beginning of **2014 December 21**. A weak storm of SYM/H = -30 nT in the middle of **2014 November 5** is suggested by a low magnetic reconnection process in the magnetosphere. In addition, the strong southward IMF Bz component and high solar wind changes in the magnetosphere system, which were a result of the X2.0 solar flare event and the CMEs on **2014 October 27**, responded to the moderate storm (SYM/H = -60 nT) at the beginning of **2014 October 28**. This dynamic physical process in the magnetosphere caused by solar wind variation is seen to excite the Earth's H-component through ultra low frequency at the ground-based magnetometers at the BCL (Vietnam), TIR (India) and SCN (Indonesia) stations during the geomagnetic storm. This study relates to seismic investigations and geomagnetic-induced current on the ground.

Study of Sudden Magnetic Storm Commencement from Observations with Second Time Resolution.

[Zagainova](#), Y.S., Gromov, S.V., Gromova, L.I. et al.

Geomagn. Aeron. 64, 313–328 (**2024**).

<https://doi.org/10.1134/S0016793224600152>

The article presents the results of a studying detection of the sudden commencement (SC) and main impulse (MI) of a magnetic storm as a function of the geographic coordinates of magnetic observatories and Universal Time, using modern data with second time resolution. The analysis was carried out for two events in which an interplanetary shock wave impacting the magnetosphere was associated with interplanetary coronal mass ejections (CMEs) with sources in different hemispheres of the Sun. The authors propose an approach to determine the time points of SC and MI detection. It is concluded that the SC and MI detection times may differ by several seconds to more than a minute at magnetic observatories located at different geographic latitudes and longitudes. For the studied events, the graphs of SC and MI detection as functions of the geographic coordinates of magnetic observatories and Universal Time revealed trends according to which, on average, the higher station the latitude, the later SC and MI are detected at the station.

The Origin of Switchbacks in the Solar Corona: Linear Theory

G. P. [Zank](#)^{1,2}, M. Nakanotani¹, L.-L. Zhao¹, L. Adhikari¹, and J. Kasper³

2020 ApJ 903 1

<https://doi.org/10.3847/1538-4357/abb828>

The origin, structure, and propagation characteristics of a switchback are compelling questions posed by Parker Solar Probe (PSP) observations of velocity spikes and magnetic field reversals. By assuming interchange reconnection between coronal loop and open magnetic field, we show that this results in the generation of upward (into the heliosphere) and downward complex structures propagating at the fast magnetosonic speed (i.e., the Alfvén speed in the low plasma beta corona) that can have an arbitrary radial magnetic field deflection, including "S-shaped." We derive the evolution equation for the switchback radial magnetic field as it propagates through the inhomogeneous supersonic solar corona. An analytic solution for arbitrary initial conditions is used to investigate the properties of a switchback propagating from launch ~ 6 to $\sim 35 R_{\odot}$ where PSP observed switchbacks during its first encounter. We provide a detailed comparison to an example event, showing that the magnetic field and plasma solutions are in accord with PSP observations. For a simple single switchback, the model predicts either a single or a double-humped structure; the former corresponding to PSP observing either the main body or the flanks of the switchback. The clustering of switchbacks and their sometimes complicated structure may be due to the formation of multiple closely spaced switchbacks created by interchange reconnection with numerous open and loop magnetic field lines over a short period. We show that their evolution yields a complex, aggregated group of switchbacks that includes "sheaths" with large-amplitude radial magnetic field and velocity fluctuations.

Twisted magnetic flux tubes in the solar wind

[Zaqarashvili](#), T.V., V"or"os, Z., Narita, Y., Bruno, R.

E-print, Feb 2014; 2014 ApJ 783 L19

Magnetic flux tubes in the solar wind can be twisted as they are transported from the solar surface, where the tubes are twisted owing to photospheric motions. It is suggested that the twisted magnetic tubes can be detected as the variation of total (thermal+magnetic) pressure during their passage through observing satellite. We show that the total pressure of several observed twisted tubes resembles the theoretically expected profile. The twist of isolated magnetic tube may explain the observed abrupt changes of magnetic field direction at tube walls. We have also found some evidence that the flux tube walls can be associated with local heating of the plasma and elevated proton and electron temperatures. For the tubes aligned with the Parker spiral, the twist angle can be estimated from the change of magnetic field direction. Stability analysis of twisted tubes shows that the critical twist angle of the tube with a homogeneous twist is 70° , but the angle can further decrease owing to the motion of the tube with regards to the solar wind stream. The tubes with a stronger twist are unstable to the kink instability, therefore they probably can not reach 1 AU.

Update on Galactic Cosmic Ray Integral Flux Measurements in Lunar Orbit With CRaTER

C. [Zeitlin](#),, [N. A. Schwadron](#), [H. E. Spence](#), [A. P. Jordan](#), [M. D. Looper](#), [J. Wilson](#), [J. E. Mazur](#), [L. W. Townsend](#)

Space Weather **Volume17, Issue7** Pages 1011-1017 2019

[sci-hub.se/10.1029/2019SW002223](https://doi.org/10.1029/2019SW002223)

We report updated measurements of the integral fluxes of energetic protons, helium ions, and heavier ions as measured by the Cosmic Ray Telescope for the Effects of Radiation (CRaTER). CRaTER is a particle telescope that has been operating aboard the Lunar Reconnaissance Orbiter since 2009. In an earlier report, we presented the methodology used to extract linear energy transfer spectra and integral fluxes for particles with sufficient energies to fully penetrate the telescope. Results were presented for the time span from late 2009 to the end of calendar year 2014, a period that encompassed the rise of solar activity from deep solar minimum to the weak maximum of Cycle 24. Here, we update the results with data obtained from that point in time through the end of 2018, in the declining phase of Cycle 24. Fluxes obtained in the most recent data are approaching the peak levels observed in late 2009 and early 2010. The results can be

used as input to models of solar modulation of galactic cosmic rays and are also relevant to human exploration of deep space.

Solar modulation of the deep space galactic cosmic ray lineal energy spectrum measured by CRaTER, 2009–2014

C. [Zeitlin](#), A. W. Case, N. A. Schwadron, et al.

Space Weather Volume 14, Issue 3 March 2016 Pages 247–258

The Cosmic Ray Telescope for the Effects of Radiation (CRaTER) is an energetic particle detector flying aboard the Lunar Reconnaissance Orbiter. Since arriving at the Moon in 2009, CRaTER has observed the deep solar minimum of solar cycle 23, the ascending phase of cycle 24, the very weak maximum of cycle 24, and in recent months, what appears to be the start of the descending phase of cycle 24. In earlier work, we presented lineal energy spectra of galactic cosmic rays (GCRs) at solar minimum for different shielding depths. The long period of CRaTER observations allows us to study the evolution of these spectra as a function of solar modulation. As solar modulation increases, the total flux of GCRs decreases, and lower-energy ions are preferentially removed from the spectrum of ions that arrive in the inner heliosphere. These effects lead to modest variations in the lineal energy spectrum as a function of time. GCR fluxes at the 2009/2010 solar minimum were high by historical standards and at solar maximum remained high compared to earlier maxima.

The solar wind during current and past solar minima and maxima

J.-L. [Zerbo](#), J. D. Richardson

JGR Volume 120, Issue 12 December 2015 Pages 10,250–10,256

This paper presents solar wind data from the last five solar cycles. We review solar wind parameters over the four solar minima and five maxima for which spacecraft data are available and show the recovery from the last very weak minimum to the current solar maximum. The solar wind magnetic field, speed, and density have remained anomalously low in this time period. However, the distributions of these parameters about the (lower than normal) average are similar to those from previous solar minima and maxima. This result suggests that the acceleration mechanism for the recent weak solar wind is probably not significantly different from earlier solar cycles. The He⁺⁺/H⁺ ratio variation with solar cycle continues to be a function of speed, but the most recent solar minimum has significantly lower ratios than in the previous solar cycle.

The properties of small magnetic flux ropes inside the solar wind come from coronal holes, active regions, and quiet Sun

Changhao [Zhai](#), [Hui Fu](#), [Jiachen Si](#), [Zhenghua Huang](#), [Lidong Xia](#)

ApJ 950 79 2023

<https://arxiv.org/pdf/2304.11802.pdf>

<https://iopscience.iop.org/article/10.3847/1538-4357/accf9a/pdf>

The origination and generation mechanisms of small magnetic flux ropes (SFRs), which are important structures in solar wind, are not clearly known. In present study, 1993 SFRs immersed in coronal holes, active regions, and quiet Sun solar wind are analyzed and compared. We find that the properties of SFRs immersed in three types of solar wind are significantly different. The SFRs are further classified into hot-SFRs, cold-SFRs, and normal-SFRs, according to whether the O7⁺/O6⁺ is 30% elevated or dropped inside SFRs as compared with background solar wind. Our studies show that the parameters of normal-SFRs are similar to background in all three types of solar wind. The properties of hot-SFRs and cold-SFRs seem to be lying in two extremes. Statistically, the hot-SFRs (cold-SFRs) are associated with longer (shorter) duration, lower (higher) speeds and proton temperatures, higher (lower) charge states, helium abundance, and FIP bias as compared with normal-SFRs and background solar wind. The anti-correlations between speed and O7⁺/O6⁺ inside hot-SFRs (normal-SFRs) are different from (similar to) those in background solar wind. Most of hot-SFRs and cold-SFRs should come from the Sun. Hot-SFRs may come from streamers associated with plasma blobs and/or small-scale activities on the Sun. Cold-SFRs may be accompanied by small-scale eruptions with lower-temperature materials. Both hot-SFRs and cold-SFRs could also be formed by magnetic erosions of ICMEs that do not contain or contain cold-filament materials. The characteristics of normal-SFRs can be explained reasonably by the two origins, from the Sun and generated in the heliosphere both.

Alpha-Proton Differential Flow of A Coronal Mass Ejection at 15 Solar Radii

Xuechao [Zhang](#), [Hongqiang Song](#), [Xiaoqian Wang](#), [Leping Li](#), [Hui Fu](#), [Rui Wang](#), [Yao Chen](#)

ApJ 2024

<https://arxiv.org/pdf/2409.10799>

Alpha-proton differential flow ($V_{\alpha p}$) of coronal mass ejections (CMEs) and solar wind from the Sun to 1 au and beyond could influence the instantaneous correspondence of absolute abundances of alpha particles ($\text{He}^{2+}/\text{H}^+$) between solar corona and interplanetary space as the abundance of a coronal source can vary with time. Previous studies based on Ulysses and Helios showed that $V_{\alpha p}$ is negligible within CMEs from 5 to 0.3 au, similar to slow solar wind ($< 400 \text{ km s}^{-1}$). However, recent new observations using Parker Solar Probe (PSP) revealed that the $V_{\alpha p}$ of slow wind increases to $\sim 60 \text{ km s}^{-1}$ inside 0.1 au. It is significant to answer whether the $V_{\alpha p}$ of CMEs exhibits the similar behavior near the Sun. In this Letter, we report the $V_{\alpha p}$ of a CME measured by PSP at $\sim 15 R_{\odot}$ for the first time, which demonstrates that the $V_{\alpha p}$ of CMEs is obvious and complex inside 0.1 au while keeps lower than the local Alfvén speed. A very interesting point is that the same one CME duration can be divided into A and B intervals clearly with Coulomb number below and beyond 0.5, respectively. The means of $V_{\alpha p}$ and alpha-to-proton temperature ratios of interval A (B) is 96.52 (21.96) km s^{-1} and 7.65 (2.23), respectively. This directly illustrates that Coulomb collisions play an important role in reducing the non-equilibrium features of CMEs. Our study indicates that the absolute elemental abundances of CMEs also might vary during their propagation.

Comparison of Ion-Proton Differential Speed between ICMEs and Solar Wind near 1 au

Xuechao Zhang, Hongqiang Song, Chengxiao Zhang, Hui Fu, Leping Li, Jinrong Li, Xiaoqian Wang, Rui Wang, Yao Chen

ApJ 2024

<https://arxiv.org/pdf/2405.00336>

The elemental abundance of ICMEs and solar wind near 1 au is often adopted to represent the abundance in the corresponding coronal sources. However, the absolute abundance of heavy ions (relative to hydrogen) near 1 au might be different from the coronal abundance due to the ion-proton differential speed (V_{ip}). To illustrate the V_{ip} characteristics and explore whether it influences the absolute abundance analysis for ICMEs and solar wind, we perform a statistical study on the V_{ip} for He^{2+} , C^{5+} , O^{6+} , and Fe^{10+} in both ICMEs and solar wind based on measurements of Advanced Composition Explorer. The results show that the V_{ip} is negligible within ICMEs and slow solar wind ($< 400 \text{ km s}^{-1}$), while obvious in the intermediate ($400 - 600 \text{ km s}^{-1}$) and fast wind ($> 600 \text{ km s}^{-1}$). Previous studies showed that the V_{ip} in ICMEs keeps negligible during propagation from 0.3 to 5 au, but in solar wind it increases with the decreasing heliocentric distance. Therefore, it might be questionable to infer the absolute abundance of coronal sources through in-situ abundance near 1 au for solar wind. Fortunately, the ion-oxygen (O^{6+}) differential speed (V_{io}) is negligible for He^{2+} , C^{5+} , and Fe^{10+} within both ICMEs and solar wind, and previous studies suggested that the V_{io} does not vary significantly with the heliocentric distance. This indicates that various heavy ions always flow at the same bulk speed and their relative abundance (relative to oxygen) near 1 au can represent the coronal abundance for both ICMEs and solar wind.

Comparison of I-ICME and M-ICME Fittings and In Situ Observation Parameters for Solar Cycles 23 and 24 and Their Influence on Geoeffectiveness.

Zhang, Z., Shen, C., Chi, Y. et al.

Sol Phys 298, 138 (2023).

<https://doi.org/10.1007/s11207-023-02225-3>

To understand the weaker geomagnetic activity in Solar Cycle 24, we present comparisons of interplanetary coronal mass ejections (ICMEs) fittings and in situ observation parameters in Solar Cycles 23 and 24. According to their in situ features, ICMEs are separated into two categories: isolated ICMEs (I-ICMEs) and multiple ICMEs (M-ICMEs). The number of I-ICMEs in Solar Cycles 23 and 24 does not show a strong difference, while the number of M-ICMEs, which have a high probability of causing intense geomagnetic storms, declines proportionally to the sunspot number in Solar Cycle 24. Despite no obvious variation in their distribution, the geoeffective ICMEs in Solar Cycle 23 have a larger average total magnetic field strength and a larger southern magnetic field than those of Solar Cycle 24. Since the average solar wind velocities of the two solar cycles differ, the geoeffective ICMEs in Solar Cycle 23 have a higher velocity and distinct speed distributions from those in Solar Cycle 24. The total magnetic flux and radius of I-ICMEs in Solar Cycle 23 are larger than those in Solar Cycle 24, while the axial magnetic field intensity is basically the same. We propose that geomagnetic activity in Solar Cycle 24 is lower than that of Solar Cycle 23, due to the smaller M-ICME number, the slower ICME speed, and absence of ICME events with significant southward magnetic field.

Nighttime Geomagnetic Response to Jumps of Solar Wind Dynamic Pressure: A Possible Cause of Québec Blackout in March 1989

T. Zhang, Y. Ebihara, T. Tanaka

Space Weather [Volume 21, Issue 11](#) November 2023 e2023SW003493

<https://agupubs.onlinelibrary.wiley.com/doi/epdf/10.1029/2023SW003493>

By performing a global magnetohydrodynamic (MHD) simulation, we investigated magnetic disturbances on the ground at high-latitudes in response to jumps in the solar wind dynamic pressure, namely a sudden commencement (SC). After the arrival of the jump, a pair of field-aligned currents (FACs), related to the preliminary impulse, develop and travel in the anti-sunward direction. Soon after another pair related to the main impulse (MI) appears and travels in the anti-sunward direction. The horizontal ionospheric current associated with the MI remains strong when propagating to the nightside. On the dawnside the MI current flows sunward (anti-sunward) resulting in northward (southward) ground magnetic disturbance at higher (lower) latitude in the post-midnight sector. These features are similar to those observed in Canada in the high-latitude post-midnight sector when the Québec blackout took place on 13 March 1989. The nighttime geomagnetic perturbations associated with the MI occur regardless of the magnitude of the solar wind dynamic pressure and IMF orientation. The amplitude of the geoelectric field, which is closely related to the geomagnetically induced currents (GICs), reaches the maximum value just before and around the maximum of the southward magnetic disturbance. This is consistent with the moment at which the blackout occurred during the southward magnetic perturbation. We suggest that the blackout in Québec could be caused by the MI-associated Hall current passing over the Hydro-Québec power system on the nightside. The nighttime polar region is shown to be sensitive to hazardous GICs for large-amplitude jumps in the solar wind dynamic pressure.

Numerical modeling of solar wind and coronal mass ejection in the inner heliosphere:

A Review

Man **Zhang**, Xueshang Feng, Huichao Li, Fang Shen, Liping Yang, and Xiaojing Liu

Front. Astron. Space Sci. 10:1105797. 2023

doi: 10.3389/fspas.2023.1105797

<https://www.frontiersin.org/articles/10.3389/fspas.2023.1105797/full>

<https://www.frontiersin.org/articles/10.3389/fspas.2023.1105797/pdf>

The predictions of plasma parameters in the interplanetary medium are the core of space weather forecasts, and the magnetohydrodynamics (MHD) numerical simulation is an important tool in the prediction of plasma parameters. Operational space weather forecasts are commonly produced by a heliosphere model whose inner boundary is set at 18 Rs or beyond. Such predictions typically use empirical/physics-based inner boundary conditions to solve the MHD equations for numerical simulation. In recent years, significant progress has been made in the numerical modeling of the inner heliosphere. In this paper, the numerical modeling of solar wind and coronal mass ejection in the inner heliosphere is reviewed. In particular, different inner boundary conditions used in the simulation are investigated since the MHD solutions are predetermined by the treatment of the inner boundary conditions to a large extent. Discussion is made on further development of the heliosphere model.

A Data-constrained Scheme for the Reconstruction of Solar Wind Parameters in the Inner Heliosphere

Man **Zhang**^{3,1}, Xueshang Feng^{3,1,2}, Liping Yang¹, and Xiaojing Liu¹

2023 ApJS 264 36

<https://iopscience.iop.org/article/10.3847/1538-4365/acaddc/pdf>

With the development of our industrial society, the reconstruction of solar wind parameters in the inner heliosphere becomes very important to understanding the interplanetary propagation of various types of space weather disturbance. However, the situ observations of solar wind parameters are only applicable to several points where spacecraft are located. Therefore, we have to rely on the numerical technologies to reconstruct the solar wind parameters. The scheme for the reconstruction of solar wind parameters can be classified into two categories: one is based on the remote-sensing data at the Sun, and the other is based on the in situ data at 1 au. In this paper, the solar wind parameters in the inner heliosphere are reconstructed with magnetohydrodynamic simulations from 20 Rs to 1 au. The inner boundary conditions are constrained by Wind observations at 1 au. The modeled results are compared with data from multispacecraft observations, such as those by Parker Solar Probe, Solar Orbiter, and the Solar Terrestrial Relations Observatory A and B. The results show that the solar wind parameters obtained with this new scheme agree with the in situ observations much better, which will provide a more realistic configuration for the study of various types of space weather disturbance in future. 31 Oct-19 Dec 2018, 2020 June 7

Numerical Study of Two Injection Methods for the 2007 November 15 Coronal Mass Ejection in the Inner Heliosphere

Man **Zhang**¹, Xueshang Feng^{1,2}, Fang Shen^{1,2}, and Liping Yang^{1,2}

2021 ApJ 918 35

<https://doi.org/10.3847/1538-4357/ac0b3f>

In this paper, we use two injection methods, i.e., coronal mass ejection (CME) with and without radial compression, to investigate the propagation of the **2007 November 15** CME in the inner heliosphere with a three-dimensional, time-dependent, numerical magnetohydrodynamic model. In order to reproduce the large-scale interplanetary magnetic field associated with the CME, the spheromak model is used to provide the intrinsic magnetic field structure of the CME. The modeled results also suggest that the CME without radial compression propagates in interplanetary space with a lower velocity and arrives at 1 au later. We interpret these differences as a result of different Lorentz forces acting on the two injection methods, which lead to different CME expansions in the heliosphere. Additionally, the model of a CME without radial compression tends to overestimate the radial extension at 1 au due to an overestimation of the CME radial size in the simulation and the modeled magnetic fields at 1 au are lower compared to the model of a CME with radial compression. The above results are all useful in understanding the dynamic process occurring between the CME and the solar wind.

Earth-affecting Solar Transients: A **Review** of Progresses in Solar Cycle 24

Jie **Zhang**, Manuela **Temmer**, Nat **Gopalswamy**, Olga **Malandraki**, Nariaki V. **Nitta**, Spiros **Patsourakos**, Fang **Shen**, Bojan **Vršnak**, Yuming **Wang**, David **Webb**, Mihir I. **Desai**, Karin **Dissauer**, Nina **Dresing**, Mateja **Dumbović**, Xueshang **Feng**, Stephan G. **Heinemann**, Monica **Laurenza**, Noé **Lugaz**, Bin **Zhuang**

Progress in Earth and Planetary Science, Volume 8, Issue 1, article id.56, **2021 File**

<https://progearthplanetosci.springeropen.com/counter/pdf/10.1186/s40645-021-00426-7.pdf>

<https://arxiv.org/ftp/arxiv/papers/2012/2012.06116.pdf> **2021**

2020 <https://arxiv.org/abs/2012.06116>

<https://arxiv.org/ftp/arxiv/papers/2012/2012.06116.pdf>

<https://doi.org/10.1186/s40645-021-00426-7>

This review article summarizes the advancement in the studies of Earth-affecting solar transients in the last decade that encompasses most of solar cycle 24. The Sun Earth is an integrated physical system in which the space environment of the Earth sustains continuous influence from mass, magnetic field and radiation energy output of the Sun in varying time scales from minutes to millennium. This article addresses short time scale events, from minutes to days that directly cause transient disturbances in the Earth space environment and generate intense adverse effects on advanced technological systems of human society. Such transient events largely fall into the following four types: (1) solar flares, (2) coronal mass ejections (CMEs) including their interplanetary counterparts ICMs, (3) solar energetic particle (SEP) events, and (4) stream interaction regions (SIRs) including corotating interaction regions (CIRs). In the last decade, the unprecedented multi viewpoint observations of the Sun from space, enabled by STEREO Ahead/Behind spacecraft in combination with a suite of observatories along the Sun-Earth lines, have provided much more accurate and global measurements of the size, speed, propagation direction and morphology of CMEs in both 3-D and over a large volume in the heliosphere. Several advanced MHD models have been developed to simulate realistic CME events from the initiation on the Sun until their arrival at 1 AU. Much progress has been made on detailed kinematic and dynamic behaviors of CMEs, including non-radial motion, rotation and deformation of CMEs, CME-CME interaction, and stealth CMEs and problematic ICMs. The knowledge about SEPs has also been significantly improved. **2008-11-03, 7 March 2011, June 30, 2012, 12-14 July 2012, 2012.10.04-05, 8-10 October 2012, 29 May 2013, 2014-06-24**

Examining the Magnetic Geometry of Magnetic Flux Ropes from the View of Single-point Analysis

Chi **Zhang**^{1,2}, Zhaojin Rong^{1,2,3}, Chao Shen⁴, Lucy Klinger⁵, Jiawei Gao^{1,2}, James A. Slavin⁶, Yongcun Zhang⁷, Jun Cui⁸, and Yong Wei^{1,2,3}

2020 ApJ 903 53

<https://doi.org/10.3847/1538-4357/abba16>

Magnetic flux ropes, characterized as magnetic field lines that wrap and rotate around a central axis, are observed ubiquitously in the space-plasma environment. Accurately examining the physical parameters (e.g., axis orientation, helical handedness, current density, curvature radius, and size) of flux ropes is essential for studying their evolution and associated dynamics. The geometric parameters of flux ropes can be resolved by a cluster of at least four spacecraft with the separation scale much smaller than the flux ropes. However, most spacecraft missions are of single-point measurements, especially for the missions on other planets (e.g., Mars, Venus, Mercury), thus, the method for investigating the flux ropes based on single-point measurements becomes particularly important. A single-point method

that infers the axis orientation of flux ropes was recently developed by Rong et al. Here, we apply this method to study two flux ropes observed by the Magnetospheric Multiscale Mission (MMS), one close to the force-free field and the other close to the non-force-free field, by comparing them with the multipoint analysis of MMS. Our study demonstrates that, apart from axis orientation, the method of Rong et al. can reasonably infer the current density, curvature radius of magnetic field, and the transverse size of flux ropes. We discussed the main error sources of calculated parameters, and suggest that it is worthwhile to widely apply the method by Rong et al. to single-point spacecraft missions for the purpose of examining the geometry and dynamics of flux ropes.

Three-dimensional MHD simulation of the 2008 December 12 coronal mass ejection: from the Sun to Interplanetary space A33

Man **Zhang**, Xue Shang Feng and Li Ping Yang

J. Space Weather Space Clim. **2019**, 9, A33

<https://www.swsc-journal.org/articles/swsc/pdf/2019/01/swsc180068.pdf>

– A three-dimensional time-dependent, numerical magnetohydrodynamic simulation is performed to investigate the propagation of a coronal mass ejection that occurred on 12 December 2008. The background solar wind is obtained by using a splitting finite-volume scheme based on a six-component grid system in spherical coordinate, with Parker's one-dimensional solar wind solution and measured photospheric magnetic fields as the initial values. A spherical plasmoid is superposed on the realistic ambient solar wind to study the 12 December 2008 coronal mass ejection event. The plasmoid is assumed to have a spheromak magnetic structure with a high-density, high-velocity, and high-pressure near the Sun. The dynamical interaction between the coronal mass ejection and the background solar wind flow is then investigated. We compared the model results with observations, and the model provide a relatively satisfactory comparison with the Wind spacecraft observations at 1 AU. We also investigated the numerical results assuming different parameters of the CME, we find that initial magnetic fields in the CME have a larger influence on the solar wind parameters at the Earth.

Editorial: Earth-affecting Solar Transients

Jie **Zhang**, Xochitl Blanco-Cano, Nariaki Nitta, Nandita Srivastava, Cristina H. Mandrini

Solar Physics May **2018**, 293:80

<https://link.springer.com/content/pdf/10.1007%2Fs11207-018-1302-9.pdf>

GIC due to storm sudden commencement in low-latitude high-voltage power network in China: Observation and simulation

J. J. **Zhang**, C. Wang, T. R. Sun, C. M. Liu, K. R. Wang

Space Weather Volume 13, Issue 10 p/ 626-642 **2015**

<http://onlinelibrary.wiley.com/doi/10.1002/2015SW001263/full>

<http://onlinelibrary.wiley.com/doi/10.1002/2015SW001263/epdf>

The impact of geomagnetically induced currents (GICs) on the power networks at middle and low latitudes has attracted attention in recent years with the increase of large-scale power networks. In this study, we report the GIC monitored at two low-latitude 500 kV substations of China during the large storm of **17 March 2015**. The GIC due to the storm sudden commencement (SSC) was much higher than that during the storm main phase. This phenomenon is more likely to happen at low-latitude locations, highlighting the importance of SSC in inducing GIC in low-latitude power networks. Furthermore, we ran a global MHD model to simulate the GIC during this SSC event by using the solar wind observation as input. The model results reproduced the main features of the GIC. The study also indicated that the eastward component of the geoelectric field is dominant for low-latitude locations during the SSC events. Further, topology and electrical parameters of the power grids make significant differences in the GIC levels.

Probabilistic forecasting analysis of geomagnetic indices for southward IMF events

X.-Y. **Zhang**, M. B. Moldwin

Space Weather [Volume 13, Issue 3](#) March **2015** Pages 130–140

Geomagnetic disturbances that drive space weather impacts such as ground-induced currents and radiation belt enhancements are usually driven by strong southward interplanetary magnetic field (IMF) intervals. However, current heliospheric models either do not predict or provide low-accuracy forecasts of IMF Bz. Here we examine the probability distribution function of geomagnetic activity indices for southward IMF intervals. We analyze the in situ plasma and

magnetic field measurements long-duration large-amplitude southward IMF intervals (called Bs events). The statistical profiles of other solar wind and IMF parameters show significant differences during the periods 1 day before the Bs events for different solar wind transients (such as interplanetary coronal mass ejections and stream interaction regions). As is well known, we find that the solar wind speed is positively correlated with geomagnetic indices and that strong southward IMF is the key in storm triggering but not necessarily for substorms. We find that the solar wind density weakly affects geomagnetic field activity, but the response depends on the type of solar wind transient that includes the strong Bs events. We also find that magnetospheric ultralow-frequency waves are induced by both strong southward IMF and solar wind dynamic pressure disturbances. We suggest that strong Bs events could be predicted from the preceding characteristics of solar wind and IMF changes and that probabilistic forecasting of geomagnetic activity occurrence is potentially useful in space weather forecasting. We present preliminary analysis to demonstrate the out-of-sample ability to predict IMF Bsevents with in situ solar wind data.

Evaluation of a Revised Interplanetary Shock Prediction Model: 1D CESE-HD-2 Solar-Wind Model

Y. **Zhang**, A. M. Du, D. Du, W. Sun

Solar Physics, Volume 289, Issue 8, pp 3159-3173 **2014**

We modified the one-dimensional conservation element and solution element (CESE) hydrodynamic (HD) model into a new version [1D CESE-HD-2], by considering the direction of the shock propagation. The real-time performance of the 1D CESE-HD-2 model during Solar Cycle 23 (February 1997 – December 2006) is investigated and compared with those of the Shock Time of Arrival Model (STOA), the Interplanetary-Shock-Propagation Model (ISPM), and the Hakamada–Akasofu–Fry version 2 (HAFv.2). Of the total of 584 flare events, 173 occurred during the rising phase, 166 events during the maximum phase, and 245 events during the declining phase. The statistical results show that the success rates of the predictions by the 1D CESE-HD-2 model for the rising, maximum, declining, and composite periods are 64 %, 62 %, 57 %, and 61 %, respectively, with a hit window of ± 24 hours. The results demonstrate that the 1D CESE-HD-2 model shows the highest success rates when the background solar-wind speed is relatively fast. Thus, when the background solar-wind speed at the time of shock initiation is enhanced, the forecasts will provide potential values to the customers. A high value (27.08) of χ^2 and low p-value (< 0.0001) for the 1D CESE-HD-2 model give considerable confidence for real-time forecasts by using this new model. Furthermore, the effects of various shock characteristics (initial speed, shock duration, background solar wind, longitude, etc.) and background solar wind on the forecast are also investigated statistically.

Alfvén waves as a possible source of long-duration, large-amplitude, and geoeffective southward IMF†

X.-Y. **Zhang**^{1,*}, M. B. Moldwin¹, J. T. Steinberg² and R. M. Skoug

JGR, Volume 119, Issue 5, pages 3259–3266, May **2014**

The southward component (Bs) of the interplanetary magnetic field (IMF) is a strong driver of geomagnetic activity. Well-defined solar wind structures such as magnetic clouds and corotating interaction regions are the main sources of long-duration, large-amplitude IMF Bs. Here we analyze IMF Bs-events ($t > 1$ hour, $B_z < -5$ nT) unrelated with any well-defined solar wind structure at 1 AU using ACE spacecraft observations from 1998 to 2004. We find that about one third of these Bs-events show Alfvénic wave features, therefore that Alfvén waves in the solar wind are also an important source of long-duration, large-amplitude IMF southward component. We find that more than half of the Alfvén wave (AW) -related Bs-events occur in slow solar wind ($V_{sw} < 400$ km/s). One third of the AW-type Bs-events triggered geomagnetic storms, and half triggered substorms.

The source, statistical properties and geoeffectiveness of long-duration southward interplanetary magnetic field intervals†

X.-Y. **Zhang**^{*}, M. B. Moldwin

JGR, Volume 119, Issue 2, pages 658–669, February **2014**

<http://onlinelibrary.wiley.com/doi/10.1002/2013JA018937/pdf>

Geomagnetic activity is strongly controlled by solar wind and Interplanetary Magnetic Field (IMF) conditions, especially the southward component of IMF (IMF Bs). We analyze the statistical properties of IMF Bs at 1 AU using in situ observations for more than a solar cycle (1995 - 2010). IMF Bs-events are defined as continuous IMF Bs intervals with varying thresholds of Bs magnitude and duration, and categorized by different solar wind structures, such as magnetic cloud (MC), interplanetary small-scale magnetic flux rope (ISMFR), interplanetary coronal mass ejection (ICME) without MC signature (ejecta), stream interacting region (SIR), and shock, as well as events unrelated with well-

defined solar wind structures. The statistical properties of IMF Bs-events and their geoeffectiveness are investigated in detail based on satellite and ground measurements. We find that the integrated duration and number of Bs-events follow the sunspot number when $B_z < -5$ nT. We also find that in extreme Bs-events ($t > 6$ hours, $B_z < -10$ nT), a majority (53 %) are related to MC and 10 % are related with ejecta, but nearly a quarter are not associated with any well-defined solar wind structure. We find different geomagnetic responses for Bs-events with comparable duration and magnitude depending on what type of solar wind structures they are associated with. We also find that great Bs-events ($t > 3$ hours, $B_z < -10$ nT) do not always trigger magnetic storms.

Simulated (STEREO) Views of the Solar Wind Disturbances Following the Coronal Mass Ejections of 1 August 2010

Y. [Zhang](#) · A.M. Du · X.S. Feng · W. Sun · Y.D. Liu · C.D. Fry · C.S. Deehr · M. Dryer · B. Zieger · Y.Q. Xie

Solar Phys (2014) 289:319–338

http://sprg.ssl.berkeley.edu/~liuxying/pubs/2014_sp_zhang.pdf

Images observed by the twin spacecraft *Solar TERrestrial RELations Observatory* (STEREO) A and B appear as complex structures for two coronal mass ejections (CMEs) on 1 August 2010. Therefore, a series of sky maps of Thomson-scattered white light by interplanetary coronal mass ejections (ICMEs) on 1 August 2010 are simulated using the Hakamada–Akasofu–Fry (HAF) three-dimensional solar-wind model. A comparison between the simulated images and observations of STEREO-A and -B clarifies the structure and evolution of ICMEs (including shocks) in the observed images. The results demonstrate that the simulated images from the HAF model are very useful in the interpretation of the observed images when the ICMEs overlap within the fields of view of the instruments onboard STEREO-A and -B.

A Comparative Study of Coronal Mass Ejections with and Without Magnetic Cloud Structure near the Earth: Are All Interplanetary CMEs Flux Ropes?

J. [Zhang](#), P. Hess, W. Poomvises

Solar Physics, May 2013, Volume 284, Issue 1, pp 89-104; **File**

An outstanding question concerning interplanetary coronal mass ejections (ICMEs) is whether all ICMEs have a magnetic flux rope structure. We test this question by studying two different ICMEs, one having a magnetic cloud (MC) showing smooth rotation of magnetic field lines and the other not. The two ICMEs are chosen in such a way that their progenitor CMEs are very similar in remote sensing observations. Both CMEs originated from close to the central meridian directly facing the Earth. Both CMEs were associated with a long-lasting post-eruption loop arcade and appeared as an elliptical halo in coronagraph images, indicating a flux rope origin. We conclude that the difference in the in-situ observation is caused by the geometric selection effect, contributed by the deflection of flux ropes in the inner corona and interplanetary space. The first event had its nose pass through the observing spacecraft; thus, the intrinsic flux rope structure of the CME appeared as a magnetic cloud. On the other hand, the second event had the flank of the flux rope intercept the spacecraft, and it thus did not appear as a magnetic cloud. We further argue that a conspicuous long period of weak magnetic field, low plasma temperature, and density in the second event should correspond to the extended leg portion of the embedded magnetic flux rope, thus validating the scenario of the flank-passing. These observations support the idea that all CMEs arriving at the Earth include flux rope drivers.

The geo-effectiveness of interplanetary small-scale magnetic fluxropes Original Research Article

X.-Y. [Zhang](#), M.B. Moldwin, M. Cartwright

JASTP, Volumes 95–96, Pages 1-14, 2013

The geo-effectiveness of Interplanetary small-scale magnetic flux ropes (ISMFRs) are studied using multiple satellites (ACE, WIND, Geotail, Cluster, THEMIS, and geosynchronous spacecraft) and ground magnetometers. We identified 16 ISMFR events during 2007–2008 that had in situ observations of the near-Earth upstream solar wind in addition to observations from ACE and Wind at 1 AU, and observations from multiple spacecraft in the inner magnetosphere. All the upstream solar wind (and in many cases magnetosheath) satellite observations showed very similar flux rope signatures indicating that the flux rope propagates from 1 AU through the bow shock. Thirteen of the 16 events were associated with substorm activity while nine of them appeared to trigger isolated substorm onsets. Combined with earlier published databases of ISMFRs from 1995 to 2005, we also examined the geo-effectiveness using 1-min AE/AL indices.

We found more than half of these events (73/141) were associated with substorms, while the rest were associated with quiet geomagnetic activity periods. Of the 73 substorm-related ISMFRs, 32 events had IMF Bz polarity signatures from south to north (SN), 31 from north to south (NS), and 10 were identified as By bipolar signature events. A superposed epoch analysis indicates that the timing of the substorm activity related to the ISMFRs is different between SN- and NS-events. Most of the ISMFRs associated with quiet geomagnetic activity were either By bipolar signature events or accompanied with complex Bz and By signatures. This study demonstrates that ISMFR with IMF Bz polarity signatures drive substorms, but not geomagnetic storms.

Sizes and relative geoeffectiveness of interplanetary coronal mass ejections and the preceding shock sheaths during intense storms in 1996–2005,

Zhang, J., W. Poomvises, and I. G. Richardson

Geophys. Res. Lett., 35, L02109, 2008, File doi:10.1029/2007GL032045.

We present a statistical study of the sizes of interplanetary coronal mass ejections (ICMEs) and the preceding shock sheath regions in near-Earth space. The 46 events studied are a subset of the events responsible for intense ($Dst \leq -100$ nT) geomagnetic storms in 1996–2005 in which only a single ICME was responsible for generating the storm. We find that the durations and radial sizes of these ICMEs range from 8.0 to 62.0 hr and 0.08 to 0.63 AU, respectively, with average values of 30.6 hr and 0.37 AU. The sheath durations and radial sizes range from 2.6 to 24.5 hr and 0.03 to 0.31 AU, with average values of 10.6 hr and 0.13 AU. On average, the ICME radial size is 2.8 times that of the sheath. In terms of their relative geoeffectiveness, ICMEs contribute on average about 71% of the total energy input (sheath + ICME) into the magnetosphere.

Interplanetary origin of multiple-dip geomagnetic storms,

Zhang, J., I. G. Richardson, and D. F. Webb,

J. Geophys. Res., 113, A00A12, 2008, File

<http://dx.doi.org/10.1029/2008JA013228>

In this paper, we have systematically investigated the interplanetary drivers of major dips during intense ($Dst \leq -100$ nT) geomagnetic storms in 1996–2006. A major dip is defined as a temporary decrease in Dst index with amplitude larger than 14.5 nT. Multiple dips result in a storm if regions of geoeffective solar wind with strong southward magnetic fields are separated by less geoeffective solar wind. Among these 90 intense storms, we found that only 34% (31 events) showed a classical “one-dip” profile, while 49% (44 events) had two dips. Another 17% (15 events) had triple or more dips. We found that of a total of 165 major dips associated with the 90 storms, about 45% (74 dips) were caused by interplanetary coronal mass ejections (ICMEs), or ejecta, and 30% (49 dips) were caused by sheaths (SHs) that lie between shocks driven by ICMEs and leading edges of the ICMEs. About 7% (11 dips) were caused by a shock driven by an ICME running into a preceding ICME and intensifying its magnetic field (PICME-SH). About 11% (18 dips) were due to corotating interaction regions (CIRs) formed by the interaction of high-speed solar wind from coronal holes with the preceding slower solar wind. Another 7% (12 dips) were caused by various solar wind structures prior the onset of the storm. Among these different types of drivers, the largest storms dips on average were produced by shocks propagating through preceding ICMEs (PICME-SH). One frequent cause of a two-dip storm is that the first dip is produced by the upstream sheath and the second dip is produced by the driving ICME. Another common cause of a two-dip or multiple-dip storm is the presence of multiple subregions of southward magnetic field within a complex solar wind flow, resulting from two successive, closely spaced ICMEs.

Statistical analysis of corotating interaction regions and their geoeffectiveness during solar cycle 23,

Zhang, Y., W. Sun, X. S. Feng, C. S. Deehr, C. D. Fry, and M. Dryer

J. Geophys. Res., 113, A08106, 2008

<http://dx.doi.org/10.1029/2008JA013095>

This is an investigation of the effects of corotating interaction regions (CIRs) in the heliosphere (<1 AU) on geomagnetic disturbances during solar cycle 23 (1996–2005). Three kinds of interplanetary structures, “pure” CIR, interaction of CIR with ICME, and “pure” ICME by transient events, are identified by using the Hakamada-Akasofu-Fry (HAF) solar wind model. Yearly occurrence of 157 “pure” CIRs has a minimum value in 2001 and a peak value in 2003

at the declining phase during the 23rd solar cycle. The maximum correlation coefficient of the daily sum of Kp indices between consecutive Carrington Rotations indicates that recurrent geomagnetic disturbances are dominant during the declining phase near solar minimum. Eighty percent of storms that are related to “pure” CIRs belong to weak and moderate storms. The statistical analysis shows that about 50% of CIRs produce classical interplanetary shocks during the descending phase and 89% of the CIR-related shocks are followed by geomagnetic storms. These results demonstrate that CIR-related shock is not a necessary condition for generating a magnetic storm, but most CIR-related shocks are related to a storm. The Dst index that corresponds to CIR-related storms has a better linear relationship with IMF B_z , E_y , and the coupling function (ϵ) when the Dst indices are higher than -100 nT. Finally, the geoeffectiveness of CIRs appears clearly to have a seasonal variation.

Solar and interplanetary sources of major geomagnetic storms ($Dst = -100$ nT) during 1996-2005,

Zhang, J. et al.

J. Geophys. Res., 112, A10102, 2007; **File**

<http://dx.doi.org/10.1029/2007JA012321>

We present the results of an investigation of the sequence of events from the Sun to the Earth that ultimately led to the 88 major geomagnetic storms (defined by minimum $Dst \leq -100$ nT) that occurred during 1996–2005.

We classify the Solar-IP sources into three broad types: (1) S-type, in which the storm is associated with a single ICME and a single CME at the Sun; (2) M-type, in which the storm is associated with a complex solar wind flow produced by multiple interacting ICMEs arising from multiple halo CMEs launched from the Sun in a short period; (3) C-type, in which the storm is associated with a CIR formed at the leading edge of a high-speed stream originating from a solar coronal hole (CH). For the 88 major storms, the S-type, M-type, and C-type events number 53 (60%), 24 (27%), and 11 (13%), respectively. For the 85 events for which the surface source regions could be investigated, 54 (63%) of the storms originated in solar active regions, 11 (13%) in quiet Sun regions associated with quiescent filaments or filament channels, and 11 (13%) were associated with coronal holes. Remarkably, nine (11%) CME-driven events showed no sign of eruptive features on the surface or in the low corona (e.g., no flare, no coronal dimming, and no loop arcade, etc.), even though all the available solar observations in a suitable time period were carefully examined. **Table** Zhang, J. et al. (2007),

Correction to Solar and interplanetary sources of major geomagnetic storms ($Dst = -100$ nT) during 1996-2005,

Zhang, J. et al. (2007),

J. Geophys. Res., 112, A12103, <http://dx.doi.org/10.1029/2007JA012891> ; **File: corrected Table**

IDENTIFICATION OF SOLAR SOURCES OF MAJOR GEOMAGNETIC STORMS BETWEEN 1996 AND 2000

J. **Zhang**,¹ K. P. Dere,² R. A. Howard,² and V. Bothmer³

The Astrophysical Journal, 582:000–000, 2003, **File**

identification of solar coronal mass ejection (CME) sources for 27 major geomagnetic storms (defined by disturbance storm time < -100 nT) occurring between 1996 and 2000.

Magnetic Flux Emergence into the Solar Corona. III. The Role of Magnetic Helicity Conservation,

Zhang, M. and Low, B. C.:

Astrophys. J., 584, 479–496, doi:10.1086/345615, 2003.

This paper treats the reconfiguration of a twisted magnetic field, from an initial two-flux system containing a current sheet to a minimum-energy state, under the conservation of total relative magnetic helicity. In the specific model presented, we assume that a fresh magnetic field of the opposite polarity has emerged into a corona containing a preexisting magnetic field, both represented by constant- α force-free fields with the same constant α . The magnetic reconnection that takes place between the two twisted magnetic flux systems during a relaxation is assumed to take the field to a minimum-energy state that keeps the total relative magnetic helicity conserved. Our calculations suggest that this kind of relaxation may result in the formation of magnetic flux ropes and may change the twist directions in flux ropes in situations where flux ropes exist in the emerging or preexisting fields. These effects are all due to the interplays between the internal magnetic helicities of the two flux systems and their mutual magnetic helicity, with redistribution of these helicities

through magnetic reconnection. In the absence of an interior current sheet, the lowest α force-free field always has the minimum magnetic energy for a given magnetic helicity, as Berger has shown. When an interior current sheet is present, this result breaks down. The lowest α force-free magnetic field with an interior equilibrium current sheet does not always have the minimum magnetic energy for a given total magnetic helicity. Implications of our results for flux emergence in the solar corona are also addressed. An alternative scenario is that from the AR a flux rope with negative twist started to rise and a right-handed MC was produced from the overlying coronal field through reconnection. Leamon et al. (2004) showed that the handedness in an AR does not necessarily imply the observation of a MC with the same handedness. A possible mechanism reversing the twist of a flux rope emerging into overlying pre-existing fields invoking reconnection is discussed in Zhang and Low (2003).

Proton Flux Measurement from Neutron Monitor Data Using Neural Networks

Pengwei **Zhao**, Jie Feng

2024

<https://arxiv.org/pdf/2412.18872>

Accurate measurements of cosmic ray proton flux are crucial for studying the modulation processes of cosmic rays during the solar activity cycle. We present a proton flux measurement method based on ground-based neutron monitor (NM) data and machine learning techniques. After preprocessing the NM data, we use a convolutional neural network (CNN) model to simulate the relationship between the NM observations and proton flux measured by the Alpha Magnetic Spectrometer (AMS-02). We obtain daily proton flux data ranging from 1GV to 100GV for the period from 2011 to 2024, showing that the measured values are in good agreement with the observed ones. In particular, we provide daily proton flux measurements for periods when AMS-02 data are unavailable due to operational reasons. We also perform wavelet analyses on the continuous proton flux data to investigate the relationship between proton flux and solar activity variations, particularly during late 2014 when AMS-02 measurements were missing.

Establishment and Application of an Interplanetary Disturbance Index Based on the Solar Wind–Magnetosphere Energy Coupling Function and the Spectral Whitening Method

Xiaowei **Zhao**^{1,2,3}, Jingsong Wang^{2,3}, Mingxian Zhao^{2,3}, Ying D. Liu^{4,5}, Huidong Hu⁴, Mingzhe Liu⁶, Tian Mao^{2,3}, and Qiugang Zong¹

2024 ApJ 970 133

<https://iopscience.iop.org/article/10.3847/1538-4357/ad5000/pdf>

We develop a preliminary interplanetary disturbance index (J_sW) by applying the spectral whitening method to an energy coupling function with solar wind measurements during the years 1998–2014 as the input, which can be used as an indicator of perturbations in the near-Earth solar wind. The correlation and temporal variation between J_sW and the geomagnetic disturbance index (J_pG) constructed from the same method have been analyzed in detail for 167 geomagnetic storms with the minimum Dst index less than or equal to -50 nT. The time delay between J_sW and J_pG is clearly observable and varies for different events, according to which J_sW is shifted backward with respect to J_pG . We obtain a fairly good negative correlation between the shifted J_sW and the J_pG indices for the majority of events, and the significance level for 88% of the events (i.e., 147 events) does not exceed 0.05. A statistical analysis of the shifted J_sW and the J_pG indices for 147 selected events reveals that larger values of J_sW and smaller magnitudes of J_pG are commonly accompanied by enhanced southward magnetic fields, which implies that more solar wind energy is entering the magnetosphere and thus causing strong geomagnetic storms. Furthermore, a linear fit of the two indices suggests that the evolution of J_pG can be predicted about 2 hr in advance based on J_sW , indicating that J_sW can provide early warnings of possible disturbances in the geomagnetic fields, which is crucial for space weather monitoring and operational forecasting.

Can We Estimate the Intensities of Great Geomagnetic Storms ($\Delta SYM-H \leq -200$ nT) with the Burton Equation or the O'Brien and McPherron Equation?

Ming-Xian **Zhao**^{1,2}, Gui-Ming Le^{1,2}, and Jianyong Lu³

2022 ApJ 928 18

<https://iopscience.iop.org/article/10.3847/1538-4357/ac50a8/pdf>

<https://iopscience.iop.org/article/10.3847/1538-4357/ac50a8/pdf>

We input the solar wind parameters responsible for the main phases of 15 great geomagnetic storms (GGs; $\Delta SYM-H \leq -200$ nT) into the empirical formulae created by Burton et al. (hereafter the Burton equation) and by O'Brien & McPherron (hereafter the OM equation) to evaluate whether these two equations can correctly estimate the intensities of GGs. The results show that the intensities of most GGs estimated by the OM equation are much smaller than the

observed intensities. The rms error between the intensities estimated by the OM equation and the observed intensities is 203 nT, implying that the estimated storm intensity deviates significantly from the observed one. The rms error between the intensities estimated by the Burton equation and the observed intensities is 130.8 nT. The relative error caused by the Burton equation for storms with intensities $\Delta\text{SYM-H} < -400$ nT is larger than 27%, implying that the absolute error will be large for storms with $\Delta\text{SYM-H} < -400$ nT. The results indicate that the two equations cannot predict the intensities of GGSs correctly. On the contrary, the intensity of a GGS estimated by the empirical formula created by Wang et al. can approximate observations better if we select the right weight for the solar wind dynamic pressure, proving that solar wind dynamic pressure is an important factor of GGS intensity. This pressure is overlooked by the ring current injection terms of the Burton and OM equations. This is the reason why the two equations do not effectively estimate GGSs.

2001 March 31, 2003 November 20

Table 1 The Intensities of GGSs (1998-2006)

Interplanetary Coronal Mass Ejections from MAVEN Orbital Observations at Mars

Dan **Zhao**¹, Jianpeng Guo^{1,2}, Hui Huang¹, Haibo Lin¹, Yichun Hong¹, Xueshang Feng², Jun Cui³, Yong Wei⁴, Yang Wang⁵, Yongyong Feng²

2021 ApJ 923 4

<https://doi.org/10.3847/1538-4357/ac294b>

The measurements from the Mars Atmosphere and Volatile Evolution spacecraft, in orbit around Mars, are utilized to investigate interplanetary coronal mass ejections (ICMEs) near 1.52 au. We identify **24 ICMEs** from 2014 December 6 to 2019 February 21. The ICME list is used to examine the statistical properties of ICMEs. On average, the magnetic field strength of 5.99 nT in ICMEs is higher than that of 5.38 nT for stream interaction regions (SIRs). The density of 5.27 cm⁻³ for ICMEs is quite comparable to that of 5.17 cm⁻³ for SIRs, the velocity of 394.7 km s⁻¹ for ICMEs is slightly lower than that of 432.8 km s⁻¹ for SIRs, and the corresponding dynamic pressure of 1.34 nPa for ICMEs is smaller than that of 1.50 nPa for SIRs. Using existing databases of ICMEs at 1 au for the same time period, we compare ICME average properties at 1.52 au with those at 1 au. The averages of the characteristic quantities decrease by a factor of 1.1–1.7 from 1 to 1.52 au. In addition, we analyze an unusual space weather event associated with the ICME on 2015 March 9–10, and propose that the extremely strong dynamic pressure with a maximum of ~18 nPa on March 8 is caused by the combined effects of the enhanced density inside a heliospheric plasma sheet (HPS), the compression of the HPS by the forward shock, and the high velocity of the sheath ahead of the ICME.

Dependence of Great Geomagnetic Storm ($\Delta\text{SYM-H} \leq -200$) on Associated Solar Wind Parameters

Ming-Xian **Zhao**, [Gui-Ming Le](#), [Qi Li](#), [Gui-Ang Liu](#) & [Tian Mao](#)

[Solar Physics](#) volume 296, Article number: 66 (2021)

<https://link.springer.com/content/pdf/10.1007/s11207-021-01816-2.pdf>

<https://doi.org/10.1007/s11207-021-01816-2>

We use $\Delta\text{SYM-H}$ to capture the variation in the SYM-H index during the main phase of a geomagnetic storm. We define great geomagnetic storms as those with $\Delta\text{SYM-H} \leq -200$ nT. After analyzing the data that were not obscured by solar winds, we determined that 17 such storms occurred during Solar Cycles 23 and 24. We calculated time integrals for the southward interplanetary magnetic field component $I(\text{Bs})$, the solar wind electric field $I(\text{Ey})$, and a combination of $I(\text{Bs})$ and the solar wind dynamic pressure $I(\text{Q})$ during the main phase of a great geomagnetic storm. The strength of the correlation coefficient (CC) between $\Delta\text{SYM-H}$ and each of the three integrals $I(\text{Bs})$ (CC = 0.73), $I(\text{Ey})$ (CC = 0.86), and $I(\text{Q})$ (CC = 0.94) suggests that Q, which encompasses both the solar wind electric field and the solar wind dynamic pressure is the main driving factor that determines the intensity of a great geomagnetic storm. The results also suggest that the impact of BsBs on the great geomagnetic storm intensity is much more significant than that of the solar wind speed and the dynamic pressure during the main phase of an associated great geomagnetic storm. The better estimation of the intensity of an extreme geomagnetic storm intensity based on solar wind parameters is also discussed. **21-22 Dec 1999, 4 Sep 2002, 15 May 2005**

Table 1 The solar wind parameters during the main phases of 32 storms (1998-2015).

Turbulence/wave transmission at an ICME-driven shock observed by Solar Orbiter and Wind

L. L. **Zhao**, [G. P. Zank](#), [J. S. He](#), [D. Telloni](#), [Q. Hu](#), [G. Li](#), [M. Nakanotani](#), [L. Adhikari](#), [E. K. J. Kilpua](#), [T. S. Horbury](#), [H. O'Brien](#), [V. Evans](#), [V. Angelini](#)

A&A **2021**

<https://arxiv.org/pdf/2102.03301.pdf>

Solar Orbiter observed an interplanetary coronal mass ejection (ICME) event at 0.8 AU on 2020 April 19. The ICME was also observed by Wind at 1 AU on 2020 April 20. An interplanetary shock wave was driven in front of the ICME.

We focus on the transmission of the magnetic fluctuations across the shock and analyze the characteristic wave modes of solar wind turbulence near the shock observed by both spacecraft. The ICME event is characterized by a magnetic helicity based technique. The shock normal is determined by magnetic coplanarity method for Solar Orbiter and using a mixed coplanarity approach for Wind. The power spectra of magnetic field fluctuations are generated by applying both a fast Fourier transform and Morlet wavelet analysis. To understand the nature of waves observed near the shock, we use the normalized magnetic helicity as a diagnostic parameter. The wavelet reconstructed magnetic field fluctuation hodograms are used to further study the polarization properties of waves. We find that the ICME-driven shock observed by Solar Orbiter and Wind is a fast forward oblique shock with a more perpendicular shock angle at 1 AU. After the shock crossing, the magnetic field fluctuation power increases. Most of the magnetic field fluctuation power resides in the transverse fluctuations. In the vicinity of the shock, both spacecraft observe right-hand polarized waves in the spacecraft frame. The upstream wave signatures fall in a relatively broad and low-frequency band, which might be attributed to low-frequency MHD waves excited by the streaming particles. For the downstream magnetic wave activity, we find oblique kinetic Alfvén waves with frequencies near the proton cyclotron frequency in the spacecraft frame. The frequency of the downstream waves increases by a factor of 7-10 due to the shock compression and the Doppler effect.

2020 April 19-20

Magnetic Helicity Signature and Its Role in Regulating Magnetic Energy Spectra and Proton Temperatures in the Solar Wind

G. Q. Zhao^{1,2}, Y. Lin³, X. Y. Wang³, H. Q. Feng¹, D. J. Wu⁴, H. B. Li¹, A. Zhao¹, and Q. Liu¹

2021 ApJ 906 123

<https://iopscience.iop.org/article/10.3847/1538-4357/abca3b/pdf>

In a previous paper, we found that perpendicular and parallel proton temperatures are clearly associated with the proton-scale turbulence in the solar wind, and magnetic helicity signature appears to be an important indicator in the association. Based on 15 yr of in situ measurements, the present paper further investigates the magnetic helicity of solar wind turbulence and its role in regulating magnetic energy spectra and proton temperatures. Results show that the presence of the helicity signature is very common in solar wind turbulence at scales $0.3 \lesssim k\rho_p \lesssim 1$, with k being the wavenumber and ρ_p the proton gyroradius. The sign of the helicity is mostly positive, indicating the dominance of right-handed polarization of the turbulence. The helicity magnitude usually increases with k and $\beta_{\parallel p}$ (the proton parallel beta) when $k\rho_p$ and $\beta_{\parallel p}$ are less than unity. As helicity magnitude increases, the power index of the energy spectrum becomes more negative, and the proton temperatures $T_{\perp p}$ and $T_{\parallel p}$ rise significantly, where $T_{\perp p}$ and $T_{\parallel p}$ are the perpendicular and parallel temperatures with respect to the background magnetic field. In particular, the rise of $T_{\perp p}$ is faster than $T_{\parallel p}$ when $\beta_{\parallel p} < 1$ is satisfied. The faster rise of $T_{\perp p}$ with the helicity magnitude may be interpreted as the result of the preferentially perpendicular heating of solar wind protons by kinetic Alfvén wave turbulence.

Detection of small magnetic flux ropes from the third and fourth Parker Solar Probe encounters

L.-L. Zhao, G. P. Zank, Q. Hu, D. Telloni, Y. Chen, L. Adhikari,

A&A 2020

<https://arxiv.org/pdf/2010.04664.pdf>

We systematically search for magnetic flux rope structures in the solar wind to within the closest distance to the Sun of 0.13 AU, using data from the third and fourth orbits of the Parker Solar Probe. We extend our previous magnetic helicity based technique of identifying magnetic flux rope structures. The method is improved upon to incorporate the azimuthal flow, which becomes larger as the spacecraft approaches the Sun. A total of 21 and 34 magnetic flux ropes are identified during the third (21 days period) and fourth (17 days period) orbits of the Parker Solar Probe, respectively. We provide a statistical analysis of the identified structures, including their relation to the streamer belt and heliospheric current sheet crossing.

Spectral Features in Field-aligned Solar Wind Turbulence from Parker Solar Probe Observations

L.-L. Zhao¹, G. P. Zank^{1,2}, L. Adhikari¹, M. Nakanotani¹, D. Telloni³, and F. Carbone⁴

2020 ApJ 898 113

<https://doi.org/10.3847/1538-4357/ab9b7e>

Parker Solar Probe (PSP) observed a large variety of Alfvénic fluctuations in the fast and slow solar wind flow during its two perihelia. The properties of Alfvénic solar wind turbulence have been studied for decades in the near-Earth environment. A spectral index of $-5/3$ or -2 for magnetic field fluctuations has been observed using spacecraft measurements, which can be explained by turbulence theories of nearly incompressible magnetohydrodynamics (NI MHD) or critical balance. In this study, a rigorous search of field-aligned solar wind is applied to PSP measurements for the first time, which yields two events in the apparently slow solar wind. The parallel spectra of the magnetic fluctuations in the inertial range show a $k_{\parallel}^{-5/3}$ power law. Probability distributions of the magnetic field show that these events are not contaminated by intermittent structures, which, according to previous studies, are known to modify spectral properties. The results presented here are consistent with spectral predictions from NI MHD theory and further deepen our understanding of the Alfvénic solar wind turbulence near the Sun.

Identification of Magnetic Flux Ropes from Parker Solar Probe Observations during the First Encounter

L.-L. [Zhao](#), [G. P. Zank](#), [L. Adhikari](#), [Q. Hu](#), [J. C. Kasper](#), [S. D. Bale](#), [K. E. Korreck](#), [A. W. Case](#), [M. Stevens](#), [J. W. Bonnell](#), [T. Dudok de Wit](#), [K. Goetz](#), [P. R. Harvey](#), [R. J. MacDowall](#), [D. M. Malaspina](#), [M. Pulupa](#), [D. E. Larson](#), [R. Livi](#), [P. Whittlesey](#), [K. G. Klein](#)

ApJ 2019

<https://arxiv.org/pdf/1912.02349.pdf>

The Parker Solar Probe (PSP) observed an interplanetary coronal mass ejection (ICME) event during its first orbit around the sun, among many other events. This event is analyzed by applying a wavelet analysis technique to obtain the reduced magnetic helicity, cross helicity, and residual energy, the first two of which are magnetohydrodynamics (MHD) invariants. Our results show that the ICME, as a large scale magnetic flux rope, possesses high magnetic helicity, very low cross helicity, and highly negative residual energy, thus pointing to a magnetic fluctuation dominated structure. Using the same technique, we also search for small-scale coherent magnetic flux rope structures during the period from 2018/10/22--2018/11/21, which are intrinsic to quasi-2D MHD turbulence in the solar wind. Multiple structures with duration between 8 and 300 minutes are identified from PSP in-situ spacecraft measurements. The location and scales of these structures are characterized by wavelet spectrograms of the normalized reduced magnetic helicity, normalized cross helicity and normalized residual energy. Transport theory suggests that these small-scale magnetic flux ropes may contribute to the acceleration of charged particles through magnetic reconnection processes, and the dissipation of these structures may be important for understanding the coronal heating processes. **2018 November 11-13**

Table 1. List of identified magnetic flux ropes from 2018/10/22 to 2018/11/21

The Relationship of Magnetic Twist and Plasma Motion in a Magnetic Cloud



Ake [Zhao](#)^{1,2}, Yuming Wang^{3,4}, Hengqiang Feng^{1,5}, Bin Zhuang³, Xiaolei Li³, Hongbo Li^{1,5}, and Hong Jia^{1,2}

2019 ApJ 885 122

[sci-hub.se/10.3847/1538-4357/ab48e5](https://arxiv.org/abs/1908.08485)

Our recent investigations indicate that interplanetary magnetic clouds (MCs) have a high-twist core and a weak-twist outer shell. Utilizing the velocity-modified uniform-twist force-free flux rope model, we further investigate the relationship between the twist profile of magnetic field lines and the distribution of the plasma poloidal angular velocity inside an MC. The poloidal velocity in the MC is 11 km s^{-1} . There are evidently positive correlations between the absolute value of the twist and the plasma poloidal angular velocity in peeled flux ropes or flux rope layers, although the correlation coefficients in flux rope layers are less than those in peeled flux ropes. This finding suggests that plasma flows are frozen-in magnetic field lines as we expected for interplanetary medium, of which the magnetic Reynolds number is large. Furthermore, based on this picture, we infer the axial velocity in the MC frame, which is less than 10 km s^{-1} and almost uniform in the cross section of the MC. Besides, it is inferred that the plasma flows velocity in the MC is much less than the local Alfvén speed.

Coalescence of Magnetic Flux Ropes Within Interplanetary Coronal Mass Ejections: Multi-cases Studies

Yan [Zhao](#)^{1,2},  [Hengqiang Feng](#)^{1,2*}, Qiang Liu^{1,2} and  [Guoqing Zhao](#)^{1,2}

Front. Phys., 7:151 2019 |

[sci-hub.se/10.3389/fphy.2019.00151](https://arxiv.org/abs/1908.08485)

Coronal mass ejections (CMEs) are intense solar explosive eruptions and have significant impact on geomagnetic activities. It is important to understand how CMEs evolve as they propagate in the solar-terrestrial space. In this paper,

we studied the coalescence of magnetic flux ropes embedded in five interplanetary coronal mass ejections (ICMEs) observed by both ACE and Wind spacecraft. The analyses show that coalescence of magnetic flux ropes could persist for hours and operate in scale of hundreds of earth radii. The two merging flux ropes could be very different in the axial orientation and the plasma density and temperature, which should complicate the progress of coalescence and have impact on the merged structures. The study indicates that coalescence of magnetic flux ropes should be an important factor in changing the magnetic topology of ICMEs. **1998 03/25, 2000 04/18, 2000 10/03, 2002 02/02, 2004 07/24**

Quantifying the Propagation of Fast Coronal Mass Ejections from the Sun to Interplanetary Space Combining Remote Sensing and Multi-Point in-situ Observations

Xiaowei [Zhao](#), [Ying D. Liu](#), [Huidong Hu](#), [Rui Wang](#)

ApJ **882** 122 **2019**

<https://arxiv.org/pdf/1908.04450.pdf>

sci-hub.se/10.3847/1538-4357/ab379b

In order to have a comprehensive view of the propagation and evolution of coronal mass ejections (CMEs) from the Sun to deep interplanetary space beyond 1 au, we carry out a kinematic analysis of 7 CMEs in solar cycle 23. The events are required to have coordinated coronagraph observations, interplanetary type II radio bursts, and multi-point in-situ measurements at the Earth and Ulysses. A graduated cylindrical shell model, an analytical model without free parameters and a magnetohydrodynamic model are used to derive CME kinematics near the Sun, to quantify the CME/shock propagation in the Sun-Earth space, and to connect in-situ signatures at the Earth and Ulysses, respectively. We find that each of the 7 CME-driven shocks experienced a major deceleration before reaching 1 au and thereafter propagated with a gradual deceleration from the Earth to larger distances. The resulting CME/shock propagation profile for each case is roughly consistent with all the data, which verifies the usefulness of the simple analytical model for CME/shock propagation in the heliosphere. The statistical analysis of CME kinematics indicates a tendency that the faster the CME, the larger the deceleration, and the shorter the deceleration time period within 1 au. For several of these events, the associated geomagnetic storms were mainly caused by the southward magnetic fields in the sheath region. In particular, the interaction between a CME-driven shock and a preceding ejecta significantly enhanced the preexisting southward magnetic fields and gave rise to a severe complex geomagnetic storm. **1997 November 4, 2000 June 6, 2001 April 2, 2001 November 4, 2001 November 22, 2005 May 13, 2006 December 13**

Table 1. Solar source information, CME propagation direction, shock arrival time and Ulysses position relative to the Earth for the 7 CMEs.

The Twist Profile in the Cross Section of Interplanetary Magnetic Clouds

Ake [Zhao](#)^{1,2}, Yuming Wang^{3,4}, Hengqiang Feng⁵, Mengjiao Xu³, Yan Zhao⁵, Guoqing Zhao⁵, and Qiang Hu⁶

2018 ApJL 869 L13 <https://doi.org/10.3847/2041-8213/aaf428>

sci-hub.tw/10.3847/2041-8213/aaf428

Magnetic flux ropes (MFRs) as a well-organized magnetic field structure embedded in space plasmas have been widely studied for several decades. The twists of magnetic field lines in MFRs can yield much information regarding the formation and stability of MFRs, yet there is still open debate about them. Here, with the aid of a uniform-twist force-free flux rope model, we study the twist profile in the cross section of an interplanetary magnetic cloud (MC) by peeling off equal azimuthal magnetic flux layer by layer from the outermost shell, just like peeling an onion. The absolute value of the average twist, $\bar{\tau}$, and the twist in each layer, τ , exhibit an almost monotonous decrease from the axis to the periphery of the MC, but τ has a larger relative error. However, they do have a coincident trend of a high-twist core and a low-twist outer shell. The twist number per unit length, $\bar{\tau}/\tau$, follows a linear trend versus $1/\pi R$, where R is the radius of each layer, with a correlation coefficient of 0.96/0.91 and slope of 0.27/0.26, which is well below the critical slope of 1 suggested by Wang et al. **2-3 Aug 2002**

Polarization properties of low frequency electromagnetic cyclotron waves associated with magnetic clouds

G. Q. [Zhao](#), H. Q. Feng, D. J. Wu, J. Huang

[Astrophysics and Space Science](#) March **2018**, 363:49

<https://link.springer.com/content/pdf/10.1007%2Fs10509-018-3271-8.pdf>

Recent studies have revealed that there are a large number of low frequency electromagnetic cyclotron waves (ECWs) occurring in and around magnetic clouds (MCs) that are common magnetic structures in interplanetary space. Using magnetic field data from the STEREO spacecraft, this paper investigates polarization properties of ECWs associated with 120 MCs. Results show that the ECWs are highly transverse, strongly polarized waves with large ellipticities.

Specifically, almost all of the waves take place with the ratios of transverse power to total power higher than 0.94, polarization degrees greater than 0.85, and ellipticities larger than 0.5. The mean values of these quantities can be up to 0.99, 0.96, 0.85, respectively. In particular, there is a tendency of ellipticities decreasing with respect to the wave normal angles for ECWs with left handed polarization. The decreasing tendency is consistent with the recent theory and simulation results. **15 January 2007**

On the Relation between the In Situ Properties and the Coronal Sources of the Solar Wind

L. **Zhao**, E. Landi, S. T. Lepri, J. A. Gilbert, T. H. Zurbuchen, L. A. Fisk, and J. M. Raines

2017 ApJ 846 135

We categorize the types of solar wind using a new classification scheme based on the location of the wind's coronal source regions in the solar atmosphere and near-solar heliosphere. We first trace the solar wind measured by ACE/SWEPAM and SWICS from 1998 to 2011 at 1 au back to a $2.5R_{\odot}$ solar surface using ballistic mapping at constant proton speed; then we map them back to their magnetic footpoints on the $1R_{\odot}$ solar surface via the potential field source surface (PFSS) model. Coronal structures are identified using a classification scheme based on the pixel brightness in the SOHO or STEREO EUV Carrington images. The angular distances between each mapped solar wind footpoint to the different coronal structure pixels are calculated and used as a criterion to identify the type of solar wind source region. Depending on the proximity of the solar wind footpoints to a given coronal or heliospheric structure, we classify the solar wind into six types: active region (AR), AR-boundary, quiet Sun (QS), coronal hole (CH), CH-boundary, and helmet-streamer associated wind. The in situ properties of these six types of solar winds are then examined and compared, and their solar cycle dependences are also discussed.

Main Cause of the Poloidal Plasma Motion Inside a Magnetic Cloud Inferred from Multiple-Spacecraft Observations

Ake **Zhao**, Yuming Wang, Yutian Chi, Jiajia Liu, Chenglong Shen, Rui Liu

Solar Physics April **2017**, 292:58

<http://link.springer.com/content/pdf/10.1007%2Fs11207-017-1077-4.pdf>

Although the dynamical evolution of magnetic clouds (MCs) has been one of the foci of interplanetary physics for decades, only few studies focus on the internal properties of large-scale MCs. Recent work by Wang et al. (J. Geophys. Res.120, 1543, 2015) suggested the existence of the poloidal plasma motion in MCs. However, the main cause of this motion is not clear. In order to find it, we identify and reconstruct the MC observed by the Solar Terrestrial Relations Observatory (STEREO)-A, Wind, and STEREO-B spacecraft during **19–20 November 2007** with the aid of the velocity-modified cylindrical force-free flux-rope model. We analyze the plasma velocity in the plane perpendicular to the MC axis. It is found that there was evident poloidal motion at Wind and STEREO-B, but this was not clear at STEREO-A, which suggests a local cause rather than a global cause for the poloidal plasma motion inside the MC. The rotational directions of the solar wind and MC plasma at the two sides of the MC boundary are found to be consistent, and the values of the rotational speeds of the solar wind and MC plasma at the three spacecraft show a rough correlation. All of these results illustrate that the interaction with ambient solar wind through viscosity might be one of the local causes of the poloidal motion. Additionally, we propose another possible local cause: the existence of a pressure gradient in the MC. The significant difference in the total pressure at the three spacecraft suggests that this speculation is perhaps correct.

Propagation Characteristics of Two Coronal Mass Ejections From the Sun Far into Interplanetary Space

Xiaowei **Zhao**, Ying D.Liu, Huidong Hu, Rui Wang

ApJ 837 4 **2017**

<https://arxiv.org/pdf/1702.04122.pdf>

Propagation of coronal mass ejections (CMEs) from the Sun far into interplanetary space is not well understood due to limited observations. In this study we examine the propagation characteristics of two geo-effective CMEs, which occurred on **2005 May 6 and 13**, respectively. Significant heliospheric consequences associated with the two CMEs are observed, including interplanetary CMEs (ICMEs) at the Earth and Ulysses, interplanetary shocks, a long-duration type II radio burst, and intense geomagnetic storms. We use coronagraph observations from SOHO/LASCO, frequency drift of the long-duration type II burst, in situ measurements at the Earth and Ulysses, and magnetohydrodynamic (MHD) propagation of the observed solar wind disturbances at 1 AU to track the CMEs from the Sun far into interplanetary

space. We find that both of the two CMEs underwent a major deceleration within 1 AU and thereafter a gradual deceleration when they propagated from the Earth to deep interplanetary space due to interactions with the ambient solar wind. The results also reveal that the two CMEs interacted with each other in the distant interplanetary space even though their launch times on the Sun were well separated. The intense geomagnetic storm for each case was caused by the southward magnetic fields ahead of the CME, stressing the critical role of the sheath region in geomagnetic storm generation, although for the first case there is a corotating interaction region involved.

TRANSIENT GALACTIC COSMIC-RAY MODULATION DURING SOLAR CYCLE 24: A COMPARATIVE STUDY OF TWO PROMINENT FORBUSH DECREASE EVENTS

L.-L. [Zhao](#)^{1,2} and H. Zhang

2016 ApJ 827 13

Forbush decrease (FD) events are of great interest for transient galactic cosmic-ray (GCR) modulation study. In this study, we perform comparative analysis of two prominent Forbush events during cycle 24, occurring on **2012 March 8** (Event 1) and **2015 June 22** (Event 2), utilizing the measurements from the worldwide neutron monitor (NM) network. Despite their comparable magnitudes, the two Forbush events are distinctly different in terms of evolving GCR energy spectrum and energy dependence of the recovery time. The recovery time of Event 1 is strongly dependent on the median energy, compared to the nearly constant recovery time of Event 2 over the studied energy range. Additionally, while the evolutions of the energy spectra during the two FD events exhibit similar variation patterns, the spectrum of Event 2 is significantly harder, especially at the time of deepest depression. These differences are essentially related to their associated solar wind disturbances. Event 1 is associated with a complicated shock-associated interplanetary coronal mass ejection (ICME) disturbance with large radial extent, probably formed by the merging of multiple shocks and transient flows, and which delivered a glancing blow to Earth. Conversely, Event 2 is accompanied by a relatively simple halo ICME with small radial extent that hit Earth more head-on.

Comparison of CME/shock propagation models with heliospheric imaging and in situ observations

Xinhua [Zhao](#), Ying D. Liu, Bernd Inhester, [Xueshang Feng](#), [Thomas Wiegelmann](#), [Lei Lu](#)

ApJ 830 48 **2016**

<http://arxiv.org/pdf/1607.05533v1.pdf>

The prediction of the arrival time for fast coronal mass ejections (CMEs) and their associated shocks is highly desirable in space weather studies. In this paper, we use two shock propagation models, i.e. Data Guided Shock Time Of Arrival (DGSTOA) and Data Guided Shock Propagation Model (DGSPM), to predict the kinematical evolution of interplanetary shocks associated with fast CMEs. DGSTOA is based on the similarity theory of shock waves in the solar wind reference frame, and DGSPM on the non-similarity theory in the stationary reference frame. The inputs are the kinematics of the CME front at the maximum speed moment obtained from the geometric triangulation method applied to STEREO imaging observations together with the Harmonic Mean approximation. The outputs provide the subsequent propagation of the associated shock. We apply these models to the CMEs on **2012 January 19, January 23, and March 7**. We find that the shock models predict reasonably well the shock's propagation after the impulsive acceleration. The shock's arrival time and local propagation speed at Earth predicted by these models are consistent with in situ measurements of WIND. We also employ the Drag-Based Model (DBM) as a comparison, and find that it predicts a steeper deceleration than the shock models after the rapid deceleration phase. The predictions of DBM at 1 AU agree with the following ICME or sheath structure, not the preceding shock. These results demonstrate the applicability of the shock models used here for future arrival time prediction of interplanetary shocks associated with fast CMEs.

Modeling transport of energetic particles in corotating interaction regions: A case study

Lulu [Zhao](#), Gang Li, R. W. Ebert, M. A. Dayeh, M. I. Desai, G. M. Mason, Z. Wu, Y. Chen

Volume 121, Issue 1 January **2016** Pages 77–92

We investigate energetic particle transport in corotating interaction regions (CIRs) through a case study. The CIR event we study occurred on **8 February 2008** and was observed by both the Advanced Composition Explorer (ACE) and the twin Solar TERrestrial Relations Observatory (STEREO) B spacecraft. An in situ reverse shock was observed by

STEREO B (1.0 AU) but not ACE (0.98 AU). Using STEREO B observations and assuming the CIR structure does not vary significantly in the corotating frame, we estimate the shock location at later times for both the STEREO B and ACE observations. Further assuming the accelerated particle spectral shape at the shock does not vary with shock location, we calculate the particle differential intensities as observed by ACE and STEREO B at two different times by solving the focused transport equation using a Monte Carlo simulation. We assume that particles move along Parker's field and experience no cross-field diffusion. We find that the modulation of sub-MeV/nucleon particles is significant. To obtain reasonable comparisons between the simulations and the observations by both ACE and STEREO B, one has to assume that the CIR shock can accelerate more particles at a larger heliocentric distance than at a smaller heliocentric distance.

Influence of a CME's Initial Parameters on the Arrival of the Associated Interplanetary Shock at Earth and the Shock Propagational Model Version 3

X. H. **Zhao** and X. S. Feng

2015 ApJ 809 44

Predicting the arrival times of coronal mass ejections (CMEs) and their related waves at Earth is an important aspect of space weather forecasting. The Shock Propagation Model (SPM) and its updated version (SPM2), which use the initial parameters of solar flare-Type II burst events as input, have been developed to predict the shock arrival time. This paper continues to investigate the influence of solar disturbances and their associated CMEs on the corresponding interplanetary (IP) shock's arrival at Earth. It has been found that IP shocks associated with wider CMEs have a greater probability of reaching the Earth, and the CME speed obtained from coronagraph observations can be supplementary to the initial shock speed computed from Type II radio bursts when predicting the shock's arrival time. Therefore, the third version of the model, i.e., SPM3, has been developed based on these findings. The new version combines the characteristics of solar flare-Type II events with the initial parameters of the accompanying CMEs to provide the prediction of the associated IP shock's arrival at Earth. The prediction test for 498 events of Solar Cycle 23 reveals that the prediction success rate of SPM3 is 70%–71%, which is apparently higher than that of the previous SPM2 model (61%–63%). The transit time prediction error of SPM3 for the Earth-encountered shocks is within 9 hr (mean-absolute). Comparisons between SPM3 and other similar models also demonstrate that SPM3 has the highest success rate and best prediction performance.

The Evolution of 1 AU Equatorial Solar Wind and its Association with the Morphology of the Heliospheric Current Sheet from Solar Cycles 23 to 24

L. **Zhao**, E. Landi, T. H. Zurbuchen, L. A. Fisk, and S. T. Lepri

2014 ApJ 793 44

The solar wind can be categorized into three types based on its "freeze-in" temperature ($T_{\text{freeze-in}}$) in the coronal source: low $T_{\text{freeze-in}}$ wind mostly from coronal holes, high $T_{\text{freeze-in}}$ wind mostly from regions outside of coronal holes, including streamers (helmet streamer and pseudostreamer), active regions, etc., and transient interplanetary coronal mass ejections (ICMEs) usually possessing the hottest $T_{\text{freeze-in}}$. The global distribution of these three types of wind has been investigated by examining the most effective $T_{\text{freeze-in}}$ indicator, the $O7+/O6+$ ratio, as measured by the Solar Wind Ion Composition Spectrometer on board the Advanced Composition Explorer (ACE) during 1998–2008 by Zhao et al. In this study, we extend the previous investigation to 2011 June, covering the unusual solar minimum between solar cycles 23 and 24 (2007–2010) and the beginning of solar cycle 24. We find that during the entire solar cycle, from the ascending phase of cycle 23 in 1998 to the ascending phase of cycle 24 in 2011, the average fractions of the low $O7+/O6+$ ratio (LOR) wind, the high $O7+/O6+$ ratio (HOR) wind, and ICMEs at 1 AU are 50.3%, 39.4%, and 10.3%, respectively; the contributions of the three types of wind evolve with time in very different ways. In addition, we compare the evolution of the HOR wind with two heliospheric current sheet (HCS) parameters, which indicate the latitudinal standard deviation (SD) and the slope (SL) of the HCS on the synoptic Carrington maps at 2.5 solar radii surface. We find that the fraction of HOR wind correlates with SD and SL very well (slightly better with SL than with SD), especially after 2005. This result verifies the link between the production of HOR wind and the morphology of the HCS, implying that at least one of the major sources of the HOR wind must be associated with the HCS.

Current status of CME/shock arrival time prediction

Xinhua **Zhao**¹ and Murray Dryer

Space Weather, Volume 12, Issue 7, pages 448–469, 2014

<http://onlinelibrary.wiley.com/doi/10.1002/SWQv11i002/pdf>

sci-hub.se/10.1002/2014SW001060 File

Review

One of the major solar transients, coronal mass ejections (CMEs) and their related interplanetary shocks have severe space weather effects and become the focus of study for both solar and space scientists. Predicting their evolutions in the heliosphere and arrival times at Earth is an important component of the space weather predictions. Various kinds of models in this aspect have been developed during the past decades. In this paper, we will present a view of the present status (during Solar Cycle 24 in 2014) of the space weather's objective to predict the arrival of coronal mass ejections and their interplanetary shock waves at Earth. This status, by implication, is relevant to their arrival elsewhere in the solar system. Application of this prediction status is clearly appropriate for operational magnetospheric and ionospheric situations including A → B → C...solar system missions. We review current empirical models, expansion speed model, drag-based models, physics-based models (and their real-time prediction's statistical experience in Solar Cycle 23), and MHD models. New observations in Solar Cycle 24, including techniques/models, are introduced as they could be incorporated to form new prediction models. The limitations of the present models and the direction of further development are also suggested.

Shock propagation model version-2 (SPM2) and its application in predicting the arrivals at Earth of interplanetary shocks during Solar Cycle 23†

X. H. **Zhao**, X. S. Feng

JGR, Volume 119, Issue 1, pages 1–10, January 2014

<http://onlinelibrary.wiley.com/doi/10.1002/2012JA018503/pdf>

The Shock Propagation Model (SPM) based on an analytic solution of blast waves has been proposed [Feng and Zhao, 2006] to predict shock arrival times (SATs) at Earth. Here to reduce the limitations of the SPM theoretical model in real applications and optimize its input parameters, a new version (called SPM2) is presented in order to enhance prediction performance. First, an empirical relationship is established to adjust the initial shock speed, which, as computed from the Type II burst drift rate, often contains observational uncertainties. Second, an additional acceleration/deceleration relation is added to the model to eliminate inherent prediction bias. Third, the propagation direction is derived in order to mitigate the isotropy limitation of blast wave theory in real predictions. Finally, an equivalent shock strength index (ESSI) at the Earth's location to judge whether or not an interplanetary (IP) shock will encounter the Earth is implemented in SPM2. The prediction results of SPM2 for 551 solar disturbance events of Solar Cycle 23 demonstrate that the success rate of SPM2 for both shock (W-shock) and non-shock (W/O-shock) events at Earth is ~ 60%. The prediction error for the W-shock events is less than 12 hours (root-mean-square) and 10 hours (mean-absolute), respectively. Comparisons between the predicted results of SPM2 and those of STOA, ISPM and HAFv.2 based on similar data samples reveal that the SPM2 model offers generally equivalent prediction accuracy and reliability compared to the existing Fearless Forecast models (STOA, ISPM and HAFv.2).

Seasonal and diurnal variation of geomagnetic activity: Russell-McPherron effect during different IMF polarity and/or extreme solar wind conditions

Zhao, H.; Zong, Q.-G.

J. Geophys. Res., Vol. 117, No. A11, A11222, 2012

The Russell-McPherron (R-M) effect is one of the most prevailing hypotheses accounting for semiannual variation of geomagnetic activity. To validate the R-M effect and investigate the difference of geomagnetic activity variation under different interplanetary magnetic field (IMF) polarity and during extreme solar wind conditions (interplanetary shock), we have analyzed 42 years interplanetary magnetic field and geomagnetic indices data and 1270 SSC (storm sudden commencement) events from the year 1968 to 2010 by defining the R-M effect with positive/negative IMF polarity (IMF away/toward the Sun). The results obtained in this study have shown that the response of geomagnetic activity to the R-M effect with positive/negative IMF polarity are rather profound: the geomagnetic activity is much more intense around fall equinox when the direction of IMF is away the Sun, while much more intense around spring equinox when the direction of IMF is toward the Sun. The seasonal and diurnal variation of geomagnetic activity after SSCs can be attributed to both R-M effect and the equinoctial hypothesis; the R-M effect explains most part of variance of southward IMF, while the equinoctial hypothesis explains similar variance of ring current injection and geomagnetic indices as the R-M effect. However, the R-M effect with positive/negative IMF polarity explains the difference between SSCs with positive/negative IMF By accurately, while the equinoctial hypothesis cannot explain such difference at the spring and fall equinoxes. Thus, the R-M effect with positive/negative IMF polarity is more reasonable to explain seasonal and diurnal variation of geomagnetic activity under extreme solar wind conditions.

Understanding the Behavior of the Heliospheric Magnetic Field and the Solar Wind during the Unusual Solar Minimum between Cycles 23 and 24

L. **Zhao**, L. Fisk

E-print, 12 Aug 2011

The properties of the heliospheric magnetic field and the solar wind were substantially different in the unusual solar minimum between Cycles 23 and 24: the magnetic-field strength was substantially reduced, as were the flow properties of the solar wind, such as the mass flux. Explanations for these changes are offered that do not require any substantial reconsiderations of the general understandings of the behavior of the heliospheric magnetic field and the solar wind that were developed in the Cycle 22-23 minimum. Solar-wind composition data are used to demonstrate that there are two distinct regions of solar wind: solar wind likely to originate from the stalk of the streamer belt (the highly elongated loops that underlie the heliospheric current sheet), and solar wind from outside this region. The region outside the streamer-stalk region is noticeably larger in the Cycle 23-24 minimum; however, the increased area can account for the reduction in the heliospheric magnetic-field strength in this minimum. Thus, the total magnetic flux contained in this region is the same in the two minima. Various correlations among the solar-wind mass flux and coronal electron temperature inferred from solar-wind charge states were developed for the Cycle 22-23 solar minimum. The data for the Cycle 23-24 minimum suggest that the correlations still hold, and thus the basic acceleration mechanism is unchanged in this minimum.

Characteristics of solar flares associated with interplanetary shock or nonshock events at Earth

Xinhua **Zhao**,^{1,2} Xueshang Feng,¹ and Chin-Chun Wu³

JOURNAL OF GEOPHYSICAL RESEARCH, VOL. 111, A09103, doi:10.1029/2006JA011784, 2006, **File**

Success rate of predicting the heliospheric magnetic field polarity with Michelson Doppler Imager (MDI) synoptic charts

Zhao, X. P.; Hoeksema, J. T.; Liu, Y.; Scherrer, P. H., J. Geophys. Res., Vol. 111, No. A10, A10108, 2006

<http://dx.doi.org/10.1029/2005JA011576>

Influence of solar flare's location and heliospheric current sheet on the associated shock's arrival at Earth

Zhao, Xinhua; Feng, Xueshang; Wu, Chin-Chun

J. Geophys. Res., Vol. 112, No. A6, A06107

<http://dx.doi.org/10.1029/2006JA012205>

Source regions and storm effectiveness of frontside full halo coronal mass ejections.

Zhao, X.P., Webb, D.F.,

2003. Journal of Geophysical Research 108, 1234, **File**.

(See Yermolaev, 2009?)

sci-hub.se/10.1029/2002JA009606

Full halo coronal mass ejections (CMEs) erupting from the side of the Sun facing Earth, i.e., frontside full halo CMEs, are considered to be a likely cause of major, transient geomagnetic storms. However, this hypothesis has not been tested over a full solar cycle. We compare all frontside full halo CMEs observed during the first half of solar cycle 23, from 1996 to the end of 2000, with moderate or larger storms at Earth. We show that the association of frontside full halo CMEs with such storms tends to decrease from 1997 to 2000, though this decreasing trend is not monotonic. We examine the locations of the frontside full halo CMEs from 1996 to 2000 with respect to two kinds of coronal closed field regions: bipolar closed field regions between opposite-polarity open field regions and unipolar closed field regions between like-polarity open field regions. We find that even during solar maximum when the occurrence frequency of the two kinds of regions is nearly the same, the central positions of the frontside full halo CMEs are mostly located under the bipolar coronal streamer belt, suggesting that most full halo CMEs originate in the bipolar coronal helmet streamers that are sandwiched between coronal holes having opposite magnetic polarity. Because the inclination of the heliospheric current sheet increases toward solar maximum, the fraction of CMEs emitted into the ecliptic decreases, and the inclination of associated flux ropes increases. These effects help to explain the solar cycle effect on the storm effectiveness of frontside full halo CMEs.

Pitch-angle distribution of accelerated electrons in 3D current sheets with magnetic islands

V. **Zharkova** and Q. Xia

A&A 648, A51 2021

https://solargsm.com/wp-content/uploads/2021/02/zharkova_xia_PADs_aa21.pdf

<https://www.aanda.org/articles/aa/pdf/2021/04/aa39220-20.pdf>

<https://doi.org/10.1051/0004-6361/202039220>

This research aims to explore variations of electron pitch-angle distribution (PAD) during spacecraft cross reconnecting current sheets (RCSs) with magnetic islands. The results can benchmark the sampled characteristic features with realistic PADs derived from in-situ observations. Particle motion is simulated in 2.5D Harris-type RCSs using particle-in-cell (PIC) method considering the plasma feedback to electromagnetic fields. We evaluate particle energy gains and PADs in different locations and under the different directions of passing the current sheet by a virtual spacecraft. The RCS parameters are comparable to heliosphere and solar wind conditions. The energy gains and the PADs of particles would change depending on the specific topology of magnetic fields. Besides, the observed PADs also depend on the crossing paths of the spacecraft. When the guiding field is weak, the bi-directional electron beams (strahls) are mainly present inside the islands and located closely above/below the X-nullpoints in the inflow regions. The magnetic field relaxation near X-nullpoint converts the PADs towards 90 degrees. As the guiding field becomes larger, the regions with bi-directional strahls are compressed towards small areas in the exhausts of RCSs. Mono-directional strahls are quasi-parallel to the magnetic field lines near the X-nullpoint due to the dominant Fermi-type magnetic curvature drift acceleration. Meanwhile, the high-energy electrons confined inside magnetic islands create PADs about 90 degrees. Our results link the electron PADs to local magnetic structures and directions of spacecraft crossings. This can help explain a variety of the PAD features reported in the recent observations in the solar wind and the Earth's magnetosphere.

Additional acceleration of solar-wind particles in current sheets of the heliosphere

Zharkova V.V. and Khabarova O.

Ann. Geophys., 33, 457-470, 2015

<http://www.ann-geophys.net/33/457/2015/angeo-33-457-2015.pdf>

Particles of fast solar wind in the vicinity of the heliospheric current sheet (HCS) or in a front of interplanetary coronal mass ejections (ICMEs) often reveal very peculiar energy or velocity profiles, density distributions with double or triple peaks, and well-defined streams of electrons occurring around or far away from these events. In order to interpret the parameters of energetic particles (both ions and electrons) measured by the WIND spacecraft during the HCS crossings, a comparison of the data was carried out with 3-D particle-in-cell (PIC) simulations for the relevant magnetic topology (Zharkova and Khabarova, 2012). The simulations showed that all the observed particle-energy distributions, densities, ion peak velocities, electron pitch angles and directivities can be fitted with the same model if the heliospheric current sheet is in a status of continuous magnetic reconnection. In this paper we present further observations of the solar-wind particles being accelerated to rather higher energies while passing through the HCS and the evidence that this acceleration happens well before the appearance of the corotating interacting region (CIR), which passes through the spacecraft position hours later. We show that the measured particle characteristics (ion velocity, electron pitch angles and the distance at which electrons are turned from the HCS) are in agreement with the simulations of additional particle acceleration in a reconnecting HCS with a strong guiding field as measured by WIND. A few examples are also presented showing additional acceleration of solar-wind particles during their passage through current sheets formed in a front of ICMEs. This additional acceleration at the ICME current sheets can explain the anticorrelation of ion and electron fluxes frequently observed around the ICME's leading front. Furthermore, it may provide a plausible explanation of the appearance of bidirectional "strahls" (field-aligned most energetic suprathermal electrons) at the leading edge of ICMEs as energetic electrons generated during a magnetic reconnection at the ICME-front current sheet.

Systematic Analysis of Machine Learning and Feature Selection Techniques for Prediction of the Kp Index

I. S. **Zhelavskaya**, **R. Vasile**, **Y. Y. Shprits**, **C. Stolle**, **J. Matzka**

Space Weather Volume17, Issue10 Pages 1461-1486 2019

<https://doi.org/10.1029/2019SW002271>

<https://agupubs.onlinelibrary.wiley.com/doi/epdf/10.1029/2019SW002271>

The Kp index is a measure of the mid-latitude global geomagnetic activity and represents short-term magnetic variations driven by solar wind plasma and IMF. The Kp index is one of the most widely used indicators for space weather alerts and serves as input to various models, such as for the thermosphere and the radiation belts. It is therefore crucial to predict the Kp index accurately. Previous work in this area has mostly employed artificial neural networks to nowcast

Kp, based their inferences on the recent history of Kp and on solar wind measurements at L1. In this study, we systematically test how different machine learning techniques perform on the task of nowcasting and forecasting Kp for prediction horizons of up to 12 hours. Additionally, we investigate different methods of machine learning and information theory for selecting the optimal inputs to a predictive model. We illustrate how these methods can be applied to select the most important inputs to a predictive model of Kp and to significantly reduce input dimensionality. We compare our best performing models based on a reduced set of optimal inputs with the existing models of Kp, using different test intervals and show how this selection can affect model performance.

Observational Evidence for Self-generation of Small-scale Magnetic Flux Ropes from Intermittent Solar Wind Turbulence

Jinlei **Zheng**¹ and Qiang Hu

2018 ApJL 852 L23

<http://iopscience.iop.org/sci-hub/tw/2041-8205/852/2/L23/>

<https://arxiv.org/pdf/1801.01771.pdf>

We present unique and additional observational evidence for the self-generation of small-scale coherent magnetic flux rope structures in the solar wind. Such structures with durations between 9 and 361 minutes are identified from Wind in situ spacecraft measurements through the Grad–Shafranov (GS) reconstruction approach. The event occurrence counts are on the order of 3500 per year on average and have a clear solar-cycle dependence. We build a database of small-scale magnetic flux ropes from 20 yr worth of Wind spacecraft data. We show a power-law distribution of the wall-to-wall time corresponding well to the inertial range turbulence, which agrees with relevant observations and numerical simulation results. We also provide the axial current density distribution from the GS-based observational analysis, which yields a non-Gaussian probability density function consistent with numerical simulation results.

Improving CME Forecasting Capability: An Urgent Need

Yihua **Zheng**

Space Weather, Volume 11, Issue 11, pages 641–642, November 2013

<http://www.readcube.com/articles/10.1002/2013SW001004?>

Forecasting propagation and evolution of CMEs in an operational setting: What has been learned

Yihua **Zheng**, Peter Macneice, Dusan Odstrcil, M. L. Mays, Lutz Rastaetter, Antti Pulkkinen, Aleksandre Taktakishvili, Michael Hesse, M. Masha Kuznetsova, Hyesook Lee and Anna Chulaki

Space Weather, Volume 11, Issue 10, pages 557–574, October 2013

<http://www.readcube.com/articles/10.1002/swe.20096?>

One of the major types of solar eruption, coronal mass ejections (CMEs) not only impact space weather, but also can have significant societal consequences. CMEs cause intense geomagnetic storms and drive fast mode shocks that accelerate charged particles, potentially resulting in enhanced radiation levels both in ions and electrons. Human and technological assets in space can be endangered as a result. CMEs are also the major contributor to generating large amplitude Geomagnetically Induced Currents (GICs), which are a source of concern for power grid safety. Due to their space weather significance, forecasting the evolution and impacts of CMEs has become a much desired capability for space weather operations worldwide. Based on our operational experience at Space Weather Research Center at NASA Goddard Space Flight Center (<http://swrc.gsfc.nasa.gov>), we present here some of the insights gained about accurately predicting CME impacts, particularly in relation to space weather operations. These include: 1. The need to maximize information to get an accurate handle of three-dimensional (3-D) CME kinetic parameters and therefore improve CME forecast; 2. The potential use of CME simulation results for qualitative prediction of regions of space where solar energetic particles (SEPs) may be found; 3. The need to include all CMEs occurring within a ~24 h period for a better representation of the CME interactions; 4. Various other important parameters in forecasting CME evolution in interplanetary space, with special emphasis on the CME propagation direction. It is noted that a future direction for our CME forecasting is to employ the ensemble modeling approach. 7 March 2011; 2012-01-18; 2012-01-22; 2013-04-11

CME Arrival Time Prediction via Fusion of Physical Parameters and Image Features

Yufeng **Zhong**^{1,2}, Dong Zhao¹, Xin Huang³, and Long Xu^{3,4}

2024 ApJS 271 31

<https://iopscience.iop.org/article/10.3847/1538-4365/ad1f5d/pdf>

Coronal mass ejections (CMEs) are among the most intense phenomena in the Sun–Earth system, often resulting in space environment effects and consequential geomagnetic disturbances. Consequently, quickly and accurately predicting CME arrival time is crucial to minimize the harm caused to the near-Earth space environment. To forecast the arrival time of CMEs, researchers have developed diverse methods over the years. While existing approaches have yielded positive results, they do not fully use the available data, as they solely accept either CME physical parameters or CME images as inputs. To solve this issue, we propose a method that extracts features from both CME physical parameters and CME images and uses the attention mechanism to fuse the two types of data. First, we design a parameter feature extraction module that extracts features from CME physical parameters. After that, we adopt an effective convolutional neural network model as our image feature extraction module for extracting features from CME images. Finally, utilizing the attention mechanism, we present a feature fusion module designed to fuse the features extracted from both parameters and images of CMEs. Therefore, our model can fully utilize and combine physical parameters and image features, which allows it to capture significant and comprehensive information about CMEs.

Geocoronal Solar Wind Charge Exchange Process Associated with the 2006-December-13 Coronal Mass Ejection Event

Yu [Zhou](#), [Noriko Y. Yamasaki](#), [Shin Toriumi](#), [Kazuhisa Mitsuda](#)

JGR 2023

<https://arxiv.org/pdf/2312.03381.pdf>

We report the discovery of a geocoronal solar wind charge exchange (SWCX) event corresponding to the well-known **2006 December 13th** coronal mass ejection (CME) event. Strong evidence for the charge exchange origin of this transient diffuse emission is provided by prominent non-thermal emission lines at energies of O7+, Ne9+, Mg11+, Si12+, Si13+. Especially, a 0.53 keV emission line that most likely arises from the N5+ 1s15p1→1s2 transition is detected. Previously, the forecastability of SWCX occurrence with proton flares has been disputed. In this particular event, we found that the SWCX signal coincided with the arrival of the magnetic cloud inside CME, triggered with a time delay after the proton flux fluctuation as the CME shock front passed through the Earth. Moreover, a spacecraft orbital modulation in SWCX light curve suggests that the emission arises close to the Earth. The line of sight was found to always pass through the northern magnetospheric cusp. The SWCX intensity was high when the line of sight passed the dusk side of the cusp, suggesting an azimuthal anisotropy in the flow of solar-wind ions inside the cusp. An axisymmetric SWCX emission model is found to underestimate the observed peak intensity by a factor of about 50. We suggest this discrepancy is related to the azimuthal anisotropy of the solar-wind flow in the cusp.

Effects of Solar Activity on Taylor Scale and Correlation Scale in Solar Wind Magnetic Fluctuations

G. [Zhou](#)^{1,2}, H.-Q. He^{1,3,4}, and W. Wan^{1,3,4}

2020 ApJL 899 L32

<https://doi.org/10.3847/2041-8213/abaaa9>

<https://iopscience.iop.org/article/10.3847/2041-8213/abaaa9/pdf>

The correlation scale and the Taylor scale are evaluated for interplanetary magnetic field fluctuations from two-point, single time correlation function using the Advanced Composition Explorer (ACE), Wind, and Cluster spacecraft data during the time period from 2001 to 2017, which covers over an entire solar cycle. The correlation scale and the Taylor scale are respectively compared with the sunspot number to investigate the effects of solar activity on the structure of the plasma turbulence. Our studies show that the Taylor scale increases with the increasing sunspot number, which indicates that the Taylor scale is positively correlated with the energy cascade rate, and the correlation coefficient between the sunspot number and the Taylor scale is 0.92. However, these results are not consistent with the traditional knowledge in hydrodynamic dissipation theories. One possible explanation is that in the solar wind, the fluid approximation fails at the spatial scales near the dissipation ranges. Therefore, the traditional hydrodynamic turbulence theory is incomplete for describing the physical nature of the solar wind turbulence, especially at the spatial scales near the kinetic dissipation scales.

Numerical study of the propagation characteristics of coronal mass ejections in a structured ambient solar wind

Yufen [Zhou](#), Xueshang Feng

JGR Volume 122, Issue 2 February 2017 Pages 1451–1462 DOI 10.1002/2016JA023053

<http://sci-hub.cc/10.1002/2016JA023053#>

Using a three-dimensional (3-D) magnetohydrodynamics (MHD) model, we analyze and study the propagation characteristics of coronal mass ejections (CMEs) launched at different positions in a realistic structured ambient solar wind. Here the ambient solar wind structure during the Carrington rotation 2095 is selected, which is the characteristics of activity rising phase. CMEs with a simple spherical plasmoid structure are initiated at different solar latitudes with respect to the heliospheric current sheet (HCS) and the Earth in the same ambient solar wind. Then, we numerically obtained the evolution process of the CMEs from the Sun to the interplanetary space. When the Earth and the CME launch position are located on the same side of the HCS, the arrival time of the shock at the Earth is faster than that when the Earth and the CME launch position are located on the opposite side of the HCS. The disturbance amplitudes for the same side event are also larger than those for the opposite side event. This may be due to the fact that the HCS between the CME and the Earth for the opposite side event hinders its propagation and weakens it. The CMEs tend to deflect toward the HCS in the latitudinal direction near the corona and then propagate almost parallel to the HCS in the interplanetary space. This deflecting tendency may be caused by the dynamic action of near-Sun magnetic pressure gradient force on the ejected coronal plasma.

Using a 3D MHD simulation to interpret propagation and evolution of a coronal mass ejection observed by multiple spacecraft: The 2010-04-03 event†

Yufen **Zhou**^{1,2,*}, Xueshang Feng¹ and Xinhua Zhao

JGR, 2014

<http://onlinelibrary.wiley.com/doi/10.1002/2014JA020347/pdf>

The coronal mass ejection (CME) event on **April 3, 2010** is the first fast CME observed by STEREO SECCHI/HI for the full Sun-Earth line. Such an event provides us a good opportunity to study the propagation and evolution of CME from the Sun up to 1 AU. In this paper, we study the time-dependent evolution and propagation of this event from the Sun to Earth using the 3D SIP-CESE MHD model. The CME is initiated by a simple spherical plasmoid model: a spheromak magnetic structure with high speed, high pressure and high plasma density plasmoid. The simulation performs a comprehensive study on the CME by comparing the simulation results with STEREO and WIND observations. It is confirmed from the comparison with observations that the MHD model successfully reproduces many features of both the fine solar coronal structure and the typical large scale structure of the shock propagation and gives the shock arrival time at Earth with an error of sim 2 hours. Then we analyze in detail the several factors affecting the CME's geo-effectiveness: the CME's propagation trajectory, span angle and velocity.

MHD numerical study of the latitudinal deflection of coronal mass ejection†

Y. F. **Zho**, X. S. Feng

JGR, 2013

In this paper, we analyze and quantitatively study the deflection of CME in the latitudinal direction during its propagation from the Corona to interplanetary (IP) space using a three-dimensional (3D) numerical magnetohydrodynamics (MHD) simulation. To this end, **12 May 1997** CME event during the Carrington rotation 1922 is selected. Firstly, we try to reproduce the physical properties for this halo CME event observed by the WIND spacecraft. Then, we study the deflection of CME, and quantify the effect of the background magnetic field and the initiation parameters (such as the initial magnetic polarity and the parameters of the CME model) on the latitudinal deflection of CMEs. The simulations show that the initial magnetic polarity substantially affects the evolution of CMEs. The "parallel" CMEs (with the CME's initial magnetic field parallel to that of the ambient field) originating from high latitude show a clear Equator-ward deflection at the beginning, and then propagate almost parallel to heliospheric current sheet (HCS), and the "anti-parallel" CMEs (with the CME's initial magnetic field opposite to that of the ambient field) deflect toward the pole. Our results demonstrate that the latitudinal deflection extent of the "parallel" CMEs is not only mainly controlled by the background magnetic field strength, but also by the initial magnetic field strength of the CMEs. There is an anti-correlation between the latitudinal deflection extent and the CME average transit speed and the energy ratio E_{cme}/E_{sw} .

Prediction for Arrival Time and Parameters of Corotation Interaction Regions using Earth–Mars Correlated Events from Tianwen-1, MAVEN, and Wind Observations

Zhihui **Zhong**¹, Chenglong Shen^{1,2}, Yutian Chi³, Dongwei Mao⁴, Bin Miao⁵, Zhiyi Fu⁴, Junyan Liu⁴, Beatriz Sánchez-Cano⁶, Daniel Heyner⁷, and Yuming Wang^{1,2,8}

2024 ApJ 965 114

<https://iopscience.iop.org/article/10.3847/1538-4357/ad2fab/pdf>

Using the Stream Interaction Regions list from the Tianwen-1/Mars Orbiter Magnetometer (MOMAG) data between 2021 November and 2021 December and from Wind observations, we present an accurate prediction for the arrival time and in situ parameters of corotating interaction regions (CIRs) when the Earth and Mars have large longitudinal separations. Since CIRs were detected earlier at Earth than at Mars during the period examined, we employ Earth-based CIR detections for predicting CIR observations at Mars. The arrival time is calculated by the Parker spiral model under the assumption of steady corotation of the Sun and coronal holes, while the in situ parameters are derived from Wind data through radial dependent scaling laws. The CIR prediction results are compared to the actual observations obtained from the MOMAG and Mars Ion and Neutral Particle Analyzer instruments onboard Tianwen-1, as well as the Magnetometer and Solar Wind Ion Analyzer instruments onboard MAVEN. The predicted arrival time is close to the observed values with relative errors less than 10%, and the expected in situ data show a good consistency with the Martian measurements. The comparison results indicate that the prediction method has good performance and will be helpful for comparative analysis with Tianwen-1 observations at Mars in the future.

Intermittencies and Local Heating in Magnetic Cloud Boundary Layers

Zilu **Zhou**, [Pingbing Zuo](#), [Xueshang Feng](#), [Yi Wang](#), [Chaowei Jiang](#)...

[Solar Physics](#) October 2019, 294:14

<https://link.springer.com/content/pdf/10.1007%2Fs11207-019-1537-0.pdf>

We perform a statistical study on the intermittency and the associated local heating in the front boundary layers (BLs) of 74 magnetic clouds (MCs). The intermittent structures are identified by the partial variance of increments (PVI) method. The probability distribution function of PVI-values reveals that the BLs are more intermittent than adjacent sheath regions, and they contain a greater concentration of strong intermittencies. These strong intermittencies are accompanied by local enhancement of the proton temperature, while the enhancement is not prominent at weaker intermittencies inside the BLs. Since the strong intermittencies are associated with magnetic reconnection (MR) processes according to previous studies, these results indicate that MR processes may account for the local heating in the MCBLs to a large extent. **10 January 1997, 28-30 October 2000, 12-13 June 2005, 08 October 2012**

Table 1 Magnetic and plasma parameters in MCBLs and sheath (1995-2015)

Using a 3-D MHD simulation to interpret propagation and evolution of a coronal mass ejection observed by multiple spacecraft: The 3 April 2010 event

Yufen **Zhou**^{1,2}, Xueshang Feng^{1,*} and Xinhua Zhao

Volume 119, Issue 12, pages 9321–9333, December 2014

<http://onlinelibrary.wiley.com/doi/10.1002/2014JA020347/pdf>

The coronal mass ejection (CME) event on 3 April 2010 is the first fast CME observed by STEREO Sun Earth Connection Coronal and Heliospheric Investigation/Heliospheric Imager for the full Sun-Earth line. Such an event provides us a good opportunity to study the propagation and evolution of CME from the Sun up to 1 AU. In this paper, we study the time-dependent evolution and propagation of this event from the Sun to Earth using the 3-D SIP-CESE (Solar-InterPlanetary Conservation Element and Solution Element) MHD model. The CME is initiated by a simple spherical plasmoid model: a spheromak magnetic structure with high-speed, high-pressure, and high-plasma density plasmoid. The simulation performs a comprehensive study on the CME by comparing the simulation results with STEREO and Wind observations. It is confirmed from the comparison with observations that the MHD model successfully reproduces many features of both the fine solar coronal structure and the typical large-scale structure of the shock propagation and gives the shock arrival time at Earth with an error of ~2 h. Then we analyze in detail the several factors affecting the CME's geo-effectiveness: the CME's propagation trajectory, span angle, and velocity.

Super-criticality of ICME and CIR shocks†

Xiaoyan **Zhou**^{1,*} and Edward J. Smith

JGR Volume 120, Issue 3 Pages 1526–1536 2015

Interplanetary Coronal Mass Ejection (ICME) and Corotating Interaction Region (CIR) shocks are characterized in terms of super-criticality introduced by Edmiston and Kennel [1984] to classify shocks based on whether dissipation is provided by electron resistivity alone or also requires ion viscosity. The condition for determining super-criticality is a critical Mach number, MC , a function of θB_n , the angle between the upstream magnetic field, B , and the normal to the shock surface, n , and β , the ratio of the plasma and magnetic pressures. The criterion was subsequently revised by Kennel [1987] to include dissipation by electron thermal as well as electrical conductivity. Two early separate studies of ICME and CIR shocks motivated our investigation that included several improvements. We use Kennel [1987], shocks identified by WIND near 1AU and Ulysses near 5 AU from the same solar cycle and provide Occurrence Probability

Distributions and statistical information for all parameters. We answer three questions: (1) Is the super-criticality of ICME and CIR shocks different? (2) If so, why? (3) Does the latter MC criterion change the answers? Our conclusions are: (1) about two-thirds of CIR shocks are supercritical as compared to one-third of ICME shocks, (2) although ICME shock speeds are typically higher than CIR shocks', the fast mode wave speeds are even higher at 1 AU than that of CIR shocks at ~5 AU causing a reduction in Mach numbers, (3) CIR shocks are also more super-critical than ICME shocks using both criteria with slight differences.

Using a 3-D spherical plasmoid to interpret the Sun-to-Earth propagation of the 4 November 1997 coronal mass ejection event

Zhou, Y. F.; Feng, X. S.; Wu, S. T.; Du, D.; Shen, F.; Xiang, C. Q.

J. Geophys. Res., Vol. 117, No. A1, A01102, 2012, **File**

<http://dx.doi.org/10.1029/2010JA016380>

We present the time-dependent propagation of a Sun-Earth connection event that occurred on **4 November 1997** using a three-dimensional (3-D) numerical magnetohydrodynamics (MHD) simulation. A global steady state solar wind for this event is obtained by a 3-D SIP-CESE MHD model with Parker's 1-D solar wind solution and measured photospheric magnetic fields as the initial values. Then, superposed on the quiet background solar wind, a spherical plasmoid is used to mimic the 4 November 1997 coronal mass ejection (CME) event. The CME is assumed to arise from the evolution of a **spheromak** magnetic structure with high-speed, high-pressure, and high-plasma-density plasmoid near the Sun. Moreover, the axis of the initial simulated CME is put at S14W34 to conform to the observed location of this flare/CME event. The result has provided us with a relatively satisfactory comparison with the Wind spacecraft observations, such as southward interplanetary magnetic field and large-scale smooth rotation of the magnetic field associated with the CME.

Large-Scale Source Regions of Earth-Directed Coronal Mass Ejections

Guiping **Zhou**, Jingxiu Wang and Jun Zhang

A&A, 445, No. 3, 1133-1141, 2006, **File**

SOLAR ORBITER REVEALS NON-FIELD-ALIGNED SOLAR WIND PROTON BEAMS AND ITS ROLE IN WAVE GROWTH ACTIVITIES

by X. Zhu¹, J. He¹, D. Duan¹, D. Verscharen², C. J. Owen², A. Fedorov³, P. Louarn³, T. Horbury⁴

Solar Orbiter nugget #16 2023 <https://www.cosmos.esa.int/web/solar-orbiter/-/science-nugget-non-field-aligned-solar-wind-proton-beam-and-its-role-in-wave-growth-activities>

Wave Composition, Propagation, and Polarization of Magnetohydrodynamic Turbulence within 0.3 au as Observed by Parker Solar Probe

Xingyu **Zhu**¹, Jansen He¹, Daniel Verscharen^{2,3}, Die Duan¹, and Stuart D. Bale

2020 ApJL 901 L3

<https://doi.org/10.3847/2041-8213/abb23e>

Turbulence, a ubiquitous phenomenon in interplanetary space, is crucial for the energy conversion of space plasma at multiple scales. This work focuses on the propagation, polarization, and wave composition properties of the solar wind turbulence within 0.3 au, and its variation with heliocentric distance at magnetohydrodynamic scales (from 10 s to 1000 s in the spacecraft frame). We present the probability density function of propagation wavevectors (PDF(k_{\parallel} , k_{\perp})) for solar wind turbulence within 0.3 au for the first time: (1) wavevectors cluster quasi-(anti-)parallel to the local background magnetic field for $k_{di} < 0.02$, where d_i is the ion inertial length; (2) wavevectors shift to quasi-perpendicular directions for $k_{di} > 0.02$. Based on our wave composition diagnosis, we find that: the outward/anti-sunward Alfvén mode dominates over the whole range of scales and distances, the spectral energy density fraction of the inward/sunward fast mode decreases with distance, and the fractional energy densities of the inward and outward slow mode increase with distance. The outward fast mode and inward Alfvén mode represent minority populations throughout the explored range of distances and scales. On average, the degree of anisotropy of the magnetic fluctuations defined with respect to the minimum variation direction decreases with increasing scale, with no trend in distance at any scale. Our results provide comprehensive insight into the scenario of transport and transfer of the solar wind fluctuations/turbulence in the inner heliosphere.

Evolution of the Radial Size and Expansion of Coronal Mass Ejections Investigated by Combining Remote and In Situ Observations

Bin Zhuang¹, Noé Lugaz¹, Nada Al-Haddad¹, Réka M. Winslow¹, Camilla Scolini¹, Charles J. Farrugia¹, and Antoinette B. Galvin¹

2023 ApJ 952 7

<https://iopscience.iop.org/article/10.3847/1538-4357/acd847/pdf>

<https://arxiv.org/pdf/2305.14339.pdf>

A fundamental property of coronal mass ejections (CMEs) is their radial expansion, which determines the increase in the CME radial size and the decrease in the CME magnetic field strength as the CME propagates. CME radial expansion can be investigated either by using remote observations or by in situ measurements based on multiple spacecraft in radial conjunction. However, there have been only few case studies combining both remote and in situ observations. It is therefore unknown if the radial expansion in the corona estimated remotely is consistent with that estimated locally in the heliosphere. To address this question, we first select 22 CME events between the years 2010 and 2013, which were well observed by coronagraphs and by two or three spacecraft in radial conjunction. We use the graduated cylindrical shell model to estimate the radial size, radial expansion speed, and a measure of the dimensionless expansion parameter of CMEs in the corona. The same parameters and two additional measures of the radial-size increase and magnetic-field-strength decrease with heliocentric distance of CMEs based on in situ measurements are also calculated. For most of the events, the CME radial size estimated by remote observations is inconsistent with the in situ estimates. We further statistically analyze the correlations of these expansion parameters estimated using remote and in situ observations, and discuss the potential reasons for the inconsistencies and their implications for the CME space weather forecasting. **17 Apr 2011, 2 Jan 2012, 13-15 Jun 2013, 9 Jul 2013, 11-12 Jul 2013**

Table 1 CME Events Observed by the Radially Aligned Spacecraft at Different Heliocentric Distances 2010-2013

Numerical Simulations on the Deflection of Coronal Mass Ejections in the Interplanetary Space

Bin Zhuang^{1,2}, Yuming Wang^{1,2}, Youqiu Hu¹, Chenglong Shen^{1,2,3}, Rui Liu^{1,2,3,4}, Tingyu Gou^{1,2}, Quanhao Zhang^{1,2}, and Xiaolei Li^{1,2}

2019 ApJ 876 73

<https://doi.org/10.3847/1538-4357/ab139e>

<https://arxiv.org/abs/1905.08139>

Deflection of coronal mass ejections (CMEs) in the interplanetary space, especially in the ecliptic plane, serves as an important factor deciding whether CMEs arrive at the Earth. Observational studies have shown evidence for deflection, whose detailed dynamic processes, however, remain obscure. Here we developed a 2.5D ideal magnetohydrodynamic simulation to study the propagation of CMEs traveling with different speeds in the heliospheric equatorial plane. The simulation confirms the existence of the CME deflection in the interplanetary space, which is related to the difference between the CME speed (v_r) and the solar wind speed (v_{sw}): a CME will propagate radially as v_r is close to v_{sw} but eastward or westward when v_r is larger or smaller than v_{sw} ; the greater the difference is, the larger the deflection angle will be. This result supports the model for CME deflection in the interplanetary space (DIPS) proposed by Wang et al., predicting that an isolated CME can be deflected due to the pileup of solar wind plasma ahead of or behind the CME. Furthermore, the deflection angles, which are derived by inputting v_r and v_{sw} from the simulation into the DIPS model, are found to be consistent with those in the simulation.

The Significance of the Influence of the CME Deflection in Interplanetary Space on the CME Arrival at Earth

Bin Zhuang^{1,2}, Yuming Wang^{1,3}, Chenglong Shen^{1,3,4}, Siqing Liu^{5,6}, Jingjing Wang^{5,6}, Zonghao Pan^{1,4}, Huimin Li⁷, and Rui Liu

2017 ApJ 845 117 DOI [10.3847/1538-4357/aa7fc0](https://doi.org/10.3847/1538-4357/aa7fc0)

[http://iopscience.iop.org/sci-hub/cc/0004-637X/845/2/117/](https://iopscience.iop.org/sci-hub/cc/0004-637X/845/2/117/)

As one of the most violent astrophysical phenomena, coronal mass ejections (CMEs) have strong potential space weather effects. However, not all Earth-directed CMEs encounter the Earth and produce geo-effects. One reason is the deflected propagation of CMEs in interplanetary space. Although there have been several case studies clearly showing such deflections, it has not yet been statistically assessed how significantly the deflected propagation would influence the CME's arrival at Earth. We develop an integrated CME-arrival forecasting (iCAF) system, assembling the modules of CME detection, three-dimensional (3D) parameter derivation, and trajectory reconstruction to predict whether or not a CME arrives at Earth, and we assess the deflection influence on the CME-arrival forecasting. The performance of iCAF is tested by comparing the two-dimensional (2D) parameters with those in the Coordinated Data Analysis Workshop

(CDAW) Data Center catalog, comparing the 3D parameters with those of the gradual cylindrical shell model, and estimating the success rate of the CME Earth-arrival predictions. It is found that the 2D parameters provided by iCAF and the CDAW catalog are consistent with each other, and the 3D parameters derived by the ice cream cone model based on single-view observations are acceptable. The success rate of the CME-arrival predictions by iCAF with deflection considered is about 82%, which is 19% higher than that without deflection, indicating the importance of the CME deflection for providing a reliable forecasting. Furthermore, iCAF is a worthwhile project since it is a completely automatic system with deflection taken into account. **3 Aug 2011**

Table 1 38 Selected Frontside Halo CMEs

Using CME Observations for Geomagnetic Storm Forecasting

A.N. **Zhukov**

Space Weather, J. Liliensten (ed.), Astrophysics and Space Science Library 344, 5--13 (2007). **File.**

Solar Sources of Geoeffective CMEs: a SOHO/EIT View

Andrei N. **Zhukov**^{1,2}

Coronal and Stellar Mass Ejections

Proceedings IAU Symposium No. 226, 2005

K. P. Dere, J. Wang & Y. Yan, eds.

See **File** at E:\Chertok_new\Library\Papers\2005\IAU_226

Observations of the low solar corona, in particular in the EUV, are an effective means of identifying the solar sources of coronal mass ejections (CMEs). SOHO/EIT, with its continuous 24 hours per day coverage, is well suited to perform this task. Source regions and start times of frontside full and partial halo CMEs (that may be geoeffective) can thus be determined. The most frequent EUV signatures of CMEs are coronal dimmings. EIT waves, eruptive filaments and post-eruption arcades are also reliable signatures. Frontside halo CMEs with source regions close to the solar disc center have the strongest chance to hit the Earth. The inspection of the EIT data together with photospheric magnetograms may give an idea about the ejected interplanetary flux rope magnetic field and, in particular, about the presence or absence of southward (geoeffective) field. If a source region is situated close to the solar limb, the corresponding CME also may be geoeffective, as the CME-driven shocks have large angular extent. In this case the storm can be produced by the sheath plasma behind the shock, provided it contains strong enough southward interplanetary magnetic field. Some implications for the operational space weather forecast are discussed. EIT and LASCO are capable to identify the solar sources of the most of geomagnetic storms. In some cases, however, the identification is uncertain, so the observations by the future STEREO mission will be needed for the investigation of similar events.

Heliospheric Propagation of Coronal Mass Ejections: Drag-Based Model Fitting

T. **Žic**, B. Vršnak, M. Temmer

2015

<http://arxiv.org/pdf/1506.08582v1.pdf>

The so-called drag-based model (DBM) simulates analytically the propagation of coronal mass ejections (CMEs) in interplanetary space and allows the prediction of their arrival times and impact speeds at any point in the heliosphere ("target"). The DBM is based on the assumption that beyond a distance of about 20 solar radii from the Sun, the dominant force acting on CMEs is the "aerodynamic" drag force. In the standard form of DBM, the user provisionally chooses values for the model input parameters, by which the kinematics of the CME over the entire Sun--"target" distance range is defined. The choice of model input parameters is usually based on several previously undertaken statistical studies. In other words, the model is used by ad hoc implementation of statistics-based values of the input parameters, which are not necessarily appropriate for the CME under study. Furthermore, such a procedure lacks quantitative information on how well the simulation reproduces the coronagraphically observed kinematics of the CME, and thus does not provide an estimate of the reliability of the arrival prediction. In this paper we advance the DBM by adopting it in a form that employs the CME observations over a given distance range to evaluate the most suitable model input parameters for a given CME by means of the least-squares fitting. Furthermore, the new version of the model automatically responds to any significant change of the conditions in the ambient medium (solar wind speed, density, CME--CME interactions, etc.) by changing the model input parameters according to changes in the CME kinematics. The advanced DBM is shaped in a form that can be readily employed in an operational system for real-time space-

weather forecasting by promptly adjusting to a successively expanding observational dataset, thus providing a successively improving prediction of the CME arrival.

Does the Time Resolution of the Geoeffective IMF Component Influence Its Annual, Semiannual and Diurnal Patterns?

Slaviša [Živković](#), [Giuliana Verbanac](#) & [Mario Bandić](#)

[Solar Physics](#) volume 298, Article number: 94 (2023)

<https://doi.org/10.1007/s11207-023-02184-9>

The geoeffective interplanetary magnetic field (IMF) component B_s , $B_s = B_z, GSM, GSM$ when $B_z, GSM < 0$, is the most commonly used at 1-hour resolution for studying solar wind–magnetosphere coupling. In this way, the fluctuation of both B_z, GSM (and thus B_s) and IMF polarity within the hour are not taken into account. We investigate whether the global patterns of B_s and B_s sorted by IMF polarity (B_s fields) change when these fluctuations are considered with respect to those based on hourly data. We have obtained B_s fields at the high 16-second resolution. In this way, the information about the existence of B_s fields within an hour is retained. The present study has shown that the initial resolution of the IMF data used to obtain B_s fields (16-seconds or 1-hour) does not affect their characteristic patterns: diurnal, annual, and semiannual variations. Regardless of the initial IMF resolution, the B_s sorted by the IMF polarity exists in all seasons. They show the two annual sinusoidal-like variations of opposite phase, the “pair of spectacles” pattern. The initial resolution affects only slightly the absolute values of B_s fields. The results have shown that hourly values of IMF data are suitable for studying their global behavior within the year and also for investigating their relationship with magnetospheric quantities.

Indirect Solar Wind Measurements Using Archival Cometary Tail Observations

Nadezhda [Zolotova](#), Yuriy Sizonenko, Mikhail Vokhmyanin, Igor Veselovsky

[Solar Physics](#) May 2018, 293:85

<https://arxiv.org/pdf/1805.04684.pdf>

<https://link.springer.com/content/pdf/10.1007%2Fs11207-018-1307-4.pdf>

This paper addresses the problem of the solar wind behaviour during the Maunder minimum. Records on plasma tails of comets can shed light on the physical parameters of the solar wind in the past. We analyse descriptions and drawings of comets between the eleventh and eighteenth century. To distinguish between dust and plasma tails, we address their colour, shape, and orientation. Based on the calculations made by F.A. Bredikhin, we found that cometary tails deviate from the antisolar direction on average by more than 10° , which is typical for dust tails. We also examined the catalogues of Hevelius and Lubieniecki. The first indication of a plasma tail was revealed only for the great comet C/1769 P1.

Two-step Dropouts of Radiation Belt Electron Phase Space Density Induced by a Magnetic Cloud Event

Zhengyang [Zou](#)¹, Pingbing Zuo¹, Binbin Ni², Zhonglei Gao¹, Geng Wang¹, Zhengyu Zhao^{1,2}, Xueshang Feng¹, and Fengsi Wei¹

2020 *ApJL* 895 L24

<https://doi.org/10.3847/2041-8213/ab9179>

<https://sci-hub.tw/10.3847/2041-8213/ab9179>

We report a two-step dropout event of radiation belt electron phase space density (PSD) induced by a typical magnetic cloud (MC) that drove an intense geomagnetic storm. The first and second steps of PSD dropout occurred, respectively, in the initial and main phases of the storm with a short-time partial recovery between the two dropouts. In this event, the initial phase after the sudden commencement lasted for near 21 hr, which gives an ideal opportunity to investigate the nature of the radiation belt electron dropout by isolating the main phase from any losses occurring during the initial phase. Detailed analysis shows that the first step of the dropout in the initial phase is likely associated with the magnetopause shadowing effect in combination with ultra-low frequency wave-induced outward transport caused by sustaining enhanced dynamic pressure activity before the MC. Comparably, the prolonged strong southward interplanetary magnetic field inside the MC that resulted in the storm main phase is supposed to play an important role in the second step of significant electron losses to the interplanetary space. Additionally, the partial recovery of electron PSD between the two steps of the dropout is possibly due to the acceleration processes via wave-particle interactions with whistler-mode chorus waves. Our study demonstrated that persistently enhanced solar wind dynamic pressure, which is frequently observed inside interplanetary coronal mass ejections and corotating interaction regions, can play an important role in modulating the radiation belt electron dynamics before the storm main phase driven by these solar wind disturbances. **2013 June 27–29**

COMPOSITION OF CORONAL MASS EJECTIONS

T. H. [Zurbuchen](#)¹, M. Weberg¹, R. von Steiger^{2,3}, R. A. Mewaldt⁴, S. T. Lepri¹, and S. K. Antiochos⁵
2016 ApJ 826 10 DOI 10.3847/0004-637X/826/1/10

We analyze the physical origin of plasmas that are ejected from the solar corona. To address this issue, we perform a comprehensive analysis of the elemental composition of interplanetary coronal mass ejections (ICMEs) using recently released elemental composition data for Fe, Mg, Si, S, C, N, Ne, and He as compared to O and H. We find that ICMEs exhibit a systematic abundance increase of elements with first ionization potential (FIP) < 10 eV, as well as a significant increase of Ne as compared to quasi-stationary solar wind. ICME plasmas have a stronger FIP effect than slow wind, which indicates either that an FIP process is active during the ICME ejection or that a different type of solar plasma is injected into ICMEs. The observed FIP fractionation is largest during times when the Fe ionic charge states are elevated above $Q_{\text{Fe}} > 12.0$. For ICMEs with elevated charge states, the FIP effect is enhanced by 70% over that of the slow wind. We argue that the compositionally hot parts of ICMEs are active region loops that do not normally have access to the heliosphere through the processes that give rise to solar wind. *We also discuss the implications of this result for solar energetic particles accelerated during solar eruptions and for the origin of the slow wind itself.*

IN-SITU SOLAR WIND AND MAGNETIC FIELD SIGNATURES OF INTERPLANETARY CORONAL MASS EJECTIONS

THOMAS H. [ZURBUCHEN](#)¹ and IAN G. RICHARDSON²

Space Science Reviews (2006) 123: 31–43, File

The heliospheric counterparts of coronal mass ejections (CMEs) at the Sun, interplanetary coronal mass ejections (ICMEs), can be identified in situ based on a number of magnetic field, plasma, compositional and energetic particle signatures as well as combinations thereof. We summarize these signatures and their implications for understanding the nature of these structures and the physical properties of coronal mass ejections. We conclude that our understanding of ICMEs is far from complete and formulate several challenges that, if addressed, would substantially improve our knowledge of the relationship between CMEs at the Sun and in the heliosphere.

ОСНОВНЫЕ ВРЕМЕННЫЕ ХАРАКТЕРИСТИКИ ВАРИАЦИЙ КОСМИЧЕСКИХ ЛУЧЕЙ И СОПУТСТВУЮЩИХ ПАРАМЕТРОВ В МАГНИТНЫХ ОБЛАКАХ

Абунина М.А., Белов А.В., Шлык Н.С., Абунин А.А., Мелкумян А.А., Прямушкина И.И., Оленева В.А., Янке В.Г.

ГИА Том: 64 Номер: 1 Год: 2024 Страницы: 29-38

Исследованы вариации основных параметров межпланетной среды, космических лучей и геомагнитной активности во время прохождения магнитных облаков мимо Земли (466 событий за период с 1967 по 2021 гг.). Рассмотрены распределения по времени указанных параметров внутри магнитных облаков. Показано, что максимальные значения скорости солнечного ветра, величины межпланетного магнитного поля и индексов геомагнитной активности чаще регистрируются в передней части магнитного облака, в то время как минимальные значения температурного индекса, плотности и экваториальной составляющей анизотропии космических лучей могут наблюдаться в любой части исследуемой структуры.

ВЫСОКОЭНЕРГИЧНЫЕ МАГНИТОСФЕРНЫЕ ЭЛЕКТРОНЫ И РАЗЛИЧНЫЕ ТИПЫ ВОЗМУЩЕНИЯ МЕЖПЛАНЕТНОЙ СРЕДЫ

[Абунин](#) А.А., Абунина М.А., Белов А.В., Гайдаш С.П., Крякунова О.Н., Николаевский Н.Ф., Прямушкина И.И., Трефилова Л.А.

ИЗВЕСТИЯ РАН Том: 83 Номер: 5 Год: 2019 Страницы: 638-640

Исследуются особенности поведения высокоэнергичных магнитосферных электронов (с энергиями более 2 МэВ) во время межпланетных возмущений, вызванных корональными выбросами плазмы и высокоскоростными потоками солнечного ветра из корональных дыр. Анализируется более чем тридцатилетний период наблюдений таких электронов (1986–2017 гг.). Показано, что корональные выбросы плазмы и высокоскоростные потоки из корональных дыр по-разному влияют на поведение высокоэнергичных электронов. В создании электронных возрастных высокоскоростных потоков из дыр эффективнее корональных выбросов.

АНАЛИЗ ВОЗМУЩЕНИЙ КОСМИЧЕСКОЙ ПОГОДЫ ОТ МОЩНЫХ

ЭРУПТИВНЫХ ВСПЫШЕК СЕНТЯБРЯ 2017 г.

Абунин^{1,2} А.А., Белов¹ А.В., Черток¹ И.М.

Астрономия-2018 Том 2 Солнечно-земная физика – современное состояние и перспективы Стр. 15

<http://www.izmiran.ru/library/eaas2018/eaas-2018-2.pdf>

УНИКАЛЬНАЯ БАЗА ДАННЫХ ТРАНЗИЕНТНЫХ ЯВЛЕНИЙ В КОСМИЧЕСКИХ ЛУЧАХ И МЕЖПЛАНЕТНОЙ СРЕДЕ

Абунин^{1,2} А.А., Абунина¹ М.А., Белов¹ А.В., Гайдаш¹ С.П.,

Ерошенко¹ Е.А., Прямушкина³ И.И., Трефилова¹ Л.А.

Астрономия-2018 Том 2 Солнечно-земная физика – современное состояние и перспективы Стр. 7

<http://www.izmiran.ru/library/eaas2018/eaas-2018-2.pdf>

ФОРБУШ-ПОНИЖЕНИЯ 19-ГО ЦИКЛА СОЛНЕЧНОЙ АКТИВНОСТИ

Абунин А.А., Абунина М.А., Белов А.В., Ерошенко Е.А., Оленёва В.А., Янке В.Г.

ИЗВЕСТИЯ РАН. СЕРИЯ ФИЗИЧЕСКАЯ, **2013**, том 77, № 5, с. 599–601

В 19-м цикле наблюдалась аномально высокая солнечная активность, но возможности ее наблюдения были ограничены. Наземные наблюдения космических лучей наряду с геомагнитной активностью среди тех немногих видов непрерывных наблюдений, которые позволяют судить о событиях 19-го цикла и сравнивать их с событиями других циклов. Сопоставление событий в космических лучах с солнечной и геомагнитной активностью показало, что количество и мощность магнитных бурь в 19-м цикле соответствует аномально высокому числу солнечных пятен. Однако в этом цикле существует определенный дефицит форбуш-понижений большой величины. Возможно, что наиболее мощные выбросы 19-го цикла имели в целом меньший размер, чем самые большие выбросы более позднего периода.

Связь параметров Форбуш-эффектов с гелиодолготой солнечных источников

Абунин А.А., Абунина М.А., Белов А.В., Ерошенко Е.А., Оленева В.А., Янке В.Г.

Геомагнетизм и Аэрономия, **2012** (в печати)

Форбуш-эффекты с внезапным и постепенным началом

Абунин А.А., Абунина М.А., Белов А.В., Ерошенко Е.А., Оленева В.А., Янке В.Г.

Геомагнетизм и Аэрономия, Т.52, №3, С.1-8, **2012**.

ФОРБУШ-ЭФФЕКТЫ, СОЗДАННЫЕ ВЫБРОСАМИ СОЛНЕЧНОГО ВЕЩЕСТВА С МАГНИТНЫМИ ОБЛАКАМИ

**АБУНИНА М. А.*1, БЕЛОВ А. В.1, ШЛЫК Н. С.1, ЕРОШЕНКО Е. А.1,
АБУНИН А. А.1, ОЛЕНЕВА В. А.1, ПРЯМУШКИНА И. И.1, ЯНКЕ В. Г.1**

Г и А Том: 61Номер: 5 Год: **2021** Страницы: 572-582

DOI: [10.31857/S0016794021050023](https://doi.org/10.31857/S0016794021050023)

Изучается влияние магнитных облаков на вариации плотности космических лучей, регистрируемые нейтронными мониторами. Из данных о 252 Форбуш-эффектах, обусловленных межпланетными возмущениями, содержащими магнитные облака, выделяются статистические закономерности и характерные особенности таких событий. Обсуждается поведение основных параметров солнечного ветра, космических лучей и геомагнитной активности во время прохождения магнитных облаков мимо Земли, а также характерные особенности внутренней структуры магнитных облаков. Было показано, что вариации космических лучей тесно связаны с максимальными параметрами солнечного ветра и межпланетного магнитного поля внутри магнитных облаков. Установлено, что по распределению времени максимальных параметров солнечного ветра чаще всего максимальная скорость внутри магнитного облака регистрируется в начале, а максимальное значение межпланетного магнитного поля – как в начале, так и в середине события. Также получено, что существует достаточно тесная корреляция вариаций плотности космических лучей в магнитном облаке с его размером, выраженным в гирорадиусах.

МЕТОД КОЛЬЦА СТАНЦИЙ В ИССЛЕДОВАНИИ ВАРИАЦИЙ КОСМИЧЕСКИХ ЛУЧЕЙ: 1. ОБЩЕЕ ОПИСАНИЕ

Абунина М.А., Белов А.В., Ерошенко Е.А., Абунин А.А., Оленева В.А., Янке В.Г., Мелкумян А.А.
ГиА Том: 60Номер: 1 Год: **2020** Страницы: 41-48

Уже более 60 лет нейтронные мониторы остаются главным, стандартным и стабильным инструментом для измерения космических лучей с энергией от 400 МэВ до сотен ГэВ. Чтобы получать достаточно полную информацию о распределении космических лучей за пределами магнитосферы, нужно иметь сеть детекторов, достаточно равномерно расположенных по земному шару. Одним из наиболее полезных методов, позволяющих получать свойства углового распределения космических лучей без разложения на гармоники, является метод кольца станций. Он позволяет получить мгновенное (точнее, ежечасное) долготное распределение интенсивности космических лучей, не прибегая к его моделированию. Главная цель данной работы – расширить использование метода кольца станций, удобного и полезного метода исследования вариаций космических лучей.

О ВАРИАЦИЯХ ПОТОКА КОСМИЧЕСКИХ ЛУЧЕЙ В КОНЦЕ 24 ЦИКЛА СОЛНЕЧНОЙ АКТИВНОСТИ

БАЛАБИН Ю.В.*¹, **БЕЛОВ А.В.²**, **ГУЩИНА Р.Т.²**, **ЯНКЕ В.Г.²**, **ЯНКОВСКИЙ И.В.³**

Известия РАН Том: 85Номер: 3 Год: **2021** Страницы: 321-325

Данные большинства нейтронных мониторов показывают, что интенсивность космических лучей еще не достигла уровня, наблюдавшегося на этих станциях в 2009 г. Однако на ряде станций (Баренцбург, Туле, Кергелен, Москва и др.) интенсивность уже превысила уровень 2009 г. Возможно, этот аномальный эффект связан с необычным поведением характеристик солнечной активности в 24 цикле.

Бархатов Н.А., Ревунова Е.А., Романов Р.В., Бархатова О.М., Ревунов С.Е. **Исследование связи параметров локализации солнечных источников магнитных облаков с их характеристиками и суббуревой активностью.**

СОЛНЕЧНО-ЗЕМНАЯ ФИЗИКА [Том 5. 2019. № 3.С. 70–80.](#) [Аннотация](#) / [Полный текст](#) (PDF)

ЗАВИСИМОСТЬ ГЕОМАГНИТНОЙ АКТИВНОСТИ ОТ СТРУКТУРЫ МАГНИТНЫХ ОБЛАКОВ

БАРХАТОВ Н. А.*¹, **ДОЛГОВА** Д. С.¹, **РЕВУНОВА** Е. А.²

ГиА Том: 59Номер: 1 Год: **2019** Страницы: 19-29

Работа посвящена изучению высокоширотной геомагнитной активности в зависимости от структурных элементов “быстрых” магнитных облаков солнечного ветра, сопровождаемых ударными волнами. Установлено условие возникновения таких облаков и возможная причина их ускорения в солнечном ветре. Предположено, что в геомагнитную активность дают вклад турбулентные оболочки облаков, параметры которых обусловлены солнечным ветром, изменившимся в результате воздействия на него ударной волны облака. Для оценки данной эволюции натекающего солнечного ветра определены локальные ориентации плоскостей ударных волн и рассчитана ожидаемая на границе магнитосферы последовательность значений геоэффективной Vz-компоненты в солнечно-магнитосферной системе координат. Сопоставление динамики AL-индекса с измеренными на КА значениями Vz-компоненты и с вычисленной последовательностью значений Vz свидетельствует о необходимости учета такой эволюции межпланетного магнитного поля (ММП) солнечного ветра на ударной волне магнитного облака за время ее переноса к магнитосфере.

ИССЛЕДОВАНИЕ ВЗАИМОСВЯЗИ ВЫСОКОШИРОТНОЙ ГЕОМАГНИТНОЙ АКТИВНОСТИ С ПАРАМЕТРАМИ МЕЖПЛАНЕТНЫХ МАГНИТНЫХ ОБЛАКОВ С ИСПОЛЬЗОВАНИЕМ ИСКУССТВЕННЫХ НЕЙРОННЫХ СЕТЕЙ

БАРХАТОВ Н.А.¹, **РЕВУНОВ** С.Е.¹, **ВОРОБЬЕВ** В.Г.², **ЯГОДКИНА** О.И.²

Геомагн. и Аэрон. Том: 58Номер: 2 Год: **2018** Страницы: 155-162

С помощью искусственных нейронных сетей исследуются причинно-следственные связи динамики высокоширотной геомагнитной активности (по AL-индексу) с типом магнитного облака солнечного ветра. Создана рекуррентная нейросетевая модель, основанная на поиске оптимальных физически связанных входных и выходных параметров, характеризующих воздействие на магнитосферу плазменного потока типа магнитного облака. Показано, что использование в качестве входных параметров нейросетей компонент ММП с учетом 90 мин предыстории, позволяет восстановить последовательность AL с точностью до ~80%. Успешность восстановления динамики AL по используемым данным указывает на наличие тесной нелинейной связи AL-индекса с параметрами облака. Созданные нейросетевые модели, с высокой эффективностью могут быть применены для восстановления AL-индекса как в периоды изолированных магнитосферных суббурь, так и в периоды взаимодействия магнитосферы Земли с магнитными облаками различных типов. Разработанная модель восстановления AL-индекса может быть использована как детектор магнитных облаков.

ПРОЯВЛЕНИЕ ОРИЕНТАЦИИ МАГНИТНЫХ ОБЛАКОВ СОЛНЕЧНОГО ВЕТРА В СЕЗОННОЙ ВАРИАЦИИ ГЕОМАГНИТНОЙ АКТИВНОСТИ

Н. А. Бархатов², Е. А. Ревунова^{1,2}, А. Б. Виноградов

Космические исследования, - том 52, № 4, Июль-Август 2014, С. 286-295

Работа посвящена анализу причин сезонной зависимости геомагнитной активности с учетом ориентации крупномасштабных плазменных структур солнечного ветра, типа магнитных облаков. Обращено внимание на вклад магнитных облаков разной ориентации в периоды равноденствия и солнцестояния. Установлено, что в периоды равноденствия геомагнитная активность увеличивается за счет выбросов с небольшими углами наклона оси к плоскости эклиптики, наиболее часто регистрируемых в околоземном пространстве. В периоды солнцестояния такие облака являются не геоэффективными структурами, вследствие уменьшения значения проекции магнитного поля оси облака на магнитный диполь Земли в такие интервалы, что отражается в снижении уровня геомагнитной активности летом и зимой.

ПРОГНОЗ ИНТЕНСИВНОСТИ ГЕОМАГНИТНЫХ БУРЬ, ВЫЗВАННЫХ МАГНИТНЫМИ ОБЛАКАМИ СОЛНЕЧНОГО ВЕТРА С УЧЕТОМ СЕЗОНА ГОДА И ИХ НАЧАЛЬНОЙ ОРИЕНТАЦИИ

Н.А. Бархатов, Е. А. Ревунова, А.Б. Виноградов

ИКИ-2014 Сессия: Солнечный ветер, гелиосфера и солнечно-земные связи

<http://plasma2014.cosmos.ru/presentations>

ФОРБУШ-ЭФФЕКТЫ И ГЕОМАГНИТНЫЕ БУРИ

БЕЛОВ А. В.¹, БЕЛОВА Е. А.¹, ШЛЫК Н. С.¹, АБУНИНА М. А.¹, АБУНИН А. А.¹, БЕЛОВ С. М.¹

ГИА Том: 64 Номер: 3 Год: 2024 Страницы: 322-335

Выделены и исследованы события Форбуш-эффектов в галактических космических лучах (по данным сети нейтронных мониторов) и сопутствующих геомагнитных возмущений за длительный период с 1957 по 2022 гг. Проанализированы статистические связи между различными параметрами вариаций потока космических лучей и индексами геомагнитной активности. Установлено, что величина Форбуш-эффектов нелинейно зависит от класса геомагнитной бури. Найдена умеренная корреляция (до 0.67) между экстремальными значениями различных индексов геомагнитной активности (Ap, Kp, Dst) и характеристиками космических лучей. Показано, что одновременная регистрация экстремальных значений параметров космических лучей и геомагнитной активности происходит далеко не всегда, а зависит от знака Vz-компоненты межпланетного магнитного поля в конкретном событии.

ПРОТОННЫЕ ВОЗРАСТАНИЯ И ФОРБУШ-ЭФФЕКТЫ С ОДНИМИ И ТЕМИ ЖЕ СОЛНЕЧНЫМИ ИСТОЧНИКАМИ

БЕЛОВ А. В.¹, ШЛЫК Н. С.¹, АБУНИНА М. А.¹, БЕЛОВА Е. А.¹, АБУНИН А. А.¹, ПАПАИОАННОУ А.²

Изв. РАН Том: 87 Номер: 7 Год: 2023 Страницы: 1005-1009

Сравниваются характеристики Форбуш-эффектов и солнечных протонных событий, вызванных одним и тем же солнечным источником (корональным выбросом массы и связанной с ним солнечной вспышкой). Выбран диапазон гелиодолгот (E04–W35), в котором вспышки ассоциированы как с Форбуш-эффектами, так и солнечными протонными событиями у Земли. Независимо рассматривались солнечные протонные события для разных энергий ($E > 10$, > 100 МэВ) и с разными порогами потоков, а также GLE (наземные возрастания солнечных космических лучей). Результаты проанализированы в сравнении с контрольной группой вспышек в той же гелиодолготной зоне, не приводивших к солнечным протонным событиям. Показано, что корональные выбросы массы, связанные с солнечными протонными событиями, с большой вероятностью вызывают значительный Форбуш-эффект на орбите Земли и геомагнитную бурю. Ускорительная и модулирующая эффективности таких солнечных явлений взаимосвязаны, что, в основном, объясняется высокими скоростями корональных выбросов массы. На практике данные результаты могут применяться для улучшения прогнозов геомагнитных бурь и Форбуш-эффектов.

ГЕОЭФФЕКТИВНОСТЬ СПОРАДИЧЕСКИХ ЯВЛЕНИЙ В 24-М СОЛНЕЧНОМ ЦИКЛЕ

БЕЛОВ А. В.¹, БЕЛОВА Е. А.^{*1}, ШЛЫК Н. С.¹, АБУНИНА М. А.^{*1}, АБУНИН А. А.¹

ГиА Том: 63Номер: 4 Год: 2023 Страницы: 534-544

Обсуждены особенности 24-го цикла солнечной активности, проявившиеся в вариациях космических лучей, характеристиках солнечных вспышек, протонных событий, корональных выбросов массы, а также уровне геомагнитной активности. Показано, что по числу солнечных пятен и других проявлений солнечной активности 24-й цикл оказался самым скромным за последние 100 лет наблюдений. Описано значительное снижение геоэффективности различных солнечных событий, проявившееся в меньшем количестве и величинах зарегистрированных на Земле Форбуш-эффектов, возрастных потоков протонов и электронов разных энергий и геомагнитных бурь.

ВЫДЕЛЕНИЕ СОЛНЕЧНО-СУТОЧНОЙ АНИЗОТРОПИИ КОСМИЧЕСКИХ ЛУЧЕЙ ЛОКАЛЬНЫМ И ГЛОБАЛЬНЫМ МЕТОДАМИ

БЕЛОВ А.В.^{*1}, ШЛЫК Н.С.^{*1}, АБУНИНА М.А.¹, АБУНИН А.А.¹, ОЛЕНЕВА В.А.¹, ЯНКЕ В.Г.¹, МЕЛКУМЯН А.А.¹

ГиА Том: 63Номер: 3 Год: 2023 Страницы: 306-320

По данным нейтронного монитора ст. Москва с помощью гармонического анализа получены характеристики солнечно-суточной анизотропии космических лучей в спокойные дни за длительный период с 1965 по 2020 гг. Установлено, что средний суточный ход вариаций космических лучей нейтронных мониторов ст. Москва практически полностью описывается двумя гармониками солнечно-суточной анизотропии и не содержит признаков других влияний. Сравнение со среднесуточными характеристиками экваториальной составляющей векторной анизотропии космических лучей, полученными по данным мировой сети нейтронных мониторов с помощью метода глобальной съемки, показало хорошее согласие результатов двух методик. Из сравнения локальных и глобальных результатов получены оценки приемных коэффициентов первой гармоники анизотропии космических лучей для нейтронного монитора ст. Москва и предложен новый экспериментальный метод расчета приемных коэффициентов отдельных детекторов. Обсуждены и обоснованы ограничения локальной методики, а также возможности продолжения и расширения данного исследования.

ИНДЕКС ДОЛГОВРЕМЕННОГО ВЛИЯНИЯ СПОРАДИЧЕСКОЙ СОЛНЕЧНОЙ АКТИВНОСТИ НА МОДУЛЯЦИЮ КОСМИЧЕСКИХ ЛУЧЕЙ

Белов А.В., Гущина Р.Т.

Г и А Том: 58Номер: 1 Год: 2018 Страницы: 3-10

Корональные выбросы вещества не только создают Форбуш-эффекты, но вносят вклад и в долговременную модуляцию космических лучей. Это делает корональные выбросы главным спорадическим проявлением солнечной активности, которое следует учитывать в моделях модуляции. В работе предложен новый вариант СМЕ-индекса, полученный на основе сопоставления данных спутниковых коронографов с Форбуш-эффектами и долговременными вариациями космических лучей.

ВЕКТОРНАЯ АНИЗОТРОПИЯ КОСМИЧЕСКИХ ЛУЧЕЙ В НАЧАЛЕ ФОРБУШ-ЭФФЕКТОВ

Белов А.В., Абунина М.А., Абунин А.А., Ерошенко Е.А., Оленева В.А., Янке В.Г.

Геомагн. и Аэрон. 57(5):584-5916 2017

Рассмотрено поведение анизотропии и плотности галактических космических лучей в первые часы Форбуш-эффектов за период 1957-2014 гг., начинавшихся с прихода ударной волны. Показано, что уже в начале события величина первой гармоники анизотропии, как правило, существенно возрастает, а ее направление заметно меняется. Изменения тем больше, чем мощнее межпланетное возмущение. Показано, что по изменениям некоторых параметров анизотропии и плотности можно судить о гелиодолготе источника возмущения, а также о дальнейшем развитии Форбуш-эффекта и геомагнитной активности.

ПОВЕДЕНИЕ ПЛОТНОСТИ ПОТОКА КОСМИЧЕСКИХ ЛУЧЕЙ В НАЧАЛЕ ФОРБУШ-ЭФФЕКТОВ

Белов А.В., Ерошенко Е.А., Абунина М.А., Абунин А.А., Оленева В.А., Янке В.Г
Г и А Том: 56 Номер: 6 Год: **2016** Страницы: 683-689

Исследовано поведение плотности потока космических лучей в начале Форбуш-эффектов, в первые часы после прихода межпланетной ударной волны. Используются данные о вариациях плотности потока космических лучей с жесткостью 10 ГВ, полученные методом глобальной съемки по наблюдениям мировой сети нейтронных мониторов в 1957–2013 гг. Выявлено большое разнообразие поведения плотности потока космических лучей после прихода ударной волны. Выделена небольшая (~1/5 от общего количества), но четко определяемая группа Форбуш-эффектов, в которых после прихода ударной волны наблюдается повышение, а не понижение плотности. В целом, наблюдается корреляция начальной вариации плотности космических лучей с полной величиной Форбуш-эффекта и мощностью сопутствующего геомагнитного возмущения.

Чем обусловлены и с чем связаны форбуш-эффекты?

Белов А.В. и др.

Известия РАН., Сер.физ. Т.65. №3. С.373-376, **2001**.

ВЛИЯНИЕ АКТИВНЫХ ОБЛАСТЕЙ НА ХАРАКТЕРИСТИКИ СОЛНЕЧНОГО ВЕТРА В МАКСИМУМЕ ЦИКЛА

БОГАЧЁВ С.А.*¹, РЕВА А.А.*¹, КИРИЧЕНКО А.С.*¹, УЛЬЯНОВ А.С.*¹, ЛОБОДА И.П.*¹

ПИСЬМА В АСТРОНОМИЧЕСКИЙ ЖУРНАЛ Том: 48 Номер: 7 Год: **2022** Страницы: 523-532

Активные области (АО) на Солнце обсуждаются как один из возможных источников медленного солнечного ветра (СВ), происхождение которого все еще является предметом споров. В настоящей работе представлены экспериментальные свидетельства возможного влияния АО на скорость и температуру СВ вблизи максимума 23-го солнечного цикла (2000–2002 гг.). Изучены отдельно характеристики СВ, сформированного в периоды, когда АО находились на центральном меридиане (ЦМ) Солнца (~40% от всего времени наблюдения), и характеристики СВ, сформированного в отсутствие АО на ЦМ (~60% времени). Скорость СВ в первом случае (в присутствии АО) в среднем оказалась примерно на 1% ниже, чем скорость СВ, сформированного в отсутствие АО (434.06 км/с против 438.09 км/с при погрешности измерений $\sigma \approx 0.37$ км/с). Для температуры СВ соответствующая разница составила около 6% (94600 К против 100500 К при погрешности $\sigma \approx 340$ К). Этот результат подтверждает в среднем более низкую скорость и температуру СВ, формирующегося в АО, по сравнению с компонентой СВ, формирующейся в корональных дырах.

СВЯЗЬ МЕЖДУ ПЛОЩАДЬЮ ПОЛЯРНЫХ КОРОНАЛЬНЫХ ДЫР И СКОРОСТЬЮ СОЛНЕЧНОГО ВЕТРА В МИНИМУМЕ МЕЖДУ 22-М И 23-М СОЛНЕЧНЫМИ ЦИКЛАМИ

Борисенко А.В., Богачёв С.А.

СОЛНЕЧНО-ЗЕМНАЯ ФИЗИКА Том: 9 Номер: 3 Год: **2023** Страницы: 122-127

https://elibrary.ru/download/elibrary_54625076_61892220.pdf

Мы использовали данные космического телескопа SOHO/EIT и спектрометра VEIS на космическом аппарате Wind, чтобы сравнить скорость солнечного ветра (СВ) около орбиты Земли с изменениями площади полярных корональных дыр (КД) на Солнце в минимуме солнечной активности 1996 г. Мы обнаружили, что в марте 1996 г. скорость СВ коррелировала с площадью южной КД с коэффициентом 0.64. В сентябре и октябре 1996 г. была обнаружена корреляция скорости СВ с площадью северной КД (коэффициенты 0.64 и 0.85 соответственно). Как мы полагаем, это подтверждает, что СВ из полярных КД может проникать в плоскость эклиптики в минимуме солнечной активности. Скорость СВ составила 460-500 км/с - это ниже, чем скорость СВ из экваториальных КД (600-700 км/с).

ВЛИЯНИЕ ПОЛЯРНЫХ КОРОНАЛЬНЫХ ДЫР НА ХАРАКТЕРИСТИКИ СОЛНЕЧНОГО ВЕТРА В МИНИМУМЕ АКТИВНОСТИ МЕЖДУ 24 И 25 СОЛНЕЧНЫМИ ЦИКЛАМИ

БОРИСЕНКО А. В.1, **БОГАЧЁВ** С. А.1

ПАЖ Том: 46Номер: [11](#) Год: **2020** Страницы: 802-813

Использованы данные SDO/AIA 193 Å и ACE/SWEPAM за 2019 г., чтобы сравнить влияние полярных и экваториальных корональных дыр (КД) на характеристики солнечного ветра (СВ) в условиях низкой солнечной активности. Как и следовало ожидать, большинство геомагнитных бурь в этот период были вызваны высокоскоростными потоками солнечного ветра (>500–600 км/с), происходящими из экваториальных корональных дыр (ЭКД). Вместе с тем показано, что в глубоком минимуме солнечной активности заметное влияние на характеристики СВ на орбите Земли могут оказывать полярные КД. Для интегральной площади полярных КД и скорости СВ в исследованный период обнаружена корреляция с коэффициентом 0.6. Особенно существенное влияние на скорость СВ оказывала южная полярная КД, для которой **весной 2019 г.** (в период максимального наклона к Земле южного полюса Солнца) найдена корреляция со скоростью СВ с коэффициентом 0.82. Северная полярная КД почти не влияла на скорость СВ. **Осенью 2019 г.**, в период наклона к Земле северного полюса Солнца, обнаружена антикорреляция площади полярных КД со скоростью СВ на земной орбите. Обсуждается возможный механизм влияния полярных КД на характеристики СВ, а также предлагаем интерпретацию полученных результатов.

СРАВНЕНИЕ ЭФФЕКТИВНОСТИ МЕТОДОВ МАШИННОГО ОБУЧЕНИЯ ПРИ ИССЛЕДОВАНИИ ВАЖНОСТИ ВХОДНЫХ ПРИЗНАКОВ В ЗАДАЧЕ ПРОГНОЗИРОВАНИЯ ГЕОМАГНИТНОГО ИНДЕКСА DST

Владимиров Р.Д., Широкий В.Р., Мягкова И.Н., Баринов О.Г., Доленко С.А.

Г и А Том: **63**Номер: **2** Год: **2023** с. **190-201**

Одним из перспективных подходов к прогнозированию значений геомагнитных индексов является использование методов машинного обучения. Однако для эффективного использования таких методов необходим отбор существенных входных признаков задачи с целью уменьшения ее входной размерности. В данной работе рассматривается алгоритм получения наиболее эффективной модели прогнозирования, основанный на понижении входной размерности данных путем постепенного отбрасывания входных признаков на основе следующих методов машинного обучения: линейная регрессия, градиентный бустинг, искусственная нейронная сеть типа многослойный перцептрон. Проводится сравнение эффективности перечисленных методов; рассматриваются направления дальнейшего развития работ.

НАБЛЮДЕНИЯ ВЫБРОСОВ КОРОНАЛЬНОЙ МАССЫ МЕТОДОМ МЕЖПЛАНЕТНЫХ МЕРЦАНИЙ ВБЛИЗИ МАКСИМУМА 24-ГО ЦИКЛА СОЛНЕЧНОЙ АКТИВНОСТИ

ГЛЯНЦЕВ А.В.1, **ТЮЛЬБАШЕВ** С.А.1, **ЧАШЕЙ** И.В.1, **ШИШОВ** В.И.

АЖ Том: 92 Номер: 1 Год: **2015** Страницы: 46

, оказывается близкой к средней скорости выброса между короной и Землей. В половине всех рассмотренных случаев точность оценки прихода возмущения на Землю составляла несколько часов. Показано, что скорости выбросов, оцененные по запаздыванию усиления мерцаний по отношению к рентгеновским вспышкам, значительно ближе к

истинным, чем скорости, найденные по ширине временных спектров мерцаний. $\frac{1}{2}$ x спектров мерцаний.

О детектировании выбросов корональной массы в межпланетной среде по наблюдениям мерцаний радиосточников

А. В. **Глянцев**, С. А. Тюльбашев, И. В. Чашей, В. И. Шишов

Астрономический журнал - **2014**, № 9 С. 713-719

Проведен анализ данных ежедневных наблюдений мерцающих радиосточников для годичной серии с июля 2011 г. по июнь 2012 г. Наблюдения проводились на радиотелескопе БСА ФИАН с 16-лучевой диаграммой на частоте 111 МГц. Вариации индексов мерцаний сопоставлялись с данными о всплесках рентгеновского излучения Солнца и возмущениях геомагнитного поля. Показано, что метод, основанный на сравнении наблюдаемых индексов мерцаний источников за текущий день с индексами мерцаний источников за предыдущий день, позволяет регистрировать подавляющую часть распространяющихся возмущений, связанных с корональными событиями класса M5.0 и выше.

Исследование методом главных компонент влияния геометрии нейтрального токового слоя гелиосферы и солнечной активности на модуляцию галактических космических лучей

Гололобов П.Ю., Кривошапкин П.А., Крымский Г.Ф., Герасимова С.К.

СОЛНЕЧНО-ЗЕМНАЯ ФИЗИКА Том 6. 2020. № 1, С. 30–35.

<https://naukaru.ru/ru/storage/viewWindow/50033>

Исследуется совокупное модулирующее воздействие геометрии нейтральной поверхности межпланетного магнитного поля и солнечной активности на распространение галактических космических лучей в гелиосфере. При помощи метода главных компонент произведена оценка роли каждого фактора в модуляции космических лучей. Применение метода к экспериментальным данным по уровню солнечной активности, углу раствора нейтральной поверхности и интенсивности космических лучей за длительный период времени с 1980 по 2018 г. позволило выявить временную динамику роли каждого фактора в модуляции. Показано, что характер модуляции сильно зависит от полярности общего магнитного поля Солнца. Результаты исследования подтверждают существующие теоретические представления о гелиосферной модуляции, а также отражают ее особенности почти за четыре полных цикла солнечной активности.

Особенности спорадических вариаций плотности и анизотропии галактических космических лучей в 24-м цикле солнечной активности.

Григорьев В. Г., Герасимова С. К., Гололобов П. Ю., Стародубцев С. А., Зверев А. С.

СОЛНЕЧНО-ЗЕМНАЯ ФИЗИКА Том 8. 2022. № 1 С. 34–38.

<https://naukaru.ru/ru/storage/viewWindow/87302>

На основе обработки данных мировой сети нейтронных мониторов и мюонных телескопов методом глобальной съемки исследуются вариации плотности и анизотропии галактических космических лучей в периоды форбуш-понижений, наблюдавшихся в 24-м цикле солнечной активности. Одновременное использование двух разнотипных детекторов позволяет рассматривать временную динамику углового распределения космических лучей в двух разных энергетических интервалах. Кроме того, по данным измерений Якутского спектрографа космических лучей им. А.И. Кузьмина проведена оценка показателя энергетического спектра в периоды больших возмущений межпланетной среды в этом цикле. Анализ полученных результатов подтверждает наши ранние утверждения, что 24-й цикл солнечной активности характеризуется повышенным уровнем турбулентности межпланетного магнитного поля. 9 марта 2012, 15 июля 2012, 15 апреля 2013, 24 июня 2013, 12 сентября 2014, 23 декабря 2014, 17 марта 2015, 23 июня 2015, 16 июля 2017, 8 сентября 2017

Мониторинг геомагнитных возмущений на основе метода глобальной съемки в реальном времени.

Григорьев В.Г., Стародубцев С.А., Гололобов П.Ю.

СОЛНЕЧНО-ЗЕМНАЯ ФИЗИКА Том 5. 2019. № 3. С. 110–115.

<https://naukaru.ru/ru/storage/view/39910>

Представлен метод прогноза геомагнитных возмущений на основе реализации метода глобальной съемки в реальном времени с использованием базы данных мировой сети нейтронных мониторов NMDB. Проведен анализ за 2013–2018 гг. поведения компонент трехмерного углового распределения космических лучей в межпланетном пространстве. Эти компоненты обусловлены первыми двумя сферическими гармониками. Установлено, что основными параметрами, реагирующими на приближение к Земле геоэффективных возмущений межпланетной среды, являются изменения амплитуд зональных (северо-южных) компонент распределения космических лучей. С целью выбора эффективных критериев определения предвестников геомагнитных возмущений и их возможной временной динамики проведен ретроспективный анализ связи поведения указанных компонент с наблюдавшимися за исследованный период геомагнитными возмущениями.

РАСПРЕДЕЛЕНИЕ КОСМИЧЕСКИХ ЛУЧЕЙ В ГЕЛИОСФЕРЕ ПО ДАННЫМ СЕТИ СТАНЦИЙ МЮОННЫХ ТЕЛЕСКОПОВ

Григорьев В.Г., Гололобов П.Ю., Кривошапкин П.А., Крымский Г.Ф., Янке В.Г.

ИЗВЕСТИЯ РАН Том: 83 Номер: 5 Год: 2019 Страницы: 606-609

В ИКФИА в 1960-х гг. был разработан метод глобальной съемки, позволяющий использовать всю мировую сеть нейтронных мониторов в качестве единого многонаправленного прибора, позволяющего получать информацию о распределении космических лучей (КЛ) в межпланетном пространстве за каждый измеряемый момент времени. По аналогии с этим подходом в данной работе представлен вариант нового метода, использующий данные измерений станций мировой сети мюонных телескопов Хобарт, Кувейт, Нагоя, Сао-Мартиньо и Якутск. Произведены расчеты приемных характеристик указанных станций, учитывающие: траектории частиц, диаграммы направленности приборов, коэффициенты связи и энергетический спектр предполагаемых вариаций КЛ. Реализация и совершенствование этого метода позволит в дальнейшем получать новую информацию о динамике распределения КЛ в удаленных областях гелиосферы.

ЯВЛЕНИЯ ГИСТЕРЕЗИСА В ОТКЛИКЕ ГЕОМАГНИТНОЙ АКТИВНОСТИ И ПАРАМЕТРОВ КОСМИЧЕСКИХ ЛУЧЕЙ НА ВАРИАЦИИ МЕЖПЛАНЕТНОЙ СРЕДЫ ВО ВРЕМЯ МАГНИТНОЙ БУРИ

ДАНИЛОВА О.А.^{✉1}, **ПТИЦЫНА Н.Г.**^{✉1}, **СДОБНОВ В.Е.**^{✉2}

[СОЛНЕЧНО-ЗЕМНАЯ ФИЗИКА](#) Том: 10 Номер: 3 Год: 2024 Страницы: 70-78

Известно, что динамика интенсивности космических лучей различна на восходящей и нисходящей ветвях 11-летнего солнечного цикла, т. е. наблюдаются явления гистерезиса. Недавно получено, что на более коротких интервалах на масштабе магнитных бурь также могут наблюдаться признаки гистерезиса в зависимостях жесткостей геомагнитного обрезания (ЖГО) космических лучей R (геомагнитных порогов) от параметров гелио- и геосферы. Параметр R - это жесткость, ниже которой поток частиц обрезан из-за геомагнитного экранирования. В настоящей работе проведен анализ зависимости геомагнитного буревого индекса Dst и вариации геомагнитных порогов ΔR от параметров межпланетного магнитного поля (ММП) и солнечного ветра (СВ) во время двухступенчатой магнитной бури 7-8 сентября 2017 г. Найлены явления гистерезиса в следующих парных рядах: (1) зависимостях Dst от параметров СВ и ММП и (2) зависимостях ΔR от параметров СВ и ММП. Найдено, что кривые на нисходящей фазе бури (главная фаза) и восходящей (фаза восстановления) не совпадают - формируются петли гистерезиса. Специфической чертой исследуемой бури является второе понижение Dst на восстановительной фазе. Картина гистерезиса отражает эту специфическую динамику бури, формируя две петли как реакцию на два понижения Dst .

ДИНАМИКА МЕЖПЛАНЕТНЫХ ПАРАМЕТРОВ И ГЕОМАГНИТНЫХ ИНДЕКСОВ В ПЕРИОДЫ МАГНИТНЫХ БУРЬ, ИНИЦИИРОВАННЫХ РАЗНЫМИ ТИПАМИ СОЛНЕЧНОГО ВЕТРА

Дремухина Л.А., **Ермолаев Ю.И.**, **Лодкина И.Г.**

Геомаг. и Аэрономия Том: 59 Номер: 6 Год: 2019 Страницы: 683-695

DOI: [10.1134/S0016794019060063](https://doi.org/10.1134/S0016794019060063)

На базе архива данных OMNI2 за 1995–2017 гг. анализируется динамика индексов геомагнитной активности (Dst , ar , AE и PC) и межпланетных параметров в периоды магнитных бурь с минимальными $Dst_{min} \leq -50$ нТл, индуцированных разными межпланетными источниками, а именно: областями взаимодействия разноскоростных потоков солнечного ветра (СВ) CIR; областями сжатия Sheath перед межпланетными CME; магнитными облаками MC и “поршнями” Ejecta. Была отобрана 181 буря с монотонным ходом Dst -индекса на главных фазах. Аналогично работам [Ермолаев и др., 2010, 2011], выполненным по данным OMNI за 1976–2000 гг., к бурям был применен двойной метод наложенных эпох с двумя опорными моментами во время начала главной фазы и минимума Dst_{min} . Такой подход позволяет выявить тенденции в динамике индексов магнитной активности и параметров СВ во время бурь с разными длительностями главных фаз и различие в этих тенденциях для бурь, вызванных разными источниками. Показано, что наибольшие средние значения индексов Dst , ar , AE и PC имеют место для Sheath-бурь, а наименьшие для Ejecta-бурь. Динамика AE и ar -индексов подобна, а полярного индекса PC существенно различается во время бурь с разными межпланетными источниками, что свидетельствует о различии в отклике полярной магнитосферы при бурях с разными источниками. Существуют заметные различия в вариациях параметров СВ для разных групп бурь: для Sheath-бурь характерен очень высокий уровень флуктуаций V и V_z ММП, для CIR-бурь он близок к среднему, а для MC и Ejecta существенно ниже среднего.

СВЯЗЬ ПАРАМЕТРОВ СОЛНЕЧНОГО ВЕТРА РАЗНЫХ ТИПОВ С ИНДЕКСАМИ ГЕОМАГНИТНОЙ АКТИВНОСТИ

Дремухина Л.А., **Лодкина И.Г.**, **Ермолаев Ю.И.**

ПАЖ Том: 56 Номер: 6 Год: 2018 Страницы: 410-419

В работе анализируются корреляционные связи между планетарными индексами геомагнитной активности Dst , ar и AE и значениями функций связи, рассчитанными по данным о параметрах плазмы и магнитного поля в четырех типах течений солнечного ветра: областях взаимодействия разноскоростных потоков CIR, межпланетных проявлениях выбросов корональной массы ICME (MC и Ejecta) и областях сжатия Sheath перед MC и Ejecta. Для отбора типов солнечного ветра используются данные из каталога <ftp://ftp.iki.rssi.ru/pub/omni/> за период 1995–2016 гг., в котором идентифицировано 744 CIR-события, 118 MC, 501 Sheath и 843 Ejecta. Функции

связи рассчитываются на основе данных базы OMNI. Проведенный анализ показал низкие значения коэффициентов корреляции ($R < 0.5$) между функциями связи и индексом Dst для всех типов солнечного ветра. Для индексов ар и АЕ получена достаточно сильная корреляционная связь с функциями связи ($0.6 < R < 0.82$) для всех типов СВ. Геоэффективность функций связи, оцениваемая по значениям коэффициентов линейной регрессии, имеет наибольшие значения для ар-индекса при типах солнечного ветра Sheath и MC. Для аврорального индекса АЕ самые высокие значения эффективностей функций связи получены для типов солнечного ветра CIR и Ejecta.

СТАТИСТИЧЕСКОЕ ИССЛЕДОВАНИЕ ВОЗДЕЙСТВИЯ СОЛНЕЧНОГО ВЕТРА РАЗНЫХ ТИПОВ НА ГЕНЕРАЦИЮ МАГНИТНЫХ БУРЬ В ПЕРИОД 1995–2016 ГГ

ДРЕМУХИНА Л.А.*1, **ЛОДКИНА** И.Г.2, **ЕРМОЛАЕВ** Ю.И.

ГиА Том: 58Номер: 6 Год: 2018 Страницы: 768-775

Настоящая работа является продолжением исследований [Николаева и др., 2015, 2017], в которых рассматривается вопрос о возможном различии в генерации магнитных бурь, вызванных разными крупномасштабными типами течений солнечного ветра: CIR, Sheath, MC и Ejecta. В этих работах по данным за период 1976–2000 гг. было показано, что при использовании функции связи Бартона и др., связывающей интегральное электрическое поле солнечного ветра $E_y = VBz$ с индексами Dst и Dst*, наибольшая геоэффективность обнаруживается для магнитных бурь, генерированных Sheath- и CIR-событиями. Использование других 12 функций связи между различными межпланетными параметрами и состоянием магнитосферы, имеющихся в литературе, показало, что их эффективность для каждого типа течения солнечного ветра зависит от вида используемой функции. В этой работе мы исследуем эффективность генерации главной фазы бури для тех же 4-х типов течений (CIR, Sheath, MC и Ejecta) на основе данных OMNI за период 1995–2016 гг., содержащий более полный набор данных о параметрах солнечного ветра. Полученные результаты подтверждают зависимость генерации магнитных бурь от типа межпланетного источника и высокую эффективность функции связи в виде интеграла от E_y для течений типа Sheath и CIR. Обсуждаются проблемы применимости используемых функций связи для прогноза магнитных бурь.

Параметры солнечного ветра на фазе роста 25-го солнечного цикла: сходства и различия с 23-м и 24-м солнечными циклами.

Ермолаев Ю.И., **Лодкина** И.Г., **Хохлачев** А.А., **Ермолаев** М.Ю., **Рязанцева** М.О., **Рахманова** Л.С., **Бородкова** Н.Л., **Сапунова** О.В., **Москалева** А.В.

СОЛНЕЧНО-ЗЕМНАЯ ФИЗИКА Том 9 № 4, 2023 С. 63–70.

<https://naukaru.ru/ru/storage/viewWindow/138051>

Солнечная активность и параметры солнечного ветра существенно снизились в 23-24-м солнечных циклах (СЦ) по сравнению с СЦ 21-22. В данной работе мы анализируем измерения солнечного ветра на фазе роста СЦ 25 и сравниваем их с аналогичными данными в предыдущих циклах. Для этого данные базы OMNI за 1976–2022 гг. были селектированы как по фазам 11-летних солнечных циклов, так и по крупномасштабным типам солнечного ветра (по каталогу [<http://www.iki.rssi.ru/pub/omni>]) и мы рассчитали средние значения параметров плазмы и магнитного поля для сформированных наборов данных. Полученные результаты свидетельствуют в пользу гипотезы о том, что продолжение этого цикла будет аналогично соответствующим фазам предыдущего цикла 24, т. е. СЦ 25 будет слабее, чем СЦ 21 и 22.

НЕКОТОРЫЕ ВОПРОСЫ ИДЕНТИФИКАЦИИ КРУПНОМАСШТАБНЫХ ТИПОВ СОЛНЕЧНОГО ВЕТРА

ЕРМОЛАЕВ М.Ю.1, **ЕРМОЛАЕВ** Ю.И.1, **РЯЗАНЦЕВА** М.О.1, **ЛОДКИНА** И.Г.1

ПАЖ Том: 56Номер: 5 Год: 2018 Страницы: 353-364

Настоящая работа является продолжением статьи [1], в которой мы обсудили некоторые некорректные подходы в идентификации крупномасштабных типов солнечного ветра и связанные с ними неправильные выводы при анализе данных по солнечно-земной физике. В данной работе мы анализируем списки 28 событий CME и 31 события CIR в 2013–2016 гг., которые были использованы Shen и др. [2] для сравнения реакции радиационных поясов Земли на различные межпланетные драйверы. Интерпретация типов солнечного ветра в этих списках отличается как от нашего каталога [3] для Sheath, ICME и CIR, так и от каталога Richardson and Cane [4] для CME. Кроме того, авторы статьи [2] не делают различий между Sheath- и ICME-индуцированными магнитными бурями, включая их в общий тип «CME-индуцированные бури». Наш анализ показал, что из 28 приведенных

событий СМЕ-индуцированных бурь 16 событий относится к Sheath, 2 события – к MC, 4 события – к Ejecta, 2 к CIR, 4 – к невозмущенному солнечному ветру с ударными волнами. В каталоге [4], который также не разделяет Sheath и ICME, содержится 18 из 28 событий СМЕ-индуцированных бурь, приведенных в работе [2]. Из приведенного авторами [2] 31 события CIR, согласно нашего анализа, 25 событий относится к CIR, 2 события к Sheath, 4 события к невозмущенному солнечному ветру. В каталоге [4] одно из 31-го события CIR из работы [2] представлено как СМЕ. Так как свойства областей сжатия CIR и Sheath близки, то выводы авторов статьи [2] о свойствах CIR-индуцированных бурь мало искажены неверной идентификацией типов течений, в то время как выводы, касающиеся СМЕ-индуцированных бурь, которые более чем на половину представляют собой Sheath-индуцированные бури, нам представляются неверными.

СТАТИСТИЧЕСКОЕ ИССЛЕДОВАНИЕ ВЛИЯНИЯ МЕЖПЛАНЕТНЫХ УСЛОВИЙ НА ГЕОМАГНИТНЫЕ БУРИ

Ю. И. Ермолаев, И. Г. Лодкина, Н. С. Николаева, М. Ю. Ермолаев
КОСМИЧЕСКИЕ ИССЛЕДОВАНИЯ, 2010, том 48, № 6, с. 499–515, File

На основе архива данных OMNI для периода 1976–2000 годов выполнен анализ 798 геомагнитных бурь с $Dst < -50$ нТл и их межпланетных источников – крупномасштабных типов солнечного ветра: CIR (145 магнитных бурь), Sheath (96); магнитные облака MC (62); Ejecta (161), источник остальных 334 магнитных бурь оказался неопределенным. Для анализа был использован двойной метод наложенных эпох, в котором за опорные времена взяты моменты начала магнитной бури и минимума Dst индекса. Подтвержден известный факт, что независимо от вида межпланетного источника начало магнитной бури наступает через 1–2 часа после поворота ММП к югу ($Bz < 0$), и окончание главной фазы бури и начало восстановительной фазы наблюдаются через 1–2 часа после исчезновения южной компоненты ММП. Также подтвержден ранее полученный результат, что наиболее эффективная генерация магнитной бури наблюдается для Sheath перед MC. На главной фазе бури параметры Bz и Ey в среднем мало изменяются между началом и концом главной фазы (минимума Dst и), в то время как Dst и монотонно уменьшаются, приблизительно пропорционально интегралу Bz и Ey по времени. Такое поведение индексов согласуется с предположением, что процесс генерации бури связан не просто с текущим значением Bz и Ey , а обладает памятью о предыстории. Полученные результаты показывают, что использованный двойной метод наложенных эпох может быть успешно применен для изучения динамики параметров на главной фазе магнитных бурь, имеющих разные длительности.

КАТАЛОГ КРУПНОМАСШТАБНЫХ ЯВЛЕНИЙ СОЛНЕЧНОГО ВЕТРА ДЛЯ ПЕРИОДА 1976–2000 ГГ

ЕРМОЛАЕВ Ю.И.1, **НИКОЛАЕВА** Н.С.1, **ЛОДКИНА** И.Г.1, **ЕРМОЛАЕВ** М.Ю.1

Косм. Исследования Том: 47Номер: 2 Год: 2009 Страницы: 99-113

Основной целью данной работы является составление каталога крупномасштабных явлений солнечного ветра за период наблюдений 1976–2000 гг. на основе измерений, представленных в базе данных OMNI. Работа включала несколько этапов. Сначала исходная база данных OMNI была дополнена некоторыми ключевыми параметрами солнечного ветра, определяющими тип течения солнечного ветра. К таким расчетным параметрам относятся плазменное отношение β , тепловое NkT и кинетическое mNV^2 давление солнечного ветра, отношение измеренной и ожидаемой температур T/T_{exp} , градиенты скорости и плотности плазмы, а также градиент магнитного поля. Результаты визуализации основных параметров плазмы, определяющих характер течения плазмы солнечного ветра, представлены на сайте ИКИ. Предварительная идентификация основных типов течений солнечного ветра (быстрые FAST и медленные SLOW течения, HCS – Heliospheric Current Sheet, CIR – Corotating Interaction Region, EJECTA (или Interplanetary CME), MC – Magnetic Cloud, SHEATH – область сжатия перед EJECTA/MC, RARE – разреженная область, IS – межпланетная ударная волна) была сделана по заданным пороговым критериям параметров плазмы и межпланетного магнитного поля с помощью программы предварительной идентификации. Окончательная идентификация проводилась путем сопоставления с результатами визуального анализа данных солнечного ветра. В заключение приведены гистограммы распределения и статистические характеристики некоторых параметров различных крупномасштабных типов солнечного ветра.

СОЛНЕЧНЫЕ И МЕЖПЛАНЕТНЫЕ ИСТОЧНИКИ ГЕОМАГНИТНЫХ БУРЬ: АСПЕКТЫ КОСМИЧЕСКОЙ ПОГОДЫ

Ю.И. Ермолаев, М.Ю. Ермолаев

ГЕОФИЗИЧЕСКИЕ ПРОЦЕССЫ И БИОСФЕРА, 2009, Т. 8, № 1, с. 5–35, File

Приведен краткий **обзор** современных представлений о солнечно-земных связях, отвечающих за передачу солнечных возмущений и генерацию магнитных бурь на Земле. Даны количественные оценки вероятности возбуждения магнитных бурь различными солнечными и межпланетными явлениями; сравнивается эффективность процессов генерации бурь различными типами течений солнечного ветра.

ФИЗИЧЕСКИЕ ОСНОВЫ ПРОГНОЗИРОВАНИЯ ВОЗМУЩЕНИЙ В ОКОЛОЗЕМНОЙ СРЕДЕ ПО ХАРАКТЕРИСТИКАМ СОЛНЦА

В.Г. Еселевич

обзор, Байкал, 2002

<http://www.kosmofizika.ru/irkutsk/eselevich.htm>

КРУПНОМАСШТАБНЫЕ ВОЗМУЩЕНИЯ СОЛНЕЧНОГО ВЕТРА ПО ДАННЫМ РАДИОПРОСВЕЧИВАНИЯ С КОСМИЧЕСКОГО АППАРАТА MARS EXPRESS И ЛОКАЛЬНЫХ ИЗМЕРЕНИЙ НА КОСМИЧЕСКОМ АППАРАТЕ WIND

ЕФИМОВ А.И.^{*1}, **СМИРНОВ В.М.**¹, **ЧАШЕЙ И.В.**², **НАБАТОВ А.С.**¹

ГиА Том: 63 Номер: 3 Год: 2023 Страницы: 275-283

Представлены результаты экспериментов радиопросвечивания околосолнечной плазмы сигналами спутника Марса Mars Express. В области гелиоцентрических расстояний прицельной точки лучевой линии 8–13 солнечных радиусов измерялись флуктуации частоты просвечивающих радиосигналов. В ходе проведения экспериментов как на восточном, так и на западном лимбах зафиксированы резкие усиления дисперсии флуктуаций частоты. В измерениях вблизи орбиты Земли на космическом аппарате Wind в смежные периоды с запаздыванием на 5–17 сут регистрировались увеличения концентрации протонов и напряженности магнитного поля, которые в 7–15 раз превышают фоновые значения. Сравнение между данными, относящимися к внутреннему и околоземному солнечному ветру, позволяет сделать вывод, что наблюдавшиеся возмущения связаны с одной и той же вращающейся с Солнцем областью солнечной короны.

НАБЛЮДЕНИЕ ВОЗМУЩЕННЫХ ПЛАЗМЕННЫХ СТРУКТУР В ОКРЕСТНОСТИ СОЛНЦА И ОКОЛОЗЕМНОМ ПРОСТРАНСТВЕ МЕТОДАМИ РАДИОЗОНДИРОВАНИЯ И ЛОКАЛЬНЫХ ИЗМЕРЕНИЙ

ЕФИМОВ А.И.^{*1}, **ЛУКАНИНА Л.А.**¹, **ЧАШЕЙ И.В.**², **КОЛОМИЕЦ С.Ф.**¹, **БЁРД М.К.**³, **ПЕТЦОЛЬД М.**⁴

Косм. Исслед. Том: 58 Номер: 6 Год: 2020 Страницы: 495-502

Эксперимент по радиозондированию околосолнечной плазмы сигналами космического аппарата Mars Express в 2013 г. был осуществлен в период с 4.III. по 31.V. Исследуемой характеристикой являлась частота сигналов сантиметрового, дециметрового диапазонов и дифференциальная частота. Зафиксирован ряд событий, когда интенсивность флуктуаций частоты зондирующей плазмы сигналов в несколько раз превышала фоновые значения. Как показал анализ наблюдений солнечной активности, таких как усиление потока рентгеновского излучения и данные коронографа SOHO LASCO, это объясняется прохождением через трассу радиосвязи КА с Землей возмущенных плазменных потоков, генерируемых в короне Солнца. Проведено сопоставление данных радиопросвечивания с результатами измерений параметров околоземной плазмы с помощью КА Wind в смежные периоды времени. В результате анализа данных о протонной концентрации выяснилось, что вблизи Земли также наблюдались резкие возрастания как средних значений, так и флуктуаций этой характеристики. Временное запаздывание между событиями, наблюдавшимися в околосолнечной и околоземной плазме, показывает, что причиной возмущений является повышенная активность одной и той же корональной области, вращающейся вместе с Солнцем.

СКОРОСТЬ ВНУТРЕННЕГО СОЛНЕЧНОГО ВЕТРА ПО ДАННЫМ КОГЕРЕНТНОГО РАДИОПРОСВЕЧИВАНИЯ

Ефимов А.И., Векслер Д., Бёрд М.К., Петцольд М., Чашей И.В., Луканина Л.А.

ПАЖ Том: 56 Номер: 6 Год: 2018 Страницы: 387-393

Представлены результаты измерений скорости движения неоднородностей плотности плазмы солнечного ветра, модулирующих частоту когерентных радиосигналов космического аппарата Galileo в S-диапазоне, выполненных методом разнесенного приема на наземных станциях слежения. Данные относятся к области гелиоцентрических расстояний от 7 до 72 радиусов Солнца на низких гелиоширотах в периоды вблизи минимума солнечной активности. Показано, что ускорение медленного солнечного ветра продолжается вплоть до расстояний около 30 радиусов Солнца. В перекрывающихся областях расстояний от Солнца результаты

находятся в качественном согласии с данными LASCO SOHO для тех же периодов времени, более ранними результатами анализа амплитудных флуктуаций сигналов аппаратов Венера-15,-16 и более поздними измерениями с помощью космического аппарата Mars Express.

ПРОГНОЗИРОВАНИЕ DST-ИНДЕКСА, ОСНОВАННОЕ НА МЕТОДАХ МАШИННОГО ОБУЧЕНИЯ

Ефиторов А.О., Доленко С.А., Широкий В.Р., Мягкова И.Н.

ПАЖ Том: 56 Номер: 6 Год: 2018 Страницы: 420-428

В работе исследуются возможности прогнозирования временного ряда геомагнитного индекса Dst. Прогноз осуществляется по параметрам солнечного ветра и межпланетного магнитного поля, измеренным в точке либрации L1 в эксперименте на космическом аппарате ACE, при помощи методов машинного обучения – искусственных нейронных сетей: классических перцептронов и рекуррентных сетей типа LSTM, а также комитетов прогнозирующих моделей. Показано, что наилучшие результаты достигаются при использовании гетерогенных комитетов на основе нейронных сетей обоих типов.

КАТАЛОГ ГЕОЭФФЕКТИВНЫХ ВСПЫШЕЧНЫХ СОБЫТИЙ ТЕКУЩЕГО 25-ГО СОЛНЕЧНОГО ЦИКЛА В СОВРЕМЕННОМ ПРЕДСТАВЛЕНИИ

ЗАБАРИНСКАЯ Л.П.¹, **ИШКОВ В.Н.**^{1,2}, **СЕРГЕЕВА Н.А.**¹

КОСМИЧЕСКИЕ ИССЛЕДОВАНИЯ Том: 61 Номер: 6 Год: 2023 Страницы: 461-465

DOI: [10.31857/S0023420623600095](https://doi.org/10.31857/S0023420623600095)

Для изучения происходящих на Солнце и в межпланетном пространстве явлений и их влияния на околоземное космическое пространство, на процессы во внешних и внутренних оболочках Земли наиболее ценными становятся результаты непрерывных многолетних наблюдений за солнечной активностью. Представительная коллекция таких длительных однородных рядов систематических наблюдений, полученных мировой сетью солнечных и астрономических обсерваторий, а также космическими аппаратами, собрана в Мировом центре данных по солнечно-земной физике в Москве. В статье приведено описание накопительного интерактивного каталога основных характеристик значимых солнечных вспышечных событий текущего 25-го цикла солнечной активности.

Мониторинг параметров анизотропии космических лучей в реальном времени и краткосрочный прогноз геомагнитных возмущений.

Зверев А.С., Григорьев В.Г., Гололобов П.Ю., Стародубцев С.А.

СОЛНЕЧНО-ЗЕМНАЯ ФИЗИКА Том 6. 2020. № 4. С. 42–45.

<https://naukaru.ru/ru/storage/viewWindow/61709>

В ИКФИА СО РАН реализованы непрерывный мониторинг динамики параметров распределения космических лучей с использованием данных международной базы нейтронных мониторов NMDB, доступных в реальном времени, и прогноз геомагнитной возмущенности на основе автоматического анализа полученных результатов. Мониторинг основан на применении метода глобальной съемки, позволяющего рассматривать мировую сеть нейтронных мониторов как единый прибор, ориентированный в каждый момент времени измерения во многих направлениях. Данный метод позволяет получать в реальном времени параметры девяти компонент первых двух угловых моментов функции распределения космических лучей за каждый час наблюдений. В работе рассматриваются методические вопросы, связанные с использованием метода глобальной съемки в реальном времени, и приводятся некоторые результаты прогноза геомагнитных возмущений за 2017–2018 гг.

СОЛНЕЧНО-ЗЕМНАЯ БУРЯ 18-20 НОЯБРЯ 2003 Г. 1. ВОЗМУЩЕНИЯ В СОЛНЕЧНОМ ВЕТРЕ ВБЛИЗИ ЗЕМЛИ

Иванов К. Г.1, Ромашец Е. П.1, Харшиладзе А. Ф.1

Геомагнетизм и аэрономия, 46(3), 291-309, 2006

Рассматриваются структура, конфигурация, динамика и солнечные источники околоземного МГД-возмущения солнечного ветра 20 ноября 2003 г. Проводятся сравнительные исследования с возмущениями 24 октября и 22 ноября, после вспышек из той же АО 10484 (10501). Впервые поле скоростей в головной части спорадического возмущения изучается в системе координат неподвижной относительно головного ударного фронта.

Обсуждается возможный сценарий физических процессов в ходе этой солнечно-земной бури в сравнении с разработанным ранее сценарием для бури 15 июля 2000 г. Показано, что: во-первых, возмущение вблизи Земли наблюдалось на секторной границе (HCS) и в ее окрестностях; во-вторых в МГД-структуру возмущения входили: сложный головной ударный слой; широкий, с пересоединяющимися полями, погранслоем на переходе

от ударной волны к магнитному облаку; магнитное облако с магнитной полостью и упакованным в ней веществом активного волокна; обратный ударный слой (предположительно). Обнаружена воспроизводимость конфигурации ударных фронтов и поля скоростей при идентичном расположении Земли относительно АО и HCS 20 ноября и 24 октября. Показано, что во всех трех бурях максимальная величина магнитной индукции в облаке удовлетворяла условию $B_t = (8\pi l_1 m \rho)^{1/2} (D - NV_1)$, т.е. определялась динамическим напором на облако [Иванов и др., 1974]. При увязке возмущения с солнечными источниками обращено внимание на параллелизм осей симметрии активного волокна, транзиентной корональной дыры, коронального выброса массы, нулевой линии коронального открытого поля (HCS) и оси околоземного магнитного облака - закономерность, ранее установленную в сценарии бури 15 июля 2000 г. [Иванов и др., 2005]. Показано, что экстремально большое значение B_t в облаке 20 октября обусловлено сильным гашением серии послевспышечных ударных волн, отраженных от гелиосферного стримера.

См. **Solar-terrestrial storm of November 18 20, 2003. 1. Near-Earth disturbances in the solar wind**

Ivanov, K. G.; Romashets, E. P.; Kharshiladze, A. F.

Geomagnetism and Aeronomy, Volume 46, Issue 3, pp.275-293, 2006, File

СОЛНЕЧНАЯ МОДУЛЯЦИЯ ИНТЕНСИВНОСТИ ГАЛАКТИЧЕСКИХ ЭЛЕКТРОНОВ И ПРОТОНОВ ВБЛИЗИ МИНИМУМА АКТИВНОСТИ 2009 ГОДА

Калинин М.С., Базилевская Г.А., Крайнев М.Б., Свиржевская А.К., Свиржевский Н.С., Филиппов М.В.

Известия РАН Том: 83 Номер: 5 Год: 2019 Страницы: 610-613

В работе представлена модель модуляции галактических космических лучей, удовлетворительно описывающая долгопериодические вариации интенсивности протонной и электронной компонент на фазе спада солнечной активности 23 цикла (2006–2009 гг.). Отличительной особенностью модели является описание временного хода энергетических спектров как электронов, так и протонов при одинаковых значениях фиксированных параметров модели. Модельные расчеты сопоставляются с измерительными данными по спектрам протонной и электронной компонент галактических космических лучей, полученными на спектрометре ПАМЕЛА.

ИСПОЛЬЗОВАНИЕ ДВМ МОДЕЛИ ДЛЯ ПРОГНОЗА ПРИХОДА КОРОНАЛЬНЫХ ВЫБРОСОВ МАССЫ К ЗЕМЛЕ

КАПОРЦЕВА К. Б.*1,2, **ШУГАЙ** Ю. С.2

КОСМИЧЕСКИЕ ИССЛЕДОВАНИЯ Том: 59 Номер: 4 Год: 2021 Страницы: 315-326

DOI: [10.31857/S0023420621040026](https://doi.org/10.31857/S0023420621040026)

<https://www.elibrary.ru/item.asp?id=45794846>

В работе анализируются результаты моделирования распространения корональных выбросов массы (КВМ) за период 2010–2011 гг., полученные с использованием входных данных из разных источников: каталогов КВМ SEEDS и SACTus, и прогнозов скорости квазистационарных потоков солнечного ветра, в качестве среды, по которой распространяются КВМ. В качестве модели квазистационарных потоков солнечного ветра используется модель прогноза скорости солнечного ветра Центра прогноза космической погоды НИИЯФ МГУ, работающая в режиме реального времени. Прогноз КВМ осуществляется с помощью Simple Drag-Based Model. Было проведено сравнение, полученных в ходе моделирования времени прихода МКВМ и их скоростей с данными из открытых каталогов МКВМ: каталога МКВМ Ричардсона и Кейн и GMU CME List. На основе сравнения сделан вывод, что более точный прогноз на фазе роста 24-го цикла солнечной активности получен на данных о параметрах КВМ из базы SACTus. Полученные ошибки прогнозирования параметров МКВМ сравнимы с ошибками других существующих моделей.

ПРОСТРАНСТВЕННАЯ ЭВОЛЮЦИЯ И СТРУКТУРА ВЫСОКОСКОРОСТНЫХ ПОТОКОВ СОЛНЕЧНОГО ВЕТРА ИЗ КОРОНАЛЬНЫХ ДЫР

Кислов Р.А., Кузнецов В.Д.

Г и А Том: 62 Номер: 6 Год: 2022 Страницы: 683-692

DOI: [10.31857/S0016794022060074](https://doi.org/10.31857/S0016794022060074)

Проанализированы природа высокоскоростных потоков из корональных дыр и механизм их коротации с источником. Показано, что распространенное представление о высокоскоростных потоках из корональных дыр как о потоках частиц, которые коротатируют с Солнцем, противоречит наблюдениям. Предложена модель, в которой спиральная структура и коротация высокоскоростных потоков из корональных дыр объясняются в рамках кинематики.

МАГНИТНАЯ БУРЯ 25–26 АВГУСТА 2018: ДНЕВНЫЕ ВЫСОКОШИРОТНЫЕ ГЕОМАГНИТНЫЕ ВАРИАЦИИ И ПУЛЬСАЦИИ

КЛЕЙМЕНОВА Н.Г.*^{1,2}, ГРОМОВА Л.И.*³, ГРОМОВ С.В.³
3, МАЛЫШЕВА Л.М.¹

ГиА Том: 59Номер: 6 Год: 2019 Страницы: 706-713

DOI: [10.1134/S0016794019060075](https://doi.org/10.1134/S0016794019060075)

Рассмотрены особенности дневных высокоширотных геомагнитных возмущений и геомагнитных пульсаций во время недавней сильной магнитной бури 25–26 августа 2018 г., произошедшей в конце фазы спада 24-го цикла солнечной активности при очень низком уровне вспышечной активности Солнца. Как правило, в эту фазу цикла солнечной активности магнитные бури вызываются высокоскоростными потоками солнечного ветра из коронарных дыр, однако магнитные бури на спаде 24-го цикла были вызваны корональными выбросами массы (СМЕ). Показано, что, несмотря на очень слабые возмущения на Солнце и низкую скорость солнечного ветра, в августе 2018 г. в магнитосфере Земли произошла достаточно сильная магнитная буря ($Dst = -171$ нТл). Внезапное начало бури (SC) с незначительным (~ 25 нТл) скачком в Dst -индексе вызвало возбуждение достаточно интенсивных дневных геомагнитных пульсаций $ipcl$ на широтах возможного положения дневного полярного каспа. Особенностью восстановительной фазы этой бури было развитие магнитосферной суббури в глобальном масштабе, т.е. появление отрицательной магнитной бухты, зарегистрированной синхронно в авроральном ночном секторе и в полярных широтах дневного сектора. Рассмотрена возможная интерпретация.

ОСОБЕННОСТИ ЖЕСТКОСТНОГО СПЕКТРА ЭФФЕКТОВ ФОРБУША

КЛЮЕВА А.И.1, БЕЛОВ А.В.2, ЕРОШЕНКО Е.А.

ГЕОМАГНЕТИЗМ И АЭРОНОМИЯ Том: 57Номер: 2 Год: 2017 Страницы: 195-207

Представлены результаты анализа вариаций жесткостного спектра первичных космических лучей во время Форбуш-эффектов, зарегистрированных в 20–24-м циклах солнечной активности. Используются данные мировой сети станций нейтронных мониторов, обработанные методом глобальной съемки. В работе изучены изменения показателя жесткостного спектра Форбуш-эффектов в зависимости от уровня солнечной активности, фазы эффекта, полярности общего магнитного поля Солнца, типа и параметров источника модуляции космических лучей и т.п. Всесторонний анализ полученных результатов выявил закономерности в динамике энергетического спектра галактических космических лучей, которые отражают динамические процессы, происходящие в межпланетном пространстве.

ИССЛЕДОВАНИЕ ФОРБУШ-ЭФФЕКТОВ ВО ВРЕМЯ МОЩНЫХ СОЛНЕЧНЫХ ВСПЫШЕК ПО ДАННЫМ МЮОННОГО ГОДОСКОПА УРАГАН

КОВЫЛЯЕВА А.А.*^{1,2}, БАРБАШИНА Н.С.¹, ГЕТМАНОВ В.Г.^{2,3}, ДМИТРИЕВА А.Н.^{1,2}, ДОБРОВОЛЬСКИЙ М.Н.², МИШУТИНА Ю.Н.¹, СОЛОВЬЕВ А.А.^{2,3}, ЧИНКИН В.Е.², ШУТЕНКО В.В.¹, ЯКОВЛЕВА Е.И.¹, ЯШИН И.И.^{1,2}

ИЗВЕСТИЯ РАН. СЕРИЯ ФИЗИЧЕСКАЯ Том: 85Номер: 4 Год: 2021 Страницы: 605-608

По данным мюонного годоскопа УРАГАН изучены Форбуш-эффекты, вызванные мощными солнечными вспышками X-класса, за период с 2007 по 2019 гг. Мюонный годоскоп УРАГАН регистрирует поток мюонов космических лучей на поверхности Земли одновременно с различных направлений. Это позволяет изучать энергетические, угловые и пространственно-временные характеристики вариаций потока мюонов космических лучей при Форбуш-эффектах. Проанализирована связь полученных характеристик Форбуш-эффектов с параметрами гелиосферных и геомагнитных возмущений.

КОСМИЧЕСКИЕ ЛУЧИ В ПЕРИОД ФОРБУШ-ЭФФЕКТОВ В МАРТЕ 1989 Г. И В МАРТЕ 1991 Г.: СПЕКТРЫ ВАРИАЦИЙ, АНИЗОТРОПИЯ И ВАРИАЦИИ ЖЕСТКОСТИ ГЕОМАГНИТНОГО ОБРЕЗАНИЯ

Кравцова М.В., Олемской С.В., Сдобнов В.Е.

Геомаг. и Аэрон. Том: 60Номер: 4 Год: 2020 Страницы: 448-456

По данным наземных измерений космических лучей на мировой сети станций методом спектрографической глобальной съемки выполнен анализ двух Форбуш-эффектов во время геомагнитных бурь в марте 1989 г. и в марте 1991 г. Приведены жесткостные спектры и спектры вариаций, питч-угловая анизотропия космических лучей на разных фазах развития Форбуш-эффектов, а также изменения планетарной системы жесткостей геомагнитного обрезания. Показано, что при аппроксимации спектров вариаций степенной функцией от

жесткости частиц в интервале 10–50 ГВ на фазе максимальной модуляции показатель спектра мягче, чем на фазах спада и восстановления интенсивности космических лучей. В рамках осесимметричной модели ограниченной магнитосферы Земли, учитывающей токи на магнитопаузе и кольцевой ток, определены расстояние до подсолнечной точки и радиус кольцевого тока, а также вклад кольцевого тока в изменения жесткости геомагнитного обрезания и в Dst-индекс во время исследуемых событий.

КОСМИЧЕСКИЕ ЛУЧИ В ПЕРИОД ГЕОМАГНИТНОГО ВОЗМУЩЕНИЯ В ЯНВАРЕ 2015 Г

КРАВЦОВА М.В.*✉1, СДОБНОВ В.Е.1

Косм. Исслед. Том: 57Номер: 1 Год: **2019** Страницы: 17-20

По данным наземных измерений космических лучей (КЛ) на мировой сети станций методом спектрографической глобальной съемки исследовано поведение интенсивности КЛ в период геомагнитного возмущения в январе 2015 г. Приведены спектры вариаций КЛ, показатели спектра этих вариаций при аппроксимации спектра степенной функцией от жесткости частиц в диапазоне жесткостей от 10 до 50 ГВ,pitch-угловая анизотропия КЛ. Показано, что показатели спектра вариаций КЛ при его аппроксимации степенной функцией от жесткости частиц в фазе максимальной модуляции больше, чем на фазах спада и восстановления интенсивности КЛ.

АНАЛИЗ ФОРБУШ-ЭФФЕКТА В ИЮНЕ 2015 Г. МЕТОДОМ СПЕКТРОГРАФИЧЕСКОЙ ГЛОБАЛЬНОЙ СЪЕМКИ

КРАВЦОВА М.В.1, СДОБНОВ В.Е.1

ИЗВЕСТИЯ РОССИЙСКОЙ АКАДЕМИИ НАУК. СЕРИЯ ФИЗИЧЕСКАЯ

Том: 81Номер: 2 Год: **2017** Страницы: 196-198

По данным наземных измерений космических лучей (КЛ) на мировой сети станций методом спектрографической глобальной съемки исследован форбуш-эффект в июне 2015 г. При аппроксимации спектров вариаций степенной функцией от жесткости частиц в интервале 10–50 ГВ на фазе максимальной модуляции показатель спектра больше, чем на фазах спада и восстановления интенсивности КЛ.

ПРОЯВЛЕНИЯ В ГЕЛИОСФЕРЕ И В ИНТЕНСИВНОСТИ ГКЛ ДВУХ ВЕТВЕЙ СОЛНЕЧНОЙ АКТИВНОСТИ

Крайнев М.Б.

[СОЛНЕЧНО-ЗЕМНАЯ ФИЗИКА Том 5 № 4, 2019](#) С 12-25

<https://naukaru.ru/ru/storage/viewWindow/43510>

Дается представление о процессах в гелиосфере и модуляции галактических космических лучей (ГКЛ) в ней как результатах действия в этом слое Солнца двух ветвей солнечной активности, называемых по топологии солнечных магнитных полей внутри Солнца тороидальной ветвью (активные области, пятна, вспышки, корональные выбросы массы и т. д.) и полоидальной ветвью (высокоширотные магнитные поля, полярные корональные дыры, зональные униполярные магнитные области и т. д.). Формулируется основная причина различного проявления обеих ветвей на поверхности Солнца и в гелиосфере — наличие в основании гелиосферы слоя, в котором основным энергетическим фактором является магнитное поле. При этом преимущество при проникновении в гелиосферу получают более крупномасштабные, хотя и менее интенсивные солнечные магнитные поля полоидальной ветви. Показана связь с полоидальной ветвью солнечной активности гелиосферных характеристик (поле скорости солнечного ветра, размер гелиосферы, форма гелиосферного токового слоя, регулярное гелиосферное магнитное поле и его флуктуации), которые, согласно современным представлениям, определяют распространение в гелиосфере ГКЛ.

О НЕКОТОРЫХ АСПЕКТАХ ВЛИЯНИЯ ГЛОБАЛЬНОГО ГЕЛИОСФЕРНОГО ТОКОВОГО СЛОЯ НА РАСПРОСТРАНЕНИЕ ГКЛ

Крайнев М.Б., Калинин М.С.

Известия РАН Том: 83Номер: 5 Год: **2019** Страницы: 614-617

Рассматривается влияние на гелиосферные характеристики, важные для распространения ГКЛ, одной из основных особенностей глобального гелиосферного токового слоя, а именно, сильной зависимости скорости солнечного ветра от расстояния до токового слоя. Предлагается простая модель скорости солнечного ветра, которая после оценки параметров по данным наблюдений может быть использована для теоретических

исследований модуляции ГКЛ. Обсуждается выбор модели гелиосферных характеристик для описания поведения ГКЛ, адекватной ситуации в период низкой и средней пятнообразовательной активности Солнца.

ИНТЕНСИВНОСТЬ ГАЛАКТИЧЕСКИХ КОСМИЧЕСКИХ ЛУЧЕЙ В ПРИБЛИЖАЮЩЕМСЯ МИНИМУМЕ ЦИКЛА СОЛНЕЧНОЙ АКТИВНОСТИ

КРАЙНЕВ М.Б.1, **БАЗИЛЕВСКАЯ** Г.А.1, **КАЛИНИН** М.С.1, **СВИРЖЕВСКАЯ** А.К.1, **СВИРЖЕВСКИЙ** Н.С.1

Геомагн. и Аэрон. Том: 58Номер: 2 Год: 2018 Страницы: 177-186

В течение длительного и глубокого минимума солнечной активности между циклами 23 и 24 в районе орбиты Земли наблюдались необычное поведение гелиосферных характеристик и повышенная интенсивность галактических лучей (ГКЛ). Максимум текущего 24-го солнечного цикла ниже, чем предыдущего, а в следующем цикле можно ожидать дальнейшего понижения солнечной, а значит, и гелиосферной активности. В этих условиях важно как для понимания процесса модуляции ГКЛ в гелиосфере, так и для прикладных целей (оценка радиационной безопасности планируемых космических полетов и т.д.) количественно оценить возможные характеристики ГКЛ около Земли в приближающемся минимуме солнечной активности (~ 2019-2020 гг.). Наша оценка основывается на прогнозе гелиосферных характеристик, важных для модуляции космических лучей, и на численных расчетах интенсивности ГКЛ. Кроме того, мы рассматриваем распределение в гелиосфере интенсивности и других характеристик ГКЛ и обсуждаем вариации от цикла к циклу интегральных для всей гелиосферы характеристик ГКЛ (суммарной и средней энергии, заряда).

ИССЛЕДОВАНИЕ ХАРАКТЕРИСТИК ФОРБУШ-ЭФФЕКТОВ, ЗАРЕГИСТРИРОВАННЫХ МЮОННЫМ ГОДОСКОПОМ УРАГАН В 2012–2017 ГГ

Ковыляева А.А., Астапов И.И., Барбашина Н.С., Борог В.В., Дмитриева А.Н., Компаниец К.Г., Мишутина Ю.Н., Петрухин А.А., Шутенко В.В., Яковлева Е.И., Яшин И.И.

Известия РАН Том: 83Номер: 5 Год: 2019 Страницы: 622-624

Приводятся результаты анализа изменений потока мюонов космических лучей во время форбуш-эффектов, зарегистрированных мюонным годоскопом УРАГАН в 2012–2017 гг. и сцинтилляционным мюонным годоскопом в период 2016–2017 гг. Анализируются характеристики форбуш-эффектов за этот период. Приведены результаты сопоставления полученных характеристик вариаций потока мюонов с различными параметрами ближней гелиосферы во время форбуш-эффектов для 11-летнего цикла солнечной активности.

О ПРОЯВЛЕНИИ КОРОТИРУЮЩИХ ОБЛАСТЕЙ ВЗАИМОДЕЙСТВИЯ СОЛНЕЧНОГО ВЕТРА В ВАРИАЦИЯХ ИНТЕНСИВНОСТИ ГКЛ

Крайнев М.Б., **Калинин** М.С., **Базилевская** Г.А., **Свиржевская** А.К., **Свиржевский** Н.С., **Луо** С., **Аслам** О.П.М., **Шен** Ф., **Нгобени** М.Д., **Подгитер** М.С.

СЗФ Том: 9Номер: 1 Год: 2023 Страницы: 10-21

https://elibrary.ru/download/elibrary_50417068_61918313.pdf

Области взаимодействия разноскоростных потоков солнечного ветра, известные как коротирующие области взаимодействия, образуют практически постоянно существующую структуру внутренней гелиосферы. Рассмотрены данные наблюдений основных характеристик гелиосферы, важных для модуляции ГКЛ, и результаты трехмерного МГД-моделирования коротирующих областей взаимодействия солнечного ветра и моделирования методом Монте-Карло рекуррентных вариаций ГКЛ. Анализируются важность коротирующих областей взаимодействия для усредненных по долготе характеристик гелиосферы и распространения ГКЛ и возможные пути описания долговременных вариаций интенсивности ГКЛ с учетом коротирующих областей взаимодействия.

ОСОБЕННОСТИ ГОДОВЫХ РАСПРЕДЕЛЕНИЙ ЧАСТОТЫ ПОЯВЛЕНИЯ БОЛЬШИХ ГЕОМАГНИТНЫХ ВОЗМУЩЕНИЙ В ЧЕТНЫХ И НЕЧЕТНЫХ СОЛНЕЧНЫХ ЦИКЛАХ

Кузнецова Т.В.

Астрономия-2018 Том 2 Солнечно-земная физика – современное состояние и перспективы С. 122
Annual distribution of disturbances with daily geomagnetic index $A_p > 190$ nT since 1932 shows

that 70% of the days occur during decline phase of odd solar cycles. Annual distribution of large disturbances with daily $A_p > 220$ nT shows further increase of contribution of the days in decline phase of odd cycles into total number of the days. Annual distribution of the disturbances with $A_p > 190$ nT also shows that 70% of the days occur near equinoxes and 20% on July and November. For the large disturbances with $A_p > 220$ nT number of the days on July and November increases but one of days near equinoxes decreases that leads to near equal probability of occurrence of the large disturbances at equinoxes and July, November. These results are discussed and compared with results based on indexes K_p , a_a , Dst .

АНАЛИЗ ЭРУПТИВНОГО СОБЫТИЯ ПОСЛЕ СОЛНЕЧНОЙ ВСПЫШКИ 7 ИЮНЯ 2011 ГОДА

КУПРЯКОВ Ю. А.*1,2, ГОРШКОВ А. Б.2, КОТРЧ П.1, КАШАПОВА Л. К.3

АЖ Том: 98Номер: [10](#) Год: **2021** Страницы: 873-880

DOI: [10.31857/S0004629921100194](#)

Мы представляем результаты анализа данных наблюдений эруптивного события 7 июня 2011 г., полученных как на космических аппаратах (SDO, LASCO), так и с помощью наземных солнечных инструментов. Эруптивное событие характеризовалось замедлением движения фронта ударной волны в первые минуты развития с 1150 км/с до 710 км/с. По данным LASCO скорость коронального выброса массы (КВМ) на временных масштабах более часа не превышала 285 км/с. Согласно спектральным наблюдениям наземного инструмента лучевые скорости наиболее быстрых деталей взрывающегося протуберанца оказались заключены между -200 км/с и 190 км/с. Особое внимание было уделено исследованию физических характеристик блоба – отдельной капли коронального дождя, которым сопровождалось данное событие. Скорость блоба по лучу зрения за 5 мин увеличилась с 207 км/с до 263 км/с, диаметр составил 5900 км, массу мы оценили в 1.8×10^{12} г, для температуры и турбулентной скорости были получены значения 7880 К и $V_{turb} = 18.7$ км/с соответственно. Отметим, что обнаружение и измерение скоростей было ограничено возможностями узкополосных фильтров и небольшим диапазоном длин волн в большинстве солнечных приборов.

ФОРБУШ-ПОНИЖЕНИЯ В ПОТОКАХ ГАЛАКТИЧЕСКИХ КОСМИЧЕСКИХ ЛУЧЕЙ ПО ДАННЫМ ЭКСПЕРИМЕНТА ПАМЕЛА






Лагойда И.А., Воронов С.А., Михайлов В.В.

Известия РАН Том: 83Номер: [8](#) Год: **2019** Страницы: 1070-1072

DOI: [10.1134/S0367676519080258](#)

Представлен анализ амплитуд форбуш-понижений, зарегистрированных в эксперименте ПАМЕЛА в период с 2006 по 2014 гг., в зависимости от характеристик межпланетного пространства, таких как величина модуля магнитного поля, скорость солнечного ветра и температура плазмы. Телескоп ПАМЕЛА, состоящий из времяпролетной системы, магнитного спектрометра, систем антисовпадений, электромагнитного калориметра и нейтронного детектора, был запущен на орбиту Земли на борту спутника “Ресурс ДК1” в июне 2006 г. и продолжал работать в течение 10 лет.

НЕКОТОРЫЕ ВОПРОСЫ ИДЕНТИФИКАЦИИ КРУПНОМАСШТАБНЫХ ТИПОВ СОЛНЕЧНОГО ВЕТРА И ИХ РОЛИ В ФИЗИКЕ МАГНИТОСФЕРЫ. 3. ИСПОЛЬЗОВАНИЕ ОПУБЛИКОВАННЫХ НЕКОРРЕКТНЫХ ДАННЫХ

ЛОДКИНА И.Г.*1, ЕРМОЛАЕВ Ю.И.*1, ЕРМОЛАЕВ М.Ю.1, РЯЗАНЦЕВА М.О.1, ХОХЛАЧЕВ А.А.1

Космич. Исслед. Том: 58Номер: [5](#) Год: **2020** Страницы: 377-395

Настоящая работа является продолжением наших работ [1, 2], в которых мы обсудили некоторые некорректные подходы в идентификации крупномасштабных типов солнечного ветра и связанные с ними неправильные выводы при анализе данных по солнечно-земной физике. В данной работе мы анализируем наборы “СМЕ-induced”, “CIR-induced” и многоступенчатых (multistep) магнитных бурь за период 1996–2004 гг. из списка Kataoka and Miyoshi [3]. Показано, что заметная часть событий в этом списке была идентифицирована неправильно, и их интерпретация отличается, как от нашего каталога Ермолаев и др. [4] (<ftp://ftp.iki.rssi.ru/pub/omni/>) для Sheath, ICME и CIR, так и от каталога Richardson and Cane [5] для ICME. Использование нескорректированного списка Kataoka and Miyoshi приводит к неправильной идентификации межпланетных драйверов магнитных бурь и ошибочным выводам, например в работе [6].

АНАЛИЗ ПРИЧИН МАГНИТНОЙ БУРИ 1-2 ДЕКАБРЯ 2023 ГОДА ПО НАБЛЮДЕНИЯМ МЕЖПЛАНЕТНЫХ МЕРЦАНИЙ НА РАДИОТЕЛЕСКОПЕ БСА ФИАН

ЛУКМАНОВ В. Р.¹, ЧАШЕЙ И. В.¹, ТЮЛЬБАШЕВ С. А.¹, СУБАЕВ И. А.¹

АЖ Том: 101 Номер: 7 Год: 2024 Страницы: 618-624

Приведены результаты анализа данных наблюдений межпланетных мерцаний, полученных на радиотелескопе Большая синфазная антенна Физического института им. П. Н. Лебедева (БСА ФИАН) перед началом, в период и после магнитной бури, произошедшей 1-2 декабря 2023 г. Проведено сравнение данных наблюдений с модельными расчетами для коротирующих и распространяющихся крупномасштабных возмущений. Результаты наблюдений мерцаний радиоисточников свидетельствуют о том, что имевшая место магнитная буря была вызвана наложением двух видов крупномасштабных возмущений солнечного ветра. В день перед началом магнитной бури наблюдались признаки взаимодействия магнитосферы Земли с коротирующей областью разноскоростных потоков солнечного ветра, тогда как позже наблюдались признаки возмущения магнитосферы выбросом корональной массы, распространяющимся после вспышки M9.8 28 ноября 2023 г.

ФОРМИРОВАНИЕ МНОЖЕСТВЕННЫХ ТОКОВЫХ СЛОЕВ В ГЕЛИОСФЕРНОМ ПЛАЗМЕННОМ СЛОЕ

МАЕВСКИЙ Е.В.¹, МАЛОВА Х.В.*², КИСЛОВ Р.А.³, ПОПОВ В.Ю.^{1,3}, ПЕТРУКОВИЧ А.А.³, ХАБАРОВА О.В.³, ЗЕЛЕНЬКИЙ Л.М.³

Космю исслед. Том: 58 Номер: 6 Год: 2020 Страницы: 445-460

При пересечении космическими аппаратами гелиосферного плазменного слоя (ГПС), разделяющего крупномасштабные магнитные сектора противоположной направленности в солнечном ветре, практически всегда наблюдаются многократные быстрые колебания знака радиальной компоненты магнитного поля, свидетельствующие о смене знака плотности азимутального тока внутри ГПС. Предложены возможные механизмы формирования многослойных токовых структур в ГПС. В рамках стационарной МГД-модели солнечного ветра проверена одна из гипотез о “вытягивании” множественных токовых слоев в солнечный ветер из пояса стримеров, ориентированного вдоль нейтральной линии гелиомагнитного поля. Исследованы самосогласованные распределения характеристик солнечного ветра в зависимости от тонкой структуры стримеров. Показано, что стримеры, одиночные и множественные, могут быть источниками многослойных токовых структур с чередующимися по направлению азимутальными токами. Значение полученных результатов для интерпретации результатов наблюдений в солнечном ветре обсуждаются

СОЛНЕЧНЫЙ ВЕТЕР И ГЕЛИОСФЕРНАЯ ТОКОВАЯ СИСТЕМА В ГОДЫ МАКСИМУМА И МИНИМУМА СОЛНЕЧНОЙ АКТИВНОСТИ

Маевский Е.В., Петрукович А.А., Попов В.Ю., Хабарова О.В., Малова Х.В., Кислов Р.А.

ПАЖ Том: 56 Номер: 6 Год: 2018 Страницы: 394-403

В рамках осесимметричной МГД-модели солнечного ветра проведен анализ магнитного поля Солнца в двух фазах солнечного цикла: минимума активности, когда доминирует дипольное магнитное поле и максимума, когда преобладает квадрупольное поле. Показано, что в период максимума солнечной активности гелиосферный токовый слой приобретает конусообразную форму и смещается в область высоких широт до 30° над плоскостью эклиптики. В противоположном полушарии на тех же широтах устанавливается второй токовый слой конической формы с азимутальным током противоположного направления. Показано, что профили основных характеристик солнечного ветра укрупняются с расстоянием от Солнца, а их амплитуды уменьшаются, причем для квадрупольного магнитного поля зависимости основных характеристик солнечного ветра имеют более сложный характер. Сравнение результатов модели с осредненными характеристиками солнечного ветра показывает хорошее соответствие между наблюдаемыми величинами и модельными параметрами.

Геомагнитные индексы ASYH и SYMH и их связь с межпланетными параметрами.

Макаров Г.А.

Солн.-земн. Физика Том 8. 2022. № 4 С. 38–45.

<https://naukaru.ru/ru/storage/viewWindow/105304>

За период времени с 1981 по 2015 г. исследуются зависимости геомагнитных индексов SYM-H и ASY-H от межпланетных параметров по их среднесуточным значениям. Исследование проводится двумя путями: первый — анализируется весь массив данных, второй — данные разбиваются на девять групп активности в соответствии со среднесуточными значениями планетарного геомагнитного индекса Ap. Выполнен корреляционный анализ индексов кольцевого тока ASY-H, SYM-H и скорости солнечного ветра, модуля и северо-южной компоненты межпланетного магнитного поля (ММП). Поиск связи индексов ASY-H и SYM-H с межпланетными параметрами оказался более успешным при рассмотрении всего массива данных, чем в случае

разбивки данных по группам магнитной активности. Определены регрессионные уравнения, связывающие ASY-H и SYM-H с межпланетными параметрами. Обнаружено, что при описании связи индексов ASY-H и SYM-H с северо-южной компонентой ММП необходимо учитывать вклад модуля ММП.

СОЛНЕЧНАЯ АКТИВНОСТЬ И ВАРИАЦИИ КОСМИЧЕСКИХ ЛУЧЕЙ В СЕНТЯБРЕ 2017 Г

Махмутов В.С., Базилевская Г.А., Стожков Ю.И., Филиппов М.В., Калинин Е.В., Морзабаев А.К., Эрхов В.А., Гиниятова Ш.

Известия РАН Том: 83Номер: 5 Год: 2019 Страницы: 602-605

В работе представлены результаты анализа данных о солнечной активности и о вариациях космических лучей вблизи минимума 24-го цикла солнечной активности в сентябре 2017 г. В этот период зарегистрировано резкое увеличение солнечной вспышечной активности, сопровождавшееся геомагнитными возмущениями, форбуш-понижением интенсивности космических лучей и появлением значительных потоков солнечных космических лучей, зарегистрированных в околоземном космическом пространстве, в земной атмосфере и на наземных установках. Отдельные характеристики указанных событий представлены в данной работе.



ФОРБУШ-ПОНИЖЕНИЯ И ГЕОМАГНИТНЫЕ ВОЗМУЩЕНИЯ: 2. СРАВНЕНИЕ СОЛНЕЧНЫХ ЦИКЛОВ 23-24 И СОБЫТИЙ С ВНЕЗАПНЫМ И ПОСТЕПЕННЫМ НАЧАЛОМ

Мелкумян А.А., Белов А.В., Шлык Н.С., Абунина М.А., Абунин А.А., Оленева В.А., Янке В.Г.

ГиА Том: 64Номер: 1 Год: 2024 Страницы: 39-54

Исследуются статистические связи между значениями геомагнитных индексов и характеристиками космических лучей и межпланетных возмущений для Форбуш-понижений с внезапным и постепенным началом, связанных с разными типами солнечных источников: а) корональными выбросами массы из активных областей, сопровождавшимися солнечными вспышками; б) волоконными выбросами вне активных областей; в) высокоскоростными потоками из корональных дыр; г) несколькими источниками. С использованием статистических методов также сравнивается зависимость геомагнитных индексов от параметров космических лучей и солнечного ветра для Форбуш-понижений в солнечных циклах 23 и 24. Полученные результаты показали: а) межпланетные возмущения, связанные с корональными выбросами из активных областей, вызывают преимущественно магнитные бури с внезапным началом; б) межпланетные возмущения, связанные с высокоскоростными потоками из корональных дыр, вызывают в основном бури с постепенным началом; в) межпланетные возмущения, связанные с волоконными выбросами вне активных областей, вызывают равновероятно бури с внезапным и постепенным началом. Для спорадических Форбуш-понижений параметры космических лучей и геомагнитной активности в среднем больше для событий с внезапным началом; для рекуррентных Форбуш-понижений характер начала события на величину этих параметров не влияет. Для всех типов солнечных источников параметры возмущенного солнечного ветра в среднем больше в событиях с внезапным началом. Геоэффективность межпланетных возмущений значительно выше в 23 цикле для событий, связанных с выбросами из активных областей; для остальных типов возмущений разница между циклами слабая.

ФОРБУШ-ПОНИЖЕНИЯ И ГЕОМАГНИТНЫЕ ВОЗМУЩЕНИЯ: 1. СОБЫТИЯ, СВЯЗАННЫЕ С РАЗНЫМИ ТИПАМИ СОЛНЕЧНЫХ И МЕЖПЛАНЕТНЫХ ИСТОЧНИКОВ

МЕЛКУМЯН А.А. ¹, **БЕЛОВ А.В.**¹, **ШЛЫК Н.С.**¹, **АБУНИНА М.А.** ¹, **АБУНИН А.А.**¹, **ОЛЕНЕВА В.А.**¹, **ЯНКЕ В.Г.**¹

ГЕОМАГНЕТИЗМ И АЭРОНОМИЯ Том: 63 Номер: 6 Год: 2023 Страницы: 699-714

DOI: [10.31857/S0016794023600503](https://doi.org/10.31857/S0016794023600503)

В работе исследуются статистические связи между геомагнитными индексами и характеристиками космических лучей и межпланетных возмущений для Форбуш-понижений, связанных с: а) корональными выбросами массы из активных областей, сопровождавшимися солнечными вспышками; б) волоконными выбросами вне активных областей; в) высокоскоростными потоками из корональных дыр; г) несколькими источниками. Для спорадических Форбуш-понижений, с использованием статистических методов, сравнивается зависимость геомагнитных индексов от параметров космических лучей и солнечного ветра при наличии или отсутствии магнитного облака. Полученные результаты показали: а) самая высокая геоэффективность характерна для межпланетных возмущений, связанных с выбросами солнечного вещества из активных областей, при наличии магнитного облака; самая низкая – для рекуррентных возмущений; б) спорадические и рекуррентные события отличаются не только величиной геомагнитных индексов и южной компоненты магнитного поля, но и характером связи между ними; в) геоэффективность транзитных возмущений солнечного ветра зависит от наличия или отсутствия магнитного облака сильнее, чем от типа солнечного источника; г) для межпланетных возмущений, связанных с волоконными выбросами вне активных областей, при наличии магнитного облака геоэффективность зависит только от южной компоненты магнитного поля, для остальных типов возмущений – и от других параметров солнечного ветра.

ФОРБУШ-ПОНИЖЕНИЯ, СВЯЗАННЫЕ С КОРОНАЛЬНЫМИ ДЫРАМИ, КОРОНАЛЬНЫМИ ВЫБРОСАМИ ИЗ АКТИВНЫХ ОБЛАСТЕЙ И ВОЛОКОННЫМИ ВЫБРОСАМИ: СРАВНЕНИЕ В СОЛНЕЧНЫХ ЦИКЛАХ 23 И 24

Мелкумян А.А., Белов А.В., Абунина М.А., Шлык Н.С., Абунин А.А., Оленева В.А., Янке В.Г.

ГиА Том: 63Номер: 5 Год: 2023 Страницы: 581-598

Исследуется сходство и различие Форбуш-понижений в солнечных циклах 23 и 24. Анализ проводился для групп событий, связанных с разными типами солнечных источников: корональными выбросами массы из активных областей, сопровождавшимися солнечными вспышками (группа СМЕ1); волоконными выбросами вне активных областей (группа СМЕ2); высокоскоростными потоками из корональных дыр (группа СН). Исследовались распределения и взаимосвязи различных параметров: амплитуды Форбуш-понижений; максимальных в течение события значений почасового уменьшения плотности космических лучей, экваториальной анизотропии космических лучей, скорости солнечного ветра, напряженности магнитного поля, а также значений скорости солнечного ветра и напряженности магнитного поля за час до начала Форбуш-понижения. Результаты показали, что количество событий, значения параметров и их взаимосвязи зависят от фазы и цикла солнечной активности. В 24-м цикле уменьшилось количество событий в группе СМЕ1, не изменилось в СМЕ2, увеличилось в СН. Значения параметров и разница между ними в разных группах событий выше в цикле 23, характеризующемся большей асимметрией и длинными "хвостами" распределений. Величина Форбуш-понижений в группе СМЕ1 в 23-м цикле зависит сильнее от скорости солнечного ветра, а в цикле 24 – от величины магнитного поля, как и в группе СМЕ2 в обоих солнечных циклах. Множественная линейная регрессия хорошо описывает зависимости параметров Форбуш-понижений в 23-м цикле в группах СМЕ1, СМЕ2, в цикле 24 – в группе СМЕ1.

РАЗВИТИЕ ФОРБУШ-ПОНИЖЕНИЙ, СВЯЗАННЫХ С КОРОНАЛЬНЫМИ ВЫБРОСАМИ ИЗ АКТИВНЫХ ОБЛАСТЕЙ И РЕГИОНОВ ВНЕ АКТИВНЫХ ОБЛАСТЕЙ

Мелкумян А.А., Белов А.В., Абунина М.А., Шлык Н.С., Абунин А.А., Оленева В.А., Янке В.Г.
Г и А Том: 62Номер: 3 Год: 2022 Страницы: 283-301

По материалам созданной и поддерживаемой в ИЗМИРАН базы данных Форбуш-эффектов и межпланетных возмущений исследовались Форбуш-понижения за период с 1997 по 2020 гг. С использованием статистических методов сравнивались Форбуш-понижения, связанные с: корональными выбросами массы из активных областей, сопровождающимися солнечными вспышками; волоконными выбросами за пределами активных областей; высокоскоростными потоками из корональных дыр; несколькими источниками. Исследовалось также различие между Форбуш-понижениями, вызванными корональными выбросами массы, когда в межпланетных возмущениях у Земли наблюдались или не наблюдались магнитные облака. Было показано, что для спорадических Форбуш-понижений распределения большинства параметров асимметричны, для рекуррентных – почти симметричны; самые сильные корреляции между параметрами Форбуш-понижений и межпланетных возмущений наблюдаются в группе корональных выбросов из активных областей, сопровождающихся солнечными вспышками и имеющих структуру магнитного облака.

ОСОБЕННОСТИ ПОВЕДЕНИЯ ВРЕМЕННЫХ ПАРАМЕТРОВ ФОРБУШ-ПОНИЖЕНИЙ, СВЯЗАННЫХ С РАЗНЫМИ ТИПАМИ СОЛНЕЧНЫХ И МЕЖПЛАНЕТНЫХ ИСТОЧНИКОВ

Мелкумян А.А., Белов А.В., Абунина М.А., Шлык Н.С., Абунин А.А., Оленева В.А., Янке В.Г.
Г и А Том: 62Номер: 2 Год: 2022 Страницы: 155-170

По материалам созданной и поддерживаемой в ИЗМИРАН базы данных Форбуш-эффектов и межпланетных возмущений исследовались Форбуш-понижения за период с 1997 по 2017 гг. – всего 1055 событий. С использованием статистических методов сравнивалось развитие Форбуш-понижений во времени для четырех групп событий: (1) связанные с корональными выбросами массы из активных областей и сопровождающиеся солнечными вспышками; (2) вызванные межпланетными возмущениями от волоконных выбросов из регионов за пределами активных областей; (3) обусловленные высокоскоростными потоками из корональных дыр; (4) вызванные двумя или более источниками с разными типами возмущений. Для сравнения использовались временные параметры развития Форбуш-понижений – время от начала события до момента регистрации: минимальной плотности космических лучей; максимального часового уменьшения плотности космических лучей; максимальной экваториальной анизотропии космических лучей; максимальной скорости солнечного ветра; максимальной индукции межпланетного магнитного поля; минимального Dst-индекса. Исследование распределений временных параметров и корреляции между ними показало, что развитие Форбуш-понижений во времени существенно различается для четырех исследуемых групп событий.

ФОРБУШ-ПОНИЖЕНИЯ В ШЕСТИ ПОСЛЕДНИХ СОЛНЕЧНЫХ ЦИКЛАХ

Мелкумян А.А., Белов А.В., Абунина М.А., Абунин А.А., Ерошенко Е.А., Оленева В.А., Янке В.Г.
Известия РАН Том: 83Номер: 5 Год: 2019 Страницы: 625-627

В данной работе мы сравниваем параметры форбуш-понижений (ФП) – величину, скорость понижения, анизотропию, продолжительность основной фазы – в солнечных циклах с 19-го по 24-й, а также в максимумах циклов 23 и 24 и минимуме между этими циклами. База данных форбуш-эффектов и межпланетных неоднородностей, созданная и поддерживаемая в ИЗМИРАН, дает возможность использовать статистические методы анализа данных. Полученные результаты показывают, что связь с солнечной цикличностью проявляется для всех параметров ФП; ФП в максимуме цикла 23 вызваны, в основном, межпланетными неоднородностями,

связанными с корональными выбросами массы, а ФП в минимуме между циклами 23 и 24 – высокоскоростными потоками из корональных дыр.

Рекуррентные и спорадические форбуш-понижения в 23-м и 24-м солнечных циклах **Мелкумян А.А., Белов А.В., Абунина М.А., Абунин А.А., Ерошенко Е.А., Оленева В.А., Янке В.Г.** **Солнечно-земная физика** Том 5 № 1, 2019, С. 39–47

<https://naukaru.ru/upload/7fd3f86c299d8e1ce467f949bdfec858/files/6c9e7573d273c9774bad309a76ce9a6c.pdf>

По материалам базы данных форбуш-эффектов и межпланетных возмущений с использованием статистических методов и большого количества экспериментального материала сравнивались рекуррентные (вызванные высокоскоростными потоками плазмы из корональных дыр) и спорадические (связанные с корональными выбросами массы) форбуш-понижения (ФП) в солнечных циклах 23 и 24, максимумах этих циклов и минимуме между ними. Результаты показали следующее: 1) в количестве и величине ФП проявляется солнечная цикличность; 2) распределения параметров ФП и солнечного ветра различаются для рекуррентных и спорадических событий; 3) в максимуме цикла 23 преобладают спорадические ФП, в минимуме между циклами — рекуррентные ФП; 4) средние значения параметров ФП выше для спорадических, чем для рекуррентных событий, причем разница значений существенно больше в максимумах циклов. Средняя величина ФП для спорадических событий увеличивается от минимума к максимумам; для рекуррентных — почти не зависит от фазы солнечной активности, что, по-видимому, связано с малым изменением основных характеристик и геоэффективности низкоширотных корональных дыр. Средняя скорость солнечного ветра выше для рекуррентных ФП, чем для спорадических, как в максимумах, так и в минимуме солнечной активности, причем для спорадических ФП скорость солнечного ветра выше в максимумах циклов, а для рекуррентных — в минимуме между циклами. Магнитное поле в неоднородностях, связанных со спорадическими ФП, значительно слабее в текущем цикле, чем в предыдущем, что, возможно, является следствием аномального расширения корональных выбросов массы, вызванного низким давлением невозмущенного солнечного ветра; в максимумах солнечных циклов средняя индукция магнитного поля выше для спорадических событий, чем для рекуррентных. Для обоих типов событий длительность главной фазы ФП в максимумах циклов 23 и 24 существенно меньше, чем в минимуме между циклами; в максимуме цикла 23 спорадические ФП развиваются существенно быстрее, чем рекуррентные.

РАСПРЕДЕЛЕНИЕ ФОРБУШ-ЭФФЕКТОВ ПО ВЕЛИЧИНЕ

МЕЛКУМЯН А.А.*1, БЕЛОВ А.В.*2, АБУНИНА М.А.2, АБУНИН А.А.2, ЕРОШЕНКО Е.А.2, ОЛЕНЕВА В.А.2, ЯНКЕ В.Г.2

ГиА Том: 58Номер: 6 Год: 2018 Страницы: 845-852

На основе большого экспериментального материала, объединенного в базу данных межпланетных возмущений и Форбуш-эффектов (ИЗМИРАН), исследовано распределение по величине Форбуш-эффектов для космических лучей жесткостью 10 ГВ, наблюдавшихся с 1957 по 2016 г. Показано, что для достаточно больших Форбуш-эффектов распределение соответствует степенному закону с показателем, близким к показателям, полученным ранее для корональных выбросов массы. Полученные распределения свидетельствуют о том, что в базе данных собраны практически все Форбуш-эффекты с величиной больше 1.4%, и они, в подавляющем большинстве, обусловлены корональными выбросами массы.

ДОЛГОПЕРИОДНЫЕ ИЗМЕНЕНИЯ КОЛИЧЕСТВА И ВЕЛИЧИНЫ ФОРБУШ-ЭФФЕКТОВ

МЕЛКУМЯН

А.А.*1, БЕЛОВ А.В.*2, АБУНИНА М.А.2, АБУНИН А.А.2, ЕРОШЕНКО Е.А.2, ОЛЕНЕВА В.А.2, ЯНКЕ В.Г.2

Г&А Том: 58Номер: 5 Год: 2018 Страницы: 638-647

По материалам базы данных Форбуш-эффектов и межпланетных возмущений, созданной в ИЗМИРАН, исследованы долговременные изменения количества и величины Форбуш-эффектов в шести последних солнечных циклах (1957–2016 гг.) для космических лучей с жесткостью 10 ГВ. Показано, что циклы солнечной активности хорошо проявляются в данных Форбуш-эффектов, особенно в событиях большой величины, которые практически исчезают в минимумах. Изменения в распределении Форбуш-эффектов и уменьшение их средних величин от максимума к минимуму солнечной активности объясняется преобладанием при низкой активности вариаций космических лучей, обусловленных воздействием корональных дыр. Обращается внимание на то, что в текущем цикле Форбуш-эффектов меньше, и они, в целом, слабее, чем в пяти предыдущих

циклах. Для каждого месяца предложен и рассчитан FD-индекс, объединяющий величину и количество Форбуш-эффектов и удобный для изучения долговременных вариаций.

См. *Астрономия-2018* Том 2 Солнечно-земная физика – современное состояние и перспективы С. 137

ПОВЕДЕНИЕ СКОРОСТИ И ТЕМПЕРАТУРЫ СОЛНЕЧНОГО ВЕТРА В МЕЖПЛАНЕТНЫХ ВОЗМУЩЕНИЯХ, СОЗДАЮЩИХ ФОРБУШ-ПОНИЖЕНИЯ

МЕЛКУМЯН А. А.*¹, **БЕЛОВ А. В.***², АБУНИНА М. А.², АБУНИН А. А.², ЕРОШЕНКО Е. А.², ОЛЕНЕВА В. А.², ЯНКЕ В. Г.²

Геомагн. и аэрон. Том: 60Номер: [5](#) Год: 2020 Страницы: 547-556

Форбуш-понижения космических лучей обусловлены двумя типами солнечных источников: корональными дырами и корональными выбросами массы. В некоторых случаях идентификация солнечного источника с межпланетным возмущением, вызывающим Форбуш-понижение, затруднена и требует тщательного и детального анализа характеристик солнечного ветра. В этих случаях полезно сопоставить поведение протонной температуры и скорости солнечного ветра. В данной работе такое сопоставление проводилось на основе большого экспериментального материала, объединенного в базы данных ИЗМИРАН. Оказалось, что зависимость температуры от скорости для спокойного солнечного ветра имеет степенной характер с более крутым спектром в области низких скоростей ($V < 425$ км/с; показатель степени 3.37 ± 0.02), чем в области высоких скоростей ($V \geq 425$ км/с; показатель степени 2.21 ± 0.02). На основе полученной $T-V$ зависимости, для каждого часа, для которого есть данные о параметрах солнечного ветра, с июля 1965 г. и по декабрь 2018 г. были вычислены ожидаемая протонная температура T_{exp} и температурный индекс $KT = T_{\text{obs}}/T_{\text{exp}}$ (T_{obs} – наблюдаемая температура). Этот индекс аномально велик в областях взаимодействия разноскоростных потоков солнечного ветра и аномально мал внутри магнитных облаков, что позволяет использовать его для выделения связанных с этими межпланетными структурами Форбуш-понижений и для идентификации их солнечных источников.

СНОВНЫЕ СВОЙСТВА ФОРБУШ-ЭФФЕКТОВ, СВЯЗАННЫХ С ВЫСОКОСКОРОСТНЫМИ ПОТОКАМИ ИЗ КОРОНАЛЬНЫХ ДЫР

МЕЛКУМЯН А.А.¹, **БЕЛОВ А.В.**², **АБУНИНА М.А.**², **АБУНИН А.А.**², **ЕРОШЕНКО Е.А.**², **ОЛЕНЕВА В.А.**², **ЯНКЕ В.Г.**²

Геомагн. и Аэрон. Том: 58Номер: [2](#) Год: 2018 Страницы: 163-176

Для того чтобы изучить особенности воздействия высокоскоростных потоков солнечного ветра из корональных дыр на космические лучи, была использована база данных Форбуш-эффектов и межпланетных возмущений, созданная в ИЗМИРАН. Были выделены 350 Форбуш-эффектов, созданных корональными дырами без других воздействий. Для различных характеристик событий этой группы найдены средние значения и распределения и проведено их сравнение со всеми Форбуш-эффектами и Форбуш-эффектами, обусловленными корональными выбросами. Несмотря на большие различия высокоскоростных потоков из корональных дыр, эта группа оказалась более компактной и однородной по сравнению с событиями, связанными с корональными выбросами. Получены регрессионные зависимости и корреляционные связи между различными параметрами событий для исследуемых групп. Показано, что Форбуш-эффекты, обусловленные корональными выбросами, значительно сильнее зависят от характеристик межпланетных возмущений по сравнению с Форбуш-эффектами, связанными с корональными дырами. Это говорит о существенном различии модуляционных механизмов Форбуш-эффектов разных типов и подтверждает выводы, сделанные ранее по косвенным данным.

ЗАВИСИТ ЛИ ГЕНЕРАЦИЯ МАГНИТНОЙ БУРИ ОТ ТИПА СОЛНЕЧНОГО ВЕТРА?

НИКОЛАЕВА Н.С.¹, **ЕРМОЛАЕВ Ю.И.**¹, **ЛОДКИНА И.Г.**¹, **ЕРМОЛАЕВ М.Ю.**¹

ГЕОМАГНЕТИЗМ И АЭРОНОМИЯ Том: 57Номер: 5 Год: 2017 Страницы: 555-561

Целью данной работы является привлечение внимания читателей к проблеме возможных различий в генерации магнитных бурь, вызванных различными крупномасштабными типами течений солнечного ветра (CB): CIR, Sheath и ICME (включая MC и Ejecta). Недавно нами было показано, что если использовать модификации формулы Бартона и др. для связи межпланетных условий с Dst и Ds^{\wedge} -индексами, то эффективность генерации

бурь типами Sheath и CIR на ~50% выше, чем генерация ICME. В литературе существует множество различных функций связи (FC) между различными межпланетными параметрами и состоянием магнитосферы, однако они не исследовались для различных типов течений СВ. В этой работе мы исследуем эффективность генерации главной фазы бури для различных потоков СВ при использовании 12 различных FC на основе данных OMNI для периода 1976-2000 гг. Полученные результаты показывают, что для большей части FC тип Sheath имеет самую высокую эффективность, а MC имеет самую низкую эффективность в соответствии с нашими предыдущими результатами. Достоверность полученных данных и возможные причины расхождений для различных FC и различных типов СВ требуют дальнейших исследований.

К ИСТОРИИ ОТКРЫТИЯ СОЛНЕЧНОГО ВЕТРА **Review**

ОБРИДКО В.Н.1, **ВАЙСБЕРГ** О.Л.

АСТРОНОМИЧЕСКИЙ ВЕСТНИК Том: 51Номер: 2 Год: 2017 Страницы: 182-186

Открытие солнечного ветра является одним из выдающихся достижений гелиофизики и космических исследований. К тому же солнечный ветер играет исключительную роль в процессах, происходящих в Солнечной системе, а в последние десятилетия он осознан как главный фактор влияющей на земные процессы космической погоды. Солнечный ветер – необыкновенная плазменная лаборатория гигантского масштаба с фантастическим набором и разнообразием параметров и режимов и отсутствием влияния стенок лабораторных плазменных установок. Он также является единственным доступным для прямых исследований экземпляром звездных ветров, исследуемых в астрофизике. История его открытия довольно драматична, и, как многие замечательные открытия, имеет нескольких родителей. И, как это обычно бывает, автором открытия остается ученый, который смог наиболее полно объяснить суть явления. Таким человеком многие заслуженно считают американского теоретика Юджина Паркера, открывшего солнечный ветер, каким мы его знаем сегодня, на кончике пера. Юджину Паркеру в 2017 г. исполняется 90 лет.

ИССЛЕДОВАНИЕ МОЩНЫХ КОРОНАЛЬНЫХ ВЫБРОСОВ МАСС, ПРОИЗОШЕДШИХ В СЕНТЯБРЕ 2017 ГОДА, ПО ДАННЫМ МЮОННОГО ГОДОСКОПА УРАГАН

Осетрова Н.В., **Астапов** И.И., **Барбашина** Н.С., **Борог** В.В., **Дмитриева** А.Н.

Известия РАН Том: 83Номер: 5 Год: 2019 Страницы: 628-630

В начале сентября 2017 г. Солнце характеризовалось аномально высокой активностью (СА), необычной для области минимума 11-летнего цикла. Произошло большое количество мощных вспышек M- и X-класса, которые сопровождалась мощными корональными выбросами масс (КВМ). Эти события вызвали на Земле сильные магнитные бури (Kp-индекс достигал значения 8, индекс Dst < -140 нТ). В работе рассматривается влияние этих выбросов на поток космических лучей (КЛ) по данным мюонного годоскопа УРАГАН (НИЯУ МИФИ). Исследование основывается на анализе вариаций потока мюонов космических лучей. Приводятся результаты обработки интенсивности потока методом фликкер-шумовой спектроскопии с целью определения предикторов геоэффективных возмущений магнитосферы Земли. Получен предиктор, опережающий появление возмущений в околоземном пространстве, связанных с распространением КВМ, более чем на сутки.

КОСМИЧЕСКАЯ ПОГОДА: ИСТОРИЯ ИССЛЕДОВАНИЯ И ПРОГНОЗИРОВАНИЕ

А. С. **Парновский**¹, Ю. И. Ермолаев², И. Т. Жук¹

Космічна наука і технологія. 2010. Т. 16. № 1. С. 90–99. File

МОДЕЛИРОВАНИЕ АНИЗОТРОПИИ ГАЛАКТИЧЕСКИХ КОСМИЧЕСКИХ ЛУЧЕЙ

Перегудов Д.В., **Соловьев** А.А., **Яшин** И.И., **Шутенко** В.В.

[СОЛНЕЧНО-ЗЕМНАЯ ФИЗИКА Том 6 № 1, 2020, С. 36–42](#)

<https://naukaru.ru/ru/storage/viewWindow/50033>

Рассматривается задача вычисления углового распределения космических лучей в данной точке гелиосферы в предположении, что из бесконечности падает изотропный поток частиц. Показано, что статическое магнитное поле не порождает анизотропии, если только точка наблюдения не находится в области захваченных частиц. Рассмотрена модель коронального выброса в виде неподвижного цилиндра с однородным магнитным полем вдоль оси. Для точек наблюдения в области захваченных частиц (внутри цилиндра) вычислены угловые распределения космических лучей. Показано, что возникает конус направлений, в котором поток ослабляется. Для той же модели с равномерно движущимся выбросом рассчитаны угловые распределения при различных положениях точки наблюдения вне цилиндра. Показано, что возникает анизотропия порядка отношения скорости выброса к скорости света. Качественно схожие распределения наблюдаются на мюонном годоскопе УРАГАН.

ПРОСТРАНСТВЕННЫЕ И ВРЕМЕННЫЕ ХАРАКТЕРИСТИКИ ПОТОКОВ ЭЛЕКТРОНОВ СУБРЕЛЯТИВИСТСКИХ ЭНЕРГИЙ В ОКОЛОЗЕМНОМ КОСМИЧЕСКОМ ПРОСТРАНСТВЕ ПО ДАННЫМ СПУТНИКА ВЕРНОВ

В. Л. Петров, А. В. Богомолов, В. В. Богомолов, В. В. Калегаев, М. И. Панасюк, С. И. Свертилов, А. А. Косенко
ГЕОМАГНЕТИЗМ И АЭРОНОМИЯ Том: 60 Номер: 2 Год: 2020 Страницы: 153-163

Изучение пространственного распределения и динамики потоков электронов субрелятивистских энергий (от нескольких десятков до сотен кэВ) проводилось в ходе космического эксперимента на спутнике Вернов. Был проведен совместный анализ данных экспериментов на спутниках Вернов и РОЕС. Получены карты глобального распределения в околоземном пространстве потоков электронов с энергиями от сотен кэВ до МэВ, а также их распределения по дрейфовым оболочкам, локальному времени и геомагнитной долготе. Показано, что значимые потоки электронов субрелятивистских энергий существуют на дрейфовых оболочках, характеризуемых значениями параметра параметра МакИлвайна $L < 1.5$. Измеренное долготное распределение потоков электронов на указанных дрейфовых оболочках свидетельствует о том, что наблюдающиеся потоки "привязаны" к этим оболочкам, а неоднородности долготного распределения обусловлены особенностями конфигурации магнитного поля на орбитах спутников.

ЭФФЕКТИВНОСТЬ МЕХАНИЗМОВ ФОРМИРОВАНИЯ СПОРАДИЧЕСКИХ ФОРБУШ-ПОНИЖЕНИЙ

Петухова А.С., Петухов И.С., Петухов С.И.

Изв. РАН Том: 87 Номер: 7 Год: 2023 1035-1037

Особенности динамики параметров среды и плотности космических лучей в сильных форбуш-понижениях, связанных с магнитными облаками.

Петухова А.С., Петухов И.С., Петухов С.И., Готовцев И.С.

СОЛНЕЧНО-ЗЕМНАЯ ФИЗИКА Том 9 № 2, 2023 С. 94–100.

<https://naukaru.ru/ru/storage/viewWindow/123147>

Диффузионный и электромагнитный механизмы определяют формирование спорадических форбуш-понижений (ФП). Диффузионный механизм влияет на амплитуду ФП (Афп) в турбулентном слое и части коронального выброса массы (КВМ), предшествующей магнитному облаку, и его эффективность зависит от уровня турбулентности магнитного поля. Электромагнитный механизм работает в магнитном облаке, и его эффективность зависит от напряженности регулярных магнитных и электрических полей. Мы анализируем параметры солнечного ветра и характеристики космических лучей, применяя метод наложенных эпох. В 1996–2006 гг. было зарегистрировано 23 сильных ФП (Афп > 5 %). Средняя амплитуда 7 % в равной степени формируется обоими механизмами. События можно разделить на две группы в зависимости от вклада механизмов в амплитуду ФП. Группа 1 включает самые сильные ФП (Афп1 = 8.5 %), образованные как диффузионным, так и электромагнитным механизмами: диффузионный механизм отвечает за 0.26Афп1, а электромагнитный — за 0.74Афп1. В группе 2 амплитуда Афп2 составляет 5.7 %, причем диффузионный механизм формирует 0.79Афп2, а электромагнитный — 0.21Афп2. Пространственные распределения средних значений параметров среды в области возмущений в группах 1 и 2 различаются. Это различие может быть объяснено тем фактом, что ФП в группах 1 и 2 формируются в центральной и периферийной частях КВМ соответственно.

ФОРБУШ-ПОНИЖЕНИЕ КОСМИЧЕСКИХ ЛУЧЕЙ В ТОРОИДАЛЬНОЙ МОДЕЛИ МАГНИТНОГО ОБЛАКА

ПЕТУХОВА А.С.¹, **ПЕТУХОВ И.С.**¹, **ПЕТУХОВ С.И.**¹, **ГРИГОРЬЕВ В.Г.**¹

ИЗВЕСТИЯ РАН. СЕРИЯ ФИЗИЧЕСКАЯ Том: 81 Номер: 4 Год: 2017 Страницы: 571-573

Выполнен расчет интенсивности космических лучей в магнитном облаке. Получено, что длительность восстановления Форбуш-понижения определяется ориентацией магнитного облака и уменьшением магнитного поля в магнитном облаке при его расширении. Установлено формирование форбуш-понижения в терминах вклада различных источников частиц.

Сильные ФП 1996-2006 гг.

ПРОЗРАЧНОСТЬ ГРАНИЦЫ МАГНИТНОГО ОБЛАКА ДЛЯ КОСМИЧЕСКИХ ЛУЧЕЙ

Петухов И.С., Петухов С.И.

ИЗВЕСТИЯ РАН. СЕРИЯ ФИЗИЧЕСКАЯ, 2013, том 77, № 5, с. 587–589

Предложена модель магнитного облака, представленного в виде тора с характерным магнитным полем, расположенным внутри межпланетного выброса корональной массы, распространяющегося от

Солнца в межпланетном пространстве. Определено магнитное поле в торе. Рассчитана прозрачность границы магнитное поле – солнечный ветер для космических лучей разных энергий.

ВЛИЯНИЕ ПАРАМЕТРОВ СОЛНЕЧНОГО ВЕТРА И ГЕОМАГНИТНОЙ АКТИВНОСТИ НА ВАРИАЦИИ ЖЕСТКОСТИ ОБРЕЗАНИЯ КОСМИЧЕСКИХ ЛУЧЕЙ ВО ВРЕМЯ СИЛЬНЫХ МАГНИТНЫХ БУРЬ

ПТИЦЫНА Н. Г. ^{*1}, ДАНИЛОВА О. А. ¹, ТЯСТО М. И. ¹, СДОБНОВ В. Е.

[ГЕОМАГНЕТИЗМ И АЭРОНОМИЯ](#) Том: 59 Номер: 5 Год: 2019 Страницы: 569-577

DOI: [10.1134/S0016794019050092](#)

Рассчитана корреляция вариаций жесткостей геомагнитного обрезания ΔR с межпланетными параметрами и Dst-индексом геомагнитной активности во время шести сильных и одной умеренной бури 23-го и 24-го солнечных циклов. Значения ΔR вычислялись с использованием двух методов: (1) метода спектрографической глобальной съемки, при котором определение жесткостей обрезания $R_{\text{сгс}}$ базируется на наблюдательных данных сети нейтронных мониторов и (2) метода, при котором для определения жесткостей обрезания $R_{\text{эф}}$ численно рассчитываются траектории частиц в модельном магнитном поле магнитосферы. В целом результаты, полученные двумя методами, хорошо согласуются между собой. Наибольшее влияние на ΔR оказывает Dst-индекс геомагнитной активности. При этом корреляция увеличивается с ростом интенсивности бури. Чувствительность ΔR к межпланетным параметрам сильно отличается для разных бурь. Наиболее геоэффективным межпланетным параметром оказалась скорость солнечного ветра V . Существенная антикорреляция ΔR и V прослеживается почти для всех бурь. Корреляция $\Delta R_{\text{сгс}}$ с V_z -компонентой межпланетного магнитного поля наблюдается только для двух бурь, 7–14.11.2003 г. и 7–8.11.2004 г., для которых абсолютная величина V_z достигала очень высоких значений (≈ 50 нТл). В то же время довольно высокая корреляция $\Delta R_{\text{эф}}$ с V_z была получена для большинства бурь. Азимутальная компонента межпланетного поля V_u и динамическое давление солнечного ветра P практически не обнаруживают связи с ΔR .

Прогнозирование геомагнитных бурь, связанных с межпланетными корональными выбросами массы

Родькин Д.Г.¹, [Слемзин В.А.](#)¹

АЖ Том 101, № 2 165-173 (2024)

Геомагнитные бури оказывают значительное влияние на работоспособность технических систем как в космосе, так и на Земле. Источниками сильных геомагнитных бурь чаще всего являются межпланетные корональные выбросы массы (МКВМ), порождаемые корональными выбросами массы (КВМ) в солнечной короне. Прогноз МКВМ основан на регулярных оптических наблюдениях Солнца, которые позволяют обнаружить КВМ на стадии формирования. Известно, что интенсивность геомагнитных бурь коррелирует с величиной южной компоненты магнитного поля (V_z) МКВМ. Однако при оперативном прогнозе произвольного КВМ заранее предсказать знак и величину V_z по солнечным наблюдениям пока не удастся. В этих условиях предварительный прогноз вероятности развития бури может быть получен в предположении, что сила бури связана с величиной магнитного потока из области эрупции, наблюдаемой как димминг. В данной работе на серии из 37 эруптивных событий 2010–2012 гг. рассматривается связь интегрального магнитного потока из области диммингов с вероятностью того, что КВМ, ассоциированные с ними, вызовут геомагнитные бури. Показано, что наблюдается общий тренд на увеличение геоэффективности МКВМ с повышением величины магнитного потока из области диммингов. Продемонстрировано, что частота наблюдения умеренных и сильных бурь повышается в случаях комплексных событий, связанных с взаимодействием КВМ с другими потоками солнечного ветра в гелиосфере.

ПОИСК СОЛНЕЧНЫХ ИСТОЧНИКОВ МЕЖПЛАНЕТНЫХ КОРОНАЛЬНЫХ ВЫБРОСОВ МАССЫ С ПОМОЩЬЮ ОБРАТНОЙ МОДЕЛИ МАГНИТОДИНАМИЧЕСКОГО ВЗАИМОДЕЙСТВИЯ СОЛНЕЧНОГО ВЕТРА В ГЕЛИОСФЕРЕ

РОДЬКИН Д. Г.^{*1}, **СЛЕМЗИН В. А.**¹, **ШУГАЙ Ю. С.**²

АЖ Том: 100 Номер: 3 Год: 2023 Страницы: 289-296

При разработке и тестировании методов прогнозирования межпланетных корональных выбросов массы (МКВМ) большое значение имеет установление их связи с источниками на Солнце – корональными выбросами массы (КВМ), наблюдаемыми коронографами. Часто применяемый обратный баллистический расчет времени старта КВМ не учитывает изменения их скорости при движении в гелиосфере и может давать неопределенность вплоть до суток. С хорошей точностью (порядка ± 10 ч) движение КВМ в гелиосфере от Солнца до Земли описывается моделью магнитодинамического взаимодействия КВМ с фоновым

солнечным ветром (drag-based model, DBM). В данной работе для поиска возможных корональных источников МКВМ, наблюдаемых у Земли, предлагается использование обратной модели магнитодинамического взаимодействия (reverse DBM, RDBM), с помощью которой по измеренным параметрам МКВМ в обратном ходе восстанавливается вероятное движение КВМ в гелиосфере и определяются их параметры на выходе из солнечной короны. В модели используются данные о скорости фонового солнечного ветра, рассчитываемые по площади корональных дыр в центральной части Солнца, представленные на сайте Центра анализа космической погоды НИИЯФ МГУ, с корректирующими коэффициентами.

КРУПНОМАСШТАБНАЯ И МЕЛКОМАСШТАБНАЯ СТРУКТУРА СОЛНЕЧНОГО ВЕТРА, ФОРМИРУЮЩАЯСЯ ПРИ ВЗАИМОДЕЙСТВИИ ПОТОКОВ В ГЕЛИОСФЕРЕ

РОДЬКИН Д.Г.

, КАПОРЦЕВА К.Б.2, ЛУКАШЕНКО А.Т.3, ВЕСЕЛОВСКИЙ И.С.3,4, СЛЕМЗИН В.А.1, ШУГАЙ Ю.С.3

Косм. Исслед. Том: 57Номер: 1 Год: **2019** Страницы: 21-31

Рассмотрена классификация потоков солнечного ветра по магнитогидродинамическим параметрам (МГД-типы) – комбинации скорости, плотности, температуры протонов и напряженности магнитного поля, в дополнение к классическому разделению солнечного ветра на высокоскоростные потоки из корональных дыр, транзитные потоки корональных выбросов массы и медленный солнечный ветер из пояса стримеров. Проведено сопоставление двух классификаций свойств солнечного ветра для событий в **августе 2010** и **мае 2011** г., когда наблюдалось взаимодействие двух корональных выбросов массы и коронального выброса массы с высокоскоростным потоком солнечного ветра из корональной дыры, соответственно. Показано, что классическое описание крупномасштабной структуры потоков ветра в масштабах часов и дней, в особенности ионного состава ветра, позволяет определить тип и источник потоков, в то время как МГД-параметры позволяют точнее описать мелкомасштабную структуру (минуты), в особенности, в случаях взаимодействия нескольких потоков в гелиосфере. Детальное исследование мелкомасштабной структуры областей взаимодействия потоков дает информацию, необходимую для развития МГД-моделей, описывающих процессы распространения и взаимодействия потоков в гелиосфере и прогнозирования их геоэффективности.

МИНИМАЛЬНАЯ ВЕЛИЧИНА ГЕЛИОСФЕРНОГО МАГНИТНОГО ПОЛЯ В 2008–2010 ГГ. ПО ДАННЫМ WIND И ACE

Свиржевский Н.С., Базилевская Г.А., Свиржевская А.К., Стожков Ю.И.

Известия РАН Том: 83Номер: 5 Год: **2019** Страницы: 618-621

В работе приводятся оценки вклада магнитных полей от коротирующих областей взаимодействия потоков быстрого и медленного ветра в величину измеряемого гелиосферного магнитного поля (ГМП) на 1 а. е. в минимуме солнечной активности 2008–2010 гг. Рассмотрена методика, позволяющая провести такие оценки, и приводятся результаты оценок, выполненных по данным КА WIND и ACE. Вклад магнитных полей от коротирующих областей взаимодействия в полное поле в минимуме 24-го цикла солнечной активности составил примерно 10%, минимальная напряженность ГМП около Земли в 2009 г. была равна 3.54 ± 0.11 нТл. Магнитные поля коротирующих областей взаимодействия играют важную роль в модуляции галактических космических лучей (ГКЛ). Эти поля оказывают влияние на спектры флуктуаций ГМП в секторной зоне, что приводит к изменению жесткостной зависимости тензора диффузии ГКЛ и, в итоге, к изменению спектров ГКЛ в гелиосфере при энергии частиц $E < 10$ ГэВ.

Модуляционное влияние коротирующей магнитной ловушки на 27-дневные вариации космических лучей в ноябре–декабре 2014 г.

Сдобнов В.Е., Кравцова М.В., Олемской С.В.

Солнечно-земная физика Том 5 № 1 , **2019**, С. 13–16

<https://naukaru.ru/upload/7fd3f86c299d8e1ce467f949bdfec858/files/a433754f1dfbb0d86c869ec0e64e0031.pdf>

По данным наземных измерений на мировой сети нейтронных мониторов и космических аппаратах GOES-15 исследована 27-дневная вариация интенсивности космических лучей (КЛ) в ноябре–декабре 2014 г. Показано, что определяющим фактором значительного различия в ее амплитудах являются существенные изменения потерь энергии при движении частиц в регулярных электромагнитных полях гелиосферы. В этот период под воздействием огромной корональной дыры на юге Солнца в межпланетном пространстве существовала долгоживущая коротирующая ловушка такой конфигурации, при которой для КЛ с энергией ~ 3 –20 ГэВ

наиболее эффективно происходила ее потеря, за счет чего в наземных измерениях интенсивности КЛ нейтронными мониторами наблюдалась аномально большая амплитуда 27-дневной вариации.

Образование и распространение плазменных потоков корональных выбросов массы в солнечной короне и гелиосфере

Review

В. А. Слемзин¹, Ф. Ф. Горяев¹, Д. Г. Родькин¹, Ю. С. Шугай², С. В. Кузин¹

2018

File

Настоящий обзор посвящен вопросам формирования в солнечной короне и распространения в гелиосфере плазменных потоков корональных выбросов массы и производных от них транзитных потоков межпланетных корональных выбросов массы в солнечном ветре. Рассматриваются основные параметры корональных выбросов массы, их отличия от других типов потоков солнечного ветра, корреляция частоты выбросов со вспышками и состоянием солнечной активности. Особое внимание уделяется формированию и моделированию ионного состава плазмы корональных выбросов массы и транзитов солнечного ветра, который является одним из ключевых факторов идентификации типов потоков и их источников, особенно в сложных комплексных структурах, образующихся в гелиосфере при взаимодействии потоков. Рассматриваются современные модели прогнозирования параметров потоков солнечного ветра по данным наблюдений. Обзор содержит перечни источников данных о корональных выбросах и баз данных о параметрах потоков солнечного ветра, а также многочисленные ссылки на работы по исследованиям рассматриваемых явлений.

О форме спектра флуктуаций интенсивности галактических космических лучей.

Стародубцев С.А.

СОЛНЕЧНО-ЗЕМНАЯ ФИЗИКА Том 8. 2022. № 2 С. 78–83.

<https://naukaru.ru/ru/storage/viewWindow/94303>

Воздействие плазмы солнечного ветра на потоки проникающих извне в гелиосферу галактических космических лучей (ГКЛ) с энергиями выше ~ 1 ГэВ приводит к возникновению вариаций интенсивности КЛ в широком диапазоне частот. Поскольку КЛ являются заряженными частицами, их модуляция происходит главным образом под воздействием межпланетного магнитного поля (ММП). Хорошо известно, что наблюдаемый спектр флуктуаций ММП в широкой области частот $\nu \sim 10\text{--}7\text{--}10$ Гц носит ярко выраженный падающий характер и состоит из трех участков — энергетического, инерционного и диссипативного. Каждый описывается степенным законом $\text{PMMP}(\nu) \sim \nu^{-\alpha}$, причем показатель α спектра ММП увеличивается с ростом частоты. При этом на каждом участке флуктуации ММП характеризуются свойствами, зависящими от их природы. Известна также установленная связь между спектрами флуктуаций ММП и ГКЛ в случае модуляции последних альфвеновскими или быстрыми магнитозвуковыми волнами. Теория предсказывает, что спектры флуктуаций КЛ должны описываться также степенным законом $\text{PKL}(\nu) \sim \nu^{-\gamma}$. Однако результаты многолетних работ сотрудников ИКФИА СО РАН по изучению природы и свойств флуктуаций интенсивности КЛ с использованием данных регистрации нейтронных мониторов на станциях с различными порогами геомагнитного обрезания $\text{RC} \sim 0.5\text{--}6.3$ ГВ показывают, что наблюдаемый спектр флуктуаций интенсивности ГКЛ при $\nu > 10\text{--}4$ Гц становится плоским, т. е. он подобен белому шуму. Этот факт требует своего понимания и объяснения. В данной работе на основе данных измерений нейтронного монитора станции Апатиты приводятся результаты изучения формы спектра флуктуаций интенсивности ГКЛ в области частот $\nu \sim 10\text{--}6\text{--}1$ Гц и их сопоставления с модельными расчетами спектров белого шума. Дано возможное физическое объяснение наблюдаемой формы спектра флуктуаций КЛ на основе известных механизмов их модуляции в гелиосфере.

Анализ солнечных, космо- и геофизических событий в сентябре 2017 г. по комплексным наблюдениям ИКФИА СО РАН

Стародубцев С.А., Баишев Д.Г., Григорьев В.Г., Каримов Р.Р., Козлов В.И., Корсаков А.А., Макаров Г.А., Моисеев А.В.

Солнечно-земная физика Том 5 № 1, 2019, С. 17–38

<https://naukaru.ru/upload/7fd3f86c299d8e1ce467f949bdfec858/files/c79f704a8899c493197f997a7f1f3fd1.pdf>

Приводятся результаты мониторинга космических лучей и геомагнитного поля вдоль 210 магнитного меридиана на территории Якутии в первой половине сентября 2017 г. Сообщается об установлении энергетического спектра наземного возрастания космических лучей 10 сентября $J = 3027E^{-1.99} \exp(-E/729 \text{ МэВ})$. Приводятся результаты прогноза и комплексного анализа магнитной бури 7–9 сентября 2017 г. с $\text{Dst} = -124$ нТл. Заблаговременность прогноза составила около суток. Рассмотрено ее влияние на изменения электрического потенциала и распространение сигналов радиостанций радионавигационной системы РСДН-20 в ОНЧ-

диапазоне. Во время магнитной бури 8 сентября 2017 г. с 12 до 20 UT в широком диапазоне периодов наблюдались иррегулярные пульсации от P₁₃ до P₁₁. При этом они сопровождались вариациями величин естественных потенциалов электротеллурического и геомагнитного полей с коэффициентом корреляции между ними $\rho(E, H) = 0.5 \div 0.9$. Эффекты магнитной бури проявились в виде повышения затухания и уменьшения фазовой задержки ОНЧ-радиосигналов.

ИЗУЧЕНИЕ 27-ДНЕВНЫХ ВАРИАЦИЙ ПОТОКА ГАЛАКТИЧЕСКИХ КОСМИЧЕСКИХ ЛУЧЕЙ ПО ДАННЫМ ЭКСПЕРИМЕНТА РАМЕЛА

Троицкая И.К., Майоров А.Г., Малахов В.В., Модзелевская Р., Роденко С.А.

Известия РАН Том: 83Номер: 5 Год: 2019 Страницы: 635-637

Спектрометры ПАМЕЛА и АРИНА на борту КА Ресурс-ДК1 с июня 2006 г. до января 2016 г. проводили прецизионные измерения потока космических лучей в широком диапазоне энергий, включая интервал от 30 МэВ до десятков ГэВ. Благодаря этому возможно получить новую информацию о характеристиках вариаций потока галактических космических лучей, включая период, амплитуду и их зависимость от энергии частиц. В работе приводятся первые предварительные результаты по данному исследованию, полученные при помощи вейвлет-анализа временных рядов потоков протонов и ядер гелия.

СРЕДНЕМАСШТАБНЫЕ ИЗМЕНЕНИЯ СОДЕРЖАНИЯ ГЕЛИЯ ВНУТРИ КОРОНАЛЬНЫХ ВЫБРОСОВ МАССЫ

Хохлачев А.А., Рязанцева М.О., Ермолаев Ю.И., Рахманова Л.С., Лодкина И.Г.

Косм. Исслед. Том: 60Номер: 6 Год: 2022 Страницы: 486-495

В работе исследуются изменения относительного содержания гелия, а также других параметров плазмы солнечного ветра и межпланетного магнитного поля на средних пространственных масштабах ($10^5 - 10^6$ км) внутри межпланетных проявлений корональных выбросов массы. Анализ проводился на основе долговременных измерений космического аппарата *WIND*. Показано, что на исследуемых масштабах отсутствует однозначная антикорреляция содержания гелия и плазменного параметра β , которая была выявлена на масштабах более 10^6 км. События со значимой положительной и отрицательной корреляцией регистрируются с одинаковой вероятностью. При этом могут наблюдаться как структуры с возрастанием содержания гелия одновременно с ростом модуля межпланетного магнитного поля, аналогичные наблюдаемому на больших масштабах, так и структуры, в которых содержание гелия растет со спадом величины межпланетного магнитного поля.

ВАРИАЦИИ СОДЕРЖАНИЯ ГЕЛИЯ В МЕЖПЛАНЕТНЫХ ВЫБРОСАХ КОРОНАЛЬНОЙ МАССЫ (ICME)

Хохлачев А. А., Ермолаев Ю. И., Лодкина И. Г., Рязанцева М. О., Рахманова Л. С.

Косм. Исслед. Том: 60Номер: 2 Год: 2022 Страницы: 93-98

На основе данных базы OMNI2 за период с 1976 по 2019 г. исследуется поведение относительного содержания ионов гелия N_α/N_p внутри ICME. Показано, что ранее обнаруженная антикорреляция между N_α/N_p и β -параметром внутри ICME в основном связана с зависимостью от магнитного давления (или величины межпланетного магнитного поля), при этом зависимость N_α/N_p от величины теплового давления является слабо падающей в MC и растущей в EJECTA. Полученные данные согласуются с ранее высказанной гипотезой о протекании обогащенного ионами гелия электрического тока внутри ICME [1–3].

ГЕОЭФФЕКТИВНЫЕ ВОЗМУЩЕНИЯ В СОЛНЕЧНОМ ВЕТРЕ ВБЛИЗИ МИНИМУМА СОЛНЕЧНОЙ АКТИВНОСТИ ПО ДАННЫМ ДВУХЛЕТНЕЙ СЕРИИ НАБЛЮДЕНИЙ МЕЖПЛАНЕТНЫХ МЕРЦАНИЙ НА РАДИОТЕЛЕСКОПЕ БСА ФИАН

ЧАШЕЙ И. В.*✉1, ЛЕБЕДЕВА Т. О.1, ТЮЛЬБАШЕВ С. А.1, СУБАЕВ И. А.1

АЖ Том: 98Номер: 11 Год: 2021 Страницы: 949-968

Совместный анализ данных мониторинга межпланетных мерцаний с солнечными и геофизическими данными показал, что на фазе спада 24 цикла солнечной активности доминирующая роль в геомагнитных возмущениях связана с коротярующими возмущениями в солнечном ветре. В 2018–2019 гг. при приближении к глубокому минимуму активности из 13 сильных магнитных бурь 12 вызвано приходом к Земле сжатой части областей взаимодействия разноскоростных потоков и только в одном событии, **11.05.2019** г., наблюдалось наложение вспышечных возмущений на коротярующее. Сравнение с результатами аналогичных данных 2016 и 2017 г. показывает существование коротярующих возмущений с временем жизни по крайней мере несколько оборотов Солнца. Подтвержден вывод о том, что за 3–4 сут до прихода сжатой части возмущения к Земле начинается ослабление вечерних и ночных мерцаний, которое может быть интерпретировано как существенное понижение уровня

мелкомасштабной турбулентности плазмы в протяженной области перед фронтальной частью возмущения. Ослабление секундных мерцаний в вечернем секторе длительностью 2–3 сут может рассматриваться как предвестник приближения к Земле коротирующего возмущения. Как и в 2016–2017 гг., одновременно с магнитной бурей происходит усиление секундных мерцаний, которое наиболее четко фиксируется, если буря происходит в вечерние или ночные часы.

КОРОТИРУЮЩИЕ И РАСПРОСТРАНЯЮЩИЕСЯ ВОЗМУЩЕНИЯ В СОЛНЕЧНОМ ВЕТРЕ ПО ДАННЫМ МОНИТОРИНГА МЕЖПЛАНЕТНЫХ МЕРЦАНИЙ НА РАДИОТЕЛЕСКОПЕ БСА ФИАН В 2017 Г

И. В. **Чашей**, Т. О. Лебедева, С. А. Тюльбашев, И. А. Субаев

[АСТРОНОМИЧЕСКИЙ ЖУРНАЛ](#) Том: 97 Номер: 1 Год: 2020 Страницы: 73–88

По данным мониторинга межпланетных мерцаний 2017 г. проведен анализ динамики уровня мерцаний в периоды, предшествующие приходу к Земле восьми крупномасштабных возмущений солнечного ветра, вызвавших сильные геомагнитные бури. Для шести событий из восьми динамика уровня мерцаний, в основном, определялась перемещением коротирующих возмущений. В двух событиях на фоне коротирующих возмущений наблюдались выбросы корональной массы, возбуждавшиеся в короне вблизи западного лимба Солнца. В одном из этих случаев магнитная буря была связана с коротирующим потоком, в другом – с мощным распространяющимся возмущением. Сравнение с результатами аналогичных данных 2016 г., также относящимися к фазе спада солнечной активности, показывает существование коротирующих возмущений с временем жизни не менее 20 оборотов Солнца. Подтвержден вывод о том, что за 3–4 дня до прихода сжатой части возмущения к Земле в вечернем секторе начинается ослабление мерцаний, которое может быть интерпретировано как существенное понижение уровня мелкомасштабной турбулентности плазмы в протяженной области перед фронтальной частью возмущения...

ЗАВИСИМОСТЬ ХАРАКТЕРИСТИК ФОРБУШ-ПОНИЖЕНИЙ ОТ ПАРАМЕТРОВ СОЛНЕЧНЫХ ЭРУПЦИЙ

И. М. **Черток**¹, А. А. Абуни¹, А. В. Белов¹, В. В. Гречнев²

ИЗВЕСТИЯ РАН. СЕРИЯ ФИЗИЧЕСКАЯ, 2013, том 77, № 5, с. 615–617

Проанализированы соотношения между характеристиками расширенного ансамбля форбуш-понижений (ФП), вызванных корональными выбросами (СМЕs) из центральной зоны солнечного диска в течение 23-го солнечного цикла, с одной стороны, и суммарным магнитным потоком диммингов и аркад, сопровождающих СМЕs, – с другой. Показано, что имеет место отчетливая прямая корреляция этого магнитного потока с величиной ФП, а также его тесная обратная корреляция с временем распространения межпланетных возмущений от Солнца до Земли. Обнаруженные корреляции свидетельствуют о том, что основные характеристики крупных нерекуррентных ФП (и геомагнитных бурь) в значительной мере определяются измеряемыми параметрами солнечных эрупций, в частности таким, как суммарный магнитный поток диммингов и аркад.

ЗАВИСИМОСТЬ ВЕЛИЧИНЫ ФОРБУШ-ПОНИЖЕНИЙ ОТ ПАРАМЕТРОВ СОЛНЕЧНЫХ ЭРУПЦИЙ

И. М. **Черток**¹, А. В. Белов¹, В. В. Гречнев²

ИЗВЕСТИЯ РАН. СЕРИЯ ФИЗИЧЕСКАЯ, 2011, том 75, № 5, с. 845–847

По материалам 23-го солнечного цикла показано, что имеет место тесная статистическая связь между количественными параметрами диммингов и аркад, вызываемых солнечными корональными выбросами (СМЕs), с одной стороны, и величиной нерекуррентных форбуш-понижений потока галактических космических лучей, а также временем распространения межпланетных возмущений от Солнца до Земли – с другой. Параметры диммингов и аркад, в частности их суммарный магнитный поток продольного поля на уровне фотосферы, определялись по данным телескопа крайнего ультрафиолетового диапазона SOHO/EIT в канале 195 Е и магнитограммам SOHO/MDI. Полученные результаты означают, что характеристики и время распространения межпланетных возмущений до Земли в значительной мере определяются измеряемыми параметрами солнечных эрупций и могут оцениваться заблаговременно по наблюдениям диммингов и аркад в крайнем УФ-диапазоне.

МОНИТОРИНГ ТУРБУЛЕНТНОГО СОЛНЕЧНОГО ВЕТРА НА МОДЕРНИЗИРОВАННОМ РАДИОТЕЛЕСКОПЕ БСА ФИАН: ПЕРВЫЕ РЕЗУЛЬТАТЫ

ШИШОВ В.И.1, ЧАШЕЙ И.В.1, ОРЕШКО В.В.1, ЛОГВИНЕНКО С.В.1, ТЮЛЬБАШЕВ С.А.1, СУБАЕВ И.А.1, СВИДСКИЙ П.М.2, ЛАПШИН В.Б.2, ДАГКЕСАМАНСКИЙ Р.Д.1
АСТРОНОМИЧЕСКИЙ ЖУРНАЛ, 2016, том 93, №12, с. 1045–1060

Кратко описаны конструктивные особенности и технические характеристики модернизированного радиотелескопа БСА ФИАН. Представлены результаты годичного цикла наблюдений межпланетных мерцаний радиоисточников на радиотелескопе БСА ФИАН с новой 96 лучевой диаграммой направленности ДН 3. В течение суток наблюдались около 5000 радиоисточников, показывающих обусловленные межпланетными мерцаниями секундные флуктуации потока излучения. Поскольку в настоящее время параметры многих из этих радиоисточников неизвестны, в качестве характеристики уровня мерцаний использовалось число источников со среднеквадратичными флуктуациями потока больше 0.2 Ян, регистрируемых в площадке неба $3^\circ \times 3^\circ$. Полученные наблюдательные данные, относящиеся к периоду максимума 24-го цикла солнечной активности, могут быть интерпретированы в рамках трехкомпонентной модели пространственной структуры солнечного ветра, состоящей из стабильного глобального компонента, распространяющихся возмущений и коротирующих структур. Глобальный компонент соответствует сферически-симметричной структуре распределения межпланетной турбулентной плазмы. На фоне глобальной структуры наблюдаются распространяющиеся от Солнца возмущения. Распространяющиеся возмущения, регистрируемые в области гелиоцентрических расстояний 0.4–1 а.е. и на всех гелиоширотах, достигают орбиты Земли через 1–2 дня после усиления мерцаний. При этом в ночное время наблюдаются усиления ионосферных мерцаний. Коротирующие возмущения имеют период повторения 27d. При приближении коронального основания коротирующей структуры к западному краю солнечного лимба наблюдаются возмущения ионосферы.

ЭМПИРИЧЕСКАЯ МОДЕЛЬ ОЦЕНКИ СКОРОСТЕЙ И ЗАПАЗДЫВАНИЙ МЕЖПЛАНЕТНЫХ КОРОНАЛЬНЫХ ВЫБРОСОВ МАССЫ

Шлык Н.С., Белов А.В., Абунина М.А., Абунин А.А.

ГИА Том: 63 Номер: 5 Год: 2023 Страницы: 599-608

Исследуется поведение скорости межпланетных корональных выбросов массы в зависимости от гелиодолготы источника (ассоциированной солнечной вспышки), начальной скорости выброса и скорости фонового солнечного ветра. В основе моделирования лежат данные о 364 выбросах солнечного вещества, сопровождавшихся вспышками и наблюдавшихся в коронографе SOHO/LASCO, межпланетные аналоги которых были впоследствии зарегистрированы у Земли в период с 1995 по 2021 гг. Описана модель, позволяющая оценивать транзитную и максимальную скорости соответствующего межпланетного возмущения, а также время его прибытия к Земле. Средняя абсолютная ошибка оценки времени распространения межпланетных корональных выбросов массы для рассмотренных 364 событий составляет 11.5 ч, а средняя относительная ошибка – 16.5%.

ФОРБУШ-ЭФФЕКТЫ, НАБЛЮДАВШИЕСЯ НА КОСМИЧЕСКИХ АППАРАТАХ МИССИИ HELIOS

Шлык Н.С., Белов А.В., Абунина М.А., Абунин А.А., Papaioannou A.

Г и А Том: 62 Номер: 4 Год: 2022 Страницы: 456-463

Выделены и исследованы Форбуш-эффекты на основе данных космических аппаратов Helios A и B, функционировавших в период с декабря 1974 по февраль 1986 гг. Составлен подробный каталог 1166 Форбуш-эффектов – Helios FD, включающий в себя характеристики космических лучей, солнечного ветра, межпланетного магнитного поля и вызвавших их межпланетных возмущений. Исследованы количество, амплитуда Форбуш-эффектов, скорость и протонная температура солнечного ветра, величина межпланетного магнитного поля на разных расстояниях от Солнца. Произведено сравнение Форбуш-эффектов, которые были зарегистрированы и космическими аппаратами Helios, и сетью нейтронных мониторов на Земле. Установлено, что величина Форбуш-эффектов определяется характеристиками межпланетных возмущений и почти не зависит от радиального расстояния от Солнца.

ВЛИЯНИЕ ВЗАИМОДЕЙСТВУЮЩИХ ВОЗМУЩЕНИЙ СОЛНЕЧНОГО ВЕТРА НА ВАРИАЦИИ ГАЛАКТИЧЕСКИХ КОСМИЧЕСКИХ ЛУЧЕЙ

Шлык Н. С., Белов А. В., Абунина М. А., Ерошенко Е. А., Абунин А. А., Оленева В. А., Янке В. Г.

ГЕОМАГНЕТИЗМ И АЭРОНОМИЯ Том: 61 Номер: 6 Год: 2021 Страницы: 694-703

DOI: [10.31857/S0016794021060134](https://doi.org/10.31857/S0016794021060134)

На основе базы данных Форбуш-эффектов и межпланетных возмущений, созданной в Институте земного магнетизма, ионосферы и распространения радиоволн, представлен анализ вариаций галактических космических лучей и изменения различных характеристик Форбуш-эффектов, связанных с влиянием на Землю взаимодействующих возмущений солнечного ветра (возмущения, временной интервал между регистрацией которых составляет менее 50 ч). Рассмотрены случаи парного взаимодействия высокоскоростных потоков из корональных дыр и корональных выбросов массы за 1995–2019 гг., приведен

анализ поведения параметров солнечного ветра, межпланетного магнитного поля и вариаций космических лучей для двух типов взаимодействующих возмущений солнечного ветра (взаимодействие следующих друг за другом корональных выбросов массы и взаимодействие коронального выброса массы с высокоскоростным потоком из корональной дыры). Установлено, что для первых из пары взаимодействующих событий уменьшаются средние времена наступления минимума Форбуш-эффекта и регистрации максимума скорости солнечного ветра и модуля индукции межпланетного магнитного поля, т.е. вторые события из пары не дают полностью развиться первым. Также установлено, что наличие взаимодействия обогащает второе событие за счет ресурсов первого, увеличивая его геомагнитную эффективность и степень модуляции космических лучей в сравнении с изолированными событиями.

ПРОГНОЗ КВАЗИСТАЦИОНАРНЫХ И ТРАНЗИЕНТНЫХ ПОТОКОВ СОЛНЕЧНОГО ВЕТРА ПО ДАННЫМ НАБЛЮДЕНИЙ СОЛНЦА В 2010 Г.

ШУГАЙ Ю.С.^{✉1}, КАПОРЦЕВА К.Б.*

Ги А Том: 61Номер: 2 Год: 2021 Страницы: 148-159

В работе представлены результаты прогноза скорости квазистационарных и транзитных потоков солнечного ветра за период с мая по декабрь 2010 года. Скорость квазистационарных потоков солнечного ветра на околоземной орбите рассчитывались с помощью эмпирической модели на основе анализа изображений солнечной короны, полученных в вакуумном ультрафиолете. Скорость и время прихода межпланетных корональных выбросов масс прогнозировались *Drag Based*-моделью. Результаты прогноза скорости квазистационарных потоков солнечного ветра использовались в качестве параметра среды, по которой распространяются и с которой взаимодействуют транзитные потоки. За период май–декабрь 2010 года было отобрано 94 корональных выброса масс из баз данных, пополняющихся в режиме близком к реальному времени. Анализ результатов прогноза показал, что у 67% из отобранных межпланетных корональных выбросов масс спрогнозированная скорость была менее 400 км/с, а 96% из них связаны со спокойной геомагнитной обстановкой ($Dst > -30$ нТл). Добавление прогноза межпланетных корональных выбросов масс к прогнозу квазистационарных потоков солнечного ветра улучшает качество прогноза. За период с мая по декабрь 2010 года среднеквадратичное отклонение между измеренными на космическом аппарате *ACE* и спрогнозированными скоростями потоков солнечного ветра с учетом как квазистационарных, так и транзитных потоков, получено равным 82 км/с, а коэффициент корреляции – 0.6.

ОСОБЕННОСТИ ПОТОКОВ СОЛНЕЧНОГО ВЕТРА В ПЕРИОД 21-28 ИЮНЯ 2015 Г. КАК РЕЗУЛЬТАТ ВЗАИМОДЕЙСТВИЯ КОРОНАЛЬНЫХ ВЫБРОСОВ МАССЫ И РЕКУРРЕНТНЫХ ПОТОКОВ ИЗ КОРОНАЛЬНЫХ ДЫР

ШУГАЙ Ю.С.^{✉1}, СЛЕМЗИН В.А.², РОДЬКИН Д.Г.²

Косм. Исслед. Том: 55Номер: 6 Год: 2017 Страницы: 399-406

В работе рассмотрены корональные источники и параметры потоков солнечного ветра во время сильного и продолжительного геомагнитного возмущения в июне 2015 года. Соответствие между корональными источниками и потоками солнечного ветра на 1 а.е. определялось на основе анализа изображений Солнца, существующих каталогов вспышек, корональных выбросов масс и параметров солнечного ветра, включая ионный состав. Источниками возмущений в рассматриваемый период была последовательность из пяти корональных выбросов масс, которые распространялись по рекуррентным потокам солнечного ветра, связанными с корональными дырами. Наблюдаемые отличия от типичных в магнитных и кинетических параметрах потоков солнечного ветра были связаны с взаимодействием разных типов солнечного ветра. Ионный состав показал себя хорошим дополнительным маркером для выделения компонент в смеси потоков СВ, которые могут быть связаны с разными корональными источниками.

ВАРИАЦИИ КОСМИЧЕСКИХ ЛУЧЕЙ РАЗНОЙ ЭНЕРГИИ В МИНИМУМАХ ЦИКЛОВ СОЛНЕЧНОЙ АКТИВНОСТИ

Янке В.Г., Белов А.В., Гущина Р.Т.

Ги А Том: 62Номер: 4 Год: 2022 Страницы: 426-435

Изменения глобального магнитного поля Солнца – основного параметра, модулирующего космические лучи приводят к изменениям характеристик солнечной активности и гелиосферного поля. В работе рассмотрен вопрос об отклике на длительное ослабление глобального магнитного поля Солнца в долговременной модуляции космических лучей разной энергии в циклах с разным направлением полярного магнитного поля Солнца. Проанализирован период 1991–2020 гг., включающий два интервала с положительным и отрицательным направлениями глобального магнитного поля Солнца. Исследование выполнено на материале непрерывных наблюдений космических лучей сетью нейтронных мониторов, телескопов и стратосферных шаров-зондов. Спектр вариаций для частиц с эффективной жесткостью $R_{eff} = 5, 10, 20$ ГВ определен с помощью разработанного нами варианта метода глобальной съемки. В минимуме 24/25 цикла, начиная с 2018 г. до настоящего времени, наблюдается плоский максимум потока космических лучей, что подтверждает дрейфовую теорию модуляции для положительного направления глобального магнитного поля на Солнце. В этот период вариации малых энергий (наблюдаемые на космических

аппаратах и в стратосфере) превышают значение вариаций базового периода (1987 г.) на ~8% и составляют 0.8 от максимальной вариации в аномальном минимуме 23/24 в 2009 г. Максимум потока частиц средних и высоких энергий, наблюдаемых на нейтронных мониторах и телескопах, на 1–2% ниже максимума 23/24. Пониманию процесса модуляции космических лучей электромагнитными полями гелиосферы способствует их моделирование. В предложенной нами многопараметрической модели долгопериодная модуляция описывается (с учетом запаздывания) рядом гелиосферных характеристик.